

3  
2  
1969  
Sci

# physics abstracts

116/72

U. of ILL. LIBRARY

AUG 21 1972

CHICAGO CIRCLE

An INSPEC Publication  
The Institution of  
Electrical Engineers



Digitized by the Internet Archive  
in 2025

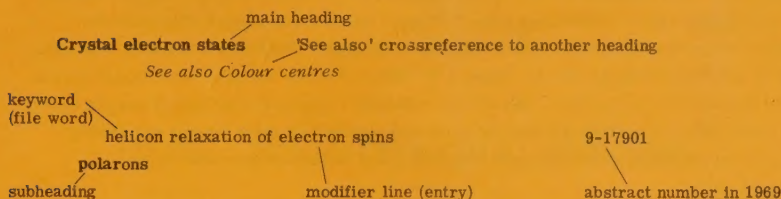


# SUBJECT INDEX—PART I

## INTRODUCTION

The entries in this index refer to the abstracts by their serial number, not by the page number. The entries are grouped under headings (printed in bold type, e.g. "**Algebra**"). If a heading for a particular subject does not appear, the subject may be in the form of a cross-reference to another heading, perhaps of a more general nature. Many of the headings are subdivided by the use of subheadings, which are indented (i.e. printed slightly to the right) and commence with a small letter.

The information contained in the subject index is illustrated by following example:



Associated with the subheading "polarons" is a 'See' crossreference as follows:

**Polarons** See *Crystal electron states/polarons*

This means that for papers on "polarons" the reader should consult the subheading "polarons" of "Crystal electron states" as displayed above.

## ARRANGEMENT OF HEADINGS AND SUBHEADINGS

The headings and crossreferences are arranged throughout the index in alphabetical order according to the "word by word" system. The subheadings are themselves arranged in alphabetical order under their respective headings.

## ARRANGEMENT OF ENTRIES UNDER HEADINGS

Entries are arranged in four distinct groups as follows:

- First group: arabic numerals
- Second group: English alphabet (A-Z), roman numerals, Greek alphabet (excluding elementary particles)
- Third group: elementary particle symbols i.e. Greek and English alphabet e.g.  $\mu$  (muon), p (proton)
- Fourth group: chemical formulae (including entries beginning with nuclei, e.g.  $^{57}\text{Fe}$ )

## CLASSIFIED LIST OF SUBJECT INDEX HEADINGS

In this list the headings are not arranged in alphabetical order, but are grouped into sections by subject, on the same basis as the arrangement in the fortnightly issues of Physics Abstracts. By using this list the reader can quickly determine all the headings which are appropriate to his subject, and then they can easily be found in the main index in their alphabetical position.

## HEADINGS WITH NO ENTRIES

All the headings in current use in a given year are printed, even those for which there are no abstracts to be recorded. The latter are followed by the announcement "No entries". This confirms that these headings have not been dropped from the index, and entries may appear under them in subsequent issues.

## NUCLEI, ELEMENTS, COMPOUNDS AND OTHER SUBSTANCES

Abstracts on nuclei whose mass number (or mass number range) is given are listed under a set of headings which begin "Nuclei with. . . ." e.g. Nuclei with  $6 \leq A \leq 19$  where A is the mass number.

The names of elements, their compounds, a few compounds of special interest (e.g. "Ruby", "Water") and a few common materials (e.g. "Wood", "Paper") are included as headings or sub-headings (e.g. "barium titanate" under "Barium compounds"). Under these, as well as under the appropriate "subject" headings, are listed any abstracts which contain significant physical information about the element, compound or substance named.

Inorganic compounds of the elements are listed under the first element in the chemical formula, and all the compounds of a given element are grouped under a single heading (e.g. "Sodium compounds"). Alloys are listed under compounds of the named constituents e.g. Au-Ag alloys under "Gold compounds" and "Silver compounds". There are also four special headings for the common alloys: "Aluminium alloys", "Copper alloys", "Iron alloys", "Nickel alloys". Organic compounds are grouped under "Organic compounds", "Polymers", "Plastics" and under special substance headings such as "Paper", "Proteins", etc.; all the latter are listed at the end of the classified list of headings. Metallic co-ordination compounds when regarded as inorganic are listed under the appropriate metallic compound heading (not under organic compounds) e.g. Ni complex, bis(dimethylglyoximate)nickel(II) under "Nickel compounds"

## CLASSIFIED LIST OF SUBJECT INDEX HEADINGS

The headings are grouped into sections on the same basis as the arrangement of the abstracts in the fortnightly issues of Physics Abstracts. A summary of the layout of these sections (these are actually further subdivided), is given below. Each section lists the headings which concern its subject and it follows that many of the headings are listed in several places.

### SUBJECT SECTIONS

- 01.00 GENERAL
- 02.00 MATHEMATICAL PHYSICS
- 03.00 MECHANICS. ELASTICITY. VIBRATION.ACOUSTICS
- 04.00 HEAT. THERMODYNAMICS
- 05.00 ELECTROMAGNETISM
- 06.00 ELECTRODYNAMICS & PARTICLE OPTICS
- 07.00 QUANTUM ELECTRONICS. QUANTUM OPTICS
- 08.00 OPTICS
- 09.00 QUANTUM FIELD THEORY
- 10.00 ELEMENTARY PARTICLES
- 11.00 ELEMENTARY PARTICLE & NUCLEAR MEASUREMENT
- 12.00 NUCLEAR PHYSICS
- 13.00 ATOMIC & MOLECULAR PHYSICS
- 14.00 FLUIDS
- 15.00 CHANGE OF STATE
- 16.00 SOLID-STATE STRUCTURE & MECHANICAL PROPERTIES
- 17.00 SOLID-STATE ELECTRICAL & MAGNETIC PROPERTIES
- 18.00 SOLID-STATE SPECTROSCOPY & OPTICAL PROPERTIES
- 19.00 PHYSICAL CHEMISTRY
- 20.00 GEOPHYSICS
- 21.00 ASTROPHYSICS
- 22.00 BIOPHYSICS
- 23.00 LABORATORY & EXPERIMENTAL TECHNIQUES



# 01.00 GENERAL

Biographies  
Collections of physical data  
History

Laboratories  
Laboratory apparatus and technique

Nomenclature and symbols  
Physics

Physics fundamentals  
Reviews

## 01.10 EDUCATION

Biographies  
History  
Laboratories

Laboratory apparatus and technique  
Physics

Physics fundamentals  
Reviews  
Teaching demonstrations

## 01.20 UNITS. MEASUREMENT AND METROLOGY

Acceleration measurement  
Anemometers  
Angle measurement  
Angular velocity measurement  
Area measurement  
Balances  
Constants  
Density measurement

Dimensions  
Force measurement  
Instruments  
Interferometry  
Length measurement  
Manometers  
Measurement errors  
Mechanical measurement

Micrometry  
Nomenclature and symbols  
Particle size  
Pressure measurement  
Recording  
Standards  
Strain gauges  
Stroboscopes

Surface measurement  
Thickness measurement  
Time interval measurement  
Time measurement  
Units  
Vapour pressure measurement  
Velocity measurement  
Volume measurement

# 02.00 MATHEMATICAL PHYSICS

Algebra  
Differential equations  
Equations  
Field theory, classical  
Fluctuations  
Fourier analysis  
Functions

Geometry  
Green's function methods  
Group theory  
Hysteresis  
Information theory  
Integral equations  
Integrals

Mathematics  
Matrices  
Probability  
Radiation  
Relaxation  
Series  
Space-time configurations

Statistical analysis/applications  
Tensors  
Transformations, mathematical  
Vectors  
Waves

## 02.10 GRAVITATION AND RELATIVITY

Gravitation  
Gravitational waves

Relativity/  
general  
special  
unified field theories  
Space-time configurations

## 02.20 QUANTUM THEORY

Collision processes  
Dispersion relations  
Indeterminacy  
Parity  
Quantum electrodynamics

Quantum theory/  
application methods  
quantization  
wave equations  
Scattering

## 02.30 STATISTICAL PHYSICS

Brownian motion  
Electron gas  
Fluctuations  
Hysteresis  
Information theory  
Kinetic theory

Lattices, theory and statistics  
Many-body problems  
Probability  
Quantum fluids/  
boson systems  
fermion systems

Quantum theory  
Radiation  
Radiative transfer  
Random processes  
Relaxation  
Statistical analysis/

applications  
Statistical mechanics/  
quantum  
Thermodynamics  
Transport processes

## 02.40 MATHEMATICAL METHODS

Calculation  
Graphs  
Nomograms

Statistical analysis  
applications  
Tables, mathematical

# 03.00 MECHANICS. ELASTICITY. VIBRATION. ACOUSTICS

Oscillations  
Vibrations  
Waves

## 03.10 MECHANICS

Ballistics  
Centrifuges  
Dynamics  
Friction  
Gravitation  
Gyroscopes  
Impact  
Kinematics

Mechanics  
Pendulums  
Pressure  
Rockets  
Rotating bodies  
Torsion  
Velocity

## 03.15 RHEOLOGY, ELASTICITY AND PLASTICITY

Bending  
Compressibility  
Damping  
Deformation  
Elastic deformation  
Elasticity  
Photoelasticity  
Plastic deformation

Plasticity  
Relaxation  
Rheology  
Stress analysis  
Stresses, internal  
Thermoelasticity  
Viscoelasticity

## 03.30 VIBRATIONS AND ELASTIC WAVES

Damping  
Elastic waves  
Magnetoelastic waves  
Membranes

Oscillations  
Piezoelectric oscillations  
Relaxation  
Resonators

Seismic waves  
Shock waves/  
effects  
Vibrating bodies

Vibrations/  
excitation  
measurement  
Waves

## 03.40 ACOUSTICS

Absorption/  
acoustic waves  
acoustic waves, ultrasonic  
Acoustic analysis  
Acoustic generators  
Acoustic impedance  
Acoustic radiators  
Acoustic receivers  
Acoustic resonators  
Acoustic streaming  
Acoustic wave propagation/  
ultrasonic  
Acoustic waves/  
effects  
Acoustical laboratories  
Acoustical measurement  
Acoustics/  
musical  
Acoustoelectric effects  
Architectural acoustics

Atmospheric acoustics  
Biological effects of radiations  
Chemical effects of radiations/  
acoustic waves  
Diffraction/  
acoustic waves  
acoustic waves, ultrasonic  
Diffusion/  
acoustic waves  
Dispersion, acoustic/  
ultrasonic  
Doppler effect  
Echo  
Helium/  
liquid, sound propagation  
Holography  
Intensity measurement/  
acoustics  
Interference/  
acoustic waves

Interferometers/  
acoustic waves  
Interferometry/  
acoustic waves  
Magnetoacoustic effects  
Microphones  
Musical instruments  
Noise/  
acoustic  
Noise abatement  
Physical effects of radiations  
Radiation pressure  
Recording  
Reflection/  
acoustic waves  
acoustic waves, ultrasonic  
Refraction/  
acoustic waves  
acoustic waves, ultrasonic  
Reverberation

Scattering/  
acoustic waves  
acoustic waves, ultrasonic  
Schlieren systems  
Sound ranging  
Sound reproduction  
Speech  
Stroboscopes  
Transducers  
Transmission/  
acoustic waves  
acoustic waves, ultrasonic  
Ultrasonics  
Velocity/  
acoustic waves  
acoustic waves, ultrasonic  
Velocity measurement/  
acoustic waves  
acoustic waves, ultrasonic

## 03.50 SHOCK WAVES

Detonation  
Explosions/  
nuclear

Schlieren systems  
Shock tubes  
Shock waves/  
effects  
Supersonic flow

## 04.00 HEAT AND THERMODYNAMICS

Bolometers  
Calorimeters  
Calorimetry  
Combustion  
Conductivity, thermal  
Convection  
Cooling  
Emissivity  
Entropy/  
properties of substances

Equations of state/  
gases  
liquids  
solids  
Flames  
Heat  
Heat conduction  
Heat transfer  
Heat treatment  
Heating

High-temperature phenomena  
and effects  
Joule-Thomson effect  
Latent heat  
Pyrometers  
Radiation/  
heat  
Radiation detectors  
Radiation pressure  
Radiation transfer  
Specific heat  
Temperature

Temperature distribution  
Temperature measurement/  
spectral methods  
Thermal expansion  
Thermal measurement  
Thermocouples  
Thermodynamic properties  
Thermodynamics/  
applications  
Thermometers/  
resistance  
Thermostats

## 05.00 ELECTROMAGNETISM

Eddy-currents  
Electromagnetism  
Electromagnetic fields  
Electromotive force  
Inductance

### 05.10 ELECTROMAGNETIC WAVES AND OSCILLATIONS

Absorption/  
electromagnetic waves  
Amplifiers  
Diffraction/  
electromagnetic waves  
Diffusion/  
electromagnetic waves  
Doppler effect  
Electromagnetic oscillations

Electromagnetic wave propaga-  
tion/  
atmosphere  
ionosphere  
guided waves  
Electromagnetic waves/  
radiators  
Interference/  
electromagnetic waves

Interferometers/  
electromagnetic waves  
Interferometry/  
electromagnetic waves  
Light/  
electromagnetic theory  
Microwave techniques and  
devices

Plasma/  
electromagnetic wave propa-  
gation  
Radiation  
Reflection/  
electromagnetic waves  
Refraction/  
electromagnetic waves  
Scattering/  
electromagnetic waves

### 05.20 RADIOFREQUENCY SPECTROSCOPY. MAGNETIC RESONANCES

Antiferromagnetic resonance  
Cyclotron resonance  
Ferrimagnetic resonance  
Ferromagnetic relaxation  
Ferromagnetic resonance

Magnetic resonance and relaxa-  
tion  
Nuclear magnetic resonance and  
relaxation/  
measurement

Nuclear quadrupole resonance  
Paramagnetic resonance and  
relaxation/  
measurement

Spectra  
Spectrometers, radio frequency  
Spectroscopy, radio frequency



## 05.30 ELECTRICAL QUANTITIES AND THEIR MEASUREMENT. CIRCUITS

Acoustoelectric effects	Electric fields/ effects	Ferroelectric phenomena	Piezoelectric oscillations
Amplifiers	Electric strength	Fluctuations	Piezoelectricity
Breakdown, electric	Electrical machines	Hall effect	Piezoresistance
Circuits	Electrical measurement	High-voltage techniques	Plasma/ diagnostics
Conductivity, electrical/ measurement	Electrical properties of sub- stances	Hysteresis	Pyroelectricity
Contacts, electrical	Electrokinetic effects	Image converters and amplifiers	Rectifiers
Counting circuits	Electroluminescence	Inductance	Relaxation
Current, electrical	Electromotive force	Magnetolectric effects	Semiconductors
Dielectric devices	Electron gas	Magnetoresistance	Skin effect
Dielectric measurement	Electrons	Noise, electrical	Space charge
Dielectric phenomena	Electro-optical effects	Oscillators	Superconductivity
Eddy-currents	Electrophoresis	Photoconductivity	Thermocouples
Electrets	Electrostatics	Photoelectricity	Thermoelectricity
Electric charge	Electrostriction	Photoelectromagnetic effects	Triboelectricity
		Photovoltaic effects	

## 05.35 DIRECT CONVERSION

Electricity, direct conversion/  
fuel cells  
magnetohydrodynamics  
solar cells  
thermionic

## 05.40 MAGNETISM

Antiferromagnetism	Gyromagnetic effect	Magnetic resonance and relaxa- tion	Magneto-optical effects
Compasses	Gyromagnetic ratio	Magnetism	Magnetoresistance
de Haas-van Alphen effect	Hall effect	Magnetization process	Magnetostriction
Diamagnetism	Magnetic devices	Magnetization state	Magnetothermal effects
Ferrimagnetism	Magnetic field measurement	Magnetoacoustic effects	Magnets
Ferromagnetism/ spin-wave theory	Magnetic fields/ effects	Magnetoelectric effects	Paramagnetism
Films, solid/ magnetic properties	Magnetic measurement	Magnetomechanical effects	Storage devices

## 06.00 ELECTRODYNAMICS AND PARTICLE OPTICS

Electrodynamics	Particle optics
Energy loss of particles	Particle velocity analysis
Particle beams	Scattering, particles

## 06.10 ELECTRON BEAMS, ELECTRON OPTICS AND TUBES

Electron beams/ effects	Electron microscopes	Electrons/ absorption	Fluctuations
Electron diffraction	Electron microscopy	ionization	Gas-discharge tubes
Electron gas	Electron optics	radiation	Image converters and amplifiers
Electron lenses/ electrostatic magnetic	Electron tubes	scattering	Noise, electrical
			Photomultipliers
			Space charge

## 06.20 ION BEAMS, ION OPTICS AND SOURCES

Ion beams/ effects	Ion velocity
Ion microscopes	Ions/ recombination
Ion optics	scattering
Ion sources	Sputtering

## 07.00 QUANTUM ELECTRONICS AND QUANTUM OPTICS

Light/  
coherence  
Optical pumping  
Photons  
Quantum optics

### 07.10 MASERS

Amplifiers  
Masers  
Optical pumping

### 07.20 LASERS

Amplifiers  
Lasers  
Light/  
coherence  
Optical pumping  
Resonators

### 07.23 Gas and Liquid Lasers

Amplifiers  
Lasers/  
gaseous  
liquid  
Light/  
coherence  
Optical pumping

## 07.25 Solid Lasers

Amplifiers  
Lasers/  
semiconductor  
solid

Light/  
coherence  
Optical pumping

## 07.27 Laser Beam Optics

Holography  
Laser beams/  
applications  
effects

Light/  
coherence  
modulation

## 08.00 OPTICS

Doppler effect  
Electro-optical effects  
Light/  
electromagnetic theory  
modulation

Light sources  
Nonlinear optics  
Optics

Photons  
Photophoresis  
Radiation

Radiation pressure  
Velocity/  
light  
Velocity measurement/  
light

## 08.10 GEOMETRICAL OPTICS

Aberrations, optical  
Dispersion, optical  
Lenses/  
aspherical  
photographic

Mirrors  
Optical images  
Optical systems  
Optics/  
geometrical

Prisms, optical  
Reflection/  
light  
Refraction/  
light

Refractive index/  
light  
Resolving power, optics  
Schlieren systems

## 08.20 PHYSICAL OPTICS

Absorption/  
light  
Diffraction/  
light  
Diffraction gratings  
Diffusion/  
light  
Dispersion, optical  
Doppler effect  
Double refraction/  
flow  
mechanical

Electro-optical effects  
Filters, optical  
Holography  
Interference/  
light  
Interferometers/  
light  
Interferometry/  
light  
Magneto-optical effects  
Optical constants  
Optical films

Optical pumping  
Optical rotation  
Photoelasticity  
Pleochroism  
Polarimeters  
Polarized light  
Reflection/  
light  
Reflectivity

Refraction/  
light  
Refractive index/  
light  
Scattering/  
light  
Transmission/  
light  
Transparency

## 08.30 PHOTOMETRY. CALORIMETRY

Bolometers  
Brightness  
Colorimetry  
Colour

Densitometry  
Emissivity  
Illumination

Photometers  
Photometry/  
light sources

Pyrometers  
Radiation detectors

## 08.40 INSTRUMENTAL OPTICS

Abberations, optical  
Dispersion, optical  
Fibres/  
optical  
Films/  
liquid  
Films, solid/  
optical properties  
Filters, optical  
Glass  
Image convertors and amplifiers

Lasers/  
gaseous  
solid  
Lenses/  
aspherical  
photographic  
Light sources  
Luminescent devices  
Microscopes  
Microscopy  
Mirrors

Optical constants  
Optical images  
Optical instrument testing  
Optical instruments  
Optical materials  
Optical systems  
Prisms, optical  
Projectors, optical  
Quartz  
Reflection/  
light

Refraction/  
light  
Refractive index/  
light  
Refractive index measurement  
Refractometers  
Resolving power, optics  
Schlieren systems  
Stroboscopes  
Telescopes

## 08.45 Spectroscopy

Astronomical spectra  
Atmospheric spectra  
Monochromators  
Spectral line breadth

Spectrochemical analysis  
Spectrometers/  
accessories  
Spectrophotometers

Spectrophotometry  
Spectroscopy/  
light sources  
Stark effect

Temperature measurement/  
spectral methods  
Zeeman effect

## 08.50 PHOTOGRAPHY

Cameras  
Cinematography  
Densitometry  
Lenses/  
photographic

Light sources  
Nuclear track emulsions  
Photographic materials/  
sensitivity

Photographic process/  
development  
Photography/  
applications  
colour  
high-speed  
Radiography



# 09.00 QUANTUM FIELD THEORY

Current algebra  
Dispersion relations  
Field theory, quantum/  
interactions  
interactions, strong  
interactions, weak  
meson field  
quantization  
scattering

Nuclear forces  
Parity  
Quantum electrodynamics  
Quantum theory/  
application methods  
quantization  
wave equations  
S-matrix theory  
Scattering

## 10.00 ELEMENTARY PARTICLES

Bosons  
Elementary particles  
Fermions

Gravitons  
Parity  
Energy loss of particles

Particle velocity analysis  
Quarks

Strange particles  
Synchrotron radiation

### 10.10 ELEMENTARY PARTICLE THEORY

Bosons  
Current algebra  
Dispersion relations

Elementary particles/  
interactions  
interactions, strong  
interactions, weak  
scattering  
symmetry  
theory

Fermions  
Nuclear forces  
Parity  
S-matrix theory  
Strange particles

### 10.20 PHOTONS, GAMMA-RAYS AND X-RAYS

Bremsstrahlung  
Cherenkov radiation  
Compton effect  
Gamma-ray spectrometers

Gamma-rays/  
absorption  
angular distribution  
detection, measurement  
effects  
scattering

Mössbauer effect  
Photons/  
interactions  
polarization  
scattering  
Synchrotron radiation

X-ray absorption  
X-ray diffraction  
X-ray measurement  
X-ray reflection  
X-ray scattering  
X-rays/  
effects

### 10.30 LEPTONS

Leptons

### 10.33 Neutrinos

Neutrinos and antineutrinos

### 10.35 Electrons

Beta-ray spectra/  
conversion electrons  
Beta-ray spectrometers  
Beta-rays/  
absorption  
angular distribution  
detection, measurement  
effects  
polarization  
scattering  
Electron pairs/  
annihilation  
production

Electron theory  
Electrons/  
absorption  
interactions  
ionization  
radiation  
scattering  
scattering, electron-proton  
Positronium  
Positrons  
Synchrotron radiation

### 10.45 Mesons

Mesons/  
absorption  
capture  
decay  
detection, measurement  
effects

Mesons/  
interactions  
magnetic moment  
mass  
production  
scattering  
spin and parity

### 10.46 Kaons

decay  
interactions

production  
scattering

### 10.47 Pions

Pions/  
decay  
interactions  
interactions, pion-nucleon  
interactions, pion-pion  
interactions, pion-proton

Pions/  
production  
scattering  
scattering, pion-nucleon  
scattering, pion-pion  
scattering, pion-proton

### 10.48 Meson Resonances

Mesons/  
resonances

### 10.51 Baryons

Baryons/  
interactions  
scattering

### 10.52 Nucleons

Nuclear forces  
Nucleons and antinucleons/  
antinucleons  
interactions  
interactions, nucleon-nucleon  
scattering  
scattering, nucleon-nucleon

### 10.40 HADRONS

Hadrons/  
current  
decay  
Quarks

### 10.41 Hadron interactions

Hadrons/  
interactions

### 10.42 Hadron scattering

Hadrons/  
scattering

## 10.53 Protons

Proton spectra  
Protons and antiprotons/  
absorption  
angular distribution  
antiprotons  
detection, measurement  
effects  
interactions  
interactions, proton-proton  
magnetic moment  
polarization  
production  
scattering  
scattering, proton-deuteron  
scattering, proton-proton

## 10.54 Neutrons

Neutron diffraction  
Neutron spectra  
Neutron spectrometers  
Neutrons and antineutrons/  
absorption  
angular distribution  
detection, measurement  
diffusion  
effects  
interactions  
moderation  
polarization  
production  
reflection  
scattering  
scattering, neutron-proton

## 10.56 Hyperons

Hypernuclei  
Hyperons/  
absorption  
capture  
decay  
detection, measurement  
effects  
interactions  
magnetic moment  
mass  
production  
resonances  
scattering  
spin and parity  
Strange particles

## 10.58 Baryon Resonances

Baryons/  
resonances  
Hyperons/  
resonances  
Nucleons

## 10.60 COMPOSITE PARTICLES

Composite particles

## 10.63 Deuterons

Deuterons/  
effects  
interactions  
photodisintegration  
polarization  
scattering

## 10.65 Tritons

Tritons/  
interactions  
scattering

## 10.67 Alpha-particles and He<sup>3</sup>

Alpha-particle spectrometers  
Alpha-particles/  
absorption  
angular distribution  
detection, measurement  
effects  
interactions  
scattering  
Helium-3  
interactions  
scattering

## 10.70 COSMIC RAYS

Cosmic rays/  
absorption  
apparatus  
composition  
alpha-particles and helium  
nuclei  
deuterons  
electrons  
mesons  
muons  
neutrinos  
neutrons  
nucleons  
photons  
protons  
X-rays

effects and interactions  
origin  
primary  
showers and bursts  
variation

## 11.00 ELEMENTARY PARTICLE AND NUCLEAR MEASUREMENT

### 11.10 APPARATUS, DETECTORS AND DETECTOR CIRCUITS

Alpha-particle spectrometers  
Amplifiers  
Beta-ray spectrometers  
Counters/  
accessories  
Cherenkov  
crystal  
Geiger  
operation technique  
proportional  
scintillation  
semiconductor  
spark  
statistical analysis

Counting circuits  
Dosimetry  
Gamma-ray spectrometers  
Ionization chambers  
Neutron spectrometers  
Nuclear bombardment targets  
Particle accelerators

Particle detectors  
Particle optics  
Particle spectrometers  
Particle velocity analysis  
Photomultipliers  
Radioactivity measurement/  
apparatus

### 11.15 Track Visualization

Bubble chambers  
Cloud chambers

Energy loss of particles  
Luminescence chambers

Nuclear track emulsions  
Particle tracks

Particle track visualization  
Spark chambers

### 11.20 PARTICLE ACCELERATORS

High-voltage techniques  
Ion sources

Particle accelerators/  
accessories  
betatrons  
cyclotrons  
linear  
synchrotrons



# 12.00 NUCLEAR PHYSICS

Nuclear physics

## 12.10 NUCLEAR STRUCTURE AND ENERGY LEVELS

Beta-ray spectra/ conversion electrons	Mössbauer effect	Nuclei with $A \leq 5$	Nucleus/ electric moment
Gamma-ray spectra	Nuclear excitation	Nuclei with $6 \leq A \leq 19$	energy level transitions
Gamma-rays/ angular distribution	Nuclear forces	Nuclei with $20 \leq A \leq 49$	energy levels
internal conversion	Nuclear isomerism	Nuclei with $50 \leq A \leq 89$	magnetic moment
Gyromagnetic ratio	Nuclear magnetic resonance and relaxation	Nuclei with $90 \leq A \leq 149$	models
Hypernuclei	Nuclear polarization	Nuclei with $150 \leq A$	size
			spin and parity theory

## 12.20 NUCLEAR DECAY AND RADIOACTIVITY

Alpha-particles	Beta-ray spectrometers	Dosimetry	Nuclear bombardment targets
Alpha-particle spectra	Beta-rays/ absorption	Fallout	Physical effects of radiations
Alpha-particle spectrometers	angular distribution	Gamma-ray spectra	Radiation monitoring
Alpha-particles/ absorption	detection, measurement	Gamma-ray spectrometers	Radiation protection
angular distribution	effects	Gamma-rays/ absorption	Radioactive dating
detection, measurement	polarization	angular distribution	Radioactive tracers
effects	scattering	detection, measurement	Radioactivity/ decay periods
scattering	Biological effects of radiations	effects	decay schemes
Beta-decay theory	Chemical effects of radiations/ ionizing radiations	internal conversion	electron capture
Beta-ray spectra/ conversion electrons		scattering	Radioactivity measurement/ apparatus
		Nuclear decay theory	Radiochemistry

## 12.30 NUCLEAR REACTIONS AND SCATTERING

Chemical analysis/ by nuclear reactions	Nuclear reactions and scattering due to/ alpha-particles	Nuclear spallation
Collision processes	cosmic rays	Nuclei with $A \leq 5$
Nuclear bombardment targets	deuterons	Nuclei with $6 \leq A \leq 19$
Nuclear excitation	electrons	Nuclei with $20 \leq A \leq 49$
Nuclear forces	helium-3	Nuclei with $50 \leq A \leq 89$
Nuclear reactions and scatter- ing/ chemical effects	hyperons	Nuclei with $90 \leq A \leq 149$
high energy $> 1\text{GeV}$	mesons	Nuclei with $150 \leq A$
	muons	Radiation monitoring
	neutrinos	Radiation protection
	neutrons	Scattering, particles
	nuclei of $Z > 2$	
	nucleons	
	photons	
	protons	
	tritons	

## 12.39 Nuclear fission and fusion

Explosions/ nuclear	Nuclear fission/ products uranium	Nuclear fusion	Plasma
		Nucleons	Thermonuclear reactions

## 12.40 NUCLEAR POWER STUDIES

### 12.43 Neutron Transport Theory

Neutrons and antineutrons/ absorption	Nuclear fission/ products
angular distribution	uranium
detection measurement	Nuclear fusion
diffusion	Nuclear reactions
effects	Thermonuclear reactions
interactions	
moderation	
polarization	
production	
reflection	
scattering	

### 12.47 Nuclear Reactors

Biological effects of radiations	Nuclear reactors, fission/ materials
Chemical analysis/ by nuclear reactions	operation
Chemical effects of radiations/ ionizing radiations	theory
Dosimetry	Nuclear reactors, fusion
Nuclear fission/ products	Physical effects of radiations
uranium	Plasma/ devices
Nuclear fusion	Radiation monitoring
Nuclear reactions/ chemical effects	Radiation protection
	Radiochemistry
	Thermonuclear reactions

## 13.00 ATOMIC AND MOLECULAR PHYSICS

Collision processes  
Orbital calculation methods  
Quantum theory

### 13.10 MASS SPECTROMETERS

Mass spectra	Mass spectrometers/ accessories applications
--------------	--

13.20 ATOMS

Atomic beams  
Atomic mass and weight  
Atoms  
  electron scattering  
  excitation  
  magnetic moment  
  structure  
Charge exchange  
Collision processes/  
  atoms

Electron emission  
  photoelectric  
Elements  
  origin  
  relative abundances  
Exchange interactions  
Gyromagnetic ratio  
Helium/  
  gas

Hydrogen/  
  ions  
  neutral atoms  
Ionization potential  
Luminescence  
  gases  
Optical pumping  
Orbital calculation methods  
Periodic system

Spectra  
  atoms  
Spectral line breadth  
Stark effect  
X-ray spectra  
  absorption  
  emission  
Zeeman effect

13.25 Isotopes

Isotope effects  
Isotope exchanges  
Isotope separation  
Isotopes  
  detection  
  relative abundances  
Mass spectra

Mass spectrometers/  
  applications  
Radioactive dating  
Radioactive tracers  
Radiochemistry  
Tracers

13.27 Mesic and Muonic Atoms

Atoms, mesic and muonic

13.30 MOLECULES

Bonds  
Chemical shift  
Chemical structure  
Exchange interactions  
Isomerism  
Jahn-Teller effect  
Luminescence/  
  gases  
Magnetic resonance and relaxa-  
  tion  
Molecular weight

Molecules/  
  configuration and dimensions  
  inorganic  
  organic  
  excitation  
  internal mechanics  
  electronic structure  
  electronic structure, inorganic  
  electronic structure, organic  
  nuclear coupling  
  relaxation  
  rotation  
  vibration  
  moments

Nuclear magnetic resonance and  
  relaxation  
Nuclear quadrupole resonance  
Optical pumping  
Orbital calculation methods  
Paramagnetic resonance and  
  relaxation  
Scattering/  
  light  
  light, Brillouin spectra  
  light, Raman spectra  
  light, Raman spectra, inorganic<sup>c</sup>  
  light, Raman spectra, organic

Spectra/  
  inorganic molecules  
  diatomic  
  diatomic, radiofrequency  
  polyatomic  
  polyatomic, radio-frequency  
  inorganic liquids and solutions  
  inorganic solids  
  radiofrequency  
  molecules  
  organic molecules and  
  substances  
  infrared  
  radiofrequency  
Spectral line breadth  
Stark effect  
Valency  
Zeeman effect

13.34 Dissociation. Free radicals

Association/  
  gases  
Free radicals  
Heat of dissociation

Molecules/  
  dissociation  
  dissociation energies

13.35 Macromolecules

Association  
Heat of formation  
Isomerism  
Macromolecules

Molecules/  
  configuration and dimensions,  
  macromolecules  
Polymers  
Proteins

13.36 Mesic and Muonic Molecules

Molecules, mesic and muonic

13.37 Intermolecular mechanics

Charge exchange  
Collision processes/  
  molecules

Molecular beams  
Molecules/  
  intermolecular mechanics

14.00 FLUIDS

Boundary layers  
Flow/  
  two-phase  
Fluids  
Hydrodynamics  
Hydrostatics

Oscillations  
Turbulence  
Viscosity  
Vortices  
Waves

14.10 MAGNETOHYDRODYNAMICS

Magnetohydrodynamics  
Shock waves/  
  effects  
Turbulence

14.20 PLASMA

Discharges, electric/  
  glows  
  high-frequency  
Nuclear fusion  
Nuclear reactors, fusion

Plasma/  
  collison processes  
  electromagnetic waves  
  magnetohydrodynamics  
  production  
  shock waves

Shock waves/  
  effects  
Space charge/  
  gas  
Thermonuclear reactions



## 14.24 Plasma Confinement, Devices and Measurements

Plasma/  
confinement  
devices  
diagnostics

## 14.26 Plasma Oscillations and Stability

Plasma/  
magnetohydrodynamics  
oscillations  
stability

## 14.30 IONIZATION

Charge exchange  
Dissociation  
Ion velocity  
Ionization/  
gases

Ionization potential  
Ionization, surface  
Ions/  
recombination  
scattering

Photoionization/  
gases  
Shock waves/  
effects  
Space charge/  
gas

## 14.40 ELECTRIC DISCHARGES

Arcs, electric  
Breakdown, electric/  
gases  
Corona, electric discharge

Discharges, electric/  
glows  
high frequency  
Gas-discharge tubes

Lightning  
Sparks, electric  
Sputtering

## 14.50 MECHANICS OF GASES

Acoustic streaming  
Aerodynamics  
Anemometers  
Compressibility/  
gases  
Condensation  
Density/  
gases

Diffusion in gases/  
thermal  
Flow/  
gases  
two-phase  
Flowmeters  
Gases  
Humidity

Hygrometers  
Jets  
Manometers  
Moisture  
Pressure  
Pumps  
Radiation pressure  
Supersonic flow

Turbulence  
Viscometers  
Viscosity/  
gases  
Vortices  
Waves

## 14.60 GASEOUS STATE

Absorption/  
acoustic waves  
acoustic waves, ultrasonic  
electromagnetic waves  
light  
Association/  
gases  
Breakdown, electric/  
gases  
Conductivity, electrical/  
gases  
measurement  
Conductivity, thermal/  
gases  
measurement  
Dielectric properties of sub-  
stances/  
gases  
Diffraction/  
acoustic waves  
acoustic waves, ultrasonic  
electromagnetic waves  
light

Diffusion/  
acoustic waves  
electromagnetic waves  
light  
Electrical properties of sub-  
stances  
Electroluminescence  
Equations of state/  
gases  
Gases  
Helium/  
gas  
Interference/  
acoustic waves  
Joule-Thomson effect  
Kinetic theory/  
gases  
Lasers/  
gaseous  
Luminescence/  
gases  
Magnetic resonance and relaxation

Molecules/  
intermolecular mechanics  
Nuclear magnetic resonance and  
relaxation  
Nuclear quadrupole resonance  
Optical properties of substances  
Paramagnetic resonance and  
relaxation  
Reflection/  
acoustic waves  
acoustic waves, ultrasonic  
electromagnetic waves  
light  
Refraction/  
acoustic waves  
acoustic waves, ultrasonic  
electromagnetic waves  
light  
Scattering/  
acoustic waves  
acoustic waves, ultrasonic  
electromagnetic waves  
light

Sorption  
Specific heat/  
gases  
Spectra  
Statistical mechanics  
Thermoluminescence  
Transmission/  
acoustic waves  
acoustic waves, ultrasonic  
light  
Velocity/  
acoustic waves  
acoustic waves, ultrasonic

## 14.65 Viscosity and Diffusion of Gases

Diffusion in gases/  
thermal

Transport processes  
Viscosity/  
gases

14.70 MECHANICS OF LIQUIDS

Acoustic streaming	Drops	Hydrodynamics	Schlieren systems
Bubbles	Elasticity/ liquids	Hydrostatics	Sprays
Capillarity	Emulsions	Jets	Surface energy
Cavitation	Films/ liquid	Liquid oscillations	Surface tension
Compressibility/ liquids	Filters	Liquid waves/ surface	Surface tension measurement
Density/ liquids	Flow/ liquids	Lubrication	Thixotropy
Diffusion in liquids thermal	two-phase	Moisture	Turbulence
Double refraction/ flow	Flowmeters	Pressure	Viscometers
	Foams	Pumps	Viscosity/ liquids
		Radiation pressure	Vortices
		Rheology	Wetting

14.80 LIQUID STATE

Liquids  
Liquid metals

14.82 Theory and Structure of Liquids and Solutions

Association/ liquids	Films/ liquid	Neutron diffraction examination of materials	Solutions
Electron diffraction examination of materials	Heat of solution	Neutrons and antineutrons/ scattering	X-ray examination of materials/ liquids
Equations of state/ liquids	Liquid crystals	Polymers	
	Liquids/ structure theory	Solubility	

14.83 Viscosity, Surface tension and Diffusion

Diffusion in liquids/ thermal	Membranes	Surface tension	Viscosity/ liquids
Filters	Osmosis	Surface tension measurement	
	Sorption	Transport processes	

14.85 Thermal properties of Liquids

Conductivity, thermal/ liquids measurement	Heat of solution	Thermal expansion
	Specific heat/ liquids	Thermodynamic properties

14.86 Acoustical Properties of Liquids

Absorption/ acoustic waves	Diffusion/ acoustic waves	Refraction/ acoustic waves	Transmission/ acoustic waves
acoustic waves, ultrasonic	Interference/ acoustic waves	acoustic waves, ultrasonic	acoustic waves, ultrasonic
Acoustic wave propagation/ ultrasonic	Reflection/ acoustic waves	Scattering/ acoustic waves	Velocity/ acoustic waves
Diffraction/ acoustic waves	acoustic waves, ultrasonic	acoustic waves, ultrasonic	acoustic waves, ultrasonic
acoustic waves, ultrasonic			

14.87 Optical Properties of Liquids

Absorption/ electromagnetic waves	Double refraction	Refraction/ electromagnetic waves	Spectra/ inorganic liquids and solutions
light	flow	light	Thermoluminescence
Chemical shift	Electroluminescence	Scattering/ electromagnetic waves	Transmission/ light
Diffraction/ electromagnetic waves	Luminescence/ liquids and solutions	light	
light	Optical pumping	light, Brillouin spectra	
Diffusion/ electromagnetic waves	Optical properties of substs.	light, Raman spectra	
light	Reflection/ electromagnetic waves	light, Raman spectra, inorganic	
	light	light, Raman spectra, organic	

14.88 Electrical and Magnetic properties of Liquids

Absorption/ electromagnetic waves	Dielectric properties of substs./ liquids and solutions	Metals
Breakdown, electric/ liquids	Electrical properties of substs.	Nuclear magnetic resonance and relaxation
Conductivity, electrical/ liquids	Ionization, liquids	Nuclear quadrupole resonance
liquids, electrolytic measurement	Liquid metals	Paramagnetic resonance and relaxation
	Magnetic properties of substs.	Semiconducting materials
	Magnetic resonance and relaxa- tion	Semiconductors



## 14.90 DISPERSIONS AND COLLOIDS

Aerosols  
Centrifuges  
Colloids  
Disperse systems  
Electrophoresis

Emulsions  
Filters  
Foams  
Gels  
Heat of solution

Membranes  
Osmosis  
Particle size  
Precipitation  
Sedimentation

Sols  
Solubility  
Solutions  
Surface phenomena  
Suspensions  
Thixotropy

## 14.95 LIQUID HELIUM

Helium/  
liquid  
liquid, sound propagation  
solid

Quantum fluids/  
boson systems  
fermion systems

## 15.00 CHANGE OF STATE

Boiling  
Boiling point  
Condensation  
Critical constants, thermal  
Distillation  
Drying

Equations of state  
gases  
liquids  
solids  
Evaporation  
Freezing  
Heat of fusion

Heat of sublimation  
Heat of transformation  
Heat of vaporization  
Humidity  
Liquefaction, gases  
Melting  
Melting point

Phase equilibrium  
Phase transformations  
Sublimation  
Supercooling  
Vapour pressure  
Vapour pressure measurement  
Vaporization

## 16.00 SOLID STATE STRUCTURE AND MECHANICAL PROPERTIES

Crystal properties  
Equations of state/  
solids

Solids/  
structure  
theory

### 16.10 NON-CRYSTALLINE STATE

Amorphous state  
Glass

Plastics  
Polymers

Rubber  
Vitreous state

Waxes

### 16.20 SURFACE AND INTERFACE PHENOMENA

Surface energy  
Surface measurement

Surface phenomena  
Surface structure

### 16.23 Films

Crystals/  
growth  
Epitaxy  
Evaporation

Films, solid/  
electrical properties  
magnetic properties  
optical properties  
Sputtering  
Sublimation

### 16.25 Adsorption

Adsorbed layers  
Adsorption

Heat of adsorption  
Sorption

### 16.30 CRYSTALLOGRAPHY

Bonds  
Charge compensation  
Crystal chemistry  
Crystal properties  
Crystallography

Crystals/  
etching  
faces  
orientation  
twinning

Isomorphism  
Minerals  
Polymorphism  
Solids/  
structure  
Surface structure

### 16.33 Crystal growth

Crystallization  
Crystals/  
growth  
whiskers

Epitaxy  
Zone melting and refining

16.35 Crystal Structures, Techniques and Apparatus

Alloys	Electron diffraction crystal-	Microscopy	X-ray crystallography/
Amorphous state	lography	Neutron diffraction crystal-	apparatus
Crystal structure/	Electron diffraction examination	lography	calculation apparatus
microstructure	of materials	Neutron diffraction examination	calculation methods
Crystal structure, atomic/	Electron microscope examination	of materials	technique
alloys	of materials	Particle size	X-ray diffraction
elements	Electron microscopy	Polymers	X-ray examination of materials
inorganic compounds	Fibres	Porous materials	microstructure
organic compounds	Granular structure	Powders	molecular structure
Density/	Ion microscopes	Radiography	X-ray measurement
solids	Metallurgy	Surface structure	X-ray monochromators
		X-ray absorption	X-ray reflection
			X-ray scattering
			X-ray tubes

16.40 DEFECT PROPERTIES OF SOLIDS

Cold working	Crystal structure	Electron microscope examina-	Plastic deformation
Creep	Crystals	tion of materials	Plastic flow
Crystal imperfections	etching	Heat treatment	Slip
dislocations	twinning	alloys	Stresses, internal
impurities	Deformation	Internal friction	Work hardening
interstitials	Elastic deformation	Neutron diffraction examination	X-ray examination of materials/
vacancies	Electron diffraction examination	of materials	microstructure
	of materials		

16.45 Colour centres

Absorption/	Colour centres
light	X-rays/
	effects

16.50 DIFFUSION IN SOLIDS

Diffusion in solids/	Permeability, mechanical
thermal	

16.60 MECHANICAL PROPERTIES OF SOLIDS

Abrasion	Elastic fatigue	Lubrication	Plasticity
Bending	Elastic limit	Magnetoelastic waves	Rheology
Brittleness	Elastic relaxation	Magnetomechanical effects	Slip
Compressibility	Elasticity	Mechanical properties of sub-	Strain gauges
Cracks	Fracture	stances	Stress analysis
Creep	Friction	Mechanical strength/	Stress effects
Deformation	Hardness	compressive	Stress/strain relations
Density/	High-pressure phenomena and	shear	Stresses, internal
solids	effects	tensile	Thermoelasticity
Elastic constants/	Hysteresis	Photoelasticity	Thixotropy
measurement	Impact	Plastic deformation	Torsion
Elastic deformation	Internal friction	Plastic flow	Viscoelasticity
			Wear

16.65 Metallurgy. Phase transformations

Adhesion	Forming processes	Phase transformations/	Precipitation
Ageing	Heat treatment/	solid-state	Sintering
Alloys	alloys	Physical effects of radiations	Solid solutions
Cold working	Metallurgy	Polymorphism	Solubility
Corrosion	Phase equilibrium	Powders	Work hardening

16.70 LATTICE MECHANICS

Crystals/	Mössbauer effect
lattice mechanics	

16.80 ACOUSTICAL PROPERTIES OF SOLIDS

Absorption/	Dispersion, acoustic/	Refraction/	Transducers
acoustic waves	ultrasonic	acoustic waves	Transmission/
acoustic waves, ultrasonic	Magnetoacoustic effects	acoustic waves, ultrasonic	acoustic waves
Acoustic wave propagation/	Reflection/	Scattering/	acoustic waves, ultrasonic
ultrasonic	acoustic waves	acoustic waves	Velocity/
Acoustoelectric effects	acoustic waves, ultrasonic	acoustic waves, ultrasonic	acoustic waves
Acousto-optical effects			acoustic waves, ultrasonic
Diffraction/			
acoustic waves			
acoustic waves, ultrasonic			

16.90 THERMAL PROPERTIES OF SOLIDS

Conductivity thermal/	Equations of state/	Specific heat/
measurement	solids	solids
solids	Heat conduction	Thermal expansion
		Thermodynamic properties



## 16.95 RADIATION INTERACTION WITH SOLIDS

Acoustic waves/ effects	Electron beams/ effects	Ion beams/ effects	Physical effects of radiations
Alpha-particles/ effects	Energy loss of particles	Mesons/ effects	Protons and antiprotons/ effects
Beta-rays/ effects	Gamma-rays/ effects	Neutrons and antineutrons/ effects	Sputtering
Deuterons/ effects	Hyperons/ effects		X-rays/ effects

## 17.00 SOLID STATE ELECTRICAL AND MAGNETIC PROPERTIES

Crystals/  
internal fields

### 17.10 ELECTRON STATES IN SOLIDS

Crystal electron states band structure excitons Fermi level Fermi surface impurity states and effects plasma polarons surface transport processes	Crystal properties Cyclotron resonance de Haas-van Alphen effect Electron beams/ effects Electron gas Electron pairs/ annihilation	Electrons absorption radiation scattering Hall effect Kondo effect Magnetoacoustic effects Magnetoresistance	Metals/ theory Piezoresistance Skin effect Solids/ theory Surface phenomena
--	---	---	---

### 17.20 ELECTRICAL PROPERTIES OF SOLIDS

Acoustoelectric effects -Conductivity, electrical/ measurement solids Contacts, electrical	Crystal electron states Eddy-currents Electrical properties of substs. Electron gas Electro-optical effects	Films, solid/ electrical properties Fluctuations Hall effect Magnetoelectric effects	Magnetoresistance Magnetothermal effects Noise, electrical Piezoelectricity Piezoresistance Space charge
--	---	--	---

### 17.22 Metallic Conducting Properties

Electron gas Hall effect Magnetoelectric effects Magnetoresistance	Metals/ theory Piezoresistance Semimetals Skin effect
---	---

### 17.24 Superconducting Properties

Storage devices Superconducting devices Superconducting magnets	Superconducting materials/ lead niobium Superconductivity/ type II
---	--

### 17.26 Semiconducting Properties

Acoustoelectric effects Contacts, electrical Electron gas Electro-optical effects Fluctuations Hall effect Magnetoelectric effects Magnetoresistance Magnetothermal effects Noise, electrical	Piezoelectricity Piezoresistance Semiconductors Space charge Semiconducting materials/ gallium arsenide germanium indium antimonide silicon
--	---

### 17.28 Semiconductor and Interface devices

Microwave techniques and devices Rectifiers	Semiconductor devices/ diodes junctions transistors tunnel and interface devices Storage devices
---	---

### 17.29 Dielectric Properties

Breakdown, electric/ solids Contacts, electrical Dielectric devices Dielectric measurement Dielectric phenomena	Dielectric properties of substs./ solids Electrets Electric charge Electric fields Electric strength	Electrostriction Ferroelectric materials/ barium titanate Ferroelectric phenomena Hysteresis Ionic conduction, solids Piezoelectric oscillations	Piezoelectricity Pyroelectricity Relaxation Rochelle salt Space charge/ solid Triboelectricity
--	---	--	--

### 17.40 THERMOELECTROMAGNETIC PROPERTIES

Magnetoelectric effects Magnetothermal effects	Thermocouples Thermoelectricity
---	------------------------------------

### 17.50 PHOTOELECTRIC PROPERTIES

Photoconducting devices Photoconductivity	Photoelectricity Photoelectromagnetic effects	Photovoltaic effects
--	--	----------------------

## 17.52 ELECTRON AND ION EMISSION BY SOLIDS

Cathodes/ oxide	Ion emission/ secondary thermionic
Electron emission field emission photoelectric secondary thermionic	Ionization/ solids Ionization, surface Work function

## 17.60 MAGNETIC PROPERTIES OF SOLIDS

Antiferromagnetism de Haas-van Alphen effect Diamagnetism Electron diffraction examination of materials Electron microscope examination of materials Exchange interactions Ferrimagnetism Ferrites Ferromagnetism/ spin-wave theory	Films, solid/ magnetic properties Gyromagnetic ratio Hall effect Hysteresis Kondo effect Magnetic devices Magnetic fields/ effects Magnetic properties of dissolved atoms in dilute alloys	Magnetic properties of subst. antiferromagnetic diamagnetic ferrimagnetic ferromagnetic paramagnetic transitions Magnetism Magnetization process Magnetization state/ domains	Magnetoacoustic effects Magnetoelastic waves Magnetoelastic effects Magneto-optical effects Magnetoresistance Magnetostriction Magnetothermal effects Neutron diffraction examination of materials Paramagnetism Zeeman effect
--	--	---	--

## 17.62 Paramagnetic Properties

Magnetic properties of sub-  
stances/  
paramagnetic  
Paramagnetism

## 17.64 Ferromagnetic Properties

Exchange interactions Ferromagnetism/ spin-wave theory Films, solid/ magnetic properties Hysteresis Magnetic devices	Magnetic properties of sub- stances/ ferromagnetic Magnetization process Magnetization state/ domains Storage devices
--	---

## 17.66 Ferrimagnetic Properties. Ferrites

Exchange interactions Ferrimagnetism Ferrites Hysteresis Magnetic devices	Films, solid/ magnetic properties Magnetic properties of sub- stances/ ferrimagnetic Storage devices
---	---

## 17.68 Antiferromagnetic Properties

Antiferromagnetism Exchange interactions	Magnetic properties of sub- stances/ antiferromagnetic
---	--

## 17.69 Magnetic Relaxation Phenomena

Ferromagnetic relaxation Magnetic resonance and relaxa- tion	Nuclear magnetic resonance and relaxation Paramagnetic resonance and relaxation
--	--

# 18.00 SOLID STATE SPECTROSCOPY AND OPTICAL PROPERTIES

Chemical shift Crystal field theory	Crystals/ hyperfine field interactions	Jahn-Teller effect Nuclear polarization
--	---	--

## 18.10 OPTICAL PROPERTIES OF SOLIDS

Absorption/ electromagnetic waves light Acousto-optical effects Diffraction/ electromagnetic waves light Diffusion/ electromagnetic waves light Dispersion, optical Double refraction/ mechanical	Electromagnetic wave propaga- tion Electro-optical effects Emissivity Films, solid/ optical properties Interference/ light Lasers/ solid Magneto-optical effects Nonlinear optics	Optical constants Optical materials Optical properties of substances Optical pumping Optical rotation Photoelasticity Pleochroism Polarized light Reflection/ electromagnetic waves light Reflectivity	Refraction/ electromagnetic waves light Refractive index/ light Scattering/ electromagnetic waves light Transmission/ light Transparency Velocity/ light
---	--	---	--

## 18.20 MÖSSBAUER SPECTRA OF SOLIDS

Crystals/  
hyperfine field interactions  
internal fields  
Mössbauer effect



18.30 OPTICAL SPECTRA OF SOLIDS

Crystals/ hyperfine field interactions	Scattering/ electromagnetic waves	Spectra/ inorganic solids	Spectral line breadth
Reflection/ electromagnetic waves	light	inorganic solids, radio	Stark effect
light	light, Brillouin spectra	frequency	X-ray spectra/ absorption
Reflectivity	light, Raman spectra	organic molecules and sub- stances	emission
	light, Raman spectra, inorganic	organic molecules and sub- stances, infrared	Zeeman effect
	light, Raman spectra, organic	organic molecules and sub- stances, radio frequency	

18.40 LUMINESCENCE SPECTRA OF SOLIDS

Colour centres	Luminescence/ solids, inorganic
Counters/ scintillation	solids, organic
Electroluminescence	Luminescent devices
	Thermoluminescence

18.50 MAGNETIC RESONANCES IN SOLIDS

Crystals/ hyperfine field interactions	Cyclotron resonance	Ferromagnetic resonance	Magnetoelastic waves
Antiferromagnetic resonance	Ferrimagnetic resonance	Gyromagnetic ratio	Magnetomechanical effects
	Ferromagnetic relaxation	Magnetic resonance and relaxa- tion	Optical pumping

18.52 Paramagnetic Resonances and Relaxation

Crystals/ hyperfine field interactions	Paramagnetic resonance and relaxation/ measurement
---	--

18.54 Nuclear Magnetic Resonance and Relaxation

Crystals/ hyperfine field interactions	Nuclear magnetic resonance and relaxation/ measurement
	Nuclear quadrupole resonance

19.00 PHYSICAL CHEMISTRY

Atomic mass and weight	Distillation	Laboratory app. and technique	Precipitation
Balances	Elements/ origin	Macromolecules	Pumps
Bonds	relative abundances	Molecular weight	Quantum chemistry
Centrifuges	Filters	Molecular weight determination	Sedimentation
Chemical structure	Isomerism	Periodic system	Valency
Chemical technology		Physical chemistry	

19.10 THERMOCHEMISTRY AND REACTIONS

Association	Crystal chemistry	Heat of adsorption	Phase equilibrium
gases	Detonation	Heat of combination	Phase transformations
liquids	Dissociation	Heat of dissociation	Polymerization
Catalysis	Exchanges, chemical	Heat of formation	Polymers
Chemical reactions	Explosions	Heat of reaction	Reaction kinetics
Combustion	Flames	Isotope exchanges	Sorption

19.15 Oxidation and Corrosion

Corrosion
Oxidation

19.20 ELECTROCHEMISTRY

Conductivity, electrical/ liquids, electrolytic	Electrochemistry electrodes	Electrolysis	Ion velocity/ electrolytic
Dissociation/ electrolytic	Electrokinetic effects	Electrolytic deposition	Ions, electrolytic
		Electrophoresis	

19.30 PHOTOCHEMISTRY AND RADIOCHEMISTRY

Chemical effects of radiations/ acoustic waves	Nuclear reactions and scattering/ chemical effects
ionizing radiations	Photochemistry
	Radiochemistry

19.40      PHYSICAL METHODS OF CHEMICAL ANALYSIS

Chemical analysis/ adsorption by mass spectrometry by nuclear reactions electrochemical radioactive X-ray	Chromatography Radioactive tracers Spectrochemical analysis Tracers
---	--

20.00      GEOPHYSICS

Earth/ age composition electricity heat rotation	Geodesy Geophysical prospecting Geophysics Glaciers	Gravity Minerals Oceanography Radioactive dating	Radioactivity Seawater Seismic waves Seismology Soil
---	--	---	--

20.10      ATMOSPHERE

Anemometers Atmosphere/ composition humidity movements precipitation radioactivity structure temperature thermodynamics Atmospheric acoustics	Atmospheric electricity Atmospheric optics Atmospheric pressure and density Atmospheric spectra Atmospherics Clouds Condensation Electromagnetic wave propaga- tion/ atmosphere	Evaporation Fallout Fog Humidity Hygrometers Ice Lightning Meteorological instruments Meteorology Rain	Rockets Satellites, artificial Sky brightness Snow Sunlight Thunderstorms Twilight Wind
---	---	---	--

20.20      UPPER ATMOSPHERE

Airglow Atmosphere/ composition movements radiation belts radioactivity structure temperature thermodynamics upper	Atmospheric electricity Atmospheric optics Atmospheric pressure and density Atmospheric spectra Atmospherics	Aurora Fallout Ionization, atmosphere Magnetosphere Meteors Rockets	Satellites, artificial Sky brightness Sunlight Twilight Zodiacal light
---	---	--	--

20.30      IONOSPHERE

Atmospherics Aurora	Electromagnetic wave propaga- tion/ ionosphere	Ionization, atmosphere Ionosphere Ionosphere measuring apparatus
------------------------	--	--

20.35      D, E and F-regions

Ionosphere/  
D-region  
E-region  
F-region

20.40      GEOMAGNETISM

Compasses Earth/ magnetic field magnetic field, variations	Magnetic storms Rock magnetism
---	-----------------------------------

20.50      SPACE RESEARCH TECHNIQUES

Rockets Satellites, artificial	Space research Space vehicles/ instrumentation
-----------------------------------	--

21.00      ASTROPHYSICS

Astronomical observations Astronomical spectra Astronomy and astrophysics	Celestial mechanics Cosmic rays Cosmology	Elements/ origin relative abundances	Gravitation Interstellar matter
---	---	--	------------------------------------



21.10 GALAXIES

Cosmic radiations, r.f.  
Galaxies/  
the Galaxy

Magnetohydrodynamics  
Nebulae

21.20 STARS

Interstellar matter  
Magnetohydrodynamics  
Novae

Stars/  
composition  
evolution  
magnetism  
radiation  
spectra  
structure  
Thermonuclear reactions

21.30 RADIOSOURCES, X-RAY AND GAMMA-RAY SOURCES

Cosmic radiations, r.f.  
Quasars  
X and gamma-ray astronomy

21.40 SOLAR SYSTEM

Comets  
Cosmic rays  
Earth/  
rotation  
Gravitation  
Interplanetary magnetic field

Interplanetary matter  
Meteorites  
Meteoroids  
Moon  
Planets  
Solar system

21.45 Sun

Cosmic rays  
Sun/  
corona  
eclipses  
flares  
magnetism  
prominences  
radiation  
radiation, corpuscular  
radiation, r.f.  
spectra

Sunspots  
Zodiacal light

21.60 ASTRONOMICAL TECHNIQUES

Astronomical instruments  
Astronomical observations

Astronomy and astrophysics  
Radioastronomy

Telescopes/  
astronomical

22.00 BIOPHYSICS

Biophysics

22.10 HEALTH AND MEDICAL PHYSICS

Biological effects of radiations  
Biological technique and instruments

Blood  
Dosimetry  
Medical science

Physiology  
Proteins  
Radiation protection

Radiography  
Zoology

22.20 HEARING AND SPEECH

Ear  
Hearing  
Noise/  
acoustic  
Speech

Eye  
Colour vision  
Vision

22.30 VISION

23.00 LABORATORY AND EXPERIMENTAL TECHNIQUES

Biological technique and instruments  
Calculating apparatus/  
analogue apparatus  
digital computers  
digital computer programmes

Chemical technology  
Heat treatment/  
alloys  
Laboratory apparatus and technique  
Leak detection

Materials  
Metallurgy  
Zone melting and refining

23.10 HIGH AND LOW TEMPERATURE TECHNIQUES

Cryostats  
High-temperature phenomena and effects

Joule-Thomson effect  
Liquefaction, gases  
Low-temperature phenomena

Low-temperature production  
Low-temperature technique  
Magnetic cooling

23.20 HIGH PRESSURE TECHNIQUES

High-pressure phenomena and effects

23.30 VACUUM TECHNIQUES

Leak detection  
Manometers  
Seals  
Sputtering

Vacuum apparatus  
Vacuum gauges  
Vacuum pumps  
Vacuum technique

23.40 X-RAY TUBES AND TECHNIQUES

Dosimetry  
High-voltage techniques  
Radiation monitoring  
Radiation protection  
Radiography

X-ray absorption  
X-ray diffraction  
X-ray examination of materials  
X-ray measurement  
X-ray monochromators

X-ray reflection  
X-ray scattering  
X-ray spectra/  
absorption  
emission

X-ray spectrometers  
X-ray spectroscopy  
X-ray tubes  
X-rays/  
effects

## Chemical elements and inorganic compounds

All the chemical elements are listed by name, followed by their compounds, e.g. "Cadmium, "Cadmium compounds".

"Hydrogen" is subdivided by the subheadings "neutral atoms", "neutral molecules" and "ions". "Deuterium" and "Tritium" are independent headings. "Hydrogen compounds" is supplemented by "Ice", "Steam" and "Water".

"Oxygen" is supplemented by "Ozone" and "Carbon" is supplemented by "Diamonds" and "Graphite"

The following inorganic compounds are further subdivided by subheadings as shown:-

Barium compounds/ barium titanate*	Nitrogen compounds/ ammonia
Cadmium compounds/ cadmium sulphide	ammonium compounds
Calcium compounds/ calcium fluoride	Potassium compounds/ potassium bromide
Gallium compounds/ gallium arsenide†	potassium chloride
Indium compounds/ indium antimonide†	Sodium compounds/ sodium chloride
Lithium compounds/ lithium fluoride	Zinc compounds/ zinc sulphide

\* Ferroelectric properties are listed under "Ferroelectric materials/barium titanate"

† Semiconducting properties are listed under the corresponding subheadings of "Semiconducting materials"

## Organic compounds

Organic compounds are grouped under headings "Organic compounds", "Polymers", "Plastics", "Proteins". "Rochelle salt" is an independent heading.

## Co-ordination compounds

Metallic co-ordination compounds are regarded as inorganic with a few exceptions and are indexed under the appropriate metallic compound heading, (not under organic compounds) e.g. Ni complex, bis (dimethylglyoximate) nickel (II) under Nickel compounds.

## Substance groups

In addition there are the following headings for groups of elements, compounds or substances:-

Actinides	Metals
Actinide compounds	Minerals
Alkali metals	Rare-earth metals
Alkali-metal compounds/ halides	Rare-earth compounds
Alkaline-earth metals	Semiconductors
Alkaline-earth compounds	Semiconducting materials/ gallium arsenide§
Ferrites	germanium§
Ferroelectric materials/ barium titanate†	indium antimonide§
Garnets	silicon§
Halogens	Superconducting materials/ lead
Inert gases	niobium
	Transition metals
	Transition-metal compounds

† Used for ferroelectric properties only

§ Used for semiconducting properties only

|| Used for superconducting properties only

## Alloys

General papers on alloys are indexed under "Alloys". Alloys of specified composition are listed under, either

- (i) special alloy headings (there are five of them: "Aluminium alloys", "Copper alloys", "Iron alloys", "Nickel alloys", "Steel"), e.g. Al-Ni alloys under "Aluminium alloys", and "Nickel alloys".
- (ii) compounds of the named elements, e.g. Mn-Zn alloys under "Manganese compounds" and "Zinc compounds". Silicon-iron under "Iron alloys" and "Silicon compounds".

## Special substances and materials

There are also the following special headings for certain common substances:-

Air	Paper
Blood	Porous materials
Ceramics	Powders
Clay	Quartz
Coal	Rubber
Concrete	Ruby
Fibres	Sand
Gelatin	Seawater
Glass	Soil
Mica	Waxes
Optical materials	Wood



**4 $\pi$  counters**

No entries

**Abacs** see *Nomograms***Aberrations, optical**

See also *Electron lenses; Ion optics; Optical instrument testing; Optics/geometrical; Particle optics*  
 chromatic, of mag. spectrometer, elimination by electrostatic mirrors, first order theory 9-13278  
 chromatic correction with single element lenses 9-2397  
 electron lenses, probe-forming and projector, spherical, rel. to distortion coeffs. 9-6479  
 in electron microscope, high resolution 9-17859  
 electron optical systems with straight optical axis 9-10596  
 gas lenses, distortion of shuttled gaussian light pulse obs. 9-5118  
 in holography 9-16790  
 Huygenian type 2-lens system 9-8643  
 i.r. materials, transmission random deviation props. 9-4510  
 lens, thin, longit. spherical aberration meas using laser 9-4504  
 photographic image quality 9-6543  
 plane diffraction gratings with non parallel concentric beams, computation by means of ray tracing formula 9-13052  
 reflector, multilayer, apparent curvature minimization 9-4511  
 spherical, infinitesimally thin lenses, analysis 9-4506  
 spherical, third-order in quadrupole lens syst. of prism spect. 9-2566  
 spherical and spherochromatic, higher orders, correction 9-6542  
 transverse geometrical, modulation transfer function, evaluation 9-10885

**Abrasion**

See also *Hardness; Wear*  
 steel, stainless, thin films, prod. of microtwins 9-3228  
 wear mechanism 9-18528  
 $\alpha$ -Al<sub>2</sub>O<sub>3</sub>, abrasion resistance rel. to ZrO 9-3457  
 ZrO, abrasion resistance rel. to  $\alpha$ -Al<sub>2</sub>O<sub>3</sub> 9-3457

**Absorption**

See also *Alpha-particles; Beta-rays; Cosmic rays; Electrons; Gamma-rays; Hyperons; Mesons; Neutrons and antineutrons; Protons and antiprotons; and also Sorption; X-ray absorption*  
 Al, anodized and blackened, heat absorption characteristics 9-5576  
 auroral, position and height deduced from v.l.f. phase measurements 9-12601  
 gas, hot and dusty, coeffs. calc. from emissivity meas. scatt. centres and radiative heat transfer factors. 9-19089  
 insulating substances, of Cs 9-5258  
 microwave and i.r. for analysis of atomic and molecular species in hypervelocity wake 9-19577  
 Mo single crystal, of O<sub>2</sub>, mass-spectroscopic investigation 9-5256  
 SrTiO<sub>3</sub>, of free carriers, using two-photon excitation, obs. 9-12199

**acoustic waves**

See also *Noise abatement; Transmission/acoustic waves*  
 acoustical excitation of nuclear spin system with I=3/2 excitation 9-1711  
 amplification, adjacent piezoelectric and semicond. crystals 9-9833  
 amplification, plasma mechanism 9-5551  
 amplification mechanisms 9-3527  
 anechoic room, averaged press. refl. coeff. meas. 9-2231  
 attenuation in solids viscosity tensor calc. 9-3522  
 near critical point 9-4326  
 cyclopropane and ethylene, rel. to vibrational relax. times, -70-150°C 9-4953  
 dielectric, infl. of elec. field on attenuation 9-19858  
 edge effect of rectang. absorber, reverberation chamber meas. 9-15463  
 ferroelectrics, uniaxial, anomalies near Curie temp. due to polarization fluctuation interaction 9-1375  
 glycerine, viscous, damping and dispersion calc. 9-19513  
 in halls, by audience and chairs, three methods of calc. 9-15473  
 ice, attenuation of multiply reflected pulses for longit. and transverse waves 9-5545  
 insulation from airborne sound, single partitions and ceilings 9-17812  
 liquids, small quantities, a resonator method 9-5155  
 liquids, with cavities prod. by ionizing particles, cavity detect. method 9-21204  
 loss of double-leaf wall construct., use and eff. of absorbent mat. 9-19073  
 magnon-elastic wave self-consistent interaction and sound absorpt. coeff. calc. 9-1647  
 metals, nearly-free electron, attenuation rel. to impurity scatt. potential 9-12045  
 methyl alcohol-cyclohexane critical mixture, freq. and temp. depend. 9-11694  
 natural sea floor sediments, 15-1500 kHz 9-8160  
 natural sea floor sediments, 15-1500 kHz 9-4031  
 nonlinear acoustic resonators, characteristics 9-2208  
 piezoelectric semiconductors, amplification by carrier drift and nonlinear amplification effects, review 9-13793  
 polycapromide oriented fibers, sound wave propagation velocity by travelling wave method in a wide range of temps. 9-5540  
 porous mat. with perforated facing, parameter calc. for max. abs. in given freq. range 9-4325  
 sawtooth, propagating and standing energy dissipation calcs. 9-12935  
 semiconductors, amplification eff. of elec. field redistribution 9-12006  
 semiconductors, many-valley, absorption and amplification of sound 9-1372  
 semiconductors, many-valley, electron contribution to absorption coeff. 9-1371  
 semiconductors, piezoelectric and ferroelectric, attenuation and amplification 9-18553  
 silicate glass: rare earth doped, range  $5 \times 10^4$ - $2 \times 10^6$  c/s 9-5544  
 silicon, vitreous, thermal treatment and impurity-ion conc. effects 9-15001  
 siren signals in built up areas, effect of buildings 9-15460  
 slots, narrow, in corners 9-19066  
 suspensions and gels, meas. for various freqs. and concs. 9-3141  
 in waveguide scattering of sound waves with resulting change of mode and absorption 9-17801  
 by wet porous medium, l.f. coeff. 9-5541  
 Al<sub>2</sub>O<sub>3</sub>:Cr<sup>3+</sup>, range  $5 \times 10^4$ - $2 \times 10^6$  c/s 9-5544  
 Cd, molten, from m.p. to 850°C, temp. depend. rel. to dilational viscosity 9-5163  
 CdS, amplification, carrier in homogeneity effect 9-1383  
 \*He liq., hypersonic, at ~650 MHz, optical method 9-14876  
 In, molten, from m.p. to 850°C, temp. depend. rel. to dilational viscosity 9-5163

**Absorption continued****acoustic waves continued**

O<sub>2</sub> with methane impurity, vibr. relax. obs. 9-21137  
 Pb, molten, from m.p. to 850°C, temp. depend. rel. to dilational viscosity 9-5163  
 SF<sub>6</sub>, rel. to vibrational relax. times, -70-150°C 9-4953  
 SF<sub>6</sub> oscillation relax., temp. depend. 10°C to 215°C 9-2879  
 Zn, molten, from m.p. to 850°C, temp. depend. rel. to dilational viscosity 9-5163

**acoustic waves, ultrasonic**  
 2-2. electrolytes solns, 0.3 to 2.8 GHz 9-18761  
 alkali halides containing CN<sup>-</sup>, attenuation and velocity 9-11996  
 amplification in gaseous plasmas 9-17097  
 amplification in transverse field 9-15003  
 aniline binary liquid mixtures, vel., absorption, compressibility meas. 9-3097  
 t-butyl alcohol-water mixtures, anal. of relax. curves at 5,25 and 45°C 9-19630  
 carbon tetrachloride, aniline liquid mixture, vel., absorption, compressibility meas. 9-3097  
 carbon tetrachloride, relax. determ. 9-3100  
 m-cresol, variation along state isotherms, isobars and isochors 9-5164  
 crystal, piezo-semiconducting, of wurtzite group, amplification coeff. derived 9-12007  
 crystal conduction electrons, mag. field effect 9-18558  
 c.w. spectroscopy, sensitivity enhancement using acoustic resonators 9-4406  
 dielectric crystals, dirty, attenuation 9-7643  
 diffraction effects in u.s. attenuation meas. devices with plane radiators 9-14385  
 ethylene glycol, variation along state isotherms, isobars and isochors 9-5164  
 ferro- and antiferromagnets, attenuation near critical point 9-5554  
 ferromagnetic spin system 9-13795  
 ferromagnets, magnetoacoustic resonance, effect of mag. alloying additions 9-5552  
 fish tissue, freshwater, by pulse-echo tech., eff. of freezing 9-4323  
 glycerol mixtures, temp. and freq. depend. 9-11693  
 H<sub>2</sub>S-CO<sub>2</sub> mixture, obs. at 300 and 500°K 9-21136  
 hydrocarbon gases, effect of temp. on rot. and vibr. relax. 9-957  
 in liquids, new meas. method 9-153  
 inert gas binary mixtures, two-fluid model 9-3054  
 iso-octane-water, emulsion, attenuation obs. 9-3139  
 isopropyl alcohol, aniline liquid mixture, vel., absorption, compressibility meas. 9-3097  
 liquids, organic, non-associated, absorpt. formula 9-5158  
 liquids under high press., eff. of press., relax. mech. interpretation 9-17205  
 Mandel'shtam-Brillouin scattering during amplification 9-5542  
 metals, liquid, rel. to relax. and disorder 9-5160  
 metals, surface states 9-18554  
 methane gas, 50-600 kHz and -30+120°C 9-5117  
 microwave phonons spectroscopy 9-9816  
 in polycrystalline metallic probe, effect of mag. field parallel to propag. direction 9-21429  
 polymethylmethacrylates in benzene, stereo and mol. wt. effects 9-1008  
 polytetrafluoroethylene, transitions and relax. pressure dependence determ. 9-3406  
 quartz, temp. depend., optical determ. 9-12001  
 quartz hypersonic attenuation by thermal Brillouin scattering 9-12000  
 rutile, hypersonic attenuation, low temp. freq. dependence and temp. dependence 9-13797  
 semiconductors, many-valley, and amplification oscills. due to inelastic scatt. of electrons 9-7644  
 semiconductors, piezoelectric, amplification in mag. field 9-3526  
 semiconductors, piezoelectric, minority carriers in amplification 9-11999  
 solid thin specimens, attenuation meas. using buffer rods 9-3520  
 superconductor, shear-wave attenuation near T<sub>c</sub>, nonlinear effect 9-7760  
 superconductors, strong coupling and impure attenuation anomaly 9-13796  
 superconductors, type II, in intermediate purity state 9-18612  
 superconductors near T<sub>c</sub> 9-3586  
 superconductors with strong e-phonon interaction, theory 9-1373  
 triglycine sulphate crystals, relax., anisotropy 9-3524  
 xylene, aniline liquid mixture, vel., absorption, compressibility meas. 9-3097  
 acetone-water mixture, rel. to relax. of conc. fluctuations 9-5167  
 Al, attenuation in normal state, electronic contribution 9-9829  
 CdS, additional signal generation in alternating elec. field 9-1382  
 CdS, attenuation, and acoustoelec. effect and trapping 9-7650  
 Co, attenuation and vel. anomalies at high temp. 9-5547  
 Cu, attenuation orientation dependence 9-9830  
 Dy, attenuation and elastic moduli rel. to mag. transition 9-7517  
 Er, attenuation and elastic moduli rel. to mag. transition 9-7517  
 Gd, attenuation and elastic moduli rel. to mag. transition 9-7517  
 H<sub>2</sub>S obs. at 300°K 9-21136  
 Hg crystals, superconducting 9-7772  
 Hg, attenuation and elastic moduli rel. to mag. transition 9-7517  
 KCl, KBr and KCl containing CN<sup>-</sup>, attenuation and US velocity 9-11996  
 KH<sub>2</sub>PO<sub>4</sub>, shear wave attenuation in paraelectric region 9-21430  
 KH<sub>2</sub>PO<sub>4</sub>, crystal, near phase transition temp. 9-1378  
 LiNbO<sub>3</sub>, n.m.r. of <sup>7</sup>Li, acoustic saturation 9-8040  
 MnF<sub>2</sub> ferro- and antiferromagnets, attenuation near critical point 9-5554  
 (NH<sub>4</sub>)<sub>2</sub>PO<sub>4</sub> 9-5162  
 NH<sub>3</sub> soln., ac., vel. depend. on conc., 1.48-10.37 MHz 9-5162  
 Na<sub>2</sub>(PO<sub>3</sub>)<sub>2</sub> soln., aq., vel. depend. on conc., 1.48-10.37 9-5162  
 NaCl containing CN<sup>-</sup>, attenuation and u.s. velocity 9-11996  
 NaNbO<sub>3</sub>, at  $\lambda$  transition 9-1369  
 Nb, attenuation anisotropy and temp. dependence in mixed state 9-7645  
 Nb, hysteresis in attenuation near H<sub>c1</sub> 9-9831  
 Ni, attenuation and vel. anomalies at high temp. 9-5547  
 RbMnF<sub>3</sub>, attenuation meas. of elastic constants 9-21431  
 Sn, attenuation meas. of superconducting energy gap pressure dependence 9-17385  
 Sn single crystals, superconducting, at 500 kHz, temp. depend. 9-21496  
 SrTiO<sub>3</sub>, anomalous hypersonic attenuation above 100°K 9-12002  
 Tb, attenuation and elastic moduli rel. to mag. transition 9-7517  
 Te freq. and temp. depend. 9-9832  
 Tl, attenuation in normal high-purity material 9-12004  
 Tl, attenuation in superconducting, high-purity material 9-12003  
 U polycrystals, attenuation meas., 4.2-300°K, of elastic moduli 9-11909

**Absorption continued****acoustic waves, ultrasonic continued**

V. (Sat.wt.%)Ta, intermediate purity type II semiconductor 9-18612

V, attenuation in mixed superconducting state 9-12005

V, attenuation near  $H_{c1}$  rel. to isolated-vortex state 9-17387

Zn, normal and superconducting, u.s. attenuation 9-1381

**electromagnetic waves***See also Spectra (radiofrequency subheadings)*cis-1,2-dichloroethylene, rel. to press.,  $0.31\text{ cm}^{-1}$  9-811atmosphere, at  $1.8\text{--}2.7\text{ cm}$  9-6079

atmosphere, at 35 GHz, humidity dependence 9-8173

atmosphere, i.r. extinction  $1\text{--}2.5\text{ }\mu$  9-17566chlorobenzene-iodobenzene-n-hexane,  $6.32\text{ to }0.75\text{ cm}$ ,  $30\text{ to }-40^\circ\text{C}$ 

9-19635

by conducting cylinder, TE and TM impulsive and unit step plane waves,

transient currents 9-20471

cosmic noise, auroral 9-21790

e.l.f., attenuation charact. with two-layered model of ionosphere 9-21809

ferrites suitability 9-17836

from plasma, magnetoactive, inclined incidence 9-879

gases, mm. and sub-mm. 9-17164

inhomogeneous media, analysis by geometric optics 9-6416

ionosphere, vertical incidence  $2.2\text{ MHz}$  (Ceylon 1964) 9-10424

ionospheric, abnormal, in auroral zone, frequency dependence 9-1961

liquids, mm. and sub-mm. 9-17164

metallic electron plasmas 9-16395

metallic filament, thin and short, absorption cross-sections 9-6431

negative absorption in quasiclassical systems 9-19133

at plasma layer, moving 9-21070

radio, by ionosphere, noon global space time var. 1957-65 obs. 9-21798

shielding, l.f. inductive, theory and calc. methods 9-4387

solar u.v. in ionosphere,  $100\text{ to }500\text{ km}$ , rocket obs. 9-21803

spectrometry, atomic, and flame emission 9-279

 $\text{CO}_2$  quadrupole interaction 9-17164 $\text{D}_2\text{O}$  at  $300\text{ GHz}$  9-17164

KCl, ultraviolet, radiation produced 9-5921

 $\text{O}_2$  sub-mm. transitions 9-17164**light***See also Atmospheric optics; Densitometry; Films, solid/optical properties; Filters, optical; Optical constants; Pleochroism; Transmission/light; Spectra* $\text{CdF}_2$ :Eu or In, spectra is range  $0.2\text{ to }15\text{ }\mu$  9-5672alkali halide crystals, F<sup>+</sup> centre rel. to formation 9-5381

alkali halide mixed phosphors, absorption spectra of isostructures, interpretation 9-15176

alkali halides, lattice effect on absorption by  $V_k$  center 9-9720

alkaline earth oxides, defect studies, review 9-9693

alkaline-earth tungstates, u.v.-induced spectral peak, wavelengths, lattice constant dependence 9-5913

aluminumborate glass: Tl, radiation-induced bands rel. to trapping mechanism 9-1777

antiferromagnet, i.r. mechanism 9-12395

atmosphere, transparency spectra,  $0.59\text{ to }15\text{ }\mu$  for paths up to  $2.6\text{ km}$ 

9-6077

benzoic acid, spectra, in polarized light 9-10214

borosilicate glass, new i.r. peak 9-17485

carbon blacks, absorbance meas. and calcs., book 9-12324

chlorophyll b, two phase system, spectra 9-16418

citrine, irradiated, colouring mechanism 9-1237

colloidal suspensions, total extinction coeff. rel. to particle size for strongly absorbing subst. 9-14865

corundum:Fe(Ni), dependence on oxidation-reduction conditions during growth 9-1132

 $\text{CoWO}_4$ , long-wave i.r., band identification and spin wave spectrum 9-1773

crystals, elec. field induced i.r. absorpt. and Raman scatt. 9-16420

crystals, second-order electric moment contrib. 9-5907

crystals, Urbach rule for localized excitations, theory 9-5905

diamond, by neutral vacancy 9-10194

diamonds, i.r. u.v. and visible spectra, participation of Al impurities 9-19987

dielectric, parameters for organic mols. 9-5869

2,3-dimethylnaphthalene single crystals, near i.r. spectra 9-5933

diphenylene oxide, frozen paraffin solns., conc., effect on absorption spectra 9-2913

diphenylstilbene, absorpt. and fluorescence spectra 9-4961

dispersed detector filter, effect on characteristics 9-262

elbaite, rel. to colour centre obs. 9-1236

film, size-quantized in quantizing mag. field, electron spectrum structure 9-16202

films, by small metallic particles, comparison with scatt. 9-15166

free-electron-like foils, absorbing power in p-polarized light 9-14022

glass, low i.r. absorpt., patent 9-8662

glass, soft, far i.r. absorpt. 9-10209

glass, spectrophotometer for meas. of attenuation coeffs. 9-2422

impurity atom or mol. in solid, antiresonance in spectra 9-1765

impurity band profiles, transitions to degenerate local levels 9-3881

insulators, exciton effects in inter-band absorpt. 9-1572

interaction of light with insulating crystals 9-12351

inversion of volume attenuation coefficient of soft particles 9-10896

i.r., impurity-induced, molecular coupling 9-7966

i.r., temperature dependence by localized vibrational modes 9-7630

layer, thin, Paynting radiation vector 9-5884

by liquids, critical abs. coeff. and nonlinear attenuation meas. 9-9512

localized, at clean metal surfaces 9-21605

Metagalaxy, average density of dust matter and non-relict origin 9-17609

metal blacks, absorbance meas. and calcs., book 9-12324

metal thin films, theoretical study 9-12368

mica, natural and synthetic, meas. rel. to elec. props.,  $4^\circ\text{--}520^\circ\text{K}$  9-12182

1-naphthol, excited, H-bonded, spectra 9-9519

near infrared, interference filter analyzer, determination of water content 9-14140

organic dielectrics, transparent, of laser radiation rel. to opacity production 9-1721

Osmium complexes with phenyl and pyridine ligands 9-7981

pharmaceutical products, u.v. spectra 9-5910

phenazine single crystals, spectra rel. to carrier generation 9-7860

photochromic spiropyran layers, coloration by u.v. laser radiation 9-18219

in plasma reflecting skin, collisionless 9-15935

**Absorption continued****light continued**

polarons, free continuum, mechanism using Landau-Pekar approach 9-21472

by polarons, small-radius, intraband and interband charact. 9-3882

polymers, biaxially oriented, polarized i.r. abs. data graphical representation 9-21606

polymethylmethacrylate, in excited state, rel. to method of polymerization 9-10217

quartz, fused, far i.r. absorpt. 9-10209

rare gas crystals, one-phonon defect-induced i.r., theory 9-5526

scattering medium, laser beam absorpt. anomalies 9-3128

semiconductor, elec.-current flow induced polarization effect, theory 9-14035

semiconductor in mag. field, exciton line excitation 9-1763

semiconductor solid solutions, width of edge 9-3880

semiconductors, rel. to non-equilibrium carrier creation during depolarisation 9-21502

silica, fused, Tl-doped, radiation-induced bands rel. to trapping mechanism 9-1777

silica, vitreous, rel. to impurity effect on ionization-radiation-induced dilatation 9-14961

silicate glass, spectra rel. to interconversion of  $\text{Eu}^{2+}=\text{Eu}^{3+}$  9-14051

solids, high pressure apparatus 9-7954

spectra, glass tinted with transition metal ions, high temperature changes 9-14052

spectrometry, review 9-2420

stilbene, absorpt. and fluorescence spectra 9-4961

styrylstilbene, absorpt. and fluorescence spectra 9-4961

total, used for natural line width determ. 9-2810

tourmaline, spectra for colour origin and change on heating 9-15171

trimethylene oxide, i.r. spectra 9-17483

Urbach's rule, theory rel. to quantum transition from vibr. sub-level to e excitation level 9-1766

Urbach's rule in electron-phonon model 9-5909

 $V_k$  colour centre in alkali halides, lattice effect. 9-9720 $\text{Y}(\text{OH})_3$ :Tb,  $\text{Tb}^{3+}$  crystal field parameters determ. 9-14019

Ag-Mn(Pd) films, rel. to resonant states 9-7937

Ag, thin films, band shift 9-17479

 $\alpha$ -AgI high-temp. phase, meas.  $8.6\text{--}10.1\text{ GHz}$ ,  $20\text{--}160^\circ\text{C}$  9-5911

Al, pseudopotential model calc. 9-14047

 $\text{Al}_2\text{O}_3$ :Co(Ti), spectra rel. to valence state of dopant 9-14908

Al thin films, expl. study and theoretical explan. 9-19986

AlP epitaxial layers on Si, spectra rel. to colour 9-19692

 $\text{AsO}_4^{3-}$  in aqueous soln., u.v. absorption,  $n\rightarrow\pi^*$  transition 9-3103 $\text{As}_2\text{S}_3(\text{Se}_2)$ , during transition from crystalline to glassy state 9-10192 $\text{As}_2\text{Se}_3$  glass, various initial purities 9-12352

Au-Fe dilute alloy, band gap var. determ. from reflectivity meas. 9-21604

Au-Pd films, rel. to resonant states 9-7937

 $\text{BaCl}_2$ , electrolytically coloured, spectrum, rel. to F centre existence 9-17279 $\text{BaF}_2$ :Nd<sup>3+</sup>, conc. dependences at  $300, 77$  and  $4.2^\circ\text{K}$  9-15161 $\text{BaTiO}_3$  powder, discoloration, grain size effects 9-21619 $\text{BaTiO}_3$  with additions of Fe, Co and Ni, H-reduced, spectra, rel. to defect structure 9-1207 $\text{BeO}$ , molten, abs. index meas. in visible spectrum 9-17210C, in wavelength region  $176\text{ to }250\text{ }\mu$  9-1769C particles in  $\text{N}_2$  stream, cross section 9-11726

CCLu, He-Ne laser beam induced index change associated with thermal blooming, interferometric observation 9-18361

 $\text{CaBa}_2$ , coeff., and extinction coeff. and refractive index from reflection meas. 9-5866 $\text{CaF}_2$ :Ho<sup>3+</sup>( $\text{Cr}^{3+}$ ), mag. circular dichroism in absorpt. bands 9-1737 $\text{CaF}_2$ :Nd<sup>3+</sup>, conc. dependences at  $300, 77$  and  $4.2^\circ\text{K}$  9-15161 $\text{CaO}^+$ , electronic absorption spectrum 9-10195 $\text{CaWO}_4$ :Tb<sup>3+</sup>, rel. to ground term energy level analysis 9-12373 $\text{Cd}_{1-x}\text{Mn}_x\text{S}$  ( $x\leq 0.4$ ), spectra and band gap composition dependence 9-1516 $\text{CdO}$ , thin films 9-3886 $\text{CdS}$ , spectra, due to intrinsic defects 9-3887 $\text{CdS}$ , three-quantum, expl. obs. of process from luminescence spectra 9-10235 $\text{CdS}_{1-x}\text{Se}_x$  films, structure defects effects 9-9973 $\text{CdTe}$ :Ti<sup>2+</sup>, and c.s.r. 9-1772

n-CdTe, free carrier mechanism 9-5916

 $\text{ClO}_2$  radical created by X-irrad. in  $\text{KClO}_3$  and  $\text{KClO}_4$  9-18737 $\text{CoO}$ , i.r. spectra, nature of nonstoichiometry 9-19989 $\text{CoO}$ , semiconducting, of small polarons in near and far i.r. 9-5929 $\text{CoO}_{1-x}\text{S}_x$ , i.r. spectra 9-19989Cs films,  $2300\text{--}11000\text{ }\text{\AA}$  9-15174

Cu-Mn(Pd) films, rel. to resonant states 9-7937

Cu films, anomalies rel. to ambient conditions 9-10198

 $\text{DyCl}_3$ , spectra in far i.r. 9-1776 $\text{ErCl}_3$ , spectra in far i.r. 9-1776

Eu chalcogenides, absorpt. edge temp. dependence 9-12328

Eu chalcogenides, mag. red shift 9-14033

Eu chalcogenides, temp. and mag. field depend. of abs. edge 9-16391

Ga films, polycrystalline, 9-3192

GaAs, edge absorption of mechanically polished surface 9-12379

n-GaAs, impurities effect,  $297^\circ\text{ to }4^\circ\text{K}$  9-21621

GaAs, inter-conduction minimum transitions 9-7932

GaAs, semi-insulating,  $\text{CO}_2$  laser radiation 9-3848

GaAs, semi-insulating, uniform elec. field effects 9-5883

GaP:N, rel. to isoelectronic impurities theory 9-7801

GaP coeff. meas. near Restrahl band 9-12326

GaS, spectra for indirect energy gap 9-18622

n-GaSb, i.r., rel. to electron masses 9-3852

GaSe, spectra for indirect energy gap 9-18622

 $\text{GaSe}_{1-x}\text{S}_x$ , spectra for indirect energy gap 9-18622

Gd, in ferromagnetic and paramagnetic states 9-16412

Ge:B, i.r. absorption for impurity vibrational modes 9-18548

n-Ge:Sb (As), electron irradiated, edge coeff. 9-10200

Ge, edge absorption of mechanically polished surface 9-12379

Ge, fundamental, effect of uniaxial deform. 9-18707

n-Ge, by grain boundaries 9-21623

Ge, i.r. lattice absorption 9-3510

Ge, u.v. rel. to spin splitting calcs. 9-13893

Ge single crystals, edge absorption rel. to temp.  $4\text{--}400^\circ\text{K}$  9-3891

Ge spectra, edge shape, electric field eff. 9-3890

Ge surface, i.r. radiation, at low temps. 9-21622

HBr, gas-phase far-u.v. spectrum 9-20929



**Absorption continued**  
**light continued**

- HI, gas-phase far-u.v. spectrum 9-20929  
 He-Ne laser, nonlinear absorpt., mode selection and self-locking 9-13015  
 Hg, liquid, electron-electron interactions eff. 9-21628  
 HgCr<sub>2</sub>S<sub>4</sub>, ferromagnetic, edge shift rel. to magnetoelastic vol. strain 9-1781  
 I<sub>2</sub> in different solvents, maxima of visible band 9-19634  
 InSb, current flow effects 9-3843  
 n-InSb, degenerate, Burstein eff. in meas. impurity conc. 9-3645  
 p-InSb, doped, fundamental absorpt. temp. dependence 9-10202  
 InSb, edge absorption of mechanically polished surface 9-12379  
 InSb films, absorption edge, thickness depend. 9-5906  
 KBr-KI:Ti type phosphors, absorption spectra of isostructures, interpretation 9-15176  
 KBr-RbBr(NaBr,KCl) solid solutions, evap. films, intrinsic spectra 9-10204  
 KBr, additionally coloured, pure and doped, effect of K colloids 9-16414  
 KBr, F-centre absorpt., temp. depend. 9-17280  
 KBr cry. with H<sup>-</sup> ions, far infrared deriv. of force const. model, abs. as function of freq. 9-10184  
 KCl:Ag, forbidden transitions 9-12381  
 KCl:Cd, coloured, u.v. and F band 9-5925  
 KCl:Mn<sup>2+</sup>, charge transfer spectra 9-3892  
 KCl:Mn<sup>2+</sup>, spectra, in range 0.1 to 15 mol% of dopant conc. 9-5923  
 KCl-KBr mixed crystal, F centre excitation, decay rate obs. 9-9721  
 KCl, of V<sub>k</sub> center, lattice effect 9-9720  
 KCl, spectra, colour centres representation 9-5920  
 KCl, X-irrad., defect production obs. 9-18462  
 KCl crystals, possible use in amplification 9-10164  
 KCl small crystals and films, i.r. absorpt. size- and shape-dependence 9-21626  
 KClO<sub>4</sub>, spectra of Cl<sub>2</sub><sup>-</sup> molecular ion, X-irradiated crystal 9-21625  
 K<sub>2</sub>CrO<sub>4</sub>, spectra, eff. of uniaxial compression, 20°K 9-10206  
 KI, fundamental band, elec. field effects 9-1783  
 KI cry. with H<sup>-</sup> ions, far-infrared, deriv. of force const. model, abs. as function of freq. 9-10184  
 KMn<sub>1-x</sub>Ni<sub>x</sub>F<sub>3</sub> single cryst., electron-magnon transitions in spectra 9-1785  
 KNO<sub>3</sub>-M(NO<sub>3</sub>)<sub>2</sub>, (M=Ba, Sr, Ca), liquid mixtures, composition depend. 9-1018  
 KNiF<sub>4</sub>, antiferromagnet, temp. dependence 77-620°K 9-1782  
 K<sub>2</sub>NiF<sub>4</sub>, comparative study with KNiF<sub>4</sub> 9-7976  
 K-Na-KCl-NaCl system, by colloidal particles 9-1725  
 LaSb films, thickness dependence 9-3897  
 LiCl of V<sub>k</sub> center, lattice effect 9-9720  
 LiF,  $\epsilon_{\text{eff}}$  increase due to X-irradiation 9-5926  
 LiF, R<sub>2</sub> zero-phonon line, 4.2°K, moment analysis of Stark effect 9-14054  
 LiF, thermal treatment effects rel. to effects on thermoluminescence 9-5969  
 Mg vapour by mols. and quasimols., 2852 Å 9-18328  
 MgAl<sub>2</sub>O<sub>4</sub>:Cr<sup>4+</sup>, spectrum 9-18708  
 MgF<sub>2</sub>, n-irradiation-induced vacuum u.v. absorpt. 9-1787  
 MgO, n irradiated and annealed, zero-phonon lines 9-5389  
 MgO, plastic deformation eff. 9-18740  
 MnO crystal film, spectra, 280-1000nm at 300°K and 77°K 9-1797  
 MoS<sub>2</sub>, hexagonal and rhombohedral crystals, props. 9-1798  
 (NH<sub>4</sub>)<sub>2</sub>CrO<sub>4</sub>, spectra, eff. of uniaxial compression, 20°K 9-10206  
 Na, interband, influence of pseudopotential Fourier coeff. V<sub>200</sub> 9-1793  
 Na, liquid and solid, electron-electron interactions eff. 9-21628  
 Na<sub>2</sub>O-Al<sub>2</sub>O<sub>3</sub>-GeO<sub>2</sub> glass, study of p-induced colour centres 9-18482  
 Na Hartree approximation and energy loss 9-3844  
 NaBr, F-centre absorpt., temp. depend. 9-17280  
 NaCl:Mn<sup>2+</sup>, spectra, in range 0.1 to 15 mol% of dopant conc. 9-5923  
 NaCl:OH<sup>-</sup>, i.r. spectrum, 0.6-4.2°K 9-16415  
 NaCl, N<sub>2</sub> zero-phonon line, strain broadening 9-1792  
 NaCl films, 25-50 eV region, substrate and exposure to air effects 9-7978  
 NaCl films, far i.r., virtual mode analysis 9-1791  
 NaF, M<sup>+</sup> centre rel. to formation kinetics 9-5392  
 NaNO<sub>2</sub> alkaline earth nitrate molten mixtures 9-13530  
 Na<sub>2</sub>O-ZnO-SiO<sub>2</sub> glasses, i.r. spectra, structural interpret. 9-3894  
 NiO, semiconducting, of small polarons in near and far i.r. 9-5929  
 $\alpha$ , autoionization effect on cross section 9-6980  
 $\alpha$ -O<sub>2</sub> crystalline, peculiarities in range 700-1150 cm<sup>-1</sup> 9-21629  
 O<sub>2</sub>, u.v. and visible absorpt. coeffs. 9-960  
 PbS and PbSe thin films, spectra 9-14021  
 PbSe epitaxial films 9-5863  
 Pb-BiCl<sub>3</sub> molten mixtures, spectra for reaction study 9-13531  
 Rb thin films 9-12384  
 RbBr:Mn<sup>2+</sup>, charge transfer spectra 9-3892  
 RbBr:Ti(Pb), spectra, new band 9-10207  
 RbCl of V<sub>k</sub> center, lattice effect 9-9720  
 RbI:Ti(Pb), spectra, new band 9-10207  
 SbI<sub>3</sub>, spectra, 95-293°K, rel. to direct and indirect transitions 9-3895  
 Sb<sub>2</sub>S<sub>3</sub>, rel. to ferroelec. phase transition 9-3711  
 SbSBr, ferro. 9-10169  
 Sb<sub>2</sub>Se<sub>3</sub>-xI mixed crystals, absorption edge position 9-12385  
 n-Si:P, i.r., dopant eff. on carrier mechanisms 9-18710  
 Si-Te vapour phase, partial press. determ. 9-7307  
 p-Si, e. irrad., oscils. in spectrum rel. to A-centres 9-18659  
 Si, i.r. lattice absorption 9-3510  
 Si, n-irrad., i.r. spectrum rel. to radiation-induced defects 9-15177  
 Si, rel. to non-equilibrium carrier creation during depolarisation 9-21502  
 SiBi<sub>2</sub>O<sub>7</sub>, rel. to darkening on exposure 9-18648  
 $\beta$ -SiC, spectra rel. to exciton states 9-3900  
 SiO<sub>2</sub> films, i.r., variation, influence of heat treatment 9-12386  
 SiO<sub>2</sub> pyrolytic films, i.r. spectra, ht. treatment dependence 9-3195  
 SiO<sub>2</sub> films, evaporated, u.v. irrad. effects 9-5868  
 SrF<sub>2</sub>:Nd<sup>3+</sup>, conc. dependences at 300, 77 and 4.2°K 9-15161  
 SrTiO<sub>3</sub>:Mo(Fe or Ni), reversible photochromic changes, model verification 9-19980  
 SrTiO<sub>3</sub>, stress induced dichroism at edge 9-3858  
 Tb(OH)<sub>3</sub>, Tb<sup>3+</sup> crystal field parameters determ. 9-14019  
 Te: Sb, i.r. spectrum 9-5930  
 Te, in fundamental absorpt. region, 10-300°K 9-21630  
 Te, i.r. edge, effect of Sb impurities 9-18711  
 TlBr, exciton sideband struct. 9-12069  
 TlCl, exciton sideband struct. 9-12069  
 TlCl, spectra in far i.r. 9-3879  
 TlSe, meas. for optical energy gap 9-3556

**Absorption continued**  
**light continued**

- V<sub>2</sub>O<sub>5</sub>, edge, temp. depend. 9-18620  
 VO<sub>2</sub> spectrum below semiconductor-metal transition point 9-18712  
 WSe<sub>2</sub>, n- and p-type, 77° to 295°K 9-5692  
 ZnAl<sub>2</sub>O<sub>4</sub>:Cr<sup>3+</sup>, spectrum 9-18708  
 ZnO, Zn excess, and discoloration rel. to ionized faulted sections 9-14059  
 ZnS:Co(Ni), bond nature effects in stacking faults 9-1796  
 ZnS:Cu single crystal, induced i.r. spectrum, 1-3 $\mu$  9-10213  
 ZnS, rel. to non-equilibrium carrier creation during depolarisation 9-21502  
 ZnS, two-photon, depend. on orientation of polarized light and crystallographic axes 9-21631  
 ZnS, two-photon spectrum near band gap 9-12388  
 ZnSnP<sub>2</sub>, chalcopyrites and sphalerites, spectra rel. to band structure 9-5931  
 ZnWO<sub>4</sub>, spectra of Cr<sup>3+</sup> ions, and i.r. emission, theory 9-14058
- Absundance ratio** see *Elements/relative abundances; Isotopes/relative abundances*
- Acceleration** see *Dynamics; Kinematics*
- Acceleration measurement**  
 See also *Velocity measurement*  
 accelerometer, diaphragm as sensing element 9-8351  
 gravitation, absolute value, Nat. Bureau Standards, USA 9-26  
 gravity at Nat. Bur. Stand., USA (June 1965), apparatus and techniques 9-12557  
 rotational motion, with linear accelerometers 9-20291
- Accelerators** see *Particle accelerators*
- Accommodation coefficient** see *Gases; Kinematic theory/gases; Surface phenomena*
- Accommodation coefficient** see *Gases; Kinetic theory/gases; Surface phenomena*
- Acids, inorganic** see *Individual compounds, and Hydrogen compounds*
- Acids, organic** see *Organic compounds*
- Acoustic amplification in solids** see *Acoustoelectric effects*
- Acoustic analysis**  
 boundary-layer section of fluid, analysis of radiation 9-18229  
 cylindrical radiators, linear row, sound field 9-4311  
 field of point source over elastic plate in moving homogeneous medium 9-4312  
 of four-terminal network closed on reactive load 9-15468  
 frequency of sound, concept 9-4307  
 loudness, automatic; instrument 9-17809  
 signal field, estimation of spectral function peak using cross-correlation function 9-16729  
 solid particle interacts in sound field, role of microstreaming 9-5192  
 sounds prod. in nest of oriental hornet, origin, phys. parameters and significance 9-8512  
 spectrum analyzer using real time Debye-Sears effect 9-2229
- Acoustic field** see *Acoustic radiators; Acoustics; Intensity measurement/acoustics*
- Acoustic generators**  
 See also *Musical instruments*  
 disk, rot., aerodynamic sound study 9-20432  
 transducers for nuclear reactor temp. and gas pressure monitoring, patent 9-6948  
 vibrating bodies sound radiation theoretical and experimental investigation 9-4335  
 KH<sub>2</sub>PO<sub>4</sub>, hyperboud generation at 10<sup>4</sup> Mc/s frequency at 4.2°K 9-18561
- Acoustic impedance**  
 ear drum, meas. apparatus 9-4150  
 electroacoustic, four-terminal network closed on reactive load 9-15468  
 fish tissue, freshwater, by pulse-echo tech. eff. of freezing 9-4323  
 piston, radiation impedance at very low freq., shape depend. 9-10735  
 plane periodic array, gain and single element impedance 9-4334  
 plate, infinite, impedance to longit. force 9-4288  
 strip, flexural vibrs. in infinite baffle 9-4287
- Acoustic mode, crystals** see *Crystals/lattice mechanics*
- Acoustic paramagnetic resonance** see *Paramagnetic resonance and relaxation*
- Acoustic radiators**  
 See also *Doppler effect*  
 baffled array, field calc. using geometrical diff. theory 9-20430  
 bubbles, gas, in liq. natural freq. 9-5156  
 convex cylinder, smooth, pulsating, short-wave asymptotic soln. 9-16733  
 cylindrical, linear row, sound field under mixed boundary conditions 9-4311  
 cylindrical shell in flow, radiation field 9-4310  
 directivity pattern 9-15467  
 elastic plate, vibrating, spatial correl. characts. of sound field near plate 9-4309  
 fields, transient, generated by arbitrary bodies, numerical and analytical solns. 9-2203  
 horn, loudspeaker, circular pipe, directivity and acoustical centre 9-14389  
 infinite elastic plate, excited by transient pt. loading, farfield press. soln. 9-10728  
 infinite plate, sound field correl. 9-4313  
 line source, random, stationary, infinite and spatially inhomogeneous, study 9-15466  
 loudspeaker, conic diaphragm, secondary resonances 9-10736  
 plane circular source, streaming buildup time 9-4322  
 plane periodic array, gain and single element impedance 9-4334  
 point source over elastic plate in moving homogeneous medium 9-4312  
 pressure distrib. at focus, meas. by echo detector 9-17808  
 pulsating rings on cylinder, amp. of vel. potential for far field 9-4308  
 sheets, thin, attenuation vibration 9-19044  
 siren, air or water operated, characts. 9-12936  
 sound field of arbitrary configuration space radiator 9-17793  
 strip, radiation impedance, flexural vibrs. in infinite baffle 9-4287  
 vibrating, cylindrical and dipole, radiation fields 9-4335  
 vibrating surface, integral eqn. for sound rad: iterative soln. and convergence 9-16730
- Acoustic receivers**  
 See also *Microphones*  
 hydrophones, international standardization 9-2227  
 noise (plane wave) rejection at acoustic arrays, anal. 9-16736  
 noise cancellation at acoustic arrays, DICANNE processor 9-19072

**Acoustic receivers continued**

performance comparison using externally sensed parameter receiver as standard 9-17806

**Acoustic resonators**

branched in silencers, optimum dimensioning 9-19067  
in c.w. u.s. spectroscopy, sensitivity enhancement 9-4406  
discand ring, stress anal., radial, torsional vibr. modes 9-4271  
nonlinear, absorpt. characteristics 9-2208  
piezoelectric, perfect, self-excited 9-12201  
superfluid Helmholtz, master eqn. 9-4337  
tube-cavity vibr. modes, math. analysis 9-2221  
u.s., high-amplitude, driven by piezoelec. disc 9-2222  
in waveguide scattering of sound waves with resulting change of mode and absorption 9-17801  
CdSe piezoelec. cryst., self-excited perfect u.s. resonator 9-12008  
Cds piezoelec. cryst., self-excited perfect u.s. resonator 9-12008

**Acoustic streaming**

buildup time, induced by plane circular source 9-4322  
microstreaming, role in interact. of solid particles in a sound field 9-5192  
pseudostationary flow, uniqueness of streamline pattern 9-14806

**Acoustic transducers see Transducers****Acoustic wave propagation**

*See also Absorption/acoustic waves; Dispersion/acoustic; Doppler effect Helium/liquid, sound propagation; Shock waves; Velocity/acoustic waves*

amplification by neutral particle flux during transition radiation 9-4333  
atmosphere, layered, ray tracing using analogue computer 9-17798  
axial ray theory in oceanic propag. 9-15461  
beam forming, digital in freq. domain, algorithm, fast Fourier transform tech. 9-4336  
in cavitating liq. 9-5154  
constant gradient medium, absence of phase change 9-2204  
continuously refracting medium, three layer model 9-2206  
crystal, i.r. e.m. wave-acoustic wave interaction 9-16389  
in dielectric crystals, eff. of finite-amplitude acoustic waves 9-11994  
diffracted beam, propag. behind obstacle 9-16732  
ducts, transmission loss at outlet openings, meas. 9-15464  
fluid, sheared 9-19511  
gas, arbitrarily moving, growth of weak discontinuities 9-5116  
geometrical-acoustic solns., frequency dependent 9-2205  
high freq., band limited waveforms, quadrature-sampling tech. for digital proc. 9-8509  
inhomogeneous media, asymptotic methods of solution 9-4316  
at liquid-gas transition, rel. to dynamics of associated critical fluctuations 9-21244  
long distance infrasonic, following explosion 9-17572  
long distance infrasonic, following explosion 9-17573  
in ocean, axial ray theory 9-15461  
ocean, signals, optimum array detection tech. 9-8161  
ocean, sound channel with parabolic profile, range focusing 9-6061  
one-dimensional, through two elastic cylinders with discontinuities 9-12934  
piezoelectric semiconducting plate in liquid, amplification 9-18556  
piezoelectric semiconductors, amplification by carrier drift and nonlinear amplification effects, review 9-13793  
pulses in homogeneous layer under inhomogeneous half-space 9-4324  
in quartz, eff. of finite-amplitude acoustic waves 9-11994  
ray tracing in layered atm. using analogue computer 9-17798  
sea, near-surface region, surface, coupled losses 9-12573  
second sound in crystal, detection by stimulated thermal scatt. 9-21427  
seismic waves generated by sonic booms, obs. 9-2239  
seismic waves generated by sonic booms, obs. 9-2236  
in semiconductors, piezoelec., nonlinear amplification and automodulation 9-12141  
shallow-water, Wood's model, sound focusing and beaming in the interference field 9-15236  
siren signals in town and country obs. wind effects 9-15460  
in stochastic media, Born series construct. for expectation of potential function 9-14384  
superposition, two coincident finite amplitude plane waves 9-2217  
thermosphere, ducted acoustic-gravity waves 9-12605  
time varying axisymmetric sources in atmosphere, computer model 9-4044  
transducers, antiferroelec. ferroelec., generation of transients in H<sub>2</sub>O, press. pulses obs. 9-4341  
transverse, in type I superconductors, theory 9-1376  
travelling wave in compressible medium, second-order terms in perturbations 9-4317  
underwater, effect of near source bottom conditions 9-12554  
underwater, ray and modal interference theory, eff. of shear flow 9-16526  
in uniaxial crystals, generalized Gruneisen parameters from third order elastic const., calc. 9-5572  
velocity measurement and coefficient of absorption in polymers by travelling wave method 9-5540  
water, shallow, asymptotic soln. for sound field 9-19061  
in waveguide of variable cross section 9-4320  
in wet porous medium, l.f., damping of transverse and longit. waves 9-5541  
Al cylinders, two, with discontinuities between 9-12934  
CdS, photoconducting, acoustic flux distrib., Brillouin scatt. meas. 9-3907  
CdS Rayleigh wave amplification theory 9-18557  
CdS surface waves with allowance for piezoelectric effect 9-18555  
H<sub>2</sub>O, generation of transients, by antiferroelec.-ferroelec. transducers, press. pulses obs. 9-4341  
He crystal, second sound and temp. pulses obs. 9-16030  
LiF crystal, second sound and temp. pulses obs. 9-16030  
in MgO dielectric cry., eff. of finite-amplitude acoustic waves 9-11994  
in MnF<sub>2</sub> dielectric cry., eff. of finite-amplitude acoustic waves 9-11994  
Ne discharge plasma, striated 9-11541

**ultrasonic**

CdSe amplification in surface layer using photostimulation 9-7647  
cell suspensions, biol. changes due to u.s. props., mechanisms for nonthermal sound eff. 9-4351  
change of cyclohexanol 9-5166  
effect on aqueous solutions of methyl iodide 9-3096  
fish tissue, freshwater, sound vel., imped., abs., by pulse-echo tech., eff. of freezing 9-4323  
hypersound, focusing in self-focusing laser beam 9-4319

**Acoustic wave propagation continued****ultrasonic continued**

intensity in liquids, electrodynamic transducer for meas. 9-9507  
liquids under high press., vel. and abs. with press. obs. 9-17205  
through optical-contact bonds at room temp. at GHz freq. 9-10730  
in piezoelectric cubic crystal using Cherenkov radiation 9-10053  
piezoquartz, using Cherenkov radiation 9-10054  
pulsed, intensity meas. with capacitor microphone, MHz freq. 9-3517  
rare-earth metals, helical spin state, u.s. attenuation, dissipation of sound energy 9-1379  
resonant system, subharmonics excitation 9-14388  
semiconductors, generation by elec. field pulses 9-3523  
semiconductors, propagation in presence of a.f. elec. field 9-11998  
semiconductors, ultrasound generation in Gunn effect 9-1524  
transversal vibration of limited width wave 9-10727  
variable gap capacitive detector for displacement amplitude meas. 9-1368  
wurtzite type crystals, surface piezoelectric waves 9-7646  
CaCO<sub>3</sub>, study of phase transition up to 20 kb and 180°C 9-9825  
CdS Lamb u.s. waves, excitation 9-5539  
n CdS piezoelectric semiconductor, generation and reception 9-3609  
CdSe, piezoelec., self-excited perfect reson. 9-12008  
CdSe, surface waves expt. method 9-7648  
Cds, piezoelec., self-excited perfect reson. 9-12008  
n-GaAs piezoelectric semiconductor, generation and reception 9-3609  
LiNbO<sub>3</sub>, hypersonic wave, second harmonic production 9-19857  
MgO:Ni<sup>2+</sup>, rotation of polarization plane 9-1380  
MnF<sub>2</sub>, attenuation near the critical point 9-7920  
Mo, prestrained, damping rel. to crystallographic directions, relax. peaks 9-5546  
N<sub>2</sub>-CO<sub>2</sub> gaseous mixtures at 95 atm., 31-100°C 9-9451  
Ta prestrained, damping rel. to crystallographic directions, relax. peaks 9-5546

**Acoustic waves**

*See also Diffraction; Interference, etc.; Elastic waves; Shock waves; Ultrasonics*

coupling with whistle mode oscillations in high press. plasma 9-2970  
detection of mechanically induced cavitation 9-11670  
in electrical discharges, pulsed, generation and detection in plasma 9-14764  
Epstein profile, general, ray theory 9-2207  
finite amplitude, rounded inverted, sawtooth waves in air, and generation 9-17797  
frequency of sound, concept 9-4307  
interaction with plasma, theory 9-2967  
interaction with plasma, theory 9-876  
internal gravity waves 9-7115  
metal surfaces, excitation by e.m. waves 9-1367  
non-piezoelectric crystals, axes directions 9-11997  
piezo-semiconductors, sonic, theory of fluctuations 9-18552  
piezoelectric semiconductors, coupling with plasma waves 9-9968  
quartz, X-cut, ultrasonic harmonics production 9-9824  
rocket chambers, acoustic anal. of v.l.f. pressure oscs. 9-6402  
scalar-wave beams, time harmonic, nearfield 9-2202  
in semiconductor, anomalous fluctuations in external electric field 9-5670  
sonic excitation of superadiative e.m. state in matter 9-14399  
spectral function peak estimated using cross-correlation function 9-16729  
U.S. pulses in inhomogeneous field, transform. into spin pulse 9-1374  
visualization of standing waves by time-averaged opt. holographic interferometry 9-10738

**effects**

*See also Chemical effects of radiations/acoustic waves*  
acoustic feedback eff. on spread and decay of supersonic air jets 9-21126  
amplification, plasma mechanism 9-5551  
amplification in piezoelectric semiconductors 9-5549  
cell suspensions, nonthermal mechanisms, biol. changes due to u.s. beams 9-4351  
compressible medium, time and co-ord. averages of perturbations 9-4317  
cylinder, rigid; transient motion produced 9-151  
degassing liqs., influence of static press. and temp. 9-5161  
heat, mass transfer processes acoustically stimulated, critical sound press. 9-5228  
image visualization in highly turbid water 9-15238  
infrasonic generated by storms, eff. on human behaviour and correlation 9-8510  
lasers, intracavity modulation using waves of two freqs. 9-4452  
liquids, u.s. cavitation intensity limit criterion 9-5136  
lycopodium particle entrainment 9-5196  
meniscus, vibr., hemispherical, radiation press. effects 9-19856  
non-linear interaction with TEM waves at micro-wave frequencies in plasma 9-15933  
propeller ducts, rot. press. distrib. and eff. of variable tip clearance 9-5103  
quartz, u.s. induced enhancement of Raman spectra 9-21636  
resonance eff. in axial flow compressor stage, excitation by wake shedding 9-17799  
on solar spectral line profiles, short period waves in photosphere 9-16617  
solid particle interacts, role of microstreaming 9-5192  
startle reaction of rats, with and without background noise 9-16643  
steel, case-hardening, insonation effects 9-19845  
on supersonic air jets, acoustic feedback eff. on spread and decay 9-21126  
temperature effects on u.s. treatment of metal surfaces 9-10739  
tobacco mosaic virus, breakage by acoustic transients, hydrodynamical model 9-12937  
ultrasonics, medical and industrial application hazards 9-4348  
u.s. fountain, liq. atomization if cavitation region in spray jet 9-5133  
u.s. visual. of tissue, new scanning and presentation methods, applic. to brain exam. 9-6220  
CdS amplification in wedge or ring crystals 9-5550  
CdS crystal, Rayleigh wave, electron interaction 9-5697  
K<sub>2</sub>Cr<sub>2</sub>O<sub>7</sub> crystn. removal from heat transfer surfaces by u.s. vibrs. 9-4347  
LiF, u.s. radiation effect on region of action of dislocation depletion mechanism 9-9764  
Ne discharge plasma, striated, 9-11541

**Acoustical laboratories**

averaged press. refl. coeff. of absorbing lay-out 9-2231  
reverberation chamber, edge effect of rectang. absorber meas. 9-15463



**Acoustical measurement**

See also *Interferometry/acoustic waves; and under separate subjects e.g. Intensity measurement/acoustics*

- airborne sound insulation, multisource sound averaging technique. 9-2230
- complex sound field meas., develop of apparatus 9-15469
- on crystals, preparatory orientation and polishing 9-3515
- diffraction effects in u.s. devices for vel. and attenuation meas. 9-14385
- dilatometer, gas-actuated, for metallic thermal expansion meas. 9-15009
- edge effect of rectang. absorber, reverberation chamber meas. 9-15463
- electroacoustical techniques on violins 9-20434
- of horizontal range, travel time, sound intensity, numerical integration tech. 9-10729
- infinite plate, sound field, caused by random press. fluctuations 9-4313
- infrasonic design of gradient microphones and windscreens 9-4342
- moving noise source, detect. in a non-stationary background 9-2223
- natural freq., gas bubbles in liq. 9-5156
- noise press. above infinite plane baffle, cross-spectral density 9-4314
- noise press. on recessed plane baffle 9-4315
- objective, or room acoustics 9-2183
- percussion response, immersed hollow spheres, cylinders 9-6385
- pitch perception of white noise, bandwidth influence 9-19069
- probe for press. fluctuations on hypersonic re-entry vehicle 9-4082
- pulse tests on architectural model 9-2234
- radiation focus, meas. of sound pressure with small echo-detector 9-17808
- reverberation meas. by integration method 9-15472
- rooms, for meas. of transmission loss at outlet openings of ducts 9-15464
- sonar signals, clipped-dig. tech. for sequential processing 9-4354
- sound press., automatic sampling and averaging 9-2230
- synchronous filtration method, applic. to petrol engine 9-15470
- underwater, international hydrophone standardization 9-2227
- u.s. absorpt. in liquids, var. of echo impulse method 9-153
- u.s. attenuation, buffer-rod syst. 9-8513
- u.s. attenuation in solid thin specimens using buffer rods 9-3520
- u.s. displacement amplitude, variable gap capacitive detector 9-1368
- u.s. pulses in liquids, electrodynamic transducer for intensity meas. 9-9507
- CaF<sub>2</sub>:Tm<sup>3+</sup> phonon detector, tunable, sensitivity and versatility 9-5524

**Acoustics**

- See also *Acoustic resonators; Architectural acoustics; Atmospheric acoustics; Hearing; Noise/acoustic; Sound reproduction; Speech; Ultrasonics; Vibrations*
- far field generated by pulsating rings on cylinder amp. of vel. potential 9-4308
- fields, transient, generated by arbitrary bodies, numerical and analytical solns. 9-2203
- lenses, cylindrical liq.-filled with large diameter-to-wavelength ratios, focusing props., comments 9-14386
- lenses, cylindrical liq.-filled with large diameter-to-wavelength ratios, focusing props., reply to comments 9-14387
- ray, intensity equations for propag. in inhomogeneous media 9-15462
- ray, new intensity expression 9-17796
- signal quality studies, reference signals 9-10726
- sound field near vib. elastic plate, spatial correl. characts. 9-4309
- sound fields frequency spectrum by laser beam 9-19062
- sound radiation field from cylindrical shell in a flow 9-4310
- supersonic transport fuselage, response to boundary layer and reverberant noise 9-20435

**musical**

- See also *Musical instruments*
- flute and organ pipe, sounding mechanism 9-2224
- pipe organ operation, time delay effects 9-4344
- violin varnish, effs. of mass, stiffness and internal friction 9-4345

**Acousto-optical effects**

- glass-N interface under transient thermal irr., mechanism 9-3181
- liquids, elasto-opt. coeff., ultrasonic light diff. method 9-7265
- radiation detector chambers, absorpt. index rel. to length and conc. of gas 9-6555
- receiver of c.m. e.m. waves, expt. and theory 9-181
- at solid-gas and liquid-vapour interfaces under thermal irr., mechanism 9-3181
- Ge phonon scatt. rel. to energy relaxation of warm carriers 9-12159
- $\alpha$ -HfO<sub>2</sub> solution-grown crystal, high figure of merit, applications 9-3865
- Hg liquid-vapour interface under transient thermal irr., mechanism 9-3181
- Si phonon scatt. rel. to energy relaxation of warm carriers 9-12159
- W-O interface under transient thermal irr., mechanism 9-3181

**Acoustoelasticity** see *Elasticity***Acoustoelectric effects**

- conductors, electron drag by ultrasound 9-1460
- electron gas randomization by trapped acoustoelectric waves 9-15439
- in magnetic fields, classical and quantizing, theory 9-1384
- piezoelectric semiconductor, sound reflection from domains 9-18559
- piezoelectric semiconductors, review 9-13793
- piezoelectric semiconductors, review 9-13793
- in polar semiconductors 9-5560
- quartz bar, x-cut, generating of two pure modes of u.s. waves at 9.4 GHz 9-5548
- second-harmonic generation, piezoelectric crystals 9-2200
- semiconductor, piezoelec., current fluctuations in nonequilib. steady state 9-5559
- semiconductor, piezoelectric, gain and current, non-linear theory 9-5558
- semiconductor, piezoelectric, gain and current, nonlinear theory 9-16173
- semiconductor, theory accounting for anisotropic dielec. and piezoelec. props. 9-12009
- in semiconductors, and acoustic wave amplification 9-5549
- semiconductors, many-valley, absorption and amplification of sound in strong elec. field 9-1372
- semiconductors, many-valley, and semimetals, in quantizing mag. fields 9-1385
- semiconductors, many-valley, interaction of sound with conduction electrons 9-1371
- semiconductors, piezoelec., nonlinear amplification and automodulation of sound 9-12141
- transducers, antiferroelec.-ferroelec., generation of transients in H<sub>2</sub>O, press. pulses obs. 9-4341
- transverse effect 9-18560

**Acoustoelectric effects continued**

- ultra and hypersound generation in cubic piezoelectric crystals using Cherenkov waves 9-10053
- u.s. wave amplification in gaseous plasmas 9-17097
- wine, 25  $\mu$ m, subject to 1  $\mu$ s pulses, excitation of longitudinal acoustic wave 9-19119
- wurtzite type crystals, surface piezoelectric waves 9-7646
- CdS, amplified acoustic flux growth, shifts in freq. of max. intensity 9-9834
- CdS, amplified acoustic oscillations, multitransit noise 9-3530
- CdS, and u.s. attenuation and trapping 9-7650
- CdS, anisotropic piezoelectric semiconductor 9-12009
- CdS, Brillouin scattering study at microwave freq. 9-12013
- CdS, domain propag. from Brillouin scatt. obs. 9-1517
- CdS, interaction, Fabry-Perot analysis 9-12010
- CdS, photoconducting platelets, h.f. currents, departure from Ohm's Law 9-13798
- CdS, piezoelectric, sound reflection from domains 9-18559
- CdS, rippled oscillations in transient of first current saturation, round trip period 9-11995
- CdS, semiconducting, domain formation 9-1515
- CdS, semiconducting, interactions rel. to high-field domain formation 9-13874
- CdS, transverse effect 9-18560
- CdS:Se<sub>1-x</sub>, photoconductive, domain formation 9-3529
- CdS crystal, Rayleigh wave, electron interaction 9-5697
- CdS platelets, h.f. currents, departure from Ohm's law 9-13798
- CdS single crystals, lamb u.s. waves, excitation 9-5539
- CdS wedge and ring crystals, current oscills. and acoustic wave amplification 9-5550
- CdS domains, direct observation 9-3528
- CdTe, transverse effect 9-18560
- GaAs, current under acoustic amplification 9-19912
- n-GaAs, domain propagation 9-9835
- on-GaAs, electroluminescence due to acoustelec. instability of current 9-7995
- GaAs, transverse effect 9-18560
- n-InSb, current oscillations, magnetic field dependence 9-5561
- n-InSb, modes origin 9-12011
- KCl, U.S. oscillations, transformation to electrical oscillations 9-12012
- KH<sub>2</sub>PO<sub>4</sub>, hyperband generation at 10<sup>4</sup> Mc/s frequency at 4.2°K 9-18561
- TiFeF<sub>3</sub>, c.m.-sound conversion by linear magnetostriction 9-16170
- ZnO, Brillouin scattering study at microwave freq. 9-12013

**Acoustomagnetic effects** see *Magnetoacoustic effects***Actinide compounds**

No entries

**Actinides**

No entries

**Actinium**

No entries

**Actinium compounds**

No entries

**Actinometry** see *Photometry***Activation analysis** see *Chemical analysis/by nuclear reactions***Active nitrogen** see *Nitrogen***Active oxygen** see *Oxygen***Adhesion**

- adhesion time of inert gases 9-21347
- aggregate and hardened cement paste, e. microscope exam. of contact 9-17337
- alcohols on water, work of adhesion calc. from spreading press. 9-9494
- bonds in armour plate and other materials, i.r. non dest. testing 9-3481
- brittle matrix composite, strengthening by chem bonding 9-19841
- contact rupture, gas discharge investig. 9-21111
- film, liquid, to cylinder, on withdrawal from Newtonian liquid baths 9-18347
- glass-metal, nonequilibrium theory 9-1335
- glass-metal oxide-metal system, rel. to atom movements and wetting 9-7599
- Johnsen-Rahbek effect, simple theory 9-16040
- metal surfaces, adhesion times for inert gases 9-21347
- metals tending to brittle fracture under combined plastic deformation without heating 9-5492
- mica, van der Waals forces, normal and retarded, direct meas. 9-18398
- phenolic resin-based adhesive films, development and testing 9-18540
- in plastics, glass reinforced, elastic and viscoelastic behaviour 9-17237
- silicates, cleaved in ultra high vacuum 9-7364
- steel and restrained expanding concrete, bond mechanism 9-18500
- Al coatings on steel, effect of condensation temp. 9-21282
- Al<sub>2</sub>O<sub>3</sub>, to metals and alloys, rel. to wettability 9-1336
- Al<sub>2</sub>O<sub>3</sub> substrates, separation force rel. to scoring and annealing 9-1307
- Au spheres, to flat cellulose or polyester surfaces, effect of immersion in water or solns. 9-9605
- Au thin films to glass 9-1337
- Fe<sub>2</sub>O<sub>3</sub> hydrous colloid, to glass, effect of stirring 9-9567

**Adiabatic demagnetization** see *Magnetic cooling***Adion** see *Adsorption***ADP (ammonium dihydrogen phosphate)** see *Nitrogen compounds/ammonium compounds***Adsorbed layers**

- albumin, bovine serum, monolayers water permeability, obs. 9-7262
- 4 amine-p-terphenyl monolayer, intermediate state 9-3208
- base and Fermi atom monolayers on cryst., thermodyn. props. 9-5255
- ethyl chloride, dielec. const. 9-12186
- gases on C surface, condensation 9-9592
- methyl chloride, dielec. const. 9-12186
- monolayers, mixed, thermodyn., mol. areas additivity rel. to components interaction 9-5253
- monomolecular films, intermediate state 9-3208
- phase transform., two-dimensional, in grain boundaries 9-11780
- phosphate on BeO, inhibition of sintering, crystallite growth obs. 9-17241
- protein monolayers water permeability, obs. 9-7262
- Sc, on W(110), structure, LEED obs. 9-1100
- thickness on single crystals, meas. by ellipsometry 9-9609
- Al, on W in field e. microscope, emission characts. 9-11784
- BaO mols. on W(113) face, electromigration obs. 9-17250
- CH<sub>4</sub> on charcoal, mol. dynamics from n scatt. spectra 9-3213

# Adsorbed layers continued

- C<sub>2</sub>H<sub>2</sub> on charcoal, mol. dynamics from n scatt. spectra 9-3213
- Cs on insulating substrates, elec. conduction mechanism 9-5641
- H<sub>2</sub> on charcoal, mol. dynamics from n scatt. spectra 9-3213
- HCl, dielec. const. 9-12186
- Kr, on C surface, two-dimens. van der Waals eqn. 9-9593
- N<sub>2</sub>-O<sub>2</sub> mixtures on anatase, activity coeffs. and deviations from Raoult's law 9-7350
- N<sub>2</sub>, on C surface, two-dimens. van der Waals eqn. 9-9593
- Na dodecyl sulphate monolayers, water permeability, obs. 9-7262
- Ni (110) surface, O monolayer oxidation on exposure to O<sub>2</sub>, stability and high temp. effects 9-12544
- O on Al evaporated film, monolayer formation obs. 9-21273
- O<sub>2</sub>, partial coverage of W (110) and (111) faces, effect on CO<sub>2</sub> adsorpt. 9-3217
- Re on W surface, diffusion, effect of elec. field 9-13707
- Th atoms on W(113) face, electromigration obs. 9-17250
- Ti on W, anomalous migration 9-5264
- Y atoms, equilib. conc., elec. field effects 9-21287

# Adsorption

See also *Chemical analysis/adsorption; Chromatography; Films Heat of adsorption; Sorption*

- $\gamma$ -Al<sub>2</sub>O<sub>3</sub>, ads. of sat. hydrocarbons, ads. energy 9-7344
- on alkali halides, of gases, effect on epitaxy of metal films 9-3199
- n alkali halides, of gases, effect on epitaxy of metal films 9-16044
- anatase, of N<sub>2</sub>-O<sub>2</sub> mixtures, activity coeffs. and deviations from Raoult's law 9-7350
- benzene on graphite, entropy of adsorpt. 9-19675
- benzene on graphite, virial treatment, errors due to hindered rot. 9-17077
- bromide on Zr, Ti and Ni, <sup>80</sup>Br nucl. isomers separation 9-18769
- cachode, gas poisoning, press. and temp. depend. 9-3753
- chemisorption isotherms meas., automatic apparatus 9-1905
- coal, carbonized and activated, rel. to microporous struct. 9-7406
- colloid, of Sb, Sb migration path, e. microscope determ. 9-1111
- rel. to contact angle and spreading on solids and liquids, model 9-7259
- cranine dye to Ag halide suspensions, surface area meas. 9-20566
- entropies and heats, determ. by gas-solid elution chromatography 9-19675
- film surface props., eff. of elastic wave excited by incident atom 9-5233
- foam film, conc. of inorganic ion meas. 9-19650
- gas-solid scattering, trapping eff. 9-3210
- gas-surface reactions, book 9-5230
- gelatin, on AgBr 9-7343
- gelatin to AgBr microcrystals 9-3214
- graphite, freshly powdered, adsorpt. of O<sub>2</sub> and H<sub>2</sub> 9-1091
- graphite, of I, and desorpt. in vacuum and Ar, 27-1100°C 9-9626
- hydrocarbon, pure and mixed, s-D equation of state, derivation and experimental data 9-9629
- isotherms, physical, at extremely low pressures 9-19674
- Langmuir theory appl. to metal outgassing at high vacuum 9-14299
- large atoms, configurational entropy 9-3209
- lipid layers, of water, iodine; dielectric const., freq. dispersion depend. obs. 9-12138
- metal, adsorbate-adsorbate interaction effect on charge of alkali atoms 9-3212
- metal-BaTiO<sub>3</sub> contact, effect of gaseous adsorption 9-7802
- migration path of adsorbed atoms. e. microscope determ. 9-1111
- model for environmental effects in fatigue crack propagation 9-3446
- oxidized carbons, characterization by gas-phase adsorption 9-8096
- physical, applications of McLachlan's theory 9-13587
- poly(dimethyl siloxane) on various surfaces, macromol. size 9-17251
- poly(methyl methacrylate) on various surfaces, macromol. size 9-17251
- polystyrene, effect of pore structure and nature of absorbent surface 9-17251
- polystyrene from carbon tetrachloride soln. on various surfaces, macromol. size 9-17251
- silica gel, effect of adsorbed H<sub>2</sub>O on elec. cond. 9-13915
- silica gel, radiolysis of adsorbed hydrocarbons 9-20063
- solid soln., ordered,  $\beta$ - brass type, in surface layers 9-3211
- at solid surface, from non-athermal polymer solns, numerical solns in parallel-layer model 9-18400
- from solution, kinetics, diffusion and adsorption-desorption antagonism 9-16045
- steel, solution of atmospheric gases during spontaneous surface cleaning 9-21283
- suction effect on adsorpt. of photosensitized H atoms 9-17247
- thermo-adsorption transfer 9-13806
- wood charcoal, of methanol, expansion effect 9-11781
- zeolite molec. sieve, of Kr at 273 and 298°K 9-7345
- Ag ordered phase of complex structure, e. diff. obs. 9-7357
- AgBr, of gelatin 9-7343
- AgCl, effects on mechanical behavior 9-13738
- C, of CO<sub>2</sub> and benzene, Dubinin theory of micropore filling 9-7346
- C, of He, rel. to press. and superficial pore sizes 9-7347
- C, of I from aqueous soln, with micropore filling 9-9625
- C (charcoal), of CH<sub>4</sub>, C<sub>2</sub>H<sub>2</sub>, C<sub>2</sub>H<sub>4</sub> and H<sub>2</sub>, mol. dynamics from n scatt. spectra 9-3213
- C blacks, gas isotherms rel. to surface area calc. and porosity 9-7348
- C films, of O, rel. to elec. resist., -196 to 450°C 9-7795
- C molecular sieves, of Kr, at 273 and 298°K 9-7345
- CO on Cu at 77°K, ads. and interac. behaviour 9-21285
- Cu, 4.2°K of He 9-19676
- Cu spherical single crystals, O<sub>2</sub> ads., surface struct. 9-5259
- Fe, of O<sub>2</sub>, effect on surface energy 9-9603
- Fe, of surface active cpds. and corrosion inhibitors, effects of deformation and heat treatment 9-18760
- Ge, of Cu from electrolyte, effect on Ge surface props. 9-5704
- Ge surface elec. props. after exposure to O<sub>2</sub> after heating in vacuo 9-3651
- H isotopes, quantum-statistical partition function 9-13586
- H<sub>2</sub>O on sugar carbon, p.m.r. relaxation times 9-5257
- Hg, of Cl<sup>-</sup>, specific, at Hg/aqueous soln. interface 9-17246
- II, liq. of atomic admixtures on quantized vortices 9-1060
- Kr on Cu at 77°K, ads. and interac. behaviour 9-21285
- MgO, adsorpt. of methanol and ethanol, i.r. spectra 9-3215
- Mo, of O, on polycryst. filaments, meas. by thermionic emission and work function changes 9-11787
- Mo of O<sub>2</sub> and H<sub>2</sub>, study by field emission retarding potential analyser 9-11782
- MoO<sub>3</sub>, of photosensitized H atoms, suction effect 9-17247
- N<sub>2</sub> on silica-supported Ir, I.R. Spectra 9-20934

# Adsorption continued

- N<sub>2</sub>O, adsorbed on NaCl, NaBr, NaI films, spectra 9-19443
  - NH<sub>3</sub>, on W(211) surface, and decomposition 9-19679
  - Na bentonite amine complexes, of H<sub>2</sub>O vapour and methanol, hydrophilic-hydrophobic props., obs. 9-5261
  - NaCl, of H<sub>2</sub>O effect of prior exposure to HCl, CO<sub>2</sub> and H<sub>2</sub>O vapour 9-19678
  - NaCl, of In, In migration path, e. microscope determ. 9-1111
  - Ni film epitaxial on NaCl, ads. of Xe 9-17248
  - O<sub>2</sub> on Cu at 77°K, ads. and interac. behaviour 9-21285
  - O<sub>2</sub> by tungsten ribbon, obs. by flash method 9-9600
  - Rep. of O, on polycryst. filaments, meas. by thermionic emission and work function changes 9-11787
  - Rn on aerosols as size meas. method 9-7287
  - Sc films on (110) face of W, rel. to electron props. 9-1115
  - TiO<sub>2</sub>-aqueous soln. interface, of H<sup>+</sup> and OH<sup>-</sup> thermodynamics, obs. 9-7351
  - TiO<sub>2</sub>, of Ag ions, in aqueous and methanolic solns. 9-10348
  - TiO<sub>2</sub>, isotherms and differential capacity curves rel. to electrochem. double level model 9-9606
  - TiO<sub>2</sub>, partially reduced, e.s.r. of adsorbed O<sub>2</sub> 9-17249
  - W, atomic binding of transition metals 9-9628
  - W, of Bi<sub>3</sub> and nucleation 9-21284
  - W, of Ba, on (100) face, eff. on work function 9-19680
  - W, of CO on (110) and (111) faces, effect of partial average with O<sub>2</sub> 9-3217
  - W, of H, field-emission patterns of phases 9-19677
  - W, of H<sub>2</sub>, field-emission patterns 9-5775
  - W, of Na, work function meas. by field-emission electron projector 9-1112
  - W, of O, on polycryst. filaments, meas. by thermionic emission and work function changes 9-11787
  - W, of O<sub>2</sub>, and desorption, meas. via thermionic emission and work function changes 9-11786
  - W, of U monolayer(113)lms on (100), ( and (110) oriented faces, work function meas. by photoelec. and contact potential diff. meas. 9-14901
  - W, of Y, and migration and evaporation 9-3216
  - W, of Y, elec. field effect on equilib. conc. 9-21287
  - W, orientated surface, adsorpt. of Ba 9-9627
  - W, single cryst., of Cs, by meas. of thermionic emission props. 9-11785
  - W (100) face, O<sub>2</sub> two-layer adsorpt. at room temp. 9-21286
  - W (110), of Na atoms, bonding between layers 9-1113
  - W(100) surface, adsorpt. and decomp. of NH<sub>3</sub> 9-1114
  - Xe on Cu at 77°K, ads. and interac. behaviour 9-21285
  - Xe on Ni films epitaxial on NaCl, comparison with data for Ni film on pyrex 9-17248
  - Xe surface, adsorpt. of Ne 9-9622
- Aerials** see *Electromagnetic waves/radiators*
- Aerodynamics**
- See also *Flow/gases; Jets; Shock waves; Supersonic flow; Turbulence*
- aerofoil, symmetric sub-critical press. distrib. at zero incidence 9-19581
  - aerofoil in exponential shear flow 9-9435
  - aerofoils in cascade, flexure torsion flutter theory and expt. 9-7219
  - air flow over water, instability 9-17154
  - ballistic vehicle meeting shock wave, interaction of turbulent region 9-19578
  - Bernoulli's principle, kinetic theory derivation 9-5099
  - blunted cones and wedges, asymptotic theory 9-9437
  - blunted wedge at hypersonic speeds, asymptotic theory 9-17153
  - boundary layer, laminar, of flat plate with sinusoidal variation of air flow 9-17149
  - boundary layer in air, gas-dynamical parameters and chemical content at high temperatures 9-13484
  - boundary layers, compressible, stability eqns. 9-11649
  - boundary layers, laminar three-dimens., mass injection effects 9-11647
  - boundary layers, turbulent, separation in front of step 9-11648
  - cascade of blades in subsonic shear flow, lifting-line theory 9-7218
  - delta wing, minimum drag in supersonic flow 9-11653
  - detached shock calculation by 2-order finite differences 9-946
  - discharge through square-edge orifice, transient effects 9-5108
  - flow behind shock wave, asymptotic expansion 9-21130
  - flow over flexible plate, nonlinear flutter theory 9-11650
  - for wind tunnels, small hypersonic, intermittent probe traversing gear 9-9436
  - high supersonic speed, vehicle design methods 9-5102
  - hypersonic wind tunnel, heat transfer obs. by i.r. camera 9-160
  - hypervelocity wake, anal. of atomic and mol. species using microwave and i.r. absorp. 9-19577
  - jet flap, ground effect influence on flowfield, linear theory 9-9432
  - laminar boundary layer, 3-dimens., conical external flow 9-19579
  - of lifted flat flame 9-20456
  - near wake flowfield of cone, injection effects rel. to species and nozzle locations 9-21128
  - panel, two-dimens., in supersonic stream, stability boundaries, Liapunov anal. 9-21127
  - pattern of 3-d supersonic flow past segment-shaped body 9-5100
  - perfect gas, equations for plane steady motion, invariant transformation 9-18323
  - profiled coupling curves, differential eqn. derivation 9-9430
  - propeller ducts, sound field, rot. press. distrib. and eff. of variable tip clearance 9-5103
  - radiation gas-dynamics, nonlinear shock wave formation 9-11651
  - rarefied gas, moments of high rank 9-18322
  - resistance of pipes with triply running spiral channels 9-15970
  - Reynolds number variation pitching model, var. with angle of attack 9-19580
  - scattering matrix on complex shapes 9-14809
  - separated flow region, press. fluct., noise sources 9-5104
  - sharp cone drag coeffs. at supersonic speed, correl. 9-7217
  - shell, cylindrical, unsteady oscils. in internal or external supersonic flow 9-7220
  - sonic, compact equation for nonideal gases, applicable for z values down to 0.80 9-13482
  - sonic bang intensities in stratified still atmosphere 9-17816
  - sonic generation by rot. disk 9-20432
  - supersonic perturbation of rotating body 9-949
  - transpiration cooled porous flat plate in stream of air or CO<sub>2</sub> 9-20453
  - transport phenomena in gas between moving strip and fixed plate 9-8460
  - turbulence characts. of Mach 3 body wake 9-11652



**Aerodynamics** continued

- turbulent boundary-layer separation ahead of cylinder, assoc. shock pattern. 9-7214
- two lifting bodies, nonlinear interaction 9-5109
- unsteady flow around cone, linear approximation 9-17155
- velocity field due to shock waves incident on stationary thin symmetric body 9-5101
- velocity meas. with heated element, or skin friction gauges 9-5106
- vibration of beam in turbulent flow, effect of random loading in time and space 9-119
- vibrational-dissociation behind shock wave 9-13483

**Aeronomy** *see Atmosphere; Meteorology*

**Aerosols**

*See also Foams*

- $\alpha$  track autoradiography of submicron aerosol particles with electron microscope 9-15693
- adsorption of radon obs. proportional to surface area 9-7287
- air pollution due to aerosols from internal combustion engines 9-8169
- atmospheric, charge equilibrium 9-18790
- atmospheric, electrophotographic picture on semicond. surface 9-4057
- atomizer with resonance chamber, patent 9-7288
- backscatter estimation and reduction in optical system 9-17571
- condensation, form. in highly supersaturated vapor 9-5197
- crystallization in ultrasonic fields 9-18374
- drops falling in elec. field, small particles capture 9-7286
- flow, laminar, in horiz. tube, gravity settling 9-5198
- holographic sub-micron particle detection 9-16789
- liquid atomization in u.s. fountain if cavitation region in spray jet 9-5133
- Lycopodium particle entrainment in acoustic field 9-5196
- medical effects of inhalation 9-4137
- nebulizer, pneumatic, for solns. spectrochem. analysis use 9-21736
- polystyrene latex, attachment coeffs. of charged and neutral  $^{212}\text{Pb}$  atoms from Rn decay 9-9565
- powders airborne in duct, mass flow meters 9-3136
- radioactive, retention in respiratory tract, obs. and simulation 9-15378
- radioactive, vertical exchanges and deposition rates above continents and oceans 9-10395
- single particles, light scatt. diagrams, influence of collecting lens aperture 9-14864
- size, number and trajectory in expts. controlled by charging 9-3137
- size and vel. distrib. by holography 9-18375
- supercooled, prob. of crystallization 9-11727
- turbidity in atmosphere, 1958-68 obs. 9-17563
- UKAERE health physics div. progress report (1967) 9-20257
- u.s. resonators aerosol conversion capabilities 9-2222
- Ag, condensation, particle surface area, obs. 9-5197
- Fe particles, thermal expansion and structural anomalies 9-5199

**Afterglow** *see Discharges, electric*

**Ageing**

- martensite, deformed and from cold-worked austenite, thermal effects 9-7595
- Nimonic alloys, recovery due to dissolution of precipitated  $\gamma'$ -phase 9-13765
- Nujol/water emulsions, stabilized, rel. to rheological changes 9-5201
- permalloy thin films, rel. to anisotropy field  $H_k$  and dispersion  $\alpha_q$  9-3471
- plastic stress relax., in time depend. 9-5433
- precipitation hardening, book 9-11951
- solid solution, variation in lattice constants, theory 9-11828
- solid solutions, lattice parameter variation, data analysis 9-11829
- steel, E1702, and quenched, effect of grain size on resistance to deform. 9-9760
- steel, Fe-ni-Si-C, eff. on martensite fracture 9-18517
- steel, martensitic, C-bearing, at room temp., heat evolution 9-1344
- steel, strain-aged, yield point directionality 9-17307
- Zircaloy-2, annealed, effect of irradiation on strain ageing 9-17330
- Ag-Cu solid solns, supersaturated, substructure changes during decomposition 9-1339
- Al-Au dilute alloys, characteristics from yield stress and elec. resistivity meas. 9-21394
- Al-Cu alloys, impure, transient effects in early stages 9-7594
- Al-Mg-Ge alloy, transformation stages 9-9782
- Al-Zn alloys Guinier-Preston zone miscibility gap obs. in precipitation reversion studies 9-21393
- Al-(10wt.%)Zn alloy, infl. of Cu addition on charact. 9-17329
- Al-Zr alloys, age-hardening 9-13762
- BaTiO<sub>3</sub>, followed by optical and electrical meas. 9-1324
- Co-Nb alloy, rel. to precip. of new phase 9-9796
- Co-75 wt.-%Pd alloys, residual resistivity rel. to short-range-order 9-12100
- Cu-Be alloys, sp. ht. temp. depend. 9-13763
- Cu-(2.5 wt.-%)Be alloy, effect of electron bombardment 9-5501
- Cu-Pd alloys, specific heat changes at low temp. induced by quenching and ageing 9-9844
- Fe-(23 at.-%)Be alloy, structure changes by transmission e. microscopy study 9-17343
- Fe-C alloys, precipitation kinetics, infl. of age-hardening rate 9-9798
- Fe-Cr alloy, at 475°C rel. to Guinier-Preston zones formation 9-9785
- Fe-Ni-Si-C steel, eff. on martensite fracture 9-18517
- Fe-Ni-Ti alloys, improvement of mechanical props. 9-11928
- Fe, electrolytic, amplitude depend. internal friction method 9-13764
- Mg-(9wt.-%)Ni alloy, hardening precipitation 9-3472
- NH<sub>4</sub>Cl dendrites, by dissolution of side arms 9-3473
- Ti alloys, age-hardenable, composition and props., patent 9-13771
- ZnS-Cu, electroluminescence ageing mechanism 9-1844

**Air**

*See also Atmosphere*

- air pollution, indoor, half-lives of HCl, SO<sub>2</sub> and smoke 9-4051
- air-CO<sub>2</sub> laser, c.w. 9-17870
- air-water system, degassing in sound field, influence of static press. and temp. 9-5161
- arc, electrodeless, at high-pressures 9-7209
- arc column, decay, effects of temp.-depend. thermal diffusivity and rad. losses 9-9423
- arc discharge, low-current, electrode vapour effect on electron conc. in plasma 9-9353
- boundary layer, gas-dynamical parameters and chemical content at high temperatures 9-13484
- boundary layer, laminar, of flat plate with sinusoidal variation of air flow 9-17149

**Air** continued

- breakdown, laser-induced, self-focusing effects 9-5090
- breakdown and prebreakdown conditions in cylindrical geometry 9-14805
- breakdown by nanosecond laser pulse, obs. 9-13470
- components modification, effect on spark counter operation 9-19231
- corona discharge, point, effect on convective heat transfer 9-5091
- density meas. by Rayleigh scatt. instrum. in rocket 9-12594
- diffusion of org. vapour, teaching expt. 9-8340
- discharge in narrow gap with nanosec rise time 9-7202
- electric discharge at atmos. pressure, X-ray production 9-5094
- flow characteristics in cylindrical vessel 9-21123
- flow of air-water mixture in tube, characteristics of disturbed region 9-18331
- flow over water, instability 9-17154
- fluorescence efficiency under e bombardment, 65 km, Ee=700 eV 9-14158
- heat transfer from solid spheres, importance of turbulence parameters 9-17162
- heated, flow in diffuser, friction and heat transfer in separation regions 9-9425
- inertia effects in pressurized gas bearing 9-21125
- initially heated, interaction with microwave field 9-7158
- interaction with sea, atmospheric motion 9-12578
- ionized by shock, conductivity meas. perpendicular to mag. field 9-915
- loading on membrane, effect on vib. configs. 9-4286
- low-temperature thermodynamic props., tables 9-3053
- mass transfer from naphthalene and phenol vibrating cylinders 9-21250
- molecules, vel. determ by effusion, intermediate laboratory expt. 9-12823
- movements followed using atmospheric radioactivity 9-17564
- oxidation of mild steel, effect of air speed 9-21694
- permittivity meas. using Maxwell's commutator bridge 9-5121
- plasma breakdown on interaction of intense r.f. fields with shock-heated air 9-9397
- spark production by train of mode-locked laser pulses 9-11636
- sparks, laser produced in 200 kG mag. field, obs. 9-7205
- supersonic dissociated, turbulent boundary-layer heat transfer 9-21120
- supersonic jets, acoustic feedback eff. on spread and decay 9-21126
- thermodynamic functions, approx. for density and sound vel. 9-10386
- turbulent, molecular backscatter of laser rad., density and vel. fluct. obs. 9-21141
- turbulent flow in rounded corner triangular duct, local friction and heat-transfer coeffs. 9-13491
- turbulent flow in tube with axially varying heat flux, Nusselt number prediction 9-13487
- turbulent jet + N<sub>2</sub>, high temp., similarities for different nozzles and temp. 9-9433
- turbulent wake behind hypervel. sharp slender cones 9-17152
- velocity meas. with heated element or skin friction gauges 9-5106
- weakly ionized, dielectric meas. in v.h.f. range 9-11584
- <sup>3</sup>H estimation by liq. scintillators, Ti target emission meas. 9-8138
- Pt surface accommodation coeff., press. depend. 9-16039

**Airglow**

- See also Atmospheric spectra; Aurora; Sky brightness, Twilight; Zodiacal light*
- day, O<sub>1</sub>(<sup>1</sup> $\Delta_g$ -<sup>3</sup> $\epsilon_g$ )O<sub>1</sub> band obs., brightness 9-14167
- dayglow of oxygen A band 9-4068
- luminous wake of Black Brant II rockets, 80-115 km altitude, obs. 9-10411
- night, measurement, instrumentation 9-21789
- night spectrum, 1.02  $\mu$ -1.13  $\mu$ , obs. 9-20101
- night tropical, O green and red emissions, mechanisms suggested 9-8191
- nightglow, polarization of line and continuum emission 9-20099
- nightglow brightness, 1957-63, maxima rel. to solar u.v. and corpuscular rad. 9-20100
- Venus, differential photometric scan of dark limb 9-2057
- O green and red emissions, mechanism suggested 9-8191
- O<sub>2</sub>(<sup>1</sup> $\Delta_g$ -<sup>3</sup> $\Sigma_g^-$ ) band, evening twilight, at 1.58  $\mu$ , interpret rel. to ozone dissociation 9-4069
- OI, 6300 Å and 5577 Å lines, night, intensity profiles 9-8192

**Albedo** *see Cosmic rays; Earth; Neutrons and antineutrons/reflection; Nuclear reactors, fission*

**Alfven waves** *see Magnetohydrodynamics; Plasma/oscillations*

**Algebra**

- C\*, automorphisms of free boson field 9-12872
- C\*, complex Banach with hermitian involution 9-20301
- C\*, generation by Weyl operators, construction props. and automorphisms studied 9-12865
- Clifford, quasi-free states description, Bogolioubov transformation representation 9-14312
- conformal mapping method, for hadron scatt. amp. 9-16854
- curvature tensor of asymptotically flat space time 9-8397
- Dirac, relationship to six-dimensional Lorentz groups 9-2133
- eigenvalue of self-coupled operator, iterative procedure for determ. 9-41
- Green's theorem in paracompact manifolds modelled on Hilbert space 9-15417
- Laplacian operator domain extension by delta functions 9-14318
- Lie, of pseudo-orthogonal and pseudo-unitary groups, construction of invariants 9-8373
- Lie, Poincare and internal symmetry Lie algebra combination, theorems deriv. 9-19187
- Lie, semi-simple, realization with quantum canonical variables 9-16802
- Lie, simple, index of representation, charact. 9-14316
- Lie algebra inhomogenizations and complex representations 9-6283
- Lie algebras and groups in inhomogenization 9-8366
- Lie groups, semisimple, induced representations 9-17697
- linear eqns., estimating perturbations during soln. 9-12868
- local, operator, in presence of superselection rules 9-14452
- matrix-valued functions of complex variables, factorization 9-14315
- von Neumann, quasi-standard, from locally normal states in quantum statistical mechanics 9-20341
- Petrov type spaces, null e.m. fields 9-10618
- pi functions, current formalism representations 9-4550
- Poincare Lie, for discussion of P, C, T 9-311
- polynomial construct. for wave functions for three-body syst. 9-15429
- SL(2C); subalgebras and contraction survival 9-42
- Vandermond determinant for soln. of linear eqns. 9-40
- W\*, book 9-12870

**Algol** *see Calculating apparatus/digital computer programmes*

**Algorithms** *see* **Calculation**

**Alignment** *see* **Mechanical measurement**

**Aliphatic compounds** *see* **Organic compounds**

### Alkali metal compounds

*See also the compounds of the individual metals*

- alkali-silicate glasses, binary and ternary, elec. cond. and dielec. props. 9-3690
- alloys, liq., Knight shift rel. to composition 9-5190
- bromides, f.c.c., valence and conduction band, Schrödinger eqn. soln., Brillouin zone symmetry 9-3554
- crystals, internal attractive press., rel. to interionic distance, derivation 9-21290
- felpars, bond lengths rel. to ordering and ionic character 9-7356
- fluorides, second order Raman spectra calc. for vibration spectra computation 9-12429
- iodides, photoemission spectra, L-bands and exciton bands 9-3759
- molybdates and Ag halides, molten, miscibility gaps 9-17192
- nitrate, fused, elec. double layers 9-21707
- salicylaldehyde complexes, i.r. spectra 9-7028
- seeded, rare gases, descriptive, theory development of positive columns 9-13469
- silicate glasses, internal friction rel. to ionic position interchange, 180°-500°C 9-3404
- sulphates, thermal decomposition and sublimation, mass spectrometric studies 9-19663

### halides

*See also the compounds of the individual metals*

- additively coloured, photocond. 9-13930
- additively-coloured crystals, electronic conductivity 9-12085
- alkali halide crystals, Debye temp. rel. to lattice props., interac. pot. calc. 9-12019
- anharmonicity and cohesive energy 9-11984
- chloride soln. in Hg cell structure, patent 9-8106
- chlorides,  $Cl^-$  L $\alpha$  absorption spectra rel. to x-ray exciton, electronic band structure and two electron excitation 9-1815
- complexes with thiourea, Madelung energy 9-9633
- crystal elec. fields due to dislocation motion in bending deformation 9-1453
- crystal growth and charact., rel. to conc. of  $OH^-$  ion 9-7374
- crystals, i.r. absorpt. rel. to lattice props., interac. pot. calc. 9-12383
- crystals with  $S^-$  trapped impurity, e.s.r. spectra 9-3954
- deformable shell model 9-3393
- dielec. dispersion obs.; lattice structure and forces calc. 9-16074
- diffusive penetration of boundaries 9-9728
- divalent cation doped, crit. shear stress, non clustering impurity ion-vacancy pairs 9-3413
- divalent cation doped, impurity-vacancy-dipole agglomerate and impurity-rich precip., rel. to critical shear stress 9-5372
- E.S.R. of  $O_2^-$  9-8010
- F $^+$  centre, prod., meas., and model 9-19756
- F $^+$  centre formation and optical absorpt. meas. 9-5381
- F centre electronic states 9-5380
- F $^-$  centre, relaxed excited, electronic props. 9-9719
- F-centre formations, exciton mechanism 9-5383
- fluorides,  $^{19}F$  n.m.r. chem. shifts in  $H_2O$   $D_2O$  solns. 9-3124
- fluorides, enthalpies of mixing of binary liq. systems 9-10324
- gas ads. effect on epitaxy of metal films 9-3199
- gas ads. effect on epitaxy of metal films 9-16044
- inert gas diff., theory 9-3386
- internal friction, time depend. 9-7530
- iodide crystals, e.s.r. of trapped  $O^-$  9-10289
- ionic crystals, shock-compressed, nonequilibrium radiation, temp.  $>1eV$  9-14970
- ionization and dissociation by e impact 9-21108
- laser induced damage and optical strength 9-16390
- laser-irradiated damage to crystals 9-1411
- light amplification, possible use of crystals 9-10164
- liquid films, periodic oscillations of impurity particles 9-9504
- luminescence decay time meas. method 9-5954
- magneto optical props. of substitutional H atoms 9-12345
- migration and trapping of inert gases 9-11891
- phosphors, mixed, absorption spectra of isostructures, interpretation 9-15176
- photoconductivity, multiphoton excitation by laser emission 9-13941
- photoconductivity of additively-coloured crystals 9-13930
- plastic deformation depend. on hydrostatic pressure 9-18503
- Raman scattering by hydroxyl ion 9-12432
- Raman spectra of  $CN^-$  ( $OH^-$ ,  $NO_2^-$ ) doped crystals 9-12407
- Raman spectra of  $O_2^-$  in crystals 9-1807
- Raman spectra of  $O_2^-$  ion 9-10220
- solid solutions containing KBr, intrinsic absorption spectra 9-10204
- solubility in organic solvent binary mixture, rel. to dielec. constant of solvent mixture 9-14834
- thallium activated, quantum efficiency of F- and  $Tl^0$ -scintillations 9-16445
- thermal expansion at melting pt., ratio of inflection pt. dist. in pot. energy curve to equil. interionic dist., comp. and correct. of calc. 9-15008
- two-quantum excitations 9-21618
- u.v. velocity and attenuation in crystals containing  $CN^-$  9-11996
- u.v. exposure of crystals with impurities photochemical reaction 9-5581
- $V_K$  colour centre lattice effect on optical absorpt. 9-9720
- Van Vleck paramagnetism 9-19947
- $Ag^+$  ions on anion sites, B centre props. 9-5387
- CN in alkali halides, electric field induced dichroism 9-3857
- $ClO_4^-$  impurity ion symmetry at temps. 300-700°C from i.r. absorpt. temp. dependence 9-18704
- Eu activated, luminesc. of red region  $\rightarrow$  blue after explosive reaction 9-7999
- and KCNS, molten mixture, eutectic comps. 9-17193
- NaCl type, elastic constants calc. from interatomic parameters 9-7518
- Zn, vibration spectra and thermodynamics 9-792

### Alkali metals

*See also the individual metals*

- atom, core polarization corrections to oscillator strengths 9-4843
- atom, ground state, rare-gas-induced gyromag. ratio shifts 9-11403
- atom adsorbed on metal, net charge 9-3212
- atom bound states obs. 9-18142
- atom reactions with halogens, harpooning dynamics 9-1888
- atom source, charge-exchange, fast 9-11415

### Alkali metals continued

- atom-rare gas collision, fine structure transitions 9-11411
- atomic beams, reactions with polyhalide mols. 9-9307
- atomic beams, reactive scatt. from polyhalide mols. 9-7096
- atoms, heavy, selection rules rel. to collisional  $m_J$ -mixing in lowest  $^2P_{3/2}$ -states 9-9147
- atoms and positive ions, charge exchange 9-3014
- charge exchange with halogen, ion-pair prod. mech. in flame detector 9-21739
- dark injection of electrons into anthracene, photoelectric effect 9-1618
- double mag. reson. signal, displacement on changing r.f. field strength 9-2823
- elastic constants, second- and third-order, calcs. and band-structure energy contrib. 9-9740
- elastic wave propagation, correlation contribution 9-5417
- Heine-Abarenkov electron-ion pseudopot. investig. by calc. thermoelec. power 9-10061
- ionic core radii calc. and orthogonality corrections 9-19682
- molecules, potential energy functions rel. to electronegativity 9-7027
- nuclear spin-lattice relax. rates and Knight shifts, electron-electron interaction effects 9-17501
- optical pumping, polarization filter 9-4830
- superconducting, electron-phonon interaction contrib. to density of states 9-19901
- superconductivity 9-5661
- vapour, permittivity at resonance frequencies 9-3057
- vapour, permittivity at resonance frequencies 9-13494
- vapour, thermal conductivity, expt. compared with gas kinetic theory 9-14817
- CBR $_4$  reactions 9-810
- Cs-Li bifluid MHD generator, parametric cycle analysis 9-10798
- H $^+$  alkali metal atomic collision with charge exchange 9-6985
- K-Li bifluid MHD generator, parametric cycle analysis 9-10798
- Na-Li bifluid MHD generator, parametric cycle analysis 9-10798
- Rb-Li bifluid MHD generator, parametric cycle analysis 9-10798

### Alkaline earth compounds

*See also the compounds of the individual metals*

- alkaline-earth chalcogenides, additive coloration technique 9-7500
- aluminate,  $Eu^{2+}$ -activated, fluorescence 9-21650
- halophosphate phosphors,  $Eu^{2+}$ -activated, prep. and luminescence 9-21643
- hydroxides, gaseous, dissoc. energies and conc. in fuel-rich  $H_2+O_2+N_2$  flames 9-17517
- nitrate- $NaNO_3$  molten mixtures absorpt. 9-13530
- oxides, computed ground state props. in molecular orbital approx. 9-7015
- oxides, defects, review 9-9693
- oxides, F-centres, Faraday rotation studies 9-3362
- oxides, thermal dissociation process 9-6002
- phosphate glasses, optical, Mossbauer and e.s.r. spectra rel. to iron valence states 9-15173
- sulphides, shear-induced coloring 9-1745
- tungstates, u.v.-induced absorpt. peak, wavelengths, lattice constant dependence 9-5913

### Alkaline earth metals

*See also the individual metals*

No entries

**Allotropes** *see* **Phase transformations; Polymorphism**

### Alloys

- See also Ageing; Crystal structure, atomic/alloys; Heat treatment/alloys; Solid solutions; Steel; and under alloys or compounds of the named elements. Alloys such as  $Au_3Cu$ ,  $Au-Cu$ ,  $Au-Cu-Zn$  are indexed under compounds of the named elements, i.e. Gold compounds, Copper alloys, Zinc compounds in these examples*
- alloys, binary, ordering energy and effective pairwise interactions 9-7696
- antiphase domains, equilib. boundaries, theory allowing for short-range order 9-1163
- b.c.c., solvent atom diffusion 9-7507
- binary, diffusion and Kirkendall shift, comments 9-9727
- binary, diffusion and Kirkendall shift, comments 9-9726
- binary, diffusion and Kirkendall shift, comments 9-18484
- binary, effect on Sn plasticity 9-9761
- binary, liquidus solidus curves 9-3150
- binary, one-dimens., electronic structure 9-7707
- binary, single-site approx. in electronic theory 9-7708
- binary and ternary, study rel. to spin subband thermoelec. power determ. 9-3718
- binary B-metal, new metastable electron phases 9-9794
- binary films, co deposition by e beam, controlling apparatus 9-11776
- binary  $\sigma$  phases, radiation damage from X-ray diff. obs. 9-11868
- corrosion in carburising gases of high-temp. alloys, factors affecting corrosion-resistance 9-17532
- creep behaviour at elevated temps. 9-7547
- d-alloys, dilute, localised mag. moments, mechanism of appearance 9-10086
- defect structures, thermally softened, response to stress 9-21335
- degassing in vacuum 9-13747
- dilute, energy spectrum and props., numerical analysis 9-3552
- dilute, low-temp. thermopower; depend. on virtual recoil of solute ions 9-1603
- dilute magnetic, free spin susceptibility, with ferromag. or antiferromag. coupling 9-10090
- dilute nonmagnetic, Kondo-Nagaoka spin-compensated state and localized spin fluctuations 9-1634
- embrittled by enrichment of boundaries with impurities, reduction in grain boundary surface energy 9-11922
- Engel Brewer theories 9-9667
- f.c.c., solid solution strengthening rel. to dislocation motion 9-7598
- ferromagnetic, coupled thin ferromagnetic layers composition, patent 9-19960
- ferromagnetic, dynamical spin states 9-16341
- ferromagnetic, electrolysis for thin film formation, patent 9-19959
- ferromagnetic, electrolysis for thin film formation, patent 9-13994
- ferromagnetic, saturation magnetostriction above room temp. 9-10125
- ferromagnetic conduction electron spin polarization range, depend. on impurity conc. determ. by neutron scatt. 9-10120
- ferromagnetic in thin film, composition and magnetostriction, patent 9-19958
- growth of single crystals, techniques 9-21291
- internal friction at large strain amplitudes 9-16118



**Alloys continued**

- junction transistor, inverse  $\alpha$  characts, reln to forward  $\alpha$  at different injection levels 9-21526  
 Laves phase cpds., Debye temp. and radius ratio of component atoms 9-9836  
 liquid, ferromagnetic behaviour 9-13540  
 liquid, thermoelec. power 9-9546  
 liquid, viscosity-concentration curves, near eutectic temp. 9-15995  
 liquid alkali, Knight shift rel. to composition 9-5190  
 magnetic dilute, conduction electron spin polarization 9-12230  
 mass-disordered lattices, displacement correlations and frequency spectra using Green's functions 9-9809  
 metal, disperse phase coalescence, diffusion-induced, kinetics 9-1243  
 metal, dispersed particles size distrib. function 9-9786  
 metallic, dilute with magnetic impurities, superconductivity below Kondo temp. 9-7779  
 monovalent, electron states distrib. 9-7705  
 multicomponent, depression of freezing pt., deviation from Raoult's law 9-17227  
 non-ferrous, grain size influence on hardness, fracture and other mech. props. 9-9653  
 non-magnetic, dil. c.-phonon effects and superconductivity 9-1495  
 ordering rate, composition depend. of A<sub>2</sub>B type 9-9790  
 phase transformations, study by hardening dilatometry 9-3484  
 precious metal, use in high-temp. resistance strain gauges 9-13723  
 pseudopotentials and residual resistivity calc. 9-5593  
 refractory, high-temp., long-time creep 9-19798  
 semiconducting, with stoichiometric vacancies, thermal conductivity 9-17358  
 semiconductor, lattice thermal conductivity 9-15015  
 spherical sample preparation 9-21403  
 standards for neutron activation anal., prod. by splat-cooling 9-16645  
 steel, strength without brittleness 9-5491  
 superalloys, vacuum melting and casting 9-5493  
 superconducting, properties review with theory 9-9946  
 superdislocation blocking in superstructure L<sub>1</sub> 9-9710  
 superlattice formation, field ion microscope obs. 9-7402  
 ternary, configurational free energy rel. to composition 9-21398  
 ternary, element redistrib. laws, rel. to diffusion 9-3381  
 transition, metal magnetic ordering, new type 9-1658  
 transition metal, magnetic ordering new type 9-13959  
 weakly ferromag., strongly paramag. near critical conc., mag. and elec. props 9-1641  
 Al-Ag, liquid quenching, depend. of Ag solid solubility 9-19831  
 Au-Cu photoluminesc., radiative recomb. obs. 9-21660  
 Au-Cu type, ordered, superdislocations 9-1216  
 C-Hf(Ta,Zr), reinforced, commercial development 9-3467  
 Cu-Sn, electron transport, Ziman theory and exptl. data comparison 9-7274  
 Cu-Zn elastic moduli var. with annealing time 9-9738  
 Fe-Cr, oxidation kinetics 9-20044  
 Fe-Si, high temp. sp. ht., mag. susceptibility temp. depend., up to 1870°K 9-7601  
 Hg<sub>1-x</sub>Cd<sub>x</sub>Te semiconductor, photoconductive i.r. detector 9-8522  
 Ir-based, dilute, spin fluctuations and superconductivity 9-1499  
 Mg<sub>2</sub>Cd type, ordering rel. to anomalous change in resistance 9-3570  
 Ni and alloys, 3d zone struct. from thermopower 9-12207  
 Pt-Co permanent magnet, improvement of mag. props. by replacement of Pt with other Pt group metals 9-12294  
 Pt-Fe permanent magnet, improvement of mag. props. by replacement of Pt with other Pt group metals 9-12294  
 U-Ti, phases, orthorhombic, metastable 9-19823  
 Zr, hydride precipitates, orientation 9-19683

**Alnico alloys** *see Nickel alloys*

**Alpha decay** *see Nuclear decay theory; Radioactivity/decay periods; Radio-activity/decay schemes*

**Alpha-particle model** *see Nucleus/models*

**Alpha-particle spectra**

*See also Nuclear decay theory*

- nucleus, even-even, decay,  $\alpha$  surface distribution determ. 9-19292  
<sup>241</sup>Am fission,  $n_{th}$  induced, long-range  $\alpha$  energy spectra meas. 9-9074  
<sup>243</sup>Fr  $\alpha$ -decay; classification of nuclei as spherical or deformed 9-563  
<sup>244</sup>Pu, fission,  $n_{th}$  induced, long-range  $\alpha$  energy spectra meas. 9-9074  
<sup>252</sup>Cf-<sup>249</sup>Cm, energy and intensity meas. 9-11251  
<sup>252</sup>Cf-<sup>250</sup>Cm energy and intensity meas. 9-11251  
<sup>255</sup>Ac  $\alpha$ -decay; classification of nuclei as spherical or deformed 9-563  
<sup>217</sup>At  $\alpha$ -decay; classification of nuclei as spherical or deformed 9-563

**Alpha-particle spectrometers**

- semiconductor, for investigation thickness dist. of a active elements in thin layer 9-8931  
 (n, $\alpha$ ) telescope involving two proportional and one scintillation counter 9-11131  
<sup>234</sup>U isotope contents, semicond. detector obs. 9-2835  
<sup>235</sup>U isotope contents, semicond. detector obs. 9-2835  
<sup>238</sup>U isotope contents, semicond. detector obs. 9-2835  
 CdTe, surface barrier and Mg, B drifted, as  $\gamma$ - and  $\alpha$ -Spectrometers 9-8937

**Alpha-particles**

*See also Cosmic rays/alpha-particles and helium nuclei; Radioactivity*

- Bragg curve shape, particle interaction effect 9-15036  
 phys. props., expt. for eval. 9-6255  
 properties calc. from matrix elements from N-N phase shifts 9-16911  
 superfluid nuclear matter, nucleons form  $\alpha$ , effective mass calc. 9-6713

**absorption**

- thickness meas. of target foil 9-2560

**angular distribution**

- solid state track detect. 9-2611  
<sup>232</sup>Th and <sup>238</sup>Ra,  $\alpha$ - $\alpha$  ang. correl of serial decay 9-6840  
<sup>13</sup>C(d, $\alpha$ )<sup>11</sup>B,  $E_d=6.3$  MeV, obs. 9-2757  
<sup>7</sup>Ge,  $\gamma$  irradiated, interpretation of spectra 9-2720  
<sup>41</sup>K(p, $\alpha$ )<sup>39</sup>Ar reaction, and excitation function obs.  $E_p=1550-2000$  keV 9-20784  
<sup>91</sup>Nb,  $\gamma$  irradiated, interpretation of spectra 9-2720  
<sup>14</sup>N(n, $\alpha$ )<sup>11</sup>B,  $E_n=14.1$  MeV, evidence for reaction mechanism 9-9039  
<sup>14</sup>N(n, $\alpha$ )<sup>11</sup>B,  $E_n=14.1$  MeV, obs. 9-11297  
<sup>16</sup>O(<sup>4</sup>Li, $\alpha$ )<sup>12</sup>F react. 4.8-13.8 MeV., analysis of yield and ang. distrib. meas. 9-11325

**Alpha-particles continued****angular distribution continued**

- <sup>16</sup>O( $\alpha+2\alpha$ )<sup>12</sup>C<sub>24</sub> correlation at  $E_\alpha \approx 25$  MeV, obs. 9-4798  
<sup>31</sup>P(p, $\alpha$ )<sup>28</sup>Si, spin mixing coeff. determ. 9-2734

**detection, measurement**

- See also Alpha-particle spectrometers+ Dosimetry; Particle detectors; Radioactivity measurement*  
 autoradiography for Pu distrib. in fuels, improved resolution 9-19374  
 concentration of long lived alpha emitters in aerosols, spectroscopic method 9-552  
 discrimination  $\alpha$ -p 9-19226  
<sup>237</sup>Np thin layer prep. methods 9-13158  
<sup>8</sup>Be-<sup>2+</sup>He, produced by 20 GeV/c proton interactions with heavy nuclei of emission 9-16955  
<sup>75</sup>Br compound nuclei from <sup>12</sup>C+<sup>63</sup>Cu, p and  $\alpha$  emission energy comparison 9-6828  
<sup>75</sup>Br compound nuclei from <sup>26</sup>O+<sup>59</sup>Co, p and  $\alpha$  emission energy comparison 9-6828  
 Si drifted detectors, pulse obs. rel. to elec. field and charge collection in detector 9-2591  
 ZnS(Ag) crystals, stability of radiation under bombard of  $\alpha$ , e. 9-11139

**effects**

*See also Nuclear reactions and scattering due to/alpha-particles*

- atom excitation, KX-radiation obs. 9-677  
 defects in irradiated material, spatial distribution 9-13668  
 dielectrics, liq., irradiated, conduction mechanism 9-5179  
 hexane, ionization current induction 9-9549  
 Monazite, metamictization, not removed by heat treatment 9-3280  
 organic films, reaction with nuclei producing diffr. patterns 9-15039  
<sup>210</sup>Po source, ion pair prod. energy for various gases 9-15951  
 Ag, Au, films, epitaxial and polycrystalline, elec. resistance and struct. 9-5240  
 Ag irradiated, black-spot damage nature 9-18459  
 Al, elec. conductivity, rel. to strain and temp. 9-7746  
 Ar-methane mixtures ionization, 1.58-5.3 MeV 9-5058  
 Ar, irradiated, yield of reson. states 9-13447  
 Au foils, quenched, irradiation effects on tetrahedra 9-7495  
 Si, high resistivity regions 9-3662  
 ZnSAg, scintillation, amplitude elec. field dependence 9-3937  
 ZnS(Ag) crystals, stability of radiation under bombard of  $\alpha$ , e. 9-11139

**interactions**

- $\alpha\alpha$ , potential, emission,  $\alpha$ -part. nuclei model, review 9-15649  
 $\gamma$ -He<sup>+</sup>He<sup>0</sup>, differential cross-sections calc. using impulse approx 9-6660

**scattering**

- $\alpha$ - $\alpha$ , D-wave phase shifts, effs. of vacuum polar 9-11119  
 $d\alpha$  14.2 MeV, obs., phenomenological pot. analysis 9-4789  
 Al thin foils, ang. distrib. meas.,  $E_\alpha=6.0, 8.8$  and 20 MeV 9-8921  
 Au thin foils, ang. distrib. meas.,  $E_\alpha=6.0, 8.8$  and 20 MeV 9-8921  
 Be thin foils, ang. distrib. meas.,  $E_\alpha=6.0, 8.8$  and 20 MeV 9-8921  
 Ni thin foils, ang. distrib. meas.,  $E_\alpha=6.0, 8.8$  and 20 MeV 9-8921

**Altimeters** *see Length measurement***Aluminium**

- adsorbed on W, in field e microscope, emission characts. 9-11784  
 anodic oxidation, and growth and struct. of Al<sub>2</sub>O<sub>3</sub> layers formed 9-4004  
 anodized and blackened, heat absorption characteristics 9-5576  
 atoms and ions, bibliography of spectra 9-13287  
 atoms spectrum, hollow cathode discharge obs. 9-18134  
 with  $\beta$  radiation pt. source, abs. dose distrib. 9-12034  
 brass-texture in polycryst., rel. to orientation changes caused by slip 9-9670  
 cathode protrusion formation during pre-breakdown conditioning 9-11633  
 coatings on steel, struct., composition and adhesion, effect of condensation temp. 9-21282  
 coatings on steel by vacuum evaporation 9-13584  
 conductivity, thermal, rel. to changeover phenomena and transverse phenomena in kinetic coeffs. of trivalent metals 9-3541  
 corrosion by CuSO<sub>4</sub> 9-20057  
 corrosion in citric acid, (chelating agent), effect of F<sup>-</sup> 9-10344  
 critical tensile strength of strain-hardened samples 9-16124  
 crystallization in liq. vibrating melt, crystallite transport and effect on structure refining 9-7375  
 cyclic work softening, effect of yield curves in tension 9-18504  
 cylinders, reln. between ultimate press. and wall thickness 9-5473  
 damping and modulus defect during plastic deform. of single crystals. 9-9744  
 dechanneling of protons at stacking faults, H accumulation 9-16102  
 deformation, stored and expended energy rel. to tensile strain and orientation 9-1283  
 deformed, 4.2°K, elec. resistivity 9-3567  
 diffusion and solubility of Pu 9-11957  
 diffusion in SiC from solns. in rare-earth metals, for p-n junction prep. 9-16056  
 diffusion of U, infinite dilution 9-17282  
 dislocation densities and configuration rel. to stress 9-21338  
 dislocation loops, climb kinetics 9-11880  
 dislocation viscous drag at high strain rate 10°K, 77°K, 300°K and 500°K 9-1214  
 e-e scatt. and resistivity low temp. depend. 9-1463  
 elastic constants, third-order, determ. from sound velocity meas. 9-9737  
 elastic constants, third-order, meas. 9-21358  
 electrode, erosion by impulse accelerator plasmas 9-9412  
 electron displacement damage in a high voltage electron microscope 9-3334  
 electron energy losses and optical data 9-16191  
 electron exoemission without photostimulation 9-5773  
 electron flux spectra for <sup>199</sup>Au and <sup>64</sup>Cu sources 9-18571  
 electron scattering, Monte Carlo calc. 9-7683  
 electron spin correlations from nuclear dipole relax. time meas. 9-7925  
 energy loss of protons and deuterons of identical velocity 9-21452  
 energy loss spectra, characteristic, of 8 keV electrons in liquid and solid  $\gamma$ -7249  
 epitaxial films, orientation dependence on substrate defects 9-1105  
 epitaxial growth on KCl, KBr and KI crystals 9-7377  
 fatigued, cell struct. and dislocation tangle obs. 9-5347  
 fatigue and annealing, low temp., resistivity changes 9-13846  
 fibre texture by X-ray and n diff. 9-5490  
 film, covered with NaCl layer, intensity of photoelectrons emitted 9-19939

# Aluminum continued

film, elec. resistance variation rel. to method of deposition 9-13582  
 film, electron energy losses rel. to thickness and surfaces 9-5588  
 film, thin, from substrate in acid soln. with fluoride ions, patent 9-19684  
 film, wavelength depend. of optical transmittance in vacuum u.v. 9-10166  
 film evaporated, O and H<sub>2</sub>O vapour interaction 9-21273  
 films, absorption study and theoretical explan. 9-19986  
 films, oxidation, effect of oxide thickness 9-18754  
 foil, for 584-Å, filter 9-6019  
 foil, refr. and refl. of fast electrons 9-17362  
 foil preparation for electron microscope exam. 9-16071  
 foils, electron energy loss 0.3-1 MeV Monte Carlo calc. 9-5587  
 foils, high-angle grain boundary structure 9-18442  
 fracture in 3% Zn amalgam, behaviour rel. to grain-size, pre-strain and strain rate 9-19806  
 grain-boundary migration effect on Xe bubble distrib. 9-657  
 Grüneisen parameter volume dependence 9-15010  
 heat capacity using adiabatic calorimeter in range 25-500°C 9-12014  
 impurities participation in i.r., u.v., and visible absorption spectra of diamonds 9-19987  
 internal friction, amplitude depend. rel. to previous thermal and mechanical treatments 9-17299  
 K<sub>α</sub> X-ray satellites in fluoresc. spectra of Mg in oxides and metals 9-3933  
 Kikuchi lines, pseudo-, obs. using e. microscope 9-9669  
 layers optical props. influence of dielectric films 9-5886  
 liquid, contact angles on sapphire, effect of nature of surfaces 9-19622  
 liquid, diffusion of Si, temp. depend. of coeff. 9-9496  
 liquid, ordered structural region size estimation by X-ray scatt. 9-17187  
 luminescence centre in SiC, recombination rates 9-5949  
 Matthiessen's rule deviations, size-dependence 9-21481  
 mean excitation potentials from stopping power data 9-9135  
 model for steel ductile fracture study when subject to compression 9-18516  
 optical interband absorption, pseudopotential model calc. 9-14047  
 optical resonance transitions, lifetime measurements, phase shift method 9-11392  
 painting, electrophoretic, rel. to paint film defects 9-4005  
 parallel plate dynode & multiplier, preparation method 9-10824  
 phonon spectrum of granular mat. from tunnelling meas. 9-9817  
 photoemission of electrons into Si<sub>3</sub>N<sub>4</sub> 9-10081  
 plastic deformation in quench-hardened single crystals 9-11924  
 plastic deformation on cutting at high velocities, specific work consumed 9-9758  
 plastically deformed, internal friction, low temp. 9-7524  
 plasticity of notched bars of intermediate thickness with small shoulder ratio, yield point 9-2195  
 plates, spinning into cone, fracture formation 9-13734  
 porous, shock response on compaction, computer simulation 9-5437  
 positron annihilation radiation, angular correlation calc. from atomic Hartree-Fock orbitals 9-5638  
 positron lifetimes, cyclic deformation effects 9-16220  
 precipitate phases, formation by ion implantation 9-11956  
 precipitation from supersaturated soln. in α-U, kinetics 9-11960  
 pseudopotential and binding energy 9-9891  
 quenched, nucleation and growth of multi-layer defects 9-3344  
 recovery, low temp., after 0.4 MeV e. irradiation 9-1323  
 recovery eff. on cell struct. and dislocation density 9-13687  
 recovery of resistivity in stages II and III after 2-MeV e. irradi. 9-9696  
 reflection coeff. diminution for laser light 9-21603  
 scattering of 9 and 15 MeV bremsstrahlung 9-11267  
 sheets, limiting speed of ductile crack propagation 9-18524  
 sintered, grain boundary maximum of internal friction 9-1266  
 sintering, in presence of liquid phase, effect of Cu additions 9-16141  
 slip band continuity across grain boundaries 9-7498  
 solar spectrum, Al I multiplets, 1-2 μ, 30 km balloon obs. 9-6190  
 solubility of H<sub>2</sub> and D<sub>2</sub>, 400-600°C, validity of square root law 9-9787  
 Sondheimer oscillations in resistivity, meas. and interpret 9-7745  
 specific heat, 330-890°K, vacancy formation contributions 9-7654  
 splash generation by detonation wave impact 9-5438  
 stage-III annealing after deuteron irradi. at different temps. 9-21389  
 strain rate history, dislocation theory of intersections 9-18498  
 strain-hardened, mechanical properties 9-16124  
 substitution partial in BaFe<sub>12</sub>O<sub>19</sub> effect on saturation magnetization 9-16366  
 superconducting film, dependence of critical temperature and energy gap on thickness 9-1497  
 superconducting film, dependence of critical temperature and energy gap on thickness 9-15080  
 target, neutron scatt. 9-591  
 texture, axial, X-ray diff. exam. 9-3289  
 thermal control surface for Mars Lander, protection from dust storm 9-1386  
 thermal radiation props., meas. by cyclic incident radiation 9-5562  
 thermodynamic props., anharmonic effects, data anal. 9-21434  
 u.s. attenuation in normal state, electronic contribution 9-9829  
 vacancies, relaxation props., under quasi-equilibrium conditions 9-19743  
 vacancy migration, applic. of potential deduced from pseudopotential theory 9-9700  
 X-ray Debye temp. from n. scatt. obs. 9-7639  
 X-ray emission spectrum, K<sub>β</sub> band-shape anode-potential dependence, 4.5-20 keV 9-1814  
 X-ray spectra, K<sub>α</sub> satellites, relative intensity 9-18717  
 α- and β- irradiated, elec. resistance meas. rel. to strain and temp. 9-7746  
 Al-Al<sub>2</sub>O<sub>3</sub>-Au structure, capacitance and I-V characs., oxide thickness depend. 9-18642  
 Al-Al<sub>2</sub>O<sub>3</sub>-Au tunnel structures, photovoltaic props., annealing effect 9-7861  
 Al-Al<sub>2</sub>O<sub>3</sub>-Bi:Pb(Te) junctions, tunnelling characs. 9-5722  
 Al-Al<sub>2</sub>O<sub>3</sub>-Bi tunnel junctions with ultrathin Bi films, I-V characs. 9-9966  
 Al-As-Ga system, thermodynamic and optical treatment of phase diagram 9-17346  
 Al-Ni powder mixtures, sintering, exothermic effs. 9-17324  
 Al-Ni powder mixtures, sintering, exothermal effs. on Al content and porosity 9-17325  
 Al-Se-Al thin film structure, negative resistance 9-13908  
 Al-SiO-Al system, I-V charact., and temp. dependence 60 to -185°C 9-1562  
 Al-SiO<sub>2</sub>-Si, injection and migration of charges in oxide 9-5741  
 Al-steel interface, heat transfer, directional effect rel. to surface conds. 9-13809

# Aluminum continued

Al, pitting and blistering on p-irrad., orientation dependence 9-9604  
 Al, plasmaron structure in soft X-ray L<sub>2,3</sub> emission spectrum 9-5943  
 Al, shell, cylindrical under axial compression; free edge buckling 9-1280  
 Al 1100 at 300°F, time-dependent uniaxial stress, strain depend. on stress history 9-21363  
 Al (III), hydrolyzed, coagulation of SiO<sub>2</sub> dispersions, kinetics and rate-determining reaction 9-9570  
 Al crystallites, lattice residual deform. distrib. and inhomogeneity of plastic deform. after uniaxial compression 9-1182  
 Al electrode erosion by impulse accelerator plasmas 9-9411  
 Al form factors of truncated at. potentials 9-9875  
 Al III, semiempirical atomic core potentials, coeffs. 9-19397  
 Al X-ray atom form factor determ. from vanishing second order reflection in high-voltage electron diff. 9-9676  
<sup>27</sup>Al, in methyl ammonium aluminium sulphate NMR rel. to phase transitions 9-3968  
<sup>27</sup>Al in equiatomic rare-earth-Al cpds., n.m.r. and susceptibility 9-3969  
<sup>27</sup>Al in Fe-Al alloys, dilute, n.m.r., rel. to <sup>57</sup>Fe 9-1874  
 Al-Al<sub>2</sub>O<sub>3</sub>-Al tunnel junctions, potential barrier shape 9-15120  
 Au, resistance and thermoelec. power, effect of high pressure 9-16306  
 C-Al barrier, electron current calc., applic. of perturbation method 9-18572  
 Cu-Al barrier, electron current calc., applic. of perturbation method 9-18572  
 α-Fe, plastic stress relax., time depend. 9-5433  
<sup>14</sup>N ions passing thro., range-energy relations 9-9869  
 Pt-Al discharge, Pt excitation inhibition, obs. 9-18134  
 strain rate history, fracture behaviour rel. to grain size, pre-strain and strain rate 9-19806

## Aluminum alloys

See also *Aluminum compounds*  
 alnico, structural states, X-ray diff. exam 9-1179  
 Alnico alloys, magnetostatic and exchange interactions between particles 9-18676  
 aluminium bronze, As-containing, CuAl5- type, fatigued, stacking fault tetrahedra 9-19752  
 concentration of Zn by photoactivation 9-1933  
 duralumin-water laminate, velocity of sound variation 9-3518  
 duralumin deformed at 77°K, thermal and elec. conductivity 9-12025  
 etching conditions, patent 9-19833  
 fatigue crack growth rate, possibility of decrease using plastic deform. 9-21381  
 fretting corrosion products 9-20053  
 impurity-dislocation interaction rel. to repeated yielding (Portevin-Le Chatelier effect) 9-11925  
 painting, electrophoretic, rel. to paint film defects 9-4005  
 Poisson's ratio during creep and recovery 9-18493  
 Portevin-Le Chatelier effect (repeated yielding) rel. to impurity-dislocation interaction 9-11925  
 production by direct reduction of aluminous ores, rel. to thermal behaviour of bauxite source material 9-11952  
 stress-corrosion and distribution, eff. of shot peening 9-17533  
 thermal conductivity calc. from that of Al and electrical resistance meas. 9-19866  
 thermal expansion, low temp. 9-19864  
 Ticonal 2000, sintered, in high coercivity state, structure 9-3302  
 Ag-Al, transition of Gd 4f electrons from bound to virtual levels 9-1462  
 Ag-Al system, hexagonal ζ-phase, stacking-fault energy calc. from thermodynamic data 9-19750  
 Ag-Al system, hexagonal ζ-phase, stacking-fault energy, exptl. determ. 9-19751  
 Al:Cr dilute low temp. impurity resistance 9-1473  
 Al/Al<sub>2</sub>O<sub>3</sub>, ductility rel. to oxide particle size 9-17305  
 Al-Ag, GP zones from X-ray small angle scattering parameters 9-13627  
 Al-Ag, liquid quenching, depend. of Ag solid solubility 9-19831  
 Al-Ag, precipitation study, use of different contrast in electron microscopy 9-7605  
 Al-Ag, soft X-ray emission spectra, interpretation 9-15181  
 Al-Ag<sub>2</sub>Al, eutectic alloy, preferred orientation development during growth 9-1123  
 Al-Al<sub>2</sub>O<sub>3</sub>, dispersion-strengthened SAP, hardness, 20-600°C 9-7577  
 Al-Au, dilute, age-hardening from yield stress and elec. resistivity meas. 9-21394  
 Al-4wt.%Au, elec. resistance rel. to plastic deform. effects 9-12098  
 Al-Be, clustering, effect of cold working 9-18458  
 Al-Cu-Cd, θ' precipitation, effect of Ag and Ge additions 9-1327  
 Al-Cu-Mg, precipitation study, use of different contrast in electron microscopy 9-7605  
 Al-(0.3at.%)Cu, recovery of resistivity in stages II and III after 2-MeV e. irradi. 9-9696  
 Al-(1.7at.%)Cu, relaxation props. of vacancies under quasi-equilibrium conditions 9-19743  
 Al-Cu, deformed, precip. and recrystallization 9-21400  
 Al-Cu, grain refinement, chemical and mechanical 9-16144  
 Al-Cu, impure, transient effects during early stages of ageing 9-7594  
 Al-Cu, lattice const., effect of lattice strains, rel. to inhomogeneity in precipitation and age hardening 9-9783  
 Al-Cu, precipitation study, use of different contrast in electron microscopy 9-7605  
 Al-Cu, θ' structure, lattice parameters determ. 9-11834  
 Al-CuAl<sub>3</sub>, eutectic, preferred orientation development during growth 9-1123  
 Al-CuO, sintering effects due to CuO reduction 9-3463  
 Al-Fe binary system, electronic structure, X-ray investigation 9-3553  
 Al-(0.3at.%)Ge, recovery of resistivity in stages II and III after 2-MeV e. irradi. 9-9696  
 Al-4.4 at.%(0.3 at.wt.%)Be, Be-vacancy interaction 9-9701  
 Al-Li, Al<sub>3</sub>Li superlattice 9-3282  
 Al-(5 wt.%)Mg-(0.4 wt.%)Ag, precipitate-free zone, light and electron microscopy obs. 9-18537  
 Al-Mg-Ge, ageing, transformation stages 9-9782  
 Al-Mg-Ge, clustering after quenching 9-17331  
 Al-Mn, dil. mag. susceptibility, 2-300°K 9-12238  
 Al-Mn, multi-faulted loops, formation and annealing 9-13686  
 Al-Mn dilute, low temp. impurity resistance 9-1473  
 Al-Mn recrystallization interaction with solid soln. decomposition 9-1153  
 Al-10 wt.%Si composites containing Ni-coated sapphire whiskers, role of Ni 9-21385



**Aluminium alloys continued**

- Al-Si eutectic, transverse band form. on directional solidification, mag. field effects 9-5313  
 Al-Sn prealloyed powders, atomizations 9-18536  
 Al-Sn prealloyed powders, pressing characteristics 9-18501  
 Al-Zn-Mg, kinetics of clustering 9-7600  
 Al-Zn-Mg, precipitation study, use of different contrast in electron microscopy 9-7605  
 Al-(10wt.%)Zn, infl. of Sn addition on ageing characters. 9-17329  
 Al-(0.3at.%)Zn, recovery of resistivity in stages II and III after 2-MeV e. irradi. 9-9696  
 Al-(78 wt.%)Zn, superplasticity, mechanism 9-21370  
 Al-Zn, dilute, n.m.r. of  $^{27}\text{Al}$ , quadrupole structure 9-12508  
 Al-Zn, eutectic, preferred orientation development during growth 9-1123  
 Al-Zn, rhombohedral distortion of transition phase, Zn content effect 9-7604  
 Al-Zn, superplastic state 9-21369  
 Al-Zn GP zones from X-ray small angle scattering parameters 9-13627  
 Al-Zn precipitation reversion studies, miscibility gap for Guinier-Preston zones obs. 9-21393  
 Al-(20 wt.%)Zn, triple point cracks nucleation and growth 9-3448  
 Al-Zr, age-hardening 9-13762  
 (93wt.%)Al-(7wt.%)Mg segregation and precipitation at grain boundaries 9-19832  
 Al-6.7 at. % Zn, Guinier-Preston zones, formation and reversion 9-13626  
 Cu-Al,  $\beta$  martensite annealing, new ordered phase 9-1350  
 $\alpha$ -Cu-Al, high-temp, vacuum tensile fatigue rel. to Al content 9-9771  
 Cu-Al, phase transformations and equilibria under high pressure 9-19837  
 Cu-Al, stacking faults, cubic type, in plastically deformed martensite 9-16103  
 Cu-Al, transition of Gd 4f electrons from bound to virtual levels 9-1462  
 Cu-Al crystals, solid soln. hardening 9-13767  
 Cu-(1wt.%)Al two-phase, high temp. creep mechanism 9-19793  
 Cu-Ti-Al alloys, hardening during slip mechanism 9-17319  
 Cu/MnAl, Heusler, low temp. sp. ht. meas. rel. to hyperfine fields 9-9841  
 Fe-Al, Mossbauer eff., electron transitions from isomeric shift and X-ray emission spectra parameters 9-3871  
 Fe-Al, oxidation in  $\text{CO}_2$ , composition and temp. dependence 9-14132  
 Fe-Al dilute, n.m.r. of  $^{57}\text{Fe}$  and  $^{27}\text{Al}$ , rel. intensities 9-1874  
 Fe-Al solid solns., heterogeneous, n-irrad. effects on elec. resistivity rel. to ordering changes 9-1465  
 Fe<sub>3</sub>Al ordered ferromag. alloys, spin-wave excitations, dispersion law, Heisenberg model 9-18674  
 Ge-Al system, surface diffusion, 'unipolar' 9-5408  
 Mg-(2wt.%)Al, complex stress creep fracture at 50°C 9-21382  
 Ni-Al-Ti, coherency hardening, comments 9-19446  
 Ni-Al, critical shear stress, conc. depend. 9-9756  
 $\beta$ -Ni-Al, Hall coeff. and magnetoresistance at liq. He temps. 9-5639  
 Ni Al, phase structure rel. to Hall coeff. 9-3582  
 Ni-Al and Ni-Al-Ti, coherency hardening 9-11945  
 Ni-Al precip. hardening mechanism 9-3469  
 Ni-Cr-Al, alloys, internal friction temp. dependence 9-14966  
 Ni-Cr-Cu-Al alloy, vacuum fractionation model. 9-7342  
 Ni-Cr-W-Co-Al-Ti, with horophylic addition, mech. props., effect of grain boundary composition 9-5475  
 Ni<sub>3</sub>Al, conduction electron scatt. by paramagnons 9-21462  
 Ni<sub>3</sub>Al, strain hardening 9-13761  
 Ti-(5wt.%)Al-(2.5wt.%)Sn hot salt cracking 9-21383  
 Ti-(6 wt.%)Al-(4 wt.%)V, fatigue-cracked, load relaxation, effect of methanol 9-19786  
 Ti-Al, binary, hot salt cracking 9-21383  
 Ti-Al  $\alpha$ -phase, single crystals, e. beam zone melting 9-11804  
 Zn-Al superplastic, microstructure and mech. behaviour 9-11858  
 Zu-Al, superplasticity 9-3428

**Aluminium compounds**

See also *Aluminium alloys*; *Ruby*

- $\gamma\text{-Al}_2\text{O}_3$ , ads. of sat. hydrocarbons, ads. energy 9-7344  
 $\text{Al}_2\text{O}_3$ , mean excitation potentials from stopping power data treatment 9-9135  
 $\text{Al}_2\text{O}_3$  films as windows for G-M counters, radioactive or photoconductive supports, patent 9-13163  
 $\text{Al}_2\text{O}_3$  refractories, creep 9-7548  
 $\text{Al}_2\text{O}_3$  mol., absorpt. spectra,  $X^{1/2}-A^{1/2}$  transition intensities 9-18173  
 alum crystals, growth rate from soln., effects of borax 9-13602  
 alumina in Ni-alumina mixture, semicond. obs. 9-13887  
 alumina-silica monoliths, hot strength 9-3435  
 aluminosilicate refractories, creep 9-16130  
 aluminosilicate catalysts, protonic active centres, exam. by pyridine adsorpt. and i.r. spectra 9-7968  
 chromium alums., classification 9-13591  
 corundum, dislocation motion, microscope obs. using decoration method 9-1215  
 corundum, strength temp. depend. rel. to stress corrosion, obs. 9-1299  
 corundum, synthetic, Tyndall scatt. rel. to microscopic and colloidal inclusions distrib. 9-1730  
 corundum ceramics, surface damage on cutting and grinding from X-ray analysis 9-13574  
 corundum doped with  $\text{Ti}^{3+}$ ,  $\text{V}^{3+}$  or  $\text{Cr}^{3+}$ , catalytic activation of  $\text{H}_2\text{-D}_2$  exchange 9-8085  
 corundum refractories, corrosion by oxides at 1500-1750°C 9-14135  
 corundum substrate for Si epitaxial layers, role in p-type contamination 9-3666  
 $\beta$  diketone chelates, emission vibronic structure 9-13342  
 leuco-sapphire, Tyndall scatt. rel. to colloidal inclusion distrib. 9-1730  
 lithium aluminosilicate, thermal expansion dependence on  $\text{TiO}_2$  catalyst content 9-13804  
 methyl ammonium aluminium sulphate,  $^{27}\text{Al}$  NMR rel. to ferroelectric phase transition 9-3968  
 sapphire, dielec. consts. 8-140 GHz, meas. accuracy of impedance method 9-3696  
 sapphire, fracture surface energy and stress corrosion on (1011) and (1010) planes 9-7571  
 sapphire, luminescence under x-irrad. 9-1839  
 sapphire, strengthening by compressive surface layers 9-1300  
 sapphire, wetting by liq. Al, effect of nature of surfaces 9-19622  
 sapphire quarter wave plate, visible achromatic 9-10925  
 sintered spinel, corrosion by oxides at 1500-1750°C 9-14135  
 spinel-corundum, corrosion by oxides at 1500-1750°C 9-14135  
 titanium-aluminium acetylacetonate, mixed cryst., spin-lattice relax. 9-16386  
 zeolite, 5A, adsorpt. of Kr 9-7345  
 zeolites, Linde-A, heats of sorption of water 9-9623  
 $\alpha$ - $\text{Al}_2\text{O}_3$  chem. vapour deposition on Ta alloy 9-1108  
 Al-Cu solid solns., superaturated and deformed elea. resistivity changes after Cu precip. 9-21482  
 Al-Mn alloys, dil.,  $^{55}\text{Mn}$  NMR rel. to electronic state 9-1871  
 Al-Y garnet,  $^{41}\text{g}_{1/2} \rightarrow ^{2}\text{P}_{1/2}$  transition in  $\text{Nd}^{3+}$ , vib. mechanism due to ion-phonon relax. 9-10186  
 Al-Zn solid solutions, resistivity during precipitation 9-21480  
 Al-mica 1M, crystal structure 9-1180  
 $\text{Al}_2\text{O}_3\text{:Co(Ti)}$ , valence state of dopant, eff. on growth and colour 9-14908  
 $\text{Al}_2\text{O}_3\text{:Cr}_2\text{O}_3\text{:SiO}_2$  system, phase equilib. data 9-19655  
 $\text{Al}_2\text{O}_3\text{:Fe}_2\text{O}_3$ , electrical cond. and thermoelec. power, effect of chemisorbed hydrogen and water vapour 9-20036  
 $\text{Al}_2\text{O}_3\text{:SiO}_2$  binary oxide film deposition on pyrolytic decomposition of trimethylsiloxy-aluminiol- isopropoxide 9-21272  
 $\text{Al}_2\text{O}_3\text{:}(0.25\text{wt.}\%) \text{MgO}$ , hot-pressed deformed, grain boundaries and dislocations obs. 9-3359  
 $\alpha$ - $\text{Al}_2\text{O}_3$ , abrasion resistance, rel. to ZrO 9-3457  
 $\text{Al}_2\text{O}_3$ , forging 9-3482  
 $\text{Al}_2\text{O}_3$ , hot-pressed deformed, grain boundaries and dislocations obs. 9-3359  
 $\text{Al}_2\text{O}_3$ , powder, initial stage sintering kinetics 9-7586  
 $\text{Al}_2\text{O}_3$ , powder mixtures, sintering kinetics 9-7585  
 $\text{Al}_2\text{O}_3$ , range of 0.5-4 KeV electrons rel. to energy 9-19872  
 $\text{Al}_2\text{O}_3$ , sapphire, wetting by liq. Al, effect of nature of surfaces 9-19622  
 $\text{Al}_2\text{O}_3$ , tensile strength rel. to microstructure 9-3434  
 $\text{Al}_2\text{O}_3$ , thermal cond. 90 to 1100°C, semi-cryst. mat. 9-21445  
 $\text{Al}_2\text{O}_3$ , thermally shocked, degree of damage 9-3437  
 $\text{Al}_2\text{O}_3$ , with compressive surface layers, residual stress meas. 9-3414  
 $\text{Al}_2\text{O}_3$  anodic coatings, structure and transforms from effluent gas detection and i.r. analysis 9-21712  
 $\text{Al}_2\text{O}_3$  anodic coatings, structural changes during anodizing and sealing, i.r. analysis 9-21711  
 $\text{Al}_2\text{O}_3$  anodic film, i.r. spectra comparison of freshly and evacuation prepared samples 9-18703  
 $\text{Al}_2\text{O}_3$  film, photoluminescence 9-18720  
 $\text{Al}_2\text{O}_3$  refractories, hot modulus, effect of selected processing variables 9-3436  
 $\text{Al}_2\text{O}_3$  sequestered phosphate soln., high temp. bonding and refractory applications 9-3460  
 $\text{Al}_2\text{O}_3$  single crystals, elastic const. press. depend. 9-3394  
 $\alpha$ - $\text{Al}_2\text{O}_3$  whiskers, Ni-coated, in Al-10% Si composites, role of Ni 9-21385  
 $\text{Al}_2\text{O}_3\cdot 2.5\text{NiO}\cdot 9\text{H}_2\text{O}$ , structure determ. and driving defects characterization 9-19707  
 $\text{Al}_2\text{SiO}_5\text{:Fe}^{3+}$  maser props. 9-14069  
 Al complexes in  $\text{AlCl}_3$ -acetonitrile solns., n.m.r. 9-5189  
 AlAs-GaAs system, coherent radiation from epitaxial heterojunction structure 9-10868  
 AlCN, mol., and possible isomers 9-753  
 $\text{AlCl}_3\text{:Ti}^{3+}(\text{Cr}^{3+})$ , e.s.r. 9-12499  
 $\text{AlCl}_3\text{:N}(\text{CH}_3)_3$ , crystal and mol. structure 9-13625  
 $\text{AlF}_3$  additive effect on strength of refractory mats. 9-9766  
 n-Al-Ga<sub>1-x</sub>As - p-GaAs heterojunction, injection properties 9-3671  
 AlH mol., absorpt. spectra,  $X^{1/2}-A^{1/2}$  transition intensities 9-18173  
 $\text{Al(III)}$  halides in N,N-dimethylformamide solutions, outer-sphere ion-pair formation obs. by NMR 9-19645  
 $\text{AlK}(\text{SO}_4)_3\cdot 12\text{H}_2\text{O}$ , crystal growth rate in fluidized bed at 32°C 9-16055  
 $\text{AlK}(\text{SO}_4)_3\cdot 12\text{H}_2\text{O}$ , crystal growth rate in fluidized bed at 32°C 9-9641  
 $\text{AlK}(\text{SO}_4)_3\cdot 12\text{H}_2\text{O}$ , crystal growth rate from soln. at 32°C 9-11799  
 $\text{AlLaO}_3\text{:Pr}^{3+}$ , visible and u.v. excitation of fluorescence 9-18724  
 $\text{Al}_2\text{MgO}_4$ , crystal structure refinement 9-1181  
 AlN, Raman spectra, excited by He-Ne laser 9-1805  
 AlN, thin film microwave acoustic transducer, vacuum deposition 9-10056  
 AlN films, pyrolytically deposited on Si, growth charact. 9-13583  
 $\text{Al}_2\text{O}_3\text{:Cr}^{3+}$ , e.p.r., elec. field effect 9-10275  
 $\text{Al}_2\text{O}_3\text{:Cr}^{3+}$ , sound absorpt. from  $5 \times 10^6\text{-}2 \times 10^8$  c/s at 300°, 77° and 4.2°K 9-5544  
 $\text{Al}_2\text{O}_3\text{:Cr}^{3+}$ , two-photon transitions in e.p.r. spectrum 9-16453  
 $\text{Al}_2\text{O}_3\text{:Cr}^{3+}$  absorption spectrum, optically pumped 9-7967  
 $\text{Al}_2\text{O}_3\text{:}^{51}\text{Cr}$ , ENDOR determ. of hyperfine splittings 9-8044  
 $\text{Al}_2\text{O}_3\text{:Ti}$ , precip. and struct. obs.,  $\text{Ti}^{3+}$  solubility 9-1340  
 $\text{Al}_2\text{O}_3\text{:V}^{4+}$ , far i.r. spectrum 9-1768  
 $\text{Al}_2\text{O}_3$ -Al system, melting curve, condensed phases, obs. 9-1341  
 $\text{Al}_2\text{O}_3$ -BaO glass ceramics, mech. and elec. props. and sintering behaviour 9-3171  
 $\text{Al}_2\text{O}_3$ -Si m.o.s.f.e.t., fabrication and characts. 9-17412  
 $\text{Al}_2\text{O}_3\text{:SiO}_2\text{:ZrO}_2$  system, phase diagrams; for Corhart-ZAC type refractories 9-13784  
 $\text{Al}_2\text{O}_3\text{:WO}_3$ , structure of compound  $\text{Al}_2(\text{WO}_4)_3$  9-3283  
 $\text{Al}_2\text{O}_3\text{-Y}_2\text{Al}_2\text{O}_3$ , microstructures formed by controlled solidification from melt 9-3285  
 AIO spectra, blue-green syst., relative band strengths 9-19426  
 AIO visible and u.v. bands, isotope shift studies 9-13341  
 AIO with metal and alkaline oxides as solid electrolyte for fuel cell, patent 9-20486  
 $\text{Al}_2\text{O}_3$ , adhesion to metals and alloys rel. to wettability 9-1336  
 $\text{Al}_2\text{O}_3$ ,  $\text{AlO}^{2+}$ , radiation-induced, electronic and crystal field interactions rel. to optical and mag. props. 9-12322  
 $\text{Al}_2\text{O}_3$ , ceramics, for electrical appl. 9-1566  
 $\beta$ - $\text{Al}_2\text{O}_3$ , crystal structure 9-11833  
 $\text{Al}_2\text{O}_3$ , detection of ferrous ions 9-12315  
 $\beta$ - $\text{Al}_2\text{O}_3$ , dielectric loss 9-1574  
 $\text{Al}_2\text{O}_3$ , double bicrystals, grain boundary strength 9-1232  
 $\text{Al}_2\text{O}_3$ , electroluminescence of films 9-5971  
 $\text{Al}_2\text{O}_3$ , fracture mechanisms rel. to structure 9-1305  
 $\alpha$ - $\text{Al}_2\text{O}_3$ , growth patterns on surface obs. 9-17260  
 $\text{Al}_2\text{O}_3$ , heat capacity using adiabatic calorimeter in range 25-500°C 9-12014  
 $\alpha$ - $\text{Al}_2\text{O}_3$ , ionic potentials, fields and gradients at lattice sites 9-10158  
 $\text{Al}_2\text{O}_3$ , isothermal bulk modulus at 295°K and second order deriv. 9-11919  
 $\text{Al}_2\text{O}_3$ , polycrystalline alumina, dielectric anisotropy dependence on crystallographic texture 9-1573  
 $\text{Al}_2\text{O}_3$ , secondary grain growth kinetics 9-1152  
 $\text{Al}_2\text{O}_3$ , X-ray emission by proton bombardment 9-7984



**Aluminum compounds continued**

- Al<sub>2</sub>O<sub>3</sub> ( $\alpha$ - and  $\gamma$ -) X-ray emission spectra, OK bands, fine struct. obs. 9-12453  
 Al<sub>2</sub>O<sub>3</sub> alumina ceramics, strength effect in shock compression 9-7563  
 Al<sub>2</sub>O<sub>3</sub> ceramic, high purity, control of elec. props. at high temp. 9-3691  
 Al<sub>2</sub>O<sub>3</sub> ceramics, electric tests up to 800°C 9-10034  
 Al<sub>2</sub>O<sub>3</sub> glass, fracture surface energy 9-1306  
 Al<sub>2</sub>O<sub>3</sub> layers formed on anodic oxidation of Al, growth an struct. 9-4004  
 Al<sub>2</sub>O<sub>3</sub> particles, dragging by migrating grain boundaries in Cu 9-1233  
 Al<sub>2</sub>O<sub>3</sub> refractories, creep 9-7549  
 Al<sub>2</sub>O<sub>3</sub> refractory, rel. to radome fabrication 9-7311  
 Al<sub>2</sub>O<sub>3</sub> sintered, mech., electrical, thermal and chemical props. rel. to comp. and microstructure 9-1256  
 Al<sub>2</sub>O<sub>3</sub> substrates, separation force rel. to scoring and annealing 9-1307  
 Al<sub>2</sub>O<sub>3</sub> surface sinusoidal grating prod., chem. method 9-4171  
 Al<sub>2</sub>O<sub>3</sub> thin layers, polarisation effects in m.i.m. and m.i.s. structures 9-3717  
 $\gamma$ -AlOOH phase transitions in electron beams 9-13773  
 Al<sub>2</sub>O<sub>3</sub>.H<sub>2</sub>O, e.p.r. of Fe<sup>3+</sup> impurity ions 9-5981  
 Al<sub>1/3</sub>(Os<sub>1-x</sub>Ru<sub>x</sub>)<sub>2</sub> monoclinic phase, supercond. 9-13852  
 AlP, vapour phase growth, lattice parameters, elec. props., opt. absorption rel. to colour 9-19692  
 AlPO<sub>4</sub>, X-ray L<sub>2,3</sub> emission bands and energy struct. 9-5944  
 AlSb, channeling of H and He ions, energy loss meas. 9-9868  
 AlSb, derivative spectrum of indirect excitons 9-18702  
 AlSb, lattice dynamics 9-11978  
 AlSb, light scattering from single particle electron and hole excitations 9-12443  
 AlSb, thermal and electrical conductivity, thermolec./power and Hall coeff. 9-7794  
 AlSiO<sub>3</sub>, kyanite, absorpt. and e microprobe obs. 9-10191  
 Aln, mean square vibration displacements and at. scatt. factors, 85-670°K 9-11993  
 CH<sub>3</sub>NH<sub>2</sub>/Al(SO<sub>4</sub>)<sub>2</sub>.12H<sub>2</sub>O, elastic moduli and internal friction in phase transition region 9-19774  
 CaO-FeO-Al<sub>2</sub>O<sub>3</sub>, solid soln., X-ray and microscopic obs. 1050° and 1200°C 9-16147  
 Cu film, epitaxially twinned, on sapphire, growth 9-1104  
 Fe-Al alloys, phase transitions rel. to ordering 9-9801  
 Mn<sub>2</sub>O-Al<sub>2</sub>O<sub>3</sub>, initial sintering, 1450-1650°C 9-18533  
 Ni-Al<sub>2</sub>O<sub>3</sub> system, grain boundary grooving at interface, kinetics const. 9-1251

**Americium**

No entries

**Americium compounds**

No entries

**Ammonia see Nitrogen compounds/ammonia****Ammonium compounds see Nitrogen compounds/ammonium compounds****Amorphous state***See also Vitreous state*

- electronic states, comparison with crystals 9-9599  
 elementary excitations in solids, dispersion relations 9-9813  
 glassy polymers, evidence from yield ion 9-14974  
 near-order parameters determination by a radial distribution curve with allowance for breaking effect 9-5224  
 porous medium, forces acting on solid phase 9-18394  
 PVC, stretched uniaxially, thermal and mechanical props. anisotropy 9-19781  
 Si-Si heterojunction between crystal and amorphous 9-3677  
 solid, interatomic potentials, deduction from low energy ion range meas. 9-5585  
 C, e.s.r. before and after air admission, linewidth and spin conc. 9-8021  
 C, g-anisotropy rel. to air adsorbed, e.s.r. study 9-8023  
 Na tallow-coconut soap, extruded, struct., e microscope obs. 9-5225  
 Ni-(14.9wt.%)P alloy, electrodeposited, structure 9-19839  
 Se, relaxation 9-19926  
 SiO film, transparent hole formation mechanism 9-19668

**Amplifiers**

- alkali halide crystals, light amplification, possible use 9-10164  
 Cockcroft-Walton voltage multipliers with arbitrary number of stages, anal. 9-17850  
 coherent, design principles and circuits, comments and author's reply 9-6458  
 d.c. voltage, for Hall effect meas. in high-resistance specimens 9-12083  
 differentiator for photoemission studies, errors origin and control 9-17846  
 f.e.t., for O<sub>2</sub> microcathode current meas. 9-17843  
 functional, amplify characteristics rel. to compensation for time-amplitude converter errors 9-11147  
 gas laser non-linear effects theory strong signals 9-6511  
 gas laser non-linear effects theory weak signals 9-4463  
 integrating, for ionising currents and charge measurement 9-8570  
 laser, high power nonlinear 9-16775  
 laser, internal beam Gaussian distortion due to saturable gain or loss 9-12993  
 of laser pulse, single mode-locked 9-6524  
 logarithmic, calibration using exponential current generator 9-17861  
 logarithmic, wideband; decay kinetics anal. 9-10792  
 nuclear preamp., influence of decay time const. on  $\gamma$  spectra resolution, pulse pile-up 9-2604  
 optical, laser beam traversal, divergence decrease 9-14439  
 power transmission to accelerating cavity of synchrotron, wideband channel 9-472  
 preamplifier using MOSFETs at liquid He temps., for use in NMR 9-6439  
 preamplifiers, charge-sensitive, capacitive sensitivity 9-19233  
 pulse, 0-4 kv for field ion microscope 9-4416  
 stabilization, multichannel analyzer, for  $\gamma$ -ray spectrometer 9-442  
 sum-delay, and gate generator 9-19120  
 thin-film hybrid comprising 4 resistances, transistor and capacitance 9-2303  
 tuned-circuit, square-wave Fourier analysis appl. 9-4224  
 CO<sub>2</sub> laser, sealed-off single frequency, characteristics 9-19143  
 CO<sub>2</sub> laser, small-signal step response and linewidth meas. 9-13005  
 CdS, acoustic, carrier inhomogeneity effect 9-1383  
 CdS, acoustic flux build-up, freq. of max. intensity 9-9834  
 CdS crystal amplification of Rayleigh waves 9-18557  
 He-Ne, optical regenerative of passing type, amplification coeff. and bandwidth 9-8615

**Amplifiers continued**

- KCl crystals, light, possible use 9-10164  
 YFe garnet rods, parametric amplification of magnetoelastic waves at room temp. 9-14967

**Analogue computers see Calculating apparatus/analogue apparatus****Analysis see Chemical analysis; Statistical analysis****Anechoic rooms see Acoustical laboratories****Anelasticity see Internal friction****Anemometers**

- hot wire, for wind vel., no moving parts 9-18791  
 hot wire probe 9-942  
 hot-wire, const. temp., nonlinear control theory 9-20084  
 hot-wire, low vel., linearizing cct. for temp. compensation 9-17847  
 hot-wire const.-temp., correction for temp. loading and high gas pressure effects 9-11643  
 sonic, comparative observations, traditional methods of vertical velocity measurement 9-15246  
 sonic, estimation of evaporation rate from water and soil surfaces 9-15243  
 sonic, turbulent kinetic energy vertical transport measurement, air layer near ground 9-15242  
 turbulence structure, small scale, meas. with hot wires 9-947

**Angle measurement**

- autocollimating technique, increased angular range, measurement of large rotations of a body 9-12847  
 fibre-optical displacement transducer 9-12846  
 goniometer to aid have X-ray orientation of single crystals 9-3261  
 goniometer sample mount, orientation and machining 9-11817  
 interferometer, confocal which points at coherent sources 9-4518  
 using plane diffraction gratings, Moire fringes 9-4216  
 plane of rotation, 2-dimens. evaluation 9-2129  
 X-ray goniometer, double crystal 9-1170  
 x-ray goniometer for cylindrical specimens partial pole figure determ. 9-11816

**Angular distribution see Gamma-rays/angular distribution; Neutrons and anti-neutrons/angular distribution; Protons and anti-protons/angular distribution****Angular momentum theory see Quantum theory****Angular velocity measurement***See also Stroboscopes*

No entries

**Annealing see Heat treatment****Annihilation of electrons see Electron pairs/annihilation****Anodic films see Electrochemistry; Films, solid****Antennas see Electromagnetic waves/radiators****Antiferroelectric materials see Ferroelectric materials****Antiferromagnetic resonance**

- biaxial crystals, line width, theory 9-10272  
 canted antiferromagnet, complex susceptibility and resonance freqs., analysis 9-7914  
 in Heisenberg antiferromag., statistical-mechanical theory 9-5979  
 nuclear spin-wave relaxation and narrowing of NMR lines 9-8037  
 oscillation transformation into elastic waves 9-1693  
 spectrometer, microwave for 1-3 mm wavelength region 9-10780  
 spin-wave scatt. by dislocations, effect on linewidth 9-3782  
 CoCl<sub>2</sub>.6H<sub>2</sub>O, relaxation, eff. of finite lattice heat capacity 9-8006  
 CoCo<sub>2</sub>, freq., mag. field strength dependence 9-1849  
 CoO, freq. determ. 9-21593  
 CoWO<sub>4</sub>, excitation identification with long-wave i.r. absorpt. bands 9-1773  
 CuCl<sub>2</sub>.2H<sub>2</sub>O single crystal, line width, comparison of theory and exptl. data 9-10272  
 EuTe, angular dependence 9-1850  
 $\alpha$ -Fe<sub>2</sub>O<sub>3</sub> (hematite), premature disappearance 9-18733  
 $\alpha$ -Fe<sub>2</sub>O<sub>3</sub>, hematite, temp. dependence with mag. field perpendicular to easy axis 9-1851  
 MnCO<sub>3</sub>, hyperfine interaction 9-14106  
 MnCO<sub>3</sub>, hyperfine interaction 9-3950  
 MnCO<sub>3</sub>, in mag. fields up to 50 kOe, freqs. 115 to 170 Gc/s 9-15197  
 MnCl<sub>2</sub>.4H<sub>2</sub>O single crystal, line width, comparison of theory and exptl. data 9-10272  
 RbMnF<sub>3</sub>, low temp. magnetization study 9-16382  
 TmFeO<sub>3</sub>, microwave absorpt meas., interpretation in two-sub-lattice model 9-7914

**Antiferromagnetism***See also Exchange interactions; Magnetic properties/antiferromagnetic*

- antiferromagnet, u.s. attenuation near critical point 9-5554  
 biaxial, potential, magnetiz., and spin thermal capacity 9-16374  
 canted antiferromagnet, complex susceptibility and resonance freqs., analysis 9-7914  
 cubic antiferromagnet, energy, effect of dynamical and kinematical interaction of spin waves 9-5852  
 exchange interactions, effective Hamiltonian 9-12251  
 free energy of interacting mag. dipoles, existence and shape in dependence, rigorous proof 9-12255  
 ground state of finite antiferromag. chain with free ends 9-1694  
 Heisenberg antiferromag., resonance phenomena, statistical-mechanical theory 9-5979  
 Heisenberg antiferromagnet, decay of thermodynamic fluctuations 9-12305  
 Heisenberg antiferromagnet, thermodynamics and correlation functions 9-10145  
 Heisenberg antiferromagnet at Neel temp. dynamic spin correlation junction 9-7915  
 Heisenberg magnet, 1/2 expansion for free energy at low temp. 9-1696  
 infinite spin dimensionality limit, spherical model 9-13955  
 itinerant electron antiferromagnet, props., effects of imperfect Fermi surface nesting 9-1695  
 line shape of spinwave sidebands 9-10104  
 magnon corrections to electron effective mass in mag. semiconductor 9-18584  
 magnon-phonon interaction rel. to e.m. wave interaction with antiferromagnet 9-1692  
 metals, mag. resonance spectrum in mag. field 9-8001  
 nuclear orientation at low-temp., static methods 9-15162  
 oscillation transformation into elastic waves 9-1693  
 spin coupling, stability against pair wise bonding 9-21592  
 spin operator extension of Heisenberg model 9-12250

**Antiferromagnetism** continued

- spin operators, Wick's theorem, proof 9-10106
- spin wave sidebands, line shape 9-16375
- spin-wave impurity states using Green's function methods 9-12307
- spin-wave instabilities, with 'easy axis' anisotropy 9-5853
- spin-wave scatt. by dislocations, theory 9-3782
- time-correlation of spins, long-time behaviour, Halperin-Hohenberg law with  $0=3/2$  9-12235
- uniaxial, ground-state energy lower bound 9-12306
- GdAlO<sub>3</sub> magnetic phase diagram 9-7918
- Sc alloys with mag. impurities, long range spin correl. 9-5856
- U<sub>1</sub>, I<sup>17</sup> nuclear quadrupole resonance 9-1885

**Antimony**

- adsorbed atoms on collodion migration path e. microscope determ. 9-1111
- alloying addition to Pb, effect on strength 9-1303
- diffusion in Ge, acceleration by u.s. irradiation 9-1247
- diffusion in ZnSb-constantan semiconductor thermoelements, X-ray microprobe analysis 9-10062
- dislocation motion mechanism during etching 9-13691
- electromechanical effect, kinetics 9-1314
- films, crystallization data from e. diff. patterns 9-5249
- in Ge, dopant periodic distrib. effects 9-5705
- solid soln. in Ag, thermoelec. powers 9-1604
- thermal conductivity, lattice, Nernst-Ettinghausen effect and sp. ht. rel. to e. scatt. mechanism 9-9856
- thermal expansion and lattice parameters 28°-220°C. obs. 9-21439
- As, current carrier conc., pressure depend 9-15069
- GaAs-Cs photocathode, effect of Sb on photoemission 9-12225
- Sb, electromechanical eff., sign inversion 9-5675
- Sb<sup>+</sup> implantation in Al, rel. to formation of precipitate phases 9-11956
- inSi, irradi., impurity vacancy pairs, c.p.r. and endor exam 9-5341
- in Sn, impurity effect on critical field curve 9-9961
- in Sn, impurity effect on residual resistivity anisotropy, ideal resistivities and deviations from Matthiessen's Rule at 77° and 273°K 9-9962
- inTe, i.r. absorpt. 9-5930

**Antimony compounds**

- alloys, dil. liq., with 3d. transition metals, mag. susceptibilities and localized impurity states 9-1043
- organic, Mossbauer eff., isomeric chem. shift 9-3874
- SbSI, polarization reversal, screening effects by non-equilibrium carriers 9-3712
- Ag-Sb alloys, hexagonal ( $\beta$ -phase), stacking-fault densities 9-1230
- Ag (10 wt.%) Mn-(1.5 wt.%) Sb alloys, solid soln. decomposition, work hardening effects 9-1326
- Ag-Sb series, X-ray spectra K $\alpha$  line shift 9-14066
- Bi-Sb-Te system, intermetallic cpds., mag. anisotropies and susceptibilities temp. dependence 9-13945
- Bi-Sb alloy, semiconductor-metal transition, rel. to mag. field and Sb conc., 4-77°K 9-1513
- Bi-Sb alloy, thermal conductivity, thermoelec. eff. and elec. resistivity 9-12026
- Bi-Sb alloy syst., energy-band parameters and relative band-edge motions near semimetal-semicond. transition 9-15053
- Bi-Sb alloys, band model 9-13831
- Bi-Sb alloys, internal friction meas. of grain boundary creep 9-16104
- Bi-Sb system, liquid state, elec. conductivity and density 9-9547
- Bi<sub>1-x</sub>Sb<sub>x</sub> alloys, mag. susceptibility and band structure 9-21565
- Bi-Sb alloy, semicond., longit. magnetoresist. anomalies in mag. fields up to 500 kOe at liq He temp. 9-1514
- Bi-Sb-Pb alloys, electron transitions, pressure-induced, 4.2-295°K 9-9892
- Cd-Sb-Zn system solid solution formation, structure and thermo-e.m.f. 9-19835
- Cu-Sb phases, supercond., and absence of antiferromagnetism in Cu<sub>2</sub>Sb 9-12122
- Sb-Sn alloys, galvanomagnetic eff. and band structure 9-3841
- Sb<sub>2</sub>S<sub>3</sub>, reflectivity spectra, polarization eff. 9-18700
- Sb<sub>2</sub>S<sub>3</sub> vitreous films, space-charge-limited currents 9-16289
- Sb<sub>2</sub>Se<sub>3</sub>, reflectivity spectra, polarization eff. 9-18700
- Sb<sub>2</sub>Te<sub>3</sub>-Bi<sub>2</sub>Te<sub>3</sub> powders, thermal conductivity, effects of grain size, impurity content and processing effects 9-19867
- SbCl<sub>3</sub>, quadrupole spin echo, 'slow beats' 9-3973
- SbI<sub>3</sub>, absorpt. spectra rel. to direct and indirect transitions 9-3895
- Sb<sub>2</sub>S<sub>3</sub>, ferroelec. phase transition from optical absorpt. temp. dependence 9-3711
- SbSBr, refractive indices and abs. coeff. 9-10169
- SbSI, Curie temp. shift due to illumination and nonequilibrium carriers 9-16300
- SbSI, ferroelec. phase transition, eff. of photoconduction 9-7845
- SbSI, ferroelec. semicond. interphase formation, eff. of nonequilibrium carriers 9-5752
- SbSI, ferroelectric transition 9-21539
- SbSI pleochroism, near ferroelectric phase transition 9-14029
- SbSI thermal cond. 6°-316°K, anomaly 9-16185
- SbS<sub>2</sub>Se<sub>1-x</sub> mixed crystals, optical, photoelec. and ferroelec. props. 9-12385
- Sb<sub>2</sub>Se<sub>3</sub>, needle-like crystals, growth, structure, mech. and elec. props. 9-1194
- SbSi, anomaly of thermal conduction 9-7674
- SbSi, ferroelectric, double hysteresis loop and spontaneous polarization 9-5649
- SbSi, space-charge-limited currents in para- and ferroelec. phases 9-10038
- Sb<sub>2</sub>Te<sub>3</sub>, mag. anisotropy and susceptibility temp. dependence 9-13945
- SbTeI, internal photoeffect 9-3728

**Antineutrinos** see *Neutrinos and antineutrinos*

**Antineutrons** see *Neutrons and antineutrons*

**Antinucleons** see *Nucleons and antinucleons*

**Antiparticles** see *corresponding particle*

**Antiphase domains** see *Alloys; Crystal structure/microstructure; Solids/structure*

**Antiprotons** see *Protons and antiprotons*

**Antireflection coatings** see *Films, solid/optical properties*

**Apodization** see *Optical images*

**Apparatus** see *Cosmic rays/apparatus; Instruments; Ionosphere measuring apparatus; Laboratory apparatus and technique; Radioactivity measurement/apparatus; Vacuum apparatus; X-ray crystallography/apparatus. Further entries describing apparatus for specific purposes are included under the headings of the appropriate subjects*

**Appearance potential** see *Ionization potential*

**Architectural acoustics**

See also *Echo; Noise abatement; Reverberation; Transmission/acoustic waves*

- absorbers comprising porous material with perforated facing, design 9-4325
- absorption by audience and chairs in large halls, three methods 9-15473
- ceiling support model, transmission meas. 9-6382
- closed rooms, regenerative reverberation assoc. with sound amplification 9-4355
- double walls with air separation and no edge coupling 9-17811
- double-leaf wall construct., eff. of using absorbent mat. on transmission loss 9-19073
- feedback, regenerative reverberation effects, obs. 9-2233
- feedback, regenerative reverberation effects, theory 9-2232
- historical review 9-4361
- insulation from airborne sound, single partitions and ceilings 9-17812
- loudspeaker-microphone reactive coupling, avoidance 9-17804
- objective meas. methods 9-2183
- practical problems of designing factors, theatres and broadcast studios book 9-20436
- pulse response of room, reln. with diffusivity of stationary field 9-4327
- pulse test meas. on model 9-2234
- reverberant room, fluctuations of sound with position, stat. at high freq. 9-10741
- single-layer floors, transmission of impact noise 9-4357
- stationary diffusivity, correl. with pulse response characts. 9-4360
- test facilities of the National Gypsum Company 9-12938
- transmission and absorption of narrow slots in corners 9-19066
- transmission of narrow slots for diffused sound 9-19065

**Arcs, electric**

- a.c., radial distrib. of gas temp., meas. 9-11637
- air, column, decay, effects of temp.-depend. thermal diffusivity and rad. losses 9-9423
- air, high-pressure, numerical analysis of electrodeless arc 9-7209
- alkali-metal-seeded rare gases, descriptive theory development of positive column 9-13469
- arcing of oxide cathode in low pressure pulse discharge 9-5777
- conductivity, elec. and thermal, and radiated power, 'inverse' soln. accuracy 9-11639
- cylindrical, whirl stabilization for new geometry 9-5095
- d.c. plasma torch, flame non-uniformity 9-21078
- electrode vapour effect on electron conc. in plasma of low-current discharge in air 9-9353
- electron density meas. using CO<sub>2</sub> laser interferometer 9-18297
- heat transfer in near electrode region 9-19565
- high pressure, temp. profiles calc. using diff. approx. for rad transfer 9-19566
- high-current, centring in coaxial chamber 9-13472
- as ion sources, obs. on Ar, Kr, Xe, W 9-232
- Krudsen, low voltage, in Cs-Ar mixtures 9-9424
- low current, motion, gas-space and electrode effects 9-931
- n, plasma, cylindrical, radiative energy transport with absorption 9-7140
- oscillator strength meas., systematic errors 9-15965
- with oxide cathode, energy equilibrium 9-3034
- positive column props. in longit. mag. field, low-pressure arcs, review 9-3022
- resistance between electrodes, effect of mag. field 9-17142
- spark transition in negative ion and free electron gases, asymmetrical fields 9-18317
- spectral line pairs, matrix effect 9-15966
- spectrochemical analysis source, continuous a.c. arc 9-18777
- spectroscopic light source, interelement effects, obs. 9-20563
- vacuum gap, decay of residual plasma after forced extinction 9-11638
- volt-amp characts. for non-stationary discharge, calc. 9-21119
- wall-stabilized columns, boundary conditions 9-932
- Ar, plasma, cylindrical, radiative energy transport with absorption 9-7140
- Cl affinity continuum u.v. region 9-9128
- Fe excited states, disc-stabilized, low pressure 9-18319
- H<sub>2</sub>-He mixture, ion, atom temp. determ. by Doppler eff. 9-5096
- He H<sub>2</sub> mixture, ion, atom temp. determ. by Doppler eff. 9-5096
- He, 10 atmospheres pressure, wall confined, investigation 9-11640
- He, low press., Doppler broadening of ion lines 9-2830
- He, low pressure, in mag. field, l.f. instabilities 9-902
- Hg, 'equiv. press.' validity, rectifier and thyatron obs. 9-13473
- Hg-Xe, far i.r. source 9-19564
- N<sub>2</sub> columns, decay, effects of temp.-depend. radiation losses and thermal diffusivity 9-9423
- SF<sub>6</sub> a.c. arc characteristics filmed by laser-Schlieren technique 9-17881

**Area measurement**

No entries

**Area measurement, porous substances** see *Surface measurement*

**Argon**

- 5p levels electronic excitation, experimental lifetimes 9-15819
- absorption struct. near L<sub>II</sub> m edge 9-4837
- arc plasma, transparent and non-transparent rad., share in total energy flux 9-7140
- atom, electron scatt. compared with Hg and Xe, rel. to Mott theory and non-relativistic approx. 9-19408
- atom, energy loss spectra for keV electrons interaction with electron shell 9-18150
- atom, energy loss spectra for keV electrons interaction with electron shell 9-11398
- atom, exchange energy of electrons 9-4834
- atom, metastable excited chem. applic. 9-825
- atom, proton excitation of 1300-A continuum 9-9133
- atom by protons, 4 MeV, continua intensity depend. on press. determ. 9-20883
- atom-electron collision integrals 9-17000
- atomic beam scatt. from Ag(111) 9-3187
- atoms, collision with He<sup>+</sup> and Ne<sup>+</sup>, optical excitation 9-6996
- atoms and ions, bibliography of spectra 9-13287
- beat frequency between axial modes, variation with cavity Q 9-8616
- bubbles in Hg, velocity of rise 9-17183



**Argon continued**

content in iron meteorites 9-6184  
 corresponding states with methane 9-9440  
 crystal, Debye-Waller factors 9-5536  
 crystal, improved self-consistent phonon approx. 9-5530  
 crystal, phonon dispersion meas. at 4.2°K 9-11985  
 crystals, review 9-13567  
 discharge, continuous spectrum in positive column at press. 1 to 10 torr 9-924  
 discharge, low pressure hot cathode, spectroscopic investigation 9-9419  
 discharges, contracted high freq. 9-3029  
 discharges, electrodeless, electron temp. distrib. 9-7206  
 dissociative recombination and molecular ion formation in decaying plasma 9-13414  
 elastic constants, at absolute zero, effect of long-range three-body forces 9-11906  
 electrical breakdown potential, influence of gas vel. and press. 9-7232  
 electron mobility, up to 42 atm. 9-17167  
 energy distrib. obs. from non-magnetic hot cathode 9-2361  
 in films, analysis by r.f. spark-source mass spectroscopy 9-15232  
 flowing, NaK seeded, I-V characts., probe meas. 9-20487  
 gas, and mixture virial coeff., second, from boiling point to room temp., from value at one temp., calc. method 9-15972  
 gas, Auger spectra of L<sub>1</sub> and L<sub>3</sub> shells 9-6978  
 gas, collision induced light scatt. 9-959  
 gas wake in shock tube, velocity meas. from induced e.m.f. 9-2238  
 gaseous Townsend discharge, e back diffusion and accel. 9-13462  
 ion irradi. effect on internal friction of Au 9-1267  
 ion laser confocal longit. mode selector for single-frequency operations. 9-8603  
 ion laser investigated 9-8605  
 ion lasers, continuous wave, study of population inversion mechanism 9-20505  
 ion lasers, pulsed, direct gain meas. 9-4466  
 ion source in arc discharge 9-232  
 ionization by  $\alpha$ -particles, energy depend., 1.58-5.3 MeV 9-5058  
 ionization probability curves for electron impact, for <sup>2</sup>P<sub>3/2</sub> and <sup>2</sup>P<sub>1/2</sub> states 9-4863  
 ionized, Boltzmann eqn. suitability for thermal conductivity calc. 9-14814  
 ions, simple and cluster, mobility at 1-100 atm., obs. 9-18310  
 ions, sputtering of Cu at 400 and 600 keV 9-7682  
 ions, sputtering of Si single crystals, detection 9-19873  
 isotope effects for study of liquid 9-11676  
 laser, f.m., freq. stabilization and noise suppression 9-13001  
 laser, frequency spectrum fluctuations 9-4467  
 laser, ion, high power single frequency operation 9-15513  
 laser, ion, new capillary structure for improved reliability and lifetime 9-15510  
 laser, ionic, u.v., 1 W continuous wave o/p 9-17868  
 laser, ionised pulsed and quasi-c.w., design and obs. 9-17867  
 laser, pumping LiNbO<sub>3</sub> to form tunable optical parametric oscillator 9-10161  
 laser, second harmonic generation to 2573 Å, efficient cw, using ADP or KDP crystals in cavity 9-20504  
 laser beam, thermal self-focussing in lead glass 9-8630  
 lasers, ion, discharge tube with Hg pool cathode 9-20506  
 line intensities of LiMM and L<sub>3</sub>MM spectra 9-4856  
 liquid, slow neutron scatt., continued fraction representation for autocorrel. function calcs. 9-13510  
 liquid, thermal neutron scattering, new model 9-11682  
 liquid, vapour press. and comparison with that of liq. Xe and Kr 9-11748  
 in liquid methane solution, acoustic wave velocity 9-5159  
 molecules, vel. determ. by effusion intermediate laboratory expt. 9-12823  
 plasma, 8 mm. interferometric results, interpretation 9-19544  
 plasma, boundary layers in shock-tube, study by quantitative schlieren tech. 9-14760  
 plasma, coronal 4412 Å emission line obs. in  $\theta$ -pinch 9-7162  
 plasma, Cs and K seeded, elec. cond. calcs., effect of multispecies ionization 9-17106  
 plasma, dense, recombination coeff. obs. 9000°K 9-5007  
 plasma, electrostatic wave transmission dispersion relms. 9-7150  
 plasma, heat transfer to water-cooled Cu pipe, elec. field eff. 9-21050  
 plasma, K-seeded, scalar conductivity and instabilities under MHD generation conditions 9-13425  
 plasma, laminar boundary layer, anal. for equilib. ionization 9-14759  
 plasma, turbulent, elec. conductivity 9-875  
 plasma discharge, low temp., radial particle distrib. profile, rel. to volume recomb. 9-11553  
 plasma electron density, feedback oscillation meas. 9-5044  
 plasma excited states, spect. studies, electron-ion recomb. coeff. 9-21057  
 plasma jet, temp. distrib., spectroscopy 9-11582  
 plasma prod. by azimuthal discharge, light radiation study 9-19539  
 plasma radial temp. distrib. by photoelec. spectroscopy in visible region 9-21051  
 positive column of low current discharge, influence of distrib. function on microwave emission and r.f. conductivity 9-19561  
 positive column unstable, radial density distrib., longit. mag. field 9-11628  
 positron annihilation rate temp. dependence 9-6604  
 pulsed discharge, time-resolved laser spectrum 9-13002  
 pulsed ion laser, role of two-step excitation 9-8606  
 refractive index and resonance line oscillator strength obs., 2300-1100 Å 9-9454  
 shock front, ionization process and relax. phenomena 9-14798  
 solid, elastic constants determ. 4.2-76.8°K from sound velocity meas. 9-7511  
 solid, infl. of lattice anharmonicity on exponential potential parameters 9-16161  
 solid, refractive index rel. to dielec. props., 3612 to 6439 Å 9-7832  
 solid, self-diffusion coeff. meas. rel. to vacancy diffusion mechanism 9-11893  
 solid, thermal conductivity temp. depend. for multiphonon interaction 9-15021  
 solubility and thermodynamic props. in water-ethylene glycol system 9-19611  
 sound vel., range depend. confirmed at very low press. 9-15973  
 spark prod. by focused subnanosec. laser pulse 9-891  
 supersonic jets, intermolecular binding 9-18179  
 supersonic molecular beam, production and temp. distribution 9-11454

**Argon continued**

thermal conductivity, expt. compared with gas kinetic theory 9-14817  
 u.v.-laser power, continuous, in Watt range 9-6512  
 weakly ionized, dielectric meas. in v.h.f. range 9-11584  
 Ar-CO<sub>2</sub>, thermal conductivity from 0° to 200°C 9-3094  
 Ar-Cs mixtures, low voltage Krundens arcs 9-9424  
 Ar-Kr(Xe) mixtures, structure factors calc. 9-11516  
 Ar-Ne gas mixture, obs. of elec. conductivity 9-929  
 Ar-O system, liquefied, sound vel. in solns. 9-9508  
 Ar-SF<sub>6</sub> plasma, oscillator strengths of 44SI and 9SII lines, 1100-2000 Å 9-7160  
 Ar, irradiated, yield of reson. states 9-13447  
 Ar<sup>+</sup> in N<sub>2</sub>, O<sub>2</sub>, CO, NO, charge-transfer proc., rate const. from drift meas., c.f. with 'nearest reson.', calc. 9-15956  
 Ar<sup>+</sup> laser, inductively excited, props. in high-current regions 9-14429  
 Ar and Xe mixture, ion pumping effect in ionization tube 9-2354  
 Ar I, II, broadening of spectral lines in spark plasma 9-5093  
 Ar I, i.r. transition arrays, transition probabilities and oscillator strengths 9-20880  
 Ar I, radiative lifetimes in resonance series 9-11390  
 Ar I, resonances obs. in photo-ionization continuum 9-13297  
 Ar I, transition probabilities meas. for 26 lines, 3000-6500 Å 9-19396  
 Ar I, i.r. lines in plasma torch sustained at h.f., Stark effect 9-9375  
 Ar II, 4p<sup>4</sup>S<sub>3/2</sub><sup>0</sup> level lifetime, absolute meas. from emission of correlated photons in cascade 9-6975  
 Ar II 4s and 4p levels population inversion mechanism, obs. 9-15817  
 Ar II line, shift and shift-to-width ratio rel. to electron temp. and density 9-5031  
 Ar II visible spectrum, relative transition probabilities 9-20876  
 Ar X-XIII, u.v. spectrum obs. 9-6972  
<sup>36</sup>Ar, inelastic n. scatt. exam. of gas dynamics near condensation 9-15971  
<sup>40</sup>Ar diffusion from KCl and microline feldspar, elec. field effects 9-11897  
 Ar<sup>2+</sup>, excitation cross section for fast e. impact 9-5057  
 ArI isoelectronic sequence, Hartree-Fock calcs. of forbidden lines rel. to the spectrum of the corona 9-15368  
<sup>40</sup>Ar-<sup>40</sup>Ca, mass diff. by high resolution mass spectrometer 9-13309  
 Ar<sup>+</sup>+D<sub>2</sub>→ArD<sup>+</sup>+D, reaction cross sections, 1-100eV 9-17075  
 Ar\*, ionizing collisions with H<sub>2</sub>, relative cross-sections for prod. gArH<sup>+</sup>, ArH<sub>2</sub><sup>+</sup> and H<sub>2</sub><sup>+</sup> 9-7188  
 Fe emission line shift, obs. 9-6963  
 H-Ar atom collisions, Lyman- $\alpha$  polarization, Born and distortion rot. approx. 9-13313  
 H<sub>2</sub>-O<sub>2</sub>-Ar mixtures, detonation initiation by incident shock waves, reaction mech. 9-14128  
 HCl-Ar interaction, intermol. dispersion pot. 9-20992  
 He and Ne mixtures, thermal cond. obs. at 296.8°K 9-19584  
 ion laser investigated 9-8605  
 K-Ar plasma, electrical conductivity 9-19532  
 K-Ar rock dating method, source of air Ar contamination 9-12571  
 K<sup>+</sup> scatt., cross-section meas. E<sub>k</sub>=150-4000 eV 9-18152  
 K scatt. in thermal energy range, total cross section meas. 9-11413  
 laser, ion, transverse modes, low order, properties 9-15512  
 microwave discharges, laser action observations 9-6513  
 N<sub>2</sub>+Ar liquid-vapour equil., 10atm. 9-17228  
 O<sub>2</sub> impurity, effect on SiO<sub>2</sub> r.f. sputtering 9-7332

**Argon compounds**

(90wt.%)Ar-(10wt.%)CH<sub>4</sub> proportional counter gas, pulse shape calcs. 9-19228  
 (90wt.%)Ar-(10wt.%)N<sub>2</sub> proportional counter gas, pulse shape calcs. 9-19228  
 Ar-methane mixtures ionization by  $\alpha$ -particles, 1.58-5.3 MeV 9-5058

**Aromatic compounds** *see Organic compounds***Arsenic**

aluminum bronze, As-containing, CuAl5-type, fatigued, effect on stacking fault tetrahedra 9-19752  
 e.s.r. of atoms trapped in inert matrices at 4.2°K, matrix perturbing effects 9-12501  
 magnetothermal and Shubnikov-de Haas oscills., obs. 9-5633  
 vaporization of single crystals, rates and coeff. 9-11750  
 As-Ga-Al system, thermodynamic and optical treatment of phase diagram 9-17346  
 As, current carrier conc., pressure depend 9-15069  
 As VII ion, vacuum u.v. spectrum 9-2813  
 in Ge, e. density modulation by impurity centre field 9-3918  
 inSi, irradi., impurity-vacancy pairs, e.p.r. and endor exam 9-5341

**Arsenic compounds**

As<sub>2</sub>S<sub>3</sub> films, e bombardment conductivity, threshold energy 9-16286  
 As<sub>2</sub>Se<sub>3</sub>, glassy, pulse I-V characts. 9-3617  
 AsI<sub>3</sub>, n.q.r. freq. calc. from electric field gradient tensor 9-20920  
 AsN, rotation structure of band rel. to new transition 9-7011  
 AsO<sub>4</sub><sup>3-</sup> in aqueous soln., u.v. absorption, n- $\pi^*$  transition 9-3103  
 As<sub>2</sub>S<sub>3</sub>-Ag<sub>2</sub>S system, phase diagram for proustite, smithite and pyrrargyrite growth 9-17255  
 As<sub>2</sub>S<sub>3</sub>, optical props. during transition from crystalline to glassy state 9-10192  
 As<sub>2</sub>S<sub>3</sub> glasses, elec. and optical props., development since 1950, review 9-3175  
 As<sub>2</sub>S<sub>3</sub> semiconductor film-Ag system, depend. of light sensitivity on thickness of semicond. layer 9-1735  
 As<sub>2</sub>S<sub>3</sub>(Se<sub>3</sub>) films, photosensitivity rel. to frequency of incident radiation 9-3731  
 AsSbS<sub>3</sub> getchellite, crystal structure, metallography and chem. props. 9-19708  
 As<sub>2</sub>Se<sub>3</sub>, optical props. during transition from crystalline to glassy state 9-10192  
 As<sub>2</sub>Se<sub>3</sub> glass, optical absorption, various initial purities 9-12352  
 Ga<sub>1-x</sub>In<sub>x</sub>As, i.r. reflection spectra, mixed cry. behaviour 9-1760  
 Ge-As solid soln., defect appearance during decay 9-14937

**Assistors** *see Conductivity, electrical; Semiconducting devices***Association**

dissociative attachment and recomb., theory 9-4967  
 electrolytes, slightly associated, thermodynamic props. predicted from elec. conductance 9-21703  
 formic acid, LCAO MO description of assoc. types 9-13385  
 ionic, influence on ground state of coronene negative ion 9-13378  
 thymine frozen soln., dimer formation 9-9297  
 N<sub>4</sub><sup>+</sup>=N<sub>2</sub><sup>+</sup>+N<sub>2</sub> equil.: const. and rates rel. to elec. field strength and press., 0.63-1.24 torr. 9-4969

**gases**

- formic acid, LCAO-MO-description of assoc. types 9-13385  
 low-temp. pressure reduction by double mols. formation 9-6265  
 Br atom recomb. in Ar, flash photolysis obs. 300°-1273°K 9-9196  
 NO, B<sup>2</sup> $\pi$  state collisional quenching rate const. determ. 9-18186  
 NO, clusters in expanding jets 9-20031  
 OH(A<sup>2</sup> $\Sigma^+$ ) form. from ground-state atoms, obs. 9-9227

**liquids**

- See also Colloids*  
 anilines, substituted 9-934  
 p- and m- chlorophenols in soln., effect on i.r. spectra 9-1024  
 effect on isotope struct. of Raman bands 9-7266  
 formic acid, LCAO-MO-description of assoc. types 9-13385  
 ion aggregates, electrolytes in nonaq. solvents 9-9514  
 molten salt mixtures 9-9484  
 TiCl<sub>4</sub>, Cl isotope effects 9-1021

**Astatine**

- No entries

**Astatine compounds**

- No entries

**Asteroids** *see Planets; Solar system***Astigmatism** *see Aberrations, optical***Astronautics** *see Space research***Astronomical instruments**

- See also Radioastronomy; Telescopes/astronomical*  
 Anacapi, solar observatory 9-21985  
 antenna array with 1'5 fan beam, for intense radio sources obs. 9-14228  
 Heinrich-Hertz Inst., solar research 9-21984  
 interferometer, for polarization distrib. in radio sources 9-12734  
 iris photometer analogue for Schmidt objective prism spectra 9-18945  
 Lyot-filter for H $\alpha$  line in sun 9-17670  
 magnetograph, photoelec., 0.5-4000 gauss 9-6193  
 magnetographs, longitudinal and transverse, polarization, analysis of effects, mag. field strengths meas. in prominences and chromosphere 9-2067  
 Malta, Cambridge Univ. solar research station 9-15372  
 microphotometer, integrating 9-10564  
 photoelectric phase dev. for registration of moment of star transit 9-2000  
 photographic zenith tube 9-21987  
 photometer, iris, new design for measurement of stellar atmospheres 9-21988  
 pinhole device for sunspot photometry 9-8291  
 radio interferometers, two-element type 9-14276  
 review of developments, (1918-68) 9-6195  
 rocket echelle-interferometer spectrograph 9-15556  
 Romer's meridian circle described 9-15373  
 solar magnetograph, photoelectric, operation rel. to Poincare sphere, photographic methods comparison 9-2066  
 spectrophotometer, single-photon counting 9-12775  
 telescope for  $\gamma$ -ray obs., at balloon altitudes 9-4684  
 CuSO<sub>4</sub> cry. as u.v. transmitting filters 9-20558

**Astronomical observations**

- See also Radioastronomy*  
 Anacapi, solar observatory 9-21985  
 atmospheric properties by inversion of occultation data 9-2047  
 coma cluster galaxies, photo. brightness profiles 9-6112  
 comets continuous spectra, forward scatt. effect 9-2058  
 continuum survey, data high-sensitivity 1415 MHz, north declinations 19° and 37° 9-6146  
 cosmology, observational, review lecture 9-18832  
 error, dimensionality determ. analysis of variance into its components 9-18941  
 Geminid meteors, photometric investigation, mass and luminosity determ. 9-2059  
 Heinrich-Hertz Inst., solar research 9-21984  
 infrared, of moon's surface 9-4117  
 intensity interferometry, recovery of information concerning brightness temp. distrib. 9-20250  
 interference from background sky brightness near satellite 9-10560  
 interferometric meas. of celestial radio spectra 9-20251  
 at i.r. wavelengths, 62 inch telescope 9-10563  
 Kepler's equation solution for Arend-Roland comet 9-17646  
 Kitt Peak National Observatory, Cerro Tololo Observatory, telescopes, instrumentation, other facilities 9-14275  
 latitude variations obs. 9-10370  
 lunar i.r. spectra, surface thermal emission, balloon-borne obs. 9-2044  
 Malta, Cambridge Univ. solar research station 9-15372  
 Mercury orbit, geometric expt. for students 9-12834  
 moon, i.r. spectra, influence of temp. depend. of mat. props. 9-2042  
 moon, Tycho crater, radar study 3.8, 70 cm wavelength 9-2043  
 negatives, reduction by local error method 9-12773  
 optical counterpart to pulsar CP1919+21, apparent variation with double period 9-6149  
 parallax determs., summary of results from past 30 years 9-14196  
 periodicity detection of unknown value in signal from an astron. source 9-20249  
 planetary nebulae, southern, observations 9-21856  
 polarimetric stars, obs. on 25 rel. to determ. of instrumental polarization in telescopes 9-12776  
 polarized starlight, technique for isolating non-interstellar component 9-18942  
 position reduction, local error method 9-21983  
 pulsating stars, possible application to spatial navigation 9-12707  
 R (interstellar absorpt. ratio) found to be valid for distances > 1 kpc 9-15284  
 radar study of moon 9-20220  
 radio, results of heterogeneities of interplanetary plasma 1965-1966 9-2062  
 radiostar scintillations, high latitude, solar modulation 9-20111  
 reduction of positions on photographic plates, errors 9-16631  
 solar activity forecasting, use of determined-probabilistic learning information syst. 9-2087  
 southern galaxies, radial velocities 9-21850  
 from spacecraft, manned, effect of light scatt. by their debris atm. 9-20124  
 spectrophotometer of faint sources by photon counting and d.c. current meas. 9-12772  
 spectroscopic methods, optical, resolution and system acceptance 9-15370

**Astronomical observations continued**

- star's diameter 9-2003  
 star distances, parallax meas., history 9-15262  
 stars and galaxies, book 9-6196  
 stellar, count data in globular clusters 9-6141  
 stellar, dwarf cepheid HD 199757, amp. of light variation period decrease 9-6138  
 stellar diameter meas., using refraction at Moon's edge 9-2002  
 stellar survey, infrared, southern sky at 2.2  $\mu$  9-6120  
 stokes instrumental vector, meas. and calc. of polarization 9-2086  
 time and latitude corrections (Nov, 1967) 9-17599  
 transit telescope, corrections for micrometer screw asymmetry 9-18943  
 venus, high-dispersion spectroscopic studies, CO<sub>2</sub> band near 1  $\mu$  9-2054  
 Venus, radius, determined by planetary radar and Mariner 5 radio tracking data 9-18915  
 venus, temp. and press. var. over surface from spectral obs. 9-2055  
 $\lambda$  Tauri, spectroscopic elements determ. 9-6135  
 Ca II K-line and H $\alpha$  line in solar spectrum, simultaneous obs., method] 9-17652  
 H II regions, absolute isophotometry in H $\alpha$  light, ratio to radio continuum rad. 9-10469  
 H $\alpha$  and CaII K-line in solar spectrum, simultaneous obs. method 9-17652

**Astronomical spectra**

- See also Atmospheric spectra; Cosmic radiations, radio-frequency; Stars/spectra; Sun/spectra; and other individual astronomical bodies*  
 continuum depth definition, 'windows' search 9-18858  
 eight-color system, based on Borgmann, for 985 bright stars 9-15308  
 interferometry with independent time standards at stations 845 km apart 9-6145  
 interstellar reddening for Cepheus 9-15324  
 interstellar reddening of Wolf-Rayet stars 9-18884  
 i.r. spectra, with Michelson interferometers, of planets 9-8298  
 isophotes for extensive astronomical objects, method of construction 9-10558  
 Mars, CO<sub>2</sub> spect. obs., approx. lab. simulation for surface press. estimation 9-20225  
 Mars, rel. to O<sub>2</sub> atm. abundance, obs. 9-8277  
 Mars, surface composition, limonite weathering model 9-2052  
 Mars, surface i.r. absorpt. bands, petrologic significance 9-17639  
 Mars, surface relief and photoelectric obs. 9-10525  
 mass effect on frequency, obs. 9-18829  
 multiplex spectrographic method 9-4539  
 nebula IC 3568, planetary, spectrophotometry 9-16560  
 OH mol. in interstellar space, r.f. spectra 9-18879  
 partial Grotrian diagrams 9-13282  
 phenidone-hydroquinone photographic developers, evaluation 9-12771  
 photometric systems, transformation between 9-18941  
 photometric telescopes, design 9-15374  
 RGU system new transformation eqns. to UVB system 9-14197  
 Schmidt objective prism, photometry 9-18945  
 Stebbins and Whitford 6-colour photometry, relation between G-R and R-I 9-15307  
 synchrotron emission obs. from ring around M81 9-10466  
 venus, rel. to atm. O<sub>2</sub> abundance, obs. 9-8277  
 Na in solid benzene, for investigation of interstellar absorpt. bands 9-18882

**Astronomical telescopes** *see Radioastronomy; Telescopes/astronomical***Astronomy and astrophysics**

- See also Cosmology; Radioastronomy*  
 astronomical unit determ. by Doppler shift of galactic spectral features of neutral hydrogen at 21 cm 9-10559  
 deep-space probes, optical tracking by refl. of sunlight from plane mirror surfaces 9-6100  
 experiments for students of astrophysics, book 9-18975  
 Hertzsprung, 1873-1967, biography 9-12822  
 high-temperature regions, cooling under cosmic conditions 9-17598  
 Japanese obs. in seventh century A.D. 9-12653  
 laboratory astrophysics, conference, Luntenen (1968) 9-15263  
 linear correlation analysis, transformation between photometric systems 9-18941  
 observations on stars and galaxies, book 9-6196  
 the Pine Mountain Observatory, Oregon, USA 9-15371  
 radio sources, extragalactic, number count formula derivation and use 9-12741  
 sky survey, twenty year programme for two Schmidt's suggested 9-18946  
 Stonehenge, its astronomical purpose 9-15265  
 wide ranging collection of 10 articles, book 9-15264

**Atmosphere**

- See also Air; Electromagnetic wave propagation/atmosphere; Ionosphere*  
 aerosol pollution from internal combustion engines 9-8169  
 air, fluorescence efficiency under e bombardment, 65 km, Ee=700eV 9-14158  
 air pollution, indoor, half-lives of HCl, SO<sub>2</sub> and smoke 9-4051  
 balloon neutron counter, in-flight calibration 9-2581  
 boundary layers, barotropic, planetary, neutral, asymptotic similarity 9-18795  
 Chandrasekhar's H( $\eta$ ) func. rel. to albedo and brightness coeff. 9-2046  
 EAS, radio pulse prod. and polarization obs. 9-11122  
 evolution, energetic study of terrestrial and Cytherean 9-21932  
 fission products precipitation  $\beta$  activity meas., Debrecen, Hungary (1966-7) 9-16533  
 inhomogeneities, effect on sonic boom strength and propag. 9-10397  
 interaction with underlying surface, momentum, heat and moisture exchange 9-20085  
 internal gravity waves, effects on ambient rates of prod., chem. losses and motion of ionization, rel. to irregularities 9-12633  
 internal gravity waves propag. in ionospheric regions, rel. to nature and movements of irregularities 9-12624  
 liquid aerosols, electrophotographic picture on semicond. surface 9-4057  
 lower, model suggested from laser backscatter results and parameters, 6943 A, up to 28 km 9-10384  
 mesosphere and above, laser scatter measurements 9-12587  
 neutral waves, interact. with F-region theory, rel. to ionization redistrib. and change in peak density 9-15256  
 parameters by inversion of satellite radiometric obs. 9-4045  
 planetary, gray optically thick, in radiative-convective equil., investing. 9-15337  
 planetary, rotational Raman scatt. 9-15335  
 planetary, solution of radiative transfer problems 9-21933



**Atmosphere continued**

- pollution, review 9-4050
- radiation, thermal, variations 9-21772
- radiation climate of Southern Norway, instrument calibration 9-8172
- radio pulses from extensive air showers, polarization obs. 9-11122
- re-entry mechanics, second-order soln. extension 9-12650
- re-entry vehicles, persistent roll resonance, boundary conds. 9-20128
- semi-infinite, albedo rel. to brightness coeff. and Chandrasekhar's  $H(\eta)$  junc. 9-2046
- star, non-equilibrium phenomena 9-21865
- $\sigma$  Boo F-star, metal deficiency determ. by spectrophotometry 9-20176
- temperature and density profiles, radar interferometric meas. 9-18804
- tropopause, laminar transport of material 9-6070
- wind power spectrum below macroscale 9-18799
- wind profiles from rocket exhaust noise 9-4054
- Na spectral line formation and radiative transfer 9-19391
- O spectral line formation and radiative transfer 9-19391

**composition**

- aerosol turbidity, 1958-68 obs. 9-17563
- estimates from vertical density distribution 9-17576
- ionized constituents model, 100-300 km region 9-12596
- ozone by absorption spectroscopy from a rocket, near sunrise 9-1946
- particle size distribution 20 km sulphate layer, lidar obs. 9-4049
- particulates in Pittsburgh air, density obs. 9-21759
- stratospheric dust, relationship to meteoric influx 9-21760
- twilight obs. of Na, K and Li, reson. emission meas., seasonal var. of abundances 9-12595
- Venus, determ. by Venus-4 space probe 9-10530
- He winter hemisphere excess, twilight emission rel. to geomagnetic activity. 9-1951
- Hg vapour, obs. over 2 year period 9-21758
- Li emission rate in upper atm., min. detectable limit obs. 9-21785
- N day time, production and loss mechanism in upper regions 9-16534
- NO day time, production and loss mechanism in upper regions 9-16534
- O, near 100 kms, seasonal variations 9-10398
- O<sub>2</sub> in lower thermosphere, Ariel 3 obs. 9-17562

**humidity**

- See also Humidity*
- effect on absorpt. of e.m. waves at 35 GHz 9-8173
- relative, profiles from i.r. spectra from satellite 9-20086

**ionosphere** *see Atmospheric electricity; Ionization, atmosphere; Ionosphere***movements**

- See also Wind*
- air-sea interaction 9-12578
- auroral disturbance, generation of atmospheric wave 9-1947
- boundary layer, planetary, vertical eddy transport estimation using vertical velocity spectrum 9-21763
- clear-air turbulence, correlation with sporadic E 9-4065
- cyclones causing crust deformation and gravity field changes 9-4034
- diffusion meas. using radioactive gas emitted from point source 9-8170
- earth's rotation, effect on 9-10371
- elec. conductive, weak discontinuity propag. 9-21761
- equatorial disturbances in embedded idealized dipole mag. field, stability 9-10388
- F-layer lunar tide height variation obs. 9-1973
- fall reversal, power and middle stratosphere, northern hemisphere 9-15244
- geostrophic eqns., total energy conservation 9-6072
- instability, nonlinear of eqns. of one-dimensional flow 9-8166
- jet-stream, eff. of earth's rot. and surface movements 9-21768
- laminar transport of material across tropopause 9-6070
- large scale, equations, mag. of terms 9-6073
- large scale, nonlinear aspects 9-20087
- macroscale windspeed fluctuations, mean and turbulent kinetic energy and power spectra 9-21762
- neutral, interaction with ionization, and real and apparent motions 9-12611
- penetrative convection, vertical mixing 9-21764
- planetary boundary layer, response to time varying pressure gradient force 9-18796
- radioactivity used to follow movements 9-17564
- stratopause circulation profiles, hemispheric similarities 9-1948
- stratosphere, large scale disturbances, summertime 9-21765
- terrestrial planets, circulation 9-6169
- tornado vortex, electrical heating 9-8175
- turbulence, buoyant subrange, measurements 9-18797
- turbulence, weak optical strength, observation 9-16531
- waves, vertically propag., in atm. with Newtonian cooling inversely proportional to density 9-4052
- wind and circulation in meteor zone 9-12599

**precipitation**

- See also Ice; Rain; Snow*
- aerosol particles charge equilibrium 9-18790
- cloud nucleations study, automated aircraft instrumentation system 9-4056
- drops, vibrating, modulation of radar echo 9-21771
- hailstones, mechanism for growth 9-6075
- hailstones, spherical, simulation of total heat transfer 9-16529
- $\beta$  activity of fission products, Debrecen, Hungary (1966-7) 9-16533

**radiation belts**

- acceleration mechanism, bimodal diffusion 9-16535
- corpuscular geomagnetic field, angular anisotropy 9-21828
- distant, energetic electrons diurnal variation and features 9-4072
- electron, bimodal diffusion 9-16536
- electron, inner belt, addition after solar flare event, expt. 9-8195
- electrons, synchrotron emission 9-12603
- electrons mirroring ( $3 < L < 5.5$ ) 9-10416
- instability, h.f., associated with loss cone 9-21794
- outer, low energy proton lifetimes 9-10415
- part., trapped, accel. in inhomogeneous magn. field, bimodal diffusion 9-222
- ring current asymmetry during mag. storm 9-21795
- synchrotron radiation calc. 9-20106

**radioactivity**

- See also Fallout*
- air movements followed using atmospheric radioactivity 9-17564
- concentration determ. from automatic dust monitor 9-8181

**Atmosphere continued****radioactivity continued**

- fallout of dry radioactive products of nuclear tests 9-8179
- fission products, large scale 9-21784
- radiocarbon transfer in nature 9-12591
- reduction following atomic weapon test suspension 9-1943
- Rn-222, short lived daughter products, conc. in atm.,  $\alpha$ -spectrometry method 9-20092
- solar neutron transport 9-10396
- <sup>212</sup>Pb atoms, neutral and charged, from Rn decay, attachment coeffs. to aerosols 9-9565
- <sup>222</sup>Rn effect on personnel dosimeters 9-12782
- <sup>10</sup>Be, <sup>7</sup>Be cosmogenic prod. rate determ. by radioactivity meas. in soil 9-4062
- <sup>14</sup>C prod. by cosmic ray neutrons 9-20123
- <sup>32</sup>Si, atmos. conc. unexpectedly high 9-21781
- <sup>89</sup>Sr and <sup>90</sup>Sr, and surface deposition 9-21783

**structure**

- computer simulation 9-18792
- ozone, vert. dist., San Francisco 9-8168
- ozone, vertical dist., rel. to thermal structure 9-6071
- pressure dist. function for model atm. 9-4058
- troposphere, study using scatter propagation meas. at 15.7 GHz 9-1942

**temperature**

- distribution from zenith sky intensity meas. during twilight 9-8183
- field, adaptation to case of sea 9-6060
- magnetosphere, temp dist. model 9-10399
- Markov chain, order of dependency, test procedure 9-8167
- nightglow [OI]6300 Å line, doppler temperature for solar cycle minimum 9-1953
- profile, determ. from outgoing radiance 9-12580
- stratosphere, middle, diurnal range 9-18794
- surface meas., using i.r. radiometers 9-2249
- thermal convection, suppression of frictional constraint on lateral boundaries 9-18793
- thermal structure, assoc. with vent. dist. of ozone 9-6071
- thermospheres, planetary, diurnal variations 9-8185
- variability near 120 km, from grenade glow cloud expts. April-May (1965) 9-17574
- variations, diurnal, and matter fluxes 9-17575
- Venus, data from 'Venus-4' 9-6180

**thermodynamics**

- baroclinic intensity, modes of kinematic generation 9-6069
- radiation balance earth atmosphere system, Nimbus 2 obs. 9-20089
- water, phase transitions in clouds, applic. of theory of irreversible proc. to expt. data, book 9-20088

**upper**

- See also Magnetosphere*
- aurora, substorm and storm regulation 9-20122
- auroral absorption, position and height deduced from v.l.f. phase measurements 9-12601
- auroral waves, fast, obs. 9-8193
- composition estimates from vertical density distribution 9-17576
- cosmic matter, dispensed, optical method of sounding 9-1945
- dayglow of oxygen A band 9-4068
- density semi-annual. var. from satellite drag, anal. (1958-1966) 9-14165
- density semi-annual var. near 1100 km, from Echo 2 orbit obs. (1964-1967) 9-14166
- density separation from drag coeffs. of satellites, expt. evidence 9-10452
- density var. near 500km, rel. to solar activity 9-1944
- equatorial counter electrojets and areas of inverted Sq currents 9-17579
- exosphere, e content response to partial solar eclipse 9-10427
- exosphere, electron content, diurnal change calcs. 9-1949
- exosphere, thermal ions, evidence of solar and geomagnetic control 9-10401
- exosphere and ionosphere, guided long e.m. waves 9-14408
- faster rotation, model including dynamo region and charged particle effects 9-12632
- glow cloud obs., effective height of Earth's shadow 9-2048
- gravity waves, effect of ohmic losses, anal. rel. to dissipation of wave modes 9-12615
- gravity waves, effects of molec. viscosity and thermal conduction 9-12598
- gravity-wave critical layers due to Doppler shifting of freq. to zero, consequences in winds and turbulence 9-12597
- heating during geomag. storms 9-21788
- ion production functions, height distribution 9-21801
- ionized constituents model, 100-300 km region 9-12596
- magnetospheric waveguide existence, conjugate echoes in satellite topside-sounder data 9-8199
- meteor zone, wind and circulation 9-12599
- molecular oxygen conc. by absorpt. spectroscopy 9-4064
- neutron fluxes, fast 9-16913
- ozonosphere, solar flare effects 9-21757
- precipitation, nocturnal, of auroral electrons, config. and displacement 9-17577
- radar research 9-6084
- radiation, terrestrial, 7-27 $\mu$ , angular and spectral distributions, Cosmos obs. 9-21786
- radiation, terrestrial 7-26 $\mu$ , spectral intensity rel. latitude, Cosmos 45 and 65 obs. 9-21787
- rocket-released probes, instantaneous orientation determ. from signal polarization anal. 9-6099
- rotation, effect on satellite orbits 9-17596
- solar activity, delay preceding density changes 9-8184
- solar particle energy dissipation, PCA 3914 and 5577 Å light emission calc. 9-20102
- stratopause circulation profiles, hemispheric similarities 9-1948
- structure and composition, advances during IQSY 9-8182
- temperature variability near 120 Km, from grenade glow cloud expts. April-May (1965) 9-17574
- temperature vars., diurnal, and matter fluxes 9-17575
- twilight obs. of Na, K and Li, reson. emission meas., seasonal var. of abundances 9-12595
- v.l.f. mag. and elect. fields, Javelin rocket obs. 9-10414
- winds, waves and drifts, conference, St. Gallen, Switzerland, (1967) 9-12593
- world data centre A, growth and future plane 9-20093
- Li emission rate, min. detectable limit >>>> obs. 9-21785
- N day time production and loss mechanism 9-16534

**Atmosphere** continued  
upper continued

NO day time production and loss mechanism 9-16534

**Atmospheric acoustics**

infrasonic waves, generated by storms, eff. on human behaviour and correlation 9-8510  
 long distance infra propag. following explosion 9-17573  
 long distance infrasonic propag. following explosion 9-17572  
 siren signals in built up areas, effect of buildings 9-15460  
 sonic boom, effects of winds and inhomogeneous atmos. on propag. and strength 9-10397  
 sonic-boom press. waveforms, spikes 9-4063  
 stratified still atm., sonic bang intensities 9-17816  
 thermosphere, ducted acoustic-gravity waves 9-12605  
 wave structure const. rel. refractive index and gradient of refractive index in surface layer 9-8174

**Atmospheric disturbances** *see* Atmosphere/movements; Thunderstorms**Atmospheric duct** *see* Electromagnetic wave propagation**Atmospheric electricity**

*See also* Atmosphere/radioactivity; Atmospherics; Aurora; Electromagnetic wave propagation/atmosphere; Ionization, atmosphere; Lightning; Thunderstorms

aerosol particles, charge equilibrium 9-18790  
 agrimeter for pot. gradients meas. 9-1940  
 charge transfer in lightning flash, magnetographic meas. 9-8177  
 charged particle concentration profile below 90 km, diurnal variation 9-18801  
 discharges, theory based on turbulent generation of electric fields 9-6469  
 electrojet, features of two main forms, and theories of origin 9-18809  
 heating, electrical, of tornado vortex 9-8175  
 source, thermally driven tidal motion in lower ionosphere 9-6080

**Atmospheric optics**

*See also* Airglow; Sky brightness; Sunlight; Twilight  
 the 'Glory', Hawaii, photographic obs. showing rings 9-14162  
 aircraft obs. at Crater Lake, Oregon, USA 9-6078  
 axially symmetric transfer of light through cloud of anisotropic scatt. particles 9-6076  
 coherent propag., parameter fluctuations rel. turbulence 9-6423  
 extinction coeff. meas. on clear atmospheres and thin cirrus clouds 9-20090  
 i.r. extinction, 1-2.5  $\mu$  9-17566  
 i.r. radiation from cirrus clouds, 8-13  $\mu$  region, physical model 9-6074  
 laser beam absorption in the lower atmosphere 9-2386  
 laser beam phase fluct., due to turbulence, interferometry 9-10869  
 laser beam scintillation under turbulence saturation 9-21774  
 laser-beam scintillation over horizontal paths from 5.5 to 145 kilometers, log-amplitude covariance 9-21775  
 l.f. fluctuations in intensity of remote sources in i.r. spectral region 9-17568  
 lidar probing techniques 9-4049  
 luminance and attenuation, Crater Lake USA, 8800-1400m 9-12586  
 modulation transfer function in turbulent air, effect of image averaging time 9-15247  
 phase and frequency of optical waves, effects of turbulent atmosphere 9-14161  
 polarization features of light reflected from natural surfaces 9-1939  
 polarization of nightglow, line versus continuum emission 9-20099  
 pressure dist. function for model atm. 9-4058  
 radiation, outgoing, temp. profile determ. from 9-12580  
 reflection, diffuse of light pulse from medium confined by underlying surface 9-17569  
 refraction angle and phase shift determ. of density 9-17560  
 scattering, small angle, phase function 9-17570  
 sky radiation, spectral distribution 9-20091  
 structure const. rel. refractive index and gradient of refractive index in surface layer 9-8174  
 transit times, r.f. and optical, simultaneous obs. 9-10770  
 transparency spectra, 0.59 to 15  $\mu$ , paths up to 2.6 km 9-6077  
 troposphere, polarization of scatt. light and zodiacal light compared 9-1938  
 turbulence, very weak optical strength 9-16531  
 twilight, colour rel. stratospheric dust, models 9-21776  
 H $\alpha$  line in night sky, obs. 9-1952

**Atmospheric pressure and density**

air density at 470 km, satellite obs. (Jan. 1967-May 1968) 9-20095  
 baroclinic intensity, modes of kinematic generation 9-6069  
 density semi-ann. var. from satellite drag, anal. (1958-1966) 9-14165  
 density semi-ann. var. near 1100 km, from Echo 2 orbit obs. (1964-1967) 9-14166  
 infrasonic long-period waves rel. to approaching cold front, obs. 9-12581  
 pressure field, anisotropic space-time correl. function 9-17561  
 profiles from radar interferometry 9-18804  
 Rayleigh scatt. instrum., rocket-borne for density meas. 9-12594  
 refraction angle and phase shift determ. 9-17560  
 refractive index variations associated with monsoon depressions 9-1941  
 solar activity, delay preceding density changes 9-8184  
 upper, density separation from drag, coeffs. of satellites, expt. evidence 9-10452  
 upper, density variations during geomag. disturbances 9-20094  
 variations, semi-ann. rel. to solar activity 9-1944  
 Venus, data from 'Venus-4' 9-6180

**Atmospheric spectra**

*See also* Atmospheric optics  
 clouds, high altitude, reflectance, models, 2.5-3.5  $\mu$  9-12582  
 diffusivity factor of band models and line shapes 9-18800  
 electron energy, secondary peak near 10 keV, inducted whistlers evidence 9-4066  
 Lyman- $\beta$ , He reson. radiation, in nightglow 9-6087  
 O emission mechanism suggested for tropical night airglow 5577 and 6300 Å 9-8191  
 polarimeter, airborne, for visible radiation studies 9-13056  
 power, of macroscale windspeed fluctuations 9-21762  
 thunder, power spectral analysis, data opposing use of single-grid hot-wire microphone 9-10385  
 transparency, 0.59 to 15  $\mu$ , paths up to 2.6 km 9-6077  
 O $_2$ ( ${}^1\Delta_g$ - ${}^3\Sigma_g^-$ ) 0.1 band obs. in day airglow, brightness 9-14167  
 [OI]  $\lambda$ 5577,  $\lambda$ 6300 auroral emissions, Antarctic night sky photometry 9-1955  
 H $_2$ O vapour,  $\lambda$  $\nu$  $^{-1}$ =12.67 cm $^{-1}$  line width and intensity 9-771  
 O emission at 6300 Å, behaviour during geomag. storms 9-21788

**Atmospheric spectra** continued

O $_2$ ( ${}^1\Delta_g$ - ${}^3\Sigma_g^-$ ) band in evening airglow, interpret rel. to ozone dissociation 9-4069  
 OI 6300 Å and 5577 Å lines, night, intensity profiles 9-8192

**Atmospherics**

decimeter radioemission from linear lightning 9-21779  
 e.l.f., SEA phenomena explanation 9-21809  
 lightning radioemission 9-21778  
 noise fluctuations in 4cm to 8mm band, radiometric meas. 9-8178  
 noise intensity, frequency dependence, 1 to 1000 kHz at low and medium latitudes 9-10390  
 radiogoniometer with c.r.t. display and automatic photographic recording 9-14163  
 r.f. emission charact. rel. to e.m. wave absorption 9-10392  
 v.l.f. emissions, Injun 3 obs. 9-10389  
 v.l.f. radio noise, spectral charact. 9-10394  
 waveform appl. to v.l.f. attenuation charact. determ. 9-12588  
 whistler and ducted echoes on topside ionograms 9-8202  
 whistler polarization, effect of propag. through lower ionosphere and earth-ionosphere guide 9-20108  
 whistlers, excitation of emissions near low hybrid frequency and their interpretation 9-12619

**Atomic beams**

*See also* Particle velocity analysis  
 alkali, fast charge exchange source 9-11415  
 alkali metal, reactions with polyhalide mols. 9-9307  
 alkali metal, reactive scatt. from polyhalide mols. 9-7096  
 in electric quadrupole fields, Mathieu functions 9-713  
 interaction with solid surface 9-3183  
 interaction with solid surfaces, theory 9-10888  
 oven with low assoc. magnetic field 9-4865  
 stopping in solids, Z $_1$  oscillations and size effect 9-5583  
 Ar scatt. from Ag(111) 9-3187  
 Au, condensation on rocksalt substrate 9-14897  
 Bi, elastic scatt. of slow electrons, ang. distrib. for energy range 5 to 1200 eV 9-4857  
 Cs fast charge exchange source 9-11415  
 Cs isotopic shift of D $_1$  line determ. 9-18137  
 98%Fe, ions produced by hypvel, impact on Ta, mass analysis 9-10084  
 Ge target, band gap effects in  ${}^{72}\text{Ge}^*$  stopping 9-5589  
 H, detection by MoO $_3$  thin film device 9-6728  
 He, 2S and 2S $^*$ , ionization of methane 9-912  
 He, charge-changing collisions in H, via metastable states 9-5071  
 Li-Hg scatt., interatomic potential 9-15827  
 Li crossed-beam reactions with Cl $_2$ , ICl $_3$ , Br $_2$ , SnCl $_4$  and PCl $_3$  9-17512  
 Na-N $_2$  beam interaction, excitation energy transfer, obs. 9-9308  
 Na, reaction with O $_2$  beams 9-909  
 Xe scatt. from Ag(111) 9-3187

**Atomic clocks** *see* Time measurement**Atomic frequency standards** *see* Time measurement**Atomic mass and weight**

*See also* Isotopes; Mass spectra  
 ${}^{40}\text{Ca}$ - ${}^{40}\text{Ar}$ , mass diff. by high resolution mass spectrometer 9-13309  
 ${}^1\text{H}$ , at. mass, high resolution spectrometer 9-11414  
 ${}^{16}\text{O}$ , at. mass, high resolution spectrometer 9-11414  
 ${}^{32}\text{S}$ , at. mass, high resolution spectrometer 9-11414

**Atomic orbitals** *see* Atoms/structure; Orbital calculation methods**Atomic scattering factors** *see* Crystal structure, atomic; X-ray crystallography; X-ray scattering**Atomic spectra** *see* Spectra/atoms**Atoms**

*See also* Atoms, mesic and muonic; Collision processes/atoms; Elements; Nucleus; Positronium  
 alkali, adsorbed on metal, net charge 9-3212  
 alkali, ground states, rare-gas-induced gyromag. ratio shifts 9-11403  
 alkali, heavy, selection rules rel. to collisional m $_j$ -mixing in lowest  ${}^2\text{P}_{3/2}$  states 9-9147  
 atomic and nuclear physics, introduction in SI units, book 9-8345  
 atomic oscillator strengths, systematic trends in isoelectronic sequences 9-19388  
 atoms, two Coulomb centres problem at large centre separ., multipole expansion for energy, quasi-crossings of curves 9-4829  
 Bethe-Goldstone eqns., soln. for electronic pair-correlation energies of ground states 9-11383  
 Born-Mayer parameters and interatomic potential for g.s. 9-20890  
 bound-state Dirac electron, 'hidden-momentum' equivalent to magnetic charges 9-669  
 coherent photon emission 9-6497  
 diamagnetic shielding factors, relativistic calc. 9-675  
 dispersion forces, second- and third-order energies 9-13273  
 electron affinities of non-transition elements 9-16994  
 electronic pair-correlation energies of ground states, soln. of Bethe-Goldstone eqns. 9-11383  
 electronic transitions in near-adiabatic collisions 9-4979  
 exchange forces, one-dimens. model 9-704  
 exchange interactions, perturbation theory 9-9108  
 experiments and projects in atomic physics, book 9-2120  
 free particle moving in one dimens., and on ring, quantum dynamical solns. 9-4866  
 inert gases, polarizability of interacting pair 9-13493  
 inert gases, repulsive potential-energy curves 9-9153  
 intense light interact., effective electronic binding pot. 9-684  
 interaction energy due to e.m. and electrostatic fields calc., quantum electrodynamics method 9-9150  
 interaction with strong e.m. field, analysis taking into account recoil 9-14663  
 ionization by electrons, ang. distrib. of outgoing electrons, eff. of identity and correlations 9-11613  
 isoelectronic sequences, electron scatt. phases by extrapolation of quantum defect data 9-4883  
 light scatt. including interference of excited states 9-683  
 monochromatic light resonant scatt. in gas, freq. distrib. and interference 9-21140  
 neutral with outer 2p and 3p electrons, ioniz. by e and proton impact, X-section calc. from Born approx. 9-4859  
 Orthopositronium-He syst., quenching rate of orthopositronium, parameter  ${}^1Z_{eff}$  meas. 9-4888  
 oscillator strengths, regularities, quantum-mech. approach 9-11377  
 overlapping multiplets of levels 9-11387



## Atoms continued

- photoeffect, relativistic, from K shell near threshold 9-690  
 photon absorption effective cross-sections, empirical formulation 9-16998  
 polarizability, field methods of calc. 9-4822  
 r.f. field interaction 9-20882  
 scattering, Harris variational method for phase shifts, analysis w.r.t. other methods 9-11404  
 scattering by superposition of two power pots, amplitude and cross-section calc. 9-4861  
 scattering theory, peaking approx., eff. on cross-sections for 1s→2s transition in H 9-13311  
 source by laser evaporation of H saturated Ti 9-11420  
 spin  $1/2$  particle, generalized Bloch eqn. extension to any multipole 9-4848  
 spin-coupled wave function Hamiltonians 9-6952  
 spin-spin contact Hamiltonian and Coulomb interaction 9-9113  
 Stark effect, review 9-13284  
 in statistical equil., ergodic Markov chain description of atomic-state populations 9-14661  
 Thomas-Fermi eqn. screening function, var. soln. 9-14662  
 transition metals, binding on W surface 9-9628  
 van der Waals forces, two-body Padé approximant of dynamical polarizability 9-13307  
 wave function corresponding to periodic electron-nucleus collisions, formation 9-15823  
 Ar refractive index and resonance line oscillator strength obs., 2300-1100 Å 9-9454  
 Au photoelec. cross sections, 30-50 KeV  $\gamma$ -rays 9-691  
 C atom trio in triangle, nonpairwise additivity in exchange energy 9-15911  
 Cl, radiative recomb. in shock waves 9-9289  
 Cl  $^2P_{3/2}$  ground-state, kinetics of overall recombination 9-19409  
 Cs, elec. dipole moment, upper limit, and for electron 9-11384  
 Cs, elec. dipole moment upper limit, obs. 9-4835  
 Cs vapour, optically oriented spin system, double refraction obs. theory 9-9115  
 Cu  $\gamma$ -scatt. cross-section calc. by subtracting photoelectric cross-section 9-710  
 D rot. ordering determ. from n.m.r. study near  $\lambda$ -transition 9-12511  
 H, Bohr-Sommerfeld identity between actual and calc. energy levels 9-4867  
 H, generalised eqn. from symmetry group of integral eqn. 9-9154  
 H, photon elastic scatt., retardation effect 9-15831  
 H depolarization while passing through mag. lens at zero field 9-2827  
 H ioniz. by fast charged part., binary encounter and Bethe theory, meas. of differential X-sections 9-4871  
 H source by laser evaporation of H saturated Ti 9-11420  
 H(2S), production by molecular dissociative excitation 9-14725  
 He-He potential near van der Waals minimum 9-7098  
 He,  $2^1S$ - $1^1S$  repulsive interaction pot., long range, calc. and obs. 9-4889  
 He, many body theory for calc. of time depend. perturbations 9-11421  
 He, metastable, formed in charge exchange of He beam in H 9-5071  
 He, optically aligned  $2^3S_1$ , gyromagnetic ratio by opt. pumping, level shifts 9-11423  
 He, van der Waals coeffs. for ground and metastable states 9-2833  
 He scattering, elastic, from He and Ar, differential cross-sections 9-727  
 He to Rn, Hartree-Fock numerical results 9-9114  
 $^3\text{He}$  interacting system, spin diffusion coeff. 9-6337  
 $^4\text{He}$ , pair distrib. function, three-particle effects 9-7225  
 Hg, diamagnetic shielding factors, relativistic calc. 9-675  
 Hg, long-range interactions 9-17002  
 I, magnetic susceptibility meas. 9-13304  
 K, intensity modulation of transmitted light, 462 MHz, at g.s. h.f. freq. 9-9130  
 Li-Hg interatomic potential from beam scatt. 9-15827  
 Li $^+$  van der Waals coeffs. for ground and metastable states 9-2833  
 Ne, splitting of  $3p_1$ ,  $3p_2$  fine structure levels, study by difference freq. reson. technique 9-2816  
 O, electron affinity calc. from dissociative electron attachment to CO $_2$  9-11614  
 Pa, level system suggested by emission spectrum  $3\mu$  to 4000 Å 9-15814  
 Pb, 280 keV  $\gamma$ -ray total cross section 9-16999  
 Pb  $\gamma$  scatt. from K shell electrons, incoherent, obs. 9-712  
 Pb photoelec. cross sections, 30-50 KeV  $\gamma$ -rays 9-691  
 Pt 280 keV  $\gamma$ -ray total cross section 9-16999  
 Pu in PuCl $_3$ -NaCl, equil. potn. depend. on temp. and conc. 9-20892  
 Sm  $\gamma$  scatt. from K shell electrons, incoherent, obs. 9-712  
 Sn  $\gamma$  scatt. from K shell electrons, incoherent, obs. 9-712  
 Sn photoelec. cross sections, 30-50 KeV  $\gamma$ -rays 9-691  
 Sn 280 keV  $\gamma$ -ray total cross section 9-16999  
 Ta  $\gamma$  scatt. from K shell electrons, incoherent, obs. 9-712  
 Th I, energy levels, odd and even, present state of anal. 9-11388  
 U photoelec. cross sections, 30-50 KeV  $\gamma$ -rays 9-691  
 W photoelec. cross sections, 30-50 KeV  $\gamma$ -rays 9-691

## electron scattering

- Ar, phase shifts compared with Hg and Xe, rel. to Mott theory and non-relativistic approx. 9-19408  
 Bethe approx. for calc. of excitation cross-section 9-701  
 close-coupling approx., trial wave function method examined 9-13276  
 collected Russian papers 9-696  
 complex at. scatt. factors for fast electrons 9-6984  
 complex atomic systems 9-2822  
 energy loss, mean, in elastic encounters 9-6983  
 excitation, theory using cross-section formula 9-682  
 high-energy, ionization cross-sections calc. 9-694  
 high-energy, ionization cross-sections calc. 9-692  
 high-energy, ionization cross-sections calc. 9-693  
 ion, resonances 9-702  
 ionization cross-section of hydrogenic atoms 9-13448  
 Mott theory and non-relativistic approx., numerical comparison 9-19408  
 multiple, fast e in thin layers, obs. ang. distrib. and single-scatt. cross-section, Thomas-Fermi model 9-6982  
 neutral, phases from extrapolation of quantum defect data along isoelectronic sequences 9-4883  
 oscillator strength, generalized, minima, rel.to nodes of radial wave functions 9-695  
 partial waves, asymptotics of functions 9-698  
 particle-bound-state scatt., compact operators method, one channel case 9-17726  
 polarization effects 9-699

## Atoms continued

## electron scattering continued

- potential approx., static, validity range 9-17001  
 quasielastic ejection from (e, 2e) 9-14669  
 s-s transitions, Coulomb. Born approx. 9-700  
 s-wave elastic scatt., variational bounds on phase shifts 9-6981  
 slow e. collisions 9-697  
 spectrometry, e impact at 25-60eV and 0°-80° 9-9142  
 spin polarization from unpolarized targets at low-energy, review 9-18148  
 variational calc. for three-electron syst., multiplets and config. 9-4884  
 Ar, interaction of keV electrons with electron shell, energy loss spectra 9-11398  
 Ar, interaction of keV electrons with electron shell, energy loss spectra 9-18150  
 Ar, Ramsauer gas kinetic collision integrals 9-17000  
 Be target, bremsstrahlung cross-section meas. 9-703  
 Be $^+$  variational calc., multiplets and config. 9-4884  
 Bi, elastic, ang. distrib. for energy range 5 to 1200 eV, ang. range 30 to 155° 9-4857  
 Ca, 9.5 and 15.5 eV, excitation cross-sections 9-13303  
 Cs, ionization cross-section 9-9400  
 Cs excitation of  $6^2P$  9-4850  
 H, elastic scatt. S-wave phase shifts, var. method calc. 9-13312  
 H, electron impact excitation of Lyman- $\alpha$  rad. in 2p state 9-19411  
 H, inclusion of strong coupling 9-718  
 H, ionization by slow electrons 9-906  
 H, ionization cross-section depend. on main quantum number 9-2826  
 H, positron elastic scatt., phase shifts using polariz. pot. method 9-20898  
 H, rearrangement collisions, eff. of core terms, nonorthogonality and conservation of particle flux on approx. theories 9-11418  
 H, resonance phenomena 9-721  
 H, triplet s-wave scatt., applic. of compact operators method 9-17726  
 e $^+$ -H collisions, positronium formation applic. of variational scatt. functions 9-18156  
 H slow collisions 9-719  
 H $^-$ , differential cross-sections of slow e at  $1/2$  and 1 Ry, deviations from Coulomb scatt., phase shifts 9-9143  
 H, e $^+$  scatt. 9-720  
 He, collision cross-sections calcs. 9-11427  
 He, elastic scatt. of zero-energy electron scatt. lengths and reciprocals from variational methods and trial function 9-4885  
 He, elastic scatt. S-wave phase shifts, var. method calc. 9-15835  
 He, in metastable  $2^3S$  state, cross-section, polarized-orbital method 9-9162  
 He, phases and scatt. lengths, from quantum defect data 9-4883  
 e $^+$ -He annihilation quanta, ang. correl., applic. of variational scatt. functions 9-18156  
 He I line broadening in plasma by electron impact, theory 9-21073  
 He phase shift, cross-section, polarization and exchange determ., 0.04 eV 9-4882  
 He $^-$  variational calc., multiplets and config. 9-4884  
 $^4\text{He}^+$ , Lamb shift obs. in N=4 state, by quantum beats from electron impact 9-724  
 Hg, 25-150eV, static pot. approx. validity 9-17001  
 Hg, differential cross-sections and spin polarizations at 3.5-500 eV 9-18149  
 Hg, e spin polarization rel. to scatt. pot. 9-11397  
 Hg, phase shifts, spin polarization compared with Ar and Xe, rel. to Mott theory and nonrelativistic approx. 9-19408  
 Hg, relativistic and exchange effects at 3.5-500 eV 9-18149  
 Hg metastable atom-electron inelastic second-order collisions 9-18153  
 Kr, interaction of keV electrons with electron shell energy loss spectra 9-11398  
 Kr, interaction of keV electrons with electron shell energy loss spectra 9-18150  
 Li isoelectronic sequence phase shifts for l=0, l=1 partial waves 9-19402  
 Li $^+$ , differential cross-sections of slow e at  $1/2$  and 1 Ry, deviations from Coulomb scatt., phase shifts, comparison with quantum defect method 9-9143  
 Na $^+$ ,  $^3S$  nonrelativistic partial wave analysis 9-18147  
 Ne, interaction of keV electrons with electron shell, energy loss spectra 9-18150  
 Ne, interaction of keV electrons with electron shell, energy loss spectra 9-11398  
 Ne $^+$ ,  $^2P$  nonrelativistic partial wave analysis 9-18147  
 O $^-$ ,  $^2P$  nonrelativistic partial wave analysis 9-18147  
 Xe, interaction of keV electrons with electron shell, energy loss spectra 9-18150  
 Xe, interaction of keV electrons with electron shell, energy loss spectra 9-11398  
 Xe, phase shifts etc. compared with Hg and Ar, rel. to Mott theory and non-relativistic approx. 9-19408

## excitation

- alkali-alkali nearly adiabatic thermal collisions, excitation transfer, Stueckelberg's formula and difficulties 9-18154  
 atomic excitation mechanisms in nonequilibrium gases up to 20000°K, classification schemes 9-19407  
 auger electron spectroscopy in LEED systems 9-4854  
 Auger ionization induced by multi-charged ions 9-13302  
 Auger K L, L, transition probabilities, relativistic calc. 9-4855  
 Beam-foil excitation method, for radiative mean-life meas. 9-14671  
 coherence radiation in ext. mag. and elec. fields 9-15815  
 double ionization, resonant mechanism 9-6974  
 by electron impact, theory using cross-section formula 9-682  
 interaction with strong e.m. field, analysis taking into account recoil 9-14663  
 KX-radiation from  $\alpha$  bombard. 9-677  
 L $_2$ MM and L $_3$ MM spectra of elements of low Z, line intensities 9-4856  
 laser spark spectroscopic source 9-18145  
 lifetime depend. on thermal motion, meas. by 2 cascade photons 9-15816  
 by light scatt., consideration of interference of excited states 9-683  
 magnetic resonances induced by modulated light, theory 9-4858  
 mean life meas. using beam foil light source 9-19405  
 metastable participation in spectrographic arc 9-680  
 multiphoton effective ionization cross-section 9-681  
 muonic X-rays in nucleus field, energy levels perturbation calc. 9-731  
 non-resonance excitation transfer on collisions induced by dipole-dipole interact. 9-11401  
 in plasma, radial distrib. meas. technique 9-13461  
 polarization corrections in optical excitation meas., elimination 9-14667

**Atoms continued****excitation continued**

- resonance fluorescence depolarisation after anisotropic collisions, theoretical study 9-9146
- resonance scatt. line splitting under strong monochromatic e.m. irradiation 9-4849
- resonances, configuration interaction theory, eff. of overlapping 9-11405
- s-s transitions due to e. scatt., Coulomb-Born approx. 9-700
- spontaneous emission, applic. of quasiparticle kinetic eqn. to order  $\lambda^6$  9-11389
- two-photon absorption rates ratio for chaotic and laser light 9-9132
- impact, of ns-n's transitions, connection to Wigner threshold law 9-13296
- <sup>20</sup>Hg, Zeeman degeneracy under non resonant light radiation 9-11393
- <sup>233</sup>Pa, KLL Auger spectra, obs. in  $\beta$ -decay 9-2817
- Ar, chem. applic. of metastable atoms 9-825
- Al, mean excitation potentials from stopping power data 9-9135
- Al optical resonance transitions, lifetime measurements, phase shift method 9-11392
- Ar, Auger spectra of L<sub>2</sub> and L<sub>3</sub> shells 9-6978
- Ar, by He<sup>+</sup> impact, spectra obs.,  $E_{\text{th}}=0.3-10$  keV 9-20887
- Ar, by protons, 4 MeV, continua intensity depend. on press. determ. 9-20883
- Ar, ionization probability curves for electron impact, for <sup>2</sup>P<sub>3/2</sub> and <sup>2</sup>P<sub>1/2</sub> states 9-4863
- Ar, L<sub>2</sub>MM and L<sub>3</sub>MM spectra, line intensities 9-4856
- Ar, proton excitation of 1300-Å continuum 9-9133
- Ar, radial distrib. of excited species in capillary discharge 9-13461
- Ar excited states, spect. studies on decaying plasmajet, electron-ion recomb. coeff. 9-21057
- Ar I, 5p levels, experimental lifetimes 9-15819
- Ar I, radiative lifetimes in resonance series 9-11390
- Ar I, resonances obs. in photo-ionization continuum 9-13297
- Ar II, 4p<sup>3</sup>S<sub>3/2</sub><sup>0</sup> level lifetime, absolute meas. from emission of correlated photons in cascade 9-6975
- Ar II 4s and 4p levels population inversion mechanism, obs. 9-15817
- B, collisional energy level and lifetime meas. 9-6959
- BII, 2p<sup>2</sup> <sup>1</sup>D lifetime meas. 9-11391
- C, laser action obs. foll. dissociative transfer 9-4851
- C III, 2p<sup>2</sup> <sup>1</sup>D level mean lifetime 9-6965
- C\*, formation in collisions between electrons and CO molecules 9-685
- Ca 5s5s<sup>3</sup>S<sub>1</sub> level, cascade transition line intensities obs. 9-9134
- Cl II ground configuration, level values and interaction parameters 9-20885
- Cl in CCl<sub>4</sub>, KLL Auger spectrum obs. 9-14668
- Cs, 6<sup>2</sup>P<sub>1/2</sub>-6<sup>2</sup>P<sub>3/2</sub> mixing induced in collisions with CH<sub>4</sub> and CD<sub>4</sub>, resulting isotope eff. 9-13298
- Cs, 6<sup>2</sup>P states 9-4850
- Cs, 7<sup>2</sup>P<sub>3/2</sub>, level, population inversion 9-686
- Cs\*-inert gas nearly adiabatic thermal collisions, excitation transfer, Stueckelberg's formula and difficulties 9-18154
- Cu, II relative transition prob. of resonance lines meas. 9-13289
- Fe population levels, current and pressure dependence 9-18319
- Fe XII transition probabilities for various excited states 9-15809
- H, 1s-2p cross-sections for excitation by electrons, post-threshold behaviour 9-717
- H, 1s-2s transition, eff. of peaking approx. on cross-sections 9-13311
- H, (2p) resonances near threshold after electron impact 9-716
- H, by fast protons from 1s to any state, asymptotic expression for cross section 9-4869
- H, by fast protons in 2s and 2p states, cross section formulae 9-4868
- H, electron-impact excitation, asymptotic form of total wave function 9-18155
- H, by protons, total cross section 9-9156
- H, radiative mean-life meas. of 2 and 3p states beam-foil excitation method 9-14671
- H by fast protons, 1s-n's excit. cross-sections 9-15830
- H ionization cross-section dependence on the main quantum number 9-2826
- H ionization cross section calc. by Monte-Carlo method 9-7186
- H Lyman- $\alpha$  rad., electron impact excitation of 2p state 9-19411
- H quenched from 25 state, polarized radiation fraction calc. 9-20896
- He, autoionizing states, Rydberg series, energies and props. 9-4877
- He, by electrons, 0.05-0.6 keV, polar, of resulting rad. 9-14674
- He, cross-section in slow collisions with He 9-687
- He, e and p using Hartree-Fock wave functions, first Born approx. X-section calc., length and velocity formulations 9-4878
- He, e bombardment, transitions obs. 3230-20582 Å 9-6994
- He, by electron beam, afterglow and fluoresc. visualization of hypersonic flow 9-21131
- He, excited states, energy 9-2831
- He, ground state to 3<sup>1</sup>D and 4<sup>1</sup>D states, by proton impact 9-726
- He, in n<sup>1</sup>P and normal states, transfer mechanism, X-section meas. for collisions 9-4880
- He, n=4 atomic states, collision cross-sections for energy transfer 9-9161
- He, oscillator strengths, generalised 9-14673
- He, by p, polarization of singlet transitions 9-6993
- He, p using wave functions accurate first Born-approx. X-sections 9-4879
- He, radiative decay processes pressure dependence 9-11425
- He, superfluid, energetic neutral excitation, prod. of charged part. at surface 9-11735
- He atom, ionization with excitation 9-908
- He by fast electrons, accurate 1st. Born approx. cross-sections 9-13317
- He by proton beam, resulting polarization of light, violation of  $\Delta S=0$  spin rule 9-9160
- He by protons, 1-150 keV, ground state to n<sup>1</sup>S, n<sup>1</sup>D and n<sup>1</sup>P, absolute cross-sections and polar. of collision-induced rad. 9-11424
- He ground to various <sup>1</sup>S, <sup>1</sup>P and <sup>1</sup>D states, Born-approx. X-sections using wave functions, accurate calc. 9-4879
- He ground to various <sup>1</sup>S, <sup>1</sup>P and <sup>1</sup>D states, Born approx. X-section calc. using Hartree-Fock wave functions 9-4878
- He I, lifetimes of S, P and D levels by delayed coincidence method 9-723
- He II, decay of the 6560 Å line 9-723
- He in plasma, state population meas., mechanism discussed 9-9340
- He n<sup>1</sup>S states (4 $\leq$ n $\leq$ 7) by impact, calc. 9-4881
- He sequence, 1sns <sup>1-3</sup>S states, relativistic correct. to eigenvalues, perturbation theory methods 9-13316
- <sup>3</sup>He metastable atoms, energy transfer during collisions 9-6995
- He\*-inert gas nearly adiabatic thermal collisions, excitation transfer, Stueckelberg's formula and difficulties 9-18154
- He(2<sup>3</sup>S)+X→He+X<sup>+</sup>+e, metastable atom collisions 9-14675

**Atoms continued****excitation continued**

- He(2<sup>3</sup>S) metastable atom destruction by Ar 9-13318
- He(2s, 2p<sup>1</sup>P) autoionizing level 9-4887
- Hg, by electron shocks, <sup>2</sup>S<sub>1</sub> state lifetime and rate of population by transition from 9, <sup>3</sup>P<sub>0</sub><sup>0</sup> 9-6976
- Hg, line profile alteration by high power laser pulse 9-11394
- Hg metastable atom, on electron inelastic second-order collision 9-18153
- I, electronic, reaction with methyl iodide 9-1924
- K, electric octupole 4<sup>3</sup>S-4<sup>3</sup>F transition from e impact 9-4839
- K, enhanced 2-photon emission between 6S and 4S levels 9-20886
- K, H<sub>2</sub> collision, resonance radiation trapping and quenching, 4<sup>2</sup>P state lifetime meas. 9-14670
- K, HD collision, resonance radiation trapping and quenching, 4<sup>2</sup>P state lifetime meas. 9-14670
- K, N<sub>2</sub> collision, resonance radiation trapping and quenching, 4<sup>2</sup>P state lifetime meas. 9-14670
- K, N<sub>2</sub> collision, resonance radiation trapping and quenching 4<sup>2</sup>P state lifetime meas. 9-14670
- K II resonance lines in slow collisions between K<sup>+</sup> and He 9-2834
- K II resonance lines in slow collisions between K<sup>+</sup> and He 9-14676
- Kr, after  $\beta$  decay, photon emission obs. 9-9136
- Kr, by He<sup>+</sup> impact, spectra obs.,  $E_{\text{th}}=0.3-10$  keV 9-20887
- Kr, ionization probability curves for electron impact, for <sup>2</sup>P<sub>3/2</sub> and <sup>2</sup>P<sub>1/2</sub> states 9-4863
- Kr, multiphonon ionization by Nd laser, role of bound states 9-910
- Li I doubly excited levels lifetime meas., beam-foil technique 9-20879
- N, laser action obs. foll. dissociative transfer 9-4851
- N II, radiative lifetimes, ultraviolet multiplets, phase shift measurement technique 9-11386
- N IV, 2p<sup>2</sup> <sup>1</sup>D level mean lifetime 9-9137
- N second positive bands, by electron impact, absolute cross-sections, relative intensities of diff. vibr. bands 9-13300
- N<sup>-</sup> metastability of <sup>1</sup>D state using first order wave function 9-9138
- N\*, formation in collisions between electrons and N<sub>2</sub> mols. 9-685
- Na 3<sup>2</sup>P resonance state natural lifetime meas. phase shift method 9-6977
- Ne, 3p<sub>4</sub> and 3p<sub>2</sub> levels, fine-structure splitting, difference-frequency resonance meas. 9-20881
- Ne, by He<sup>+</sup> impact, spectra obs.,  $E_{\text{th}}=0.3-10$  keV 9-20887
- Ne I, II, III ions, radiative lifetimes, u.v. obs. 9-4844
- O, absorpt. cross section, effect of autoionization 9-6980
- O, ionospheric e temp. cooling explanation 9-12607
- O\*, formation in collisions between electrons and CO, O<sub>2</sub> mols. 9-685
- Pb, muonic, new dynamical effect 9-4891
- Pb reson. interaction with Pt, discharge obs. 9-18134
- Pt, inhibition by Al and reson. with Pb, discharge obs. 9-18134
- Rb\* from <sup>85</sup>Kr  $\beta$  decay, dipole transitions from excited states, lifetimes obs 9-9140
- Rb\*-inert gas nearly adiabatic thermal collisions, excitation transfer, Stueckelberg's formula and difficulties 9-18154
- Si ground configuration, level values and interaction parameters 9-20885
- Si, mean excitation potentials from stopping power data 9-9135
- V IV, V spectra determ. from hollow cathode discharge 9-2820
- Xe, by He<sup>+</sup> impact, spectra obs.,  $E_{\text{th}}=0.3-10$  keV 9-20887
- Xe, e impact, 1470 Å resonance line obs. 9-4853
- Xe, luminescence gain in elec. field, geometrical props. 9-689
- Xe, multiphonon ionization by Nd laser, role of bound states 9-910
- Xe, time correlation of emitted photons 9-13301
- Xe minima of generalized oscillator strength 9-695
- Zn 4s5s<sup>3</sup>S<sub>1</sub> level, cascade transition line intensities obs. 9-9134

**magnetic moment***See also Gyromagnetic ratio*

- Ba, odd isotopes, quadrupole moment 9-6961
- Ho ion, obs. from HoFeO<sub>3</sub> spectrum 9-21624
- Li, dipole polarizability and antishielding factor, many-body calc. 9-4842
- O of (2p<sup>4</sup>)<sup>3</sup>P<sub>4</sub> and (2p<sup>3</sup>)<sup>3</sup>P<sub>2</sub> terms 9-18143

**structure***See also Nucleus; Spectra/atoms*

- 7/2- multiplet, correct mass calculation 9-20874
- alkali, core polarization rel. to oscillator strengths of low-lying transitions 9-4843
- alkali atoms, well-separated, induced dipole moment calc. 9-15826
- auto-ionizing states, bounds on energy levels and lifetimes 9-20893
- ch.YG factors of 6s6p <sup>1</sup>P<sub>1</sub> and 6s6p <sup>3</sup>P<sub>1</sub> states 9-15812
- correlated pair functions, calc. from pseudopotential transform. of orthogonal projection operator 9-663
- correlated wavefunctions, symmetry props. 9-6950
- correlation energy, degeneracy effects, second-row atoms 9-9116
- diamagnetism of atoms with unpaired electrons 9-20866
- dipole moments induced betw. well-separated atoms, theory 9-15826
- distinguishable electron method calc. 9-8412
- effective potential eqns. with oscillatory correction 9-2808
- electron correlation calcs. 9-4819
- electron rearrangement in Hartree-Fock scheme 9-4826
- electronic struct. calc., Van Vleck's method 9-8411
- electrons in atoms, matrix fabrications for Coulomb interaction 9-20872
- energetic transitions, independent-part. model, difficulties and correct. 9-18133
- energy level population thermodynamic equilibrium shifts calc. 9-6956
- excited states, variational upper bounds to energies 9-2156
- f<sup>2</sup> configuration levels, mag. params. 9-4831
- four-body S-state coordinates 9-9117
- fractional parentage coeffs. and LL-coupling 9-20867
- ground states, Bopp two-matrix, Pauli-principle restriction 9-15807
- Hartree and Hartree-Fock Hamiltonians, perturbation expansions of at. non-relativistic eigenfunctions 9-4827
- Hartree-Fock, time-dependent, new deriv. 9-11379
- Hartree-Fock approx. for 2p<sup>3</sup>3p configurations, orthogonality assumption 9-4824
- Hartree-Fock scheme, field calc. on 3rd row periodic syst., ioniz. energies eval. and pot. comparison 9-4826
- Hartree-Fock theory, dipole shielding factor 9-16992
- Hartree-Fock  $\rho_{\text{a}}$  modified perturbation theory 9-6949
- heavy atoms, inclusion of mag. interaction in energy level calc. 9-11382
- helium-like isoelectronic sequence, Two-photon decay rate calc. for singlet and triplet metastable states 9-20870
- hypervirial theorems, off-diagonal constraints 9-2159
- integrals, evaluation 9-12866
- from ionization potential 9-5056
- KandL shells, radiative decay rate of vacancies 9-18132



**Atoms continued**  
**structure continued**

- M-shell, internal conversion coeff. allowing for screening, semiempirical method, applic. to Z=65 9-9127
- muonic atoms, nuclear polarization effects 9-13319
- neutral atom, many-electron interaction calc. 9-11381
- np<sup>2</sup> config., coupling coeffs determ. from expt. g factors, fine struct, and elec. dipole transitions 9-668
- pair correlation, review of papers 9-14665
- paramagnetic, statistical model 9-12243
- pseudopotentials in struct. calcs. 9-6958
- R4 group applied to energy level separations and correlation energies 9-13283
- radial integrals for many-body problem 9-16993
- rare earths, trivalent aquo ions, electronic energy levels 9-16017
- scalar model nonlinear field theory, limit cycle soln., applic. to Hartree eigenvalue eqn. 9-11378
- SCF functions with minimal basis sets 9-2802
- screening parameters, new method 9-13281
- Slater transform functions, construct. 9-19389
- soft-sphere model for closed-shell atoms and ions 9-6986
- spin-orbit coupling and dispersion of gyromagnetic ratio 9-20871
- spin-orbit interaction of  $1^2-1^1\Pi$  configuration in L-S coupling 9-13274
- spin-other-orbit matrix elements for f<sup>3</sup> configs. 9-16991
- Thomas-Fermi eqn. for +ve valence differences, calc. by iterative numerical method 9-20875
- Thomas-Fermi model, e scatt. target 9-6982
- transition elements, Slater-Condon integrals, calc. 9-4823
- transition metals ground states, config. and truncated orbital bases 9-2815
- wave functions, accurate, without exchange terms, perturbation calc. 9-4832
- Z=114, 126, 140, electron binding and K, L X-ray energies, relativistic calc. 9-4833
- AR by absorpt. spectra near L<sub>II, III</sub> edge 9-4837
- Al III, semiempirical core potentials, coeffs. 9-19397
- Ar, exchange energy of electrons 9-4834
- Ar II, 4p<sup>5</sup>3s<sup>2</sup> level lifetime, absolute meas. from emission of correlated photons in cascade 9-6975
- Au incoherent scatt. of 662 keV  $\gamma$  by K electrons, differential cross section 9-9120
- B, lifetimes and levels of collisionally excited ions 9-6959
- B, spin-extended Hartree-Fock functions 9-671
- B, spin densities calc. 9-672
- BII, 2p<sup>2</sup> <sup>1</sup>D lifetime meas. 9-11391
- Ba, 6s5d config., g factors obs. 9-18135
- Ba II, semiempirical core potentials, coeffs. 9-19397
- C III, 2p<sup>2</sup> <sup>1</sup>D level mean lifetime 9-6965
- C IV, semiempirical core potentials, coeffs. 9-19397
- Ca II, semiempirical core potentials, coeffs. 9-19397
- Co, core-electron energy levels and state density, X-ray photoelectron obs. 9-1813
- Cu, core-electron energy levels and state density, X-ray photoelectron obs. 9-1813
- Cu<sup>+</sup> ion, Hartree-Fock exchange potentials for electrons, comparison of different methods 9-18138
- ErIV 4f<sup>11</sup> free-ion levels, from LaCl<sub>3</sub>:Nd<sup>3+</sup> spectra and calc. 9-4831
- Eu<sup>3+</sup> in aq. soln., electronic energy levels 9-16006
- Fe, core-electron energy levels and state density, X-ray photoelectron obs. 9-1813
- Fe group doubly ionized atoms, config. 3d<sup>4</sup>4p in 3rd spectra, energy levels, interac. parameters 9-18139
- Fe series, ground states configs. and truncated orbital bases 9-2815
- H-like, quasiclassical approx. for oscillator strengths and effective crossings of radar transitions 9-17003
- H, bounds on polarizability, perturbation calc. 9-8410
- H, Green function calc. 2nd-order perturbation 9-9106
- H, ground state, applic. of Slater transform functions 9-19389
- H, relativistic discrete spectrum realizes representation of O(4,2)@SU(2), classification by O(4,2) 9-15828
- He, bounds on polarizability, perturbation calc. 9-8410
- He, expectation values of correl. wavefunctions 9-14672
- He, Green function 9-9105
- He, lower bounds for various powers of r<sub>1</sub> and r<sub>12</sub>, quantum mech. calc. 9-6992
- He, perturbation calc. with correlation in zeroth order 9-6991
- He, three-particle forces eff., diamagnetic correction for 2<sup>3</sup>S<sub>1</sub> state 9-4876
- He ground state, Slater transform functions appl. 9-20900
- He multiplets with non-orthogonal orb., Hartree-Fock eqn. and perturbation treatment, Hellmann-Feynmann formula anal. 9-4875
- He to Ne, screening parameters for ground and excited states, applic. of new method 9-13281
- He<sup>+</sup>, <sup>4</sup>P<sub>3/2</sub> state autoionization, final state distortion effects 9-11615
- <sup>3</sup>He, hyperfine levels of 2<sup>3</sup>P state 9-9159
- HeI, first excited levels local thermodynamic equilib., validity criteria 9-11426
- He-like ions, 2s<sup>2</sup>1S weakly quantized state, Hartree-Fock eqn., perturbation treatment 9-11422
- F<sup>-</sup>, orbital wave functions, reduced basis set expansions 9-11385
- K<sup>+</sup>, exchange energy of electrons 9-4834
- K<sup>+</sup>, antishielding factor and dipole polarizability, many-body calc. 9-4842
- Li, doubly excited states 9-13299
- Li, ground-state h.f.s., many-body perturbation calc. 9-4841
- Li, hyperfine splitting of ground state 9-2819
- Li, isoelectronic sequence, dipole transitions between 1s<sup>2</sup>3<sup>2</sup>L<sup>2</sup> states, oscillator strengths by perturbation theory 9-9125
- Li ground state, Hartree-Fock eqn., Z<sup>-1/2</sup> expansion 9-4828
- Li and other atoms Green function 9-9107
- Mg II, semiempirical core potentials, coeffs. 9-19397
- N 4s<sub>3/2</sub> ground state, hyperfine constant calc. by Brueckner-Goldstone method 9-18141
- N V, semiempirical core potentials, coeffs. 9-19397
- NO<sub>2</sub><sup>-</sup> anisotropic polarizability 9-3855
- Na, transitions between fine structure levels in Na-He collisions 9-11411
- Nd<sup>4+</sup> electronic levels in Nd(IV) complexes 9-16416
- NdIV 4f<sup>4</sup> free-ion levels, from LaCl<sub>3</sub>:Nd<sup>3+</sup> spectra and calc. 9-4831
- Ne, 1s<sub>1</sub> metastable states, spatial distribution in auxiliary active discharge 9-20520
- Nel 3d-4f lines meas. 2p<sup>2</sup>5f config. derived. 9-15813
- Ni, core-electron energy levels and state density, X-ray photoelectron obs. 9-1813

**Atoms continued**  
**structure continued**

- O VI, semiempirical core potentials, coeffs. 9-19397
- Os<sup>4+</sup> in cubic crystals, at 4.2°K 9-14055
- P, d orbitals in sp<sup>3</sup>d, sp<sup>2</sup>d<sup>2</sup> and p<sup>3</sup>d<sup>2</sup> configs. 9-9131
- P, hyperfine structure, Brueckner-Goldstone many-body theory, core-polarization effect 9-678
- PrIII 4f<sup>3</sup> energy levels, mag. params. 9-4831
- Pt, core-electron energy levels and state density, X-ray photoelectron obs. 9-1813
- Rb, transitions between fine structure levels in Rb-He collisions 9-11411
- Si IV, semiempirical core potentials, coeffs. 9-19397
- Tb, internal conversion coeff. in M-shell allowing for screening, semiempirical method 9-9127
- U, M emission spectrum, meas. and comparison 9-6968
- Xe I, 5p<sup>2</sup>(6s+5d) and 5p<sup>2</sup>(6p+7p) configurations and hyperfine structure 9-20878
- Xe III, Hartree-Fock parameters for the <sup>1</sup>D and <sup>1</sup>S terms of configuration 5s<sup>2</sup>5p<sup>4</sup> 9-9129
- Yb, photoionization, 1350-2000Å 9-5065
- Atoms, mesic and muonic**
- Lamb shift and vacuum polarization correction 9-11431
- muon residual polarization calc. during cascade transitions for nuclear spin from 0 to 1/2 9-15837
- muonic, with odd-mass nuclei, single particle excitation effect on spectra 9-18162
- muonic X-rays, energy levels perturbation calc. 9-731
- muonium, hyperfine splitting and fine struct. const. 9-4870
- muonium-antimonium conversion, search 9-6610
- nuclear polarization effects on level scheme estimated 9-13319
- vacuum polarisation contribution to nuclear polarisation 9-13320
- $\pi$ -mesic, elementary props. and formation, review 9-14678
- <sup>190</sup>Os muonic isomer shifts rel. to nuclear charge distrib. 9-2836
- <sup>192</sup>Os muons isomer shifts rel. to nuclear charge distrib. 9-2836
- <sup>152</sup>Sm muonic isomer shifts rel. to nuclear charge distrib. 9-2836
- <sup>182</sup>W muonic isomer shifts rel. to nuclear charge distrib. 9-2836
- <sup>153</sup>Eu nuclear rotation and single particle excitation effects on X-ray spectrum 9-11432
- <sup>203</sup>Tl, magnetic hyperfine splitting of ground and first excited states, shell model anal. 9-9052
- <sup>203</sup>Tl nuclear  $\gamma$  ray mag. hyperfine splitting 9-2837
- <sup>184</sup>W muonic isomer shifts rel. to nuclear charge distrib. 9-2836
- <sup>205</sup>Tl, magnetic hyperfine splitting of ground and first excited states, shell model anal. 9-9052
- <sup>203</sup>Tl nuclear  $\gamma$  ray mag. hyperfine splitting 9-2837
- <sup>206</sup>Pb, muonic X-ray emission, weak transitions meas., nuc. polarization by  $\mu$  9-17009
- <sup>186</sup>W muonic isomer shifts rel. to nuclear charge distrib. 9-2836
- <sup>107</sup>Ag, muonic X-ray spectra, isotope shift of K lines and RMS radius, comparison with opt. spect. 9-6794
- <sup>108</sup>Os muonic isomer shifts rel. to nuclear charge distrib. 9-2836
- <sup>108</sup>Ag, muonic X-ray spectra, isotope shift of K lines and RMS radius, comparison with opt. spect. 9-6794
- <sup>11</sup>B, formed from Be<sup>11</sup>, hyperfine effect 9-11208
- <sup>23</sup>Na 2p-1s transition, energy and natural linewidth 9-6813
- pb transition intensity calc. of Elsberg Kessler type 9-11430
- Si-Sn, K $\alpha$  isotope shifts used to calc. nuclear charge radii. 9-535

**Attenuation** *see Absorption***Auger effect** *see Atoms/excitation; Atoms, mesic and muonic; Radioactivity***Auger showers** *see Cosmic rays/showers and bursts***Aurora**

- See also Airglow; Atmospheric spectra*
- absorption, cosmic radio noise bays, time lag 9-21790
- absorption, electron and positive ion density meas. 9-21810
- absorption, position and height deduced from v.l.f. phase measurements 9-12601
- atmospheric wave generated in supersonic auroral disturbance 9-1947
- cinematography, image intensifier-vidicon system 9-14168
- e and p intensity in mag. disturbance, rocket meas. 9-4070
- electron and proton flux spectrometer, calibration 9-8219
- electron flux obs., 1-10 MeV 9-20103
- electrons, nocturnal precip., config. and displacement 9-17577
- excitation and emission rate profiles of spectral lines and heating effects, calc. 9-21792
- flaming, observed with auroral image orthicon TV systems 9-10413
- flickering, at 10Hz in bright auroras 9-8194
- intensity ratio I(4278)/I(5577), variations 9-20105
- ionosphere, F-region, ionization drift during mag. disturbances 9-21822
- ionosphere, ion-acoustic instabilities, ion-neutral collisions effect 9-21806
- ionospheric, Explorer 22 radio obs. 9-8206
- Jovian, search for limb aurorae 9-21938
- light bursts, correlation with v.l.f. hiss, X-rays, obs. (March 1966) 9-14170
- low latitude emissions, intensities correlated to different geomagnetic indices 9-1954
- optical, h.f. radar, and electron precipitation, spatial relationship 9-14169
- optical emissions, variations with time, magnetic activity and solar cycle 9-21791
- particle acceleration, rel. to interact of plasma waves and particles in magnetosphere 9-20097
- polar ionosphere, review 9-18808
- radio, review and bibliography 9-17578
- regulation by upper atmosphere 9-20122
- r.f. refraction in developing forms rel. to creation energy input 9-6088
- solar particle energy dissipation, PCA 3914 and 5577 Å light emission calc. 9-20102
- spectra, N and O bands obs., brightness determ., 1.02-1.13  $\mu$  9-20104
- spectroscopic studies since 1960, review 9-15251
- substorm obs., magnetic conditions determ. 9-12602
- v.h.f. fades, high latitude, rel. to auroral disturbance 9-2026
- waves, fast, obs. 9-8193
- [OI]  $\lambda$ 5577,  $\lambda$ 6300 emissions, Antarctic night sky photometry 9-1955

**Austenite** *see Iron alloys; Steel***Autoionization** *see Ionization***Avagadro's number** *see Constants***Axicons** *see Lenses***Backscattering** *see Scattering, particles; and under 'scattering' subheadings of the appropriate particles*

**Backward wave oscillations** *see* *Electromagnetic oscillations; Electron tubes*

## Balances

- force (magnetic), automatic with photocell for gravimetric and magnetic analysis 9-18978
- magnetic, servo-type, for routine thermomagnetic analysis 9-14414
- microbalance, vacuum, pivot type 9-10612
- piston-cylinder, performance in h.p. meas. 9-12807
- precision, laboratory and factory 9-8349
- Stanton thermobalance, attachments for thermogravimetric and differential thermal analysis 9-4020
- thermobalance, symmetrical, for corrosive atms. 9-4019
- thermobalance for use in flowing gas 9-3978

## Ballistics

- See also Impact*
- gun, isothermal soln., new gas density function assumed 9-2189
- perforation limits for thin plates, for cylindrical projectiles, simple determ. method 9-20381
- plasticine projectiles, impact on plasticine laminated targets obs. 9-19014
- projectile impact on clamped plates, plastic deform. 9-1279
- projectile vel. gauge 9-2130

**Band theory of solids** *see* *Crystal electron states/band structure; Solids/theory*

**Bardeen-Cooper-Schrieffer theory** *see* *Nucleus/theory; Superconductivity*

## Barium

- absorption oscil. strengths Ba-II, 1400-2000 Å and 4100-4600 Å 9-6960
- adsorbed on (100) face of W, eff. on work function 9-19680
- adsorption on oriented W surfaces 9-9627
- atom, 6s5d config., g factors obs. 9-18135
- contacts on Si, prep. and barrier height 9-13907
- electron prod. in H<sub>2</sub>-N<sub>2</sub>-O<sub>2</sub> flames, meas. by enthalpy changes and equilib. consts. 9-12534
- energy-band struct. and Fermi surface under press. 9-15054
- liquid, surface tension and density, temp. dependence obs. 9-5149
- odd isotopes, quadrupole moment 9-6961
- solar abundance determ., including hyperfine structure 9-14249
- vacancy relaxations in b.c.c. crystals 9-9702
- Au on Ba, double film on Nb contact potential difference 9-1093
- Ba I, two-electron spectra, config. mixing and oscillator strengths 9-19398
- Ba II, resonance lines, 6p<sup>2</sup>P<sub>3/2,1/2</sub>-s<sup>2</sup>S<sub>1/2</sub>, h.f.s. 9-6961
- Ba II, semiempirical atomic core potentials, coeffs. 9-19397
- Ba<sup>+</sup>, ionization to Ba<sup>2+</sup> by e impact, cross-section rel. to energy 9-5064
- Ba<sup>2+</sup> in KBr, thermoelec. power and ionic conductivity 9-1607

## Barium compounds

- barite, cryst. form rel. to cryst. struct. 9-16064
- ferrite polycrystals, h.f. conductivity and Seebeck coeff. 9-12086
- ferrites, hexagonal, mag. relax. 9-12314
- ferrites, hexagonal, magneto-optical and optical props. 9-12343
- hydroxides, gaseous, dissoc. energies and conc. in fuel-rich H<sub>2</sub>+O<sub>2</sub>+N<sub>2</sub> flames 9-17517
- Ba<sub>1-x</sub>La<sub>2x/3</sub>TiO<sub>3</sub>:Fe<sub>2</sub>O<sub>3</sub>, semiconducting properties, polycrystalline, contrast to barium bismuth titanate 9-3608
- Ba<sub>2</sub>TiGe<sub>2</sub>O<sub>8</sub>, isomorphous with Ba<sub>2</sub>TiSi<sub>2</sub>O<sub>8</sub>, fluoresc. 9-14083
- Ba type A zeolite, stability and cation self-diffusion obs. 9-5400
- Ba WO<sub>4</sub>, phototropy, pink after irradi. by u.v. light 9-3866
- BaAl<sub>2</sub>SiO<sub>6</sub>, crystal structure of new phase in BaO-Al<sub>2</sub>O<sub>3</sub>-SiO<sub>2</sub> system 9-14987
- BaBaO<sub>19</sub>-Eu<sup>2+</sup> activated, fluorescence 9-20004
- BaBrF, Raman spectra 9-5934
- BaCl<sub>2</sub>, electrolytically coloured, F centre study 9-17279
- BaClF, Raman spectra 9-5934
- BaCo<sub>2</sub>TiFe<sub>4</sub>O<sub>12</sub>, magnetization anisotropy 9-18684
- BaCo<sub>2</sub>Ti<sub>2</sub>Fe<sub>12</sub>O<sub>19</sub>, hexagonal ferrite, mag. exchange anisotropy 9-10136
- BaD, absorption spectra 4000-3000 Å, extension of F<sup>2</sup>Σ→X<sup>2</sup>Σ system 9-4917
- BaF<sub>2</sub>:Er<sup>3+</sup>, luminescence spectra 9-3916
- BaF<sub>2</sub>:Eu<sup>2+</sup>, e.p.r., hyperfine coupling constant of <sup>151</sup>Eu<sup>2+</sup>, temp. depend. 9-12502
- BaF<sub>2</sub>:Nd<sup>3+</sup> interaction mechanism of Nd<sup>3+</sup> ions and nature of conc. quenching 9-15161
- BaF<sub>2</sub>:CaF<sub>2</sub> eutectic, wettability of graphite 9-7326
- BaF<sub>2</sub>, anharmonic temp. factors from n. diff. 9-3514
- BaF<sub>2</sub>, e.p.r. of Tb<sup>3+</sup> 9-20014
- BaF<sub>2</sub> diffusion of <sup>89</sup>Sr 9-3379
- BaF<sub>2</sub>:BaCl<sub>2</sub>, crystal growth by indirect flux method 9-18422
- BaF<sub>2</sub>, dislocation structure around indentation 9-5357
- BaF<sub>2</sub>, elastic constants, pressure and temp derivatives 9-1262
- BaF<sub>2</sub>, etch pits orientation variation on (111) surface 9-11793
- BaF<sub>2</sub>, hyperfine consts. of F-centre, endor meas. 9-1234
- BaF<sub>2</sub>, impurity precipitation at dislocations, display by selective etch methods 9-13680
- BaF<sub>2</sub>, optical, spectrochem. meas. of metal impurities 9-16513
- BaF<sub>2</sub>, pure and Eu<sup>2+</sup>-doped, spin-lattice relax. at low and high temps 9-5859
- BaF<sub>2</sub> films, chemisorption of p-benzoquinone, i.r. spectra 9-8084
- BaFe<sub>12</sub>-xAl<sub>2</sub>O<sub>19</sub> saturation magnetization variation with Al substitution 9-16366
- BaFe<sub>12</sub>O<sub>19</sub>, <sup>57</sup>Fe n.m.r., powdered crystals, spin-echo 9-1872
- BaFe<sub>12</sub>O<sub>19</sub> ferrite, magnetostriiction 9-14004
- BaFe<sub>2</sub>TiO(Si<sub>2</sub>O<sub>7</sub>)(OH)<sub>2</sub>, bafertisite, crystal structure determ. by Fourier transformation of minimum function 9-11831
- BaH, absorption spectra 4000-3000 Å, extension of F<sup>2</sup>Σ→X<sup>2</sup>Σ system 9-4917
- BaI<sub>2</sub>.2H<sub>2</sub>O apparent molal expansibility and volume obs. 9-986
- BaMF<sub>4</sub> (M=Mn, Fe, Co and Ni) antiferromagnetic piezoelectric crystals 9-12308
- Ba<sub>2</sub>MgGe<sub>2</sub>O<sub>7</sub>:Nd<sup>3+</sup>, optical spectra and laser action 9-5914
- Ba(NO<sub>3</sub>)<sub>2</sub>-Sr(NO<sub>3</sub>)<sub>2</sub>-Ca(NO<sub>3</sub>)<sub>2</sub> binary phase systems, Raman spectra obs. of structure 9-17186
- Ba(NO<sub>3</sub>)<sub>2</sub>, morphological symmetry 9-1125
- Ba(NO<sub>3</sub>)<sub>2</sub>, permittivity and loss-angle tangent, impurities effect 9-1575
- Ba(NO<sub>3</sub>)<sub>2</sub>.H<sub>2</sub>O, n.q.r. of <sup>14</sup>N, temp. depend. between 77°K and 300°K 9-10303
- Ba<sub>2</sub>NaNb<sub>5</sub>O<sub>12</sub>, elastic props. 9-7531
- Ba<sub>2</sub>NaNb<sub>5</sub>O<sub>15</sub>, gain coeffs. for stimulated Raman scattering 9-5936
- Ba<sub>2</sub>NaNb<sub>5</sub>O<sub>15</sub> growth of single crystals for optical appl. 9-13597

## Barium compounds continued

- BaO-Al<sub>2</sub>O<sub>3</sub>-SiO<sub>2</sub> system, crystal structure of new BaAl<sub>2</sub>SiO<sub>6</sub> phase 9-14987
- BaO, A Σ→X<sup>2</sup>Σ band syst. spectrum, Franck-Condon factors 9-13344
- BaO, electromigration of adsorbed mols. on W(113) face 9-17250
- BaO, F-centres, Faraday rotation studies 9-3362
- BaO films, e.s.r. abs., band I 9-8011
- α-Ba(OH)<sub>2</sub>, crystal data 9-11837
- BaS:Cu electron trap depth determ. from thermoluminescence decay 9-1840
- BaS, radiation-damage centres, e.s.r. obs. 9-13697
- BaS, shear-induced coloration, obs. 9-1745
- BaSO<sub>4</sub>, barite, etch patterns, effect of heat 9-13594
- BaSO<sub>4</sub> optical sphere paint, luminous reflectance 9-5875
- BaSe:Fe<sub>12</sub>-xO<sub>19</sub>(M), helicoidal antiphase spin ordering, neutron diffraction 9-16367
- BaSO<sub>4</sub>, synthetic, cleavage face etching rel. to dislocation structure 9-1127
- Ba<sub>1-x</sub>Sr<sub>x</sub>RuO<sub>3</sub>, phase transforms rel. to press and composition x 9-5510
- BaTiO<sub>3</sub> soft phonon dispersion 9-18547
- BaTiO<sub>3</sub>, dielectric and optical properties 9-5745
- BaTiO<sub>3</sub>, tetragonal-orthorhombic transformation, lattice parameters rel. to temp. 9-1183
- BaV<sub>3</sub>, atomic structure and electrical props. 9-7747
- Ba<sub>2</sub>Zn<sub>2</sub>Al<sub>2</sub>:Fe<sub>3</sub>O<sub>12</sub>, n. diff. study of cell parameters and configuration 9-5314
- Eu-Ba, Mossbauer effect 9-7957
- hexaferrites, rotating moment curves in case of uniaxial ferromag. anisotropy 9-1666

## barium titanate

- See also Ferroelectric materials/barium titanate*
- defect structure, H-reduced crystal with additions of Fe, Co and Ni 9-1207
- dislocations, axial screw, detection in whiskers using K<sub>α</sub> X-radiation 9-14944
- electrical conductivity, rel. to O partial press., 800-1200°C 9-1512
- film, thin, prep. by electrophoresis after annealing or melting 9-9610
- light emission accompanying each polarization reversal 9-1843
- light generation at electrode interface during polarization reversal 9-12346
- metal-BaTiO<sub>3</sub> contact, effect of gaseous adsorption 9-7802
- paraelectric, thermocurrents rel. to point defects 9-5756
- Raman spectrum, single domain crystal 9-3902
- rare-earth doped, thermolum. and paramagnetic hole centres 9-10252
- semiconductor effect 9-3618
- BaTiO<sub>3</sub>-PbTiO<sub>3</sub> single cryst. solid solns., dielec. and elastic props. 9-12196
- BaTiO<sub>3</sub>, chain structure 9-11818
- La<sup>3+</sup> doped gravimetric studies of disorder 9-3224
- Nb<sup>5+</sup> doped gravimetric studies of disorder 9-3224

**Barkhausen effect** *see* *Magnetization process*

**Barnett effect** *see* *Gyromagnetic effect*

## Baryons

- See also Hyperons; Nucleons and antinucleons*
- No entries

## interactions

- meson-baryon, QQ $\bar{Q}$  model, with vector meson prod. 9-2490
- meson-baryon charge exchange reaction anal., Reggeized supermultiplet theory 9-14481
- quark model for short-range repulsion 9-6680
- quintet on pseudoscalar mes. decouplet in C<sub>2</sub> 9-19199
- septet 7 (<sup>1</sup>/<sub>2</sub>)<sup>+</sup> on pseudoscalar mes. septet 7 (0<sup>-</sup>) in G<sub>2</sub> 9-19199
- SU(3) symm. model, Pauli-Kusaka mixture 9-15595
- BB and BB vector meson exchange pots. 9-6687

## resonances

- <sup>3</sup>/<sub>2</sub><sup>+</sup>, decay widths from relativistic quark strong-coupling consts. 9-13108
- decay modes 9-20674
- decays, O(3,1) model and obs. comparison 9-14527
- decuplet of <sup>3</sup>/<sub>2</sub><sup>+</sup>, rates of <sup>3</sup>/<sub>2</sub><sup>+</sup>→<sup>1</sup>/<sub>2</sub><sup>+</sup>+0<sup>-</sup> calc. 9-11111
- with exotic quantum numbers, higher multiplets from reson. saturation hypothesis 9-17992
- J=1 nonstrange sequence, calc. of masses from bound-state theory 9-6629
- on leading trajectories stability to decay at high spin 9-346
- lowest mass, -ve parity; reanalysis using symmetric quark model 9-8911
- N\*(1400)-ππ<sup>+</sup>, ππ prod. in pp→pN\*, one prior exchange model, isospin <sup>1</sup>/<sub>2</sub> 9-11113
- negative parity, comparison of decay ratios with SU<sub>w</sub>(6) predictions 9-13147
- new scheme for classification 9-2543
- nucleons, of spin <sup>3</sup>/<sub>2</sub> and isospin <sup>1</sup>/<sub>2</sub>, off-mass-shell self-consistency approach 9-16890
- parity doublets of nucleon resonances 9-20652
- Regge trajectory, new reson. prediction from symmetry props. 9-6684
- strong decays, off mass shell approach 9-2544
- SU(3) 27-plet for classification 9-4649
- SU(3) sym. breaking, representation mixing in <sup>1</sup>/<sub>2</sub><sup>-</sup> octet 9-18012
- SU(3) symm. breaking, octet coupling sum rules 9-11110
- S<sub>1/2</sub>\*(1935) of odd parity, decay branching ratio determ. 9-20675
- Δ<sup>++</sup> photoprod. on p, expl. comparison with intermediate isobar model E<sub>π</sub>≤1.8 GeV 9-19207
- Δ production pp→π<sup>+</sup>Δ<sup>++</sup> 9-16909
- Δ<sup>+</sup>, p<sup>2</sup>Δ<sup>0</sup> associated prod. in π<sup>+</sup>d interac. at 5 GeV/c 9-17998
- Δ<sup>++</sup>, prod. in pp→ppπ<sup>+</sup>π<sup>+</sup> 9-16901
- Δ<sup>++</sup>-ppπ<sup>+</sup>, prod. in high-multiplicity p-p interac. at 10 GeV/c 9-6694
- Δ(1236), prod. in pp→ppπ<sup>+</sup> 9-16901
- Δ<sup>++</sup>(1236)π<sup>+</sup> from pp, theory discussed, low energies 9-11049
- Δ<sup>++</sup>(1238) prod. in π<sup>+</sup>p reaction, O<sub>3</sub> symmetry analysis 9-427
- Δ(1920)-ppN<sub>ρ</sub>N branching ratio, vector-meson dominance model 9-18013
- Δ(2420)-ppN<sub>ρ</sub>N branching ratio, vector-meson dominance model 9-18013
- Δδ Regge trajectories 9-8915
- γN→Δ(1920)-p<sup>+</sup>N cross section, vector-meson dominance model 9-18013
- γN→Δ(2420)-p<sup>+</sup>N cross section, vector-meson dominance model 9-18013
- γ interactions in H<sub>2</sub> bubble chamber, 0.3-5.8 GeV, Δ obs. 9-11071
- K<sup>-</sup>n→Λπ<sup>+</sup>π<sup>+</sup>π<sup>+</sup>, Y\*, reson. at 1616 MeV 9-15648



**Baryons** continued**resonances** continued

- $\Lambda(1405) \rightarrow Y_p$ , estimated width of radiative decay; and dispersion sum rules 9-429
- $\Lambda(1520) \rightarrow Y_p$ , estimated width of radiative decay; and dispersion sum rules 9-429
- $N_{1/2}^*(1518)$  of odd parity, decay branching ratio determ. 9-20675
- $NK\pi$ ,  $S=+1$ , from  $\pi\pi \rightarrow NKK\pi$ , 3.25 GeV/c 9-2514
- $N^*(1470)$  from ed scatt., search,  $M_3=1578$  MeV 9-18089
- $N^*$  and  $N\pi$ ,  $\Delta\pi$  decay widths, mass spectrum paraquark harmonic-oscill. model 9-8913
- $N^*$  prod. in  $\nu N \rightarrow N^*\ell$ , polarization eff. 9-20601
- $N^*$  prod. in  $pp \rightarrow pN^*$ , review of data up to 30 GeV/c 9-6696
- $N^{*+}$  prod. in  $\pi p \rightarrow N^{*+} \rightarrow \pi^0 p \pi^+$ , cross-section obs. to be  $0.4 \pm 0.06$  mbarn 9-15624
- $N^{*3/2}(1520)$  isobar, prod. in  $\pi\pi \rightarrow \pi^+\pi^-\pi$  9-20676
- $N^*(1236)$  from  $\pi\pi N$  scatt., possibility of resonance generating mechanism 9-11065
- $N^*(1470)$  admixtures, accounting for mag. moment anomaly in  $^3H$  and  $^3He$  9-14563
- $N^*\omega$  production by  $\pi^+p$ , joint decay statistical tensors, quark-model predictions 9-8914
- $N^*\rho$  production by  $\pi^+p$ , joint decay statistical tensors, quark-model predictions 9-8914
- $N(1400)$  mass doubted, using self-consistency conditions 9-2544
- $N^*(1518)$  and (1688) excited in p-p collisions, 19.2 GeV/c 9-11114
- $N(1700) \rightarrow N(1400)\pi$  decay width of 24 MeV using self-consistency conditions 9-2544
- $N\pi$  Regge trajectories 9-8915
- $N(1400)$  prod. and representation mixing in algebra of vertex strengths 9-10994
- $p\Lambda$  9-8912
- $\pi$ , describes by group theory 9-6586
- $\phi^*$ , (1385, 1660) prod. in K $^-$ p scatt., rescatt. model 9-8918
- $\Xi^*$ , search from K $^-$ p 4.25 GeV/c interaction 9-11041
- $\Xi(1815)$  with strangeness  $S=-2$ , evidence for existence 9-11116
- $\Xi(2030 \rightarrow 10\text{MeV})$ , evidence for existence 9-11116
- $\Xi(2430 \rightarrow 20\text{MeV})$ , evidence for existence 9-11116
- $Y_0^*(1830)$  of odd parity, decay branching ratio determ. 9-20675
- $Y_1^*(1660)$ , two, from K $^-$ p react.  $\sim 2.6$  GeV/c 9-19208
- $Y_1^*(1660)$  of odd parity, decay branching ratio determ. 9-20675
- $Y_1^*(1765)$  of odd parity, decay branching ratio determ. 9-20675
- $Y^*$  from K $^-$ p scatt., spin and parity assignments, 1.4-2.4 GeV/c 9-428
- $Y_0^*5$ , existence of metastable  $J^P=1/2^+$  unitary singlet state 9-11115
- $Y_0^*(1520)$  prod. in K $^-$ p scatt., rescatt. model 9-8918
- $Y_1^*$ , at 1616 MeV, in  $\Lambda\pi^+$  mass spectrum 9-15648
- $Y_1^*(1385)\pi \rightarrow \Lambda\pi\pi$  9-4619
- $Y^*(1520) \rightarrow \Lambda\gamma$  ang. distrib. and  $\Lambda$  polarisation consistent with pure electric dipole transition 9-8917
- $Y_1^*(1765)$  mass, width, elasticity parameter, spin and parity 9-4619
- $Y_1^*(1660)$  mass, width, elasticity parameter, spin and parity 9-4619
- $Y_0^*5$  decay distrib., from obs. K $^-$ d-K $^-$  $\pi\pi$  react. 2.24 GeV/c 9-15614
- in  $^3H$ , admixtures description of mag. moment anomaly 9-14563
- in  $^3He$ , admixtures description of mag. moment anomaly 9-14563
- $\Delta^+(1236)$  prod. at high energy Toller pole parameters and  $O(3,1)$  symmetry experimental fit. 9-8916
- $N^*$  band structure and paraquark harmonic oscillator shell model 9-19206
- $N^*(1400)$ ,  $\bar{N}^*(1400)$  enhancements in  $\bar{p}(p) \rightarrow \bar{p}p\pi^+\pi^-(n)$  reaction at 2.8 GeV/c 9-11112
- $N_{1/2}^*(1400)\pi\pi$  decay mode, obs. 9-6708

**scattering**

- baryon-pseudoscalar mes. applic. of relativistic Schrodinger eqn., broken SU(3) sym. model 9-11028
- meson-baryon, charge and hypercharge exchange, Regge pole analysis 9-6638
- meson-baryon, decouplet exchange superconvergence relns. and cuts in complex  $j$ -plane 9-4609
- meson-baryon,  $U(6)4WU(6)$  Reggeized theory, trajectory exchange contrib. 9-18004
- meson-baryon elastic-scatt. proc., new superconvergent sum rules for product of factorized amp. 9-14496
- Regge trajectories, sum rule constraints assuming parity doubling 9-2525
- Regge trajectories, symmetry rel. new reson. prediction, spin-parity of hyp. reson. 9-6684
- Regge-pole model for forward-scatt. amp., comparison with quark model 9-13117
- tensor trajectories, rel. to energy-momentum tensor, use of Regge and quark models 9-13117
- BB,  $U(6)4WU(6)$  Reggeized theory, trajectory exchange contrib. 9-18004
- $\pi$ -baryon, backward, dispersion sum rules at  $u=0$  9-17983
- $\pi N$  symmetric amplitude, constraints on asymptotic behaviour 9-385

**Barysphere** *see Earth***Bauschinger effect** *see Deformation***Bayard-Alpert gauges** *see Vacuum gauges***Bays** *see Earth/magnetic field; Magnetic storms***BCS theory** *see Nucleus/theory; Superconductivity***Bells** *see Musical instruments***Bending***See also Stress analysis; Torsion*

- alkali halide crystals, dislocation movement and elec. field production 9-1453
- angle section beam, instability under applied moment 9-20388
- bar, behaviour of photoelastic interference fringes 9-20397
- beam, curved, central concentrated loading, stability 9-10698
- beam, elastic; subject to randomly moving load 9-131
- beam, free-pinned, dynamic stresses during impact 9-16703
- beam, thin-walled, suspended at both ends, lateral buckling theory 9-8494
- beams, continuous, deflection determ. 9-8479
- buckling, free-edge, heterogeneous shells, cylindrical, in axial compression 9-20389
- buckling conditions for columns supported laterally by side-rails 9-20387
- cantilever beams, tapered, with perpendicular load, computer analysis 9-17762
- circular plate with one-sided ribs subjected to antisymmetric bending, strength 9-20391
- cosserat plates, load-induced stress singularities 9-12915
- creep buckling of circular cylindrical shells 9-17761

**Bending** continued

- direct stiffness soles. in structural anal., round off errors in computation 9-8474
- elastic plate containing crack, plate thickness eff. 9-17760
- elastic plates, variable thickness, large deflexion 9-20400
- elastic-plastic behaviour of plates 9-17772
- flat spring in measuring instruments 9-8482
- inhomogeneous anisotropic cyl. shells, buckling analysis 9-20384
- layered plates, thin, theory 9-10701
- micropolar plates, infinite, clamped along 2 edges, uniformly distributed load 9-4270
- micropolar plates, shear and rotation inertia corrections 9-4269
- mirrors, circular, with linearly var. thickness, supported at central hole, deflection 9-10696
- multilayer sandwich beam, and inc. bending rigidity of face layers 9-20393
- orthotropic simple solid, supported by surface traction 9-19027
- parallelogram plate element, stiffness matrices and stress anal. 9-16713
- plastic, beams of unequal angle section 9-10707
- plastic, of anisotropic plate, anal. using max. shear stress yield conds 9-4279
- plate, conforming quartic triangular element 9-8483
- plate, problems comparing various finite element methods 9-8468
- plate, refined triang. finite element 9-15451
- plate, sandwich with light core, nonlinear, theory 9-8493
- plates, large deflection anal. by finite element method 9-8485
- plates, Reissnerian algorithms in refined theories 9-14374
- rectangular plates, moderately thick, bending, stiffness matrix, finite element, analysis 9-20398
- shell, helicoidal, stresses, stiffness coeff. calc. 9-19024
- shells, cylindrical and spherical, buckling under press., analysis 9-20399
- strip, by continuous stress distrib. 9-19787
- thick plates, multi moment theory of equilibrium 9-10690
- torus, pressurized, role of initial displacements in stress analysis 9-134
- AgCl single crystals, rel. to introduction of dislocations of minority sign 9-5497
- C fibres,  $7\mu$  diam., at room temp., stress-strain curve 9-7564

**Bending of light** *see Gravitation; Light***Berkelium**

No entries

**Berkelium compounds**BkF<sub>4</sub>, lattice parameter determ. 9-17264**Beryllium**

- atom, e bombard. at 1.0, 2.0 MeV, obs. 9-703
- atoms and ion, bibliography of spectra 9-13287
- cosmogenic prod. rate determ. of  $^{10}Be$  and  $^7Be$  9-4062
- defect prod. and recovery, irradi. induced, study by elec. resistivity and stored energy meas. 9-16091
- deformation, compressive, investg. 9-11926
- diffusion in Fe and Ni, 1100-1350°C and 1020-1400°C, resp. 9-5403
- elastic shear constants, first principle pseudopotential calc. 9-11904
- electronic pair-correlation energies of ground states, soln. of Bethe-Goldstone eqns. 9-11383
- film, structure and supercond. by e diff. 9-13863
- graphite, plasmon obs. in X-ray scatt. 9-1818
- lattice dynamics, h.c.p. structure 9-3506
- moderators, equilib. neutron, spectra meas., expt. installation and results 9-19378
- n irradiated at 4.2°K, damage and recovery up to 350°K from elec. resist. meas. 9-5578
- neutron diffusion in slabs 9-20833
- neutron reflections simulated by multiple Bragg reflection 9-9662
- n.m.r. in pure metal, of  $^9Be$ , quadrupole split spectrum, pulse method study 9-3971
- oxidation in water vapour, 600-800°C blistering and film break away obs. 9-6011
- plastic deformation in high-purity crystal, 4.2-300°K 9-1282
- purification by vacuum melting followed by distillation and simultaneous deposition to sheet in e beam furnace 9-13748
- Raman scatt. from optical modes, freq. 9-1804
- range and dE/dx of C, N, O, F, and Ne at 500 keV to 2 MeV 9-9871
- recovery data of mechanical and physical props. from kinetics of He evolution temp. depend. 9-13710
- resistance oscillations in superconducting magnet 9-9877
- solar abundance, lower than previously admitted 9-15353
- in solar atm. abundance 9-14271
- stars, Balmer emission line half-widths 9-10486
- stars, envelopes model 9-21871
- vacancy interaction in Al-Zn-Be alloy 9-9701
- variational calc., multipeaks and config. 9-4884
- Be, n thermalization in large buckling range 9-19334
- BeO, X-ray absorpt. spectra, and energy-loss of 20 keV electrons 9-15182

**Beryllium compounds**

- alloy, conc. of Zi by photoactivation 9-1933
- Al-Be alloy, clustering, effect of cold working 9-18458
- Al-(4.4 at.%)Zn-(0.3 at. wt.%)Be, alloy, Be-vacancy interaction 9-9701
- Be-Co alloy in vacuum, friction, rel. crystal structure and atomic ordering 9-19814
- Be brass photocathode for He lines meas. on HL<sub>a</sub> background 9-15560
- BeF, Frank-Condon factors r-centroids for  $A^2\Pi \rightarrow X^2\Sigma$  system 9-7016
- BeF<sub>2</sub> glass, activated, spectral props. rel. to chem. bonds and ligand fields 9-10193
- BeH, molecular, theoretical calc. 9-757
- BeH<sub>2</sub>, LCAO-MO SCF calc. 9-15849
- BeO:Li, radiation-induced paramagnetic centre structure 9-1868
- BeO, computed ground state props. in molecular orbital approx. 9-7015
- BeO, molten, absorption index meas. in visible spectrum 9-17210
- BeO, polycrystalline, fracture energy 9-19807
- BeO, range of 0.5-4 KeV electrons rel. to energy 9-19872
- BeO, X-ray absorpt. spectra, and energy-loss of 20 keV electrons 9-15182
- BeO crystal, inversion twin boundaries from X-ray diff. contrast 9-3356
- BeO particles in Cu single crystals, tensile deformation 9-17306
- BeO powders, crystallite growth obs. of sintering and inhibition by adsorbed phosphate 9-17241
- BeSO<sub>4</sub>.4H<sub>2</sub>O, crystal structure refinement 9-14915
- BeSO<sub>4</sub>.4H<sub>2</sub>O, crystal structure from n. diff. exam. 9-13628
- Cu-Be alloys, sp. ht. temp. depend. during ageing 9-13763

**Beryllium compounds continued**

- Cu (2.5 wt.%)Be alloys, decomposition, effect of electron bombardment 9-5501  
 Fe (23 at.%)Be alloy, structure changes during ageing, transmission e. microscopy study 9-17343  
 Fe-Be solid solution, Mossbauer eff., elec. field gradient variation 9-17477  
 LiF-BeF<sub>2</sub>-ZrF<sub>4</sub> system, equilib. phase diagram, 350-1000°C 9-16031

**Bessel functions** *see Functions***Beta-decay theory**

- See also Nuclear decay theory*  
 coupling const., ratio determ. from  $p$  spectrum during  $n$  decay 9-6832  
 Fermi's (1934) paper, complete translation 9-15409  
 heavy nuclei, hindrance factors and influence of giant dipole reson. 9-14591  
 isospin forbidden transitions, higher contributions and nuclear structure effects 9-13207  
 neutron, radiative correction to axial vector coupling constant, divergent parts 9-8904  
 nuclear, relativistic quark model 9-17969  
 radiative corrections rel. to equal-time current commutators 9-8740  
 $\beta^+$ , forbidden transition probability functions 9-553  
 $e$  pair competition between decay emission and internal formation emission 9-6833  
 $n$ , correl. functions and relativistic corrections to recoil spectrum 9-4642  
 $n$ , polarized, time-parity violation search 9-4641  
 $n \rightarrow p e \bar{\nu}$  radiative corrections 9-417  
 $^{130}\text{Cs} \rightarrow ^{130}\text{Xe}$   $\beta$  spectra obs., energy levels calc. 9-4733  
 $^{130}\text{I} \rightarrow ^{130}\text{Xe}$   $\beta$  spectra obs., energy levels calc. 9-4733  
 $^{58}\text{Co}$ , (475 keV,  $2^+ \rightarrow 2^+$ ,  $\beta^+$ ) (0.810 MeV,  $\gamma$ ), Fermi/Gamow-Teller matrix element ratio 9-15743  
 $^{85}\text{Kr}$ , photon emission obs., bound atomic states excited 9-9136  
 $^{16}\text{N} \rightarrow ^{16}\text{O}$   $0^+$  state, deformed admixtures obs. 9-8986  
 $^{46}\text{Sc}$ , (357 keV,  $4^+ \rightarrow 4^+$ ,  $\beta^-$ ) (1.121+0.889 MeV,  $\gamma$ ), Fermi/Gamow-Teller matrix element ratio 9-15743

**Beta-ray spectra**

- See also Nuclear decay theory*  
 $^{170}\text{Tm}$ , decay, form of transitions  $1^- \rightarrow 0^+$  9-16948  
 $^{114}\text{In}$ , obs. by Siegbahn-Slater intermediate image spectrometer 9-15690  
 $^{234}\text{Pa}(\text{UZ})$  decay into energy levels of  $^{234}\text{U}$  9-2678  
 $^{146}\text{Pr}$  24 min. 9-2698  
 $^{186}\text{Re}$ , decay, form of transitions  $1^- \rightarrow 0^+$  9-16948  
 $^{286}\text{Re} \rightarrow ^{186}\text{Os}$ ,  $1^- \rightarrow 2^+$  transition obs. 9-14575  
 $^{116}\text{Sb} \rightarrow ^{116}\text{Sn}$ , decay scheme determ. 9-11249  
 $^{116}\text{Te} \rightarrow ^{116}\text{Sb}$ , decay scheme determ. 9-11249  
 $^{188}\text{Re} \rightarrow ^{188}\text{Os}$ ,  $1^- \rightarrow 2^+$  transition obs. 9-14575  
 $^{188}\text{Re}$ , decay form of transitions  $1^- \rightarrow 0^+$  9-16948  
 Al, flux spectra for  $^{198}\text{Au}$  and  $^{64}\text{Cu}$  sources 9-18571  
 $^{47}\text{Ca}$ , intensities of inner  $\beta$  groups 9-565  
 $^{62}\text{Co}$  isomers, decay schemes determ. 9-14589  
 $\text{Ni}$ ,  $e$  pair emission in decay, competition from internal formation 9-6833  
 $^{22}\text{Na}$ , and rest mass of  $\nu$  connected with  $\beta^+$  decay 9-9010  
 $^{32}\text{P}$  obs. by Siegbahn-Slater intermediate image spectrometer 9-15690  
 $^{73}\text{Se}$ , isomer states lifetimes calc. 9-2690  
 $^{90}\text{Y}$   $e$  pair emission in decay, competition from internal formation 9-6833  
 $^{95}\text{Zr} \rightarrow ^{95}\text{Nb}$ , decay period determ. 9-15744

**conversion electrons**

- $^{198}\text{Tl} \rightarrow ^{198}\text{Hg}$  energy levels determ. 9-4740  
 K conversion coeffs., high energy 9-8969  
 Kelman-type mag. spectrometer, Bucharest, appl. 9-2572  
 M-shell, internal conversion coeff. allowing for screening, semiempirical method, applic. to Z=65 9-9127  
 separation from  $\gamma$  lines in Ge diode coincidence counter 9-6724  
 $^{147}\text{Pd} \rightarrow ^{109}\text{Ag}$ , K conversion coeffs. rel. to  $^{109}\text{Ag}$  energy levels 9-19274  
 $^{217}\text{Th}$ , E, G, H and L line energies, obs. 9-2696  
 $^{192}\text{Ti} \rightarrow ^{192}\text{Hg}$ , energy levels determ. 9-4740  
 $^{164}\text{Dy}$ , radiative  $n$  capture, incident emission obs. analysis 9-522  
 $^{154}\text{Gd}$  from  $^{154}\text{Eu}$  decay,  $e$  intensities meas. 9-13210  
 $^{194}\text{Ti} \rightarrow ^{194}\text{Hg}$ , energy levels determ. 9-4740  
 $^{176}\text{Lu}(n, \gamma)^{176}\text{Lu}$ , internal conversion electron spectrum 9-2745  
 $^{106}\text{Rh}$ , decay obs. 9-555  
 $^{116}\text{Sb}$ , rel. to 103.2 keV transitions 9-6799  
 $^{116}\text{Sn}$ , rel. to 134.5 keV transition 9-6799  
 $^{196}\text{Ti} \rightarrow ^{196}\text{Hg}$ , energy levels determ. 9-4740  
 $^{137}\text{Cs}$ ,  $\beta$ -branching ratio and K conversion coeffs. 9-4762  
 $^{151}\text{Gd}(n, p)^{151}\text{Gd}$ , conversion electron spectrum 9-15764  
 $^{129\text{m}}\text{Te} \rightarrow ^{129\text{I}}$ , rel. to excited states of  $^{129}\text{I}$  9-15717  
 $^{57}\text{Fe}$  K-conversion  $e$  meas., by Si detector and parallel FET preamp. 9-20703  
 Tb, internal conversion coeff. in M-shell allowing for screening, semiempirical method 9-9127  
 $^{51}\text{V}$ , in 320 keV transition obs. 9-6823

**Beta-ray spectrometers**

- $\beta$ - $\gamma$  coincidence meas., adaptation of intermediate imaging  $\beta$  spectrometer 9-443  
 cylindrical electrostatic, focusing and geometry 9-20693  
 dual phosphor scin., background rate 1.7 cpm for 0.1-4 MeV 9-2571  
 for  $e$  pair prod. due to  $\gamma$ -rays, obs. 9-10976  
 intermediate-image, for precision anal., resolution correlation method 9-18031  
 Kelman-type, high-resolution magnetic, built in Bucharest 9-2572  
 magnetic, flat type; design, construction and performance 9-2570  
 magnetic, luminosity improvement by azimuthally variable field 9-2564  
 magnetic, semi-circular for momentum analysis 9-6720  
 magnetic, spectral shape energy depend. 9-6721  
 mylar, film preparation to 200  $\mu\text{g}/\text{cm}^2$  9-3207  
 on-line work with cyclotron 9-19220  
 sector type double focusing, new 9-13159  
 Siegbahn-Slater intermediate image, continuous spectra obs. 9-15690  
 $4\pi\beta$ , with Li-Si counters, improvement by preamplifier cooling 9-4666  
 Si surface-barrier, large area 9-4681  
 Si(Li), energy resolution, effect of inhomogeneities 9-14530

**Beta-rays**

- See also Electrons*  
 phys. props., expt. for eval. 9-6255

**absorption**

- See also Electrons/absorption*  
 dose attenuation in different media, empirical formula 9-4145  
 dose distrib. of around pt. source in Al and C<sub>18</sub>H<sub>21</sub> plastic 9-12034

**angular distribution**

- $^{186}\text{Ho}$ ,  $\beta$ - $\gamma$  ang. correl.  $P_4(\cos \theta)$  depend. 9-6844  
 Au-Pb activated alloys, rel. to interstitial sites 9-3332

**detection, measurement**

- See also Beta-ray spectrometers; Dosimetry; Particle detectors; Radioactivity measurement*  
 coincidence methods, double or triple, in activity meas., statistical errors 9-20757  
 isotopes, low-energy, activity meas., phosphoresc. and afterpulsing disturbances 9-20754  
 organic scintillator response, photomultiplier meas. 9-6722  
 scintillation guard detectors, plastic, for low-activity meas. 9-13168  
 source energy release evaluation by G-M counter 9-9003  
 spectrometer, sector type double focusing 9-13159  
 $^{170}\text{Tm}$ ,  $\beta$ - $\gamma$  correl. in first forbidden decay 9-15738  
 $^{241}\text{Pu}$  monitoring, liq. scintillation technique 9-18082  
 Li glass scintillation characts. 9-449  
 Si surface barrier detectors, sensitivity 9-14532

**effects**

- See also Electron beams/effects; Nuclear reactions and scattering due to/ electrons*  
 benzene and other liquids subject to high intensity electron pulses, H yield 9-1925  
 dielectrics, liq., irradiated, conduction mechanism 9-5179  
 hexane, ionization current induction 9-9549  
 semiconductors, recombination radiation, instrument for study 9-12157  
 sources exciting luminous radiation, applications 9-554  
 X-rays, characteristic, excitation, intensity calc. and obs. 9-19996  
 Al, elec. conductivity, rel. to strain and temp. 9-7746  
 CsI, luminesc. kinetics 9-16448  
 CsI photocathode u.v. quantum efficiency, 1-2 MeV 9-12224  
 CsTe photocathode u.v. quantum efficiency, 1-2 MeV 9-12224  
 CuI photocathode u.v. quantum efficiency, 1-2 MeV 9-12224  
 W photocathode u.v. quantum efficiency, 1-2 MeV 9-12224

**polarization**

- spin self-, radiational, during spiral motion in mag. field 9-2468  
 transverse, produced on scatt. by thick foils 9-4589  
 transverse polarization of electron, storage ring determ. 9-20604  
 $^{141}\text{Ce}$  meas. By-CP, deduced  $\beta$ -decay matrix element ratio 9-2685  
 $^{198}\text{Au}$ , longit. depolarization within source 9-15740  
 $^{42}\text{K}$   $\beta$ -circular polar. correlation 9-2685  
 $^{86}\text{Rb}$ , B- $\gamma$ -CP 9-2685

**scattering**

- See also Electrons/scattering*  
 transverse polarization production on scatt. by thick foils 9-4589

**Betatron** *see Particle accelerators/betatron***Bethe-Salpeter equation** *see Field theory, quantum***Bethe-Uhlenbeck equations** *see Statistical mechanics***Bevatron** *see Particle accelerators***Binary stars** *see Stars***Binding energy, solid state** *see Bonds; Solids***Bingham plastics and solids** *see Rheology***Biographies**

- Hertzprung, astronomer (1873-1967) 9-12822

**Biological effects of radiations**

- $\alpha$  particle energy loss in tissue 9-6203  
 bone-tissue interface, n-irrad., recoil p dose 9-15379  
 cell suspensions, sound eff., nonthermal mechanisms 9-4351  
 chromosomes damage 9-17671  
 D.N.A., alkali denaturation by capture 9-8300  
 DNA, double-strand scission 9-21991  
 enzymes, noncavitating u.s. effects 9-4140  
 fast neutron beam LET distrib. in tissues, calc. 9-18948  
 hearing hazard from 0.22 in weapons, obs. 9-4159  
 mammalian cells, survival after exposure to ultra-high X-ray dose rates 9-15380  
 molecule specific structure loss, spontaneous and rad.-induced, comparison 9-8302  
 population injury probability for random re-entry of satellite carrying radioactive mats. 9-20127  
 rat embryo, X-ray eff. obs. 9-21992  
 tissue, energy loss of  $\alpha$  particles 9-6203  
 ultrasonic, medical application hazards 9-4348  
 ultrasonic cleaning and cutting, health aspects 9-18947  
 from X-ray diffraction equipment, hazards and precautions 9-16633  
 $\pi^-$  beam therapy in cancer treatment 9-12779  
 $\pi^-$  capture in light elements, calcs. and comparison with cancer radiotherapy expts. 9-13233

**Biological technique and instruments**

- bacteria identification by differential light scatt. 9-12780  
 blood plasma Fe clearance, radioactive meas. method 9-15382  
 cell counter, automatic, for population growth monitoring 9-4173  
 clotting tests, end point times detection apparatus, patent 9-20256  
 echoencephalography, A-scan, transducer alignment device 9-6208  
 electrical stimulation of brain, localization without probes 9-4135  
 electroanesthesia, four-sequential-output generator for current focussing 9-4138  
 electron microprobe analysis 9-8131  
 electron microscope, scanning 9-2349  
 flowmeter, e.m. for blood 9-6202  
 image formation from detectors with incident  $\gamma$  flux 9-2089  
 i.r. camera for breast cancer detection 9-2254  
 i.r. radiation thermometer, portable 9-4131  
 laser interferometer, for meas. of submicroscopic displacement amp. and phases in small biol. struct. 9-15383  
 laser interferometer, for meas. submicroscopic displacement amplitudes of cat's tympanic membrane 9-10576  
 light beam, shadowless; method of direction to operating table, patent 9-10567  
 membrane cell, perspex, for Na transport studies across frog's skin 9-12778  
 MeV linear electron accel. for X-ray and electron irradiation 9-2093  
 microphone, intracardiac, calibration by two devices 9-4340  
 ophthalmoscope, laser, focusing method, patent 9-19156  
 phosphorescent instrument, multipurpose, for turbid biological materials 9-18725  
 recording, intensity-modulated, for u.s. diagnosis 9-6205  
 sample holder, irradiation of suspensions with protons 9-2096



**Biological technique and instruments continued**

- serum, electrophoresis medium for improved resolution, patent 9-10566  
skin-friction gauge for blood-flow meas. 9-5106  
sound masking, shifts with time, expt. 9-4160  
specimen holder for potato section, thermal diffusivity meas. 9-15394  
specimens, unstained, polytropic montage for electron microscopy 9-17262  
steady-state system, occupancy principle for radioactive tracers 9-17672  
submersible for bioacoustic obs., masking of biol. signals with vehicle's self-noise 9-15239  
temp. and radiance meas. of night flying moths 9-4132  
tissue preparation for liquid scintillation radioactivity counting 9-16635  
u.s. diagnostics of eye, intraocular distances, improvement in meas. 9-10577  
u.s. immersion scanner, use in symmetrical scanning of head 9-6207  
u.s. two-dimensional visual, design and use in medical diagnosis 9-6204  
u.s. visual, of images of brain, eff. of skull in echoencephalographic B and C scans 9-6206  
u.s. visual syst. for tissue, new scanning and presentation methods, applie. to brain exam. 9-6220  
vessel for irradiation of organic mats. 9-6200  
 $\gamma$ -irradiation plant for seeds 9-328  
e probe microanalyser and its applications to medicine 9-4142  
 $\gamma$  camera system, image quality 9-2088  
K in human body,  $^{40}\text{K}$   $\gamma$  emission meas. 9-10568  
 $\text{O}_2$  microcathode currents, meas. by f.e.t. amplifier 9-17843

**Biology**

- See also Medical science; Physiology; Zoology*  
cell suspensions, sound eff., nonthermal mechanisms 9-4351  
photosynthesis, e transfer mechanisms, obs. 9-16490

**Biophysics**

- aeromedical electronic stethoscope 9-4144  
bacteria suspensions in salt soln., osmotic responses and light scatt. 9-14867  
biomagnetism reviewed 9-8299  
biomedical instrum., Physics Exhibition, London 1968 review 9-4136  
biopolymers, collective proton tunneling mode coupling 9-7090  
cardiovascular flow 9-18334  
cat ears, losses in cochlear microphonic sensitivity, from 5 kHz stimulation 9-15389  
cat ears, tympanic membrane, submicroscopic displacement amplitudes by laser interferometer 9-10576  
chlorophyll-water aggregates, EPR studies 9-15377  
chromophore identification and conc. determ. by absorption 9-18713  
chromosomes damage 9-17671  
D.N.A., alkali denaturation by capture 9-8300  
electroencephalogram  $\alpha$ -occurrence rel. to target visibility 9-15392  
electroretinogram, signals 9-18957  
environmental chamber, with programmed temp. control to simulate daily temp. changes for plants 9-4380  
enzyme assay, radiochemical, review 9-14148  
fish tissue, freshwater, high-freq. u.s. props. 9-4323  
hemolysis kinetics, analogue comp. simulation 9-4139  
hen egg-white lysozyme, NMR studies 9-17068  
hornet, oriental, nature of sounds prod. in nest 9-8512  
human vertex pot., effect of changing stimulus frequency, intensity 9-4133  
insect obs. by means of time-lapse cinematography 9-289  
noncavitating ultrasound, effect on selected enzymes 9-4140  
organisms in hot springs 9-10565  
photosynthesis, entropy balance 9-16632  
primate vocalizations and human linguistic ability 9-15386  
tobacco mosaic virus, breakage by acoustic transients, hydrodynamical model 9-12937  
tobacco mosaic virus-III soln., distrib. curve from light scatt. in elec. field 9-14860  
trace element analysis in biological mats., peak fraction method of interpretation 9-4660  
whales, gray, migrating, underwater sounds 9-4350  
yeast cells in water, small ang. depend. of light scatt., comparison with the predictions 9-14868  
 $^{137}\text{Cs}$  in human body following atomic tests, possible sources in bread and milk 9-1943  
Na transport across living frog's skin, perspex membrane cell 9-12778

**Biot-Savart law** *see Electromagnetism***Birefringence** *see Double refraction***Bismuth**

- as lowpass n vel. filter, transparency determ.,  $\lambda_n=1.5\text{\AA}$  9-11105  
atoms, elastic scatt. of electrons, ang. distrib. for energy range 5 to 1200 eV 9-4857  
charge carrier densities and mobilities temp. dependence, 50-90°K 9-12046  
charge carrier relax. time variation with mag field from Alfvén wave obs. 9-12047  
complex in boiling mixture separation by chromatography followed by spectrophotometric determ. 9-18779  
crystal-melt system surface temp. distrib. meas. device rel. to solidification obs. 9-3237  
deformation potentials calc. 9-13824  
electromechanical effect, kinetics 9-1314  
energy loss spectra, characteristic, of 8 keV electrons in liquid and solid 9-7249  
film, critical conducting thickness, 100 400°K 9-3577  
film, deposition on mica, orienting action of substrate 9-21275  
film, evaporated, stress during and after deposition 9-5449  
films, optical transmission rel. to quantum size effect 9-7969  
implanted layers in Si, elec. behaviour 9-7810  
lattice dynamics 9-21424  
liquid, containing halide ions, elec. resistivity 9-11715  
magnetic quantum level motion in high fields Alfvén wave propag. obs. 9-7710  
magnetic surface layers 9-15068  
magnetic susceptibility lattice and charge carrier components 9-7876  
magnetoacoustic attenuation anisotropy rel. to deformation potential tensor component determ. 9-5556  
melt struct., Mg impurities, nucl. reson. fluoresc. study 9-7278  
multipole spectral lines, hyperfine structure 9-15810  
Raman scattering by optical modes, linewidths temp. depend. 9-12442  
residual twins, hysteresis props. 9-13978

**Bismuth continued**

- solid-liquid interfacial free energies, absolute determ. 9-11759  
superconducting film, resistive transition thickness dependence 9-9955  
thermal conduction, effects at intermediate fields 9-15022  
thermoelectric and thermomagnetic props. at low temp. 9-10059  
thermoelectric props. at phase transitions, effect of impurities 9-18368  
twinned interlayer growth rate temp. dependence, 123-293°K 9-5289  
Al-Al<sub>2</sub>O<sub>3</sub>-Bi tunnel junctions with ultrathin Bi films, I-V characts. 9-9966  
As, current carrier conc., pressure depend 9-15069  
Bi-MnBi composite, structural and mag. props. 9-9671  
Bi-Zn binary liquid metal mixture, critical inelastic slow neutron scatt. 9-19607  
Bi<sup>3+</sup> in Sc<sub>2</sub>O<sub>3</sub> and Y<sub>2</sub>O<sub>3</sub>, fluorescence spectra 9-3927

**Bismuth compounds**

- cBiTeI, prep of crystals 9-1131  
chlorides, fused, structure obs. from Raman spectra 9-21215  
perovskites, high-pressure synthesis and structure 9-18452  
Bi-Pb alloys, dilute, differential Shubnikov-de Haas effect 9-7726  
Bi-Sb-Te system, intermetallic cpds., mag. anisotropies and susceptibilities temp. dependence 9-13945  
Bi-Sb alloy, semiconductor-metal transition, rel. to mag. field and Sb conc., 4-77°K 9-1513  
Bi-Sb alloy, thermal conductivity, thermoelec. eff. and elec. resistivity 9-12026  
Bi-Sb alloy syst., energy-band parameters and relative band-edge motions near semimetal-semicond. transition 9-15053  
Bi-Sb alloys, band model 9-13831  
Bi-Sb alloys, internal friction meas. of grain boundary creep 9-16104  
Bi-Sb system, liquid state, elec. conductivity and density 9-9547  
Bi-Se alloy, vitreous, thermal props. 9-3153  
Bi- $\alpha$ -Sb<sub>2</sub> alloys, mag. susceptibility and band structure 9-21565  
Bi<sub>2</sub>Te<sub>3</sub>-Sb<sub>2</sub>Te<sub>3</sub> powders, thermal conductivity, effects of grain size, impurity content and processing effects 9-19867  
Bi<sub>2</sub>Te<sub>3</sub>, n and p type, band struct. 9-3637  
Bi<sub>2</sub>Te<sub>3</sub> molten, optical props. rel. to electronic struct. 9-16002  
Bi<sub>2</sub>Sb<sub>2</sub>, band structure 9-16209  
Bi<sub>2</sub>Sb<sub>2</sub>, nonohmic conductivity, 4.2°K 9-3619  
Bi<sub>2</sub>Te<sub>3</sub>-S, semimetal to semiconductor transition by size effect quantization 9-16230  
Bi complex, tris(dimethylammonium) hexabromobismuthate, crystal structure 9-21309  
BiBr emission spectrum, band structure, dissociation energy 9-2858  
BiBr mol. visible A-X system, rotational anal. 9-18176  
BiCl mol., analysis of bands of A'-X system 9-4918  
BiCl<sub>3</sub> fused, elec. conductance meas., by two-probe d.c. method 9-17845  
BiCl<sub>3</sub>-Pb molten mixtures, absorption spectra for reaction study 9-13531  
BiCrO<sub>3</sub>, mag. props. and crystal distortions 9-10112  
BiF, rot. struct. of 3050-3250 Å syst., electronic state struct. deduced 9-4919  
BiI emission spectra new B-a transition obs. 9-7017  
BiI<sub>3</sub> crystals, absorption spectra 9-3884  
BiMnO<sub>3</sub>, mag. props. and crtions 9-10112  
Bi(OH)<sub>3</sub>, polynuclear metal complex vib. spectra obs. 9-11455  
Bi- $\alpha$ -Sb<sub>2</sub>, magnetic susceptibility lattice and charge carrier components 9-7876  
Bi-Sb<sub>2</sub>, (x=97,90; y=3,10), band parameters from galvanomag. meas. 9-1533  
n-Bi<sub>2</sub>Te<sub>3</sub>, de Haas-van Alphen effect 9-9913  
Bi<sub>2</sub>Te<sub>3</sub>, mag. anisotropy and susceptibility temp. dependence 9-13945  
n-Bi<sub>2</sub>Te<sub>3</sub>, quantum oscillations of transport and photomag. coeffs. 9-12144  
BiTeBr, semiconducting, semiconducting, band structure from elec. and optical props. 9-21512  
Bi-Pb alloys, electron transitions, pressure-induced, 4.2-295°K 9-9892  
Bi-Sb alloy, semicond. longit. magnetoresist. anomalies in mag. fields up to 500 kOe at liq. He temp. 9-1514  
Bi-Sb-Pb alloys, electron transitions, pressure-induced, 4.2-295°K 9-9892  
Bi-Sn alloys, electron transitions, pressure induced, 4.2-295°K 9-9892  
n-Bi<sub>2</sub>Te<sub>3</sub>, Fermi surface shape discrepancy, galvanomag. data recal. 9-1427  
Na-Bi liquid alloy, density meas. 9-5145  
PrBi nuc. mag. cooling, hyperfine enhanced, low-temp prod. 9-4185

**Bitter patterns** *see Magnetization state/domains***Bitumen** *see Materials***Bloch walls** *see Ferromagnetism; Magnetization state/domains***Boiling**

- clotting tests, end point times detection apparatus, patent 9-20256  
flowmeter, e.m. 9-6202  
velocity meas. with heated element or skin friction gauges 9-5106  
white cell separation by electronically sensed vol. 9-11728  
 $^{57}\text{Fe}$  in plasma, determ. using liquid scintillation counting 9-16634  
 $^{59}\text{Fe}$  in plasma, determ. using liquid scintillation counting 9-16634
- Boiling** *See also Distillation*  
acetone carbon tetrachloride binary system, superheat temp. 9-18388  
Arcton 11, pool boiling, high press. and accel. effects 9-13560  
bubble separation from heated surface 9-3155  
Chloroform-carbon tetrachloride binary system, superheat temp. 9-18388  
in fuel rod bundles, departure from nucleate type and uncertainties in heat flux evaluation 9-9092  
gasoil decomposition products deposition vel. depend. on wall temp. 9-17230  
heat transfer in transition boiling method of study 9-19660  
liquid, local temp. fluctuations 9-19661  
metals, voids, X-ray meas. 9-9468  
nucleate, site instability 9-1072  
nucleate bulk, loss of hydrodynamic stability, effect of viscosity of liq. phase 9-7305  
pool boiling, principal crisis mechanism at high heat fluxes 9-13561  
superheated liquids, bubble growth meas. 9-21176  
transition, heating surface effects 9-16032  
water, pool boiling, high press. and accel. effects 9-13560  
water, saturated, crisis in pool boiling at high heat fluxes, principal mechanism 9-13561  
K, voids, X-ray obs. 9-9468  
Na, heat transfer with natural convection, obs. 9-17231

**Boiling continued**

- UF<sub>6</sub>-WF<sub>6</sub> mixture, liquid-vapour phase equilib. determ., 1520-2660 mm Hg 9-21246  
 WF<sub>6</sub>-UF<sub>6</sub> mixture, liquid-vapour phase equilib. determ., 1520-2660 mm Hg 9-21246

**Boiling point**

- hydrocarbons, substituted, correlation with skeletal deformation freq. 9-21249

**Bolometers**

- automatic, stability and accuracy 9-15477  
 Ge single cryst., very-far i.r. region 9-15551  
 superconducting, temp. stabilization by electronic means 9-12952  
 Ni, production and properties 9-10750

**Boltzmann equation** *see* *Transport processes***Bonding of materials** *see* *Adhesion***Bonds***See also* *Molecules*

- aliphatic secondary amines, H-bonding from p.m.r. obs. 9-19455  
 alkali feldspars, lengths rel. to ordering and ionic character 9-7356  
 alkali halides, anharmonicity and cohesive energy 9-11984  
 alkali-alumino-silicate glasses, chem. bonding using X-ray emission spectroscopy 9-1117  
 alkyl acetates, skeletal, scission probabilities in mass spectra 9-14698  
 alternation, and Overhauser phase in long-chain mols. 9-4972  
 antiferromagnetic, pair-wise bonding us. spin coupling 9-21592  
 aromatic hydrocarbon bases, H-bonded complexes 9-4942  
 aziridine, 1-substituted, interproton coupling consts. from <sup>13</sup>C-H satellite n.m.r. 9-13543  
 azulene, ground and doubly excited states, bond orders, SCF calc. 9-20951  
 benzenes, alkyl-substituted, proton-donor effects 9-11698  
 benzo-2,1,3-oxadiazole and derivatives, p mag. reson. rel. to bond order, obs. 9-15882  
 benzo-2,1,3-selenodiazole and derivatives, p mag. reson. rel. to bond order, obs. 9-15882  
 benzo-2,1,3-thiadiazole and derivatives, p mag. reson. rel. to bond order, obs. 9-15882  
 book, specialized topics 9-14903  
 borosilicate films, B-O bond, infl. of moisture on bond strength 9-17485  
 breaking in adiabatic proc., significance of SCF MO calc. on electr. struct. of methyl fluoride 9-17057  
 carbon tetrabromide, force constant calculation 9-18175  
 carbon tetrachloride, force constant calculation 9-18175  
 carbonates, calcite-type, relation between carbon-O distance and properties 9-19681  
 carboxylic acid dimer configuration, planarity 9-7018  
 chloroethylenes, substituted, C-Cl bonds 9-2906  
 chloroform - triethylamine system, enthalpy of H bond 9-1039  
 covalent, condensed matter, free positron lifetime and effective number of electrons per atom 9-5637  
 crystals, interatomic, thermal expansion 9-7659  
 2,6-dimethyl-1,4-phenylpyridine, lengths between rings from absorpt. spectra 9-9273  
 1,8-dimethyl-5,12-dimethylene biphenyl, twisted C-C double bond, optical activity meas., electronic structure proposal 9-9274  
 dimethylamine, C-N bond lengths and molec. struct. 9-18210  
 effective ionic radii, for bond and unit cell calc. 9-7354  
 electrostatics of finite charge distrib. 9-12039  
 ethane, theory 9-9265  
 ethylenes, H bond study from NMR and i.r. obs. 9-18751  
 ethylenimine, N bonds 9-20962  
 ethylphenylphosphine, geminal coupling consts., n.m.r. anal. 9-13546  
 glass, flint, enthalpy evaluation and sputtering rates 9-17361  
 in graphite oxide, rel. to struct. model 9-7352  
 group IIIA monohalides, nature of binding 9-20919  
 H, cryst. two-dims. transfer matrix rel. to anisotropic Heisenberg chain 9-1120  
 H, intermolecular, of cumene hydroperoxide 9-2903  
 hydrocarbons, calc. method 9-4952  
 hydrogen-bonded crystals, i.r. spectra, theory 9-15170  
 I beams, lateral buckling beyond limit of proportionality 9-14379  
 inductive effect in saturated mol., var.-perturbation theory, geminal method 9-11443  
 inorganic complexes, linkage isomerism 9-9194  
 ionic radii, concept and determ. from density minima 9-14904  
 length changes on ioniz., mechanisms 9-20916  
 Lifshitz-van der Waals forces between graphite masses, deviations from pairwise additivity 9-3220  
 ligand-ENDOR spectrometer 9-2290  
 magnesia refractory, creep rel. to microstructure, bonding and composition, 1450-1550°C 9-3423  
 manganous formate dihydrate, H bonding from n.-diff. data 9-7455  
 metal fluorides, solid, stability rel. to anode behaviour of metal in HF 9-18763  
 metal-ligand, information from electronic spectrum, book 9-11453  
 metals, monovalent, cohesion 9-11788  
 methane, halogen substituted, polarizability theory rel. to calc. of Raman intensities 9-13387  
 mica, normal and retarded van der Waals forces 9-18398  
 moisture, in concrete, shape and type, depend. on solidification method 9-17345  
 molecular, condensed matter, effective number of annihilation electrons per atom for free positrons 9-5637  
 molecules, breaking-energies connection with Monte-Carlo calculated dissociation energies 9-7076  
 monomer-dimer problem, series expansion 9-8424  
 monoorganosilanes, Si-H bond props., n.m.r. obs. 9-19475  
 naphthalene, ground and doubly excited states, bond orders, SCF calc. 9-20951  
 1-naphthol, excited, H-, and level reversal 9-9519  
 nickelocene 9-15900  
 niobates thermal expansion of interatomic bonds 9-7659  
 n-nitroaniline, proton-donor effects, obs. from spectra in o-xylol 9-11698  
 novel, effect on atom images in field-ion microscope 9-5306  
 in octafluorocyclohexa-1,3-dieneion tricarbanol 9-1198  
 orders in completely filled MO shells 9-9186  
 organic cpds., energies and lengths of C, S, O and N 9-798  
 oxides, from X-ray K-emission spectroscopy of crystals 9-13589

**Bonds continue**

- pentane isomer, deductions from kinetic energy of fragments after electron impact 9-7087  
 in perchlorylamide ion, length effect on normal vibrs. 9-7046  
 perovskite structure, Madelung potential calc. for various sites for any ion charges 9-7355  
 phenols, two-substituted, NO<sub>2</sub> group vibrs. rel. to H bond form., i.r. obs. 9-15896  
 polystyrene, proton-donor effects, obs. from spectra in benzene 9-11698  
 quartz, H-bonded OH, characts. from i.r. spectra 9-5267  
 quartz, valence bond approximation; applic. to u.v. spectrum anal. 9-5266  
 $\pi$ -H in naphthols 9-17059  
 rutile, lattice energy, anion dipole contrib. 9-9630  
 salicylic acids, substituted, intramol. H-bonding in lowest excited singlet states 9-19474  
 salts, lattice energies and chemical significance 9-18406  
 sandwich cpds. 9-15900  
 semiconductors, binary, lattice bond energy rel. to atomic displacement energies 9-12133  
 silica, vitreous, contrib. to configurational entropy of random network model 9-14887  
 silicates, from X-ray K-emission spectroscopy of crystals 9-13589  
 sulphates, rel. to S L<sub>2,3</sub> X-ray emission, obs. 9-20940  
 sulphides, rel. to S L<sub>2,3</sub> X-ray emission, obs. 9-20940  
 symmetry eff. teaching article 9-14302  
 tetrachloroethylene, bond length changes on ioniz., mechanisms 9-20916  
 tetracyano complexes, inter-planar bonding 9-18441  
 thiourea ionic complexes, Madelung energy 9-9633  
 trans-cyclooctene twisted C-C double bond, optical activity meas., electronic structure proposal 9-9274  
 transition metal carbonyls, back donation depend. 9-19448  
 transition metals, bonding and structures 9-18577  
 s-triazine mol., comparative X-ray and n. diff. obs. 9-11502  
 trifluoroacetic acid, C-F, chemical shift anisotropy from <sup>19</sup>F NMR spectrum obs. 9-9286  
 trimethylamine, C-N bond lengths and molec. struct. 9-18210  
 trimethylphosphinoallylnickel (II) chloride, bonding, phys. and chem. predictions 9-19469  
 vanadocene 9-15900  
 water, rel. to diamagnetism 9-5188  
 X-ray temperature parameters, introduction of systematic errors 9-3274  
 zinc acetate dihydrate, H bonding scheme investing by PMR 9-1121  
<sup>197</sup>Au chemical bond, n.q.r. spectroscopic obs. 9-4916  
 Al, binding energy and pseudopotential 9-9891  
 Al<sub>2</sub>O<sub>3</sub> sequestered phosphate soln., high temp. bonding and refractory applications 9-3460  
 B<sub>3</sub>N<sub>2</sub>H<sub>6</sub>, bond lengths BN, BH, NH, from CNDO/2 calc. on  $\pi$ -electron system 9-20922  
 BB<sub>3</sub>, force constant calculation 9-18175  
 BC<sub>3</sub>, force constant calculation 9-18175  
 C-H aliphatic groups, bond polarization 9-7044  
 C<sub>2</sub>, isoelectronic series, charge distrib. and binding 9-2876  
 CCl<sub>4</sub>, bond moments and derivative 9-2860  
 CF<sub>4</sub>, bond moments and derivative 9-2860  
 CH bond moments of aromatic hydrocarbons, depend. on bond angle 9-7069  
 CO<sub>2</sub> model from orbital theory 9-14301  
 CaF<sub>2</sub>, covalency evidence in Tm<sup>3+</sup> and Yb<sup>3+</sup> 9-11791  
 Ca(NO<sub>3</sub>)<sub>2</sub>-Ba(NO<sub>3</sub>)<sub>2</sub>-Sr(NO<sub>3</sub>)<sub>2</sub> binary fused systems, from Raman scatt. 9-17186  
 Co-N, lengths from crystal structure obs. of hexaamminecobalt (III) iodide 9-13631  
 CoSe<sub>2</sub>, X-ray spectroscopic study 9-20931  
 CrO halide complexes, ligand hyperfine interactions 9-17498  
 Cs-graphite cpds, lamellar, Mossbauer study 9-7353  
 Cu, cohesive energy, correlation and orthogonality corrections 9-18407  
 DIO<sub>3</sub>, from piezoelectric and elastic props. obs. 9-12202  
 GeCl<sub>4</sub>, bond moments and derivative 9-2860  
 H-bond distances in cry., rel. to i.r. stretching freq. 9-11449  
 H-bond energies, var. with intermol. distance, perturbation calc. 9-11447  
 H, in HCl-dimethyl ether vapour system, n.m.r. 9-7021  
 H, weak, effect of lone-pair hybridization on stability 9-2887  
 H in chlorosubstituted alcohol, i.r. spectra obs. 9-9243  
 HCN $\pi$  angle determ. from ESR spectrum in KCl 9-13358  
 HF chemical bond, minimal basis SCGF calc. 9-13353  
 HIO<sub>3</sub>, from piezoelectric and elastic props. obs. 9-12202  
 KBr:Ti<sup>4+</sup>, binding energy of Ti<sup>4+</sup> with light foreign anions and lattice distortion 9-3297  
 KCl:Ti<sup>4+</sup>, binding energy of Ti<sup>4+</sup>, binding energy of Ti<sup>4+</sup> with foreign anions and lattice distortion 9-3296  
 KCl:Ti<sup>4+</sup>, binding energy of Ti<sup>4+</sup> with foreign anions and lattice distortion 9-3296  
 KI:Ti<sup>4+</sup>, binding energy of Ti<sup>4+</sup> with foreign anions and lattice distortions 9-3297  
 Li mols. bonding energy, geminal calc. 9-4909  
 Mn-C alloys, rel. to resistance comp. dependence 1000-1400°C 9-12088  
 Mn<sup>2+</sup> in fluoroberyllate glasses, chem. bonding with ligands effect on luminesc. 9-1845  
 MnSe<sub>2</sub>, X-ray spectroscopic study 9-20931  
 MoO halide complexes, ligand hyperfine interactions 9-17498  
 N 1s electron binding energies correl. with CNDO charges 9-11451  
 N<sub>2</sub>, isoelectronic series, charge distrib. and binding 9-2876  
 N<sub>2</sub> molecule as ligand in nitrogenpentammineruthenium (II) dichloride and related salts 9-7448  
 NSF<sub>3</sub> from i.r. absorpt. and Raman obs. 9-15862  
 Na films on W(110), between adsorbed layers 9-1113  
 Ni K $\beta$ ' lines, effect of chem. bonding 9-19998  
 O<sub>2</sub> model from orbital theory 9-14301  
 PbZrO<sub>3</sub>, covalency from <sup>57</sup>Fe resonance meas. 9-7625  
 Pt(CO)Cl<sub>2</sub>, Pt-Cl, metal-ligand vibr., i.r. and Raman obs. 9-15868  
 Pt(NH<sub>3</sub>)Cl<sub>2</sub>, metal-ligand vibr., i.r. and Raman obs. 9-15868  
 Se-S<sub>8</sub> energy diff. and force consts.,  $\rho$ -parameter potential function 9-20941  
 SeO<sub>2</sub>, monoclinic, electrostatic energy and anion ordering 9-11790  
 Si phenyl cpds., n.m.r. spectra obs. 9-11499  
 SiCl<sub>4</sub>, bond moments and derivative 9-2860  
 SiF<sub>4</sub>, bond moments and derivative 9-2860  
 Sn-transition metal, nature 9-16048



**Bonds** continued

- VO<sup>2+</sup> complexes,  $\pi$ -bonding by equatorial O, study by proton n.m.r. 9-13590  
VOF<sub>3</sub> complexes 9-14114  
ZnS, wurtzite, effective ionic charge magnitude estimation 9-9631

**Bone** *see* **Materials****Bootstrap theory** *see* **Elementary particles; Field theory, quantum****Bordoni effect** *see* **Acoustic wave propagation/ultrasonic; Damping; Internal friction****Boron**

- acceptors in carbon black P33, effect on e.s.r. in range 1800°-2400°C 9-8019  
addition to graphite, effect on nucleation pattern of rad. damage 9-7477  
atom, spin densities calc. 9-672  
atom, spin-extended Hartree-Fock functions 9-671  
atoms and ion, bibliography of spectra 9-13287  
conductivity, electrical, freq., and temp. dependence 9-1454  
diffusion in Si in oxygen ambient rel. to transistor fabrication 9-14959  
diffusion in Si or SiO<sub>2</sub>, 1070 to 1190°C 9-13708  
electronic pair-correlation energies of ground states, soln. of Bethe-Goldstone eqns. 9-11383  
film prep. on Si substrate 9-13585  
foil, preparation and electron microscope obs. of defects 9-5247  
in graphite, effects on transport props 9-7848  
implantation in Si, range and distribution by capac. method 9-5709  
lifetimes and levels of collisionally excited ions 9-6959  
magnetoconductivity, -60° to +50°C, 0 to 2000 Gauss 9-16221  
magnetoconductivity, -60° to +50°C, 0 to 2000 Gauss 9-16222  
poisonin H<sub>2</sub>O, decay of thermal neutrons 9-14644  
in pyrolytic graphite, effect on mech. and physical props. 9-7515  
semiconducting props. in breakdown region 9-12143  
solar abundance, lower than previously admitted 9-15353  
<sup>11</sup>B, n.m.r. in CaB<sub>2</sub>O<sub>4</sub> 9-1873  
BII, 2p<sup>2</sup> L<sup>1</sup> lifetime meas. 9-11391  
Ba Q plasma, optical study 9-14783  
Bi lifetime of 2s2p<sup>2</sup>D<sub>3/2,5/2</sub>-states, from level crossing expts. 9-6964  
in Ge, impurity vibrational modes by i.r. absorption 9-18548  
Si implantation with improved elec. activity and profiles 9-16277  
in SiC, electroluminescent energy spectrum, 77-300°K 9-18727

**Boron compounds**

- borides of transition metals, physical and mechanical props. 9-7510  
borosilicate glasses, thermo-optical properties over wide range of temperature and wavelength 9-14027  
diborene hydrazine i.r. spectra for struct. 9-11463  
diborates, methyl substituted, sum rules for frequencies and squares of frequencies of vibration 9-19428  
halide mols. BXY<sub>2</sub> type, const.  $\zeta$  element var. determ. 9-7012  
halides, pure and mixed, force consts. transfer, i.r. spectra obs. 9-7014  
B<sub>2</sub>H<sub>6</sub>, n.m.r. and mag. nonequivalence 9-755  
B<sub>2</sub>N<sub>2</sub>H<sub>6</sub>,  $\sigma$ - and  $\pi$ -electron system, CNDO/2 calc. 9-20922  
B<sub>2</sub>C, fast n. space, energy and angular distrib. 9-19329  
BBr<sub>3</sub>, force constant calculation 9-18175  
BBr<sub>3</sub> liquid plasma jet analysis for metal impurities 9-6028  
BCl<sub>3</sub>, force constant calculation 9-18175  
BCl molecule, potential energy curve of  $\Sigma$  and  $\Sigma'$  states 9-754  
BCl<sub>3</sub> laser 9-4468  
BF<sub>3</sub>, rotational analysis of 14900 cm<sup>-1</sup> band, assignment as e<sup>2</sup> $\Sigma^{\prime\prime}$  $\Sigma^{\prime}$  transition 9-13343  
BF<sub>3</sub>, viscosity coeff. depend. on B isotopic composition and temp. 9-21146  
BF<sub>3</sub> isotopes spectra,  $\nu_3$  bands meas., rotn. fine structure determ. 9-17027  
<sup>10</sup>BF<sub>3</sub> graphite moderated counter, design and efficiency 9-2575  
BH, pair correl. energies and unitary transf., SCF orbital depend. 9-19427  
BH<sub>4</sub><sup>-</sup>, n.m.r. isotope chem. shifts 9-7013  
BN, band structure 9-5609  
BN, cubic, synthetic growth mechanism rel. to that of synthetic diamond 9-7368  
BN, electroluminescence brightness voltage- and freq.-dependence 9-12484  
BN, etching and microscopic examination 9-5271  
BN, Raman spectra, excited by He-Ne laser 9-1805  
BN and BN composite, oxidation and compatibility,  $\leq 2000^\circ\text{C}$  9-3995  
BNH<sub>4</sub>, umbrella vs. bridged geometries 9-756  
BO<sub>2</sub><sup>-</sup> molecular ion, i.r. absorption in alkali halide crystals 9-14685  
<sup>10</sup>BO<sub>2</sub><sup>-</sup> and <sup>11</sup>BO<sub>2</sub><sup>-</sup> migration, isotope effect 9-17200  
B<sub>2</sub>O<sub>3</sub>, viscosity, 10<sup>4</sup>-10<sup>6</sup> poise, rel. to struct. 9-3083  
B<sub>2</sub>O<sub>3</sub> glass, relax. times spectrum temp. depend. 9-3850  
B<sub>2</sub>O<sub>3</sub>, molten, inadequacies of viscosity theories 9-9493  
B<sub>2</sub>O<sub>3</sub> particles, dragging by migrating grain boundaries in Cu 9-1233  
BP, Raman spectra, excited by He-Ne laser 9-1805  
Bi, adsorption and nucleation on W 9-21284  
Pd-B alloys, mag. susceptibility and H<sub>2</sub> diff. 9-7889  
Si-Ge-B alloy, thermolec. props. and conductivity 9-15133

**Bormann effect** *see* **X-ray diffraction****Bose gas** *see* **Quantum fluids/boson systems****Bosons**

- See also Gravitons; Mesons; Photons; Quantum fluids/boson systems; Statistical mechanics/quantum*  
boson field, self-interacting in 2D, in periodic box, semiboundedness of Hamiltonian 9-14457  
boson fields, two coupled massive, bound states 9-2157  
boson-fermion scatt., removal of square-root singularity from amplitude 9-17935  
field, free, C\*-algebra and automorphisms 9-12872  
field, nonlinear self-interacting, dynamical invariance 9-2448  
high spin,  $>2$ , spectral representation, mass eigenvalues, sum rules 9-4564  
interactions, weak, vector boson mediated, models 9-8725  
mass, coupling const. determ. from model of interactions with leptons 9-16824  
operator realization obtaining state vectors of unitary groups U<sub>n</sub> 9-17693  
pair-conjugate and CPT nonconservation 9-20615  
parity tests, non-dynamical, decay mechanism 9-4562  
radiation in plane wave e.m. field, classical and quantum theory analysis 9-6414  
Regge trajectories, boson, parity doubling 9-2493  
resonance formation in pp scattering 9-409

**Bosons** continued

- resonances, higher spin and radiative decay, O(4, 2) group representation 9-2520  
scattering, vertex function, N/D coincident zeros and Levinson's theorem scalar bosons 9-15606  
scattering of three identical through zero-range pair potentials 9-17936  
spinless with arbitrary isospin, free-field theories and locality 9-8716  
transformation props. from wave func. to 4-vector func., relativistic eqn. 9-8710  
 $m^2$ , single mass, compactness of integral operator of Bethe-Salpeter eqn. 9-8721  
W-bosons, intermediate, hadron disintegrations 9-15607  
weak, rel. to  $\nu$  quasi-elastic interactions and weak angle 9-4585

**Boundary layers**

- air, gas-dynamical parameters and chemical content at high temperatures 9-13484  
bleed drag of flow at supersonic speed 9-19510  
bubble, hot inert gas in chemically reactive liquid stream 9-17182  
between cold plasma and confined mag. field effect of transverse plasma vel. component 9-21829  
compressible, stability equations 9-11649  
compressible laminar three-dimens., mass injection effects 9-11647  
diffusion, from forward stagnation point of sphere to separation point, for mass transfer 9-13495  
dissipative, rel. to vorticity in gas flow 9-14808  
dissociated gas flow past catalytic surface, rel. to surface reaction rates 9-12540  
equation for spreading of jet along porous wall 9-973  
flow on blunted cone at angle of attack, three-dimens. laminar eqns. 9-17595  
in flow near trailing edge of flat plate 9-967  
in flow over rotating disc, effect of circular mag. field imposed on disc. 9-9324  
in flow with separation, soln. of three-dimens. laminar eqns. 9-7107  
graphite particle pseudo-fluidized bed, elec. resistance 9-9314  
heat and momentum convection in viscous fluid 9-20999  
heat transfer bibliography 9-19085  
hydromagnetic stability at large Reynolds number 9-7109  
hypersonic, heating solid mat., determ. of rate of sublimation 9-7309  
hypervelocity flat plate flow, effects of thermal rad. 9-19576  
impulsive motion of flat plate in viscous fluid 9-17089  
jet flow along curved surface, for small curvature 9-7244  
laminar, 3-dimens., aerodynamics conical external flow 9-19579  
laminar, close to Falkner-Skan rel. profile, description rel. to const. press. grad. 9-14747  
laminar, free convection, vertical plate with constant suction 9-15979  
laminar, in three-dimens. non-stationary flow, approx. treatment 9-9463  
laminar, of flat plate with sinusoidal variation of air flow 9-17149  
laminar, over flat plate, thermal response to step change in wall temp. or flux 9-13488  
laminar, stability, effect of temp.-depend. viscosity 9-11687  
in laminar accelerating film flow down wall, growth and decrease rel. to mathematical soln. 9-18349  
laminar flow, appl. of Galerkin-Kantorovich-Dorodnitsyn method 9-21027  
laminar in exponential flow along flat plate 9-12203  
light scatt. layer, optical conds. near back boundary 9-265  
liquid, laminar, stability on elastic surface 9-14822  
with mass transfer, expt. studies 9-19496  
MHD, at surface of plate for arbitrary orientation of mag. field, properties 9-9329  
MHD, Blasius problem, Laplace transfrom appl. 9-2953  
MHD, use of Karman-Pohlhausen method with fourth deg. polynomial vel. profile 9-7116  
neutral, barotropic, planetary, asymptotic similarity 9-18795  
ocean flows, two-dimens., eqn. 9-8159  
planetary, response to time varying pressure gradient force 9-18796  
planetary, vertical eddy transport estimation using vertical velocity spectrum 9-21763  
plasma flow in perpendicular mag. field 9-9357  
plasma MGD viscous channel flow, heat conduction approximation 9-21059  
above porous medium, conjugate heat transfer with blowing 9-9503  
power-law fluid, laminar three-dimens., similarity solns. 9-11523  
rotating fluid, Kelvin-Helmholtz stability problem, correction to soln. of eigenvalue eqn. 9-17088  
semiconductor-vacuum interface plasma heated by h.f. field 9-13428  
semiconductor-vacuum interface plasma heated by h.f. field 9-880  
separation of viscous, non-isothermal effects 9-968  
shock-induced, frictional stress and heat transfer at wall, and recovery factors 9-21129  
suction of fluid from surface analysis of acoustic radiation 9-18229  
supersonic, turbulent, effect of wall curvature on heat transfer 9-14811  
thermal, unsteady, 2-dimens. low-speed flows, soln. 9-18230  
transition at low Reynolds numbers 9-11527  
transition point on flat plate, change on appl. of electrostatic field 9-7108  
transverse curvature eff. due to laminar, incompressible, longitudinal flow over cylinder 9-14823  
turbulent, calc. for MHD channel with non-conducting wall 9-7128  
turbulent, drag coeffs. on plates, evaluation of Coles' theory 9-17145  
turbulent, flow with press. grad., heat transfer and possibly mass transfer 9-17144  
turbulent, on rough plate, skin friction coeff. 9-18338  
turbulent, pressure pulsations on plate surface 9-971  
turbulent, separation in front of step 9-11648  
turbulent, turbulence intensities 9-9319  
turbulent, viscous region 9-18246  
turbulent, viscous sublayer, longit. intensity eqn. 9-21166  
turbulent free flows, spreading and contraction at boundaries 9-21016  
turbulent separation ahead of cylinder, associated shock pattern 9-7214  
turbulent-equilibrium, prediction for Prandtl mixing length distrib. 9-21026  
vapour condensation on supercooled high velocity jet turbulent boundary layer parameters 9-19659  
wake behind inclined flat plate at arbitrary angle of attack 9-17170  
water, laminar, with adverse press. grad., heat flow 9-21163  
Ar plasma, laminar flow, anal. for equilib. ionization 9-14759  
Ar plasma in shock-tube, study by quantitative schlieren tech. 9-14760

**Bragg reflection** *see* **X-ray crystallography****Brass** *see* **Copper alloys**

**Bravais lattice** *see Crystal structure, atomic*

### Breakdown, electric

*See also Discharges, electric; Electric strength*  
cathode protrusions formation during pre-breakdown conditioning electron optical obs. 9-11633  
dust on electrodes, effect 9-928  
plasma, thermal 9-9358  
propane-oxygen flame 9-933  
surface creepage flashover discharge, effects of conducting metallic barrier 9-10041  
suspensions, mechanism 9-11724  
vacuum, caused by anode evaporation 9-5088  
vacuum, desorption mechanism 9-7203  
vacuum, initiation by e injection 9-11632  
vacuum, initiation with extended electrodes 9-5087  
Ne, streamer, exptl. investigation of development 9-930  
W cathode protrusions formation during pre-breakdown conditioning electron optical obs. 9-11633

### gases

1.5 mtorr, high frequency applied elec. field with and without mag. field, due to secondary electron resonance 9-9418  
air, and prebreakdown conditions in cylindrical geometry 9-14805  
air, by nanosecond laser pulse, obs. 9-13470  
air, laser induced, self focusing effects 9-5090  
arc columns, wall-stabilized, in boundary regions 9-932  
electronegative, dielectric, in uniform field rel. to characterization of gas 9-5120  
ignition probability theory 9-5086  
laser-irradiated, for plasma production 9-11578  
molecular gases, medium and high vacuum, plane electrode arrangement breakdown voltage 9-5085  
perfluorobutane, ionization and attachment coeffs. 9-913  
photo-electric effect on high-intensity laser light irradiation 9-7201  
r.f. diffusion controlled, evaluation 9-7200  
spark transition in negative ion and free electron gases, asymmetrical fields 9-18317  
streamer, mechanism of secondary processes 9-11631  
Ar-Ne mixture, obs. 9-929  
Ar, velocity and press. influence on potential 9-7232  
D<sub>2</sub>, by nanosecond laser pulse, obs. 9-13470  
H<sub>2</sub>, cylindrical positive corona discharges, breakdown voltage, comments 9-7204  
He ignition characts., plane electrodes, theory and obs. 9-13467  
Ne increase with applied a.c. voltage 9-3032

### liquids

n-hexane with series of dielectric admixtures 9-5185  
oil, mineral, electronegative dissolved gas effects 9-11711  
underwater sparks, laser induced 9-9420  
He, at 4.2°K, dielectric 9-1055

### solids

coal, energy characts. of impulse discharge 9-10042  
dielectric voids, partial discharge 9-18650  
dielectrics, e-irradiated at 1 MeV, rel. to e. emission processes 9-10077  
dielectrics, time taken meas. 9-12178  
mica, natural, thermal, and hopping elec. conduction 9-12182  
minerals, energy characts. of impulse discharge 9-10042  
polymers, dielectric, multistage mechanism 9-7841  
polythene, dielectric, time taken meas. 9-12178  
Schottky barriers, microprocesses 9-18634  
wires, enamelled, high-temp. and damp storage effects 9-7842  
B, semiconducting props., in breakdown region 9-12143  
CaTiO<sub>3</sub>, prebreakdown processes 9-18651  
CdS-n-Ge, photosensitive junction 9-5723  
CdSe-n-Ge, photosensitive junction 9-5723  
GaAs-metal point contact 9-3686  
Ge, impact ionization of impurities 9-15105  
KBr, dielectric, time taken meas. 9-12178  
LiF, energy characts. of impulse discharge 9-10042  
NaCl cleaved surface, visualization 9-9638  
NaCl plates with polyethylene barrier, discharge development 9-1586  
Si p-n junctions, discrete nature and effect on reverse I-V characteristics 9-21520  
SiC films, microwave-discharge-prepared 9-21601  
SiO-Al condensers, breakdown voltage rel. to thickness 9-17430  
SiO films, rel. microscopic surface roughness 9-21531

**Breaking strength** *see Mechanical strength*

**Breeders** *see Nuclear reactors, fission*

from O plasma, statistical props. 9-7133

### Bremsstrahlung

*See also Electrons/radiation; Gamma-ray spectra; Gamma-rays; X-ray spectral/emission; X-rays*  
betatron targets, comparison, obs. 9-15697  
coherent spikes prod. from Si target, collimation tests 9-13103  
cosmic ray, e.m. cascade in Fe, 10<sup>12</sup> eV 9-20683  
double, from e collisions, hard end of spectrum 9-10973  
energies, max., of electron accelerators, scale calibration with photoproton spectrometer 9-2628  
glass, scatt. obs. 9 and 15 MeV 9-11267  
in nuclear charge distrib., calc. of cross-section 9-484  
induced emission, polarization eff. and photon intensity 9-8747  
intensity rel. to energy of electron beam 9-19193  
internal, rel. to identification of mechanism of binary direct reactions 9-13214  
Linac thick-target spectra meas. with large NaI scintillation spectrometer 9-16926  
low approx. arbitrary tensor components 9-10975  
multipole momenta of particles in process with soft  $\gamma$ -quanta determ. 9-10974  
off-mass-shell effects absent in collision of two identical particles with  $g=1$  9-20599  
photons, soft, emission amplitude, quantum and classical low freq. limits 9-8746  
at plasma frequency, calc. 9-2993  
from plasma  $\theta$ -pinch, 0.25-25  $\mu$  9-11565  
polarization in induced emission 9-8747  
potential model, soft-photon theorem 9-16816  
radiation spectrum, rel. to plasma electron distrib. function determ. 9-13422  
relativistic particles, quasiclassical theory 9-8745

### Bremsstrahlung continued

spectra from thick target e irradiation calc., high energy collimation 9-17943  
spectrum, effect of structure of medium 9-8744  
ep test for quantum electrodynamics 9-16807  
K $\rightarrow\pi\pi\pi$  decays, spectra 9-354  
inel collisions, calc. 9-15581  
ip test for quantum electrodynamics 9-16807  
N-N interaction of nuclear potential model anal. 9-18057  
NN $\rightarrow$ NN $\gamma$ , amp. determ. 9-11087  
p-p at 47 MeV, cross section obs. 9-10972  
p-p scatt. cross section obs., 3.2 MeV 9-412  
pp at 99 MeV, cross-section meas., photon ang. distrib. 9-8900  
pp co- and noncoplanar, pot. model calc., kinematic analysis 9-6692  
pp $\rightarrow$ pp $\gamma$ , theory, at 3.2 and 10 MeV 9-13143  
Al glass, scatt. obs. 9 and 15 MeV 9-11267  
<sup>27</sup>Al 3.00 MeV level  $\gamma$  width calc. from nuclear resonant scatt. 9-4744  
Be atom, e bombard. at 1.0, 2.0 MeV, obs. 9-703  
<sup>12</sup>C superallowed positron decay 9-20733  
Fe glass, scatt. obs. 9 and 15 MeV 9-11267  
<sup>31</sup>P 3.13 MeV level  $\gamma$  width calc. from nuclear resonant scatt. 9-4744  
Pb glass, scatt. obs. 9 and 15 MeV 9-11267

### Brightness

*See also Illumination*  
equivalent luminance of any light, as function of scotopic and photopic luminances 9-14446  
field-ion image, comparison for different metals 9-6495  
glare impression, influence of geometry and high luminance light 9-12798  
holographic image, increase by using density relief of photographic emulsion 9-10877  
holography, Fourier luminosity obs. 9-2391  
luminance and spatial factor rel. visual excitability 9-12790  
optimum signal luminance for normal and proton observers 9-4169  
of ramp stimuli, rel. to plateau and gradient widths 9-12791  
visual discrimination with stabilized retinal image 9-12794  
ZnS-Mn(Cu,Cl) films, electroluminescence waves, effect of elec. polarization 9-10261

**Brillouin scattering** *see Scattering/light, Brillouin spectra*

**Brillouin zones** *see Crystal electron states/band structure*

### Brittleness

*See also Breaking strength*  
materials testing of stress states 9-1272  
powder, inorganic crystalline, shock-wave prep., patent 9-9668  
steel alloys, strength 9-5491  
steel casting, embrittlement due to welding, effects of conditions and structure 9-17317  
AgCl, embrittlement, adsorption-sensitive 9-13738  
Cr, temp. threshold, gaseous impurity effect 9-1309  
Cr n irradiation effects on ductility 9-1310  
Fe-(3wt.%)Si alloy polycrystals, twinning effects 9-1124  
Fe and Fe-Si, cold rolling effect on embrittlement 9-1311  
Mo, following neutron irradiation 9-19808  
Mo, temp. threshold, gaseous impurity effect 9-1309  
NiSi<sub>3</sub>, embrittlement mechanism during annealing at 600°C 9-3443  
Sn in contact with binary alloy, brittle rupture temp. and alloy comp. dependence 9-9761  
W, temp. threshold, gaseous impurity effect 9-1309  
Zr-Cu alloys, above 400°C, embrittlement due to O<sub>2</sub> diffusion and reaction 9-11940

### Bromine

atom recomb. in Ar, flash photolysis obs. 300°-1273°K 9-9196  
chemisorption on diamond, heat of wetting, e.s.r. and i.r. spectrum 9-8083  
ions, equilib. charge states in solids and gases in energy range, 10-180 MeV 9-11620  
photochemical reaction with H<sub>2</sub> at room temp. 9-1917  
Br<sub>2</sub>, shock-wave dissoc. in Ar, rate determ. 9-19480  
Br<sub>2</sub>, dissoc. in shock waves 9-13395  
Br<sub>2</sub>, shock-wave dissoc. in Ar, rate determ. 9-13394  
Br<sub>2</sub> in soft carbons, residual lamellar cpds. after heat treatment 9-7362

### Bromine compounds

adsorption on Zr, Ti, Ni, <sup>80</sup>Br nucl. isomers separation 9-18769  
BrF<sub>3</sub>, molecular force field 9-20923  
BrF<sub>3</sub>, coriolis coupling coeffs. 9-18177

### Brownian motion

density field, fluctuating, representation by Markovian process 9-47  
Fokker-Planck eqn., microscopic derivation from Liouville eqn. 9-12894  
nucleation theory, reconsideration 9-7303  
particle diffusion in gases and liquids, analogy with spin diffusion in ferromagnets 9-12895  
Schrödinger-type prob. amplitude in phase-space 9-12893  
sphere in fluid, coupled translational and rot. motions 9-3066  
weak convergence of isotropic scatt. transport 9-17748  
e, displacement in mag. field, probability density calc. 9-8427

**Brush discharges** *see Corona, electric discharge*

### Bubble chambers

120-liter, with magnet for heavy liquids 9-2613  
computer-controlled film, measuring system 9-461  
cryogenic, book 9-6739  
data analysis event selection method 9-6737  
direction measurement variance determination 9-459  
fiducial marks and cameras reconstruction, utilization simultaneous of available photographs 9-11154  
growth of bubbles, expt. exam. 9-6738  
heavy liquid, book 9-6739  
illumination and photography 9-6739  
largest in world, review 9-19248  
one-meter, J.I.N.R. Dubna, six-objective stereoscopic camera 9-2612  
pressure gauge calib. and limit of sensitivity of hydrogen 9-8942  
propane, allowing for Coulomb scatt. and bremsstrahlung in track analysis 9-11153  
pulsed magnetic field 9-19249  
range energy relations for  $\pi$ , K, p. 9-458  
H, liquid, 50 cm diameter, description 9-11152  
He liquid, 80cm for use with Nimrod 9-4691  
He liquid, Northwestern University, 50 cm 9-460  
He liquid utilization 9-8318



**Bubbles***See also Foams*

- air, in water, device for exam. formation and development 9-17181  
 boundary layer treatment of hot inert gas bubbles in chemically reactive liquid stream 9-17182  
 cavitation, collapse velocity rel. to surface tension and viscosity 9-9467  
 cavitation, rectified diffusion, acoustic threshold phenomena 9-5139  
 collapse in compressible fluid 9-19601  
 contact angle with liquid, investigation using deflection of light beam 9-21178  
 gas, in solids, stability 9-21339  
 gas, moving in unbounded viscous medium, shape 9-974  
 gas hold-up and water axial dispersion coeff. in bubble columns 9-21175  
 gas in liq. natural freq. 9-5156  
 growth in bubble chamber, expt. exam. 9-6738  
 growth meas. in uniformly superheated liquids 9-21176  
 growth rate in superheated pure liquids and binary mixtures, expt. 9-21180  
 growth rate in superheated pure liquids and binary mixtures, theory 9-21179  
 incipient fluidizing velocity in gas fluidized beds 9-21010  
 inert gas, nucleation and behaviour in reactor fuels 9-624  
 methanol-water system, mass transfer from single bubbles under distillation conditions 9-18329  
 radius of separation from heated surface during boiling 9-3155  
 size distrib. effect on liq. phase efficiency 9-19600  
 spherical, diffusion of real gas 9-18345  
 vapour void in liq. metals, 0.5 mm probe 9-3074  
 velocity in bounded liquids rel. to surface wave velocity 9-19598  
 Ar in Hg, velocity of rise 9-17183  
 He II, e bubble mobility, calc. 9-9581  
 in  $\text{UO}_2$  after irradi., microstructure, transmission e microscopy 9-11856

**Burgers vector** *see Crystal imperfections/dislocations***Cadmium**

- carrier scatt. between adjacent branches of hole surface 9-12106  
 crystal, hexagonal, hexagonal crystal, thermal and electronic attenuations and dislocation drag 9-19853  
 cyclotron resonance and r.f. dimension effects on drifting effective electrons 9-1442  
 diffusion in CdTe, self-diffusion mechanism 9-1244  
 effusion of gases atoms, ang. number distrib. 9-3062  
 electrodeposition method, patent 9-8108  
 electron-phonon mass enhancement, determ. usieudopot. approaches 9-13827  
 Fermi surface from r.f. size effect meas. 9-5610  
 in GaP, thermal ionization energy 9-5696  
 interfacial energy during growth from melt. 9-18401  
 ion vapour laser, continuous wave 9-17872  
 lasers, ion, CW oscillation at 3250 Å 9-20509  
 molten, sound absorpt. temp. depend. showing existence of dilational viscosity 9-5163  
 poisonin  $\text{H}_2\text{O}$ , non-1/v absorber, decay of thermal neutrons 9-14644  
 r.f. size effect on electrons during cyclotron period 9-3562  
 separation from Cu, Zn by pyrophosphate complex precipitation 9-18748  
 single crystal, cellular substructure, metallographic study 9-7435  
 slip relation for basal glide, primary and secondary, in single crystals 9-3345  
 solid soln. in Ag, thermoelec. power 9-1604  
 spectra, holographic, obtained with Lloyd's mirror 9-4496  
 spin-lattice relax. temp. dependence in metal 9-12510  
 thermal switch for mag. refrigerator 9-175  
 $^{111}\text{Cd}$ , optical pumping with resonance line  $5^1\text{S}_0-5^1\text{P}_1$ , nuclear orientation depend. on mag. field 9-20884  
 $\text{Cd}^+$  mobility calc. in parent vapour 9-5067  
 $\text{Cd}^{2+}$ , complex combinations with the ions  $\text{SO}_4^{2-}$ ,  $\text{Cd}^{2+}$  SCN and the amines aniline, benzidine,  $\beta$ -naptyl amine, o-toluidine and m-toluidine, infrared spectra 9-6969  
 $\text{Cd}^{2+}$  diff. in cubic  $\text{Li}_2\text{SO}_4$ , 600-800°C 9-17288  
d (II), efficient CW laser oscillation at 4416 Å 9-6530  
in In, impurity effect on In phonon spectrum 9-5533  
in Sn, impurity effect on residual resistivity anisotropy, ideal resistivities and deviations from Matthiessen's Rule at 77° and 273°K 9-9962

**Cadmium compounds**

- Au-Cd alloys, phase transforms and structures 9-11835  
 complexes of triphenylphosphine, i.r. spectra 9-20944  
 oscillatory lifetime obs. through photoconductive decay 9-3734  
 wurtzite type, piezoelectric surface oscils. 9-7646  
 Al-Cu-Cd,  $\phi'$  precipitation, effect of Ag and Ge additions 9-1327  
 Au-(47.5 wt.%)Cd, martensitic transformation mechanism 9-5509  
 Cd-CdSe graded single crystal prep. 9-3232  
 Cd-Sb-Zn system solid solution formation, structure and thermo-e.m.f. 9-19835  
 Cd-Zn alloy, carrier scatt. between adjacent branches of hole surface 9-12106  
 cd,  $\text{Hg}_{1-x}\text{Te}$  graded gap structures, photocarrier transport 9-18619  
 Cd complex, bis(hydrazinecarboxylato- N',O) cadmium monohydrate, crystal and mol. structure 9-13630  
 $\text{Cd}_3\text{As}_2$ -ZnAs $_2$  system, solid-soln. growth and semicond. props. 9-13882  
 $\text{CdAs}_2$ , tetragonal, reflectivity spectra 9-19983  
 $\text{Cd}_3\text{As}_2$ , non-parabolic conduction band 9-9893  
 $\text{CdBr}_2$ , first-order lattice Raman spectra 9-12412  
 $\text{CdCl}_2$ , first-order lattice Raman spectra 9-12412  
 $(\text{CdCl}_6^{4-})_x(\text{CH}_3)_2\text{NH}_2^+$ , dielec. props. at two temps., 400-8500 MHz 9-11710  
 $\text{CdCr}_2\text{Se}_4$ , conduction band edge shift near Curie temp. 9-7712  
 $\text{CdCr}_2\text{Se}_4$ , growth by reversible chemical transport 9-18412  
 $\text{CdCr}_2\text{Se}_4$ :Ag, ferromag. resonance 9-16451  
 $\text{CdCr}_2\text{Se}_4$ :Ga initial permeability, photomag. change 9-12215  
 $\text{CdCr}_2\text{Se}_4$ , ferromagnetic, Raman scattering 7°-295°K 9-12409  
 $\text{CdCr}_2\text{Se}_4$ , ferromagnetic, Raman scattering 9-12410  
 $\text{CdCr}_2\text{Se}_4$ , Raman scatt. 9-16421  
 $\text{CdCr}_2\text{Se}_4$  ferromagnetic semiconducting spinel, single crystal p-n junction fabrication and characts. 9-10014  
 $\text{CdF}_2$ :Eu or In, optical and electrical props. 9-5672  
 $\text{CdF}_2$ : $\text{Er}^{3+}$ , impurity exchange interaction probability temp. dependence 9-1716  
 $\text{CdF}_2$ : $\text{Er}^{3+}$ , luminescence spectra 9-3916  
 $\text{CdF}_2$ :at  $1\text{Er}^{3+}$  blue fluorescence, excitation mechanisms, opt. double resonance proc. 9-3925

**Cadmium compounds continued**

- $\text{CdF}_2$ : $\text{Yb}^{3+}$ , optical and e.s.r. spectra 9-1771  
 $\text{CdFe}$  garnet, sublattice magnetization by  $^{57}\text{Fe}$  n.m.r. 9-21671  
 $\text{CdGeAs}_2$ , conductivity, effect of In, Te, Cu and Ga 9-18618  
 $\text{CdGeAs}_2$ , radiative recombination 9-5951  
 $\text{CdGe}(\text{As}_2\text{P}_{1-x})_2$  glasses, optical and thermal carrier activation energies 9-17394  
 $\text{CdGeP}_2(\text{As})_2$ , semicond., generation of second harmonic 9-9969  
 CdI band spectra, 4130-4800 Å, electronic transition  $(B)^2\Sigma^-(X)^2\Sigma$ , spectrographic obs. 9-4920  
 CdI $_2$ , nucleation and epitaxial growth 9-13609  
 $\text{CdIn}_2\text{S}_4$ : $\text{Nd}^{3+}$  or  $\text{Er}^{3+}$  fluorescence 9-14081  
 $\text{CdIn}_2\text{S}_4$ , photoconductivity spectra 9-3733  
 $\text{CdIn}_2\text{S}_4$  photoconductivity 9-3732  
 CdMg alloys, degree of ordering of  $y_a$  and  $y_b$  of  $\alpha$  and  $\beta$  sites, determ. 20-250°C 9-7434  
 $\text{CdMg}$  alloy, order-disorder, 10° to 185°C, obs. 9-11971  
 $\text{Cd}_{1-x}\text{Mn}_x\text{S}$  ( $x \leq 0.4$ ), elec. and opt. props. 9-1516  
 $\text{Cd}(\text{NO}_3)_2$ , soln.,  $\beta$  backscatt. rel. to conc. 9-10367  
 $\text{CdO-B}_2\text{O}_3$ : $\text{SiO}_2$  photocond. glasses, optimization of props. 9-7853  
 CdO, kinetics, knudsen effusion study 9-3158  
 CdO, reflectivity, absorption of thin films, freq. depend. of opt. const., rel. to band struct. 9-3886  
 CdO thin films, optical phonons by e tunneling obs. 9-9814  
 $\text{CdP}_2$ , tetragonal, reflectivity spectra 9-19983  
 $\text{CdP}_2$ , field emission 9-13939  
 $\text{CdS:Au:S}_2$ , impurity diffusion and solubility, vapour pressure investigation 9-3380  
 $\text{CdS:In}$  degenerate, evaporated films, mobility studies 9-12145  
 $\text{CdS:Tm}(\text{Cu})$  phosphors fired in S atmosphere i.r. luminescence 9-5977  
 CdS, exciton transitions, phonon-assisted 9-5966  
 $\text{CdS,Se}_{1-x}$ , photoconductive, acoustoelec. domain 9-3529  
 $\text{CdS,Se}_{1-x}$ , refractive index and birefringence dispersion 9-18691  
 CdS wedge or ring crystals, current oscils. and acoustic amplification 9-5550  
 $\text{CdS}_{1-x}\text{Se}_x$ , spin resonance, photo-induced, of trapped electrons 9-16454  
 $\text{CdS}_{1-x}\text{Se}_x$  single crystals, e.p.r. of  $\text{Mn}^{2+}$  9-3955  
 $\text{CdS,Se}_{1-x}$  graded films, photoconduction 9-3735  
 CdSb, Ag doped, field emission 9-3751  
 CdSb, doped, conductivity, Hall effect and magnetoresistance, 2.2-77°K 9-9972  
 CdSb, optical reflectivity spectra, 300° and 77°K 9-14042  
 CdSb, valence band investigation using transverse thermoelec. power meas. 9-16269  
 CdSb alloy with Fe, Ni, Mn, La and liq. mag. susceptibility 9-16328  
 CdSb molten, optical props. rel. to electronic struct. 9-16002  
 $\text{CdSe-MnSe}$ , phase diagrams 9-19656  
 CdSe, bound exciton-donor complexes, excited terminal states 9-21471  
 CdSe, diffusion and solubility of P, 900 and 950°C, Cd partial pressure dependence 9-11895  
 CdSe, exciton transitions, phonon-assisted 9-5966  
 CdSe, i.r. absorpt. and reflection spectra, rel. to effective masses of conduction electrons 9-10197  
 CdSe, photo-induced e.p.r. of  $^{251}\text{In}$ -state impurity centres 9-20017  
 CdSe, photocurrent saturation mechanism, relaxation oscillations 9-5762  
 CdSe, piezoelec., self-excited perfect u.s. reson. 9-12008  
 CdSe, sensitization to light as result of etching, investig. 9-3917  
 CdSe, surface waves, mech. characts. 9-5439  
 CdSe, u.s. surface wave amplification, expt. method 9-7648  
 CdSe emission of thermal and electroluminescent radiation after applic. of a.c. elec. field 9-3939  
 CdSe film, encapsulated, Hall effect 9-3649  
 CdSe film, encapsulated, Hall effect 9-3649  
 CdSe films, epitaxial growth on NaCl(111) surface 9-7338  
 CdSe mechanism of  $\lambda_m=0.82 \mu$  photoluminescence and parameters of luminescence centres 9-10234  
 CdSe surface u.s. wave amplification using photostimulation 9-7647  
 $\text{CdSiAs}_2$ , radiative recombination 9-5951  
 $\text{CdSiAs}_2$ , semicond., generation of second harmonic 9-9969  
 n-CdSnAs $_2$ , conduction band anisotropy from galvanomagnetic tensor components 9-9984  
 $\text{CdSnP}_2$ , semicond., generation of s 9-9969  
 $\text{CdSnP}_2$  laser, e beam excited 9-245  
 $\text{CdTe:Li}$ , Hall coeff. and elec. conductivity, temp. depend. meas. rel. to effect of dopant 9-12156  
 p-CdTe:P film, resistivity meas. 9-15089  
 $\text{CdTe:Ti}^{2+}$ , optical absorption and e.s.r. 9-1772  
 CdTe, acoustoelec. effect, transverse 9-18560  
 CdTe, atomic displacements and nature of band edge radiative emission 9-16429  
 CdTe, band structure, Green's function method calc. 9-21467  
 CdTe, carrier mobility, Hall mobility and magnetoresistance rel. to elec. and mag. field intensities 9-3622  
 CdTe, diffusion and solubility of Cu, 97-300°C rel. to  $\text{Cu}_2\text{Te}$  film formation 9-11896  
 CdTe, diffusion and solubility of P, 800-1000°C, Cd partial pressure dependence 9-11895  
 CdTe, electrical conductance temp. dependence rel. to ambient partial pressure 9-3644  
 CdTe, exciton transitions, phonon-assisted 9-5966  
 p-CdTe, excitons interactions with opt. phonons in photoconductivity 9-10069  
 CdTe, hexagonal, band structure 9-13826  
 n-CdTe, high-resistivity, elec. and photoelec. props. 9-3621  
 CdTe, light scattering from single particle electron and hole excitations 9-12443  
 CdTe, mean square displacements for sub-lattices 9-19711  
 n-CdTe, optical absorpt. by free carriers 9-5916  
 n-CdTe, photoconductivity, oscillatory, from shallow donors 9-5763  
 n-CdTe, photoelec. props. of surface in contact with electrolytes 9-3727  
 CdTe, self diffusion mechanisms of Cd and Te 9-12444  
 CdTe counters, surface barrier and Mg, B doped, as p- and  $\alpha$ -spectrometers, as p- and  $\alpha$ -spectrometers 9-8937  
 CdTe crystals,  $\text{Hg}^+$  bombardment in formation of  $\text{Hg}_{1-x}\text{Cd}_x\text{Te}$  layers 9-14898  
 CdTe molten, optical props. rel. to electronic struct. 9-16002  
 CdTe semiconductor for p-ray pulse registration 9-6729  
 CdTe, acceptor levels 9-1428  
 $\text{CdTiO}_3$ , preparation and dielectric props. 9-18647

**Cadmium compounds continued**

- CdWO<sub>4</sub>, Co<sup>2+</sup> e.p.r. line half-width, elec. field eff., angular dependence 9-20016  
 Cd<sup>2+</sup>-Co<sup>2+</sup> nitrate soln.,  $\beta$  backscatt. rel. to percentage comp. 9-10367  
 Hg-(0.5-2at%)Cd liq., struct. from X-ray diff. 9-7251  
 In-Cd dilute alloy, In phonon spectrum, effect of Cd impurity 9-5533  
 Mg-Cd alloy, order-disorder phase transition, change in props. 9-16155  
 Mg-Cd alloy, ordering speed, effect on props. 9-16156  
 Mg-Cd alloys, Zenes relaxation, rel. to internal friction 9-11913  
 Mg-Cd single crystal, solid solution hardening investig., conc. and temp. depend. 9-21378  
 Se-CdSe p-n junction, Cl impurity effects on characts. 9-10010  
 Se-CdSe p-n junctions, Tl impurity conc. eff. on characts. 9-5721  
 SiC-CdSe p-n junction, production technology and props. 9-10013

**cadmium sulphide**

- absorption, three-quantum, exptl. obs. of process from luminescence spectra 9-10235  
 acoustic amplification, carrier inhomogeneity effect 9-1383  
 acoustic flux distrib., Brillouin scatt. meas. 9-3907  
 acoustic performance of evaporated films, n.-irrad. effects 9-15002  
 acoustoelectric currents, h.f., and departures from Ohm's Law in thin platelets, linear behaviour 9-13798  
 acoustoelectric domain propag. from Brillouin scatt. obs. 9-1517  
 acoustoelectric domains, direct observation 9-3528  
 acoustoelectric eff., Brillouin scattering study at microwave freq. 9-12013  
 acoustoelectric effect, transverse 9-18560  
 acoustoelectric effect, u.s. attenuation and trapping 9-7650  
 acoustoelectric effect of amplified acoustic oscillations, multitransit noise 9-3530  
 acoustoelectric interaction, Fabry-Perot analysis 9-12010  
 amplified acoustic flux growth, in freq. of max intensity 9-9834  
 Brillouin scattering, stimulated, laser-induced 9-3906  
 conductivity storage, model 9-13929  
 contact resistance with In and In-Ga 9-3613  
 crystals with edge emission, i.r. effects on luminescence, photocond., and conductivity glow curves 9-21644  
 current noise induced by electron-phonon interaction 9-5686  
 dislocations, electronic energy states 9-7487  
 edge emission, green and blue, at 4.2°K 9-14074  
 edge emission bands 9-15188  
 electron beam pumping, 260 keV, stimulated emission to  $3 \times 10^8$  W/cm<sup>2</sup> 9-20523  
 electron microscope obs. 9-7453  
 electron microscopic images and anomalous bend extinction in a single crystal 9-3287  
 electron mobility in high electric fields 9-13825  
 electron-hole direct recomb., photoexcitation 9-16261  
 electronic energy states of dislocations 9-7487  
 epitaxial films, vapour phase chemical reaction growth technique 9-9616  
 epitaxial growth on InSb and CdS substrates, cubic CdS 9-14910  
 e.p.r., photo-induced, of <sup>71</sup>Si<sub>112</sub>-state impurity centres 9-20017  
 e.s.r. meas. 9-5983  
 exciton complexes, bound, excited states 9-9904  
 exciton emission oscs in excitation spectra 9-12489  
 excitons, dynamical behaviour, correlation between intrinsic absorpt. and emission 9-14049  
 film, photovoltages, larger-than-bandgap., generation and decay mechanism 9-15136  
 film, thin, surface props., u.h. vacuum system for preparation and expt. 9-16038  
 films, photoconductivity recombination centres 9-10068  
 Hall mobility of photoelectrons 9-5761  
 hole mobility, field effect photocurrent obs. 9-1612  
 internal friction temp. dependence, 300-700°K and mechanism 9-1268  
 ionic surface states from band-edge method 9-5618  
 Lamb u.s. waves, excitation 9-5539  
 laser, electron-beam-pumped, standing waves and single-mode room temp. laser emission 9-19151  
 luminescence, green edge, mechanism and luminescence centre parameters 9-14075  
 luminescence, long-wavelength bands, flash excitation 9-16427  
 optical absorption due to intrinsic defects 9-3887  
 opto-electronic (slow) phenomena, photochemical interpretation 9-21547  
 oscillations, rippled, in transient of first current saturation, round trip period 9-11995  
 phosphors, i.r. luminescence and role of cation vacancies 9-12467  
 photoconductive, depolarization field eff. on electro-elastic props. 9-17439  
 photoconductive, negative resistance and relax. effect of conductivity at low temp. 9-5764  
 photoconductivity, oscillatory phase 9-1613  
 photoconductivity in vicinity of absorption edge 9-1611  
 photoconductors, g-r noise dependence on light penetration depth 9-12211  
 photocurrent, isothermal decay, trap mechanism 9-18655  
 photoluminescence, orange red and i.r., mechanism, and centre parameters 9-5976  
 photosensitive, field-effect 9-10067  
 plate-shaped crystals, inclusions and Si contamination, electron microprobe and e microscope investig. 9-5343  
 polarity, crystallographic, A wurtzite, He<sup>+</sup> ion. scatt. obs., 2 keV 9-9635  
 polarization, spontaneous estimation from refractive indices and Pockels coeff. 9-7936  
 radiation recombination excited by fast electrons 9-3915  
 Raman scattering, spin-flip mechanism 9-12413  
 Raman scattering, spin-flop 9-10219  
 Raman spectra cross sections, temp. depend. 9-12428  
 Rayleigh wave amplification theory 9-18557  
 resonant Raman eff. 9-12411  
 semiconducting, acoustoelec. effect rel. to anisotropic dielec. and piezoelec. props. 9-12009  
 semiconducting, spatial and time variation of elec. fields 9-13874  
 single crystal phosphorescence, photoconductivity and trap distrib. 9-16440  
 stacking faults, Hg diffusion-induced 9-7496  
 substrate, ZnTe epitaxial film prep. by vapour transport method 9-5245  
 surface states and photocurrent pinch off effect 9-7855  
 surface waves, mech. characts. 9-5439  
 surface waves with allowance for piezoelectric effect 9-18555

**Cadmium compounds continued****cadmium sulphide continued**

- thermal conductivity anisotropy, in annealed electron-irrad. CdS, low temp. obs. 9-9853  
 thin film solar cell, design and space applic. 9-2319  
 thin films, optical phonons by e tunneling obs. 9-9814  
 transducer, multilayer piezoelec. method of c axes flipping 9-10055  
 trap depth and density determ. by space-charge-limited currents 9-10070  
 u.s. resonance, self-excited perfect, in piezoelec. cryst. 9-12008  
 u.s. wave generation by u.s. pulses traversing crystal in alternating elec. field 9-1382  
 , semiconducting, acoustoelec. domain formation 9-1515  
 CdS:Cl, impurity conduction at low temperatures 9-3620  
 CdS:Li<sup>+</sup>, habit change on increasing Li<sup>+</sup> content 9-1184  
 CdS:Na, growth in form of hollow hexagonal pyramids 9-13599  
 CdS MnS, phase diagrams 9-19656  
 CdS, laser action involving free excitons and LO-phonon-assisted transitions, theory 9-6522  
 CdS oriented films, semicond. charact., use of surface vib. meas. method 9-18625  
 Cd(S<sub>0.9</sub>Se<sub>0.1</sub>), photoconductivity gain, steady-state and pulse meas. 9-7854  
 CdS<sub>1-x</sub>Se<sub>x</sub> films, structure defects on optical and elec. props. 9-9973  
 Cd<sub>1-x</sub>Se<sub>x</sub>, u.v. reflectivity spectra at 90°K 9-10187  
 crystal, Rayleigh wave, electron interaction 9-5697

**Caesium**

- absorption on insulating substances 9-5258  
 addition to liquid Na, effect on e.p.r. 9-13541  
 adsorbed on insulating substrates, elec. conduction mechanism 9-5641  
 adsorption on W, meas. via thermionic emission props. 9-11785  
 atom, doublet suppression in foreign gases 9-13288  
 atom, e excitation of 6<sup>2</sup>P states 9-4850  
 atom, elec. dipole moment; upper limit, and for electron 9-11384  
 atom, electron-impact ionization 9-9400  
 atom source, charge-exchange, fast 9-11415  
 atoms, elec. dipole moment upper limit, obs. 9-4835  
 c liquid, isothermal compressibility 9-19596  
 conductivity, electrical, temp. var. calc., comparison with expt. 9-16231  
 contacts on Si, prep. and barrier height 9-13907  
 diode, thermionic converter 9-6465  
 Electronic structure calcs. using Wigner-Seitz cell method and polymorphic transitions 9-5614  
 films, optical props., rel. to thickness, 2300-11000 Å 9-15174  
 isotope shift in D<sub>1</sub> line, atomic beam meas. 9-18137  
 laser, chemical reaction with I vapour for depletion of ground state population, patent 9-8618  
 metal, oxygen concentration by vacuum distribution 9-648  
 molecular beam reaction with RbCl 9-10310  
 photoelectrons ejection by circularly polarized light, spin orientation meas. 9-20888  
 plasma, current carrying, ion wave propagation 9-11546  
 plasma, drift waves 9-11600  
 plasma, ion acoustic waves 9-17124  
 plasma, ionic diagnostics using grid probe 9-5039  
 plasma, low temp., optical and probe obs. comparison 9-11588  
 plasma, magnetically confined, radial diffusion, radial electric field effect 9-14758  
 plasma, thermally generated, non-linear interactions of e.m. waves 9-7159  
 plasma in Q machine, confinement time meas. 9-14782  
 plasma production from Ta cavity, 1400°K 9-11591  
 population inversion during optical excitation of <sup>71</sup>P<sub>1/2</sub> level 9-686  
 reaction with C blocks, 350°-550°C 9-6004  
 second doublet, broadening by inert gases 9-2814  
 spectral line broadening due to Ar, Ne presence 9-19400  
 thermally ionized plasma, destruction of coherent motion 9-17129  
 vacancy-produced lattice distortion, calc. by method of lattice states 9-21332  
 vapour, charge exchange with H<sup>+</sup>, 0.5-20 keV obs. 9-13314  
 vapour, optically oriented spin system, theory of double refraction 9-9115  
 vapour, photon echoes 9-10848  
 vapour cells as hyperfine filters for optical pumping 9-19406  
 vapour injection into vacuum device, O<sub>2</sub> and water vapour trapping 9-10585  
 vapour with impurity, plasma decay at elevated pressure in inert gases 9-4998  
<sup>133</sup>Cs, isotope shift in resonance lines of CsI spectra, against <sup>133</sup>Cs 9-6962  
<sup>133</sup>Cs atom collisions, spin-exchange cross-section obs. 9-9152  
<sup>133</sup>Cs reson. in zeolites, chem shift 9-4924  
<sup>133</sup>Cs in human body following atomic tests, possible sources in bread and milk 9-1943  
 Ag, Cs/Cl, NO<sub>3</sub> liquid-liquid and solid-liquid equilibria 9-18380  
 Cs:Pt:ZnS forward biased Schottky barrier electron emission 9-16317  
 Cs-Ar mixtures low voltage Krundens, arcs 9-9424  
 Cs thermionic diodes, e. beam reflections effects 9-8584  
 Cs<sup>+</sup> ions, scatt. by W surface 9-5231  
 Cs<sub>2</sub>, i.r. absorpt. spectrum 9-4923  
 Cs<sup>+</sup>-inert gas nearly adiabatic thermal collisions, excitation transfer, Stuckelberg's formula and difficulties 9-18154  
 GaAs-Cs photocathode, photoemission, effect of Sb(Te) on surface 9-12225

**Caesium compounds**

- CsF sp. ht., phonon branches calc. from shell model lattice dynamics 9-7633  
 CsI sp. ht., phonon branches calc. from shell model lattice dynamics 9-7633  
 halides, Debye-Waller factors of <sup>133</sup>Cs and <sup>129</sup>I 9-11986  
 pollicite, crystal, location of Na, Cs and water mols. 9-7436  
 (Ag+Rb or Cs)NO<sub>3</sub>, molten, thermoelec. power 9-3119  
<sup>35</sup>Cl, r.f. Stark spectrum, mol. beam elec. resonance meas. 9-7036  
 Cs-C black system, phase equilibria, CS content rel. to press. 9-7620  
 Cs-Sb photocathodes, processing on glass substrates, photoresponse and build-up time meas. 9-15146  
 Cs<sub>2</sub>HfCl<sub>6</sub>:Os<sup>4+</sup>, optical spectra at 4.2°K 9-14055  
 Cs<sub>2</sub>ZrCl<sub>6</sub>:Os<sup>4+</sup>, optical spectra at 4.2°K 9-14055  
 Cs<sub>2</sub>BeF<sub>4</sub>, crystal structure 9-13633  
 CsAu, electronic band struct. and metallic character 9-15055  
 CsBr, dissoc., invented population 9-822  
 CsBr, F-to-M colour centre photochem. conversion mechanism 9-5384



**Caesium compounds continued**

- CsBr, specific heat, meas. and related thermodynamic props., 20°-300°K. 9-5568  
 CsBr, thermal expansion temp. dependence 9-12022  
 CsBr colour centre formation and conversion mechanism 9-7501  
 CsBr sp. ht., phonon branches calc. from shell model lattice dynamics 9-7633  
 CsBr(l), heat capacity analysis in terms of lattice freq. spectrum 9-9839  
 CsCl:Ba<sup>2+</sup>, ionic conductivity 9-3701  
 CsCl, elec. cond. obs. rel. to phase transform. kinetics 9-11963  
 CsCl, lattice dynamics and sp. ht. 9-7634  
 CsCl, sp. ht., phonon branches calc. from shell model lattice dynamics 9-7633  
 CsCl, stress-optical dispersion meas. 9-5873  
 CsCl colour centre formation and conversion mechanism 9-7501  
 CsCl effusion, ang. number distrib. 9-3063  
 CsCl effusion, ang. number distrib. 9-9460  
 CsCl finite ellipsoid, low-temp. behaviour of dielec. consts., quasi-harmonic approx. 9-10027  
 CsCl<sub>4</sub>(SCN<sub>2</sub>H<sub>4</sub>).H<sub>2</sub>O crystal structure 9-3288  
 Cs<sub>2</sub>CoCl<sub>4</sub> cryst., n.m.r. of <sup>133</sup>Cs 9-17503  
 CsCr(SO<sub>4</sub>)<sub>2</sub>.12H<sub>2</sub>O, crystal structure and classification 9-7445  
 Cs<sub>2</sub>CuCl<sub>4</sub> (or Br<sub>4</sub>), cryst., n.m.r. of <sup>133</sup>Cs 9-17503  
 CsF, r.f. Stark spectrum, mol. beam elec. resonance meas. 9-7036  
 CsF, second-order Raman spectra calc. for vibration spectra computation 9-12429  
 CsI:Mn<sup>2+</sup>(Eu<sup>2+</sup>), thermal treatment, e.p.r. spectra comparison with luminescence of CsI 9-20028  
 CsI, luminescence rel. to TI conc. 9-7987  
 CsI:Ti, X-ray luminescence, excitation intensity dependence 9-16442  
 CsI, Debye-Waller factors of <sup>137</sup>I 9-11986  
 CsI, energy band calcs., using Green's function method 9-1429  
 CsI, exciton peaks shift with press. and deform. potentials 9-12067  
 CsI, impurity additions effect on strength 9-18514  
 CsI, luminesc. kinetics 9-16448  
 CsI, photoemission spectra, L-bands and exciton bands 9-3759  
 CsI, recoilless fraction of 26.8 keV transition of <sup>129</sup>I, calc. using Debye model of phonon spectrum 9-12359  
 CsI, second order Raman scattering spectrum 9-17481  
 CsI, stress-optical dispersion meas. 9-5873  
 CsI photocathode tube containing channel electron multiplier 9-17894  
 CsI(Tl)<sup>+</sup> e.p.r. spectra obs., trapped holes determ. in CsI luminescence 9-20028  
 CsI(Tl) optical nonuniformity obs. 9-12482  
 CsI(Tl) stopping power and luminescent-response calcs. 9-12035  
 Cs<sub>2</sub>LiCo(CN)<sub>6</sub>, crystal structure 9-13632  
 CsMnCl<sub>4</sub>.2H<sub>2</sub>O, antiferromagnetism, linear chain type 9-14010  
 Cs<sub>2</sub>MnCl<sub>4</sub>.2H<sub>2</sub>O, cryst. elec.-field-gradient determ. by n.q.r. 9-8047  
 CsMnF<sub>3</sub>, antiferromagnet, critical fluctuations, e.p.r. studies 9-18735  
 CsNO<sub>2</sub>:VO<sup>2+</sup>, e.p.r. 9-3961  
 CsNO<sub>3</sub> molten salt, <sup>137</sup>Cs mobility meas. by paper electrophoresis 9-19614  
 CsNO<sub>3</sub>, interdiffusion in dilute solns. of AgNO<sub>3</sub> 9-7261  
 CsNO<sub>3</sub>, crystal structure 9-1185  
 CsOH, matrix-isolated i.r. spectra 9-761  
 CsPbCl<sub>3</sub>, formation in vaporization of PbCl<sub>2</sub>+CsCl mixtures, thermodynamic props. from mass spectra 9-19442  
 CsPbCl<sub>3</sub>, superstructure phase transition 9-21407  
 Cs<sub>2</sub>Sb, films, photoemissive quantum yield and phase transition 9-3756  
 Cs<sub>2</sub>Sb, thin films production electrical and optical properties 9-5246  
 CsTe photocathode u.v. quantum efficiency, e.-irrad. effects, 1-2 MeV 9-12224  
 Cs<sub>2</sub>UBr<sub>6</sub>, electronic and vibronic structure from Zeeman effect obs. 9-7972  
 Cs<sub>2</sub>UCl<sub>6</sub>, electronic and vibronic structure from Zeeman effect obs. 9-7972  
 Cs<sub>2</sub>(UO<sub>2</sub>)NO<sub>3</sub>, exciton migration and quenching during cooling 9-5620  
 Cs<sub>2</sub>ZnCl<sub>4</sub>:Fe<sup>2+</sup>, e.s.r. determ. of interstitial dopant sites 9-8025  
 Cs<sub>2</sub>ZnCl<sub>4</sub> cryst., n.m.r. of <sup>133</sup>Cs 9-17503  
 Cs-graphite cpds, lamellar, Mossbauer study of chem. bonding 9-7353

**Calcium**

- atom, electron impact excitation, cross-section, 9.5 and 15.5 eV 9-13303  
 atoms and ions, bibliography of spectra 9-13287  
 Ca<sup>2+</sup> in NaCl, vacancy conc. determ. by density change 9-9703  
 diffusion in CaF<sub>2</sub>, process during uptake of excess Ca 9-9729  
 electron prod. in H<sub>2</sub>-N<sub>2</sub>-O<sub>2</sub> flames, meas. by enthalpy changes and equilib. consts. 9-12534  
 energy-band struct. and Fermi surface under press. 9-15054  
 excitation of 5s6s<sup>2</sup>S<sub>1</sub> level, cascade transition line intensities obs. 9-9134  
 liquid, surface tension and density, temp. dependence obs. 9-5149  
 oxidation, reaction kinetics 9-10340  
 solar chromosphere, H, K and subordinate lines formation 9-21979  
 in solar spectrum, red auto-ionizing lines 9-15355  
 stopping power for 5-12 MeV protons and deuterons 9-17364  
 vaporization mass spectrometric study 9-19386  
 X-ray K-absorpt. fine structure obs. 9-21639  
 Ca I, two-electron spectra, config. mixing and oscillator strengths 9-19398  
 Ca II, semiempirical atomic core potentials, coeffs. 9-19397  
 Ca II emission in spectra of  $\gamma$  Virginis 9-21885  
 Ca II K-line and H $\alpha$  line in solar spectrum simultaneous obs. method 9-17652  
 Ca III, spectrum, revised and extended anal. 9-18136  
 Ca XIII-XV, u.v. spectrum obs. 9-6972  
 Ca<sup>2+</sup> diff. in cubic Li<sub>2</sub>SO<sub>4</sub>, 600-800°C 9-17288  
<sup>40</sup>Ca-<sup>40</sup>Ar, mass diff. by high resolution mass spectrometer 9-13309

**Calcium compounds**

- CaCO<sub>3</sub>, twinning dislocations repeated reciprocal motion, initial fatigue stages 9-18468  
 calcia, elastic constants at 16 GHz and 4.2°K 9-17296  
 calcite, dielec. const. and loss, variation with temp. and freq. 9-10026  
 calcite, elastic constants temp. dependence, 160°-300°K 9-14963  
 calcite, stimulated Raman scatt. 9-1770  
 CaO-Nb<sub>2</sub>O<sub>5</sub>-TiO<sub>2</sub> system, phase equilibrium study 9-3496  
 heat treated with C under press., effect on C (002) diff. profiles 9-10595  
 hydroxides, gaseous, dissoci. energies and conc. in fuel-rich H<sub>2</sub>+O<sub>2</sub>+N<sub>2</sub> flames 9-17517  
 hydroxy apatite, dielec. relax. 9-7837  
 lime refractories, sintered and fused, props. 9-3461  
 CaPt(CN)<sub>4</sub>.5H<sub>2</sub>O isotopic structure 9-21310

**Calcium compounds continued**

- Ca<sub>10</sub>(CeO<sub>3</sub>)CrO<sub>3</sub>, polycrystalline, dielectric const. and resistivity, temp. depend. 9-18645  
 Ca<sub>10</sub>(PO<sub>4</sub>)<sub>6</sub>F<sub>2</sub>, Davydov splittings of PO<sub>4</sub><sup>3-</sup> vib. 9-16167  
 Ca<sub>11</sub>N, crystal structure 9-14916  
 Ca<sub>3</sub>(PO<sub>4</sub>)<sub>2</sub>:F:Nd<sup>3+</sup>, absorpt., luminescence spectra and stimulated emission 9-18709  
 Ca V Bi Fe garnet, conduction mechanism by conductivity and thermoelec. power meas. 9-1458  
 Ca V garnets, preparation rel. to device applications 9-7910  
 Ca(NH<sub>2</sub>SO<sub>3</sub>)<sub>2</sub>, Raman and i.r. spectra 9-12458  
 CaAl<sub>2</sub>Si<sub>2</sub>O<sub>8</sub>, <sup>27</sup>Al NMR obs. at high temp. 9-10293  
 Ca<sub>3</sub>Al<sub>2</sub>(SiO<sub>4</sub>)<sub>2</sub>, garnet, grossularite, <sup>27</sup>Al n.m.r. 9-12509  
 CaB<sub>6</sub>, refractive index, extinction coeff. and absorpt. coeff. from reflection meas. 9-5866  
 CaB<sub>2</sub>O<sub>4</sub>, polycryst., <sup>11</sup>B n.m.r. 9-1873  
 CaCO<sub>3</sub>, Ca<sup>2+</sup> K-absorpt. fine structure obs. 9-21639  
 CaCO<sub>3</sub>, Ca<sup>2+</sup> K-absorpt. fine structure obs. 9-21639  
 CaCO<sub>3</sub>, elastic const. and force fields 9-19780  
 CaCO<sub>3</sub> calcite, deformed, colour centre form. by X-rad. 9-3364  
 CaCO<sub>3</sub> calcite, deformed, colour centre form. by X-rad. 9-16105  
 CaCO<sub>3</sub>, phase transitions, ultrasonic vel. study to 20 kb and 180°C 9-9825  
 CaCl<sub>2</sub>-KCl-H<sub>2</sub>O soln., isopiestic vapour press. meas., osmotic and activity coeffs. 9-21187  
 CaCO<sub>3</sub>:Mn<sup>2+</sup> e.s.r., superhyperfine interaction of Mn<sup>2+</sup> with <sup>13</sup>C 9-5987  
 Ca<sub>2</sub>(CrO<sub>4</sub>)<sub>2</sub>(PO<sub>4</sub>)<sub>2</sub>Cl, 80°K cryst. spectrum 9-3885  
 CaF<sub>2</sub>:Ce<sup>3+</sup>-H<sup>+</sup>(D<sup>+</sup>), e.s.r. spectra, interstitial location of ions, charge compensators 9-1857  
 CaF<sub>2</sub>:Dy<sup>3+</sup> solid laser, sun-pumped, 130 mW power output 9-13031  
 CaF<sub>2</sub>:Er<sup>3+</sup>, luminescence spectra 9-3916  
 CaF<sub>2</sub>:Nd<sup>3+</sup>(H<sup>+</sup>), e.s.r. spectra, interstitial location of ions, charge compensators 9-1857  
 CaF<sub>2</sub>:U<sup>3+</sup>, nuclear spin diffusion coeff. meas. 9-17467  
 CaF<sub>2</sub>:Ho<sup>3+</sup>, X-irrad., optical emission 9-21657  
 CaF<sub>2</sub>:La,Ce,Gd,Tb, linear dichroism of absorption band 9-14048  
 CaF<sub>2</sub>, rare-earth doped, photochromic parameters for electro-optic applications 9-19978  
 CaF<sub>2</sub> single crystals mixed with SrF<sub>2</sub> or BaF<sub>2</sub> single crystals, microhardness 9-11942  
 CaF<sub>2</sub>-SrF<sub>2</sub> mixed crystal, Raman scattering from point defects 9-12408  
 CaH<sub>2</sub>, crystal structure by X-ray diff. 9-18542  
 CaH<sub>2</sub> vaporization mass spectrometric study 9-19386  
 Ca(H<sub>2</sub>PO<sub>4</sub>)<sub>2</sub>.H<sub>2</sub>O and deuterated analogue, H<sub>2</sub>PO<sub>4</sub><sup>-</sup> and H<sub>2</sub>O vibr., 4000-200 cm<sup>-1</sup> 9-15872  
 CaH mol. absorpt. spectra, A<sup>2</sup> $\Pi$ -X<sup>2</sup> $\Sigma$  and B<sup>2</sup> $\Sigma$ -X<sup>2</sup> $\Sigma$  systems study 9-18180  
 CaI<sub>2</sub>.4H<sub>2</sub>O apparent molal expansibility and volume obs. 9-986  
 Ca(Mg, Fe)<sub>3</sub>(PO<sub>4</sub>)<sub>6</sub>, stanfieldite, in meteorites, Mg:Fe ratio obs. 9-12758  
 Ca<sub>1-x</sub>Mg<sub>x</sub>(PO<sub>4</sub>)<sub>2</sub>:Eu<sup>2+</sup>, luminescence 9-3914  
 CaMoO<sub>4</sub>, refractive index, pressure dependence 9-16393  
 Ca(NO<sub>3</sub>)<sub>2</sub>-Ba(NO<sub>3</sub>)<sub>2</sub>-Sr(NO<sub>3</sub>)<sub>2</sub> binary fused systems, Raman spectra obs. of structure 9-17186  
 CaNi(CN)<sub>4</sub>.5H<sub>2</sub>O, isotopic structure 9-21310  
 CaO:Tm<sup>3+</sup>, reduction of Tm<sup>3+</sup> to Tm<sup>2+</sup> on  $\gamma$ - and e-irrad., e.s.r. obs. 9-10277  
 CaO-Al<sub>2</sub>O<sub>3</sub>-MgO-BaO-B<sub>2</sub>O<sub>3</sub> glasses, Na-vapour resistant up to 700°C 9-4001  
 CaO-FeO-Al<sub>2</sub>O<sub>3</sub>, solid soln., X-ray and microscopic obs. 1050° and 1200°C 9-16147  
 CaO-MgO-Al<sub>2</sub>O<sub>3</sub>-SiO<sub>2</sub> glasses, crystallization kinetics, iron oxide addition effects 9-19688  
 CaO-Sb and CaO-Bi phosphors with wide forbidden zone, radical recombination luminescence, mech. 9-16428  
 CaO-Ta<sub>2</sub>O<sub>5</sub>-SiO<sub>2</sub> system, phase diagram for melting relations 9-7300  
 CaO, additively colored, F<sup>+</sup> and F centre obs. 9-13698  
 CaO, computed ground state props. in molecular orbital approx. 9-7015  
 CaO, deformations under press. and temp. 9-5448  
 CaO, dense, fracture and strength 9-7567  
 CaO, F-band obs. by Faraday rotation and Faraday rotation-e.s.r. 9-21342  
 CaO, F-centres, Faraday rotation studies 9-3362  
 CaO ceramic crystals, recrystn. in forging and annealing 9-3482  
 CaO coloured crystal, fluorescence of 3.7 eV F-centre absorption band 9-3924  
 CaO microcrystal, lattice const. and energies study 9-17270  
 CaO stabilizing additive to ZrO<sub>2</sub> ceramics, volatilization 9-21252  
 CaO+, electronic absorption spectrum 9-10195  
 12CaO.7Al<sub>2</sub>O<sub>3</sub> fluoride derivative, crystal structure 9-17265  
 Ca<sub>3</sub>(PO<sub>4</sub>)<sub>2</sub>:Eu<sup>2+</sup>, luminescence in  $\alpha$ - and  $\beta$ -phases 9-3914  
 Ca<sub>10</sub>(PO<sub>4</sub>)<sub>6</sub>(OH)<sub>2</sub>, hydroxy apatite, dielec. relax. 9-7837  
 CaPd(CN)<sub>4</sub>.5H<sub>2</sub>O, isotopic structure 9-21310  
 CaPd(CN)<sub>4</sub> crystals, dichroism 9-16396  
 CaS:Ce, thermally stimulated currents and trap depths 9-21546  
 Ca(S:Se):Mn<sup>2+</sup> luminescent props. and EPR 9-3957  
 CaS, shear-induced coloration, obs. 9-1745  
 CaSO<sub>4</sub>.2H<sub>2</sub>O, dispersed porous mat., microstresses on pressing giving plastic deform., X-ray exam. 9-1276  
 CaSO<sub>4</sub>.2H<sub>2</sub>O (gypsum), birefringence study by 9 mm. interferometry rel. to electrical axis and permittivities 9-7943  
 CaS<sub>2</sub>O<sub>6</sub>.4H<sub>2</sub>O, optical activity in vibration-transition region 9-7941  
 CaSnO<sub>3</sub>, suitable source for Mossbauer studies 9-12358  
 CaSn(OH)<sub>6</sub>, crystal structure from n. diff., i.r. absorpt. and n.m.r. 9-19709  
 CaTiGeO<sub>3</sub>, synthetic, cryst. struct., unit cell and space group compared with CaTiSiO<sub>3</sub> 9-5317  
 CaTiO<sub>3</sub>, prebreakdown processes 9-18651  
 CaTiSiO<sub>3</sub>, synthetic, cryst. struct., unit cell and space group, compared with CaTiGeO<sub>3</sub> 9-5317  
 CaUF<sub>6</sub>, X-ray powder diffraction investigation of structure 9-11838  
 CaV garnet, Curie pt. rel. to crystal chemistry 9-14005  
 CaWO<sub>4</sub>:Ce<sup>3+</sup>, e spin echo envelope modulation by very small alternating mag. field 9-10282  
 CaWO<sub>4</sub>:Nd<sup>3+</sup> solid laser, sun-pumped, 130 mW power output 9-13031  
 CaWO<sub>4</sub>:Tb<sup>3+</sup>, ground term energy level analysis 9-12373  
 CaWO<sub>4</sub>-Al fluorescent screen for high stress conditions, vacuum evaporated 9-13069  
 CaWO<sub>4</sub>:Nd<sup>3+</sup>, Lande factor of excited state by Cotton-Mouton eff. 9-18698  
 CaWO<sub>4</sub>, e.p.r. of Er<sup>3+</sup>, spin-Hamiltonian parameters determ. 9-12500

**Calcium compounds continued**

- CaWO<sub>4</sub>, phototropy, reddish-purple after irradiation by U.V. light 9-3866  
 CaWO<sub>4</sub>, refractive index, pressure dependence 9-16393  
 CaWO<sub>4</sub>, single crystal, defect states, origin, thermoluminescence investigation 9-12042  
 CaWO<sub>4</sub>, paramagnetic thermoluminescent colour centres 9-19757  
 CaZr(PO<sub>4</sub>)<sub>2</sub>, thermal decomposition, 1450-1700°C 9-3989  
 Cu-Al, transition of Gd 4f electrons from bound to virtual levels 9-1462  
 FeO-CaO thermoelectric power, 1150-1470°C 9-1606

**calcium fluoride**

- covalency evidence in Tm<sup>3+</sup> and Yb<sup>3+</sup> 9-11791  
 diffusion of <sup>89</sup>Sr 9-3379  
 diffusion processes during uptake of excess Ca 9-9729  
 dosimeter thermoluminescent, using powder 9-2599  
 edge dislocation mobility stress-temperature dependence 9-14945  
 elastic constants, pressure and temperature derivatives 9-1262  
 endor ultrasonic of U<sup>4+</sup>, absorption line broadening by superhyperfine interaction 9-15209  
 e.p.r. line of <sup>47</sup>Ti, for valency determination 9-10276  
 F centre hyperfine interactions, endor measurements 9-1234  
 free induction decay, theory and experiment, comparison 9-5982  
 interaction mechanism of Nd<sup>3+</sup> ions and nature of concentration quenching 9-15161  
 optical transition energy 1s-2p for F-centres 9-3363  
 phonon detector, acoustical, using Tm<sup>3+</sup> impurity ion 9-5524  
 seal to steel, high pressure and temperature 9-6233  
 thermoluminescence relative to colour centres and d.c. resistivity in irradiated crystals 9-14092  
 Ca<sup>19</sup>F<sub>2</sub>:Ce<sup>3+</sup>, Yb<sup>3+</sup>, presence of F<sup>-</sup> confirmed by ENDOR OBS. 9-8045  
 CaF<sub>2</sub>:D<sup>2+</sup> crystal, giant pulses, generation using LiNbO<sub>3</sub> crystal, electro-optical shutter 9-1723  
 CaF<sub>2</sub>:Er<sup>3+</sup>, impurity exchange interaction probability temperature dependence 9-1716  
 CaF<sub>2</sub>:Eu<sup>2+</sup>, relaxation effect from e.s.r. signals using optical Faraday rotation 9-7945  
 CaF<sub>2</sub>:Eu<sup>2+</sup>:Ho<sup>3+</sup>, fluorescent decay of Eu<sup>2+</sup> as function of Ho concentration 9-15187  
 CaF<sub>2</sub>:Eu<sup>2+</sup>, microwave-modulated fluorescence, 9.5 GHz 9-1828  
 CaF<sub>2</sub>:Gd<sup>3+</sup>, Zeeman data of Gd<sup>3+</sup> in sites of cubic symmetry 9-10196  
 CaF<sub>2</sub>:Ho<sup>3+</sup>(<sup>2+</sup>), magnetic circular dichroism in absorption bands 9-1737  
 CaF<sub>2</sub>:V<sup>3+</sup>, electron-nuclear double resonance 9-16472  
 CaF<sub>2</sub>:Eu<sup>2+</sup>, Zeeman effect and fluorescent lifetime measurements, temperature dependence 9-14050

**Calculating apparatus**

- See also *Fourier analysis*; *X-ray crystallography/calculational apparatus*  
 bidimensional data acquisition system 9-4180  
 conditioner with integrated circuits, for *n* time-of-flight experiment, data selection 9-2565  
 hardware and software for nuclear physics 9-22014  
 multiscale analysis, for periodic signals incommensurate with the timing signal 9-20278  
 on-line programmed desk, use with pulse height analyzer for peak integration 9-2603  
 simulation of one-dimensional counting spectra 9-6225  
 stacking register, simultaneous input/output buffer, description 9-4419

**analogue apparatus**

- See also *Nomograms*  
 amplitude ratio of two signals, analogue measurement method 9-20482  
 chemical kinetics experiment, analogue simulation for college students 9-17679  
 contour mapping circuit for display of scanned information 9-14289  
 conversion of analogue voltage in dual no., improved method 9-4176  
 on-line computation of reactivity using integrating system 9-9101  
 ray tracing in layered atmosphere, computation 9-17798  
 statistical analyser with up-dated histogram display 9-2182

**digital computer programmes**

- alkanes, linear, dimensions calculation and use in theory of diffusion in liquid solution 9-17046  
 atomic orbitals 9-9131  
 Bragg X-ray intensity correction for thermal diffuse scattering 9-19702  
 CHAFFER, for chemical reactions thermodynamic data evaluation 9-20279  
 coincidence circuit triple, statistical parameters 9-20707  
 colour, luminance and true temperatures, solution of conversion relationships 9-8538  
 for configurational interaction calculation of molecular excited states 9-17019  
 Copolymerization behaviour, binary and ternary, calculations 9-17522  
 copolymers and terpolymers, chemical reactions calculations 9-10337  
 for crystal band structure population analysis 9-9887  
 crystal structure amplitude sign determination by Karle-Hauptmann method 9-13623  
 DICANNE processor for noise cancellation at receiving arrays 9-19072  
 electric circuit transient state analysis, application 9-6456  
 elementary particle interactions, Monte Carlo method investigation 9-10965  
 e.p.r. spectra in solution, least squares curve fitting analysis 9-11720  
 Fortran II, conducting sequence distribution calculation in copolymers 9-17069  
 Gunn diodes with above critical *naL* products, direct series operation conditions 9-5734  
 integrals, Coulomb, in Slater-type atomic orbitals 9-15802  
 integrals, overlap, in Slater-type atomic orbitals 9-15801  
 light scattering functions, heterodisperse systems of isotropic spheres 9-11725  
 linear programming for quantum mechanical perturbation theory 9-8410  
 macromolecules, translational and rotational frictional coefficients calculation 9-17066  
 nuclear experiment, software controlled multiple scanner of 6 quantities 9-22016  
 on-line data processing, self-consuming program 9-6224  
 plate bending, conforming quartic triangular element, subroutine program 9-8483  
 POISSON, for stray field of magnets calculation 9-16763  
 polymer latexes, particle size, computer analysis 9-17223  
 polymerization, relative reactivity ratio calculation from composition conversion data 9-17524  
 pressure waves, time-varying axisymmetric sources in atmosphere, computer model 9-4044  
 propagation of finite amplitude wave distorted by reflection 9-2212  
 radiation damage in f.c.c. and b.c.c. crystals, mathematical modelling 9-13669

**Calculating apparatus continued****digital computer programmes continued**

- rigid rotor energy levels computer program for calculation 9-20911  
 spectrum stripping, use in *n* activation analysis with  $\gamma$  spectra 9-4170  
 structural group analysis of polyatomic molecules, from i.r. spectra 9-6998  
 surface-barrier detector evaluation from fission-fragment energy spectrum 9-2773  
 vinyl terpolymerization patterns, composition calculation 9-17523  
 X-ray diffraction, line profile analysis, deformed polycrystalline material 9-18438  
 X-ray powder photograph indexing and cell dimensions refinement 9-5311  
 Si p-i-n junction diodes, avalanche-induced relaxation oscillations 9-16281  
**digital computers**  
 for spectrogram reductions 9-4179  
 automated tutorial, discontents, special relativity application 9-7  
 digital transformations, pseudo-random 9-19245  
 digital word generator using transistor for each word digit 9-14288  
 galactic model, for evolution subject and gravitation 9-20148  
 for high energy physics data analysis, present techniques, future trends 9-13154  
 information retrieval system SARC1, application to graphite research program 9-6249  
 multistorey structure oscillation analysis 9-10724  
 neutron diffractometer data assessment 9-19699  
 PDP-8 in 2000 channel pulse height analyser 9-19243  
 Permalloy films, optimization of properties for magnetic memories 9-13995  
 use in simulation of secondary residue effect, pitch shift 9-6217  
 tape storage, data compression circuit 9-8313  
 telescope, photometric, automatic control 9-14277  
 transformation, pseudo-random, for pulse height analysers 9-19244

**Calculation**

- See also *Graphs*; *Nomograms*  
 'ravine' method for following functional valleys 9-12910  
 A-P algorithm for matrix analysis of damped dynamical systems 9-20373  
 algorithm for reducing products of  $\gamma$  matrices 9-17688  
 celestial mechanics, analytical and numerical methods 9-6109  
 convergence of approximate solutions, least-squares and Bubnov-Galerkin methods 9-12908  
 division, analogue, novel circuit 9-4263  
 experimental functions expansion in series of descending exponentials 9-15442  
 heat equation, adiabatic, mixed boundary problem numerical solution by tracking 9-12944  
 iteration procedure, quadratically convergent 9-9109  
 local variation method applied to complex operator  $L(u)=f$  9-12907  
 minimization algorithm for calculation of minimum impulse orbital transfer 9-10451  
 Neville's repetitive linear interpolation of estimates, extension 9-6348  
 n.m.r. high-resolution spectra 9-16756  
 operator lower bound determination by method of decomposition, speed of convergence 9-12909

**Calculus** see *Differential equations*; *Integrals*; *Mathematics***Californium**

- <sup>246</sup>Cf, spontaneous fission half-life measurements 9-620  
<sup>248</sup>Cf, spontaneous fission half-life measurements 9-620

**Californium compounds**

No entries

**Calorimeters**

- adiabatic, for temperature range 25-500°C, relative to heat capacities of Al<sub>2</sub>O<sub>3</sub>, Al and Pb 9-12014  
 adiabatic, high temperature (300°K-1900°K), with continuous operation under inert gas 9-9838  
 black horn, laser beam energy measurements 9-19155  
 differential scanning for study of temperature induced solid decomposition 9-12522  
 gasket seal, low-mass, vacuum tight in 0.8 to 400°K range 9-2271  
 graphite, adiabatic, for high intensity electron pulses 9-1925  
 for laser absolute energies, spherical cavity 9-10852  
 for laser output energy measurements in wide power range 9-10851  
 laser-cone, calibration 9-2268  
 liquid load, for far i.r. laser power measurements 9-17875  
 simple reaction, in solution chemistry, design 9-6409  
 specific heat, dynamic measurements, 4-150°K 9-19860  
 specific heat of liquids measurement 9-13523  
 wire cone for absolute laser control wave radiation-power measurements 25  $\mu$ W-25 mW 9-4453

**Calorimetry**

- See also *Heat of adsorption, etc*; *Specific heat*  
 differential flow, block of plane reactive cells 9-10761  
 differential scanning, for thermal properties of cholesterol 9-13799  
 discharge, anode fall determination 9-3027  
 experimental methods and apparatus, book 9-4381  
 filters, interference, use with Unicam SP1300 colorimeter 9-272  
 flow, for enthalpy measurement in natural gases, in range -320°F to +100°F and pressure up to 2000 p.s.i.a. 9-13490  
 ion beam intensity measurements, errors due to non-turbulent coolant flow 9-2269  
 low temperature, tan  $\delta$  measurements, at 4.2K 50Hz, thick insulating materials 9-1565  
 martensite, deformed and from cold-worked austenite, thermal effects of ageing 9-7595  
 metals, 300-1900°K 9-9838  
 microcalorimetry, analogue milliwatt-hourmeter 9-2299  
 steady state, a-c temperature 9-7653  
 wire, energy dissipated during fatigue cycling, study 9-13717  
 K vapour, heat capacity observations 9-17161

**Cameras**

- ballistic, in artificial satellites, method of determination of geographical coordinates 9-20573  
 convolution, to reveal periodicities in electron micrographs 9-16072  
 Debye-Scherrer, <sup>57</sup>Fe source of Mn K $\alpha$  X-rays, diffraction study 9-3265  
 Debye-Scherrer, for high-temperature X-ray crystallography 9-3260  
 double Schmidt sky survey programme 9-18946  
 electron diffraction, review 9-230  
 eye movement recording 9-6219  
 image converter, streak, calibration technique 9-19174  
 i.r. industrial and medical applications 9-2254  
 iris diaphragms, linear scale, graphical design 9-13079  
 multiple-spark-gap, for dynamic photoelasticity 9-6363  
 radioisotope, pinhole collimator theory 9-11428  
 rotating-mirror, multiple-image objective system 9-10950



**Cameras continued**

- scintillation, output recording method 9-10948  
 stereoscopic, six-objective for one-meter bubble chamber 9-2612  
 streak, with continuously moving film 9-10949  
 X-ray microcamera for phase anal. of microsegregations 9-22025  
 X-ray spectrographic, 0.5-7Å, non-destructive sample analysis 9-2432

**Candoluminescence** *see Luminescence***Capillarity**

- See also Bubbles; Drops; Films/liquid; Foams; Surface tension*  
 capillary waves, longitudinal, theory 9-21172  
 circular ring centralized when wetted by liquid in cylindrical hole 9-3073  
 dielectric cylinder, in viscous fluid, instability calc. 9-11674  
 membrane transport model 9-997  
 moisture transfer in capillary-porous substances 9-18336  
 polar molecules, surface force action and i.r. determ. of interfacial region thickness 9-13515  
 pyrrrole between polyethylene supports, surface forces and i.r. determ. of interfacial region thickness 9-13515

**Capture cross-sections** *see Nuclear reactions and scattering and subheadings***Caratheodory's principle** *see Thermodynamics***Carbon**

- See also Diamonds; Graphite*  
 with A-centres, from sugar and PVC, temp. depend. of e.s.r. 9-8022  
 absorption coeffs. in wavelength region 17.6 to 250 Å 9-1769  
 abundance in Population II 9-12677  
 acetylene black, electronic props. rel. to graphitization and heat treatment temp. 9-7738  
 active, chemisorption of SO<sub>2</sub> 9-8081  
 adsorbed gas condensation 9-9592  
 adsorption of He at room temp., rel. to superficial pore sizes and preferential press. domains 9-7347  
 adsorption of I from aqueous soln., with micropore filling 9-9625  
 aggregates, shape and bulkiness factors from electron microscopy 9-7421  
 amorphous, e.s.r. linewidth and spin conc., before and after air admission 9-8021  
 amorphous, g-anisotropy rel. to adsorbed air, e.s.r. study 9-8023  
 anthracite, influence of oxygen sorption on e.p.r. 9-10273  
 atom trio in triangle, nonpairwise additivity in exchange energy 9-15911  
 atoms and ion, bibliography of spectra 9-13287  
 black, electron momentum density, X-ray determ. 9-18581  
 blacks, oxidized rel. to microstruct. of inside and outside of particle 9-7419  
 blacks optical props., book 9-12324  
 blocks, reaction with Cs, 350°-550°C 9-6004  
 build-in during Si fabrication 9-3667  
 charcoal, mol. dynamics of adsorbed gases, from n scatt. spectra 9-3213  
 charcoal in contact with HD mols. at 20°C dynamic polarization of nuclei 9-7270  
 chemisorption of SO<sub>2</sub> on O<sub>2</sub>-free active surface 9-8081  
 coalesced mesophase in coal-tar pitch carbonization, microstructs. 9-7418  
 coke, irreversible expansion in baking, suppressive effect of Fe<sub>2</sub>O<sub>3</sub> additive in filler 9-7591  
 comet Rudnicki (1966e), C<sub>2</sub> emission band ratios, obs. 9-6182  
 compacting carbon blacks without binder, Hall effect and magnetoresistance 9-7735  
 crystalline order characts. from X-ray exam. 9-7426  
 cycle in stellar energy prod. 9-6126  
 diatomic, new simple band spectrum 9-4985  
 diatomic and triatomic, in comets, radius of existence 9-4123  
 diffusion in Fe-Si(Ni)(Cr)-C ternary alloys, rel. to element redistrib. laws. 9-3381  
 diffusion in UC, and mechanism, 1266 1684°C 9-11899  
 disordered, reaction with C saturated V carbide melts, rel. to catalytic graphitization 9-12531  
 disordered, reaction with V carbide melt to form ordered graphite 9-7617  
 dissociative excitation transfer, laser action obs. 9-4851  
 donor doped, (Na or K), temp. depend of Hall coeff. and magnetoresistivity 9-7752  
 electronic pair-correlation energies of ground states, soln. of Bethe-Goldstone eqns. 9-11383  
 e.s.r., effect of B acceptors and Na donors in range 1800°-2400°C in carbon black P33 9-8019  
 e.s.r. in carbon blacks, P33 and Thermax, temp. depend. and n irradi. effects 9-8018  
 e.s.r. linewidth and spin conc. in amorphous carbon, before and after air admission 9-8021  
 e.s.r. of C blacks, P33 and Thermax, temp. depend. and neutron irradi. effects 9-8012  
 e.s.r. of deposits on Al<sub>2</sub>O<sub>3</sub> 9-20015  
 evaporation from Th dispenser cathode in Auger emission spectroscopy 9-7867  
 fibre, MP, suitable pitch mats. for prod. 9-8054  
 fibres, 7µ diam-in loop, bending behaviour and tensile failure 9-7564  
 fibres, carbonized cellulose, microfibrillar and micropore struct. 9-7417  
 fibres, carbonized cellulose, preferred orientation 9-7359  
 fibres, high strength and modulus, prod. by stretching heated C yarn 9-7514  
 fibres from cellulose pyrolysis, preferred orientation after heat treatment 9-8072  
 fibres obtained from petroleum sulfol. prep. and phys. props. 9-8060  
 film, adsorption of O rel. to elec. resist., -196 to 450°C 9-7795  
 film, anisotropic cryst. growth on heat treatment to 2500°C 9-7335  
 films, e transmission expts. electron microscope 9-6488  
 films, evaporated, grain size and at. struct., obs. 9-13576  
 films, thickness estimation by e. microscopy of transverse sections and optical density meas. 9-11766  
 in flames, chemical reactions 9-3991  
 glass-like, prod. by pyrolysis of non-melting resins, study at various states of heat treatment 9-7319  
 glassy, industrial applies, in Japan 9-7316  
 glassy, tensile creep rate, stress depend., 2500-2900°C 9-7550  
 glassy carbon, total cross-section from 0.001-0.1 eV 9-20824  
 glassy monofilament obtained by spinning and quenching condensates of thermo-setting resins 9-7320  
 granular, thermal, contact resistance at container walls 9-15023  
 graphitic carbons, pore struct. 9-1077  
 graphitization accel. under high press. by elec. spark shock 9-7606  
 green bodies, baking process rel. to pyrolysis kinetics 9-7589

**Carbon continued**

- Hall coeff., field depend. rel. to acceptor doping and heat treatment 9-7751  
 Hall coeff. and magnetoresistivity, temp. depend. 9-7749  
 heat treatment under press. in presence of Ca cpds, (002) diffraction profiles 9-10595  
 interaction of different types at high temps. 9-8061  
 interstitial atoms in soft carbons, rel. to classifications 9-7473  
 ions III, IV, V, photoionisation cross sections, calc., 39.1-867.9 Å 9-6979  
 lamp blacks, binder content req. for products 9-7590  
 magnetoresistivity, field depend-rel. to acceptor doping and heat treatment 9-7751  
 membranes, graphitization during annealing, and charact. variation 9-7609  
 membranes, prep., strength, crystallog. characts. elec. and optical props. 9-11777  
 microporosity rel. to Dubinin theory of pore filling in adsorpt. 9-7346  
 monolithic articles, prod. using low press. semi-isostatic moulding tech. 9-8309  
 non-graphitic, preferred orientation, effect on X-ray scatt. 9-7360  
 non-graphitic, struct. from X-ray meas., significance rel. to hexagonal layer struct. 9-7425  
 non-graphitizing, (002) X-ray refl. characts., 2400-3000°C 9-5315  
 non-graphitizing type, X-ray characts and composite profiles 9-9672  
 oxidation by atomic O, temp. depend. and amount of surface oxide from 0-400°C 9-8097  
 oxidation of carbon black, effect of metallic salts on surface 9-8092  
 oxidized by CO<sub>2</sub>, effects of struct, temp., impurities etc. on resultant carbons 9-8096  
 parallel plate dynode e multiplier, preparation method 9-10824  
 particles form. in vapour-phase pyrolysis, theory 9-8067  
 particles in N<sub>2</sub> stream, transmittance and absorption cross sections 9-11726  
 petroleum coke, graphite cryst. form. and struct. changes in desulphurization, obs. 9-7431  
 phenol-formaldehyde resin carbons, microstruct. rel. to graphitizability, obs. 9-7429  
 from phenol-formaldehyde resins, contact pot. difference rel. to heat treatment temp. 9-7324  
 positron-electron ranges 9-12036  
 powder, actual Hall effect calc. from meas. of apparent one 9-7737  
 powder, graphitic, e.p.r. line at  $\nu \approx 10$  GHz, width, shape and position 9-8013  
 powder, sintering and graphitization by elec. spark discharge 9-7610  
 powdered, graphitic, e.p.r. determ. of g-factor anisotropy 9-8014  
 pyrocarbons, B doped, elec. and mag. props. rel. to B content 9-7736  
 pyrocarbons, compressed samples, reproducible, prep. and props. 9-7596  
 pyrocarbons, paramag. resonance 9-8020  
 pyrolytic, dimensional changes during neutron irradi., descriptive model 9-7651  
 pyrolytic, dimensional changes induced by high temp. neutron irradi. 9-7409  
 pyrolytic, rubbed, surface orientations development and reln. to friction and wear 9-11758  
 radiocarbon, transfer in nature 9-12591  
 range and dE/dx in Be from 500 keV and 2 MeV 9-9871  
 range and dE/dx of O and Ne at 500 keV to 2 MeV 9-9871  
 reduction of UO<sub>2</sub> to metal U in vacuum 9-14134  
 reflection coeff. diminution for laser light 9-21603  
 resistance thermometer, new interpolation formula 9-2261  
 small crystallite type, microstruct. variations by electron microscopy 9-7420  
 soft, Hall coeff. and magnetoresistivity rel. to acceptors and heat treatment 9-7750  
 soft, residual lamellar cpds. (H<sub>2</sub>SO<sub>4</sub> and Br<sub>2</sub>) 9-7362  
 solubility in  $\alpha$ -Fe 9-9788  
 soot production in laminar ethylene diffusion flames, rel. to diluents 9-15214  
 soot yields from mixed ethylene-acetylene flames burning in O<sub>2</sub> and N<sub>2</sub>O 9-12535  
 species present in r.f. discharges of binary mixtures of CO, CO<sub>2</sub>, methane, He and O<sub>2</sub> 9-8120  
 spectra, p<sup>2</sup>-ps transition line oscillator strength in isoelectronic sequence 9-9122  
 spheres, internal burning, order of reaction and temp. limit of reaction zones 9-8076  
 spheres, internal burning, tech. for determ. depth of reaction 9-8075  
 spiral and whisker growth from pyrolysis of methane 9-8073  
 stars at south galactic pole cap, obs. 9-21886  
 in steel, martensitic, interaction with dislocations 9-1218  
 steel, martensitic stainless, effect on grindability 9-17323  
 in steel, redistrib. during austenitic transforms 9-3490  
 structure, atomic radial distrib. functions rel. to stacks and layers 9-7405  
 surface, reversible oxygen exchange between CO<sub>2</sub> and CO, kinetics 9-8051  
 surface groups, nature and distrib., anal. via vacuum pyrolyses 9-7325  
 surface reactivity 9-8058  
 thermal, contact resistance at container walls 9-15023  
 thermal cond. meas. by flash tech., crit. evaluation 9-7662  
 transfer from unstabilized to stabilized steel by corrosion in Na liq. 9-10345  
 vitreous, disordered, role and nature of localized electronic states 9-7711  
 vitreous, oxidation by CO<sub>2</sub> and O<sub>2</sub>/Ar mixtures at 1500-3000°K 9-8091  
 vitrocabon, elec., mech. and thermal props. rel. to heat treatment temp. 9-7318  
 wood charcoal, expansion due to methanol adsorpt. and elastic props. 9-11781  
 C-Al barrier, electron current calc., applic. of perturbation method 9-18572  
 C<sub>2</sub>, analysis of Swan bands 9-14686  
 C<sub>2</sub> electronic transition moment of Swan bands determ. in CO<sub>2</sub>-Ar shock tube 9-19429  
 C<sub>2</sub> radical, rot. distrib. obs. in low-press. plasma 9-20983  
 C<sup>++</sup>, excitation-heating of ions, magnetically confined vacuum arcs 9-18271  
 C<sup>+</sup> reaction with N<sub>2</sub> and O<sub>2</sub> 9-14122  
 C III, 2p<sup>2</sup> 1D level mean lifetime 9-6965  
 C IV, absolute oscillator strengths for important transitions 9-15808  
 C IV, semiempirical atomic core potentials, coeffs. 9-19397  
 C<sub>2</sub>, molec. charge distrib. and chem. binding 9-2876

**Carbon continued**

- C<sub>2</sub> interstitials in graphite lattice, self-energy and deform. 9-7407  
 C<sub>2</sub> molecule, swan system, additional rot. perturbations of A<sup>3</sup>Π<sub>g</sub> state 9-11457  
 C<sub>2</sub> radical in plasma discharge appl. to identification of C-C groups in org. cpds 9-9370  
 C<sub>4</sub>, C<sub>5</sub> and C<sub>6</sub>, bending and stretching freqs. 9-9199  
 C\* formation from collisions between electrons and CO mols. 9-685  
 fabric-Ta foil, multilayer thermal insulation systems 9-3543  
 in Fe-C alloys, deformed, effect on annealing stages above room temp. 9-13754  
 in α-Fe dipole strength 9-9739  
 glassy, order, resistance and thermal props. rel. to fabrication techs. 9-7317  
 Na-doped blacks, Hall coeff. and dramag. susceptibility 9-7739  
 in Ni-Fe alloys, effect on Curie pt. and spontaneous magnetization 9-13984  
 pyrolytic, tensile creep rate, stress depend., 2500-2900°C 9-7550  
 U-Zr-C phase diagram, 1700-2000°C 9-11976  
 in U<sub>3</sub>Si alloys, approx., effect on δ peritectoid reaction 9-16158

**Carbon compounds***See also Organic compounds*

- basic surface oxide complexes, form by chemisorpt. and dissociation 9-8080  
 C<sub>2</sub>S<sub>2</sub> force constants determ. and mean amplitudes of vibration 9-20924  
 C-Fe solid solutions, electrical resistivity recovery mechanism after e irradi. 9-18991  
 carbides, refractory, crystal structure high temp. 9-7433  
 carbide of transition metals, physical and mechanical props. 9-7510  
 carbonates, calcite-type, relation between carbon-O distance and properties 9-19681  
 carboxylic acid dimer configuration, planarity 9-7018  
 CO<sub>2</sub>, rotational relax. time, direct meas. 9-2852  
 CO<sub>2</sub> near crit. point, depolarization of scatt. light and Krishnan effect 9-961  
 CO gas, i.r. spectral transmission function 9-17031  
 cyanide, complexes, double, Pt, diamagnetic susceptibility 9-19946  
 graphite nitrates, λ transform. at H-21°C, struct., elec. and thermodynamic aspects 9-7607  
 graphite oxide, chemistry, struct. model, bonding and grouping 9-7352  
 graphite-nitrate residue cpds, electronic props. rel. to band model approx. 9-7740  
 phosgene, thermodynamic props. up to 600°K, 150 atm. 9-7263  
 refractory carbides, thermodynamics and diffusion data 9-7506  
 struct. and physical props. rel. to use as depolarizer in dry cells of c blacks 9-8105  
 surface oxide, amount formed from 0-400°C by atomic O 9-8097  
 C-H(Ta,Zr) alloys, reinforced, commercial development 9-3467  
 C<sub>2</sub>N<sub>2</sub>, solid, lattice vibr. 9-16164  
 C particles form. in vapour-phase pyrolysis, theory 9-8067  
 C<sup>14</sup> O<sup>18</sup>O<sub>2</sub> laser transitions, obs. and calcs. 9-6514  
 CCl<sub>4</sub> molecule, infrared absorption bands obs., bond moments calc. 9-2860  
 CF<sub>4</sub> molecule, infrared absorption bands obs., bond moments calc. 9-2860  
 CH, valence excited states and transition probabilities 9-2875  
 CH<sub>2</sub>, orbit depend. on spin for singlet, triplet states 9-20982  
 CH radicals, proton hyperfine splittings, theory 9-827  
 CN, ground state in active N flames, optical absorpt. 9-826  
 CN, in comet Rudnicki (1966e), emission band ratios, obs. 9-6182  
 CN, temp. meas. from nonresolved spectra, obs. 9-8531  
 CN halides, photodissociation, bond energies 9-17062  
 CN radical, ht. of formation 9-825  
 CN<sup>-</sup> in alkali halides, Raman spectra 9-12407  
 CN<sup>-</sup> in RbCl, tunneling states 9-10040  
 C<sub>2</sub>N<sub>2</sub>, photodissociation, bond energy 9-17062  
 C<sub>2</sub>N<sub>2</sub>, photoionization 9-9398  
 CO<sub>2</sub>-A(N<sub>2</sub>) 9-3094  
 CO<sub>2</sub>-CO mixtures, oxidation and reduction of UO<sub>2</sub>, surface controlled, 977-1400°C 9-3998  
 CO<sub>2</sub>-He static laser, cw, long life 9-15518  
 CO<sub>2</sub>-N<sub>2</sub>-He laser, gain at 10.6 μ 9-15517  
 CO<sub>2</sub>-N<sub>2</sub> solid solns., equilibrium vapour press. meas. 9-21253  
 CO<sub>2</sub>-N<sub>2</sub>, laser, vibrational relax. data, kinetic model, review 9-15509  
 CO<sub>2</sub>-N<sub>2</sub> gas laser system, simultaneous laser action of CO<sub>2</sub> and N<sub>2</sub>O mols. 9-8608  
 CO<sub>2</sub>-N<sub>2</sub> gaseous mixtures, u.s. wave propag. at 95 atm., 31-100°C 9-9451  
 CO<sub>2</sub> (A<sup>1</sup>Π-X<sup>1</sup>Σ<sup>+</sup>) syst. in absorption at high resolution in vacuum u.v. 9-18178  
 CO<sub>2</sub> adsorption and interac. on Cu, 77°K 9-21285  
 CO<sub>2</sub> dipole moment and mag. props. 9-2859  
 CO<sub>2</sub> electr. transition moment integrals for first ioniz., r-centroid approx. limits 9-20925  
 CO<sub>2</sub> high-resolution widths of self-broadened lines 9-13346  
 CO<sub>2</sub> influence on CO<sub>2</sub> laser performance 9-20507  
 CO<sub>2</sub> ionization and fragmentation by 5-45 keV protons, mass spect. investigation, X-section meas. 9-5060  
 CO<sub>2</sub> liq. and solid, p.-radiolysis 9-10359  
 CO<sub>2</sub> mobility of CO<sup>+</sup>, CO<sub>2</sub><sup>+</sup> and C<sub>2</sub>O<sub>2</sub><sup>+</sup> 9-917  
 CO<sub>2</sub> self-broadening coeffs. determination by CO<sub>2</sub> laser radiation 9-4921  
 CO<sub>2</sub> solid, sp. ht. anomaly due to O<sub>2</sub> impurity 9-1392  
 CO<sub>2</sub> transitions B-X, c-X and J<sup>1</sup>-X<sup>1</sup>, in high resolution u.v. absorpt. spectra 9-11456  
 CO<sub>2</sub>, abs. band at 6970 cm<sup>-1</sup> 9-758  
 CO<sub>2</sub>, abundance in Martian atmosphere 9-18910  
 CO<sub>2</sub>, heat transfer at supercritical pressure 9-20998  
 CO<sub>2</sub> removal from He coolant by molecular sieves 9-19373  
 CO<sub>2</sub>, self and N<sub>2</sub> broadenings of rot. lines of 15 and 4.3 μ bands, width meas. 9-19494  
 CO<sub>2</sub>, significant structure theory applied to correlation of thermodynamic props. in terms of molecular parameters 9-19605  
 CO<sub>2</sub>, supersonic jets, intermolecular binding 9-18179  
 CO<sub>2</sub> vibr. relax. in shock-tube 9-759  
 CO<sub>2</sub> vibration excitation by electron impact 9-760  
 CO<sub>2</sub><sup>+</sup>, X<sup>2</sup>Π<sub>g</sub> and A<sup>2</sup>Π<sub>g</sub> states, spin-orbit coupling constants calc. 9-15845  
 CO<sub>2</sub> gas, i.r. rad., large path length limit 9-19585  
 CO<sub>2</sub> ionization by low-energy heavy ions 9-904  
 CO<sub>2</sub> laser, discharge e. energy distrib. and effect of He 9-18298  
 CO<sub>2</sub> laser, sealed-off single freq., characteristics 9-19143

**Carbon compounds continued**

- CO<sub>2</sub> laser, sealed, heated Pt wire effects 9-16235  
 CO<sub>2</sub> model from orbital theory 9-14301  
 CO<sub>2</sub> oxidation of Fe-Al alloys, composition and temp. dependence 9-14132  
 CO<sub>2</sub> oxidation resistance of Zr-Nb alloys 9-20050  
 CO<sub>2</sub> oxidation resistance of Cu-Zr alloys 9-20049  
 CO<sub>2</sub> plasma, d.c., slight dispersion forward waves, 4.7 to 9 torr 9-18311  
 CO<sub>2</sub> reaction with O<sup>+</sup>D atom, ozone quantum yield 9-21719  
 CO<sub>2</sub> spect. obs. in Mars atmospheres, approx. lab. simulation 9-20225  
 CO<sub>2</sub> vibration energy transfer mechanism in collision between isotopes 9-18227  
 CO<sub>2</sub> with organic impurities as gas coolant mixture, patent 9-20859  
 CO<sup>+</sup>+N<sub>2</sub>, near-resonant transfer of vibr. energy. 9-20996  
 CO<sup>+</sup>, A-X transition, electr. transition moment integrals eval. 9-20925  
 CO<sup>+</sup> plasma envelopes of comets, fountain model of dynamics 9-21949  
 CO<sub>2</sub> differential scatt. cross-section for 25-60 eV e impact 9-9142  
 CO dissociation by electronic collision in solar photosphere 9-17662  
 CO gas, i.r. large path length limit 9-19585  
 CO ioniz. transitions, use of Franck-Condon factors 9-4934  
 CO liq., linear, and ang.-momentum autocorrel. functions 9-3076  
 CO molecule, collision with electron rel. to formation of highly excited atoms 9-685  
 CO on C surface, reversible exchange of O into CO<sub>2</sub> 9-8051  
 CO spectra, branching ratio investigation, 1500 to 2600 Å 9-11460  
 CO<sub>2</sub>, 0°C, vapour pressure meas., dynamic method 9-3037  
 CO<sub>2</sub>, 4.3 μ absorpt. and emission obs. 9-9200  
 CO<sub>2</sub>, abundances of O isotopes, calc. from mass spectrometric meas. 9-11429  
 CO<sub>2</sub>, abundance in atmosphere of Venus 9-6179  
 CO<sub>2</sub>, adsorption on carbon, rel. to Dubinin theory of pore filling 9-7346  
 CO<sub>2</sub>, atmospheric, <sup>14</sup>C content measurement 9-15248  
 CO<sub>2</sub>, collisional relaxation from ν<sub>3</sub> vibr. 9-4922  
 CO<sub>2</sub>, dimerization rel. to quadrupole moment 9-4908  
 CO<sub>2</sub>, i.r. band low resolution emissivity, theory and expt. 9-17028  
 CO<sub>2</sub>, influence on surface tension of NaF-ZrF<sub>4</sub>-ZrO<sub>2</sub> and 3NaF-Al<sub>2</sub>F<sub>3</sub>-Al<sub>2</sub>O<sub>3</sub> melts 9-11689  
 CO<sub>2</sub>, laser, generation bands rel. to rotational lines, effect of pumping 9-8610  
 CO<sub>2</sub>, migration of second layer in W, with trapping on first layer sites 9-11900  
 CO<sub>2</sub>, oxidation of C, effects of temp., gas flow rate etc. on resultant carbons 9-8096  
 CO<sub>2</sub>, photolysis in far u.v. 9-10351  
 CO<sub>2</sub>, resonance capture of very slow electrons 9-9399  
 CO<sub>2</sub>, review 9-15514  
 CO<sub>2</sub>, stearate, oleic acid and 3β-cholestanol multilayer permeabilities, obs. 9-5415  
 CO<sub>2</sub>, synthesis, and purification using Cu on SiO<sub>2</sub>-MgO support 9-12526  
 CO<sub>2</sub>, ultrasonic relaxation in gas mixture with O<sub>2</sub> 9-2901  
 CO<sub>2</sub>, vibrational level population inversion in laser 9-13008  
 CO<sub>2</sub> adsorption on W(110) and (111) faces, effect of partial coverage with O<sub>2</sub> b//c// 9-3217  
 CO<sub>2</sub> conductometric determ., improvement 9-10365  
 CO<sub>2</sub> content in Venus atmosphere 9-2056  
 CO<sub>2</sub> frosts on Cat-A-Lac black paint and Cu surfaces, spectral reflectance 0.36 to 1.15 μ 9-10188  
 CO<sub>2</sub> laser, 20 watt, single frequency 9-15519  
 CO<sub>2</sub> laser, c.w., characts. for CO<sub>2</sub> and air-CO<sub>2</sub> obs. 9-17870  
 CO<sub>2</sub> laser, enhancement of third harmonic generation in InSb 9-257  
 CO<sub>2</sub> laser, frequency control by BCl<sub>3</sub> filter 9-15515  
 CO<sub>2</sub> laser, high power c.w. 9-8609  
 CO<sub>2</sub> laser, investigation of pulsed excitation 9-13012  
 CO<sub>2</sub> laser, investigation of pulsed excitation 9-2373  
 CO<sub>2</sub> laser, linewidth by step response meas. 9-8607  
 CO<sub>2</sub> laser, mode-locking 9-15516  
 CO<sub>2</sub> laser, rot. level competition 9-13004  
 CO<sub>2</sub> laser, single-mode high-power 9-13006  
 CO<sub>2</sub> laser, small-signal step response and linewidth meas. 9-13005  
 CO<sub>2</sub> laser, unsaturated gain meas. in gas discharge 9-13007  
 CO<sub>2</sub> laser level relax. induced by chopped 10.6 μm radiation 9-17871  
 CO<sub>2</sub> laser light chirped pulses generation at 10.6 microns 9-4500  
 CO<sub>2</sub> laser power increase on proton irradiation 9-15507  
 CO<sub>2</sub> meas. i.r. gas analyser calibration 9-4027  
 CO<sub>2</sub> mixed with Ne, afterglow, microwave and mass spectrometric study of recombination, diffusion 9-9341  
 CO<sub>2</sub> molecule formation of O<sup>-</sup> by electron coeff. affinity attachment 9-11614  
 CO<sub>2</sub> molecules, spectra calc. rel. obs. 9-4927  
 CO<sub>2</sub> on C surface, reversible exchange of O with CO 9-8051  
 CO<sub>2</sub> on Mars, abundance and temp. 9-4120  
 CO<sub>2</sub> oscillator, ultrastable 9-15520  
 CO<sub>2</sub> Q-switched laser, non-linear amplification characts. 9-10860  
 CO<sub>2</sub> quadrupole interaction 9-17164  
 CO<sub>2</sub> reorientation cross-section from depolarized Rayleigh line width meas. 9-13345  
 CO<sub>2</sub> supersonic jet, e diff. for existence of crystals and free molecules 9-11459  
 CO<sub>2</sub> wet, mixture with N<sub>2</sub>, thermal relax. obs. using Kundt's tube 9-13492  
 CO<sub>2</sub>, geometry and electronic struct. 9-13347  
<sup>11</sup>CO preparation of gas for medical use 9-21990  
<sup>12</sup>C<sup>18</sup>O molecule, Angstrom bands in visible region 9-9197  
<sup>12</sup>C<sup>18</sup>O<sub>2</sub>, i.r. spectra, and vib.-rot. bands 9-13348  
<sup>12</sup>C<sup>18</sup>O, spin rot. and rot. mag. moment 9-9198  
<sup>12</sup>C<sup>18</sup>O<sub>2</sub>, i.r. spectra, and vib.-rot. bands 9-13348  
 COS, significant structure theory applied to correlation of thermodynamic props. in terms of molecular parameters 9-19605  
 CO<sup>+</sup>+D<sub>2</sub>→COD<sup>+</sup>+D, reaction cross sections, 1-100 eV 9-17075  
 CS-C black system, CS content rel. to press. and phase equilibria 9-7620  
 CS<sub>2</sub>-CCl<sub>4</sub> mixtures, volume relax. 9-3095  
 CS<sub>2</sub>, dipole moment in ground and first excited vib. state 9-11458  
 CS<sub>2</sub>, significant structure theory applied to correlation of thermodynamic props. in terms of molecular parameters 9-19605  
 CS<sub>2</sub>, stimulated Raman scatt., periodic fine struct. 9-21212  
 CS<sub>2</sub>, thermodynamic props., temp.-entropy diagram up to 750°K, 300 atm. 9-21134  
 CS<sub>2</sub>, photoionization and electron impact 9-17131  
 CS<sub>2</sub>, Raman band intensities, influence of solvent 9-13528



**Carbon compounds** continued

- CS<sub>2</sub>, Raman scatt., stimulated by focussed low power ruby laser beam 9-5171  
 ClF<sub>3</sub>, coriolis coupling coeffs. 9-18177  
 Co<sub>2</sub>-N<sub>2</sub>-He laser, output 80W 9-17869  
 Fe-C alloys, deformation mechanism, 77° to 300°K 9-5458  
 Fe-C alloys, magnetoresistivity, 4.2 and 78°K 9-15070  
 Fe-C alloys, phase transformations during tempering, eff. of prior plastic deform. 9-13777  
 Fe-C alloys, precipitation kinetics, infl. of age-hardening rate 9-9798  
 Fe-Ni-C alloys, ferromagnetic f.c.c., plastic deform. 9-13727  
 (90wt.%)Kr-(10wt.%)CO<sub>2</sub> proportional counter gas, pulse shape calcs. 9-19228  
 Mn-C alloys, resistance comp. dependence, 1000-1400°C, rel. to chem. bonds. 9-12088  
 Na<sub>2</sub>Fe(CN)<sub>6</sub> affect on NaCl crystal growth and characteristics 9-18415  
 O<sup>15</sup>O preparation of gas for medical use 9-21990  
 (90wt.%)Xe-(10wt.%)CO<sub>2</sub> proportional counter gas, pulse shape calcs. 9-19228

**Carbon tetrachloride (CCl<sub>4</sub>)** *see Organic compounds***Carcinotrons** *see Electromagnetic oscillations; Electron tubes***Carrier mobility** *see Crystal electron states/transport processes; Semiconducting materials; Semiconductors***Carrier scattering** *see Crystal electron states/transport processes; Semiconducting materials; Semiconductors***Catalysis**

- See also Reaction kinetics*  
 corundum doped with Ti<sup>3+</sup>, V<sup>3+</sup> or Cr<sup>3+</sup>, H<sub>2</sub>-D<sub>2</sub> exchange activation 9-8085  
 dissociated gas flow past catalytic surface, study of laminar boundary layer 9-12540  
 ethylene, hydrogenation on metal catalysts 9-10336  
 graphite deposition, by BCl<sub>3</sub> catalyst, effects of gaseous impurities 9-8062  
 heterogeneous gas reactions, mass transfer factors calc. 9-21690  
 oxidation for waste gas purification, patent 9-20043  
 porcelain enamels, catalyst bearing, effect on soil removal by oxidation 9-1910  
 porous catalysts, average pore radius and effective diffusivity 9-13702  
 refractory metals and alloys, oxidation, retardation by Li<sub>2</sub>O presence 9-3994  
 Ag, work function O<sub>2</sub> or ethylene atm.,  $\gamma$  irradi. effects 9-12219  
 NH<sub>4</sub>ClO<sub>4</sub>, thermal decomposition, effect of Cu chromite 9-12528  
 NO- catalysed recombination of radicals in premixed flames 9-14121  
 Ni-Cr<sub>2</sub>O<sub>3</sub> catalyst, rel. to h<sub>2</sub>O-H isotopic exchange, H desorpt., obs. 9-16046  
 Ni on SiO<sub>2</sub>-Al<sub>2</sub>O<sub>3</sub>, prep. and particle size 9-1909  
 O<sub>2</sub> reduction mechanism on noble metal cathodes 9-18758  
 Pt black, activity rel. to particle size, defects and stored energy 9-5325  
 Pt catalyst, alumina-supported, ave. crystallite size and crystalline content 9-17271  
 Pt catalysts, Warren-Averbach tech. for X-ray characterization 9-5326

**Cataphoresis** *see Electrophoresis***Cathode rays** *see Electron beams***Cathode-ray oscillographs** *see Electrical measurement***Cathode-ray tubes** *see Electron tubes***Cathodes**

- See also Electron emission*  
 contamination effects in h.v. glow discharge 9-11625  
 discharge initiation by negative ion desorption 9-21114  
 electrolytic cell, protection from corrosion, patent 9-8107  
 hair pin, pointed and oxide, characts. rel. to e beam line broadening 9-16768  
 luminescence, electron microprobe study 9-20007  
 photocathode cooling using Peltier effect 9-4444  
 photocathode S-20, near i.r. sensitivity enhancement by field assisted photoemission 9-12223  
 poisoning by adsorbed gas, press. and temp. depend. 9-3753  
 protrusions formation during pre-breakdown conditioning electron optical obs. 9-11633  
 sputtering reduced in discharge expts. 9-7197  
 sublimation meas. by quartz crystal oscillator 9-3755  
 thermionic, hollow, for Ar ion laser 9-15511  
 thermionic, hollow, for gas laser use 9-15508  
 tube techniques, conference 9-3747  
 tube techniques, conference 9-7862  
 tube techniques, conference 9-3748  
 tungstate matrix, emission and life props. rel. to composition 9-5780  
 uniform field, for use in discharge chamber of restricted size: design and performance 9-13164  
 Ag-Cs-O photocathode, increased sensitivity using optical effects 9-19938  
 Al electrode erosion by impulse accelerator plasmas 9-9412  
 Al electrode erosion by impulse accelerator plasmas 9-9411  
 Be brass photocathode for He lines meas. on HL<sub>a</sub> background 9-15560  
 Cs-Sb photocathodes, processing on glass substrates, photoresponse and build-up time meas. 9-15146  
 CsI photodiode, u.v. quantum efficiency, e-irrad. effects, 1-2 MeV 9-12224  
 CsTe photodiode, u.v. quantum efficiency, e-irrad. effects, 1-2 MeV 9-12224  
 Cu electrode erosion by impulse accelerator plasmas 9-9412  
 Cu electrode erosion by impulse accelerator plasmas 9-9411  
 Cu electrode erosion in spark discharge under Ar atmos. 9-17141  
 CuI photodiode, u.v. quantum efficiency, e-irrad. effects, 1-2 MeV 9-12224  
 LiF photocathode for He lines meas. on HL<sub>a</sub> background 9-15560  
 Mo electrode erosion by impulse accelerator plasmas 9-9411  
 Ni, prep. and thermionic parameters of (111), (100) and (110) faces 9-1625  
 TaB<sub>2</sub>, thermionic properties 9-5778  
 Th dispenser, for Auger emission spectroscopy, C evaporates 9-7867  
 ThC, thermionic emission props. 9-3754  
 ThC thermionic emission props. 9-3754  
 W, protrusions formation during pre-breakdown conditioning, electron optical obs. 9-11633  
 W atom-emission stabilization by Ge coating 9-21551  
 W photodiode, u.v. quantum efficiency, e-irrad. effects, 1-2 MeV 9-12224

**oxide**

- arcing in low pressure pulse discharge 9-5777  
 electron emission energy distribution 9-21553  
 emission rel. fall 9-3024  
 surface conduction due to Ba adsorpt., behaviour 9-3752  
 unified model; role of localized surface states on small crystals. 9-5776

**Cathodoluminescence** *see Luminescence***Causality** *see Physics fundamentals***Cavitation***See also Vortices*

- bubbles, collapse velocity rel. to surface tension and viscosity 9-9467  
 bubbles, rectified diffusion acoustic threshold phenomena 9-5139  
 erosion, analogy with jet impact 9-5138  
 erosion and cavity flow, relationship 9-19595  
 hydrodynamic, acoustic noise rel. to erosion 9-7100  
 hydroerosion of metals, effect of surface-active agents 9-9775  
 hydrofoils in cascade, fully cavitating, Munk's integral appl. 9-13506  
 incompressible fluid with small cavitation numbers, flow past solid of revolution 9-18241  
 liquid, caused by cylinder, noise intensity 9-5157  
 luminescence, thermal quality 9-5175  
 mechanically induced, acoustic detection 9-11670  
 metals, boiling, void dynamics, X-ray meas. 9-9468  
 noise, and acoustic noise, relationship btw. statistical charac. 9-5152  
 noise spectra, statistical 9-5134  
 nuclei, prod. in liq. by ionizing particles, detect. by sound absorpt. obs. 9-21204  
 plate under tension with elliptic inclusion 9-19029  
 propagation of sound waves, cavitating liqs. 9-5154  
 radius, max., of cavitation void, calc. 9-5135  
 due to underwater explosion, calc. of propagation 9-17178  
 u.s., criterion for evaluating intensity limit 9-5136  
 u.s. fountain, in spray jet region rel. to atomization process 9-5133  
 Cu, cavity formation in early stages of creep 9-13731  
 K, boiling, void dynamics, X-ray obs. 9-9468  
 K ferrioxalate reduction, oxidation processes, u.s. wave instigated 9-6025

**Cavity resonators** *see Acoustic resonators; Electromagnetic oscillations***Celestial mechanics**

- analytical and numerical methods, book 9-6109  
 binary collisions, numerical regularization 9-20142  
 binary collisions in N-body problem, regularization anal. 9-6107  
 clusters, open, 25-48 stars, under influence of galactic field 9-20191  
 collisionless astronomical systems, variational treatment 9-20137  
 dynamical friction in the approx of general relativity 9-12716  
 earth orbit mecs. using pulsars proposed 9-8268  
 encounters, applic. of non-equilibrium statistical mechanics 9-20145  
 FORMAC computer language, application 9-10460  
 four-body problem, earth-sun-moon-satellite system, stability of close binary with third component 9-18834  
 four-body problem, periodic solns. as perturbation of restricted three-body problem 9-8224  
 galactic evolution, computer model 9-20148  
 galactic star cloud encounters, calc. of effect on stellar distributions 9-15274  
 galaxies as gravitational lenses 9-10467  
 gas flow from galactic centre 9-15376  
 gravitational impact of astronomical systems 9-20143  
 gravitational instability theory, evidence from the rotation of the Galaxy 9-12662  
 gravitationally interacting particles, collisionless syst., Liouville and Poisson eqns., locally isotropic solns. 9-18833  
 Hamiltonian reduction by successive approximations, uniformity 9-15271  
 intermediate orbits in the study of natural satellites of the planets 9-10519  
 introductory book including comprehensive account of satellite orbits 9-14188  
 Lie series application to perturbation studies 9-17608  
 moon elliptic motion, periodic soln. of plane 3-body problem 9-17637  
 n-body problem, round-off errors for systems of up to 10<sup>6</sup> bodies 9-20146  
 outer satellites of Jupiter, trajectory integration by modified Cowell's method 9-15341  
 perturbation theory for strongly perturbed dynamical syst. 9-6106  
 restricted three-body problem, expansion of natural families of periodic orbits of the first kind 9-6108  
 Schwarzschild mass, gravitational radiation explosion 9-1987  
 self-gravitating systems, violent relax. phase, equilibrium considerations 9-21875  
 solar system, distrib. of mean motions, tidal hypothesis 9-16607  
 solar system satellites, orbital period relns. and commensurability 9-16608  
 spherical stationary systems with purely radial velocities 9-12680  
 stable orbits about Earth-Moon triangular points, sun perturbed 9-10449  
 stars, encounters and escapes 9-20144  
 strongly perturbed syst. formal series soln. orbit differential correct. 9-6106  
 three-star system, evolution 9-10495  
 triple system Zeta Aquarii, orbit computation, effects of coupling, stability of configuration 9-6143  
 Trojan librations, short-period, stability characts. in sun-Jupiter restricted three-body problem 9-17642  
 two fixed centres force function for earth's potential 9-10520  
 two-body problem, reducing the error in numerical solutions 9-15270  
 two-body problem with variable masses, eccentricity var. eqn. 9-10461  
 visual binaries, dynamical parallaxes, new elements, orbit computations 9-6144

**Cell model** *see Liquids, theory***Centrifuges**

- Beckman model E, analytical, electronic speed control 9-20029  
 fields, centrifugal, creation and use 9-10686  
 speed control, electronic, for Beckman model E analytical centrifuge 9-20029

**Ceramics**

- brick, max. firing rate rel. to structure and thermodynamic props. 9-3462  
 brick plant, automatic 9-4172  
 ceramic-metal composites, thermal shock resistance 9-1273  
 ceramics, semivitreous extruded, dry rupture modulus and shrinkage response surfaces 9-3166  
 cermets, high-temperature, wetting and fabrication 9-18535  
 characterization uncertainty rel. to variability of exptl. results 9-7313

**Ceramics continued**

- Clevite Ceramic B, pyroelec. coeffs., d.c. dielec. consts., vol. resist., obs. 4.2 to 300 K 9-19100  
 coating deposition of porcelain enamel 9-1913  
 coatings, thermal control surface for Mars Lander, protection from dust storm 9-1386  
 with compressive surface layers, residual stress meas. 9-3414  
 control of properties 9-18539  
 corundum, surface damage on cutting and grinding from X-ray analysis 9-13574  
 crack interaction with microstructural features, meas. 9-3445  
 crystals, forging and recrystn. 9-3482  
 electroceramics, intrinsic props., prep-effects 9-1563  
 electron microscope exam., 3 dim. and stereo scanning 9-3278  
 electrophoretic deposition, thickness control using probe electrode technique 9-12966  
 experimental results variability rel. to characterization uncertainty 9-7313  
 ferrites, microwave latching devices 9-1679  
 ferroelectric mirror, wideband interference light modulator 9-13051  
 fired props. rel. to raw particulates, struct. and comp. 9-7312  
 fuel elements, pore migration in thermal grad., shape change 9-18483  
 glass, transmission micrographs, thickness errors, analysis 9-3174  
 glass bonded cordierite bodies sintered from devitrifiable frit 9-7315  
 glass-ceramic coatings for metals, elec. and mech. props. improvement 9-3189  
 glass-crystal systems, flow props. rel. to deform. in firing 9-3417  
 heat and mass transfer kinetics, thermal anal. apparatus and technique 9-19084  
 laser separation, controlled 9-3441  
 lithium aluminosilicate, thermal expansion dependence on TiO<sub>2</sub> catalyst content 9-13804  
 nuclear, microstructure of mech. thinned specimens 9-3279  
 porcelain, toughness meas. 9-3432  
 porcelain enamels, catalyst bearing, effect on soil removal by oxidation 9-1910  
 porcelain enamels, electrostatic spraying 9-1095  
 PZT-4, pyroelec. coeffs., d.c. dielec. consts., vol. resist., obs. 4.2 to 300 K 9-19100  
 PZT-5A, pyroelec. Coeffs., d.c. dielectric. consts., vol. resist., obs. 4.2 to 300 K 9-19100  
 reactor fuel, evolution and high burn up behaviour 9-2787  
 semivitreous, extruded, fired rupture modulus response surface rel. to particle size and firing rate 9-3164  
 sintered, mech. and elec. props., microporosity effects 9-3431  
 sintering, solid-state, research review 9-7582  
 sintering, vol., grain boundary and surface diffusion contributions 9-1246  
 spherical sample preparation 9-21403  
 spinel, corrosion by oxides at 1500-1750°C 9-14135  
 spinel in chromium, reaction with nitrogen in chromium 9-20032  
 super plasticity 9-7541  
 thermal-stress resistance 9-1275  
 thyatron pulse generator appl. for wire spark chamber 9-8943  
 titanates, superconductivity, review 9-3598  
 toughness meas. 9-3432  
 transducer, piezo-ceramic, mech. response calc. 9-13921  
 with water, chem. combined, blackcoring combating by additives 9-8050  
 white thermal control coatings in space, stability model 9-1096  
 Al<sub>2</sub>O<sub>3</sub>, electric tests to 800°C 9-10034  
 Al<sub>2</sub>O<sub>3</sub>, for electrical applic. 9-1566  
 Al<sub>2</sub>O<sub>3</sub>, high purity, control of elec. props. at high temp. 9-3691  
 Al<sub>2</sub>O<sub>3</sub> with BaO glasses, mech. and elec. props. and sintering behaviour 9-3171  
 Gd<sub>2</sub>(MoO<sub>4</sub>)<sub>3</sub>, preparation and X-ray analysis 9-18446  
 Laba field ion images, description 9-12988  
 MgO-Al<sub>2</sub>O<sub>3</sub>-SiO<sub>2</sub> phase composition and cordierite formation, 800-1400°C 9-21409  
 NaKNbO<sub>3</sub>, ferroelectric, polarized optical retardation 9-1743  
 PbO-based polymorphic systems 9-12457  
 PbZrO<sub>3</sub>-PbTiO<sub>3</sub>, reaction kinetics in PbO-ZrO<sub>2</sub>-TiO<sub>2</sub>-Nb<sub>2</sub>O<sub>5</sub> system 9-8098  
 Pb(Zr<sub>1-x</sub>Ti<sub>x</sub>)O<sub>3</sub>, ferroelectric, polarized optical retardation 9-1743  
 $\beta$ -SiC field ion images, description 9-12988  
 SrTiO<sub>3</sub>, superconductivity, review 9-3598  
 TiO<sub>2</sub>, surface spark discharges, influence of voltage polarity 9-10157  
 ZrO<sub>2</sub>, stabilizing additives, Y<sub>2</sub>O<sub>3</sub> and CaO and their volatilization 9-21252

**Cerenkov radiation** *see Cherenkov radiation***Cerium**

- f.c.c.  $\rightarrow$  d.h.c.p. martensitic transform., effect of plastic deform. 9-3487  
 isomorphism; P-T phase equilib. diag. 9-5268  
 isomorphism theory rel. to anomalous phys. props. 9-3225  
 semivitreous extruded, dry modulus and shrinkage response surfaces 9-3165  
 spin-lattice relax. of 4f-electrons 9-12316  
 supercond. under press. 9-3595  
 Ce<sup>3+</sup> in La(Cl,Br), modified Orbach relax. process 9-12317  
 Ce<sup>3+</sup> in LaCl<sub>3</sub>, pair-interaction e.p.r. meas. 9-10283  
 La-Ce system, elec. conductivity temp dependence 9-1455

**Cerium compounds**

- Ce<sub>1.05</sub>CO<sub>2-x</sub>Cu<sub>0.75</sub> alloy, permanent mag. props. and prep. 9-3795  
 Ce-Mg nitrate, mag. thermometers, powders compared with cryst. sphere 9-172  
 CeAl<sub>3</sub>, Laves phase cpd., antiferromag. props. and exchange interactions 9-12247  
 CeAl<sub>3</sub>, magnetic characteristics between 2.2 and 300°K 9-5798  
 CeB<sub>6</sub>-M, (M=Hf, Ta, W and Re), elec. props. temp. dependence 9-9920  
 CeB<sub>6</sub>-M, (M=Hf, Ta, W and Re), elec. props. 9-9919  
 CeCl<sub>3</sub>, active phonon Raman spectra 9-3903  
 CeCl<sub>3</sub>, electronic Raman eff. 9-12356  
 CeCo<sub>5</sub>-CeCu<sub>4</sub> alloy of high coercivity, microstructure 9-11839  
 CeCo<sub>2</sub> phase, supercond. at high and zero press. 9-3594  
 CeCrO<sub>3</sub>, polycrystalline, dielectric const. and resistivity, temp. depend. 9-18645  
 Ce<sub>1-x</sub>Eu<sub>x</sub>Al<sub>3</sub>, Laves phase cpd., mag. props. comp. dependence at 4°K 9-12247  
 Ce(IV) in H<sub>2</sub>SO<sub>4</sub> solns., radiolysis due to <sup>18</sup>B(n, $\alpha$ )<sup>7</sup>Li reaction 9-15229  
 CeMg<sub>2</sub>(NO<sub>3</sub>)<sub>12</sub>, thermometers, shape factors from demagnetizing factors meas. 9-15395  
 CeO<sub>2</sub>, dielectric films, influence on opt. props. of In and Al layers 9-5886

**Cerium compounds continued**

- CeAl<sub>3</sub>, magnetic characteristics between 2.2 and 300°K 9-5798  
 La-Ce film, Kondo effect obs. 9-3581  
 La-Ce superconducting transition temperature, pressure dependence 9-1486  
 Y-Ce alloys, non-dilute, h.c.p., resistance minima rel. to spin-compensated state 9-15063
- Cermets** *see Ceramics; Metals*
- Change of state** *see Boiling; Condensation; Freezing; Melting; Phase transformations; Sublimation; Vaporization*
- Characteristic temperature** *see Specific heat*
- Charcoal** *see Carbon*
- Charge** *see Electric charge*
- Charge carriers** *see Crystal electron states; Semiconducting materials; Semiconductors*
- Charge compensation**  
 ion configuration in spinels 9-9632  
 spinels, ion configuration 9-9632  
 spinels, ion configuration 9-9632  
 BaTiO<sub>3</sub>:La<sup>3+</sup> (Nb<sup>5+</sup>), disorder, gravimetric studies 9-3224
- Charge exchange**  
 (p,n) reactions on light nuclei, compound nucleus effects 9-9024  
 alkali atomic beam source device 9-11415  
 alkali positive ions with alkali atoms 9-3014  
 anthracene mol., excited, electron transfer react. 9-17076  
 halogen and alkali metal ion-pair prod. mech. in flame detector 9-21739  
 inert-gas ions with N<sub>2</sub>, and dissoc. charge-transfer 9-15957  
 ion and gas mol. charge-transfer collisions, eff. on diff. of ions in strong elec. field 9-15977  
 ion beam prod. by collisions between 5-40 KeV proton beam and metal vapour beams 9-233  
 ion-atom collisions, high-energy scatt. eqns., coupling potentials, amplitudes 9-11406  
 low-kinetic energy collision-induced dissoc. 9-9406  
 in meson-baryon scatt., Regge pole analysis 9-6638  
 molecular complexes, characts. in excited state 9-15844  
 noble metals, model for ion-ion repulsive interaction 9-17252  
 rare gas solids, model for ion-ion repulsive interaction 9-17252  
 resonance, symmetric, of multicharged ions 9-14801  
 resonance, symmetric, of multicharged ions 9-3013  
 K $\pi$  react., Regge quark-model description 9-13127  
 PB $\rightarrow$ PB\* or PB, Reggeized (6,6) $\otimes$ (6,6), supermultiplet theory anal.  $\mu_{\text{eff}}=4-13\text{ GeV/c}$  9-14481  
 pp $\rightarrow$ nn at 5.6, 7.9, GeV/c 9-8891  
 $\pi^-$ , double on <sup>28</sup>Ni at 15 MeV 9-15773  
 $\pi^+$ -p $\rightarrow$ n $\pi^0$  react., polar obs., existence of Regge cuts 9-14512  
 $\pi^+$  scatt. on nuclei, form factor eff. 9-15771  
 $\pi^0$  scatt., high energy, polarization, Lorentz-pole model 9-11060  
 $\pi$ p react., Regge quark-model description 9-13127  
 Ar, electron capture cross sections, from <sup>2</sup>P<sub>3/2</sub> to <sup>2</sup>P<sub>1/2</sub> states 9-4863  
 Ar in N<sub>2</sub>O, CO, NO, charge-transfer proc., rate const. from drift meas., c.f. with "nearest reson." calc. 9-15956  
 Au complex, dicyanodihaloaurate, transfer spectra 9-20921  
 CO<sub>2</sub> with Ne<sup>+</sup> below 250 eV 9-7193  
 Cd cross sections for Cd<sup>+</sup> mobility calc. 9-5067  
 D<sup>+</sup>-D cross-section, eff. of apparatus geom. 9-4872  
 D<sub>2</sub>O $\rightarrow$ OD<sup>+</sup>+H<sub>2</sub>, cross section for incident ion energies near 2eV 9-921  
 H<sup>+</sup>-D cross-section, eff. of apparatus geom. 9-4872  
 H<sup>+</sup>-H cross-section, eff. of apparatus geom. 9-4872  
 H, atoms and ions, in low energy scatt. at metal surface 9-2828  
 H<sup>+</sup>+H<sub>2</sub>O $\rightarrow$ OH<sup>+</sup>+H<sub>2</sub>, cross-section for incident ion energies near 2eV 9-921  
 H<sup>+</sup>-beam prod. by p charge exchange on H target 9-12987  
 H<sup>+</sup>, charge exchange with Cs vapour, 0.5-20 keV, cross section obs. 9-13314  
 H<sup>+</sup>, electron capture, diff. cross-sections for neutral atomic targets 9-5069  
 H<sup>+</sup>, alkali metal vapour collisions 9-6985  
 H<sub>1</sub><sup>+</sup>, transformation to high energy neutral atoms in supersonic Li vapour jet 9-4445  
 H<sub>2</sub><sup>+</sup>, electron capture on impact with Ne 9-9407  
 H<sub>2</sub><sup>+</sup>, transformation to high energy neutral atoms in supersonic Li vapour jet 9-4445  
 H<sub>3</sub><sup>+</sup>, electron capture on impact with Ne and Ar 9-9407  
 H<sub>3</sub><sup>+</sup>, transformation to high energy neutral atoms in supersonic Li vapour jet 9-4445  
 in He<sup>+</sup>-Cs collisions, 1.5-25 keV 9-4890  
 He-He atomic charge exchange scatt. meas. 400-2000 e. V. 9-18158  
 He<sup>+</sup>+2He $\rightarrow$ He<sup>+</sup>+He, charge and dissociative charge-transfer proc., rate const. from drift data 9-15956  
 He<sup>+</sup> in N<sub>2</sub>, charge and dissociative charge-transfer proc., rate const. from drift data 9-15956  
 He beams in H<sub>2</sub>, via form. and destruction of metastable He atoms 9-5071  
 He<sup>+</sup> one- and two-electron loss in H<sub>2</sub>, He and Ne, 400-1500 keV 9-5072  
 He(1s<sup>2</sup>)+H<sup>+</sup> $\rightarrow$ He<sup>+</sup>(1s)+H(1s), perturbed stationary state calc. 9-5070-7  
 Hg cross-sections for Hg<sup>+</sup> mobility calc. 9-5067  
 Kr electron capture cross-section from <sup>2</sup>P<sub>3/2</sub> to <sup>2</sup>P<sub>1/2</sub> states 9-4863  
 Li neutral atoms from transformation of H<sub>1</sub><sup>+</sup>, H<sub>2</sub><sup>+</sup>, H<sub>3</sub><sup>+</sup> ions 9-4445  
 N<sub>2</sub><sup>+</sup> with H<sub>2</sub> and D<sub>2</sub>, cross-sections at 20 and 1000 eV 9-15958  
 Ne<sup>+</sup> with N<sub>2</sub>, O<sub>2</sub> and 71cc CO<sub>2</sub> charge exchange with Ne<sup>+</sup> below 250 eV optical CO<sub>2</sub> below 250 eV, optical excitation) Mol. excitation [cc N<sub>2</sub> charge exchange with Ne<sup>+</sup> below 250eV optical excitation] [cc O<sub>2</sub> charge exchange with Ne<sup>+</sup> below 250 eV optical82z/032e342e23u3m3.3(05343.0 0008022 03000000000005072 9-7193  
 SrTiO<sub>3</sub>, transition metal doped, photoinduced reversible processes 9-7955  
 TiO<sub>2</sub>, transition metal doped, photoinduced reversible processes 9-7955  
 Zn cross-sections for Hg<sup>+</sup> mobility calc. 9-5067
- Chelates** *see Molecules; Organic compounds. For inorganic chelates see under metal compound headings*
- Chemical analysis**  
*See also Spectrochemical analysis*  
 clay raw materials, mineral anal. 9-4018  
 deoxygenation determ., intermol. photo-reduction method 9-10364  
 electron microprobe, cathodoluminesc. attachment 9-18782  
 field-flow fractionation, nonequilibrium theory 9-848  
 gases, optico-acoustic analyzer 9-14141  
 glass contact refractories, staining for metal ions detection 9-4017  
 gravimetric with automatic mag. balance 9-18978



**Chemical analysis continued**

- hexafluoroacetone, quenching addends during photolysis, identification 9-1922  
 isotopic, negative surface ionization method, applications 9-20067  
 manganous formate dihydrate, thermogravimetric analysis, extraction of kinetic parameters 9-16506  
 o Moon, by Surveyor VI, preliminary obs. 9-21927  
 of Moon, Surveyor VII prelim. obs. 9-17640  
 NMR probe into flowing liquid 9-20065  
 oxygen analyser, patent 9-21730  
 physical methods, physics exhibition London, 1968 review 9-4021  
 polymer solutions, turbidimetric titration, conc. determination by angular light scattering 9-14870  
 residual thiosulphate in gelatin, colorimetric analysis 9-6563  
 semiconductor materials, book 9-8114  
 thermobalance, symmetrical, for corrosive atms. 9-4019  
 thermogravimetric analysis, extraction of kinetic parameters 9-16506  
 thermogravimetric and differential thermal attachments for Stanton thermobalance 9-4020  
 of volatile liquid, using counterflow of gas and vapour through microporous membrane 9-12550  
 C surface groups, by pyrolytic volatile anal. and i.r. spectrometry 9-7325  
 CO<sub>2</sub> conductometric determ., improvement 9-10365  
 Cd(NO<sub>3</sub>)<sub>2</sub> soln.,  $\beta$  backscatt. rel. to conc. 9-10367  
 Cd<sup>2+</sup>-Co<sup>3+</sup> nitrate soln.,  $\beta$  backscatt. rel. to percentage comp. 9-10367  
 Co(NO<sub>3</sub>)<sub>2</sub> soln.,  $\beta$  backscatt. rel. to conc. 9-10367  
 Co<sup>2+</sup>-Hg<sup>2+</sup> nitrate soln.,  $\beta$  backscatt. rel. to percentage comp. 9-10367  
 Cs metal, oxygen determ. by vacuum distillation 9-648  
 Fe corrosion prods. by Mossbauer backscatt. spectroscopy 9-10363  
 $\beta$ -FeOOH on steel by Mossbauer backscatt. spectroscopy 9-10363  
 Hg(NO<sub>3</sub>)<sub>2</sub> soln.,  $\beta$  backscatt. rel. to conc. 9-10367  
 Hg<sup>2+</sup>-Cd<sup>2+</sup> nitrate soln.,  $\beta$  backscatt. rel. to percentage comp. 9-10367  
 KCl, irradiated and additively coloured, method for investigating electronic colour centres 9-16109  
 NaCl, irradiated and additively coloured, method for investigating electronic colour centres 9-16109  
 Nb-H, impurity contamination on electrolytic charging of Nb with H 9-13750  
 O<sub>2</sub> detection in laboratory furnaces with Zr strip 9-8316  
 Pu amperometric titration 9-17544  
 Pu in organic solns., inadequacy of radiometric methods 9-1929  
 Pu research using laser microprobe 9-4023  
 Th complex of thiocyanate, paper chromatographic method for separation and identification 9-18772  
 Ti complex of thiocyanate, paper chromatographic method for separation and identification 9-18772  
 U complex of thiocyanate, paper chromatographic method for separation and identification 9-18772  
 U in organic solns., inadequacy of radiometric methods 9-1929  
 YFe garnet:Hf, Fe<sup>2+</sup> characterization 9-16388  
 Zr complex of thiocyanate, paper chromatographic method for separation and identification 9-18772

**adsorption**

See also *Chromatography*  
 No entries

**by mass spectrometry**

See also *Mass spectrometers/applications*

- limitations, review 9-728  
 liquid impurities determ. 9-8116  
 Pb isotopes 9-8115  
 photolysis, flash: vessel designed for fast gas phase reactions 9-4009  
 residual atmospheres in vacuum systems 9-8119  
 shock tube contents sampling 9-21110  
 spark source with pressed electrodes having graphite powder support 9-8117  
 Ar in thin films by r.f. spark-source mass spectrography 9-15232  
 C deposition in r.f. discharges of binary mixtures of CO, CO<sub>2</sub>, methane, He and O<sub>2</sub>, species involved 9-8120  
 Na, spark source mass spectrographic anal. 9-8121

**by nuclear reactions**

- activation anal. *in vivo* using 5 MeV neutrons 9-21746  
 activation analysis  $\gamma$ -spectrograms, improved treatment of digital data 9-4686  
 air, tritium content meas. from Ti-<sup>3</sup>H target emission of <sup>3</sup>H 9-8138  
 concentration use in high sensitivity activation analysis determ. by reaction 9-4029  
 element 110, search in Pt ore, neutron-induced fis., obs. 9-18160  
 neutron activation anal., 14 Mev, use of double irradiation technique 9-21745  
 neutron activation analysis for metals in solutions 9-1931  
 neutron capture  $\gamma$  meas., sensitivity 9-21744  
 neutron resonance analysis, apparatus 9-17548  
 nuclear chemistry, book 9-8948  
<sup>115m</sup>In conc. in mineral samples, using ( $\gamma, \gamma'$ ) reactions 9-1934  
 F by <sup>19</sup>F( $\gamma, p$ )<sup>17</sup>N+<sup>16</sup>O+n, use in high sensitivity activation analysis 9-4029  
<sup>7</sup>Li isotopic analysis 9-1930  
<sup>7</sup>Li( $p, \gamma$ )<sup>4</sup>Be, for Li concentration determ. 9-12553  
 Se content in biological mats., instrumental neutron-activation anal. 9-21743  
 Si, semiconductor, non-destructive neutron activation analysis 9-20074

**electrochemical**

polarography, book 9-15231

**radioactive**

See also *Radiochemistry*

- Chinese test 28 Dec, 1966, quantitative investigation of fallout sample 9-6082  
 enzyme assays, review 9-14148  
 isotope dilution analysis, review 9-18784  
 labelled, organic compounds, review of stability 9-14145  
 labelled compounds, stability and storage, review 9-14146  
 manganese montmorillonite, Szilard-Chalmers reaction 9-10368  
 minerals, presence of K, calibration coeffs. 9-1932  
 neutron activation anal., prod. of sput-coated alloy standards 9-16645  
 purity of labelled compounds, review 9-14147  
 tracers, review of methods 9-20072  
 urine analysis for <sup>239</sup>Pu 9-20073  
<sup>210</sup>Pb, direct determ. either, separated or in mixture with daughters 9-10369

**Chemical analysis continued****radioactive continued**

- <sup>233</sup>Pa, rapid determ. and chem. yield 9-21742  
<sup>64</sup>Cu in biological materials by n activation, simul. <sup>56</sup>Mn meas. 9-18783  
 K in minerals, calibration coeffs. 9-1932  
<sup>56</sup>Mn in biological materials by n activation simul. <sup>64</sup>Cu meas. 9-18783  
 SiO<sub>2</sub>, Na ion contamination, expt. results rel. to theory 9-17547
- X-ray**  
 See also *X-ray examination of materials*  
 alite composition in Portland cement clinker 9-18393  
 cement, Portland, clinker, belite analysis by e. probe microanalysis 9-16515  
 diffusion in solids, radiographic surface analysis 9-14953  
 electron microprobe analysis, alloy microstructure, quantitative evaluation methods 9-8130  
 electron microprobe analysis of biological spec. 9-8131  
 electron probe microanalyser for quantitative analysis 9-8135  
 electron probe microanalysis, absorption edge effects 9-8129  
 electron probe microanalysis, atomic number effect correction 9-8128  
 electron probe microanalysis, industrial applic. 9-8136  
 electron probe microanalysis, model for scattering and deceleration 9-8127  
 electron probe microanalysis, quantitative, a progress report 9-8123  
 electron probe microanalysis, quantitative, calculation corrections 9-8124  
 electron probe microanalysis, quantitative, formula structure for fluorescence 9-8126  
 electron probe microanalysis, quantitative, theory 9-8125  
 electron probe microanalysis, stopping power and backscatter eff., calc. 9-20071  
 emission from e excited targets, computational methods 9-8337  
 films, thin, electron-probe microanalysis 9-14143  
 fluorescence, sample area effects on intensity meas. 9-8132  
 geological samples, with matrix mass absorpt. correction 9-21741  
 irradiated oxide fuels, identification of unknown constituent in inclusion 9-17546  
 microanalyser, various techniques 9-8134  
 microanalysers, design considerations 9-8133  
 microanalysis, industrial applic. 9-8137  
 source-target assembly for X-ray spectrophotometry 9-6033  
 spectrochemical, error minimization in sample prep., theory 9-4025  
 spectrochemical, inter-element effects, computer prediction 9-4026  
 steel, mild, fluorescent technique 9-6034  
 e probe microanalyser and its applications to medicine 9-4142

**Chemical effects of radiations**

See also *Nuclear reactions and scattering/chemical effects; Photochemistry*

- anthracene, X-rays, low energy, from optical and e.s.r. meas. 9-6020  
 anthracene in cyclohexane, radiation-induced fluorescence, elec. field effects 9-18765  
 benzene and other liquids subject to high intensity electron pulses, H yield 9-1925  
 chloral hydrate aq. soln., e.p.r. obs. 9-21224  
 duren radiolysis, production of radical with 13 equiv. protons 9-8078  
 ethane, liquid solns.,  $\gamma$ -radiolysis at -78°C, products obs. 9-21726  
 ethylene in aq. soln., radiolysis products 9-21725  
 ethylene polymerization 9-17541  
 fluorocarbons, aromatic, radiolysis 9-20061  
 investigations at Institute for Radium Research and Nuclear Physics, Austria 9-12549  
 1,5-pentanediol, liquid, products produced under  $\gamma$ -radiation 9-4015  
 petroleum products, radiolysis with <sup>60</sup>Co  $\gamma$  and 19 MeV e, G values for H<sub>2</sub> and methane 9-8111  
 polypropylene, radiolytic cross-linking 9-18767  
 proteins, in vacuo and with oxygen and adenine, mechanism of secondary radical formation 9-4013  
 pyrene in cyclohexane, radiation-induced fluorescence, elec. field effects 9-18765  
 structure materials, thermal n irradiation, effect on corrosion and electrochem. props. 9-1912  
 styrene,  $\gamma$ -induced polymerization 9-20037  
 CaO:Tm<sup>3+</sup>, reduction of Tm<sup>3+</sup> to Tm<sup>2+</sup> on  $\gamma$ - and e-irrad., e.s.r. obs. 9-10277  
 CrO<sub>4</sub>K<sub>2</sub>  $\gamma$  and n irradi., CrO<sub>4</sub><sup>2-</sup> form., e.s.r. obs. 9-20062  
 CrO<sub>4</sub>(NH<sub>4</sub>)<sub>2</sub> and n irradi., Cr(V), Cr(III) form., e.s.r. obs. 9-20062  
 N<sub>2</sub>-methane mixture, fission fragment prod. of H<sup>14</sup>CN 9-18770  
 NaCl, n-irradiated, behaviour of <sup>35</sup>S 9-6023  
 SrCl<sub>2</sub>:Tm<sup>3+</sup>, reduction of Tm<sup>3+</sup> on  $\gamma$ - and e-irrad., e.s.r. obs. 9-10277

**acoustic waves**

K ferrioxalate reduction, oxidation processes, u.s. wave instigated 9-6025

**ionizing radiations**

- benzene, liq., radiolysis by low energy <sup>4</sup>He ions 9-17542  
 n-butane, H formation in liq. radiolysis 9-16503  
 cyclopropane, gas-phase radiolysis 9-10355  
 hydrazinium hydrogenoxalate, N<sub>2</sub>H<sub>4</sub><sup>+</sup> in  $\gamma$ -irrad. cryst. 9-1927  
 hydrocarbons, liq., chem. determ. of free-ion yields 9-6024  
 hydrocarbons, liq. radiolysis, elec. cond. and molec. struct. 9-16022  
 hydrocarbons, liq. radiolysis, ion yield and molec. struct. 9-1926  
 hydrocarbons adsorbed on silica gel, mechanism 9-20063  
 ice, pulse-irrad., transient solvated electron, hydroxyl radicals 9-10360  
 methanol glasses,  $\gamma$ -irrad., spatial distrib. of trapped electrons 9-4014  
 methyltetrahydrofuran glasses,  $\gamma$ -irrad., spatial distrib. of trapped electrons 9-4014  
 naphthalene in ether. solns., pulse radiolysis, solute excited states and radicals formation 9-21728  
 naphthalene in hydrocarbon glass pulse radiolysis, triplet-states yield 9-17543  
 perfluoroalkanes,  $\gamma$ -irrad. products obs. 9-18766  
 propionaldehyde, liq.,  $\gamma$  radiolysis 9-14139  
 radiolysis model, electrons in aq. and organic media 9-10358  
 resin, ion-exchange, heat and  $\gamma$  effects 9-6021  
 tetrafluoroethylene, e.s.r. spectra of fluorocarbon radicals 9-21727  
 water, e.s.r. detect. of hydrated electrons 9-1044  
 CO, liq. and solid,  $\gamma$ -radiolysis 9-10359  
 Cl(IV) in H<sub>2</sub>SO<sub>4</sub> solns., radiolysis due to <sup>10</sup>B(n, $\alpha$ )<sup>7</sup>Li reaction 9-15229  
 Cl<sup>2</sup>-prod. in polycryst. matrix, e.s.r. 9-8024  
 HO<sub>2</sub> in irradi. H<sub>2</sub>O<sub>2</sub>-H<sub>2</sub>O solns., e.s.r. 9-7081  
 H<sub>2</sub>SO<sub>4</sub> solns.,  $\gamma$ -radiolysis at high press. 9-10361  
 NH<sub>4</sub>ClO<sub>4</sub>, effects on thermal decomp. 9-4012  
 NH<sub>4</sub>ClO<sub>4</sub>, effects on thermal decomp. 9-4011  
 Te aqueous solns.,  $\gamma$ -radiolysis 9-15230

**Chemical equilibrium** *see* *Chemical reactions*

**Chemical exchanges** *see* *Exchanges, chemical*

**Chemical kinetics** *see* *Reaction kinetics*

**Chemical reactions**

*See also* *Exchanges, chemical; Heat of formation; Heat of reaction; Oxidation; Photochemistry; Polymerization; Reaction kinetics*  
 acenaphthylene, pyrolysis, mechanism and residues 9-10330  
 acetylene prod. in flame reaction, patent 9-12533  
 alkyl radical reactions, chem. induced dyn. nucl. polarization 9-17222  
 alkyl radicals, chem. induced dynamic nuclear polarization 9-2921  
 alkylbenzenes, proton affinity and basicity 9-8071  
 aromatic anhydride mixtures, graphitization by copolyolysis with benzene precursors 9-8055  
 branched chain, as basis of chemical laser 9-8592  
 carbonization, e.s.r. of aromatic free radical intermediates 9-7088  
 carbons of different types, interact. at high temp. 9-8061  
 cellulose fibres, pyrolysis and fibrillar struct. 9-8072  
 cements, hydration 9-14123  
 chelates of ammonium aurintricarboxylate with U(VI), Th(IV), stepwise stability const. 9-16481  
 chlorination of polyethylene film 9-17520  
 copolymers and terpolymers, computer calcs. 9-10337  
 desulfurization of petroleum coke, structural changes 9-7431  
 diamino- and dihydroxy-aromatic cpds. heated, prod. of cokes showing N-puffing 9-8070  
 equilibrium under elec. and mag. fields effects in closed system free from ferroelec. and ferrimag. constituents 9-1895  
 ethylene, hydrogenation on metal catalysts 9-10336  
 ethylenes with OH-containing cpds., NMR and i.r. study 9-18751  
 exothermic, involving mol. or molec. ions, interchange rates, calc. by 'nearest resonance' method 9-6000  
 flames, C formation 9-3991  
 freely suspended single droplets, instantaneous exchange rate meas. 9-21192  
 gas, chemiluminescent emission at low conc. 9-10329  
 gas mixtures, three-component, reacting with finite rate, effective thermal cond. coeff. 9-9442  
 graphite, intercalation isotherm of FeCl<sub>3</sub> vapour from 300 to 350°C 9-8066  
 graphite, pyrolytic deposition, BCl<sub>3</sub> catalyzed, effects of gaseous impurities 9-8062  
 graphite, surface complexes formed during irradiation in CO<sub>2</sub>/CH<sub>4</sub> mixtures 9-8065  
 graphite, ZTA, with gases at 1400° to 3000°K, rates and kinetics 9-8064  
 graphite pyrolysis using acetylene as main gas source 9-8063  
 graphite with liq. Na, dilation effects rel. to previous irradiation and stress 9-6003  
 graphite-pyroc carbon composite bodies obtained by thermal cracking of natural gas, nuclear radiation effects 9-9861  
 inert-gas atoms with organic solids 9-1906  
 inert-gas atoms with organic solids 9-1907  
 i.r. spectroscopy, sample holder 9-20280  
 laser effects in H+Cl<sub>2</sub> or NOCl reactions 9-6521  
 liquid-gas, infrared high-pressure, cell construct. 9-22019  
 methane pyrolysis, spiral and whisker growth of C 9-8073  
 methane synthesis and purification of <sup>13</sup>C meas. 9-12526  
 muonium, classification and reaction rate 9-10316  
 o-, m- and p- nitroaniline, spectroscopic study of chelation and complex formation 9-17060  
 nitrogen-spinel, in chromium 9-20032  
 in nuclear reactors 9-21729  
 organic cpds., orbital calc. method, MOLKAO, applic. 9-20946  
 oxydo-reduction reactions and homogeneous electron transfer 9-20042  
 packed column, effective interfacial area as function of flow rate 9-21155  
 petroleum coke, desulfurization, struct. changes 9-7611  
 phenyl radical reactions, chem. induced dyn. nucl. polarization 9-17222  
 photochemical, conference, Munich (1967) 9-16488  
 polyanilines, oligomeric, chem. props. 9-19641  
 polyethylene, Phillips-type, reactions at terminal vinyl group, mech. props. 9-17516  
 of polymers, critical factors 9-17511  
 of polymers, symposium 9-17509  
 p- polyphenylene, compressed, pyrolysis yielding laminated struct. 9-8074  
 polystyrene, living, reaction with some natural polymers and their analogs 9-17526  
 propane, pyrolysis below 500°C, product form. study 9-1900  
 pyrolysis apparatus for liqs. 9-18750  
 rate-determining step: non-uniform reactivity of intermediates 9-21677  
 reactors, continuous flow, calorimetric expts. 9-5126  
 reactors, continuous flow mixing, attaining scaling-up 9-5125  
 reactors, efficiency of continuous flow mixer 9-5124  
 refractories, mineralogy of reactions, rel. to synthetic blast furnace slags 9-3980  
 salts, significance of lattice energies 9-18406  
 sea water-LiH, high-pressure, gas prod., obs. 9-20041  
 solid decomposition, temp. induced, study by differential scanning calorimeter 9-12522  
 solid-gas, kinetic and diffusional models 9-21680  
 soot production in laminar ethylene diffusion flames, rel. to diluents 9-15214  
 specimen chamber for electron microscope, for high temp. gas reactions 9-2346  
 steel, decarburization and graphitization on contact with Na at 600°C 9-16150  
 thermodynamic data evaluation computer program, CHAFFER 9-20279  
 unimolecular, Kassel theory extension to Markovian critical osc. energy, model 9-8442  
 BN and BN composite, static oxidation and compatibility, <2000°C 9-3995  
 C, glasslike, formation by pyrolysis of non-melting resins 9-7319  
 C, radical reactions on surface, surface groups obs. 9-7589  
 C blocks with Cs, composition rel. to pressure, isotherms 350°-550°C 9-6004  
 C compounds vapour-phase pyrolysis, C particles form., theory 9-8067  
 C green bodies, pyrolysis kinetics influence on baking process 9-7589  
 C surface oxide complexes, dissociation 9-8080  
 CBR<sub>4</sub> with alkali-metal atoms 9-810  
 CO<sub>2</sub> synthesis, and purification for <sup>14</sup>C meas. 9-12526  
 CaZr(PO<sub>4</sub>)<sub>2</sub>, thermal decomposition 9-3989

**Chemical reactions continued**

CdS, epitaxial films, vapour phase growth technique 9-9616  
 Cl+HCl→Cl<sub>2</sub>+H→3Cl, shock tube obs. 9-8077  
 Cr<sub>2</sub>O<sub>3</sub>, interaction with MgO, mechanism 9-3987  
 Cs with C blocks, composition rel. to pressure, isotherms 350°-550°C 9-6004  
 Cu<sub>2</sub>Te formation on diffusion of Cu in CdTe 9-11896  
 D<sub>2</sub>+X<sup>+</sup>→D+XD<sup>+</sup>, reaction cross-sections, 1-100eV 9-17075  
 Fe, carburization under vacuum 9-14124  
 Gd<sub>2</sub>O<sub>3</sub>, solid state with WO<sub>3</sub>, for stabilization 9-17326  
 Ge(OCH<sub>3</sub>)<sub>4</sub> vs. Ge(SCH<sub>3</sub>)<sub>4</sub> substituent exchange, <sup>1</sup>H n.m.r. obs. 9-6005  
 Ge(SCH<sub>3</sub>)<sub>4</sub> vs. GeZn(Z=Cl, Br, I, NCO), substituent exchange, <sup>1</sup>H n.m.r. obs. 9-6005  
<sup>3</sup>H (recoil) with n-butane, n-pentane and neo-pentane, kinetic theory calc., reactivity integral 9-21684  
 K+CH<sub>3</sub>I system, complex optical potential calc. 9-10322  
 Li-C system, compound formation 9-14992  
 LiF·FeO<sub>3</sub>, preparation attempts 9-16480  
 LiH-sea water, high-pressure, gas prod., obs. 9-20041  
 MgO, interaction with Cr<sub>2</sub>O<sub>3</sub>, mechanism 9-3987  
 NH<sub>3</sub>, adsorp. and decomp. on W(100) surface 9-1114  
 NH<sub>4</sub>ClO<sub>4</sub> thermal decomposition, role of point defects 9-20033  
 NO+(O+M)→NO<sub>2</sub><sup>+</sup>+(M), chemiluminescent, three-body mechanism 9-16478  
 N+NO<sub>2</sub>=N<sub>2</sub>O+O, vibr. excited N<sub>2</sub>O modes, obs. 9-10326  
 NaO<sup>+</sup>, prod. from Na+O, in merged beams 9-909  
 Nb, H addition by electrolytic charging in prep. of pure Nb-H 9-13750  
 Nd<sub>2</sub>O<sub>3</sub>, solid state with WO<sub>3</sub>, for stabilization 9-17326  
 O, atoms, molecules, ozone, review of kinetics 9-15212  
 O, with free radicals in  $\gamma$ -irrad. propionamide, n-butyramide and isobutyramide 9-12538  
 O<sub>2</sub>(Z<sub>2</sub>) formation, reaction and deactivation obs. 9-8069  
 Pu and U separation by fractional sublimation following chlorination 9-20857  
 SO + O<sub>2</sub> = SO<sub>2</sub> + O<sub>2</sub>, excited SO<sub>2</sub> mol. distrib. obs. 9-10328  
 SO<sub>2</sub> with free radicals in  $\gamma$ -irrad. propionamide n-butyramide and isobutyramide 9-12538  
 Si nitridation in preparing Si<sub>3</sub>N<sub>4</sub> films 9-21281  
 SiCl<sub>4</sub>-H<sub>2</sub> vapour-gas system, conc. ratio in saturator of epitaxial equipment 9-21301  
 Sm<sub>2</sub>O<sub>3</sub>, solid state with WO<sub>3</sub>, for stabilization 9-17326  
 Sn, surface reactions with aq. thiourea soln. 9-21702  
 Th hydrolysis in NaNO<sub>3</sub> and NaClO<sub>4</sub> solns., obs. 9-12529  
 Ti, addition to brazes for oxide wetting promotion 9-3180  
 U and fission products, separation by eutectic freeing of uranyl nitrate-hexahydrate 9-18749  
 UC, reactions with aqueous NaOH soln. 9-16482  
 U<sub>2</sub>C<sub>3</sub> form. in UC-UC<sub>2</sub> melt, and grain orientation effects, 1350°C 9-12530  
 UO<sub>2</sub>, rare earth oxides, high temp. stability in H atm 9-3979  
 UO<sub>2</sub>-PuO<sub>2</sub> reactor fuel, with Na and stainless steel rel. to stoichiometry 9-2789  
 UO<sub>2</sub>, reprocessing of irradiated fuels, by fluorinating with BrF<sub>3</sub> and F<sub>2</sub> 9-6944  
 UOCl<sub>2</sub> dissolved in molten UCl<sub>4</sub>, thermal decomposition, cry. UO<sub>2</sub> prep. 9-19686  
 V carbide melt, C saturated, with disordered carbons, rel. to catalytic graphitization 9-12531  
 W ribbons, chemisorption of O<sub>2</sub> 9-12539  
 (ZrO)<sub>2</sub>P<sub>2</sub>O<sub>7</sub>, thermal decomposition, 1450-1700°C 9-3989  
 ZrP<sub>2</sub>O<sub>7</sub>, thermal decomposition, 1450-1700°C 9-3989

**Chemical shift**  
 alkyl radicals, Cl h.f.s., e.p.r. 9-2884  
 amines, aromatic, and derived amides, in p.m.r. spectra 9-19456  
 aryl fluorides, <sup>19</sup>F n.m.r. 9-802  
 ethyl formate, formyl group, temp., solvent depend. 9-17054  
 ethylenes, unsymmetrically substituted, cis-trans effect on <sup>13</sup>C shifts 9-9266  
 methane, n.m.r. isotope shifts 9-7013  
 N, theoretical calc. 9-2886  
 nitrobenzene in CCl<sub>4</sub>, n.m.r., effect of addition of tetra-n-butylammonium salts 9-7281  
 n.m.r. moments and line shapes in rigid lattice 9-1869  
 pentafluorophenyl cpds. of group IV elements, <sup>19</sup>F n.m.r. 9-14716  
 pentafluorostyrene: <sup>19</sup>F,  $\alpha$ -methyl group introduction effects 9-12518  
 perfluorodimethyl acetylene in nematic solvents, n.m.r. anisotropy 9-13545  
 polyhalobenzenes in cyclohexane and carbon tetrachloride, additivity scheme 9-19646  
 triaetadomethane, <sup>13</sup>C, meas. 9-9282  
 trifluoroacetic acid, anisotropy meas. in F mag. shielding for C-F bonds 9-9286  
 in <sup>31</sup>P NMR spectra of P(CN)<sub>3</sub>, P<sub>2</sub>O<sub>10</sub> and P<sub>2</sub>S<sub>10</sub>, anisotropies 9-20936  
<sup>205</sup>Tl, in n.m.r. of Tl borate glasses 9-8041  
 Ag-Sb series, X-ray spectra, K $\alpha$  line shift 9-14066  
 BH<sub>4</sub><sup>-</sup>, n.m.r. isotope shifts 9-7013  
 o<sup>13</sup>Cs reson. in zeolites 9-4924  
 Cu, X-ray K-absorption edge, shift due to chemical combination 9-12454  
 Eu in Eu<sub>2</sub>O<sub>3</sub> and lower valence states, e.s.r. spectroscopic meas. 9-15852  
<sup>19</sup>F n.m.r. alkali fluorides in K<sub>2</sub>O·D<sub>2</sub>O solns. 9-3124  
 Fe cpds., Mossbauer spectroscopy, standard ref. mat. 9-3872  
 Hg, in X-ray L<sub>III</sub> absorption edge of <sup>201</sup>Hg 9-14068  
 HgO, <sup>201</sup>Hg X-ray spectra L<sub>III</sub> absorption edge 9-14068  
 NH<sub>4</sub><sup>+</sup>, n.m.r. isotope shifts 9-7013  
 N<sub>2</sub>[Fe(CN)<sub>6</sub>]NO 9-3872  
 Ni(II) in methanol, p.m.r. and solvation 9-9554  
<sup>17</sup>O n.m.r., in Co(II) solns. 9-3123  
 Rb<sup>+</sup> in aqueous soln., obs. 9-6971  
 Sb-organic cpds., Mossbauer eff., isomeric chem. shift 9-3874  
 Tl, in X-ray L<sub>III</sub> absorption edge of <sup>205</sup>Tl 9-14068  
 TlBr, <sup>205</sup>Tl X-ray spectra L<sub>III</sub> absorption edge 9-14068  
 Tl(NO<sub>3</sub>)<sub>3</sub>, <sup>205</sup>Tl X-ray spectra L<sub>III</sub> absorption edge 9-14068

**Chemical structure**  
*See also* *Bonds*  
 n-chlorodiazobenzenes, tautomerism and crystal structure 9-3320  
 ionicity model, Wolfsberg-Helmholtz calc. with Madelung corrections 9-11448  
 Linde Y zeolite, cation distrib. and selective exchange from Mn<sup>2+</sup> e.s.r. obs. 9-1889



**Chemical structure continued**

- n-methyldiazoaminobenzene tautomerism 9-3320
- molar ratio curves, new plotting method 9-17506
- organic, applications of e.p.r. 9-17507
- 2-phenyl indole, effect on fluoresc. 9-17214
- 2-phenyl indole, effect on scintillation props. 9-17213
- Al(III) halides in N,N-dimethylformamide solutions, outer-sphere ion-pair formation obs. by NMR 9-19645
- Cu minerals containing complex sulphides 9-13593
- KH<sub>2</sub>PO<sub>4</sub>:Cu<sup>2+</sup>, impurity position and co-ordination from e.p.r. spectra 9-1860
- Mn(II) complexes, stereochemistry from e.s.r. 9-18185
- Na<sub>2</sub>O-SnO<sub>2</sub>-SiO<sub>2</sub> glass, Sn valence states from Mossbauer effect 9-1751
- Si<sub>3</sub>N<sub>4</sub> films, prep. by SiH<sub>4</sub>+NH<sub>3</sub> gas phase reaction, from i.r. spectroscopy rel. to cracking mechanism 9-3194

**Chemical technology**

- ceramics with chem. combined H<sub>2</sub>O, blackcoring combating by additives 9-8050
- chemical reactor, differential test with reactive jet and internal circulation 9-5997
- dictionary of chemistry 9-4212
- fractionation device for prod. of gas-free liquids 9-14291
- gas-liquid reactors, occurrence of min. stirring rates 9-21675
- molecular sieves, for removal of H<sub>2</sub>O and CO<sub>2</sub> from He coolant 9-19373
- oil contamination in water on-line monitoring, fluoresc. detector 9-4022
- reactors, continuous flow, colorimetric expts. 9-5126
- reactors, continuous flow mixing, attaining scaling-up 9-5125
- reactors, efficiency of continuous flow mixer 9-5124
- C, glassy, fabrication factors rel. to characts. and thermal props. 9-7317
- C fibre prod. from petroleum sludge 9-8060
- CO<sub>2</sub> and methane purification without regeneration and high temp. 9-12526
- H isotope effects, test for transition-state models 9-12525
- U bearing liquid metal-immiscible solvent metal system, mass transfer meas. rel. to extraction processes 9-16473
- ZnS:Cu phosphor prep. 9-7991

**Chemiluminescence** *see* Chemical reactions; Luminescence**Chemisorption** *see* Chemical reactions; Sorption**Cherenkov radiation**

- See also* Counters/Cherenkov; Electrons/radiation
- EAS, flash, fluctuations obs. in 1300 events 9-15660
- from EAS detection review 9-16915
- electron emission and absorption, radiative equilibrium 9-4429
- e.m., in moving medium, Green's functions derived 9-14402
- energy loss of relativistic muons in water 9-2554
- from charge moving along axis of helical waveguide, energy spectrum 9-4395
- in dielectric, periodic laminar, spectrum and angular distrib. rel. to particle vel. 9-4582
- in inhomogeneous media, asymptotic theory 9-2277
- from moving charge train 9-10766
- occurrence with electron retardation by e.m. field in thin foils 9-7689
- and transition rad. of charge crossing betw. two regions of different elec. props. 9-19105
- ultra and hypersound generation in cubic piezoelectric crystals 9-10053
- ultra and hypersound generation in piezoquartz 9-10054
- Vavilov-Cherenkov, hard, possibility of exptl. obs. 9-8748
- Vavilov-Cherenkov hard radiation at moderate energies, probability and kinematics 9-331

**Chirality** *see* Elementary particles; Field theory, quantum**Chlorine**

- affinity continuum, u.v. region 9-9128
- atom, <sup>23</sup>Cl ground-state, kinetics of overall recombination 9-19409
- atom, neutral, Stark broadening of four multiplets 9-6966
- atom, radiative recomb. in shock waves 9-9289
- atoms and ions, bibliography of spectra 9-13287
- chemisorption on diamond, heat of wetting, e.s.r. and i.r. spectrum 9-8083
- chlorination of polyethylene films, eff. on mech. props. 9-17520
- diffusion in p-PbTe, 700°C, junction formation 9-19767
- ions as groundwater tracers for kaolinitic clay in acid soil detection 9-18787
- laser, effects in H+Cl<sub>2</sub> or NOCl reactions 9-6521
- pressure effect on Ag/AgCl electrode e.m.f. 9-6462
- solar abundance, first obs. 9-15354
- trace determ. in uranyl salts 9-8113
- Zeeman quadrupole spectra obs. in 2, 4-dichloroaniline 9-20958
- Ag, Cs/Cl, NO<sub>2</sub> liquid-liquid and solid-liquid equilibria 9-18380
- p-Cl<sub>2</sub>-φ, Zeeman effect, intensity rel. to static mag. field 9-15211
- p-Cl<sub>2</sub>-φ mono- and polycrystals, in n.q.r., effect of elastic actions and mag. field 9-15211
- Cl<sub>2</sub>, radiative recombination spectrum studied 9-20891
- Cl<sub>2</sub><sup>-</sup> in KClO<sub>4</sub>, e.p.r. and optical absorption study 9-21625
- Cl II ground configuration, level values and interaction parameters 9-20885
- Cl IX-XIII, u.v. spectrum obs. 9-6972
- <sup>35</sup>Cl n.q.r. freqs. in conjugated mols. 9-7061
- Cl<sup>2-</sup>, e.s.r. in polycryst. matrix 9-8024
- in Se-CdSe p-n junctions, impurity effects on characts. 9-10010
- ZnS:Cu,Mn,Cl film, electroluminescence, excitation mechanism 9-5974

**Chlorine compounds**

- ClO<sub>2</sub> radical created by X-irrad. e.p.r. in KClO<sub>3</sub> and KClO<sub>4</sub> 9-18737
- ClO<sub>4</sub><sup>-</sup> in alkali halides, symmetry at temps. 300-700°C from i.r. absorpt. temp. dependence 9-18704
- ClO<sub>2</sub><sup>-</sup>, electronic struct. from X-ray spectra 9-7019
- ClO<sub>4</sub><sup>-</sup>, electronic struct. from X-ray spectra 9-7019
- CuCl optical, non-linear phenomena 9-10160
- HClO<sub>4</sub>-H<sub>2</sub>O, p.m.r. and molec. states 9-11721
- NaCl crystal growth, effect of Na<sub>4</sub> Fe (CN)<sub>6</sub> 9-18415

**Chondrites** *see* Meteorites**Chromatic aberration** *see* Aberrations, optical**Chromatography**

- See also* Adsorption; Chemical analysis/adsorption
- flame detector, halogen sensitized, mechanism determ. 9-21739
- flue gases, power station instrument 9-16505
- gas, combined with mass spectrometry, for organic substances analysis 9-1887
- gas detector, radiation emission from sensitized flame meas. 9-21740

**Chromatography continued**

- gas-solid elution, rel. to determ. of entropies and heats of adsorption 9-19675
- gel permeation type, for molec. distrib. determ. of graphite binder mats. 9-8122
- hydrocarbon type analysis, fluorescent indicators 9-6031
- ionization detector to increase utility of gas chromatograph 9-21732
- separating column of large diameter, design, patent 9-20066
- valve, fine-regulation, for gas flow rate 9-15968
- Pb, Cu, Bi in boiling mixture separation by chromatography followed by spectrophotometric determ. 9-18779
- Ti complex of thiocyanate, paper chromatographic method for separation and identification 9-18772
- U complex of thiocyanate, paper chromatographic method for separation and identification 9-18772
- Zr complex of thiocyanate, paper chromatographic metho for separation and identification 9-18772

**Chromium**

- antiferromagnet, de Haas-van Alphen obs. of Q-vector truncating effect on Fermi surface 9-17461
- brittleness temp. threshold, gaseous impurity effect 9-1309
- diffusion in Fe and low C steel 9-5407
- diffusion in Fe and low C steel 9-5406
- diffusion in Fe-Cr alloy 9-5404
- diffusion in Nb, 953°-1435°C 9-13706
- diffusion Zircaloy-2 9-19761
- dislocation redistribution during annealing and deformation 9-13688
- electrical resistivity-temp dependence curve, second minimum near Neel temp. 9-12099
- electron-spin susceptibility from Knight shift meas. in liquid binary alkali metal alloys 9-13542
- evaporation rate from molten iron under vacuum 9-19658
- in ruby, conc. dependent spectral line shifts 9-1767
- lattice relaxation due to rapid heating through Neel temp. 9-21417
- magnetostriction stress-cooling effects rel. to ordering obs. 9-1700
- plating Ti alloys, effect on fatigue strength 9-3442
- powder, long range magnetic order by n diff. 9-14009
- recoil atoms in V, stopping 9-19875
- replacement of W in alloys 9-19842
- in ruby, ion pair e.p.r. spectrum 9-18734
- with spinel dispersed phase and nitrogen, spinel-nitrogen reaction 9-20032
- in steel, Kh12ND, welds, effect on structure and props. 9-14984
- thermal conductivity, elec. resistivity and Seebeck coeff., 77 to 400°K 9-15024
- X-ray emission spectra, K and L<sub>III</sub> bands rel. to band structure 9-1821
- X-ray interference, 293-1100°K 9-21312
- Al-SiO-Al structure, I-V, and temp. dependence, 60 to -185°C 9-1562
- Cr<sup>2+</sup> in MgO, acoustic paramag. resonance 9-21666
- Cr<sup>3+</sup> in α-MgMoO<sub>4</sub>, pseudo-Stark e.p.r. line splitting 9-18739
- Cr<sup>3+</sup> in ZnWO<sub>4</sub>, absorpt. and i.r. emission, theory 9-14058
- Cr diffusion layers on Fe materials, structure and metallography 9-11769
- Cr I, II absolute g<sub>v</sub>-values, shock tube radiation source 9-19399
- Cr<sup>3+</sup> in ZnS, decay behaviour of photo-induced e.s.r. 9-10290
- Cr<sup>2+</sup> in MgO, spin lattice relax. anisotropy theory 9-12318
- Cr<sup>3+</sup>, paramagnetic resonance in layer structure of NaInS<sub>2</sub> 9-8029
- Cr<sup>3+</sup> doped corundum, catalytic activation of H<sub>2</sub>-D<sub>2</sub> exchange 9-8085
- Cr<sup>3+</sup> in Al<sub>2</sub>O<sub>3</sub>, optically pumped, absorption spectrum 9-7967
- Cr<sup>3+</sup> in AlCl<sub>3</sub>, e.s.r. 9-12499
- Cr<sup>3+</sup> in Li<sub>2</sub>Ge<sub>2</sub>O<sub>7</sub>, R lines, width and position temp. dependence 9-5963
- Cr<sup>3+</sup> in Li<sub>2</sub>Ge<sub>2</sub>O<sub>7</sub>, energy transfer between nonequivalent sites 9-5964
- Cr<sup>3+</sup> in MgO, spectral line shift temp. dependence interpretation 9-12470
- Cr<sup>3+</sup> in NaInS<sub>2</sub>, layered crystal, e.p.r. rel. to hyperfine structure with coplanar In<sup>3+</sup> ions 9-10287
- Cr<sup>2+</sup> in ruby, e.p.r. absorpt., laser induced changes meas. by double resonance technique 9-10163
- Cr<sup>2+</sup> in Sr TiO<sub>3</sub>, R lines spectral shift 4 kV/cm electric field, 4.2°K 9-3709
- Cr(III,V) radiolytic form, in CrO<sub>4</sub>(NH<sub>4</sub>)<sub>2</sub>, e.s.r. obs. 9-20062
- MgO:Cr X-irrad., Cr<sup>2+</sup> phonon scatt., thermal cond. meas. 9-5535
- in SrTiO<sub>3</sub>, photoluminescence 9-21648

**Chromium compounds**

- alloys, magnetic susceptibility 9-7916
- chromium alums., classification 9-13591
- halides, band structure and charact. energy losses from continuous X-ray spectrum at high freq. limit 9-16210
- metal-like, X-ray spectra obs. rel. to band structure calcs. 9-3912
- 9-5513
- <sup>203</sup>Cr, Curie point anisotropy 9-12248
- Al-Cr alloy, dilute, low-temp. impurity resistance 9-1473
- Au-Cr thermoelectricity, positive hump of power 9-3720
- Cr-Fe alloys, dil. from Fe impurity e.p.r. 9-1858
- Cr-Ni alloys, thermoelectric power and resistivity, max. due to ordering for low Ni content 9-3721
- Cr-SiC system, composition and phases 9-1328
- Cr<sub>2</sub>O<sub>3</sub>-Fe<sub>2</sub>O<sub>3</sub>, electrical cond. and thermoelec. power, effect of chemisorbed hydrogen and water vapour 9-20036
- Cr<sub>2</sub>O<sub>3</sub>-La<sub>2</sub>O<sub>3</sub>, phase diagram up to 1,700°C 9-16152
- Cr<sub>2</sub>O<sub>3</sub>-SiO<sub>2</sub>-Al<sub>2</sub>O<sub>3</sub> system, phase equilib., data 9-19655
- Cr<sub>2</sub>O<sub>3</sub>, i.r. and Raman spectra 9-18705
- Cr(III) complexes, luminescence, temp. depend. 9-14076
- Cr complex, [Cr(urea)<sub>6</sub>](ClO<sub>4</sub>)<sub>3</sub>, cryst. and in soln., temp. depend. of luminesc. 9-12469
- Cr complex., [Cr(antipyrene)<sub>6</sub>](ClO<sub>4</sub>)<sub>3</sub>, cryst. and in soln., temp. depend. of luminesc. 9-12469
- Cr oxide, sintering and calcination study 9-1320
- CrB<sub>2</sub> irradiated by thermal neutrons, investigation of stability 9-1409
- Cr(CO)<sub>6</sub>, negative-ion metastable transitions 9-3015
- Cr<sub>11</sub>Ge<sub>19</sub>, mag. susceptibility and elec. conductivity meas., 80-1000°K 9-5799
- CrI<sub>3</sub>, internal field obs. from <sup>129</sup>I Mossbauer effect 9-21609
- CrIII tri-acetylacetonate, n irrad. and anneal., <sup>51</sup>Cr species, obs. 9-16504
- CrLaO<sub>3</sub>, crystal structure 9-16152
- Cr<sub>2</sub>O<sub>3</sub>-α-Fe<sub>2</sub>O<sub>3</sub>-La<sub>2</sub>O<sub>3</sub>, ternary phase diagram 9-13774
- Cr<sub>2</sub>O<sub>3</sub>-Fe<sub>2</sub>O<sub>3</sub> solid solutions, reduction behaviour at high temp. 9-17332
- CrO<sub>3</sub><sup>-</sup> radiolytic form, in CrO<sub>4</sub>K<sub>2</sub>, e.s.r. obs. 9-20062
- CrO<sub>4</sub>K<sub>2</sub>, n and p irrad., CrO<sub>3</sub><sup>-</sup> form., e.s.r. obs. 9-20062
- CrO<sub>4</sub>(NH<sub>4</sub>)<sub>2</sub>, n and p irrad., (Cr(V), Cr(III)) form., e.s.r. obs. 9-20062
- CrO halide complexes, ligand hyperfine interactions 9-17498

**Chromium compounds** continued

- Cr<sub>2</sub>O<sub>3</sub>, interaction with MgO, mechanism 9-3987  
 Cr<sub>2</sub>O<sub>3</sub>, reactions with MgO, effect of processing parameters on kinetics 9-3986  
 Cr<sub>1-x</sub>S with  $x \leq 0.12$ , structural and mag. phase transitions 9-13783  
 Cr<sub>2</sub>S<sub>3</sub>, structural and mag. phase transitions, vacancy ordering, obs. of trigonal superstruct. 9-13783  
 Cr<sub>2</sub>WO<sub>4</sub>, ordered trirutile, mag. ordering at 4.2°K from n.-diffr. exam 9-1701  
 Cr<sub>2</sub>WO<sub>4</sub>, ordered trirutile, mag. ordering at 4.2°K from n.-diffr. exam 9-1701  
 Cr-O system, phase diagram 9-18382  
 (8.2 wt.%)Cr-Fe alloy, polymorphic transform., effect on kinetics and phase equilb. temp. 9-5513  
 2Cr(en)<sub>3</sub>Cl<sub>2</sub>·6H<sub>2</sub>O, luminescence, temp. depend. 9-14076  
 Cu-Cr, susceptibility and specific heat obs., Kondo transition 9-19942  
 Cu-Cr alloy, f.c.c., effect of precip. hardening and recrystallization on texture 9-21391  
 Cu-Cr ESR, transmission conduction 9-8030  
 Fe-Cr-Al-Y alloy, oxide film formed in CO<sub>2</sub>, struct.- and composition 9-11779  
 Fe-Cr-Mn alloy, structure effect on oxidation resistance 9-5503  
 Fe-Cr-Ni, austenitic, in oxidizing acids, effect of Si content on corrosion resistance 9-17535  
 Fe (18 wt.%)Cr, alloy, increased oxidation at 1223°K due to Ni additions 9-20045  
 Fe-Cr, interdiffusion investigation in powder alloys 9-5405  
 Fe-Cr alloy, ageing, 475°C, rel. to Guinier-Preston zones formation 9-9785  
 Fe-Cr alloy, b.c.c., <sup>59</sup>Fe diffusion rel. to solvent atom diff. mechanism 9-7507  
 Fe-Cr alloy, diffusion of Cr 9-5404  
 Fe-Cr alloy, virtual spin-wave state below and above Curie pt 9-16343  
 Fe-Cr alloy Mossbauer spectra, use of Zero point calibration technique 9-19973  
 Fe-Cr alloys, itinerant electron ferromagnetism evidence 9-3797  
 Fe-Cr alloys, oxidation kinetics 9-20044  
 Fe-Cr alloys, oxide growth and spalling 9-18755  
 Fe-Cr alloys, self-diffusion of <sup>59</sup>Fe in para- and ferromag. temp. ranges 9-1245  
 Fe-Cr systems, diffusion, vacancy mechanism, specific features 9-9730  
 Fe (16wt.%)Cr crystal, corrosion pit nucleation, e. microprobe exam. 9-21697  
 Fe-Ni-Cr alloys, magnetization intensity and susceptibility rel. to heat treatment 9-12288  
 Fe<sub>2</sub>Cr superlattice alloys, isothermal magnetic annealing effects on magnetization and magnetostriction at high and room temperatures 9-15153  
 Fe-30 wt% Cr, stress-strain relations 9-1286  
 Hf-Cr system, phase diagram based on microscopic, X-ray and thermal analysis 9-14996  
 Ni-Cr-Al alloys, internal friction temp. dependence 9-14966  
 Ni-Cr-Cu-Al alloy, vacuum fractionation model. 9-7342  
 Ni-Cr-Ti alloys, internal friction temp. dependence 9-14966  
 Ni-Cr-W-Co-Al-Ti alloy, with horophilic addition, mech. props. effect of grain boundary composition 9-5475  
 Ni-Cr alloys, electrodeposition from aq. electrolytes 9-4007  
 Ni-Cr alloys, X-ray study of thermal expansion up to 900°C 9-21438  
 Ni-Cr dilute alloy, oxidation mechanism 9-20047  
 Ni-Cr films, bias-sputtered, preferred orientation 9-21265  
 Ni-Cr white castiron, heat treatment for improving mech. props., patent 9-13757  
 Ni (20wt.%)Cr wires of different lifetimes, oxidation 9-21695  
 NiCr films, resistivity change due to neutrons and γ rays 9-17378  
 Pd-Cr alloy films, e. diff. obs. rel. to elec. characts. 9-17242  
 Ti-Cr alloys, β-stabilized, resistance anomaly, 4.2°-473°K 9-12104

**Chromosphere** *see* Sun**Chronographs** *see* Time measurement**Cinematography***See also* Cameras

- auroral, image intensifier-videon system 9-14168  
 continuous film motion camera 9-10949  
 film viewing, still stroboscopic system 9-2431  
 time-lapse equipment for insect study 9-289  
 SF<sub>6</sub> a.c. arc characteristics filmed by laser-Schlieren technique 9-17881

**Circuits***See also* Amplifiers; Counting circuits; Oscillators

- a.c. conductor, for blocking low pot. galvanic currents of any polarity 9-8564  
 acoustic bridge for static and dynamic impedance meas. of eardrum 9-16637  
 acoustic bridge for static and dynamic impedance meas. of eardrum 9-16638  
 amplitude-to-time fast pulse converter, GHz equipment clock rate 9-4421  
 analog differentiation, instrumentation at I.F. 9-17848  
 autodyne for e.p.v. observations in weak fields 9-2295  
 batteries connected in parallel 9-6444  
 bridge for direct reading of a Pt resist. thermometer 9-15481  
 closed loop mode control of mag. field modulation 9-10796  
 Cockcroft-Walton voltage multipliers with arbitrary number of stages, anal. 9-17850  
 comparator for u.s. pulse echo attenuation 9-10734  
 condenser, under compression, current and elec. relax. calc. 9-200  
 current generator, four-sequential, for Electroanesthesia research 9-4138  
 current sweep circuit with sweep speed feedback 9-205  
 curve tracer for ferroelectric measurements, compensable and virtually grounded 9-1588  
 decay time const., rapid and accurate meas. method 9-10791  
 digital recording, de Haas-Van Alphen eff. meas. 9-17849  
 discriminator, fast leading-edge, 20 mV-I. V. threshold, 0.5 ns resolution 9-18041  
 discriminator and low-level linear gate for detection channeling equipment 9-4418  
 discriminator of amplitude and zero crossing detector, tunnel diode circuit 9-18040  
 double injection, noise and equivalent circuit 9-15115  
 dual input null networks utilizing RC ladders 9-20484  
 electric signal traces formation optical analogy 9-258  
 electrometer, vibr. reed transistorized, for demonstrations 9-2117  
 exploding wires, interaction with elec. circuit 9-6443

**Circuits** continued

- feedback oscillation excitation, metals internal friction automatic recording 9-1265  
 ferromagnetic system with saturable core coil, hysteresis losses 9-4409  
 flyback syst. for const. vel. Mossbauer drive 9-10793  
 frequency changes, small, meas. and appl. to thin film thickness determ. 9-12968  
 frequency sweep, uniform, for n.m.r. 9-4408  
 frequency synthesizer, unattended controller composed of I.C. and Si controlled rectifiers 9-10794  
 grounding switch, timed, low level signals after large transients, obs. 9-2306  
 Hall effect square root extractor, positive and negative signals, study 9-6457  
 heat and mass transfer analogue circuits 9-17822  
 inductor, variable, infinite Q 9-204  
 integrated, design and components, applic. of thin film technology, book 9-18402  
 limiter of fast pulses of 2 ns, delay correction 9-6460  
 linear gate, fast bipolar, dc-coupled, 3 ns switching time 9-20485  
 linearizing, temp. compensated, for low vel. hot-wire anemometry 9-17847  
 magic-T for meas. of transient variations in impedance 9-19119  
 with magnetic alloy cores, tape-wound 9-12975  
 micro, thin metal film on curved substrate, etching technique 9-8571  
 microcircuits, i.r. techniques for temp. meas. 9-4375  
 modulator-demodulator, optimal performance 9-14412  
 non-linear as analogues for soln. of non-linear fields 9-48  
 nonlinear, modeling of heat wave distrib. 9-20444  
 oscillator-detector, for programmed laboratory sequencers 9-10790  
 phase meter for subnanosecond electronic processes in semiconductors 9-20483  
 point diodes, equivalent circuit with microwave freq. dependent components 9-13903  
 pulse generation, high voltage, versatile 9-2304  
 pulse shapes from nuclear detector, meas. device 9-4420  
 pulse shaping unit, 10 ns resolving time, 100ns-2μs width 9-6733  
 readout systems for proportional multiwire chamber 9-4692  
 r.f. generator for quadrupole mass spectrometer 9-18129  
 simulation of boundary conds. in unsteady state heat and mass transfer 9-20443  
 sing-around velocimeter, reversal time effect of sound vel. meas. in liqs. 9-5153  
 sinusoidal waveform generation from sawtooth waveform 9-2305  
 spark timer, synchronous, solid-state 9-6455  
 stacking register, simultaneous input/output buffer, description 9-4419  
 switch for magnetic flux stabilizer, fail-safe 9-206  
 switching, characteristic parameters statistical evaluation of noise, threshold 9-6459  
 time measuring, fast nuclear lifetime spectroscopy 9-4417  
 timing, for rotating-prism Q-switched lasers 9-2364  
 transient state analysis by digital computer 9-6456  
 transient voltage decoupling elements, thyatron generator inexact timing 9-2307  
 transistor, dual, as thermometer probe 9-10797  
 transmission line pulse, low-impedance high-voltage, coaxial 9-10795  
 voltage divider, low-resistance, for photomultiplier 9-4442

**Clathrates** *see* Molecules; Organic compounds**Clay**

- analysis of raw materials and manufacturing props. correlation 9-4018  
 ceramic props. rel. to mineral composition 9-3163  
 clay-water foamed systems for lightweight aggregate prod. 9-3140  
 colloids role in deflocculation, rheology and casting 9-3134  
 electron micrograph of structure 9-3271  
 hectorite solutions, light scatt. in elec. fields rel. to rod-like struct. of particles and elec. props. 9-14861  
 illite, i.r. absorpt. spectrum, 3800-700 cm<sup>-1</sup> obs. and identification 9-12372  
 kaolin, i.r. absorpt. spectrum, 3800-700 cm<sup>-1</sup> obs. and identification 9-12372  
 montmorillonite, i.r. absorpt. spectrum, 3800-700 cm<sup>-1</sup> obs. and identification 9-12372  
 plasticity of clay-liq. mixtures, characterization using torque meas. rheometer 9-3425  
 sericite, i.r. absorpt. spectrum, 3800-700 cm<sup>-1</sup> obs. and identification 9-12372  
 Na bentonite amine complexes, H<sub>2</sub>O vapour and methanol adsorpt., hydrophilic-hydrophobic props., obs. 9-5261

**Cleavage** *see* Crystals/faces; Fracture**Clebsch-Gordan coefficients** *see* Field theory, quantum;*Nucleus/theory; Quantum theory***Climatology** *see* Meteorology**Clock paradox** *see* Relativity**Clocks** *see* Time measurement**Cloud chambers**

No entries

**Clouds**

- anisotropic scatt. particles, axially symmetric refl. and transmission functions of light 9-6076  
 cirrus, extinction coeff. meas. 9-20090  
 cirrus, i.r. raiance, 8-1 μ, physical model 9-6074  
 cirrus rel. i.r. sky radiance 9-16530  
 drops, collision efficiencies, theoretical calculations, experimental test 9-14159  
 electrification study from charge transfer between uncharged water drops in free fall in electric field 9-14160  
 ice, laboratory, near-infrared reflectivity 9-12584  
 ice, Venus, consistent with polarimetric obs. 9-8282  
 multiple-scattering calculations, sensitivity to single-scattering phase function 9-21770  
 noctilucent 1963-7 obs. 9-21769  
 nucleation study, automated aircraft instrumentation system 9-4056  
 spectra, refl., of high altitude clouds, models, 2.5-3.5 μ 9-12582  
 structure from i.r. sunlight refl. obs. 9-12583  
 supercooled, ice crystal dielec. polarity rel. to temp. 9-12183  
 Venus, composition 9-10528  
 volcanic smoke 9-6083  
 water, photographic obs. of the 'Glory', light scatt. phenomena, Hawaii 9-14162



**Clouds** continued

water droplets and ice crystals, behaviour, interpret. by applic. of thermodynamics of irreversible proc., book 9-20088

**Clusius-Dickel columns** *see Isotope separation***Co-ordination complexes** *see For inorganic complexes see under appropriate metal compound heading***Coal**

absorption bend at 1600  $\text{cm}^{-1}$  in i.r. spectra, rel. to aromatic strucls or conjugated chelated carbonyls 9-7964  
anthracite, carbonized and activated with  $\text{H}_2\text{O}$  vapour, microporous struct. 9-7406  
anthracite, influence of oxygen sorption on e.p.r. 9-10273  
electric discharge causing breakdown, energy characs. 9-10042  
humic acid for adsorption of radioactive materials 9-6008  
lean, carbonized and activated with  $\text{H}_2\text{O}$  vapour, microporous struct. 9-7406

**Cobalt**

addition to  $\text{Ni}_3\text{Mn}$  alloy, effect on props 9-12278  
addition to oxide glasses, effect on e.p.r. of  $\text{Cu}^{2+}$  9-18736  
atom, core-e energy levels and density of states, X-ray photoelectron spectrum 9-1813  
cast, galvanomag. effects rel. to  $\epsilon=\gamma$  transition 9-3578  
 $\text{Co}^{2+}$  in glass, optical absorption spectra obs., structural features determ. 9-10193  
coherent particles, interaction with dislocations, in Cu matrix 9-1213  
conductivity, thermal, calc. 290-1710°K from thermal diffusivity meas., 950-1710°K and elec. resistivity meas., 290-1710°K 9-1403  
crystal and nuclei growth and formation rate after deformation and annealing 9-19836  
diffusion in liquid Ga 9-13516  
diffusion of Fe and Ni and diffusion in Fe and Ni, heterodiffusion coeff., 1136-1370°C 9-19763  
f.c.c., ferromagnetic and paramagnetic props., comparison from theoretical eqns. 9-3787  
Film, growth on Ni, f.c.c. structure 9-7341  
films, electrodeposited, magnetocrystalline and uniaxial anisotropies 9-1678  
hexagonal phase, temp. depend. of magnetostriction coeff. 9-7903  
magnetic domain patterns rel. to magnetization process 9-16353  
magnetic domain walls in thin crystals 9-16354  
magnetic eqn. of state near Curie pt. 9-10127  
magnetic remanence, strain-induced 9-7905  
magnetic remanent domain struct., infl. of crystal thickness 9-5819  
magnetostriction infl. on domain structure 9-17453  
martensite platelets, shear-induced, geometrical form 9-9795  
morphology of vapour-deposited foils, eff. of deposition rate and temp. 9-14927  
precipitated particles in Cu-Co solid solns., distribution function rel. to mag. behaviour 9-5803  
in rock, spectrophotometric estimation 9-16525  
self-shielding factors for neutron resonances, scatt. dominant 9-18123  
solar abundance determ., including hyperfine structure 9-14249  
thermal conductivity, by Jain and Krishnan method, 1200°-1500°K 9-13807  
u.s. attenuation and vel. anomalies at high temp. 9-5547  
In  $\text{Al}_2\text{O}_3$ , effect of valence state on growth and colour 9-14908  
Co, anodic behaviour in acid and alkali solns. 9-12546  
 $\text{Co}^{2+}$ , e.p.r. in  $\text{CdWO}_4$ , elec-field eff. and angular dependence of line half-width 9-20016  
 $\text{Co}^{2+}$  in  $\text{ZnWO}_4$ , mag. props. anisotropy 9-16326  
 $\text{Co}^{2+}$  ions, isothermal diff. in pure NaCl cry., Soret eff. 9-21348  
Co ferromagnetic thin films, mag. birefringence 9-14034  
 $\beta$ -Co film, thick, preparation 9-11778  
 $\text{Co}^{2+}$ , e.p.r. in X-irrad.  $\text{K}_2\text{Co}(\text{CN})_6$  crystals. 9-10278  
 $\text{Co}^{2+}$ , paramagnetic ion in  $\text{Co}(\text{NH}_4)(\text{SO}_4)_2 \cdot 6\text{H}_2\text{O}$ , hyperfine interactions from NMR and EPR exam 9-8038  
 $\text{Co}^{2+}$  in glass, EPR spectra obs., structural features determ. 9-10193  
 $\text{Co}^{2+}$  in  $\text{MgF}_2$ , far i.r. spectrum of  $\text{Co}^{2+}$  ion pairs 9-1788  
 $\text{Co}^{2+}$  in  $\text{MgO}$ , spin lattice relax. anisotropy theory 9-12318  
 $\text{Co}^{2+}$  in  $\text{MgSeO}_4 \cdot 6\text{H}_2\text{O}$ , e.s.r. 9-1856  
 $\text{Co}^{2+}$  in KCl, F-centres, growth and bleach at room temp. 9-5386  
 $\text{Co}(\text{II})$ , solvation determ. by  $^{17}\text{O}$  n.m.r. 9-3123

**Cobalt compounds**

alloys, with Fe and Co, friction rel. crystal structure and atomic ordering 9-19814  
alnico, structural states, X-ray diff. exam 9-1179  
cobalt-rare earth intermetallic cpds., mag. resonance at 9.3 GHz 9-14100  
disilicide-nickel disilicide solid solns., lattice parameters, densities, thermal expansion and elec. conductivity 9-3480  
magnetostatic and exchange interactions between particles 9-18676  
Pt-(52 wt.%)Co alloy, ordered, magnetic anisotropy, 298° and 77°K 9-21583  
Ticonal 2000, sintered alloy in high coercivity state, structure 9-3302  
tris-dipyridyl  $\text{Co}(\text{III})$  perchlorate trihydrate,  $^{59}\text{Co}^{3+}$ -doped thermal exchange and annealing 9-9779  
tris-dipyridyl  $\text{Co}(\text{III})$  perchlorate trihydrate, n-irrad., thermal exchange and annealing 9-9779  
Au-Co alloys, liquid, ferromagnetism 9-13540  
 $\text{Ce}_{1.05}\text{Co}_{0.25}\text{Cu}_{0.75}$  alloy, permanent mag. props. and prep. 9-3795  
Co-Al intermetallic, mag. susceptibility and n.m.r. study 9-7888  
Co-Cu alloys, hexagonal, mag. moments rel. to e. transfer 9-12274  
Co-Cu mixed crystals, nucleus formation at dissociation 9-14988  
Co-Fe alloy, cold rolling to give constricted mag. hysteresis loop, patent 9-13759  
Co-In system, liquid immiscible behaviour 9-21241  
Co-Nb alloy, precip. of new phase after ageing 9-9796  
Co-Ni-Fe films, vapour deposited nonmagnetic mag. props. 9-5837  
 $^{57}\text{Co}$ -Pd experimental Mossbauer source prod 9-11898  
Co-Pt alloy, ordered, nature of coercive force 9-10118  
Co-Pt alloys, magnetic ordering, effect of thermomagnetic treatment 9-3767  
Co-V alloys, n.m.r. of  $^{59}\text{Co}$  9-15204  
Co(II) thiourea complex, subnormal mag. moment 9-18194  
Co complex,  $[\text{CoX}_2 \cdot 2\text{L}]$  and  $[\text{CoL}_4] (\text{ClO}_4)_x$  ( $\text{X}=\text{Cl}, \text{Br}, \text{I}$  and  $\text{L}=2$ -thiazolidine) i.r. and electronic spectral studies 9-20926  
Co complex, bis(1,2,3,4-tetrachlorobenzene-5,6-dithiolato)cobaltate, crystal and molec. struct. 9-17266  
Co complex, cis-cobalt diazobisethylenediamine nitrate, crystal structure 9-11840

**Cobalt compounds continued**

Co complex, hexaamminecobalt (III) iodide, crystal structure rel. to Co-N bond lengths 9-13631  
Co oxides, Mossbauer study of Fe atoms behaviour, crystal structure interpretation 9-5887  
 $\text{CoCl}_2 \cdot 6\text{H}_2\text{O}$ , colour changes with temp. 9-20559  
 $\text{CoCl}_2$ , specific heat, 1.8-4°K, rel. to mag. props. of lamellar antiferromagnets 9-1393  
 $\text{CoCl}_2 \cdot 2\text{H}_2\text{O} \cdot \text{Mn}^{2+}$  antiferromagnetic, exchange interactions 9-3834  
 $\text{CoCl}_2 \cdot 2\text{H}_2\text{O} \cdot \text{Mn}^{2+}$ , exchange contribution to D-parameter 9-3776  
 $\text{CoCl}_2 \cdot 2\text{H}_2\text{O}$ , proton spin lattice relaxation time, anomaly in angular dependence 9-3840  
 $\text{CoCl}_2 \cdot 6\text{H}_2\text{O}$ , antiferromagnetic relaxation, eff. of finite lattice heat capacity 9-8006  
 $\text{CoCo}_3$ , antiferromag. resonance, freq., mag. field strength dependence 9-1849  
 $\text{CoF}_2$ , Raman scattering spectra and two-magnon absorption, Green's function method 9-12435  
 $\text{CoF}_2$ , spin-optical phonon interaction, obs. 9-10146  
 $\text{CoF}_2 \cdot 5\text{HF}_6\text{H}_2\text{O}$ , magnetic anisotropy and susceptibility 9-7878  
 $\text{Co}_2\text{Fe}_{1-x}$ , induced anisotropy const., Co content eff. 9-5847  
 $\text{Co}(\text{II})$  complexes, isotropic proton mag. reson. shifts 9-13349  
 $\text{CoMn}_2\text{Fe}_{1-x}\text{O}_4$  charge distrib. from Mossbauer spectra 9-1119  
 $\text{Co}(\text{NH}_4)_2(\text{SO}_4)_2 \cdot 6\text{H}_2\text{O}$ , paramag.  $\text{Co}^{2+}$  hyperfine interactions, NMR and EPR exam. 9-8038  
 $\text{Co}(\text{NO}_3)_2$ , soln.,  $\beta$  backscatt. rel. to conc. 9-10367  
 $\text{Co}_{1-x}\text{Ni}_x\text{S}_2$ , itinerant d-electron type ferromagnetism 9-1674  
 $\text{CoO}$ -Li elec. conductivity and thermoelec. power rel. press. and temp. 9-21506  
 $\text{Co}_3\text{O}_4$ - $\text{Mn}_3\text{O}_4$  (or  $\text{Fe}_3\text{O}_4$ ) solid solns., interaction and substitutional disorder 9-17333  
 $\text{CoO}$ ,  $^{57}\text{Fe}$  relaxation rates, limitations 9-1749  
 $\text{CoO}$ , antiferromagnetic resonance and symmetry 9-21593  
 $\text{CoO}$ , cryst. struct., rebuttal of Schroer-Tritshauer interpretation 9-1178  
 $\text{CoO}$ , electrical conductivity and thermogravimetric studies for defect conc. 9-3569  
 $\text{CoO}$ , heats of formation of point defects 9-17276  
 $\text{CoO}$ , nature of nonstoichiometry from i.r. absorption spectra 9-19989  
 $\text{CoO}$ , semiconducting, optical absorpt. of small polarons in near and far i.r. 9-5929  
 $\text{CoO}_{1-x}$ , i.r. absorption spectra 9-19989  
 $\text{Co}_2\text{P}_2\text{O}_7$ , monoclinic, crystallographic data 9-5324  
 $\text{CoSe}_2$ , chemical bonding, X-ray spectroscopic study 9-20931  
 $\text{CoWO}_4$ , long-wave i.r. absorpt. band identification and spin wave spectrum 9-1773  
 $\text{Co}_2\text{Zr}$ , anisotropy of paramagnetic line point 9-12248  
 $\text{Co}_2\text{Zn}_{0.5}\text{Fe}_{0.5}\text{O}_4$ , paramagnetic susceptibility maximum at Curie point 9-16368  
 $\text{Co}^{2+}$ - $\text{Hg}^{2+}$  nitrate soln.,  $\beta$  backscatt. rel. to percentage comp. 9-10367  
 $\text{CrF}_2$ , exchange integrals in paramagnetic phase 9-1643  
CsI photocathode u.v. quantum efficiency, e-irrad. effects, 1-2 MeV 9-12224  
Fe-Co, alloys, ferromagnetism and order 9-3788  
Fe-Co alloy, lattice parameters and Curie point anomalies 9-18444  
Fe-Co alloy (Permuend), V addition, magnetic anisotropy 9-12281  
Fe-Ni-Co alloys, monocrystalline thin films, epitaxial growth and coercive force 9-12298  
Ni-Co-Si alloy, Nicosi, magnetostrictive, anisotropy, static and dynamic props. 9-5830  
Ni-Co alloy, deformed, positron annihilation 9-21477  
Ni-Co alloys, absolute thermo e.m.f., eff. of plastic deformation 9-21543  
Ni-Co alloys, dil. ferromag., elec. resistivity and screening 9-5645  
Ni-Co thin films, strain insensitive, 17 to 50 at.%Ni 9-5843  
Ni-Cr-W-Co-Al-Ti alloy, with horophilic addition, mech. props. effect of grain boundary composition 9-5475  
Ni-Zn-Co alloy Procopieff effect in bar sample 9-3832  
Pd-Co alloys, ferromag., specific heat, 1.4 to 4.2°K 9-16178  
Pt-Co alloys, ferromagnetic, specific heat, 1.4 to 4.2°K 9-16178  
Pt-Co alloys, low temp. susceptibility, anomalous 9-13966  
Pt-Co permanent magnetic alloy, improvement of mag. props. by replacement of Pt by Pt groups metals 9-12294  
Pt-Co alloys, superlattice formation, field-ion microscope obs. 9-7402  
W-Co alloys, compressive creep deformation at elevated temps. 9-7555  
Zr-Co alloy, spot cooled, new non-crystalline phases 9-5523

**Cochlea** *see Ear***Coherence** *see Electromagnetic waves; Lasers; Light/coherence; Masers***Cohesive energy** *see Bonds; Solids***Coincidence circuits** *see Counting circuits***Cold working**

*See also Plastic deformation; Slip; Work hardening*

Bauschinger effect, yield strength rel. to cold-forming state-of-stress 9-5457  
ferromagnetic articles, hardening depth from non-destructive test model 9-17327  
metals tending to brittle fracture, adhesion under combined plastic deformation 9-5492  
recovery, stage III in cold worked metals, kinetics 9-5500  
steel, 12% Mn, austenitic-martensitic transformation obs. by transmission electron microscopy 9-5516  
Ag, f.c.c., rolling texture formation by slip and mech. twinning 9-19815  
Al-Be alloy, effect on clustering 9-18458  
Al, cyclic work softening, effect on yield curves in tension 9-18504  
Au, internal friction, cold-worked and irradiated at low temp. 9-5430  
Au phase V restoration 9-19827  
AuMn, phase transform.,  $\beta$ -martensitic f.c.c., caused by cold work and subsequent heating 9-3486  
Co-Fe alloy, cold rolling to give constricted mag. hysteresis loop, patent 9-13759  
Co, crystal nuclei growth and formation rate 9-19836  
Cu, f.c.c., rolling texture formation by slip and mech. twinning 9-19815  
Cu, rolling texture form. by slip, orientation changes and deform. bands 9-9777  
Fe-(30 wt.%)Ni-(5 wt.%)Nb austenitic alloy, phase transform. 9-9802  
Fe and Fe-Si, rolling effect on embrittlement 9-1311  
Fe powders, compressibility increase by cold rolling, patent 9-13749  
LiF crystallite size and microstrains, evaluation from X-ray diff. line profiles 9-13640  
Zr-(2.5 wt.%)Nb corrosion resistance, cold deformation effect 9-647

**Collections of physical data**

*Only comprehensive works of reference are listed here*

- formulae and data of use to first year engineering students 9-14303  
 homopolymers, linear, physical constants, book 9-11756  
 ionospheric observations, Dec. 1967 9-4073  
 ionospheric observations, Feb. 1968 9-6089  
 ionospheric observations, Jan. 1968 9-4074  
 Magnetic Observatory at Baker Lake, Canada, obs. record, 1966 9-8207  
 metals and semiconds., tabular reduction of cryst. chem. information 9-16073  
 molten salts, electrical conductance, density and viscosity data 9-11714  
 for nuclear reaction analysis, graphs and tables 9-13216  
 theoretical derivations, formulae and data, pocket-book 9-4203  
 thermodynamic and thermochemical tables 9-3053  
 upper atmosphere geophysics, world data centre A, growth and future plans 9-20093  
 X-ray diffraction powder patterns, standard 9-11809

**Collective model** *see* **Nucleus/models****Collision processes**

*See also* **Atoms/electron scattering; Charge exchange; Elementary particles; Field theory, quantum/interactions; Ionization; Nuclear forces; Nuclear reactions and scattering; Scattering, particles; and under the individual particles**

No entries

**atoms**

- absorption spectra, effect of dispersion on exponential dipole moment model 9-4860  
 Alkali<sup>+</sup>-alkali nearly adiabatic thermal collisions, excitation transfer, Stueckelberg's formula and difficulties 9-18154  
 alkali, heavy, selection rules rel. to  $m_j$ -mixing in lowest  $^2P_{1/2}$  states 9-9147  
 alkali metal-rare gas, fine structure transitions 9-11411  
 binary-encounter and Bethe theory, applic. to meas. of differential X-sections of H atom by fast charged part. 9-4871  
 close-coupling approx., trial wave function method examined 9-13276  
 collected Russian papers 9-696  
 Coulomb interac., extension of integral formulation of scatt. theory 9-17725  
 cross-section behaviour near threshold for reaction in attractive Coulomb field 9-708  
 depolarization effect on resonance fluoresc. 9-706  
 diabatic and adiabatic representations 9-18151  
 elastic scattering induced perturbation, Landau-Zener-Stueckelberg formula applic. 9-6987  
 electronic transitions in near-adiabatic collisions 9-4979  
 with electrons, rel. to diffusion in inert gas atmosphere 9-15975  
 excitation transfer, non-reson., in collisions induced by dipole-dipole interaction. 9-11401  
 films, solid, interaction causing elastic waves, eff. on adsorption props 9-5233  
 high-energy ion-atom with electron exchanges, scatt. eqns. and amp., coupling potentials 9-11406  
 high-energy neutral atoms prod. by scatt. of ions, rel. to sputtering 9-2806  
 inelastic, angular distrib. 9-9149  
 interatomic potentials, deduction from low energy ion range meas. in amorphous solids 9-5585  
 inverse problem in atom-atom scatt. in WKB approach 9-9148  
 ion-atom, parametric treatments comparison for low and high impact vel. 9-11407  
 K X-radiation excitation by  $\alpha$ -bombard. obs. 9-677  
 Kr electron capture cross sections, from  $^2P_{1/2}$  to  $^2P_{1/2}$  states 9-4863  
 matrix elements incorporating momentum transfer 9-15824  
 mechanism under gas-kinetic conditions 9-20889  
 metastable-ionic ground states, mag. resonance obs. 9-11400  
 molecular systems, nuclear and electronic motion separation approx., accuracy 9-20914  
 with multi-charged ions, rel. to Auger ionization 9-13302  
 neutral with outer 2p and 3p electrons, ioniz. by e and proton impact, X-section calc. from Born approx. 9-4859  
 particle flux conservation 9-709  
 Penning ionization, e energy analysis 9-903  
 periodic, electrons with nucleus, wave function formation possibility 9-15823  
 photon scattering, quantum interpretation of resonances 9-20869  
 Q values, influence on scatt. cross sections 9-11408  
 radial eqns. 9-707  
 reactive, in thermal gas, dynamics 9-12524  
 recoil atoms in solids, slow, stopping 9-19875  
 repulsive inverse-power potential, scatt. cross-sections calc. 9-705  
 resonance fluorescence depolarization, theoretical study 9-9146  
 review 9-6988  
 scattering, Harris variational method for phase shifts, analysis w.r.t. other methods 9-11404  
 scattering, stepfunction model for total cross-section calcs. 9-20995  
 spectral line broadening, role of repulsive forces 9-13305  
 in stellerator, containment 9-886  
 superposition of two power pots, scatt. amplitude and total cross-section 9-4861  
 two-body syst., separable series expansion for off-shell two-body t matrix with Coulomb pot. 9-13306  
 van der Waals interactions of two and three atoms, upper bounds 9-15825  
 X-ray prod. from 20-80 keV ion beam collisions with C target 9-9151  
<sup>85</sup>Rb, spin-exchange cross-section obs. 9-9152  
<sup>217</sup>Pb, charged and neutral, attachment coeffs. to polystyrene latex aerosols 9-9565  
<sup>133</sup>Cs, spin-exchange cross-section obs. 9-9152  
 Ar, electron capture cross sections, from  $^2P_{1/2}$  to  $^2P_{1/2}$  states 9-4863  
 Ar, K<sup>+</sup> scatt., cross section meas.,  $E_k=150-4000$  eV 9-18152  
 Ar, K scatt. in thermal energy range, total cross section meas. 9-11413  
 Ar, polarizability induced, and light scatt. 9-959  
 Ar excitation by He<sup>+</sup>, spectra obs.,  $E_{ex}=0.3-10$  keV 9-20887  
<sup>26</sup>Ar, inelastic n. scatt. exam. of gas dynamics near condensation 9-15971  
 B, lifetimes and levels of collisionally excited ions 9-6959  
 C target various ion beams, 20-80 keV, K X-ray prod., mol. orbit mechanism 9-9151  
 Cl,  $^2P_{1/2}$  ground state, kinetics of overall recombination 9-19409  
 Cr, radioactive, in V, stopping of slow recoil atoms 9-19875  
 Cs<sup>+</sup>-inert gas nearly adiabatic thermal collisions, excitation transfer, Stueckelberg's formula and difficulties 9-18154  
**Collision processes** continued  
**atoms continued**  
 Cu, radioactive, in Zn, stopping of slow recoil atoms 9-19875  
 D<sup>+</sup>-D charge-exchange cross-sections, eff. of apparatus geom. 9-4872  
 H<sup>+</sup>-D charge-exchange cross-sections, eff. of apparatus geom. 9-4872  
 H H Coulomb interaction matrix elements and pots. calc. 9-18157  
 H H spin-exchange cross section, meas. by variation of T<sub>1</sub> and T<sub>2</sub> with at. density 9-11419  
 H<sup>+</sup>-H charge-exchange cross-sections, eff. of apparatus geom. 9-4872  
 H-He, Ne, Ar; polar. of Lyman  $\alpha$  rad., Born and distortion rotational approx. 9-13313  
 H-He van der Waals interaction rel. to hyperfine press. shift 9-4873  
 H, and ions, low energy scatt. at metal surface 9-2828  
 H, differential X-sections for ioniz. by fast charged part., binary-encounter and Bethe theory 9-4871  
 H, K and L shell electron ejection probability in collision with other atoms 9-13450  
 H elastic scattering of photons, retardation effects 9-15831  
 H van der Waals const. computation 9-722  
 H<sup>+</sup>, charge exchange with Cs vapour, 0.5-20 keV, cross section obs. 9-13314  
 H<sup>+</sup>, double electron capture cross section obs. on various targets, 75-250 keV 9-13315  
 H<sup>+</sup> alkali metal vapour, charge exchange 9-6985  
 H-H<sub>2</sub> (para and ortho) collisional excitation of rot. levels calc. up to J=15, and for  $10 \leq T \leq 10^4$  K 9-14227  
 He-Ar mixtures, collision-induced absorpt. spectrum 9-2829  
 He<sup>+</sup>-Cs, charge exchange, 1.5-25 keV 9-4890  
 He<sup>+</sup>-He elastic and inelastic X-sections at 500-3000 eV., differential scatt. meas. 9-4887  
 He-He with charge exchange, cross-section meas., 400-2000 eV. 9-18158  
 He-Ne laser, broadening effect on transition linewidths 9-10861  
 He-Ne laser, with impurity gas (Ar, Kr or Xe) 9-19145  
 He,  $2^2S_1/2$ - $1^1S_0$  repulsive interaction pot., long range calc. and obs. 9-4889  
 He, energy transfer between n=4 states, cross-sections 9-9161  
 He, K scatt. in thermal energy range, total cross section meas. 9-11413  
 He, of second kind in n<sup>+</sup>P and normal states, X-section meas. 9-4880  
 He and zero-energy e, elastic, scatt. lengths and reciprocals calc. and data 9-4885  
 He beam in H, charge-exchange and metastable He form. 9-5071  
 He oriented metastable atoms, with Ne, polarization transfer 9-711  
 He with He, excitation cross section 9-687  
 He with proton beam, resulting polarization of light, violation of  $\Delta S=0$  spin rule 9-9160  
<sup>3</sup>He, metastable, diffusion and excitation transfer 9-6995  
 He<sup>+</sup> on Ne, analysis using differential cross-section formulae 9-9149  
 He<sup>+</sup> with Ar and Kr, 5 to 300 eV, optical excitation 9-6996  
 He-K<sup>+</sup> excitation of KII resonance lines 9-14676  
 He-K<sup>+</sup>, excitation of KII resonance lines 9-2834  
 He<sup>+</sup>-inert gas, nearly adiabatic thermal collisions, excitation transfer, Stueckelberg's formula and difficulties 9-18154  
 He( $2^2S$ )+X→He<sup>+</sup>X<sup>+</sup>+e cross-sections 9-14675  
 He( $2^2S$ ) metastable atom destruction by Ar 9-13318  
 Hg-Hg multiple scatt. and collisions, effect on resonant light backscattered by  $6^3P$  state 9-674  
 Hg metastable atom-electron inelastic second-order collisions 9-18153  
 K,D<sub>2</sub>; resonance radiation trapping and quenching,  $4^2P$  state lifetime meas. 9-14670  
 K,H<sub>2</sub>; resonance radiation trapping and quenching,  $4^2P$  state lifetime meas. 9-14670  
 K,H,D; resonance radiation trapping and quenching  $4^2P$  state lifetime meas. 9-14670  
 K,N<sub>2</sub>; resonance radiation trapping and quenching,  $4^2P$  state lifetime meas. 9-14670  
<sup>39</sup>K, spin exchange cross-section obs. 9-9152  
 Kr-Kr, meas. of total ionization cross section of Kr 9-13456  
 Kr, polarizability induced, and light scatt. 9-959  
 Kr<sup>+</sup>-Kr coincidence meas. 9-11410  
<sup>7</sup>Li<sup>+</sup>, scatt. by free atoms and mols. 9-13308  
 N-He, short-range effects rel. to hyperfine const. press. shift 9-4864  
 N-He van der Waals interaction rel. to hyperfine press. shift 9-6989  
 N<sub>2</sub>-He atom collisions resonances in cross section obs. 9-7034  
 Na-He, transitions between fine structure levels in Na, cross section 9-11411  
 Na-N<sub>2</sub> beam interaction, excitation energy transfer, obs. 9-9308  
<sup>23</sup>Na, spin exchange cross-section obs. 9-9152  
 Ne-Ne, meas. of total ionization cross section of Ne 9-13456  
 Ne, diff. cross section meas., intermolecular potential determ. 9-11412  
 Ne, K scatt. in thermal energy range, total cross section meas. 9-11413  
 Ne, with oriented metastable He atoms, polarization transfer 9-711  
 Ne excitation by He<sup>+</sup>, spectra obs.,  $E_{ex}=0.3-10$  keV 9-20887  
 Ne<sup>+</sup> with Ar and Kr, 5 to 300 eV, optical excitation 9-6996  
 Rb-He, transitions between fine structure levels in Rb, cross section 9-11411  
<sup>87</sup>Rb, spin-exchange cross section obs. 9-9152  
 Rb<sup>+</sup>-inert gas nearly adiabatic thermal collisions, excitation transfer, Stueckelberg's formula and difficulties 9-18154  
 W, surface scattering of slow Cs<sup>+</sup> ions 9-5231  
 Xe, K scatt. in thermal energy range, total cross section meas. 9-11413  
**molecules**  
 acetylene, gas, electron drift vel., momentum transfer and energy loss calc. 9-17166  
 atom-mol. scatt., quenching of glory extrema 9-839  
 benzene, gas, ion mol. react., ion disappearance rate const. 9-17078  
 cross-section, new contrib. due to ang. depend. part in London dispersion forces 9-11513  
 diagrammatic representation of resonances 9-7006  
 diatomic, vibr.-vibr. translational energy transfer 9-840  
 diatomic mol. with atom, distorted, wave theory 9-9305  
 diatomic mol. with atom, quantum mech. 9-4977  
 dichloroethylene+C<sub>2</sub>H<sub>2</sub>Cl<sub>2</sub> (or Cl<sub>2</sub>)→C<sub>2</sub>H<sub>2</sub>+neutral prods., direct processes 9-4984  
 differential eqns. 9-2933  
 dimethyl ether, gas, electron drift vel., momentum transfer and energy loss calc. 9-17166  
 dissociation of homopol diatomic mol., proper choice of final state wave function 9-9288  
 electron ejection, surface effects 9-19936  
 electronic transitions in near-adiabatic collisions 9-4979  
 electronic transitions in near-adiabatic collisions 9-4979  
 energy transfer in distorted wave approx. 9-4978



**Collision processes continued****molecules continued**

- ethane, gas, electron drift vel., momentum transfer and energy loss calc. 9-17166  
 ethylene gas, electron drift vel., momentum transfer and energy loss calc. 9-17166  
 Franck-Condon principle violation 9-13402  
 gases, range of 5-50keV heavy ions 9-14739  
 inelastic scatt., diagonalization of phase shift matrix 9-2929  
 infrared absorption in rare gas mixtures 9-4914  
 interactions rel. to elec. field intensity for Kerr effect 9-13525  
 ion-molecule, computer plots 9-3012  
 liquid, contributions to optically induced nonlinearities 9-13524  
 macromolecular solutions, critical opalescence 9-16027  
 methane, press. broadening and shift of 3.39  $\mu$  line perturbed by inert gases 9-15891  
 methanol, gas, electron drift vel., momentum transfer and energy loss calc. 9-17166  
 methyl chloride, gas, electron drift vel., momentum transfer and energy loss calc. 9-17166  
 microwave triple resonance,  $\Delta J=2$  induced transitions 9-17073  
 molecular beams, transformation relationships from c.-of-m. to lab. obs. 9-2932  
 N<sub>2</sub>-Na beam interaction, excitation energy transfer, obs. 9-9308  
 near-resonant collisions, energy transfer 9-20996  
 neutron scatt. from C<sub>3</sub> mols. 9-4892  
 nonreactive subexcitation, adiabatic approx. 9-836  
 oil in diffusion pump vapour jet, mol. velocity distrib. after impact 9-20994  
 phosphine, gas, electron drift vel., momentum transfer and energy loss calc. 9-17166  
 propane gas, electron drift vel., momentum transfer and energy loss calc. 9-17166  
 quenching of glory undulations 9-2934  
 reactive collisions, perturbed Morse oscillator calc. 9-16479  
 reflection from surface, kinetic and spatial distrib. in rarefied atmos. 9-11654  
 resonances in rotational excitation 9-837  
 scattering amplitude and rot. ang. depend., elastic collisions 9-17074  
 spectral line broadening, influence of proper vol. 9-2839  
 toluene, gas, ion-mol. react., ion disappearance rate const. 9-17078  
 transition probabilities for rotational excitation, exact eval. vs. variational computation 9-11512  
 triatomic mol. with atom, intramol. vib.-vib. energy transfer 9-11440  
 in turbomolecular pump, accommodation process 9-937  
 vibration-translation energy transfer, coupled eqns. 9-838  
 vibrational and rotational energy transfer 9-4981  
 vibrational transitions, preferential orientations 9-13401  
 vibronic states, energy transfer per collision, three-level model 9-15910  
 xylenes, gas, ion-mol. react., ion disappearance rate 9-17078  
 CO<sub>2</sub>-O<sub>2</sub> relaxation time meas. 9-4922  
 CO<sub>2</sub>-CO<sub>2</sub> quadrupole-quadrupole interac., rot. line widths of 15 and 4.3  $\mu$  bands 9-19494  
 CO<sub>2</sub>-N<sub>2</sub> quadrupole-quadrupole interac., rot. line widths of 15 and 4.3  $\mu$  bands 9-19494  
 CO<sub>2</sub> vibration energy transfer mechanism in collision between isotopes 9-18227  
 CO<sub>2</sub>+N<sub>2</sub>, near-resonant transfer of vibr. energy 9-20996  
 CO<sub>2</sub> relaxation time from  $\nu_3$  vibr., variation with temp. 9-4922  
 D<sub>2</sub>+X<sup>+</sup>→D+XD<sup>+</sup>, reaction cross-sections, 1-100eV 9-17075  
 H<sub>2</sub><sup>+</sup>(H<sub>2</sub>, Ar, Xe), dissociation proc. by meas. of energy distrib. of prod. protons 9-4968  
 H<sub>2</sub>-H<sub>2</sub>, two-body potential and elastic scatt., quantum theory 9-2936  
 H<sub>2</sub><sup>+</sup>-N<sub>2</sub>, N<sub>2</sub><sup>+</sup> rot. excitation, 0.4-3.0 keV 9-4982  
 H<sub>2</sub> in liq. Ar, collision-induced absorpt., liq. cell model 9-21214  
 H<sub>2</sub> in liq. Ar, collision-induced absorpt., liq. cell model 9-21213  
 o-p H<sub>2</sub> scattering cross-sections 9-20997  
 H<sub>2</sub>, K scatt. in thermal energy range, total cross section meas. 9-11413  
 H<sub>2</sub> with Li<sup>+</sup> ions, vibrational excitation 9-7097  
 H<sub>2</sub> and D<sub>2</sub>, with slow K<sup>+</sup>, vibr. excitation and fragmentation 9-2937  
 HBr-HBr, vibrational transitions P<sub>1,0</sub> probabilities 9-11514  
 HCl-rare gas, cross-section, new contrib. due to ang. depend. part in London dispersion forces 9-11513  
 HD<sup>+</sup>, dissociation by inert gases 9-7077  
 HF-H<sub>2</sub>, He, Ar; vibrational transitions P<sub>1,0</sub> probabilities 9-11514  
 HI-Ar, Hi; vibrational transitions P<sub>1,0</sub> probabilities 9-11514  
 H-H<sub>2</sub> (para and ortho) collisional excitation of rot. levels calc. up to J=15, and for 10<T<10<sup>4</sup>K 9-14227  
 HCl-HCl and H<sub>2</sub>Cl-H<sub>2</sub>Cl, vibrational transitions P<sub>1,0</sub> probabilities 9-11514  
 K<sup>+</sup>-r<sub>2</sub> reactive collisions in molec. beams, theory 9-10323  
 N<sub>2</sub>-He atom collisions resonances in cross section obs. 9-7034  
 N<sub>2</sub> with inert-gas ions, charge transfer and dissociation 9-15957  
 N<sub>2</sub> with heavy ions, excitation of 3914A N<sub>2</sub><sup>+</sup> rad. 9-18187  
 N<sub>2</sub>, excited in ion-mol. collisions, Franck-Condon principle violated below a certain projectile vel. 9-13402  
 N<sub>2</sub><sup>+</sup> dynamics of reaction with H<sub>2</sub>, D<sub>2</sub>, and HD 9-17513  
 NH<sub>3</sub>, inert-gas collision-induced transitions between rot. levels 9-11469  
 Na-D<sub>2</sub>, Na/3<sup>2</sup>P<sub>1/2</sub>=3<sup>2</sup>P<sub>3/2</sub> excitation transfer cross sections, obs. 9-9309  
 Na-H<sub>2</sub>, Na/3<sup>2</sup>P<sub>1/2</sub>=3<sup>2</sup>P<sub>3/2</sub> excitation transfer cross sections, obs. 9-9309  
 Na-HD, Na/3<sup>2</sup>P<sub>1/2</sub>=3<sup>2</sup>P<sub>3/2</sub> excitation transfer cross sections, obs. 9-9309  
 Na-N<sub>2</sub>, Na/3<sup>2</sup>P<sub>1/2</sub>=3<sup>2</sup>P<sub>3/2</sub> excitation transfer cross sections, obs. 9-9309  
 O<sub>2</sub>, electron collision, 0-200eV, vac.u.v. emission 9-17040

**Collision processes, plasma** *see Plasma/collision processes***Colloids**

- See also Electrophoresis; Emulsions; Gels; Sols; Thixotropy*  
 capillary porous, moisture diffusion coeff. at all drying temps. 9-21243  
 clay slips, rel. to deflocculation, rheology and casting 9-3134  
 conference, 1968, Chicago, USA 9-14863  
 dimethyldodecylamine oxide micelle surface pot., long-chain alkyl and small ions effects 9-7289  
 extinction index of colloidal suspensions for magnetic fields examination 9-1051  
 graphite, optical transmission in magnetic field 9-1050  
 magneto-optical cross effects, laser light induced 9-3133  
 nonlinear laser light scatt. effects, rel. to shape and size of particles 9-14866  
 nonlinear Poisson Boltzmann boundary-value problems, variational solns. 9-21048  
 proton self-diffusion, by spin echo 9-3127  
 resonance absorpt. of  $\gamma$ -quanta, effect of viscosity 9-3138

**Colloids continued**

- supracolloidal suspensions, coagulation behaviour, study using Coulter counter and particle size distrib. 9-9562  
 suspensions, light absorption and scatt., extinction coeff. rel. to particle size, for strongly absorbing subst. 9-14865  
 thermodynamics of charged and polarized layers, book 9-10662  
 AgBr, in Sc(NO<sub>3</sub>)<sub>3</sub> soln, critical coagulation and stabilization concs. 9-9569  
 AgCl, radiation-produced colloids, phonon scattering investig. 9-9692  
 Au, lamellar crystal growth from soln. 9-11800  
 Au in water, power spectrum of scatt. laser light, as test of self-beating spectrometer 9-14875  
 Fe<sub>2</sub>O<sub>3</sub>, hydrous, adhesion to glass, effect of stirring 9-9567  
 Fe<sub>2</sub>O<sub>3</sub> soln. in mag. field, aggregate dissociation, mag. forces linking 9-5200  
 Fe(OH)<sub>3</sub>, oxidation, Cu(II) effects, obs. 9-6014  
 K, in additionally coloured KBr, pure and doped, optical, e.s.r. and elec. studies 9-16414  
 K-Na-KCl-NaCl system, absorpt. of light 9-1725  
 SiO<sub>2</sub>, coagulation with hydrolyzed Al(III), kinetics rel. to destabilization and particle collisions 9-9570

**Colorimeters** *see Colorimetry***Colorimetry**

- See also Spectrochemical analysis; Spectrophotometry*  
 analysis of residual thiosulphate in gelatin 9-6563  
 CIE primaries, transformation relationships 9-20555  
 color equivalent luminance meas. 9-20554  
 colour changes with temp., cell for obs. 9-20559  
 contrast phenomenon, design and calibration for meas. 9-6554  
 correlated colour temperature and distribution temperature of light source, computer calculations 9-10913  
 differences in colour rel. illuminant change CIE C to D<sub>6500</sub> 9-10914  
 diffuse reflectance spectroscopy, reflectometers, colorimeters and reflectance attachments 9-18773  
 isotope identification by  $\gamma$  radiation 9-729  
 matching and adaptation, large field 9-10915  
 mixers, continuous flow, colorimetric expts. 9-5126  
 references, annotated 9-20553  
 review 9-6551  
 TiO<sub>2</sub>, rutile and anatase forms 9-15169

**Colour***See also Photography/colour*

- alkaline-earth sulphides, shear-induced colouring 9-1745  
 anils, photochromism and thermal reactions 9-10353  
 differences rel. illuminant change CIE C to D<sub>6500</sub> 9-10914  
 glasses by rare earth oxides 9-3856  
 photochromic spiropyran layers, coloration by u.v. laser radiation 9-18219  
 temperature, rel. to luminance and true temps., two-colour pyrometer obs. 9-8538  
 Al<sub>2</sub>O<sub>3</sub>:Co(Ti), eff. of valence state of dopant 9-14908  
 AlP epitaxial layers on Si, from absorption spectra 9-19692  
 BaS, shear-induced coloration, obs. 9-1745  
 BaTiO<sub>3</sub> powder, discoloration, grain size effects 9-21619  
 BaWO<sub>4</sub>, phototropy, pink after irradiation, by u.v. light 9-3866  
 Ca WO<sub>4</sub>, phototropy, reddish-green after irradiation, by u.v. light 9-3866  
 SrS, shear-induced coloration, obs. 9-1745  
 SrWO<sub>4</sub>, phototropy, green after irradiation, by u.v. light 9-3866  
 TiO<sub>2</sub>, opacified porcelain enamels, role of P<sub>2</sub>O<sub>5</sub> 9-3854  
 zCaS, shear-induced coloration, obs. 9-1745

**Colour centres**

- alkali halide crystals; F centre electronic states 9-5380  
 alkali halide crystals, F' centre formation and absorpt. meas. 9-5381  
 alkali halides, B centres due to neg. Ag ions on anion sites, model and props. 9-5387  
 alkali halides, F' centre, prod., meas., and model 9-19756  
 alkali halides, thallium activated, quantum efficiency of F- and Ti<sup>0</sup>-scintillations 9-16445  
 alkaline earth oxides, review 9-9693  
 alkaline-earth chalcogenides, additive coloration technique 9-7500  
 citrine, irradiated, formation 9-1237  
 elbaite 9-1236  
 ENDOR high press. cavity design and meas. 9-10785  
 ENDOR obs. in F centres, optical pumping and monitoring 9-21673  
 F to M conversion, impurity effects in NaF 9-5391  
 F-, relaxed excited, electronic problem 9-9719  
 F-centre formation, exciton mechanism, defect-free parts of ionic crystals 9-5383  
 F-centres, pair singlet-triplet splitting ionic crystal 9-5379  
 F-centres in alkali halides, Raman spectra 9-12404  
 F-F' non-radiative transition, quantum yield 9-3361  
 glass-H<sub>2</sub> gas high pressure systems, destruction of irradiation-produced centres 9-3365  
 ion size effect calcs. 9-18478  
 KCl, F<sub>2</sub> band and two new bands 9-9722  
 KCl, F and M centres, luminescent excitation spectra 9-7988  
 lithium tourmaline, (elbaite) 9-1236  
 $\alpha$ -quartz,  $\gamma$ -irrad., nonthermoluminescent smoky, nature and formation mechanism 9-5393  
 $\alpha$ -quartz,  $\gamma$ -irrad., smoky centre formation, thermoluminescence and dielec behaviour 9-13701  
 ruby, nature 9-5382  
 from sodalite (synthetic) interaction with Na vapour 9-5262  
 thermal ionization of KBr F' centres 9-3366  
 U centre, lattice vibrational Faraday rotation, obs. poss. 9-14032  
 U-centre sidebands, eff. of local mode self-energy 9-18479  
 V<sub>k</sub> lattice effect on optical absorpt. 9-9720  
 AgCl:I<sup>-</sup>, excited state structure of I 9-12057  
 BaCl<sub>2</sub>, electrolytically coloured, F centre study 9-17279  
 BaF<sub>2</sub>:rare earth, paramag. holes, interpret. of thermoluminescence 9-10252  
 BaF<sub>2</sub>, F-centre hyperfine interacts, endor meas. 9-1234  
 BaO, F-centres, Faraday rotation studies 9-3362  
 BaS, F centre production by n. irrad., e.s.r. obs. 9-13697  
 CaCO<sub>3</sub> calcite, deformed, X-rad. 9-16105  
 CaCO<sub>3</sub> calcite, deformed, X-rad. 9-3364  
 CaF<sub>2</sub>:(La,Ce,Gd,Tb) F-centres 9-14048  
 CaF<sub>2</sub>, F-centres, 1s 2p optical transition energy 9-3363  
 CaF<sub>2</sub>, irrad., rel. to thermoluminescence 9-14092

**Colour centres continued**

- CaF<sub>2</sub>, F-centre hyperfine interacts, endor meas. 9-1234  
 CaO, 3.7 eV F-centre, fluorescence of absorption band 9-3924  
 CaO, additively coloured, F' and F centre obs. 9-13698  
 CaO, F-band obs. by Faraday rotation and Faraday rotation-e.s.r. 9-21342  
 CaO, F-centres, Faraday rotation studies 9-3362  
 CaWO<sub>4</sub>, paramagnetic thermoluminescent centres 9-19757  
 in Cd, S and Se compound doped glasses, structural changes during heat treatment 9-13699  
 CsBr, F-to-M photochem. conversion mechanism 9-5384  
 CsBr(Cl), formation and conversion mechanism 9-7501  
 KBr:OH<sup>-</sup>, U<sub>2</sub> decomposition 9-18480  
 KBr, F-to-M photochem. conversion mechanism 9-5384  
 KBr, F', thermal ionization 9-3366  
 KBr, M'-centre electronic states theory, F<sub>2</sub>'-model 9-19758  
 KBr, temp. depend. of F-centre absorpt. 9-17280  
 KBr, X-irrad., Frenkel defect production and volume expansion obs. in coloration process 9-21331  
 KCl:(Ca, Sr or Ba), fluorescence of Z<sub>1</sub> centres 9-5962  
 KCl:Ca, Z<sub>1</sub>-centres, thermoluminescence after X-irradiation 9-14088  
 KCl:Ca, coloured, optical, e.s.r. and elec. studies 9-5925  
 KCl:Co<sup>2+</sup>, F-centres, growth and bleach at room temp. 9-5386  
 KCl:Mn, bleaching, optical and thermal, effects on u.v. band shifts rel. to those in highly pure KCl 9-14053  
 KCl:Mn F, suppressed by Mn presence, thermoluminescence meas. 9-3893  
 KCl:OH<sup>-</sup>, U<sub>2</sub> decomposition 9-18480  
 KCl:Sr, Z<sub>1</sub>-centres, circular dichroism 9-18692  
 KCl-KBr mixed crystal, F thermal stability and decay rate obs. 9-9721  
 KCl-LiCl, mixed crystal, A-centres ENDOR 9-12519  
 KCl, F-centre, hyperfine and quadrupole interactions, ENDOR determ. 9-5385  
 KCl, F-centre production by u.v. irrad. 9-1235  
 KCl, F-centres, surface, state of localized electrons 9-16108  
 KCl, F-to-M photochem. conversion mechanism 9-5384  
 KCl, F, by electron radiation, u.v. absorption 9-5921  
 KCl, F, M and R, electric field eff. at liquid N<sub>2</sub> temp. 9-3367  
 KCl, F-centres, EPR obs. 9-20020  
 KCl, irrad., rel. to thermoluminescence 9-14092  
 KCl, irradiated and additively coloured, chemical method for investigating electronic colour centres 9-16109  
 KCl, M'-centre electronic theory, F<sub>2</sub>'-model 9-19758  
 KCl, N<sub>1</sub> centre 9-7502  
 KCl, photoconductive sensitivity changes during bleaching 9-5768  
 KCl, R-centres, circular dichroism 9-7975  
 KCl, representation in absorption spectra 9-5920  
 KCl, V<sub>1</sub> centres, optical reorientation temp. dependence 9-16106  
 KCl, X-ray-induced, optical absorpt. meas. 9-18462  
 KCl(Br), F-centre experiment for ENDOR spectrum effs. explanation 9-15208  
 KCl(Ca) X-ray coloration mechanism, model 9-14951  
 KI, u.v. centres, vibrational spectra 9-5388  
 KI, u.v. irrad., defect formation 9-14952  
 KBr-KCl mixed crystals, X-irrad., Frenkel defect production and volume expansion obs. in coloration process 9-21331  
 Kce:NaCl, F-centres in additive coloration 9-21344  
 LaF<sub>3</sub>:Mg,Ca, thermoluminescence obs. 9-21658  
 LiF, F-centre experiment for ENDOR spectrum effs. explanation 9-15208  
 LiF, F<sub>3</sub><sup>+</sup>, linear Stark eff. of no-phonon transitions 9-19759  
 LiF, irrad., rel. to thermoluminescence 9-14092  
 LiF, irradiated, nature of paramagnetic imperfections 9-16107  
 LiF,  $\gamma$ -irrad., F band thermal bleaching, plastic deform. effects 9-7503  
 LiF, R<sub>2</sub> zero-phonon line, Stark effect, 4.2°K 9-14054  
 Li<sub>2</sub>GeO<sub>5</sub>:5:Cr<sup>3+</sup>, R lines, width and position temp. dependence 9-5963  
 MgF<sub>2</sub>, photochemical mechanism in radiation-damage process 9-5390  
 MgO, trigonal, spin-orbit coupling and stress spectra 9-5389  
 NH<sub>4</sub>Br, radiation-induced NH<sub>4</sub>Br defect centre, e.p.r. 9-9723  
 NH<sub>4</sub>Cl, radiation-induced NH<sub>4</sub>Cl defect centre, e.p.r. 9-9723  
 Na<sub>2</sub>O-Al<sub>2</sub>O<sub>3</sub>-GeO<sub>2</sub> glass,  $\gamma$ -induced, e.s.r., optical absorption and thermoluminescence study 9-18482  
 Na silicate glasses, photochromic, kinetic behaviour 9-3369  
 6(NaAlSiO<sub>4</sub>)<sub>8</sub>H<sub>2</sub>O, interaction with Na vapour and sorption 9-5262  
 NaBr, f-centre Raman spectra 9-12431  
 NaBr, F-centres, Raman spectra 9-12404  
 NaBr, temp. depend. of F-centre absorpt. 9-17280  
 NaCl, F-centre production by u.v. irrad. 9-1235  
 NaCl, F-centres, surface, state of localized electrons 9-16108  
 NaCl, F-colouring, x- or  $\gamma$ -ray irrad., room temp. 9-3368  
 NaCl, irrad., rel. to thermoluminescence 9-14092  
 NaCl, irradiated and additively coloured, chemical method for investigating electronic colour centres 9-16109  
 NaCl, N<sub>1</sub> zero-phonon line, strain broadening 9-1792  
 NaCl, thermal activation, electron emission 9-1626  
 NaCl F-centres,  $\gamma$ -induced, bleaching by laser irrad., 10.6  $\mu$  9-11889  
 NaCl whiskers, F- and M-centre radiational accumulation kinetics, effect of whisker size and origin 9-13700  
 NaF, complex electron-type, elec. field effects on no-phonon lines and point symmetry 9-18481  
 NaF, F<sub>3</sub><sup>+</sup>, linear Stark eff. of no-phonon transitions 9-19759  
 NaF, impurity effects on F to M conversion 9-5391  
 NaF, irrad., rel. to thermoluminescence 9-14092  
 NaF, M' formation kinetics and optical props. 9-5392  
 NaF, R<sub>2</sub> zero-phonon absorpt. line, moment anal. of uniaxial stress eff. 9-7504  
 SdF<sub>2</sub>:Ca, Raman scattering of green coloured crystals 9-12438  
 Si:P, A and E centres, influence on minority-carrier density dependence on neutron dose 9-1549  
 Si, E-centre annealing kinetics, activation energy and entropy 9-7505  
 p-Si, e. irrad., A-centres associated with oscillations in photoconductivity and absorpt. spectra 9-18659  
 SrF<sub>2</sub>, F-centre hyperfine interacts, endor meas. 9-1234  
 SrO, F-centres, Faraday rotation studies 9-3362  
 Y<sub>2</sub>Si<sub>2</sub>(Eu, Yb)<sub>0.9</sub>Al<sub>0.1</sub>O<sub>12</sub>, formation by optical zone melting 9-1238  
 ZnS crystals grown, Zn or S vapour excess, I carrier, luminescence meas. 9-21345

**Colour photography** *see* **Photography/colour****Colour vision**

afterimage matching study 9-18961

**Colour vision continued**

- dim flashes viewed foveally, rel. to origin of dark noise 9-15391  
 discrimination under reduced angular subtense and luminance 9-22006  
 Mach band phenomena, search 9-10579  
 matching functions, large-field, additivity 9-12795  
 model, parameter values for non-ideal detectors 9-20275  
 motion contingent after effect 9-8308  
 orientation specific colour adaptation 9-22007  
 photodichroism in frog's frozen retina 9-20276  
 primates, physiology of visual systems 9-18962  
 underwater, visibility, behaviour of different pigments 9-19302

**Columbium** *see* **Niobium****Coma** *see* **Aberrations, optical****Combustion**

- See also Explosions; Flames; Heat of combustion; Reaction kinetics*  
 acetylene burning in O<sub>2</sub> and N<sub>2</sub>O, comparative soot yields 9-12535  
 composite solid propellants, phalanx flame model 9-15213  
 droplet, liq. fuel, burning in oxidising atm., variable prop. effs. 9-21688  
 droplet in small Peclet number flow, decomposition burning, soln. 9-21687  
 ethylene, diffusion flame in O<sub>2</sub>-Ar and O<sub>2</sub>-N<sub>2</sub>, polycyclic aromatic hydrocarbon prod. in soot, rel. to O<sub>2</sub> conc. 9-12536  
 ethylene burning in O<sub>2</sub> and N<sub>2</sub>O, comparative soot yields 9-12535  
 ethylene flames, laminar diffusion type, soot prod. rel. to diluents 9-15214  
 ethylene-air diffusion flame, addition of H<sub>2</sub> to ethylene rel. to polycyclic aromatic hydrocarbon prod. 9-12537  
 flame in condensed phase, rate of burning 9-8530  
 flames, electron role from temp. elec. field dependence obs. 9-6403  
 gas, and its plasma, thermodynamic and elec. props. 9-19095  
 gas sampling valve, hydraulically actuated 9-8311  
 gases in annular combustion zone, stability conditions 9-20455  
 hexane, effect of olefins at different oxidation stages leading to ignition 9-14126  
 inhibition, two step process 9-19096  
 knock, flame accel. or spontaneous ignition of end gas, expt. data 9-12532  
 olefins, preflame and ignition behaviours, effect on hexane combustion 9-14126  
 propionaldehyde, gas phase, 155° to 220°C, study of rate and products 9-10333  
 rocket chambers, acoustic anal. of v.l.f. pressure oscs. 9-6402  
 stability in annular gas combustor 9-20455  
 C spheres, internal burning, depth of reaction determ., expt. tech. 9-8075  
 C spheres, internal burning, order of reaction and temp. limit of reaction zones 9-8076  
 NH<sub>4</sub>ClO<sub>4</sub>, deflagration, surface temp. meas. from orthorhombic-cubic transition thickness 9-10755  
 U, 20% enriched, ignition in O<sub>2</sub> and air, irrad. effects, obs. 9-10332

**Comets**

- 1966e, obs. 9-12756  
 1967 observations 9-17647  
 1967d, obs. 9-12756  
 1967f, obs. 9-12756  
 Alcock 1963b, brightness variations 9-21948  
 Arend-Roland, solution of Kepler's equations 9-17646  
 diffusion equation, existence of soln. 9-18918  
 flow, two-phase with evaporation, in comas, simulation 9-18920  
 long-period, major axis distribution 9-20231  
 major plasma envelopes, fountain model of dynamics 9-21949  
 Morehouse 1908 III, waviness in tail rel. to strength and direction of solar wind 9-14256  
 periodic, motions rel. to existence of comet belt beyond Neptune 9-15347  
 periodic, orbital elements, catalogue (1967) 9-20230  
 photometry and chemical physics, book 9-4123  
 Rudnicki (1966e), C<sub>2</sub> and CN emission band ratios, obs. 9-6182  
 Schwassmann-Wachmann, revised orbit by recal. of perturbations etc. 9-20229  
 spectra, continuous, forward scatt. effect 9-2058  
 statistics and perihelia 9-18919  
 total energy change on passing through solar system 9-10533  
 zodiacal light, their contrib. 9-20239  
 CO<sup>+</sup> plasma envelope, fountain model of dynamics 9-21949

**Communications, optical** *see* **Laser beams/applications****Compasses**

- pivot, surveying, transmitting and gyro-magnetic compasses, book 9-10803

**Complementarity** *see* **Physics fundamentals; Quantum theory****Composite particles**

- See also Alpha-particles; Deuterons; Helium-3; Tritons*  
 baryons, elementarity and compositeness distinguished in crossed channels 9-18014  
 Bethe-Salpeter bootstrap eqns., some solns. 9-2545  
 compositeness conditions for poles in partial wave amplitudes scatt. amplitudes 9-16847  
 compositeness criteria based on vanishing renormalization constants 9-18014  
 coupled state of three particle, allowance for Coulomb interaction 9-8975  
 e.m. form factors asymptotic behaviour 9-8919  
 energy lowest estimate in Schroedinger eqn. framework 9-11117  
 interactions, electromagnetic, of loosely-bound syst. 9-16910  
 many-channel description and Z-0 condition 9-6710  
 multichannel collisions, exact effective two-particle eqns by quasi particle method 9-6591  
 theory, connection with  $\rho$ -meson and  $\pi$ -N scatt. 9-8844  
 three and four nucleon systems, spatial symmetry and wave function 9-19209  
 three-nucleon system scatt. problem 9-2464  
 trineutron, bound state existence possibility, N-N interaction in  $p$  wave 9-6709  
 zitterbewegung for infinite component theories is analog of Bohn radius 9-13148

**Compressibility**

- See also High-pressure phenomena and effects*  
 alkali halides ionic crystals, shock-compressed, nonequilibrium radiation, temp. above 1 eV 9-14970  
 buckling, creep, of circular cylindrical shell under compression 9-19030  
 buckling, free-edge, heterogeneous shells, cylindrical, in axial compression 9-20389  
 calcite, from elastic constants temp. dependence, 160-300°K 9-14963



**Compressibility** continued

- ceramic crystals, forging and recrystallisation 9-3482
- concrete, failure surface in compression 9-16132
- Coulomb material, short cylinders, analysis 9-20386
- crystal, uniaxial stress vice 9-1165
- cylinder on flat surface, formulae and meas. apparatus 9-10700
- earth models 9-12568
- graphite, synthetic polycryst., effect of pore struct. accessibility 9-5455
- graphite powder, compactibility into reactor fuel rods 9-2797
- ionic crystals, shock-compressed, nonequilibrium radiation, temp. above 1 eV 9-14971
- metals, solid and liq., rel. to self-diffusion activation energy, near melting point 9-11890
- metals compressed by liqs., theory of props. 9-5446
- polymer organic solids effect 9-21366
- PVC, stretched uniaxially, thermal and mechanical props. anisotropy 9-19781
- rocks and minerals, measurement at high static pressure 9-12572
- solids, linear, meas. device 9-3416
- solids, shock, compression Hugoniot, correlation of two universal expressions 9-5434
- steel cylinders, at high strain rate, meas. 9-21365
- steel ductile fracture criteria, study using AI model 9-18516
- tensile plastic instability and ductile fracture criteria in uniaxial compression tests 9-20412
- transition from compressible to incompressible materials 9-16714
- AgI, hexagonal, linear for 8 cryst. directions 9-7540
- Al<sub>2</sub>O<sub>3</sub>, isothermal compression at 295°K to 1 megabar 9-11919
- Ce, anomalous, rel. to isomorphism theory 9-3225
- Cs, liquid, isothermal 9-19596
- CsI, impurity additions effect 9-18514
- Cu, porous, shock compression 9-11920
- Fe porous, shock compression in region of incomplete compaction 9-11948
- Fe powders, increase by cold rolling, patent 9-13749
- Ge:As(Sb), under uniaxial compression, effect on long-wavelength intrinsic 'tail' 9-12466
- Ge:As(Sb), under uniaxial compression, radiative recombination 9-10239
- K, liquid, isothermal 9-19596
- N<sub>2</sub> crystals, from sound velocity meas. 9-3519
- Na, liquid isothermal 9-19596
- O<sub>2</sub> crystals, from sound velocity meas. 9-3519
- Rb, liquid, isothermal 9-19596

**gases**

- boson, divergence with falling temp., rel. to off diagonal long-range order 9-16697
- homogeneous model, asymptotic behaviour of linear oscillations 9-13474
- nonadiabatic restrained expansion, arbitrary energy losses or release 9-14812
- Ar and methane, corresponding states 9-9440

**liquids**

- electrolytes, simple and complex ternary systems, rel. to molar conc. 9-15998
- H<sub>2</sub>SO<sub>4</sub>, aqueous mixture, molecular, and sound vel. 9-16000

**Compressive strength** *see Mechanical strength/compressive***Compton effect**

- carbon black, profile meas. in e. momentum density determ. 9-18581
- diamond, profile meas. in e. momentum density determ. 9-18581
- forward-spin-averaged amplitudes, current commutators and e.m. mass differences 9-8740
- graphite, profile meas. in e. momentum density determ. 9-18581
- inducing interaction between intense radiation and plasma 9-9351
- mass in region smaller than Compton wavelength, alteration to concept 9-14464
- photon, polarized, scattering by polarized particle with spin 1/2, theory 9-15579
- photon scatt., amplitude theorem derivation 9-17941
- photon scatt. in gas of electrons 9-20597
- quadratic, mixed-freq. incident wave 9-8739
- quadratic, scatt. cross-section for arbitrarily polarized monochromatic radiation 9-8738
- on relativistic electrons 9-6598
- scattering amplitude expansion to e<sup>4</sup>, low-energy theorem 9-17939
- scattering sum rules, high energy assumption and subtraction consts. 9-16819
- spin, arbitrary, of target, low-energy theorem for matrix elements 9-17942
- spin-zero systems, Feynman graphs for calc. of low energy theorems 9-6597
- stimulated scatt. possibility for laser generation 9-12998
- subtraction consts. for scatt. dispersion relations and vector meson dominance 9-8741
- theorems, low energy, for scatt., to fourth order in e 9-326
- unfolding iterative, of Compton spectra 9-19223
- virtual amplitude, using Regge theory rel. to hadron mass difference 9-2478
- virtual proton, with 3-3 resonance, contrib. to bremsstrahlung variable rel. to quantum electrodynamics 9-16807
- $\gamma\gamma \rightarrow p\bar{p}$  by polarised photons, in c.m. system and first reson. region, differential cross sections, comparison with isobaric model 9-16822
- $K^+ - K^-$  mass difference, calc. from finite energy sum rules, for virtual Compton scatt. amplitude 9-13122
- N nuclear Compton scatt., low-energy, invariant amplitude calc. 9-13102
- p, dispersion relations and obs.,  $\geq 300$  MeV 9-16823
- p scatt., sum rules 9-15642
- $\pi$  and N Compton scatt. invariant amplitudes 9-8735
- $\pi$  Compton scatt. low-energy, invariant amplitude calc. 9-13102

**Computation** *see Calculation***Computer memories** *see Calculating apparatus/digital computers; Magnetic devices; Storage devices; Superconducting devices***Computers** *see Calculating apparatus***Concrete**

- aggregate and hardened cement paste contact, e. microscope exam. 9-17337
- bearing strength on loading through rigid plates 9-18513
- columns, creep stability and buckling strength 9-17310
- compressive strength, effect of mix proportions and aggregate dust 9-17312
- failure surface in compression 9-16132

**Concrete** continued

- fatigue, and effect upon prestressed beams, review 9-18519
- microcracks interaction 9-5482
- photon penetration and back-scatter 9-2712
- porous structure, shape and type of moisture bond, solidification method depend. 9-17345
- steel in restrained expanded concrete, bonding 9-18500
- stress-strain curves for short-term loading and deformation 9-16121
- thermal conductivity measurement problems 9-18567
- X-ray absorpt., 6MV primary radiation 9-7681
- yield criterion for isotropically reinforced slabs 9-18502

**Condensation***See also Drops; Fog*

- adsorbed gases on homogeneous C surface 9-9592
- ethyl chloride adsorbed layers, heat of adsorption 9-9594
- lattice formation from mol. base-gas, anal. 9-4247
- metal film condensation effect of vapor subcooling 9-19662
- metal vapour, m.h.d. gas conductivity enhancement 9-14413
- molar surface entropy rel. to homogeneous nucleation of liquid 9-14884
- Nasselt relations, explicit solns. 9-21245
- nucleation theory, reconsideration 9-7303
- nuclei production, influence of mono 9-6066
- phase rule for two-dimens. phases 9-11747
- on supercooled high velocity jet, turbulent boundary layer parameters 9-19659
- vapour, prediction based on microscopic theory 9-5219
- vapour on cold surfaces, conds. for fog formation with thermal boundary layers 9-9591
- vapour on rotating disc, heat transfer coeff. 9-14883
- of water and methanol in turbulent air flow 9-1070
- Ar+N<sub>2</sub> liquid-vapour equil., syst., condensation press. variation obs. 9-17228
- Au, on Si(111) surface 9-1094
- Au atomic beam on rocksalt substrate 9-14897
- g, dropwise, heat transfer rel. to temp. head 9-17229
- H<sub>2</sub>O, surface free energy of embryonic droplet in nucleation theory 9-7304
- Hg vapour, coeff. 9-1071
- Kr, multilayer adsorpt. on C surface, two-dimens. van der Waals eqn. 9-9593
- Kr adsorbed layers, heat of adsorption 9-9594
- N<sub>2</sub>, multilayer adsorpt. on C surface, two-dimens. van der Waals eqn. 9-9593
- N<sub>2</sub> adsorbed layers, heat of adsorption 9-9594
- N<sub>2</sub>+Ar liquid-vapour equil., syst., condensation press. variation obs. 9-17228
- O, on NiO coeff., and self-diffusion 9-3387
- Sb film, internal stress obs. 9-21266

**Condensation of gases** *see Liquefaction, gases***Conduction, electrical** *see Conductivity, electrical***Conduction, heat** *see Heat conduction***Conduction, ionic, solids** *see Ionic conduction, solids***Conduction bands** *see Crystal electron states/band structure***Conduction electron scattering** *see Crystal electron states/transport processes***Conductivity, electrical**

- See also Ionic conduction, solids; Kondo effect; Semiconducting materials; Semiconductor; Skin effect; Superconducting materials; Superconductivity*
- charged plasma in magnetic field 9-18283
- dimethacrylate-bis-mono, di, triethyleneglycolphthalates, polymerization meas. 9-15219
- DNA periodic models, deform. pot. approximation 9-19485
- graphite particle pseudo-fluidized bed, resistance to 900°C rel. to particle size 9-9314
- metal, influence of small-angle scatt. 9-236
- metals, general tensor props., magnetoresist. theory 9-18594
- nonlinear, kinetic theory, Ohm's law correct. in weak field domain, slow and high speed part. study 9-6452
- nonlinear, kinetic theory, Ohm's law correct. in weak field domain, slow and high speed part. study 9-6452
- Ohm's Law, classical aspects 9-16197
- Onsager relations and Pauli eqn. 9-8439
- phenol-sulfonic cation-exchange membrane, transport numbers determ. 9-9501
- plasma, turbulent, verification of Buneman formula 9-875
- polyamides, aromatic; depend. on vapour sorption 9-7094
- polymers, organic semiconductors, film meas. 9-14730
- posistor, sensitivity to heat transfer condition change 9-203
- sphere, resistance as function of diameter of elec. contacts, theory 9-6445
- structure beneath Iceland, magnetotelluric sounding expt. 9-14154
- superconductor, 2-dimens., temp. depend. near T<sub>c</sub> 9-21490
- two-phase materials, bounds on transport coeffs. 9-4259
- Ag film, thickness depend. from Fuchs-Sondheimer theory 9-7331
- Au film, thickness depend. from Fuchs-Sondheimer theory 9-7331
- In, small angle scatt., influence of 9-236
- UO<sub>2</sub> heated, local meas. for fission prod. diffusion profile determ. 9-5647

**gases**

- air, ionized by shock, meas. perpendicular to mag. field 9-915
- arcs, 'inverse' soln. accuracy 9-11639
- ionized gas calc. in alternating field 9-5066
- ionized suspensions, in MHD system 9-3132
- m.h.d., enhancement by condensing metal vapour 9-14413
- plasma, from kinetic eqn. 9-19522
- plasma, fully ionized, in mag. field, calc. 9-15930
- plasma, highly nonequilib., kinetic theory 9-11537
- positive column of low current discharges in Ne and Ar, influence of distrib. function 9-19561
- variation, ionized gas in initial section of plane duct 9-3056
- Ar-K plasma, at low current densities as function of gas temperature 9-19532
- Ar-Ne mixture, obs. 9-929
- N<sub>2</sub> plasma, K-seeded, under conditions of MHD accelerator 9-7151

**liquids**

- alcohols, semicond., 20°C 9-13538
- alcohols of common purity, characteristics of ions 9-19642
- amines of common purity, characteristics of ions 9-19642
- benzene, injected charge-carrier drift mobility 9-11713

**Conductivity, electrical continued****liquids continued**

- electron liq., degenerate, conductivity tensor calc. using Maxwell's eqns. 9-20367  
 n-hexane with series of dielectric admixtures, pre-breakdown 9-5185  
 Hg containing halide ions 9-11715  
 insulating, electric wind and its reaction at a sharp point 9-5184  
 metals, electroconductance and thermo-e.m.f., correlation in approximation of weakly bound electrons theory 9-3117  
 molten salts, data collection 9-11714  
 naphthalene, molten, photocurrent from triplet state generation by light 9-9533  
 nitrobenzene and electrochemical props. 9-21221  
 non-polar, natural and ionization, temp. effect 9-9545  
 polar and aprotic dielectrics, mechanism 9-21221  
 polyanilines, oligomeric 9-19641  
 polymer solns., molecular theory of ion mobility 9-18369  
 solutions of polymeric dielectrics 9-21222  
 3d-transition metals in liq. Sn, and thermopowers 9-16021  
 Au-Ga, elec. resist., electronic struct. 9-16020  
 Bi-Sb system 9-9547  
 Bi, containing halide ions 9-11715  
 Cu-Ge, elec. resist., electronic struct. 9-16020  
 H<sub>2</sub>O, changes near 4°C, rel. to phase transform. 9-11681  
 Hg alloys, resistivity model 9-5187  
 HgCl<sub>2</sub>-Hg<sub>2</sub>Cl<sub>2</sub> molten system 9-14856  
 HgI<sub>2</sub>-Hg<sub>2</sub>I<sub>2</sub> molten system 9-14856  
 La-Ce system, temp. dependence 9-1455  
 Li, m.p. to b.p. 9-21197  
 PbBr<sub>2</sub>, molten, specific conductivity, 370°-900°C 9-19640

**liquids, electrolytic**

- See also *Chemical analysis/electrochemical; Ion velocity/electrolytic*  
 electrolyte + liquid aromatic hydrocarbon syst., criteria necessary for photocond. 9-17219  
 hydrocarbons, radiation-induced, depend. on molec. struct. 9-16022  
 polyelectrolyte solns., dielectric dispersion props. at 25°C and 40-100 kHz 9-16018  
 slightly associated solns., thermodynamic props. prediction 9-21703  
 Wien effect in non-assoc. electrolytes 9-8100  
 KClO<sub>4</sub> in dioxane-water mixtures at 25°C, obs. rel. to ion-solvent interactions 9-11717  
<sup>6</sup>LiNO<sub>3</sub>, <sup>7</sup>LiNO<sub>3</sub>, 280-440°C 9-8103  
<sup>6</sup>LiCl, <sup>7</sup>LiCl, 620-780°C 9-8103  
 NaCl-glycerol solns. 9-9548  
 NaClO<sub>4</sub> in dioxane-water mixtures at 25°C, obs. rel. to ion-solvent interactions 9-11717

**measurement**

- cryostat for resist. meas., 4°K to 350°K 9-14294  
 films, thin, sheet resist. meas. by four point probe method, theor. anal. 9-16042  
 flames, hydrocarbon/O<sub>2</sub>/N<sub>2</sub> 9-18249  
 foil samples, high press. and varying temps., compact device 9-10789  
 fused salt conductance, two-probe d.c. method 9-17845  
 Hall effect high resistivity meas. 9-6454  
 impedance, transient variations meas. with modified magic-T 9-19119  
 insulating crystals, without using contact electrodes 9-7836  
 low temperature, 5-100°K, device 9-2301  
 metals, resistivity changes during and after irradiation, meas. method 9-19888  
 methane-O<sub>2</sub> flame combustion products 9-18752  
 milliohm meter, 1.1 × 10<sup>-3</sup> to 1.0 × 10<sup>-1</sup> ohms 9-4410  
 phase transformation tracing by means of h.f. a.c. meas. using Q-meter 9-5506  
 rocks and minerals, at high static pressure 9-12572  
 Ag single crystal films, size effect 9-5640  
 BiCl<sub>3</sub> fused, two-probe d.c. method 9-17845  
 KCl:Mn activation energy for cation vacancy migration determ. 9-3893  
 NaNO<sub>3</sub> fused, two-probe d.c. method 9-17845

**solids**

- alkali halides, additively-coloured, anal. 9-12085  
 alkali-silicate glasses, binary and ternary, meas. 9-3690  
 alloys, residual resistivity and pseudopotentials 9-5593  
 alloys, resistivity change near critical conc. for strong paramag.→weak ferromag. 9-1641  
 conductors, electron drag by ultrasound 9-1460  
 copper sandstone, temp. dependence 9-10036  
 cylindrical wires, size effects 9-12082  
 d-alloys, dilute, mechanism 9-10086  
 disordered systems, static, non-perturbative evaluation 9-15059  
 DNA, sodium salt 9-1459  
 duraluminium deformed at 77°K 9-12025  
 earth's crust, resistivity 9-16522  
 earth, model, integration of equations of Lahiri and Price 9-14155  
 electron-phonon self-energy contributions temp. depend., calc. 9-16199  
 f.c.c. metals, deformed, resistivity at 4.2°K 9-3567  
 ferrites, resist., cooling rate depend. rel. to cation conc. 9-12193  
 ferrites, spin type, resistivity behaviour near Curie point 9-21478  
 ferromagnetic alloys, resistivity, magnon drag eff., low temp. 9-13951  
 ferromagnetic metals, rel. to temp. and s.catt. by spin waves 9-12094  
 ferromagnetic metals, transport calcs. at high temp. using spin wave method 9-3576  
 film, metal, in longit. mag. field 9-5650  
 glass, soda-lead-oilica, rel. to soda content 9-13913  
 glasses, binary silicate, rel. to metastable crystn. 9-1081  
 glasses, chalcogenide, rel. to energy levels and progressive crystn. model 9-3611  
 graphite, effect of B (to 1% ppm) on resistivity, temp. depend. 9-7848  
 graphite, impregnated, resistivity changes under neutron irradi. 9-7667  
 graphite, irradiated with electrons at 80°K, rel. to annealing 9-18534  
 graphite, pile irradi., rel. to annealing temp. 9-7587  
 graphite, pyrolytic, e-irrad., recovery of resistivity below 6°K 9-9931  
 graphite, resistivity and stored energy changes on neutron or electron irradi. 9-7741  
 graphite, resistivity at 80°K rel. to crystallite sizes 9-7672  
 graphite nitrates, near λ transform, at ~21°C, rel. to struct. 9-7607  
 graphite-nitrate residue cpds, resistivity anal. rel. to band model approx. 9-740  
 graphites, polycryst., rel. to X-ray anisotropy factors 9-7428  
 hopping conduction, meas. by a.c. method, model 9-15084  
 ice, guarded potential probe method 9-3692

**Conductivity, electrical continued****solids continued**

- Ice, nature of charge carriers 9-1579  
 inhomogeneous crystal with carriers of one sign, real part of impedance 9-19885  
 insulating crystals, meas. without using contact electrodes 9-7836  
 insulating films 9-21530  
 lipid film, bilayers and rel. to semicond. props. 9-12138  
 macromolecular compounds subject to gas doping 9-15065  
 metal, rel. to plastic deformation 9-12093  
 metal, residual-resistance impurity detection 9-17377  
 metal films, surface roughness effects on resistivity thickness dependence 9-9928  
 metal films sputtered at low voltages 9-12097  
 metal films with arbitrarily oriented ellipsoidal Fermi surfaces, size effect 9-7744  
 metal surface layer, stationary states of electrons, in weak mag. field 9-15068  
 metal wires, shape factor of resistance rel. to non-conductive second phases 9-5648  
 metals, antiferromagnetic, anomalous, near Neel point 9-9927  
 metals, ferro- and antiferromagnetic, resistivity anomaly, near mag. ordering point 9-12096  
 metals, nearly-free electron, rel. to impurity scatt. potential 9-12045  
 metals, non-local, band structure effects 9-13840  
 metals, phonon-limited resistivity 9-9926  
 metals, resistivity, infl. of dislocations 9-12095  
 metals with paramagnetic impurities, electron interactions effects 9-9876  
 mica, natural and synthetic, hopping conduction and thermal breakdown 9-12182  
 Naphthazarine-Cu Chelate 9-3636  
 nickel-cobalt disilicide solid soln. rel. to lattice parameters 9-3480  
 Ohm's law violation in semiconductors 9-7786  
 olefin oxide polymers 9-16293  
 organic cpds. with metallic conduction props. 9-7756  
 organic semiconductors, mechanism 9-9982  
 organic semiconductors, pre-exponential factor 9-13888  
 oxides, effect of pressure 9-1522  
 poly(ethylene oxide) 9-16293  
 polyamides, N-substituted 9-18600  
 polymers, p conduction 9-1451  
 p-polyphenyl and oligomers, temp. time and thickness depend. 9-9924  
 polyurethane, p conduction 9-1451  
 pyrocarbons, B-doped, resistivity rel. to B content 9-7736  
 pyrocarbons, reproducible compressed samples, resistivity in a and c crystallographic directions 9-7596  
 quantum theory, rel. to non-degenerate electron gas in high elec. and mag. fields 9-21476  
 quartz, natural and synthetic, in constant elec. field 9-1569  
 rare earth germanides, charact. change with temp. 9-12091  
 rare-earth cpds., cond. character 9-16226  
 resistivity of supercond. in normal state near transition temp., Ginzburg-Landau theory 9-3657  
 semiconductor and semimetal thin plates, many-valley energy spectrum of carriers 9-9925  
 semiconductor films, quantum oscillations rel. to mag. field 9-5679  
 semiconductor surface space charge 9-21459  
 semiconductors, high permittivity, depend. on elec. field intensity 9-17366  
 semiconductors, inhomogeneous, theory 9-21504  
 semiconductors in strong electric and magnetic fields 9-15088  
 silica gel with adsorbed H<sub>2</sub>O 9-13915  
 snow and glacier ice, electrolytic 9-12570  
 soda-lead-silica, glass, rel. to soda content 9-13913  
 steel, austenitic, resist. changes accompanying γ/precipitation 9-1319  
 above superconducting transition, anomalies 9-17380  
 surface resistance 9-5659  
 tetracyanoquinodimethane-phenazine complex, conduction mechanism 9-18599  
 tetrasilicates, interpretation of results 9-15062  
 thermally stimulated curves, extensions to method of trap analysis 9-5595  
 transition metals, dil. metallic solns; anomalous resistivity 9-16229  
 transition metals, rel. to electronic structure 9-10078  
 vitrocrown, resistivity rel. to heat treatment temp. 9-7318  
 n-Ge, negative differential conductance 9-13891  
 Ag-Au:Yb alloys, Kondo effect in resistivity 9-9929  
 Ag, deformed at room temp., resistance rel. to temp. 9-19890  
 Ag and p-n semicond. composites 9-16260  
 Ag alloys, resist.-conc. depend. 9-16223  
 Ag thin films, resistivity change due to neutrons and γ rays 9-17378  
 Al-Au dilute alloys, meas. rel. to ageing charact. 9-21394  
 Al-4wt.%Au alloy, plastic deformation effects 9-12098  
 Al-Cr alloys, dilute, low temp. impurity resistance 9-1473  
 Al-Cu solid solns., supersaturated and deformed, changes after Cu precip. 9-21482  
 Al-Mn alloys, dilute, low temp. impurity resistance 9-1473  
 Al-Zn solid solutions, resistivity during precipitation 9-21480  
 Al, α- and β- irradiation effects rel. to strain and temp. 9-7746  
 Al, e-scatt. and resistivity low temp. depend. 9-1463  
 Al, Matthiessen's rule deviations, size-dependence 9-21481  
 Al, resistance and thermoelec. power, effect of high pressure 9-16306  
 Al, resistivity, deformed at 4.2°K 9-3567  
 Al, Sondheimer oscillations in resistivity, meas. and interpret. 9-7745  
 Al and alloys, resistivity, recovery in stages II and III after 2-Mev e. irradi. 9-9696  
 Al and alloys rel. to calc. of thermal conductivity in Al alloys 9-19866  
 Al fatiguing and annealing, resist. changes 9-13846  
 Al small angle scatt., influence of 9-236  
 Al thin films, resistivity change due to neutrons and γ rays 9-17378  
 AlP epitaxial layers on Si, resistivity for indication of n-type material 9-19692  
 AlSb, 2°-500°K 9-7794  
 As, current carrier conc., pressure depend 9-15069  
 Au-Cu alloys, resistivity meas. of short-range order 9-19804  
 Au, resistance and thermoelec. power, effect of high pressure 9-16306  
 Au, resistivity, deformed at 4.2°K 9-3567  
 Au alloys, (with Pt, Cu, In,) resistivity, 1.5-40°K rel. to phonon-assisted impurity scatt. 9-13847  
 Au alloys, resist.-conc. depend. 9-16223  
 Au binary alloys, quenched in resistivity due to solute vacancy pairs 9-18601



**Conductivity, electrical continued**  
**solids continued**

Au deformed at room temp., resistance rel. to temp. 9-19890  
 Au film, epitaxial, size effects in temp. variation 9-9930  
 Au thin films, resistivity change due to neutrons and  $\gamma$  rays 9-17378  
 $\text{Au}_3\text{Mn}_2$ , resistivity temp. depend., antiferromag. anomalies 9-15157  
 B,  $-60^\circ$  to  $+50^\circ\text{C}$ , magnetocond., 0 to 2000 Gauss 9-16222  
 B,  $-60^\circ$  to  $+50^\circ\text{C}$ , magnetocond., 0 to 2000 Gauss 9-16221  
 B, freq. and temp. dependence 9-1454  
 Ba ferrite polycrystals, at h.f.,  $\text{Fe}^{2+}$  content dependence 9-12086  
 $\text{BaTiO}_3$ , rel. to O partial press., 800-1200°C 9-1512  
 $\text{BaTiO}_3$ , resistivity rel. to point defect conc. and sintering kinetics 9-1589  
 $\text{BaVS}_3$ , resistivity below 130°K 9-7747  
 Be, n irradiated at 4.2°K, resist. meas. rel. to damage and recovery up to 350°K 9-5578  
 Be, resistance oscillations in superconducting magnet 9-9877  
 Bi-Sb alloy, resistivity 9-12026  
 Bi-Sb alloy, semiconducting to metal transition, rel. to mag. field and Sb conc., 4-77°K 9-1513  
 Bi, current carrier conc., pressure depend 9-15069  
 Bi, film, critical conducting thickness, 100 400°K 9-3577  
 $\text{Bi}_2\text{Sb}_3$ , nonohmic conductivity, K 9-3619  
 Bi film, evaporated, rel. to thickness and stress during and after deposition 9-5449  
 C, soft, resistance 1.5-300°K, after acceptor introd. and heat treated 1800-3000°C 9-7750  
 C, soft and hard, resistance temp depend., 1.5 to 300°K, rel. to heat treatment 9-7749  
 C films, resist., O adsorp. effects, -196 to 450°C 9-7795  
 Ca V Bi Fe garnet, conduction mechanism by conductivity and thermoelec. power meas. 9-1458  
 $\text{CaF}_2$ , irradi., d.c. conductivity rel. to thermoluminescence 9-14092  
 $\text{CdF}_2$ :Eu, over broad temp. range 9-5672  
 $\text{CdF}_2$ :In, over broad temp. range 9-5672  
 $\text{CdS}$ :Cl, low temperature impurity conduction 9-3620  
 $\text{CdS}$ , photoconductive, negative resistance and relax. effect at low temp. 9-5764  
 $\text{CdSb}$ , doped, 2.2-77°K 9-9972  
 $\text{CdTe}$ :Li temp. depend. meas. rel. to effect of dopant 9-12156  
 $\text{CdTe}$ , conductance, temp. dependence rel. to ambient partial pressure 9-3644  
 $\text{CeB}_6$ -M, (M=Hf, Ta, W and Re), temp. dependence 9-9920  
 $\text{CeB}_6$ -M, (M=Hf, Ta, W and Re), comp. dependence 9-9919  
 Co, 1200°-1500°K 9-13807  
 Co, meas. 290-1710°K in thermal conductivity calcs. 9-1403  
 $\text{CoO}$ :Li rel. press. and temp. 9-21506  
 $\text{CoO}$ , for defect conc. rel. to partial press., temp. depend. 9-3569  
 Cr-Ni alloys, resistivity, max. due to antiferromagnetic ordering for low Ni content 9-3721  
 Cr, resistivity, 77 to 400°K 9-15024  
 Cr, second minimum in resistivity-temp. dependence curve near Neel temp. 9-12099  
 Cr, stress-cooling effects rel. to ordering obs. 9-1700  
 $\text{Cr}_{11}\text{Ge}_{19}$ , 80-1000°K 9-5799  
 Cs adsorbed on insulating substrates, conduction mechanism 9-5641  
 Cs temp. var. calc., comparison with expt. 9-16231  
 CsCl, obs. rel. to phase transform. kinetics 9-11963  
 Cu-75 wt.%Pd alloys, residual resistivity rel. to short-range order 9-12100  
 Cu-Fe dilute alloy, low-temp., and magnetoresistance 9-18602  
 Cu-GaAs supersaturated solid solns., for decomposition study 9-5511  
 Cu-Ni alloys, resistivity change due to cyclic deformation 9-3579  
 Cu-Si solid soln., deformed, resistivity decrease 9-16224  
 Cu-Zn alloys at different compositions 9-1464  
 Cu, eff. of creep on resistance 9-13730  
 Cu, electron irradiated, rel. to stage III recovery behaviour 9-13671  
 Cu, polycrystalline wires, resistivity under tension and in transverse mag. fields 9-7753  
 Cu, resistivity, deformed at 4.2°K 9-3567  
 Cu and Cu alloys, phonon-drag effect 9-5652  
 Cu alloys, resist.-conc. depend. 9-16223  
 Cu small angle scatt., influence of 9-236  
 $\text{Cu}_2\text{O}$ , polycrystalline, high-resistivity, combined prep. and low temp. meas. device 9-3742  
 $\text{Cu}_2\text{O}$  rel. press. and temp. 9-21506  
 Cu<sub>2</sub>Se, rel. to phase transformation 9-17390  
 Dy, Lorenz function from elec. and thermal conductivity meas. 9-7673  
 Er, Lorenz function from elec. and thermal conductivity meas. 9-7673  
 $\text{Eu}_{0.95}\text{Gd}_{0.05}\text{S}$  obs. rel. to band conduction and critical scatt. 9-9886  
 Fe-Al solid solns., heterogeneous, n-irrad. effects rel. to ordering changes 9-1465  
 Fe-C alloys, in mag. fields at 4.2°K and 78°K 9-15070  
 Fe-Mn alloys, temp. and comp. dependence 9-9921  
 Fe-Si alloys, temp. and comp. dependence 9-9921  
 Fe-V alloys, temp. and comp. dependence 9-9921  
 Fe, dynamic resistivity obs. of high pressure phase transformation 9-14991  
 Fe, thin films, resistivity change in planar magnetic fields above 4 kOe 9-18682  
 $\text{Fe}_2\text{O}_3$ :Al<sub>2</sub>O<sub>3</sub>, effect of chemisorbed water vapour and hydrogen 9-20036  
 $\text{Fe}_2\text{O}_3$ :Cr<sub>2</sub>O<sub>3</sub>, effect of chemisorbed water vapour and hydrogen 9-20036  
 $\text{Fe}_2\text{O}_3$ , effect of chemisorbed water vapour and hydrogen 9-20036  
 $\text{FeSe}_8$ , metallic type, band magnetism interpretation 9-21484  
 $\text{FeCr}_2\text{Se}_4$  rel. to effect of interactions between d shells of transition element 9-16253  
 $\text{Fe}_2\text{O}_3$ :Ti rel. press. and temp. 9-21506  
 $\text{Fe}_2\text{O}_4$ , depend. on reflection coeff. 9-10171  
 $\text{Fe}_2\text{O}_4$ , pressure effects, and metal-nonmetal transition 9-1467  
 Fe-C solid solutions, resistivity recovery after e irradi. 9-19891  
 p-GaAs, infl. of constant elec. field 9-3650  
 n- and p-GaAs, resistivity, temp. and press. depend. 9-7799  
 n-GaAs, temp. depend., influence of  $\gamma$ -radiation 9-13875  
 GaAs high resistance layer occurrence due to epitaxial film growth on surface 9-11773  
 $\text{GaAs}_{1-x}\text{P}_x$ , Sand Te doped, rel. temp. 55 to 400°K 9-12150  
 n-GaAs<sub>1-x</sub>P<sub>x</sub>S(Te), press. depend. of resistivity at 77° 9-16266  
 GaP, 2°-500°K 9-7794  
 n-l GaSb:Te, rel. to transport props. 9-10177  
 p-Ge:Ga, mechanism of changes during e-irrad. and annealing 9-5703  
 Ge:Mu, effect of heat on Mn incorporation 9-3658  
 Ge:Sb, resistivity rel. to temp. 9-3656

**Conductivity, electrical continued**  
**solids continued**

Ge, charge transport in low angle grain boundaries 9-3657  
 Ge, ion bombardment effects 9-7807  
 n-Ge meas. rel. to non-equilib. depletion effects at electrolyte interface 9-13895  
 H-Pd, resistivity, 2-300°K 9-3580  
 $\text{Hg}_{1-x}\text{Cd}_x\text{Te}$  layers formed by Hg<sup>+</sup> bombardment of CdTe crystals, conductivity 9-14898  
 HgSe, from helicon wave resonance meas. at 77°K 9-7723  
 HgSe, Lorenz number, 80°-440°K 9-5642  
 n-HgTe, in strong elec. field 9-3626  
 In, e-e scatt. and resistivity low temp. depend. 9-1463  
 In, in normal state from meas. on superconductor 9-9933  
 In, very-high-purity, temp. dependence, 1.5-4.2°K, in mag. fields 9-12101  
 In films, electrotransport obs. 9-15061  
 $\text{In}_{1-x}\text{Ga}_x\text{As}$ , solid solutions, resistivity meas. for energy structure and Debye temp. calc. 9-3640  
 InSb, barrier mechanism, temp. depend. interpretation 9-12146  
 p-InSb, eff. of dislocations, 50° to 200°K 9-21505  
 InSb, optical absorption effects in a semiconductor 9-3843  
 p-InSb, temp. dependence rel. to dislocation density 9-3631  
 n-InSb anodic oxide films, resistivity 9-11770  
 K, e-e scatt. and resistivity low temp. depend. 9-1463  
 K, temp. var. calc., comparison with expt. 9-16231  
 KBr, additively coloured, pure and doped, enhancement due to K colloidal particles 9-16414  
 KBr dislocation on boundary conduction 9-3355  
 KCl: Cd, coloured, ratio, room temp. to 500°K 9-5925  
 KCl: SrCl<sub>2</sub> and Cl<sup>-</sup> diffusion, ionic transport eqns. derived from five-defect model 9-13914  
 KCl, and Cl<sup>-</sup> diffusion, ionic transport eqns. derived from five-defect model 9-13914  
 KCl, irradi., d.c. conductivity rel. to thermoluminescence 9-14092  
 $x\text{K}_2\text{O} \cdot (1-x) \text{Na}_2\text{O} \cdot 4\text{SiO}_2$  glasses, resist. rel. to composition 9-3693  
 La-Ce system, temp. dependence 9-1455  
 $\text{Li}_{0.5}\text{Fe}_{2.5-x}\text{Al}_x\text{O}_4$ , eff. on ferromagnetic resonance line width 9-18730  
 Li temp. var. calc., comparison with expt. 9-16231  
 LiF:Ca, low temp. meas. 9-19928  
 LiF, irradi., d.c. conductivity rel. to thermoluminescence 9-14092  
 LiF, meas. without using contact electrodes 9-7836  
 LiF, pressure and temp. dependence, 50-5300 bars, 400-780°C 9-7839  
 Lu, Lorenz function from elec. and thermal conductivity meas. 9-7673  
 Mg-Cd alloy, order-disorder phase transition, changes 9-16155  
 Mg, deformed, meas. of generation and recovery of lattice defects 9-7478  
 $\text{Mg}_2\text{Cd}$  type alloys, anomalous change in resistance on ordering 9-3570  
 Mg Mn ferrite, depend. on reflection coeff. 9-10171  
 Mn-C alloys, resistance comp. dependence, 1000-1400°C, rel. to chem. bonds 9-12088  
 Mn-Fe spinel, effect of Mn<sup>3+</sup> clusters on resistivity 9-1206  
 MnP, temp. dependence, 4.2-500°K rel. to s-d exchange interaction 9-1456  
 MnZn ferrites of stoichiometric compositions, specific resistance, rel. to composition 9-16079  
 Mo, size effect meas. rel. to Fermi surface area estimation 9-12062  
 Mo single cryst. obtained by electron beam zone melting, meas. rel. to impurity distrib. 9-5344  
 Mo thin films, on NaCl, infl. of thickness and substrate temp. 9-5238  
 Na, e-e scatt. and resistivity low temp. depend. 9-1463  
 Na, temp. var. calc., comparison with expt. 9-16231  
 NaCl, irradi., d.c. conductivity rel. to thermoluminescence 9-14092  
 NaF, irradi., d.c. conductivity rel. to thermoluminescence 9-14092  
 Nb-C composite, resistivity, effect of particle size and C source powders 9-3391  
 Nb<sub>2</sub>O<sub>3</sub> thin films, voltage controlled negative resistance 9-12089  
 Nb<sub>2</sub>S<sub>4</sub>, metallic conduction rel. to crystal structure 9-9681  
 Ni-Co alloys, dil. ferromag., resistivity for each spin direction and screening 9-5645  
 Ni-Cu alloys, near Curie point, and thermal conductivity 9-7755  
 Ni-Cu alloys, resistivity meas., 100-700°K and mag. resistivity 9-21485  
 Ni-Fe alloys, dil. ferromag., resistivity for each spin direction and screening 9-5645  
 Ni, resistivity meas., 100-700°K and mag. resistivity 9-21485  
 Ni, temperature (1.85-20.1°K) and thickness (1.005-0.041 mm) dependences 9-1468  
 Ni, thin films, resistivity change in planar magnetic fields above 4 kOe 9-18682  
 Ni<sub>3</sub>Al, conduction electron scatt. by paramagnons 9-21462  
 Ni alloy, dilute low-temp., two-current conduction, implications on pure ferromagnets 9-3583  
 Ni and Ni alloys, meas. and interpret., 1-120°K 9-7754  
 Ni Fe ferrite, depend. on reflection coeff. 9-10171  
 Ni film, vacuum deposited, and temp. coeff., rel. to electron mean free paths 9-17369  
 Ni films, ultra-thin, tunneling mechanism rel. to structure 9-5644  
 Ni magnetic component of resistance at low temp. 9-13845  
 Ni Zn Fe ferrite, depend. on reflection coeff. 9-10171  
 NiCr<sub>2</sub>Se<sub>4</sub> rel. to effect of interactions between d shells of transition element 9-16253  
 NiCr thin films, resistivity change due to neutrons and  $\gamma$  rays 9-17378  
 $\text{Ni}_{1-x}\text{Fe}_x^{2+}\text{Fe}_x^{3+}\text{O}_4$ , resistivity vs.  $\text{Fe}^{2+}$  concentration (x) curves 77-373°K 9-12090  
 $\text{Ni}_3\text{Fe}_{1-x}\text{Te}_x$ , in strong microwave fields 9-12092  
 NiO:Li rel. press. and temp. 9-21506  
 NiO, high-temp., and defect props. 9-3571  
 NiO, holes in O<sub>2</sub> 2p band and primarily localized 3d states 9-1469  
 $(\text{Ni}_x\text{Zn}_{1-x})_2\text{Fe}_2\text{O}_4$ , in strong microwave fields 9-12092  
 NpN, anomaly near Curie point 9-5817  
 Pb, in normal state from meas. on superconductor 9-9933  
 Pb films, resistive transition rounding 9-16232  
 p-PbSe, temp. dependence for band structure determ. 9-3643  
 $\text{Pb}_2\text{Sn}_{1-x}\text{Te}_x$ , temp. dependence, 4-300°K rel. to band inversion 9-13890  
 p-PbTe:Fe,Mn, temp. depend. obs. 9-13876  
 n-PbTe:Gd,Mn, temp. depend. obs. 9-13876  
 $\text{Pb}(\text{Zr}_{1-x}\text{Ti}_x)\text{O}_3$ , charge transport mechanism, 650-1000°K 9-19932  
 Pd:Fe alloys, rel. to ferromag. ordering 9-5818  
 Pd-Au alloys, resistivity, high temp. 9-15027  
 Pd-Cr alloy films, rel. to e. diff. obs. 9-17242  
 $\text{Pm}_2\text{O}_3$ :Sm<sub>2</sub>O<sub>3</sub>, resistivity, rel. to  $^{147}\text{Pm}$  as power source 9-2790  
 Pt-Pd Au alloys, resistivity, high temp. 9-15027  
 Rb resist. rel. to conduction electron mean free path, obs. 9-18582

**Conductivity, electrical continued**  
**solids continued**

- Rb temp. var. calc., comparison with expt. 9-16231  
 Rb thin wires, deviation from Matthiessen rule, liq. He temp. 9-16233  
 RbNO<sub>3</sub>, rel. to phase transformations 9-16254  
 Re, resistance rel. to Hall eff. and Pauli susceptibility, temp. depend. 9-15072  
 RuO<sub>2</sub>, rel. to phases, comp. and O<sub>2</sub> partial pressure, -190°C -1000°C 9-1470  
 Sb, current carrier conc., pressure depend 9-15069  
 Se<sub>2</sub>O<sub>3</sub>, rel. to defects, 700-1600°C 9-1583  
 Se, amorphous, temp. depend rel. to heat treatment and Na admixtures 9-3572  
 Se, crystallized nonthermally, X-ray induced 9-9806  
 Se, metallic impurities effects in phase transition region 9-12103  
   Se film, amorphous, photogeneration, field controlled and free-carrier transport 9-3729  
 Se thin films 9-12191  
 Si: Au, step-like recovery after majority carrier sweep-out by trapped space charge 9-18615  
 n-Si, deviations from Ohm's law in high electric fields 9-16275  
 Si, infl. of e bombardment 9-3663  
 Si, irradi. with deuterons and  $\alpha$ -particles, high resistivity regions 9-3662  
 Si<sub>3</sub>N<sub>4</sub> films, d.c. conduction 9-19927  
 Si crystal, filamentary growth from soln. in tin, resistivity 0.01 ohm-cm 9-9644  
 Si laser-induced resistivity changes 9-7812  
 Si resistivity, predicting fast neutron induced changes at room temp. 9-1550  
 Si semiconducting, depend. on dislocations 9-1548  
 SiN, processes of Frenkel-Poole emission, field ionization and trap hopping 9-7834  
 Si<sub>3</sub>N<sub>4</sub>, produced from stain films on Si, resistivities 9-3205  
 SiO film in m.i.m. structure, voltage and temp. dependences 9-1562  
 Sn, in normal state from meas. on superconductor 9-9933  
 Sn film, critical conducting thickness, 100-400°K 9-3577  
 SnO<sub>2</sub>, cassiterite powder, press. depend. to 90 kg/cm<sup>2</sup> 9-13877  
 SnTe-Sb<sub>2</sub>Te<sub>3</sub> system, composition and temp. dependence 9-12153  
 Sr, metal-semiconductor transition at high pressure 9-18605  
 Ta films, cathode-sputtered, resistance changes rel. to structural changes 9-3196  
 Te single crystals, anisotropy 9-19911  
 Th, anisotropy and temp. dependence rel. to mag. props. 9-13843  
 ThB<sub>6</sub> polycrystals, carrier conc. obs. 9-1471  
 ThB<sub>4</sub> polycrystals, carrier conc. obs. 9-1471  
 ThC-UC solid solns., resist. meas., and Hall coeff. and thermoelec. power 9-3573  
 Ti-Cr alloys,  $\beta$ -stabilized, resistance anomaly, 4.2°-473°K 9-12104  
 Ti-V alloy, variation during decomposition of martensite on continuous heating 9-5494  
 Ti thin films, on NaCl, infl. of thickness and substrate temp. 9-5238  
 TiO<sub>2</sub>, doped, electronic conductivity rel. to optical props. 9-9706  
 Ti<sub>2</sub>O<sub>3</sub>, pure and doped, at 4.2, 77 and 273°K rel. to stoichiometry and purity 9-5646  
 Ti<sub>2</sub>(Se)<sub>2</sub> cpds, MTi<sub>2</sub>X<sub>4</sub> (M=Fe, Co, Ni), resistivity meas. and structural props. 9-9934  
 Ti, e. mean free path calc. from residual resistance diam. dependence 9-1422  
 n-TiBite<sub>2</sub>, specific conductivity temp. dependence 9-21507  
 TiCrO<sub>4</sub>, 200-600°C, rel. to change of structure 9-17375  
 Tm, temp. dependence, 5-300°K rel. to Neel temp. and mag. superzones 9-14014  
 $\alpha$ -U, Matthiessen's Rule, deviations from, n irradi. defects 9-16089  
 U n irradiated, length and electrical changes 9-3574  
 UN, resistivity, rel. to electronic and lattice contrib. to thermal conductivity, 77-400°K 9-7675  
 UO<sub>2</sub>-SiO<sub>2</sub> system, effect of fission fragments 9-7743  
 UO<sub>2</sub>, n-irrad. flux dependence 9-1457  
 V<sub>2</sub>O<sub>5</sub>, semicond. resistivity, depend. on uniaxial stress and hydrostatic pressure 9-18620  
 V oxides, crystalline and glassy, mechanism and reln. to structure 9-3702  
 VCr<sub>2</sub>Se<sub>4</sub>, rel. to effect of interactions between d shells of transition element 9-16253  
 VO<sub>2</sub>, semicond. to metal phase transition, resist. jump 9-16255  
 W-(26 wt.%) Re alloy, resistivity 300 to 2200°C 9-15035  
 W, size effect meas. rel. to Fermi surface area estimation 9-12062  
 $\beta$ -W compounds, resistivity 9-18604  
 WSe<sub>2</sub>, n- and p-type, 77°-295°K 9-5692  
 Y-Ce alloys, non-dilute, h.c.p., resistance minima rel. to spin-compensated state 9-15063  
 Y, anisotropy, 300-3°K 9-15064  
 Y, metal-semiconductor transition at high pressure 9-18605  
 Y Fe garnet:Hf, conduction mechanism by conductivity and thermoelec. power meas. 9-1458  
 Zn<sub>2</sub>Fe<sub>1-x</sub>Fe<sub>2x</sub>O<sub>4</sub> in strong microwave fields 9-12092  
 ZnO, thin films, resistivity 9-5252  
 ZnO, Zn excess, temp. dependence, 20-250°C rel. to discoloration 9-14059  
 ZnO films, dependence on parameters of growth process from saturated condensate current 9-1103  
 ZnSb, anisotropy 9-9923  
 Zr-Nb alloys, normal state resistivity 9-18606  
 Zr-U-H system, resistivity meas. for phase boundaries investigation 9-14995  
 Zr, resistance rel. to Hall eff. and Pauli susceptibility, temp. depend. 9-15072  
 ZrO<sub>2</sub>, and thermoelec. power rel. to defects, 800-1600°C 9-3703

**Conductivity, thermal***See also Heat conduction*

- disperse layers at high temp., separation of radiant component 9-9561  
 Fermi liq., transport coeffs. expressed as rapidly converging series 9-105  
 film, 1-dimens. growth from vapour, heat transfer 9-21248  
 in flame 9-17828  
 heat transfer bibliography 9-19085  
 hollow cylinder, temp. fields for boundary conds. of fourth kind on external surface 9-8529  
 hot-wire method, approx. to exact soln. for practical use 9-19090  
 laminated medium, transient heat conduction 9-165  
 lattice, model with phonon scatt., Umklapp proc., predicted exponential temp. behaviour 9-3500  
 porous medium, saturated, in presence of percolation 9-7666

**Conductivity, thermal continued**

- ratio, solid mass and fluid, convective equilibrium stability definition 9-17825  
 reference mats., new meas. comment and reply 9-162  
 resistance due to unique contact of circular cross section 9-14394  
 teaching demonstration using interferometry 9-8338  
 temperature distribution of body under non-linear conditions 9-14397  
 thermoelasticity, heating through boundary layer, and of surface of half space 9-19041  
 thin film infrared receiver performance, effect 9-6395  
 two-phase systems 9-14844  
 A-CO<sub>2</sub>, from 0° to 200°C 9-3094  
 Al<sub>2</sub>O<sub>3</sub>, rel. to purity and microstructure 9-1256  
 H plasma, in transverse mag. field, 10,000-50,000°K 9-7139  
 H plasma, infinite column, press. increase and total thermal cond. calc. 9-11540  
 Hg, supercritical, variation as example of nonmetal-metal transition 9-11692  
 N<sub>2</sub>-CO<sub>2</sub>, from 0° to 200°C 9-3094

**gases**

- alkali metal vapours, expt. compared with gas kinetic theory 9-14817  
 arcs, 'inverse' soln. accuracy 9-11639  
 bead thermistor apparatus and some expt. results 9-19583  
 carbon tetrachloride, expt. results compared with predictions 9-21135  
 chemically reacting mixture, heat transport theory studied 9-7227  
 compressed, density dependence 9-14815  
 deuterium - inert gas mixtures, comp. and temp. dependences 40-90°C 9-956  
 diethyl ether-nonpolar gas mixtures 9-14818  
 diphenyl, expt. results compared with predictions 9-21135  
 Eucken factor determ. 9-953  
 external field depend, theory 9-9445  
 hot radiating stagnant layer, transient energy transfer to surrounding cold gas 9-11659  
 hydrocarbons, gaseous, at normal pressures 9-9444  
 ionized, Boltzmann eqn. suitability for calc. 9-14814  
 Joule energy dissipation rel. to heating of medium 9-3052  
 measurement methods 9-14813  
 mixture, new model 9-7228  
 non-metallic elements, literature information analysis 9-15012  
 ozone, thermally decomposing, heat transfer study 9-3051  
 polar rotational relax. 9-9447  
 polar-nonpolar mixtures, theoretical predictions 9-9441  
 polyatomic, binary, ternary and quaternary mixtures 9-14816  
 polyatomic, multicomponent mixtures, calc. methods 9-18324  
 for pressure meas. up to 1 atm. using multifoil thermocouple 9-6273  
 Senftleben-Beenakker effect in gases of regular octahedral mols. 9-9446  
 three-component reacting mixtures, effective coeff. 9-9442  
 toluene, expt. results compared with predictions 9-21135  
 Ar-He mixture, obs. at 296.8°K 9-19584  
 Ar-Ne mixture, obs. at 296.8°K 9-19584  
 Ar, expt. compared with gas kinetic theory 9-14817  
 Ar, ionized, Boltzmann eqn. suitability for calc. 9-14814  
 H, ionized, Boltzmann eqn. suitability for calc. 9-14814  
 o-p-H<sub>2</sub> mixtures, Eucken factor determ. 9-953  
 H<sub>2</sub>, arc, 2000° to 7000°K 9-5114  
 HCl 9-9447  
 HF<sub>2</sub>, in crossed elec. and mag. field, reson. decrease of transfer coeffs. 9-9448  
 H<sub>2</sub>S 9-9447  
 He, meas. using hot-wire type of thermal diffusion column, 350-1350°K 9-5115  
 Hg, variation as example of nonmetal-metal transition 9-11692  
 N, ionized, Boltzmann eqn. suitability for calc. 9-14814  
 NH<sub>3</sub> 9-9447  
 N<sub>2</sub>O<sub>4</sub>=2NO<sub>2</sub>, He and Ar diluents, heat transport theory studied 9-7227  
 Ne-He mixture, obs. at 296.8°K 9-19584  
 SF<sub>6</sub>, Senftleben-Beenakker effect 9-9446  
 UF<sub>6</sub>, Senftleben-Beenakker effect 9-9446

**liquids**

- albumen dilute solns., non-Newtonian, rel. to displacement vel. 9-9506  
 alcohols, data considerations for standard reference materials 9-14847  
 chlorofluorohydrocarbons, FC-78 and Freons, C51-12 and 113 9-14848  
 crystals, nematic 9-21186  
 DNA dilute solns., non-Newtonian, rel. to displacement vel. 9-9506  
 heated body dissolving in free fluid 9-1005  
 inert gases, transport theory 9-9490  
 non-metallic elements, literature information analysis 9-15012  
 organic, pure, 15-130°C 9-14846  
 organic coolants for reactors, turbulent heat transfer 9-643  
 pressure, temp. and molecular struct. depend. 9-14843  
 sodium carboxymethylcellulose aqueous soln., non-Newtonian, rel. to displacement vel. 9-9506  
 two-phase systems, liq.-liq. and liq.-solid 9-14844  
 He, near superfluid transition S.V.P., critical exponent 9-1054  
 He, size dependence near  $\lambda$  point, along vapor press. curve 9-1053  
 He I, rel. to second sound velocity in He II and scaling laws near superfluid transition 9-11739  
<sup>3</sup>He in superfluid He<sup>4</sup> and pure He<sup>4</sup>, 0.035-0.5°K 9-3145  
 Hg, variation as example of nonmetal-metal transition 9-11692  
 InTe, temp. dependence, 670-950°K 9-1405  
 Li, m.p. to b.p., and thermal diffusivity and Prandtl number 9-21197

**measurement**

- calorimeter type cell, heat loss prediction 9-14393  
 concrete, problems 9-18567  
 crystals with paramag. ions, phonon mean free path calc. 9-9854  
 electric models for transient problems with variable boundary conditions in solids 9-1401  
 flash tech. for manufactured C and graphite, crit. evaluation 9-7662  
 gases, bead thermistor apparatus and results 9-19583  
 guarded hot-plate, error effs. 9-15017  
 i.r. transient method for solids 9-5573  
 solids, 90-200°K, apparatus based on axial flow technique 9-15016  
 solids, using electron beam 9-7665

**solids**

- apparatus based on axial flow technique for meas. between 90 and 200°K 9-15016  
 coatings, thin, by method of pulverization 9-9851  
 concrete, measurement problems 9-18567



**Conductivity, thermal continued****solids continued**

dense, quadrupole-quadrupole interact. eff. on initial press. depend. 9-5112  
dielectrics, nonlinearity under conditions of viscous flow of phonon gas 9-18566  
duraluminium deformed at 77°K 9-12025  
ferrites and garnets, polycrystalline 9-3535  
ferromagnetic alloys, resistivity, magnon drag eff., low temp. 9-13951  
glass beads, in vacuum, 100 to 500°K 9-15020  
glass beads, low range standard 9-15014  
graphite, anisotropic and near-isotropic, rel. to high-temp. irradi. 9-7663  
graphite, crystallite boundaries influence, and elastic const.  $C_{44}$  9-7671  
graphite, effect of point defects on basal cond., calc. for isotopes and vacancies 9-7668  
graphite, flash tech. of meas., crit. evaluation 9-7662  
graphite, impregnated, reduction under neutron irradi., 300-1500°K 9-7667  
graphite, polycryst., at two mutually perpendicular directions, rel. to crystallite sizes 9-7669  
graphite, polycryst., in perpendicular directions, 100-900°K. rel. to crystallite sizes 9-7672  
graphite, pyrolytic, expanded and brazed, up to 700°K 9-18565  
graphite, SX-5, from -100°K to 2600°K 9-7670  
graphites, polycryst., rel. to X-ray anisotropy factors 9-7428  
high temp. standard development 9-15013  
i.r. transient method of determination 9-5573  
Kapitza resistance between liquid  $^4\text{He}$  and metals, review 9-18379  
lattice, for one- dimens., harmonic, isotopically disturbed crystal 9-18568  
magnetic lattice near Curie point, contribution of diffuse modes 9-12266  
metal silicides, electric and grid 9-21443  
metals, apparatus, 90 to 200°K 9-15016  
metals with paramagnetic impurities, electron interactions effects 9-9876  
non-metallic elements, literature information analysis 9-15012  
plastics, apparatus, 90 to 200°K 9-15016  
potato section, specimen holder design 9-15394  
praseodymium ethylsulphate, mag. field dependence, 0.4-4°K, anomalies 9-13811  
PVC, stretched uniaxially, thermal and mechanical props. anisotropy 9-19781  
pyrocarbons, reproducible compressed samples, in a and c crystallographic directions 9-7596  
quartz, pure fused, precise determ., 0-500°K 9-15028  
response time of long uniform specimens 9-3540  
rocks, rel. to thermal piercing 9-15019  
rocks, ring heat source probes for rapid determ. 9-15018  
sand, dry 9-3539  
sandstones, calc. for unconsolidated sand, phase distrib. 9-3542  
SbSi, anomaly 9-7674  
semiconducting alloys with stoichiometric vacancies 9-17358  
semiconductor alloys, rel. to lattice parameters 9-15015  
silica, vitreous, critical evaluation of published literature 9-15029  
sintered semiconductor alloys 9-16183  
spin-wave scatt. by dislocations effect 9-3782  
at steel-Al interface, directional heat transfer rel. to surface conds. 9-13809  
superconductor, type II, in mixed state 9-21442  
superconductors, anomalies due to impurity spin ordering 9-12108  
tetra cyanquinodimethane derivatives, rel. to moving excited states 9-12505  
thermal and elastic waves at hypersonic freqs., unified theory 9-11914  
thermo-adsorption transfer 9-13806  
thin films, phenomenological theory 9-3538  
transient problems with variable boundary conditions, electric models 9-1401  
two-phase granular systems 9-3539  
two-phase system, liq.-solid 9-14844  
AgCl, irradiated, 2°-250°K, rel. to colloid prod. 9-9692  
Al, changeover phenomena and transverse phonons in kinetic coeffs. of trivalent metals 9-3541  
Al<sub>2</sub>O<sub>3</sub>, semi-cryst., temp. range 90 to 1100°K 9-21445  
Al alloys, 293°-673°K, calc. from elect. resistance and thermal conductivity 9-18866  
AlSb, phonon, 2°-500°K 9-7794  
Ar, multiphonon interaction from temp. depend. 9-15021  
Bi-Sb alloy, electronic cond. calc. 9-12026  
Bi effects at intermediate fields 9-15022  
C, granular, contact resistance at container walls 9-15023  
C, manufactured, flash method of meas., crit. evaluation 9-7662  
C fabric-Ta foil, multilayers for thermal insulation systems 9-3543  
Cd<sub>3</sub>As<sub>2</sub>-Zn<sub>3</sub>As<sub>2</sub> system, of solid solns. grown 9-13882  
CdS, annealed electron-irrad., anisotropic low temp. cond., obs. 9-9853  
Co, by Jain and Krishnan method, 1200°-1500°K 9-13807  
Co, calc., 290-1710°K from thermal diffusivity meas. 950-1710°K and elec. resistivity meas., 290-1710°K 9-1403  
Cr, 77 to 400°K 9-15024  
Cu chalcogenides, temp. dependence rel. to heat transfer mechanisms 9-12027  
Dy, and Lorenz functions 9-7673  
Er, and Lorenz functions 9-7673  
EuO, 50°-300°K 9-16184  
Fe, diffusivity, 900-1660°K 9-13808  
Fe<sub>3</sub>O<sub>4</sub>, (magnetite), thin films 9-1404  
GaP, phonon, 2°-500°K 9-7794  
GeTe alloys, 2.5°K to 110°K 9-5757  
GeTe alloys, 2.5°K to 110°K 9-5757  
Ge, change under n-irrad., 5-300°K 9-1402  
 $^3\text{He}$  with  $^4\text{He}$  impurity variational calc. of exchange constant and thermal conductivity 9-13554  
 $^4\text{He}$  high density, 1.1-7°K 9-21239  
HgSe, Lorenz number, 80°-440°K 9-5642  
In-Pb superconducting alloys, meas. down to 0.4°K rel. to phonon scatt. mechanism 9-21444  
In, very-high-purity, temp. dependence, 1.5-4.2°K, in mag. fields 9-12101  
InTe, temp. dependence, 950-1450°K 9-1405  
Kr, multiphonon interaction from temp. depend. 9-15021  
Lu, and Lorenz functions 9-7673  
Mg<sub>2</sub>Su, 80 to 700°K 9-15025  
MgO:Cr<sup>2+</sup> phonon scatt., meas. of phonon scatt., 1°-4°K 9-5535  
MgO:Fe<sup>2+</sup>, < room temp. 9-1406  
MgO dense powder, in N<sub>2</sub> gas 9-15026

**Conductivity, thermal continued****solids continued**

MnCl<sub>2</sub>·4H<sub>2</sub>O, magnetic field depend. rel. to magnon-phonon coupling 9-1421  
multilayer thermal insulation systems for high-temp. nonoxidising environments 9-3543  
Nb, pure, lattice component 9-9855  
Ni-Cu alloy, near Curie point, and elec. conductivity 9-7755  
Ni, and diffusivity at 900-1670°K 9-5574  
p-PbTe:Fe,Mn, temp. depend. obs. 9-13876  
n-PbTe:Gd,Mn, temp. depend. obs. 9-13876  
Pd-Au alloys, high temp. 9-15027  
Pm<sub>2</sub>O<sub>3</sub>-Sm<sub>2</sub>O<sub>3</sub>, rel. to  $^{147}\text{Pm}$  as power source, 70-1030°K 9-2790  
Pt-Pd-Au alloys, high temp. 9-15027  
Pt, by Jain and Krishnan method, 1200-1700°K 9-18569  
Pt, calc. from data on sp. ht., density and linear expansion coeff. 9-5575  
PuC, diffusivity, USNRDL flash technique 9-15032  
Sb, lattice thermal cond. rel. to e. scatt. mechanism 9-9856  
Sb<sub>2</sub>Te<sub>3</sub>-Bi<sub>2</sub>Te<sub>3</sub> powders, grain size, impurity content and processing effects 9-19867  
SbSI, 6°-316°K, anomaly 9-16185  
Se:Ge, amorphous, 100-300°K, phonon thermal cond. 9-1407  
Si, change under n-irrad., 5-300°K 9-1402  
SiO<sub>2</sub>, vitreous, critical evaluation of literature 9-15029  
SiO<sub>2</sub> glass, 0.5 to 4.2 K 9-19868  
Sn, pure and impure, normal and supercond. state 9-15030  
Sn, superconducting energy-gap effect, calc. 9-9857  
TaC, electron beam meas. technique, <2250°K 9-7665  
Tb, polycryst. and single cryst.,  $^1\text{K}$ , anomalies 9-9858  
Tb:Sb, 100-600°K, mechanism 9-13810  
Th, anisotropy and temp. dependence rel. to mag. props. 9-13843  
ThO<sub>2</sub> (1.3 wt.%)UO<sub>2</sub>, irradi. induced changes, annealing 9-7676  
ThO<sub>2</sub> powder, in various gases 9-15031  
Tm, temp. dependence, 5-300°K rel. to Neel temp. and mag. superzones 9-14014  
UC, arc cast and sintered radiation eff., 150-1600°K 9-15034  
UC, diffusivity, USNRDL flash technique 9-15032  
UN, electronic and lattice contrib., 77-400°K 9-7675  
UO<sub>2</sub>-SiO<sub>2</sub> system, and thermal resist., 100-800°K 9-16186  
UO<sub>2</sub>, sintered, radiation eff., 150-1600°K 9-15034  
UO<sub>2</sub>, with cracks, diffusivity, flash method suitability 9-15033  
W (26 wt.%) Re alloy, 300 to 2200°K 9-15035  
W-Sm oxide cermet, electron beam meas. technique, <2000°K 9-7665  
W, phonon cond. from thermal and elec. magnetoresists., 80-130°K 9-5636  
Xe, multiphonon interaction from temp. depend. 9-15021  
Y, anisotropy, 300 3°K 9-15064  
ZrO<sub>2</sub>, low density, monolithic structure for thermal insulation systems 9-3543  
ZrO<sub>2</sub> paper-Mo foil, multilayers for thermal insulation systems 9-3543

**Confinement of plasma** *see Plasma/confinement***Constants**

fundamental, numerical relations 9-6268  
gravitation, NPL-Trieste meas. 9-8347  
YFe granet, magneto-elastic, meas. by microwave techniques 9-10142

**Contact angle** *see Capillarity; Surface tension; Wetting***Contacts, electrical**

brush, mechanical stability 9-8573  
cathode-control-grid contact potential of receiving valves, meas. 9-231  
contact resistance effect on e.m. flowmeter readings, reducing method 9-7110  
metal-BaTiO<sub>3</sub>, effect of gaseous adsorption 9-7802  
metal-GaAs point contact, rectifying barrier structure 9-12163  
metal-photoconductor, carrier conc. rel. to illum. 9-16312  
metals in liq. environment, p.d. meas. 9-19889  
phenol-formaldehyde resin carbons, contact pot. difference rel. to heat treatment temp. 9-7324  
switch solid dielectric, fast metallic contact, high voltage, current 9-1602  
Au on Ba, double film on Nb, contact potential difference 9-1093  
Au on PbTe, elec. props. 9-3652  
Ba on Si, prep. and barrier height 9-13907  
Cs on Si, prep. and barrier height 9-13907  
GaAs ohmic contacts, vacuum dusting on to hot substrate 9-12161  
In and In-Ga on CdS, resistive props. 9-3613  
KCl, contact electrification by metals 9-10029  
Ni on Si, contact resistance 9-19892  
W films, vacuum deposited, on glass and polycryst. foil, contact p.d. between, and structure 9-5239

**Continuous creation hypothesis** *see Cosmology***Convection**

advances in free convection, book 9-6399  
boundary layer flow with organic surface sublimation 9-17147  
in cavity of conductivity fluid mag. field colinear to gravitational 9-19514  
elements in rotating medium, thermal growth conservation laws 9-19094  
film, 1-dimens. growth from vapour, heat transfer 9-21248  
flow, stability, horizontal fluid layer with permeable boundaries 9-12950  
flow, steady; instability, hydrodynamic and thermal; angular variation w.r.t. gravity 9-12949  
flow in sphere, toroidal and poloidal vel. field representation 9-20454  
in fluid, rot., flows in free convection, numerical calc. 9-11520  
in fluid, viscous, incompressible, in finite vessel, soln. by topological method 9-19627  
fluid flow, convective, in heated rotat. annulus, effect of radial barrier 9-21013  
fluid in enclosed rectangular cavity 9-19091  
fluids, hydrodynamic flow, stability 9-14744  
forced, vortex, two-phase spheroidal heat transfer to Hg 9-2260  
free convection from flat plate, solns. 9-21018  
free convection mass transfer at vertical mesh electrodes 9-14137  
free in horizontal layers, hydrodynamic liquid flow patterns obs. 9-21195  
in geology, dynamical 9-14153  
heat and momentum, in viscous fluid, boundary layer soln. 9-20999  
heat transfer, effect corona point discharge 9-5091  
heat transfer bibliography 9-19085  
heat transfer from rotating disc, effect of Prandtl number 9-6400  
hexagonal cell formation, flow in horizontal fluid layer 9-10754  
instabilities, penetrative convective 9-11519  
instabilities and counter-rot. cylinders analogy 9-11518  
instability, convective, of horizontal fluid layers bounded by thermal interaction 9-17825

**Convection continued**

- invariant group solutions of motions problems 9-17826
- laminar boundary layers, vertical plate with constant suction 9-15979
- laminar flow and temp. field in rotating radial circular pipes 9-13518
- laminar free, from heated vertical plate in stagnant radiating gas 9-7229
- laminar natural, from vertical circular cylinder 9-19092
- non-Newtonian mass transfer of plate 9-845
- paramagnetic fluids, insulating, magnetothermal 9-7233
- planetary interiors, thermal and nonthermal, combined effects 9-21934
- rotating-fluid sphere containing heat sources thermal instability 9-4371
- solar photospheric motions 9-21970
- thermal, atmosphere, suppression of frictional constraint on lateral boundaries 9-18793
- thermal and nonthermal, combined effects, planetary interiors 9-21934
- thermal leak, numerical calc. of soln. 9-8523
- in variable viscosity fluid layer, anal. 9-6039
- water, heat transfer from vertical circular cylinder 9-19093
- water, turbulent free convection boundary layer formed near hot plate, structure 9-21167
- Hg, laminar natural, effect of mag. field 9-18252
- in  $\text{NaNO}_3$ , liquid oscillatory temp. instability 9-14845

**Conversion electrons** see Beta-ray spectral/conversion electrons;**Gamma-rays/internal conversion****Cooling**

- See also Joule-Thomson effect; Low-temperature production; Magnetic cooling; Supercooling
- crystal growth, single, spherical, dendritic of high melting point metals 9-19689
- field ion microscope, by He gas 9-6496
- film cooling by gas, effect of strong adverse pressure gradients 9-17158
- high-temperature regions, cooling under cosmic conditions 9-17598
- immersion cooler using liq. vapour phase transitions 9-18966
- liquid flows, by thermal battery, efficiency rel. to geometry of elements 9-21544
- metal film condensation effect of vapor subcooling 9-19662
- nuclear reactor containers, spray cooling 9-20849
- Peltier effect cooling device for photocathodes 9-4444
- plane multilayer wall with inner heat generation, min. heat flow into cooling liq. 9-20445
- reactor, heat transfer from fuel rod array to turbulent flow 9-639
- reactor, liquid  $\text{N}_2$  lines, poor thermal insulation 9-19361
- semi-infinite wall, with temp. depend. thermophys. props., soln. with second-order approx. 9-10753
- splat, preparation of neutron activation analysis standards 9-16645
- thermoelectric, baffles for rotary pump 9-4196
- transpiration, wall-temp. distrib. calc., effect of Mach number 9-20457
- transpiration cooled porous flat plate in stream of air or  $\text{CO}_2$  9-20453
- YAl garnet, optical refrigeration 9-1831
- $\text{CO}_2$  with organic impurities, for nuclear reactor, patent 9-20859
- $^3\text{He}$  solid/liquid mixture, adiabatic compression, to 2.5 mK. 9-21234
- Na, in reactor, contamination by hydride thermal dissoc. 9-650

**Copper**

- additions to Al, effect on sintering 9-16141
- adhesion time of inert gases 9-21347
- adsorption of He on surface at 4.2°K 9-19676
- adsorption on Ge from electrolyte, effect on surface props. 9-5704
- alloying addition to Pb, effect on strength 9-1303
- alloying in Zn, effect on brittle fracture of Zn 9-9772
- atom, p-scatt. cross-section calc. by subtracting photoelectric cross-section 9-710
- atom, core-e energy levels and density of states, X-ray photoelectron spectrum 9-1813
- atomic collisions along [100] and [110] directions 9-5538
- Brinell hardness, fast neutron integrated dose, peak annealing temp. determ. 9-21401
- cathode protrusion formation during pre-breakdown conditioning 9-11633
- cellular method for band structure calc., test 9-12050
- cohesive energy, correlation and orthogonality corrections 9-18407
- cold-rolled, three-dimens. orientation distrib. function of crystallites 9-11841
- complex in boiling mixture separation by chromatography followed by spectrophotometric determ. 9-18779
- corrosion by  $\text{CuSO}_4$  9-20057
- creep, cavity formation in early stages 9-13731
- creep eff. on elec. resistance and mechanical props. 9-13730
- d-band optical density of states, photoemission study 9-1629
- deformation, stored and expended energy rel. to tensile strain and orientation 9-1283
- deformation in easy glide 9-5373
- deformed, 4.2°K, elec. resistivity 9-3567
- deformed dislocation arrangement in stress applied state electron microscope obs. 9-14946
- deformed polycrystalline small angle scattering of subthermal neutrons 9-3346
- density of states, accurate computation 9-15050
- diffused in n-GaAs, photoconductive lifetime, temp. depend. 9-5765
- diffusion and solubility in CdTe rel. to  $\text{Cu}_2\text{Te}$  film formation 9-11896
- diffusion and solubility in InP 9-5410
- diffusion in GaAs, coeff. meas. by u.s. method 9-14955
- diffusion in GaAs, impurity atom interaction 9-17286
- diffusion in KCl and NaCl, temp. dependence, 350°C-650°C, rel. to ion size effects 9-1250
- diffusion of Fe, direct obs. by Mossbauer effect 9-5401
- diffusion of Zn and resulting dislocation arrangements from etch-pit exam. 9-5359
- dislocation density growth during homogenization quenching 9-1217
- dislocation-pinning, activation energies meas. using electron irradiation at 78°K 9-5360
- dislocations, visibility, effect of degree of deviation from Bragg condition 9-13689
- dislocations in Cu matrix, interaction with coherent Co particles 9-1213
- dopant diffusion in ZnSb constant semiconductor thermoelements, X-ray microprobe analysis 9-10062
- drawn through die, microband development separating main deform. bands 9-9674
- elastic constants, higher-order, from finite deform. meas. 9-5419
- electrode, erosion by impulse accelerator plasma 9-9412
- electrode erosion in spark discharge under Ar atmos. 9-17141
- electrodeposition on graphite, grain clustering and projections 9-8101

**Copper continued**

- electrolytic dissolution in  $\text{H}_3\text{PO}_4$ , effects of heat transfer 9-21706
- electron emission, secondary, multiple distrib. 9-5782
- electron scattering, Monte Carlo calc. 9-7683
- electronic band structures, approx. calc. 9-12059
- electronic structure, calc. at two values of lattice const. 9-5611
- electronic structure, calc. at two values of lattice const., model Hamiltonian 9-5612
- epitaxial growth on cleavage face of mica 9-5242
- epitaxial growth on KCl, KBr and KI crystals 9-7377
- epitaxial growth of Te on (111) surface, LEED study 9-21270
- evaporation rate from molten iron under vacuum 9-19658
- fatigue at low amplitudes, influence of surfaces 9-16135
- fatigue hardening mechanism 9-13737
- fatigue-hardened foils, dislocation loss and rearrangement, effect of neutron irradi. 9-11882
- f.c.c., fatigue mechanism at u.s. freqs. 9-13735
- f.c.c., rolling texture formation by slip and mechanical twinning 9-19815
- Fermi surface and optical properties 9-18585
- Fermi surface band structure wave functions 9-9894
- Fermi surface determ. by positron annihilation 9-21465
- fibre texture by X-ray and n diff. 9-5490
- film, energy loss in  $\text{H}^{1+} \rightarrow \text{H}^{1,0}$  and  $\text{H}^{1,0} \rightarrow \text{H}^{1+}$  conversions in range 7-40 keV 9-17363
- film, epitaxial twinned, on sapphire, growth 9-1104
- film,  $\text{H}_2\text{O}$  chemisorption, 77° and 273°K 9-17519
- film, polycryst., creep rate rel. to film thickness 9-5467
- films, anomalous optical absorpt. rel. to ambient conditions 9-10198
- films, electron channelling at 50 keV 9-1413
- films, nucleation, growth and structure in obs. in e. microscope 9-19673
- foil preparation for electron microscope exam. 9-16071
- Frenkel pairs, e. irradi. induced, effects of annealing 9-3330
- Gantmakher effects at microwave freqs. 9-12076
- gettering from Si 9-3668
- grain boundaries migration rel. to dragging of small oxide particles 9-1233
- Hall, coeff. determ. 4.2-300°K 9-5651
- hyperfine struct. in  $4p\ ^2P_{3/2}$  state, level-crossing and Stark effect meas. 9-4836
- impurities in ZnS, internal friction reduction 9-5429
- impurity distribution in ZnS crystals grown from melt 9-18429
- internal friction peak  $P_1$ , impurity effects 9-7528
- interstitial defects, infl. on irradiation damage rate, 80°K 9-3329
- ionic core radii calc. and orthogonality corrections 9-19682
- isotope abundance ratio meas., surface ionization method 9-19416
- lattice distortion produced by interstitial Cu atom, lattice statics calcs. 9-13679
- lattice nuclei of equilibrium form, two dimensional nucleation process 9-14909
- lattice parameter changes on defect formation on quenching and  $\gamma$ -irradiation 9-1186
- liquid, diffusion of O, electrochem. meas. 9-11690
- liquid, thermal capacity at high temperatures 9-9505
- magnetomechanical behaviour associated with dislocation slip during fatigue deformation 9-17308
- magnetoresistance, longit. temp. depend. of saturation ratio 9-1446
- magnetoresistances, elec. and thermal, 80-130°K 9-5636
- melting, possible vacancy mechanism 9-5215
- monocrystal, secondary slip from compression deformation parameters 9-3427
- Mossbauer eff. of  $^{57}\text{Fe}$ , high pressure eff. at room temp. 9-21610
- neutron irradiated, hardening, thermally activated obstacles 9-11943
- outgassing at  $10^{-7}$   $10^{-10}$  torr 9-14299
- oxidation, influence of cryst. orientation 9-12543
- oxidation rate, effect of small Li addition at room temp. 9-3996
- oxidation rate at room temp., eff. of applied elec. current 9-15224
- phonon dispersion 9-5532
- photoneutron cross section 9-7691
- plastic deformation of polycrystals at 373-573°K 9-1284
- porous, shock compression 9-11920
- positron annihilation rel. to Fermi surface 9-7730
- positron lifetimes, cyclic deformation effects 9-16220
- powder particle formation during atomization by gas stream 9-5221
- quenching defects and hardness increase in polycrystalline sample 9-9774
- recoil atoms in Zn, stropping 9-19875
- recovery, isochronal, after cyclic deform. at 78°K 9-16119
- recovery, stage III, of e irradiated sample 9-13671
- relaxation time calc. from energy transfer between electron and phonon system 9-5599
- resistivity, elec., phonon-drag effect 9-5652
- resistivity of polycrystalline wires under tension and in transverse mag. fields 9-7753
- rods, cold worked, dislocation arrangement 9-9712
- rolling textures formed by slip 9-9777
- sintered, stress-deformation behaviour 9-17301
- solar abundance determ. 9-13289
- solar abundance determ., including hyperfine structure 9-14249
- solid, heat transfer from Ar plasma 9-21050
- solid and liquid, mag. susceptibility; apparatus, technique and temp. depend. 9-21563
- specific heat, 1-30°K 9-9843
- specific heat, excess, temp. dependence, 300-1200°K, analysis 9-1394
- specific heat and Gruneisen parameter calcs. 9-9842
- sputtering by 400 and 600 keV Ar ions, mechanism 9-7682
- stacking fault energy, formation from dislocation loop dissociation during plastic deformation 9-3343
- in steel, effect on graphite precipitation 9-19838
- strain hardening study 9-18499
- stress-induced ordering of point defects near 10°K following p irradi. 9-9755
- surface self-diffusion, infl. of Pb vapour 9-17284
- surface terrace vacancies, relaxation, migration and formation enies 9-21330
- tensile deformation of single crystals containing BeO particles 9-17306
- texture, axial, X-ray diff. exam. 9-3289
- thermal conductivity, new meas. rel. to reference standard, comment 9-162
- thermal radiation props. meas. by cyclic incident radiation 9-5562
- thermodynamic props. evaluation and literature data analysis, 0°-300°K 9-12015



**Copper continued**

- thermopower calcs. 9-12204  
thin films, light scattering, 2200 to 5400 Å 9-17478  
tubes, pitting corrosion, cause and counter-measures 9-17534  
U.S. attenuation orientation dependence 9-9830  
vacuum-smelted, recrystallization diagram 9-5287  
vapour laser, MHD, electrically accelerated, pulse broadening 9-20510  
X-ray absorption, fine structure obs. by bent crystal X-ray spectrograph 9-3910  
X-ray K-absorption edge, shift due to chemical combination 9-12454  
X-ray spectra and electronic structure 9-14067  
yield strength depend. on temp. 9-21371  
Young's modulus variation after plastic deformation 9-16117  
 $\gamma$  scatt., photoelectric cross sections, theor., expt. comparison, 50-412 keV 9-5579  
Al electrode erosion by impulse accelerator plasmas 9-9411  
Au-Cu alloy photoluminescence, radiative recomb. obs. 9-21660  
in CdGeAs<sub>2</sub>, effect on conductivity 9-18618  
Cd(PO<sub>3</sub>)<sub>2</sub>, crystal structure 9-19710  
Cu-Fe<sup>57</sup> lattice dynamics using Mossbauer effect 9-7638  
Cu-Pt(Pd), high speed dislocations, effect of impurity atoms on frictional force 9-3397  
Cu/Mg electric exploded wire, temp. and e. density distrib. in later stages 9-9346  
Cu-Ag-Se system, thermodynamics 9-18562  
Cu-Al barrier, electron current calc., applic. of perturbation method 9-18572  
Cu-GaAs supersaturated solid soln., precipitation 9-5511  
Cu-Zn alloy, elastic moduli var. with annealing time 9-9738  
Cu<sup>+</sup> ion, Hartree-Fock exchange potentials for electrons, comparison of methods 9-18138  
Cu<sup>2+</sup>, e.p.r. in borate, phosphate and silicate glasses 9-14111  
Cu<sup>2+</sup>, e.p.r. in oxide glasses, eff. of Co addition 9-18736  
Cu helicon window, Gantmakher oscillations due to magnetic field 9-1440  
Cu VII-XII, Hartree-Fock calcs. rel. to Sun's coronal spectrum 9-15368  
<sup>67</sup>Cu, prep. by <sup>67</sup>Zn(n,p)<sup>68</sup>Cu in reactor 9-16502  
Cu<sup>+</sup> implantation in Al, rel. to formation of precipitate phases 9-11956  
Cu<sup>2+</sup> in KH<sub>2</sub>PO<sub>4</sub>, chem. structure from e.p.r. spectra 9-1860  
Cu<sup>2+</sup> ion, interac. betw. 3d<sup>8</sup>, 4p, 3d<sup>9</sup> configs. under T<sub>d</sub> symm., eff. 9-17468  
Cu<sup>2+</sup> in ZnWO<sub>4</sub>, e.p.r. line half-width angular dependence 9-1866  
Cu,II relative transition prob. of resonance lines meas. 9-13289  
rel. to Δ Fe(OH)<sub>2</sub> colloid oxidation, Cu(II) effects, obs. 9-6014  
in Ge, effect on n-irrad. induced defects generation rate 9-5335  
O<sub>2</sub>, Xe, Kr, CO adsorption and interac., 77°K 9-21285  
O<sub>2</sub> adsorption on spherical single crystals, surface struct. 9-5259  
Pb-Cu-Pb sandwiches, resist. studies with Pb in supercond. state 9-13862  
in Si, effect on n-irrad. induced defects generation rate 9-5335  
ZnS:Cu,Mn,Cl film, electroluminescence, excitation mechanism 9-5974

**Copper alloys***See also Copper compounds*

- α-brass, fibre texture by X-ray and n diff. 9-5490  
aluminum bronze, As-containing, CuAl<sub>5</sub>-type, fatigued, stacking fault tetrahedra 9-19752  
brass: (5 wt.%)Zn, rolling texture, deform. rate depend. 9-1330  
brass, (70/30), fracture behaviour rel. to grain size, pre-strain and strain rate 9-19806  
brass, corrosion by CuSO<sub>4</sub> 9-20057  
α-brass, f.c.c., fatigue mechanism at u.s. freqs. 9-13735  
β-brass, quenched, anti-phase domain growth rate and final size 9-3335  
α brass, stress dependence of dislocation velocity 9-5358  
composition, prob. and props., patent 9-13768  
constantan-ZnSb semiconductor thermoelements, diffusion phenomena and phase transitions, X-ray probe analysis 9-10062  
Cu-In, discontinuous precipitation kinetics 9-9797  
β-Cu-Sn martensitic transformation 9-1338  
outgassing at 10<sup>-7</sup> 10<sup>-10</sup> torr 9-14299  
resistivity, elec., phonon-drag effect 9-5652  
resistivity-conc. dependence 9-16223  
thermal expansion, low temp. 9-19864  
welding joints with steel, crack formation and melting of base materials 9-21397  
Ag-Cu hollow cathode discharge, spect. study 9-19559  
Ag-Cu solid solns, supersaturated, substructure changes during decomposition 9-1339  
Al-Cu-Cd,  $\theta'$  precipitation, effect of Ag and Ge additions 9-1327  
Al-(0.3at.%)Cu, recovery of resistivity in stages II and III after 2-MeV e. irradi. 9-9696  
Al-(1.7at.%)Cu, relaxation props. of vacancies under quasi-equilibrium conditions 9-19743  
Al-Cu, deformed, precip. and recrystallization 9-21400  
Al-Cu, grain refinement, chemical and mechanical 9-16144  
Al-Cu, lattice const., effect of lattice strains, rel. to inhomogeneity in precipitation and age hardening 9-9783  
Al-Cu,  $\theta'$  structure, lattice parameters determ. 9-11834  
Al-CuAl<sub>3</sub>, eutectic, preferred orientation development during growth 9-1123  
Au-Cu, order-disorder props. rel. to partial substitution of Ni or Ga 9-5522  
Au-Cu, Zener relaxation and resistivity meas. of short-range order 9-19804  
Au-Cu on Au, two-layer films, Moiré patterns and misalignment dislocations 9-3200  
Au-Cu<sub>3</sub>, order-disorder props. rel. to partial substitution of Ni or Ga 9-5522  
AuCu type, ordered, superdislocations 9-1216  
Ce<sub>0.05</sub>Co<sub>0.25</sub>Cu<sub>0.75</sub> alloy, permanent mag. props. and prep. 9-3795  
Co-Cu, hexagonal, mag. moments rel. to e. transfer 9-12274  
Cu-Ag, brazing for metal-to-ceramic seals 9-13766  
Cu-Ag, precipitation assoc. with stacking faults growth 9-11958  
Cu-Al, annealed, near-order parameters, conc. dependence 9-3479  
Cu-Al, Brinell hardness comparison with Cu, fast neutron integrated dose 9-21401  
Cu-Al, β martensite annealing, new ordered phase 9-1350  
α-Cu-Al, high-temp. vacuum tensile fatigue rel. to Al content 9-9771  
Cu-Al, stacking faults, cubic type, in plastically deformed martensite 9-16103  
Cu-Al crystals, solid soln., hardening 9-13767  
Cu-(1wt.%)Al two-phase, high temp. creep mechanism 9-19793

**Copper alloys continued**

- Cu-Au, dislocation formation during ordering, e. microscopic exam. 9-11881  
Cu-75 wt.-%Pd, residual resistivity rel. to short-range order 9-12100  
Cu-Be, sp. ht. temp. depend. during ageing 9-13763  
Cu-(2.5 wt.-%)Be, decomposition, effect of electron bombardment 9-5501  
Cu-Co mixed crystals, nucleus formation at dissociation 9-14988  
Cu-Cr, f.c.c., effect of precip. hardening and recrystallization on texture 9-21391  
Cu-Cr ESR, transmission conduction 9-8030  
Cu-Cr Kondo transition, susceptibility and specific heat obs. 9-19942  
Cu-Fe, dil., sp. ht. meas. 9-18563  
Cu-Fe dilute, magnetoresistance and low-temp. resist. 9-18602  
Cu-Ga single crystal, work-hardening curve, transition from stage I to stage II, X-ray investig. 9-13760  
Cu-Gd dilute, e.s.r. of Gd 9-14110  
Cu-Ge, liquid, elec. resist., electronic struct. 9-16020  
Cu-He, stress-rupture characts. rel. to grain boundary degeneration 9-16133  
Cu-(2.4 wt.-%)Mg, precipitation hardening mechanism 9-1329  
Cu-Mn, <sup>63</sup>Cu spin lattice relax. meas. 9-14015  
Cu-Mn, liquid, partial and integral thermodynamic props. 9-21199  
Cu-Mn, magnetic props. rel. to structural state, applied field intensity and temp. 9-10147  
Cu-Mn solid solutions, stacking fault energies 9-7492  
Cu-Mn film, transmission, reflection and absorpt. coeffs., rel. to resonant states 9-7937  
Cu-(20at.-%)Ni-(20at.-%)Mn ordering process, 400-450°C 9-1342  
Cu-Ni-Zn, yield point and plastic deformation rel. to degree of ordering 9-19794  
Cu-Ni, corrosion rate, effect of Fe 9-4000  
Cu-Ni, damping behaviour 9-3398  
Cu-Ni, damping behaviour, miscibility gap existence 9-3400  
Cu-Ni, electrical resistivity change due to cyclic deformation 9-3579  
Cu-Ni, electron band structure 9-12058  
Cu-Ni, lattice constant temp. dependence over conc. range 9-19955  
Cu-Ni, plastically deformed, internal friction 9-13720  
Cu-Ni oxidation kinetics, scale formation 9-21693  
Cu-Ni resistance alloys for high temp. strain gauges 9-3409  
Cu-Pd, ordered and disordered, magnetoresistance variation 9-21483  
Cu-Pd, specific heat changes at low temps. from changes in short-range order 9-9844  
Cu-Pd film, transmission, reflection and absorpt. coeffs., rel. to resonant states 9-7937  
Cu-Sb phases, supercond., and absence of antiferromagnetism in Cu<sub>2</sub>Sb 9-12122  
Cu-Si Brinell hardness comparison with Cu, fast neutron integrated dose 9-21401  
Cu-Si solid soln., deformed, elec. resistivity decrease 9-16224  
Cu-Sn, equilibrated, grain boundary segregation, electron microprobe obs. 9-11843  
Cu-Sn, isomeric shift of <sup>119</sup>Sn in Mossbauer spectrum 9-5888  
Cu-Sn, liquid, electron transport, Ziman theory and exptl. data. comparison 9-7274  
Cu-Su, grain boundary segregation, electron microprobe obs. 9-5378  
Cu-Ti-Al alloys, hardening during slip mechanism 9-17319  
Cu-Ti, hardening during slip mechanism 9-17319  
Cu-Zn, α<sub>1</sub>-plates, morphology and crystallography correlation 9-11842  
Cu-Zn, characteristic temp., Grüneisen eqn., Debye function 9-19861  
β<sub>1</sub>-Cu-Zn, martensitic transformation, effect of n irradiation, heat treatment and deform. 9-5512  
Cu-Zn specific resistance for different compositions 9-1464  
Cu-(30 at.wt.-%)Zn, shock-induced deform. faults 9-13681  
CuAu I, ordered, deformation and mechanism 9-13726  
Cu<sub>3</sub>Au, magnetic susceptibility as function of order 9-13946  
Cu<sub>2</sub>MnAl(Sn), Heusler, low temp. sp. ht. meas. rel. to hyperfine fields 9-9841  
CuSi, stacking fault energy meas., composition and temp. dependence 9-11887  
Cu-<sup>62</sup>Ni, clustering, n. scatt. meas. 9-9673  
Fe-Cu systems, diffusion, vacancy mechanism, specific features 9-9730  
(48.2-57.0 at.-%)Ni-(51.8-43.0 at.-%)Cu, short-range dissoc. 9-17344  
Ni-Cr-Cu-Al alloy, vacuum fractionation model. 9-7342  
Ni-(30wt.-%)Cu, with interstitial occluded hydrogen, spontaneous magnetization temp. dependence 9-16361  
Ni-Cu, conductivity, elec. and thermal, near Curie point 9-7755  
Ni-Cu, Hall effect, magnetic resistivity and mag. susceptibility 9-21485  
Ni-Fe-Cu-Mo rolled from sintered compacts, high mag. permeability 9-13965  
Ti-Cu alloys, spot-cooled, new non-crystalline phases 9-5523  
ZnS-Cu, luminophors, dependence of three kinds of the Gudden-Pole effect on the light sum 9-5960  
Zr-Cu, oxidation by CO<sub>2</sub>, resistance behaviour 9-20049  
Zr-Cu, oxidation resistant for use as a coolant 9-20852  
Zr-Cu alloys (<5wt.-%Cu), phase transforms after quenching and tempering from β phase 9-11970  
Zr-Cu on ductile-brittle transition 9-11940  
Zr-Cu spot-cooled, new non-crystalline phases 9-5523

**Copper compounds***See also Copper alloys*

- chalcogenides, thermal conductivity temp. dependence rel. to heat transfer mechanisms 9-12027  
chalcopyrite, Mossbauer effect study, 80-700°K 9-5889  
complex of α-hydroxy-carboxylic acid, i.r. absorption spectra obs. 9-15851  
copper acetate monohydrate, anomalous magnetic susceptibility and optical behaviour interpretation 9-7043  
copper formate tetrahydrate, antiferroelec. props. 9-12200  
copper (II) salicylate adducts, e.p.r. and mag. susceptibility 9-17500  
Cu complex, dichlorobis(pyridine-N-oxide) oxide) copper(II), mag. susceptibility and exchange integral 9-16330  
CuO, microhardness anisotropy rel. to dislocations motion, obs. 9-3454  
halides lattice, vibration modes and force constants 9-13788  
minerals containing complex sulphides, crystal chemistry 9-13593  
oxide films, ellipsometric meas. of thickness and reflection eqns. 9-16043  
trichite, torsion of reticular planes 9-19792  
Al-Cu alloy, impure, transient effects during early stages of ageing 9-7594  
CdF<sub>2</sub>, e.s.r. of Mn<sup>2+</sup>, obs. 9-14112

**Copper compounds continued**

- Cu-Ag solid solutions, supersaturated, discontinuous precip. kinetics, investigation 9-21399
- Cu-Al solid solns., supersaturated and deformed, elec. resistivity changes after Cu precip. 9-21482
- Cu-Co solid solns., distribution function of precipitated Co particles 9-5803
- Cu-Ge solid solutions, mechanical twinning, structure and distribution 9-17254
- Cu-Sn bronzes, electrodeposition from Cyanide stannate bath 9-4006
- Cu-Sn  $\gamma$  solid solns., structural changes during eutectoid decomposition 9-7613
- Cu-Sn solid solns., Mossbauer effect, plastic deform. and annealing effects 9-1750
- Cu<sub>2</sub>O, nuclear spin-lattice relax. of <sup>63</sup>Cu, press. depend. 9-18687
- Cu<sub>2</sub>O elec. conductivity and thermoelec. power rel. press. and temp. 9-21506
- Cu<sub>2</sub>O photoresistors, characts. 9-16316
- Cu<sub>2</sub>O single cryst. layer, space-charge-limited current 9-16262
- Cu<sub>2</sub>TeO<sub>4</sub>, crystal structure 9-21311
- Cu acetylacetonate complex, u.v. and visible spectra, Wolfsberg-Helmholtz calc. 9-17029
- Cu chromite, catalysts of NH<sub>4</sub>ClO<sub>4</sub> thermal decomp. 9-12528
- Cu complex, bis-L-histidine copper (II) dinitrate dihydrate, crystal structure 9-13634
- Cu complex, copper monochloroacetate 2.5 hydrate, mag. susceptibility and exchange integral 9-16330
- Cu complex, Cu-8-hydroxyquinolate, effect of host lattice on e.p.r. 9-10279
- Cu complex, dichloromonoquo- (pyridine-N-oxide) copper(II), mag. susceptibility and exchange integral 9-16330
- Cu complex, N-salicylidene-glycinatoaquocopper (II) tetrahydrate, crystal structure 9-13635
- Cu complex, pyruvidene- $\beta$ -alaninatoaquocopper (II) dihydrate, crystal and mol. structure 9-7437
- Cu complex, triphenylmethylphosphonium bis(3-1,2-dicarbolyl) cuprate(III), crystal and molecular struct. 9-19712
- Cu complexes, trinuclear, containing transition metals, antiferromag. 9-10148
- Cu halide complexes with n- heterocyclic ligands, diffuse reflectance and far i.r. spectra 9-14043
- Cu II chelates, mixed, absorpt. spectra study 9-13350
- Cu II complexes, mol., Jahn-Teller eff. 9-18181
- Cu<sub>15</sub>Au<sub>0.25</sub> solid solns., Mossbauer effect, plastic deform. and annealing effects 9-1750
- Cu<sub>1</sub>Au, work hardening rel. to superlattice structure 9-13758
- CuBr-CuCl solid solns., exciton absorpt. and emission spectra at 8 and 80°K 9-1775
- CuBr, electric field gradient, spin echo meas. 9-10028
- Cu<sub>3</sub>Cd<sub>3</sub>Fe<sub>2</sub>O<sub>4</sub><sup>57</sup>Fe Mossbauer spectra, 4.2-1000°K in appl. ext. mag. fields 9-7956
- Cu<sub>2</sub>CdSi<sub>4</sub>, crystal structure 9-17267
- CuCl, electro-optic effect of excitons 9-3863
- CuCl, far i.r. phonon processes 9-1774
- CuCl, Faraday rotation spectra, sign reversal 9-12374
- CuCl, refractive index from thin-film interference spectra, temp. dependence 9-1728
- CuCl, second order Raman-laser spectrum 9-12421
- CuCl, Zeeman eff. on excitonic refl. spectrum, low temp. 9-14044
- CuCl mol., spectra, r-centroid and Franck-Condon eff. determ. 9-4925
- CuCl optical, non-linear, phenomena 9-10160
- CuCl radiative recomb., low temp., laser u.v. excitation 9-16430
- CuCl single crystals, photoconductivity, 10 to 150°K 9-10071
- CuCl in ZnS, effect on electroluminescence freq. characts. 9-3941
- CuCl<sub>2</sub>·2H<sub>2</sub>O, i.r. vibrations, study 9-7973
- CuCl<sub>2</sub>·4H<sub>2</sub>O single crystal, antiferromag. reson. line width 9-10272
- CuCr<sub>2</sub>Te, Mossbauer effect, of <sup>121</sup>Te, internal mag. field at iodine impurities 9-16400
- CuCr<sub>2</sub>Y<sub>2</sub> (X=S, Se and Te, Y=Cl, Br and I), magnetic props. 9-1639
- Cu(C<sub>2</sub>SO<sub>4</sub>)<sub>2</sub>·6H<sub>2</sub>O, orthorhombic g-tensors and orientations, e.p.r. determ. 9-12240
- CuFe<sub>2</sub>O<sub>4</sub><sup>57</sup>Fe, Mossbauer spectra, 4.2-1000°K in appl. ext. mag. fields 9-7956
- CuFe<sub>2</sub>O<sub>4</sub>, mag. props. 9-1680
- CuFeS<sub>2</sub>, Mossbauer effect obs. discrepancy with previous work 9-10182
- CuFeS<sub>2</sub> (chalcopyrite, Mossbauer effect study, 80-700°K 9-5889
- CuHPO<sub>3</sub>·2H<sub>2</sub>O, crystal structure 9-14917
- Cu<sub>2</sub>HgI<sub>4</sub>, photoelectric properties 9-12216
- CuI, Cu NMR up to 465°K rel. to  $\alpha$ ,  $\beta$  and  $\alpha'$  phases 9-8039
- CuI, electric field gradient, spin echo meas. 9-10028
- CuI, high pressure polymorphism, temp. depend. 9-3488
- CuI, photocathode, u.v. quantum efficiency, e-irrad. effects, 1-2 MeV 9-12224
- $\gamma$ -CuI films, internal stresses rel. to thermal expansion coeff. incompatibility with substrate, obs. 9-16126
- Cu(II) complexes, bis(thiosemicarbazone) Cu(II) and others, molec. props. 9-2861
- CuK<sub>2</sub>(SO<sub>4</sub>)<sub>2</sub>·6H<sub>2</sub>O, solid dilution with ZnK<sub>2</sub>(SO<sub>4</sub>)<sub>2</sub>·6H<sub>2</sub>O effect on spectra 9-10199
- CuMnSb, antiferromagnetism 9-3835
- (Cu<sub>2</sub>Mn<sub>1-x</sub>)<sub>2</sub>·5H<sub>2</sub>O mixed crystal, e.p.r. 9-5984
- Cu(NH<sub>4</sub>)<sub>2</sub>Br<sub>2</sub>·2H<sub>2</sub>O, b.c.c. Heisenberg ferromagnet, spontaneous magnetiz. meas. 9-18673
- CuO-Al, sintering effects due to CuO reduction 9-3463
- CuO mol. spectrum, especially orange-red bands 9-20927
- Cu<sub>2</sub>O, bound states at 110°K 9-12375
- Cu<sub>2</sub>O, optical transitions to n=1 exciton, elec. field effects 9-12376
- Cu<sub>2</sub>O, polycrystalline, high-resistivity, combined prep. and low temp. meas. device 9-3742
- Cu<sub>2</sub>O, single crystals, even photomagnetic effect 9-1623
- CuO mono- and polycrystals, in n.q.r., effect of elastic actions and mag. field 9-15211
- Cu<sub>2</sub>P<sub>2</sub>O<sub>4</sub>, monoclinic, crystallographic data 9-5324
- Cu(RbSO<sub>4</sub>)<sub>2</sub>·6H<sub>2</sub>O, orthorhombic g-tensors and orientations, e.p.r. determ. 9-12240
- Cu<sub>2</sub>S, spec. heat, -70 to 550°K 9-5566
- Cu<sub>2</sub>S Cu NMR up to 465°K rel. to  $\alpha$  and  $\beta$  phases 9-8039
- Cu<sub>2</sub>S layers, i.r. refl. and transmission rel. to elec. cond. and stoichiometry 9-1736
- CuSO<sub>4</sub>, corrosion of metals 9-20057

**Copper compounds continued**

- CuSO<sub>4</sub> cry. as u.v. transmitting filters 9-20558
- CuSO<sub>4</sub>·5H<sub>2</sub>O, i.r. vibrations, study 9-7973
- CuSO<sub>4</sub>·5H<sub>2</sub>O, magnetothermodynamics, 0.4° 4.2°K 9-9840
- Cu<sub>2</sub>Sb, absence of antiferromagnetism and supercond. of Cu-Sb phases 9-12122
- Cu<sub>2</sub>Sb, n.m.r., evidence of absence of antiferromagnetism 9-16376
- Cu<sub>2</sub>Se, electrical conductivity rel. to phase transformations 9-17390
- Cu(TiSO<sub>4</sub>)<sub>2</sub>·6H<sub>2</sub>O orthorhombic g-tensors and orientations, e.p.r. determ. 9-12240
- Cu<sub>2</sub>Zn<sub>0.5</sub>Fe<sub>0.5</sub>O<sub>4</sub><sup>57</sup>Fe, Mossbauer spectra, 4.2-100°K in appl. ext. mag. fields 9-7956
- (Cu+Zn)K<sub>2</sub>(SO<sub>4</sub>)<sub>2</sub>·6H<sub>2</sub>O crystals, magnetically dilute, e.p.r. line width, theory and expt. 9-15201
- Ni-Cu alloys, interstitial H occlusion 9-17278
- Ni-Fe-Cu layers, mag. and struct. props., influence of annealing 9-3821
- ZnS:Cu single crystal, induced i.r. absorption spectra obs., 1-3  $\mu$  9-10213
- ZnS-Cu, lumiphosphors, temperature dependence of three kinds of the Gud-Pole effect 9-5959
- Corbino effect** see *Current, electrical*
- Coriolis forces** see *Dynamics*
- Cornea** see *Eye*
- Corona, electric discharge**  
See also *Breakdown, electric*  
in air point, effect on convective heat transfer 9-5091  
counters of scintillating particles, integral noise spectrum formation mechanism 9-2595  
d.c., electron attaching impurities role 9-11634  
d.c., on smooth conductors in air, ionization layer anal. 9-11635  
heat transfer props. of fine wire, effect of corona 9-17140  
I-V characteristics, electrode temp. dependence 9-9421  
impulse type to impulseless, transition 9-3033  
positive, d.c. and pulse, comparison 9-15964  
propulsion system performance, theory and expt. 9-11619  
H<sub>2</sub>, breakdown voltage, comments 9-7204
- Corona, solar** see *Sun/corona*
- Coronagraphs** see *Sun/corona*
- Corpuscular streams** see *Cosmic rays; Sun/radiation, corpuscular*
- Correspondence principle** see *Quantum theory*
- Corrosion**  
Al alloys, stress-corrosion and distribution, eff. of shot peening 9-17533  
alloys, high-temperature, in carburising gases, factors affecting corrosion-resistance 9-17532  
alloys, relevance of surface composition due to chem. modification 9-16037  
brass, by CuSO<sub>4</sub> 9-20057  
corundum, stress corrosion rel. to temp. depend. of strength, obs. 9-1299  
corundum refractories, by oxides at 1500-1750°K 9-14135  
electrolytic cell cathode protection, patent 9-8107  
fatigue, control, anodic protection 9-20052  
graphite cylinder attacked by water vapour, diffusion-convective soln. 9-9095  
group VAla metal composite mats., effects of W replacement by Mo or Cr 9-19842  
intergranular, applic. of solute clustering mechanism of grain boundary hardening 9-3358  
metal electrode, dissolution during yield under stress 9-1914  
refractories, by blast furnace slags, mineralogies 9-3980  
sapphire, stress corrosion and fracture surface energy on (1011) and (1101) planes 9-7571  
sintered spinel, by oxides at 1500-1750°K 9-14135  
spinel-corundum, by oxides at 1500-1750°K 9-14135  
stainless-steel tube, vented, exposed to CO<sub>2</sub>-CO mixture in nuclear reactor 9-15221  
steel, 18-10, welded joints, corrosion resistance enhancement by quenching 9-16142  
steel, 60KH3G8N8V, hot working effects on stress-corrosion cracking susceptibility 9-3449  
steel, austenitic, Cr-Ni, following neutron irradiation 9-21701  
steel, austenitic Cr-Ni stainless, pitting, in H<sub>2</sub>SO<sub>4</sub> containing H<sub>2</sub>S 9-20054  
steel, by organic acids 9-20056  
steel, ferritic Cr, by S at 600-1000°K 9-18759  
steel, high strength, stress-corrosion cracking 9-9757  
steel, in Na melt, transfer of C from unstabilized to stabilized sample 9-10345  
steel, mild, by sulphate-reducing bacteria 9-17537  
steel, outdoor exposure, eff. of orientation of specimens 9-20055  
steel, stainless, behaviour in high temp. water and superheated steam 9-17536  
steel, stainless, pit nucleation, effect of sulphide inclusions 9-21700  
steel as melting pot material for reactor 9-651  
steel in H<sub>2</sub>SO<sub>4</sub> soln., from polarization data 9-21698  
steel powders, pressed and sintered 9-17339  
steelpipe, under flow conditions, mass transfer correlation with temp. effects 9-21696  
structure materials, effect of thermal n irradiation 9-1912  
Al, by CuSO<sub>4</sub> 9-20057  
Al, in citric acid., effect of F<sup>-</sup> 9-10344  
Al alloys, fretting products 9-20053  
CaO-Al<sub>2</sub>O<sub>3</sub>-MgO-BaO-B<sub>2</sub>O<sub>3</sub> glasses, Na-vapour resistant up to 700°K 9-4001  
Cu-Ni alloys, effect of Fe on rate 9-4000  
Cu, by CuSO<sub>4</sub> 9-20057  
Cu electrode erosion in spark discharge under Ar atmos. 9-17141  
Cu in H<sub>2</sub>PO<sub>4</sub>, electrolytic dissolution, effects of heat transfer 9-21706  
Cu tubes, pitting, cause and counter-measures 9-17534  
Fe-Cr-Ni alloy, austenitic, in oxidizing acids, effect of Si content on resistance 9-17535  
Fe-(16wt.%)Cr crystal, pit nucleation, e. microprobe exam. 9-21697  
Fe, cast, by CuSO<sub>4</sub> 9-20057  
Fe, high-purity, stress-corrosion cracking in NH<sub>4</sub>NO<sub>3</sub> soln. 9-14981  
Fe, in Li<sub>2</sub>SO<sub>4</sub>-K<sub>2</sub>SO<sub>4</sub> eutectic at 600°K, thermodynamics 9-15222  
Fe, inhibition by phenylthiourea 9-12545  
Fe, inhibitor action rel. to effects of deformation and heat treatment on metal 9-18760  
Fe<sub>2</sub>O<sub>3</sub>, magnetic, film nucleation and growth on Fe in high-temp. water 9-21276  
Fe in HClO<sub>4</sub>, transition state of inhibition by org. cpds. 9-15223  
Fe in NH<sub>4</sub>NO<sub>3</sub>-NH<sub>3</sub>-N<sub>2</sub>O system 9-21699



**Corrosion continued**

- Ni-Mo alloys, anodic props., mag. field effects 9-21709  
 Ni alloys as melting pot material for reactor 9-651  
 Ni anodic props., mag. field effects 9-21709  
 Ni electrodes, anodic dissolution and pitting in NiCl<sub>2</sub> soln. 9-21713  
 Sn, surface reactions with aq. thiourea soln. 9-21702  
 TaO<sub>2</sub> protective film on Ta in high temp. HNO<sub>3</sub> acid and ag. CuCl<sub>2</sub> soln. 9-21267  
 Ti-(5wt.%) Al-(2.5wt.%) Sn alloys, hot salt cracking 9-21383  
 Ti-Al alloys, binary, hot salt cracking 9-21383  
 Ti-Sn alloys, binary, hot salt cracking 9-21383  
 Ti alloys, stress cracking, electrochemical mechanism 9-19813  
 U-(10 wt.%) Mo alloy, stress-corrosion cracking, effects of heat treatment and ambient atmospheres 9-21384  
 U fuel element with defective Zircalloy-2 cladding, in steam - H<sub>2</sub>O, 285°C 9-11361  
 Zn, by CuSO<sub>4</sub> 9-20057  
 Zr-(2.5 wt.%) Nb corrosion resistance, cold deformation effect 9-647  
 Zr alloys with improved corrosion resistance, composition, patent 9-13745

**Cosmic dust** see *Interplanetary matter; Interstellar matter; Meteorites*

**Cosmic noise** see *Cosmic radiations, radiofrequency*

**Cosmic radiations, radiofrequency**

See also *Quasars; Radioastronomy; Sun/radiation, radiofrequency*

- 3°K, for earth's velocity calc. 9-17559  
 3°K region, photon prod. by inverse Compton eff. 9-18886  
 3C 273, polarization, 9.55 mm 9-20205  
 3C 305 radiogalaxy red shift obs. with contact image-converter tube 9-12733  
 3C 371 radiogalaxy red shift obs. with contact image-converter tube 9-12733  
 3C 390.3 radiogalaxy red shift obs. with contact image-converter tube 9-12733  
 3C 84, polarization, 9.55 mm 9-20205  
 3C and 3CR catalogues, 560 sources obs. at 86 MHz 9-10504  
 4C sources obs. at 408 MHz, mean spectral index depend. on flux 9-15331  
 234 sources, brightness distrib. at 2695 MHz 9-12738  
 γ-source correl. with optical nebulosity, postulated supernova remnant or star 9-16597  
 antipodic, rel. to information on universe 9-20140  
 background, crowave antenna noise temp. meas. 9-8223  
 background contribution of i.r. galaxies 9-6156  
 black-body, in universe 9-16548  
 blackbody radiation, obs. and cosmological interpretation 9-6102  
 Cas-A, obs. with 1' fan beam in 3.75 MHz 9-20210  
 Cassiopeia A, emission 9-12689  
 Cassiopeia A scintillation inversion rel. to source size 9-12740  
 catalogue of 615 radiosources in continuum near 1420 MHz declinations -5° to +70° 9-12739  
 continuum survey, data high-sensitivity 1415 MHz, north declinations 19° and 37° 9-6146  
 cosmological black-body, and expanding Universe evolution 9-18831  
 CP 1133, Cerenkov night sky detector obs. 9-16604  
 CP 1919, pulsating source, simultaneous obs. over 5000 km. baseline 9-18890  
 crab nebula, radio source of small angular dims. 9-2036  
 Cyg-A, obs. with 1' fan beam in 3.75 MHz 9-20210  
 Cygnus A scintillation inversion rel. to source size 9-12740  
 in diapasone, frequency spectrum 9-4112  
 east-west brightness distrib. and structure at 1425 MHz 9-12737  
 excitation wave due to light flare 9-20204  
 flux densities of sources at 10.03 MHz, correlation for ionospheric effects 9-17631  
 galactic anticentre, observations at 70, 60 and 40 cm wavelengths 9-6154  
 galactic centre region lunar occultations in 1667-MHz OH line 9-6110  
 galactic radio noise freq. spectrum rel. to cosmic ray electron flux 9-12730  
 galaxies, bright, fan-beam detection of 408 MHz emission, correl. with optical props. 9-16558  
 galaxies, normal, 39 obs. at 430 and 611 MHz 9-20208  
 galaxies at 1415 MHz, calc. of structure and evolution 9-15276  
 galaxies at 1415 MHz, ratio of radio to optical diameters, interpretation 9-15275  
 galaxies radioluminosity contrib. to metagalaxy background rad. 9-1989  
 IC443, radio spectra obs. 9-1999  
 intensity distrib. in homogeneous, anisotropic models 9-2034  
 interplanetary plasma 1965-1966, heterogeneities 9-2062  
 Jupiter, polarization, 9.55 mm 9-20205  
 Jupiter, radii emission, and e.m. wave prod. by plasma 9-11558  
 linear polarization meas. method, corrections 9-6155  
 moon thermal conditions of upper cover and integral radioemission during the eclipse 9-4114  
 nebulae, emission, high resolution obs. at 408 MHz 9-20165  
 NGC 7293; accumulation of radial filaments and nebulae envelope 9-1993  
 noise, auroral absorption bays time lag 9-21790  
 Orion A, polarization, 9.55 mm 9-20205  
 Parkes obs. corrected by those at Molonglo 9-16598  
 planetary nebulae, radio obs. on 84 at 5000 MHz 9-12670  
 polarization, high resolution measurements at 408 MHz of region around  $\theta^1=140^\circ$ ,  $\theta^{II}=10^\circ$  9-21860  
 in a pulsar corona 9-4095  
 pulsar CP1919, statistical props. 9-16599  
 pulsar CP 1919+21, possible optical counterpart 9-6149  
 pulsar freq. shift and general relativity 9-8395  
 pulsar in constellation Vulpecula 9-16601  
 pulsar models based on vibrating white dwarfs 9-18889  
 pulsar obs., meas. on CP 0328, CP 0808, HP 1506, PSR 1749-28 and PSR 2045-16 9-16603  
 pulsars, applic. to test general relativity 9-8268  
 pulsars, discovery and props. 9-15332  
 pulsars, discovery and props. 9-16605  
 pulsars, obs. on two at 3 MHz 9-6150  
 pulsars, positions of four 9-17634  
 pulsars in southern hemisphere sky, discovery of two 9-17633  
 pulsars obs. at 113MHz, pattern of variability 9-6153  
 pulsating radio source, distances 9-16600  
 pulsating source, new 9-17632  
 pulsating sources in declination range +44° <  $\delta$  < 90° 9-21914

**Cosmic radiations, radiofrequency continued**

- pulsating sporadically, two near Crab Nebula 9-18892  
 quasar, 3C273, A and B components, 3.9 cm 9-4109  
 radio sources, log N-Log S relation and luminosity functions in Friedmann universes 9-20133  
 radiogalaxies spectra 9-1990  
 radiosource, supernova remnant in Centaurus 9-15328  
 radiosources, supernova remnants, polar, distrib., 1418 MHz 9-15329  
 redshifts and intrinsic powers of 89 identified sources from 3C revised catalogue 9-17630  
 relativistic effects from astrophysical sources rel. to energy sources of quasars and radio galaxies 9-18885  
 Sagittarius A lunar occultations obs. 230-2400 MHz, spectral index calc. 9-16595  
 scintillating sources, optical identification 9-21915  
 slope of log N-log S diagram, determ. from radio-source counts 9-12731  
 small-diameter sources, 18 cm obs. 9-8269  
 in solar particle events (23 and 27 May 1967) 9-18939  
 source counts and spectral index distrib. dependence on observing freq. derived 9-10506  
 source W3, spectral line interferometry with independent time standards at stations 845 km apart 9-6145  
 sources, 11, near 55 MHz, obs. 9-2033  
 sources, 13, distrib. of linear polarization at 21.2 cm wavelength 9-2030  
 sources, 45, linear polarization at 6 cm wavelength 9-2031  
 sources, 67, accurate position meas. and identification between +20° and +27° 9-2032  
 sources, high freq., not listed in 4C catalogue, investigation 9-14231  
 sources in clusters of galaxies 9-4104  
 sources in Monoceros 9-16562  
 sources opposite quasars as cosmological test 9-20211  
 southern sky, brightness distrib. of radio noise at 10.02 MHz 9-15330  
 SP 0808, CP 0328 and HP 1506, corrected dispersion values 9-16602  
 special relativity application for the investigation of nature of some cosmic radio sources 9-4107  
 supernova remnants as radio sources 9-12704  
 synchrotron emissivity 9-4106  
 synchrotron radiation polarization, effect of ionized medium 9-12726  
 Tau-A, obs. with 1' fan beam in 3.75 MHz 9-20210  
 Taurus A, polarization, 9.55 mm 9-20205  
 Vela X in Stromlo 16, optical spectrum 9-1994  
 W28, 1720 MHz OH emission position and polarization 9-4111  
 W44, 1720 MHz OH emission position and polarization 9-4111  
 W49 radiosource, neutral H line reduced brightness at  $\lambda=21$  cms 9-2035  
 W63 obs. shell structure no optical identification, probably supernova remnant 9-12742  
 W 49 (3C 398) obs. of thermal and non-thermal component (a supernova remnant 9-20209  
 H, W49 radiosource, region of reduced brightness of neutral line,  $\lambda=21$  cm 9-2035  
 H II regions, galactic, southern hemisphere, 5 GHz continuum obs., 28 maps 9-15280  
 H  $\alpha$  lines, 28 obs. from Orion nebula, electron temp. determ. 9-16564  
 H56 $\alpha$  recombination line, from Omega nebula 9-16563  
 OH-emission sources, positions and Stokes parameters 9-16593  
 OH 1665 MHz wideband emission, new type, Carina region 9-16596  
 OH mol. in interstellar space, r.f. absorpt. and emission 9-18879

**Cosmic rays**

- $\gamma$  exponent, contradiction in assumed value 9-20680  
 data handling by paper tape 9-4650  
 diffusion tensor and its variation observed by Mariner IV 9-10459  
 galactic, life, explanation in stochastic model of mag. field 9-20150  
 galactic, low energy, intensity meas. 1961-5 obs. 9-12663  
 galactic, solar modulation 9-14185  
 in gold mines, neutrino detection 9-18015  
 in gold mines, neutrino detection 9-18015  
 heating rate in interstellar He from detect. of metastable He, possibility 9-18878  
 intensity gradient perpendicular to ecliptic, estimate from seasonal variation due to earth's movement from equatorial plane 9-11120  
 intensity increase, 28 Jan., 1967 9-12646  
 intensity underground, review 9-16912  
 in interplanetary mag. field, eff. of random walks of lines of force 9-21952  
 interplanetary region, distrib. and motion of the gas particles 9-14245  
 in interstellar medium, shock wave structure 9-1988  
 penetrating component at mountain altitudes, energy spectrum and angular distrib. 9-4652  
 Propagation through interstellar matter, diffusion and nuclear reaction 9-12661  
 quarks, relativistic  $e/3$  and  $2e/3$ , search at sea level, and upper limits of flux 9-2553  
 solar, low-energy, latitude-intensity structure and pitch-angle distrib. 9-10441  
 solar, screening by outer magnetosphere 9-14254  
 sub, acceleration and high frequency turbulence spectra of a plasma 9-2976  
 sub, acceleration and high frequency turbulence using spectra of a plasma 9-14775  
 time-of-flight meas. with scin. detect., direction distinguishing 9-8934  
 trajectories in galactic disc, radiation transfer estimation for protons  $E=10^{18}$  eV 9-8924  
 universal microwave radiation upper limit below  $\lambda=1.7$  mm 9-17607  
 zenith angle distrib. determ. for 60 GeV particles 9-15651  
 He spectrum intensity var., 60-500 MeV/ 60-500 MeV/ nucleon, 1963-5 obs. 9-12663

**absorption**

- atmospheric, explanation of events with energy  $10^{11}$ - $10^{12}$  ev 9-18021  
 atmospheric, using fireball model for very high energy NN interactions 9-2529  
 muon absorpt., underground laboratory, depth determ. 9-10987  
 shower particles, strongly interacting, 70 m w.e. underground, search 9-14529  
 Cu mass number depend. of interaction cross-section investigated at Nor-Amberd 9-15683  
 Fe, of cascade showers, obs. at Tyan-Shan 9-15686  
 Pb mass number depend. of interaction cross-section investigated at Nor-Amberd 9-15683

**alpha-particles and helium nuclei**

See also *Quasars; Radioastronomy; Sun/radiation r.f.*  
 magnetosphere spectral obs., penetration to geomagnetic equator 9-1978

**Cosmic rays continued apparatus**

See also *Particle detectors*

for bursts, automatic recording 9-20678

EAS geomagnetic effect meas. 9-2550

hodoscope, pulse-powered gas-discharge counters with large no. cells 9-433

ionization calorimeter, principles and applic. 9-13166

ionization calorimeter electron- photon cascades, radiation unit for Fe 9-20683

Lexan polycarbonate detectors, response rel. to ionization rate of heavy nuclei 9-434

neutron monitor intensity, effect of snow 9-19211

scintillation counter for mass and energy meas. 9-11134

super n monitor, variations of mean recorded multiplicity 9-2549

telescope, mobile, for vertical flux intensity 9-19212

Wilson chambers (2) in field of an electromagnet, ionization chamber and 6 trays of Geiger/counters 9-20679

Ne flash-tube hodoscope for e.a.s. 9-4561

**composition**

EAS Cherenkov radiation detection, review 9-16915

heavy stable triplets, search 9-6716

interplanetary negatron and positron spectra, 12-220 MeV, balloon obs. 9-20141

leptonic quarks, underground search obs. 9-15653

neutral particle search, highly penetrating at 40 m.w.e. underground 9-18017

in nuclear interactions,  $\sim 10^6$  GeV 9-20771

nuclei,  $16 \leq Z \leq 30$ , energy spectra obs. by high-altitude balloon emulsions 9-8925

nuclei,  $20 \leq Z \leq 30$ , energy spectra analysis rel. to He spectra 9-8926

particles  $> 2$  BeV/C<sup>2</sup>, search at sea level 9-2551

review at Cambridge Conference, July 1968 9-15269

He-Fe, energy spectra and abundances obs. by OGO-I satellite, (Oct 1964-Nov 1965) 9-11121

**deuterons**

No entries

**effects and interactions**

See also *Nuclear reactions and scattering due to cosmic rays*

$1.5 \times 10^{12}$  eV with C nuclei, obs. of photon cascade 9-15677

$10^{13}$ - $10^{15}$  eV, N- nucleus interaction 9-15688

100-1000 GeV, analysis of 73 meson prod. interac. at Pamir and Tyan-Shan 9-15674

$10^{12}$  eV and above, N with emulsion nuclei 9-15671

atmospheric, explanation of events with energy  $10^{11}$ - $10^{12}$  eV 9-18021

cross-section calc. at high energy for N,  $\pi$ , K 9-15755

cross-section depend. on mass number investigated in cosmic ray expts. at Nor-Amberd 9-15683

D-region ionization by galactic and solar rays 9-1969

e.m. cascade from bremsstrahlung,  $10^{12}$  eV 9-20683

energy spectrum of nuclear active particles recorded at Aragats mountain station 9-15676

energy transferred to  $\pi^0$ , meas. 9-18023

fireball + N<sup>+</sup> prod., with W<sup>+</sup> + N<sup>+</sup> +  $\pi^+$ , analysis 9-15680

fireball with large Lorentz factor, obs. of e- $\gamma$  cascades  $> 10^{14}$  eV 9-15670

fireballs, existence and props., discussion 9-15672

with graphite, ang. distrib., obs. of secondaries 9-18022

hydrodynamic model modified 9-15679

interaction function determ. by inverse problem method 9-15666

necessity of knowing momenta of all secondaries for analysis 9-15687

nuclear emulsion obs. on Aragats mountain 9-15675

with nucleus, including many-particle interactions 9-15681

paleomagnetic field reversals 9-10444

$\pi$ -nuclei at 200 GeV 9-6662

unitary statistical model of multiple particle production 9-15746

$\gamma\gamma \rightarrow N\pi$ , photomeson prod. by universal rad. field 9-438

$\mu$  scatt. on nuclei, calc. of probable upward backscatter at sea-level 9-15689

$\mu e$  collisions, calc. of bremsstrahlung 9-15581

N  $\sim 10^{14}$  eV, obs with aircraft-borne X-ray films 9-15678

N $\pi$  + N $\pi$ , analysis 9-15680

$10^{14}$  eV particles with Pb, cross section and interaction free path 9-18025

A1 cross-section depend. on mass number investigated in cosmic ray expts. at Nor-Amberd 9-15683

$^{10}\text{Be}$ ,  $^7\text{Be}$  prod. rate determ. by radioactivity 9-4062

C nuclei interac. distrib. of shower particles, obs. 9-15673

C, obs. with Wilson cloud chambers system at Tskhira-Tsharo 9-20679

C 100GeV cosmic ray obs. at Nor-Amberd 9-15684

$^{14}\text{C}$  prod. by cosmic ray neutrons 9-20123

C(n,p),  $10^{10}$ - $10^{12}$  eV, cross-section obs. on satellites Proton 1 and 2 9-18024

Cu, with prod. of  $\Lambda^0$ ,  $K^0$ ,  $\Sigma^+$ , depend. on target mass number 9-18026

Cu cross-section depend. on mass number investigated in cosmic ray expts. at Nor-Amberd 9-15683

Fe,  $10^9$  GeV cosmic rays, cross-section obs. at Tyan-Shan 9-15685

Fe,  $5 \times 10^{10}$ - $10^{12}$  eV cross-section obs. at Tskhira-Tskaro 9-15682

Fe, electron-photon cascade, due to bremsstrahlung from cosmic rays 9-20683

He nuclei ejected from nuclear emulsions by 2.26, 9 and 19.5 GeV p and 2.23 GeV p, importance of cascade N 9-15758

Pb with prod. of  $\Lambda^0$ ,  $K^0$ ,  $\Sigma^+$ , depend. on target mass number 9-18026

Sn with prod. of  $\Lambda^0$ ,  $K^0$ ,  $\Sigma^+$ , depend. on target mass number 9-18026

**electrons**

in cascade ang. distrib. calc. for different depths 9-15663

EAS with fixed e component variation in energy flux 9-15658

energy spectrum compared with galactic r.f. noise 9-12730

equilibrium flux from eqns. for differential flux in cascade prod. e 9-20682

excess in e.m. cascade showers 9-15662

in the Galaxy, magnetic fields, obs. w.r.t. background radio emission 9-18837

intensity and energy spectrum, Canada, diurnal variations 9-4079

solar flare events 9-17661

**jets**

see *Cosmic rays/showers and bursts*

**mesons**

No entries

**muons**

at 200 m.w.e., obs. 9-15669

altitude determ. in showers 9-15656

**Cosmic rays continued****muons (continued)**

angular variation, underground,  $1500\text{Hg}/\text{cm}^2$ , M prod. in TeV region 9-1981

Cherenkov energy loss of relativistic  $\mu$  in water 9-2554

current model 9-435

direct prod. or via very short-lived parent? 9-6714

direct prod. rate, limit 9-437

EAS, fluctuation of  $N_e$  and age parameter s, with fixed  $N_e$  9-15659

EAS, muonic components, effect of multiplicity of secondary particle created in high energy nuclear interactions 9-19215

EAS with fixed  $\mu$  component, variation in energy flux 9-15658

energy and ang. distrib. obs. 9-15667

intensity at  $80^\circ$  to zenith spectrographic meas., 4-500 GeV 9-19213

ionization energy loss in plastic scintillator 9-2555

nuclear backscatter calc. at sea level 9-15689

penetrating component obs. 20 and 40 m.w.e. underground 9-15652

in photomultiplier, astronomical, cause of dark noise component 9-12772

production new processes for  $\approx 10^{12}$  eV, implausibility of U and W part, hypotheses 9-15650

review 9-6607

underground inelastic scatt. from emulsion nuclei 9-6718

**neutrinos**

detection in gold mines 9-18015

earth surface, no. decrease due to  $\nu e \rightarrow \nu \mu$ , lepton nonconservation 9-14528

review 9-4584

**neutrons**

$10^{14}$  eV, interactions, obs. on X-ray films carried by aircraft 9-15678

daily component variation due to geomagnetic disturbances 9-8213

fast fluxes in atmosphere 9-16913

monitor intensity, effect of snow 9-19211

solar, neutron transport in Earth's atmosphere 9-10396

super n monitor, mean recorded multiplicity, variations for period 1965-67 9-2549

variation with latitude and solar activity 9-20123

C 100GeV cosmic ray obs. at Nor-Amberd 9-15684

NuNu very high energy interactions, fireball model 9-2529

**nucleons**

No entries

**origin**

galactic, prod. in Ap and Am stars 9-8236

review at Cambridge Conference, July 1968 9-15269

single close source superimposed on general background 9-19214

$\mu$ , direct prod. or via very short-lived parent? 9-6714

**photons**

$5 \times 10^{10}$ - $10^{14}$  eV, Proton 1 and Proton 2 obs. 9-13152

atmospheric production, obs. on X-ray films carried by aircraft 9-15678

cascade produced by  $1.5 \times 10^{12}$  eV interactions with graphite 9-15677

crab nebula emission, detection by digitized spark chamber 9-8232

Cygnus constellation source, detection expt. 9-8272

equilibrium flux from eqns. for differential flux in cascade prod.  $\gamma$ -quanta 9-20682

Galaxy,  $\gamma$ -rays, high-energy, and particles lifetime 9-1985

Galaxy, particles lifetime and high energy  $\gamma$ -rays 9-1985

galactic field over polar cap from incoming proton fluxes 9-10379

interplanetary, temperature estimates, Venera 3 space probe, (1965) 9-18923

magnetosphere spectral obs., penetration to geomagnetic equator 9-1978

mass composition at  $> 10^8$  GeV 9-16914

nuclei,  $16 \leq Z \leq 30$ , energy spectra obs. by high-altitude balloon emulsions 9-8925

nuclei,  $20 \leq Z \leq 30$ , energy spectra analysis rel. to He spectra 9-8926

search, Queensland, 26 Nov 1966,  $E_p > 100$  MeV 9-18016

trajectories in galactic disc, radiation transfer estimation,  $E_p = 10^{18}$  eV 9-8924

$\gamma$ , detection by spark chamber counter system 9-6715

$\gamma\gamma \rightarrow N\pi$ , photomeson prod. by universal rad. field 9-438

**primary**

No entries

**protons**

No entries

**showers and bursts**

angular distrib. calc. in multiple scatt. approx. in shower initiated by primary with finite energy 9-15664

asymmetry due to presence of a few extra energetic particles 9-15655

cascades, electrons and  $\gamma$ -quanta prod., equil. flux obs. 9-20682

Cherenkov flash fluctuations obs. in 1300 events 9-15660

EAS, apparatus for meas. of geomagnetic effect 9-2550

EAS, arrival-time distrib. and energy content at large core distances 9-8927

EAS, muonic components, effect of multiplicity of secondary particle created in high energy nuclear interactions 9-19215

EAS, nuclear active particles in energy range  $5.10^{12}$ - $10^{13}$  eV anomaly in distrib. 9-18019

EAS, prominent em cascades 9-2552

E.A.S. energy spectrum,  $\Gamma$  determ. 9-18020

EAS radio pulse prod., polarization obs. 9-11122

EHS, obs. near axis, underground 9-15657

electron-photon showers, scintillation counter investig. 9-13153

e.m., particle number fluctuation theory 9-15665

e.m. cascade, electron excess 9-15662

e.m. cascade from cosmic ray bremsstrahlung 9-20683

e.m. shower in Pb, obs. of 87 events 9-15661

emulsion stack obs. 9-15671

hodoscope, extensive air showers, core study 9-433

from interactions with graphite, ang. distrib., obs. 9-18022

inverse problem theory applied to determ. of interaction functions 9-15666

jets, effective mass analysis, rel. to models of multiple particle prods. in high energy region 9-436

jets  $> 10^{14}$  eV, analysis in transforms of Lobachevskii-Einstein space 9-18018

magnetic monopole, bound pairs production 9-11123

Pb, e.m. shower, obs. of 87 events 9-15661

penetrating component obs. at 130 m.w.e., two separate maxima 9-15668

recording instrument for, automatic 9-20678

solar flares, associated ionospheric disturbances 9-16539

e- $\gamma$  cascade,  $> 10^{14}$  eV, obs. on Roentgen film, probably due to fireball 9-15670



**Cosmic rays continued****showers and bursts continued**

- e ang. distrib. in cascade, calc. of expression 9-15663
- with e component fixed, fluctuation in energy flux 9-15658
- $\mu$ , energy and ang. distrib. obs. 9-15667
- $\mu$  component fluctuation w.r.t. to fixed number of e and age parameters  $\lambda$  9-15659
- $\mu$  obs. at 200 m.w.e. 9-15669
- $\mu$  production altitude determ. 9-15656
- with  $\mu$  component fixed, fluctuation in energy flux 9-15658
- Fe, electron cascade, calc. of equilibrium ang. distrib. function 9-15664
- Fe absorpt. obs. at Tyan-Shan 9-15686
- Ne flash-tube hodoscope detection 9-4561
- Pb, electron cascade calc. of equilibrium ang. distrib. function 9-15664

**variations**

- anisotropy in galactic rays, obs. on four possible causes 9-1986
- cut-offs, magnetospheric, and vars. 9-15261
- diurnal at Fort Churchill Canada 9-4079
- due to earth's deviation from solar equatorial plane 9-11120
- Forbush-decrease rel. to v.l.f. emission May 1967 9-1979
- Forbush-decrease, analysis, transit time of modulating cloud 9-1980
- H and He implantation into olivine and enstatite 9-4651
- intensity fluctuations, 14-15 July, 1961 9-21835
- intensity increase, 28 Jan. 9-12646
- latitude and solar activity effects obs. in balloon flights 9-20123
- during meteor showers and rel. amplitude to solar activity 9-21833
- modulation spectrum in interplanetary space 9-17606
- radial anisotropy for energy 7.5-45 MeV 9-8922
- second harmonic of daily variation, rel. to particle density grad. perpendicular to ecliptic plane 9-21834
- solar modulation, possible anisotropy w.r.t. helio-latitude 9-21832
- solar wind, dynamical origin 9-17660
- temporal, persistent and transient anisotropies, world-wide results studied 9-8923
- temporal and spatial, at low satellite altitudes 9-10441
- N component, daily, rel. to geomagnetic disturbances 9-8213

**X-rays**

- isotropic background, 50-290 keV, upper atm. obs. 9-6717
- X-rays, 7.7-210 keV, OSO-III satellite (1967) obs. 9-18930

**Cosmogony see Cosmology****Cosmology***See also Elements, origin*

- $3^{\circ}\text{K}$  radiation rel. to earth's velocity meas. 9-17559
- 1917-1967, review 9-17604
- Bianchi type I, with uniform mag. field, solns. 9-12654
- constants, fundamental, numerical relations 9-6268
- continuous creation, mass stability against gravitational decay 9-21838
- cosmic blackbody radiation, interpretation 9-6102
- cosmic time functions, condition of stable causality 9-6104
- de Sitters universe shown to be consistent with Mach's principle 9-4084
- dust grains rotation and orientation 9-10453
- dyadic formalism applied to spatially homogeneous world models 9-4231
- Einstein universe, supercharge-scale model 9-12657
- elimination of  $M_2$  and  $A_2$  models using red shift data 9-16550
- energy conservation and time reversal 9-17601
- equivalence principle in second and higher orders in Newtonian gravitational constant, possible verification 9-1984
- event horizons, static axially sym. points, singularity 9-17603
- evolution, review 9-15272
- expansion and observation, anisotropy of early stages 9-14183
- expansion of Universe 9-18828
- fireball, primeval, exact theory for anisotropy 9-17602
- Friedman models of Universe including non-interacting radiation 9-12656
- Friedmann universes, Log N-Log S relation and luminosity functions for radio sources 9-20133
- galaxy formation, initial inhomogeneities 9-16559
- gravitation radiation in expanding Friedmann universe 9-6103
- gravitational collapse of rot. bodies 9-8222
- gravitational instability in expanding universe 9-12660
- history of universe 9-10457
- homogeneous models class, Einstein's eqns. soln. 9-21839
- Hubble universe initial dimension 9-2450
- kinetic theory 9-18830
- Lemaître models non consistent with distributions of both radio-galaxies and quasars 9-16551
- luminosity distance, apparent size, number counts, background radiation for any model universe 9-16549
- mass in region smaller than Compton wavelength, alteration to concept 9-14464
- massless scalar field propag. in closed universe rel. to topology 9-6105
- Melvin's universe, absolute stability under non-radial small perturbation 9-12658
- metagalactic rotation as explanation of red-shift of quasars 9-4110
- microwave radiation upper limit below  $\lambda=1.7$  mm 9-17607
- Milne's problem, soln. by Duhamel's principle giving Hopf-Bronstein reln. 9-10456
- model, anisotropic,  $3^{\circ}\text{K}$ . radio intensity distrib. 9-2034
- model, plane symmetric perfect fluid, universe expanding with time 9-14186
- model, with radiation and dust, relativistic, general theory 9-14187
- models, anisotropic, effects of neutrino viscosity 9-10462
- models, elementary review assuming constancy of physical laws 9-1983
- neutral H period, necessity in evolution of universe 9-6101
- neutrino sea, universal degenerate Fermi, eff. on electromagnetism 9-16825
- neutrinos as a clue 9-4584
- neutrinos in anisotropic cosmological solutions 9-17605
- Newton-Liouville eqns; for system of gravitating particles, all solns. 9-14184
- Newtonian, isotropic and Vlasov eqn. models 9-12655
- Newtonian, rel. of locally isotropic solns. of Liouville and Poisson eqns. for gravitationally interacting part. 9-18833
- observational, review lecture 9-18832
- origin of Universe, redirection of research 9-14181
- particle creation processes, quantum field theory essential 9-1982
- photon storms in the hot universe 9-4085
- Poincaré recurrence theorem and gravitational collapse 9-14182
- quantities rel. to elementary particle interaction characts. 9-6585
- quantization, general covariant 9-8396

**Cosmology continued**

- radiation, cosmic,  $3^{\circ}\text{K}$ , and mass creation 9-21840
- Riemannian metric which satisfies field eqns. of gravitation 9-8388
- religion and astronomy 9-15267
- Schwarzschild solution, extension 9-17709
- self-gravitating gas, approach to equilibrium 9-20136
- spherical inhomogeneities model in vel. dispersion obs. of Coma Cluster 9-20132
- Taub soln, separation of background gravitational radiation 9-16674
- thermodynamics, statistical mechanics and the universe 9-15268
- universe, anisotropic models of Bianchi type I 9-17600
- universe, expanding; observable horizons and photon propagation 9-10455
- Universe, expanding, evolution and black-body radiation 9-18831
- universe, information from antipode ratio sources 9-20140
- universe filled with black-body radiation 9-16548
- universes, uniform, self-consistent models 9-10454
- universes with positive cosmological const., screening of distant objects 9-20134

**Cosmotron see Particle accelerators****Costa Ribeiro effect see Dielectric phenomena; Phase transformations****Cotton-Mouton effect see Magneto-optical effects****Cottrell atmosphere see Crystal imperfections/dislocations****Couette flow see Flow; Hydrodynamics****Counters***See also Ionization chambers*

- corona, inherent noise spectrum formation mechanism 9-2595
- dead-time method of prompt  $n$  decay constant meas. 9-11129
- discriminator of amplitude, zero crossing detector, tunnel diode circuit 9-18040
- gas discharge, for electrons, 30 KeV, recording in circumlunar space using Luna-11 satellite 9-18899
- gas-flow, detection and study of short emissions in extreme ultraviolet 9-5043
- infrared quantum, effect of multiphonon relaxation in laser materials on design 9-13024
- ion, large, battery operated 9-19240
- particles suspended in transparent fluid, patent 9-21230
- photoelectron, techniques and applications 9-6498
- precision and  $S^2/B$  criterion 9-18027
- quantometer for SLAC photon beam, 10 kW power level 9-6731
- solid-state track recorders for absolute fission rate meas. 9-11142
- type I and IV models 9-16916
- X-ray diffraction meas., review 9-2593
- N,  $\beta$ -emitting self-powered detectors 9-8938
- p recoil, with collimator, n beam flux determ., 1-30 MeV 9-20689

**accessories***See also Counting circuits*

- digital transformation, pseudo-random, for pulse height analysers 9-19244
- digital transformations, pseudo-random 9-19245

**Cherenkov**

- EAS, Cherenkov radiation detection 9-16915
- EAS detection method, review 9-16915
- long, of perspex and freon, investigation of 120 to 320 MeV/c  $\pi$  beams 9-2584
- with plexiglas radiator for separation of e.m.  $\pi$  beams 9-11140

**crystal**

- i.r. quantum counters, thermal noise 9-6499
- stilbene for  $\gamma$  spectrometry against n background 9-11138
- Nal(Tl), detection of fast n in time-of-flight app. 9-13170
- Nal(Tl) for automatic monitoring of radioactive waste drums 9-2776

**Geiger**

- correction for finite resolving time 9-440
- Geiger-Muller probe in hybrid radiation survey meter 9-2596
- low-intensity thermionic e emission meas. 9-12221
- for ultra high vacuum systems 9-18033
- $\beta$  source energy release evaluation 9-9003
- Ag, for n burst 9-444
- $\text{Al}_2\text{O}_3$  film as window, patent 9-13163

**operation technique***See also Counting circuits*

- aperture size, influence on meas. of differential cross-section 9-2559
- TANC detectors of high energy part. 9-2594

**proportional**

- position sensitive, for undergraduate laboratory 9-12841
- position-sensitive, appl. of risetime meas. 9-445
- pulse risetimes, calc. method for point and extended ionisation tracks 9-19228
- re-entrant well gas flow for solutions with radioactive nuclei 9-15733
- spectrum stabilizer design 9-15691
- X-ray, background reduction by pulse shape discrimination 9-19229
- X-ray, pulse rise time discrimination system 9-8940
- X-rays, cosmic dust particles 9-16919
- (90wt.%)Ar-(10wt.%) $\text{CH}_4$  counter gas, pulse shape calcs. 9-19228
- (90wt.%)Ar-(10wt.%)N<sub>2</sub> counter gas, pulse shape calcs. 9-19228
- $^{10}\text{BF}_3$  graphite moderated, design and efficiency 9-2575
- (90wt.%)Kr-(10wt.%) $\text{CO}_2$  counter gas, pulse shape calcs. 9-19228
- (90wt.%)Xe-(10wt.%) $\text{CO}_2$  counter gas, pulse shape calcs. 9-19228

**scintillation**

- adapter for wells for direct meas. of radioactivity, patent 9-15692
- alkali halides, thallium activated, quantum efficiency of F- and  $\text{Tl}^{\text{po}}$ -scintillations 9-16445
- association with semiconductor detector for  $\gamma$  transitions obs. 9-2567
- for blood plasma with  $^{55,59}\text{Fe}$  9-16634
- $\gamma$ -radiation dose, measurement by organic scintillators with an impurity 9-8935
- $\gamma$ -ray spectrometer amplifier stabilization according to working spectrum channel peak counting rates difference 9-442
- characteristics, with FEU-66, as functions of temperature 9-450
- discrimination of fast pulses, use of with charge storage diodes in coincidence syst. 9-2609
- dual phosphor  $\beta$  spect. background rate 1.7 cpm for 0.1-4 MeV 9-2571
- with electron photomultiplier in connection with scintillating medium, detection efficiency 9-13167
- foreelectrons, 30 KeV, recording in circumlunar space using Luna-11 satellite 9-18899

**Counters continued**  
**scintillation continued**

- fast decay time meas., use and design of high resolution time-amp. converter 9-8933
- fast discriminator with minimal time jitter 9-2580
- in gas target for operation with slow mesons, gas pressure up to 100 atm. 9-2561
- guard detectors, plastic, for low-activity  $\beta$  meas. 9-13168
- integral eqn., matrix method of approx. error analysis 9-2578
- liquid,  $\beta$ -ray activity meas. by coincidence methods, statistical errors 9-20757
- liquid, direct meas. of  $^{14}\text{CO}_2$  9-20764
- liquid, for low level  $^3\text{H}$  meas. in homogeneous systems 9-20696
- liquid, requirements for radioactivity meas. 9-2579
- liquid, solvent synthesis for sensitivity enhancement of low level activities 9-11247
- liquid, volume-responses of the counting efficiency 9-8932
- liquid counters, sample preparation, book 9-13169
- liquid scintillation counter NE214 in n spectrometer with n-p discrimination 9-18029
- liquid water-dioxane scintillator 9-451
- neutron detector using time-of-flight method 9-18036
- organic, response to e.p.d. meas. with photomultiplier 9-6722
- organic, with an impurity,  $\gamma$ -radiation dose measurement 9-8935
- organic for  $\gamma$  spectrometry against n background 9-11138
- organic for n spectrometry, calibration 9-5860
- organic scintillators, appl. of luminesc decay to pulse shape discrimination 9-10255
- plastic, polymer bases, props. 9-11135
- plastic ionization energy loss in plastic scintillator 9-2555
- plastic large area, response uniformity 9-2582
- plastic scintillators based on cross-linked epoxy resins, prod. and characts. 9-10256
- preamplifier and power supply for self-contained unit 9-448
- quaterphenyl cpd. in toluene, fast response and high efficiency for  $\gamma$ -rays 9-16007
- quench correction techniques 9-4668
- sample holder for automatically presenting successive samples to photomultiplier, patent 9-10582
- scintillator-photodiode detectors, high energy charged particles 9-20697
- spectrometric, to meas. mass and energy of cosmic rays 9-11134
- spectrum stabilizer design 9-15691
- in time-of-flight high resolution meas. to distinguish cosmic rays and charged part. 9-8934
- $\beta$ , efficiency increase using 1,4-di(2-(5-tolyloxazoly))-benzene 9-18035
- d as detectors for fast n spectrum analysis 9-11137
- $\gamma$  spect. used to determine conc. of Z in alloys 9-1933
- $\gamma$  spectrometer, background, shielding and collimation 9-20691
- $\gamma$  spectrometer, background, shielding and collimation 9-20691
- $\gamma$  stopping, at 160 MeV, energy resolution and output var. meas. 9-11136
- CsI(Tl) for balloon obs. in-flight calibration 9-2581
- CsI(Tl) optical nonuniformity obs. 9-12482
- CsI(Tl) stopping power and luminescent-response calcs. 9-12035
- $^3\text{H}$  low level meas., liq. scintillation counting 9-20696
- Li glass, characteristics for neutron,  $\beta$  and  $\gamma$  ray detection. 9-449
- $^6\text{Li}$  glass, for neutrons, effect of  $^{23}\text{Na}$  impurity 9-2583
- $^6\text{LiF-ZnS(Ag)}$ -polyethylene,  $\gamma$ -insensitive, for subcritical thermal n flux 9-6723
- NaI, in Linac thick target bremsstrahlung spectra meas. 9-16926
- NaI, response to neutrons determ. 9-20699
- NaI unactivated design and performance 9-19232
- NaI(Tl), Compton spectrometer, electronic cct., response and theor. calc. 9-19239
- NaI(Tl) crystals, response as a function of size 9-2577
- NaI(Tl)  $\gamma$  background monitor for field meas. 9-4670
- NaI(Tl) optical nonuniformity obs. 9-12482
- NaI(Tl) stopping power and luminescent-response calcs. 9-12035
- ZnS(Ag) crystals, stability of radiation under bombard of  $\alpha$ , e. 9-11139

**semiconductor**

- association with scintillator for  $\gamma$  transitions obs. 9-2567
- $\gamma$ -spectrometer, Compton 9-468
- collection-time variations, error reduction by area-to-amp. conversion 9-2588
- development performance and prospects 9-4672
- filters, time-variant, application to time analysis 9-19236
- impulse forms 9-4671
- ion-implantation proc., anneal characteristics of implanted atoms 9-2586
- muonic X-ray efficiency calibration by a Ge(Li) detector 9-19234
- use in nuclear lifetimes meas., twin-target technique by Doppler shift method 9-2640
- particle identifier with  $\Delta E \times E$  solid state telescope 9-8936
- photon detector incorporating internal multiplication 9-19237
- preamplifiers, charge-sensitive, capacitive sensitivity 9-19233
- radioactivity measurement, characteristics 9-452
- for reactor incore neutron flux density meas. 9-662
- resolution, carrier capture dependence 9-2585
- review 9-16921
- surface barrier, high resolution, used for energy levels of  $^{89}\text{Y}$  and  $^{27}\text{Al}$  9-14581
- surface-barrier, evaluation from fission-fragment energy spectrum 9-2773
- transistor ring with tunnel diodes 9-2587
- n with  $\gamma$  rays, detection 9-19238
- CdTe,  $\gamma$ -ray pulse detection 9-6729
- CdTe, surface barrier and Mg, B drifted, as  $\gamma$ - and  $\alpha$ -spectrometers 9-8937
- Ge, compensated by irradiation defects 9-19235
- Ge, optimal thickness of sensitive layers 9-10073
- Ge, with compensation by Li-ion drifting, fabrication methods, bibliography 9-20702
- Ge diode separation of conversion electron and  $\gamma$  lines 9-6724
- Ge(Li)-diode, for low (500 keV)  $\gamma$  activities 9-4678
- Ge(Li) ultra high resolution spectrometer, 6 keV-2 MeV 9-4679
- Ge(Li), ang. correl. and distrib. attenuation coeffs. 9-6727
- Ge(Li), anomalous effect at 77°K 9-6730
- Ge(Li), calibration by muonic X-rays 9-19234
- Ge(Li), coincident summing effects 9-2590
- Ge(Li), for neutron resonance and capture  $\chi$ -sections meas. 9-6878
- Ge(Li),  $\gamma$  detection efficiency calibration, 20-100 keV 9-2589
- Ge(Li), meas. of  $\gamma$ -transitions in  $^{135}\text{Sn}$  and  $^{133}\text{Ba}$  decay 9-2695
- Ge(Li) and NaI(Li) detectors in pair and escape-suppressed  $\gamma$  spectrometer 9-4665

**Counters continued****semiconductor continued**

- Ge(Li) characts. and basic expts. with them for undergraduates 9-12824
- Ge(Li) cylindrical, coaxially-drifted, large sensitive volume, construction 9-6726
- Ge(Li) detector system error in pair peak method 9-4680
- Ge(Li) diode detector, drift control method 9-4677
- Ge(Li) efficiency eqn, form, up to 200 keV 9-4675
- Ge(Li) for n-capture  $\gamma$ -ray activation analysis 9-4682
- Ge(Li) in  $\gamma$  spectrometer system 9-19224
- Li-Si,  $\pi$ -interactions, spark chamber trigger, 6 GeV/c 9-20701
- Li drifted Ge detectors for  $\gamma$ -ray spectrometer 9-16918
- Li sandwich spectrometer, triton energy response function 9-19225
- NaI(Li) and Ge(Li) detectors in pair and escape-suppressed  $\gamma$  spectrometer 9-4665
- NaI(Tl) detector of  $^{22}\text{Na}$  K and  $^{65}\text{Zn}$  L capture peak, 1 keV 9-4676
- Si, e backscatt. and bremsstrahlung pulse height distrib., 300-1200 keV 9-11141
- Si, with compensation by Li-ion drifting, fabrication methods, bibliography 9-20702
- Si avalanche diode as  $\gamma$  detector 9-13171
- Si detector and parallel FET preamp., internal conversion e meas. 9-20703
- Si drifted, elec. field determ. from pulse obs. 9-2591
- Si surface-barrier for  $\beta$  spectroscopy 9-4681
- Si surface barrier,  $\beta$  sensitivity 9-14532
- Si surface barrier, high resistivity, holes preferential trapping 9-6725
- Si(Li), boundary var. of drift region, expt. and theory 9-4674
- Si(Li),  $\beta$ -spectrometer, energy resolution, effect of inhomogeneities 9-14530
- Si(Li) drifted p.i.n. types, fabrication and testing 9-14531
- Si(Li) high voltage operation, improved charge collection 9-4673
- spark**
- air components modification and effects on operation 9-19231
- $\gamma$  cosmic ray detection from crab nebula 9-8232
- $\gamma$  cosmic rays detection apparatus 9-6715
- statistical analysis**
- $\gamma$ - $\gamma$  probe, calibration by Monte-Carlo methods 9-4661
- dead-time correction, Poisson and negative-binomial statistics 9-19217
- maximum likelihood tech. for fitting counting distrib., applic. to ang. distrib. 9-8929
- maximum likelihood tech. for fitting counting distrib., applic. to sum of two exponentials with const. background 9-13156
- on-line computer applications, nuclear electronics advanced modular systs 9-6734
- pulse height analyzer digital data analysis, improvements to Covell's method 9-4686
- rare events, search statistics with 2 scanners, general case brief discussion 9-4659
- Rossi- $\alpha$  experiment, correlation amplitude 9-20687
- scanning efficiency, detection of inhomogeneity 9-20688
- signal/background quality criterion, applicability rel. to signal rate 9-20686
- spectral line distortion effects 9-4655
- spruans pulses (after discharges) probability 9-11125
- square root display with small computer 9-4658
- $\gamma$ , Monte Carlo calc. and linear energy transform. 9-18028
- $\gamma$  spectra from pulse height, response matrix formation for iterative unfolding 9-4657

**Counting circuits**

- analogue digital converter of high resolution 9-456
- analyzer, 8-channel for multi-parameter spectroscopy 9-457
- use of bidimensional data acquisition syst., dead time losses calc. 9-4180
- $4\pi$  coincidence,  $\gamma$  sensitivity correction as function of discrimination level 9-20708
- coincidence, double or triple in  $\beta$ -ray activity meas., statistical errors 9-20757
- coincidence, fast-slow system 9-4689
- coincidence, involving Ge diode, method of separation of conversion electron and  $\gamma$  lines 9-6724
- coincidence, nanosecond time analyzer for  $\mu$ - $\pi$  decay 9-2608
- coincidence, parameter estimation method 9-19246
- coincidence syst., delayed, digital stabilization by light pulsing 9-2606
- converter, high resolution time-amp., for meas. of fast decay time of scintillators 9-8933
- discriminator, high-rate highly stable 9-11127
- discriminator, slope of pulse height distrib. 9-2610
- Esaki diode pair applic. 9-2602
- fast coincidence, use of charge storage diode discriminator 9-2609
- fast pulse-d.c. integrator, description and applic. 9-2601
- gated linear chain, positive current pulses applic. 9-2605
- integral bias summing coincidence for correlation meas. 9-4688
- light pulsing syst., applic. to digital stabilization of delayed coincidence syst. 9-2606
- live-timer method of automatic dead-time correction 9-11126
- multichannel analyzer, Mossbauer spectra smoothing 9-20706
- Multiscaler for Mossbauer spectrometer 9-13174
- peak integration, background subtraction, use of interface with desk calculator and pulse height analyzer 9-2603
- pulse analyzer for random nanosecond pulses 9-4685
- pulse height analyzer, 2000 channel with PDP-8 computer 9-19243
- pulse height analyzer, interface with programmable desk calculator, peak integration with background subtraction 9-2603
- pulse height analyzer, single channel, of gain sweep type 9-11148
- pulse height analyzer digital data analysis, improvements to Covell's method 9-4686
- pulse rise time discrimination system for X-ray proportional counters 9-8940
- pulse-height analysis, collection-time variation, error reduction by area-to-amp. conversion 9-2588
- ratemeter, true random, with automatic dead-time correction for duty factors  $\leq 99\%$  9-11128
- spectrum stabilizer based on single channel analyzer 9-15691
- time analyzer using binary scalars 9-4687
- time-amplitude converter errors, compensation 9-11147
- time-lag, nanosecond, random, automatic meas. 9-6719
- time-to-pulse height converter, Larmor freq. of excited nuclei, p meas. 9-20705
- triparametric device and associated electronics for nuclear physics 9-18037



**Counting circuits** continued

triple coincidence, statistical parameters using computer programme 9-20707  
 $\gamma$ - $\gamma$  directional correl. syst., automation and appl. 9-2607

**CPT (charge, parity, time) conservation** *see* *Elementary particles/symmetry; Kaons/decay; Parity*

**Cracks**

Al, fatigue induced, electron microscope examination 9-5347  
 beam stress conc., photoelastic obs. and analysis 9-16136  
 brittle, propagation in crystal with dislocations 9-19810  
 brittle materials, crack propagation testing 9-1272  
 ceramics, interaction with microstructural features, meas. 9-3445  
 checkerboard array, interaction estimate 9-3447  
 cleavage, nucleation rel. to dislocation 9-1212  
 coating film on base metal, crack restraint due to binding 9-18520  
 concrete, microcracks interaction 9-5482  
 diamond-type crystals, Hertzian fracture 9-7575  
 elastic plate, thickness eff. on bending 9-17760  
 equilibrium cracks under harmonic loading 9-10697  
 fatigue, contact, propagation rel. to lubrication effects 9-13736  
 fatigue, i.r. detection 9-3444  
 fatigue, mode two growth rel. to cryst. orientation, dislocation model 9-5481  
 fatigue in tensioned plate rel. to aeroplane fuselage 9-15458  
 fatigue propagation, adsorption model for environmental effects 9-3446  
 glass, fracture energy, slow and rapid growth 9-11941  
 Griffith, stress intensity factors for asymmetrically loaded surfaces 9-18523  
 growth in notch fatigue rel. to stress in intensity factor 9-1313  
 metals, fatigue propagation, mechanism analysis 9-11938  
 metals, hot cracking resistance on solidification, quantitative determ. 9-21396  
 microcracks, dead-end, stress fields 9-18521  
 polymethylmethacrylate, damage under extreme loads during laser-illumination 9-16137  
 polystyrene, damage under extreme loads during laser illumination 9-16137  
 polystyrene, kinetics of cracking and major crack growth obs., mass spectrometric investigation 9-18522  
 pressurized penny-shaped, initiation of ductile fracture 9-17314  
 propagating ductile crack, limiting speed estimate 9-18524  
 propagation, nonlinear model 9-16709  
 relaxed, expanding, model 9-1312  
 Robertson crack arrest test 9-19809  
 steel, 60Kh3G8N8V, hot working effects on stress-corrosion cracking susceptibility 9-3449  
 steel, AISI 4340, environmental cracking 9-19812  
 steel, austenitic, nucleation and growth during creep 9-13740  
 steel, growth in H and water environments, comments 9-5484  
 steel, high strength, stress-corrosion cracking 9-9757  
 steel, 1.4%Mn, grain boundary carbide film cracking 9-19811  
 steel, Mn, low C, Nb-treated, rolled, susceptibility to cracking in heat-affected zone props. 9-19819  
 steel, of 'flocule' type in fracture surfaces, metallographic and X-ray diffraction investigation 9-5483  
 steel sheets, propagation limiting speed 9-18524  
 steel welds, hot cracks, review 9-13739  
 weakening of solid by external circular crack, rel. to thermal stresses 9-17302  
 weld cracking 9-18532  
 Al-(20 wt.%)Zn, alloy triple point cracks, nucleation and growth 9-3448  
 Al<sub>2</sub>O<sub>3</sub>, thermally shocked, degree of damage 9-3437  
 Al alloy, fatigue growth rate, possibility of decrease using plastic deform. 9-21381  
 Al sheets, propagation limiting speed 9-18524  
 Cu alloys and steel joints, formation during welding 9-21397  
 Fe, Armco, dislocation structure and peculiarities of development 9-3450  
 Fe, high-purity, stress-corrosion cracking in NH<sub>4</sub>NO<sub>3</sub> soln. 9-14981  
 LiF, spontaneous propag. 9-3451  
 Mg alloy disk with circular hole, creep rupture under uniform radial tension 9-7554  
 Mg alloy disk with circular hole, creep rupture under uniform radial tension 9-7554  
 Si<sub>3</sub>N<sub>4</sub> films, prep. by SiH<sub>4</sub>+NH<sub>3</sub> gas phase reaction, mechanism rel. to mol. structure 9-3194  
 SrMoO<sub>4</sub>, scheelite-type, laser radiation damage 9-1825  
 Ti-(5wt.%)Al-(2.5wt.%)Sn alloys, hot salt cracking 9-21383  
 Ti-(6 wt.%)Al-(4 wt.%)V alloy, fatigue-cracked, load relaxation, effect of methanol 9-19786  
 Ti-Al alloys, binary, hot salt cracking 9-21383  
 Ti-Sn alloys, binary, hot salt cracking 9-21383  
 Ti alloys, stress-corrosion, electrochemical mechanism 9-19813  
 U-(10 wt.%)Mo alloy, stress-corrosion cracking, effects of heat treatment and ambient atmospheres 9-21384  
 Zr, nucleation and propag. rel. to hydride precipitates and deform. 9-3452

**Cracking model** *see* *Nucleus/theory*

**Creation of electron pairs** *see* *Electron pairs*

**Creep**

*See also Slip*

Al<sub>2</sub>O<sub>3</sub> refractories, 1450-1515°C 9-7548  
 aluminosilicate refractories 9-16130  
 buckling, by bending and axial compression, of circular cylindrical shells 9-17761  
 buckling, creep, of circular cylindrical shell under compression 9-19030  
 concrete columns, stability and buckling strength 9-17310  
 constant-stress testing devices 9-5464  
 crystal, under irradiation, system of eqns. with allowance for formation of gas atoms 9-5466  
 crystalline solids at elevated temps 9-7547  
 cylinder, thick-walled, under internal pressure, uniaxial tension, rate determ. 9-17309  
 deformation meas. device with particular ref. to necking 9-19797  
 disk with circular hole, rupture under inform. radial tension 9-7554  
 disk with circular hole, under equal biaxial loading 9-5469  
 double-resonator method for meas. of Young's mod. during tests 9-11911  
 graphite, rad. induced, under const. tensile and compressive stresses 9-7553  
 graphite, rate rel. to stress-strain relns. and temp. 9-7551

**Creep continued**

graphite, tensile and compressive, stress depend. and activation energies 9-7552  
 graphite in reactor, neutron irradiation, stress and crystal dimension changes 9-20851  
 indentation creep in crystals 9-5465  
 magnesia refractories 9-16130  
 magnesia refractory, rel. to microstructure, bonding and composition, 1450-1550°C 9-3423  
 mechanical systems vibrations depend., random excitation 9-21377  
 mechanism by jogged screw dislocations thermally activated motion 9-5356  
 metals, fine grained, strength, diffusion effect 9-9763  
 Nimonic 80A, tertiary-creep behaviour, 750°C 9-18510  
 Nujol/water emulsions, stabilized, compliance rel. to aging 9-5201  
 polymer materials, vibrational 9-3424  
 refractory alloys, high-temp., long-time creep 9-19798  
 shell, cylindrical, axisymmetric, theory of buckling 9-8473  
 steel, austenitic, crack nucleation and growth 9-13740  
 steel, Kh18N10T, by deformation with ball 9-5468  
 steels, mild and Cr-Mo comparison of multiaxial stress creep theory with obs. for pressurized cylinders 9-18509  
 strain gauge for in-pile meas. on reactor pressure tubes 9-4818  
 strainometer for remote high temp. meas., >2100°C of refractory oxides 9-3421  
 stress analysis, elastic analogue for all time-independ. boundary conditions 9-21376  
 viscoplastic ductile, failure under complex stress 9-8495  
 Al (20 wt.%)Zn, alloy, test rel. to nucleation and growth of triple point cracks 9-3448  
 Al-(78 wt.%)Zn alloy, rel. to superplastic deformation 9-21370  
 Al, single cryst., damping and modulus defects, double-resonator meas. 9-9744  
 Al alloy, Poisson's ratio, and during recovery 9-18493  
 Al<sub>2</sub>O<sub>3</sub> refractories, 1450-1515°C 9-7549  
 Bi-Sb alloys, grain boundary creep, internal friction obs. 9-16104  
 C, pyrolytic and glassy, stress depend. of tensile creep rate 9-7550  
 Cu-(1wt.%)Al two-phase alloy, high temp. creep mechanism 9-19793  
 Cu, cavity formation in early stages 9-13731  
 Cu, eff. on elec. resistance and mechanical props. 9-13730  
 Cu film, polycryst., rel. to film thickness 9-5467  
 Fe-(7.5 at.%) Si rate control by thermally activated screw dislocation 9-5402  
 $\alpha$ -Fe temperature range 220-900°C 9-1290  
 Ir, polycrystalline, up to 2000°C at low freq. 9-14965  
 KCl, deformed crystals, dislocation processes 9-1223  
 LiF, polycrystalline, behaviour under const. stress, 300° to 550°C 9-11933  
 LiF, u.s. radiation effect on region of action of dislocation depletion mechanism 9-9764  
 Mg-(2wt.%)Al alloy, complex-stress creep fracture at 50°C 9-21382  
 Mg alloy disk with circular hole, rupture under uniform radial tension 9-7554  
 Mg disk with circular hole, under equal biaxial loading 9-5469  
 Mg powder, compacted with 1% O, high temp. props. 9-17311  
 MgO, effects of varying porosity, grain size and impurity addition 9-1292  
 MgO, stress, temp., and strain rate 9-19799  
 Mg(OH)<sub>2</sub> powder compacts, compressive creep rel. to dehydroxylation rate 9-1291  
 Mo, polycrystalline, up to 2000°C at low freq. 9-14965  
 Na stearate -19.7 to 35.7% H<sub>2</sub>O, shear creep rel. to struct., 5-60°C 9-5470  
 NaCl, at elevated temps. 9-1293  
 NaCl, deformed crystals, dislocation processes 9-1223  
 Nb-base alloys, creep-rupture props., response to ht. treatment 9-14976  
 Nb-base alloys, creep rupture props., eff. of ht. treatment 9-14975  
 Ni-Cr-W-Co-Al-Ti alloy with horophilic additions, effect of grain boundary composition 9-5475  
 Ni-base alloy, wrought, stress cycling effect on behaviour at 955°C 9-18511  
 Ni, internal friction, 823-1023°K 9-13721  
 Ta-base alloys, creep-rupture props., comparative mech. behaviour 9-14977  
 Ta, polycrystalline, up to 2000°C at low freq. 9-14965  
 $\alpha$ -U, and internal stresses rel. to surface oxidation, obs. 9-9765  
 U, viscous displacement at grain boundaries during creep, conditions and study 9-19800  
 V-Ti-Nb alloys, and stress-rupture behaviour 9-19801  
 V-Ti alloys, and stress-rupture behaviour 9-19801  
 W polycrystals, high temp., stress and grain size effects 9-13733  
 WC-Co alloys, compressive deformation at elevated temps. 9-7555

**Critical constants, thermal**

alkanes, temp. and press., rel. to acentric factor and molec. struct. 9-18381  
 discontinuities in thermodynamic quantities at crit. pt. of analytical fluid 9-9583  
 fluctuation theory and critical phenom. 9-9587  
 inequalities for critical indices near crit. pt. 9-19654  
 specific heat near crit. pt. 9-1067  
 substances at critical point, properties 9-9586  
 tables 9-3053  
 water substance, equation of state with limited no. of constants 9-980  
 He-H<sub>2</sub> liq.-vapour equilib. at 100 atm. 9-9590  
 He II, liq., critical heat flux close to  $\lambda$  transition 9-18378

**Critical mixtures** *see* *Solutions*

**Critical opalescence** *see* *Phase transformations; Solutions*

**Crowdions** *see* *Crystal imperfections/interstitials*

**Cryogenics** *see* *Cryostats; Low-temperature/phenomena; Low-temperature production; Low-temperature technique*

**Cryopumping** *see* *Vacuum pumps; Vacuum technique*

**Cryoscopy** *see* *Freezing; Low-temperature production; Low temperature technique*

**Cryostats**

double chamber, electronic temp. control, for resist. meas. 9-14294  
 E.S.R. meas. below 4.2°K 9-6436  
 intrachannel cooling of Be slow-neutron filter 9-4189  
 liquid cell with thermistor amplifier feedback 9-6438  
 metal, collapsible, for magnetooptical research at temps. to 1.2°K 9-4188  
 polymer components sp. ht., 1.7-4°K 9-2925  
 provision for internal application of small forces to contacts 9-22018

**Cryostats continued**

<sup>3</sup>He and ESR spectrometer, relax. times  $1 \mu$  sec. meas. 0.24-4.2°K  
9-4190

**Cryotrons** *see Superconducting devices***Crystal chemistry**

alkali metals, ionic core radii calc. and orthogonality corrections 9-19682  
alkaline earth phosphate glasses, iron valency states from optical, e.s.r. and Mossbauer spectra 9-15173  
Ba<sub>1-x</sub>Sr<sub>x</sub>RuO<sub>3</sub> system, structural changes, press.-induced 9-5510  
book, specialized topics 9-14903  
effective ionic radii, for bond and unit cell calc. 9-7354  
graphite oxide, struct. model, bonds and groups rel. to method of preparation 9-7352  
hydration of ions, enthalpies 9-14904  
ionic radii, concept and determ. from e density minima 9-14904  
metals, geom. factor, near-neighbour diagrams 9-19703  
noble metals, ionic core radii calc. and orthogonality corrections 9-19682  
oxides, bonding from X-ray K-emission spectroscopy 9-13589  
silicates, bonding from X-ray K-emission spectroscopy 9-13589  
tabulation of information on metals and semiconductors 9-16073  
transition metal carbides and nitrides, ordering structures 9-17272  
BaTiO<sub>3</sub>:La<sup>3+</sup>(Nb<sup>5+</sup>), gravimetric studies of disorder 9-3224  
BaTiO<sub>3</sub>:OH stoichiometry effect on ferroelectric transition 9-10048  
CaO:Tm<sup>3+</sup>, reduction of Tm<sup>3+</sup>, to Tm<sup>2+</sup> on  $\gamma$ - and e-irrad., e.s.r. obs. 9-10277  
CoMn<sub>2</sub>Fe<sub>2</sub>O<sub>4</sub> charge distrib. from Mossbauer spectra 9-1119  
CoO, nature of nonstoichiometry from i.r. absorption spectra 9-19989  
Cu minerals containing complex sulphides 9-13593  
Fe, eff. of alloying elements on polymorphism 9-16049  
Li<sub>0.5</sub>Fe<sub>1.5-x</sub>Al<sub>x</sub>O<sub>4</sub>, cation distrib., n.diffr. obs. 9-21316  
LiF:Fe<sub>2</sub>O<sub>3</sub>, preparation attempt 9-9634  
Mu ferrites cation distribution equilibrium position by i.r. spectral analysis 9-3876  
Ni<sub>2</sub>Fe<sub>1-x</sub>Fe<sub>2-x</sub>O<sub>4</sub>, ion valence state obs. from X-ray absorpt. spectra comp. dependence 9-21640  
Ni<sub>2</sub>Zn<sub>1-x</sub>Fe<sub>2-x</sub>O<sub>4</sub>, ion valence state obs. from X-ray absorpt. spectra comp. dependence 9-21640  
ScO<sub>2</sub>, monoclinic, electrostatic energy and anion ordering 9-11790  
SrCl<sub>2</sub>:Tm<sup>3+</sup>, reduction of Tm<sup>3+</sup> to Tm<sup>2+</sup> on  $\gamma$ - and e-irrad., e.s.r. obs. 9-10277  
Y<sub>3</sub>Al<sub>5-x</sub>Ga<sub>x</sub>O<sub>12</sub>, garnet, cation distrib. 9-11857  
ZnMn<sub>2</sub>Fe<sub>2-x</sub>O<sub>4</sub> charge distrib. from Mossbauer spectra 9-1119

**Crystal classes** *see Crystallography: Crystal structure, atomic***Crystal counters** *see Counters, crystal***Crystal electron states**

*See also Colour centres*

adiabatic potential calc., use of perturbation theory 9-10637  
alloys, monovalent, distrib. 9-7705  
alloys, pseudopotentials and residual resistivity calc. 9-5593  
anthracene doped with tetracene shallow hole trap activation energy and cross section determ. 9-7376  
antiferromag. lattice of 2N one-electron atoms, excitation energies, insulator-to-metal transitions 9-15046  
aromatic hydrocarbons in boric acid glass, u.v. irrad., traps and thermoluminesc. 9-17493  
bismuth-type metals, quasi local level effects on de Haas-van Alphen effect 9-1444  
bound states, polarization waves excitation, electron energy loss techniques 9-18575  
C, vitreous, nature and role of localized states 9-7711  
calculation by MAPW method 9-16203  
carbon black, e. momentum density, X-ray determ. 9-18581  
charge separation due to hydrostatic pressure 9-19876  
coherent states props., connection with magnetic translation symmetry 9-18576  
conduction electron gas with embedded heavy particle gas, rel. to deriv. of Suhl's eqns. for Kondo effect 9-9885  
conductivity, e phonon self-energy contribution temp. depend., calc. 9-16199  
consequences of transition to amorphous state 9-9599  
correlation contribution to elastic props. of normal metals 9-5417  
deformation potential tensor components from magnetoacoustic attenuation anisotropy meas. 9-5556  
density fluctuations and ground state for system of electrons in strong mag. field 9-21455  
diamond, e. momentum density, X-ray determ. 9-18581  
diamond, semiconducting, nature of acceptor centre 9-12135  
Dirac Hamiltonian, transformation to  $k \cdot p$  nonrel. eqn. 9-16813  
electron-impurity system, Titeica-type formula for transverse cond. in mag. field 9-5601  
electron-phonon system, elec. cond. oscs. in mag. field 9-7700  
electrons, localization in ordered and disordered systems, percolation of classical particles 9-10678  
energy migration, exchange-phonon mechanism 9-9883  
energy transfer between electron and phonon system 9-5599  
ferromagnetic semiconductor, helicon waves, film thickness effect 9-1539  
Gantmakher effects at microwave freqs. 9-12076  
Goldstone's theorem, demonstration by Green's function methods, advantages 9-12041  
graphite, e. momentum density, X-ray determ. 9-18581  
graphite, pyrolytic, localized states, nature and role 9-7711  
harmonic oscillator, one-dimens., effects of finite boundaries 9-5794  
Heine-Abarenkov model potential, modified, optimum form 9-5594  
helicon damping at tipped mag. field rel. to Fermi surface anisotropy 9-7709  
helicon propagation in metal, quantum oscillations, mechanism 9-1439  
holes, role in photographic proc. 9-17901  
Hubbard model, degenerate mass operator perturbation theory 9-14345  
Hubmodel, for correlation and mag. eff. in narrow energy bands 9-12054  
ice, pure, binding of electron using polaron model 9-5613  
III-V compounds, spin-orbit splittings, from refl. spectra, 3.5-7.5 eV 9-5899  
with intra-atomic coupling, strong, electron correlations and magnetic ordering 9-1415  
layered system, drifting carriers, interaction with surface elastic waves 9-5435  
level widths of Coulomb centre in strong mag. field 9-9873  
light bound e interactions and quasiparticles kinetic eqn. 9-1416  
local states in shallow potential well due to strong mag. field 9-1425

**Crystal electron states continued**

localized and weakly metallic electrons, correlations 9-15046  
localized states of surface and line defects using band theory 9-12065  
magnetoacoustic dispersion and attenuation, expt. rel. to free electron theory 9-5553  
metal, electron sound 9-13820  
metal, electron sound 9-3548  
metals, conduction-electron polarization rel. to exchange coupling 9-21561  
metals, dispersed, thermodynamics and paramag. props. 9-13829  
metals, electronic component of dislocation drag 9-13684  
metals, electronic props., literature and teaching aids review 9-8343  
metals, monovalent, distrib. 9-7705  
metals, real, effective mass of positron 9-16207  
mixed molecular crystals, dispersion and attenuation of e.m. waves 9-9872  
n-semiconductors, electron-phonon interaction and l.f. oscillations 9-7790  
one-electron wave function calc. including many-body aspects 9-5608  
organic, exciton and electron-hole pairs ionization 9-18589  
p-n-p alloy junction transistor, minority carrier lifetime in base 9-1558  
phase transition for strong electron-phonon interaction 9-9884  
phosphors, e trap depth determ. from decay of thermoluminescence 9-1840  
polaritons, role in Raman scatt. in polyatomic crystals 9-12392  
polyacene solid solns., energy transfer, bibliography for 1967 9-7986  
pseudopotentials, theoretical foundation 9-9874  
use of pseudopotentials, validity 9-13360  
 $\alpha$ -quartz, polariton Raman scattering intensities 9-12436  
rare gases, condensed, wave scatt. theory applic. to electron mobility maxima in conduction band 9-8376  
relaxation time of high density electrons, freq. depend. 9-1437  
RKKY interaction, soluble model 9-13818  
semiconductor, carrier interaction with neutral centre 9-19881  
semiconductor, polar, zero field mobility calc. 9-9977  
semiconductor devices, electron theory of operation, book 9-18631  
semiconductors, charge carrier recombination mechanism 9-3549  
semiconductors, high permittivity, phonon drag by electrons, theory 9-17366  
semiconductors, Landau level Raman scattering 9-12398  
semiconductors, Landau level Raman scattering 9-12397  
semiconductors in strong electric and magnetic fields 9-15088  
semimetal-semicond. transition, possible anomalies 9-15045  
spin-orbit coupling, calc. Clebsch-Gordan coeffs. 9-2135  
superconducting alkali metals, electron-phonon interaction contrib. to density of states 9-19901  
superconductivity carrying in spin-wave state 9-7763  
superconductivity transition temp., one-body interaction eff. 9-9950  
superconductors, type II, density of states, theory 9-12115  
transfer processes for normal collisions of quasi-particles 9-16200  
trap analysis, extensions to method by thermally stimulated conductivity curves 9-5595  
Urbach's rule in electron-phonon model 9-5909  
Ag-Mn alloys, phonon-electron scattering coeff. from electronic thermal conductivity 9-3505  
Al, electronic props. and band structure 9-13830  
Al, pseudopotential and binding energy 9-9891  
Al form factors of truncated at. potentials 9-9875  
Al<sub>2</sub>O<sub>3</sub>:V<sup>4+</sup>, energy levels 9-1768  
Be, resistance oscillations in superconducting magnet, mag. field depend. 9-9877  
Bi, charge carrier contribution to mag. susceptibility 9-7876  
Bi, deformation potentials calc. 9-13824  
Bi-Sb, charge carrier contribution to mag. susceptibility 9-7876  
Bi-Pb, Bi-Sn and Bi-Sb-Pb alloys, electron transitions, pressure-induced, 4.2-295°K 9-9892  
 $\beta$ -InAs, energy depend. of wave vector in forbidden gap 9-1537  
Cd, r.f. size effect on electrons during, cyclotron period 9-3562  
CdS, electronic energy states 9-7487  
CdSe, effective mass of electrons, from i.r. absorpt. and refl. spectra 9-10197  
CdTe, carrier mobility rel. to electric and magnetic field intensities 9-3622  
Cu, Gantmakher effects at microwave freqs. 9-12076  
Fe halides, ferrous, 3d delocalization from Mossbauer meas. 9-14036  
GaAs, laser transitions and photon energy 9-3847  
GaAs, n-type epitaxial films, hot electron magneto phonon effect 9-16265  
GaP, breakdown oscillations, induced impurity, and obs. of traps higher than indirect band edge 9-5695  
GaP, coherent excitation of polaritons by nonlinear parametric process 9-12326  
GaP, symmetry of bound states 9-1520  
Ge:Mn, carrier conc. and mobility, variation due to heat treatment 9-3658  
n-Ge, depletion effects, non-equilib., at electrolyte interface 9-13895  
Ge, hole-phonon coupling conc. determ. by cyclotron reson. 9-3551  
Ge, oscillator, frequency of helical intensities 9-1561  
n-Ge, transmission of helicon waves, liq. He temp. 9-16270  
Ge, valence band quantum eff. 9-12068  
n-Ge current instability due to intervalley redistrib. of electrons on heating by elec. field, n-type 9-1545  
Ge density of states, changes rel. to disordering, photoemission obs. 9-9994  
n-Ge phonon drag eff., inf. of e scatt. anisotropy 9-19917  
Ge slice, carrier injection, transverse mag. field eff. 9-5706  
In, helicon velocity oscs. and damping determ. 9-7724  
InP, electron effective mass depend. on their density 9-9979  
InSb, electron-optical phonon interact., effects on combined resonance spectra 9-1742  
n-InSb, helicons, bounded 9-16256  
n-InSb, interaction between drifting carriers and slow e.m. waves 9-9978  
InSb, Landau levels of holes 9-5632  
p-InSb, temp. dependence of carrier mobility rel. to dislocation density 9-3631  
K, Landau Fermi-liquid parameters 9-9912  
KI:Tl, electron-hole mechanism of scintillations 9-20008  
Li conduction e shift,  $\delta g$  theoretical estimate 9-12061  
MnCl<sub>2</sub>·4H<sub>2</sub>O, magnon-phonon coupling from mag. field depend. of thermal conductivity 9-1421  
Na, Landau Fermi-liquid parameters 9-9912  
NaI:Tl, electron-hole mechanism of scintillations 9-20008



**Crystal electron states continued**

- NaI phonon frequency press. depend. meas. 9-7713  
 NiO, antiferromag., low-lying surface-spin-wave band prediction 9-21595  
 Pb, nuclear-spin interactions, indirect, relativistic calcs. and theory 9-9880  
 PbO- based polymorphic systems, charge carrier pair formation energy 9-12457  
 PbSe, scattering mechanism of current carriers 9-7702  
 PbTe-PbS solid solns., effective density-of-states mass rel. to carrier density and temp. 9-9897  
 PbTe, helicon propag., high-field anisotropy 9-5631  
 PbTe vacancies, new model 9-19744  
 Rb, conduction electron mean free path, obs. 9-18582  
 S, carrier transport and generation 9-7703  
 Si, hot-e-electron effective mass, field depend 9-1431  
 Sc, electron structure, spin density distrib. rel. to diamag. susceptibility 9-1878  
 Si:P, influence of A and E centres on dependence of majority-carrier density on neutron dose 9-1549  
 Si, 10 MeV electron damage annealing, carrier conc. and lifetime recovery 9-17399  
 Si, applic. of Kohn potential 9-1417  
 n-Si, dislocation acceptor level energy, from dislocation vel. obs. 9-9713  
 Si diodes, n irradiated, majority and minority carrier trapping by capacitance recovery 9-17408  
 n-Si phonon drag eff., inf., of e scatt. anisotropy 9-19917  
 Sn film, Cu added, tunnel junction meas. for critical temp. determ. 3.5-7°K 9-7776  
 SrTiO<sub>3</sub> free carrier absorpt. obs. using two-photon excitation 9-12199  
 Te, electron and hole heating by light causing quantum oscillations of photomagnetic effect 9-1624  
 VO<sub>2</sub>, electronic phase transitions and nature of 'metallic' state 9-15048  
 Zn in Si, ionization energy levels, existence problem 9-15058  
 ZnS, two photon absorption spectra near band gap 9-12388  
 ZnSe, emission in excitation spectra, oscillations 9-12489

**band structure**

- 'muffin-tin' approximation in calc. 9-5605  
 alkali halides, of F centre 9-5380  
 alkali metals, energy contrib. to second- and third-order elastic constants 9-9740  
 alloys, binary, one-dimens., electronic structure 9-7707  
 alloys, binary, single-site approx. in electronic theory 9-7708  
 alloys of non-transition metals of Cu<sub>3</sub>Au type, W-like dependence of critical temp. on number of valence electrons 9-12123  
 anisotropic insulating crystals, rel. to opt. spectra 9-10185  
 anthracene, broad band existence, confirmation by photoemission of electrons from alkaline earth contacts 9-5616  
 approximate calculation, improvement 9-12059  
 Auger recombination model modification 9-7800  
 augmented plane wave method, description 9-1426  
 band-tail spreading energy in semiconductors using lasers 9-1541  
 cellular method for calc., test 9-12050  
 chemical shear, electron-hole complexes localized near charged impurities 9-5607  
 chromium halides, from continuous X-ray spectrum, at high freq. limit 9-16210  
 correlation and mag. eff. in narrow bands 9-12054  
 curvature and effective masses 9-16206  
 diamond-type cpds., complex structure of hole bands rel. to X-ray emission spectra 9-1812  
 DNA, low-lying collective energy loss, or basis of  $\pi$  electron band structs. for periodic models 9-12064  
 effective mass approx. from pseudopotential method 9-12052  
 electron mass temp. dependence from sp. ht. and cyclotron resonance 9-16217  
 energy levels of H like system in mag. field, variational calc. 9-12049  
 F centre, relaxed excited 9-9719  
 graphite,  $\pi$ -electron interband transitions and dielec. function 9-1567  
 group IB alloys,  $\alpha$ -phase, anisotropic relax. times from Hall coeff. meas., 10-300°K 9-13844  
 group II-VI compounds, Green's function method calc. 9-21467  
 Hubbard's theory of Mott transition nonexistence of Fermi Surface 9-12056  
 hybrid bands, electron correlated motion, model 9-5604  
 n-InSb, rel. to photoconductivity due to cyclotron absorpt. 9-5767  
 intraband effects on orbital diamagnetism of nearly free electrons 9-1637  
 LEED theory, OPW method appl. 9-1171  
 localized versus band model of e in solids 9-16205  
 magnetic energy model from translational symmetry of Bloch electron in mag. field 9-12053  
 magnetic levels with inversion asymmetry splitting 9-7706  
 magnetic semiconductor, magnon corrections to electron effective mass 9-18584  
 magnetic susceptibility of electrons with energy spectrum having degeneracy point 9-12233  
 metal, Schrodinger eqn. soln. 9-13828  
 metal-nonmetal transition due to cryst. distortion 9-16204  
 metal-semiconductor-metal junctions, effect on tunnelling 9-13901  
 metals, effect on nonlocal conductivity and anomalous skin effect 9-13840  
 metals, quantum mag. trap formation 9-7875  
 Mott-insulator and paramag. metal ranges of narrow energy band, Hubbard Hamiltonian 9-15051  
 narrow energy-band model, correlated, generalized spin susceptibility 9-12051  
 one dimensional indefinite periodic models, analogue method 9-21464  
 one-dimensional periodic systems, nonadiabatic transitions 9-1423  
 one-electron wave functions, modulus and phase eqns. 9-16208  
 polyethylene, ideal chain, LCAO calc. 9-2928  
 population analysis, data program 9-9887  
 P.V.K., by photoemission of holes from metal interface obs. 9-5739  
 quantum size effect to determine Landau band form and Fermi surface areas 9-16202  
 rare earth intermetallic cpds., interband mixing, exptl. evidence 9-14116  
 rare-earth chlorides, far i.r. energy levels, electronic Raman eff. 9-12356  
 relativistic, applic. of Kapur-Peiris resonance theory 9-9890  
 s-band model, onset of local correlation 9-12055  
 s/f coupling, effect of range on the relaxation rate  $1/T_1$  9-5858  
 Sb<sub>2</sub>Se<sub>3</sub>, needle-like crystals 9-1194

**Crystal electron states continued  
band structure continued**

- Schottky barrier, ellipsoidal energy surface effect on differential resistance 9-13904  
 self-consistent pair correlations 9-15051  
 semiconductor, two-valley, stability of state with negative differential conductivity under small perturbations 9-16268  
 semiconductor and semimetal thin plates, many-valley energy spectrum of carriers 9-9925  
 semiconductors, graded mixed, electronic states and transport, theory 9-21511  
 semiconductors, many-valley, two-stream instability in hot-electron systems 9-15096  
 semiconductors, from thermoreflectance meas. 9-14041  
 sphalerite-type cpds., complex structure of hole bands rel. to X-ray emission spectra 9-1812  
 superconductors t-band, infl. of normal d band on s band 9-16240  
 transition metal cpds., metal-like, theoretical calc. rel. to exptl. X-ray spectra 9-3912  
 transition metals, correlation with elastic moduli 9-19773  
 transition metals, spin orbit coupling and mag. props. 9-16201  
 transition metals electron heat rel. to d-electrons per atom 9-3534  
 transition metals rel. to work function, resistivity and Hall constant 9-10078  
 two-band, superconductor, infl. of normal d band on s band 9-16240  
 Ag-In alloys, dil., determ. by Kohn Rostoker method within virtual crystal approx. 9-15052  
 Ag, calc. at two values of lattice const., model Hamiltonian 9-5612  
 Ag, calc. at two values of lattice const., model Hamiltonian 9-5611  
 AgCl-Tl, excited state structure of I centre 9-12057  
 Al-Fe binary system, electronic structure, X-ray investigation 9-3553  
 Al, changes on melting from charact. energy losses of 8 keV electrons in liquid and solid 9-7249  
 AlPO<sub>4</sub>, from X-ray L<sub>2,3</sub> emission bands 9-5944  
 Au-Fe dilute alloys, band gap var., 3-6 eV absorption, reflectivity meas. 9-21604  
 Au, calc. at one value of lattice const. 9-5611  
 Au, calc. at one value of lattice const., model Hamiltonian 9-5612  
 Au, changes on melting from charact. energy losses of 8 keV electrons in liquid and solid 9-7249  
 BN, orthogonal plane wave method 9-5609  
 Ba under pressure, by pseudopotential like approx. 9-15054  
 Bi-Sb alloy syst., energy-band parameters and relative band-edge motions near semimetal-semicond. transition 9-15053  
 Bi-Sb alloys 9-13831  
 Bi, changes on melting from charact. energy losses of 8 keV electrons in liquid and solid 9-7249  
 Bi, mag. quantum level model, Alfven wave propag. obs. in high mag. fields 9-7710  
 Bi<sub>1-x</sub>Sb<sub>x</sub> alloys, mag. susceptibility and band structure 9-21565  
 Bi<sub>2</sub>Te<sub>3</sub>, n and p type 9-3637  
 Bi<sub>2</sub>Se<sub>3</sub>, from Shubnikov-De Haas data 9-16209  
 Bi<sub>2</sub>Sb<sub>3</sub>, ( $x=97.90$ ; $y=3, 10$ ), parameters from galvanomag. meas. 9-1533  
 n-Bi<sub>2</sub>Te<sub>3</sub>, and carrier density meas. by de Haas-van Alphen effect 9-9913  
 BiTeBr, semiconducting, from elec. and optical props. 9-21512  
 Ca under pressure, by pseudopotential-like approx. 9-15054  
 Cd<sub>3</sub>As<sub>2</sub>, non-parabolic conduction band 9-9893  
 CdCr<sub>2</sub>Se<sub>4</sub>, conduction band edge shift near Curie temp. 9-7712  
 CdGe(As<sub>2</sub>P<sub>2</sub>)<sub>2</sub>, glasses, optical and thermal activation energies 9-17394  
 CdO, freq. depend. of opt. constants rel. to band struct. 9-3886  
 CdS, of dislocations in semiconductors 9-7487  
 CdSb, doped, from elec. props. at 2.2-77°K 9-9972  
 CdSb, valence band investigation using transverse thermoelec. power meas. 9-16269  
 n-CdSnAs<sub>2</sub>, conduction band anisotropy from galvanomagnetic tensor components 9-9984  
 CdTe, Green's function method calc. 9-21467  
 CdTe, hexagonal, from reflection spectrum 9-13826  
 n-CdTe, optical absorpt. by free carriers 9-5916  
 CdTe, acceptor levels 9-1428  
 CeCl<sub>3</sub>, for i.r. energy levels, electronic Raman eff. 9-12356  
 $\gamma$ -Fe<sub>2</sub>N, e. diff. exam. 9-1430  
 Co-Cu alloys, hexagonal, e. transfer rel. to mag. moments 9-12274  
 Cr, cpds., metal-like theoretical calc. rel. to exptl. X-ray spectra 9-3912  
 Cr, X-ray emission spectral determ. using K and L<sub>III</sub> bands 9-1821  
 Cs, at volume dependence, Wigner-Seitz cell calcs. rel. to polymorphic transitions under pressure 9-5614  
 CsAu, band-theoretic study of metallic character 9-15055  
 CsI, Green's function method calc. 9-1429  
 Cu-Ni alloys 9-12058  
 Cu, approx. calc. method 9-12059  
 Cu, calc. at two values of lattice const., model Hamiltonian 9-5612  
 Cu, calc. at two values of lattice const., model Hamiltonian 9-5611  
 Cu, d-band optical density of states, photoemission study 9-1629  
 Cu, density of states, accurate computation 9-15050  
 Cu to Se elements, at end of first long period, and X-ray spectra 9-14067  
 Cu<sub>3</sub>Au-type alloys of non-transition metals, W-like dependence of critical temp. on number of valence electrons 9-12123  
 Cu<sub>2</sub>O, bound states at 110°K 9-12375  
 Dy, conduction e. density at nucleus 9-16211  
 Eu chalcogenides, spin-polarized energy bands rel. to mag. and optical props. 9-12328  
 Fe-base dilute alloys, electronic sp. ht. rel. to origin of ferromagnetism 9-13800  
 Fe, approx. calc. method 9-12059  
 FeCr<sub>2</sub>Se<sub>4</sub> effect of interaction between d shells of transition elements on physical props. 9-16253  
 GaAs:Si, epitaxial films, deduction from luminescence spectra 9-5701  
 n-GaAs, 'freezing-out' of electrons 9-12147  
 GaAs, L<sub>1</sub> and X<sub>3</sub> minima location, photoemission determ. 9-9895  
 n-GaAs, luminescence from donor-acceptor pair recombination involving the first excited state of donor 9-12465  
 GaAs, from photoemissive yields, spectral analysis 9-5917  
 GaAs, uniaxially stressed, inter-valence-band transitions 9-18706  
 n-GaAs intermediate donor level activation energy by temp dependence of Hall effect 9-3653  
 GaP:O<sup>-</sup>, i.r. radiative capture of electrons at ionized oxygen donors 9-12464  
 GaP, Auger model impurity band and quenching of luminescence 9-8000  
 GaS, indirect energy gap by opt. absorption spectra 9-18622

**Crystal electron states continued  
band structure continued**

- n-GaSb-InSb mixed crystal, conduction bands, resistivity, Hall effect and piezoresistance investigation 9-5690  
GaSb, nonlocal pseudopotential calc. 9-1534  
GaSb cond. bands from free carrier Faraday rot. obs. 9-13889  
GaSe, 1-s, indirect energy gap by opt. absorption spectra 9-18622  
GaSe, indirect energy gap by opt. absorption spectra 9-18622  
Ge, 2-3 eV range, by electron beam modulated reflectance 9-9989  
Ge, effects and many-particle scatt. corrections in far u.v. spectra 9-12378  
n-Ge, Schottky barrier, ellipsoidal energy surface effect on differential resistance 9-13904  
Ge, spin splitting rel. to u.v. absorpt. 9-13893  
Ge, uniaxially stressed, inter-valence-band transitions 9-18706  
Ge amorphous electronic struct. and reflect. spectrum model 9-13894  
Ge dislocations, from radiative recombination 9-15183  
Hg, effective electron mass temp. dependence from sp. ht. and cyclotron resonance 9-16217  
p-HgTe, effective hole mass at 95°K 9-9985  
InAs, effective mass carrier density dependence at 78°K 9-3639  
In<sub>1-x</sub>Ga<sub>x</sub>As, solid solutions, energy structure calc. for elec. resistivity and Hall coeff. meas. 9-3640  
InSb, effective electron mass pressure dependence from magnetoresistance and thermoelec. power meas. 9-1536  
InSb, g-value of Landau levels in conduction band 9-1538  
n-InSb radiation absorption, mm. and sub-mm., 2.1 and 4.2°K qualitative interpretation 9-16413  
K, at volume dependence, Wigner-Seitz cell calcs. rel. to polymorphic transitions under pressure 9-5614  
K, ground state determ. from de Haas-van Alphen freq. meas. 9-18593  
KCl, orthogonalized-plane-wave calcs. 9-13832  
Li, calcs. rel. to elastic consts. value 9-5420  
LiAl, band-theoretic study of metallic character 9-15055  
LiCl, orthogonalized-plane-wave calcs. 9-13832  
MgO, X-ray spectral study 9-18586  
MnF<sub>2</sub>, Brillouin zone and exciton states thermodynamic distinction 9-1434  
NaCl, effect of potentials used in investigations 9-15056  
NaCl, orthogonalized-plane-wave calcs. 9-13832  
Na<sub>3</sub>PO<sub>4</sub>, from X-ray L<sub>2,3</sub> emission bands 9-5944  
Nb<sub>3</sub>Sn, from temp. dependent isomer shift of <sup>119</sup>Sn meas. by Mossbauer effect 9-7960  
Ni, d-band in 1s coupling 9-9896  
Ni, d-band optical density of states, photoemission study 9-1629  
Ni, electronic specific heat calc., 0-300°K 9-16177  
Ni, ferromagnetic, and spin-orbit splitting of 0.7-eV transition 9-7948  
Ni<sub>2</sub>Fe(Mn)-based ternary alloys with transition metal 9-19834  
Ni and alloys, 3d zone struct. from thermopower 9-12207  
Ni and Ni alloys, 3d-zone structure rel. to thermo-e.m.f. 9-16310  
NiCr<sub>2</sub>Se<sub>4</sub>, effect of interactions between d shells of transition elements on physical props 9-16253  
NiO, rel. to elec. cond. 9-1469  
NiSi<sub>2</sub>, (x=1, 2), Ni 3d-band structure from X-ray spectra 9-3911  
P, red and black, from X-ray L<sub>2,3</sub> emission bands 9-5944  
PbS, electro-optical meas. 9-7953  
PbSe, conduction band dispersion relation 9-3642  
PbSe, electro-optical meas. 9-7953  
p-PbSe, from temp. depend. of elec. props. 9-3643  
Pb<sub>1-x</sub>Sn<sub>x</sub>-Te inversion model rel. to resistivity and Hall coeff. temp. dependence, 4-300°K 9-13890  
PbTe-PbS solid solution, valence band, from Hall coeff. elec. conductivity and thermoelec. power meas. 9-21514  
PbTe, band gap temp. depend. and Debye-Waller factors 9-9898  
PbTe, electro-optical meas. 9-7953  
n-PbTe, electron spin-flip Raman scatt. 9-18715  
Pd, d-band in 1s coupling 9-9896  
Pd, density of states curve rel. to spin susceptibility field dependence 9-16333  
Pt, d-band in 1s coupling 9-9896  
Rb, at volume dependence, Wigner-Seitz cell calcs. rel. to polymorphic transitions under pressure 9-5614  
RbCl:CN<sup>-</sup>, tunneling states of CN<sup>-</sup> ions 9-10040  
RbCl, valence and conduction band, Schrodinger eqn. soln., Brillouin zone symmetry 9-3554  
Sb-Sn alloys, galvanomagnetic coeff., band struct. interpretation 9-3841  
Sc augmented-plane-wave method, Fermi surface 9-7714  
Si SiO<sub>2</sub>, diagram construction 9-18587  
Si, effective mass approx. for acceptor states 9-18630  
Si, effects and many-particle scatt. corrections in far u.v. spectra 9-12378  
Si, electron states at dislocations 9-16274  
Si deep levels introduced into band structure by 300 KeV electron irradi. 9-7809  
Sm, conduction e. density at nucleus 9-16211  
Sn gray 9-13833  
Sn grey, conduction and valence bands at k=0, excitonic transition, critical temp. 9-15047  
SnO<sub>2</sub>, from magnetoresistance meas., weak-field 9-9981  
Sr under pressure, by pseudopotential-like approx. 9-15054  
SrTiO<sub>3</sub>:Nb by magnetoresistance 9-7788  
Tb, rel. to mag. ordering 9-16212  
Tl, valence band, from Shubnikov-de Haas effect 9-7729  
Ti, X-ray emission spectral determ. using K and L<sub>II</sub> bands 9-1821  
Ti and TiC, rel. to X-ray emission spectra 9-10229  
Ti cpds., metal-like, theoretical calc. rel. to exptl. X-ray spectra 9-3912  
Ti cpds. rel. to X-ray L<sub>III</sub> spectra from pure metal, oxides, nitride, carbide and boride 9-19999  
TiO<sub>2-x</sub>, reduced rutile, from sp. ht. and paramag. susceptibility meas. 9-21436  
TiSe, model, absorption edge 9-5903  
TiSe, optical energy gap 9-3556  
V, cpds., metal-like theoretical calc. rel. to exptl. X-ray spectra 9-3912  
V, X-ray emission spectral determ. using K and L<sub>III</sub> bands 9-1821  
V, VCo<sub>88</sub>, VN and VO, rel. to X-ray emission spectra 9-10229  
V<sub>2</sub>O<sub>5</sub>, from reflection spectra 9-19984  
VCr<sub>2</sub>Se<sub>4</sub>, effect of interactions between d shells of transition elements on physical props. 9-16253  
VO<sub>2</sub>, from reflection spectra 9-19984  
VO<sub>2</sub>, and opt. props. 9-12329  
VO<sub>2</sub>, high density-of-states band near Fermi level, evidence from photoemission data 9-12227

**Crystal electron states continued  
band structure continued**

- Y, from positron annihilation meas. 9-18597  
Zn, compensation in anomalous size effects in galvanomagnetic props. 9-13848  
Zn<sub>1-x</sub>Hg<sub>x</sub>-Te solid solns., from elec. and optical data 9-7716  
ZnS, Green's function method calc. 9-21467  
ZnSe, computation from reflectivity data, rel. to freq. 9-18701  
n-ZnSe, from piezoresistance and piezo-Hall effect meas. 9-5693  
ZnSe, Green's function method calc. 9-21467  
ZnSnP<sub>2</sub>, chalcopyrites and spherulites, from optical spectra 9-5931  
ZnTe, effective mass of holes, valence band parameters from cyclotron reson. meas. 9-3635  
ZnTe, Green's function method calc. 9-21467  
ZnTe, photoemission obs. 9-7866  
Zr, from positron annihilation meas. 9-18597

**excitons**

- alkali halides, two-quantum excitations 9-21618  
anisotropic, diffusion tensor 9-9901  
anthracene, crystalline, interactions 9-1418  
anthracene, singlet excitons, diffusion and surface reactions 9-13835  
anthracene, triplet type, review 9-5623  
anthracene in naphthalene solid soln., two exciton transfer mechanisms, fluorescence decay pattern obs. 9-12471  
anthracene molecular cry., exciton configs. construct. from orbitals, mixing obs. 9-21617  
cooperative states in crystals with two mols. per unit cell 9-16214  
exchange interaction in two-body representation and effect on spectrum 9-12066  
exciton-phonon bound state, new quasiparticle 9-12319  
F-centre formation in defect-free pairs of ionic crystals, exciton mechanism 9-5383  
generation in nonmetallic crystals by fast electrons 9-19880  
ground state energy depend. on electron hole mass ratio 9-18590  
insulators, effects in inter-band absorpt. 9-1572  
laser action involving free excitons and LO-phonon assisted transitions, theory 9-6522  
magnetic insulator, exciton-magnon interact., coupling const. determ. 9-1706  
mechanism of superconductivity, high-temp. possibilities 9-7757  
molecular complexes, excitation energy, Green's function method 9-17371  
molecular cry., exciton configs. construct. from orbitals, mixing obs. 9-21617  
molecular cryst., damping obs. w.r.t. trapping and radiationless transition 9-21469  
molecular cryst. with impurity, diagonalization of Hamiltonian 9-16215  
naphthalene, pure cryst. 9-1838  
naphthalene in anthracene solid soln., two exciton transfer mechanisms, fluorescence decay pattern obs. 9-12471  
naphthalene evap. films, exciton diff. 9-7718  
polyadenic acid, triplet exciton dynamics 9-9300  
polyadenic acid, triplet exciton dynamics 9-14733  
polymers, theory, u.v. absorpt. spectra 9-10216  
rauping of Frenkel excitons in molec. crystals 9-9902  
rare-earth exciton migration rates in trichloride crystals 9-10243  
resonance energy transfer in condensed media from many-particle viewpoint 9-5621  
rocksalt, formation rel. to luminescence in 800-1000 V fields 9-16433  
semiconductor, interaction with charged centre 9-19881  
semiconductor in mag. field, line excitation on light absorpt. 9-1763  
semiconductors, A<sup>1</sup>B<sup>VI</sup>, transitions, phonon-assisted 9-5966  
semiconductors, bound, spectra 9-21470  
semiconductors, recombination through exciton states, kinetics 9-14071  
semiconductors, rel. to optical absorpt. in crossed elec. and strong mag. fields 9-10174  
small-radius, superfluid state in molecular crystals 9-18588  
TCNQ complex salts, energy levels of triplet excitons by ESR 9-19883  
tetracene, bimolecular radiationless transitions, import, as fluor. quenching channel 9-14085  
AgCl absorpt. spectra, existence of direct excitons 9-9903  
AlSb, derivative spectrum of indirect excitons 9-18702  
alkali iodides, L-bands and exciton bands 9-3759  
CdS, absorption, infl. of strong elec. field 9-19988  
CdS, bound complexes, excited states 9-9904  
CdS, dynamical behaviour, correlation between intrinsic absorpt. and emission 9-14049  
CdS, emission in excitation spectra, oscillations 9-12489  
CdS, laser action involving free excitons and LO-phonon-assisted transitions, theory 9-6522  
CdS, transitions, phonon-assisted 9-5966  
CdSe, bound exciton-donor complexes, excited terminal states 9-21471  
CdSe, transitions, phonon-assisted 9-5966  
p-CdTe, interaction with opt. phonons in photoconductivity 9-10069  
CdTe, transitions, phonon-assisted 9-5966  
CsI, peak shift with press. and deform. potentials 9-12067  
Cu<sub>2</sub>(UO<sub>2</sub>)<sub>2</sub>, exciton migration and quenching during cooling 9-5620  
CuBr-CuCl solid solns., in absorpt. and emission spectra at 8 and 80°K 9-1775  
CuCl, linear electro-optic effect 9-3863  
CuCl, refl. spectrum, Zeeman eff., low temp. 9-14044  
CuCl, transitions in sign reversal effect in Faraday rotation spectra 9-12374  
CuCl radiative recomb., laser, u.v. excitation, biexcitonic decomp. theory 9-16430  
Cu<sub>2</sub>O, optical transitions to n=1 exciton, elec. field effects 9-12376  
GaAs, free- and bound- excitons in radiative recombination 9-14077  
n-GaAs interaction with opt. phonons in photoconductivity 9-10069  
GaP, binding energies of excitons to single and double nitrogen impurities 9-7801  
Ge, absorpt. rise rel. to magnetabsorpt. intensity 9-5919  
Ge, diamag., structure obs. from electroabsorpt. obs. 9-7951  
Ge, ionization of diamagnetic excitons in valence band 9-12068  
Ge, rel. to magnetabsorpt. oscils, assoc. with interband transitions 9-5918  
Ge, Mott transition from many-electron system to metallic conductivity state 9-3659  
Ge, in photocurrent formation 9-7858  
InSb, effects at hyperbolic crit. pts. 9-5901  
KBr, structure from energy loss spectrum of electrons 9-5591  
KI:TL, photomodelling of scintillation mechanism 9-20008



**Crystal electron states continued**

- excitons continued**  
 LiBr, Jahn-Teller effect in  $\Gamma$  exciton splitting 9-19882  
 MnF<sub>2</sub>, thermodynamic distinction between states and Brillouin zone 9-1434  
 MnF<sub>2</sub> absorpt. in 4000 Å region, exciton-magnon bound state and exciton dispersion obs. 9-1707  
 MoS<sub>2</sub>, rel. to optical absorption props. 9-1798  
 MoS<sub>2</sub> thin crystals, photovoltage rel. to dissociation of excitons 9-13934  
 NaCl models 9-1432  
 NaI:Ti, photomodelling of scintillation mechanism 9-20008  
 NaI, energy transfer to Q and Ti centres during luminescence 9-20000  
 NaI, intrinsic photoluminescence 9-3943  
 RbI differential magnetorefractance for right and left-hand circularly polarized light 9-7949  
 RbMnF<sub>3</sub>, absorpt. in 4000 Å region, exciton dispersion obs. 9-1707  
 $\beta$ -SiC, free and bound excitons, rel. to absorption and luminescence spectra 9-3900  
 Sn grey, excitonic transition, critical temp. 9-15047  
 SnO<sub>2</sub>, Zeeman effect and symmetry of exciton 9-1433  
 TiBr<sub>3</sub>, direct band gap assoc., sideband struct. 9-12069  
 TiCl<sub>3</sub>, direct band gap assoc., sideband struct. 9-12069  
 UO<sub>2</sub>(NO<sub>3</sub>)<sub>2</sub>·6H<sub>2</sub>O, migration and quenching during cooling 9-5620  
 Xe, excitonic struct. and plasma loss from energy loss meas. on electrons 9-7694  
 ZnSe, excitonic structure from anomalous electro-reflectance near fundamental edge 9-16409  
 ZnSe, interaction with opt. phonons in photoconductivity 9-10069

**Fermi level**

- alloys, monovalent, effective mass interpret. rel. to electron states, distrib. 9-7705  
 magnetoacoustic investigation 9-18558  
 metals, monovalent, effective mass interpret. rel. to electron states, distrib. 9-7705  
 r.f. methods of study 9-18583  
 Cu, magnetoresist. theory 9-18594  
 GaP-Zn, hole concentration function, 1040°C solid solubility isotherm of Zn 9-7715  
 Ge, electron-irrad. at 50 MeV, effect on ultimate position 9-12154  
 Se thin films 9-12191  
 Si, location, dopant dependency 9-13896  
 Si, stabilization and surface states at interfaces of (1,1,1) surfaces and insulating layers 9-3555

**Fermi surface**

- anisotropic, helicon damping at tipped mag. field 9-7709  
 anisotropic, in electron fluid, existence of weakly decaying spin waves 9-1438  
 n-Bi<sub>2</sub>Te<sub>3</sub>, surface shape discrepancy, galvanomagnetic data recal. 9-1427  
 curvature and effective masses 9-16206  
 itinerant electron antiferromagnet, props., effects of imperfect Fermi surface nesting 9-1695  
 Li, positron annihilation study 9-18596  
 metal, Schrodinger eqn. soln. 9-13828  
 metal films, arbitrarily oriented, rel. to size effect in elec. conductivity 9-7744  
 metals, localized Umklapp scatt., effect on galvanomagnetic props. 9-9918  
 metals, positron annihilation study 9-18596  
 nearly ferromag. syst., spin-orbit interac., sp. ht. temp. depend., impurity scatt. 9-1657  
 potential curves, effects of screened exchange and self-energy processes 9-12075  
 scattering distribution function disturbance var. rel. to resistance 9-236  
 sound, electron in metal 9-3548  
 sound, electron in metal 9-13820  
 transition metals, structure rel. to anomalous Hall effect 9-1461  
 Bi-Pb alloys, dilute, shift of Fermi energy due to Pb content 9-7726  
 Ca under pressure, de Haas-van Alphen periods cyclotron meas., press. depend. of elec. resistivity 9-15054  
 Cd, characteristics by dimension and cyclotron resonance effects on drifting effective electrons 9-1442  
 Cd, from r.f. size effect meas. 9-5610  
 Cd, s-character at low temps. from spin-lattice relax. temp. dependence meas. 9-12510  
 Cr, antiferromag. Q-vector truncating effect, from de Haas-van Alphen effect obs. 9-17461  
 Cr, antiferromagnetic spin density wave effects from high-field galvanomag. meas. 9-17462  
 Cu, in thermopower calcs. 9-12204  
 Cu, band structure wave functions 9-9894  
 Cu, deformation rel. to u.s. attenuation orientation dependence 9-9830  
 Cu, Fourier expanded model Hamiltonian 9-18585  
 Cu, rel. to positron annihilation 9-7730  
 Cu, from positron annihilation meas. 9-21465  
 Hg, Azbel-Kaner cyclotron resonance obs. 9-13838  
 In-Pb alloys, interactions eff. on temp. depend. of axial ratio and supercond. transition 9-21491  
 n-InSb, anisotropy, null deflection barque magnetometer obs. 9-3641  
 K, calc. from de Haas-van Alphen osc. 9-1443  
 K, helicon Doppler-shifted cyclotron resonance meas. 9-12060  
 La, d.h.c.p., rel. to mag. ordering, crystal structure 9-5615  
 Mo, area, exptl. estimation from size effect meas. 9-12062  
 Na, helicon Doppler-shifted cyclotron resonance meas. 9-12060  
 Nb, rel. to de Haas-van Alphen oscs. 9-7727  
 Nb, from galvanomagnetic high field props. 9-3770  
 Nd, d.h.c.p., rel. to mag. ordering, crystal structure 9-5615  
 Ni, anisotropies in de Haas-van Alphen effect data. 9-12063  
 Pr, d.h.c.p., rel. to mag. ordering, crystal structure 9-5615  
 Scr, energy bands using augmented-plane-wave method 9-7714  
 Sn, tension effects 9-15057  
 Te, from obs. of Shubnikov-De Haas eff. 9-9915  
 Te, from Shubnikov-De Haas effect 9-7729  
 Th, de Haas-van Alphen eff. obs., electron structure study 9-21466  
 V, anisotropy from magnetoresistance 9-12105  
 W, area, exptl. estimation from size effect meas. 9-12062  
 W, geometrical model, rel. to de Haas-van Alphen freqs. 9-3565

**impurity states and effects**

- alloys, dil, host ion displacement, contrib. to residual resistivity and elec. field gradients in dil. alloys 9-5600  
 alloys, dil, magnetic, spin correlations at low temps. 9-21562

**Crystal electron states continued**

- impurity states and effects continued**  
 alloys, dil, non-magnetic, impurity-induced changes in low temp. sp. ht. and T, e-phonon effects 9-1495  
 alloys, dilute, 'non-magnetic', localized spin fluctuations causing mag. behaviour 9-12234  
 charged, near electron-hole complexes, chemical shear of energy levels 9-5607  
 classical impurity spin interacting with free electron gas, exact solution 9-16216  
 conduction electron spin polarization range, depend. on impurity conc. determ. by neutron scatt. 9-10120  
 D<sup>-</sup>-band based on Hubbard's theory and mag. field effect 9-16407  
 decay modes with coherent resonant-energy transfer between deep impurities 9-9889  
 diamond, semiconducting, nature of acceptor centre 9-12135  
 Dyson equation in many-impurity problems, solution for extended impurity potential 9-17368  
 Dyson equation solution in many-impurity problems 9-18580  
 electron scatt. by impurities, kinetic eqn. 9-17367  
 Fermi syst., spin-orbit interac., impurity scatt., sp. ht. temp. depend. 9-1657  
 Friedal oscs., modification by mag. field 9-5627  
 group IB alloys,  $\alpha$ -phase, anisotropic relax. times from Hall coeff. meas., 10-300°K 9-13844  
 host ion displacement, contrib. to residual resistivity and elec. field gradients in dil. alloys 9-5600  
 hybrid bands, electron correlated motion, model 9-5604  
 n-InSb, rel. to photoconductivity due to cyclotron absorpt. 9-5767  
 intersystem crossing and multiple tunnelling model 9-18719  
 light emission by impurity centres from non-equilibrium vibrational states 9-14073  
 linear molec. crystals 9-9888  
 magnetic alloys, dil., spin relax. and transport 9-17466  
 many-impurity problems, self-energy and T-matrix relation 9-16196  
 metals, energy spectrum and props., numerical analysis 9-3552  
 metals, nearly-free electron, scatt. potential from elec. resistivity and acoustic attenuation 9-12045  
 metals with paramagnetic impurities, electron interaction effects 9-9876  
 metals with transition element impurities, localised mag. mom. 9-7874  
 molecular mixed crystal, discrete and zone states 9-5622  
 one-dimensional periodic systems, nonadiabatic transitions 9-1423  
 optical transitions to degenerate local levels 9-3881  
 Poole-Frenkel effect with compensation present 9-13821  
 resonance energy transfer in condensed media from many-particle viewpoint 9-5621  
 semicond., band conduction with strong electron correlations 9-7704  
 semiconductor, charged surface impurity shallow levels and capture cross-section 9-16213  
 semiconductor, model for metal-nonmetal transition 9-15098  
 semiconductor capture levels determ. by thermally stimulated currents 9-19879  
 semiconductors, isoelectronic impurities, Koster-Slater one-band-one-site approx. 9-7801  
 semiconductors, Raman scattering of shallow impurity states, mag. field eff. 9-12396  
 shallow surface states, variational calc. using orthogonal functions 9-21468  
 superconductor with classical spin, impurity band growth in energy gap 9-5606  
 superconductors, fluctuations 9-7764  
 superconductors, impurity spin ordering effects on electronic thermal conductivity 9-12108  
 superconductors with nonmag. impurities, upper critical field in two-band model 9-16241  
 traps, thermal activation emptying mechanism 9-18579  
 traps in semiconductor, eff. on m.o.s. transistor characts. 9-5732  
 vibrational structure from radiation spectrum 9-16408  
 vibronic spectrum of impurity absorpt./ emission of light due to electron-localized vibration interaction, analysis 9-1762  
 Ag-Al alloy, transition of Gd 4f electrons from bound to virtual levels 9-1462  
 Ag-Au alloys, electronic sp. ht. below 3°K 9-12018  
 Al-Mn alloys, dil., from <sup>55</sup>Mn NMR 9-1871  
 Al<sub>2</sub>O<sub>3</sub>, of AlO<sub>3</sub><sup>-</sup>, radiation-induced, rel. to optical and mag. props. 9-12322  
 Au alloys, (with Pt, Cu, In), phonon-assisted impurity scatt. 9-13847  
 Bi-Sb alloys 9-13831  
 CaF<sub>2</sub>:Er<sup>3+</sup>, intercentre interaction probability temp. dependence 9-1716  
 CaWO<sub>4</sub> single cry., defect states, glow peaks prod., origin from thermolum. investg. 9-12042  
 Cd<sub>1-x</sub>Mn<sub>x</sub>S (x<0.4), elec. and opt. props. 9-1516  
 CdF<sub>2</sub>:Er<sup>3+</sup>, intercentre interaction probability temp. dependence 9-1716  
 CdGeAs<sub>3</sub>, effect of In, Te, Cu and Ga on conductivity 9-18618  
 CdS, donor props. from excited states of bound exciton complexes 9-9904  
 CdS, in slow (opto-electronic) phenomena, photochemical interpretation 9-21547  
 CdS, trap depth and density determ. by space-charge-limited currents 9-10070  
 CdS, trap mechanism of isothermal decay of photocurrent 9-18655  
 CdSe, bound exciton-donor complexes, excited terminal states 9-21471  
 n-InSb, degenerate, conc. meas. using Burstein eff. 9-3645  
 Co-Cu alloys, hexagonal, e. transfer rel. to mag. moments 9-12274  
 Cu-Al alloy, transition of Gd 4f electrons from bound to virtual levels 9-1462  
 Eu<sub>0.95</sub>Gd<sub>0.05</sub>S critical scatt. and band conduction 9-9886  
 GaAs:Sn, rel. to deep-level luminescence 9-12463  
 GaAs, band- and donor-acceptor and Auger recombination in luminescence spectrum 9-14077  
 n-GaAs, donor band states from cathodoluminescence 9-12479  
 n-GaAs, luminescence from donor-acceptor pair recombination involving the first excited state of donor 9-12465  
 GaAs double injection diodes, doping effects on characts. rel. to trapping levels 9-18636  
 GaP:O<sup>-</sup>, i.r. radiative capture of electrons at ionized oxygen donors 9-12464  
 GaP, vapour-grown, rel. to substrates 9-12148  
 Ge:Cu, spectral levels, rel. to impurity effects during n-irrad. 9-5335  
 Ge:Zn, e. scatt. by neutralized Zn acceptors, stress effects, 1.5-4.2°K 9-1546

**Crystal electron states continued****impurity states and effects continued**

- Ge, impurity impact ionization 9-15105  
 Ge surface recombination centres, nature 9-17443  
 GaP:B, Zn, reactions in doping in photolum. and electrolum. mechanisms 9-3940  
 InAs: Cd, Cd ionization energy conc. dependence 9-3646  
 n-InSb, mag. field dependence of donor ionization energy by Hall eff. meas. 9-13885  
 KBr, M<sup>+</sup>-centre, F<sub>2</sub> theoretical treatment 9-19758  
 KCl, F-centres, surface, state of localized electrons 9-16108  
 KCl, M<sup>+</sup>-centre, F<sub>2</sub>-theoretical model 9-19758  
 MgO: Fe<sup>2+</sup>, thermal cond. < room temp. rel. to Fe<sup>2+</sup> spin-phenon. scatt. 9-1406  
 NaCl, F-centres, surface, state of localized electrons 9-16108  
 Ni-Co alloys, dil. ferromag., elec. resistivity and screening 9-5645  
 Ni-Fe alloys, dil. ferromag., elec. resistivity and screening 9-5645  
 PbTe, donor and acceptor, on microhardness 9-1316  
 Pd-Ag alloys, dil., from mag. susceptibility meas. 9-13986  
 Pd-Rh alloys, dil., from mag. susceptibility meas. 9-13986  
 Se-CdSe p-n junction, Cl impurity effects on characts. 9-10010  
 Se-CdSe p-n junctions, Tl impurity conc. eff. on characts. 9-5721  
 Se single cry., space-charge limited currents, trapping levels and density obs. 9-21479  
 Si: Cu, spectral levels, rel. to impurity effect during n-irrad. 9-5335  
 n-Si: P, dopant eff. on carrier mechanism of i.r. absorption 9-18710  
 Si: Sb, carrier density and elec. active impurity reduction by Sb solid soln. precip. 9-1333  
 Si-Au alloys, i.r. impurity photocond. 9-15140  
 Si, ground state energy of P donor, corrected 9-12160  
 Si, radiative spectra from shallow donor-acceptor electron transfer 9-18722  
 TiO<sub>2</sub>, reduced rutile, from sp. ht. and paramag. susceptibility meas. 9-21436  
 ZnS: Cu, trap levels with electrons excited by modulated light, dynamic study of behaviour 9-17487  
 ZnTe, isoelectronic oxygen trap from isotopic substitution and Zeeman expts. 9-18723  
 BeO: Li, radiation-induced paramagnetic centre structure 9-1868  
 CaF<sub>2</sub>, F-centres, 1s-2p optical transition energy 9-3363  
 CdS, S<sub>1/2</sub>-state impurity centres, photo-induced e.p.r. 9-20017  
 CdSe, S<sub>1/2</sub>-state impurity centres, photo-induced e.p.r. 9-20017  
 n-CdTe, high-resistivity, photosensitizing centre 9-3621  
 GaP: Cd (Zn), thermal ionization energies of acceptors 9-5696  
 Ge: As, e, density modulation by impurity centre field 9-3918  
 p-Ge: Ga, Li, ion pair effects on interimpurity radiative recombination 9-3919  
 Si: Bi implanted layers, elec. behaviour by sheet Hall effect meas. 9-7810  
 ZnO: Li, radiation-induced paramagnetic centre structure 9-1868

**plasma**

- diffraction grating surface-plasmon resonance effect 9-4520  
 electron gas in phonon field, plasma freq., second random phase approx. 9-12073  
 electron-hole, pinch effect I-V characts. 9-1436  
 e.m. waves amplification 9-9910  
 e.m. waves in metallic electron plasmas 9-16395  
 Fermi-liquid effects on propagation in metals 9-7719  
 films, thin, acoustic waves 9-9911  
 fluctuations, dispersion relation 9-5626  
 graphite, plasmon obs. in X-ray scatt. 9-1818  
 helicon amplification in Fabry-Perot geometry 9-9908  
 helicon waves in non-resistive cylinders, spheres, principal mode wave fields calc. 9-9907  
 light scattering in mag. field 9-16397  
 metal, disintegration of vol. and surface plasmons, probability calc. 9-12070  
 metal, Fermi liquid effects on propagation 9-7719  
 metal particle, oscillations induced by fast incident electron 9-13439  
 metallic particle, plasma oscillations excited by fast electron 9-9906  
 metals, electron relaxation time determ. using weakly-damped helicon waves 9-9909  
 metals, plasma waves and transition rad. due to oblique incidence electron bombard. 9-7722  
 metals, plasmons, virtual excitation, contrib. to vertex corrections to effective lattice pseudopotential 9-12072  
 multilayers, surface oscs., dispersion relns. 9-7721  
 multilayers, surface oscs., dispersion relations 9-5628  
 optical props. of anisotropic plasma, microscopic theory 9-21602  
 plasmon lifetime in degenerate electron gas, degenerate electron gas, dielectric const. depend. 9-10677  
 plasmon mechanism of superconductivity in degenerate semiconds. and semimetals 9-15077  
 plasmons, volume and surface, disintegration, and excitation of electron-hole pair 9-12070  
 scattering of light 9-16425  
 semiconductor, degenerate pinch, stationary state and parameters 9-9983  
 semiconductor, edge reflection meas. rel. to carrier conc., effective mass, scattering time and conductivity determ. 9-7792  
 semiconductor, overheating instability, theory 9-3607  
 semiconductor, transition to paramag. 9-3606  
 semiconductors, many-valley, two-stream instability in hot-electron systems 9-15096  
 semiconductors, piezoelectric, coupled acoustic-plasma waves 9-9968  
 semiconductors, pinch-like instabilities and turbulence 9-5694  
 semiconductors, plasmon-phonon interaction in Raman scatt., theory 9-3901  
 semiconductors, Raman scattering from magnetoplasma waves 9-12415  
 semiconductors p-type, magnetoplasma wave propag. in two carrier system 9-5681  
 sound amplification, mechanism 9-5551  
 space harmonics, effect of electron drift 9-3558  
 surface plasmons, tangential, radiative decay 9-7720  
 waves, in metals, propag. and absorpt. 9-18583  
 Ag, surface waves, nonradiative, excitation by total reflection method 9-5602  
 Ag film, surface plasmons, light emission 9-17373  
 Al, plasmaron structure in soft X-ray L<sub>2,3</sub> emission spectrum 9-5943  
 Be, plasmon obs. in X-ray scatt. 9-1818  
 Cu helicon window, Gantmakher oscillations due to magnetic field 9-1440  
 GaAs: Te, longitudinal-optical-phonon-plasmon coupling 9-21615

**Crystal electron states continued****plasma continued**

- n-GaAs, e plasma in mag. field Raman scatt. 9-14060  
 GaAs, light scattering from plasmons and phonons 9-12353  
 GaAs, Raman scattering, from magnetoplasma waves 9-12415  
 p-Ge, transport props. study using magnetoplasma waves 9-5681  
 p-Ge, electron-hole plasma double injection 9-7804  
 InAs, magneto plasma-phonon interaction from Kramers-Kronig analysis of reflection spectra 9-12363  
 n-InSb, aftervoltage effect 9-5629  
 n-InSb, instability, mag. field effect on 70 MHz component 9-5630  
 K film, optical plasma resonance emission and transmission 9-12382  
 KBr, plasmon struct., from energy loss spectrum of electrons 9-5591  
 Li, plasmon obs. in X-ray scatt. 9-1818  
 PbTe, coupled plasmon-phonon modes, magneto-reflection spectra 9-18699  
 Sr, plasmon excitation energies from electron energy loss meas. 9-3547
- polarons**
- F<sup>+</sup> non-radiative transition, quantum yield 9-3361  
 ferromagnetic, small-radius polarons, mobility at low temps. 9-1648  
 integral function method applie. 9-13837  
 intermediate-coupling, effective mass calc. 9-5624  
 ionic crystals, polaron absorpt. process 9-11980  
 light absorption mechanism by free continuum, Landau-Pekar approach 9-21472  
 multi-valley cryst., weak interaction between electron and polarization oscillations of lattice 9-13836  
 optical absorption by small-radius polarons, intraband and interband characts. 9-3882  
 runaway mode, renormalization of Hamiltonian 9-17372  
 rutile, reduced, interaction with paramag. centres 9-1864  
 semiconductors, model for heat transport 9-7791  
 semiconductors with polarons as charge carriers, Hall effect 9-18616  
 small-radius, mobility, theory 9-1435  
 small-radius, relaxation time 9-9905  
 CoO, semiconducting, optical absorpt. of small polarons in near and far i.r. 9-5929  
 NiO, semiconducting, optical absorpt. of small polarons in near and far i.r. 9-5929
- surface**
- anthracene, eff. of surface purity on photo-generation of charge carriers 9-15049  
 anthracene, existence, density, depth and props. 9-1540  
 dipole centre, model, spectrum of 'fast' and 'slow' states 9-9900  
 ionic states from band-edge method 9-5618  
 localized states of surface and line defects using band theory 9-12065  
 metal, clean, optical absorption 9-21605  
 metal, energy exchange processes, non-equilibrium distribution 9-21550  
 metal, free electron, surface pot. in random phase approx. 9-12074  
 metal surface layer, stationary states of electrons, in weak mag. field 9-15068  
 metals, ultrasonic attenuation by mag. surface states 9-18554  
 m.i.s. structures, density of surface states, eff. of e irrad. 9-12171  
 m.o.s. structures, high density by capacity var. rel. to frequency 9-21528  
 multilayers, plasma oscs., dispersion relns. 9-7721  
 multilayers, plasma oscs., dispersion relns. 9-5628  
 potential curves, effects of screened exchange and self-energy processes 9-12075  
 quantum states and impedance oscs. in weak mag. field, numerical analysis 9-5617  
 recombination rate, non-equilib. carrier density dependence 9-5698  
 semiconductor, shallow levels and capture cross-section of charged surface impurity 9-16213  
 semiconductor oxides, e traps rel. to adsorbed Ag photolytic reduction, visible and i.r. 9-6017  
 semiconductors, intrinsic, carrier waves 9-15101  
 semiconductors, recombination velocity, flying spot method, improved 9-3647  
 semiconductors, two-dimensional transport 9-18624  
 shallow impurity states, variational calc. using orthogonal functions 9-21468  
 spectrum and damping in a magnetic field 9-13834  
 spectrum and damping in a magnetic field 9-3557  
 structure determ. methods, surface bound states eff. 9-21256  
 Ag, plasma waves, nonradiative, excitation by total refl. method 9-5602  
 Ag, transitions between mag. surface states 9-7717  
 Ag film, surface plasmons, light emission 9-17373  
 Au-CaF<sub>2</sub>-CdSe m.i.s. capacitors, obs. 9-5740  
 Au-SiO<sub>2</sub>-CaF<sub>2</sub>-CdSe m.i.s. capacitors, obs. 9-5740  
 Au-SiO<sub>2</sub>-CdSe m.i.s. capacitors, obs. 9-5740  
 Au-n-Si surface barrier diodes, rectification characts. rel. to surface states 9-21525  
 BaTiO<sub>3</sub>, chemisorption of O<sub>2</sub> causing change in electron affinity 9-3648  
 CdS, ionic states from band-edge method 9-5618  
 CdS, photosensitive, rel. to field-effect 9-10067  
 CdS, surface states and photocurrent pinch-off 9-7855  
 GaAs, ionic states from band-edge method 9-5618  
 GaSe-metal barriers on layer semiconductors 9-5699  
 n-Ge, electron heating in strong const. elec. field, n-type 9-9991  
 Ge, non-equilibrium charging 9-21516  
 Ge, recombination centres, nature 9-17443  
 Ge diode, alloyed, velocity of surface recombination in base, dependence on injection level 9-18637  
 Ge recombination studies using Suhl effect and light injection 9-9988  
 Ge thin plates, rel. to elec. instabilities at 20.4°K 9-5702  
 p-InSb, field-effect at 88°K 9-5700  
 InSb, intrinsic, carrier waves 9-15101  
 Li deformed crystal, states 9-9899  
 NaCl, ionic states from band-edge method 9-5618  
 Si-Au alloys, i.r. impurity photocond. 9-15140  
 Si, stabilization using Si<sub>3</sub>N<sub>4</sub> 9-7811  
 n-Si, tilted mag. field effects on two-dimens. electron gas props. 9-5619  
 Si, treated with gaseous HF, elec. props. 9-3661  
 ZnO space charge layers, electroreflectance obs. 9-16290
- transport processes**
- in strong electric field due to fixed space charges 9-5596  
 alloys, dil. non-magnetic, e-phonon effects on low temp. sp. ht. and T<sub>c</sub> 9-1495  
 anthracene, carrier, and prod. 9-17445  
 anthracene, eff. of surface purity on photo-generation of charge carriers 9-15049



**Crystal electron states continued**  
**transport processes continued**

- anthracene, hole and electron photogeneration mechanisms 9-1617  
anthracene crystals, hole injection from electronically excited iodine mols. 9-16313  
anthracene crystals, optical activation of traps. 9-19934  
aromatic semiconductors, electrode injection of charge carriers 9-21509  
bulk-polarization, range controlled, analytical soln. 9-5597  
carrier, non-equilibrium, creation during depolarisation and radiation absorpt. 9-21502  
carrier density, non-equilib. effect on surface recombination rates 9-5698  
carrier transport in elec. field, flux method applic. 9-5677  
CdS, direct e-hole recomb., photoexcitation 9-16261  
conductors, electron drag by ultrasound 9-1460  
copper phthalocyanine, e. drift mobilities 9-17393  
copper phthalocyanine, semiconducting, hopping and band conduction mechanisms 9-19915  
dielectric, e-phonon scatt. in elec. strength thickness dependence theory 9-3689  
diodes, meas., effect of recombination and deceleration field in base on diffusion current 9-17405  
dynamics of electrons in external fields 9-21457  
electron motion in external fields 9-12044  
electron-phonon interaction, h.f. effect on superconductors 9-13853  
electron-phonon interaction, h.f. effect on superconductors 9-3589  
electron-phonon interaction, modified tight-binding approx. 9-16198  
electron-phonon systems amplification of discontinuity waves 9-6368  
ferroelectric semiconductor, carrier drift causing amplification of transverse optical phonons 9-19929  
ferroelectric semiconductors, electric induction waves at temps. above first order transition 9-16258  
ferromagnetic metals, e. scatt. on spin-waves in thermo-e.m.f. calcs. allowing for interzone transitions 9-3719  
film with nonideal boundary, electron spectrum and mobility 9-13873  
fluctuation spectrum of electrons in non-equilibrium stationary state 9-9881  
ferroelectric semiconductors, elec. induction wave theory 9-16257  
Ge, mobility of hot e. and holes, 300°K 9-17398  
graphite, intercarrier scatt. effects and trigonal warping of bands rel. to Hall coeff. calc. 9-7748  
Hall effect and semiconductor physics fundamentals, book 9-13880  
hot electrons, resonance variation of mobility in a h.f. magnetic field 9-13823  
hot electrons, resonance variation of mobility in a h.f. magnetic field 9-3550  
Ice, nature of charge carriers 9-1579  
image potential for medium with wavevector freq. dependent dielec. function 9-9882  
lifetimes meas. short, of excess carriers from fluorescence phase shift 9-1529  
magnesium phthalocyanine, semiconducting, hopping and band conduction mechanisms 9-19915  
magnetic alloys, dil., spin relax. and transport 9-17466  
metal films, mean free path of conduction electrons 9-13925  
metals, anharmonic, Green's function theory 9-13822  
metals, localized Umklapp scatt., effect on galvanomagnetic props. 9-9918  
metals, phonon-limited resistivity 9-9926  
m.i.m. dielectric properties, traps, transfer ratio 9-1419  
n-type epitaxial films on p<sup>+</sup> substrates, hole diffusion length meas. using laser 9-3616  
nonlinear effects rel. to partially filled bands and external field freq. 9-1420  
Ohm's Law, classical aspects 9-16197  
organic semiconductors, conductivity mechanism 9-9982  
organic semiconductors, hopping and band conduction mechanisms 9-19915  
phthalocyanine, metal-free, transfer integrals 9-12048  
Poole-Frenkel effect, three-dimensional model 9-7698  
Poole-Frenkel effect with compensation present 9-13821  
quantum theory, rel. to non-degenerate electron gas in high elec. and mag. fields 9-21476  
quantum theory of transport coeffs. 9-13819  
rare-earth halides, energy transport mechanism by e.p.r. of coupled ions 9-7697  
resonance scatt. in type II superconductors, eff. on mag. props. 9-15086  
semiconductor, galvanomagnetic effects in presence of small number of free carriers 9-13878  
semiconductor, nondegenerate, steady-state diffusion eqns. in space-charge regions with large elec. fields 9-16259  
semiconductor, two-valley, stability of state with negative differential conductivity under small perturbations 9-16268  
semiconductor equilibrium carrier density in presence of 2 types of local level 9-5678  
semiconductor field effect and photoconductivity relax. phenomena 9-10064  
semiconductor h.f. effects with carriers inelastically scattered on optical phonons 9-1528  
semiconductor h.f. effects with carriers inelastically scattered on optical phonons 9-13879  
semiconductor surface space charge conductivity 9-21459  
semiconductors, anisotropic scatt. of current carriers 9-1526  
semiconductors, elec.-current-flow induced polarization effect on optical absorption, theory 9-14035  
semiconductors, electron-hole scattering at high injection levels 9-5676  
semiconductors, electrothermal domains, theoretical analysis 9-13871  
semiconductors, flexure-drift resonance 9-18617  
semiconductors, graded mixed, electronic states and transport, theory 9-21511  
semiconductors, heat transport, polaron model 9-7791  
semiconductors, instability of hot electrons in crossed elec. and mag. field 9-21501  
semiconductors, many-valley, inelastic scatt. of electrons and u.s. absorpt. and amplification oscils. 9-7644  
semiconductors, many-valley, two-stream instability in hot-electron systems 9-15096  
semiconductors, n-bombarded, carrier scattering from defects 9-17389  
semiconductors, nondegenerate, effect of collisions between carriers 9-15129  
semiconductors, nuclear polarization by hot carrier flow in crossed static and mag. fields 9-15042

**Crystal electron states continued**  
**transport processes continued**

- semiconductors, piezoelectric, minority carriers in u.s. amplification 9-11999  
semiconductors, polar, microwave electron mobility 9-1525  
semiconductors, spin polarized e. scatt. from cyclotron resonance obs. 9-9993  
semiconductors, superconducting behaviour 9-19894  
semiconductors velocity saturated, coupled-mode instabilities 9-13881  
semiconductr surfaces, two-dimensional transport 9-18624  
SnSe<sub>2</sub> film, charge carrier mobility 9-13883  
spectrum and damping in a magnetic field 9-13834  
spectrum and damping in a magnetic field 9-3557  
superconducting films 9-7758  
superconductivity, photoinduced, theory 9-5656  
superconductors, Cooper pair density relax. rel. to approach to equilibrium 9-7789  
superconductors, strong e.-phonon interaction rel. to u.s. absorpt. 9-1373  
in surface-charge and space-charge fields, rel. to metal oxidation kinetics 9-9620  
tetracyanquinodimethane-phenazine complex, conduction mechanism 9-18599  
transition metal alloys, variation in number of 3p 3d electrons meas. 9-19877  
tunnel junction, electronic interactions model for examining collective excitations spectroscopy 9-12169  
Ag, attenuation length of hot electrons, meas. 9-12043  
AgBr, electron mobility determ. 9-15123  
Al-SiO<sub>2</sub>-Si, injection and migration of charges in oxide 9-5741  
Al, electron component of thermal conductivity 15-573°K, theory 9-3541  
Al, normal state, electronic contribution to u.s. attenuation 9-9829  
As, current carrier conc., press. depend. 9-15069  
Au alloys, (with Pt, Cu, In) phonon-assisted impurity scatt. 9-13847  
B, conductivity and charge carrier conc. meas. in breakdown region 9-12143  
Ba ferrite polycrystals, from h.f. conductivity and Seebeck coeff. meas. 9-12086  
Bi-Sb-Te system, intermetallic cpds., in mag. anisotropy and susceptibility phenomena 9-13945  
Bi, charge carrier densities and mobilities temp. dependence, 50-90°K 9-12046  
Bi, charge carrier relax. time variation with mag. field 9-12047  
Bi, current carrier conc., press. depend. 9-15069  
Bi Alfvén wave transmission obs. for carrier relax. time calcs. 9-12047  
Bi<sub>2</sub>Te<sub>3</sub>, in, mag. anisotropy and susceptibility temp. dependence 9-13945  
CaWO<sub>4</sub> single cry. impure state, excitation mechanism of charge-carrier prod. 9-12042  
Cd-Zn alloy, carrier scatt. between adjacent branches of hole surfaces 9-12106  
Cd, carrier scatt. between adjacent branches of hole surface 9-12106  
cd,Hg<sub>1-x</sub>Te graded gap structures, photocarrier transport 9-18619  
CdGeAs<sub>2</sub>, effect of In, Te, Cu and Ga impurities 9-18618  
CdS:In degenerate, evaporated films, mobility studies 9-12145  
CdS, e. mobility in high electric fields 9-13825  
CdS, hole mobility, field effect photocurrent obs. 9-1612  
Cu, electron-phonon interaction, contribution to u.s. attenuation 9-9830  
Cu and alloys, phonon-drag effect on elec. cond. 9-5652  
pGe:Ga, [during e. irradi. and annealing 9-5703  
Eu- chalcogenide alloys, anomalous opt., mag. and transport phenomena 9-9878  
Eu<sub>0.95</sub>Gd<sub>0.05</sub>S band conduction, onset reported 9-9886  
GaAs-Pd Schottky diodes, electron-phonon coupling in barrier 9-7825  
GaAs, Auger recombination 9-15090  
GaAs, carrier distrib., equilb., photoluminescent meas. method 9-9974  
N- GaAs, electron heating effects on Hall coeff. 9-12149  
GaAs, expt. obs. 9-5689  
n- GaAs, free carrier Faraday effect 9-3864  
n- GaAs, heavily doped, electron mobility 9-17391  
GaAs, hot electron energy relaxation time 9-9975  
GaAs<sub>0.5</sub>PO<sub>0.5</sub>: Fe trapping phenomena 9-16263  
GaAs dislocation free, electronic transport props. 9-16099  
GaP, vapour-grown, rel. to substrates 9-12148  
n- GaSb:Te, from Faraday effect, Hall effect and conductivity meas. 9-10177  
GaTe film, charge carrier mobility 9-13883  
Grap, electroluminescent diodes, minority carrier lifetime 9-12491  
Ge:Zn, e. scatt. by neutralized Zn acceptors, stress effects, 1.5-4.2°K 9-1546  
Ge-metal contacts, e. and phonon tunneling spectroscopy 9-13909  
Ge, carrier density gradient, associated instability 9-5707  
Ge, deformed, carrier mobility 9-18628  
n- Ge, electron-electron, effect on mobility of warm electrons at 78°K 9-9990  
Ge, hole low-field mobility and galvanomagnetic props rel. to phonon scatt. 9-5708  
p-Ge, hole mobility in strong elec. fields 9-21515  
p-Ge, hole recombination at shallow acceptors 9-3655  
n-Ge, phonon-drag effect anisotropy parameter of thermoelec. power 9-12205  
p-Ge, props. study using magnetoplasma waves 9-5681  
Ge, spin polarized e. scatt. from cyclotron resonance obs. 9-9993  
Ge, charge transport in low angle grain boundaries 9-3657  
Ge diode, alloyed, velocity of surface recombination in base, dependence on injection level 9-18637  
Ge relaxation of warm carriers 9-12159  
GeTe, carrier-conc. dependence of superconductivity, rel. to intervalley transitions 9-21494  
n- Ge, magnetophonon oscils. in drag thermoelec. power 9-3722  
n-Hg<sub>1-x</sub>Cd<sub>x</sub>Te ionized-impurity scattering of conduction electrons at 4.2°K, calcs. 9-13884  
HgS, e-drift mobility determs. 9-5691  
HgSe helicon waves obs. at 77°K 9-7723  
I, electron and hole mobilities 9-17424  
InAs:Cd compensated, intrinsic, e. density lifetime temp. dependence rel. to recombination at Cd levels 9-3630  
InSb, Bloch electron anomalous velocity in mag. field and combined resonances 9-21460  
n- InSb, carrier conc. depend. of far i.r. resonant photoconductivity 9-17444  
InSb, carrier freeze-out effects in strong mag. field 9-1531

**Crystal electron states continued**  
**transport processes continued**

- n-InSb, phonon drag effects on thermoelec. power in transverse quantizing mag. field 9-3723  
 n-InSb free carrier Faraday effect 9-3864  
 KCl, electron drift mobility 9-19878  
 p-MnO, Hall mobility of electrons and holes at high temp. 9-12152  
 Na, liquid and solid, electron-electron interactions eff. on optical absorption 9-21628  
 Ni, effective hole-hole interaction, magnetization dependence 9-21461  
 Ni, mean free paths of 4s electrons 9-17370  
 Ni<sub>3</sub>Al, conduction electron scatt. by paramagnons 9-21462  
 Ni Fe ferrite, hopping model explanation of conductivity 9-3632  
 Ni film, vacuum deposited, electron mean free paths 9-17369  
 p-PbSe, carrier mobilities 9-3633  
 Pb(Zr,Ti...)<sub>2</sub>O<sub>3</sub>, charge transport mechanism, 650-1000°K 9-19932  
 Pd, electron-phonon interband scatt. 9-21463  
 p-PbSe, carrier density dependence of thermopower 9-3724  
 Pt, conduction-electron g factor, anisotropy 9-1445  
 Pt, electron-phonon interband scatt. 9-21463  
 S, liquid and solid, charge carrier transport 9-5603  
 Sb, current carrier conc., press. depend. 9-15069  
 Sb, electron scatt. mechanism from thermal props. 9-9856  
 SbSi, Curie temp. shift due to illumination and nonequilibrium carriers 9-16300  
 SbSi, non-equilibrium carriers screening effects on polarization reversal 9-3712  
 Sb<sub>2</sub>Te<sub>3</sub>, in, mag. anisotropy and susceptibility temp. dependence 9-13945  
 Si:Au, majority carrier sweep-out by trapped space charge, conductivity recovery 9-18615  
 Si:Au, recombination of hot electrons 9-9997  
 Si:Li, electron-irradiated, recombination velocity, Li impurity effects 9-9998  
 Si, abrupt p-n junctions, avalanche multiplication, theoretical analysis 9-7819  
 Si, Au doped, conductivity and lifetime of excess carriers anomaly 9-16273  
 Si, electron drift velocity at high elec. field, temp. depend. 9-10002  
 n-Si, Hall mobility and carrier repopulation at high elec. fields 9-16278  
 Si, non-equilibrium carrier creation during depolarisation and radiation absorpt. 9-21502  
 Si, spin polarized e. scatt. from cyclotron resonance obs. 9-9993  
 n-Si electron-electron, effect on mobility of warm electrons at 78°K 9-9990  
 n-Si electron elements 9-7814  
 Si electrons and holes drift velocity, at very low temp. 9-10003  
 Si high field anisotropy, role of inter-valley scatt. 9-10001  
 Si p-type layers formed by Ga ion-implantation, charge carrier conc. annealing temp. dependence 9-15108  
 Si relaxation of warm carriers 9-12159  
 Sn-grey 9-13833  
 SnO<sub>2</sub>, from magnetoresistance meas., weak-field 9-9981  
 SnSx, pellets obtained by compression electronic props. 9-19887  
 SnTe, carrier conc., dependence of superconductivity, rel. to intervalley transitions 9-21494  
 TiO<sub>2</sub>, doped, electronic conductivity rel. to optical props. 9-9706  
 Ti, e. mean. free path calcs. from residual resistance diam. dependence 9-1422  
 Ti, in u.s., attenuation mechanism in normal high-purity material 9-12004  
 V<sub>2</sub>O<sub>3</sub>, from, Hall effect in metallic conduction region at 200°-320°K 9-18603  
 ZnS, non-equilibrium carrier creation during depolarisation and radiation absorpt. 9-21502

**Crystal energy** *see Bonds; Crystals; Solids/structure***Crystal field theory**

- electrostatic potential of point charge systems, potential expansion symmetry 9-4910  
 ion-size effect in colour centres 9-18478  
 magnetic susceptibility in random dilute systems, molec. field theory extension 9-12246  
 praseodymium ethyl sulphate, high resolution of lines in far i.r. 9-5862  
 pseudopotential method rel. to effective mass approx. 9-12052  
 rare earth magnesium nitrates, high resolution of lines in far i.r. 9-5862  
 rare earths trivalent ions in Yb<sub>3</sub> crystal, effect of cubic crystal field on mag. props. 9-16327  
 rutile, e.p.r. of ions with d<sup>1</sup> shells rel. to internal fields 9-16460  
 trigonal bipyramidal environment, crystal field-spin orbit perturbation calcs. 9-21598  
 AlCl<sub>3</sub>:Ti<sup>3+</sup>, Orel. to 9-12499  
 BaF<sub>2</sub>, interaction mechanism of Nd<sup>3+</sup> ions and nature of conc. quenching 9-15161  
 CaF<sub>2</sub>, interaction mechanism of Nd<sup>3+</sup> ions and nature of conc. quenching 9-15161  
 Cu<sup>2+</sup> ion, interac. betw. 3d<sup>8</sup>, 4p, 3d<sup>9</sup> configs. under T<sub>d</sub> symm., eff. 9-17468  
 Gd<sub>2</sub>O<sub>3</sub>:Eu<sup>3+</sup>, luminescence and emission spectra, interpretation 9-10205  
 KH<sub>2</sub>AsO<sub>4</sub>, electric-field-gradient tensor at As site from p. relax. meas. 9-17469  
 Lu<sub>2</sub>O<sub>3</sub>:Eu<sup>3+</sup>, luminescence and emission spectra interpretation 9-10205  
 MgO:Cr<sup>3+</sup>, energy level symmetry from acoustic paramag. resonance 9-21666  
 SrF<sub>2</sub>, interaction mechanism of Nd<sup>3+</sup> ions and nature of conc. quenching 9-15161  
 Tb<sup>3+</sup> in hydroxides, crystal field parameters from absorpt. and fluorescence meas. 9-14019  
 YAsO<sub>4</sub>:Gd<sup>3+</sup>, parameters from e.p.r. spectrum 9-21668  
 Y<sub>2</sub>O<sub>3</sub>:Eu<sup>3+</sup>, luminescence and emission spectra, interpretation 9-10205  
 YPO<sub>4</sub>:Gd<sup>3+</sup>, parameters from e.p.r. spectrum 9-21668  
 YVO<sub>4</sub>:Gd<sup>3+</sup>, parameters from e.p.r. spectrum 9-21668

**Crystal fields** *see Crystals/internal fields***Crystal imperfections**

- See also Colour centres*  
 alkali feldspars, exsolved, appl. of theory of optimal phase boundaries 9-3360  
 alkali halides: divalent cation, crit. shear stress, non clustering impurity ion-vacancy pairs 9-3413  
 alkaline earth oxides, review 9-9693  
 alloys, defect structures, thermally softened, response to stress 9-21335  
 aluminium bronze, As-containing, CuAlSi: type, fatigued, stacking fault tetrahedra 9-19752

**Crystal imperfections continued**

- antiphase boundary tubes, stability 9-7485  
 b.c.c., radiation damage, mathematical modelling 9-13669  
 b.c.c. crystals, intrinsic stacking faults 9-5374  
 b.c.c. metals, field-ion microscopic contrast from stacking faults 9-18465  
 b.c.c. metals, packing defects {110} plane effect on X-ray scatt. 9-13677  
 binary  $\sigma$  phases, radiation damage from X-ray diffraction obs. 9-11868  
 $\beta$ -brass, quenched, anti-phase domain growth rate and final size 9-3335  
 bubbles in solids, stability 9-21339  
 cavity growth during thermal cycling, mechanism 9-19772  
 l-chloro-2,3,5,6-tetramethyl benzene, orientational disorder 9-17273  
 clusters, unrelaxed, determ. of number of unique configs. 9-13674  
 corundum, synthetic, microscopic and colloidal inclusions distrib. from Tyndall scatt. 9-1730  
 cubic lattice with line defect, Mossbauer effect 9-12354  
 dynamics of simple lattices with line defects, theory 9-1356  
 effects, photoconductive properties of II-VI semiconductors 9-1622  
 elastic interactions of defects 9-19739  
 epitaxial layer misorientation from stacking fault geometry 9-11771  
 etch pits, slope 9-21341  
 f.c.c., radiation damage, mathematical modelling 9-13669  
 f.c.c. metals, stacking fault conc. 9-13693  
 Frenkel and Schottky-Frenkel and Schottky defects, derivation of the number in solid 9-12840  
 glass, soft, rel. to far i.r. absorpt. 9-10209  
 glasses, two-component,  $\gamma$ -irrad., atomic displacement section 9-3321  
 grain boundary glide mechanism 9-3357  
 grain boundary hydride habit in Zircaloy 2 9-19754  
 grain boundary struct. in metals 9-5377  
 grain boundary torque effect on spherical particle rotation rates 9-13751  
 grain size, effect on activation energy for serrated yielding 9-11917  
 grain-boundary triple junction and corner-twinned junctions, transmission e. microscope exam. 9-13696  
 graphite, bending of layers prod. translational deviations 9-7425  
 graphite, effects on thermal conductivity 9-7668  
 graphite, irradiation defects and self-diffusion mechanism, thermal annealing studies 9-5337  
 graphite, mosaic character. shown by oxidation, crystallite sizes and boundaries 9-7497  
 graphite, polycryst., void fractions rel. to temp. depend. of Young's modulus 9-7519  
 graphite, pyrolytic, parallel layer stacking 9-7422  
 graphite, rad. damage, effect of B addition on nucleation patterns 9-7477  
 graphite boronated, struct. faults influence on oxidation 9-8094  
 inclusions, semi-metallic or semicond., rel. to supercond. enhancement 9-9940  
 intergranular corrosion, applic. of solute clustering mechanism 9-3358  
 intersection jogs in L<sub>1</sub> structure 9-16094  
 ionic, intrinsic defect depletion and accumulation near interface with aq. solns 9-14890  
 jump rates for point-defect paths between equivalent sites around a trap, relative magnitudes 9-14938  
 lattice defects obs., small diam. wire temp. control, ~350°C 9-10760  
 leuco-sapphire, colloidal inclusion distrib. from Tyndall scatt. 9-1730  
 lines of dilation, electron microscope images and props., micrograph construct. 9-21326  
 martensite, deformed and from cold-worked austenite, rel. to thermal effects of ageing 9-7595  
 metals, cold worked, stage III recovery kinetics 9-5500  
 metals, f.c.c. and h.c.p., intrinsic and extrinsic faults in field-ion micrographs, distinction 9-13670  
 metals, grain boundaries effect on distrib. of vacancies and vacancy pairs 9-3322  
 metals, point defects 9-19740  
 metals, structural defects autoradiographic obs. 9-9707  
 metals and alloys, lattice rel. to positron annihilation 9-12078  
 microdefects, development under stress field rel. to crack system formation 9-3447  
 ordering forces range in struct. with long range order 9-1162  
 Ostwald ripening and related phenomena, exptl. verification of mass transport anal. 9-1251  
 p-n junctions, defects in structure 9-13900  
 phase boundaries, optimal, theory appl. to exsolved alkali feldspars 9-3360  
 point defects, elastic strength calc. 9-9767  
 point defects, mechanical interactions using elasticity theory 9-13675  
 point defects and phase stability of transition metal compounds 9-5332  
 point defects in cubic lattices, long wavelength phonon scattering 9-13785  
 point defects in special positions held by trap of noncubic symm., jump rates and equivalence 9-21328  
 quadrupole shift of n.m.r. lines, lattice defect effects 9-12506  
 quartz, defects revealed by etching and Ag decoration in elec. field 9-13682  
 quartz, fused, rel. to far i.r. absorpt. 9-10209  
 radiation defects, spatial distribution in materials irradiated with beams of monoenergetic particles 9-13668  
 rare gas crystals, defect-induced one-phonon i.r. absorption, theory 9-5526  
 ruby, lattice defects, e.p.r. and X-ray investigation 9-9694  
 rel. semiconductor structural props. 9-19919  
 semiconductors, structural defects rel. to Kikuchi line anomalies 9-18445  
 specific heat, eff. on singularity nature near second kind phase transition points 9-9837  
 stacking fault energy calc. with energy wave-number characteristic 9-5375  
 stacking fault energy determ. from Frank dislocation loops and tetrahedra 9-14949  
 stacking fault energy meas. by different techniques 9-13694  
 stacking fault X-ray topography fringe contrast, application of Takagi's dynamical theory 9-3353  
 steel, Cr-Mn-N, austenitic, X-ray meas. of stacking faults 9-18476  
 steel, stainless 304 film, twin-grain boundary intersections, energy ratios 9-1231  
 structural defect-phonon coupling in H-bonded system 9-21422  
 substitutional defects, shell model treatment of vibrations: defect-induced one phonon absorpt. 9-13787  
 surface and line defects, localized states calc. using band theory 9-12065  
 thin films, defects produced by deformation 9-7544



**Crystal imperfections continued**

- transfer of defects from deformed seed crystals to grown crystals 9-13606
- transition metal compounds, point defects and phase stability 9-5332
- twin lamellae, small static, numerical analysis of deformation behaviour 9-14950
- twinned stacking faults, deformational, X-ray diffr. analysis 9-1229
- u.s. wave prod. in mag. field, transducerless for det. 9-7469
- wedge shaped parts rel. to fine structure of spots in electron diffraction 9-13620
- whiskers, lattice defects, diffracting plane shapes from Laue technique 9-9659
- Ag-Al system, hexagonal  $\zeta$ -phase, stacking-fault energy calc. from thermodynamic data 9-19750
- Ag-Al system, hexagonal  $\zeta$ -phase, stacking-fault energy, exptl. determ. 9-19751
- Ag-Cu solid solns, supersaturated, substructure changes, during decomposition 9-1339
- Ag-Mn solid solutions, stacking fault energies 9-7492
- Ag-Pd alloys, falling in severely cold-worked filings, X-ray meas. 9-7493
- Ag-Sb alloys, hexagonal ( $\beta$ -phase), stacking-fault densities 9-1230
- Ag-Zn alloys, stacking fault energy meas. by different techniques 9-13694
- Ag, grain-boundary diffusion of In, temp. dependence, 180-100°C 9-3375
- Ag, irradiated, black-spot damage, nature 9-18459
- Ag, stacking fault energy meas. by different techniques 9-13694
- AgCl radiation-produced colloids, phonon scattering investig. 9-9692
- Al-Be alloy, clustering, effect of cold working 9-18458
- Al-Mg-Ge alloy, clustering after quenching 9-17331
- Al, electron displacement damage 9-3334
- Al, grain-boundary migration rel. to Xe bubble distrib. 9-657
- Al, grain boundaries, slip band continuity 9-7498
- Al, quenched-hardened, slip-bands behaviour in plastic deformation 9-11924
- Al, stacking faults, H accumulation on dechannelling of protons 9-16102
- Al<sub>2</sub>O<sub>3</sub>.2.5NiO.9H<sub>2</sub>O, driving defects characterization 9-19707
- Al, fatiguing and annealing, low temp., defects rel. to resistivity changes 9-13846
- Al nucleation and growth of multi-layer defects 9-3344
- Al<sub>2</sub>O<sub>3</sub>, double bicrystals, grain boundary strength 9-1232
- Au-Mg alloys near Au<sub>3</sub>Mg, long periodic stacking order 9-9716
- Au foils, quenched,  $\alpha$ -irradiation effects on tetrahedra 9-7495
- Au quenched from 900°, double stacking fault tetrahedra 9-7494
- B foils, preparation and electron microscope obs. of defects 9-5247
- BaS, radiation-damage centres, e.s.r. obs. 9-13697
- BaSO<sub>4</sub>, barite, rel. to etch patterns 9-13594
- BaTiO<sub>3</sub>, paraelectric, thermocurrents rel. to point defects 9-5756
- BaTiO<sub>3</sub>, point defect conc. rel. to resistivity and sintering kinetics 9-1589
- BaTiO<sub>3</sub> with additions of Fe, Co and Ni, H-reduced, defect structure 9-1207
- Be, irradi. induced, prod. and recovery, study by elec. resistivity and stored energy meas. 9-16091
- Be,  $n$  irradiated at 4.2°K, damage and recovery up to 350°K from elec. resist. meas. 9-5578
- BeO, inversion twin boundaries, X-ray diffr. contrast 9-3356
- Bi-Sb alloys, grain boundary creep, internal friction obs. 9-16104
- CdS, stacking faults, Hg diffusion-induced 9-7496
- CdS plate-shaped crystals, inclusions and Si contamination, electron microprobe and e microscope investig. 9-5343
- Co<sup>2+</sup>, in ZnS, spectra, bond nature eff. in stacking faults 9-1796
- CoO, heats of formation of point defects 9-17276
- Cu-Ag alloys, stacking faults growth, rel. to precip. 9-11958
- Cu-Al alloy, stacking faults, cubic type, in plastically deformed martensite 9-16103
- Cu-He alloys, grain boundary degeneration rel. to stress-rupture characts. 9-16133
- Cu-Mn solid solutions, stacking fault energies 9-7492
- Cu-Si alloy, stacking fault energy meas., composition and temp. dependence 9-11887
- Cu-Su alloys, grain boundary segregation, electron microprobe obs. 9-5378
- Cu-(30 at.wt%)Zn alloy, deform. faults, shock-induced 9-13681
- Cu, deformation in easy glide 9-5373
- Cu, electron displacement damage 9-3334
- Cu, electron irradiated, stage III recovery behaviour 9-13671
- Cu, grain boundaries migration rel. to dragging of small oxide particles 9-1233
- Cu, p-irrad., point defects stress-induced near 10°K 9-9755
- Cu, point defect states, infl. on irradiation damage rate, 80°K 9-3329
- Cu polycrystalline, stacking fault conc. rel. to quenching of defects 9-9774
- Cu polycrystalline, stacking fault energy calc. from stress/strain drag, during plastic deformation 9-1284
- Fe-C solid soln., point defects studied by mag. after-effect meas. 9-5333
- Fe-6.5%Si, rel. to  $n$  induced mag. viscosity, obs. 9-19952
- $\alpha$ -Fe, dipolar strains of C and N 9-9739
- Fe, high-purity, deformation-produced defect network elimination 9-9697
- Fe,  $n$  irradiated, defects, saturation and exposure depend. 9-11929
- FeO, heats of formation of point defects 9-17276
- Fe-C solid solutions, elec. resistivity study 9-19891
- n-GaAs, <sup>60</sup>Co  $\gamma$  irradiation induced 9-13875
- GaAs, structural defects rel. to Kikuchi line anomalies 9-18445
- GaAs<sub>1-x</sub>P<sub>x</sub> epitaxial layers on GaAs defect distrib. in Zn diffusion front 9-14895
- GaSb, undoped, e-irrad. damage, orientation and energy dependence 9-5334
- Gd, e. and  $n$ . irradi. produced point defects and recovery 9-11870
- Ge-Cu,  $n$ -irrad. induced defects generation rate, effect of impurities and dislocations 9-5335
- Ge-As solid soln., defect appearance during decay 9-14937
- Ge, defect formation and annealing on Xe ion bombardment, e. emission exam. 9-18662
- n-Ge, electron damage, orientation and temp. depend. 9-13672
- n-ge, grain boundaries, optical absorpt. obs. 9-21623
- Ge,  $n$ -irrad. induced defects, small-angle X-ray scatt. exam. 9-5331
- Ge, neutron irradiated, electron microscopic obs. 9-16090
- Ge, point defects, dilatometric study at thermodynamic equilibrium 9-3331

**Crystal imperfections continued**

- n-Ge, radiation annealing and modification of 35° and 65°K defects at 7°K 9-9695
- Ge, radiation defects, enhanced diffusion study 9-13705
- Ge, thermal defects conc., inf. of dislocation density 9-5346
- Ge wafers, X-ray diffraction topography 9-9677
- In-Tl martensitic alloys, stacking faults as twin nuclei during deformation 9-13728
- InP, epitaxial films, stacking disorder 9-9617
- InP clean surface, photoelec. yield near threshold 9-16319
- InSb, defect structure from X-ray topography 9-1208
- KBr, defects, rel. to nucleation 9-18425
- KBr, volume change due to point defects after X-irrad. 9-18460
- KCl, defects, rel. to nucleation 9-18425
- KI, u.v. irradi., defect formation 9-14952
- Li defect complex in e irradi. Si, i.r. spectroscopic study 9-13673
- LiF,  $\gamma$ -irrad., point defects annealing 9-19821
- LiF and LiF:Mg<sup>2+</sup> effect of defects on mech. props. 9-1257
- Mg (3 wt.%)Zn alloy, clustering kinetics and precip. 9-5505
- Mg, plastically deformed, generation and recovery, from elec. resist. meas. 9-7478
- Mn-Fe spinel, effect of Mn<sup>3+</sup> clusters on physical props. 9-1206
- MnO, heats of formation of point defects 9-17276
- NH<sub>4</sub>ClO<sub>4</sub> thermal decomposition, role of point defects 9-20033
- NaCl:Mn<sup>2+</sup>, impurity-vacancy assoc. from ionic conductance and diffusion meas. 9-1202
- NaCl, complex boundaries, barrier effect 9-19755
- NaCl, defects, rel. to nucleation 9-18425
- Nb-Ti(VZr) alloys, rel. to deformation effects, X-ray powder diffraction study 9-11930
- Ni-Al<sub>2</sub>O<sub>3</sub> system, grain boundary grooving at interface, kinetics const. 9-1251
- Ni, fast  $n$  irradi., voids,  $5 \times 10^{19}$  n/cm<sup>2</sup> 9-7499
- Ni, high-purity, deformation-produced defect network elimination 9-9697
- Ni, lattice microdistortions rel. to ferromag. reson. line width variation during plastic deform. and annealing 9-14103
- Ni,  $n$  irradi., small-angle X-ray scatt. from voids, obs. 9-9718
- Ni alloys, rel. to self-diffusion of Ni from autoradiographic obs. 9-9707
- Ni<sup>2+</sup> in ZnS, spectra, bond nature eff. in stacking faults 9-1796
- NiO, heats of formation of point defects 9-17276
- NiO, high temp. defect. struct. 9-3571
- NiO films, eff. of structural defects on growth 9-9621
- Pb, impurity-drag eff. on grain growth 9-11888
- Pb stacking fault energy calc. 9-5375
- Pt quenching and radiation doping 9-7479
- Pt black catalysts, stacking faults and stored energy rel. to activity 9-5325
- Ru, deformed, domain size distrib. from X-ray line profiles 9-7447
- n-Si, e. irradi., defect reorientation, stress-induced, obs. by photoconductivity meas. 9-21340
- Se<sub>2</sub>O<sub>3</sub>, elec. conductivity dependence, 700 1600°C 9-1583
- p-Si:B,  $\gamma$ -irrad., radiation defects in recombination 9-3665
- Si:B, P, radiation defects, kinetics of thermal annealing 9-21327
- Si:Cu,  $n$ -irrad. induced defects generation rate, effect of impurities and dislocations 9-5335
- Si:P, A and E centres, influence on minority-carrier density dependence on neutron dose 9-1549
- Si:P, point defects and microhardness, reln. 9-5486
- Si, divacancy-associated energy levels: photoconductivity study 9-3327
- Si, effect of defects on channelling of P ions 9-9708
- Si, irradiated by 15 to 45 MeV electrons, defect cluster formation 9-17400
- Si, neutron bombard, activation energy  $1.2 \pm 0.1$  eV obs. 100-156°C 9-17275
- Si, p-irrad., fringe contrast on X-ray topograph, application of Takagi's dynamic theory 9-3354
- Si, paramagnetic stacking faults causing one line in e.p.r. spectrum 9-1862
- Si, stress patterns on X-ray micrographs, analytical description 9-11873
- Si, structural defects rel. to Kikuchi line anomalies 9-18445
- p-Si  $n$  irradiation induced defect clusters from Hall effect and conductivity meas. at 76°K 9-17401
- Ta<sub>2</sub>O<sub>5</sub>, stacking faults bounded by partial dislocations 9-9714
- $\alpha$ -Ti, grain size effect on deformation dynamics 9-3420
- Ti alloys, rel. to self-diffusion of Ni from autoradiographic obs. 9-9707
- TiO, heats of formation of point defects 9-17276
- TiO<sub>2</sub>, domain boundaries and stacking faults 9-5376
- $\alpha$ -U, radiation defects and Matthiessen's rule 9-16089
- U, void formation during thermal cycling between 400 and 600°C 9-19771
- UO<sub>2</sub> fuel pellets, after irradi., defects, gas bubbles and grain growth 9-11856
- UO<sub>2</sub>, s, defect ordering and temp. dependence, statistical model 9-1203
- V, point defects, rel. to elec. resistivity recovery peak 9-11871
- VO, heats of formation of point defects 9-17276
- W, stacking faults, from field-ion micrograph analysis 9-9717
- YFe garnet, growth defects effects on domain structure 9-12302
- Zn, slope of etch pits 9-21341
- ZnS:Co(Ni), bond nature effects in stacking faults 9-1796
- ZnS:Co(Ni), in stacking faults, effect on spectra 9-1796
- ZnS, influence on I V characts. and built-in field formation 9-15093
- ZnS, twist boundaries and rotational slip 9-5348
- Zr (2.7 wt.%) Nb, irradiation strengthening, effect of Nb 9-5479
- ZrO<sub>2</sub>, dependence of elec. conductivity, ionic conduction and thermoelec. power, 800-1600°C 9-3703

**dislocations**

- aa Ag, loops, dissociation during plastic deformation forming stacking fault tetrahedra 9-3343
- alkali halide, movement in bending deform. rel. to elec. field production 9-1453
- alkali halides, presence with dissociated cores, compatibility with pressure effect 9-18503
- alloys, f.c.c., motion rel. to solid soln. strengthening 9-7598
- anisotropic, analytic solns. for stress fields 9-7481
- annealed from vacancies, kinetics 9-16092
- annealed from vacancies, kinetics 9-13678
- atomic displacements around loops 9-14942
- b.c.c. metals, field-ion microscopic contrast from partial dislocations 9-18465
- $\alpha$  brass, stress dependence of dislocation velocity 9-5358

**Crystal imperfections continued**  
**dislocations continued**

- brittle crack propagation mechanism 9-19810  
charge-carrier mobility in m.o.s. inversion layers misfit disloc. consideration 9-3339  
continuum theory, constitutive and strain compatibility eqns. 9-11878  
continuum theory, geometry and boundary conditions 9-16097  
contrast in field-ion images: origin of cross-over effect 9-11877  
corundum, motion, microscope obs. using decoration method 9-1215  
and cracks, fatigue, micro scope rel. to cryst. orientation 9-5481  
cyclotrimethylene trinitramine, solution grown, etching for habit faces 9-18475  
dechanneling effect on particle, cylinder simulation 9-12033  
density determining factors during growth by Czochralski method 9-3338  
detection technique using  $K_{\alpha}$  X-radiation for axial screw dislocations in whiskers 9-14944  
dipole in half-space, stability 9-5354  
dissociated, pile-up, and strength-grain size relationship 9-18464  
dissociated perfect, in field ion image 9-16100  
dynamics and impact response 9-21336  
edge, correlated and uncorrelated diffusion 9-9724  
edge dipole clusters, transient work hardening phenom. 9-1322  
edge dislocation strain field analysis 9-3341  
electron microscope technique, error rel. to diffraction vector assumption 9-18469  
escape from bound states by tunneling 9-14943  
f.c.c. and b.c.c. crystals, generalized splittings 9-21337  
f.c.c. metals, glide dissociation into Shockley partials, energy changes 9-11874  
f.c.c. metals, split width, eff. of surface-active additions 9-13683  
ferromagnet, effect of local and quasilocal levels (due to dislocation) on magnetization 9-1673  
field ion microscope, problem interpretation 9-3340  
fine structure of electron diffraction spots 9-13620  
fracture markings, transverse, generated by unsteady cleavage velocities 9-1211  
glide-dislocation arrays, coaxial circular associated stress fields 9-5351  
grain boundaries in generation mechanism 9-19747  
grain boundary glide mechanism caused by dislocation motion 9-3357  
h.c.p. metals,  $c^+$  +  $a^-$  reactions 9-13685  
hexagonal metals, description using 3-index and cartesian coordinate system 9-3342  
interacting segments in long-wave approximation, vibrational spectrum 9-16095  
interaction with rad. induced point defects, rel. to damping and internal friction 9-7525  
jogged screw, thermally activated motion, creep mechanism 9-5356  
in Kirkendall effect mechanism 9-19762  
lineage structures, origin and growth, melt-grown crystals 9-1225  
loop motion in ionic crystal subjected to ext. elec. field 9-11875  
loops, conversion from depletion zones 9-7480  
loops, self stresses and line tensions 9-19748  
metal f.c.c. crystal, secondary, in plastic deform., sources 9-11879  
metals, electronic component of dislocation drag 9-13684  
metals, infl. on elec. resistivity and galvanomagnetic effect 9-12095  
metals, low-density, growth techniques 9-21295  
mobility in internally stressed solid 9-7483  
mobility of groups, stress driven 9-11876  
Moire fringe pattern 9-13617  
moving edge, width, calc. with Nabarro force law 9-7482  
node size meas. in stacking fault energy meas. 9-13694  
non-screw, dissociation in b.c.c. lattices 9-18467  
parallel edge, self-vibrations 9-3355  
partial twinning, obs. of sources and reactions on X-ray topographs 9-7484  
pile-up in non-uniform stress fields 9-5352  
pinning of impurity atoms, distribution funct. for time depend. of amplitude dependent internal friction 9-5426  
planar arrays, continuous and discrete distribution, analyses 9-1212  
plates with notches and holes, dislocation singularities rel. to stress and strain 9-5440  
polygon displacement field 9-3337  
quartz, in u.s. induced enhancement of Raman spectra 9-21636  
random distribution causing internal stresses 9-5447  
randomly distributed in infinite elastic anisotropic medium, fields 9-2193  
Rochelle salt, effect on dielec. props. 9-7486  
screw, dynamic atomic model 9-9711  
slip trace analysis in e. microscope and foil thickness determ. without specimen tilt determ. 9-7330  
solid solutions, multi-component substitutional, resistance to motion, effect of short-range order 9-9709  
spin-wave scatt., in ferro- and antiferromagnetic crystals 9-3782  
split, starting stress in superstructure 9-14941  
steel, austenitic stainless, rel. to Widmannstätten  $M_{23}C_6$  precip., nucleation and growth 9-1331  
steel, martensitic, interaction with carbon 9-1218  
steel, N36KH12TYU, produced on deform. ageing 9-3347  
steel, transformer, single crystals, structure, depend. of coercive force 9-13988  
steel, V, tempering, high dislocation density as preferential nucleation sites 9-17328  
stress field in inhomogeneous, anisotropic medium 9-3336  
stress fields, anisotropic media, analytic solns. 9-7481  
superdislocation behaviour in work hardening 9-13758  
superdislocation blocking in superstructure  $L1_2$  9-9710  
superdislocations, stability of antiphase boundary tubes 9-7485  
tilt boundary-edge disloc. interaction 9-16096  
in twin lamellas, small static, numerical analysis of deformation behaviour 9-14950  
velocity, pinning centre conc. and shear stress dependence, statistical analysis 9-1209  
vibration and phonon scattering 9-3502  
wave scattering, micromag. calc. for ferromag. resonance 9-12492  
wedge, counterpart of deformation twin 9-18466  
wedge-like twinned layers, shape rel. to dislocation density 9-19753  
X-ray diffraction, method of moments, applic. 9-13618  
Ag-Au diffusion couples, in Kirkendall effect mechanism 9-19762  
Ag, diffusion of In, temp. dependence, 180-100°C 9-3375  
AgCl single crystals, slightly bent, annealing behaviour, rel. to sub-structure 9-5497

**Crystal imperfections continued**  
**dislocations continued**

- Al-Mn alloys, multi-faulted loops, formation and annealing 9-13686  
Al-(78 wt.%)Zn alloy, rel. to superplastic deformation 9-21370  
Al, densities and configuration rel. to stress 9-21338  
Al, fatigued, form of patches and loops 9-5347  
Al, loops, climb kinetics 9-11880  
Al, recovery eff. on density and cell structure 9-13687  
Al, theory of intersections rel. to strain rate history 9-18498  
Al, viscous drag at high strain rate, 10°K, 77°K, 300°K and 500°K 9-1214  
Al<sub>2</sub>O<sub>3</sub> (0.25wt.%) MgO, hot-pressed deformed, and grain boundary sliding obs. 9-3359  
Al<sub>2</sub>O<sub>3</sub>, hot-pressed deformed, and grain boundary sliding obs. 9-3359  
Al alloy, commercial, impurity-dislocation interaction rel. to repeated yielding (Portevin-Le Chatelier effect) 9-11925  
Al<sub>2</sub>O<sub>3</sub> rel. to fracture 9-1305  
Au-Cu alloy on Au, two-layer films, misalignment 9-3200  
Au, electron irradiated at low temp., pinning, rel. to internal friction changes 9-11912  
Au, loops, dissociation during plastic deformation forming stacking fault tetrahedra 9-3343  
AuCu type alloy, ordered, superdislocations 9-1216  
 $\alpha$ -U, energies and easy glide parameters rel. to slip systems 9-1226  
BaF<sub>2</sub>, impurity precipitation, display by selective etch methods 9-13680  
BaSO<sub>4</sub>, synthetic, cleavage face dislocation structure from etching 9-1127  
BaTiO<sub>3</sub> whiskers, axial screw dislocations, detection using  $K_{\alpha}$  X-radiation 9-14944  
CaCO<sub>3</sub>, repeated reciprocal motion, initial fatigue stages 9-18468  
CaF<sub>2</sub>, edge-disloc. mobility stress temp. dependence 9-14945  
Cd, single, slip relation for basal glide, primary and secondary 9-3345  
GaAs Czochralski growth method 9-3348  
Co films grown on Ni, associated stacking faults 9-7341  
Cr, redistribution during annealing and deformation 9-13688  
CsI, impurity additions effect on rosette ray length and dislocation velocity 9-18514  
Cu:Pt(Pd) impurity atoms effect on frictional force 9-3397  
Cu:Zn, arrangements arising from Zn diffusion, etch-pit exam. 9-5359  
Cu-Au alloys, formation during ordering, e. microscope exam. 9-11881  
Cu-Ga single crystal, deformed, disloc. layer parallel to glide plane at transition from stage I to II 9-13760  
Cu-Si alloy, node size meas. in stacking fault energy determ. 9-11887  
Cu, deformed, arrangement in stress-applied state, electron microscope obs. 9-14946  
Cu, density growth during homogenization quenching 9-1217  
Cu, dislocation-phonon interaction, contribution to u.s. attenuation 9-9830  
Cu, easy glide, rel. to deform. 9-5373  
Cu, fatigue-hardened foils, loss and rearrangement, effect of neutron irradiation 9-11882  
Cu, in fatigue hardening mechanisms 9-13737  
Cu, loops, dissociation during plastic deformation forming stacking fault tetrahedra 9-3343  
Cu, pinning, activation energies meas. using electron irradiation at 78°K 9-5360  
Cu, visibility, effect of degree of deviation from Bragg condition 9-13689  
Cu coldworked crystals, invest. by small angle scattering of sub thermal neutrons 9-3346  
Cu matrix, interaction with coherent Co particles 9-1213  
Cu polycrystalline, in plastic deformation controlling mechanism 9-1284  
Cu rods, cold worked, disloc. arrangement 9-9712  
Cu<sub>2</sub>Au, superdislocation behaviour in workhardening 9-13758  
CuO, motion rel. to microhardness anisotropy obs. 9-3454  
Fe-(23 at.%)Be alloy, network formation during ageing, transmission e. microscopy study 9-17343  
Fe-Si, network eff. on plastic strain 9-16098  
Fe-Si, structure, rel. to coercive forces and mag. susceptibility 9-16360  
Fe-Si alloys, velocity stress dependence, temp. and comp. effects 9-7488  
Fe-(7.5 at.%) Si creep rate control by thermally activated screw dislocations 9-5402  
Fe, a <1007> field-ion microscope evidence for existence 9-5361  
Fe, Armo, structure and peculiarities of viscous crack development 9-3450  
Fe, deformed, recovery mechanism models 9-18470  
 $\alpha$ -Fe, dislocation visibility, error in electron microscope technique 9-18469  
Fe, false peaking causing damping near Snoek peak 9-9749  
Fe, high purity, dissolution in stress-corrosion cracking in  $NH_4NO_3$  soln. 9-14981  
Fe, produced by strain, two beam dark field electron micrographs 9-7539  
Fe, rel. to strain rate depend. of resistance to plastic deform. 9-9759  
Fe, vel. from electron microscope obs. 9-10823  
Fe interaction with impurities 9-5353  
GaAs, removal of dislocations., props. 9-16099  
GaAs epitaxial layers, using selective etching 9-1219  
GaF<sub>3</sub>, structure around indentation 9-5357  
GaP, before and after electric erosion 9-5350  
GaP, etch pits 9-14947  
Gd climb due to thermal diffusion 9-3349  
Ge:Cu, effect on n-irrad. induced defect generation rate and spectral levels 9-5335  
Ge, band model for carrier mobility after deformation 9-18628  
Ge, band structure from radiative recombination 9-15183  
Ge, before and after electric erosion 9-5350  
Ge, charge transport in low angle grain boundaries 9-3657  
Ge, density infl. on thermal defect conc. 9-5346  
Ge, rel. to l.f. damping 9-5432  
Ge dislocations and dislocation diodes, bilateral microscopy 9-7806  
Ge monocrystal, space charge display by scanning e beam 9-7390  
Ge ribbons, distrib. 9-1227  
HgTe, formation during annealing in Hg vapour 9-1220  
HgTe, surface, from etch pits on differently oriented crystals 9-9639  
InAs-Cu(Au,Ag) solid solutions, effect on precipitation 9-11967  
In<sub>2</sub>O<sub>3</sub>, in growth mechanism from PbO-B<sub>2</sub>O<sub>3</sub> melt rel. to habit changes 9-17257  
InSb, and other defects from X ray topography 9-1208  
p-InSb, density increase, infl. on temp. dependence of Hall coeff., elec. conductivity and carrier mobility 9-3631  
p-InSb, eff. on electrical props., 50° to 200°K 9-21505  
InSb, velocity 9-7489  
Ir, dissociated perfect, in field-ion image 9-16100



**Crystal imperfections continued**  
**dislocations continued**

- Ir, Schockley loops, glissile, occurrence in field-ion specimens 9-5362  
 K:Al<sub>2</sub>(SO<sub>4</sub>)<sub>3</sub>.24H<sub>2</sub>O (potash alum.), direct obs. 9-11883  
 KBr decoration and dislocation conduction 9-3355  
 KCl:Ba<sup>2+</sup>, mobility and yield point, temp. depend. 9-5363  
 KCl:(Cu), behaviour on applied stress from X-ray luminescence exam. 9-3932  
 KCl:Pb, macrodislocations in single slip line 9-14948  
 KCl, deformed, processes during creep and heating 9-1223  
 KCl, effects on anomalous X-ray transmission 9-1746  
 KCl, melt-grown crystals, low density 9-16101  
 KCl, photomobility in irradiated crystals 9-21548  
 KCl etching soln. for revealing 9-1221  
 LiF, behaviour during dynamical cleavage 9-13741  
 LiF, depletion mechanism region of action, effect of u.s. radiation 9-9764  
 LiF, mobility, n irradi. eff. 9-11885  
 LiF, slip band structure during annealing 9-11886  
 LiF, structure after slip deformation 9-5364  
 LiF, structure formation near surface during annealing 9-11884  
 LiF, u.s. deformed, role in internal stress behaviour 9-16128  
 LiF motion in electric field 9-5365  
 Mg foils, growth from oxidation vacancies, struct. obs. by e. micro. 9-18471  
 MgO, motion rel. to microhardness anisotropy obs. 9-3454  
 MnFe<sub>2</sub>O<sub>4</sub>, structure from etch pits 9-3231  
 Mo, redistribution during annealing and deformation 9-13688  
 Mo, structure and multiplication of disloc. during thermal cycling 9-5366  
 Mo, velocity temp. dependence 9-7490  
 NaCl: Sr<sup>2+</sup>, velocity 9-1222  
 NaCl, deformed, processes during creep and heating 9-1223  
 NaCl, edge, core-structure, core-energy and Peierls-stress, atomic calc. 9-13690  
 NaCl, edge and screw for mixed boundary, barrier eff. 9-19755  
 NaCl, edge dislocation, abrupt jog energies 9-18473  
 NaCl, edge dislocation kinks, born model calc. 9-18472  
 NaCl, effect on evaporation rates 9-11751  
 NaCl, Gyulai-Hartly interaction affecting ionic cond. 9-12194  
 NaCl, intergranular substructure, formation during growth from melt 9-21296  
 NaCl, movement in electric field 9-3350  
 NaCl crystals, deformed along cube plane, etch pits 9-5367  
 NaNO<sub>2</sub>, ferroelec., etching rel. to polarization 9-15125  
 Nb-Ti alloy, structure after annealing at 1250-1500°C 9-5368  
 Nb-Ti(V)(Zr) alloys, rel. to deformation effects, X-ray powder diffraction study 9-11930  
 Nb single crystals, relaxations 9-3351  
 Ni, structure, rate of loading effects, e. microscope exam 9-3352  
 Ni foil, interstitial Frank dislocation loops after n and e irradi. 9-3326  
 Ni<sub>3</sub>Fe, superdislocation behaviour in workhardening 9-13758  
 NiO, motion rel. to microhardness anisotropy obs. 9-3454  
 Sb, motion mechanism during etching 9-13691  
 Si-Cu, effect on n-irrad. induced defect generation rate and spectral levels 9-5335  
 Si, before and after electric erosion 9-5350  
 n-Si, dislocation acceptor level energy, from dislocation vel. obs. 9-9713  
 Si, edge, effect of contamination on elec. props. 9-5712  
 Si, electron states at dislocations 9-16274  
 Si, epitaxial layers, partial screw dislocations, obs. 9-5369  
 Si effect on elec. conductivity 9-1548  
 Si monocrystal, space charge display by scanning e beam 9-7390  
 Si single crystals, generation and concentration during growth 9-1224  
 SiC, screw clusters rel. to Frank's growth mechanism 9-18477  
 strain produced, two beam dark field electron micrographs 9-7539  
 TaC<sub>0.75</sub>, bounding stacking faults 9-9714  
 Ti-(47 wt.%)Nb alloy, superconducting props., changes attributed to formation of Ti atom clusters on dislocations 9-13865  
 α-U, parameters rel. to slip modes 9-1228  
 V steel, high density as preferential nucleation sites for hardening on tempering 9-17328  
 W, 'horseshoes' in field-ion micrographs 9-9715  
 W, n irradiated and annealed, vacancy loops 9-7491  
 W, redistribution during annealing and deformation 9-13688  
 Zn, basal slip, incorporation in {1012} twins 9-18474  
 Zn, chemically attacked, Berg-Barrett X-ray obs. 9-19749  
 Zn, mobility in {1122} <1123> slip system 9-5371  
 Zn, single, slip relation for basal glide, primary and secondary 9-3345  
 ZnS, density, by X-ray oscillating film method, crystals from melt under 50 atm. pressure 9-5329  
 ZnS, pinned dislocations oscillations causing internal friction 9-5429

**impurities**

- alkali halides: divalent cations, impurity-vacancy-dipole agglomerate and precip. 9-5372  
 alkali halides, OH<sup>-</sup> ion conc. from u.v. absorpt. spectra 9-7374  
 alkali iodides, e.s.r. of trapped O<sup>-</sup> 9-10289  
 alkaline earth oxides, review 9-9693  
 aluminium bronze, As-containing, CuAl<sub>5</sub>-type, fatigued, effect on stacking fault tetrahedra 9-19752  
 anthracene crystal doped with tetracene as a hole trap 9-7376  
 Coulomb interactions between two impurity charges in an atomic dielectric 9-7831  
 decay modes with coherent resonant energy transfer between deep impurities 9-9889  
 defect centres and role in bulk props. of crystals 9-20001  
 diamond, one-phonon band-mode i.r. absorption by impurity resonances 9-5915  
 diamond lattice, diffusion mechanism, correlation factor calc. 9-21346  
 diffusion in α-Zr 9-3389  
 Fe, interaction with dislocations 9-5353  
 force-constant changes, effect on incoherent n. scatt. 9-9822  
 ice, dissolved impurities effect on mechanical props. 9-13711  
 inclusion, two-dimensional, circular 9-18463  
 ionic transport, five defect model 9-13914  
 linear molec. crystals, impurity electronic states 9-9888  
 magnetically coupled, in Heisenberg linear chain ferromagnet 9-16338  
 metal, residual elec. resistance detection 9-17377  
 metals, energy spectrum and props., numerical analysis 9-3552  
 metals with paramagnetic impurities, electron interaction effects 9-9876  
 minerals, liquid-CO<sub>2</sub> bearing inclusions, mass spectra, microscope exam. and geochemistry 9-14940  
 molecular cryst., diagonalization of exciton Hamiltonian 9-16215

**Crystal imperfections continued**  
**impurities continued**

- molecular cryst. with complicated elementary cell, impurity molecule, discrete states 9-1205  
 optical spectra, local oscillations and broadening of phonon-free lines 9-7961  
 paramagnetic, in superconductors, electron interaction, effect on transition temp. and gap 9-1476  
 quartz, elastic consts., temp. depend., impurity eff. 9-5424  
 Raman scattering in impurity-containing crystals microscopic theory 9-12402  
 Raman scattering in solids, impurity induced 9-12401  
 semiconductor, effect on electron energy spectrum 9-15095  
 silica, vitreous, effect on ionizing radiation induced dilation 9-14961  
 silica, vitreous, ion conc. effect on acoustic props. 9-15001  
 solid solns., Al-, Ag-, Au- and Zn-rich, vacancy-impurity binding energies 9-9698  
 solid solutions, -drag effect rel. to grain growth kinetics 9-5342  
 trace, effect on X ray diffraction 9-7475  
 Xe, bombardment temp. effect on trapping in oxides and halides 9-19746  
 Al alloy, commercial, impurity-dislocation interaction rel. to repeated yielding (Portevin-Le Chatelier effect) 9-11925  
 Al and alloys, role in stage II and III recovery after 2-MeV e. irradi. 9-9696  
 Al in diamonds, participation in i.r., u.v., and visible absorption spectra 9-19987  
 alkali halides: CN<sup>-</sup> (OH<sup>-</sup>, NO<sub>2</sub><sup>-</sup>), Raman spectra 9-12407  
 B, in artificial diamonds, effect on phosphorescence and thermoluminescence 9-21651  
 BaF<sub>2</sub>, precipitation at dislocations, display by selective etch methods 9-13680  
 Ba(NO<sub>3</sub>)<sub>2</sub>, effect on permittivity and loss-angle tangent 9-1575  
 CN<sup>-</sup> in alkali halides, Raman spectrum 9-12407  
 CaF<sub>2</sub>-SrF<sub>2</sub> mixed crystal, Raman scattering from point defects 9-12408  
 CdS: Au: Sn, diffusions solubility, vapour press. investigation 9-3380  
 CdS plate-shaped crystals, Si contamination and inclusions, electron microprobe and e microscope investig. 9-5343  
 ClO<sub>4</sub><sup>-</sup> in alkali halides, symmetry at temps. 300-700°C from i.r. absorpt. temp. dependence 9-18704  
 Cr, gaseous impurity effect on brittleness temp. threshold 9-1309  
 CsI, effect on strength 9-18514  
 Cu, effect on internal friction peak P<sub>1</sub> 9-7528  
 Fe, alloying additions effect on strength, dislocation density and recrystallization 9-11962  
 Ga in HgTe, effect on h.p. phase transition 9-11966  
 GaAs, atom interaction at Cu diffusion 9-17286  
 Gd, phase transitions, high order, effect near T<sub>c</sub> from thermal expansion data 9-1399  
 Ge:As, impurity-vacancy complex formation kinetics 9-9992  
 Ge:Cu, effect on n-irrad. induced defect generation rate and spectral levels 9-5335  
 Ge:In(Tl,Sb,Bi,Pb) dopant lattice location by C ions backscattering technique 9-18629  
 Ge, electrically active, infl. on plastic deformation 9-18505  
 n-Ge, neutron irradiated, photoconductivity kinetics 9-10072  
 HgTe, effect of Ga on h.p. phase transition 9-11966  
 In-Hg(Cd) dilute alloys, In phonon spectrum, effect of Hg (Cd) impurities 9-5533  
 KBr: impurity defects, far i.r. absorpt., discontinuities obs. 9-19990  
 KBr, distrib. coeff. during zone melting 9-3239  
 KCl-KBr solid solns., removal of divalent cations by introduction of anions 9-16053  
 KCl, (I)<sup>+</sup>-centre, lattice distortion and binding energy 9-3333  
 KCl, distrib. coeff. during zone melting 9-3239  
 KH<sub>2</sub>PO<sub>4</sub>:Cu<sup>2+</sup>, chem. structure from e.p.r. spectra 9-1860  
 KI, removal by double and zone-melting recrystallization 9-3240  
 LiF, growth conditions and effects on density 9-1133  
 LiNO<sub>3</sub>, effect in permittivity and loss-angle tangent 9-1576  
 LiTa(Nb)O<sub>3</sub>, rel. to reduction in laser-induced refractive index inhomogeneity 9-5870  
 Mo, distrib. in single crystals obtained by electron beam zone melting 9-5344  
 Mo, gaseous impurity effect on brittleness temp. threshold 9-1309  
 NO<sub>2</sub><sup>-</sup> in alkali halides, Raman spectrum 9-12407  
 NaBr, distrib. coeff. during zone melting 9-3239  
 NaCl:Mn<sup>2+</sup>, impurity-vacancy assoc. from ionic conductance and diffusion meas. 9-1202  
 NaCl, distrib. coeff. during zone melting 9-3239  
 NaCl, effect of Ca<sup>2+</sup> on evaporation rates 9-11751  
 NaI:Cl<sup>-</sup> anharmonicity assoc. with reson. mode by Stark effect 9-7637  
 Ni-W solid solns, impurity atom causing distortion of matrix lattice 9-5345  
 OH<sup>-</sup> in alkali halides, Raman spectrum 9-12407  
 PbTe, donor and acceptor, effect on microhardness 9-1316  
 Pt:Cu, n. scatt. for defect mode detection at 300, 570, 930°K 9-7476  
 Sb, effect on i.r. absorpt. edge of Te 9-18711  
 Si:As(Sb), irradi., impurity-vacancy pairs, e.p.r. and endor exam 9-5341  
 Si-Cu, effect on n-irrad. induced defect generation rate and spectral levels 9-5335  
 Si, atom impurity distribution meas. by differential capacitance technique 9-3664  
 Si, Au, doped, conductivity and lifetime of excess carriers anomaly 9-16273  
 Si, contamination of edge dislocations, effect on elec. props. 9-5712  
 Si, one-phonon band-mode i.r. absorption by impurity resonances 9-5915  
 Ti, surface impurity effects in pore formation in welds 9-16146  
 W, gaseous impurity effect on brittleness temp. threshold 9-1309  
 Zn<sup>2+</sup>-vacancy complex formation, free energy of association determ. from solubility data 9-17277  
 ZnS, distribution of Fe, Cu and Ag in crystals grown from melt 9-18429

**interstitials**

- diffusion, quantum effects 9-3370  
 distribution near interface in ion crystal 9-17274  
 ferromagnet, spin-wave theory 9-5809  
 graphite, after neutron irradi., rel. to lattice parameter changes 9-7471  
 graphite, pyrolytic, loop prod. at twist boundaries on neutron irradi. 9-7472  
 point defect, neutron scatt. cross-section in a relaxed lattice calc. method 9-19741  
 semiconductors, formation of Frenkel pairs under hard radiation 9-3328

**Crystal imperfections continued**  
**interstitials continued**

- structure, energies and mobilities review 9-13676
- vacancy-interstitial reactions in f.c.c. lattice, diffusion controlled, unified formalism 9-1201
- Al and alloys, role in stage II and III recovery after 2-MeV e. irradi. 9-9696
- Au-Pb alloys, sites from e. emission angular distrib. of activated mat. 9-3332
- Au atoms, annealing by Ar<sup>+</sup> irradi. 9-1267
- C<sub>2</sub> mol. in graphite lattice, self-energy and deform. 9-7407
- Ca<sup>19</sup>F<sub>2</sub>:Ce<sup>3+</sup>, Yb<sup>3+</sup>, presence of F<sup>-</sup> confirmed by ENDOR OBS. 9-8045
- CdS intrinsic optical absorption spectra 9-3887
- C atoms in soft carbons, rel. to classification of cokes 9-7473
- C<sub>5</sub>ZnCl<sub>3</sub>:Fe<sup>2+</sup>, dopant sites from e.s.r. 9-8025
- Cu, formation on  $\gamma$ -irrad, effect on lattice parameters 9-1186
- Cu, Frenkel pairs, e-irrad. induced, effects of annealing 9-3330
- Cu, infl. on irradiation damage rate, 80°K. 9-3329
- Cu, lattice distortion produced by interstitial Cu atom, lattice statics calcs. 9-13679
- Ge:In(Tl,Sb,Bi,Pb) dopant lattice location by C ions backscattering technique 9-18629
- Ge, Frenkel defects, dilatometric study at thermodynamic equilibrium 9-3331
- Ge thermal defects, conc., migration and annealing, dislocation density influence 9-5346
- H impurities in V and Ta, effect on elastic props. 9-21334
- KCl, X-ray induced, optical absorpt. meas 9-18462
- Mo, formation on  $\gamma$ -irrad., effect on lattice parameters 9-1186
- Mo, impurity content effect on stresses for favorable orientation 9-5452
- Ni-Cu alloys, interstitial H occlusion 9-12728
- Ni, formation on  $\gamma$ -irrad, effect on lattice parameters 9-1186
- n-Si:P,  $\gamma$ -irradiated, rel. to thermal donor formation 9-21333
- n-TiO<sub>2</sub>, doped, e.p.r. exam. 9-9704
- TiO<sub>2</sub>, doped, from optical and elec. props. 9-9706
- TiO<sub>2</sub>, Li<sup>+</sup> diffusion 9-9705
- $\alpha$ -U rel. to neutron-induced growth mechanism 9-19870
- UO<sub>2+x</sub>, oxygen ions, in stable association with oxygen vacancies and U<sup>5+</sup> ions 9-1203
- W, e. irradiated at 240 MeV, and 10 Å cavity conc. 9-1204

**vacancies**

- alkali halides; divalent cations, impurity-vacancy-dipole agglomerate and precip. 9-5372
- annealed to dislocations, kinetics 9-13678
- annealed to dislocations, kinetics 9-16092
- b.c.c. crystals, relaxations 9-9702
- binary crystals, ordering theory 9-21303
- coalescence nonstationary homogeneous 9-11872
- diamond, optical absorption by neutral vacancy 9-10194
- diamond lattice, rel. to correlation factor for impurity diffusion 9-21346
- diffusion, from scattering theory 9-7470
- distribution near interface in ion crystal 9-17274
- f.c.c. metal 3-dimens. voids, density change expt. method 9-11869
- ferrites, mixed, cation vacancy density rel. to disaccommodation 9-3323
- generation, and kinetics of oxidation 9-12541
- graphite, after neutron irradi. rel. to lattice parameter changes 9-7471
- graphite, pyrolytic, lood prod. in crystallites on neutron irradi. 9-7472
- hydrated crystals, Schottky, in mechanism of mol. water diffusion 9-1241
- ionic crystal, change in spherical pore form due to vacancy diffusion 9-21329
- in Kirkendall effect mechanism 9-19762
- melting mechanism 9-5215
- metals, and pairs, effect of grain boundaries on distrib. 9-3322
- metals, clustering and annealing 9-5336
- motion persistence 9-9699
- relaxation of crystal lattice near vacancy 9-19742
- semiconducting alloys with stoichiometric vacancies, thermal conductivity 9-17358
- solid solns., Al-, Ag-, Au- and Zn-rich, vacancy-impurity binding energies 9-9698
- steel, austenitic stainless, rel. to Widmannstätten M<sub>23</sub>C<sub>6</sub> precip., nucleation and growth 9-1331
- structure, energies and mobilities review 9-13676
- vacancy-interstitial reactions in f.c.c. lattice, diffusion controlled, unified formalism 9-1201
- Ag-Au diffusion couples, in Kirkendall effect mechanism 9-19762
- Ag, bound divacancies, infl. on self diffusion isotope eff. 9-18487
- Al-(1.7at.%)Ca, relaxation props. under quasi-equilibrium condition 9-19743
- Al-Cu alloys, impure, migration rel. to transient effects in early stages of ageing 9-7594
- Al-(4.4 at.%)Zn-(0.3 at.wt.%)Be, alloy, Be-vacancy interaction 9-9701
- Al, migration, applic. of potential deduced from pseudopotential theory 9-9700
- Al, relaxation props. under quasi-equilibrium condition 9-19743
- Al, sp. heat contributions, 330-890°K 9-7654
- Al alloy, commercial, in impurity-dislocation interaction rel. to repeated yielding (Portevin-Le Chatelier effect 9-11925
- Al and alloys, role in stage II and III recovery after 2-MeV e. irradi. 9-9696
- Ar, solid in self-diffusion mechanism 9-11893
- Au-(50 at. %)Ag alloy, quenched in, short range order 9-3324
- Au, furnace coated, density change investigation expt. method 9-11869
- Au, melting mechanism, press. depend. of melting point, explanation 9-5215
- Au, parameters, interpretation 9-3378
- Au binary alloys, solute vacancy pairs, quenched in elec. resistivity 9-18601
- Ba, b.c.c. crystals, relaxations 9-9702
- CdS intrinsic optical absorption spectra 9-3887
- CdS phosphors, cation, rel. to i.r. luminescence 9-12467
- CoO, defect conc. from electrical conductivity and thermogravimetric studies 9-3569
- Cr<sub>2</sub>S<sub>3</sub>, vacancy ordering 9-13783
- Cs, lattice distortion calc. by method of lattice statics 9-21332
- Cu, formation on quenching and irradi., effect on lattice parameters 9-1186
- Cu, infl. on irradiation damage rate, 80°K. 9-3329
- Cu, melting mechanism, press. depend. of melting point, explanation 9-5215

**Crystal imperfections continued**  
**vacancies continued**

- Cu, surface terrace vacancies, relaxation, migration and formation energies 9-21330
- Fe-Cu(Cr) systems, diffusion mechanism, specific features 9-9730
- Fe, b.c.c. crystals, relaxations 9-9702
- Fe, melting mechanism, press. depend. of melting point, explanation 9-5215
- Fe<sub>1-x</sub>O ion-vacancy cluster structures 9-14939
- Ge:As, impurity-vacancy complex formation kinetics 9-9992
- Ge thermal defects, conc., migration and annealing, dislocation density influence 9-5346
- Ge vacancy diff. determ. 9-16093
- HgTe, Hg vacancies causing nature change in elastic vibrations 9-9678
- K, lattice distortion calc. by method of lattice statics 9-21332
- KBr, vacancy-breakdown under self-diffusion 9-18461
- KBr, X-irrad., Frenkel defect production and volume expansion obs. in coloration process 9-21331
- KBr-KCl, X-irrad., Frenkel defect production and volume expansion obs. in coloration process 9-21331
- KCl-KBr system, interdiffusion process, role of anion-cation pair vacancies 9-5411
- KCl, in five-defect model of ionic transport 9-13914
- KCl, vacancy-breakdown under self-diffusion 9-18461
- KCl, X-ray-induced, optical absorpt. meas. 9-18462
- KCl in five-defect model of ionic transport 9-13914
- KCl thermal, conc. 9-3325
- Li, migration, applic. of potential deduced from pseudopotential theory 9-9700
- LiF, in excess elec. charge formation mechanism 9-1568
- Mg, melting mechanism, press. depend. of melting point, explanation 9-5215
- Mg foil, growth of dislocation loops 9-18471
- Mg<sub>1-x</sub>Fe<sub>2x</sub>O<sub>4</sub>, solid solution decay in ferrosinels 9-5339
- Mo, formation on quenching and irradi., effect on lattice parameters 9-1186
- Na, b.c.c. crystals, relaxations 9-9702
- Na, lattice distortion calc. by method of lattice statics 9-21332
- NaCl:Ca<sup>2+</sup>, conc. by density change 9-9703
- NaCl:Mn<sup>2+</sup>, impurity-vacancy assoc. from ionic conductance and diffusion meas. 9-1202
- NaCl, defects determ. from electron centres form. 9-7474
- NaCl, vacancy-breakdown under self-diffusion 9-18461
- Ni, formation energy after liquid He-II quenching 9-5338
- Ni, formation on quenching and irradi., effect on lattice parameters 9-1186
- Ni foil, tetrahedral voids, after n and e irradi. 9-3326
- Pb, relaxation props. under quasi-equilibrium condition 9-19743
- PbTe states, new model 9-19744
- Pd, bound divacancies, infl. on self-diffusion isotope eff. 9-18487
- Pt wires, recovery after quenching in Ar and water 9-19745
- Rb, lattice distortion calc. by method of lattice statics 9-21332
- Si:As(Sb), irradi., impurity-vacancy pairs, e.p.r. and endor exam 9-5341
- n-Si:P,  $\gamma$ -irradiated, rel. to thermal donor formation 9-21333
- Si,  $\gamma$ -irrad. induced, generation rates 9-5340
- p-Si,  $\gamma$ -irradiated, stable defects, elec. props. changes 9-21518
- TiO<sub>2</sub>, changes in conc. due to quenching 9-21392
- Ti<sub>2</sub>Se<sub>3</sub>(Se)<sub>2</sub> cpds, MTi<sub>2</sub>X<sub>4</sub>, (M=Fe, Co, Ni), rel. to elec. props. 9-9934
- UO<sub>2+x</sub>, oxygen vacancies and U<sup>5+</sup> ions, in stable association with oxygen ions 9-1203
- W, n irradiated and annealed, dislocation loops 9-7491
- Zn<sup>2+</sup>-vacancy complex formation, free energy of association determ. from solubility data 9-17277
- ZnS phosphors, cation, rel. to i.r. luminescence 9-12467

**Crystal properties**

- alkali thalides, internal attractive press. rel. to interionic distance, derivation 9-21290
- diamond, atomic vib., heat capacity, opt. and spect. props. 9-18443
- elastic const., formulae efficiency comparison 9-9738
- ferromagnetic oxides, control by composition var. 9-21308
- ferromagnetic spinels, lattice parameter and volume rel. press. 9-11844
- ion configuration in spinels 9-9632
- ionic crystals, thermodyn. functions 9-17253
- laminated, applic. to neutron diff. and scatt. monochromator 9-17263
- macroscopic responses rel. to symmetry 9-3222
- plastic, wear resistance tests 9-11947
- polymers, structure and mechanical props. 9-21325
- spinel, ion configuration 9-9632
- Ar, review 9-13567
- CdS wurtzite, crystall. polarity He<sup>+</sup> ion scatt. obs., 2 keV 9-9635
- Kr, review 9-13567
- NaCl, thermodyn. functions 9-17253
- Ne, review 9-13567
- Ti<sub>2</sub>VS<sub>4</sub> basic props. 9-3219
- Xe, review 9-13567

**Crystal structure**

- See also Polymorphism*
- D.L. arabinol, crystal structure 9-9685
- barite, cryst. form rel. to cryst. struct. 9-16064
- binary crystals with vacancies, ordering theory 9-21303
- binary  $\alpha$  phases, radiation damage from X-ray diff. obs. 9-11868
- book, specialized topics 9-14903
- carbonaceous mats., prep. for optical and electron microscopy 9-8314
- electron diffraction, low energy, from surface, matrix formulation 9-5302
- epitaxial layers, by X-ray diffraction 9-3198
- ferroelectric photoconductors, lamellar structure on illumination near phase transition temp. 9-15135
- $\beta$ -fluoronaphthalene-naphthalene, block structure 9-1334
- graphite, book 9-13566
- graphite, cigar shaped crystals, with conical struct., obs. 9-7430
- graphite, dilution on exposure to liq. Na, rel. to irradi. dose and stress 9-6003
- graphite, dimensional effects of long-term radiation 9-6945
- graphite, dynamic changes during heating, study with replication tech. 9-7424
- graphite, hexagonal layer struct. and imperfections 9-7425
- graphite, isotropic, bulk dimensional changes under irradi., 300 to 1400°C 9-7410
- graphite, lattice expansion during neutron irradi. anal. 9-7412
- graphite, pyrolytic, anisotropy correl. with spectral emissivity 9-7970
- graphite, pyrolytic, parallel layer stacking 9-7422



**Crystal structure continued**

- graphite oxide, model, bonds and groups rel. to method of preparation 9-7352
- Lang topographs of crystals strained by thin films, contrast asymmetries 9-5292
- lattice const. comparison for two crystals using Weissenberg goniometer modification 9-13619
- lattice formation from mol. base-gas, anal. 9-4247
- mag. anisotropy, uniaxial, in electrodeposited thin films, due to lattice distortion 9-9611
- metallographic exam. using interferential films 9-5296
- metals, high melting point, electron optics apparatus using thermal electrons 9-3247
- Mossbauer study, environment effect on nuclear energy levels 9-18695
- perovskite, Madelung potential calc. for various sites for any ion charges 9-7355
- petroleum coke, changes during desulphurization 9-7611
- petroleum coke, graphite cryst. form. and struct. changes in desulphurization, obs. 9-7431
- polyamide fibres, arranged contribution of macromolecules by magnetic susceptibility and anisotropy 9-21557
- polyethylene, change due to redrawing 9-17238
- PVC, plate-like, twisted to fibrillar structure 9-16088
- pyrophyllite, natural and synthetic, rel. to polytypism with mica-like minerals 9-1192
- representation, exact  $\Gamma$  matrices and projection operators 9-7382
- salol films, control during growth process from supersaturated condensate current 9-1103
- soda-lime-silica glass, rel. to Ca coordination 9-1079
- space group,  $D_{4h}^{14}$ , little group irreducible representations 9-1164
- space-time groups, Bravais classes and lattice systems, summary 9-21304
- structure factor of centric and acentric crystals, effect of large numbers of heavy atoms 9-1161
- talc, rel. to polytypism with mica-like minerals 9-1192
- teaching model 9-14902
- torsional pendulum studies 9-5291
- 2PbO.SiO<sub>2</sub> glass in temp. range 300-650°C 9-7321
- Al-Li, Al<sub>3</sub>Li superlattice 9-3282
- Al, refining in l.f. vibrating melt during crystallization, effect of crystallite transport stage 9-7375
- Al<sub>3</sub>Li in Al-4.5 wt.% Li alloy, superlattice 9-3282
- Al<sub>2</sub>O<sub>3</sub>.Ti, and precip. obs. 9-1340
- Au-Mg alloys near Au<sub>3</sub>Mg, long periodic stacking order 9-9716
- Ba(NO<sub>3</sub>)<sub>2</sub>, morphological symmetry 9-1125
- Be thin films, amorphous, superconductivity below 7°K by e diff. 9-13863
- Bi-MnBi composite grown from eutectic melts 9-9671
- C, non-graphitic, hexagonal layer struct. and other parameters 9-7425
- C, pyrolytic, apparent crystallite height changes after neutron irradi. 9-7409
- C, pyrolytic, dimensional behaviour during neutron irradi., descriptive model 9-7651
- C membranes, interlayer spacing and ordering 9-11777
- Cd-Sb-Zn system solid solns. 9-19835
- Cd<sub>3</sub>As<sub>2</sub>.Zn<sub>3</sub>As<sub>2</sub> system, of solid solns. grown 9-13882
- CdS-Li<sup>+</sup>, habit change on increasing Li<sup>+</sup> content 9-1184
- CdS, cubic, epitaxial growth on InSb and CdS substrates 9-14910
- Co, martensite platelets, shear-induced during  $\alpha \rightarrow \beta$  transform., geometrical form 9-9795
- CoMn<sub>2</sub>Fe<sub>2</sub> xO<sub>2</sub> charge distrib. from Mossbauer spectra 9-1119
- Cu-Al alloy,  $\beta$  martensite, new ordered phase 9-1350
- Cu-Sn  $\gamma$  solid solns, structural changes during eutectoid decomposition 9-7613
- Cu-Zn alloy,  $\alpha_1$ -plates, morphology and crystallography correlation 9-11842
- Cu halide complexes with n-heterocyclic ligands, distortion obs. via spectra 9-14043
- Fe-30wt.%Ni-5 wt.%Nb austenitic alloy, on phase transform during hardening by heat treatment and cold working 9-9802
- Ge, Chokirai'skii-grown 9-1122
- $\gamma$ -Hg evidence for a third phase 9-3077
- In<sub>2</sub>O<sub>3</sub>, habit changes in growth from PbO-B<sub>2</sub>O<sub>3</sub> melt 9-17257
- La, d.h.c.p., mag. ordering rel. to Fermi surface 9-5615
- Li<sub>2</sub>O-SiO<sub>2</sub> glasses, crystallization stages, X-ray obs. 9-1080
- Ln<sub>2</sub>Me<sup>4+</sup>Me<sup>6+</sup>O<sub>8</sub>, Ln=La, Gd, Y; Lu; Me<sup>4+</sup>=Si, Ge, Ti; Me<sup>6+</sup>=Mo, W) 9-13638
- $\alpha$ -Mn<sub>2</sub>O<sub>3</sub>-Fe<sub>2</sub>O<sub>3</sub> system, and mag. transitions 9-17464
- Nb-C system, effect on sp. ht., Debye temp. and supercond. T<sub>c</sub> from ht. capacity meas. 9-1397
- Nd, d.h.c.p., mag. ordering rel. to Fermi surface 9-5615
- Ni electrodeposited thin films, uniaxial mag. anisotropy due to lattice distortion 9-9611
- NiCr<sub>2</sub>O<sub>4</sub>, tetragonal-cubic phase transform 9-1347
- Pb-7 at.%Sn, rel. to cellular reaction kinetics 9-14906
- Pr, d.h.c.p., mag. ordering rel. to Fermi surface 9-5615
- Pt base alloys, field ion microscope imaging 9-14924
- Sb<sub>2</sub>Se<sub>3</sub>, needle-like, rel. to mech. and elec. props. 9-1194
- SnI<sub>4</sub> type, theoretical morphology 9-9637
- Ta-C system, effect on sp. ht., Debye temp. and supercond. T<sub>c</sub> from ht. capacity meas. 9-1397
- Ta-N, sputtered highly nitrated films, e diff. exam. 9-13578
- Ti-CrO<sub>4</sub>, rel. to elec. conductivity 9-13735
- UO<sub>2</sub>, changes at para-antiferromag. transition, X-ray diff. obs. 9-7890
- ZnMn<sub>2</sub>Fe<sub>2</sub> xO<sub>2</sub> charge distrib. from Mossbauer spectra 9-1119
- ZnO layers, cathode-deposited, rel. to prep. conditions 9-1102

**microstructure**

- See also X-ray examination of materials/microstructure
- alkali feldspars, exsolved, appl. of theory of optimal phase boundaries 9-3360
- alloys, electron microprobe analysis 9-8130
- alloys, non-ferrous, grain size influence on hardness, fracture and other mech. props. 9-9653
- alnico alloys, structural states, X-ray diff. exam 9-1179
- C fibres, carbonized cellulose, microfibrillar and micropore struct. 9-7417
- carbides, and mechanical behaviour, review 9-19704
- cementite, hypereutectoid, in white cast iron, spheroidization on annealing at 900°C 9-5496
- ceramics, interaction of microstruct. features with cracks 9-3445
- cermets, high temperature 9-18535
- clay, micrograph 9-3271

**Crystal structure continued****microstructure continued**

- coal, carbonized and activated, microporous struct. 9-7406
- coal-tar pitch carbonizations, bubbles and defects in coalesced mesophase 9-7418
- diamonds, shock-synthesized 9-5316
- domain formation and structure on phase transformations with spontaneous decomposition 9-16062
- foils with coherent distortion free particles, extinction contrast 9-7334
- grain boundaries, two dimensional phase transform. 9-11780
- grain boundary, large-angle free energy and migration models 9-1160
- grain boundary hardening, appl. to intergranular corrosion 9-3358
- graphite, changes due to creep strain at 2500°C 9-7545
- graphite, compacts, rel. to pitch binder content 9-7413
- graphite, crystallite boundaries effect on principal thermal cond. 9-7671
- graphite, crystallite sizes from thermal cond. and elec. resistivity meas. 9-7672
- graphite, crystallite sizes from thermal cond. meas. at two mutually perpendicular directions 9-7669
- graphite, from uncalcined coke, influence of pitch-binder content on neutron irradi. changes 9-7432
- graphite, moulded, change rel. to high-temp. irradiation 9-7414
- graphite, nuclear porosity changes under thermal and radiolytic oxidation 9-7408
- graphite, rad. induced contraction, effects of process temps. 9-7411
- graphite resolution during microautoradiography 9-3246
- graphite transparent specimens, transmitted light study of pore systems 9-7423
- graphites, polycryst., X-ray anisotropy functions rel. to thermal and elec. props. 9-7428
- ice, micrograph 9-3271
- magnesia refractory, rel. to creep behaviour 9-3423
- magnetic materials, soft, grain size depend. of mag. props. 9-12237
- magnetite, ordered phase, electron microscopy 9-7439
- metals, b.c.c., deformation textures 9-19791
- metals, grain boundary dislocations 9-5377
- metals, non-ferrous, grain size influence on hardness, fracture and other mech. props. 9-9653
- metals deformed at high temp., micrographic studies of changes, appls. of stereogrammetry 9-16065
- nuclear ceramics, mech. thinned specimens 9-3279
- phase boundaries, optimal, theory appl. to exsolved alkali feldspars 9-3360
- polyethylene, biaxially oriented crystallite orient. distrib. 9-3221
- polyethylene, drawn and annealed lamellar structure and molecular orientation 9-19738
- proteins, by e. diff. 9-14936
- rare earth oxy. fluorides rel. to absorpt. spectra, 220-5000 cm<sup>-1</sup> 9-16411
- solid solutions, grain growth kinetics rel. to impurity-drag effect 9-5342
- steel, grain growth rel. to recrystallization process, vacuum metallographic exam. 9-1154
- steel, Mn, low C, Nb-treated, rolled, in heat-affected zones produced by welding 9-19819
- steel, transformer, free energy of grain boundaries, variation rel. to crystal misalignment angle 9-3291
- steel, transformer, texture effects on sp. losses mag. induction amplitude dependence 9-1676
- texture development during rolling rel. to stacking fault energy determ. 9-13694
- thin films, nondestructive thickness meas. (10 nm-10  $\mu$ m) 9-3191
- Ticonal 2000, sintered alloy in high coercivity state 9-3302
- triglycine sulphate, deformation around 180° domain walls 9-16301
- UO<sub>2</sub>, swaged, changes on irradi. tracks of fission products 9-11358
- welded clad metal diffusion layer structure 9-18485
- X-ray grating for electron probe microanalysis 9-9661
- <sup>147</sup>Pm<sub>2</sub>O<sub>3</sub> microspheres, high density, production by r.f. induction plasma heating 9-2795
- Ag, f.c.c., rolling texture formation by slip and mechanical twinning 9-19815
- Ag films, size effect on elec. resist. 9-5640
- Al-Si alloy, eutectic, transverse banding rel. to mag. field, in directional solidification 9-5313
- Al-Zn alloys Guinier-Preston zone miscibility gap obs. in precipitation reversion studies 9-21393
- Al-6.7 at.% Zn alloys, Guinier-Preston zones, formation and reversion 9-13626
- Al, fatigued, cell struct. form. 9-5347
- Al, recovery eff. on cell struct. and dislocation density 9-13687
- Al, sintered, grain boundary maximum of internal friction 9-1266
- Al<sub>2</sub>O<sub>3</sub>-(0.25wt.% MgO, hot-pressed, deformed, grain boundaries, and dislocations obs. 9-3359
- Al<sub>2</sub>O<sub>3</sub>, hot-pressed, deformed, grain boundaries, and dislocations obs. 9-3359
- Al<sub>2</sub>O<sub>3</sub>, rel. to tensile strength 9-3434
- Al<sub>2</sub>O<sub>3</sub> refractories, rel. to hot modulus of rupture 9-3436
- Al alloys, Guinier-Preston zones from X-ray small angle scattering parameters 9-13627
- Al crystallites, lattice residual deform. distrib. and inhomogeneity of plastic deform. after uniaxial compression 9-1182
- Al Guinier-Preston zones from X-ray small angle scattering parameters 9-13627
- Al<sub>2</sub>O<sub>3</sub>-Y<sub>3</sub>Al<sub>2</sub>O<sub>3</sub>, solidification from melt 9-3285
- Al<sub>2</sub>O<sub>3</sub>, sintered, mech., thermal, electrical and chemical props. 9-1256
- BaTiO<sub>3</sub>, grain boundary contrib. to optical dielec. const. 9-17432
- BeO powders, crystallite growth obs. of sintering and inhibition by adsorbed phosphate 9-17241
- C, non-graphitizing, crystallite size or thickness, correl. with interlayer spacing d(002) 9-5315
- C, small crystallite type, variations in crystallite size and orientation 9-7420
- C blacks, external layer of crystallites and closed porosity interior of lower order 9-7419
- C deposits on Al<sub>2</sub>O<sub>3</sub>, e.s.r. obs. 9-20015
- C prep. from phenol-formaldehyde resins, rel. to graphitizability, obs. 9-7429
- CaO, microcry., lattice const. and energies study 9-17270
- Cd, cellular substructure, metallographic study 9-7435
- CdS, e. microscope obs. 9-7453
- CdSe films on NaCl, rel. to cleavage surface 9-7338
- CeCo<sub>5</sub>-CeCu<sub>4</sub> alloy of high coercivity 9-11839
- Ce<sub>1.05</sub>Co<sub>4.25</sub>Cu<sub>0.75</sub> alloy, and permanent mag props. 9-3795

**Crystal structure continued**  
**microstructure continued**

- Co, vapour-deposited foils, eff. of deposition rate and temp. on morphology 9-14927
- Cu-Si alloy, texture meas. in stacking fault energy determ. 9-11887
- Cu-Sn alloys, equilibrated, grain boundary segregation, electron microprobe obs. 9-11843
- Cu-(30 at.wt.%)Zn alloy, rel. to shock induced deformation faults 9-13681
- Cu, cold-rolled, three-dimens. orientation distrib. function of crystallites 9-11841
- Cu, drawn through die, development of microbands separating main deform. bands 9-9674
- Cu, f.c.c., rolling texture formation by slip and mechanical twinning 9-19815
- Cu, rolling texture formed by slip, orientation changes and deform. bands 9-9777
- Cu, vacuum-smelted, data for recrystallization diagram 9-5287
- Ge, lattice parameter expansion calc. from fast n irradiation 9-1189
- Ge wafers, X-ray diffraction topography 9-9677
- KCl, microcry., lattice const. and energies study 9-17270
- LiF, cold-worked, crystallite size and microstrains, evaluation from X-ray diff. line profiles 9-13640
- MgO, microcry., lattice const. and energies study 9-17270
- MgO, rel. to creep 9-1292
- MgO brick, microstructure and phases 9-3170
- Na stearate soap, extruded, e microscope obs. 9-5225
- NaCl, microcry., lattice const. and energies study 9-17270
- Nb-H, rel. to electrolytic charging of Nb with H 9-13750
- Nb-Ti alloys, influence on superconductivity 9-12125
- Nb-(44wt.%)Ti superconducting wire 9-18450
- Ni-Cr-W-Co-Al-Ti alloy with borophilic additions, effect of grain boundary composition on mech. props. 9-5475
- Ni-Fe-Cu layers, influence of annealing 9-3821
- Ni-Fe film, electrodeposited, crystallite size effect on coercive force 9-7909
- Ni<sub>3</sub>Mo, ordered, contrast variation, in field-ion images 9-16077
- Ni<sub>3</sub>Mo, ordered, field ion images 9-14922
- Ni<sub>3</sub>P, effect on Hall effect 9-9922
- Pb zone-refined, grain growth kinetics, mechanisms 9-3304
- Si, lattice parameter expansion calc. from fast n irradiation 9-1189
- SiC epitaxial layers, X-ray topographical analysis 9-3202
- SiC filaments, continuous vapour deposited, obs. 9-9683
- Sm<sub>2</sub>O<sub>3</sub> microspheres, high density, production by r.f. induction plasma heating 9-2795
- Ta-H(D) solid solns., n scatt. study 9-7449
- Ti, vapour-deposited foils, eff. of deposition rate and temp. on morphology 9-14927
- TiO<sub>2</sub>, ordered and disordered, rel. to growth faults 9-5376
- (U, Pu)O<sub>2</sub> microspheres, techniques for ceramography and alpha autoradiography 9-3309
- UC, dihedral angles of U inclusions in grain boundaries, rel. to annealing temp. 9-11855
- UO<sub>2</sub>, grain growth and fission- gas release around 2000°C 9-13250
- UO<sub>2</sub> fuel pellets, after irradi., defects, gas bubbles and grain growth 9-11856
- W compacts, grain growth during sintering 9-7583
- Y<sub>2</sub>O<sub>3</sub>-Zr dispersions, grain boundaries and sizes, stability 9-1318
- Zn-Al alloy, superplastic, and mech. behaviour 9-11858
- ZnO, control during growth process from supersaturated condensate current 9-1103
- ZnO, densification and grain growth during sintering 9-19825
- ZnO, pore growth during final stages of sintering 9-19826
- ZnS, e. microscope obs. 9-7453
- ZnSnP<sub>2</sub>, position of P atom in ordered struct., Debye temp., Hall mobility 9-3310

**Crystal structure, atomic**

- See also *Crystal electron states; Crystals/lattice mechanics; Electron diffraction crystallography; Neutron diffraction crystallography; X-ray crystallography*
- 3-index and cartesian coordinate system for dislocation description in hexagonal metals 9-3342
- antiphase domains, equilib. boundaries, theory allowing for short-range order 9-1163
- atomic factors, general harmonic expansions 9-5295
- B-B phases, systematics 9-16063
- Bond's method for lattice parameter determ., specimen and beam tilt 9-7384
- channeling of high-energy particles 9-16189
- close packing in b.c.c. and simple cubic systems 9-21302
- effective ionic radii, for bond and unit cell calc. 9-7354
- electron density computation by anomalous dispersion method, wrong scale factor effects 9-3273
- electron density distributions, scale and phase angle errors, and rel. to structures with non-crystallographic mol. symmetry 9-3276
- electron diffraction determ., review 9-5304
- Fourier transformation of minimum function in determ. 9-11831
- images in field-ion microscope, effect of bond number 9-5306
- lattice atoms, mean square displacement determ. methods 9-7403
- lattice const., determ. from single cryst. X-ray photographs 9-5299
- lattice parameter relative meas. new double crystal arrangement technique 9-21305
- lattice sites of atoms of nearly equal X-ray scatt. power from X-ray K-absorpt. spectral data 9-14065
- lattice spacing determ. by successive reflections of n beam from two crystal specimens 9-11826
- magnetic groups of cubic symmetry, co-representation with simple lattice 9-1632
- metals and semiconds., tabular reduction of cryst. chem. information 9-16073
- modulated structures, X-ray scatt. 9-5301
- molecular mixed crystal, discrete and zone states 9-5622
- monoclinic noncentrosymmetric crystals, program for NE 803B computer 9-3223
- orientation determ. by selected area electron diffraction, accuracy 9-5303
- phase computation by anomalous dispersion method, wrong scale factor effects 9-3273
- with planar molecules, modified 2-dimens. data construction 9-18440
- plane point groups of colour symmetry and other kinds of antisymmetry 9-13614

**Crystal structure, atomic continued**

- point groups, fourth-order polarizability tensor, transformation props. 9-11810
- point groups, non-cubic, double-valued rep. using projection operators method 9-13615
- precipitated phase, three-dimensional macroperiodic lattices formed by regularly distrib. occlusions, theory 9-3245
- primary solid solutions, class for law of corresponding states 9-5293
- refinement rel. to non-crystallographic mol. symmetry 9-3275
- review of electron diffraction determ. 9-5304
- and screw dislocation model 9-9711
- similarity symmetry groups, three-dimensional, derivation 9-7381
- Simplex method appl. to determ. 9-7400
- space group representation in classification of principal vibrations 9-1358
- space group representations, Zak's method and self-conjugate groups 9-14911
- space groups, direct determ. of irreducible representations 9-18984
- symmetry operations, demonstration model 9-18431
- thermal expansion of interatomic bonds 9-7659
- X-ray diffraction powder patterns, standard 9-11809
- C grains in evaporated films, obs. 9-13576
- $\gamma$ -CuI films, lattice params. rel. to internal stresses, obs. 9-16126
- Sb thermal expansion and lattice parameters 28°-220°C obs. 9-21439
- Si highly doped, lattice parameter relative to undoped sample, meas. technique 9-21305
- Ta, thin and very thin films 9-1101

**alloys**

- ageing solid solutions, parameter variation, data analysis 9-11829
- Engel-Brewer theories 9-9667
- Nickel Invar and its anomalous expansion coefficient 9-3243
- nickel-cobalt disilicide, solid soln., lattice parameters and densities 9-3480
- ordering forces range in struct. with long range order 9-1162
- solid solutions, ageing variation in lattice constants, theory 9-11828
- superlattice formation, field ion microscope obs. 9-7402
- $\psi$ -Cd, Ahexagonal, phase rel. to transforms 9-11835
- Al-Cu, effect of lattice strains on const., rel. to precipitation and age hardening inhomogeneities 9-9783
- Al-CuO, lattice parameter, sintering effects due to CuO reduction 9-3463
- Au-Cu, short-range order, Zener relaxation and resistivity meas. 9-19804
- CdMg, degree of ordering of  $y_a$  and  $y_b$  of  $\alpha$  and  $\beta$  sites, determ. 20-250°C 9-7434
- Co-Nb, new phase of Cu<sub>3</sub>Au type, precip. on ageing 9-9796
- Cu-Al alloys, annealed, near-order parameters, conc. dependence 9-3479
- Cu-75 wt.%Pd, short-range-order effects on residual resistivity 9-12100
- Cu-Ni, lattice constant temp. dependence over conc. range 9-19955
- Cu-<sup>62</sup>Ni, clustering, n. scatt. meas. 9-9673
- Fe-Co, lattice parameters and Curie point anomalies 9-18444
- Fe-Ni, hysteresis loops, constant-field, effect of atomic arrangement and anisotropy 9-5825
- In-Pb, axial ratio temp. depend. rel. to Fermi surface interactions 9-21491
- Ni-Fe, evaporated film, lattice parameter composition dependence 9-14986
- 2a/0Ni-Pt, short-range order, field ion microscope investigation 9-3305
- Ni<sub>3</sub>Fe(Mn)-based ternary alloys with transition metal, ordering process 9-19834
- 2a/0 Au-Pt, short-range order field ion microscope investigation 9-3305
- PtCo, superlattice formation, field-ion microscope obs. 9-7402
- Sn-Ni, electrodeposited, and thermal stability rel. to acid bath conditions 9-14926

**elements**

- diamond, symmetry study from spectra obs. 9-18443
- graphite, lattice and dimensional changes on neutron irradi. 9-7471
- graphite, lattice deform. by interstitial C<sub>2</sub> mol., and self-energy 9-7407
- graphite, model parameters from inelastic thermal neutron scatt. data 9-19855
- Hittorf's phosphorus 9-13646
- metals, Engel-Brewer theories 9-9667
- metals, geom. factor, near-neighbour diagrams 9-19703
- Al polycrystals, brass-texture rel. to orientation changes caused by slip 9-9670
- Al X-ray atom form factor determ. from vanishing second order reflection in high-voltage electron diff. 9-9676
- C, amorphous films, e. diff. patterns, 9-5237
- C, polyrotic, linear dimension and layer spacing changes due to neutron irradi. 9-7409
- C, radial distrib. functions rel. to stacking and layering 9-7405
- Cu, lattice parameter changes on defect formation due to quenching and irradiation 9-1186
- D, above and below  $\lambda$  transition 9-9675
- $\alpha$ -F 9-3290
- Fe, lattice constant rel. to ferromagnetic props. 9-13982
- Fe, lattice parameter anomalies at Curie point 9-5569
- Fe lattice atoms, mean square displacement determ. 9-7403
- Fe X-ray atom form factor determ. from vanishing second order reflection in high-voltage electron diff. 9-9676
- Ga, from pseudopotential and second-order perturbation theory 9-5319
- Ge, heavily doped, periodicity meas., X-ray diffraction exam. 9-5320
- Hg, stereographic anal. of  $\alpha$  to  $\gamma$  martensitic transformation 9-5519
- Mo, lattice parameter changes on defect formation due to quenching and irradiation 9-1186
- Mo, thin films, infl. of thickness and substrate temp. 9-5238
- Ni, lattice parameter changes on defect formation due to quenching and irradiation 9-1186
- Ni films evap. on glass, struct. depend. on thickness 9-7337
- Ni lattice atoms, mean square displacement determ. 9-7403
- Ni X-ray atom form factor determ. from vanishing second order reflection in high-voltage electron diff. 9-9676
- P, Hittorf's 9-13646
- Rh thermal expansion and lattice parameter determ., X-ray diffraction, 28-587°C 9-16182
- Si, heavily doped, periodicity meas., X-ray diffraction exam. 9-5320
- Ti, thin film, infl. of thickness and substrate temp. 9-5238

**inorganic compounds**

- alkali feldspars, exsolved, appl. of theory of optimal phase boundaries 9-3360
- alkaline-earth tungstates, lattice constants rel. to u.v.-induced absorpt. peak wavelengths 9-5913
- amarantite, Fe (SO<sub>4</sub>)OH.3H<sub>2</sub>O 9-1188
- carbides, refractory, high temp. 9-7433



**Crystal structure, atomic continued****inorganic compounds continued**

carbones, calcite-type, relation between cation-O distance and parameters  $a_0$ ,  $c_0$  9-19681  
chromium alums., classification 9-13591  
diethylammonium palladium cyanide, 001 Fourier synthesis 9-21320  
eveite, mineral from Langban, Sweden 9-18449  
fluorides, ternary 9-7438  
getchellite,  $\text{AsSbS}_3$  9-19708  
 $\gamma$ - $\text{Hg}_2\text{S}_2\text{Cl}_2$  9-11847  
hocartite,  $\text{Ag}_2\text{SnFeS}_4$  9-19705  
holmquistite, orthorhombic amphibole 9-13639  
ice Ic, neutron diff. 9-16076  
ice II, neutron diff. 9-16075  
ice III 9-7441  
ice IX, neutron diff. determ. 9-5321  
ice polymorphs, proton and deuterium n.m.r. 9-16463  
Kurrol salt, type A,  $(\text{NaPO}_3)_x$ , refinement 9-11851  
lanthanides, trifluorides, melt grown 9-9648  
Metamic, heat treatment not successful in reducing metamictization 9-3280  
Monazite, heat treatment not successful in reducing metamictization 9-3280  
niobates, thermal expansion of interatomic bonds 9-7659  
nitrides, refractory, high temp. 9-7433  
parwelite, mineral from Langban, Sweden 9-16078  
penfieldite,  $\text{Pb}_2(\text{OH})\text{Cl}_3$  9-18451  
perovskite type crystals, structural phase transitions, temp. depend. of rot. angle and soft-mode freq. below  $T_c$  9-3281  
perovskites, classification 9-13592  
perovskites, high-pressure synthesized 9-18452  
pollucite, location of Na, Cs and water mol. 9-7436  
potassium periodates obtained from aqueous soln. at 25°C 9-19720  
potassium selenites obtained from aqueous soln. at 25°C 9-19720  
rare earth manganites of perovskite-type, and mag. ordering 9-19717  
refractory materials, high temp. 9-7433  
serpentine,  $\text{Ca}(\text{Cu}, \text{Zn})_4(\text{OH})_6(\text{SO}_4)_2 \cdot 3\text{H}_2\text{O}$  9-3286  
sodium periodates obtained from aqueous soln. at 25°C 9-19720  
sodium selenites obtained from aqueous soln. at 25°C 9-19720  
tetracyano complexes, inter-planar bonding 9-18441  
tolan phase in tolan-diphenylmercury system, mol. packing 9-1200  
transition metal carbides and nitrides 9-17272  
 $\text{InZrO}_2\text{Sc}_2\text{O}_3$ , of intermediate phases  $\text{Zr}_3\text{Sc}_2\text{O}_{11}$  and  $\text{Zr}_3\text{Sc}_4\text{O}_{12}$  9-3311  
 $\text{Ag}_2\text{SnFeS}_4$ , hocartite 9-19705  
 $\alpha$ - $\text{Ag}_2\text{S}$  crystal structure, analogy with  $\beta$  phase 9-19706  
 $\alpha$ - $\text{Ag}_2\text{Se}$  crystal structure, analogy with  $\beta$  phase 9-19706  
 $\alpha$ - $\text{Ag}_2\text{AuS}$  crystal structure, analogy with  $\beta$  phase 9-19706  
 $\alpha$ - $\text{Ag}_2\text{AuSe}_2$  crystal structure, analogy with  $\beta$  phase 9-19706  
 $\alpha$ - $\text{Ag}_2\text{AuTe}_2$  crystal structure, analogy with  $\beta$  phase 9-19706  
Ag lutidine nitrate complex, space group and unit cell dims. 9-11832  
Ag lutidine nitrate complex, unit cell dims. from powder diff. data 9-13624  
Al-Cu alloy,  $\theta'$  structure, lattice parameters determ. 9-11834  
Al-mica 1M, and refinement 9-1180  
 $\text{Al}_2\text{O}_3$  single crystals, lattice parameters, press. depend. 9-3394  
 $\text{Al}_2\text{O}_3 \cdot 2.5\text{NiO} \cdot 9\text{H}_2\text{O}$ , hexagonal lattice parameters 9-19707  
 $\text{AlCl}_3 \cdot \text{N}(\text{CH}_3)_3$ , and mol. structure 9-13625  
 $\text{Al}_2\text{MgO}_4$ , refinement 9-1181  
in  $\text{Al}_2\text{O}_3 \cdot \text{WO}_3$ , of compound  $\text{Al}_2(\text{WO}_4)_3$  9-3283  
 $\beta$ - $\text{Al}_2\text{O}_3$  9-11833  
AlP, lattice parameters of epitaxial layers grown on Si by vapour transport reaction 9-19692  
 $\text{AsSbS}_3$ , getchellite 9-19708  
 $\alpha$ - $\alpha\text{-Te}$  crystal structure, analogy with  $\beta$  phase 9-19706  
 $\text{BaF}_2 \cdot \text{BaCl}_2$ , primitive unit cell dimensions, crystal grown by indirect flux method 9-18422  
 $\text{BaFe}_2\text{TiO}$  [ $\text{Si}_2\text{O}_7$ ](OH) $_2$ , bafertsite, determ. by Fourier-transformation of minimum function 9-11831  
 $\text{BaO} \cdot \text{Al}_2\text{O}_3 \cdot \text{SiO}_2$  system, new  $\text{BaAl}_2\text{SiO}_6$  phase 9-14987  
 $\alpha$ - $\text{Ba}(\text{OH})_2$  9-11837  
 $\text{BaTiO}_3$ , chain structure 9-11818  
 $\text{BaTiO}_3$  parameters rel. to temp. of tetragonal-orthorhombic transformation 9-1183  
 $\text{BaVS}_3$ , space group, cell dimensions, low temp. distortion 9-7747  
 $\text{Ba}_2\text{ZnAl}_3\text{Fe}_5\text{O}_{22}$ , n diff. study of cell parameters and configuration 9-5314  
 $12\text{CaO} \cdot 7\text{Al}_2\text{O}_3$  fluoride derivative 9-17265  
 $\text{CaPt}(\text{CN})_4 \cdot 5\text{H}_2\text{O}$  isotopic structure 9-21310  
 $\text{BeSO}_4 \cdot 4\text{H}_2\text{O}$ , refinement 9-14915  
 $\text{BeSO}_4 \cdot 4\text{H}_2\text{O}$ , n. diff. exam. 9-13628  
 $\text{Bi}_2\text{Te}_{3-x}\text{Se}_x$ , mixed-crystal region, composition depend. 9-14985  
Bi complex, tris(dimethylammonium) hexabromobismuthate 9-21309  
Bi perovskites, high-pressure synthesized 9-18452  
 $\text{BiCrO}_3$ , crystal distortions and mag. props. 9-10112  
 $\text{BiMnO}_3$ , crystal distortions and mag. props. 9-10112  
 $\text{BkF}_4$ , lattice parameter determ. 9-17264  
 $\text{Ca}_{11}\text{N}_8$  9-14916  
 $\text{CaH}_2$ , X-ray diff. 9-18542  
 $\text{CaNi}(\text{CN})_4 \cdot 5\text{H}_2\text{O}$  isotopic structure 9-21310  
CaO microcry., lattice const. and energies study 9-17270  
 $\text{CaPd}(\text{CN})_4 \cdot 5\text{H}_2\text{O}$  isotopic structure 9-21310  
 $\text{CaSn}(\text{OH})_2$ , film n. diff., i.r. absorpt. and n.m.r. 9-19709  
 $\text{CaTiGeO}_3$ , synthetic, unit cell and space group, compared with  $\text{CaTiSiO}_3$  9-5317  
 $\text{CaTiSiO}_3$ , synthetic, unit cell and space group, compared with  $\text{CaTiGeO}_3$  9-5317  
 $\text{CaUF}_6$  X-ray powder diffraction investigation of structure 9-11838  
Cd complex, bis(hydrazinecarboxylate- $\text{N}'$ , O) cadmium monohydrate, and mol. structure 9-13630  
 $\text{Cd}(\text{PO}_3)_2$  9-19710  
CdTe, mean square displacements for sub-lattices 9-19711  
Co complex, bis(1,2,3,4-tetrachlorobenzene-5,6-dithiolato)cobaltate 9-17266  
Co complex, cis-cobalt diazobisethylenediamine nitrate 9-11840  
Co complex, hexaamminecobalt (III) iodide, rel. to Co-N bond lengths 9-13631  
Co oxides, interpretation of Mossbauer study of Fe atoms behaviour 9-5887  
CoO, rebuttal of microcry. model of Schroerer and Trifshausen 9-1178  
 $\text{Co}_2\text{P}_2\text{O}_4$ , monoclinic, crystallographic data 9-5324  
 $\text{CrLaO}_3$  9-16152

**Crystal structure, atomic continued****inorganic compounds continued**

$\text{Cs}_2\text{Bef}_4$  9-13633  
 $\text{CsCl}_4(\text{SCN}_2\text{H}_4) \cdot \text{H}_2\text{O}$  9-3288  
 $\text{CsCrO}$  (9-7445)  
 $\text{Cs}_2\text{LiCo}(\text{CN})_6$  9-13632  
 $\text{CsNO}_3$  9-1185  
 $\text{Cu}_2\text{TeO}_6$  9-21311  
Cu complex, bis-L-histidine copper (II) dinitrate dihydrate 9-13634  
Cu complex, N-salicylidene-glycinatoaquocopper (II) tetrahydrate 9-13635  
Cu complex, pyruvidene- $\beta$ -alaninatoaquocopper (II) dihydrate, and mol. structure 9-7437  
Cu complex, triphenylmethylphosphonium bis((3)-1,2-dicarbolyl)-cuprate(III) 9-19712  
 $\text{Cu}_2\text{CdSiS}_4$  9-17267  
 $\text{CuFeS}_2$ , possible second kind 9-10182  
 $\text{CuHPO}_3 \cdot 2\text{H}_2\text{O}$  9-14917  
 $\text{Cu}_2\text{P}_2\text{O}_4$ , monoclinic, crystallographic data 9-5324  
DyP, lattice deformation at Neel pt. 9-12309  
 $\text{EuCl}_3$  9-11850  
 $\text{Fe}_2\text{AlB}_2$  9-13133  
 $\text{Fe}_2(\text{CO})_{11}\text{P}(\text{C}_6\text{H}_5)_3$ , 3 dims. X-ray data 9-21314  
 $\text{Fe}_2\text{Se}_8$  9-21484  
 $\text{Fe}(\text{SO}_4)\text{OH} \cdot 3\text{H}_2\text{O}$  (amarantite) 9-1188  
Fe complex, bis(cyclooctatetraene)iron 9-17268  
Fe complex, tris-(2-dimethylaminoethyl)amineiron (II) bromide 9-3299  
 $\text{Fe}(\text{CO})_4$  powder, at scatt. factor corrections for surface roughness and porosity 9-11845  
 $\text{FeCl}_3$ , transition h.c.p.-f.c.c., Mossbauer evidence 9-5515  
 $\text{FeCr}_2\text{Se}_4$  lattice constants rel. to effect on physical props. of interactions between d shells of transition element 9-16253  
 $\epsilon$ - $\text{Fe}_2\text{N}$ , electron diffraction 9-5318  
 $\zeta$ - $\text{Fe}_2\text{N}$ , electron diffraction 9-5318  
 $\delta$ - $\text{FeOOH}$  9-19713  
 $\text{Fe}_2\text{Zr}$ , near stoichiometric composition 9-7440  
GaAs, distribution of electrons 9-3292  
 $\text{Gd}(\text{MoO}_4)_3$  ceramic and single-crystal, prep. and X-ray analysis 9-18446  
 $\text{GdCl}_3$  9-11850  
 $\text{HBr} \cdot 4\text{H}_2\text{O}$  9-1190  
 $\text{HClO}_4 \cdot 2\text{H}_2\text{O}$  9-3293  
 $\text{H}_2\text{O}_2$ , space group determ. by X-ray diff. rel. to double refraction effect errors 9-11846  
 $\text{H}_2\text{S}$  and  $\text{D}_2\text{S}$ , phase III 9-5935  
(Hg Cd)Te solid solns. mean square displacements for sub-lattices 9-19711  
HgSe, X-ray diff. exam. 9-3294  
HgTe, mean square displacements for sub lattices 9-19711  
HgTe, X-ray diff. study, bond weakening due to Hg vacancies 9-9678  
 $\text{HoZn}_3$  9-3295  
IBr 9-11848  
 $\text{K}_1[\text{Ni}(\text{CS})_3]_n$ , magnetic susceptibility and config. 9-18667  
 $\text{K}_1\text{Fe}(\text{CN})_6$ , crystallography and paramag. anisotropy, 95° and 300°K 9-21343  
 $\text{K}_1\text{Fe}(\text{CN})_6$ , crystallography and paramag. anisotropy, 95° and 300°K 9-21315  
KBr-TiBr solid solutions, lattice parameter composition dependence 9-13637  
KCl microcry., lattice const. and energies study 9-17270  
 $\text{KI-Tl}^+$  lattice distortion and binding energy of  $\text{Tl}^+$  with light foreign anions 9-3297  
 $\text{K}_1\text{Li}_2\text{Nb}_2\text{O}_{15}$ , growth and characts. 9-11803  
 $\text{K}_2\text{Mn}(\text{SO}_4)_2 \cdot 4\text{H}_2\text{O}$ , space group and structure refinement using n. diff. 9-3277  
 $\text{KNbO}_3$ , chain structure 9-11818  
( $\text{K Pb}_2$ )-( $\text{K Sr}_2$ ,  $\text{Na Ba}_3$ ) $\text{Nb}_2\text{O}_{15}$  parameters rel. to ferroelec. transition temp. 9-1594  
 $\text{KSr}_2\text{Nb}_2\text{O}_{15}$ , parameters rel. to ferroelec. transition temp. 9-1594  
 $\alpha$ - $\text{KZnBr}_2 \cdot 2\text{H}_2\text{O}$  9-7442  
 $\text{K}[\text{Au}(\text{CN})_2]\text{H}_2\text{O}$ , solid soln., X-ray investigation 9-13636  
 $\text{kbr}:\text{tl}^+$ , lattice distortion and binding energy of  $\text{Tl}^+$  with foreign anions 9-3296  
 $\text{kCl}:\text{tl}^+$  lattice distortion and binding energy of  $\text{Tl}^+$  with foreign anions 9-3296  
 $\text{La}_2\text{Re}_6\text{O}_{19}$  9-19715  
 $\text{LaCl}_3$  9-11850  
 $\text{Li}_2\text{Fe}_{2-x}\text{Al}_x\text{O}_4$ , n. diff. obs. 9-21316  
 $\text{Li}_2\text{O} \cdot \text{Al}_2\text{O}_3 \cdot \text{n SiO}_2$  ( $4 \leq n \leq 10.0$ ), solid solns., rel. to thermal expansion anisotropy 9-3537  
 $\text{Li}_2\text{WO}_4 \cdot \text{Fe}$ , cubic 9-18447  
Li ferrite, and Li loss effects, 20°C 9-1686  
 $\text{LiCd}(\text{MoO}_4)\text{OH}$ , monoclinic cell parameters 9-5322  
LiF, X-ray scatt. factors using approx. model for overlap charge density 9-3298  
 $\text{LiNbO}_3$  9-7443  
 $\text{Li}_2\text{Ni}_{1-2x}\text{O}$  system, lattice parameter comp. dependence 9-1191  
 $\text{Ln}_2\text{Me}^{4+}\text{Me}^{6+}\text{O}_8$ ,  $\text{Ln}=\text{La}, \text{Gd}, \text{Y}; \text{Li}; \text{Me}^{4+}=\text{Si}, \text{Ge}, \text{Ti}; \text{Me}^{6+}=\text{Mo}, \text{W}$  9-13638  
 $\text{MgBr}_2 \cdot 4\text{C}_2\text{H}_5\text{O}$ , tetrahydrofuran complex 9-19716  
 $\text{MgF}_2$  ionic binding nature determ. 9-18448  
 $\text{MgO}$  microcry., lattice const. and energies study 9-17270  
 $\text{Mg}(\text{OH})_2(\text{HO}_2)_2$  hexaquoque nitrate 9-13641  
 $\text{Mg}_2\text{P}_2\text{O}_4$ , monoclinic, crystallographic data 9-5324  
 $\text{MgWO}_4$  9-13642  
( $\text{Mn}, \text{Mg}$ ) $_2\text{Sb}(\text{Si}, \text{As})_2\text{O}_{10-11}$ , parwelite, mineral from Langban, Sweden 9-16078  
 $\text{Mn}_2(\text{OH})(\text{AsO}_4)$ , eveite, mineral from Langban, Sweden 9-18449  
Mn complex, tris-(2-dimethylaminoethyl)aminemanganese (II) bromide 9-3299  
 $\text{MnAsO}_4 \cdot \text{P}_{0.1}$ , 4.2 to 660°K, and mag. props. 9-16357  
 $\text{Mn}_2\text{Cr}_{1-x}\text{HoO}_3$ , rel. to mag. struct. 9-17269  
 $\text{MnF}_2 \cdot \text{Fe}^{2+}$  M1- active local mode at 94  $\text{cm}^{-1}$  9-3949  
 $\alpha$ - $\text{MnOOH}$ , groutite, A-MnOOH, refinement 9-7444  
 $\alpha$ - $\text{MnOOH}$ , groutite, refinement 9-7444  
 $\text{Mn}_2\text{P}_2\text{O}_4$ , monoclinic, crystallographic data 9-5324  
 $\text{MnZn}$  ferrites of stoichiometric compositions, lattice const. rel. to composition 9-16079  
 $\text{MoNi}_4$ , close-packed ordered structures 9-19718  
 $\text{MoS}_2$ , Kikuchi patterns, intensity anomaly 9-14918  
 $\text{MoS}_2$ , Kikuchi patensity anomaly 9-9679

**Crystal structure, atomic continued  
inorganic compounds continued**

- MoZn<sub>2</sub>Zr<sub>2</sub>, from X-ray powder data 9-19719  
 NH<sub>4</sub>Br and ND<sub>4</sub>Br, modifications III and IV, -56° to -192°C 9-16153  
 N<sub>2</sub>H<sub>5</sub>UF<sub>6</sub>, unit cell dimens. from powder pattern 9-9682  
 Na<sub>2</sub>CD<sub>3</sub>[Si<sub>3</sub>O<sub>10</sub>], crystal structure 9-21317  
 Na<sub>2</sub>ZrO<sub>3</sub>, X-ray and optical data 9-19721  
 NaBF<sub>4</sub>, refinement 9-11852  
 NaBa<sub>2</sub>Nb<sub>2</sub>O<sub>15</sub>, parameters rel. to ferroelec. transition temp. 9-1594  
 Na<sub>2</sub>B<sub>2</sub>F<sub>4</sub>, rel. to <sup>19</sup>F NMR temp. dependence meas. 9-16466  
 Na<sub>2</sub>Cd<sub>2</sub>[Si<sub>3</sub>O<sub>10</sub>], rel. to existence of [Si<sub>3</sub>O<sub>10</sub>] group 9-5323  
 NaCl, static Green's tensor function 9-7446  
 NaCl, X-ray scatt. factors using approx. model for overlap charge density 9-3298  
 NaCl microcry. lattice const. and energies study 9-17270  
 NaCr(oSo<sub>4</sub>)<sub>2</sub>, 12H<sub>2</sub>O, and classification 9-7445  
 NaF, X-ray scatt. factors using approx. model for overlap charge density 9-3298  
 NaH<sub>2</sub>(SeO<sub>3</sub>)<sub>2</sub> 9-3300  
 Na<sub>2</sub>Mn<sub>2</sub>Si<sub>2</sub>O<sub>7</sub>, synthetic, determ. by Fourier-transformation of minimum function 9-11831  
 NaNiF<sub>3</sub>, lattice const. determ. from single cryst. X-ray photographs 9-5299  
 Na<sub>2</sub>·NiO<sub>1.8</sub> 9-13644  
 (NaPO<sub>3</sub>)<sub>2</sub>, Kurrol salt, type A, refinement 9-11851  
 Na<sub>2</sub>Ti<sub>2</sub>(Si<sub>2</sub>O<sub>6</sub>)<sub>2</sub>·[Si<sub>2</sub>O<sub>6</sub>]<sub>2</sub>·nH<sub>2</sub>O, vinogradovite, determ. by Fourier-transformation of minimum function 9-11831  
 NaVMoO<sub>4</sub>, and isotypism 9-14919  
 Na<sub>2</sub>Y(WO<sub>4</sub>)<sub>3</sub> and growth 9-1150  
 Na<sub>2</sub>ZnGeO<sub>4</sub>, synthetic D phase 9-13643  
 Nb<sub>2</sub>Co<sub>2</sub>Si<sub>2</sub> 9-13645  
 NbNiB 9-1193  
 Nb<sub>2</sub>S<sub>4</sub>, and prep. and props. 9-9681  
 NdCl<sub>3</sub> 9-11850  
 NdMnO<sub>3</sub>, and antiferromagnetic ordering 9-19717  
 Ni<sub>4</sub>Mo, ordered, field ion images 9-14922  
 Ni complex, bis(thioacetamide) nickel (II) (thiocyanate, and mol. structure 9-3301  
 Ni complex diaquobis-(2,2'-biimidazole)nickel(II)dinitrate, and mol. structure 9-21319  
 Ni complex tetra (thiourea) nickel (II) thiosulphate monohydrate, and mol. structure 9-14920  
 NiAl<sub>3</sub>, applic. of powder pattern indexing procedure 9-11813  
 NiCr<sub>2</sub>Se<sub>4</sub>, lattice constants rel. to effect on physical props. of interactions between d shells of transition element 9-16253  
 Ni<sub>2</sub>P<sub>2</sub>O<sub>4</sub>, monoclinic, crystallographic data 9-5324  
 β-PaBr<sub>3</sub> 9-14923  
 Pb(OH)Cl, penfieldite 9-18451  
 Pb perovskites, high-pressure synthesized 9-18452  
 PbTiO<sub>3</sub>, and decomposition 9-19722  
 PrMnO<sub>3</sub>, and antiferromagnetic ordering 9-19717  
 Pr<sub>2</sub>Pd<sub>4</sub>, X-ray crystallography 9-19723  
 PuNi<sub>2</sub>-type cpds, unit cell constants 9-7451  
 Rb<sub>2</sub>FeF<sub>6</sub> rel. to <sup>19</sup>F NMR temp. dependence meas. 9-16466  
 Rb<sub>2</sub>Mn<sub>2</sub>Ti<sub>2</sub>·xO<sub>4</sub> (0.60 < x < 0.80), and isomorphs 9-3306  
 RbPaF<sub>6</sub> 9-14925  
 Rh complex, RhCl(C<sub>4</sub>H<sub>8</sub>)<sub>2</sub>, and mol. structure 9-13647  
 Ru, deformed, domain size distrib. form X-ray line profiles 9-7447  
 Ru complex, nitrogenpentammineruthenium (II) dichloride and related salts 9-7448  
 Sb<sub>2</sub>Te<sub>3-5</sub>Se<sub>5</sub>, mixed-crystal region, composition depend. 9-14985  
 Se<sub>2</sub>O<sub>3</sub>, refinement 9-21321  
 Si complex, tetrafluorobispyridinesilicon (IV), and mol. structure 9-13648  
 SiC, type 120R, direct determ. 9-19724  
 SiC structure of 6H types 9-16080  
 Si<sub>2</sub>·xMg<sub>2</sub>·P<sub>2</sub>O<sub>7</sub> system 9-18453  
 SrFe<sub>1-x</sub>La<sub>x</sub>O<sub>10</sub> rel. to variation in saturation magnetiz. with Ga substitution 9-16373  
 TaC, rel. to strain due to comp. gradient, X-ray meas. 9-1271  
 TaNiB 9-1193  
 TbP, lattice deformation at Neel pt. 9-12309  
 Th<sub>2</sub>(N<sub>2</sub>O)<sub>2</sub>X, (X=P, As, Se and S) 9-14928  
 Ti-Pd system, of Ti<sub>2</sub>Pd<sub>3</sub>, Ti<sub>3</sub>Pd<sub>2</sub>, TiPd<sub>2</sub>, TiPd<sub>2</sub> 9-19725  
 Ti-Pt system, of Ti<sub>3</sub>Pt<sub>2</sub> 9-19725  
 TiO<sub>2</sub>, changes in lattice parameters due to quenching 9-21392  
 Ti<sub>2</sub>S<sub>4</sub>(Se<sub>2</sub>)<sub>2</sub>, MTi<sub>2</sub>X<sub>4</sub> (M=Fe, Co, Ni), rel. to elec. props. 9-9934  
 KBr:Ti<sup>3+</sup> lattice distortion and binding energy of Ti<sup>3+</sup> with light foreign anions 9-3297  
 TiH<sub>2</sub>PO<sub>4</sub>·4(SCN·H<sub>2</sub>) 9-3308  
 TiSe, X-ray diff. patterns for tetragonal lattice parameters 9-3556  
 (U, Zr)C solid solns., lattice param. rel. to comp., obs. 9-11976  
 U<sub>2</sub>N<sub>2</sub>X, (X=P, S, Se and As) 9-14928  
 U<sub>3</sub>O<sub>8</sub>, superlattice reflections 9-7450  
 U<sub>3</sub>O<sub>8</sub> foils, e. microscope obs. at 20°C, 300-1000°C 9-11854  
 US<sub>1.5</sub> to US<sub>3</sub>, homogeneity and phases 9-16081  
 US<sub>6</sub> to US<sub>8</sub>, homogeneity and phases 9-16081  
 VCr<sub>2</sub>Se<sub>4</sub>, lattice constants rel. to effect on physical props. of interactions between d shells of transition element 9-16253  
 VS, in phase transition 9-9807  
 W<sub>2</sub>C, WC in field ion microscope 9-1175  
 WCl<sub>6</sub> 9-19726  
 Y<sub>2</sub>Al<sub>2</sub>-Ga<sub>2</sub>O<sub>12</sub> garnet, cation distrib. 9-11857  
 Y<sub>2</sub>TiO<sub>5</sub>, orthorhombic, rel. to mixed seven- and five-fold coordination 9-7452  
 YbH<sub>2</sub>, by X-ray diff. for study of orthorhombic to cubic phase transition 9-18542  
 Zn complex, tris-(2-dimethylaminoethyl)aminezinc (II) bromide 9-3299  
 ZnNH<sub>4</sub>PO<sub>4</sub>, two forms 9-21322  
 Zn<sub>2</sub>P<sub>2</sub>O<sub>4</sub>, monoclinic, crystallographic data and polymorphism 9-5324  
 ZnS, obtained from melt under 50 atm. pressure, X-ray investig. 9-5329  
 ZnSn(OH)<sub>6</sub>, from n. diff., i.r. absorpt. and n.m.r. 9-19709  
 Zr-Pt system, of ZrPt<sub>8</sub> 9-19725  
 Zr 0.61-0.66 wt % H, rel. to phase boundaries, obs. 9-16160

**organic compounds**

- DL-α-amino-n-butyric acid, A and B modifications 9-19728  
 p-bromoacetanilide 9-3316  
 15,15'-dehydrocanthaxanthin 9-11863  
 o-diaminobenzene 9-13653  
 4,4'-diamino-3,3'-dimethylbiphenyl 9-3317  
 1,8-diazacyclotetradecane-2,7-dione 9-16084  
 2-dimethylsulfonylidenemalononitrile, and mol. structure 9-13655

**Crystal structure, atomic continued  
organic compounds continued**

- DL-2-methyl-7-oxododecanoic acid 9-19735  
 trans-perhydrotriphenylene, adducts with cyclohexane and dioxane 9-7465  
 2,4,6-trinitrophenetole-caesium (potassium) ethoxide complexes, (Meisenheimer salts), and mol. structure 9-7467  
 4-acetyl-2'-chlorobiphenyl 9-3313  
 l-amino cyclopentane carboxylic acid hydrobromide, X-ray diff. obs. 9-18454  
 anisaldehyde azine 9-19729  
 D,L-arabinitol 9-9685  
 L-ascorbic acid, n. diff. analysis 9-19727  
 L-aspartic acid, and mol. structure 9-7458  
 DL-aspartic acid, symbolic addition method 9-5330  
 8-azaguanine monohydrate, refinement 9-11860  
 azobenzene-2-sulphenyl cyanide, and mol. structure 9-11861  
 benzene-dinitrogen tetroxide equimolec. complex 9-11862  
 benzotrifluorane, phase refinement 9-3314  
 bicyclo (1.1.1) pentane derivative, correl. with n.m.r. spectrum 9-15205  
 5-bromo veratric acid 9-18455  
 β-bromopicrotoxinin, direct determ. 9-3315  
 calcium tartrate tetrahydrate, and mol. structure 9-19737  
 canthaxanthin, and mol. structure 9-9686  
 carbazole 9-16083  
 carbon tetrachloride, phase II 9-1023  
 catecholamine, dopamine hydrochloride 9-19730  
 cembrene, and mol. structure 9-13650  
 n-chlorodiazoaminobenzene, and tautomerism 9-3320  
 1-chloro-2,3,5,6-tetramethylbenzene, orientational disorder 9-17273  
 2'-chlorobiphenyl-4-carboxylic acid 9-13651  
 cholesteric liquid cry. film, internal helical structure pitch depend. on comp. position 9-18352  
 copper acetate-quinoline cpd., and refinement 9-1197  
 copper formate dihydrate, re-refinement 9-7455  
 cycloheptaamyllose complexes with small organic mols., interrelated space groups 9-7456  
 cyclohexane, phase II 9-1801  
 L-cysteic acid monohydrate 9-13652  
 L-cystinediamide dihydrochloride, and mol. structure 9-19731  
 4,4'-diamino-3,3'-dichlorobiphenyl, and mol. structure 9-9687  
 4,8-dichloro-2,6-diethylbenzo (1,2,4,5-bisoxazole, unit cell and space group 9-7459  
 2,2'-dichlorotrimethylene sulphate, and mol. structure 9-19732  
 β,17α-dihydroxy-16β-bromo-5αpregnen-11,20-dione, and mol. structure 9-13654  
 N,N-dimethyl-p-phenylenediamine bromide, Wursters red bromide 9-7460  
 2,2'-di(1,4-naphthoquinone, and mol. structure 9-13656  
 diphenyl-Δ<sup>2</sup>-pyrazoline 9-3318  
 N,N-diphonylacetic acid, 9-7461  
 dopamine hydrochloride, catecholamine 9-19730  
 ellagic acid 9-19733  
 ethylmagnesium bromide dietherate, obs. 9-9688  
 ferrocenium triiodide 9-9689  
 glycine silver nitrate, obs. 9-1199  
 hexaphenylbenzene modification 9-7462  
 2,2,4,4,6,6-hexaphenylcyclotriphosphazatriene 9-13657  
 hydrazinium hydrazinedithiocarbonylate, and mol. structure 9-13658  
 indole 9-16083  
 π-indocyclopentadienyltetraphenylcyclobutadienylcobalt, lattice constants and space group 9-7463  
 1-isopropyl-4,8,12-trimethyl-2,4,7,11-cyclotetradecatetraene, and mol. structure 9-13650  
 maleimides and maleamic acid, γ-irrad., e.p.r. spectra study 9-21323  
 manganous formate dihydrate, H atom positions from n. diff. data 9-7455  
 K-D-mannitol 9-19734  
 Meisenheimer salts, 2,4,6-trinitrophenetole-caesium (potassium) ethoxide complexes, and mol. structure 9-7467  
 2-mercapto-6-methyl-purine monohydrate 9-11864  
 methanesulfonic acid, and mol. structure 9-14929  
 6-methoxy-8-nitro-5(1H)-quinoline, and mol. structure 9-13660  
 n-methyldiazaminobenzene, and tautomerism 9-3320  
 methylene bromide, from polarized i.r. spectrum 9-17480  
 methylglyoxal bisguanyldiazone dihydrochloride monohydrate, and mol. structure 9-3319  
 2-methylnaphthalene-1,4-diol, and mol. structure 9-21324  
 neopentylalcohol, unit cell and space group 9-16085  
 ninhydrin 9-14930  
 3-nitroperchlorylbenzene, and mol. structure 9-3312  
 ophiobolin methoxybromide 9-7466  
 8,16-oxides-cis-[2,2]metacyclophane 9-14931  
 palladium n-propyl mercaptide 9-11865  
 pentaerythritol, n.m.r. determ. 9-9690  
 trans-perhydrotri-phenylene 9-9691  
 phenanthridine 9-16083  
 2,3-phenanthro, 4,5-naphtho furan, X-ray diffraction data 9-18456  
 p-phenylenediamine dihydrochloride 9-13659  
 phthalocyanine, metal-free, polymorph. spectroscopic characterization 9-19736  
 poly(dimethyl Ketene) 9-19490  
 polyacrylonitrile, non-grafting, and of random-layer line profiles 9-7401  
 polymers, eff. on dielectric props., review 9-19925  
 polymers, supramolecular complexity 9-21325  
 trans-polyptenamer, from X-ray fiber spectra 9-14934  
 polypropylene, syndiotactic, cell constants determ. from fiber spectra 9-14935  
 potassium allantoinate, and mol. structure 9-11859  
 potassium citrates obtained from aqueous soln. at 25°C 9-19720  
 protein phase refinement with Karle-Hauptmann tangent formula 9-13667  
 proteins, by e. diff. 9-14936  
 rauvioxine, absolute config. 9-16086  
 RNA bacterial transfer, probable unit cell dimensions from X-ray power photographs 9-16059  
 sarcosine hydrochloride 9-11866  
 sodium citrates obtained from aqueous soln. at 25°C 9-19720  
 sodium D-tartrate dihydrate 9-7464  
 sodium hydrogen fumarate 9-18457



**Crystal structure, atomic continued**  
**organic compounds continued**

- strontium tartrate trihydrate, and mol. structure 9-19737  
 terpenoid, C<sub>25</sub>, ophiobalin methoxybromide 9-7466  
 tetra  $\alpha$ -pico M-fluoroborates, (M=Ni, Co, Zn or Cd), X-ray diffraction data 9-18456  
 tetramethylammonium sulphate tetrahydrate 9-16087  
 thioacetanilide-S-oxide, and mol. structure 9-13662  
 2-thiohydantoin 9-13661  
 thiosemicarbazide, and mol. structure 9-13663  
 thiourea nitrate 9-7454  
 thorium acetate, isomorphism with U(IV) acetate 9-14932  
 thunbergene, and mol. structure 9-13650  
 thymine photodimer E, and mol. structure 9-14933  
 O-tolidine 9-3317  
 1,2,4-triazole, and mol. structure at -160°C 9-13665  
 trimelic acid 9-13664  
 Uranium(IV) acetate, isomorphism with Th acetate 9-14932  
 ureas., symmetric disubstituted, unit cells and space groups 9-7468  
 D,L-valine 9-13666  
 Vitamin C, n. diff. analysis 9-19727  
 Wurster's red bromide 9-7460  
 UCOs, and other PuNi<sub>2</sub>-type cpds, unit-cell constants 9-7451

**Crystal symmetry** *see* **Crystallography; Crystal structure, atomic**

**Crystallites** *see* **Crystal structure/microstructure**

**Crystallization**

*See also* **Crystals/growth**

- 4,4'-bis dimethylaminodiphenylamine radical iodide, flow 9-11801  
 of aerosols in ultrasonic fields 9-18374  
 of aerosols when supercooled 9-11727  
 austenite recrystallization in slightly hypoeutectoid carbon steel during hot working 9-16145  
 column, separations, determ. of causing and limiting mechanisms 9-16058  
 condensed phases 9-21679  
 cristobalite, internally nucleated in vitreous silica, kinetics 9-18426  
 dielectric thin film, crystallization state evolution, e. diff. study 9-11768  
 Einstein solid, temp. depend. of specific heat 9-7367  
 of elastomers, device for dilatometric meas. 9-21293  
 epitaxial, kinetics during rapid cooling of melt 9-13613  
 glass, differential thermal analysis system 9-13568  
 glasses, binary silicate, heat treated, metastable phases 9-1081  
 ice nucleation by meteoritic material 9-11745  
 of ice subliming in vacuum 9-17234  
 merwinite from melilitite composition 9-18541  
 metal, stable solid nucleus growth in supercooled melts 9-13559  
 nonequilibrium distrib. coeffs., theory 9-16054  
 nucleation and condensing in binary condensed phases, computer simulation 9-5283  
 nucleation growth nucleus, shape stability 9-11805  
 nucleation growth nucleus, shape stability 9-17258  
 nucleation orientation during recrystallization 9-5286  
 nuclei prod. at surface of aqueous soln. by spark discharge 9-18428  
 nuclei production in presence of seed crystal 9-13610  
 polycarbonate of bisphenol A, vapour induced 9-18420  
 polymers, under shear stress, rel. to unstable flow mechanism 9-17236  
 polyoxymethylene, morphology 9-9645  
 potassium dipicrylamine, aqueous system, and reaction kinetics in condensed phases 9-21679  
 RNA bacterial transfer 9-16059  
 rubbers, chloroprene, kinetics obs. 9-11796  
 secondary recrystallization matrix, critical grain size 9-9792  
 solid solutions, new phase nucleation, theory 9-1151  
 solidification, isothermal, in thin layers during combined spontaneous and induced crystallization, statistical theory 9-1142  
 steel, structural recrystallization studies by vacuum metallography 9-1154  
 steel, transformer, cold-rolled, recrystallization 9-1155  
 steel, transformer, commercial grade, secondary recrystallization, role of surface energy 9-13752  
 thin film polymers, spherulite size depend. on film thickness 9-21271  
 A<sup>118</sup>B<sup>119</sup> single crystals under pressure from melt 9-3236  
 Al-Cu alloy, chemical and mechanical grain refinement 9-16144  
 Al-Mn alloys, recrystallization interaction with solid soln. decomposition 9-1153  
 Al, crystallite transport stage and effect on structure refining in l.f. vibrating melt 9-7375  
 Au film, recrystallization rel. to prod. of large single crystals 9-19691  
 Au films nucleation density on colour-centred NaCl. obs. 9-9615  
 CaO-MgO-Al<sub>2</sub>O<sub>3</sub>-SiO<sub>2</sub> glasses, kinetics, iron oxide addition effects 9-19688  
 CaO ceramic crystals, forging and recrystn. 9-3482  
 Co, deformed, nuclei growth and formation rate 9-19836  
 Cu, two-dimensional nucleation of equilibrium lattice nuclei 9-14909  
 Cu, vacuum-smelted, recrystallization diagram 9-5287  
 Fe,  $\gamma$ - $\alpha$  transformation, anisotropic and heterogeneous 9-3489  
 Fe, recrystall. study by isochronal strength curves, effect of alloying additions 9-11962  
 Ge film recrystallized by electron beam, mobility and conc. of current carriers, effect of substrate temp. 9-16271  
 KBr, nucleation centres of condensed phase 9-18425  
 KCl, nucleation centres of condensed phase 9-18425  
 K<sub>2</sub>Cr<sub>2</sub>O<sub>7</sub> u.s. removal from heat transfer surfaces 9-4347  
 KI, double and zone refining for removal of impurities 9-3240  
 Li<sub>2</sub>O-SiO<sub>2</sub> glasses, metastable and equil. phases, X-ray obs. 9-1080  
 LiAlSiO<sub>4</sub>, eucryptite, high temp. form 9-1134  
 MgAl<sub>2</sub>O<sub>4</sub> ceramic crystals, forging and recrystn. 9-3482  
 MgO ceramic crystals, forging and recrystn. 9-3482  
 MgSO<sub>4</sub>·7H<sub>2</sub>O nuclei production in presence of seed crystal 9-13610  
 Mo wines, recrystallization phenomena, investigation using simple electron optics apparatus 9-3247  
 NH<sub>4</sub>Cl dendrites, ageing by dissolution of side arms 9-3473  
 NaCl, nucleation centres of condensed phase 9-18425  
 NiO<sub>2</sub> film, and grain growth, by transmission electron microscopy 9-5251  
 PuO<sub>2</sub> film, and grain growth, by transmission electron microscopy 9-5251  
 Sb films, data from e. diff. patterns 9-5249  
 Se, nonthermally, structure and props. 9-9806  
 Si, front fluctuation during growth by Czochralski technique 9-5280

**Crystallization continued**

- Si film, epitaxial chemically grown, nucleation kinetic meas. on (100) surfaces, using molecular beam techniques 9-21298  
 ThO<sub>2</sub> film, and grain growth, by transmission electron microscopy 9-5251  
 TiC ceramic crystals, forging and recrystn. 9-3482  
 UO<sub>2</sub> crystallization from melt by electrolysis 9-19690  
 W wines, recrystallization phenomena, investigation using simple electron optics apparatus 9-3247

**Crystallography**

- See also* **Electron diffraction crystallography; Isomorphism; Neutron diffraction crystallography; X-ray crystallography**  
 chromium alums., classification 9-13591  
 cleavage to produce miniature circular samples 9-3229  
 dispersion law in f.c. rhombic lattices 9-9665  
 electron density computation by anomalous dispersion method, wrong scale factor effects 9-3273  
 electron density distributions, scale and phase angle errors, and rel. to structures with non-crystallographic mol. symmetry 9-3276  
 ferromagnetic oxides, control of properties by composition variation 9-21308  
 goniometer which allows tilting to 20° at liquid nitrogen temp. 9-5305  
 ion configuration in spinels 9-9632  
 Kagome lattice, modified Slater model 9-5265  
 magnetic groups of cubic symmetry, co-representation with simple lattice 9-1632  
 monoclinic noncentrosymmetric crystals, program for NE 803B computer 9-3223  
 perovskites, classification 9-13592  
 phase computation by anomalous dispersion method, wrong scale factor effects 9-3273  
 proton blocking in cubic crystals 9-19697  
 proton scatt. microscope for crystallography 9-3272  
 replicas, use in materials investigation 9-7396  
 all-trans retinal data 9-3218  
 similarity symmetry groups, three-dimensional, derivation 9-7381  
 Simplex method appl. to direct determ. structure 9-7400  
 small angle scatt., resolution errors, correction using Hermite function 9-11811  
 space group representation in classification of principal vibrations 9-1358  
 space groups, calc. of Clebsch-Gordan coeffs. 9-2135  
 space groups, non equivalent syst. of non-primitive translations 9-21289  
 space groups, plane, dichromatic, magnetic, derived from representation theory of conventional space groups 9-21558  
 specimen preparation 9-7395  
 structure refinement rel. to non-crystallographic mol. symmetry 9-3275  
 symmetry conditions for jump rates of point defects in special positions held by noncubic symm. trap 9-21328  
 symmetry rel. to macroscopic responses 9-3222  
 H, solid contrib. from short range molecular correlations at higher temp. 9-11789  
 KH<sub>2</sub>PO<sub>4</sub>, modified Slater model for Kagome lattice 9-5265

**Crystals**

*See also* **Liquid crystals**

- cleavage apparatus for production of clean film in vacuum 9-1097  
 crystallites, superconducting, coated with polarizable material 9-5654  
 field symmetry, rel. to Eu Raman spectra, scatt. tensor of transitions 9-21634  
 Glan-Thompson and Rochon prisms, modified forms, polarizers and polarizing beam splitters 9-10905  
 molecular, life time measurements of delayed luminescences, use of spectro-photographic phosphoroscope 9-5961  
 onmoon surface 9-18900  
 nonlinear optical, systematic approach for finding new materials 9-18690  
 nonmagnetic, dislocation model of ferromagnetism 9-1659  
 nonmagnetic, dislocation model of ferromagnetism 9-13960  
 polymer, deformed, morphology of fibres pulled from them 9-18395  
 $\alpha$ -quartz optical rotary power, variation due to pressure and temperature 9-12341  
 soft carbons, heat treated, residual lamellar cpds. of H<sub>2</sub>SO<sub>4</sub> and Br<sub>2</sub> 9-7362  
 soluble, cutting using string saw 9-16066  
 from solution, origin of new phase in low temp. hydrocarbon, continuous ultramicroscope obs. 9-3235  
 thiourea ionic complexes, Madelung energy 9-9633  
 FeBO<sub>3</sub>, calcite struct., stability 9-5272  
 He liquid, for resistance thermometer calibration 9-2265  
 LiNbO<sub>3</sub>, holographic storage medium 9-15536  
 SiC crystallites on Si(111) surface obs. by electron diffraction 9-5288  
 TmGa garnet, phonon spectra, laser induced 9-12439  
 U inclusions in grain boundaries of UC, dihedral angles rel. to annealing temp. 9-11855

**electron states** *see* **Crystal electron states**

**etching**

- cyclotrimethylene trinitramine, solution grown, dislocation etching 9-18475  
 diamond, trigons on (111) faces 9-7365  
 quartz, and Ag decoration in elec. field, rel. to defect obs. 9-13682  
 quartz, selective etchants 9-1128  
 rotating anode device which also washes and polishes 9-6015  
 slope of etch pits 9-21341  
 Al alloys, extruded, conditions, patent 9-19833  
 Al thin film from substrate in acid soln. with fluoride ions, patent 9-19684  
 BN etch pits formation, microscopic examination 9-5271  
 BaF<sub>2</sub>, etch pits orientation variation on (111) surface 9-11793  
 BaF<sub>2</sub>, selective display of impurity precipitation at dislocations 9-13680  
 BaSO<sub>4</sub>, barite, patterns, heat effects 9-13594  
 BaSO<sub>4</sub>, synthetic, cleavage faces rel. to dislocation structure 9-1127  
 CdSe, rel. to sensitization to light, investig. 9-3917  
 Ge, surface, parameters rel. to structure, impurities and effect of dislocations on surface roughness 9-3230  
 HgTe, dislocation pits on surface of differently oriented crystals 9-9639  
 KCl, solutions for revealing dislocations 9-1221  
 MnFe<sub>2</sub>O<sub>3</sub>, rel. to dislocation patterns 9-3231  
 NaCl, dislocation etch pits observed on crystals deformed along a cube plane 9-5367  
 NaCl (100) surfaces, thermal etch pits types 9-7366

**Crystals continued****etching continued**

- NaNO<sub>2</sub>, ferroelectric, etching of domains and dislocations rel. to polarization 9-15125  
 Si etch rate using <sup>31</sup>Si tracer 9-16051  
 n-Si specimen prep. for electron damage obs. 9-13815  
 SiO<sub>2</sub>, pyrolytic films, rate dependence on ht. treatment 9-3195  
 U-Nb alloys, electrolytic etching in conc. aqueous citric acid 9-1129  
 Zn, slope of etch pits 9-21341

**excitons** *see Crystal electron states/excitons***faces**

- cyclotrimethylene trinitramine, solution grown, dislocation etching for habit faces 9-18475  
 diamond, dodecahedral form, (111) face due to interrupted growth 9-11795  
 graphite fibres, co-existence of cryst. graphite and turbostratic C phases 9-7363  
 metals, faceted surfaces, LEED patterns 9-11794  
 quartz, growth of first order prisms, microtopographical studies 9-9636  
 silicates cleaved in ultra high vacuum, adhesion 9-7364  
 solid soln., ordered  $\beta$ -brass type, adsorpt. in surface layer 9-3211  
 Ag, (111) face faceting, e. diff. method 9-7357  
 BaF<sub>2</sub>, (111), etch pits orientation variation 9-11793  
 Ba(NO<sub>3</sub>)<sub>2</sub>, morphological symmetry 9-1125  
 BaSO<sub>4</sub>, synthetic, cleavage face etching rel. to dislocation structure 9-1127  
 CdS wurtzite, crystal polarity, He<sup>+</sup> ion scatt. obs., 2 keV 9-9635  
 Ge (111) cleaved surface, opt. detection of surface states 9-1544  
 NaCl, dislocation etch pits observed on crystals deformed along a cube plane 9-5367  
 NaCl cleaved surface electrical microbreakdown, visualization 9-9638  
 NaCl substrate for epitaxial Al films, defect effects on film orientation 9-1105  
 Ni, thermionic parameters of (111), (100) and (110) faces 9-1625  
 Sn single crystals growing from liquid, cellular structure 9-1126  
 SnI<sub>4</sub> structure type, theoretical morphology 9-9637  
 W(100), NH<sub>3</sub> adsorpt. and decomposition obs. 9-1114

**Crystals** *see Crystallization; Epitaxy; Zone melting and refining***Crystals****growth**

*See Also Crystallization; Epitaxy; Zone melting and refining*

- alkali halides, OH<sup>-</sup> conc. from u.v. absorpt. spectra 9-7374  
 alloys, metallic, single crystals, techniques 9-21291  
 alloys, small spherical crystal prep. from melted powders 9-17256  
 alum, from soln., effect of borax on rate 9-13602  
 anthracene, oriented nucleation in elec. field 9-21299  
 anthracene doped with tetracene from melt impurity distrib. determ. 9-7376  
 benzophenone, collision breeding from melt 9-18421  
 $\beta$ -brass, quenched, anti-phase domain growth rate and final size 9-3335  
 cementite particles in tempered iron martensite, X-ray exam. 9-19714  
 chemical reaction growth, mechanism 9-21294  
 citric acid aqueous solutions, nucleation characts. 9-18427  
 collision breeding of crystal nuclei 9-18421  
 corundum:Fe(Ni), composition dependence on oxidation-reduction conditions during growth 9-1132  
 crystalliser with batch-wise or continuous operation, patent 9-13607  
 cyclotrimethylene trinitramine, from solution, dislocation etching for habit faces 9-18475  
 Czochralski, tri-arc furnace with cold crucible 9-1141  
 Czochralski method, dislocation density determining factors 9-3338  
 defects transfer from deformed seed crystal 9-13606  
 dendritic theory for isenthalpic solidification kinetics 9-1156  
 diamond, interrupted growth, study of (111) face 9-11795  
 diamond, synthetic, from graphite, patent 9-13598  
 diamond, synthetic, mechanism rel. to synthetic cubic BN crystals 9-7368  
 4,4'-bis dimethylaminodiphenylamine radical iodide, from solution 9-11801  
 equilibrium shape rel. to bulk free energy 9-13595  
 f.c.c. metals, formation on alkali halides, influence of impurities 9-21268  
 ferrites, hexagonal, preparation by coprecipitation 9-5277  
 fundamental rate equation, theory 9-18409  
 in gels 9-16052  
 glasses, spinodal decomposition, critical temp. depend. on fluctuation wavelength 9-1130  
 graphite, cigar shaped crystals with conical struct., obs. 9-7430  
 graphite, cigar-shaped conical crystals, by heating impure carbon 9-7369  
 graphite, from C-saturated metal solns. 9-7372  
 graphite, rotation boundary angles 9-13629  
 high pressure, high temp. system 9-21292  
 ice:NaCl, interfacial free energy mechanism 9-18410  
 ice, in supercooled aqueous solns. 9-9643  
 ice, on lake, surface growth marks, obs. 9-18414  
 ice, polycrystalline, interfacial free energy mechanism 9-18410  
 ice replicator 9-7370  
 impurity effects, reln. to pH of solution 9-13601  
 impurity influence on formation of single-crystal films 9-21268  
 isenthalpic solidification, theoretical analyses 9-1157  
 lanthanides, trifluorides, from melt 9-9648  
 liquid epitaxy, solvent distribution in unstirred melt, eff. on growth rate 9-18430  
 liquid films, periodic oscillations of impurity particles 9-9504  
 magnetite, from borax flux 9-18413  
 from melt, transient effects, theory 9-1143  
 melt lineage structures origin and growth 9-1225  
 melt-grown, oscillatory temp. instabilities in liquid effects 9-14845  
 melt-grown single crystals, mechanism 9-13600  
 metal, stable solid nucleus growth in supercooled melts 9-13559  
 metal single crystals, bicrystals and tricrystals, from solid state 9-21300  
 metals, low-dislocation-density 9-21295  
 metals, techniques, book 9-21387  
 needle crystal stability 9-16060  
 noble metal alloys, small spherical crystal prep. from melted powders 9-17256  
 nucleating ability of substrate grain boundaries during electrodeposition of Ag from aqueous solution 9-20060  
 organic, and mechanism for melt-grown single crystals 9-13600  
 orientated mat. deposition on single crystals 9-5284  
 oxide film on Ir field-ion specimens 9-21280  
 oxide films on Fe-Fe<sub>3</sub>C 9-1110  
 p-n junctions, epitaxial by UHV sublimation 9-13899  
 planar interface, solution where diffusion coeff. is conc. dependent 9-1087  
 polycarbonate of bisphenol A, vapour induced crystallization 9-18420  
 polymer single crystals, in soln., kinetics study by light scatt. 9-15168  
 polyoxymethylene, morphology of crystallization 9-9645  
 polytypic crystals, nucleation and epitaxial growth 9-13609  
 pulling, temp. distribution analysis 9-11802  
 quartz, first order prism faces, microtopographical studies 9-9636  
 quartz, hydrothermal synthesis in Fe-lined vessel 9-13605  
 quartz solid solutions in MgO-Al<sub>2</sub>O<sub>3</sub>-SiO<sub>2</sub> glass 9-11797  
 salal, surface temp. under unidirectional cooling 9-18424  
 sintered bodies, exaggerated grain growth, mechanism 9-11798  
 solidification, atomic kinetics using Peltier heating and cooling 9-3152  
 from solution, rake 9-9640  
 solution growth, importance of surface diffusion 9-18418  
 spherical dendritic single crystals of high melting point metals 9-19689  
 spherical nuclei, time-depend. theory 9-18411  
 surface temperature of crystals growing from melt 9-18424  
 technology for standardization of growth of monocrystals 9-5273  
 Ti, single crystals growth, using electron beam technique 9-11804  
 1,2,4-trichlorobenzene, surface temp. unidirectional cooling 9-18424  
 triglycine selenate, deuterated, dielectric properties 9-1136  
 triglycine sulphate, domain nucleation and growth, topography 9-16301  
 triglycine sulphate, effect of conditions on dielec. props. 9-10050  
 ulvospinel single crystals from melt in depression in Pt strip 9-5279  
 vanadium oxides, from oxychloride hydrolysis 9-3234  
 vapour transport growth, mechanism 9-21294  
 water, step growth during freezing 9-5216  
 para-xylene, surface temp. under unidirectional cooling 9-18424  
 zone melting and pulling, diffusion effects 9-19687  
 in2PbO<sub>2</sub>SiO<sub>2</sub> glass, from 300-650°C, from i.r. spectra and electron microscopy 9-7321  
 Ag<sub>2</sub>S-As<sub>2</sub>S<sub>3</sub> system, proustite, smithite and pyrrargyrite growth from phase diagram 9-17255  
 Al-Zn (CuAl<sub>2</sub>, Ag<sub>2</sub>Al) eutectic alloys, development of preferred orientation 9-1123  
 Al, crystallite transport stage and effect on structure refining in l.f. vibrating melt 9-7375  
 Al<sub>2</sub>O<sub>3</sub>:Co(Ti), eff. of valence state of dopant 9-14908  
 Al film, elec. resistance variation rel. to method of deposition 9-13582  
 Al film evaporated, O and H<sub>2</sub>O vapour interaction 9-21273  
 Al quenched, multi-layer defects nucleation 9-3344  
 AlK(SO<sub>4</sub>)<sub>2</sub>·12H<sub>2</sub>O, fluidized bed crystallizer, rate obs. at 32°C 9-16055  
 AlK(SO<sub>4</sub>)<sub>2</sub>·12H<sub>2</sub>O, fluidized bed crystallizer, rate obs. at 32°C 9-9641  
 AlK(SO<sub>4</sub>)<sub>2</sub>·12H<sub>2</sub>O, from soln., rate obs. at 32°C 9-11799  
 $\alpha$ -Al<sub>2</sub>O<sub>3</sub>, mechanism from surface growth pattern obs. 9-17260  
 Al<sub>2</sub>O<sub>3</sub>, secondary grain growth kinetics 9-1152  
 AlP epitaxial layers on Si by vapour transport reaction 9-19692  
 Au colloidal, lamellar from soln. e microscopy, diff. obs. 9-11800  
 Au condensation on Si 9-1094  
 Au films, on KCl in high vacuum 9-21274  
 Au large single crystal, from recrystallization of films 9-19691  
 Bi<sub>3</sub> nucleation on W 9-21284  
 BN, cubic, mechanism rel. to synthetic diamond 9-7368  
 BaF<sub>2</sub>·BaCl<sub>2</sub>, indirect flux method 9-18422  
 Ba<sub>2</sub>NaNb<sub>2</sub>O<sub>15</sub> single crystals for optical appl. 9-13597  
 BaTiO<sub>3</sub>, melt, dielectric and optical properties 9-5745  
 Bi, melt-grown, temp. distrib. on crystal-melt system surface meas. apparatus rel. to solidification obs. 9-3237  
 Bi, twinned interlayer growth rate temp. dependence, 123-293°K 9-5289  
 BiTeI, prep 9-1131  
 in C films, anisotropic growth during heat treatment to 2500°C 9-7335  
 Cd-CdSe graded single crystal prep. 9-3232  
 Cd, from melt, interfacial energy 9-18401  
 Cd<sub>3</sub>As<sub>2</sub>-Zn<sub>3</sub>As<sub>2</sub> system, solid soln. growth 9-13882  
 CdCr<sub>2</sub>Se<sub>4</sub>, reversible chemical transport 9-18412  
 CdI<sub>2</sub>, nucleation and epitaxial 9-13609  
 CdS:Na, hollow hexagonal pyramid form 9-13599  
 CdS, cubic, epitaxial growth on InSb and CdS substrates 9-14910  
 CdS epitaxial films, vapour phase chemical reaction technique 9-9616  
 CdSe, epitaxial, on NaCl (111) surface 9-7338  
 CdTiO<sub>3</sub>, melt-grown prep. and dielectric props. 9-18647  
 Co film on Ni, f.c.c. structure 9-7341  
 Cu film, epitaxially twinned, on sapphire 9-1104  
 Fe-Ni-Co monocrystalline alloy thin films epitaxy and coercive force 9-12298  
 Fe-Ni-Mn alloy, nucleation rate of isothermal martensitic transformation 9-14990  
 Fe(III) hydroxide gels, nucleation obs. 9-5285  
 $\alpha$ -FeO(OH), needle shape preservation for Y-Fe<sub>2</sub>O<sub>3</sub> mag. tape preparation, patent 9-9642  
 GaAs dislocations, Czochralski growth method 9-3348  
 GaIO<sub>3</sub>, from melt by Czochralski technique, possible laser host 9-1144  
 Ge, Chokhrals'kii growth, effect on structure 9-1122  
 Ge, epitaxial deposition onto GaAs by GeH<sub>4</sub> pyrolysis 9-19670  
 Ge, rotating crucible method 9-1145  
 Ge epitaxial film, from supercooled droplets 9-13580  
 Ge epitaxial layers on Si substrates, by vacuum evaporation 9-3201  
 Ge epitaxial mirror smooth layers on GaAs by disproportionation reaction 9-19671  
 Ge thin films, zone melting method using SiO<sub>2</sub> and glass coatings 9-3238  
 HfO<sub>2</sub>, hydrothermal, temp. and solvent effects 9-1139  
 In film thermal evaporation on amorphous substrates 9-21279  
 In<sub>2</sub>O<sub>3</sub>, from PbO-B<sub>2</sub>O<sub>3</sub> melts, mechanism rel. to habit changes 9-17257  
 InSb single crystal 9-1147  
 K whiskers, rate in critical saturation region 9-16061  
 KBr, collision breeding from aqueous soln. 9-18421  
 KCl-KBr solid solns., removal of divalent cations by introduction of anion-replacing impurities 9-16053  
 KCl, collision breeding, from aqueous soln. 9-18421  
 KCl, from melt, free of grain boundaries and with low density dislocations 9-16101  
 KCl, high purity, by heat treatment followed by zone melting 9-18423  
 K<sub>2</sub>Li<sub>2</sub>Nb<sub>2</sub>O<sub>15</sub>, and crystallographic characts. 9-11803  
 Li ferrite in SiO<sub>2</sub> glasses, kinetics and mag. props. 9-1146  
 LiF-NaF, by Czochralski method, preferred <100> texture 9-1123  
 LiF, impurity-doped 9-1133



**Crystals continued****growth continued**

- LiF, skeletal cavities formation on melting 9-13611  
 LiNbO<sub>3</sub>, hydrothermal synthesis of single domain crystals by transport reactions 9-19685  
 melt-grown, temp. distrib. on crystal-melt system surface meas. apparatus rel. to solidification obs. 9-3237  
 MgSO<sub>4</sub>·7H<sub>2</sub>O, collision breeding from aqueous soln. 9-18421  
 MoO<sub>3</sub>, from vapour, plates 9-1137  
 NH<sub>4</sub>H<sub>2</sub>PO<sub>4</sub>, shape, effects of pH 9-13604  
 NaCl, effect of Na<sub>2</sub>Fe(CN)<sub>6</sub> on growth and characteristics 9-18415  
 NaCl, from melt, formation of intergranular dislocation substructure 9-21296  
 Na<sub>2</sub>SbS<sub>4</sub>·9H<sub>2</sub>O, from solution, pH and temp. dependence 9-13603  
 Nb<sub>2</sub>O<sub>5</sub>, single crystals large enough for dielec. studies, by careful control of halogen transport 9-3695  
 Ni evap. films on glass, X-ray texture investigation 9-7336  
 Ni films evap. on glass, struct. depend. on thickness 9-7337  
 NiO, solar furnace fusion 9-13608  
 NiO films, eff. of structural defects 9-9621  
 NpO<sub>2</sub> film, grain, and crystallization 9-5251  
 Pb-7 at. %Sn, cellular reaction kinetics 9-14906  
 Pb, melt-grown, temp. distrib. on crystal-melt system surface meas. apparatus rel. to solidification obs. 9-3237  
 Pb film thermal evaporation on amorphous substrates 9-21279  
 PbTe film on KCl, epitaxial, mechanism 9-1106  
 PbTiO<sub>3</sub>, conditions effect on ferroelec. props. 9-19931  
 PbTiO<sub>3</sub>, hydrothermal production kinetics 9-1138  
 Pb(Zr-Ti)O<sub>3</sub>, by flux method 9-1148  
 Pd<sub>2</sub>O<sup>4-</sup>, ternary oxide, (a<sub>2</sub>PdO)<sub>3</sub>, A=rare earth or In, pyrochlore struct., prep. at 3 kbar 9-5274  
 Pt depression used for growth of single crystals 9-5279  
 Pt<sub>2</sub>O<sup>4-</sup>, ternary oxide, (A<sub>2</sub>Pt<sub>2</sub>O)<sub>3</sub>, A=rare earth or In, pyrochlore struct., prep. at 3 kbar 9-5274  
 PuO<sub>2</sub> film, grain, and crystallization 9-5251  
 Sb<sub>2</sub>Se<sub>3</sub>, needle like, rel. to structure, mech. and elec. props. 9-1194  
 Si, crystallization front fluctuation during growth by Czochralski technique 9-5280  
 Si, epitaxial, light irradiation effects 9-11808  
 Si, epitaxial on Si substrates, heater, patent 9-21269  
 Si, filamentary, from soln. in tin, resistivity 0.01 ohm-cm 9-9644  
 Si, mosaic, for semicond. devices, low dislocation density, prod., patent 9-13596  
 Si, semiconductor grade 9-9651  
 Si epitaxial technology advances 9-7339  
 Si layer, highly alloyed, by PCl<sub>3</sub> diffusion 9-17245  
 Si on (111) Si, in ultrahigh vacuum, surface processes 9-5276  
 Si single crystal, dislocation generation and concentration 9-1224  
 Si web, processes and defects, thermal interaction effects 9-9646  
 SiBi<sub>2</sub>O<sub>10</sub>, melt grown prep. 9-18648  
 SiC, Frank's mechanism, screw dislocation clusters 9-18477  
 SiC, recrystallization by floating solvent method using molten rare-earth metals 9-16056  
 n-SiC, sublimation, eff. of time and temp. 9-18416  
 SiC, sublimation process, eff. of time and temp. 9-18416  
 SiC whiskers 9-3241  
 from SiCl<sub>4</sub>-H<sub>2</sub> vapour-gas system, conc. ratio in saturator of epitaxial equipment 9-12101  
 SiN, vapour growth from SiH<sub>4</sub>-NH<sub>3</sub>-H<sub>2</sub> and SiCl<sub>4</sub>-NH<sub>3</sub>-H<sub>2</sub> systems 9-5250  
 Sn, melt-grown, temp. distrib. on crystal-melt system surface meas. apparatus rel. to solidification obs. 9-3237  
 Sn film thermal evaporation on amorphous substrates 9-21279  
 Sn from liquid, surface cellular structure 9-1126  
 SnO<sub>2</sub>, sublimation process for new electrochrom. material 9-15193  
 SrTiO<sub>3</sub>, from silica flux 9-14907  
 Te, epitaxial on Cu(111) surface, LEED study 9-21270  
 ThO<sub>2</sub> film, grain, and crystallization 9-5251  
 Ti-Al, α-phase, single crystals, growth using electron beam technique 9-11804  
 α-U, under irradi. at 25°C 9-7371  
 UO<sub>2</sub>, by solar furnace 9-16057  
 UO<sub>2</sub> by thermal decomposition of UOCl<sub>2</sub> dissolved in molten UCl<sub>4</sub> 9-19686  
 UO<sub>2</sub> single crystal prepared by induction heating of rod, with rotation and elevation 9-21297  
 WC monocrystals, from Co flux by Czochralski technique 9-5281  
 WO<sub>3</sub>, from vapour, plates 9-1137  
 Y Fe garnet, flux, Fe<sup>2+</sup>-Fe<sup>4+</sup> equilibrium model 9-1149  
 Y Fe garnet, from Na<sub>2</sub>WO<sub>4</sub> melts 9-1150  
 YFe garnet, defects effects on domain structure 9-12302  
 YVO<sub>4</sub>, Verneuil process 9-18417  
 ZnO, thin films 9-5252  
 ZnO, zincite, Fe entry during hydrothermal growth 9-18419  
 3 ZnO·P<sub>2</sub>O<sub>5</sub>·4H<sub>2</sub>O (hopeite), from ZnPO<sub>4</sub> cements in humid atm. 9-3233  
 ZnS, from melt, distribution of Fe, Cu and Ag impurities 9-18429  
 ZnS in Zn or S vapour excess, I carrier, luminescence meas. 9-21345  
 Zr, single crystals growth, using electron beam technique 9-11804  
 ZrO<sub>2</sub>, hydrothermal, temp. and solvent effects 9-1139

**hyperfine field interactions**

- alkali halide crystals, of S<sup>-</sup> trapped impurity 9-3954  
 alkali metals, electron-electron interaction effect on nuclear spin-lattice relax rates and Knight shifts 9-17501  
 γ-optical transitions, laser-stimulated in determining hyperfine structure of ions of Mossbauer nuclei 9-18696  
 degenerate electron systems and impurity centres 9-16399  
 Eu<sub>2</sub>O<sub>3</sub>, isomer shift, temp. variation, non-linearity and hysteresis effects 9-1718  
 ferromagnet, rel. to longit. relax. time near Curie pt. 9-3838  
 ferromagnetic host with rare earth nuclei, anomalous fields in unresolvable time period 9-7929  
 ions, <sup>6</sup>S<sub>1/2</sub> in cubic crystal, energy levels 9-16452  
 molecular crystals, hyperfine structure of stabilized foreign atoms, effect of multipoles of matrix mols. 9-1717  
 noble metals, electron-electron interaction effect on nuclear spin-lattice relax rates and Knight shifts 9-17501  
 nuclear quadrupole coupling constant in solids, obs. disproved 9-10301  
 nuclear spin exchange interaction effect on dynamic nuclear polarization 9-1719  
 pyrene, excimer interaction potential 9-1834  
 RKKY interaction between two mag. moments, soluble model 9-13818

**Crystals continued****hyperfine field interactions continued**

- spin coords transformation, soln. of Hamiltonian for orthorhombic paramag. center in rigid lattice 9-10274  
 spin Hamilton of two equivalent nuclei, appl. to I<sub>2</sub><sup>-</sup> centres 9-5986  
 spin-spin interaction constants from hyperfine structure of coupled ion pairs 9-21599  
 static field parallel to external polarizing field, hypothesis justified on time scale starting at 1 nsec 9-7929  
<sup>151</sup>Eu, isomer shift, chemical effects 9-3842  
<sup>153</sup>Eu in Sm intermetallic cpds. 9-14040  
 Al<sub>2</sub>O<sub>3</sub>:<sup>53</sup>Cr, ENDOR determ. 9-8044  
 Al<sub>2</sub>O<sub>3</sub>, of AlO<sub>3</sub><sup>-</sup>, radiation-induced, rel. to optical and mag. props. 9-12322  
 As atoms trapped in inert matrices at 4.2°K, matrix perturbing effects 9-12501  
 Au(II) diethyldithiocarbamate, single cry., ESR spectra, quadrupole eff. on hyperfine struct. 9-14109  
 BaF<sub>2</sub>:Eu<sup>2+</sup>, e.p.r., hyperfine coupling constant of <sup>151</sup>Eu<sup>2+</sup>, temp. depend. 9-12502  
 BaF<sub>2</sub>, F centre electron interact. with four nearest F shells, endor meas. 9-1234  
 BaFe<sub>12</sub>-...Al<sub>2</sub>O<sub>3</sub> of <sup>57</sup>Fe nuclei, var. with Al substitution 9-16366  
 Ca<sub>3</sub>Al<sub>2</sub>(SiO<sub>4</sub>)<sub>2</sub> garnet, grossularite, <sup>27</sup>Al quadrupole coupling constant 9-12509  
 CaCO<sub>3</sub>:Mn<sup>2+</sup>, superhyperfine interaction of Mn<sup>2+</sup> e.s.r. with <sup>13</sup>C 9-5987  
 CaF<sub>2</sub>, F centre electron interact., with four nearest F shells, endor meas. 9-1234  
 Co(NH<sub>4</sub>)<sub>2</sub>(SO<sub>4</sub>)<sub>6</sub>·6H<sub>2</sub>O, of paramag. Co<sup>2+</sup>, NMR and EPR exam. 9-8038  
 CrI<sub>3</sub>, internal field coupling constants determ from <sup>129</sup>I Mossbauer effect 9-21609  
 Cu, rel. to Fermi-surface electron and prediction of Knight's ratio 9-9894  
 CuCr<sub>2</sub>Te, Mossbauer effect of <sup>129</sup>I, mechanism of hyperfine interaction at anion 9-16400  
 Cu<sub>2</sub>MnAl(Sn), Heusler alloys, from low temp. sp. ht. and NMR data 9-9841  
 EuFe garnet, of 21.7 keV level of <sup>151</sup>Eu from Mossbauer meas. 9-16401  
 Fe<sub>2</sub>B, ferromagnetic, from n.m.r. and Mossbauer effect obs. 9-21670  
 Fe<sub>2</sub>Zr, ferromagnetic, from n.m.r. and Mossbauer effect obs. 9-21670  
 Fe<sup>3+</sup> ions in ice and FeCl<sub>3</sub>·6H<sub>2</sub>O, elec. quadrupole h.f.s., Mossbauer determ. 9-14037  
 Fe<sup>57m</sup>, nuclear quadrupole moment from α-Fe<sub>2</sub>O<sub>3</sub> data 9-7930  
 FeS, near stoichiometric, temp. depend. 9-5892  
 GdFe garnet, temp. and mag. field dependence of hyperfine field at Fe nuclei, by <sup>57</sup>Fe spin echo n.m.r. 9-21671  
 GdFe<sub>2</sub>, at <sup>115</sup>Gd rel. to absence of induced mag. field 9-17470  
 H atoms trapped in inert matrices at 4.2°K, matrix perturbing effects 9-12501  
 HfO<sub>2</sub> elec. quadrupole interaction 9-3972  
 Ho, specific heat meas. 0.03-0.5°K 9-21600  
 I<sub>2</sub><sup>-</sup> centre, derivation of spin Hamiltonian of two equivalent nuclei 9-5986  
 I<sub>2</sub>O<sub>4</sub>, quadrupole splitting of <sup>129</sup>I Mossbauer level at 80°K 9-16403  
 LuFe garnet, temp. and mag. field dependence of hyperfine field at Fe nuclei, by <sup>57</sup>Fe spin echo n.m.r. 9-21671  
 MgO:Fe<sup>2+</sup>, spin-lattice coupling constants 9-14016  
 MgO:<sup>51</sup>V<sup>2+</sup>, spin Hamiltonian of <sup>51</sup>V<sup>2+</sup> from ENDOR 9-12520  
 Mn<sup>2+</sup> in CdF<sub>2</sub>, interplay of fine, hyperfine and superfine interac., ESR 9-14112  
 MnO, rel. to <sup>17</sup>O NMR shift 9-1876  
 Mn<sub>2</sub>P, paramagnetic, at P sites from susceptibility and Knight shift meas. 9-16379  
 N atoms trapped in inert matrices at 4.2°K, matrix perturbing effects 9-12501  
 NaCl:Mn<sup>2+</sup>, X-irrad., from e.p.r. spectrum 9-21667  
 NaCl-NaBr:<sup>23</sup>Na, interaction with elec. quadrupole moment of neighbour nuclei 9-8048  
 NaF:Li, from ENDOR spectrum of self-trapped hole associated with Li<sup>+</sup> impurity 9-10286  
 NaF, from ENDOR spectrum of V<sub>k</sub> centre 9-10285  
 NaInS<sub>2</sub>:Cr<sup>3+</sup>, of Cr<sup>3+</sup> with coplanar In<sup>3+</sup>, from e.p.r. obs. 9-10287  
 NaInS<sub>2</sub> with Cr<sup>3+</sup> substitutions 9-8029  
 Nb<sub>2</sub>Sn, temp.-dependent isomer shift of <sup>119</sup>Sn from Mossbauer effect meas. 9-7960  
 NpO<sub>2</sub>, of <sup>237</sup>Np, from Mossbauer effect rel. to antiferromag. ordering 9-1708  
 P atoms trapped in inert matrices at 4.2°K, matrix perturbing effects 9-12501  
 Pt-Co alloys, nuclear orientation meas. of field at <sup>60</sup>Co nuclei 9-13966  
 Sm<sub>2</sub>Co<sub>17</sub>:<sup>153</sup>Eu, Mossbauer effect exam. 9-14040  
 SmFe<sub>2</sub>:<sup>153</sup>Eu, Mossbauer effect exam. 9-14040  
 Sm<sub>2</sub>Ni<sub>17</sub>:<sup>153</sup>Eu, Mossbauer effect exam. 9-14040  
 SrF<sub>2</sub>:Eu<sup>2+</sup>, e.p.r., hyperfine coupling constant of <sup>151</sup>Eu<sup>2+</sup>, temp. depend. 9-12502  
 SrF<sub>2</sub>, F centre electron interact. with four nearest F shells, endor meas. 9-1234  
 SrFe<sub>12</sub>-...Ga<sub>2</sub>O<sub>9</sub>, orientation angle between Fe<sup>3+</sup> mag. moments 9-16373  
 Tb, specific heat meas., 0.03-0.5°K 9-21600  
 ThO<sub>2</sub>:<sup>152</sup>Gd<sup>3+</sup>, hyperfine coupling, temp. dependence 9-8031  
 Tm Ga garnet, from NMR of <sup>167</sup>Tm at 4°K 9-1880  
 TmFe garnet, temp. and mag. field dependence of hyperfine field at Fe nuclei, by <sup>57</sup>Fe spin echo n.m.r. 9-21671  
 V<sup>2+</sup> in cubic fields, phonon-induced hyperfine coupling 9-5531  
 YFe garnet, temp. and mag. field dependence of hyperfine field at Fe nuclei, by <sup>57</sup>Fe spin echo n.m.r. 9-21671

**imperfections see Crystal imperfections****internal fields**

- See also *Crystal field theory*  
 alkali halide, elec. fields due to dislocation motion in bending deformation 9-1453  
 CdS, semiconducting, spatial and time variation of elec. fields 9-13874  
 electric field gradient asymmetry parameter rel. to nuclear quadrupole spin echo slow beats 9-3973  
 electric-field-gradient tensors determ. by n.q.r. 9-8047  
 electron-phonon mass enhancement, determ. usieudopot. approaches 9-13827  
 electrostatic potential of point charge systems, potential expansion symmetry 9-4910  
 electrostatics of finite charge distrib. 9-12039

**Crystals continued****internal fields continued**

- fluorides, field grads. at  $^{19}\text{F}$  nuclei from quadrupole moment of excited  $5/2^+$  state 9-4730
- induced moment systems, mag. props. and cryst. elec. field 9-16334
- inorganic, elastic const. calc. from force field const. 9-19778
- methyl ammonium aluminium sulphate, from  $^{27}\text{Al}$  NMR rel. to ferroelec. phase transitions 9-3968
- phthalocyanine iron (II), elec. field gradient at Fe nucleus, Mossbauer spectrum obs. 9-10100
- rare-earth halides, stabilization energy rel. to spin-orbital interaction 9-21453
- ruby, crystal-field parameters, isotope effects 9-12040
- rutile, e.p.r. of ions with  $d^1$  shells 9-16460
- $\alpha\text{-Al}_2\text{O}_3$ , ionic potentials, fields and gradients at lattice sites 9-10158
- $\text{Cs}_2\text{MnCl}_4 \cdot 2\text{H}_2\text{O}$ , elec. field-gradient determ. by n.q.r. 9-8047
- Cu-8-hydroxyquinolate, host lattice effects 9-10279
- Cu, hyperfine field rel. to Fermi-surface electron and prediction of Knight's ratio 9-9894
- $\text{CuBr}$ , electric field gradient, spin echo meas. 9-10028
- $\text{CuCr}_2\text{Te}$ , Mossbauer effect, of  $^{125}\text{I}$ , internal mag. field at iodine impurities 9-16400
- CuI, electric field gradient, spin echo meas. 9-10028
- Eu ion in octacoordinate sites, symmetry, potential and level splittings 9-14018
- $^{19}\text{F}$  in polycryst. fluorides, static nuclear quadrupole-interact. parameters, and field grads. 9-4730
- GdAs surface field modulation of reflectance spectra 9-10172
- $\text{Ga}^{3+}$ , direct determ. in  $\text{YVO}_4$  and  $\text{YPO}_4$  from variable-freq. e.p.r. 9-5985
- $\text{K}_2\text{Fe}(\text{CN})_6$ , crystallography and paramag. anisotropy,  $95^\circ$  and  $300^\circ\text{K}$  9-21315
- $\text{K}_2\text{Fe}(\text{CN})_6$ , crystallography and paramag. anisotropy,  $95^\circ$  and  $300^\circ\text{K}$  9-21343
- KF, field grads. at  $^{39}\text{K}$  nuclei 9-1884
- $\text{MgO}$ , crystal-field parameters, isotope effects 9-12040
- $\text{MgO}$ , internal potential meas. by interferential microscopy 9-5861
- $\text{MnF}_2$ , mag. dipole optical absorpt. 9-1789
- $\text{Mo}(\text{IV})\text{Cl}_6$ , electronic spectra 9-7982
- $\text{Os}^{3+}$  in cubic crystals, at  $4.2^\circ\text{K}$  9-14055
- $\text{Pd}_2\text{MnSn}$  Heusler alloy at  $^{119}\text{Sn}$  site 9-16404
- $\text{Pr}^{3+}$ , shielding at rare-earth ions 9-7695
- $\text{PrCl}_3$ , charge penetration and covalency contribs. 9-10159
- $\text{Tm}^{3+}$ , shielding at rare-earth ions 9-7695
- $\text{TmAl}_3$ , mag. props. and cryst. elec. field 9-16334

**lattice mechanics***See also Mossbauer effect*

- p-dichlorobenzene, librational amplitudes 9-10224
- Al, changeover phenomenon and transverse phonons in kinetic coeffs. rel. to thermal conductivity 9-3541
- alkali halides, anharmonicity and cohesive energy 9-11984
- alkali halides, Debye temp. calc., interac. pot. approach 9-12019
- alkali halides, i.r. absorpt. calc., interac. pot. approach 9-12383
- alkali halides, one-phonon relax. of  $\text{OH}^-$  9-5534
- amine-halogen charge-transfer complexes 9-2892
- anharmonic, thermal motions and eqns. 9-3499
- anharmonic contribution to free energy 9-21420
- anharmonic crystal, phonon frequency change with temp. increase causing melting 9-19848
- anharmonic effects in thermodynamic props. of solids 9-21434
- anharmonic effects in thermodynamics props. of solids 9-12014
- anharmonic interaction in lattice with impurities, quasi-local vibrations 9-11979
- anharmonic phonon shifts and widths for a centro symmetrical potential 9-7627
- anharmonicity and thermal accommodation coeff. 9-9602
- anthracene, vibr. intensities, Raman obs. 9-18551
- benzene, vib. spectra, splittings due to intermolec. forces 9-5932
- caesium halides, Debye-Waller factors of  $^{133}\text{Cs}$  and  $^{129}\text{I}$  9-11986
- calcite structured crystals, lattice vibrations 9-5525
- carbazole, vibr. assignm. 9-9252
- cerium ethyl sulphate, anomalous phonon effects, on sp.ht., spin-lattice relax. 9-7658
- copper halides, vibration modes and force constants 9-13788
- covalent crystals, bond charge model 9-9808
- cubic crystals, rel. to Debye characteristic temp. at  $T=0$  9-5565
- cubic metals, thermal vibrations mean square displacements at melting point 9-11743
- damping anharmonic of Rayleigh surface modes 9-3503
- Debye-Waller factor for small cubes and thin films 9-7623
- Debye-Waller factors of  $^{133}\text{Cs}$  and  $^{129}\text{I}$  in Cs halides 9-11986
- diamond, one-phonon band-mode i.r. absorption by impurity resonances 9-5915
- dielectric, internal photoeffect with atomic centres 9-10231
- dielectric anharmonic, phonon transport eqn. and hydrodynamic applic. 9-21421
- dielectrics, phonon gas viscous flow in thermal conductivity nonlinearities 9-18566
- dimers on rectangular lattice, matrix equations 9-4246
- dipolar coupling and molec. vibr., theory 9-3501
- dislocations, interacting system, vibrational spectrum in long-wave approximation 9-16095
- dislocations and phonon scattering 9-3502
- disordered harmonic lattices, normal-mode spectra for abnormal arrays 9-9812
- disordered solids, vibration spectra 9-11981
- disorders, effect on supercond. transition temp. 9-5655
- displacive-ferroelectric, impurity phonon modes frequency rel. to temp. 9-18546
- Einstein phonons, interac. by Green's function method, soln. of chain of coupled eqns. 9-3498
- electron diffraction, dynamic, in ideal vibrating crystals 9-13792
- electron-vibrational systems with e. degeneracy, optical bands 9-15172
- electronic and vibrational spectra, unified presentation 9-1757
- e.m. radiation interac. with LO phonons in ionic cry., effs on dielec. props. 9-11990
- entropy of small classical crystals. 9-3531
- exchange-phonon mechanism of energy migration 9-9883
- f.c.c. metals, angular forces 9-5528
- ferroelectric materials, rel. to Kanizg's regions dimensions 9-21534
- ferroelectricity, review 9-13917

**Crystals continued****lattice mechanics continued**

- ferroelectrics, displacement-type, soft-mode-freq. calcs. in statistical theory 9-21535
- ferroelectrics, displacement-type, soft-mode-frequency calcs. from statistical theory 9-21536
- ferroelectrics, thermal oscils. anomalies near phase transition 9-1364
- ferromagnet, spin-phonon interaction effects on specific heat 9-12017
- ferromagnetic films, dipolar effects in spin-wave eigenfrequencies and eigenfunctions 9-21588
- films, local modes and Mossbauer eff. 9-18544
- films, metallic, layered, supercond. enhancement by phonon freq. lowering 9-7765
- force-constant changes, effect on incoherent n. scatt. from cubic crystals with impurities 9-9822
- frequency shift effects on multiphonon structure in absorpt. and emission spectra 9-16410
- garnets: rare-earth, electronic and vibrational Raman eff. obs. 9-12434
- graphite, phonon freq. distrib. from inelastic thermal neutron scatt. 9-19855
- harmonic approx., freq. spectra, normal modes and coordinates, thermodynamic functions calc. 9-21423
- h.c.p., dispersion relations 9-18545
- h.c.p. metals 9-3506
- Heisenberg ferromagnet, spin-phonon interaction and magnetic excitations 9-16387
- ice, dynamical model of lattice rel. to interpretation second order Raman spectra 9-12418
- ice, light water, phonon spectrum and thermal neutron scattering 9-21426
- III-V cpds., dispersion curves, freq. distrib. functions eff. calorimetric and X-ray Debye temp. 9-11978
- imidazole, l.f. lattice vibr. 9-16424
- impurity crystals, vibrational structure of vibronic spectrum, double adiabatic approximation 9-17349
- impurity-induced i.r. absorpt., mol. coupling, theory 9-7966
- inert gases, infl. of lattice anharmonicity on exponential potential parameters 9-16161
- insulators, optical phonon freq. and mag. order 9-7626
- ionic, optical vibrational 9-11980
- i.r. resonant-mode freq. shifts on uniaxial stress 9-5922
- lanthanum cobalt nitrate, phonon mean free paths, spin-lattice interac. strengths from magneto-thermal-conductivity meas. 9-9854
- laser action involving free excitons and LO-phonon assisted transitions, theory 9-6522
- light scatt. by phonons in presence of heat flow 9-16162
- linear chain with second-neighbour interaction, surface effect 9-14998
- local mode self-energy eff. on U-centre sidebands 9-18479
- localized modes, temp. depend. and i.r. absorption 9-7630
- long wavelength phonon scattering by point defects in cubic lattices 9-13785
- mass-disordered lattices, displacement correlations and frequency spectra using Green's functions 9-9809
- matrix-trapped diatomic mol., effect of localized vibr. on spectra 9-3883
- metal, optical phonons, inelastic scatt., Raman effect 9-1759
- metals, anharmonicity effect on transport props., Green's function theory 9-13822
- metals, phonon-limited resistivity 9-9926
- microwave phonons spectroscopy 9-9816
- $\text{MnF}_2$ , rutile structure, vibrational spectra, critical dipole frequency behaviour 9-7636
- molecular crystals, peak width in single phonon scattering of neutrons 9-14997
- molecular crystals, torsional vibrs. 9-7628
- n-semiconductors, electron-phonon interaction and l.f. oscillations 9-7790
- naphthalene, low freq. phonons near Brillouin zone boundaries 9-19854
- naphthalene, phonon structure in emission spectra 9-18714
- naphthalene, vib. spectra, splittings due to intermolec. forces 9-5932
- naphthalene, vibr. intensities, Raman obs. 9-18551
- neutron dispersion in system of one-dimensional anharmonic oscillators, exact results 9-11992
- $\alpha\text{NiSO}_4 \cdot 6\text{H}_2\text{O}$ , internal energy,  $0.4^\circ\text{K}$ ,  $0.90\text{ kG}$  fields 9-19862
- non-crystalline solids, elementary excitations, dispersion relations 9-9813
- nonlinear, optical excitations 9-1357
- one dimensional, harmonic, isotopically disturbed crystal, lattice thermal conductivity 9-18568
- one-dimensional periodic systems, nonadiabatic transition probability vibrational spectrum dependence 9-1423
- optical phonon-magnon interaction rel. to e.m. wave interaction with antiferromagnet 9-1692
- perchlorylamide ion, normal vibrs., effect of bond lengths and state 9-7046
- phonon gas, heat-pulse propag. theory 9-9852
- phonon mass operator, imaginary part freq. dependence at high temps. 9-21574
- phonon mass operator, real part determ. 9-20358
- phonon means free paths, spin lattice interac. strengths, from magneto-thermal-conductivity meas. 9-9854
- phonon propagator structure, anharmonic crystal 9-5527
- phonon spectra of metallic and non-metallic crystals rel. to dielectric screening approach 9-9811
- phonon spectrum changes in small particle layers, supercond. enhancement 9-5529
- phonon spectrum for cubic lattice with interstitial atom 9-19847
- phonon system, interacting, linear response and transport eqns. 9-7632
- phonons, LO, interac. with e.m. rad. in nonuniform field, eff on dielec. props. 9-11990
- phonons, thermal, effect on high-temp. supercond. 9-1484
- phonons in time-dependent Hartree approx., appl. to order-disorder ferroelectrics 9-9810
- phonons treated as renormalised Einstein phonons 9-3498
- in piezoelectric vibrating resonators, using neutron diffraction 9-1355
- polar lattice vibrations causing first-order Raman scattering 9-12391
- polycrystals, inelastic n. scatt. cross section calc. in one-phonon approx 9-11991
- polyethylene, intermolecular vibrations 9-5537
- polyethylene, l.f. vibrs. 9-1366
- polyethylene terephthalate, intermolecular vibrations 9-5537
- polymer, long helical, Umklapp process rel. to optical rot. 9-5879
- polyoxymethylene, hexagonal, orthorhombic, deuterio, vib. assignments from Raman spectra 9-14064
- polypropylene, isotactic, dispersion curves and freq. distribs. 9-9302



## Crystals continued

## lattice mechanics continued

- praseodymium ethylsulphate, phonon scatt. in thermal resistivity anomalies <1°K 9-13811
- proton-phonon coupling in H-bonded system 9-21422
- pyrazine, i.r. vibr. 9-1363
- quartz, coherent optical phonons of 100 W, generation 9-12320
- quartz, one- and two-phonon excitations coupling evidence 9-1361
- $\alpha$ -quartz, polariton Raman scattering intensities 9-12436
- quartz transducers, coherent phonon fusion for u.s. second harmonic generation 9-3511
- quasi-local vibrations, anharmonicity infl. on spectral distribution 9-19846
- Raman scattering by polaritons in polyatomic crystals 9-12392
- Raman scattering in impurity-containing crystals, microscopic theory 9-12402
- Raman scattering tensor for combinations and overtones 9-12394
- rare gas crystals, defect-induced one-phonon i.r. absorption, theory 9-5526
- rare-gas, many-body van der Waals forces effect on lattice dynamics 9-13786
- Rayleigh surface modes, anharmonic damping calculation 9-3503
- resonance energy transfer in condensed media from many-particle view-point 9-5621
- reststrahlen and symmetry, elemental 9-7629
- rutile, phonon processes in hypersonic attenuation 9-13797
- rutile structure crystals, vibrational spectra, dipole freq. behaviour 9-18549
- rutile structure crystals, vibrational spectra, dipole freq. behaviour 9-7636
- second-order electric moment contrib. to optical absorption 9-5907
- semiconductors, longit. optical phonon-plasmon interaction in Raman scatt., theory 9-3901
- simple lattices with line defects, theory 9-1356
- simple microscopic model for thermal conductivity 9-3500
- sodium halides, rel. to ionic deformation 9-13791
- solid solutions, boundary scatt. of phonons 9-1359
- spectral symmetry in model, vib. modes and applic. 9-19849
- surface phonon vibrations, phase shift solution 9-21418
- tetragonal crystals, freq. distrib. function calcs. 9-7631
- thermal cond., model with phonon scatt., Umklapp proc., predicted exponential temp. behaviour 9-3500
- thermal diffuse scatt. in measured integrated intensities from cubic single crystals 9-18543
- thermal motions in anharmonic cry., phonon Green's function, propag. and damping of phonons thro' freq. range 9-3499
- tungstates, dipole-dipole interactions 9-1362
- two-phonon scattering of light, electronic terms in spectrum 9-11982
- Urbach rule for localized excitations, theory 9-5905
- urea, vibrations, from i.r. and Raman meas. 9-17351
- vibration spectra in system with coinciding ferroelec. and ferromag. axes, from motion of polarization and magnetization vectors 9-16163
- vibrational Faraday rotation of U centre, obs. poss. 9-14032
- vibrational relaxation of excited luminescence centre, Raman. spectra 9-12403
- vibrational structure of impurities from radiation spectrum 9-16408
- vibrations, classification by irreducible space group representation 9-1358
- vibrations, shell model treatment, cryst. with substitutional defects: defect-induced one-phonon absorpt. 9-13787
- vibronic spectrum of impurity absorpt./ emission of light due to electron-localized vibration interaction, analysis 9-1762
- Wigner lattice and related dipole lattices, dielec. props. 9-21419
- Ag-Mn alloys, phonon-electron scattering coeff. from electronic thermal conductivity 9-3505
- Ag, phonon dispersion meas. 9-11983
- Al, X-ray Debye temp. from n. scatt. obs. 9-7639
- Al granular, phonon spectrum from tunneling meas. 9-9817
- AlSb, dispersion curves, freq. distrib. functions eff. calorimetric and X-ray Debye temp. 9-11978
- Aln, mean square vibration displacements and at. scatt. factors, 85-670°K 9-11993
- Ar, containing D<sub>2</sub> molecules, phonons rel. to induced fundamental vibration band 9-14687
- Ar, Debye-Waller factors 9-5536
- Ar, improved self consistent phonon approx. 9-5530
- Ar, infl. of lattice anharmonicity on exponential potential parameters 9-16161
- Ar, phonon dispersion meas. at 4.2°K 9-11985
- Au alloys, (with Pt, Cu, In) phonon-assisted impurity scatt. 9-13847
- BaBrF, Raman vibr. 9-5934
- BaClF, Raman vibr. 9-5934
- BaF<sub>2</sub>, anharmonic temp. factors from n. diff. 9-3514
- BaF<sub>2</sub>, pure and Eu<sup>3+</sup>-doped, spin lattice relax. at low and high temps 9-5859
- BaTiO<sub>3</sub> soft phonon dispersion 9-18547
- BaTiO<sub>3</sub>, mode damping from Raman spectr. 9-3902
- Be, h.c.p. structure 9-3506
- Bi, phonon dispersion curves at 75°K 9-21424
- C<sub>2</sub>N<sub>2</sub>, vibr. freq. 9-16164
- Ca<sub>10</sub>(PO<sub>4</sub>)<sub>6</sub>F<sub>2</sub>, Davydov splittings of PO<sub>4</sub><sup>3-</sup> vib. 9-16167
- Cd electron-phonon mass enhancement, determ. using pseudopot. approaches 9-13827
- Cd hexagonal crystal, thermal and electronic attenuations and dislocation drag 9-19853
- CdO thin films, optical phonons by e tunneling obs. 9-9814
- CdS, laser action involving free excitons and LO-phonon-assisted transitions, theory 9-6522
- CdS phonon-assisted exciton transitions 9-5966
- CdS thin films, optical phonons by e tunneling obs. 9-9814
- CdS, Se<sub>1-x</sub>S<sub>x</sub>, phonon peaks, broadening and freq. shift, temp. depend. 9-12437
- CdSe phonon-assisted exciton transitions 9-5966
- CdTe, atomic displacements and nature of band edge radiative emission 9-16429
- CdTe, phonon-assisted exciton transitions 9-5966
- CoF<sub>2</sub>, spin-optical phonon interaction, obs. 9-10146
- Cr, relaxation due to rapid heating through Neel temp. 9-21417
- Cr<sub>2</sub>O<sub>3</sub>, vibr. spectra 9-18705
- Cs, statics in calc. of lattice distortion produced by vacancies 9-21332
- CsBr phonon branches, sp. ht. calc. from shell model 9-7633

## Crystals continued

## lattice mechanics continued

- CsBr(I), freq. spectrum in thermal props analysis 9-9839
- CsCl, and sp. ht. 9-7634
- CsCl phonon branches, sp. ht. calc. from shell model 9-7633
- CsF phonon branches, sp. ht. calc. from shell model 9-7633
- CsI, phonon spectrum Debye model, use in calc. of recoilless fraction of 26.8 keV transition in <sup>129</sup>I 9-12359
- CsI phonon branches, sp. ht. calc. from shell model 9-7633
- Cu:Fe<sup>57</sup>, using Mossbauer effect 9-7638
- Cu, collisions chains along [100] and [110] direction 9-5538
- Cu, lattice distortion produced by interstitial Cu atom, lattice statics calcs. 9-13679
- Cu phonon dispersion 9-5532
- CuCl, far i.r. phonon processes 9-1774
- Dy, lattice sp. ht. calc. from phonon freq. distrib. curves 9-16165
- Dy, lattice sp. ht. calc. from phonon freq. distrib. curves 9-7635
- Er, lattice sp. ht. calc. from phonon freq. distrib. curves 9-16165
- Er, lattice sp. ht. calc. from phonon freq. distrib. curves 9-7635
- FeCl<sub>3</sub>, thermal shift, precision Mossbauer meas., 83-350°K 9-16402
- FeF<sub>2</sub>, rutile structure, vibrational spectra, critical dipole frequency behaviour 9-18549
- FeF<sub>2</sub>, rutile structure, vibrational spectra, critical dipole frequency behaviour 9-18549
- FeF<sub>2</sub>, rutile structure, vibrational spectra, critical dipole frequency behaviour 9-7636
- Ga<sub>2</sub>Fe<sub>3-x</sub>O<sub>4</sub>, magnon dispersion relation 9-21581
- GaAs:Te, longitudinal-optical-phonon-plasmon coupling 9-21615
- GaAs, dispersion curves, freq. distrib. functions eff. calorimetric and X-ray Debye temp. 9-11978
- GaAs, phonon peaks, broadening and freq. shift, temp. depend. 9-12437
- GaAs, P<sub>1-x</sub>, Raman scattering from lattice vibrations 9-12416
- GaP, dispersion curves, freq. distrib. functions eff. calorimetric and X-ray Debye temp. 9-11978
- GaP, i.r. two-phonon spectra 9-12446
- Gd, lattice sp. ht. calc. from phonon freq. distrib. curves 9-16165
- Gd, lattice sp. ht. calc. from phonon freq. distrib. curves 9-7635
- Ge:B, impurity vibrational modes by i.r. absorption 9-18548
- Ge, anharmonicity and Grueneisen parameter 9-14999
- Ge, i.r. lattice absorption 9-3510
- n-Ge, phonon drag eff., infl. of e scatt. anisotropy 9-19917
- n-Ge, phonon role in intraband radiation of hot electrons 9-3638
- H, equation of state at absolute zero over wide range of densities 9-19850
- H<sub>2</sub> solid below 4.2°K, NMR obs. 9-1118
- H<sub>2</sub>S and D<sub>2</sub>S, Raman vibr. of three phases 9-5935
- \*He, h.c.p., phonon spectrum, 1.0°K 9-5211
- \*He, h.c.p., self-consistent phonon spectrum calc. 9-9818
- HgTe, elastic vibrations nature change due to increase in Hg vacancies, X-ray diff. study 9-9678
- In-Hg(Cd) dilute alloys, In phonon spectrum, effect of Hg(Cd) impurities 9-5533
- In-Pb superconducting alloy, phonon scatt. mechanisms from thermal conductivity meas. down to 0.4°K 9-21444
- InAs, magneto-plasma-phonon interaction from Kramers-Kronig analysis of reflection spectra 9-12363
- InSb, dispersion curves, freq. distrib. functions eff. calorimetric and X-ray Debye temp. 9-11978
- K, statics in calc. of lattice distortion produced by vacancies 9-21332
- KAg(CN)<sub>2</sub> vibr. spectrum and Ag(CN)<sub>2</sub><sup>-</sup> sites symmetry, obs. 9-16166
- KBr:Li<sup>+</sup>, far i.r. resonant-mode freq. shifts on uniaxial stress 9-5922
- KBr:NO<sub>2</sub><sup>-</sup>, vibration structure in absorpt. and luminescence spectra at 4.2°K 9-16432
- KBr:S<sup>2-</sup> vibronic centre freq. and anharmonicity from lum. spectra at 4.2°K 9-14078
- KBr, i.r. eigenfrequency pressure dependence, 1-35 kbar 9-5897
- KCl:Eu<sup>2+</sup>, lattice freq. shift effects on multiphonon structure in absorpt. and emission spectra 9-16410
- KCl:NO<sub>2</sub><sup>-</sup>, vibration structure in absorpt. and luminescence spectra at 4.2°K 9-16432
- KCl:S<sup>2-</sup> vibronic centre freq. and anharmonicity from lum. spectra at 4.2°K 9-14078
- KCl, decomposition time of NO<sub>2</sub><sup>-</sup> impurity local vibration quantum into phonons 9-15000
- KCl, i.r. eigenfrequency pressure dependence, 1-35 kbar 9-5897
- KCl, one-phonon relax. of OH<sup>-</sup> 9-5534
- KCl, thermal lattice vibrations 9-21425
- KH<sub>2</sub>PO<sub>4</sub>, oscillations rel. to dielectric phase transitions 9-12422
- KI:Ag<sup>+</sup>, far i.r. resonant-mode freq. shifts on uniaxial stress 9-5922
- KI:(Br<sup>-</sup>, Cl<sup>-</sup>), frequency spectrum, statistical calc. 9-5312
- KI:NO<sub>2</sub><sup>-</sup>, vibration structure in absorpt. spectra at 4.2°K 9-16432
- KI, vibrational spectra of U<sup>+</sup> centres 9-5388
- KMgF<sub>3</sub>-KNiF<sub>3</sub> mixed crystals, long-wavelength optical lattice vibrations 9-13789
- KNO<sub>3</sub>, vibration modes from Raman scatt. obs. in phases I, II, III 9-14061
- KNO<sub>3</sub>, oscillations rel. to dielectric phase transitions 9-12422
- K<sub>2</sub>PtCl<sub>6</sub>, NQR exam. 9-11987
- KTaO<sub>3</sub>, phonon modes in elec-field-induced Raman scatt. 9-5938
- Kr, Debye-Waller factors 9-5536
- Kr, infl. of lattice anharmonicity on exponential potential parameters 9-16161
- Kr atoms in clathrate, Mossbauer determ. 9-3513
- LaAlO<sub>3</sub>, lattice vibrations, x-ray study 9-3504
- LiF, lattice vibrations causing spectral emission 9-7977
- LiF, multiple-phonon processes in Raman spectra from ultra microscopic scatt. centres 9-5937
- LiF thin cry., nonuniform e.m. field treatment of i.r. props. 9-17352
- LiH, from phonon dispersion curve meas. 9-19851
- Mg, h.c.p. structure 9-3506
- MgF<sub>2</sub>, rutile structure, vibrational spectra, critical dipole frequency behaviour 9-18549
- MgF<sub>2</sub>, rutile structure, vibrational spectra, critical dipole frequency behaviour 9-7636
- MgO:Cr<sup>2+</sup> phonon scatt., thermal cond. meas. 1°-4°K 9-5535
- MgO:Cr<sup>3+</sup>, Van Vleck orbit-lattice interaction for all phonon wave vectors in interpretation of spectral line shift temp. dependence 9-12470
- MgO:Fe<sup>3+</sup>, phonon-photon double quantum transitions freq. depend. 9-1360
- MgO:M<sup>2+</sup>, (M=Co, Ni, Cr paramag. ions), spin lattice relax. anisotropy, theory 9-12318

**Crystals continued****lattice mechanics continued**

- MgO:Ni microwave, acoustic phonon bottleneck, direct obs. by Brillouin scatt. 9-9819  
 MgO, rel. n. scatt. 9-9821  
 MgO, vibrational spectra, phonon density of state curves 9-11988  
 MgO, vibrational spectra, phonon density of state curves 9-9820  
 MnF<sub>2</sub>, rutile structure, vibrational spectra, critical dipole frequency behaviour 9-18549  
 MnO, phonon dispersion relations for acoustic branches along [100], [011] and [111] 9-13790  
 Mo(IV)Cl<sub>6</sub>, vibr. spectra 9-7982  
 NH<sub>4</sub>Br vibrational Raman spectrum of order-disorder transition 9-11973  
 NH<sub>4</sub>Cl, vibrational Raman spectrum of order-disorder transition 9-11973  
 NH<sub>4</sub>H<sub>2</sub>PO<sub>4</sub>, oscillations rel. to dielectric phase transitions 9-12422  
 NO<sub>2</sub><sup>-</sup> in potassium halides, vibration structure in absorpt. and luminescence spectra at 4.2°K 9-16432  
 Na, anharmonic contribs. to thermodynamic props., simplified theory 9-7652  
 Na, statics in calc. of lattice distortion produced by vacancies 9-21332  
 Na absorption and energy loss in the Hartree approximation 9-3844  
 NaCl, dispersion curves, on basis of simple shell model 9-11989  
 NaCl, pair model, determ. of thermodynamic props. 9-16174  
 NaCl, thermal lattice vibrations 9-21425  
 NaCl films, virtual mode analysis of far i.r. absorpt. spectra 9-1791  
 NaF:H<sup>-</sup> thin film, localized mode frequency shift by surface polarization 9-19852  
 NaNO<sub>3</sub>, two-phonon absorpt. spectrum 9-16169  
 NaNO<sub>3</sub>, vibrations, and i.r. spectrum 9-21614  
 NaNO<sub>3</sub>, temp. dependent vibrational modes 9-5902  
 NaSH, elec. dipole-dipole interact. bet. SH ions 9-17038  
 Nb, X-ray Debye temp. from n. scatt. obs. 9-7639  
 Nb<sub>2</sub>Sn, anharmonic binding of <sup>119</sup>Sn from Mossbauer-effect meas. 9-7960  
 NaCl, effective density of phonon states from vibronic spectra and appl. to ion-lattice interactions 9-17350  
 Nd<sub>2</sub>Mg<sub>3</sub>(NO<sub>3</sub>)<sub>12</sub>·24H<sub>2</sub>O, spin-phonon relax. field dependence 9-10156  
 Ne, containing H<sub>2</sub> molecules, phonons rel. to induced fundamental vibration band 9-14687  
 Ne, Debye-Waller factors 9-5536  
 Ne, improved self-consistent phonon approx. 9-5530  
 Ne, single, isotope effects in lattice constant and thermal expansion 9-7624  
 Ne thermodynamic props evaluation using improved self-consistent phonon theory 9-12016  
 Ni, normal oscill. freq., 300-700°K 9-3507  
 Os<sup>4+</sup> in cubic crystals, at 4.2°K 9-14055  
 PNaI and PNaI 9-1794  
 Pb, Gruneisen parameters, phonon freq. press. depend. calc. from pseudopotential models 9-7640  
 Pb, three-body forces in pseudopotential calc. of phonon frequencies 9-16168  
 Pb, X-ray Debye temp. from n. scatt. obs. 9-7639  
 PbI<sub>2</sub>, phonon freq. calc. from temp. dependence of diffuse streak patterns 9-11853  
 PbZrO<sub>3</sub> soft lattice mode obs. from <sup>57</sup>Co resonance meas. 9-7625  
 Pd:Fe<sup>57</sup>, using Mossbauer effect 9-7638  
 Pt:Fe<sup>57</sup>, using Mossbauer effect 9-7638  
 Rb, statics in calc. of lattice distortion produced by vacancies 9-21332  
 RbCl:S<sub>2</sub><sup>-</sup> vibronic centre freq. and anharmonicity from lum. spectra at 4.2°K 9-14078  
 RbCl phonon branches, sp. ht. calc. from shell model 9-7633  
 S<sub>2</sub><sup>-</sup> vibronic centre in alkali halides, freq. and anharmonicity from lum. spectra at 4.2°K 9-14078  
 Se, x<sub>2</sub>Te, i.r. active lattice bands 9-12365  
 Se, phonons, optical and dynamic charge in trigonal systems 9-3508  
 semiconductors, A<sup>II</sup> B<sup>VI</sup> phonon-assisted exciton transitions 9-5966  
 Si, i.r. lattice absorption 9-3510  
 Si, one-phonon band-mode i.r. absorption by impurity resonances 9-5915  
 Si, phonon peaks, broadening and freq. shift, temp. depend. 9-12437  
 n-Si phonon drag eff., infl. of e scatt. anisotropy 9-19917  
 SiC, phonon dispersion curves by Raman scattering, polytypes 9-3509  
 β-Sn, white tin, freq. distrib. function calcs. 9-7631  
 SnI<sub>4</sub>, Mossbauer determ. 9-1365  
 SrClF, Raman vibrs. 9-5934  
 SrF<sub>2</sub>:Sm<sup>2+</sup>(Eu<sup>2+</sup>), vibronic transitions and Zeeman effect 9-10212  
 TiO<sub>2</sub>, rutile structure, vibrational spectra, critical dipole frequency behaviour 9-18549  
 TiI, phonon frequency shifts from results of Raman spectra pressure depend. 9-18716  
 V<sup>2+</sup> in cubic fields, effect of dynamic phonon interaction on hyperfine fields 9-5531  
 W, phonon cond. from thermal and elec. magnetoresists., 80-13K 9-5636  
 WO<sub>3</sub>, vibration spectrum 9-18550  
 Xe, Debye-Waller factors 9-5536  
 Xe, infl. of lattice anharmonicity on exponential potential parameters 9-16161  
 Y:Al<sub>2</sub>O<sub>3</sub>, garnet, optical phonons by infrared reflection spectra 9-3512  
 YtO<sub>2</sub>, rutile structure, vibrational spectra, critical dipole frequency behaviour 9-7636  
 Zn electron-phonon mass enhancement, determ. using pseudopot. approaches 9-18327  
 ZnF<sub>2</sub>, rutile structure, vibrational spectra, critical dipole frequency behaviour 9-18549  
 ZnF<sub>2</sub>, rutile structure, vibrational spectra, critical dipole frequency behaviour 9-7636  
 ZnO thin films, optical phonons by e tunneling obs. 9-9814  
 ZnS, e diff. diffuse spot energy loss due to electron-phonon interaction 9-9607  
 ZnS thin films, optical phonons by e tunneling obs. 9-9814  
 Zu, h.c.p. structure 9-3506

**orientation**

- CdSe films on NaCl (111) surface 9-7338  
 1-chloro-2,3,5,6-tetramethyl benzene, orientational disorder 9-17273  
 rel. to cracks, fatigue, mode two growth, dislocation model 9-5481  
 cubic materials, uniaxial textures 9-11792  
 ferrimagnetic single sphere by mag. dev. 9-5270  
 graphite, rotation boundary angles and growth 9-13629  
 group II-IV cpds., by optical reflection method 9-18408  
 hydride precipitates in Zr alloys 9-19683

**Crystals continued****orientation continued**

- ice VII, orientational disorder 9-10201  
 Laue, high precision technique 9-3227  
 plate-like particles, correction for preferred orientation in diffractometric powder analysis 9-11812  
 polyethylene, biaxially oriented crystallite orient. distrib. 9-3221  
 preferred, effect on intensity distrib. of X ray (hk) interferences 9-7360  
 steel, tempered, alloyed with W, orientation of carbide phases 9-5504  
 for ultrasonic meas. 9-3515  
 Ag-S system, surface energy variation 9-9624  
 Al-Zn CuAl<sub>2</sub>, Ag<sub>2</sub>Al eutectic alloys, preferred, development during growth 9-1123  
 Al, pitting and blistering on p. irradi., orientation dependence 9-9604  
 Al polycrystals, changes caused by slip, rel. to brass-texture 9-9670  
 Al<sub>2</sub>O<sub>3</sub>, polycrystalline alumina, dependence of dielectric constant 9-1573  
 Au films on colour-centred NaCl, obs. 9-9615  
 BaF<sub>2</sub>, etch pits, variation on (111) surface 9-11793  
 Bi film, grown on mica, effect of substrate 9-21275  
 C fibres of carbonized cellulose, preferred orient. 9-7359  
 Cu, changes after rolling, rel. to slip 9-9777  
 Cu, influence on oxidation 9-12543  
 Cu, rel. to stored and expended energy during deformation 9-1283  
 Cu, U.S. attenuation, dependence 9-9830  
 Fe-(3wt %Si), magnetoelastic attenuation of vibrations rel. to orientation 9-11915  
 Ni-Cr films, bias-sputtered, preferred orientation 9-21265  
 PbO.6Fe<sub>2</sub>O<sub>3</sub>, preferred, increased by sintering 9-19817  
 Sn, white, preferred, investig. by galvanomagnetic effects 9-16050  
 rel. to U<sub>2</sub>C<sub>3</sub> form. reactions in UC-UC<sub>2</sub> melt, 1350°C 9-12530  
 UO<sub>2</sub> rel. to plastic flow and slip planes, 600-1800°C 9-9762

**polareons see Crystal electron states/polareons****twinning**

- deformation behaviour of small, static, twin lamellas, numerical analysis 9-14950  
 deformation twin, wedge disloc. counterpart 9-18466  
 dislocations, obs. of sources and reactions on X-ray topographs 9-7484  
 stacking faults, deformational, X-ray diff. analysis 9-1229  
 steel, stainless, thin films, microtwins prod. by mechanical abrasion 9-3228  
 wedge-like twinned layers, shape and stress field calc. 9-19753  
 Ag, f.c.c., mechanical, in rolling texture formation 9-19815  
 Ag, rolling texture formation 9-3426  
 Al<sub>2</sub>O<sub>3</sub> (0.25wt %) MgO, hot-pressed deformed, obs. 9-3359  
 Al<sub>2</sub>O<sub>3</sub>, hot-pressed deformed, obs. 9-3359  
 Bi, growth rate temp. dependence, 123-293°K 9-5289  
 Bi, hysteresis props. of residual twins 9-13978  
 Cu-Ge solid solutions, structure and distribution 9-17254  
 Cu, f.c.c., mechanical, in rolling texture formation 9-19815  
 CuAu I, ordered alloy, rel. to deform. mechanism 9-13726  
 Fe-(3wt %Si) alloy polycrystals, and effect on brittleness 9-1124  
 Fe, shock hardened, and complementary twins 9-13695  
 Gd, mechanical, origin and growth 9-7361  
 GdAlO<sub>3</sub>, during growth from melt by Czochralski technique 9-1144  
 Ni films, epitaxially grown, secondary twinning in e. diff. patterns 9-9618  
 Pt black catalysts, rel. to activity 9-5325  
 Ti during deformation caused by drawing 9-19802  
 Zn, [1012], incorporation of basal slip dislocations 9-18474

**whiskers**

- C, and spirals, growth from pyrolysis of methane 9-8073  
 diamonds, growth on single crystal 9-11806  
 growth from vapour phase, mechanism and morphology 9-21294  
 lattice defects, diffracting plane shapes from Laue technique 9-9659  
 α-Al<sub>2</sub>O<sub>3</sub> whiskers, Ni-coated, in Al-10% Si composites, role of Ni 9-21385  
 α-Al<sub>2</sub>O<sub>3</sub>, growth patterns on surface obs. 9-17260  
 BaTiO<sub>3</sub>, axial screw dislocation detection using K<sub>α</sub> X-radiation 9-14944  
 K, growth rate in critical saturation region 9-16061  
 NaCl, 4-50 μ thick, ionic cond. 150°-600°C obs. 9-15124  
 NaCl, size and origin effects on F- and M-centre radiational accumulation kinetics 9-13700  
 PdCl<sub>2</sub>, preparation and properties 9-17259  
 SiC, growth 9-3241  
 Ti, growth method 9-9652

**Curie temperature see Ferroelectric materials; Ferroelectric phenomena; Magnetic properties of substances****Curie-Weiss law see Magnetic properties of substances/paramagnetic; Paramagnetism****Curium**

No entries

**Curium compounds**

Cm<sub>2</sub>O<sub>3</sub>, melting pt. redetermination 9-13558

**Current, electrical**

- alternating, excitation in quasi-static systems by motion of ionized medium 9-194  
 ampere, (A), definition 9-10606  
 axial to cylindrical plasma column, subjected anomalous behaviour 9-21075  
 benzene single crystal, temp. depend. 9-3575  
 benzene single crystal, temp. depend. 9-16227  
 blocking low pot. galvanic currents with a.c. conductor 9-8564  
 constitution determ. from asymptotic behaviour of electroproduction cross sections 9-11279  
 critical densities in supercond. Nb films reactively sputtered in presence of N<sub>2</sub> 9-7742  
 current pulse due to laser radiation incident on target in gas 9-1627  
 distribution in smeared transition zones between two elec. cond. phases, instabilities 9-20478  
 energy conservation in circuits with capacitances 9-2296  
 ionizing, integrating amplifier measurement 9-8570  
 peak, of pulses, meas. using meter with tunnel diode sensing element 9-16759  
 profiles, holographic meas. technique 9-15537  
 pulsed, and associated mag. field, by Faraday eff. 9-4426  
 pulses, high-current, production by capacitor bank discharge 9-6442  
 in superconducting thin strip, analytical soln. for distrib. 9-9938  
 in thin conductor, passive and transmitting aerial 9-16753



**Current, electrical** continued

- CdS, saturation, rippled oscillations in transient, round trip period 9-11995  
O<sub>2</sub> microcathode, meas. by f.e.t. amplifier 9-17843

**Current algebra**

- Adler-Fubini sum rule, inconsistency of modification 9-10990  
asymptotic sum rules for hadron scatt. 9-16843  
basic commutation relation for current divergences 9-14474  
C.C.R., quasi-free states and Bogoliubov transf. 9-16811  
consequences of Fubini-Nashen-Gell-Mann sum rules for all t-channel helicity amp. 9-6617  
conserved currents, gradient terms, saturation and commutator matrix elements equal time limit 9-17906  
constraints imposed on  $\pi N$  strong interaction amplitudes 9-6665  
current formalism, ordering theorems using  $II$  functions 9-4550  
current formalism, S-matrix in perturbation theory using  $\pi$  functions 9-4551  
currents integrated over lightlike hyperplane 9-15586  
dynamical theory, equal-time commutators and Lorentz co-variance 9-17919  
fixed J-plane singularities, Kronecker deltas in all t-channel helicity amp. 9-6617  
for form factors in  $K \rightarrow \pi \nu$  9-6644  
hadron, relations between e.m. quantities, agreement with quark model 9-2475  
hadron-current ops. and bootstrap theory reln. 9-11022  
hadrons, recent developments 9-14489  
hadrons, SU(3) approx., infinite momentum and sum rules 9-19196  
hard-pion, calc. of meson processes, N-point functions 9-8858  
isospin and local space-time rotations, relation 9-19184  
isospin-factored at infinite momentum, saturation 9-306  
J-plane fixed poles anal. 9-15603  
for  $K^+A$  photoproduction ang. distrib. analysis by PCAC and current algebra 9-8818  
for  $K_L$  form factors calc. 9-8810  
local tensor fields and energy momentum operator 9-6612  
mass shell calc., for leptonic K decays of hadrons 9-16832  
mesons, in free effective quark model 9-20629  
multichannel case, S-wave scatt. lengths unitarity correct. 9-4599  
off-mass-shell correct., in calc. of  $\pi N$  S wave scatt. lengths 9-16881  
and PCAC derivation of  $BB\pi$  nonleptonic  $\Delta S=0$  and  $\Delta S=1$  amplitudes 9-16836  
and pole-dominance and meson coupling constants 9-6618  
quark meson model, general form of densities 9-2473  
quasi-free states of C.C.R. algebra, Bogoliubov transf. 9-16811  
Regge trajectory for  $\pi$  scatt., choice of Toller quantum number 9-374  
spectral function sum rules for tensor currents 9-14473  
SU(2) $\times$ SU(2) results for 3-, 4-pt function, virtual-photon pion scatt. 9-17987  
SU(3)  $\times$  SU(3) chiral algebra approx. saturation, in hadrons classification scheme 9-15591  
sum rules and Stueckelberg fields 9-8688  
sum rules involving  $\pi\rho$  and  $A_1$  deriv. from chiral SU(2) $\times$ SU(2) 9-16886  
theory 9-13107  
three-point functions, hard-pion, applic. to  $\pi, \rho, A_1$  and  $\rho$  data 9-16893  
three-point functions, hard-pion calc. of meson vertex functions 9-16892  
vector-dominance model, test by forward and backward  $\rho^0$  pion prod. 9-4627  
vertex functions, vector, analytic props. 9-8708  
vertex functions in pole-dominance approx., use of Bjorken limit, applic. to  $\omega\rho\pi$  syst. 9-16894  
and weak interactions 9-19197  
 $A_1 \rightarrow \pi\rho$ , decay prob. and partial width determ. 9-11046  
commutation relations and PCAC tech., for  $\pi\pi$  photoprod. 9-16872  
 $\gamma N \rightarrow N\pi$  photoprod., modified PCAC hypothesis 9-6661  
 $\gamma\rho \rightarrow \pi^0\rho$ , test for current algebra 9-2504  
 $K^+ \rightarrow \pi^+ e^+ \nu$ , vector form factor determ. 9-17976  
 $KN$  complex scatt. length calc. 9-17979  
pole-dominance approx. and Bjorken limit, applic. to  $\pi\rho$  scatt. 9-16895  
 $\pi \rightarrow e\nu\gamma$ , decay prob. determ. 9-11046  
 $\pi N$  scatt., radiative, applic. 9-13129  
 $\pi\pi$  scatt. length calc. 9-16884  
 $\pi\Sigma$  S-wave scatt. length calc., consistency with forward dispersion rel., unitarity correct. 9-4599

**Curvature measurement** see *Mechanical measurement***Cutting** see *Forming processes***Cyanogen (C<sub>2</sub>N<sub>2</sub>)** see *Carbon compounds***Cyclotron resonance**

- absorption of radiation injected into plasma, magnetic mirror compression experiment 9-21077  
acetonitrile, ion-mol. reactions 9-20034  
description and dims. effect, appl. to Fermi level determ. 9-18583  
e. heating of alkali plasma 9-17109  
electron mass temp. dependence determ. 9-16217  
electrons in plasma, s.h.f. power produced, particle conc. and electron temp. 9-21052  
electrons produced during chemi-ionization 9-3999  
film, thin 9-1441  
freq. rel. to plasma-wave echoes 9-2998  
generalized electron, in weakly ionized plasmas 9-2963  
hydromagnetic waves, instability 9-3002  
ion, detection using e energy modulation 9-3058  
ion ejection, spectroscopy for ion-mol. reaction study 9-10830  
ionosphere and lab. plasma, obs. 9-9364  
metals, electron relaxation-time determ. using weakly-damped helicon waves 9-9909  
plasma, beam plasma syst., instability near electron cyclotron harmonics 9-19554  
plasma, effect on helicon waves 9-15929  
plasma, non-uniformly magnetized, ion cyclotron resonance acceleration 9-15920  
plasma, nonlinear oscillations near electron cyclotron harmonics 9-19547  
plasma r.f. electron heating enhancement 9-11543  
plasma trapping and heating in mirror geometries, non-adiabatic and stochastic mechanism 9-21076  
semiconductors, spin polarized e. scatt. obs. 9-9993  
width theory 9-3560  
Cd and r.f. dimension effects on drifting effective electrons 9-1442  
Ge, hole-phonon coupling const. determ. 9-3551

**Cyclotron resonance** continued

- Ge,  $M_j=1/2$  valence bands, free-hole g factor determ. 9-1543  
Ge, spin polarized e. scatt. obs. 9-9993  
Ge valence bands quantum effects meas. using c.w. HCN laser 9-14070  
Hg, effective electron mass temp. dependence determ. 9-16217  
Hg crystals, Azbel-Kaner, rel. to Fermi surface model 9-13838  
n-InSb, far i.r. resonant photoconductive props. 9-17440  
n-InSb, photoconductivity due to cyclotron absorpt. 9-5767  
InSb holes, Landau levels 9-5632  
K, helicon Doppler-shifted, in Fermi surface determ. 9-12060  
Na, helicon Doppler-shifted, in Fermi surface determ. 9-12060  
RuO<sub>2</sub>, Azbel-Kaner, in  $[110]$  plane 9-7725  
Si, doped, between 1.5 and 4.2°K 9-3561  
Si, spin polarized e. scatt. obs. 9-9993  
ZnTe, from thermally excited holes 9-3635

**Cyclotrons** see *Particle accelerators/cyclotrons***Czocharalski method** see *Crystals, growth***D-layer** see *Ionosphere/D-region***Damping**See also *Internal friction*

- anti-vibration instrument mounting 9-20281  
drift waves in inhomogeneous plasma 9-17123  
e. plasma waves in cylindrical plasma column 9-17104  
elastic dumbbell satellite, via linear force acting on higher freq. mode 9-14179  
ion acoustic waves in quiescent plasma 9-14791  
pendulum, horiz., mag. suspended, gravity-induced energy losses 9-120  
second-order oscillator, necessary and sufficient conditions 9-20375  
surface electron states in magnetic field 9-13834  
surface electron states in magnetic field 9-3557  
suspension meas. method, elimination of energy absorption by strings 9-5427  
turbulence, mechanism to account for effect of added soluble polymers 9-7242  
vibration reducing mats., in construct. industry, performance and economics 9-17782  
viscoelastic, of symmetrical multilayer beam, flexural vib. 9-16726  
waves, proper, in plate with rough walls 9-50  
Cu-Ni alloys, behaviour interpretation, miscibility gap existence 9-3400  
Fe, strain-induced, near Snoek peak 9-9749  
Ge, lif. 9-5432

**Dark space** see *Discharges, electric***Data tables** see *Collections of physical data; Tables, mathematical***Dating** see *Earth/age; Radioactive dating***Daughter** see *Nucleus; Radioactivity***Dawn chorus** see *Atmospherics; Ionosphere***Dayglow** see *Airglow***de Haas-van Alphen effect**See also *Diamagnetism; Magnetic properties/diamagnetic*

- bismuth-type metals, quasi-local level effects 9-1444  
digital instrum. for recording in impulsive mag. field 9-17849  
experimental aspects 9-13839  
magnetic interaction, weak and strong, of two frequencies 9-5634  
magneto-oscillatory effect analysis by Fourier method 9-16219  
metals, field modulation meas., technique and theory 9-19884  
metals, meas. techniques and instrumentation up to 62 kG, down to 0.3°K 9-3563  
Ag, mag. interaction effects, obs. 9-5635  
Ag, magnetization state domains, n.m.r. obs. 9-1664  
n-Bi-Te, band structure and carrier density determ. 9-9913  
Ca under pressure, periods cyclotron meas. 9-15054  
Cr antiferromagnetic Q-vector truncating effect on Fermi surface, obs. 9-17461  
n-HgSe, in strong mag. fields 9-16218  
HgSe pulsed peak obs. up to 200 kG 9-9914  
In, rel. to helicon velocity oscills, and damping determ. 9-7724  
InSb, pulsed peak obs. up to 200 kG 9-9914  
K, absolute freq. meas. rel. to electronic ground state determ. 9-18593  
K, phase var. with crystal rotation rel. to Fermi surface area anisotropy 9-1443  
Nb, rel. to fermi surface 9-7727  
Ni, Fermi surface anisotropy 9-12063  
Pt, conduction electron g factor, anisotropy 9-1445  
ReO<sub>3</sub>, meas. 9-7728  
Sn Fermi surface, effects of tension, meas. 9-15057  
Th, electronic and Fermi surface structure determ. 9-21466  
W, frequency detail, using large impulsive mag. fields 9-3565  
Zn, in pulsed mag. field, oscillation amplitudes meas. 9-10094  
Zn, magneto-oscillatory effect analysis by Fourier method 9-16219

**Debye temperature** see *Specific heat***Debye-Huckel theory** see *Conductivity, electrical/liquids, electrolytic; Electrochemistry; Solutions***Debye-Scherrer cameras** see *Cameras; X-ray crystallography/apparatus***Debye-Waller factors** see *Crystals/lattices mechanics; Electron diffraction crystallography; X-ray crystallography***Decay periods** see *Hyperons/decay; Kaons/decay; Mesons/decay; Pions/decay; Radioactivity/decay periods***Decay schemes** see *Hyperons/decay; Kaons/decay; Mesons/decay; Pions/decay; Radioactivity/decay schemes***Decomposition** see *Dissociation***Decomposition, thermal** see *Chemical reactions***Decoration techniques** see *Crystal imperfections/dislocations; Crystals/etching***Defects** see *Crystal imperfections***Deformation**See also *Bending; Elastic deformation; Plastic deformation*

- alkali halides, shell model 9-3393  
brass: (5 wt.%) Zn, rate depend. of rolling texture 9-1330  
buckling, creep, of circular cylindrical shell under compression 9-19030  
buckling, free-edge, heterogeneous shells, cylindrical, in axial compression 9-20389  
buckling conditions for columns supported laterally by side-rails 9-20387  
buckling of circular cylindrical shells under axial compression 9-16710  
buckling of inhomogeneous anisotropic cyl. shells by bending 9-20384  
buckling of twisted columns with complex loads 9-16707  
concrete, short-term, stress-strain curves 9-16121

**Deformation continued**

- copper trichite, torsion of reticular planes 9-19792  
 cylinders, ring-supported, edge restraint coupling effect on buckling 9-20395  
 cylindrical shell under concentrated loading 9-20385  
 diaphragm, circular, in electrosark forming, anal. 9-19828  
 dielectric spherical shell, compressible, radial deforms. 9-125  
 duraluminium, at 77°K, effect on thermal and elec. conductivities 9-12025  
 elastic-plastic behaviour of plates 9-17772  
 f.c.c. metal, solid solutions anomalous after-effect 9-1325  
 f.c.c. metals, elec. resistivity measurements 9-3567  
 ferromagnetic spinels, volume rel. press. 9-11844  
 glass-crystal systems, during firing 9-3417  
 graphite, effect of B on nucleation pattern of rad. damage 9-7477  
 I beams, lateral buckling beyond limit of proportionality 9-14379  
 I beams, lateral buckling beyond limit of proportionality 9-14379  
 inhomogeneous anisotropic cyl. shells, buckling due to bending 9-20384  
 instability under applied moment of angle section beam 9-20388  
 large, superimposition of small displacements 9-4274  
 magnetic, deformation velocity and material constants 9-3800  
 membranes, elastic axially symmetric, dynamic deformation 9-16722  
 metal surfaces, damage due to micron sized particle cloud hypervel. impingement 9-9859  
 metals, b.c.c., texture formation 9-19791  
 metals, variation in work absorbed during fatigue 9-13718  
 metals rel. to friction at low temps. 9-16139  
 olivine, in stony meteorites 9-6185  
 polyethylene films with spherulitic structures 9-17240  
 polyethylene terephthalate, bands prod. by tensile and shear tests 9-5463  
 polyethylene terephthalate, behaviour 9-1287  
 polymer systems containing spherulites, diff. Hv patterns, sensitive central spot 9-12336  
 polymers, Young's modulus dependence, mechanism 9-16116  
 polypropylene, uniaxially drawn isotactic films, quantitative characterization 9-21375  
 post-buckling behaviour of elastic structures 9-17763  
 precritical, of thin elastic shells, correlation theory 9-17767  
 shell, cylindrical, in electrosark forming, anal. 9-19828  
 shell, spherical, buckling, rotationally symmetric, post-buckling behaviour 9-19017  
 specimen profile meas. device 9-19797  
 steel, austenitic, cyclic loading causing exoelectron emission 9-13937  
 steel, creep tests by deformation with ball 9-5468  
 steel, E1702, aged and quenched, effect of grain size on resistance to deform. 9-9760  
 steel, N36KH12TYU, aged, resistance temp. dependence anomaly 9-21372  
 steel plates, mild, on thermal cycling 9-5450  
 stress-strain relations and analysis, book 9-14973  
 thin films, production of defects 9-7544  
 triglycine sulphate, around 180° domain walls, topography 9-16301  
 twin lamellae, small static, numerical analysis of deform. behaviour 9-14950  
 yield, limit analysis 9-19803  
 Ag-Pd alloys, faulting in severely cold-worked filings, X-ray meas. 9-7493  
 AgCl, pressure-induced rel. to photoluminescence 9-12462  
 Al-Be alloy, effect on ageing rel. to clustering formation 9-18458  
 Al-Cu alloys, precip. and recrystallization 9-21400  
 Al, stored and expended energy rel. to tensile strain and orientation 9-1283  
 Cd, slip relation for basal glide, primary and secondary, in single crystals 9-3345  
 CsI, with hydrostatic press., pots for shift of exciton peaks 9-12067  
 Cu-Ni alloys, cyclic, causing electrical resistivity change 9-3579  
 Cu-Si solid soln., elec. resistivity decrease 9-16224  
 $\beta$ -Cu-Zn, effect on martensitic transformations 9-5512  
 Cu, dislocation arrangement in stress-applied state, electron microscope obs. 9-14946  
 Cu, drawn, development of microbands separating main deform. bands 9-9674  
 Cu, in easy glide 9-5373  
 Cu, by rolling, texture form. by slip 9-9777  
 Cu, stored and expended energy rel. to tensile strain and orientation 9-1283  
 Cu matrix, rel. to interaction of dislocations with coherent Co particles 9-1213  
 Cu monocrystal, compression parameters rel. to secondary slip 9-3427  
 Cu single crystals containing BeO particles 9-17306  
 Cu yield strength depend. on temp. 9-21371  
 CuAu I, ordered alloy, and mechanism 9-13726  
 Fe-C alloy, mechanism, 77° to 300°K 9-5458  
 Fe-(0.2 wt.%)Zr, alloys, mechanism 9-5458  
 Fe, Armco, rel. to dislocation structure and peculiarities of viscous crack development 9-3450  
 Fe, effect on adsorption and corrosion inhibitor action 9-18760  
 Fe, high-purity, defect network production and recovery 9-9697  
 Fe, shock-hardened, twins and complementary twins 9-13695  
 Ge, uniaxial, effect on fundamental absorpt. 9-18707  
 In-Tl martensitic alloys, stacking faults as twin nuclei 9-13728  
 K<sub>1</sub> and fracture 9-1308  
 Li crystal, rel. to surface states 9-9899  
 LiF causing dislocations, structure obs. 9-5364  
 Mg<sub>2</sub>Cd, polycryst., basal slip 9-5459  
 Mg(OH)<sub>2</sub> powder compacts, compressive creep rel. to dehydroxylation rate 9-1291  
 Nb-Ti(V) (Zr) alloys, effects, X-ray powder diffraction studies 9-11930  
 Nb-W alloys, mechanism temp. depend. 9-3411  
 Ni, high-purity, defect network production and recovery 9-9697  
 Ni, loading rate effects on defect structure 9-3352  
 Ni ribbon, effect on K<sup>+</sup> and Na<sup>+</sup> thermionic emission 9-21554  
 NiAl, modes of intermediate phase 9-5462  
 NiTi, prestrain effect on tensile props., 150° to 370°C 9-18491  
 Pt ribbon, effect on K<sup>+</sup> and Na<sup>+</sup> thermionic emission 9-21554  
 Ti, by drawing, slip and twinning mech. 9-19802  
 $\alpha$ -Ti, grain size effect on dynamics 9-3420  
 WC-Co alloys, compressive creep at elevated temps. 9-7555  
 Zn, slip relation for basal glide, primary and secondary, in single crystals 9-3345

**Deformation continued**

- Zn single crystals, at high strain rates 9-18512  
 Zr, with hydride precipitates, rel. to crack nucleation and propag. 9-3452
- Delay lines, ultrasonic** *see Acoustics; Ultrasonics*
- Delbruck scattering** *see Photons/scattering*
- Demagnetization** *see Magnetization process*
- Dember effect** *see Photoelectromagnetic effects*
- Demonstrations** *see Teaching/demonstrations*
- Dendrites** *see Crystallization; Crystals/growth*
- Densitometry**  
 evaporographic method for measuring energy field of flash lamps 9-4534  
 spectra, nonresolved, for temp. meas. 9-8531  
 C films, optical density meas. in thickness meas. 9-11766
- Density**  
 dry bulk, correction of n moisture gauge 9-3065  
 one-component system near critical point, vertical distrib. 9-18387
- gases**  
 air, approximation for, in terms of f press. and enthalpy 9-10386  
 axisymmetric interferogram determ. by meas. of fringe shift 9-17143  
 in hypervelocity nozzles, atom mass fraction meas. 9-9434  
 vapour density meas. apparatus for student use 9-20286
- liquids**  
 densimeter, mag., using optical sensing 9-18353  
 hydrocarbon mixtures, light, liq. density, -165°C 9-17195  
 N-methylpropionamide solutions, apparent molal volumes 9-19620  
 mixture, binary, of low density 9-7238  
 molten salts, data collection 9-11714  
 Ba, temp. dependence obs. 9-5149  
 BaI<sub>2</sub>.2H<sub>2</sub>O, apparent molal expansibility and volume 9-1007  
 Bi-Sb system 9-9547  
 Ca, temp. dependence obs. 9-5149  
 CaI<sub>2</sub>.4H<sub>2</sub>O apparent molal expansibility and volume 9-1007  
 He, superfluid, temp. depend. eqn. for  $1.2^\circ\text{K} \leq T \leq T_\lambda$  9-7297  
 He II, increase due to turbulent flow 9-5208  
 He II, superfluid, size effects 9-21236  
 Li, m.p. to b.p. 9-21197  
 LiI.2H<sub>2</sub>O, apparent molal expansibility and volume 9-1007  
 Mg, temp. dependence obs. 9-5149  
 Na-Bi alloy, meas. rel. to bimetallic galvanic cells 9-5145  
 Na-Pb alloy, meas. rel. to bimetallic galvanic cells 9-5145  
 RbI apparent molal expansibility and volume 9-1007  
 S, discontinuity near 160°C  $\lambda$ -transition 9-9479  
 Sr, temp. dependence obs. 9-5149  
 ZnI<sub>2</sub> apparent molal expansibility and volume 9-1007
- solids**  
 cavity growth during thermal cycling, mechanism 9-19772  
 graphite, area density fluctuation 147 MeV proton beam meas. 9-19693  
 graphite, bulk, nondestructive quality control for rocket motors 9-11936  
 lattice dilatation due to dislocation loops 9-14942  
 pyrocarbons, reproducible compressed samples, apparent density 9-7596  
 shock-compressed, empirical reln. with press. and sound vel. 9-4362  
 silica, checking by statistical method 9-13712  
 silica, vitreous, ionizing-radiation-induced dilatation, impurity effect 9-14961  
 steel powders, pressed and sintered 9-17339  
 surface density gauge, influence of air gap 9-5227  
 As<sub>2</sub>Se<sub>3</sub>-metal oxide semicond. glasses, rel. to comp. and temp., obs. 9-1521  
 BaTiO<sub>3</sub>-PbTiO<sub>3</sub> single cryst. solid solns. 9-12196  
 C, pyrolytic, changes due to neutron irradi. 9-7409  
 C fibre, from petroleum sludge, specific gravity 9-8060  
 Cr oxide, calcined samples 9-1320  
 KBr-KCl mixed crystals, X-irrad., volume expansion rel. to Frenkel defect production in coloration process 9-21331  
 KBr, X-irrad., volume expansion rel. to Frenkel defect production in coloration process 9-21331  
 LiCd[MoO<sub>4</sub>]OH, monoclinic cell parameters 9-5322  
 LiF, decrease due to X-irradiation 9-5926  
 LiF, impurity effects 9-1133  
 MnZn ferrites of stoichiometric compositions, rel. to composition 9-16079  
 NaCl:Ca<sup>2+</sup>, change for vacancy conc. determ. 9-9703  
 SiBi<sup>12</sup>O<sub>20</sub>, specific gravity 9-18648  
 SiO<sub>2</sub>, vitreous silica, radiation compaction 9-11921  
 TiO<sub>2</sub>, changes due to quenching 9-21392  
 U, changes on thermal cycling between 400 and 600°C 9-19771  
 UO<sub>2</sub>, densification, powder morphology and energy effects 9-3465  
 VS, in phase transition 9-9807
- Density measurement**  
 atmosphere, rocket-borne Rayleigh scatt. instrument 9-12594  
 fibres, vibroscope, fixed frequency, evaluation tests 9-6370  
 gas, by fringe shift meas. in axisymmetric interferograms 9-17143  
 unar surface, by automatic station Luna 13 9-6158  
 lunar soil, meter-penetrometer of automatic lunar station Luna-13 9-6157  
 oxide films on Al<sub>2</sub>O<sub>3</sub>, using charact. X-ray production by 100-keV protons 9-13575  
 vapour density meas. apparatus for student use 9-20286
- Desorption** *see Sorption*
- Detonation**  
*See also Explosions; Shock waves*  
 explosive, velocity meas. multichannel intervalometer 9-155  
 explosive in external fields 9-10745  
 front, in gases, temp. meas. behind 9-2240  
 heat source in infinite tube, effects of heat transfer and friction on flowfield of gas 9-7210  
 normal wave propagation, 3D gas flow by regions of rest 9-21124  
 solid explosives, behaviour behind plane and spherical detonation waves 9-20440  
 in solid explosives, converging, fluid-dynamic eqns. with changing co-ordinate system 9-12943  
 viscosity infl. on LVD stability 9-16737  
 wave propagation in space with conical cutout 9-13476  
 wave structure under transverse mag. field influence 9-17817  
 Al splash generation by wave impact 9-5438  
 H-O, explosive gas, transverse flame-shock interacts. 9-1901  
 H-O mixtures, propagation in supersonic flow 9-19582  
 H-O mixtures, speed of products meas. 9-10743



**Detonation continued**

H<sub>2</sub>O<sub>2</sub>-Ar mixture, initiation by incident shock waves, reaction mech. 9-14128

**Deuterium**

auto-ionic emission and surface ionization in strong elec. field, rel. to neut-  
ron prod. 9-16322  
breakdown by nanosecond laser pulse, obs. 9-13470  
gas mixtures with inert gases, thermal conductivities 9-956  
ionization by short pulse laser, theoretical exam. 9-9383  
ionization under action of short pulse laser 9-3005  
plasma seed targets for laser irradi. 9-2991  
solid, struct. above and below  $\lambda$  transition, neutron diffusion 9-9675  
solubility in pure Al, 400-600°C, validity of square root law 9-9787  
solvent isotope effs. in water, transfer and exchange contrib. 9-21678  
D<sup>+</sup>-D charge-exchange cross-sections, eff. of apparatus geom. 9-4872  
D<sup>+</sup>+D<sup>+</sup>→OD<sup>+</sup>+D<sub>2</sub>, cross-section for incident ion. energies near 2eV  
9-921  
D<sup>+</sup> in Ti, backscattering energy distrib. 9-12037  
D<sub>2</sub> vibration-rotation band fundamental, in elec. field induced spectra, lines  
in press. range 0-600 psi 9-13354  
D<sub>2</sub><sup>+</sup>, dissociation energy 9-2920  
D<sub>2</sub>O substitution effect on fluorescence lifetime of uranyl salts 9-1830  
D<sub>2</sub>+O<sub>2</sub>, rate const., and kinetics of branching step 9-14129  
D<sub>2</sub>+X<sup>+</sup>→D<sub>2</sub>+XD<sup>+</sup>, reaction cross-sections, 1-100eV 9-17075  
HD<sup>+</sup> beam intensity automatic meas. 9-17863

**Deuterium compounds** *see Hydrogen compounds***Deuterons**

*See also Cosmic rays/deuterons; Nuclear reactions and scattering due to deuterons*  
beam, time structure study by electronic method 9-13149  
binding energy, wave functions, mag. and quadrupole moments, eff. range,  
and e.m. form factors from calc. on low-energy N-N interac. 9-11086  
Bragg curve shape, particle interaction effect 9-15036  
electrodisintegration near threshold, at low momentum transfer 9-13191  
energy losses compared with protons 9-21452  
n.m.r., rot. ordering determ. near  $\lambda$ -transition 9-12511  
optical potential calc. by 3 body model 9-9055  
organic scintillator response, photomultiplier meas. 9-6722  
plasmoids from coaxial injector, struct. and impurities obs. 9-13417  
singlet state, DWBA anal. of (p,pn) reactions 9-14607  
structure from  $\pi$ d interaction cross section meas. 9-17981  
transition metals, (Z=21-30), stopping power meas. at 5-12 MeV  
9-17364  
Ca, stopping power meas. at 5.12 MeV 9-17364  
<sup>2</sup>H(n, $\gamma$ )<sup>3</sup>H  $\gamma$  polarization and ang. distrib. asymm. expressed in terms of  
NN interac. 9-15767

**effects**

deuteration in 2-naphthaldehyde, eff. on radiationless decay proc.  
9-19472  
spin-lattice relax. in PH<sub>4</sub>I and Pd<sub>4</sub>I 9-16385  
Al, irradi. at different temps., rel. to stage-III annealing 9-21389  
Pt, defects injected by quenching and radiation 9-7479  
Si, high resistivity regions 9-3662

**interactions**

elastic scatt. Glauber theory corrections, BeV energies 9-8920  
 $\pi^+$ d-pp in Regge-pole theory, residue functions, rel. to low-energy models  
9-16874  
dd-dpn, final state interacts and scatt. for 51.5 MeV 9-6711  
dd-n<sup>+</sup>He, as 14 MeV n pulse generator 9-11101  
dp-ppn, final state interacts and scatt. for 51.5 MeV d 9-6711  
 $\gamma$ d- $\pi^+$ pp,  $\gamma$ d- $\pi^+$ nn, ratio of  $\pi$  production for varying momentum transfers,  
8 and 16 GeV 9-15620  
K<sup>-</sup> d- $\Lambda$  $\pi$ p,  $\Lambda$ p invariant mass enhancement at 2130 MeV, M<sub>K</sub>~1  
GeV/c 9-20637  
K<sup>+</sup>d-K<sup>+</sup>(892) prod. and decay ang. distrib. obs. M<sub>K</sub>=3 GeV/c 9-16897  
nd cross section obs., 14 MeV, charge symmetry comparison with np  
results 9-6700  
nd- $\gamma$ <sup>2</sup>H, and parity nonconservation 9-4643  
nd-nnp, 14 MeV 9-19210  
pd, elastic, polarisation obs. at 22.7 MeV 9-8899  
Pd scatt. at 198MeV, cross-section and polarization obs. 9-6698  
p<sup>+</sup>d-<sup>3</sup>He $\pi^0$  diff. cross section, p<sup>+</sup>d<sup>3</sup>He vertex form factor meas. Ep=1.515  
BeV 9-8895  
 $\pi$ d rel to  $\pi$ N interac. 9-2511  
 $\pi$ d total cross section depend. on d alignment, Glauber approx. 9-17981  
 $\pi^+$ d-ppn, Glauber corrections, spin and isospin at 5.1 GeV/c 9-2546  
 $\pi^+$ d- $\pi^+$ pp 2.15 BeV/c for  $|\mathbf{k}|10u^2$  obs., comparison with  $\pi^+\pi^-$  prod.,  
meas. of  $2\pi^0$  cross section 9-2509  
 $\Sigma^-$ d- $\Sigma^0$ nn- $\Lambda$ nn, relation between states using SU(3) symmetry 9-6707  
Nd cross section spin depend., Glauber approx. 9-11118

**photodisintegration**

for photon energies 100 to 300 MeV, recoil p detect. and effects of more  
complex reactions 9-2655  
proton polarization obs., E<sub>p</sub>=282 to 405 MeV 9-17938  
retardation functions 9-2547

**polarization**

recoil-d vector polar. meas. for e scatt. from unpolar. d target, test of  
time-reversal invariance for e.m. interac. 9-4588  
tensor, meas. from <sup>7</sup>Be (p,d) <sup>8</sup>Be react. at 1.6-3.8 MeV 9-9031  
in pd elastic scatt. at 22.7 MeV 9-8899

**scattering**

*See also Protons and antiprotons/scattering, proton-deuteron*  
<sup>2</sup>H(p,p)<sup>2</sup>H cross section calc., separable S-interaction, E=100 MeV  
9-13223  
 $\alpha$ , phase shifts, ang. distrib. and polarization 9-432  
N-d, elastic in GeV region, first-order dispersive impulse approx. 9-4634  
nd, differential cross sections, elastic and inelastic at 14.1 MeV 9-8906  
Pd, D wave eff., at high energy 9-8901  
Pd-Pd cross section and d final state polarization meas., scatt. amplitude  
determ. 9-8836  
by  $\pi$  in 2 nucleon exchange, glauber multiple- scatt. expansion correction  
9-20677  
 $\pi^+$  d Fermi motion at high energies, expt. and glauber theory comparison  
9-8842  
 $\pi$ d, 895 MeV/c, cross section dis. 9-8835  
 $\pi$ d Glauber theory extended to include spin variables 9-11062  
 $\pi$ d- $2n$ p, n-n scatt. length calc. 9-2507  
 $\pi$ d- $\pi$ d cross section and d final state polarization meas., scatt. amplitude  
determ. 9-17982

**Development, photographic** *see Photographic process/development***Diamagnetic resonance** *see Cyclotron resonance***Diamagnetism**

*See also Cyclotron resonance; de Haas-van Alphen effect; Magnetic properties/diamagnetic*  
atoms and mol. with unpaired electrons 9-20866  
electrons in weak periodic potential, orbital diamagnetism rel. to intraband  
effects 9-1637  
Fermi gas, magnetized, mag. moment 9-8450  
metals, susceptibility, theory 9-21567  
nuclear orientation at low-temp., static methods 9-15162  
susceptibility, statistical model 9-10096  
tiltmeter suspension, horizontal pendulum type 9-2140  
H plasma, due to ion pressure 9-19551  
He hyperfine structure, 3 particle forces eff., <sup>2</sup>S<sub>1/2</sub> state correction 9-4876  
Pt, based double cyanide complexes, mean diamagnetic susceptibility  
determ. by Faraday method. 9-19946

**Diamonds**

artificial, with B impurity, phosphorescence and thermoluminescence  
9-21651  
book 9-13565  
chemisorption of H, F, Cl, Br and O, heats of wetting, e.s.r. and i.r. spectra  
9-8083  
dodecahedral form, (111) face due to interrupted growth 9-11795  
electro-optical effects, i.r. 9-12348  
electron momentum density, X-ray determ. 9-18581  
etching of trigons on (111) faces 9-7365  
hexagonal, synthesis by heat and press treatments of graphite 9-7612  
natural, luminescence-excitation elec. field modulated in range 5.0-6.0 eV  
9-5950  
one-phonon band-mode i.r. absorption by impurity resonances 9-5915  
optical absorption by neutral vacancy 9-10194  
phosphorescence and thermoluminescence of artificial diamonds with B  
impurity 9-21651  
Raman scattering, elec. field eff. 9-12406  
semiconducting natural, nature of acceptor centre 9-12135  
shock-synthesized, microstructure 9-5316  
structure and properties 9-18443  
synthetic, growth from graphite, patent 9-13598  
synthetic, growth mechanism rel. to that of synthetic cubic BN crystals  
9-7368  
synthetic, thermoluminescence, disperse nitrogen impurity effects 9-3935  
whisker growth on single crystal 9-11806

**Dichroism** *see Pleochroism***Dielectric devices**

capacitor, ferroelectric, hysteresis loop tracer 9-8312  
capacitor, ideal, apparent nonconservation of energy in discharge 9-4415  
condenser, thin film, based on SiO<sub>2</sub> elec. strength 9-10043  
condensor circuit, under compression, current and elec. relax. calc. 9-200  
diaphragm press. transducer for differential vacuum gauge 9-6226  
diode, transient processes at high electric field strengths 9-16295  
diode, trapping transit time, impedance 9-16304  
for displacement meas., capacitive transducer 9-2128  
displacement meter, capacitive 9-25  
film electroluminescent capacitors on ZnS-Cu, Mn base 9-18653  
heated sensor for water vapour pressure meas. 9-18389  
m.i.m. system, influence on angular emission of electrons 9-3687  
n films with different optical properties, polarization of light by refraction,  
theory 9-7939  
pyroelectric i.r. receiver, sensitivity 9-19933  
pyroelectric i.r. receiver, sensitivity 9-19933  
quadrant electrometer, frequency meas. appl. 9-6270  
resonators with layered dielec. walls, tolerance determ. in construction  
9-15485  
resonators with multilayer dielectric walls, effects of large power super-high  
freq. field on characts. 9-8565  
switch solid dielectric, fast metallic contact, high voltage, current 9-1602  
transducer, piezoelec. for stress on bolted joint 9-8352  
ALN, thin film microwave acoustic transducer, vacuum deposition  
9-10056  
LiNbO<sub>3</sub>, acoustic surface wave transducers and delay lines 9-10057  
SiO<sub>2</sub>-Al condensers, breakdown voltage rel. to thickness 9-17430  
SiO<sub>2</sub> condenser film, breakdown rel. microscopic surface roughness  
9-21531

**Dielectric loss** *see Dielectric phenomena; Dielectric properties of substances***Dielectric measurement**

0.4Hz-5×10<sup>-1</sup>Hz 9-195  
cavity discharge, interpretation 9-7196  
cavity Q-factor meas. method 9-6415  
complex dielectric const., meas. schemes in far i.r. 9-10788  
complex permittivity, analysis and method 9-10033  
conducting liqs., bridge and sample cell r.f. methods 9-11709  
cyclohexyl amine +o-cresol molecular complex formation due to H-bond-  
ing 9-5744  
dibenzyl amine + phenol, molecular complex formation due to H-bonding  
9-5744  
cis-1,2-dichloroethylene vapor, elec. susceptibility rel. to press. at 9231  
MHz 9-11660  
dielectric const., complex of liqs. containing polar mois. with rotating  
groups 9-11708  
electrical parameters of heated dielectrics in 8mm wavelength range  
9-8566  
ferroelectric hysteresis curve tracer with virtual grounding 9-1588  
H-bonded, complexes formation, constant var. method applied 9-5744  
high r.f. region, variable geometry cell 9-199  
insulating crystals, conductivity meas. without using contact electrodes  
9-7836  
interferometric technique 9-12181  
liquid permittivity, standing-wave methods 9-7269  
liquids, dielectric const. determ., modification of freq. meas. method  
9-11707  
low-loss materials, 8-140 GHz, meas. accuracy of impedance method  
9-3696  
Michelson type interferometer in overmoded waveguide for liquids  
9-5182  
permittivity, complex, short-circuited line method, improvement 9-6447  
permittivity and conductivity meas., freq. limit by 'electrodeless' method  
9-14853  
plasma, feedback oscillator determ. from e density 9-5044

**Dielectric measurement continued**

- pyridine + o-cresol molecular complex formation due to H-bonding 9-5744  
 sample holder, electrode spacing calibration 9-4182  
 stress in static field, approximate method 9-20479  
 weakly ionized gas, in v.h.f. range 9-11584  
 Al<sub>2</sub>O<sub>3</sub> ceramics, electric tests up to 800°C 9-10034

**Dielectric phenomena**

- See also Electric strength*  
 alkali halides, dispersion obs.; lattice structure and forces calc. 9-16074  
 discharges, partial, in voids 9-18650  
 dispersion in O<sub>2</sub>- and m- hydroxy anilines 9-7835  
 elastic dielectric, small finite deformations 9-8488  
 elastic dielectric, surface stress definition 9-6450  
 electro-elasticity, thermodynamics of non-linear relations 9-17294  
 electrostatic energy calc. from model of interacting polar mols. 9-20480  
 e.m. waves changes in polarization 9-12337  
 energy transfer of thermal radiation between two dielectrics, low temperatures 9-7677  
 ferromagnetic dielectrics, u.s. reflection plane of polarization rot. and ellipticity appearance 9-3525  
 field, internal, calc. from freq. shift in cavity resonator 9-5743  
 high-field domain parameters, eff. of bias, voltage change 9-12195  
 o-m- hydroxy anilines, const. and loss determ., r.f. - microwave region 9-7835  
 image potential for medium with wavevector freq. dependent dielec. function 9-9882  
 internal fields in dipole lattices, Fortran program for calculation 9-1452  
 lipid layers; 1, H<sub>2</sub> adsorption depend. obs. 9-12138  
 liquids, polar and aprotic, conduction mechanism and electrochem. 9-21221  
 losses at temps in poly (4 methyl pentene-1) 9-12189  
 m.i.m. system, influence on angular emission of electrons 9-3687  
 m.i.m. traps, emission, transfer ratio 9-1419  
 nonlinear, non-dispersive e.m. wave propagation 9-20469  
 optical characteristics of shock-compressed, condensed dielectric, review 9-16285  
 optical coherence in nonlinear media 9-10846  
 paraelectric resonance spectroscopy 9-13916  
 polarization and population difference, in 2 level quantum mechanical systems with amplitude mod. e.m. field 9-20467  
 relaxation, book 9-2298  
 relaxation, diatomic rotators in lig. and solids, ang. correls. 9-15841  
 relaxation, of liqs. containing polar mols. with rotating groups 9-11708  
 relaxation, of o-, m-dihalobenzenes 9-9543  
 relaxation in NaCl and KCl with Ni<sup>2+</sup> and Cu<sup>2+</sup> 9-1577  
 solid insulating materials at 4.2°K 9-1565  
 susceptibility tensors, isothermal, adiabatic and isolated static, bounds 9-5793  
 synthetic insulators, resist to leakage currents 9-18646  
 thin films at low frequency under intense electric field, non-linearity 9-1585  
 thin layers, dispersion of phase shift of refl. light, use of Kramers-Kronig relns. 9-1734  
 transmission and reflection complex coeffs. of film, plasma diagnostic applic. 9-19116  
 transport, electronic and ionic, in large surface-charge and space-charge fields, rel. to metal oxidation kinetics 9-9620  
 Wigner lattice and related dipole lattices 9-21419  
 Ag halides, dispersion obs.; lattice structure and forces calc. 9-16074  
 Al<sub>2</sub>O<sub>3</sub> films, 500 to 6000 Å,  $\gamma$  irradiated, traps study using thermoluminescence glow curves, 30 to 300°C 9-17429  
 H liquid, and cold gaseous, study 9-1036  
 He liquid, breakdown at 4.2°K 9-1055  
 KBr:O<sup>2-</sup> loss meas. and dipole moment 9-3698  
 KCl:O<sup>2-</sup> loss meas. and dipole moment 9-3698  
 KH<sub>2</sub>PO<sub>4</sub>, phase transitions from Raman spectra 9-12422  
 KNO<sub>3</sub>, phase transitions from Raman spectra 9-12422  
 NH<sub>4</sub>H<sub>2</sub>PO<sub>4</sub>, phase transitions from Raman spectra 9-12422  
 NaCl:O<sup>2-</sup> loss meas. and dipole moment 9-3698  
 SiO<sub>2</sub> films, 500 to 6000 Å,  $\gamma$  irradiated, traps study using thermoluminescence glow curves, 30 to 300°C 9-17429  
 Te- insulating substrate (mica, glass, teflon), field effect relax. obs. 9-7840  
 Tl halides, dispersion obs.; lattice structure and forces calc. 9-16074  
 Zn, liquid, effective ion-ion interaction and dielectric screening 9-18350

**Dielectric phenomena** *see Ferroelectric phenomena***Dielectric properties of substances**

- See also Electric strength*  
 ceramics, sintered, strength and loss factors, rel. to microporosity 9-3431  
 Coulomb interactions between two impurity charges in an atomic dielectric 9-7831  
 electroceramics, intrinsic props., prep-effects 9-1563  
 ethyl chloride in adsorbed state 9-12186  
 ferroelectric to antiferroelec. phase transitions and composition, thermodynamic relations 9-19930  
 film, elec. conduction 9-21530  
 graphite, transverse and longit. const., spectra in u.v., visible and i.r. regions 9-7971  
 hexadecane-diol-1,16-urea, phase and abs. changes 9-16288  
 hexadecanol-1-urea, phase and abs. changes 9-16288  
 hydrocarbons, MO theory of polarizabilities 9-9238  
 i.e., pure and doped, depolarization of thermocurrents method 9-16287  
 insulators, exciton effects in inter-band absorpt. 9-1572  
 literature digest on dielectrics 9-10787  
 metal-dielectric-metal cathode, eff. on energy distribution of e emission 9-18661  
 metal-nonmetal transition, description 9-15121  
 metal-nonmetal transitions in transition metal oxides and sulfides, mechanisms 9-15122  
 methyl chloride in adsorbed state 9-12186  
 permeability, effective, of randomly inhomogeneous media, analytic props 9-201  
 permittivity, complex, meas. by improved short-circuited line method 9-6447  
 plasma, electron, near cyclotron reson., relativistic influence on permittivity 9-11563  
 poly(methyl methacrylate), comparison with dynamic birefringences obs. 9-18693  
 semiconductor calculation of complex dielectric constant 9-5668

**Dielectric properties of substances continued**

- susceptibility tensors, isothermal, adiabatic and isolated static, bounds 9-5793  
 Al<sub>2</sub>O<sub>3</sub>, ceramics, for electrical applic. 9-1566  
 Al<sub>2</sub>O<sub>3</sub>, rel. to purity and microstructure 9-1256  
 Al<sub>2</sub>O<sub>3</sub> (corundum) ceramic capacitors, dissipation factor, dielec. const. and vol. resist. 9-3691  
 BaTiO<sub>3</sub>, melt-grown, optical props. 9-5745  
 HCl, in adsorbed state 9-12186  
 InSb electron abs. Urbach's law, perturbative and nonperturbative calc. application 9-3603  
 KD<sub>2</sub>PO<sub>4</sub>, polarization relax. and susceptibility in ferro- and para elec. regions 9-1595  
 N<sub>2</sub>, press.-induced microwave absorpt. 9-9455  
 NaCl absorption and reabsorption currents in single crystals 9-10037
- gases**  
 air permittivity meas. using Maxwell's commutator bridge 9-5121  
 alkali vapour, permittivity at resonance frequencies 9-13494  
 alkali vapour, permittivity at resonance frequencies 9-3057  
 constant for fully ionized gases 9-13459  
 cis-1,2- dichloroethylene vapor, elec. susceptibility rel. to press. at 9231 MHz 9-11660  
 electron, degenerate, h.f. const. and plasmon lifetime depend. 9-10677  
 electron-ion plasma, statistical polarization 9-9342  
 electronegative, characterization using test cell based on breakdown in uniform field 9-5120  
 inert gases, second dielec. virial coeff. 9-13493  
 quadrupole-quadrupole interact., effect on initial press. depend. of viscosity and thermal cond. 9-5112  
 H<sub>2</sub> permittivity at resonance frequencies 9-13494  
 H<sub>2</sub> permittivity at resonance frequencies 9-3057  
 chloroform-triethylamine system 9-1039

**liquids and solutions**

- $\epsilon$ - aminocaproic acid, dispersion obs. 70-2000 MHz 9-19638  
 1,3- dibromopropane in benzene paraffin mixtures, relaxation times, viscosity depend. 9-11712  
 acetone-chloroform mixtures, x-band microwave obs. 9-3116  
 alkali halide in organic solvent binary mixture, dielec. constant of solvent mixture rel. to solubility 9-14834  
 anilines, substituted, molar polarization and assoc. 9-934  
 anisol p-aminoazobenzene liq. cry. phase, static dielec. const., influence of mag. and elec. fields 9-11684  
 D- camphor, during phase transition 9-3148  
 carboxylic acid- water mixture, anomalous var. of constant and loss 9-7271  
 chloroform, microwave relax. 9-9542  
 cholesteryl ester crystal, static const. temp. var., heating, cooling cycles comparison 9-9539  
 complex permittivity measurements, X-band transmission method 9-9540  
 conduction mechanism after irradiation with  $\alpha$  and  $\beta$  particles 9-5179  
 conducting drops in dielec. medium of uniform elec. field stability criteria 9-9566  
 conducting liqs., dielec. const., r.f. meas. 9-11709  
 1,4- dibromobutane in benzene paraffin mixtures, relaxation times, viscosity depend. 9-11712  
 o- m- dibromobenzene, dielec. relax. 9-9543  
 o- m- dichlorobenzene, dielec. relax. 9-9543  
 dielectric const. determ., modification of freq. meas. method 9-11707  
 o- m- diiodobenzene, dielec. relax. 9-9543  
 diethylether-chloroform mixtures, x-band microwave obs. 9-3116  
 dimethylformamide in polar solvent, large viscosity range relax. obs. 9-5183  
 dipolar organic, microwave absorpt., const. and losses meas. 9-5181  
 ethyl chloride, complex dielec. const. 9-12186  
 hexane, ion mobility, effect of liq. motion 9-13536  
 heterocyclic amines, molecular relaxation 9-20947  
 holy (4-methyl pentene-1), dielectric loss at cryogenic temps. 9-12189  
 ion pair, overlapping hydration shells, interact., spheroidal cavity mode 9-14858  
 ion pair with overlapping hydration shells interact., truncated-spheres model 9-14857  
 jet in longit. elec. field, stability 9-9538  
 methyl chloride, complex dielec. const. 9-12186  
 using Michelson type interferometer in overmoded waveguide 9-5182  
 molecules containing librating polar groups, microwave relax. 9-21220  
 m- nitrotoluene and its solns. in benzene, saturation, effect of hydrostatic pressure 9-5180  
 nitrobenzene, pure, and in solution, dipolar interactions from elec. birefringence meas. 9-9544  
 non-polar, conductivity, natural and ionization, temp. effect 9-9545  
 nonpolar, 2.1 mm wavelength 9-7268  
 n- octanethiol 9-16019  
 octanol isomers, sterically hindered, rel. to intermol. associatin 9-19495  
 permittivity and conductivity meas., freq. limit by 'electrodeless' method 9-14853  
 permittivity at meter and decimeter wavelengths, standing-wave methods of meas. 9-7269  
 polyelectrolyte solns., dielectric dispersion props. at 25°C and 40-100 kHz 9-16018  
 polymer solns., damped torsional oscillator model 9-21188  
 polymeric dielectric soln., electroconductivity 9-21222  
 polymers in non-polar solvents, spherical suspension model 9-14855  
 pressure dependence of dielec. const. 9-17216  
 pressure effect, 1-750 kp/cm<sup>2</sup>, on dielec. const., 30° and 50°C 9-17215  
 proline, aqueous, and hydroxyproline solns., dispersion obs., 80-2000 MHz 9-19639  
 relaxation of liqs. containing polar mols. with rotating groups 9-11708  
 solvated electrons, dielec. model 9-1035  
 surface waves on horiz. layer of viscous fluid with normal electrostatic field at surface 9-17217  
 tetra- n-butyl ammonium picrate soln., dispersion 9-1038  
 wind, electric, and its reaction at a sharp point 9-5184  
 H<sub>2</sub>O, shock-induced polarization, mechanism 9-1037  
 HCl, complex dielec. const. 9-12186  
 HD mols. at 20°K in contact with charcoal, dynamic polarization of nuclei 9-7270  
 NaCl-glycerol solns., relax. 9-9548  
 (CdCl<sub>6</sub><sup>4-</sup>),{(CH<sub>3</sub>)<sub>4</sub>NH<sub>2</sub><sup>+</sup>}<sub>4</sub> at two temperatures, 400-8500 MHz 9-11710



**Dielectric properties of substances continued**  
**liquids and solutions continued**

- H<sub>2</sub>O, permittivity and conductivity meas., freq. limit by 'electrodeless' method 9-14853  
KCl, permittivity and conductivity meas., freq., limit by 'electrodeless' method 9-14853  
Na-NH<sub>3</sub> solns., microwave dielec. const., temp.-variation studies, nonmetal-to-metal transition 9-14854

**solids**

- 4.2°K, 50Hz, tan $\delta$  meas. 9-1565  
2- 9-14888  
aggregates, permittivity and porosity 9-7282  
alkali-silicate glasses, binary and ternary, meas. 9-3690  
aromatic crystals, internal polarization as function of temp. and elec. field 9-17425  
BaTiO<sub>3</sub> thin film, vacuum deposited, presentation of properties and formulations of thermodynamic model 9-12197  
benzene sorbed on silica gel, dielec. isotherm, analysis 9-21288  
breakdown time meas. 9-12178  
calcite, loss and const., variation with temp. and freq. 9-10026  
D camphor, during phase transition 9-3148  
capacitance, temp. coeff. 9-1571  
cholesteryl ester crystal, static const. temp. var., heating, cooling cycles comparison 9-9539  
copper formate tetrahydrate, antiferroelec. 9-12200  
copper sandstone, loss meas. temp. dependence 9-10036  
electrical parameters of heated dielectrics in 8m.m. wavelength range, measuring equipment 9-8566  
ethyl chloride, complex dielec. const. 9-12186  
film, polystyrol, discharge effects 9-10032  
glasses, binary silicate, rel. to metastable crystn. 9-1081  
graphite function due to  $\pi$  electron interband transitions 9-1567  
Gunn effect under s.c.l. conditions 9-1510  
heterogeneous material, dielec. constant meas. for porosity determ. 9-17422  
homogeneous submicron layers 9-1564  
ice, conductivity by guarded potential probe method 9-3692  
ice crystals from supercooled cloud, polarity rel. to temp. 9-12183  
insulating crystals, charge during LEED 9-12179  
insulating crystals, conductivity meas. without using contact electrodes 9-7836  
insulating sheets submitted to d.c. voltage, temp. effect on transverse conductivity 9-12180  
internal photoemission technique 9-17423  
ionic cry., effs of nonuniform e.m. fields on dielec. props. 9-11990  
ionic crystals, dielec. saturation 9-1582  
6 methoxy 8 nitro-5(1H) quinoline, rel. to mol. structure 9-13660  
methyl chloride complex dielec. const. 9-12186  
molecular cryst., cubic, dipole response and dielec. const. 9-21529  
Perovskite-type crystals, and neutron scatt. 9-13910  
petroliferous grit, dielec. constant meas. for porosity determ. 9-17422  
phenanthrene, capacitance temp. dependence, 25 79°C 9-10031  
polymers, 8-140GHz, meas. accuracy of impedance method 9-3696  
polymers, infl. of glass transition temp., m.p., impurities and at. struct., review 9-19925  
quartz, 8-140GHz, meas. accuracy of impedance method 9-3696  
 $\alpha$  quartz,  $\gamma$ -irrad., rel. to smoky centre formation 9-13701  
quartz, natural and synthetic, conductivity in constant elec. field 9-1569  
quinol hydrogen cyanide clathrate, phase transition 9-1578  
relaxation, anomalous, antiferroelectric Cu(HCO<sub>2</sub>)<sub>2</sub>.4H<sub>2</sub>O 9-3715  
review, including loss and relaxation mechanisms 9-13911  
Rochelle salt, dielec. constant temp. dependence, from meas. at 9 GHz. 9-10051  
Rochelle salt, dielec. const. temp. var. 9-3700  
Rochelle salt, effect of lattice defects 9-7486  
Sapphire, 8-140GHz, meas. accuracy of impedance method 9-3696  
semiconductor, h.f. permittivity, spatial dispersion 9-19908  
semiconductors, dielec., function 9-19909  
synthetic insulators, resist. to leakage currents 9-18646  
transient processes at high electric field strengths 9-16295  
triglycine sulphate, effect of growth conditions 9-10050  
triglycine sulphate cryst., const., role of surface layers 9-5753  
triglycine sulphate crystals, permittivity, temp. hysteresis 9-10052  
wires, enamelled, breakdown at high temp. and after damp storage 9-7842  
zeolite, synthetic Linde 5-A-water system, permittivity and loss factor 9-17426  
zeolite, synthetic Linde type-A with adsorbed water, permittivity and loss factors 9-17427  
Ag, electroreflectance changes in constants, modulated ellipsometric meas. 9-10035  
AgBr, electron mobility determ. 9-15123  
Al<sub>2</sub>SiO<sub>5</sub>:Fe<sup>3+</sup> host crystal 9-14069  
 $\beta$ -Al<sub>2</sub>O<sub>3</sub>, dielectric loss 9-1574  
Al<sub>2</sub>O<sub>3</sub>, polycrystalline alumina, constant rel. to crystallographic texture 9-1573  
Al<sub>2</sub>O<sub>3</sub> thin layers, polarisation effects in m.i.m. and m.i.s. structures 9-3717  
Ar. rel. to refractive index between 3612 and 6439 Å 9-7832  
As<sub>2</sub>S<sub>3</sub> films, e bombardment conductivity, threshold energy 9-16286  
As<sub>2</sub>Se<sub>3</sub> metal oxide, semicond. glasses, obs. 9-1521  
Au, electroreflectance changes in constants, modulated ellipsometric meas. 9-10035  
Ba(NO<sub>3</sub>)<sub>2</sub>, permittivity and loss-angle tangent, impurities effect 9-1575  
BaTiO<sub>3</sub>-PbTiO<sub>3</sub> single cryst. solid solns. 9-12196  
BaTiO<sub>3</sub>, constant, ageing characs. 9-10049  
BaTiO<sub>3</sub>, constant, optical, contrib. of grain boundary 9-17432  
BaTiO<sub>3</sub>, permittivity peak suppression at transition point by substitution elements for Ba and Ti 9-1183  
Ca<sub>0.7</sub>Ce<sub>0.3</sub>CrO<sub>3</sub>, polycrystalline, const. and resistivity, temp. depend. 9-18645  
CaSO<sub>4</sub>.2H<sub>2</sub>O (gypsum) film, principal permittivities and elec. axis from 9 mm. interferometry study 9-7943  
CaTiO<sub>3</sub>, prebreakdown processes 9-18651  
CdTiO<sub>3</sub>, permittivity and loss-tangent meas., 20-600°C, 0.1-20 MHz 9-18647  
CeCrO<sub>3</sub>, polycrystalline, const. and resistivity, temp. depend. 9-18645  
CsCl finite ellipsoid, low-temp. behaviour of dielec. const. quasi-harmonic approx. 9-10027  
CuBr, electric field gradient, spin echo meas. 9-10028  
Cu(HCO<sub>2</sub>)<sub>2</sub>.4H<sub>2</sub>O, relaxation, anomalous, antiferroelectric 9-3715

**Dielectric properties of substances continued**  
**solids continued**

- CuI, electric field gradient, spin echo meas. 9-10028  
p GaAs, infl. of constant elec. field on capacitance 9-3650  
GaAs, piezobirefringence, dispersion 9-13922  
HCl, complex dielec. const. 9-12186  
n-InSb anodic oxide films, dielec. constant 9-11770  
KBr:KOH, pressure depend. of relaxation 9-5746  
KBr:OH, paraelec. dipole equilibrium directions and elec. moments by electro-caloric eff. 9-21532  
KBr, u.v. absorpt. of amide ions rel. to paraelec. and paraelastic orientation 9-5747  
KCl:Li, paraelec. dipole equilibrium directions and elec. moment by electro-caloric eff. 9-21532  
KCl, contact electrification by metals 9-10029  
KCl, paraelectric resonance spectroscopy, theory and expt. 9-13916  
KCl, u.v. absorpt. of amide ions rel. to paraelec. and paraelastic orientation 9-5747  
KH<sub>2</sub>PO<sub>4</sub>, elastic Curie Weiss law from u.s. velocity and attenuation meas. 9-21430  
KI, ionic conductivity, 200-700°K 9-16292  
KI, paraelastic relaxation, mass depend. 9-9752  
KI, u.v. absorpt. of amide ions rel. to paraelec. and paraelastic orientation 9-5747  
KNbO<sub>3</sub>, and neutron scatt. 9-13910  
K<sub>2</sub>NiF<sub>4</sub> single crystals, dielec. constant and loss calc., eff. of static biasing field 9-12184  
K<sub>2</sub>SrNb<sub>2</sub>O<sub>13</sub> high constant 9-1594  
Kr. rel. to refractive index between 3612 and 6439 Å 9-7832  
LaCl<sub>3</sub>, dispersion function adjusting poles and zeros to fit reststrahlen data 9-5876  
Ca<sub>10</sub>(PO<sub>4</sub>)<sub>6</sub>(OH)<sub>2</sub>, hydroxy apatite, relax. meas. 9-7837  
LiF, conductivity meas. without using contact electrodes 9-7836  
LiF, excess elec. charges, statistical analysis and formation mechanism 9-1568  
LiNO<sub>3</sub>, permittivity and loss-angle tangent, impurities effect 9-1576  
Li<sub>2</sub>O-Si<sub>2</sub>O<sub>2</sub> glasses, heat treated, n irradiation effects 9-7833  
Mg ferrites, quenching temp. effect on complex permittivity tensor components 9-19967  
MnO:Li, loss and dipole relaxation 9-12187  
MnZn ferrites of stoichiometric compositions, permittivity and loss, rel. to composition 9-16079  
NaBa<sub>2</sub>Nb<sub>2</sub>O<sub>15</sub>, high constant 9-1594  
NaD<sub>3</sub>(SeO<sub>3</sub>)<sub>2</sub>, ferroelectric transitions from NMR temp. dependence meas. 9-17435  
NaD<sub>3</sub>(SeO<sub>3</sub>)<sub>2</sub>, for low temp. phase transition study 9-17434  
NaD<sub>3</sub>(SeO<sub>3</sub>)<sub>2</sub>, ferroelectric transitions from NMR temp. dependence meas. 9-17435  
NaI ionic cryst., dielec. saturation 9-1582  
Nb<sub>2</sub>O<sub>5</sub>, B-modification, capacity depend. on impurity conc., and a.c. polarization 9-3694  
Nb<sub>2</sub>O<sub>5</sub>, lattice const. rel. to atom polarisability 9-3695  
Nb<sub>2</sub>O<sub>5</sub>:Cl, dielec. constants, refractive index and optical band gaps for principal crystal axes 9-10030  
Ni Fe ferrite, conduction mechanism 9-3632  
Pb(Mg<sub>1/3</sub>Nb<sub>2/3</sub>)O<sub>3</sub>-PbTiO<sub>3</sub>-PbZrO<sub>3</sub> system, antiferro-ferroelec. and ferroelec. 1-2 phase boundaries, obs. 9-7844  
PbO thin film const., forbidden gap width deduced 9-10167  
PbO thin films, anomaly rel. to possible ferroelectricity 9-17437  
Pb(Zr,Sr,Ti)O<sub>3</sub> solid solutions, with properties depending on applied elect. field, expt. study 9-10046  
PbZrO<sub>3</sub>:Nb<sub>2</sub>O<sub>5</sub> with properties depending on applied elect. field, experimental study 9-10046  
PbZrO<sub>3</sub>-PbTiO<sub>3</sub>, sputtered ferroelec. films, dielectric loss and strength 9-1596  
PbZrO<sub>3</sub>, effect of impurity on phase 9-17436  
PbZrO<sub>3</sub>, relaxation and spontaneous polarization 9-5748  
PrCl<sub>3</sub>, dispersion function, adjusting poles and zeros to fit reststrahlen data 9-5876  
RbCl:Ag, paraelec. dipole equilibrium directions and elec. moment by electro-caloric eff. 9-21532  
RbCl:CN<sup>-</sup>, tunneling states of CN<sup>-</sup> ions 9-10040  
Sb<sub>2</sub>S<sub>3</sub> vitreous films, space-charge-limited currents 9-16289  
SbSI, space-charge-limited currents in para- and ferroelec. phases 9-10038  
Se, relaxation in crystalline and amorphous states 9-19926  
Si<sub>3</sub>N<sub>4</sub> films, complex constant 9-19927  
SiBi<sub>2</sub>O<sub>7</sub>, permittivity and resistivity 9-18648  
SiC films, microwave discharge prepared, IV characs. 9-21601  
SiN, Frenkel-Poole emission, field ionization and trap hopping processes in elec. cond. 9-7834  
SiO<sub>2</sub>, pyrolytic films, I-V characs. in m.i.s. structure, dependence on ht. treatment 9-3195  
SiO<sub>2</sub> structure influence on m.o.s. system 9-7830  
SiO<sub>x</sub> films, evaporated, u.v. irrad. effects 9-5868  
SiO<sub>2</sub> thin layers, polarisation effects in m.i.m. and m.i.s. structures 9-3717  
 $\alpha$  Sn, singularity in long wave length limit 9-3697  
SrTiO<sub>3</sub>:rare-earths, relaxation, activation energy, obs. 9-3699  
TiO<sub>2</sub>, reduced, variations of dielectric constant and loss 9-1601  
TiO<sub>2</sub>, rutile, effect of H on elec. props. 9-1584  
TiO<sub>2</sub> single cry. at room temp., dielec. const. and loss variation at diff. freq., abs. peaks and relax. 9-12188  
Xe, rel. to refractive index between 3612 and 6439 Å 9-7832  
Y<sub>3</sub>Al<sub>5</sub> garnet, optical phonons by infrared reflection spectra 9-3512  
ZnO single crystal, differential capacitance between nonsymmetric contacts 9-17428  
ZnS:Cu, Cl photodielectric effect due to photoconduction in grains 9-1570

**solids, ferroelectric** see *Ferroelectric materials*

**Dielectric relaxation** see *Dielectric phenomena; Dielectric properties of substances*

**Dielectric strength** see *Electric strength*

**Differential analysers** see *Calculating apparatus*

**Differential equations**

aerodynamic profiled coupling curves, derivation 9-9430

bound condition change, estimation of error 9-36

boundary problem of second degree, soln. by method of finite differences 9-12863

boundary value problems for second order elliptic eqns., book 9-18982

boundary-value problems, nonlinear, asymptotic behaviour 9-12862

**Differential equations continued**

- Cauchy problem singular perturbations and boundary value problems 9-20302  
 eigen and boundary value problems, Ritz finite difference method 9-4220  
 extended energy-integral technique 9-6281  
 factorization method extended 9-6280  
 finite difference methods, stability 9-34  
 flow, viscous, incompressible, existence theorems for partial differential eqn. 9-7240  
 Hamiltonian analytic system asymptotic soln. 9-16655  
 heat, linear and weakly nonlinear, first boundary value problem periodic soln. 9-14391  
 infinite order, bending of plates 9-14374  
 integro-differential eqn. soln., straight line convergence method 9-16654  
 inverse problem, chapter in book 9-12861  
 Klein-Gordon, non-linear discussion including physical realisation, for undergraduates 9-12829  
 Lax's method for solving numerically hyperbolic systems 9-5097  
 linear, functional, soln. representations 9-20300  
 linear, ordinary, with exponential coeffs., soln. 9-17689  
 molecular collisions 9-2933  
 non-autonomous nonlinear, periodic soln., perturbation method 9-10615  
 nonlinear, stability of solns., differentiability w.r.t. initial conditions 9-10614  
 nonlinear Dirichlet problems, use of finite difference analogues 9-18981  
 orbits, ultimate behaviour with respect to an unstable critical point 9-20294  
 partial, for heat cond., elec. analogue soln. error analysis 9-10617  
 perturbation, iterative soln. procedure 9-6324  
 quasilinear systems, non-autonomous, two deg. of freedom, periodic solns. 9-8359  
 Ritz finite difference method for boundary and eigenvalue problems 9-4220  
 Schrodinger operator, periodic, perturbation by vanishing potential 9-14311  
 in second order approx. for a point on edge of base of finite cylinder of revolution 9-17687  
 second order approximation for fluid turbulence 9-11669  
 second-order nonlinear, quadrature soln. 9-17686  
 Sturm-Liouville of VIII order 9-37  
 third-order system, with rapidly rotating phase 9-2188

**Diffraction**

- aperture, patterns, effect of phase term in mutual coherence function 9-15544  
 induced wave in solid by aerial shock wave, polariscopic investigation 9-19077  
 of scalar waves by circular diaphragms 9-51  
 stress wave, by solids and photoelastic expt. representation 9-6380  
 of waves, textbook 9-10716

**acoustic waves**

- at compliant cylinder, inhomogeneous, of gas or liq. with N-layers 9-4329  
 by cone, infinite circular: axisymmetrical case 9-17803  
 grating with finite number of bands 9-17805  
 holography with scanning source and stationary point detector 9-8633  
 by moving fluid cylinder, scatt. wave characteristics, magnitudes and rad. patterns, eff. of var. in angle of incidence 9-4331  
 plane pulses, arbitrary cross-section obstacles, impedance boundary condition 9-2219  
 propagation behind obstacle 9-16732  
 theory and appl. to field of baffled array calc. 9-20430

**acoustic waves, ultrasonic**

- in ultrasonic devices for vel. and attenuation meas. in gases and liqs. 9-14385

**electromagnetic waves**

- angular spectrum of plane waves representation, equivalence to a Rayleigh integral transform 9-10902  
 by rocket exhausts, v.h.f. and C-band 9-186  
 fields expressible by plane-wave expansions containing only homogeneous waves, props. 9-256  
 fraunhofer, by two ships obs. rel. to Huygens and Kirchhoff obliquity factors 9-4393  
 groundwave by terrain features, two-dimensional analysis 9-8551  
 half-plane, boundary wave formation near edge, radiation losses 9-6421  
 impedance system of cylinder on plane, boundary problem 9-20472  
 microwave, atomic stacking models for expts. 9-16  
 microwave apertures, sectoral and annular, focal region fields 9-8550  
 ObyO plane, unidirectionally conducting strip, Weiner-Hopf eqn., surface-wave excitation and scattering at edges 9-2279  
 on arbitrarily moving surface, theory 9-8549  
 parabolic eqn. soln. by finite difference method 9-12959  
 in plasma, anisotropic, cylindrical wave diff. at an impedance wedge 9-19535  
 quadrupole radiation, on perfectly conducting wedge 9-19109  
 radiation problem, solution 9-4394  
 resonator, open, with large Fresnel diffraction number, proper freqs. and diffraction losses 9-12955  
 by slit aperture formed by two inclined planes 9-10773  
 wedge diffraction functions, use in quasioptics 9-10775  
 Weiner-Hopf simultaneous eqns., appl. 9-187

**electrons see Electron diffraction****light**

- See also Holography*  
 angular spectrum of plane waves representation, equivalence to a Rayleigh integral transform 9-10902  
 coherent imaging using pseudo-random coded diffuser 9-8652  
 convolution method to reveal periodicities in electron micrographs 9-16072  
 diffraction-limited lens, problems in photo at diff. limit 9-20564  
 efficiency comp. for double and single exposure holograms 9-2387  
 Fresnel images correl. by collinear heterodyning of Fresnel images 9-10887  
 Fresnel zone plates, theory 9-15545  
 inverse for monochromatic scalar wave field, new reciprocity theorem 9-10900  
 iterated, of  $(\sin x)/x$  pattern by slit grating, local intensity vars. 9-17888  
 liquids, elasto-opt. coeff., ultrasonic light diff. method 9-7265  
 losses in optical confocal and semiconfocal resonators 9-4461

**Diffraction continued****light continued**

- Moire fringes from superposition of Cornu's grating and Soret's zone plate 9-264  
 Moire patterns due to superposition of Cornu gratings 9-263  
 due to monochromatic source, distribution formulation 9-20547  
 non-linear, theory and expt. verification 9-4519  
 optical and X-ray effects demonstration by laser source 9-15405  
 pattern role in microscope resolving power, demonstration 9-12839  
 phase grating spectra produced by u.s. waves, interferometric meas. method 9-10903  
 plane waves, generalized angular spectrum and diffraction transform 9-20548  
 polymer systems containing spherulites, Hv patterns, deformation sensitive central spot 9-12336  
 production, new and simple method 9-13050  
 radial lines on visual and photographic star images 9-8653  
 scalar, optical filter synthesis by holographic methods 9-10924  
 spherical optical resonator, effects 9-8598  
 by superposed ultrasonic waves, calc. 9-17889  
 surface plasmon resons. in gratings 9-4520  
 surface structure analysis by optical simulation of LEED patterns 9-13570  
 u.s. diffraction modulation in crystals, loss effects 9-10162  
 u.s. grating, audio spectrum angle using real time Debye-Sears effect 9-2229  
 by u.s. waves, investigation using holographic method 9-2406  
 LaF<sub>3</sub>, Bragg diff. for sound velocity meas. 9-9826  
 YFe garnet, diffraction of light from magnetoelastic waves 9-12342

**neutrons see Neutron diffraction****X-rays see X-ray diffraction****Diffraction by acoustic waves see Acoustic waves/effects; Diffraction/light****Diffraction gratings**

- array space factors, synthesis in main beam and grating lobes 9-10774  
 chemical prod. on Al<sub>2</sub>O<sub>3</sub> surface 9-4171  
 cornu's superimposed Moire patterns 9-263  
 Cornu spiral superimposed on Soret's zone plane, Moire fringes 9-264  
 crossed, as pseudo-random coded diffuser for coherent imagery 9-8652  
 Czerny-Turner and Ebert spectrometers, dispersion 9-10933  
 dichromated gelatin holographic system, high resolution, properties 9-4541  
 holographic, bleaching for max. efficiency 9-19157  
 immersion grating 9-13053  
 lamellar, far i.r. 9-10899  
 Lyman ghosts, intensity and removal 9-10929  
 non-parallel concentric beams, computation of aberrations 9-13052  
 phase, spectra produced by u.s. waves, interferometric meas. method 9-10903  
 plane, for measurement of small angles, Moire fringes 9-4216  
 radiation emission from neighbouring particles, review 9-15486  
 reflection efficiencies in soft X-ray region in Rayleigh-Fano theory 9-10901  
 reflectivity in ultrasoft  $\gamma$  ray region 9-6549  
 ruling methods, props. and appls. 9-6548  
 Wood's anomalies as local phenomena 9-14445  
 Al coated, surface plasmon reson. effects 9-4520  
 Au coated, surface plasmon reson. effects 9-4520

**Diffraction/scopy see Diffraction/light; Optical images****Diffusion**

- See also Neutrons and antineutrons/diffusion; for diffusion of matter, see Diffusion in gases; Diffusion in liquids; Diffusion in solids*  
 binary coeff., critical assessment 9-1240  
 chemical reactions, diffusion-controlled, theory 9-8057  
 comet, soln. of equation 9-18918  
 convective, in capillaries, transient props. 9-21193  
 cosmic rays, interplanetary, Mariner IV obs. 9-10459  
 earth's electron belt 9-16536  
 in earth's radiation belts rel. acceleration mechanism 9-16535  
 equation with nonlinear boundary condition, periodic solution 9-6344  
 ferromagnets, magnetic moment diffusion and entropy production 9-10108  
 field-flow fractionation, nonequilibrium, theory 9-848  
 in finite region with moving boundary, solution to problem 9-10680  
 in flame 9-17828  
 flames, buoyant, from liquid pools, effect of merging on burning rate 9-16746  
 fluids, almost classical, theory 9-841  
 ion exchangers, diff. and reaction coupling 9-17510  
 ions in solar corona, theory 9-10557  
 of magnetic field, stream variant variant of finite difference approach 9-110  
 magnetoplasma, fully ionized, drift waves effect on transverse diffusion 9-17103  
 multicomponent coeffs., predictive theory 9-112  
 multicomponent coeffs., predictive theory 9-111  
 Onsager's reciprocal relations, with coeffs. depend. on intensive props. 9-16701  
 plasma, particles diffusion across magnetic lines 9-17101  
 plasma expansion from inductive high frequency discharges 9-13463  
 plasma in magnetic field, law 9-18286  
 polycrystals, relax. theory 9-3403  
 relativistic eqn. 9-6343  
 spin, effect on spin echo signals in inhomogeneous alternating rot. solenoid field 9-4913  
 teaching demonstration using interferometry 9-8338  
 tensor of particles in r.f. fields with stochastic parameters 9-221  
 ternary coefficients, analytical determ. 9-6345  
 transpiration cooled porous flat plate in stream of air or CO<sub>2</sub> 9-20453  
 unsteady transport equation, fundamental soln. in solid geometry 9-17750  
 Cs plasma, magnetically confined, radial electric field effect 9-14758  
 K magneto-plasma, meas. 9-17102  
 Na-P zeolite, self-diffusion of water 9-5130  
 Pm<sub>2</sub>O<sub>3</sub>-Sm<sub>2</sub>O<sub>3</sub>, thermal diffusivity, rel. to <sup>147</sup>Pm as power source 9-2790

**acoustic waves**

- See also Scattering/acoustic waves*  
 diffusivity of stationary field, reln. with pulse response of room 9-4327  
 stationary diffusivity in rooms, correl. with pulse response characts. 9-4360



**electromagnetic waves**

*See also Scattering/electromagnetic waves*  
 creeping-wave analysis of sphere, Poynting vector approach 9-6422  
 in plasma layer for large amplitude 9-21072

**light**

*See also Reflectivity; Scattering/light*  
 coherent imagery, pseudo-random coded diffuser 9-8652  
 fluorescent temp. diffuser construction, patent 9-8657  
 holographic image of diffuse object, effects of film nonlinearities 9-10875  
 theory of scatt. media 9-2405  
 · transmission, diffuse, through spherical, inhomogeneous, scatt. shell 9-8654

**Diffusion columns** *see Diffusion in gases/thermal; Isotope separation*

**Diffusion in gases**

*See also Flow/gases*  
 air, mass transfer from naphthalene and phenol vibrating cylinders 9-21250  
 analogy with spin diffusion in ferromagnets 9-12895  
 binary, krypton ethylchloride, non-polar mixtures, unlike interactions 9-21147  
 binary krypton-methylene chloride, non-polar mixtures, unlike interactions 9-21147  
 binary single-phase and multiphase systems, interdiffusion coeff. calc. 9-19760  
 chemically reacting mixture, binary coeff. var. 9-7227  
 controlled afterglows, electron decay, plasma 9-923  
 effusion from Knudsen cells with conical channels 9-15976  
 flow in commercial catalysts, at pressure levels above atmospheric 9-9459  
 inert, of slow electrons, in presence of inelastic collisions 9-15975  
 inert gases, transport coeff. calc. from Boltzmann eqn. 9-13496  
 ion motion under const. elec. field, stochastic computer simulation 9-7235  
 ionosphere F2 layer, global diff. eqn. soln. 9-21824  
 of ions in strong elec. fields, under influence of charge-transfer collisions 9-15977  
 isotope separation efficiency, surface diffusion eff. 9-7236  
 jet, supersonic separation of gas mixture 9-21145  
 organic vapour in air, teaching expt. 9-8340  
 plasma, turbulent, rel. to elec. field fluctuations and particle orbits 9-11548  
 symmetric coeffs., kinetic theory 9-11662  
 three-component mixture, in transition region between Knudsen and molecular diffusion, equations soln. 9-3059  
 transition region at const. pressure, effects of different structures of porous solids 9-9666  
 turbulent mass diffusion in mixing of two coaxial streams, small press. grads. 9-7234  
 vapour migration in capillary-porous bodies 9-962  
 Cd effusion, ang. number distrib. 9-3062  
 CsCl effusion, ang. number distrib. 9-9460  
 CsCl effusion, ang. number distrib. 9-3063  
 H<sub>2</sub>-O<sub>2</sub> diffusion flame structure 9-19098  
 H<sub>2</sub> separation from gaseous mixture, method and apparatus, patent 9-13481  
 He, electron lateral diff., and first Townsend coeffs. 9-15978  
 He of He(2<sup>3</sup>S<sub>1</sub>) rel. to 2<sup>3</sup>S<sub>1</sub>-1<sup>3</sup>S<sub>0</sub> repulsive interaction pot., obs. 9-4889  
 He plasma, in mag. field, obs. 9-9349  
<sup>3</sup>He metastable atoms, rel. to excitation transfer during collisions 9-6995  
 K plasma, non-uniform, of instabilities 9-11609  
 N, N\*, N<sub>2</sub><sup>+</sup>, longitudinal and transverse diffusion coeff., 12-300×10<sup>-27</sup> Vcm<sup>2</sup> 9-918  
 O<sub>2</sub>, through Ag membrane, mass spectra comparison of evolved and diffused gas 9-11663

**thermal**

air arc column, temp.-depend. diffusivity rel. to decay 9-9423  
 apparatus for coeff. determ. in gas mixtures 9-19590  
 electron, kinetic theory study, temp. depend. of density 9-3060  
 hydrocarbon systems, pressure change meas. 9-964  
 polyatomic gases, nonspherical interactions 9-3061  
 specific molar compositions, identification of meas. factors 9-5123  
 Ar-He system, N-stage swing-separator, back diffusion correction evaluation 9-7237  
 H<sub>2</sub>-He mixtures, comp. and temp. depend. 9-17168  
 He-N<sub>2</sub> mixture, coeff. determ. 9-19590  
 He column rel. to thermal conductivity meas., 350-1350°K 9-5115  
 N<sub>2</sub> arc column, temp.-depend. diffusivity effect on decay 9-9423

**Diffusion in liquids**

*See also Flow/liquids*  
 in adsorption from solution kinetics 9-16045  
 alcohols, of gas, low temp. 9-21194  
 alkanes, linear, use of computer calculation of dimensions in theory 9-17046  
 analogy with spin diffusion in ferromagnets 9-12895  
 binary diffusion coefficient, composition dependence 9-3088  
 binary single-phase and multiphase systems, interdiffusion coeff. calc. 9-19760  
 binary soln. through potential-energy profile 9-9499  
 colloids, proton self-diffusion, by spin echo 9-3127  
 diaphragm cell method of meas. up to 60°C 9-995  
 effect on crystal growth by pulling and zone melting 9-19687  
 electrochemical with rotating electrodes 9-20058  
 freely suspended single droplets, instantaneous exchange rate meas. 9-21192  
 gels, of electrolytes, coeff. meas. 9-21233  
 jets, laminar liquid absorption expts 9-15997  
 macromolecules, flexible-coil, rel. to light scatt. 9-3101  
 macromolecules, optically anisotropic, rel. to light scatt. 9-1011  
 metal, cell for multiple time isothermal meas. on diffusivities 9-996  
 metals, self-diffusion activation energy rel. to compressibility and charact. temp., near melting point 9-11890  
 multicomponent, use and limitations of effective binary diffusion coeff. concept 9-19613  
 phase permeabilities of displacing and displaced liquids 9-18354  
 phenanthrene-acridine soln., effect on fluoresc. decay 9-5178  
 phenol-water system, const. rel. to temp., photon correlation method 9-9497  
 polyethacrylate in toluene, coeff. determ. in cell 9-14840  
 polymer solutions, diffusion coefficients variation 9-3091

**Diffusion in liquids continued**

polymethacrylate in acetone, coeff. determ. in cell 9-14840  
 polymethacrylate in benzene, coeff. determ. in cell 9-14840  
 power-law, mass transport from rotating disc 9-19624  
 real gas in spherical bubble 9-18345  
 rectified in cavitation bubbles, acoustic threshold phenomena 9-5139  
 rotational, in solutions 9-9488  
 sodium polystyrenesulfonate, tracer coeffs., counterion binding in aqueous solutions 9-18355  
 solute dispersion in m.h.d. laminar flow between parallel plates 9-17094  
 ternary diffusion measurement, steady state method, apparatus 9-3087  
 transparent liqs., interdiff. coeff. meas. by plane source method 9-5150  
 u.s. standing wave freezing-in by conc. zone effect 9-18358  
 Ag, of O, electrochem. meas. 9-11690  
 AgNO<sub>3</sub> dilute solns., interdiffusion in alkali nitrates 9-7261  
 Al, of Si, temp. depend. of coeff. 9-9496  
<sup>10</sup>BO<sub>3</sub><sup>-</sup> and <sup>11</sup>BO<sub>3</sub><sup>-</sup>, migration, isotope effect 9-17200  
 CsNO<sub>3</sub>, molten salt diff. coeff. of <sup>137</sup>Cs meas. 9-19614  
 Cu, of O, electrochem. meas. 9-11690  
 D<sub>2</sub>O, of H<sub>2</sub>O, examined by neutron radiography 9-11367  
 Ga, of Zn, Ag and Co 9-13516  
 H halides in cyclohexane, rotational diffusion 9-9488  
 Na, self, volume and pressure constant 9-3089  
 NaNO<sub>3</sub> molten salt diff. coeff. of <sup>23</sup>Na meas. 9-19614  
 SiO<sub>2</sub> gels, rel. to pore size anal. 9-9572  
 Sn-Zn foreign diff. coeffs. 9-17201  
 Sn self-diffusion, applic. of 'fluctuation' theory 9-5151

**thermal**

tetrabromoethane-tetrachloroethane solns. 9-9498  
 thermogravimational, revised formula 9-9495

**Diffusion in solids**

*See also Permeability, mechanical*  
 alkali halides, diffusive penetration of boundaries 9-9728  
 alkali halides, inert gas diff., theory 9-3386  
 alloys, binary, and Kirkendall shift, comments 9-9727  
 alloys, binary, and Kirkendall shift, comments 9-9726  
 alloys, binary, and Kirkendall shift, comments 9-18484  
 b.c.c. alloys, solvent atom diffusion 9-7507  
 b.c.c. metals, of H, activation energy 9-3385  
 bimetallic systems, vacancy mechanism, specific features 9-9730  
 binary coeff., critical assessment 9-1240  
 binary single-phase and multiphase systems, interdiffusion coeff. calc. 9-19760  
 capillary-porous mats., moisture diff. coeff. at all drying temps. 9-21243  
 ceramic fuel elements, pore migration and shape change in thermal grad. 9-18483  
 chemical reactions in porous media 9-1904  
 Cl<sup>-</sup> diffusion and elec. conductivity, transport eqns. derived from five-defect model 9-13914  
 correlated and uncorrelated, via edge dislocations 9-9724  
 diamond lattice, correlation factor for impurity diffusion 9-21346  
 1,4- dioxane, molecular mobility, n.m.r. study 9-11901  
 discrete lattice, diff. controlled reaction kinetics 9-1201  
 epitaxial doping density vs. depth meas. 9-18623  
 exponential tempering function appl. 9-3179  
 ferrites, mixed of ions rel. to cation vacancy density determ. 9-3323  
 in finite region with moving boundary, solution to problem 9-10680  
 gels, of electrolytes, coeff. meas. 9-21233  
 glass, of Li, increase in mechanical and thermal resistance 9-21379  
 glass, of separated phases, coeff. meas. by light scatt. 9-14954  
 glass, sodium disilicate, of iron oxides, dissolution and diffusion kinetics 9-19766  
 graphite, self-diffusion in single crystals, 2000-2600°C 9-16110  
 graphite, self diffusion mechanism rel. to thermal annealing studies of irradiation defects 9-5337  
 heat of transport rel. to effective valency 9-5396  
 humidity, into insulating material in form of plate 9-1239  
 hydrated crystals, of water mols., effect on NMR spectrum 9-1241  
 interface growth, solution where diffusion coeff. is conc. dependent 9-1087  
 interstitial, quantum effects 9-3370  
 ion crystals, of inclusions, motion under temp. and elec. field 9-17281  
 ionic crystal, of vacancies causing change in spherical pore form 9-21329  
 ionic crystals, of inert gases, migration and trapping 9-11891  
 Kirkendall effect mechanism 9-19762  
 metal alloys, diffusion- induced disperse phase coalescence kinetics 9-1243  
 metal surfaces, inert gas diff. coeffs. 9-21347  
 metals, of H, interstitial, quantum effects 9-3370  
 metals, rel. to structural defects, autoradiographic obs. 9-9707  
 metals, self, high pressure effects 9-3384  
 metals, self-diffusion activation energy rel. to compressibility and charact. temp., near melting point 9-11890  
 mica, of Au and Ag, migration activation energy along natural cleavage surface 9-11892  
 Mossbauer effect direct obs. 9-5401  
 multi-phase, one- dimensional, Fick's 2nd law soln. 9-3372  
 multicomponent couples, interdiffusion phenom. 9-3371  
 naphthalene in polymethylmethacrylate, diffusional fluoresc. quenching 9-12477  
 naphthalene evap. films, exciton diff. 9-7718  
 Ostwald ripening and related phenomena, exptl. verification of mass transport anal. 9-1251  
 oxides as sources for semicond. device fabrication 9-5394  
 porous catalyst pellets, effective diffusivity and average pore radius 9-13702  
 Pyrex glass, of Na<sup>+</sup> and Ag<sup>+</sup>, and exchange between two-phase structure of glass 9-14958  
 quartz, decorated paths 9-18488  
 reactive gases, kinetic and diffusional models 9-21680  
 refractory carbides, data 9-7506  
 solid soln., binary metallic, interdiffusion coeff., conc. depend. 9-3374  
 solid-liquid interfacial reaction between 18-8 stainless steel and aluminium 9-1089  
 statistical theory of process 9-13703  
 steel, low C, of Cr 9-5407  
 steel, low C, of Cr 9-5406  
 steel, of C during austenitic transforms. rel. to redistrib. laws 9-3490  
 surface, importance in crystal growth from solution 9-18418  
 surface, theoretical study of laws 9-9725

**Diffusion in solids continued**

ternary coefficients, analytical determ. 9-6345  
 ternary systems, rel. to element redistribution laws 9-3381  
 vacancy, from scattering theory 9-7470  
 Vacancy motion persistence 9-9699  
 water molecules in hydrates and NMR spectra 9-1242  
 water molecules in hydrates and NMR spectra 9-13704  
 welded clad metal diffusion layer structure, diffusion activation energy and coeff. of reactive diffusion 9-18485  
 X-ray fluorescence radiographic surface analysis 9-14953  
 Zircaloy-2, of Cr and Fe 9-19761  
 in zone melting process for crystal production, mathematical model 9-9649  
 $\alpha$  emitters in foils, meas. using  $\alpha$  spectrometer 9-8931  
 Ag-Au couples, Kirkendall effect mechanism 9-19762  
 Ag, of In, grain boundary and dislocation mechanism, temp. dependence, 180-100°C 9-3375  
 Ag, self-diffusion, effect of electron bombardment 9-5398  
 Ag, self-diffusion, infl. of bound divacancies on isotope eff. 9-18487  
 Ag, self-diffusion, influence of traces of O<sub>2</sub> and S 9-3376  
 Ag, self-diffusion in polycryst. 9-5397  
 Ag compacts, surface diffusivity, effect of O<sub>2</sub> 9-5498  
 Al, of Pu 9-11957  
 Al, of U, at infinite dilution 9-17282  
 Ar self-diffusion coeff. meas. rel. to vacancy diffusion mechanism 9-11893  
<sup>40</sup>Ar, from KCl and microcline feldspar, elec. field effects 9-11897  
 Au (54.4at.%)Ag alloy, surface self-diffusion 9-17283  
 Au-Pd film, coeff., 400-600°C, electron diffraction study 9-5399  
 Au, of Fe, measurement using Mossbauer effect 9-3377  
 Au, self-, on naturally rough surfaces, 870-970°C 9-11894  
 Au, self, interpretation 9-3378  
 Au, surface self-diffusion 9-21349  
 Au in Li, 45-150°C 9-7509  
 Ba type A zeolite, stability and cation self-diffusion obs. 9-5400  
 BaF<sub>2</sub> of <sup>89</sup>Sr 9-3379  
 CaF<sub>2</sub> of <sup>89</sup>Sr 9-3379  
 CaF<sub>2</sub>, of excess Ca, process eqns. 9-9729  
 CdS: Au: S<sub>2</sub>, of impurity, vapour pressure investigation 9-3380  
 CdSe, of P, and solubility meas., 900 and 950°C, Cd partial pressure dependence 9-11895  
 CdTe, of Cd and Te, self-diffusion mechanisms 9-1244  
 CdTe, of Cu, and solubility meas., 97-300°C rel. to Cu<sub>2</sub>Te film formation 9-11896  
 CdTe, of P, and solubility meas., 800-1000°C, Cd partial pressure dependence 9-11895  
<sup>57</sup>Co-Pd experimental Mossbauer source prod 9-11898  
 Co, of Fe and Ni, 1136-1370°C 9-19763  
 Cr diffusion layers on Fe materials, structure and metallography 9-11769  
 Cu, of Fe, direct obs. by Mossbauer effect 9-5401  
 Cu, of Zn and resulting dislocation arrangements from etch-pit exam. 9-5359  
 Cu, surface self-diff., infl. of Pb vapour 9-17284  
 Cu, surface terrace vacancies, migration energies 9-21330  
 deuterium in Nb; relaxation process, coeff. determined 9-1248  
 Fe-Cr, interdiffusion investigation in powder alloys 9-5405  
 Fe-Cr, of <sup>59</sup>Fe self-diffusion in para- and ferromag. temp. ranges 9-1245  
 Fe-Cr alloy, of Cr 9-5404  
 Fe-Cr alloys, b.c.c., of <sup>59</sup>Fe rel. to solvent atom diff. mechanism 9-7507  
 Fe-Cu(Cr) systems, vacancy mechanism, specific features 9-9730  
 Fe-Si(Ni)(Cr)-C ternary alloys, of C, rel. to element redistrib. laws. 9-3381  
 Fe-V alloy, of Cr 9-5404  
 Fe (7.5 at%) Si, magnetic effect, contrib of Young's mod. 9-5402  
 $\alpha$ -Fe, of <sup>59</sup>Fe and <sup>55</sup>Fe, elementary jump process 9-3382  
 Fe, of Be, 1100-1350°C 9-5403  
 Fe, of Co and Ni, 1136-1370°C 9-19763  
 Fe, of Cr 9-5406  
 Fe, of Cr 9-5407  
 Fe, pure, self-diffusion 9-21350  
 Fe, self-, and electrotransport, 1000-1350°C rel. to degree of ionization 9-1581  
 Fe and Fe<sub>2</sub>O<sub>3</sub>, of vol., grain boundaries and surface in sintering 9-1246  
 GaAs, improved by exposure to radiation, patent 9-21354  
 GaAs, of Cu, coeff. meas. by u.s. method 9-14955  
 GaAs, of Cu, impurity atom interaction 9-17286  
 GaAs, of Zn, mechanism 9-16111  
 GaAs, of Zn under arsenic pressure 9-3383  
 GaAs of Zn for producing laser diodes p-n junctions 9-17285  
 Ge-Al system, 'unipolar' surface 9-5408  
 Ge, enhanced, rel. to radiation defects 9-13705  
 Ge, improved by exposure to radiation, patent 9-21354  
 Ge, of Sb, acceleration by u.s. irradiation 9-1247  
 H, in Nb; relaxation process, coeff. determined 9-1248  
 $\beta$ -Hf, self, 1785-2185°C 9-9732  
 HgTe crystals, of Hg on annealing in Hg vapour, rel. to dislocation formation 9-1220  
 In films, electrotransport obs. 9-15061  
 InAs, improved by exposure to radiation patent 9-21354  
 InAs, self-diffusion meas. 9-14957  
 InAs of Zn, conc. depend. 9-7508  
 InP, of Au, 600° to 900°C, and solubility 9-14956  
 InP, of Cu, 600° to 900°C 9-5410  
 InP of Ag, volume coeff. 9-5409  
 InSb, improved by exposure to radiation patent 9-21354  
 InSb, of Se 9-18486  
 KCl: SrCl<sub>2</sub>, Cl<sup>-</sup> diffusion and elec. conductivity, transport eqns. derived from five-defect model 9-13914  
 KCl-KBr system, interdiffusion process, role of anion-cation pair vacancies 9-5411  
 KCl, of Cu ions, temp. dependence, 350°C-650°C, rel. to ion size effect 9-1250  
 KCl, self-diffusion induced vacancy-breakdown 9-18461  
 K<sub>2</sub>O-SrO-SiO<sub>2</sub> glass, of <sup>45</sup>K and <sup>85</sup>Sr 9-1249  
 KBr, self-diffusion induced vacancy-breakdown 9-18461  
 Kr, tracer diffu bs. by isotope exchange technique, 90°<T<115°K 9-9731  
 Li, <sup>114m</sup>In diff., 75°-170°C 9-17290  
 (LiAg)<sub>2</sub>SO<sub>4</sub>.b.c.c., Li<sup>+</sup> and Ag<sup>+</sup> diff. coeffs., 470-550°C 9-17287  
 LiF, of Li<sup>+</sup> self-diffusion, 650-800°C 9-21351

**Diffusion in solids continued**

LiF, of vol., grain boundaries and surface in sintering 9-1246  
 Li<sub>2</sub>SO<sub>4</sub>, cubic, Mg<sup>2+</sup>, Zn<sup>2+</sup>, Ca<sup>2+</sup>, Cd<sup>2+</sup>, Pb<sup>2+</sup> diff. coeffs., 600-800°C 9-17288  
 Mo, electrotransport and Soret effect, 1650-1900°C 9-16112  
 MoF<sub>6</sub>, of molecules, from <sup>19</sup>F n.m.r. 9-16468  
 NaCl, of Mu<sup>+</sup>, for impurity-vacancy assoc. determ. 9-1202  
 NaCl, of Cu ions, temp. dependence, 350°C-650°C, rel. to ion size effect 9-1250  
 NaCl, self-diffusion induced vacancy breakdown 9-18461  
 NaCl, surface heterodiffusion rel. to coalescence of Au particles 9-19765  
 Nb, of <sup>91</sup>Zr, 953°-1435°C 9-13706  
 Ni-Al<sub>2</sub>O<sub>3</sub> system, grain boundary grooving at interface, kinetics const. 9-1251  
 Ni (8at.%)Mo alloy, of Mo ions and electrotransport process 9-1253  
 Ni, of Be, 1020-1400°C 9-5403  
 Ni, of Fe and Co, 1136-1370°C 9-19763  
 Ni, of O, to and from surface at high temp., rel. to oxidation process. 9-12544  
 Ni, of surface chemisorbed H 9-1086  
 Ni alloys, Ni self-diffusion rel. to structural defects, autoradiographic obs. 9-9707  
 Ni H, at 78°K following 35 KeV implantation 9-21352  
 NiO, of O, self, and condensation coeff. 9-3387  
 Ni<sub>2</sub>Zn<sub>1-2</sub>Fe<sub>2</sub>O<sub>4</sub>, of Ni 9-1252  
 p-PbTe, of Ni and Cl, 700°C, junction formation 9-19767  
 Pd-B, alloys, H<sub>2</sub> diff., 50-175°C 9-7889  
 Pd, self-diffusion, infl. of bound divacancies on isotope eff. 9-18487  
 Pu in Ni 9-19768  
 RbNO<sub>3</sub>, ionic, by n.m.r. linewidth rel. to temp. 9-19770  
 inSi:P, p-irradiated, of O, rel. to thermal donor formation 9-21333  
 Si, improved by exposure to radiation, patent 9-21354  
 Si, of Au, conductivity and lifetime of excess carriers anomaly 9-16273  
 Si, of B, in oxygen ambient rel. to transistor fabrication 9-14959  
 Si, of Be, thermal, resulting elec. and opt. props. of Si 9-10004  
 Si, of Ga, retardation 9-5413  
 Si, of Ga, retarded 9-5412  
 Si, or PCl<sub>3</sub> rel. to prod. of highly alloyed n<sup>+</sup>-type layer 9-17245  
 SiC, of Al from solns. in rare earth metals, for p-n junction prep. 9-16056  
 SiO<sub>2</sub>, permeation of H molecules and ions 9-3388  
 SiO<sub>2</sub> glass, of Na, 170-1000°C 9-17291  
 SrF<sub>2</sub> of <sup>89</sup>Sr 9-3379  
 Ta, surface self-diffusion, field e microscope obs., 1200-1400°K 9-1255  
 ThO<sub>2</sub>, of <sup>230</sup>Th, rel. to grain size. 9-3390  
 Ti-Mo alloys, U diffusion 9-19769  
 Ti, of Ag ions, mobility, 1123-1623°K 9-9733  
 Ti, of H, at 78°K following 35 KeV implantation 9-21352  
 $\beta$ -Ti, self, 900-1580°C 9-9732  
 Ti alloys, Ni self-diffusion rel. to structural defects, autoradiographic obs. 9-9707  
 TiO<sub>2</sub>, of interstitial Li<sup>+</sup> ions 9-9705  
 TiNO<sub>3</sub>, ionic by n.m.r. linewidth rel. to temp. 9-19770  
 UC, of U and C, and mechanisms, 1266-1863°C 9-11899  
 UO<sub>2</sub>, cation self-diff. 9-16113  
 UO<sub>2</sub> fuels, redistrib. mechanism of O 9-11360  
 V, of Fe and isotope-effect parameter of <sup>55</sup>Fe and <sup>59</sup>Fe 9-9734  
 W, second layer migration of H<sub>2</sub>, N<sub>2</sub> and CO<sub>2</sub> with trapping on first layer sites 9-11900  
 W effect of electric field, of Re adsorbed on surface 9-13707  
 ZnO, bulk coeff. calc. 9-7593  
 ZnO, diffusivity calc. during sintering in air and oxygen 9-19825  
 ZnO, improved by exposure to radiation, patent 9-21354  
 ZnO, rel. to pore growth during final stages of sintering 9-19826  
 ZnO, zincite, of Fe, during hydrothermal growth 9-18419  
 ZnSb-constantan, semiconductor thermoelements of Sb, Ni, and Cu, Sn dopants, X-ray microprobe analysis 9-10062  
 ZnTe, of Zn and Te, self-diffusion 9-14960  
 Zr, of H, examined by neutron radiography 9-11367  
 $\alpha$ -Zr, self-diffusion 9-5414  
 $\alpha$ -Zr, self and impurity 9-3389  
 $\beta$ -Zr, thermal mass transport and electromigration 9-13709  
 ZrO<sub>2</sub>, hypostoichiometric, of O ions, 600-850°C 9-17292  
 ZrO<sub>2</sub> films, growing, of O<sub>2</sub>, 400-500°C 9-9735

**thermal**

i.r. transient method of determination 9-5573  
 mass transport, driving forces 9-3373  
 Co<sup>2+</sup> ions in pure NaCl cry., isothermal diff., Soret eff. 9-21348  
 Gd dislocation climb production 9-3349  
 (LiAg)<sub>2</sub>SO<sub>4</sub>.b.c.c., +0.5% alkali sulphates, 450-550°C 9-17289  
 LiNaSO<sub>4</sub>, b.c.c., 546-588°C 9-17289  
 Li<sub>2</sub>SO<sub>4</sub>, f.c.c., + small amts. alkali sulphates, 590-750°C 9-17289  
 Mo, Soret effect and electrotransport, 1650-1900°C 9-16112  
 Si, of B, using BBr<sub>3</sub> liquid source, 1100-1200°C 9-1254  
 Si or SiO<sub>2</sub>, of B at 1070 to 1190°C 9-13708  
 Sr<sup>2+</sup> ions in pure NaCl cry., isothermal diff., Soret eff. 9-21348  
 UC, of C into Mb and W, 1000-1800°C 9-19764  
 UN, 20 to 1000°C, by laser pulse method 9-13269

**Diffusion pumps** see Vacuum pumps**Digital computers** see Calculating apparatus/digital computers**Dilatometers** see Length measurement; Volume measurement**Dimensions**

See also Units  
 analysis, determination of mathematical relations in physics and technology 9-4262

**Dimers** see Molecules; Polymers**Dineutrons** see Neutrons**Diodes** see Electron tubes; Plasma devices; Rectifiers; Semiconducting devices/diodes and tunnel and interface devices**Dipole moments** see Molecules/moments; Nucleus/electric moment; Nucleus/magnetic moment**Diquarks** see Quarks**Dirac electron theory** see Electron theory**Dirac equation** see Quantum theory/wave equations**Discharge tubes** see Electron tubes; Gas-discharge tubes; Ion sources; Particle accelerators; X-ray tubes



**Discharges, electric**

See also *Arcs, electric; Breakdown, electric; Corona, electric discharge; Plasma; Sparks, electric*

'optical', produced by single laser pulses on non absorbing surface 9-5785

ablation of dielectric channel 9-19558

acoustical spectra 9-5078

air, X-ray production at atmos. pressure 9-5094

air gaps, narrow, with nanosec rise time 9-7202

alkali-metal-seeded rare gases, descriptive theory development of positive column 9-13469

anode, thermal processes and evaporation 9-19557

anode fall, calorimetric determ. 9-3027

anode fall meas., calorimetric method 9-3017

binary mixtures of CO, CO<sub>2</sub>, methane He and O<sub>2</sub>, species involved in C deposition 9-8120

capacitor, ideal, apparent nonconservation of energy 9-4415

cathode shielding to minimize sputtering in discharge expts. 9-7197

cathode spot reverse motion 9-21112

cavity in solid dielec., meas. interpretation 9-7196

chamber, restricted size, design and performance of uniform field electrode 9-13164

commutator, pulsed with radioactive stabilization 9-11624

current-growth expts., rel. to determ. of ionization and attachment coeffs., detachment and ion-mol. reactions effects 9-11612

in dielectric voids, partial 9-18650

electrodeless, electron temp. distrib., determ. by spectrometric techs. 9-7206

electron density variation during change of state 9-9410

excess point discharge, developed local potential gradient 9-19563

excess point-discharge currents, local potential grad. around point 9-21118

film, polystyrol, effect on dielec. and mech. props. 9-10032

focussed, noncylindrical, axial striograms 9-17138

gas, detector for digitization of ionizing particle distrib. 9-13165

gas, during rupture of adhesive contact 9-21111

gas, e energy distrib. by Markov random flight soln. 9-5080

gas, microwave, harmonic radiation exptl. studiey 9-11622

gas, Townsend; e back diffusion and accel. 9-13462

gases, streamer breakdown, mech. of secondary processes 9-11631

h.f. voltage of oscillator rel. to anode voltage 9-3016

hollow cathode, excitation temp. in negative glow light, meas. 9-9413

hollow-cathode, basis of ion laser 9-4464

hot-cathode, h.f. instability in mag. field 9-21104

initiation by cathode desorbed negative ions 9-21114

investigation from 10<sup>-8</sup> torr - 4 atmos., apparatus 9-3019

Langmuir paradox 9-9422

light source, pulsed, due to discharges in halogens 9-6557

liquid, pulse discharge theory 9-3118

low voltage, u.v. light source 9-2414

noble gas ion lasers, calc. of max. inversion density and power output 9-4465

noble gases, medium pressure, positive column, application of diffusion theory 9-21116

noble gases, medium pressures, experimental results 9-21115

oxide cathode fall rel. emission 9-3024

partial, pulse analyser, multi-channel 9-9414

Penning, drift-dissipative plasma instability 9-5053

Penning, microwave emission from plasma in inhomogeneous mag. field 9-5028

Penning, sputtering type for analysis of low charge state metallic ions 9-3020

plasma, acoustic wave generation and detection 9-14764

plasma, electronegative, with moving striations, radial ambipolar field reversal 9-21062

plasma ion outflow in 100 kOe mag. field 9-9348

point, atmospheric charge transfer 9-18802

positive column, ion waves, drift waves and instabilities 9-21106

positive column, magnetised, effect of conducting wall 9-3025

positive column theory including space-charge effects 9-5079

positive column with moving striations Langmuir probe meas., phase reference necessity 9-3026

pre-breakdown currents from non-metallic emitting sites in cathode 9-17137

pulsed, spectroscopic, sampling technique for time-resolved meas. 9-10930

Rayleigh-Taylor Z pinch instability in constriction process, soln. 9-2977

r.f., probe current meas., frequency analysis 9-19567

r.f., sputtering of insulating film on to substrate 9-3204

screening by auxiliary electrodes of the spiral in the direction of positive column 9-21117

similitude laws concerning geometrical parameters and disruptive field, experimental verification 9-927

striation, moving, critical mag. field for disappearance 9-14803

striations, fast moving type 'r' ionization freq. depend. on electron mean energy 9-7173

striations, forward positive moving, theory 9-11621

striations, moving, probe and microwave meas. validity 9-5084

striations, moving, probe meas., rel. to electron energy distrib. 9-866

striations, review 9-15961

striations in plasma, review 9-15945

trigatron spark gap, with long time lags to breakdown 9-13460

<sup>198</sup>Hg at low press., photon correlation meas. 9-9339

Ag-Cu alloy hollow cathode discharge, eff. of mat. composition current and He press., spect. study 9-19559

Ar-Ne mixture, obs. 9-929

Ar, electrodeless, determ. of electron temp. distribts. 9-7206

Ar, low pressure, hot cathode discharge, spectroscopic investigation 9-9419

Ar, positive column, continuous spectrum obs. 9-924

Ar, positive column, influence of distrib. function on microwave emission and r.f. conductivity 9-19561

Ar, Townsend diagram, e back diffusion and accel. 9-13462

Ar<sup>+</sup> laser, study of properties to determine inversion mechanism 9-20505

Ar capillary, radial distrib. of excited species 9-13461

Ar energy distrib. obs. from non-magnetic hot cathode 9-2361

Ar laser, pulsed, time-resolved spectrum 9-13002

Ar plasma, low temp., radial particle distrib. profile, rel. to volume recomb. 9-11553

**Discharges, electric continued**

Ar positive column unstable, radial density distrib., longit. mag. field 9-11628

CO<sub>2</sub>, electron energy distrib. and effect of He 9-18298

CO<sub>2</sub> d.c., slight dispersion forward waves, 4.7 to 9 torr 9-18311

CO<sub>2</sub> laser, unsaturated gain meas. 9-13007

Cs vapour light sources, radiation charact. 9-17893

Cu-Ag alloy hollow cathode discharge, eff. of mat composition, current and He press., spect. study 9-19559

Cu electrode erosion in spark discharge under Ar atmos. 9-17141

H, electron e torch, h.f., and <1 atm. discharges, ionization mechanism, obs. 9-15959

He-Ne, optical pumping of metastable (<sup>3</sup>P<sub>2</sub>) Ne atoms 9-688

He-Ne, population inversion distrib. rel. to He:Ne ratio, obs. 9-18312

He-Ne mixture, 6328 Å Ne line, homogeneous linewidth meas., using non-linear travelling wave interaction technique 9-2824

He, continuum rad., mol. origin 9-19562

He, ignition characts., plane electrodes, theory and obs. 9-13467

He, low-temperature, diffusion- dominated, electrons energy distribution 9-18275

He, positive column, elec. and optical props rel. to press, theory testing 9-925

He, X-ray poduction at atos. pressure 9-5094

He I lines, mag. enhancement, spectral series depend. 9-19530

He system removal of H impurities by gettering on Ti film and pumping through Pd membrane 9-3021

<sup>3</sup>He gas in mag. field, nuclear polarization meas. 9-9417

Hg meniscus discharge, e. bunching obs. 9-5089

Hgg ion mechanism formation in the column at low press., spectroscopic study 9-5083

K vapour light sources, radiation charact. 9-17893

Li vapour light sources, radiation charact. 9-17893

N<sub>2</sub>, plasma, ionization waves dispersion waves 9-13418

N<sub>2</sub>, electron energy distrib. 9-18298

N<sub>2</sub>, and afterglows, intensity of first neg. bands reduced by O<sub>2</sub> traces 9-5111

Na vapour, low pressure characts. 9-21113

Na vapour light sources, radiation charact. 9-17893

NaCl plates with polyethylene barrier, development 9-1586

Ne, low-temperature, diffusion- dominated, electrons energy distribution 9-18275

Ne, plasma params. in slow- moving striations 9-3031

Ne, positive column, influence of distrib. function on microwave emission and r.f. conductivity 9-19561

Ne, positive plasma columns at moderate pressure 9-14762

Ne, streamer breakdown, exptl. investigation of development 9-930

Ne 6328 Å line, homogeneous linewidth meas., using nonlinear travelling wave interaction technique 9-2824

Ne hollow cathode obs. at 0.5, 1, 2, 5 torr. 9-922

O, Gunn-instabilities, positive columns, generation of T-layers 9-19560

O<sub>2</sub> preparation 9-3018

Rb vapour light sources, radiation charact. 9-17893

Xe, continuum radiation decay rate 9-926

Zn II lines de-excitation in pulsed discharges with Zn binetal electrodes, obs. 9-15963

**glows**

after glow, diff. and recomb., electron density decay, continuity equation 9-923

anomalous, field linearity in cathode fall space 9-5081

cathode pot. drop, theory and obs. 9-13466

cathode space processes 9-3023

collisional-radiative recombination, two-electron, depend. of emitted light on charge density 9-11623

controlled propagation along divided cathode 9-11626

d.c., segregation of gases in positive column due to axial ion flow, deriv. of expressions 9-11627

electron reflection from anode, influence on cathode voltage drop 9-7198

Faraday dark spaces, continuity equns. soln. for idealized geometry 9-13464

fractional glow curve automatic meas. apparatus 9-18314

hollow-cathode, plasma current and radiation intensities, mag. field influence 9-14804

h.v., cathode contamination effects 9-11625

low-pressure, rel. to Fresnel dragging of 3 cm. microwaves by drift of electron gas 9-9365

N afterglow, prod. and loss of N<sub>2</sub><sup>+</sup> 9-13465

negative, recombination and diffusion losses 9-9416

negative glow carrier density and ion current extrapolation in Langmuir probe meas. 9-18313

organic molecular gases, expt. study 9-11630

planar afterglow with reflecting walls, decay of resonance radiation 9-9415

plasma striation, h.f., high-pressure 9-2994

positive column with moving striations, electron energy transfer and thermal relax. length 9-7199

relaxation length of electron temp. in positive column 9-17139

sheath capacitance of plasma, freq. conversion 9-11572

time depend. at parameter changes in nanoseconds range 9-3028

Ar-4%O<sub>2</sub> afterglow, source of O<sub>2</sub>(A<sup>3</sup>Σ<sub>u</sub><sup>+</sup>-X<sup>3</sup>Σ<sub>g</sub><sup>-</sup>) Herzberg I band system 9-4933

H, perturbed, study of atomic transitions and self-absorpt. of line rad. 9-5032

H<sub>2</sub>, H-ion comp. in positive column 9-15962

H cathode pot. drop, theory and obs. 1mm Hg obs. 9-13466

He, low-binding energy e at 77°K 9-868

He, negative glow and positive column rel. to recombination hypothesis for He<sub>2</sub> 9-5082

He, relaxation length of electron temp. in positive column 9-17139

He afterglow, mol. origin of 1.08 μ atomic line 9-19562

He afterglow late-time light due to mutual ionization of two metastable mols. 9-13468

He low-pressure afterglow, time-depend. behaviour of 10830 Å line 9-18315

He(2<sup>3</sup>S) metastable atom destruction by Ar 9-13318

Hg, inert gases mixture, optical, elec. characts. of positive column 9-3030

I, 2062 Å emission line at 0.5 torr, monochromatic lamp devel. 9-4535

N<sub>2</sub>H<sub>4</sub>, decomp. reaction 9-14125

Ne, p-type striations generated by external excitation 9-19552

Ne, relaxation length of electron temp. in positive column 9-17139

**Discharges, electric** continued**glows** continued

- Ne positive column with moving striations, electron thermal relax. length, obs. 9-7199  
Xe pulse lamps, double current pulses, emission 9-2415

**high frequency**

- coal, impulse causing breakdown, energy characts. 9-10042  
experiments in ionized environments, scaling laws 9-7200  
high-pressure 9-2994  
ion-molecule reactions in 50MHz discharge 9-9350  
light intensity produced by induced h.f. discharge, variation with gas pressure 9-14802  
minerals, impulse causing breakdown, energy characts. 9-10042  
plasma expansion 9-13463  
rf-induced, prod. of high-energy neutral atoms by scatt. of ions, sputtering 9-2806  
striations, phase velocity influenced by an H.F. disturbance 9-2973  
theta-pinch, 0.5-1 MHz, meas. methods and analysis 9-11575  
u.h.f. discharge in atmospheric-pressure gas, characteristics 9-9338  
Ar, electron radial distrib., contracted column theory 9-3029  
Ar, microwave excited, laser action observations 9-6513  
H<sub>2</sub>, electrodeless ring, 10MHz, 0.1-0.3 torr electron energy, density meas. 9-15960  
HCl gas oxidation in microwave range 9-3035  
LiF, impulse, causing rupture, energy characts. 9-10042  
N<sub>2</sub>, dissoci. in weak discharge 9-9293

**Disintegration** see *Beta-decay theory; Nuclear decay theory; Radioactivity*

**Disintegration energies** see *Radioactivity*

**Dislocations** see *Crystal imperfections/dislocations*

**Dispersions relations**

See also *Field theory, quantum; S-matrix theory*  
No entries

**Disperse systems**

See also *Aerosols; Colloids; Emulsions; Foams; Powders; Sols; Suspensions*

- aggregates, porosity and permittivity 9-7282  
anisodiametric particle solns., distrib. curves from intensity decay of elec. light scatt. 9-14860  
clay-liquid mixtures, plasticity characterization using torque meas. rheometer 9-3425  
counting particles in fluid, apparatus, patent 9-21230  
drops falling in elec. field, small particles capture 9-7286  
fluidised beds, liq., solids movement; axial mixing coeffs., meas. 9-19649  
fluidised beds, liq., solids movement; particle vel. distrib. 9-19648  
gas-solid particle system, loss in working capacity due to irreversible heat transfer 9-1048  
gas-solids stream, suspension of spheres, dispersed phases contribution 9-3130  
graphite, colloidal, optical transmission in magnetic field 9-1050  
ground paste-like materials, heat and mass transfer 9-17823  
hectorite solutions, light scatt. in elec. fields rel. to rod-like struct. of particles 9-14861  
heterodisperse systems of isotropic spheres, light scatt. functions, computer calc. 9-11725  
layer, thermal conductivity at high temp., separation of radiant component 9-9561  
light scatt. by particles in turbulent fluid 9-16026  
rel. to light-scattering photometer calibration 9-271  
liquid atomization in u.s. fountain if cavitation region in spray jet 9-5133  
macromolecular solutions, critical opalescence 9-16027  
IN metal alloys, diffusion-induced coalescence kinetics 9-1243  
metal alloys, dispersed particles size distrib. function 9-9786  
mixed monodisperse systems, coagulation kinetics, study using Coulter counter 9-9562  
natural sea floor sediments, 15-1500 kHz acoustic wave vel. and absorpt. 9-4031  
natural sea floor sediments, 15-1500 kHz acoustic wave vel. and absorpt. 9-8160  
non-Newtonian hydromechanics 9-18373  
particle size meas. using laser homodyne spectrometer 9-17224  
particles in oscillating fluids, velocity retardation 9-21227  
photochromic dispersion in thermoplastic resin, patent 9-8676  
phthalic acid diester dispersions for photographic prints, patent 9-6565  
polydispersion, particle size from light extinction photometry 9-3135  
polymer latexes, particle size, computer analysis 9-17223  
polymers in good solvent, polydispersity index from light scatt. 9-14862  
poly-r-methylstyrene solns., light scatt. rel. to radius of gyration 9-14874  
polystyrene in cyclohexane, macromolecular solutions, critical opalescence 9-16027  
solid and liquid phase particles, penetration in gas jets 9-1047  
solid particle interacts in sound field, role of microstreaming 9-5192  
thermal anal., apparatus and technique 9-19084  
turbid medium boundary, illuminated by narrow beam, anisotropic scattering 9-5193  
two-phase, granular materials and liquid, determ. of thermal conductivity 9-3539  
Ag, colloidal, in KCl, optical extinction coeff., effect of annealing 9-5924  
C particles in N<sub>2</sub> stream, transmittance and absorption cross sections 9-11726  
Dy<sub>2</sub>O<sub>3</sub> in W, ZrO<sub>2</sub>, and UO<sub>2</sub> near their melting points 9-3476  
KI in uranin soln., rel. to polarization of fluorescence 9-9537  
LaB<sub>6</sub> powder, gas suspended, as MHD generator working fluid 9-2220  
Y<sub>2</sub>O<sub>3</sub> in Zr, uniform, struct., stability and props. 9-1318

**Dispersion, acoustic**

- composite materials, elastic constants calc. from dispersion relations 9-13714  
ocean, signal proc., optimum array detection tech. 9-8161  
velocity, in Brillouin scatt. of hypersonic waves 9-10732  
He II, critical region, and second-sound vel. 9-5209  
SF<sub>6</sub> oscillation relax., temp. depend. 10°C to 215°C 9-2879

**ultrasonic**

- inert gas binary mixtures, two-fluid model 9-3054  
isooctane-nitroethane solutions, rel. to conc. fluctuations near critical stratification pt. 9-984  
H<sub>2</sub> and H<sub>2</sub>-He mixture, normal, interferometric method 9-3055

**Dispersion, optical**

See also *Optical constants; Refractive index/light*  
anomalous, of refractive index of absorbing body, meas. method 9-7934  
crown glass, blue spectrum 9-4527

**Dispersion, optical** continued

- Fresnel convection coeff. in dispersive medium 9-17  
glass, reduction with unaltered refractive index, patent 9-8663  
glass, silicate and borosilicate, rel. to chem. composition over wide temp. and wavelength range 9-14027  
Kramers-Kronig eqns, validity for liquid vibration spectra 9-3104  
liquid, anomalous, third-harmonic generation 9-21205  
medium with spatial dispersion, equations 9-4505  
multiple, in Czerny-Turner and Ebert spectrometer 9-10933  
Ohara glass, between Fand C lines, use of Hg 'e' line as mean reference index 9-7935  
prism, small angled, Rayleighs expression for F and C lines 9-6541  
radiowaves, for rain of various origins 9-6081  
rotatory dispersion in transparent media demonstration expt. 9-20287  
in strong absorpt. band region, determ. from refl. and transmission data, applicability of method 9-259  
GaAs, of piezobirefringence 9-13922  
GaP, in nonlinear susceptibility near the reststrahl band 9-7962  
He gas, theory and meas. method 9-21138  
NaF, curves determ. by diffuse X-rays scattering 9-1731

**Dispersion relations**

See also *Field theory, quantum; S-matrix theory*

- Alfvén waves, compressional, propagation below ion cyclotron frequency, meas. 9-21097  
asymptotic sum rules for three-pt functions 9-16891  
baryon Compton scatt., sum rules contribution from higher resonances 9-429  
Compton scatt., vector meson dominance 9-8741  
e.m. corrections for  $\pi$ N scatt. 9-11063  
e.m. wave propagation normal to mag. field in anisotropic plasma 9-18290  
hypersonic waves, temporally absorbed, in Brillouin scatt. 9-10732  
lasers, semiclassical theory 9-6504  
modified, applic. to KN scatt. amp. 9-16868  
multilayer surface plasma oscillations 9-7721  
N/D eqns., inversion formalism Regge-pole hypothesis, self-clamping mechanism, S-matrix threshold behaviour 9-4597  
and nuclear forces with ref. to N-N scatt. 9-6759  
off mass shell, self consistency conditions for decay of baryon resonances 9-2544  
once-subtracted, use in calc. of K $\pi$ - $\pi$  form factors 9-16863  
perturbation theory for strong interactions 9-13113  
plasma, correlational contrib. to h.f. branch 9-11549  
plasma layer e.m. waves 9-21072  
plasma oscillations in constant electric field 9-17121  
for pp, pp real part forward amplitude calc. 9-8897  
superconvergent relations for product of factorized amp. in mes.-baryon scatt. proc 9-14496  
superconvergent sum rule from Gell-Mann factorization 9-6593  
surface plasma oscs. of multilayers 9-5628  
Vlasov eqn. for quasiparticles in dense classical systems 9-8429  
K $\pi$  scatt., calc. of real part of amplitude 9-13124  
K $\pi$  p scatt. to test Kim's coupling constant for low-energy  $\bar{K}\pi$  interactions 9-6652  
N-d elastic scatt., first order impulse approx. 9-4634  
 $\pi$ , photoproduction from nucleons with fixed u, sum rules 9-2501  
 $\pi$ N scatt., violation of causality obs. 9-2443  
 $\pi$ N scatt., Coulomb interference problem 9-2518  
 $\pi$ - $\pi$  used to calc.  $g_{\pi\pi\pi}$  9-4613  
 $\pi$  scatt. S-wave, Weinberg prediction 9-2519  
 $\pi$  forward, S-wave scatt., length consistency 9-4599  
sum rules for Pomeranchuk parameters in KN scatt. 9-14502

**Dispersions** see *Disperse systems*

**Displacement measurement** see *Length measurement; Strain gauges*

**Dissociation**

- See also *Heat of dissociation; Ionization; Molecules/dissociation*  
alkali metal sulphates, thermal decomposition and sublimation, mass spectrometric studies 9-19663  
alkali-earth metal oxides, thermal process 9-6002  
b.c.c. crystals, of non-screw dislocations 9-18467  
formation of highly excited atoms in collisions between electrons and CO, O<sub>2</sub> and N<sub>2</sub> mol. 9-685  
gases, diatomic, vibr.-dissoc. relax. behind shock wave 9-13483  
hexafluoroacetone vapour, photodecomp., temp., wavelength, detone conc and inert added effects 9-1920  
Cu-(2.5 wt.%)Be alloy, decomposition, effect of electron bombardment 9-5501  
NH<sub>4</sub>ClO<sub>4</sub>, thermal, product yield, effect of Cu chromite catalysis 9-12528  
Pm (III) oxalate, decomposition, and formation of oxide, thermal analyses 9-2790  
Ti V alloy, decomposition of martensite during continuous heating 9-5494

**electrolytic**

- See also *Ions; Electrolytic*  
steel corrosion in H<sub>2</sub>SO<sub>4</sub> soln., from polarization data 9-21698  
Wien dissoci. as a rate process 9-21704  
HClO<sub>4</sub>-H<sub>2</sub>O 9-11721  
HNO<sub>3</sub>-H<sub>2</sub>O 9-11721

**Dissolution** see *Solubility; Solutions*

**Distillation**

- See also *Isotope separation*  
methanol-water system, mass transfer from single bubbles under distillation conditions 9-18329  
UO<sub>2</sub>, reprocessing of irradiated fuels, by fluorinating with BrF<sub>3</sub> and F<sub>2</sub> 9-6944

**DNA** see *Macromolecules*

**Domains** see *Ferroelectric phenomena; Magnetization state; Superconductivity*

**Domains, antiphase** see *Alloys; Crystal structure/microstructure; Solid structure*

**Doping** see *Semiconducting materials; Semiconductors*

**Doppler effect**

- complex, radiation field analysis of oscillating source in motion in dispersive medium 9-4400  
differential, satellite signal ionospheric electron density irregularities determ. 9-6095  
Dopplermeter, laser, new theoretical model 9-12848



**Doppler effect continued**

- electro-optical, laser beam modulation, spectrum anal. 9-4497  
 gases, absorb. spectrum saturation 9-958  
 non-coherent, Doppler redistribution functions in moving atmosphere 9-16565  
 particle size meas. using shift of scattered laser light 9-17224  
 plane wave scattering by moving conducting bodies 9-188  
 plasma diagnostics, relativistic effects 9-17115  
 second-order, rel. to Mossbauer resonance strength in zero-point velocity determ. 9-14020  
<sup>238</sup>U(n,  $\gamma$ ) reaction in U<sub>3</sub>O<sub>8</sub>, obs. 300°-2000°K 9-654  
 in H $\alpha$  solar spectra investigation vel. field of chromosphere 9-18940  
 He II, spectra line broadening in low pressure arc 9-2830

**Dosimetry**

- See also *Radiation monitoring; Radioactivity measurement; X-ray measurement*  
<sup>137</sup>Cs  $\gamma$ -ray beams, of practice 9-18950  
<sup>60</sup>Co  $\gamma$ -ray beams, code of practice 9-18950  
 $\gamma$ , with fluorocarbons 9-19242  
 $\gamma$ -ray, by anthracene triplet-triplet annihilation emission 9-12472  
 $\gamma$ -rays, low energy, in water, point source dose build-up factors obs. 9-20259  
 chloral hydrate, aqueous solutions 9-21224  
 code of practice for absorbed dose at a point in water 9-18950  
 dose fields of mixed radiation behind steel shielding 9-2091  
 dosimeter, thermoluminescent, dose and dose-rate dependences, theoretical interpret. 9-5978  
 electroscope type dosimeter, patent 9-10583  
 fast n flux by <sup>238</sup>U(n, 2n) reaction and thermal flux by <sup>238</sup>U(n,  $\gamma$ ) reaction 9-6934  
 Fricke dosimeter, source of error in its appl. 9-18034  
 glass dosimeters, high-dose-level, with low dependence on energy 9-16924  
 glass elements, high sensitivity, low energy depend., patent 9-11145  
 ion-chamber dosimeters, neutron detection 9-454  
 LiF pellet 9-6210  
 neutron detection by ion-chamber dosimeters 9-454  
 oxalic acid in light and heavy water as in-pile chemical dosimeter 9-20864  
 p-n junction diode application 9-14534  
 photoluminescent dosimeter, readout using pulsed u.v. laser, patent 9-13173  
 photon, electron and neutron radiations 9-453  
 pocket, for  $\beta$ -,  $\gamma$ - and X-rays; ionization chamber, patent 9-8930  
 polytetrafluoroethylene as possible base, formation of free radicals in reaction to radiation 9-2558  
 pulsed radiation, strain gauge measurement of thermal expansion of irradiated material 9-16923  
 radioactive aerosols, retention in respiratory tract, obs. and simulation 9-15378  
 scintillation  $\gamma$  dosimeters, extension of useful energy range 9-455  
 thermoluminescent, book 9-11144  
 thermoluminescent, noise limitations for low radiation dosage 9-14533  
 thermoluminescent, solid state Bragg-Gray cavity chamber appl. 9-20704  
 thermoluminescent, with LiF, design of reader 9-2090  
 tissue preparation for liquid scintillation radioactivity counting 9-16635  
 trabecular bone, of  $\beta$ -particles, point source calc. method 9-20261  
 UKAERE health physics div. progress report (1967) 9-20257  
 whole-body, stable, low-background counter, uniform detection geom. 9-20260  
 x-ray/u.v., FD-P8-3 glass dosimeter, response, 23.40 keV 9-8939  
 X-rays, 2 to 35 Mv, code of practice 9-18950  
 $\beta$  dose attenuation in different media, empirical formula 9-4145  
 $\beta$  particles, in trabecular bone 9-20261  
 e pulses high intensity, comparison of liquid samples with graphite adiabatic calorimeters 9-1925  
 $\gamma$  monitor Ar badges, calibration apparatus 9-20756  
 $\gamma$  penetration through heterogeneous barriers, perturbation calc. 9-20842  
 n, spectroscopy appls. 9-12784  
 n, thermal and fast, and  $\gamma$ , personal dosimeter,  $3 \times 10^{-2}$ - $10^3$  rem 9-11146  
 n flux density around and within a phantom 9-2092  
 n thermal fluxes dosimetry 9-6732  
<sup>222</sup>Rn, atmospheric, effect on personnel dosimeters 9-12782  
<sup>224</sup>Ra determ. of purity of samples used on patients 10 years ago from patent-monitoring 9-12783  
 CaF<sub>2</sub> thermoluminescent dosimeter 9-2599  
<sup>60</sup>Co cylindrical source with shell-shaped shield, dose buildup factor 9-19380  
 Li<sub>2</sub>B<sub>4</sub>O<sub>7</sub>:Mn as material for thermoluminescent dosimetry 9-20006  
 LiF thermoluminesc. dosimeters, isotopic effect 9-14091  
 LiF thermoluminesc. dosimeters, influence of pre-annealing on precision meas., statistical anal. 9-14090  
 LiF thermoluminesc. toxicity 9-15384  
 LiF thermoluminesc. dosimeters, thermal history influence, pre-annealing technique for precision meas. 9-14089  
 W detector in reactor water shield,  $\gamma$ -heating 9-12038

**Double refraction**

- See also *Electromagnetic wave propagation; Optical constants; Optical rotation; Polarised light*  
 barite crystal, dispersion meas. using Soleil-Babinet compensator 9-5880  
 crystals, anisotropic, meas. by Soleil-Babinet compensator method 9-5880  
 electric, in macromol. soln., orientation factor tables 9-9541  
 extinction index of colloidal suspensions for magnetic fields examination 9-1051  
 iodates, noncentric (MIO<sub>3</sub> where M=H<sup>+</sup>, Li, Ti<sup>4+</sup>, K<sup>+</sup> and NH<sub>4</sub><sup>+</sup>), nonlinear and electro opt. props. 9-867  
 liquids with large Kerr constants, spectral broadening of light in self-trapped filaments 9-13526  
 magnetic, of paramag. complexes in solution, quantum theory for Cotton-Mouton eff., influence of ligand symmetry on anisotropy 9-9183  
 nitrobenzene Kerr effect utilized in fast light shutter 9-8672  
 optical, rotation, quantum field theory 9-268  
 Osmium complexes with phenyl and pyridine ligands, dichroism 9-7981  
 poly (methyl methacrylate), 16-10<sup>-2.5</sup> Hz, and -130 to +140°C 9-18693  
 quantum field theory 9-17206  
 quantum field theory 9-11696  
 CaSO<sub>4</sub>.2H<sub>2</sub>O (gypsum), birefringence study by 9 mm. interferometry rel. to electrical axis and permittivities 9-7943  
 CdS, Se<sub>1-x</sub>, birefringence dispersion 9-18691

**Double refraction continued**

- Co ferromagnetic thin films, mag. birefringence 9-14034  
 Cs vapour, optically oriented spin system, theory 9-9115  
 Fe ferromagnetic thin films, mag. birefringence 9-14034  
 Fe<sub>2</sub>O<sub>3</sub> colloidal soln. in mag. field, aggregate dissociation time depend. 9-5200  
 GaAs, piezobirefringence, dispersion 9-13922  
<sup>4</sup>He, modulated birefringence signals in mag. resonance 9-2832  
 LiTaO<sub>3</sub>, light extinction theory 9-10178  
 Ni-(19 wt.%)Fe ferromagnetic thin films, mag. birefringence 9-14034  
 RbI magneto-reflection dichroism, Zeeman effect irregularity 9-7949  
 ZnS crystal, faulted, phenomenological explanation of the origin of striations 9-3859

**electric flow**

- in-alkanes, liq., flow birefringence, var. with temp. 9-17207  
 errors in Senarmont meas. method 9-10907  
 polydiphenylpropene - polystyrene graft copolymers 9-994  
 polymethylmethacrylate - polystyrene graft copolymers 9-994

**magnetic mechanical**

- See also *Photoelasticity*  
 atomic-electronic polarization effects 9-7942

**Double resonance** See *Nuclear magnetic resonance and relaxation; Paramagnetic resonance and relaxation***DPPH (Diphenylpicrylhydrazyl)** See *Free radicals; Organic compounds***Drawing** See *Forming processes***Drops**

- apparatus for projecting with given velocity 9-975  
 cloud, collision efficiencies 9-14159  
 coalescence when at different electric potentials, rel. to separation 9-976  
 conducting in dielectric medium, stability criteria 9-9566  
 decomposition burning of droplet in small Peclet number flow, soln. 9-21687  
 film boiling from sphere to flowing saturated liquid, heat transfer coefficient 9-3093  
 formation, direct contact heat transfer between two immiscible phases 9-21177  
 formation through circular orifice, effect of plate wettability 9-18344  
 liquid, coalescence, effect of oscillating elec. fields 9-19599  
 liquid, in air stream, photograph tech. for rel. meas. 9-18346  
 liquid, moving in unbounded viscous medium, shape 9-974  
 liquid, revolving, shape and energy 9-14825  
 liquid, revolving, stability 9-14826  
 liquid, vibrating, modulation of radar echo 9-21771  
 liquid fuel droplet burning in oxidising atm., combustion charact. 9-21688  
 mass transfer and wake phenomena 9-15983  
 mass transfer effect on formation 9-3070  
 mean size from injection of liquid jet into gas stream 9-17184  
 nucleation theory, embryonic droplet surface free energy 9-7304  
 profile calc. from closed-form solution of young-Laplace equation 9-9474  
 sessile, contact angle computation from max. radius rad. at plane of contact and interfacial tension 9-9475  
 splashing on shallow liquid surface 9-11675  
 water, uncharged, in free fall in electric field, charge transfer between drops 9-14160  
 water droplets applic. of electrostatic theory of dielec. sphere 9-12826

**Drying**

- capillary-porous materials by ferromag. elements in e.m. field, kinetics 9-17827  
 capillary-porous mats, moisture diffusion coeff. determ. at all drying temps. 9-21243  
 cellulose films, regenerated, effect on i.r. spectra, rel. to 25°C phase transition 9-11509  
 ceramics, semivitreous extruded, shrinkage response surface 9-3165  
 ceramics, semivitreous extruded, shrinkage response surface 9-3166  
 ground paste-like materials, heat and mass transfer 9-17823  
 heat and mass transfer criteria in liq. media 9-3154  
 pneumogas dryer parameters, influence of initial moisture content of materials 9-14881  
 temperature field, evaporation zone movement, anal. by conjugate heat cond. with moving boundary 9-7302

**Ductility** See *Plastic flow; Plasticity***Dusts** See *Aerosols; Powders***Dynamics**

- See also *Ballistics; Kinematics; Rotating bodies; Vibrations*  
 angular and action variable for general systs. 9-15445  
 artificial satellite motion, stability and influence of space environment, book 9-20380  
 body oriented by electrodynamic forces 9-17753  
 canonical invariance and three-body problem 9-19010  
 central force motion, mech. and pot. energies calc. 9-2185  
 conservation laws, gravito-inertial field interpretation 9-10625  
 discrete structural systems, non-linear perturbation analysis 9-17759  
 elastic collisions, demonstrations using superballs 9-4206  
 for inelastic collisions demonstration, locking air track glider bumpers 9-4209  
 gaseous, mag. mass, influence of radiative effect 9-21091  
 harmonic oscillators, class of exact invariants 9-14347  
 impulse experiment with linear air track 9-4265  
 linear air track, double sparker 9-2118  
 motion of space vehicles while approaching and meeting on orbits 9-4268  
 nonlinear system, approx. freq. calc. 9-17754  
 open systems, equations of motion, force and momentum change, discussion 9-12835  
 oscillating mass on wheels, minimum free-energy, applic. to statistically steady turbulent motion 9-20379  
 plates, symbolic approach to problems 9-2190  
 relativistic, of disperse materials with heat transfer 9-17705  
 relativistic particle orbits. 9-2186  
 satellites, theory of flight, book 9-4081  
 spherical planet containing falling body, isochronous props., inverse square law 9-16706  
 superball collision problems, matrix representations 9-4266  
 textbook for upper forms at school 9-10604

**Dynamics continued**

- threadline, travelling, non-linear vibrations 9-6374
- three body mass syst. moving in ellipses, double collision with infinite mass possibility, closed path obs. 9-19011
- three-body problem, and canonical invariance 9-19010
- vibration of beam in turbulent flow, effect of random loading in time and space 9-119

**Dynamometers** *see Force measurement***Dynamos** *see Electrical machines***Dysprosium**

- conduction e. density at nucleus from isomer shifts 9-16211
- elastic moduli and u.s. attenuation rel. to mag. transitions 9-7517
- lattice sp. ht. calc. from phonon freq. distrib. curves 9-7635
- lattice sp. ht. calc. from phonon freq. distrib. curves 9-16165
- thermal conductivity and Lorenz function 9-7673
- u.s. attenuation in helical spin state, inc. below Neel temp. 9-1379
- CaF<sub>2</sub>:Dy<sup>2+</sup> solid laser, sun-pumped, 130 mW power output 9-13031
- Dy<sup>3+</sup> activation in rare earth vanadates, luminescence spectra 9-20003
- Dy<sup>3+</sup> in YVO<sub>4</sub>, e.p.r. 9-16461
- Dy<sup>3+</sup> in La<sub>2</sub>Mg<sub>3</sub>(NO<sub>3</sub>)<sub>13</sub>, relaxation and polarization 9-10298

**Dysprosium compounds**

- Dy<sub>2</sub>O<sub>3</sub> in W, ZrO<sub>2</sub>, UO<sub>2</sub> near their melting points 9-3476
- DyAl, n.m.r. of <sup>27</sup>Al, Knight shift and susceptibilities, temp. depend. 9-3969
- DyAu, magnetization and susceptibility in as-cast state 9-3768
- DyCl<sub>3</sub>, abs. spectra in far i.r. 9-1776
- DyFe garnets, high-field magnetization 9-15154
- DyFeO<sub>3</sub>, absorpt. spectra, 1.2 ≤ T ≤ 4.2°K and T = 77°K 9-21620
- DyFeO<sub>3</sub>, metamagnetic props. 9-16383
- DyFeO<sub>3</sub>, perovskite ferrite, magnetization model 9-1681
- Dy<sub>2</sub>O<sub>3</sub>, n diffraction for <sup>160</sup>Dy coherent scatt. amplitudes determ. 9-4735
- DyP, lattice deformation at Neel pt. 9-12309

**E-layer** *see Ionosphere/E-region***Ear***See also Hearing*

- auditory canal, transform. of freq. characts. 9-2094
- cat. tympanic membrane, submicroscopic displacement amplitudes by laser interferometer 9-10576
- cochlea, guinea pig, combination tones distrib. pattern 9-18956
- cochlea, guinea pig, harmonic distrib. pattern 9-16644
- cochlear microphonic, losses in sensitivity due to high-intensity sound, 5 kHz stimulation in cats 9-15389
- drum, acoustic impedance, meas. apparatus 9-4150
- ear drum impedance, static and dynamic, meas. by acoustic bridge 9-16638
- ear drum impedance, static and dynamic meas. by acoustic bridge 9-16637
- frequency discrimination, difference limens, mechanisms for duration and pitch discrim. 9-10574
- guinea pig, apical cochlear responses to pulse trains, obs. 9-4165
- guinea pigs, two-tone stimulation, microphone response 9-10575
- human, sensitivity and analytical props., masking phenom. and response of cochlea 9-8305
- organ of Corti, negative resting pot. rel. to damage by electrodes 9-4151
- peripheral auditory syst. as spectra analyzer, time-scaling, rel. to short-time Fourier integral 9-8364
- pitch perception per and poststimulatory fatigue 9-10572
- preservation of temporal information, jitter discrimination test 9-4162
- seniorneural deafness recovery rate from TTS by use of hearing-aids 9-10573
- sensitization of auditory and tactile syst. after stimulation 9-10571
- sound analyzer, summary 9-4152
- sound exposure, eff. on subsequent detect. var. of data 9-6218

**Earphones** *see Transducers***Earth** *see Geodesy; Geophysics***Earth***See also Geodesy; Geophysics*

- Africa, rotation in Tertiary, from palaeomagnetic data 9-21750
- Africa, rotation in Tertiary, from palaeomagnetic data 9-17557
- bow shock-wave, fluctuating elec. field detect. by OGO-5 satellite 9-10521
- core structure from P wave velocity distribution 9-17551
- core-mantle boundary props. rel. PcP waves 9-8143
- crust, exterior origin and evolution, theory 9-10377
- crust, exterior origin and evolution, theory 9-10378
- crust deformation due to cyclones 9-4034
- crystal thickness, reln. to relief, demonstrated by Alpine folding ridges 9-17552
- earth's magnetotail electrons obs., E<sub>e</sub> ≥ 45keV 9-12759
- Earth-Moon system, history, effect of tidal friction 9-6171
- flute marks and flute separation in rocks, rel. to flow 9-17558
- free oscillation period, partial derivatives 9-12566
- gravitational potential, determination from satellite, observed and model anomalies 9-14149
- ground propagation, definition for certain pulsations of mag. field 9-15260
- ground propagation, definition for certain pulsations of mag. field 9-20117
- hydrostatic figure, theory re-evaluation 9-6051
- interior model, anelasticity and the spectra of body waves 9-12567
- ionosphere/cavity resonances, fine structure 9-4077
- latitude variation, data anal. by two methods, (1899-1967) 9-16524
- light sources, terrestrial, satellite comparison 9-21751
- mass substitution by mass points 9-6057
- model after 10<sup>6</sup> random trials 9-6058
- models giving mechanical parameters rel. depth 9-12568
- orbit mecs. using pulsars proposed 9-8268
- Permian radius calc., by palaeomeridian method 9-17553
- strain meas. laser interferometry 9-4038
- structure, model derived from free oscillation data 9-8154
- structures and isostatic adjustment, hydrodynamics 9-16520
- tectonic deformation in crust, role of gravity, fundamental dynamic theory, book 9-16521
- two fixed centres force function for earth's potential 9-10520
- upper mantle, rel. to p wave station anomalies 9-16517
- upper mantle partial melting, effect on seismic variables 9-8145
- viscosity variation of mantle, rel. to slow thermal convection 9-6039
- volcanic formations, Kamchatka, comparative morphology of moon craters 9-2041

**Earth continued**

- volume rel. gravitational const. time changes 9-12558
- energy spectra in radiation belt, rocket probe meas. 9-12604

**age***See also Radioactive dating*

No entries

**composition**

- basalt magma generation, melting study of a peridotite nodule 9-8150
- cascade Range pyroelastics, neutron activation analysis 9-21752
- core and lower mantle, empirical equations of state 9-21748
- crustal structure, seismic refraction method, Missouri 9-8149
- crustal structure, seismic refraction method, Missouri 9-10376
- elastic props. of CaO under pressure and temp. 9-5448
- ferromagnesian spinels in mantle 9-11844
- hornblende stability in upper mantle and low velocity zone model 9-20078
- limestone, rate of the 15 kb phase transition 9-8153
- models obtained by Monte Carlo inversion 9-6050
- rare earth abundances in some basic rocks 9-8152
- surface, amount of <sup>90</sup>Sr, rel. to fallout rate 9-17555
- virarais, miocene volcanoc series, evidence for intermediate magnetic polarity lava 9-15235

**electricity**

- conductivity model, integration of equations of Lahiri and Price 9-14155
- crust, continental, high conductivity rel. water saturation 9-12569
- crust, resistivity 9-16522
- electrolytic conductivity of snow and glacier ice 9-12570
- e.m. impedance 9-6052
- e.m. induction for spherical model 9-17554
- geoelectric field over polar cap from incoming proton fluxes 9-10379
- resistivity of rocks, effects of pressure 9-6053
- resistivity structure from magnetotelluric deep sounding expt., Iceland 9-14154
- rocks and minerals, measurement of conductivity at high static pressures 9-12572

**heat**

- flow from interior, USA 9-6040
- organisms in hot springs 9-10565
- rocks and minerals, measurement of thermal conductivity at high static pressures 9-12572
- slow thermal convection and variation of viscosity of mantle 9-6039
- thermal history, possible role of water 9-6041

**magnetic field**

- anomaly source separation by depth of occurrence 9-17593
- Baker Lake Magnetic Observatory, Canada, obs. record, 1966 9-8207
- charge separation due to hydrostatic pressure, contrib. 9-19876
- conductor sheet, nonuniform, resonant behaviour of e.m. induced currents 9-21826
- confinement, boundary layer with cold plasma when plasma not normally incident on boundary 9-21829
- dipole model 9-17585
- dynamo, nonsteady Bullard-Gellman model 9-21827
- dynamo model 9-15258
- effect on ionospheric effects due to acoustic-gravity wave propag. 9-12635
- equipment, at resolute Bay Magnetic Observatory 1966 for 3-component meas. 9-8208
- equipment at Mould Bay Magnetic Observatory 1966 9-8209
- GSFC(12/66) field model analysis 9-12640
- hydromagnetic structure of neutral sheet in magnetotail 9-8211
- idealized dipole embedded in nonuniform atm., equatorial disturbance stability 9-10388
- induction anomaly in northern part of Greenland, external sources non-random effect 9-20121
- inversion in Kerguelen Islands during Miocene period 9-10442
- local gradient rel. underground conductivity structure 9-17594
- in magnetopause at synchronous alt., obs. 9-10404
- measurement by miniature rubidium vapour magnetometer, self-oscillating 9-18817
- meteor trains, height depend. of geomag. field effects, obs. 9-12757
- modelling, analytic 9-17586
- moving lines, identification 9-8574
- multipole anal., geomag multipoles 1965.0 9-1975
- multipole analysis, secular variation field 9-16542
- rel. noctilucent clouds, 1963-7 obs. 9-21769
- in oceans, anomalous 9-21830
- Operation Magnet, aerial mapping of field, description of flight 9-12639
- origin 9-8210
- polar substorm and electron 'islands' in mag. tail 9-8212
- potential; eccentric dipole, orientation depend. algorithm calc. 9-12641
- quartz variometers, reliability under unfavourable weather conditions 9-21825
- shipborne proton magnetometer, f.m. of signal due to hydrodynamic instability 9-6097
- Sicily, 1300 to 1800, orientation, from data on magnetization of lavas of Etna 9-17591
- solar wind, interaction, pioneer 6 obs. 9-1977
- stationary, corpuscular radiation, angular anisotropy 9-21828
- tesseral harmonics, effect on long-period behaviour of satellite orbits 9-10448
- virtual poles 9-10443
- virtual poles 9-8215
- world map, differences at conjugate areas 9-12642

**magnetic field, variations***See also Magnetic storms*

- 16 month periodicity in quiet-day range and in sunspot number 9-1976
- 26 month periodicity in horizontal force and in sunspot number 9-1976
- due to Nuclear bursts, high altitude, m.h.d. wave generation model 9-10440
- Baker Lake Magnetic Observatory, Canada, obs. record, 1966 9-8207
- diurnal, amplitudes at various points in Japan, special noise 9-15259
- diurnal, combination of analytical and numerical method of analysis 9-12643
- DP2 fluctuations, correl. interplanetary mag. variations 9-10536
- effect on cosmic-ray nucleon component daily var. 9-8213
- effect on F<sub>2</sub> ionization 9-1974
- geomagnetic impulses and solar wind relation 9-10439
- ground propagation definition for certain pulsations 9-20117
- ground propagation definition for certain pulsations 9-15260



**Earth continued****magnetic field, variations continued**

- mag. anomaly on continental rise, Cape Hatteras, interpretation 9-6098  
 magnetic observatory, Ellesmere Island, Canada, 1965-6 obs. 9-6047  
 at magnetic storm sudden commencement, declination change rel. to local time and season 9-12644  
 magnetogram processing, simplification 9-17588  
 micropulsations, amplitude spectrum determination 9-20119  
 micropulsations, possible mechanisms 9-20118  
 micropulsations, unattended recording station design 9-12645  
 motion of pole in 1846-1891.5 on the box of observations in Pulkovo, Greenwich and Washington 9-4080  
 Parkinson's vector in N.W. Africa and S. Spain, obs. 9-12638  
 P12, excitation by magnetosphere Alfvén waves 9-17590  
 pulsations, latitude-dependent periods 9-20120  
 S<sub>2</sub> and ionosphere current system, determ. 9-21831  
 secular, fluctuations in var. and rel. earthquake phenomena 9-17587  
 secular decay, free, non-dipole components 9-16543  
 v.l.f. in upper atmosphere, Javelin rocket obs. 9-10414  
 He, emission at twilight rel. to geomagnetic activity 9-1951

**rotation**

- eff. on atmospheric movements 9-21768  
 encounter irregularity, conversion into new syst. of fundamental const. coeffs. 9-21749  
 latitude variation due to polar movement data anal. (1899-1967) 9-16524  
 pole secular motion, rel. to var. of latitude, longitude and azimuth of point 9-1936  
 velocity, influence of atmospheric circulation 9-10371  
 velocity, w.r.t. 3°K cosmic radiation, by anisotropy meas. 9-17559  
 velocity characts. 1965 to 1968, by time scales comparison 9-21931

**Earth satellites** *see* **Satellites, artificial****Earthquakes** *see* **Seismology****Eberhard effect** *see* **Photographic materials****Ebullition** *see* **Boiling****Echelons** *see* **Diffraction gratings****Echo**

- See also Architectural acoustics; Reverberation; Sound ranging*  
 acoustic scattering from ellipsoids and cylinders, pulse form 9-2220  
 detector used to meas. sound pressure at focus of radiation 9-17808  
 ducted on topside ionograms, whistlers at middle latitude 9-8202  
 immersed spheres and cylinders, hollow, percussion response 9-6385  
 from internal reflections in solid metal targets, formation, charact., geom. location 9-17802  
 pulses, f.m., from scatt. sound pulses by spherical elastic shells, cross-correlation tech., freq. depend. 9-4332  
 NH<sub>3</sub>, microwave 9-13362

**Eclipses** *see* **Moon; Sun/eclipses****Eddy-currents**

No entries

**Edge emission** *see* **Luminescence/solids, inorganic; Luminescence/solids, organic****Education** *see* **Teaching****Effusion** *see* **Flow/gases****Eightfold way** *see* **Elementary particles/symmetry; Field theory, quantum****Einstein-de Haas effect** *see* **Gyromagnetic effect****Einsteinium**

No entries

**Einsteinium compounds**

No entries

**Elastic constants**

*See also Compressibility; Stress/strain relations*

- alkali metals, second- and third-order, calcs. and band-structure energy contrib. 9-9740  
 calcia, at 16 GHz and 4.2°K 9-17296  
 calcite, temp. dependence, 160-300°K 9-14963  
 cellulose, natural, cryst., in chain direction, and via H bonds, in others 9-1261  
 ceramics, sintered, rel. to microporosity 9-3431  
 chalcogenide i.r. optical mats. 9-14962  
 composites, prediction from model 9-18492  
 crystal anharmonic, isothermal const. reln. with static self-energy in long-wavelength limit 9-9736  
 crystals, fourth and fifth order, for 32 classes b// c// 9-3392  
 cubic crystals, rel. to Debye characteristic temp. at T=0 9-5565  
 cubic materials, rel. to uniaxial textures 9-11792  
 dynamic, of cylindrical and prismatic samples, from meas. of dynamic stiffness 9-5425  
 graphite, B pyrolytic, Youngs mod. and Poisson's ratio rel. to B content 9-7515  
 graphite, C44, effect on principal thermal conds. 9-7671  
 graphite, polycryst., Young's mod. rel. to cryst. orientation, modified model 9-7520  
 graphite, pyrolytic, compression annealed, shear mod. change with neutron irradiat. 9-7513  
 graphite, pyrolytic, shear modulus rel. to short neutron irrads. 9-7521  
 graphite, RVD, dynamic moduli, to 5500°F 9-7537  
 graphite, shear modulus change after neutron irradiat. 9-7513  
 graphite, static shear modulus meas. with basal plane uniaxial stress 9-7512  
 graphite, Youngs mod. temp. depend. rel. to void fraction 9-7519  
 graphites, polycryst., rel. to X-ray anisotropy factors 9-7428  
 graphites dynamic elastic modulus and internal friction, 4-750°K 9-7527  
 ice single crystals, anomalous temp. depend. 9-18496  
 magnesia, at 16 GHz and 4.2°K 9-17296  
 metals, plasticity modulus 9-17293  
 microstrain studies, modulus reduction and reverse strain 9-16122  
 naphthalene, +20 to -180°C 9-16115  
 Poisson's ratio during creep and recovery 9-18493  
 polycrystalline aggregates, corrections to calc. rel. to dislocation arrangements etc. 9-11903  
 polycrystalline media, third order, rel. to single crystal constants 9-21357  
 polymers, Young's modulus deformation and stress relaxation dependence, mechanism 9-16116  
 porosity effects 9-17295  
 PVC, stretched uniaxially, thermal and mechanical props. anisotropy 9-19781  
 α-quartz, calc. from force field const. 9-19779

**Elastic constants continued**

- quartz, from velocity meas. of u.s. waves generated at 9.4 GHz in x-cut bar 9-5548  
 quartz., temp. depend., impurity eff. 9-5424  
 quartz fibres, fused, higher-order, from finite deform. meas. 9-5419  
 shear modulus parameter in solid solution hardening theory 9-3470  
 silica, vitreous, from acoustic props., thermal treatment and impurity-ion conc. effects 9-15001  
 spinel, at 16 GHz and 4.2°K 9-17296  
 third order, rel. to calc. of generalized Gruneisen parameters for acoustic waves in uniaxial crystals. 9-5572  
 transition metals, correlation between moduli and band structure 9-19773  
 vitrocabon, dynamic Young's mod. rel. to heat treatment temp. 9-7318  
 wood charcoal, before and after methanol adsorpt. 9-11781  
 Ag, higher-order, from finite deform. meas. 9-5419  
 Al, single crystals., modulus defects during plastic deform. 9-9744  
 Al, third-order, from sound velocity meas. 9-9737  
 Al, third-order, meas. 9-21358  
 Al<sub>2</sub>O<sub>3</sub> single crystals, press. depend. 9-3394  
 Al alloy, Poisson's ratio during creep and recovery 9-18493  
 Al<sub>2</sub>O<sub>3</sub>-Y<sub>2</sub>Al<sub>2</sub>O<sub>3</sub>, Youngs modulus, rel. to microstruct. 9-3285  
 AlO with metal and alkaline oxides as solid electrolyte, patent 9-20486  
 Al<sub>2</sub>O<sub>3</sub>, isothermal bulk modulus at 295°K and second order deriv. 9-11919  
 Ar, at absolute zero, effect of long-range three-body forces 9-11906  
 Ar crystal, 4.2-76.8°K from sound velocity meas. 9-7511  
 Au/Mn, Young's modulus temp. depend., antiferromag. anomalies 9-15157  
 B, pyrolytic graphite, Young's mod. and Poisson's ratio rel. to B content 9-7515  
 BaF<sub>2</sub>, pressure and temp. derivatives at 195 and 298°K 9-1262  
 BaTiO<sub>3</sub>-PbTiO<sub>3</sub> single cryst. solid solns. 9-12196  
 Be first principle pseudopotential calc. 9-11904  
 C fibres, stretched in prod., Young's modulus 9-7514  
 CH<sub>3</sub>NH<sub>2</sub>Al(SO<sub>4</sub>)<sub>2</sub>·12H<sub>2</sub>O, in phase transition region 9-19774  
 CaCO<sub>3</sub>, calc. from force field const. 9-19780  
 CaF<sub>2</sub>, pressure and temp. derivatives at 195 and 298°K 9-1262  
 Cu-Zn crystal, var. with annealing time 9-9738  
 Cu, higher-order, from finite deform. meas. 9-5419  
 Cu, Young's modulus variation after plastic deformation 9-16117  
 DIO<sub>3</sub>, and piezoelectric props. rel. to bonding 9-12202  
 Dy, from u.s. attenuation meas. rel. to mag. transitions 9-7517  
 ET, from u.s. attenuation meas. rel. to mag. transitions 9-7517  
 Fe-7.5 at% Si, Young's mod. contrib. to 'magnetic effect', from creep expts 9-5402  
 Fe, higher-order, from finite deform. meas. 9-5419  
 α-Fe<sub>2</sub>O<sub>3</sub> polycrystalline, function of pressure to 3 kilobars 9-11902  
 Fe-(30wt.%)Ni alloy, rel. to martensitic transformation 9-7516  
 GaAs, heavily doped, temp. depend. 9-9742  
 Gd, from u.s. attenuation meas. rel. to mag. transitions 9-7517  
 HfO<sub>3</sub>, and piezoelectric props. rel. to bonding 9-12202  
 HfB<sub>2</sub>, rel. to porosity and grain structure 9-1259  
 Ho, from u.s. attenuation meas. rel. to mag. transitions 9-7517  
 Ir, polycrystalline, dynamic modulus, up to 2000°C at low freq. 9-14965  
 KBr, paraelastic orientation of amide ions from u.v. absorpt. 9-5747  
 KCl, 20-700°C, by audio freq. reson. method 9-5423  
 KCl, by static, reson. and u.s. techniques 9-5422  
 KCl, paraelastic orientation of amide ions from u.v. absorpt. 9-5747  
 KI, paraelastic orientation of amide ions from u.v. absorpt. 9-5747  
 KMgF<sub>3</sub>, from elastic wave velocity meas., and temp. dependence, 120-300°K 9-1258  
 Kr, at absolute zero, effect of long-range three-body forces 9-11906  
 Li, from band-structure calcs. 9-5420  
 LiF, 20-700°C, by audio freq. reson. method 9-5423  
 LiF, by static, reson. and u.s. techniques 9-5422  
 LiF, third-order 9-19775  
 Mg, third order and second order pressure derivatives 9-18495  
 MgO, polycrystalline, Poisson's ratio porosity dependence by resonant sphere method 9-18494  
 MgO, water vapour effects on Young's modulus 9-18506  
 Mo-Re alloys, -190 to +100°C 9-11905  
 Mo, polycrystalline, dynamic modulus, up to 2000°C at low freq. 9-14965  
 N<sub>2</sub> crystals, from sound velocity meas. 9-3519  
 NaCl, 20-700°C, by audio freq. reson. method 9-5423  
 NaCl, by static, reson. and u.s. techniques 9-5422  
 NaCl type alkali halides calc. from inter atomic parameters 9-7518  
 NaF, audio freq. reson. method, 20-700°C 9-5423  
 NaF, static, reson. and u.s. techniques 9-5422  
 NaNO<sub>3</sub>, calc. from force field const. 9-19780  
 NbC-C composite, effect of particle size and C source powders 9-3391  
 NbC-graphite composite system, and rupture moduli, rel. to effect of processing parameters 9-3161  
 Ne, at absolute zero, effect of long-range three-body forces 9-11906  
 Ni-Fe alloys, f.c.c., and sp. heats, 4.2°K 9-5421  
 Ni-Zn ferrite, 80-303°K, meas. 9-1260  
 Ni, and sp. hts., 4.2°K 9-5421  
 NiFe-based alloys, changes on isothermal ordering 9-9741  
 O<sub>2</sub> crystals, from sound velocity meas. 9-3519  
 Pd, YouC 9-14964  
 Pu, ε phase, cubic centred 9-21359  
 RbMnF<sub>3</sub>, from u.s. attenuation meas. 9-21431  
 Se, trigonal, tensor 9-17297  
 SiC-HfB<sub>2</sub> (ZrB<sub>2</sub>) mixtures, rel. to porosity and grain structure 9-1259  
 SnTe, from sound velocity meas., 4.2-300°K 9-11907  
 Ta, anomalies due to interstitial hydrogen impurities precipitation 9-21334  
 Ta, polycrystalline, dynamic modulus, up to 2000°C at low freq. 9-14965  
 Tb, from u.s. attenuation meas. rel. to mag. transitions 9-7517  
 Te, Young's modulus of square rods, torsional modulus of circular rods 9-19776  
 p-TeO<sub>2</sub>, new piezoelec. material 9-7846  
 Ti-V alloy, variation during decomposition of martensite on continuous heating 9-5494  
 Ti, cold-rolled, anisotropy of Young's modulus 9-11908  
 Ti and β-Ti alloy, VT15, eff. of hydrogen addition 9-11910  
 U polycrystals, from u.s. attenuation meas., 4.2-300°K 9-11909  
 UO<sub>2</sub>, Mo cermet, isothermal Young's modulus 9-19777  
 UO<sub>2</sub>, Young's modulus, cylindrical samples Forster technique 9-1264  
 UO<sub>2</sub>, cermet, isothermal Young's modulus 9-19777

**Elastic constants** continued

- UO<sub>2</sub>-ZrO<sub>2</sub>, Young's modulus, cylindrical samples Forster technique 9-1264  
 V, anomalies due to interstitial hydrogen impurities precipitation 9-21334  
 Xe, at absolute zero, effect of long-range three-body forces 9-11906  
 Y<sub>2</sub>O<sub>3</sub>, polycrystalline, Young's and shear moduli, porosity dependence 9-17298  
 ZrB<sub>2</sub>, rel. to porosity and grain structure 9-1259

**measurement**

- adhesive banded joints, napkin-ring torsion apparatus 9-3395  
 composite materials, from acoustic wave dispersion obs. 9-13714  
 dynamic, by stiffness meas. of cylindrical and prismatic samples with rigidly fixed ends 9-5425  
 inorganic cry., calc. from force field const. 9-19778  
 liquid crystals, twist determ. from phase transition magnetically induced 9-14831  
 standards, dynamic meas. 9-1263  
 testing machine, hydraulic, for medium strain rates 9-9743  
 Young's modulus, complex, continuous meas. during creep and tensile tests by double-resonator method 9-11911  
 Young's modulus, determ. by flexural vibrations, errors due to shear and rotatory inertia 9-13713  
 Young's modulus rel. to temp., freq., strain amplitude, apparatus 9-5428  
 NaBrO<sub>3</sub> single crystal, ultrasonic pulse echo method, obs. 9-13715  
 NaClO<sub>3</sub> from u.s. vels. along arbitrary directions 9-7522

**Elastic deformation**

- See also Bending; Stress/strain relations; Torsion*  
 anisotropic media, plane elastostatic dislocation problems, theory 9-1210  
 circular arch, strongest, perturbation soln. 9-19026  
 Cosserat surface, compatibility eqns. in infinitesimal theory 9-6364  
 curvilinearly aeolotropic cylinder with elastic symmetry, torsion, Saint-Venant problem 9-19019  
 cylinder, finite length, hollow, exact analysis 9-666  
 cylinder, viscoelastic hollow in elastic casting, inner surface ablation, axial plane strain 9-17320  
 dielectric, small finite deformations 9-8488  
 finite, Menabrea's theorem appl. 9-17770  
 flexural impedance and wave propag. in nonuniform rods 9-4302  
 'freezing' method in photoelastic stress analysis 9-14378  
 inhomogeneous isotropic body, plane deform. calc. 9-14375  
 load-displacement relations. Betti reciprocal theorem 9-12922  
 magnetic, production of stable strain-induced magnetic remanence 9-7905  
 magnetoelastic buckling of thin plate in transverse magnetic field 9-132  
 mirrors, curved, dynamic relax. meas. 9-10695  
 orthotropic shells of revolution, prestressed, under axisymmetric loading, anal. 9-20394  
 plane, of incompressible mat., class of exact solns. by suitable choice of strain energy function 9-10692  
 plane frames, failure loads evaluation 9-126  
 plate, circular, deflection under central load 9-12918  
 plates, stability, direct matrix analysis 9-17758  
 plates, thin circular transverse flexure under symmetrical loading 9-127  
 polyethylene film, chlorinated, eff. 9-17520  
 polymers, rubber-like, non-linear deformation, evaluation of Rivlin's strain energy function 9-19784  
 self-gravitating globes, thermoelastic deform., explicit form of governing eqns. 9-6170  
 shear wave propagation in finite strain 9-10704  
 shearing of orthotropic simple solid, supported by surface traction 9-19027  
 shell theory, Reissner nonlinear eqns. soln. for nonshallow symmetrically loaded shells of revolution 9-15454  
 shells, circular cylindrical, symmetric deformations 9-135  
 shells, cylindric and spherical, buckling under press., analysis 9-20399  
 shells, oval cylindrical; buckling and initial postbuckling under axial compression 9-133  
 solid, porous, small superimposed motions, flow theory 9-11665  
 solids, elastic, isotropic mixture, linearized plane strain determ. 9-15452  
 steel, thin-walled cylindrical shell, external press., collapse press. and failure modes determ. 9-18490  
 stretching of orthotropic simple solid, supported by surface traction 9-19027  
 structure, dynamically loaded, displacement upper bounds determ. 9-16718  
 viscoelastic, additive, kinematics of fluid media 9-12923  
 wedge, sharp, obtuse, impressed on plane 9-10699  
 Cu sintered compacts 9-17301  
 Fe in remanent state, elastic tensile stress effects on magnetostrictive props. 9-1956  
 Fe sintered compacts 9-17301  
 Ge/Sb, effect on activation energy 9-3656  
 n-Ge, inf., on low temp. thermomagnetic props. in phonon-drag eff. region 9-21542  
 LiF, by ultrasound, internal stress behaviour rel. to disloc. mechanism 9-16128  
 Mg(OH)<sub>2</sub>, dispersed porous mat., microstresses on pressing, X-ray analysis 9-1276  
 SiO<sub>2</sub> epitaxial films on Si, lattice distortion of edges, from contrast fields on X-ray topographs 9-1107

**Elastic fatigue**

- $\alpha$ -brass, mechanism at u.s. freqs. 9-13735  
 of brittle materials, testing 9-1272  
 concrete and effect upon prestressed beams, review 9-18519  
 corrosion fatigue, control, anodic protection 9-20052  
 crack propagation, adsorption model for environmental effects 9-3446  
 cracks, contact, propagation rel. to lubrication effects 9-13736  
 cracks, mode two growth rel. to cryst. orientation, dislocation model 9-5481  
 cycle dependent, research progress review 9-19783  
 f.c.c. metals, mechanism at u.s. freqs. 9-13735  
 Hounsfield tensometer modification for push-pull fatigue 9-9747  
 limit loads of non-standard materials 9-12917  
 metals, crack propagation, mechanism analysis 9-11938  
 metals, variation in deformation work absorbed 9-13718  
 notch, crack growth, rel. to stress 9-1313  
 resistance of metals, heat treatments 9-9748  
 steel, cast, repair welded 9-17316  
 steel, low C, strength under composite stress including h.f. vib. 9-5474  
 in welded structures, damage accumulation law 9-14980

**Elastic fatigue** continued

- wire, energy dissipated during cycling, calorimetric study 9-13717  
 Al, torsional low temp., resistivity changes rel. to induced defects 9-13846  
 Al alloy, crack growth rate, possibility of decrease using plastic deform. 9-21381  
 CaCO<sub>3</sub>, initial stages due to repeated reciprocal motion of twinning dislocations 9-18468  
 Cu, hardened foils, neutron irradiation effect on dislocation loss and rearrangement 9-11882  
 Cu, deformation, magnetomechanical behaviour associated with dislocation slip 9-17308  
 Cu, f.c.c., mechanism at u.s. freqs. 9-13735  
 Cu, hardening mechanisms 9-13737  
 Cu, at low amplitudes, influence of surfaces 9-16135  
 Cu, recovery, isochronal 78°K 9-16119  
 Ni-Cr white castiron, impact fatigue life improvement treatment, patent 9-13757  
 Ni, deformation, magnetomechanical behaviour associated with dislocation slip 9-17308  
 Ti-6 wt.%Al-4 wt.%V alloy, -cracked, effect of methanol on load relaxation 9-19786  
 Ti alloys, high-strength, fatigue strength loss on Ni and Cr plating 9-3442

**Elastic limit**

- See also Slip*  
 concrete slabs, isotropically reinforced, yield criterion 9-18502  
 Moon outer layer, determination 9-21922  
 permalloy films, vacuum deposited 9-3412  
 polycrystalline h.c.p. metals, crystallographic studies 9-21367  
 yielding serrated, apparent activation energy 9-11917  
 Al-Au dilute alloys, yield stress curves rel. to ageing characts. 9-21394  
 Al<sub>2</sub>O<sub>3</sub> alumina ceramics, Hugoniot EL in shock compression 9-7563  
 Cu, effect of creep on yield point 9-13730  
 Fe, irradiated, yield stress, saturation and exposure depend. 9-11929  
 NiAl, sheet solid solns., yield stress, e. irradi. eff. 9-5502

**Elastic losses** *see Internal friction***Elastic relaxation**

- See also Creep*  
 graphite, tensile stress relax., 2000° 2700°K 9-7532  
 polymers, thermodynamic description 9-9754  
 polymers, Young's modulus stress relax. dependence, mechanism 9-16116  
 in polymers quantitative rules 9-14731  
 Fe, damping near Snoek peak 9-9749

**Elastic waves**

- See also Acoustic waves; Magnetoelastic waves; Seismic waves*  
 alkali metals, propagation, correlation contribution 9-5417  
 anisotropic materials, load speed > stable wave speed 9-20429  
 axisymmetric, propagation in shells of revolution 9-12933  
 axisymmetric stress wave propag. across cylindrical solid-fluid interface 9-3182  
 compressional, incident on rigid quarter-space, diffraction and reflection theory 9-20424  
 in crystals, pure transverse modes 9-16120  
 cubic structure discrete body, spin elastic surface waves soln. 9-4306  
 cylinder, rigid; transient motion produced 9-151  
 damping, in ferromagnet, eff. of second sound 9-13961  
 elastic plastic longitudinal, resonance in finite bar 9-8507  
 elastic-plastic, propagation in solid media, numerical soln. 9-17792  
 elastic-plastic stress waves in semi-infinite bar 9-8506  
 elastoplastic propag. along bar heated at one end 9-19057  
 in electrical conductors, perturbation due to applied nonuniform magnetic field 9-14150  
 in fiber-reinforced composites, free harmonic wave propag., dispersion 9-20422  
 flexural, propag. and impedance in nonuniform rods 9-4302  
 flexurally vibr. non-uniform rods, reson. freqs. calc. by impedance method 9-4289  
 h.f. stress waves in bars and plates under damped sinusoidal loading, photoelastic anal. 9-19058  
 at interface, reflection-refraction, associated critical angles 9-14383  
 loading and unloading in nonhomogeneous elastic-visco-plastic medium 9-6379  
 longitudinal, in rods, dispersion dependences calc. 9-16728  
 longitudinal propag., in thin rods, higher modes analysis 9-4303  
 magnon-elastic wave self-consistent interaction and sound absorpt. coeff. calc. 9-1647  
 non-piezoelectric crystals, acoustic axes directions 9-11997  
 nonlinear energy transfer 9-6376  
 normal plate modes in strip with transverse curvature 9-4299  
 optical mode in finite body with rotational degrees of freedom 9-6378  
 optical mode surface waves in continuum with rotational degrees of freedom 9-6377  
 at piezoelectric crystal surface under conducting grating, dispersion relation 9-15126  
 plane harmonic, propag. in fiber-reinforced composites, dispersion 9-20422  
 polymer solids, sinusoidal strain excitation obs. with X-ray diffractometer 9-7536  
 propagation, Green's tensor matrix factorization 9-14315  
 quartz surface waves attenuation, 316 and 1047 MHz, 4.2-300°K 9-9745  
 $\alpha$ -quartz, second-harmonic generation at surface 9-11916  
 in quartz, u.s. attenuation, calc. 9-3405  
 Rayleigh's expansion, analogy with finite rotation operator 9-75  
 Rayleigh, due to surface press. over homogeneous elastic medium, displacements and solns. 9-20426  
 Rayleigh, on curved surfaces 9-20425  
 scatt., by penny-shaped crack, soln. of axisymmetric eqn. 9-4304  
 scattering by rigid obstacles, retarded pot. calc. 9-2199  
 in solids, and thermal waves at hypersonic freqs., unified theory 9-11914  
 on spherical shell, math. anal. 9-12931  
 stress production in solid by pulsed energy input, thermoelastic mechanism 9-13725  
 stress pulse, longitud., propag. in free-free bar with variable cross-section 9-17791  
 stress wave diffraction by solids and photoelastic expt. representation 9-6380  
 surface, interaction with drifting carriers in layered system 9-5435  
 surface, on layered anisotropic crystals, propagation characts. 9-9751



**Elastic waves continued**

- thermoelastic, discontinuities in one-dimens. propag. in inhomogeneous half-space 9-20423
- thermoelastic stress wave generation by absorpt. of impulse e.m. rad. 9-16723
- thin inhomogeneous elastic strip, longitudinal propag. 9-17789
- torsional, impinging on penny-shaped crack, soln. of axisymmetric wave eqn. 9-4304
- transient stress waves in layered media, numerical soln. 9-19055
- transient waves on surface of transversely isotropic half-space, soln. 9-19056
- transmission through plane half-wave layer 9-4300
- transverse and longitudinal, coupling in 3-element viscoelastic string, subject to transverse impact 9-20427
- vibrations, longit., momentum conservation law 9-2201
- in visco-elasto-plastic half-space, reflected irrotational wave as plastic stress wave 9-12932
- viscoelastic medium, propag. equation 9-17790
- waveguide effects in solid layered media 9-4301
- Ba<sub>2</sub>NaNb<sub>3</sub>O<sub>12</sub>, propagation attenuation 9-7531
- CdS, surface waves, mech. characts. 9-5439
- CdSe, surface waves, mech. characts. 9-5439
- KMgF<sub>3</sub>, velocities, 120-300°K, and moduli determ. 9-1258
- in SiO<sub>2</sub>, fused, u.s. attenuation, calc. 9-3405
- Y<sub>2</sub>FeO<sub>12</sub> crystals, damping freq. dependence 9-1274

**Elasticity**

- See also Compressibility; Mechanical strength; Stresses, internal; Thermoelasticity; Viscoelasticity*
- bar, impact on infinite beam 9-6358
- beam, clamped or free, semi-infinite, transverse motion 9-19047
- beam, curved, central concentrated loading, stability 9-10698
- beam bending under randomly moving concentrated force 9-131
- bending of layered plates 9-10701
- bidimensional problem, normal null tension 9-12921
- buckling of cylindrical shells, axially compressed, influence of small imperfections 9-19031
- cantilever, rectangular, torsional stability when subject to axial loading 9-147
- circular shell, cylindrical, radial displacement under random press., statistical characts. 9-6371
- constant meas., proposed standard 9-1263
- constitutive eqns. of isotropic mats. with memory, use of symmetry 9-128
- constitutive inequalities for simple materials 9-17764
- contact impedances rel. to indenter vibrating on surface of semi-infinite elastic body 9-17766
- contact of strip between two cylinders 9-19022
- contact problem of layered bodies, two-dimens. theory 9-10702
- cylinder, curvilinearly aeolotropic, finite oscillation calc. 9-8489
- cylinder, orthotropic, torsional rigidity bounds 9-8490
- cylinder, solid, elastostatic boundary region 9-10703
- cylindrical shell, collapse under radial press. difference, elastic-plastic anal. 9-17771
- cylindrical shell, finite curved element, stiffness matrix and load vectors 9-16712
- cylindrical shell, plane-strain dynamic response 9-19023
- dielectric, small finite deformations 9-8488
- dielectric, surface stress definition 9-6450
- dipolar field eqns. for elastic isotropic surface 9-19028
- discrete structural systems, non-linear perturbation analysis 9-17759
- dynamic, boundary value problems, perturbation method 9-15455
- earth interior model, anelasticity and body wave spectra 9-12567
- elastic embedded filament under longitudinal force, shear stresses and discontinuities 9-16711
- elastic half plane with variable Poisson's ratio, theory 9-4273
- elastic-plastic boundaries, speed restrictions in longit. and torsional plastic wave propag. 9-19059
- elastic-plastic Prandtl-Reuss solids, stability conditions 9-10705
- elastic-plastic torsion, numerical methods 9-19033
- elastic-visco-plastic medium, propag. of loading and unloading waves 9-6379
- elasto-geometric characts. generalized, of inhomogeneous envelopes, invariance 9-16720
- elasto-plastic matrix, formulation using 'initial stress' finite element approach 9-8484
- elastoplastic bodies, nonuniformly heated, shakedown theory analysis 9-2194
- elastoplastic medium pressure restoration during filtration 9-136
- e.m. field local interaction with polarizable elastic medium in theory of gravitation 9-4226
- equilibrium cracks under harmonic loading 9-10697
- extension of space containing plane annular slit 9-17768
- finite element method, convergence 9-19021
- flow over flexible plate, nonlinear flutter theory 9-11650
- half-space with spherical inclusion, torsion problems 9-130
- heterogeneous cone under axial load, equilibrium, associated stresses and displacements 9-20402
- high polymer molecules, mechanical entanglements 9-19488
- impact of bars, semi-infinite, 2D, asymptotic study 9-17769
- inclusion, eccentric circular, in a circular region 9-2191
- inclusion, two-dimensional, circular 9-18463
- infinite anisotropic medium, field of randomly distrib. disloc. and force dipoles 9-2193
- laminates, continuum theory and harmonic wave propag. 9-20428
- linear, transition from compressible to incompressible materials 9-16714
- linear bodies, vibs., inversion of Laplace transform. for soln. 9-17787
- linear bodies with microstructure, models presented and discussed 9-4278
- linear elastodynamics, displacement boundary-value problem, uniqueness of soln. 9-19020
- materials with microstructure, linear theory, uniqueness theorem 9-18489
- membrane, plane stress anal., finite difference solns. 9-19015
- membranes, elastic axially symmetric, dynamic deformation 9-16722
- Menabrea's theorem, appl. to finite deformations 9-17770
- metals, normal, correlation contribution to elastic props. 9-5417
- multilayer sandwich beams, rigidity of face layers inc. in bending anal. 9-20393
- non-simple materials, thermodynamics, with two temperatures 9-17820
- numerical approximate soln. of theory rel. to interaction of checkerboard array of cracks 9-3447
- numerical treatment of two dimens. mixed boundary value problems 9-15448

**Elasticity continued**

- parallelogram plate element, bending anal. and stiffness matrices 9-16713
- pendulums, asymptotic and analog computer solns. 9-16727
- plane, integral methods, mech. interpretation and classification 9-15449
- plane, integral methods, mech. interpretation and classification 9-14376
- plane deformations of incompressible mat., exact solns. by suitable choice of strain energy function 9-10692
- plastic-elastic behaviour of plates 9-17772
- plastics, glass reinforced, behaviour with reference to adhesion 9-17237
- plate, circular, partially resting on elastic foundation, loading 9-10693
- plate, thick circular, three-dimens. stress, stability 9-8481
- plates, anisotropic, two with different elastic props. bonded, extension soln. 9-16716
- plates, dynamical problems, symbolic approach 9-2190
- plates, pyramidal, folded and uniformly loaded, behaviour 9-8486
- plates, stability, direct matrix analysis 9-17758
- plates, variable thickness, large deflexion 9-20400
- plates with two opposite simply supported ends, analysis by finite strip method 9-4277
- point defects, elastic strength calc. 9-9767
- post-buckling behaviour of elastic structures 9-17763
- potential distrib. in structure using matrix displacement method 9-16717
- Poynting-effect problem, numerical soln. 9-5444
- rectangular plates, moderately thick, bending, stiffness matrix, finite element, analysis 9-20398
- rubber network, statistical mech. of crosslink orientation 9-16114
- semi-infinite body, three-dimens. stress conc. round cyl. hole, soln. and boundary values 9-20403
- semi-infinite body, three-dimens. stress conc. round cyl. hole, soln. and boundary values 9-20404
- shell, cylindrical, response to const.-press-rel. wave, soln. near load front 9-14377
- shell, shallow, sufficient condition for stability 9-8487
- shell filled with non-viscous compressible fluid, axially symm. vibrations 9-15457
- shell theory, equilibrium modes of rubber spherical shell under internal pressure 9-12920
- shell theory, nonlinear equations of motion, variational methods 9-2192
- shell theory, nonshallow spherical dome stability 9-12919
- shell theory, Reissner nonlinear eqns. soln. for nonshallow symmetrically loaded shells of revolution 9-15454
- shells, non-linear theory 9-16719
- shells, nonlinear theory, tensor eqs. of equilibrium 9-19025
- shells, stress around curvilinear holes 9-4272
- shells, translation, elastic theory 9-20405
- small displacements superposed on large deformations, anal. 9-4274
- spherical shell under uneven loadings, asymptotic behaviour 9-129
- spin-lattice interaction, effect on mag. phase transitions 9-16336
- stability loss due to shell edge clamping imperfection 9-4276
- stability theory, accuracy of Kirchhoff-Love hypothesis in critical force determ. 9-6362
- static problems, finite difference scheme for solution 9-8491
- stress determ. without intermediate calc. of constraining forces 9-17756
- stress distribution around loaded bolt in axially loaded bar 9-16721
- strip, circularly notched, under tension, numerical method of soln. 9-16715
- strip in contact with two rollers 9-20382
- surface isotropic with cylindrical hole, stress concentration using dipolar field eqns. 9-19028
- tank, natural oscillations of sloshing liquid 9-9471
- theory rel. to mechanical interactions of point defects 9-13675
- thermodynamics, relativistic of elastic media, separation of mechanical and heat transfer tensors 9-10746
- thick shells, linear theory 9-20407
- thin elastic shells precritical deformation, correlation theory 9-17767
- thin shells, finite-element analysis for static small-deflection behavior 9-20392
- time independent materials, convexity conditions and energy theorems 9-17765
- transient stress distrib. in layered media, numerical soln. 9-19055
- two dissimilar materials bonded over one face, stress analysis when subject to normal and shear loading 9-20406
- variational principles, generalized, derivation 9-8480
- waves, transverse in an elastic medium due to surface forces, use of Heaviside function 9-8505
- wedge, sharp, obtuse, impressed on plane 9-10699
- workhardening solid, stress-strain relations 9-18497
- yield point loads of plates, upper and lower bounds, numerical anal. 9-19032
- Ba<sub>2</sub>NaNb<sub>3</sub>O<sub>12</sub>, props. 9-7531
- CaO, under press. and temp. 9-5448
- KMgF<sub>3</sub>, temp. dependence, 120-300°K and anisotropy 9-1258
- N<sub>2</sub> crystals, elastic props. from sound velocity meas. 9-3519
- O<sub>2</sub> crystals, elastic props. from sound velocity meas. 9-3519
- Ti and  $\beta$ -Ti alloy, VT15, eff. of hydrogen addition 9-11910

**liquids**

- See also Compressibility/liquids*
- elasto-viscous, flow between rotating spheres, asymptotic soln. 9-9469
- polydimethylsiloxane melts 9-15981

**Elastometers** *see Rubber***Elastoplasticity** *see Plasticity***Elastoresistance** *see Piezoresistance***Electrets***See also Electrostatics*

- hysteresis eff. on teflon, polarizing field and temp. depend. 9-8567
- teflon, hysteresis eff., polarizing field and temp. depend. 9-8567

**Electric breakdown** *see Breakdown, electric***Electric charge***See also Space charge*

- atmosphere, below 90 km, charged particle concentration profile, diurnal variation 9-18801
- distrib., surface of parallel conductors 9-8
- insulating crystals, charge during LEED 9-12179
- integrating amplifier measurement 9-8570
- potential representations by multipole potentials 9-2297
- surface-charge fields, transport phenomena rel. to metal oxidation kinetics 9-9620
- KCl, contact electrification by metals 9-10029

**Electric discharges** *see Discharges, electric*

**Electric fields***See also Electromagnetic fields*

- atmosphere, pot. gradient meas. agrimeter 9-1940
- in collisionless plasma, Green's tensor 9-5027
- dielectric stress meas., approximate method 9-20479
- energy-field strength in electrostatic field, simple proof 9-18
- explosions in external field 9-10745
- internal, in dipole lattices, Fortran program for calculation 9-1452
- ion flux affected field, soln. of its equation by numerical analysis 9-8563
- mapping, teaching expts. and computer program 9-2124
- m.i.m. structures, penetration, and film thickness fluctuations 9-3688
- penetration into magnetoactive plasma 9-872
- plasma, transverse from longit. fluctuations, nonlinear generation 9-871
- plasma microfield, collective part and distrib. 9-7149
- potential representations by multipole potentials 9-2297
- in random medium, bounds on fluctuations 9-8568
- rotation-induced, near metals 9-198
- rotor surface potential 9-207
- static, disc electrodes, integral equations method of solution 9-6448
- transverse, in conductor carrying steady current 9-176
- two-dimensional, general integral formula 9-4383
- visualization, appl. of NH<sub>4</sub>Cl fog 9-202
- v.l.f. in upper atmosphere, Javelin rocket obs. 9-10414
- D, auto-ionic emission and surface ionization, rel. to neutron prod. 9-16322

**effects**

- acoustic waves, amplification mechanisms 9-3527
- anthracene, photocond. 9-3738
- anthracene in cyclohexane, excitation from radiation-induced fluorescence obs. 9-18765
- atom interaction with r.f. field 9-20882
- chemical equilibrium in closed system free from ferroelec. and ferrimag. constituents 9-1895
- d.c. field-induced opt. second harmonic generation by multipolar mol. 9-13038
- diamond, natural, luminescence-excitation modulation in range 5.0-6.0 eV 9-5950
- diamond, on Raman scattering 9-12406
- dielectric, infl. on sound velocity, attenuation and second harmonic generation, sp. heat and thermal expansion 9-19858
- dielectric fluid, viscous, surface instabilities 9-17217
- dielectric fluid flow in pipes 9-9330
- drops, liquid, effect of oscillating fields on coalescence 9-19599
- dyes, elec. field effect on optical absorpt. of mols. 9-7075
- dyes, elec. field effect on optical absorpt. of mols. 9-7041
- electric induction in hydrodynamic flow, electrodynamic diffusion coefficient 9-6469
- electromechanical effect, kinetics 9-1314
- electrostatic field, change in boundary-layer transition point 9-7108
- on EPR spectra of radicals 9-21225
- flame temperature 9-6403
- gas, perfectly conducting, two-dimensional flow in crossed elec. and mag. field 9-2957
- guard ring shielding, ionization chamber collecting vol. instability eliminated 9-2576
- heat-transfer from plasma to solid Cu 9-21050
- ion motion in gas, stochastic computer simulation 9-7235
- ionic crystal, dislocation loop motion 9-11875
- latent photographic image destruction in nuclear emulsion 9-4694
- MHD channel with non-conducting wall, turbulent boundary layer calc. 9-7128
- phase transitions, cholesteric-nematic, prod. by weak fields 9-9483
- plasma oscillations of electron beam 9-2999
- positronium formation in matter 9-6606
- pyrene in cyclohexane, excitation from radiation-induced fluorescence obs. 9-18765
- Q-machines 9-14777
- radial field effects in Q-machines 9-14778
- Raman scattering, field induced 9-12400
- rocksalt, luminescence, in 800-1000 V fields 9-16433
- scintillators, liq., luminesc. enhancement 9-19636
- semiconductor, mag., e.m. wave and slow neutron scattering by anomalous fluctuations of spin waves 9-5814
- semiconductor, ultrasound damping in h.f. elec. field, oscillatory charact. 9-1377
- semiconductor with magnetic field, conductivity 9-15088
- semiconductors, on magneto-absorpt. rel. to exciton states 9-10174
- semiconductors, redistribution eff. on sound amplification 9-12006
- Stark emission line broadening, effect of time fluctuations of microscopic field 9-19383
- thermal cond. in fluid of rough spheres 9-9445
- triboelectric enhancement 9-5755
- triglycine sulphate, ferroelec. phase transition, and high pressure effects 9-1598
- water drops, uncharged, in free fall, charge transfer between drops 9-14160
- Al film, on growth 9-13582
- Al<sub>2</sub>O<sub>3</sub>:Cr<sup>3+</sup>, on e.p.r. 9-10275
- <sup>40</sup>Ar diffusion flux from KCl and microcline feldspar 9-11897
- Au, modulation of attenuated total reflection spectrum 9-5900
- Au thin film, inf. of elec. field 9-17442
- BaTiO<sub>3</sub> domain structure changes 9-13918
- CN<sup>-</sup> in alkali halides, induced dichroism 9-3857
- CdS, exciton absorption, inf. of strong elec. field 9-19988
- CdWO<sub>4</sub>, e.p.r. of Co<sup>2+</sup>, on line half-width 9-20016
- Cs plasma, magnetically confined, radial diffusion, radial field effect 9-14758
- Cu<sub>2</sub>O, on optical transitions to n=1 exciton 9-12376
- Fe<sub>2</sub>Ga<sub>2</sub>xO<sub>3</sub>, on ferrimagnetic resonance 9-18732
- p-GaAs, infl. on conductivity and capacitance 9-3650
- GaAs, semi-insulating, uniform field effect on optical absorption 9-5883
- GaAs and GaSb tunnel diodes, I-V characts. in high crossed elec. and mag. fields 9-10019
- GaP, exciton luminescence intensity 9-16431
- Ge, carrier distrib. and type, Hall effect study 9-17396
- n-Ge, current instability in crossed elec. and mag. field 9-7805
- n-Ge, electron heating at surface 9-9991
- n-Ge, field induced e.m.f. 9-13892
- p-Ge, hole mobility 9-21515
- Ge, photoluminescence in presence of crossed fields 9-14097

**Elasticity continued  
effects continued**

- Ge tunnel diodes, I-V characts. in high crossed elec. and mag. fields 9-10019
- HF<sub>2</sub>, thermal conductivity in crossed elec. and mag. field, reson. decrease of transfer coeffs. 9-9448
- InSb, Raman scatt., by LO phonons, field induced, resonance enhanced 9-12420
- n-InSb surfaces, relaxation phen. at high fields 9-19916
- KBr:Li<sup>+</sup>, far i.r. resonance line shift 9-1784
- KCl, F, M and R colour centres at liquid N<sub>2</sub> temp. 9-3367
- KI, on fundamental absorption band 9-1783
- NaCl layers, luminescence production 9-3921
- NaF, electron colour centres, on no-phonon lines and point symmetry 9-18481
- Re adsorbed on W, surface diffusion 9-13707
- n-Si, deviations from Ohm's law 9-16275
- SrTiO<sub>3</sub>:Cr<sup>3+</sup>, R line shift due to 4kV/cm at 4.2°K 9-3709
- Ta<sub>2</sub>O<sub>5</sub> thin films, induced shift of interference peaks 9-19975
- Te, electromechanical effect 9-18525
- Y adsorbed atoms in equilb. conc. on W point 9-21287
- ZnS:Mn<sup>2+</sup>, e.s.r. 9-17499
- ZnSg, amplitude of scintillations due to  $\alpha$ -particles 9-3937

**Electric strength***See also Breakdown, electric*

- polymers, volume dependence 9-12190
- polystyrols, mol. wt. dependence 9-3704
- solid dielectric, thickness dependence, theory 9-3689
- SiO films in thin film condensers, thickness dependence 9-10043

**Electrical conduction** *see Conductivity, electrical***Electrical current** *see Current, electrical***Electrical machines**

- brush contacts, mechanical stability 9-8573
- commutation losses of brushes estimated 9-8572
- electrode, rotating disc., metal deposition from nonaqueous solvent obs. 9-2308
- induction, linear, optimal efficiency 9-12969

**Electrical measurement***See also Entries describing measurement methods for specific electrical quantities and effects may also be found listed under the various headings for the subjects concerned*

- admittance, complex, automatic recording method 9-6453
- amplitude ratio of two signals, analogue meas. method 9-20482
- analogue voltage in dual no., improved method for conversion 9-4176
- current, peak, of pulses, meter using tunnel diode sensing element 9-16759
- current sweep circuit for I-V characteristics of Josephson tunnel junction 9-205
- electrometer, vibr. reed transistorized, for demonstrations 9-2117
- electrostatic voltmeter, cylindrical, built around air track 9-4202
- experiments and projects, book 9-2119
- impedance, complex, vector meter for undergraduate laboratory 9-12832
- impedance at low temps., suitable coaxial lines 9-8315
- ionising currents and charges, integrating amplifier measurement 9-8570
- microcalorimetry power inputs, analogue milliwatt-hourmeter 9-2299
- Physics Exhibition, London, 1968 review 9-2300
- probe for p-n junctions meas. design 9-10012
- resistance variations at low temps., elementary expt. for students 9-12842
- response time of linear amplifying elements 9-15494
- solar-powered digital integrating recorder 9-10075
- voltage, current and resistance, book 9-6267
- Ni-Cd batteries, state of charge meas. 9-17844

**Electrical properties of substances***See also individual properties, e.g. Conductivity, electrical; Dielectric properties of substances, etc.*

- acetylene black, rel. to graphitization and heat treatment temp. 9-7738
- alkali metal nitrates, fused, elec. double layers 9-21707
- benzene, liq., course of electrostatic pot., meas. 9-7275
- benzene single cryst., temp. depend. of elec. current 9-3575
- benzene single cryst., temp. depend. of elec. current 9-16227
- crystals, inhomogeneous, impedance calcs. 9-1450
- DPPH iodine complex magnetic props. 9-5797
- electrostatic dynamic 2D channel flow, relaxation time of ion diffusion 9-19587
- electron drift velocities in quadrupolar and polar gases 9-17166
- electrons, localization in ordered and disordered systems, percolation of classical particles 9-10678
- electrophoresis medium with improved resolution for serum proteins, patent 9-10566
- films, metal and semiconductor 9-3568
- gas, combustion, and its plasma 9-19095
- gases, current-growth expts., rel. to determ. of ionization and attachment coeffs., detachment and ion-mol. reactions effects 9-11612
- glass-ceramic coating for metals, improvements 9-3189
- graphite, book 9-13566
- graphite, pile irradi., behaviour rel. to annealing temp. 9-7587
- hectorite solutions, anisotropy and dipole moment rel. to rod-like struct. 9-14861
- Ising model, modified admittance, perpendicular susceptibilities, transform. of corals. 9-17734
- liquid transition metal alloys 9-5186
- particles, thermionic, in space charge, rate of charging 9-17165
- phenol-formaldehyde resin carbons, contact pot. difference rel. to heat treatment temp. 9-7324
- polar liquids, injection of ions 9-7272
- potential, surface of conductors and semicond., probe for meas. 9-4413
- rare earth compounds with group V anions, review 9-18598
- solid state phenomena, effect on electronics 9-5592
- steel, elec. sheet, volt amp. meas. accuracy, air flux correction 9-1466
- switching, reversible, in disordered semiconductors 9-12140
- transition metal borides, carbides and nitrides 9-7510
- Al<sub>2</sub>O<sub>3</sub>:BaO glass ceramics, rel. to glass composition 9-3171
- Al<sub>2</sub>O<sub>3</sub>, rel. to purity and microstructure 9-1256
- Al<sub>2</sub>O<sub>3</sub> refractory, modified, rel. to radome applications 9-7311
- Ar, electron mobility up to 42 atm. 9-17167
- As<sub>2</sub>S<sub>3</sub> glasses, development since 1950, review 9-3175
- Au contacts on PbTe 9-3652
- Bi implanted layers in Si, by sheet Hall effect meas. 9-7810
- C blacks, rel. to use in depolarizing mixture of Leclanche type dry cells 9-8105



**Electrical properties of substances continued**

- CdS, photocurrent pinch-off and surface states 9-7855  
 Fe<sub>3</sub>O<sub>4</sub>, metal-nonmetal transition, press. effects 9-1467  
 Ge dislocations and dislocation diodes, bilateral microscopy 9-7806  
 H<sub>2</sub>, electron mobility up to 42 atm. 9-17167  
 He, electron mobility up to 42 atm. 9-17167  
 Hg resistivity and equation of state at elevated temperatures and pressures 9-3075  
 HgTe, conductivity character and basic characteristic parameters 9-5643  
 I<sub>2</sub> crystal, dark injection of defect electrons from electrolyte contacts 9-4002  
 KNO<sub>3</sub>, molten, electromigration of K ions, temp. depend. of isotope effect 9-11716  
 K<sub>2</sub>NiF<sub>4</sub> single crystals, charge transfer study, elec. cond. calc. 9-12184  
 N<sub>2</sub>, electron mobility up to 42 atm. 9-17167  
 Ni, thin films, prep. and study of props. 9-1109  
 Ni films, ultra-thin, rel. to structure and tunneling mechanism of conduction 9-5644  
 NiS, hexagonal form, metal-to-semicond. transition 9-12084  
 SO<sub>2</sub> cryst., spontaneous elec. polarization 9-13842  
 SiO<sub>2</sub> in m.o.s. devices, effect of water 9-7838  
 SnS<sub>2</sub>, pellets obtained by compression 9-19887  
 TiO<sub>2</sub> elec. transition, semiconductor-semimetal model 9-15060  
 TiO<sub>2</sub>, rutile, effect of hydrogen 9-1584  
 W filaments, electrotransport and life 9-15071  
 Zn, liquid, rel. to structure 9-7248

**Electrical units** *see Units***Electricity**

No entries

**Electricity, direct conversion**

- biphenyl, working fluid for Rankine cycle power conversion, thermal stability 9-3092  
 conference, Boulder, Colorado, (1968) 9-2309  
 conference, Boulder, Colorado, (1968) 9-6461  
 conference, Boulder, Colorado, (1968) 9-2310  
 electrofluidynamic colloid generator 9-2311  
 electrogasdynamic generators, relaxation time of ion diffusion 9-19587  
 energy sources of the future, survey 9-2765  
 galvanic cells, meas. of density of liquid alloys 9-5145  
 nuclear fusion power, feasibility 9-19121  
 phenyl ether-biphenyl eutectic, working fluid for Rankine cycle power conversion, thermal stability 9-3092  
 radioisotope electrogenerators, basic design considerations 9-2312  
 Rankine cycle system, thermal stability of org. working fluids 9-3092  
 Ag-sulphurization cells 9-17538

**fuel cells**

- electrode made by pressing in powdered form a transition metal with a transition metal compound, patent. 9-12970  
 introductory book 9-21  
 status for large scale power generation 9-2313  
 Ag/AgCl electrode e.m.f. dependence on Cl pressure 9-6462

**magnetohydrodynamic**

- conference, Vienna, Austria, 1966 9-15495  
 converters with longitudinal and transverse loads, power charact. 9-6463  
 dynamo problem, exact solutions 9-21041  
 EHD power generators, with segmented electrodes, radial elec. field parameter 9-10800  
 fluid properties charges rel. to Hall effect, channel wall interaction 9-210  
 gas conductivity enhancement by condensing metal vapour 9-14413  
 generator cryogenic and superconducting magnet optimization 9-17852  
 Hall generators, linear and disk types, electrical charact. 9-210  
 heat transfer meas. in water-cooled channel 9-209  
 linear induction machine, optimization considering longit. end effect 9-16758  
 liquid metal flow in channel with segmented electrodes 9-7121  
 liquid metal power generation 9-2317  
 liquid vein and linear machines, study of elec. model 9-10799  
 magnet system optimization for MHD generators 9-17853  
 magnetoplasmadynamic closed loop energy conversion system 9-2315  
 oil-fired MHD generator, wall losses by radiation 9-15496  
 plasma power generation 9-2316  
 pollution-free hybrid fossil-nuclear fueled power cycle 9-2314  
 segmented duct, current distrib. from two-dimens rel. profile 9-10801  
 segmented electrodes generation, effect of local non equilib. ionization 9-6464  
 semi-hot wall channel materials 9-208  
 shock tube method, meas. 9-20488  
 status for large-scale power generation 9-2313  
 superconducting magnet model for MHD generators 9-15497  
 superconducting saddle-shaped magnets for generator 9-19903  
 superionic MGD generators, transient acoustical response to natural disturbances 9-19122  
 synchronous generator with pulsating elect. conductivity of the medium 9-17855  
 synchronous induction generator, striated flow 9-17854  
 thermal radiation from flames used in MHD conversion 9-17851  
 Ar-K plasma, efficiency rel. to scalar conductivity and onset of instabilities 9-13425  
 Ar flow, NaK seeded, I-V charact. using electrostatic probe 9-20487  
 He-K plasma, efficiency rel. to scalar conductivity and onset of instabilities 9-13425  
 LaB<sub>6</sub> powder, gas suspended, as generator working fluid 9-220  
 Rb-Li bifid generator, parametric cycle analysis 9-10798

**solar cells**

- near-sun missions, particle radiation effects 9-4424  
 introductory book 9-21  
 CdS thin film, design and space applic. 9-2319  
 Si single crystals, development survey 9-2320  
 Si, 1 MeV electron damage 9-4422  
 Si, charact. rel. to temp. and solar intensity 9-4423  
 Si, fabrication, performance and terrestrial applications 9-2318  
 p-n Si, Li containing, e-irradiated, room temp. recovery kinetics 9-17407

**thermionic**

- introductory book 9-21  
 in Knudsen regime, transverse mag. field effect 9-20489  
 plasma, semiconductor thermocouple analogy 9-17856  
 single emitter diodes, static potential dist. 9-16760  
 Cs converters, high power direct flight 9-6465

**Electro-deposition** *see Electrolytic deposition***Electro-optical effects***See also Electroluminescence; Optical constants*

- anisotropic crystals, electric field, calc. 9-3862  
 n-butane parameters calc. from i.r. spectra absolute intensities 9-4960  
 coefficient meas., interferometric 9-12181  
 crystal, thermodynamic description, temp. depend. 9-10176  
 crystal dielectric in plane condenser, edge eff. of control field 9-6449  
 diamagnetic molecules, quantum theory of electric birefringence, applics. 9-746  
 diamagnetic molecules, quantum theory of electric birefringence 9-745  
 diamond, i.r. 9-12348  
 ethane, Kerr constant determ., from quantum theory 9-746  
 Faraday, negative, beats in i.r. ring lasers 9-4470  
 n-hexane parameters calc. from i.r. spectra absolute intensities 9-4960  
 image storage, tube, for optoelectronic computing 9-14287  
 inert gases Kerr eff. obs. at various pressures, second Kerr virial coeffs. obtained 9-21144  
 iodates, noncentric (MIO<sub>3</sub> where M=H<sup>+</sup>, Li, Ti<sup>+</sup>, K<sup>+</sup> and NH<sub>4</sub><sup>+</sup>) nonlinear opt. props. 9-3867  
 Kerr cell, light modulation, nonlinear distortion calc. 9-4488  
 Kerr consts. of macromols. in soln., table 9-16004  
 Kerr effect, required field intensity rel. to mol. interactions 9-13525  
 Kerr effect apparatus for liquid state studies 9-7264  
 Kerr effect in non-polar liq., hyperpolarizability contrib. 9-17218  
 Kerr effect induced by elec. field at optical frequency, dispersion props. 9-8660  
 Kerr-effect microscopy of mag. domains, picture improvement by laser 9-16352  
 laser beam modulation by Doppler shift, spectrum anal. 9-4497  
 liquid crystals, nematic, dynamic scatt. due to ion transport, obs. 9-9510  
 magnetoelectric-optical effects in cubic crystals 9-14031  
 methane, Kerr constant determ., from quantum theory 9-746  
 nematic liq. cry., guest-host interacts. and orientation of dichroic dye mols. 9-9481  
 nitrobenzene Kerr effect utilized in fast light shutter 9-8672  
 optical amplitude modulator used as signal-frequency converter 9-13039  
 optical consts., rel. to interband transitions at critical points 9-1741  
 n-pentane parameters calc. from i.r. spectra absolute intensities 9-4960  
 Pockels cell light modulator, r.f. operation, wide angle rad. 9-12347  
 propane, parameters calc. from i.r. spectra absolute intensities 9-4960  
 semiconductors, absorpt., elec.-current flow induced polarization effect, theory 9-14035  
 semiconductors, electroreflectance, anomalous Franz-Keldysh eff. 9-1511  
 in semiconductors, internal, investigation by condenser method 9-13926  
 shutter, subnanosecond risetime, for Nd glass laser system 9-17882  
 u.s. light modulators, random elec. excitation 9-2392  
 Ag, electroreflectance changes in dielec. constants, modulated ellipsometric meas. 9-10035  
 Au, electroreflectance changes in dielec. constants, modulated ellipsometric meas. 9-10035  
 BaTiO<sub>3</sub>-electrode interfaces, light generation during polarization reversal 9-12346  
 CdS, Pockels coeff. for spontaneous polarization estimation 9-7936  
 CuCl, Faraday rotation spectra, sign reversal 9-12374  
 CuCl, linear, of excitons 9-3863  
 D<sub>2</sub>O, Kerr constants temp. dependence, 5-55°C at 365 mμ and 436 mμ 9-19632  
 n-GaAs, Faraday effect of free carriers 9-3864  
 GaAs, Franz-Keldysh eff. with Gunn domains 9-7798  
 n-GaAs, high resistivity, obs. of moving high field domains by Franz-Keldysh effect 9-9976  
 GaAs, semi-insulating, uniform field effects on absorpt. 9-5883  
 p-GaP photoluminescence, voltage pulse modulation 9-5758  
 n-GaSb:Te, Faraday effect at 20°K rel. to transport props. 9-10177  
 Gd<sub>2</sub>(MoO<sub>4</sub>)<sub>3</sub>, ferroelectric, temp. dependence 9-12349  
 (93.5-6.5at%)Ge-(7.6-92.4at%)Si, electroreflectance spectra 9-14045  
 Ge, electroabsorpt. spectrum rel. to diamag. exciton structure obs. 9-7951  
 H<sub>2</sub>, Kerr constant determ. from quantum theory 9-746  
 H<sub>2</sub>O, Kerr constants temp. dependence, 5-55°C at 365 mμ 9-19632  
 HgI<sub>2</sub>, electroabsorption and electroreflectance near fundamental edge 9-12350  
 p-n InAs, electroreflectance spectra behaviour 9-9987  
 InSb, combined resonance spectra, effects electron-optical-phonon interact. 9-1742  
 InSb, current flow on optical absorption 9-3843  
 n-InSb, Faraday effect of free carriers 9-3864  
 KH<sub>2</sub>PO<sub>4</sub>, crystal, radiation frequency of a parametric laser 9-14424  
 KSr<sub>2</sub>Nb<sub>2</sub>O<sub>7</sub>, good properties 9-1594  
 LiNbO<sub>3</sub>-based electro-optical shutter, Q-modulation for giant pulses on CaF<sub>2</sub>:Dy<sup>3+</sup> 9-1723  
 LiTaO<sub>3</sub>, light modulation, cryst. quality rel. to extinction ratio 9-10178  
 Mg<sub>2</sub>Ge, electroreflectance spectra, 1.5-4.5 eV 9-12364  
 Mg<sub>2</sub>Si, electroreflectance spectra, 1.5-4.5 eV 9-12364  
 Mg<sub>2</sub>Sn, electroreflectance spectra, 1.5-4.5 eV 9-12364  
 Na polyethylenesulphonate solns., transient elec. birefringence 9-16004  
 NaBa<sub>2</sub>Nb<sub>2</sub>O<sub>7</sub>, good properties 9-1594  
 NaKNbO<sub>3</sub> ferroelectric ceramics, polarized retardation 9-1743  
 PbI<sub>2</sub>, electroabsorption and electroreflectance near fundamental edge 9-12350  
 PbMg<sub>1/3</sub>Ta<sub>2/3</sub>O<sub>3</sub>, -150° to +120°C 9-7952  
 PbNi<sub>1/3</sub>Nb<sub>2/3</sub>O<sub>3</sub>, -150° to +120°C 9-7952  
 PbS, band structure measurements 9-7953  
 PbTe, band structure measurements 9-7953  
 PbZn<sub>1/3</sub>Nb<sub>2/3</sub>O<sub>3</sub>, -150° to +120°C 9-7952  
 Pb(Zr<sub>1-x</sub>Ti<sub>x</sub>)O<sub>3</sub>, ferroelectric ceramics, polarized retardation 9-1743  
 SF<sub>6</sub>, Kerr eff. obs. at various pressures, second Kerr virial coeffs. obtained 9-21144  
 SiBi<sub>2</sub>O<sub>7</sub>, constants 9-18648  
 SrTiO<sub>3</sub> transition metal doped, photoinduced charge exchange processes 9-7955  
 TiO<sub>2</sub> transition metal doped, photo-induced charge exchange processes 9-7955  
 ZnS(O), Pockels coeff. for spontaneous polarization estimation 9-7936  
 ZnSe, anomalous electro-reflectance signals near fundamental edge 9-16409

**Electroacoustic transducers** *see Transducers***Electrocataphoresis** *see Electrophoresis*

**Electrochemistry**

- See also *Chemical analysis/electrochemical; Electrolysis; Electrolytic deposition*
- electrical double layers in fused alkali metal nitrates 9-21707
- electrical forces between uncharged plates in ionic solns. 9-16484
- electrolytes, ion distrib. 9-10346
- electron emitters manuf., point filaments, by etching 9-16767
- energy conversion, elementary introduction 9-21
- galvanic cell for meas. of O diffusion in liquid Cu and Ag 9-11690
- ionic solutions, charged square-well model 9-19603
- Leclanche type dry cells, props. of C blacks rel to use in depolarizing mixture 9-8105
- molten carbonate electrolytes as acid-base solvents 9-10347
- nitrobenzene and elect. conduction props. 9-21221
- phenol-sulfonic cation-exchange membrane, transport numbers and ratios of tracer fluxes 9-9501
- photocurrents due to electron transfer between SnO<sub>2</sub> electrode and optically excited mol. in soln. 9-16486
- polarography, book 9-15231
- polishing, etching and washing, rotating anode device 9-6015
- structure materials, thermal n irradiation, effect on corrosion and electrochem. props. 9-1912
- thermodynamics of charged and polarized layers, book 9-10662
- transport props. of electrolytic solns. 9-21705
- velocity gradient at wall meas. for flow around solid objects, Reynolds numbers 60 to 360 9-17086
- Ag-sulphurization cells 9-17538
- n-CdTe, photoelec. props. of surface in contact with electrolytes 9-3727
- Co, anodic behaviour in acid and alkali solns. 9-12546
- Cu in H<sub>2</sub>PO<sub>4</sub>, dissolution, effects of heat transfer 9-21706
- Fe, soft, anodic polarization in conc. electrolytes 9-15225
- HClO<sub>4</sub>-H<sub>2</sub>O, p.m.r. and molec. states 9-11721
- HNO<sub>3</sub>-H<sub>2</sub>O, p.m.r. and molec. states 9-11721
- I<sub>2</sub> crystal, dark injection of defect electrons from electrolyte contacts 9-4002
- K-graphite lamellar cpds., thermodynamics, from solid-state e.m.f. 9-1391
- Ni-Cd batteries, state of charge meas. 9-17844
- Ni-Mo alloys, anodic props., Mag. field effects 9-21709
- Ni-Mo alloys in H<sub>2</sub>SeO<sub>4</sub>, anodic behaviour, effect of mag. transform 9-21708
- Ni, anodic props., mag. field effects 9-21709
- Ni in H<sub>2</sub>SeO<sub>4</sub>, anodic behaviour, effect of mag. transform 9-21708
- O<sub>2</sub> reduction mechanism on noble metal cathodes 9-18758
- (Pd-H) electrodes oxidation in H<sub>2</sub>SO<sub>4</sub>, mass transport obs. 9-16485
- SiO<sub>2</sub> film passivation of Si surfaces 9-18404
- Ti alloy, mechanism for stress-corrosion cracking 9-19813
- TiO<sub>2</sub>, double layer model study from differential capacity curves and adsorpt. isotherms 9-9606
- U-Nb alloys, electrolytic etching in conc. aqueous citric acid 9-1129

**Electrodes**

- adiabatic electrode proc. with bond-breaking, significance of SCE MO calc. on electr. struct. of methyl fluoride 9-17057
- Billiter pot., Ag dipping electrode expts. 9-15227
- electrode + liquid aromatic hydrocarbon syst., criteria necessary for photocond. 9-17219
- electrolyte-conductor interface, eff. of elec. double layer on reflectance and ellipsometry 9-14136
- glow, during electrolysis, investigation 9-10349
- glow and H<sub>2</sub>-O<sub>2</sub> liberation, prelim. report 9-12548
- membrane, ion exchange, prod., patent 9-14138
- metal, dissolution during yield under stress 9-1914
- metals, anodic behaviour in HF, rel. to stability of solid-state metal fluorides 9-18763
- noble metal, reduction of O<sub>2</sub> in acid solution 9-18758
- photocurrents in metals in various organic solns. 9-1916
- reversible, general electrocapillary eqn., depend. of surface tension on chem. potentials 9-12547
- rotating, disc and annular, material transport 9-20058
- vertical mesh type, free convection mass transfer 9-14137
- Ag/AgCl cell e.m.f. dependence on Cl pressure 9-6462
- Ag dipping electrode, Billiter pot. 9-15227
- Al-O<sub>2</sub> anodic coatings, structure and transforms from effluent gas detection and i.r. analysis 9-21712
- Al-O<sub>2</sub> anodic coatings, structural changes during anodizing and sealing, i.r. analysis 9-21711
- Hg film for electrode surface and amalgam decomposer, patent 9-21717
- Ni/NiF<sub>2</sub> anode in pulsed electrolysis of wet HF, electrochem. behaviour 9-21716
- Ni, anodic dissolution and pitting in NiCl<sub>2</sub> soln. 9-21713
- Pb anode, mechanism of dissolution in aqueous solns. 9-21714
- Pt, dynamic behaviour of oxygen-peroxide couple 9-8104
- SnO<sub>2</sub>, transparent, electron transfer with optically excited mol. in soln., photocurrent obs. 9-16486
- TiO<sub>2</sub>, adsorption of Ag ions in aqueous and methanolic solns 9-10348

**Electrodes** see *Cathodes; Electrochemistry/electrodes***Electrodynamics**

- See also *Eddy currents; Quantum electrodynamics*
- in accelerated systems of reference 9-16764
- m axially symm. e.m. field soln. for charged particle motion 9-2331
- charged particles, electrode design for radial accel. 9-8944
- charged particles, motion in slightly damped sinusoidal pot. wave 9-6470
- charged particles in multipole 2D magnetic fields 9-2323
- classical and quantum, of relativistic charge radiating in e.m. field 9-6414
- crystal with fluctuating parameters 9-18578
- diffusion tensor, in r.f. fields with stochastic parameters 9-221
- direct interparticle action theory, correspondence with field theories 9-16677
- electric induction in hydrodynamic flow, electrodynamic diffusion coefficient 9-6469
- in electric quadrupole fields, Mathieu functions 9-713
- electron, Abraham-Lorentz, and special relativity 9-6468
- electron ring trapping in pulsed mag. mirror field 9-4430
- electron spin-polarization effect in uniform mag. field, classical interpretation 9-6471
- electrons in medium, equilibrium between Cherenkov emission and absorpt. 9-4429
- electrons in metals, magnetoresist. theory 9-18594
- e.l.f. e.m. wave cause of particle motion in constant mag. field 9-8583
- external field of radiating charged particle in general relativity 9-17710

**Electrodynamics continued**

- Hamilton Jacobi function, perturbation expansion 9-115
- hidden momentum in magnets and interaction energy 9-10816
- image potential for medium with wavevector freq. dependent dielec. function 9-9882
- intensity fluctuations in random mag. field 9-8582
- isolated charged body, soln. in isotropic co-ords. 9-20316
- Klein-Gordon and Dirac eqns., time-dependent, soln. for infinite uniform elec. field 9-10815
- Levinson theorem for single-channel scatt., Coulomb field, quantum defect, meas. 9-6316
- mag. interac., between charged part. applic. in H atoms 9-2329
- Minkowski's eqns. for moving media, useful relations derived 9-2333
- of moving media, relativistic effects 9-4384
- multipole, e.m., non-gravitating relativistic behaviour 9-17716
- particle in spatially modulated mag. field, invariants of motion 9-12976
- particle in uniform field, Green's function behaviour 9-2330
- point charge in mag.-monopole field, consts. of motion, interpretation 9-20492
- Poynting's integral theorem, S-ambiguity eliminated by conceptual expts. with pulsed currents 9-15499
- rel. between quantum and classical, in presence of randomly fluctuating field 9-16808
- of quasi permanent states, book 9-179
- radiation emission, inhomogeneous periodic medium 9-12977
- relativistic charged particle in mag. field, damping with self-interaction 9-17857
- solids in external fields 9-21457
- stochastic autoresonant acceleration 9-223
- substances with simultaneous -ve  $\epsilon$ ,  $\mu$  9-16750
- superconductors, type II, London eqn. in Schubnikov state 9-9954
- transition, rad. and Cherenkov eff. of charge crossing betw. two regions of different elec. props. 9-19105
- trapped particles in mag. field, bimodal diffusion accel. 9-222
- two-body problem of classical particles with charge, spin and mag. moment 9-8581

**Electroendosmosis** see *Electrophoresis***Electrojet** see *Atmosphere/upper; Atmospheric electricity; Ionosphere***Electrokinetic effects**See also *Electrophoresis*

- electrical forces between uncharged plates in ionic solns. 9-16484
- transient electro-osmosis in capillary tubes 9-13517

**Electroluminescence**

- anthracene, delayed, normal fluoresc. prod. by recombination of holes and electrons 9-16437
- aromatic hydrocarbons, electrochemilum., cation-anion annihilation study 9-14701
- diode clamp type holder 9-12799
- film electroluminescent capacitors on ZnS-Cu, Mn base 9-18653
- gases, brightness and current intensity study 9-9171
- polarization, field depend. of radiation energy 9-15191
- radiation converter, electroluminescent-photoluminescent 9-14098
- rare earth, transition metal mols., in II-VI compounds, by e impact 9-5975
- resonance 9-1842
- rigid organic solid solutions, electrophotoluminescence 9-16447
- semiconductor, electron-hole recomb. and diode optical emission efficiency 9-12139
- sulphide phosphors, governing role of activator 9-17495
- works in review 9-10065
- AgBr, spectrum and mechanism, 80°K 9-12483
- AgCl, spectrum and mechanism, 80°K 9-12483
- Al<sub>2</sub>O<sub>3</sub>, films 9-5971
- BN, brightness voltage- and freq.-dependence 9-12484
- BaTiO<sub>3</sub>, accompanying each polarization reversal 9-1843
- CdSe, band at 1.77 eV after applic. of a.c. elec. field 9-3939
- epitaxial film, spectra rel. to band struct. determ. 9-5701
- n-GaAs, due to acoustoelectric instability of current 9-7995
- GaAs<sub>1-x</sub>P<sub>x</sub> epitaxial layers on GaAs, rel. to compositional inhomogeneities effects 9-14895
- p-GaAs alloyed diode, props. 9-7996
- GaAs diode clamp type holder allowing continuous generation of coherent radiation 9-12799
- p-GaAs diodes, 300°K and 77°K 9-21659
- GaAs epitaxial p-n structures, high-efficiency 9-15192
- GaP-B, Zn, mechanism rel. to reactions in doping 9-3940
- p-n GaP:N<sub>2</sub> junctions green light 9-3938
- p-GaP:O-Zn diode, epitaxial growth, patent 9-10257
- KCl electrophotoluminesc. at room temp. 9-12485
- Na:ZrSiO<sub>3</sub> 9-10258
- SiC-B: p-n junctions, 77-300°K 9-18727
- SiC epitaxial films 9-5972
- SiC p-n junctions, diffused and grown, 77-300°K 9-16056
- SnO<sub>2</sub>, new material, sublimation growth and cond. increase 9-15193
- ZnS:Cu, Al, electroluminescent regions, radiation characs. 9-3942
- ZnS:Cu, effect on non-additivities 9-7998
- ZnS:Cu, Mn, Cl luminophors, X-ray induced enhancement 9-10262
- ZnS:Cu, polarization effect, confirm. of theory 9-21499
- ZnS:Cu, Al, brightness wave temp. and freq. dependence 9-10260
- ZnS:Cu, Mn, Cl film, excitation mechanism 9-5974
- ZnS:Cu capacitors, characs. and use 9-15195
- ZnS:Cu spectra, freq. depend. 9-10259
- ZnS-Mn(Cu,Cl) films, brightness waves, effect of elec. polarization 9-10261
- ZnS, electron emission meas. 9-16446
- ZnS, frequency characs. rel. to CuCl and Mn doping 9-3941
- ZnS, i.r. enhanced, temp. depend 9-14095
- ZnS phosphor, brightness wave-current relations 9-12487
- ZnS phosphors, on short-pulse excitation 9-12486
- ZnS polarization, field depend. of radiation energy 9-15191
- ZnS positive-hole lifetimes and i.r. enhancement 9-14094
- Zn(Si<sub>100-x</sub>Se<sub>x</sub>)(Cu, I), spectra compared with photoluminesc. 9-10263
- ZnS:Cu ageing mechanism 9-1844
- ZnSe-Mn thin films 9-20009
- ZnSe, low-resistivity crystals 9-5973
- ZnTe:Al alloyed junctions, injection-type, efficiencies 9-15194
- ZnTe junctions 9-7997



**Electrolysis**

- See also *Conductivity, electrical/liquids, electrolytic; Dissociation/electrolytic; Electrochemistry; Electrolytic deposition; Ion velocity/electrolytic*
- alkali metal chloride aq. soln. in Hg cell structure, patent 9-8106
- anthracene chemiluminesc. in N, N-dimethylformamide soln. 9-21219
- cell, cathode protection from corrosion, patent 9-8107
- charging of electroplated Ni and H, effect on magnetocrystalline anisotropy 9-15152
- electrode glow, investigation 9-10349
- electrolytes, simple and complex ternary, u.s. vel. rel. to molar. conc. 9-15998
- electrophotographic process, patent 9-20059
- Faraday, resume of values 9-4003
- film, thin, ferromagnetic, formation patent 9-13994
- film, thin, ferromagnetic, formation patent 9-19959
- organic additives, eff. on Fe-HClO<sub>4</sub> system 9-21718
- water, ion product const. determ. 9-16487
- AlO with metal and alkaline oxides as solid electrolyte for fuel cell, patent 9-20486
- Fe-H<sub>2</sub>O system, eff. of organic additives 9-21718
- H<sub>2</sub>Cr<sub>2</sub>O<sub>7</sub>, regeneration from Cr<sub>2</sub>(SO<sub>4</sub>)<sub>3</sub> 9-6016
- HF-H<sub>2</sub>O solution, pulsed electrolysis, behaviour of Ni/NiF<sub>2</sub> anode 9-21716
- HF-H<sub>2</sub>O solution, pulsed electrolysis 9-21715
- Hg film for electrode surface and amalgam decomposer, patent 9-21717
- Nb, electrolytic charging with H in prep. of pure Nb-H 9-13750
- SiO<sub>2</sub> layer on Si 9-4008

**Electrolytes, theory** see *Electrochemistry; Solutions***Electrolytic conductivity** see *Conductivity, electrical/liquids, electrolytic***Electrolytic deposition**

- on graphite, of Cu and PbO<sub>2</sub>, grain clustering and projections 9-8101
- metal film, thickness meas. 9-11763
- metal from nonaqueous soln., rotating disc electrode study 9-2308
- <sup>237</sup>Np thin layer prep. methods for neutron detectors and  $\alpha$ -counters 9-13158
- Ag, from aqueous solution, nucleating ability of substrate grain boundaries 9-20060
- Ag oxides anodically formed in KOH solns., texture, growth and orientation 9-17539
- Al<sub>2</sub>O<sub>3</sub> layers formed on anodic oxidation of Al, growth an struct. 9-4004
- Cd method, patent 9-8108
- Cu-Sn bronzes, from cyanide stannate bath 9-4006
- Ni-Cr alloys, from aq. electrolytes 9-4007
- Pd ductile 9-15228
- Sn-Ni alloys, acid bath conditions, effect on structure and thermal stability 9-14926
- Ti alloys, Ni and Cr plating effect on fatigue strength 9-3442
- UO<sub>2</sub> crystallization from melt by electrolysis 9-19690

**Electrolytic tanks** see *Calculating apparatus; analogue apparatus***Electromagnetic fields**

- angular spectrum representation, equivalence to a Rayleigh integral transform 9-10902
- arbitrary media characterization in fields 9-177
- axially symmetric time-dependent, electrodynamics of harmonic oscillator 9-2331
- in cavities, effect of rot. movement on field 9-10762
- coherence and radiation source structure 9-19103
- coherent states, prop. 9-178
- continuation theory, spectral method 9-6413
- cylindrical electrovac fields, stationary props, extension of Weyl's theorem 9-14332
- distribution in MHD channels with semi-infinite electrodes 9-9323
- E and H field boundary conditions, another derivation 9-6410
- generalized coherent states rel. to average field and e scatt. amplitudes 9-8689
- h.f., stabilizing effect on screw-type plasma instability 9-899
- in conducting plane layer, and temp. distrib. 9-182
- intensity meas. apparatus 9-10767
- interaction, local, with polarizable elastic medium in theory of gravitation 9-4226
- interaction with atom, analysis taking into account recoil 9-14663
- in matter, covariant field equations 9-12954
- microwave, interaction with initially heated air 9-7158
- moving conducting strip, tooth shaped inducer surface effects on field distrib. 9-20466
- non-static, in general relativity, Rainich UFT eqns. considered 9-8398
- nonuniform, effs. on dielec. props. of cry. 9-11990
- nonuniform, effs. on i.r. props. of LiF 9-17352
- null, in algebraically special Petrov type spaces 9-10618
- permittivity of a random medium 9-10764
- spherically stratified medium, exact potential functions, radial variations 9-16749
- stationary, in general relativity, Einstein-Maxwell equations soln. 9-14337
- teaching, classical theory, undergraduate expts. 9-2121
- transient, of conducting permeable sphere in uniform external field 9-19104
- two-dimensional, general integral formula 9-4383
- vector potential expansion, elim. of monopole term. 9-11

**Electromagnetic oscillations**

- See also *Magnetohydrodynamics; Masers; Plasma/oscillations*
- in conducting plane layer, and temp. distrib. 9-182
- resonator, microwave active Fabry Perot, use of plasma impedance element 9-8545
- LiNbO<sub>3</sub>, tunable optical parametric oscillator using c.w. Ar laser as pump 9-10161

**Electromagnetic radiation** see *Electromagnetic waves; Gamma-rays; Light; Radiation; X-rays***Electromagnetic wave propagation**

- See also *Absorption; Diffraction, etc.; Plasma/electromagnetic waves*
- beam forming, digital in freq. domain, algorithm, fast Fourier transform tech. 9-4336
- Cherenkov, in inhomogeneous media, asymptotic theory 9-2277
- classical theory of nonideal, coherent beams 9-2278
- classical theory of nonideal, coherent beams 9-12956
- crystal, acoustic-i.r. e.m. wave interaction 9-16389
- crystal with fluctuating parameters 9-18578

**Electromagnetic wave propagation continued**

- delta operator for treatment of e.m. wave propag. in moving refractive media 9-6418
- dielectric, centrosymmetric, circular polarization calc. 9-8547
- dielectric, nonlinear, alteration in polarization 9-12337
- dielectric media modulated by harmonic pump components, sonic region 9-19106
- ferromagnets, magnetostatic wave excitation by e.m. waves in ferromagnets 9-16337
- frequency change during propag. on earth's surface, not due to its mass 9-17702
- Ge slice, microwave emission in transverse mag. field 9-15104
- group vel., stored energy, dispersion reln. for anisotropic e. m. media 9-17833
- in gyro-anisotropic media 9-4388
- gyrotropic media, rel. to comets and meteors 9-4123
- high freq., band limited waveforms, quadrature-sampling tech. for digital proc. 9-8509
- inhomogeneous media, asymptotic methods of solution 9-4316
- isotropic, centro-symm. nonabsorptive and nondissipative materials, with applied elec. field 9-14401
- light, intense beam, in nonlinear medium 9-2399
- light beam, theory, algorithmic Monte-Carlo method applic. 9-2398
- light signal analysis after propag. through turbulent atmos. 9-8646
- in metal slabs 9-17376
- in metals, in mag. field, review 9-5625
- mixed molecular crystals, dispersion and attenuation 9-9872
- non-dispersive, in nonlinear dielectric 9-20469
- nonlinear media, theory 9-4389
- Paynting vector for inner thin layer 9-5884
- at plasma layer, moving 9-21070
- radiation from moving charge train 9-10766
- radiation in moving medium, Green's functions derived 9-14402
- in random medium, book 9-19107
- random medium, log-normal distrib. for fluctuations of flux regardless of receiving aperture 9-14400
- ray displacement in turbulent medium 9-6417
- self-focussing, linear, theory 9-10776
- semiconductor with carriers inelastically scattered on optical phonons, h.f. effects 9-13879
- semiconductor with carriers inelastically scattered on optical phonons, h.f. effects 9-1528
- shielding, l.f. inductive, theory and calc. methods 9-4387
- space vehicle radio communication during re-entry 9-21837
- substance electrodynamics, simultaneously -ve  $\epsilon$ ,  $\mu$  9-16750
- subsurface, experimental techniques and results, review 9-6419
- superdirectivity in aperture radiation 9-4397
- transit times, r.f. and optical, simultaneous meas. 9-10770
- turbulent layer, sub-mm region, atmosphere amplitude and phase fluctuations 9-10391
- in turbulent medium, book 9-19108
- Al<sub>2</sub>O<sub>3</sub> refractory radome, transmission efficiency 9-7311

**atmosphere**

- 3cm waves at Cairo, obs. 9-16532
- absorption at 35GHz, humidity dependence 9-8173
- absorption calc. 9-10392
- aerosol backscatter, estimation and reduction in optical system 9-17571
- attenuation and emission in 4cm to 8mm band, radiometric meas. 9-8178
- attenuation of v.l.f. waves, from atmospheric waveforms 9-12588
- auroral forms, developing r.f. refr. rel. to creation energy input 9-6088
- Doppler effect, differences of frequencies, radio waves emitted by earth satellite, numerical analysis 9-21793
- earth-ionosphere waveguide, v.l.f. refl. modes, step model 9-4401
- fine structure, microwave propag. obs. 9-21780
- India, refractivity in lowest km 9-4060
- laser light, parameters fluctuations dependent on turbulence 9-6423
- long-wave radiation of obs. at Waltair 9-18803
- meteor ionization 39.3 MHz forward transmission obs. (1965-6) 9-2060
- radar echo modulation by vibrating drops 9-21771
- radar in upper atmos. research 9-6084
- radar reflectivity and refractive index fluctuations, relationship 9-10393
- radio, dispersion and weakening for rain of various origins 9-6081
- refractive index and attenuation rel. to N climatology and radio meteorology, book 9-18805
- refractive index variations associated with monsoon depressions 9-1941
- scatter meas. at 15.7 GHz for troposphere structure study 9-1942
- telemetry signal strength variations from balloon-borne equipment and their use 9-12589
- whistler mode, magnetosphere 9-20096

**guided waves**

- cavity, Q-factor meas. method plotting dispersion curve on oscilloscope 9-6415
- dielectric layer, normal modes and lateral wave charact. 9-8555
- earth-ionosphere, effect on whistler polarization 9-20108
- earth-ionosphere cavity resonances, fine structure 9-4077
- ferrite-filled coaxial cavity, dynamical modes and appl. to ferrite material-parameter meas. at mm waves 9-8556
- horn, conical, biconical and quasi-pyramidal 9-10778
- hybrid EH waves in periodic trough waveguide 9-2281
- inhomogeneous plasma column, axially symmetric and dipolar surface modes, quasistatic theory 9-7154
- light, tubular ray, props. 9-8647
- magneto-active plasma waveguide excitation 9-21069
- microwave apertures, sectoral and annular, focal region fields 9-8550
- microwave cavity containing magnetoplasma dielec., resonance freq. and fields 9-14406
- optical waveguide, coherent interaction with lasers 9-14434
- rectangular, loaded with semiconductor thin film, microwave 9-16752
- transient, in moving media 9-6430
- v.l.f. mode conversion in earth-ionosphere waveguide 9-10422
- waveguide, group velocities rel. to energy 9-6429
- waveguide, oversized, reflection coeff. meas., higher order modes effects 9-8557
- waveguide internal dimens. meas., noncontacting air gauges 9-10777
- waveguides, plasma-filled, power flow 9-14405
- SiO<sub>2</sub> optical waveguide, formed by proton channeling changing refractive index 9-20556

**ionosphere**

- absorption, abnormal, in auroral zone, frequency dependence 9-1961
- absorption at 2.2 MHz, vertical incidence (Ceylon 1964) 9-10424

**Electromagnetic wave propagation continued**  
**ionosphere continued**

- absorption rel. high latit. radiostar scintillation, solar modulation 9-20111  
artificial fading records, correl. with vels. obtained in Mitra type drift expts. 9-18810  
coherence ratio meas. 9-10425  
D1 fading drift obs., evaluated by method of similar fades 9-12620  
E<sub>1</sub> parameters rel. radio absorption 9-21811  
E-layer, nighttime, I.f. ionograms (50-2000 kHz) 9-12622  
E-sporadic reflection, v.h.f. expt. 9-8198  
earth-ionosphere waveguide, v.l.f. refl. modes, step model 9-4401  
electrostatic waves, excited around lower hybrid reson. freq. 9-14174  
e.l.f., in constant mag. field rel. to particle motion 9-8583  
F2 critical freq. diurnal and seasonal vars. rel. to neutral winds, calc. 9-12629  
f<sub>o</sub>E<sub>1</sub>, fE<sub>2</sub> and f<sub>o</sub>E<sub>3</sub>, physical significance 9-10435  
F region, spread and oblique reflections 9-21817  
F-region drifts obs. by radio star scintillation, dispersion tests 9-12634  
fading of waves returned from E<sub>1</sub> 9-16540  
fading radio echoes, on adjacent freqs., cross-correl. function of amplitudes 9-15254  
Faraday rot. polarized lunar echoes [Jan-Dec 1963] 9-20113  
from rocket radio propagation expt. 9-14173  
guided, for long wave 9-14408  
gyrotropic layer, multiple wave numbers case, polarization and energy charact. 9-6091  
ionograms containing conjugate echo traces, Alouette-2 topside-sounder data 9-8199  
lens effect on waves reaching moon from distant source 9-1962  
l.f., m.f. propag., effects of ionosphere 9-6092  
l.f. drift meas. for continuous obs. of night-time winds 9-12612  
lower, and earth-ionosphere waveguide propag., effect on whistler polarization 9-20108  
oblique ionograms, synthesis, quasi-linear ionospheric model and spherical earth-ionosphere geometry 9-6432  
partial refl. technique for ionization increases due to small solar proton events 9-14175  
partial reflection theory for D-region meas. 9-10434  
radio absorption, noon global, space-time var. 1957-65 obs. 9-21798  
radio drift meas. of neutral wind direction, comparison with expt. profiles 9-15255  
radio star scintillation inversion rel. to source size 9-12740  
ray trajectories in anisotropic plasma near resonance 9-10421  
reflected waves horizon focusing effects 9-4392  
reflected waves polarization, secular and diurnal vars., Ahmedabad, 164kHz 9-1970  
reflection, specular component, statistical variation 9-10426  
reflection in v.l.f./l.f. range, rel. to periodic structure near 90 km 9-12609  
refractive index vars. 9-21799  
resonator, earth-ionosphere, natural freq. diurnal var. rel. mag. field 9-21797  
r.f., polarization rot. rel. to group path, e density meas. appls. 9-14172  
scintillation occurrence, slab thickness and electron content, results from three stations 9-20110  
self-focusing possibility 9-4402  
short wave radio signals, P'-f. curve from fading records near max. usable freq. 9-12608  
signals oblique reflection, statistical model 9-4390  
spaced receiver drift meas., cross-correl. curves, shape variation with receiver separation 9-15252  
three-station method of drift determ., validity rel. to anal. of vel. and charact. vel. 9-12618  
v.l.f. emission and other phenomena during the great disturbance, May 1967 9-1979  
v.l.f. refl. signal fluctuations rel. to off-path irregularities movement 9-14171  
whistler and ducted echoes on topside ionograms 9-8202  
whistler mode, presence of longitudinal electrostatic field 9-10423

**Electromagnetic waves**

- See also Diffraction; Reflection, etc.; Light/electromagnetic theory*  
in antiferromagnet, interaction rel. to optical phonon-magnon coupling 9-1692  
blackbody radiation, scalar representation of coherence props. 9-20468  
from charged particles in ferrite 9-5845  
collision with isolated photon, rel. to electron-positron pair creation 9-15583  
current in thin conductor, passive and transmitting aerial 9-16753  
exact potential functions in spherically stratified media, radial variations 9-16749  
excitation by ultrasound 9-14399  
field components E and H in Maxwell boundary value problems, simplified calc. 9-6412  
free radiation, correspondence between classical and quantum theory 9-8546  
Gooss-Hanchen shift by Poynting vector calc.: prediction of shift for elliptically polarized incident wave 9-12958  
impulsive, in elastic half-space, generation of thermoelastic stress-waves 9-16723  
metal surfaces, sound excitation 9-1367  
microwave second harmonic generation and sum and difference frequency at low temperatures in semiconductors 9-3604  
opticoacoustic receiver of cm. waves, expt. and theory 9-181  
piezo-semiconductors, coupled longit., theory of fluctuations 9-18552  
polarization Stokes params., derivation and values 9-2276  
radiation emission by fast charged particle in inhomogeneous periodic medium 9-12977  
resonance systems, ponderomotive effects when mech systems freq.  $\ll$  e.m. waves freq. 9-183  
submillimeter wave techniques 9-180  
textbook 9-10716  
track-to-train communication of binary coded telegram 9-2275  
transition, rad. and Cherenkov eff. of charge crossing betw. two regions of different elec. props. 9-19105  
transition radiation, transient aspects 9-10768

**radiators**

- antenna arrays, circular, consisting of tangential dipoles 9-14407  
antenna disposition for underground communications 9-10779  
aperture, superdirectivity, physical limitations 9-4397  
auto-oscillating system, fluctuation-effect, averaged equations 9-4399  
charge accelerated in gravitational field, equivalence principle 9-2274  
current loop inside infinite dielec. cylinder, field calc. 9-8558

**Electromagnetic waves continued**  
**radiators continued**

- dipole rad. in periodically stratified dielec. medium, formal soln. 9-6420  
from charge moving along axis of helical waveguide, energy spectrum 9-4395  
helix, narrow tape, Smith-Purcell rad., self-consistent investig. 9-12961  
high-order sub-harmonics in optical range, generation 9-4385  
oscillating electric dipole in motion in dispersive medium, complex Doppler effect analysis 9-4400  
oscillating electric dipole moving in dispersive medium 9-189  
planar arrays above stratified medium 9-4398  
in plasma, compressible and anisotropic, radiation characteristics 9-5029  
surface radiation props., hemispherical emissivity 9-20470  
Weiner-Hopf simultaneous eqns., appl. 9-187

**Electromagnetism**

- See also Electrodynamics; Quantum electrodynamics*  
circularly polarised incident beam, lateral shift by total reflection, theor. prediction 9-16751  
conducting strip progressively moving in constant mag. field, e.m. processes 9-8540  
conductor carrying steady current, transverse electric field 9-176  
displacement current derived without assuming charge conservation 9-4382  
E and H field boundary conditions, another derivation 9-6410  
Einstein-Maxwell eqn, Godel-type soln using equiv. Rainich eqns. 9-6308  
fields of arbitrary spin, correspondence with direct particle fields 9-16677  
fluid electromagnetodynamics, fundamental eqns. and consequences 9-7105  
induced currents and electromagnetic action, book 9-179  
Kaluza-Klein theory generalized for non-abelian gauge group 9-17832  
Lorentz transformation 9-6411  
magnetic field of cylinder moving in field of current-carrying coil 9-10763  
Maxwell's equations, eff. of degenerate neutrino sea 9-16825  
Maxwell's equations, geometric optics approx. in general case of inhomogeneous and nonstationary media with freq. and space dispersion 9-8543  
metallic sphere detection by e.m. induction, limitations 9-8542  
monopole search 9-2273  
monopole theory, action integral field formulation rel. to monopole props. 9-14398  
moving conducting strip, e.m. field distrib., tooth-shaped inducer surface effects 9-20466  
moving conductive cylinder in travelling mag. field of finite length cylindrical inductor 9-20465  
eff. of neutrino sea, degenerate Fermi 9-16825  
Poynting's integral theorem, S-ambiguity eliminated by conceptual expts. with pulsed currents 9-15499  
Poynting's theorem for a moving conductor medium 9-10765  
prospecting, double-dipole half-plane model 9-20075  
relativistic treatment of Maxwell's equations, clarifying displacement current 9-4384  
rotation symmetric, pulsed mag. fields calc. 9-20147  
superradiative state in matter, sonic excitation 9-14399  
three-phase axial-symmetric system with travelling mag. field, calc. 9-20464  
units, humorous note 9-15413  
vector pot., vanishing of monopole term 9-6262  
vector potential effect 9-8544

**Electromagnets** *see Magnets***Electromechanical effects** *see Electrostriction; Piezoelectricity***Electrometers** *see Electrical measurement***Electromotive force**

- batteries connected in parallel 9-6444  
induced, rel. to vel. meas. of gas wake in shock tube 9-2238  
metals, liquid, thermoelectric, correlation with electroconductance, approximation of weakly bound electrons theory 9-3117  
Procopiu effect, conditions required 9-14410  
Ag/AgCl electrode, dependence on Cl pressure 9-6462  
**Electron affinity** *see Atoms; Ionization; Molecules; Solids*  
**Electron annihilation** *see Electron pairs/annihilation*  
**Electron avalanches** *see Breakdown, electric*  
**Electron beams**

- See also Electron optics; Particle accelerators*  
of 1.5 GeV synchrotron, variation in transverse dimensions 9-475  
accelerator output, radial-angular characteristics determination 9-2618  
broadening due to beam current, cathode charact. 9-16768  
bunched, phase distribution analysis 9-14416  
carbon, penetration range at 1.77 MeV 9-12036  
charge density increase using high permeance 3 electrode gun with longitudinal compression 9-6478  
collimation in a betatron 9-6748  
collision machine, absolute luminosity meas. system 9-12981  
crossover region, parameter and profile measuring device 9-4436  
difference freqs. of two beams resulting beat freq. defi.-descript. by wave optics 9-4437  
energy analyser with retarding pot. filter 9-12031  
energy losses, characteristic, classification and line profile 9-1412  
energy losses in Al films, rel. to thickness and surface effects 9-5588  
gas-focused, and background media, electrostatic-energy analyzer 9-2332  
gun for evaporation 9-12979  
guns, three-electrode high-permeance, exptl. theory of checking by modelling 9-6477  
in O plasma, magnetoactive, relax., quasilinear theory 9-874  
injection from vacuum into gas through gasdynamic window 9-2337  
instabilities, thresholds, exptl. investigation 9-901  
instabilities due to virtual cathodes 9-2336  
instability due to nonsymmetrical field in linear accelerator 9-19255  
light emission at diff. grating, quantum theory 9-4435  
metals, penetration range at 1.77 MeV 9-12036  
monovelocity source 9-6476  
in plasma, instability near electron cyclotron harmonics 9-19554  
plasma oscillations in external elec. field 9-2999  
for plasma turbulence expts. 9-7182  
point-focused, appl. to zone melting of refractory metals 9-9647  
polarization of electrons in mag. field 9-16769  
polarized, field emission from ferromagnets, theory 9-7865  
potential probe information display by contour mapping, examples 9-14289



**Electron beams continued**

- quasi-shock wave propag. 9-227  
 rare earth metals, penetration range at 1.77 MeV 9-12036  
 reflection, inelastic and transmission coeff. calcs., at moderate energies 9-1410  
 trochoidal monochromator in axial mag. field 9-2340  
 velocity-modulated, r.f. energy distrib meas. and calc. 9-4434  
 in  $e^-e^+$  in colliding beams, meson resons. prod. and decays 9-17993  
 Al, liquid and solid, charact. energy losses at 8 keV 9-7249  
 Al<sub>2</sub>O<sub>3</sub>, range rel. to energy, 0/5-4 KeV 9-19872  
 Au, liquid and solid, charact. energy losses at 8 keV 9-7249  
 BeO, range rel. to energy, 0.6-4 KeV 9-19872  
 Bi, liquid and solid, charact. energy losses at 8 keV 9-7249  
 Cu films, channeling at 50 keV 9-1413  
 Ga, liquid, charact. energy losses at 8 keV 9-7249  
 Hg, charact. energy losses at 8 keV 9-7249  
 In, liquid, charact. energy losses at 8 keV 9-7249  
 LaB<sub>6</sub> cathode gun, characteristics 9-15500  
 Mg, range rel. to energy, 0.5-4 KeV 9-19872  
 MgO, range rel. to energy, 0.5-4 KeV 9-19872  
 Sr, energy loss meas. 9-3547

**absorption** *see* **Electrons/absorption****effects**

- See also Beta-rays/effects*  
 bremsstrahlung intensity rel. to e beam energy 9-19193  
 cathode luminescence, of chondrite and achondrite meteorites, microprobe obs. 9-20007  
 co-deposition of binary alloy films, controlling apparatus 9-11776  
 dielectrics, e. emission processes at 1 MeV irradiation 9-10077  
 dose deposition profiles determ. from mega-volt spectra 9-17360  
 graphite, irradiated at 80°K, annealing 9-18534  
 graphite, pyrolytic, recovery of elec. resistivity below 6°K 9-9931  
 graphite, released energy profile and elec. resistivity changes 9-7741  
 heating of surface, impulsive 9-21446  
 on helix, narrow tape, Smith-Purcell rad., self-consistent investig. 9-12961  
 ion-source application 9-2358  
 metal surface, high-vacuum bombardment, pot. behaviour 9-12229  
 metal surface, oblique incidence, transition rad. rel. to plasma waves 9-7722  
 m.i.s. structures, density of surface states 9-12171  
 m.o.s.f.e.t.'s, bias-temperature treatments investigation of electron irradiation damage 9-17421  
 organic liquids, scintillation 9-9530  
 plasma, acceleration on scatt. strong beam of electrons rel. to production of high-energy particles 9-15925  
 on plasma, cold, stability, in presence of external mag. field 9-11602  
 plasma, electron heating by beam-plasma interaction in uniform mag. field 9-11543  
 plasma, inhomogeneous, interaction with 9-18273  
 on plasma, magnetoactive, cold 9-13442  
 plasma heating in adiabatic trap 9-873  
 probe for meas. potential on flat conducting or semiconducting surfaces 9-4413  
 reflection and modulation, for low energy due to transverse charge gradients near target 9-12980  
 relativistic, helical stream, interaction with cold magnetoactive plasma 9-13442  
 semiconductors, induced conductivity, terminal voltage change 9-5682  
 silica, vitreous, ionizing-radiation- induced dilatation, impurity effect 9-14961  
 solids, pulsed beam, dynamic effs. 9-9864  
 spectra, mega-volt, rel. to dose deposition profiles calc. 9-17360  
 transverse dispersion in stationary electric field with rotational axial symmetry 9-228  
 welding, penetration depth 9-6229  
 transition rad. in opt. region from passing Al and Ag foils, relativistic 9-9860  
 Ag, bombardment rel. to self-diffusion 9-5398  
 Ag particles, micron-sized, temp. rise due to heating in e. microscope 9-11822  
 Al, 0.4 MeV e. irradiated, low-temp. recovery 9-1323  
 Al and alloys, 2 MeV irrads., resistivity, recovery in stages II and III 9-9696  
 on Al foil, refr. and refl. 9-17362  
 Al foils, energy loss, 0.3-MeV Monte Carlo calc. 9-5587  
 γ-AIOOH, phase transitions 9-13773  
 As<sub>2</sub>S<sub>3</sub> films, e bombardment conductivity, threshold energy 9-16286  
 Au, electron energy loss rel. to sample thickness 9-3545  
 Au, irradiated, Stage III annealing process 9-21390  
 Au, low temp. irradiated, internal friction meas. rel. to dislocation pinning 9-11912  
 Au, stage III annealing post-irrad. at 3 MeV at 7.7°K 9-12029  
 Ba<sup>+</sup>, ionization to Ba<sup>2+</sup>, cross-sections rel. to energy 9-5064  
 Be, defect prod. and recovery, study by elec. resistivity and stored energy meas. 9-16091  
 Be distillation and simultaneous deposition to sheet after vacuum melting 9-13748  
 C-Al barrier, current calc., applic. of perturbation method 9-18572  
 CaO:TM<sup>2+</sup>, TM<sup>3+</sup> production, e.s.r. obs. 9-10277  
 CdS, anisotropic thermal cond., low temp. obs. 9-9853  
 CdS, radiation recombination excited by fast electrons 9-3915  
 CdS platelets pumping, stimulated emission to  $3 \times 10^8$  W/cm<sup>2</sup> 9-20523  
 CdTe, irradiated and non-irradiated, rel. to nature of band edge radiative emission and atomic displacements 9-16429  
 Cu-Al barrier, current calc., applic. of perturbation method 9-18572  
 Cu-(2.5 wt.%)Be alloy, bombardment effect on decomposition 9-5501  
 Cu, dislocation-pinning, irradiation rel. to activation energies meas., 78°K 9-5360  
 Cu, Frenkel pairs, effects of annealing 9-3330  
 Cu, stage III recovery behaviour of irradiated sample 9-13671  
 Fe-C solid solutions, electrical resistivity recovery mechanism 9-19891  
 GaAs and GaAs<sub>1-x</sub>P<sub>x</sub>, radiation damage, cathodoluminescence study 9-18570  
 GaAs semiconductor laser, output power and efficiency 9-2381  
 GaP, energy loss intensities, deviations at low energies 9-7692  
 GaP, radiation damage, cathodoluminescence study 9-18570  
 GaSb, radiative recombination excitation 9-21645

**Electron beams continued****effects continued**

- GaSb, undoped, irrads. damage, orientation and energy dependence 9-5334  
 Gd, point defect production and recovery 9-11870  
 p-Ge:Ga, on conduction mechanism 9-5703  
 n-Ge:Sb (As), irradiated, absorpt. edge 9-10200  
 n-Ge, damage, orientation and temp. depend. 9-13672  
 Ge, Fermi level, ultimate position on 50 MeV e.-irrad. 9-12154  
 Ge, induced conductivity, terminal voltage change 9-5682  
 Ge, irradiated and plastically deformed, photoconductivity spectra 9-15137  
 n-Ge, radiation annealing and modification of 35° and 65°K defects at 7°K 9-9695  
 Ge, stored-energy release after irrads. 9-7656  
 Ge film recrystallized by zone melting, mobility and conc. of current carriers, effect of substrate temp. 9-16271  
 H to Ca atoms and ions, ionization cross-section and rate coeffs. 9-5061  
 H<sub>2</sub>, excitation of triplet states, low-energy, ang. depend. 9-17032  
 He atom excitation by fast electrons, accurate first Born approx. cross sections 9-13317  
 He hypersonic flow, visualization by excited fluoresc. and afterglow 9-21131  
 InSb thin films, heating for zone melting 9-14893  
 KCl, surface dissociation at low temps. 9-7327  
 Li<sup>+</sup>, ionization to Li<sup>2+</sup>, cross-sections rel. to energy 9-5064  
 N atom, impact excitation of second positive bands, cross sections 9-13300  
 Ni foils, interstitial Frank dislocation loops and tetrahedral voids 9-3326  
 Ni<sub>3</sub>Al, sheet solid solns., yield stress 9-5502  
 O<sub>2</sub>, high resolution energy-loss spectrum 9-784  
 O<sub>2</sub>, excitation, 0-200eV, vac.u.v. emission 9-17040  
 Si:As(Sb), irrads., impurity-vacancy pairs, e.p.r. and endor exam 9-5341  
 Si:Li, recombination velocity on irrads., Li impurity effects 9-9998  
 Si, 10 MeV irradiation damage annealing, carrier conc. and lifetime recovery 9-17399  
 Si, influence on conductivity 9-3663  
 Si, irradiated by 15 to 45 MeV electrons, defect cluster formation 9-17400  
 p-n Si, Li containing diodes and solar cells, e-irradiated, room temp. recovery kinetics 9-17407  
 Si, Li defect complex, i.r. spectroscopic study 9-13673  
 p-Si, oscillations induced in photoconductivity and absorpt. spectra and association with A-centres 9-18659  
 Si deep levels introduced into band structure by 300 KeV electron irrads. 9-7809  
 Si p-n-p transistors, effect of Si<sub>3</sub>N<sub>4</sub> passivation 9-17417  
 Si solar cells, 1 MeV damage 9-4422  
 SiO<sub>2</sub>, 0 to 30keV, space charge buildup and release, obs. 9-12192  
 SrCl<sub>2</sub>:Tm<sup>3+</sup>, Tm<sup>3+</sup> production, e.s.r. obs. 9-10277  
 W, cavity production and interstitial conc. on 240 MeV bombardment 9-1204  
 Xe excitation 1470 Å resonance line obs. 9-4853  
 ZnS(Ag) crystals, stability of radiation under bombard of α, e. 9-11139
- ionization** *see* **Electrons/ionization**
- Electron capture** *see* **Ions/recombination; Radioactivity/electron capture**
- Electron diffraction**  
 camera adapted for study of molecular structure 9-11452  
 cameras, review 9-230  
 cellular method for complex monolayers and multilayers, low energy e diffraction theory 9-7391  
 at crystal surfaces, generalization of Darwins dynamical theory 9-11819  
 double diffraction picture, anal. with dynamical theory of diffraction at crystal surfaces 9-11820  
 LEED, resonance effects in crystals 9-3268  
 LEED theory, OPW energy band calc. method appl. 9-1171  
 low energy, review 9-15501  
 molecules and crystals in molecular crystals 9-17025  
 patterns, phase distribution 9-2338  
 resonance effects by crystals 9-3268  
 Pb cryst. surface, specular LEED 9-11760  
 Pd cryst. surface, specular LEED 9-11760  
 Pt cryst. surface, specular LEED 9-11760
- Electron diffraction crystallography**  
*See also Crystal structure, atomic*  
 diffraction process in terms of transfer matrices involving scatt. props. of atom layers 9-11819  
 diffractometer- collected data, least squares weighting schemes, effect of random setting errors 9-13621  
 double diffraction picture, anal. using dynamical theory 9-11820  
 dynamic, in ideal vibrating crystals 9-13792  
 dynamic, intensity calc. by analog computer 9-3267  
 h.v., vanishing second order reflection in X-ray atom form factor determ. 9-9676  
 insulating crystals, charge during LEED 9-12179  
 integral intensity of reciprocal spot, no. of beams in calc. 9-3266  
 lattice diffraction of s-wave scatterers 9-1173  
 Laue zones, use in interpretation of diffraction patterns 9-16068  
 LEED, resonance intensity profile temp. dependence 9-17261  
 low energy, review 9-15501  
 many-beam dynamical theory, averaged intensities, nondegenerate charact. values 9-1172  
 pattern interpretation, book 9-5290  
 review of cry. struct. determ. 9-5304  
 small angle scattering, convolution and deconvolution 9-13616  
 solid solutions with short range order and size effects, kinematical theory 9-3251  
 stereo plotting of 3-dimens. e. density 9-13622  
 surface structure analysis by optical simulation of LEED patterns 9-13570  
 Al, pseudo Kikuchi line obs. using e. microscope 9-9669  
 Au polycrystalline foils, anomalous e transmission 9-11836  
 Ni, atomic scatt. factor and rigid lattice interf. function 9-9660  
 PbI<sub>2</sub>, diffuse streak-patterns, temp. depend. 9-11853
- Electron diffraction examination of materials**  
 atomic struct. determ. 9-7392  
 Burgers vectors, size rel. to visibility of dislocations 9-18469

**Electron diffraction examination of materials continued**

- cements, composition and hydration 9-14123  
 crystal surface, low energy study, matrix formulation 9-5302  
 dielectric thin film, crystallization state evolution 9-11768  
 ellipsometer for LEED chamber 9-1174  
 f.c.c metals, epitaxial growth on KCl, KBr, and KI crystals 9-7377  
 fibres from deformed polymer crystals 9-18395  
 film, thin metal, e microscope decharger design 9-6483  
 fine structure of spots caused by wedge shaped crystal parts 9-13620  
 foils with coherent distortion free particles, extinction contrast 9-7334  
 Laue zones, use in interpretation of diffraction patterns 9-16068  
 magnetic scatt., elastic, and mechanism of polarization of scatt. beam 9-12256  
 metal overlayers, LEED 9-1085  
 metals, faceted surfaces, patterns 9-11794  
 orientation determ. from selected area patterns, accuracy 9-5303  
 oxide film on Fe-Si alloy crystals, structure 9-21278  
 Permalloy, magnetic analysis 9-12277  
 proteins, structure analysis 9-14936  
 steel, stainless 304 film, interfacial free energies 9-1231  
 surface structure analysis by optical simulation of LEED patterns 9-13570  
 Ag, (111) face surface state variation 9-7357  
 Ag, inelastic scatt. in LEED obs. 9-21451  
 Ag, on (111) face for apparent Debye temp. 9-3532  
 Ag overlayer on Cu(100), LEED 9-1085  
 Au films, discontinuous, evaporated on CdI<sub>2</sub> substrate 9-18433  
 Be thin films, structure and superconductivity below 7°K 9-13863  
 C, amorphous films, atomic struct. 9-5237  
 Cu, cold-rolled, three-dimens. orientation distrib. function of crystallites 9-11841  
 e-Fe<sub>2</sub>N, electronic structure study 9-5318  
 (-Fe<sub>2</sub>N, electronic structure study 9-5318  
 γ'-Fe<sub>2</sub>N, electronic structure 9-1430  
 Ge monocrystal, dislocation space charge display by scanning beam 9-7390  
 In condensed films of subcritical thickness, melting characts. 9-18383  
 InP, epitaxial films, stacking disorder 9-9617  
 MoS<sub>2</sub>, Kikuchi lines, intensity anomaly 9-14918  
 MoS<sub>2</sub>, Kikuchi lines, intensity anomaly 9-9679  
 MoS<sub>2</sub> films, transmission of electrons, anomalous 9-9680  
 NH<sub>3</sub> adsorption and decomposition on W(211) surface 9-19679  
 NH<sub>3</sub> and OD<sub>3</sub>, molec. struct. 9-7032  
 NaAlSi<sub>3</sub>O<sub>8</sub>-KAlSi<sub>3</sub>O<sub>8</sub> system, incipient exsolution and inversion phenomena 9-21318  
 Nb (110) surface, rel. to hydrogen chemisorption 9-15215  
 Ni (19 wt.% Fe ferromagnetic film, investig. of domain walls 9-13997  
 Ni film, epitaxially grown, polycryst., double diffraction 9-5244  
 Ni films, epitaxially grown, secondary twinning in patterns 9-9618  
 NiO, antiferromag., coherent exchange scatt. 9-1698  
 PbI<sub>2</sub>, diffuse streak-patterns, temp. depend. 9-11853  
 Pd-Cr alloy films, rel. to elec. characts. 9-17242  
 Rh-Pd-Ag alloy, energy loss spectra obs., E<sub>0</sub>=200-800 eV 9-16194  
 Sb films, crystallization data 9-5249  
 Si (111) surface structure, Ni induced, LEED study 9-21262  
 Si (111) surface structure, Ni induced, LEED study 9-21261  
 Si monocrystal, dislocation space charge display by scanning beam 9-7390  
 Si surface struct., (111) LEED pattern indicating impurity presence 9-5327  
 SiC crystallites on Si(111) surface obs. by electron diffraction 9-5288  
 TaN<sub>x</sub> sputtered, highly nitrided films, structure determ. 9-13578  
 TaO<sub>2</sub> protective film on Ta in high temp. HNO<sub>3</sub> acid and ag. CuCl<sub>2</sub> soln. 9-21267  
 Te clean surfaces 9-21263  
 Te. epitaxial growth on Cu(111) surface, LEED study 9-21270  
 U<sub>2</sub>O<sub>8</sub>, e, microscope obs., 20°C, 300-1000°C 9-11854  
 ZnS, diffuse patterns from cleaved face 9-9607

**Electron emission**

- See also Noise/electrical; Photoelectricity*  
 atomic-particle induced, probability distrib. 9-7868  
 from crystals, angular distrib. mass dependence, transition to classical limit 9-7863  
 current pulse due to laser radiation incident on target in gas 9-1627  
 dielectrics, MeV e. irradiated, mechanism 9-10077  
 exo-electron decay curves, mathematical treatment 9-15143  
 glow discharge cathode space processes 9-3023  
 metal surface, energy exchange processes, non-equilibrium distribution 9-21550  
 metal-dielectric-metal cathode, eff. of dielec. props. on energy distributions 9-18661  
 metallic surface, polycrystalline, distribution function of work function 9-19937  
 m.i.m. system, dielectric influence on angular emission 9-3687  
 multipliers, channel, characts. and use as secondary standards in vacuum u.v. region 9-17894  
 rel. oxide cathode falls 9-3024  
 probe, characteristics depend. for low plasma densities 9-13936  
 steel, austenitic, exoemission during cyclic loading 9-13937  
 surface effects, ejection by electronically excited molecules 9-19936  
 Al, exoemission without photostimulation 9-5773  
 C evaporation from Th dispenser cathode in Auger emission spectroscopy 9-7867  
 Ge, on Xe ion bombardment rel. to defect formation and annealing 9-18662  
 LiF, exo-emission in high vacuum, due to surface states and volume traps 9-7864  
 Mo, bombarded by rare gas ions, and ion reflection 9-12218  
 NaCl thermal activation, emission mechanism 9-1626  
 O, absorpt. cross section, effect of autoionization 9-6980  
 U auger spectra, K.L.M. obs. 9-9141  
 W, auto, stabilization by Ge coating 9-21551  
 ZnS, meas. during electroluminescence 9-16446

**field emission**

- asperities, 10<sup>-4</sup> cm, surface density mapping technique 9-3750  
 emitters, point filaments, manufacture by electrochemical etching 9-16767  
 energy analyzers, resolution determination 9-3749  
 from ferromagnets, polarized beam production theory 9-7865  
 microscope, effect of Al adsorbed on W 9-11784

**Electron emission continued****field emission continued**

- from particles, solid negatively charged 9-5774  
 photocathode S-20, field assisted photoemission rel. to near i.r. sensitivity enhancement 9-12223  
 retarding potential analyser, rel. to adsorption study on O<sub>2</sub> and H<sub>2</sub> on Mo 9-11782  
 Schottky barriers, normalized thermionic-field emission 9-15144  
 semiconducting field emitter, field distrib. and rate of pot. fall calc. 9-17447  
 CdP<sub>2</sub>, illumination intensity dependence 9-13939  
 CdSb, Ag doped 9-3751  
 Eu<sub>1-x</sub>Gd<sub>x</sub>S, use as possible source of polarized beams 9-7865  
 Gd, ferromag., prod. of beam with 8% spin polarization 9-7865  
 In<sub>2</sub>S<sub>3</sub>, field distrib. and rate of pot. fall calc. and compared with expt. 9-17447  
 LaB<sub>6</sub> crystals for emitters, construction and performance 9-13938  
 W, patterns for H<sub>2</sub> adsorption 9-5775  
 W, patterns of phases rel. to H adsorption 9-19677  
 W tip, heated, effect of O<sub>2</sub> on electron current 9-12220  
 ZnS:Pr:Cs forward-biased Schottky barrier 9-16317

**photoelectric**

- alkali iodides, spectra, L-bands and exciton bands 9-3759  
 alkali metals, dark injection into anthracene 9-1618  
 from alkaline earth contacts into anthracene broad conduction band existence confirmation 9-5616  
 butadiene-based glow-discharge polymer films, photoionization potential 9-12228  
 carbon tetrafluoride, He(I) reson. photoelec. spectra, band assignments from orbital obs. 9-19462  
 critical-point structure in energy distrib. 9-13940  
 gases, on high-intensity laser light irradiation 9-7201  
 internal, technique for study of insulators 9-17423  
 K shell cross-sections for 145 keV γ in elements of 47 ≤ Z ≤ 82, obs. 9-11395  
 laser-induced non-linear photoeffect, discrimination from thermionic emission by time response meas. 9-16318  
 metal foils, laser induced spontaneous, evidence for 9-16320  
 metal foils laser induced spontaneous, evidence against 9-5781  
 naphthalene-based glow-discharge polymer films, photoionization potential 9-12228  
 photocathode S-20, field assisted photoemission rel. to near i.r. sensitivity enhancement 9-12223  
 photocathodes absolute quantum output, meas., 550-200 nm 9-18664  
 photoelectron energy distrib. meas. and applic. 9-18663  
 phthalocyanines 9-2914  
 porphyrins 9-2914  
 AgPd, electron energy distribution meas. 9-1628  
 Al, electrons in Si<sub>3</sub>N<sub>4</sub> 9-10081  
 Al thin film covered with NaCl layer, intensity meas. by electron camera 9-19939  
 Au, laser-induced non-linear photoeffect, discrimination from thermionic emission by time response meas. 9-16318  
 BaTiO<sub>3</sub>, heat treated in O atmosphere, yield rel. to chemisorbed O 9-7802  
 Cs-Sb photocathodes, processing on glass substrates, photoresponse and build-up time meas. 9-15146  
 Cs, ejection by circularly polarized light, spin orientation meas. 9-20888  
 Cs<sub>2</sub>Sb, films, quantum yield and phase transition 9-3756  
 Cu, d-band optical density of states 9-1629  
 GaAs-Cs photocathode, effect of Sb(Te) on surface 9-12225  
 GaAs, rel. to conduction-band minima, L<sub>1</sub> and X<sub>3</sub>, location 9-9895  
 Ge density of states, changes rel. to disordering, by photoemission 9-9994  
 GeF<sub>4</sub>, He (I) carbon tetrafluoride, He(I) reson. photoelec. spectra, band assignments from orbital obs. 9-19462  
 He<sup>+</sup> collision with Ar and Kr, 5 to 300 eV 9-6996  
 In, 215-280 nm, quantum yield over photon energy range 4.1 to 5.6 eV 9-12226  
 InP clean surface, photoelec. yield near threshold 9-16319  
 KF(Cl), spectra, evidence for L-bands 9-3757  
 K<sub>2</sub>Sb, three-photon eff. 9-10080  
 LiF:Mg, spectrum 9-3758  
 Ne<sup>+</sup> collision with Ar and Kr, 5 to 300 eV 9-6996  
 Ni, d-band optical density of states 9-1629  
 SiF<sub>4</sub>, He (I) carbon tetrafluoride, He(I) reson. photoelec. spectra, band assignments from orbital obs. 9-19462  
 Si, electrons and holes into Si<sub>3</sub>N<sub>4</sub> thin layers 9-10081  
 from VO<sub>2</sub> quantum yield and energy distrib. curves 9-12227  
 ZnTe, electronic structure determ. 9-7866

**secondary**

- device for recording efficiency 9-21555  
 following ionization 9-13449  
 high-energy neutral atoms prod. in rf-induced discharge 9-2806  
 of resistance strips, coated glass, as function of primary energy 9-18665  
 scattering components in non-equilibrium zones near planar interface on X-irrad. 9-1630  
 solids, due to atom bombard., review 9-16321  
 solids, due to atom bombard., review 9-3760  
 Ag, multiple distrib., prod. by electrons with energies in range 60-960 eV 9-5782  
 Ar atom, metastable impact on W surface, rel. to work function 9-11409  
 Au, multiple distrib., prod. by electrons with energies in range 60-960 eV 9-5782  
 Cu, multiple distrib., prod. by electrons with energies in range 60-960 eV 9-5782  
 Gd secondary emission of electrons as n detector 9-2562  
 MgO, temp. dependence, excess Mg effects 9-1631  
 MgO surface preparation by baking and dipping 9-7869  
 Mo, multicharged ion-bombarded target, rel. to ion charge 9-21556  
 Pt, multiple distrib., prod. by electrons with energies in range 60-960 eV 9-5782  
 Xe atom, metastable impact on W surface, rel. to work function 9-11409

**thermionic**

- See also Cathodes*  
 laser-induced, discrimination from non-linear photoeffect by time response meas. 9-16318  
 low-intensity, Geiger-Müller counting 9-12221  
 oxide cathodes, energy distribution 9-21553  
 refractory materials, in vacuum, Ar and caesium vapours, measurement 9-12222  
 saturation current evaluation method based on Fowler's eqn. 9-21552



**Electron emission continued****thermionic continued**

- Schottky barrier diodes, Richardson const. and tunneling eff. mass 9-21524  
 Schottky barrier diodes, Richardson constant 9-15145  
 Schottky barriers, normalized thermionic-field emission 9-15144  
 tungstate matrix cathode, rel. to composition 9-5780  
 Au, laser-induced, discrimination from non-linear photoeffect by time response meas. 9-16318  
 Mo, CO<sub>2</sub> laser induced 9-10079  
 Mo, polycryst., meas. of O adsorption and desorption 9-11787  
 Ni, parameters of (111), (100) and (110) faces 9-1625  
 Re, polycryst., meas. of O adsorption and desorption 9-11787  
 TaB<sub>3</sub> cathodes, properties 9-5778  
 ThC cathode props 9-3754  
 ThC cathode props. 9-3754  
 Ti evaporation controlled from thermoelectronic emission 9-12811  
 W, CO<sub>2</sub> laser induced 9-10079  
 W, in Cs vapour, rel. to adsorpt. of Cs atoms 9-11785  
 W, in O<sub>2</sub>, effect of press. and temp., rel. to O adsorpt. and desorption 9-11786  
 W, polycryst., meas. of O adsorption and desorption 9-11787  
 W pyrolytic coatings 9-5779  
 ZrC pyrolytic coatings 9-5779

**Electron energy states** *see Crystal electron states***Electron gas**

*See also Metals/theory; Plasma; Solids/theory; Superconductivity*

- classical, pair distrib. function asymptotic behaviour 9-10674  
 conduction, with embedded heavy-particle gas, Suhl's eqns. for Kondo effect 9-9885  
 $\delta$ -function, ferromag. transition, effects of correlations 9-12260  
 degenerate, h.f. dielec. const., plasmon lifetime 9-10677  
 electron solid, ferromagnetic props. 9-6340  
 energy, ground-state, parametric approach 9-10675  
 equations of state, numerical evaluation for pair creation 9-19005  
 films, thin, acoustic plasma waves 9-9911  
 Friedal oscills, modification by mag. field 9-5627  
 heating, rel. to e.m. oscillation instability 9-3607  
 inhomogeneous, perturbation-theoretic treatment 9-21473  
 interaction with classical impurity spin, exact solution 9-16216  
 in magnetic field, linear response theory 9-18591  
 in magnetic field, non-uniform state for degenerate Coulomb gas 9-21474  
 magnetization, spontaneous, of noninteracting gas 9-8450  
 in metal, surface potential, effects of correl. 9-12074  
 metals, dispersed, statistical thermodynamics 9-13829  
 metals, second sound existence prediction 9-18592  
 motion in a random electric field 9-2423  
 non-degenerate, electrical transport in high elec. and mag. fields, quantum theory 9-21476  
 phase transitions of electron fluid 9-14357  
 in phonon field, plasma freq., second random phase approx. 9-12073  
 photon scatt., Compton eff. 9-20597  
 quantum mech. distrib. functions 9-4255  
 random phase approx., quasielectron props. 9-2177  
 randomization by trapped electro-acoustic waves 9-15439  
 relativistic, in intense mag. field, quantum theory 9-8453  
 in semiconductors, light scattering, theory 9-1744  
 specific heat, displacement and collective variables calc. method, low temp. 9-21475  
 spin waves in degenerate electron fluid 9-1438  
 superconductivity in spin density wave state 9-7763  
 surface potential, effects of screened exchange and correl. 9-12075  
 transport eqns. for weakly ionized gas in d.c. mag. field 9-10676  
 two-dimensional, effects of tilted mag. field 9-5619  
 Wigner, dielectric props. 9-21419  
 n-Si, two-dimens., effects of tilted mag. field 9-5619

**Electron guns** *see Electron beams***Electron lenses**

*See also Electron microscopes; Electron optics*  
 geometrical principles rel. to microscope 9-6489  
 image aberrations for straight optical axis, calc. method 9-10596  
 immersion objective, pot. distrib. and e trajectories 9-19124  
 probe-forming and projector, spherical aberration rel. to distorton coeffs. 9-6479  
 quadrupolar, acceptance of antisymmetric quadruplet in phase plane 9-6472  
 quadrupole, spherical aberration 9-20494  
 quadrupole and octopole system, evaluation by third order aberration equations 9-6480  
 superconducting, with Ho poles, cardinal elements and aberration coeffs. 9-14417

**electrostatic**

- double aperture immersion, pot. distrib. and other calcs. 9-10819  
 three-aperture, variable energy image prod. at fixed position 9-2339  
 three-electrode cathode lens, resolution limit for ion generated e 9-6481

**magnetic**

- cryogenic solenoid objective, electron-optical properties 9-2342  
 cylindrical, for e. energy analysis 9-2335  
 depolarization of hydrogen atoms while passing through mag. lens at zero field 9-2827  
 for double second-order focusing and double-focusing spectrometers 9-6482  
 field axis location 9-4438  
 flux density distrib. determ. 9-2341  
 pole piece saturation effect on axial field distribution 9-2341  
 transgaussian trajectories determ. for lens with symmetry of revolution 9-19132

**Electron microscope examination of materials**

*See also Ion microscopes*

- adsorbed atoms migration path determ. 9-1111  
 aggregate and hardened cement paste contact 9-17337  
 ALBA thinning machine, improvements 9-7394  
 biological unstained specimens, polytopic montage 9-17262  
 cathode protrusion formation during pre-breakdown conditioning 9-11633  
 channelling patterns, crystal orientation depend., optimum conditions for generation 9-19696  
 crystals, isotropic, images of lines of dilation, props., micrograph construct. 9-21326

**Electron microscope examination of materials continued**

- dark field microscopy and strain meas. 9-7539  
 deformation studies on thin films, production of defects 9-7544  
 ferromagnetic films, domain wall thickness meas. 9-12297  
 fibres from deformed polymer crystals 9-18395  
 foil preparation from 0.01" diam. wires, longitudinal and transverse sections 9-16071  
 glass and ceramics., 3 dim. and stereo scanning 9-3278  
 glass fragment preparation for transmission e. microscopy 9-18434  
 grain-boundary triple junction and corner-twinned junctions 9-13696  
 height differences, microscopic, by reflection electron microscopy 9-4217  
 magnetic structures, by Lorentz microscopy, Fresnel mode 9-5836  
 magnetite, orthorhombic ordered phase structure 9-7439  
 megavolt, possibility of using thicker sections 9-6487  
 patterns varying with crystal orientation and due to electron channeling effects 9-19695  
 polymers, relaxation mechanisms 9-7535  
 polymers in ultrathin sections, beam-induced contrast in images 9-11867  
 replicas, use in materials investigation 9-7396  
 review 9-2343  
 scanning system for use with e microprobe X-ray analyzer 9-11821  
 siloxane elastomers, submolecular structure rel. to mech. strength, -80 to +20°C 9-9770  
 slip trace analysis and foil thickness determ. without specimen tilt determ. 9-7330  
 solution, high polymer, mol. wt. determ. 9-14836  
 specimen preparation 9-7395  
 steel, austenitic-martensitic transformation obs. 9-5516  
 steel, 1.4%Mn, grain boundary carbide film cracking 9-19811  
 steels, welded high-strength structural, occurrence of massive ferrite in heat-affected zones which corrode in sea-water 9-21402  
 stress measurable tensile device 9-3407  
 sugar coke, heat treated, prod. d graphite and turbostratic C particles 9-7358  
 superconducting vortex line obs. using transmission microscopy 9-7393  
 triglycine sulphate, domain structure from exam. of elec. decorated surfaces 9-1599  
 water-containing mats., method of study 9-3271  
 X-ray grating for electron probe microanalysis 9-9661  
 Ag films, vacuum-deposited, sulphuration obs. 9-11765  
 Ag particles, micron-sized, temp. rise due to e. beam heating in e. microscope 9-11822  
 Al-(5 wt.%)Mg-(0.4 wt.%) Ag alloy, precipitate-free zone 9-18537  
 (93wt.%)Al-(7wt.%)Mg alloy, segregation and precipitation at grain boundaries 9-19832  
 Al, electron displacement damage 9-3334  
 Al, fatigued, form of cell structs. and dislocation patches 9-5347  
 Al, pseudo Kikuchi line obs. 9-9669  
 Al, quenched-hardened, plastic deformation 9-11924  
 Al alloys, transmission, rel. to X-ray small angle scattering parameters for GP zones 9-13627  
 Au films, nucleation, growth and structure 9-19673  
 Au polycrystalline foils, anomalous e transmission 9-11836  
 B foils, rel. to defects 9-5247  
 C, small crystallite type, study of microstruct. variations 9-7420  
 C black aggregates, shape and bulkiness factors 9-7421  
 C film thickness estimation from microscopy of transverse sections 9-11766  
 CdS, crystal single, anomalous bend extinction contours 9-3287  
 CdS crystals 9-7453  
 CdS plate-shaped crystals, Si contamination and inclusions 9-5343  
 Cu-Au alloys, dislocation formation during ordering 9-11881  
 Cu-Sn alloy, equilibrated, microprobe obs. of grain boundary segregation 9-11843  
 Cu, dislocation arrangement in stress-applied state 9-14946  
 Cu, electron displacement damage 9-3334  
 Cu films, nucleation, growth and structure 9-19673  
 Fe-(23 at.%)Be alloy, structure changes during ageing 9-17343  
 Fe-Si alloys, thin foils, antiphase boundaries contrast in superlattice reflections 9-11849  
 Fe, high-purity, stress-corrosion cracking in NH<sub>4</sub>NO<sub>3</sub> soln. 9-14981  
 Fe, two beam dark field, strain and dislocations produced 9-7539  
 Fe<sub>3</sub>O<sub>4</sub>, magnetite, film nucleation and growth on Fe in high-temp. water 9-21276  
 Fe film nucleation, growth and structure 9-19672  
 Fe films, nucleation, growth and structure 9-19673  
 GaAs<sub>1-x</sub>P<sub>x</sub> epitaxial layers on GaAs, compositional inhomogeneities 9-14895  
 ge, neutron irradiated, defect obs. 9-16090  
 Ir, radiation damage exam., explt. technique 9-5580  
 MnAl, domain structure 9-13967  
 MoS<sub>2</sub>, Kikuchi patterns, intensity anomaly 9-14918  
 MoS<sub>2</sub>, Kikuchi patensity anomaly 9-9679  
 MoS<sub>2</sub>, Kikuchi patensity anomaly 9-9679  
 Na soaps, structure 9-5225  
 Ni-Ti, equi-atomic, martensite behaviour 9-7615  
 Ni, defect structure, rate of loading effects 9-3352  
 Ni<sub>3</sub>Mn alloy, antiphase boundaries and dynamic effects under high voltage 9-14921  
 Ni cylindrical crystal, stray mag. field above Bloch walls, investig. 9-13974  
 NpO<sub>2</sub> film, grain growth and crystallization 9-5251  
 PuO<sub>2</sub> film, grain growth and crystallization 9-5251  
 Si:P diodes, laser-irrad.-produced, structural characts. 9-18638  
 SiO amorphous film, transparent hole formation mechanism 9-19668  
 TaO<sub>2</sub> protective film on Ta in high temp. HNO<sub>3</sub> acid and ag. CuCl<sub>2</sub> soln. 9-21267  
 ThO<sub>2</sub> film, grain growth and crystallization 9-5251  
 U<sub>3</sub>O<sub>8</sub> at 20°C, C 9-11854  
 V film, nucleation, growth and structure 9-19672  
 ZnS crystals 9-7453  
 ZnSe, cathodoluminescence by scanning electron microscope in single crystals 9-3944  
 Zr alloys, thin oxide films formed by oxidation 9-20051

**Electron microscopes**

*See also Ion microscopes*

- beam temp. obs. 9-10823  
 decharger design for thin metal films study by e diffraction 9-6483  
 design and construction of 1 MV type, advantages in thicker specimens, reduced aberration 9-7380

**Electron microscopes continued**

- emission, electrostatic three- electrode cathode lens charact. 9-6481  
 emission and scanning, relief contrasts of uneven specimen surfaces, formation 9-6490  
 field, emission, effect of Al adsorbed on W 9-11784  
 focusing method using image scanning signals 9-12984  
 grid holder for shadow casting unit to achieve near zero angle of incidence 9-12983  
 high resolution chromatic aberration and axial astigmatism 9-17859  
 high voltage 9-17860  
 Jem 7, magnification, camera const. and image rot. calibrations 9-2345  
 lens principle for use in microscope 9-6489  
 magnification calibration, accurate method using Cu mesh 9-10821  
 megavolt, possibility of using thicker sections 9-6487  
 modifications for ultrahigh vacuum work 9-6485  
 Muller, modification for 19- $\mu$ m, surface asperity mapping 9-3750  
 with Quantimet image analyzer for quantitative metallography 9-12982  
 scanning, using field emission gen. without auxiliary lenses, design and operation 9-19126  
 scanning, h.v. supply 9-2347  
 scanning, mag. field meas. 9-8578  
 scanning, role in life sciences 9-2349  
 scattering contrast meas. 17-1200 KeV, expts. on C, Ge and Pt. films. 9-6488  
 secondary e emission, image contrast studies via current density meas. 9-6484  
 Siemens Elmiskop I, modification to Ward anticontamination trap 9-19125  
 specimen chamber for high temp. gas reactions 9-2346  
 stereophotographic techniques 9-15198  
 transmission, high-resolution scanning 9-14418  
 transmission, with ARL microprobe 9-2348  
 with TV display system 9-10822  
 e impact rel. var. by varying pot. 9-2344  
 Al-Ag(Cu) alloys, precipitation study, use of different forms of contrast 9-7605  
 In condensed films, subcritical thickness meas. 9-18383  
 Mo foils, rel. to deform., slip geometry study 9-5460

**Electron microscopy**

- See also Crystal structure, atomic*  
 applications and instrumentation review 9-2343  
 calibration film, instant, prefabricated, to give known diff. patterns on every specimen 9-16070  
 carbonaceous mats., prep. of specimens 9-8314  
 ceramics, transmission micrographs, thickness errors, analysis 9-3174  
 dark field microscopy and strain meas. 9-7539  
 electropolishing, jet, of specimens, modification 9-16069  
 foil preparation for transmission work, modified technique 9-4439  
 foil thickness determ. from slip trace analysis without specimen tilt determ. 9-7330  
 glass fragment preparation for transmission e. microscopy 9-18434  
 goniometer which allows tilting to 20° at liquid nitrogen temp. 9-5305  
 graphite, replication tech. for exam. dynamic changes during heat treatment 9-7424  
 high-resolution, cryogenic solenoid objective, properties 9-2342  
 metal foils prep., electrolytic grinder 9-3269  
 microfurnace for specimens in vacuum and inert atmos. 9-14292  
 Moire pattern for crystal containing dislocation 9-13617  
 patterns varying with crystal orientation and due to electron channeling effects 9-19695  
 periodicities in micrographs, revealed by optical convolution method 9-16072  
 reflection, rel. to microscopic height differences 9-4217  
 replicas, carbon, improved method of removing plastic backing 9-6486  
 replication, plastic- carbon of optically pre-selected areas 9-3270  
 scanning, applies. to mat. and device sciences, book 9-12985  
 scanning, review 9-10820  
 scanning extension using varying retarding field 9-2344  
 with TV display system 9-10822  
 uneven extended surfaces, relief contrast formation for emission and scanning types 9-6490  
 wave diffraction patterns, phase distribution 9-2338  
 Ag particles, micron-sized, temp. rise due to e. beam heating in e. microscope 9-11822

**Electron mobility, solids** *see Crystal electron states/transport processes*

**Electron multiplier phototubes** *see Photomultipliers*

**Electron multipliers** *see Electron tubes; Photomultipliers*

**Electron nuclear double resonance (ENDOR)** *see Nuclear magnetic resonance and relaxation; Paramagnetic resonance and relaxation*

**Electron optics**

- See also Beta-ray spectrometers; Electron lenses; Ion optics; Particle optics*  
 difference freqs of two e waves, deflection descript by wave optics 9-4437  
 dynamics in injection accelerator with waveguide prebuncher, focusing problems 9-4697  
 ellipsometer for low energy electron diffraction chamber 9-1174  
 image aberrations for straight optical axis, calc. method 9-10596  
 microscope focusing, method using image scanning signals 9-12984  
 principles 9-6489  
 spectrometer, cylindrical, electrostatic; focusing and geometry 9-20693  
 systems with rectilinear axis of symmetry or asymmetry, potentials modeling device 9-229

**Electron pairs**

- See also Positronium*  
 one electron, less than half of 9-9110  
 in e<sup>+</sup>e<sup>-</sup> in colliding beams, meson resons. prod. and decays 9-17993  
 e<sup>+</sup>e<sup>-</sup> decay mode of  $\rho$  mes., branching-ratio meas. 9-8870  
 e<sup>+</sup>e<sup>-</sup> $\rightarrow\pi A_2$  cross section expression and depend. on lepton polarization determ. 9-11084

**annihilation**

- condensed matter with molec. or covalent bonds, free positron lifetime, effective number of e per atom 9-5637  
 e<sup>+</sup>e<sup>-</sup> $\rightarrow\nu\bar{\nu}$ , rel. to astrophysics, energy loss rate and  $\nu$  luminosity 9-10477  
 Fermi energy and Doppler- broadened radiation 9-14472  
 ice-water system,  $S^+$ - $S^-$  conversion of positronium in positron annihilation mechanism 9-12079  
 in-flight, 80-300 MeV photon spectra 9-16821  
 ionic cpds., positrons 9-9916

**Electron pairs continued****annihilation continued**

- metals and alloys, positron annihilation rel. to physical conditions 9-12078  
 polytetrafluoroethylene (Teflon), irradiated, positron lifetime meas. study 9-13841  
 positronium decay $\rightarrow 3\gamma$ ,  $^1S_0$  C-forbidden and  $^1S_1$  C-allowed, obs. separation 9-10985  
 semiconductors, positron annihilation 9-17374  
 two-photon radiation, angular correlations calc. from atomic Hartree-Fock orbitals 9-5638  
 in unsymmetrical valence type substances, positron lifetime 9-1448  
 e<sup>+</sup>e<sup>-</sup> $\rightarrow\pi^+\gamma$  cross section calc.,  $\rho^0\rightarrow\pi^+\gamma$  decay width prediction 9-20605  
 e<sup>+</sup>e<sup>-</sup> $\rightarrow\nu\bar{\nu}$ , diff. and total cross sections formulae determ. 9-10983  
 e<sup>+</sup>e<sup>-</sup> $\rightarrow\pi^+\gamma$ ,  $\omega$ - $p$  interference and rare  $\omega$ - $p$  decay modes 9-394  
 e<sup>+</sup>e<sup>-</sup> $\rightarrow\pi^+\pi^-$ ,  $\omega$ - $p$  interference and rare  $\omega$ - $p$  decay modes 9-394  
 e<sup>+</sup>e<sup>-</sup> $\rightarrow\pi^+\pi^-$ , in  $p$  resonance region, max. cross-section calc. 9-15585  
 Al, positron lifetimes, cyclic deformation effects 9-16220  
 Al, two- photon radiation, angular correlat. from atomic Hartree-Fock orbitals 9-5638  
 Ar, positron annihilation rate temp. dependence 9-6604  
 Cu, positron annihilation meas. of Fermi surface 9-21465  
 Cu, positron annihilation rel. to Fermi surface 9-7730  
 Cu, positron lifetimes, cyclic deformation effects 9-16220  
 Ga, positron lifetimes in solid and liquid 9-7731  
 Gd, ferromagnetic, polarized positron annihilation 9-9917  
 Ge, two- photon radiation, angular correlations calc. from atomic Hartree-Fock orbitals 9-5638  
 Na, positron lifetimes in solid and liquid 9-7731  
 Ni-Co alloy, positron annihilation rel. to plastic deformation 9-21477  
 Ni-Fe alloy, positron annihilation rel. to plastic deformation 9-21477  
 Pb, radiationless 9-12081  
 Se, two- photon radiation, angular correlations calc. from atomic Hartree-Fock orbitals 9-5638  
 Si, two- photon radiation, angular correlations calc. from atomic Hartree-Fock orbitals 9-5638  
 Y, positron annihilation rel. to electronic structure 9-18597  
 Zn single crystals, C, S angular correlation of radiation 9-1449  
 Zr, positron annihilation rel. to electronic structure 9-18597

**production**

- by  $\gamma$ , 2-20 MeV, in nuclear field 9-11265  
 Coulomb field, total Born approximation cross-section 9-13104  
 rel. to electron eqns. of state numerical evaluation 9-19005  
 in nuclear charge distrib., calc. of cross-section 9-484  
 nuclear photographic emulsion, automatic scanning device for trident detection 9-18048  
 photon interaction with plane e.m. wave 9-15583  
 showers due to  $\gamma$  bombard. of liquid Xe, 100, 200, 500, 2000 MeV 9-15584  
 e<sup>+</sup> spectra, total cross section in atom field calc., photon energy  $\leq 2.5$  MeV 9-8755  
 $\gamma$  rays, 2.62, 13 MeV on various targets 9-10976  
 $\gamma$ C-e<sup>+</sup>e<sup>-</sup>C meas., use as validity test of quantum electrodynamics at small distances 9-6575  
 Ag, target, 2.62 MeV  $\gamma$  rays obs. 9-10976  
 Al target, 2.62 23 MeV  $\gamma$ -rays obs. 9-10976  
 Au 2.62 13 MeV  $\gamma$ -rays, obs. 9-10976  
 c( $\gamma$ e<sup>+</sup>e<sup>-</sup>)c wide-angle pairs, rel. to quantum electrodynamics validity, 250-650 MeV/c<sup>2</sup> 9-8754  
 in Cu Coulomb field, 5.5 and 32 MeV, diff. cross sections 9-6857

**Electron paramagnetic resonance** *see Paramagnetic resonance and relaxation*

**Electron probe analysis** *see Chemical analysis/X-ray*

**Electron resonance** *see Cyclotron resonance; Paramagnetic resonance and relaxation*

**Electron spin resonance** *see Paramagnetic resonance and relaxation*

**Electron states in solids** *see Crystal electron states*

**Electron structure of solids (crystallography)** *see Crystal structure, atomic*

**Electron structure of solids (energy structure)** *see Crystal electron states*

**Electron theory**

- See also Quantum electrodynamics*  
 Abrahm-Lorenz model and special relativity 9-6468  
 bound-state Dirac electron, 'hidden- momentum' equivalent to magnetic charges 9-669  
 Dirac, Heisenberg extended picture, Frenkel-Kramers model and Zitterbewegung 9-333  
 Dirac-PPPP Pavli eqn. exact solns. and polarization precession 9-332  
 H atom, energy levels in Dirac eqn., influence of boundary conditions 9-11417

**Electron theory of metals** *see Crystal electron states; Metals/theory*

**Electron traps** *see Crystal electron states/impurity states and effects*

**Electron tubes**

- See also X-ray tubes*  
 dynode multiplier arrays, ratio of incident secondary calc. 9-18038  
 electronographic image tubes, mica windows 9-12978  
 flame, rectifying effect on electrodes 9-226  
 graphite cylinder, vacuum-tight device allowing expansion of heated element 9-19127  
 image analyzer tube targets from thin Si films, development 9-8587  
 image storage, tube, for optoelectronic computing 9-14287  
 klystron, two-cavity, freq. control for double resonance studies 9-15502  
 magnetic e multipliers, anode current time sampling method 9-10825  
 magnetron with mag. field inclination 9-6491  
 microwave beam-plasma devices, input and output coupling 9-13438  
 receiving valves, contact potential, grid and cathode work functions, meas. 9-231  
 reflex klystron, oscillations initiation study 9-2350  
 secondary emission from MgO, surface preparation by baking and dipping 9-7869  
 technology, conference 9-3748  
 technology, conference 9-7862  
 technology, conference 9-3747  
 thermionic conduction stabilization by space charge effects against cathode temp. change 9-16770  
 TV image analyzer target using alloyed junction mosaics on Si 9-8586  
 TWT, electron deceleration effect on flux deformation 9-4440  
 Cs thermionic diodes, e. beam reflections effects 9-8584  
 Hg vapour rectifiers and thyratrons, equivalent press. concept validity, obs. 9-13473



**Electron-phonon interactions** *see* *Crystal electron states/transport processes; Crystals/lattice mechanics*

## Electrons

*See also* *Beta-rays; Cosmic rays/electrons; Crystal electron states; Noise/electrical; Nuclear reactions and scattering due to electrons; Photoelectricity; Plasma; Positronium; Positrons; Space charge*  
*This heading includes both negative and positive electrons when the differences between them are of no special significance*  
 atmospheric, trapped, obs. at low and high alt. 9-10416  
 in atoms, matrix factorizations for Coulomb interaction 9-20872  
 auroral, flux obs., 1-10 MeV 9-20103  
 bubble in superfluid He, mobility 9-9581  
 correlation functions, interelectronic, condition removing degeneracy 9-20327  
 detection with ZnS(Ag) scintillating crystal, instability of radiation 9-11139  
 diffusion in He, lateral diff. and first Townsend coeffs. 9-15978  
 elec. dipole moment, new upper limit 9-11384  
 electric dipole moment of free electrons, upper limit, obs. 9-4835  
 energy analysis by cylindrical mag. lens 9-2335  
 energy distrib. in gas discharge by Markov random flight soln. 9-5080  
 energy loss in thin foils with e.m. retardation, occurrence Cherenkov rad. 9-7689  
 high density, freq. depend. of relax. time 9-1437  
 hydrated, e.s.r. detect. in water 9-1044  
 $m_e > 500$  MeV, possible existence 9-10977  
 magnetic moment, anomalous 9-14470  
 magnetic moments, gyromag. ratio with muon, calc. of sixth-order contrib. from fourth-order vacuum polar. 9-16826  
 magnetic monopole moment, upper limit obs. 9-8751  
 mobility in Ar, He, N<sub>2</sub>, H<sub>2</sub> up to 42 atm. 9-17167  
 motion in collisional plasma in mag. field, conductivity calc. 9-18281  
 negatrons in interplanetary cosmic rays, spectra 12-220 MeV, balloon obs. 9-20141  
 one, less than half pair 9-9110  
 polarization in mag. field 9-16769  
 propagator, consistency with Ward's identity 9-10959  
 in solar particle streams, discussion 9-16620  
 solvated, dielec. model 9-1035  
 solvated, in pulse irradiated ice 9-10360  
 spin polarization by low-energy scatt. from unpolarized targets, review 9-18148  
 states in quantum electrodynamics, Rayleigh-Ritz procedure for determ. 9-6574  
 trajectory and mass shift in radiation pulse from Hamilton-Jacobi eqn. 9-17948  
 C<sub>2</sub>H<sub>6</sub>, slow electron drift velocity 9-3011

## Absorption

*See also* *Beta-rays/absorption*  
 electroluminescence of rare earth and transition metal mols. in II-VI compounds 9-5975  
 metal films, self-supporting as thickness meas. 9-9608  
 radiative equilibrium between Cherenkov emission and absorption 9-4429  
 semiconductors, abs. coeffs., Urbach's law, perturbative and nonperturbative calc., weak and strong interac. 9-3603  
 Ge single crystal coeff. meas. temp. depend. 9-7808  
 Si single crystal coeff. meas. temp. depend. 9-7808

## Interactions

cascade theory test in nuclear track emulsions, 180-2000 BeV 9-17946  
 Compton effect on relativistic electrons 9-6598  
 electron-phonon, superconductivity high temp., Green's functions 9-1484  
 with hypothetical radiation, range of coupling constants based on energy balance of sum 9-10978  
 with hypothetical zero-mass pseudoscalar meson, range of coupling constants based on energy balance of sum 9-10978  
 magnetic, quantum kinetic eqn. 9-97  
 metals with paramagnetic impurities, effects 9-9876  
 neutral atom, many-electron interaction calc. 9-11381  
 in superconductors with paramag. impurities, effect on transition temp. and gap 9-1476  
 $e^+e^- \rightarrow (2n+1)\pi$  in tests for  $|\Delta I| \leq 1$  in e.m. interactions 9-6621  
 $e^+e^- \rightarrow \gamma\gamma\gamma$  at high energies, distrib. meas. 9-6605  
 $e^+e^- \rightarrow \pi^+\pi^-$ , pion e.m. form factor compared with vector meson decay data 9-393  
 $eN \rightarrow eN\pi$ , threshold  $\pi$  prod., current algebra calc. 9-8830  
 $e^-p \rightarrow e^-\pi^+$ , asymmetry calc. by  $\pi$ -e.m. form 9-11000  
 $e^-p \rightarrow e^-A_2$  cross section expression and depend. on lepton polarization determ. 9-11084  
 $\mu e$  collisions, calc. of bremsstrahlung 9-15581  
 $\nu_e e \rightarrow \nu_e e$  interac., e.m. renormalization of vector part 9-8750  
 He ionization near threshold by e impact 9-5062  
 Si detector, backscatt. and bremsstrahlung, pulse height distrib., 300-1200 keV 9-11141

## Ionization

carbohydrates and O derivs., ionization cross-sections 9-7191  
 organic Si chlorides, neg. ion form. 9-3008  
 SiC<sub>4</sub> neg. ion. form. 9-3008

## Radiation

*See also* *Bremsstrahlung; Cherenkov radiation; Electrodynamics; Synchrotron radiation*  
 beams, light emission at diff. grating, quantum theory 9-4435  
 circumlunar space, 30 KeV ELECTRONS RECORDING USING Luna-11 satellite 9-18899  
 dosimetry, physical basis 9-453  
 in e.m. field, classical and quantum theory analysis 9-6414  
 equilibrium between Cherenkov emission and absorption 9-4429  
 polarization, 500 1000 Å, 6 GeV 9-10979  
 spin self-polarization, radiational, in spiral motion in mag. field 9-2468  
 synchrotron polarization Stokes params. 9-2276

## Scattering

*See also* *Atoms/electron scattering Beta-rays/scattering*  
<sup>4</sup>He target, influence of nucleon-nucleon correls. 9-4772  
 angular distrib. for resonant scatt. by molecules 9-4895  
 backscattering phen., single-energy beam between 50 and 1200 keV 9-10980  
 gaseous targets, spin polarization rel. to scatt. pot. 9-11397  
 high-energy, by nuclei with nucleon knockout 9-579

## Electrons continued

### scattering continued

hydrocarbons, condensed aromatic, monochromatic e energy loss 9-13539  
 inelastic, and point-like structure inside proton 9-17994  
 Kapitza-Dirac eff. theory with no limitations 9-6601  
 for low gas pressure meas. 9-12849  
 magnetic, elastic, and mechanism of polarization of scatt. beam 9-12256  
 many-channel, by localized potential, total displaced charge 9-5598  
 by molecular beams 9-2856  
 molecules, quantum defect method 9-767  
 momenta in Monte-Carlo transport codes 9-4260  
 multiple, fast e in thin layers, obs. ang. distrib. and single-scatt. cross-section, target atom 9-6982  
 multiple, solution of kinetic equation for continuous energy loss approx. 9-334  
 photons in electron gas, Compton eff. 9-20597  
 by polar gas molecules, screened, eff. of exponential attenuating factor 9-15846  
 by polar molecules, thermal e, cross-sections and drift vel. data 9-13335  
 Ramsauer-Townsend effect, teaching demonstration using Xe thyratron 9-2125  
 recoil-d vector polar. meas. for e scatt. from unpolar. d target, test of time-reversal invariance for e.m. interac. 9-4588  
 reflection by standing wave of giant pulse laser 9-6602  
 spin polarization from unpolarized targets at low-energy, review 9-18148  
 in storage rings, polarized, in bunches 9-19264  
 superelastic, from ally excited N<sub>2</sub> mols. 9-9224  
 in water vapour, collision freq. calc. 9-13352  
 ed quasielastic, rel. to n farm factors, 0.27-4.47 (BeV/c)<sup>2</sup> 9-8752  
 e<sup>+</sup>e<sup>-</sup>, cross-sections rel. to Bhabha exchange effects 9-6603  
 e<sup>+</sup>p, renormalizable theory of weak interaction 9-335  
 Ag, inelastic, in LEED obs. 9-21451  
 Al, Monte Carlo calc. 9-7683  
 in Al foil 9-17362  
 Cu, Monte Carlo calc. 9-7683  
 e<sup>+</sup>e<sup>-</sup>, Bhabha formula verified, 1.52-2.62 MeV 9-10982  
 H<sub>2</sub><sup>+</sup>, phase-shifts calc. 9-766  
 H<sub>2</sub><sup>+</sup>, quantum defect method 9-767  
 HgSe, inelastic 40°-400°K, elastic >400°K 9-5642  
 NiO, antiferromag., low-lying surface-spin-wave band prediction 9-21595

**scattering, electron-proton**  
 cross section meas., resonances determ. 9-17947  
 p-odd correlations calc., Tanikawa-Watanabe renormalizable theory 9-10981  
 polarization-odd effects, E<sub>e</sub> ≈ 10 GeV 9-14471  
 radiative corrections, review 9-20603  
 time-reversal invariance test in inelastic scatt. e from polar. p target 9-2467  
 e<sup>+</sup>p →  $\Lambda$  $\bar{\Lambda}$ , weak scatt., cross-sections, time-reversal invariance, PCAC, Cabibbo hypothesis 9-20602  
 e<sup>+</sup>p → e<sup>+</sup>n<sup>+</sup> for 1236 MeV isobar transverse and longitudinal cross-sections 9-6659  
 ep → eN\*, nonrelativistic symmetric quark model 9-8753

**Electrophoresis**  
 ceramic deposition, thickness control using probe electrode technique 9-12966  
 gelatin gels, struct. studies 9-19651  
 liquids of low permittivity with field-induced polarization 9-16025  
 medium for improved resolution of serum proteins, patent 9-10566  
 porcelain enamel, ceramic coating deposition 9-1913  
 theory, macroscopic transport equations applic. 9-19588  
 Al and alloys, painting rel. to paint film defects 9-4005  
<sup>10</sup>BO<sub>2</sub><sup>-</sup> and <sup>11</sup>BO<sub>2</sub><sup>-</sup>, migration, isotope effect 9-17200  
 BaTiO<sub>3</sub> film, prep. by electrophoresis after annealing or melting 9-9610  
 Mg coating of nuclear fuel elements, patent 9-9097

### Electrophotography *see* *Photography*

### Electrophotoluminescence *see* *Electroluminescence*

### Electropolishing *see* *Surface structure*

### Electroproduction *see* *Beta-rays/effects; Electrons; Nuclear reactions and scattering/due to electrons*

### Electrostatic generator *see* *High voltage techniques; Particle accelerators/linear*

### Electrostatic lenses *see* *Electron lenses/electrostatic; Ion optics*

### Electrostatics

*See also* *Electrets; Electric charge; Electric fields*  
 benzene, liq., course of electrostatic pot., meas. 9-7275  
 capacitor, plane, edge eff. of control field, transverse electrooptical eff. 9-6449  
 conductors, parallel with steady currents, surface charge distrib. 9-8  
 Coulomb interactions between two impurity charges in an atomic dielectric 9-7831  
 crystals, finite charge distrib. 9-12039  
 cylinders, coax. circular and square e.s. potential between, and capacitance 9-20481  
 differential equation in second order approx. for a point on edge of base of finite cylinder of revolution 9-17687  
 electrified disc in infinite cylinder, asymmetric mixed boundary value problems 9-196  
 electrostatic energy calc. from model of interacting polar mols. 9-20480  
 exact potential functions in spherically stratified media, radial variations 9-16749  
 fields, disc electrodes, integral equations method of solutions 9-6448  
 forces between uncharged plates in ionic solns. 9-16484  
 Johnsen-Rahbek effect, simple theory 9-16040  
 linear distribution of charges equivalent to elongated ellipsoid of revolution 9-19117  
 liquid dielectric jet in longitud. elec. field, stability 9-9538  
 mirror for mag. spectrometer, elimination of chromatic effects, first order theory 9-13278  
 plates, semicond., elec. connected, force between, free energy method 9-15492  
 point charge, electrostatic pot. 9-6451  
 potential due to two point charges at spherical cavity centres, in dielec. medium 9-14411  
 potential in cylindrical electrode partially submerged in conducting medium 9-197  
 potential of point charge, Legendre polynomial expansion validity 9-4412  
 potential representations by multipole potentials 9-2297

**Electrostatics** continued

- printing, screen with charging of article and use of toner particles, patent 9-12967
- problems, approx. methods 9-15493
- pump, efficiency 9-9461
- space charge clouds, expansion and shrinkage 9-10786
- sphere, dielec., near conducting plane, field and force anal., water droplet applic. 9-12826
- teaching demonstrations with vibrating reed electrometer 9-2117

**Electrostriction**

See also *Piezoelectricity*

- current-striction in many valley n-type Ge and Si, theory 9-9995
- liquids, cause of anomalies in refractive index meas. on laser-illumination 9-9511
- n-Ge, many valley, current-striction, theory 9-9995
- Ge electromechanical eff., sign inversion 9-5675
- Sb electromechanical eff., sign inversion 9-5675
- n-Si, many valley, current-striction, theory 9-9995

**Electroviscous effect** see *Colloids; Viscosity***Elementary particles**

See also *Baryons; Energy loss of particles; Field theory, quantum; Hadrons; Leptons; Nucleons and antinucleons; Nucleus; Particle detectors; Quantum theory; Quarks; Strange particles; and individual particles, e.g. Electrons, Mesons*

- angular momentum theory, topological characteristics 9-10642
- classical field theory for structure 9-8685
- compositeness, Majorana eqns., revival 9-2548
- decay into three particles, Faddeev-type relativistic eqns. 9-13094
- decay modes of high-spin parts on linearly rising trajectory 9-346
- elementary review 9-4560
- e.m. mass splittings and equal-time commutators, relationship analyzed 9-8731
- experiments, use of computers 9-13154
- factorization principle of Gell Mann, applic. to construction of superconvergent sum rule 9-6593
- Galilei space gauge props., and connections with Liouville group 9-15573
- gauge invariance and analytic regularization 9-8706
- magnetic monopole, bound pairs production in cosmic ray emulsions 9-11123
- mass diff. of 2 superposed spin states rest energy calc. from Kemmers' eqn 9-8719
- massless, relativistic kinematics 9-8711
- monopole search 9-2273
- negative mass, and the theory of relativity, book 9-12877
- new, non-strongly interacting, prod. by  $<18$  Gev  $\gamma$ -rays, search 9-8743
- non-existence of self-conjugate particles with half-integral spin 9-2442
- nonidentical, interference 9-13095
- nonidentical, interference 9-2452
- and nuclear physics, two different subjects? 9-8947
- peripheral events, Monte Carlo generation method 9-20607
- review 9-20588
- review of progress (1932-67) 9-8704
- Schrodinger's difference eqn. for two relativistic particles 9-20595
- stable, de Sitter model 9-309
- superconvergent sum rule, construction using Gell-Mann's factorization principle 9-6593
- urbaryon interactions in hyperon decay 9-2540
- wave and particle experiments for students 9-4211
- Yang-Mills, massive fields; perturbation theory using Bell-Treiman transformation 9-15574

**interaction, strong**

- C-invariance test 9-313
- dispersion formulae, perturbation theory 9-13113
- high energy and peripheral processes 9-4556
- N/D eqns., inversion formalism Regge-pole hypothesis, self-clamping mechanism, S-matrix threshold behaviour 9-4597
- spinor space, internal quantum numbers, SU theory 9-2455

**interactions**

See also *Field-theory, quantum/interactions; Nuclear reactions and scattering. Entries on interactions involving named particles are listed under the particles concerned, e.g. Mesons/interactions; Cosmic rays/effects and interactions*

- $10^4$  GeV region, fireball covariant statistical model for multiparticle production 9-16815
- amplitudes, phenomenological, construction and relativistic particle wave functions 9-17933
- amplitudes and between polarizations for asymptotically large energies and transferred momenta, a possible relation 9-4572
- any spin formalisms, construct. of invariant amp., relativistic part. wave-functions for bispinor case, vertex functions and two-body scatt. amp. obs. 9-4568
- Bethe-Salpeter abnormal soln. and S-matrix poles, two spinless equal-mass particles 9-4571
- Bethe-Salpeter bootstrap, SU(3), hadron classification 9-2484
- Bethe-Salpeter eqn. for bound state of two spin- $1/2$  particles, accurate soln. 9-6588
- bethe-salpeter eqn. for two spinless plates, differential eqn. treatment and soln. 9-20594
- Bethe-Salpeter eqn. integral operator compact for all values of total energy 9-8721
- Bethe-Salpeter equation solution 9-20593
- differential cross-sections equalities at large energies 9-10964
- elastic, high-energy, phenomenological fits connection 9-4201
- electrical/gravitational force ratio rel. to cosmological quantities 9-6585
- e.m. and gravit. of massless particles, and Schwinger terms 9-10967
- Fermi, polar,  $\mu$ , radiative correct. and parameter meas. 9-6609
- final state of 3 particles, physical region on plane of 2 invariant momentum transfers 9-8724
- form factors, e.m., asymptotic behaviour in composite models 9-8715
- group description in terms of Lie groups 9-6586
- high energy branching ratios, statistical model 9-8722
- introductory book 9-17932
- Lee model, Tamm-Dancoff method in  $2\nu$  sector 9-8720
- massless particle, kinematic singularity structure of amp. for 4-part. process 9-17931
- Monte Carlo method investigation, FORTRAN program 9-10965
- multichannel amplitudes, unitary representations 9-10966
- with n final particles, helicity amplitudes crossing relations and rel. to multi-Regge model 9-317

**Elementary particles continued****interactions** continued

- n-particle kinematics and generalized partial-wave analysis 9-8723
- n-particle prod. cross section, multi-Regge model 9-316
- polarization and amplitudes for asymptotically large energies and transferred momenta or possible relation 9-4572
- Pomeranchuk pole exchange in fireball model for very high energy NN interactions 9-2529
- potential model, bremsstrahlung matrix element, soft-photon theorem 9-16816
- primary and universal, coupling constant 9-319
- quark model with factorizability and two-body inelastic processes 9-4570
- quasi-two-body react., parity exchange, splitting of cross-section 9-4569
- resonances, Jackson's formula for parametrization near, threshold 9-16814
- space-time description 9-15576
- symmetries from Schwinger's action principle 9-2449
- tachyons, quantum field theory construct. 9-16812
- three-particle collision, cross-section for particle exchange from ground state to ground state 9-4578
- transcendental and polynomial, Langrangians, correlations and radiative correct., applic. to chiral models 9-16817
- transcendental and polynomial Langrangians, correlations and radiative correct. 9-16817
- two-body, transversity amplitudes, kinematical singularities 9-318
- two-particle, in potential, treatment using Lippmann-Schwinger eqn. 9-14467
- unrenormalizable in local and nonlocal theories, construction of Green's functions in momentum space 9-2454

**interactions, weak**

- broken mirror symmetry treatment of nonconservation of parity 9-13097
- CP violation 9-13093
- CP-invariance violation in weak radiative decays 9-314
- four-fermion and bilinear, interrelation 9-4574
- high energy, cross section limits and W-pair strong interaction model 9-8749
- Mandelstam representation, large- angular-momentum partial wave amplitudes 9-8727
- and Sakaton model 9-4590
- universality concept and radiative decay  $\pi \rightarrow l^+ \nu_l$  9-16870
- V-A, sixth interaction 9-20631
- vector boson mediated, models 9-8725
- $K^+ \rightarrow e^+ \nu_e / \mu^+ \nu_\mu$  rel. rate meas., agreement with universal V-A theory prediction 9-11036
- NN, from  $p$  polarization and ang. distrib. asymm. in  $^2\text{H}(n,p)^3\text{H}$  9-15767

**scattering**

- amplitude, elastic, at fixed momentum transfer, lower limit 9-13099
- amplitude at high energies, inelastic channels contrib. 9-10968
- amplitudes, helicity, free from kinematical singularities and constraints 9-17935
- arbitrary spin, Regge-pole conspiracy trajectories, Feynman diagram 9-2486
- Bethe-Salpeter amplitudes, degenerate multi-pole, normalization 9-4576
- Bethe-Salpeter eqn., expectation value calc., variational technique 9-2459
- Bethe-Salpeter eqn. for amplitude and relativistic Regge theory 9-4575
- Bjorken limit, generalization by making it covariant 9-2458
- Born approx., correct. to potential arising from direct-channel strips, low-energy applic. 9-6675
- charged, elastic scatt. from polar. quadrupole moment, DWBA and WKB techniques 9-2642
- delay, operative definition 9-15577
- diffraction peak, lower bound of width 9-15578
- elastic, by weak central potentials, modified Born approx. 9-320
- elastic at large angles, unitary conditions and shape of diffraction peak 9-11004
- equal-mass conspiracy relations as unequal-mass case limit 9-8728
- fermion-fermion, invest. in covariant spinor formalism 9-4565
- Feynman amplitudes O(4) symmetry at zero invariant mass 9-8733
- helicity amplitudes constraints and kinematic singularities 9-8729
- high energy review of models 9-6578
- high-energy, multiple Coulomb scatt. in nuc. emulsions 9-4637
- impact-parameter representation using  $J_0(kb \sin \theta)$  9-6590
- inverse problem, random variable approach 9-17934
- inverse problem, soln. by Gel'fand-Levitan eqns., using half-off-energy-shell matrix element 9-2456
- jet model, uncorrelated 9-6578
- many-body, nonperturbative T-matrix study 9-2463
- model for neutral self-conjugate field 9-6589
- multichannel collisions, exact effective two-particle eqns by quasi-particle method 9-6591
- N/D equations, singular, with inelastic unitary, soln. 9-6594
- N/D method, Froissart's, threshold behaviour 9-11009
- O(4) off-shell formalism 9-6691
- one-particle exchange model 9-6578
- optical model reviewed 9-6578
- partial-wave expansion in Mandelstam variables 9-2462
- phase contour method, high energy behaviour at fixed angles 9-2461
- Pomeranchuk theorem, a new proof 9-4579
- quasiclassical, high energies, S-matrix 9-13100
- quasiclassical, high energies, S-matrix 9-2466
- radiative correct., i.r. contrib., separ. in terms of exponential factor, modification for gen. exptl. conditions 9-13098
- Regge amplitudes Argand analysis and resonances 9-2488
- Regge asymptotics rel. to resonance parameters 9-2489
- Regge cuts contrib. calc. from absorpt. model 9-321
- Regge parameters and Cerulus-Martin lower bound, high-energy 9-8734
- Regge phenomenology of virtual Compton scatt., rel. to hadron e.m. mass difference 9-2478
- Regge pole amplitudes, absorptive corrections and singularities 9-324
- Regge trajectories, indefinitely rising, generalized interference model 9-6595
- Regge trajectories, infinitely rising, asymptotic behaviour 9-325
- Regge trajectories eval. using Ladder approx. in perturbation theory 9-4603
- Regge trajectory families, perturbation formulae, algebraic struct. 9-15598
- Regge-pole model 9-6578
- Regge-pole model, distinguish from others 9-4569
- S-matrix formulation of broken internal symmetries 9-8732
- S-matrix theory mass-shell, causality conditions and consequences 9-16818



**Elementary particles continued**  
**scattering continued**

- scalar, two-body elastic scatt., self-consistent vacuum trajectory 9-322  
 spiral amplitude, relativistically invariant expansion 9-14455  
 statistical model 9-6578  
 three particles, transition amplitudes and partial wave soln. 9-2465  
 three-body, breaking up wave function 9-17936  
 three-body rearrangement amplitudes, Born series convergence 9-8417  
 three-nucleon system scatt. problem 9-2464  
 three-particle collision, cross-section for particle exchange from ground state to ground state 9-4578  
 two-body, model with crossing symmetry and minimal inelastic effects 9-8730  
 two-point functions 9-8726  
 unstable particles, generalized scatt. amplitudes 9-10969  
 Yukawa potential, simple writing of S-matrix, residue function at Regge poles 9-2457  
 by d, elastic, Glauber theory corrections, BeV energies 9-8920  
 by  $\pi$  in 2 nucleon exchange in d, glauber multipole-scatt. expansion correction 9-20677

**symmetry**

- Amer. J. Phys. resource letter 9-6584  
 baryon resons, negative parity, comparison of decay ratios with SU<sub>w</sub>(6) predictions 9-13147  
 bosons, parity tests using decay mechanisms 9-4562  
 broken mirror symmetry treatment of nonconservation of parity 9-13097  
 C<sub>P</sub>, 'counter-particles' and their props. 9-4594  
 C-invariance in strong e.m. interactions test 9-313  
 chiral-symmetry breaking Lagrangian, Weinberg's eqn. general soln. 9-8713  
 compact group, arbitrary, internal symmetry crossing 9-341  
 Conspiracy problem, minimal solutions, Regge-pole families classification 9-4605  
 coupling of space-line and internal symmetry groups 9-6582  
 CP, models for breakdown 9-315  
 CP invariance, violation in some neutral kaon decays? 9-11033  
 CP nonconservation, expt. proof, and its irrelevance 9-19188  
 CP nonconservation effect in hyperon nonleptonic decay 9-423  
 CP nonconservation included in K $\rightarrow\pi\pi$  parameters theor. formulation 9-16865  
 CP noninvariance effects and K $\rightarrow\pi^+\pi^0$  9-8813  
 CP violation, K $^0$  mixed beam coherent decay 9-17972  
 CP violation and K $\rightarrow\pi^+\pi^0$  decay rate violation reln., SU(3) model 9-20634  
 CP violation in K $^0\rightarrow\pi^0\pi^0$ , branching ratio obs. 9-11037  
 CP violation in weak interactions 9-13093  
 CP violation weak interaction Lagrangian, possible shapes 9-20591  
 CP-conserving and violating weak interac. unified theory, applic. to intermediate vector mes. 9-2447  
 CP-invariance isolation in weak radiative decays 9-314  
 CPT, invariance test from K- $\ell\ell(\pi)$  polarization and ang. distrib. 9-17977  
 CPT invariances, consequences and test 9-8712  
 CPT nonconservation and pair-conjugate bosons 9-20615  
 CPT violation in K $^0$  decay 9-15610  
 current theory of symmetry breaking without extra currents 9-312  
 $\Delta I=1/2$  rule, violation in K decay 9-11031  
 $\Delta I=1/2$  rule, test in K $^0$  leptonic and nonleptonic decay branching ratios 9-6643  
 $\Delta S=\Delta Q$  rule expt. investigation in K $^0\rightarrow\pi^+\pi^-p$  9-17973  
 $\Delta S=\Delta Q$  rule violation in K decay, Ree obtained 9-14501  
 $\Delta S=\Delta Q$  violation in K decay 9-11032  
 Re  $\epsilon$  obtained from K<sub>L</sub> decays in extended Cabibbo model 9-14501  
 fermion-fermion scatt., invest. in covariant spinor formalism, meas. invariant amp., transformation matrices 9-4565  
 fermions, parity tests using decay mechanisms 9-4562  
 and high energy scatt. 9-6578  
 invariance, conditional, theory and application 9-73  
 invariant amp construction for interac. of part. with any spin 9-4568  
 isospin and local space-time rotations, relation 9-19184  
 isospin-nonconservation in  $^{12}\text{C}(\alpha,\alpha')^{12}\text{C}$ , cross section meas. 9-20804  
 isospin-nonconservation in  $^{16}\text{O}(\alpha,\alpha')^{16}\text{O}$ , cross section meas. 9-20804  
 Lie algebras, direct sums, generalized symmetries and deform. 9-20589  
 MacDowell 9-17929  
 Mach's principle considerations 9-20592  
 manifolds, internal, exact and broken symmetries 9-20612  
 mass spectrum from space curvature 9-2450  
 multiplets with differing mass particles, free field Langrangians 9-307  
 noncompact groups, reduction of n-fold tensor product representations 9-19186  
 O(3,1) applied to coupling of pseudoscalar mesons 9-6586  
 O(4,1) to coupling between photons and baryons 9-6586  
 O(4,2) model of Baryon structure 9-2533  
 O(4) symmetry and effects of particle mixing 9-20616  
 P, C, T, in terms of extensions of Poincare Lie algebra 9-311  
 parity nonconservation and the reaction  $n\bar{d}\rightarrow\gamma^*\text{H}$  9-4643  
 parity-violating weak interaction pot. 9-6623  
 PC violation in K decay 9-11032  
 Poincare and internal symmetry Lie algebra combination, theorems deriv. 9-19187  
 Poincare and SU(3) groups simultaneously acting 9-20612  
 positronium decay  $\rightarrow 3\gamma$ ,  $^3\text{S}_0$  C-forbidden and  $^1\text{S}_1$  C-allowed, obs. separation 9-10985  
 Regge-pole families, classification, minimal solutions to conspiracy problem 9-4605  
 relativistic and internal symmetries, combination, general theorems deriv. 9-19187  
 relativistic invariance without ang.-momentum conservation 9-15593  
 S(3), Bethe-Salpeter bootstrap model 9-2484  
 Schwinger's action principle used for derivation. 9-2449  
 SU(2,C) group, convolution integral of Fourier transforms 9-19185  
 SO(p,1) and ln(SO(p,1)), Pauli spin motion, extension 9-15419  
 SU(2, 1), Fourier analysis 9-8367  
 SU(2)  $\times$  SU(2) for N-N scatt. amplitudes 9-2531  
 SU(2), 3j symbols, Regge symmetry 9-308  
 SU(2) generalization to SU(3) in quark model taking symmetry breaking into account 9-344  
 SU(2) $\otimes$ SU(2), implied relation between 2 $^+$  and 2 $^-$  mesons 9-2476  
 SU(3) $\times$ SU(3) breaking weak nonleptonic amplitude divergences 9-6622

**Elementary particles continued**  
**symmetry continued**

- SU(3) 27-plet for baryon resonances 9-4649  
 SU(3)  $\otimes$  SU(3) breaking vel. to KN scattering 9-14498  
 SU(3) and chiral symm. breaking parameters, spectral representation 9-2477  
 SU(3) chiral dynamics from generalization of SU(2) using quark model 9-344  
 SU(3) decay predictions; importance of  $n\pi$  decay mode in split A<sub>2</sub> decay 9-20661  
 SU(3) irreducible representation derivation 9-4592  
 SU(3) symm., breaking effect on baryon magnetic moment 9-6683  
 SU(3)-symm. breaking applied to baryon-reson. octet coupling sum rules 9-11110  
 SU theory, spinor space and strong interac. 9-2455  
 T reversal in K $^0\rightarrow\pi\pi$  9-353  
 tensor decomposition of transition operator 9-6616  
 three-body syst., wave functions, construct. of polynomials 9-15429  
 time-parity violation search in polarized n  $\beta$ -decay 9-4641  
 time-reversal invariance test in inelastic scatt. e from polar. p target 9-2467  
 time-reversal invariance tested in e-d elastic scatt. 9-4588  
 U(4) model with urbaryon interactions for nonleptonic hyperon decay 9-2540  
 U(6) $\times$ U(6), Reggeization of quark number 9-6634  
 zcp invariance and K $^0$  decay 9-6641  
 $\beta$ - $\gamma$ - $\gamma$  ang. correlation test of time-reversal invariance in  $^{106}\text{Rh}$ - $^{106}\text{Pd}$  9-4732  
 K $^{\pm}\rightarrow\pi\pi\pi$ ,  $\tau$  spectra comparison, CP violation 9-11038  
 K $^0\rightarrow\pi^+\pi^-\pi^0$ , search for CP-nonconserving asymm. in momentum spectra 9-8807

**theory**

- Adler-Fubini sum rule, inconsistency of modification 9-10990  
 Adler-Fubini sum rule, modification due to finite Schwinger term 9-305  
 arbitrary spin part., Low-Burnet-Kroll theorem for soft-photon emission, proof 9-17930  
 Bethe-Salpeter bootstrap eqns., some solns. 9-2545  
 bootstrap concept, scientific status 9-20596  
 Casimir model for charged particle and quantum e.m. zero point energy of conducting spherical shell 9-16809  
 causality violation obs. in  $\pi\text{N}$  scatt. 9-2443  
 charged, coherent states in a magnetic field 9-13096  
 charged, coherent states in a magnetic field 9-2453  
 complex higher-order poles and generalized unstable particles for resonance description 9-4598  
 composite model, p-nucleus scatt. 1-21 GeV 9-2725  
 compositeness conditions in Bronzan's version of Lee model 9-6580  
 coupling const. in spinor, scalar fields; Dyson eqn. soln. 9-2444  
 covariant polarization matrix of particles with spin 2 9-4559  
 current algebra, isospin factored saturation at infinite momentum 9-306  
 Dirac eqn. Foldy Wouthuysen formalism, decoupled 2-component eqn. in Weyl rep. 9-16813  
 equivalence principle, test for unstable particles 9-4567  
 Faddeev equations, relativistic, decoupled and covariantly reduced 9-8705  
 faster-than-light particles, local quantum field theory and Lorentz invariance 9-8709  
 Feynman-diagram models for Regge-pole conspiracies 9-2486  
 form factors, properties 9-8714  
 $g_{\text{strong}}$  coupling constant determ 9-4613  
 Goldstone representation of gravitons 9-55  
 Green's functions construction in momentum space for unrenormalizable interac. 9-2454  
 isospin transformation in e.m. interactions of up to 3 hadrons 9-6621  
 Lagrangian, weak interaction, with CP violation, possible shapes 9-20591  
 lectures in theoretical high-energy physics, book 9-8341  
 Lee model, Bronzan's version, compositeness, conditions 9-6580  
 Lee model, N-quantum approx., reformulation 9-2441  
 Lee model, third sector, reduction to Fredholm integral eqn. 9-2446  
 Lorentz groups and representation theory 9-13091  
 Low-Burnett-Kroll theorem, proof for part. of arbitrary spin 9-17930  
 M functions, high-spin covariant in Dirac-Ravita-Schwinger formalism 9-8718  
 Majorana eqns. for composite systems, deduced from Bethe-Salpeter eqn., applied to H atom 9-2548  
 mass arising from Zitterbewegung, two-component fermion theory 9-14464  
 mass quantum, existence 9-2451  
 Poincare group, zero-mass representations, reduction with respect to O(3,1) 9-2445  
 Poincare group and invariant relativistic equations for massive particles, connection 9-14465  
 preludes in theoretical physics, book 9-8342  
 Regge symmetry of 3j symbols in SU(2) 9-308  
 Schwinger terms restrictions due to Lorentz covariance 9-20587  
 spectral representation and mass eigenvalues for high spin bosons 9-4564  
 spin and statistics rel., fundamental theorem for connection with Bose and Fermi fields 9-17926  
 spin density matrix, measurability 9-4566  
 spin quantization by path integration 9-17916  
 spin wave function, covariant arbitrary, and helicity couplings 9-10963  
 spin wave functions and helicity couplings 9-10963  
 spinor partial-wave amplitudes, def. parity 9-304  
 SU(3) and SU(2,1), generating functions and characters of irreducible representations 9-14466  
 SU(3) mixing restrictions implied by exchange degeneracy 9-310  
 SU(3) representation functions from 'Euler' decomposition 9-20590  
 Sugawara's theory of currents, canonical representation 9-6567  
 vector fields and current commutators, assumptions 9-6581  
 Watson's theorem rel. to final state with three strongly interacting particles 9-8717  
 wave eqns. for neutral particles and arbitrary spin, covariance and quantization 9-6579  
 wave functions for particles with higher spin 9-4563  
 Weinberg's sum rules, symmetry breaking based on Okubo's ansatz 9-6611  
 Yukawa and Fermi Hamiltonians compared 9-303  
 Zitterbewegung, origin, rel. to particle mass 2-component fermion theory 9-14464  
 e and photon as bound states of e $^+$  and e $^-$  9-4555

**Elements**

light, isotopic ratio meas. 9-19414  
 in solar system, age and r-process intensity 9-21919  
 trans-Uranium elements, unexpected oxidation states 9-12542  
 transplutonium, bibliography 9-16938

**origin**

See also *Cosmology; Thermonuclear reactions*  
 heavy nuclei 9-20139  
 heavy nuclei, empirical abundance distrib. 9-6770  
 synthesis in stars, rel. to obs. on halo stars 9-14180

**relative abundances**

110, in Pt ore neutron-induced fission, obs. 9-18160  
 in RT Aurigae, and anal. of stellar atm. parameters 9-20186  
 (CrB)Ap, star, and distrib. 9-20180  
 HD 109995 brighter horizontal branch A star, analysis 9-15301  
 HD 86986 brighter horizontal branch A star, analysis 9-15301  
 metals in globular cluster M69 rel. to colour-magnitude diagram 9-6139  
 of Moon, Surveyor VII prelim. obs. 9-17640  
 in sun's photosphere, with ground state configurations  $s^2$ ,  $s^2p$ ,  $s^2p^2$  9-12768  
 Sun, Li, Be, B, results lower than previously admitted 9-15353  
 $\alpha$  Boo atmosphere metal deficiency determ. 9-20176  
 Ba on Sun, hyperfine structure eff. 9-14249  
 Be in solar atm. 9-14271  
 CO<sub>2</sub> spect. obs. in Mars atmospheres, approx. lab. simulation 9-20225  
 Ca on Sun, hyperfine structure eff. 9-14249  
 Cl in Sun 9-15354  
 Co on Sun, hyperfine structure eff. 9-14249  
 Cu in sun 9-13289  
 Fe, in solar photospheric spectrum, forbidden Fe II lines meas. 9-14258  
 Fe in 3C 273 radiosource using models of emission-line region 9-16594  
 H $\alpha$ /NII ratio in Rosette nebula, interferometry 9-18842  
 H in 3C 273 radiosource using models of emission-line region 9-16594  
 He, primordial, in horizontal branch stars and field RR Lyrae 9-21880  
 He in 3C 273 radiosource using models of emission-line region 9-16594  
 He in young Galactic objects 9-18836  
 He solar, upper rel. to lower limit, use of estimates for nuc. cross-section 9-2075  
 K, upper atmospheric, twilight reson. emissions obs. 9-12595  
 Li, upper atmospheric, twilight reson. emissions obs. 9-12595  
 Mg in 3C 273 radiosource using models of emission-line region 9-16594  
 Mg in B stars, calc. 9-8237  
 Mn on Sun, hyperfine structure eff. 9-14249  
 N, nebular abund. 9-20162  
 Na, upper atmospheric, twilight reson. emissions obs. 9-12595  
 Ne, nebular abund. 9-20162  
 Ne in 3C 273 radiosource using models of emission-line region 9-16594  
 O, nebular abund. 9-20162  
 O in 3C 273 radiosource using models of emission-line region 9-16594  
 O<sub>2</sub> in Mars and Venus, atms., obs. 9-8277  
 V, on Sun, hyperfine structure eff. 9-14249

**Emission spectra** see *Luminescence; Spectra; X-ray spectra/emission*

**Emissivity**

graphite, pyrolytic, visible to i.r. range, correl. with struct. anisotropy 9-7970  
 i.r. by non-black plates eff. on radiative transfer by a gas 9-19080  
 i.r. spectra, from particulate surfaces of various grain types 9-7965  
 metals, rel. to optical and elec. parameters 9-21433  
 Moon and Venus, microwave rel. surface roughness 9-21947  
 random band models with pure Doppler shaped lines, behaviour for several irradiance distrib. 9-10932  
 Bi<sub>2</sub>Te<sub>3</sub> molten, photon, energy 0.5-4 eV, rel. to electronic struct. 9-16002  
 CdSb and CdTe molten, photon, energy 0.5-4 eV, rel. to electronic struct. 9-16002  
 W, thermal radiation in normal and off-normal directions, surface roughness effects 9-5577

**Emulsions**

See also *Colloids*

coagulation and emulsification, Markov process model 9-13547  
 emulsification and coagulation, Markov process model 9-13547  
 holographic, method reducing movement during processing 9-13037  
 i.r. sensitive, hypersensitization and astrophotometric applicability 9-4544  
 iso-octane-water, u.s. attenuation obs. 9-3139  
 Nujol/water, stabilized, rheological changes in aging 9-5201  
 oil-in-water, globule-size distrib., from specific turbidity and matched spectra 9-14869  
 photodevelopable silver halide, optically sensitized method, patent 9-8680  
 photographic, Eastman Kodak Ila, performance data 9-4543  
 photographic, thick, holographic props. 9-253  
 plate, electron sensitive, prep. in lab. 9-4695  
 polystyrene, polymerization due to  $\gamma$  irradiation 9-21686  
 water-oil type, stability of conducting drops in uniform elec. field 9-9566  
 Ag halide emulsions for oscillograph recording, preparation, patent 9-21232

**Emulsions, nuclear** see *Nuclear track emulsions*

**Emulsions, photographic** see *Nuclear track emulsions; Photographic materials*

**ENDOR (electron nuclear double resonance)** see *Nuclear magnetic resonance and relaxation; Paramagnetic resonance and relaxation*

**Energy bands** see *Crystal electron states/band structure; Metals/theory; Semiconducting materials; Semiconductors*

**Energy gaps** see *Crystal electron states/band structure; Semiconducting materials; Semiconductors; Superconducting materials; Superconductivity*

**Energy levels** see *Atoms/structure; Molecules; Nucleus/energy levels; Spectra*

**Energy loss of particles**

(Z)<sub>1</sub> oscs. in stopping and size effect 9-5583  
 $\alpha$  particles in tissue 9-6203  
 absorbed  $\beta$  energy distrib. around pt. source in Al and C<sub>19</sub>H<sub>21</sub> plastic 9-12034  
 amorphous solid, low energy ion range meas., rel. to deduction of interatomic potentials 9-5585  
 Bragg curve shape, particle interaction effect 9-15036  
 in bubble chamber, formulae for  $\pi$ , K, p 9-458  
 carbon, positron-electron ranges 9-12036  
 channeling in crystals, classical theory and review of types of expts. 9-7685

**Energy loss of particles continued**

chromium halides, charact. losses from continuous X-ray spectrum at high freq. limit 9-16210  
 cosmic ray muons, Cherenkov energy loss in water 9-2554  
 cosmic ray muons, ionization energy loss in plastic scintillator 9-2555  
 crystal, thin, proton channelling 9-7686  
 in crystals, planar blocking intensities correlated with continuum potentials 9-16190  
 in crystals, single, positively charged 9-1414  
 defects in irradiated-material, spatial distribution rel. to particle range 9-13668  
 DNA, low-lying collective loss, on basis of  $\pi$  electron band structs. for periodic models 9-12064  
 electron, in collision with molecules, calc. 9-13339  
 electron energy loss, mean, in elastic encounters 9-6983  
 electrons, classification and line profile 9-1412  
 electrons, excitation of polarization waves in bound states 9-18575  
 electrons in thin foil, with retardation of e.m. field 9-7689  
 equilibrium charge distribution in heavy element ion beams after passing through solids 9-10834  
 fast charged, channelling, correspondence principle 9-7687  
 fast neutron beam LET distrib. in tissues, calc. 9-18948  
 gases, range of 5-50 keV heavy ions 9-14739  
 glass, flint, rel. to enthalpy evaluation and sputtering ratios 9-17361  
 H<sub>1</sub><sup>+</sup>-H<sub>1</sub><sup>0</sup> and H<sub>1</sub><sup>0</sup>-H<sub>1</sub><sup>+</sup> conversions in energy range 7-40 keV, use of metallic film 9-17363  
 hydrocarbons, condensed aromatic, monochromatic e energy loss 9-13539  
 inert gas ions, low-energy, penetration and capture in polycryst. W. 9-5590  
 ionization of KCl coating on foils used to meas. energy of ultrarelativistic part. 9-11143  
 ions, channelled, scattering effects 9-5586  
 ions, heavy, electronic stopping cross section, periodic dependence 9-7688  
 ions, heavy, stopping power theory in gases and solids 9-920  
 ions, periodicity rel. to nuclear charge 9-9867  
 KCl(Br), high-energy protons channelling 9-7680  
 light particles channelled through crystal 9-5584  
 liquid lines for reactor, poor thermal insulation 9-19361  
 metals, positron-electron ranges 9-12036  
 Monte Carlo calcs. of particle motion in 3-dimensional space 9-16690  
 negatively charged particles, lattice directed trajectories 9-12032  
 nuclear emission, due to ionization, 5-24 GeV/c p and 5 GeV/c  $\pi$  comparison 9-18047  
 polymer film, photoresist, ion beam, scatt. effects 9-13813  
 protons and deuterons of identical velocity 9-21452  
 range effect in  $p$ - $\nu$  angular correlation experiment 9-19191  
 rare earth metals, positron-electron ranges 9-12036  
 relativistic charged particle in mag. field, damping with self-interaction 9-17857  
 straggling distrib. in extremely large energy losses 9-2709  
 thickness meas. by  $\alpha$  energy loss 9-2560  
 tissue, of  $\alpha$  particles 9-6203  
 transition metals, (Z-21-30), stopping power meas. at 5-12 MeV 9-17364  
 transition metals, charact. electron energy loss spectra 9-15040  
 e energy analyser with retarding pot. filter 9-12031  
 $\pi^-$  beam in water, LET spectrum and Bragg curve calc. 9-21223  
<sup>235</sup>U fission fragments, range determ. in Lexan detector 9-20820  
 Ag, electron energy-loss spectra from inelastic scattering in LEED obs. 9-21451  
 Al, e energy losses and optical data 9-16191  
 Al, liquid and solid, charact. loss spectra of 8 keV electrons 9-7249  
 Al, proton dechannelling at stacking faults, H accumulation 9-16102  
 Al<sub>2</sub>O<sub>3</sub>, range of electrons rel. to energy, 0.5-4 KeV 9-19872  
 Al films, charact. losses of electrons, rel. to thickness, influences of surfaces 9-5588  
 Al foils, 0.3-1 MeV e beam, Monte Carlo calc. 9-5587  
 AlSiB, in channelling of H and He ions 9-9868  
 Ar atom, spectra for keV electrons interaction with electron shell 9-18150  
 Ar atoms, spectra for keV electrons interaction with electron shell 9-11398  
 Au, <110> channelled alpha-recoil atoms 9-3546  
 Au, electrons, rel. to sample thickness 9-3545  
 Au, energy structure in axial channelling of 30 keV protons 9-7690  
 Au, liquid and solid, charact. loss spectra of 8 keV electrons 9-7249  
 Be, of 20 keV electrons, rel. to K edge 9-15182  
 Be, range and dE/dx of C, N, O, F, and Ne at 500 keV to 2 MeV 9-9871  
 BeO, of 20 keV electrons, rel. to K edge 9-15182  
 BeO, range of electrons rel. to energy, 0.5-4 KeV 9-19872  
 Bi, liquid and solid, charact. loss spectra of 8 keV electrons 9-7249  
 C-Al barrier, electron current calc., applic. of perturbation method 9-18572  
 C, range and dE/dx of O and Ne at 500 keV to 2 MeV 9-9871  
 Ca, 5-12 MeV protons and deuterons, stopping power 9-17364  
 CsI(Tl), stopping power and luminescent-response calc. 9-12035  
 Cu-Al barrier, electron current calc., applic. of perturbation method 9-18572  
 Ga, liquid, charact. loss spectra of 8 keV electrons 9-7249  
 GaP, e energy losses and optical data 9-16191  
 in GaP, loss intensities of 50 keV electrons, deviations at low energies 9-7692  
 GaSb, in channelling of H and He ions 9-9868  
 Ge, e energy losses and optical data 9-16191  
 Ge, proton transmission along (100) and (110) channels in crystal lattice, energy and angular distributions 9-16192  
 Ge, tunnelling of 6.72 MeV protons 9-21448  
 Ge\* atoms in Ge target, band gap effects 9-5589  
 H ion, stopping power Z depend. in arbitrary medium, 0.5-8 MeV/a.m.u. 9-6990  
 He ion, stopping power, Z depend. in arbitrary medium, 0.5-8 MeV/a.m.u. 9-6990  
 Hg, charact. loss spectra of 8 keV electrons 9-7249  
 In, liquid, charact. loss spectra of 8 keV electrons 9-7249  
 InAs, in channelling of H and He ions 9-9868  
 InSb, in channelling of H and He ions 9-9868  
 KBr, e energy losses and optical data 9-16191  
 KBr, of electrons, rel. to band struct. and optical consts. 9-5591  
 KBr, tunnelling of 6.72 MeV protons 9-21448  
 KCl, tunnelling of 6.72 MeV protons 9-21448



**Energy loss of particles continued**

- Kr atom, spectra for keV electrons interaction with electron shell 9-18150  
 Kr atom, spectra for keV electrons interaction with electron shell 9-11398  
 Li ions, vel. depend., method and mathematical anal. 9-21450  
 Mg, range of electrons rel. to energy, 0.5-4 KeV 9-19872  
 MgO, range of electrons rel. to energy, 0.5-4 KeV 9-19872  
 NaCl, high-energy protons channelling 9-7680  
 NaCl layer on Al film, mean free path of electrons 9-19939  
 NaI(Tl), stopping power and luminescent response calc. 9-12035  
 Ne, atoms spectra for keV electrons interaction with electron shell 9-18150  
 Ne, atoms spectra for keV electrons interaction with electron shell 9-11398  
 O<sub>2</sub>, high resolution electron energy-loss spectrum 9-784  
 Pb, 10<sup>11</sup>eV, cosmic rays, interaction free path calc. 9-18025  
 Rh-Pd-Ag, alloy, energy loss spectra obs., E<sub>e</sub>=200-800 eV 9-16194  
 Si, heavy particle range- energy table 9-7693  
 Si, p. energy-loss straggling 9-13816  
 Si, proton transmission along {100} and {110} channels in crystal lattice, energy and angular distributions 9-16192  
 Si tunnelling of 6.72 MeV protons 9-21448  
 Sr, of electrons 9-3547  
 Ti, D<sup>+</sup> backscattering energy distrib. 9-12037  
 Xe, solid, of 51 keV electrons, rel. to excitonic spectra and optical consts. 9-7694  
 Xe atom, spectra for keV electrons interaction with electron shell 9-11398  
 Xe atom, spectra for keV electrons interaction with electron shell 9-18150

**Enthalpy** see *Thermodynamic properties*

**Enthalpy measurement** see *Calorimetry*

**Entropy**

See also *Thermodynamics*

- and 'exergy', confusion of terms 9-2244  
 Bose and Fermi atom adsorbed monolayers on cryst. 9-5255  
 crystals, small classical 9-3531  
 diagram, curved axes, thermodynamic evolutions calculations, flow of perfect gas mixtures 9-5113  
 ΔS=0?, comment 9-15475  
 error parameters 9-8348  
 evolution in spin systems and non Markovian effects 9-20356  
 ferromagnets, magnetic moment diffusion and entropy production 9-10108  
 Gibbs entropy as measure of uncertainty at microscopic level 9-6328  
 gravitating gas of point particles, absence of maximal entropy state 9-20138  
 ideal, organic compounds, estimation 9-3050  
 liquid, from intermolec. potential 9-979  
 non-equilibrium function 9-15434  
 periodic systems of hard disks and spheres, solid phase 9-8459  
 photosynthesis, entropy balance 9-16632  
 production inequality, thermodynamics of directed continuous media 9-20345  
 statistical theory of production in non-isolated system 9-20353  
 thermodynamic classical, of irreversible processes as a special case of entropy-free thermodynamics 9-8518  
 Al, anharmonic effects, data anal. 9-21434  
 Pb, anharmonic effects, data anal. 9-21434

**properties of substances**

- acetaldehyde, temp.-entropy diagram 9-18325  
 adsorbed large atoms, configurational 9-3209  
 ethyl chloride, temp. - entropy diagram 9-18326  
 hydrocarbons, saturated liquid prediction 9-19629  
 molar surface, rel. to homogeneous nucleation of liquid 9-14884  
 silica, vitreous, configurational entropy of random network model 9-14887  
 CS<sub>2</sub> temp.-entropy diagram up to 750°K, 300 atm. 9-21134  
 CuSO<sub>4</sub>.5H<sub>2</sub>O, in mag. fields, 0.4°-4.2°K 9-9840  
 D<sub>2</sub>O, dimerization, 150°-500°K 9-7224  
<sup>3</sup>He-<sup>4</sup>He liquid mixtures, light scatt. by entropy fluctuation 9-5204  
 Ne on Xe surface 9-9622  
 α-NiSO<sub>4</sub>.6H<sub>2</sub>O, 0.4°-4.2°K, 0-90 kG fields 9-19862  
 Si, E-centre annealing kinetics 9-7505  
 TiO<sub>2</sub>-aqueous soln. interface double layer, obs. 9-7351  
 UO<sub>2</sub>, mag. entropy 9-9846

**Epitaxy**

See also *Crystals/growth*

- AlAs-GaAs heterojunction structures, coherent radiation 9-10868  
 crystallization kinetics during rapid cooling of melt 9-13613  
 doping density vs. depth meas. 9-18623  
 f.c.c. metals, growth on KCl cleaved in u.h. vacuum, surface defects effects 9-5241  
 f.c.c. metals, formation on alkali halides, influence of impurities 9-21268  
 f.c.c. metals, growth on KCl, KBr, and KI crystals 9-7377  
 film, thermolec. power, theory 9-15130  
 impurity influence on formation of single-crystal films 9-21268  
 layers, obs. by X ray diffraction 9-3198  
 liquid, solvent distribution in unstirred melt, eff. on growth rate 9-18430  
 metal film growth on alkali halides, effect of gas ads. 9-3199  
 metal films growth on alkali halides, effect of gas ads. 9-16044  
 misorientation from stacking fault geometry 9-11771  
 p-n junctions, growth by UHV sublimation 9-13899  
 polyamides on quartz 9-1158  
 polytypic crystals, nucleation and epitaxial growth 9-13609  
 salicylic acid, on muscovite 9-1159  
 Si, growth in horizontal reactors, theory 9-7378  
 substrate temperature on hotplate used for growth 9-11807  
 Ag, f.c.c., growth on cleavage face of mica 9-5242  
 Al films, orientation dependence on substrate effects 9-1105  
 Au, f.c.c., growth on cleavage face of mica 9-5242  
 Au films, elec. conductivity, size effects in temp. variation 9-9930  
 Au films on colour-centred NaCl, obs. 9-9615  
 Au films on MoS<sub>2</sub>, angular distribution of Au nuclei 9-9614  
 Au on KCl, KBr, KI in u.h. vac. 9-7310  
 CdI<sub>2</sub>, epitaxial growth 9-13609  
 CdS, cubic, growth on InSb and CdS substrates 9-14910  
 CdS films, vapour phase chemical reaction growth technique 9-9616

**Epitaxy continued**

- Cu, f.c.c., growth on cleavage face of mica 9-5242  
 Cu film, epitaxially twinned, on sapphire, growth 9-1104  
 Fe-Ni-Co monocrystalline alloy films, growth and coercive force 9-12298  
 n-GaAs, heavily doped, electron mobility 9-17391  
 GaAs<sub>1-x</sub>P<sub>x</sub> layers on GaAs, compositional inhomogeneities 9-14895  
 GaAs film growth on GaAs substrate causing high resistance layer 9-11773  
 GaAs films, impurity transfer in vapour growth and carrier-conc. profiles 9-11772  
 n-GaAs films, photoluminescence 9-10265  
 GaAs layers, dislocations 9-1219  
 GaAs p-n structures, high-efficiency electroluminescence 9-15192  
 GaAs substrate, annealing effects, 800-1200°C 9-11950  
 GaAs tunnel diodes, high-power, prep. and characts. 9-12167  
 p-GaP-O-Zn electroluminescent diode, patent 9-10257  
 Ge film, growth from supercooled droplets 9-13580  
 Ge layers on GaAs by GeH<sub>4</sub> pyrolysis 9-19670  
 Ge mirror smooth layers on GaAs by disproportionation reaction 9-19671  
 InP, films, stacking disorder 9-9617  
 InP, growth on GaAs in open flow system 9-5243  
 Ni film, polycryst., double diffraction 9-5244  
 Ni films, secondary twinning in c. diff. patterns 9-9618  
 PbTe film on KCl, growth mechanism 9-1106  
 Pd, f.c.c., growth on cleavage face of mica 9-5242  
 Si, growth, light irradiation effects 9-11808  
 Si, technology advances 9-7339  
 Si film, chemically grown, nucleation kinetic meas. on (100) surfaces, using molecular beam techniques 9-21298  
 Si film, growth, continuous method, and thermodynamical anal. 9-14896  
 Si film growth equilibria of nuclei formed during H<sub>2</sub> reduction of SiCl<sub>4</sub> 9-11774  
 Si film on spinel, mech. and elec. props. 9-7815  
 Si growth on Si substrates, heater, patent 9-21269  
 Si vapour, applic. to semiconductor device technology 9-13612  
 SiC crystallites on Si(111) surface obs. by electron diffraction 9-5288  
 SiC films, blue photo- and electroluminescence 9-5972  
 SiC p-n junctions, solution grown 9-13902  
 SiCl<sub>4</sub>-H<sub>2</sub> vapour-gas system in crystal growth, conc. ratio in saturator of epitaxial equipment 9-21301  
 ZnTe films on CdS, prep. by vapour transport method 9-5245  
 ZrO<sub>2</sub> films on Zr in O<sub>2</sub> atm., 300°C 9-9619

**Equations**

See also *Differential equations; Integral equations*

- Bethe-Salpeter, partial-wave, soln. and reduction to linear systems 9-13106  
 Bethe-Salpeter, use of algebraic structure, treatment of singularities 9-17909  
 Boltzmann and transport eqns., solns. 9-8421  
 Boltzmann eqn., quantum-mechanical description, avoidance of singular and non-physical terms 9-19336  
 Boltzmann spectrum of hard sphere gas 9-4256  
 Burger's eqn., harmonic analysis, spectral form estimated 9-8361  
 cubic, computation of roots, book 9-8363  
 cubic secular eqn. for mol. vib., extremal force consts. 9-11439  
 diffusion, relativistic 9-6343  
 e<sup>2</sup>=e<sup>2</sup>e<sup>2</sup>, soln. where x, y are non-commuting operators 9-8360  
 eikonal, geometric-acoustics, frequency dependent solns. 9-2205  
 gap eqn. in supercond. theory, existence proof 9-19895  
 of heat transfer, non-linear system 9-17821  
 iterative solns. using trial operators 9-10616  
 Korteweg-de Vries, conservation laws, constants of motion, relation to Sturm-Liouville eigenvalue problem 9-6279  
 Korteweg-de Vries, transformation relating solns. to a similar nonlinear eqn. 9-6278  
 Laplace Cauchy problem, chapter in book 9-12861  
 linear, of mathematical physics, variational formulation 9-20374  
 linear, use of Vandermonde determinant to accelerate iterative method of soln. 9-40  
 linear homogeneous, group props. 9-8368  
 linear system, iterative process for soln. 9-35  
 Liouville eqn. for collisionless syst. of gravitationally interact. part., soln. 9-18833  
 Lippman-Schwinger, partial-wave, soln. and reduction to syst. of linear eqns. 9-13090  
 Margules, multicomponent 9-108  
 motion of space vehicles while approaching and meeting on orbits 9-4268  
 Nambu, infinite component, similarity transformation between two models 9-6317  
 neutron transport, numerical methods of solution using P<sub>n</sub> approximation 9-11344  
 Newton-Liouville for system of gravitating particles, all solns. 9-14184  
 partial wave eqn. for low energy π-π scatt., approx. solns. 9-14513  
 Poisson, for system of gravitating particles, all solns. 9-14184  
 Poisson eqn. for collisionless syst. of gravitationally interact. part., soln. 9-18833  
 Poisson-Boltzmann, variational soln. 9-7252  
 quartic, factorization method of soln., book 9-8363  
 spreading loss for rays specularly reflected from curved surface 9-2214  
 Sturm-Liouville, eigenfunctions, stability of functionals 9-12864  
 Van der Pol, cycle asymptotic representation for small damping 9-8362  
 wave, non linear, vibr. membrane anal. 9-6375  
 wave, of sound in viscous media, lumped element transmission line model 9-18359  
 Weiner Hopf, simultaneous, and appl. to diff. in e.m. wave theory 9-187  
 H atom, generalised, from symmetry group of integral eqn. 9-9154

**Equations of state**

See also *Thermodynamics*

- empirical, for earth's lower mantle and core 9-21748  
 finite difference method for soln. 9-1066  
 fluid, pure chemical, PVT eqns. review 9-11740  
 fluids, exponential virial eqn. 9-14741  
 hard-sphere square-well systems, N depend. in Monte Carlo calc. 9-14369  
 ionized monolayers at air/water and oil/water interfaces, low surface press. 9-9500  
 many-body systems, classical, rigorous bounds 9-20363  
 Morse potential parameters, estimation from critical constants and acentric factor 9-9438

**Equations of state continued**

- plasma, fully ionized quantum 9-860
- star, superdense, possible 'third' family 9-8251
- virial coeffs., interrelation 9-952
- wafer 9-980
- water substance from 100 to 1000°C, simplified 9-981

**gases**

- <sup>4</sup>He, third virial coeff. calc. from Wiener integrals 9-7225
- Boltzmann, for hard-sphere gas, reduction of singular integral eqn., to Fredholm eqns., use of Cauchy-type singularities 9-8456
- electron, numerical evaluation for pair creation 9-19005
- gas-surface second virial coeff., quantum corrections 9-9601
- inert gases, second dielec. virial coeff. 9-13493
- methanes, halogen-substituted, 2nd virial coeff. determ. 9-7070
- mixtures, nonuniform, nonequilib. theory 9-11658
- naphthalene in compressed ethane and N<sub>2</sub>O 9-13485
- plasma, second virial coeff., general expression 9-9344
- second virial coeff. determ. from sound velocity 9-21235
- statistical mech., use of graphs 9-92
- virial coeff., fifth, quantum correction 9-13486
- virial coeff., second, from boiling point to room temp., from value at one temp., calc. method 9-15972
- virial coefficients and calc. of thermodynamic props. at press > 12kbar, temp., > 700°K 9-21133
- virial coeffs., second, of non-polar mats. 9-17157
- volumetric props. review 9-9439
- Ar and mixture, virial coeff., second, from boiling point to room temp., from value at one temp., calc. method 9-15972
- Ar and methane, corresponding states 9-9440
- D<sub>2</sub>O, virial coeffs., 150°-500°C 9-7224
- Kr and mixture virial coeff., second, from boiling point to room temp., from value at one temp., calc. method 9-15972

**liquids**

- cybotactic group, C<sub>v</sub> deduced, molecular interact. ignored 9-7247
- water, Rice and Walsh eqn., limitations and extensions 9-11680
- Hg electrical resistivity, elevated temperatures and pressure 9-3075

**solids**

- cubic, generalizations 9-1388
- Mie-Grunisen, simple derivation 9-1400
- periodic systems of hard disks and spheres 9-8459
- polyethylene, P, v, T eqn. 9-17239
- Co, magnetic, near Curie pt. 9-10127
- H, quantum theory 9-19850

**Erbium**

- elastic moduli and u.s. attenuation rel. to mag. transitions 9-7517
- ions, ErIV 4f<sup>11</sup> free-ion levels from LaCl<sub>3</sub>:Nd<sup>3+</sup> spectra and calc. 9-4831
- lattice sp. ht. calc. from phonon freq. distrib. curves 9-16165
- lattice sp. ht. calc. from phonon freq. distrib. curves 9-7635
- magnetic structure and form factor meas. by n. diff. 9-13971
- silicate glass coactivation with Ho and Yb 9-4476
- thermal conductivity and Lorenz function 9-7673
- Er,<sup>119</sup>Sn, Mossbauer spectra, hyperfine mag. fields 9-5890
- Er<sup>3+</sup>, Zeeman effect in GdCl<sub>3</sub> 9-3888
- Er<sup>3+</sup> in Ca(Cd)F<sub>2</sub>, exchange interaction 9-1716
- Er<sup>3+</sup> in divalent fluorides, luminescence spectra 9-3916
- Er<sup>3+</sup> in CaWO<sub>4</sub>, e.p.r., spin-Hamiltonian parameters determ. 9-12500
- Er<sup>3+</sup> in CdF<sub>2</sub>, blue fluorescence, competitive excitation mechanisms 9-3925
- Er<sup>3+</sup> in La(Cl,Br), modified Orbach relax. process 9-12317
- Er<sup>3+</sup> in SrCl<sub>2</sub>, e.s.r. 9-1863
- Er<sup>3+</sup> in YVO<sub>4</sub>, e.p.r. 9-16461
- Er<sup>3+</sup> in ZnS, fluorescence 9-10244

**Erbium compounds**

- E-FeO<sub>3</sub>, domain-wall energy meas. at 25°C 9-14001
- ErAl, mag. props. and mag. struct. 9-1702
- ErAl, n.m.r. of <sup>27</sup>Al, Knight shift and susceptibilities, temp. 9-3969
- ErAl<sub>2</sub>, mag. props. 9-7898
- ErCl<sub>3</sub>, abs. spectra in far i.r. 9-1776
- ErCo<sub>5</sub>, ferrimag., magnetization, 4.2-1250°K, up to 30 kOe 9-5848
- Er<sub>2</sub>Co<sub>7</sub>, ferrimag., magnetization 4.2-1250°K, up to 30 kOe 9-5848
- Er<sub>2</sub>Co<sub>7</sub>, ferrimag., magnetization, 4.2-1250°K, up to 30 kOe 9-5848
- ErFeO<sub>3</sub>, domain wall energy, direct meas. method 9-3824
- ErFeO<sub>3</sub>, metamagnetic props. 9-16383
- Er<sub>2</sub>O<sub>3</sub>, magnetic structures 9-17463
- Sc-Ho alloys, mag. structure comp. dependence 9-5802

**Ergodic theorem** *see* Statistical mechanics**Errors** *see* Measurement errors; Random processes**Esaki diodes** *see* Semiconducting devices/tunnel and interface devices**Esaki effect** *see* Semiconducting devices/junctions**Etalons** *see* Interferometers**Etching** *see* Crystals/etching**Ether drift** *see* Relativity/special; Velocity/light**Ettinghausen effect** *see* Magnetothermal effects**Europium**

- ion in octacoordinate sites, symmetry, potential and level splittings 9-14018
- magnetic transition, first order obs. from Mossbauer effect meas. 9-15148
- muonic atom, effects of rotation and excitation of nucleus on spectrum 9-11432
- <sup>151</sup>Eu, isomer shift, chemical effects 9-3842
- CaF<sub>2</sub>:Eu<sup>2+</sup> microwave-modulated fluorescence, 9.5 GHz 9-1828
- in Ca<sub>3</sub>(Mg<sub>13</sub>(PO<sub>4</sub>)<sub>13</sub>), luminescence 9-3914
- in Ca<sub>3</sub>(PO<sub>4</sub>)<sub>2</sub>, luminescence in  $\alpha$ - and  $\beta$ -phases 9-3914
- Eu<sup>2+</sup> in alkaline earth halophosphate phosphors, prep. and luminescence 9-21643
- Eu<sup>2+</sup>-activated alkaline-earth aluminates, fluorescence 9-21650
- Eu<sup>2+</sup>-activated BaB<sub>2</sub>O<sub>7</sub>, fluorescence 9-20004
- Eu<sup>2+</sup>-activated silicates, fluorescence 9-21649
- Eu<sup>2+</sup>-Eu<sup>3+</sup> interconversion in silicate glasses, absorption spectra 9-14051
- Eu<sup>3+</sup>, in POCl<sub>3</sub>-SnCl<sub>4</sub> soln., fluorescence spectra and radiative lifetimes 9-21217
- Eu<sup>3+</sup>, Raman spectra, scatt. tensor of transitions rel. to hosts crystal field symmetry 9-21634
- Eu<sup>3+</sup> activated in rare earth vanadates, luminescence spectra 9-20003
- Eu<sup>3+</sup> activated thorium, alkali metal vanadates, luminescence 9-20002
- Eu<sup>3+</sup> in aq. soln., electronic energy levels 9-16006
- Eu<sup>3+</sup> in EuAlO<sub>3</sub>, crystal-field splitting 9-21570

**Europium continued**

- Eu<sup>3+</sup> in rare earth-oxygen-sulphur cpds., prep. and luminescence 9-21647
- Eu<sup>2+</sup> in SrF<sub>2</sub>, vibronic transitions and Zeeman effect 9-10212
- Eu<sup>2+</sup> in CaF<sub>2</sub>, e.s.r. effect on opt. Faraday rotation, saturation phenomena and relaxation effects 9-7945
- Eu<sup>2+</sup> in BaF<sub>2</sub>, e.p.r., hyperfine coupling constant of <sup>151</sup>Eu<sup>2+</sup>, temp. depend. 9-12502
- Eu<sup>2+</sup> in CaF<sub>2</sub>:Eu<sup>2+</sup>, Ho<sup>3+</sup>, fluorescent decay, Ho conc. dependence 9-15187
- Eu<sup>2+</sup> in KCl, absorption and emission spectra, multiphonon structure, lattice freq. shift effects 9-16410
- Eu<sup>2+</sup> in Sr<sub>2-x</sub>Eu<sub>x</sub>(PO<sub>4</sub>)<sub>3</sub>:SiO<sub>2</sub>, energy transfer between non-equivalent sites 9-15189
- Eu<sup>2+</sup> in SrF<sub>2</sub>, e.p.r., hyperfine coupling constant of <sup>151</sup>Eu<sup>2+</sup>, temp. depend. 9-12502
- Eu<sup>2+</sup> in Yb, e.p.r., g-shift and exchange integral calc. 9-12504
- Eu<sup>3+</sup> in BaF<sub>2</sub>, spin-lattice relax. at low and high temp. 9-5859
- Eu<sup>3+</sup> in KTaO<sub>3</sub> and KTa<sub>0.9</sub>Nb<sub>0.1</sub>O<sub>3</sub>, fluorescence 9-10242

**Europium compounds**

- chalcogenides, Faraday effect 9-5878
- chalcogenides, mag. and optical props. 9-12328
- chalcogenides, mag. red shift of absorpt. spectrum 9-14033
- chalcogenides, optical investigation 9-16391
- Eu in Eu<sub>2</sub>O<sub>3</sub> and lower valence states, chem. shift 9-15852
- europium dibenzylmethanate, luminesc. in alcohol solns., level transition rates, obs. 9-18367
- EuSe, optical constants 9-7933
- isomer shifts, chemical effects 9-3842
- theonyltrifluoroacetate, luminescence props. 9-16016
- chalcogenides, exchange magnetostriction 9-7904
- chelates in polymethylmethacrylate, luminesc. under strong excitation 9-2899
- Eu-chalcogenide alloys, anomalous opt., mag. and transport phenomena 9-9878
- Eu-Al intermetallic cpds., mag. props. 9-10095
- Eu-Yb(Ba) alloys, Mossbauer effect 9-7957
- Eu<sub>2</sub>O<sub>3</sub>, semicond. 9-7796
- Eu Ga garnet: Fe<sup>3+</sup>, exchange interaction orbital anisotropy 9-1682
- Eu<sup>3+</sup> chelates, <sup>241</sup>Am-doped,  $\alpha$ -particle fluoresc. 9-1829
- EuAlO<sub>3</sub>, paramagnetic anisotropy and crystal-field splittings 9-21570
- EuBa, polaron ferromagnetism 9-1660
- EuCl<sub>3</sub>, cryst. struct. 9-11850
- EuFe garnet, hyperfine field interac. of 21.7 keV level of <sup>151</sup>Eu from Mossbauer meas. 9-16401
- Eu<sub>0.95</sub>Gd<sub>0.05</sub>N, band conduction and critical scatt. 9-9886
- Eu<sub>2-x</sub>Gd<sub>x</sub>S, ferromag. possible source for prod. of polarized electron beams by field emission 9-7865
- Eu<sub>2-x</sub>Gd<sub>x</sub>S, magneto-optic and magnetic props., origin and mechanisms 9-7879
- EuLu<sub>2</sub>O<sub>4</sub>, mag. props., 1.7-300°K 9-3778
- EuO-4at.%Gd alloy, Curie temp. pressure dependence rel. to exchange interactions 9-18672
- EuO, optical phonons in ferromagnetic insulators, temp. depend. wavelength shift 9-7946
- EuO, photoconduction 9-7856
- EuO, semicond. 9-7797
- EuO Kerr effect, on mirror substrates 9-3860
- EuO magnetic effects on photoconduction 9-19935
- EuO photoconductivity, low-temp., magnetic effects 9-12212
- EuO resonance linewidth, temp. dependence, 2-300°K 9-10269
- EuO thermal cond., 50°-300°K 9-16184
- Eu<sub>2</sub>O<sub>3</sub>, isomer shift, temp. variation, non-linearity and hysteresis effects 9-1718
- EuS, diffuse scatt. of light by ferromag. domains 9-10180
- EuS, photoconduction 9-7856
- EuS, spin corrls. 9-13964
- EuS films, mag. hysteresis meas., thickness dependence 9-18678
- EuS photoconductivity, low-temp., magnetic effects 9-12212
- EuS scaling laws and impurity effects near critical point 9-16345
- EuSe, mag. struct. from n. diff. expts 9-14011
- EuSe, metamagnetic transitions, field- and temp.-depend. 9-7899
- EuSe, photoconduction 9-7856
- EuSe, work function and cathodoluminescence 9-5970
- EuTe, antiferromagnetic resonance, angular dependence 9-1850
- EuTe, optical constants 9-7933

**Evaporation***See also* Vaporization

- anode, under pulse regime 9-19557
- cyclotron target, separation of radioactive elements 9-18392
- of dielectric channel due to pulsed elec. discharge 9-19558
- droplets in spheroidal state on hot surface, rate expression 9-21247
- electron gun application 9-12979
- metal particle prep. in Xe gas 9-5220
- processes, and energy characteristics mass spectral study of relatively involatile materials 9-664
- source, folded baffled boat 9-7328
- tungstate matrix cathode, rel. to composition 9-5780
- vapour, meteorological meanings in literature 9-12579
- water and soil surfaces, rate estimation with sonic anemometer 9-15243
- zone movement in drying process, anal. by conjugate heat cond. with moving boundary 9-7302
- Ag film, temperature 9-17243
- C from Th dispenser cathode in Auger emission spectroscopy 9-7867
- Fe-Cr alloy, of Cr, under vacuum, kinetics 9-19658
- Fe-Cu alloy, of Cu under vacuum, kinetics 9-19658
- Fe-Mn alloy, of Mn under vacuum, kinetics 9-19658
- Fe-S alloy, of S, under vacuum, kinetics 9-19658
- Fe-Si alloy, of S, under vacuum, kinetics 9-19658
- Fe-Sn alloy, of Sn, under vacuum, kinetics 9-19658
- NaCl, single crystals, mechanism 9-11751
- Ni-Cr-Cu-Al alloy, vacuum fractionation model. 9-7342
- NiCr, thin film resistors, flash evaporation 9-15393
- Pb film, by ionization gauges 9-21264
- Si film, by vacuum-arc discharge 9-17244
- Sn film, rate meas. by ionization gauges 9-21264
- ThC cathode, rate calc. 9-3754
- Ti film, through thermoelectronic emission 9-12811
- W, field, in ion microscope, surface atoms cohesion 9-5784
- W carrier, evaporation of larger amount of metal 9-11749
- Y from W, rel. to adsorption and evaporation 9-3216



**Evershed effect** see *Sunspots*

**Examination of materials** see *Electron diffraction examination of materials; Electron microscope examination of materials; Neutron diffraction examination of materials; X-ray examination of materials*

### Exchange interactions

alloys, dil., e.p.r. theory using freq.-dependent susceptibility interpretation 9-12497  
 alloys, dil. magnetic, spin correlations at low temps. 9-21562  
 Alnico alloys, and magnetostatic interactions between particles 9-18676  
 Anderson model, ground-state energy calc. by cluster variation method 9-13944  
 aromatic mol. in sol., electron exchange rate const., NMR meas. 9-20950  
 atoms, two Coulomb centres problem at large centre separ., multipole expansion for energy, quasi-crossings of curves 9-4829  
 atoms or mols., perturbation theory 9-9108  
 p-benzoquinone-p-benzoquinone radical anion in sol., electron exchange rate const., NMR meas. 9-20950  
 classical impurity spin interacting with free electron gas, exact solution 9-16216  
 conduction electron spin-impurity- electron spin correlation function using t-matrix formalism 9-21560  
 duroquinone-duroquinone radical anion in sol., electron exchange rate const., NMR meas. 9-20950  
 effective, estimation using Anderson model 9-13942  
 electron correlations over whole range of metallic densities 9-12071  
 electronic spin polarization around mag. impurity calc. using perturbation theory 9-7872  
 excitons, two-body representation, and effect on spectrum 9-12066  
 ferromagnetic metals, s-d contrib. to thermo-e.m.f. 9-3719  
 ferromagnets, effective Hamiltonian and spin wave energy 9-12251  
 impurity e.p.r. in metals, theory using freq.-dependent susceptibility interpretation 9-12497  
 ion-atom, high-energy collision with electron exchanges, scatt. eqns. and amp., coupling potentials 9-11406  
 magnetic alloy, dilute s-d model in Hall anomaly calc. 9-16228  
 in magnetic electron scatt., elastic, and in mechanism of polarization of scatt. beam 9-12256  
 magnetic ions, indirect exchange of localized spins via conduction electrons with separated Fermi spheres 9-1635  
 magnetic moments, indirect exchange interactions 9-16340  
 metals, coupling integral rel. to conduction-electron polarization 9-21561  
 nuclear spin, effect on dynamic nuclear polarization 9-1719  
 rare earth intermetallic cpds., interband mixing, exptl. evidence 9-14116  
 between rare earth ions, indirect 9-1715  
 rare earth metals, anisotropic and anisotropy of mag. props 9-1645  
 rare-earth ions in La halides 9-1697  
 Ruderman-Kittel-Kasuya-Yosida (RKKY), mag. field dependence 9-5792  
 rutile, reduced, paramag. centre-charge carrier interaction 9-1864  
 s-band, strongly correlated, translationally uniform mag. solns., using modified RPA 9-1633  
 s-d interaction Hamiltonian, cluster variation calc. method 9-17451  
 transition metal complexes, unrestricted Hartree-Fock molecular-orbital treatment 9-12232  
 Au-Fe alloys, dil., magnetoresistance rel. to s-d scatt. model 9-5805  
 Au-Mn alloys, dil., magnetoresistance rel. to s-d scatt. model 9-5805  
 BaFe<sub>12</sub>-xAl<sub>2</sub>O<sub>19</sub> rel. to var. of saturation magnetization with Al substitution 9-16366  
 CaF<sub>2</sub>:Er<sup>3+</sup>, intercentre exchange probability temp. dependence 9-1716  
 CdF<sub>2</sub>:Er<sup>3+</sup>, intercentre exchange probability temp. dependence 9-1716  
 Ce, rel. to spin-lattice relax. of 4f electrons 9-12316  
 CeAl<sub>2</sub>, Laves phase cpd., 9-12247  
 β-Co epitaxial films, spin-wave resonance 9-20011  
 Cr-Fe alloys, dil. from Fe impurity e.p.r. 9-1858  
 CrF<sub>2</sub>, integrals, in paramagnetic phase 9-1643  
 Cu-Fe alloys, dil., and Ising model in sp. ht. meas. interpretation 9-18563  
 Cu complexes, trinuclear, containing transition metals, antiferromag. interaction 9-10148  
 Cu<sup>2+</sup> ion, interac. betw. 3d<sup>8</sup>, 4p, 3d<sup>9</sup> configs. under T<sub>d</sub> symm., eff. 9-17468  
 Eu Ga garnet:Fe<sup>3+</sup>, strong orbital anisotropy 9-1682  
 Eu<sub>1-x</sub>Gd<sub>x</sub>Se, explanation for anomalous magneto-optic and mag. props. 9-7879  
 EuO 4at.% Gd alloy, effect on Curie temp. pressure dependence 9-18672  
 Fe epitaxial films, spin-wave resonance 9-20011  
 FeF<sub>2</sub>, integrals, in paramagnetic phase 9-1643  
 H-H spin-exchange cross section, meas. by variation of T<sub>1</sub> and T<sub>2</sub> with at. density 9-11419  
 He, e scatt., phase shift, cross section, polarization determ., 0.04 eV 9-4882  
<sup>3</sup>He crystals, exchange frequency temp. and density calcs. 9-21240  
 He<sup>3</sup>, solid, nuclear spin, effect on dynamic nuclear polarization 9-1719  
 Hg atom electron scatt., 3.5-500 eV, differential cross-sections and spin polarizations obs. 9-18149  
 Ho<sub>2</sub>Sm<sub>1-x</sub>FeO<sub>3</sub> orthoferrites, effect on ordering of Ho ions 9-16371  
 K<sub>2</sub>MnCl<sub>6</sub> 9-16456  
 KNiF<sub>3</sub>, superexchange 9-14012  
 KNiF<sub>3</sub>, unrestricted Hartree-Fock molecular-orbital treatment 9-12232  
 MgF<sub>2</sub>:Co<sup>2+</sup>, isotropic and anisotropic parameter from far i.r. spectrum 9-1788  
 Mn<sub>21-x</sub>Fe<sub>x</sub>F<sub>2</sub>, from Neel temp. composition dependence obs. 9-21594  
 Mn<sup>2+</sup> in CoCl<sub>2</sub>.2H<sub>2</sub>O, D-parameter exchange contribution 9-3776  
 MnCl<sub>2</sub>.4H<sub>2</sub>O, modulation, rel. to strong magnon-phonon coupling 9-1421  
 MnP, s-d, from resistivity and thermoelec. power temp. dependence, 4.2°-500°K 9-1456  
 MnS, between second neighbours, variation rel. to distance 9-18685  
 N donors in SiC 9-19972  
 NaNiF<sub>3</sub>, antisymmetric interaction responsible for weak ferromagnetism 9-5855  
 Ni<sub>3</sub>Fe(Mn) based ternary alloys with transition metal 9-19834  
 Ni epitaxial films, spin-wave resonance 9-20011  
 Ni<sub>3</sub>Mn, character and features of atomic distrib., eff. of Co and Fe additions 9-12278  
 RbMnF<sub>3</sub>, between excited Mn<sup>2+</sup> and unexcited ions, calc. from Zeeman effect meas. 9-1795  
 RbNiF<sub>3</sub>, 15°-300°K, using Ar laser 9-10222  
 SrFe<sub>12-x</sub>Ga<sub>x</sub>O<sub>19</sub> superexchange rel. to variation in saturation magnetiz. with Ga substitution 9-16373  
 YFe garnet, in sublattice magnetization calc. by Oguchi method 9-10144

### Exchange interactions continued

Yb e.p.r. of dissolved Eu<sup>2+</sup>, exchange integral calc. 9-12504

### Exchanges, chemical

See also *Isotope exchanges*  
 bimolecular, statistical theory, rederivation 9-10307  
 exothermic interchange reaction rates, calc. by 'nearest resonance' method 9-6000  
 halogen atom-mol., short-range attraction 9-10309  
 hexafluoroacetone photolysis, intersystem crossing efficiency 9-1919  
 ion exchangers, diff. and reaction coupling 9-17510  
 kinetics, demonstration of n.m.r. application 9-8344  
 Linde Y zeolite, of cation sites, Mn<sup>2+</sup> e.s.r. obs. 9-1889  
 methanol system, proton exchange rates 9-9560  
 molecular partition functions, isotopic effects 9-15847  
 n.m.r. indirect spin saturation 9-16755  
 rates determ. by n.m.r. 9-5996  
 solutions, proton-transfer reactions, quantum-mech. tunnelling through parabolic energy barriers 9-20030  
 C surface, O reversible exchange between CO<sub>2</sub> and CO, rates and activation energy 9-8051  
 Cs+RbCl, mol. beam mass spectrometric obs. 9-10310  
 Ge(OCH<sub>3</sub>)<sub>4</sub> vs. Ge(SCH<sub>3</sub>)<sub>4</sub> substituent exchange, <sup>1</sup>H n.m.r. obs. 9-6005  
 Ge(SCH<sub>3</sub>)<sub>4</sub> vs. GeZ<sub>4</sub>(Z=Cl, Br, I, NCO), substituent exchange, <sup>1</sup>H n.m.r. obs. 9-6005  
 H<sub>2</sub>, transition state 9-10319  
 H+H<sub>2</sub>, theoretical H<sub>2</sub> potential surface 9-10311  
 K-Li ion exchange syst., diff. and reaction coupling 9-17510  
 K+RbCl mol. beam mass spectrometric obs. 9-10310  
 Ni(II) ions in dimethyl sulphoxide solns. 9-9555

**Excimers** see *Molecules/excitation*

**Excitation** see *Atoms/excitation; Molecules/excitation; Nuclear excitation; Vibrations/excitation*

**Excitons** see *Crystal electron states/excitons*

**Excitons, molecular** see *Molecules; Polymers*

**Exoelectron emission** see *Electron emission*

**Exosphere** see *Atmosphere/upper*

**exp-6 potential** see *Kinetic theory; Molecules/intermolecular mechanics*

**Expanding universe** see *Cosmology*

**Expansion, thermal** see *Thermal expansion*

### Explosions

See also *Detonation; shock waves*  
 aerial, seismic effect 9-6042  
 detonations in solid explosives, fluid-dynamic eqns with changing co-ordinate system 9-12943  
 electric wire, later stages, temp. and e. density distrib. 9-9346  
 exploding wires, confined, optical and elec. meas. 9-18287  
 in external elec. field 9-10745  
 causing long distance infrasonic propag. 9-17572  
 causing long distance infrasonic propag. 9-17573  
 in magnetic flux compression, recoil phase 9-12972  
 seismic effect of above ground explosions 9-8141  
 shock wave prod., rel. to radio wave reflections 9-156  
 of solids, behaviour behind detonation waves, plane and spherical 9-20440  
 underground, intense, dynamics, mathematical model 9-19079  
 under water, at small depths, calc. of cavitation propag. 9-17178  
 underwater, spectra of acoustic and seismic signals 9-6046  
 wires, electrically exploded, interaction with elec. circuit 9-6443  
 wires, wires in very dense plasma production 9-9381  
 D-O<sub>2</sub> mixtures, lower limits, rate consts. and kinetics of branching step 9-14129  
 H<sub>2</sub>-Cl<sub>2</sub> laser 9-2374  
 H-O<sub>2</sub> mixtures, lower limits, rate consts. and kinetics of branching step 9-14129  
 Li wires, self-broadening of reson. line emitted 9-16996

### nuclear

Chinese 1966, fallout particles in ground level air 9-12592  
 Chinese of 9 May 1966, fallout fractionation  $\gamma$  spectrometry 9-8180  
 Chinese test 28 Dec, 1966, quantitative investigation of fallout sample 9-6082  
 high-altitude, m.h.d. wave generation model 9-10440  
 high-altitude, prod. of acoustic-gravity waves, effects in ionosphere 9-12635  
 underground, intense, dynamics, mathematical model 9-19079  
 yield of underground explosions, peak-stress gauge for meas. 9-10744  
 n source, hot sample changer and transfer cask, material irradiation 9-20810

**Extensive air showers** see *Cosmic rays/showers and bursts*

**Extensometers** see *Strain gauges; Thermal expansion*

**Extra-terrestrial radiation** see *Cosmic radiations, radiofrequency; Sun/radiation*

**Extrusion** see *Forming processes*

### Eye

See also *Vision*  
 cat. recordings from optic tract fibers 9-18963  
 elements, role in determ. of retinal image 9-10578  
 intraocular distances, u.s. diagnostics, improvement in meas. 9-10577  
 lens, dynamic visco-elastic props. 9-18958  
 Limulus, lateral; inhibitory fields 9-10580  
 movements recorded by special camera 9-6219  
 photoreceptor discs, fine structure obs. 9-12796  
 single cone response recording site, electrode marking technique 9-12797

**F-centres** see *Colour centres*

**F-layer** see *Ionosphere/F-region*

**Faculae** see *Sun*

### Fallout

See also *Atmosphere/radioactivity; Nuclear reactions and scattering; Radioactivity*  
 3<sup>rd</sup> Chinese nuclear test obs. at Chiba, Japan 9-4061  
 automatic dust monitor, radioactivity conc. determ. 9-8181  
 Chinese test 28 Dec, 1966 quantitative investigation of sample 9-6082  
 dry radioactive dust obs. in Central Asia 9-8179  
 fifth Chinese nuclear explosion, 28 Dec 1966, activities of various radionuclides determ. 9-21782  
 fractionation from Chinese nuclear explosion 9 May 1966,  $\gamma$  spectrometry of ten nuclides 9-8180  
 ground level air particles from Chinese nuclear explosion 1966 9-12592

**Fallout continued**

- radioactive aerosols, vertical exchanges and deposition rates above continents and oceans 9-10395
- radioactive particles, separation for microscopic examination 9-15249
- rate, from amount of  $^{90}\text{Sr}$  on Earth's surface 9-17555
- $^{137}\text{Cs}$  annual variation at Vilnius (1966) 9-12590
- $^{137}\text{Cs}$  in human body following atomic tests, possible sources in bread and milk 9-1943
- $^{14}\text{C}$  in atmospheric  $\text{CO}_2$ , measuring technique and results 9-15248
- $\text{Ge}(\text{Li})$  diode meas. 9-550
- $^{93}\text{Nb}$ , to  $^{91}\text{Zr}$ , ratio over-ocean 9-18806

**Faraday effect** *see* Magneto-optical effects**Fatigue** *see* Elastic fatigue**Fermi gas** *see* Quantum fluids/fermion systems**Fermi level** *see* Crystal electron states/Fermi level**Fermi surface** *see* Crystal electron states/Fermi surface**Fermion systems** *see* Quantum fluids/fermion systems**Fermions**

- See also Elementary particles; Quantum fluids/Fermion systems; Statistical mechanics/quantum*
- Bethe-Salpeter eqn. reduction for zero-mass fermion-antifermion system 9-14463
- Bethe-Salpeter equation solution 9-20593
- boson-fermion scatt., removal of square-root singularity from amplitude 9-17935
- Fermion superselection rule, proof without T invariance assumption 9-20331
- N-fermion system, ground state energy calc. via lower-bound shell model 9-2176
- Fermion-antifermion system bound by vector exchange, accurate soln. of Bethe-Salpeter eqn. 9-6588
- field, broken-symmetry condition 9-13092
- Hamiltonian compared with Yukawa Hamiltonian 9-303
- interacting 1-dimens. syst., Luttinger model 9-13083
- interacting in one-dimension, remarks on theory 9-17743
- interactions, weak, four-fermion and bilinear, interrelation 9-4574
- Mach's principle considerations 9-20592
- meson photprod. amplitudes asymptotic props. 9-8801
- meson-spin- $1/2$  fermion, reaction amplitude calc. in 4th order perturbation theory 9-2491
- parity number, assignation and phys. consequences 9-6583
- parity tests, non-dynamical, decay mechanism 9-4562
- Regge exchange in backward  $\Lambda$  associated prod. 9-4648
- scatt., general fermion-fermion, invest. in covariant spinor formalism, meas. invariant amp. 9-4565
- scatt. process prob., polarization states described 9-2460
- SU group representation using fermion operator realization 9-14475
- two-component theory for particle mass and the origin of Zitterbewegung 9-14464

**Ferrim**

No entries

**Ferrim compounds**

No entries

**Ferrimagnetic resonance***See also Ferromagnetic resonance*

- ferrites for resonance apparatus in m.m. wavelength with weak mag. fields 9-14003
- linewidth measurement errors, single-crystal ferrites, due to nonideal microwave components 9-10271
- spin, magneto-crystalline anisotropy effect elimination, patent 9-19962
- $\text{Fe}_2\text{Ga}_2\text{-xO}_3$ , electric fields eff. 9-18732
- Mg-Mn polycrystalline ferrite spinel, line broadening mechanism and temp. dependence 9-1852
- Ni-Zn polycrystalline ferrite spinel, line broadening mechanism and temp. dependence 9-1852
- $\text{Ni}_0.5\text{Zn}_{0.5}\text{Fe}_2\text{O}_4$  ferrite, spectrum temp. dependence 9-21662
- $\text{RbNiF}_3$ , uniaxial ferrimagnet, 77-200°K 9-12496
- YFe garnet:Hf,  $\text{Fe}^{2+}$  characterization 9-16388

**Ferrimagnetism***See also Ferromagnetism*

- Neel ferrimagnets, high-field magnetization analysis 9-15154
- spin wave coherent amplification in ferrites 9-16365
- spin-wave attenuation in Mg, Mn and Mg-Mn ferrites 9-17458

**Ferrites***See also Magnetic properties of substances*

- alloyed,  $\text{N}_2$  solubility 9-5395
- anisotropy constants, magnetometer for automatic meas. 9-17456
- barium, hexagonal, mag. relax. 9-12314
- barium, hexagonal, magneto-optical and optical props. 9-12343
- barium, h.f. conductivity and Seebeck coeff. 9-12086
- ceramic, microwave latching devices 9-1679
- Conference, Intermag., Washington, D.C., April 1968 9-3773
- Conference, Intermag., Washington, D.C., April 1968 9-3774
- Conference, Intermag., Washington, D.C., April 1968 9-7883
- crystal properties control by composition variation 9-21308
- disaccommodation and con diffusion 9-3323
- for e.m. wave absorption 9-17836
- excitation of exchange oscils. by moving charged particles 9-5845
- ferromagnetic resonance,  $\gamma$ -n irrad. effects 9-14105
- ferromagnetic resonance linewidth variations with mat. characs. 9-12493
- ferromagnetic resonance meas. resonator method theory 9-16450
- grains, monodomain interacting, remanent props. and Preisach diagrams 9-14000
- hexagonal, preparation by coprecipitation 9-5277
- magnesium, quenching temp. effect on mag. permeability and complex dielec. permittivity tensor components 9-19967
- magnetoacoustic resonance 9-16172
- magnetoelastic instability, quantum investigation 9-3823
- magnetoresistance of spinel-type ferrites, obs. 9-12087
- material-parameter meas. at mm-waves using dynamical modes in ferrite-filled coaxial cavity 9-8556
- in microwave filters, magnetically tunable with high quality factors 9-10769
- ortho-, cylindrical domains, properties 9-3825
- ortho-, domain wall energy, direct meas. method 9-3824
- orthoferrites, domain-wall energy meas. 9-14001
- permeability mechanism 9-14002
- permivar, mag. ordering stability 9-10138

**Ferrites continued**

- porous and anisotropic polycrystalline, absorption and dispersion at microwave frequencies 9-3945
- preparation for h.f. field operation 9-12299
- rare earth orthoferrites, metamagnetic props. 9-16383
- rare earth orthoferrites, weak field magnetization 9-19969
- rare-earth orthoferrites, antiferromagnetism vector reorientation 9-15159
- rare-earth orthoferrites, u.v. meas. of complex polar Kerr effect 9-1738
- remnance in monodomain grains obs. on Neel thermal activation theory 9-3791
- resistivity, cooling rate depend. rel. to cation conc. 9-12193
- resistivity behaviour near Curie point 9-21478
- for resonance apparatus in m.m. wavelength with weak mag. fields 9-14003
- single-crystal, linewidth measurement errors due to nonideal microwave components 9-10271
- spherical sample preparation 9-21403
- spin wave coherent amplification 9-16365
- spinel type, resistivity behaviour near Curie point 9-21478
- thermal expansion and conductivity of polycrystalline ferrites 9-3535
- YFe garnet, magneto-elastic constants, meas. by microwave techniques 9-10142
- Ba, fine-milled, saturation magnetization temp. dependence between -195°C and Curie temp. 9-3826
- Ba, fine particle assemblies, coercive force variation with packing 9-3796
- Ba hexaferrites, rotating moment curves in case of uniaxial ferromag. anisotropy 9-1666
- $\text{BaCo}_2\text{TiFe}_{14}\text{O}_{37}$ , magnetization anisotropy 9-18684
- $\text{BaCo}_2\text{TiFe}_{12-2x}\text{O}_{39}$ , hexagonal, mag. exchange anisotropy 9-10136
- $\text{BaFe}_{12}\text{O}_{19}$ , magnetostriction 9-14004
- $\text{BaFe}_{12-2x}\text{Al}_x\text{O}_{19}$  saturation magnetization variation with Al substitution 9-16366
- $\text{BaSc}_2\text{Fe}_{12-2x}\text{O}_{19}(\text{M})$ , helicoidal antiphase spin ordering, neutron diffraction 9-16367
- $(\text{Li}_{0.5}\text{Fe}_{1.5}\text{O}_3)_x$ , I:3 type ordering, temp. effects 9-14006
- $\text{Co}_2\text{Fe}_{1-x}\text{O}_4$ , induced anisotropy const., Co content eff. 9-5847
- $\text{Co}_{0.7}\text{Zn}_{0.3}\text{Fe}_2\text{O}_4$ , paraprocess susceptibility maximum at Curie point 9-16368
- $\text{CuFe}_2\text{O}_4$ , mag. props. 9-1680
- $\text{DyFeO}_3$ , metamagnetic props. 9-16383
- $\text{DyFeO}_3$ , perovskite, magnetization model 9-1681
- $\text{E-FeO}_3$ , domain-wall energy meas. at 25°C 9-14001
- $\text{ErFeO}_3$ , domain wall energy, direct meas. method 9-3824
- $\text{ErFeO}_3$ , metamagnetic props. 9-16383
- Fe, polycrystalline, directional order below order-disorder transformation point 9-17457
- $\text{FeNiCo}$ , thermomagnetically induced anisotropy 9-19963
- $(\text{FeO})_{0.38}(\text{NiO})_{0.62-x-y}(\text{CoO})_x(\text{ZnO})_y$  ferrite system, mag. ordering stability 9-10138
- Gd garnet, magnetic sublattice interactions 9-16369
- $\text{Gd}_3\text{Fe}_5\text{O}_{12}$ , magnetothermal effect, anomalous sign in compensation pt. region 9-1683
- $\text{GdFeO}_3$  metamagnetic props. 9-16383
- $\text{Ho}_0.5\text{Sm}_{0.5}\text{FeO}_3$  orthoferrites, exchange interaction effect on ordering of Ho ions 9-16371
- Li, alignment and microwave props. 9-1685
- Li, Ca substituted, mag. props. structure and sintering 9-1684
- Li, saturation magnetization and lattice strcut., 20°C 9-1686
- $\text{Li}_{0.5}\text{Fe}_{2.5-x}\text{Al}_x\text{O}_4$ , lattice structure and cation distrib., n. diff. obs. 9-21316
- $\text{Li}_{0.5}\text{Fe}_{2.5-x}\text{Al}_x\text{O}_4$ , ferromag. resonance line width rel. to elec. cond. 9-18730
- $\text{Li}_{0.5}\text{Mn}_{0.5}\text{Mn}_2\text{V}_2\text{Fe}_2\text{O}_4$  core with square hysteresis loop, production method, patent 9-19966
- $\text{LiO} \cdot (2.2 \text{ wt.}\%) \text{Fe}_2\text{O}_3$  9-19965
- Li ferrite growth in  $\text{SiO}_2$  glasses and composite mag. props. 9-1146
- LiCo, ferromagnetic resonance 9-18731
- LiGa, magneto-crystalline anisotropy by ferromag. resonance 9-19964
- $\text{Li}_2\text{O} \cdot 2.2\text{Fe}_2\text{O}_3 \cdot 2.8\text{Cr}_2\text{O}_3$  longit. and transverse magnetoresistance, anomalies around compensation temp. 9-19965
- $\text{Li}_2\text{O} \cdot 2.5\text{Fe}_2\text{O}_3 \cdot 2.5\text{Cr}_2\text{O}_3$  magnetothermal effect, anomalous sign in compensation pt. region 9-1683
- Mg-Mn-Zn-, microwave, resonance line width and scalar susceptibility 9-5811
- Mg-Mn polycrystalline spinel, ferrimag. reson. line broadening mechanism and temp. dependence 9-1852
- Mg-Mn spin-wave attenuation -150°C-300°C obs. in single crystals 9-17458
- Mg, spin-wave attenuation -150°C-300°C obs. in single crystals 9-17458
- Mg Mn, alignment and microwave props. 9-1685
- Mg Mn, optical props. and conduction mechanisms 9-10171
- MgMn, ferrite, single crystal film, ferromagnetic resonance 9-15196
- MgMn, pulse and hysteresis props., eff. of annealing conditions 9-17459
- Mn-Mg-Fe, after-effect,  $\text{Mg}^{2+}$ ,  $\text{Mn}^{2+}$  role, obs. 9-14007
- Mn-Zn, elastic moduli, 80-303°K, meas. 9-1260
- Mn-Zn, permeability rel. to comp., magnitude and temp. dependence, sintering atmosphere effect 9-1687
- Mn cation distribution equilibrium position by i.r. spectral analysis 9-3876
- Mn spin-wave attenuation -150°C-300°C obs. in single crystals 9-17458
- $\text{MnFe}_2\text{O}_4$ , etch pits 9-3231
- $\text{Mn}_2\text{Fe}_{1-x}\text{O}_4$  ferromagnetic linewidth inhomogeneous broadening 9-3947
- $\text{Mn}_2\text{Fe}_{1-x}\text{O}_4$ , electronic magnetic relaxation, 20-500 K/s, 80-350°K 9-14017
- $\text{Mn}_2\text{Fe}_{1-x}\text{O}_{4.5}$ , electron relaxation processes 9-10154
- $\text{MnFe}_2\text{-xSc}_x\text{O}_4$  X-ray investigation of K absorption edge 9-5945
- MnZn, Cd-for-Zn substitution, effect on mag. props. 9-17460
- MnZn, magnetization at near saturation 9-15155
- MnZn high permeability, temp. insensitive 0 to 60°C 9-3830
- MnZn of stoichiometric compositions, props. 9-16079
- Ni-Co-Zn, Procopiu effect in bar sample 9-3832
- Ni-Fe, rotational losses 9-3831
- Ni-Fe single crystal, ferromag. resonance line breadth rel. to mag. field-induced anisotropy 9-12494
- Ni-Fe single crystals containing Co, stabilized-domain walls, effect on hysteresis loop shape 9-5849
- Ni-Zn-Co, Procopiu effect in bar sample 9-3832
- Ni-Zn, elastic moduli, 80-303°K, meas. 9-1260



**Ferrites continued**

- Ni<sub>2</sub>Zn, magnetic transition parameters, chemical homogeneity eff. 9-7911  
 Ni<sub>2</sub>Zn polycrystalline spinel, ferrimag. reson. line broadening mechanism and temp. dependence 9-1852  
 Ni, alignment and microwave props. 9-1685  
 Ni, hysteresis, mag. of u.s. velocities 9-9828  
 Ni<sub>0.5</sub>Zn<sub>0.5</sub>Fe<sub>2</sub>O<sub>4</sub>, magnetic resonance spectrum 9-21662  
 Ni<sub>2</sub>Fe<sub>1-x</sub>Fe<sub>2</sub><sup>3+</sup>O<sub>4</sub>, X-ray absorpt. spectra comp. dependence 9-21640  
 Ni<sub>2</sub>Zn<sub>1-x</sub>Fe<sub>2</sub>O<sub>4</sub>, X-ray absorpt. spectra comp. dependence 9-21640  
 Ni Co, alignment and microwave props. 9-1685  
 Ni Fe, conductivity mechanism 9-3632  
 Ni Fe, optical props. and conduction mechanisms 9-10171  
 Ni u.s. vel. minimum, depend. on temp. and mag. polarization 9-9827  
 Ni Zn Fe, optical props. and conduction mechanism 9-10171  
 NiCo piezomag. coeffs, temp. depend. 9-5846  
 Ni<sub>1-x</sub>Fe<sub>x</sub>Fe<sub>2</sub><sup>3+</sup>O<sub>4</sub>, resistivity vs. Fe<sup>2+</sup> concentration (x) curves 77-373°K 9-12090  
 NiMn piezomag. coeffs, temp. depend. 9-5846  
 NiZn, magnetization at near saturation 9-15155  
 SmFeO<sub>3</sub>, spin re-orientation phase transition 9-16372  
 Sr, fine-milled, saturation magnetization temp. dependence between -195°C and Curie temp. 9-3826  
 SrCo<sub>1-x</sub>Ti<sub>x</sub>Fe<sub>9</sub>O<sub>19</sub>, hexagonal, mag. exchange anisotropy 9-10136  
 SrFe<sub>12-x</sub>Ga<sub>x</sub>O<sub>19</sub>, saturation magnetization depend. on Ga substitution 9-16373  
 TbFeO<sub>3</sub>, metamagnetic props. 9-16383  
 YFe garnet, interaction of longitudinal phonons with spin waves 9-12304  
 YFe garnet rods, magnetoelastic longit. waves, obs. 9-9746  
 Sr<sub>0.8</sub>Ba<sub>0.2</sub>(1/3)ZnFe<sub>2</sub>O<sub>4</sub>, angular spin ordering from neutron diffraction meas. 9-10140

**Ferroacoustic resonance** see *Crystals/lattice mechanics; Ferromagnetic resonance*

**Ferroelectric devices** see *Dielectric devices*

**Ferroelectric materials**

- acoustic attenuation and amplification in ferroelec. semiconductors 9-18553  
 acoustic-i.r. e.m. wave interaction 9-16389  
 antiferroelectric, Cu(HCO<sub>2</sub>)<sub>2</sub>·4H<sub>2</sub>O, anomalous dielectric relaxation 9-3715  
 ceramic mirror, wideband interference light modulator 9-13051  
 chalcogens, new materials <sup>75</sup>As n.g.r. study 9-18747  
 displacement, statistical theory 9-21535  
 displacement, statistical theory, applic. to LiNbO<sub>3</sub> expt. results 9-21537  
 displacement, statistical theory rel. to specific heat and soft-mode-freq. calcs. 9-21536  
 dispersive, impurity phonon modes frequency rel. to temp. 9-18546  
 guanidinium aluminium sulphate hexahydrate, e.p.r. of Mn<sup>2+</sup> 9-18744  
 hydrogen-bonded, transverse and longit. correlations 9-21538  
 Kanzig's regions dimensions rel. to lattice dynamics 9-21534  
 low-temperature effects of the tunneling integral, hydrogen bonded 9-7843  
 methyl ammonium aluminium sulphate, phase transition, <sup>27</sup>Al NMR exam. 9-3968  
 order-disorder type, critical behaviour of pseudospin model 9-17431  
 phonons in time-dependent Hartree approx., appl. to order-disorder type 9-9810  
 photoconductors, lamellar structure on illumination near phase transition temp. 9-15135  
 Raman scattering from soft optic mode 9-12405  
 Rochelle salt, dielec. const. temp. dependence from meas. at 9 GHz 9-10051  
 Rochelle salt, dielec. const. temp. var. 9-3700  
 Rochelle salt, i.r. absorpt. spectra in thin crystal textures, -195 to 51°C 9-1803  
 Rochelle salt, Ising model with two phase transitions 9-5754  
 Rochelle salt, lattice defects effect on dielec. props. 9-7486  
 with semiconducting props., possible instability 9-5666  
 semiconductor, transverse optical phonon amplification by carrier drift 9-19929  
 semiconductors, elec. induction wave theory 9-16257  
 semiconductors, electric induction waves at temps. above first order transition 9-16258  
 temperature stable, high dielec. constant materials, preparation 9-1591  
 thermal oscillations and Mossbauer effect near phase transition 9-1364  
 transducers, antiferroelec.-ferroelec., acoustic transients generation 9-4341  
 triglycine selenate, deuterated, dielectric properties 9-1136  
 triglycine selenate, high temp. structural transitions 9-13920  
 triglycine sulphate: vandy, switching effect obs. by e.p.r. 9-3713  
 triglycine sulphate, 180° domains, topography of deformation, nucleation and growth 9-16301  
 triglycine sulphate, critical exponents, expt.-determ. 9-1597  
 triglycine sulphate, domain structure, e. microscope exam. of elec. decorated surfaces 9-1599  
 triglycine sulphate, domain switching induced temp. instabilities 9-21541  
 triglycine sulphate, high temp. structural transitions 9-13920  
 triglycine sulphate, i.f. Raman spectra near Curie point 9-1808  
 triglycine sulphate, phase transition, high pressure and elec. fields effects 9-1598  
 triglycine sulphate, props., effect of growth conditions 9-10050  
 triglycine sulphate cryst., surface layers rel. to dielec. const. 9-5753  
 triglycine sulphate crystals, permittivity, temp. hysteresis 9-10052  
 triglycine sulphate type, optical indicatrix tensor orientation, high temp. 9-21540  
 tunneling integral for hydrogen bonded ferroelectrics, low-temp. effects 9-7843  
 tunneling phenomena 9-3706  
 uniaxial, polarization fluctuation-acoustic wave interaction rel. to anomalous sound absorpt. near Curie pt. 9-1375  
 vibration spectra in system with coinciding ferroelec. and ferromag. axes, from motion of polarization and magnetization vectors 9-16163  
 Bi<sub>2</sub>TiO<sub>5</sub> crystals, optically induced refractive index changes, obs. with internally formed holograms 9-19976  
 Cu(HCO<sub>2</sub>)<sub>2</sub>·4H<sub>2</sub>O, antiferroelectric, anomalous dielectric relaxation 9-3715  
 Gd<sub>2</sub>(MoO<sub>4</sub>)<sub>3</sub>, switching and electro-optical props. 9-12349  
 Gd<sub>2</sub>(MoO<sub>4</sub>)<sub>3</sub>, spontaneous polarization from elastic instability 9-1593  
 KD<sub>2</sub>PO<sub>4</sub>, polarization relax. time and dielec. susceptibility 9-1595  
 KH<sub>2</sub>PO<sub>4</sub>, elastic Curie-Weiss law from u.s. velocity and attenuation meas. 9-21430

**Ferroelectric materials continued**

- KH<sub>2</sub>PO<sub>4</sub>, H<sub>2</sub>PO<sub>4</sub><sup>-</sup> ion structure from Raman scatt. spectra in ferroelec. and paraelec. states 9-18652  
 KH<sub>2</sub>AsO<sub>4</sub>, electric-field-gradient tensor at As site from p. relax. meas. 9-17469  
 KH<sub>2</sub>PO<sub>4</sub>, P<sup>31</sup> spin-lattice relax. time anomalous decrease near Curie point 9-1713  
 KH<sub>2</sub>PO<sub>4</sub>, phase transition, Brillouin scattering study 9-12198  
 KH<sub>2</sub>PO<sub>4</sub>, KD<sub>2</sub>PO<sub>4</sub> press. depend. of ferroelec. props. 9-13919  
 KNO<sub>3</sub>, phase III, Raman scatt. from obs. in phase-transition cycle 9-14061  
 KNbO<sub>3</sub>, neutron scatt. and dielec. props. 9-13910  
 (KPb<sub>2</sub>-(KSR<sub>2</sub>, NaBa<sub>2</sub>)/NbO<sub>5</sub>) transition temp. rel. to lattice structure 9-1594  
 KSr<sub>2</sub>NbO<sub>5</sub>, transition temp. rel. to lattice structure 9-1594  
 LiNbO<sub>3</sub>:Mn<sup>2+</sup> e.p.r. spectrum obs. 9-16458  
 LiNbO<sub>3</sub>, crystal structure 9-7443  
 LiTaO<sub>3</sub>:Mn<sup>2+</sup> e.p.r. spectrum obs. 9-16458  
 LiTaO<sub>3</sub>, applic. of statistical theory of displacement ferroelectrics to experimentally determined props. 9-21537  
 (NH<sub>4</sub>)<sub>2</sub>H<sub>2</sub>IO<sub>6</sub>, antiferroelec. props. 9-16302  
 NH<sub>4</sub>HSO<sub>4</sub>, p-T diag. 9-3710  
 NaBa<sub>2</sub>NbO<sub>5</sub>, transition temp. rel. to lattice structure 9-1594  
 NaD<sub>2</sub>(SeO<sub>3</sub>)<sub>2</sub>, transitions from NMR temp. dependence 9-17435  
 NaH<sub>2</sub>(SeO<sub>3</sub>)<sub>2</sub>, transitions from NMR temp. dependence 9-17435  
 NaKNbO<sub>3</sub>, ceramics, polarized optical retardation 9-1743  
 NaNO<sub>2</sub>, etching of domains and dislocations rel. to polarization 9-15125  
 NaNO<sub>2</sub>, temp. dependent vibrational modes 9-5902  
 Pb(Mg<sub>1/3</sub>Nb<sub>2/3</sub>)O<sub>3</sub>-PbTiO<sub>3</sub>-PbZrO<sub>3</sub> system, antiferro-ferroelec. and ferroelec. 1-2 phase boundaries, obs. 9-7844  
 PbMg<sub>1/3</sub>Ta<sub>2/3</sub>O<sub>3</sub>, electro-opt. eff., -150° to +120°C 9-7952  
 PbNi<sub>1/3</sub>Nb<sub>2/3</sub>O<sub>3</sub>, electro-opt. eff., -150° to +120°C 9-7952  
 PbO thin films, possibility rel. to dielec. anomaly 9-17437  
 PbTiO<sub>3</sub>, transition temp. and effect of growth conditions on props. 9-19931  
 PbZr<sub>1/3</sub>Nb<sub>2/3</sub>O<sub>3</sub>, electro-opt. eff., -150° to +120°C 9-7952  
 Pb(Zr,Sn,Ti)O<sub>3</sub> solid solutions, with properties depending on applied elect. field, expt. study 9-10046  
 Pb(Zr,Ti<sub>1-x</sub>)O<sub>3</sub>, charge transport mechanism, 650-1000°K 9-19932  
 PbZrO<sub>3</sub>:Nb<sub>2</sub>O<sub>5</sub> with properties depending on applied elect. field, experimental study 9-10046  
 PbZrO<sub>3</sub>-PbTiO<sub>3</sub>, sputtered films, dielectric loss and strength 9-1596  
 PbZrO<sub>3</sub>, impurity effects on dielec. phase 9-17436  
 PbZrO<sub>3</sub> solid solns., ferroelec.-antiferroelec. phase changes rel. to elec. field and temp. 9-5751  
 PbZr<sub>(1-x)</sub>Ti<sub>x</sub>O<sub>3</sub>, ceramics, polarized optical retardation 9-1743  
 Sb<sub>2</sub>S<sub>3</sub>, phase transition from optical absorpt. temp. dependence 9-3711  
 SbSI, Curie temp. shift due to illumination and nonequilibrium carriers 9-16300  
 SbSI, phase transition, eff. of photoconduction 9-7845  
 SbSI, polarization, spontaneous and double hysteresis loop 9-5649  
 SbSI, transition dependence on polarization and crystal symmetry 9-21539  
 SbSI pleochroism near phase transition 9-14029  
 SbSI thermal cond. 6°-316°K, anomaly 9-16185  
 Sb<sub>2</sub>Se<sub>3</sub>-I mixed crystals, transition from paraelec. state 9-12385  
 SbSi, polarization reversal, screening effects by non-equilibrium carriers 9-3712  
 SbSi, semicond. interphase boundary formation, eff. of non-equilibrium carriers 9-5752  
 SbSi, space-charge-limited currents in para- and ferroelec. phases 9-10038  
 Sr<sub>1-x</sub>Ba<sub>x</sub>Nb<sub>2</sub>O<sub>6</sub> infrared detector, fast and sensitive 9-3714  
 SrTiO<sub>3</sub>:Cr<sup>3+</sup>, Cr R lines spectral shift, 4 kV/cm electric field, 4.2°K 9-3709  
 SrTiO<sub>3</sub>:rare-earth, relaxation, activation energy, obs. 9-3699  
 SrTiO<sub>3</sub>, 110°K phase transition, soft phonon modes and interactions 9-11968  
 SrTiO<sub>3</sub>, Raman spectrum, spatial variation below 110°K 9-16423  
 SrTiO<sub>3</sub>, two-photon excited free carrier absorpt. obs. 9-12199  
 YMnO<sub>3</sub>, dynamic fatigue, rel. to free loads 9-10045

**barium titanate**

- aging, followed by optical and electrical meas. 9-1324  
 conductivity, electrical and sintering kinetics, point defect conc. estimation 9-1589  
 dielectric const., ageing characts. 9-10049  
 dielectric const. rel. to initial soak before sintering 9-3708  
 dipolar relaxation phenomena 9-10047  
 domain structure, constant elec. field effects 9-13918  
 180° domain-wall energies 9-17433  
 grain boundaries rel. to dielec. props., reflectance spectra obs. 9-3707  
 melt grown, dielectric and optical properties 9-5745  
 paraelectric range, thermocurrents rel. to point defects 9-5756  
 permittivity peak suppression at transition point by substitution elements for Ba and Ti 9-1183  
 Raman scattering from soft optic mode 9-12405  
 Raman spectrum, single domain crystal 9-3902  
 repolarisation processes in sinusoidal fields rel. to domain structure 9-1592  
 Schottky diode, photosensitive 9-18660  
 thin film, properties and thermodynamic model 9-12197  
 thin films and structures, characteristics and applications 9-16298  
 BaTiO<sub>3</sub>-PbTiO<sub>3</sub> single cryst. solid solns., dielec. and elastic props. 9-12196  
 BaTiO<sub>3</sub>-SrSnO<sub>3</sub> system, high dielectric const. rel. to temp. 9-1591  
 OH radical and stoichiometry effect on transition 9-10048  
 Ta<sub>2</sub>O<sub>5</sub> doped, sintering characts. rel. to electrical props. 9-1590

**Ferroelectric phenomena**

- crystals, lattice dynamics, review 9-13917  
 domain walls and secondary effect phenomena 9-21533  
 energy conversion technique, electro-mechanical application 9-16299  
 ferroelectric-antiferroelectric phase changes, effect of elec. field 9-5751  
 hysteresis loop tracer for capacitors 9-8312  
 hysteresis curve tracer with compensation and virtual sample grounding 9-1588  
 magnetic moment ordering in ferroelects. 9-16339  
 non-collinear ferroelectrics and antiferroelectrics 9-16296  
 phase transition, second-order, Ehrenfest relations, new deriv. 9-8441  
 phase transition to antiferroelec., thermodynamic relations with composition 9-19930

**Ferroelectric phenomena continued**

- polarization change, factors influencing 9-3705
- revival 9-10044
- soft vibrational modes, freq. dependence on elec. field 9-1587
- switching current pulse representation 9-5749
- thermal diffusivity, electrocaloric effect, thermocurrents, meas. 9-16297
- triglycine sulphate: vandy, switching effect obs. by c.p.r. 9-3713
- $\text{KH}_2\text{PO}_4$ , phase transition, Brillouin scattering study 9-12198
- $\text{KH}_2\text{PO}_4$  Brillouin-scatt. study transition paraelec. phase and piezoelec. coupling analysis. 9-5750
- $\text{NaD}_3(\text{SeO}_3)_2$ , low temp. phase transition from study of dielec. and opt. props. 9-17434
- $\text{NaH}_2(\text{SeO}_3)_2$  second order transition at Curie point high thermal expansion coeff. 9-9849
- SbSI, phase transition, eff. of photoconduction 9-7845
- SbSi, semicond. interphase boundary formation, eff. of non-equilibrium carriers 9-5752

**Ferromagnetic relaxation**

- $\text{Mn}_x\text{Fe}_{3-x}\text{O}_{4.1p}$ , magnetic loss factors from 2 to 360°K 9-10154

**Ferromagnetic resonance**

*See also Ferrimagnetic resonance*

- crystals with dislocations, micromag. calc. of scattered wave 9-12492
- ferrites,  $\gamma$ -n effects 9-14105
- ferrites, meas. by resonator method theory 9-16450
- ferrites, porous and anisotropic polycrystalline, absorption and dispersion at microwave frequencies 9-3945
- films, thin, surface peak 9-5834
- Heisenberg ferromagnet, precession line width 9-5808
- line width and scalar susceptibility in ferrites 9-5811
- linewidth meas. methods, variation with mat. characts. and applic. to ferrites exam. 9-12493
- magnetoacoustic resonance in ferromagnets, effect of mag. alloying additions 9-5552
- magnetostatic modes and pinning, generalized 9-10268
- in metal considered as plasma, review 9-21661
- nonlinear, energetic equilibrium mechanics 9-3946
- nonlinear, second order, line shape obs. and theory 9-8003
- nuclear spin-wave relaxation and narrowing of NMR lines 9-8037
- Permalloy films, linewidth thickness depend. 9-8005
- permalloy films, X-band obs. by reflecto-polarimetric exam. 9-10270
- spheroids, magnetostatic modes rel. to magnetization direction 9-14102
- spin, magneto-crystalline anisotropy effect elimination, patent 9-19962
- spin-wave scatt. by dislocations, effect on linewidth 9-3782
- spinel, ferrimag., main relaxation mechanisms 9-14101
- uniform precession mode of main peak 9-8002
- $\text{CdCr}_2\text{Se}_4$ :Ag dopant effects 9-16451
- $\gamma$ -Co films, spin-wave resonance and exchange interactions 9-20011
- $\text{EuO}$ , linewidth temp. dependence, 2-300°K 9-10269
- Fe-Si alloys, 294 and 77°K 9-8004
- Fe films, spin-wave resonance and exchange interactions 9-20011
- $6\text{Fe}_2\text{O}_3\cdot\text{PbO}$ , magnetoplumbite, powder, intrinsic, at 40.1Gc/s 9-1848
- $\text{Li}_0.5\text{Fe}_{2.5-x}\text{Al}_x\text{O}_4$ , line, width rel. to elec. conductivity 9-18730
- LiCo ferrite single crystals 9-18731
- LiGa ferrites, meas. of magnetocrystalline anisotropy 9-19964
- MgMn ferrite, single crystal films 9-15196
- Mn-Fe spinel, effect of  $\text{Mn}^{3+}$  clustering on linewidth 9-1206
- $\text{Mn}_x\text{Fe}_{3-x}\text{O}_4$  linewidth inhomogeneous broadening 9-3947
- $\text{Mn}_x\text{Fe}_{3-x}\text{O}_{4.1p}$ , magnetic loss factors from 2 to 360°K 9-10154
- Ni-Fe ferrite single crystal, line breadth rel. to mag. field-induced anisotropy 9-12494
- Ni, films, spin-wave resonance and exchange interactions 9-20011
- Ni, line width variation rel. to lattice microdistortions during plastic deformation and annealing 9-14103
- Ni film, field, shift rel. to magnetostrictive transverse phonon generation 9-10126
- Ni polycrystals, as function of angle between static mag. field and sample surface 9-14104
- Pd-Co alloy dil. 9-3948
- Pd-Fe alloy, dil. 9-3948
- Pt-Co alloy 9-3948
- YFe garnet,  $\gamma$ -n radiation effects 9-14105
- YFe garnet, nonlinear instability 9-12495

**Ferromagnetics** *see Magnetic properties of substances/ferromagnetic*

**Ferromagnetism**

*See also Antiferromagnetism; Exchange interactions; Ferrimagnetism; Ferromagnetic relaxation; Ferromagnetic resonance; Magnetic properties/ferromagnetic; Magnetization process; Magnetization state*

- alloys, dilute, 'non-magnetic', mag. behaviour due to localized spin fluctuations 9-12234
- anisotropic spontaneous magnetization and anisotropy energy in orthorhombic ferromagnets at 0°K 9-12286
- balanced distrib. of magnetization around spherical cavity 9-13970
- Barkhausen effect and irreversible magnetization processes 9-13977
- conduction electron spin polarization range, depend. on impurity conc. determ. by neutron scatt. 9-10120
- $\delta$ -function gas, ferromag. transition, correlations effects 9-12260
- DeBlois experiment, theory rel. to effect of small coil 9-10102
- DeBlois experiment, theory rel. to surface imperfection in infinite coil 9-10103
- dielectrics, ferromagnetic, u.s. reflection plane of polarization rot. and ellipticity appearance 9-3525
- dislocation model in nonmagnetic crystals 9-1659
- dislocation model in nonmagnetic crystals 9-13960
- Dzialoshinskii vector  $\vec{D}$ , calc. via stat. mechanics 9-1656
- elastic wave damping, eff. of second sound 9-13961
- electron ferromagnet at transition point, spin-spin correlation function 9-3784
- electron mag. scatt., elastic, mechanism of polarization of scatt. beam 9-12256
- electron solid, ferromagnetic props. 9-6340
- exchange interactions, effective Hamiltonian 9-12251
- ferromagnet, u.s. attenuation near critical point 9-5554
- field electron emission, prod. of polarized beams, theory 9-7865
- ground state in mag. systems 9-16342
- Heisenberg, critical fluctuations, estimate of error terms in dynamical theory 9-21577
- Heisenberg, n. scatt. phenomenology 9-12254
- Heisenberg anisotropic model, domain struct. 9-10116
- Heisenberg lattice, impure, magnon low-energy resons. 9-5813

**Ferromagnetism continued**

- Heisenberg linear chain, anisotropic, free energy lower bound 9-12263
- Heisenberg model, anisotropic, analyticity props. 9-19000
- Heisenberg model, dipole-dipole forces, free energy depend. on sample shape 9-12252
- Heisenberg models, spherical and classical, Pade approximant results 9-12261
- Heisenberg ferromagnet near Curie temp., effect of dipole-dipole interaction on thermodynamic props. 9-1389
- insulators, optical phonon freq. and mag. order 9-7626
- Ising, random on square lattice exhibiting spontaneous magnetization 9-8425
- Ising and Heisenberg model theorems 9-10645
- Ising lattice with three transition temperatures 9-3785
- Ising model, difference eqn. solns. 9-4244
- Ising model, Lee-Yang model proved in spin 1 case 9-12265
- Ising model, non simultaneous decouplings 9-5807
- Ising model, one-dimensional, with general spin 9-1650
- Ising model, quantum one-dimensional, soln by quantum statistical spectral density technique 9-98
- Ising model, three-dimensional, critical behaviour of specific heat below  $T_c$  9-21573
- Ising model, two-dimens., with random impurities, thermodynamics 9-12253
- Ising model, validity of recent phenomenological theory 9-18670
- Ising model, with spin  $1/2$  and nearest neighbour interaction, second random phase approx. 9-12264
- Ising problem, eff. of impurities on Curie temp. 9-13952
- isotropic, spontaneous magnetization, critical behaviour 9-10122
- lattice near Curie point, contribution of diffuse modes to thermal conductivity 9-12266
- liquid alloys 9-13540
- magnetic moment diffusion and entropy production 9-10108
- magnetic moments, indirect exchange interactions 9-16340
- magnetostatic wave excitation by e.m. waves in ferromagnets 9-16337
- magnon corrections to electron effective mass in mag. semiconductor 9-18584
- magnons, short-wave, damping below  $T_c$  9-1655
- metals, elec. conductivity rel. to temp. and e. scatt. by spin waves 9-12094
- neutron inelastic scattering by imperfect ferromagnets, temperature dependence 9-10111
- nuclear orientation at low-temp., static methods 9-15162
- ordered structures 9-13969
- relaxation time, longit. near Curie pt. rel. to isotope hyperfine interac. 9-3838
- specific-heat curves for infinite chains with interactions of range  $n(n \leq 7)$  9-17733
- spin correlation functions of the X-Y model 9-7893
- spin susceptibility, generalized, in correlated narrow energy-band model 9-12051
- susceptibility in random dilute systems, molec. field theory extension 9-12246
- theory, allowing for s-d transitions and electron exchange interaction 9-7896
- theory, first order Green function 9-18669
- u.s. absorption by spin system of ferromagnet 9-13795
- vibration spectra in system with coinciding ferroelec. and ferromag. axes, from motion of polarization and magnetization vectors 9-16163
- $\text{Cu}(\text{NH}_4)\text{Br}_2\cdot 2\text{H}_2\text{O}$ , b.c.c. Heisenberg ferromagnet, spontaneous magnetiz. meas. 9-18673
- Fe-base alloys, dilute, rel. to band struct. from electronic sp. ht. 9-13800
- Pd-Fe alloys, ordering temp. by resist. obs. 9-5818

**spin wave theory**

- acoustic oscillation effect in monocrystals 9-3803
- alloys, dynamical spin states 9-16341
- band model, magnetization and susceptibility, review 9-19950
- contribution to neutron scatt., apparatus 9-19701
- correlation function  $S_{zz}(\omega)$  for weakly coupled impurity atom spin 9-3786
- critical slowing down in anisotropic material 9-16347
- diffusion of spins, analogy with particle diffusion in gases and liquids 9-12895
- dislocation scatt. of spin-waves, theory 9-3782
- dynamics of critical fluctuations in kinetic Ising model and anisotropic ferromagnets 9-10109
- elasticity effects on mag. phase transition 9-16336
- electron gas in spin density wave state as carrier of superconductivity 9-7763
- energy of spin waves by Green's function method 9-12251
- exchange model, non-simultaneous decoupling method 9-16346
- Fermi systems, spin-orbit interac., impurity scatt., sp.ht. temp. depend. 9-1657
- ferromagnet with magnetic interstitial impurities 9-5809
- films, dipolar effects in spin-wave eigenfrequencies and eigenfunctions 9-21588
- films, non-planar, spin-wave and magnetization calcs. 9-21589
- fluctuations and slow n and e.m. wave scatt. processes rel. to weak anisotropy 9-18677
- free energy of interacting mag. dipoles, existence and shape in dependence, rigorous proof 9-12255
- Green function theory of spin- $1/2$  Heisenberg ferromagnet 9-16348
- Heisenberg ferromagnet, dynamics at low temps. 9-7895
- Heisenberg ferromagnet, semi-infinite anisotropic, surface waves 9-12257
- Heisenberg ferromagnet, spin wave energy width 9-10105
- Heisenberg ferromagnet, spin-phonon interaction 9-16387
- Heisenberg ferromagnet statistical mechanics 9-21579
- Heisenberg ferromagnets on B-site spinel lattice, critical props. 9-13957
- Heisenberg linear chain ferromag., mag. coupled impurities 9-16338
- Heisenberg model, anisotropic, high temp. critical indices 9-13956
- Heisenberg model, Curie pt. estimations for small particles and thin layers 9-13962
- Heisenberg model, extension to antiferromagnets 9-12250
- Heisenberg model, free energy 9-1654
- Heisenberg model, spin correlation functions in paramag. temp. range 9-3780
- Heisenberg model, resonance freq. rel. to temp. 9-18671
- Heisenberg spin system irreversibility, kinetic eqn. for autocorrelation function at finite temp. 9-21575
- Heisenberg spin system irreversibility, time-dependent fluctuations at Curie pt. 9-21576



**Ferromagnetism continued**

**spin wave theory continued**

- Heisenberg model, Dyson equation for magnons 9-16344  
infinite spin dimensionality limit, spherical model 9-13955  
Ising, order parameter calc. 9-12262  
Ising chain with long-range interaction, phase transition existence 9-12259  
Ising ferromagnets on B-site spinel lattice, critical props. 9-13957  
Ising model, 2-dimens., partial weak clustering states, symmetry groups 9-17692  
Ising model, two-dimensional, Toeplitz determinants and spin correlations, theory 9-5812  
Ising model appl. to magnetization process in spinel lattice 9-1652  
Ising model with higher spin, zeros of partition coeff. 9-10107  
Ising model with two and three phase transitions 9-5754  
Ising one-dimens. ferromagnet, phase transition 9-21572  
Lenz-Ising model 9-21578  
line shape of spinwave sidebands 9-10104  
magnetic diode interaction for Heisenberg ferromagnet sublattice 9-5808  
magneto-elastic interactions, effect of elastic anisotropy 9-3804  
magnetoelastic waves, coupled, props. in mag. mats. without centre of inversion 9-21559  
magnon density fluctuations in Heisenberg ferromagnet 9-17450  
magnon-elastic wave self-consistent interaction and sound absorpt. coeff. calc. 9-1647  
mass operator for phonons, imaginary part freq. dependence at high temps. 9-21574  
mass operators for phonons and magnons, real part determ. 9-20358  
metals, appl. to transport phenomena at high temp. 9-3576  
metals, c. scatt. on spin-waves in thermo-e.m.f. calcs. 9-3719  
neutron inelastic scatt. by spin waves 9-7892  
neutron scatt. in thin films, angular distrib. rel. to spin wave freq. 9-16349  
neutron scattering temp. shift of maximum,  $\langle \sin^2 \theta \rangle / r$  spin correlation discussion 9-12258  
nonlinear effects in isotropic ferromagnet due to spin wave instability in case of arbitrary orientation of alternating and static mag. fields 9-1649  
paramagnons, existence in strongly anisotropic ferromag. crystals 9-10101  
polar states in metals 9-7894  
polarons, small-radius, mobility at low temps. 9-1648  
Raman scatt. of hypersound in ferromagnet with strong magnetostriction 9-5543  
scaling laws and impurity effects near critical point 9-16345  
semiconductors, spin wave amplification 9-10110  
spin-lattice interaction in effect of elasticity on phase transitions 9-16336  
spin-phonon interaction, influence on sp. ht. of ferromagnet 9-12017  
spin-Raman susceptibility by means of spin-wave instabilities 9-10143  
thin film, magnetic domain struct. 9-5833  
time-correlation of spins, long-time behaviour, Halperin-Hohenberg law with  $0=5/2$  9-12235  
uniaxial, parametric resonance threshold, anisotropy effects 9-3781  
uniaxial system, Green function approach 9-1651  
Wick's theorem for spin operators, proof 9-10106  
XY ferromagnets on B-site spinel lattice, critical props. 9-13957  
Fe-Pd alloy, dilute, spin-wave stiffness, by neutron scattering technique 9-12268  
Fe<sub>2</sub>Al ordered alloys, dispersion law for spin-wave excitations, Heisenberg model 9-18674  
FeSi ordered alloys, dispersion law for spin-wave excitations, Heisenberg model 9-18674  
Gd, magnetocrystalline anisotropy 9-5815  
<sup>3</sup>He, liquid, spin-wave spectrum, paramagnon model 9-5206  
Ni, long wavelength, energy computation 9-12271  
Tb, rel. to temp. depend. of magnetization and mag. specific heat 9-12292

**Ferromagnets** see *Magnetic properties of substances/ferromagnetic*

**Feynman diagrams** see *Field theory, quantum/interactions*

**Fibre optics** see *Fibres/optical*

**Fibres**

- acoustic wave velocity and absorption 9-5540  
C, MP, suitable pitch mats. for prod. 9-8054  
cellulose, preferred orientation, effect of thermal decomp. 9-8072  
cotton, finishing with chloroacetamide 9-17515  
density meas. with vibroscope, fixed frequency, evaluation tests 9-6370  
diameter meas. using cell interferometer and Edser-Butler fringes 9-4213  
filamentary composites, fabrication, props. and applications 9-1076  
flexible, dynamic phenomena at free end 9-123  
glass, strength, irradiation effect 9-11934  
graphite, co-existence of cryst. graphite and turbostratic C phases 9-7363  
in plastics as reinforcements, model for plasticity 9-1278  
polyamide, arranged contribution of macromolecules by magnetic susceptibility and anisotropy 9-21557  
polycaprolactam, photomechanical, degradation and lifetime 9-11937  
polyethylene terephthalate monofibres, effect of orientation of visco-elastic properties 9-9750  
polyethyleneterephthalate, oriented, supermol. struct. rel. to thermoplasticizing elongation, obs. 9-11757  
from polymer crystals, deformed, fine structure by electron diff. and microscopy 9-18395  
polyvinyl chloroformate, preparation 9-17527  
polyvinylalcohol, oriented, supermol. struct. rel. to thermoplasticizing elongation, obs. 9-11757  
reinforced composites, free harmonic wave dispersion 9-20422  
silk, photomechanical degradation and lifetime 9-11937  
thin layer mats., optical coeffs. 9-1726  
wooden, microrheometer for meas. tensile stress 9-5472  
C, 'ordinary' and high modulus, microstruct. 9-7417  
C, 7  $\mu$  diam., in loop, bending behaviour and tensile failure 9-7564  
C, from petroleum sludge, prep. and phys. props. 9-8060  
C, high strength and modulus, with good graphite layer alignment 9-7514  
C, preferred orientation of carbonized cellulose, X-ray study 9-7359  
C glassy monofilaments, obtained from thermo-setting resins 9-7320  
Ta, tensile props. of 10-fibre bundles at 1000°F 9-18515  
W, tensile props. of 10-fibre bundles at 1000°F 9-18515

**optical**

- contiguous, for carrying thermal information from welds 9-6228  
frequency constant charact. of fibre assembly 9-15548  
glass, angular displacement transducer 9-12846  
glass compatibility 9-13066  
glass-fibre waveguides e.m. coupling with Nd<sup>3+</sup>-doped laser resonators 9-14434

**Fibres continued**

**optical continued**

- light transmissivity, effect of interdiffusion of glass 9-13065

**Field emission** see *Electron emission/field emission*

**Field emission microscopes** see *Electron microscopes; Ion microscopes*

**Field theory, classical**

- See also *Electromagnetism; Gravitation; Relativity*  
boson field, free, C\*-algebra and automorphisms 9-12872  
density field, fluctuating, representation by Markovian process 9-47  
faster-than-light motion, consistency with Lorentz-invariance of S-matrix 9-16670  
generating function of tree graph approx. for quantum field theory 9-6577  
gravitational, Einstein's eqns., Schwarzschild's interior soln., nonstatic analogs 9-16676  
gravitational, Einstein eqns., axially symmetric soln. 9-16666  
gravitational, Kerr family, global struct. causal behaviour 9-16679  
gravitational, Kerr family, global struct. causal behaviour 9-6310  
gravitational, Kerr family, global struct. causal behaviour 9-6310  
Hamilton's principle, modification with natural boundary and initial conditions 9-14324  
Hamiltonian, relativistic derived by octonion methods 9-2141  
harmonic force fields, conservative system motion 9-20310  
inverse square problems in potential theory, for spherical shells 9-16663  
linear thermo-viscoelasticity theory, correspondence principle, mixed boundary value problems 9-16662  
non-linear fields, electrical analogues made from non-linear elements 9-48  
particle-like solns., interaction, exact calcs. 9-6293  
potential theory, inverse square problems and spherical shells 9-16663  
Riemann surfaces of field extensions 9-17698  
vector fields, Hamiltonian, ang. and action variable 9-15445

**Field theory, quantum**

- See also *Dispersion relations; Elementary particles; Physics fundamentals; Quantum theory*  
2(2s+1) component fields, bilinear expressions and spin kinetic moment currents 9-17950  
A<sup>4</sup>-coupling, direction-depend. singularities, eff. in local field eqn. 9-19176  
algebra of observables, continuous representations of symmetry groups 9-45  
algebras of test functions, positive functionals 9-299  
angular momentum separation into spin and orbital parts 9-10954  
angular momentum waves RPA in solid o-H<sub>2</sub> 9-20580  
axiomatic, consistent bootstrap 9-11023  
axiomatic, renormalization of field operator 9-300  
Bethe-Salpeter eqn., bootstrap solns. 9-2545  
Bethe-Salpeter eqn., for calc. asymptotic behaviour of hadron form factors 9-16830  
Bethe-Salpeter eqn., partial-wave, soln. and reduction to linear systems 9-13106  
Bethe-Salpeter eqn., stationary expectation value calc. 9-2459  
Bethe-Salpeter eqn. and dynamical groups 9-16804  
Bethe-Salpeter eqn. reduction for zero-mass fermion-antifermion system 9-14463  
bilocaf field eqns., Greens function with special reference to Regge pole  
Green's function with special reference to Regge pole term 9-2435  
binary inelastic processes, amplitudes asymptotic behaviour 9-6569  
bootstrap and pole dominance formulation for hadron scatt. amp. and form factors 9-6636  
bootstraps, field theoretic formulation 9-17966  
Bose local free infinite-component fields, TCP-invariance invalidity 9-20576  
boson field, nonlinear self-interacting, dynamical invariance 9-2448  
boson fields, two coupled massive, bound states 9-2157  
bosons, spinless with arbitrary isospin, free-field theories and locality 9-8716  
bremsstrahlung amplitude for soft photon emission, low freq. limit 9-8746  
canonical anticommutation relations, representations and adjoints 9-6576  
canonical commutation reln. nonequivalent representations 9-17923  
Cauchy data and particle states for theories with higher order derivatives 9-8681  
chiral-dynamical Lagrangian for baryons of arbitrary spin and isospin 9-16899  
chiral-invariant effective Lagrangian for S- and P-wave noneptonic hyperon decay 9-14524  
Clebsch-Gordan coeffs. of different SU(n) groups, relationship 9-8692  
complex self interacting scalar field theory with positive-definite energy density, particle-like solns. 9-8684  
coupling constant, analytical structure 9-4549  
coupling of space-line and internal symmetry groups 9-6582  
critical phenomena description 9-83  
critical phenomena description 9-12888  
current commutators in perturbation theory, singular equal-time behaviour 9-10953  
currents and densities as coordinates in nonrelativistic quantum mechanics 9-8690  
currents dynamical theory, equal-time commutators and Lorentz covariance 9-17919  
de Sitter space-time, scalar field, quantum theory, quasiclassical motion condition 9-17904  
differential cross-sections equalities at large energies 9-10964  
Dirac isotopic current operator in Yang-Mills theory 9-337  
Dirac spinor in 6-dimens. space 9-17920  
Einstein field eqn., axial symmetric stationary soln. for vacuum 9-17907  
electromagnetic zero-pt. energy and retarded dispersion forces, relation to classical mech. field 9-16808  
e.m. field generalized coherent states rel. to average field and e scatt. amplitudes 9-8689  
equations coupled by  $\alpha/r^2$  potential, model and threshold law 9-4237  
e.s.r. of impurities in metals (dil. mag. alloys), applic. of Abrikosov diags. for spin operators 9-12497  
essential for cosmic particle creation calc. 9-1982  
Faddeev equations, relativistic, decoupled and covariantly reduced 9-8705  
faster-than-light particles, local field theory and Lorentz invariance 9-8709  
Federbush model, existence of Green's functions 9-8686  
Fermi local free infinite-component fields, TCP-invariance invalidity 9-20576

**Field theory, quantum continued**

- fermion field broken-symmetry condition 9-13092
- fermion interacting syst., 1-dimens., Luttinger model 9-13083
- Fermion non-relativistic field, time displacements and auto morphism 9-290
- Feynman amplitudes analytic renormalization 9-14461
- Feynman diagram method for nuclear tunnelling reactions 9-11263
- Feynman diagrams, instructive simple example 9-4557
- Feynman integrals, type-II singularities, struct. 9-20584
- Feynman rules for e.m. and Yang-Mills fields from gauge-independent formalism 9-15571
- Feynman rules for gravitational field from co-ordinate independent formalism 9-10961
- Feynman-diagram models for Regge pole conspiracies 9-2486
- Finsler spaces 9-20585
- form factors, properties 9-8714
- free e.m. radiation, correspondence with classical theory 9-8546
- free theories of arbitrary spin and isospin particles 9-17911
- gauge field, non-Abelian, internal charge 9-13084
- general relativistic theories, equivalence 9-16806
- generalized unstable particle, complex higher order poles 9-4598
- Green's functions construction in momentum space for unrenormalizable interac. 9-2454
- Hamiltonian describing two-level system coupled to Bose gas with Einstein spectrum, exact diagonalization, simple method 9-20365
- Hamiltonian formalism for free particles of any spin and non-zero mass. 9-16801
- hard-core potential and two-body  $t$  matrix expansion 9-4706
- Hilbert spaces, continuous tensor products in field construction 9-14317
- hyperplanes, spacelike, coupling between Poincare group and space-time reflections 9-16669
- hyperplanes, spacelike, timelike reflection, coupling between time reserval and Poincare group 9-16668
- infinite component field theory, Lagrangian approach 9-13086
- infinite multiplets, interaction and specific props., matrix of finite Lorentz transformation, formulation of Feynman rules 9-4558
- infinite-component fields, TCP-invariance invalidity 9-20576
- infrared divergences, soft-photon asymptotic states, Green's functions, reduction formulae 9-16810
- intrinsic invariance groups, mass operators and linear wave eqns. for free spinning particle 9-8698
- isospin violation in direct and compound nuclear reactions 9-573
- Jacobi matrix representation of models 9-8683
- Kallen distributions, analyticity 9-293
- Lagrangian, nonlinear, chiral symmetry 9-16852
- Lagrangian formulation of Joos-Weinberg equations for spin- $s$  particles 9-10996
- Lee model, Galilean invariant, local Hamiltonian existence 9-15567
- Lee model, mass renormalization, composite effects 9-295
- Lee model, N-quantum approx., renormalization procedure 9-2441
- Lee model,  $Z \rightarrow 0$  limits 9-8772
- Lie algebra, nonintegral, and charge quantization 9-10956
- Lie algebra, semi-simple, realization with quantum canonical variables 9-16802
- Lie algebra representations, first order deform., classification using cohomology group 9-6282
- Lippman-Schwinger eqn., partial-wave, for superposition of Yukawa pot., soln. and reduction to linear systems 9-13090
- local, and covariant version of Bjorken limit 9-2458
- local, rel. to Carruthers theorem of Carruthers and positronium decay 9-10984
- local operator algebras in presence of superselection rules 9-14452
- Lorentz and isospin-covariant field eqn., non-existence of self-conjugate particles with half-integral isospin 9-2442
- Lorentz group extension, covariant currents and Dirac spinors over finite field 9-17922
- Lorentz-covariant complex scalar theories with minimal gauge invariant e.m. coupling, positive definite energy density existence of particle like solns 9-8685
- LSZ, rigorous formulation 9-19180
- magnetic moments and charge radii for states described by infinite component wave equation 9-20609
- Maxwell-Einstein-Klein-Gordon fields, static 9-20575
- meson processes, hard-pion current algebra calc., N-point func. 9-8858
- model with three fixed sources, bound states and resonances 9-14456
- molecular approx., Weiss, formal structure anal., fields and partition function determ. 9-20579
- $\lambda\phi^4$  self-interaction of  $\phi$  scalar field, 2-dimens. space-time, dynamics construction 9-20577
- N-quantum approx. of Greenberg, renormalization procedure 9-2441
- nonlinear real scalar field, determ. of mass spectrum 9-13082
- nonzero-mass theory, renormalizable conditions 9-2436
- operators commutation relations 9-19178
- optical birefringence 9-17206
- optical birefringence 9-11696
- optical birefringence, application to linear, nonlinear optical rotation 9-268
- optical model, phys. significance of field comparison of classical and quantum-mechanical descriptions 9-14419
- particle localization props. 9-291
- perturbation theory equal-time commutation reln. of renormalizable currents 9-14451
- perturbative, finite formulation for obtaining S-operator 9-13085
- plane graph asymptotics, simplified method 9-20586
- plasma in magnetic field, nonlinear phenomena considered 9-11539
- plasma in magnetic field, nonlinear phenomena considered 9-9345
- Poincare generators, structure 9-2439
- position-space analytic func. dual to Feynman integral, mass-superpositions 9-8691
- potential, bound states asymptotic behaviour, in large coupling limit 9-15569
- quasi-particle, transposition into ideal space, canonical transf., boson method 9-14542
- R(11) current commutation relations 9-16828
- Rarita-Schwinger spin- $1/2$  field; interaction, quantization and subsidiary conditions 9-17918
- Reeh-Schlieder theorem, weak additivity-property in deriv. 9-19183
- Regge trajectories, intersecting, high-energy perturbation theory calc. 9-17962

**Field theory, quantum continued**

- relativistic, symmetry operations rel. to spontaneously broken symmetries 9-16805
- relativistic, TCP theorem breakdown in odd-dimen. space-time 9-17925
- relativistic invariant distributions and space-time props. 9-294
- relativistic wave eqn. 5-dimens. formalism, De Sitter group representation 9-10955
- renormalization groups and transforms props. and consequences 9-301
- S-matrix amplitude, Heisenberg field and T-product representation technique 9-6570
- scalar fields, null and pseudonull data 9-17910
- scalar model, cut-off depend. operator soln. and Wightman functions 9-19177
- scalar model nonlinear theory, limit cycle solns., applic. to Hartree eigenvalue eqn. 9-11378
- scattering lengths for static potentials, upper and lower bounds 9-17917
- Schrodinger theory, random fluct., connection with classical mechanics 9-16808
- self-composed field dynamics in 1-dimens. space-time 9-13081
- self-conjugate isofermion theories of arbitrary spin are nonlocal 9-17911
- with spacelike momentum spectra and isospin, relativistic 9-8696
- spherical top in internal space second-quantized theory 9-8707
- spin, statistics and kinks 9-14453
- spin and statistics rel., fundamental theorem for connection with Bose and Fermi fields 9-17926
- Stueckelberg fields and current-algebra sum rules 9-8688
- Sugawara's theory of currents, canonical representation 9-6567
- symmetry Amer. J. Phys. resource letter 9-6584
- TCP theorem, breakdown in odd-dimen. space-time 9-17925
- time invariant, in covariant Hamiltonian formalism 9-16801
- transcendental and polynomial Langrangians, correlations and radiative correct. 9-16817
- tree-graph approx., classical field generating functional 9-6577
- two-dimensional, time-ordered products 9-8686
- u.v. divergences, regularization, and analytic functionals 9-2440
- vacuum polarization in an oscillatory gauge 9-10959
- $\Phi^4$  3-dimens. interaction of boson field 9-17905
- Wigner 9j symbols, relationships and identities 9-292
- Yang-Mills field, free, e.m. part, asymptotic identification 9-14462
- Zachariasen-Thirring model, asymptotic condition 9-8682
- Zachariasen-Thirring model with 2 coupling const., reduction formulae applic. 9-15566
- zero rest-mass field eqns. in flat space-time, solns. 9-17908
- npd vertex functions, eff. on form factors in calc. 9-15588
- H atom relativistic model, helicity symmetry group SU(2), Dirac quantum no. double degenerate 9-6571

**electromagnetic field see Quantum electrodynamics****interactions**

- See also *Elementary particles/interactions; Nuclear reactions and scattering. Entries on interactions involving named particles are listed under the particles concerned*
- atoms, neutral hydrogenic, e.m. and electrostatic contribution to energy 9-9150
- Bethe-Salpeter eqn., algebraic structure and singularities 9-17909
- Bethe-Salpeter equation, fourth order, solns. 9-15572
- Bethe-Salpeter eqn., soln. for bound state of two spin- $1/2$  particles 9-6588
- boson field, self-interacting in 2D, in periodic box, semiboundedness of Hamiltonian 9-14457
- composite systems, loosely-bound, e.m. interac., Dirac interac. validity 9-16910
- distortion operator method generalization 9-10952
- e.m., free Yang-Mills field, asymptotic identification 9-14462
- Heisenberg picture field operators for Yukawa interac. in infinite vol. 9-17924
- Lee model, 2V sector, dispersion methods 9-16844
- Lee model, 2V sector, LSZ formalism used to solve entire sector 9-2434
- non-linear fields, variational method for obtaining forces 9-2433
- with  $n$  final particles, helicity amplitudes crossing relations and rel. to multi-Regge model 9-317
- $n$ -particle prod. cross section, multi-Regge model 9-316
- particles with elec. and mag. charges, soluble nonrelativistic model 9-17913
- self-conjugate isofermion fields 9-6566
- set of fields belonging to internal symm. group, commutation relations 9-17912
- Su(3) strong breaking and dynamical asymmetry 9-8769
- tachyons, construct. of Lorentz-invariant theory 9-16812
- two-body, transversity amplitudes, kinematical singularities 9-318
- Yang-Mills interaction with gravitational field 9-17832
- Yukawa interac. in infinite vol., Heisenberg picture field operators 9-17924
- $p$  atoms, hyperfine structure, many-body perturbation theory 9-678

**interactions, strong**

- See also *Elementary particles/interactions, strong*
- $A(x)$  model, N-quantum approx., reformulation 9-2441
- coupling theory, new formulation 9-15570
- perturbations, cal. divergent integrals analytic continuation 9-8781
- spinor space, SU theory 9-2455
- two-nucleon  $s$ -wave phase shift, attraction and repulsion of single separable potential 9-4553
- unitary Padé approximants in nucleon-nucleon syst. 9-20667

**interactions, weak**

- See also *Elementary particles/interactions, weak*
- renormalizable field theory 9-20578
- time-reversal apparent violation in higher-order interactions 9-4573

**meson field**

- See also *Mesons; Nuclear forces*
- coupled with fermion field, behaviour of classical solns. near light cone 9-6587
- nucleon-nucleon scatt. obs., nuclear forces considered, 25-310 MeV 9-4707
- in photons and gravitons presence, single-particle singularities 9-8697
- pseudoscalar-pseudoscalar coupling model calc. of  $p, s$ -wave scatt. lengths in  $\pi$ N scatt. 9-16879
- scalar, coupling to trace of energy-momentum tensor, nonpolynomial interac. Langrangian 9-16827
- scalar, zero-mass Einstein eqns., axially symmetric soln. 9-16666



**Field theory, quantum continued****meson field continued**

- vector field with non-zero mass, relativistic eqns., invariant expansion of solns. 9-15631
- vector massless precise form factors 9-8799
- Yukawa potentials, superposition, soln. of partial-wave Lippman-Schwinger eqn. 9-13090

**quantization**

See also *Quantum theory/quantization*

- infinite multiplets 9-4558
- para field theory, procedure 9-19179
- polarization operator 9-8703
- radiation fields, phase- and amplitude-size rel. to meas. method 9-6568
- scalar-mes., coupling to trace of energy-momentum tensor, nonpolynomial interac. Langrangian 9-16827

**scattering**

See also *Elementary particles/scattering*

- amplitude, false poles in models 9-17921
- amplitude, restrictions on high energy behaviour 9-8694
- axiomatic analyticity properties of spin particles, proof of superconvergence relations 9-16841
- central potentials, amplitude convergence and bounds considered 9-8695
- compositeness conditions for particles with identical quantum numbers 9-15568
- Einstein's opt. scatt. eqn., microscopic extensions 9-13331
- Einstein's opt. scatt. eqn., microscopic theory 9-13330
- elastic transition matrix, unitarized Born approx., soln. 9-4577
- Feynman amplitudes  $O(4)$  symmetry at zero invariant mass 9-8733
- field operators, asymptotic, multiparticle, for phenomenological pots. 9-8693
- impact-parameter representation of high energy amplitude 9-4552
- Klein-Gordon eqn., nonlinear, time and local energy decay 9-302
- Lee model, 2V sector, LSZ formalism used to solve entire sector 9-2434
- particles, angular momentum, tensor form 9-16803
- relativistic kinematics, constraints among partial waves 9-338
- s matrix elements, second order 9-2440
- SL(2C); subalgebras and contraction survival 9-42
- spiral amplitude, relativistically invariant expansion 9-14455
- $\pi\pi$ , low-energy S-wave, model with rigorous constraints 9-8864

**Films**

- Bose, transition from  $\approx$  to  $\Xi$  behaviour 9-19002
- on cellulose gel, wet, monolayer coating by transfer from aqueous sub-phase 9-9573
- dielectric, applic. of complex transmission and reflection coeffs. to plasma diagnostics 9-19116
- dielectric, inhomogeneous, light reflection and transmission, theory 9-15542
- gas, for cooling, effect of strong adverse pressure gradients 9-17158
- photographic, sensitivity, absolute determination in vacuum ultraviolet 9-20570
- polyvinyl chloroformate, preparation, reaction props. 9-17527
- resistive thin, residual gases during deposition, mass spectroscopy 9-1099
- vapour, 1-dimens. growth, uniform thickness 9-21248
- Fe, corrosion inhibition, transition state in inhibitor ionc. versus surface coverage 9-15223
- SiO<sub>2</sub>, resistance-heat and e-gun evaporated, comparison of props. 9-3206

**liquid**

See also *Adsorbed layers; Contact angle; Helium/liquid;*

*Superfluidity; Surface tension*

- adhering to cylinder withdrawing from Newtonian liquid baths, props., thickness meas. 9-18347
- alcohols, 1- and 2-, on water surface, dissolution rate 9-5144
- alcohols on water, spreading press. rel. to interfacial tension, work of adhesion and solubility 9-9494
- alkali halides, periodic oscillations of impurity particles 9-9504
- black film, contact angles with bulk liq., and expansion kinetics 9-19602
- bovine serum albumin at air-water interface, thickness rel. to adsorb or spreading 9-9477
- bubble contact angle with liquid, investigation using deflection of light beam 9-21178
- cetane, ignition by reflected shock waves in air or O<sub>2</sub> 9-14127
- docosyl triethylammonium bromide, ionized monolayers at air/water interface, eqns. of state 9-9500
- falling along vertical solid surface, mass transfer 9-14827
- foam, black, stability due to work of desorbing H<sub>2</sub>O mols. 9-19650
- free, dynamics 9-977
- gas absorbing with time depend. density gradients, stability 9-21182
- immiscible, co-current flow with surface evaporation, direct contact heat transfer with change of phase 9-19086
- interfacial, hydrodynamic effects 9-18348
- laminar accelerating flow down vertical wall, soln. rel. to growth of boundary layer and film thickness 9-18349
- mass transfer coefficient from bubbles, estimation 9-19600
- nematic, structure distortion under mag. field 9-9482
- non-Newtonian, flow on surface of rotating disc., vel. and thickness calc. 9-21181
- oscillations of a viscous thick film in the gravitational field 9-21002
- sodium lauryl sulphate, at different NaCl conc., black film contact angles with bulk liq. 9-19602
- splitting behaviour between two parallel disks/dynamics 9-9476
- surface square mesh patterns due to vibration 9-998
- surfactant layer at cellulose acetate membrane saline soln. interface, effect on reverse osmosis 9-9502
- viscous, flowing down, flexible boundary stability characteristics 9-3072
- Ga, optical props. 9-3192
- He, Bose-Einstein and hard sphere gas models 9-3142
- He, unsaturated, superfluidity without superflow 9-19653
- He superfluid, critical vel. determ. by third sound 9-21237

**Films, solid**

See also *Thickness measurement*

- acoustic plasma waves 9-9911
- adsorption layers on single crystals, meas. by ellipsometry 9-9609
- Al<sub>2</sub>O<sub>3</sub> film as support, patent 9-13163
- alloys, binary, co-deposition by e beam, controlling apparatus 9-11776
- antireflection coating, attenuation increase of off-axis laser modes 9-4459
- antireflection coatings, broadband, refractive indices 9-14028
- BaF<sub>2</sub>, chemisorption of p-benzoquinone, i.r. spectra 9-8084
- binding of coating to metal base restraining crack propagation 9-18520
- borosilicate glass, new i.r. absorption peak 9-17485
- $\beta$ -cholestanol multilayers, CO<sub>2</sub>, N<sub>2</sub> and He permeabilities, obs. 9-5415

**Films, solid continued**

- coating on rough surface, thickness meas., luminescent method 9-10609
- with coherent distortion-free particles, extinction contrast 9-7334
- collision of atom, theory 9-5233
- condensed, internal stresses, obs. during condensation and annealing 9-21266
- crystal cleavage apparatus for production of clean film in vacuum 9-1097
- cyclotron resonance 9-1441
- Debye-Waller factor, size dependence 9-7623
- defects produced by deformation 9-7544
- dielectric, crystallization state evolution, e. diff. study 9-11768
- dielectric, elimination of reflectance of solid laser materials 9-10864
- dielectric, sputtering yield and thickness meas. 9-13581
- dielectric nonlinearity under intense elct. field at low freq. 9-1585
- electron diff. calibration film, instant, prefabricated 9-16070
- electron scattering, (e, 2e), quasielastic ejection 9-14669
- electron-probe X-ray microanalysis 9-14143
- energy loss of fast electrons with retardation of e.m. field 9-7689
- epitaxial, thermoelec. power, theory 9-15130
- evaporated, surface roughness effect on thickness meas. by Tolansky method 9-5235
- f.c.c. metals, epitaxial growth on KCl cleaved in u.h. vacuum, surface defects effects 9-5241
- f.c.c. metals, formation on alkali halides, influence of impurities 9-21268
- ferrites, for e.m. wave absorption 9-17836
- foil thickness meas., by Coulomb back scatt. of heavy ions 9-5234
- formation, material props. rel. to electronic use, applic. to integrated circuits, book 9-18402
- garnet, prep. by sputtering 9-5248
- glass, preparation, applic. to phase separation study 9-5226
- glass-ceramic coatings for metals, elec. and mech. props. improvement 9-3189
- graphite, membranes, density, tensile strength, crystallog. parameters, elec. and optical props. 9-11777
- growth from vapour phase, mechanism and morphology 9-21294
- impurity influence on formation of single-crystal films 9-21268
- interferential, for metallographic exam. 9-5296
- lattice dynamics, local modes and Mossbauer eff. 9-18544
- lubricant, pressure effects on friction coeff. 9-16138
- metal epitaxial film on alkali halides, effect of gas ads. 9-16044
- metal epitaxial film on alkali halides, effect of gas ads. 9-3199
- metal film condensation effect of vapor subcooling 9-19662
- metal self-supporting, thickness meas by e transmission 9-9608
- metallic, formation and physical properties influence of residual gases 9-3203
- metallic, layered, supercond. enhancement 9-7765
- metallic, thin, on curved substrates, etching technique for microcircuit prod. 9-8571
- metallic, vacuum deposition techniques, review 9-7340
- metals, fracture strength 9-7559
- metals, oxidation kinetics investigation 9-10338
- metals, thermoelec. and mean free path effects 9-13925
- mylar, preparation to 200  $\mu\text{g}/\text{cm}^2$  9-3207
- naphthalene, evap., exciton diff. 9-7718
- oleic acid multilayers, CO<sub>2</sub>, N<sub>2</sub> and He permeabilities, obs. 9-5415
- optical coatings, instrument for estimating hardness 9-13743
- organic, diffraction patterns produced by nuclear reactions 9-15039
- organic, particle detector, sensitivity effects of O<sub>2</sub> and humidity 9-20710
- orientated mat. deposition on single crystals 9-5284
- oxide, on Fe-Si alloy crystals, growth kinetics, optimal exam. 9-21277
- oxide, on Cu, ellipsometric meas. of thickness and reflection eqns. 9-16043
- oxide, on Fe-Fe<sub>3</sub>C, growth 9-1110
- oxide, thickness determ. by triton irradi. 9-2758
- oxide growth on metals, kinetics rel. to electronic and ionic diffusion in large surface-charge and space-charge fields 9-9620
- oxide surface-density meas. based on charact. X-ray production by 100-keV protons 9-13575
- paint, on Al and alloys, defects rel. to electrophoretic deposition 9-4005
- paraffin lubricant on steel, pressure effects on friction coeff. 9-16138
- permalloy, ageing and stabilization 9-3471
- permalloy, stresses, annealing and substrate temp. effects 9-13724
- permalloy, vacuum deposited, elastic limit and tensile strength 9-3412
- phenolic resin-based adhesive films, development and testing 9-18540
- phonon spectrum changes, supercond. enhancement 9-5529
- polyethylene, chlorination and eff. on mech. props. 9-17520
- polyethylene, drawn, orientation distrib. functions by broad line n.m.r. 9-12517
- polymer photoresist, ion beam exposure, scattering effects 9-13813
- polymer thin films, crystn. process 9-21271
- polymers, surface treatment by r.f. plasma reactor 9-11579
- polypropylene, uniaxially drawn isotactic films, quantitative characterization of deform. 9-21375
- polystyrol, mech. effects of discharges 9-10032
- polyurethane, chem. struct. eff. on resistance to various forms of degradation 9-14983
- porcelain enamels, electrostatic spraying 9-1095
- quantum size effect in determining electron spectrum structure 9-16202
- reduced oxide, structure, on electrochemical hot-rolled steel 9-6012
- salol, structure control during growth process from supersaturated condensate current 9-1103
- semiconductor, charact., use of surface elastic vib. meas. method 9-18625
- skin effect, anomalous 9-1447
- stearate multilayers, CO<sub>2</sub>, N<sub>2</sub> and He permeabilities, obs. 9-5415
- steel, Cr-Ni, nitride layer formation in intermediate stages of  $\gamma$ - $\alpha$  transformation 9-13775
- steel, stainless, microtwins prod. by mechanical abrasion 9-3228
- steel, stainless 304 film, interfacial free energies investig. by electron transmission and diff. microscopy 9-1231
- structure and props. control during growth process for supersaturated condensate current 9-1103
- superconducting, inhomogeneity of transport current distrib. 9-7758
- superconducting thin film, type II, current distrib. 9-13858
- superconducting transition temp., effect of lattice disorders 9-5655
- thermal conductivity, phenomenological theory 9-3538
- thermoplastic thin, time measuring of mechanical relaxation 9-5436
- thickness, x-ray direct counting precision method 9-1098
- thickness determ. from slip trace analysis in e. microscope without specimen tilt determ. 9-7330

## Films, solid continued

- thickness determ. using small freq. change meas. circuit 9-12968  
 thickness meas., nondestructive, of transparent films on microstructures 9-3191  
 thickness meas. by electron microprobe analyzer 9-3190  
 thickness meas. method for electrolytically deposited films 9-11763  
 thickness meas. technique for films grown on rough surfaces 9-5236  
 thickness meas. using quartz oscillator 9-11764  
 thickness meas. using quartz-crystal monitors, acoustic wave analysis of operation 9-11761  
 transparent, on reflective substrates, thickness determ., phase-shift corrections 9-7329  
 vacuum deposited, electron gun for evaporation 9-12979  
 vacuum deposition, differential ion pumping 9-12816  
 vacuum deposition wing CO<sub>2</sub> laser 9-11775  
 vacuum-deposited, thickness meas. 9-5232  
 welded clad metal diffusion layer structure 9-18485  
 white thermal control coatings in space, stability model 9-1096  
 Ag, Au, epitaxial and polycrystalline, props., influence of  $\alpha$  irradiation 9-5240  
 Ag, epitaxial growth on cleavage face of mica 9-5242  
 Ag, resistivity change due to neutrons and  $\gamma$  rays 9-17378  
 Ag, temperature during evaporation 9-17243  
 Ag, vacuum-deposited, electron microscope obs. on sulphuration 9-11765  
 Al, energy losses of electrons, rel. to thickness and surfaces 9-5588  
 Al, evaporated, O and H<sub>2</sub>O vapour interaction 9-21273  
 Al, growth, effect of elec. field 9-13582  
 Al, high-angle grain boundary structure 9-18442  
 Al, oxidation, effect of oxide thickness 9-18754  
 Al, refr. and refl. of fast electrons 9-17362  
 Al<sub>2</sub>O<sub>3</sub>-SiO<sub>2</sub>, binary oxide, deposition on pyrolytic decomposition of trimethylsiloxyl-aluminium-isopropoxide 9-21272  
 Al<sub>2</sub>O<sub>3</sub> anodic coatings, structural changes during anodizing and sealing, i.r. analysis 9-21711  
 Al<sub>2</sub>O<sub>3</sub> anodic coatings, structure and transforms from effluent gas detection and i.r. analysis 9-21712  
 $\alpha$ -Al<sub>2</sub>O<sub>3</sub> on Ta alloy by chem. vapour deposition 9-1108  
 Al coatings on steel, structure and composition, effect of condensation temp. 9-21282  
 Al coatings on steel by vacuum evaporation 9-13584  
 Al covered with NaCl layer, intensity of photoelectrons emitted 9-19939  
 Al epitaxial, orientation dependence on substrate defects 9-1105  
 Al etching from substrate in acid soln. with fluoride ions, patent 9-19684  
 AlN, microwave acoustic transducer, vacuum deposition 9-10056  
 AlN, pyrolytically deposited on Si, growth charact. 9-13583  
 Al<sub>2</sub>O<sub>3</sub>, 500 to 6000 Å, traps, study using thermoluminescence glow curves in range 30 to 300°C 9-17429  
 Al<sub>2</sub>O<sub>3</sub> layers formed on anodic oxidation of Al, growth an struct. 9-4004  
 Ar impurity analysis by r.f. spark-source mass spectrography 9-15232  
 Au-Cu alloy on Au, two-layer, Moiré patterns and misalignment dislocations 9-3200  
 Au-Pd, diffusion coeff., 400-600°C, electron diffraction study 9-5399  
 Au, condensation of atomic beam on rocksalt substrate 9-14897  
 Au, discontinuous, evaporated on CdI<sub>2</sub> substrate, electron diffraction pattern interpretation 9-18433  
 Au, epitaxial growth on cleavage face of mica 9-5242  
 Au, grown on rough surfaces, thickness meas. technique 9-5236  
 Au, growth on KCl in high vacuum 9-21274  
 Au, lubricant on steel, pressure effects on friction coefficient 9-16138  
 Au, nucleation, growth and struct. obs. in e. microscope 9-19673  
 Au, recrystallization rel. to prod. of large single crystals 9-19691  
 Au, thin, adhesion to glass 9-1337  
 Au epitaxy on KCl, KBr, KI in u.h. vac. 9-7310  
 Au on colour-centred NaCl, nucleation density epitaxy and orientation, obs. 9-9615  
 Au on MoS<sub>2</sub>, epitaxial, angular distribution of nuclei 9-9614  
 Au resistivity change due to neutrons and  $\gamma$  rays 9-17378  
 B, prep. on Si substrate 9-13585  
 B, preparation and electron microscope obs. of defects 9-5247  
 BaTiO<sub>3</sub>, characteristics and applications 9-16298  
 BaTiO<sub>3</sub>, prep. by electrophoresis after annealing or melting 9-9610  
 Bi, critical conducting thickness, 100-400°K 9-3577  
 Bi, evaporated, stress during and after deposition 9-5449  
 Bi, on mica, orienting action of substrate 9-21275  
 C, amorphous, atomic struct. from e. diffraction patterns 9-5237  
 C, e transmission expts. 9-6488  
 C, evaporated, grain size and at. struct., obs. 9-13576  
 C, heat treated to 2500°C, anisotropic cryst. growth 9-7335  
 C, thickness estimation by e. microscopy of transverse sections and optical density meas. 9-11766  
 C, vacuum-evap., annealing effect on e.s.r. after n-irrad. 9-8017  
 c Al, resistivity change due to neutrons and  $\gamma$  rays 9-17378  
 C membranes, density, tensile strength, crystallog. parameters, elec. and optical props. 9-11777  
 CdS, evaporated, n. irrad. effects on acoustic performance 9-15002  
 CdS, surface props., u.h. vacuum system for preparation and expt. 9-16038  
 CdS epitaxial, vapour phase chemical reaction growth technique 9-9616  
 CdS oriented films, semicond. charact., use of surface vib. meas. method 9-18625  
 CdS solar cells, design and space applic. 9-2319  
 CdS, Se<sub>1-x</sub>S<sub>x</sub>, structure defects effects on elec. and optical props. 9-9973  
 CdSe, epitaxial growth on NaCl (111) surface 9-7338  
 CeO<sub>2</sub>, dielec., influence on opt. props. of In and Al 9-5886  
 Co, growth on Ni, f.c.c. structure 9-7341  
 $\beta$ -Co, thick, preparation 9-11778  
 Co vapour-deposited foils, eff. of deposition rate and temp. on morphology 9-14927  
 Cr-Ni steel, formation of nitride layers in intermediate states of  $\gamma$ - $\alpha$  transformation 9-13775  
 Cr diffusion layers on Fe materials, structure and metallography 9-11769  
 Cs<sub>3</sub>Sb, production by Cs vapour action on vacuum evaporated Sb films 9-5246  
 Cu, electron channeling at 50 keV 9-1413  
 Cu, energy loss in H<sub>1</sub><sup>0</sup>→H<sub>1</sub><sup>+</sup> and H<sub>1</sub><sup>0</sup>→H<sub>1</sub><sup>+</sup> conversions in range 7-40 keV 9-17363  
 Cu, epitaxial growth on cleavage face of mica 9-5242  
 Cu, fatigue-hardened, dislocation loss and rearrangement, effect of neutron irradiation 9-11882  
 Cu, nucleation, growth and struct. obs. in e. microscope 9-19673

## Films, solid continued

- Cu, on sapphire, epitaxial twinned, growth 9-1104  
 Cu, polycryst., creep rate, rel. to thickness 9-5467  
 Cu on graphite, electrodeposited, grain clustering and projections 9-8101  
 $\gamma$ -CuI, internal stresses rel. to thermal expansion coeff. incompatibility with substrate, obs. 9-16126  
 Cu<sub>2</sub>Te, chemical formation on diffusion of Cu in CdTe 9-11896  
 Fe<sub>2</sub>O<sub>3</sub>, (magnetite, thermal conductivity meas. 9-1404  
 Fe-Cr-Al-Y alloy, oxide film formed in CO<sub>2</sub>, struct. and composition 9-11779  
 Fe-Ni alloys, grain size variation, X-ray diffraction study 9-13577  
 Fe-Si alloy, oxide film effect on max. permeability 9-10092  
 Fe-Si alloys, thin foils, antiphase boundaries contrast in superlattice reflections 9-11849  
 Fe, nucleation, growth and structure obs. in e. microscope 9-19673  
 Fe, nucleation, growth and structure obs. in e. microscope 9-19672  
 Fe<sub>2</sub>O<sub>4</sub>, magnetite, nucleation and growth on Fe in high-temp. water 9-21276  
 $\beta$ -FeOOH on steel, thickness meas. by Mossbauer backscatt. spectroscopy 9-10363  
 Ga, 10-170°K development of mech. stresses 9-16127  
 Ga, amorphous and cryst., mech. stresses 9-5451  
 Ga, structure rel. to growth 9-3192  
 GaAs, epitaxial, growth on GaAs substrate causing high resistance layer 9-11773  
 GaAs, impurity transfer in vapour growth and carrier-conc. profiles 9-11772  
 GaAs, n-type epitaxial films, hot electron magnetophonon effect 9-16265  
 GaAs<sub>1-x</sub>P<sub>x</sub> epitaxial layers on GaAs, compositional inhomogeneities 9-14895  
 GaAs epitaxial layers, dislocations 9-1219  
 Gd dislocation climb due to thermal diffusion 9-3349  
 Gd Fe garnet, prep. by sputtering 9-5248  
 Ge, epitaxial growth from supercooled droplets 9-13580  
 Ge, photovoltaic eff. mechanism 9-12214  
 Ge, photovoltaic effect, high-voltage, study 9-15141  
 Ge, semiconducting, crystallization by zone melting technique using SiO<sub>2</sub> and glass coatings 9-3238  
 Ge e transmission expts. electron microscope 17-1200 keV 9-6488  
 Ge epitaxial layer growth on GaAs by disproportionation reaction 9-19671  
 Ge epitaxial layer growth on GaAs 9-19670  
 Ge epitaxial layers on Si substrates, growth by vacuum evaporation 9-3201  
 Hg<sub>1-x</sub>Cd<sub>x</sub>Te, formation by Hg ion bombardment of CdTe crystals and composition thickness dependence 9-14898  
 In, thermal evaporation on amorphous substrates, growth characteristics 9-21279  
 In condensed, of subcritical thickness, e. diffraction exam. of melting 9-18383  
 n-In<sub>2</sub>O<sub>3</sub>, photoconductivity 9-15138  
 InP, epitaxial, stacking disorder 9-9617  
 InP, epitaxial growth on GaAs in open flow system 9-5243  
 n-InSb, prep. and props. 9-11770  
 InSb zone melting by e beam heating 9-14893  
 LiF, dielec., influence on opt. props. of In and Al 9-5886  
 Mg foil, growth of dislocation loops 9-18471  
 Mo, on NaCl single crystal, structure, infl. of thickness and substrate temp. 9-5238  
 Mo foils, deformation under electron microscope, study of slip geometry 9-5460  
 Mo on Si, chemical deposition, rel. to Schottky diode fabrication 9-6010  
 MoO<sub>3</sub>, for H beam detection 9-6728  
 MoS<sub>2</sub>, lubricant on steel, pressure effects on friction coefficient 9-16138  
 MoS<sub>2</sub>, transmission of electrons, anomalous 9-9680  
 Na adsorbed on W(110), bonding between layers 9-1113  
 NaF:H<sup>+</sup>, frequency shift of localized mode by surface polarization 9-19852  
 NaF, chemisorption of p-benzoquinone, i.r. spectra 9-8084  
 Ni-Cr bias-sputtered, preferred orientation 9-21265  
 Ni-Fe alloy, evaporated, lattice parameter composition dependence 9-14986  
 Ni, epitaxially grown, polycryst., double diffraction 9-5244  
 Ni, epitaxially grown, secondary twinning in e. diffraction patterns 9-9618  
 Ni, mean free paths of 4s electrons 9-17370  
 Ni, on Fe-Si alloys, effect on mag. props. 9-13990  
 Ni, oxide growth on (110) surface, rel. to O atom adsorption and diffusion 9-12544  
 Ni evap. on glass, struct. depend. on thickness 9-7337  
 Ni on glass, X-ray texture investigation 9-7336  
 NiCr, resistivity change due to neutrons and  $\gamma$  rays 9-17378  
 NiCr, thin film resistors, flash evaporation 9-15393  
 NiO, growth, eff. of structural defects 9-9621  
 NpO<sub>2</sub>, grain growth and crystallization, by transmission electron microscopy 9-5251  
 oxide, on Fe-Si alloy crystals, structure 9-21278  
 Pb, evaporation rate and thickness meas. by ionization gauges 9-21264  
 Pb, vacuum deposited, oxidation, 227-307°C 9-20048  
 Pb, thermal evaporation on amorphous substrates, growth characteristics 9-21279  
 PbO based polymorphic systems 9-12457  
 PbO, red, vapour-deposited layers, space-charge limited photocurrent 9-15139  
 PbO<sub>2</sub> on graphite, electrodeposited, grain clustering and projections 9-8101  
 PbS and PbSe, spectral absorptions, structure and phase composition 9-14021  
 PbTe on KCl, epitaxial growth mechanism 9-1106  
 Pd-Cr alloy, e. diffraction obs. rel. to elec. charact. 9-17242  
 Pd, epitaxial growth on cleavage face of mica 9-5242  
 Pt, on W(110) face, structure from LEED 9-1135  
 Pt e transmission expts. electron microscope, 17-1200 keV 9-6488  
 Pt e transmission expts. electron microscope, 17-1200 keV 9-6488  
 PuO<sub>2</sub>, grain growth and crystallization, by transmission electron microscopy 9-5251  
 Sb, crystallization data from e. diffraction patterns 9-5249  
 Se, on (110) face of W, electron and absorption props. 9-1115  
 Se, on W(110), structure, LEED obs. 9-1100  
 Si, electron microscope obs., 700-1000°C 9-14899  
 Si, epitaxial growth, continuous method, and thermodynamical anal. 9-14896



**Films, solid continued**

- Si, epitaxial growth, equilibria of nuclei formed during  $H_2$  reduction of  $SiCl_4$  9-11774  
 Si, epitaxial layers, partial screw dislocations, obs. 9-5369  
 Si, epitaxial layers on corundum, p-type contamination source 9-3666  
 Si, evaporation by vacuum-arc discharge 9-17244  
 Si, for use as image analyzer tube targets 9-8587  
 Si, paramagnetic stacking faults, c.p.r. 9-1862  
 $Si_3N_4$ , preparation by direct nitridation of Si substrates 9-21281  
 Si epitaxial, chemically grown, nucleation kinetic meas. on (100) surfaces, using molecular beam techniques 9-21298  
 Si epitaxial film on spinel, mech. props. 9-7815  
 Si layer, highly alloyed, growth by  $PCl_3$  diffusion 9-17245  
 Si with  $SiO_2$  surface films dynamical diff. effects rel. to induced strain, obs. 9-9612  
 SiC epitaxial layers, structure analysis by X-ray diff. 9-3202  
 $SiN_x$ , vapour growth from  $SiH_4-NH_3-H_2$  and  $SiCl_4-NH_3-H_2$  systems 9-5250  
 $Si_3N_4$ , prep. by  $SiH_4 + NH_3$  gas phase reaction, mol. structure and cracks 9-3194  
 $Si_3N_4$ , production from stain films on Si 9-3205  
 $SiO_2$ , characteristics on preparation by  $SiH_4$  oxidation and applic. to Si surface passivation 9-18404  
 $SiO_2$ , low-temp deposition by  $NO_2$  process 9-18403  
 $SiO_2$ , low-temp deposition by decomposition of organo silicate 9-18405  
 $SiO_2$ , on Si, band structure, diagram 9-18587  
 $SiO_2$ , on Si, epitaxial, elastic anisotropy of edges from contrast fields on X-ray topographs 9-1107  
 SiO amorphous, transparent hole formation mechanism 9-19668  
 SiO deposition, magnetic thin element preparation, patent 9-19669  
 $SiO_2$ , 500 to 6000 Å, traps, study using thermoluminescence glow curves in range 30 to 300°C 9-17429  
 $SiO_2$ , pyrolytic, prop. changes on heat treatment 9-3195  
 $SiO_2$ , thickness meas. over small geometries 9-11767  
 $SiO_2$  layer, prep. by thermal oxidation of Si, interdepend. between thickness and exptl. condns. 9-3993  
 $SiO_2$  on Si, electrolysis 9-4008  
 Sn evaporation rate and thickness meas. by ionization gauges 9-21264  
 Sn thermal evaporation on amorphous substrates, growth characteristics 9-21279  
 Ta, cathode-sputtered, structure 9-3196  
 Ta, deposition in reactive cathodic pulverisation and three-dimens. equilib. diag. 9-3197  
 Ta, thin and very thin, structure 9-1101  
 $Ta_2O_5$  ionic conduction mechanism for high field 9-16291  
 $TaN_x$ , sputtered, highly nitrided, prep., props. and structure 9-13578  
 $TaO_2$  protective film on Ta in high temp.  $HNO_3$  acid and ag.  $CuCl_2$  soln. 9-21267  
 $Ta_2O_5$ , deposition in reactive cathodic pulverisation and three-dimens. equilib. diag. 9-3197  
 Te, orientation from X-ray analysis 9-14894  
 Te, epitaxial growth on  $Cu(111)$  surface, LEED study 9-21270  
 $ThO_2$ , grain growth and crystallization, by transmission electron microscopy 9-5251  
 Ti, on NaCl single crystal, structure, infl. of thickness and substrate temp. 9-5238  
 Ti film evaporation for getter ion pump, control through thermoelectron emission 9-12811  
 Ti for gettering H impurities in He tube 9-3021  
 Ti vapour-deposited foils, eff. of deposition rate and temp. on morphology 9-14927  
 V, nucleation, growth and struct. obs. in e microscope 9-19672  
 $V_2Si_3$  on Si, transmission e. microscope exam. 9-1613  
 W, vacuum-deposited, on glass and polycryst. foil, structure and contact p.d. between 9-5239  
 YFe garnet, epitaxial film on YAl garnet, shear wave generation at micro-wave freqs. 9-10141  
 $ZnO$ , cathode-deposited, crystal structure rel. to prep. conditions 9-1102  
 $ZnO$ , structure and props., control during growth process from supersaturated condensate current 9-1103  
 $ZnO-Si$  resin electrophotographic films, characts. 9-15564  
 ZnTe epitaxial, on CdS, prep. by vapour transport method 9-5245  
 Zr alloys, thin oxide films formed by oxid., eff. of alloying mat. on struct. and morphology 9-20051  
 Zr on graphite, metallographic exam. 9-13579  
 $ZrO_2$  on Zr in  $O_2$  atm., struct. and epitaxy, 300°C 9-9619

**electrical properties**

- butadiene-based glow-discharge polymer, photoionization potential 9-12228  
 conductivity in longit. mag. field, thin metal 9-5650  
 cylindrical wires, size effects in elec. conductivity 9-12082  
 electron energy spectrum and mobility 9-13873  
 glass-ceramic coatings for metals, elec. props. improvement 9-3189  
 Hall effect, transverse in electric quantum limit 9-7732  
 insulating, conduction 9-21530  
 lipid bilayers, semiconducting depend. on electrical conductivity 9-12138  
 metal, sputtered at low voltages 9-12097  
 metal, surface roughness effects on resistivity thickness dependence 9-9928  
 metal, using e.m. field 9-3568  
 metal, with arbitrarily oriented Fermi surfaces, size effect, in elec. conductivity 9-7744  
 metal-InSb metal structures, V-I characts. 9-18641  
 n-type epitaxial, on  $p^+$  substrates, hole diffusion length meas. 9-3616  
 naphthalene-based flow-discharge polymer, photoionization potential 9-12228  
 polymers, organic semiconductors, props. description 9-14730  
 polystyrol, dielec. effects of discharge 9-10032  
 resistivity, sheet, four-point probe correction factors relationship, theor. anal. 9-16042  
 rhodamine-B, semicond., linear and quadratic recombination of photocarriers 9-12213  
 semiconducting, using e.m. field 9-3568  
 semiconductor, conductivity, quantum oscillations rel. to mag. field 9-5679  
 semiconductor dye films, photoconductivity spectra, polarization changes and external field effects 9-1616  
 superconducting, carrying current 9-16239  
 superconducting, superposed, coupled motion of vortices 9-7777  
 superconducting critical fields 9-13854

**Films, solid continued**

- electrical properties continued**  
 superconducting critical fields 9-1485  
 superconducting proximity effect, tunneling model 9-17379  
 superconducting proximity effect theory, exptl. tests 9-17384  
 superconductor, in surface parallel mag. fields, eqn. for crit. field 9-7767  
 Ag, epitaxial, resist., temp. depend. and influence of  $\alpha$  irradi. 9-5240  
 Ag, Hall coeff., normalized conductivity, thickness depend. from Fuchs-Sondheimer theory 9-7331  
 Ag, single crystal, size effect in resist. 9-5640  
 AgBr, photocurrent maxima and their origin 9-21545  
 AgCl, photocurrent maxima and their origin 9-21545  
 AgI, photocurrent maxima and their origin 9-21545  
 Al-InSb-Al structure, V-I characts. 9-18641  
 Al-Se-Al structure, negative resistance 9-13908  
 Al, resistance variation rel. to method of deposition 9-13582  
 Al, size-dependent deviations from Matthiessen's rule 9-21481  
 Al, Sondheimer oscillations in resistivity 9-7745  
 Al superconducting, dependence of critical temperature and energy gap on thickness 9-15080  
 Al superconducting, dependence of critical temperature and energy gap on thickness 9-1497  
 $Al_2O_3$  thin layers, polarisation effects in m.i.m. and m.i.s. structures 9-3717  
 $As_2S_3$ , e bombardment conductivity, threshold energy 9-16286  
 $As_2Se_3$ , glassy, pulse I-V characts. 9-3617  
 $As_2S_3(Se_2)$ , photosensitivity rel. to frequency of incident radiation 9-3731  
 Au-InSb-Au structure, V-I characts. 9-18641  
 Au, epitaxial, conductivity, size effects in temp. variation 9-9930  
 Au, epitaxial, resist., temp. depend. and influence of  $\alpha$  irradi. 9-5240  
 Au, Hall coeff., normalized conductivity, thickness depend. from Fuchs-Sondheimer theory 9-7331  
 Au, photoelec. eff., infl. of elec. field 9-17442  
 Au on Ag, photoelec. eff. 9-17441  
 $BaTiO_3$ , vacuum deposited, presentations of properties and formulations of thermodynamic model 9-12197  
 Be, superconductivity below 7°K by e diff. 9-13863  
 Bi, superconducting resistive transition thickness dependence 9-9955  
 C, elec. resist. rel. to O adsorpt., -196 to 450°C 9-7795  
 $CaSO_4 \cdot 2H_2O$  (gypsum), principal permittivities and elec. axis from 9 mm. interferometry study 9-7943  
 CdS, In degenerate, evaporated, mobility studies 9-12145  
 CdS, photoconductivity recombination centres 9-10068  
 CdS, photovoltages, larger-than-bandgap., generation and decay mechanism 9-15136  
 $CdS_{1-x}Se_x$ , structure defects effects 9-9973  
 $CdS_{1-x}Se_x$  graded, photoconduction 9-3735  
 CdSe Hall effect, encapsulated 9-3649  
 p-CdTe:P, resistivity 9-15089  
 $Cs_3Sb$ , conductivity, electrical, as function of mass and thickness 9-5246  
 $Cs_3Sb$ , photoemissive quantum yield and phase transition 9-3756  
 Cu  $H_2O$  chemisorption effect, 77° and 273°K 9-17519  
 Fe,  $H_2O$  chemisorption effect, 77° and 273°K 9-17519  
 GaAs:Si, epitaxial, band structure from luminescence spectra 9-5701  
 GaAs, epitaxial extrinsic far i.r. photocond. 9-7857  
 GaAs film-substrate interface, vapour epitaxial, occurrence of high resistance layer 9-5674  
 GaP, photovoltage effect, anomalous 9-3741  
 GaP, vapour-grown, rel. to substrates 9-12148  
 GaTe, charge carrier mobility 9-13883  
 n-Ge, photoelec. props. 9-3736  
 Ge, recrystallized in electron beam, mobility and conc. of current carriers, effect of substrate temp. 9-16271  
 Ge, thermoelectric props. and use as thermoelements 9-16308  
 Ge epitaxial layers on Si, vacuum-deposited, I-V characts. of heterojunction 9-3201  
 Ge layers, voltage photosensitivity 9-10074  
 Ge radiation detectors, optimal thickness of sensitive layers 9-10073  
 Ge thin plates, instabilities at 20.4°K 9-5702  
 $Hg_{1-x}Cd_xTe$  layers formed by  $Hg^+$  bombardment of CdTe crystals, conductivity 9-14898  
 In/Th superimposed, superconducting proximity effect 9-17384  
 In, electrotransport obs. 9-15061  
 InAs, epitaxial, e. mobility and conc., thickness dependence 9-1532  
 InAs, magnetoresistance 9-9980  
 InSb, epitaxial, e. mobility and conc., thickness dependence 9-1532  
 InSb, and structural and galvanomagnetic properties 9-3193  
 InSb, transport parameters temp. depend. interpretation 9-12146  
 n-InSb anodic oxide, resistivity and dielec. const. 9-11770  
 La-Ce, Kondo effect obs. 9-3581  
 Mo on NaCl, conductivity, infl. of thickness and substrate temp. 9-5238  
 Na, photoelectric and optical props., rel. to electronic structure 9-17472  
 Nb, reactively sputtered, superconductive transition temps., process parameter dependence 9-5662  
 Nb, supercond., reactively sputtered in presence of  $N_2$ , critical current densities 9-7742  
 NbN, superconducting, energy gap meas. 9-12127  
 $Nb_2O_5$ , thin, voltage controlled negative resistance 9-12089  
 Ni, prep. and study of props. 9-1109  
 Ni, ultra-thin, rel. to structure and tunneling mechanism 9-5644  
 Ni, vacuum deposited, and mean free paths of electrons 9-17369  
 $Ni_3P$ , Hall effect, structure depend. 9-9922  
 Pb/Th superimposed, superconducting proximity effect 9-17384  
 Pb, resistive transition rounding 9-16232  
 Pb, superconducting, critical temp. gradient and critical current density 9-18609  
 Pb superconducting transitions 9-7780  
 PbO, dielec. anomaly rel. to possible ferroelectricity 9-17437  
 PbS, photo e.m.f., angular dependence 9-1615  
 PbSe, evaporated, O effect on photosensitivity 9-5770  
 $PbZrO_3$ - $PbTiO_3$ , sputtered ferroelec., dielectric loss and strength 9-1596  
 Pd-Cr alloy, rel. to e. diff. obs. 9-17242  
 Rb, resist. rel. to conduction electron mean free path, obs. 9-18582  
 $Sb_2S_3$ , vitreous, space-charge-limited currents 9-16289  
 Se, photogeneration, field controlled and free-carrier transport 9-3729  
 Se, space charge limiting currents, conduction, Fermi level 9-12191  
 Se glassy, thermally stimulated conductivity 9-3726  
 Si, epitaxial, on spinel, and mech. props. 9-7815  
 $Si_3N_4$ , d.c. conduction and complex dielec. constant 9-19927  
 SiC, microwave-discharge-prepared, IV characts. and breakdown 9-21601

**Films, solid continued****electrical properties continued**

- Si<sub>3</sub>N<sub>4</sub>, produced from stain films on Si, resistivities 9-3205  
 SiO-Al condensers, breakdown voltage rel. to thickness 9-17430  
 SiO, in m.i.m. structure, elec. conductivity 9-1562  
 SiO, in m.i.m. structure, elec. conductivity 9-1562  
 SiO, in the film condensers, elec. strength thickness dependence 9-10043  
 SiO elec. breakdown rel. microscopic surface roughness 9-21531  
 SiO<sub>2</sub> thin layers, polarisation effects in m.i.m. and m.i.s. structures 9-3717  
 SiO<sub>2</sub>, evaporated, u.v. irr. effects on dielec. props. 9-5868  
 Sn, critical conducting thickness, 100-400°K 9-3577  
 Sn, Cu added, tunnel junction meas. for critical temp. determ. 3.5-7°K 9-7776  
 Sn, disordered, invest. by superconducting tunnelling 9-13868  
 Sn, superconducting, depairing 9-1506  
 Sn, superconducting, quantum size effects 9-5832  
 Sn, superconducting, superposed, coupled motion of vortices 9-7777  
 Sn, superconducting magnetic transition 9-7775  
 Sn superconducting, type II, switch from thin to bulk behaviour 9-16249  
 SnSe, charge carrier mobility 9-13883  
 superconducting, type I, critical temp. gradient and critical current density 9-18609  
 Ta, cathode-sputtered, resistance changes rel. to structural changes 9-3196  
 TaN<sub>x</sub>, sputtered, highly nitrided, thickness and sputtering cathode-current density dependence 9-13578  
 Te, contact with lead, photovoltaic effect 9-17446  
 Te, on insulating substrates (mica, glass, teflon) field effect relax. obs. 9-7840  
 Te, semicond. props., activation energy; temp resistance coeff. thickness depend. 9-7803  
 Ti on NaCl, conductivity, infl. of thickness and substrate temp. 9-5238  
 β-W, superconductivity 9-13869  
 W, vacuum-deposited, on glass and polycryst. foil, structure and contact p.d. between 9-5239  
 Zn, anomalous size effects in galvanomagnetic props. caused by compensation 9-13848  
 ZnO, control during growth process from supersaturated condensate current 9-1103  
 ZnO, thin resistivity 9-5252  
 ZnS:Cu, Cl photoelectric effect due to photoconduction in grains 9-1570

**magnetic properties**

- 'fanning' magnetization reversal and exchange stiffness 9-19954  
 anisotropy constant meas. using rotating sample magnetometer 9-2321  
 biaxial anisotropy, shape induced 9-3808  
 coercive force increment in mag. coupled structs., applic. to memories 9-3811  
 composite, specifications and yields for high density memory 9-3810  
 Conference, Intermag., Washington, D.C., April 1968 9-7883  
 Conference, Intermag., Washington, D.C., April 1968 9-3773  
 Conference, Intermag., Washington, D.C., April 1968 9-3774  
 domain struct., spin wave theory 9-5833  
 domain wall, high speed creep effects 9-3807  
 domain wall creep measurements in thin films using high-speed pulses 9-10128  
 domain wall energy, combined Bloch and Neel type 9-18683  
 domain wall structure calcs. 9-13993  
 ferromagnetic, alloy composition and magnetostriction, patent 9-19958  
 ferromagnetic, alloy electrolysis at const. current density, temp., patent 9-19959  
 ferromagnetic, alloy electrolysis at const. current density, temp., patent 9-13994  
 ferromagnetic, mag. birefringence 9-14034  
 ferromagnetic, magneto-optic apparatus for domain wall visualization 9-18681  
 ferromagnetic, surface resonance peak 9-5834  
 ferromagnetic coupled layers composition, patent 9-19960  
 ferromagnetic domain wall thickness by defocused electron optical pictures 9-12297  
 ferromagnetic thin films, props. explained 9-19957  
 hysteresisgraph for meas. in films for fast computer memories 9-16762  
 hysteresis loop meas. in rotating field using automatic magnetometer 9-12296  
 moment motion detection by Mossbauer spectroscopy, r.f. field eff. 9-15147  
 neutron scatt. by spin waves, angular distrib. rel. to freq. 9-16349  
 non-planar thin films, magnetization and spin-wave calcs. 9-21589  
 permalloy, <sup>3</sup>He irr. effects on anisotropy-field inhomogeneity and coercive force 9-7908  
 permalloy, angular dependence of magnetic annealing effects 9-10131  
 permalloy, anisotropy field H<sub>a</sub> and dispersion α<sub>a</sub>, rel. to ageing 9-3471  
 permalloy, anisotropy inhomogeneity, origin 9-5838  
 Permalloy, coercive force and anisotropy field, effect of crystallite size 9-13996  
 permalloy, creeping mechanism of magnetization 9-5842  
 permalloy, domain tip motion control 9-5841  
 Permalloy, ferromag. reson., linewidth thickness depend. 9-8005  
 permalloy, ferromag. resonance, X-band obs. by reflecto-polarimetric exam. 9-10270  
 permalloy, hysteresis loop meas. in rotating field, using automatic magnetometer 9-12296  
 Permalloy, magneto-resist. rel. to torque 9-7906  
 Permalloy, optimization of props. for mag. memories 9-13995  
 permalloy, rotational hysteresis 9-10134  
 permalloy, supercritical, thickness effects 9-1677  
 permalloy, uniaxial anisotropy, origin 9-3815  
 permalloy tapes, annealed below recrystallization temp. 9-3814  
 permalloy thin film pairs with large separations, domain wall coupling 9-10132  
 permalloy-on-glass, remagnetization in rotating mag. fields 9-21590  
 planar structures with one infinite dimension, demagnetizing field 9-3809  
 pulse reversals by uniform rot., parameters of phenomenological eqn. 9-3806  
 remagnetization in rotating mag. fields 9-21590  
 reversal of new type propagating at high speed 9-10087  
 spin wave resonance, uniform precession mode 9-8002  
 spin waves, dipolar effects 9-21588  
 stripe domains, theoretical explan. 9-3812  
 structures, by Lorentz electron microscopy, Fresnel mode 9-5836  
 superconducting magnetization, phase transitions 9-12231

**Films, solid continued****magnetic properties continued**

- switching, effect of crystallite interactions 9-10129  
 torque acting on ferromag. layer in quasi static mag. field 9-3805  
 Tyablikov-Bogolyubov diagonalization method, applic. 9-5835  
 uniaxial anisotropy due to lattice distortion, electrodeposited 9-9611  
 BaO evap., e.s.r. abs., band I 9-8011  
 Co-Ni-Fe, vapour deposited, nonmagnetostrictive 9-5837  
 Co, domain walls 9-16354  
 Co, electrodeposited, magnetocrystalline and uniaxial anisotropies 9-1678  
 Co, ferromagnetic, mag. birefringence 9-14034  
 β Co, spin-wave resonance and exchange interactions 9-20011  
 EuS, hysteresis meas., thickness dependence 9-18678  
 Fe-Ni Co monocrystalline alloy films, epitaxial growth and coercive force 9-12298  
 (19wt.%Fe)-(81wt.%Ni) films, anhysteretic behaviour, 20°C 9-13992  
 Fe, ferromagnetic, mag. birefringence 9-14034  
 Fe, negative magnetoresistance anisotropy 9-18682  
 Fe, spin-wave resonance and exchange interactions 9-20011  
 Fe with (100) surface orientation, spatial magnetization distribution 9-19961  
 Fe longitudinal Kerr rotations and figures of merit 9-3813  
 82.5 wt% Ni-(17.5 wt%) Fe permalloy film, Faraday and Kerr effect 9-16364  
 InSb, galvanomagnetic, structural and electrical properties 9-3193  
 MgMn ferrite, single crystal, ferromagnetic resonance 9-15196  
 Mn/Permalloy double-layer with exchange anisotropy, stabilisation of ferromag. domain structures 9-10130  
 Ni 20% Fe annealing in rotating mag. field 9-3817  
 Ni-Co, strain insensitive, 17 to 50 at% Ni 9-5843  
 Ni-(17 wt.%Fe)/EuS double layers, hysteresis meas., thickness dependence 9-18678  
 Ni-Fe-Cu layers, influence of annealing 9-3821  
 Ni-Fe-Pd alloys, composition and deposition for use as storage elements, patent 9-13998  
 Ni-Fe annealing, cylindrical 9-5839  
 Ni-(19 wt.%Fe), ferromagnetic, mag. birefringence 9-14034  
 Ni-(19wt.%Fe), energy of combined Bloch and Neel type domain wall 9-18683  
 Ni-Fe, double, coupling between 9-3816  
 Ni-Fe, electrodeposited on Cu, coercive force rel. to crystallite size 9-7909  
 Ni-Fe, magnetization-ripple, crystallite-size and film-thickness dependence 9-7907  
 Ni-Fe, transverse Kerr effect, 0.3 to 3.0 μ 9-5840  
 Ni-Fe, uniaxial, analog. storage using non-uniform fields 9-5844  
 Ni-Fe alloy, magnetostriction meas. method 9-13985  
 Ni-Fe domain wall streaming, creeping and parade motion, hard axis pulse excitation 9-3820  
 Ni-Fe susceptibility, effect of strain, polycrystalline 9-3818  
 Ni-(19 wt.%Fe) ferromag., domain walls, low-angle electron diffraction investig. 9-13997  
 Ni, electrodeposited, magnetocrystalline and uniaxial anisotropies 9-1678  
 Ni, magnetostrictive generation of transverse phonons at zero field 9-10126  
 Ni, negative magnetoresistance anisotropy 9-18682  
 Ni, produced by chem. reduction method, anisotropy 9-16358  
 Ni, spin-wave resonance and exchange interactions 9-20011  
 Ni, uniaxial mag. anisotropy due to lattice distortion electrodeposited 9-9611  
 Ni-Fe coupled with stripe domain films 9-10133
- optical properties**  
 antireflection coatings of small optical elements, cathode sputtering methods 9-13049  
 cellulose, regenerated, i.r. spectra, drying and temp. effects rel. to 25°C phase transition 9-11509  
 dielectric films, reflected light, dispersion of phase shift, use of Kramer-Kronig relns. 9-1734  
 fibrous thin-layer mats, total solar spectrum coeffs 9-1726  
 free-electron-like foils 9-14022  
 granular metallic, parameters ν<sub>1</sub>, χ and d 9-16398  
 interference thickness computer calc., thermal radiation screening 9-4513  
 Lippmann, recording by transmission and reflection, patent 9-8678  
 measurement technique for films grown on rough surfaces 9-5236  
 metal, absorption, theoretical study 9-12368  
 metal, ellipsometric determ. using transmitted light 9-3849  
 metal, in island form, effective consts. 9-12327  
 with metallic particles, small, light scatt. and absorpt. 9-15166  
 multilayer anti-reflection coatings for high refractive index materials 9-5874  
 multilayer reflecting surfaces, minimization of apparent curvature 9-4511  
 optical phonons by e tunneling obs. group II-VI compound films 9-9814  
 oxide, on Fe-Si alloy crystals, rel. to growth kinetics 9-21277  
 oxide on metal composites, hemispherical reflectances, spectral data 9-19985  
 Paynting radiation vector 9-5884  
 photochromic film on polyester, patent 9-8675  
 polymer, scatter of polarized light, model of annular spherulites 9-7940  
 reflection and transmission formulae rel. to refractive index 9-12333  
 sputtered multilayer dielectric mirrors, optical properties 9-4528  
 transient luminescence kinetics 9-8648  
 transparent, on reflective substrates, phase-shift corrections in thickness determ. 9-7329  
 Ag-Mn(Pd), rel. to resonant states 9-7937  
 Ag, absorption band shift 9-17479  
 Ag, anomalous absorpt., rel. to grain size 9-5912  
 Ag, granular, parameters ν<sub>1</sub>, χ and d 9-16398  
 Ag, second harmonic excitation, eff. of thickness 9-19974  
 Ag film, surface plasmons, light emission 9-17373  
 Ag island films, light scatt. and absorpt. rel. to struct. 9-15166  
 Al, absorption study and theoretical explan. 9-19986  
 Al<sub>2</sub>O<sub>3</sub>, photoluminescence 9-18720  
 Al<sub>2</sub>O<sub>3</sub> anodic, i.r. spectra comparison of freshly and evacuation prepared samples 9-18703  
 Al 90 nm thick, wavelength depend. of transmittance in vacuum u.v. 9-10166  
 Al<sub>2</sub>O<sub>3</sub>, electroluminescence of films 9-5971  
 As<sub>2</sub>S<sub>3</sub> semiconductor film-Ag system, light sensitivity depend. on thickness of semicond. layer 9-1735  
 Au-Pd, rel. to resonant states 9-7937  
 Au, electromodulation 9-5900



**Films, solid continued****optical properties continued**

- Au, grown on rough surfaces, meas. technique 9-5236  
 BaTiO<sub>3</sub>, vacuum deposited, presentations of properties and formulations of thermodynamic model 9-12197  
 Bi, transmission rel. to quantum size effect 9-7969  
 C, density meas. in thickness estimation 9-11766  
 CdO, abs., reflectivity, freq., depend. of opt. consts. rel. to band struct. 9-3886  
 CdSe, Se<sub>x</sub>, structure defects effects 9-9973  
 Co, ferromagnetic thin films, mag. birefringence 9-14034  
 Cs, absorpt. spectrum rel. to thickness, 2300-11000 Å 9-15174  
 Cs<sub>2</sub>Sb, transparency as function of mass and thickness 9-5246  
 Cu-Mn(Pd), rel. to resonant states 9-7937  
 Cu, anomalous absorpt. rel. to ambient conditions 9-10198  
 Cu, scattering of light, 2200 to 5400 Å 9-17478  
 EuO Kerr effect, on mirror substrates 9-3860  
 Fe ferromagnetic thin films, mag. birefringence 9-14034  
 Ga, rel. to structure 9-3192  
 n-GaAs epitaxial, photoluminescence 9-10265  
 GaP, vapour-grown, rel. to substrates 9-12148  
 GaP doped, epitaxial, photoluminescence 9-10237  
 Ge wavelength depend. of transmittance in vacuum u.v. 9-10166  
 InSb, absorption edge, thickness depend. 9-5906  
 K, transmittance, ultraviolet 9-5867  
 K optical plasma resonance emission and transmission of thin film 9-12382  
 KBr-RbBr(NaBr.KCl) solid solutions, intrinsic absorption spectra 9-10204  
 KBr, emission in far i.r. 9-15175  
 KCl, i.r. absorpt., size- and shape-dependence 9-21626  
 LASb, absorpt., thickness dependence 9-3897  
 Li, transmittance, ultraviolet 9-5867  
 Mg wavelength depend. of transmittance in vacuum u.v. 9-10166  
 MgF<sub>2</sub>, evaporated film, refractive index inhomogeneity 9-5872  
 MnO, absorpt. spectra 9-1797  
 Na, and photoelectric props., rel. to electronic structure 9-17472  
 Na, transmittance, ultraviolet 9-5867  
 NaCl, absorption in 25-50 eV region, substrate and exposure to air effects 9-7978  
 NaCl, emission in far i.r. 9-15175  
 NaCl, far i.r. absorpt. spectra, virtual mode analysis 9-1791  
 NaCl, luminescence in strong elec. fields 9-3921  
 Ni, (19 wt.%) Fe ferromagnetic thin films, mag. birefringence 9-14034  
 PbO, thin, dielectric const., forbidden gap width meas. 9-10167  
 PbSe, epitaxial 9-5863  
 Rb, absorption 9-12384  
 RbBr, emission in far i.r. 9-15175  
 RbCl, emission in far i.r. 9-15175  
 Se amorphous, reflectance, refractive index and absorption in vacuum u.v. 9-12335  
 Se wavelength depend. of transmittance in vacuum u.v. 9-10166  
 SiC, epitaxial, blue photo- and electroluminescence 9-5972  
 SiC, microwave-discharge- prepared, i.r. transmission and refractive index 9-21601  
 SiO<sub>2</sub>, i.r. abs. variation, influence of heat treatment 9-12386  
 SiO<sub>x</sub>, evaporated, u.v. irr. effects on absorption 9-5868  
 Ta<sub>2</sub>O<sub>5</sub> interference peaks, elec. field induced shift 9-19975  
 TaN<sub>x</sub>, sputtered highly nitrated, energy gap, film thickness and sputtering cathode current density dependence 9-13578  
 Te wavelength depend. of transmittance in vacuum u.v. 9-10166  
 ZnO, control during growth process from supersaturated condensate current 9-1103  
 ZnS:Cu,Mn,Cl electroluminescence, excitation mechanism 9-5974  
 ZnS-Mn(Cu,Cl) electroluminescence brightness waves, effect of elec. polarization 9-10261  
 ZnSe-Mn, electroluminescence 9-20009  
 ZnSe epitaxial, photoluminescence 9-5956

**Filters**

- in elasto-plastic medium, pressure restoration and relief waves during filtration 9-136  
 glass fibre, multicomponent, properties rel. to pressure drop 9-21009  
 glass fibre, single component, properties rel. to pressure drop 9-21008  
 liquid, fabric dry-cleaning, perforated centre tube and annular chambers, patent 9-19625  
 microwave, using resonant cavity with one coupling element 9-4414  
 non-linear flow, soln. through elec. analogue 9-48  
 time analysis application, variant and invariant 9-19236  
 X-rays, soft, reflection by multilayer absorbing system 9-10772

**Filters, electrical** *see Circuits***Filters, optical**

*See also Absorption/light; Films, solid/optical properties*

- 584-Å, Al foil 9-6019  
 achromatic, triple layer, transmission flat extreme 0.8-1.1 μ, design discussed 9-8667  
 achromatic wave plates for visible spectrum 9-10925  
 density meas. with Cary 14R spectrophotometer 9-6556  
 differential reflection, for dispersionless spectral anal. of soft X-rays 9-2104  
 diffraction, use of Soller system 9-6545  
 hyperfine, Cs vapour cell, for optical pumping 9-19406  
 interference, i.r., fabrication material props. discussed 9-4532  
 interference, parasitic radiation transmission 9-10742  
 interference, type, narrow band, effective refractive index as performance criterion 9-8664  
 interference, use with Unicam SP 1300 colorimeter 9-272  
 interference analyzer, determination of water content by near infrared absorption 9-14140  
 i.r. (far), interference waveguide type 9-10923  
 i.r. dispersion, background rel. to particle size 9-15549  
 Lyot-filter for H $\alpha$  line in sun 9-17670  
 Lyot-Ohman filters, line profiles 9-14449  
 polarization, for optical pumping of alkali metals 9-4830  
 quarter-wave cut off, multilayers 9-2413  
 rocks with radioactive impurities, Pb-Cu-Cd filter for obs. of  $\gamma$ -spectra 9-6054  
 Ross, balancing method for X-ray diff. of liq. 9-15986  
 for selective photoelectric radiation detector 9-2410  
 synthesis by holographic methods 9-10924  
 total internal refl., transient processes calc. 9-2412  
 CuS<sub>4</sub> cry. as, u.v. transmitting filters 9-20558

**Filters, optical continued**

InSb, infrared spectral region 9-4533

**Finlay-Freundlich red-shift hypothesis** *see Astronomical spectra; Cosmology; Gravitation; Relativity*

**Fireball model** *see Cosmic rays; Elementary particles; Field theory, quantum/ Interactions; Nuclear reactions and scattering*

**Fission** *see Nuclear fission*

**Flames**

- acceleration, or spontaneous ignition of end gas, rel. to 'knock', expt. study 9-12532  
 acetylene, soot yields on burning in O<sub>2</sub> and N<sub>2</sub>O; rel. to conc. of polyacetylenes 9-12535  
 acetylene prod. process, patent 9-12533  
 acetylene-air, as primary temp. standard, (2.600 $\pm$ 3K) 9-10757  
 acetylene-air, as secondary temp. standard, line reversal at 2500( $\pm$ 2)K 9-12951  
 acetylene-N<sub>2</sub>O+air, for atomic absorpt. spectroscopy 9-10944  
 composite solid propellants, phalanx flame model for combustion 9-15213  
 condensed phase, calc. of temp. and concentration fields, and rate of burning 9-8530  
 d.c. arc plasma torch, non-uniformity 9-21078  
 diffusion, buoyant, from liquid pools, effect of merging on burning rate 9-16746  
 diffusion and thermal conduction 9-17828  
 emission spectroscopic analysis, advances 9-6032  
 ethylene, diffusion, in O<sub>2</sub>-Ar and O<sub>2</sub>-N<sub>2</sub>, polycyclic aromatic hydrocarbon prod. rel. to O<sub>2</sub> conc. 9-12536  
 ethylene, laminar diffusion type, soot prod. rel. to diluents 9-15214  
 ethylene, soot yields on burning in O<sub>2</sub> and N<sub>2</sub>O; rel. to conc. of polyacetylenes 9-12535  
 ethylene-air diffusion type, effect of H<sub>2</sub> on prod. of polycyclic aromatic hydrocarbons 9-12537  
 hydrocarbon/O<sub>2</sub>/N<sub>2</sub> reaction zone, electrical conductivity meas. 9-18249  
 inhibition, two step process 9-19096  
 laminar, in stagnation flows 9-20035  
 lifted flat, aerodynamic properties 9-20456  
 low pressure, quantitative addition of metals by exploding wire 9-17896  
 methane-68.7%FI, temp., calc. and obs. 9-15561  
 methane-O<sub>2</sub>, combustion products, invest of ionization and conductivity 9-18752  
 MHD conversion, thermal radiation meas. 9-17851  
 neglecting action on gridded electrode 9-226  
 propagation across liq. surface, induction period 9-4372  
 propagation across liq. surface, steady-state conditions 9-6404  
 propagation across liq. surface, theoretical model 9-4373  
 propagation in supersonic premixed flows of H and air 9-16747  
 propagation velocity and temp. determ. 9-4374  
 propane-butane-N<sub>2</sub>O, for atomic absorpt. spectroscopy 9-10944  
 propane-oxygen, electric breakdown 9-933  
 sound recording, photometric 9-16734  
 stability rel. to action of Lorentz forces 9-6401  
 temperature, elec. field dependence 9-6403  
 temperature meas., line reversal method, appl. problems 9-16744  
 temperature meas. of low pressure flames, line reversal and excitation temp. 9-9449  
 turbulent, premixed, structure and burning vel. 9-19097  
 C formation, chemistry 9-3991  
 H<sub>2</sub>-N<sub>2</sub>-O<sub>2</sub>, electron prod. by Cd, Sr and Ba, meas. by enthalpy changes and equilib. consts. 9-12534  
 H<sub>2</sub>-N<sub>2</sub>-O<sub>2</sub> temp. profile at atm. press. using thermocouple probe and optical method 9-15480  
 H-O, transverse interact. with shock waves in explosive gas 9-1901  
 H<sub>2</sub>-O<sub>2</sub> diffusion flame structure 9-19098  
 H<sub>2</sub>, low pressure, line reversal and excitation temp. 9-9449  
 H<sub>2</sub>+O<sub>2</sub>+N<sub>2</sub>, fuel-rich, conc. and dissoc. energies of alkaline earth hydroxides 9-17517  
 MgO radiative temp. meas. 9-6405  
 N active, determ. of ground state CN conc. 9-826  
 N<sub>2</sub>O-acetylene, temp. distrib. obs. 9-15562  
 NO<sub>2</sub>-Acetylene, for atomic absorption spectroscopy impurities 9-6030  
 N<sub>2</sub>O-acetylene, appl. in atomic absorpt. spectrochem. analysis 9-10366

**Flare stars** *see Stars***Flares, solar** *see Sun/flares***Flash photolysis** *see Photochemistry***Flicker noise** *see Electron tubes; Noise/electrical***Floating zone refining** *see Zone melting and refining***Flocculation** *see Sedimentation***Flow**

- See also Boundary layers; Diffusion; Jets; Plastic flow; Turbulence; Viscosity*  
 - 9-17172  
 acoustic, separated behind thin fence, press. fluct., noise sources 9-5104  
 around plate in applied magnetic field 9-18259  
 in axial turbo machines with varying boundary shapes, compressible flow, two-parameters theory 9-4989  
 axisymmetric boundary-layer eqns., class of solns. with mass transfer 9-21006  
 birefringence by Senarmont method, errors 9-10907  
 boundary layer bleed drag at supersonic speed 9-19510  
 boundary layers, turbulent-equilibrium, prediction for Prandtl mixing length distrib. 9-21026  
 channel type, theoretical turbulence spectrum using 'kinetic damping force' 9-9427  
 co-current, of immiscible films with surface evaporation, direct contact heat transfer 9-19086  
 compressible fluid, aligned flow past slender body in circular wind tunnel 9-15916  
 compressible laminar boundary-layer eqns., approx. soln. using integral relations method 9-21005  
 conducting fluid, eff. on mag. field of dipole in centre of sphere 9-21029  
 continuous systems, residence time distribution 9-21011  
 in convection, free, in rot. fluid, numerical calc. 9-11520  
 convective, horizontal fluid layer with permeable boundaries, stability 9-12950  
 convective, in horizontal fluid layer, hexagonal cell formation 9-10754  
 convective, in sphere, toroidal and poloidal vel. field representation 9-20454

## Flow continued

- convective, steady; instability, hydrodynamic and thermal; at various inclinations 9-12949  
 convective in heated rotat. annulus, effect of radial barrier 9-21013  
 couette, fluid, var. with mag. field, press. gradient 9-2958  
 Couette, normal mode expansion, stability and perturbation bound 9-21022  
 Couette, unsteady of conducting incompressible fluid bet. two parallel plates under a transverse mag. field 9-21040  
 curve determ. of non-Newtonian fluids by cone and plate viscometer 9-4991  
 around cylinder, velocity grad. at wall, electrochem. meas. for Reynolds numbers 60 to 360 9-17086  
 detached, axisymmetric, with small cavitation numbers, past slender solid of revolution 9-18241  
 dielectric fluids in pipes, elec. field eff. 9-9330  
 field-flow fractionation, nonequilib. theory 9-848  
 flame, stagnation flow in burner 9-20035  
 fluid, compressible, computation by Kernel function application 9-21021  
 fluid, non-Newtonian, steady slow motion through tapered tube, theory 9-11524  
 fluid, second order, incompressible, integration of equations of motion 9-9316  
 fluid, steady turbulent motion, analogy of oscillating mass on wheels 9-20379  
 fluid, viscoelastic, down inclined plane, stability 9-2944  
 fluid, viscoelastic steady laminar flow, permeability depend. parallel uniformly porous walls 9-5128  
 fluid, viscous, incompressible, time-depend. Navier-Stokes eqn. soln. 9-21159  
 fluid, viscous, through pipe orifice, low Reynolds no., Navier-Stokes eqn. soln. 9-19502  
 fluid, viscous incompressible, steady laminar flow through tube with X-section as intersection of two circles 9-21160  
 fluids, 2-dimens., heat and momentum convection, boundary layer soln. 9-20999  
 fluids, hydrodynamic, stability of 2-dimens. convection 9-14744  
 fluids, laminar, between parallel walls, circular pipe, suction eff. on forced convection 9-4990  
 fluids, laminar, in pipes, rheology 9-853  
 fluids, laminar, over flat plate, non-equilib. dynamics 9-18245  
 fluids, non-Newtonian, mixing 9-844  
 fluids, in pipe in transverse mag. field, anal. with uniform radial heat flux 9-13408  
 fluids, secondary, and viscous drag in granular beds 9-13406  
 fluids, viscous, relativistic 9-18243  
 free boundary layer stability at large Reynolds number 9-7109  
 free convection flow from flat plate, solns. 9-21018  
 in front of shock wave, at infinity 9-19060  
 gas-solids suspensions, turbulent flow study at high Reynolds number 9-3131  
 glass-crystal systems, props. rel. to deform. in firing 9-3417  
 heat, moving source in two-dimensional infinite media, theory 9-10747  
 hydromagnetic, in rotating straight pipe 9-13409  
 hydromagnetic, in rotating straight pipe 9-9325  
 hypersonic viscous flow over slender bodies with sharp leading edges, solns. 9-18236  
 hypersonic viscous flow past semi-infinite flat plate with sharp leading edge, analysis 9-21004  
 impulsive motion of flat plate in viscous fluid 9-17089  
 inviscid stratified fluid, steady two-dimens. flow in channel over obstacle, theory 9-14748  
 jet, along curved surface, similarity soln. by transform. of straight surface soln. 9-7244  
 jet, turbulent, pressure field characteristics determ. 9-19574  
 jet injection at small angle into uniform flow, linear theory, soln. by Wiener-Hopf tech. 9-17085  
 jets, round, one-row system in limited transverse stream 9-18244  
 Kelvin-Helmholtz and gravitational instability in relative motion of two fluids 9-17091  
 Kelvin-Helmholtz instability of two superposed fluids in relative motion, mag. field effects 9-14750  
 laminar, between rotating and stationary discs, radial inflow 9-9320  
 laminar, between rotating discs, asymptotic soln. 9-970  
 laminar, in open circular channels and symmetrical lenticular tubes 9-15915  
 laminar, incompressible, longitudinal over cylinder, transverse curvature eff. on boundary layer 9-14823  
 laminar, of viscous conducting liquid between parallel walls, travelling magnetic fields 9-18260  
 laminar boundary layer with const. press. grad. and rel. profile close to Falkner-Skan eqn. 9-14747  
 laminar in cocurrent flow heat exchangers, heat transfer in entrance region 9-13520  
 laminar flow and temp. field in rotating radial circular pipes 9-13518  
 linear viscous shear flow, lift tensor for three-dimens. body, maximum dissipation 9-17084  
 liquid, through filter, perforated centre tube and annular chambers, patent 9-19625  
 liquid metal, resistance, channels in transverse magnetic field 9-21032  
 liquid metal in MHD channel with segmented electrodes 9-7121  
 liquid metals in tubes in transverse mag. field, shear stresses and turbulent exchange coefficients 9-7124  
 loss-cone velocity distribution, negative energy waves association 9-2938  
 low-speed, 2-dimens., unsteady thermal boundary layers, soln. 9-18230  
 mass transfer with plate in non-Newtonian plastic fluid 9-845  
 MHD, axially-symmetric, in vortex chamber for large Hartmann numbers 9-7126  
 MHD, fluid kinematic props. 9-2952  
 m.h.d., steady electrically driven, flat plate considered 9-18261  
 m.h.d., tensor conductivity eff. on flow 9-18257  
 MHD and OHD, nonanalyticity at surface of fluid 9-19507  
 MHD duct, uniqueness theorem 9-18262  
 MHD jets with variable conductivity, theory 9-7118  
 micropolar fluids, shearing, plane Couette and Poiseuille flow behaviour 9-18238  
 mixing of parallel subsonic streams, momentum eqn. integration 9-9317  
 non-Newtonian, analogue 9-3129  
 non-Newtonian, combined laminar free and forced convection 9-846  
 non-Newtonian fluid, unsteady, velocity-profile development 9-11528

## Flow continued

- non-Newtonian hydromechanics of disperse systems 9-18373  
 non-viscous fluid, anisotropically conducting, symmetric flow analysis 9-7129  
 OHD and MHD, nonanalyticity at surface of fluid 9-19507  
 one dimensional, magnetized incompressible, non viscous conducting fluid 9-18253  
 one-dimensional hydrostatic fluid with gravity, model for earth's atmospheres 9-8166  
 periodic in rigid circular tube, pulsating vel. field 9-4994  
 plane Couette, suction, injection and heat transfer 9-11170  
 plane steady, of perfect compressible fluid, invariant transformations of Euler eqns. 9-21020  
 plasma, collisionless, over wedge, ion saturation current predictions 9-21054  
 Poiseuille, theory of lateral migration of solid particles 9-19501  
 polymers, unstable flow mechanism involving crystallization of molten polymers under shear stress 9-17236  
 through porous solid, small motions superimposed on large static deform. 9-11665  
 in porous tubes, frictional and heat transfer characts. for laminar flow 9-13498  
 in precessing spheroidal shell, steady fluid flow 9-19505  
 pressure drop across multicomponent glass fibre filters 9-21009  
 pressure drop across single component glass fibre filters 9-21008  
 Rayleigh-Taylor instability of two superposed fluids on relative motion, mag. field effects 9-17090  
 relativistic, of viscous fluids 9-18243  
 Reynolds no. similarity argument, in pipe and channel 9-18240  
 in rotating annulus, transition from axisymmetric to nonaxisymmetric flow 9-18239  
 rotating fluid, Kelvin-Helmholtz stability problem, correction to soln. of eigenvalue eqn. 9-17088  
 second order fluid, stability between two concentric cylinders 9-7101  
 secondary, of non-Newtonian fluids, comparison of constitutive eqns. 9-9318  
 separation, rel. to flute marks and flute separation in rocks 9-17558  
 solid, heavy, moving in fluid, integrable cases 9-18231  
 solid boundaries, eff. of suspended particles 9-18508  
 sonic, inviscid, 2-dimens., blunt symmetrical body, marching procedure soln. 9-19509  
 sonic flow about axisymm. object at large distance behind shock wave 9-19074  
 spiral, between rotating cylinders, stability 9-7111  
 stability of time-periodic azimuthal flows between coaxial, circular cylinders 9-17087  
 steady laminar, of viscous incompressible fluid through tube with X-section as intersection of two circles 9-21160  
 steady separated flow past bluff objects, exptl. obs. 9-21017  
 Stewartson layers in transient rotating fluid flows 9-19506  
 Stokes solns. for slow rotation of sphere about a diameter parallel to plane wall 9-19499  
 stratified fluid through curved screens 9-19504  
 subsonic, plane, indirect approach 9-21015  
 superfluid, through channels, thermodynamic stability 9-18377  
 suspensions, pipeline, conc. gradient meas. by  $\gamma$ -radiation technique 9-9563  
 suspensions through tubes, pulsatile and oscill. flow, particle interactions 9-5195  
 suspensions through tubes, pulsatile and oscill. flow, particles radial migration 9-5194  
 with Taylor's vortices in wide gap, heat exchange, analytical investigation 9-15479  
 three-dimensional, in variable profile channels with symmetry plane 9-9331  
 three-dimensional boundary layer eqns., solns. with press. grads and flow separation 9-7107  
 three-dimensional in centrifugal compressor, photographic study 9-851  
 transfer coefficient, effect of inhomogeneity localisation in medium 9-13407  
 transonic, plane, then rotational, at large distance from non-level surface 9-21014  
 transonic, computation by Lax scheme 9-15914  
 in tube, smooth, theory 9-7113  
 turbulence, eqns. of motion and Heisenberg's statistical theory 9-7112  
 turbulent, anomalous wall effects and associated drag reduction 9-21007  
 turbulent, confined equilib., shear stress distrib. 9-19594  
 turbulent, exciting vibrs. in flat rectang. plate, anal. 9-12928  
 turbulent, heat transfer in annulus with internal heat generation 9-8525  
 turbulent, heat transfer rel. to temp. depend. phys. props., for high heat fluxes 9-12946  
 turbulent, in duct, velocity profile Reynolds no. depend. from Von Karman similarity hypothesis 9-21012  
 turbulent, swirling inlet in circular pipe, theoretical conditions 9-17176  
 turbulent, through smooth pipes, friction coeff. 9-14746  
 turbulent boundary layer, drag coeffs. on plate evaluation of Coles' theory 9-17145  
 turbulent boundary layer with press. grad., heat transfer and possibly mass transfer 9-17144  
 turbulent free flow, spreading and contraction at transition boundaries 9-21016  
 turbulent in concentric annuli, rel. profile, and reln. between friction factor and Reynolds number 9-11522  
 turbulent spectral data, large scale boundary layers with different roughnesses 9-19508  
 two dimensional, anisotropically conducting, incompressible liquid in axisymmetric channels in magnetic field 9-21039  
 unsteady centred, integral of motion 9-21019  
 unsteady torsional flows of simple fluids 9-19500  
 through vane profiles in moving turbines, calc. 9-18237  
 vector potential and boundary conditions, 3-dimens. hydrodynamics 9-18242  
 velocity field without discontinuities for axisymmetric extrusion through conical dies, theory 9-21395  
 viscoelastic, through tubes, efflux perturbation 9-15913  
 viscometric, of non-Newtonian fluids, book 9-11529  
 viscometric, power-law fluid, heat generation and temp. depend. viscosity 9-9457  
 viscous, slow, asymmetrical due to motion of 2 equal spheres almost in contact 9-11525



**Flow continued**

- viscous, slow stationary, past surface of revolution of Booth's lemniscate 9-847  
 viscous conductive fluid in axis-symmetric MHD system 9-9332  
 viscous fluid, past flat plate, boundary layer approx. neat trailing edge 9-967  
 viscous fluid, problems of nonisothermal steady flow 9-2947  
 viscous region of turbulent boundary layer 9-18246  
 viscous sublayer instability 9-842  
 vortex, conjugate solutions 9-19503  
 vortex core, maximum swirl angle rel. to breakdown behaviour 9-17146  
 water, laminar boundary layers with adverse press. grad., heat transfer 9-21163  
 Ga liquid in channels with conducting walls, resistance during transition from laminar to turbulent flow 9-9336  
 Hg, non stationary open channel flow, transverse magnetic field 9-21038

**gases**

- See also *Acoustic streaming; Aerodynamics; Anemometers; Supersonic flow*  
 aerodynamic resistance of pipes with triply running spiral channels 9-15970  
 air, over water surface, instability 9-17154  
 air, turbulent in rounded corner triangular duct, local friction and heat transfer coeffs. 9-13491  
 annular gap of irregular shape, flow rate calc. 9-3044  
 asymmetric two-dimens. orifice, force defect. coeff. method appl. 9-9426  
 over blunt cone at angle of attack, three-dimens. boundary-layer eqns. 9-17595  
 boundary conds. in transition region, from Boltzmann eqn. 9-5098  
 boundary layer, convective with organic sublimation 9-17147  
 characteristics in cylindrical vessel 9-21123  
 conducting dusty, plane parallel, in transverse mag. field 9-13410  
 in conical nozzle, viscous heat cond. gas, soln. with heat extraction 9-11641  
 counterflow phenomenon used for quantitative analysis of volatile liquid 9-12550  
 detonation wave propagation in space with conical cutout 9-13476  
 dissociated, past catalytic surface, laminar boundary layer rel. to surface reaction rates 9-12540  
 dusty conducting gas, plane parallel flow 9-9326  
 effusion from circular orifice, ang. number distrib. 9-9460  
 effusion from effusion oven, vapour-solid interactions 9-940  
 effusion from Knudsen cells with conical channels 9-15976  
 electrodynamic channel flow, elec. field distrib., math. anal. 9-5119  
 in e.m. shock tube 9-14765  
 engine cylinder numerical soln. 9-19571  
 entropy diagram, thermodynamic evolutions calculations 9-5113  
 on flat plate, laminar boundary layer stability, influence of temp. depend. viscosity 9-11687  
 flowfield induced by subsonic heat source, effects of friction and heat transfer 9-7210  
 fluidized beds, model 9-3041  
 from galactic centre 9-15376  
 heated air in diffusers, friction in pre-separation and heat transfer in separation regions 9-9425  
 high-temperature gas dynamics and gas physics, book 9-11645  
 hypersonic, over wedge, of diatomic gas 9-19572  
 laminar boundary layer, 3-dimens., conical external flow 9-19579  
 Lax's numerical method for soln. of hyperbolic systems 9-5097  
 low density, nozzle beam mapping technique 9-11644  
 through lyophobic microporous membranes, induced by volatile liquids 9-21122  
 mass transfer using porous spheres 9-939  
 Maxwell gas between two infinite parallel planes 9-3040  
 MGD channel, viscous, boundary layer approx. with heat conduction 9-21059  
 MHD aligned flow past slender body in wind tunnel 9-9327  
 molecular conductance and flow as temp. indep. substitutes for gaseous conductance and flow 9-8323  
 n-component gas in chemical disequilib., inside boundary layer on rot. sphere 9-13478  
 noise, acoustic, spoiler generated in jet pipe, obs. and analytical model 9-15471  
 nonisothermal, at finite Reynolds numbers, friction and heat transfer, extension of asymptotic relative laws 9-3046  
 nonviscous, three-dimensional hypersonic flow 9-14807  
 one-dimensional, with discontinuities, second-order accurate schemes for solution 9-941  
 plane steady motion of perfect gas, invariant transformation of equations 9-18323  
 plasma, cold non-equilibrium, charge particle concentration variation 9-14757  
 plasma, interaction with mag. barrier to form shock 9-21064  
 Poiseuille, in transition regime, with mol. mean free path related to tube diameter 9-943  
 Poiseuille, in transition regime, with tube radius near collision mean free path 9-944  
 in porous materials and vacuum systems, obs. 9-7213  
 pressurized bearing, air inertia effects 9-21125  
 profile meas. using ring lasers 9-19569  
 pseudostationary, uniqueness of streamline pattern 9-14806  
 pumping process in turbomolecular pumps, accommodation coefficient 9-937  
 radiating grey gas behind hypersonic shock layer, eff. of rad. ht. transfer on shock, soln. 9-21121  
 rarefied, past circular cylinder at low Mach numbers, Knudsen layer kinetic theory 9-15969  
 rarefied mixtures, critical mass flow through slit nozzle 9-18320  
 rotational, two-dimensional, integral invariants 9-3045  
 secondary, causing circular distrib., theor. treatment 9-19570  
 servocontrolled inbled syst. for high vacuum calibration chamber, design and development 9-19575  
 sonic, compact equation for nonideal gases, applicable for z values down to 0.80 9-13482  
 sonic, past body, behind shock wave 9-13477  
 in sonic nozzle throat, effects of downstream geometry changes, for transition flow regime 9-9429  
 round sphere, mass transfer and development of diffusion boundary layer 9-13495  
 stability study in plane pipes of large but finite length 9-945

**Flow continued****gases continued**

- subsonic inviscid stream, steady flow through statistically roughened wall ducts 9-3042  
 supersonic stream round blunt body finite difference calc. 9-948  
 three-dimensional, adjacent to regions of rest 9-21124  
 in transition and free molec. regions, boundary conds. 9-5098  
 turbulent, frequency spectrum by laser beam 9-19062  
 turbulent, heat transfer rel. to variability of physical props. 9-9443  
 turbulent, in tube with axially varying heat flux distrib., Nusselt number prediction 9-13487  
 turbulent air across vertical cylinders, condensation of methanol and water 9-1070  
 turbulent boundary-layer heat transfer in supersonic dissociated air, exptl. investig. 9-21120  
 turbulent in circular adiabatic pipe efficiency of gas screen 9-938  
 turbulent mixing of two coaxial streams, mass diffusion processes 9-7234  
 turbulent wakes, determ. of molecular mixing lengths 9-7211  
 two-dimensional, in crossed elec. and mag. fields 9-2957  
 upstream from shock waves due to object at sonic speed, asymptotic theory 9-8515  
 valve, fine regulation, for use in gas chromatography 9-15968  
 velocity meas. of gases with variable fluid props. 9-15967  
 velocity meas. using thermistor gauge 9-5105  
 velocity variation ionizing shock waves 9-18321  
 vorticity layer, dissipative boundary layer 9-14808  
 wind tunnel, viscous region of turbulent boundary layer 9-18246  
 Ar, velocity and press. influence on elec. breakdown potential 9-7232  
 Ar, wake in shock tube, vel. meas. from induced e.m.f. 9-2238  
 Cd effusion from cylindrical orifice 9-3062  
 CdO, vaporization, knudsen effusion study 9-3158  
 CsCl effusion from circular orifice 9-3063  
 CsCl effusion from circular orifice 9-9460  
 He, low-density, afterglow and fluoresc. visualization, excited by electron beam 9-21131  
 N<sub>2</sub>, rarefied, in sonic nozzle throat, effects of downstream geometry changes 9-9429  
 O<sub>2</sub>, round graphite sphere, taking chemical reactions into account 9-13478  
 Xe, wake in shock tube, vel. meas. from induced e.m.f. 9-2238

**liquids**

- See also *Acoustic streaming; Double refraction/flow; Hydrodynamics; Superfluidity*  
 albumen dilute solns., non-Newtonian, displacement vel. rel. to thermal cond. 9-9506  
 annulus, concentric, analysis of fully developed turbulent flow 9-18337  
 in annulus with rot. inner cylinder 9-18335  
 axially symmetric, ideal and viscous fluids 9-969  
 binary soln. through potential-energy profile 9-9499  
 cavity flow and cavitation erosion, relationship 9-19595  
 through cement paste, effective cross-sectional area, electrical meas. 9-15980  
 conducting, immiscible, two, between two moving parallel porous plates, under transverse mag. field 9-17173  
 creeping flow in rectangular duct with partition 9-21158  
 around cylinder, velocity grad. at wall, electrochem. meas. for Reynolds numbers 60 to 360 9-17086  
 dielectric streams, round charged spheres and cylinders, displacement current streamlines 9-5127  
 dispersion coeffs. on perforated plates with downcomers 9-21162  
 DNA dilute solns., non-Newtonian, displacement vel. rel. to thermal cond. 9-9506  
 droplet formation through circular orifice, min. size function of flow rate 9-18344  
 droplet in small Peclet number flow, decomposition burning, soln. 9-21687  
 ducts, contracting, throat profiles, containing incompressible, irrotational flows 9-21153  
 elastic, linear and nonlinear behaviour, expt. meas. and theory 9-18332  
 elastico-viscous, between rotating spheres asymptotic soln. 9-9469  
 elastico-viscous, in corrugated pipe 9-9464  
 excess pressure drop through sudden contraction, non-Newtonian liquids 9-9462  
 exponential, along infinite flat plate with uniform suction, laminar boundary layers 9-12203  
 film, accelerating down vertical wall, soln. rel. to boundary layer growth and film thickness 9-18349  
 fingering in oil-water displacement process with capillary press., statistical behaviour 9-11667  
 on flat plate, laminar boundary layer stability, influence of temp. depend. viscosity 9-11687  
 fluctuating, through right angled isosceles triangular channels, for 2nd order liq. 9-9465  
 free solid with liquid filling, circular motion stability in force field of two stationary attracting centres 9-12913  
 hydromagnetic, nonisotropic, rectilinear 9-19518  
 inviscid, pressure on spindle 9-11664  
 laminar, free convection, vertical plate with constant suction 9-15979  
 laminar, of homogeneous viscous liq. in pipe at low and moderate reynolds number 9-17171  
 laminar, of viscous liq., flow pattern visualization by phosphorescence method 9-21157  
 laminar, over rectangular slots, control expt. rel. to disturbances and vortex flow 9-13499  
 laminar, past paraboloid of revolution, anal. 9-18333  
 laminar boundary layer flow, appl. of Galerkin-Kantorovich-Dorodnitsyn method 9-21027  
 laminar boundary layer stability on elastic surface 9-14822  
 laminar co-current flow of two liqs., conc. distrib. and local mass-transfer coeffs. 9-13501  
 laminar source flow, between two parallel coaxial rotating porous discs 9-17174  
 laminar-turbulent transition in two-dimens. channel 9-13505  
 metal, dynamic hold-up in irrigated packed beds 9-21164  
 mixer, continuous flow, working efficiency 9-5124  
 mixer continuous flow, attaining scaling up 9-5125  
 mixers, continuous flow, colorimetric expts. 9-5126  
 naphthene oil, upward and downward motion in filter paper 9-5131  
 noise, temperature, measurement, in out-of-pile heat transfer loop 9-20863

**Flow continued**  
**liquids continued**

- non-Newtonian, film on surface of rotating disc, vel. and thickness calc. 9-21181  
 non-Newtonian, mass transfer from rotating disc 9-16705  
 non-stationary, laminar boundary layers, approximate treatment 9-9463  
 Nonvolatile, upward and downward motion in absorbent porous solid 9-5131  
 ocean flows, two-dimens., boundary layer eqn. 9-8159  
 packed column, effective interfacial area as function of flow rate 9-21155  
 paraffin, upward and downward motion in filter paper 9-5131  
 phase permeabilities of displacing and displaced liquids 9-18354  
 polybutene, creeping flow in rectangular duct with partition 9-21158  
 porous media, in 3D channels 9-3067  
 in porous media, stability conditions for displacement processes 9-11666  
 power-law liquid, motion and energy equations 9-3081  
 Prandtl equation, soln. in vicinity of critical point 9-13513  
 pressure pulsations on plate surface below a turbulent boundary layer, characteristics computation 9-971  
 rotational, in right-angle bends, 'frozen vorticity' theory 9-13504  
 rotational, of some elasto-viscous liqs., non-Newtonian effects 9-18330  
 scintillation camera meas. 9-10948  
 secondary, effect on viscosity meas. using cone-and-plate viscometer 9-19615  
 shear, eff. in underwater acoustics 9-16526  
 sodium carboxymethylcellulose aqueous soln., displacement vel. rel. to thermal cond. 9-9506  
 stagnation region behaviour of resistance thermometer 9-6062  
 statistical theory of turbulence for large Reynolds' number 9-13503  
 statistical theory of turbulence for large Reynolds number 9-3068  
 thickness and rate, film adhesion on cylinder withdrawal from Newtonian liquid 9-18347  
 turbulent, in tube, fluidization onset, h.f. oscillations and heat transfer 9-9466  
 visco elastic, in cored channels, non-Newtonian eff. 9-21023  
 viscous, due to impulsive pressure gradient 9-14821  
 viscous, existence theorems for nonlinear partial differential eqn. 9-7240  
 viscous, flexible boundary, long-wave disturbances, stability characteristics 9-3072  
 viscous about parabolic object 9-21161  
 viscous drag and secondary flow in granular beds 9-13406  
 viscous heating in plane and circular flow between moving surfaces 9-987  
 viscous incompressible plane, around an object, solns. to Navier-Stokes eqn. 9-21154  
 wake, boundary effects behind inclined flat plate at arbitrary angle of attack 9-17170  
 water in open channels; unsteady 9-7241  
 water jet, conical confined, momentum transfer 9-18342  
 water swirling conical pressure nozzles, measurement of rotational velocity 9-18343  
 water-[25%] carboxymethylcellulose soln, non-Newtonian, on rotating disc surface 9-21181  
 Weissenberg rheogoniometer self-aligning platens 9-3064  
 He, superfluid, energy dissipation and critical vel. obs. 9-11736  
 He II, turbulent, rel. to density increase 9-5208  
 He superfluid, critical flow rate through narrow pores 9-11737  
 HeII critical vel. and supercritical flow 9-13550

**two-phase**

- aerosols, in horiz. tube, gravity settling, in laminar flow 9-5198  
 air-water mixture in tube, characteristics of disturbed region 9-18331  
 annular, gas core study, velocity distribution and droplet flow rate after injection through axial jet 9-21156  
 bubble growth meas. in uniformly superheated liquids 9-21176  
 in capillary serial model 9-5223  
 cometary comas, with evaporation, simulation 9-18920  
 diffusional resistance to mass transfer 9-13501  
 fluid; in permeable annulus; fully developed soln. obtained 9-852  
 gas with liquid particles, limits on slip factor value 9-3038  
 gas with particles in suspension distrib. 9-3039  
 Graetz problem, multiregion generalization 9-21003  
 heat transfer bibliography 9-19085  
 incipient fluidizing velocity in gas fluidized beds 9-21010  
 in jet, analysis 9-9473  
 jet injection at small angle into uniform flow, linear theory, soln. by Wiener-Hopf tech. 9-17085  
 liquid presence, movement detection by transducer 9-5129  
 in porous medium, Green functions 9-17083  
 steam vol. fraction of mixture in channel,  $\leq 2000$  psi 9-11646  
 surface tension variation effects 9-21151  
 upward in vertical tubes, frictional pressure drop and void fraction 9-9322  
 upward in vertical tubes, heat transfer coeff. obs. 9-7114  
 upward in vertical tubes, interface shear stress obs. 9-9321  
 void-meter studies 9-3043  
 vortex, gas-jet driven, velocity distrib. model 9-4993  
 water-air layers, measuring device 9-17181  
 CO<sub>2</sub> supersonic jet, e. diff. for existence of crystals and free molecules 9-11459

**Flow birefringence** *see Double refraction/flow***Flowmeters***See also Anemometers*

- bimetal flow control element 9-5132  
 e.m., reducing contact resistance effect 9-7110  
 e.m. for blood 9-6202  
 n.m.r., optimum detectors, discussion 9-19592  
 open channel meas. with radioactive tracers 9-19593  
 thin-film heated element or skin friction gauges 9-5106  
 turbulence structure, small scale, meas. with hot wires 9-947  
 Venturi, velocity coeff. theoretical expression 9-17175  
 void-meter, electric, used to study two-phase flow 9-3043

**Fluctuations** *see Brownian motion; Random processes***Fluctuations***See also Brownian motion; Random processes*

- amplitude, of plane light wave moving in randomly nonuniform medium 9-260  
 critical, estimate of error terms in dynamical theory 9-21577  
 critical point phenomena, theory 9-9587  
 electron beam instabilities due to virtual cathodes 9-2336  
 Gunn effect, explanatory account 9-5683  
 laser beam phase, in turbulent atm. interferometry 9-10869

**Fluctuations continued**

- light wave amplitude and random caustics 9-13040  
 light wave amplitude and random caustics 9-2396  
 liquid-gas transition, dynamics of associated critical fluctuations 9-21244  
 magnetic field square nonlinearity, nonlinear resonance in proton synchrotron 9-480  
 plasma, turbulent, of elec. field, rel. to particle orbits and diffusion coeffs. 9-11548  
 plasma turbulence, spectrum, calc. 9-5001  
 in semiconductors, LSA mode 9-5684  
 in superconductor, contrib. to e.m. response function for small freqs. and wave numbers 9-9951  
 superconductors, order parameter, due to paramag. impurities 9-7764

**Fluid flow** *see Flow***Fluid mechanics** *see Hydrodynamics***Fluidized powders** *see Flow; Fluids; Powders***Fluids***See also Gases; Liquids*

- acoustic oscillations, non-linear, in spherical cavity, soln. 9-18247  
 almost classical, kinetic theory 9-841  
 boundary layer above porous medium, conjugate heat transfer with blowing 9-9503  
 Burgers model, a successive approximation for turbulence 9-2946  
 capillary-gravity waves, weak reson. interaction, variational method 9-21024  
 cell model, thermodynamic props. 9-14743  
 cell model with infinite pot., evaluation of partition function 9-14742  
 charged-parti. equilibrium props. 9-8454  
 classical, generalized Vlasov eqn. derivation from Liouville eqn. 9-8440  
 classical non-polar, triple-dipole pot. contrib. to parameters 9-13403  
 collapsing or exploding cyl. shell of conducting fluid in mag. field, stability 9-19520  
 compressible flow in axial turbomachines, two- parameters theory 9-4989  
 conducting, surface waves obs. using microwave resonator method 9-2941  
 conducting incompressible bet. two parallel plates under a transverse mag. field, unsteady Couette flow 9-21040  
 convection, 2-dimens., stability of hydrodynamic flow 9-14744  
 convection in enclosed rectangular cavity 9-19091  
 dielectric, flow in pipes, elec. field eff. 9-9330  
 dynamics, teaching in USA 9-2109  
 dynamics, theory for large spatial gradients and long memory 9-9315  
 elasto-viscous, damping force on oscillating body calc. 9-14745  
 electromagnetodynamics, fundamental eqns. and consequences 9-7105  
 field-flow fractionation, nonequilib. theory 9-848  
 flow, computation by Kernel function application 9-21021  
 flow, laminar, in pipes, rheology 9-853  
 flow, laminar, over flat plate, non-equilib. dynamics 9-18245  
 flow, MHD and OHD, nonanalyticity at surface 9-19507  
 flow, steady turbulent motion, analogy of oscillating mass on wheels 9-20379  
 flow, unsteady centred, integral of motion 9-21019  
 flow, viscous, through pipe orifice, low Reynolds no., Navier-Stokes eqn. soln. 9-19502  
 flow between parallel plates in transverse field, stabilization 9-7123  
 flow in rotating annulus, transition from axisymmetric to nonaxisymmetric flow 9-18239  
 flow of second order incompressible fluid, integration of eqns. of motion 9-9316  
 fluid, viscous incompressible, steady laminar flow through tube with X-section as intersection of two circles 9-21160  
 fluid mechanics, book 9-2945  
 fluidized beds, mechanism 9-13404  
 free convection from flat plate, solns. 9-21018  
 gas-liquid crit. pt., inequalities for critical indices 9-19654  
 glycerine, viscous, acoustic wave damping, dispersion calc. 9-19513  
 graphite particle pseudo-fluidized bed, elec. resistance to 900°C rel. to particle size 9-9314  
 hard spheres, mixture of two sizes excess free energy 9-2178  
 hard-core, 1D, translational invariance props. 9-17745  
 hard-sphere and square-well molcs., free-path distrib. and collision rates 9-8457  
 heat transfer, turbulent, in channel 9-17081  
 heat transfer fluid in channel, transient temp. fields considering wall metal 9-14841  
 heated body dissolving in free fluid 9-1005  
 heterogeneous layer heated from above, stability 9-7102  
 incipient fluidizing velocity in gas fluidized beds 9-21010  
 inert-gas binary mixture, structure factors calc. 9-11516  
 interaction of ideal fluid with gravitational field 9-8389  
 inverse problem, picking distrib. function and determ. pot. which could give rise to it 9-12898  
 laminar flow between parallel walls, circular pipe, suction eff. on forced convection 9-4990  
 laminar pipe flow in transverse mag. field, anal. with uniform radial heat flux at wall 9-13408  
 Lax's numerical method for soln. of hyperbolic systems 9-5097  
 layer heated from above, stability 9-11530  
 layer with time-depend. density gradients, stability 9-21182  
 light scatt. by particles turbulent fluid 9-16026  
 mass transfer with plate in non-Newtonian plastic fluid 9-845  
 MHD flows, kinematic props. 9-2952  
 micropolar, shearing, plane Couette and Poiseuille flow behaviour 9-18238  
 mixtures, separation, parametric pumping technique 9-2943  
 Navier-Stokes eqns., canonical form derived using Clebsch transformation 9-21002  
 nearest neighbour, difference eqn. solns. 9-4244  
 Newtonian, identification by right circular cyl. solns. 9-19035  
 non-Newtonian, combined laminar free and forced convection 9-846  
 non-Newtonian, cone and plate viscometer for flow curve determs 9-4991  
 non-Newtonian, flow, mixing 9-844  
 non-Newtonian, secondary flow, comparison of constitutive eqns. 9-9318  
 non-Newtonian, steady slow motion through tapered tube, theory 9-11524  
 non-Newtonian hydromechanics of disperse systems 9-18373  
 non-relativistic, thermodynamics, energy tensors 9-17738  
 non-viscous, post-Newtonian eqn. of hydrodynamics in Brans-Dicke theory 9-19497



**Fluids continued**

- Ornstein-Zernike rel. for disordered fluid 9-14740  
 perfect, Cauchy's problem for general relativistic eqns. 9-10629  
 plane vortex sheet, stability rel. to compressibility and mag. field applic. 9-21101  
 polar and dipolar, theories and thermodyn. 9-11517  
 power-law, laminar three-dimens. boundary layer eqns., similarity solns. 9-11523  
 quantum deviations from classical behaviour, effs. of using perturbation theory 9-10643  
 relativistic motion, eqn. with stress force term. 9-7099  
 relativistic scalar, thermodynamics 9-6330  
 rotating, contained and unbounded, theory, book 9-11521  
 rotating, Ekman layer, m.h.d. 9-18250  
 rotating, thermal convection, suppression of frictional constraint on lateral boundaries 9-18793  
 rotating sphere containing heat sources, thermal instability 9-4371  
 second order, stability between two concentric cylinders 9-7101  
 second-order, differential type, constitutive eqn. 9-6366  
 sheared, acoustic wave propag. 9-19511  
 specific heat near crit. pt., theory 9-1067  
 sphere, relativistic, at mech. and thermal equilibrium 9-7104  
 spheres, general relativistic, regularity and boundary conditions 9-8384  
 supercritical press., heat transfer coeffs. 9-20998  
 thermodynamics of irreversible processes 9-8518  
 turbulence, Burger's model, correl. function, functional integral numerical calc. 9-11526  
 turbulence, decaying isotropic, distortion of energy spectrum due to suspended particles 9-2948  
 turbulent, transport props., prediction using simple model 9-11661  
 turbulent flow, heat transfer rel. to temp. depend. phys. props., for high heat fluxes 9-12946  
 turbulent flow in pipes in magnetic field, unified semiempirical theory 9-7122  
 two-dimensional, correlation functions, geometrical sum rule 9-11515  
 virial eqn. of state, exponential 9-14741  
 viscoelastic, flow down inclined plane, stability 9-2944  
 viscoelastic, kinematics, with finite deformations 9-12923  
 viscoelastic, steady laminar flow, permeability depend. parallel uniformly porous walls 9-5128  
 viscometric flow, non-Newtonian, book 9-11529  
 viscous, finite elec. cond., incompressible, magnetohydrodynamic disturbances due to oscillating dipole introduction 9-11532  
 viscous, flow past flat plate, boundary layer approx. net trailing edge 9-967  
 viscous, general relativistic props. 9-18232  
 viscous, heat and momentum natural convection, boundary layer soln. 9-20999  
 viscous, incompressible, axisymmetric flow, time-depend. Navier-Stokes eqn. soln. 9-21159  
 viscous, incompressible, in finite vessel, free convection soln. by topological method 9-19627  
 viscous, nonisothermal steady flow, problems 9-2947  
 viscous, relativistic flow 9-18243  
 viscous conductive, flow in axis-symmetric MHD system 9-9332  
 viscous drag and secondary flow in granular beds 9-13406  
 viscous sublayer instability 9-842  
 vortex, jet-driven, hydromagnetic stabilization 9-21043  
 waves, long, in stratified compress. fluid over channel 9-21025  
 weakly compressible, stability study of flows in plane pipes 9-945  
 LaB<sub>6</sub> powder, gas suspended, as MHD generator working fluid 9-220  
 Xe, isochores, motor polarization temp., density depend. 9-4939

**Fluorescence** *see Luminescence***Fluorescent screens** *see Luminescent devices***Fluorimetry** *see Chemical analysis***Fluorine**

- atoms and ion, bibliography of spectra 9-13287  
 chemisorption on diamond, heat of wetting, e.s.r. and i.r. spectrum 9-8083  
 electronic pair-correlation energies of ground states, soln. of Bethe-Goldstone eqns. 9-11383  
 fluorination of irradiated reactor fuels for re-use 9-6944  
 I 9-9871  
 methane-68.7%FI flame, temp., calc. and obs. 9-15561  
 $\alpha$ -F, cryst. struct. 9-3290  
 F<sup>-</sup>K<sup>+</sup> ion pair, overlapping hydration shells, interact., spheroidal cavity model 9-14858  
 F<sup>-</sup>, in citrate soln., influence on corrosion of Al 9-10344  
 F<sup>-</sup> ion, interstitial in Ca<sup>19</sup>F<sub>2</sub>:Ce<sup>3+</sup>, Yb<sup>3+</sup>, ENDOR obs. 9-8045  
<sup>19</sup>F, hole-particle states using <sup>14</sup>N(<sup>7</sup>Li,t)<sup>18</sup>F reaction 9-8978  
<sup>19</sup>F, n.m.r. in cpds. with F 9-762  
<sup>19</sup>F, n.m.r. in paramag. single cryst. PrF<sub>3</sub>, temp. depend. of component shift 9-1877  
<sup>19</sup>F n.m.r., chemical shifts of alkali fluorides in H<sub>2</sub>O-D<sub>2</sub>O solns. 9-3124

**Fluorine compounds**

- fluorides, ternary, cryst. lattice struct. and mag. props. 9-7438  
 trifluorides of lanthanides, melt growth 9-9648  
 CaF<sub>2</sub>:Dy<sup>3+</sup> solid laser, sun-pumped, 130 mW power output 9-13031  
 CaF<sub>2</sub> single crystals mixed with SrF<sub>2</sub> or BaF<sub>2</sub> single crystals, microhardness 9-11942  
 F<sup>35</sup>Cl/F<sup>37</sup>Cl, O<sup>-</sup>← $\Sigma$ <sup>+</sup> system investigation, 5200-4600 Å 9-2862

**Foams**

- See also Bubbles*  
 clay-water, for lightweight aggregate prod. 9-3140  
 film, black, conc. of adsorbed inorganic ions obs. 9-19650  
 generation by fire-fighting equipment, patent 9-9568

**Focasons** *see Crystals/lattice mechanics; Sputtering***Focussed collision sequences** *see Sputtering***Fog**

- dissipation using CO<sub>2</sub> laser 9-4055  
 formation conditions near cool surfaces 9-9591  
 NH<sub>4</sub>Cl, elec. field visualization appl. 9-202

**Fokker-Planck equation** *see Transport processes***Foldy-Wouthuysen transformation** *see Field theory, quantum***Forbush decreases** *see Cosmic rays/variations***Force** *see Dynamics***Force constants** *see Molecules/vibration***Force measurement**

- balance, magnetic, automatic with photocell for gravimetric and magnetic analysis 9-18978  
 frictional, during vibration 9-6349  
 interference dynamometer 9-6271  
 magnetoelastic transformer-type transducers, error reduction 9-8353  
 stress on bolted joint, piezoelec. transducer 9-8352

**Form factors** *see Elementary particles/theory***Forming processes**

- ceramics, preparation of spherical samples 9-21403  
 cermets, high-temperature, fabrication 9-18535  
 corundum ceramics, cutting and grinding rel. to surface damage production 9-13574  
 electrospar, cylindrical shell and circular diaphragm deformation anal. 9-19828  
 ferrites, preparation of spherical samples 9-21403  
 friction measurement in drawing, extrusion and rolling 9-13719  
 graphite powder, compactibility into reactor fuel rods 9-2797  
 graphite sphere elements for pebble bed reactors 9-6940  
 hot cracking resistance of solidifying metal, quantitative determ. 9-21396  
 metal shaping, contemporary techniques 9-19829  
 metallic alloys, preparation of spherical samples 9-21403  
 metals, cutting at high velocities, specific work consumed in plastic deformation 9-9758  
 moulding of nuclear fuel elements, patent 9-20858  
 polychloroprene uniaxially stretched, length of statistical segment calc. 9-19781  
 polyethylene, drawn and annealed lamellar structure and molecular orientation 9-19738  
 polyethylene, redrawing causing structure change 9-17238  
 polyethyleneterephthalate fibres, oriented, thermoplasticizing drawing rel. to supermol. struct., obs. 9-11757  
 polyvinylalcohol fibres, oriented, thermoplasticizing drawing rel. to supermol. struct., obs. 9-11757  
 PVC, stretched uniaxially, thermal and mechanical props. anisotropy 9-19781  
 PVC, structural changes due to mechanical and heat treatments 9-21416  
 pyrocarbons, reproducible compressed samples, prep. and props. 9-7596  
 quartz comminution, net energy input rel. to fineness 9-7597  
 rod, axisymmetric extrusion through conical dies, theory 9-21395  
 rubber, uniaxially stretched, length of statistical segment calc. 9-19781  
 sheet metal drawing, plastic anisotropy eff. 9-19830  
 steel, Kh12ND, structure and properties of welds, effect of Cr content 9-14984  
 steel, Mn, low C, Nb-treated, rolled, weldability 9-19819  
 steel casting, embrittlement due to welding effects of conditions and structure 9-17317  
 steel welds, hot cracks, review 9-13739  
 weld cracking 9-18532  
 welded steel box columns, ultimate strength 9-14979  
 welding, spot cold, stress and strain states in welding area of brittle mats. 9-21362  
 welding, under vacuum 9-18530  
 Al cutting at high velocities, specific work consumed in plastic deformation 9-9758  
 Be purification by vacuum melting followed by distillation and simultaneous deposition to sheet in a beam furnace 9-13748  
 C, glassy, characts. and thermal props. rel. to fabrication factors 9-7317  
 C fibres, by stretching yarn, high strength and high modulus prod. 9-7514  
 C monolithic articles, prod. using low-pressure semi-isostatic tech. 9-8309  
 C steel, slightly hypoeutectoid, austenite recrystallization during hot-working 9-16145  
 Cu-Ag alloy brazing for metal-to-ceramic seals 9-13766  
 Cu, drawing through die, change of submicroscopic struct. 9-9674  
 Cu alloys and steel, welding joints, crack formation and melting of base materials 9-21397  
 Nb alloys with improved ease of fabrication 9-13770  
 Ti, drawing, slip and twinning during deformation 9-19802  
 Ti welding, pore formation, surface impurity effects 9-16146  
 U metal production by C reduction of UO<sub>3</sub> in vacuum 9-14134

**Fortran** *see Calculating apparatus/digital computer programmes***Fountain effect** *see Helium-liquid; Superfluidity***Fourier analysis**

- See also X-ray crystallography/calculation methods*  
 binary hologram synthesis from three-dimens. object, transform method 9-20536  
 diethylammonium palladium cyanide, structure, 001 Fourier synthesis 9-21320  
 Gerstner wave decomposition and related identities 9-7243  
 optical transform and holography 9-270  
 plane waves, generalized angular spectrum and diffraction transform 9-20548  
 scalar wave diffraction applic. 9-51  
 of square wave, using tuned circuit 9-4224  
 of SU(2,1) group 9-8367  
 textbook 9-20  
 textbook 9-10716  
 use in time-scaling and short-time spectral analysis 9-8364  
 Zn magneto-oscillations 9-16219

**Fourier series** *see Series; Transformations, mathematical***Fourier-transform spectroscopy** *see Fourier analysis; Spectroscopy***Fractionation** *see Distillation***Fracture**

- See also Mechanical strength*  
 brass (70/30), in Hg, behaviour rel. to grain size, pre-strain and strain rate 9-19806  
 brittle, effect of inhomogeneities 9-7576  
 ceramics, controlled laser separation 9-3441  
 concrete, in compression 9-16132  
 diamond-type crystals, Hertzian fracture 9-7575  
 ductile, initiated by pressurized penny-shaped crack 9-17314  
 ductile criteria in uniaxial compression tests 9-20412  
 glass, brittle fracture, effect of inhomogeneities 9-7576  
 glass, energy, determ. using double-cantilever cleavage technique 9-11941  
 glass, fracture front straightening 9-7574  
 graphite, resistance to thermal rupture, direct meas. 9-7572  
 graphite, under torsional and biaxial stresses, at room temp. 9-7565

**Fracture continued**

- internal, control rel. to obtaining juvenile surfaces: plastic extrusion method 9-13572  
 internal, control rel. to obtaining juvenile surfaces: plastic casing method 9-13571  
 markings, transverse, generated by unsteady cleavage velocities 9-1211  
 martensite in Fe-Ni-Si-C steel, eff. of plate size, ageing and temp. 9-18517  
 metal films, strength 9-7559  
 metals, surface energy rel. to plastic deform. 9-11922  
 polymethylmethacrylate, and yield, 78°-350°K 9-13729  
 Robertson crack arrest test 9-19809  
 sapphire, surface energy and stress corrosion on (10 $\bar{1}$ 1) and (10 $\bar{1}$ 0) planes 9-7571  
 steel, 0.16-0.2C, 0.65-0.75Mn, Al-killing effect 9-19795  
 steel, compression induced, study using Al model 9-18516  
 steel, fatigue, surface topography under repeated bending, rotation and tension 9-5480  
 steel, Fe-Ni-Si-C, fracture of martensite, eff. of plate size, ageing and temp. 9-18517  
 steel, fracture behaviour, subject to pressure 9-18518  
 steel, mild and low-C, Mn, effect of hydrostatic stress on cleavage fracture 9-17318  
 steel, Mn, low C, Nb-treated, rolled, susceptibility to cracking in heat-affected zone props. 9-19819  
 steel, stainless, ductile, localized deformation obs. 9-17315  
 steel, surfaces with cracks of 'flocule' type, metallographic and X-ray diffraction investigation 9-5483  
 WC, during fast n irradi., 10<sup>21</sup> n/cm<sup>2</sup> 9-9862  
 Zr-Se alloys, hydrided, effects of Se and H contents 9-19805  
 Al in 3% Zn amalgam, behaviour rel. to grain size, pre-strain and strain rate 9-19806  
 Al plates, formation during spinning into core 9-13734  
 Al<sub>2</sub>O<sub>3</sub>, mechanisms rel. to structure 9-1305  
 Al<sub>2</sub>O<sub>3</sub> glass, surface energy 9-1306  
 BeO, polycrystalline, energy 9-19807  
 CaO, dense, mechanisms and H<sub>2</sub>O effects 9-7567  
 Fe-Ni-Si-C steel, fracture of martensite, eff. of plate size, ageing and temp. 9-18517  
 Ir field-ion specimen, rel. to glissile Schockley loop occurrence 9-5362  
 K, and deformation 9-1308  
 LiF, surface energy ratio rel. to spontaneous crack propag. 9-3451  
 LiF dynamical cleavage, fracture surface energies, dislocation processes and transverse fracture markings 9-13741  
 Mg-(2wt.%)Al alloy, complex-stress creep fracture at 50°C 9-21382  
 MgO, hot extruded, and strength up to 1315°C 9-1302  
 MgO, water vapour effects on fracture stress 9-18506  
 MgO single cryst. with magnesioferrite precipitates, rel. to particle size 9-7573  
 NbC, during fast n irradi., 10<sup>21</sup> n/cm<sup>2</sup> 9-9862  
 Pb glass, surface energy 9-1306  
 Sn in contact with binary alloy, brittle rupture temp. and alloy comp. dependence 9-9761  
 TaC, during fast n irradi., 10<sup>21</sup> n/cm<sup>2</sup> 9-9862  
 TiC, during fast n irradi., 10<sup>21</sup> n/cm<sup>2</sup> 9-9862  
 W, cast, intergranular fracture, influence of oxygen 9-16134  
 Zn, brittle, alloying effects 9-9772  
 Zn, rupture and plastic deform. for forbidden basal slip 9-11932  
 ZrC, during fast n irradi., 10<sup>21</sup> n/cm<sup>2</sup> 9-9862

**Francium**

No entries

**Francium compounds**

No entries

**Franck-Condon factors** *see Spectra***Frank-Read sources** *see Crystal imperfections/dislocations***Fraunhofer lines** *see Astronomical spectra; Spectra; Sun/spectra***Free field rooms** *see Acoustical laboratories***Free radicals**

- alkoxybenzene radical anions, e.s.r. and electronic struct. 9-7085  
 alkyl, chem. induced dynamic nuclear polarization 9-2921  
 alkyl radical reactions, chem. induced dyn. nucl. polarization 9-17222  
 9-alkylxanthyls, e.s.r. 9-9295  
 inp-azoxanisole liq. crystals, e.p.r. study 9-7086  
 benzene anion, removal of orbital degeneracy at 4.2°K 9-14727  
 benzene anion, T<sub>1</sub>/T<sub>2</sub> and spin relax. 9-15904  
 benzene negative ion, e.s.r., effects of deuterium substitution 9-2895  
 benzophenone, fluorinated, anion radicals, e.s.r. 9-4970  
 benzophenone ion, high resolution transient e.s.r. spectra 9-20954  
 benzyl, doublet electronic states 9-9247  
 1,1' and 2,2'-biazulenyl anion radicals, ESR spectra 9-20986  
 n-butylamide single crystals, X-irradiated, e.s.r. spectra 9-9294  
 carbon radical, e.p.r. spectra from resolution of PVC spectrum 9-17496  
 cation with inert-gas shell, empirical formula for radius 9-19482  
 chloranil radical anion, optical spectrum 9-5173  
 cytosine-5-<sup>3</sup>H, free radicals formed by decay of constituent T atom 9-1928  
 diazomethyl, trapped radical, vibrational absorption 9-20970  
 durenne radiolysis, production of radical with 13 equiv. protons 9-8078  
 dynamic nuclear polarization in fluorocarbon solns. 9-21226  
 ENDOR in randomly oriented paramag. mofs. 9-5995  
 e.p.r., weak field, of radical solutions, hyperfine struct. 9-9550  
 e.s.r. of aromatic intermediates in pyrolysis 9-7088  
 fluorocarbons in  $\gamma$ -irrad. tetrafluoroethylene, e.s.r. spectra 9-21277  
 in Group-IV and V hydrides in inert matrices at low temps., e.s.r. 9-12498  
 hydrocarbons, conjugated, spin densities, LCAO-MO calc. 9-13396  
 ice, pulse-irrad. 9-10360  
 iminoxy, formed from tetranitromethane and 1,3-dicarbonyl cpds., structure from e.s.r. 9-20987  
 ionization potentials meas. in mass spectrometer 9-15950  
 isobutyramide single, crystals, X-irradiated, e.s.r. spectra 9-9294  
 mass spectrometry of v. fast reactions 9-10334  
 methylstannylium, ionization by electron impact 9-17133  
 1-methylthymine H-addition radical, conformation 9-828  
 peroxy, ESR obs. of decay during grafting of styrene on to poly(tetrafluoroethylene) 9-20040  
 peroxy radical, e.p.r. spectra from resolution of PVC spectrum 9-17496  
 phenoxy, in solid ion-exchange resins, inhomogeneous e.p.r. line broadening 9-829  
 phenoxy-nitroxide biradical, ESR 9-13397

**Free radicals continued**

- phenyl radical reactions, chem. induced dyn. nucl. polarization 9-17222  
 phenyldibiphenyl methyl, calc. of electron spin density by valence-bond method 9-830  
 9-phenylxanthyl, e.s.r., spatial config. 9-13398  
 polyenic radicals, odd linear, applic. of stability conditions for Hartree-Fock eqn. to  $\pi$ -electron model 9-20917  
 polyethylene terephthalate, photo-induced post-irrad. radical conversion, e.s.r. 9-10357  
 polyradicals, C and N, preparation 9-17518  
 in polytetrafluoroethylene, due to irradiation, possible dosimeter base 9-2558  
 propionamide single crystals, X-irradiated, e.s.r. spectra 9-9294  
 propyl rupture in chem. activated radicals 9-1890  
 in proteins due to x-irradiation 9-4013  
 $\pi$ -electron radicals, proton hyperfine splittings, theory 9-827  
 radical ion and intermediates from  $\alpha$ -methylstyrene in org. glasses, ESR and opt. studies 9-20988  
 recombination reactions in flames, catalysis by NO 9-14121  
 semiquinones, fluorinated, anion radicals, e.s.r. spectra 9-4971  
 succinic acid,  $\gamma$ -irrad. crystals, e.s.r. 9-16462  
 tetramethyl-2, 2, 6, 6-piperidinol-4-oxyl-1, in polyisoprene and polybutadiene 9-9296  
 2,2,6,6-tetramethyl-4-hydroxypiperidine-1-oxyl, mag. props., 1.8°K to 300°K 9-10115  
 thienyl-phenyl ketones, radical anions, ESR study 9-20989  
 tribiphenyl methyl, calc. of electron spin density by valence bond method 9-830  
 tribromomethyl, i.r. spectrum in solid Ar 9-810  
 vanadyl acetylacetonate dissolved in p-azoxanisole, alignment by elec. field, eff. on EPR spectrum 9-21225  
 xanthyl, e.s.r. 9-7089  
 xanthyl, spin densities, unrestricted Hartree-Fock calc. 9-11506  
 in  $\gamma$ -irrad. propionamide, n-butylamide and isobutyramide, reactions with O<sub>2</sub> and SO<sub>2</sub> 9-12538  
 C<sub>2</sub>, rotational distrib. obs. in low-pressure plasma 9-20983  
 C polycrystal, preparation 9-17518  
 CH<sub>2</sub>CH( $\alpha$ )-CH<sub>2</sub> in polyethylene, e.s.r. spectra, hyperfine constant 9-15203  
 CH, proton hyperfine splittings, theory 9-827  
 CH<sub>2</sub>, orbit depend. on spin for singlet, triplet states 9-20982  
 CH<sub>3</sub> motion in polyarylates during heating 9-21415  
 CH<sub>3</sub>, ESR studies during redox polymerization 9-15217  
 CH<sub>2</sub>Cl photodissociation primary products, energy distrib. in vibr. excitation 9-10350  
 CHO\*, heat of formation 9-21685  
 CN, ground state in active N flames, optical absorpt. 9-826  
 CN, ht. of formation 9-825  
 Cl<sub>2</sub> in KClO<sub>4</sub>, e.p.r. and optical absorption study 9-21625  
 Cl<sup>-</sup> e.s.r. in polycryst. matrix 9-8024  
 ClO<sub>2</sub> in KClO<sub>4</sub> and KClO<sub>3</sub>, created by X-irradiation 9-18737  
 HO<sub>2</sub>, e.s.r. in solns. of H<sub>2</sub>O<sub>2</sub> in H<sub>2</sub>O at 77°K 9-7081  
 MnO<sub>4</sub> vacuo u.v. spectra, bands inductive MO description and behaviour 9-19483  
 N polyradical, preparation 9-17518  
 NCO gas-phase electron reson. spectrum 9-17063  
 NS, gas phase e.s.r. 9-7082  
 -OCH, H.F.S.-zero field e.p.r. 9-11505  
 OD, chemiluminescent, predissociation behavior determ. 9-18221  
 OH, (0,0) (A $\rightarrow$ X) u.v. transition, collision broadening cross-sections, line-widths, low temp. 9-19484  
 OH, chemiluminescent, predissociation behavior determ. 9-18221  
 OH, Hanle eff. in <sup>2</sup> $\Sigma^+$ ( $\nu=0$ ) state obs., g-factor-lifetime product determ. 9-20984  
 OH, interatomic force in  $\beta^2\Sigma^+$  obtained 9-20981  
 OH, rotational distrib. obs. in low-pressure plasma 9-20983  
 OH(A<sup>2</sup> $\Sigma^+$ ,  $\nu=0$ , K') quenching and rotational relax. 9-7083  
 PO<sub>2</sub>, e.p.r. in X-irrad. Na<sub>2</sub>HPO<sub>3</sub>.5H<sub>2</sub>O crystals 9-14113  
 RO<sub>2</sub> vacuo u.v. spectra, bands inductive MO description and behaviour 9-19483  
 SO, microwave spectrum, low-field Zeeman effect 9-13399  
 SiCl<sub>2</sub> matrix-isolation, vacuum u.v. photolysis 9-10352  
 SiF<sub>2</sub>, matrix-isolated i.r. and u.v. spectra 9-15903  
 SiH<sub>2</sub>, absorpt. spectrum in visible region, rotational struct. anal. of three bands 9-7084  
 TeO<sub>4</sub> vacuo u.v. spectra, bands inductive MO description and behaviour 9-19483

**Freezing***See also Melting; Supercooling*

- crystal-melt system surface temp. distrib. meas. device 9-3237  
 deformation method in photoelastic stress analysis 9-14378  
 eutectic growth front stability 9-3149  
 isenthalpic solidification, theoretical analyses 9-1157  
 isenthalpic solidification kinetics, dendritic growth theory 9-1156  
 nucleation theory, reconsideration 9-7303  
 separation of U from fission products by eutectic freezing 9-18749  
 solidification, atomic kinetics using Peltier heating and cooling 9-3152  
 solidification, isothermal, in thin layers during combined spontaneous and induced crystallization, statistical theory 9-1142  
 systems of several solutes, deviation from Raoult's law 9-17227  
 temperature difference curves 9-1068  
 transient temp. in growing solid, calcs. 9-18386  
 water, step growth on ice 9-5216  
 Al<sub>2</sub>O<sub>3</sub>-Y<sub>2</sub>Al<sub>2</sub>O<sub>3</sub>, solidification from melt, microstructure formation 9-3285  
 Bi-Se alloy, vitreous, glass transition temp. rel. to composition 9-3153  
 H<sub>2</sub>O, supercooled, homogeneous nucleation temp. 9-7301  
 I<sub>2</sub>-gasoline vapour mixture, ice nuclei prod. 9-9595  
 Su, solidification, thermal wave technique 9-5217

**Frenkel defects** *see Crystal imperfections/interstitials***Frequency** *see Time measurement***Friction***See also Internal friction*

- aerodynamic resistance of pipes with triply running spiral channels 9-15970  
 brittle solids, scale factor effect on mech. strength under complex compressive and tensile loading 9-7558  
 dry, oscillations anal. 9-14382  
 force meas. during vibration 9-6349



**Friction** continued

- four-ball lubricant testing machine with three wear tracks 9-6223
- gas flow, nonisothermal, at finite Reynolds numbers, extension of asymptotic relative law 9-3046
- ground surfaces, effect of rock type, press., strain rate and stiffness 9-8151
- lubricant, solid film, pressure effects 9-16138
- in metal drawing, extrusion and rolling, measurement procedure 9-13719
- metals, role of oxygen in eff. of additive surface-active substances 9-18529
- metals rel. to deformation at low temps. 9-16139
- paraffin film lubricant on steel, pressure effects 9-16138
- polyethylene, oriented crystalline, props., and dynamic props. 9-21361
- polytetrafluoroethylene, and wear 9-5488
- rubber on wet surfaces 9-3458
- static, time dependence 9-16704
- stick-slip oscillations threshold velocity investigation, metal-metal and plastic-metal surfaces 9-5489
- in turbulent flow through smooth pipes 9-14746
- Au film lubricant on steel, pressure effects 9-16138
- Be-Co alloy in vacuum, rel. crystal structure and atomic ordering 9-19814
- C, pyrolytic, rubbed, rel. to surface orientations 9-11758
- FeCo alloy in vacuum, rel. crystal structure and atomic ordering 9-19814
- MoS<sub>2</sub> film lubricant on steel, pressure effects 9-16138

**Frictional electricity** *see* **Electric charge; Electrostatics**

**Fuel cells** *see* **Electricity, direct conversion/fuel cells**

**Fugacity** *see* **Diffusion in gases; Kinetic theory/gases**

**Functions**

- Ax<sup>n</sup>, simulation network calc. diagram 9-6347
- Bessel's rel. to finite rotation operator and partial wave expansion 9-75
- Bessel, asymptotic expansion 9-12858
- Bessel, spherical, and vector harmonics in spherical co-ordinates, addition theorems 9-27
- Bessel, two, inverse function of product, appl. to pot. scatt. 9-14325
- Bessel and Gegenbauer polynomials, addition theorem as representation of complex Euclidean group 9-6286
- continuations, analytic, of analytic and harmonic functions, chapter in book 9-12861
- correlation, 3-state for Ising problems 9-4245
- correlation, props. of irreducible tensor operators 9-20297
- correlation functions, asymptotic forms 9-13556
- diagonal coherent state weight functional, convergence of Sudarshan expansion 9-6275
- entire, classification 9-6277
- exp (-x), tables for calc. activity changes with time of radioactive isotopes 9-11248
- generating, for exact soln. of the transport equation 9-17728
- harmonic, under boundary conditions, uniqueness and comparison theorems 9-8358
- Hermite polynomial, operational representations 9-14305
- minimisation, descending algorithm procedure 9-29
- modified functions of higher orders and applications to structural problems 9-17684
- modified functions of higher orders and applications to structural problems 9-17685
- non-analytic, for which deviation from analyticity is a generalised analytic function 9-32
- nonlinear functionals for transport theory 9-109
- nonperiodic, extension of Euler's quadrature formulae 9-28
- pair distrib. in degenerate Bose system 9-4251
- prolate spheroidal, image enhancement, truncation effect 9-20543
- special, book for physicists and chemists 9-12860
- special, identities from representation of complex Euclidean group in 3-space 9-8372
- tempering, exponential, applic. to diffusion and desorption processes 9-3179
- time-correlation, phase-space analysis 9-12881

**Fundamental concepts** *see* **Physics fundamentals**

**Fundamental constants** *see* **Constants**

**Fundamental particles** *see* **Elementary particles**

**Furnaces** *see* **Heating**

**Furry theorem** *see* **Quantum electrodynamics**

**Fusion** *see* **Heat of fusion; Melting; Nuclear fusion**

**g-factor** *see* **Elementary particles; Gyromagnetic ratio; Nucleus; Spectra**

**G-matrix** *see* **Molecules/internal mechanics**

**Gadolinium**

- absorption bands in ferromagnetic and paramagnetic states 9-16412
- dislocation climb due to thermal diffusion 9-3349
- doping of n-PbTe, thermoelec. power, thermal and elec. cond. effects 9-13876
- elastic moduli and u.s. attenuation rel. to mag. transitions 9-7517
- e.p.r. in dilute Cu-Gd alloy 9-14110
- ferromagnetic, polarized position annihilation 9-9917
- ferromagnetic, prod. of partially polarized electron beams by field emission 9-7865
- garnet, static and dynamic props. meas. 9-10139
- impurities eff. on high order phase transitions near T<sub>c</sub>, from thermal expansion data 9-1399
- internal friction spectrum, analysis of  $\alpha$  and  $\beta$  peaks 9-5431
- lattice sp. ht. calc. from phonon freq. distrib. curves 9-7635
- lattice sp. ht. calc. from phonon freq. distrib. curves 9-16165
- magnetization, direction of easy magnetization 9-21585
- magnetization, temp. depend. below 50°K 9-13983
- magnetocrystalline anisotropy, spin-wave theory 9-5815
- NMR in LaNi<sub>5</sub> rel. to dynamic effects, g shift 9-10280
- point defect production on e. and n. irradi. 9-11870
- twinning, mechanical, origin and growth 9-7361
- <sup>160</sup>Gd crystal, neutron diffraction study rel. to mag. props. 9-10114
- <sup>155</sup>Gd<sup>3+</sup> in ThO<sub>2</sub>, hyperfine coupling constant, temp. dependence 9-8031
- Gd<sup>3+</sup> in YVO<sub>4</sub>, YPO<sub>4</sub> and YAsO<sub>4</sub>, e.p.r. 9-21668
- Gd<sup>3+</sup>, cryst. field, direct determ. from variable freq. e.p.r. 9-5985
- Gd<sup>3+</sup>, zero-field reson. in YVO<sub>4</sub> and YPO<sub>4</sub> 9-8026
- Gd<sup>3+</sup>, zero field splitting in rare-earth ethyl sulphates 9-1859
- Gd<sup>3+</sup> in CaF<sub>2</sub>, Zeeman effect in sites of cubic symmetry 9-10196
- Gd<sup>3+</sup> in ThO<sub>2</sub>, e.p.r., low field spectrum 9-12503

**Gadolinium compounds**

- ferrite garnet, magnetic sublattice interactions 9-16369
- Cu-Gd dilute alloy, e.s.r. of Gd 9-14110
- EuO-4at.%Gd alloy, Curie temp. pressure dependence rel. to exchange interactions 9-18672
- Gd-GdFe<sub>2</sub> phase mixtures, magnetic ordering, 285-800°K 9-5820
- Gd-(2at.%)Sn alloy, mag. field at <sup>115</sup>Sn 9-12282
- Gd<sub>2</sub>(MoO<sub>4</sub>)<sub>3</sub> ceramic and single-crystal, prep. and X-ray analysis 9-18446
- Gd Fe garnet film, prep. by sputtering 9-5248
- GdAl, n.m.r. of <sup>27</sup>Al, Knight shift and susceptibilities, temp. depend. 9-3969
- GdAl<sub>3</sub>, thermoelec. power temp. dependence, ferromag. ordering effects 9-16307
- GdAlO<sub>3</sub>:<sup>27</sup>Al NMR obs. 9-5992
- GdAlO<sub>3</sub>:Eu<sup>3+</sup>, fluorescent emission 9-12490
- GdAlO<sub>3</sub>, growth from melt by Czochralski technique, possible laser host 9-1144
- GdAlO<sub>3</sub> antiferromagnetism and the magnetic phase diagram 9-7918
- GdCl<sub>3</sub>:Er<sup>3+</sup>, Zeeman effect 9-3888
- GdCl<sub>3</sub>, magnetic susceptibility, freq.-dependent, and renormalized spin-wave energies 9-16363
- GdCl<sub>3</sub>, cryst. struct. 9-11850
- GdCl<sub>3</sub>, magnetic eff. between rare-earths 9-12270
- GdCl<sub>3</sub> magnon density obs. in optical spectrum 9-7947
- GdCrO<sub>3</sub>, specific heat at low temps. rel. to  $\lambda$  transitions in mag. ordering 9-7655
- GdFe<sub>2</sub>, induced mag. fields at <sup>115</sup>Gd, absence 9-17470
- GdFeO<sub>3</sub>, metamagnetic props. 9-16383
- Gd<sub>2</sub>Fe<sub>2</sub>O<sub>7</sub>, magnetothermal effect, anomalous sign in compensation pt. region 9-1683
- Gd<sub>2</sub>(MoO<sub>4</sub>)<sub>3</sub> ferroelectric switching and electro-optical props. 9-12349
- Gd<sub>2</sub>(MoO<sub>4</sub>)<sub>3</sub>, ferroelec. props from new mechanism 9-1593
- Gd<sub>2</sub>O<sub>3</sub>:Eu<sup>3+</sup>, fluorescent emission 9-12490
- Gd<sub>2</sub>O<sub>3</sub>:Eu<sup>3+</sup>, luminescence and emission spectra, crystal field interpretation 9-10205
- Gd<sub>2</sub>O<sub>3</sub>, rare earth traces meas. by X-ray excited fluoresc. spectra 9-16514
- Gd<sub>2</sub>O<sub>3</sub>, structural stabilization with WO<sub>3</sub> 9-17326
- Ho-Gd alloy, ferromag. <sup>165</sup>Ho 9-16464
- La-Gd superconducting transition temperature, pressure dependence 9-1486
- Sc-Gd alloys, n.m.r. and mag. susceptibility, rel. to conduction-electron polarization 9-12513

**Galaxies**

*See also* **Nebulae**

- 3C120 Seyfert, light curve irregular var. 9-4087
- 3C273 X-ray luminosity obs. 9-12744
- Abell 2199 cluster, static props. 9-12667
- antiretro, radio emission, observations at 70, 60 and 40 wavelengths 9-6154
- barred and Magellanic spiral, stellar orbits 9-20158
- bright, fan-beam detection of radio emission at 408 MHz, correl. with optical props. 9-16558
- clusters, average opt. thickness for blue and red rays 9-17609
- clusters associated with supergiant, cluster orientation, age 9-12668
- coma cluster, photo, brightness profiles proc. for calib. and reduction, physical and geom. parameters 9-6112
- Coma Cluster, vel. dispersion using spherical inhomogeneities model 9-20132
- in Coma cluster central field, peculiar opt. struct. 9-21851
- compact, bright, blue and small, a list 9-20161
- computer model, evaluation through barred to cylindrical form 9-20148
- computer two-dimensional model with up to 4000 members, evolution 9-20149
- cosmic rays, life, explanation in stochastic nature of mag. field 9-20150
- Cygnus A, radio-emission mechanism 9-1992
- diameter, linear, function of absolute luminosity and its type 9-20157
- dwarf spheroidal, of Local Group, bibliography 9-21844
- evolution, quasar stage 9-15327
- evolution, review 9-12669
- field, UVB determ. of metallicity index Q, comparison with cluster galaxies 9-10464
- gas heating rel. to neutral H period in evolution of universe 9-6101
- gravitational lens action, theory 9-10467
- gravitational lenses acting on light from other galaxies and producing quasar like effects 9-6152
- H II regions, Ly- $\alpha$  radiation transfer 9-6117
- Haro, blue, four, radial vels. 9-14193
- H II regions, interstellar reddening and existing stars Lyman-visual colours, obs. 9-6118
- H II regions, ionized, temp. struct. and emission props. 9-8233
- i.r., contribution to cosmic background 9-6156
- kinematics of distant objects, local solar motion method 9-18839
- M67, color-magnitude diagram interpretation, He content obs. 9-20155
- M81, luminous ring due to synchrotron emission 9-10466
- M82, eruption, book 9-8220
- M87, peculiar, hard X-ray flux upper limit 9-18930
- M87 jet, detailed photometry 9-10465
- M87 X-ray luminosity obs. 9-12744
- M 31, H II region photoelectric study, temp., chemical abundance determ. 9-21852
- M 32, H II region photoelectric study, temp., chemical abundance determ. 9-21852
- M 51, H II region photoelectric study, temp., chemical abundance determ. 9-21852
- M 81, H II region photoelectric study, temp., chemical abundance determ. 9-21852
- magnetic field, stochastic nature, applic. to cosmic-ray life 9-20150
- magnetic field generation by viscous forces in non-uniformly rotating plasma 9-6114
- Metagalaxy, average density of dust matter and non-relict origin 9-17609
- NGC 1068, small dia. radio and optical features, relationship 9-14192
- NGC 1275, small dia. radio and optical features, relationship 9-14192
- NGC 4027, unusual velocity field 9-20158
- NGC 4486 small dia. radio and optical features, relationship 9-14192
- NGC 1052, 178 MHz flux density meas., 2-component source model suggestion 9-6113
- NGC 1672, possible variations of radio emission 9-21849

**Galaxies continued**

- NGC 1832, spiral, rotation and mass 9-15277  
 NGC 188, chemical comp., model 9-20154  
 NGC 188, color-magnitude diagram interpretation, He content obs. 9-20155  
 NGC 2276, second supernova obs. 9-20184  
 NGC 4194 and its peculiarities 9-21846  
 NGC 4214, Magellanic, vel. field, spectroscopic study 9-20160  
 NGC 4278, 178MHz flux density meas., shape depend. on thermal absorption 9-6113  
 NGC 4486, radio-emission mechanism 9-1992  
 NGC 4486, special relativity applic. for determ. of nature of radiation 9-4107  
 NGC 6946, spiral, neutral-H content and kinematic props. 9-21845  
 normal, 39 obs. at 430 and 611 MHz 9-20208  
 normal at 1415 MHz, ratio of radio to optical diameters, interpretation 9-15275  
 observations, book 9-6196  
 optical half-thickness, causes of systematic error and contradictory obs. 9-20159  
 origin, initial homogeneities 9-16559  
 protogalaxies, formation, 'photon whirls' hypothesis 9-17610  
 radio, energy sources from obs. of relativistic effects of non-thermal cosmic sources 9-18885  
 radio, optical positions 9-18887  
 radio, r.f. spectra 9-1990  
 radio, spectra compared with quasars' 9-20207  
 radio, X-radiation 9-4108  
 radioluminescence function, contrib. to metagalaxy background rad. 9-1989  
 radioresources in clusters of galaxies 9-4104  
 satellites, dwarfish: Palomar Atlas optical pairs 9-1991  
 SB(r) galaxies, ring structure investigated 9-20158  
 Seyfert 9-18840  
 Seyfert, and related objects, conference, Arizona (1968) 9-14191  
 Seyfert, compact and N-type radio, H $\beta$  emission line width rel. to ionization mech. 9-6111  
 Seyfert galaxies nuclei, spectrophotometric study 9-18838  
 shock wave influence on degree of gas ionization in cluster 9-4088  
 southern, radial velocities 9-21850  
 spiral, density-wave theory implications 9-20153  
 spiral arm distortion 9-21848  
 stellar systems, radial mass flow 9-2021  
 structure and evolution, calc. from assumed diffusion of particles in mag. field 9-15276  
 supernova explosion freq. in galaxy clusters 9-12705  
 triplet, austral 9-4086  
 Virgins-A radiogalaxy, nucleus spectrum, H $\alpha$  line obs. 9-21847  
 H atom, neutral, content in 32 small ang. dia. galaxies 9-12666  
 H II regions, southern hemisphere, 5 GHz continuum radiation obs., 28 maps 9-15280  
 H II regions structure rel. to OH 18 cm stimulated radiation 9-12727

**the Galaxy**

- absorbing matter in spiral arm, evidence from dispersion of two-colour diagrams 9-10498  
 age from U decay obs. 9-16554  
 Aql constellation, colour excess study for obs. of dust matter in galactic plane 9-21842  
 bending oscillations of rot. disks, dynamics, applic. to warp origin 9-20151  
 centre region, lunar occultations in 1667MHz OH line 9-6110  
 classical Cepheids, fundamental data catalogue 9-6137  
 continuum survey of southern Milky Way, 1410 MHz 9-10463  
 cosmic ray electrons magnetic fields and background radio emission study 9-18837  
 cosmic rays, particles lifetime and high energy  $\gamma$ -rays 9-1985  
 cosmic rays, solar modulation 9-14185  
 Cyg constellation, colour excess study for obs. of dust matter in galactic plane 9-21842  
 disc trajectories of cosmic protons, radiation transfer estimation 9-8924  
 dust layer, space struct. problem, rel. to visible brightness of Milky Way 9-21842  
 extended source obs. from infrared survey 9-6120  
 galactic plane positions, rectangular coordinates on Palomar sky atlas 9-18835  
 galactic X-ray sources in hydromag. waves 9-20213  
 gas flow from centre 9-15376  
 giant M stars, space distrib. and density rel. to Galactic disk distrib. 9-20152  
 halo, observational test 9-21843  
 halo, transient nature 9-15273  
 magnetic field investigation by spherical harmonic anal. of interstellar polarization 9-12665  
 Milky Way, northern, OB stars distrib. 9-8234  
 Milky Way, visible brightness, rel. of space struct. of dust layer 9-21842  
 orbits and integrals calc. in spiral field 9-20156  
 Perseus spiral arm in dirn Cassiopeia A mag. fields of order  $2 \times 10^{-5}$  G determ. 9-2025  
 radio emission, background, obs. w.r.t. cosmic ray electrons mag. fields 9-18837  
 radio halo, existence 9-16557  
 radio noise freq. spectrum rel. to cosmic ray energy spectrum 9-12730  
 rotation agrees with gravitational instability theory in cosmology 9-12662  
 star cloud encounters, calc. of effect on stellar distributions 9-15274  
 stars, proper-motion, blue objects and eclipsing binaries near south pole, UVB obs. 9-8225  
 stellar orbit perturbation by gas cloud, motion inclined to galactic plane 9-16555  
 structure, from space distrib. of Classical Cepheids 9-12664  
 Wolf-Rayet stars distrib. in galactic plane 9-16556  
 H II regions, absolute isophotometry in the H $\alpha$  light, ratio to radio continuum rad. 9-10469  
 H II regions, opacity and structure 9-20167  
 He abundance in young objects 9-18836  
 OH 18 cm absorpt. lines obs. 9-14190

**Gallium**

- diffusion in Si, retarded 9-5412  
 energy loss spectra, characteristic, of 8 keV electrons in liquid 9-7249  
 film, amorphous and cryst., mech. stresses 9-5451  
 films, 10-170°K, development of mech. stresses 9-16127

**Gallium continued**

- films, structure and optical props of solid and liq. films 9-3192  
 ion-implantation of Si to form p-type layers, penetration depth rel. to charge carrier conc. annealing temp. dependence of layers 9-15108  
 liquid, diffusion of Zn, Ag and Co 9-13516  
 liquid, flow in tube in trans. mag. field 9-9328  
 liquid, thermal capacity at high temperatures 9-9505  
 partial substitution in AuCu or AuCu $_3$  alloys, effect on order-disorder transforms 9-5522  
 specific heat meas. near melting point 9-21435  
 structure and phase changes from pseudopotential and second-order perturbation theory 9-5319  
 in CdGeAs $_2$ , effect on conductivity 9-18618  
 diffusion in Si, retarded 9-5413  
 Ga-Al-As system, thermodynamic and optical treatment of phase diagram 9-17346  
 positron lifetimes in solid and liquid 9-7731  
 substitution partial of Fe in SrFe $_{12}$ O $_{19}$ , effect on saturation magnetization 9-16373

**Gallium compounds**

- co n-GaSb, i.r. absorption and reflection, rel. to electron masses 9-3852  
 Ga $_2$ O $_3$  natural abundance and isotopically enriched, for  $^{69m}$ Zn prod. 9-18075  
 I 9-12300  
 Au-Ga liq. alloy, elec. resist., electronic struct. 9-16020  
 Cu-Ga single crystal, work-hardening curve, transition from stage I to stage II, X-ray investig. 9-13760  
 n-Ga $_1-x$ P $_x$ Te, Se, Hall effect, of two kinds of carriers 9-3623  
 Ga $_2$ Se $_3$ , thermal expansion rel. to temp. 9-18564  
 Ga $_2$ Fe $_{1-x}$ O $_4$ , spin wave spectrum from inelastic n. scatt. 9-21581  
 GaAs, lattice dynamics 9-11978  
 GaAs, semi-insulating, precision thermal expansion meas., 25-325°C 9-5570  
 GaAs, substrate for mirror smooth Ge epitaxial layers by disproportionation reaction 9-19671  
 GaAs $_{1-x}$ P $_x$ Se, props. from temp. depend. of Hall effect 9-21500  
 GaAs $_{1-x}$ P $_x$ , electron radiation damage, cathodoluminescence study 9-18570  
 GaAs substrate for Ge epitaxial layers deposition by GeH $_4$  pyrolysis 9-19670  
 GaAs dislocation free, electronic transport props. 9-16099  
 GaAs $_{1-x}$ P $_x$ S, S and Te doped, Hall coeff. and resist. rel. temp., 55 to 400 °K 9-12150  
 GaAs $_2$ P $_{1-x}$ , Raman scattering from lattice vibrations 9-12416  
 Ga $_2-x$ Fe $_x$ O $_3$ , mag. props. 9-5826  
 Ga $_1-x$ In $_x$ As, i.r. reflection spectra, mixed cry. behaviour 9-1760  
 Ga $_2$ In $_{1-x}$ As alloys, E $_i$  interband transition energies 9-9987  
 GaN, sublimation, kinetic energy of vapour mols. 9-1074  
 GaP-B, Zn, photoluminescence and electroluminescence mechanisms rel. to reactions in doping 9-3940  
 GaP-Cd (Zn), thermal ionization energies of acceptors 9-5696  
 GaP-N, isoelectronic impurities theory 9-7801  
 p-n GaP-N, junctions, green electroluminescence 9-3938  
 p-GaP-O-Zn epitaxial growth, patent 9-10257  
 GaP-O $_2$ , i.r. radiative capture of electrons at ionized oxygen donors 9-12464  
 n-GaP-S(Te) and undoped, epitaxial, edge luminescence, intrinsic and extrinsic, 80°-300°K 9-12480  
 GaP-Zn, Fermi levels as a function of hole concentration function, 1040°C solid solubility isotherm of Zn 9-7715  
 GaP, bound electron states, symmetry 9-1520  
 GaP, breakdown oscillations, induced impurity, and obs. of traps higher than indirect band edge 9-5695  
 GaP, Brillouin, Raman and i.r. spectra 9-12446  
 GaP, coherent excitation of polarons by nonlinear parametric process 9-12326  
 GaP, dislocation etch pits 9-14947  
 GaP, dispersion in the nonlinear susceptibility near the reststrahl band 9-7962  
 GaP, e energy losses and optical data 9-16191  
 GaP, ejection patterns in low-energy sputtering, 50-525°C, orientation dependence 9-9866  
 GaP, electron radiation damage, cathodoluminescence study 9-18570  
 GaP, energy loss intensities of 50 kV electrons, deviations in low energy region 9-7692  
 GaP, exciton luminescence intensity elec. field and temp. dependences 9-16431  
 GaP, gaseous, dissociation energy 9-11504  
 GaP, lattice dynamics 9-11978  
 GaP, luminescence concentration quenching and the impurity-band Auger model 9-8000  
 GaP, luminescence near indirect transition in multiphoton excitation case, 4.2°K and 77.3°K 9-10236  
 n-GaP, Mossbauer spectra of  $^{57}$ Fe 9-5893  
 GaP, photovoltage effect, anomalous 9-3741  
 GaP, Raman spectra cross sections, temp. depend. 9-12428  
 GaP, vapour-grown, elec. and optical props. 9-12148  
 GaP, X-ray-K absorption edge shifts 9-21638  
 GaP diode sources of red radiation, prep. and characts. 9-3679  
 GaP donor-acceptor electron recombination luminescence, multipole field effects 9-10266  
 GaP doped epitaxial films, photoluminescence 9-10237  
 GaP electroluminescent diodes, minority carrier lifetime 9-12491  
 GaP p-n structures, radiation spectrum control 9-5952  
 GaP plastic deformation, single crystals, rel. elec. erosion 9-5350  
 GaS, indirect energy gap by opt. absorption spectra 9-18622  
 GaS, photoconductivity and photo Hall effect 9-1614  
 n-GaSb-Te, Faraday effect at 20°K rel. to transport props. 9-10177  
 n-GaSb-InSb mixed crystal, conduction bands, resistivity, Hall effect and piezoresistance investigation 9-5690  
 GaSb, band structure calc. using nonlocal pseudopotential 9-1534  
 GaSb, channeling of H and He ions, energy loss meas. 9-9868  
 GaSb, microhardness, eff. of doping 9-5485  
 GaSb, radiative recombination excited by 20 KeV electron beam 9-21645  
 GaSb, spec. ht., 1-30°K 9-9843  
 GaSb, undoped, e-irrad. damage, orientation and energy dependence 9-5334  
 GaSb, X-ray-K-absorption edge shifts 9-21638  
 GaSb tunnel diodes, I-V characts. in high crossed elec. and mag. fields 9-10019



**Gallium compounds continued**

- GaSe-metal surface barriers on layer semiconductors 9-5699  
 GaSe, indirect energy gap by opt. absorption spectra 9-18622  
 GaSe<sub>1-x</sub>S<sub>x</sub>, indirect energy gap by opt. absorption spectra 9-18622  
 GaSe monocrystal absorption spectra fine structure, photoelectric determ. 77°K 9-10203  
 GaTe film, charge carrier mobility 9-13883  
 GnP, thermal and electrical conductivity, thermoelec. power and Hall coeff. 9-7794  
 Mn-Ca alloy powders, magnetization and coercive force, particle size depend. 9-12239  
 Mn-Ga alloys high-coercivity state 9-1636  
 TmGa garnet, oriented crystal, phonon spectra, laser induced 9-12439

**gallium arsenide**

- See also Semiconducting materials/gallium arsenide*  
 acoustoelectric effect, transverse 9-18560  
 conduction-band minima, L<sub>1</sub> and X<sub>3</sub>, location, photoemission determ. 9-9895  
 diffusion improved by exposure to radiation, patent 9-21354  
 diffusion of Cu, coeff. meas. by u.s. method 9-14955  
 diffusion of Cu, impurity atom interaction 9-17286  
 diffusion of Zn under arsenic pressure 9-3383  
 dislocations in Czochralski growth method 9-3348  
 dislocations in epitaxial layers 9-1219  
 edge absorption of mechanically polished surface 9-12379  
 elastic constants, temp. depend. 9-9742  
 electroluminescence due to acoustoelectric instability of current, n-type 9-7995  
 electroluminescent allowing continuous generation of coherent radiation 9-12799  
 electron distribution, X-ray study 9-3292  
 electron plasma in mag. field, Raman spectra light 9-14060  
 epitaxial films, photoluminescence 9-10265  
 excitons interactions with opt. phonons in photoconductivity free-carrier and exciton radiation recombination 9-10238  
 hot electron magnetophonon effect in n-type epitaxial films 9-16265  
 inter-valence-band transitions in uniaxially stressed samples 9-18706  
 ionic surface states from band-edge method 9-5618  
 Kikuchi line anomalies rel. to structural defects 9-18445  
 lasers, CW, correlation between laser emission noise and voltage noise 9-20528  
 light scattering from plasmons and phonons 9-12353  
 light scattering from single particle electron and hole excitations 9-12443  
 luminescence, at 1.2eV and 77°K, effect of heat treatment 9-5953  
 n-type, luminescence from donor-acceptor pair recombination involving the first excited state of donor 9-12465  
 photoconductive lifetime of n-type, diffused with Cu, temp. depend. 9-5765  
 photoconductivity, h.f. phase shift meas., n-type 9-18656  
 photoconductivity and far i.r. absorption spectra, shallow donor interpretation 9-12377  
 photoconductivity enhancement, elec. and optical, in semi-insulating crystals 9-5766  
 photoemissive yields, spectral analysis 9-5917  
 piezobirefringence dispersion 9-13922  
 Raman scattering, from electron spin-density fluctuations 9-12414  
 reflectance modulation by surface field obs. 9-10172  
 semi-insulating, uniform elec. fields effects on optical absorpt. 9-5883  
 specific heat, 1/30°K 9-9843  
 sputtering at low energies, ejection patterns, 50-525°C, orientation dependence 9-9866  
 substrate, epitaxial growth of InP in open flow system 9-5243  
 substrate crystals for epitaxial growth expts., annealing effects, 800°-1200°C 9-11950  
 substrate for Ge epitaxial layers, plastic deform. 9-19796  
 ultrasonic transducer application 9-17795  
 X-ray-K-absorption edge shifts 9-21638  
 Cu-GaAs supersaturated solid soln., precipitation 9-5511  
 diffusion of Zn, mechanism 9-16111  
 GaAs:Sn, luminescence rel. to impurity band structure and effects 9-12463  
 GaAs:Te, longitudinal-optical-phonon-plasmon coupling 9-21615  
 GaAs<sub>1-x</sub>P<sub>x</sub> epitaxial layers on GaAs, compositional inhomogeneities 9-14895

**Galvanomagnetic effects** *see Magnetolectric effects***Galvanothermoelectric effects** *see Magnetolectric effects; Magnetothermal effects***Gamma-ray astronomy** *see X- and gamma-ray astronomy***Gamma-ray sources** *see Gamma-rays***Gamma-ray spectra***See also Nuclear decay theory*

- 80-300 MeV, from positron annihilation in flight 9-16821  
<sup>16</sup>O  $\gamma$ -ray branching in decay of 6.92, 7.12, 8.88 and 13.10 MeV states 9-2651  
<sup>196</sup>Tl-<sup>196</sup>Hg energy levels determ. 9-4740  
 $\gamma$ -activation method of spectroscopy of  $\gamma$ -ray sources 9-20731  
 cascades, double and multiple, obs., using association of semicond. counter and scintillator 9-2567  
 Compton, iterative unfolding 9-19223  
 difference- $\gamma$ -spectrometry, theor. and exptl. investigations 9-13162  
 fallout from Chinese nuclear explosion (9 May 1966) 9-8180  
 graphical method of analysis 9-8742  
 and internal conversion electrons, separation, using Ge diode 9-6724  
 peak fraction method of interpretation 9-4660  
 polarization, linear, of isotropically emitted  $\gamma$ 's for nuclei spin determ. 9-11218  
 pulse height analyzer digital data analysis, improvements to Covell's method 9-4686  
 from reactor materials bombard. by 14 MeV n 9-652  
 resolution, influence of nuc. preamp. decay time const. 9-2604  
 rocks with radioactive impurities, energy distrib. 9-8157  
 rocks with radioactive impurities, Pb-Cu-Cd filter for obs. of  $\gamma$ -spectra 9-6054  
 self-inversion of  $\gamma$  lines 9-8972  
 solar flares, indication of atm. composition 9-10550  
 thermal (n, $\gamma$ ) energy and intensity obs., compendium 9-9033  
 (n,n' $\gamma$ ) on low atomic no. foils, obs. of  $\gamma$ -spectra 9-16961  
 (n,n' $\gamma$ ) on low atomic no. foils, obs. of  $\gamma$ -spectra 9-9035  
 $n$  capture, giant dipole resonance meas. 9-8968

**Gamma-ray spectra continued**

- $P$  capture, giant dipole resonance meas. 9-8968  
 $\pi^+p \rightarrow \pi^+\pi^+\gamma$ ,  $E_\pi=340$  MeV 9-11059  
 $\pi^-\pi^+\pi^0$ , spin and parity assignments, levels determ. 9-4745  
<sup>41</sup>Ar obs. using Ge(Li) detector 9-13202  
<sup>200m</sup>Au 18.7h isomer decay 9-2673  
<sup>140</sup>Ce, energy, intensity and decay sequences calc. 9-11224  
<sup>130a</sup>-<sup>130</sup>Xe, energy level determ. 9-4733  
<sup>160</sup>Tb decay to levels in <sup>160</sup>Dy 9-2701  
<sup>111</sup>Ag from <sup>111</sup>Pd, <sup>111m</sup>Pd decay, energy levels, spin and parity determ. 9-20760  
<sup>231</sup>Pa-<sup>227</sup>Ac, levels, transitions, rotational structure determ. 9-14579  
<sup>141</sup>Pr, energy, intensity and decay sequences calc. 9-11224  
<sup>141</sup>Pr(n,n' $\gamma$ ), energy levels determ.,  $E_n=0.5-2.3$  MeV 9-14613  
<sup>112</sup>Cd from <sup>112</sup>Ag decay,  $\gamma$  spectra meas. 9-13208  
<sup>252</sup>Cf nuclear fission fragments obs. 9-6923  
<sup>142</sup>Nd, energy, intensity and decay sequences calc. 9-11224  
<sup>142</sup>Nd, thermal-n capture,  $\gamma$  emission, transition schemes determ. 9-14569  
<sup>152</sup>Sm, thermal n capture, study of following  $\gamma$  spectra 9-18066  
<sup>192</sup>Tl-<sup>192</sup>Hg, energy levels determ. 9-4740  
<sup>133</sup>Ba-<sup>133</sup>Cs decay, obs. 9-557  
<sup>113m</sup>In, e.m. decay, search for double electron ejection 9-6796  
<sup>142</sup>Nd, thermal-n capture,  $\gamma$  emission, transition schemes determ. 9-14569  
<sup>113</sup>Sn(n, $\gamma$ ), E1, M1 transitions meas. 9-13228  
<sup>133</sup>Xe-<sup>133</sup>Cs, half-life determ. 9-15718  
<sup>194</sup>Ir-<sup>194</sup>Pt,  $E_\gamma \leq 1.4$  MeV, intensity meas. 9-15739  
<sup>154</sup>Gd from <sup>154</sup>Eu decay, E0 transitions, internal conversion coeffs. determ. 9-13210  
<sup>154</sup>Gd from Eu isotopes decay energy levels determ. 9-4734  
<sup>142</sup>Nd, thermal-n capture,  $\gamma$  emission, transition schemes determ. 9-14569  
<sup>144</sup>Pm-<sup>144</sup>Nd, energy level determ. from decay scheme 9-517  
<sup>214</sup>Po, 1.1 to 3.3 MeV, 4-5 keV resolution 9-13211  
<sup>124</sup>Sb-<sup>124</sup>Te, partial decay scheme proposal, levels determ. 9-18079  
<sup>154</sup>Sm (<sup>16</sup>O, <sup>16</sup>O $\gamma$ ) 2<sup>+</sup> states  $\gamma$  emission ang. distrib., hyperfine interactions 9-15781  
<sup>194</sup>Tl-<sup>194</sup>Hg, energy levels determ. 9-4740  
<sup>142</sup>Nd, thermal-n capture,  $\gamma$  emission, transition schemes determ. 9-14569  
<sup>115</sup>Sb-<sup>115</sup>Sn, energy levels determ. 9-14592  
<sup>115</sup>Sn from <sup>115</sup>Sb decay, energy levels determ. 9-14592  
<sup>135</sup>Xe-<sup>135</sup>Cs half-life determ. 9-15718  
<sup>136</sup>I  $\beta$  decay, energy levels, lifetime determ. 9-20762  
<sup>146</sup>Nd, thermal-n capture,  $\gamma$  emission, transition schemes determ. 9-14569  
<sup>106</sup>Pd, energy levels, spin and parity determ. 9-13193  
<sup>146</sup>Pr 24 min,  $\gamma$ - $\gamma$  and  $\beta$ - $\gamma$  coincidence 9-2698  
<sup>106</sup>Rh, decay obs. 9-555  
<sup>116</sup>Sb-<sup>116</sup>Sn, decay scheme determ. 9-11249  
<sup>116</sup>Te-<sup>116</sup>Sb, decay scheme determ. 9-11249  
<sup>227</sup>Ac from <sup>231</sup>Pa decay; levels, transitions, rotational structure determ. 9-14579  
<sup>197</sup>Au(n, $\gamma$ )<sup>198</sup>Au obs. near 4.9 eV resonance 9-2746  
<sup>137</sup>Ba(n, $\gamma$ )<sup>138</sup>Ba, energy level determ. 9-6881  
<sup>177</sup>Hf(n,e $\gamma$ )<sup>177</sup>Hf, transitions in range 70-2000 keV 9-16939  
<sup>177</sup>Hf(n, $\gamma$ )<sup>177</sup>Hf, levels determ.,  $E_n=0.06-8.8$  eV 9-13195  
<sup>127</sup>( $\alpha$ , $\alpha'$ ) Coulomb excitation, E2 transition prob. determ.,  $E_\alpha=3.5-5$  MeV 9-20737  
<sup>127</sup>(p,p' $\gamma$ ) Coulomb excitation, E2 transition prob. determ.,  $E_p=3.5-5$  MeV 9-20737  
<sup>117</sup>Sb-<sup>117</sup>Sn, energy levels, spin and parity determ. 9-13194  
<sup>147</sup>Sm, thermal n capture, study of following  $\gamma$  spectra 9-18066  
<sup>198</sup>Au(n, $\gamma$ ) transition strengths to final states, 0.2-1.2MeV obs., 10-60keV 9-529  
<sup>178</sup>Hf from <sup>177</sup>Hf(n, $\gamma$ ), levels determ.,  $E_n=0.06-8.8$  eV 9-13195  
<sup>118</sup>In isomeric state decay, levels, spin and parity determ. 9-19276  
<sup>148</sup>Nd (<sup>16</sup>O, <sup>16</sup>O $\gamma$ ) 2<sup>+</sup> states  $\gamma$  emission ang. distrib., hyperfine interactions 9-15781  
<sup>128</sup>Sn, energies of twelve  $\gamma$  lines 9-11335  
<sup>198</sup>Tl-<sup>198</sup>Hg energy levels determ. 9-4740  
<sup>238</sup>U(n, $\gamma$ ), decay scheme determ. 9-15769  
<sup>129m</sup>Te-<sup>129</sup>I, energy levels, spin and parity determ. 9-18080  
<sup>129</sup>La, energy, intensity and decay sequences calc. 9-11224  
<sup>129</sup>I from <sup>129m</sup>Te decay, energy levels, spin and parity determ. 9-18080  
<sup>139</sup>La(n,n' $\gamma$ ), energy levels determ.,  $E_n=0.5-2.3$  MeV 9-14613  
<sup>149</sup>Sm, thermal n capture, study of following  $\gamma$  spectra 9-18066  
<sup>119</sup>Te isomers, decay scheme from  $\gamma$ - $\gamma$  coincidence spectra 9-4754  
<sup>72</sup>As-<sup>72</sup>Ge energy levels determ. 9-20750  
<sup>119</sup>(<sup>16</sup>O, $\alpha$ )<sup>119</sup>B, e.m. branching ratio determ. 9-14559  
<sup>10</sup>C-<sup>10</sup>B, ft values and branching ratios determ. 9-18086  
<sup>40</sup>Ca from <sup>39</sup>K(p, $\gamma$ ), resonances decay, levels and lifetimes determ.,  $E_p=1.1-2.5$  MeV 9-15729  
<sup>44</sup>Ca from <sup>44</sup>K decay, levels determ. 9-19299  
<sup>44</sup>Ca-<sup>44</sup>Sc decay obs. 9-20767  
<sup>77</sup>Cl, from <sup>36</sup>S(p, $\gamma$ );  $\gamma$  spectrum recorded and levels determ. 1147 keV 9-540  
<sup>58</sup>Co, (475 keV, 2<sup>+</sup>→2<sup>+</sup>,  $\beta^+$ ) (0.810 MeV,  $\gamma$ ) 9-15743  
<sup>60</sup>Co, obs. using Ge(Li) detector 9-13202  
<sup>60</sup>Co isomers, decay schemes determ. 9-14589  
<sup>62</sup>Co-<sup>62</sup>Ni, decay scheme determ. 9-16950  
<sup>53</sup>Cr(n, $\gamma$ )<sup>54</sup>Cr, using second-escape peak method 9-13202  
<sup>59</sup>Cu, 81 $\mu$  decay 9-20768  
 decay,  $\gamma$ - $\gamma$  directional correlation 9-19295  
<sup>53</sup>Fe<sup>53m</sup>, rel. level schemes of Fe<sup>53</sup> and Mn<sup>53</sup> 9-19285  
<sup>56</sup>Fe, ang. correl. obs. following  $\gamma$  scatt. rel. to level props. 9-14588  
<sup>72</sup>Ga-<sup>72</sup>Ge, energy levels determ. 9-20750  
<sup>72</sup>Ge from <sup>72</sup>As decay, energy levels determ. 9-20750  
<sup>72</sup>Ge from <sup>72</sup>Ga decay, energy levels determ. 9-20750  
 from <sup>75</sup>Ge decay, assignment of transitions in level scheme of <sup>75</sup>As 9-11256  
 from <sup>77</sup>Ge decay, assignment of transitions in level scheme of <sup>77</sup>As 9-11256  
<sup>40</sup>K,  $\gamma$ -ray energy meas. 9-20747  
<sup>27</sup>Mg decay, Ge(Li) spectrometer obs. 9-14595  
<sup>26</sup>Mg(p, $\gamma$ )<sup>27</sup>Al,  $\gamma$  and coincidence spectra obs. 2322 keV 9-533  
<sup>99</sup>Mo-<sup>99</sup>Tc, decay scheme determ. 9-15731  
<sup>99</sup>Mo-<sup>99</sup>Tc, energy levels determ. from  $\gamma$  internal conversion spectra 9-11258  
<sup>93</sup>Nb(n $\gamma$ , $\gamma$ ) <sup>94</sup>Nb, energy levels determ. and resonances spin assignment 9-6890  
<sup>60</sup>Ni(n, $\gamma$ )<sup>61</sup>Ni, reaction, intensities and energies of  $\gamma$  lines 9-603  
<sup>62</sup>Ni(n, $\gamma$ )<sup>63</sup>Ni, reaction, intensities and energies of  $\gamma$  lines 9-603

**Gamma-ray spectra continued**

- <sup>31</sup>P from <sup>30</sup>Si(p,  $\gamma$ ), resonance levels, spin and parity determ.,  $E_p=0.8-2.2$  MeV 9-18069  
<sup>46</sup>Sc, (357 keV,  $4^+ \rightarrow 4^-$ ;  $\beta^-$ ) - (1.121+0.889 MeV,  $\gamma$ ),  $\beta$ - $\gamma$  circular polarization meas. 9-15743  
<sup>28</sup>Si( $\alpha$ ,  $\gamma$ )<sup>32</sup>S, levels and spin determ.,  $E_\alpha=3.7-3.9$  MeV 9-18070  
<sup>34</sup>S(p,  $\gamma$ )<sup>34</sup>S,  $\gamma$ 's and reaction excitation function obs. 9-567  
<sup>51</sup>V( $\alpha$ ,  $3n$ )<sup>54</sup>Mn cascade models with quadrupole transitions studied, 32-51 MeV 9-20807  
<sup>95</sup>Zr-<sup>95</sup>Nb, decay period determ. 9-15744

**Gamma-ray spectrometers**

- See also *Beta-ray spectrometers; X-ray spectrometers*  
 amplifier stabilization, use of multichannel analyzer 9-442  
 $\beta$ - $\gamma$  coincidence meas., adaptation of intermediate imaging  $\beta$  spectrometer 9-443  
 calibration for soil radioactivity meas. 9-18030  
 cascades, double and multiple, obs., using association of semicond. counter and scintillator 9-2567  
 coincidence, integral bias summing, for directional correlation meas. 9-4688  
 coincidence- Mossbauer tech., inclusion of finite resolution time in anal. 9-441  
 Compton, with semiconductor detector 9-468  
 difference, theor. and exptl. investigations 9-13162  
 high resolution, with Li drifted Ge detectors 9-16918  
 magnetic, pair ionization and bremsstrahlung loss meas. 9-20690  
 Mossbauer, increased capacity using tape recorder 9-2568  
 Mossbauer, module for slow multiscaling 9-13174  
 NaI(Tl) scintillation, low-energy  $\gamma$ -ray spectral analysis 9-15580  
 pair and escape-suppressed, using Ge(Li) and NaI(Li) detectors 9-4665  
 scintillation crystals sensitivity, expt. and theor. calc. 9-20698  
 scintillation meas., background, shielding and collimation 9-20691  
 scintillation meas., background shielding and collimation 9-20691  
 sum-coincidence methods for use in determ. branching ratios 9-20684  
 unfolding iterative, of Compton spectra 9-19223  
 with n background, single crystal organic scintillator 9-11138  
 Pulse from Ge(Li) detector, shape and distrib. obs. 9-4664  
 CdTe, surface barrier and Mg, B drifted, as  $\gamma$ - and  $\alpha$ -Spectrometers 9-8937  
 Ge(Li)-diode, for low (500 keV)  $\gamma$  activities 9-4678  
 Ge(Li) ultra high resolution spectrometer, 6 keV-2 MeV 9-4679  
 Ge(Li) detectors, collimated  $\gamma$  beams study 9-2569  
 Ge(Li) detectors in  $\gamma$  spectrometer system 9-19224  
 Ge(Li) relative detect. efficiency calibration at 20-100 keV 9-2589  
 Ge(Li) total absorption, sensitivity 330 to 1300 keV 9-20692  
 NaI(Tl) counter, Compton eff., electronic cct., response and theor. calc. 9-19239

**Gamma-rays**

- See also *Cosmic rays/photons*  
 in concentration gradient meas. in pipeline flow of suspensions 9-9563  
 in displacement meas., remote 9-15414  
 irradiation plant for laboratories 9-327  
 irradiation plant for seeds 9-328  
 lunar rocks, composition according to results of Lunar-10 experiment 9-18898  
 polarization rel. to space parity violation effects in e.m. transitions 9-498  
 production, 4-10 MeV, by n capture in IEAR-1 swimming pool reactor, targets 9-20841  
 radiation transfer, higher order perturbation calc. 9-16820  
 shielding, leakage through zig-zag slit in Pb shield 9-15381  
 source, 45 MeV behind graphite shield, ang. distrib. obs. 9-330  
 sources, build-up factors for Al, Fe barriers 9-329  
 streaming about annular duct, distrib. of flux and dose rate rel. to rad. shields 9-13272  
 transport eqn. Monte Carlo integration 9-19356  
 (n, xy), 14.1 MeV n interaction with Na, Mg, S, Si, Mn, Fe 9-600  
<sup>132</sup>I, new high energy, obs. 9-18081

**absorption**

- See also *Mossbauer effect*  
 by heterogeneous barriers, perturbation calc. 9-20842  
 Lorentzian line transmission through Lorentzian absorbers 9-6599  
 non-Mossbauer substs. resonance absorpt. obs. of phase transition 9-11961  
 polyethylene, transmission through slab obs. 9-21447  
 in reactor vertical channel, use of polyethylene, volume absorbed 9-661  
 in water, dose build-up factors for low energy point sources 9-20259  
 Fe Pb laminated shield, Fe thickness depend. on abs. rate 9-2782  
 Fe transmission through slab obs. 9-21447  
 Pb Fe laminated shield, Fe thickness depend. on abs. rate 9-2782  
<sup>32</sup>S, cross section in giant dipole resonance region meas., 10-30 MeV 9-14583

**angular distribution**

- from aligned nuclei, coeff. tables 9-6781  
 $p$ - $\gamma$  ang. correlations,  $p$  ang. distrib., Butler theory agreement, 955 keV  $\gamma$  comparison 9-2755  
 $\gamma$ - $\nu$  angular correlation experiment, range effect 9-19191  
<sup>130</sup>Xe,  $p$ - $\gamma$  directional correlation meas. rel. to spin assignments 9-8980  
<sup>172</sup>Lu-<sup>172</sup>Yb decay, sign of  $\delta$  for E2+M1 multipole mixture in  $\gamma$  transition, 1093 KeV 9-561  
<sup>154</sup>Gd, 692KeV level  $2^+ \rightarrow 2^+ \rightarrow 0^+$  cascade obs., transition pure E2 9-11226  
<sup>235</sup>U fission, two dimens. depend. of quanta anisotropy on kinetic energy 9-626  
<sup>166</sup>Ho,  $\beta$ - $\gamma$  ang. correl.  $P_4(\cos \theta)$  depend. 9-6844  
<sup>187</sup>Re-<sup>187</sup>W, ang. correlation meas. 9-20766  
<sup>12</sup>B 995 keV, distrib. polar. method for  $\gamma$ , e.m. transitions 9-2646  
 from <sup>11</sup>B( $p$ ,  $\gamma$ ) radiative capture obs., 14-27MeV 9-16956  
<sup>83</sup>Br decay,  $\gamma$  directional correls. 9-11257  
<sup>35</sup>Cl, spin and parity assigned to 3.01, 2.65 MeV levels 9-538  
<sup>181</sup>Fr-<sup>181</sup>Ta,  $\gamma$ - $\gamma$  ang. correl. and quadrupole interaction 9-3972  
 Ge(Li) detector, directional correl., attenuation factors 9-16922

**detection, measurement**

- See also *Dosimetry; Gamma-ray spectrometers; Particle detectors; Radioactivity measurement*  
 100-1000 Å, use of metal film (Bi, In or Ti) with inert gas ionization chamber 9-12227  
<sup>11</sup>B( $p$ ,  $\gamma$ ), radiative capture obs., excitation functions and ang. distrib. meas. 9-16956

**Gamma-rays continued****detection, measurement continued**

- anthracene dosimeter, by means of triplet-triplet annihilation emission 9-12472  
 calibration, of detector, effect of scattered radiation 9-2600  
 camera compared with two-head scanner 9-4654  
 detector response functions Monte Carlo calc. with linear energy transform. 9-18028  
 dosimetry, with fluorocarbons 9-19242  
 image formation from detectors with incident  $\gamma$  flux 9-2089  
 low-energy, spectral analysis with NaI(Tl) scintillation spectrometer 9-15580  
 multidecade survey meter combining ionization chamber, electrometer amplifier with Geiger-Muller probe 9-2596  
 neutron capture chem. analysis, sensitivity 9-21744  
 pinhole collimator for scintillation camera 9-14536  
 probes,  $\gamma$ - $\gamma$ , calibration curve established by Monte-Carlo method 9-4661  
 prompt-fission, obs. in reactor rel. to fission rate fluctuations and kinetic parameters 9-14651  
 in reactor vertical channel, use of polyethylene, volume absorbed 9-661  
 in reactor vertical channels, use of cellulose diacetate 9-660  
 scintillation  $\gamma$  dosimeters, extension of useful energy range 9-455  
 scintillation camera, output recording method 9-10948  
 scintillator, organic with an impurity 9-8935  
 semiconductor counters for detect. of n with  $\gamma$  9-19238  
 semiconductor detector with internal multiplication 9-19237  
 spark chamber ten cm. gap used to investigate resonance radiation decay 9-11156  
 telescope for balloon altitudes 9-4684  
 time resolved exposure rates, paired detector techniques 9-19247  
 two-head scanner compared with camera 9-4654  
 (n,n' $\gamma$ ) on low atomic no. foils, obs. of  $\gamma$ -spectra 9-16961  
 (n,n' $\gamma$ ) on low atomic no. foils, obs. of  $\gamma$ -spectra 9-9035  
<sup>170</sup>Tm,  $\beta$ - $\gamma$  correl. in first forbidden decay 9-15738  
<sup>119</sup>Sn source, quanta correlation in X-ray band 9-20598  
 in <sup>212</sup>Bi decay, at high energies 9-11254  
 CdTe, semiconductor for pulse registration 9-6729  
<sup>60</sup>Co  $4\pi$  coincidence counter,  $\gamma$  sensitivity correction 9-20708  
 Ge(Li)-diode, for low (500 keV)  $\gamma$  activities 9-4678  
 Ge(Li) detector, directional correl., attenuation factors 9-16922  
 Ge(Li) detector system error in pair peak method 9-4680  
 Ge(Li) n capture activation analysis 9-4682  
 Li detector with B-10 or Li-6 shield, patent 9-20700  
 Li glass scintillation characts. 9-449  
<sup>54</sup>Mn,  $4\pi$  coincidence counter,  $\gamma$  sensitivity correction 9-20708  
 NaI(Tl) scintillation background monitor 9-4670  
 Si avalanche diode application 9-13171

**effects**

- See also *Nuclear reactions and scattering due to photons*  
 Ag thin films, resistivity change 9-17378  
 anthracene single crystals and paramagnetic center 9-3963  
 bipolar transistors, low dose ionization-induced failures 9-17411  
 on calibration of detectors by scattered radiation 9-2600  
 ethylene, polymerization, eff. of alcohols 9-20039  
 ethylene polymerization, induced by  $\gamma$ -irradiation 9-17541  
 ferrites, on ferromagnetic resonance 9-14105  
 films, commercial photographic, response 0.667 to 1.25 MeV 9-15694  
 fluorocarbons, aromatic, radiolysis 9-20061  
 glass, organic, photo- and  $\gamma$ -ionization compared by e.p.r. spectroscopy 9-10082  
 glasses, alkali-silicate, e.p.r. spectra 9-15200  
 glasses, two-component,  $\gamma$ -irrad., atomic displacement section 9-3321  
 heating of solids studied 9-19874  
 K-shell photoelec. cross-sections,  $E_b=145$  keV,  $47^\circ \leq Z \leq 82$ , obs. 9-11395  
 maleic anhydride, cryst., ion radical pairs 9-10291  
 maleimides and maleamic acid e.p.r. spectra 9-21323  
 methanol glasses, trapped electrons 9-4014  
 methyltetrahydrofuran glasses, trapped electrons 9-4014  
 Na<sub>2</sub>O-Al<sub>2</sub>O<sub>3</sub>-GeO<sub>2</sub> glass, colour centre production 9-18482  
 paramagnetic centres in Anthracene single crystals 9-3963  
 1,5-pentanediol, liquid, products produced under  $\gamma$ -radiation 9-4015  
 Perspex effective atomic number determ., 30-1332 keV 9-9865  
 poly-4-vinylpyridine 9-18226  
 poly-2-vinylpyridine 9-18226  
 polyethylene, n- $\gamma$  reactor radiation effect on e.p.r. and spin-lattice relax. 9-21669  
 polystyrene, polymerization in emulsion 9-21686  
 polytetrafluoroethylene (Teflon), irradiated, positron lifetime meas. study 9-13841  
 propionaldehyde, liq.,  $\gamma$  radiolysis 9-14139  
 purine nucleotides, irradi. resistance 9-11718  
 pyrimidine nucleotides, irradi. resistance 9-11718  
 $\alpha$ -quartz, smoky centre formation, thermoluminescence and dielec. behaviour 9-13701  
 resin, ion-exchange, irradi. effect 9-6021  
 Rochelle salt single crystal and E.S.R. analysis of centre no.1 9-3953  
 silica, vitreous, ionizing-radiation-induced dilatation, impurity effect 9-14961  
 solid elements, K-shell X-ray prod. and absorpt. meas. 9-18172  
 styrene, polymerization 9-20037  
 succinic acid, e.s.r. of  $\gamma$ -irrad. crystals 9-16462  
 tetraethylammonium iodide, irradiated, e.s.r. study 9-20978  
 tetrahydronaphthalene frozen solid, EPR spectra temp. depend 9-8034  
 $\gamma$ N- $\pi$  photoprod., modified PCAC hypothesis 9-6661  
 $\gamma$ p- $\Delta^{++}(1236)\pi^-$ , theory discussed, low energies 9-11049  
 Ag catalyst work function, oxygen or ethylene atm., 20 and 120°C 9-12219  
 Ag photoelectric cross sections, comparison of theor. expt. values, 50-412 keV 9-5579  
 AgCl, colloid production, phonon scattering investig. 9-9692  
 Al thin films, resistivity change 9-17378  
 Al<sub>2</sub>O<sub>3</sub> films, 500 to 6000Å, traps, study using thermoluminescence glow curves in range 30 to 300°C 9-17429  
 Au thin films, resistivity change 9-17378  
 CO, liq. and solid, radiolysis 9-10359  
 CaO-Tm<sup>3+</sup>, Tm<sup>3+</sup> production, e.s.r. obs. 9-10277  
 Cs<sup>137</sup>, ion formation energy in ethylene and acetylene 9-9409  
 Cu, defect formation and effect on lattice parameters 9-1186  
 Cu photoelectric cross section, comparison theor. expt. values, 50-412 keV 9-5579



**Gamma-rays continued effects continued**

- n-GaAs, defect introduction by  $^{60}\text{Co}$   $\gamma$  quanta 9-13875  
 Ge:As, Ga, bombardment, quenching of nonradiative interimpurity recombination, 4.2°K 9-21646  
 Ge:As, recombination centres 9-17397  
 n-Ge:Sb, radiation-induced carrier mobility changes 9-5705  
 H<sub>2</sub>O, effective atomic number determ. 30-1332 keV 9-9865  
 H<sub>2</sub>SO<sub>4</sub> solns., radiolysis at high press. 9-10361  
 Mo, defect formation and effect on lattice parameters 9-1186  
 NaCl, F-colouring 9-3368  
 Ni, defect formation and effect on lattice parameters 9-1186  
 NiCr thin films, resistivity change 9-17378  
 Pb glasses, e.s.r. 9-3958  
 Pt photoelectric cross sections, comparison of comparison of theor., expt. values, 50-412 keV 9-5579  
 p-Si:B,  $\gamma$  irradi., radiation defects in recombination 9-3665  
 n-Si:P, irradiated, thermal donor formation 9-21333  
 Si, irradi., recombination luminescence 9-7989  
 p-Si, irradiated, elec. props. changes 9-21518  
 Si, p-n junction, effect on parameters and structure 9-16280  
 Si, vacancy generation rates 9-5340  
 Si transistors, recovery of gamma dose failures during life testing 9-17418  
 Si(Li) junctions, recovery behaviour after  $\gamma$ -irrad 9-15111  
 SiO<sub>2</sub> films, 500 to 6000Å, traps, study using thermoluminescence glow curves in range 30 to 300°C 9-17429  
 SrCl<sub>2</sub>:Tm<sup>3+</sup>, Tm<sup>3+</sup> production, e.s.r. obs. 9-10277  
 Te aqueous solns., radiolysis 9-15230  
 W thin, heating 9-12038  
 YFe garnet, on ferromag. resonance 9-14105  
 Y<sub>2</sub>O<sub>3</sub>:Eu(Dy), induced thermoluminescence 9-12478  
 Zr alloys oxidation in high temp. H<sub>2</sub>O, review 9-10343

**internal conversion**

- See also Beta-ray spectra/conversion electrons*  
 $^{129m}\text{Te} \rightarrow ^{129}\text{I}$ , excited states of  $^{129}\text{I}$  9-15717  
 electronic shell effect 9-13186  
 K conversion coeffs., high energy 9-8969  
 K/L<sub>3</sub> ratio for E2 transitions for mass numbers 152 to 198, energy interval 480-500 keV 9-4757  
 L-shell coeffs. distortion effects due to nuclear quadrupole moment 9-2641  
 nuclei with  $6 < Z < 95$ , threshold energy, coeffs. 9-6783  
 in  $^{114}\text{Cd}$  transitions, 1-9 MeV, coeffs. 9-2663  
 $^{180}\text{Hf}$  energies and relative coeffs. obs. 9-525  
 $^{160}\text{Tb}$ , from  $^{159}\text{Tb}$  (n, $\gamma$ ), relative K,L,M, (N+O+P) line intensities of pure E2 transitions 9-11253  
 $^{170}\text{Tm}$ , from  $^{169}\text{Tm}$  (n, $\gamma$ ), relative M line intensities in pure E2 transitions 9-6838  
 $^{170}\text{Tm}$ , from  $^{169}\text{Tm}$  (n, $\gamma$ ), relative K,L,M, (N+O+P) line intensities of pure E2 transitions 9-11253  
 $^{187}\text{Ta}$ , from  $^{187}\text{Ta}$  (n, $\gamma$ ), relative M line intensities in pure E2 transitions 9-6838  
 $^{187}\text{Ta}$ , from  $^{187}\text{Ta}$  (n, $\gamma$ ), relative K,L,M, (N+O+P) line intensities of pure E2 transitions 9-11253  
 $^{133}\text{Ba} \rightarrow ^{133}\text{Cs}$  spin assignments, spectra obs. and K conversion coeffs. calc. 9-8981  
 $^{193}\text{Ir}$  from  $^{193}\text{Os}$  energy levels determ. from  $\gamma$ - $\gamma$  meas. 9-11229  
 $^{193}\text{Os} \rightarrow ^{193}\text{Ir}$ , energy levels determ. from  $\gamma$ - $\gamma$  meas. 9-11229  
 $^{203}\text{Tl}$ ,  $\alpha_K$  of 279, 404 keV transitions, obs. 9-15726  
 $^{203}\text{Tl}$ , K-conversion coeff. of 279 keV level, obs. 9-20744  
 $^{154}\text{Eu}$  440 to 1280 keV transitions, K conversion coeffs. 9-2700  
 $^{164}\text{Er}$  from  $^{164}\text{Ho}$ , K shell coeff. for the 91.5 keV transition. 9-2669  
 $^{154}\text{Gd}$  from  $^{154}\text{Eu}$  decay, conversion coeff. determ. from  $\gamma$  spectra meas. 9-13210  
 $^{154}\text{Gd}$  K intensities, evidence for new O<sup>+</sup> level 9-2668  
 $^{224}\text{Ra}$  total internal conversion coeffs. from E2 transitions 9-2675  
 $^{234}\text{U}$  total internal conversion coeffs. from E2 transitions 9-2675  
 $^{160}\text{Ho}$ , from  $^{165}\text{Ho}$  (n, $\gamma$ ) relative M line intensities in pure E2 transitions 9-6838  
 $^{160}\text{Ho}$ , from  $^{165}\text{Ho}$  (n, $\gamma$ ), relative K,L,M, (N+O+P) line intensities of pure E2 transitions 9-11253  
 $^{236}\text{U}$  total internal conversion coeffs. from E2 transitions 9-2675  
 $^{227}\text{Th} \rightarrow ^{223}\text{Ra}$ , rel. to  $^{223}\text{Ra}$  energy level transitions 9-6812  
 $^{228}\text{Th}$  total internal conversion coeffs. from E2 transitions 9-2675  
 $^{119m}\text{Sn}$  23.9 deV g.s. transition coeff. obs. 9-6800  
 $^{25}\text{Al}$  decay of T<sub>1/2</sub> states obs. 9-4743  
 $^{7}\text{Ge}$  spectrum obs., level scheme determ. 9-8981  
 $^{99}\text{Mo} \rightarrow ^{99}\text{Tc}$ , energy levels determ. from  $\gamma$  internal conversion spectra 9-11258  
 $^{86m}\text{Rb}$ , coeffs. and half life meas. 9-9000  
 $^{95}\text{Nb}$ , M4 assignment theor. calc. from  $\gamma$  meas. 9-15744  
 $^{51}\text{V}$ , decay of T<sub>1/2</sub> states obs. 9-4743  
 $^{51}\text{V}$ , s-electrons, coeff. meas. 9-14596

**scattering**

- See also Compton effect*  
 atoms, collision density functional by Monte Carlo sampling method 9-11396  
 boson targets, non-abelian, Compton effect obs. 9-10971  
 at boundary of medium, formation of radiation field 9-574  
 glass of 9 and 15 MeV bremsstrahlung 9-11267  
 incoherent, of 662 keV  $\gamma$  by K electrons of Au, differential cross-section 9-9120  
 perturbation by small hollow, Monte-Carlo calc. 9-19190  
 Al of 9 and 15 MeV bremsstrahlung 9-11267  
 Cu atom, cross-section calc. by subtracting photo-electric cross-section 9-710  
 Fe of 9 and 15 MeV bremsstrahlung 9-11267  
 Pb atom, incoherent, from K shell electron, obs. 9-712  
 Pb atoms, 280 keV  $\gamma$ -ray total cross section 9-16999  
 Pb of 9 and 15 MeV bremsstrahlung 9-11267  
 Pt-Rh alloys, photoelectric  $\gamma$  cross-section, by dis. and calc. 9-18654  
 Pt atoms, 280 keV  $\gamma$ -ray total cross section 9-16999  
 Sm atom, incoherent, from K shell electron, obs. 9-712  
 Sn, diffraction of resonant radiation in Bragg scattering by nuclei and electrons 9-21612  
 Sn atom, incoherent, obs. on K-shell electrons 9-712  
 Sn atoms, 280 keV  $\gamma$ -ray total cross section 9-16999  
 Ta atom, incoherent, from K shell electron, obs. 9-712  
 Zr, Thomas-Fermi model for electron binding eff. 9-18146

**Gamow-Teller transitions** *see Beta-decay theory; Nucleus/energy levels*

**Garnets**

*See also Ferrites*

- films, prep. by sputtering 9-5248  
 grossularite,  $^{27}\text{Al}$  NMR 9-12509  
 Photomag. effect 9-16315  
 rare-earth doped, electronic and vibrational Raman eff. obs. 9-12434  
 thermal expansion and conductivity of polycrystalline garnets 9-3535  
 Y Ga Fe, magnetoacoustic resonance at 3- and 10-cm bands 9-5557  
 YAl:Nd, optical refrigeration 9-1831  
 Al-Y,  $^{197}\text{Au} \rightarrow ^{197}\text{Pt}$  transition in Nd<sup>3+</sup>, vib. mechanism due to ion-phonon relax. 9-10186  
 Ca V, preparation rel. to device applications 9-7910  
 Ca V Bi Fe, conduction mechanism by conductivity and thermoelec. power meas. 9-1458  
 Ca<sub>3</sub>Al<sub>2</sub>(SiO<sub>4</sub>)<sub>3</sub>, grossularite,  $^{27}\text{Al}$  n.m.r. 9-12509  
 CaV, Curie pt. rel. to crystal chemistry 9-14005  
 CdK<sub>2</sub>, sublattice magnetization by  $^{57}\text{Fe}$  n.m.r. 9-21671  
 DyFe, high-field magnetization 9-15154  
 Eu Ga: Fe<sup>3+</sup>, exchange interaction, strong orbital anisotropy 9-1682  
 EuFe hyperfine field interac. of 21.7 keV level of  $^{151}\text{Eu}$  from Mossbauer meas. 9-16401  
 Gd, static and dynamic props. meas. 9-10139  
 Gd Fe, film, prep. by sputtering 9-5248  
 Gd Fe, magnetothermal effect, anomalous sign in compensation pt. region 9-1683  
 Gd ferrite, magnetic sublattice interactions 9-16369  
 Ho Fe, Faraday effect, effect of mag. field 9-1740  
 Ho ferr garnet Faraday effect and reversal of mag. sublattices 9-1739  
 LuFe, sublattice magnetization by  $^{57}\text{Fe}$  n.m.r. 9-21671  
 Ni<sub>1-x</sub>GexFe<sub>2-x</sub>O<sub>4</sub>, anisotropy field, effect of heat treatment 9-5850  
 Sm Fe, sub-lattice magnetization sign reversal 9-1691  
 TbAl garnet, electronic Raman transitions 9-10223  
 Tm Ga,  $^{169}\text{Tm}$  NMR at 4°K 9-1880  
 TmFe, sublattice magnetization by  $^{57}\text{Fe}$  n.m.r. 9-21671  
 TmGa garnet, oriented crystal, phonon spectra, laser induced 9-12439  
 Y Al, (containing 0.5 wt.% Nd), luminescence and laser emission threshold, temp. depend. 9-5955  
 Y Al garnet:(Eu, Yb), colour centre formation in optical zone melting 9-1238  
 Y Fe:Hf, conduction mechanism by conductivity and thermoelec. power meas. 9-1458  
 Y Fe, Al-Gd substituted, alignment and microwave props. 9-1685  
 Y Fe, Faraday eff. rotation rel. to mag. field intensity 9-7950  
 Y Fe, Faraday effect, effect of mag. field 9-1740  
 Y Fe, magnetoacoustic resonance at 3- and 10-cm bands 9-5557  
 Y Fe, type cpds., spin wave theory 9-1690  
 Y Fe crystals, elastic wave damping freq. dependence 9-1274  
 Y Fe garnet:Gd<sup>3+</sup>, Al<sup>3+</sup>, and Cr<sup>3+</sup>, reaction kinetics and mag. props. 9-1688  
 Y Fe garnet, crystal growth from Na<sub>2</sub>WO<sub>4</sub> melts 9-1150  
 Y Fe garnet, Fe<sup>2+</sup>-Fe<sup>3+</sup> equilibrium in flux growth, model 9-1149  
 Y Fe garnet powder, strain induced by various milling treatments 9-5453  
 Y Fe magnetoelastic waves, excitation and amplification 9-1689  
 YAl:Nd laser, non-mode-locked, two photon fluorescence displays 9-6527  
 YAl garnet, laser Raman spectra 9-10223  
 Y<sub>3</sub>Al<sub>5</sub>-Ga<sub>2</sub>O<sub>12</sub>, cation distrib. 9-11857  
 YFe<sup>3+</sup> spin-Raman susceptibility by means of spin wave instabilities 9-10143  
 YFe, Hf doped, characterization of Fe<sup>2+</sup> 9-16388  
 YFe, magnetoelc. effect 9-12303  
 YFe:Si l.r. irradi., photomag. anneal props. by torque meas. 9-10137  
 YFe:Tb, Bloch wall mobili Tb ct 9-13975  
 YFe, ferromag. resonance,  $\gamma$ -n irradi. effects 9-14105  
 YFe, light diffraction probing of magnetoelastic waves 9-12342  
 YFe, magnetic eqn. of state near Curie point 9-7913  
 YFe, magnetoacoustic resonance 9-16172  
 YFe, nonlinear ferromag. resonance instability 9-12495  
 YFe, nonlinear phenom. during excitation of magnetoelectric waves 9-19970  
 YFe, polycrystalline, magnetostriction effects, control 9-3833  
 YFe, rods, parametric amplification of magnetoelastic waves at room temp. 9-14967  
 YFe, sublattice magnetization by  $^{57}\text{Fe}$  n.m.r. 9-21671  
 YFe, sublattice magnetization calc. by Oguchi method 9-10144  
 YFe domain structure and growth defects effects 9-12302  
 YFe rods, polycrystalline, axially magnetized, magneto-static modes at 9.96 GHz 9-5851  
 YGa garnet:Cr<sup>3+</sup>, e.p.r. 9-1865  
 YGd, magnetoacoustic resonance 9-16172  
 YbFe, high-field magnetization 9-15154  
 Yelctronic Raman transition selection rules rel. to double group, D<sub>2</sub> 9-3905

**Gas analysis** *see Chemical analysis*

**Gas flow** *see Flow/gases*

**Gas-discharge tubes**

*See also Counters; Ion sources*

- anode fall, calorimetric determ. 9-3027  
 backscattering of emitted electrons by cathode 9-19526  
 low-noise, for elimination of discharge modulation noise in He-Ne lasers 9-20517  
 pre-breakdown currents from non-metallic emitting sites in cathode 9-17137  
 screening by auxiliary electrodes of the spiral in the direction of positive column 9-21117  
 thyatron, Hg vapour, characts rel. to equivalent pressure 9-13473  
 thyatron pulse generator, ceramic, use with wire spark chambers 9-8943  
 Ar, laser action, microwave excited, in modified TR tube 9-6513  
 Hg thyatron and rectifier characts. rel. to 'equiv. press'. use, obs. 9-13473  
 Ne hodoscope for cosmic ray showers 9-4561  
 Xe, pulsed, series and parallel connection, obs. 9-11629

**Gases**

*See also Kinetic theory/gases*

- arbitrarily moving, anisotropic nonlinear wave propag. 9-5116  
 Boltzmann eqn. soln. for rigid sphere gas 9-8455  
 charged particles transport theory and experiment 9-19588  
 classical, dense, new kinetic theory 9-951  
 combustion, and its plasma thermodynamic and elec. props. 9-19095  
 compressed, collision-induced infrared absorption 9-4914

**Gases continued**

- dense, transport processes 9-21132  
 dilute, hydrodynamic equations of grad-theory, statistical derivation 9-3036  
 dipolar, equilib. and transport props. 9-5110  
 discharge, microwave, harmonic radiation exptl. studies, 34 GHz 9-11622  
 electron beam injection from vacuum through gasdynamic window 9-2337  
 electronegative, dielectric, characterization using test cell based on breakdown in uniform field 9-5120  
 energy exchange through inelastic collisions of gases at different temps. 9-950  
 enthalpy measurement of natural gases, in range  $-320^{\circ}\text{F}$  to  $+100^{\circ}\text{F}$  and pressure up to 2000 p.s.i.a., flow calorimeter method 9-13490  
 expansion nonadiabatic restrained, arbitrary energy losses or release 9-14812  
 Faraday effect meas. 9-21143  
 flue gas in power stations analysis by chromatographic instrument 9-16505  
 gas particle mixture, shock wave propag. eff. of finite particle volume 9-9450  
 Gibbs paradox, general solution and applic. to diffusing ideal gas mixture 9-11657  
 hot, transport coeffs, contrib. of nonelastic collisions of atoms and mols. 9-14819  
 humidity and vapour content meas., adiabatic saturation psychrometer 9-935  
 hydrocarbon, elementary steps in oxidation 9-21692  
 interaction of coherent and incoherent light in mag. field, appl. of Bloch-type formalism 9-4848  
 ion motion under const. elec. field, stochastic computer simulation 9-7235  
 ionized, elec. conductivity variation in initial section of plane duct 9-3056  
 mechanical equilibrium eqns. 9-10663  
 methane, u.s. absorpt. 50-600 kHz and  $-30$  to  $+120^{\circ}\text{C}$  9-5117  
 mixtures, nonuniform, nonequilibrium, theory 9-11658  
 molecular vel. determ. by effusion, intermediate laboratory expt. 9-12823  
 molecules vel. determ. by effusion, intermediate laboratory expt. 9-12823  
 neutron rethermalization in heavy gas 9-9080  
 neutron scattering, quasi-ideal approximation and total cross-section 9-9303  
 non-grey absorbing gas between parallel plates radiative transfer 9-19006  
 nonequilibrium, atomic and mol. excitation mechanisms, review 9-19407  
 optico-acoustic gas analyzer, design 9-14141  
 perfect mixtures, flow and thermodynamic evolution from entropy diagrams 9-5113  
 perfectly conducting, two-dimensional flow in crossed elec. and mag. fields 9-2957  
 pressure, low, determ. by electron scatt. meas. 9-12849  
 radiant, temp. distrib., Monte Carlo calc. 9-7226  
 radiative transfer, between parallel plates eff. of surface emissivity 9-19080  
 range of 5-50keV heavy ions 9-14739  
 rarefied, linearized heat transfer for inverse Knudsen nos. 0-10, influence of accommodation coeff. 9-13489  
 rarefied, weakly, moments of high rank 9-18322  
 relaxation by vibr. vibr. exchange 9-3048  
 relaxation by vibr. vibr. exchange in binary mixtures 9-7221  
 relaxing, shock waves (plane, cylindrically or spherically symm.) prod. 9-19568  
 resonant scattering of monochromatic light in gases 9-18327  
 sampling value, hydraulically actuated for internal combustion engine 9-8311  
 sphere, empty, collapse 9-936  
 streamer breakdown, mechanism of secondary processes 9-11631  
 temperature meas. behind detonation fronts 9-2240  
 temperature meas. by spectral method in hot systems 9-7230  
 temperature meas. of low pressure flames, line reversal and excitation temp. 9-9449  
 vibrational energy transfer in system of radiating oscillators 9-3049  
 volumetric props., review 9-9439  
<sup>36</sup>Ar, dynamics near coexistence region, inelastic n. scatt. exam. 9-15971  
 H<sub>2</sub>, temp. meas. of low pressure flames, line reversal and excitation temp. 9-9449  
 methane-Ar mixture, thermalization times of positrons 9-15974  
 N<sub>2</sub>-Ar mixture, thermalization times of positrons 9-15974

**Gegenschein** *see* **Zodiacal light****Geiger counters** *see* **Counters/Geiger****Gelatin**

- adsorption on AgBr 9-7343  
 adsorption to AgBr microcrystals 9-3214  
 gels, struct. studies by electrophoresis and depolariz. of fluor. 9-19651  
 macromolecule, photographic props., bibliography 9-6564  
 photographic, colorimetric analysis of residual thiosulphate 9-6563

**Gels**

- acoustic attenuation rel. to freq. and conc. 9-3141  
 cellulose, wet, transfer of monolayers of Ca stearate and polymer from aqueous sub-phase 9-9573  
 cellulose acetate, dilatometric, rheological and optical studies 9-17225  
 crystal growth 9-16052  
 electrolyte diffusion coeff. meas. 9-21233  
 gelatin, struct. studies by electrophoresis and depolariz. of fluor. 9-19651  
 poly(vinyl alcohol), dilatometric, rheological and optical studies 9-17225  
 polymeric micro-cryst. gels, rheological props. rel. to particle size distrib., with high yield values 9-9571  
 silica, elec. cond. effect of adsorbed H<sub>2</sub>O 9-13915  
 silica, radiolysis of adsorbed hydrocarbons 9-20063  
 silica, sorption and dielec. behaviour of benzene 9-21288  
 silica gel, surface structure 9-19667  
 Fe(III) hydroxide, crystal nucleation obs. 9-5285  
 SiO<sub>2</sub>, diffusion coeffs. rel. to pore size anal. 9-9572

**Generators** *see* **Electrical machines****Geochemistry** *see* **Earth/composition****Geochronology** *see* **Earth/age; Radioactive dating****Geodesy***See also* **Gravity**

- completeness rel. to general relativity 9-63  
 gravitational potential field, canonical correl. analysis 9-6038  
 Love's number derived from satellite orbits 9-15234

**Geoelectricity** *see* **Earth/electricity****Geomagnetism** *see* **Earth/magnetic field****Geometrical optics** *see* **Optics/geometrical****Geometry**

- finite geometry, approx. Euclidean rotation Lorentz and Poincare groups 9-8371  
 four-body S-state coordinates 9-9117  
 modified functions of higher orders and applications to structural problems 9-17685  
 modified functions of higher orders and applications to structural problems 9-17684  
 shell of revolution, shape optimization w.r.t. vol. and wt. 9-18980  
 shell to fit into circular cylinder, shape optimization w.r.t. mass and vol. 9-18980  
 structures related to complex vector space structure 9-38

**Geons** *see* **Gravitation****Geophysical prospecting**

- compressional waves velocity in porous media at permafrost temperatures 9-4035  
 displacement processes in porous media, stability conditions 9-11666  
 electromagnetic, double-dipole half-plane model 9-20075  
 fingering in oil-water displacement process with capillary press., statistical behaviour 9-11667  
 geoaoustic applic. of electroseismic sources 9-12560  
 groundwater reservoirs, induced electrical polarization equipment, applicability and limitations 9-8155  
 Rn/Th ratio in soil gas, meas. 9-1935  
 sea floor deposits, location and exam, physical techs. involved 9-18788  
 seismic detonator which automatically disarms, for marine use, patent 9-12564  
 sounding, e.m., by transient method using grounded dipole 9-20077  
 water in lower crust, continental, saturation rel. elec. conductivity 9-12569  
 U, Pb isotopic composition as guide 9-20079  
 U ore, mathematical methods appl. 9-4036

**Geophysics***See also* **Atmosphere; Earth; Oceanography; Siesmology**

- conductor sheet, nonuniform, resonant behaviour of e.m. induced currents 9-21826  
 continuation of e.m. fields, theory, spectral method 9-6413  
 crust, exterior origin and evolution, theory 9-10378  
 crust, exterior origin and evolution, theory 9-10377  
 data correl. with seismic delay times 9-12563  
 earth's crust, elec. resistivity 9-16522  
 earth's crust, present day experimentation lecture 9-20288  
 earth models giving mechanical parameters r. depth 9-12568  
 elect. resistivity of rocks, effects of pressure 9-6053  
 electron content measurements in ionosphere, satellite radio beacon trans missions 9-20109  
 frictional sliding on ground surfaces, effect of rock type, press., strain rate and stiffness 9-8151  
 geology, dynamical, role of convection 9-14153  
 global structures and isostatic adjustment, hydrodynamics 9-16520  
 Gruneisen parameter, volume dependence 9-6049  
 igneous rocks, light scatt., Stokes parameters, spectral obs. 9-17476  
 IQSY and solar-terrestrial research 9-8287  
 i.r. images of natural subjects 9-4366  
 latitude variations obs. 9-10370  
 limestone, rate of the 15 kb phase transition 9-8153  
 magnetic and seismic observatory, equipment and observations, Ellesmere Island, Canada (1965-6) 9-6047  
 patterns, moving random, correl. analysis 9-12555  
 patterns, moving random, dispersion analysis 9-12556  
 rocks with radioactive impurities, energy distrib. of  $\gamma$  spectra 9-8157  
 rocks with radioactive impurities, Pb-Cu-Cd filter for obs. of  $\gamma$ -spectra 9-6054  
 sea floor spreading and continental drift 9-12565  
 sulphate-water system, oxygen isotope behaviour 9-8156  
 tectonic movements, global, relationships with seismology 9-8142  
 theory and computers conference, Trieste Italy, 1967 9-8139  
 volcanic smoke clouds 9-6083  
 U underground leaching from water-bearing deposits 9-20081

**Germanium***See also* **Semiconducting devices; Semiconducting materials/germanium**

- absorption, fundamental, effect of uniaxial deform. 9-18707  
 absorption edge shape, electric field eff. 9-3890  
 additions to Al-Cu-Cd alloy, effect of  $\theta'$  precip. 9-1327  
 amorphous, electronic struct. and reflect. spectrum model 9-13894  
 anharmonicity and Gruneisen parameter 9-14999  
 Chokirai'ski-grown, structure 9-1122  
 coating of W electrode for auto-emission stabilization 9-21551  
 crystal growth in rotating crucible 9-1145  
 crystal lattice parameter expansion due to fast n irradiation 9-1189  
 damping, i.f. 9-5432  
 defects at 35°K and 65°K, radiation annealing and modification at 7°K 9-9695  
 density of states, changes rel. to disordering, photoemission obs. 9-9994  
 diffusion, enhanced, rel. to radiation defects 9-13705  
 diffusion improved by exposure to radiation, patent 9-21354  
 diffusion of Sb, acceleration by u.s. irradiation 9-1247  
 edge absorption, infl. of temp., 4-400°K 9-3891  
 edge absorption of mechanically polished surface 9-12379  
 electromechanical effect, kinetics 9-1314  
 electromechanical effect existence 9-1315  
 electron energy losses and optical data 9-16191  
 epitaxial deposition on GaAs by GeH<sub>4</sub> pyrolysis 9-19670  
 epitaxial films, growth from supercooled droplets 9-13580  
 epitaxial layer, X-ray diffraction for structure 9-3198  
 epitaxial layer on Si, growth by vacuum evap. and elec. props. 9-3201  
 epitaxial mirror smooth layers on GaAs by disproportionation reaction 9-19671  
 exciton states in photocurrent formation 9-7858  
 film, photovoltaic eff. mechanism 9-12214  
 film, thermoelectric props., and use as thermoelements 9-16308  
 film, wavelength depend. of optical transmittance in vacuum u.v. 9-10166  
 films n-type photoelec. props. 9-3736  
 heavily doped, lattice periodicity meas., X-ray diffraction exam. 9-5320  
 hole-phonon coupling const. determ. by cyclotron reson. 9-3551  
 inter-valence-band transitions in uniaxially stressed samples 9-18706  
 internal friction below room temp. 9-1270



**Germanium** continued

- ion implantation, dopant lattice location by C ions backscattering technique 9-18629
- i.r. lattice absorption 9-3510
- irradiated by inert gas ions, cathode sputtering coeffs. 9-15037
- isotopes, neutron cross sections and strength functions 9-592
- magnetoabsorption oscillations associated with interband transitions rel. to exciton states 9-5918
- microwave emission in transverse mag. field 9-15104
- n-type, radiation annealing and modification of 35° and 65°K defects at 7°K 9-9695
- neutron irradiated, electron microscopic obs. of defects 9-16090
- neutron irradiation induced defects, small angle X-ray scatt. exam. 9-5331
- neutron reflections simulated by multiple Bragg reflection 9-9662
- optical absorption by grain boundaries in n-type material 9-21623
- optimal constants, measurements with polarized light 9-12334
- photosensitivity in thin layers 9-10074
- plastic deformation, infl. of electrically active impurities 9-18505
- plastic deformation, single crystals, rel. elec. erosion 9-5350
- plastic deformation of epitaxial layers on GaAs 9-19796
- point defect, dilatometric study at thermodynamic equilibrium 9-3331
- positron annihilation radiation, angular correlation calc. from atomic Hartree-Fock orbitals 9-5638
- proton transmission along {100} and {110} channels in crystal lattice, energy and angular distributions 9-16192
- proton tunnelling, 6.72 MeV 9-21448
- radiation detectors, optimal thickness of sensitive layers 9-10073
- neutron energy incident as a function of partition of deposited energy 9-7684
- solid soln. in Ag, thermoelec. powers 9-1604
- spectra, far u.v., band structure effects and many-particle scatt. corrections 9-12378
- stored-energy release after e. irradi. 9-7656
- surface, absorption of i.r. radiation at low temps. 9-21622
- surface evolution by H atoms and their effect on latent image formation in photographic emulsions 9-18045
- thermal defects, conc., migration and annealing, dislocation density influence 9-5346
- thermodesorption, real surface 9-5260
- thermoelectric power, phonon drag effect anisotropy parameter 9-12205
- thermoelectric props. at low temp., infl. of elastic deformations in phonon-drag eff. region 9-21542
- vacancy diff. determ. 9-16093
- X-ray anomalous transmission, integrated characts. 9-3889
- X-ray L spectra 9-19997
- X-ray spectra, comparison between pure and doped with Ga or Sb 9-1816
- X-ray spectra and electronic structure 9-14067
- n diffraction from monocrystal, temp. and press. eff. on mosaic spread, 1.884 Å 9-5307
- dislocation distrib. in ribbon crystals 9-1227
- Ge:As, acoustic paramag. resonances 9-10281
- Ge:B, impurity vibrational modes by i.r. absorption 9-18548
- Ge:Sb, far i.r. photoconductivity, two types 9-18657
- Ge:Si, n-irrad. induced defects generation rate, effect of impurities and dislocations 9-5335
- Ge:Zn, excitation spectrum and stress behaviour 9-7974
- Ge, magnetoabsorption intensity rel. to exciton absorpt. rise 9-5919
- Ge, photoluminescence in presence of crossed fields 9-14097
- Ge, uniaxially compressed, photoionization of acceptor impurities 9-1610
- Ge surface recombination centres, nature 9-17443
- Ge(Li) detectors, collimated  $\beta$  beams study 9-2569
- Ge(Li) efficiency eqn. form, up to 200 keV 9-4675
- Mn<sup>2+</sup>-Ge, e.p.r., effect of heat treatment on struct. state 9-16459
- in Se, amorphous phonon thermal conductivity, 100-300°K 9-1407
- Si, photoelectron mobility, variation with photon energy 9-13927
- n-Si phonon drag eff., inf. of e scatt. anisotropy 9-19917
- Xe ion bombarded, e. emission and defect formation and annealing 9-18662

**Germanium compounds**

- defect appearance during decay 9-14937
- Al-(0.3at.%)Ge alloy, recovery of resistivity in stages II and III after 2-MeV e. irradi. 9-9696
- Al-Mg-Ge alloy, ageing, transformation stages 9-9782
- Al-Mg-Ge alloy, clustering after quenching 9-17331
- Cu-Ge liq. alloy, elec. resist., electronic struct. 9-16020
- Fe-Ge alloy, oxidation, high temp. study 9-6013
- (93.5-6.5at.%)Ge (7.6-92.4 at%) Si, electroreflectance spectra 9-14045
- Ge-Cu solid solutions, mechanical twinning, structure and distribution 9-17254
- Ge-Si alloys, n-irrad. effects on thermoelec. props. 9-7849
- GeCl, new band system, vibr. anal. 9-763
- GeCl<sub>4</sub> molecule, infrared absorption bands, obs., bond moments calc. 9-2860
- GeCo, dissociation energy 9-9290
- GeCr, dissociation energy 9-9290
- GeCu, dissociation energy 9-9290
- GeF<sub>4</sub>, carbon tetrafluoride, photoelec. spectrum, band assignments from orbital obs. 9-19462
- GeF<sub>3</sub>, gas, u.v. absorpt. spectrum rel. to bending freqs. 9-13351
- GeF<sub>4</sub>, vib. force constants determ. 9-13326
- GeFe, dissociation energy 9-9290
- GeH<sub>3</sub>NCO, microwave spectrum for Ge-N-C angle determ. 9-19430
- GeI, u.v. absorption spectra, new band obs. 9-17030
- GeO<sub>2</sub> particles, dragging by migrating grain boundaries in Cu 9-1233
- Ge(OCH<sub>3</sub>)<sub>4</sub> vs. Ge(SCH<sub>3</sub>)<sub>4</sub> substituent exchange, <sup>1</sup>H n.m.r. obs. 9-6005
- GeO<sub>2</sub>-SiO<sub>2</sub> glass, binary, structure 9-3172
- Ge(SCH<sub>3</sub>)<sub>4</sub> vs. GeZ<sub>4</sub>(Z=Cl, Br, I, NCO), substituent exchange, <sup>1</sup>H n.m.r. obs. 9-6005
- GeTe-GaAs tunnel junction, neg. resistance Schottky-type barrier props. 9-15119
- GeTe-MnTe alloys, thermoelec. power and thermal cond. 2.5 to 110°K 9-5757
- GeTe, superconductivity carrier-conc. dependence 9-21494
- GeTe alloys, thermoelec. power and thermal cond. 2.5 to 110°K 9-5757
- Si-Ge-B alloy, thermoelec. props. and conductivity 9-15133

**Getters** see Adsorption; Electron tubes; Vacuum technique**Giant pulsations** see Earth/magnetic field; Magnetic storms**Gibbs function** see Thermodynamic properties**Ginzberg-Landau theory** see Superconductivity**Glaciers**

- thickness measurement using radar method 9-6055

**Glass**

See also Optical materials; Vitreous state

- adhesion of Au thin films 9-1337
- adhesion of colloidal hydrous Fe<sub>2</sub>, effect of stirring 9-9567
- aliphatic hydrocarbon, containing naphthalene, triplet-states yield in pulse radiolysis 9-17543
- alkali, mixed, ionic transport 9-13912
- alkali silicate, internal friction, rel. to ionic position interchange, 180-500°C 9-3404
- alkali-alumino-silicate, chemical bonding wing X-ray emission spectroscopy 9-1117
- alkali-silicate, binary and ternary elec. cond. and dielec. props. 9-3690
- alkali-silicate,  $\gamma$ -irrad., e.p.r. spectral form 9-15200
- alkaline earth phosphate, optical, Mossbauer and e.s.r. spectra rel. to iron valence states 9-15173
- aluminoborate, Ti-doped, trapping mechanism and luminescence centres 9-1777
- beads, low thermal conductivity range standard 9-15014
- beads, thermal conductivity in vacuum, 100 to 500°K 9-15020
- $\alpha$ -benzalazo-anisal- $\alpha'$ -naphthylamine, liq. cryst. characts. from spectral lines 9-7980
- borate, e.s.r. of Cu<sup>2+</sup> 9-14111
- borosilicate, Fe-activated, luminesc. spectra and absorpt. bands 9-10264
- borosilicate films, new i.r. absorption peak 9-17485
- borosilicate glass-mild steel composite, thermal shock resistance 9-1273
- brittle fracture, effect of inhomogeneities 9-7576
- cathodoluminescent screens, high resolution, variable spectrum 9-14093
- ceramics, lithium aluminosilicate, thermal expansion dependence on TiO<sub>2</sub> catalyst content 9-13804
- chalcogenide, e props. rel. to semicond. and photocond. props. 9-3611
- chalcogenide, optical props. considered for i.r. interference filter fabrication 8-20  $\mu$ m 9-4532
- coated, resistance strip, secondary electron emission rel. to primary energy 9-18665
- coatings used in crystallization of Ge semiconducting thin films by zone melting 9-3238
- crystallization process, differential thermal analysis system 9-13568
- deformation under point loading, role of densification 9-19790
- diffraction grating, reflection efficiencies in soft X-ray region 9-10901
- dosimeter, FD P8-3, for X-ray/u.v., response, 23-40 keV 9-8939
- dosimeters, high-dose-level, with low dependence on energy 9-16924
- electrical conductivity, effect of structural changes in transform. range 9-18649
- electron microscope exam., 3 dim. and stereo scanning 9-3278
- EPR and absorption spectra obs., structural features determ. 9-10193
- e.p.r. of Cu<sup>2+</sup>, eff. of Co 9-18736
- in fiber optics, compatibility 9-13066
- fibre-optical angular displacement transducer 9-12846
- fibres, effect of radiation on strength 9-11934
- film prep. and phase separation study 9-5226
- flint, bond enthalpy evaluation and sputtering ratios 9-17361
- fluoroberyllate, luminesc., effect of Mn<sup>2+</sup> chem. bonding with ligands 9-1845
- formation, rel. to Madelung const. 9-1082
- fracture energy, using double-cantilever cleavage technique 9-11941
- fracture front straightening 9-7574
- Glan-Thompson and Rochon prisms, modified forms, polarizers and polarizing beam splitters 9-10905
- glass-ceramic coatings for metals, elec. and mech. props. improvement 9-3189
- glass-fibre optical waveguide, e.m. coupling with Nd<sup>3+</sup>-doped laser resonators 9-14434
- glass-H<sub>2</sub> gas system, colour centres, irradiation-produced, destruction 9-3365
- glass-metal adhesion theory 9-1335
- glass-metal oxide metal system, atom movements, adhesion and wettability 9-7599
- hardness, slow loading indentation meas. 9-3453
- heat and mass transfer kinetics, thermal anal. apparatus and technique 9-19084
- heat capacity in glassy and supercooled liq. state, inorganic glasses 9-13801
- high refractivity, extension of critical angle measurement range of refractometers 9-13064
- high-borate, for Na vapour lamp, patent 9-8666
- inorganic, heat capacity in glassy and supercooled liq. state 9-13801
- inorganic, radioluminescence, nuclear and other radiation fields effects 9-12481
- interdiffusion, effect on light transmissivity of fiber elements 9-13065
- ionic transport in mixed alkali glasses 9-13912
- K108, LK6 and T411, refractive indices at liquid hydrogen temperature 9-14026
- leached layer formation on surface, kinetics 9-13573
- linear heterogeneity effect on ray path in prism 9-10889
- low i.r. absorpt. mixture, patent 9-8662
- matrix for 1,2,5,6 dibenzanthracene, phosphoresc. compared with polymeric matrix 9-21654
- met surface light reflection radiation scatt. matrix in diffraction approx. 9-8548
- mechanical and thermal resistance increase due to Li diffusion 9-21379
- metal ions detection by chem. staining 9-4017
- microhardness, indentation tests 9-18527
- Nd laser, continuous shift in emission band 9-15529
- Ohara optical type, dispersion between F and C lines, used Hg 'e' line as reference 9-7935
- optical, composition and screening studies 9-20557
- optical, crown, high relative dispersion in blue spectrum 9-4527
- optical, spectral lines for refractometry 9-14447
- optical attenuation coeff. meas. with spectrophotometer 9-2422
- optical with reduced dispersion but unaltered refractive index, patent 9-8663
- organic, photo- and  $\gamma$ -ionization compared by e.p.r. spectroscopy 9-10082
- organic, radical ion and intermediates from  $\alpha$ -methylstyrene 9-20988
- organic, thermal expansion, 10-300°K 9-21437
- phase-separated, light scatt. rel. to diffusion coeffs. 9-14954

## Glass continued

- phosphate, e.s.r. of  $\text{Cu}^{2+}$  9-14111  
 phosphate, Fe-activated, luminesc. spectra and absorpt. bands 9-10264  
 polymers, yield 9-14974  
 polymethylmethacrylate, thermoelastic destruction by laser beam 9-19869  
 Pyrex, interdiffusion and exchange between two-phase structure of  $\text{Na}^+$  and  $\text{Ag}^+$  9-14958  
 quartz, e.p.r. of  $\text{Ti}^{3+}$  9-21664  
 Raman spectra of low-expansion CER-VIT, fused silicon, ULE and Corning heat absorbing glass 9-12417  
 rare earth oxide colouration, obs. 9-3856  
 refraction measurements on goniometer, differential technique 9-12331  
 reinforced plastics, elastic and viscoelastic behaviour, role of adhesion 9-17237  
 scattering light, stimulated, thermal, in picosecond regime 9-11697  
 scattering of 9 and 15 MeV bremsstrahlung 9-11267  
 selenium, prep., props. and structure 9-17235  
 semiconducting, chalcogenide and transition metal oxide 9-1523  
 silica, fused, Ti-doped, trapping mechanism and luminescence centres 9-1777  
 silicate, absorption spectra, rel. to interconversion of  $\text{Eu}^{2+}=\text{Eu}^{3+}$  9-14051  
 silicate, binary, metastable crystallization in heat treatment 9-1081  
 silicate, e.s.r. of  $\text{Cu}^{2+}$  9-14111  
 silicate, Fe-activated, luminesc. spectra and absorpt. bands 9-10264  
 silicate, light scatt., spectral line fine structure 9-3908  
 silicate, Sn containing, properties 9-13569  
 silicate and borosilicate, thermo-optical properties over wide range of temperature and wavelength 9-14027  
 silicate glass: rare earth doped, sound absorpt. in range  $5 \times 10^6$ - $2 \times 10^8$  c/s 9-5544  
 sintering kinetics, effect of particle shape 9-19820  
 sintering of powder compacts, effect of particle shape 9-7314  
 soda lime: rare earths, visible fluorescence 9-3926  
 soda-lead-silica, ionic transport 9-13913  
 soda-lime-silica, structure and Ca coordination 9-1079  
 sodium disilicate, dissolution and diffusion of iron oxides, kinetics 9-19766  
 soft, far i.r. absorpt. 9-10209  
 sorption vacuum pump 9-8329  
 spinodal decomposition, critical temp. depend. on fluctuation wavelength 9-1130  
 stones and seeds in discs, simple photometric device to measure rel. amounts 9-3173  
 structure rel. to pair correlation functions 9-1078  
 sulphide, prep., props. and structure 9-17235  
 surface damage, laser-induced, mechanisms 9-14891  
 surface damage by laser radiation 9-3176  
 surface structure, deposited films, mass spectrographic studies 9-7333  
 thermal conductivity of beads in vacuum, 100 to 500°K 9-15020  
 thermal deformation of glass-crystal systems 9-3417  
 tinted with transition metal ions, spectral absorption, high temperature changes 9-14052  
 transmission e. microscopy fragment preparation 9-18434  
 two-component,  $\gamma$ -irrad., atomic displacement section 9-3321  
 vacuum systems, heat shrinkable sleeve in lubricant-free connector 9-16649  
 viscosity in softening and annealing range 9-5147  
 viscous flow in glass-forming liquids 9-3084  
 X-rays reflected by mirrors, spectra distribution in proper absorption region 9-21637  
 xx  $\text{K}_2\text{PO}_3\text{-V}_2\text{O}_5$  semicond., effect of thermal treatment on a.c. props. 9-3612  
 2PbO.SiO<sub>2</sub> structure and phase transforms, 300-650°C 9-7321  
 Al<sub>2</sub>O<sub>3</sub> and Pb:fluorine surface energy 9-1306  
 As<sub>2</sub>S<sub>3</sub> elec. and optical props., development since 1950, review 9-3175  
 As<sub>2</sub>Se<sub>3</sub>-metal oxide, semicond., structure and cond. mechanism 9-1521  
 As<sub>2</sub>Se<sub>3</sub>, optical absorption, various initial purities 9-12352  
 B<sub>2</sub>O<sub>3</sub>, relax. times spectrum, temp. depend. 9-3850  
 B<sub>2</sub>O<sub>3</sub> molten, inadequacies of viscosity theories 9-9493  
 Bi-Se alloy, transition temp. rel. to composition 9-3153  
 C, flaw-free, monolithic, thermal props. etc. rel. to fabrication techs. 9-7317  
 CaO-Al<sub>2</sub>O<sub>3</sub>-MgO-BaO-B<sub>2</sub>O<sub>3</sub>, Na-vapour resistant up to 700°C 9-4001  
 CaO-MgO-Al<sub>2</sub>O<sub>3</sub>-SiO<sub>2</sub>, crystallization kinetics, iron oxide addition effects 9-19688  
 Cd, S and Se compound doped, structural changes of colour centers during heat treatment 9-13699  
 CdGe(As<sub>2</sub>P<sub>1-x</sub>)<sub>2</sub> system, optical and thermal carrier activation energies 9-17394  
 CdO-B<sub>2</sub>O<sub>3</sub>-SiO<sub>2</sub> photocond., optimization of props. 9-7853  
 GeO<sub>2</sub>-SiO<sub>2</sub> binary, structure 9-3172  
 GeO<sub>2</sub> glass, spectrum of relaxation times, refractive index var. 9-3851  
 K<sub>2</sub>O-SrO-SiO<sub>2</sub>, diffusion of <sup>85</sup>Sr and <sup>87</sup>K 9-1249  
 K<sub>2</sub>O-(1-x)Na<sub>2</sub>O.4SiO<sub>2</sub>, elec. resist. and structure rel. to composition 9-3693  
 Li<sub>2</sub>O-SiO<sub>2</sub> glasses, crystallization phases, X-ray obs. 9-1080  
 Li<sub>2</sub>O-Al<sub>2</sub>O<sub>3</sub>-4SiO<sub>2</sub>, struct. and comp. rel. to temp., i.r. obs. 9-16036  
 Li<sub>2</sub>O-SiO<sub>2</sub>-P<sub>2</sub>O<sub>5</sub>, phase separation, direct obs. 9-5226  
 Li<sub>2</sub>O-SiO<sub>2</sub> heat treated, n irradiation effects on dielec. and d.c. props. 9-7833  
 Li<sub>2</sub>O-SiO<sub>2</sub>-Li<sub>2</sub>O-Al<sub>2</sub>O<sub>3</sub>-4SiO<sub>2</sub>, isostructure and correlation 9-21254  
 Li<sub>2</sub>O-SiO<sub>2</sub>-Li<sub>2</sub>O-Al<sub>2</sub>O<sub>3</sub>-4SiO<sub>2</sub>, isostructure and correlation 9-3177  
 MgO-Al<sub>2</sub>O<sub>3</sub>-SiO<sub>2</sub>, growth of quartz solid solutions 9-11797  
 -N interface, acousto-optical effect under thermal irrad., mechanism 9-3181  
 Na<sub>2</sub>B<sub>4</sub>O<sub>7</sub>-SiO<sub>2</sub> system, phase separation rel. to thermal expansion 9-1083  
 Na<sub>2</sub>O-Al<sub>2</sub>O<sub>3</sub>-GeO<sub>2</sub>,  $\gamma$ -induced colour centres 9-18482  
 Na silicate, photochromic colour centres, kinetics 9-3369  
 Na<sub>2</sub>O-ZnO-SiO<sub>2</sub>, i.r. absorpt. spectra, structural interpret. 9-3894  
 Na<sub>2</sub>O-SnO<sub>2</sub>-SiO<sub>2</sub>, Sn valence states from Mossbauer effect 9-1751  
 Nd, laser, two channel, single pulse, 180 joule output 9-19160  
 Nd laser, 1 GW, design 9-4479  
 Pb, borate and silicate,  $\gamma$  irrad., e.s.r. 9-3958  
 PbO-SiO<sub>2</sub>-K<sub>2</sub>O system, u.v.-induced luminescence at 120°K 9-10267  
 Rb silicate, viscosity, stress depend.,  $10^{14}$ - $10^{16}$  poise 9-3422  
 SiO<sub>2</sub>-Li ferrite growth and composite mag. props. 9-1146  
 SiO<sub>2</sub> glass, thermal cond., 0.5 to 4.2 K 9-19868  
 SiO<sub>2</sub>, diffusion of Na, 170-1000°C 9-17291

## Glass continued

Tl borate, n.m.r., <sup>205</sup>Tl chem. shift 9-8041

Glass-metal seals see *Seals*Glow discharges see *Discharges, electric/glow*Goks see *Hypernuclei*

## Gold

- adhesion of thin films to glass 9-1337  
 adhesion to cellulose or polyester, effect of immersion in water, or solns. of surfactants or alkaline salts 9-9605  
 attenuated total reflection, electromodulation 9-5900  
 coalescence of particles on NaCl cleaved surface rel. to surface heterodiffusion 9-19765  
 cold-worked, phase V restoration 9-19827  
 colloid, in water, power spectrum of scatt. laser light 9-14875  
 colloidal, lamellar cry. growth from soln. e microscopy, diffr. obs. 9-11800  
 condensation of atomic beam on rocksalt substrate 9-14897  
 condensation on Si(111) surface 9-1094  
 crystal, 3-dimens. voids, density change expt. method 9-11869  
 deformed, 4.2°K, elec. resistivity 9-3567  
 deformed at room temp., elec. resistance rel. to temp. 9-19890  
 dielectric constants, electroreflectance changes, modulated ellipsometric meas. 9-10035  
 diffusion and solubility in InP, 600° to 850°C 9-14956  
 diffusion in CdS, vapour pressure investigation 9-3380  
 diffusion in Li, 45-150°C 9-7509  
 dope in Si, anomaly in conductivity and lifetime of excess carriers anomaly 9-16273  
 electron emission, secondary, multiple distrib. 9-5782  
 electron energy loss rel. to sample thickness 9-3545  
 electron irradiated, Stage III annealing process 9-21390  
 electron irradiated at low temp., internal friction meas. 9-11912  
 electron transmission, anomalous, in polycryst. foils 9-11836  
 electron-irradiated, stage III annealing 9-12029  
 electronic structure, calc. at one value of lattice const. 9-5611  
 electronic structure, calc. at one value of lattice const., model Hamiltonian 9-5612  
 energy loss of  $\langle 110 \rangle$  channelled  $\alpha$ -recoil atoms 9-3546  
 energy loss spectra, characteristic, of 8 keV electrons in liquid and solid 9-7249  
 epitaxial film on MoS<sub>2</sub>, angular distribution of nuclei 9-9614  
 epitaxial films on KCl, KBr and KI in u.h. vacuum 9-7310  
 epitaxial growth on cleavage face of mica 9-5242  
 epitaxial growth on KCl, KBr and KI crystals 9-7377  
 film, epitaxial, elec. conductivity, size effects in temp. variation 9-9930  
 film, Hall coeff., normalized conductivity, thickness depend. from Fuchs-Sondheimer theory 9-7331  
 film, recrystallization rel. to prod. of large single crystals 9-19691  
 film lubricant on steel, pressure effects on friction coefficient 9-16138  
 films, discontinuous, evaporated on CdI<sub>2</sub> substrate, electron diff. pattern interpretation 9-18433  
 films, nucleation, growth and structure in obs. in e. microscope 9-19673  
 films grown on rough surfaces, thickness and optical meas. technique 9-5236  
 films growth on KCl in high vacuum 9-21274  
 films on colour-centred NaCl, nucleation density, epitaxy and orientation, obs. 9-9615  
 foils, quenched,  $\alpha$ -irradiation effects on tetrahedra 9-7495  
 foils, quenching methods and rate meas., review 9-11949  
 gettering from Si 9-3668  
 Hall, coeff. determ. 4.2-300°K 9-5651  
 internal friction, cold-worked and irradiated at low temp. 9-5430  
 internal friction, effect of Ar<sup>+</sup> irrad. 9-1267  
 internal friction after e. irrad. at low temp. 9-11912  
 ionic core radii calc. and orthogonality corrections 9-19682  
 magnetoresistances, elec. and thermal, 80-130K 9-5636  
 melting, possible vacancy mechanism 9-5215  
 metal contracts on PbTe, elect. props. 9-3652  
 migration activation energy along natural cleavage surface in mica 9-11892  
 optical props, electromodulation 9-5900  
 photoeffect, non-linear, laser-induced, discrimination from thermionic emis. by time response meas. 9-16318  
 proton channelling, axial, at 30 keV, energy structure 9-7690  
 quenched from 900°, double stacking-fault tetrahedra 9-7494  
 self diffusion and vacancy props., interpretation 9-3378  
 self diffusion on naturally rough surfaces, 870-970°C 9-11894  
 sol., light scatt., and absorpt., comparison with theory 9-15166  
 sol., particle-diameter distrib., X-ray scatt. determ. 9-14873  
 solid soln. in Ag, thermoelec. power 9-1604  
 specific heat and Gruneisen parameter calcs. 9-9842  
 stacking fault energy, formation from dislocation loop dissociation during plastic deformation 9-3343  
 substrate for Au-Cu alloy, two-layer film formation, Moire patterns and misalignment dislocations 9-3200  
 surface self diffusion 9-21349  
 surface stress determ. 9-21259  
 thermal expansion, anomalous, below 8°K and lattice Gruneisen gamma 9-16180  
 thermionic emission, laser-induced, discrimination from non linear photoeffect by time response meas. 9-16318  
 thermodynamic props. evaluation and literature data analysis, 0°-300°K 9-12015  
 thin films, photoelec. eff., inf. of elec. field 9-17442  
 thin films on Ag, photoelec. eff. 9-17441  
 Ag-Au diffusion couples, Kirkendall effect mechanism 9-9762  
 Au-Cu alloy photoluminescence, radiative recomb. obs. 9-21660  
 Au-GaAs surface barrier junctions, elec. props. 9-10009  
 Au GaAs Schottky barriers, capacitance meas. 9-5720  
 Au, quench hardening mechanism 9-19818  
 Au, resistance and thermoelec. power, effect of high pressure 9-16306  
 Au III spectrophotometric determ. with o-phenylenediamine 9-12551  
 Au incoherent scatt. of 662 keV  $\gamma$  by K electrons, differential cross section 9-9120  
 of Au single cry., (111) surface, under bombardment by heavy ions, directional eff. 9-13814  
 Au-n-Si surface barrier diodes, rectification characts. rel. to surface states 9-21525  
 Au(100) surface, atomic arrangement 9-1084



**Gold** continued

- on Ba, double film on Nb, contact potential difference 9-1093
- Fe diffusion, measurement using Mossbauer effect 9-3377
- $^{15}\text{N}$  ions passing thro., range-energy relations 9-9869

**Gold compounds**

- alloys, binary, quenched in elec. resistivity due to solute vacancy pairs 9-18601
- alloys, (with Pt, Cu, In) phonon-assisted impurity scatt. 9-13847
- alloys, resist.-conc. depend. 9-16223
- (ii) diethyldithiocarbamate, single cry., ESR spectra, quadrupole eff. on hyperfine struct. 9-14109
- Au-(50 at. %)Ag alloy, short range order, quenched-in vacancies 9-3324
- Au-Mn alloys, dil., magnetoresistance 9-5805
- $^{197}\text{Au}$  chemical bond, n.q.r. spectroscopic obs. 9-4916
- Ag-Au:Yb, Kondo effect 9-9929
- Ag-Au alloys, sp. ht. below  $3^\circ\text{K}$  9-12018
- Al-Au dilute alloys, age-hardening from yield stress and elec. resistivity meas. 9-21394
- Al-4wt.%Au alloys, elec. resistance rel. to plastic deform. effects 9-12098
- Au-(54.4at.%)Ag alloy, surface self-diffusion 9-17283
- Au-Ag alloy film on n Si Schottky barrier, characts 9-3675
- Au-(47.5 wt.%)Cd, martensitic transformation mechanism 9-5509
- Au-CaF<sub>2</sub> CdSe m.i.s. capacitors, surface states, obs. 9-5740
- $\beta$ -Au-Cd alloys, phase transforms and structures 9-11835
- Au-Co alloys, liquid, ferromagnetism 9-13540
- Au-Cr thermoelectricity, positive hump of power 9-3720
- Au-Cu alloy on Au, two-layer films, Moire patterns and misalignment dislocations 9-3200
- Au-Cu alloys, effect of Ni or Ga partial substitution on order-disorder props. 9-5522
- Au-Cu alloys, Zener relaxation and resistivity meas. of short-range order 9-19804
- Au-Cu<sub>3</sub> alloys, partial substitution of Ni or Ga, effect on order-disorder props. 9-5522
- Au-(0.03 at.%)Fe alloy, thermoelec. power,  $0.35^\circ\text{K}$ - $10^\circ\text{K}$ , mag. field (0-77 kOe) dependence 9-1605
- Au-Fe alloys, dil., magnetoresistance 9-5805
- Au-Fe dilute alloys, band gap var. determ. from light reflectivity meas. 9-21604
- Au-Ga liq. alloy, elec. resist., electronic struct. 9-16020
- Au-Mg alloys near Au<sub>3</sub>Mg, long periodic stacking order 9-9716
- Au-Pb alloys, interstitial sites from e. emission angular distrib. of activated mat. 9-3332
- Au-Pd alloy film, transmission, reflection and absorpt. coeffs., rel. to resonant states 9-7937
- Au-Pd film, diffusion coeff., 400-600°C, electron diffraction study 9-5399
- 2a/oAu-Pt short range order field ion microscope investigation 9-3305
- Au-Sb alloys, metastability of phase prepared by splat cooling 9-3478
- Au-Se system, phase relationships 9-21411
- Au-SiO<sub>2</sub>-CaF<sub>2</sub>-CdSe m.i.s. capacitors, surface states, obs. 9-5740
- Au-SiO<sub>2</sub>-CdSe m.i.s. capacitors, surface states, obs. 9-5740
- Au-V dil. alloys, mag. props. temp. dependence 9-12267
- Au complex, dicyanodihaloaurate, charge transfer spectra 9-20921
- AuAl<sub>3</sub>, Raman scatt. from optical modes, freq. 9-1804
- AuCu type alloy, ordered, superdislocations 9-1216
- AuGa<sub>2</sub>, Knight shift, spin-lattice relax., susceptibility, temp. depend. and relationship 9-10292
- AuMn, Neel temp. pressure dependence from susceptibility, sp. ht. and thermal expansion meas. 9-1699
- AuMn, phase transform.,  $\beta$ -martensitic f.c.c., caused by cold work and subsequent heating 9-3486
- Au<sub>2</sub>Mn, metamagnetic pressure induced transition, ferromag. Curie temp. pressure depend. 9-17452
- Au<sub>5</sub>Mn<sub>2</sub>, antiferromagnetic, susceptibility, elec. resistivity and Young's modulus rel. to temp. 9-15157
- $\beta'$ -AuZn, b.c.c., slip geometry from optical microscopy studies 9-13692
- Cu-Au alloys, dislocation formation during ordering, e. microscopic exam. 9-11881
- CuAu I, ordered alloy, deformation and mechanism 9-13726
- Cu<sub>3</sub>Au, magnetic susceptibility as function of order 9-13946
- Pd-Au alloys, high temp. transport props. 9-15027
- Pt-Pd-Au alloys, high temp. transport props. 9-15027
- Si-Au alloys, i.r. impurity photocond. of Si surface 9-15140

**Grain boundaries** *see* *Crystal imperfections; Crystal structure/microstructure*

**Gramophones** *see* *Sound reproduction*

**Granato-Lucke theory** *see* *Crystal imperfections/dislocations*

**Granular structure**

- Fe electrolytic, eff. of grain size on microhardness 9-11944
- grain boundary dislocations in metals 9-5377
- grain boundary glide mechanism caused by dislocation motion 9-3357
- grain boundary segregation, electron microprobe obs. 9-5378
- grain growth data analysis use of log-log plots 9-14914
- graphite, rhombohedral, rel. to mag. susceptibility 9-7877
- metals, creep strength rel. to grain size 9-9763
- photographic, stat. model 9-19173
- recrystallization matrix, secondary, initial grain size 9-9792
- starch granules, fluctuations in anisotropy from light scatt. meas. 9-15167
- steel, E1702, aged and quenched, grain size effect on resistance to deform. 9-9760
- steel, mild, explosively loading grain size effect on dynamic yielding 9-3439
- two-phase, thermal cond. calc. 9-3539
- Ag film, anomalous absorpt. of light, rel. to grain size 9-5912
- Al<sub>2</sub>O<sub>3</sub>-(0.25wt.%) MgO, hot-pressed deformed, grain boundaries and dislocations dos. 9-3359
- Al<sub>2</sub>O<sub>3</sub>, hot-pressed deformed, grain boundaries and dislocations dos. 9-3359
- Al foils, high angle boundaries 9-18442
- Al<sub>2</sub>O<sub>3</sub>, secondary grain growth kinetics 9-1152
- BaTiO<sub>3</sub>, grain boundary contribution to dielec. props., reflectance spectra obs. 9-3707
- C films, evaporated, and grains at. struct., obs. 9-13576
- Cu-Sn alloy, equilibrated, microprobe obs. of grain boundary segregation 9-11843
- Fe-Ni alloys, grain size variation, X-ray diffr. study 9-13577
- KCl, melt-growth of crystals, free of grain boundaries 9-16101

**Granular structure** continued

- Li ferrites, Ca substituted, grain growth uniformity and size reduction 9-1684
- MgO:Fe<sub>2</sub>O<sub>3</sub>, hot pressed, grain growth rel. to purity and porosity, 1100-1400°C 9-3169
- MgO, hot pressed, grain growth rel. to purity and porosity, 1100-1400°C 9-3169
- NaCl, intergranular dislocation substructure, formation during growth from melt 9-21296
- Pb-Tl alloys, causing flux pinning in type II superconductors 9-3597
- Pb, grain growth, impurity-drag, eff. 9-11888
- ThO<sub>2</sub>, diffusion of  $^{230}\text{Th}$ , rel. to grain size 9-3390
- $\alpha$ -Ti, grain size effect on deformation dynamics 9-3420
- UO<sub>2</sub>, sintered, exaggerated grains and growth mechanism, obs. 9-11798

**Graphite**

- acoustic emission under compressive stress 9-7641
- adsorption of I and desorpt. in vacuum and Ar, 27-1100°C 9-9626
- aligned layers in stretched C fibres, rel. to strength and elasticity 9-7514
- annealing, after electron irradiation at  $80^\circ\text{K}$  9-18534
- artificial, damaged by n irradi., e.s.r. change on annealing 9-8017
- binder mats., molec. distrib. determ. by gel permeation chromatography 9-8122
- block, area density fluctuations, 147 MeV proton beam meas. 9-19693
- boronated, oxidation, rate rel. to form of B<sub>2</sub>O<sub>3</sub> 9-8093
- cigar-shaped conical crystals., growth by heating carbon from dissolution of martensite 9-7369
- from cokes yielded by interacts of diamino- and dihydroxy-aromatic cpds. 9-8070
- colloidal, optical transmission in magnetic field 9-1050
- commercial, relaxation of tensile stress in across-grain specimens, 2000-2700°C 9-7533
- compacts from uncalcined coke, vol., microstruct. and porosity changes under high-temp. irradi. 9-7432
- compressibility, effect of pore struct. accessibility 9-5455
- contraction, neutron irradi. induced, rel. to processing temp. 9-7679
- contraction, rad. induced, effect of binder graphitization and process temps. 9-7411
- cosmic ray interactions obs., ang. distrib. of secondaries 9-18022
- creep, tensile and compressive, of highly-oriented samples, stress depend. and activation energies 9-7552
- creep and recovery, time laws rel. to stress/strain relns. and temp. 9-7551
- creep under const. tensile and compressive stresses, neutron irradi. induced 9-7553
- crystal growth by precipitation from C-saturated metal solns. 9-7372
- crystalline moderator, neutron wave propag. 9-13261
- crystalline order characts. from X-ray exam. 9-7426
- crystallite sizes from meas. of thermal cond. 9-7669
- crystals, cigar shaped with conical struct., obs. 9-7430
- dense, isotropic bodies, prod. by hot-isostatic compaction of powders from 1650 to 2700°C 9-7588
- densified by thermal cracking of natural gas, pore size distrib. meas. 9-7416
- dielectric const., longit. and transverse, spectra in u.v., visible and i.r. regions 9-7971
- dielectric function due to  $\pi$  electron interband transitions 9-1567
- dilation on exposure to liq. Na after neutron irradi. 9-7661
- dilation on exposure to liq. Na rel. to irradi. dose effect of stress 9-6003
- dosimeter for high intensity electron pulses, adiabatic calorimeter 9-1925
- dynamic struct. changes during heating, study by replication tech. 9-7424
- electrodeposition of Cu and PbO<sub>2</sub>, nucleation and growth 9-8101
- electron momentum density, X-ray determ. 9-18581
- erosion and shock resistant, quality techs for rocket motors 9-7568
- erosion resistant for rocket motors quality control, nondestructive tech-niques 9-11936
- e.s.r. at 9.3 GHz and 335 MHz, linewidth and spin-lattice relax. time, temp. depend. 9-8015
- fibres, co-existence of cryst. graphite and turbostratic C phases 9-7363
- fibres from carbonized cellulose, micro fibrillar and micro pore struct. 9-7417
- flakes, absolute thermoelec. power, 77 to 300°K, and galvanomag. effects 9-7847
- flexural strength and breaking strain, effect of gaseous environment 9-7566
- fusion curves up to 60 kbars, meas. by optical techniques 9-7299
- g-factor, spin-resonance, theory and calc. for two-dimens. graphite 9-8016
- graphite, plasmon obs. in X-ray scatt. 9-1818
- graphite-nitrate residue cpds, electronic props. rel. to band model approx. 9-7740
- graphite-pyroc carbon composite bodies obtained by thermal cracking of natural gas, nuclear radiation effects 9-9861
- graphitic carbons, pore struct. 9-1077
- Graphon, activated, chemisorption of O<sub>2</sub>, kinetics 9-8079
- Graphon, cleaned activated surface, chemisorpt. of O<sub>2</sub> from 25 to 400°C 9-10335
- Graphon, degassed, room-temp. chemisorption of oxygen 9-8082
- Hall coeff., low-temp., calc. using trigonal symmetry of bands and inter-carrier scatt. effects 9-7748
- hardness before and after n-irrad., annealing effects 9-7578
- hexagonal layer struct. and imperfections 9-7425
- high current device, vacuum-tight allowing expansion of heated element 9-19127
- high-temperature surface, error in pyrometry due to soot 9-8535
- impregnated thermal cond. and elec. resistivity changes under irradi. 9-7667
- interactions with benzene, analysis w.r.t. virial treatment of phys. ads. 9-17077
- intercalation isotherm of FeCl<sub>3</sub> vapour from 300 to 350°C 9-8066
- internal friction and dynamic elastic modulus, 4-750°K 9-7527
- internal friction and resonant freq. rel. to annealing temp. after n-irrad. 9-7525
- internal friction peak near room temp., height rel. to crystallite size and previous history 9-7526
- irradiation defects and self-diffusion mechanism, thermal annealing studies 9-5337
- isotopic, thermal expansion and bulk dimensional changes under neutron irradi. 9-7410
- isotropic monolithic articles, prod. using semi-isostatic techs. 9-8309
- lattice deform. by interstitial C; mols. 9-7407

**Graphite continued**

lattice expansion coeffs. and anal. of thermal expansion during neutron irradi. 9-7412  
 lattice parameter and dimensional changes on n irradi. 300 to 1350°C 9-7471  
 Lifshitz-van der Waals forces between masses, deviations from pairwise additivity 9-3220  
 localized electronic states, nature and role 9-7711  
 membranes, prep., strength, crystallog. characts. elec. and optical props. 9-11777  
 membranes, turbostratic layer spacing on annealing C membranes 9-7609  
 microstructure changes after creep strain at 2500°C 9-7545  
 moderators, equilib. neutron spectra meas., expt. installation and results 9-19378  
 mosaic charact. shown by oxidation, determ. of crystallite sizes and reactivity 9-7497  
 moulded, high temp. irradiation behaviour, influence of pitch binder content 9-7414  
 moulded microstruct. and porosity rel. to pitch binder content 9-7413  
 MTR reflector, struct. and stored energy tested after 112550 MWD of operation 9-6946  
 natural, effect of neutron irradi. on shear modulus and mech. props. 9-7513  
 natural U graphite lattice, infinite multiplication factor 9-13266  
 neutron detection, meas. with graphite prism 9-14523  
 neutron diffusion in slabs 9-20833  
 neutron irradiated, diffuse X-ray diff. obs. 9-7404  
 neutron irradiation in reactor, stress, creep and crystal dimension changes 9-20851  
 neutron moderation times, resonance-filter meas. 9-6930  
 neutron scatt. characts. for reactor-grade, initial energies to 0.611 eV 9-13225  
 neutron thermalization calc. 9-9094  
 neutron wave propag., effects of Bragg cut-off 9-13255  
 neutron wave propag. in parallelepipeds, interpret. of expt. results 9-9083  
 nitrates,  $\lambda$  transform. at  $\approx 21^\circ\text{C}$ , struct., elec. and thermodynamic aspects 9-7607  
 nucleation pattern of rad. damage, effect of B addition 9-7477  
 ordered form, from V carbide melt reaction with disordered C 9-7617  
 oxidation, nonuniform, boronated graphite, influence of struct. faults 9-8094  
 oxidation, on heating in inert gas and then exposing to air, unsteady mass transfer effects 9-8089  
 oxidation by air along vertical channel, effect of in-pore mass transport 9-8090  
 oxidation by water vapour at high temp., initial stages and activation energy 9-8095  
 oxidation in CO<sub>2</sub> and O<sub>2</sub>/Ar mixtures at 1500-3000°K, compared with vitreous C 9-8091  
 oxidation of boronated graphite rel. to form. of B<sub>2</sub>O<sub>3</sub> 9-8093  
 oxidation resistance, improvement to transpiration cooling, composite tech. and coating 9-10339  
 oxidation resistance, strength and thermal expansion rel. to B content and heat-treatment temp. 9-7608  
 oxidized radiolytically and thermally degassed, stability of surface complexes rel. to thermal oxidation 9-8087  
 particle formation in C type Mira variable stars 9-18853  
 particle pseudo-fluidized bed, elec. resistance to 900°C rel. to particle size 9-9314  
 in petroleum coke, crystals, form. during desulphurization, obs. 9-7431  
 physical properties, book 9-13566  
 pile-irradiated, elec. and mag. props rel. to annealing temp. 9-7587  
 polycrystalline, replica preparation 9-7396  
 polycrystalline, Young's mod. and thermal expansion coeff. rel. to cryst. orientation, modified models 9-7520  
 porosity determ. by Hg methods, stat. anal. rel. to pore size distrib. 9-7415  
 porosity texture changes due to thermal and radiolytic oxidations 9-7408  
 powder compactibility to form reactor fuel rods 9-2797  
 powder mixtures, particle size distrib. and shape factor, statistics 9-7427  
 powder support for pressed electrode of spark source mass spectrograph 9-8117  
 powdered, e.p.r. lines, shape and position at  $\nu \approx 10\text{GHz}$  9-8013  
 powdered, surface struct. and adsorption H<sub>2</sub> 9-1091  
 production in sugar coke heat treated to 2200°C 9-7358  
 purified, thermal oxidation rate, effect of pre-irrad. 9-8086  
 pyrolytic, B, cylinders, elastic consts., density and thermal expansion rel. to B content 9-7515  
 pyrolytic, B, graphitization study via Co lattice spacings 9-8059  
 pyrolytic, compression-annealed, effect of neutron-irrad. on shear modulus 9-7513  
 pyrolytic, e. irrad., recovery of elec. resistivity below 6°K 9-9931  
 pyrolytic, expanded and brazed, thermal conductivity up to 700°C 9-18563  
 pyrolytic, hot-worked, shear-modulus, increase one to neutron irradi. 9-7521  
 pyrolytic, interstitial loop prod. at twist boundaries on neutron irradi. 9-7472  
 pyrolytic, parallel layer stacking, characts. 9-7422  
 pyrolytic, prod. using acetylene as main gas source, deposition rate and phys. props. 9-8063  
 pyrolytic, struct. anisotropy correl. with spectral emissivity, visible to i.r., near 800° 9-7970  
 pyrolytic deposition with BCl<sub>3</sub> catalysts, effects of gaseous impurities 9-8062  
 radiation effects, long term, on dimensions 9-6945  
 random-layer line profiles, Fourier transform methods of anal. 9-7401  
 reactions with gases of ZTA type, 1400° to 3000°K, rates 9-8064  
 released energy profile on neutron or electron irrad., resistivity changes 9-7741  
 research prog., information retrieval system SARC1 9-6249  
 rhombohedral, mag. susceptibility rel. to granular struct. 9-7877  
 rotation boundary angles and growth 9-13629  
 RVD type, tensile and compressive stress/strain curves, elastic consts., to 5500°F 9-7537  
 Seebeck coeff. of pyrolytic graphite, temp. depend. above room temp. 9-10060  
 self-diffusion in single crystals., 2000-2600°C 9-16110  
 shield for 4.5 MeV  $\beta$ -source, ang. distrib. obs. 9-330

**Graphite continued**

SP-1, compacted, effect of B resistivity, thermo- elec. props and Hall const 9-7848  
 specific heat, 13°-300°K 9-16175  
 spectral reflectance, high temp. 9-20560  
 sphere, flow of O<sub>2</sub> around, taking chemical reactions into account 9-13478  
 spherical fuel elements for pebble bed reactors, fabrication 9-6940  
 spheron 6, surface complexes formed by contact with air at high temp. 9-8088  
 static shear modulus meas. of natural single cryst., uniaxial stress along basal plane 9-7512  
 steam graphite corrosion, diffusion-convective soln. rel. to reactors 9-9095  
 in steel, precipitation, effect of Ca 9-19838  
 structure resolution during microautoradiography 9-3246  
 surface, interaction potentials for polar mol. 9-1090  
 surface complexes formed on irradi. in CO<sub>2</sub>/CH<sub>4</sub> mixtures at 300°C 9-8065  
 SX-5 type, thermal cond. from -100°C to 2600°C 9-7670  
 synthetic diamond growth, patent 9-13598  
 technological aspects of modern usage 9-14886  
 tensile stress at 2000°-2700°C, relax. times 9-7532  
 thermal, elec. and elastic props. rel. to X-ray anisotropy functions, polycryst. graphites 9-7428  
 thermal cond., effects of point defects, isotopes and vacancies 9-7668  
 thermal cond. in perpendicular directions, 100-900°K, rel. to crystallite size anal. 9-7672  
 thermal cond. meas. by flash tech., crit. evaluation 9-7662  
 thermal cond. of SX-5 type, -100°C to 2600°C 9-7670  
 thermal cond. rel. to anal. of crystallite sizes 9-7669  
 thermal conds., principal, effect of crystallite boundaries and elastic const. C<sub>44</sub> 9-7671  
 thermal expansion and cond. rel. to high-temp. irradi., for anisotropic and near isotropic samples 9-7663  
 thermal expansion coeffs., linear, decrease under high temp. neutron irradi. 9-7660  
 thermal expansion hysteresis in polycryst., 1000-2400°C cycling 9-3536  
 thermal neutron inelastic scatt., rel. to phonon freq. and lattice model 9-19855  
 thermal rupture resistance, direct meas. on thin discs 9-7572  
 thermalized n pulse decay 9-9019  
 torsional and biaxial stress-strain rels. fracture at room temp. 9-7565  
 transition to hexagonal diamond 9-7612  
 transmitted light microscopy, rel. to filler-binder constituents and porosity 9-7423  
 triple point press and temp., and solidus-liquidus interface, to 1000 atm. 9-1092  
 two-dimensional, theory and calc. of spin-resonance g-factor 9-8016  
 wettability by BaF<sub>2</sub>-CaF<sub>2</sub> eutectic 9-7326  
 ZTA specimens, Youngs modulus temp. depend. rel. to void fraction 9-7519  
 ZTA type, reactions with gases at 1400° to 3000°K, rates 9-8064  
<sup>235</sup>U, graphite critical assemblies, leakage anal. and cross-sections 9-18122  
 B pyrolytic graphite, cylinders, elastic consts., density and thermal expansion rel. to B content 9-7515  
 B pyrolytic graphite, graphitization study via C<sub>2</sub> lattice spacings 9-8059  
 C prep. from phenol-formaldehyde resins, graphitizability rel. to microstruct., obs. 9-7429  
 C<sub>5</sub>-graphite cpds, lamellar, Mossbauer study of chem. bonding 9-7353  
 K, graphite lamellar cpds., thermodynamics, from solid-state c.m.f. 9-1391  
 NbC graphite composite system, effect of processing parameters 9-3161  
 U, graphite assemblies, enriched, accurate criticality meas. 9-18121

**Graphs**

See also *Nomograms*

analysis of  $\gamma$  spectra 9-8742  
 Lorentzian func. and differentiated func., graphical analysis 9-8464  
 Mercedes graph as superposition of simpler graphs 9-12906  
 reflection echelon, line-shape parameters determ., graphic technique 9-4517  
 spectral line breadth, Voigt parameter, graphical determ. 9-2810  
 statistical mech., types used 9-92

**Gratings** see *Diffraction gratings; X-ray diffraction***Gravimeters** see *Gravity***Gravitation**

See also *Gravitons; Relativity*

asymptotic field of 'electron' 9-4238  
 classical particle system 9-21000  
 collapse, precise initial conditions from triggering physical process 9-12659  
 collapse of neutron stars, critical radius 9-2013  
 collapse of rotating bodies, inertial frames induced rot. 9-8222  
 collisionless, self gravitating systems, two dims. computer model 9-20320  
 collisionless astronomical systems, variational treatment 9-20137  
 constant, NPL-Trieste meas 9-8347  
 constant, secular decrease expt. evidence 9-10372  
 decay stability of continuously created mass 9-21838  
 dynamics, conservation laws, gravito-inertial field interpretation 9-10625  
 Eddington's fundamental theory, space-time frame formulation 9-12874  
 Einstein's field eqns., Schwarzschild's interior soln., nonstatic analogs 9-16676  
 Einstein field eqn. maths. structure exam. 9-10626  
 Einstein theory, proposed verification by means of earth orbiting gyroscopes 9-10634  
 Einstein-Liouville eqns, isotropic solns. 9-14358  
 e.m. field interaction with polarizable elastic medium 9-18990  
 e.m. field interaction with polarizable elastic medium within theory 9-4226  
 equations in homogeneous, completely anisotropic model, soln. 9-4230  
 equatorial, in gravitational field, anomalistic and sidereal period in co-ordinate and proper time 9-10446  
 equipotential areas and directional singularities 9-15425  
 field, Einstein eqns., axially symmetric soln. 9-16666  
 field, first-order equation 9-4233  
 field, heuristic foundation of tetrad theory 9-6294  
 field eqn. in empty space, canonical form 9-17700



**Gravitation continued**

- field eqn. static solns., Aharonov-Bohm effect analogues 9-15421
- field eqns. for general spherically symmetric metric form 9-15426
- field equation, possible generalization 9-20318
- field equations in general relativity 9-14340
- field equations in neighbourhood of particle, in conformal theory 9-69
- field in static spherical shell of matter, exact soln. 9-10624
- field interacting with generalized Yang-Mills field 9-17832
- field spin struct., global existence 9-6300
- field theory, 4D, action principle and gauge parameter 9-70
- fields, axisymmetric stationary, classification 9-67
- fields, empty, generation of radiation fields 9-60
- fields of arbitrary spin, correspondence with direct particle fields 9-16677
- fluid layer, incompress., with Hall effect magneto-gravit. stability 9-7117
- free solid with liquid filling, circular motion stability in force field of two stationary attracting centres 9-12913
- galactic model with up to 4000 members, computer model 9-20149
- galaxies as lenses distorting light from other galaxies and producing effect of quasars 9-6152
- gas, generalized kinetic eqn. obtained 9-14756
- gas of gravitating point particles, absence of maximal entropy state 9-20138
- gas relativistic, gravitating, collective motions 9-20135
- geodesic motion of rotating source in field 9-14328
- geon, Klein Gordon, do not undergo collapse 9-8221
- geons, Klein-Gordon; stability and unsymmetrical gravitational collapse 9-10458
- gravitons, production from photons in photon field 9-61
- gravitor source theory 9-8394
- harmonic force fields, conservative system motion 9-20310
- ideal fluid interaction 9-8389
- impact, gravitational, of astronomical systems 9-20143
- induction field communications expt., 1660 Hz 9-18991
- induction field communications expt., 1660Hz 9-8381
- inertial gravitational field, eqns 9-8385
- instability in expanding universe 9-12660
- instability in rotating stellar syst. 9-17611
- Kerr fields, global struct., collapse, killing horizons, causal behaviour, geodesics 9-16679
- Kerr fields, global struct., collapse, killing horizons, causal behaviour, geodesics 9-6310
- Killing fields, appl. to spaces containing gravitation radiation 9-17711
- laser beam self-focussing analogy 9-14423
- light bending, gravitational lens simulator for demonstration purposes 9-12836
- Liouville and Poisson eqns. for collisionless syst. of interacting part., locally isotropic solns. 9-18833
- of magnetic field, cylindrically symmetric 9-6305
- mass sources 9-6057
- Maxwellian form of field eqns. in agreement with special relativity 9-15444
- microwave background variations prod. by nonthermal gravitational radiation 9-20131
- near-field transfer of energy for quasi-static axisymmetric systems 9-16678
- Newton's gravit. constant, light vel. independ. formula 9-2146
- Newton's law derived from general relativity 9-8391
- Newton-Liouville eqns. for system of gravitating particles, all solns. 9-14184
- Newtonian const., equivalence principle in second and higher orders, possible verification 9-1984
- non-Newtonian forces round spinning elastic sphere 9-68
- non-Newtonian theories test by lunar laser ranging Brans-Dicke correction terms 9-8380
- non-static fluid spheres without energy flow 9-17713
- nonlinear, teaching example 9-6297
- opt. path of phonons in field of sun, general-relativistic correct., shift of pulsar freq. 9-8395
- Petrov classification of most cylindrically symmetric space time 9-8465
- plane wave space, Maxwell eqns. satisfy Huygens principle 9-20314
- plasma, anisotropic, rotating; instability, finite Larmor radius eff. inclusion 9-14189
- Poincare recurrence theorem, gravitational collapse 9-14182
- Poisson eqn. for system of gravitating particles, all solns. 9-14184
- primordial black-body rad., present temp. 9-15266
- quantization, general covariant 9-8396
- quantum fluctuation and a possible elem. part. mass spectrum 9-2450
- quantum theories, canonical and covariant 9-18992
- quantum theory, locality postulate 9-14334
- quantum theory, supplementary conditions 9-2139
- radiation in expanding universe 9-6103
- radiation successive approx. approach 9-6299
- radio-wave frequency change during propag. on earth's surface, not due to its mass 9-17702
- Reimannian metric which satisfies field eqns. of gravitation 9-8388
- scalar tensor theory compatibility with Mach's principle 9-4232
- scalar-tensor field eqns. posing of Cauchy problem 9-8390
- Schwarzschild mass, imploding quadrupole wave, tail of gravitational wave 9-1987
- self-gravitating gas, approach to equilibrium 9-20136
- self-gravitating medium in quasi-static equilibrium, physics of, using phenomenological approach of thermodynamics 9-10501
- space-time matrix, special type related to plane matter source 9-10633
- spheres, gravitating, restricted motion 9-17707
- spheres, uniform, radial motion, and gravitational 'bounce' 9-16675
- spherical planet containing falling body, isochronous props., inverse square law 9-16706
- stars, rotating anisotropic systems; stability 9-2004
- stellar systems, applic. of non-equilibrium statistical mech. 9-20145
- tensor fields, massive and massless, gauge theories 9-85
- theory, improved, action principle, conservation laws, energy and field interacts 9-2147
- theory, improved classical, and particle and astrophysics appls. 9-4229
- three body mass syst. moving in ellipses, double collision with infinite mass possibility, closed path obs. 9-19011
- unstable elementary particles, gravitational coupling, equivalence principle test 9-4567
- weightlessness, demonstration 9-8379
- weightlessness demonstration 9-16667

**Gravitational collapse** *see Gravitation***Gravitational red shift** *see Relativity/general***Gravitational waves**

- background separation for long wavelengths 9-16674
- imploding quadrupole behind wave exploding from Schwarzschild source 9-1987
- laser simulation by liquid waves 9-8597
- primordial black-body rad., present temp. 9-15266
- radiation from vibrating axisymmetric source, double-series approx. method, exact soln. 9-8387
- radiation successive approx. approach 9-6299
- radiative, energy impulse tensor applic. 9-10631
- reality considerations 9-10632
- shock in generalized space-times 9-16672
- from stellar models, general-relativistic with non-radial pulsations props. 9-18849

**Gravitons**

- generation and detection by lasers, interaction with external gravit. field 9-10872
- as Goldstone particles 9-55

**Gravity***See also Geophysical prospecting*

- acceleration meas. at Nat. Bur. Stand., USA (June 1965) apparatus and techniques 9-12557
- earth vol. rel. gravitational const. time changes 9-12558
- field changes due to air masses 9-4034
- geopotential field, canonical correl. analysis 9-6038
- gravitational const., secular decrease, expt. evidence 9-10372
- and heat transfer 9-6399
- odd zonal harmonics in geopotential, new evaluation 9-18785
- potential of earth, determination from satellite, observed and model anomalies 9-14149
- role in tectonic deformation of earth's crust, dynamic theory, book 9-16521
- tiltmeter, utilizing diamagnetic suspension 9-2140
- waves, long, on rot. earth, e.m. analogies of eqns. 9-17550
- waves in  $F$ -region, internal, observed by means of electron density profiles 9-12636

**Green's function methods**

- alloys, dil., e.p.r. in metals, theory using freq.-dependent susceptibility interpretation 9-12497
- anharmonic crystals, free energy calc. using double-time Green's function 9-21420
- antiferromagnets, magnon sideband shapes 9-12313
- atomic and molec. calc. 9-9106
- atomic and molec. calc. 9-9107
- atomic and molec. calc. 9-9105
- in atomic line broadening in plasmas 9-19523
- band structure calc. of group II-VI compounds 9-21467
- Bose fluid, phase transition of second kind and diagram technique near Curie pt. 9-12900
- cerium ethyl sulphate, anomalous phonon effects on sp.ht., spin-lattice relax. 9-7658
- charged particle in uniform e.m. field, behaviour 9-2330
- in Coulomb problems for H-atom 9-17004
- dielectric anharmonic crystal, phonon transport equation 9-21421
- e.m. waves in moving simple media 9-14402
- ethylene molecular vibrations 9-11477
- ferroelectrics, hydrogen-bonded, transverse and longit. correlations 9-21538
- ferromagnet, spin- $1/2$  Heisenberg model 9-16348
- ferromagnet, uniaxial, appl. 9-1651
- ferromagnet with mag. interstitial impurities, spin-wave theory 9-5809
- ferromagnetism, first order Green function theory 9-18669
- field eqns., bilocal, Regge pole term 9-2435
- Goldstone's theorem demonstration, advantages 9-12041
- Heisenberg model, anisotropic, Green's function study 9-20336
- rel. to Hubbard Hamiltonian degenerate mass operator perturbation theory 9-14345
- hydrodynamical approximation for ordinary fluid 9-12853
- impurity e.p.r. in metals, theory using freq.-dependent susceptibility interpretation 9-12497
- induced moment system, excitation spectra and magnetization investig. 9-5791
- interacting particles system, nonanalytic points 9-20357
- for Kondo effect, proof of complete equivalence with s-matrix approach 9-7701
- Kondo problem at zero temp., anomalous Green's function method 9-21458
- lattice, randomly doped, electronic state approx. and vib. spectrum calc. 9-9879
- local modes in diatomic chain 9-12854
- Lorentz-invariance, off-shell scatt. field theory, Wightman functions, causal equal-time commutators 9-16670
- magnetism, higher order functions 9-10089
- many-time, calc. using resolvent operator 9-6333
- mass-disordered lattices, displacement correlations and freq. spectrum calcs. 9-9809
- metals, anharmonic, transport props., theory 9-13822
- metals, quasi-particles, determ. of spectral functions and generalization of results 9-7734
- metals, soln. of many body problem and Ansatz for spectral functions 9-7733
- molecular complexes, collective excitations 9-17371
- in molecular constants eval. for tetrahedral  $XY_4$  type mol. and substituted derivatives 9-11441
- multiphoton effective ionization cross-section, using perturbed function 9-681
- n.m.r. line profile of paramagnetic ion nuclei in solid 9-20027
- nonuniform medium, short wave asymptotics 9-8378
- pairing correlations of deformed atomic nuclei, const. compared with BCS-theory 9-4713
- paramagnets, non reduction of unbonded diagrams in fermion presentation of spin operation 9-16329
- perturbation expansion for real-time functions, transport processes 9-4222
- phonon functions for theory of nuclear quadrupole spin-lattice relax. 9-5857
- phonon hydrodynamics in solids 9-21421
- phonon spectrum for cubic lattice with interstitial atom 9-19847
- quantum Fermi systems of charged colliding particles 9-4252

**Green's function methods** continued

- Sherrington's density field formalism used to obtain diagrammatic expansions for density correlation function 9-15438  
 spin density wave, density and thermodynamic behaviour 9-5790  
 spin-density waves, stability and thermodynamic behaviour 9-7871  
 for superconductivity of dil. metallic alloys with mag. impurities 9-7779  
 superconductors with nonmag. impurities, applic. to two-band model in upper critical field theory 9-16241  
 textbook 9-20  
 thermodynamic, Ising chain calc. 9-14352  
 three-particle correl. calc. in nuclear matter 9-6768  
 two-magnon absorption and Raman spectra 9-12435  
 two-phase flow in porous medium 9-17083  
 u.s. attenuation response calc. and applic. to strong coupling and impure superconductors 9-13796  
 X-ray emission spectra, theory 9-7985  
 CsI, energy band calcs. 9-1429  
 Cu, cohesive energy, correlation and orthogonality corrections 9-18407  
 Fe film with (100) surface orientation, spatial magnetization distribution 9-19961  
 H atom bound-state calc., reduced Coulomb function 9-20895  
 MnF<sub>2</sub>, rel. to line shape of spin wave sidebands 9-16375  
 NaCl, cryst., static Green's tensor function 9-7446  
 RbMnF<sub>3</sub>, antiferromagnetic, magnon sideband shapes 9-12313  
 Y Fe garnet-type cpds., spin wave theory applic. 9-1690

**Grey atmosphere** *see* Radiative transfer; Stars/radiation**Grinding** *see* Forming processes**Group theory**

- Abelian group violation in second-order transitions 9-10657  
 Affine group, unitary representations 9-2134  
 algebra of observables, continuous representations of symmetry groups 9-45  
 analysis of n.m.r. spectra 9-17024  
 Burnside metabelian groups 9-18986  
 C<sub>2</sub>, role in symmetry theory of strong interac. 9-19199  
 chiral SU(3) ⊗ SU(3) algebra, 3-point functions structure of vector, axial-vector currents 9-10998  
 classical groups, relations between inner and outer multiplicities 9-43  
 Clebsch-Gordan coeffs. calc. for space groups 9-2135  
 cohomology group, use in classifying first order deforms. of Lie algebras 9-6282  
 complex Euclidean in 3-space, identities for special functions derived from representation 9-8372  
 conformal and Young and Mills field 9-16657  
 crystal, representation by exact Γ matrices and projection operators 9-7382  
 crystallography, non-primitive translations in space groups 9-21289  
 use in degeneracy, conditional invariance 9-73  
 dynamical, limitable groups in quantum mechanics 9-17719  
 Euclidean 3-group representation, addition theorem for Bessel functions and Gegenbauer polynomials 9-6286  
 Euclidean complex group in three-space, special function identities 9-14322  
 Euclidean group representations related to representations having position observables 9-8400  
 extension theorem, non-compact groups, representations 9-2136  
 factorizability theory proof, conjectured by Sciarrino and Toller 9-17696  
 finite, applic. to quantum mechanical systems, book 9-6292  
 finite geometry, approx. Euclidean rotation Lorentz and Poincare groups 9-8371  
 finite order groups, representations and classes 9-8369  
 G<sub>2</sub>, role in symmetry theory of strong interac. 9-19199  
 Galilei group in classical mechanics, canonical representation 9-8467  
 group representations, algorithm for reduction 9-17695  
 group representations, algorithm for reduction 9-6285  
 harmonic oscillators, shell model 9-18985  
 inhomogeneous pseudo-orthogonal and pseudo-unitary groups, Lie algebra, construction of invariants 9-8373  
 integral eqns. symmetry group forming generalized eqns. for H atom 9-9154  
 international symmetry symbols, desirable modifications 9-6291  
 isomorphism theorem extensions 9-20306  
 Lagrange formalism and symmetry theory 9-20304  
 Lie algebras, direct sums, generalized symmetries and deform. 9-20589  
 Lie group F<sub>4</sub>, representation ring 9-10620  
 Lie groups, semisimple, induced representations 9-17697  
 Lie groups and algebras inhomogenizations 9-8366  
 with Lie subgroup of index two irreducible corepresentations 9-14321  
 linear homogeneous eqn., establishment of props. 9-8368  
 Lorentz, relationship to Dirac algebra 9-2133  
 Lorentz and representation theory 9-13091  
 Lorentz covariant distrib. of four-vector variables 9-14314  
 Lorentz groups, unitary representations, reduction of supplementary series 9-16660  
 many-body problems 9-20362  
 matrices, internal symmetry crossing rel. to arbitrary compact group 9-341  
 Minkowski 3-dimens. space, rotation groups 9-20303  
 molecular systems, classification of states 9-14679  
 noncompact groups, multiplicity problem for their compact subgroups 9-14320  
 noncompact groups, reduction of n-fold tensor product representations 9-19186  
 O'Raifeartaigh's theorem, dilation in any semi-simple Lie algebra with a Poincare subalgebra 9-18983  
 O(3,1), pseudoscalar mesons coupling description 9-10993  
 O(4,2), composite relativistic model applic. to hadron weak decay amplitude 9-14477  
 O(4,2), photon-baryon coupling description 9-10993  
 O(4) expansion of off-shell scatt. amplitude, unequal-mass, arbitrary-spin particles 9-17959  
 O(4) representations and Wigner coeff. 9-20305  
 O(4) symmetry, π in bound NN syst., M-function expansion from Bethe-Salpeter eqn. 9-17980  
 optical interactions applic., book 9-14023  
 orthomodular lattices satisfying chain condition, structure 9-20309  
 overlapping group methods for asymptotic spectra in multiregion reactor 9-19346  
 partial weak clustering states, symmetry groups 9-17692  
 particle group functions treatment of many body problem 9-15437

**Group theory** continued

- permutation groups characts. and branching, modified Frobenius eqn. 9-46  
 plethysm applied to atomic spectroscopy 9-9118  
 Poincare and internal symmetry Lie algebra combination, gen. theorems deriv. 9-19187  
 Poincare group, Lorentz basis 9-6290  
 Poincare groups, generalized, unitary representations construction 9-17694  
 polyatomic many-electron systems, rel. to determ. of allowed multiplets 9-13338  
 R4 group applied to energy level separations and correlation energies 9-13283  
 Regge symm. origin for Wigner coeffs. of SU(2) 9-12871  
 renormalization groups and transforms, props and consequences 9-301  
 rotation group, five-dimensional generators in natural and physical bases 9-6289  
 rotational group, five-dimensional, irreducible representation 9-6288  
 S<sub>6</sub>, broken, for baryon e.m. props. calc. 9-16898  
 semidirect product group K<sub>n</sub>=A<sub>n</sub>:S<sub>n</sub>, harmonic-oscillator shell model 9-2137  
 semigroup perturbation theory, appl. to wave eqn. integration 9-8406  
 SL(2,C), convolution integral of Fourier transforms 9-19185  
 SL(2C); subalgebras and contraction survival 9-42  
 SL(3,C) representations, intertwining operators and equivalence rel. 9-8374  
 SL(n,C), class I representations operators matrix elements 9-8370  
 SO(p,1) and In(SO(p,1)), Pauli spin motion, extension 9-15419  
 space groups, direct determ. of irreducible representations 9-18984  
 SU(2,1), irreducible representations 9-16658  
 SU<sub>3</sub> breaking and e.m. mass splittings of baryons, connection 9-18005  
 SU<sub>∞</sub> symmetry, deriv. of spectral function sum rules for tensor currents, extensions to SU<sub>∞</sub> 9-14473  
 SU<sub>∞</sub>, state labelling of irreducible representations 9-16659  
 SU(2, 1), Fourier analysis 9-8367  
 SU(2, 2), unitary irreducible representations 9-14319  
 SU(2)×SU(2) current algebra hard-pion three-point functions, applic. to π, ρ, A<sub>1</sub> and ρ data 9-16893  
 SU(2)×SU(2) chiral-dynamical Lagrangian 9-16899  
 SU(2)×SU(2) charge-charge algebra, deriv. of sum rules involving π, ρ and A<sub>1</sub> 9-16886  
 SU(2)×SU(2) current algebra results for 3-, 4-pt function, virtual photon-pion scatt. 9-17987  
 SU(2) generators for free particle, single valuedness conditions 9-10685  
 SU(2) symmetries combined, variable-mass problem of hadrons 9-343  
 SU(2) Wigner coeffs., Regge symm. origin 9-12871  
 SU(2)×SU(2) spectral function sum rules derivation for hadrons 9-19196  
 SU(3)×SU(3), expressed as spectral-function sum rules, for hard-kaon processes 9-16864  
 SU(3)×SU(3) breaking weak nonleptonic amplitude divergences 9-6622  
 SU(3)×SU(3) charge algebra, chiral, for deriv. of intermultiplet-mass formulas 9-16829  
 SU(3)×SU(3) chiral algebra approx. saturation, in hadrons classification scheme 9-15591  
 SU(3)×SU(3) for hadron current divergences 9-8770  
 SU(3), asymptotic, and Kez decay form factors 9-11034  
 SU(3), Gell Mann's λ matrices, d- and f-tensors, octets and parametrizations 9-17691  
 SU(3), hadrons scatt., Mandelstam variables simultaneous partial-wave expansion 9-17957  
 SU(3), spontaneous strong breaking, Cabibbo angle deriv. 9-20613  
 SU(3) and SU(2,1), generating functions and characters of irreducible representations 9-14466  
 SU(3) approx., current algebra, infinite momentum and sum rules for hadrons 9-19196  
 SU(3) breaking, nonleptonic weak interac. matrix elements depend. 9-16837  
 SU(3) crossing reln. and Regge pole theory for meson-nucleon scatt. 9-16859  
 SU(3) group, representation coefficients 9-20307  
 SU(3) irreducible representation derivation 9-4592  
 SU(3) multiplets in vector mesons, splitting, mixing and small perturbations 9-16888  
 SU(3) nuclear model, rotational bands assignment, validity 9-18059  
 SU(3) rep., Beltrami-Laplace operator eigenfunctions and values 9-14323  
 SU(3) representation, correlation, between ellipsoidal pairs 9-6284  
 SU(3) representation functions from 'Euler' decomposition 9-20590  
 SU(3) scheme, equal spacing rule in masses in decuplet 9-15590  
 SU(3) sym. breaking, representation mixing in 1/2- baryon octet 9-18012  
 SU(3) symmetry; vector and tensor Regge poles degeneracy in meson photoproduction 9-391  
 SU(3) symmetry, combining with exchange degeneracy to form single parameter fit to mes.-Nu scatt. 9-16839  
 SU(3) symmetry for relation between Σ<sup>+</sup>, Σ<sup>0</sup>n and Σ<sup>+</sup>Λn states 9-6707  
 SU(3)×SU(3) 3-point function 9-8800  
 SU(6) symmetry and structure of weak interaction AN→NN 9-425  
 SU(N,1), unitary irreducible representations classification 9-17690  
 SU group representation using fermion operator realization 9-14475  
 symmetry point groups and characters of its irreducible representations, survey 9-44  
 symplectic groups, degenerate representations 9-6287  
 Tannaka duality theorem, generalization and proof 9-20308  
 three-dimensional rotation group, representation in terms of direction and angle of rotation 9-14371  
 U<sub>3</sub> multiplets of radially excited mesons, relativistic formalism 9-20630  
 U<sub>3</sub> bases for representations in the chain U<sub>3</sub>→U<sub>2</sub>→U<sub>1</sub> 9-16661  
 U<sub>3</sub>×U<sub>3</sub> symmetry for radially excited mesons 9-20630  
 U(6)×U(6), representation function for degenerate baryon series 9-18001  
 U(6)×U(6) Reggeized theory, trajectory exchange contrib. for meson-baryon, BB scatt. 9-18004  
 U(n), hook patterns for maximal and semimaximal states 9-17693  
 for unequal-mass scatt. amplitude of two-particle 9-14488  
 unitary symmetry complementary groups, induced representation in generalized spherical harmonics 9-15420  
 use in det. normal modes of symmetrical vib. syst. 9-9  
 SU(3), 10, 10\*, 27 representations, decay into baryon and antibaryon, B=0 enhancements 9-404  
 H atom, generalised eqn. from group props. of integral eqn. 9-9154  
 O(4,2) classification of states of relativistic H atom 9-15828  
 O(4,2)×SU(2) representation of spectrum of H atom 9-15828



**Group theory** continued

- Su(6) invariance in s-wave meson-baryon scatt. 9-8791
- Gruneisen coefficient** *see* *Specific heat; Thermal expansion*
- Gudden-Pohl effect** *see* *Electroluminescence*
- Guiner-Preston zones** *see* *Crystal structures/microstructure*
- Gunn devices** *see* *Microwave techniques and devices; Semiconductor devices*
- Gunn effect** *see* *Crystal electron states/plasma; Semiconducting materials; Semiconductors*
- Gyromagnetic effect**  
No entries
- Gyromagnetic ratio**  
bremsstrahlung amplitude in collision of two identical particles with  $g=1$ , absence of off-mass-shell effects 9-20599  
cb.YG factors of  $6s6p\ ^3P_1$  and  $6s6p\ ^1P_1$  states 9-15812  
dispersion about mean value as function of spin-orbit coupling parameter 9-20871  
graphite, two-dimens., g-factor, theory and calc. 9-8016  
graphitic carbon, powder, g-factor anisotropy, e.p.r. determ. 9-8014  
shifters, rare-gas-induced, in ground states of alkali atoms 9-11403  
silicon iron, meas. using magneto-optical effect 9-12344  
 $\mu$  and  $e$ , sixth-order contrib., calc. from fourth-order vacuum polar. 9-16826  
 $^{156}\text{Gd}$ , g factors of two-quasi-particle state at 1513 keV and  $4^+$  state of ground state 9-6804  
 $\text{AlCl}_3:\text{Ti}^{3+}$ , crystal field theory of  $\text{Ti}^{3+}$  in trigonal environment 9-12499  
C. amorphous, g-anisotropy rel. to air adsorbed, e.s.r. study 9-8023  
 $^{13}\text{C}^{16}\text{O}$  rotational, molec.-beam mag.-reson. determ. 9-9198  
 $\text{Cu}(\text{C}_2\text{SO}_4)_2 \cdot 6\text{H}_2\text{O}$ , orthorhombic g-tensors and orientations, e.p.r. determ. 9-12240  
 $\text{Cu}(\text{RbSO}_4)_2 \cdot 6\text{H}_2\text{O}$ , orthorhombic g-tensors and orientations, e.p.r. determ. 9-12240  
 $\text{Cu}(\text{TISO}_4)_2 \cdot 6\text{H}_2\text{O}$  orthorhombic g-tensors and orientations, e.p.r. determ. 9-12240  
He atoms,  $2^3\text{S}_1$ , optical pumping method, level shifts 9-11423  
 $\text{or}^{19}\text{Ne}$  first excited state 9-16936  
Pt, conduction-electron g factor, anisotropy 9-1445  
 $^{85}\text{Rb}$  atoms nuclear and electronic g factors ratio, obs. 9-6971  
 $^{87}\text{Rb}$  atoms nuclear and electronic g factors ratio, obs. 9-6971  
YFe garnet, of  $^{57}\text{Fe}$ ,  $4.2^\circ\text{K}$ , from n.m.r. 9-21671  
Yb, e.p.r. of dissolved  $\text{Eu}^{3+}$ , g-shift calc. 9-12504

**Gyroscopes**

- conducting, in magnetic field, expt. 9-15447  
drift, for rotational oscillations of vehicle 9-19012  
earth orbiting, proposed verification of Einstein's theory of gravitation 9-10634  
motion in uniform gravitational field, equivalence principle application 9-8472

**Hadrons**

- 2(2s+1) component fields, bilinear expressions and spin kinetic moment currents 9-17950  
'counter-particles' and their props. 9-4594  
amp., current algebra and dispersion treatment, vertex functions 9-6630  
Bargman-Wigner type eqn. for mesons and baryons from nonlinear quark eqn. 9-345  
Bethe-Salpeter eqn., partial-wave, soln. and reduction to linear systems 9-13106  
Breit double system, helicity amplitudes crossing relation 9-339  
canonical commutation reln., creation and annihilation operators, orthogonal group of even dimensions 9-15587  
chiral  $\text{SU}(3) \times \text{SU}(3)$  charge algebra, for deriv. of intermultiplet mass formulas 9-16829  
chiral  $\text{SU}(3) \times \text{SU}(3)$  dynamics 9-19195  
chiral  $\text{SU}(3) \otimes \text{SU}(3)$  algebra, 3-point functions structure of vector, axial-vector currents 9-10998  
chiral  $\text{SU}(3) \otimes \text{SU}(3)$  symmetry spontaneous breakdown, Hamiltonian determ. 9-20614  
classification, induced by an internal manifold, props. 9-14476  
classification in relativistic non-invariance symmetries of local current generation 9-8767  
classification scheme for lower states and  $\text{SU}(3) \times \text{SU}(3)$ , chiral algebra approx. saturation 9-15591  
compact group, arbitrary, internal symmetry crossing 9-341  
compact-group recoupling theory and graphical formulation 9-342  
complex higher-order poles and generalized unstable particles for resonance description 9-4598  
composite model, convergence func. condition 9-10989  
composites,  $\text{SU}(3)$  symmetry, Bethe-Salpeter bootstrap model 9-2484  
coupling of space-line and internal symmetry groups 9-6582  
D/F ratio,  $\mathcal{R}^*(1400)$  prod. and representation mixing in algebra of vertex strengths 9-10994  
disintegrations of intermediate W-bosons 9-15607  
e.m. mass difference, Reggeized and cancellation of divergences 9-17951  
e.m. mass sum rule, corrections to Coleman-Glashow theory 9-8776  
e.m. quantities, agreement between current algebra and quark model 9-2475  
energy-momentum tensor trace, scalar fields coupled calc. 9-16827  
form factors, eff. of npd vertex functions calc. 9-15588  
form factors, in Bethe-Salpeter model, asymptotic props. 9-16830  
form factors in weak interactions, subtractions and off-shell continuation 9-11002  
fundamental particles, quarks and unit charges review 9-15589  
 $G_\pi$  parity defn., eigenstates, extension to  $G_\pi$  parity 9-4607  
Gedanken expt., not asymptotic scatt., suggested 9-340  
group dynamics, coupling description 9-10993  
hadron scattering 9-350  
Heisenberg-type scalar field theory model, particle-antiparticle two-quanta states 9-8761  
helicity amplitude of double and multiple Breit-system 9-15594  
infinite component field theory, Lagrangian approach 9-13086  
intermediate vector mes., weak and ordinary  $\text{SU}(3)$  space contrast 9-2447  
internal manifold as classification scheme, props. 9-14476  
isobar prod. using multiple-scattering formalism 9-8775  
Joos-Weinberg equations for spin-s particles, Lagrangian formulation 9-10996  
Lanczos spin tensor, spinor approach 9-13111  
Lee model, Z-0 limits 9-8772  
Lee model for C, P, T conservation, interpretation of  $C_\pi$ , props. of 'counter-particles' 9-4594

**Hadrons** continued

- magnetic and quadrupole momenta determ. from ang. distrib. of  $\gamma$ -quanta in radiative decays 9-10974  
magnetic moments and charge radii for states described by infinite component wave equation 9-20609  
manifolds, internal, exact and broken symmetries 9-20612  
mass and spin spectrum derivation from Majorana rep. and de Sitter model 9-8759  
mass difference, e.m., using Regge theory of virtual Compton amplitude 9-2478  
mass formulas, intermultiplet, from chiral  $\text{SU}(3) \times \text{SU}(3)$  charge algebra 9-16829  
model, global aspects of collisions, thermo. behaviour and boiling 'pt. 9-4596  
multiplet mass differences 9-8766  
multiplets, infinite, and representations of SU generated gauge group 9-13110  
N-particle functions, integral representations 9-13105  
O(4) broken symmetry and analyticity, constraints on trajectory functions 9-8777  
in O partial symmetry, e.m. props. 9-2479  
particle fusion, theory based on 5-dimensional scheme 9-8758  
peripheral events, Monte Carlo generation method 9-20607  
photoproduction on p up to 5 GeV, total cross section 9-2472  
Pomeranchukon, quark model, relativistic, Regge trajectory constraints and const. residue 9-15605  
production amplitude, Reggeized resonance model 9-14479  
quarks, form factor of proton, harmonic oscillator states for three-particle systems 9-20610  
relativistic invariance without ang.-momentum conservation 9-15593  
resonances, elementary system representation 9-8768  
S-matrix theory internal symmetries: isotopic spin G2, C2 and  $\text{SU}(3)$  9-8771  
Sakaton model and weak interactions 9-4590  
scatt., relativistic kinematics, constraints among partial waves 9-338  
spectral rep. and matrix elements of equal-time current commutators, perturbation theory 9-10991  
spectral sum rules for 3-point functions involving soft  $\pi$  9-17949  
 $\text{SU}(2,1)$ , irreducible representations 9-16658  
 $\text{SU}(2)$  internal, external symmetries combined variable-mass problem 9-343  
 $\text{SU}(2) \otimes \text{SU}(2)$ , implied relation between  $2^+$  and  $2^-$  mesons 9-2476  
 $\text{SU}(3)$ , spontaneous strong breaking, Cabibbo angle deriv. 9-20613  
 $\text{SU}(3)$  and chiral symm. breaking parameters, spectral representation 9-2477  
 $\text{SU}(3)$  chiral dynamics from generalization of  $\text{SU}(2)$  9-344  
 $\text{SU}(3)$  irreducible representation derivation 9-4592  
 $\text{SU}(3)$  mixing restrictions implied by exchange degeneracy 9-310  
 $\text{SU}(3)$  scheme, equal spacing rule in masses in decuplet 9-15590  
SU group representation using fermion operator realization 9-14475  
SU theory, chiral  $\text{SU}(3) \times \text{SU}(3)$  charge algebra, for deriv. of intermultiplet mass formulas 9-16829  
symmetry, Bethe-Salpeter eqn., dynamical groups 9-16804  
symmetry, current commutation relations in  $\text{R}(11)$ ,  $\text{SU}(6)$  model 9-16828  
t-channel helicity amp., current-algebra and fixed J-plane singularities 9-6617  
vector charges, additivity and algebra, quark model framework 9-14478  
Veneziano's formula, generalization to the five point function 9-10995  
Veneziano's formula, generalization to the five point function 9-10995  
Yang-Mills field, free, e.m. part, asymptotic identification 9-14462  
npd vertex functions, eff. on form factors in calc. 9-15588
- current**  
baryons and pseudo scalar mes., e.m.-mass sum rules from deriv. current algebra 9-4593  
bootstrap principle for equal-time commutators of current ops. 9-11022  
Cabibbo parameter determ. from baryon decays 9-2483  
commutation relations in  $\text{R}(11)$ ,  $\text{SU}(6)$  symmetry 9-16828  
coupling constants, axial-vector, calc. method for leptonic decays 9-16831  
current algebra on mass shell 9-16832  
current commutators, equivalence to divergence conditions for vector fields 9-6581  
current commutators matrix elements taken between vacuum and vector and axial-vector states 9-6618  
current-current picture for  $|\Delta I|=1/2$  rule in nonleptonic weak decays 9-14482  
current-density-current density commutators rel. to VVP couplings 9-10997  
current-field identification and Schwinger term 9-397  
currents integrated over lightlike hyperplane 9-15586  
derivation from phenomenological strong-interaction Lagrangian 9-4595  
Dirac isotopic operator in Yang-Mills theory 9-337  
divergences, basic commutation relation 9-14474  
divergences behaviour under  $\text{SU}(3) \times \text{SU}(3)$ , energy density studied 9-8770  
electromagnetic sum rules, deriv. from equal-time current commutators 9-4593  
e.m., properties between algebra of currents and algebra of fields 9-17952  
e.m., quark dominance assumption tested in Regge-pole model for  $\gamma p \rightarrow \pi^+ \Delta^{++}$  9-16909  
nonleptonic, divergences of weak amp., effect of  $\text{SU}(3) \times \text{SU}(3)$  breaking 9-6622  
PCAC for  $\pi\pi$  scatt. length, corrections 9-16884  
 $\text{R}(11)$  model commutation relations,  $\text{SU}(6)$  symmetry 9-16828  
Sugawara's theory of currents, canonical representation 9-6567  
sum rules, infinite momentum, and current algebra,  $\text{SU}(3)$  approx. 9-19196  
sum rules, new asymptotic 9-16843  
tensor, applic. of spectral function sum rules 9-14473  
weak second-class, existence in  $\eta$  prod. off nucleons by neutrinos, pion-pole contrib. 9-16860
- decay**  
amplitudes, weak; form factor and mass Corrections from  $\text{O}(4,2)$  model 9-14477  
 $|\Delta I|=1/2$  rule in nonleptonic weak decays, current current picture 9-14482  
hard meson analysis of photon decays of  $\pi^0$ ,  $\eta$  and vector mesons 9-6640  
leptonic, and third neutrino hypothesis 9-8773  
leptonic, u.v. divergences in radiative corrections 9-8774  
nonleptonic, phenomenological Lagrangian for weak interac., method of obtaining weak Lagrangian from strong 9-4595  
nonleptonic weak,  $|\Delta I|=1/2$  rule, current-current picture 9-14482

**Hadrons continued****decay continued**

- and number of wave functions of particles 9-20617
- strong, of resonances, coupling consts. calc. by contracted projectors method 9-15592
- three-hadron, final state interaction enhancement 9-8760

**interactions**

- amplitude, invariant, analytic continuation 9-16834
- angular momentum 9-16803
- Cabibbo angle, weak self-masses and broken  $SU(2) \times SU(2)$  9-11001
- Cabibbo angle deriv. from spontaneous strong breaking of  $SU(3)$  9-20613
- $|\Delta I|=1/2$  rule in nonleptonic weak decays, current current picture 9-14482
- dynamic interpretation of weak, e.m. and strong interactions and value of  $\theta$  9-10999
- e.m., free Yang-Mills field, asymptotic identification 9-14462
- e.m., test for  $|\Delta I| \leq 1$ , using storage rings 9-6621
- fifth interaction possibility 9-6619
- high-energy, global aspects., thermo. behaviour and boiling pt. 9-4596
- high-energy, transverse momentum distrib. of part., interpretation 9-13112
- inelastic at high energy, use of Reggeized multiperipheral model 9-6631
- isotopic invariance of strong interactions, expt. test suggestion 9-2482
- multiple particle prod., unitary-symmetrical statistical model 9-16833
- nonleptonic, divergences of weak amp., effect of  $SU(3) \times SU(3)$  breaking 9-6622
- Pauli-Kusaka mixture 9-15595
- peripheral and central collisions distinction 9-14480
- peripheral reactions, branching ratios and sum rules 9-6625
- perturbations, cal. divergent integrals analytic continuation 9-8781
- photo-hadron, chiral dynamics 9-347
- Regge model, multiple, for two particles, determ. of bounds for coupling constants 9-2481
- Regge pole and K-matrix models for 2 particles 9-8784
- Reggeized multiperipheral model for prod. proc., distrib. variation rel. to multiplicity, incoming energy and q-numbers of final part. 9-6631
- Reggeized multiperipheral model including reson. prod., method, applic. 9-20618
- resonance term, dynamical separation from background term 9-2480
- spectral-junction sum rules, unitarity corrections to pole dominance 9-8778
- spinless, equal mass particles; eigen vectors for partial-wave crossing matrices 9-8779
- stress-tensor-current commutators, e.m. and weak corrections, and sum rules 9-8780
- strong, perturbation theory in dispersion formulae 9-13113
- strong coupling theory, new formulation 9-15570
- strong-coupling consts., relativistic quark model 9-13108
- $SU(3)$  strong breaking and dynamical asymmetry 9-8769
- two-particle, light-part-resonances produced, identification by Lorentz factor 9-6624
- vector meson exchange scatt. lengths comparison with expt., low energy 9-6620
- velocity space transform method of analysis 9-15654
- weak, also sum rules 9-19197
- weak, CP-conserving and violating proc. unified theory, intermediate vector mes. applic. 9-2447
- weak,  $|\Delta I|=1/2$  rule in nonleptonic decays, current-current picture 9-14482
- weak, internucleon pot., parity violation 9-6623
- weak, lagrangians, parity-nonconserving potential 9-16835
- weak, nonleptonic, structure, matrix elements and divergences 9-16837
- weak Hamiltonian density, models, sum rules to distinguish 9-16836
- $BB\pi$  nonleptonic  $\Delta S=0$  and 1 amplitudes, sum rules, current algebra and PCAC derivation 9-16836
- $pp$  total hadronic cross sections at 75 GeV 9-4581
- $p\bar{p} \rightarrow PB^* \rightarrow PB$  charge exchange, Reggeized supermultiplet theory anal.  $p_{lab}=4-13 \text{ GeV}/c$  9-14481

**scattering**

- albedo problem, inverse thin-slab, iterative proc. for scatt. kernel, applic. to one-speed isotropic scatt. 9-11103
- amp. crossing-symmetric, Regge-behaved, construct. for linearly rising trajectories 9-6632
- amplitude, invariant, for elastic unitarity in  $S$  channel 9-8782
- amplitude, off-shell,  $O(4)$  group expansion, 2 unequal-mass, arbitrary-spin particles 9-17959
- amplitudes, helicity, kinematic singularity structure and Regge-pole contributions 9-13116
- amplitudes, Regge behaviour, dynamical scheme 9-20627
- amplitudes, spinless scatt., Lorentz expansion 9-11013
- amplitudes and asymptotic form factors use of field theoretic formulation of bootstrap and pole dominance 9-6636
- arbitrary compact group, tensor decomposition of transition operator 9-6616
- arbitrary-mass scatt. of spinless part. with analyticity and Regge-pole dominance, Lorentz pole behaviour of amp. 9-14493
- Argand diagram loops for partial wave pole 9-11012
- baryon-pseudoscalar meson in broken  $SU(3)$  symmetry model, relativistic Schrödinger eqn. applic. 9-8790
- Bjorken limit and pole dominance 9-16894
- bootstrap, consistent, in axiomatic field theory 9-11023
- bootstrap calc. using Regge pole vs. reson. duality 9-15599
- bootstrap model based on duality 9-16851
- bootstrap principle for equal-time commutators of had.-current ops. 9-11022
- bootstrap theory of static pion-baryon scatt., connections with strong-coupling theory 9-6635
- bootstraps, field theoretic formulation 9-17966
- bosons, scalar, vertex function, N/D coincident zeros and Levinson's theorem 9-15606
- bound on amplitude deriv. for particle with spin 9-6626
- chiral symmetry, in nonlinear pion and pion-nucleon Lagrangians construct., divergence requirements 9-16852
- compositeness conditions for poles in partial wave amplitudes 9-16847
- Compton, Regge phenomenology rel. to e.m. mass difference 9-2478
- conspiracy, equal-mass conditions Regge-pole residues factorization 9-17954
- coupled channel process, inelastic unitarity and J-plane singularities 9-14483
- covariant spin operators and their transformations 9-17967
- crossing-symmetric finite-energy sum-rules, conds. needed, effect on Regge behaviour 9-8797

**Hadrons continued****scattering continued**

- current algebra, recent developments 9-14489
- damping of large transverse momenta, unitarity reln. 9-17955
- daughter trajectories, rel. to fixed poles, Regge behaviour 9-15597
- daughters, conspiracies and Lorentz symmetry, Freedman-Wang prescription, arbitrary-spin case 9-8789
- diffraction, at high-energies, and quark model of particle interaction 9-11006
- diffraction, fixed cuts in  $t$ -plane 9-11003
- dispersion treatment of mass extrapolation, vertex functions for phys.  $\pi$  9-6630
- double charge-exchange proc., Regge model 9-6627
- eikonal approx. for Bethe-Salpeter eqn. 9-6628
- elastic at large angles, unitarity conditions and shape of diffraction peak 9-11004
- factorization, kinematic singularities and conspiracies 9-20623
- field theory, quantum scattering, T matrix at zero momenta and classical Lagrangian correction 9-8687
- finite energy sum rules including Regge cut amplitudes 9-11016
- fixed-angle elastic amplitudes, eff. of asymptotic unitarity 9-20619
- forward dispersion relations in presence of Regge cut, asymptotic behaviour 9-4606
- four-point functions, Bjorken limit and pole-dominance approx. for current algebra eqns. 9-16895
- hadron-nucleon, total, cross sections, isospin and U-spin depend., quark-model predictions 9-16855
- helicity amplitudes, kinematic constraints, deriv. from analyticity props. 9-16856
- helicity amplitudes, kinematical constraints deriv., transitions between sets of  $S=O$  constraints 9-16857
- hybrid model for elastic scatt. 9-13114
- inelastic, high-energy, model 9-13115
- J-plane, analyticity of fixed poles 9-15603
- ladder diagrams, calc. using Sudakov kinematic variables 9-20620
- Lagrangians, nonlinear pion and pion-nucleon with chiral invariance, construct. and divergence requirements 9-16852
- Lee model, 2V sector, dispersion methods 9-16844
- Lee model, V0 sector, stable and unstable states 9-349
- linearly rising trajectories, construct. of crossing symmetric, Regge-behaved amp. 9-6632
- Lorentz pole behaviour of analytic amp. of spinless part. with arbitrary masses and Regge-pole dominance 9-14493
- Lorentz poles, infinite family possibility, Bethe-Salpeter eqn. soln. 9-17960
- MacDowell symmetry 9-17929
- meson-nucleon, elastic using baryon trajectories 9-13119
- meson-nucleon, forward react., single-parameter fit, from  $SU(3)$  and exchange degeneracy 9-16839
- model, Glauber equivalent, for new density function at high-energy 9-8788
- Multi-Regge model contrib. to two-body elastic amp., from high-energy form of unitarity eqn. 9-20620
- multichannel case, calc. S-wave scatt. length, current algebra tech., dispersion rel. 9-4599
- multiperipheralism and multi-Regge-Poles 9-17961
- multiple, inverse thin-slab albedo problem, iterative proc. for scatt. kernel, applic. to one-speed isotropic scatt. 9-11103
- multiple-scattering formalism, isobar prod. 9-8775
- N-point function, infinite series representation in generalized Veneziano model 9-14486
- N-point function construction, in generalized Veneziano model 9-14485
- N/D eqns., inversion formalism Regge-pole hypothesis, self-clamping mechanism, S matrix threshold behaviour 9-4597
- N/D factorization for spinless equal-mass particles, Levinson's theorem 9-16845
- N/D method, Froissart's, threshold behaviour 9-11009
- N/D P-wave eqns., nonrelativistic, threshold-behaviour conditions 9-14490
- neutral particle, upper bounds of relativistic scatt. amplitude 9-17956
- off-mass-shell scatt., bound states in framework of Pade approximants 9-17953
- orbiting and resonance states, quantum mech. investig. 9-8783
- overlap function structure and production processes peripherality 9-15596
- peripheral and central collisions distinction 9-14480
- polarizations prod. in inelastic collision, properties 9-11018
- Pomeranchuk pole problem, strong coupling 9-8796
- Pomeranchuk pole props., rel. to branch pts., small momentum transfer 9-14494
- Pomeranchuk quasistable pole and diffraction scatt. at superhigh energies 9-11020
- Pomeranchuk singularity, evidence for factorizability 9-4602
- Pomeranchuk theory, contribution of cuts not small 9-20628
- Pomeranchuk trajectory props. 9-15604
- Pomeranchukon exchange, multiple-scatt. correct. 9-4604
- from potentials square, extremely strong, many-level formula 9-16838
- production amplitudes multi-Reggeon behaviour 9-20625
- quark model multiple-scatt. contributions rel. to high energy cross sections 9-8787
- quasi-2-part., absorption corrections for double peripheral model 9-11005
- Regge amp. and superconvergence factorization 9-2485
- Regge amplitudes Argand analysis and resonances 9-2488
- Regge asymptotic behaviour and Bethe-Salpeter eqn. 9-20624
- Regge asymptotics rel. to resonance parameters 9-2489
- Regge behaviour, kinematical singularities and fixed poles 9-15597
- Regge cut amplitudes in finite energy sum rules 9-11016
- Regge cuts, energy depend. effective trajectory definition 9-15601
- Regge cuts, use of DCEX proc. and model 9-6627
- Regge daughter poles, trajectory and residue functions, general parametrization 9-16850
- Regge daughters mass formula, residue expressions determ. 9-14491
- Regge model, conspirators and daughters for nonzero-spin 9-2487
- Regge O-pole contrib. of 2 spinless particles 9-4601
- Regge pole amplitudes, problem of dips 9-11017
- Regge pole analysis of charge and hypercharge exchange in meson-baryon scatt. 9-6638
- Regge pole analysis of  $\pi^+p \rightarrow \pi^+p^*$  9-2512
- Regge pole conspiracy, Feynman diagram model 9-2486



**Hadrons continued****scattering continued**

- Regge pole families classification, minimal solutions to conspiracy problem 9-4605
- Regge pole model for comparison of pn and pp scatt. amplitudes 9-2531
- Regge pole model for  $\pi^+n \rightarrow \omega p$  9-15627
- Regge pole parameters for  $\pi N$  scatt. 9-4629
- Regge pole term in Green's function for bilocal field eqns. 9-2435
- Regge pole vs. resonance duality in bootstrap calc. 9-15599
- Regge poles, condition on number using impact parameter representation 9-6590
- Regge poles, symm. props, conspiracy and evasion 9-19197
- Regge poles and Argand-diagram loops 9-18010
- Regge poles and cuts, leading singularity may not be simple pole 9-6633
- Regge poles and their residues for a general class of singular pots 9-8792
- Regge poles connection to analytic continuation of Khuri amp.,  $u=0$  9-11011
- Regge pot. theory, inverse problem 9-16846
- Regge rep., daughters and conspiracy constraint phenomena 9-15600
- Regge residue function and conspiracy, factorisation and kinematic factors 9-15602
- Regge residue functions,  $t=0$  kinematical constraints and factorization 9-17965
- Regge secondary trajectories,  $j$  plane additional singularities, isospin-one exchange reactions 9-16849
- Regge theory confirmed at large angle and high energy in p-p scatt. 9-15644
- Regge theory of  $10+10^*$  and 27 mesons 9-11070
- Regge theory, reduction in number of parameters through use of quark number 9-6634
- Regge trajectories, baryon sum rule constraints 9-2525
- Regge trajectories, boson, parity doubling 9-2493
- Regge trajectories, crossing-symmetric, corrections for resonance exchange 9-8794
- Regge trajectories and poles, two-dimensional expansions of relativistic amplitudes 9-11019
- Regge trajectories bootstrap models 9-11021
- Regge trajectories eval. using Ladder approx. in perturbation theory 9-4603
- Regge trajectories for Bethe-Salpeter eqn., stationary expectation values and slopes 9-2459
- Regge trajectories intersecting in field-theory model 9-17962
- Regge trajectories of opposite normality connected by  $\pi$  emission must have same slope 9-11015
- Regge trajectory cancellation by representing amplitude as sum of terms of Veneziano type 9-11014
- Regge trajectory conspiracies 9-14492
- Regge trajectory domination quark effect 9-20608
- Regge-behaved amplitudes, crossing-symmetric, consistency condition 9-17964
- Regge-pole contributions, direct-channel, sum and crossing symmetry 9-17963
- Regge-pole model for forward-scatt. amp., comparison with quark model 9-13117
- Regge-pole theory, factorization and constraints near zero momentum transfer 9-8793
- Reggeon exchange, inclusion of diffraction dissociation 9-8795
- resonance parameters rel. to Regge asymptotics 9-2489
- S-matrix, analytic, strong interaction dynamics, book 9-11008
- Schrodinger scatt. of spin 0 particle, inverse problem 9-16846
- with single-meson prod.,  $SU(6) \times O(3)$  quark model 9-8762
- spin particles, helicity amplitudes, axiomatic analyticity props., superconvergence relations 9-16841
- spin-zero, equal-mass, amplitude calc. by conformal mapping 9-16854
- SU(3) group, Mandelstam variables simultaneous partial-wave expansion 9-17957
- sum rules, finite-energy rel. to  $\rho\eta\eta'$  couplings 9-4600
- sum rules, new asymptotic 9-16843
- superconvergence relations incomplete in 2-particle scatt. 9-14487
- t-channel Regge poles, n-fold s-channel iterations from high energy form of unitarity eqn. 9-20620
- three-body theory and eqns., relativistic 9-16842
- three-part bound-state eqns. for two  $\pi$  and one baryon syst. equivalence of model to phys. dressed baryon one,  $J=1$  reson. marres calc. 9-6629
- three-particle, recent work on nonrelativistic theory, review 9-19198
- three-particle amplitudes, off-and on-shell analyticity 9-20622
- time-reversal invariance tests, effects and final state interac. 9-16853
- Toller pole parameters, in  $\Delta^{++}(1236)$  prod. at high energy 9-8916
- Toller quantum no. M and s-channel helicity amp. factorization connection 9-17958
- Toller  $\omega$  depend. on 2-Reggeon-one-particle vertex function, test 9-20626
- two-body off-shell potential scatt., amplitude calc., Padé approximants 9-20621
- two-body relativistic, Klein-Gordon treatment 9-16840
- two-particle relativistic, generalized Moller operators constructed 9-8786
- unequal-mass scatt. amplitude of two-particle, group theoretical approach 9-14488
- unitarity eqn., high energy form, applic. 9-20620
- upper bounds for forward and fixed-momentum-transfer scatt. amplitudes at high energies 9-8785
- vacuum Regge exchange, role of third pole  $P''$  9-11010
- vector and tensor trajectories, universality hypothesis 9-15604
- Veneziano's model, trajectories study 9-8798
- Veneziano form extension to N-particle amplitudes 9-14484
- Veneziano model with crossing symmetry and Regge asymptotic behaviour, mass relations 9-16848
- p-C, nuclei equiv. to elem. part., high energy 9-348
- pp at large s, t, Regge trajectory dynamics anomaly due to fifth interaction 9-6619
- $\rho\eta\eta'$  couplings, fermion Regge pole behaviour, finite-energy sum rules, superconvergence relations for  $\pi\eta$  amp. 9-4600
- Su(6) invariance in s wave meson-baryon scatt. 9-8791
- Superconvergent sum rule for combination of four elastic channels 9-11007

**Haemoglobins** see *Proteins***Hafnium**

- infinite dilution resonance absorption integrals 9-19372
- superconductivity, absence in bulk material 9-12124
- $\beta$ -Hf, self-diffusion, 1785-2185°C 9-9732

**Hafnium compounds**

- HfO<sub>2</sub> crystal, hydrothermal growth, temp. and solvents effects 9-1139

**Hafnium compounds continued**

- C-Hf alloy, reinforced, commercial development 9-3467
- CeB<sub>6</sub>-Hf, elec. props. 9-9919
- CeB<sub>6</sub>-Hf, elec. props. temp. dependence 9-9920
- HfO<sub>2</sub> elec. quadrupole interaction 9-3972
- Hf-Cr system, phase diagram based on microscopic, X-ray and thermal analysis 9-14996
- HfB<sub>3</sub>, bend strength rel. to grain structure 9-1259
- HfC-10 vol.% HfB<sub>3</sub>, hot-pressed, plasticity and fracture strength  $\leq 2635^\circ\text{C}$  9-1301
- HfC, hot-pressed, plasticity and fracture strength,  $\leq 2635^\circ\text{C}$  9-1301
- Pu (1.5at% Hf,  $\beta \rightarrow \alpha$  transformation kinetics 9-11977

**Half-lives** see *Radioactivity/decay periods***Hall effect**

See also *Semiconducting materials; Semiconductors*

- conducting fluid rotating in vertical mag. field, effects of Hall currents on thermal instability 9-7145
- glasses, chalcogenide, rel. to energy levels and progressive crystn. model 9-3611
- graphite, low-temp., calc. using trigonal symmetry and intercarrier scatt. effects 9-7748
- graphite, pile irradi., Hall coeff. rel. to annealing temp. 9-7587
- graphite-nitrate residue cpds, anal. in band model approx. 9-7740
- graphites, polycryst., rel. to X-ray anisotropy factors 9-7428
- in gravitating fluid layer, incompress., rel. to stability 9-7117
- group IB alloys  $\alpha$ -phase, coeff. meas., 10-300°K, rel. to anisotropic relaxation times 9-13844
- Hall current influence on dynamics of plasmoids in spatially periodic mag. fields 9-5013
- Hall probe for meas. of magnetization 9-4425
- high resistivity meas. methods 9-6454
- inhomogeneous materials, resistivity variations, variety of effects 9-3730
- Kelvin-Helmholtz plasma instability 9-9390
- magnetic alloy, dilute, coefficient field-dependence calc. from s-d model 9-16228
- magnetic metal, compensated, resistance proportional to  $MB^2$  in high-field limit 9-21456
- measurement in high-resistance specimens, d.c. voltage amplifiers 9-12083
- metal-NH<sub>3</sub> solns. 9-1041
- m.h.d. flow, tensor conductivity eff. on flow 9-18257
- photo- in inhomogeneous materials, resistivity variations, variety of effects 9-3730
- plasma, gravitational stability, Hall current destabilizing effect 9-7178
- plasma accelerator, design 9-19541
- polaron semiconductors 9-18616
- pyrocarbons, rel. to B content between 0.04 and 0.2% 9-7736
- and semiconductor physics fundamentals, book 9-13880
- semiconductors, heavily doped, at low temp. 9-12155
- semiconductors, intrinsic, theory of isothermal Hall effect corrected 9-7787
- sphere, diam. dependence, theory 9-6445
- square root extractor, positive and negative signals, study 9-6457
- superconductor, type II, core model explanation 9-12117
- transition metals, anomalous, rel. to Fermi surface structure 9-1461
- transition metals, rel. to electronic structure 9-10078
- transverse in thin layer, quantum limit 9-7732
- turbulent MHD 9-9335
- Ag, coeff. determ. 4.2 300°K 9-5651
- Ag film, coeff. depend. on thickness from Fuchs-Sondheimer theory 9-7331
- AlP epitaxial layers on Si, indication of n-type material 9-19692
- AlSb, power, 2° 500°K 9-7794
- Au, coeff. determ. 4.2-300°K 9-5651
- Au film, coeff. depend. on thickness from Fuchs-Sondheimer theory 9-7331
- Bi<sub>2</sub>Te<sub>3</sub>, n and p type., Hall coeff. 9-3637
- n-Bi<sub>2</sub>Te<sub>3</sub>, quantum oscillations 9-12144
- C, donor doped, (Na and K), temp. depend 9-7752
- C, mdg. field depend. at various temp., rel. to acceptor doping and heat treatment 9-7751
- C, soft and hard, temp. depend. from 1.5 to 300°K, after heat treatment to 3000°K 9-7749
- C, soft heat treated from 1800°-3000°K after acceptor introduction 9-7750
- C blacks, compacted without a binder 9-7735
- C blacks, effect of Na on coefficient 9-7739
- C powders, calc. of actual effect from meas. apparent one 9-7737
- Cd<sub>3</sub>As<sub>2</sub>, non-parabolic conduction band from magneto-Seebeck and Hall coeff. meas. 9-9893
- CdF<sub>2</sub> containing In or Eu centres, Hall coeff. over broad temp. range 9-5672
- CdS, mobility of photoelectrons 9-5761
- CdSb, doped, 2.2-77°K 9-9972
- CdSe film, encapsulated 9-3649
- n-CdSnAs<sub>2</sub>, isotropic, rel. to conduction band anisotropy 9-9984
- CdTe:Li, temp. depend. meas. rel. to effect of dopant 9-12156
- CdTe Hall mobility rel. to electric and magnetic field intensities 9-3622
- Cu-GaAs supersaturated solid solns., for decomposition study 9-5511
- Cu, coeff. determ. 4.2 300°K 9-5651
- Cu<sub>2</sub>O, polycrystalline, high-resistivity, combined prep. and low temp. meas. device 9-3742
- Euo.<sub>95</sub>Gd<sub>0.05</sub>S obs. rel. to band conduction and critical scatt. 9-9886
- Fe-Mn alloys, temp. and comp. dependence 9-9921
- Fe-Si alloys, temp. and comp. dependence 9-9921
- Fe-V alloys, temp. and comp. dependence 9-9921
- Fe<sub>2</sub>Se<sub>3</sub>, rel. to change in mag. order at 200°K 9-19886
- n-Ga<sub>1-x</sub>P<sub>x</sub>-Te, Se, effects of two kinds of carriers 9-3623
- GaAs<sub>1-x</sub>P<sub>x</sub>-Se, temp. depend., rel. to activation energy of Se 9-21500
- p-GaAs:Ni, temp. depend., rel. to props. 9-15099
- n-GaAs, 300° to 900°K 9-16264
- n-GaAs, coeff. shift rel. to magnetoresistance oscillations 9-5687
- N-GaAs, electron heating effects on Hall coeff. 9-12149
- n- and p-GaAs, temp. depend. 9-7799
- n-GaAs, temp. depend., influence of  $\gamma$ -radiation 9-13875
- n-GaAs, temp. depend., rel. to 'freezing-out' of electrons, 4.2-20°K 9-12147
- n-GaAs temp. depend. intermediate donor level activation energy 9-3653
- GaAs<sub>1-x</sub>P<sub>x</sub>, S and Te doped, rel. temp., 55 to 400°K 9-12150
- GaP, 2°-500°K 9-7794

**Hall effect** continued

- GaS, photo. meas. 9-1614  
 n- GaSb,  $\text{Te}$ , rel. to transport props. 9-10177  
 n- GaSb, InSb mixed crystal, rel. to conduction bands 9-5690  
 Ge:Mu, variation of carrier conc. and mobility by heat treatment 9-3658  
 Ge, carrier distrib. and type, under elec. field 9-17396  
 p-Ge, longit. 9-15103  
 n-Ge, meas. rel. to non-equilib. depletion effects at electrolyte interface 9-13895  
 Ge, mobility after deformation, dislocation band model 9-18628  
 Ge, mobility after deformation, dislocation band model 9-18628  
 Ge film recrystallized by electron beam, meas. rel. to mobility and conc. of current carriers, effect of substrate temp. 9-16271  
 HgSe, from helicon wave resonance meas. at 77°K 9-7723  
 n-HgTe, in strong elec. field, obs. 9-3626  
 InAs, 4.2°K, doped, cond. band 9-1535  
 InAs, anomalous 9-15091  
 InAs film used in Hall e.m.f. transducers 9-10007  
 In<sub>0.5</sub>Ga<sub>0.5</sub>As, solid solutions, coeff. meas. for energy structure and Debye temp. calc. 9-3640  
 n-InP, compensated, mag. field dependence 9-3627  
 p-InSb, eff. of dislocations, 50° to 200°K 9-21505  
 n-InSb, increase in Hall coeff., mag.-field depend. activation energy, energy gap interpretation 9-15100  
 n-InSb, mag. field dependence of donor ionization energy 9-13885  
 InSb, mobility, temp. depend. interpretation 9-12146  
 p-InSb, temp. dependence rel. to dislocation density 9-3631  
 n-InSb temp. and elec. field dependence of coeff. 9-3628  
 p-MnO, mobility of electrons and holes at high temp. 9-12152  
 $\beta$ -Ni-Al, and transverse magnetoresist. at liq. He temps. 9-5639  
 Ni-Al alloy, coeff. sign change rel. to phase structure 9-3582  
 Ni-Cu alloys, 100-700°K and spontaneous coeff. in paramag. region 9-21485  
 Ni, 100-700°K and spontaneous coeff. in paramag. region 9-21485  
 Ni, temperature (1.85-20.1°K) and thickness (1.005-0.041 mm) dependences 9-1468  
 Ni-Fe ferrite, mobility, freq. depend., rel. to conduction mechanism 9-3632  
 Ni<sub>3</sub>P, Hall effect, structure depend. 9-9922  
 p-PbSe, temp. dependence for band structure determ. 9-3643  
 Pb<sub>2</sub>Sn<sub>1-x</sub>Te, temp. dependence, 4-300°K rel. to band inversion 9-13890  
 PbTe-PbS, solid solutions, coeff. meas. rel. to valence band structure 9-21514  
 Pd-Ag alloys, low-temp. 9-12102  
 Re, coeff. rel. to Pauli susceptibility and elec. resistance, temp. depend. 9-15072  
 Si:Bi implanted layers, elec. props. meas. 9-7810  
 Si, electron states at dislocations 9-16274  
 n-Si, mobility and carrier repopulation at high elec. fields 9-16278  
 Si surface inversion layer, electron mobility 9-5711  
 Sn, white, anisotropy at 4.2°K, rel. to preferred orientation investig. 9-16050  
 SnO<sub>2</sub>, rel. to electronic props. 9-9981  
 SnTe-Sb<sub>2</sub>Te<sub>3</sub> system, composition and temp. dependence 9-12153  
 ThB<sub>4</sub> polycrystals, Hall coeff. obs. 9-1471  
 ThB<sub>6</sub> polycrystals, Hall coeff. obs. 9-1471  
 ThC<sub>0.4</sub>UC solid solns., and elec. resist. and thermoelec. power 9-3573  
 Ti-Te, liquid, composition and temp. dependence, 340-640°K 9-13537  
 n-TiBiTe<sub>2</sub>, temp. dependence 9-21507  
 TiCl<sub>3</sub> galvanomagnetic effect 9-3772  
 TiTe<sub>2</sub>, semiconducting, rel. to optical energy gap determ. 9-14046  
 V<sub>2</sub>O<sub>3</sub>, in metallic conduction region, at 200-320°K 9-18603  
 WSe<sub>2</sub>, n- and p-type, coeffs., 77°-295°K 9-5692  
 Zn, anomalous size effects caused by compensation 9-13848  
 ZnO films, dependence on parameters of growth process from saturated condensate current 9-1103  
 ZnSb, anisotropy 9-9923  
 n-ZnSe, piezo-, and piezoresistance 9-5693  
 ZnSnP<sub>2</sub>, mobility of holes rel. to ordering 9-3310  
 Zr, coeff. rel. to Pauli susceptibility and elec. resistance, temp. depend. 9-15072

**Hall generators** see *Electricity/direct conversion; Semiconducting devices*

**Hall mobility** see *Semiconducting materials; Semiconductors*

**Halogens**

- atom-mol. exchange reactions, short-range attractions 9-10309  
 charge exchange with alkali metal, ion-pair prod. mech. in flame detector 9-21739  
 discharge, as rapid recovery pulsed light source 9-6557  
 reactions with alkali atoms, harpooning dynamics 9-1888  
 spectral lines, intensity reln., with S lines 9-9126

**Hamidashi effect** see *Ferroelectric materials; Ferroelectric phenomena*

**Hard-sphere gases** see *Quantum fluids; Statistical mechanics*

**Hardness**

- See also *Abrasion; Work hardening*  
 cermets, high-temperature 9-18535  
 electromechanical effect, kinetics 9-1314  
 glass, microhardness, indentation tests 9-18527  
 glasses, slow loading indentation meas. 9-3453  
 graphite, Vickers hardness before and after n-irrad., annealing effects 9-7578  
 group IV B and V B carbides, stoichiometry depend. 9-21374  
 group VIa metal composite mats., effects of W replacement by Mo or Cr 9-19842  
 hot-microhardness test equipment, 10° to 1400°C, loads up to 1 Kg 9-18526  
 international uniformity of measurement 9-9773  
 kinematic hardening, generalization for nonlinear stress/strain law 9-20408  
 MgO, Knoop anisotropy rel. to dislocations motion, obs. 9-3454  
 Nimonic alloy, precip. hardening mechanism 9-3469  
 of optical coatings, instrument for estimation 9-13743  
 radiation hardening, saturation, model 9-16143  
 steel, austenitic stainless, strain hardening due to phase transform, strengthening eff. 9-5499  
 steel, case hardening, insonation effects 9-19845  
 transition metal carbides, stoichiometry dependence 9-21374  
 Ag<sub>2</sub>GeSe<sub>4</sub>, microhardness rel. to loading, illum. and temp. 9-14982  
 AgCl, Rebinder effects 9-13738  
 Ag<sub>2</sub>SnS<sub>4</sub>, microhardness rel. to loading, illum. and temp. 9-14982

**Hardness** continued

- Al-Al<sub>2</sub>O<sub>3</sub> alloys, dispersion-strengthened SAP, 20-600°C 9-7577  
 Al-Cu, age hardening inhomogeneities, correl. with lattice const. and lattice strains 9-9783  
 Al-Cu, sintering effects rel. to CuO reduction 9-3463  
 Al-10 wt.%Si composites containing Ni-coated sapphire whiskers, role of Ni 9-21385  
 Al, yield curves in tension, effect of cyclic work softening 9-18504  
 Al<sub>2</sub>O<sub>3</sub>-BaO glass ceramics, rel. to glass composition 9-3171  
 Au, quench hardening mechanism 9-19818  
 CaF<sub>2</sub> single crystals mixed with SrF<sub>2</sub> or BaF<sub>2</sub> single crystals 9-11942  
 Cu-Al crystals, solid soln. hardening 9-13767  
 Cu-GaAs supersaturated solid solns., microhardness meas. for decomposition study 9-5511  
 Cu-(2.4 wt.%Mg) alloy, precipitation hardening mechanism 9-1329  
 Cu-Ti-Al alloys, hardening during slip mechanism 9-17319  
 Cu-Ti alloys, hardening during slip mechanism 9-17319  
 Cu, fatigue hardening mechanisms 9-13737  
 Cu, neutron irradiated, hardening, thermally activated obstacles 9-11943  
 Cu, strain hardening study 9-18499  
 Cu polycrystalline, microhardness increase due to quenching 9-9774  
 CuO, Knoop anisotropy rel. to dislocations motion, obs. 9-3454  
 Fe-30wt.%Ni-5wt.%Nb austenitic alloy, of phases formed by heat treatment and cold working 9-9802  
 Fe, electrolytic, eff. of grain size on microhardness 9-11944  
 GaSb, microhardness, eff. of doping 9-5485  
 Ge, electromechanical effect existence 9-1315  
 InSb, microhardness, eff. of doping 9-5485  
 LiF, microhardness, n-irrad. eff. 9-11885  
 Mg-Cd single crystal, solid soln. hardening investig., conc. and temp. depend. 9-21378  
 Mo, following neutron irradiation 9-19808  
 NaCl:BaCl<sub>2</sub>, concentration dependence 9-3455  
 Nb(M<sub>1-x</sub>N<sub>x</sub>) solid solns., (M<sub>1</sub>=Al, Ga, Ge, In, Sn), microhardness reln. to supercond. transition 9-5664  
 Ni-Al-Ti alloys, coherency hardening, comments 9-11946  
 Ni-Al alloys, precip. hardening mechanism 9-3469  
 Ni-Al and Ni-Al-Ti alloys, coherency hardening 9-11945  
 Ni-Cr white castiron, improvement treatment, patent 9-13757  
 Ni-base alloys,  $\gamma'$  precipitation-hardened slip and climb processes 9-7579  
 Ni<sub>3</sub>Al, strain hardening, stage separation by stress/strain diagram 9-13761  
 NiO, Knoop anisotropy rel. to dislocations motion, obs. 9-3454  
 Ni-(12 at wt.%)Ti alloy, age-hardening Caand0600°C 9-11959  
 Pb, strain hardening, eff. of strain rate 9-13744  
 PbS-PbSe solid solns., microindentation hardness rel. to comp., obs. 9-7580  
 PbS-PbTe solid solns., microindentation hardness rel. to comp., obs. 9-7580  
 PbTe, microhardness, donor and acceptor impurity dependence 9-1316  
 Si-P, microhardness and point defects, reln. 9-5486  
 SiBi<sub>2</sub>O<sub>7</sub> 9-18648  
 Te, electromechanical effect 9-18525  
 $\alpha$ -Ti, strain hardening, effect of strain rate, temp. and purity 9-5487  
 Ti alloys, age-hardenable, composition and props., patent 9-13771  
 Y<sub>2</sub>O<sub>3</sub>-ThO<sub>2</sub> solid solutions 9-3456

**Hardness, magnetic** see *Magnetic properties of substances/ferromagnetic*

**Harmonic analysis** see *Acoustic analysis; Calculating apparatus; Fourier analysis*

**Harmonic generation, optical** see *Lasers; Optics*

**Harmonic oscillators** see *Quantum theory*

**Hartree-Fock method** see *Atoms/structure; Solid/structure*

**Hearing**

See also *Ear; Speech*

- acoustic sensations, equivalence law of variation of loudness, pitch and tonal roughness 9-8306  
 aids, use of in recovery from TTS assoc. with sensorineural deafness 9-10573  
 amplitude modulated tones, frequency regions distinguished 9-6214  
 asynchrony thresholds, differential, for auditory pulse trains 9-21996  
 auditory excitation from cubic difference tone meas. 9-6213  
 auditory-flutter fusion threshold rel. to signal envelope, obs. 9-4156  
 binaural, interaural amplitude effects 9-4146  
 binaural, marking-level differences at low signal freq., eff. of marker spectrum level 9-12788  
 cat cochlear nucleus, unit responses to amplitude-modulated stimuli 9-21997  
 cochlear combination tones distrib. pattern of guinea pig 9-18956  
 cochlear harmonic distrib. pattern of guinea pig 9-16644  
 cochlear microphonics, longit. distrib. in cochlear duct (Guinea pig) 9-8307  
 critical bands in human auditory processing 9-18953  
 deafness due to impulse noise 9-2095  
 detectability of binaural tone masked by another of same freq. 9-14281  
 detection after-eff. masking due to sound exposure var. of data 9-6218  
 direction of sound pulses, threshold for reversal perception 9-16639  
 distance estimation of 0° or apparent 0°-orientated speech signals in a-choic space 9-16640  
 evoked response from vertex, eff. of intersignal interval 9-15388  
 frequency discrimination, difference limens, mechanisms for duration and pitch discrim. 9-10574  
 frequency discrimination, eff. of harmonic components 9-10570  
 frog, leopard, auditory units in eighth nerve, responses 9-17675  
 guinea pigs, two-tone stimulation, microphone response 9-10575  
 Haas effect, comments on historical background 9-20266  
 hazard from 0.22 in weapons, obs. 9-4159  
 high-intensity sound, functional changes, prod. in ear 9-15389  
 human, masking phenom. and signal response 9-8305  
 impairments, correl. with sound levels at work 9-16641  
 eff. of impulsive noise, duration and temporary threshold shift 9-15387  
 intensity discrimination of Rayleigh noise 9-14280  
 localization of sound, role of signal onset 9-17674  
 loss due to steady-state noise 9-4164  
 loudness discomfort level, auditory fatigue rel. to sound-press. and sensation levels 9-4161  
 masked tonal thresholds for bottlenosed porpoise 9-4166  
 masking, multiple, release from , effect of interaural tune disparities 9-20264



**Hearing** continued

- masking by broadband noise, sinusoidal tone or both, 3 dimens. representation 9-20265
- masking monaural temporal, of transients, latency-intensity conversion hypothesis 9-10569
- matching range, vowel acoustic parameters from speech synthesizers 9-6212
- noise pitch determ. by noise bands 9-18954
- perception of acoustic roughness and fluctuation strength of amplitude modulated pure tone 9-6215
- pitch, contralateral and monaural difference limen investig. 9-20267
- pitch matching in interrupted white noise, periodicity theory substantiated? 9-16642
- pitch perception per and poststimulatory fatigue 9-10572
- pitch shift, secondary residue eff. simulation by dig. comp 9-6217
- readaptation of ear after interrupted traffic noise 9-6216
- semivowels, synthetic, rel. to first-formant locus freq. and transition shape 9-4153
- seniorineural deafness recovery rate from TTS by use of hearing-aids 9-10573
- sensitization of auditory and tactile syst. after stimulation 9-10571
- signal in gated and continuous noise, rel. to duration, obs. 9-4158
- signal in masking noise, lateral localization threshold, obs. 9-4157
- sonic bangs, eff. on visual task performance 9-15474
- sound masking, shifts with time, expt. 9-4160
- speaker authentication and identification, comparisons of spectrographic and auditory presentations of material 9-12789
- speech signals, 0°-oriented, lateral localization, obs. 9-4155
- startle reaction of rats, with and without background noise 9-16643
- threshold shifts, temporary, recovery rel. to test and exposure freqs. 9-18955
- tinnitus, induced temporarily by noise, pitch and freq. study 9-12787
- two-state threshold theory, multiple-look k-alternative forced choice expt. 9-4163
- Two-tone stimulation, microphone response of guinea-pig 9-10575
- vowel intelligibility rel. to duration and freq. distortion jobs. 9-4154
- white noise, bandwidth influence on pitch perception 9-19069

**Heat**

- See also Radiation/heat; Thermodynamics*
- adiabatic eqn. mixed type boundary problem numerical soln. 9-12944
- energy conversion, elementary book 9-21
- model from theory of inherently macroscopic processes 9-17737
- moving source, two dimensional heat flow theory 9-10747
- thermal analysis review 9-2241

**Heat capacity** *see Specific heat***Heat conduction**

- See also Conductivity, thermal*
- n circular bars and slabs, with various internal geometries, shape factors rel. to heat flow 9-12948
- coeff. with singularity, finite difference approach 9-167
- conjugate problem with moving boundary, applic. to anal. of drying process 9-7302
- cylinder, finite composite hollow circular, flow problem 9-17824
- diffusivity into double layer infinite slab 9-14395
- equation, explicit solution 9-164
- equation, explicit solution 9-4370
- equation, linear and weakly nonlinear, first boundary value problem periodic soln. 9-14391
- fluid of rough spheres, external field depend 9-9445
- heat insulated devices, paradoxical props. 9-4369
- loss prediction in calorimeter type thermal conductivity cell 9-14393
- multicomponent finite regions, theory 9-16743
- partial differential eqns., elec. analogue soln. error analysis 9-10617
- plane-radial problem in cylindrical system with thermal resistance 9-21441
- plasma MGD viscous channel flow, heat conduction approximation 9-21059
- propagating stress jumps, influence of conduction 9-16708
- solid-solid interface, calc. of thermal resistance 9-1408
- solution using finite integral transform, for general boundary conds. 9-8528
- in spin systems, negative 9-12896
- temperature distrib. in solid and liquid phases and position of interface as function of time 9-9588
- theorems relating changes in charact. parameters to average temp. in all regions 9-166
- thermocouple sample in isotropic medium, temp. distrib. and heat balance eqn. 9-15011
- time functions, trigonometric, in law representing approach to thermal steady state, paradoxical props 9-6397
- transient combined cond. rad. in optically thick semi infinite grey medium 9-6393
- U fuel element and can, calc. of thermal resistance 9-1408

**Heat exchange** *see Heat transfer***Heat flow** *see Convection; Heat conduction; Heat transfer***Heat losses** *see Heat transfer***Heat measurement** *see Calorimeters; Calorimetry***Heat of adsorption**

- cathode, effect on gas poisoning mechanism 9-3753
- determination by gas-solid elution chromatography 9-19675
- ethyl chloride, two dimens. condensation 9-9594
- zeolites, Linde-A type, water sorption, enthalpies and entropies 9-9623
- Kr, two dimens. condensation 9-9594
- N<sub>2</sub> on silica supported Ir 9-20934
- N<sub>2</sub>, two dimens. condensation 9-9594
- Ne on Xe surface 9-9622
- Xe on Ni films epitaxed on NaCl, comparison with data for Ni films on pyrex. 9-17248
- Zn, ht. of chemisorption of O<sub>2</sub> 9-17530

**Heat of combustion**

No entries

**Heat of crystallization** *see Crystallization***Heat of dissociation**

- methy halides photoionization mass spectrometric obs., ionization threshold to 600Å 9-3004
- HCl photoionization mass spectrometric obs., ionization threshold to 600Å 9-3004

**Heat of formation**

- methylaniline, H-bond formation 9-10215
- pyrene-N,N-dimethylaniline Heteroexcimer 9-13389
- UP<sub>2</sub>, enthalpies of formation, qualitative method of differential thermal analysis 9-19368
- CHO<sup>+</sup> 9-21685
- CN radical 9-825
- CN 9-17062
- CoO point defects 9-17276
- CsPbCl<sub>3</sub>, in vaporization of PbCl<sub>2</sub>+CsCl mixture 9-19442
- FeO point defects 9-17276
- H<sub>2</sub>S ions 9-905
- K-graphite lamellar cpds., from solid-state e.m.f. meas. 9-1391
- KPbCl<sub>3</sub>, in vaporization of PbCl<sub>2</sub>+KCl mixture 9-19442
- MnO point defects 9-17276
- NaPbCl<sub>3</sub>, in vaporization of PbCl<sub>2</sub>+NaCl mixture 9-19442
- NiO point defects 9-17276
- RbPbCl<sub>3</sub>, in vaporization of PbCl<sub>2</sub>+RbCl mixture 9-19442
- SO<sub>2</sub> ions 9-905
- Te-Tl alloys, enthalpies 9-17514
- ThN 9-824
- TiO point defects 9-17276
- UP<sub>2</sub>, enthalpies of formation, qualitative method of differential thermal analysis 9-19368
- VO point defects 9-17276
- ZrN 9-823

**Heat of fusion**

- cholesterol, and purity, by differential scanning calorimetry 9-13799
- Ag<sub>3</sub>AsS<sub>4</sub>, entropy of fusion 9-13782
- <sup>3</sup>He-<sup>4</sup>He solns., during HeI-He II transition 9-9576
- UO<sub>2</sub>, and enthalpy, 1200-3260°K 9-3151

**Heat of mixing** *see Heat of solution***Heat of reaction**

- calorimeter design for solution chemistry 9-6409
- diethyl ether-chloroform, rel. to chemical interaction 9-10312
- hydration of ions, enthalpies 9-14904
- nitromethane sulphuric acid, rel. to chemical interaction 9-10312
- water sorption on zeolites 9-9623
- FeCl<sub>3</sub>, intercalation isotherm with graphite from 300 to 350°C 9-8066

**Heat of solution**

- alkali fluorides, mixing of binary liq. systems 9-10324
- methane-Ar, gaseous, heat of mixing, 170-2930°K 9-954
- methane-N<sub>2</sub>, gaseous, heat of mixing, 170-2930°K 9-954
- H<sub>2</sub>-methane, gaseous, heat of mixing, 170-2930°K 9-954
- He-Ar, gaseous, heat of mixing, 170-2930°K 9-954
- He-methane, gaseous, heat of mixing, 170-2930°K 9-954
- LiPO<sub>3</sub>+NaPO<sub>3</sub>, surface heat of mixing calc. from surface tension 9-21191
- NaPO<sub>3</sub>+Ca(PO<sub>3</sub>)<sub>2</sub>, surface heat of mixing calc. from surface tension 9-21191
- NaPO<sub>3</sub>+KPO<sub>3</sub>, surface heat of mixing calc. from surface tension 9-21191

**Heat of sublimation**

- PrF<sub>3</sub> 9-9597
- PuO<sub>2</sub> to PuO and PuO<sub>2</sub>, partial heats 9-3160
- ThN 9-824
- U, from vapour press. obs. 9-16033
- ZrN 9-823

**Heat of transformation**

- metals, calorimetric determ., 300-1900°K 9-9838
- steel, martensitic, C-bearing, heat evaluation during room-temp. ageing 9-1344
- NaNbO<sub>3</sub>, Boersma type calorimeter meas. at 372, 527, 576 and 640°C 9-14993

**Heat of vaporization**

- U, from UN vaporization reactions 9-7308
- UC, thermal dissociation 9-1897

**Heat of wetting** *see Wetting***Heat pumps** *see Heat transfer***Heat radiation** *see Radiation/heat***Heat transfer**

- See also Convection; Heat conduction; Radiation/heat; Radiative transfer*
- air, heat transfer from solid spheres, importance of turbulence parameters 9-17162
- air, in turbulent flow in vertical rounded corner triangular ducts 9-13491
- arc for plasma generator, near-electrode region 9-19565
- bibliography 9-161
- bibliography 9-19085
- bibliography of Japanese works (1967) 9-12947
- in biotechnology 9-6399
- blackbody, ideal, behavior 9-19082
- in boiling, transitions, method of study 9-19660
- boundary layer, turbulent, with press. gradient 9-17144
- in channels considering fluid flow and wall metal, transient temp. fields 9-14841
- characteristics and design data for offset rectangular plate-fin surfaces 9-163
- chemically reacting gas mixture, theory from thermal conductivity data 9-7227
- co-current flow of immiscible films with surface evaporation 9-19086
- co-current flow heat exchangers, in thermal entrance region 9-13520
- composite, in non-gray medium 9-6394
- condensing vapour on rotating disc, coeff. 9-14883
- conducting liquid, rotationally advancing, in magnetic field 9-13521
- convection from rotating disc, effect of Prandtl number 9-6400
- convective effect of point corona discharge 9-5091
- convective flow in heated rotat. fluid, effect of radial barrier 9-21013
- convective temp. and laminar flow field in rotating radial circular pipes 9-13518
- critical sound press. for acoustically stimulated processes 9-5228
- cylinder, aeolotropic with rigid insulation, thermal stress calc. 9-10714
- diffusion in cylinder, soln. by Meijer's G-function and Gauss' hypergeometric function 9-16742
- direct contact, between two immiscible phases during drop formation 9-21177
- disperse materials, relativistic dynamics 9-17705
- dispersed and fused substances, combined thermal anal., apparatus and technique 9-19084
- double layer, variational phenomena 9-2258
- drying in liq. media 9-3154

**Heat transfer continued**

in drying of ground paste-like materials 9-17823  
 electrical analogue circuit, also mass transfer 9-17822  
 electrically conducting fluid, unsteady forced-convection MHD in parallel plate channel 9-18264  
 equations, non-linear system for 11 dimen. problems 9-17821  
 exchange in flow with Taylor's vortices in wide gap 9-15479  
 exchanger, vibrating, calc. at luminar regime of main flow 9-2256  
 of fluid, electrically conducting in perpendicular elec. and mag. field 9-18251  
 fluid flowing in channel, turbulent heat transfer coeff. calc. 9-17081  
 fluid laminar flow between parallel walls, circular pipe, suction eff. 9-4990  
 fluids, non-Newtonian, combined laminar free and forced convection 9-846  
 fluids at supercritical pressure 9-20998  
 free-convection, and mass transfer, limiting cases 9-16740  
 Freons with supercritical parameters 9-1004  
 gas, hot radiating stagnant layer, transient transfer to and from surrounding cold gas 9-11659  
 gas, turbulent, effect of variability of physical props. 9-9443  
 gas flow, nonisothermal, at finite Reynolds numbers, extension of asymptotic relative law 9-3046  
 in gas flow in conical nozzle, class of exact solns. of Navier-stokes eqn. 9-11641  
 in gas flow induced by const. rel. heat source, effects on flow 9-7210  
 in gas flow round sphere, development of thermal boundary layer 9-13495  
 gas screen in adiabatic pipe with turbulent flow efficiency 9-938  
 in gas-solid particle system 9-1048  
 gas-vapour mixture, dynamic process and mass transfer, calc. 9-20447  
 gravitational effects 9-6399  
 gray scattering medium, absorption coeff. calc. 9-19089  
 hailstones, spherical, simulation of total heat transfer 9-16529  
 heat exchangers, countercurrent, steady-state and transient behaviour eqns. 9-16741  
 heat rate controller for thermoluminescent studies 9-2267  
 heat-generating polygonal cylinder with central circular hole 9-20450  
 heterogeneous layer between two media 9-20449  
 high-intensity, nonlinear unsteady-state, eqn. reduction to equivalent linear ones 9-20444  
 hypersonic wind tunnel, paraboloid obs. with i.r. camera 9-160  
 in hypervelocity nozzles, at stagnation point, rel. to viscosity, Reynolds number and atom conc. meas. 9-9434  
 ice sublimation in vacuum 9-17233  
 from isothermal cylinder, spray cooled, analytical investigation 9-6398  
 jet, 2D, on circular cylinder 9-19597  
 in laminar boundary layer in contact with porous medium with blowing 9-9503  
 in laminar boundary layer over plate, response to step change in wall temp. or flux 9-13488  
 in laminar flow in porous tube 9-13498  
 in laminar pipe flow in transverse mag. field, anal. for uniform radial heat flux 9-13408  
 loop, out-of-pile, measurement of temperature noise 9-20863  
 and mass transfer from suspended bodies in shear flow 9-20452  
 MHD, in crossed-field couette flow 9-854  
 MHD channel, water cooled, meas. 9-209  
 non-stationary, scientific and technological appl. 9-2259  
 nonlinear, in orthogonal coord. systems, Kirchhoff transformation 9-8524  
 nonlinear diffusion, rel. to heating and cooling problems 9-10753  
 Nusselt number for heat transfer in turbulent tube flow with axially varying heat flux 9-13487  
 8a110/24/1 9-643  
 in phonon gas, pulse propag., theory 9-9852  
 pipe bundle, threaded-profile, under cross-sectional air flow 9-2257  
 plane Couette flow with suction or injection 9-11170  
 plane multilayer wall with internal heat generation, cooling conds. 9-20445  
 in plasma 9-6399  
 polymer soln. dilute, showing drag reduction 9-1006  
 to quadratic shear profile 9-19088  
 radiant, in adiabatic tubular reactor containing gray gas 9-12945  
 radiant, in spherically symmetric medium, calc. by planar slab tech. and differential approx. 9-8519  
 radiation interaction in nongray boundary layers near lower stagnation point. 9-19087  
 radiative, in plane layer of absorbing medium 9-2180  
 rarefied gas, inverse Knudsen nos. 0-10, influence of accommodation coeff. 9-13489  
 reactor coolant channel axial temp. distrib. 9-19344  
 reactor fuel element temperature distribution from heat transfer eqns. 9-19363  
 reactor fuel rod array, to turbulent coolant flow 9-639  
 rel. to reactors, between semiopen channels in square lattice, obs. 9-15795  
 in regular fluid-solid packings 9-5229  
 relativistic pressure invariance, invalidity 9-8527  
 review 9-20446  
 rough and smooth tubes, obs. 9-19102  
 in separation region of turbulent boundary layer in diffuser with hot air flow 9-9425  
 shock-induced boundary layer at wall, rel. to recovery factors 9-21129  
 solid-gas studies, plasma jet facility 9-2982  
 stagnation-point, effect of external vorticity at high Prandtl number 9-20448  
 at steel-Al interface, directional effect rel. to surface conds. 9-13809  
 supersonic boundary layer, turbulent, effect of streamwise wall curvature 9-14811  
 supersonic flow to cavity, mass addition eff. 9-159  
 surface, synthesis technique 9-20451  
 tensor in relativistic thermodynamics of elastic media 9-10746  
 thermal leak, numerical calc. of soln. 9-8523  
 thermal radiation between two dielectrics 9-7677  
 time functions, trigonometric, in law representing approach to thermal steady state, paradoxical props 9-6397  
 transient combined cond.-rad. in optically thick semi-infinite grey medium 9-6393  
 tube, eigenvalue problem with two turning points 9-8526  
 turbulent, temp. profiles in rifted pipe 9-20442

**Heat transfer continued**

turbulent, to viscoelastic polyacrylamide and carboxymethyl cellulose, coeff. determ. 9-19628  
 turbulent boundary-layer ht. transfer in supersonic dissociated air, exptl. investig. 9-21120  
 in turbulent flow in annulus with internal heat generation 9-8525  
 in turbulent fluid flow, influence of temp. depend props. for high heat fluxes 9-12946  
 turbulent liquid flow in tube, onset of fluidization and h.f. oscs. 9-9466  
 turbulent sublayer, effect of transpiration at wall 9-13519  
 two-phase flow upward in vertical tubes, obs. 9-7114  
 two phase spheroidal, to Hg in vortex forced convection 9-2260  
 unsteady forced-convection MHD ht. transfer of elec. conducting fluid in parallel plate channel 9-18264  
 unsteady-state, elec. simulation of boundary conditions 9-20443  
 vapour film of uniform thickness, 1-dimens. growth 9-21248  
 variational principle, first and second kind of boundary value problem 9-6342  
 water laminar boundary layers with adverse press. grad. 9-21163  
 to wavy wall in hypersonic flow 9-11642  
 wire, energy dissipated during fatigue cycling, calorimetric study 9-13717  
 wire, fine, effect of corona discharge 9-17140  
 Ag particles, micron-sized, temp. rise due to e beam heating in e. micro-scope 9-11822  
 Ar plasma to water-cooled copper pipe under the influence of elec. field, obs. 9-21050  
 CO<sub>2</sub> at supercritical pressure 9-20998  
 Cu in H<sub>3</sub>PO<sub>4</sub>, effect on electrolytic dissolution 9-21706  
 Hg, best value of condensation coeff. 9-1071  
 Hg, in dropwise condensation, rel. to temp. head 9-17229  
 Hg liquid when conducting elec. and in mag. field 9-21198  
 Na, boiling, with natural convection, obs. 9-17231

**Heat treatment**

annealing, thermal and radiation, after neutron irradiation, 'peculiar' behaviour 9-21388  
 annealing kinetics of vacancies to dislocations 9-16092  
 annealing kinetics of vacancies to dislocations dislocations 9-13678  
 carbon from dissolution of martensite, yielding graphite cigar-shaped crystals. 9-7369  
 carbons, non-graphitizing, X-ray composite profiles and characts. 9-9672  
 coal-tar pitch, carbonization, microstructs. in coalesced mesophase 9-7418  
 coke, use of Fe<sub>2</sub>O<sub>3</sub> additive in filler for suppression of irreversible expansion in baking 9-7591  
 cyclic growth, thermal ratchet mechanism 9-5495  
 fatigue, elastic, resistance of metals 9-9748  
 firing, maximum rate rel. to structure and thermodynamic props. 9-3462  
 glass, Cd, S and Se compounds doped, effect on colour centres 9-13699  
 graphite, annealing studies of irradiation defects and self-diffusion mechanism 9-5337  
 graphite, B containing, temp. effects on strength and expansion coeffs. 9-7608  
 graphite, irradiated with electrons at 80°K annealing 9-18534  
 graphite, pile irradi., annealing temp. rel. to elec. and mag. props. 9-7587  
 graphite, pile irradi., annealing temp. rel. to internal friction and resonant freq. 9-7525  
 graphite, pyrolytic, e.-irrad., recovery of resistivity below 6°K 9-9931  
 graphite, temp. and degree of binder graphitization rel. to rad. induced contraction 9-7411  
 graphite, thermal rupture resistance, direct meas. 9-7572  
 graphite, Vickers hardness before and after n-irrad., annealing effects 9-7578  
 graphite powders, hot-isostatic compaction to form dense, isotropic bodies, 1650 2700°C 9-7588  
 graphite reflector, MTR, stored energy releasable after 200°C anneal. 9-6946  
 lamp blacks as raw mat. for C products, amount of binder needed 9-7590  
 metal single crystals, bicrystals and tricrystals, recrystallization from solid state 9-21300  
 metals, annealing rel. to vacancy clustering 9-5336  
 metallic crystals, heat treatment not successful in reducing metamictization 9-3280  
 permalloy thin tapes annealed below recrystallization temp., mag. props. 9-3814  
 perthites, homogenisation during routine thermal treatment of powders 9-18531  
 phenolic-nylon, ablation study 9-20125  
 polyurethane films, resistance to degradation improved by high cross-link density, chem. content effect 9-14983  
 PVC, structural changes due to mechanical and heat treatments 9-21416  
 pyrocarbons, compressed reproducible samples, prep. and props. 9-7596  
 quenching methods and rate meas., review 9-11949  
 sapphire, quenching method for strengthening 9-1300  
 Si p-type layers formed by Ga ion-implantation, annealing temp. effects on charge carrier conc. 9-15108  
 silica, vitreous, effect on acoustic props. 9-15001  
 soft carbons, study of residual lamellar cpds. (H<sub>2</sub>SO<sub>4</sub> and Br<sub>2</sub>) 9-7362  
 steel, E1702, quenched and aged, effect of grain size on resistance to deform. 9-9760  
 sugar coke, perfect graphite and turbostratic C prod. at 2200°C 9-7358  
 Teflon, ablation study 9-20125  
 thermal cycling, rel. to cavity growth 9-19772  
 tris-dipyridyl Co(III) perchlorate trihydrate, <sup>57</sup>Co<sup>++</sup>-doped, thermal exchange and annealing 9-9779  
 tris-dipyridyl Co(III) perchlorate trihydrate, n-irrad., thermal exchange and annealing 9-9779  
 undervacuum, metallurgy 9-18530  
 vitrocarbon, temp. rel. to elec. resistivity, elastic consts., strength and expansion coeff. 9-7318  
 welding, electron beam 9-6229  
 wires, small dia., programmable temp. control 9-10760  
 e-microscope specimens, microfurnace, vacuum or inert atmospheres 9-14292  
 AgCl single crystals, slightly bent, annealing behaviour, rel. to sub-structure 9-5497  
 Al-Al<sub>2</sub>O<sub>3</sub>-Au tunnel structures, annealing effect on photovoltaic props. 9-7861  
 Al-Cu alloys, deformed, recrystallization and precip. 9-21400  
 Al-Cu solid solns., heated and aged, elec. resistivity changes rel. to Cu precip. 9-21482



**Heat treatment continued**

- Al-Mg-Ge alloy, clustering after quenching 9-17331  
 Al-Mn alloys, multi faulted loops, formation and annealing 9-13686  
 Al, effect of pretreatment on amplitude depend. internal friction 9-17299  
 Al, quenched, annealing kinetics of dislocation loops 9-11880  
 Al, stage-III annealing after deuteron irradiat. at different temps. 9-21389  
 Al<sub>2</sub>O<sub>3</sub>, thermally shocked, degree of damage 9-3437  
 Al annealing after low temp. fatiguing resistivity changes rel. to induced defects 9-13846  
 AlP epitaxial layers on Si colour change rel. to annealing atmosphere 9-19692  
 Au-Sb alloys, sput cooling, metastability of phases formed 9-3478  
 Au, e. irradi., Stage III annealing process 9-21390  
 Au, electron irradiated, stage III annealing 9-12029  
 Au, quench hardening mechanism 9-19818  
 Au foils, quenched,  $\alpha$ -irradiation effects on tetrahedra 9-7495  
 Au foils, quenching methods and rate meas., review 9-11949  
 Au quenched from 900°C, double stacking-fault tetrahedra 9-7494  
 BaSO<sub>4</sub>, barite, effect on etch patterns 9-13594  
 BaTiO<sub>3</sub> film, prep. by electrophoresis after annealing or melting 9-9610  
 C, glass-like, props. at various stages in pyrolysis of non-melting resins 9-7319  
 C, temp. range Rel. to field depend of Hall coeff. and magnetoresistivity 9-7751  
 C, under press. in presence of Ca cpds., composite (002) diffraction profiles 9-10595  
 C blacks, 1400 to 3000°C. effect on e.s.r. 9-8012  
 C films, to 2500°C, anisotropic cryst. growth 9-7335  
 C green bodies, baking, kinetics and critical parameters 9-7589  
 C monofilaments, spinning and quenching condensates from thermo-setting resins 9-7320  
 CaO ceramic crystals, recrystn. in forging and annealing 9-3482  
 Cr, vacuum annealing, eff. on dislocation structure 9-13688  
 Cu-Cr alloy, f.c.c., recrystallization texture formation effect of precip. 9-21391  
 $\beta$ -Cu-Zn, martensitic transformations, effect of thermal cycling and annealing 9-5512  
 Cu, dislocation density growth during homogenization quenching 9-1217  
 Cu, quenching in vacancy formation and effect on lattice parameters 9-1186  
 Fe, effect on adsorption and corrosion inhibitor action 9-18760  
 GaAs, luminescence, at 1.2 eV and 77°K, annealing effects 9-5953  
 GaAs substrate crystals for epitaxial growth expts., annealing effects, 800°-1200°C 9-11950  
 GaP doped epitaxial films, effect on photoluminescence 9-10237  
 Gd<sub>2</sub>O<sub>3</sub>, solid state reaction with WO<sub>3</sub> for stabilization 9-17326  
 p-Ge:Ga, e. irradi., annealing effects on conduction mechanism 9-5703  
 Ge:Mn, effect of heat on Mn incorporation 9-3658  
 Ge-As, solid soln., defect appearance during decay 9-14937  
 H<sub>2</sub>TeO<sub>6</sub>, annealing of  $\beta$ - $\gamma$  decay and isomeric transition recoil products 9-7584  
 HgTe crystals, annealing in Hg vapour rel. to dislocation formation 9-1220  
 K<sub>2</sub>PO<sub>3</sub>-V<sub>2</sub>O<sub>5</sub> semicond. glasses, effect on a.c. props. 9-3612  
 KCl, annealing effect on optical extinction coeff. of colloidal Ag 9-5924  
 KCl, dislocation processes during creep deform. and heating 9-1223  
 KCl, followed by zone melting for high purity crystals 9-18423  
 LiF, dislocation structure formation near surface during annealing 9-11884  
 LiF, effects on optical absorpt. and thermoluminescence 9-5969  
 LiF,  $\gamma$ -irrad., annealing point defects 9-19821  
 LiF dosimeters, influence of pre-annealing on precision meas., statistical anal. 9-14090  
 LiF dosimeters, to stabilize thermoluminescence 9-14089  
 Li<sub>2</sub>O:SiO<sub>2</sub>-Li<sub>2</sub>O:Al<sub>2</sub>O<sub>3</sub>:4SiO<sub>2</sub>, isostructure and correlation 9-21254  
 Li<sub>2</sub>O:SiO<sub>2</sub>-Li<sub>2</sub>O:Al<sub>2</sub>O<sub>3</sub>:4SiO<sub>2</sub>, isostructure and correlation 9-3177  
 Mg ferrites, quenching temp. effect on mag. permeability and complex dielec. permittivity tensor components 9-19967  
 MgAl<sub>2</sub>O<sub>4</sub> ceramic crystals, recrystn. in forging and annealing 9-3482  
 MgMn ferrites, annealing conditions eff. on pulse and hysteresis props. 9-17459  
 MgO ceramic crystals, recryst. in forging and annealing 9-3482  
 Mn<sup>2+</sup>:Ge, e.p.r., effect of heat treatment on struct. state 9-16459  
 Mo, quenching in vacancy formation and effect on lattice parameter 9-1186  
 Mo, thermally cycled, dislocation structure and multiplication of dislocations 9-5366  
 Mo, vacuum annealing, eff. on dislocation structure 9-13688  
 NaCl:Pb, thermal annealing eff. on scattering of luminous flux at ambient temp. 9-19979  
 NaCl, dislocation processes during creep deform. and heating 9-1223  
 NaCl (100) surfaces, etch pit production 9-7366  
 Nd<sub>2</sub>O<sub>3</sub>, solid state reaction with WO<sub>3</sub> for stabilization 9-17326  
 Ni-Fe-Cu layers, annealing, influence on mag. and struct. props. 9-3821  
 Ni, annealing, ferromag. reson. line width variation rel. to lattice microdistortions 9-14103  
 Ni, quenching in vacancy formation and effect on lattice parameter 9-1186  
 Ni, vacancy formation energy after liq. He-II quenching 9-5338  
 Ni<sub>1-x</sub>Fe<sub>x</sub>:Ge, Fe<sub>2-x</sub>O<sub>4</sub>, effect on anisotropy field 9-5850  
 Pb<sub>0.5</sub>Sn<sub>0.5</sub>-Te, cation-rich, excess carrier conc., annealing temp. and comp. dependence 9-3634  
 Pt, eff. on thermal props. 9-5575  
 Pt wires, quenching in Ar and water, vacancy recovery 9-19745  
 Pt wires, quenching methods and rate meas., review 9-11949  
 Sb film, internal stress obs. during annealing 9-21266  
 p-Si:B,  $\gamma$ -irrad., radiation defects in recombination from annealing 9-3665  
 Si:B, P, thermal annealing of radiation defects, kinetics 9-21327  
 Si:Sb, annealing and precip. of Sb solid soln. 9-1333  
 Si:SiO<sub>2</sub> interface, C-V characts., freq. depend. 9-7813  
 Si:SiO<sub>2</sub> interface, in H. effect on recombination carrier velocity 9-12170  
 Si, e-centre annealing kinetics, activation energy and entropy 9-7505  
 Si n-p-n planar transistors, n-pulse irradiated, rapid annealing data 9-17413  
 SiO<sub>2</sub>, pyrolytic films, props. changes 9-3195  
 SiO<sub>2</sub> films, influence on i.r. abs. variation 9-12386  
 Sm<sub>2</sub>O<sub>3</sub>, solid state reaction with WO<sub>3</sub> for stabilization 9-17326

**Heat treatment continued**

- SrTiO<sub>3</sub>:Mo(Fe or Ni), reversible photochromic changes, model verification 9-19980  
 ThO<sub>2</sub> (1.3 wt.%)UO<sub>2</sub>, thermal cond. changes, irradi. induced, annealing 9-7676  
 TiC ceramic crystals, recrystn. in forging and annealing 9-3482  
 TiO<sub>2</sub>, quench effs. on properties 9-21392  
 U(Fe,Al),  $\beta$ -quenched, recrystallization kinetics on annealing 9-3466  
 U (10 wt.%)Mo alloy, effect on stress-corrosion cracking, field emission microscope investig. 9-21384  
 (U, Pu)C, synthesis from U-Pu alloy, involving sintering 9-2791  
 U, irradi., annealing in NaK under high hydrostatic press. and temps., technique 9-19824  
 U, post-irrad. annealing behaviour of fission gas bubble distrib. 9-11336  
 U, thermally cycled between 400 and 600°C, density changes 9-19771  
 W, vacuum annealing, eff. on dislocation structure 9-13688
- alloys**
- binary B metal, rapid quenching, rel. to study of new metastable electron phases 9-9794  
 cementite, hypereutectoid, in white cast iron, spheroidization on annealing at 900°C 9-5496  
 f.c.c. metal, solid solutions, anomalous after-effect 9-1325  
 permalloy film, annealing effect on stresses 9-13724  
 steel, 18-10, welded joints, quenching effects on corrosion resistance 9-16142  
 steel, 60K3G8N8V, hot working effects on stress-corrosion cracking susceptibility 9-3449  
 steel, annealing effects on Mossbauer spectra 9-16151  
 steel, austenitic, thermal cycling effects on oxidation in CO<sub>2</sub> 9-17528  
 steel, austenitic, to improve corrosion resistance, patent 9-13755  
 steel, Mn, low C, Nb treated, rolled, heat-affected zone props. 9-19819  
 steel, OKh32N8, quench-hardened,  $\delta$ -ferrite decomp. during tempering 9-1343  
 steel, Si, commercial grade sheets, mag. field annealing eff. 9-13753  
 steel, transformer, commercial grade, secondary recrystallization, role of surface energy 9-13752  
 steel, V, tempering, high dislocation density as preferential nucleation sites 9-17328  
 steel, zero change in length at austempering 9-9778  
 steel plates, mild, elastoplastic stress and deformation on thermal cycling 9-5450  
 V steel, tempering, high dislocation density as preferential nucleation sites 9-17328  
 Ag-Sn solid solns., annealing after plastic deform. and effect on Mossbauer spectrum 9-1750  
 Au (50 at.%)Ag annealing, rel. to quenched-in vacancies b//c// 9-3324  
 C steel, slightly hypoeutectoid, austenite recrystallization during hot-working 9-16145  
 Cr-Mn-N steel, cold-worked, structural changes during annealing 9-13776  
 Cu-Pd, specific heat changes at low temp. induced by quenching and ageing 9-9844  
 Cu-Sn solid solns., annealing after plastic deform. and effect on Mossbauer spectrum 9-1750  
 Cu<sub>0.75</sub>Al<sub>0.25</sub> solid solns., annealing after plastic deform. and effect on Mossbauer spectrum 9-1750  
 Fe-Cr, oxide spalling, hot stage microscope obs. 9-18755  
 Fe-Ni-Cr, eff. on magnetization intensity and susceptibility 9-12288  
 Fe-(30 wt.%)Ni-(5 wt.%)Nb austenitic alloy, phase form. 9-9802  
 Fe-c, deformed, effect of C on annealing stages above room temp. 9-13754  
 Fe-Cr superlattice, isothermal magnetic annealing effect on magnetization and magnetostriction at high and room temperatures 9-15153  
 Mg-Cd, annealed, rel. to props. 9-16156  
 Nb-Ti, annealed at 1250-1500°C, dislocation structure 9-5368  
 Nb-base, eff. on creep-rupture props. 9-14975  
 Ni-Cr white castiron, for improving mech. props., patent 9-13757  
 oxides, wetting promotion by Ti addition to brazes 9-3180  
 Si steel, commercial grade sheets, mag. field annealing eff. 9-13753  
 steel, Cr-Mn-N, cold-worked, phase transformations during annealing 9-13776  
 Ti-V, decomposition of martensite during continuous heating 9-5494  
 U-Ti, phases, orthorhombic, metastable 9-19823  
 Zr-Cu, (<5wt%Cu), quenching from  $\beta$  phase, phase transforms, effect of tempering 9-11970
- Heating**
- alkali plasmas, e. cyclotron resonance heating 9-17109  
 cylinder, solid, by solar radiation, temp. distrib. 9-10758  
 dielectric, sensor for water vapour pressure meas. 9-18389  
 furnace, convection heated, for X-ray diffractometry thermal expansion meas. 9-13803  
 furnace, tri-arc with cold crucible for Czochralski growth of crystals 9-1141  
 furnace-cell multipliers, high temperature for spectroscopy 9-283  
 medium as result of Joule energy dissipation 9-3052  
 microfurnace for e-microscope specimens in vacuum and inert atmospheres 9-14292  
 plasma, inhomogeneous collisional, by magnetic pumping 9-15922  
 plasma ions, turbulent, anomalously rapid, rel. to ion-ion instabilities 9-21105  
 polyarylates, CH<sub>3</sub>-group motion and glass transition 9-21415  
 radiator in heating system with one feed, working characts. 9-2245  
 semi-infinite wall, with temp. depend. thermophys. props., soln. with second-order approx. 9-10753  
 solids and liquids, interference due to low-power heating 9-12323  
 solids by  $\gamma$  irradiation 9-19874  
 surface effects on transition boiling 9-16032  
 turbulent, of ions in plasma by MHD waves 9-870  
 in u.s. treatment of metal surfaces 9-10739  
 viscous, in plane and circular flow between moving surfaces 9-987  
 CH<sub>3</sub> motion in polyarylates during heating 9-21415
- Heaviside layer** see *Ionosphere*  
**Heavy water** see *Water*  
**Height measurement** see *Length measurement*  
**Heisenberg model** see *Ferromagnetism; Statistical mechanics*  
**Helicity** see *Elementary particles; Field theory, quantum*  
**Helicons** see *Crystal electron states*  
**Helions** see *Alpha particles; Helium-3*  
**Heliotron** see *Plasma devices*

## Helium

abundance in young Galactic objects 9-18836  
 adsorption by C, rel. to press and superficial pore sizes 9-7347  
 adsorption on Cu surface, 4.2°K 9-19676  
 afterglow at 77°K, low-binding energy 9-868  
 atom,  $2s^21s$  weakly quantized state Hartree-Fock eqn., perturbation treatment 9-11422  
 atom, collisional energy transfer between  $n=4$  states 9-9161  
 atom, differential cross-section for 25-60 eV e scatt. 9-9142  
 atom, e. elastic scatt. S-wave phase shifts, var. method calc. 9-15835  
 atom, energy of excited states 9-2831  
 atom, excitation by 0.05-6 keV electrons, polar. of. of resulting rad. 9-14674  
 atom, excitation by fast electrons, accurate 1st Born approx. cross sections 9-13317  
 atom, excitation by proton beam, resulting polarization of light, violation of  $\Delta S=0$  spin rule 9-9160  
 atom, Green function 9-9105  
 atom, h.f.s., 3 particle forces eff.,  $2^3S_1$  correction 9-4876  
 atom, ionization near threshold energy 9-7189  
 atom, ionization with excitation 9-908  
 atom, lower bounds for various powers of  $r_1$  and  $r_{12}$ , quantum mech. calc. 9-6992  
 atom, many body theory for calc. of time depend. perturbations 9-11421  
 atom, metastable  $2^3S$  state, elastic scatt. of electrons, cross-section meas. by polarised-orbital method 9-9162  
 atom, oriented metastable, collision with Ne atoms, polarization transfer 9-711  
 atom, oscillator strengths, generalised 9-14673  
 atom, p-excited, polarization of singlet transitions 9-6993  
 atom, perturbation calc. with correlation in zeroth order 9-6991  
 atom excitation, generalised oscillator strengths 9-14673  
 atom ground state, Slater transform functions appl. 9-20900  
 atom n S states ( $4\leq n\leq 7$ ) excitation by p impact, calc. 9-4881  
 atom-K<sup>+</sup> collisions, excitation of KII resonance lines 9-2834  
 atom-K<sup>+</sup> collisions, excitation of KII resonance lines 9-14676  
 atoms,  $2^3S_1$ , Gyromagnetic ratio by opt. pumping, level shifts 9-11423  
 atoms,  $2^3S_1$ -a<sup>3</sup>S<sub>0</sub> repulsive interaction pot., long range, calc. and obs. 9-4889  
 atoms, collisions of second kind, X-section meas., excitation transfer mechanism 9-4880  
 atoms, elastic scatt. of zero-energy e. scatt. lengths and reciprocals from variational methods and trial function 9-4885  
 atoms, van der Waals coeffs. for ground and metastable states 9-2833  
 atoms and ion, bibliography of spectra 9-13287  
 atoms in plasma, excited state population meas., mechanism discussed 9-9340  
 $\beta\beta$ -cholestanol multilayer permeability, obs. 9-5415  
 diatomic, energy levels of  $^1\Sigma_u^+$  and  $^3\Sigma_u^+$  states calc. 9-4928  
 discharge tube, removal of H impurities by gettering on Ti film and pumping through Pd membrane 9-3021  
 dissociative recombination and molecular ion formation in decaying plasma 9-13414  
 eigenvalues of  $1s2s$   $1^3S$  states of He sequence, relativistic corrections 9-13316  
 electric discharge at atmos. pressure, X-ray production 9-5094  
 electron collision cross-sections calc. 9-11427  
 electron scatt., phases from anal. of quantum defect data 9-4883  
 excitation, by e and p using Hartree-Fock wave functions, first Born approx. X-section calc., length and velocity formulations 9-4878  
 excitation, ground state to  $3^1D$  and  $4^1D$  states, by proton impact 9-726  
 excitation cross-section for He atom in slow collisions with He 9-687  
 Franck-Condon factors calc. for  $D^1\Sigma_u^+B^1\Pi_g$  band system transition prob. 9-9215  
 gyromagnetic ratio of  $2^3S_1$  atoms, opt. pumping method, level shifts 9-11423  
 Hartree-Fock eqn. for multiplets with non-orthogonal orb. 9-4875  
 implantation into olive and enstatite 9-4651  
 ion beam, stationary, 0.15 A, 75 keV, injector for prod. 9-10832  
 ion channeling in InAs, GaSb, AlSb, InSb, energy loss meas. 9-9868  
 ionic species in topside ionosphere 9-4076  
 ionization pot. rel. to SCF eigenvalue 9-4874  
 ionized, recomb. coeff. variation rel. to pressure 9-17136  
 ions, He<sup>+</sup>-Cs charge exchange collisions, 1.5-25 keV 9-4890  
 isoenergetic series, K-electron loss cross sections on collision with H and He atoms 9-907  
 liquid, 50 cm bubble chamber at Northwestern Univ. 9-460  
 liquid, 80 cm bubble chamber 9-4691  
 liquid, cryostat for resistance thermometer calibration 9-2265  
 magnetoplasma, highly-ionized, l.f. instabilities 9-902  
 metastable  $2^3S$  state, possibility of detect. in interstellar and intergalactic space 9-18878  
 metastable atom form in charge-changing collisions of He beam with H 9-5071  
 multiplets with non-orthogonal orb., Hartree-Fock eqn. and perturbation treatment, Hellmann-Feynman formula anal. 9-4875  
 neutral, in sun, u.v. reson. lines intensity calc. 9-12763  
 oleic acid multilayer permeability, obs. 9-5415  
 Omicron Andromedae variable, and H abundance 9-14218  
 orthopositronium He atom syst., quenching rate of orthopositronium, parameter  $^1Z_{eff}$  meas. 9-4888  
 p excitation, first Born-approx. X-sections, length and velocity formulations 9-4879  
 plasma, Cs and K seeded, elec. cond. calcs., effect of multispecies ionization 9-7106  
 plasma, K-seeded, MHD generation rel. to scalar elec. cond. and onset of instabilities 9-13425  
 plasma, laser-produced, collision processes in post-discharge 9-7141  
 plasma, neutralized ion beam, harmonics of ion oscillations 9-11601  
 plasma, recombination, study of afterglow 9-11547  
 plasma electron vel. generated by e beam, analysis using Boltzmann eqn. 9-13420  
 plasma expansion 9-13463  
 plasma radiation at low temps., l.f. intensity oscillations 9-7176  
 positron-He annihilation quanta, ang. correl. 9-18156  
 recombination lines, r.f. rest freq. from radioastronomy meas. 9-12732  
 scattering, elastic, from He and Ar, differential cross sections 9-727  
 single electron capture by slow H<sup>+</sup>, perturbed stationary state calc. 9-5070  
 solar abundance rel. to  $\nu$  flux 9-2075

## Helium continued

in solar wind, ioniz. stages 9-14255  
 spectrum intensity var. of galactic cosmic rays, 1963-5 obs. 9-12663  
 star atoms. early-type, non-local thermodyn. equilib. statistical mechs. 9-6123  
 stars, model atmospheres constructed, 16,000-30,000°K; He, Si spectra computed 9-8239  
 stearate multilayer permeability, obs. 9-5415  
 thermal desorption spectra, high resolution, from Re and Pt 9-11783  
 variational calc., multiplets and config. 9-4884  
 e scatt., phase shift, cross section, polarization and exchange determ., 0.04 eV 9-4882  
 Ar and Ne mixtures, thermal cond. obs. at 296.8°K 9-19584  
 atom, expectation values of correl. wavefunctions 9-14672  
 CO<sub>2</sub>-He mixture used for CO<sub>2</sub> laser, e. energy distrib. 9-18298  
 H He atom collisions, Lyman- $\alpha$  polarization, Born and distortion rot. approx. 9-13313  
 HCl-He interaction, intermol. dispersion pot. 9-20992  
 He-Ar mixtures, collision-induced absorpt. spectrum 9-2829  
 He-H<sub>2</sub> liq.-vapour equilb. at 100 atm. 9-9590  
 He-H<sub>2</sub> mixture, arc discharge, ion, atom temp. determ. by Doppler eff. 9-5096  
 He-He atomic charge exchange scatt. meas. 400-2000 e. V. 9-18158  
 He-He potential near van der Waals minimum 9-7098  
 He<sup>+</sup> He collision, elastic and inelastic X-sections at 500-3000 ev., differential scatt. meas. 9-4887  
 He Ne d.c.-laser, transitions of 2 modes to same lower level, mutual influence 9-6517  
 He-Ne discharge, population inversion distrib. rel. to He:Ne ratio, obs. 9-18312  
 He-Ne laser, 3.39  $\mu$ , state mixing effects prod. by optical freq. fields 9-2816  
 He-Ne laser, anomalous circular polarization of 1.523  $\mu$  line 9-6520  
 He-Ne laser, dynamics of optical mixing 9-12850  
 He-Ne laser, freq. fluctuations and determ. of natural width of spectral line 9-14428  
 He-Ne laser, Michelson type interferometer, deformable bodies collision processes obs. 9-20535  
 He-Ne laser, mode-coupling effects in mode-selection expts. 9-4471  
 He-Ne laser as absolute wavelength standard, problem 9-13014  
 He-Ne laser with 3 mirror resonator, radiation generation at 0.63 and 3.39  $\mu$  9-6519  
 He-Ne multimode laser, gain interaction and dynamical behaviour 9-8613  
 He-like ions, 2s2p 3P and <sup>3</sup>P states, Hartree-Fock eqns. 9-15833  
 He<sub>2</sub>, bare-nucleus and screened-nucleus perturbation theory 9-20930  
 He<sup>+</sup> excitation by electron impact, wave function expansion for  $1s-2s$  excitation cross-section 9-15834  
 He<sup>+</sup> ions scattered from semicrystalline targets, energy distributions 9-21449  
 He I, 2  $^3P$ ,  $^3P$ ,  $^3D$ ,  $^3F$  transitions, electron and ion Stark broadening 9-20899  
 He I, lifetimes of S, P and D levels 9-723  
 He I line broadening in plasma by electron impact, theory 9-21073  
 He II, damping and decay of 6560 Å line 9-723  
 He II, interference between fine structure levels, interpret. 9-20897  
 He molecular ions, drift velocities in He gas 9-919  
 He,  $^4P_{3/2}$  state autoionization, final state distortion effects 9-11615  
<sup>3</sup>He, hyperfine struct. of  $2^3P$  level 9-9159  
<sup>3</sup>He atom, fine struct. and h.f.s. of  $2^3P$  states 9-9158  
<sup>3</sup>He cryostat and ESR spectrometer relax. times 1  $\mu$  sec. meas. 0.24-4.2°K 9-4190  
<sup>3</sup>He interacting system of atoms, spin diffusion coeff. 9-6337  
<sup>3</sup>He<sup>+</sup>, PIG source for Van de Graaff accelerator 9-2355  
<sup>4</sup>He, magnetic resonance, modulated birefringence 9-2832  
<sup>4</sup>He<sup>+</sup>, Lamb shift in  $n=4$  state, quantum beats obs. from e impact 9-724  
 He<sup>+</sup> collision with Ar and Kr, optical excitation 9-6996  
 He<sup>+</sup> on Ne, scattering, analysis using differential cross-section formulae 9-9149  
 He<sup>+</sup>, role in radiative decay processes of helium 9-11425  
 HeI, first excited levels local thermodynamic equilb., validity criteria 9-11426  
 He-Ne laser with 4 mirror T form, longitudinal vibration selection 9-20518  
 He-Ne ring laser, optimum gas mixture ratio 9-15522  
 He\*-inert gas nearly adiabatic thermal collisions, excitation transfer, Stueckelberg's formula and difficulties 9-18154  
 He\*, ionizing collisions with H<sub>2</sub>, relative cross-sections for prod. of HeH<sup>+</sup>, HeH<sub>2</sub><sup>+</sup> and H<sub>3</sub><sup>+</sup> 9-7188  
 He(2S)+X→He+X<sup>+</sup>+e, collision cross-sections and Penning ioniz. 9-14675  
 He(2S) metastable atom destruction by Ar 9-13318  
 He(2s, 2p) autoionizing level, excitation 9-4887  
 ion stopping power Z depend. in arbitrary 0.5-8 MeV/a.m.u. 9-6990  
 Ne-He mixture, 6328 Å Ne line, homogeneous linewidth meas., using non-linear travelling wave interaction technique 9-2824

## gas

afterglow, low-pressure, time-depend. behaviour of 10830 Å line 9-18315  
 afterglow, mol. origin of 1.08  $\mu$  atomic line 9-19562  
 afterglow late-time light due to mutual ionization of two metastable mols. 9-13468  
 arcs, 10 atmospheres pressure, wall confined, investigation 9-11640  
 coolant, removal of H<sub>2</sub>O and CO<sub>2</sub> by cosorption on molec. sieves 9-19373  
 cooling of field ion microscope 9-6496  
 discharge, continuum rad., mol. origin 9-19562  
 discharge, positive column, elec. and optical props. rel. to press., test of theory 9-925  
 discharge ignition characts., plane electrodes, theory and obs. 9-13467  
 electron lateral diff. and first Townsend coeffs. 9-15978  
 electron mobility, up to 42 atm. 9-7167  
 excitation by protons, 1-150 keV, ground state to n'S, n'D and n'P, absolute cross-sections and polar. of collision-induced rad. 9-11424  
 gas, quantum deviations from classical behaviour, effs. of using perturbation theory 9-10643  
 He-Ne laser with mixture of Ne isotopes in gain tube, saturated absorption by neon 9-20513  
 hypersonic flow visualization by electron beam excited afterglow and fluorescence 9-21131  
 ionization, yields, X-sections and loss functions 9-5054



**Helium continued**  
**gas continued**

- ions, He<sup>+</sup> one- and two-electron loss in H<sub>2</sub>, He and Ne, 400-1500 keV 9-5072
- leak detector, sensitivity improvement by turbo-molecular pump 9-22022
- liquefaction, principles and practice 9-7294
- metastable molecules (<sup>3</sup>Σ<sub>u</sub><sup>+</sup>) and atoms (<sup>3</sup>S) in afterglow, decay 9-15832
- molecules, vel. determ. by effusion intermediate laboratory expt. 9-12823
- orthopositronium scatt. and pick-off quenching 9-4886
- plasma, discharge, mag. enhancement of He I lines, spectral series depend. 9-19530
- radiative decay processes pressure dependence 9-11425
- refractivity and dispersion, meas. method 9-21138
- relaxation length of electron temp. in positive column of glow discharge 9-17139
- Rydberg series of autoionizing states converging to n=2 level of He<sup>+</sup>, props. and energies 9-4877
- singly ionized, Stark-mixing signals in n=4 term 9-20901
- sparks, laser produced in 200 kG mag. field, obs. 9-7205
- sputter-ion pump effectiveness in He atmosphere 9-8326
- in stars, six early type, ratio with abundance 9-14206
- thermal conductivity meas. using hot-wire type of thermal diffusion column, 350-1350°K 9-5115
- thermal diffusion in H<sub>2</sub>-He mixtures 9-17168
- thermometer determ. of thermodynamic scale, -183° to +100°C 9-17829
- thermophysical props. 3-300°K, 0.5-100 atm. 9-7293
- twilight emission rel. to geomagnetic activity, excess in winter hemisphere 9-1951
- vapour press. bulb, thermal relax. obs. 9-13563
- e bombardment excitation, transitions obs. 3230-20582 Å 9-6994
- CO<sub>2</sub>-N<sub>2</sub>-He laser, output 80W 9-17869
- Fe emission line shift, obs. 9-6963
- He-N<sub>2</sub> mixture, coeff. of thermal diffusion determ. 9-19590
- He-Ne, 6328 Å laser, incorporating Ne absorption, single-mode power 9-20514
- He-Ne active discharge, radial profile of Ne 1s<sub>2</sub> atoms and lens effect on lasing at 6401 Å 9-20520
- He-Ne amplifiers, optical regenerative of passing type, amplification coeff. and bandwidth 9-8615
- He-Ne d.c. laser, transitions of 2 modes to same lower level, mutual influence 9-6516
- He-Ne intensity of single-mode as a function of cavity Q deviations explicitly-Lamb theory 9-8617
- He-Ne laser, atomic collisions with impurity gas (Ar, Kr or Xe) 9-19145
- He-Ne laser, competing-wavelength interaction 9-10862
- He-Ne laser, emission line intensities modification rel. to population inversion, obs. 9-17873
- He-Ne laser, nonlinear absorpt., mode selection and self-locking 9-13015
- He-Ne laser, oscill. freq. shift by discharge current increase 9-6518
- He-Ne laser, power saturation at 6328 Å 9-2375
- He-Ne laser, transition linewidths, meas. vid mag. resonance 9-10861
- He-Ne laser in confocal split resonator, mode formation and selection 9-8596
- He-Ne laser mode self-locking obs. 9-8602
- He-Ne laser tubes, negative Faraday effect obs. at 3.39 μ 9-4470
- He-Ne lasers, discharge tube, low-noise, for elimination of discharge modulation noise 9-20517
- He-Ne lasers, single-mode oscillations, buildup at excitation levels significantly above threshold 9-20516
- He, liquifier construction and operation 9-11731
- He<sup>+</sup> in N<sub>2</sub>, charge and dissociative charge-transfer proc., rate consts. from drift data 9-15956
- He<sup>+</sup>+2He→He<sub>2</sub><sup>+</sup>+He, charge and dissociative charge-transfer proc., rate consts. from drift data 9-15956
- He I line intensity meas. of electronic temp. 9-5042
- <sup>3</sup>He in electric discharge in mag. field, nuclear polarisation meas. 9-9417
- <sup>4</sup>He, pair distrib. function, three-particle effects 9-7225
- He<sup>+</sup> form. by e impact on He 9-5062
- He<sub>2</sub>, excitation of band spectrum in discharge and recombination 9-5082
- K scatt. in thermal energy range, total cross section meas. 9-11413
- laser, He-Ne beat frequency between axial modes, variation with cavity Q 9-8616

**liquid**

- See also Quantum fluids; Statistical mechanics/quantum; Superfluidity*
- applications to superconducting magnets, accelerators, bubble chambers, and pumping 9-8318
- conductivity, thermal near superfluid transition critical exponent 9-1054
- critical phenomena, dynamical 9-9575
- dielectric breakdown 9-1055
- films, Bose-Einstein and hard sphere gas models 9-3142
- films, unsaturated, superfluidity without superflow 9-19653
- heat capacity obs. by differencing method 20-150 m°K 9-13548
- liquefaction, principles and practice 9-7294
- neutron scatt. at large energy and momentum transfers 9-1052
- optical processes, theory 9-11734
- optical windows of fused silica for Dewar 9-7290
- phonon dispersion from hydrodynamic Hamiltonian 9-5203
- refrigeration, dilution, principles and methods 9-8320
- resources, production, conservation 9-7291
- safety in handling 9-7296
- second critical velocity in narrow annulus 9-1057
- storage, distribution and handling 9-7295
- superfluid, critical flow rate through narrow pores 9-11737
- superfluid, density, temp. depend. eqn. for 1.2°K≤T<T<sub>λ</sub> 9-7297
- superfluid, energetic neutral excitation, prod. of charged part. at surface 9-11735
- superfluid, energy dissipation in flow, critical vel. obs. 9-11736
- superfluid, hard-sphere Bose gas model 9-3143
- superfluid, possibility of two critical velocities 9-2959
- superfluid, rot., trapped negative ions mobility on vortices, 0.8-1.6°K 9-5207
- superfluid, rotating, escape of trapped ions at <1°K 9-14878
- superfluid rotating, lifetime of trapped -ve ions meas. 9-9582
- superfluid rotating under press., trapping lifetime of negative ions 9-13551
- temperature controller, integrated semicond. circuits 9-11733
- temperature meas. with Ce-Mg nitrate powder and single-cryst. mag. thermometers 9-172
- theory, at zero temp. 9-14877

**Helium continued**  
**liquid continued**

- thermophysical props. 3-300°K, 0.5-100 atm. 9-7293
- vortex line, quantized, model for core 9-9580
- vortex ring creation by positive ions, 1.0°-1.5°K, critical vel. 9-9579
- vortices, quantized lines and rings, model many-body wave functions, energy and velocity calc. 9-11732
- asn polarimeter 9-4645
- conductivity, thermal, size depend. near λ point 9-1053
- He<sup>3</sup> in He<sup>4</sup>, dilute mixture, applic. of soln. of Boltzmann eqn. 9-14367
- He I, thermal conductivity, rel. to second sound velocity in He II and scaling laws near superfluid transition 9-11739
- He II, critical heat flux close to λ transition 9-18378
- He II, density increase due to turbulent flow 9-5208
- He II, e bubble mobility, calc. 9-9581
- He II, fluctuations and correlations, review 9-21238
- He II, stimulated Mandelstam-Brillouin scatt. 9-14879
- He II, superfluid, applic. of thermodynamic stability criterion 9-18377
- He II, thermal expansion, 0.85-2°K, from capacitance meas. 9-16028
- He II negative ion mobility obs. T≤0.5K, inelastic phonon scatt. contrib. 9-1059
- He II size effects on transition temp. shift, sp. ht. and superfluid density near T<sub>λ</sub> 9-21236
- <sup>3</sup>He, ion mobility near critical pt. 9-7292
- <sup>3</sup>He, Landau theory of transport coeffs., finite temp. corrections 9-12902
- <sup>3</sup>He, transition studies rel. to molar volume and thermal expansion coeffs. 9-13552
- <sup>3</sup>He in <sup>4</sup>He, dilute solns., effect of mag. field on osmotic pressure 9-11730
- <sup>3</sup>He solid/liquid mixture, adiabatic compression, cooling to 2.5 mK 9-21234
- <sup>3</sup>He spin-wave spectrum, paramagnon model 9-5206
- <sup>3</sup>He surface phenomena at zero temp. 9-104
- <sup>4</sup>He, ground-state struct. factor and sound vel., calc. 9-5205
- <sup>4</sup>He, ground state calc. by variational methods 9-9577
- <sup>4</sup>He, logarithmic corrections to theory of λ-transition 9-16029
- <sup>4</sup>He, transition studies rel. to molar volume and thermal expansion coeffs. 9-13552
- <sup>4</sup>He, viscosity, 14-31°K and pressures up to 100 atm. 9-1056
- <sup>4</sup>He and metal boundary, Kapitza resistance, review 9-18379
- He<sup>3</sup> dilute sol. in superfluid He<sup>4</sup>, thermal conductivity meas., 0.035-0.5°K 9-3145
- <sup>3</sup>He/<sup>4</sup>He dilution refrigerator 9-16646
- <sup>3</sup>He-<sup>4</sup>He derivative of <sup>3</sup>He mass w.r.t. pressure 9-13549
- <sup>3</sup>He-<sup>4</sup>He mixture, phase separation curve and molar density obs. at SVP, 0.024-1.25°K 9-9578
- <sup>3</sup>He-<sup>4</sup>He mixture vol. occupied by <sup>3</sup>He atom in liquid <sup>4</sup>He 9-13549
- <sup>3</sup>He-<sup>4</sup>He mixtures, at low temp., limiting solubility at 0°K 9-13549
- <sup>3</sup>He-<sup>4</sup>He mixtures at critical pt., hydrodynamic modes and damping 9-11729
- <sup>3</sup>He-<sup>4</sup>He solutions, thermodynamic props. during HeI-He II transition 9-9576
- <sup>3</sup>Hein<sup>4</sup>He, dil. solns., osmotic pressure theory 9-9574
- HeII, critical heat flux near λ-transition 9-1058
- HeII, mutual friction near superfluid transition, evidence from heat flow obs. 9-11738
- HeII vortex energy near boundary, critical vel. and supercritical flow 9-13550
- <sup>3</sup>He-<sup>4</sup>He interface, surface tension 9-18376
- <sup>3</sup>He-<sup>4</sup>He mixtures, light scatt. by entropy fluctuations and second sound 9-5204
- II, atomic admixtures, adsorpt. on quantized vortices 9-1060
- refrigerations, survey 9-8321

**liquid, sound propagation**

- critical region second-sound vel. 9-5209
- hypersonic absorpt. at ~650 MHz, optical method 9-14876
- second-sound damping in T<sub>λ</sub> region 9-3146
- superflowing film critical vel. determ. by third sound 9-21237
- superfluid Helmholtz resonator, master eqn. 9-4337
- He II, excitation by light waves 9-14879
- He II, second sound obs. from critical heat flux close to λ transition study 9-18378
- He II, second sound velocities near τ<sub>1</sub> 9-7298
- He II second sound velocity rel. to thermal conductivity in He I and scaling laws near superfluid transition 9-11739
- <sup>4</sup>He, vel. meas., 2nd virial coeff. of gas determ. 9-21235
- <sup>4</sup>He, velocity rel. to density 9-9577
- <sup>4</sup>He velocity and ground-state struct. factor calc. 9-5205
- <sup>3</sup>He-<sup>4</sup>He solns., second sound 9-1061
- <sup>3</sup>He-<sup>4</sup>He solution, in narrow channels, vel. and absorpt. coeffs. of first, second and fourth 9-13553

**solid**

- crystal, second sound and temp. pulse propagation obs. 9-16030
- quasicrystal approx., ground state energy calc. 9-13555
- <sup>3</sup>He, b.c.c. and h.c.p., Debye-Waller factor with short range correlations 9-5212
- <sup>3</sup>He, melting curve to 12 m°K 9-19652
- <sup>3</sup>He crystals, spin Hamiltonian, exchange and nuclear relax. 9-21240
- <sup>3</sup>He with <sup>4</sup>He impurity variational calc. of exchange constant and thermal conductivity 9-13554
- <sup>4</sup>He, b.c.c., instability modes prior to melting 9-1063
- <sup>4</sup>He, b.c.c. and h.c.p. Debye-Waller factor with short range correlations 9-5212
- <sup>4</sup>He, h.c.p., high density, thermal conductivity, 1.1-7°K 9-21239
- <sup>4</sup>He, h.c.p., phonon spectrum, 1.0°K 9-5211
- <sup>4</sup>He, h.c.p., self-consistent phonon spectrum calc. 9-9818
- <sup>4</sup>He, melting curve below 300 m°K 9-19652
- <sup>3</sup>He-<sup>4</sup>He mixtures, isotopic phase separation temp. 9-1064
- <sup>3</sup>He-<sup>3</sup>He dilute solns, mag. susceptibility 9-1062

**Helium compounds**

- Cu-He alloys, stress-rupture characts. rel. to grain boundary degeneration 9-16133
- He-Ar, gaseous, heat of mixing, 170-2930°K 9-954
- He-Ar gaseous mixtures, excess enthalpy at high densities 9-955
- He-methane, gaseous, heat of mixing, 170-2930°K 9-954
- He-methane gaseous mixtures, excess enthalpy at high densities 9-955
- HeH<sup>+</sup>, bare-nucleus perturbation calc. 9-9214
- HeH<sup>2+</sup>, ground-state energy, perturbation calc., comparison of two results 9-2870
- HeH<sup>2+</sup> and HeH<sup>+</sup>, one-centre MO's with variable origin 9-13359

**Helium-3**

- polarization meas. using optical method 9-6712  
solid, nuclear spin exchange interaction effect on dynamic nuclear polarization 9-1719  
Fermi liquid, Landau parameter estimated from quasiparticle transport eqn.  $T \rightarrow 0$  9-106

**interactions**

- permalloy films, irradiated effects on anisotropy-field inhomogeneity and coercive force 9-7908

**scattering**

- elastic, from react. of light nuclei, ang. distrib., opt. model analysis, eff. of spin-orbit term 9-9063  
metastable atoms, diffusion and excitation transfer during collisions 9-6995

**Hellmann-Feynman theorem** *see Quantum theory***High voltage techniques**

- Cockcroft-Walton voltage multipliers with arbitrary number of stages, anal. 9-17850  
piezoelectric power supply for i.r. image converter tube 9-10751  
power supply for scanning e microscopes 9-2347  
pulse generator, ceramic thyatron, for use with wire spark chambers 9-8943  
pulse generator, coaxial cable discharge 9-2304

**High-pressure phenomena and effects**

- apparatus for phase transformation expts. 9-17338  
aromatic hydrocarbons, fluoresc. lifetimes 9-14084  
autoclave, with Ar atm. for use up to 4500b and 1600°C 9-6234  
crystal growth system 9-21292  
crystallization from melt 9-3236  
edge zone yielding in pressure vessels 9-17775  
Electronic structure calcs. using Wigner-Seitz cell method and polymorphic transitions 9-5614  
EPR spectrometer for work up to  $10^4$  kg/cm<sup>2</sup> 9-10783  
force generation by Slyphon bellows 9-4192  
gas, pressure > 12kbar, temp., > 700°K, comparative anal. of calc. methods 9-21133  
halonaphthalenes, phosphoresc. decay in polymethylmethacrylate 9-17491  
hemin, Mossbauer effect 9-9202  
infrared high-pressure cell for liq./gas chem. react. 9-22019  
isopentane, refractive index 9-5170  
leak detection in high pressure gas system by <sup>85</sup>Kr 9-12806  
liquid dielectrics, permittivity at 30° and 50°C, pressure depend. 1-750 kg/cm<sup>2</sup> 9-17215  
luminescence studies of solids, apparatus 9-7954  
mesitylene, refractive index 9-5170  
metal, h.c.p., strength and ductility obs. 9-5478  
metals, self-diffusion 9-3384  
microbomb, multipurpose, for applic. of hydrostatic pressure up to 11 kbar 9-6235  
naphthalene fluoresc. in polymethylmethacrylate 9-12477  
piston-cylinder balance performance 9-12807  
plugs for introducing current leads into high pressure vessels 9-6236  
polymers, amorphous, glass-forming, 40 kbar and 300°C 9-3178  
polymers, solid organic 9-21366  
powders, compaction, effect on ejection pressure 9-5476  
on propylene radical polymerization kinetics 9-17521  
rocks and minerals, physical properties 9-12572  
seal between CaF<sub>2</sub> and steel at high temp. 9-6233  
steel, tensile fracture behaviour 9-18518  
steel powder pressing 9-17339  
on styrene, cation polymerization kinetics 9-17521  
tensile testing of soft crystals 9-7560  
triglycine sulphate, ferroelec. phase transition, and elec. field. effect 9-1598  
on trioxane polymerization in solid state 9-17521  
on X-ray interference intensities 9-5294  
Al, thermoelectric power and resistance, up to 4 kbar 9-16306  
Ar, electron mobility up to 42 atm. 9-17167  
Ar, simple- and cluster-ion mobility obs., 1-100 atm. 9-18310  
Au, thermoelectric power and resistance, up to 4 kbar 9-16306  
Cs, polymorphic transitions and electronic structure calcs. using Wigner-Seitz cell method 9-5614  
Cu-Al alloys, phase transformations and equilibria 9-19837  
Fe phthalocyanine, Mossbauer effect 9-9202  
Fe<sub>2</sub>(CO)<sub>9</sub> and Fe<sub>3</sub>(CO)<sub>12</sub>, Mossbauer effect 9-10183  
H<sub>2</sub>, electron mobility up to 42 atm. 9-17167  
H<sub>2</sub>SO<sub>4</sub> solns.,  $\gamma$ -radiolysis 9-10361  
He-H<sub>2</sub> liq. vapour equilib. at 100 atm. 9-9590  
He, electron mobility up to 42 atm. 9-17167  
Hg differential manometer 9-6272  
Hg equation of state and elec. resistivity 9-3075  
Hg melting curve up to  $15 \times 10^8$  N/m<sup>2</sup> 9-9589  
HgTe phase transition, Ge impurity eff. 9-11966  
In alloys, Ginzburg-Landau parameters, pressure depend. 9-7881  
K, polymorphic transitions and electron structure calcs using Wigner-Seitz cell method 9-5614  
KNO<sub>3</sub>, III-II transition 9-9803  
<sup>85</sup>Kr, leak detection in high pressure gas system 9-12806  
N<sub>2</sub>, electron mobility up to 42 atm. 9-17167  
N<sub>2</sub>, microwave absorpt. 9-9455  
Ni, thermoelectric power, up to 4 kbar 9-16306  
Pt, thermoelectric power, up to 4 kbar 9-16306  
Rb, polymorphic transitions and electron structure calcs. using Wigner-Seitz cell method 9-5614  
Sn, superconducting, effect on energy gap 9-12129  
SnO<sub>2</sub>, cassiterite powder, elec. cond., press. depend. to 90 kg/cm<sup>2</sup> 9-13877  
Sr, metal-semiconductor transition 9-18605  
U, irradiated, annealing in NaK under high hydrostatic press. and temps., technique 9-19824  
Y, metal-semiconductor transition 9-18605  
ZrO<sub>2</sub>, phase transition, high-pressure induced 9-19840

**High-speed photography** *see Cinematography; Photography/high speed***High-temperature phenomena and effects**

- furnace attachment for X-ray goniometer 9-5298  
investigation using laser beam interaction 9-20531

**High-temperature phenomena and effects continued**

- measurement diagrams from Stark effect shifts in plasma spectral lines 9-8539  
metals, structural changes, apparatus 9-3247  
phase diagrams, equipment and techniques development 9-7618  
quartz, critical, opalescence, obs. and interpretation 9-10181  
refractory metals, vapour press. meas. in shock tube 9-9596  
seal between CaF<sub>2</sub> and steel at high pressure 9-6233  
virial coeff., second, quantum corrections 9-17746  
wires, enamelled, dielec. breakdown after damp storage 9-7842  
Hg equation of state and elec. resistivity 9-3075  
O<sub>2</sub> detection in laboratory furnaces with Zr strip 9-8316  
U, irradiated, annealing in NaK under high hydrostatic press. and temps., technique 9-19824  
ZrB<sub>2</sub> protective sheath for thermocouples, production 9-15483

**History**

- accomplishments of six scientists having anniversaries in 1969 9-12821  
of architectural acoustics 9-4361  
Boskovic, R.J., (1748), solid state theory 9-16034  
Copernican theory described 9-15333  
measurements at NPL, review 9-8346  
navigational instruments (1918-68) 9-2107  
Newton's math. and 'Principia' 9-15400  
Poincare, and his math. contributions to relativity 9-15399  
quantum chemistry, inception 9-10306  
relativity, influence of Poincare 9-6248  
Romer's meridian circle described 9-15373  
semiconductor investigations at Leningrad Physicotechnical Institute from 1918 9-7785  
Stonehenge, its astronomical purpose 9-15265  
x-ray wavelength x unit 9-4214

**Hodoscopes** *see Cosmic rays/apparatus; Particle detectors***Hole theory of liquids** *see Liquids/theory***Holes** *see Crystal electron states; Semiconducting materials; Semiconductor***Hollow cathode** *see Discharges, electric***Holmium**

- elastic moduli and u.s. attenuation rel. to mag. transitions 9-7517  
hyperfine interactions from specific heat meas., 0.03-0.5°K 9-21600  
nuclear magnetic dipole moment 9-15821  
silicate glass coactivation with Er and Yb 9-4476  
u.s. attenuation in helical spin state, inc. below Neel temp. 9-1379  
Ho<sup>3+</sup> in CaF<sub>2</sub>, optical emission following X-irrad. 9-21657  
Ho<sup>3+</sup> in CaF<sub>2</sub>:Eu<sup>2+</sup>, Ho<sup>3+</sup>, fluorescent decay of Eu<sup>2+</sup>, Ho conc. dependence 9-15187  
Ho<sup>3+</sup> ion in silicate glass, laser action 9-4476  
in Ho<sub>2</sub>Sm<sub>1-x</sub>FeO<sub>3</sub>, orthoferrites, exchange interaction effect on ordering of ions 9-16371

**Holmium compounds**

- Ho (80 wt.%)Tb alloy single crystal, antiferromagnetism 9-16377  
Ho-Gd alloy, ferromag., <sup>165</sup>Ho n.m.r. 9-16464  
Ho Fe garnet, Faraday effect, effect of mag. field 9-1740  
Ho ferrite garnet, Faraday effect and reversal of mag. sublattices 9-1739  
HoAl, n.m.r. of <sup>27</sup>Al, Knight shift and susceptibilities, temp. 9-3969  
HoCl<sub>3</sub>,  $\beta$ - $\gamma$  correlation, attenuation factor, solid and liquid, comparison 9-560  
HoCl<sub>3</sub>, differential mag. susceptibility, transition at T=2.15°K 9-7880  
HoFeO<sub>3</sub>, absorpt. spectra, near i.r. T=1.2, 4.2, 20 and 77°K 9-21624  
Ho(La)Cl<sub>3</sub>, differential mag. susceptibility, obs. of phonon-bottleneck 9-7880  
HoN, specific heat 9-5567  
Ho<sub>2</sub>Sm<sub>1-x</sub>FeO<sub>3</sub> orthoferrites, exchange interaction effect on ordering of Ho ions 9-16371  
Ho(Y)Cl<sub>3</sub>, differential mag. susceptibility 9-7880  
HoZn<sub>3</sub>, crystal structure 9-3295  
Sc Ho alloys, mag. structure comp. dependence 9-5802

**Holography**

- aberrations 9-16790  
acoustic, historical development and appl. 9-2388  
acoustic, with scanning source and stationary point detector 9-8633  
aerosol size and vel. distrib., holographic technique 9-18375  
binary holograms, synthesis from three-dimens. objects by Fourier-transform method 9-20536  
bioholography, model of information processing 9-14441  
chromatism, two-lens corrector 9-17884  
coherence limitations 9-10881  
computer synthesis of holograms for 3-D display 9-251  
contour map of diffusely reflecting surface, generation using immersion method 9-2390  
current profile meas. appl. 9-15537  
diffraction gratings, bleaching for max. efficiency 9-19157  
double exposure, use for study of self-trapped laser beams 9-13035  
double-exposure interferometry with separate ref. beams 9-4494  
emulsions, method reducing movement during processing 9-13037  
emulsions, thick photographic, colour and directional selectivity, second wave suppression 9-253  
extended source holograms, compensation 9-6535  
Foucault knife edge test for optical elements of arbitrary design 9-2417  
Fourier, luminosity obs. 9-2391  
and Fourier transform spectroscopy 9-270  
high index fringe recording in hol. reconstruction of vib. plates 9-4291  
hologram exposure times reduction 9-2403  
hologram making and reconstruction 9-6536  
hologram microscopy, carrier suppression and restoration 9-20537  
holograms, storing on photochromic films 9-13036  
hyperstereoscopic and hypostereoscopic hologram images 9-10874  
image brightness increase by using density relief of photographic emulsion 9-10877  
image depth contours generation 9-8631  
image of diffuse object, effects on film nonlinearities 9-10875  
image radiance, comparison of expt. and theoretical values 9-10876  
and integral photography 9-20534  
interference microscope applics. 9-4493  
interferogram with longitudinally reversed shear, theory 9-20545  
interferograms, multiple display techniques 9-4515  
interferograms of laser induced spark 9-5092  
interferometer for photoelastic stress analysis 9-6365  
interferometry, for vibration analysis of sonar transducer 9-4353



**Holography** continued

- interferometry, time-averaged, for visualiz. of standing acoustic waves 9-10738
- interferometry using two reference beams 9-4495
- laser light field, spatial distribution, reconstruction 9-20539
- lens images correction 9-8632
- for light diff. by u.s. waves investigation 9-2406
- Lippmann-Bragg holograms of >10% efficiency 9-10878
- microscopic three-dimens. sample reconstruction 9-4492
- multiple and single exposure, diffraction efficiency comp. 9-2387
- negative image reconstruction 9-4491
- noisy images, optimum nonlinear processing 9-14450
- optical and x-ray, multiplexing and three-dimens. reconstruction 9-2389
- optical filter synthesis 9-10924
- optical imaging systems achieving aperture synthesis from non-conventional optics by a posteriori lensless Fourier-transform holography 9-15539
- phase holograms recording in dichromated gelatin 9-10873
- photographic film (Agfa-Gevaert type 10E70), characts. 9-4545
- reconstruction in back diffraction field 9-14442
- reflexion microscopic, technique 9-6534
- review 9-252
- scatter-plate, three beam 9-20538
- scene motion eff. on image, fringe position feedback control 9-10880
- sound instead of light 9-17883
- source scanning 9-10879
- speckle noise, elimination in holograms with redundancy 9-4490
- spectra obtained with Lloyd's mirror 9-4496
- stereo-radiography using holog. techniques 9-14440
- stroboscopic holographic interferometry for vibr. analysis 9-8634
- sub-micron particle detection 9-16789
- surface wave, inhomogeneous, reconstruction and interference 9-15538
- three-beam using scattering to divide beam 9-20538
- three-dimens., scatter plates appls. 9-2404
- transmission of holograms using television channel 9-8635
- transparent objects, holograms 9-4489
- unfiltered radiation holograms, from Hg and incandescent lamp 9-20540
- vibration meas., verification of holographic technique 9-4285
- wave front freqs. spatial to temporal conversion and reconversion 9-8649
- wavelength selective reconstruction in new type hologram 9-8636
- X-ray, three-dimensional 9-12781
- $\text{Bi}_4\text{Ti}_3\text{O}_{12}$  crystals, optically induced refractive index changes, obs. with internally formed holograms 9-19976
- Cd spectra from holograms obtained with Lloyd's mirror 9-4496
- Hg spectra from holograms obtained with Lloyd's mirror 9-4496
- $\text{LiNbO}_3$ , as holographic storage medium 9-15536
- $\text{LiNbO}_3$ , holographic storage medium 9-15536

**Hot-atom chemistry** *see* **Chemical analysis/radioactive; Nuclear reactions and scattering/chemical effects; Radiochemistry****Hubble model** *see* **Cosmology****Hugoniot diagrams** *see* **Equations of state****Humidity**

- See also Atmosphere/humidity; Hygrometers; Moisture*
- adiabatic saturation psychrometer 9-935
- diffusion into insulating material in form of plate 9-1239
- gas mixture, determ. from i.r. absorption spectra 9-4915
- organic foil particle detector sensitivity effect 9-20710
- $\text{SeO}_2$  electrolytic probe 9-4174
- $3 \text{ ZnO} \cdot \text{P}_2\text{O}_5 \cdot 4\text{H}_2\text{O}$  (hopeite) cryst. cements, effect on growth from  $\text{ZnPO}_4$  9-3233

**Hydrodynamics**

- See also Flow/liquids; Jets; Liquid oscillations; Liquid waves; Magneto-hydrodynamics; Viscosity/liquids*
- advances, review 9-15241
- Boltzmann linearized eqn., initial and boundary conditions, normal solns. 9-19498
- commutation relation 9-15912
- convective flow, steady; instability variation with angle w.r.t. gravity 9-12949
- convective instabilities, penetrative 9-11519
- Couette flow, normal mode expansion, stability and perturbation bound 9-21022
- detonations in solid explosives, fluid-dynamic eqns with changing co-ordinate system 9-12943
- drag-reduction by fine suspensions, vortex stretching mechanism 9-19591
- ducts, contracting, throat profiles, containing incompressible, irrotational flows 9-21153
- electrohydrodynamic waves 9-9311
- equations of grad-type, statistical derivation 9-3036
- evolution criterion for dissipative mechanically reversible processes 9-21148
- film, interfacial, surface tension and shear force effects 9-18348
- fluids, viscous, non-homogeneous, in container, decay of oscills. 9-18248
- gas bearings, stability 9-7103
- high polymer molecules, mechanical entanglements 9-19488
- high-temperature phenomena, and physics of shock waves, book 9-11645
- hydroelastic forces on bluff cylinder in flow 9-9313
- hydrofoils in cascade, fully cavitated, Munk's integral appl. 9-13506
- inviscid, homogeneous liq. in cylindrical tank with flexible bottom 9-21149
- laminar flomber 9-17171
- layered global system in gravity field 9-16520
- liquid motion in turbomachines, three-dimens. field 9-21150
- Navier-Stokes eqn., analyticity and unique continuation theorem 9-9312
- non-conservative system, equations 9-9310
- non-linear flow, soln. through elec. analogue 9-48
- non-Newtonian, disperse systems 9-18373
- non-viscous fluid, post-Newtonian eqn. in Brans-Dicke theory applic. to dynamic instability problems 9-19497
- polymer solns., bead and spring model 9-7255
- pressure field, subsonic inviscid stream flowing through roughened wall ducts 9-3042
- ray theory in Cauchy problem 9-965
- relativistic motion of fluids, eqn. with stress force term. 9-7099
- Reynolds no. similarity argument, in pipe and channel flow 9-18240
- rotating fluid, contained and unbounded, theory, book 9-11521
- rotating fluid, Kelvin-Helmholtz stability problem, correction to soln. of eigenvalue eqn. 9-17088
- scalar, classical particle system 9-21000

**Hydrodynamics** continued

- second order fluid, stability between two concentric cylinders 9-7101
- slow rotation of sphere about a diameter parallel to plane wall, Stokes flow solns. 9-19499
- solid, heavy, moving in fluid, integrable cases 9-18231
- space-periodic motions 9-2939
- sphere in fluid, coupled translational and rot. motions 9-3066
- sphere moving along axis of cylinder containing viscous liquid 9-17169
- sphere moving unsteadily along circular path in viscous fluid, forces acting and eqn. of motion 9-19618
- spherical structure in viscous fluid with one degree of freedom, motion 9-21152
- stability loss in nucleate bulk boiling, effect of viscosity of liq. phase 9-7305
- stratified fluid, wake collapse scaling characts. 9-4988
- supersonic jet, impact on flat plate 9-18234
- surf board behaviour 9-7239
- surface wave in conducting fluid obs. using microwave resonator method 9-2941
- tube, steady motion of incompressible fluid 9-18334
- vector potential and boundary conditions for incompressible flow 9-18242
- velocity profiles, heated rotating annulus 9-966
- viscous fluid, flow past flat plate, boundary layer approx. neat trailing edge 9-967
- wake behind inclined flat plate at arbitrary angle of attack 9-17170
- wake examples, undergraduate level book 9-22
- $\text{D}_2\text{O}$ , modes of motion study by slow-neutron inelastic scatt. 9-13500
- $^4\text{He}$  liquid, phonon dispersion from hydrodynamic Hamiltonian 9-5203
- $^3\text{He}$ - $^4\text{He}$  mixtures at critical pt., hydrodynamic modes and damping 9-11729
- Hg wave, oscillation and damping frequency, Navier Stokes eqn. 9-2942

**Hydrogen**

- See also Deuterium; Protons and antiprotons; Tritium*
- accumulation at stacking faults in Al on dechannelling of protons 9-16102
- adsorbed isotopes, hindered rot., quantum-statistical partition function 9-13586
- adsorption on Mo, study by field emission retarding potential analyser 9-11782
- adsorption on W, field-emission patterns of phases 9-19677
- adsorption on W by field-emission patterns 9-5775
- atom,  $\text{H}_2$ , test of Stark-broadening, high electron density 9-714
- atom, relativistic model, helicity symmetry group  $\text{SU}(2)$ , Dirac quantum no. double degenerate 9-6571
- atom  $\text{H}_2$  test of Stark-broadening, high electron density 9-715
- atoms and ion, bibliography of spectra 9-13287
- bond, weak, effect of lone-pair hybridization on stability 9-2887
- bond distances in cry., rel. to i.r. stretching freq. 9-11449
- bubble chamber, limit of sensitivity 9-8942
- as buffer in water vapour sub-mm. laser 9-20512
- charge exchange with He beam leading to metastable He atoms 9-5071
- chemisorption on diamond, heat of wetting, e.s.r. and i.r. spectrum 9-8083
- chemisorption on Nb (110) surface, LEED exam. 9-15215
- compressed, scattering and broadening of intense laser radiation spectrum 9-13291
- cryogenic pumping in ultrahigh vacuum systems 9-6238
- discharges, <1 atm., and h.f. electron torch, ionization mechanism, obs. 9-19599
- electrolytic charging of electroplated Ni, effect on magnetocrystalline anisotropy 9-15152
- electrolytic charging of Nb in prep. of pure Nb-H 9-13750
- environment for slow crack growth in steels 9-5484
- galactic HII regions, ionized, temp. struct. and emission props. 9-8233
- gas mixture  $\text{H}_2$ - $\text{N}_2$  separation in supersonic jet 9-21145
- glow discharge, cathode pot. drop, theory and obs. 1mm Hg obs. 9-13466
- glow discharge, H-ion comp. in positive column 9-15962
- implantation into olivine and enstatite 9-4651
- impurity in He discharge tube, removal by gettering and pumping 9-3021
- ion beam, stationary, 0.5 A, 115 keV, injector for prod. 9-10832
- in ion source with hot filament, behaviour at press. near  $10^{-11}$  Torr rel. to appl. as meas. instrument 9-10591
- ioniz. transitions, use of Franck-Condon factors 9-4934
- ionization, yields, X-sections and loss functions 9-5054
- ionization and fragmentation by 5-45 keV protons, mass spect. investigation, X-section meas. 9-5060
- ionized, Boltzmann eqn. suitability for thermal conductivity calc. 9-14814
- isotope effects, test for chem. kinetics transition-state models 9-12525
- Knight shift for adsorbed atoms on Pd 9-17505
- laser effects in  $\text{H} + \text{Cl}_2$  or  $\text{NOCl}$  reactions 9-6521
- lines in gaseous nebulae, eff. of self-absorption and internal dust on intensities 9-20163
- liquid, dielectric phenomena 9-1036
- maser oscillations with external gain 9-10849
- migration of second layer in W, with trapping on first layer sites 9-11900
- $n\sigma$  lines, 28 obs. from Orion nebula, electron temp. determ. 9-16564
- in nebulae, diffuse and H II regions  $\text{Ly}-\alpha$  transfer 9-6117
- parahydrogen, 77°K, e drift and diff. 9-9405
- permeation rate through Pd-Alg alloy tube for ion sources 9-21353
- plasma, infinite column, press. increase and total thermal cond. calc. 9-11540
- plasma, thermal conductivity meas. in transverse mag. field, 10,000-50,000°K 9-7139
- plasma decay parameter meas. 9-7168
- plasma radial temp. distrib. by photoelec. spectroscopy in visible region 9-21051
- recombination lines, r.f. rest freq. from radioastronomy meas. 9-12732
- reduction of hematite dense sphere, rate calcs. using mathematical model 9-20046
- scattering, low energy, at metal surface 9-2828
- solid, equation of state, quantum theory 9-19850
- solid, high density,  $10^4$  to  $10^6$  g/cm<sup>3</sup>, possible nuclear ferromagnetism 9-21582
- solid, para-ortho transitions 9-1345
- solid, phase transition, intermolecular interactions, Ising model 9-3492
- solid metallic phase, possible high temp. superconductor 9-9956
- solid phase transitions at higher temps. 9-11789

**Hydrogen continued**

- solubility, solid, in  $\alpha$ -Zr, obs. 9-16148  
 solubility in pure Al, 400 600°C, validity of square root law 9-9787  
 solubility in Zircaloy-4, rel. to dissolution kinetics of hydride platelets 9-17336  
 spectral line widening by plasma electrons 9-2010  
 in transition metals, high-melting, gaseous impurity effect on brittleness temp. dependence 9-1309  
 W49 Zr-source, neutral H line reduced brightness at  $\lambda=21$  cms 9-2035  
 in Zr-Se alloys, effect on mech. props. 9-19805  
 $\pi^-$  capture in chem. cpds. 9-14505  
 9-1584  
 H<sub>2</sub>-He mixture, arc discharge, ion atom temp. determ. by Doppler eff. 9-5096  
 H<sub>2</sub>-He mixture press.-induced i.r. spectrum, vel. and force correlations, deriv. of moment relations 9-9203  
 H-O, explosive mixture, transverse flame-shock interactions 9-1901  
 H-O mixtures, detonation propagation in supersonic flow 9-19582  
 H-O mixtures, speed of products of detonations 9-10743  
 H<sub>2</sub>-O<sub>2</sub> Ar mixtures, detonation initiation by incident shock waves, reaction mech. 9-14128  
 H<sub>2</sub> solid below 4.2°K, mol. motion, NMR meas. 9-1118  
 H<sup>+</sup> and H from impulse source, intensity increase 9-20496  
 H atomic beam oscillator with multichannel source output 9-4450  
 H II regions, galactic, southern hemisphere, 5 GHz continuum obs., 28 maps 9-15280  
 H II regions, IC 1805 and 1848, low-freq. absorption 9-20166  
<sup>1</sup>H, at. mass using high resolution spectrometer 9-11414  
 H<sup>+</sup> irradiation of metal oxides, darkening 9-12370  
 H<sub>1</sub><sup>+</sup> transformation to high energy neutral atoms in supersonic Li vapour jet 9-4445  
 H<sub>2</sub>, molecular vacuum u.v. laser theory 9-15521  
 o-H<sub>2</sub> solid, f.c.c., orientational thermodynamics 9-1390  
 H<sub>2</sub> permittivity at resonance frequencies 9-3057  
 H<sub>2</sub> permittivity at resonance frequencies 9-13494  
 H<sub>2</sub><sup>+</sup> transformation to high energy neutral atoms in supersonic Li vapour jet 9-4445  
 H<sub>3</sub><sup>+</sup> transformation to high energy neutral atoms in supersonic Li vapour jet 9-4445  
 H+H<sub>2</sub> exchange reaction theory 9-10311  
 H+O<sub>2</sub>→OH+Δ, rate consts., and kinetics of branching step 9-14129  
 H $\alpha$  line obs. in 951 stars, suggested luminosity indicator 9-12690  
 H $\alpha$  profiles of  $\beta$  Orionis, time variation 1966-67 9-10487  
 He-H<sub>2</sub> liq.-vapour equil. at 100 atm. 9-9590  
 in Ni-(30wt.%)Cu alloy, interstitially occluded, effect on spontaneous magnetization temp. dependence 9-16361  
 NiSO<sub>4</sub>/(NH<sub>4</sub>)<sub>2</sub>SO<sub>4</sub> soln., gas reduction, effect of surface active agent 9-18757  
 Si-SiO<sub>2</sub> heat treated in H<sub>2</sub>, reduction in recombination carrier velocity 9-12170  
 in SiCl<sub>4</sub> reduction, conc. ratio in vapour-gas system in saturator of epitaxial equipment 9-21301  
 in SiO<sub>2</sub>, permeation of molecules and ions 9-3388  
 in  $\alpha$ -Ti, effect on relax. spectrum 9-7534  
 Zr-H phase boundaries and lattice params., 0.61-0.66 wt.% H 9-16160

**ions**

- beam deflection and rotation, rel. to obtaining high power beams 9-17864  
 channeling in InAs, GaSb, AlSb, InSb, energy loss meas. 9-9868  
 composition in positive column of H<sub>2</sub> glow discharge 9-15962  
 diffusion in Ni, Ti, at 78°K following 35 KeV implantation 9-21352  
 extragalactic objects H $\beta$  emission line width rel. to ionization mech. 9-6111  
 ion, stopping power Z depend. in arbitrary medium, 0.5-8 MeV/a.m.u. 9-6990  
 neutral atom excitation, 1s-ns, cross-sections 9-15830  
 oscillator strength sum rules, upper and lower bounds determ. 9-8407  
 plasma, magneto-acoustic waves, diamagnetic eff. 9-19551  
 plasma, partially ionized, equilibrium theory 9-13413  
 plasma, thermonuclear, prod. by field emission discharge irradi. of D-T target 9-5047  
 plasma, turbulent, elec. conductivity 9-875  
 plasma glow discharge, perturbed, atomic transitions and self-absorpt. of line rad. 9-5032  
 plasma prod.  $1 \times 10^{17}$  ions/cm<sup>3</sup> 9-7170  
 scattering, low energy, at metal surface 9-2828  
 spectral absorption coeffs. 9-19410  
 D<sub>2</sub><sup>+</sup>, dissociation energy 9-2920  
 H<sup>+</sup>, alkali metal atom collision with charge exchange 9-6985  
 H<sub>2</sub><sup>+</sup>-H<sub>3</sub><sup>+</sup> partition functions of ground electronic states 9-867  
 H<sub>2</sub><sup>+</sup> e. scatt. 9-766  
 H<sub>2</sub><sup>+</sup> e. scatt., quantum defect method 9-767  
 H<sub>2</sub><sup>+</sup>, collision-induced dissoci., 0.7-2 keV, non-vertical transitions 9-15901  
 H+H<sub>2</sub>O→OH+H<sub>2</sub>, cross-section for incident ion energies near 2eV 9-921  
 H I, interference between fine structure levels, interpret. 9-20897  
 H II galactic regions, absolute isophotometry in H $\alpha$  light, ratio to radio continuum rad. 9-10469  
 H II galactic regions, ionization fronts, effect of interstellar mag. field on stability 9-12729  
 H II regions, fronts, H I clouds, densities, calcs. 9-18883  
 H<sub>2</sub>, dissociation equil. in stellar atmos. rel. to continuous thermal rad. 9-17612  
 H<sub>2</sub>, slow e. elastic scatt., differential cross-section calc. 9-9143  
 H<sup>+</sup> beam, intense, prod. from pulsed H arc 9-12987  
 H<sup>+</sup>, charge exchange with Cs vapour, 0.5-20 keV, cross section obs. 9-13314  
 H<sup>+</sup>, double electron capture cross section obs. on various targets, 75-250 keV 9-13315  
 H<sup>+</sup>, electron capture, differential cross-sections for neutral atomic targets 9-5069  
 H<sup>+</sup>, prod. by collisions of excited rare gas atoms with H<sub>2</sub>, and isotope effect 9-7188  
 H<sup>+</sup>, single electron capture in He, perturbed stationary state calc. 9-5070  
 H<sup>+</sup> at TiO<sub>2</sub> aqueous soln. interface, adsorpt., obs. 9-7351  
 H<sup>+</sup> beam, intense, prod. from pulsed H arc 9-12987  
 H<sub>2</sub><sup>+</sup>, dissociative collisions with H<sub>2</sub>, Ar, and Xe, energy distrib. of prod. protons 9-4968  
 H<sub>2</sub><sup>+</sup>, electron capture on impact with Ne 9-9407

**Hydrogen continued****ions continued**

- H<sub>2</sub><sup>+</sup>, energy expectation values and integral Hellmann-Feynman theorem 9-2867  
 H<sub>2</sub><sup>+</sup>, Green function calc., 2nd-order perturbation 9-9106  
 H<sub>3</sub><sup>+</sup>, config.-interaction calc., expanded basis 9-9210  
 H<sub>3</sub><sup>+</sup>, electron capture on impact with Ne and Ar 9-9407  
 H<sub>3</sub><sup>+</sup>, natural orbital, electron-population, and energy anal. 9-17017  
 H<sub>3</sub><sup>+</sup>, wave function expansion, overlap matrix elements, related integrals, correl. functions 9-11462  
 HD<sup>+</sup>, collision-induced dissoci. by inert gases 9-7077  
 HD<sup>+</sup> beam intensity automatic meas. 9-17863  
 H $\alpha$  and Ca II K-line in solar spectrum, simultaneous obs. method 9-17652
- neutral atoms**  
 1s-2s or 2p, long-range interaction, second-order perturb. theory 9-9157  
<sup>2</sup>P<sub>3/2,1/2</sub>-<sup>2</sup>S<sub>1/2</sub> transition, oscillator strength expt. estimate 9-11416  
 in alkali halides, magneto optical props. 9-12345  
 Balmer lines in strong mag. field in plasma, Stark-broadening obs. 9-17110  
 beam, detection by MoO<sub>3</sub> thin film device 9-6728  
 Bethe-Salpeter eqn. and dynamical groups 9-16804  
 bound-state calc., reduced Coulomb Green's function, g.s. perturbations 9-20895  
 content in 32 small ang. dia. galaxies 9-12666  
 Coulomb problems, O(4) symmetry and Green's function methods, use of Lamb shift 9-17004  
 depolarization while passing through magnetic lens at zero field 9-2827  
 differential X-sections for ioniz. by fast charged part., calc. from binary-encounter and Bethe theory 9-4871  
 diffusion, long range in Nb, relaxation process, coeff. determined 9-1248  
 diffusion in b.c.c. metals, activation energy 9-3385  
 diffusion in metals, interstitial, quantum effects 9-3370  
 diffusion in Zr, examined by means of n radiography 9-11367  
 electron excitation, 1s-2p cross-sections, post-threshold behaviour 9-717  
 electron-exchange scatt., rearrangement collisions, eff. of core terms, nonorthogonality and conservation of particle flux on approx. theories 9-11418  
 energy levels, actual and calc. by old quantum theory, Bohr-Sommerfeld identity 9-4867  
 energy levels in Dirac eqn., influence of boundary conditions 9-11417  
 equation, generalised, from symmetry group of integral eqn. 9-9154  
 e.s.r. of atoms trapped in inert matrices at 4.2°K, matrix perturbing effects 9-12501  
 excitation 1s→2s transition, eff. of peaking approx. on cross-sections 9-13311  
 excitation by electron impact of Lyman- $\alpha$  rad. in 2p state 9-19411  
 excitation by fast protons, 1s-ns exc. cross-sections 9-15830  
 excitation by fast protons, cross section formulae in 2s and 2p states 9-4868  
 excitation by fast protons from 1s to any state, asymptotic expression for cross section 9-4869  
 excitation by protons, total cross section 9-9156  
 excitation resonances near (2p) level, after electron impact 9-716  
 excited, ionization cross-section dependence on the main quantum number 9-2826  
 ground state, applic. of Slater transform functions 9-19389  
 H+H+M→H<sub>2</sub>+M thermomolecular recombination, resonance theory 9-17005  
 hyperfine pressure shifts in Kr and Xe 9-9155  
 ionization by slow electrons 9-906  
 ionization cross-section calc. using Monte-Carlo method 9-7186  
 ionization cross-section using plane-wave approx. 9-914  
 isotope separation by Pd in desiccant column, patent 9-9163  
 mag. interac. between charged part. 9-2329  
 magneto optical props. in alkali halides 9-12345  
 Majorana eqns. for composite systems, deduced from Bethe-Salpeter eqn., applied to H atom 9-2548  
 multiphoton ionization by laser beam 9-13451  
 O(4) symmetry, Green's function methods for soln. of Coulomb problems, Lamb shift and Bethe logarithm 9-17004  
 olefin reactions, rate const. determ. from Lyman- $\alpha$  re-emission 9-12527  
 Omicron Andromedae variable, and He abundance 9-14218  
 optical polarisability, magnitude 9-2825  
 oscillator strength sum rules, upper and lower bound determ. 9-8407  
 photographic emulsion latent image formation when evolved from Si, Ge and other metal surfaces 9-18045  
 photoionization, anisotropic cross-sections, ang. distrib. of photoelectrons 9-15829  
 photon elastic scatt., retardation effect 9-15831  
 photosensitized, adsorpt. on MoO<sub>3</sub> surface, suction effect 9-17247  
 plasma pinch in Tokamak TM-3 machine, conc. meas. method 9-7144  
 polarization bounds 9-8410  
 polarized radiation calc. on quenching from 25 metastable state 9-20896  
 positron elastic scatt., phase shifts using polariz. pot. method 9-20898  
 positron-H scatt., positronium formation 9-18156  
 radiative mean-life, meas. of 2 and 3p states, beam-foil excitation method 9-14671  
 recombination lines, partial maser effect in nebular plasma 9-8231  
 scattering by H<sub>2</sub>, two-body potential 9-2936  
 scattering problems, misuse of peaking approx. 9-17006  
 sorption at gas electrode in u.s. field, thermodynamic interpretation 9-5165  
 spectral absorption coeffs. 9-19410  
 spectrum, discrete, of relativistic atom realizes representation of O(4,2)@SU(2), classification by O(4,2) 9-15828  
 spin-exchange cross section for H-H<sub>2</sub>, meas. by variation of T<sub>1</sub> and T<sub>2</sub> with at. density 9-11419  
 Stark effect, energy levels determined 9-20894  
 in stars, six early type, ratio with He abundance 9-14206  
 triplet s-wave scatt., applic. of compact operators method 9-17726  
 two-photon bound-bound transitions in a Coulomb field 9-13310  
 van der Waals const. computation, London potential 9-722  
 e<sup>+</sup> scatt. 9-720  
 e scatt., resonance phenomena 9-721  
 e scatt., slow 9-719  
 e scatt., with strong coupling 9-718  
 e. elastic scatt. S-wave phase shifts, var. method calc. 9-13312  
 in Ar, hyperfine splitting press. shift, obs. 9-4870  
 desorption on Ni-Cr<sub>2</sub>O<sub>3</sub> catalyst rel. to H<sub>2</sub>O-H isotopic exchange, obs. 9-16046



**Hydrogen continued**

- neutral atoms continued**  
 H-Al spin-change collision cross sections calc. 9-11402  
 H-C<sup>+</sup> spin-change collision cross sections calc. 9-11402  
 H<sup>+</sup>-D charge-exchange cross-sections, eff. of apparatus geom. 9-4872  
 H-H Coulomb interaction matrix elements and pots. calc. 9-18157  
 H-H spin-exchange cross section, meas. by variation of T<sub>1</sub> and T<sub>2</sub> with at. density 9-11419  
 H<sup>+</sup>-H collision, charge-exchange cross-sections, eff. of apparatus geom. 9-4872  
 H-He,Ne,Ar collisions, polar. of Lyman  $\alpha$  rad., Born and distortion rotational approx. 9-13313  
 H-Si<sup>+</sup> spin-change collision cross sections calc. 9-11402  
 H, electron impact excitation, asymptotic form of total wave function 9-18155  
 H I clouds, densities near H II region fronts, calcs. 9-18883  
 H II region photoelectric study, temp., chemical abundance in nebula and galaxies 9-21852  
 H<sub>1</sub><sup>+</sup>→H<sub>1</sub><sup>0</sup> and H<sub>1</sub><sup>0</sup>→H<sub>1</sub><sup>+</sup> conversions in energy range 7.40 keV, use of metallic film 9-17363  
 H-H<sub>2</sub> (para and ortho) collisional excitation of rot. levels calc. up to J=15, and for 10<sup>3</sup>T≤10<sup>4</sup>K 9-14227  
 H+Br<sub>2</sub>→HBr+Br, perturbed Morse oscillator calc. 9-16479  
 H+Br<sub>2</sub>→HBr+Br, quantum mechanical calc. 9-10313  
 H+H<sub>2</sub> reactive scatt., quantum mechanics 9-10317  
 H(2S), production by molecular dissociative excitation 9-14725  
 H56 $\alpha$  recombination radio line detect. in Omega nebula 9-16563  
 H $\alpha$  solar line, wing obs. for population of n=2 and n=3 levels 9-12764  
 in He, hyperfine press. shift rel. to van der Waals interaction 9-4873  
 maser with large storage box for reduced wall effect 9-17865  
 in Ni Cu alloys, interstitial occlusion 9-17278

**neutral molecules**

- air mixture, supersonic premixed flow, flame propag. 9-16747  
 desorption from metal surfaces, angular distrib. 9-7349  
 differential cross-section for 25-60eV e scatt. 9-9142  
 discharge, electrodeless ring, 10 MHz, 0.1-0.3 torr electron energy, density meas. 9-15960  
 dissociation rates behind shock wave 9-1902  
 e.m. interaction theory, nuclear shielding const. calc. 9-7025  
 escape rate from CO<sub>2</sub> planetary atm., Monte Carlo calc. 9-12747  
 in ethylene-air diffusion flame, effect on prod. of polycyclic aromatic hydrocarbons 9-12537  
 excitation by electron impact, cross-sections calc., semiclassical method 9-19433  
 gas, press. induced pure rot. spectrum, analysis of i.r. abs. band 9-11461  
 gas, quantum deviations from classical behaviour, effs. of using perturbation theory 9-10643  
 ground-state dissoci. energies rel. to long-range interaction theory 9-9157  
 ground-state energy calc. 9-769  
 o H<sub>2</sub> solid intermediate double h.c.p. struct. in phase transition 9-13778  
 in glasses, colour centres, irradiation-produced, destruction 9-3365  
 interstellar, photodissociation mechanism 9-18880  
 ionization by electron impact, cross-section calc., semiclassical method 9-19433  
 Kerr constant determ. from quantum theory 9-746  
 liquid, level meas. using spaced C resistors 9-6269  
 in localized regions, formation mechanism 9-16590  
 mixtures with inert gases, N<sub>2</sub>, methane, refr. index rel. to long-range atom-mol. interactions 9-9304  
 molecular transitions calc., applic. of Coulomb approx. 9-13333  
 ortho, solid, angular momentum waves RPA 9-20580  
 ortho-para mixtures, thermal cond. 9-953  
 quantum crystal, wide range of physical and computational utility 9-15436  
 quasi-molecules continuous absorpt. rel. to stellar spectra 9-6189  
 refined calc. with Weinbaum functions 9-17033  
 reorientation cross-section from depolarized Rayleigh line width meas. 9-13345  
 residual atm. in sputter-ion and non-evaporable getter pumped systems 9-14297  
 Rydberg and scatt. states 9-766  
 scattering by H atoms, two-body potential 9-2936  
 separation from gaseous mixture, method and apparatus, patent 9-13481  
 spectral absorption coeffs. 9-19410  
 spectroscopic excitation of doubly excited electronic states 9-2868  
 spectrum with new photoelectron spectroscope 9-17898  
 thermal conductivity from 2000° to 7000°K 9-5114  
 thermal diffusion in H<sub>2</sub>-He mixtures 9-17168  
 vibration, induced fundamental band in dil. solid soln. of Ne, at 4°K 9-14687  
 vibration-rotation band fundamental, in elec. field induced spectra, lines in press. range 0-600 psi 9-13354  
 vibrational excitation in central collisions with Li<sup>+</sup> beams 9-7097  
 $\pi$ -transfer in mixture of H<sub>2</sub> and other gases 9-14620  
 D<sub>2</sub> vibration, induced fundamental band in dil. solid soln. of Ar, at 77°K 9-14687  
 DH, spectra, elec. field induced, 0-600 psi, fundamental vib.-rot. band lines 9-13354  
 gas, electron mobility, up to 42 atm. 9-17167  
 H<sub>2</sub>-D<sub>2</sub> exchange, catalytic activation on corundum doped with Ti<sup>3+</sup>, V<sup>3+</sup> or Cr<sup>3+</sup> 9-8085  
 H<sub>2</sub>-N<sub>2</sub>-O<sub>2</sub> flame, electron prod. by Ca, Sr and Ba 9-12534  
 H<sub>2</sub>-N<sub>2</sub>-O<sub>2</sub> flame, temp. profile at atm. press. 9-15480  
 H<sub>2</sub>-H<sub>2</sub> bimolec. exchange reaction 9-770  
 H<sub>2</sub> exchange and Coulomb energy, perturbation calc. 9-765  
 H<sub>2</sub> Raman intensity theory 9-733  
 H<sub>2</sub> continuous spectrum, transition absorption coeff. calc. 9-19431  
 O-H<sub>2</sub> in dilute solid solution with HD, spin relax time calc. 9-21596  
 H<sub>2</sub> in liq. Ar, collision-induced absorpt., liq. cell model 9-21213  
 H<sub>2</sub> in liq. Ar, collision-induced absorpt., liq. cell model 9-21214  
 o-p H<sub>2</sub> scattering cross-sections 9-20997  
 H<sub>2</sub>-O<sub>2</sub> diffusion flame structure 9-19098  
 H<sub>3</sub>, energy surface, superposition of configs. calc. 9-768  
 H<sub>4</sub>, ground and excited states, diatomics-in-mols. calc. 9-770  
 H<sub>2</sub>, excited vibr. states in adiabatic approx. 9-2844  
 H<sub>2</sub> + inert gases, photoionization ion-mol. reactions 9-17132  
 H<sub>2</sub> and D<sub>2</sub>, vibr.-rot. effects in Franck-Condon factors calc. 9-5059  
 H<sub>2</sub> and D<sub>2</sub>, vibr. excitation and fragmentation in collisions with slow K<sup>+</sup> 9-2937  
 H<sub>2</sub> lowest triplet states, excitation by low-energy electrons 9-17032  
 H<sub>2</sub> Raman lines collisions, line width of S<sub>0</sub>(0) and S<sub>0</sub>(1) 9-2864
- Hydrogen contigued**  
**neutral molecules continued**  
 H<sub>2</sub> solid, pair interaction between ortho-molecules, p.m.r. obs. 9-17504  
 HD, at 20°K in contact with charcoal, dynamic polarization of nuclei 9-7270  
 H-H<sub>2</sub> (para and ortho) collisional excitation of rot. levels calc. up to J=15, and for 10<sup>3</sup>T≤10<sup>4</sup>K 9-14227  
 H+H<sub>2</sub> reactive scatt., quantum mechanics 9-10317  
 H<sub>2</sub>+I<sub>2</sub>, low-temp. reaction mechanism 9-10320  
 H<sub>2</sub>+I<sub>2</sub> reaction, transition state 9-10319  
 H<sub>2</sub>+I<sub>2</sub> reaction mechanism 9-10321  
 K scatt. in thermal energy range, total cross section meas. 9-11413  
 N<sub>2</sub><sup>+</sup>+D<sub>2</sub>, product energy and ang. distrib. obs. 2.3 to 11.6 eV 9-10325  
 N<sub>2</sub><sup>+</sup>+H<sub>2</sub>, product energy and ang. distrib. obs. 2.3 to 11.6 eV 9-10325  
 N<sub>2</sub><sup>+</sup>+HD, product energy and ang. distrib. obs. 2.3 to 11.6 eV 9-10325  
 Pd-B alloys, H<sub>2</sub> diff. 9-7889
- Hydrogen compounds**  
*See also Ice; Steam; Water*  
 DIO<sub>3</sub>, piezoelectric and elastic props. rel. to bonding 9-12202  
 H<sub>2</sub>Cl collisions with H<sub>2</sub>Cl, vibrational transitions P<sub>1,0</sub> probabilities 9-11514  
 H<sub>2</sub>S-CO<sub>2</sub> mixture, sound absorpt. obs. at 300 and 500°K 9-21136  
 halides in cyclohexane, rotational motion 9-9488  
 HBr collisions, with HBr, vibrational transitions P<sub>1,0</sub> probabilities 9-11514  
 HCl collisions with HCl, vibrational transitions P<sub>1,0</sub> probabilities 9-11514  
 hydride precipitates in Zr alloys 9-19683  
 hydrides precip. in  $\alpha$ -Zr, obs. 9-16148  
 phosphoric acid organic solvent-water, liquid-liquid equilibria rel. to selectivity of phosphoric acid 9-15989  
 transition metal, as reactor moderating material 9-14655  
 D<sub>2</sub>O mixed with water and paramagnetic ions, proton relaxation time obs. 9-1045  
 D<sub>2</sub>P(BH<sub>3</sub>)<sub>2</sub><sup>-</sup> vibr. modes, i.r., Raman and n.m.r. obs. 9-18183  
 D<sub>2</sub>S, pure rot. absorpt. spectra, analysis 9-20928  
 DCl, i.r. bands, higher J rotational struts. 9-13357  
 DF<sub>2</sub><sup>-</sup>, potential energy const. and mean amplitudes of vibration 9-4838  
 DNCO, extreme centrifugal distortion, interpretation rel. to Q-branch freqs. 9-13356  
 DNCS, extreme centrifugal distortion, interpretation rel. to Q-branch freqs. 9-13356  
 D<sub>2</sub>O vapour, new laser emission 9-6515  
 D<sub>2</sub>S, ground state inertia defects, Coriolis coupling constants 9-9212  
 D<sub>2</sub>Se, Coriolis coupling constants, ground state inertia defects 9-9212  
 H-Pd electrical resistivity, 2/300°K 9-3580  
 H<sub>2</sub>-methane, gaseous, heat of mixing 170-2930°K 9-954  
 H<sub>2</sub>-methane gaseous mixtures, excess enthalpy at high densities 9-955  
 H<sub>2</sub>O, mol., mag. susceptibility calc. 9-744  
 H<sub>2</sub>O vapour, width and intensity of  $\lambda_{H^+}$ =12.67cm<sup>-1</sup> spectral line 9-771  
 H<sub>2</sub>PO<sub>4</sub><sup>-</sup> in KH<sub>2</sub>PO<sub>4</sub>, structure from Raman scatt. spectra in ferroelec. and paraelec. states 9-18652  
 H<sub>2</sub>P(BD<sub>3</sub>)<sub>2</sub><sup>-</sup> vibr. modes, i.r. Raman and n.m.r. obs. 9-18183  
 H<sub>2</sub>P(BH<sub>3</sub>)<sub>2</sub><sup>-</sup> vibr. modes, i.r., Raman and n.m.r. obs. 9-18183  
 H<sub>2</sub>S, anal. of pure rot. absorpt. spectra 9-20928  
 H<sub>2</sub>S, photoionization 9-905  
 H<sub>2</sub>S, sound absorpt. obs. at 300°K 9-21136  
 H<sub>2</sub>SO<sub>4</sub>, aqueous mixture, molecular sound velocity and compressibility 9-16000  
 H<sup>14</sup>CN meas. in HCN from N<sub>2</sub>-methane fission fragment irradi. 9-18770  
 H<sup>79</sup>Br, dipole matrix elements for 2-0 vib.-rot. band lines 9-15853  
 HBr, gas-phase far u.v. absorpt. spectrum 9-20929  
 HBr.4H<sub>2</sub>O, cryst. struct., H-bonding 9-1190  
 HCN, photodissociation, bond energy 9-17062  
 HCN laser, duration by pulsed discharge in seal-off tube 9-16782  
 HCN laser, emission line at 12.85  $\mu$ m 9-2869  
 HCN laser, long time operation by pulsed discharges in seal-off tube 9-20511  
 HCN—in KCl magnetic parameters completely determ. 9-13358  
 H<sub>2</sub>CO<sub>3</sub>, gas, transmission function calc., 1-7  $\mu$  9-2866  
 HCP, rotational line intensities in <sup>13</sup>C-<sup>15</sup>N electronic transitions 9-2880  
 HCl-Ar interaction, intermol. dispersion pot. 9-20992  
 HCl-He interaction, intermol. dispersion pot. 9-20992  
 HCl-Ne interaction, intermol. dispersion pot. 9-20992  
 HCl-dimethyl ether, vapour system, n.m.r. and H bonding 9-7021  
 HCl, decomposition via chlorine exchange reaction, shock tube obs. 9-8077  
 HCl, dielec. const. in liq. solid and adsorbed states 9-12186  
 HCl, photoionization efficiency curves, mass spectrometric study, ionization threshold to 600A 9-3004  
 HCl, thermal cond. and rotational relax. 9-9447  
 HCl, vibration-rotation spectrum, density and linewidth 9-18182  
 HCl and DCL explosion laser 9-2374  
 HCl i.r. bands, higher J rotational struts. 9-13357  
 HCl i.r. spectra, press.-induced shifts, j-depend., elastic cross-section expansion 9-17012  
 HCl liq., inelastic scatt. of neutrons at 183°K, intensity meas. 9-15987  
 HCl liq., proton relax. and scalar spin-spin coupling 9-9553  
 HCl n.m.r. of aq. solns., hydration determ. 9-17220  
 H<sup>35</sup>Cl and H<sup>37</sup>Cl, nuclear mag. hyperfine spectra 9-9206  
 HClO<sub>4</sub>, n.m.r. of aq. solns., hydration determ. 9-17220  
 HClO<sub>4</sub>.2H<sub>2</sub>O, cryst. struct., H-bonding 9-3293  
 H<sub>2</sub>Cr<sub>2</sub>O<sub>7</sub> electrolytic regeneration from Cr<sub>2</sub>(SO<sub>4</sub>)<sub>3</sub> 9-6016  
 HD-O-H<sub>2</sub> solid solutions, dilute, spin relax time calc. 9-21596  
 HD mol. elec. dipole moment, radial matrix elements J depend. 9-2863  
 HF-H<sub>2</sub>O solution, pulsed electrolysis 9-21715  
 HF, i.r. bands, higher J rotational struts. 9-13357  
 HF, impurity in ice, effect on mechanical props. 9-13711  
 HF<sup>+</sup> mol. X<sup>2</sup> $\Pi$ , A<sup>2</sup> $\Sigma^+$  Hartree-Fock level calc. 9-19434  
 HF chemical bond, minimal basis SCGF calc. 9-13353  
 HF collisions with H<sub>2</sub>, He, Ar, vibrational transitions P<sub>1,0</sub> probabilities 9-11514  
 HF<sub>2</sub><sup>-</sup>, potential energy const. and mean amplitudes of vibration 9-4838  
 HF<sub>2</sub>, thermal conductivity in crossed elec. and mag. field, reson. decrease of transfer coeffs. 9-9448  
 HI, flash photolysis with deuterated hydrocarbons 9-8109  
 HI, gas-phase far-u.v. absorpt. spectrum 9-20929  
 HI, h.f.s. of rot. spectrum in sub-mm region 9-9204  
 HI collisions with Ar and HI, vibrational transitions P<sub>1,0</sub> probabilities 9-11514  
 HIO<sub>3</sub>, piezoelectric and elastic props. rel. to bonding 9-12202  
 $\alpha$ -HIO<sub>3</sub> acousto-optic device applications, high figure of merit 9-3865

Hydrogen compounds continued

H<sup>+</sup>IO<sub>3</sub>, electro-optical and nonlinear optical props. 9-3867  
HI+DI→2I+HD reaction, energy requirements 9-8068  
HN<sub>3</sub>, photodissoc. in vac. u.v. 9-7078  
HNCO, and D derivs., rotational constns., study by far i.r. spectra 9-13355  
HNCO, extreme centrifugal distortion, interpretation rel. to Q-branch freqs. 9-13356  
HNCS, and D derivs., rotational constns., study by far i.r. spectra 9-13355  
HNCS, extreme centrifugal distortion, interpretation rel. to Q-branch freqs. 9-13356  
HNO<sub>2</sub>, H<sub>2</sub>O, p.m.r. and molec. states 9-11721  
HNO<sub>2</sub>, NO<sub>2</sub> force constns. and (D<sup>2</sup>) in gas and liq. 9-764  
HNO<sub>2</sub>, trans. vibration amplitude, coriolis coupling coeff. determ. 9-4929  
HNO<sub>2</sub>, vibration spectra at 77°K 9-7029  
HN<sub>3</sub>, and D derivs., rotational constns., study by far i.r. spectra 9-13355  
HO<sub>2</sub>, e.s.r. in solns. of H<sub>2</sub>O<sub>2</sub> in H<sub>2</sub>O at 77°K 9-7081  
H<sub>2</sub>O, vibrational states, Hamiltonian constns., eff. on spectrum 9-7024  
H<sub>2</sub>O vapour laser, proposed transition assignments, expt. test 9-8611  
H<sub>2</sub>O<sub>2</sub>, abs. coeff., 1200 2000Å 9-7022  
H<sub>2</sub>O<sub>2</sub>, space group determ. by X-ray diff. rel. to double reflexion effect errors 9-11846  
H<sub>2</sub>O<sub>2</sub> decomposition, study of intermediates formed after u.v. irradiation 9-17034  
H<sub>2</sub>O<sub>2</sub> decomposition, study of intermediates formed after u.v. irradiation 9-9213  
H<sub>2</sub>O<sub>2</sub> absorpt. spectra and kinetics in HClO<sub>4</sub> soln. 9-9515  
H<sub>2</sub>O<sup>+</sup> ion in SO<sub>3</sub> solution, vibration spectra 9-2865  
H<sub>2</sub>S, extremal props. of force constns. 9-7023  
H<sub>2</sub>S, ground state inertia defects, Coriolis coupling constants 9-9212  
H<sub>2</sub>S, homogeneous reaction with D<sub>2</sub> 9-3981  
H<sub>2</sub>S, thermal cond. and rotational relax. 9-9447  
H<sub>2</sub>S and D<sub>2</sub>S, Raman spectra of poly. cryst. phases 9-5935  
H<sub>2</sub>S rotational absorption spectrum, 10-125 cm<sup>-1</sup> obs., comparison with theory 9-7026  
H<sub>2</sub>S<sub>2</sub> and D<sub>2</sub>S<sub>2</sub>, mm-wave rot. spectrum 9-9211  
in H<sub>2</sub>SO<sub>4</sub>(Pd-H) electrodes oxidation, mass transport, obs. 9-16485  
H<sub>2</sub>SO<sub>4</sub> in soft carbons, residual lamellar cpds, after heat treating 9-7362  
H<sub>2</sub>SO<sub>4</sub> solns., γ-radiolysis at high press. 9-10361  
H<sub>2</sub>Se, ground state inertia defects, Coriolis coupling constants 9-9212  
H<sub>2</sub>TeO<sub>4</sub>, annealing of β<sup>-1</sup> decay and isomeric transition recoil products 9-7584  
KH<sub>2</sub>PO<sub>4</sub>, refractive index, pressure dependence 9-16393  
Kr-D<sub>2</sub> mixtures, ionisation consts. of KrD<sup>+</sup> ions 9-7187  
NH, electronic excitation in vac. u.v. photodissoc. of HN<sub>3</sub> 9-7078  
NH<sub>4</sub>H<sub>2</sub>PO<sub>4</sub>, refractive index, pressure dependence 9-16393

Hydrogen ion concentration see Electrochemistry

Hydromagnetics see Magnetohydrodynamics

Hydrometry see Flowmeters

Hydrophones see Oceanography; Transducers

Hydrostatics

No entries

Hygiene see Medical science

Hygrometers

adiabatic saturation psychrometer 9-935

Hyperfine structure see Crystals/hyperfine field interactions; Paramagnetic resonance and relaxation; Spectra

Hyperfragments see Hypernuclei

Hypernuclei

<sup>Λ</sup>14C, anal., using Λ-Λ interactions determined from <sup>ΛΛ</sup>He anal. 9-19273  
A=3 to 14, hyperfragments binding energy and π<sup>±</sup> decay 9-18065  
B<sub>Λ</sub> binding energy, Green function formulae 9-8973  
decay lifetimes of heavy spallation fragments meas. 9-11206  
heavy hyperfragments, multi nucleon stimulated decay, Monte Carlo computer program tech. 9-18063  
hyperfragment prod. in 5 GeV/c  $\bar{p}$  interact. with ionographic emulsion nuclei 9-20781  
hyperfragments, prod. from interact. of 3.0 GeV/c K<sup>-</sup> in nuc. emulsion 9-20639  
production, strangeness s=-2 9-16935  
Λ binding energy to nuclear matter, variational calc. 9-6704  
Λ<sup>+</sup> binding energy and π<sup>±</sup> decay 9-18065  
Λ<sup>+</sup>He<sup>+</sup>, binding energy and π<sup>±</sup> decay 9-18065  
Λ<sup>0</sup>B, π<sup>±</sup> decay 9-15715  
Λ<sup>0</sup>Be, π<sup>±</sup> decay 9-15715  
ΛH<sup>3</sup> prod. from 3.0 GeV/c K<sup>-</sup> interact. in nuc. emulsion 9-20639  
Λ<sup>+</sup>H-3Heπ<sup>+</sup>, energy spectra and particle angular correlations obs. 9-2661  
Λ<sup>+</sup>He-3Heπ<sup>+</sup>, energy spectra and particle angular correlations obs. 9-2661  
Λ<sup>+</sup>He-4Heπ<sup>+</sup>, energy spectra and particle angular correlations obs. 9-2661  
Λ<sup>0</sup>Li mesonic decay to ≥4 particles obs. 9-20735  
Λ, well depth in nuclear matter, invalidity of current estimations 9-8974

Hyperons

See also Mesons; Nuclear reactions and scattering due to hyperons  
Λ, potential depth in nuc. matter 9-20639  
Λ binding energy of light hyperfragments 9-18065  
Λ-Z splitting of baryon octet and SU(6) mass formula calc. 9-8880  
Λ<sub>1</sub> nondegenerate mass, applic. in πΣ scatt. length calc., πΣ→πΛ amp. and KN data 9-4599  
Λ binding energy to nuclear matter, variational calc. 9-6704  
πΣΛ and πΣΣ coupling constants determ. 9-13126  
Σ, nondegenerate mass. calc. πΣ S-wave scatt. length, consistency with forward dispersion rel. 9-4599

absorption

No entries

capture

No entries

decay

Λ→Bγlν, form factors related to A→Bllν decay 9-6681  
leptonic, vector current form-factors, quark model applic. to additivity and algebra 9-14478  
low-energy theory theorem 9-6703  
non-leptonic, Δ<sub>3/2</sub>-type weak interaction and E.T.C. terms 9-20672  
non-leptonic, tadpole model 9-355  
nonleptonic, CP nonconservation effect, β/α for Σ<sup>+</sup> mode effect 9-423

Hyperons continued

decay continued

nonleptonic, S- and P-wave amplitudes, with chiral-invariant effective Lagrangian 9-14524  
nonleptonic, S-P current × current Hamiltonian 9-11107  
nonleptonic, two-body urbaryon interaction in U(4)model 9-2540  
quark model for nonleptonic, p-wave amplitude ambiguities 9-2541  
S-wave, K<sup>±</sup> and baryon-pole models 9-16907  
semileptonic for calc. of Cabibbo parameters 9-2483  
B→B<sup>+</sup>γ(ΔS=1) radiative, expansion of exact amp. in powers of ω, pole model-comparison 9-6703  
Λ→pe<sup>+</sup>ν, renormalized axial-vector coupling const. recalcul. 9-15647  
Λ→pe<sup>+</sup>em, T-odd correlations calc. 9-2542  
Λ→ππ<sup>+</sup>, radiative corrections due to ΔT=1/2 rule 9-11108  
Λ→ππ and O(4) symmetry 9-20616  
Λ(1405)→Yγ, width estimate 9-429  
Λ(1520)→Yγ, width estimate 9-429  
ω<sup>+</sup>→e<sup>+</sup>e<sup>+</sup>ν, T-odd correlations calc. due to final e.m. interact., T violation 9-13146  
Σ<sup>0</sup>→ne<sup>+</sup>ν, renormalized axial-vector coupling const. recalcul. 9-15647  
Σ<sup>0</sup>→e<sup>+</sup>γγ/Σ<sup>0</sup>→e<sup>+</sup>γγ branching ratio, magnetic moments of Σ<sup>0</sup> 9-16908  
Σ→ne<sup>+</sup>em, T-odd correlations calc. 9-2542  
Σ(1660)→KN, Σπ, Λπ, Σππ and Λππ branching ratios determ. from K p interact. 9-14526  
Σ(1660)→Λ(1405)π upper limit for decay determ. 9-11043  
Σ(1660)→Σ(1385)π→Λππ from K<sup>-</sup>N reaction, Σ(1660) spin and parity determ. 9-8910  
Σ(1940) from K<sup>-</sup>p, Σπ mode obs. 9-20673  
Σ(2280) from K<sup>-</sup>p, decay modes obs. 9-20673  
Σ<sup>+</sup>→Σ<sup>0</sup>π<sup>+</sup>; Σ<sup>+</sup>→Λπ<sup>+</sup>π<sup>+</sup>, comparison; transition amplitude obs. and unitary symmetry checked 9-426  
Σ<sup>+</sup>→Σ<sup>0</sup>π<sup>0</sup>; Σ<sup>+</sup>→Λπ<sup>0</sup>π<sup>+</sup>, comparison; transition amplitude obs. and unitary symmetry checked 9-426  
Σ<sup>+</sup>→Λπ and O(4) symmetry 9-20616  
Y<sub>1</sub>(1660)<sup>+</sup>→Σ<sup>0</sup>π<sup>±</sup>(Λ<sup>0</sup>π<sup>±</sup>) spin and parity of 3/2<sup>-</sup> 9-430  
Λ→p+π<sup>+</sup>, meas. of β parameter 9-4647

detection, measurement

Λγ peak, 1350 MeV, in π<sup>-</sup>p interact. 9-14525  
Λ, well depth in nuclear matter, invalidity of current estimations 9-8974

effects

No entries

interactions

See also Hypernuclei

ΛN→NN, structure of weak interaction and SU(6) symmetry 9-425  
p from π<sup>-</sup>Λ, mass spectrum obs. for centre of mass energy 2050-3500 MeV 9-11093  
Σ<sup>+</sup>d→Σ<sup>0</sup>nn→Λnn, relation between states using SU(3) symmetry 9-6707  
N, potential 9-6687

magnetic moment

Ω<sup>-</sup>, rel. to proton mag. moment 9-2479  
Σ<sup>0</sup>, from branching ratio meas. of (Σ<sup>0</sup>→Λ<sup>0</sup>+γ+γ)/(Σ<sup>0</sup>→Λ<sup>0</sup>+γ) 9-16908  
Σ<sup>+</sup>, meas. by obs. of polar vector impuised mag. field 9-6705

mass

No entries

production

Λ in yp→ΛK<sup>+</sup> near threshold in Born approx. 9-8908  
photoformation in yp reaction, pole reson. model, <1200 MeV 9-8355  
Λ<sup>+</sup> backward in π<sup>-</sup>p→ΛK<sup>0</sup>, polar eff. Regge fermion exchange 9-4648  
Λ in πp→ΛΛn, at 7 and 12 GeV/c 9-6667  
Λ<sup>0</sup> in cosmic ray interact. with Cu, Sn, Pb targets, mass no. depend. 9-18026  
ΛΛ peripheral prod. in πp→ΛΛn, at 7 and 12 GeV/c 9-11057  
Λγ peak, 1350 MeV, in π<sup>-</sup>p interact. 9-14525  
Λp invariant mass enhancement at 2130 MeV from K<sup>-</sup>d, 1 GeV/c 9-20637  
Λππ in K<sup>-</sup>p(n), structure from 1600 to 1740 MeV 9-369  
NN→YY, conspiracy relation 9-424  
NN→YY+mπ, m<sub>π</sub>≥0, review of data 9-6690  
Σ in K<sup>-</sup>p→Σπ 9-13145  
Σ<sup>±</sup> in cosmic ray interact. with Cu, Sn, Pb targets, mass no. depend. 9-18026  
Σ<sup>0</sup>, associative, in π<sup>-</sup>p, ang. distrib. 9-6706  
Σ<sup>0</sup> in yp→Σ<sup>0</sup>K<sup>+</sup>, near threshold in Born approx. 9-8908  
Σ(1385) from K<sup>-</sup>p, high energy 9-20673  
Σ(1660) from K<sup>-</sup>p, high energy 9-20673  
Σ(1940) from K<sup>-</sup>p, high energy, Σπ decay mode obs. 9-20673  
Σ(2280) from K<sup>-</sup>p, high energy, decay modes determ. 9-20673

resonances

Regge trajectory study, spin-parity predictions 9-6684  
K p→Σπ, interference effects between Λ and Σ 9-13145  
Σ<sup>+</sup> mass 1930 MeV, S=-2, Γ=80 MeV 9-431  
Y<sub>1</sub>(1660)<sup>+</sup>→Σ<sup>0</sup>π<sup>±</sup>(Λ<sup>0</sup>π<sup>±</sup>) spin and parity of 3/2<sup>-</sup> 9-430

scattering

Λp elastic, rel. to Λ-N interaction, 120-320 MeV/c 9-8909  
Λπ cross sections meas., MΛ=110-330 MeV/c 9-11109  
ΛΣ (0,3/2<sup>+</sup>), (2,3/2<sup>+</sup>) possible resonance search, amplitude superconvergence reln. 9-17988  
πΣ vector dominance sum rules for invariant amplitudes 9-6672

spin and parity

Λ, new classification with spin 1 9-15593  
Ω<sup>-</sup>, parity meas. possibility 9-18011  
Σ, new classification with spin 1 9-15593  
Σ(1660) from K<sup>-</sup>N reaction, partial wave analysis 9-8910  
Σ, new classification with spin 3/2<sup>-</sup> 9-15593  
Y<sub>1</sub>(1660)<sup>+</sup>→Σ<sup>0</sup>π<sup>±</sup>(Λ<sup>0</sup>π<sup>±</sup>) spin and parity of 3/2<sup>-</sup> 9-430

Hypersonics see Ultrasonics

Hypertritons see Hypernuclei; Tritons

Hyperpervial theorem see Quantum theory

Hypochromism see Absorption/light; Polymers

Hysteresis

See also Dielectric phenomena; Dielectric properties of substances; Ferroelectric phenomena; Magnetization process  
cholesteric ester crystal static dielectric const. temp. var., heating, cooling curve comparison 9-9539  
curve traces for ferroelectric measurements, compensable and virtually grounded 9-1588  
domain-wall motion, rel. to nature of material perturbations 9-15150  
electret, teflon: polarizing field and temp. depend. 9-8567



**Hysteresis** continued

- ferroelectric capacitor, hysteresis loop tracer 9-8312  
 ferromagnetic substances, magnetization charact. and directional properties 9-16359  
 ferromagnetic circuits with saturable core coils 9-4409  
 grains, monodomain, synthetic and natural, props. 9-13976  
 grains, monodomain interacting, remanent props. and Preisach diagrams 9-14000  
 hysteresigraph for meas. in thin cylindrical magnetic films for fast computer memories 9-16762  
 hysteresigraph for permanent magnet mats. 9-3794  
 loop in ferromagnetic thin films 9-19957  
 loop tracer, magnetization vs. temp. continuous recording apparatus 9-14286  
 loop tracer, quasistatic for ferroelectric capacitors 9-8312  
 permalloy films, rotational hysteresis 9-10134  
 permalloy fine wires, Nb addition, materials parameters affecting reentrancy 9-5824  
 permalloy thin films, loop meas. in rotating field using automatic magnetometer 9-12296  
 permanent magnets, charact. meas. using analogue precision method 9-12974  
 permanent magnets, deviations in operating lines of hysteresis loop 9-10812  
 rotational due to perpendicularly superimposed continuous and alternating field 9-10123  
 steel, internally oxidized electrotechnical, loops 9-13989  
 in superconductors, hollow cylinders of Type-I, effect of surface energies on shielding and field retaining properties 9-7768  
 thin films, loop meas. in rotating field using automatic magnetometers 9-12296  
 triglycine sulphate crystals, temp. of elec. permittivity 9-10052  
 Bi, props. of residual twins 9-13978  
 Co Fe alloy, constricted loop produced by cold rolling method, patent 9-13759  
 Eu-O<sub>2</sub>, effect in temp. variation of isomer shift 9-1718  
 Fe-Ni, constant field loops, effect of anisotropy and atomic arrangement. X-ray exam. of textures 9-5825  
 Fe Si, magnetization reversal mechanism for single crystal picture frames 9-13981  
 Fe, amrcio, mag., meas. rel. to shock wave effects on residual props. 9-13980  
 Li ferrite-SiO<sub>2</sub> glass composites, d.c. obs. 9-1146  
 MgMn ferrites, eff. of annealing conditions 9-17459  
 Nb, in u.s. attenuation near H<sub>c1</sub> 9-9831  
 Ni above Curie temp. obs. 9-7902  
 Ni ferrites, of u.s. velocities 9-9828  
 SbSi, ferroelectric, spontaneous polarization 9-5649

**Ice**

- See also Glaciers; Snow*  
 attenuation of multiply reflected acoustic pulses for longit. and transverse waves 9-5545  
 clouds, laboratory, near-infrared reflectivity 9-12584  
 clouds, Venus, consistent with polarimetric obs. 9-8282  
 conductivity, elec., nature of charge carriers 9-1579  
 conductivity by guarded potential probe method 9-3692  
 crystals from supercooled cloud, dielec. polarity rel. to temp. 9-12183  
 elastic constants, anomalous temp. depend. 9-18496  
 electrical props. by depolarization of thermocurrents method 9-16287  
 electron micrograph of structure 9-3271  
 glacier, electrolytic conductivity 9-12570  
 grain growth in polycrystalline ice 9-18410  
 growth in supercooled aqueous solns. 9-9643  
 growth marks on surface of ice layer on lake, obs. 9-18414  
 hailstones, spherical, simulation of total heat transfer 9-16529  
 hexagonal, proton spin-lattice relax. time meas., 0.125-6.57 kOe, -10 to -80°C 9-16384  
 ice Ic, neutron diffr. 9-16076  
 ice II, struct. from neutron diffr. 9-16075  
 ice II, V and IX, far-i.r. spectra 9-1778  
 ice III, structure 9-7441  
 ice IX, struct. neutron diffr. determ. 9-5321  
 ice VI, i.r. spectrum 9-10201  
 light water, phonon spectrum and thermal neutron scattering 9-21426  
 Mars, ice retention 9-21943  
 mechanical properties, effect of dissolved impurities 9-13711  
 neutron decay and diffusion parameters, effect. of temp. 9-18573  
 nucleation by meteoritic material 9-11745  
 Nuclei prod. from I<sub>2</sub>-gasoline vapour mixture 9-9595  
 polycrystalline, grain growth mechanism 9-18410  
 polymorphs, p.m.r. and d.m.r. 9-16463  
 positron annihilation mechanism involving <sup>3</sup>S→<sup>1</sup>S conversion of positronium in ice water system 9-12079  
 pulse-irradiated, transient solvated electron and free radicals 9-10360  
 pure, binding of electron using polaron model, and calc. of absorpt. props. 9-5613  
 pure and doped, elec. props. by depolarization of thermocurrents method 9-16287  
 Raman spectra, second order, dynamical model of lattice 9-12418  
 replicator 9-7370  
 sound produced in breaking ice 9-17556  
 sound reflection coeff. at rough boundary 9-4328  
 spectral reflectance, 0.36 to 1.15 $\mu$ , rel. to thickness, incidence angle and Cu and black paint substrates 9-10188  
 strain relaxation, exptl. investigation 9-16129  
 sublimation and crystallization in vacuum 9-19665  
 sublimation in vacuum 9-19664  
 sublimation in vacuum, crystn. on subliming layer surface 9-17234  
 sublimation in vacuum, heat and mass transfer mechanisms 9-17233  
 surface structure, revised model 9-9478  
 thymine frozen soln., dimer formation 9-9297  
 Venus polar caps, radar obs. 9-18917  
<sup>26</sup>Al radioactivity in Greenland, obs. 9-10380  
<sup>10</sup>Be radioactivity in Greenland, obs. 9-10380  
 NaCl-doped, grain growth mechanism 9-18410

**Ignition** *see Combustion***Illumination***See also Brightness*

- from linear light sources, meas. 9-6553  
 optimum signal luminance for normal and proton observers 9-4169

**Image converters and amplifiers**

- analyzer tube targets from thin Si films, development 9-8587  
 camera, streak, calibration technique 9-19174  
 in cinematography system for auroral recording 9-14168  
 electronographic image tubes, mica windows 9-12978  
 eye-piece, cross-wire, digitized and telecontrolled, for nuclear emulsion meas. 9-2416  
 intensifier for X-ray diffr. pattern 9-3263  
 i.r.. device characteristics 9-2246  
 i.r. converter tube, piezoelec. power supply 9-10751  
 i.r. rare earth, 1-2  $\mu$  9-10927  
 i.r. to visible for ranges 0.5-1.0  $\mu$ , 3.0-5.5  $\mu$ ; 8-14  $\mu$  9-2253  
 neutron radiography, results display by direct viewing of scintillating plate 9-10951  
 photocathode cooling using Peltier effect 9-4444  
 properties computed from analytic potential representation 9-6492  
 Quantimet image analyzer, combination with e microscope in quantitative metallography 9-12982  
 radionuclide imaging in nuclear medicine 9-2352  
 signal-frequency, optical amplitude modulator 9-13039  
 single transients, use of Pim-3's compensated electronic shutter 9-278  
 TV image analyzer target using alloyed junction mosaics on Si 9-8586  
 u.s., use of electrokinetic target for reception 9-4346

**Image intensifiers** *see Image converters and amplifiers***Image orthicons** *see Electron tubes***Impact***See also Ballistics*

- beam, free-pinned, dynamic stresses and bending 9-16703  
 beam, stresses due to elastic bar 9-6358  
 cylindrical projectile on thin plate, simple determ. of perforation limits 9-20381  
 elastic, semi-infinite bars, 2D, asymptotic study 9-17769  
 gravitational, of astronomical systems 9-20143  
 impulse experiment with linear air track 9-4265  
 indentation problem, Prandtl's solns. 9-19789  
 jet, analogy with cavitation erosion 9-5138  
 liquid solid, pressure and shock wave velocity 9-8516  
 particle cloud impingement on metals, micron sized, damaging effects 9-9859  
 plasticine projectiles, impact on plasticine laminated targets obs. 9-19014  
 Prandtl's solns. of indentation problem 9-19789  
 response and dislocation dynamics of materials 9-21336  
 sensitivity test data, interpretation techniques 9-19009  
 steel, Kh12ND, welds, impact strength, effect of Cr content 9-14984  
 steel plates, clamped, of projectile, plastic deform. anal. 9-1279  
 supersonic jet on flat plate 9-18234  
 zirconia, thermal shock resistance, phase comp. effect 9-13742  
 Al splash generation by detonation wave impact 9-5438

**Impedance, acoustic** *see Acoustic impedance***Imperfections in solids** *see Alloys; Crystal imperfections; Solids/structure***Impurities** *see Crystal imperfections/impurities; Crystals/growth; Semiconducting materials***Impurity electron states and effects** *see Crystal electron states/impurity states and effects***Independent particle model** *see Nucleus/models***Indeterminacy**

- measuring instrument role 9-12882  
 quantum mechanical description using Jaynes' irreversible statistical mech. 9-20323  
 quantum theory propositions as a set of evolving filters on a particle beam 9-18995  
 uncertainty products, minimization by coherent states 9-80  
 inter-electronic correl. functions, condition removing degeneracy 9-20327

**Indium**

- concentration in mineral samples using ( $\gamma,\gamma'$ ) reactions 9-1934

**Indium compounds**

- chlorides, fused, structure obs. from Raman spectra 9-21215  
 Ginzburg-Landau parameters, pressure depend. 9-7881  
 In-Pb alloys, superconducting, magnetic moment as function of ext. field 9-10093  
 InAs, X-ray-K-absorption edge shifts 9-21638  
 Raman spectra at photon energies near E<sub>g</sub> energy gap 9-1806  
 semimetal, negative magnetoresist. and localized spins 9-9932  
 $\gamma$ -InAs, wave vector in forbidden gap, energy depend. 9-1537  
 (86 at %)(14 at %) TL mech. effects, type II superconds. 9-16245  
 Ag-In alloys, dil., band structure 9-15052  
 Co-In system, liquid immiscible behaviour 9-21241  
 Cu-In alloys, discontinuous precipitation kinetics 9-9797  
 Ga<sub>1-x</sub>In<sub>x</sub>As, i.r. reflection spectra, mixed cry. behaviour 9-1760  
 Hg-In amalgam, optical constants obs. 9-16392  
 In-Ga, contact resistance on CdS single cryst. 9-3613  
 In-Hg(Cd) dilute alloys, In phonon spectrum, effect of Hg (Cd) impurities 9-5533  
 In-Pb alloy, supercond., upper critical field, anomalous values 9-1498  
 In-Pb alloys, axial ratio and supercond. transition rel. to Fermi surface interactions 9-21491  
 In-Pb superconducting alloy, thermal conductivity meas. down to 0.4°K rel. to phonon scatt. mechanism 9-21444  
 In-Pb superconducting alloys, type II, specific heat temp. dependence, 1.5-4.2°K rel. to Maki parameter determ. 9-21493  
 In-Pb system, pressure depend. of superconducting critical temp. 9-16246  
 In-Tl all, deformation, stacking faults as twin nuclei 9-13728  
 In-Tl alloy, supercond., upper critical field, anomalous values 9-1498  
 InS<sub>2</sub>:Nd<sup>3+</sup> or Er<sup>3+</sup> fluorescence 9-14081  
 In<sub>2</sub>Te, thermal expansion rel. to temp. 9-18564  
 InAs:Cd, Cd ionization energy conc. dependence 9-3646  
 n-InAs:Te, injection laser, self modulation obs. 9-254  
 n-InAs:Te, Mossbauer spectra of <sup>57</sup>Fe 9-5893  
 InAs-Cu(Au, Ag) solid solutions, precipitation, effect of dislocations 9-11967  
 InAs, 4.2°K, doped, cond. band 9-1535  
 InAs, channeling of H and He ions, energy loss meas. 9-9868  
 InAs, channeling of H and He ions, energy loss meas. 9-9868  
 InAs, coupled collective cyclotron excitation- longitudinal optical phonon modes, reflectivity meas. 9-12151  
 InAs, diffusion improved by exposure to radiation, patent 9-21354  
 InAs, diffusion of Zn, conc. depend. 9-7508

**Indium compounds continued**

- InAs, effective mass carrier density dependence at 78°K 9-3639  
 InAs, electroreflectance spectra behaviour, p- to n- like changeover 9-9987  
 InAs, electrol, anomalous 9-15091  
 InAs, magneto plasma-phonon interaction from Kramers-Kronig analysis of reflection spectra 9-12363  
 n-InAs, magnetoresistance oscill. maxima fine structure at 1.6°K 9-1530  
 n-InAs, quantum thermomagn. effects 9-3629  
 InAs, self diffusion meas. 9-14957  
 InAs, spec. ht., 1/30°K 9-9843  
 InAs epitaxial films, elec. props. thickness dependence 9-1532  
 InAs films, magnetoresistance 9-9980  
 InAs Raman spectra of optical phonons, Ar laser excitation 9-12419  
 In<sub>1-x</sub>Ga<sub>x</sub>As, solid solutions, elec. resistivity and Hall coeff. meas. for energy structure and Debye temp. calc. 9-3640  
 In<sub>1-x</sub>Ga<sub>x</sub>P, photoluminescence, i.r. and visible 9-12488  
 In<sub>2</sub>O<sub>3</sub>, growth mechanism from PbO-B<sub>2</sub>O<sub>3</sub> melts rel. to habit changes 9-17257  
 n-In<sub>2</sub>O<sub>3</sub> film, photoconductivity 9-15138  
 n-InP, compensated, magnetoresistance and Hall effect 9-3627  
 InP, diffusion and solubility of Au, 600° to 850°C 9-14956  
 InP, diffusion and solubility of Ag 9-5409  
 InP, diffusion and solubility of Cu 9-5410  
 InP, electron effective mass depend. on their density 9-9979  
 InP, epitaxial films, stacking disorder 9-9617  
 InP, epitaxial growth on GaAs in open flow system 9-5243  
 InP, field ionized, stimulated emission obs. 9-15533  
 InP, light scattering from single particle electron and hole excitations 9-12443  
 InP, time-resolved photoluminescence spectroscopy for donor-acceptor recombination evidence 9-18729  
 InP clean surface, photoelec. yield near threshold 9-16319  
 InP Raman spectra of optical phonons, Ar laser excitation 9-12419  
 In<sub>2</sub>Pd<sub>2</sub>O<sub>7</sub>, pyrochlore struct., prep. at 3 kbar 9-5274  
 In<sub>2</sub>Pt<sub>2</sub>O<sub>7</sub>, pyrochlore struct., prep. at 3 kbar 9-5274  
 InS, gas, vaporization and dissociation energy, also other sulphides 9-19481  
 InS<sub>2</sub> semiconducting field emitter, field distrib. and rate of pot. fall calc. 9-17447  
 InSb-NiSb, anisotropic, as i.r. detector 9-6396  
 n-InSb, e.p.r. rel. to impurity 9-8027  
 InSb, lattice dynamics 9-11978  
 InSb, microhardness, eff. of doping 9-5485  
 n-InSb, photoconductivity under electron heating conditions 9-10063  
 n-InSb acoustoelect. current oscills. rel. mag. field 9-5561  
 InSb films, absorption edge, thickness depend. 9-3906  
 InSe, gas, vaporization and dissociation energy also other selenides 9-19481  
 InSe, photoconductivity, kinetic and stationary characts. 9-18658  
 InTe, gas, vaporization and dissociation energy, also other tellurides 9-19481  
 In<sub>2</sub>Te<sub>3</sub>, thermal conductivity, 670-1450°K 9-1405  
 (Sn at.%) Pb-(2 at.%) In supercond. type-II, flux jump size distrib. 9-1480  
 In-Al alloys, superconductivity; resonant freq. of tank cct. with specimen as core and a.c. mag. susceptibility 9-16237

**indium antimonide**

*See also Semiconducting materials/indium antimonide*

- Bloch electron anomalous velocity in mag. field and combined resonances 9-21460  
 defect structure from X-ray topography 9-1208  
 diffusion improved by exposure to radiation, patent 9-21354  
 diffusion of Se 9-18486  
 dislocation velocity 9-7489  
 edge absorption of mechanically polished surface 9-12379  
 exciton effects at hyperbolic crit. pts. 9-5901  
 far i.r. detector, response enhancement by near i.r. irradi. 9-3746  
 far i.r. resonant photoconductive props. due to cyclotron resonance, n-type 9-17440  
 film, formation and props. 9-11770  
 film, transport parameters temp. depend. interpretation 9-12146  
 film, zone melting by e beam heating 9-14893  
 filter, infrared spectral region 9-4533  
 n-type, far i.r. resonant photoconductive props. due to cyclotron resonance 9-17440  
 n.m.r., impurity states detection 9-10297  
 photoelectromagnetic effect, short-circuited Demer voltage effects 9-5772  
 preparation, purification and single crystal growth 9-1147  
 Raman scattering by LO phonons, resonance enhanced, elec. field induced 9-12420  
 reflection spectra 9-3877  
 specific heat, 1-30°K 9-9843  
 superconducting, with anisotropic upper critical field, props. 9-21492  
 thermoelectric power, depend. on carrier density 9-16309  
 p-InSb, doped, fundamental absorpt. temp. dependence 9-10202  
 n-InSb, radiation absorption, mm. and sub-mm., 2.1 and 4.2°K 9-16413

**INDOR (internuclear double resonance)** *see Nuclear magnetic resonance and relaxation*

**Inductance**

- $LiL \gg M^2$ , derivation and physical significance 9-12825

**Inert gases**

*See also the individual gases*

- alkali-metal-seeded, constricted positive columns of arc discharges, descriptive theory development 9-13469  
 atom bound states obs. 9-18142  
 atom reactions with organic solids 9-1906  
 atom reactions with organic solids 9-1907  
 atoms, repulsive potential-energy curves 9-9153  
 condensed, theory, quantum effects and props. 9-13509  
 crystals, absorption, one-phonon defect-induced i.r., theory 9-5526  
 desorption from W(100) surface on heating 9-5263  
 dielec. const., theory 9-13493  
 diethyl ether-inert gas mixtures, thermal conductivity 9-14818  
 diffusion in alkali halides, theory 9-3386  
 diffusion in ionic crystals, migration and trapping 9-11891  
 diffusion of slow electrons, in presence of inelastic collisions 9-15975  
 discharges, positive column, diffusion theory application 9-21116  
 discharges, positive column, medium pressure results 9-21115

**Inert gases continued**

- electron transport coeff. calc. from Boltz eqn. 9-13496  
 infrared absorption, collision induced in mixtures 9-4914  
 ion bombardment of Mo, electron emission and ion reflection 9-12218  
 ion lasers, calc. of maximum inversion density and power output 9-4465  
 ionization chamber with metal film for 100-1000 Å photon detection 9-19227  
 ions, bombardment of Ge, cathode sputtering coeffs. 9-15037  
 ions, charge-transfer collisions with N<sub>2</sub> 9-15957  
 ions, low-energy, penetration and capture in polycryst. W. 9-5590  
 liquid, shear viscosity theory 9-9490  
 metal surfaces, diffusion coeffs. and adhesion time 9-21347  
 mixture with other gases, reaction kinetics 9-1893  
 mixtures with deuterium, thermal conductivities 9-956  
 mixtures with H<sub>2</sub>, N<sub>2</sub>, methane, refr. index rel. to long-range atom mol. interactions 9-9304  
 mixtures with H<sub>2</sub>, photoionization ion-mol. reactions 9-17132  
 perturbation of methane 3.39 μ line, breadth and shift 9-15891  
 plasma decay at an elevated pressure 9-4998  
 Rayleigh scattering, cage model 9-21139  
 solid, electron. mobility maxima in conduction band, applic. of theory of wave scatt. by fluctuating potentials system 9-8376  
 solid, ion-ion repulsive interactions 9-17252  
 solid, lattice dynamics, many-body van der Waals forces effect 9-13786  
 solids, infl. of lattice anharmonicity on exponential potential parameters 9-16161  
 troilite from Great Namaqualand, inert gas anomalies 9-6187  
 u.s. waves absorpt. and dispersion in binary mixtures, two-fluid model 9-3054  
 Cs spectrum second doublet broadening effects 9-2814  
 O<sub>2</sub> mixtures, ion recomb. temp. depend. 205-690°K 9-5076  
 SF<sub>6</sub>, Kerr eff. obs. at various pressures, second Kerr virial coeffs. obtained 9-21144

**Inflammability** *see Combustion*

**Information theory**

- See also Entropy; Random processes; Statistical analysis/applications*  
 axiomatic definition in quantum mechanics 9-12885  
 dynamic programming applications 9-10621  
 energy intensity, anal. 9-4223  
 optical imaging systems 9-20541  
 random probability distrib. 9-4242

**Infrared detectors** *see Bolometers; Radiation detectors*

**Infrared sources** *see Light sources; Radiation/heat*

**Infrared spectra** *see Spectra*

**Instruments**

- See also Laboratory apparatus and technique; Measurements; Recording; and under specific subjects, e.g. Astronomical instruments; Some specific instruments are listed separately, e.g. Spectrometers; Thermometers. Where no separate headings exist, entries describing instruments may be found included under the headings of the appropriate quantities or subjects*  
 agrimeter for atm. elec. pot. gradient 9-1940  
 interference dynamometer 9-6271  
 kinematometers, magnetic measurement scales 9-8350

**Insulating materials, acoustic** *see Noise abatement*

**Insulating materials, electrical** *see Dielectric properties of substances*

**Insulating materials, thermal** *see Conductivity, thermal*

**Integral equations**

- Abarzumian's for stellar velocities, generalization to n dimensions 9-33  
 boundary value problem integrals, collocation method of soln. 9-12855  
 coupled, Lee model, calc. of S-matrix 9-6592  
 elastic free-free body, natural freq. and modes 9-4292  
 Fredholm, complementary variational principles and bounds 9-14310  
 Fredholm in third sector of Lee model 9-2446  
 integro-differential transport eqns. solns. 9-8421  
 Kirkwood-Riseman theory of macromolecules, numerical soln. 9-16656  
 optimisation principle for Monte Carlo methods 9-12857  
 for plane wave scatt. by singular potentials 9-53  
 Romberg integration, appl. of Neville's process 9-6348  
 singular, Muskhelishvili-type, book on Boundary value problems 9-18982  
 for sound radiation from vib. surface, iterative solns. and convergence 9-16730  
 symmetry group of eqn forming generalised eqns. for H atom 9-9154  
 transport and nonlinear functionals 9-109  
 Volterra and delay eqn., boundedness and oscillation 9-20299

**Integrals**

- See also Calculus; Green's function methods*  
 atomic, evaluation 9-12866  
 Coulomb and hybrid related to overlap 9-6276  
 Feynman, convergent, asymptotic estimates 9-14308  
 Feynman, renormalization 9-18979  
 Feynman-Cameron, approximation for generalized Schrodinger eqn. 9-8413  
 finite integral transforms for forced vib. of circular plates 9-19051  
 functional, for many boson systems 9-8447  
 gas kinetic electron-Ar collisions 9-17000  
 molecular, over Hermite-Gaussian functions 9-17018  
 overlap, in Slater-type atomic orbitals 9-15801  
 overlap to express Coulomb and hybrid integrals 9-6276  
 radial, for atomic many-body problem 9-16993  
 tabulated, book 9-10683  
 two-centre, α-function technique 9-2132  
 two-centre Coulomb, between Slater-type atomic orbitals 9-15802  
 two-centre hybrid, over Slater-type atomic orbitals 9-15800  
 wave equation, perturbation theory of semigroups 9-8406

**Intensity measurement**

- c.m. fields, apparatus 9-10767  
 light sources, terrestrial, by satellite 9-21751

**acoustics**

- impulse sound level meter, required properties 9-2226  
 loudness analyser, Zwicker-type analysis 9-17809  
 by numerical integration tech. 9-10729  
 PbZrO<sub>3</sub>-PbTiO<sub>3</sub> Piezoelec. transducers for broad-band noise, 10-100 kHz 9-2228

**Interatomic forces, between bound atoms** *see Bonds; Molecules/internal mechanics; Solids*

**Interatomic forces, between free atoms** *see Collision processes/atoms*



**Interface tension** *see Surface tension*

**Interference**

NGC 7000, electron temp., high resolution interference method 9-18844  
particles, nonidentical 9-13095  
particles, nonidentical 9-2452

**acoustic waves**

coincident, finite amp., plane waves of different freqs. 9-2217  
in Wood's model shallow-water propag. expts., sound focusing and beam-  
ing 9-15236

**electromagnetic waves**

X-ray interference intensities, pressure effect 9-5294

**light**

*See also Films, solid/optical properties*  
crystal with dislocation, Moire pattern 9-13617  
filter analyzer, determination of water content by near infrared absorption  
9-14140  
filters, i.r., materials 9-4532  
filters, narrow band, effective refractive index as performance criterion  
9-8664  
fringes from bending bar, behaviour 9-20397  
in gas, density determ. by fringe shift meas. in axisymmetric interfero-  
grams 9-17143  
hook fringe prod., Jamin interferometer method 9-15543  
irradiance fluctuations, correl. function, rel. to fourth order coherence func-  
tions 9-10842  
laser beams, failure of Fresnel laws 9-2369  
laser expts. rel. to wave- particle model for light 9-6500  
Moire fringes, measurement of small angles using plane diffraction grat-  
ings 9-4216  
Moire phenomena, photographic peculiarity 9-20546  
multiple wave phenom. using identical scatterers 9-19163  
production, new and simple method 9-13050  
random structure superposition 9-6547  
solids and liquids, effects due to low-power laser heating 9-12323  
from thermal light source by superposition of light from two independent  
sources 9-10843  
three-beam, optimum intensity distrib. 9-10898  
wave front freqs. spatial to temporal conversion and reconversion 9-8649  
wideband modulator, ferroelectric ceramic mirror 9-13051  
Cd spectra, holographic, obtained with Lloyd's mirror 9-4496  
Hg spectra, holographic, obtained with Lloyd's mirror 9-4496  
Ta<sub>2</sub>O<sub>5</sub> thin films, peaks, elec. field induced shift 9-19975

**Interference spectroscopy** *see Spectroscopy*

**Interferometers**

Fabry-Perot, automatic recording wavelength modification, press. control  
by voltage 9-2402  
laser, for earth strain meas. 9-4038  
Mach Zehnder, for electron density in rapidly varying plasma 9-19543  
reflection echelon, line-shape parameters determ., graphic technique  
9-4517

**acoustic waves**

u.s., dispersion in normal H<sub>2</sub> and normal H<sub>2</sub>-He mixture 9-3055

**electromagnetic waves**

10<sup>3</sup> wavelength baseline, for radioastronomy 9-12774  
astronomical, for radio source polarization distrib. meas. 9-12734  
Fabry-Perot resonator for plasma density meas. 9-888  
Michelson type in overmoded waveguide for liquid dielectric measure-  
ments 9-5182  
quasi-optic imaging resonator for plasma diagnostics 9-21080  
radar system for atm. temp. and density profiles 9-18804  
radio astronomy application 9-14276

**light**

active, for laser pulse frequency modulation 9-16794  
alignment meas., high accuracy 9-4514  
for aspherical surfaces quality control 9-4512  
autocollimator errors determ. 9-2401  
confocal for pointing at coherent source, alternative to theodolite 9-4518  
Fabry-Perot, appl. to repetitive Q-switching in continuously pumped  
Nd:YAl garnet laser 9-13033  
Fabry-Perot, electrostrictively scanning 9-15552  
Fabry-Perot, equi- inclination bands rel. to light coherence 9-8651  
Fabry-Perot, thermal scanning 9-2425  
holographic for photoelastic stress analysis 9-6365  
installation on high resolution grating spectrometer for precise calibration  
9-17897  
Jamin, prod. of hook fringes 9-15543  
laser, for earth strain meas. 9-10373  
laser, He-Ne gas, Michelson type, deformable bodies collision processes  
obs. 9-20535  
laser beam scanner 9-19158  
as level 9-4215  
multi-beam, used as light modulator 9-2395  
HCN laser beam as source for plasma decay study 9-7166

**Interferometry**

dye soln. fluorescence spectra detection method, 720-900 nm 9-9241  
hologram, using two reference beams 9-4495  
laser beams, intensity interferometry by two- photon excitation of  
fluorescence 9-20532  
laser determination of dynamic response of solids induced by charged  
particle interaction 9-17348  
laser for length meas. 9-2127  
plasma diagnosis by interferometric methods 9-14784  
resonator interferometry of pulsed gaseous submillimeter wave lasers  
9-20292  
teaching experiments in optics and at super-high frequencies 9-8338  
X-ray, rel. to 'Angstrom ruler' 9-10608  
Youngs experiment at super-high freqs., teaching demonstration 9-8338  
CaSO<sub>4</sub>.2H<sub>2</sub>O (gypsum) film, 9 mm. study rel. to principal permittivities and  
elec. axis 9-7943

**acoustic waves**

holographic, opt., vibr. analysis of sonar transducer 9-4353  
holographic, time- averaged optical, for visualiz. of standing acoustic  
waves 9-10738  
teaching expt. demonstrating phase relations 9-8338

**electromagnetic waves**

intercontinental-baseline radioastronomy 9-17627  
microwave, H plasma decay meas. 9-7168  
in radioastronomical obs. of celestial spectra 9-20251

**Interferometry continued**

**electromagnetic waves continued**

velocity meas. appl. to light 9-8642

**light**

brittle materials, testing 9-1272  
dielectric property meas. in solids 9-12181  
distance meas., high precision 9-10610  
Edser-Butler fringes used to meas. fibre diameters 9-4213  
fringe strength meas. 9-10908  
holographic, method reducing movement of emulsion during processing  
9-13037  
holographic, stroboscopic, for vibrs. analysis 9-8634  
holographic interference microscope applics. 9-4493  
intensity interferometry in astronomy 9-20250  
interference dynamometer 9-6271  
interferogram with longitudinally reversed shear, holography applic.,  
theory 9-20545  
interferograms, multiple display using holographic techniques 9-4515  
laser, in far i.r., for electron density meas. 9-14780  
with lasers, gaseous 9-19142  
Moire, with embedded grids, effect of refraction 9-19164  
phase changes, small, improved accuracy determ. 9-10898  
phase fluctuations of laser beam through turbulent atm. 9-10869  
reflectors, with indep. variable wavelength and reflectance 9-8650  
rough surface, using CO<sub>2</sub> laser source 9-4516  
spectrochemical analysis with Fabry-Perot etalon, spectrograph combina-  
tion 9-18776  
streak, laser beam expansion by prisms 9-4485  
vibration analysis by projected fringes 9-6369  
vibrations of a plate, meas. method 9-15456  
SiO<sub>2</sub> films, thickness meas. over small geometries 9-11767

**Intergalactic matter** *see Galaxies*

**Intermetallic compounds** *see Alloys; Semiconducting materials and under the compounds and alloys of the individual metals*

**Intermolecular forces** *see Molecules; intermolecular mechanics*

**Internal conversion** *see Beta-ray spectra/conversion electrons; Gamma-rays/internal conversion*

**Internal friction**

alkali halides, deformed crystal, time depend. 9-7530  
alkali silicate glasses, rel. to ionic position interchange, 180-500°C  
9-3404  
alloys, at large strain amplitudes 9-16118  
amplitude dependent, time depend. by distribution funct. of dislocation  
pinning 9-5426  
graphite, n-irrad., rel. to annealing temp., damping anal. 9-7525  
graphite, peak rel. to crystallite size, destroyed by annealing or neutron  
irrad. 9-7526  
graphites, and dynamic elastic modulus, 4-750°K 9-7527  
group III-V compounds, below room temp. 9-1270  
intercrystallite thermoelastic Karman correlation function 9-3396  
measurement, anal. of compound piezoelec. vibrator 9-7523  
measurement rel. to temp. freq, strain amplitude, apparatus 9-5428  
metals, at large strain amplitudes 9-16118  
metals, automatic recording apparatus 9-1265  
steel, martensitic, amplitude dependence rel. to carbon-dislocation interac-  
tion 9-1218  
suspension meas. method, elimination of energy absorption by strings  
9-5427  
weld metal, -30° to +300°C 9-19782  
Al, amplitude depend. rel. to previous thermal and mechanical treatments  
9-17299  
Al, plastically deformed, low temp. 9-7524  
Al, single crysts., damping during plastic deform. 9-9744  
Al, sintered, grain boundary maximum 9-1266  
Au, effect of Ar<sup>+</sup> irrad. 9-1267  
Au, electron irradiated at low temp., changes rel. to dislocation pinning  
9-11912  
Au, internal friction, cold-worked and irradiated at low temp. 9-5430  
Bi-Sb alloys, grain boundary creep meas. 9-16104  
CH<sub>3</sub>NH<sub>2</sub>Al(SO<sub>4</sub>)<sub>3</sub>.12H<sub>2</sub>O, in phase transition region 9-19774  
CdS, temp. dependence, 300-700°K and mechanism 9-1268  
Cu:Pt(Pd) force on dislocations, effect of impurity atoms 9-3397  
Cu-Ni alloy, damping behaviour miscibility gap existence 9-3400  
Cu-Ni alloys, plastically deformed 9-13720  
Cu, peak P<sub>1</sub>, impurity effects 9-7528  
Fe-3wt %Si, magnetoelastic internal friction, infl. of temp. on amplitude  
depend. 9-11915  
Fe, electrolytic, ageing by amplitude depend. method 9-13764  
Fe whiskers, and plastic deform. and recovery 9-1269  
Gd, spectrum, analysis of  $\alpha$  and  $\beta$  peaks 9-5431  
Ge, below room temp. 9-1270  
Ge, dislocation-fuse samples, l.f. damping 9-5432  
Ir, polycrystalline, up to 2000°C at low freq. 9-14965  
LiF, temp. dependence, 150-300°K 9-3399  
Mg-Cd alloys, meas. for Zener relaxation determ. 9-11913  
Mo, polycrystalline, up to 2000°C at low freq. 9-14965  
NaCl:CaCl<sub>2</sub>, rel. to temp., freq., strain amplitude, apparatus 9-5428  
NaCl, rel. to temp., freq., strain amplitude, apparatus 9-5428  
NaCl, temp. dependence, 150-300°K 9-3399  
Ni-Cr-Al alloys, temp. dependence 9-14966  
Ni-Cr-Ti alloys, temp. dependence 9-14966  
Ni, during creep, 823-1023°K 9-13721  
Ta, polycrystalline, up to 2000°C at low freq. 9-14965  
 $\alpha$ -Ti, relaxation spectrum, effect of H content 9-7534  
V-N solid solns., l.f. meas. 9-19788  
V-O solids solns., l.f. meas. 9-19788  
W, freq. dependence at 1400-2500°K 9-3401  
Zns. amplitude depend. pinned dislocations oscillations reduction due to Cu  
impurities 9-5429

**liquids** *see Liquids; Viscosity/liquids*

**Internal stresses** *see Stresses, internal*

**Intruclear double resonance (INDOR)** *see Nuclear magnetic resonance and relaxation*

**Interplanetary magnetic fields**

discontinuities on mesoscale possibly not of solar origin 9-20235  
fluxgate magnetometer sensor, high stability with time and temp. 9-4124  
and geomagnetic DP2 fluctuations, correl. 9-10536  
guiding centre drifts in time-dependent meridional magnetic fields  
9-21954  
effect on hydromag. interplanetary shock waves 9-8286

**Interplanetary magnetic fields continued**

lines of force, random walks and stochastic aspects 9-21952  
 map, sector formation from solar induced magnetic loops 9-15351  
 meridional component shape, field props. studied 9-14246  
 particle, charged, dynamics in spiral field, drift velocity determ. 9-21955  
 solar wind interaction, Pioneer 6 obs. 9-2063  
 spacecraft obs. during IQSY 9-8285

**Interplanetary matter**

boundary with, and transition from outer ionosphere 9-17581  
 charged particles, scattering by random e.m. fields 9-16773  
 cometary statistics and perihelia 9-18919  
 cosmic dust collection, Luster flight (1965) 9-6188  
 cosmic dust grains rotation and orientation 9-10453  
 cosmic ray modulation 9-17606  
 cosmic ray radial anisotropy, implication of obs. 9-8922  
 earth's magnetotail electrons obs.,  $E \geq 45$  keV 9-12759  
 electron content meas. by radio propag. effect 9-10535  
 electrostatic charge of grains 9-20234  
 flare plasma transport from Sun to earth 9-2078  
 grains, electrostatic charge 9-20234  
 particle distribution function near ecliptic 9-17648  
 plasma, heterogeneities, 1965-1966 9-2062  
 plasma, ionization processes in expanding solar corona 9-8290  
 proton outward flow from Earth's bow shock 9-8188  
 proton temperature estimates, Venera 3 space probe, (1965) 9-18923  
 self-gravitating globes, thermoelastic deforms., explicit form of governing eqns. 9-6170  
 solar flare electrons  $>40$  keV, propagation obs. 9-10552  
 solar radiation press. effects and particle nature 9-21953  
 solar wind electrons, Vela 4 meas. 9-10545  
 solar wind particles, direct obs. (1962-67) 9-15358  
 spacecraft obs. during IQSY 9-8285  
 zodiacal light dust particles, detection of motion 9-17649

**Interstellar matter**

absorption bands, due to reson. lines of impurity atoms? 9-18882  
 absorption in Kapteyn's Selected Area 19, obs. 9-16589  
 Aql constellation, colour excess study for obs. of dust matter in galactic plane 9-21842  
 atmosphere, plane-parallel finite Rayleigh-scatt., rad. field construct. and soln. 9-18877  
 atmospheres, spectra, line-blanketing eff. for pure abs. and non-coherent scatt. 9-16587  
 axisymmetric dynamo model 9-8265  
 Cepheus region, extinction law 9-10500  
 clouds, interaction with stars to give 'r.r. stars' 9-6136  
 clouds, mass spectrum rel. to vels. and cross sections 9-8264  
 clouds, star formation studying using virial theorem 9-20200  
 cosmic dust grains rotation and orientation 9-10453  
 cosmic ray diffusion and nuclear reaction effects 9-12661  
 cosmic ray medium, shock wave structure 9-1988  
 Cyg constellation, colour excess study for obs. of dust matter in galactic plane 9-21842  
 dielectric spherical grain model, agreement with far u.v. extinction data 9-18881  
 dust, distrib., explanation of starlight polarization variability 9-15322  
 dust layer, space struct. problem, rel. to visible brightness of Milky Way 9-21842  
 electron density, suggested determ. using pulsars 9-8268  
 extinction curves for arrays of polycyclic aromatic mols. 9-15323  
 n galactic latitudes, faint blue objects obs., nature 9-16552  
 galactic mag. field, stochastic nature, applic. to cosmic ray life 9-20150  
 gas, gravitationally condensed, star motion 9-17625  
 gas cloud collapse, equation of hydrodynamics with gravitation, suitable for numerical methods 9-12728  
 gas cloud collapse analysis 9-20175  
 gas cloud perturbing stellar orbit, motion inclined to galactic plane 9-16555  
 gas clouds, dissociation and ionization front 9-8246  
 gas into stars conversion, disruption forces, dynamical theory 9-21909  
 gas orbit under non-gravitational and gravitational forces 9-12683  
 gas relativistic, gravitating, collective motions 9-20135  
 gravitational gas, generalized kinetic eqn. obtained 9-14756  
 IC 1805 and 1848, low-freq. absorption, electron temp. and non-thermal emission obs. 9-20166  
 infinite cyl. with var. density, radial pulsation calc. 9-8235  
 interaction with stars, density distrib. law near star and its appl. 9-21910  
 mass and vel. distrib., anal. 9-20201  
 Metagalaxy, average density of dust matter and non-relict origin 9-17609  
 Milky Way, visible brightness, rel. of space struct. of dust layer 9-21842  
 obscuration and reddening of Wolf-Rayet stars 9-18884  
 Perseus spiral arm in dirn Cassiopeia A mag. fields of order  $2 \times 10^{-5} \text{ G}$  determ. 9-2025  
 plasma, cosmic; nonlinear ion waves with rot. mag. vector 9-2022  
 plasma, gravitational instability with Hall effect 9-7178  
 plasma, non-uniform rot., generation by viscous forces 9-6114  
 plasma, relativistic, anisotropic, stability in mag. field, growth of Alfvén type waves 9-14552  
 polarization of radiation of the turbulent plasma under cosmic conditions 9-2023  
 R (interstellar absorpt. ratio) found to be valid for distances  $>1 \text{ kpc}$  9-15284  
 reddening material, distrib. within few kiloparsecs of sun 9-12725  
 reddening of Cepheus region 9-15324  
 self-gravitating gas, approach to equilibrium 9-20136  
 self-gravitating masses, oscillations and stability in axial mag. field 9-17624  
 self-gravitating medium in quasi-static equilibrium, physics of, using phenomenological approach of thermodynamics 9-10501  
 self-gravitating system in extended phase, relaxation eff. 9-16571  
 sun environs, dust distribution determ. by photometry 9-8247  
 synchrotron radiation polarization, effect of ionized medium 9-12726  
 synchrotron radiation reabsorption 9-10502  
 universe, expanding; observable horizons and photon propagation 9-10455  
 variable  $\lambda$  4430 absorption 9-20202  
 wind, interaction with diffuse nebulae 9-8229  
 CH mol., photodissociation mechanism 9-18880  
 H<sub>2</sub> mol., photodissociation mechanism 9-18880

**Interstellar matter continued**

H gas clouds, formation structure and propagation of R-fronts and the Stromgren sphere 9-16553  
 H I clouds, densities near H II region fronts, calcs. 9-18883  
 H II regions, abundances 9-20162  
 H II regions, electron temp., high resolution interference method 9-18844  
 H II regions, fronts, H I clouds, densities, calcs. 9-18883  
 H II regions, galactic, southern hemisphere, 5 GHz continuum obs., 28 maps 9-15280  
 H II regions, IC 1805 and 1848, low-freq. absorption, electron temp. and non-thermal emission obs. 9-20166  
 H II regions, molecular in form, gas speed determ. 9-20203  
 H II regions, obs. and contour maps 9-21859  
 H II regions, opacity and structure 9-20167  
 H II regions, stability of ionization fronts, effect of interstellar mag. field 9-12729  
 H interstellar clouds, densities 9-2024  
 H<sub>2</sub> in localized regions, formation mechanism 9-16590  
 HII region, OH radiolines obs. for W3,49,51,75, NGC 6334 and On A 9-18845  
 H-H<sub>2</sub> (para and ortho) collisional excitation of rot. levels calc. up to J=15, and for  $10 \leq T \leq 10^4 \text{ K}$  9-14227  
 He, metastable <sup>2</sup>S state, possibility of detect. 9-18878  
 NH<sub>3</sub> mols. detection by microwave emission 9-8266  
 NO molecules, radiolines obs. 9-17626  
 OH-emission sources, positions and Stokes parameters 9-16593  
 OH 18 cm radiation, stimulated elementary model 9-12727  
 OH excitation mechanism 9-16591  
 OH mol. r.f. absorpt. and emission 9-18879  
 OH radio lines emission in W3, 49, 51, 75, NGC 6334 and On A 9-18845

**Interstitials** *see* *Crystal imperfections/interstitials*

**Invariance (CP, CPT)** *see* *Elementary particles/symmetry*

**Iodine**

adsorption by C from aqueous soln., with micropore filling 9-9625  
 adsorption on graphite and desorpt. in vacuum and Ar, 27-1100°C 9-9626  
 atom, mag. susceptibility meas. 9-13304  
 charge-transfer spectra with H<sub>2</sub>S and benzene in solid matrices 9-12380  
 discharge electric, 2062 Å emission line at 0.5 torr, monochromatic lamp devel. 9-4535  
 electronically excited atoms, reaction with methyl iodide 9-1924  
 impurities in CuCr<sub>2</sub>Te ferromag. spinel, internal mag. field determ. from Mossbauer effect 9-16400  
 ionic cond. in single crystals. 9-10039  
 ions, cross-sections for electron loss in N, 13.7-64 MeV 9-3006  
 ions, equilib. charge states in solids and gases in energy range, 10-180 MeV 9-11620  
 laser, chemical reaction with Cs vapour for depletion of ground state population, patent 9-8618  
 mobilities of electrons and holes 9-17424  
 radioiodine recoils in KIO<sub>3</sub>,  $\pi$  irradiated 9-16193  
 solid, X-ray L<sub>III</sub> absorpt. spectrograms 9-12455  
 I<sub>2</sub>-gasoline vapour mixture, ice nuclei prod. 9-9595  
 I<sub>2</sub> formation in photodissociation laser, effect of stimulated emission 9-15902  
 I<sub>2</sub> in different solvents, absorption maxima of visible band 9-19634  
 I<sub>2</sub> in hydrocarbon solvents, contact charge-transfer spectra 9-19435  
 I<sup>-</sup>, orbital wave functions, reduced basis set expansions 9-11385  
 I<sup>-</sup> aq. medium, interaction energy, 25°C 9-11719  
 I<sub>2</sub> crystal, defect electrons, dark injection from electrolyte contacts 9-4002  
 I<sup>-</sup> centre, derivation of spin Hamiltonian of two equivalent nuclei 9-5986  
 I<sub>2</sub>(<sup>3</sup>I<sub>g</sub>), direct predissociation 9-9291  
 in Sb<sub>2</sub>Se<sub>3</sub>, needle-like crystals, doping effects on conductivity and photoconductivity 9-1194

**Iodine compounds**

DPPH iodine complex, magnetic and electrical props. 9-5797  
 iodates, noncentric, electro-optical and nonlinear optical props. 9-3867  
 IBr, crystal structure 9-11848  
 IF<sub>3</sub>, force consts., vibration amplitudes, shrinkage effect, Coriolis consts., calcs. 9-9216  
 IF<sub>7</sub>, vibr. spectra 9-2871  
 I<sub>2</sub>O<sub>4</sub>, quadrupole splitting of <sup>129</sup>I Mossbauer level at 80°K 9-16403  
 IOF<sup>-</sup> force consts., vibration amplitudes, shrinkage effect, coriolis consts., calcs. 9-9216

**Ion beams**

*See also* *Energy loss of particles; Ion optics; Mass spectrometers; Particle accelerators; Sputtering*  
 channelled, stopping powers from scattering effects 9-5586  
 in crystals, planar blocking intensities correlated with continuum potentials 9-16190  
 cyclotron reson., spectroscopy and ejection for ion-mol. reaction study 9-10830  
 duoplasmatron pulsed ion beam composition meas., for continuous and pulsed gas feed 9-234  
 duoplasmatron pulsed ion beam composition meas., for continuous and pulsed gas feed 9-6494  
 emission current regulator to 0.1% of electron impact source 9-2359  
 extraction by magnetic shielding in cyclotron 9-19260  
 heavy element, equilibrium charge distribution 9-10834  
 heavy ions, subharmonic acceleration in cyclotron 9-20719  
 instabilities, threshold, explt. investigation 9-901  
 light, accelerator with vacuum target chamber 9-11165  
 metallic, prod. from sputtering type Penning discharge 9-3020  
 N<sub>2</sub><sup>+</sup>+D<sub>2</sub><sup>+</sup>→N<sub>2</sub>D<sup>+</sup>+D, reaction cross sections, 1-100 eV 9-17075  
 negative, prod. with energies below 10 eV, apparatus 9-10833  
 plasma source; high intensity, low energy spread for chem. accelerators 9-10829  
 position detector of charged particle beam 9-447  
 range meas., low energy in amorphous solids, rel. to deduction of interatomic potentials 9-5585  
 AlSiB, channeling of H and He ions, energy loss meas. 9-9868  
 Ar<sup>+</sup> energy distrib. obs. from non-magnetic hot cathode 9-2361  
 Ar<sup>+</sup>+D<sub>2</sub><sup>+</sup>→ArD<sup>+</sup>+D, reaction cross sections, 1-100 eV 9-17075  
 Br, equilib. charge states in solids and gases in energy range, 10-180 MeV 9-11620  
 CO<sup>+</sup>+D<sub>2</sub><sup>+</sup>→COD<sup>+</sup>+D, reaction cross sections, 1-100 eV 9-17075  
 GaSb, channeling of H and He ions, energy loss meas. 9-9868



**Ion beams continued**

- H, deflection and rotation, rel. to obtaining high power beams 9-17864  
 H and H from impulse source, intensity increase 9-20496  
 HD<sup>+</sup>, intensity automatic meas. 9-17863  
 He<sup>+</sup> scattered from semicrystalline targets, energy distributions 9-21449  
 I, equilib. charge states in solids and gases in energy range, 10-180 MeV 9-11620  
 InAs, channeling of H and He ions, energy loss meas. 9-9868  
 InSb, channeling of H and He ions, energy loss meas. 9-9868  
 Li, charge distrib. after passage through gas or foil, 0.5-2 MeV 9-16772  
 Li from charge exchange by 5-40 KeV p 9-233  
 Mg from charge exchange by 5-40 KeV p 9-233  
 Mo, reflection and electron emission on bombardment by rare gas ions 9-12218  
 N<sub>2</sub>, D<sub>2</sub> reactions, product energy and ang. distrib. meas., 25-135 eV 9-7035  
 N<sub>2</sub>, H<sub>2</sub> reactions, product energy and ang. distrib. meas., 25-135 eV 9-7035  
 N<sub>2</sub>, HD reactions, product energy and ang. distrib. meas., 25-135 eV 9-7035  
 NO<sup>+</sup>, abundance of excited ions 9-8589  
 Na from charge exchange by 5-40 KeV p 9-233  
 P, channelling in Si, effect of defects 9-9708  
 Ti, D<sup>+</sup> backscattering energy distrib. 9-12037  
 Zn from charge exchange by 5-40 KeV p 9-233

**effects**

- in crystals, single, positively charged 9-1414  
 implantation for semiconductor doping 9-5669  
 inert gas, low energy, penetration and capture in polycryst. W. 9-5590  
 inert gases, bombardment of Ge, cathode sputtering coeffs. 9-15037  
 material processing (etching, drilling etc) apparatus 9-235  
 metal attack by bombardment 9-5296  
 phase formation kinetics, dose dependence 9-3483  
 polymer film, photoresist, scattering effects 9-13813  
 rare gases, electron emission and ion reflection from Mo target 9-12218  
 X-ray prod. from 20-80 keV ion beam collisions with C target 9-9151  
 Xe, bombardment temp. effect on trapping in oxides and halides 9-19746  
 Ar, proton excitation of 1300-A continuum 9-9133  
<sup>40</sup>Ar, monoenergetic, bombardment on (111) surface of single Au cry., directional eff. of sputtering 9-13814  
 Au, internal friction, Ar<sup>+</sup> eff. 9-1267  
 on Au single cry., (111) surface, directional eff. of sputtering 9-13814  
<sup>11</sup>B, monoenergetic, bombardment on (111) surface of single Au cry., directional eff. of sputtering 9-13814  
 Be, range and dE/dx of C, N, O, F, and Ne at 500 keV to 2 MeV 9-9871  
 C, range and dE/dx of O and Ne at 500 keV to 2 MeV 9-9871  
 D + D<sub>2</sub>O → OD + D<sub>2</sub>, cross-section for incident in energies near 2 eV 9-921  
 Ge:In(Tl,Sb,Bi,Pb) ion implantation, dopant lattice location by C ions back-scattering technique 9-18629  
 Ge, elec. conductivity 9-7807  
 Ge, irradiated by inert gases, cathode sputtering coeffs. 9-15037  
<sup>1</sup>H, monoenergetic, bombardment on (111) surface of single Au cry., directional eff. of sputtering 9-13814  
 H<sup>+</sup>, darkening of metal oxides 9-12370  
 H<sup>+</sup> + H<sub>2</sub>O → OH + H<sub>2</sub>, cross-section for incident ion energies near 2 eV 9-921  
<sup>4</sup>He, monoenergetic, bombardment on (111) surface of single Au cry., directional eff. of sputtering 9-13814  
 Hg<sub>1-3</sub>Cd<sub>2</sub>Te layers, formation by Hg<sup>+</sup> bombardment of CdTe crystals 9-14898  
 Ir, radiation damage, field ion microscope exam., exptl. technique 9-5580  
 Li<sup>+</sup>, vibrational excitation of H<sub>2</sub> mols in central collisions 9-7097  
 Mo target bombardment, secondary e. emission dependence on ion charge 9-21556  
<sup>14</sup>N, monoenergetic, bombardment on (111) surface of single Au cry., directional eff. of sputtering 9-13814  
<sup>20</sup>Ne, monoenergetic, bombardment on (111) surface of single Au cry., directional eff. of sputtering 9-13814  
 Ni<sup>2+</sup> absorpt. spectra in three Tutton salt crystals 9-12369  
 Pb, self-sputtering energy efficiency 9-9870  
 Si, implantation doping of B and P ions, thermal annealing of radiation defects, kinetics 9-21327  
 p-Si, P-bombard. at 30 keV, effects on elec. props. 9-9999  
 Si single crystals, sputtering by Ar ions, detection 9-19873  
 Xe bombardment of Ge, e. emission and defect formation and annealing 9-18662

**Ion counters** *see Counters***Ion emission**

- from crystals, angular distrib. mass dependence, transition to classical limit 9-7863  
 discharge initiation by negative ion desorption 9-21114  
 D, auto-ionic, in strong elec. fields, rel. to neutron prod. 9-16322  
 Ir, field-evaporated atoms charge state, obs. 9-10085  
 Ir, field-evaporated atoms charge state, obs. 9-5783  
 Ir field-ion specimens, study of oxide film growth 9-21280  
 Ta, by hypervelocity impact of micron size Fe particles, mass analysis 9-10084  
 W, field evaporated atoms charge state, obs. 9-5783  
 W, field-evaporated atoms charge state, obs. 9-10085  
 W, field evaporation in ion microscope surface atoms cohesion 9-5784  
 W, positive, further obs. 9-19940

**secondary**

- application to volume processes in solids exam. 9-16187  
 formation and emission mechanism during sputtering 9-18666  
 metals, angular distribution and ion yield 9-7870

**thermionic**

- Ni ribbon, deformation effect on K<sup>+</sup> and Na<sup>+</sup> emission 9-21554  
 Pt ribbon, deformation effect on K<sup>+</sup> and Na<sup>+</sup> emission 9-21554

**Ion exchange** *see Exchanges, chemical; Ions, electrolytic***Ion microscopes**

- b.c.c. metals, contrast from partial dislocations and stacking faults 9-18465  
 field, 0-4 kv pulse amplifier 9-4416  
 field, atom images, effect of bond number 9-5306  
 field, carburizing of tungsten 9-1175  
 field, image development, of two stoichiometric ceramics 9-12988  
 field, variable temp., He gas cooling 9-6496  
 field for short range order in 2a/Ou-Pt and 2a/Ou-Ni-PPt 9-3305

**Ion microscopes continued**

- field ion, image interpretation 9-3340  
 field-ion image, brightness comparison for different metals 9-6495  
 field-ion micrographs, intrinsic and extrinsic faults, distinction 9-13670  
 proton scatt. microscope for crystallography 9-3272  
 scanning, with ion probe, possibility investigation 9-235  
 Fe, dislocation, a <100>, evidence for existence 9-5361  
 He-H gas mixture, eff. of added Ne on images 9-21107  
 Ir, field, exam. of heavy ion radiation damage, exptl. technique 9-5580  
 W, field evaporation, surface atoms cohesion 9-5784

**Ion mobility** *see Ion velocity***Ion optics**

- See also Alpha-particle spectrometers; Ion microscopes; Mass Spectrometers; Particle optics.*  
 apparatus for producing ion probes 9-235  
 cathode spot edge field, motion in 9-21112  
 drift space calcs. for high current accelerators, theorem 9-19131  
 electrode design for disc-constrained particle beam acceleration 9-8944  
 magnetic prism, quantum description 9-2362  
 mass spectrometer, normal incidence on mag. fields 9-11372  
 mass spectrometers, oblique incidence on mag. fields 9-13277  
 rotational focussing system, analysis of element placement errors 9-10835  
 transgaussian trajectories determ. for lens with symmetry of revolution 9-19132

**Ion pumps** *see Vacuum pumps***Ion sources**

- See also Ion emission/thermionic*  
 atoms, high energy, by transforming ions in a supersonic vapour jet 9-4445  
 C<sup>4+</sup>, for the IPCR cyclotron 9-19130  
 coaxion, design 9-10831  
 drift tube, transport model for converting charged species 9-20495  
 emission current regulator for e impact 9-2359  
 with hot filaments, behaviour of H<sub>2</sub> at press. near 10<sup>-11</sup> Torr rel. to appl. as meas. instrument 9-10591  
 impulse, H<sup>+</sup> and H beam intensity increase 9-20496  
 ionization by electroc collision, calc. of limiting efficiency 9-8588  
 magnetron, intense hot- cathode; discharge charact. for getter-ion pumping applic. 9-2353  
 mass selector for primary and secondary beams 9-665  
 mass spectral study of energy characteristics of molecules 9-664  
 for mass spectrometer 9-2357  
 mass spectrometer for electron ionization cross-section meas. 9-5055  
 O<sup>5+</sup>, for the IPCR cyclotron 9-19130  
 Penning, self controlled pulsing 9-12986  
 plasma, of high melting elements, survey 9-2981  
 plasmoid from c.m. plasma gun 9-10828  
 polarized, strong field ionizer 9-2356  
 r.f., measurement of ion current as a function of probe voltage and gas flow 9-6493  
 r.f. for electrostatic thrusters 9-17862  
 upper atmosphere, height distribution 9-21801  
 vacuum vibrator type, ion emitting charact. 9-10827  
 d, polarized, weak field ionizer for 9-2360  
 e bombardment, for low-energy beams 9-2358  
 Ar in arc discharge, obs. 9-232  
 Ar<sup>+</sup> hot cathode discharge, beam energy distrib. obs. 9-2361  
 H, 0.5 A, 115 keV, injector for providing stationary beam 9-10832  
 H device for deflection and rotation of beams 9-17864  
 H<sup>+</sup> beam, intense, prod. from pulsed H arc 9-12987  
 H<sup>+</sup> beam, intense, prod. from pulsed H arc 9-12987  
 He, 0.15 A, 75 keV, injector for providing stationary beam 9-10832  
<sup>3</sup>He<sup>2+</sup>, PIG source for Van de Graaff accelerator 9-2355  
 Kr-D<sub>2</sub> mixture, ionization curves of KrD<sup>+</sup> 9-7187  
 Kr in arc discharge, obs. 9-232  
 N<sup>4+</sup>, for IPCR cyclotron 9-19130  
 N<sup>5+</sup>, for the IPCR cyclotron 9-19130  
 Pd-Ag alloy tube, H<sub>2</sub> permeation rates 9-21353  
 W in arc discharge, obs. 9-232  
 Xe in arc discharge, obs. 9-232

**Ion velocity**

- corona discharge propulsion, theory and expt. 9-11619  
 electrogasdynamic 2D channel flow, relaxation time of ion diffusion 9-19587  
 hexane, liq., mobility, effect of liq. motion 9-13536  
 polymer solns., during electroconduction rel. to ion solvation on polymer chains 9-18369  
 in polymeric dielectric solns., role in electroconduction 9-21222  
 rate const., from drift meas. of ion-mol. react. 9-15956  
 stopping power theory for heavy ions 9-920  
 in Ar, simple and cluster, mobility at 1-100atm., obs 9-18310  
 Ar<sup>+</sup> in N<sub>2</sub>, O<sub>2</sub>, CO, NO, charge-transfer proc., rate const., from drift data 9-15956  
 C<sub>2</sub>H<sub>6</sub>, slow electron drift velocity 9-3011  
 CO gas, mobility of CO<sup>+</sup>, CO<sub>2</sub><sup>+</sup> and C<sub>2</sub>O<sub>2</sub><sup>+</sup> 9-917  
 Cd<sup>+</sup> in parent vapour, mobility from charge exchange 9-5067  
 CsNO<sub>3</sub> molten salt, <sup>137</sup>Cs mobility meas. by paper electrophoresis 9-19614  
 p-H<sub>2</sub>, 77°K, e drift and diff. 9-9405  
 He<sup>+</sup> in N<sub>2</sub>, charge and dissociative charge-transfer proc., rate const., from drift data 9-15956  
 He<sup>+</sup> + 2He → He<sub>2</sub><sup>+</sup> + He, charge and dissociative charge-transfer proc., rate const., from drift data 9-15956  
 He molecular ions, drift velocities in He gas [cc He molecular ions, drift velocities in He gas] Helium [-] b//c// 9-919  
 He molecular ions, drift velocities in He gas 9-919  
 He molecular ions, in He gas, drift velocities 9-919  
 in He superfluid, trapped negative ions mobility on vortices, 0.8-1.6 K 9-5207  
<sup>3</sup>He, liq., near critical pt. 9-7292  
 Hg<sup>+</sup> in parent vapour, mobility from charge exchange 9-5067  
 Li, dependence of energy loss in matter 9-21450  
 NaNO<sub>3</sub> molten salt, <sup>22</sup>Na mobility meas. by paper electrophoresis 9-19614  
 O<sup>2+</sup>, drift vel. in O, diff. coeff. data, X-section and binding energy meas. 9-5068  
 Zn<sup>+</sup> in parent vapour, mobility from charge exchange 9-5067

**Ion velocity continued****electrolytic**

See also *Conductivity, electrical/liquids, electrolytic; Electrophoresis*

K<sub>2</sub>SO<sub>4</sub>-Li<sub>2</sub>SO<sub>4</sub> (41-90 equiv.%), molten isotope effects of electro-migration

9-8102

<sup>6</sup>Li, <sup>7</sup>Li in molten LiCl, internal mobilities 9-8103

**Ionic conduction, solids**

ferrites, resist., cooling rate depend. rel. to cation conc. 9-12193

f.e.t., thin film, mobility in insulator layer 9-3681

glass, alkali-metal, mobilities rel. to temp. 9-13912

glass, soda-lead-silica, rel. to soder content 9-13913

glass, transform. range, effect of structural changes 9-18649

olefin oxide polymers 9-16293

olefin oxide polymers 9-16293

poly(ethylene oxide) 9-16293

polyvinylchloride, and glass transition 9-16294

soda-lead-silica, glass 9-13913

in surface charge and space-charge fields, rel. to metal oxidation kinetics

9-9620

CsCl:Ba<sup>2+</sup>, high impurity conductivity 9-3701

Fe, electrotransport, 1000-1350°C, rel. to degree of ionization 9-1581

I<sub>2</sub> single crysts, p-phenylenediamine-doped 9-10039

KBr:Ba<sup>2+</sup>, rel. to thermoelec. power meas. 9-1607

KCl:SrCl<sub>2</sub>, transport eqns. derived from five-defect model 9-13914

KCl, transport eqns. derived from five-defect model 9-13914

KI, 200-700°K 9-16292

LiF:Ca, low temp. meas. 9-19928

NaCl:Mn<sup>2+</sup>, rel. to impurity-vacancy assoc. determ. 9-1202

NaCl crystal, Gyalai-Hartly effect of disloc. interaction 9-12194

NaCl whiskers, 4-50  $\mu$  thick, 150°-600°C obs. 9-15124

Ni(8at.%)Mo alloy, Mo ion diffusion and electrotransport process

9-1253

Pb(Zr<sub>1-x</sub>Ti<sub>x</sub>)O<sub>3</sub>, charge transport mechanism, 650-1000°K 9-19932

RbNO<sub>3</sub>, metal ion diffusion 9-19770

Se<sub>2</sub>O<sub>3</sub>, rel. to defects, 700-1600°C 9-1583

Ta<sub>2</sub>O<sub>5</sub> films, mechanism at high fields 9-16291

TiNO<sub>3</sub>, metal ion diffusion 9-19770

V oxides, crystalline and glassy, rel. to structure 9-3702

ZrO<sub>2</sub>, rel. to defects, 800-1600°C 9-3703

**Ionization**

See also *Dissociation; Electrons/ionization; Photoionization*

air, shock-heated, breakdown on interaction of intense r.f. fields with

shock-heated air 9-9397

atoms, by electrons, angular distrib. of outgoing electrons and effects

9-11613

atoms, by high-energy cross-sections calc. 9-692

atoms, by high-energy e. cross sections calc. 9-693

atoms, by high-energy e. cross-sections calc. 9-694

atoms, multiphoton effective cross-section 9-681

Auger, induced by multi-charged ions 9-13302

auto-ionizing states, bounds on energy levels and lifetimes 9-20893

bond length changes in ioniz., mechanisms 9-20916

contact, review 9-7322

cross section behaviour in high energy collision of electrons with hydrogenic

atoms 9-13448

detection for gas chromatography 9-21732

double, resonant mechanism 9-6974

efficiency curves, fine struct. 9-9395

electron mass spectrometer ion source design 9-5055

electronic, angular distrib. of outgoing electrons and effects 9-11613

gas discharge detector for digital reproduction of ionizing particle distrib.

9-13165

halogenated aliphatic hydrocarbons, electron attachment 9-3010

HCl photoionization mass spectrometric obs., ionization threshold to

600A 9-3004

interplanetary plasma, by expanding solar corona 9-8290

ionizer, strong field, for polarized ion source 9-2356

ions with  $1 \leq Z \leq 22$ , pair production in methane at energies 10-120 keV

9-17134

K and L shell electrons, semiclassical ejection prob., as a result of p

collisions 9-13450

metal carbonyls, negative-ion metastable transitions 9-3015

methane-O<sub>2</sub> flame combustion products, meas. 9-18752

methyl halides photoionization mass spectrometric obs., ionization thresh-

old to 600A 9-3004

molecules, electronically excited, surface effects in ejection of electrons

9-19936

negative-ion formation in polyatomic mol., mass spect. investig. 9-20909

neutral atoms with outer 2p and 3p electrons, by e and proton impact,

X-sections calc. from Born approx. 9-4859

phthalate cpds., electron affinities 9-17135

positive ions, by charged-part. impact, binary-encounter model calc.

9-18144

primary, specific, in streamer chamber, meas. of relativistic increase

9-464

by radiation due to heating of substance in laser beam focus and ionized

plasma production 9-7185

secondary electron production examined 9-13449

tetrachloroethylene, bond length changes on ioniz., mechanisms 9-20916

weak field ionizer for polarized d source 9-2360

Ba, in H<sub>2</sub>-N<sub>2</sub>-O<sub>2</sub> flames, electron prod. meas. by enthalpy changes and

equilib. const. 9-12534

CO, electr. transition moment integrals for first ioniz., r-centroid approx.

limits 9-20925

Ca, in H<sub>2</sub>-N<sub>2</sub>-O<sub>2</sub> flames, electron prod. meas. by enthalpy changes and

equilib. const. 9-12534

Fe, ioniz. equilibrium in low-density plasma 9-15820

H, by fast charged part., binary-encounter and Bethe theory, meas. of

differential X-sections 9-4871

H, cross-section calc, using plane-wave approx. 9-914

H<sub>2</sub>, by electron impact, cross-sections calc., semiclassical method

9-19433

H by slow electrons 9-906

H to Ca, atoms and ions, rate coeffs. and cross-sections for electron

impact 9-5061

He atom, accompanied by excitation 9-908

He by slow-electrons near threshold energy 9-7189

He mol., mutual of two metastable mols. in afterglow 9-13468

Kr, in Kr-Kr beam collisions beam-gas target collisions meas. 9-13456

**Ionization continued**

N<sub>2</sub>, by electron impact, cross-sections calc., semiclassical method

9-19433

NaO<sup>+</sup>, prod. from Na+O<sub>2</sub> in merged beams 9-909

Ne, in Ne-Ne beam-gas target collisions meas. 9-13456

Ne, ioniz. equilibrium in low-density plasma 9-15820

O, ioniz. equilibrium in low-density plasma 9-15820

O<sup>-</sup> by dissociative electron attachment to CO<sub>2</sub>; calc. of O electron affinity

9-11614

Si, ioniz. equilibrium in low-density plasma 9-15820

Si, neutral and singly ionized, relative oscillator strengths of spectral lines

9-19404

Sr, in H<sub>2</sub>-N<sub>2</sub>-O<sub>2</sub> flames, electron prod. meas. by enthalpy changes and

equilib. const. 9-12534

Ti, in shock waves in Ti-Ar mixtures 9-19556

**ionization****gases**

See also *Charge exchange; Plasma*

acetonitrile, ion-mol. reactions, ion cyclotron reson. 9-20034

acetylene, by electron impact, Franck-Condon principle validity 9-19453

acetylene, fine struct. in ioniz. efficiency curves 9-9395

acetylene, ion formation energy for  $\gamma$  radiation of Cs<sup>137</sup> 9-9409

alkali halides, and dissociation by e impact 9-21108

n-butane for bombardment by atomic and molecular ions 9-7080

carbohydrates and O derivs., ionization cross-sections 9-7191

cascade, in high-intensity light field 9-15952

from current-growth expts., effects of detachment and ion-molecule reac-

tions 9-11612

dense, rel. of degree of ionization to gas density 9-11611

electrical parameter calc. in alternating field 9-5066

ethyl alcohol, Townsend coeff. and excitation potential 9-18308

ethylene, ion formation energy for  $\gamma$  radiation of Cs<sup>137</sup> 9-9409

fluorocarbons, alicyclic and aromatic, transient negative-ion states

9-7192

fragmentation by 5-45 keV protons during passage thro' thin targets, mass

spect. investigation, X-section meas. 9-5060

helium-like ions, K-electron loss cross sections on collision with H and He

atoms 9-907

h.f. voltage corresponding to saturation proportional to ionization poten-

tial 9-3016

hydrocarbon chemi-ionization, electron cyclotron reson. 9-3999

hypervelocity wake, anal. of atomic and mol. species using microwave and

i.r. absorp. 9-19577

ion pair prod. energy for <sup>210</sup>Po  $\alpha$ -part., obs. 9-15951

ion-molecule collisions, computer plots 9-3012

ion-molecule reactions, spectator mechanism 9-10314

ion-molecule reactions in 50MHz discharge 9-9350

ion-molecule reactions in flowing afterglow system 9-3983

by laser beam, intensive 9-17879

low-kinetic energ collision-induced dissoci. 9-9406

luminous flow around bodies, exptl. data 9-5107

methane, ionizing photolysis 9-6019

methane and methane-d<sub>4</sub> by <sup>23</sup>S and <sup>23</sup>S He atoms 9-912

methane fragmentation by 5-45 keV protons, mass spect. investigation,

X-section meas. 9-5060

molecular beams striking various surfaces 9-9396

negative-ion hydration 9-1896

nonequilibrium theory of partially ionized mixtures 9-11658

organic Si chlorides, neg. ion form. by electron impact 9-3008

Penning processes, energy of electrons released analysis, interaction forces

9-903

perfluorobutane, ionization and attachment coeffs. 9-913

perfluoromethylcyclohexane, thermal electron attachment rates 9-3007

photon momentum distrib., nonrelativistic 9-13458

plasma, magnetoactive, chemical rate equation for reactive nonequilib.

9-13411

plasma sheath, effects on transition domain of flow 9-14776

radiation spectrum based on Planck's law 9-13459

resonance, symmetric, charge exchange of multicharged ions 9-3013

resonance, symmetric, charge exchange of multicharged ions 9-14801

structure and nonlinear wave propag. mech. for ionization fronts 9-14797

suspensions, recombination coeffs. and transport props. 9-3132

time-of-flight meas. for ions in open gases 9-15949

Townsend's coeff. of ioniz., drifting and diffusing e pulse 9-9404

velocity variation ionizing shock waves 9-18321

yields, X-sections and loss functions 9-5054

Ar-methane mixtures, by  $\alpha$ -particles, energy depend., 1.58-5.3 MeV

9-5058

Ar, by electron impact, probability curves for <sup>2</sup>P<sub>3/2</sub> and <sup>2</sup>P<sub>1/2</sub> states

9-4863

Ar, pulsed and quasi-c.w. laser design 9-17867

Ar, relax. phenomena in ionized shock front 9-14798

Ar<sup>+</sup>, excitation cross section for fast e. impact 9-5057

Ba<sup>+</sup>, by e impact to Ba<sup>2+</sup>, cross-sections 9-5064

C<sub>2</sub>H<sub>2</sub>, by 25-50 keV, H<sup>+</sup>, O<sup>+</sup> and Ar<sup>+</sup> 9-904

C<sub>2</sub>H<sub>4</sub>, by 25-50 keV, H<sup>+</sup>, O<sup>+</sup> and Ar<sup>+</sup> 9-904

C<sup>+</sup> reaction with N<sub>2</sub> and O<sub>2</sub> 9-14122

CO, fragmentation by 5-45 keV protons, mass spect. investigation, X-section

meas. 9-5060

CO<sub>2</sub>, by 25-50 keV, H<sup>+</sup>, O<sup>+</sup> and Ar<sup>+</sup> 9-904

CO transitions, Franck-Condon factors 9-4934

CO<sub>2</sub>, resonance capture of very slow electrons 9-9399

CS<sub>2</sub>, by electron impact 9-17131

Cs, electron-impact cross-section 9-9400

D<sub>2</sub>, by short pulse laser, theoretical exam. 9-9383

D<sub>2</sub> ionization under action of short pulse laser 9-3005

D<sup>+</sup>+D<sub>2</sub>O<sup>+</sup>→OD<sup>+</sup>+D<sub>2</sub>, cross-section for incident ion energies near 2 eV

9-921

Fe<sup>m+</sup>, (8≤m≤15), collisional cross-sections rel. to temp. of solar corona

9-10556

H, cross section calc. using Monte-Carlo method 9-7186

H<sub>2</sub>, transport coefficients at 0.01, 0.1 and 10 atm. pressures and up to

5000°K 9-18309

H and rare gases, multiphoton ionization 9-13451

H by electron, cross-section depend. on main quantum number 9-2826

H electron torch, h.f. and <1 atm. discharges, mechanism, obs. 9-15959

H<sub>2</sub>, by collisions with excited rare gas atoms, isotope effect 9-7188

H<sub>2</sub>, fragmentation by 5-45 keV protons, mass spect. investigation, X-section

meas. 9-5060

H<sub>2</sub>, yields, X-sections and loss functions 9-5054



**ionization continued**  
**gases continued**

- H<sub>2</sub> and D<sub>2</sub>, Franck-Condon factors calc., vibr.-rot. effects 9-5059  
 H<sub>2</sub> transitions, Franck-Condon factors 9-4934  
 H + H<sub>2</sub>O → OH + H<sub>2</sub>, cross-section for incident ion energies near 2 eV 9-921  
 He, field ionization, H and H-Ne promoted 9-21107  
 He, recomb. coeff. variation rel. to pressure 9-17136  
 He, Rydberg series of autoionizing states converging to n=2 level of He\*, energies and props. 9-4877  
 He, singly ionized, Stark-mixing signals in n=4 term 9-20901  
 He, yields, X sections and loss functions 9-5054  
 He near threshold by e impact 9-5062  
 He<sup>-</sup>, <sup>4</sup>P<sub>3/2</sub> state autoionization, final state distortion effects 9-11615  
 He(2<sup>3</sup>S) + X → He + X<sup>+</sup> + e, Penning ioniz. reactions 9-14675  
 Hg, up to 9+, by repeated e collisions at <150 eV 9-5063  
 Kr-D<sub>2</sub> mixtures, ionisation curves of KrD<sup>+</sup> ions 9-7187  
 Kr, by electron impact, probability curves for <sup>2</sup>P<sub>3/2</sub> and <sup>2</sup>P<sub>1/2</sub> states 9-4863  
 Kr, multi-photon, by Nd laser, role of bound states 9-910  
 Kr<sup>+</sup> by e collisions rel. to ion excitation energy, obs. 9-11616  
 Kr<sup>2+</sup>, excitation cross section for fast e. impact 9-5057  
 Li<sup>+</sup>, by e impact to Li<sup>2+</sup>, cross-sections 9-5064  
 N, N<sup>1</sup>, N<sup>2</sup>, longitudinal and transverse diffusion coeff., 12-300×10<sup>-27</sup> Vcm<sup>2</sup> 9-918  
 N, waves dispersion curves in plasma discharge 9-13418  
 N<sub>2</sub>, dissociative, due to vibrational mode excitation 9-14799  
 N<sub>2</sub>O, three body electron capture 9-15953  
 N<sub>2</sub>, fragmentation by 5-45 keV protons, mass spect. investigation, X-section meas. 9-5060  
 N<sub>2</sub>, yields, X-sections and loss functions 9-5054  
 N<sub>2</sub><sup>+</sup> reaction with H<sub>2</sub>, D<sub>2</sub>, and HD 9-17513  
 NO transitions, Franck-Condon factors 9-4934  
 NO<sup>+</sup>(A<sup>1</sup>Σ<sup>+</sup>-X<sup>1</sup>Σ<sup>+</sup>) band system, Franck-Condon factors in transitions 9-4934  
 Ne, primary coeff. 9-911  
 Ne<sup>2+</sup>, excitation cross section for fast e. impact 9-5057  
 O- low-energy reactions with H<sub>2</sub> and D<sub>2</sub> 9-9401  
 O<sub>2</sub>, electron collision, 0-200 eV, vac.u.v. emission 9-17040  
 O<sub>2</sub>, fragmentation by 5-45 keV protons, mass spect. investigation, X-section meas. 9-5060  
 O<sub>2</sub>, yields, X-sections and loss functions 9-5054  
 O<sub>2</sub> equil. calc. at various temp., O VI emission from sun, presence in corona 9-2081  
 O<sub>2</sub> transitions, Franck Condon factors 9-4934  
 PbCl<sub>2</sub> + ACl (A=Na, K, Rb or Cs), electron impact 9-9408  
 SF<sub>6</sub>, thermal electron attachment rates 9-3007  
 SiCl<sub>4</sub> neg. ion ferm. by electron impact 9-3008  
 SiH<sub>4</sub><sup>+</sup> formation in ionized SiH<sub>4</sub>-CH<sub>4</sub> mixtures 9-13452  
 Xe, autoionization processes on e. impact 9-14800  
 Xe, by X-rays, ion average change and abund. determ. 9-11618  
 Xe, multi-photon, by Nd laser, role of bound states 9-910  
 Xe<sup>+</sup>, fine struct. in ioniz.-efficiency curves 9-9395  
 Zn vapour vacuum u.v. spectrum, photo- and auto-ioniz. proc., abs. cross-section meas. 9-13453

**Ionization****liquids**

- aromatic hydrocarbons in soln., bimolec. ionization of triplet state 9-3120  
 hexane, currents induced by α or β particles 9-9549  
 hydrocarbons, chem. determ. of free-ion yields 9-6024  
 hydrocarbons, radiation-induced, depend. on molec. struct. 9-16022  
 ion pair, overlapping hydration shells, interact., spheroidal cavity mode 9-14858  
 ion pair with overlapping hydration shells interact., truncated-spheres model 9-14857  
 monovalent isolated ion, interact. in aq. medium, 25°C 9-11719  
 water, ion product const. determ., thermodynamics considered 9-16487  
 HClO<sub>4</sub>-H<sub>2</sub>O, p.m.r. and molec. states 9-11721  
 HNO<sub>3</sub>-H<sub>2</sub>O, p.m.r. and molec. states 9-11721

**solids**

- dielectric polymers, breakdown, multistage mechanism 9-7841  
 photo, 'optical' discharge produced by single laser pulses on non absorbing surface 9-5785  
 quasiclassical approx. of tunnel effect 9-1580  
 Fe, degree from diffusion and electrotransport obs., 1000-1350°C 9-1581  
 I<sub>2</sub> single crysts. p-phenylenediamine-doped 9-10039  
 In<sub>2</sub>S<sub>3</sub>, field emitter mechanism responsible for electron multiplication 9-17447  
 Ni-(8at.%)Mo alloy, of Mo sign and degree from diffusion and electrotransport 9-1253

**Ionization, atmosphere**

- See also Atmosphere/radioactivity; Ionosphere*  
 abnormal diurnal variation of total ionization 9-16537  
 D-region by cosmic rays, galactic and solar 9-1969  
 exosphere, electron content, diurnal change calcs. 9-1949  
 in F region, auroral, drift durin mag. disturbances 9-21822  
 by meteors, 39.3 MHz forward transmission obs. (1965-6) 9-2060  
 NmF<sub>2</sub> region, day and night reversal, transequatorial neutral wind effects 9-18815  
 plasma wave and particle interacts, and auroral particle precipitation 9-20097  
 rates and recombination, 100 to 500 km, rocket obs. 9-21803

**Ionization, surface**

- See also Electron emission/thermionic; Ion emission/thermionic; Work function*  
 ion formation and emission during sputtering, mechanism 9-18666  
 isotope abundance ratio meas. on trace sample, method 9-19415  
 metal, high vacuum e bombardment, pot. behaviour 9-12229  
 molecular beams striking various surfaces 9-9396  
 negative, isotopic analysis method, applications 9-20067  
 Ar atom, metastable impact on W, rel. to work function 9-11409  
 Cu, isotope abundance ratio meas. method 9-19416  
 D, in strong elec. fields, rel. to neutron prod. 9-16322  
 H<sub>2</sub>, metastable mol. impact on W, rel. to work function 9-11409  
 Li, isotope abundance ratio meas. method 9-19416  
 N<sub>2</sub>, metastable mol. impact on W, rel. to work function 9-11409  
 Ni anticathode, function of at. number and accel. voltage 9-5946  
 Pb anticathode, function of at. number and accel. voltage 9-5946  
 Rb on Pt, absolute determ. of coeff. between 1200 and 1700°K 9-5786  
 Rb on W, maximum coeff. at approx. 1150°K 9-5786

**Ionization, surface continued**

- Ti anticathode, function of at. number and accel. voltage 9-5946  
 U, isotope abundance ratio meas. method 9-19416  
 Xe atom, metastable impact on W, rel. to work function 9-11409  
 ZnO, crystal, electroluminescence study of space charge layers, conductivity depend. 9-16290  
**Ionization chambers**  
 1383A, calibration for <sup>132</sup>I 9-19230  
 1383A standard, calibration for <sup>87m</sup>Sr 9-20695  
 for 100-1000 Å radiation using Bi, In or Ti film on inert gas ionization chamber 9-19227  
 β-ray backscatter intensity meas., radioisotopic coat thickness gauge 9-4667  
 calorimeter for cosmic rays energy determ. up to 10<sup>14</sup>eV 9-13166  
 discharge, of restricted size, design and performance of uniform field electrode 9-13164  
 dosimetry of radiations under non-equilibrium conditions 9-11133  
 in hybrid radiation survey meter 9-2596  
 instability of collecting vol. eliminated by guard ring shielding 9-2576  
 parallel-plate free-air, ion recombination processes 9-11132  
 for pocket dosimeter for β-, γ- and X-rays, patent 9-8930  
 position detector of charged particle beam 9-447  
 as X-ray monitor in hospital work 9-18971  
 for β-emitting gases internal meas., calibration and characts. 9-16920  
 x-ray meas., 10-30 kV 9-2105  
 H discharge cloud, construction 9-446

**Ionization gauges** *see Vacuum gauges***Ionization potential**

- allene 9-9403  
 atoms field calc. on 3rd row periodic syst., Hartree-Fock pot. comparison 9-4826  
 azulene, ground and doubly excited states, SCF calc. 9-20951  
 butadiene 9-9403  
 cis-1,3-butadiene 9-9402  
 carbon tetrafluoride, by photo electron spectroscopy, comp. with INDO-MO calc. 9-13457  
 carbonyl cpds., conjugated, lone-pair and π pot. calc., Pariser-Parr-Pople methods, comparison with vertical pot. 9-9253  
 ethyl alcohol, Townsend coeff. and excitation potential 9-18308  
 free radicals, in mass spectrometer 9-15950  
 measurement, mols. and free radicals, by electron impact in mass spectrometer 9-15950  
 methane in 10-50 Å range 9-15955  
 methylstannyl radicals, electron impact 9-17133  
 molecules, in mass spectrometer 9-15950  
 naphthalene, ground and doubly excited states, SCF calc. 9-20951  
 organic mols., from photoelectron spectra 9-21109  
 and periodicity of atomic props., electronic configurations 9-5056  
 phthalate cpds. 9-17135  
 propyne 9-9403  
 water, three distinct smaller than 21.22 eV 9-17895  
 He rel. to SCF eigenvalue 9-4874  
 Hg<sup>+</sup>, obs. 9-5063  
 Kr<sup>+</sup> through Kr<sup>2+</sup>, from coincidence meas. of Kr<sup>+</sup>-Kr collisions 9-11410  
 NO, higher potentials, photoelectron spectroscopy meas. 9-11467  
 O<sub>2</sub> first IP determ. 9-15954

**Ionized gases** *see Ionization/gases; Plasma***Ionosondes** *see Ionosphere measuring apparatus***Ionosphere**

- See also Electromagnetic wave propagation/ionosphere*  
 abnormal diurnal variation of total ionization 9-16537  
 absorption meas. for distribution of X-ray emission from sun 9-16618  
 acoustic-gravity waves ducted in thermosphere 9-12605  
 Alfvén waves, polarization 9-15942  
 ambient electrons, presunrise heating due to conjugate photoelectrons 9-20115  
 artificial plasma clouds released by rocket 9-6090  
 auroral, ion-acoustic instabilities, ion-neutral collisions effect 9-21806  
 conductivity, elec. 105-125 km from solar daily quiet geomag. var. 9-1957  
 current field asymmetric development and conductivity var. 9-1956  
 current systems, international quiet day, N hemisphere plots 9-21804  
 cyclotron resonance, higher order, obs. 9-9364  
 disturbances associated with solar cosmic-ray flares 9-16539  
 drift meas. by spaced receivers, movement of pattern of signal strength over ground for reflected wave 9-15252  
 drift measurements on adjacent aerial arrays 9-10432  
 drift variation and anisotropy parameters during magnetically disturbed days 9-20114  
 drifts, conference, St. Gallen, Switzerland, (1967) 9-12593  
 e content, response to partial solar eclipse 9-10427  
 earth cavity resonances, fine structure 9-4077  
 electrojet, features of two main forms, and theories of origin 9-18809  
 electron content, slab thickness and scintillation occurrence 9-20110  
 electron content and slab thickness, changes during magnetic storm in June 1965 9-10420  
 electron content diurnal var. from Faraday rot. polarized lunar echoes 9-20112  
 electron content in equat. region under mag. quiet and active conditions, latitude, variations 9-8196  
 electron content measurements from satellite radio beacon transmissions 9-20109  
 electron temp. meas. using two probes separated by small voltage 9-1967  
 e.f. wave attenuation coeff with two-layered model 9-21809  
 far i.r. night sky background radiation, obs. 9-6086  
 fine structure, effect of ion-acoustic wave excitation 9-17583  
 frontal horizontally-moving irregularities at high latitudes 9-1965  
 frontal surfaces of travelling disturbances, rel. to ohmic losses of gravity waves and mode dissipation 9-12615  
 gravity waves, effect of ohmic losses, rel. to frontal surfaces of travelling disturbances 9-12615  
 hiss v.f.f. correlation with auroral light and X-ray bursts., obs. (March 1966) 9-14170  
 hydrodynamic wave propag. normal to mag. field, influence of currents 9-19516  
 hydromagnetic waves propagation, current density effects 9-10410  
 ion production functions, height distribution 9-21801

**Ionsphere continued**

- ion temperature, diurnal variation, results from Thomson scatter spectra, Arecibo 9-10417
- ions, positive, concentration rel. height obs. 9-8186
- ions and neutral particles, momentum transfer collision frequency expression 9-21800
- IQSY (1964-65), summary of measurements 9-6093
- irregularities, deduced from Beacon satellite obs. 9-10428
- irregularities, induced by gravity waves, apparent transport by wind, for critical layers 9-12597
- irregularities, movement, discussion 9-16538
- irregularities, off-path, movement from v.l.f. refl. signal fluctuations 9-14171
- irregularities, origin and movements, meas. methods 9-12611
- irregularities, rel. to dispersion of space charge waves in plasma, and drift instability 9-12616
- irregularities, satellite scintillation at high latitudes, possible relation to precipitation of soft particles 9-10429
- irregularities, spatial, and their variations with time, ionosonde program 9-21807
- irregularities deduced from beacon satellite observations 9-10428
- irregularities over Europe, height, spaced receiver meas. 9-1964
- layer tilts and horizontal irregularities, radio obs. 9-10431
- lens effect on radio waves reaching moon from distant source 9-1962
- lower, electron conc. meas. method 9-21808
- lower, winds, solar cycle dependence 9-10430
- lower hybrid reson. noise, electrostatic wave origin 9-14174
- lunar tides near magnetic equator, height distribution 9-10419
- Mitra type drift expts., anal. of artificial fading records rel. to velocities 9-18810
- motion, drift vel. and charact. vel., validity of determ. by three stations method 9-12618
- movements measurements, statistics of time shifts 9-1966
- neutral and ionized components, 100-500 km, rocket obs. 9-21803
- night, negative ions and continuous sub e.l.f. emissions 9-17582
- night-time, maintenance and mean change  $10^\circ$  to  $60^\circ$  latitude 9-1958
- night-time winds, continuous obs. using closely spaced receiver l.f. drift meas. 9-12612
- observations, Dec. 1967 9-4073
- observations, Feb. 1968 9-6089
- observations, Jan. 1968 9-4074
- outer, and transition into interplanetary medium 9-17581
- parameter vars. during SC, rel. solar and mag. activity, obs. 9-17580
- periodic structure, near 90 km, determ. by spaced receiver studies of reflected radio waves 9-12609
- polar, winter anomalies and noctilucent clouds, review 9-18808
- radio signals obs. Oct. 31 1967, change in amp. scintillations struct., rel. to simultaneous meteorological data 9-18812
- reaction studies, laboratory techniques 9-1960
- reflection level and group retardation from rocket radio propagation expt. 9-14173
- research based on Arecibo backscatter sounder obs. 9-20107
- resonant responses, satellite ionosonde obs. 9-18811
- review of the last ten years 9-4075
- $S_x$  vars. and current system, determ. 9-21831
- satellite trail, kinetic analysis 9-12606
- scintillation index, scaling method 9-18814
- temperatures of different components ionospheric plasma, popular, paper 9-21796
- tilted layer, -mode, ray-tracing 9-10418
- topside, positive ion composition, computer anal. of Ariel I data 9-21802
- topside over Japan, electron density distrib. from a louette II 9-8200
- topside sounding, review 9-18813
- travelling disturbances 9-21805
- travelling disturbances, study by network of h.f. CW Doppler sounders 9-12614
- travelling disturbances due to gravity waves, effects of molec. viscosity and thermal conduction 9-12598
- travelling irregularities, effect on data obtained by sweep-frequency ground back scatter sounders 9-12610
- upper, plasma scale height variations at sunrise 9-8197
- whistler mode propagation, presence of longitudinal electrostatic field 9-10423
- whistlers, excitation of emissions near low hybrid frequency and their interpretation 9-12619
- wind profiles, dynamic model 9-4078
- wind profiles, mid latitude, 90-150 km, anal. rel. to turbulence and wavelength of dominant wave 9-12617
- zonal winds, 70-100 km, seasonal variation in S. hemisphere from drift meas. 9-12613
- e density profile from rocket radio propagation expt. 9-14173
- e temp., cooling eff. due to  $O^+$  fine structure levels excitation 9-12607
- $He^+$ , in topside ions. 9-4076
- $O^+$  fine structure levels excitation, e temp. cooling 9-12607
- $O_2^+$ , dissociative recombination coefficient with electrons, lab. meas. 9-1959

**D-region**

- cosmic ray ionization, galactic and solar sources 9-1969
- D1 fading drift obs., evaluated by method of similar fades 9-12620
- electron and positive ion density meas during auroral absorption cond. 9-21810
- electron conc. 70-90 km, from partial reflections at varying pulsewidths 9-20116
- electron density and temp. meas. on anomalous winter day using rockets 9-12621
- electron density distrib., regular variations 9-16541
- ion and e density, night-time, models 9-14176
- ionization by galactic and solar cosmic rays 9-1969
- ionization increases caused by small solar proton events, partial refl. obs. (Feb. 1965) 9-14175
- partial reflection theory 9-10434
- wind, Fourier anal. of data and interpret. 9-15253
- X-ray source on Sun identified during 12 Nov. 1966 eclipse, using D layer ionization 9-18929

**E-region**

- drift, simultaneous obs. with meteor winds, and rel. to bulk motion of matter 9-12623
- $E_s$ , determ. from electron conc. profile computation 9-21814
- $E_s$  analysis, appl. correl. methods 9-21815
- $E_s$  parameters rel. radio absorption 9-21811

**Ionsphere continued****E-region continued**

- $f_oE_s$ ,  $fE_s$  and  $f_oE_s$ , physical significance 9-10435
  - fading of radio waves returned from  $E_s$  9-16540
  - fading radio echoes on adjacent freqs., cross-correl. of amplitudes 9-15254
  - horizontal drifts at Waltair (India), spaced phase path technique 9-21813
  - irregularities, classes and formation rel. to internal gravity waves, and movements 9-12624
  - irregularities producing radio scintillations 9-8205
  - neutral wind profiles, comparison with radio drift meas. 9-15255
  - neutral wind shears, daily, seasonal and solar-cycle variations deduced from blanketing  $E_s$  9-12625
  - nighttime, mean variations 9-12622
  - spaced fading records, time shifts variability 9-21812
  - sporadic, formation time, theory 9-8204
  - sporadic ionisation, electron density over Miedzeszyn 9-8203
  - sporadic reflection, v.h.f. expt. 9-8198
  - sporadic E activity, correlation obs. with clear air turbulence 9-4065
  - wind, Fourier anal. of data and interpret. 9-15253
  - $N_2$  and e vibrational temp. 9-1971
  - $O_2^+$  and  $NO^+$  abundances, analysis of rocket-measured profiles 9-10436
- F-region**
- acoustic-gravity wave propag., effects, geomag. field depend. 9-12635
  - Antarctica, spread-F irregularities 9-10438
  - auroral, ionization drift during mag. disturbances 9-21822
  - auroral and middle latitudes, Explorer 22 radio obs. 9-8206
  - diffusion eqn., time-depend., soln. in terms of arbitrary scale-height factor 9-12631
  - drift meas. by radio star scintillation, test for dispersion 9-12634
  - electron content and slab thickness, seasonal variation 9-1968
  - electron density and temp. fluctuations on quiet days 9-15257
  - electron density irregularities, classification and parameters 9-6095
  - equatorial irregularity belt, observed from scintillation satellite transmissions 9-12637
  - F1-ionograms, overlay analysis problems 9-12628
  - F2, critical freq. vars. and mean square deviations 9-21816
  - F2, effects of SSC mag. storms 9-21823
  - F2, equatorial anomaly at local noon, IGY and IQSY 9-21819
  - NmF2, ionization day and night reversal, transequatorial neutral wind effects 9-18815
  - $f_oF_2$ , lunar tidal variations, American zone, geomag. anomaly eff. 9-18816
  - F2, plasma excited by neutral gas movements, global distribution of drifts 9-21818
  - F2 critical freq. and height, diurnal and seasonal vars. rel. to neutral winds, calc. 9-12629
  - F2 critical freq. var. with stationary primary ionization flux 9-21820
  - F2 disturbance, electronic computer simulation 9-21820
  - F2 electrodynamic drifts, time dependent effects evaluation 9-21824
  - $\Phi F_2$ , defined by computer 9-12630
  - $f_oF_2$  diurnal characteristics 9-10437
  - $F_2$  ionization and geomagnetic disturbance 9-1974
  - fading radio echoes on adjacent freqs., cross-correl. of amplitudes 9-15254
  - gravity waves, internal, observed by means of electron density profiles 9-12636
  - h'F obs. before and in relation to spread F 9-6096
  - index IF2 and simspot number relationship 9-6094
  - ion diffusion and charge exchange in  $F_2$ -region 9-1972
  - ionic production and recombination rates, diurnal variation, Thomson scatter study 9-12627
  - irregularities, classes and formation rel. to internal gravity waves, and movements 9-12624
  - irregularities, rel. to internal gravity waves eff. on prod. rates, chem. losses, and motion of ionization 9-12633
  - lunar tide height variation obs. 9-1973
  - nighttime behavior, study using incoherent scatter sounder 9-17584
  - plasma diffusion ion. effects of Coriolis force, rel. to faster eastern motion of upper atmos. 9-12632
  - response to neutral atmos. wave types, calc. of ionization redistrib. and change in peak e density 9-15256
  - seasonal and magnetic-storm behaviour 9-12626
  - solar corpuscular radiation effect, day and night (Mar 21-5, 1966) 9-21821
  - structure, effect of field aligned currents 9-10433

**Ionsphere measuring apparatus**

- adjacent aerial arrays, drift measurements 9-10432
- closely spaced receiver l.f. drift meas., obs. of night-time winds 9-12612
- probe for plasma parameters 9-8201
- probes separated by small voltage for electron temp. determ. 9-1967
- rocket-released probes, instantaneous orientation determ. from signal polarization anal. 9-6099
- sweep-frequency back scatter sounders, influence of irregularities on data, from computer simulation 9-12610

**Ions**

- See also Atoms; Ion emission/thermionic; Molecules; Plasma*
- with  $1 \leq Z \leq 22$ , ionization in methane at energies 10-120 keV 9-17134
- adsorption in black foam film 9-19650
- alcohols of common purity, characteristics of ions 9-19642
- amines of common purity, characteristics of ions 9-19642
- atmospheric, large battery operated counter 9-19240
- collector with movable slits for mass spectrometer 9-11374
- coronene negative ion, ground state, influence of ionic assoc. 9-13378
- cyclotron centre, space charge and vertical motion 9-4699
- cyclotron resonance detection using e energy modulation 9-3058
- diamagnetic shielding factors, relativistic calc. 9-675
- dichloroethylene- $C_2H_2Cl_2$  (or  $CH_2 \rightarrow Cl^+$  + neutral prods., direct processes 9-4984
- diffusion in solar corona, theory 9-10557
- dipoles, molecules, binary distribution functions systems 9-4980
- electronic partition functions, 1500-7000°K, 73 elements 9-20873
- electrostatic accelerator, high-freq. neutron wave production 9-19259
- fluorocarbons, alicyclic and aromatic, transient negative-ion states 9-7192
- force consts., Coriolis coupling consts. mean amplitude  $ZXY_1(C_{2s})$  and  $ZXY_1(C_{3s})$  type 9-7010
- heavy, 5-50keV, range in various gases 9-14739
- injection into polar liquids 9-7272
- ionsphere, frictional forces and collision frequency with neutral particles 9-21800



## Ions continued

- ionosphere, night, negative ions and continuous sub. e.l.f. emissions 9-17582  
macroion molec. beams 9-9298  
macroions of rigid core, thermodynamic functions 9-2922  
metallic, low charge state, prod. and analysis from sputtering type Penning discharge 9-3020  
negative, cause of stationary electrostatic configurations in plasma 9-17098  
paramagnetic, statistical model 9-12243  
positive, in topside ionosphere, computer anal. of Ariel I data 9-21802  
positive, ioniz. by charged-part. impact, binary-encounter model calc. 9-18144  
produced by laser interaction with solids, mass spectrometer invest 9-9380  
resonances in e scatt. 9-702  
in shock tube, mass spectrometric sampling 9-21110  
solute, virtual recoil and depend. on dilute alloys low-temp. thermopower 9-1603  
thermal in exosphere, evidence of solar and geomagnetic control 9-10401  
transition elements, Slater-Condon integrals, calc. 9-4823  
Two-electron systems, 2s2p 3p and 'P states, Hartree-Fock eqns. 9-15533  
(*pup*)<sup>+</sup>, L=1 ortho bound state h.f.s., calc. 9-4976  
Ar and Xe mixture, pumping effect in ionization tube 9-2354  
Ar II 4s and 4p levels population inversion mechanism, obs. 9-15817  
Ar pulsed laser, role of two-step excitation 9-8606  
BII, 2p<sup>2</sup> <sup>1</sup>D lifetime meas. 9-11391  
Be<sup>2+</sup>, relativistic shifts for 1sns <sup>1,3</sup>S states, prediction 9-13316  
C, O<sub>2</sub><sup>+</sup>, mobility in CO gas 9-917  
C III, IV, V, cross sections, calc., 39.1 867.9 Å 9-6979  
CH<sub>3</sub><sup>+</sup>, geometry investigation, CNDO method 9-19461  
CO<sub>2</sub><sup>+</sup>, mobility in CO gas 9-917  
CO<sup>+</sup>, mobility in CO gas 9-917  
Cu<sup>+</sup>, Hartree-Fock exchange pot. for electrons, comparison of methods 9-18138  
D:P(BH<sub>3</sub>)<sub>2</sub> vibr. modes, i.r. Raman and n.m.r. obs. 9-18183  
D<sup>+</sup>, dissociation energy 9-2920  
DF<sub>2</sub><sup>+</sup>, potential energy consts. and mean amplitudes of vibration 9-4838  
Eu<sup>2+</sup>: CaF<sub>2</sub>, microwave modulated fluorescence, 9.5 GHz 9-1828  
H<sub>2</sub>P(BD)<sub>2</sub><sup>+</sup> vibr. modes, i.r. Raman and n.m.r. obs. 9-18183  
H<sub>2</sub>P(BH<sub>3</sub>)<sub>2</sub><sup>+</sup> vibr. modes, i.r. Raman and n.m.r. obs. 9-18183  
H<sup>+</sup> adsorption at TiO<sub>2</sub>-aqueous soln. interface obs. 9-7351  
HCN<sup>-</sup> in KCl magnetic parameters completely determ. 9-13358  
HD<sup>+</sup>, collision induced dissociation by inert gases 9-7077  
HF<sub>2</sub><sup>+</sup>, potential energy consts. and mean amplitudes of vibration 9-4838  
He<sup>+</sup>-Cs charge exchange collisions, 1.5-25 keV 9-4890  
He-like, 2s2p, 3p and 'P states Hartree-Fock eqns. 9-15833  
He<sup>+</sup> electron impact excitation, wave function expansion for 1s-2s excitation cross section 9-15834  
He<sup>-</sup>, <sup>4</sup>P<sub>3/2</sub> state autoionization, final state distortion effects 9-11615  
He<sup>+</sup> one- and two-electron loss in H<sub>2</sub>, He and Ne, 400-1500 keV 9-5072  
He, low energy, radiolysis of liq. benzene 9-17542  
He<sup>+</sup> collision with Ar and Kr, optical excitation 9-6996  
He<sup>+</sup> form. by e impact on He 9-5062  
Ho, mag. moment from HoFeO<sub>3</sub> spectrum 9-21624  
I<sup>+</sup>, orbital wave functions, reduced basis set expansions 9-11385  
Ir, field-evaporated, charge state, obs. 9-10085  
Ir, field-evaporated, charge state, obs. 9-5783  
K, electromigration in molten KNO<sub>3</sub>, temp. depend. of isotope effect 9-11716  
K<sup>+</sup>, Ar scatt., cross section meas., E<sub>k</sub>=150-4000 eV 9-18152  
Kr<sup>+</sup> ionization by e collisions rel. to excitation energy, obs. 9-11616  
Li energy loss in matter, vel. depend. 9-21450  
<sup>7</sup>Li<sup>+</sup>, scatt. by free atoms and molcs. 9-13308  
Li<sup>+</sup>, relativistic shifts for 1sns <sup>1,3</sup>S states, prediction 9-13316  
Li<sup>+</sup>, van der Waals coeffs. for ground and metastable states 9-2833  
N<sup>+</sup>, N<sub>2</sub><sup>+</sup> in N, longitudinal and transverse diffusion coeff., 12-300×10<sup>-27</sup> Vcm<sup>2</sup> 9-918  
N<sup>2+</sup>, probability of 1'S<sub>0</sub>-2<sup>3</sup>P<sub>1</sub> transition 9-916  
N III, IV, V, photoionisation cross sections, calc., 39.1-867.9 Å 9-6979  
N IV, 2p<sup>2</sup> <sup>1</sup>D level mean lifetime 9-9137  
N<sup>+</sup> metastability of <sup>1</sup>D state using first order wave function 9-9138  
N<sub>2</sub><sup>+</sup> in nitrogen afterglow, prod. and loss. 9-13465  
N<sub>2</sub><sup>+</sup> rot. excitation in H<sub>2</sub><sup>+</sup>-N<sub>2</sub> collisions, 0.4-3.0 keV 9-4982  
N<sub>2</sub><sup>+</sup>, mass spectrometric identification in h.f. discharge 9-9223  
NO<sup>+</sup>, excited electronic states 9-774  
Na<sup>+</sup>=N<sub>2</sub><sup>+</sup>+N<sub>2</sub> equilb.: const. and rates rel. to elec. field strength and press., 0.63-1.24 torr. 9-4969  
NdIV 4f<sup>3</sup> free-ion levels from LaCl<sub>3</sub>:Nd<sup>3+</sup> spectra and calc. 9-4831  
Ne, II, III, IV, V, photoionisation cross sections, calc., 39.1-867.9 Å 9-6979  
Ne I, II, III states radiative lifetimes, u.v. obs. 9-4844  
Ne<sup>+</sup> collision with Ar and Kr, optical excitation 9-6996  
O<sup>6+</sup>, probability of 1'S<sub>0</sub>-2<sup>3</sup>P<sub>1</sub> transition 9-916  
O III, IV, V, photoionisation cross sections, calc., 39.1-867.9 Å 9-6979  
O formation, due to dissociative electron attachment to CO<sub>2</sub>, temp. depend. 9-11614  
O<sup>2</sup> in O, drift vel. meas., diff. coeff. data, X-section and binding energy meas. 9-5068  
O<sub>2</sub><sup>+</sup> and NO<sup>+</sup> abundances in E region, analysis of rocket-measured profiles 9-10436  
OH<sup>-</sup> adsorption at TiO<sub>2</sub>-aqueous soln. interface obs. 9-7351  
OH<sup>+</sup> singlet-triplet intercombination separation, calc. 9-2874  
PrIII 4f<sup>3</sup> energy levels, mag. params. 9-4831  
Rb<sup>+</sup>, free, nuclear moment obs. 9-11399  
SH<sup>+</sup> singlet triplet intercombination separation, calc. 9-2874  
SiH<sub>3</sub><sup>+</sup> formation in ionized SiH<sub>4</sub> CH<sub>4</sub> mixtures 9-13452  
SiO<sup>+</sup>, spectral band struct. 9-4938  
W, field-evaporated, charge state, obs. 9-10085  
W, field-evaporated, charge state, obs. 9-5783  
Xe III, Hartree-Fock parameters for the <sup>1</sup>D and <sup>1</sup>S terms of configuration 5s<sup>2</sup> 5p<sup>4</sup> 9-9129

## recombination

- dissociative recomb. and attachment, theory 9-4967  
electron decay in controlled afterglows 9-923  
Ne dissociative recombination and molecular ion formation in decaying plasma 9-13414  
in parallel-plate free-air ioniz. chambers 9-11132  
in plasma, high pressure with electron temp. exceeding gas temp. 9-13421

## Ions continued

## recombination continued

- in semiconductor following electron bombardment, monument for spectral study 9-12157  
three-body, diff. and effective gradient treatment methods, modifications and accuracy 9-5073  
two-electron collisional-radiative, depend. of emitted light on charge density 9-11623  
Ar dense plasma, recombination coeff. obs. 9000°K 9-5007  
Ar dissociative recombination and molecular ion formation in decaying plasma 9-13414  
Ar plasma excited states, spect. studies, electron-ion recomb. coeff. 9-21057  
CO<sub>2</sub>-Ne afterglow plasma, obs. 9-9341  
H<sup>+</sup>, electron capture cross-sections for neutral atomic targets 9-5069  
H+H+M→H<sub>2</sub>+M, thermomolecular recomb. kinetics, resonance theory 9-17005  
He, electron-ion recombination, coeff. variation rel. to pressure 9-17136  
He dissociative recombination and molecular ion formation in decaying plasma 9-13414  
NO-Ne afterglow plasma, obs. 9-9341  
NO<sup>+</sup>+NO<sub>2</sub>→N<sub>2</sub>O<sub>3</sub> rate determ. in various gases 9-7194  
O<sub>2</sub><sup>+</sup>-electron, in O<sub>2</sub>-rare gas mixtures, temp. depend., 205-690°K 9-5076  
O<sub>2</sub>-ion ion dissociative recomb. calc. 9-5075  
O<sub>2</sub><sup>+</sup>, electron-ion recomb., quantum mech. calc. 9-5074  
O<sub>4</sub><sup>+</sup>+O<sub>2</sub>→O<sub>6</sub>, rate determ. in O<sub>2</sub> 9-7194

## scattering

- ion-ion collisions, effect on plasma resistive drift mode 9-17122  
polymer film, photoresist, beam exposure 9-13813  
<sup>10</sup>B scatt. of <sup>16</sup>O ions, elastic, obs. and anal. of results 9-15503  
<sup>9</sup>Be scatt. of <sup>16</sup>O ions, elastic, obs. and anal. of results 9-15503  
<sup>12</sup>C scatt. of <sup>16</sup>O ions, elastic, obs. and anal. of results 9-15503  
p-H<sub>2</sub>, 77°K, e drift and diff. 9-9405  
He<sup>2+</sup> by wurtzite CdS rel. to crystal. polarity meas. 2 keV 9-9635  
<sup>16</sup>O on <sup>9</sup>Be, <sup>10</sup>B and <sup>12</sup>C, elastic, obs. and anal. of results 9-15503

## Ions, electrolytic

- See also Conductivity, electrical/liquids, electrolytic; Dissociation/electrolytic  
aggregates, electrolytes in nonaq. solvents 9-9514  
alkoxybenzene radical anions, e.s.r. and electronic struct. 9-7085  
benzene anion, T<sub>1</sub>/T<sub>2</sub> and spin relax. 9-15904  
p-benzoquinone-K, e.s.r. and ion pair assoc. 9-19644  
cation with inert gas shell, empirical formula for radius 9-19482  
chloranil radical anion, optical spectrum 9-5173  
coronene dimer cation, e.s.r. 9-2902  
counterions, and polyions in polyelectrolyte, different forms of association 9-15226  
distribution in conc. electrolytes 9-18762  
distribution in electrolytes 9-10346  
ion-ion-pair-solvent equilibria, isothermal, independent of dielec. constant 9-8099  
phenol-sulfonic cation-exchange membrane, determ. of transport numbers 9-9501  
rare earths, trivalent, electronic energy levels 9-16017  
rare-earth, in aq. soln., nonradiative energy transfer 9-9524  
selection by membrane system, patent 9-19626  
Ag, absorption on TiO<sub>2</sub> in aqueous and methanolic solns. 9-10348  
<sup>10</sup>BO<sub>2</sub><sup>-</sup> and <sup>11</sup>BO<sub>2</sub><sup>-</sup>, migration, isotope effect 9-17200  
Co(II), solvation determ. by <sup>17</sup>O n.m.r. 9-3123  
Eu<sup>3+</sup> in aq. soln., electronic energy levels 9-16006  
HCl, hydration determ. by n.m.r. 9-17220  
HClO<sub>4</sub>, hydration determ. by n.m.r. 9-17220  
Na<sub>2</sub>Al<sub>6</sub>, cryolite, liq. complex ion identification 9-1017  
NaClO<sub>4</sub>, hydration determ. by n.m.r. 9-17220

## Irasers see Lasers

## Iridium

- dislocations, dissociated perfect, in field ion image 9-16100  
field ion specimens, oxidised, structure of oxide films 9-21280  
internal friction, dynamic modulus and creep up to 2000°C at low freq. 9-14965  
ions, field-evaporated, charge state, obs. 9-5783  
ions, field-evaporated, charge state, obs. 9-10085  
radiation damage, heavy ion, field ion microscope exam., exptl. technique 9-5580  
Schockley loops, glissile, occurrence in field-ion specimens 9-5362  
silica-supported, adsorption of N<sub>2</sub>, i.r. spectra 9-20934  
Iridium compounds  
Ir-Rh alloys, mag. susceptibility comp. and temp. dependence, 6-1850°K 9-13947  
Ir-based dilute alloys, spin fluctuations and superconductivity 9-1499  
IrC, gaseous, dissociation energies, mass spect. determination 9-14726  
IrF<sub>6</sub>, electronic spectrum, Jahn-Teller progressions 9-772

## Iron

- α-γ phase transition revealed by hysteresis in thermoelectric e.m.f. 9-17340  
abundance in solar photospheric spectrum, forbidden Fe II lines meas. 9-14258  
acid corrosion, inhibition by phenylthiourea 9-12545  
addition to Ni<sub>3</sub>Mn alloy, effect on props 9-12278  
adsorption of surface active cpds. and corrosion inhibitors, effects of deformation and heat treatment 9-18760  
ageing by amplitude depend. internal friction 9-13764  
anode polarization of soft wires in conc. electrolytes 9-15225  
armco, residual mag. props., effect of shock waves 9-13980  
Armco, viscous crack development, dislocation structure and peculiarities 9-3450  
atom, core-e energy levels and density of states, X-ray photoelectron spectrum 9-1813  
atomic beam impact on Ta, resulting ions mass analysis 9-10084  
blood plasma <sup>59</sup>Fe clearance meas. 9-15382  
carburization under vacuum 9-14124  
cast, corrosion by CuSO<sub>4</sub> 9-20057  
corrosion in HClO<sub>4</sub>, transition state of inhibition by org. cpds. 9-15223  
corrosion in Li<sub>2</sub>SO<sub>4</sub>-K<sub>2</sub>SO<sub>4</sub> eutectic at 600°C, equilb. pots. rel. to activity of P O<sub>2</sub><sup>-</sup> 9-15222  
corrosion in NH<sub>4</sub>NO<sub>3</sub>-NH<sub>3</sub>-H<sub>2</sub>O system 9-21699  
corrosion prods. analysis by Mossbauer backscatt. spectroscopy 9-10363  
in corundum, content and oxidation state rel. to synthesis and optical absorpt. 9-1132  
Curie point, temp. depend. obs. by critical scatt. of neutrons 9-12269

## Iron continued

damping near Snoek peak 9-9749  
 defect network, deformation-produced, in high-purity mat., elimination 9-9697  
 deformation behaviour in single crystals at upper yield point 9-3418  
 desorption of H<sub>2</sub> mols., angular distrib. 9-7349  
 diffusion in Cu, direct obs. by Mossbauer effect 9-5401  
 diffusion in V and isotope-effect parameter of <sup>55</sup>Fe and <sup>59</sup>Fe 9-9734  
 diffusion in zincite during hydrothermal growth 9-18419  
 diffusion of Be, 1100-1350°C 9-5403  
 diffusion of Co and Ni and diffusion in Co and Ni, heterodiffusion coeff., 1136 1370°C 9-19763  
 diffusion of Cr 9-5406  
 diffusion of Cr 9-5407  
 diffusion Zircaloy-2 9-19761  
 dislocation, a <100> field-ion microscope evidence for existence 9-5361  
 dislocation recovery mechanism models 9-18470  
 dislocation vel. obs. with e microscope 9-10823  
 dislocations, strain produced, two beam dark field electron micrographs 9-7539  
 divalent, S=1 spin state, investigation of Mossbauer spectrum of <sup>57</sup>Fe in phthalocyanine iron (II) 9-10100  
 doping of p-PbTe, thermoelec. power thermal and elec. cond. effects 9-13876  
 elastic constants, higher order, from finite deform. meas. 9-5419  
 electrolytic, ageing by amplitude depend. internal friction 9-13764  
 electrolytic, eff. of grain size on microhardness 9-11944  
 electronic band structures, approx. calc. 9-12059  
 e.m. cascade from cosmic ray bremsstrahlung 9-20683  
 e.m. phenomena, internal, investigation with improved B-H characteristic 9-16350  
 embrittlement, effect of cold rolling 9-1311  
 emission line shift prod. by Ar and He, obs. 9-6963  
 f.c.c., ferromagnetic and paramagnetic props., comparison from theoretical eqns. 9-3787  
 ferrovac-E, plastic strain through macroscopic yielding 9-17347  
 ferromagnetic props. rel. to lattice constant 9-13982  
 at ferromagnetic transition point, props. from Landau-type theory 9-7901  
 film, H<sub>2</sub>O chemisorption, 77° and 273°K 9-17519  
 film, negative magnetoresistance anisotropy 9-18682  
 film with (100) surface orientation, spatial magnetization distribution 9-19961  
 films, nucleation, growth and structure in obs. in e. microscope 9-19673  
 films, nucleation, growth and structure obs. in e. microscope 9-19672  
 flow stress, 10-300°K 9-13732  
 group doubly ionized atoms, 3rd spectra, config. 3d<sup>4</sup>p 9-18139  
 impurity distribution in ZnS crystals grown from melt 9-18429  
 interaction between impurities and dislocations 9-5353  
 interdomain wall thickness temp. depend., numerical results 9-12276  
 ionization degree from diffusion and electrotransport, 1000-1350°C 9-1581  
 ionization equilibrium in low-density plasma 9-15820  
 irradiated, yield stress, saturation and exposure depend. 9-11929  
 lattice atoms, mean square displacement determ. 9-7403  
 lattice parameter anomalies at Curie point 9-5569  
 Luders from propagation accompanying yield-point phenomena, stress-strain distrib. 9-19785  
 magnetic domain patterns rel. to magnetization process 9-16353  
 magnetic film longitudinal Kerr rotations and figures of merit 9-3813  
 magnetization of polycrystals, interpretation near Curie temp. using Landau-Ginzburg-Lifshitz theory 9-12291  
 magnetocrystalline energy consts. K<sub>1</sub>, K<sub>2</sub> and K<sub>3</sub>, temp. depend. 20 to 800°K 9-3789  
 magnetostrictive props. in remanent state, elastic tensile stress effects 9-19956  
 martensite, growth and X-ray exam. of cementite particles 9-19714  
 melting, possible vacancy mechanism 9-5215  
 meteorites responsible for lunar mascons 9-18904  
 Mossbauer eff. of <sup>57</sup>Fe, high pressure eff. at room temp. 9-21610  
 neutron attenuation, extended source 9-422  
 neutron irradi., work hardening characts. 9-3468  
 oxidation of foils obs. with e microscope 9-10823  
 particles, thermal expansion and structural anomalies 9-5199  
 phase transformation, high-pressure, dynamic elec. resistivity obs. 9-14991  
 plastic strain through macroscopic yielding 9-17347  
 Polymorphism, eff. of alloying elements 9-16049  
 porous, shock compression in region of incomplete compaction 9-11948  
 powders, compressibility, increase by cold rolling patent 9-13749  
 recrystallization, influence of alloying additions, obs. by isochronal strength curves 9-11962  
 resistance to plastic deform., effect of strain rate 9-9759  
 rotational hysteresis due to perpendicularly superimposed continuous and alternating fields 9-10123  
 scattering of 9 and 15 MeV bremsstrahlung 9-11267  
 self diffusion 9-21350  
 shock-hardened, twin and complementary twins 9-13695  
 sintered, stress-deformation behaviour 9-17301  
 sintering, vol., grain boundary and surface diffusion contributions 9-1246  
 slip, activation parameters rel. to neutron irradiation 9-1296  
 soft, anode polarization in conc. electrolytes 9-15225  
 specific heat, mag. fields effects near Curie temp. 9-13802  
 stress-corrosion cracking in NH<sub>4</sub>NO<sub>3</sub> soln. 9-14981  
 surface energy, effect of O<sub>2</sub> adsorption 9-9603  
 target, neutron scatt. 9-591  
 thermal diffusivity and conductivity, 900-1660°C 9-13808  
 vacancy relaxations in b.c.c. crystals 9-9702  
 whiskers, internal friction, plastic deform. and recovery 9-1269  
 wire, Barkhausen discontinuities propag. 9-12290  
 e cosmic ray cascade calc. of equilibrium ang. distrib. function 9-15664  
 γ-δ transformation, anisotropic and heterogeneous nucleation 9-3489  
 γ transmission (from <sup>60</sup>Co source) in polyethylene 9-21447  
 A) X-ray atom form factor determ. from vanishing second order reflection in high-voltage electron diff. 9-9676  
 Ba. fine particle assemblies, coercive force variation with packing 9-3796  
 Cr-Fe alloys, dil., Fe impurity e.p.r. 9-1858  
 diffusion in Au, measurement using Mossbauer effect 9-3377  
 α-Fe, dipole strength of C and N 9-9739  
 α-Fe, dislocation visibility, error in electron microscope technique 9-18469

## Iron continued

α-Fe, plastic stress relax., time depend. 9-5433  
 α-Fe, self-diffusion of <sup>59</sup>Fe and <sup>55</sup>Fe, isotope eff. 9-3382  
 α-Fe, solid solubility of C 9-9788  
 Fe<sup>2+</sup>, e.p.r. in MgO, by saturation by u.s. waves 9-21665  
 Fe<sup>2+</sup>, Mossbauer spectra, hyperfine structure, rel. to spin-lattice relax. study 9-18688  
 Fe<sup>2+</sup> in SrTiO<sub>3</sub>, e.p.r. spectrum, cubic splitting temp. dependence, 123-773°K 9-18742  
 Fe<sup>2+</sup> in V<sub>2</sub>O<sub>5</sub>, Mossbauer exam. using <sup>57</sup>Fe 9-21613  
 Fe complex, tris (2-dimethylaminoethyl) amineiron (II) bromide, crystal structure 9-3299  
 α-Fe creep, temperature range 220-900°C 9-1290  
 Fe ferromagnetic thin films, mag. birefringence 9-14034  
 Fe I and Fe II sunset lines curve of growth calcs., equivalent widths interpretation 9-21971  
 Fe I spectra, absolute oscillator strength of reson. line λ=3720 9-18140  
 Fe IX-XIV, identification of 3d-4p and 3d-4f transitions in solar spectrum 9-6191  
 Fe population levels, current and pressure dependence 9-18319  
 Fe XII, transition probabilities for various excited states 9-15809  
<sup>57</sup>Fe, self-diffusion in α-Fe 9-3382  
<sup>57</sup>Fe, Mossbauer and Rayleigh scatt. interference, spin-depend. of Rayleigh scatt. 9-7959  
<sup>57</sup>Fe, Mossbauer spectrum 9-501  
<sup>57</sup>Fe in BaFe<sub>12</sub>O<sub>19</sub>, n.m.r. 9-1872  
<sup>57</sup>Fe in CoO, relaxation rates, limitations 9-1749  
<sup>57</sup>Fe in Cu, Pd, Pt, Mossbauer effect for lattice dynamics 9-7638  
<sup>57</sup>Fe in Fe-Al alloys, dilute, n.m.r., rel. to <sup>27</sup>Al 9-1874  
<sup>57</sup>Fe in oxide spinels containing Cu and Fe, Mossbauer spectra 9-7956  
<sup>57</sup>Fe, self diffusion in α-Fe 9-3382  
<sup>59</sup>Fe, self diffusion in para- and ferromag. temp. ranges of Fe-Cr alloys 9-1245  
 Fe<sup>2+</sup> in AgCl, e.s.r. 9-5980  
 Fe<sup>2+</sup> in Al<sub>2</sub>O<sub>3</sub>, ground-state and spin-lattice relaxation 9-12315  
 Fe<sup>2+</sup> in CsZnCl<sub>3</sub>, interstitial sites, e.s.r. determ. 9-8025  
 Fe<sup>2+</sup> in MgO, phonon-photon double quantum transitions, freq. depend. 9-1360  
 Fe<sup>2+</sup> in MgO thermal cond. < room temp. 9-1406  
 Fe<sup>2+</sup> in YFe garnet, characterization 9-16388  
 Fe<sup>2+</sup>, e.p.r. in Al<sub>2</sub>O<sub>3</sub>·H<sub>2</sub>O 9-5981  
 Fe<sup>2+</sup> angle between mag. moments in SrFe<sub>12-2x</sub>Ga<sub>x</sub>O<sub>19</sub> 9-16373  
 Fe<sup>2+</sup> activating phosphate, borosilicate and silicate glasses, luminesc. spectra and absorpt. bands 9-10264  
 Fe<sup>2+</sup> in MgO, spin-lattice coupling constants 9-14016  
 Fe<sup>2+</sup> in SnO<sub>2</sub>, e.s.r. spectrum 9-17497  
 Fe<sup>2+</sup> in methylamine alum, e.p.r. rel. to spin-Hamiltonian coeffs. determ., 77°K 9-5990  
 Fe<sup>2+</sup> in zeolite molecular sieve, superparamagnetism evidence, magnetic and Mossbauer eff. studies 9-5810  
 Fe<sup>m+</sup>, (8≤m≤15), collisional ionization cross-sections and temp. of solar corona 9-10556  
 Fe(III) tetrahedral ions, Mossbauer hyperfine interactions 9-1748  
 Fe<sub>2</sub>O<sub>3</sub> fine powders, magnetization reversal, particle agglomeration effect 9-3822  
 Fe-NaCl system, complex e.s.r. spectra after X irradi. 9-20023  
 Fe<sup>2+</sup>, Mossbauer effect obs. in chalcopyrite 9-10182  
 ions, eff. on photographic process 9-20567  
 MgO:Fe<sup>2+</sup>, absorption bands, pressure shift, and dynamic Jahn-Teller effect 9-5927  
 Mo content determ. using vacuum spectrometer 9-20069  
 in Ni, state at grain boundaries from Mossbauer effect 9-21611

**Iron alloys**  
*See also Iron compounds; Steel*  
 armco iron, interface tension at boundary with fluxes 9-14889  
 Armco iron, yield and flow stresses, temp. and strain-rate dependence at low temps. 9-1285  
 cementite, hypereutectoid, in white cast iron, spheroidization on annealing at 900°C 9-5496  
 dilute with transition elements, electronic sp. heat for band struct. rel. to origin of ferromagnetism 9-13800  
 Invar alloys, mag. contrib. to low temp. thermal expansion and Curie temp. pressure dependence 9-21580  
 neutron embrittlement at high temps. 9-19369  
 Permalloy, magnetic analysis by electron diffraction 9-12277  
 Permalloy, thin films, hysteresis loop meas. 9-12296  
 Permalloy film, coercive force and anisotropy field, eff. of crystallite size 9-13996  
 Permalloy film, ferromag. reson., linewidth thickness depend. 9-8005  
 permalloy film, supercritical, thickness effects on mag. props. 9-1677  
 permalloy films, <sup>4</sup>He irradi. effects on anisotropy field inhomogeneity and coercive force 9-7908  
 permalloy films, ferromag. resonance, X-band obs. by reflecto-polarimetric exam. 9-10270  
 Permalloy films, optimization of props. for computer memories 9-13995  
 permalloy films, rotational hysteresis 9-10134  
 permalloy films, stresses, annealing and substrate temp. effects 9-13724  
 permalloy films, vacuum deposited elastic limit and tensile strength 9-3412  
 permalloy fine wires, Nb addition, materials parameters affecting reentrancy 9-5824  
 permalloy thin film pairs with large separations, domain wall coupling 9-10132  
 permalloy thin films, ageing and stabilization 9-3471  
 permalloy thin films, angular dependence of magnetic annealing effects 9-10131  
 permalloy thin films, angular dependence of magnetic annealing effects 9-10131  
 permalloy thin films, anisotropy inhomogeneity, origin 9-5838  
 permalloy thin films, uniaxial anisotropy, origin 9-3815  
 permalloy thin tapes annealed below recrystallization temp., mag. props. 9-3814  
 permalloy/Mn double layer films with exchange anisotropy, stabilisation of ferromag. domain structures 9-10130  
 silicon iron, gyromagnetic constant meas. using magneto-optical effect 9-12344  
 thermal expansion, low temp. 9-19864  
 Al Fe binary system, electronic structure, X-ray investigation 9-3553  
 Au-Fe, dilute, band gap var. determ. from light reflectivity meas. 9-21604  
 Au-Fe dil., magnetoresistance 9-5805



**Iron alloys continued**

- Au-(0.03at.%)Fe, thermoelec. power, 0.35°K-10°K, mag. field (0-77 kOe) dependence 9-1605
- (8.85 wt.%) Cr-(1.0 wt.%) Ni-Fe, polymorphic transform., effect of high pressure on kinetics and phase equilb. temp. 9-5513
- CdSb-Fe, mag. susceptibility 9-16328
- Co-Fe, cold rolling to give constricted mag. hysteresis loop, patent 9-13759
- Co-Ni-Fe films, vapour deposited nonmagnetic mag. props. 9-5837
- (8.2 wt.%) Cr-Fe, polymorphic transform., effect of high pressure on kinetics and phase equilb. temp. 9-5513
- Cu-Fe, dil., sp. ht. meas. 9-18563
- Cu-Fe dilute, magnetoresistance and low temp. resist. 9-18602
- Fe-Al, Mossbauer eff., electron transitions from isomeric shift and X-ray emission spectra parameters 9-3871
- Fe-Al, oxidation in CO<sub>2</sub>, composition and temp. dependence 9-14132
- Fe-Al, phase transitions rel. to ordering 9-9801
- Fe-Al dilute, n.m.r. of <sup>57</sup>Fe and <sup>27</sup>Al, rel. intensities 9-1874
- Fe-Al solid solns., heterogeneous, n.-irrad. effects on elec. resistivity rel. to ordering changes 9-1465
- Fe-(23 at.%)Be, structure changes during ageing, transmission e. microscopy study 9-17343
- Fe-C, deformation mechanism, 77° to 300°K 9-5458
- Fe-C, deformed, affect of C on annealing stages above room temp. 9-13754
- Fe-C, magnetoresistivity, 4.2 and 78°K 9-15070
- Fe-C, phase transformations during tempering, eff. of prior plastic deform. 9-13777
- Fe-C, precipitation kinetics, infl. of age-hardening rate 9-9798
- Fe-C solid soln., point defects studied by mag. after-effect meas. 9-5333
- Fe-Ca-Si addition to steel, effect on graphite precipitation 9-19838
- Fe-Co, ferromagnetism and order 9-3788
- Fe-Co, lattice parameters and Curie point anomalies 9-18444
- Fe-Co (Permudivco), V addition, magnetic anisotropy 9-12281
- Fe-Cr-Al-Y, oxide films formed in CO<sub>2</sub>, struct. and composition 9-11779
- Fe-Cr-Mn, structure effect on oxidation resistance 9-5503
- Fe-Cr-Ni, austenitic, in oxidizing acids, effect of Si content on corrosion resistance 9-17535
- Fe-(18 wt.%)Cr, increased oxidation at 1123°K due to Ni additions 9-20045
- Fe-Cr, ageing, C<sub>5</sub> rel. to Guinier-Preston zones formation 9-9785
- Fe-Cr, b.c.c., <sup>59</sup>Fe diffusion rel. to solvent atom diff. mechanism 9-7507
- Fe-Cr, diffusion of Cr 9-5404
- Fe-Cr, evaporation rate of Cr under vacuum 9-19658
- Fe-Cr, interdiffusion investigation in powder alloys 9-5405
- Fe-Cr, oxide growth and spalling 9-18755
- Fe-Cr, self-diffusion of <sup>59</sup>Fe in para- and ferromag. temp. ranges 9-1245
- Fe-Cr, virtual spin-wave state below and above Curie pt. 9-16343
- Fe-Cr Mossbauer spectra, use of zero point calibration technique 9-19973
- Fe-(16wt.%)Cr crystal, corrosion pit nucleation, e. microprobe exam. 9-21697
- Fe-(30 wt.%)Cr aged at 475°C, plastic deform., activation parameters 9-1286
- Fe-Cr(V), itinerant electron ferromagnetism evidence 9-3797
- Fe-Cu, evaporation rate of Cu under vacuum 9-19658
- Fe-Cu(Cr) systems, diffusion, vacancy mechanism, specific features 9-9730
- Fe-3 wt.%Si with Goss-texture, irreversible magnetization process and Barkhausen effect 9-13977
- Fe-Ge, oxidation, high temp. study 9-6013
- Fe-Mn, evaporation rate of Mn under vacuum 9-19658
- Fe-Mn, ferromagnetic behaviour 9-18679
- Fe-Mn, Hall effect and resistivity temp. and comp. dependence 9-9921
- γ-Fe-Mn paramag. n. scatt. 9-1644
- Fe-Mo, ferromagnetic magnetization 9-18679
- Fe-Mo, wetting with molten Ag 9-13508
- Fe-N, phase transformations during tempering, eff. of prior plastic deform. 9-13777
- Fe-Ni-Co, monocrystalline thin films, epitaxial growth and coercive force 9-12298
- Fe-Ni-Cr, magnetization intensity and susceptibility rel. to heat treatment 9-12288
- Fe-Ni-Mn, isothermal martensitic transformation nucleation rate 9-14990
- Fe-Ni-Mn, uniaxial mag. anisotropy in martensitic transform 9-1667
- Fe-Ni-Ti, mechanical props. improvement by ageing 9-11928
- Fe-30wt.%Ni-5wt.%Nb austenitic, structure and hardening on heat treatment and cold working 9-9802
- Fe-Ni, f.c.c. Curie temp. pressure dependence 9-12289
- Fe-Ni, hysteresis loops, constant field, effect of anisotropy and atomic arrangement, X-ray exam. of textures 9-5825
- Fe-Ni, Invar effect 9-1662
- Fe-Ni, magnetic anisotropy and ordering 9-3792
- Fe-Ni, martensitic transform., effect of additions 9-9799
- Fe-Ni, martensitic transform. rel. to change in mech. of transform. 9-5514
- Fe-Ni, uniaxial mag. anisotropy in martensitic transform 9-1667
- Fe-Ni invar., Curie point, effect of third component 9-10113
- Fe-Ni thin films, grain size variation, X-ray diff. study 9-13577
- Fe-(30 wt.%)Ni, elastic moduli, rel. to martensitic transformations 9-7516
- Fe-30at.%Ni, martensitic transformation, mag. fields effect 9-3491
- Fe-Pd, coercive force rel. to ferromag. domain ordering 9-12275
- Fe-Pd, dil. mag. magnetization distrib. 9-7900
- Fe-Pd, dilute, spin-wave stiffness by neutron scattering technique 9-12268
- Fe-Pd, f.c.c., Curie temp. pressure dependence 9-12289
- Fe-Pt, f.c.c., Curie temp. pressure dependence 9-12289
- Fe-Rh, e.s.r. meas. rel. to antiferromag.-ferromag. transition 9-16455
- Fe-S, evaporation rate of S under vacuum 9-19658
- Fe-Si-S, evaporation rate of S under vacuum 9-19658
- Fe-Si-Zn system, constitution anal. using mag. and X-ray techs. 9-11975
- Fe-Si, Barkhausen discontinuities due to mech. stresses 9-5827
- Fe-Si, coercive forces and mag. susceptibility 9-16360
- Fe-Si, crystals, oxidation kinetics, optical exam. 9-21277
- Fe-Si, dislocation, velocity stress dependence, temp. and comp. effects 9-7488
- Fe-Si, eff. of dislocation network on plastic strain 9-16098
- Fe-Si, eutectic crystal behaviour below eutectic pts. 9-5213

**Iron alloys continued**

- Fe-Si, ferromag. resonance 9-8004
- Fe-Si, grain oriented, basic expts. on nature of anomalous losses 9-12242
- Fe-Si, grain oriented, magnetostriction meas. using ceramic displacement transducers 9-12293
- Fe-Si, with Gross or cube texture, hysteresis losses rel. to grain size 9-12237
- Fe-Si, Hall effect and resistivity temp. and comp. dependence 9-9921
- Fe-Si, high temp. sp. ht., mag. susceptibility temp. depend., up to 1870°K 9-7601
- Fe-Si, magnetic props., anisotropy, eff. of surface Ni films 9-13990
- Fe-Si, magnetization reversal mechanism for single crystal picture frames 9-13981
- Fe-Si, oxide film effect on max. permeability 9-10092
- Fe-Si, phase diagram 900-1200°C for 30 to 40 at.%Si 9-11974
- α-Fe-Si, superlattice phases, equilb. and transforms. 9-11965
- Fe-Si, thin films, antiphase boundaries contrast in superlattice reflections 9-11849
- Fe-Si, X-ray fluorescence 9-14080
- Fe-Si crystals, oxide film structure 9-21278
- Fe-Si embrittlement, effect of cold rolling 9-1311
- Fe-(3wt.%)Si, magnetoelastic attenuation of vibrations eff. of temp. 9-11915
- Fe-(3wt.%)Si polycrystals, twinning and effects on brittleness 9-1124
- Fe-Si(Ni)(Cr)-C ternary, diffusion of C rel. to element redistrib. laws 9-3381
- Fe-Sn, evaporation rate of Cr under vacuum 9-19658
- Fe-Ta, ferromagnetic behaviour 9-18679
- Fe-Ti, Laves phase magnetism, conc. depend. 9-7897
- Fe-V, diffusion of Cr 9-5404
- Fe-V, Hall effect and resistivity temp. and comp. dependence 9-9921
- Fe-W, wetting with molten Ag 9-13508
- Fe-(0.2 wt.%)Zr, deformation mechanisms, 77° to 300°K 9-5458
- Fe-6.5%Si, zero magnetostriction, n. induced mag. viscosity, obs. 9-19952
- Fe-(7.5 at.%)Si, self-diffusion near Curie temp., activation energy rel. to elastic modulus 9-5402
- (19wt.%)Fe-(8.1wt.%)Ni films, anhyseretic behaviour, 20°C 9-13992
- Fe-28 wt.% Ni 0.04 wt.% C, martensite grain substructure (fragmented structure) 9-1187
- FeAl, coercive force, magnetization, susceptibility and magnetostriction rel. to order-disorder 9-21584
- FeAl ordered ferromag. alloys, spin-wave excitations, dispersion law, Heisenberg model 9-18674
- FeSi ordered ferromag. alloys, spin-wave excitations, dispersion law, Heisenberg model 9-18674
- FeCo in vacuum, friction rel. crystal structure and atomic ordering 9-19814
- Fe/Cr superlattice, isothermal magnetic annealing effect on magnetization and magnetostriction at high and room temperatures 9-15153
- Fe-Ni-C, ferromagnetic f.c.c., plastic deform. 9-13727
- MnF<sub>2</sub>:Fe<sup>2+</sup> M1-active local mode at 94 cm<sup>-1</sup> 9-3949
- Ni-Cr white castiron, heat treatment for improving mech. props., patent 9-13757
- Ni-(17 wt.%)Fe/EuS double layers, mag. hysteresis, thickness dependence 9-18678
- Ni-Fe-Cu-Mo rolled from sintered compacts, high mag. permeability 9-13965
- Ni-Fe-Cu layers, mag. and struct. props., influence of annealing 9-3821
- Ni-Fe-Pd, films, composition and deposition for use as magnetic storage elements, patent 9-13998
- Ni-(35 wt.%)Fe, ferromagnetic domain structures 9-13973
- Ni-(19 wt.%)Fe ferromagnetic thin films, mag. birefringence 9-14034
- Ni-Fe, absolute thermo e.m.f., eff. of plastic deformation 9-21543
- Ni-Fe, dil. ferromag., elec. resistivity and screening 9-5645
- Ni-Fe, effects of radiation on magnetic props. 9-1661
- Ni-Fe, evaporated film, lattice parameter composition dependence 9-14986
- Ni-Fe, f.c.c., elastic const. and sp. hts., 4.2°K 9-5421
- Ni-Fe, Kerr magneto optic effect, longit., and optical const. 9-10175
- Ni-Fe, solute C effects on Curie pt. and spontaneous magnetization 9-13984
- Ni-(19 wt.%)Fe ferromagnetic film, domain walls, low-angle electron diffraction investig. 9-13997
- Ni-Fe double films, coupling between 9-3816
- Ni-Fe ferrite single crystals containing Co, stabilized-domain walls, effect on hysteresis loop shape 9-5849
- Ni-Fe film, domain boundary propag., slow to intermediate speed. Kerr magneto optical obs. 9-3819
- Ni-Fe film, domain wall streaming, creeping and parade motion, hard axis pulse excitation 9-3820
- Ni-Fe films, electrodeposited, coercive force rel. to crystallite size 9-7909
- Ni-Fe films, magnetization-ripple, crystallite-size and film-thickness dependence 9-7907
- Ni-Fe films, magnetostriction meas. method 9-13985
- Ni-Fe films, transverse Kerr effect, 0.3 to 3 μ 9-5840
- Ni-Fe films, uniaxial, analog, storage using non-uniform fields 9-5844
- Ni-Fe films coupled with stripe domain films, mag. props. 9-10133
- Ni-(19wt.%)Fe magnetic films, energy of combined Bloch and Neel type domain wall 9-18683
- 82.5 wt.% Ni-17.5 wt.% Fe permalloy film, Faraday and Kerr effect 9-16364
- NiFe-based ternary alloys with transition metal, electronic structure and ordering processes 9-19834
- NiFe-based, isothermal ordering effects on elastic constants and deformational hardening 9-9741
- Ni-Fe, deformed, positron annihilation 9-21477
- Pd-Fe, dil., microwave ferromagnetic resonance 9-3948
- Pt-Fe, Mossbauer effect, mag. structure rel. to ordering 9-12362
- Pt-Fe permanent magnetic alloy, improvement of mag. props. by replacement of Pt by Pt group metals 9-12294

**Iron compounds**

*See also Ferrites; Iron alloys; Steel*

- dimeric, Mossbauer effect, relaxation effects 9-18697
- FeOOH, Fe<sub>2</sub>O<sub>3</sub> system, chemical remanent magnetization 9-16546
- ferrites, directional order below order-disorder transformation point 9-17457
- ferrocene in glassy soln., 77°K phosphoresc. 9-3111
- halides, ferrous, anhydrous, 3d electron delocalization from Mossbauer meas. 9-14036

**Iron compounds continued**

hematite, specular, pure crystal ferromagnetic exchange interactions obs. 9-10149  
 magnetite, growth from borax flux 9-18413  
 magnetite, magnetic remanence, strain-induced 9-7905  
 magnetite, orthorhombic phase, electron microscopy 9-7439  
 magnetites, low temp. oxidation mechanism 9-15220  
 Mossbauer spectra, standard ref. mat. for chemical shift 9-3872  
 oxide addition to CaO-MgO-Al<sub>2</sub>O<sub>3</sub>-SiO<sub>2</sub> glasses, effect on crystallization kinetics 9-19688  
 oxides, diffusion and dissolution in sodium disilicate glass, kinetics 9-19766  
 perminvar ferrites, mag. ordering stability 9-10138  
 6 Fe<sub>2</sub>O<sub>3</sub>·PbO, magnetoplumbite, zigzag domain obs. 9-1663  
 CaO-FeO-Al<sub>2</sub>O<sub>3</sub> solid soln., X-ray and microscopic obs. 1050° and 1200°C 9-16147  
 Fe-rare earth intermetallics, cubic Laves, Mossbauer study of hyperfine fields 9-7958  
 Fe-Al intermetallic, mag. susceptibility and n.m.r. study 9-7888  
 Fe-Be solid solution, Mossbauer eff., elec. field gradient variation 9-17477  
 Fe-C martensite, diffusional magnetic viscosity effect 9-3801  
 Fe-Fe<sub>3</sub>C growth of oxide films 9-1110  
 Fe-I-boracite small spontaneous lattice strain determ. by X-ray strain-meter 9-3262  
 Fe-Si frame in monocystal, negative Barkhausen jumps, occurrence during magnetization 9-1672  
 Fe-Si sheet, coarse grain, pole figure by neutron diff. 9-19698  
 Fe-Ti oxides in basalts, composition 9-16545  
 Fe<sub>0.85</sub>S and Fe<sub>0.9</sub>S natural pyrrhotite thermomag. investigation 9-18821  
 Fe<sub>1-x</sub>O ion-vacancy cluster structures 9-14939  
 (Fe<sub>1-x</sub>Y<sub>x</sub>)<sub>2</sub>Ge, magnetic susceptibility up to 1000°C 9-19948  
 Fe<sub>2</sub>AlB<sub>2</sub> crystal structure 9-21313  
 Fe<sub>2</sub>B, ferromagnetic, n.m.r. and Mossbauer effect obs. 9-21670  
 Fe<sub>2</sub>O<sub>3</sub>-Ti elec. conductivity and thermoelec. power rel. press. and temp. 9-21506  
 Fe<sub>2</sub>O<sub>3</sub>-Al<sub>2</sub>O<sub>3</sub> electrical cond. and thermoelec. power, effect of chemisorbed hydrogen and water vapour 9-20036  
 Fe<sub>2</sub>O<sub>3</sub>-Cr<sub>2</sub>O<sub>3</sub> electrical cond. and thermoelec. power, effect of chemisorbed hydrogen and water vapour 9-20036  
 Fe<sub>2</sub>O<sub>3</sub>, additive to coke filler, for suppression of irreversible expansion in baking 9-7591  
 Fe<sub>2</sub>O<sub>3</sub> electrical cond. and thermoelec. power, effect of chemisorbed hydrogen and water vapour 9-20036  
 α-Fe<sub>2</sub>O<sub>3</sub> (hematite), antiferromag. reson., premature disappearance 9-18733  
 α-Fe<sub>2</sub>O<sub>3</sub> (hematite), n.m.r. of <sup>57</sup>Fe, freq. and signal intensity rel. to temp. 9-14115  
 Fe<sub>2</sub>TiO<sub>4</sub>-Fe<sub>2</sub>O<sub>3</sub> solid soln., initial susceptibility of fine grain assembly, rel. axial stress 9-18680  
 Fe<sub>2</sub>Zr, ferromagnetic, n.m.r. and Mossbauer effect obs. 9-21670  
 Fe<sub>3</sub>O<sub>4</sub>, magnetite, film nucleation and growth on Fe in high-temp. water 9-21276  
 Fe<sub>3</sub>(CO)<sub>12</sub>P(C<sub>6</sub>H<sub>5</sub>)<sub>3</sub>, crystal structure determ. by n diffraction and X-ray data 9-21314  
 Fe<sub>3</sub>Se<sub>8</sub>, Hall effect and transverse magnetoresistance 9-19886  
 Fe<sub>3</sub>Se<sub>9</sub>, preparation, crystal structure, elec. conductivity, sp. ht. component 9-21484  
 Fe<sub>3</sub>Ga<sub>2-x</sub>O<sub>3</sub>, ferrimagnetic resonance, electric fields eff. 9-18732  
 Fe(OH)<sub>2</sub>, colloid, oxidation, Cu(II) effects, obs. 9-6014  
 Fe(SO<sub>4</sub>)OH·3H<sub>2</sub>O (amarantite), crystal structure 9-1188  
 Fe complex, [Fe(salen)Cl]<sub>2</sub>, Mossbauer effect, relaxation effects 9-18697  
 Fe complex, bis(cyclooctatetraene)iron cryst. struct. 9-17268  
 Fe phthalocyanine, h.p. Mossbauer effect 9-9202  
 Fe<sub>0.9</sub>Mn<sub>0.9</sub>Ge, mag. structure 9-3827  
 Fe<sup>3+</sup> ions in ice and FeCl<sub>3</sub>·6H<sub>2</sub>O, paramag. and elec. quadrupole hyperfine interactions 9-14037  
 Fe<sub>3</sub>Al, phase transitions rel. to ordering 9-9801  
 FeBO<sub>3</sub>, calcite struct., stability, mag. props. and i.r. spectra 9-5272  
 Fe<sub>3</sub>BO<sub>4</sub>, norbergite struct., stability and mag. props. 9-5272  
 Fe(CO)<sub>4</sub> powder, surface roughness and porosity effects on X-ray integrated intensities 9-11845  
 Fe<sub>2</sub>(CO)<sub>9</sub>, Mossbauer spectrum, press. effect 9-10183  
 Fe<sub>2</sub>(CO)<sub>12</sub>, Mossbauer spectrum, press. effect 9-10183  
 FeCl<sub>3</sub>, sp. ht. meas. rel. to mag. props. of lamellar antiferromagnets 9-1393  
 FeCl<sub>3</sub>, intercalation isotherm on graphite from 300 to 350°C 9-8066  
 FeCl<sub>3</sub>, Mossbauer evidence for an h.c.p.-f.c.c. transition 9-5515  
 FeCl<sub>3</sub>, Mossbauer precision meas. of thermal shift, 83-350°K 9-16402  
 Fe(ClO<sub>4</sub>)<sub>3</sub> frozen soln., Mossbauer spectra, mag. relax. eff. obs. 9-12360  
 Fe<sub>1-x</sub>Co<sub>x</sub>S<sub>2</sub>, itinerant d-electron type ferromagnetism 9-1674  
 FeCr<sub>2</sub>Se<sub>4</sub>, physical props., effect of interactions between d shells of transition element 9-16253  
 FeF<sub>3</sub>:Mn<sup>2+</sup>, spin wave impurity states 9-12307  
 FeF<sub>3</sub>, rutile structure, vibrational spectra, critical dipole frequency behaviour 9-7636  
 FeF<sub>3</sub>, rutile structure, vibrational spectra, critical dipole frequency behaviour 9-18549  
 FeF<sub>3</sub>, exchange integrals in paramagnetic phase 9-1643  
 FeF<sub>2</sub>, two-magnon Raman spectra 9-12425  
 FeF<sub>3</sub>, ferromagnetic anomalous behaviour near Curie temp. 9-1665  
 Fe<sub>1-x</sub>Ga<sub>x</sub>O<sub>4</sub>, ion distribution from magnetic reflections 9-3828  
 FeGe, cubic, mag. susceptibility meas., 4.2-520°K 9-16356  
 FeGe, cubic, Mossbauer exam. of mag. props., 80-300°K 9-16355  
 Fe(III) hydroxide gels, crystal nucleation obs. 9-5285  
 Fe<sub>2-x</sub>Mn<sub>x</sub>As, antiferromagnetic to ferromagnetic transition, pulsed field measurement 9-1703  
 ε-Fe<sub>2</sub>N, electronic structure by electron diffraction 9-5318  
 ζ-Fe<sub>2</sub>N, electronic structure by electron diffraction 9-5318  
 γ'-Fe<sub>2</sub>N, electronic structure from e. diff. 9-1430  
 FeNiCo ferrites, thermomagnetically induced anisotropy 9-19963  
 FeO-CaO, thermoelec. power, 1150-1470°C 9-1606  
 Fe<sub>3</sub>O<sub>4</sub>-Co<sub>3</sub>O<sub>4</sub> (or Mn<sub>3</sub>O<sub>4</sub>) solid solns., interaction and substitutional disorder 9-17333  
 Fe<sub>3</sub>O<sub>4</sub>-Co<sub>3</sub>O<sub>4</sub> spinel solid soln., thermodynamics 9-13769  
 Fe<sub>3</sub>O<sub>4</sub>-Cr<sub>2</sub>O<sub>3</sub> solid solutions, reduction behaviour at high temp. 9-17332  
 α-Fe<sub>2</sub>O<sub>3</sub>-La<sub>2</sub>O<sub>3</sub>-Cr<sub>2</sub>O<sub>3</sub>, ternary phase diagram 9-13774  
 FeO-MgO solid solutions, magnetic susceptibility 9-5806  
 Fe<sub>3</sub>O<sub>4</sub>-Mn<sub>3</sub>O<sub>4</sub> spinel solid soln., thermodynamics 9-13769  
 FeO-SiO<sub>2</sub>, thermoelec. power, 1150-1470°C 9-1606

**Iron compounds continued**

FeO, heats of formation of point defects 9-17276  
 FeO, thermoelec. power, 1150-1470°C 9-1606  
 α-Fe<sub>2</sub>O<sub>3</sub>, haematite, domain interactions 9-7917  
 α-Fe<sub>2</sub>O<sub>3</sub>, hematite, antiferromag. resonance temp. dependence with mag. field perpendicular to easy axis 9-1851  
 Fe<sub>2</sub>O<sub>3</sub>, hydrous, colloidal, adhesion to glass, effect of stirring 9-9567  
 Fe<sub>2</sub>O<sub>3</sub>, interaction with MgO, kinetics 9-3988  
 α-Fe<sub>2</sub>O<sub>3</sub>, nuclear quadrupole moment for Fe<sup>57m</sup> 9-7930  
 α-Fe<sub>2</sub>O<sub>3</sub>, piezomagnetism, microscopic origin 9-1704  
 Fe<sub>2</sub>O<sub>3</sub>, sintering, vol., grain boundary and surface diffusion contributions 9-1246  
 Fe<sub>2</sub>O<sub>3</sub> (hematite), antiferromag. with weak ferromagnetism, effect of hydrostatic press. on mag. anisotropy 9-3836  
 Fe<sub>2</sub>O<sub>3</sub> (hematite), magnetoelastic, coupling consts. from magnetostriction meas., 100-300°K up to 150 kOe 9-7529  
 α-Fe<sub>2</sub>O<sub>3</sub> microcrystals, Mossbauer quadrupole interaction 9-3870  
 α-Fe<sub>2</sub>O<sub>3</sub> polycrystalline, elastic constant rel. to pressure up to 3 Kbar 9-11902  
 Fe<sub>3</sub>O<sub>4</sub> (magnetite), thermal conductivity meas. 9-1404  
 Fe<sub>3</sub>O<sub>4</sub>, conductivity and metal-nonmetal transition, press. effects 9-1467  
 Fe<sub>3</sub>O<sub>4</sub>, memory and remanence 9-3798  
 Fe<sub>3</sub>O<sub>4</sub>, optical props. and conduction mechanism 9-10171  
 Fe<sub>3</sub>O<sub>4</sub> colloidal soln. in mag. field, optical transmission and birefringence obs. 9-5200  
 Fe<sub>3</sub>O<sub>4</sub> fine powders, magnetization reversal, particle agglomeration effect 9-3822  
 δ-FeOOH, structure 9-19713  
 α-Fe(OH) crystal, needle shape preservation for Y-Fe<sub>2</sub>O<sub>3</sub> mag. tape prep., patent 9-9642  
 β-FeOOH on steel, detect. by Mossbauer backscatt. spectroscopy 9-10363  
 (Fe<sub>2</sub>O<sub>3</sub>)<sub>0.38</sub>(NiO)<sub>0.42-x-y</sub>(CoO)<sub>x</sub>(ZnO)<sub>y</sub> ferrite, mag. ordering stability 9-10138  
 6Fe<sub>2</sub>O<sub>3</sub>·PbO, magnetoplumbite, powder, intrinsic ferromag. resonance 9-1848  
 FePO<sub>4</sub>, antiferromagnet, anisotropy const. meas. by Mossbauer effect 9-5854  
 FeS, miscibility gap with Fe<sub>1-x</sub>S 9-21408  
 FeS, near stoichiometric, hyperfine interactions, temp. depend. 9-5892  
 Fe<sub>2</sub>S<sub>8</sub>, Mossbauer study of magnetic structure 9-10119  
 FeS<sub>2</sub>B<sub>2</sub>O<sub>4</sub>, paramagnetic, quadrupole splitting of Mossbauer spectra, 50 to 817°K 9-14038  
 Fe<sub>2</sub>Si, formation in Fe-Si at 1215°C, making eutectic with α<sub>2</sub> and FeSi 9-11974  
 Fe<sub>2</sub>TeO<sub>4</sub>, ordered trirutile, mag. ordering at 4.2°K from n. diff. exam. 9-1701  
 Fe<sub>2</sub>Zr, crystal structure and mag. props 9-7440  
 Fe-C solid solutions, electrical resistivity recovery mechanism after irradiation 9-19891  
 Fe<sub>3</sub>sm from Mossbauer obs. 9-10135  
 Gd<sub>3</sub>Fe<sub>2</sub>O<sub>12</sub>, anomalous magnetocaloric effect 9-16370  
 Ge-Al system, surface diffusion, 'unipolar' 9-5408  
 Li<sub>2</sub>O<sub>2</sub>(7.2.5)Fe<sub>2</sub>O<sub>3</sub>2.3(2.5)Cr<sub>2</sub>O<sub>3</sub> anomalous magnetocaloric and magnetoelec. effect 9-16370  
 Mo-Fe alloys, dil., superconductivity and Kondo effect 9-1500  
 Na<sub>2</sub>Fe(CN)<sub>6</sub> effect on NaCl crystal growth and characteristics 9-18415  
 Ni-Fe films susceptibility, effect of strain, polycrystalline 9-3818  
 Ni-Fe film annealing, cylindrical 9-5839

**Irradiation effects** see *Biological effects of radiations; Chemical effects of radiations; Physical effects of radiations*

**Ising lattice** see *Lattices, theory and statistics*

**Ising model** see *Alloys; Ferromagnetism*

**Isomerism**  
 See also *Nuclear isomerism*  
 1,2-dibromofluoroethane, stable configs. in liq. and vapour phases 9-14706  
 1-chloro-1, 2-dibromo-2-iodoethane, internal rot., rotational, n.m.r. 9-807  
 1,2-chlorofluoroethane, stable configs. in liq. and vapour phases 9-14706  
 cyclopropylcarbinyl chloride, conformational 9-794  
 diethyl ether and deuterated analogues, vibr. spectra of conformers 9-14708  
 trans-1,4-diiodocyclohexane, rotational isomerism and vibr. spectra 9-17482  
 1,2-diiodotetrafluoroethane, rot. isomers, i.r. obs. 9-15887  
 ethylenes, unsymmetrically substituted, cis-trans effect on <sup>13</sup>C chem. shifts 9-9266  
 1-fluoro-2-haloethanes, rot. isomers 9-812  
 linkage, in inorg. complexes 9-9194  
 methyl isocyanide, <sup>13</sup>C bombardment, thermal isomerization 9-8112  
 propyl radical isomerization in propane pyrolysis 9-1900

**Isomerization** see *Isomerism*

**Isomorphism**  
 Ba<sub>2</sub>TiGe<sub>2</sub>O<sub>8</sub> with Ba<sub>2</sub>TiSi<sub>2</sub>O<sub>8</sub>, comparison of fluoresc. 9-14083  
 Ce, P-T phase equilib. diag., rel. to theory 9-5268  
 Ce, p-V-T relationship, theory, rel. to anomalies in phys. props. 9-3225  
 NaVMoO<sub>4</sub> isotypism and crystal structure 9-14919  
 Sr<sub>2</sub>TiSi<sub>2</sub>O<sub>8</sub> with Ba<sub>2</sub>TiSi<sub>2</sub>O<sub>8</sub>, comparison of fluoresc. 9-14083

**Isotope effects**  
 aromatic hydrocarbons, singlet-ground-state transitions 9-11480  
 benzene negative ion, e.s.r. 9-2895  
 chloroethanes, kinetic effects in unimolec. reactions 9-3990  
 chlorinated tetrahadral cpds., i.r. spectra 9-2900  
 chloroform, Raman spectra 9-7266  
 for diffusion of Fe in V, parameter using <sup>55</sup>Fe and <sup>59</sup>Fe 9-9734  
 ethylene d<sub>3</sub> and -d<sub>4</sub>, vapour press. 9-17232  
 kinetic, in oxidation of light and heavy water by peroxydisulphate 9-18756  
 methane, n.m.r. chem. shifts 9-7013  
 molecules spectra freq. shifts and partition functions 9-15847  
 naphthalene, phosphores, triplet lifetime, deuterium substitution effects 9-14086  
 ruby, crystal-field parameters 9-12040  
 spectra var. in heavy elements, review 9-19394  
 trichloromethyl cyanide, Raman spectra 9-7266  
 trichloromethyl fluoride, Raman spectra 9-7266  
<sup>133</sup>Cs, isotope shift in resonance lines of spectra, against <sup>133</sup>Cs 9-6962  
 Ag, for self-diffusion, infl. of bound dislocations 9-18487  
 AlO visible and u.v. bands, isotope shift studies 9-13341



**Isotope effects continued**

- BH<sub>4</sub><sup>-</sup>, n.m.r. chem. shifts 9-7013  
<sup>10</sup>BO<sub>2</sub><sup>-</sup> and <sup>11</sup>BO<sub>2</sub><sup>-</sup>, migration 9-17200  
 Ba, shift of odd isotopes w.r.t. <sup>138</sup>Ba 9-6961  
 C-H in tetrahedrally hybridized carbons, deuterium substitution eff. on <sup>13</sup>C<sub>α</sub> coupling const. 9-17043  
 Cs, 6<sup>2</sup>P<sub>1/2</sub>-6<sup>2</sup>P<sub>3/2</sub> mixing, induced in collisions with CH<sub>4</sub> and CD<sub>4</sub> collisions 9-13298  
 Cs isotopic shift of D<sub>1</sub> line determ. 9-18137  
 α-Fe, of <sup>59</sup>Fe and <sup>55</sup>Fe 9-3382  
 H, adsorbed isotopes, hindered rot. 9-13586  
 H, test for chem. kinetics transition-state models 9-12525  
<sup>35</sup>Cl and <sup>37</sup>Cl, nuclear mag. hyperfine spectra 9-9206  
<sup>3</sup>He-<sup>4</sup>He mixtures, solid, phase separation temp. 9-1064  
 in K, liq., temp. depend., investigation 9-9491  
 K ions, electromigration in molten KNO<sub>3</sub>, temp. depend. 9-11716  
 K<sub>2</sub>SO<sub>4</sub>-Li<sub>2</sub>SO<sub>4</sub> (41-90 equiv.%), molten, electromigration 9-8102  
<sup>6</sup>Li, <sup>7</sup>Li in molten LiCl, internal mobilities 9-8103  
 LiF dosimeter absorpt. coeff., mass stopping power, isotope content effect. 9-14091  
 MgO, crystal-field parameters 9-12040  
 NH<sub>3</sub> and ND<sub>3</sub>, electron diff. and molec. struct. 9-7032  
 NH<sub>4</sub><sup>+</sup>, n.m.r. chem. shifts 9-7013  
 NO photolysis, <sup>15</sup>N-enriched N<sub>2</sub> formation 9-16491  
 Ne, single crystals, in lattice constant and thermal expansion 9-7624  
 P<sup>16</sup>O u.v. and visible bands, shift obs. of band systems 9-18190  
 P<sup>18</sup>O u.v. and visible bands, shift obs. of band systems 9-18190  
 Pd, for self-diffusion, infl. of bound divacancies 9-18487  
 in Rb, liq., temp. depend., investigation 9-9491  
 TiCl<sub>4</sub>, molec. assoc. in liq. 9-1021  
 α-U superconductivity 9-1487  
 Xe, shifts of 20 i.r. laser lines 9-15811  
 Xe I, spectrum, isotope shift in visible lines 9-16997

**Isotope exchanges**

- alkoxybenzoic acids, liq. crystals, H D isotope effect 9-3982  
 deuterium solvent eff. in water, transfer and exchange contrib. 9-21678  
 diffusion method modification for investigation 9-21676  
 nitromethane hydrocarbon binary systems, effect of isotopic substitution on demixing temps. 9-10308  
 proton-transfer reactions in solution, quantum-mech. tunnelling through parabolic energy barriers 9-20030  
 rate determ. in solution without separation of components 9-8053  
 rhenium thiocyanate complexes, structural investigations 9-8052  
<sup>204</sup>Tl(I)-Ti(III) system, electron transfer 9-12523  
 HD exchange, Kr, Xe-photosensitized, mechanism 9-16476  
 H<sub>2</sub>O+D<sub>2</sub>O, disproportionation 9-1891  
 H<sub>2</sub>S, homogeneous reaction with D<sub>2</sub> 9-3981  
 Kr, solid, tracer diffusion obs., 90°<T<115°K 9-9731

**Isotope separation**

- See also Radiochemistry*  
 e.m., beam handling by magnetic quadrupole lenses, line and spot focus 9-20903  
 e.m., for laboratory purposes, review 9-13161  
 fission products, system for rapid chemical separation and spectroscopic examination 9-8111  
 gaseous diffusion method, surface diffusion eff. 9-7236  
 nuclides of high specific alpha activity, cells and equipment 9-14677  
 radio-frequency, review 9-13161  
 radioactive elements in cyclotron target, optimum evaporative separation conditions 9-18392  
 separator, electromagnet, high voltage regulation circuit 9-730  
 techniques, review 9-20904  
 yield calc. using ion exchanger with the dynamic irradiation-elution method 9-18161  
 H, by Pd in desiccant column, patent 9-9163  
<sup>87</sup>Kr, β decay, 1.3 h., to levels in <sup>87</sup>Rb 9-13213  
<sup>87</sup>Kr, β decay, 2.8 h., to levels in <sup>88</sup>Rb 9-13213  
<sup>88</sup>Rb, β decay, 15 min., to levels in <sup>88</sup>Sr 9-13213  
 Sn, from fission products, extraction method 9-11335

**Isotope shifts** *see Isotope effects; Spectra***Isotopes**

- (<sup>17</sup>O, <sup>18</sup>O), rotation spectra of SO<sub>2</sub> molecules 9-20939  
 deuterium diffusion, long range in Nb, relaxation process, coeff. determined 9-1248  
 formation cross-sections by proton with E<sub>p</sub>=0.5-2.9 GeV 9-19310  
 neutron irradiat. prod. of radioisotope generator fuel 9-19316  
 production and energy conversion efficiency 9-9164  
 radioactive isotope dilution analysis, review 9-18784  
 radioisotope camera, theory of pinhole collimator 9-11428  
 (u.g.) pairs with I=<sup>3</sup>/<sub>2</sub>, relaxation behaviour and Schmidt correlation 9-17007  
<sup>176</sup>Re, first prod. from <sup>165</sup>Ho(<sup>16</sup>O, Sn) and <sup>159</sup>Tb(<sup>22</sup>Ne, Sn) 9-14633  
<sup>64</sup>Ar, inelastic n. scatt. exam. of gas dynamics near condensation 9-15971  
<sup>64</sup>Cu prod. by (n,p) reaction purity investigated 9-18159  
<sup>19</sup>F in cooling water due to <sup>18</sup>O(p,n)<sup>18</sup>F 9-16985  
<sup>18</sup>O used in study of orange-red system in CuO spectrum 9-20927  
<sup>32</sup>P prod. by <sup>32</sup>S(n,p)<sup>32</sup>P, <sup>33</sup>P contamination determ. 9-15836  
<sup>87</sup>Rb, zero-field level crossing resonances and very weak magnetic field detection 9-15822  
<sup>33</sup>SO<sub>2</sub>, rotation spectra in fundamental state 9-19446  
 Th, new assignments 213≤A≤217 9-14578

**detection**

- See also Mass spectra; Radioactivity*  
 element 110, search in Pt ore, neutron-induced fis., obs. 9-18160  
 identification of γ-radiation colorimetry 9-729  
 radioactive in dilute solutions, apparatus, patent 9-17008  
<sup>234</sup>U by α spectra 9-2835  
<sup>235</sup>U by α spectra 9-2835  
<sup>238</sup>U by α spectra 9-2835  
<sup>17</sup>C, combined time-of-flight particle-identification technique obs. 9-2653

**relative abundances**

- See also Elements/relative abundances*  
 light elements, measurement 9-19414  
 by mass spectroscopy, review 9-728  
 measurement methods, symposium (Tokyo, 1966) 9-19412  
 measurement problems 9-19413  
 trace sample meas., surface ionization method 9-19415  
 Cu, surface ionization method of meas. 9-19416  
 Li, surface ionization method of meas. 9-19416

**Isotopes continued****relative abundances continued**

- O, in CO<sub>2</sub>, calc. from mass spectrometric meas. 9-11429  
 O compounds, calc. in <sup>18</sup>O tracer applications 9-6035  
 Pb, common, equal-atom and radiogenic isotopic standards, abund. ratios 9-20902  
 Pb analysis methods, review 9-8115  
 S, balance method of meas., problems 9-19417  
 U, surface ionization method of meas. 9-19416
- Jahn-Teller effect**  
 interaction and stable potential minima 9-751  
 optical transitions, J-T induced, theory 9-7928  
 AgCl:I<sup>-</sup>, excited-state structure of I centre 9-12057  
 CCl<sub>4</sub>, molecule symmetry lowered, Raman spectrum obs. 9-4950  
 Cu II complexes 9-18181  
 IrF<sub>6</sub>, electronic spectrum, Jahn-Teller progressions 9-772  
 K<sub>3</sub>Co(CN)<sub>6</sub>, X-irrad. crystals, e.p.r. 9-10278  
 in LiBr Γ exciton splitting 9-19882  
 MgO:Fe<sup>2+</sup>, absorption bands pressure shift 9-5927  
 Ti complex, hexaurea Ti(III) trioxide, crystal spectra 9-14057

**Jet stream** *see Atmosphere/movements***Jets***See also Sprays*

- aerosol, resonance-chamber atomizer, patent 9-7288  
 asymmetric two-dimens. orifice, force defect. coeff. method appl. 9-9426  
 axial, velocity distribution and droplet flow rate after injection 9-21156  
 axisymmetrical, in cross-wind, mixing processes 9-18233  
 bending, transversal stream and Archimedes force 9-2940  
 bounded turbulent jet, mixing characts. 9-21173  
 on circular cylinder, heat transfer coeff. 9-19597  
 of conducting liquid adjacent to walls in transverse magnetic fields 9-21034  
 fan-shaped, turbulent, spreading distrib. along plane and concave solid surfaces 9-9472  
 flow, shear, turbulent, pressure field characteristics determ. 9-19574  
 flow over flat plate in bounded jet 9-17170  
 gas mixtures, rarefied, critical mass flow through slit 9-18320  
 gaseous, penetration of solid and liquid phase particles 9-1047  
 heated free, variable viscosity, dynamics 9-5137  
 impact, analogy with cavitation erosion 9-5138  
 injection into flow of lower total head, linearization for small angles, soln. by Wiener-Hopf tech. 9-17085  
 et flap, ground effect influence on flowfield, linear theory 9-9432  
 laminar, incompressible, flow along curved surface for small curvature, similarity soln. 9-7244  
 laminar liquid diffusion 9-15997  
 liquid, injection into gas stream, mean drop size 9-17184  
 liquid, spreading along a porous wall 9-973  
 liquid dielectric in longit. elec. field, stability 9-9538  
 MHD, 2-d steady, infl. of thermal radiation 9-7119  
 MHD, flat, with variable conductivity, theory 9-7118  
 MHD, laminar submerged jet 9-4995  
 MHD, with variable conductivity 9-2954  
 mixing of turbulent half-jet along curved streamline 9-14749  
 plane turbulent wall jet in moving stream, mean and fluctuating props., meas. 9-19573  
 plasma, non-isothermal, I.f. current oscills. resonance 9-21093  
 plasma, ultraviolet emission, study using spectrograph 9-5030  
 round, one-row system in limited transverse stream 9-18244  
 submerged laminar, theory 9-7106  
 supersonic, impact on flat plate 9-18234  
 supersonic, separation of gas mixture 9-21145  
 supersonic air, eff. of acoustic feedback on spread and decay 9-21126  
 swirling flow of water through conical pressure nozzles measurement of rotational velocity 9-18343  
 turbulent, conducting liquid, axial symmetry in a longitudinal magnetic field 9-21045  
 turbulent, conducting liquid, axis-symmetric, distribution of pulsation energy, longitudinal magnetic field 9-21046  
 turbulent conical confined, water; momentum transfer 9-18342  
 turbulent mixing in coflowing stream 9-21001  
 two-phase flow analysis 9-9473  
 two-stream mixing region, turbulent, similarity parameter 9-7216  
 vapour condensation on supercooled high velocity jet turbulent boundary layer parameters 9-19659  
 Ar, supersonic, intermolecular binding 9-18179  
 CO<sub>2</sub>, supersonic, intermolecular binding 9-18179  
 CO<sub>2</sub> supersonic, e. diff. for existence of crystals and free molecules 9-11459  
 H<sub>2</sub>-N<sub>2</sub> supersonic, separation of gases 9-21145  
 N<sub>2</sub> with C particles, transmittances and absorption cross sections 9-11726  
 NO+O chemiluminesc. in expanding flow, effect of molec. clusters 9-20031  
 N<sub>2</sub>+ air, 4000-6000°K, total press. profiles for round and rectangular nozzles 9-9433  
 O supersonic flow through nonsymmetric nozzle 9-13480  
 Xe, supersonic, intermolecular binding 9-18179
- Jets, cosmic-ray** *see Cosmic rays/showers and bursts*  
**Jogs** *see Crystal imperfections/dislocations*  
**Johnsen-Rahbek effect** *see Adhesion; Electrostatics*  
**Johnson noise** *see Noise/electrical*  
**Jordan-Thiry field** *see Cosmology; Relativity/general*  
**Josephson junction** *see Superconducting devices*  
**Josephson tunnelling effect** *see Superconductivity; Superconducting devices*  
**Joshi effect** *see Discharges, electric/glows*  
**Joule-Thomson effect**  
 paramagnets 9-12244  
**Jupiter** *see Planets*  
**K-capture** *see Radioactivity/electron capture*  
**Kaons**  
 e.m. props., form factors 9-6642  
 f<sub>0</sub>/f<sub>π</sub> sum rules and m<sub>K</sub> and κ width 9-14500  
 form factor, determ. from Chou-Yang high-energy scatt. model 9-14520  
 form factors and e.m. props. 9-6642  
 new classification with spin 1/2 9-15593  
 K<sup>0</sup>-K<sup>+</sup> mass difference, scalar and tensor tadpole contributions 9-2497  
 K<sup>0</sup>-K<sub>s</sub><sup>0</sup> mass difference meas., gap method 9-6651  
 K<sup>0</sup> mass differences, pole-dominance model 9-2496

## Kaons continued

- $K^0$ , phenomenological theory and decay 9-6641  
 $K^0 \rightarrow K^0_l$  e.m. transition radius meas. from  $K^0_l \rightarrow \pi^+ \pi^- e^+ e^-$  decay rate obs. 9-6648  
 $K^+ \rightarrow \mu^+ \mu^0 \nu / K^+ \rightarrow \pi^0 e^+ \nu$  branching ratio, rel. to  $K_{\mu 3}^+$  form factor ratio 9-357  
 $K^0_l$ - $K^0_s$  mass difference deserved 9-6650  
 $K^+$ - $K^0$  mass difference, calc. from finite energy sum rules, for virtual Compton scatt. amplitude 9-13122  
 $K^+$ - $K^0$  e.m. mass difference sign 9-360  
 $K$ - $\pi$  2-charged particles, production, effective mass and decay distrib. at 2.63, 2.70 GeV/c 9-8820

## decay

- CP invariance violation? 9-11033  
 CP nonconservation, expt. proof, and its irrelevance 9-19188  
 current algebra tech. calc. 9-16832  
 $K \rightarrow \pi \mu (e) D$  form factors, using once-subtracted dispersion relations and current algebra 9-16863  
 $K \rightarrow \pi \mu (e) \nu$ , form factor depend. 9-6645  
 non-leptonic, tadpole model 9-355  
 nonleptonic, chiral vector meson model, violation of  $\Delta I=1/2$  rule 9-11031  
 $f_K/f_\pi$ , determ. in terms of pseudoscalar nonet masses, sum rules 9-6637  
 $K \rightarrow \pi \mu (e)$  form factors and intermediate mesons decay consts. determ. 9-8806  
 $K^0 \rightarrow \pi^+ e^- \nu / K^0 \rightarrow \pi^+ e^- \bar{\nu}$  violation of  $\Delta S=\Delta Q$  rule predicted Re $e$  obtained 9-14501  
 $K^+ \rightarrow \pi^+ \pi^0$  rate and CP violation reln., SU(3) model 9-20634  
 $K^- \rightarrow \pi^0 e^- \nu$ , field current identity and form factor 9-356  
 $K^- \rightarrow \pi^0 \mu^- \nu$ , field current identity and form factor 9-356  
 $K^0$ , non-exponential character, theory 9-6641  
 $K^0$ , PC,  $\Delta S=\Delta Q$  violation 9-11032  
 $K^0$ , unitarity sum rule for meas. of relations betw. parameters, comparison with CPT-violation method 9-15610  
 $K^0$  mirror production possibility 9-362  
 $K^0$  mixed beam,  $\pi^+ \pi^- \pi^0 \pi^0$  coherent decays, CP violation 9-17972  
 $K^0_l \rightarrow \pi^+ \pi^- e^+ e^-$ , use in radius of e.m. transition meas. 9-6648  
 $K^0 \rightarrow \pi \nu$ ,  $\pi$  energy depend of  $f^+$  form factor determ. 9-11045  
 $K^0 \rightarrow \pi^+ \pi^- \nu$   $\Delta S/\Delta Q$  rule expt. investigation 9-17973  
 $K^0 \rightarrow \pi^0 e^+ \nu$  branching ratio and positron momentum spectrum 9-16864  
 $K^0 \rightarrow \pi \mu (e) \nu$  chiral SU(3)@SU(3) 3-point functions 9-8800  
 $K^0 \rightarrow \pi \pi$  time depend. compared to  $K^0 \rightarrow \pi \pi$  9-6649  
 $K^0 \rightarrow \pi \pi$  time depend. compared to  $K^0 \rightarrow \pi \pi$  9-6649  
 $K^0 \rightarrow \pi \pi$  time reversal 9-353  
 $K^0 \rightarrow \pi \pi \pi$ ,  $\Delta T=1/2$  violation, experimental evidence 9-359  
 $K^0 \rightarrow e^+ \mu^- \nu / \mu^+ \nu$  rel. rate meas. 9-11036  
 $K^+ \rightarrow \mu^+ \pi^0$  total polar. meas., form-factor analysis 9-4615  
 $K^+ \rightarrow \pi^0 e^+ \nu$ , field current identity and form factor 9-356  
 $K^+ \rightarrow \pi^0 \mu^+ \nu$ , field current identity and form factor 9-356  
 $K^+ \rightarrow \pi^+ \mu^+ \nu$ , form factor ratio, from branching ratio rel. to  $K_{e3}$  9-357  
 $K^+ \rightarrow \pi^+ \pi^- e^+ \nu$ , vector form factor calc. by current algebra 9-17976  
 $K^+ \rightarrow \pi^+ \pi^- \pi^0$  energy spectra obs., estimation of max. decay asymmetry due to CP noninvariance 9-8813  
 $K^2 \rightarrow \pi \pi \pi$ ,  $\tau$  spectra comparison, CP violation 9-11038  
 $K^0 \rightarrow \pi \pi$ , chiral vector meson model, violation of  $\Delta I=1/2$  rule 9-11031  
 $K^0 \rightarrow \gamma \gamma$ , pole-dominance model 9-2496  
 $K^0 \rightarrow 2\gamma$ , pole model calc. 9-8808  
 $K^0 \rightarrow \pi^+ \pi^- \pi^0$ ,  $K^0 \rightarrow K^0_l$  transition e.m. radius in matrix element 9-11039  
 $K^0 \rightarrow \pi \pi$ , due to weak nonlinearity of electrodynamic field Lagrangian eqn. 9-297  
 $K^0 \rightarrow \pi \pi \pi$ , final-state  $\pi \pi$  interactions, domination by  $\rho$  and  $S$  mesons 9-8812  
 $K \rightarrow \pi \nu$  form factors, current-algebra calc., spectral function sum rules 9-16864  
 $K \rightarrow \pi \pi$ , CPT invariance study from polarization and ang. distrib. meas. 9-17977  
 $K \rightarrow \mu \nu$ , sum rules, derived treatment of vertex functions 9-6630  
 $K \rightarrow \nu \nu$ , weak, sum rules and axial-vector, vector contributions 9-8809  
 $K \rightarrow \pi \nu$ , Callan-Treiman relation consistency with soft theorems on  $K \rightarrow \pi \nu$  9-6647  
 $K \rightarrow \pi \nu$  form factors and rel. to current algebra 9-6644  
 $K \rightarrow \pi \nu$  vector current form-factors, quark model applic. to additivity and algebra 9-14478  
 $K \rightarrow \pi \pi \nu$  soft  $\pi$  theorems, consistency with Callan-Treiman relation on  $K \rightarrow \pi \nu$  9-6647  
 $K \rightarrow \pi^+ \pi^- \nu$ , axial vector form factor due to  $e, \eta \nu$  mixing 9-17970  
 $K \rightarrow \pi \nu$  form factor, renormalization calc. 9-4616  
 $K \rightarrow \pi \nu$  form factors, soft  $\pi$  calc. and applic. of near  $\kappa$ - $K$  mass degeneracy 9-13121  
 $K \rightarrow \pi \mu (e) \nu$  form factors and weak decay parameters 9-2495  
 $K \rightarrow \pi \mu (e) \nu$ , form factors by combining three theories 9-358  
 $K \rightarrow \pi \mu (e) \nu$  form factors, current algebra hard- $\pi$  hard- $K$  calc. 9-8810  
 $K \rightarrow \pi \mu (e) \nu$  form factors, new sum rules 9-13120  
 $K \rightarrow \pi \mu (e) \nu$  form factors from  $K \pi S$ -wave phase shifts 9-6671  
 $K \rightarrow \pi \pi$  parameters theor. formulation, CP nonconservation inclusion 9-16865  
 $K \rightarrow \pi \pi$  spectra obs., final-state interactions studied 9-8805  
 $K \rightarrow \pi \pi \nu$ , momentum depend. form factors determ. from SU(3)@SU(3) algebra 9-11035  
 $K \rightarrow \pi \pi \nu$  form factors, soft  $\pi$  calc. and applic. of near  $\kappa$ - $K$  mass degeneracy 9-13121  
 $K \rightarrow \pi \pi \pi$ , bremsstrahlung spectra 9-354  
 $K \rightarrow \pi \pi \pi$ , production correction factors from decay structure 9-8811  
 $K \rightarrow \pi \pi \pi$ , structure from linear matrix-element and spectrum approx. 9-17975  
 $K \rightarrow \pi \pi \pi$  integral eqn., two subtractions, final state  $\pi \pi$  interactions 9-6646  
 $K^0 \rightarrow \pi^+ \pi^-$  radiative corrections due to  $\Delta T=1/2$  rule 9-11108  
 $K^0 \rightarrow K^+ \pi^-$ , current-algebra calc., spectral function sum rules 9-16864  
 $K_0$  current-algebra calc., spectral function sum rules 9-16864  
 $K_{\text{eff}}$  decay, form factors, SU(3) asymptotic, 9-11034  
 $K^0 \rightarrow \pi^+ \pi^- \nu / K^0 \rightarrow \pi^+ \pi^- \bar{\nu}$  branching ratio meas. rel. to CP violation 9-11037  
 $K^0 \rightarrow 2\gamma / K^0 \rightarrow 3\pi^0$  ratio meas. 9-8814  
 $K^0 \rightarrow 3\pi^0 / K^0 \rightarrow \pi^+ \pi^- \pi^0$ , ratio, tests of  $\Delta I=1/2$  rule 9-6643  
 $K^0 \rightarrow 3\pi^0 / K^0 \rightarrow \pi^+ \pi^- \pi^0$ , ratio, tests of  $\Delta I=1/2$  rule 9-6643  
 $K^0 \rightarrow \gamma \gamma / K^0 \rightarrow \pi^+ \pi^- \pi^0$  branching ratio measurement 9-368  
 $K^0 \rightarrow \gamma \gamma / K^0 \rightarrow \pi^+ \pi^- \pi^0$  branching ratio measurement 9-367  
 $K^0 \rightarrow \gamma \gamma$  branching ratio meas. 9-11040  
 $K^0 \rightarrow \pi^+ \mu^- \nu$ ,  $\mu$  polarization meas. 9-17974  
 $K^0 \rightarrow \pi^0 \pi^+ \pi^-$ , possible connection with  $K^0 \rightarrow \pi^+ \pi^- \gamma$  9-16862

## Kaons continued

## decay continued

- $K^0 \rightarrow \pi^+ \pi^- \gamma$  upper limit, connections with other decay processes, CP  $\pi^+ \pi^- \gamma$ ,  $D K^0 \rightarrow \pi^+ \pi^- \gamma$  possible connection with  $K^0 \rightarrow \pi^+ \pi^- \gamma$  9-16862  
 $K^0 \rightarrow \pi^+ \pi^- \pi^0$ , search for CP-nonconserving asymm. in momentum spectra 9-8807  
 $K^0 \rightarrow \pi \mu \nu / K^0 \rightarrow \pi \nu$  ratio, tests of  $\Delta I=1/2$  rule 9-6643  
 $K \rightarrow \pi^+ \pi^- \pi^0$ ,  $\pi$  energy spectra study 9-8815  
 $K_l \rightarrow \pi^0 l l$ , consequences of momentum conservation and neutral lepton current  $\gamma S$  invariance 9-8816  
 $K_{\text{eff}} \rightarrow \pi^+ \pi^- \gamma$ , possible connection with  $K^0 \rightarrow \pi^+ \pi^- \gamma$  9-16862  
 $\pi \pi$  scatt. length calc. 9-17991  
 $K^+ \rightarrow \pi^+ \pi^+ \pi^-$ , ratio meas., search for CP violation,  $\pi$  interactions 9-8817

## interactions

- $K^* \rightarrow K^0 \pi^+ \pi^- \pi^0$ ,  $k \pi \pi$  spin and parity near 1.3 GeV 9-13135  
 $K^* \rightarrow Y_1^* \pi^0$  (1660) $\pi^+$ , evidence for two  $Y_1^*(1660)$  resons. at  $E_K \approx 2.6$  GeV/c 9-19208  
 2 body interact with meson resonance production use of Pade approximants 9-2522  
 $K^- \rightarrow d \Lambda \pi \pi$ ,  $\Lambda p$  invariant mass enhancement at 2130 MeV,  $M_K \approx 1$  GeV/c 9-20637  
 $K^+$  in nuclear emulsion, 3.0 GeV/c, hyperfragment prod. 9-20639  
 $K^- \rightarrow K^0 \pi^0$ , isospin- $1/2$   $K \pi$  mass enhancement of 1160 MeV obs.,  $M_K \approx 3.9$  GeV/c 9-20638  
 $K^* \rightarrow K_0^* \pi$ , Regge-pole model description, coupling obs. 9-14519  
 $K^* \rightarrow K^* \pi$ , quark model expt. test, hi high energies 9-20633  
 $K^* \rightarrow \Lambda(n-1)\pi$ , applic. of Reggeized multiperipheral model including reson. prod. 9-20618  
 $K^* \rightarrow \Sigma$  decay modes obs. 9-20673  
 $K^* \rightarrow \Sigma(1660)$ ,  $\Sigma$  decay modes branching ratios determ. 9-14526  
 $K^* \pi$ , multi-body final states studied,  $K_K \approx 5$  GeV/c 9-19200  
 $K^* \rightarrow K^* N^*$ ,  $\pi$  trajectory quantum numbers determ.,  $O(3,1)$  symmetry,  $P_{\text{lab}}=3.5-5$  GeV/c 9-20635  
 $K^* \pi$ , axial-vector-meson prod. in Regge-pole model 9-14519  
 $K^0$  in  $\pi^+ \pi^- \rightarrow K^0 \bar{K}^0$  backward, polar. eff., Regge fermion exchange 9-4648  
 $K N$  inelastic processes above 1.4 GeV/c with more than two particles in final or intermediate state, reviews 9-11042  
 $K N \rightarrow K^* N$ ,  $K^* \pi$  mass spectra low-mass enhancement, Deck model calc. of double charged syst. 9-20636  
 $K N$ , obs. of  $K^0 \pi^0$  enhancement NuNu/interac.  $[-] b/c$  9-8819  
 $K^- \rightarrow \Sigma \pi$ , total cross sections meas.,  $M_K \approx 0.6-1.2$  GeV/c 9-11043  
 $K^- \rightarrow Y_1^*(1385) \pi^- \Lambda \pi \pi$  sequential react., partial wave anal. 9-4619  
 $K N$ , hyper-fragment prod., decay and non-mesic absorpt., bubble chamber obs. 9-364  
 $K^- \rightarrow p \rightarrow K^0 N^{*+}$  (1236), density matrix elements,  $t$ -distributions, 12.7 GeV/c 9-15613  
 $K^- \rightarrow \Sigma^+ \pi^-$  angular distrib. and cross sections, 4.07 and 5.47 GeV/c 9-6653  
 $K^- \rightarrow K^- \pi \pi$ , as representative of  $K^- \rightarrow K^- \pi \pi$ , reson. prod. obs., cross-sections,  $Y_0^*(1520)$  decay distrib., 2.24 GeV/c 9-15614  
 $K^- \rightarrow \Lambda \pi \pi$ ,  $\Lambda \pi$  enhancement near  $\bar{K} N$  threshold 9-4618  
 $K^- \rightarrow d K^* \pi$ ,  $K^*(890)$  prod., 4.5 GeV/c 9-13136  
 $K^- \rightarrow d K^*(892)$  prod. and decay ang. distrib. obs.,  $M_K \approx 3$  GeV/c 9-16897  
 $K^- \rightarrow K^- \pi \pi$ , represented by  $K^- \rightarrow K^- \pi \pi$ , 2.24 GeV/c, reson. prod., cross-sections,  $Y_0^*$  decay distrib. 9-15614  
 $K^- \rightarrow \Lambda \pi \pi$ ,  $W^*$ , reson. obs. at 1616 MeV 9-15648  
 $K^- \rightarrow \Lambda \pi \pi$ ,  $\Lambda \pi \pi$  structure from 1600 to 1740 MeV 9-369  
 $K^0 \rightarrow K^0 \pi$ , forward scatt. amplitude, real-to-imaginary ratio 9-376  
 $K p$ , low energy, coupling constant tested in dispersion relation for  $K^+ p$  scatt. 9-6652  
 $K p$  charge-exchange react., Regge quark-model description of differential cross sections 9-13127  
 $K p$ , search for  $\Xi^0$  resonances with strangeness  $-2$ , of  $\theta$  meson mass obs., 4.25 GeV/c 9-11041  
 $K^* \pi$ , total and differential cross sections, 10 GeV/c 9-4617  
 $K^* \rightarrow \Delta + (n-1)\pi$  at high energy, use of Reggeized multiperipheral model for data analysis 9-6631  
 $k^* \rightarrow K^- N^+ \pi^+ \pi^0$  at 4.6 and 5.0 GeV/c] 9-6655  
 $K^* \rightarrow K^* \pi$ , cross section determ.,  $M_K \approx 777-1226$  MeV/c 9-15612  
 $K^* \rightarrow K^* \pi^+ \pi^- \pi^0$  at 4.6 and 5.0 GeV/c. obs. 9-6655  
 $K^* \rightarrow K^* \pi$ , kinematics of momentum transfer 9-350  
 $K^* \rightarrow K^* \pi$ , cross section meas.,  $M_K \approx 7.7$  GeV/c 9-17978  
 $K^* \rightarrow K^* \pi$ , forward scatt. amplitude, real-to-imaginary ratio 9-376  
 $K^* \rightarrow K^* \pi$  charge exchange, multiple-Regge pole model 9-8852  
 $K^* \rightarrow K^* \pi$  Regge pole analysis 9-6638  
 $K^* \rightarrow K^* \pi$ , cross section determ.,  $M_K \approx 777-1226$  MeV/c 9-15612  
 $K^* \rightarrow K^0(890) \pi$ , cross sections obs., spark chamber expt., 11.2 GeV/c 9-363  
 $K^* \rightarrow K^0 \pi^+ \pi^- \pi^0$   $K^- \pi^+ \pi^- \pi^0$  at 5.5 BeV/c, spin-parity analysis of low-mass  $K^* \pi$  system 9-16866  
 $K^* \rightarrow K^*(1420) \pi$ , spin density matrix elements, prod. mech.,  $M_K \approx 4.57$  BeV/c 9-17999  
 $K^* \rightarrow K^*(890) \pi$ , spin density matrix elements, prod. mech.,  $M_K \approx 4.57$  BeV/c 9-17999  
 $K^* \rightarrow \Lambda \pi^+ \pi^-$ ,  $C \pi \pi$  structure from 1600 to 1740 MeV 9-369  
 $K^* \rightarrow \Lambda \pi^+ \pi^- \pi^0$ ,  $X^0$  decay prod. 1 GeV peak 9-365  
 $K^* \rightarrow \Lambda \pi^0$ ,  $\Sigma^+ \pi^-$  cross sections determ.  $M_K \approx 777-1226$  MeV/c 9-15611  
 $K^* \rightarrow \Sigma^+ \pi^-$ , kinematics of momentum transfer 9-350  
 $K^* \rightarrow \Sigma^+ \pi^-$ , two-meson exchange contrib. for anomalous behaviour in ang. distrib. 9-13123  
 $K^* \rightarrow \Sigma \pi$ , hyperon resonance interference effects 9-13145  
 $K^* \rightarrow \Sigma \pi$  partial-wave analysis, resonance formation in mass region, 1.6-1.8 GeV 9-8822  
 $K^* \rightarrow Y_1^*(1385) \pi^0$  boson reson. of mass 980 MeV, at 5.5 GeV/c 9-8869  
 $K^* \rightarrow \eta \Lambda(\Sigma^0)$  cross-section 9-6638  
 $K^* \rightarrow \rho \pi$ , strange boson prod. cross section obs., 565 670 MeV 9-8821  
 $K^* \rightarrow \pi^+ \Sigma^-$  Regge pole analysis 9-6638  
 $K^* \rightarrow \pi^0 \Lambda$  Regge pole analysis 9-6638  
 $K^* \pi$ , K matrix formalism application at 1 BeV/c 9-8784  
 $K^* \pi$ ,  $S=+1$  baryonic resonances search 9-2498  
 $K^* \pi$  search for new meson resonances, 12.7 GeV/c 9-6654  
 $K^* \rightarrow K^+ \pi^+ \pi^- \pi^0$ ,  $K^*(1400)$  interf. and at 5.5 BeV/c 9-13134  
 $K^* \rightarrow K^+ \pi^+ \pi^- \pi^0$ , 1450 MeV  $\pi^+ \pi^-$  enhancement at 5.5 BeV/c 9-11078  
 $K^* \rightarrow K^0(890) N^{*+}$  (1236), density matrix elements,  $t$ -distributions, 12.7 GeV/c 9-15613  
 $K^* \rightarrow p K^*(890)$ , density matrix elements,  $t$ -distributions, 12.7 GeV/c 9-15613

## production

- associative, from  $\pi^+ \pi^-$ , pole-reson. model, <1200 MeV 9-8355



**Kaons** continued**production** continued

- in cosmic ray interac. with Cu, Sn and Pb targets, mass no. depend. 9-18026
- $K^0$ -nucleus interaction amplitudes, spin dependence of regeneration amplitude 9-361
- $K^+$  photoprod. from hydrogen, search for  $S=+1$  baryon states 9-13138
- $K^0$ ,  $K^0$  enhancement in  $K^+-N$  interactions 9-8819
- $K^0$  mirror, from  $K$ -meson decays; expt. search possibility 9-362
- $K^0$ ,  $K^0/S^0$  interference and mass difference between original and regenerated Kaons 9-6649
- $K^0$  associative, in  $\pi^+-p$ , ang. distrib. 9-6706
- $K^+\Lambda$  photoproduction ang. distrib. analysis by PCAC and current algebra 9-8818
- $K\pi$  isospin- $1/2$  mass enhancement of 1160 MeV obs.,  $M_K=3.9$  GeV/c 9-20638
- NN $\rightarrow$ KK $+\pi\pi$ , review of data 9-6690
- pp $\rightarrow$ KK\*(KK\*), search for  $K^*$  below  $K\pi$  threshold 9-402

**resonances** *see Mesons/resonances***scattering**

- $K^-\pi$ , elastic cross section calc.,  $M_K=4.6$  GeV/c 9-20640
- KN, generalized superconvergence relns. rel. to rho meson trajectory 9-4620
- vector, tensor trajectory hypothesis 9-15604
- $K^+\pi$ , hard core and single imag. Yukawa pot. term fit,  $E_K=2-20$  GeV/c 9-14503
- KK  $s$ -wave scatt. lengths estimation, scalar density term and sym.-breaking parameter 9-16869
- KN, crossing-even Pomeranchuk parameters using modified dispersion relations 9-14502
- KN, generalized superconvergence relns. rel. to rho meson trajectory 9-4620
- $K^+-N$ , invariance in  $S$ -wave meson-baryon scatt. 9-8791
- KN, invariance in  $s$ -wave meson-baryon scatt. 9-8791
- KN, low energy, effective Lagrangian 9-366
- KN charge-exchange, high-energy, model 9-13115
- KN complex scatt. length calc. from soft-meson current algebra 9-17979
- KN forward crossing-even amplitudes, applic. of modified dispersion relations 9-16868
- KN including symmetry breaking of chiral SU(3) $\otimes$ SU(3) 9-14498
- KN isospin-0, partial cross-sections around 1 BeV/c 9-8825
- KN Regge poles and finite-energy sum rules 9-15615
- KN reviewed up to 30 GeV/c 9-11030
- KN $\rightarrow$ KN, superconvergent sum rules 9-8823
- KN+ $K^+$ N, superconvergent sum rules 9-11007
- $K\pi\rightarrow k\pi$ , superconvergent sum rules 9-8823
- $K^+d$ , partial cross-sections around 1 BeV/c 9-8825
- KN, forward, invariant amplitudes, study of superconvergence 9-19201
- $K^+\pi\rightarrow K^0p$  charge-exchange scatt., Be target, 0.97 BeV/c 9-8802
- $K^0$  elastic, multiple Regge-pole model 9-8852
- $K\pi$ , Regge pole parameters from total cross sections 9-11044
- Kp and structure of  $p$  9-18009
- $K^-\pi$ , differential cross-section, ang. distrib., elastic at 9.7 and 13.6 GeV/c 9-11066
- $K^-\pi$ , polarization meas., fit to 5 Regge-pole model,  $M^*=2-2.4$  GeV/c 9-16867
- $K^-\pi$ ,  $Y^*$  spin and parity assignments, 1.4-2.4 GeV/c 9-428
- $K^+$ , resonance in  $p_{1/2}$  state, energy depend. phase-shift analysis 9-4030
- $K^+\pi$  backward, 1.0 to 2.5 GeV/c 9-2499
- $K^+\pi$  elastic, backward direction, 2.76 BeV/c 9-4621
- $K^+\pi$  low energy  $s$ -wave dynamics, singularities contribution calc. 9-8824
- $K^+\pi$ , cross sections meas.,  $E_K=3-3.5$  GeV/c 9-16883
- $K^+\pi$ , partial-wave projections of Regge fits, Argand-diagram loops 9-18010
- $K^+\pi$ , real part of amplitude calc. using dispersion relations 9-13124
- $K^+\pi$  elastic, multiple Regge-pole model 9-8852
- $K^+\pi$  superconvergent dispersion relation to test self consistency of coupling constant for Kp interactions 9-6652
- $K^+\pi$  with single-meson prod.,  $SU(6)\times O(3)$  quark model 9-8762
- $K\pi$  phase shift calc. using  $\pi$ -pole dominance model 9-6671
- $K\pi$   $s$ -wave scatt. lengths estimation, scalar density term and sym.-breaking parameter 9-16869
- Fe, compressibility increase by cold rolling, patent 9-13749
- $K^+$ , partial wave analysis of KN data applic. to  $\pi\pi$   $S$ -wave scatt. lengths 9-4599

**KDP** *see Potassium compounds***Keratin** *see Proteins***Kerr effect** *see Electrico-optical effects; Magneto-optical effects***Kicksorters** *see Counting circuits***Kikuchi lines** *see Electrons/scattering***Kinematics**

- ball, elastic, motion on regularly corrugated surface 9-6259
- baseball catching, vel. and elevation angle var. 9-121
- body with fixed point, interpretation of motion 9-12914
- degrees of freedom, demonstration model 9-17755
- hadron coll., global and boiling pt. aspects 9-4596
- helical motions in fluid of body bounded by multiply connected surface 9-10689
- Lagrange's eqn., intrinsic geometry of coordinate systems derivation 9-122
- Lagrangian and Hamiltonian form of eqns. of motion, algebraic equivalence 9-6260
- nonlinear theory of viscoelasticity 9-843
- of nuclear reactions, book 9-2710
- oscillator, time-dependent, new soln. 9-2331
- perpendicular harmonic motions, compounding 9-15446
- relativistic, Ehrenfest's paradox resolved 9-10684
- relativistic, of massless particles 9-8711
- resonant forced non-linear oscillatory and rotary motions 9-2188
- simple harmonic motion, elliptic 9-6264
- spatial four-bar mechanisms, synthesis with cylindric and spheric pairs 9-6356
- spatial four-bar mechanisms, synthesis with two spheric pairs 9-6357
- systems with multiple relative motion, generalized vector derivatives 9-124
- three-body problem, escape and temporary capture 9-19013
- viscoelastic fluids with additive deformations 9-12923

**Kinetic theory**

- Boltzmann eqn. extended proof, solns. of models 9-2163
- Boltzmann eqn. for bounded medium, wall boundary condition model 9-8420
- Boltzmann gas, dil., kinetic eqn. for the self-correlation function  $G_s(r,t)$  9-12889
- of cosmology 9-18830
- electron fluids, action density equation 9-21096
- electron plasma, model equation 9-18267
- electron plasma waves and ion wave, three-wave interaction, equations 9-7135
- Fermi fluid, normal charged, eqns. in theory 9-8452
- fluids, almost classical 9-841
- gas, low pressure calc. from electron scatt. meas. 9-12849
- molecular vel., determ. by gas effusion, intermediate laboratory expt. 9-12823
- perturbation theory and local compressibility approx. 9-90
- plasma, eqn. formed from g soln. 9-858
- plasma, inhomogeneous, one-component, ring approx. 9-14755
- plasma, with e.m. interaction 9-11542
- plasmas, special equation derived and solved for fully ionized plasma 9-19522
- radiating systems, nonequilibrium, time-dependent behaviour 9-10652
- self-consistent approximations 9-4986
- simple liquids 9-11676
- space depend. problem, one neutron-energy group model 9-15789
- Vlasov eqn. soln., inhomogeneous system results similar to those for homogeneous system 9-14756

**gases**

- See also Association/gases; Brownian motion; Collision processes; Diffusion in gases; Equations of state/gases; Joule-Thomson effect; Molecules/intermolecular mechanics*
- application to diatomic mol. high-temp. thermal dissoc. 9-19479
- Boltzmann's H function, alternation in sign of time derivatives 9-8422
- Boltzmann eqn., operator soln. 9-14810
- Boltzmann eqn., unique soln. to Couette problem 9-20342
- classical, dense, new theory 9-951
- density expansion of 2-pticle distrib. fn. 9-8445
- flow of Maxwell gas between two infinite parallel planes 9-3040
- gas-surface reactions, book 9-5230
- high vacuum system with adsorbing walls 9-7222
- interatomic collisions, theoretical analysis 9-20889
- ionized, thermal diffusion of electrons, density temp. depend. 9-3060
- Lennard-Jones potential, superiority of 18.6 over 12.6 form 9-15972
- mixtures, models, collision integrals rel. to Boltzmann operator 9-11656
- molecules reflected from surface, kinetic and spatial distrib. in rarefied atmos. 9-11654
- particles with spin, dil., relax. coeffs. 9-16700
- plasma, highly nonequilib., elec. cond. and supersonic states 9-11537
- polyatomic, Boltzmann eqn. formulation 9-17156
- rarefied, book 9-7223
- relativistic reciprocal relations betw. transport phen. 9-11655
- symmetric diffusion coeffs. 9-11662
- transition and free molec. regions, boundary conds. 9-5098
- HF<sub>3</sub>, thermal conductivity in crossed elec. and mag. field, reson. decrease of transfer coeff. 9-9448

**liquids** *see Liquids/theory***Kink bands** *see Crystal imperfections/dislocations; Plastic deformation***Kirkendall effect** *see Diffusion in solids; Precipitation***Klystrons** *see Electron tubes; Microwave techniques and devices***Knight shift** *see Nuclear magnetic resonance and relaxation***Knudsen number** *see Flow; Hydrodynamics***Kohn effect** *see Crystal electron states; Crystals/lattice mechanics***Kondo effect**

- 'non-magnetic' dilute alloys, due to localized spin fluctuations 9-12234
- Green function, anomalous, method for problem at zero temp. 9-21458
- low temperature, electrons decoupled in lowest random-phase approx. 9-7699
- $S$ -matrix and Greens function approach, proof of complete equivalence 9-7701
- spin correlations at low temps. about localized impurity moment 9-21562
- Suhl eqns. deriv. from impurity model of heavy-particle gas embedded in cond. electron gas 9-9885
- zero temperature, anomalous Green's function method 9-21458
- Ag-Au-Yb alloys 9-9929
- Cu-Cr, susceptibility and sp. ht. obs. 9-19942
- La-Ce film. obs. 9-3581
- Mo-Fe alloys, dil., rel. to superconductivity 9-1500
- Y-Ce alloys, non-dilute, h.c.p., resistance minima rel. to spin-compensated state 9-15063

**Kramers-Kronig relations** *see Dielectric phenomena; Optical properties of substances***Krypton**

- adsorption and interac. on Cu, 77°K 9-21285
- adsorption on carbon molec. sieves and 5A zeolite 9-7345
- atom, energy loss spectra for keV electrons interaction with electron shell 9-11398
- atom, energy loss spectra for keV electrons interaction with electron shell 9-18150
- atoms, collision with He<sup>+</sup> and Ne<sup>+</sup>, optical excitation 9-6996
- crystal, Debye-Waller factors 9-5536
- crystalline, thermal expansion near triple point 9-9848
- crystals, review 9-13567
- elastic constants, at absolute zero, effect of long-range three-body forces 9-11906
- excitation after  $\beta$  decay, photon emission obs. 9-9136
- gas, and mixture virial coeff., second, from boiling point to room temp., from value at one temp., calc. method 9-15972
- gas, collision induced light scatt. 9-959
- ion source in arc discharge 9-232
- ionization, multiphonon, by Nd laser, role of bound states 9-910
- ionization in low energy Kr-Kr atomic collisions 9-13456
- ionization probability curves for electron impact, for  $^2P_{3/2}$  and  $^2P_{1/2}$  states 9-4863
- liquid, vapour press. and comparison with that of liq. Xe, Ar 9-11748
- krx, molecular Rydberg states of ethylene, obs. 9-14710
- muonium formation and fraction press. shift of its hyperfine structure interval 9-20905

**Krypton continued**

- photoionization by soft C-rays, 200-1500 eV, sub-shell contribs. 9-13455  
 photoionization subshell cross-sections obs. X-ray 9-13454  
 photosensitization of HD exchange reaction, mechanism 9-16476  
 solid, infl. of lattice anharmonicity on exponential potential parameters 9-16161  
 solid, Mossbauer recoilless fraction 9-12361  
 solid, refractive index rel. to dielec. props., 3612 to 6439 Å 9-7832  
 solid, thermal conductivity temp. depend. for multiphonon interaction 9-15021  
 solid, tracer diffusion obs. by isotope exchange technique,  $90^\circ < T < 115^\circ \text{K}$  9-9731  
 sorption in UC, fission induced, mechanism 9-16047  
 specific surface determ. of solids, applic. 9-21255  
 thermal expansion of crystalline Kr near triple point 9-9848  
 u.v.-laser power, continuous, in Watt range 9-6512  
 ion laser investigated 9-8605  
 Kr<sup>+</sup> laser, basic data 9-19146  
 Kr I, visible 5s-5p array, transition probabilities and oscillator strengths 9-20880  
 Kr<sup>+</sup> ionization by e collisions rel. to excitation energy obs. 9-11616  
 Kr<sup>2+</sup>, excitation cross section for fast e. impact 9-5057  
 Kr<sup>+</sup>-Kr collisions, coincidence meas. 9-11410  
 Kr<sup>8+</sup>, ionizing collisions with H<sub>2</sub>, relative cross-sections for prod. of KrH<sup>+</sup>, KrH<sub>2</sub><sup>+</sup> and H<sub>2</sub><sup>+</sup> 9-7188  
 N<sub>2</sub> adsorbed layers, heat of adsorpt., two-dimens. condensation 9-9594  
 N<sub>2</sub> multilayer adsorpt. on C surface, two-dimens. van der Waals eqn. 9-9593

**Krypton compounds**

- Kr-D<sub>2</sub> mixtures, ionisation curves of KrD<sup>+</sup> ions 9-7187  
 (90wt.%)Kr-(10wt.%)CO<sub>2</sub> proportional counter gas, pulse shape calcs. 9-19228  
 Kr clathrate, dynamics of trapped atoms, Mossbauer effect 9-3513

**Kuhn-Thomas sum rule** *see Molecules/electronic structure***Kurie plots** *see Beta-decay theory; Beta-ray spectra***Kypoupolos method** *see Crystals/growth***Laboratories**

- See also Acoustical laboratories*  
 plan and curricula 9-1  
 undergraduate temp. control system for low temp. work 9-8319

**Laboratory apparatus and technique**

- acceleration due to gravity, Nat. Bureau Standards, USA 9-26  
 adiabatic rotation of sample in magnetic field, liquid He temps. 9-4181  
 Al<sub>2</sub>O<sub>3</sub> film as support, patent 9-13163  
 anti-vibration instrument mounting 9-20281  
 atomic beam oven with low mag. field 9-4865  
 autographic attachment for dilatometer 9-22015  
 ballistic pendulum, use of blowgun 9-14  
 benzene synthesis, for sensitivity enhancement in <sup>14</sup>C and tritium dating 9-11247  
 biological specimen holder for potato section, thermal diffusivity meas. 9-15394  
 Cahn electrobalance, new method for mag. susceptibility meas. 9-3765  
 carbonaceous mats, prep. for optical and electron microscopy 9-8314  
 chart recorders, erasable trace methods reviewed 9-12801  
 chemical analysis physical methods, Physics Exhibition, London 1968 review 9-4021  
 clamp-type holder for lasers or electroluminescent diodes 9-12799  
 coloration, additive, technique for alkaline-earth chalcogenides 9-7500  
 computers for nuclear physics 9-22014  
 conical pendulum expt. 9-12  
 constant true strain rate apparatus 9-4177  
 contrast enhancements of vibrating samples, retroreflective materials 9-4178  
 creep testing, constant-stress devices 9-5464  
 deformation meas. device with particular rel. to necking 9-19797  
 design and role for student teaching 9-6253  
 Dewar, modification for freezing nitrogen 9-5  
 dielectric sample holder, calibration of electrode spacing 9-4182  
 diffusion coeff. determ. for electrolytes in gels 9-21233  
 digital reader of oscilloscope trace photographs 9-286  
 discharge investigation, 300kV, 10<sup>-8</sup> torr to 4 atmos. 9-3019  
 electron temp., direct display, magnetised and time varying plasmas 9-2986  
 electronics course, expt. and bib. 9-10  
 electropolishing, jet, of e microscope specimens, modification 9-16069  
 environmental chamber, with programmed temp. control to simulate daily temp. changes for plants 9-4380  
 evaporation source, folded baffled boat 9-7328  
 experimental design technique 9-8310  
 experiments for students of astrophysics, book 9-18975  
 foils of Mn, preparation technique 9-4184  
 four-ball lubricant testing machine with three wear tracks 9-6223  
 gas-free liquids, fractionation device for prod. 9-14291  
 glass contact refractories, chem. staining for metal ions detection 9-4017  
 graphite, erosion resistant for rocket motors, nondestructive quality control techs. 9-1936  
 graphite, oxidation resistance improvement 9-10339  
 grating sinusoidal, on Al<sub>2</sub>O<sub>3</sub> surface, chemical prod. method 9-4171  
 heat-reflecting filters composition, for light sources, patent 9-13068  
 indicator for recording Hg manometer levels at regular intervals 9-6227  
 ion-molecule reaction rates monitoring by venetian blind particle multiplier appl. 9-1886  
 ionospheric reaction studies 9-1960  
 i.r. source of uniform intensity 9-8521  
 Kerr effect apparatus for liquid state studies 9-7264  
 kinetic motion simulator, evaporation and distillation expt. 9-15403  
 laser beam target projector, retracting-pedestal 9-2365  
 level maintenance device for liquid N<sub>2</sub> in Dewar 9-6222  
 linear air track, double sparker 9-2118  
 machining of flat double spiral channels, method 9-18965  
 magneto-optical apparatus for ferromagnetic thin films domain wall visualisation 9-18681  
 metallurgical lab. at Polytechnic of Denmark 9-6221  
 microbomb, multipurpose, for applic. of hydrostatic pressure up to 11 kbar 9-6235  
 microwave diff. expts., atomic stacking models 9-16

**Laboratory apparatus and technique continued**

- neutron source, hot sample changer and transfer cask, material irradiation 9-20810  
 oscillator-detector circuit for programmed laboratory sequencers 9-10790  
 particulate rad., expt. for eval. of phys. props. 9-6255  
 pendulum, ball, using spring gun 9-15402  
 plan and curricula 9-1  
 pneumogas dryer parameters, influence of initial moisture content of mats. 9-14881  
 porosimeter, Hg, for meas. of pore size distrib. heterogeneities 9-7416  
 radioactive foil, transportation to counters by converted slide projector 9-13206  
 reaction vessel, diamond prod. 9-12800  
 recording high-speed processes, photographic tech. and equipment, book 9-17903  
 right-angle drive, compact, using flexible wheel 9-14290  
 sample changer in radioactive meas., use of slide projector 9-22017  
 sample holder for i.r. spectroscopy 9-20280  
 sample holder for sequential presentation to photomultiplier, patent 9-10582  
 sampling value, hydraulically actuated for internal combustion engine 9-8311  
 shielded γ-irradiation plant 9-327  
 silica optical windows, strain-free in Dewar for optical expts. on liquid He 9-7290  
 solenoid for general use 9-6467  
 solid compressibility meas. device 9-3416  
 stopcock for gas mixing of solution 9-22013  
 string saw for cutting large soluble crystals 9-16066  
 sublimation, large-scale, modified cold finger apparatus 9-21251  
 temperature distrib. of crystal-melt system surface, meas. device 9-3237  
 thermogravimetry in flowing gas, errors and thermobalance 9-3978  
 transducers and circuits in student labs. 9-6252  
 TV closed-circuit system for instrum. reading 9-4175  
 vacuum (ultra-high) multiple rotor, manual or automatic op. 9-4200  
 vapour density meas. apparatus for student use 9-20286  
 vertical force table 9-15  
 wire, fine, gripping during mechanical tests 9-4183  
 zone melting, patent 9-14285  
 Al<sub>2</sub>O<sub>3</sub> ceramics, electric tests up to 800°C. 9-10034  
 C blacks, compaction without binder, for study of electronic props. 9-7735  
 C monolithic articles, prod. using low press. semi-isostatic moulding tech. 9-8309  
<sup>14</sup>C in atmospheric CO<sub>2</sub>, measurement 9-15248  
 Ge, chemical polishing apparatus for flat, clean, strain-free surfaces 9-14284  
 Mn, foils, technique for preparation 9-4184  
 NiCr, thin film resistors, flash evaporation 9-15393  
<sup>18</sup>O tracer investigations, data handling 9-6035  
 SiC<sub>4</sub> synthesis, for sensitivity enhancement of <sup>14</sup>C dating 9-11247  
 Ti film sorption of N<sub>2</sub>, all-metal meas. apparatus 9-13588

**Lamb shift** *see Spectra/atoms***Lambda (λ) point** *see Helium/liquid; Phase transformations***Lamps** *see Light sources***Landé splitting factor** *see Spectra; Zeeman effect***Langmuir probes** *see Discharges, electric; Plasma/diagnostics; Space vehicles/instrumentation***Lanthanides** *see Rare earth metals***Lanthanons** *see Rare earth metals***Lanthanum**

- crystal, d.h.c.p., Fermi surface, rel. to mag. ordering and structure 9-5615  
 La-Ce system, elec. conductivity temp. dependence 9-1455

**Lanthanum compounds**

- intermetallic, localized mag. moment obs. 9-16331  
 lanthanum cobalt nitrate, phonon mean free paths, spin-lattice interact. strengths, from magneto-thermal conductivity meas. 9-9854  
 phosphor, cathodoluminescent, patent 9-10254  
 CdSb-La, mag. susceptibility 9-16328  
 La-Ce film, Kondo effect obs. 9-3581  
 La-Ce(Gd) superconducting transition temperature, pressure dependence 9-1486  
 La-Tb, dil. alloys, n, diff. and susceptibility meas. 9-17454  
 La<sub>2</sub>Mg<sub>3</sub>(NO<sub>3</sub>)<sub>12</sub>·Ce<sup>3+</sup>, Pr<sup>3+</sup>, e.p.r., coupling of two spin species by resonant phonons 9-18738  
 La<sub>2</sub>O<sub>3</sub>-Cr<sub>2</sub>O<sub>3</sub>, phase diagram up to 1,700°C 9-16152  
 La<sub>2</sub>-Gd<sub>2</sub>Al, superconducting transition temp., anomalous behaviour 9-7773  
 La<sub>2</sub>ReO<sub>9</sub>, crystal structure 9-19715  
 LaAl, n.m.r. of <sup>27</sup>Al, Knight shift and susceptibilities, temp. depend. 9-3969  
 LaAlO<sub>3</sub>:Eu<sup>3+</sup>, fluorescent emission 9-12490  
 LaAlO<sub>3</sub>, phase transitions and lattice vibrations, x-ray study 9-3504  
 LaAlO<sub>3</sub>, trigonal rot. of AlO<sub>6</sub> octahedra as charact. struct. transition 9-1349  
 LaB<sub>3</sub> irradiated by thermal neutrons, investigation of stability 9-1409  
 LaB<sub>6</sub> electron gun, characteristics 9-15500  
 LaB<sub>6</sub> field ion images, description 9-12988  
 LaB<sub>6</sub> powder, gas suspended, as MHD generator working fluid 9-220  
 LaBr<sub>3</sub>, Ce<sup>3+</sup> and Nd<sup>3+</sup> pairs, anisotropic superexchange interact. 9-1697  
 LaBr<sub>3</sub>, Raman spectrum 9-3904  
 LaBr<sub>3</sub> strain-modified spin lattice relax. rates 9-7927  
 LaCl<sub>3</sub>:Ce<sup>3+</sup>, pair interaction e.p.r. meas. 9-10283  
 La(Cl,Br)<sub>3</sub>:Ce(Er)<sup>3+</sup>, modified Orbach relax. process 9-12317  
 LaCl<sub>3</sub>, adjusting poles and zeros of dielec. dispersion to fit reststrahlen 9-5876  
 LaCl<sub>3</sub>, Ce<sup>3+</sup> and Nd<sup>3+</sup> pairs, anisotropic superexchange interact. 9-1697  
 LaCl<sub>3</sub>, cryst. struct. 9-11850  
 LaCl<sub>3</sub> strain modified spin-lattice relax. rates 9-7927  
 LaErO<sub>3</sub>, antiferromag. struct., n diffraction study 9-12310  
 LaF:Mg,Ca, thermoluminescence and colour centres 9-21658  
 LaF<sub>3</sub>:Nd<sup>3+</sup>, deform. and dipole dipole broadening of Nd<sup>3+</sup> lines 9-1786  
 LaF<sub>3</sub>, sound vel. meas. using Bragg diff. of light 9-9826  
 LaF<sub>3</sub> vapour discharge spectra, band system obs., 3000-3350 Å 9-9217  
 LaMg nitrate, strain-modified spin-lattice relax. rates 9-7927  
 La<sub>2</sub>Mg<sub>3</sub>(NO<sub>3</sub>)<sub>12</sub>:Dy<sup>3+</sup>, electronic and nuclear relaxation and polarization 9-10298



**Lanthanum compounds continued**

- La<sub>2</sub>Mg<sub>3</sub>(NO<sub>3</sub>)<sub>12</sub>·24H<sub>2</sub>O:Mn<sup>2+</sup>, ENDOR study of quadrupole splitting 9-1883  
 LaNbO<sub>3</sub>, e.p.r. and spin-lattice relaxation of Nd<sup>3+</sup> 9-20021  
 LaNi<sub>5</sub>, NMR of Gd, dynamic effects, g shift 9-10280  
 La<sub>2</sub>O<sub>3</sub>:Eu<sup>3+</sup>, fluorescent emission 9-12490  
 La<sub>2</sub>O<sub>3</sub>-Cr<sub>2</sub>O<sub>3</sub>-α-Fe<sub>2</sub>O<sub>3</sub>, ternary phase diagram 9-13774  
 LaSb films, opt. absorpt. thickness dependence 9-3897  
 LaSn<sub>3</sub>:Gd, supercond. critical temp. reln. with normal-state mag. props. 9-1478  
 Pr-La alloys, mag. susceptibility rel. to temp. and field strength 9-17449  
 Pr and Tm doping effect on supercond. 9-13857

**Laser beams**

- absorption anomalies in scatt. medium 9-3128  
 angular distrib., inhomogenous plane mirror resonator 9-2367  
 atmospheric absorption review 9-2386  
 atmospheric propagation, parameters fluctuations dependent on turbulence 9-6423  
 coherence, temporal and spatial, appl. high resolution spectroscopy to meas. 9-15556  
 deflection by KDP crystal in electric field close to Curie temp. 9-10854  
 divergence decrease on traversal of optical amplifier 9-14439  
 energy meas. with "black horn" calorimeter 9-19155  
 expansion in one dimension by prisms, for streak interferometry 9-4485  
 fast i.r. pulses, detection by thin film thermocouple 9-8637  
 fluctuations near threshold, sixth order correlations 9-249  
 focussed Gaussian beam through random medium, fluctuation distribution 9-16792  
 focussing power of hyperbolic-type gas lens, limitation 9-16787  
 frequency modulation by active interferometer 9-16794  
 in gas, diffusing beam narrowing and propag. path reduction 9-15535  
 incoherent wide-angle beam prod. devices, 10.6 μ 9-10917  
 intensity interference by two-photon excitation of fluorescence 9-20532  
 interaction with atoms, effective electronic binding pot. 9-684  
 interferometer freq. response, fringe pattern depend. on external resonator 9-14437  
 light pulse narrowing 9-4499  
 light pulses, short and low-energy calorimeter meas. 9-255  
 light statistics 9-15534  
 mode-locked, optical frequency shifting 9-15540  
 modulated, photon counting distributions 9-248  
 modulation by electrooptic Doppler shift, spectrum anal. 9-4497  
 multimode radiation, propagation and focusing 9-4487  
 optical breakdown threshold lowering in laser focus by superimposing microwave field 9-6533  
 optical heterodyne system with pyroelectric detectors 9-14443  
 optical receivers, broadband signal and noise performance 9-19159  
 phase fluctuations through turbulent atm., interferometric study 9-10869  
 picosecond pulse display, two-photon fluorescence technique 9-6537  
 in plasma, hot, net absorpt. coeff. allowing for stimulated emission 9-2974  
 power and polarization plane control device, 10<sup>-6</sup>-10<sup>3</sup>ω 9-237  
 profile recording using foamed polystyrene 9-13010  
 propagation in liquids, opt. permittivity, molecular angular correlations 9-11695  
 pulsed, attenuation meas., differential transformer method 9-16791  
 Q-switched pulse, evolution from noise 9-20499  
 reflection from media with inversion symmetry, second harmonic generation, intensity and polarization 9-19140  
 ruby, focused low-power, rel. to stimulated Raman scatt. of liqs. 9-5171  
 in ruby, interaction of radiation from double-resonance meas. 9-10163  
 ruby, spectrum of pulse observed at output of photodetector 9-4477  
 sampling techniques and parameter meas., book 9-16788  
 scattering, microsystems, optical saturation theory 9-20530  
 self-focussing, analogy with gravitational theory 9-14423  
 self-focussing in org. liqs. and effect on stimulated scattering 9-14438  
 self-trapped filaments, spectral broadening by sinusoidal phase modulation 9-4498  
 shutter, subnanosecond risetime, for Nd glass laser system 9-17882  
 space coherence atmos. turbulence dependence 9-2385  
 time distortion of intense pulses due to self-focussing effect 9-10871  
 trapped filaments in liquids, anti-Stokes generation 9-3102  
 Ar, thermal self-focussing in lead glass 9-8630  
 CO<sub>2</sub> laser, profile recording using foamed polystyrene 9-13010  
 GaAs laser with nonlinear passive element in resonator, charact. features of radiation 9-17878  
 PbS<sub>1-x</sub>Se<sub>x</sub>, generation of coherent laser radiation, 4-6.5 μ range 9-2384

**applications**

- "optical" discharges produced by single laser pulses on non absorbing surfaces 9-5785  
 arc electron density meas. using CO<sub>2</sub> laser interferometers 9-18297  
 atmosphere, lidar probing techniques 9-4049  
 biomedical, book 9-4134  
 ceramics, controlled separation 9-3441  
 communication system, coherent and noncoherent detect., 0.6328 μ and 10.6 μ 9-10882  
 diffusion length meas. in epitaxial films 9-3616  
 Dopplermeter, new theoretical model 9-12848  
 earth strain meas. interferometer 9-4038  
 earth-moon separation determ. and test of non-Newtonian gravitational theories 9-8380  
 gas flow profile meas. 9-19569  
 gas irradiation for plasma production 9-11578  
 high-temperature and plasma phenomena 9-20531  
 interferometer, Michelson type, He-Ne gas, deformable bodies collision processes obs. 9-20535  
 interferometers, laser beam scanner 9-19158  
 interferometry, far i.r., for electron density meas. 9-14780  
 interferometry, rough surface 9-4516  
 introductory lecture 9-6502  
 length meas. interferometry 9-2127  
 methane, 3.39 μ line, press. shift and broadening, laser-saturated mol. absorbt. study 9-11496  
 molecules, translational, vib. and rot. motion determ. by scatt. 9-19421  
 moon's light location 9-250  
 NASA educational presentation 9-19138  
 nonlinear scattering from colloids rel. to particle size and shape 9-14866  
 object illumination under low atmospheric transparency, photographs 9-4548

**Laser beams continued****applications continued**

- ophthalmoscope, focusing method, patent 9-19156  
 optical image quality improvement by eliminating coherence 9-10890  
 organic dye lasers characts. as tunable light sources for nsec absorption spectroscopy 9-20562  
 particle size meas. 9-7283  
 particle size meas. using laser homodyne spectrometer 9-17224  
 photolysis and spectroscopy for nanosecond reactions 9-6559  
 photon-graviton interaction, detection in external gravit. field 9-10872  
 plasma creation, dynamic parameters in magnetic field 9-21086  
 plasma density meas. by CO<sub>2</sub> laser interferometer 9-5006  
 plasma production, high density and temp. by large power laser 9-17119  
 plasma production and density meas. by light scatt. 9-2989  
 plasma production and heating, theory and experiments, review 9-19546  
 plasma production by focussed CO<sub>2</sub> laser radiation 9-890  
 radar return, meteorological problems 9-10870  
 Raman effect, stimulated, high conversion efficiency, quantitative investigation 9-20533  
 Raman spectrograph, S<sub>0</sub> fundamental modes determ. 9-20941  
 Raman spectroscopy, 50 cps ruby laser excited, signal-noise ratio improvement 9-6560  
 Raman spectroscopy, apparatus with laser excitation 9-16798  
 Raman spectroscopy of single crystals, chemical implications with examples 9-21633  
 Rayleigh scattering and depolarization in liqs., rel. to molec. interactions 9-14850  
 refractive index meas. in liquids showing self focussing and electrostriction 9-9511  
 seismic strain meas., interferometer system 9-10373  
 self-beating technique in light scatt. rel. to translational motions and transport props. of solutions 9-14875  
 semiconductor band-tail spreading energy 9-1541  
 solid irradiation for plasma production 9-11578  
 spark production by train of mode-locked laser pulses 9-11636  
 spark source of highly ionized atom spectra 9-18145  
 spectroscopy, nanosecond absorption using laser photolysis 9-19170  
 thermonuclear plasma production from focussing on LiD surface, n. obs. expts. 9-7171  
 thickness meas. of Cr coatings on brass, from flash spectra produced by laser interaction 9-11762  
 triggering of pressurized spark gap 9-13471  
 u.v. pulsed, use in photoluminescent dosimeter readout, patent 9-13173  
 YAl garnet, Nd doped, opt. refrigeration, fluorescent quantum efficiency 9-1831  
 Ar, 4880 Å, Raman effect of glycerol 9-15890  
 CO<sub>2</sub>, interferometer, plasma density meas. 9-5006  
 CO<sub>2</sub>, vacuum deposition of thin films 9-11775  
 CO<sub>2</sub> laser, fog dissipation 9-4055  
 D<sub>2</sub> ionization, theoretical exam. 9-9383  
 Ge, quantum effects in cyclotron resonance using c.w. HCN laser 9-14070  
 HCN, for e.p.r. abs. in O<sub>2</sub> 9-786  
 HCN, interferometer source for plasma decay study 9-7166  
 He-Ne, in Kerr effect mag. domain microscopy, picture improvement technique 9-16352  
 He-Ne, optical sampling of pulse by Nd:glass laser 9-6531  
 N<sub>2</sub>O, vibr. relax. determ. 9-7030  
 Nd:glass, optical sampling of He-Ne pulse 9-6531  
 Nd pulsed laser, range finding 9-15526  
 Nd rad., clearing of bromophthalocyanine solns. 9-1015  
 Pu inclusions analysis using laser microprobe 9-4023  
 SF<sub>6</sub> a.c. arc characteristics filmed by laser-Schlieren technique 9-17881  
 Si:P diode preparation 9-18638  
 YFe garnet, magnetoelastic waves, optical probing 9-12342
- effects**
- alkali halide crystals, damage 9-1411  
 alkali halide crystals, multiphoton excitation of photoconductivity 9-13941  
 alkali-halide crystals, laser-induced damage 9-16390  
 brittle homogeneous transparent medium, thermoelastic destruction 9-19869  
 γ-optical transition stimulation in determining hyperfine structure of ions of Mossbauer nuclei 9-18696  
 current pulse due to radiation incident on target in gas 9-1627  
 gases, photoelectric effect on high-intensity light irradi. 9-7201  
 Gaussian distortion due to saturable gain or loss 9-12993  
 glass surface damage 9-3176  
 glasses, surface damage, mechanisms 9-14891  
 harmonic generation, third, phase-matched, in anomalously dispersive liq. 9-21205  
 heating of substances and resultant radiation ionizing action 9-7185  
 instabilities in Raman-active media 9-11699  
 interaction of two beams, failure of Fresnel laws 9-2369  
 ionization by radiation due to heating substance in laser beam focus 9-7185  
 ionization of gaseous medium 9-17879  
 ions produced by interaction with solids, mass spectrometer investigation 9-9380  
 laser induced Raman spectra of crystalline Lysozyme, pepsin and α-Chymotrypsin 9-5940  
 liquid cry., second harmonic generation, origin, applic. to struct. study 9-21207  
 liquid media, change in refractive indices, use of double exposure holography 9-13035  
 molecules, diatomic, electron transitions 9-781  
 organic dielectrics, transparent, opacity production 9-1721  
 photochromic spiropyran layers, coloration by u.v. laser radiation 9-18219  
 photodissociation of iodoheptafluorobutane mol. rel. to formation of I<sub>2</sub> 9-15902  
 photoeffect, non-linear, discrimination from thermionic emission by time response meas. 9-16318  
 plasma, partially-ionized, light absorpt. increase at high intensities 9-7161  
 plasma, production, radiation pressure effects 9-18299  
 plasma interaction with laser radiation, Compton effect induced 9-9351  
 plasma production, prebreakdown bubble phenomena 9-9382  
 plasma production with high ionization degree 9-7185  
 plasma torch, pulsed, production and characts. 9-887  
 polyethylmethacrylate, laser-induced damage temp. dependence meas. Q-switching dye 9-9863

**Laser beams continued**  
**effects continued**

- polymethylmethacrylate, damage under extreme loads during laser-illumination 9-16137  
 polystyrene, damage under extreme loads during laser-illumination 9-16137  
 Raman scattering 9-12390  
 reflection coefficients diminution for solid surface 9-21603  
 refractive index change in  $\text{CCl}_4$  associated with thermal blooming, interferometric observation 9-18361  
 scintillation over horizontal paths from 5.5 to 145 kilometers, log-amplitude covariance 9-21775  
 scintillation under atmospheric turbulence, saturation 9-21774  
 self-focusing, focusing of hypersound 9-4319  
 self-focusing, laser induced air breakdown 9-5090  
 self-trapping, filament diameter calc. 9-4486  
 semiconductor reflectivity enhancement by Q-switched ruby lasers 9-15163  
 solids and liquids, interference due to low-power heating 9-12323  
 sparks in air, butane, He, in mag. field 9-7205  
 stimulated Raman effect, theory 9-9169  
 stress, production in solids, thermoelastic mechanism 9-13725  
 thermal self-defocusing and self-focusing in liquids and solids, self-actions in liquids with flows 9-17880  
 thermionic emission from metals induced by  $\text{CO}_2$  laser 9-10079  
 underwater sparks, induction 9-9420  
 vanadyl phthalocyanine, laser-induced damage temp. dependenc-switching dye 9-9863  
 Ar. spark prod. by focused sub. nanosec. pulse, press. depend. 9-891  
 Au, induced non-linear photoeffect, discrimination from thermionic emission by time response meas. 9-16318  
 CdS induced stimulated Brillouin scattering 9-3906  
 $\text{Co}_2$ , absorption in semi-insulating GaAs 9-3848  
 D<sub>2</sub> ionization under action of short pulse laser 9-3005  
 H and rare gases, multiphoton ionization 9-13451  
 Hg, profile alteration by high power pulse 9-11394  
 InSb third harmonic generation enhancement using  $\text{CO}_2$  laser, magneto interband contrib. 9-257  
 K,Sb photoelectric emission induced by Nd-glass laser, three photon eff. 9-10080  
 LiD surface, thermonuclear neutron emission at focus 9-13245  
 $\text{LiNbO}_3$ , second harmonic generation by Nd, glass psec pulses 9-10173  
 N, spark prod. by focused sub. nanosec. pulse, press. depend. 9-891  
 NaCl F-centres,  $\gamma$ -induced, bleaching,  $10.6 \mu$  9-11889  
 Ne atom fluorescence polarization 9-13292  
 Si, resistivity changes 9-7812  
 $\text{SrMoO}_4$ , scheelite-type, two-photon excitation of luminescence and damage processes 9-1825

**Lasers***See also Light/coherence*

- 10.6  $\mu$ , large volume TEM<sub>00</sub> mode techniques 9-16777  
 amplifier, high power nonlinear 9-16775  
 amplifier internal beam, Gaussian distortion due to saturable gain or loss 9-12993  
 attenuation increase of off-axis modes, application of antireflection coating 9-4459  
 backscatter meas. of lower atmosphere up to 28 km, 6943 Å 9-10384  
 beam, as frequency standard, construction possibilities 9-8593  
 bibliography, with indexes, Apr-Dec 1967 9-19139  
 bleach-out effect, nonlinear wave equations description 9-10840  
 chemical, based on branched chain reactions 9-8592  
 clamp-type holder 9-12799  
 composite cavity, single-frequency, stabilization 9-12845  
 with convex mirrors, transverse mode selection 9-6506  
 c.w. oscillator, cross relaxation effect on spectral flux and population inversion distribution 9-12999  
 diffraction effects, optical and X-ray, demonstration 9-15405  
 dispersion theory, semiclassical 9-6504  
 electrooptical effect with a  $\text{KH}_2\text{PO}_4$  crystal 9-14424  
 energy output meas. using calorimeter 9-10851  
 energy output meas. using spherical cavity calorimeter 9-10852  
 Faraday cell as decoupling element 9-10855  
 frequency locking to time standard 9-8590  
 frequency tuning by organic dye, appl. high resolution spectroscopy to meas. 9-15556  
 generation peaks, suppression using Kerr cell 9-6508  
 graviton generation and detection by interaction with external gravit. field 9-10872  
 IEEE region six conf. Portland (1968) 9-6247  
 IEEE region six conf. Portland (1968) 9-2106  
 for inducing phonon spectra in thulium gallium garnet oriented crystal 9-12439  
 interference, correlation meas. rel. to fourth order coherence functions 9-10842  
 international electron devices meeting, conference, Washington, USA, 1967 9-14421  
 introductory lecture 9-6502  
 ionic, thermionic hollow-cathode discharge basis 9-4464  
 i.r. and submm. wave, dielectric tube resonators 9-2368  
 i.r. ring, beats produced by negative Faraday effect 9-4470  
 light statistics 9-15534  
 metal foil spontaneous electron emission, laser induced, evidence for 9-16320  
 metal foil spontaneous electron emissions, laser induced, evidence against 9-5781  
 mirror transmittivity optimization 9-4455  
 mode interactions rel. to spatial matter inhomogeneities 9-4462  
 model, spatially nonuniform 9-12997  
 modulation, intracavity, by u.s. waves of two freqs. 9-4452  
 noise, generalized van der Pol -eq. not limited to threshold region 9-239  
 with nonlinear absorbing gas cell in resonator, freq. stabilization effects 9-241  
 optical generators, combined 9-20502  
 optical line irradiation, doublet line shape depend. on relaxation const. calc. 9-6955  
 oscillation, nonresonant continuous, in visible 9-6509  
 oscillation forms due to light scatt. deform. stat. anal. 9-8599  
 parameter measurement techs, energy, gain, coherence, stability and modulation, book 9-16788  
 photon number and amplitude fluctuations quantum mechanical calc., inhomogeneous broadened atomic line 9-6503

**Lasers continued**

- population inversion using flash tube, patent 9-16776  
 power of cont. wave, wire cone calorimeter design for meas., 25  $\mu\text{W}$ -25 mW 9-4453  
 pulse duration and line breadth determ. from transient Raman scatt. 9-13527  
 pulse width control technique 9-19136  
 pulses, giant, generation effects 9-12994  
 pulses, ultrashort, generation with a nonlinear absorber 9-14426  
 pulses, ultrashort, generation with a nonlinear absorber 9-240  
 Q-switched, inverted population condition in two elements, patent 9-16778  
 Q-switched beam focused on single solid target, plasma studied 9-2365  
 Q-switched emission, calc. using fluctuating dipole model 9-20499  
 quantum theory, introductory lecture 9-14425  
 radiation instability, transverse 9-8591  
 Raman, pulses, temporal shape analysis using steady state theory 9-19141  
 Raman spectroscopy, rapid scanning, excitation techniques 9-10938  
 with resonance loss modulation, limiting parameters of emitted ultra-short pulses 9-8594  
 resonant cavity for increased coherence 9-8595  
 forresonator field distrib. meas. in i.r. laser, thermotransducer 9-15506  
 ring, accelerated rotating, shift of light freq. 9-238  
 ring, spectra of beats between adjacent oscillating modes 9-20500  
 ring, unidirectional, patent 9-19137  
 rotating-prism Q-switched, timing circuit 9-2364  
 ruby:  $\text{Cr}^{3+}$  inversion coeff. meas. using double-cavity device 9-10853  
 with saturable absorber as Q-switch, time behaviour 9-4458  
 scatter measurements in mesosphere and above 9-12587  
 self-pumping phenomena 9-4454  
 simulation by gravitational waves on liquid surface 9-8597  
 statistical model for light 9-10847  
 stimulated Compton scatt, possibility 9-12998  
 technique and multiple applications 9-19138  
 theory, nonstationary nonlinear optical effects, ultrashort light pulse formation 9-12995  
 threshold, inhomogeneously widened at. lines 9-13295  
 t.w., Q-switched, giant pulse generation process with population and field variations along cavity, calc. 9-12996  
 two-photon fluorescent display technique, contrast ratio rel. to mode-locking effects 9-10858  
 ultrashort optical pulses, methods of generation and amplification 9-12992  
 unified theory based on kinetic equations, book 9-2366  
 wavelength selection device 9-10857  
 $\text{H}_2\text{O}$ , emission lines at 4.77  $\mu\text{m}$ , 11.83  $\mu\text{m}$  and 11.96  $\mu\text{m}$  9-2869  
 He-Ne, medium in confocal resonator showing mode selection 9-8596  
 $\text{KH}_2\text{PO}_4$ , crystal, electrooptical effect on the radiation frequency 9-14424
- gaseous**
- action obs. in C and N atoms foll. dissociative excitation transfer 9-4851  
 amplifier, non-linear effects theory, weak signals 9-4463  
 amplifier, non-linear effects theory strong signals 9-6511  
 annular with anisotropic element, rad. polarization and freq. characts. 9-243  
 cathodes, thermionic, hollow, investigation of usage 9-15508  
 $\text{CO}_2$ , frequency control by  $\text{BCl}_3$  filter 9-15515  
 collision broadening, role of interatomic repulsion 9-13305  
 continuous, in near u.v. and violet operation 9-17681  
 with coupled modes, emission line width meas. 9-20503  
 c.w., phase pulsations and combination tones in output, observation using interferometer 9-16780  
 c.w., sub-m.m., high power output 9-16779  
 elliptically polarized dual-polarization, freq. discrimination characts. 9-13000  
 emission single mode, radiation polarization and freq. 9-8601  
 fabrication techniques and materials 9-2372  
 frequency fluctuations and determ. of natural width of spectral line 9-14428  
 He-Ne, with mixture of Ne isotopes in gain tube, saturated absorption by neon 9-20513  
 intensity of single mode as a function of cavity Q 9-8617  
 interferometry 9-19142  
 ion, high power, construction 9-17866  
 ionic, thermionic hollow-cathode discharge basis 9-2371  
 mirror, inteval, improved mounting 9-10859  
 mode selector for single-freq. operation, using confocal cavity 9-8603  
 mode self-locking, Lamb theory approx. 9-8602  
 molecular backscatter of laser rad. from turbulent air 9-21141  
 multimode, phase-locking by means of l.f. cavity-length modulation 9-6510  
 in noble gas discharge, max. inversion density and power output calc. 9-4465  
 noise, generalized van der Pol -eq. not limited to threshold region 9-239  
 oxygen pure 9-8619  
 resonator interferometry of pulsed gaseous submillimeter wave lasers 9-20292  
 single-mode, theory 9-16781  
 tubes, Brewster-angle grinding of windows to reduce loss 9-2370  
 u.v.-power, continuous, in watt range 9-6512  
 water vapour, sub-mm., with H as buffer 9-20512  
 water-vapour, monochromatic rad., strongly linearly polarized, 118.6  $\mu$  9-19144  
 wavelength stability meas. 9-8600  
 A/r ionic, u.v., 1 W continuous wave o/p 9-17868  
 Ar-ion, discharge tube with Hg pool cathode 9-20506  
 Ar, continuous u.v.-power in Watt range 9-6512  
 Ar, continuous u.v.-power in watt range 9-6512  
 Ar, excitation and discharge mechanism - radial distrib. of excited species in capillary discharge 9-13461  
 Ar, frequency spectrum fluctuations 9-4467  
 Ar, ion using three mirror cavity, for high power single frequency operation 9-15513  
 Ar, ionised, pulsed and quasi-c.w., design and obs. 9-17867  
 Ar, ionized, microwave excited 9-6513  
 Ar, new high-power stable modes of operation 9-8604  
 Ar, pulsed, time-resolved spectrum in visible region 9-13002  
 Ar, second harmonic generation to 2573 Å, efficient cw, using ADP or KDP crystals in cavity 9-20504  
 Ar, spectroscopic system for low intensity sources 9-15559



**Lasers continued****gaseous continued**

- Ar, thermal self-focussing in lead glass 9-8630  
 Ar<sup>+</sup>, inductively excited, props. in high-current regions 9-14429  
 Ar<sup>+</sup> continuous wave, study of mechanism of population inversion 9-20505  
 Ar con laser investigated 9-8605  
 Ar f.m., freq. stabilization and noise suppression 9-13001  
 Ar ion, beat frequency between axial modes, variation with cavity Q 9-8616  
 Ar ion, mode selection using confocal cavity 9-8603  
 Ar ion, pulsed, direct gain meas. 9-4466  
 Ar ion, pulsed, role of two-step excitation 9-8606  
 Ar ion, transverse modes, low order, properties 9-15512  
 Ar ion, using thermionic hollow cathode, operation 9-15511  
 Ar ion laser, new capillary structure for improved reliability and lifetime 9-15510  
 BCl<sub>3</sub> 9-4468  
 C<sup>14</sup> O<sup>18</sup>O<sub>2</sub>, transitions, obs. and calcs. 9-6514  
 CO<sub>2</sub>-He, static, cw, long life 9-15518  
 CO<sub>2</sub>-N<sub>2</sub>-He, gain, on individual rotation-vibration transitions at 10.6  $\mu$  9-15517  
 CO<sub>2</sub>-N<sub>2</sub>, simultaneous laser action of CO<sub>2</sub> and N<sub>2</sub>O mols. 9-8608  
 CO<sub>2</sub>-N<sub>2</sub>, vibrational relax. data, kinetic model, review 9-15509  
 CO<sub>2</sub>, electron energy distrib. in discharges used for CO<sub>2</sub> lasers 9-18298  
 CO<sub>2</sub>, use of focussed radiation for plasma production 9-890  
 CO<sub>2</sub>, influence of CO on performance 9-20507  
 CO<sub>2</sub>, sealed system, heated Pt wire effects 9-16235  
 CO<sub>2</sub> laser, sealed-off single frequency amplifier, characteristics 9-19143  
 CO<sub>2</sub>, beam profile recording using foamed polystyrene 9-13010  
 CO<sub>2</sub>, C.W., characts. for CO<sub>2</sub> and air-CO<sub>2</sub>, obs. 9-17870  
 CO<sub>2</sub>, for self broadening coeffs. of CO 9-4921  
 CO<sub>2</sub>, generation intensity distrib. along rotational lines, effect of pumping 9-8610  
 CO<sub>2</sub>, high power c.w. 9-8609  
 CO<sub>2</sub>, investigation of pulsed excitation 9-13012  
 CO<sub>2</sub>, investigation of pulsed excitation 9-2373  
 CO<sub>2</sub>, Lamb dip and rotational competition study, stabilization and gas absorption coeff. meas. appln. 9-13009  
 CO<sub>2</sub>, level relax. induced by chopped 10.6  $\mu$ m radiation 9-17871  
 CO<sub>2</sub>, linewidth by step response meas. 9-8607  
 CO<sub>2</sub>, mode-locking by intercavity loss modulation 9-15516  
 CO<sub>2</sub>, power increase on proton irradiation 9-15507  
 CO<sub>2</sub>, Q-switching techniques, effects on output pulses 9-13003  
 CO<sub>2</sub>, review 9-15514  
 CO<sub>2</sub>, rotational level competition 9-13004  
 CO<sub>2</sub>, single-frequency, 20-watts, using master oscillator-power amplifier technique, for high-frequency stability and high power 9-15519  
 CO<sub>2</sub>, small-signal step response and linewidth meas. 9-13005  
 CO<sub>2</sub>, vibrational levels population inversion calcs. 9-13008  
 CO<sub>2</sub> Q-switched, nonlinear amplification characts. 9-10860  
 CO<sub>2</sub> unsaturated gain meas. in gas discharge 9-13007  
 CO<sub>2</sub> with Xe and H<sub>2</sub> additives, life and power output studies 9-13011  
 CO<sub>2</sub>-N<sub>2</sub>-He, output 80W 9-17869  
 Cd 4416Å, <sup>112</sup>Cd, <sup>114</sup>Cd and <sup>116</sup>Cd isotope shifts meas. using enriched isotopes 9-20508  
 Cd ion, CW oscillation at 3250 Å 9-20509  
 Cd ion vapour, continuous wave 9-17872  
 Co oscillator, ultrastable 9-15520  
 Co: single-mode high-power 9-13006  
 Cu vapour, MHD, electrically accelerated, pulse broadening 9-20510  
 D<sub>2</sub>O vapour, new emission 9-6515  
 D<sub>2</sub>-Cl<sub>2</sub> explosion, and DCl 9-2374  
 H<sub>2</sub>, Raman, pulses, temporal shape analysis using steady state theory 9-19141  
 H<sub>2</sub>, molecular vacuum u.v. theory 9-15521  
 HCN, duration by pulsed discharge in seal-off tube 9-16782  
 HCN, emission line at 12.85  $\mu$ m 9-2869  
 HCN, long-time operation by pulsed discharges in seal-off tube 9-20511  
 HCl-CO<sub>2</sub>, for excited vib. fluorescence of HCl mixtures 9-15854  
 H<sub>2</sub>O vapour, proposed transition assignments, exp. test 9-8611  
 H<sub>2</sub>O vapour, pulsed Brewster window, operating between 20 and 120  $\mu$  9-13013  
 H<sub>2</sub>O vapour, relaxation phenom. 9-8612  
 He-Ne, 3.39  $\mu$ m, state mixing effects prod. by optical freq. fields 9-2816  
 He-Ne, 6328 Å, incorporating Ne absorption, single-mode power 9-20514  
 He-Ne, as absolute wavelength standard, problem 9-13014  
 He-Ne, anomalous circular polarization of 1.523  $\mu$ m line 9-6520  
 He-Ne, atomic collisions with impurity gas (Ar, Kr or Xe) 9-19145  
 He-Ne, competing-wavelength interaction 9-10862  
 He-Ne, discharge tube, low-noise, for elimination of discharge modulation noise 9-20517  
 He-Ne, freq. of oscill. shift, by discharge current increase 9-6518  
 He-Ne, frequency fluctuations and determ. of natural width of spectral line 9-14428  
 He-Ne, frequency reproducibility stabilizati on at 0.63  $\mu$ m 9-13016  
 He-Ne, linewidth of transition, collision broadening effect, mag. reson meas. 9-10861  
 He-Ne, longitudinal and transverse modes, simultaneous phase-locking 9-6505  
 He-Ne, Michelson type interferometer, deformable bodies collision processes obs. 9-20535  
 He-Ne, mode-locking by regenerative r.f. feedback 9-4469  
 He-Ne, negative Faraday rotation obs. and Doppler line width derived, 3.39  $\mu$ m 9-4470  
 He-Ne, optical mixing dynamics in i.r. detection 9-12850  
 He-Ne, optical sampling of pulse by Nd:glass laser 9-6531  
 He-Ne, phase locking phenomena of multitransverse, longitudinal modes 9-13017  
 He-Ne, power saturation at 6328 Å 9-2375  
 He-Ne, ring and normal, mode-power spectra obs. 9-20515  
 He-Ne, self locking of three modes 9-8614  
 He-Ne, single-mode oscillations, buildup at excitation levels significantly above threshold 9-20516  
 He-Ne, stimulated emission at 6401 Å, lens effect of Ne 1s<sub>5</sub> metastable states 9-20520  
 He-Ne, transitions of 2 modes to same lower level, mutual influence 9-6517  
 He-Ne, transitions of 2 modes to same lower level, mutual influence 9-6516

**Lasers continued****gaseous continued**

- He-Ne, with 3 mirrors, radiation generation at 0.63 and 3.39  $\mu$ m 9-6519  
 He-Ne beat frequency between axial modes, variation with cavity Q 9-8616  
 He-Ne intensity of single-mode as a function of cavity Q deviations explicacly-Lamb theory 9-8617  
 He-Ne mode-coupling effects in mode-selection expts. 9-4471  
 He-Ne multimode, gain interaction and dynamical behaviour 9-8613  
 He-Ne with Ne absorption discharge cell in cavity, mode selection and self-locking 9-13015  
 He-Ne, emission line intensities modification rel. to Ne population inversion, obs. 9-17873  
 He-Ne ring, optimum gas mixture ratio 9-15522  
 He-Ne with 4 mirror T form resonator, longitudinal vibration selection 9-20518  
 I, c.w. emission at eight wavelengths between 3.0 and 9.0  $\mu$ m 9-13018  
 I and Cs vapour, chemical reactions used for depletion of ground state population, patent 9-8618  
 Kr, continuous u.v.-power in watt range 9-6512  
 Kr, continuous u.v.-power in Watt range 9-6512  
 Kr<sup>+</sup>, upper laser states 9-19146  
 Kr ion laser investigated 9-8605  
 N<sub>2</sub>, second positive system, laser transitions in 0-0 band 9-19422  
 N<sub>2</sub>O, c.w. oscillations in rotation-vibration transitions 9-20519  
 N<sub>2</sub>, high power, design considerations 9-10863  
 N<sub>2</sub>O molecular, parameters meas., compared with CO<sub>2</sub> laser 9-13019  
 Ne, 3.39  $\mu$ m line width from Lamb-dip 9-17874  
 SO<sub>2</sub>, with He addition, submillimeter, generating at 0.141 and 0.193 mm 9-244  
 Xe, gas pressure control method 9-13020  
 Xe, isotope shift of 20 i.r. lines 9-15811
- liquid**  
 cryptocyanine dyes, polarized emission of laser radiation 9-4473  
 dye, temperature tuning Q-switched ruby laser pump 9-2376  
 dye solution flashlamp-pumped, frequency and time dependent gain characteristics 9-4472  
 dye-solution, pumped by a dye laser 9-2377  
 organic dye, characteristics 9-15523  
 organic dye, characts. as tunable light sources for nsec absorption spectroscopy 9-20562  
 organic dye, flashlamp pumped, theoretical and experimental studies 9-13021  
 organic pigment solns. generation intensity, calc. 9-18366  
 organic pigment solns. generation intensity in reson. transverse mode, calc. 9-15524  
 organic-dye, continuously tunable picosec. pulse 9-8620  
 phthalimide in pyridine solns., wideband quantum output 9-9536  
 Q-switching, Bragg refl., from phase grating 9-8629  
 rhodamine, cooled alcohol solns. laser action 9-2378  
 H<sub>2</sub>O, power meas. in far i.r. using liq. load calorimeter 9-17875  
 I, Q-switched, energy increase by Zeeman splitting 9-19147  
 ND<sup>+</sup>/SeOCl<sub>2</sub>, soln. prep. 9-14431  
 Nd:SeOCl<sub>2</sub> as high-power nonlinear amplifier 9-16775  
 Nd<sup>3+</sup>:SeOCl<sub>2</sub>, operating props. 9-13023  
 Nd<sup>3+</sup>:SeOCl<sub>2</sub>, Q-switching and mode-locking 9-8621  
 Nd<sup>3+</sup>:POCl<sub>3</sub> 9-14430  
 Nd in SeOCl<sub>2</sub>, circulating, components and characts. 9-13022  
 Nd<sup>3+</sup> in SeOCl<sub>2</sub> aprotic solvent, quantum yield and quenching 9-17876
- semiconductor**  
 axial modes self-synchronization with external mirror 9-13034  
 diodes spontaneous emission linewidth rel. to temp. 9-246  
 emission spectra, temp. effect 9-20527  
 with external resonator, rel. to power and directivity of coherent radiation 9-14436  
 impact ionization and radiative recombination of ionized particles, device configuration, patent 9-16786  
 with non-uniform excitation, threshold characts. 9-17877  
 picosecond pulse generation 9-13034  
 pulsed injection, with Fabry-Perot cavity, theoretical max. of power efficiency 9-6528  
 spectrally inhomogeneous, generation 9-4481  
 AlAs GaAs system, coherent radiation from epitaxial heterojunction structure 9-10868  
 CdS electron-beam-pumped, standing waves and single-mode room temperature laser emission 9-19151  
 GaAs:Te(Zn diffusion) injection, threshold current density doping conc. dependence 9-8626  
 GaAs-InAs diodes solid-soln., separate lines in rad. spectrum 9-8628  
 GaAs, bistable operation characts. 9-2382  
 GaAs, C.W. correlation between laser emission noise and voltage noise 9-20528  
 GaAs, c.w., noise 9-247  
 GaAs, e. beam excited, output power and efficiency 9-2381  
 GaAs, electron-beam pumped, threshold current density and emission spectra, temp. depend. 9-4483  
 GaAs, junction, gain factor and internal loss, annealing and compensation eff. 9-4482  
 GaAs, laser transitions and photon energy 9-3847  
 GaAs, modulation in an external resonator 9-19153  
 GaAs, Zn diffusion gr p-n junction production 9-17285  
 GaAs injection, characts. 9-19154  
 GaAs injection, construction for cw operation at high temps. 9-8627  
 GaAs injection, threshold current density, effect of external optical coupling 9-4484  
 GaAs junction, resonant modes, comparison of theoretical and experimental results 9-19152  
 GaAs p-n junction, with nonlinear passive element in resonator, charact. features of radiation 9-17878  
 GaAs p-n junction injection, characts., obs. 9-15531  
 In-AlAs:Te, injection laser, self modulation obs. 9-254  
 InAs diode lasers, generation threshold dependence on resonator length 9-15532  
 InAs use in i.r. detector response time meas. 9-2383  
 InP, field injected, stimulated emission obs. 9-15533  
 pbi-xSn<sub>2</sub>Te:Bi diode with low threshold currents 9-20529  
 PbS<sub>1-x</sub>Se<sub>x</sub>, generation of coherent laser radiation, 4-6.5  $\mu$ m range 9-2384  
 PbSe hydrostatic pressure tuning from 8-22  $\mu$ m 9-6529
- solid**  
 fluorescent material, beam of narrow elongate cross section, patent 9-16784

**Lasers continued**  
**solid continued**

- glass, neodymium-doped, exposure to nuclear radiations, efficiency increment study 9-19150
- glass, Q-switched, as high-power nonlinear amplifier 9-16775
- glass rod, compensation for pump induced distortion 9-19148
- light pulses, ultra-short, from fluctuation intensity spikes 9-13027
- mode selection, off axial, caused by nonuniformity of excitation 9-20521
- Nd, pulsed, rangefinding appl. 9-15526
- operation with non-parallel mirrors 9-15525
- plural fiber, energy output beam of uniform conditions, patent 9-16783
- pulsed, four-level, operating characteristics 9-4474
- pumping chambers, spherical and ellipsoidal, optimum design 9-10865
- radiation, nonstationary, and effect of energy redistribution between modes 9-4475
- rare-earth and transition-metal ions in crystals, multiphonon orbit-lattice relaxation of excited states 9-13024
- Rayleigh scatt. of ruby light in neutral gases, depolarization raton determ. 9-9453
- review 9-13026
- ruby; losses, passive and active, meas. 9-8625
- ruby, 'Czochralski', degradation of energy output of a long pulse 9-15528
- ruby, assembly, two-frequency generation, near and far zones 9-8624
- ruby, Czech made, basic parameters and properties 9-13030
- ruby, diffraction modulator utilizing standing ultrasonic waves 9-13029
- ruby, experimental upper limit to time of nonradiative relaxation between  $^4\text{T}_2$  and  $^2\text{E}$  states 9-12851
- ruby, exposure to nuclear radiation, efficiency increment study 9-19150
- ruby, mode locking and ultrashort pulses induced by molecular liquids 9-6523
- ruby, mode-locked, achievement of minimum attainable pulse duration 9-20501
- ruby, optical homogeneity rel. to radiation divergence 9-5885
- ruby, Q-switched, enhancement of reflectivity of semiconductors 9-15163
- ruby, Q-switched, prod. 300 MW pulse 9-10866
- ruby, Q-switched, single-mode passive, dynamic behaviour 9-14432
- ruby, Rayleigh scatt. by neutral gases and depolarization 9-14435
- ruby, saturable dye filte, behaviour study 9-13028
- ruby, self Q-switching at 77°K 9-12852
- ruby, spectrum of pulse observed at output of photodetector 9-4477
- ruby, spherical resonator, generation astrophysics 9-15527
- ruby, two-rod assembly, reln. between output and design parameters 9-8623
- ruby component generation 9-14433
- ruby crystals, optical homogeneity, surface and volume scattering, surface-damage connection with laser-emission characteristics 9-20522
- ruby spectrum narrowing, internal freq. modulation 9-4478
- single mode, with reflecting cavity and polariser, patent 9-16785
- spiking, characts. and analysis 9-2379
- subharmonic generation, and prod. of difference freq. in far i.r. 9-6532
- theory, book 9-14023
- theory of action involving free excitons and LO-phonon assisted transitions 9-6522
- ultrashort-light pulse generation and meas. by mode-locking of Nd:glass laser with saturable dye 9-14427
- zero reflectance of laser materials by use of thin dielectric films 9-10864
- $\text{CaF}_2:\text{Dy}^{2+}$  and  $\text{CaWO}_4:\text{Nd}^{3+}$  crystals, sun-pumped, 130 mW power output. 9-13031
- $\text{CaF}_2:\text{Dy}^{2+}$  cryst, giant pulses, generation using  $\text{LiNbO}_3$  cryst. electro-optical shutter 9-1723
- $\text{CaF}_2:\text{Sm}^{2+}$ , loss evaluation rel. to light scatt. effect 9-8599
- Cd (II), efficient CW oscillation at 4416 Å 9-6530
- CdS, 260 keV electron beam pumping, stimulated emission to  $3 \times 10^{16} \text{ W/cm}^2$  9-20523
- CdS, theory of action involving free excitons and LO-phonon-assisted transitions 9-6522
- CdSnP<sub>2</sub> laser, e beam excited 9-245
- $\text{Ho}^{3+}$  ions, in silicate glass, coactivated by Ho, Er, Yb 9-4476
- Nd:CaWO<sub>4</sub>, slowly Q-switched, output characts. 9-10867
- Nd:glass, giant pulse production using harmonic pumping 9-19149
- Nd:glass, optical sampling of He-Ne pulse 9-6531
- Nd:glass, subpicosecond structure in relax. oscills. 9-20525
- Nd:glass oscillator, spectral control by secondary light sources 9-13032
- Nd:YAl garnet, repetitive Q-switching in continuously pumped laser using Fabry-Perot interferometer 9-13033
- Nd:glass, single mode-locked optical pulse selection and amplification 9-6524
- Nd:glass, time energy characts. and peak separation effect d focusing elements in resonator 9-6526
- Nd:glass, two channel, single pulse, 180 joule output 9-19160
- Nd:glass, two rod assembly, reln. between output and design parameters 9-8623
- Nd:glass emission, rel. to generation in polymethine dye solns. 9-1014
- Nd, dynamic emission under nonuniform broadening conditions 9-4480
- Nd, glass, circularly polarised modes in resonator 9-2380
- $\text{Nd}^{3+}:\text{Ca}_3(\text{PO}_4)_2$ , stimulated emission at 300°K 9-18709
- $\text{Nd}^{3+}$  doped, active resonator, e.m. coupling with glass fibre waveguide 9-14434
- $\text{Nd}^{3+}$  glass, passive transverse mode locking by dye technique 9-20524
- Nd 6-Gigawatt 9-13025
- Nd glass, 1 GW, design 9-4479
- Nd glass, compression of picosecond light pulses 9-6525
- Nd glass, continuous shift in emission band 9-15529
- Nd glass, plasma production, optical measurements 9-18294
- Nd glass system, electro-optical shutter, subnanosecond risetime 9-17882
- Nd pumping efficiency, effect of rare gas spectra 9-15530
- $\text{Nd}^{3+}$  in Ba<sub>2</sub>MgGeO<sub>7</sub>, and optical spectra 9-5914
- $\text{SrF}_2:\text{Dy}^{2+}$ , threshold and quantum efficiency rel. to Dy conc. and distrib. 9-7990
- YAl garnet:Nd, non-mode-locked, two photon fluorescence displays 9-6527
- YAl garnet:Nd<sup>3+</sup>, efficiency, influence of pump-power level and pump light spectral filtering 9-20526
- $\text{Y}_2\text{Al}_2\text{O}_7:\text{Nd}^{3+}$ , laser emission threshold 9-5955

**Latent heat** *see Heat of adsorption, etc.; Thermodynamic properties***Latent heat**  
*See also Heat of adsorption; Thermodynamic properties*  
No entries**Latent image** *see Photographic process***Lattice constants** *see Crystal structure, atomic***Lattice dynamics** *see Crystals/lattice mechanics***Lattice energy** *see Bonds; Crystals; Solids***Lattice gas** *see Statistical mechanics***Lattices theory and statistics**

- antiferromagnet, uniaxial, ground-state energy lower bound 9-12306
- Bethe, using one-dimensional Ising model with general spin 9-1650
- carbonates, calcite-type, relation between cation-O distance and vibration frequency  $\nu_4$  9-19681
- dimer problem reformulation 9-87
- dimers and monomers on rectangular lattice, matrix equations 9-4246
- dynamic response of solids induced by charged particle interaction, laser interferometric determination 9-17348
- ferromagnet, Heisenberg anisotropic, domains 9-10116
- formation from molecular base-gas, anal. 9-4247
- gas, hard square, phase transitions 9-20369
- Heisenberg anisotropic model, reduced density matrices, integral eqns. determ. 9-17732
- Heisenberg ferromagnet, impure, magnon low-energy resons. 9-5813
- Heisenberg model, anisotropic, Green's function study 9-20336
- international symmetry symbols, desirable modifications 9-6291
- Ising, pair correls. asymptotic props. at critical point 9-6327
- Ising chain, nearest neighbour one-dimensional extended for arbitrary finite range 9-17733
- Ising membranes, stochastic growth, form and steady-state props. 9-20337
- Ising model, calc. of three-state correlation functions 9-4245
- Ising model, difference eqn. solns. 9-4244
- Ising model, Lee-Yang model proved in spin-1 case 9-12265
- Ising model, modified admittance, perpendicular susceptibilities, transform. of correls. 9-17734
- Ising model, near transition point, magnetization decay on removal of magnetic field 9-3783
- Ising model, one-dimensional, with general spin 9-1650
- Ising model, theory 9-17735
- Ising model, zeros of partition function lie on unit circle 9-10645
- Ising model for helix-coil transitions of helical macromols. 9-19486
- Ising model in one dimension with arbitrary spin, low temperature behaviour 9-2166
- Ising model with non-magnetic impurities, decorated, exact solution 9-4248
- Ising problems, spin-1/2 and spin-1, weak graph method of obtaining series expansion 9-8424
- Ising spin system, dilute, temperature dependent distribution of field and magnetic susceptibility 9-7884
- Ising system approximate method 9-2165
- iteration calc., parametric speeding-up method 9-12869
- Kagome lattice, modified Slater model 9-5265
- lattice gas, 1D, stat. mech. 9-14351
- linear, eqns. of motion, soln. in Schrodinger co-ords. 9-8414
- long range potential system, rigorous treatment 9-20338
- phonon propagator structure, anharmonic crystal 9-5527
- quasilattice, uncoherent, and fixed-point theorem for snake-wise-connected spaces 9-12890
- random, exact form of first-order self energy 9-2167
- random spin systems interacting via Heisenberg or Ising interaction 9-8425
- spin correlation functions of the X-Y model 9-7893
- spin system, Hamiltonians of Ising and Heisenberg 9-2164
- vector lattice, properties 9-8426
- weak sub-graphs, combinatorial theorem for p generating functions 9-12892
- weak graph method for obtaining series expansions 9-8424
- Ar crystal, improved self-consistent phonon approx. 9-5530
- Ne crystal, improved self-consistent phonon approx. 9-5530

**Laves phases** *see Alloys; Phase transformations/solid-state***Lawrencium**

No entries

**Lawrencium compounds**

No entries

**LCAO calculations** *see Molecules/electronic structure; Orbital calculation methods***Lead***See also Superconducting materials/lead*

- anodic dissolution, in aqueous solutions 9-21714
- anticathode, primary X-ray emission, distrib. in depth 9-5946
- atom,  $\gamma$ -ray total cross sections, 280 keV 9-16999
- atom, incoherent  $\gamma$ -scatt. on K shell electron obs. 9-712
- atom, nuclear orientation attempt by optical pumping 9-9139
- atoms spectrum, hollow cathode discharge obs. 9-18134
- complex in boiling mixture separation by chromatography followed by spectrophotometric determ. 9-18779
- conductivity in normal state from meas. on superconductor 9-9933
- crystal Gruneisen parameters, phonon freq. press. depend. calc. from pseudopotential models 9-7640
- crystal-melt system surface temp. distrib. meas. device rel. to solidification obs. 9-3237
- evaporation rate and film thickness meas. by ionization gauges 9-21264
- film, vacuum deposited, oxidation, 227-307°K 9-20048
- films, resistive transition rounding 9-16232
- grain growth, impurity-drag eff. 9-11888
- heat capacity using adiabatic calorimeter in range 25-500°K 9-12014
- isotope analysis, review 9-8115
- isotopic standards, common, equal-atom and radiogenic, abundance ratios 9-20902
- lattice dynamics, three-body forces in calc. 9-16168
- liquid, ordered structural region size estimation by X-ray scatt. 9-17187
- melt struct., Mg impurities, nucl. reson. fluoresc. study 9-7278
- molten, sound absorpt. temp. depend. showing existence of dilatational viscosity 9-5163
- muonic atom, new dynamical effect 9-4891
- muonic atom, transition intensity calc. of Eisenberg-Kessler type 9-11430
- neutron radiographic scatter factors 9-2801
- neutron scatt., extinction of Bragg reflection, temp. depend. 9-21306
- nuclear spin interactions, indirect, relativistic calcs. and theory 9-9880
- phonon/neutron cross section 9-7691
- photo voltaic effect of contact with tellurium thin film 9-17446
- position annihilation, radiationless 9-12081
- powder particle formation during atomization by gas stream 9-5221
- scattering of 9 and 15 MeV bremsstrahlung 9-11267



**Lead continued**

- self-sputtering energy efficiency 9-9870  
 solid and liq. mag. susceptibility 9-21563  
 stacking fault energy calc. with energy wave-number characteristic 9-5375  
 strain hardening, eff. of strain rate 9-13744  
 strength, alloying additions (Sb, Cu, Te) effect 9-1303  
 superconducting thin films, critical temp. gradient and critical current density 9-18609  
 superconducting transition temp. pressure dependence 9-9959  
 superconductor, d.c. Josephson effect rel. to strong-coupling 9-12131  
 superconductor, type II magnetic flux penetration depend. on surface condition 9-13861  
 surface, specular low-energy electron beam scatt. 9-11760  
 thermodynamic props., anharmonic effects, data anal. 9-21434  
 vacancies, relaxation props., under quasi-equilibrium conditions 9-19743  
 vapour infl. on Cu surface self-diffusion 9-17284  
 weak transitions meas., nuc. polarization by  $\mu$ , muonic x-ray emission 9-17009  
 X-ray absorpt., 6MV primary radiation 9-7681  
 X-ray Debye temp. from n. scatt. obs. 9-7639  
 zone-refined, grain growth kinetics, mechanisms 9-3304  
 $\epsilon$  cosmic ray cascade calc. of equilibrium ang. distrib. function 9-15664  
<sup>210</sup>Pb, chemical determ. by radioactive analysis 9-10369  
<sup>212</sup>Pb, charged and neutral, attachment coeffs. to polystyrene latex aerosols 9-9565  
 ions, eff. on photographic process 9-20567  
 Pb/Th superimposed films, superconducting proximity effect 9-17384  
 Pb-H<sub>2</sub>O system n yield under bombard. by 400, 500 and 660 MeV p 9-19364  
 Pb\* implantation in Al rel. to formation of precipitate phases 9-11956  
 Pb<sup>2+</sup> diff. in cubic Li<sub>2</sub>SO<sub>4</sub>, 600-800°C 9-17288  
 PbSe laser tuning by hydrostatic pressure from 8.22  $\mu$  9-6529  
 Pb-BiCl<sub>3</sub> molten mixtures, absorption spectra for reaction study 9-13531  
 Pt-Pb discharge, atoms reson. interaction, obs. 9-18134

**Lead compounds**

- $\infty$  Ab(Zr,Sn,Ti)O<sub>3</sub> solid solutions, with properties depending on applied elect. field, expt. study 9-10046  
 $\beta$ -diketon chelates, emission vibronic structure 9-13342  
 glass, thermal self focussing of Ar laser beam 9-8630  
 perovskites, high-pressure synthesis and structure 9-18452  
 2PbO.SiO<sub>2</sub> glass, struct. and phase transforms.C,0from $\alpha$ .r. spectra 9-7321  
 Au-Pb alloys, interstitial sites from e. emission angular distrib. of activated mat. 9-3332  
 BaTiO<sub>3</sub>.PbTiO<sub>3</sub> single cryst. solid solns., dielec. and elastic props. 9-12196  
 Bi-Pb alloys, dilute, differential Shubnikov-de Haas effect 9-7726  
 Bi-Pb and Bi-Sb-Pb alloys, electron transitions, pressure-induced, 4.2-295°K 9-9892  
 Hg-(0.5-1at%)Pb liq., struct. from X-ray diffr. 9-7251  
 In-Pb alloy, supercond., upper critical field, anomalous values 9-1498  
 In-Pb alloys, axial ratio and supercond. transition rel. to Fermi surface interactions 9-21491  
 In-Pb superconducting alloy, thermal conductivity meas. down to 0.4°K rel. to phonon scatt. mechanism 9-21444  
 In-Pb superconducting alloys, type II, specific heat temp. dependence, 1.5-4.2°K rel. to Maki parameter determ. 9-21493  
 In-Pb system, pressure depend. of superconducting critical temp. 9-16246  
 Mg-Pb molten alloys, structure 9-14829  
 Na-Pb liquid alloy, density meas. 9-5145  
 Pb-In(Bi) alloys, dirty type II superconductors, h.f. surface impedance in surface-sheath regime 9-12113  
 (98 at.%) Pb-(2 at.%) In supercond. type-II, flux jump size distrib. 9-1480  
 Pb-Ni alloys, radiation-induced scatt., small angle X-ray and n. scatt. meas. 9-9805  
 Pb-Sn alloy, liquid, ordered structural region size estimation by X-ray scatt. 9-17187  
 Pb-(1.89wt.%) Tl superconducting alloy with Ginzburg Landau parameter near 1/ $\sqrt{2}$ , flux line lattices in intermediate state 9-16248  
 Pb-Tl alloys, type II superconductors, flux pinning by grain boundaries 9-3597  
 Pb-7 at.% Sn cellular reaction kinetics 9-14906  
 (Pb, Sr)-(Ti, Zr)O<sub>3</sub> solid solutions, reaction formation 9-1892  
 Pb<sub>1-x</sub>Sn<sub>x</sub>Te:Bi diode laser with low threshold currents 9-20529  
 Pb<sub>2</sub>(OH)Cl<sub>3</sub>, penfieldite, crystal structure 9-18451  
 Pb<sub>2</sub>Sn<sub>1-x</sub>Te alloys, cation-rich, excess carrier conc., comp. and annealing temp. dependence 9-3634  
 Pb as TlOs, supercond. thermal dissipation 9-1490  
 Pb glass, fracture surface energy 9-1306  
 PbBr, molecule, emission spectrum up to 6100 Å, dissociation energy calc. 9-4936  
 PbBr<sub>2</sub>, molten, specific elec. conductivity, 370°-900°C 9-19640  
 PbBr mols. A-X system rot. analysis, obs. 9-4935  
 PbCl<sub>2</sub>+ACl, (A=Na, K, Rb, Cs), mixtures, mass spectra of vapours rel. to thermodynamic props. 9-19442  
 PbCl<sub>2</sub>, thermoluminesc. and luminesc. 9-10253  
 PbCl<sub>2</sub>+ACl, (A=Na, K, Rb or Cs), electron-impact ionization 9-9408  
 PbCrO<sub>4</sub>, natural and artificial single crystals, optical props. 9-17473  
 PbF<sub>2</sub>, u.v. absorpt. spectra 9-9236  
 PbF<sub>2</sub> as low-pass n. vel. filter, high transmission  $\lambda_0=1.35\text{Å}$  9-11105  
 PbHg, type II superconductor, interaction between vortex lines and ferro-mag. inclusions 9-9958  
 PbI<sub>2</sub>, electroabsorption and electroreflectance near fundamental edge 9-12350  
 PbI<sub>2</sub>, electron diffraction patterns, streak intensity meas., temp. depend. 9-11853  
 Pb(Mg<sub>1/3</sub>Nb<sub>2/3</sub>)O<sub>3</sub>-PbTiO<sub>3</sub>-PbZrO<sub>3</sub> system, antiferro-ferroelec. and ferroelec. 1-2 phase boundaries, obs. 9-7844  
 PbMg<sub>1/3</sub>Ta<sub>2/3</sub>O<sub>3</sub>, electro-opt. props., -150° to +120°C 9-7952  
 PbNe, photo e.m.f. meas. 9-10066  
 PbNi<sub>1-x</sub>Nb<sub>x</sub>O<sub>3</sub>, electro-opt. props., -150° to +120°C 9-7952  
 PbO, based polymorphic systems 9-12457  
 PbO-SiO<sub>2</sub>-K<sub>2</sub>O glasses, u.v.-induced luminescence at 120°K 9-10267  
 PbO, red, vapour-deposited layers, space-charge- limited photocurrent 9-15139  
 PbO, two-phase crystals, photoelec. sensitivity spectra temp. dependence 9-3737  
 PbO thin films, dielec. anomaly rel. to possible ferroelectricity 9-17437

**Lead compounds continued**

- PbO thin films, optical const., forbidden gap width meas. 9-10167  
 PbO<sub>2</sub>, electrodeposition on graphite, nucleation, grain clustering and projections 9-8101  
 PbO.6Fe<sub>2</sub>O<sub>3</sub>, orientation, preferred, increased by sintering 9-19817  
 Pb(OH)Cl formation, i.r. absorption spectra and thermogravimetric anal. 9-21532  
 PbS-PbSe, solid solns., microindentation hardness rel. to comp., obs. 9-7580  
 PbS-PbTe, solid solns., microindentation hardness rel. to comp., obs. 9-7580  
 PbS, electro-optic measurements of band structure 9-7953  
 PbS films, photo e.m.f., angular dependence 9-1615  
 PbS polycrystalline photoresistors, V-I, luminous charact. and absolute spectral sensitivity 9-13935  
 PbS thin films, spectral absorption structure and phase composition 9-14021  
 p-PbSe, carrier mobilities 9-3633  
 PbSe, conduction band dispersion relation 9-3642  
 PbSe, electro-optic measurements of band structure 9-7953  
 PbSe, epitaxial films, optical props. 9-5863  
 PbSe, evaporated films, O<sub>2</sub> effect on photosensitivity 9-5770  
 PbSe, scattering mechanism of current carriers 9-7702  
 p-PbSe, thermopower power dependence on carrier density 9-3724  
 PbSe thin films, spectral absorption structure and phase composition 9-14021  
 Pb<sub>1-x</sub>Sn<sub>x</sub>Te single crystal, photoconductivity, 77°K-4.2°K 9-5769  
 Pb<sub>2</sub>Sn<sub>1-x</sub>Te, resistivity and Hall coeff. temp. dependence, 4-300°K, rel. to band-inversion 9-13890  
 PbTe-PbS solid solns., effective density-of-states mass rel. to carrier density and temp. 9-9897  
 PbTe-PbS solid solutions, valence band structure, from elec. meas. 9-21514  
 PbTe, band gap temp. depend. and Debye-Waller factors 9-9898  
 p-PbTe, diffusion of Ni and Cl, 700°C, junction formation 9-19767  
 PbTe, electro-optic measurements of band structure 9-7953  
 n-PbTe, electron spin-flip Raman scatt. 9-18715  
 PbTe, helicon propag., high-field, anisotropy 9-5631  
 PbTe, intraband Faraday and Voigt eff., behaviour of coeffs.  $g'$ -17475  
 PbTe, microhardness, donor and acceptor impurity dependence 9-1316  
 PbTe, Nerst-Ettingshausen effect, transverse, in mixed conduction region 9-15132  
 PbTe, sublimation data for weight loss at high temps. 9-3159  
 PbTe, thermoelectric design parameters 9-3725  
 PbTe, with Au contacts, elect. props. 9-3652  
 PbTe film on KCl, epitaxial growth mechanism 9-1106  
 PbTe vacancy states, new model 9-19744  
 PbTiO<sub>3</sub>, crystal structure and decomposition 9-19722  
 PbTiO<sub>3</sub> crystals, hydrothermal production kinetics 9-1138  
 PbTiO<sub>3</sub> ferroelec. props. 9-19931  
 PbTiO<sub>3</sub>, Raman spectra 9-12433  
 Pb<sub>60</sub>Tl<sub>40</sub> resistance minimum in supercond. 9-1490  
 PbZn<sub>1/3</sub>Nb<sub>2/3</sub>O<sub>3</sub>, electro-opt. props., -150° to +120°C 9-7952  
 Pb(Zr-Ti)O<sub>3</sub>, crystal growth by flux method 9-1148  
 Pb(Zr-Ti)O<sub>3</sub>, ferroelec., dielectric const. ageing characts. 9-10049  
 Pb(Zr<sub>1-x</sub>Ti<sub>x</sub>)O<sub>3</sub>, charge transport mechanism, 650-1000°K 9-19932  
 PbZrO<sub>3</sub>:Nb<sub>2</sub>O<sub>3</sub> with properties depending on applied elect. field, experimental study 9-10046  
 PbZrO<sub>3</sub>-PbTiO<sub>3</sub>, ferroelec. films, dielectric loss and strength 9-1596  
 PbZrO<sub>3</sub>-PbTiO<sub>3</sub>, reaction kinetics in PbO-ZrO<sub>2</sub>-TiO<sub>2</sub>-Nb<sub>2</sub>O<sub>3</sub> system 9-8098  
 PbZrO<sub>3</sub>-PbTiO<sub>3</sub>, vapourization of hot-pressed pellets, 780-1250°C 9-3156  
 PbZrO<sub>3</sub>-PbTiO<sub>3</sub> piezoelec. transducers for broad-band acoustic noise meas. 10-100 kHz 9-2228  
 PbZrO<sub>3</sub>, lattice dynamic and chemical bonding aspects 9-7625  
 PbZrO<sub>3</sub>, effect of impurity on dielec. phase 9-17436  
 PbZrO<sub>3</sub>, relaxation and spontaneous polarization 9-5748  
 PbZrO<sub>3</sub> solid solns., ferroelec.- antiferroelec. phase changes rel. to elec. field and temp. 9-5751  
 Pb(Zr<sub>1-x</sub>Ti<sub>x</sub>)O<sub>3</sub>, ferroelectric ceramic, polarized optical retardation 9-1743  
 polynuclear metal complex vib. spectra obs. 9-11455

**Leak detection**

- principles and properties of detectors 9-12815  
 He, mass spectrometer, using an electric quadrupole mass filter description 9-8334  
 He, sensitivity improvement by turbo- molecular pump 9-22022  
 He leakproofing control 9-18970  
<sup>85</sup>Kr application in h.p. gas system 9-12806

**Leather** *see* **Materials****Lee model** *see* **Field theory, quantum****LEED** *see* **Electron diffraction; Electron diffraction crystallography; Electron diffraction examination of materials****Length measurement**

- See also Micrometry; Strain gauges; Thickness measurement*  
 'Angstrom ruler', use of X-ray interferometer 9-10608  
 air gauges, noncontacting, for internal dims. of waveguides and transmission lines 9-10777  
 compensation for linear thermal expansion 9-10611  
 displacement meter, capacitance type 9-25  
 displacement transducer, thermally operated 9-24  
 interferometric, using laser 9-2127  
 interferometry, optical, in high precision techniques 9-10610  
 level, using interference 9-4215  
 metre, (m), definition 9-10606  
 metrology methods comparison 9-10605  
 rangefinding with pulsed Nd laser 9-15526  
 transducers, capacitive high resolution 9-2128  
 $\gamma$ -ray source for remote meas. of displacement 9-15414  
 Nd laser, pulsed, rangefinding appl. 9-15526  
 U, n irradiated, change in length 9-3574

**Length standards** *see* **Standards****Lennard-Jones and Devonshire theory** *see* **Liquids/theory****Lennard-Jones potential** *see* **Kinetic theory; Molecules/intermolecular mechanics****Lenses**

- See also Electron lenses*  
 aberration, longit. spherical, meas. using laser 9-4504

**Lenses continued**

- acoustic, cylindrical liq.-filled with large diameter-to-wavelength ratios. focusing props., reply to comments 9-14387  
 acoustic, cylindrical liq.-filled with large diameter-to-wavelength ratios. focusing props., comments 9-14386  
 acoustic, Luneburg, variable density, theory 9-19064  
 acoustic, perfect focusing, spherically symm., characts. 9-19063  
 apochromatic plano-objectives, non-immersion type, design 9-13043  
 compensating eyepieces for flut field microscope objectives, design 9-4530  
 eye, dynamic viscoelasticity 9-18958  
 eye-piece, cross-wire, digitized and telecontrolled, for nuclear emulsion meas. 9-2416  
 eyepiece syst., Huygenian and Ramsden, constructional parameters tolerance 9-8644  
 gas, distortion of shuttled gaussian light pulse, obs. 9-5118  
 gas, hyperbolic-type, focussing power limitation 9-16787  
 gravitational, simulator for demonstration purposes 9-12836  
 holographic Foucault knife edge test 9-2417  
 Huygenian type 2-lens system primary aberrations 9-8643  
 infinitesimally thin, extreme values of spherical aberration, analysis 9-4506  
 ion beam focusing, principles dimensions 9-235  
 magnetic, quadrupole, circular aperture, excitation winding effect on mag. field nonlinearity 9-2328  
 magnetic, quadrupole doublets, periodically arranged, particle transportation channel calcs. 9-225  
 magnetic, system design for particle focusing 9-224  
 magnetic, with longitudinal mag. field 9-225  
 magnetic with sloping circular edges, influence of vertical motion on horiz. 2nd order aberrations 9-6474  
 nonastigmatic, for spectacles, instrument for measuring vertex power 9-4526  
 quadrupole syst. in prism spect., opt. diagrams, spherical aberration 9-2566  
 single element for correction of chromatic aberration 9-2397

**aspherical**

No entries

**photographic**

diffraction-limited lens, problems in photo at diff. limit 9-20564

**Leptons**

- See also Electrons; Mesons; Muons; Neutrinos and antineutrinos*  
 heavy with spin  $1/2$ , observation possibilities 9-10977  
 interaction with  $B^+$ ,  $C^+$  bosons, mass and coupling consts. determ. 9-16824  
 interactions, high energy behaviour of differential cross section 9-4583  
 interactions,  $\pi$  as intermediate boson 9-20600  
 nonconservation, decrease in solar  $\nu$  detection at earth's surface 9-14528  
 quarks in cosmic rad., underground search obs. 9-15653  
 scattering, polarization depend., by hadrons at high energy, review 9-17944  
 scattering due to 4-fermion interaction, nonperturbative treatment 9-17945  
 triplets existence possibility 9-15589  
 weak interactions, high energy, cross section limits 9-8749  
 weak interactions, renormalizable theory 9-335

**Lie groups** *see Group theory. For applications see Elementary particles; Field theory, quantum*

**Ligands** *see Bonds; Molecules*

**Light**

*See also Diffraction; Interference, etc.; Doppler effect; Radiation*

- beam propagation theory, algorithmic Monte-Carlo method 9-2398  
 flux meas. by photon counting 9-10844  
 focussed Gaussian beam through random medium, fluctuation distribution 9-16792  
 gas ionization, cascade, in high-intensity light field 9-15952  
 Gaussian, intensity-fluctuation distrib., choice of observable 9-2393  
 generation at  $BaTiO_3$ -electrode during polarization reversal 9-12346  
 interaction with gases in mag. field, appl. of Bloch-type formalism 9-4848  
 laser, statistical model 9-10847  
 luminance pre-determination in room by digital, analogue and model techniques 9-6538  
 propagation, self-consistent, in resonant medium 9-2394  
 pulses, picosecond, shape asymmetry meas. method 9-8641  
 radiometric scales, international comparison 9-10911  
 resonant scattering of monochromatic light in gases 9-18327  
 Signal analysis after prop. through turbulent atmos. 9-8646  
 tubular ray, wave guide props. 9-8647  
 wave+particle model and laser interference expts. 9-6500  
 wave, plane, strong amplitude fluctuations on moving in randomly nonuniform medium 9-260  
 CdS, exciton, inf. of strong elec. field 9-19988

**coherence**

*See also Lasers*

- aperture-diffraction patterns, when illuminated by partially coherent light 9-15544  
 dielectric medium nonlinear, coherence props. of optical field 9-10846  
 elimination, laser-produced image quality improvement 9-10890  
 e.m. coupling between glass-fibre waveguides and  $Nd^{3+}$ -doped laser resonators 9-14434  
 e.m. field and radiation source structure 9-19103  
 Fabry-Perot interferometers, rel. to equi-inclination bands 9-8651  
 fourth-order functions of fields with phase fluctuations, expt. study 9-10842  
 Gaussian incoherent beam heterodyned with coherent beam, statistics rel. to detection 9-15504  
 and holographic limitations 9-10881  
 interference effect produced by superposition of light from two independent thermal light sources 9-10843  
 laser beam, temporal and spatial appl. high resolution spectroscopy to meas. 9-15556  
 laser light statistics 9-15534  
 laser radiation, space coherence atmos. turbulence dependence 9-2385  
 partial, quasimonochromatic, mutual coherence function of field 9-10926  
 photon emission by many atoms 9-6497  
 pulse propagation in inhomogeneously broadened medium 9-16774  
 quartz, generation of 100W coherent optical phonons 9-12320  
 scattered in many level system, resonance variation of props. 9-8638

**Light continued****coherence continued**

- scattering, known coherence function, eqn. for intensity derived 9-8655  
 surface properties, reln. with radiometric props. 9-10910  
 temporal, complex degree, phase determ. from modulus meas. 9-10841  
 thermodynamical formulation of optical field 9-10839  
 ultrashort pulse generation and meas. by mode-locking of Nd: glass laser with saturable dye 9-14427

**electromagnetic theory**

- 'source-free' wave fields, expansion and props. 9-256  
 angular spectrum of plane waves representation, equivalence to a Rayleigh integral transform 9-10902  
 classical theory of nonideal, coherent beams 9-2278  
 classical theory of nonideal, coherent beams 9-12956  
 coherence of e.m. field and radiation source structure 9-19103  
 field components E and H in Maxwell boundary value problems, simplified calc. 9-6412  
 scattering, known coherence function, eqn. for intensity derived 9-8655  
 scattering, transient luminescence of optical layers, kinetics analyzed 9-8648

**modulation**

- atom mag. resonance induction, theory 9-4858  
 in filaments, trapped, self-modulation, self-steepening and spectral development 9-13526  
 frequency, of spectra, device 9-6561  
 frequency, of spectra, device 9-15557  
 Fresnel images correl. by collinear heterodyning of Fresnel images 9-10887  
 laser, self-trapped filaments, sinusoidal phase modulation 9-4498  
 laser beam, by electrooptic Doppler shift, spectrum anal. 9-4497  
 laser beam, photon counting distributions 9-248  
 lasers, by u.s. waves of two freqs. 9-4452  
 multi-beam interferometer application 9-2395  
 optical amplitude modulator used as signal-frequency converter 9-13039  
 optical rad. nonlinear distortion by Kerr cell 9-4488  
 Pockels cell, r.f., wide angle rad. 9-12347  
 pulse shape distortion by self-focusing 9-10871  
 ruby laser, internal freq. modulation and spectrum narrowing 9-4478  
 sequential encoding with multislit spectrometers 9-10884  
 signal detection optimum shape, limited peak power 9-8640  
 u.s., operation of modulator under random elec. excitation 9-2392  
 u.s. diffraction modulation in crystals, loss effects 9-10162  
 $^{44}S^{2+}$  Zcut, temp. depend. of modulation degree 9-12338  
 CO<sub>2</sub> laser, chirped pulses generation at 10.6 microns 9-4500  
 GaAs diode laser, modulation in an external resonator 9-19153  
 GaAs reflectance, modulation by surface field obs. 9-10172  
 n-InAs:Te, injection laser, self modulation obs. 9-254  
 K, transmitted intensity modulation at 462 MHz 9-9130  
 LiNbO<sub>3</sub>-based electro-optical shutter, Q-modulation for giant pulses on CaF<sub>2</sub>:Dy<sup>3+</sup> 9-1723  
 LiNbO<sub>3</sub>, second harmonic generation by Nd:glass laser, psec pulses 9-10173  
 $^{87}Rb$  vapour, optically pumped, microwave modulation 9-679

**quantum theory** *see Photons; Quantum electrodynamics; Quantum theory*

**velocity** *see Velocity/light*

**Light guides** *see Optical instruments*

**Light modulation** *see Light/modulation*

**Light sources**

- See also Lasers; Monochromators; Photometry/light sources; Spectroscopy/light sources*  
 3-aminophthalhydrazide, chemilum. applic. to sensitometry 9-20565  
 correlated colour temperature and distribution temperature, computer calculations 9-10913  
 flash lamp, demountable, for photolysis work 9-13067  
 flash lamps, evaporographic study of energy field 9-4534  
 heat-reflecting filters composition, patent 9-13068  
 high-borate glass for Na vapour lamp, patent 9-8666  
 hollow cathode discharge lamp, excitation temp. in negative glow light 9-9413  
 luminescent semicond. junctions 9-17486  
 milliwatt, for use with precision photometer 9-20552  
 pulsed illuminator of rapid rate, using halogen discharge 9-6557  
 quartz- $\Sigma$ , W filament lamp, polarization anisotropy, obs. 9-276  
 quasimonochromatic, partially coherent, mutual coherence function of field 9-10926  
 semiconductor diodes 9-12166  
 terrestrial, satellite comparison 9-21751  
 u.v., low-voltage discharge source 9-2414  
 u.v., pulsed, radiation energy calibration, obs. 9-15550  
 vacuum u.v. gas mixture flow lamps, microwave excited 9-8665  
 $^{13}C$ s point source near air-ground interface, scattered photons spectral obs. 9-19189  
 $^{60}Co$  point source near air-ground interface, scattered photons spectral obs. 9-19189  
 Cs vapour discharge, radiation charact. 9-17893  
 GaAs:P semiconductor diode 9-12166  
 GaP semiconductor diode 9-12166  
 I monochromatic lamp devel., 2062Å emission line at 0.5 torr. 9-4535  
 K vapour discharge, radiation charact. 9-17893  
 Li vapour discharge, radiation charact. 9-17893  
 Na vapour discharge, radiation charact. 9-17893  
 Xe discharge tubes, pulsed, series and parallel connection, obs. 9-11629  
 Xe pulse lamps, double current pulses, emission 9-2415  
 ZnTe with photo-n-p junctions, light-emitting mechanism 9-10083

**Lighting** *see Illumination*

**Lightning**

- ball, and radioemission from linear 9-21778  
 charge transfer, atmospheric, by point discharge 9-18802  
 charge transfer, magnetographic meas. 9-8177  
 discharges rel. to atmospheric press. var., hot wire microphones obs. 9-10385  
 excess point-discharge currents, local potential grad. around point 9-21118  
 leader, stepped, slitless spectrograph obs. 9-21777  
 linear, decimeter radioemission 9-21779  
 relaxation theory of stepped leaders, lab. corroboration 9-4059  
 stepped leader stroke, verification of space wave of potential gradient 9-8176  
 stroke, pressure pulse 9-14164

**Linear accelerators** *see Particle accelerators/linear*



**Linewidths** *see Spectral line breadth*

**Liouville equation** *see Statistical mechanics*

### Liquefaction, gases

*See also Low-temperature production*

method involving heat transfer which reduces cost, patent 9-16647

He, liquifier construction and operation 9-11731

He, methods, types of liquefier and facilities in the U.S. 9-7294

### Liquid crystals

alkoxybenzoic acids, H-D isotope effect 9-3982

anisol p-aminoazobenzene, static dielec. const., influence of mag. and elec. fields 9-11684

p-azoxyanisole, e.p.r. study of radicals 9-7086

benzenes, ortho-disubstituted, dissolved in nematic phase, n.m.r. 9-7280

cholesteric phase, relevance of optical effects to thermal mapping 9-3098

cholesteric, 2-component film, internal helical structure pitch depend. on composition 9-18352

cholesteric, reflective optical storage, electric field control 9-3099

cholesteric, some thermal effects 9-19608

cholesteric mesophase struct. study using second harmonic generation of light 9-21207

cholesteric-to-nematic phase transition, magnetically induced, optical obs. 9-14831

cholesteryl myristate, mesophases, light scatt. rel. to orientation 9-14851

cholesteryl myristate mesophases, photographic scattering 9-19633

cholesteryl propionate, positron lifetimes 9-3079

dimethyl-acetylene in nematic solvents, n.m.r. 9-13545

disclination loops 9-17188

electro-optic dynamic scatt. in nematic crystals, obs. 9-9510

nematic, guest-host interacts, and orientation of guest dichroic dye mols. 9-9481

nematic, in mag. field, alignment inversion walls 9-5143

nematic, n.m.r. spectroscopy of dissolved mols. 9-19609

nematic, nuclear relaxation and resonance freq. 9-18370

nematic, reflective optical storage, electric field control 9-3099

nematic, thermal conduction and heat dissipation 9-21186

nematic film, structure distortion under mag. field 9-9482

nematic mesophase struct. study using second harmonic generation of light 9-21207

NMR, as method for determ. mol. struct. 9-18171

n.m.r. in nematic phase, relaxation 9-18370

optical second harmonic generation, origin, applic. to struct. study 9-21207

par-azoxyanisole twist elastic const. determ. from magnetically induced phase transition 9-14831

perfluorodimethyl-acetylene in nematic solvents n.m.r. 9-13545

phase transitions, cholesteric-nematic, elec. field strength rel. to helix pitch 9-9483

pyridazine oriented in a nematic phase, NMR studies 9-18371

pyridine oriented in a nematic phase, NMR studies 9-18371

pyridine oriented in nematic phase, N.M.R. spectrum, inter-p distance ratios obs. 9-9277

smectic mesophase struct. study using second harmonic generation of light 9-21207

thermal mapping of aerospace materials 9-2252

vanadyl acetylacetonate dissolved in p-azoxyanisole, alignment by elec. field, eff. on EPR spectrum 9-21225

vinyl oleate phase transition, radiation-induced polymerization 9-14734

X-ray structural investigations, design of camera and sample container 9-13512

**Liquid flow** *see Flow/liquids*

**Liquid helium** *see Helium/liquid*

**Liquid lasers** *see Lasers/liquid*

### Liquid metals

Alfven-wave resonances, non-viscous state 9-21036

Bi, charact. energy losses of 8 keV electrons rel. to electronic structure 9-7249

binary systems, props. rel. to structure, bibliography 9-21184

calorimetry, up to 1900°K 9-9838

correspondence to gaseous metals 9-7273

Cs, isothermal compressibility 9-19596

flow, turbulent charact., mag. field eff. 9-7125

flow in MHD system, velocity and momentum 9-9332

flow in tubes in transverse mag. field, shear stresses and turbulent exchange coefficients 9-7124

hold-up, dynamic, in irrigated picked beds 9-21164

impurity states, localized, elec. resistivities and thermopowers 9-16021

ion-ion interactions and electron energy levels 9-11676

isotope thermotransport, temp. depend. 9-9491

magnetic susceptibility, up to 800°C, apparatus for meas. 9-21563

MHD flow in channel with segmented electrodes 9-7121

MHD pressurization of bearing, centrifugal effects 9-4996

network of holes suggested as structure 9-21183

non-viscous, Alfven-wave resonances 9-21036

nuclear spin relaxation, quadrupole mechanism 9-16023

optical constants, meas. apparatus 9-5168

packed beds, static hold-up, rel. to aqueous solns. 9-17180

self-diffusion activation energy rel. to compressibility and charact. temp., near melting point 9-11890

solubility, limited mutual conditions 9-17189

surface tension, temp. depend. 9-17199

thermo-e.m.f. and electroconductance, correlation in approximation of weakly bound electrons theory 9-3117

thermodynamics of dil. metallic solutions, use of polynomials 9-14842

transition, elec. and mag. props. 9-5186

void detection, up to 900°C, 0.5 mm diam. probe 9-3074

Al, diffusion of O, electrochem. meas. 9-11690

Al, charact. energy losses of 8 keV electrons rel. to electronic structure 9-7249

Al, diffusion of Si, temp. depend. of coeff. 9-9496

Au, charact. energy losses of 8 keV electrons rel. to electronic structure 9-7249

Bi-Zn binary mixture, critical inelastic slow neutron scatt. 9-19607

Bi containing halide ions, elec. resistivity 9-11715

Cd, molten, sound absorpt. rel. to dilational viscosity 9-5163

Cs-Li bifluid MHD generator, parametric cycle analysis 9-10798

Cu, diffusion of O, electrochem. meas. 9-11690

Ga, charact. energy losses of 8 keV electrons rel. to electronic structure 9-7249

Ga, diffusion of Zn, Ag and Co 9-13516

### Liquid metals continued

Ga, flow in conducting circular tubes in transverse mag. fields, pressure losses due to contact resistance 9-9328

Ga, positron lifetimes 9-7731

Hg, characteristic energy losses of 8 keV electrons rel. to electronic structure 9-7249

Hg, conductivity and density meas., nonmetal-metal transition 9-11692

Hg containing halide ions, elec. resistivity 9-11715

In, charact. energy losses of 8 keV electrons rel. to electronic structure 9-7249

In, molten, sound absorpt. rel. to dilational viscosity 9-5163

K-Li bifluid MHD generator, parametric cycle analysis 9-10798

K, isothermal compressibility 9-19596

Li, thermophysical props., compilation 9-21197

Na-Li bifluid MHD generator, parametric cycle analysis 9-10798

Na, Alfven-wave resonances 9-2955

Na, dilation effect on neutron irradiation, graphite 9-7661

Na, e.p.r., eff. of Rb, Tl and Cs additions 9-13541

Na, isothermal compressibility 9-19596

Na, positron lifetimes 9-7731

Na, solubility of O<sub>2</sub> 9-19610

Pb, molten, sound absorpt. rel. to dilational viscosity 9-5163

Rb-Li bifluid MHD generator, parametric cycle analysis 9-10798

Rb, isothermal compressibility 9-19596

Sb alloys, dil. with 3d-transition metals, localized impurity states and mag. susceptibilities 9-1043

Sn, self-diffusion, applic. of 'fluctuation' theory 9-5151

Tl-Te, Hall coeff. and mobility, composition and temp. dependence, 340-640°C 9-13537

Zn, effective ion-ion interaction and dielectric screening 9-18350

Zn, molten, sound absorpt. rel. to dilational viscosity 9-5163

Zn, structure and elec. props. 9-7248

### Liquid oscillations

in circular cylinder with flexible bottom 9-9470

sloshing in elastic tank, natural freqs. 9-9471

surface, in small tank, effect of drainage and viscosity 9-11671

water in shallow channel 9-972

### Liquid waves

*See also Acoustic waves*

capillary-gravity, nonlinear, periodic, finite depth liquid 9-11673

cnoidal, mass transfer 9-8163

laser simulation by gravitational waves 9-8597

ocean, bottom and surface, due to submarine disturbance 9-6059

shear, thermally excited prod. peaks in light scatt. spectra 9-21211

water, due to heaving circular cylinder, surface tension effect 9-21171

water, potentials expansion at great distances 9-18341

wind-wave interact., wind profile surveys, drift current and water surface obs. 9-21169

### surface

*See also Oceanography*

capillary waves, longitudinal, theory 9-21172

dielectric fluid, viscous, instabilities with normal electrostatic field at surface 9-17217

fluctuations of free surface, thermal equilibrium 9-18339

free liquid films, dynamics 9-977

hydromagnetic, with alternating mag. field, propag., damping and dispersion 9-17092

inviscid fluid, effect of drainage from tank, and viscosity 9-11671

ocean, refraction, grid and projection problems in numerical calc. 9-21754

ocean, wind generated, spectrum autocorrelation functions 9-14824

oceanic ridge waveguide, model 9-6068

in rotating liqs. 9-21170

shallow, wave patterns and role of surface tension 9-18340

in shallow water, velocity pot. and surface elevation for arbitrary surface disturbances 9-11672

velocity in bounded liquids rel. to bubble velocity 9-19598

water, instability on air flow over surface 9-17154

wind driven, onset, tunnel test 9-6065

wind-wave interact., wind profile surveys, drift current and water surface obs. 9-21169

**Liquid-drop model** *see Nucleus/models*

### Liquids

*See also Association/liquids; Diffusion in liquids; Solutions*

absorbing, stimulated thermal light scatt. in picosecond regime 9-11697

activity coefficient, using light scatt. data 9-9487

Arcton 11, pool boiling, effects of high press. and accel. 9-13560

boiling, local temp. fluctuations 9-19661

burning rate from pools, effect of flame merging 9-16746

carboxylic acid-water mixture, polymer-dimer and dimer-monomer equilibria 9-3126

compressible, sealed by circular plate, stress analysis 9-8476

compression of metals 9-5446

degassing in a sound field, influence of static press. and temp. 9-5161

diffusion systems, u.s. standing wave freezing-in by conc. zone effect 9-18358

elastic, linear and nonlinear behaviour, expt. meas. and theory 9-18332

evaporation rate of droplets in spherical state on hot surface 9-21247

free positron lifetime, effective no. of annihilation electrons per atom 9-5637

gas-free, fractionation device for production 9-14291

impurities, mass spectrograph determ. 9-8116

inert gases, condensed, theory and props. 9-13509

laser beam thermal self-defocusing and self-focusing in liquids, self-actions in liquids with flows 9-17880

laser beams, self-trapping effect, use of double-exposure holography 9-13035

light scattering, time-dependent autocorrelation functions 9-19631

methane, props., obs. review 9-13509

mixtures, binary, of low density, summation of partial surface tensions 9-7238

molecular interactions, evidence from Rayleigh light scatt. 9-14850

molecular thermodynamics 9-1001

molecular thermodynamics 9-1002

molecular thermodynamics 9-1003

organic, i.r. absorption band width temp. depend. 9-9517

phosgene, thermodynamic props. up to 600°K, 150 atm. 9-7263

polar, injection of ions 9-7272

polar, u.r.f. and far i.r. absorpt. 9-1016

**Liquids continued**

- proton n.m.r., cross-relax. processes 9-3121  
 pulse discharge theory 9-3118  
 Raman scattering, stimulated in focused low power ruby laser beam 9-5171  
 relaxing, light scatt. by density fluctuations 9-1010  
 simulator, oil-covered ball bearings on vibrating rough-molded glass 9-11677  
 thermophysical props., estimation 9-999  
 u.s. absorption, formula for organic, non-associated, liq. 9-5158  
 viscous, hydrodynamic equations of grad-type, statistical derivation 9-3036  
 H<sub>2</sub> level meas. using spaced C resistors 9-6269

**structure**

- acetylenes, substituted, molec. rot. motion 9-9557  
 n-alkanes, elongated chain orientation, from molec. optical anisotropy 9-14830  
 benzene, X-ray anal. 9-5142  
 binary metal systems, bibliography 9-21184  
 borates, binary, rel. to viscosity 9-3083  
 carbon tetrachloride, l.f. motions 9-9518  
 chloroform, dipole moment 9-17185  
 condensing vapours at solid surfaces 9-18351  
 cybotactic group: partition func. and eqn. of state determ. 9-7247  
 diatomic, linear- and ang.-momentum autocorrel. functions 9-3076  
 dipole moment of anisotropic mols. 9-17185  
 glycerine, partially deuterated, quasi-elastic cold neutron scattering 9-7250  
 metal melts, <sup>24</sup>Mg impurity, nucl. reson. fluoresc. study 9-7278  
 monovalent ion in water, dipole moment in first hydration shell 9-5077  
 near-solid association suggested for metals 9-21183  
 nonpolar, intermolec. forces 9-7268  
 from optical molecular anisotropy temp. depend. 9-14849  
 order disorder equil., vacancy struct., temp. and polarity depend. 9-15985  
 orientational relax., from Rayleigh scatt. 9-1009  
 polymethylene liquids, chain shortening 9-13511  
 sulphates, molten, vibr. spectra 9-16005  
 water, cell theory applic. with electrostatic intermolec. pot., free volume calc. 9-19606  
 water, revised model 9-9478  
 water, super, and props., theory 9-14828  
 Al, ordered structural region size estimation by X-ray scatt. 9-17187  
 Ar, thermal neutron scattering, new model 9-11682  
 B<sub>2</sub>O<sub>3</sub>, rel. to viscosity 9-3083  
 CO, linear- and ang.-momentum autocorrel. functions 9-3076  
 CO<sub>2</sub>, significant structure theory applied to correlation of thermodynamic props. in terms of molecular parameters 9-19605  
 COS, significant structure theory applied to correlation of thermodynamic props. in terms of molecular parameters 9-19605  
 CS<sub>2</sub>, significant structure theory applied to correlation of thermodynamic props. in terms of molecular parameters 9-19605  
 Ca(NO<sub>3</sub>)<sub>2</sub>:Ba(NO<sub>3</sub>)<sub>2</sub>:Sr(NO<sub>3</sub>)<sub>2</sub> binary fused systems, from Raman scatt. 9-17186  
 H<sub>2</sub>O-NH<sub>3</sub> solns., X-ray diffraction 9-3078  
<sup>4</sup>He, ground-state struct. factor, calc. 9-5205  
 Hg, Hg-Cd, Hg-Pb dil. alloys, X-ray diff. 9-7251  
 Hg evidence for a third phase 9-3077  
 Lu, ordered structural region size estimation by X-ray scatt. 9-17187  
 KNO<sub>3</sub>-AgNO<sub>3</sub> molten mixtures 9-1019  
 Mg-Pb molten alloys 9-14829  
 Pb-Sn alloy, ordered structural region size estimation by X-ray scatt. 9-17187  
 Pb, ordered structural region size estimation by X-ray scatt. 9-17187  
 Sn, ordered structural region size estimation by X-ray scatt. 9-17187  
 Zn, rel. to elec. props. 9-7248  
 Zn, from n diff. expts. 9-14011

**theory**

- See also *Dielectric phenomena; Equations of state/liquids*  
 cell model, thermodynamic props. 9-14743  
 cell model with infinite pot., evaluation of partition function 9-14742  
 classical, cybotactic group hypothesis 9-11678  
 classical, rel. autocorrel. and density-density correl. functions 9-5140  
 classical, zero-sound approach to current-current correl. 9-100  
 co-operative modes of motion in simple model 9-15984  
 equilibrium theories, solns. of integral eqns. for distrib. functions, Monte Carlo studies of models 9-11676  
 free energy and entropy, from intermolec. potential 9-979  
 inert, gases, condensed, quantum effects 9-13509  
 intermolecular potential, medium-depend. 9-979  
 ionic solutions, charged square-well model 9-19603  
 metal-ammonia solns., props. and existence of metal-nonmetal transition 9-14833  
 metals, hard sphere model, density depend. pots. 9-19604  
 molecular theory of liquids and mixtures 9-11679  
 molten salts, significant-struct. theory 9-978  
 neutron scatt., slow, continued fraction representation for autocorrel. function calcs. 9-13510  
 organic, energy migration at high temps. 9-7246  
 resonance energy transfer in condensed media from many-particle view-point 9-5621  
 spin dynamic polarization, unitary theory 9-17471  
 statistical, coherence time concept 9-20364  
 surface, stimulated light scatt. 9-1012  
 surface tension of binary mixtures 9-7245  
 Viasov eqn., dispersion rels. 9-8429  
 Ar, neutron scatt., slow, continued fraction representation for autocorrel. function calcs. 9-13510  
 Cu-Sn, electron transport, Ziman theory and exptl. data comparison 9-7274  
 H<sub>2</sub> in liq. Ar, collision-induced absorpt., liq. cell model 9-21213  
 H<sub>2</sub> in liq. Ar, collision-induced absorpt., liq. cell model 9-21214  
 H<sub>2</sub>O, surface free energy of droplet, in nucleation theory of condensation 9-304  
 H<sub>2</sub>O, vibr. dynamics 9-13529  
 S, charge carrier transport 9-5603  
 Zn, effective ion-ion interaction and dielectric screening 9-18350

**Lithium**

- <sup>116m</sup>Li diff., 75°-170°C 9-17290  
 addition to Cu rel. to oxidation rate at room temp. 9-3996

**Lithium continued**

- atom, dipole polarizability and antishielding factor, many-body calc. 9-4842  
 atom, doubly excited states 9-13299  
 atom, Green function 9-9107  
 atom, ground-state h.f.s., many-body perturbation calc. 9-4841  
 atom, hyperfine splitting of ground state 9-2819  
 atomic beam reactions with Cl<sub>2</sub>, ICl, Br<sub>2</sub>, SnCl<sub>4</sub> and PCl<sub>5</sub> 9-17512  
 atoms and ion, bibliography of spectra 9-13287  
 conductivity, electrical, temp. var. calc., comparison with expt. 9-16231  
 defect complex in e irradi. Si, i.r. spectroscopic study 9-13673  
 diffusion in glass, increase in mechanical and thermal resistance 9-21379  
 elastic constants from band-structure calcs. 9-5420  
 fluorescence quenching from 2p<sup>2</sup>P state, in H<sub>2</sub>O flame, diluted with Ar, N<sub>2</sub> and CO<sub>2</sub> 9-676  
 graphite, plasmon obs. in X-ray scatt. 9-1818  
 ground state, Hartree-Fock eqn., Z<sup>-1/2</sup> expansion 9-4828  
 ion, energy loss in matter, vel. depend 9-21450  
 ion beam charge distrib. after passage through gas or foil, 0.5-2 MeV 9-16772  
 ion beam production by charge exchange with 5-40 KeV p beam 9-233  
 isotope abundance ratio meas., surface ionization method 9-19416  
 liquid, thermophysical properties, compilation 9-21197  
 melt struct., Mg impurities, nucl. reson. fluoresc. study 9-7278  
 MPD arc thruster, efficiency at 3×10<sup>-6</sup> torr 9-9376  
 neutron angular and space-energy distrib. 9-19331  
 resonance line emitted by exploding wire, self-broadening calc. 9-16996  
 salts, non-aqueous soln., U.S. vel., molal and adiabatic compressibility determ. 9-7254  
 solar abundance, lower than previously admitted 9-15353  
 spectra, absorption, in noble-gas matrices, 3500-8000 Å, 4.2-40.0°K 9-4840  
 supersonic vapour jet, high energy neutral atom prod. by transformation of H<sub>1</sub><sup>+</sup>, H<sub>2</sub><sup>+</sup> and H<sub>3</sub><sup>+</sup> ions 9-4445  
 surface states of deformed crystal 9-9899  
 thin film, ultraviolet transmittance 9-5867  
 in upper atmosphere, min. detectable limit of emission rate 9-21785  
 upper atmospheric, twilight obs., seasonal var. of abund. 9-12595  
 vacancy migration, applic. of potential deduced from pseudopotential theory 9-9700  
 e, conduction, g shift,  $\delta g$  theoretical estimate 9-12061  
 neutron sandwich spectrometer, triton energy response function 9-19225  
 Au diff., 45-150°C 9-7509  
 in BeO, radiation induced paramagnetic centre structure 9-1868  
 K-Li ion exchange syst., diff. and reaction coupling 9-17510  
 Li<sup>+</sup> interstitial ion diffusion in TiO<sub>2</sub> 9-9705  
 Li-Hg atom beams scatt., interatomic potential 9-15827  
 Li<sup>+</sup> diffusion in LiF, 650-800°C 9-21351  
 Li<sup>+</sup> low energy ions, sputtering of diatomic compounds 9-7678  
 Li I doubly excited levels lifetime meas., beam-foil technique 9-20879  
<sup>7</sup>Li, n.m.r. in LiNbO<sub>3</sub>, acoustic saturation 9-8040  
<sup>7</sup>Li isotopic analysis using  $\alpha$  scatt. 9-1930  
<sup>7</sup>Li<sup>+</sup> scatt. by free atoms and mols. 9-13308  
 Li<sup>+</sup>, aq. medium, interaction energy, 25°C 9-11719  
 Li<sup>+</sup>, ionization by e impact to Li<sup>2+</sup>, cross-section rel. to energy 9-5064  
 Li<sup>+</sup>, van der Waals coeffs. for ground and metastable states 9-2833  
 Li<sup>+</sup> in CdS, crystal, habit change on increasing Li<sup>+</sup> content 9-1184  
 Li<sub>2</sub>, use of pseudopotentials, validity 9-13360  
 Li<sub>3</sub>, diatomics in mols. theory of stable mol. 9-9218  
 Li<sub>2</sub>Ni<sub>1-x</sub>O<sub>2</sub> system, lattice parameter comp. dependence 9-1191  
 molecules bonding and correl. energies, geminal calc. 9-4909  
 i, n Si, effect on recombination velocity due to e-irrad. 9-9998  
 Si(Li) junctions, recovery behaviour after p-irrad 9-15111  
 in ZnO, radiation-induced paramagnetic centre structure 9-1868

**Lithium compounds**

- acetate, dehydrate, Raman effect meas. in polarized light 9-10225  
 ferrite, alignment and microwave props. 9-1685  
 ferrite, saturation magnetization and lattice struct., 20°C 9-1686  
 ferrite growth in SiO<sub>2</sub> glasses and composite mag. props. 9-1146  
 glass, scintillation characteristics for neutron,  $\beta$  and  $\gamma$  ray detection 9-449  
 halide molec. species, l.f. absorpt. spectra 9-9220  
 lithium aluminosilicate, thermal expansion dependence on TiO<sub>2</sub> catalyst content 9-13804  
 magnetothermal effect, anomalous sign in kn in compensation pt. region 9-1683  
 Ca, substituted ferrites, mag. props. structure and sintering 9-1684  
 (Li<sub>1-x</sub>Fe<sub>x</sub>)<sub>2</sub>O<sub>4</sub>, 1:3 type ordering, temp. effects 9-14006  
 KNO<sub>3</sub>-LiNO<sub>3</sub> liquid, dis. of u.s. vel. 9-1007  
 Li-C system, compound formation 9-14992  
 Li-Mg binary alloy, ordering energy and effective pairwise interactions 9-7696  
 Li-Si detector for spark-chamber triggering 9-20701  
 (Li<sub>1-x</sub>Ag<sub>x</sub>)<sub>2</sub>SO<sub>4</sub>, b.c.c.+0.5% alkali sulphates, thermal diff. 450-550°C 9-17289  
 (Li<sub>1-x</sub>Ag<sub>x</sub>)<sub>2</sub>SO<sub>4</sub>, b.c.c., Li<sup>+</sup> and Ag<sup>+</sup> diff. coeffs., 470-550°C 9-17287  
 Li<sub>0.5</sub>Fe<sub>2.5-x</sub>Al<sub>x</sub>O<sub>4</sub>, lattice structure and cation distrib., n. diff. obs. 9-21316  
 Li<sub>0.5</sub>Fe<sub>2.5-x</sub>Al<sub>x</sub>O<sub>4</sub>, ferromagnetic resonance line width rel. to elec. conductivity 9-18730  
 Li<sub>2</sub>BaO<sub>4</sub>:Mn as material for thermoluminescent dosimetry 9-20006  
 Li<sub>2</sub>BaO<sub>4</sub>:Mn thermoluminesc. emission spectra, apparatus and results 9-18726  
 Li<sub>2</sub>O-SiO<sub>2</sub> glasses, crystallization phases, X-ray obs. 9-1080  
 Li<sub>2</sub>O-Al<sub>2</sub>O<sub>3</sub>-nSiO<sub>2</sub> (4 ≤ n ≤ 10.0) solid solns., thermal expansion behaviour 9-3537  
 Li<sub>2</sub>O-Al<sub>2</sub>O<sub>3</sub>:4SiO<sub>2</sub>, glass form., i.r. obs. 9-16036  
 Li<sub>2</sub>SO<sub>4</sub> polycryst., thermal expansion 200-550°C and 600-750°C 9-7664  
 Li<sub>2</sub>WO<sub>4</sub>:Fe, cubic, crystal structure 9-18447  
 LiAg, electronic band struct. and metallic character 9-15055  
 LiAlD<sub>4</sub>, polycrystalline, deuteron quadrupole coupling const. 9-11464  
 LiAlSiO<sub>4</sub> (eucryptite) high temp. form, crystallization and polymorphism 9-1134  
 LiBr: Ag<sup>+</sup> solns., absorpt., luminesc. and excitation spectra 9-1020  
 LiBr Jahn-Teller effect in  $\Gamma$  excitation splitting 9-19882  
 LiCd[MoO<sub>4</sub>]OH, cell parameters, density 9-5322  
 LiCl: Ag<sup>+</sup> solns., absorpt., luminesc. and excitation spectra 9-1020  
 LiCl: Ag e.p.r. of stabilized Ag atoms 9-14108  
 LiCl-H<sub>2</sub>O system, liq.-liq. immiscibility at low temp. 9-15988  
 LiCl, orthogonized-plane-waves calc. 9-13832  
 LiCl molecule, rot., vibr. and pot. constants by microwave meas. 9-18184



**Lithium compounds continued**

- LiCl optical absorption of  $V_K$  center, lattice effect 9-9720  
 LiCl solns., nuclear spin-lattice relax. 9-1046  
 $^6\text{LiCl}$ ,  $^7\text{LiCl}$  molten, internal mobilities and elec. cond. 9-8103  
 $\text{LiCo}$  ferrite, ferromagnetic resonance 9-18731  
 $\text{LiD}$  surface, laser-induced thermonuclear plasma and n. obs. 9-7171  
 $\text{LiD}$  surface, thermonuclear neutron emission at Nd glass laser beam focus 9-13245  
 $^6\text{LiD}$ , rot. line  $J=0 \rightarrow 1$  in ground vibr. and first excited states, microwave obs. 9-13361  
 $^7\text{LiD}$  rot. line  $J=0 \rightarrow 1$  in ground vibr. and first excited states, microwave obs. 9-13361  
 $\text{LiF}$  crystals, tensile strength 9-5454  
 $\text{LiF}$  dosimetry, design of reader 9-2090  
 $\text{LiF}$  pellet dosimeter 9-6210  
 $\text{LiF}$  thermoluminesc. emission spectra, apparatus and results 9-18726  
 $\text{LiF.Fe}_2\text{O}_3$ , preparation attempts 9-16480  
 $\text{Li}_2\text{Fe}_2\text{O}_4\text{Fe}_2\text{CuO}_4$ , molecular magnetic moment variation with quenching temps. 9-3769  
 $\text{LiFePO}_4$ , magnetoelec. coeff. temp. dependence in a.c. field 9-14013  
 $\text{LiGa}$  ferrites, magnetocrystalline anisotropy by ferromag. resonance 9-19964  
 $\text{Li}_2\text{GeO}_5\text{:Cr}^{3+}$ , energy transfer between nonequivalent sites 9-5964  
 $\text{Li}_2\text{GeO}_5\text{:S:Cr}^{3+}$ , R lines, width and position temp. dependence 9-5963  
 $\text{LiH}$  seawater react., high-pressure, gas prod., obs. 9-20041  
 $\text{LiH}$ , calc. of mol. constants from microwave obs. of  $\text{LiD}$  9-13361  
 $\text{LiH}$ , correl. energy calc. and unitary transforms. 9-773  
 $\text{LiH}$ , fast n. space, energy and angular distrib. 9-19329  
 $\text{LiH}$ , lattice dynamics, from phonon dispersion curve meas. 9-19851  
 $\text{LiH}$ , low-lying electronic states, theoretical calc. 9-9219  
 $\text{LiH}$ , use of pseudopotentials, validity 9-13360  
 $\text{LiH}$ , valence electron calc. 9-17035  
 $\text{LiH}$  e.m. interaction theory, nuclear shielding const. calc. 9-7025  
 $\text{LiH}$  torpedo-recovery system 9-20041  
 $\text{LiIO}_3$ , electro-optical and nonlinear optical props. 9-3867  
 $\text{Li}_2\text{ZnO}$  apparent molal expansibility and volume obs. 9-986  
 $\text{LiNO}_3$ , interdiffusion in dilute solns. of  $\text{AgNO}_3$  9-7261  
 $\text{LiNO}_3$ , magnetoelec. eff. 9-1600  
 $\text{LiNO}_3$ , permittivity and loss-angle tangent, impurities effect 9-1576  
 $^6\text{LiNO}_3$ ,  $^7\text{LiNO}_3$  280-440°C, elec. cond. 9-8103  
 $\text{LiNaSO}_4$ , b.c.c., thermal diff. 546-588°C 9-17289  
 $\text{LiNbO}_3\text{:Mn}^{2+}$  e.p.r. spectrum obs. 9-16458  
 $\text{LiNbO}_3$ , hypersonic wave, second harmonic production 9-19857  
 $\text{LiNbO}_3$  single domain crystals, hydrothermal synthesis by transport reactions 9-19685  
 $\text{LiNbO}_3$ , acoustic surface wave transducers and delay lines 9-10057  
 $\text{LiNbO}_3$ , Brillouin scattering 9-12452  
 $\text{LiNbO}_3$ , crystal structure 9-7443  
 $\text{LiNbO}_3$ , n.m.r. of  $^7\text{Li}$ , acoustic saturation 9-8040  
 $\text{LiNbO}_3$ , nonlinear coeffs.  $d_{31}$  and  $d_{32}$  opposite signs obs. 9-10165  
 $\text{LiNbO}_3$ , reduction in laser-induced refractive index inhomogeneity rel. to OH content 9-5870  
 $\text{LiNbO}_3$ , second harmonic generation by Nd:glass laser psec pulses 9-10173  
 $\text{LiNbO}_3$ , tunable optical parametric oscillator using c.w. Ar laser as pump 9-10161  
 $\text{LiNbO}_3$  cryst. electro-optical shutter, rel. to generation of giant pulses in  $\text{CaF}_2\text{:Dy}^{3+}$  crystals 9-1723  
 $\text{LiNbO}_3$  holographic storage medium 9-15536  
 $^{14}\text{NbO}_3$ , gain coeffs. for stimulated Raman scattering 9-5936  
 $\text{Li}_2\text{O-SiO}_2\text{-P}_2\text{O}_5$  glass film, prep. and phase separation study 9-5226  
 $\text{Li}_2\text{O-SiO}_2$  glasses, heat treated, n irradiation effects on dielec. and d.c. props. 9-7833  
 $\text{Li}_2\text{O}$ , presence in refractory metals and alloys causing oxidation retardation 9-3994  
 $\text{Li}_2\text{O-2.2Fe}_2\text{O}_3\text{-2.8Cr}_2\text{O}_3$ , ferrite, longit. and transverse magnetoresistance, anomalies around compensation temp. 9-19965  
 $\text{LiPO}_3\text{-NaPO}_3$ , and  $\text{LiPO}_3$  surface tension of molten mixture obs., surface heat of mixing estimated 9-21191  
 $\text{Li}_2\text{SO}_4\text{-K}_2\text{SO}_4$  eutectic, corrosion of Fe, thermodynamics 9-15222  
 $\text{Li}_2\text{SO}_4$ , cubic,  $\text{Mg}^{2+}$ ,  $\text{Zn}^{2+}$ ,  $\text{Ca}^{2+}$ ,  $\text{Cd}^{2+}$ ,  $\text{Pb}^{2+}$  diff. coeffs., 600-800°C 9-17288  
 $\text{Li}_2\text{SO}_4$ , f.c.c., +other sulphates, thermal diff. 590-750°C 9-17289  
 $\text{Li}_2\text{SO}_4(41-90 \text{ equiv.}\%)\text{-K}_2\text{SO}_4$  molten isotope effects of electromigration 9-8102  
 $\text{LiSb}$ , n.m.r., powder 9-1875  
 $\text{LiTaO}_3\text{:Mn}^{2+}$  e.p.r. spectrum obs. 9-16458  
 $\text{LiTaO}_3$ , ferroelectric, displacement-type, applic. of statistical theory to expt. results 9-21537  
 $\text{LiTaO}_3$ , light extinction in light modulation 9-10178  
 $\text{LiTaO}_3$ , reduction in laser-induced refractive index inhomogeneity rel. to OH content 9-5870

**lithium fluoride**

- cleavage, dynamical, fracture surface energies, dislocation processes and transverse fracture markings 9-13741  
 cold-worked, crystallite size and microstrains, evaluation from X-ray diff. line profiles 9-13640  
 conduction electrons, spin reson. 9-1861  
 conductivity, elec., pressure and temp. dependence, 50-5300 bars, 400-780°C 9-7839  
 conductivity meas. without using contact electrodes 9-7836  
 cracks, spontaneous propag. 9-3451  
 creep, effect of u.s. radiation on region of action of dislocation depletion mechanism 9-9764  
 creep behaviour under const. stress, 300° to 550°C 9-11933  
 crystal, second sound and temp. pulse propagation obs. 9-16030  
 dielectric films, influence on opt. props. of In and Al layers 9-5886  
 diffusion of  $\text{Li}^+$ , 650-800°C 9-21351  
 dislocation mobility, n irradi. eff. 9-11885  
 dislocation motion in electric field 9-5365  
 dislocation structure and mechanical props. after slip deformation 9-5364  
 dislocation structure formation near surface during annealing 9-11884  
 elastic constant, third-order 9-19775  
 elastic const., meas. by audio freq. reson. method, 20-700°C 9-5423  
 elastic const., meas. by static, reson. and u.s. techniques 9-5422  
 electric discharge causing breakdown, energy characts. 9-10042  
 electrical charges excess statistical analyses and formation mech. 9-1568  
 ENDOR meas. of self-trapped hole 9-10284  
 ENDOR spectrum, F-centre experimental explanation 9-15208

**Lithium compounds continued****lithium fluoride continued**

- exoelectron-emission in high vacuum, from surface states and vol. traps 9-7864  
 F band thermal bleaching in  $\gamma$ -irrad. crystals, plastic deform. effects 9-7503  
 impurity-doped, growth conditions and props. 9-1133  
 internal friction temp. dependence, 150-300°K 9-3399  
 line at 4.2°K, moment analysis of Stark effect 9-14054  
 mechanical props. of pure cryst. and doped with  $\text{Mg}^{2+}$ , effect of lattice defects 9-1257  
 molecule, Rot., vibr. and pot. constants by microwave meas. 9-18184  
 $\text{NaF.F}_3^+$  colour centres, linear Stark eff. of no-phonon transitions 9-19759  
 optical absorption and density, effect of X-irradiation 9-5926  
 optical absorption and thermoluminescence, thermal treatment effects 9-5969  
 paramagnetic imperfections in irradiated crystal 9-16107  
 photocathode for He lines meas. on  $\text{HL}_\alpha$  background 9-15560  
 point defects annealing in gamma-irradiated material 9-19821  
 Raman effect of ideal lattice, generation by anomalous polarization scatt. at surface of ultramicroscopic scatt. centres 9-16422  
 Raman spectra of ultramicroscopic centres, laser-excited, multiple-phonon processes 9-5937  
 for recovering and purifying  $\text{PuF}_6$  gas by sorption 9-5254  
 relaxation effects at low freqs., 30°-180°C 9-12185  
 sintering, Vol., grain boundary and surface diffusion contributions 9-1246  
 skeletal cavities formation on melting 9-13611  
 slip band dislocation structure during annealing 9-11886  
 slip in one plane, production by selective hardening 9-1294  
 slip line structure determ. using layered polishing and etching and stat. analysis 9-1297  
 spectral emission due to lattice vibrations 9-7977  
 strength, tensile, rel. to ionic polarizability and slip systems interpenetrability, 300-700°C 9-3440  
 thermoluminescence characts. after reactor irradiation, rel. to dose 9-17492  
 thermoluminescence rel. to colour centres and d.c. resistivity in irradiated crystals 9-14092  
 thermoluminescent dosimetry, toxicity 9-15384  
 thermoluminescent emission spectra, meas. 9-16444  
 u.s. deformed, internal stress behaviour 9-16128  
 X-ray scatt. factors using approx. model for overlap charge density 9-3298  
 $\text{LiF:Ca}$ , elec. conductivity at low temps. 9-19928  
 $\text{LiF:Fe}_2\text{O}_3$ , preparation attempt 9-9634  
 $\text{LiF:Mg}$ , photoemission spectrum 9-3758  
 $\text{LiF-BeF}_2\text{-ZrF}_4$ , equilb. phase diagram, 350-1000°C 9-16031  
 $\text{LiF-NaF}$ , growth by Czochralski technique, preferred <100> texture 9-1123  
 $^6\text{LiF-Zn(Sg)}_2$ -polyethylene scintillation detector for subcritical thermal n flux 9-6723  
 thin cry., nonuniform e.m. field treatment of i.r. props. 9-17352

**Lithosphere see Earth****Localized states see Crystal electron states****Loges (molecular bonds) see Bonds; Molecules/electronic structure****Lorentz transformation see Relativity/special****Lorentz-Lorenz relation see Dielectric phenomena****Lorenz number see Conductivity, electrical/solids; Conductivity, thermal/solids****Loschmidt number (= Avogadro number) see Constants****Loudness see Hearing; Intensity measurement, acoustics****Loudspeakers see Acoustic radiators****Love waves see Elastic waves; Seismic waves****Low-temperature phenomena**

See also Helium/liquid; Helium/solid; Joule-Thomson effect; Superconducting materials; Superconductivity; Superfluidity

benzophenone, phosphoresc. and triplet-singlet absorpt. at 4.2°K 9-10251

dielectric properties of solid insulating materials 9-1565

energy transfer of thermal radiation between two dielectrics 9-7677

in ferroelectrics, hydrogen-bonded, tunneling integral 9-7843

gases, press. reduction by double mols. formation 9-6265

Heisenberg antiferromagnet free energy, 1/2 expansion 9-1696

Kapitza resistance between liquid  $^4\text{He}$  and metals 9-18379

m.o.s. capacitors, hysteresis effects caused by surface-state trapping 9-18644

new phase origin in hydrocarbon 9-3235

production, meas. and handling and props. of low temp. mats., book 9-20282

resistance variations, elementary expt. for students 9-12842

Al-Cr alloy, dilute, low-temp. impurity resistance 9-1473

Al-Mn alloy, dilute, low-temp. impurity resistance 9-1473

$\text{CuSO}_4\cdot 5\text{H}_2\text{O}$ , magnetothermodynamics, 0.4°-4.2°K 9-9840

h liquid, dielectric phenomena study 9-1036

He, liquid dielectric breakdown at 4.2°K 9-1055

He II, critical region second-sound vel. 9-5209

He plasma, recombination, study of afterglows 9-11547

K $\alpha$   $\text{MnCl}_2$ , e.p.r. and mag. susceptibility 9-16456

$\alpha\text{-NiSO}_4\cdot 6\text{H}_2\text{O}$ , 0.4°-4.2°K, 0-90 kG fields magnetothermodynamics 9-19862

$\text{U}_3\text{O}_8$ , ht capacity 1.6°-24°K, mag. entropy 9-9846

**Low-temperature production**

See also Joule-Thomson effect; Liquefaction/gases; Magnetic cooling

2.5 mK  $^3\text{He}$  solid/liquid mixture, adiabatic compressional cooling 9-21234

absorption cell, long path, for spectroscopic studies 9-6232

accuracy of 0.001°K, any temp between 4°-3°K and 300°K 9-2097

cold trap, controlled-temp., -196°-0°C 9-2098

Dewar for controlled-temp. spectroscopy >77°K 9-2099

dilution refrigeration using liquid He, principles and methods 9-8320

immersion cooler using liq.-vapour phase transitions 9-18966

refrigeration, dilution, expts. on intrinsic limitations 9-4187

refrigerator, magnetic, use of Cd thermal switch 9-175

Re refrigerations, survey 9-8321

$^3\text{He}/^4\text{He}$  dilution refrigerator 9-16646

nuc. adiabatic demag. method, rare-earth ions suitability 9-4185

**Low-temperature technique**

- 77°K and above, temp. control system suitable for undergraduates 9-8319  
 applies, to physics biology, chemistry and engineering, book 9-4191  
 cell, for u.v. and visible region absorpt. spectroscopy 9-15558  
 coaxial lines, low-loss, produced with polystyrene bead core 9-8315  
 cryoelectronics review 9-8317  
 dilution refrigerator, thermal contact to mixing chamber 9-20284  
 electrical resistivity meas. device, 5-100°K 9-2301  
 E.S.R. meas. below 4.2°K 9-6436  
 flow rate, temp., and moisture content variation, hydrocarbon 9-3235  
 liquid N<sub>2</sub> lines, poor thermal insulation, for reactor 9-19361  
 magnetic sample adiabatic rotation 9-4181  
 optical Dewar for two-beam expts. 9-2411  
 Physics Exhibition, London 1968, review 9-4186  
 pressure or uniaxial force generation by Sylphon bellows 9-4192  
 production, meas. and handling and props. of low temp. mats., book 9-20282  
 pyroelectric thermometer 9-19100  
 safety in handling liquid He 9-7296  
 sample rotator with right-angle drive using flexible wheel 9-14290  
 solders, supercond. meas. table given 9-12805  
 spectrophotometer attachment for liq. spectra meas. down to -96°C 9-10943  
 stabilization of working temperature of superconducting bolometer, electronic instrument 9-12952  
 temperature regulation using Zener diodes 9-20283  
 X-ray scatt., small angle, meas. device 9-3259  
 Ce<sub>2</sub>Mg<sub>3</sub>(NO<sub>3</sub>)<sub>12</sub> thermometers, shape factors from demagnetizing factors meas. 9-15395  
 H liquid dielectric phenomena investigation, meas. apparatus 9-1036  
 He liquid, purification, transport, storage 9-7291  
 He liquid, storage, distribution and handling 9-7295  
 He liquid applications to superconducting magnets, accelerators, bubble chambers, and pumping 9-8318  
 N<sub>2</sub>, liq., level control in dewar, instrument description 9-12804

**LS coupling** *see Atoms; Spectra/atoms*

**Lubrication**

- See also Friction*  
 fatigue crack propagation rel. to lubrication effects 9-13736  
 four-ball lubricant testing machine with three wear tracks 9-6223  
 metal bearing, liq., MHD pressurization, centrifugal effects 9-4996  
 metals, role of oxygen in eff. of additive surface-active substances 9-18529  
 paraffin film lubricant on steel, pressure effects on friction coeff. 9-16138  
 solid film lubricants, pressure effects on friction coeff. 9-16138  
 turbulent, possibilities of universal velocity laws 9-11668  
 Au film lubricant on steel, pressure effects on friction coefficient 9-16138  
 MoS<sub>2</sub> film lubricant on steel, pressure effects on friction coefficient 9-16138

**Ludwig-Soret effect** *see Diffusion in solids*

**Luminescence**

- See also Electroluminescence; Luminescent devices; Thermoluminescence*  
 640 phosphor rel. to photometry appls. as optical converter 9-15547  
 anti-Stokes, at T=O°K, rel. to impurity centres 9-14073  
 aromatic molecules, short fluoresc. lifetime, relevant factors 9-9240  
 atoms, anisotropic collisions resonance fluorescence depolarisation, theoretical study 9-9146  
 1-azatriphenylene, fluorescence, spectral analysis 9-9243  
 benzene in cyclohexane, quasiline spectra, mol. symmetry determ., 77°K 9-4948  
 5,6-benzoquinoline rel. to  $\pi$  transitions and N effects on mol. levels, 77°K 9-15899  
 bound electron capture in models 9-15293  
 carbazole-pyridine (triethylamine) system, phosphorescence 9-7056  
 centre, multilayer model 9-9166  
 crystal light amplification by centre with Stokes shift 9-10232  
 crystals with impurity centres, mechanism 9-20001  
 9,10-dichloroanthracene dimer, fluorescence, temp. depend. 9-13322  
 dimeric syst., weakly coupled, fluorescence, temp. depend. 9-13322  
 dye fluorescence quenching by inorganic salt, soln. structure depend. 9-9174  
 emission by impurity centres from non-equilib. vibrational states, theory 9-14073  
 film coating thickness meas. method for rough surface 9-10609  
 fluorescence, excited by continuum 9-7992  
 fluorescence, formula structure, quantitative electron probe microanalysis 9-8126  
 fluorescence, structural and environmental factors, polarization 9-6997  
 fluorescence monitoring by glass dosimeter specimens, patent 9-12461  
 fluorescence spectroscopy of proteins 9-18224  
 fluorometer for study of molecular lifetimes 9-747  
 gelatin gels, depolar. of fluorescence studies of mol. behaviour 9-19651  
 hexatriene substituted in heptane, toluene; fluorescent props. comparison, temp. depend. 200-350°K 9-4956  
 hydrocarbons, polyeyelic, rel. to chem. analysis, obs. 9-18780  
 intersystem crossing and multiple tunnelling model 9-18719  
 laser-beam scintillation over horizontal paths from 5.5 to 145 kilometers, log-amplitude covariance 9-21775  
 laser-beam scintillation under atmospheric turbulence, saturation 9-21774  
 light-diffusing layer, absorption index depend. on exciting radiation density 9-5948  
 metalorganic phenyls, O atm. and metal at. wt. effects, 77 and 290°K 9-15848  
 4,5-methylenepheneanthrene react. with alkali metal, fluor. spect. investig. of carbanions MH<sup>-</sup> and H<sub>2</sub>MH<sup>-</sup> 9-19468  
 molecular dimers, vibronic energy calc. 9-736  
 molecule, fluorescence decay time variation with proximity of mirror 9-15838  
 moon, lab. simulation, powdered rock sample, proton and u.v. irradiation 9-20221  
 2-naphthaldehyde, phosphorescence radiationless decay proc., deuteration eff. 9-19472  
 naphthalene, rel. to quinoline and 5,6-benzoquinoline, 77°K 9-15899  
 1-naphthol, excited, H-bonded, fluorescence and phosphorescence spectra 9-9519  
 optical layers, transient, kinetics 9-8648  
 organic dyes, wide-angle interference and multipole fluorescence 9-15839  
 parametric, quantum mech. of noncollinear interactions 9-14096

**Luminescence continued**

- phenanthrene, rel. to quinoline and 5,6-benzoquinoline, 77°K 9-15899  
 phosphorescence, disturbance in low-energy  $\beta$  isotope activity meas. 9-20754  
 phosphorescent mols. of short lifetime, e.p.r. 9-8007  
 phosphorescent instrument, multipurpose, for turbid biological materials 9-18725  
 phosphors with electronic transitions in localized centres, photoluminescent efficiency 9-21641  
 porphyrins, intercombination transitions quantum output meas. using heavy atom effect, obs. 9-15877  
 proteins, fluorescence and phosphorescence under u.v. excitation 9-15905  
 pyrazine phosphorescent state, ESR 9-14719  
 quinoline rel. to  $\pi$  transitions and N effects on mol. levels, 77°K 9-15899  
 radiation spectrum of impurities, vibrational structure 9-16408  
 resonance fluorescence, Ar laser spectroscopic system 9-15559  
 rock, powder sample, proton and u.v. irradiation for moon lum. lab. simulation 9-20221  
 semiconductors, recombination through exciton states kinetics 9-14071  
 spectrophospho-fluorimeter, sensitive, construction details 9-15554  
 theory, book 9-12460  
 transient phenom. evaluation by freq. characts. 9-12459  
 triboluminescence, symposium, Berlin (1967) 9-18728  
 X-ray fluorescent screens, random noise 9-12817  
 Al  $\beta$ -diketone chelates, emission vibronic structure 9-13342  
 H<sub>2</sub>O<sub>2</sub> decomposition, study of intermediates formed after u.v. irradiation 9-9213  
 H<sub>2</sub>O<sub>2</sub> decomposition, study of intermediates formed after u.v. irradiation 9-17034  
 K vapour, resonance radiation trapping and quenching, <sup>42</sup>P state lifetime meas. 9-14670  
 OD chemiluminescent, breaking-off pts. on limiting curve of predissociation 9-18221  
 OH chemiluminescent, breaking-off pts. on limiting curve of predissociation 9-18221  
 Pb  $\beta$ -diketone chelates, emission vibronic structure 9-13342
- gases**  
 air, fluorescence efficiency under e bombardment, 65 km, Ee=700 eV 9-14158  
 atoms, resonance fluoresc., effects of collisions on polarization 9-706  
 benzene vapour, <sup>1</sup>B<sub>2u</sub>-<sup>1</sup>A<sub>1g</sub> transition, fluorescence obs. 9-19450  
 benzene vapour, quenching by olefins 9-2896  
 biacetyl in vapour phase, photoluminescence and phosphorescence spectrum 9-793  
 chemiluminescence in low-conc. reactions 9-10329  
 fluorescence rotation depolarization in mirror, fluid vacancy theory 9-13321  
 hexafluoroacetone, quenching by O<sub>2</sub>, NO and hydrocarbons 9-799  
 hexafluoroacetone vapour, fluoresc. and phosphoresc. rel. to ketone pressure and excitation 9-1921  
 indazole, fluorescence 9-15898  
 isoquinoline, fluorescence 9-15898  
 methane, vibr. energy transfer 9-2935  
 modulation excitation of vibronic states, relax. theory 9-20910  
 optical r.f. double reson. technique 9-8559  
 pyrazine, fluorescence and phosphorescence 9-15898  
 pyrimidine, fluorescence 9-15898  
 toluene vapour, electronic energy relax. 9-9283  
 HCl-CO<sub>2</sub> mixture, laser-excited vib. fluorescence, energy transfer rates 9-15854  
 HCl-HI mixture, laser-excited vib. fluorescence, energy transfer rates 9-15854  
 HI-CO<sub>2</sub> mixture, laser-excited vib. fluorescence, energy transfer rates 9-15854  
 He, radiative decay processes pressure dependence 9-11425  
 K<sub>2</sub> vapour, laser-induced 9-15856  
 Li in H-O flame, fluoresc. quenching by Ar, N<sub>2</sub> and CO<sub>2</sub> from 2p<sup>2</sup>P state, cross-sections 9-676  
 NO<sub>2</sub> fluorescence, radiative lifetime and collisional quenching, nature of air afterglow 9-15861  
 N<sub>2</sub>O, laser-induced 9-7030  
 N<sub>2</sub>O, vibr.-vibr. energy transfer in gas mixtures 9-4983  
 NO+O chemiluminesc. in expanding flow, effect of molec. clusters 9-20031  
 NO+O+(M) $\rightarrow$ NO<sub>2</sub>+(M), chemiluminescent reaction, three body mechanism 9-16478  
 Na-D<sub>2</sub> sensitised luminesc., Na 3<sup>2</sup>P<sub>1/2</sub> $\rightarrow$ 3<sup>2</sup>P<sub>1/2</sub> excit. transfer, obs. 9-9309  
 Na-H<sub>2</sub> sensitised luminesc., Na 3<sup>2</sup>P<sub>1/2</sub> $\rightarrow$ 3<sup>2</sup>P<sub>1/2</sub> excit. transfer, obs. 9-9309  
 Na-HD, sensitised luminesc., Na 3<sup>2</sup>P<sub>1/2</sub> $\rightarrow$ 3<sup>2</sup>P<sub>1/2</sub> excit. transfer, obs. 9-9309  
 Na-N<sub>2</sub> sensitised luminesc., Na 3<sup>2</sup>P<sub>1/2</sub> $\rightarrow$ 3<sup>2</sup>P<sub>1/2</sub> excit. transfer, obs. 9-9309  
 Ne, discharge formation of metastable atoms, optical absorption meas. of density 9-6967  
 Ne fluorescence polarization, laser beam interaction 9-13292  
 NO,  $\epsilon$ -fluorescence, mean lifetime in D<sup>2</sup> $\Sigma^+$  state 9-17037  
 SO<sub>2</sub>, electronic excitation chemiluminescence obs. 9-10328  
 SO<sub>2</sub>, fluoresc. and phosphoresc. 9-9233  
 SO<sub>2</sub> fluorescence from lowest excited electronic state, lifetime obs. 9-7038  
 SO<sub>2</sub> 9-2881  
 Xe, continuum emission induced by 1470 Å radiation 9-19401  
 Xe, light gain in elec. field, geometrical props. 9-689
- liquids and solutions**  
 acetone, monomer and excimer emission 9-16011  
 anthracene, electrogenerated chemiluminesc. in soln. 9-21219  
 anthracene in cyclohexane, radiation-induced fluorescence, elec. field effects 9-18765  
 anthracene and mesoderivs. in soln, fluoresc. quenching by 'heavy atom quenchers' 9-9529  
 aromatic fluoresc., relative yield rel. to wavelength, conc. and higher excimer states 9-5176  
 aromatic solvents with low solute concs. down to 0.005g/lg radiative transfer rel. to luminesc. yield 9-9525  
 arylethylenes, sterically hindered, spectrum and polarization rel. to viscosity 9-20948  
 benzene, fluoresc. quenching by biacetyl at 28°C, rel. to dilution in hexane and cyclohexane 9-16014  
 benzene, quenching by carbon tetrachloride, solvent excimers 9-7267  
 benzene, radiationless decay of triplet state 9-803  
 benzene, solvent and temp. effects on quantum yield 9-16012  
 benzene and derivatives, foreign quenching and energy migration 9-1030



**Luminescence continued****liquids and solutions continued**

- benzene and derivatives, self-quenching and energy migration 9-1029  
benzene and liq. derivatives, electron-impact excitation 9-9530  
benzene in cyclohexane, aggregation effects 9-2556  
benzene in cyclohexane, quenching by O<sub>2</sub> and CCl<sub>4</sub> 9-3112  
benzene plus *p*-terphenyl solns., scintillation efficiency 9-16013  
benzene solns with trans-stilbene and diphenyloxazole, excitation energy transfer and quenching 9-3113  
benzoxazole derivs. as fluorese. solutes for liq. scintillators 9-16009  
biacetyl, fluorese. sensitization with 2-aminopyridine 9-1031  
1,4'-bis (2-butyl-octyloxy)-*p*-quaterphenyl in toluene, fast response and high efficiency 9-16007  
 $\beta$ -carotene, fluorescence and phosphorescence 9-17212  
in cavitating liquids 9-5175  
coupled resonance system as model of centre, relax. in nonadiabatic transitions 9-1027  
cryptocyanine dyes, polarized emission of laser radiation 9-4473  
cyclohexane scintillator systems, fluorese. decay curves after high-energy excitation 9-11703  
cyclohexane systems, energy transfer kinetics 9-9531  
diacetyl excitation by methylethylketone oxidation, transition prob. obs. 9-9527  
trans 1,2-diarylethylenes, as scintillator solutes in toluene, fluorese. spectra 9-11704  
diazanaphthalenes, solvent effects 9-9281  
4-dimethylamino 4'-nitrodiphenyl+acetone in frozen decaline soln., fluorescence obs. 9-7071  
4-dimethylamino 4'-nitrodiphenyl+propyl alcohol in frozen decaline soln., fluorescence obs. 9-7071  
dioxane base scintillator solns., quenching props. of alcohols rel. to molec. weight 9-9528  
diphenylene oxide soln., fluorescence spectra conc. depend. 9-9279  
diphenylstilbene, absorpt. and fluorescence spectra 9-4961  
divinylbenzene soln., fluorese. 9-801  
dye soln. stimulated fluorescence interferometry 9-9241  
emission spectroscopy, time-resolved nanosec., for interpretation of spectral shifts due to solvent-solute relax. 9-13534  
energy radiative transfer processes characterization by fluorescence spectra 9-13532  
enhancement in scintillators by elec. fields 9-19636  
eosin-blue, absorption and fluorescence spectra obs., dipole moment determ. 9-13535  
europium dibenzylmethanate in alcohols, levels population and transition rates, obs. 9-18367  
europium theonyltrifluoroacetate 9-16016  
ferrocene in glassy soln., 77°K phosphoresc. 9-3111  
fluorescein, rel. to species, 80 and 300°K 9-1034  
fluorescence decay studies of emission spectral shifts due to solvent-solute relax. 9-13534  
fluorescence emission band shift with excitation wavelength 9-19637  
fluorescence radiative lifetime determ., nanosecond phase fluorometer 9-13533  
fluorescence response functions, for org. solns., and scintillation pulse shapes 9-5177  
fluorescence rotation depolarization in mirror, fluid vacancy theory 9-13321  
*p*-hydroxybenzaldehyde, emission and proton transfer 9-9532  
naphthalene, mten, migration of triplet excitons from excitation region to anode 9-9533  
naphthalene derivatives, substituted, intermol. fluorescence quenching 9-20972  
naphthalene liq. derivatives, electron-impact excitation 9-9530  
1-naphthol, excited, H-bonded, fluorescence and phosphorescence spectra, 293°K 9-9519  
naphthols in soln.,  $\pi$ -H bonding 9-17059  
oil contamination in water, on-line monitoring method 9-4022  
*p*-oligophenylene series, scintillator solute, correl. between molec. struct. and luminesc. props. 9-9534  
organic, energy migration at high temps. 9-7246  
organic, scintillations, tail quenching and decay time shortening by O and bromobenzene 9-9526  
organic phosphors rel. to activator conc. and excitation wavelength, obs. 9-16010  
organic scintillators, luminesc. decay, appl. to pulse shape discrimination of particles 9-10255  
organic solns. high solute conc., self-quenching struct. correls. 9-16008  
organic systems, high-energy-induced, ionic processes 9-1028  
oric scintillators, fluorese. and energy transfer rel. to high temp. 9-11702  
1,3,4-oxadiazole derivs., as fluorese. solutes for liq. scintillators, characts. 9-16009  
oxadiazoles, fluorese. and scintillation rel. to use as secondary solute 9-9535  
oxazoles, fluorese. and scintillation rel. to use as secondary solute 9-9535  
phenanthrene, fluorese. decay, effect of diffusion in presence of acridine 9-5178  
2-phenyl indole solns., u.v. excitation, conc. depend. 9-17214  
2-phenyl indole solns. fast-electron excitation, conc. depend. 9-17213  
phthalimide, fluorescence polarisation 9-3114  
phthalimide in pyridine solns., rad. spectral width 9-9536  
phthalimide in vitrifying solvent, limit fluorescence polarization determ. 9-16015  
pyrazoles, fluorese. and scintillation rel. to use as secondary solute 9-9535  
pyrene in ethanol soln., xcimer and molec. fluorese. intensities rel. to triplet-triplet annihilation 9-11705  
pyrene excimer, fluorescence yield and lifetime 9-15897  
pyrene in cyclohexane, radiation-induced fluorescence, elec. field effects 9-18765  
quinoxaline, solvent effects 9-9281  
rare-earth ions in aq. soln., nonradiative energy transfer 9-9524  
resonance transfer of excitation energy between compound mols. 9-9522  
rubrene, triplet-triplet fluorese. in soln. 9-3115  
samarium dibenzoylmetanate 9-16016  
scintillators in aliphatic solvents, high-energy excitation, ionic processes 9-21218  
solute quenching. Validity of Perrin's eqn., effect of quencher addition 9-9523  
stilbene, absorpt. and fluorescence spectra 9-4961  
styrylstilbene, absorpt. and fluorescence spectra 9-4961  
terephthalic acid, aldehyde and acid chloride, phosphoresc. 9-801

**Luminescence continued****liquids and solutions continued**

- thymine in alkali soln., fluorese. excitation spectrum, wavelength depend. of quantum yield 9-11706  
toluene base scintillator solns. quenching props. of alcohol rel. to molec. weight 9-9528  
Toluene in *n*-hexane, fluorescence, mol. and excimer, obs. of lifetimes and quantum yields for eval. of parameters 9-4964  
toluene solns., triplet-triplet transfer to chelates through an intermediary 9-1032  
triacylbenzene soln, phosphoresc. 9-801  
Uranin, aggregate fluorescence obs. 9-1033  
uranin, rel. to species, 80 and 300°K 9-1034  
uranin soln. containing KI, polarization of fluorescence 9-9537  
*p*-xylene in cyclohexane, aggregation effects 9-2556  
*p*-xylene in cyclohexane, quenching by O<sub>2</sub> and CCl<sub>4</sub> 9-3112  
*p* xylol solns with trans-stilbene and diphenyloxazole, excitation energy transfer and quenching 9-3113  
Cr complex, [Cr(antipyrine)<sub>3</sub>](ClO<sub>4</sub>)<sub>3</sub> 9-12469  
Cr complex., [Cr(urea)<sub>6</sub>](ClO<sub>4</sub>)<sub>3</sub> solns., temp. depend. 9-12469  
LiBr: Ag<sup>+</sup>, spectra, and absorpt. and excitation spectra 9-1020  
LiCl: Ag<sup>+</sup>, spectra, and absorpt. and excitation spectra 9-1020  
NaBr: Ag<sup>+</sup>, spectra, and absorpt. and excitation spectra 9-1020  
NaCl: Ag<sup>+</sup>, spectra, and absorpt. and excitation spectra 9-1020  
Pb<sup>2+</sup> in SeOCl<sub>2</sub>: aprotic solvent rel. to laser appls. 9-17876  
POCl<sub>3</sub>-SnCl<sub>4</sub> mixture, fluorescence spectra and radiative lifetimes of Nd<sup>3+</sup>, Eu<sup>3+</sup>, Tb<sup>3+</sup> in soln. 9-21217
- solids, inorganic**  
alkali halides, delayed coincidence method of meas. decay time 9-5954  
alkali halides, Eu activated, red  $\rightarrow$  blue after explosive reaction 9-7999  
alkali halides, thallium activated, quantum efficiency of F- and Tl<sup>0</sup>-scintillations 9-16445  
alkaline earth halophosphate phosphors, Eu<sup>2+</sup>-activated, prep. and luminescence 9-21643  
alkaline earth oxides, defect studies, review 9-9693  
alkaline-earth aluminates, Eu<sup>2+</sup>-activated, fluorescence 9-21650  
aluminoborate glass: Tl, centres and trapping mechanism 9-1777  
anthracene, emission decay time and singlet exciton diffusion 9-1847  
borosilicate glass, Fe<sup>3+</sup> activated, comparison with silicates and phosphates 9-10264  
chondrite and achondrite meteorites, bombarded with 40 keV electrons, obs. microprobe 9-20007  
decay time of lumidimeters after excitation by u.v. flash 9-20010  
diamond, natural, elec. field modulation of excitation in range 5.0-6.0 eV 9-5950  
diamonds, artificial, with B impurity, phosphorescence and thermoluminescence 9-21651  
elbaite, rel. to colour centre obs. 9-1236  
excited centre vibrational relaxation, Raman spectra 9-12403  
fluorescence, charact. broadband, concentration quenching, considerations and expts. 9-3923  
fluorescent phosphors preparation, patent 9-15186  
fluoroberyllate glasses, effect of chem. bonding of Mn<sup>2+</sup> with ligands 9-1845  
GaAs:Sn, rel. to impurity band structure and effects 9-12463  
*p*-GaP voltage pulse modulation 9-5758  
glass, radioluminescence, nuclear and other radiation fields effects 9-12481  
glass screens, cathodoluminescent, high resolution, variable spectrum 9-14093  
group II-VI compounds: Ni, model for emission process mechanism 9-14072  
KI: Tl, scintillations, electron-hole and exciton mechanisms, photomolelling 9-20008  
phosphate glass, Fe<sup>3+</sup> activated, comparison with silicate and borosilicates 9-10264  
pyrene single crystals, excimer fluorescence spectra, 4 353°K 9-1834  
rare earth-oxygen sulphur cpds., Eu<sup>3+</sup>-activated, and prep. 9-21647  
rare-earth i.r. lifetimes in trichloride crystals. 9-10243  
rocksalt, in 800 1000 V fields 9-16433  
ruby, self-absorpt. of R-lines, 4.2-300°K 9-16435  
sapphire, under x irradi. 9-1839  
semiconductor solid solutions, edge width and band broadening 9-3880  
silica, fused, Tl-doped, centres and trapping mechanism 9-1777  
silicate glass, Fe<sup>3+</sup> activated, comparison with phosphates and borosilicates 9-10264  
silicates, Eu<sup>2+</sup>-activated, fluorescence 9-21649  
soda lime glass: rare earths, visible fluorescence 9-3926  
theory, book 9-14023  
thorium alkali metal vanadates, Eu<sup>3+</sup> activated 9-20002  
transient phenom. evaluation by freq. characts. 9-12459  
transition metal chelates 9-1837  
YAl garnet, Nd-doped, opt. refrigeration, laser rad. fluorescent quantum efficiency 9-1831  
ZnS, phosphors, characteristics of pair emission types 9-5958  
Ag film, surface plasmons, light emission 9-17373  
AgCl: Mn<sup>2+</sup>, temp. depend. 9-21642  
AgCl, pressure-induced photoluminescence 9-12462  
AgCl crystals, temp. and press. dependence 9-3913  
Ag<sub>2</sub>O bands obs. 9-1823  
Al<sub>2</sub>O<sub>3</sub> film, photoluminescence 9-18720  
Al optical resonance transitions, lifetime measurements, phase shift method 9-11392  
AlhaO<sub>3</sub>: Pr<sup>3+</sup>, visible and u.v. excitation of fluorescence 9-18724  
Au-Cu alloy photoluminescence, radiative recomb. obs. 9-21660  
Au photoluminescence, radiative recomb. obs. 9-21660  
Ba<sub>2</sub>TiGe<sub>2</sub>O<sub>8</sub>, fluorese., compared with isomorphous Ba<sub>2</sub>TiSi<sub>2</sub>O<sub>8</sub> 9-14083  
BaB<sub>2</sub>O<sub>7</sub>: Eu<sup>2+</sup> activated, fluorescence 9-20004  
BaF<sub>2</sub>: Er<sup>3+</sup>, Stark structure analysis 9-3916  
BaF<sub>2</sub>: Nd<sup>3+</sup>, conc. dependences at 300, 77 and 4.2°K 9-15161  
Ca<sub>3</sub>(PO<sub>4</sub>)<sub>2</sub>: F: Nd<sup>3+</sup>, spectral meas. at 300, 77 and 4.2°K 9-18709  
CaF<sub>2</sub>: Er<sup>3+</sup>, Stark structure analysis 9-3916  
CaF<sub>2</sub>: Eu<sup>2+</sup>, Ho<sup>3+</sup>, fluorescent decay of Eu<sup>2+</sup> as function of Ho conc. 9-15187  
CaF<sub>2</sub>: Eu<sup>2+</sup> microwave-modulated fluorescence, 9.5 GHz 9-1828  
CaF<sub>2</sub>: Nd<sup>3+</sup>, conc. dependences at 300, 77 and 4.2°K 9-15161  
CaF<sub>2</sub>: Eu<sup>2+</sup>, fluorescent lifetime meas. and Zeeman eff., temp. depend. 9-14050  
CaF<sub>2</sub>: Ho<sup>3+</sup>, X-irrad., phosphorescence spectral distrib. 9-21657  
Ca<sub>1.5</sub>Mg<sub>1.5</sub>(PO<sub>4</sub>)<sub>2</sub>: Eu<sup>2+</sup> emission max., quantum efficiency and energy conversion efficiency 9-3914

### Luminescence continued

#### solids, inorganic continued

- CaO-Sb and CaO-Bi phosphors with wide forbidden zone, radical recombination, mech. 9-16428
- CaO coloured crystal, fluorescence of 3.7 eV F-centre absorption band 9-3924
- Ca<sub>3</sub>(PO<sub>4</sub>)<sub>2</sub>:Eu<sup>2+</sup>, emission peaks in  $\alpha$ - and  $\beta$ -phase 9-3914
- Ca(SiSe):Mn<sup>2+</sup>, phosphors 9-3957
- CaWO<sub>4</sub>:Tb<sup>3+</sup>, fluorescence rel. to ground term energy level analysis 9-12373
- CaWO<sub>4</sub>-Al fluorescent screen for high stress conditions, vacuum evaporated 9-13069
- CdF<sub>2</sub>:Er<sup>3+</sup>, Stark structure analysis 9-3916
- CdF<sub>2</sub>:at 1%Er<sup>3+</sup> blue fluorescence, opt. double-resonance proc. 9-3925
- CdGeAs<sub>2</sub>, radiative recombination 9-5951
- CdIn<sub>2</sub>S<sub>4</sub>:Nd<sup>3+</sup> or Er<sup>3+</sup> fluorescence 9-14081
- CdS:TM(Cu) phosphors fired in S atmosphere line emission in i.r. region 9-5977
- CdS, e.-irrad., recombination radiation 9-3915
- CdS, edge emission bands 9-15188
- CdS, exciton emission in excitation spectra, oscs. 9-12489
- CdS, green edge, mechanism, and luminescence centre parameters 9-14075
- CdS, spectra, rel. to exptl. obs. of three-quantum absorpt. process 9-10235
- CdS crystals with edge emission, i.r. effects, and temp. depend. of photoluminescence 9-21644
- CdS edge emission, green and blue, at 4.2°K 9-14074
- CdS phosphors, i.r., and role of cation vacancies 9-12467
- CdS photoluminescence, orange, red and i.r., mechanism, and centre parameters 9-5976
- CdS single crystal phosphorescence and trap distrib. 9-16440
- CdS slow phenomena, photochemical interpretation 9-21547
- CdS single crystals, long-wavelength bands, flash excitation 9-16427
- CdSe, mechanism of  $\lambda_m=0.82 \mu$  photoluminescence, and parameters of luminescence centres 9-10234
- CdSe, sensitization as result of etching, investigation 9-3917
- CdSiAs<sub>2</sub>, radiative recombination 9-5951
- CdTe, band edge radiative emission, nature, and atomic displacements 9-16429
- CdTe, photoluminescence and cathodoluminescence rel. to displacement energies of Te and Cd 9-16429
- Cr(III) complexes, temp. depend. of emission bands 9-14076
- Cr complex, [Cr(turea)<sub>6</sub>](ClO<sub>4</sub>)<sub>3</sub>, temp. depend. of fluoresc. and phosphoresc. 9-12469
- Cr complex, [Cr(antipyrine)<sub>6</sub>](ClO<sub>4</sub>)<sub>3</sub>, temp. depend. of fluoresc. and phosphoresc. 9-12469
- 2Cr(en)<sub>3</sub>Cl<sub>2</sub>.KCl.6H<sub>2</sub>O, temp. depend. of emission bands 9-14076
- CsI:Ti, impurity conc. depend. 9-7987
- CsI:Ti, X-ray luminescence, excitation intensity dependence 9-16442
- CsI, kinetics, excitation by  $\beta$  particles, u.v. and i.r. pulses 9-16448
- CsI(Tl) optical nonuniformity obs. 9-12482
- CsI(Tl) scintillation-response and stopping power calcs. 9-12035
- Cu photoluminescence, radiative recomb. obs. 9-21660
- CuCl radiative recomb., low temp., laser u.v. excitation 9-16430
- Eu chalcogenides, photo- and cathodoluminescence 9-12328
- Eu<sup>3+</sup> chelates, <sup>241</sup>Am-doped,  $\alpha$ -particle fluoresc. 9-1829
- EuSe, work function and cathodoluminescence 9-5970
- Fe-Si alloys, X-ray fluorescence 9-14080
- GaAs:Si epitaxial films, spectra for band structure determ. 9-5701
- GaAs, at 1.2eV and 77°K, heat treatment effects 9-5953
- GaAs, bound- and free- exciton, band- and donor-acceptor, and Auger recombination 9-14077
- n-GaAs, cathodoluminescence rel. to donor band states 9-12479
- n-GaAs, donor-acceptor pair recombination involving the first excited state of donor 9-12465
- GaAs, free-carrier and exciton radiation recombination 9-10238
- GaAs, photoluminescent meas. method rel. to equilib. carrier distrib. 9-9974
- GaAs and GaAs<sub>1-x</sub>P<sub>x</sub>, cathodoluminescence studies of electron radiation damage 9-18570
- n-GaAs epitaxial films, photoluminescence 9-10265
- GaP:B, Zn, photoluminescence rel. to reactions in doping 9-3940
- GaP:O<sup>-</sup>, i.r. radiative capture of electrons at ionized oxygen donors 9-12464
- n-GaP:S(Te) and undoped, epitaxial, cathodoluminescence spectra, 80°-300°K 9-12480
- GaP, cathodoluminescence studies of electron radiation damage 9-18570
- GaP, concentration quenching and the impurity-band Auger model 9-8000
- GaP, exciton luminescence intensity elec. field and temp. dependences 9-16431
- GaP, near indirect transition in multiphoton excitation case, 4.2°K and 77.3°K 9-10236
- GaP donor-acceptor electron recombination luminescence, multiple field effects 9-10266
- GaP doped epitaxial films, photoluminescence 9-10237
- GaP p-n structures, radiation spectrum control 9-5952
- GaSb, radiative recombination excited by 20 KeV electron beam 9-21645
- GdAlO<sub>3</sub>:Eu<sup>3+</sup>, fluorescent emission 9-12490
- Gd<sub>2</sub>O<sub>3</sub>:Eu<sup>3+</sup>, crystal field interpretation 9-10205
- Gd<sub>2</sub>O<sub>3</sub>:Eu<sup>3+</sup>, fluorescent emission 9-12490
- Gd<sub>2</sub>O<sub>3</sub> rare earth traces meas. by X-ray excited fluoresc. spectra 9-16514
- GdVO<sub>4</sub>, activated by Sm<sup>3+</sup>, Eu<sup>3+</sup> and Dy<sup>3+</sup> 9-20003
- p-Ge:Ga, Li, interimpurity radiative recombination, Li-Ga ion pair effects 9-3919
- Ge:As, Ga, nonradiative interimpurity recombination, 4.2°K 9-21646
- Ge:As, p-irradiated, recombination centres 9-17397
- Ge:A., recombination radiation impurity conc. dependence rel. to e. density modulation 9-3918
- Ge:As(Sb), under uniaxial compression, radiative recombination 9-10239
- Ge:As(Sb), under uniaxial compression, effect on long-wavelength intrinsic 'tail' 9-12466
- p-Ge:Ga, Li, interimpurity radiation recombination, Li-Ga ion pair effects 9-3919
- Ge, photoluminescence in presence of crossed fields 9-14097
- Ge, radiative recombination at dislocations 9-15183
- In<sub>2</sub>S<sub>3</sub>:Nd<sup>3+</sup> or Er<sup>3+</sup> fluorescence 9-14081
- In<sub>2</sub>-Ga<sub>2</sub>P, photoluminescence, i.r. and visible 9-12488
- InP, time-resolved photoluminescence for donor-acceptor recombination evidence 9-18729

### Luminescence continued

#### solids, inorganic continued

- KBr:NO<sub>2</sub><sup>-</sup>, vibration structure in spectra at 4.2°K 9-16432
- KBr:S<sub>2</sub><sup>-</sup>, spectra at 4.2°K rel. to S<sub>2</sub><sup>-</sup> centre local vibrations freq. and anharmonicity 9-14078
- KBr, decay time of O<sub>2</sub><sup>-</sup> centres, effect of pressure 9-15184
- KCl:(Ca, Sr or Ba), fluorescence of Z<sub>1</sub> centres 9-5962
- KCl:(Cu), X-irrad., external stress dependence 9-3932
- KCl:Eu, radical recombination, atomic H excited 9-3920
- KCl:NO<sub>2</sub><sup>-</sup>, vibration structure in spectra at 4.2°K 9-16432
- KCl:S<sub>2</sub><sup>-</sup>, spectra at 4.2°K rel. to S<sub>2</sub><sup>-</sup> centre local vibrations freq. and anharmonicity 9-14078
- KCl:Tb<sup>3+</sup>:S<sub>2</sub><sup>-</sup> 9-1846
- KCl:Tb<sup>3+</sup>:Se<sup>2-</sup>, models of lum. centres 9-1846
- KCl-Eu and KCl-Sb phosphors with wide forbidden zone, radical recombination, mech. 9-16428
- KCl, excitation of F and M centres 9-7988
- KCl, with quasi-colloidal K centres 9-18721
- KCl electrophotoluminesc. at room temp. 9-12485
- KI:S<sub>2</sub><sup>-</sup> 9-14082
- KI:Se<sub>2</sub><sup>-</sup> 9-14082
- KI:Se<sub>2</sub><sup>-</sup> 9-14082
- KTa<sub>2</sub>Nb<sub>1-x</sub>O<sub>7</sub>:Eu<sup>3+</sup>(Sm<sup>3+</sup>), fluorescence 9-10242
- KTaO<sub>3</sub>:Eu<sup>3+</sup>(Sm<sup>3+</sup>), fluorescence 9-10242
- K<sub>2</sub>UO<sub>2</sub>SO<sub>4</sub>.2H<sub>2</sub>O fluorescence lifetime, effect of D<sub>2</sub>O substitution 9-1830
- Ka cpts. as useful cathodoluminescent phosphors, patent 9-10254
- LaAlO<sub>3</sub>:Eu<sup>3+</sup>, fluorescent emission 9-12490
- La<sub>2</sub>O<sub>3</sub>:Eu<sup>3+</sup>, fluorescent emission 9-12490
- LaVO<sub>4</sub>, activated by Sm<sup>3+</sup>, Eu<sup>3+</sup> and Dy<sup>3+</sup> 9-20003
- Li<sub>2</sub>GeO<sub>4</sub>:Cr<sup>3+</sup>, energy transfer between nonequivalent sites 9-5964
- Li<sub>2</sub>GeO<sub>4</sub>:Cr<sup>3+</sup>, R lines, width and position temp. dependence 9-5963
- Ln:Me<sup>+</sup>Me<sup>+</sup>O<sub>4</sub> fluoresc., (Ln=La, Gd, Y; Lu; Me<sup>+</sup>=Si, Ge, Ti; Me<sup>+</sup>=Mo, W) 9-13638
- Lu cpts. as useful cathodoluminescent phosphors, patent 9-10254
- Lu<sub>2</sub>O<sub>3</sub>:Eu<sup>3+</sup>, crystal field interpretation 9-10205
- MgAl<sub>2</sub>O<sub>4</sub>:Cr<sup>3+</sup>, fluorescence spectrum 9-18708
- MgO:Cr<sup>3+</sup> spectral line shift temp. dependence interpretation 9-12470
- Mn<sub>2</sub>TiO<sub>4</sub>, spinel struct., co-ord. of Mn<sup>2+</sup> centres 9-20005
- MnF<sub>2</sub>, antiferromagnet, enhancement in mag. fields 9-1824
- NO<sub>2</sub><sup>-</sup> in potassium halides, vibration structure in spectra at 4.2°K 9-16432
- Na rare-earth tungstates, quenching interactions of rare-earth ions 9-16436
- NaCl:Ag, activator glow output and X-ray lum. spectra temp. dependence, 77-600°K 9-3922
- NaCl, quenching, ionic temp. mechanism, decay law 9-3928
- NaCl layers, in strong elec. fields 9-3921
- NaI:TL, scintillations, electron-hole and exciton mechanisms, photomodeling 9-20008
- NaI, excitonic energy transfer to Q and T centres 9-20000
- NaI, intrinsic photoluminescence, exciton states 9-3943
- NaI(Tl), scintillation-response and stopping power calcs. 9-12035
- NaI(Tl) optical nonuniformity obs. 9-12482
- PbCl<sub>2</sub> 9-10253
- PbO-SiO<sub>2</sub>-K<sub>2</sub>O glasses, u.v. irrad. at 120°K., spectra 9-10267
- RbBr:S<sub>2</sub><sup>-</sup>, spectra at 4.2°K rel. to S<sub>2</sub><sup>-</sup> centre local vibrations freq. and anharmonicity 9-14078
- RbF(U) temp. var. of total intensity,  $\alpha_0$ ,  $\Delta E_1$ ,  $\Delta E_2$  calc., 3650 Å 9-10240
- RbMnF<sub>6</sub>, antiferromagnet, enhancement in mag. fields 9-1824
- S<sub>2</sub><sup>-</sup> centre in alkali halides, spectra at 4.2°K rel. to local vib. freq. and anharmonicity 9-14078
- SO<sub>2</sub>, phosphorescence intensity depend. on temp., 4-100°K, intersystem crossing 9-15190
- Se<sub>2</sub>O<sub>3</sub>:B<sup>3+</sup>, fluorescence spectra 9-3927
- Si, p- and n-irrad., recombination luminescence 9-7989
- Si, radiative spectra from shallow donor-acceptor electron transfer 9-18722
- SiC:Al, dependence of recombination rates on the intensity of the light excitation 9-5949
- $\alpha$ -SiC, photoluminescence and phosphorescence quantum yields 9-3929
- $\beta$ -SiC, spectra rel. to exciton states 9-3900
- n-SiC, u.v.-excited, rel. to photoconduction, 77°K 9-13932
- SiC diffusional p-n junctions, light sum relax. 9-10241
- SiC epitaxial films, blue photo luminescence 9-5972
- SiC p-n junctions, near-i.r. region 9-16056
- Sr<sub>2</sub>TiSi<sub>2</sub>O<sub>8</sub>, fluoresc., compared with isomorphous Ba<sub>2</sub>TiSi<sub>2</sub>O<sub>8</sub> 9-14083
- Sr<sub>2</sub>(Eu(PO<sub>4</sub>))<sub>2</sub>SiO<sub>4</sub>, emission colour composition (x) dependence rel. to energy transfer between Eu<sup>3+</sup> in non-equivalent sites 9-15189
- SrF<sub>2</sub>:Dy<sup>3+</sup>, rel. to Dy conc. and distrib. 9-7990
- SrF<sub>2</sub>:Er<sup>3+</sup>, Stark structure analysis 9-3916
- SrF<sub>2</sub>:Nd<sup>3+</sup>, conc. dependence at 300, 77 and 4.2°K 9-15161
- SrMoO<sub>4</sub>, scheelite-type, two-photon laser excitation 9-1825
- STiO<sub>2</sub>, photoluminescence in undoped and Sm- and Cr-doped crystals 9-21648
- Tb<sup>3+</sup> chelates, <sup>241</sup>Am-doped,  $\alpha$ -particle fluoresc. 9-1829
- Tb(OH)<sub>3</sub>, Tb<sup>3+</sup> crystal field parameters determ. from fluorescence 9-14019
- UO<sub>2</sub>SO<sub>4</sub>.3H<sub>2</sub>O fluorescence lifetime, effect of D<sub>2</sub>O substitution 9-1830
- Xe, cathodoluminescence in u.v. region 9-1841
- YAl garnet:Nd laser, non-mode-locked, two photon fluorescence displays 9-6527
- Y<sub>2</sub>Al<sub>2</sub>O<sub>7</sub>:Nd<sup>3+</sup>, temp. depend. 9-5955
- Y<sub>2</sub>O<sub>3</sub>:Bi<sup>3+</sup>, fluorescence spectra 9-3927
- Y<sub>2</sub>O<sub>3</sub>:Eu<sup>3+</sup>, crystal field interpretation 9-10205
- Y<sub>2</sub>O<sub>3</sub>, rare earth traces meas. by X-ray excited fluoresc. spectra 9-16514
- Y<sub>2</sub>O<sub>3</sub>, rare earth traces X-ray excited fluoresc., interelement effects, obs. 9-16443
- Y(OH)<sub>3</sub>:Tb, Tb<sup>3+</sup> crystal field parameters determ. from fluorescence 9-14019
- YVO<sub>4</sub>, activated by Sm<sup>3+</sup>, Eu<sup>3+</sup> and Dy<sup>3+</sup> 9-20003
- Zn<sub>2</sub>TiO<sub>4</sub>:Mn, spinel struct., co-ord. of Mn<sup>2+</sup> centres 9-20005
- ZnA, crystals grown, Zn or S vapour excess, I carrier, luminescence meas. 9-21545
- ZnAl<sub>2</sub>O<sub>4</sub>:Cr<sup>3+</sup>, fluorescence spectrum 9-18708
- ZnIn<sub>2</sub>S<sub>4</sub>:Nd<sup>3+</sup> or Er<sup>3+</sup> fluorescence 9-14081
- ZnO, decay times of u.v. and green emission lines 9-1826
- ZnO films, dependence on parameters of growth process from saturated condensate current 9-1103
- ZnS-Co(Ni), bond nature effects in stacking faults 9-1796
- ZnS-Cu, (I,Cl,Al or Ga) blue-Cu, polarization 9-16449
- ZnS-Cu, photoluminesc., effect of u.v. rad. intensity 9-7998



**Luminescence continued****solids, inorganic continued**

- ZnS:Cu, trap levels with electrons excited by modulated light, dynamic study of behaviour 9-17487  
 ZnS:Cu phosphor prep. 9-7991  
 ZnS:Er<sup>3+</sup> fluorescence 9-10244  
 (ZnS-CdS):Cu, recombination luminescence, temp.-time depend. 9-15185  
 ZnS-Cu, Gudden-Pole effect on light sum of luminophors and its dependence 9-5960  
 ZnS-Cu, Gudden-Pole effect, three kinds, temperature dependence 9-5959  
 ZnS-Cu phosphors, effect of coactivators 9-3930  
 ZnS, recombination luminescence, temp.-time depend. 9-15185  
 ZnS activatorless luminors, band edge emission, electro and photoexcitation 9-10233  
 ZnS phosphors, i.r. and role of cation vacancies 9-12467  
 ZnS phosphors, spectrum shift during decay and with excitation intensity 9-5957  
 ZnSag, scintillation due to  $\alpha$ -particles, amplitude elec. field dependence 9-3937  
 ZnS(Ag) single crystals photo luminescence obs. 9-12468  
 ZnS(Ag) under  $\alpha$  bombardment, instability of radiation 9-11139  
 Zn(S<sub>100-x</sub>Se<sub>x</sub>)(Cu,I) photoluminesc. spectra comparison with electroluminesc. 9-10263  
 ZnSe, cathodoluminescence by scanning electron microscope in single crystals 9-3944  
 ZnSe, exciton emission in excitation spectra, oscs. 9-12489  
 ZnSe epitaxial films, photoluminescence 9-5956  
 ZnSe unactivated single crystals,  $\lambda_m=0.63 \mu$  band 9-14079  
 ZnSnP<sub>2</sub>, chalcopyrites and sphalerites, photoluminescence rel. to band structure 9-5931  
 ZnTe, isoelectronic oxygen trap from isotopic substitution and Zeeman expts. 9-18723

**solids, organic**

- afatoxins B<sub>1</sub> and G<sub>1</sub>, fluorescence and phosphorescence for presence determin. 9-6201  
 3-aminophthalhydrazide, chemilum. applic. to sensitometry 9-20565  
 anils., photochromic 9-10353  
 anthracene, delayed fluoresc., ionic energy levels and charge-transfer exciton state 9-16437  
 anthracene, fluorescence quenching for study of exciton conc. with excitation depth 9-13835  
 anthracene, triplet exciton quenching by paramag. impurities, field depend. 9-1832  
 anthracene, triplet lifetime as monitor in zone refining 9-5282  
 anthracene, triplet-triplet annihilation emission, as indicator of low  $\gamma$ -ray dose 9-12472  
 anthracene in naphthalene, solid soln., fluorescence decay pattern 9-12471  
 anthracene soln. in polyethylene matrices, spectra for various concs. at 77°K 9-17211  
 aromatic hydrocarbons, phosphoresc. growth and decay 9-10249  
 aromatic hydrocarbons, press. effect on fluoresc. lifetimes 9-14084  
 aromatic hydrocarbons, singlet-ground-state transitions 9-11480  
 aromatics, in frozen solns., triplet-state energy transfer 9-17488  
 1,2-benzanthracene, triplet formation, quantum yield, fluoresc. and phosphoresc. 9-16438  
 benzene, lifetime, solvent and temp. effects 9-10250  
 benzene, nonexponential decay 9-1835  
 benzene, triplet formation, quantum yield, fluoresc. and phosphoresc. 9-16438  
 benzophenone, at 4.2°K 9-10251  
 benzophenone, triplet level energy transfer rel. to phenanthrene and phenazine additives 9-3931  
 benzophenone crystals, pure and impure, phosphorescence, temp. depend 9-16441  
 benzophenone in mixed crystals., temp. and host effects 9-10248  
 benzophenone-naphthalene, solid soln., phosphorescence decay at K 9-12476  
 5,6-benzoquinoline boric acid phosphor, props. 9-1827  
 biphenyls, phosphoresc., eff. of partial deuteration 9-17489  
 4-bromo-testosterone acetate, singlet-triplet states 9-11487  
 carbazole 9-9252  
 chlorophyll b, two phase system, fluorescence spectra and lifetimes 9-16418  
 chrysene, triplet formation, quantum yield, fluoresc. and phosphoresc. 9-16438  
 chrysene-biphenyl crystals., fluoresc. and phosphoresc. obs. rel. to triplet-triplet annihilation kinetics 9-16439  
 crystal scintillators, luminesc. decay, appl. to pulse shape discrimination of particles 9-10255  
 delayed, life-time measurements, use of spectrophotographic phosphoroscope 9-5961  
 1,2,5,6-dibenzanthracene in polymeric matrices, phosphoresc., compared with glass matrix 9-21654  
 diphenylmethylen., fluoresc. lifetime 9-1833  
 electrophotoluminescence 9-16447  
 genzene, phosphoresc. polarization and triplet level energy transfer 9-1836  
 halonaphthalenes in compressed polymethylmethacrylate, triplet decay 9-17491  
 hexahelicene, low-temp. 9-15165  
 high pressure apparatus 9-7954  
 3-methylcholanthrene solns., quasi-line and i.r. absorpt. spectra, 77°K 9-16434  
 Mixed crystals., temp. and host effects on phosphoresc. triplet state 9-10248  
 naphthalene, deuterium substitution effects on triplet lifetime 9-14086  
 naphthalene, fluoresc. decay rel. to temp and thickness, lifetimes of two Davydov-components 9-10246  
 naphthalene, pure cryst. 9-1838  
 naphthalene, triplet formation, quantum yield, fluoresc. and phosphoresc. 9-16438  
 naphthalene in compressed polymethylmethacrylate, oxygen quenching 9-12477  
 naphthalene phosphoresc., vibr. assignment 9-5967  
 naphthalene-biphenyls, fluoresc. and phosphoresc. obs. rel. to triplet-triplet annihilation kinetics 9-16439  
 1-naphthol, excited, H-bonded, fluorescence and phosphorescence spectra, 77°K 9-9519  
 naphthalene in anthracene, solid soln., fluorescence decay pattern 9-12471

**Luminescence continued****solids, organic continued**

- phenanthrene, triplet formation, quantum yield, fluoresc. and phosphoresc. 9-16438  
 phenanthrene in EPA, phosphoresc. rise and decay curves at 77°K 9-14087  
 phenanthrene-biphenyl crystals., fluoresc. and phosphoresc. obs. rel. to triplet-triplet annihilation kinetics 9-16439  
 phenazine single crystals, fluorescence spectra rel. to carrier generation 9-7860  
 phosphorescence, anti-Stokes problem 9-21653  
 phosphorescent triplet states, zero field transitions, opt. detection 9-12474  
 phthalic acid diester dispersions for photographic prints, patent 9-6565  
 phthalimide uronic acid, solid soln., phosphoresc. with foreign NiCl<sub>2</sub>, KBr or KI mols. 9-7994  
 polyacene solid solns., energy transfer, bibliography for 1967 9-7986  
 polystyrene-9,10-diphenyl anthracene+quencher fluoresc. quenching and energy transfer 9-10247  
 polystyrene+quencher, fluoresc. quenching and energy transfer 9-10247  
 polystyrene, pure and with anthracene or diphenyl-oxazole, fluoresc. rel. to excitation wavelength 9-12473  
 porphyrin, degree of polarization of fluorescence depend. on emission wavelength 9-5965  
 pyrene excimer, fluorescence yield and lifetime 9-15897  
 pyrene trapped in methylcyclopentane, fluorescence spectrum at 88°K 9-17490  
 quinoxaline in durene cryst. 9-5968  
 salicylic acid, phosphoresc. polarization and triplet level energy transfer 9-1836  
 scintillation pulse shapes 9-5177  
 sodium salicylate, absolute quantum efficiency for extreme ultraviolet 9-21652  
 tetraene, bimolecular radiationless transitions of excitons as fluorescence quenching channel 9-14085  
 theory, book 9-14023  
 Eu chelates in polymethyl methacrylate, strong excitation characts. 9-2899

**Luminescence chambers**

- pinhole imaging of  $\gamma$ -rays 9-14536  
 test method using radioactive sources 9-6740

**Luminescent devices**

- See also Counters/scintillation*  
 cathodoluminescence attachment for electron microprobe anal. 9-18782  
 diode, electroluminescent, efficiency and electron-hole recomb. 9-12139  
 dosimeter, thermoluminescent, dose and dose-rate dependences, theoretical interpret. 9-5978  
 electroluminescent condenser, brightness wave-current relations 9-12487  
 film electroluminescent capacitors on ZnS-Cu, Mn base 9-18653  
 lumidosimeters, decay time of luminescence after excitation by u.v. flash 9-20010  
 phosphor, La, Lu<sup>3+</sup>cpd., cathodoluminescent, patent 9-10254  
 radiation converter, electroluminescent-photoluminescent 9-14098  
 screen, fluorescent, for monochromatic X-ray diffr. pattern on polaroid film 9-3264  
 CaF<sub>2</sub> thermoluminescent dosimeter 9-2599  
 CaWO<sub>4</sub>-Al fluorescent screen for high stress conditions, vacuum evaporated 9-13069  
 p-GaP:O-Zn electroluminescent diode, epitaxial growth, patent 9-10257  
 GaP diode sources of red radiation, prep. and characts. 9-3679  
 GaP electroluminescent diodes, minority carrier lifetime 9-12491  
 ZnS:Cu electroluminescent capacitors, characts. and current rectification applic. 9-15195  
 ZnS activatorless luminors, band edge emission, electro- and photoexcitation 9-10233

**Lumino(pho)rs** *see Luminescences/solids, inorganic; Luminescence/solids, organic; Luminescent devices***Lutetium**

- thermal conductivity and Lorenz function 9-7673

**Lutetium compounds**

- phosphor, cathodoluminescent, patent 9-10254  
 LuFe garnet, sublattice magnetization by <sup>57</sup>Fe n.m.r. 9-21671  
 LuN, specific heat 9-5567  
 Lu<sub>2</sub>O<sub>3</sub>:Eu<sup>3+</sup>, luminescence and emission spectra, crystal field interpretation 9-10205

**Luxemburg effect** *see Electromagnetic wave propagation/ionosphere***M-centres** *see Colour centres***M-regions** *see Sun***Mach's principal** *see Relativity***Mach number** *see Aerodynamics; Shock waves; Supersonic flow***Machines, electrical** *see Electrical machines***Macromolecules** *see Molecules/configurations and dimensions, macromolecules; Polymers; Proteins***Madelung constant** *see Solids/structure***Maggi-Righi-Leduc effect** *see Magnetothermal effects***Magnesium**

- alloy, hydrostatic press. and temp. eff. on strength and ductility 9-5478  
 atoms and ions, bibliography of spectra 9-13287  
 conduction e.s.r. obs. 9-16457  
 deformed, generation and recovery of cryst. defects, from elec. resist. meas. 9-7478  
 disk with circular hole, creep under equal biaxial loading 9-5469  
 dislocation loops in foil, growth and structure 9-18471  
 film, wavelength depend. of optical transmittance in vacuum u.v. 9-10166  
 ion beam production by charge exchange with 5-40 KeV p beam 9-233  
 K $\alpha$  X-ray satellites in fluoresc. spectra of Mg in oxides and metals 9-3933  
 lattice dynamics, h.c.p. structure 9-3506  
 liquid, surface tension and density, temp. dependence obs. 9-5149  
 melting, possible vacancy mechanism 9-5215  
 powder, compacted with 1% O, high temp. creep 9-17311  
 powder patterns from hexagonal crystals, temp. diffuse scatt. 9-11814  
 Raman scattering by optical modes, linewidths temp. depend. 9-12442  
 range of 0.5-4 KeV electrons rel. to energy 9-19872  
 second order pressure derivatives and third order elastic constants 9-18495  
 solar spectrum, MgI multiplets, 1-2  $\mu$ , 30 km balloon obs. 9-6190  
 in stars, B, abundance 9-8237  
 thermolec. power, 5-300°K 9-12206

**Magnesium continued**

- vaporization mass spectrometric study 9-19386  
 X-ray spectra,  $K\alpha_{1,2}$  satellites, relative intensity 9-18717  
 X-ray spectra, ultrafast 9-18718  
 Cu/Mg electric exploded wire, temp. and e. density distrib. in later stages 9-9346  
 $Mg_2$  mols. and quasimols. absorpt., 2852 Å 9-18328  
 Mg II, semiempirical atomic core potentials, coeffs. 9-19397  
 $Mg^{2+}$  diff. in cubic  $Li_2SO_4$ , 600-800°C 9-17288  
 MgI, radiation, Stark and van der Waals level broadening constants 9-13293  
 in MgO, as impurity, effect on secondary e. emission temp. dependence 9-1631  
 MgO, n. scatt. obs. and calcs. from lattice-dynamical model 9-9821

**Magnesium compounds**

- MgO, water vapour effect on mech. props. 9-18506  
 alloy, conc. of Zn by photoactivation 9-1933  
 alloys, thermoelec. power 9-12206  
 ferrite, spin-wave attenuation -150°C-300°C obs. in single crystals 9-17458  
 ferrites, quenching temp. effect on mag. permeability and complex dielec. permittivity tensor components 9-19967  
 magnesia, elastic at 16 GHz and 4.2°K 9-17296  
 magnesia refractories, creep 9-16130  
 magnesia refractory, creep, rel. to microstructure, bonding and composition, 1450-1550°C 9-3423  
 magnesite-chrome refractories, fine grain, hot strength and thermal shock resist. 9-3438  
 MgO ceramic crystals, recrystn. in forging and annealing 9-3482  
 sintered spinel, corrosion by oxides at 1500-1750°C 9-14135  
 spinel, elastic constants at 16 GHz and 4.2°K 9-17296  
 spinel in chromium, reaction with nitrogen in chromium 9-20032  
 spinel-cordunum, corrosion by oxides at 1500-1750°C 9-14135  
 Al-(5 wt.%)Mg-(0.4 wt.%) Ag alloy, precipitate-free zone, light and electron microscopy obs. 9-18537  
 Al-Mg-Ge alloy, ageing, transformation stages 9-9782  
 Al-Mg-Ge alloy, clustering after quenching 9-17331  
 Al-Zn-Mg alloy, kinetics of clustering 9-7600  
 (93 wt.%)Al-(7 wt.%)Mg alloy, segregation and precipitation at grain boundaries 9-18832  
 Au-Mg alloys near  $Au_3Mg$ , long periodic stacking order 9-9716  
 CdMg alloys, degree of ordering of  $y_a$  and  $y_b$  of  $\alpha$  and  $\beta$  sites, determ. 20-250°C 9-7434  
 CdMg $_2$  alloy, order-disorder, 10° to 185°C. obs. 9-11971  
 FeO-MgO solid solutions, magnetic susceptibility 9-5806  
 Li-Mg binary alloy, ordering energy and effective pairwise interactions 9-7696  
 Mg-(2 wt.%)Al alloy, complex stress creep fracture at 50°C 9-21382  
 Mg-Cd alloy, order-disorder phase transition, change in props. 9-16155  
 Mg-Cd alloy, ordering speed, effect on props. 9-16156  
 Mg-Cd alloys, Zenes relaxation, rel. to internal friction 9-11913  
 Mg-Cd single crystal, solid solution hardening investig., core and temp. depend. 9-21378  
 Mg-Mn-Zn-ferrites, microwave, resonance line width and scale susceptibility 9-5811  
 Mg-Mn polycrystalline ferrite spinel, ferrimag. reson. line broadening mechanism and temp. dependence 9-1852  
 Mg-(9 wt.%)Ni, age hardening precipitation 9-3472  
 Mg-Pb molten alloys, structure 9-14829  
 Mg-Te system, MgTe: phase formation 9-17341  
 Mg-(3 wt.%)Zn, clustering kinetics and precip. 9-5505  
 Mg $_2$ Si, thermal expansion, linear, coeff. 25-300°K 9-18564  
 Mg $_2$ Sn, thermal conductivity, 80 to 700°K 9-15025  
 Mg $_2$ Sn, thermal expansion, linear, coeffs. 25-300°K 9-18564  
 Mg $_2$ As $_2$ , semicond. props. 9-16267  
 Mg $_2$ Cd type alloys, anomalous change in resistance on ordering 9-3570  
 Mg-Mn ferrite, optical props. and conduction mechanism 9-10171  
 MgAl $_2$ O $_4$ :Cr $^{3+}$ , optical absorption and fluorescence spectrum 9-18708  
 MgAl $_2$ O $_4$  ceramic crystals, recrystn. in forging and annealing 9-3482  
 MgAl $_2$ O $_4$  spinel, active, powder characteristics and sintering 9-3464  
 MgAl $_2$ O $_4$  spinel powders, prep. by decomposition 9-3242  
 MgAl $_2$ O $_4$  powders, initial sintering kinetics 9-1321  
 MgBr $_2$ ·4C $_4$ H $_8$ O, tetrahydrofuran complex, crystal structure 9-19716  
 Mg $_2$ Cd, ordering rate, composition depend. 9-9790  
 Mg $_2$ Cd, polycrystalline, deform. 9-5459  
 MgCl $_2$ · $\frac{1}{2}H_2O$ , rot. anal. of  $A^2\Pi_{1/2} \rightarrow X^2\Sigma^+$  system,  $\lambda\lambda$ 3950-3600LB 9-11465  
 MgCr $_2$ O $_4$ -MgFe $_2$ O $_4$  system, spinel characteristics 9-19843  
 MgF $_2$ :Co $^{2+}$ , far i.r. spectrum of Co $^{2+}$  ion pairs 9-1788  
 MgF, configurations for first excited electronic state 9-4930  
 MgF, Franck-Condon factors and r centroids for B-X and C-X systems 9-11466  
 MgF $_2$ , ionic binding nature determ. 9-18448  
 MgF $_2$ , rutile structure spectra, critical dipole frequency behaviour 9-7636  
 MgF $_2$ , rutile structure spectra, critical dipole frequency behaviour 9-18549  
 MgF first excited electronic state, calc. and empirical arguments using matrix Hartree-Fock eqns. 9-4930  
 MgF $_2$ , colour centre formation 9-5390  
 MgF $_2$ , evaporation film, refractive index inhomogeneity 9-5872  
 MgF $_2$ , n-irradiation-induced vacuum u.v. absorpt. 9-1787  
 Mg $_2$ Fe $_2$ O $_7$ : $Fe_2O_3$ , anisotropy induced at higher temperatures 9-3829  
 Mg $_2$ Fe $_2$ O $_7$ , structural vacancies and solid solution decay in ferros-pinel 9-5339  
 Mg $_2$ Ge, electroreflectance spectra, 1.5-4.5 eV 9-12364  
 MgMn ferrite, single crystal film, ferromagnetic resonance 9-15196  
 MgMn ferrites, alignment and microwave props. 9-1685  
 MgMn ferrites, pulse and hysteresis props., eff. of annealing conditions 9-17459  
 $\alpha$ -MgMoO $_4$ :Cr $^{3+}$ , pseudo-Stark e.p.r. line splitting 9-18739  
 MgO:Cr $^{2+}$ , acoustic paramag. reson. 9-21666  
 MgO:Cr-X-irrad., Cr $^{2+}$  phonon scatt., thermal cond. meas. 9-5535  
 MgO:Cr $^{3+}$  spectral line shift, temp. dependence interpretation 9-12470  
 MgO:Fe $^{2+}$ , absorption bands, pressure shift, and dynamic Jahn-Teller effect 9-5927  
 MgO:Fe $^{2+}$ , phonon-photon double quantum transitions freq. depend. 9-1360  
 MgO:Fe $^{3+}$ , thermal cond. < room temp. 9-1406  
 MgO:Fe $^{3+}$ , spin-lattice coupling constants 9-14016

**Magnesium compounds continued**

- MgO:Fe $_2$ O $_3$ , hot pressed, grain growth rel. to purity and porosity, 1100-1400°C 9-3169  
 MgO:M $^{2+}$ , (M=Co, Ni, Cr paramag. ions), spin lattice relax. anisotropy, theory 9-12318  
 MgO:Ni microwave, acoustic phonon bottleneck, direct obs. by Brillouin scatt. 9-9819  
 MgO:Ni $^{2+}$ , rotation of polarization plane of u.s. wave 9-1380  
 MgO:V $^{3+}$ , hyperfine fields, effect of dynamic phonon interaction 9-5531  
 MgO: $^{51}V^{3+}$ , spin Hamiltonian of  $^{51}V^{3+}$  from ENDOR 9-12520  
 MgO-Al $_2$ O $_3$ -Cr $_2$ O $_3$  cryst. solns., precip. kinetics 9-3493  
 MgO-Al $_2$ O $_3$ -SiO $_2$  ceramic, phase composition and cordierite formation, 800-1400°C 9-21409  
 MgO-Al $_2$ O $_3$ -SiO $_2$  glasses, growth of quartz solid solutions 9-11797  
 MgO-FeO-Fe $_2$ O $_3$  phase equilibria 9-21412  
 MgO, adsorp. of methanol and ethanol, i.r. spectra 9-3215  
 MgO, colour centres, spin-orbit coupling and stress spectra 9-5389  
 MgO, computed ground state props. in molecular orbital approx. 9-7015  
 MgO, creep, effects of varying porosity, grain size and impurity addition 9-1292  
 MgO, creep, stress, temp., and strain rate 9-19799  
 MgO, crystal-field parameters, isotope effects 9-12040  
 MgO, ENDOR spectra for  $V_{oh}$  centre 9-8046  
 MgO, e.p.r. of Fe $^{2+}$ , by saturation by u.s. waves 9-21665  
 MgO, fine structure of spots caused by wedge shaped crystal parts, exptl. rel. to theory 9-13620  
 MgO, hot extruded, strength and fracture up to 1315°C 9-1302  
 MgO, hot pressed, grain growth rel. to purity and porosity, 1100-1400°C 9-3169  
 MgO, interaction with Cr $_2$ O $_3$ , mechanism 9-3987  
 MgO, interaction with Fe $_2$ O $_3$ , kinetics 9-3988  
 MgO, internal potential meas. by interferential microscopy 9-5861  
 MgO, microhardness anisotropy rel. to dislocations motion, obs. 9-3454  
 MgO, optical absorption, e.s.r. and thermoluminescence, eff. of plastic deformation 9-18740  
 MgO, polycrystalline sound velocity and Poisson's ratio porosity dependence 9-18494  
 MgO, range of 0.5-4 KeV electrons rel. to energy 9-19872  
 MgO, reactions with Cr $_2$ O $_3$ , effect of processing parameters on kinetics 9-3986  
 MgO, secondary e. emission temp. dependence, excess Mg effects 9-1631  
 MgO, secondary electron emitting surface preparation by baking and dipping 9-7869  
 MgO, ultrasoft X-ray spectra 9-18718  
 MgO, vibrational spectra, Raman spectra, photon density of state curves 9-11988  
 MgO, vibrational spectra, Raman spectra, phonon density of state curves 9-9820  
 MgO, X-ray spectral study of energy structure 9-18586  
 MgO as lowpass n vel. filter, transparency determ.,  $\lambda_m=1.5\lambda$  9-11105  
 MgO brick, microstructure and phases 9-3170  
 MgO dense powder, thermal conductivity in N $_2$  gas 9-15026  
 MgO dielectric cry., eff. of finite-amplitude acoustic waves 9-11994  
 MgO flame, radiative temp. meas. 9-6405  
 MgO microcrystal, lattice const. and energies study 9-17270  
 MgO shock wave expt. 9-16516  
 MgO single crystal with magnesioferrite precipitates, fracture rel. to particle size 9-7573  
 Mg(OH) $_2$ , dispersed porous mat., microstresses on pressing giving reversible elastic deform., X-ray exam. 9-1276  
 Mg(OH) $_2$ , powder compacts, compressive creep rel. to dehydroxylation rate 9-1291  
 Mg(OH) $_2$ (NO $_3$ ) $_2$ , crystal structure 9-13641  
 Mg $_2$ P $_2$ O $_7$ , monoclinic, crystallographic data 9-5324  
 MgSO $_4$ ·7H $_2$ O, collision breeding from aqueous soln. 9-18421  
 MgSO $_4$ , growth, impurity effects, rel. to pH of soln. 9-13601  
 MgSO $_4$ ·7H $_2$ O, crystallization nuclei production in presence of seed crystal 9-13610  
 MgSeO $_4$ ·6H $_2$ O:Co $^{2+}$ , e.s.r. 9-1856  
 Mg $_2$ Si, electroreflectance spectra, 1.5-4.5 eV 9-12364  
 Mg $_2$ Sn, electroreflectance spectra, 1.5-4.5 eV 9-12364  
 Mg $_2$ SnO $_4$ , thermal neutron capture, chem. and Mossbauer study 9-17549  
 MgWO $_4$ , crystal structure 9-13642
- Magnetic amplifiers** see *Amplifiers; Magnetic devices*  
**Magnetic anisotropy** see *Magnetic properties of substances; Magnetization state*  
**Magnetic bays** see *Earth/magnetic field, variations; Magnetic storms*  
**Magnetic bottles** see *Magnetic fields; Plasma confinement*  
**Magnetic cooling**  
 low-temp. prod., nuc. adiabatic damag., rare-earth ions suitability 9-4185  
 by paramagnetic salt demagnetisation, reversibility 9-14293  
 Ce $_2$ Mg $_2$ (NO $_3$ ) $_2$ , thermometers, shape factors from demagnetizing factors meas. 9-15395
- Magnetic devices**  
 balance for susceptibility meas., calibration of pole times 9-4428  
 ballistic scales with short period pulses for meas. of susceptibility 9-12236  
 ceramic ferrite, microwave latching devices 9-1679  
 circuit with large air-gap for field switch-off 9-8580  
 coils, experimental aspects, book 9-12971  
 crystal ferrimagnetic single sphere orientation method 9-5270  
 densimeter, for liq. mixtures, using optical sensing 9-18353  
 hysteresigraph for meas. in thin cylindrical mag. films for fast computer memories 9-16762  
 kinematometer, measurement scales 9-8350  
 ens, quadrupole, circular aperture, excitation winding effect on mag. field nonlinearity 9-2328  
 lense system design for particle focusing 9-224  
 lenses, with longitudinal mag. field, particle transportation channel 9-225  
 magnetization coil field, increase of homogeneity 9-214  
 magnetometer, rubidium vapour self-oscillating, miniature 9-18817  
 magnetometers for geomag. micropulsations meas. in unattended stations 9-12645  
 mirror with pulsed field, e ring trapping 9-4430  
 particle in viscous medium, motion 9-13999  
 solenoid for general use 9-6467  
 superconducting solenoids 9-18610  
 suspension densimeter 9-10814  
 suspensions for pendulums, energy losses induced by gravity 9-120



**Magnetic devices continued**

- tape recorder to increase capacity of Mossbauer spectrometers 9-2568
- tape-wound cores of soft mag. alloys for power circuits 9-12975
- transducer, magnetoelastic transformer-type error reduction 9-8353
- Ni-Fe-Pd alloy films, storage element use rel. to composition and deposition, patent 9-13998
- SiO thin film element, deposition patent 9-19669

**Magnetic domains** *see Magnetization state/domains***Magnetic field measurement**

- components, two, simultaneous local meas. and sum of squares 9-10810
- earth's, quartz variometers, reliability under unfavourable weather conditions 9-21825
- electronic magnetometer using magnetoresistance transducers 9-212
- EPR signal of DPPH used as sensor, 700-3500G 9-10808
- experimental methods, book 9-12971
- geomagnetic micropulsations, unattended recording station design 9-12645
- magnetometer, automatic torque for meas. anisotropy constants of ferrites 9-17456
- magnetometer, nuclear maser, oscillator type, precise tuning 9-10805
- magnetometer, optical, based on total internal reflection prevention, patent 9-20490
- magnetometer, quartz D 9-20491
- magnetometer, rubidium vapour self-oscillating, miniature 9-18817
- magnetometers, in book 9-10803
- minor components calc., large aperture applic. in part. physics 9-2322
- moving mag. field line identification 9-8574
- probe, used in n.m.r. spectrometer 9-12962
- proton magnetometer, shipborne, freq. mod. of signal 9-6097
- pulsed, calibration 9-215
- pulsed, up to 20 kG, by Faraday eff. 9-4426
- quantum interference magnetometer response to magnetic Johnson (thermal) noise from conducting environment 9-7783
- r.f., using field-locked n.m.r. spectrometers 9-218
- using scanning e microscope 9-8578
- search coil, magnetometer data from OGO 3 at 6.6 R<sub>e</sub> 9-10409
- solar, by photoelec. magnetograph, comparison with photographic methods 9-2066
- stray fields, calc. using POISSON program 9-16763
- strengths, book 9-6267
- superconducting low-pass filter 9-10811
- from <sup>87</sup>Rb zero-field level crossing resonances to detect fields ~10<sup>-9</sup> gauss 9-15822
- Rb magnetometer, self oscillating, long term stability 9-15498

**Magnetic fields**

- See also Earth/magnetic field; Electromagnetic fields; Interplanetary magnetic fields; Sun/magnetism*
- ambient, compensation for null field 9-14415
- anomalies and demagnetization effects caused by bodies of arbitrary shape, rapid computation 9-4427
- capture and plasma containment in expts. with collisionless shock wave 9-15932
- in collisionless plasma, Green's tensor 9-5027
- current distrib. in terms 9-217
- current loop, steady, acceleration 9-19123
- of cylinder moving in field of current-carrying coil 9-10763
- cylindrically symmetric, gravitation 9-6305
- electromagnet with Fe core, increase of homogeneity of field 9-219
- electron spin self-polarization during spiral motion in mag. field 9-2468
- fluctuations of square nonlinearity, nonlinear resonance in proton synchrotron 9-480
- flux compression by explosion, recoil phase 9-12972
- force-free magnetic fields, behaviour, rel. to sunspots 9-10548
- Galactic, investigation by spherical harmonic anal. of interstellar polarization 9-12665
- generation, switching by explosive syst., MJ range 9-10809
- generation of megoersted fields 9-12973
- guiding field of Julich isochronous cyclotron 9-14540
- homogeneous, magnet assemblies for production, patent 9-10813
- interstellar, estimation from galactic noise freq. spectrum and cosmic ray flux 9-12730
- lines of force, motion of, times characteristic 9-15917
- magnetization coil field, increase of homogeneity 9-214
- metals, rel. to e.m. wave propag., review 9-5625
- modulation, automatic distortionless control 9-10796
- neighbourhood of corners of transformer with nonlinear permeability 9-213
- in nonlinear media, convergence of method of soln. 9-10804
- plasma, non-uniform rot., generation by viscous forces 9-6114
- plasma moving in field, occurrence of strong discontinuities 9-13423
- prism. quantum description 9-2362
- production, book 9-2325
- production as rectangular pulse, and applic. to relax. process study in ruby 9-10807
- production method by air cored coils, for 80 cm diameter 9-6466
- pulsed, by rotation symmetric coils, calc. 9-20147
- spatial variation due to instabilities 9-216
- spatially modulated, invariants of motion of a charged particle 9-12976
- strong, transport phenomena, semiclassical and quantum theories, applic. to polar opt.-phonon scatt. 9-8461
- sun, Rossby-wave, field reversals 9-6194
- switch-off using large air-gap device 9-8580
- transient intense, prod. by increasing flux density using metal sheet compressed by capacitor discharge 9-10806
- transport phenomena, semiclassical and quantum theories, applic. to polar opt.-phonon scatt. 9-8461
- turbulent medium, dynamics 9-8541
- two-dimensional, general integral formula 9-4383
- two-dimensional, useful props. 9-2323
- vector potential expansion, elim. of monopole term. 9-11
- Nb<sub>3</sub>Sn superconducting magnet, optimum field for particular form 9-7771
- Ni cylindrical crystal, stray field above Bloch walls, electron-optical investigation, 9-13974

**effects**

- acoustic waves, u.s., vel. and absorpt. 9-21429
- acoustoelectric effect, theory 9-1384
- alternating, hydromagnetic surface wave prod., propag. study 9-17092

**Magnetic fields continued****effects continued**

- chemical equilibrium in closed system free from ferroelec. and ferrimag. constituents 9-1895
- coherent states of a charged particle 9-13096
- coherent states of a charged particle 9-2453
- conducting strip progressively moving in constant mag. field, e.m. processes 9-8540
- conductivity, elec. thin metal film in longit. field 9-5650
- crystals, liq. nematic, alignment-inversion wall prod. 9-5143
- D<sup>-</sup> band model, calc., by Hubbard's theory 9-16407
- damping of relativistic charged particle with self-interaction 9-17857
- elastic body, electrically conductive, in mag. field, asymm. stress possibility 9-21564
- elastic wave motion in electrical conductors, perturbation by applied magnetic field 9-14150
- electron spin echo envelope modulation by very small alternating fields 9-10282
- electron spin polarization in uniform field, classical interpretation 9-6471
- ferrite, magnetization under simultaneous a.c. circular field and longitudinal constant one 9-3832
- ferromagnet with domain struct. threshold 9-13968
- Friedel oscills, modification 9-5627
- gas, perfectly conducting, two-dimensional flow in crossed elec. and mag. field 9-2957
- graphite, colloidal, optical transmission 9-1050
- hollow-cathode negative glow, current and radiation intensities 9-14804
- hot electron mobility, resonance variation 9-13823
- hot electron mobility, resonance variation 9-3550
- inhomogeneous, trapped part. accel. by bimodal diffusion 9-222
- on Kelvin-Helmholtz and gravitational instability in self-gravitating fluid layer 9-17091
- on Kelvin-Helmholtz instability of two superposed fluids in relative horizontal motion 9-14750
- Knight shift dependence 9-20026
- on laser prod. sparks in air, butane and He 9-7205
- liquid metal flow, turbulent charact. 9-7125
- magnetoelastic buckling of thin plate in transverse magnetic field 9-132
- manganese acetate tetrahydrate, heat capacity, 0.4-20°K 9-12020
- metal surface layer, rel. to stationary state of conductivity electrons 9-15068
- metals, u.s. reflection plane of polarization rot. and ellipticity appearance 9-3525
- MHD boundary layer at surface of plate for arbitrary orientation, properties 9-9329
- MHD channel with non-conducting wall, turbulent boundary layer calc. 9-7128
- monopole field, eff. on motion of point charge 9-20492
- motion and polarization interaction of a plasma in field of a multipole 9-5011
- nematic film, on structure 9-9482
- on nonlocal superconductor, theory 9-7766
- paramagnetic system, steady-state thermodynamics 9-14353
- photocurrent amplification by mag. field 9-5759
- photomultiplier gain shift in  $\gamma$ -ray circular polarisation meas., elimination 9-19192
- plane vortex sheet, or stability, rel. to parallel or transverse applic. 9-21101
- on plasma, cold, stability, traversed by two e beams, in const. external field 9-11602
- plasma, cylindrical, radial penetration 9-19531
- plasma, laser produced, expansion in mag. field 9-9355
- plasma, rarefied cold, propag. of nonstationary cylindrical waves of finite amplitude 9-3001
- primordial on spatially homogeneous cosmological models 9-12654
- random, intensity fluctuations of moving charged particles 9-8582
- on Rayleigh-Taylor instability of two superposed fluids in relative horizontal motion 9-17090
- on resistance between electrodes in current conducting channel 9-17142
- Ruderman-Kittel-Kasuya-Yosida (RKKY), mag. field dependence exchange interaction 9-5792
- semiconductor films, conductivity, quantum oscillations 9-5679
- semiconductor with electric field, conductivity 9-15088
- semiconductors, on Raman scattering of shallow impurity states 9-12396
- semiconductors, piezoelectric, u.s. amplification 9-3526
- Sentfleben-Beemakker effect on heat conductivity of gases of regular octahedral mols. 9-9446
- solid-state physics in megagauss fields 9-16323
- spark discharge formation time 9-18316
- steel, Si, commercial grade sheets, annealing 9-13753
- superconducting current ring supported in mag. field, stability 9-19896
- superconducting tubes, enhancement 9-15075
- superconductivity, surface, in critical field 9-3588
- superconductivity, surface, in critical field 9-15073
- superconductors, type II, effect on pinning force 9-12118
- superconductors, type II, peak effect 9-1492
- surface electron states, spectrum and damping 9-13834
- surface electron states, spectrum and damping 9-3557
- thermal cond. in fluid of rough spheres 9-9445
- thermionic converter in Knudsen state 9-20489
- torque acting on thin ferromag. layer 9-3805
- transverse, acoustoelectric current oscillation in n-InSb 9-5561
- transverse, fluid flow between parallel plates, reduction of effective length of entrance region 9-7123
- visco-elastic rod, disturbance propagation 9-21360
- e Brownian motion, displacement and diffusion const. calc. 9-8427
- Al-Si alloy, eutectic, on transverse banding in directional solidification 9-5313
- Au-(0.03 at.%)Fe alloy, thermoelec. power, 0.35°K-10°K, mag. field (0-77 kOe) dependence 9-1605
- Be, resistance oscillations in superconducting magnet 9-9877
- Bi-Sb alloy, rel. to semiconducting-metal transition 9-1513
- Bi, charge carrier relax. time 9-12047
- Cu helicon window, Gantmakher oscillations 9-1440
- Fe-30at.%Ni, martensitic transformation, mag. fields effect 9-3491
- Fe, specific heat near Curie temp. 9-13802
- GaAs and GaSb tunnel diodes, I-V characts. in high crossed elec. and mag. fields 9-10019
- n-GaAs e plasma Raman scatt. 9-14060
- n-GaAs Gunn diode, on l.f. oscillations 9-5737
- Ge, slice, transverse eff. on carrier injection 9-5706

**Magnetic fields continued**  
**effects continued**

- Ge tunnel diodes, I-V characts. in high crossed elec. and mag. fields 9-10019
- Hf<sub>1</sub>, thermal conductivity in crossed elec. and mag. field, reson. decrease of transfer coeffs. 9-9448
- He plasma, diffusion obs. 9-9349
- <sup>3</sup>He in <sup>4</sup>He, dilute solns., effect on osmotic pressure 9-11730
- Hg heat transfer of liquid reduced 9-21198
- Hg laminar natural convection 9-18252
- Hg pipe flow, friction factor and transition Reynolds number rel. to field strength, stability effects 9-14753
- Ho Fe garnet, rel. to Faraday effect 9-1740
- n-InSb, current oscillations, 77°K 9-15092
- n-InSb, instability, 70 MHz component 9-5630
- n-InSb, localization of electrons 9-15100
- MnCo<sub>2</sub>, antiferromag. reson. in fields up to 50 kOe, at freqs. 115 to 170 Gcs 9-15197
- MnF<sub>2</sub>, antiferromagnet, luminescence enhancement 9-1824
- Nb, type II, J<sub>0</sub>STATIC MAG. FIELD EFFECTS 9-1501
- NbTi wire, superconducting, type II, effect on pinning force 9-12118
- Nb<sub>3</sub>Zr wire, superconducting, type II, effect on pinning force 9-12118
- Ni-Fe ferrite single crystal, mag. anisotropy, effect on ferromag. resonance line breadth 9-12494
- Ni-Mo alloys, on anodic props 9-21709
- Ni, on anodic props 9-21709
- Ni, specific heat near Curie temp. 9-13802
- $\alpha$ -NiSO<sub>4</sub>·6H<sub>2</sub>O, magneto-thermodynamics, low-temp 9-19862
- RbMnF<sub>3</sub>, antiferromagnet, luminescence enhancement 9-1824
- ScF<sub>3</sub>, Senfleben-Beenakker effect on heat conductivity 9-9446
- n-Si, tilted effects on two- dimens. electron gas props. 9-5619
- Si steel, commercial grade sheets, annealing eff. 9-13753
- UF<sub>6</sub>, Senfleben-Beenakker effect on heat conductivity 9-9446
- UN, sp. ht., 1.3-4.6°K 9-17357
- Y Fe garnet, rel. to Faraday effect 9-1740
- Y<sub>2</sub>Fe<sub>2</sub>O<sub>7</sub>, intensity effect on Faraday rotation 9-7950
- Zn, de Haas-van Alphen effect in pulsed field, oscillation amplitudes meas. 9-10094
- n-Ge, current instability in crossed elec. and mag. field 9-7805

**Magnetic films** see *Films, solid/magnetic properties***Magnetic flux** see *Magnetic field measurement; Magnetic fields***Magnetic hysteresis** see *Magnetization process***Magnetic lenses** see *Electron lenses/magnetic; Ion optics***Magnetic measurement**

- See also *Magnetic field measurement. Entries describing measurement methods for specific magnetic quantities and effects may also be found listed under the various headings for the subjects concerned*
- adiabatic rotation of sample in magnetic field, liquid He temps. 9-4181
- anisotropy constant meas. using rotating sample magnetometer 9-2321
- anisotropy meter 9-8576
- balance, magnetic, automatic with photocell for gravimetric and magnetic analysis 9-18978
- balance, servo-type, for routine thermomagnetic analysis 9-14414
- Faraday balance for susceptibility 9-7873
- ferrites, ferromagnetic resonance meas. resonator method theory 9-16450
- ferrometer with high sensitivity 9-8577
- Hall probe for meas. of magnetization 9-4425
- hysteresigraph for meas. in thin cylindrical mag. films for fast computer memories 9-16762
- induction meas. of screened fields, equipment and methods 9-8575
- magnetometer, automatic torque for meas. of anisotropy constants 9-17456
- magnetometer, vibrating coil, for Type II superconductors 9-1491
- magnetoresistance, compensation method for meas. in alternating fields 9-12287
- permanent magnets, charact. meas. using analogue precision method 9-12974
- susceptibility, by Cahn electrobalance 9-3765

**Magnetic memories** see *Calculating apparatus; Magnetic devices***Magnetic mirrors** see *Magnetic fields; Plasma/confinement***Magnetic properties of dissolved atoms in dilute alloys**

- Anderson model, ground-state energy calc. by cluster variation method 9-13944
- d-alloys, localised moments, mechanism of appearance 9-10086
- electronic spin polarization calc. using perturbation theory 9-7872
- Hall anomaly, s-d model 9-16228
- magnetization distribts. 9-7900
- metals with transition element impurities, localised mag. mom. 9-7874
- spin resonance theory of impurities in metals, freq.-dependent susceptibility interpretation 9-12497
- spin correlations at low temps. about localized impurity moment 9-21562
- superconductor with mag. impurities antiferromagnetically coupled, ultrahigh critical field 9-21488
- , Sb, liq., with 3d-transition metals, susceptibilities rel. to localized impurity states 9-1043
- Al-Mn, susceptibility, 2.300°K 9-12238
- Au-Mn, anomalous scatt. of conduction electrons from magnetoresistance 9-5805
- Cr-Fe alloys, dil., from Fe impurity e.p.r. 9-1858
- Cu-Fe, mag. contrib. to sp. ht. 9-18563
- Eu<sub>0.95</sub>Gd<sub>0.05</sub>S critical scatt. and band conduction onset 9-9886
- Fe-Pd magnetization distribts. 9-7900
- La-Tb, n. diff. and susceptibility meas. 9-17454
- LaCl<sub>3</sub>:Ce<sup>3+</sup>, pair-interaction meas. e.p.r. 9-10283
- Ni-Cu alloys, susceptibility rel. to Hall effect and elec. resistivity 9-21485
- Pd-Ag, susceptibility meas. rel. to impurity scatt. and electron density of states 9-13986
- Pd-Rh, susceptibility meas. rel. to impurity scatt. and electron density of states 9-13986
- Pt-Co low temp. susceptibility, anomalous 9-13966
- Co particles in Cu-Co solid solns., distribution function in superparamagnetic range 9-5803

**Magnetic properties of substances**See also *Films, solid/magnetic properties*

## No entries

**antiferromagnetic**See also *Antiferromagnetism*

- alloys, dilute, coupling effect on free spin susceptibility 9-10090
- atoms, spin broadening of Mossbauer lines 9-3869

**Magnetic properties of substances continued**  
**antiferromagnetic continued**

- biaxial, thermodynamic potential, magnetiz., and spin thermal capacity 9-16374
- canted antiferromagnet, complex susceptibility and resonance freqs., analysis 9-7914
- goethite, thermomagnetic magnetization at Neel temp. 9-10150
- h.f. susceptibility in strong mag. field 9-19971
- magnon sideband shapes, Green function theory 9-12313
- metal, e.m. wave propagation 9-4388
- metals, anomalous elec. resistivity near Neel point 9-9927
- metals, elec. resistivity anomaly near ordering point 9-12096
- rare earth orthoferrites, metamagnetic props. 9-16383
- rare earth orthoferrites, vector reorientation 9-15159
- semiconductor, e.m. wave and slow neutron scattering by anomalous fluctuations of spin waves in elec. field 9-5814
- two spin-wave Raman scattering and i.r. absorption 9-12395
- AuMn, Neel temp. pressure dependence from susceptibility, sp. ht. and thermal expansion meas. 9-1699
- AuMn, metamagnetic pressure induced transition 9-17452
- AuMn<sub>2</sub>, susceptibility, elec. resistivity and Young's modulus temp. depend. 9-15157
- BaMF<sub>3</sub> piezoelectric crystals, M= Mn, Fe, Co and Ni 9-12308
- BiCrO<sub>3</sub>, below 123°K 9-10112
- COF<sub>2</sub>, two magnon absorption, Raman spectra 9-12435
- CeAl<sub>3</sub>, Laves phase cpd., 9-12247
- Ce<sub>1-x</sub>Eu<sub>x</sub>Al<sub>3</sub>, Laves phase cpd.,  $\chi$ >0.8 at 4°K 9-12247
- CoCl<sub>2</sub>·2H<sub>2</sub>O·Mn<sup>2+</sup>, e.s.r. and exchange interactions 9-3834
- CoF<sub>2</sub>, spin-optical phonon interaction, obs. 9-10146
- CoW<sub>2</sub>O<sub>8</sub>, symmetry corepresentations 9-21593
- CoW<sub>2</sub>O<sub>8</sub>, spin wave spectrum from i.r. absorpt. band identification 9-1773
- Cr-Fe alloys, dil., from Fe impurity e.p.r. 9-1858
- Cr-Ni alloys, thermoelectric power and resistivity, max. due to ordering for low Ni content 9-3721
- Cr, magnetostriction on stress-cooling rel. to ordering obs. 9-1700
- Cr, Q vector truncating effect on Fermi surface from de Haas-van Alphen effect obs. 9-17461
- Cr, second minimum in elec. resistivity-temp. dependence curve near Neel temp. 9-12099
- Cr, spin-density wave effects on Fermi surface from high field galvanomagnetic meas. 9-17462
- Cr alloys, susceptibility 9-7916
- Cr powder, long range order by n. diff. 9-14009
- Cr<sub>2</sub>TeO<sub>6</sub>, ordered trirutile, mag. ordering at 4.2°K from n.-diff. exam 9-1701
- Cr<sub>2</sub>WO<sub>6</sub>, ordered trirutile, mag. ordering at 4.2°K from n.-diff. exam. 9-1701
- CsMnCl<sub>2</sub>·2H<sub>2</sub>O, linear chain props. 9-14010
- CsMnF<sub>3</sub>, critical fluctuations, e.p.r. studies 9-18735
- Cu-Mn rel. to structural state, applied field intensity and temp. 9-10147
- Cu complexes, trinuclear, containing transition metals 9-10148
- CuMnSb 9-3835
- CuSb, absence of antiferromagnetism n.m.r. evidence 9-16376
- DyFeO<sub>3</sub> metamagnetic props. 9-16383
- DyP, lattice deformation at Neel pt. 9-12309
- ErAl, metamag. preps. <10°K, and mag. struct. 9-1702
- ErFeO<sub>3</sub>, metamagnetic props 9-16383
- Er<sub>2</sub>O<sub>3</sub>, structures from n. diff. exam 9-17463
- Eu, first order transition obs. from Mossbauer effect meas. 9-15148
- EuSe, domains effect on light scatt. 9-12328
- EuSe, mag. struct. from n. diff. expts 9-14011
- EuTe, domains effect on light scatt. 9-12328
- Fe-Ti alloy system, Laves phase, conc. depend. 9-7897
- Fe<sub>0.95</sub>S natural pyrrhotite thermomag. investigation 9-18821
- FeF<sub>2</sub>:Mn<sup>2+</sup>, spin wave impurity states 9-12307
- FeO·MgO, solid solns, susceptibility 9-5806
- $\alpha$ -Fe<sub>2</sub>O<sub>3</sub>, haematite, domain interactions 9-7917
- $\alpha$ -Fe<sub>2</sub>O<sub>3</sub>, piezomagnetism, microscopic origin 9-1704
- Fe<sub>2</sub>O<sub>3</sub> (hematite), with weak ferromagnetism, effect of hystrostatic pressure on mag. anisotropy 9-3836
- FePO<sub>4</sub>, anisotropy const. meas. by Mossbauer effect 9-5854
- Fe<sub>2</sub>TeO<sub>6</sub>, ordered trirutile, mag. ordering at 4.2°K from n.-diff. exam 9-1701
- GdCrO<sub>3</sub>,  $\lambda$ transition in mag. ordering from low temp. sp. ht. 9-7655
- GdFeO<sub>3</sub>, metamagnetic props 9-16383
- Ho (80 wt.%)Tb alloy single crystal 9-16377
- Ho<sub>8</sub>Smi<sub>2</sub>-xFeO<sub>3</sub> orthoferrites, Ho ion ordering, exchange interaction effects 9-16371
- KMnCl<sub>3</sub>, from e.s.r. spectra of MnCl<sub>2</sub>-alkali chloride fused mixtures 9-13948
- KMnCl<sub>3</sub>·2H<sub>2</sub>O, transition to antiferromag. state at 2.70°K, from sp. ht. meas. 9-1395
- KMnF<sub>3</sub>, critical fluctuations, e.p.r. studies 9-18735
- KMnF<sub>3</sub>, near phase transition, temp. behaviour of 2-phonon transition 9-7919
- K<sub>2</sub>MnF<sub>4</sub>, zero-point spin deviation from n.m.r. and e.s.r. obs. 9-10151
- KMn<sub>1-x</sub>Ni<sub>x</sub>F<sub>4</sub> single cryst., electron- magnon transitions in absorpt. spectra 9-1785
- KNiF<sub>3</sub>, superexchange interactions 9-14012
- KNiF<sub>3</sub>, unrestricted Hartree-Fock molecular-orbital treatment 9-12232
- LaBr<sub>3</sub>, supercharge interact. between pairs of Ce<sup>3+</sup> and Nd<sup>3+</sup> pairs 9-1697
- LaCl<sub>3</sub>, supercharge interact. between pairs of Ce<sup>3+</sup> and Nd<sup>3+</sup> pairs 9-1697
- LaErO<sub>3</sub>, mag. struct. n. diffraction study 9-12310
- LiFePO<sub>4</sub>, magneto-elec. coeff. temp. dependence in a.c. field 9-14013
- MnF<sub>2</sub>:Fe<sup>2+</sup>, localised mag. excitations, obs. by Raman scatt. 9-10221
- MnF<sub>2</sub>:Ni<sup>2+</sup>, localised mag. excitations, obs. by Raman scatt. 9-10221
- MnF<sub>2</sub>:Ni, magnons, localised, obs. by Raman scatt. 9-14062
- Mn<sub>2</sub>P, ordering at 110°K from susceptibility meas. 9-16379
- Mn-Pd alloys,  $\gamma$ -phase 9-12311
- Mn<sub>21-x</sub>Fe<sub>2</sub>F<sub>22</sub>, exchange interactions from Neel temp. composition dependence obs. 9-21594
- Mn<sub>2</sub>GeSb<sub>1-x</sub> system, antiferromag.-ferrimag. transitions for y>0.19 9-19968
- MnAu<sub>2</sub>, structure from n. diff. exam. 9-10152
- MnCO<sub>3</sub>, ferromag. component spin density distribution, covalency and exchange polarization 9-15156
- Mn<sub>1-x</sub>Co<sub>x</sub>F<sub>2</sub>, mixed crystals, electron-magnon transitions 9-15158
- Mn<sub>2</sub>Cr<sub>1-x</sub>HoO<sub>3</sub>, temp. and composition depend. 9-17269



# Magnetic properties of substances continued

## antiferromagnetic continued

- MnF<sub>2</sub>:Fe<sup>2+</sup> M1-active local mode at 94 cm<sup>-1</sup>, linear splitting of abs. line and g factor 9-3949
- MnF<sub>2</sub>, line shape of spin wave sidebands 9-16375
- MnF<sub>2</sub>, ultrasonic attenuation near the critical point 9-7920
- MnF<sub>2</sub> absorpt. in 4000 Å region, exciton-magnon bound state and exciton dispersion obs. 9-1707
- MnF<sub>2</sub> insulator, exciton-magnon interact., coupling const. determ. 9-1706
- Mn<sub>1-x</sub>Ni<sub>x</sub>F<sub>2</sub>, mixed crystals, electron-magnon transitions 9-15158
- α-Mn<sub>2</sub>O<sub>3</sub>-Fe<sub>2</sub>O<sub>3</sub> system, temp. and phase comp. dependence 9-17464
- MnS<sub>2</sub>, Neel temp. rel. to pressure, volume anomaly at 0°K 9-18685
- MnS<sub>2</sub>, low temp. susceptibility, indicating antiferromag.-paramag. transition 9-12312
- MnSe, susceptibility temp. dependence, 80-260°K and field strength dependence 9-1705
- MnTe<sub>2</sub>, low temp. susceptibility, indicating antiferromag.-paramag. transition 9-12312
- MnTiO<sub>3</sub>, mag. ht. capacity, 30° to 300°K 9-3533
- NaCrS<sub>2</sub>, at 18°K 9-7921
- NaNiF<sub>3</sub>, structure 9-5855
- Nd<sub>2</sub>Dy<sub>1-x</sub>Sb system, mag. props. of single crystals 9-16380
- NdMnO<sub>3</sub>, ordering and crystal structure 9-19717
- Ni complex, benzene amino-nickel cyanide clathrate 9-1710
- NiF<sub>2</sub>, spin wave contrib. to sp. ht., 0.36-50°K 9-15006
- NiF<sub>2</sub>, space group corepresentations and magnon dispersion relations 9-16381
- NiO, coherent exchange scatt. in electron diffraction 9-1698
- NiO low-lying surface spin-wave band prediction 9-21595
- NpCo<sub>0.95</sub>, 190 to 317°K 9-5817
- NpO<sub>2</sub>, ordering from <sup>237</sup>Np Mossbauer spectra 9-1708
- PrMnO<sub>3</sub>, order and crystal structure 9-19717
- Pt-Fe alloy, ordered, Mossbauer effect rel. to structure 9-12362
- Rb<sub>2</sub>MnCl<sub>4</sub>·2H<sub>2</sub>O, nuclear spin lattice relax. of <sup>87</sup>Rb, <sup>35</sup>Cl and <sup>1</sup>H 9-21597
- Rb<sub>2</sub>FeF<sub>4</sub>, planar, susceptibility and long-range order 9-7922
- RbMnCl<sub>3</sub>, from e.s.r. spectra of MnCl<sub>2</sub>-alkali chlorides fused mixture 9-13948
- RbMnF<sub>3</sub>, magneto-elastic props. from u.s. attenuation meas. 9-21431
- RbMnF<sub>3</sub>, absorpt. in 4000 Å region, exciton dispersion obs. 9-1707
- RbMnF<sub>3</sub>, critical fluctuations, e.p.r. studies 9-18735
- RbMnF<sub>3</sub>, domains 9-17465
- RbMnF<sub>3</sub>, magnon sideband shapes, Green function theory 9-12313
- RbMnF<sub>3</sub>, spin wave theory and low temp. magnetization 9-16382
- RbMnF<sub>3</sub>, two-magnon absorption, Raman spectra 9-12435
- RbMnF<sub>3</sub>, Zeeman effect anisotropy 9-1795
- Rb<sub>2</sub>MnF<sub>4</sub>, structure rel. to optical transitions 9-10208
- SiC, exchange interactions of N donors 9-19972
- SmAlO<sub>3</sub>, A transition in mag. ordering from low temp. sp. ht. 9-7655
- TbFeO<sub>3</sub>, metamagnetic props. 9-16383
- TbP, lattice deformation at Neel pt. 9-12309
- Th, from transport properties 9-13843
- TiFe<sub>2</sub>, Ti excess, temp. depend. of Curie temp. and saturation magnetization 9-3799
- Tm, superzones in interpretation of transport props. anomalies near Neel temp. 9-10414
- TmFeO<sub>3</sub>, microwave absorpt meas., interpretation in two-sub-lattice model 9-7914
- UAs, neutron diffraction study 9-3837
- UFeO<sub>4</sub>, Mossbauer and neutron diffraction study of ordering 9-3873
- UN, mag. contribution to sp. ht. values, 1.3-4.6°K 9-17357
- Yb<sub>2</sub>O<sub>3</sub>, structures from n. diffraction exam. 9-17463
- (Zr<sub>1-x</sub>Nb<sub>1-x</sub>)Fe<sub>2</sub>, study using Mossbauer technique 9-16406

## diamagnetic

- See also *Haas-van Alphen effect*; *Diamagnetism*
- aromatic hydrocarbons, anisotropy, MO calc. 9-17048
- p-chloronitrobenzene, susceptibilities and anisotropies 9-18668
- constants, tabular form, book 9-3777
- p-dinitrobenzene, susceptibilities and anisotropies 9-18668
- metals, magnetization-density-wave state, thermodynamic pot. determ. 9-17448
- metals, susceptibility, statistical model 9-10096
- metals, susceptibility, theory 9-21567
- Semiconductors, susceptibility, statistical model 9-10096
- semimetal with electron-hole pairing, isotropic model 9-10097
- susceptibility of semiconductor and semimetal 9-10097
- water, temp. depend. 9-5188
- C blacks, susceptibility, effect of Na doping 9-7739
- CO, Hartree-Fock calc. 9-2859
- <sup>13</sup>C<sup>18</sup>O, susceptibility calc. 9-9198
- CdSb alloyed with Fe, Ni, mag. susceptibility 9-16328
- CdSb liq., mag. susceptibility 9-16328
- HgI<sub>2</sub>, susceptibility obs. 9-1638
- Ni<sup>2+</sup> in benzene amino-nickel cyanide clathrate, from saturation magnetization at low temps. 9-1710

## ferrimagnetic

- See also *Ferrimagnetism*
- anisotropy, magneto-crystalline, elimination method, patent 9-19962
- crystal single sphere orientation, magnetic dev. 9-5270
- grains, monodomain interacting, remanent props. and Preisach diagrams 9-14000
- manganese acetate tetrahydrate, from heat capacity meas. in mag. field, 0.4-20°K 9-10200
- Neel ferrimagnets, high-field magnetization analysis 9-15154
- Neel model, temp. depend. of paramag. susceptibility 9-1640
- NiO-ZnO-Fe<sub>2</sub>O<sub>3</sub>, MnO-ZnO-Fe<sub>2</sub>O<sub>3</sub>, Procopiu effect, obs. 9-16225
- orthoferrites domain-wall energy meas. 9-14001
- perminvar ferrites, mag. ordering stability 9-10138
- Procopiu effect in ferrite bar 9-3832
- spinel, relax. and resonance line breadth 9-14101
- BaCo<sub>2</sub>TiFe<sub>4</sub>O<sub>17</sub>, anisotropy 9-18684
- BaCo<sub>2</sub>Ti<sub>2</sub>Fe<sub>12</sub>-xO<sub>19</sub>, hexagonal, exchange anisotropy 9-10136
- (Li<sub>0.5</sub>Fe<sub>1.5</sub>)O<sub>4</sub>, 1:3 type ordering, temp. effects 9-14006
- Co<sub>2</sub>Fe<sub>2-x</sub>, induced anisotropy const., Co content eff. 9-5847
- Co<sub>2</sub>Zn<sub>0.3</sub>Fe<sub>0.7</sub>O<sub>4</sub>, paraprocess susceptibility maximum at Curie point 9-16368
- CuFe<sub>2</sub>O<sub>4</sub>, and temp. dependences 9-1680
- DyFe garnet, high-field magnetization 9-15154
- E-FeO<sub>3</sub>, domain-wall energy meas. at 25°K 9-14001
- ErCo<sub>6</sub>, magnetization, 4.2-1250°K, up to 30 kOe 9-5848

# Magnetic properties of substances continued

## ferrimagnetic continued

- Er<sub>2</sub>Co<sub>7</sub>, magnetization, 4.2-1250°K, up to 30 kOe 9-5848
- Er<sub>2</sub>Co<sub>7</sub>, magnetization, 4.2-1250°K, up to 30 kOe 9-5848
- Fe<sub>0.88</sub>S natural pyrrhotite thermomag. investigation 9-18821
- Fe<sub>0.9</sub>Mn<sub>0.1</sub>Ge, structure determ. 9-3827
- Fe<sub>2-x</sub>Ga<sub>x</sub>O<sub>4</sub>, ion distribution from magnetic reflections 9-3828
- FeNiCo 9-19963
- (Fe<sub>2</sub>O<sub>3</sub>)<sub>0.58</sub>(NiO)<sub>0.42-x-y</sub>(CoO)<sub>x</sub>(ZnO)<sub>y</sub> ferrite system, mag. ordering stability 9-10138
- Ga<sub>2</sub>Fe<sub>2-x</sub>O<sub>5</sub>, (x=0.89), anisotropic spontaneous magnetization 9-12300
- Gd ferrite garnet, sublattice interactions 9-16369
- Gd garnet, hysteresis logs rectangularity v.s. temp. 9-10139
- Gd<sub>2</sub>Fe<sub>3</sub>O<sub>12</sub>, anomalous magnetoacoustic effect 9-16370
- Ho ferrite garnet, Faraday effect and reversal of mag. sublattices 9-1739
- Li ferrite, saturation magnetization and Li loss effects, 20°K 9-1686
- Li<sub>2</sub>O<sub>2</sub>·7 Fe<sub>2</sub>O<sub>3</sub>·2.3 Cr<sub>2</sub>O<sub>3</sub> magnetoelastic effect 9-16370
- Li<sub>2</sub>O<sub>2</sub>·5 Fe<sub>2</sub>O<sub>3</sub>·2.5 Cr<sub>2</sub>O<sub>3</sub> anomalous magnetoacoustic effect 9-16370
- Mg ferrites, quenching temp. effect on permeability tensor components 9-19967
- MgMn ferrites, pulse and hysteresis props., eff. of annealing conditions 9-17459
- Mn-Mg-Fe ferrites, after-effect, Mg<sup>2+</sup>, Mn<sup>2+</sup> role, obs. 9-14007
- Mn<sub>2</sub>G<sub>2</sub>Sb<sub>2</sub>, system, helical-ferrimag. transitions for y≤0.08 9-19968
- MnZn ferrite, magnetic susceptibility variation 9-15155
- MnZn ferrites, effect of Cd-for-Zn substitution 9-17460
- MuV<sub>2</sub>O<sub>4</sub>, Bloch wall motion, n. scatt. study 9-12301
- Ni-Fe ferrites, rotational losses 9-3831
- NiZn ferrite, magnetic susceptibility variation 9-15155
- RbMg<sub>1-x</sub>Co<sub>x</sub>F<sub>3</sub>, x=0.35-0.68, obs. 9-7912
- SmFeO<sub>3</sub>, spin re-orientation phase transition 9-16372
- SrCo<sub>2</sub>Ti<sub>1-x</sub>Fe<sub>x</sub>O<sub>10</sub>, hexagonal, exchange anisotropy 9-10136
- Y<sub>2</sub>In<sub>2</sub>Ga<sub>2</sub>Fe<sub>2-x</sub>O<sub>12</sub>, Fe sublattices, four, Mossbauer and neutron diffraction investg. 9-21591
- Y Fe garnet-type cpds., spin wave theory 9-1690
- YFe garnet, domain structure and growth defects effect 9-12302
- YFe garnet, eqn. of state near Curie point 9-7913
- YFe garnet, rods, polycrystalline, axially magnetized, magneto-static modes at 9.96 GHz 9-5851
- YFe garnet, sublattice magnetization calc. by Oguchi method 9-10144
- YFe garnet interaction of longitudinal phonons with spin waves 9-12304
- YbFe garnet, high-field magnetization 9-15154
- YFe garnet, spin-Raman susceptibility by means of spin-wave instabilities 9-10143
- Sn<sub>0.8</sub>Ba<sub>0.2</sub>Li<sub>2</sub>Zn<sub>2</sub>Fe<sub>2</sub>O<sub>41</sub>, angular spin ordering from neutron diffraction meas. 9-10140

## ferromagnetic

- See also *Ferromagnetic relaxation*; *Ferromagnetic resonance*; *Ferromagnetism*; *Magnetization process*; *Magnetization state*
- alloys, dilute, coupling effect on free spin susceptibility 9-10090
- alloys, for tape-wound cores for power circuits 9-12975
- alloys, magnon drag eff. on elec. and thermal resistivity and thermo e.m.f., low temp. 9-13951
- alloys, saturation magnetization above room temp. 9-10125
- alloys, weakly ferromag., strongly paramag., behaviour near critical conc. 9-1641
- anisotropy, infl. on sp. ht., Hisenberg model 9-18671
- anisotropy meter 9-8576
- core coil, saturable in ferromagnetic circuit 9-4409
- domain nucleation 9-18675
- dysprosium ethyl sulphate, anisotropic dipole interact. below 0.13°K 9-1670
- electron solid, correction of Carr calc. 9-6340
- f.c.c., magnon impurity modes of pair defect 9-13954
- f.c.c. lattices, symmetric Bloch walls, thickness and energy, infl. of domain width 9-19951
- FeO (hematite), antiferromag. with weak ferromagnetism, effect of hydrostatic pressure on mag. anisotropy 9-3836
- Fe, rotational hysteresis due to perpendicularly superimposed continuous and alternating fields 9-10123
- Fe-Co alloys, rel. to order-disorder transformation 9-3788
- ferrites, permeability mechanism 9-14002
- ferroelectrics, ordering of mag. moments 9-16339
- ferrometer with high sensitivity 9-8577
- film, 'fanning' magnetization reversal and exchange stiffness 9-19954
- films, magneto-optic apparatus for domain wall visualization 9-18681
- films, spin waves, dipolar effects 9-21588
- fluctuations anisotropy and e.m. wave scatt. processes rel. to weak anisotropy 9-18677
- hematite, specular, pure crystal exchange interactions obs. 9-10149
- impurities, spin broadening of Mossbauer lines 9-3869
- inclusions in type II superconductor, interaction with vortex lines 9-9958
- insulators phonon wavelength temp. depend. shift 9-7946
- interdomain wall thickness, temp. depend., numerical results for Fe 9-12276
- Invar alloys 9-3793
- Invar alloys, mag. contrib. to low temp. thermal expansion and Curie temp. pressure dependence 9-21580
- Ising model, time depend. susceptibility and n. scatt. cross section 9-13953
- lanthanum intermetallic cpds localized mag. moment obs. 9-16331
- liquid alloys 9-13540
- magnetite, Curie point, after growth from borax flux 9-18413
- magnetite, stable strain-induced remanence 9-7905
- magneto-elastic interactions, effect of elastic anisotropy 9-3804
- magneto-optical observations, interpret. 9-16335
- magnetoacoustic resonance, effect of mag. alloying additions 9-5552
- magnetoelastic wave amplification in a semiconductor 9-5829
- metals, effect accompanying galvanomagnetic effect: Matteucci spontaneous effect 9-12249
- metals, elec. resistivity anomaly near ordering point 9-12096
- metals, magneto-opt. eff., theory 9-17474
- monocrystals, effect of spin waves with acoustic oscillations 9-3803
- Ni, electroplated, magnetocrystalline anisotropy, effect of electrolytic charging with H 9-15152
- Ni, magnetocrystalline anisotropy, Mossbauer study 9-12279
- ordered structures 9-13969
- permalloy, creeping mechanism of magnetization 9-5842
- permalloy, domain tip motion control 9-5841
- Permalloy film, coercive force and anisotropy field, eff. of crystallite size 9-13996

**Magnetic properties of substances continued**

**ferromagnetic continued**  
 permalloy films,  $^3\text{He}$  irradiat. effects on anisotropy-field inhomogeneity and coercive force 9-7908  
 Permalloy films, optimization for computer memories 9-13995  
 permalloy films, rotational hysteresis 9-10134  
 permalloy films, supercritical, thickness effects 9-1677  
 permalloy fine wires, Nb addition, materials parameters affecting reentrancy 9-5824  
 permalloy thin films, anisotropy inhomogeneity, origin 9-5838  
 permalloy thin films, uniaxial anisotropy, origin 9-3815  
 permalloy thin tapes annealed below recrystallization temp., 9-3814  
 pinning and magnetostatic modes, generalized 9-10268  
 planar film structures with one infinite dimension, demagnetizing field 9-3809  
 polycrystalline, directional properties 9-1671  
 polycrystalline, directional properties 9-16359  
 Procopiu effect with cylindrical sample free at one end 9-13958  
 Pt-(52 wt.%)Co alloy, ordered, anisotropy, 298° and 77°K 9-21583  
 rare earth cobalt epds., permanent mag. behaviour 9-13963  
 rare earth compounds with group V anions, review 9-18598  
 rare earth metals, structure and form factor meas. by n. diff. 9-13971  
 reversible magnetiz. curve and magnetostriction of uniaxial crystal with internal stresses 9-13979  
 semiconductor, c.m. wave and slow neutron scattering by anomalous fluctuations of spin waves in elec. field 9-5814  
 semiconductors, spin wave amplification 9-10110  
 with small magnetic anisotropy, anomalous scattering of slow neutrons and c.m. waves 9-13972  
 specific heats, Pd-Ni alloys, dilute 9-1398  
 steel, internally oxidized electrotechnical, magnetization curves, hysteresis loops and magnetostriction 9-13989  
 steel, transformer, single crystals, coercive force, depend. on dislocation structure 9-13988  
 steel, transformer, sp. losses mag. induction amplitude dependence, texture effects 9-1676  
 structures, by Lorentz electron microscopy, Fresnel mode 9-5836  
 superconductor, effect of impurities on existence of inhomogeneous state 9-9943  
 2,2,6,6-tetramethyl-4-hydroxypiperidine-1-oxyl, susceptibility, 1.8°K to 300°K 9-10115  
 thin films, biaxial anisotropy, shape induced 9-3808  
 thin films, description 9-19957  
 threshold mag. fields and temperatures for uniaxial ferromagnet with domain struct. 9-13968  
 titanomagnetite, pressure remanent magnetization and related phenomena 9-19953  
 torque acting on thin layer in quasi-static mag. field 9-3805  
 transition metal alloys, ordering, new type 9-1658  
 transition metal alloys, ordering, new type 9-13959  
 vibration spectra in system with coinciding ferromag. and ferromag. axes, from motion of polarization and magnetization vectors 9-16163  
 wire, magnetization rel. to internal Barkhausen effect 9-5823  
 zeolite molecular sieve,  $\text{Fe}^{3+}$  introduction, superparamagnetism evidence, magnetic and Mossbauer effect studies 9-5810  
 $^151\text{Gd}$  crystal, neutron diffraction study up to room temp. 9-10114  
 $^6\text{Fe}$  wires, annealed, Armo, remagnetization effects 9-15151  
 $\text{AgF}_2$ , magnetic long-range ordering 9-10117  
 Au-Co alloys, liquid, susceptibility temp. dependence 9-13540  
 Au-V alloys, temp. dependent rel. to model of localization for AuV 9-12267  
 Au-Mn, Curie temp. pressure depend. 9-17452  
 Ba ferrite fine particle assemblies, coercive force variation with packing 9-3796  
 Ba hexaferrites, rotating moment curves in case of uniaxial anisotropy 9-1666  
 Bi-MnBi composite, anisotropy field and Curie pt. determ. 9-9671  
 Bi, hysteresis props. of residual twins 9-13978  
 BiMnO<sub>3</sub>, below 103°K 9-10112  
 CdCr<sub>2</sub>Se<sub>4</sub>, transition from paramagnetic state, conduction band edge shift 9-7712  
 CdCr<sub>2</sub>Se<sub>4</sub>:Ga initial permeability, photomag. change 9-12215  
 CdCr<sub>2</sub>Se<sub>4</sub>, ferromagnetic, Raman scattering 9-12410  
 CdCr<sub>2</sub>Se<sub>4</sub>, Raman scattering, 7.295°K, magnon scatt. 9-12409  
 Ce<sub>1-x</sub>Co<sub>x</sub>, CO<sub>1-x</sub>Co<sub>x</sub>, liquid, permanent mag. props. and prep. 9-3795  
 Co-Cu alloys, hexagonal, mag. moments rel. to c. transfer 9-12274  
 Co-Fe alloy, constricted hysteresis loop produced by cold rolling method, patent 9-13759  
 Co-Pt alloy, ordered, nature of coercive force 9-10118  
 Co, domain patterns rel. to magnetization process 9-16353  
 Co, eqn. of state near Curie pt. 9-10127  
 Co, f.c.c., compared with paramag. prop. from theoretical eqns. 9-3787  
 Co, films, electrodeposited, magnetocrystalline and uniaxial anisotropies 9-1678  
 Co, magnetostriction infl. on domain structure 9-17453  
 Co, remanent domain struct., infl. of crystal thickness 9-5819  
 Co, stable strain induced remanence 9-7905  
 Co<sub>1-x</sub>Ni<sub>x</sub>S<sub>2</sub>, itinerant d-electron type, evidence 9-1674  
 CrI<sub>3</sub>, internal field obs. from  $^{121}\text{Mossbauer}$  effect 9-21609  
 Cu-Co solid solns., Co particles in superpara. range, distribution function 9-5803  
 Cu-Fe alloys, dil. Ising model and s-d exchange theory in spec. heat meas. interpretation 9-18563  
 Cu-Mn alloy, rel. to structural state, applied field intensity and temp. 9-10147  
 CuCr<sub>2</sub>Te spinel, Mossbauer, effect of  $^{121}\text{I}$ , internal mag. field study 9-16400  
 Er, form factor meas. by n. diff. 9-13971  
 ErAl<sub>2</sub>, from n. diff. and susceptibility meas. 9-7898  
 EuB<sub>6</sub>, polaron ferromagnetism 9-1660  
 EuLu<sub>2</sub>O<sub>4</sub>, 1.7 to 300°K 9-3778  
 EuO 4at.%Gd alloy, Curie temp. pressure dependence rel. to exchange interactions 9-18672  
 EuO, mag. effects on low-temp. photoconductivity 9-12212  
 EuO phonon wavelength temp. depend. shift 9-7946  
 EuS, domains, diffuse scatt. of light 9-10180  
 EuS, domains effect on light scatt. 9-12328  
 EuS, mag. effects on low-temp. photoconductivity 9-12212  
 EuS, scaling laws and impurity effects near critical point 9-16345  
 EuS, spin corals. 9-13964  
 EuS films, hysteresis meas., thickness dependence 9-18678

**Magnetic properties of substances continued**

**ferromagnetic continued**  
 EuSe, metamagnetic transitions, field- and temp.-depend. 9-7899  
 Fe-C martensite diffusional magnetic viscosity effect 9-3801  
 Fe-C solid soln., point defects studied by mag. after effect meas. 9-5333  
 Fe-Co alloy (Permuend), V addition, magnetic anisotropy 9-12281  
 Fe-Cr alloy, virtual spin-wave state below and above Curie pt. 9-16343  
 Fe-Cr(V), itinerant electron ferromagnetism evidence 9-3797  
 Fe-3 wt.%Si with Goss-texture, irreversible magnetization process and Barkhausen effect 9-13977  
 Fe-Mn alloys, mass magnetization as function of internal mag. field 9-18679  
 Fe-Mo alloys mass magnetization as function of internal mag. field 9-18679  
 Fe-Ni-Co epitaxial growth and coercive force 9-12298  
 Fe-Ni-Cr alloys, magnetization intensity and susceptibility rel. to heat treatment 9-12288  
 Fe-Ni-Mn alloys, uniaxial anisotropy in martensitic transforms 9-1667  
 Fe-Ni, hysteresis loops, constant-field, effect of anisotropy and atomic arrangement, X-ray exam. of texture 9-5825  
 Fe-Ni alloys, anisotropy and ordering 9-3792  
 Fe-Ni alloys, f.c.c., Curie temp. pressure dependence 9-12289  
 Fe-Ni alloys, Invar effect 9-1662  
 Fe-Ni invar. alloys, Curie point, effect of third component 9-10113  
 Fe-Ni alloys, uniaxial anisotropy in martensitic transforms 9-1667  
 Fe-Pd alloy, dilute, spin-wave stiffness, by neutron scattering technique 9-12268  
 Fe-Pd alloys, coercive force rel. to domain ordering 9-12275  
 Fe-Pd alloys, f.c.c., Curie temp. pressure dependence 9-12289  
 Fe-Pt alloys, f.c.c., Curie temp. pressure dependence 9-12289  
 Fe-Si, grain oriented, basic expts. on nature of anomalous losses 9-12242  
 Fe-Si, magnetization reversal mechanism for single crystal picture frames 9-13981  
 Fe-Si, susceptibility and coercive forces 9-16360  
 Fe-Si alloys, anisotropy, eff. of surface Ni films 9-13990  
 Fe-Si frame monocrystal, negative Barkhausen jumps, occurrence during magnetization 9-1672  
 Fe-Ta alloys, mass magnetization as function of internal mag. field 9-18679  
 Fe-Ti alloy system, Laves phase, conc. depend. 9-7897  
 Fe-6.5%Si, zero magnetostriction, n induced mag. viscosity, obs. 9-19952  
 Fe-7.5 at.% Si, elastic mod. contrib. to 'magnetic effect', from creep expts. 9-5402  
 Fe, at transition point, props. from Landau-type theory 9-7901  
 Fe, Curie point, temp. depend. obs. by critical scatt. of neutrons 9-12269  
 Fe, domain patterns rel. to magnetization process 9-16353  
 Fe, f.c.c. compared with paramag. props. from theoretical eqns. 9-3787  
 Fe, interdomain wall thickness, temp. depend., numerical results 9-12276  
 Fe, lattice constant effect 9-13982  
 Fe, mag. field effects on specific heat near Curie temp. 9-13802  
 Fe, magnetocrystalline energy consts. K<sub>1</sub>, K<sub>2</sub> and K<sub>3</sub>, temp. depend. 20 to 800°K 9-3789  
 Fe, Ni, Procopiu effect obs. 9-16225  
 (Fe<sub>1-x</sub>Y<sub>x</sub>)-G, susceptibility up to 1000°K 9-19948  
 FeAl alloy, coercive force, magnetization, susceptibility and magnetostriction rel. to order-disorder 9-21584  
 Fe<sub>2</sub>Se<sub>3</sub>, band magnetism interpretation of elec. conductivity and electronic component of sp. ht. 9-21484  
 Fe<sub>2</sub>Se<sub>3</sub>, mag. order change at 200°K rel. to Hall effect and transverse magnetoresistance 9-19886  
 Fe<sub>2</sub>armco, effect of shock waves on residual props. 9-13980  
 Fe film with (100) surface orientation, spatial magnetization distribution 9-19961  
 Fe fine particle assemblies, coercive force variation with packing 9-3796  
 Fe fine powders, magnetization reversal, particle agglomeration effect 9-3822  
 Fe in remanent state, elastic tensile stresses effects on magnetostrictive props. 9-19956  
 Fe polycrystals, magnetization plots interpretation near Curie temp. using Landau-Ginzburg-Lifshitz theory 9-12291  
 Fe solid bodies, internal e.m. phenomena investigation with improved B-H characteristic 9-16350  
 Fe wire, Barkhausen discontinuities propag. 9-12290  
 $^{57}\text{Fe}$  spin relax. in domain walls via magnon interactions 9-7926  
 Fe film, longitudinal Kerr rotations and figures of merit 9-3813  
 FeBO<sub>3</sub>, polycryst., below 115°K 9-5272  
 Fe<sub>1-x</sub>Co<sub>x</sub>S<sub>2</sub>, itinerant d-electron type, evidence 9-1674  
 Fe<sub>3</sub>Cr superlattice alloys, isothermal magnetic annealing effect on magnetization and magnetostriction at high and room temperatures 9-15153  
 FeF<sub>3</sub>, anomalous behaviour near Curie temp. 9-1665  
 FeGe, cubic, susceptibility meas., 4.2-520°K 9-16356  
 FeO<sub>4</sub>, memory and remanence 9-3798  
 Fe<sub>3</sub>O<sub>4</sub> fine powders, magnetization reversal, effect of particle agglomeration 9-3822  
 Fe<sub>3</sub>S<sub>8</sub>, structure study using Mossbauer eff. 9-10119  
 Fe<sub>2</sub>Zr phase alloys, and crystal structure 9-7440  
 Fe-Ni-C alloys, f.c.c., rel. to plastic deform. 9-13727  
 Feism from Mossbauer obs. 9-10135  
 films, vapour deposited, nonmagnetostrictive 9-5837  
 Ga<sub>2</sub>Fe<sub>2</sub>O<sub>7</sub>, spin wave spectrum from inelastic n. scatt. 9-21581  
 Ga<sub>2</sub>xFe<sub>2</sub>O<sub>7</sub>, comp. and temp. dependence 9-5826  
 Gd-GFe<sub>2</sub> phase mixtures, ordering, 285-800°K 9-5820  
 Gd, absorption bands in ferromag. state 9-16412  
 Gd, direction of easy magnetization 9-21585  
 Gd, magnetization, temp. depend. below 50°K 9-13983  
 Gd, magnetocrystalline anisotropy, spin wave theory 9-5815  
 Gd, polarized positron annihilation 9-9917  
 GdAl<sub>3</sub>, ordering effects on thermoelec. power temp. dependence 9-16307  
 GdCl<sub>3</sub>, freq.-dependent susceptibility and renormalized spinwave energies 9-16363  
 GdCl<sub>3</sub>, eff. between rare-earths 9-12270  
 H solids, density 10<sup>4</sup> to 10<sup>6</sup> g/cm<sup>3</sup>, possible nuclear ferromag. 9-21582  
 Ho-(80 wt.%)Tb alloy, stable simple ferromag. struct. at low temps., minimum effective spin prediction 9-16377  
 Mg<sub>0.78</sub>Fe<sub>0.22</sub>O<sub>4</sub>, anisotropy induced at higher temperatures 9-3829  
 Mn/Permalloy double-layer films with exchange anisotropy, domain structures stabilisation 9-10130  
 MnAl, domain structure e. microscope examination 9-13967  
 MnAs<sub>0.9</sub>P<sub>0.1</sub>, 4.2 to 660°K, and crystallographic studies 9-16357  
 Mn<sub>2</sub>Cr<sub>1-x</sub>Ho<sub>x</sub>O<sub>3</sub>, temp. and composition depend. 9-17269  
 MnP, Curie point, effect of hydrostatic pressure 9-15149



**Magnetic properties of substances continued**

- ferromagnetic continued**  
 Mn<sub>3</sub>Sb<sub>2</sub>, anisotropy constants from magnetization meas. at 77°K and 288°K 9-1675  
 MnSi, n.m.r. study at 4.2°K 9-16467  
 (48.2-57.0 at%)Ni- (51.8-43.0 at%) Cu, susceptibility, 150-300°K 9-17344  
 Ni-20% Fe annealing in rotating mag. field 9-3817  
 Ni-Cu alloys, effect of H occlusion 9-17278  
 Ni-Cu alloys, susceptibility rel. to Hall effect and elec. resistivity 9-21485  
 Ni-(30wt.%)Cu alloy with interstitial occluded hydrogen, spontaneous magnetization temp. dependence 9-16361  
 Ni-Fe-Cu-Mo alloy, rolled from sintered compacts, high permeability 9-13965  
 Ni-Fe-Pd alloy films, composition and deposition for use as storage elements, patent 9-13998  
 Ni-Fe, effects of radiation on magnetic props. 9-1661  
 Ni-Fe alloys, solute C effects on Curie pt. and spontaneous magnetization 9-13984  
 Ni-Fe alloys with 50 to 60% Ni after isothermal treatment with mag. field, permeability obs. 9-5831  
 Ni-Fe double films, coupling between 9-3816  
 Ni-Fe film, domain wall streaming, creeping and parade motion, hard axis pulse excitation 9-3820  
 Ni-Fe films, magnetization-ripple crystallite-size and film-thickness dependence 9-7907  
 Ni-Fe films, transverse Kerr effect, 0.3 to 3.0  $\mu$  9-5840  
 Ni-Fe films, uniaxial, analog, storage using non-uniform fields 9-5844  
 Ni-Fe film, domain boundary propagation, slow to intermediate speed, Kerr magneto optical study 9-3819  
 Ni-Fe films susceptibility, effect of strain, polycrystalline 9-3818  
 Ni-(19wt.%)Fe films, energy of combined Bloch and Neel type domain wall 9-18683  
 Ni-Rh, mag. behaviour 9-16351  
 Ni-Ta(Nb) alloy system, galvanomagnetic eff. 9-3790  
 (63wt.%)Ni-(37wt.%)Rh anomalous low sp. ht. near crit. conc. for ferromag. 9-16176  
 Ni-(17 wt.%) Fe/EuS double layers, hysteresis meas., thickness dependence 9-18678  
 Ni, anisotropy constants temp. dependence at low temps. 9-12285  
 Ni, anisotropy energy in (111) plane 9-12283  
 Ni, domain patterns rel. to magnetization process 9-16353  
 Ni, domain structures, plastic deform. effects 9-12280  
 Ni, effective hole-hole interaction, magnetization dependence 9-21461  
 Ni, f.c.c., compared with paramag. props. from theoretical eqns. 9-3787  
 Ni, Kerr effect rel. to spin-orbit splitting of 0.7-eV transition and electron structure 9-7948  
 Ni, long wavelength spin wave energy computation 9-12271  
 Ni, mag. field effects on specific heat near Curie temp. 9-13802  
 Ni, mag. hysteresis above Curie temp. 9-7902  
 Ni, magnetic after-effect of n. irradi. and plastic deformation 9-3802  
 Ni, magnetocryst. anisotropy energy, 4.2-296°K 9-1668  
 Ni, memory, coercive force, isothermal remanent magnetization, variation with internal stress 9-5828  
 Ni, plastic deformation of single crystal 9-5461  
 Ni, stable strain-induced remanence 9-7905  
 Ni, susceptibility rel. to Hall effect and resistivity 9-21485  
 Ni, uniaxial anisotropy, formation by plastic deformation 9-12295  
 Ni, X-ray interferences in the Curie point neighbourhood, temperature dependence 9-5816  
 Ni alloys, f.c.c., ferromag. quantities, calc. in band model 9-1662  
 Ni film, produced by chem. reduction method, anisotropy 9-16358  
 Ni film, transverse phonon generation at zero field by mech. stresses 9-10126  
 Ni films, electrodeposited, magnetocrystalline and uniaxial anisotropies 9-1678  
 Ni magnetic component of elec. resistance at low temp. 9-13845  
 Ni<sub>3</sub>B<sub>2</sub>O<sub>7</sub>, spin arrangements 9-17455  
 NiMn, mean mag. moment per. atom, and ordering effects, effect of Fe and Co additions 9-12278  
 Ni-(35 wt.%)Fe alloy, domain structures 9-13973  
 Ni-Fe films coupled with stripe domain films 9-10133  
 Ni-Fe film annealing, cylindrical 9-5839  
 NiCo<sub>0.55</sub>, susceptibility, Curie temp. 9-5817  
 NiPn, susceptibility, Curie temp. 9-5817  
 PbHg, ferromag. inclusions in type II superconductor, interaction with vortex lines 9-9958  
 PbO(Fe<sub>2</sub>O<sub>3</sub>)<sub>2</sub>, stiffness field dependence rel. to domain behaviour 9-13991  
 Pd-Ni dilute specific heat of nearly magnetic centres 9-1398  
 PdF<sub>3</sub>, weak ferromagnetism 9-10124  
 PrAl<sub>3</sub>, from n. diff. and susceptibility meas. 9-7898  
 Pt-Co alloys, low temp. susceptibility, anomalous 9-13966  
 Pt-Co permanent magnetic alloy, improvement of mag. props. by replacement of Pt by Pt group metals 9-12294  
 Pt-Fe alloy, disordered, Mossbauer effect rel. to structure 9-12362  
 Pt-Fe permanent magnetic alloy, improvement of mag. props. by replacement of Pt by Pt group metals 9-12294  
 RbFeF<sub>3</sub>, magnetization in strong pulsed fields, 4.2-106°K 9-16362  
 RbNi<sub>1-x</sub>Co<sub>x</sub>F<sub>3</sub>, magnetization in strong pulsed fields, 77-4.2°K 9-16362  
 Re-rare earth metal, compounds 9-13949  
 Si-Fe sheets, common and grain orientated, remagnetization domain effects 9-15151  
 Tb, anisotropic, spin fluctuations decay rates 9-16347  
 Tb, form factor meas. by n. diff. 9-13971  
 Tb, ordering rel. to band structure 9-16212  
 TiFe<sub>2</sub>, Fe excess, temp. depend. of Curie temp. and saturation magnetization 9-3799  
 Tm<sub>3</sub>Ni 9-3775  
 YFeO<sub>3</sub>, Mossbauer and neutron diff. study of ordering 9-3873  
 YFe garnet-Si i.r. irr., photomag. anneal props. by torque meas. 9-10137  
 ZrFe<sub>2</sub>, throughout homogeneity range, temp. depend. of Curie temp. and saturation magnetization 9-3799  
 (Zr<sub>1-x</sub>Nb<sub>x</sub>)Fe<sub>2</sub>, study using Mossbauer technique 9-16406  
 ZrZn<sub>2</sub>, Invar type, mag. contrib. to low temp. thermal expansion and Curie temp. pressure dependence 9-21580  
 ZrZn<sub>2</sub>, high purity, Curie temps. for low conc. Fe contamination 9-12272

**paramagnetic**

See also *Paramagnetic resonance and relaxation; Paramagnetism*  
 alkali halides, Van Vleck component 9-19947

**Magnetic properties of substances continued**

- paramagnetic continued**  
 alloys, strongly paramag., weakly ferromag., behaviour near critical conc. 9-1641  
 anthracene single crystals, centres when  $\gamma$ -irradiated 9-3963  
 axial crysts., susceptibility, spin Hamiltonian derivation 9-5804  
 copper calcium acetate hexahydrate, susceptibility obs., 90-300°K 9-7891  
 ferrimagnetic Neel model, temp. depend. of susceptibility 9-1640  
 fluids, insulating, magnetothermal convection 9-7233  
 heat conduction, negative, in spin systems 9-12896  
 induced moment systems, effect of cryst. elec. field 9-16334  
 ionic crystals, Van Vleck components 9-19947  
 lanthanide aluminides, Ln<sub>2</sub>Ln'<sub>1-x</sub>Al<sub>3</sub>, Laves phase cpds. 9-12247  
 lanthanide aluminides, Ln<sub>2</sub>Ln'<sub>1-x</sub>Al<sub>3</sub>, Laves phase cpds. 9-12247  
 lanthanum cobalt nitrate, phonon mean free paths, spin-lattice interac. strengths from magneto-therm. conductivity meas. 9-9854  
 lanthanum intermetallic cpds, localized mag. moment obs. 9-16331  
 metals, dispersed, and thermodynamics 9-13829  
 organic, conformation determ. by e.p.r. 9-17507  
 organic cpds., constants, tabular form, book 9-3777  
 pyrocarbons, B-doped, rel. to B content 9-7736  
 pyrocarbons, B-doped, rel. to B content 9-7736  
 quartz, susceptibility obs., and Suprasil 9-19949  
 rare earth gallates, garnet-structure-type, magnetostriction, 4.2-60°K 9-21571  
 rare earth germanates, garnet-structure-type, magnetostriction, 4.2-60°K 9-21571  
 rare earth intermetallic cpds, susceptibility meas. rel. to interband mixing 9-14116  
 rare earth metals, anisotropy and exchange interactions 9-1645  
 scattering of slow neutrons and e.m. waves in strong magnetic field 9-21568  
 slow-neutron scattering, solids subjected to strong mag. fields., cross section 9-12028  
 Suprasil, susceptibility obs., and quartz 9-19949  
 tetracyanoquinodimethane-phenazine complex, susceptibility temp. dependence rel. to conduction mechanism 9-18599  
 2,2,6,6-tetramethyl-4-hydroxypiperidine-1-oxyl, susceptibility, 1.8°K to 300°K 9-10115  
 CaWO<sub>4</sub>, thermoluminescent colour centres 9-19757  
 CdCr<sub>2</sub>Se<sub>4</sub>, transition to ferromagnetic state, conduction band edge shift 9-7712  
 Ce<sub>1-x</sub>Eu<sub>x</sub>Al<sub>3</sub>, Laves phase cpd., 0.2 $\times$ 0.6 at 4°K 9-12247  
 Co-Al intermetallic cpds., susceptibility 9-7888  
 Co, eqn. of state near Curie pt. 9-10127  
 Co, f.c.c., compared with ferromag. props. from theoretical eqns. 9-3787  
 CrF<sub>2</sub>, exchange integrals in paramagnetic phase 9-1643  
 Cu complex, copper monochloroacetate 2.5 hydrate, susceptibility and exchange integral 9-16330  
 Cu complex, dichlorobis(pyridine-N-oxide) copper(II), susceptibility and exchange integral 9-16330  
 Cu complex, dichloromonoaquo-(pyridine-N-oxide), copper (II), susceptibility and exchange integral 9-16330  
 ErAl<sub>3</sub>, from n. diff. and susceptibility meas. 9-7898  
 Eu, first order transition obs. from Mossbauer effect meas. 9-15148  
 EuAlO<sub>3</sub>, anisotropy and crystal field splittings 9-21570  
 EuLu<sub>2</sub>O<sub>4</sub>, 1.7 to 300°K 9-3778  
 Fe-Al intermetallic cpds., susceptibility 9-7888  
 Fe-Cr(V), susceptibility meas. giving evidence for itinerant electron ferro magnetism 9-3797  
 $\gamma$ -Fe-Mn alloy, from n. scatt. 9-1644  
 Fe, f.c.c., compared with paramag. props. from theoretical eqns. 9-3787  
 (Fe<sub>1-x</sub>Y<sub>x</sub>)<sub>2</sub>Ge, susceptibility up to 1000°K 9-19948  
 FeF<sub>3</sub>, exchange integrals in paramagnetic phase 9-1643  
 FeO-MgO solid solns, dil. antiferromagnet, paramag. susceptibility 9-5806  
 FeSb<sub>2</sub>O<sub>4</sub>, Mossbauer spectra quadrupole splitting, 50 to 817°K 9-14038  
 Gd, absorption bands in paramag. state 9-16412  
 Gd, direction of easy magnetization 9-21585  
 I: single crysts. p phenylenediamine-doped 9-10039  
 K<sub>2</sub>Fe(CN)<sub>6</sub>, crystallography and paramag. anisotropy, 95° and 300°K 9-21343  
 K<sub>2</sub>Fe(CN)<sub>6</sub>, crystallography and paramag. anisotropy, 95° and 300°K 9-21315  
 K<sub>2</sub>MnCl<sub>6</sub>, susceptibility, 1.4°-300°K 9-16456  
 La-CdSb mag. susceptibility 9-16328  
 Mn-CdSb mag. susceptibility 9-16328  
 MnAs<sub>0.9</sub>Po<sub>0.1</sub>, and crystallographic studies, 4.2 to 660°K 9-16357  
 Mn<sub>2</sub>Cr<sub>1-x</sub>Ho<sub>x</sub>O<sub>3</sub>, temp. and composition depend. 9-17269  
 Mn<sub>2</sub>P, hyperfine fields at P sites from susceptibility and Knight shift meas. 9-16379  
 MnS<sub>2</sub>, low temp. susceptibility, indicating antiferromag.-paramag. transition 9-12312  
 MnSi<sub>1.7</sub>, susceptibility, 20-1100°K 9-16332  
 MnTe<sub>2</sub>, low temp. susceptibility, indicating antiferromag.-paramag. transition 9-12312  
 NaCrS<sub>2</sub>, phase transition at 0K 9-7921  
 Nb<sub>3</sub>S<sub>4</sub>, rel. to crystal structure 9-9681  
 Ni-Al intermetallic cpds., susceptibility 9-7888  
 Ni-Cu alloys, susceptibility rel. to Hall effect and elec. resistivity 9-21485  
 Ni-on-Si catalysts, finely divided in direct and alternating fields, superparamagnetism 9-21569  
 Ni, effective hole-hole interaction, magnetization dependence 9-21461  
 Ni, f.c.c., compared with ferromag. props. from theoretical eqns. 9-3787  
 Ni, mag. hysteresis above Curie temp. 9-7902  
 Ni<sub>3</sub>Al, paramagnon scatt. of conduction electrons 9-21462  
 Ni<sup>2+</sup> in benzene amino-nickel cyanide clathrate, from saturation magnetization at low temps. 9-1710  
 Pd-B alloys, mag. susceptibility 9-7889  
 Pd-H system, susceptibility rel. to Knight shift for adsorbed H 9-17505  
 Pd-(1at.%)MnH system, susceptibility rel. to Knight shift for adsorbed H 9-17505  
 Pd, spin susceptibility field dependence 9-16333  
 Pr-La alloys, susceptibility rel. to temp. and field strength 9-17449  
 Pr-Y alloys, susceptibility rel. to temp. and field strength 9-17449  
 Pr doping of Th and La cpds., effect on supercond. 9-13857  
 PrAl<sub>3</sub>, from n. diff. and susceptibility meas. 9-7898  
 R<sub>1/2</sub>Na<sub>1/2</sub>MoO<sub>4</sub>, R=Gd, Tb, Dy, Ho, Er, Tm, and Yb, susceptibility 9-3779

**Magnetic properties of substances continued**  
**paramagnetic continued**

- Re, Pauli susceptibility rel. to Hall coeff. and elec. resistance, temp. depend. 9-15072  
 Sc, susceptibility, form with two overlapping bands 9-10098  
 Si:P, susceptibility, 1.5 to 500°K 9-10000  
 n-Si:P, susceptibility, and piezoresistance 9-16276  
 Sm<sub>2</sub>Ni, weak and independ. of temp 9-3775  
 TiO<sub>2-x</sub>, reduced rutile, susceptibility stoichiometry dependence rel. to band structure 9-21436  
 TiO<sub>2</sub>, orthorhombic (Brookite), Van Vleck mechanism 9-10099  
 Tm doping of Th and La cpds, effect on supercond. 9-13857  
 TmAl<sub>3</sub>, effect of cryst. elec. field 9-16334  
 UO<sub>2.18</sub>, xThO<sub>2</sub>, nonstoichiometric, temp. independ. term, rel. to U valency 9-13950  
 Y<sub>2</sub>Ni, weak and independ. of temp 9-3775  
 Zr, Pauli susceptibility rel. to Hall coeff. and elec. resistance, temp. depend. 9-15072

**transitions**

- $\delta$ -function gas, ferromag. transition, correlations effects 9-12260  
 elasticity of lattice effects, rel. to spin-lattice interaction 9-16336  
 Fe-Pt alloys, f.c.c., Curie temp. pressure dependence 9-12289  
 induced-moment system, excitation spectra and magnetization investig. using Green's functions 9-5791  
 Invar alloys, ferromagnetic contrib. to Curie temp. pressure dependence 9-21580  
 in Ising chain with long-range ferromagnetic interaction 9-12259  
 MnTiO<sub>3</sub>, entropy of antiferromag. transition 9-3533  
 second-order, critical behaviour of singular quantities in neighbourhood 9-16195  
 semiconductor plasma, diamag. to paramag. 9-3606  
 AuMn, Neel temp. pressure dependence from susceptibility, sp. ht. and thermal expansion meas. 9-1699  
 AuMn, metamagnetic, pressure induced 9-17452  
 CaV garnets, Curie pt. rel. to crystal chemistry 9-14005  
 (Li<sub>0.5</sub>Fe<sub>0.5</sub>)O<sub>3</sub>, ferro-paramagnetic and order-disorder from temp. effect on 1:3 ordering obs. 9-14006  
 Cu-Ni alloys, ferro- to paramag., rel. to lattice constant temp. dependence 9-19955  
 Dy, rel. to u.s. attenuation and elastic moduli 9-7517  
 DyP, lattice deformation at Neel pt. 9-12309  
 Er, rel. to u.s. attenuation and elastic moduli 9-7517  
 ErAl<sub>2</sub>, Curie temp. determ. 9-7898  
 Eu-Al intermetallic cpds. 9-10095  
 Eu, first order transition obs. from Mossbauer effect meas. 9-15148  
 EuO-4at.%Gd alloy, Curie temp. pressure dependence rel. to exchange interactions 9-18672  
 EuO thermal cond. across Curie temp. 69°K 9-16184  
 EuSe, metamagnetic, field- and temp.-dependences 9-7899  
 Fe-Co alloy, lattice parameter in Curie point regions 9-18444  
 Fe-Ni alloys, f.c.c., Curie temp. pressure dependence 9-12289  
 Fe-Ni invar. alloys, Curie point, effect of third component 9-10113  
 Fe-Pd alloys, f.c.c., Curie temp. pressure dependence 9-12289  
 Fe-Rh alloy, antiferromag.-ferromag., rel. to e.s.r. meas. 9-16455  
 Fe, Curie point, temp. depend. obs. by critical scatt. of neutrons 9-12269  
 Fe, ferromag.-paramag., associated lattice parameter anomalies 9-5569  
 Fe, ferromag., mag. and thermal props. from Landau-type theory 9-7901  
 Fe polycrystals, Curie temp. from extrapolated magnetization data using Landau-Lifshitz-Ginzburg theory 9-12291  
 FeGe, cubic, Curie pt. from susceptibility meas., 4.K 9-16356  
 FeGe, cubic, from Mossbauer effect, 80 300°K 9-16355  
 Fe<sub>2-x</sub>Mn<sub>x</sub>As, antiferromagnetic to ferromagnetic, pulsed field measurement 9-1703  
 Fe<sub>2</sub>O<sub>3</sub> (hematite), ferromag. to antiferromag., effect of hydrostatic pressure 9-3836  
 Gd, rel. to u.s. attenuation and elastic moduli 9-7517  
 Ho, rel. to u.s. attenuation and elastic moduli 9-7517  
 Mn<sub>2</sub>GeSb<sub>1-y</sub> systems, antiferromag.-ferromag. transitions for y>0.19 9-19968  
 $\alpha$ -Mn<sub>2</sub>O<sub>3</sub>-Fe<sub>2</sub>O<sub>3</sub> system, and crystallographic transitions 9-17464  
 MnP, Curie point, effect of hydrostatic pressure 9-15149  
 MnS<sub>2</sub>, antiferromag.-paramag. transition, from low-temp. susceptibility meas. 9-12312  
 MnTe<sub>2</sub>, antiferromag.-paramag. transition, from low-temp. susceptibility meas. 9-12312  
 Ni-Fe alloys, solute C effects on Curie pt. and spontaneous magnetization 9-13984  
 Ni-Mo alloys, effect on anodic behaviour in H<sub>2</sub>SeO<sub>4</sub> 9-21708  
 Ni-Zn, magnetic transition parameters, chemical homogeneity eff. 9-7911  
 Ni, effect on anodic behaviour in H<sub>2</sub>SeO<sub>4</sub> 9-21708  
 PrAl<sub>3</sub>, Curie temp. determ. 9-7898  
 SnFeO<sub>3</sub>, spin re-orientation 9-16372  
 TiAl<sub>3</sub> (T=rare earth metal), ferromag.-antiferromag. at low temp. 9-1646  
 Tb, rel. to u.s. attenuation and elastic moduli 9-7517  
 TbP, lattice deformation at Neel pt. 9-12309  
 Tm, Neel temp. from transport process 9-14014  
 UO<sub>2</sub>, para-antiferromag., crystallographic changes from X-ray diff. obs. 9-7890  
 ZrZn<sub>2</sub>, Invar-type ferromagnet, mag. contrib. to Curie temp. pressure dependence 9-21580

**Magnetic resonance and relaxation**

- See also Antiferromagnetic resonance; Ferrimagnetic resonance; Ferromagnetic relaxation; Ferromagnetic resonance; Nuclear magnetic resonance and relaxation; Paramagnetic resonance and relaxation*  
 alkali metals, double res. signal, displacement on changing r.f. field strength 9-2823  
 anthracene crystals, spin-lattice relax. of protons 9-16470  
 antiferromagnetic metals, spectrum in mag. field 9-8001  
 atom, induced by modulated light, theory 9-4858  
 atom, ionic ground state, exchange collisions 9-11400  
 cerium ethyl sulphate, spin-lattice relax., anomalous phonon effects 9-7658  
 cobalt-rare earth intermetallic cpds., at 9.3 GHz 9-14100  
 c.w. u.s. spectroscopy, sensitivity enhancement using acoustic resonators 9-4406  
 diatomic rotators in ligs. and solids, ang. correls., determ. 9-15841  
 dispersion-mode curves, modulation effects 9-8560  
 ferrites, magnetoacoustic resonance 9-16172  
 ferromagnet, longit. relax. time 9-3838  
 ferromagnet, spin-phonon interaction effects on specific heat 9-12017  
 Hertzian resonance obs., optical methods 9-9144

**Magnetic resonance and relaxation continued**

- Lorentzian absorpt. lines, unsaturated, effect of modulation broadening on shape 9-4404  
 magnetic alloys, dil., spin relax. and transport 9-17466  
 magneto-optical props. of optically pumped medium with near-reson. r.f. irradi. 9-2407  
 measurement, signal noise ratio optimization 9-2282  
 modulated birefringence of spin assembly 9-2832  
 nuclear quadrupole spin-lattice relax. in anharmonic crystals. 9-5857  
 optical detection in optically pumped vapour 9-9452  
 plasma, cold, magneto acoustic reson., nonlinear excitation eff., theory and expt. 9-19521  
 quantum theory of relaxation applied to mag. resonance phenomena 9-15428  
 ruby, relaxation process study, applic. of mag. field prod. as rectangular pulse 9-10807  
 spin diffusion, effect on spin echo signals in inhomogeneous alternating rot. solenoid field 9-4913  
 spin-lattice relax. study based on hyperfine structure of Fe<sup>3+</sup> Mossbauer spectra 9-18688  
 spin-relax. theory, generalized cumulant expansions 9-752  
<sup>201</sup>Hg, optical pumping, transients 9-9145  
 Ba ferrites, hexagonal, relax. Fe<sup>3+</sup> content dependence 9-12314  
 BaF<sub>2</sub>, pure and Eu<sup>2+</sup>-doped, spin-lattice relax. at low and high temps 9-5859  
<sup>13</sup>C<sup>16</sup>O, molec. beam, spin rot. and rot. mag. moment determ. 9-9198  
 Ce, spin-lattice relax. of 4f-electrons 9-12316  
 Co(II) complexes, isotropic proton mag. reson. shifts 9-13349  
 Fe(ClO<sub>4</sub>)<sub>3</sub> frozen soln., relax. eff. from Mossbauer spectra obs. 9-12360  
 H<sup>35</sup>Cl and H<sup>37</sup>Cl, nuclear hyperfine spectra 9-9206  
 He-Ne laser, transition linewidths meas., collision broadening eff. 9-10861  
<sup>4</sup>He, optically pumped, birefringence signals modulated at  $\omega$ ,  $\omega$  and  $2\omega$  9-2832  
 InSb, combined resonances rel. to Bloch electron anomalous velocity in mag. field 9-21460  
 KH<sub>2</sub>PO<sub>4</sub>, P<sup>31</sup> spin-lattice relax. time anomalous decrease near Curie point 9-1713  
 LaBr strain modified spin-lattice relax. rates 9-7927  
 LaCl<sub>3</sub> strain-modified spin-lattice relax. rates 9-7927  
 LaMg nitrate, strain modified spin-lattice relax. rates 9-7927  
 Ni(II) complexes, isotropic proton mag. reson. shifts 9-13349  
 No, <sup>2</sup>H<sub>1/2</sub>, v=0, J=1/2 state, hyperfine perturbations, resonance transitions 9-11468  
 PdAl, proton and deuteron spin-lattice relax. times 9-16385  
 PHAl, proton and deuteron spin-lattice relax. times 9-16385  
 Rb magnetometer, self oscillating long term stability, simultaneous mag. netic field measurements 9-15498  
 VO<sub>2</sub>, metal-semiconductor transition study 9-1552  
 YFe garnet, magnetoacoustic resonance 9-16172  
 YG garnet, magnetoacoustic resonance 9-16172

**Magnetic storms**

- atmosphere, upper, density variations 9-20094  
 auroral emissions, variations 9-21791  
 Chapman-Ferraro model of magnetosphere, absence of disturbance amplification mechanism 9-1950  
 declination change at sudden commencement rel. to local time and season 9-12644  
 effect on heating of upper atmos. and O emission at 6300 Å 9-21788  
 rel. electron flux, solar, ATS-1 omnidirectional spectrometer obs. 9-21968  
 energetic e flux meas. by ATS 1, Jan 13-14, 1967 9-8187  
 energetic e fluxes at 6.6 R<sub>s</sub>, Jan 13-14, 1967 9-10407  
 F-region, daily behaviour 9-12626  
 ionosphere electron content and slab thickness during June 1965 storm 9-10420  
 ionosphere parameters vars. during SC rel. solar and mag. activity, obs. 9-17580  
 magnetopause penetration during storm 9-10403  
 magnetosphere, high latitude night Elektron 2 obs. 9-17589  
 magnetospheric at synchronous alt. acceleration of energetic electrons 9-8189  
 noise spectrum production 9-14408  
 polar substorm and electron 'islands' in Earth's mag. tail 9-8212  
 regulation by upper atmosphere 9-20122  
 ring current asymmetry during 9-21795  
 in solar particle events (23 and 27 May 1967) 9-18939  
 solar wind and magnetosheath obs. from Vela satellites 9-10408  
 SSC, F2 layer effects 9-21823  
 thermospheric wind obs. 9-4053

**Magnetic traps** *see Plasma confinement***Magnetic wells** *see Plasma confinement***Magnetism**

- See also Antiferromagnetism; Diamagnetism; Earth/magnetic field; Exchange interactions; Ferrimagnetism; Ferromagnetism; Gyromagnetic effect; Magnetohydrodynamics; Paramagnetism; Rock magnetism; Stars/magnetism; Sun/magnetism*  
 Anderson model, effective Hamiltonian 9-13942  
 anomalies and demagnetization effects caused by bodies of arbitrary shape, rapid computation 9-4427  
 balanced distrib. of magnetization around spherical cavity 9-13970  
 biomagnetism reviewed 9-8299  
 charge density, pseudoscalar, method of obtaining 9-16761  
 classical theories and descriptions, rel. to solid state electronics, book 9-18631  
 experimental methods, book 9-12971  
 ferrite, under simultaneous a.c. circular field and longitudinal constant one 9-3832  
 flux gain calcs. of cores in equilibrium 9-211  
 Green functions, higher order, calc. 9-10089  
 groups of cubic symmetry, co-representation with simple lattice 9-1632  
 hidden momentum in magnets and interaction energy 9-10816  
 induced-moment system, two kinds 9-5791  
 magnetic charge, photon source model 9-10597  
 metals, non-ferromag., spin waves and other excitations 9-13943  
 monopole sphere 9-2273  
 monopoles, unexpected props. rel. e.m. theory formulation 9-14398  
 reversal of new type propagating at high speed 9-10087



**Magnetism continued**

- s-band, strongly correlated, translationally uniform mag. solns., using modified RPA 9-1633
- spin susceptibility, generalized, in correlated narrow energy-band model 9-12051
- spin-density waves, density and thermodynamic behaviour, correlation theory 9-5790
- spin-density waves, stability and thermodynamic behaviour, Hartree-Fock theory 9-7871
- translation symmetry, connection with coherent states props. 9-18576
- MnCl<sub>2</sub>·4H<sub>2</sub>O, magnon-phonon coupling from mag. field depend. of thermal conductivity 9-1421

**Magnetization process**

See also *Ferromagnetic relaxation*

- Alnico alloys, magnetostatic and exchange Interactions between particles 9-18676
- anomalies and demagnetization effects caused by bodies of arbitrary shape, rapid computation 9-4427
- Barkhausen discontinuities, long. due to mech. stresses 9-5827
- Barkhausen effect and irreversible magnetization processes 9-13977
- Curie point, radio frequency method for determ. 9-1653
- curve representation by rational-fraction approximations 9-10802
- DeBlois experiment, theory rel. to effect of small coil 9-10102
- DeBlois experiment, theory rel. to surface imperfection in infinite coil 9-10103
- domain pattern behaviour 9-16353
- electron gas, noninteracting, spontaneous magnetization 9-8450
- FeOOH·Fe<sub>2</sub>O<sub>3</sub> system, chemical remanent 9-16546
- ferromagnet, isotropic, critical behaviour of spontaneous magnetization 9-10122
- ferromagnetic crystals, uniaxial, with internal stresses, reversible curve, and magnetostriction 9-13979
- ferromagnetic film, "fanning" reversal and exchange stiffness 9-19954
- ferromagnetic wire, internal Barkhausen effect 9-5823
- ferromagnets, orthorhombic, anisotropic spontaneous magnetization and anisotropy energy at 0°K 9-12286
- films, remagnetization in rotating mag. fields 9-21590
- hard substs., normalized parameters for demagnetization and restoration 9-8579
- Ising model, near transition point, magnetization decay on removal of magnetic field 9-3783
- magnetite and Ni, stress control, implications for rock magnetism 9-21586
- measurement of small changes at low temp. using ballistic technique 9-5822
- Neel ferrimagnets, high-field magnetization analysis 9-15154
- permalloy, Barkhausen discontinuities due to mech. stresses 9-5827
- permalloy films on glass, remagnetization in rotating mag. fields 9-21590
- planar film structures with one infinite dimension, demagnetizing field 9-3809
- pressure remanent magnetization and related phenomena 9-19953
- reversal mechanism for single crystal picture frames 9-13981
- around spherical cavity, balanced distrib. 9-13970
- spinel lattice, Ising model appl. 9-1652
- spontaneous, temp. depend., Heisenberg model 9-18671
- superconducting films 9-12231
- superconductors, type II, behaviour using flux-trapping model 9-3593
- susceptibility in random dilute systems, molec. field theory extension 9-12246
- variations by boundary moving due to elastic mechanical stresses 9-3763
- BaFe<sub>12</sub>xAl<sub>1-x</sub>O<sub>19</sub> saturation magnetization variation with Al substitution 9-16366
- Co, rel. to domain patterns 9-16353
- Cu(NH<sub>4</sub>)<sub>2</sub>Br<sub>2</sub>·2H<sub>2</sub>O, b.c.c. Heisenberg ferromagnet, spontaneous magnetiz. meas. 9-18673
- DyFe garnet, in high-fields 9-15154
- DyFeO<sub>3</sub>, perovskite ferrite, model 9-1681
- Fe-3 wt.%Si with Goss-texture 9-13977
- Fe-Mn alloy, mass magnetization as function of internal mag. field 9-18679
- Fe-Mo alloy, mass magnetization as function of internal mag. field 9-18679
- Fe-Si, Barkhausen discontinuities due to mech. stresses 9-5827
- Fe-Si, reversal mechanism for single crystal picture frames 9-13981
- Fe-Si frame monocystal, occurrence of negative Barkhausen jumps 9-1672
- Fe-Ta alloy, mass magnetization as function of internal mag. field 9-18679
- (19wt.%)Fe-(81wt.%)Ni films, anhysteretic behaviour, 20°C 9-13992
- Fe, rel. to domain patterns 9-16353
- Fe, spontaneous, spatial fluctuations at transition point 9-7901
- Fe fine powders, reversal, particle agglomeration effect 9-3822
- Fe polycrystals, Curie temp. from extrapolated data using Landau-Lifshitz-Ginzburg theory 9-12291
- Fe<sub>2</sub>Cr superlattice alloys, isothermal magnetic annealing effects 9-15153
- Fe<sub>2</sub>O<sub>3</sub> fine powders, reversal, particle agglomeration effect 9-3822
- Gd, direction of easy magnetization 9-21585
- Gd, temp. depend. below 50°K 9-13983
- KMnF<sub>3</sub> near phase transition, temp. behaviour of 2-phonon transition 9-7919
- Mn-Ga alloys in high-coercivity state 9-1636
- Ni-(30wt.%)Cu alloy with interstitial occluded hydrogen, spontaneous magnetization temp. dependence 9-16361
- Ni-Fe alloys, solute C effects on spontaneous magnetization 9-13984
- Ni, Barkhausen discontinuities due to mech. stresses 9-5827
- Ni magnetic hysteresis above Curie temp. 9-7902
- Ni rel. to domain patterns 9-16353
- RbMnF<sub>3</sub>, low temp. 9-16382
- SrFe<sub>12</sub>xGa<sub>1-x</sub>O<sub>19</sub> saturation magnetization effect of substitution of Fe<sup>3+</sup> by Ga<sup>3+</sup> 9-16373
- YbFe garnet, in high-fields 9-15154

**Magnetization state**

- application of micromagnetics to boundless plate, comments and authors' reply 9-10058
- dilute systems, mag. and exchange field distrib. 9-7900
- ferromagnetic cryst. effect of local and quasilocal levels (due to dislocation) on magnetization 9-1673
- films, non-planar, computer calcs. 9-21589
- goethite, thermoremanence at Neel temp. 9-10150
- induced moment system, two kinds 9-5791

**Magnetization state continued**

- Ising spin model with 5 transition points 9-5795
- Ising spin system, dilute, temperature dependent distribution of field and magnetic susceptibility 9-7884
- l 9-12300
- lattice near Curie point, contribution of diffuse modes to thermal conductivity 9-12266
- magnetite, after growth from borax flux 9-18413
- ordered structures 9-13969
- periodic configurations, effect of internal magnetostriction on formation 9-13987
- polarity reversal rel. oxidation state in rocks 9-18819
- Preisach-Neel model of interacting single domain grains, exptl. test 9-3764
- rare earth orthoferrites, weak field 9-19969
- remanent, rel. uniaxial compression 9-18822
- superconducting hollow tube in sheath state 9-1483
- superconductor, Type II, vibrating coil magnetometer 9-1491
- susceptibility meas. with magnetic balance, calibration 9-4428
- thermal conductivity of lattice near Curie point, contribution of diffuse modes 9-12266
- transition metal alloys, ordering, new type 9-1658
- transition metal alloys, ordering, new type 9-13959
- variation with temp., continuous recording apparatus for hysteresis loop tracer 9-14286
- Ba, fine-milled saturation, temp. dependence between -195°C and Curie temp. 9-3826
- BaCo<sub>2</sub>TiFe<sub>4</sub>O<sub>12</sub> anisotropy 9-18684
- CdFe garnet, sublattice magnetization by <sup>57</sup>Fe n.m.r. 9-21671
- DyAu, in as-cast state 9-3768
- Fe-Ni-Cr alloys, intensity rel. to heat treatment 9-12288
- Fe-Pd alloys dil. mag. and exchange field distrib. 9-7900
- Fe-6.5%Si, zero magnetostriction, n induced mag. viscosity, obs. 9-19952
- Fe, armco, curves meas. rel. to shock wave effects on residual mag. props. 9-13980
- FeAl alloy, residual, eff. of annealing time and temp. rel. to order-disorder 9-21584
- Fe in remanent state, elastic tensile stresses effects on magnetostrictive props. 9-19956
- Fe wire, Barkhausen discontinuities propag. 9-12290
- Fe<sub>2</sub>O<sub>4</sub>, memory and remanence 9-3798
- LaSn<sub>3</sub>Gd, normal-state, reln. with supercond. critical temp. 9-1478
- LuFe garnet, sublattice magnetization by <sup>57</sup>Fe n.m.r. 9-21671
- Mg<sub>0.78</sub>Fe<sub>2.22</sub>O<sub>4</sub>, anisotropy induced at higher temperatures 9-3829
- Mn-Fe spinel, effect of Mn<sup>2+</sup> clusters on magnetization, anisotropy const. and induced anisotropy 9-1206
- Ni-Fe films, ripple crystallite-size and film-thickness dependence 9-7907
- Ni, effective hole-hole interaction rel. to ferromag. and paramag. 9-21461
- Ni, magnetocryst. anisotropy energy, 4.2.296°K 9-1668
- Ni, magnetocrystalline anisotropy, Mossbauer study 9-12279
- Ni memory, coercive force, isothermal remanent magnetization, variation with internal stress 9-5828
- Ni<sub>1-x</sub>Ge<sub>x</sub>Fe<sub>2-x</sub>O<sub>4</sub>, anisotropy field, effect of heat treatment 9-5850
- Sm-Fe garnet, sub-lattice magnetization sign reversal 9-1691
- Sn-In alloy, a.c. susceptibility rel. to resonant freq. of tank cct. with specimen as core 9-16237
- Sr, fine-milled, saturation, temp. dependence between -195°C and Curie temp. 9-3826
- Th, and mag. specific heat 9-12292
- TmFe garnet, sublattice magnetization by <sup>57</sup>Fe n.m.r. 9-21671
- YFe garnet, sublattice magnetization by <sup>57</sup>Fe n.m.r. 9-21671

**domains**

- disprosium ethyl sulphate, anisotropic mag. dipole interacts, below Curie point, influence on low-field props. below Curie temp. 9-1670
- ferromagnet with domain struct., threshold mag. field and temp. 9-13968
- ferromagnetic f.c.c. lattices, symmetric Bloch walls, thickness and energy, infl. of domain width 9-19951
- ferromagnetic thin films 9-19957
- ferromagnetic thin films, wall visualization by magneto-optical apparatus 9-18681
- film, energy of combined Bloch and Neel type domain wall 9-18683
- films, new stripe domains, theoretical explan. 9-3812
- films, rel. to remagnetization in rotating mag. fields 9-21590
- grains, monodomain, synthetic and natural, hysteretic props. 9-13976
- grains, monodomain interacting, Preisach diagrams and remanent props. 9-14000
- Heisenberg anisotropic ferromagnet 9-10116
- interdomain wall thickness, temp. depend. 9-12276
- Kerr-effect microscopy using rotating diffusing screen for speckle elimination 9-16352
- nucleation in ferromagnetic 9-18675
- orthoferrites, cylindrical domains, properties 9-3825
- orthoferrites domain-wall energy meas. 9-14001
- patterns rel. to magnetization process 9-16353
- Permalloy, analysis by electron diffraction 9-12277
- permalloy films on glass, rel. to remagnetization in rotating mag. fields 9-21590
- remnance in monodomain grains obs. on Neel thermal activation theory 9-3791
- thin-films, magnetic domain struct., spin wave theory 9-5833
- wall, high speed creep effects 9-3807
- wall coupling in permalloy thin film pairs with large separations 9-10132
- wall creep measurements in thin films using high-speed pulses 9-10128
- wall motion hysteresis, rel. to nature of material perturbations 9-15150
- wall structures in films 9-13993
- wall thickness determ. by defocused electron optical pictures of films 9-12297
- wall topography rel. to initial susceptibility 9-5789
- 6Fe<sub>2</sub>O<sub>3</sub> PbO, magnetoplumbite, zigzag domain obs. 9-1663
- Al, due to de Haas-van Alphen magnetization, n.m.r. obs. 9-1664
- Co, magnetostriction infl. on domain structure 9-17453
- Co, patterns rel. to magnetization process 9-16353
- Co, remanent struct., infl. of crystal thickness 9-5819
- Co crystals, thin, walls 9-16354
- E-FeO<sub>3</sub>, domain-wall energy meas. at 25°C 9-14001
- Eu chalcogenides, effects on light scatt. 9-12328
- EuS, diffuse scatt. of light by domains 9-10180
- (19wt.%)Fe-(81wt.%)Ni films, anhysteretic behaviour, 20°C 9-13992
- Fe, interdomain wall thickness, temp. depend. 9-12276
- Fe, patterns rel. to magnetization process 9-16353

**Magnetization state continued**  
**domains continued**

- Fe wires, annealed, Armco, discontinuities distrib. on remagnetization 9-15151  
 $\alpha$ -Fe<sub>2</sub>O<sub>3</sub>, haematite, interactions 9-7917  
 Mn/Permalloy double-layer films, with exchange anisotropy, ferromag. structures stabilisation 9-10130  
 MnAl, c. microscope examination 9-13967  
 Ni (19wt.%)Fe films, energy of combined Bloch and Neel type domain wall 9-18683  
 Ni-Fe, Kerr magneto-optic effect, study 9-10175  
 Ni (19 wt.%)Fe ferromagnetic film, walls, low-angle electron diffraction investig. 9-13997  
 Ni, patterns rel. to magnetization process 9-16353  
 Ni, plastic deform. effects 9-12280  
 Ni cylindrical crystal, stray mag. field above Bloch walls, rel. to struct. 9-13974  
 Ni-(35 wt.%)Fe alloy, ferromag. structures 9-13973  
 PbO(Fe<sub>2</sub>O<sub>3</sub>), rel. to magnetic stiffness field dependence 9-13991  
 RbMnF<sub>3</sub>, antiferromagnetic domains 9-17465  
 Si-Fe sheets, common and grain orientated, discontinuities distrib. on remagnetization 9-15151  
 YFe garnet; Bloch wall mobility, Tb doping effect 9-13975  
 YFe garnet, structure and growth defects effects 9-12302

**Magneto-optical effects**

- See also Optical constants; Zeeman effect*  
 1.2°K, collapsible metal crystal 9-4188  
 alcohols, rotation and magnetic rotary dispersion 9-15878  
 birefringence, quantum field theory 9-11696  
 Faraday, and inverse effect, quantum field theory 9-17206  
 Faraday cell as decoupling element in laser 9-10855  
 Faraday eff., pulsed current and mag. field meas. 9-4426  
 Faraday effect, free-carrier, in piezoelec. semiconductors, at microwave freq. 9-14030  
 Faraday effect, measurement by generation of topography mag. field 9-7944  
 Faraday rotation, lattice vibrational, of U-centre, obs. poss. 9-14032  
 Faraday rotation effect on polarization of normal Zeeman triplet, appl. to sunspots 9-12769  
 ferromagnetic metals, Hall conductivity freq. eff. 9-17474  
 ferromagnetic thin films, apparatus for domain wall visualization 9-18681  
 ferromagnets, interpretation of obs. 9-16335  
 gas interact. with light in mag. field, appl. of Bloch-type formalism 9-4848  
 gases, Faraday effect meas., pulsed-field technique 9-21143  
 H atoms in alkali halides, props. 9-12345  
 insulators, ferromagnetic, optical phonon wavelength shift temp. depend. 9-7946  
 Kerr coefficient, measurement and relationships 9-15546  
 laser light induced, measurable cross effects in isotropic media 9-3133  
 magnetoelectric-optical effects in cubic crystals 9-14031  
 molecules, mag. moments from mag. circular dichroism 9-9184  
 inoptically pumped medium with near-reson. r.f. irradi. 9-2407  
 paramag. complexes in soln., quantum theory for Cotton-Mouton eff. 9-9183  
 polarization switch, latching 9-19977  
 rare-earth orthoferrites, u.v. meas. of complex polar Kerr effect 9-1738  
 semiconductor, piezoelec., free-carrier Faraday effect at microwave freq. 9-14030  
 semiconductors, far-i.r. difference-freq. generation 9-18694  
 semiconductors, magneto-absorpt. in elec. fields rel. to exciton states 9-10174  
 semiconductors, nonlinear phenomena associated with free carriers 9-5881  
 silicon iron, in gyromagnetic constant meas. 9-12344  
 Ba ferrite, hexagonal, polar Faraday and Kerr effects 9-12343  
 BaO, F-centres, Faraday rotation studies 9-3362  
 CaF<sub>2</sub>:Eu<sup>2+</sup>, opt. Faraday rotation from e.s.r. signals for relaxation eff. 9-7945  
 CaF<sub>2</sub>:Ho<sup>3+</sup>, opt. mag. circular dichroism in absorpt. bands 9-1737  
 CaO, F-band obs. by Faraday rotation and Faraday rotation-e.s.r. 9-21342  
 CaO, Faraday rot. study of F-centres 9-3362  
 CaWO<sub>4</sub>:Nd<sup>3+</sup>, Lande factor of excited state by Cotton Mouton eff. 9-18698  
 Co ferromagnetic thin films, mag. birefringence 9-14034  
 CoF<sub>3</sub>, spin-optical phonon interaction, obs. 9-10146  
 Eu chalcogenides, mag. red shift of absorpt. spectrum 9-14033  
 Eu<sub>2</sub>, xGd<sub>2</sub>Se, origin and mechanisms 9-7879  
 EuO, optical phonon wavelength shift temp. depend. 9-7946  
 EuO Kerr effect, on mirror substrates 9-3860  
 Fe ferromagnetic thin films, mag. birefringence 9-14034  
 Fe<sub>2</sub>O<sub>3</sub>, colloidal soln. in mag. field, particle size determ. 9-5200  
 GdCl<sub>3</sub> magnon density obs. in optical spectrum 9-7947  
 Ge, magnetoabsorpt. oscillations associated with interband transitions, and exciton states 9-5918  
 Ge, magnetoabsorption intensity rel. to exciton absorpt. rise 9-5919  
 Ho Fe garnet, Faraday effect, effect of mag. field 9-1740  
 Ho ferrite garnet Faraday effect and reversal of mag. sublattices 9-1739  
 n-InAs, magnetoreflection in far i.r. near optical phonon freq. 9-12151  
 NO, mag.-rot. spectra of I-O vibr. rot. band 9-9221  
 NO, near i.r. mag. rot. spectrum calc. 9-2877  
 N(XYZ), mols., where X, Y, Z = H or R. 9-780  
 Ni-Fe, Kerr longit. eff., and optical constants 9-10175  
 Ni-Fe, Kerr longit. eff., and mag. birefringence 9-14034  
 Ni (19 wt.%)Fe, ferromagnetic thin films, mag. birefringence 9-14034  
 Ni, ferromagnetic, Kerr effect rel. to spin-orbit splitting of 0.7-eV transition and electron structure 9-7948  
 Ni-(35 wt.%)Fe alloy, Kerr effect rel. to domain structures 9-13973  
 PbTe, intraband Faraday and Voigt eff., behaviour of coeffs. 9-17475  
 PbTe, magneto-reflection spectra of coupled plasmon-phonon modes 9-18699  
 RbFeF<sub>3</sub>, Cotton-Mouton effect and mag. structures at 77 and 200°K 9-3771  
 Rbl magnoreflexion dichroism, Zeeman effect irregularity 9-7949  
 RbNiF<sub>3</sub>, Co substituted, properties 9-5882  
 Se amorphous, Faraday effect 9-3861  
 SiO<sub>2</sub>, F-centres, Faraday rotation studies 9-3362  
 Y Fe garnet, Faraday effect, effect of mag. field 9-1740  
 YFe garnet:Si i.r. irradi., photomag. anneal props. by torque meas. 9-10137  
 Y<sub>2</sub>Fe<sub>2</sub>O<sub>12</sub>, Faraday eff. rotation rel. to mag. field intensity 9-7950

**Magnetoacoustic effects**

- antiferromagnets, resonance rel. to oscillation transformation into elastic waves 9-1693  
 crystal conduction electrons u.s. absorpt. coeff., mag. field effect 9-18558  
 dispersion and attenuation, expt. rel. to free-electron theory 9-5553  
 ferrites, resonance 9-16172  
 ferromagnetic medium, magneto-elastic interactions, elastic anisotropy effect 9-3804  
 ferromagnetic single crystals, spin waves-acoustic interaction 9-3803  
 ferromagnets, resonance, effect of mag. alloying additions 9-5552  
 flaw det. using transducerless u.s. generation 9-7469  
 magnetosonic waves, reflection from boundary of magnetosphere, magneto-spheric resonances 9-18807  
 plasma, cold, resonance, nonlinear excitation eff., theory and expt. 9-19521  
 semimetals, field instability at low temps. and waves 9-15004  
 waves, generation by stellar wind-surrounding gas interaction 9-21861  
 Bi, attenuation anisotropy rel. to deformation potential tensor component determ. 9-5556  
 Ge:As, u.s. spin reson. of donors 9-5555  
 H plasma, waves obs. 9-19551  
 Hg crystals 9-21432  
 InSb, amplification, quantum theory 9-16171  
 InSb, third harmonic generation using CO<sub>2</sub> laser enhancement in mag. field 9-257  
 K and free electron theory 9-7649  
 Ni ferrites, hysteresis of u.s. vel. 9-9828  
 Y Ga Fe garnet, resonance at 3- and 10-cm bands 9-5557  
 YFe garnet, resonance 9-16172  
 YFe garnet, resonance at 3 and 10-cm bands 9-5557  
 YFe garnet epitaxial film on YAl garnet, shear wave generation at micro-wave freqs. 9-10141  
 YGd garnet, resonance 9-16172

**Magnetocaloric effects** *see Magnetochemical effects***Magnetocrystalline anisotropy** *see Magnetic properties of substances; Magnetization state***Magnetoelastic effects** *see Magnetochemical effects; Magnetoelastic waves***Magnetoelastic waves**

- amplification in a ferromagnetic semiconductor 9-5829  
 coupled, props. in mag. mats. without centre of inversion 9-21559  
 dispersion relation of long transversely magnetized cylinder with metal boundary 9-10121  
 excitation and amplification 9-1689  
 ferrites, instability, quantum investigation 9-3823  
 fluid-filled cylindrical cavity, vibrations in infinite solid medium 9-4305  
 oscillation transformation into elastic waves 9-1693  
 parametric amplification in YFe garnet rods 9-14967  
 pulses in inhomogeneous field, transform. coeff. 9-1374  
 Fe-(3wt.%)Si alloy, vibration attenuation, eff. of temp. and orientation 9-11915  
 Y Fe garnet, excitation and amplification 9-1689  
 YFe garnet, light diffraction 9-12342  
 YFe garnet rods, longit. waves, obs. 9-9746  
 YFe garnets, excitation, nonlinear phenom. 9-19970

**Magnetolectric effects**

- See also Hall effect; Magnetoresistance*  
 cylindrical wires, magnetomagnetic oscils. in elec. conductivity 9-12082  
 electron-impurity system, Titeica-type formula for transverse cond. in mag. field 9-5601  
 electron-phonon system, oscs. in elec. cond. in mag. field, calc. 9-7700  
 galvanomagnetic eff. meas., a.c. technique 9-19118  
 graphite flakes, galvanomag. effects. 77 to 300°K 9-7847  
 n-InSb, galvanometric props. meas. 0.4-4°K 9-12137  
 metals, ferromagnetic, effect accompanying galvanomagnetic effect: Mat-teucci spontaneous 9-12249  
 metals, infl. of dislocations on galvanomag. effects. 9-12095  
 metals, localized Umklapp scatt. effect on galvanomag. props. 9-9918  
 Procopiu effect, conditions required 9-14410  
 Procopiu effect with cylindrical ferromagnet free at one end 9-13958  
 rare-earth metals, galvanomag. effects below Neel temp. 9-1709  
 semiconductor, galvanomagnetic effects in presence of small number of free carriers 9-13878  
 semiconductor, nondegenerate, steady-state galvanomagnetic effect, coupled current densities 9-13872  
 semiconductors, polar, hot-electron galvanomagnetic coeffs. 9-5680  
 B, -60° to +50°K, magnetocond., 0 to 2000 Gauss 9-16222  
 B, -60° to +50°K, magnetocond., 0 to 2000 Gauss 9-16221  
 Bi MnBi composite, galvanomag. props. 9-9671  
 Bi<sub>2</sub>Sb<sub>3</sub>, (x=97.90;y=3.10), band parameters from galvanomag. meas. 9-1533  
 Bi-Pb, Bi-Sn and Bi-Sb-Pb alloys, galvanomag. props., effect of pressure up to 20 ktm., 4.2-295°K 9-9892  
 Co cast, galvanomag. effects rel. to  $\epsilon$ - $\gamma$  transition 9-3578  
 Cr, antiferromag., high-field eff. meas. rel. to Fermi surface 9-17462  
 Fe, procopiu effect, obs. 9-16225  
 n-GaAs, galvanomagnetic effects of hot electrons 9-3624  
 n-InSb, galvanomagnetic phenomena, quantization effects 9-13886  
 LiFePO<sub>4</sub>, coeff. temp. dependence in a.c. field 9-14013  
 LiNO<sub>3</sub> 9-1600  
 Li:O<sub>2</sub>:7Fe:O<sub>2</sub>:3Cr:O<sub>3</sub> 9-16370  
 MnO-ZnO-Fe<sub>2</sub>O<sub>3</sub>, Procopiu effect, obs. 9-16225  
 MnP, galvanomag. eff., hydrostatic pressure eff. on Curie temp. 9-15149  
 Nb, galvanomagnetic, high-field 9-3770  
 Ni-Ta(Nb) ferromagnetic alloy system, galvanomagnetic eff. 9-3790  
 Ni, Procopiu effect, obs. 9-16225  
 NiO-ZnO-Fe<sub>2</sub>O<sub>3</sub>, Procopiu effect, obs. 9-16225  
 Sb Sn alloys, galvanomagnetic coeff., band struct. interpretation 9-3841  
 Si, metal-nonmetal transition, galvanomag. investigation 9-1472  
 Sn, white, galvanomagnetic effects rel. to preferred orientation of crystal 9-16050  
 TiCl<sub>3</sub>, galvanomagnetic effect 9-3772  
 YFe garnet 9-12303  
 Zn, anomalous size effects caused by compensation 9-13848

**Magnetogasdynamics** *see Magnetohydrodynamics***Magnetohydrodynamic generators** *see Electricity, direct conversion/magnetohydrodynamic***Magnetohydrodynamic waves** *see Magnetohydrodynamics; Plasma/magnetohydrodynamics; Plasma/oscillations*



**Magnetohydrodynamics**

- See also *Plasma/magnetohydrodynamics*  
 accelerator, pulsed, hot-shot gas source 9-11531  
 Alfvén-wave resonances in non-viscous liq. metals 9-21036  
 aligned flow of compressible fluid past slender body in wind tunnel 9-9327  
 atmosphere, elec. conductive, weak discontinuity propag. 9-21761  
 augmented shock tube, meas. techniques 9-17813  
 axially-symmetric flow in vortex chamber for large Hartmann numbers 9-7126  
 axis-symmetric channels, viscous conductive fluid flow 9-9332  
 Bernoulli equation for relativistic case 9-21042  
 Blasius problem, application of Laplace transform to solution of boundary layers equations 9-2953  
 body of revolution, insulating, rot. in conducting fluid 9-15919  
 boundary layer at surface of plate for arbitrary orientation of mag. field, properties 9-9329  
 boundary layer eqns. with transverse mag. field and arbitrary press. gradient, solns. 9-18263  
 boundary layers, soln. by Karman-Polhausen method with fourth degree polynomial vel. profile 9-7116  
 canonical form of MHD eqns. 9-21028  
 channel with non-conducting wall, turbulent boundary layer calc. 9-7128  
 channels with semi-infinite electrodes, edge effects analysis 9-9323  
 chemi-ionization phenomena, utilization prospects 9-18249  
 collapsing or exploding cyl. shell of conducting fluid in mag. field, stability 9-19520  
 compressible fluid, aligned, flow past slender body in circular wind tunnel 9-15916  
 conducting fluid, eff. of flow on mag. field of dipole in centre of sphere 9-21029  
 conducting fluid rotating in vertical mag. field, effects of Hall currents on thermal instability 9-7145  
 conducting incompressible fluid between two parallel plates under a transverse mag. field, unsteady Couette flow 9-21040  
 conducting liquid, rotationally advancing, in magnetic field, heat transfer and resistance to movement 9-13521  
 convection in cavity with variable upper wall temp. 9-19514  
 Couette, stationary, accelerated and pulsating flows between parallel plates 9-2951  
 Couette flow, between coaxial rotating cylinders, instability 9-856  
 couette fluid flow var., pressure gradient 9-2958  
 cylindrical sys., least stable mode 9-4997  
 dielectric fluid flow in pipes, elec. field eff. 9-9330  
 dissipative conservation laws 9-2949  
 duct flows, uniqueness theorem 9-18262  
 dusty conducting gas, plane parallel flow 9-9326  
 dynamo problem, exact solutions 9-21041  
 Ekman layer in rotating fluid 9-18250  
 electrically conducting fluid, unsteady forced-convection ht. transfer in parallel plate channel 9-18264  
 electrically driven flows, theory and expt. 9-21031  
 electrodynamic turbulence in conducting media, e.m. field behaviour 9-7130  
 electrodynamic turbulence in conducting media, e.m. field behaviour 9-7131  
 e.m. flowmeter readings, reducing contact resistance effect 9-7110  
 equations governing flow of conducting fluid in high mag. field, propulsion applications 9-21037  
 flow, nonanalyticity at surface of fluid 9-19507  
 flow, nonisotropic, rectilinear 9-19518  
 flow, steady electrically driven, flat plate considered 9-18261  
 flow around a plate in applied magnetic field 9-18259  
 flow in equilateral triangle in transverse mag. field 9-15918  
 flow in rotating straight pipe 9-13409  
 flow in rotating straight pipe 9-9325  
 flow of fluid with periodically changing elect. conductivity 9-17855  
 flow over rotating disc with circular mag. field imposed, soln. 9-9324  
 flow past an inclined plate at non zero incidence 9-19519  
 fluid flow between parallel plates in transverse field, stabilization 9-7123  
 fluid flows, kinematic props. 9-2952  
 fluid laminar pipe flow in transverse mag. field, anal. with heat transfer 9-13408  
 fluid motion and disturbances due to sudden introduction of oscillating dipole 9-11532  
 gas, conducting dusty, plane parallel flow 9-13410  
 gas, perfectly conducting, two-dimensional flow in crossed elec. and mag. fields 9-2957  
 gravitating fluid layer, incompress., with Hall effect, stability 9-7117  
 heat transfer in crossed-field couette flow 9-854  
 heat transfer of fluid flowing in a parallel plate non-conducting channel 9-18251  
 Hg, non stationary open channel flow, transverse magnetic field 9-21038  
 hydraulic friction, fluid flow in travelling magnetic field 9-21033  
 hydromagnetic surface waves with alternating mag. field, propag., damping and dispersion 9-17092  
 inhomogeneous flow, Rayleigh-Taylor instability and turbulent diffusion effects 9-18265  
 interchange instabilities theory, and driving energy forces 9-5052  
 intrinsic equation 9-18258  
 jet, 2-d steady, infl. of thermal radiation 9-7119  
 jet driven vortex flow, hydromagnetic stabilization 9-21043  
 jet flow with variable conductivity, theory 9-7118  
 jets of conducting liquid adjacent to walls in transverse magnetic fields 9-21034  
 jets with variable conductivity 9-2954  
 Kelvin-Helmholtz instability, horizontal and vertical mag. fields effects 9-14750  
 Kelvin-Helmholtz and gravitational instability, combined effect on self-gravitating fluid layer 9-17091  
 laminar flow between parallel plates, dispersion of soluble matter, analytical soln. 9-17094  
 laminar flow of viscous conducting liquid between parallel walls, travelling magnetic fields 9-18260  
 laminar submerged jet, characteristics 9-4995  
 linearized magneto-fluid-mechanics, theory 9-14752  
 lines of force, motion of, times characteristic 9-15917  
 liquid metal flow, turbulent velocity pulsations, mag. field eff. 9-7125  
 liquid metal flow in channel with segmented electrodes 9-7121

**Magnetohydrodynamics continued**

- liquid metal flow in transverse mag. field, shear stresses and turbulent exchange coefficients 9-7124  
 Mangler's transformation 9-17093  
 metal bearing, liquid, pressurization, centrifugal effects 9-4996  
 metals, liquid non-viscous, Alfvén-wave resonances 9-21036  
 MGD steady flow in finite region, aligned fields 9-17095  
 non-viscous fluid, anisotropically conducting, symmetric flow analysis 9-7129  
 one dimensional flow of magnetized incompressible, non viscous conducting fluid 9-18253  
 overheating instability, effect of walls of channel 9-2956  
 particles in a high frequency component field 9-2950  
 penetration of magnetic field through shock-wave front 9-18254  
 plasma, anisotropic, rotating; gravitational instability, finite Larmor radius eff. inclusion 9-14189  
 in protogalaxies formation 9-17610  
 Rayleigh flow past an infinite porous plate 9-21165  
 Rayleigh-Taylor instability, horizontal and vertical mag. fields effects 9-17090  
 Rayleigh-Taylor instability of conducting fluid in varying mag. field 9-855  
 relativistic, Bernoulli equation 9-21042  
 relativistic, ray theory 9-965  
 relativistic, shock waves time orientation and compressibility hypothesis 9-21030  
 resistance of liquid metal flow in channels in transverse magnetic field 9-21032  
 self-gravitating masses, oscillations and stability in axial mag. field 9-17624  
 shallow-liquid, weak discontinuities 9-14751  
 shock relations, reduced, for jump conditions 9-15931  
 shock waves in non-viscous fluids, structure 9-7127  
 shocks in two fluid plasma, critical Alfvén-Mach numbers 9-18280  
 striated flow in synchronous induction generator 9-17854  
 surface stability of liquid metal levitated in vacuum by alternating magnetic field, effects of dissipative processes in casing 9-18256  
 teaching review 9-15412  
 tensor conductivity eff. on flow 9-18257  
 three-dimensional duct flows with strong transverse magnetic fields, obstacles in constant area channel 9-19515  
 three-dimensional flow in variable profile channels with symmetry plane 9-9331  
 transfer coefficients for inhomogeneous systems in e.m. fields 9-18255  
 turbulence, effect on Lorentz field strength and Hall coeff. 9-9335  
 turbulence, two-dimens., in Ohm's law governed system 9-11533  
 turbulence suppression by transverse magnetic fields in special shaped tubes, investigation 9-21044  
 turbulent flow in pipes, unified semiempirical theory 9-7122  
 turbulent jet of conducting liquid, axial symmetry in a longitudinal magnetic field 9-21045  
 turbulent jet of conducting liquid, axis-symmetric, distribution of pulsation energy, longitudinal magnetic field 9-21046  
 turbulent motion, differential equation of second order approx. 9-11669  
 two dimensional flow, anisotropically conducting, incompressible liquid in axis-symmetric channels in magnetic field 9-21039  
 two-dimensional steady flow, perturbation stream function 9-9333  
 unsteady forced-convection MHD ht. transfer of elec. conducting fluid in parallel plate channel 9-18264  
 variational methods in steady magnetogasdynamics 9-9334  
 vibration treatment of liquid metals by e.m. forces 9-21035  
 viscous flow around spherical shell 9-7120  
 wave generation by high altitude nuclear bursts, model 9-10440  
 wave propag. normal to mag. field, as in ionosphere and magnetosphere, current influence 9-19516  
 wind velocity var. with height in turbulent elec. conducting atmosphere 9-21766  
 Cu vapour laser, electrically accelerated, pulse broadening 9-20510  
 Ga, liquid metal flow in conducting circular tubes in transverse mag. fields, pressure losses due to contact resistance 9-9328  
 Ga liquid flow in channels with conducting walls, resistance during transition from laminar to turbulent flow 9-9336  
 Hg, laminar natural convection, influence of mag. field 9-18252  
 Hg pipe flow, strong longit. mag. field effects, transition region and turbulence struct. 9-14753  
 Na, liquid, Alfvén-wave reson. 9-2955

**Magnetomechanical effects**

- See also *Gyromagnetic effect; Magnetoelastic waves; Magnetostriction*  
 elastic body, electrically conductive, in mag. field, asymm. stress possibility 9-21564  
 elastic waves in electric conductors, effect of magnetic field 9-14150  
 magnetite bearing rocks and Ni polycrystallites, remanent magnetization rel. uniaxial compression 9-18822  
 oscillations, magnetostrictively induced longit., e.m. aspect 9-13958  
 piezomagnetization, ferromagnetics, susceptibility of fine grain assemblage rel. uniaxial compression 9-21587  
 thermo-magneto-microelasticity 9-10711  
 Co, behaviour during fatigue deformation, associated with dislocation slip 9-17308  
 Fe<sub>2</sub>TiO<sub>4</sub>-Fe<sub>2</sub>O<sub>3</sub> solid soln., initial susceptibility of fine grain assembly, rel. axial stress 9-18680  
 Fe in remanent state, elastic tensile stresses effects on magnetostrictive props. 9-19956  
 Ni, behaviour during fatigue deformation, associated with dislocation slip 9-17308  
 NiCo ferrites, piezomag. coeff. temp. depend. 9-5846  
 NiMn ferrites, piezomag. coeff. temp. depend. 9-5846

**Magnetometers** see *Magnetic field measurement***Magnetoreflexion** see *Magneto-optical effects***Magnetoresistance**

- See also *Magnetoelectric effects*  
 compensation method for meas. in alternating fields 9-12287  
 ferrites of spinel type, obs. 9-12087  
 graphite-nitrate residue cpds, anal. in band model approx. 9-7740  
 metals, effect of breakdown and spin-orbit coupling 9-12077  
 metals, theory 9-18594  
 metals localised Umklapp scatt. effect 9-9918  
 Permalloy film, rel. to torque 9-7906  
 semiconducting cpds., group III-V magnetophonon effect 9-21513

**Magnetoresistance continued**

- semiconductors, rel. to Hall effect, book 9-13880  
 semimetals 9-15066  
 Shubnikov-de Haas eff. meas., a.c. technique 9-19118  
 weak field, approximation for kinetic transport coeff. of organic semiconductors 9-21508  
 OCu, elec. and thermal, 80-130°K 9-5636  
 Ag, elec. and thermal, 80-130°K 9-5636  
 As, Shubnikov-de Haas and magnetothermal oscills., obs. 9-5633  
 Au-Fe alloys, dil. rel. to conduction e. anomalous scatt. 9-5805  
 Au-Mn alloys, dil. rel. to conduction e. anomalous scatt. 9-5805  
 Au, elec. and thermal, 80-130°K 9-5636  
 Bi-Pb alloys, dilute, differential Shubnikov-de Haas effect 9-7726  
 Bi<sub>2</sub>Te<sub>3</sub>, n and p type, Shubnikov-de Haas oscills. 9-3637  
 Bi<sub>2</sub>Sb<sub>3</sub>, Shubnikov-de Haas meas. of band structure 9-16209  
 n-Bi<sub>2</sub>Te<sub>3</sub>, quantum oscillations 9-12144  
 Bi-Sb alloy, semicond., longit. anomalies in mag. fields up to 500 kOe at liq. He temp. 9-1514  
 C, donor doped (Na and K), temp. depend. of negative effect 9-7752  
 C, mdg-field depend. at various temp., rel. to acceptor doping and heat treatment 9-7751  
 C, soft and hard, temp. depend. from 1.5 to 300°K, after heat treatment to 3000°K 9-7749  
 C, soft heat treated from 1800°-3000°K after acceptor introduction 9-7750  
 C blacks, compacted without a binder 9-7735  
 CdSb, doped, 2.2-77°K 9-9972  
 n- CdSnAs<sub>2</sub>, meas. in mag. fields rel. to effective anisotropy coeff. 9-9984  
 CdTe, rel. to electric and magnetic field intensities 9-3622  
 Cu-Fe dilute alloy, and low-temp resist. 9-18602  
 Cu-Pd solid solutions, ordered and disordered, variation 9-21483  
 Cu, longitudinal, temp. depend. of saturation ratio 9-1446  
 Cu, polycrystalline wires, transverse 9-7753  
 Fe-C alloys, 4.2 and 78°K 9-15070  
 Fe, thin films, negative anisotropy 9-18682  
 Fe<sub>2</sub>Se<sub>3</sub>, transverse magnetoresistance rel. to change in mag. order at 200°K 9-19886  
 n-GaAs:Cr, negative 9-19913  
 n- GaAs, magnetophonon effect 9-21513  
 n- GaAs, temp. depend., rel. to 'freezing-out' of electrons, 4.2-20°K 9-12147  
 n-GaAs, transverse oscillatory component, Shubnikov-de Haas eff. 9-5687  
 n-GaAs, undoped, at low temperatures 9-3610  
 n- Ge, transverse, magnetophonon oscillations 9-12158  
 n-HgSe, Shubnikov-de Haas eff. in strong mag. fields 9-16218  
 InAs, 4.2°K, doped, cond. band 9-1535  
 n-InAs, magnetophonon effect 9-21513  
 n-InAs, oscill. maxima fine structure at 1.6°K 9-1530  
 n-InAs, Shubnikov-de Haas oscills. in thermomag. effect 9-3629  
 InAs films 9-9980  
 n-InP, compensated, mag. field, temp. and sample geom. dependence 9-3627  
 InSb, in effective electron mass pressure dependence determ. 9-1536  
 n- InSb, magnetophonon oscillations in strong elec. fields 9-19914  
 n-InSb, magnetophonon effect 9-21513  
 n-InSb, quantization effects, 4.2°, 50° and 77°K 9-13886  
 InSb, semimetal, negative, rel. to localized spins 9-9932  
 n-InSb, Shubnikov-de Haas oscills. in thermomag. effect 9-3629  
 Li<sub>2</sub>O.2.2Fe<sub>2</sub>O<sub>3</sub>.2.8Cr<sub>2</sub>O<sub>3</sub> longit. and transverse magnetoresistance, anomalies around compensation temp. 9-19965  
 n-NgTe, quantum oscills., 9-3625  
 β-Ni-Al, and Hall coeff. at liq. He temps. 9-5639  
 Ni, temperature (1.85-20.1°K) and thickness (1.005-0.041 mm) dependences 9-1468  
 Ni, thin films, negative anisotropy 9-18682  
 RuO<sub>2</sub>, transverse meas. 9-16234  
 Si, longit., in mixed conduction region 9-15106  
 Sn grey, Shubnikov-de Haas oscills. 9-13833  
 Sn, white, 'Shubnikov-de Haas' oscillations, explanation in terms of mag. breakdown 9-3564  
 Sn, white, rel. to preferred orientation investig., 4.2°K 5-16050  
 SnO<sub>2</sub>, weak-field, meas. rel. to electronic props. 9-9981  
 SrTiO<sub>3</sub>:Nb rel. to conduction band structure 9-7788  
 Te, negative, at low temps. 9-3566  
 Te, Shubnikov-de Haas eff. obs. 9-9915  
 Te, Shubnikov-de Haas effect 9-7729  
 Ti<sub>2</sub>O<sub>3</sub>, pure and doped, at 4.2, 77 and 273°K rel. to stoichiometry and purity 9-5646  
 TiCl galvanomagnetic effect 9-3772  
 V, rel. to Fermi surface anisotropy 9-12105  
 W, elec. and thermal, rel. to phonon cond., K 9-5636  
 Zn, anomalous size effects caused by compensation 9-13848  
 Zn, effect of breakdown and spin-orbit coupling 9-12077

**Magnetosphere**

- Alfvén waves excitation of Pi2 pulsations 9-17590  
 artificial plasma clouds released by rocket 9-6090  
 Chapman-Ferraro model, dynamics 9-1950  
 cosmic-ray cut-offs, and vars. 9-15261  
 disturbance field, high latitude night Elektron 2 obs. 9-17589  
 diurnal variations of size, estimation from pressure balance considerations 9-15250  
 electron density deduced from nose whistlers 9-6085  
 electron flux, energetic, ATS 1 Jan 13-14, 1967 obs. 9-8187  
 electron fluxes, energetic at 6.6 R<sub>J</sub> Jan 13-14, 1967 obs. 9-10407  
 electrons, moving along mag. field lines, synchrotron radiation 9-12603  
 electrons, trapped, drift rel. auroral cosmic radio noise absorption time lags 9-21790  
 electrostatic field asymmetric development and conductivity var. 9-1956  
 energetic e acceleration obs. at synchronous alt. during mag. storms 9-8189  
 hydrodynamic wave propag. normal to mag. field, influence of currents 9-19516  
 hydromagnetic waves propagation, current density effects 9-10410  
 induced whistler and ambient plasma interaction 9-4066  
 magnetic fields in magnetopause at synchronous alt. 9-10404  
 magnetodynamic toroidal waves, existence and validity of magnetodynamic approx. 9-19549  
 magnetopause, nose region, oscillatory motion 9-4067

**Magnetosphere continued**

- magnetopause at 6.6 R<sub>J</sub>, OGO 3 search coil magnetometer data, Jan 14, 1967 9-10409  
 magnetopause boundary layer transfer processes 9-10402  
 magnetopause penetration beyond 6.6 R<sub>J</sub> during mag. storm 9-10403  
 magnetopause structure at 6.6 R<sub>J</sub> in terms of 50-150 keV electrons, Jan 14, 1967 obs. 9-10406  
 magnetosheath, outward flow of p 9-8188  
 magnetosheath during geomagnetic storm, Vela satellite obs. 9-10408  
 magnetosonic waves, reflection from boundary, magnetospheric resonances 9-18807  
 magnetotail, hydromagnetic structure of neutral sheet 9-8211  
 and micropulsations due to solar wind interaction 9-20118  
 moving mag. field line identification 9-8574  
 particles and fields, review 9-8190  
 plasma flow 9-10400  
 plasma flow directions at magnetopause, Jan 13-14, 1967 9-10405  
 plasma waves and particle interactions and auroral precipitation 9-20097  
 solar cosmic rays screening 9-14254  
 tail, shape and mag. field, effect of neutral sheet currents 9-20098  
 temp. dist. model 9-10399  
 v.l.f. e.m. field, FR 1 satellite obs., interpretation 9-20096

**Magnetostriiction**

- deformation velocity and material constants in case of mag. deformation 9-3800  
 ferromagnetic alloys, saturation, above room temp. 9-10125  
 ferromagnetic crystals, uniaxial, with internal stresses, and reversible magnetization curve 9-13979  
 internal, effect on formation of periodic magnetization configurations 9-13987  
 magnetite, volume 9-21836  
 rare earth gallates, paramagnetic with garnet structures, 4.2-60°K 9-21571  
 rare earth germanates, paramagnetic with garnet structures, 4.2-60°K 9-21571  
 steel, internally oxidised electrotechnical, longitudinal 9-13989  
 in superconductors, type II 9-5658  
 superconductors, type II, surface current eff. 9-19893  
 BaFe<sub>12</sub>O<sub>19</sub> ferrite 9-14004  
 Co, hexagonal phase, coeff. temp. depend. 9-7903  
 Co, infl. on domain structure 9-17453  
 Cr, stress-cooling effect rel. to ordering obs. 9-1700  
 Cu-Ni alloys, effects on lattice constant conc. dependence at -189°C, 20°C and 400°C 9-19955  
 Eu chalcogenides, exchange 9-7904  
 Fe Si, grain oriented, meas. using ceramic displacement 9-12293  
 Fe Si alloys, surface Ni films, eff. on anisotropy 9-13990  
 Fe<sub>2</sub>Al alloy, eff. of annealing time and temp. rel. to order-disorder 9-21584  
 Fe in remanent state, elastic tensile stresses effects on magnetostrictive props. 9-19956  
 Fe<sub>2</sub>Cr superlattice alloys, isothermal magnetic annealing effects 9-15153  
 In alloys, Ginzburg Landau parameters, pressure depend. 9-7881  
 MnSe, temp. and field strength dependence 9-1705  
 Ni-Co Si alloy, 'Nicolosi', sensitivity, magnetomech. coupling and mag. anisotropy 9-5830  
 Ni-Fe alloy films, meas. method 9-13985  
 Ni, electroplated, magnetocrystalline anisotropy, effect of electrolytic charging with H 9-15152  
 Ni ferrites, piezomag. coeff. temp. depend. 9-5846  
 Ni film, transverse microwave phonon generation at zero field 9-10126  
 Pd-Ni alloy, paramagnetic, exchange enhancement, localised, vol. derivative, Pd contrast 9-1642  
 Pd exchange enhancement, localised, vol. derivative, Pd:Ni alloy contrast 9-1642  
 TiFeF<sub>3</sub>, linear, in e.m.-sound conversion 9-16170  
 YFe garnet, polycrystalline control of effects 9-3833

**Magnetothermal effects**

- balance, servo-type, for routine thermomagnetic analysis 9-14414  
 lanthanum cobalt nitrate, conductivity meas. for phonon mean free paths 9-9854  
 paramagnetic fluids, insulating magnetothermal convection 9-7233  
 photomagnetic effect in quantizing mag. fields during electron heating by light 9-3744  
 semiconductors, Nernst-Ettinghausen eff. 9-7791  
 semiconductors, nondegenerate, Nernst-Ettinghausen effect, effect of collisions between carriers 9-15129  
 superconductors, type II, heat current operator 9-9953  
 Ag, magnetoresists., thermal and elec., 80-130°K 9-5636  
 As, magnetothermal and Shubnikov-de Haas oscills., obs. 9-5633  
 Au, magnetoresists., thermal and elec., 80-130°K 9-5636  
 AuGa<sub>3</sub>, Knight shift, spin-lattice relax., susceptibility, temp. depend. and relationship 9-10292  
 Bi, props. at low temp. 9-10059  
 CdAs<sub>2</sub>, non-parabolic conduction band from magneto-Seebeck and Hall coeff. meas. 9-9893  
 Co-Pt alloys, effect of thermomagnetic treatment on ordering 9-3767  
 Cu, magnetoresists., thermal and elec., 80-130°K 9-5636  
 FeNiCo ferrites, thermomagnetically induced anisotropy 9-19963  
 Gd<sub>2</sub>Fe<sub>2</sub>O<sub>11</sub>, anomalous sign in compensation pt. region 9-1683  
 Gd<sub>2</sub>Fe<sub>2</sub>O<sub>11</sub>, anomaly 9-16370  
 n-Ge, elastic deformations infl. in phonon-drag eff. region, low temp. 9-21542  
 HgTe galvanothermoelectric effects and conductivity 9-5643  
 n-InAs, quantum effects 9-3629  
 n- InSb, photoeffect in quantizing mag. fields during electron heating by light 9-3744  
 n-InSb, quantum effects 9-3629  
 Li<sub>2</sub>O.2.5Fe<sub>2</sub>O<sub>3</sub>.2.5Cr<sub>2</sub>O<sub>3</sub>, anomaly 9-16370  
 Li<sub>2</sub>O.2.5Fe<sub>2</sub>O<sub>3</sub>.2.5Cr<sub>2</sub>O<sub>3</sub>, anomalous sign in compensation pt. region 9-1683  
 α-NiSO<sub>4</sub>.6H<sub>2</sub>O, 0.4°-4.2°K, 0-90 kG fields 9-19862  
 p-PbSe, Nernst Ettinghausen eff., temp. dependence for band structure determ. 9-3643  
 PbTe, Nernst-Ettinghausen effect, transverse, in mixed conduction region 9-15132  
 Sn Nernst-Ettinghausen effect rel. to e. scatt. mechanism 9-9856  
 W magnetoresists., thermal and elec., and phonon cond., 80-130°K 9-5636  
 ZnSb, transverse Nernst-Ettinghausen eff. anisotropy 9-9923



**Magnetrons** see *Electron tubes; Microwave techniques and devices*

## Magnets

See also *Superconducting magnets*

- assemblies for high homogeneity fields, patent 9-10813
- construction, Cu and teflon interlaced spirals, 2000 Hz, 10 kG 9-2327
- cryogenic and superconducting, for MHD generators, optimization 9-17852
- cryogenic and superconducting, optimization for MHD generators 9-17852
- electromagnet for NMR work, design and construction 9-17840
- electromagnet with Fe core, increase of homogeneity of field 9-219
- ferrite  $\text{Li}_{0.3}\text{Mn}_{0.7}\text{Fe}_2\text{O}_4$  core with square hysteresis loop, production method, patent 9-19966
- field modulators, amplitude stabilizer 9-2324
- flux stabilizer, fail-safe switch cct. 9-206
- gradient, of strong focusing synchrotron, pole shape study 9-16928
- misch metal-Co powders as permanent magnet 9-5788
- with nonlinear characteristics, applic. of conformal mapping for evaluation or design 9-2326
- optimum design for MHD generators 9-17853
- permanent, charact. meas. using analogue precision method 9-12974
- permanent, deviations in operating lines of hysteresis loop 9-10812
- permanent, magnetostatic and exchange interactions between particles 9-18676
- permanent, materials, review 9-3762
- rare earth cobalt cpds., permanent magnets 9-13963
- with sloping circular edges, influence of vertical motion on horiz. 2nd order aberrations 9-6474
- stray fields, calc. using POISSON program 9-16763
- superconducting, for high-energy physics 9-12121
- superconducting, n.m.r. spectrometer appl. 9-12962
- cryogenic, using liquid Helium 9-8318
- Nb<sub>3</sub>Sn, permanent superconducting, possibilities, advantages and disadvantages 9-7771

**Magnons** see *Ferromagnetism*

**Magnus effect** see *Aerodynamics*

**Majorana effect** see *Magneto-optical effects*

**Majorana forces** see *Nuclear forces*

**Malter effect** see *Electron emission/secondary; Photomultipliers*

**Mandelstam representation** see *Elementary particles/scattering*

## Manganese

- doping of PbTe, thermoelec. power, thermal and elec. cond. effects 9-13876
- evaporation rate from molten iron under vacuum 9-19658
- foils, preparation technique 9-4184
- self-shielding factors for neutron resonances, scatt. dominant 9-18123
- solar abundance determ., including hyperfine structure 9-14249
- in Ge, change in state of Mn by heat treatments 9-3658
- Mn<sup>2+</sup>:Ge, e.p.r., effect of heat treatment on struct. state 9-16459
- Mn/Permalloy double-layer films with exchange anisotropy, stabilisation of ferromag. domain structures 9-10130
- $\alpha$ -Mn, heat capacity from 0.2 to 0.4°K 9-7657
- Mn<sup>2+</sup>, e.p.r. in guanidinium aluminum sulphate, hexahydrate 9-18744
- Mn<sup>2+</sup> in AgCl, luminescence and e.p.r. spectra, temp. depend. 9-21642
- Mn<sup>2+</sup> in CdF<sub>2</sub>, ESR, Mn<sup>2+</sup>-F<sup>-</sup> interac. parameters, interplay of fine, superfine and hyperfine interact. 9-14112
- Mn<sup>2+</sup> in NaCl, X-irrad., e.p.r. spectrum 9-21667
- Mn I spectrum in long period variables 9-21894
- <sup>55</sup>Mn, NMR in Al-Mn dil. alloy rel. to electronic state 9-1871
- Mn<sup>2+</sup> at cation vacancies of KCl, superhyperfine struct. in e.p.r. spectrum 9-5988
- Mn<sup>2+</sup>, e.p.r. in ZnWO<sub>4</sub>-MnWO<sub>4</sub> system, 1.5° to 300°K 9-5989
- Mn<sup>2+</sup>, e.s.r. in calcite, superhyperfine interaction with <sup>13</sup>C 9-5987
- Mn<sup>2+</sup> in KCl and RBr, charge transfer spectra 9-3892
- Mn<sup>2+</sup> in CdS<sub>1-x</sub>Se<sub>x</sub>, e.p.r. 9-3955
- Mn<sup>2+</sup> in CoCl<sub>2</sub>·2H<sub>2</sub>O, antiferromag., e.s.r. and exchange interactions 9-3834
- Mn<sup>2+</sup> in CoCl<sub>2</sub>·2H<sub>2</sub>O, D-parameter exchange contribution 9-3776
- Mn<sup>2+</sup> in fluoroborate glasses, chem. bonding with ligands, effect on luminesc. 9-1845
- Mn<sup>2+</sup> in glass, EPR spectra obs., structural features determ. 9-10193
- Mn<sup>2+</sup> in K<sub>2</sub>MnF<sub>4</sub>, e.s.r. obs. of zero-point spin deviations 9-10151
- Mn<sup>2+</sup> in Linde Y zeolite, e.s.r. rel. to cation distrib. and selective exchanges 9-1889
- Mn<sup>2+</sup> in Zn(ClO<sub>4</sub>)<sub>2</sub>·6H<sub>2</sub>O, e.s.r. 9-8032
- Mn<sup>2+</sup> ions in calcite lattice, e.p.r., origin of forbidden spectra 9-15199
- Mn<sup>2+</sup> in KCl, absorption spectra, in range 0.1 to 15 mol% of dopant conc. 9-5923
- Mn<sup>2+</sup> in La<sub>2</sub>Mg<sub>3</sub>(NO<sub>3</sub>)<sub>12</sub>·24H<sub>2</sub>O, quadrupole interaction parameter, ENDOR study 9-1883
- Mn<sup>2+</sup> in NaCl, absorption spectra, in range 0.1 to 15 mol% of dopant conc. 9-5923
- Mn<sup>2+</sup> in NaCl, impurity-vacancy assoc. determ. from ionic conductance and diffusion meas. 9-1202
- Mn<sup>2+</sup> in ZnS, e.s.r. effect of elec. field 9-17499
- Mn<sup>3+</sup> clusters, effect on physical props. of Mn-Fe spinels 9-1206
- Mn-S complexes, e.p.r. in KCl 9-20019
- ZnS:Cu,Mn,Cl film, electroluminescence, excitation mechanism 9-5974
- ZnS:Mn, electroluminescence freq. characts. 9-3941

## Manganese compounds

- Au-Mn alloys, dil., magnetoresistance 9-5805
- ferrite, spin-wave attenuation -150°C-300°C obs. in single crystals 9-17458
- ferrites, i.r. spectra analysis for equilibrium position in cation distribution 9-3876
- manganese acetate tetrahydrate, heat capacity, 0.4-20°K 9-12020
- manganous formate dihydrate, kinetic parameters from thermogravimetric analysis 9-16506
- montmorillonite, Szilard Chalmers reaction 9-10368
- Ag-Mn alloy film, transmission, reflection and absorpt. coeffs., rel. to resonant states 9-7937
- Ag-Mn alloys, phonon-electron scattering coeff. from electronic thermal conductivity 9-3505
- Ag-Mn solid solutions, stacking fault energies 9-7492
- Ag(10 wt.%) Mn(1.5 wt.%) Sb alloys, solid soln. decomposition, work hardening effects 9-1326
- Al-Mn alloy, dilute, low-temp. impurity resistance 9-1473
- Al-Mn alloys, dil., <sup>55</sup>Mn NMR rel. to electronic state 9-1871
- Al-Mn alloys, multi-faulted loops, formation and annealing 9-13686

## Manganese compounds continued

- Al-Mn alloys, recrystallization interaction with solid soln. decomposition 9-1153
- Al-Mn dil. alloys, mag. susceptibility, 2 300°K 9-12238
- Bi-MnBi composite, structural and mag. props. 9-9671
- CdSb-Mn, mag. susceptibility 9-16328
- Cu-Mn alloy, <sup>63</sup>Cu spin lattice relax. meas. 9-14015
- Cu-Mn alloy, magnetic props. rel. to structural state, applied field intensity and temp. 9-10147
- Cu-Mn alloy film, transmission, reflection and absorpt. coeffs., rel. to resonant states 9-7937
- Cu-Mn solid solutions, stacking fault energies 9-7492
- Cu<sub>2</sub>MnAl(Sn), Heusler alloys, low temp. sp. ht. meas. rel. to hyperfine fields 9-9841
- (Cu<sub>2</sub>Mn<sub>1-x</sub>)<sub>5</sub>Si<sub>2</sub>O mixed crystal e.p.r. 9-5984
- Fe-Cr-Mn alloy, structure effect on oxidation resistance 9-5503
- Fe-Mn alloys, ferromagnetic magnetization 9-18679
- Fe-Mn alloys, Hall effect and resistivity temp. and comp. dependence 9-9921
- Fe-Ni-Mn alloy, isothermal martensitic transformation nucleation rate 9-14990
- Fe-Ni-Mn alloys, uniaxial mag. anisotropy in martensitic transform 9-1667
- MgMn ferrites, pulse and hysteresis props., eff. of annealing conditions 9-17459
- Mn-C alloys, resistance comp. dependence, 1000-1400°C, rel. to chem. bonds. 9-12088
- Mn-Ca alloy powders, magnetization and coercive force, particle size depend. 9-12239
- Mn-Cu liquid alloys, partial and integral thermodynamic props. 9-21199
- Mn-Fe spinel, effect of Mn<sup>3+</sup> clusters on physical props. 9-1206
- Mn-Ga alloys high-coercivity state 9-1636
- Mn-Mg-Fe ferrites, after-effect, Mg<sup>2+</sup>, Mn<sup>2+</sup> role, obs. 9-14007
- Mn-Ni alloys,  $\gamma$ -phase, antiferromagnetism 9-12311
- Mn-Pd alloys,  $\gamma$ -phase, antiferromagnetism 9-12311
- Mn-Zn ferrite, elastic moduli, 80-303°K, meas. 9-1260
- Mn-Zn ferrites, permeability rel. to comp., magnitude and temp. dependence, sintering atmosphere effect 9-1687
- (Mn,Mg)Sb(Si,As)<sup>10-11</sup>, parawelite, mineral from Langban, Sweden, crystal structure 9-16078
- Mn<sub>21-x</sub><sup>2+</sup>Fe<sub>2</sub>F<sub>2</sub>, exchange interactions 9-21594
- Mn<sub>2</sub>GeSb<sub>1-x</sub> system, magnetic transitions rel. to conc. 9-19968
- Mn<sub>2</sub>(OH)(AsO<sub>4</sub>) crystal structure 9-18449
- Mn<sub>2</sub>TiO<sub>4</sub> phosphor, spinel struct., co-ord. of Mn<sup>4+</sup> luminesc. centres 9-20005
- Mn<sub>2</sub>O<sub>3</sub>-Al<sub>2</sub>O<sub>3</sub>, partial sintering, 1450-1650°C 9-18533
- Mn complex, tris-(2-dimethylaminoethyl) aminemanganese (II) bromide, crystal structure 9-3299
- Mn oxides, extended fine structure near K absorpt. edge, applic. of model 9-5942
- Mn<sub>2</sub>, dissociation energy 9-9292
- MnAs<sub>0.9</sub>PO<sub>1.1</sub>, magnetic and crystallographic studies, 4.2 to 660°K 9-16357
- MnAu<sub>2</sub>, mag. structure from n. diff. exam. 9-10152
- MnCO<sub>3</sub>, antiferromagnetic, hyperfine interactions on antiferromagnetic and nuclear resonance 9-14106
- MnCO<sub>3</sub>, antiferromag. reson. in mag. fields up to 50 kOe, freqs. 115 to 170 Gc/s 9-15197
- MnCO<sub>3</sub>, antiferromagnetic hyperfine interactions on antiferromagnetic and nuclear resonance 9-3950
- MnCO<sub>3</sub>, e.p.r. and n.m.r., uniaxial pressure depend., rel. to magnetoelectric anisotropy, 4.12°K and 20.0°K 9-8028
- MnCO<sub>3</sub>, ferromag. component spin density distribution, covalency and exchange polarization 9-15156
- MnCl-alkali chloride fused mixtures, mag. props. 9-13948
- MnCl<sub>2</sub>·4H<sub>2</sub>O, magnon-phonon coupling from mag. field depend. of thermal conductivity 9-1421
- MnCl<sub>2</sub>·4H<sub>2</sub>O single crystal, antiferromag. reson. line width 9-10272
- Mn<sub>1-x</sub>Co<sub>x</sub>F<sub>2</sub>, antiferromagnetic mixed crystals, electron-magnon transitions 9-15158
- Mn<sub>2</sub>Cr<sub>1-x</sub>Ho<sub>x</sub>O<sub>4</sub>, crystal structure and magnetic props. 9-17269
- MnF<sub>2</sub>:Fe<sup>2+</sup> M1 active local mode at 94 cm<sup>-1</sup> 9-3949
- MnF<sub>2</sub>:Fe<sup>2+</sup> 9-10221
- MnF<sub>2</sub>:Ni, Raman scattering from magnons localized on Ni ions 9-12426
- MnF<sub>2</sub>:Ni<sup>2+</sup> Raman scatt. from localised mag. excitation 9-10221
- MnF<sub>2</sub>:Ni<sup>2+</sup>(Fe<sup>3+</sup>), Raman scattering from magnetic excitations 9-12427
- MnF<sub>2</sub>:Ni Raman scatt. weak, localised magnon obs. 9-14062
- MnF<sub>2</sub>, rutile structure, vibrational spectra, critical dipole frequency behaviour 9-18549
- MnF<sub>2</sub>, rutile structure, vibrational spectra, critical dipole frequency behaviour 9-7636
- MnF<sub>2</sub>, antiferromagnet, luminescence enhancement in mag. fields 9-1824
- MnF<sub>2</sub>, line shape of spin wave sidebands 9-16375
- MnF<sub>2</sub>, mag. dipole optical absorpt. 9-1789
- MnF<sub>2</sub>, two-magnon Raman spectra 9-12425
- MnF<sub>2</sub>, ultrasonic attenuation near the critical point 9-7920
- MnF<sub>2</sub>, ultrasonic attenuation mechanism 9-5554
- MnF<sub>2</sub>, absorpt. in 4000 Å region, exciton-magnon bound state and exciton dispersion obs. 9-1707
- MnF<sub>2</sub>, Brillouin zone and exciton states, thermodynamic distinction 9-1434
- MnF<sub>2</sub>, dielectric cry., eff. of finite-amplitude acoustic waves 9-11994
- MnF<sub>2</sub>, magnetic insulator, exciton-magnon interact., coupling const. determ. 9-1706
- MnFe<sub>2</sub>O<sub>4</sub>, etch pits 9-3231
- Mn<sub>2</sub>Fe<sub>1-x</sub>O<sub>4</sub> linewidth inhomogeneous broadening 9-3947
- Mn<sub>2</sub>Fe<sub>1-x</sub>O<sub>4</sub>, electronic magnetic relaxation, 20-500 Kc/s, 80-350°K 9-14017
- Mn<sub>2</sub>Fe<sub>1-x</sub>O<sub>4</sub>, electron relaxation processes 9-10154
- MnFe<sub>2-x</sub>Sc<sub>x</sub>O<sub>4</sub> X-ray investigation of K absorption edge 9-5945
- MnH<sub>2</sub> vaporization mass spectrometric study 9-19386
- Mn(II) complexes, stereochemistry from e.s.r. 9-18185
- Mn(II) complexes in methanol, e.s.r. and n.m.r. 9-9551
- Mn<sub>1-x</sub>Ni<sub>x</sub>F<sub>2</sub>, antiferromagnetic mixed crystals, electron-magnon transitions 9-15158
- MnO:Li dipole relaxation 9-12187
- Mn<sub>2</sub>O<sub>3</sub>-Co<sub>2</sub>O<sub>3</sub> spinel solid soln., thermodynamics 9-13769
- $\alpha$ -Mn<sub>2</sub>O<sub>3</sub>-Fe<sub>2</sub>O<sub>3</sub> system, mag. and crystallographic transitions 9-17464
- Mn<sub>2</sub>O<sub>3</sub>-Fe<sub>2</sub>O<sub>4</sub> (or Co<sub>2</sub>O<sub>4</sub>) solid solns., interaction and substitutional disorder 9-17333

**Manganese compounds continued**

- p-MnO, Hall mobility of electrons and holes at high temp. 9-12152  
 MnO, heats of formation of point defects 9-17276  
 MnO, hyperfine interactions and  $^{10}\text{O}$  NMR shift 9-1876  
 MnO, lattice dynamics 9-13790  
 MnO<sub>2</sub>, vacuo u.v. spectra study 9-19483  
 MnO crystal film, absorpt. spectra 9-1797  
 Mn<sub>2</sub>O<sub>7</sub>, value as oxidizing agent 9-6006  
 MnOCl<sub>2</sub>, preparation and props. 9-6006  
 MnO<sub>2</sub>Cl<sub>2</sub>, preparation and props. 9-6006  
 MnO<sub>2</sub>Cl<sub>2</sub>, preparation and props. 9-6006  
 $\alpha$ -MnOOH, groutite, crystal structure refinement 9-7444  
 MnP, Curie temp., hydrostatic pressure eff., magnetoelec. eff. and thermal expansion 9-15149  
 MnP, resistivity and thermoelec. power temp. dependence 9-1456  
 MnP single crystal, thermal expansions, anisotropic linear, rel. to change in atomic dist. and mag. ordering 9-16181  
 Mn<sub>2</sub>P, mag. susceptibility and  $^{31}\text{P}$  n.m.r. meas. 9-16379  
 Mn<sub>2</sub>P<sub>2</sub>O<sub>4</sub>, monoclinic, crystallographic data 9-5324  
 Mn<sub>2</sub>P<sub>2</sub>O<sub>7</sub>, mag. susceptibility, 4.2-300°K 9-12241  
 MnS-CdS, phase diagrams 9-19656  
 $\alpha$  MnS, e.s.r. absorption in single crystals 9-3875  
 MnS, volume magnetic anomaly at 0°K, Neel temp. rel. to pressure 9-18685  
 MnS<sub>2</sub>, antiferromagnetic-paramagnetic transition, from susceptibility data 9-12312  
 MnSO<sub>4</sub> D<sub>2</sub>O liquid foils, non-perturbing, for thermal n flux meas. 9-9099  
 Mn<sub>3</sub>Sb<sub>2</sub>, magnetic anisotropy constants from magnetization meas. at 77°K and 288°K 9-1675  
 MnSe CdSe, phase diagrams 9-19656  
 MnSe, magnetic susceptibility and magnetostriction obs. 9-1705  
 MnSe<sub>2</sub>, chemical bonding, X-ray spectroscopic study 9-20931  
 MnSi, n.m.r. study at 4.2°K 9-16467  
 MnSi<sub>1.77</sub>, magnetic susceptibility, 20-1100°K 9-16332  
 MnTe<sub>2</sub>, antiferromagnetic-paramagnetic transition, from susceptibility data 9-12312  
 MnTiO<sub>3</sub>, ht. capacity, 30° to 300°K 9-3533  
 MnZn ferrite, high permeability, temp. insensitive 0-60°K 9-3830  
 MnZn ferrite, magnetization at near saturation 9-15155  
 MnZn ferrites, Cd-for-Zn substitution, effect on mag. props. 9-17460  
 MnZn ferrites of stoichiometric compositions, props. 9-16079  
 MnV<sub>2</sub>O<sub>4</sub>, Block wall motion, n scatt. study 9-12301  
 Ni-Mn, NMR study of  $^{55}\text{Mn}$  9-8042  
 Ni<sub>3</sub>Mn-based ternary alloys with transition metal, electronic structure and ordering processes 9-19834  
 Ni<sub>3</sub>Mn alloy, electron microscope obs. of antiphase boundaries and dynamic effects under high voltage 9-14921  
 Pd<sub>3</sub>MnSn Heusler alloy, internal field at  $^{119}\text{Sn}$  site 9-16404  
 RbMnF<sub>3</sub>, absorpt. in 40000 Å region, exciton exciton dispersion obs. 9-1707  
 V-Mn alloys,  $^{51}\text{V}$  and  $^{55}\text{Mn}$  Knight shift 9-21672

**Manometers** *see Vacuum gauges*

**Manometers**

- See also Vacuum gauges*  
 digital recording mechanism for three Hg manometers 9-6227  
 Hg h.p. differential instrument 9-6272

**Many-body problems**

- atomic, radial integrals 9-16993  
 atomic, two-body syst., separable series expansion for off-shell two-body t matrix with Coulomb pot. 9-13306  
 atomic systems, theory for time depend. perturbations calc. 9-11421  
 binary collisions in N-body problem, regularization anal. 9-6107  
 Bogoliubov gas, evolution of probability distributions and correlation functions 9-2179  
 Brueckner-Goldstone method applied to calc. of hyperfine constant for N 9-18141  
 canonical point transform, reformulation of classical hard-core potential 9-99  
 classical, rigorous bounds for eqn. of state and pair correlation function 9-20363  
 classical system direct space-time correl. function 9-10667  
 computer expt., high-speed soln. technique 9-20361  
 cybotactic group, partition function and equation of state determ. 9-7247  
 density matrices, correlations in many-fermion syst. 9-20359  
 electron-ion system, circular one- dimen. model, random phase approx. 9-10665  
 electron-ion system, circular one- dimen. model, random phase approx. 9-10664  
 elem. syst., position operator defn. 9-6332  
 N-fermion system, ground state energy calc. via lower-bound shell model 9-2176  
 five particle kinematics, physical regions in invariant variables 9-6846  
 fluid, classical, one-dimens., Yang-Lee distrib. of zeros 9-8443  
 fluids, polar and dipolar, theories 9-11517  
 four-body problem, periodic solns. as perturbation of restricted three-body problem 9-8224  
 galactic model with up to 4000 members, computer model 9-20149  
 gas slip coeff. depend. on collision freq. 9-14360  
 global existence and uniqueness theorem for classical mech. of one-dimens. interact. system 9-6336  
 Green's Functions, real-time, perturbation expansion 9-4222  
 group theory 9-20362  
 harmonic oscillator shell model, group theory 9-18985  
 lattice dynamics harmonic approx., freq. spectra and thermodynamic functions calc. 9-21423  
 liquids, monatomic, cybotactic group assumed, C<sub>v</sub> and equat. of state determ. 9-7247  
 liquids statistical theory, coherence time concept 9-20364  
 metallic densities, electron correlations 9-12071  
 molecule, polyatomic, 'multiple- scatt.' model of electronic structure 9-14684  
 N free electrons and N free protons, average thermal energy 9-21049  
 n-body problem, round-off errors for systems of up to 10<sup>6</sup> bodies 9-20146  
 n-particle, with spin-orbit and Coulomb interac., resolvent study, modified Fredholm theory 9-17739  
 nearly-periodic Hamiltonian system, adiabatic invariant 9-14359  
 nuclear, wave Functions Form., review 9-14548  
 nuclear reaction theory, single- particle shell model with configuration mixing 9-4764  
 nuclear wave functions for rotational states and spurious CM 9-495
- Many-body problems continued**  
 particle density matrix, integral eqns. 9-17741  
 particle group functions treatment 9-15437  
 phase transitions of electron fluid 9-14357  
 scattering amplitudes, nonrelativistic, integral eqns. derivation 9-14361  
 scattering theory, Hilbert-space version of classical mech. 9-17740  
 scattering theory, nonperturbative T-matrix study 9-2463  
 Schrodinger many-particle operator with combined Zeeman and Stark eff. 9-20330  
 stellar clusters, open, 25-48 stars, under influence of galactic field 9-20191  
 three-body, symm. representation for motion in space 9-8415  
 three-body problem, and canonical invariance 9-19010  
 three-body syst. with local Yukawa pot., comparison of variational results and solns. of Faddeev eqn. 9-19003  
 three-nucleon syst., photodisintegration cross-sections, sum-rule cal. 9-16953  
 three-nucleon system scatt. problem 9-2464  
 three-particle, cross-section for particle exchange from ground state to ground state 9-4578  
 three-particle scatt., transition amplitudes and partial waves 9-2465  
 three-particle syst., wave functions, construct. of polynomials 9-15429  
 Vlasov eqn. for quasiparticles in dense classical systems 9-8429  
 He liquid films, hard sphere gas model 9-3142
- Many-particle systems** *see Statistical mechanics/quantum*
- Markov processes** *see Statistical analysis*
- Mars** *see Planets*
- Masers**  
 analog with oscillating rigid pendulum and coupled loaded gyroscope 9-2363  
 atomic hydrogen, design and performance 9-12991  
 bibliography, with indexes, Apr-Dec 1967 9-19139  
 detuning effect of two-cavity molecular beam masers, quantum-mechanical explanation 9-10850  
 dynamically wide-range maser-effect on inversion (tunneling) levels, possibility 9-12321  
 low-temp. maser amplifier 9-8317  
 nebular plasma, partial maser effect in recombination lines of H atoms 9-8231  
 nuclear maser magnetometer, precise tuning 9-10805  
 oscillations with external gain 9-10849  
 preamplifier for e.p.r. spectrometer, justification 9-10782  
 preamplifier for e.p.r. spectrometer, justification 9-10781  
 radiometer system for 84 ft radio telescope, Onsala, Sweden 9-8296  
 ruby, with optical pumping, generated power rel. to pumping intensity 9-4451  
 ruby broad-band traveling-wave, intrinsic spot noise temp., spectral charact. 9-6501  
 proton spin, with 2 emission coils, prepolarized liq. coupling, theory 9-20497  
 Al<sub>2</sub>SiO<sub>5</sub>:Fe<sup>3+</sup> X-band three level and F-band push-pull 9-14069  
 H<sub>2</sub> oscillations with external gain 9-10849  
 H<sub>2</sub> with large storage box for reduce wall effect 9-17865  
 H atomic beam oscillator with multichannel source output 9-4450  
<sup>85</sup>Rb, regenerative oscillators, freq. stability 9-15505  
<sup>85</sup>Rb optically pumped vapour, 0-0 transition theory and expt. arrangement 9-4449
- Masers** *see Lasers; Optical pumping*
- Mass spectra**  
*See also Chemical analysis/by mass spectrometry*  
 alkyl acetates, scission probabilities of skeletal radicals 9-14698  
 cosmic ray jets, anal. rel. to models of multiple particle prod. in high energy region 9-436  
 L(+)- dihydrodesoxyxystreptose, structure obs. 9-18203  
 flash desorption, NH<sub>3</sub> adsorption and decomposition on W(211) surface 9-19679  
 fluorocarbons, photoioniz. 9-18206  
 metal carbonyls, negative-ion metastable transitions 9-3015  
 of nonlinear real scalar field, using Ritz's variational methods 9-13082  
 paraffin-water syst., study of ion-mol. reaction 9-18228  
 peak shapes, computed 9-11373  
 polyatomic mol., negative-ion formation obs. 9-20909  
 tetrahydropteroberberine alkaloids 9-19477  
 trifluoromethyl halides, photoioniz. 9-18206  
 of <sup>235</sup>U fission fragments due to 14.8 MeV neutrons 9-15786  
 C<sub>2</sub>H<sub>2</sub>O<sup>+</sup> ion in mass spectra of Z-alkanois, struct. 9-15885  
 C<sup>+</sup> reaction with N<sub>2</sub> and O<sub>2</sub> 9-14122  
 CH<sub>3</sub> vaporization study 9-19386  
 CO<sub>2</sub> isotope abundances of O, rel. to calcs. 9-11429  
 Ca vaporization study 9-19386  
 CsPbCl<sub>3</sub>, in vapour of PbCl<sub>2</sub> + CsCl mixture rel. to thermodynamic props. 9-19442  
 H<sub>2</sub>S, photoionization 9-905  
 H ions in positive column of H<sub>2</sub> glow discharge 9-15962  
 KPbCl<sub>3</sub>, in vapour of PbCl<sub>2</sub> + KCl mixture rel. to thermodynamic props. 9-19442  
 Mg vaporization study 9-19386  
 MnH<sub>3</sub> vaporization study 9-19386  
 N<sub>2</sub><sup>+</sup>, identification in h.f. discharge 9-9223  
 NO<sub>2</sub> clusters in expanding jets 9-20031  
 NaPbCl<sub>3</sub>, in vapour of PbCl<sub>2</sub> + NaCl mixture rel. to thermodynamic props. 9-19442  
 O<sub>2</sub>, comparison of evolved and diffused gas through Ag membrane 9-11663  
 Pb isotopic standards, common, equal-atom and radiogenic, abundance ratios 9-20902  
 PbCl<sub>2</sub> + AlCl<sub>3</sub> (A=Na, K, Rb or Cs) 9-9408  
 RbPbCl<sub>3</sub>, in vapour of PbCl<sub>2</sub> + RbCl mixture rel. to thermodynamic props. 9-19442  
 SO<sub>2</sub>, photoionization 9-905  
 SnPbTe<sub>2</sub>, equilb. sublimation study 9-18391  
 UNO, gaseous mol. obs. 9-790  
 Yb, photoionization, 1350-2000 Å 9-5065
- Mass spectrometers**  
*See also Ion optics*  
 cyclotron, with trapezoidal alternating pulses, multi-modulation 9-18131  
 investigation of ions produced by laser interaction with solids 9-9380  
 ion optics, normal incidence on mag. fields 9-11372  
 ion optics, oblique incidence on mag. fields 9-13277



**Mass spectrometers continued**

- ion source, simultaneous introduction and meas. of sample and reference standard 9-2357
- magnetic, chromatic effects elimination by electrostatic mirrors, first order theory 9-13278
- measurement accuracy and sensitivity improvement 9-2804
- measurements, automatic control with scan repetition and cycle selection 9-19384
- miniature, for identification of oil vapours in vacuum systems 9-8333
- monopole, characteristics by analysis of ion trajectories 9-2805
- with parallel chambers for simultaneous sample introduction and retrieval standard 9-11376
- producing primary and secondary ions in medium current range 9-665
- with programmable mag. field and on-line data processing 9-18128
- quadrupole, for rocket 9-8186
- quadrupole, simple design 9-18130
- reaction vessel, after flash photolysis 9-4009
- r.f., aperiodic, four stage, theor. anal. 9-13279
- sensitivity, review 9-728
- techniques and applications, book 9-13280
- time-of-flight, geometric mass discrimination effect 9-11375
- Kr-D<sub>2</sub> mixtures, ionisation curves of KrD<sup>+</sup> ions 9-7187

**accessories**

*See also Ion sources*

- electric quadrupole mass filter for high vacuum meas. 9-8334
- electrostatic mirrors to eliminate chromatic effects, first order theory 9-13278
- Ilford Q<sub>5</sub>A071 plate as ion detector, plate-to-plate eff. on darkening 9-14660
- ion beam instability eliminated by metal coating on Teflon valve 9-6953
- ion collector with movable slots which does not disturb vacuum when changing isotopes 9-11374
- ion source, IE-06, energy characteristics of molecules 9-664
- for powdered samples 9-8117
- power supply, simultaneous observation of two groups of lines 9-4820
- r.f. generator for quadrupole spectrometer 9-18129
- u.v. monochromator combination for photoionization obs. 600-1000 Å 9-7195
- valve, variable leak, modification to permit continuous high temp. operation 9-19385

**applications**

*See also Chemical analysis/by mass spectrometry*

- atom reaction kinetics, v. fast, time-of-flight 9-21681
- binding energy and isotope masses of nuclei determ. 9-2635
- chemistry, biology and medicine, book 9-13280
- chemical reactions, very fast 9-10334
- electric quadrupole mass filter for high vacuum meas. 9-8334
- electron ionization cross-section meas., ion source design 9-5055
- evaporation processes and energy characteristics of relatively involatile materials 9-664
- films on glass surfaces, study 9-7333
- ionization potentials of mols. and free radicals 9-15950
- liquids, impurities determ. 9-8116
- methyl halides, photoionization efficiency curves from ionization threshold to 600 Å 9-3004
- molecular beams, background effect reduction 9-6954
- nuclear and reactor physics, in book 9-13280
- oil industry, instrument with parallel chambers for simultaneous sample introduction 9-11376
- organic substances analysis, combination with gaschromatograph 9-1887
- polystyrene, cracking kinetics and major crack growth obs. 9-18522
- quantitative mass spectrography, plate-to-plate eff. on darkening of Ilford Q<sub>5</sub> as ion detect. 9-14660
- reaction rate const. from transient conc. profile 9-16477
- residual atmosphere analysis in vacuum systems 9-8119
- review 9-2803
- rocketborne, for upper atmosphere ion concentration 9-8186
- semiconductors, in book 9-13280
- space science, geology and cosmology, book 9-13280
- <sup>40</sup>Ca-<sup>40</sup>Ar mass diff., high resolution spectrometer 9-13309
- <sup>1</sup>H, <sup>16</sup>O and <sup>32</sup>S at. masses, high resolution 9-11414
- HCL, photoionization efficiency curves from ionization threshold to 600 Å 9-3004
- InS, vapour, dissociation energy determ. 9-19481
- Na analysis by spark source mass spectrograph 9-8121

**Mass standards** *see Standards***Mass transfer** *see Transport processes***Master equation** *see Transport processes***Materials**

*See also Individual materials (if separately named) e.g. Ruby*

- binder mats, for graphite, molec. distrib. determ. by gel permeation chromatography 9-8122
- bone, trabecular, point-source  $\beta$  dose calc. 9-20261
- carbonaceous, prep. for optical and electron microscopy 9-8314
- cement, Portland, clinker, belite analysis by e. probe microanalysis 9-16515
- cement, Portland, hydration and mechanical strength 9-16131
- cement paste, effective cross-sectional area for liquid flow, elec. meas. 9-15980
- cordierites, sintering and props. 9-21404
- for gas lasers, and fabrication techniques 9-2372
- graphites, technological aspects of modern usage 9-14886
- initial moisture content influence of parameters of pneumogas dryer 9-14881
- i.r. nondestructive testing 9-6231
- meteoritic, ice nucleation 9-11745
- pitch, suitable for prod. of MP carbon fibres 9-8054
- plastic scintillators based on cross-linked epoxy resins, prod. and characts. 9-10256
- research progress, book 9-21386
- rock, homogeneous, plastic flow analysis under lubricated punch 9-1288
- rock, plane-strain plastic flow under pointed punch 9-1289
- starch granules, light scatt. rel. to fluctuations in anisotropy 9-15167
- C black aggregates, shape and bulkiness factors 9-7421
- C green bodies, baking, kinetics and critical parameters 9-7589

**Materials testing** *see Mechanical strength***Mathematical methods** *see Calculation; Statistical analysis***Mathematics**

- 'ravine' method for following functional valleys 9-12910

**Mathematics continued**

- Algorithms for random number generation 9-31
- beam systems, vibr. transmission, three methods of soln. 9-8498
- Bessel functions, two, inverse functions of their product, appl. to pot. scatt. 9-14325
- binomial coefficient identities 9-14306
- boundary value problem integrals, collocation method of soln. 9-12855
- Cauchy problem for scalar-tensor gravitational theory 9-8390
- closed formula for 3nj coefficients of R<sub>3</sub> (Racah coefficient) 9-20865
- complex harmonic and electromechanical analyses, book 9-12912
- convergence of linear operator in Banach space 9-12859
- courses for scientists, USA national requirement study 9-4204
- difference eqn. solns. to Ising model and nearest neighbour fluid 9-4244
- Doppler broadening integrals and error function relatives, Voigt functions computation 9-15415
- Dyson's formula, generalization 9-17682
- elasto-plastic matrix, formulation using 'initial stress' finite element approach 9-8484
- elastostatics, numerical treatment of two dims. mixed boundary value problems 9-15448
- ellipsoidal pairs, correlation in SU(3) theory 9-6284
- finite difference method, stream variant 9-110
- finite difference soln. for infinite value of coeff. of heat conductivity 9-167
- finite element method in the theory of elasticity 9-19021
- finite element methods in solid mechanics 9-8468
- Gaussian processes, canonical representations 9-20293
- generating functions for exact soln. of the transport equation 9-17728
- integration of fundamental equations, new formulation of stochastic theory and quantum mechanics 9-20329
- integro-differential eqn. soln., straight line convergence method 9-16654
- iteration calcs. in a general space of variables, speeding up method 9-12869
- iterative procedure for obtaining polynomials 9-30
- Klein-Gordon non-linear partial differential eqn., discussion 9-12829
- Markov chain, convergence of approximants 9-14309
- mathematical physics, book of worked examples 9-22
- method of Moments applied to calc. of permittivity of a random medium 9-10764
- MHD equations governing flow of conducting fluid in high mag. field, propulsion applications 9-21037
- Monte Carlo methods for modelling Markov chains 9-12857
- Newton's conception and form of 'Principia' 9-15400
- null e.m. fields in algebraically special Petrov type spaces 9-10618
- operator decomposition, speed of convergence 9-12909
- operator in Banach space, speed of convergence 9-12859
- plate bending, conforming quartic triangular element 9-8483
- plate bending, large deflection anal. by finite element method 9-8485
- plate bending, refined triang. finite element 9-15451
- polynomials, iterative procedure for obtaining 9-30
- problems improperly posed in the Hadamard sense 9-12861
- Riemann surfaces of field extensions 9-17698
- scatt., potential, high energy fixed angle 9-14326
- Schwarz-Christoffel conformal mapping of hexagon on circle, integration 9-19345
- space-time transformations rel. to Lorentz group 9-8383
- spectra, measured; unfolding method 9-4219
- system analysis, nonlinear, new numerical technique 9-6274
- trigonometric series, algebra of computer programs to perform. 9-8356
- unfolding measured distributions 9-20298
- zeta function for flows and diffeomorphisms, convergence 9-20295

**Matrices**

- aerodynamic scattering on complex shapes 9-14809
- angular momentum, traces of products 9-15418
- Bopp two-matrix for atomic ground states, Pauli-principle restriction 9-15807
- $\gamma$ , contracted products, algorithmic reduction 9-17688
- diagonalization method 9-39
- ensembles of random matrices, method of predicting nuclear energy levels, calc. of nearest neighbour spacing distrib. 9-8949
- Gell-Mann  $\lambda$ -matrices of SU(3), algebraic props. 9-17691
- in quantum mech., matrix methods appl. 9-2158
- internal symmetry crossing, arbitrary compact group, reduced amplitude interpretation, Racah coefficients rel. to 9-341
- matrix mechanics, numerical techniques 9-76
- matrix-valued functions of complex variables, factorization 9-14315
- Mueller, for analysis of polarized light optical systems, operational notation 9-20551
- nuclear-spin-density eqns. 9-16755
- one-dimensional quantum-mech. problems 9-12883
- random probability distrib. 9-4242
- simplified method for statistical mech. of linear systems 9-8432
- special unitary 3x3 matrices of SU(3), algebraic props. 9-17691
- spin-other-orbit matrix elements for  $f^2$  configs. 9-16991
- statistical two-particle density matrix 9-9112
- t matrix, off-shell two-body, separable expansion with Coulomb pot. 9-13306
- t-matrix, two-particle, separable representation, three-nucleon problem 9-13151
- textbook 9-20
- unitary group, specific unitary representation and props. 9-12867

**Matrix-isolation methods** *see Free radicals; Molecules***Matteucci effect** *see Magnetolectric effects; Magnetomechanical effects***Maxwell effect** *see Double refraction/flow***Maxwell equations** *see Electromagnetism***Maxwell-Boltzmann distribution** *see Kinetic theory; Statistical mechanics***Measurement**

- See also Instruments; Recording; Standards; Units; Acoustical measurement; Dielectric measurement; Electrical measurement; Magnetic measurement; Mechanical measurement; Radioactivity measurement; Thermal measurement; X-ray measurement. Some specific quantities are listed separately, e.g. Calorimetry; Density measurement. Where no separate heading exists, measurement methods and instruments are included among the other entries under the heading of the appropriate quantity or subject*
- background dependence of observables in finite space-time regions 9-14304
- Daneri-Loinger-Prosperi quantum theory 9-18976
- local states coherent superposition 9-10607

**Measurement continued**

- of moments of inertia by means of single-wire torsional pendulums 9-10687
- NPL standards, historical review 9-8346
- space charge layer thickness, plasma capacitor method 9-9378

**errors**

- See also Statistical analysis*
- entropy error parameters 9-8348
- focussing error detection in optical paths 9-8645
- thermal conductivity, guarded hot-plate meas., effects of edge insulation and ambient temperatures 9-15017
- transit telescope, asymmetry of micrometer screw action 9-18943
- Young's modulus determ. by flexural vibrations, errors due to shear and rotatory inertia 9-13713

**Mechanical measurement**

- Individual quantities and instruments are listed separately e.g. Length measurement*
- alignment interferometer 9-4514
- curvature radius with ring spherometer, accuracy and calibration curves 9-23
- flat spring bending analysis in instruments 9-8482
- kilogramme, (kg), definition 9-10066

**Mechanical properties of substances**

- See also Individual properties, e.g., Abrasion; Elastic deformation; Mechanical strength; Plastic deformation; Slip; Wear; etc.*
- ablation materials, rapidly charred, testing technique 9-11935
- alloys, non-ferrous, influence of grain size 9-9653
- carbides, behaviour, and microstructure, review 9-19704
- elastic solids, constitutive inequalities 9-17764
- electromechanical effect, kinetics 9-1314
- film, polystyrol, elec. discharge effects 9-10032
- glasses, binary silicate, rel. to metastable crystn. 9-1081
- graphite, book 9-13566
- graphite, erosion and shock resistant, quality control for rocket motors 9-7568
- ice, effect of dissolved impurities 9-13711
- lime refractories, sintered and fused, props. 9-3461
- metals, non-ferrous, influence of grain size 9-9653
- metals subjected to mechanical stress at high temp. and n. irradiation, long term props. 9-21380
- Permalloy film, torque rel. to magnetoresist. 9-7906
- polymers, glassy, with aromatic groups in side chain or backbone, molecular motions 9-19666
- polymers, relaxation mechanisms 9-7535
- polymers, relaxation mechanisms e microscopic obs. 9-7535
- polyoxymethylene, dynamic 9-17321
- powders, model for fundamental aspects of behaviour 9-21355
- relaxation of thin thermoplastic layers, time meas. 9-5436
- silica composite, prestressed and reinforced with W wires, props. 9-7569
- strain amplitude, critical, temp. depend 9-3408
- thin plate, perforation limits for cylindrical projectiles, simple determ. 9-20381
- transition metal borides, carbides and nitrides 9-7510
- Al-Al<sub>2</sub>O<sub>3</sub> alloys, dispersion-strengthened SAP, rel. to hardness, 20-600°C 9-7577
- Al<sub>2</sub>O<sub>3</sub>-BaO glass ceramics, rel. to glass composition 9-3171
- Al<sub>2</sub>O<sub>3</sub>, rel. to purity and microstructure 9-1256
- Be, irradi., recovery data from kinetics of the evolution temp. depend. 9-13710
- Cu, eff. of creep on strain and yield point 9-13730
- Cu, recovery isochronal, after cyclic deform. at 78°K 9-16119
- Fe-Ni-Ti alloy, improvement by ageing followed by hot rolling 9-11928
- Ge, electromechanical effect existence 9-1315
- LiF and LiF:Mg<sup>2+</sup>, effect of lattice defects 9-1257
- Mg, Cd alloy, order-disorder phase transition, changes 9-16155
- Ni-Cr-W-Co-Al-Ti alloy with horophilic additions, effect of grain boundary composition 9-5475
- NiTi, tensile, 150° to 370°C, effect of room temp. prestrain 9-18491
- Si epitaxial film on spinel, and elec. props. 9-7815
- Ta-Hf-C microcomposite, thermal shock resist., and development 9-3168
- TaC-C thermal shock resist. hypereutectic, and development 9-3168
- Y<sub>2</sub>O<sub>3</sub>-ThO<sub>2</sub> solid solutions 9-3456

**Mechanical strength**

- See also Elasticity; Hardness*
- ablation materials, rapidly charred, testing technique 9-11935
- alumina-silica monoliths, hot strength 9-3435
- b.c.c. metals, limiting strength produced by solution hardening 9-7562
- b.c.c. metals, limiting strength produced by solution hardening 9-7561
- brittle matrix composite, strengthening by chem. bonding 9-19841
- brittle solids, under complex compressive and tensile loading, effect of loading sequence and scale factor 9-7558
- cement, Portland 9-16131
- ceramic, semivitreous, extruded, fired rupture modulus response surface rel. to particle size and firing rate 9-3164
- ceramics, semivitreous extruded, dry rupture modulus, response surface 9-3166
- ceramics, semivitreous extruded dry modulus, response surface 9-3165
- ceramics, sintered, rel. to microporosity 9-3431
- ceramics, toughness meas. 9-3432
- ceramics, with compressive surface layers, residual stress meas. 9-3414
- cermets, high-temperature, transverse rupture strengths 9-18535
- circular arch, strongest, perturbation soln. 9-19026
- circular plate with one-sided ribs subjected to antisymmetric bending 9-20391
- concrete columns, creep stability and buckling strength 9-17310
- concrete loaded through rigid plates, bearing strength 9-18513
- cordierites, sintered, bending strength 9-21404
- corundum, temp. depend. rel. to stress corrosion, obs. 9-1299
- glass, increase caused by Li diffusion 9-21379
- glass fibre, following irradiation 9-11934
- glass-ceramic coatings for metals, improvements 9-3189
- graphite, erosion and shock resistance, determ. rel. to rocket nozzle inserts prod. 9-7568
- graphite, flexural, and breaking strain, effect of gaseous environment 9-7566
- graphite, rel. to B content and heat treatment temp. 9-7608
- graphite compacts, rel. to pitch binder content 9-7413
- group VIa metal composite mats., effects of W replacement by Mo or Cr 9-19842

**Mechanical strength continued**

- magnesium-chrome refractories, fine grain, hot strength and thermal shock resist. 9-3438
  - metal, h.c.p., hydrostatic press. and temp. effects 9-5478
  - metal films, fracture 9-7559
  - metals, fine grained, effect of diffusion creep 9-9763
  - metals, under stress at high temp. and on n. irradi. 9-21380
  - plane frames, failure loads evaluation using elastic and plastic load-deform. characts. 9-126
  - point defects, elastic strength calc. 9-9767
  - porcelain, toughness meas. 9-3432
  - refractory mats., effect of AlF<sub>3</sub> additives 9-9766
  - resin, low-temp. fatigue characteristics 9-11939
  - sapphire, strengthening by compressive surface layers 9-1300
  - silica composite, prestressed and reinforced with W wires, props. 9-7569
  - siloxane elastomers, -80 to +20°C, rel. to submolecular structure 9-9770
  - steel, austenitic stainless, by strain hardening due to phase transform 9-5499
  - steel, K<sub>h</sub>12ND, welds, impact strength, effect of Cr content 9-14984
  - steel, low c. fatigue props. under composite stress including h.f. vib. 9-5474
  - steel, mild, explosively loaded dynamic yielding rel. to grain size 9-3439
  - steel, Mn, low C, Nb-treated, rolled, in heat affected zones produced by welding 9-19819
  - steel, stainless, fuel cladding, burst strength rel. to thickness and defects obs. 9-15799
  - steel alloys, unbrITTLE 9-5491
  - steel box columns, welded, ultimate 9-14979
  - yield, limit analysis 9-19803
  - Zircaloy-2 fuel cladding, burst strength rel. to thickness and defects obs. 9-15799
  - Al<sub>2</sub>O<sub>3</sub>, ceramics, with compressive surface layers, residual stress meas. 9-3414
  - Al<sub>2</sub>O<sub>3</sub>, thermally shocked, degree of damage 9-3437
  - Al<sub>2</sub>O<sub>3</sub> refractories, hot modulus, effect of selected processing variables 9-3436
  - Al cylinders, reln. between ultimate press. and wall thickness 9-5473
  - Al<sub>2</sub>O<sub>3</sub>, adhesion to metals and alloys, interfacial strength rel. to wettability 9-1336
  - Al<sub>2</sub>O<sub>3</sub>, double bicrystals, grain boundary strength 9-1232
  - Al<sub>2</sub>O<sub>3</sub> substrates, separation force rel. to scoring and annealing 9-1307
  - CaO, dense, H<sub>2</sub>O effects 9-7567
  - CsI, impurity additions effect 9-18514
  - Cu-He alloys, stress-rupture characts. rel. to grain boundary degeneration 9-16133
  - Cu-(30 at.wt.%)Zn alloy, shock deformed 9-13681
  - Cu yield strength depend. on temp. 9-21371
  - HfB<sub>2</sub>, bend strength rel. to grain structure 9-1259
  - HfC and HfC·(10vol%)HfB<sub>2</sub>, hot-pressed, and plasticity <2635°C 9-1301
  - MgO, hot extruded, and fracture up to 1315°C 9-1302
  - Nb alloys with improved elevated temp. strengths 9-13770
  - NbC composite, flexural, effect of particle size and C source powders 9-3391
  - Ni-Cr-W-Co-Al-Ti alloy with horophilic additions, effect of grain boundary composition on impact strength 9-5475
  - Pb, alloying additions (Sb, Cu, Te) effect 9-1303
  - SiC HfB<sub>2</sub>(ZrB<sub>2</sub>), mixtures, bend strength rel. to grain structure 9-1259
  - SiO<sub>2</sub>, sintered fused silica, fluorination strengthening 9-1304
  - Ti alloys, high-strength, fatigue strength loss on Ni and Cr plating 9-3442
  - V-Ti-Nb alloys, stress-rupture behaviour 9-19801
  - V-Ti alloys, stress-rupture behaviour 9-19801
  - Y<sub>2</sub>O<sub>3</sub>-ThO<sub>2</sub> solid solutions 9-3456
  - Zr-(2.7 wt.%)Nb, n. irradiated, effect of Nb 9-5479
  - ZrB<sub>2</sub>, bend strength rel. to grain structure 9-1259
- compressive**
- axial compression of circular cylindrical shells, creep buckling 9-17761
  - axial compression of circular cylindrical shells, effects of unreinforced circular cutouts on buckling 9-16710
  - concrete, effect of mix proportions and aggregate dust 9-17312
  - powders, effect of compacting pressures 9-5476
  - pressure vessel consisting of cylindrical and toroidal shells and rigid circular plate 9-6359
  - testing machine, hydraulic, for medium strain rates 9-9743
  - Al<sub>2</sub>O<sub>3</sub> alumina ceramics, effect in shock compression 9-7563
- shear**
- adhesive bonded joints, napkin-ring torsion apparatus 9-3395
  - deformed solids, temp. and press. depend. 9-7556
  - graphite, fracture under torsional and biaxial stresses 9-7565
  - minerals, pressure and temp. dependence 9-5477
  - orthotropic simple solid, supported by surface traction 9-19027
  - shaft assembly, press-fitted, improvement 9-7557
  - Ni-Al alloy, critical stress, conc. depend. 9-9756
  - Sb<sub>2</sub>Se<sub>3</sub>, needle-like crystals 9-1194
- tensile**
- alloys, non-ferrous, influence of grain size 9-9653
  - loading device for Kossel microdiffraction and metallography 9-11918
  - metals, non-ferrous, influence of grain size 9-9653
  - permalloy films, vacuum-deposited 9-3412
  - polyethylene film, chlorinated, eff. 9-17520
  - powders, effect of compacting pressures 9-5476
  - single crystal testing apparatus for press. of 30 kilobars 9-7560
  - steel, fracture behaviour, subject to pressure 9-18518
  - steel, notch effect rel. to inclination angle 9-9769
  - steel cylinder, Bridgman's observational relationship between strain parameters 9-9768
  - steel powders, pressed and sintered 9-17339
  - testing machine, hydraulic, for medium strain rates 9-9743
  - wooden fibres, microheometer for meas. 9-5472
  - Zr-Se alloys, hydrided, effects of Se and H contents 9-19805
  - Al, critically strain-hardened, properties 9-16124
  - Al<sub>2</sub>O<sub>3</sub>, microstructural anomalies 9-3434
  - C fibres, 7μ diam., failure at room temp., at one half per cent strain 9-7564
  - C fibres, high strength rel. to stretch in prod. 9-7514
  - C membranes, rel. to graphitization 9-11777
  - α-Cu-Al alloys, high-temp. vacuum tensile fatigue rel. to Al content 9-9771
  - Cu single crystals with dispersed BeO particles, strengthening and deformation 9-17306



**Mechanical strength** continued**tensile** continued

- LiF, rel. to ionic polarizability and slip systems interpenetrability, 300-700°C 9-3440  
 LiF crystals, effects of certain factors 9-5454  
 Mo, following neutron irradiation 9-19808  
 Ni-Cr white castiron, toughness improvement treatment, patent 9-13757  
 Sb<sub>2</sub>Se<sub>3</sub>, needle-like crystals 9-1194  
 Ta-W solid solution alloy system, monotonic strengthening 9-3433  
 Ta 10-fibre bundles at 1000°F 9-18515  
 W 10-fibre bundles at 1000°F 9-18515  
 W wire, high temp. vacuum tensile fatigue, temp. depend. 9-7570  
 Zr(1wt%)Nb, effect of H<sub>2</sub> and extension rates, 30 to 600°C 9-17313

**Mechanics***See also Dynamics*

- angular velocity of orthogonal curvilinear frame, mnemonic 9-6350  
 chemical reactions in two dimensions, classical treatment 9-8056  
 classical, canonical representations of Galilei groups 9-8467  
 classical system, dissipative; time- translational invar. equation of motion 9-2187  
 complex harmonic and electromechanical analyses, book 9-12912  
 conservation law constructed from an invariance 9-8466  
 continuous medium growth phenomenon, general uniform growth 9-116  
 control system, deviation of motion in presence of noise 9-114  
 cylindrical hole, in elastic matrix, mixed boundary value problem, soln. 9-17818  
 Dirac bracket, structure in classical mechanics 9-117  
 elastic dumbbell satellite, damping via nonlinear resonance 9-14179  
 finite element methods for solid continua 9-8468  
 fluid mechanics, book 9-2945  
 generalised, comments 9-2115  
 Hamilton Jacobi function, perturbation expansion 9-115  
 invariance constructed from conservation law 9-8466  
 Jacobi's identity, classical derivation 9-2184  
 Lagrange multipliers and system constraints, geometrical basis 9-12911  
 membrane statics, conservation laws 9-20378  
 modified functions of higher orders and applications to structural problems 9-17684  
 modified functions of higher orders and applications to structural problems 9-17685  
 N-particle syst., scattering theory, Hilbert-space formulation 9-17740  
 Newton's math. and 'Principia' 9-15400  
 nonlinear, review 9-20376  
 of continuous media, using calculus of variations and Banach space 9-16702  
 Ostrogradsky's mechanics, quantization, ambiguity 9-8402  
 particle in plane restrained by two springs 9-4267  
 platform supported by vertical columns, collapse modes 9-20377  
 rational university level textbook 9-10603  
 statics, book for students 9-4821  
 Statics, collapse analysis of framework systematic selection of redundant force 9-118  
 steel cylinders, mild, reln. between ultimate press. and wall thickness 9-5473  
 structural problem, Shingo modified functions table 9-4264  
 SU(2) generators for free particle, single valuedness conditions 9-10685  
 three-dimensional rotation group, representation in terms of direction and angle of rotation 9-14371

**Mechanics of gases** *see Aerodynamics***Mechanics of liquids** *see Hydrodynamics***Medical science***See also Physiology; Radiation protection*

- aerosol inhalation effects 9-4137  
 aflatoxins B<sub>1</sub> and G<sub>1</sub>, fluorescence and phosphorescence for presence determ. 9-6201  
 biomedical instrum., Physics Exhibition, London 1968 review 9-4136  
 brain exam. using u.s. visual syst. 9-6220  
 brain structure by symmetrical scanning of head with ultrasound 9-6207  
 diagnosis, u.s., intensity- modulated recording 9-6205  
 diagnosis, u.s., two-dimensional visual, design and tech. 9-6204  
 eye, intraocular distances, u.s. diagnostics 9-10577  
 glucose kinetics of human body, analog, computer study 9-20254  
 nuclear medicine, radionuclide imaging 9-2352  
 obstetrics and gynecology, u.s. diagnostics 9-6209  
 radioactive aerosols, retention in respiratory tract, obs. and simulation 9-15378  
 radioactive gases, short lived, preparation 9-21990  
 renograms, radioisotope, quantitative evaluation method 9-20255  
 scintillation camera, output recording method 9-10948  
 sensorineural deafness, recovery rate from TTS by use of hearing aids 9-10573  
 spectrophotometer, automatic scanning, for Na, K, Ca, Mg in clinical samples 9-16512  
 thermography, diagnostic 9-4141  
 tinnitus, induced temporarily by noise, pitch and freq. study 9-12787  
 UKAERE health physics div. progress report (1967) 9-20257  
 u.s. visual. of images of brain, eff. of skull in echoencephalographic B and C scans 9-6206  
 u.s. wave intensity meas. in liquids with electrodynamic transducers 9-9507  
 $\pi^-$  beam therapy in cancer treatment 9-12779  
 Ca, whole body, proposed 5 MeV neutron activation anal. method 9-21746  
 Cl, whole body, proposed 5 MeV neutron activation anal. method 9-21746  
 Na, whole body, proposed 5 MeV neutron activation anal. method 9-21746

**Meissner effect** *see Superconductivity***Melting***See also Zone melting and refining*

- anharmonic crystal, caused by phonon frequency change with temp. increase 9-19848  
 cubic metals, thermal vibrations mean square displacements at melting point 9-11743  
 elements, low temp., under high pressure, rel. to position in periodic table 9-5214  
 graphite fusion curves up to 60 kbars, meas. by optical technique 9-7299  
 heating curve and melting point meas. using solar furnace 9-13557

**Melting** continued

- ionic solids, thermal expansion at melting pt., ratio of inflection pt. dist. in pot. energy curve to equil. interionic dist., comp. and correc. of calc. 9-15008  
 Lindemann's law and Kreb's model 9-1069  
 Lindemann hypothesis, thermodynamic consequences 9-19657  
 orthonitrophenol crystals, in saturated vapour of camphor, anisotropy 9-18384  
 photometric recording for single crystals 9-11744  
 polypropylene, disappearance of 998 cm<sup>-1</sup> l.r. band 9-12389  
 polystyrene, melt viscosity, eff. of press., analysis 9-18385  
 reactive metal vacuum-induction melting in water-cooled crucibles 9-13746  
 temperature difference curves 9-1068  
 vacancy mechanism, possibility 9-5215  
 Al<sub>2</sub>O<sub>3</sub>-Al system, curve, condensed phases, obs. 9-1341  
 Au, possible vacancy mechanism 9-5215  
 CaO-Ta<sub>2</sub>O<sub>5</sub>-SiO<sub>2</sub> system, relations using phase diagram 9-7300  
 Cu, possible vacancy mechanism 9-5215  
 Cu alloys and steel joints, during welding 9-21397  
 Fe, possible vacancy mechanism 9-5215  
<sup>3</sup>He, curve to 12 m°K 9-19652  
<sup>4</sup>He, b.c.c., prior instability modes 9-1063  
<sup>4</sup>He, curve below 300 m°K 9-19652  
 Hg, curve up to 15×10<sup>8</sup> N/m<sup>2</sup> 9-9589  
 In condensed films, of subcritical thickness, e diff. exam. 9-18383  
 LiF, rel. to skeletal cavities formation 9-13611  
 Mg, possible vacancy mechanism 9-5215  
 Pt fusion curves up to 40 kbars, meas. by optical technique 9-7299

**Melting point**

- cholesterol, and purity, by differential scanning calorimetry 9-13799  
 compounds, inorganic hot stage microscopy determ. 9-14880  
 cubic metals, mean square displacements of atoms thermal vibrations 9-11743  
 lanthanides, trifluorides, melt grown 9-9648  
 organic materials, environment eff. on temp. depend. of constant pressure viscosity 9-14839  
 polymers, eff. on dielectric props., review 9-19925  
 solar furnace measurement 9-13557  
 rel. to superconductive transformation point 9-16236  
 thallous halides, pressure effect on the polymorphism 9-7622  
 transition metal borides, carbides and nitrides 9-7510  
 Cm<sub>2</sub>O<sub>3</sub>, redetermination 9-13558  
 Ga specific heat determ. 9-21435  
 NaF-ZrF<sub>4</sub> mixtures, depression by ZrO<sub>2</sub> additions 9-17194  
 Pm<sub>2</sub>O<sub>3</sub>-Sm<sub>2</sub>O<sub>3</sub>, rel. to <sup>147</sup>Pm as power source 9-2790  
 SiBi<sub>11</sub>O<sub>20</sub> 9-18648  
 SrO-ZrO<sub>2</sub> system, phase equilibria, eutectics 9-1352  
 Y<sub>2</sub>O<sub>3</sub>, meas. using solar furnace 9-13557  
 ZrO<sub>2</sub>, meas. using solar furnace 9-13557

**Membranes**

- cellulose acetate/saline soln. interface, effect of surfactant layer on reverse osmosis 9-9502  
 curved, stress anal. 9-6354  
 elastic, axially symmetric, dynamic behaviour 9-16722  
 elastic shell, circular, displacement field, statistical parameters rel. to load parameters 9-6371  
 flow of binary soln., thermodynamic eqns. 9-9499  
 ion exchange electrode, prod., patent 9-14138  
 ion separation and concentrationend method, patent 9-19626  
 Ising lattice, stochastic growth, form and steady-state props. 9-20337  
 Ising lattice membranes, steady-state props. 9-88  
 living cell, electric and ionic problems 9-8301  
 lyophobic, microporous, induced by volatile liquids 9-21122  
 perspex cell, for Na transport studies across frog's skin 9-12778  
 phenol-sulfonic cation-exchange membrane, transport numbers determ. 9-9501  
 plates, rigid plastic and dynamically loaded; bending moments and membrane forces considered 9-137  
 shells, small perturbations, approx. eqns. 9-19025  
 skew, natural frequencies and mode shapes 9-10718  
 spinning membrane disks, large amp. axisymmetric transverse vib. 9-19050  
 statics, conservation laws 9-20378  
 stress analysis, plane, finite difference solns. 9-19015  
 temperature field and stress determination 9-14380  
 transport characts. of ultrafine capillaries 9-997  
 vibration, non linear wave equation anal. 9-6375  
 vibrations when loaded with air layer, configs. 9-4286  
 Ag, mass spectra comparison of evolved and diffused O<sub>2</sub> 9-11663  
 C, graphitization during annealing between 700 and 3000°C 9-7609  
 Pd for pumping H impurities out of He discharge tube 9-3021

**Memory devices** *see Calculating apparatus; Magnetic devices; Storage devices; Superconducting devices***Mendelevium**

- heat conduction coeff. with singularity finite difference approach 9-167

**Mendelevium compounds**

No entries

**Mercury**

- 'e' line, use as mean reference index for dispersion between F and C lines of Ohara glass 9-7935  
 acousto-optical effect at liquid-vapour interfaces under thermal irradiation, mechanism 9-3181  
 arc, 'equiv. press.' validity, rectifier and thyatron obs. 9-13473  
 atmosphere vapour, obs. over 2 year period 9-21758  
 atom, e. scatt, spin polarization rel. to scatt. pot. 9-11397  
 atom, electron scatt., 25-150eV, static pot. approx. validity 9-17001  
 atom, electron scatt. compared with Ar and Xe, rel. to Mott theory and non-relativistic approx. 9-19408  
 atom, electron scatt. 3.5-500 eV, relativistic and exchange effects 9-18149  
 atom, long-range interactions 9-17002  
 atom, metastable, electron inelastic second-order collision 9-18153  
 atom excitation, by electron shocks, <sup>75</sup>Si, state lifetime and rate of population by transition from <sup>9</sup>P<sub>1/2</sub><sup>0</sup> 9-6976  
 cell structure for alkali metal chloride aq. soln. electrolysis, patent 9-8106  
 condensation, dropwise, heat transfer rel. to temp. head 9-17229  
 convection, laminar, natural, effect of mag. field 9-18252  
 crystalline,  $\alpha$  to  $\gamma$  martensitic transformation, crystallography 9-5519

**Mercury continued**

- crystals, Azbel-Kaner cyclotron resonance rel. to Fermi surface model 9-13838  
 crystals, magnetoacoustic effect 9-21432  
 differential h.p. manometer 9-6272  
 diffused into CdS, rel. to induced defects 9-7496  
 diffusion in HgTe on annealing in vapour rel. to dislocation formation 9-1229  
 discharge in inert gases mixture, positive column characts. 9-3030  
 electrolytic cell, film for electrode surface and amalgam decomposer, patent 9-21717  
 electron mass temp. dependence from sp. ht. and cyclotron resonance 9-16217  
 energy loss spectra, characteristic, of 8 keV electrons 9-7249  
 equati on of state and electrical resistivity at elevated temperatures and pressures 9-3075  
 exploding wires in very dense plasma production 9-9381  
 gas, conductivity and density meas., nonmetal-metal transition 9-11692  
 heat transfer of liquid when conducting elec. and in mag. field 9-21198  
 ion mechanism formation in the column low-press. discharge, spectroscopic study 9-5083  
 ionization up to  $9+$ , by repeated e collisions at  $<150\text{eV}$  9-5063  
 liq., conductivity and density a, nonmetal-metal transition 9-11692  
 liquid, containing halide ions, elec. resistivity 9-11715  
 liquid, electron-electron interaction eff. on optical absorption 9-21628  
 liquid, thermoelectric power, vol. depend. meas., pressure up to 1000 bars,  $20\text{--}120^\circ\text{C}$  9-1040  
 magnetic depolarization of resonant light backscattered by  $6^3\text{P}$ , state, effect of Hg Hg collisions 9-674  
 melting curve up to  $15 \times 10^6 \text{ N/m}^2$  9-9589  
 meniscus discharge, e. bunching obs. 9-5089  
 non stationary open channel flow, transverse magnetic field 9-21038  
 pipe flow in strong longit. mag. field, transition region and turbulence struct. 9-14753  
 spectra, holographic, obtained with Lloyd's mirror 9-4496  
 structure study of liq., X-ray diff. 9-7251  
 superconducting crystals, ultrasonic attenuation 9-7772  
 supercritical, conductivity and density meas., nonmetal-metal transition 9-11692  
 triboelectric effect between Hg and insulator, enhancement due to applied electric field 9-5755  
 vapour, condensation coeff. 9-1071  
 X-ray  $L_{III}$  absorption edge of  $^{80}\text{Hg}$ , chemical shift 9-14068  
 $^{201}\text{Hg}$ , optical pumping, transient phenomena in mag. resonance 9-9145  
 $^{201}\text{Hg}$ , vapour, effect of detecting light beam on modulated absorption and dispersion signals 9-673  
 $^{201}\text{Hg}$  atoms, Zeeman degeneracy under non resonant light radiation 9-11393  
 Ar bubbles in mercury, velocity of rise 9-17183  
 Hg $^+$  bombardment of CdTe crystals in formation of Hg $_{1-x}\text{Cd}_x\text{Te}$  layers 9-14898  
 $\gamma$ -Hg evidence for a third phase 9-3077  
 Hg vapour drag effect in pressure region of transition flow, accurate meas. 9-6237  
 Hg $^+$  mobility calc. in parent vapour 9-5067  
 Hg $^{2+}$ , complex combinations with the ions  $\text{SO}_4^{2-}$ ,  $\text{Cd}^{2+}$  SCN and the amines aniline, benzidine,  $\beta$ -naptyl-amine, o-toluidine and m-toluidine, infrared spectra 9-6969  
 Hg-Xe arcs, far i.r. source 9-19564  
 in  $\text{In}$ , impurity effect on  $\text{In}$  phonon spectrum 9-5533

**Mercury (planet) see Planets****Mercury compounds**

- alloys, liq. based, resist. 9-5187  
 complexes of triphenylphosphine, i.r. spectra 9-20944  
 halides, far i.r. cryst. spectra 9-1780  
 Hg $_{1-x}\text{Cd}_x$  superconducting crystals, ultrasonic attenuation 9-7772  
 Hg in amalgam, optical constants obs. 9-16392  
 Hg (0.5-1at%)Pb liq., struct. from X-ray diff. 9-7251  
 Hg (0.5-2at%)Cd liq., struct. from X-ray diff. 9-7251  
 Hg $_{1-x}\text{Cd}_x\text{Te}$  layers, formation by Hg $^+$  bombardment of CdTe crystals 9-14898  
 Hg(CN) $_2$ , far i.r. cryst. spectra 9-1780  
 (HgCd)Te solid solns., mean square displacements for sub-lattices 9-19711  
 Hg $_{1-x}\text{Cd}_x\text{Te}$  alloy, photoconductive i.r. detector 9-8522  
 Hg $_{1-x}\text{Cd}_x\text{Te}$  phase diagrams, (P,T) for  $x=0.2$  and segregation coeff. data given 9-5518  
 n-Hg $_{1-x}\text{Cd}_x\text{Te}$  ionized impurity scattering of conduction electrons at  $4.2^\circ\text{K}$ , calcs. 9-13884  
 HgCl $_2$ , Hg $_2\text{Cl}_2$ , elec. cond. of molten system 9-14856  
 HgCr $_2\text{S}_4$ , ferromagnetic, absorption edge shift, diffuse reflectance spectrum 9-1781  
 HgH, analysis of spectrum 9-14689  
 HgI $_2$ -HgI $_2$ , elec. cond. of molten system 9-14856  
 HgI $_2$ , electroabsorption and electroreflectance near fundamental edge 9-12350  
 HgI $_2$ , mag. props. 9-1638  
 Hg(NO $_3$ ) $_2$ , soln.,  $\beta$  backscatt. rel. to conc. 9-10367  
 HgO, far i.r. cryst. spectra 9-1780  
 HgO, X-ray spectra  $L_{III}$  absorption edge of  $^{80}\text{Hg}$ , chemical shift 9-14068  
 HgS, e-drift mobility determ. 9-5691  
 HgS, far i.r. cryst. spectra 9-1780  
 HgS, optical, non-linear, pmena 9-10160  
 $\gamma$ -HgS, Cl $_2$ , crystal structure 9-11847  
 HgS, Se $_2$ , ( $0.8 \times 0.4$ ) solid solns., kinetic props., investigation 9-1332  
 n-HgSe, de Haas-Van Alphen and Shubnikov-De Haas eff. in strong mag. fields 9-16218  
 HgSe, Lorenz number 9-5642  
 HgSe, X-ray diff. exam. 9-3294  
 HgSe De Haas-Van Alphen effect, obs. using pulsed peaks up to 200 kG 9-9914  
 HgSe helicon waves obs. at  $77^\circ\text{K}$  9-7723  
 HgTe, dislocation etch pits on surface of differently oriented crystals 9-9639  
 p-HgTe, effective hole mass at  $95^\circ\text{K}$  9-9985  
 n-HgTe, elec. conductivity in strong field 9-3626  
 HgTe, electrical properties, conductivity character and basic characteristic parameters 9-5643  
 HgTe, lattice parameter using X-ray diff. 9-9678  
 n-HgTe, magnetoresistance quantum oscills. 9-3625

**Mercury compounds continued**

- HgTe, mean square displacements for sub-lattices 9-19711  
 HgTe crystals, dislocation formation on annealing in Hg vapour 9-1220  
 Hg $^{2+}$ -Cd $^{4+}$  nitrate soln.,  $\beta$  backscatt. rel. to percentage comp. 9-10367  
 In-Hg dilute alloys,  $\text{In}$  phonon spectrum, effect of Hg impurity 9-5533

**Mesic atoms see Atoms, mesic and muonic****Mesic molecules see Molecules, mesic and muonic****Mesomorphic state see Liquid crystals****Meson field theory see Field theory, quantum/meson field****Mesons**

- See also Atoms, mesic and muonic; Cosmic rays/mesons; Hyperons; Kaons; Molecules, mesic and muonic; Pions*  
 $2^+2^-$  relation implied by  $\text{SU}(2)_C \times \text{SU}(2)$  9-2476  
 annihilation, relativistic quark model description 9-14495  
 coupling of pseudoscalar described by  $\text{O}(3,1)$  9-6586  
 current algebra in free effective quark model 9-20629  
 current algebra, hard-pion tech. for vertex functions 9-16892  
 decay to lepton pairs, eff. on rate by continuum contributions 9-393  
 eigenstates of  $G$ -parity, defin. 9-4607  
 evolution of quantum states with finite number of particles 9-4234  
 excited, radially, formalism for  $U_3$  multiplets and interac.,  $U_6 \times U_6$  symmetries 9-20630  
 form factors 9-8799  
 hard-pion, calc. of meson processes, N point functions 9-8858  
 instable, characterization 9-11025  
 mass and spin spectrum derivation from Majorana rep. and de Sitter model 9-8759  
 meson-baryon couplings, rescattering eff. in quark model 9-17968  
 nonet assignment of axial-vector using modified Weinberg sum rules 9-6611  
 production amplitude, Reggeized resonance model 9-14479  
 pseudoscalar, coupling description by  $\text{O}(3,1)$  9-10993  
 pseudoscalar, UFT,  $0^-$  2 families existence prediction 9-11024  
 quark model 9-10992  
 quark model, current algebra representations 9-2473  
 quark model, relativistic 9-14495  
 quark model, relativistic, Regge trajectory constraints in NID calc. method 9-15605  
 quark-antiquark, Heisenberg type scalar field theory model 9-8761  
 radial  $U_3$  multiplets and interac.,  $U_6 \times U_6$  symmetries 9-20630  
 scalar field, zero-mass, Einstein eqns., axially symmetric soln. 9-16666  
 strangeness-carrying isospinor scalar existence from spectral sum rules 9-4614  
 three point functions, Ward identities calc. 9-19203  
 vertex functions, hard pion current algebra calc. 9-16892  
 $\phi$ -KK,  $\text{SU}(3)$  prediction modified by continuum contributions 9-393  
 Yang-Mills nonlinear eqn. obtained from compensating fields theory 9-345  
 $\eta$  generation of 3-body forces in nuclear matter 9-14545  
 $1/s/t_c$  sum rules for determ. 9-6637  
 $\kappa$  existence doubted 9-2495  
 $\rho$ , trajectory parameters deduced from KN and  $\bar{\text{K}}\text{N}$  scatt. superconvergence relns. 9-4620  
 $\rho$  Regge pole exchange in  $\pi^+\pi^-\omega\omega$  9-15627  
 W self-conjugate isofermion field 9-6566  
 Z $^0$  evidence for in  $p_{1/2}$  state from  $\text{K}^+\text{p}$  scatt. data 9-4030

**absorption**

No entries

**capture***See also Nuclear reactions and scattering due to/mesons*

No entries

**decay**

- chiral  $\text{SU}(3)_C \times \text{SU}(3)$  3-point functions, strong and weak decays 9-8800  
 constants in nonlinear quark theory 9-20611  
 $\eta$ , photon, hard mes. analysis PCAC breakdown 9-6640  
 in quark model, recoil and rescatt. eff. in strong decays, width meas. 9-16858  
 quark model, relativistic 9-17969  
 resonances,  $2^{++}$  widths from relativistic quark strong-coupling consts. 9-13108  
 tensor meson decay, soft meson approx. 9-4632  
 Vector, photon hard mes. analysis, PCAC breakdown 9-6640  
 Weinberg's sum rules, symmetry breaking based on Okubo's ansatz 9-6611  
 $2^+ \rightarrow 0^-0^-$  and universality hypothesis for vector and tensor trajectories 9-15604  
 $\Lambda_1$ - $\rho$  system, hard and soft- $\pi$  approach, asymptotic sum rules, Bjorken tech. 9-16891  
 $\Lambda_1 \rightarrow \pi^+\sigma$ , hard-pion current-algebra predictions 9-16893  
 $\Lambda_1 \rightarrow \pi\gamma$ , hard-pion current-algebra predictions 9-16893  
 $\Lambda_1 \rightarrow \pi\rho$ , hard-pion current algebra calc. 9-16893  
 $\Lambda_1 \rightarrow \rho\pi$ , sum rules derivation from chiral  $\text{SU}(2) \times \text{SU}(2)$  charge-charge algebra 9-16886  
 $\Lambda_1 \rightarrow \rho\pi$  rate, asymptotic chiral symmetry calc. 9-8875  
 $\Lambda_1 \rightarrow \rho\pi$  s- and d-wave decay, Weinberg mass relation 9-17997  
 $\alpha \rightarrow \pi\pi$ , hard-pion current algebra calc. 9-16893  
 $D^0 \rightarrow \pi^+\pi^-$  evidence from  $\eta^0\pi^+$  reson. obs. 9-14518  
 $\eta$ , and  $\pi\pi$  scatt. length calc. 9-17991  
 $\eta \rightarrow 2\rho$ , rate rel. to integrally charged quarks 9-2500  
 $\eta \rightarrow \pi^0\pi^0\pi^0/\eta \rightarrow \pi^+\pi^-\pi^0$  branching ratio determ., final-state interactions studied 9-8805  
 $\eta \rightarrow \pi^+\pi^-\pi^0$ , asym. due to  $\eta$  and nonresonant background,  $3\pi$  amp. interference 9-17971  
 $\eta \rightarrow \pi^+\pi^-\gamma$ , matrix element 9-4612  
 $\eta \rightarrow \pi^+\pi^-\pi^0$ , Dalitz diagram 9-4611  
 $\eta \rightarrow \pi^+\pi^-\pi^0$ , s-wave  $\pi\pi$  phase shift obs. 9-20632  
 $\eta \rightarrow \pi^+\pi^-\pi^0/\eta \rightarrow \pi^02\pi$  branching ratio, by  $\omega$ -meson-dominant and current algebra calc. 9-14497  
 $\eta \rightarrow \pi^+\pi^-\pi^0$ , vector-meson dominance rel. to current algebra calc. 9-14497  
 $\eta \rightarrow \pi^+\pi^-\pi^0$  direct search, branching ratios obs. 9-2494  
 $\eta \rightarrow \pi\pi\pi$ , chiral dynamics exam., PCAC violation for a suggestion 9-8803  
 $\eta \rightarrow \pi\pi\pi$ , dynamics exam., PCAC violation for  $\eta$  suggestion 9-15609  
 $\eta \rightarrow \pi\pi\pi$ , structure from linear matrix-element and spectrum approx. 9-17975  
 $\eta \rightarrow \pi\pi\pi$ , two-pole model 9-8804  
 $\eta \rightarrow \pi\pi\pi$  final-state  $\pi\pi$  interactions, domination by  $\rho$  and S mesons 9-8812  
 $\eta \rightarrow \pi\pi\pi$  integral eqn., two subtractions, final state  $\pi\pi$  interactions 9-6646



**Mesons continued**  
**decay continued**

$\eta \rightarrow \pi\pi/\eta \rightarrow K\bar{K}$  small branching ratio due to  $e, \eta$  mixing 9-17970  
 $i^0 \rightarrow \pi^+\pi^-\pi^0$  obs. 9-8871  
 $\eta \rightarrow \pi\pi\pi$ , spectrum correction factors from decay structure 9-8811  
 $\kappa$ , isospinor scalar, deter. of const. from spectral-function sum rules 9-4614  
 $\kappa \rightarrow K\pi$  width calc. 9-2495  
 $\omega^0 \rightarrow e^+e^-$  and  $\mu^+\mu^-$ , partial width, NN composite model 9-2524  
 $\omega \rightarrow \pi\gamma$ , vector gauge field anal., current mixing and octet breaking 9-392  
 $\omega \rightarrow \pi\gamma$  vertex function, current algebra tech. 9-16894  
 $\omega \rightarrow \pi\pi\pi$ , vector gauge field anal., current mixing and octet breaking 9-392  
 $\omega \rightarrow \pi\pi\pi$  vertex function, current algebra tech. 9-16894  
 $P \rightarrow \pi\pi$ , hard-pion current-algebra calc. 9-16893  
 $\pi\pi\pi$  mode of isosinglet resonance phase-space distrib. 9-2521  
 $\phi$ , leptonic, branching-ratio of  $e^+e^-$  mode 9-8870  
 $\phi \rightarrow K+K$ , current-algebra calc., spectral function sum rules 9-16864  
 $\phi \rightarrow \rho\pi$  and  $O(4)$  symmetry 9-20616  
 $\rho^-$ , spin density matrix elements, prod. in  $\pi^-p$  at 2.26 GeV/c 9-11080  
 $\rho^0 \rightarrow e^+e^-$  and  $\mu^+\mu^-$ , partial width, NN composite model 9-2524  
 $S \rightarrow \pi\gamma$  vertex function, current algebra tech. 9-16894  
 $\phi \rightarrow e^+e^-$  9-6639  
 $X^0$ , amplitude parity relevance 9-15632

**detection, measurement**

$\delta^+$  evidence for existence from narrow  $\eta^0\pi^+$  reson. obs. 9-14518

**effects**

$\pi$  transition rad. in opt. region from passing Al and Ag foils, relativistic 9-9860

**interactions**

See also *Nuclear reactions and scattering due to mesons*  
 decouplet on baryon quintet in  $C_2$  9-19199  
 $g_{\pi NN}$  coupling constant determ. 9-4613  
 gas target for slow mesons, pressure up to 100 atm., 9-2561  
 intermediate vector mes. phenomena, CP-conserving and violating proc. unified theory, SU(3) space 9-2447  
 meson-baryon, QQQ model, with vector meson prod. 9-2490  
 meson-baryon charge exchange reaction anal., Reggeized supermultiplet theory 9-14481  
 meson-nucleon, forward react., single-parameter fit, from SU(3) and exchange degeneracy 9-16839  
 meson-spin- $1/2$  fermion, reaction amplitude calc. in 4th order perturbation theory 9-2491  
 $\lambda\phi^4$  model, SU(3) extension with  $O(8)$  symmetry 9-8905  
 scalar-mes. field coupled with fermion field, behaviour of classical solns. near light cone, q-number theory connection 9-6587  
 septet  $7(O^-)$  on baryon septet  $7(1/2^+)$  in  $G_2$  9-19199  
 with solids, capture rel. to atomic number 9-2492  
 SU(3) symm. model, Pauli-Kusaka mixture 9-15595  
 V-A, sixth interaction 9-20631  
 weak, nonleptonic, structure, matrix elements and divergences 9-16837  
 $pp \rightarrow \pi\pi$ , Regge-pole conspiracy trajectories, Feynman diagram 9-2486  
 $Li$  fragments production, energy spectra, angular distribution 9-15772

**magnetic moment**

in quark theory, nonlinear 9-20611  
 $A_1$ , anomalous mag. moment from Weinberg mass relation calc. 9-17997

**mass**

pseudoscalar, mass splitting, self-consistent calc. and parameters 9-16889  
 pseudoscalar nonet used to express  $f_K/f_\pi$  coupling constants 9-6637  
 quark model 9-2526  
 spin-orbit splitting rel. to quark model 9-4608  
 vector, mass splitting, self-consistent calc. and parameters 9-16889  
 Weinberg's sum rules, symmetry breaking based on Okubo's ansatz 9-6611  
 $\eta^0\pi^+$  and  $\eta^0\pi^-\pi^0$  effective mass distrib., peak obs., interpretations as decay of  $\delta^+$  mes. and  $D^0 \rightarrow \pi^+\pi^-$  9-14518  
 $f_0$ , double bootstrap calc. 9-8872  
 $K^0, K^+$  mass difference, scalar and tensor tadpole contributions 9-2497  
 $K^0 \rightarrow K^0, K^0$  obs. in regeneration 9-6649  
 $K$ - $K$  mass degeneracy in soft  $\pi$  calc. on  $K \rightarrow \pi l \nu$  form factors 9-13121  
 $\kappa$ , 1300 MeV or more 9-2495  
 $\kappa$ , isospinor scalar, existence from spectral-function sum rules 9-4614  
 $\rho$ , double bootstrap calc. 9-8872  
 $\rho$  mass and width determ. from  $e^+e^- \rightarrow \pi\pi$  9-15585

**production**

amplitude, Reggeized resonance model 9-14479  
 axial-vector-mesons, in  $\pi^+p$  and  $K^+p$  collisions, Regge-pole model obs. 9-14519  
 cosmic ray interac., 100-1000 GeV, analysis of 73 events at Pamir and Tyan-Shan 9-15674  
 from fermions, photoprod. amplitudes asymptotic props. 9-8801  
 photomeson, via  $u$  channel, and meson-nucleon elastic scatt. 9-13119  
 photoproduction by polarized photons, Primakoff effect, coherent and incoherent 9-11027  
 production amplitude, Reggeized resonance model 9-14479  
 pseudoscalar, by photons on nucleons; Regge-pole model and SU(3) symmetry 9-391  
 pseudoscalar, quark model, proton antiproton annihilation 9-11026  
 $\pi^+\pi^-\pi^0$ , in  $\pi^0d$  at 8 GeV/c 9-13138  
 vector, high energy production rel. to quark model prediction 9-20658  
 in  $e^+e^-$  colliding beams, resons. prod. and decays 9-17993  
 $\eta$ , weak, off nucleons by neutrinos via  $S_{11}$  reson., cross-section meas., existence of second-class currents 9-16860  
 $\eta$  in  $pp \rightarrow p\eta$ , differential cross section 0.8 to 1.45 GeV 9-352  
 $\eta$  in  $X^0 \rightarrow \pi^+\pi^-\eta$  9-6678  
 $\eta^0$ , photoprod. at 4 GeV 9-351  
 $g_1^-(1640)$  in  $\pi p$  at 6 GeV/c 9-13118  
 $\gamma p \rightarrow \pi^+\pi^0 p$  with 16 GeV bremsstrahlung 9-401  
 $K^*(890)$  in  $K^-d \rightarrow K^0\pi^+$ , 4.5 GeV/c 9-13136  
 $O^-$  and heavy resonances by  $\pi^-p$  at 17 GeV, stars in nuclear emulsion obs. 9-20648  
 $\phi$ , anomalous nuclear photoprod. rel. to vector-dominance and quark models, 9.16 GeV/c 9-8873  
 $\phi$ , photoproduction, suppression, vector dominance and  $\omega\phi$  mixing 9-13132  
 $\rho, \beta$ -decay coupling const., meas. by high energy neutrinos 9-11077  
 $\rho^0, \omega$ , photopions, results used for vector meson dominance validity test 9-19202  
 $\rho^+$  prod. in  $\pi^+p \rightarrow pp^+ \rightarrow \pi^+\pi^0$ , cross-section obs. to be  $1.2 \pm 0.2$  mbarn 9-15624

**Mesons continued**

**production continued**

$\rho^+\Delta^0$  associated prod. in  $\pi^+\pi^0$  interac. at 5 GeV/c 9-17998  
 $W^+$ , in  $\gamma p \rightarrow nW^+$  cross-section, mag. and T-violating elec. dipole moment 9-16887

**resonances**

$2^{++}$ , decay widths from relativistic quark strong-coupling const. 9-13108  
 $10^+ 10^+$ , existence and Regge pole theory 9-11070  
 $2^+$  existence and Regge pole theory 9-11070  
 $A_1\rho^*$  system, information from current-commutator algebra and divergence equations 9-11082  
 arbitrary spin,  $\pi\pi$  and  $NN$  vertex form factors 9-15630  
 axial-vector-meson prod. in  $\pi^+p$  and  $K^+p$  collisions, Regge-pole model obs. 9-14519  
 as baryon-antibaryon bound states in coupling constant bootstrap calcs. 9-2523  
 bootstraps for unnatural-parity states, finite-energy sum rules 9-20657  
 classification of exchange-degenerate trajectories, quark theory consistency 9-20655  
 current-mixing model, connection with dominance hypothesis and spectral function sum rule 9-6677  
 decay, radiative, of higher-spin boson resonances,  $O(4, 2)$  group representation 9-2520  
 dominance hypothesis, connection with spectral-function sum rule and current mixing model 9-6677  
 with exotic quantum numbers, higher multiplets from reson. saturation hypothesis 9-17992  
 form factors for massless vector mes. field 9-8799  
 heavy, prod. by  $\pi^+p$  at 17 GeV stars in nuclear emulsion obs. 9-20648  
 inelastic, broad, obs. of two-peak structure 9-399  
 isosinglet, decay mode, phase distrib. 9-2521  
 mass splitting, self-consistent calc. 9-16889  
 new, search in  $K^+p$  interac. at 12.7 GeV/c 9-6654  
 nucleon-nucleon data explanation by one-boson-exchange potential 9-6754  
 nucleus interaction ratios rel. to pion photoproduction 9-2501  
 PCAC, integral form between  $\pi$  and  $A_1$  mesons 9-4622  
 photoproduction, modified coherent-droplet model 9-20656  
 photoproduction cross section calc., vertex-strength-algebra treatment 9-11075  
 photoproduction on nucleons Regge-pole model 9-391  
 photoproduction on  $p$ , in Regge pole model, high-energy 9-11074  
 pole dominance and asymptotic symmetry for axial vector and vector currents 9-8867  
 pole dominance appl. to scatt. amplitude calc. 9-8834  
 production in  $\pi$ -N collisions, Regge model 9-11072  
 $\pi_1(980)$  from  $K^-p \rightarrow Y_1^*(1385)\pi^0\eta$  9-8869  
 spectral function sum rule, connection with dominance hypothesis and current-mixing model 9-6677  
 SU(3) multiplets, splitting, mixing and small perturbations 9-16888  
 tensor meson decay, soft meson approx. 9-4632  
 vector, high energy production rel. to quark model prediction 9-20658  
 vector and tensor nonets, SU(3) mixing restrictions 9-310  
 vector dominance and  $\phi$ -meson photoproduction 9-13132  
 vector dominance for hadron e.m. current tested in  $\gamma p \rightarrow K^+\Delta^+$  9-16909  
 vector dominance validity 9-17994  
 vector field with non-zero mass, relativistic eqns., invariant expansion of solns. 9-15631  
 vector meson dominance, validity test using  $\rho^0, \omega$  and photopion prod. results 9-19202  
 vector meson-baryon coupling constants, bootstrap calc. 9-2523  
 vector particles interac. of spin- $1/2$  particle-antiparticle syst., compositeness conditions 9-14516  
 Veneziano's model, trajectories study 9-8798  
 $4\pi$ , spin-parities, test 9-390  
 $A_1$ - $\rho$ - $\pi$  decay system, hard and soft- $\pi$  approach, asymptotic sum rules, Bjorken tech. 9-16891  
 $A_1$ , anomalous mag. moment, calc. 9-8879  
 $A_2$ , split, importance of  $\pi\pi$  decay mode to SU(3) decay predictions 9-20661  
 $A_2$  double-peaked structure, 2 poles in complex  $s$ -plane, resonance scatt. 9-14517  
 $A_2$  exchange domination, Regge theory test of  $\pi^+\pi^-\eta\eta$  9-14506  
 $A_2 \rightarrow \pi\gamma$  hard-pion current-algebra predictions 9-16893  
 $A_2 \rightarrow \pi\gamma$  hard-pion current-algebra calc. 9-16893  
 $A_2 \rightarrow \pi\sigma$  hard-pion current-algebra predictions 9-16893  
 $A_2$  scatt., invariant amplitudes, asymptotic behaviour, partial wave anal. 9-4633  
 $A$  enhancement in  $\pi^-\rho^+$  mass spectrum 9-2513  
 $A_1$ , sum rules derivation from chiral SU(2) $\times$ SU(2) charge-charge algebra 9-16886  
 $A_1$ , Weinberg mass relation from  $\pi^+\pi^- \rightarrow \pi^+A_1^+$  obs. with Veneziano formula 9-17997  
 $A_1 \rightarrow \pi\pi$ , decay prob. and partial width determ. from current algebra 9-11046  
 $A_1 \rightarrow \pi\pi$ , sum rules derivation from chiral SU(2) $\times$ SU(2) charge-charge algebra 9-16886  
 $A_1 \rightarrow \pi\pi$  rate, asymptotic chiral symmetry calc. 9-8875  
 $A_1 \rightarrow \pi\pi$  s- and d-wave decay, Weinberg mass relation 9-17997  
 $A_1 \rightarrow \pi\pi$  width and  $\pi$  charge radius calc. from Weinberg sum rules 9-395  
 $A_2$  prod. in e.m. process, cross section expression determ. 9-11084  
 $A_2$  spin and parity determ. in reaction  $\pi^+\pi^-\rho^0$  9-6679  
 $A_2$  splitting, confirmed, shape in  $\pi^+\pi^-\rho^0$ , 2.6 GeV/c 9-11058  
 $A_2^0 \rightarrow K\bar{K}^0$  interference, mixing in decay channel with  $\rho^0 \rightarrow K\bar{K}^0$  9-17996  
 $A_2 \rightarrow \pi\rho$ ,  $A_2$  quantum numbers determ. 9-11081  
 $A_1$  1660 MeV resonance production from  $\pi^+\pi^-$  interac. at 8 GeV/c 9-8876  
 $A_2'$ , intermediate prod. in  $\pi^-\pi^+ \rightarrow \pi^+\pi^0\eta$ , 2.26 GeV/c with  $J^P=2^{++}$  9-14509  
 $B-\rho'$  conspiracy, evidence from  $\pi$  photoprod. sum rules 9-20660  
 $B(\omega^-)$ , in  $\pi N$  scatt., Regge struct. at large momentum transfer 9-11079  
 $B \rightarrow \omega\pi$  decay, eval. using spectral function sum rules for tensor currents 9-14473  
 $\chi^{--}$ ,  $I=2$ , search in reactions of type  $\pi^-p \rightarrow p\chi^{--}$  9-388  
 $\delta$  in  $\pi N$  S-wave interactions using  $\pi$ -pole dominance model 9-6670  
 $e$  reson. width narrowing and Pomeranchuk theorem for partial waves 9-8874  
 in  $e^+e^-$  colliding beams, prod. and decays 9-17993  
 $\eta^0\pi^+$  existence at 975 MeV, interpretation as decay of  $\delta^+$  mes. 9-14518  
 $\rho^0 \rightarrow K\bar{K}^0$ , interference, mixing in decay channel with  $A_2^0 \rightarrow K\bar{K}^0$  9-17996  
 $\rho^0$  mass and width, double bootstrap calc. 9-8872  
 $\pi\pi, \rho\pi\pi$  vertices connection by spectral function sum rule 9-20659

## Mesons continued

## resonances continued

- $\eta$  interactions in  $H_2$  bubble chamber, 0.3-5.8 GeV,  $\Delta$  obs. 9-11071  
 $K^*$ -exchange diagram, role in  $\Sigma K^0$  prod. 9-6706  
 $K^*$ -pole model, for calc. of S-wave hyperon decay 9-16907  
 $K^* \rightarrow K + \pi$ , current-algebra calc., spectral function sum rules 9-16864  
 $K^*(1400)$  interf. anal. using  $K^* \rightarrow K^* \pi^* \pi^* p$  at 5.5 BeV/c 9-13134  
 $K^*(1420)$  prod. from  $K^* \pi$  interac., spin density matrix elements, prod. mech.,  $K_1 = 4.57$  BeV/c 9-17999  
 $K^*(890)$  photoprod., Regge pole model, conspiracy reln., factorization and kinematic constraints 9-18000  
 $K^*(890)$  prod. from  $K^* \pi$  interac., spin density matrix elements, prod. mech.,  $M_1 = 4.57$  BeV/c 9-17999  
 $K^*(890)$  prod. in  $K^* d \rightarrow K^* \pi^* n$ , 4.5 GeV/c, density matrix elements calc. 9-13136  
 $K^*(892)$  prod. from  $K^* d$ , decay ang. distrib. obs. 9-16897  
 $K^*$  low-mass system, spin-parity analysis, from  $K^* p \rightarrow K^* \pi^* p$  at 5.5 BeV/c 9-16866  
 $K^* \pi$  syst. from KN interac., Deck-model calc. of double charged syst. 9-20636  
 $K \pi \pi^- = T=1/2$  system near 1.3 GeV, spin and parity 9-13135  
 $\omega$ - $\phi$  mixing angle and  $\omega \rightarrow e^+ e^-$  made 9-8868  
 $\omega$ - $\phi$  mixing models, connecting with dominance hypothesis and spectral function sum rule 9-6677  
 $\omega \eta$  coupling const. determ., vector meson dominance hypothesis 9-14515  
 $\omega$  and Regge residues universal coupling, const. estimation 9-17995  
 $\omega$  form factor, determ. from Chou-Yang high-energy scatt. model 9-14520  
 $\omega$  isotopic singlet, Kawarabayashi-Suzuki reln. analogy 9-15633  
 $\omega$  photoproduction from  $\gamma p$  reaction, via diffraction and elementary  $\pi$  exchange 9-15635  
 $\omega$  photoproduction from  $\gamma p$  reaction, Regge pole model description 9-15608  
 $\omega \rightarrow e^+ e^-$  and direct determ. of  $\omega$ - $\phi$  mixing angle 9-8868  
 $\omega \rightarrow \pi^+ \pi^- e^+ e^- \rightarrow \pi^+ \pi^- \pi^0 \gamma$  coherent  $\omega$ - $\rho$  interference information for  $\omega$  decay 9-394  
 $\omega$ - $\phi$  mixing and  $\phi$ -meson photoproduction 9-13132  
 $\omega \rho \pi$  coupling const., eval. using spectral function sum rules for tensor currents 9-14473  
 $\pi^+ \pi^-$  1450 MeV enhancement in  $K^* p \rightarrow K^* \pi^* \pi^* p$  react. at 5.5 BeV/c 9-11078  
 $\pi^+ \pi^-$  enhancement in  $pp \rightarrow pp \pi^+ \pi^-$  at 24.8 GeV/c 9-8878  
 $\pi$  and K two body interactions, appl. of Padé approximants 9-2522  
 $\pi_c$  Regge pole pion conspirator, implications in meson spect. 9-400  
 $\pi N$  scattering, multi-resonance structure in  $P_{11}$  state 9-20651  
 $\pi^+ p \rightarrow \pi^+ \pi^+ \pi^- n$   $A_1, A_2$  prod. cross sections and decay ang. distrib. 9-398  
 $\pi^+ \pi^+, I=0$  at mass 1.06 GeV, obs. 9-8877  
 $\pi^+ \pi^-$  enhancement at  $M=1.05$  GeV in  $\pi N$  interaction 9-11083  
 $\pi^+ \pi^+ \pi^-$  prod. in  $\pi^+ d$  reacts, at 8 GeV/c 9-13133  
 $\pi \pi \pi \pi$  decaying into  $4\pi$ , spin, symmetry and polarization effects 9-6676  
 $\pi \pi \pi \pi$  decaying into  $4\pi$ , spin symmetry and polarization effects 9-13131  
 $\phi$ , anomalous nuclear photoprod. rel. to vector-dominance and quark models, 9-16 GeV/c 9-8873  
 $\phi \eta$  coupling const. determ., vector meson dominance hypothesis 9-14515  
 $\phi$  form factor, determ. from Chou-Yang high-energy scatt. model 9-14520  
 $\phi$  isotopic singlet, Kawarabayashi-Suzuki reln. analogy 9-15633  
 $\phi$  leptonic decay, branching-ratio of  $e^+ e^-$  mode 9-8870  
 $\phi$  mass meas. from  $K^* p$  4.25 GeV/c interaction 9-11041  
 $\phi$  photoproduction, suppression, and vector dominance and  $\omega$ - $\phi$  mixing 9-13132  
 $\phi$  photoproduction from  $\gamma p$  reaction, Regge pole model description 9-15608  
 $\phi \rightarrow e^+ e^-$  mode, obs. 9-6639  
 $\phi \rightarrow \pi^+ \pi^-$  and O(4) symmetry 9-20616  
 $\rho$ - $A_2$  trajectory dynamics of high-spin members, implications of results on decay widths 9-16896  
 $\rho$ , dipole model rel. to  $1/Q^4$  behaviour of nucleon form factor 9-8886  
 $\rho$ , mass and width, double bootstrap calc. 9-8872  
 $\rho^-$  backward prod. from  $\pi^+ p$  interaction; 8.16 GeV/c 9-20647  
 $\rho^-$  backward prod. from  $\pi^-$  interactions, Regge pole anal. 9-20663  
 $\rho^0$  prod. from  $\pi^+ p$  interac., ang. distrib. meas.,  $E_\pi = 2.7, 3$  GeV/c 9-14508  
 $\rho^0$  photoproduction, high energy, from  $^1H$  and  $^2H$  9-20664  
 $\rho^0$  photoproduction from complex nuclei 9-20665  
 $\rho^0$  backward prod. from  $\pi^+ p$ ; density matrix elements calc.,  $M_\pi = 4$  GeV/c 9-20646  
 $\rho^0$  photoprod. from complex nuclei,  $\rho \gamma$  coupling calc.,  $E_\pi = 8.8$  BeV 9-20662  
 $\rho \eta$  coupling const. determ., vector meson dominance hypothesis 9-14515  
 $\rho$  composite part. theory connection 9-8844  
 $\rho$  coupling const. current-field identification and Schwinger terms 9-397  
 $\rho$  dipole model rel. to nucleon and pion form factors 9-8887  
 $\rho$  field in massless limit, current-field identification and Schwinger terms 9-397  
 $\rho$  form factor, determ. from Chou-Yang high-energy scatt. model 9-14520  
 $\rho$  mass and width determ. from  $e^+ e^- \rightarrow \pi \pi$  9-15585  
 $\rho^-$  decay, spin density matrix elements, prod. in  $\pi^+ p$  at 2.26 GeV/c 9-11080  
 $\rho^-$  production from  $\pi^+ p \rightarrow \pi^+ \pi^0 p$ , decay const.,  $M_\pi = 2.77$  GeV/c 9-17984  
 $\rho^0$  non-forward coherent photoproduction and wave function 9-396  
 $\rho^0$  photoproduction from  $\gamma p$  reaction, Regge pole model description 9-15608  
 $\rho^0 \rightarrow e^+ e^-$  and  $\mu^+ \mu^-$ , partial width, NN composite model 9-2524  
 $\rho^0 \rightarrow \pi^+ \pi^- e^+ e^- \rightarrow \pi^+ \pi^- \pi^0 \gamma$  coherent  $\omega$ - $\rho$  interference information for  $\rho$  decay 9-394  
 $\rho^+$  prod. in  $\pi^+ p \rightarrow pp^+ \rightarrow \pi^+ \pi^0 p$ , cross-section obs. to be  $1.2 \pm 0.2$  mbarn 9-15624  
 $\rho_1$ , sum rules derivation from chiral  $SU(2) \times SU(2)$  charge-charge algebra 9-16886  
 $\rho \rightarrow \pi \gamma$ , vertex function, current algebra tech. 9-16894  
 $\rho \rightarrow \pi \pi$ ,  $\rho$  width and  $\pi$  charge radius calc. from Weinberg sum rules 9-395  
 $\rho \rightarrow \pi \pi$  hard-pion current-algebra calc. 9-16893  
 $\rho^0$ , from  $\pi p$ , vector-dominance model test 9-4627  
 $\rho^0: \Delta^2 < \mu^2$ , prod. and decay obs., Chew-Low extrapolation, 8 GeV/C 9-381  
 $\rho^2 \Delta^0$  associated prod. in  $\pi^+ d$  interac. at 5 GeV/c 9-17998

## Mesons continued

## resonances continued

- $\rho N \rightarrow \pi N \rightarrow \pi \Delta$  system giving good representation of  $D_{13}$  amplitude below 700 MeV 9-8848  
 $\rho$  scatt., invariant amplitudes, asymptotic behaviour, partial wave anal. 9-4633  
 $\sigma \rightarrow \pi \pi$  hard-pion current-algebra calc. 9-16893  
 $W$  pairs photoproduction, cross section analytical expression, mass=2, 2.5, 3 GeV 9-11073  
 $W^0 \rightarrow e^+ e^-$  and  $\mu^+ \mu^-$ , partial width, NN composite model 9-2524  
 $W^0$  production, from  $\gamma p \rightarrow \pi W^0$  semiweak process 9-16887  
 $W \rightarrow \pi \gamma$ , vertex function, current algebra tech. 9-16894  
 $W(\rho \gamma)/W(A_2 \rightarrow \gamma \gamma)$ , ratio of amplitudes of two-phonon decays for  $2^+$  tensor mesons 9-389  
 $X^0 \rightarrow \gamma \gamma$  from  $\pi^+ p$  reaction,  $E_\pi = 1.93$  GeV/c 9-15634  
 $X^0 \rightarrow \pi^+ \pi^- \eta$  decay 9-6678  
 $X^0$  decay, amplitude parity relevance 9-15632
- scattering**  
baryon-pseudoscalar mes. appl. of relativistic Schrodinger eqn., broken  $SU(3)$  sym. model 9-11028  
from baryons, exchange degeneracy and  $SU(3)$  for baryons 9-20666  
meson-baryon, charge and hypercharge exchange, Regge pole analysis 9-6638  
meson-baryon, decouplet exchange superconvergence relns. and cuts in complex  $j$ -plane 9-4609  
meson-baryon,  $U(6)/4WU(6)$  Reggeized theory, trajectory exchange contrib. 9-18004  
meson-baryon elastic scatt. proc., new superconvergent sum rules for product of factorized amp. 9-14496  
meson-meson, finite-energy sum rules 9-4625  
meson-nuclear,  $SU(3)$  crossing relation and Regge pole theory rel. to obs., 6-18 GeV/c 9-11029  
meson-nucleon, elastic, and photomeson prod. via  $u$  channel 9-13119  
meson-nucleon, Regge-pole model for invariant functions 9-15638  
meson-nucleon, review, of data including charge exchange up to 30 GeV/c 9-11030  
nucleon-meson,  $SU(3)$  crossing reln. and Regge pole theory 9-16859  
pseudo-scalar-pseudo-scalar, saturation of superconvergence relations by one-particle states 9-4610  
Regge trajectories, boson, parity doubling 9-2493  
Regge-pole model for forward-scatt. amp., comparison with quark model 9-13117  
Reggeized resonance model for prod. amp. 9-14479  
scalar, field, coupling to trace of energy-momentum tensor, nonpolynomial interac. Langrangian 9-16827  
scalar, vertex function, N/D coincident zeros and Levinson's theorem 9-15606  
tensor trajectories, rel. to energy-momentum tensor, use of Regge and quark models 9-13117  
vector meson-proton, momentum transfer dependence, elastic, from photoprod. data 9-11076  
 $\eta$ , Regge trajectories bootstrap models 9-11021  
 $\rho$ - $A_2$  trajectory dynamics of high-spin members, implications of results on decay widths 9-16896
- spin and parity**  
 $\pi$  produced in decay of isosinglet resonances 9-13131  
 $\pi$  produced in decay of isosinglet resonances 9-6676  
 $A_2'$  intermediate prod. in  $\pi \pi \rightarrow \pi \eta$ , 2.26 GeV/c with  $J^P = 2^+ 5^-$  9-14509  
 $pp \rightarrow \pi^+ \pi^+ \pi^- \pi^0$  phase space distrib., spin and parity of resonance 9-2521  
 $\rho$ - $A_2$  trajectory dynamics of high-spin members, implications of results on decay widths 9-16896  
 $X^0$  decay, amplitude parity relevance 9-15632

## Mesosphere see Atmosphere

## Metal-insulator-metal structures see Semiconducting devices/tunnel and interface devices

## Metal-insulator-semiconductor structures see Semiconducting devices/tunnel and interface devices

## Metallo-organic compounds see appropriate metal compound headings

## Metallurgy

- See also Ageing; Zone melting and refining  
adhesion under combined plastic deformation without heating in metals tending to brittle fracture 9-5492  
Al alloys, stress-corrosion and distribution, eff. of shot peening 9-17533  
alloy standards, radiochem. pure, spiat. cooling for neutron activation anal. 9-16645  
armco iron, interface tension at boundary with fluxes 9-14889  
brass: (5 wt.%) Zn, rolling texture, deform. rate depend. 9-1330  
drawing of sheet metal, plastic anisotropy effect 9-19830  
firing, maximum rate rel. to structure and thermodynamic props. 9-3462  
fluxes surface tension 9-14889  
friction measurement in drawing, extrusion and rolling 9-13719  
gun mix, resin bonded, research and development 9-3162  
laboratory, at Polytechnic of Denmark 9-6221  
magnesium-chrome refractories, fine grain, hot strength and thermal shock resist. 9-3438  
metallographic exam. using interferential films 9-5296  
of meteorites, review 9-6186  
particle coarsening theory, further applic. 9-11954  
particle coarsening theory, further applic., comments 9-11955  
powder bed, bottom pressure with applied ext. pressure 9-17322  
pyrophyllite, thermal-chemical props. and applications 9-3459  
reactive metal vacuum-induction melting in water-cooled crucibles 9-13746  
recovery, stage III in cold worked metals, kinetics 9-5500  
Robertson crack arrest test 9-19809  
shaping techniques 9-19829  
sintering, elementary review 9-3474  
spark cutter, electronic 9-6230  
steel, austenitic, heat treatment to improve corrosion resistance, patent 9-13755  
steel, case-hardening, insonation effects 9-19845  
steel, fracture surfaces with cracks of 'flocuic' type, metallographic investigation 9-5483  
steel, martensitic, ferritization by 1% Ti addition 9-16140  
steel, martensitic stainless, grindability, effect of C content 9-17323  
steel, tempered, alloyed with W, orientation of carbide phases 9-5504  
steel, zero change in length at hardening and austempering 9-9778  
steel aluminumized by vacuum evaporation 9-13584



**Metallurgy** continued

steel casting, embrittlement due to welding, effects of conditions and structure 9-17317  
 structural changes at high-temp., apparatus for high-melting point metals 9-3247  
 surface phenomena, vacuum 9-8324  
 tensile loading device for Kossel microdiffraction 9-11918  
 vacuum, thermodynamic aspects 9-8325  
 vacuum degassing of alloys and steels 9-13747  
 vacuum melting and casting 9-5493  
 vacuum metallurgy, physical-chemistry aspects 9-18530  
 vibration treatment of liquid metals by e.m. forces 9-21035  
 welded clad metal diffusion layer structure 9-18485  
 welded structures, fatigue damage accumulation law 9-14980  
 welds, thermal information transmission through optical fibres 9-6228  
 Al(5 wt.%)Mg-(0.4 wt.%) Ag alloy, precipitate-free zone, light and electron microscopy obs. 9-18537  
 Al-Mg-Ge alloy, clustering after quenching 9-17331  
 Al alloy, crude, production by direct reduction of aluminous ores, rel. to thermal behaviour of bauxite source material 9-11952  
 Al coatings on steel by vacuum evaporation 9-13584  
 Au-Sb alloys, metastability of phases prepared by splat cooling 9-3478  
 Be purification by vacuum melting followed by distillation and simultaneous deposition to sheet in e. beam furnace 9-13748  
 C steel, slightly hypoeutectoid, austenite recrystallization during hot-working 9-16145  
 Cr, diffusion layers on Fe materials, structure and metallography 9-11769  
 Cu-Cr alloy, f.c.c., recrystallization texture formation, effect of precip. 9-21391  
 Cu alloys, composition, prod. and props., patent 9-13768  
 Cu alloys and steel joints, crack formation and melting of base materials during welding 9-21397  
 Fe, carburization under vacuum 9-14124  
 Ni-Cr white castiron, heat treatment for improving mech. props., patent 9-13757  
 Ni and alloys, prep., props. and uses, review 9-7581  
 Ti alloys, age hardenable, composition and props., patent 9-13771  
 (U. Pu)C, synthesis from U-Pu alloy and fabrication of pellets 9-2791  
 U metal production by C reduction of  $\text{UO}_3$  in vacuum 9-14134  
 ( $\text{U}_{0.8}\text{Pu}_{0.2}$ )C pellets, low density, prep. 9-6938  
 W-Re alloys, prod., patent 9-13772  
 Y Fe garnet, powder, strain induced by various milling treatments 9-5453  
 Zr alloys with improved corrosion resistance, composition, patent 9-13745

**Metals**

See also *Alloys; Semiconductors; Semimetals*

adhesion under combined plastic deformation without heating in metals tending to brittle fracture 9-5492  
 angular distribution and ion yield in secondary emission 9-7870  
 anharmonic, transport props., Green's function theory 9-13822  
 antiferromagnetic, anomalous elec. resistivity near Neel point 9-9927  
 antiferromagnetic, mag. resonance spectrum in mag. field 9-8001  
 attack by bombardment 9-5296  
 b.c.c., deformation textures 9-19791  
 b.c.c., diffusion of H, activation energy 9-3385  
 b.c.c., flow stress, 10-300°K 9-13732  
 b.c.c., packing defects on {110} plane effect on X-ray scatt. 9-13677  
 blacks optical props., book 9-12324  
 boiling, voids, X-ray, meas. 9-9468  
 calorimetry, 300-1900°K 9-9838  
 carbon, ductility and strength depend. on hydrostatic press. and temp. 9-5478  
 cold-worked, stage III recovery kinetics 9-5500  
 compressed by liqs., theory of props. 9-5446  
 condensation, film effect of vapor subcooling 9-19662  
 contact potential difference meas., in liq. environment 9-19889  
 creep behaviour at elevated temps. 9-7547  
 crystal chem. information, tabular reduction 9-16073  
 crystal growth, single, spherical, dendritic of high melting point metals by cooling 9-19689  
 de Haas-van Alphen eff., meas. techniques up to 62 kG, down to 0.3°K 9-3563  
 de Haas-van Alphen spectra, field modulation meas., technique and theory 9-19884  
 diffusion of H, interstitial, quantum effects 9-3370  
 dispersed, thermodynamics and paramag. props. 9-13829  
 drawing of sheet metal, plastic anisotropy effect 9-19830  
 elastic props. of normal metals, correlation contribution 9-5417  
 electric fields, rotation-induced, near metals 9-198  
 electrical conductivity and galvanomagnetic eff., infl. of dislocations 9-12095  
 electrolytically deposited films, thickness meas. method 9-11763  
 electron-bombarded at oblique incidence, transition rad. rel. to plasma waves 9-7722  
 e.m. wave propag. in mag. field, review 9-5625  
 e.m. wave propagation through finite slab 9-17376  
 epitaxial films on alkali halides, effect of gas ads. 9-3199  
 epitaxial films on alkali halides, effect of gas ads. 9-16044  
 f.c.c., epitaxial growth on KCl cleaved in u.h. vacuum, surface defects effects 9-5241  
 faceted surfaces, LEED patterns 9-11794  
 fatigue, elastic, resistance, heat treatments 9-9748  
 fatigue crack propagation, mechanism analysis 9-11938  
 f.c.c., 3-dimens. voids, density change expt. method 9-11869  
 f.c.c., fatigue mechanism at u.s. freqs. 9-13735  
 f.c.c., stacking fault conc. 9-13693  
 f.c.c., width of slip dislocations, eff. of surface-active additions 9-13683  
 f.c.c. and h.c.p., intrinsic and extrinsic faults in field-ion micrographs, distinction 9-13670  
 f.c.c. crystal, secondary dislocations in plastic deform., sources 9-11879  
 f.c.c. crystals, work hardening, Kuhlmann-Wilsdorf theory of analysis, new formulation 9-9780  
 ferromagnetic, effect accompanying galvanomagnetic effect: Matteucci spontaneous effect 9-12249  
 ferromagnetic, elec. conductivity rel. to temp. and e scatt. by spin waves 9-12094  
 ferromagnetic, magneto-opt. eff., theory 9-17474  
 ferromagnetic resonance review 9-21661

**Metals** continued

field-ion image, brightness comparison for different metals 9-6495  
 film, electric props. e.m. field meas. 9-3568  
 film, thin, determ. of optical constants using transmitted light 9-3849  
 film in island form, effective optical consts. 9-12327  
 films, thermoelec. and mean free path effects 9-13925  
 films sputtered at low voltages, elec. props. 9-12097  
 films surface roughness effects on resistivity thickness dependence 9-9928  
 fine grained, strength, effect of diffusion creep 9-9763  
 flaw det. using transducerless u.s. generation 9-7469  
 friction, lubrication and wear, role of oxygen in eff. of additive surface-active substances 9-18529  
 friction measurement in drawing, extrusion and rolling 9-13719  
 friction rel. to deformation at low temps. 9-16139  
 growth of single crystals low-dislocation-density 9-21295  
 h.c.p.,  $c^+$  +  $a^+$  dislocation reactions 9-13685  
 h.c.p., interfacial free energy, anisotropy 9-21257  
 h.c.p., lattice dynamics 9-3506  
 high melting point, apparatus for high temp. structural changes investigation 9-3247  
 hot cracking resistance on solidification, quantitative determ. 9-21396  
 hydroerosion, effect of surface-active agents 9-9775  
 impure, energy spectrum and props., numerical analysis 9-3552  
 impurity scatt. potential in nearly-free electron metals, from elec. resistivity and acoustic attenuation 9-12045  
 internal friction, automatic recording apparatus 9-1265  
 internal friction at large strain amplitudes 9-16118  
 isotope thermotransport, temp. depend. 9-9491  
 liquid, hard sphere model, density depend. pots. 9-19604  
 magnetic susceptibility, up to 800°K, apparatus for meas. 9-21563  
 magnetization-density-wave state, thermodynamic pot. determ. 9-17448  
 mechanical props., long term, subjected to mechanical stress at high temp. and n. irradiation 9-21380  
 monovalent, cohesion 9-11788  
 monovalent, electron states distrib. 9-7705  
 noble, ion-ion repulsive interactions 9-17252  
 noble, nuclear spin-lattice relax. rates and Knight shifts, electron-electron 9-17501  
 noble, s-d mixing by impurity, calc. of charge displaced by localized perturbation on many-channel system 9-5598  
 non-ferromagnetic, spin waves and other magnetic excitations 9-13943  
 non-ferrous, grain size influence on hardness, fracture and other mech. props. 9-9653  
 oxidation, controlled by surface reaction, logarithmic law 9-14131  
 oxidation kinetics rel. to electronic and ionic diffusion in large surface-charge and space-charge fields 9-9620  
 with paramagnetic impurities, electron interaction effects 9-9876  
 particle, interaction with fast incident electron rel. to plasma oscillations 9-13439  
 particle prep. by evaporation in Xe gas 9-5220  
 phase transitions, isomorphic, T-P diag. 9-9793  
 photoconductor-metal contact investigation 9-16312  
 plastic behaviour of close-packed crystals, factors effecting initial behaviour 9-21368  
 plastic deformation on cutting at high velocities, specific work consumed 9-9758  
 plastic wave propag., u.s. probing 9-11923  
 plastic-metal and metal-metal surfaces stick-slip threshold velocity investigation 9-5489  
 plasticity modulus 9-17293  
 point defects 9-19740  
 polycrystalline h.c.p., crystallographic study of yield condition 9-21367  
 positron effective mass in real metals 9-16207  
 positron-electron ranges 9-12036  
 preparation and handling techniques, book 9-21387  
 reactive, vacuum-induction melting in water-cooled crucibles 9-13746  
 refractory, zone melting by point-focused e beams 9-9647  
 residual elec. resistance detection of impurities 9-17377  
 resistivity, elec., rel. to plastic deform 9-12093  
 resistivity changes during and after irradiation, meas. method 9-19888  
 second sound existence, prediction 9-18592  
 self-diffusion, high-pressure effects 9-3384  
 self-diffusion activation energy rel. to compressibility and charact. temp., near melting point 9-11890  
 sheets, coarse grain, texture studies by neutron diffr. 9-19698  
 sintering, vol., grain boundary and surface diffusion contributions 9-1246  
 solid soln., binary, conc. depend. of interdiffusion coeff. 9-3374  
 solid-liquid interfacial free energies, absolute determ. 9-11759  
 solutions in  $\text{NH}_3$ , Hall effect 9-1041  
 structural changes in metals deformed at high temp., micrographic studies, applies of stereogrammetry 9-16065  
 superplasticity 9-7541  
 superconducting, properties review with theory 9-9946  
 surface diffusion of inert gases and adhesion time 9-21347  
 texture, axial, X ray diffr. exam. 9-3289  
 thermal conductivity, apparatus, 90 to 200°K 9-15016  
 thermal expansion meas. by gas-actuated acoustic dilatometer 9-15009  
 thermal radiation rel. to optical and elec. props. 9-21433  
 thermometry, optical and thermoelec., of small spherical crystals 9-20462  
 transition element impurities, localised mag. mom. 9-7874  
 u.s. reflection in strong mag. fields, plane of polarization rot. and ellipticity appearance 9-3525  
 vacancies and vacancy pairs, effect of grain boundaries on distrib. 9-3322  
 vacancy clustering and annealing 9-5336  
 viscosity, solid effect on dynamic load factor 9-4280  
 waves, plastic torsional, velocity expt. determ. 9-16724  
 welding, spot cold, stress and strain states in welding area of brittle mats. 9-21362  
 wire, elec. resistance shape factor rel. to non-conductive second phases 9-5648  
 X-ray emission spectra, soft, anomalies in edges 9-1817  
 GaAs-metal point contact, rectifying barrier structure 9-12163  
 GaAs point contact, breakdown 9-3686  
 Ge-metal contacts, e. and phonon tunneling spectroscopy 9-13909  
 semiconductor-metal transition in Bi-Sb alloy, mag. field and Sb conc. depend., 4-77°K 9-1513  
 Si, metal-nonmetal transition, resistivity and Hall effect study 9-1472

**liquid** see *Liquid metals*

**Metals** continued  
**theory***See also Crystals; Electron gas; Plasma*

- alloys, binary, one-dimens., electronic structure 9-7707  
 alloys, binary, ordering energy and effective pairwise interactions 9-7696  
 alloys, binary, single-site approx. in electronic theory 9-7708  
 alloys, pseudopotentials and residual resistivity calc. 9-5593  
 b.c.c., limiting strength produced by solution hardening 9-7561  
 b.c.c., limiting strength produced by solution hardening 9-7562  
 cellular method for band structure calc., test 9-12050  
 charge separation due to hydrostatic pressure 9-19876  
 cohesive energy, structural expansion in effective Hamiltonian approx. 9-21454  
 conduction *e* free-energy shift, *s-d* exchange interaction with localized impurity spin  $b//c//$  9-15043  
 conduction-electron polarization rel. to exchange coupling 9-21561  
 Coulomb gas, degenerate, non-uniform state in strong mag. field 9-21474  
 crystal chemistry, geom. factor, near-neighbour diagrams 9-19703  
 diamagnetic susceptibility 9-21567  
 diamagnetic susceptibility, statistical model 9-10096  
 dislocation drag, electronic component 9-13684  
 effective lattice pseudopotential, vertex corrections, contrib. of virtual excitation of plasmons 9-12072  
 electron correlations over whole range of metallic densities 9-12071  
 electron relaxation-time determ. using weakly-damped helicon waves 9-9909  
 energy transfer between electron and phonon system 9-5599  
 Engel-Brewer theories 9-9667  
 e.p.r., frequency-dependent mag. susceptibility interpretation 9-12497  
 exchange scatt., Suhli's integral eqns. for T-matrices 9-15044  
 f.c.c., angular forces in lattice dynamics 9-5528  
 ferro- and antiferromagnetic, elec. resistivity anomaly near mag. ordering point 9-12096  
 films, anomalous skin effect 9-1447  
 films with arbitrarily oriented ellipsoidal Fermi surfaces, size effect in elec. conductivity 9-7744  
 free-electron-like foils optical props. 9-14022  
 galvanomagnetic props., effect of localized Umklapp scattering 9-9918  
 harmonic oscillator, one-dimens., effects of finite boundaries 9-5794  
 Heine-Abarenkov model potential, modified, optimum form 9-5594  
 Heine-Abarenkov pseudopot. investigated through thermoelec. power 9-10061  
 helicon propagation quantum oscillations, mechanism 9-1439  
 homogeneous model, Hamilton operator and Ansatz for spectral functions of Green's functions 9-7733  
 image potential for medium with wavevector *q* freq. dependent dielec. function 9-9882  
 Landau Fermi-liquid parameters, sum rule 9-3559  
 lattices, random, exclusion effect and self-contained first-order approx. 9-9879  
 liquid, u.s. attenuation rel. to relax. and disorder 9-5160  
 liquid and gaseous, correspondence behaviour 9-7273  
 magnetic, compensated, Hall effect proportional to  $MB^2$  in high-field limit 9-21456  
 magnetoacoustic dispersion and attenuation, expt. rel. to free-electron theory 9-5553  
 metal-ammonia solns., props. and existence of metal-nonmetal transition 9-14833  
 metal-nonmetal transition, conference 9-15067  
 metal-nonmetal transition, description 9-15121  
 metal-nonmetal transition due to cryst. distortion 9-16204  
 models for small-angle scatt. dependence of conduction 9-236  
 plasticity at elevated temps., expt. approach 9-14972  
 positrons, effective mass calcs. 9-1424  
 pseudopotentials, theoretical foundation 9-9874  
 quasi-particle model, determ. of Green's-functions spectral functions and generalization of results 9-7734  
 Raman scattering by opt. vibration modes 9-12399  
 resistivity, phonon-limited 9-9926  
 Ruderman-Kittel-Kasuya-Yosida (RRKY) exchange interaction mag. field dependence 9-5792  
 Schrodinger eqn., band struct. and Fermi surface theory 9-13828  
 semimetal semicond. transition, possible anomalies 9-15045  
 sound velocity model 9-21428  
 surface, energy exchange processes, non-equilibrium distribution 9-21550  
 surface potential in random phase approx. for interact. system, effects of correl. 9-12074  
 surface quantum states and impedance oscils. in weak mag. field, numerical analysis 9-5617  
 surface sound excitation by e.m. waves 9-1367  
 transition metals, bonding and structures 9-18577  
 Al form factors of truncated at. potentials 9-9875  
 CsAu, band-theoretic study of metallic character 9-15055  
 Ga, positron lifetimes in solid and liquid 9-7731  
 H-Pd electrical resistivity 9-3580  
 Hg, nonmetal-metal transition 9-11692  
 K, Landau Fermi-liquid parameters 9-9912  
 K, pseudopotential calc. of thermal expansion coeff. 9-12023  
 Li-Mg binary alloy, ordering energy and effective pairwise interactions 9-7696  
 LiAg, band-theoretic study of metallic character 9-15055  
 Na, Landau Fermi-liquid parameters 9-9912  
 Na, positron lifetimes in solid and liquid 9-7731  
 Na, pseudopotential calc. of thermal expansion coeff. 9-12023  
 NiS, hexagonal form, metal-to-semicond. transition 9-12084  
 Sb alloys, dilute liq., with 3d- transition metals, localized impurity states, and mag. susceptibilities 9-1043  
 Ti, u.s. attenuation in normal high-purity material 9-12004  
 VO<sub>2</sub>, 'metallic' state 9-15048  
 Zn, liquid, effective ion-ion interaction and dielectric screening 9-18350

**Metamagnetism** *see* **antiferromagnetism; Ferromagnetism****Meteorites***See also Meteors*

- chondrite and achondrite cathode luminescence, for electron bombardment, microprobe obs. 40 keV 9-20007  
 chondrites, <sup>139</sup>Xe formation intervals, cooling rates and dating 9-6183  
 chondritic, on Moon, contrary evidence from soil structure 9-10517  
 Deelfontein, abundance of rare gases in metal, troilite and graphite phases 9-8284

**Meteorites** continued

- Denver, USA (July 1967) 9-20233  
 use in examining ancient events 9-8220  
 falls, binomial distrib. and probabilities w.r.t. lunar hour angle 9-21951  
 heating of parent bodies and planets by dynamo induction from a pre-main sequence T Tauri solar wind 9-15350  
 iron, K and Ar contents 9-6184  
 luminescence due to proton irradiation, lab. simulation of moon lum. 9-20221  
 lunar, responsible for mascons 9-18904  
 lunar impacts rel. seismicity 9-17638  
 metallurgy and structure, review 9-6186  
 meteoroid distribution near the ecliptic 9-17648  
 micrometeorites and their simulation 9-20232  
 olivine deformation 9-6185  
 pyroxene deformation 9-6185  
 radioactivity, conclusions from 0.5 to 2.9 GeV *p* reaction obs. 9-19310  
 stratospheric dust, relationship to meteoric influx 9-21760  
 tektites, physical model of origin 9-10534  
 troilite from Great Namaqualand, inert gas anomalies 9-6187  
<sup>244</sup>Pu/<sup>138</sup>Xe decay intervals of chondrite dark phases 9-2061  
<sup>129</sup>I/<sup>129</sup>Xe decay intervals of chondrite dark phases 9-2061  
 Ca<sub>2</sub>(Mg,Fe)<sub>2</sub>(PO<sub>4</sub>)<sub>2</sub>, stanfieldite, Mg:Fe ratio obs. 9-12758  
 NaMg<sub>2</sub>CrSiO<sub>6</sub>, kranovite, obs. in meteorites 9-18922  
 Xe heavy isotope abundance attributed to <sup>244</sup>Pu decay 9-6925

**Meteoroids** *see* **Meteorites****Meteorological instruments***See also Anemometers; Hygrometers; Ionosphere measuring apparatus*

- 1918, 1968, review 9-4046  
 airborne automatic system for cloud nucleation study 9-4056  
 for electrical meas. in snowstorms 9-16528  
 event recorder, digital, multichannel, for field appls. 9-16527  
 ozonesonde, electrochem. 9-4047  
 thermocouple voltage linearization 9-2266

**Meteorology**

- air earth currents, conduction and convection 9-10387  
 air-sea interaction 9-12578  
 atmospheric interaction with underlying surface, momentum, heat and moisture exchange 9-20085  
 computer simulation of the atmosphere 9-18792  
 ionospheric event of Oct. 31 1967 interpretation 9-18812  
 laser radar return, determ. of physical props. of atmos. droplets 9-10870  
 Markov chain, order of dependency, test procedure 9-8167  
 radiation balance of earth-atmosphere system, Nimbus 2 obs. 9-20089  
 radio meas., lower atmos. effects on radio propag., book 9-18805  
 rotating annulus, transition from axisymmetric to nonaxisymmetric flow, quasi-geostrophic model 9-18239  
 satellite observations, problems 9-21756  
 satellites, role in observing and forecasting atm. behaviour 9-21755  
 semi-diurnal lunar harmonic term in met. data using only 3 values each day 9-4048  
 snowstorms, electrical currents and characts. meas. 9-16528  
 snowstorms, measurements of electrical characteristics 9-12577  
 vapour, meanings of term in literature 9-12579  
 wind and temperature profiles above Sardinia, results from ESRO Skylark launches, Sept. and Oct. 1965 9-12576

**Meteors***See also Meteorites*

- 11 Canis Minorid stream obs. 9-14244  
 1963 Geminids, radio echo 9-4123  
 asteroid explanation of fireball 25 April (1966) 9-18921  
 drift of meteor trains 9-4123  
 echoes, radar obs., calc. of mass distrib. of meteoroids 9-15348  
 fireball, 25 April 1966, photographic obs. orbit determ. 9-18921  
 Geminid, photometric investigation, mass and luminosity determ. 9-2059  
 geomagnetic field effect on trains, height depend., obs. 9-12577  
 ionization forward transmission, Oct. 1965-Sept. 1966, count rates 9-2060  
 from Leonid shower, 1966, spectrum 9-18053  
 meteoroid hazard to lunar orbiting vehicles 9-21950  
 meteoroids, mass distrib. from radar obs. of underdense meteor trails 9-15348  
 reflections, long duration, and transient ionizations 9-2060  
 showers, earth cosmic ray var. during 9-21833  
 spectrum photography, 74 spectra 9-15349  
 sporadic photographic, velocity distribution 9-16614  
 stimulated, spectral meas. and features 9-16613  
 visual over Waltair, Nov.-Jan. inclusive 1964-7 9-8283  
 wind trains, simultaneous obs. with *E*-region ionospheric drift, anal. rel. to bulk motion of matter 9-12623

**Metrology** *see* **Measurement; Mechanical measurement****Mica**

- cleavage face, epitaxial growth of Cu, Ag, Au and Pd 9-5242  
 electrical conduction, hopping, and thermal breakdown, in natural and synthetic cryst. 9-12182  
 fission track ages of various minerals 9-16523  
 fission track ages of various minerals 9-4037  
 migration activation energy of Au and Ag atoms along natural cleavage surface 9-11892  
 muscovite, salicylic acid epitaxy 9-1159  
 natural and synthetic, hopping electrical conduction and thermal breakdown 9-12182  
 oxidation zone 9-1911  
 pre etched, use in track recorder for absolute fission rate meas. 9-11142  
 substrate, deposition of Bi film, orienting action 9-21275  
 surface temperature of substrate on hotplate used for epitaxial growth 9-11807  
 van der Waals forces, normal and retarded, direct meas. 9-18398  
 windows for electronographic tubes 9-12978  
 Al-mica 1M, crystal structure 9-1180

**Micelle systems** *see* **Colloids****Microanalysis** *see* **Chemical analysis****Microhardness** *see* **Hardness****Micrometeorites** *see* **Meteorites****Micrometry***See also Interferometry; Strain gauges; Thickness measurement*

- microscopic height differences by reflection electron microscopy 9-4217



**Microphones***See also Transducers*

capacitor, calibration, press, and field-free response, coupler versus electrostatic methods 9-4343  
 directional pattern, doughnut shape 9-4339  
 infrasonic orthogonal biquad array, low-freq. design and meas., appl. to windscreens 9-4342  
 intracardiac, calibration by two devices 9-4340  
 loudspeaker reactive coupling, avoidance 9-17804  
 single grid hot-wire, data opposing use in power spectral analysis of thunder 9 10385

**Microphotometers** *see Densitometry***Microprobe analysis** *see Chemical analysis/X-ray***Micropulsations** *see Earth/magnetic field variations; Magnetic storms***Microscopes***See also Electron microscopes; Ion microscopes*

amplitude contrast, with soot rings between objective lenses 9-14448  
 continuous ultramicroscope, for origin of new phase in low temp. hydrocarbon 9-3235  
 eye-piece, cross-wire, digitized and telecontrolled, for nuclear emulsion meas. 9-2416  
 flat field objectives, compensating eyepieces, design 9-4530  
 i.r., for temp. meas. of microstructures 9-2262  
 objectives, u.v. measurement of transmission, fluorescent converter 9-13063  
 optical, resolving power, demonstration of role of diff. pattern 9-12839  
 refinements for semiconductor device production 9-8661  
 X-ray shadow, visual image 9-6244

**Microscopy***See also Electron microscopy*

carbonaceous mats., use of H ion bombard. and masks in prep. of specimens 9-8314  
 ceramics, transmission micrographs, thickness errors, analysis 9-3174  
 corundum, dislocation motion obs. using decoration method 9-1215  
 field-ion, appl. to superlattice formation obs. 9-7402  
 field-ion image of dissociated perfect dislocations 9-16100  
 field-ion images, contrast from dislocations: origin of cross-over effect 9-11877  
 field-ion micrographs, intrinsic and extrinsic faults, distinction 9-13670  
 flash fluorescence, taking colour photo-micrographs 9-10921  
 graphite, transmitted light, constituent identification and interrel. with pore systems 9-7423  
 hologram, carrier suppression and restoration 9-20537  
 holography applied to reflexion microscopy 9-6534  
 hot stage, inorganic compounds 9-14880  
 interference reflectors with independ. variable wavelength and reflectance 9-8650  
 Kerr-effect, in mag. domain obs., picture improvement technique 9-16352  
 metals, deformed at high temp., micrographic studies of structural changes, appls. of stereogrammetry 9-16065  
 meteoritic mats, photomicrographic exam. rel. to ice nucleation 9-11745  
 p-n junctions exam. of inhomogeneities 9-13900  
 radioactive fallout, particle separation for examination 9-15249  
 refractive index, determ., subnanogram particles 9-12330  
 steel, structural recrystallization studies by vacuum metallography 9-1154  
 stereogrammetry, appls. in micrographic studies of structural changes in metals deformed at high temp. 9-16065  
 stereophotography with light and electron microscopes 9-15198  
 AsSb<sub>3</sub>, getchellite, metallography 9-19708  
 BN, metallographic exam. of etched faces 9-5271  
 Ir, field-ion image of dissociated perfect dislocations 9-16100  
 Ni<sub>3</sub>Mo, ordered, field-ion images, contrast variation 9 16077  
 Ni<sub>3</sub>Mo, ordered, field ion images 9-14922  
 Pt-Co alloys, superlattice formation, field-ion microscope obs. 9-7402  
 Si:P diodes, laser-irrad.-produced, optical microscope exam. of structural characts. 9-18638  
 W, field-ion micrograph analysis of stacking faults 9-9717

**Microstructure of crystals** *see Crystal structure/microstructure; X-ray examination of materials/microstructure***Microtomes** *see Biological technique and instruments; Laboratory apparatus and technique; Microscopy***Microtrons** *see Particle accelerators***Microwave spectra** *see Spectra***Microwave spectrometers** *see Spectrometers, radiofrequency***Microwave techniques and devices**

apertures, sectoral and annular, focal region fields obs. 9-8550  
 atomic stacking models, diff. expts. 9-16  
 cavity containing magnetoplasma dielec., resonance freq. and field 9-14406  
 cavity for far u.v. intensity calibration 9-17891  
 cylinder with variable surface impedance, axial-symmetric excitation theory 9-4396  
 cylindrical TM<sub>10</sub> cavity determ. of electron density 9-11552  
 ferrite-filled coaxial cavity, dynamical models and appl. to ferrite material-parameter meas. at mm waves 9-8556  
 filters, magnetically tunable with high quality factors 9-10769  
 frequency markers on microwave spectrum 9-2283  
 Gunn generators, freq. and power modulation 9-5733  
 Gunn generators, tunability, noise and synchronization 9-5733  
 IMPATT diodes, passivated metal-semiconductor, microwave oscills. 9-15117  
 klystron, two-cavity, freq. control for double resonance studies 9-15502  
 plasma decay parameter meas. 9-7168  
 plasma reflection to determ. electron density, boundary effect 9-17114  
 reflection coeff. meas., effect of higher order modes in oversized waveguide 9-8557  
 resonator, active Fabry-Perot, use of plasma impedance element 9-8545  
 resonator, cylindrical, oscillation and damping frequencies 9-2942  
 resonator, cylindrical, TE and TM electromagnetic mode results, applications 9-2941  
 Rochelle salt, dielec. constant temp. dependence from meas. at 9 GHz 9-10051  
 selective filters, using resonant cavity with one coupling element 9-4414  
 semiconductor, non-ohmic microwave conductivity meas. 9-15102  
 semiconductor oscillator, generalization of theory 9-5715  
 Stark modulation absorption system for high temp. molecular spectroscopy 9-6435

**Mie theory** *see Scattering***Milky way** *see Galaxies/the Galaxy***Mineralogy** *see Minerals***Minerals***See also Mica; Quartz; Ruby*

akermite-gehlenite merwinite system, X-ray analysis of liquidus surface 9-18541  
 alite composition in Portland cement clinker 9-18393  
 alkali feldspars, bond lengths rel. to ordering and ionic character 9-7356  
 alkali feldspars, exsolved, appl. of theory of optimal phase boundaries 9-3360  
 amaranite, Fe(SO<sub>4</sub>)OH.3H<sub>2</sub>O, crystal structure 9-1188  
 argyrodite, (Ag<sub>8</sub>GeS<sub>6</sub>), microhardness and photochem. effect 9-14982  
 barfettisite, crystal structure determ. by Fourier-transformation of minimum function 9-11831  
 basic rocks, rare earth abundances 9-8152  
 bauxite, thermal behaviour as source material in crude Al alloy production by direct reduction 9-11952  
 canfieldite (Ag<sub>3</sub>SnS<sub>3</sub>), microhardness and photochem. effect 9-14982  
 cascade Range pyroelastics, neutron activation analysis 9-21752  
 cements, composition and hydration 9-14123  
 chalcopyrite, Mossbauer effect study, 80-700°K 9-5889  
 chondrites, amounts of fission Xenon 9-16615  
 copper sandstone, elec. conductivity and dielec. loss temp. dependence 9-10036  
 copper trichite, torsion of reticular planes 9-19792  
 corundum, dislocation motion, microscope obs. using decoration method 9-1215  
 corundum, synthetic, Tyndall scatt. rel. to microscopic and colloidal inclusions distrib. 9-1730  
 diopside, shear strength pressure and temp. dependence 9-5477  
 dunite, phase changes 9-16516  
 elbaite, colour centres 9-1236  
 electric discharge causing breakdown, energy characts. 9-10042  
 eucryptite, (LiAlSiO<sub>4</sub>), high temp. form, crystallization and polymorphism 9-1134  
 eveite, Mn<sub>2</sub>(OH)(AsO<sub>4</sub>), from Langban, Sweden, crystal structure 9-18449  
 ferromagnezian spinels, lattice parameter and volume rel. press. 9-11844  
 getchellite, AsSbS<sub>3</sub>, crystal structure, metallography and chem. props. 9-19708  
 goethite, antiferromag. thermoremanence at Neel temp. 9-10150  
 groutite, A-MnOOH, crystal structure refinement 9-7444  
 haematite content, sediments, mag. determination 9-12647  
 hematite, magnetoelastic coupling const. from magnetostriction meas., 100-300°K, up to 150 kOe 9-7529  
 hematite, specular, pure crystal ferromagnetic exchange interactions obs. 9-10149  
 hocartite, Ag<sub>3</sub>SnFeS<sub>4</sub>, comp., structure and reflectivity 9-19705  
 hornblende, orthorhombic amphibole, crystal structure 9-13639  
 hornblende stability in upper mantle and low velocity zone model 9-20078  
 illite clay, i.r. absorpt. 3800-700 cm<sup>-1</sup> obs. 9-12372  
 inclusions, liquid-CO<sub>2</sub>, bearing, mass spectra, microscope exam. and geochemistry 9-14940  
 kaolin clay, i.r. absorpt. 3800-700 cm<sup>-1</sup> obs. 9-12372  
 labradorite, shear strength pressure and temp. dependence 9-5477  
 leuco-sapphire, Tyndall scatt. rel. to colloidal inclusion distrib. 9-1730  
 limonite, weathering model for Martian surface coloration 9-2052  
 lithium tourmaline, (elbaite), colour centres 9-1236  
 lunar surface, Surveyor 5 expt. 9-21925  
 magnetite, stress control of magnetization, implications 9-21586  
 magnetite, volume magnetostriction 9-21836  
 Martian surface, stability 9-6176  
 merwinite, crystallization from melilitite compositions 9-18541  
 mica, dating of fission tracks 9-16523  
 mica, dating of fission tracks 9-4037  
 microline feldspar, <sup>40</sup>Ar diffusion flux, elec. fields effects 9-11897  
 monodomain grains, remanence coercivity meas. 9-13976  
 olivine, deformation in stony meteorites 9-6185  
 olivine, plastic deformation 9-5456  
 olivine, shear strength pressure and temp. dependence 9 5477  
 parawellite, (Mn,Mg)<sub>2</sub>Sb(Si,As)<sub>2</sub>O<sub>10-11</sub>, from Langban, Sweden, crystal structure 9-16078  
 penfieldite, Pb<sub>2</sub>(OH)Cl<sub>3</sub>, crystal structure 9-18451  
 physical characteristics meas. production at high static pressures 9-12572  
 potash alum., dislocations, direct obs. 9-11883  
 prospecting on and below sea-floor, physics techniques required 9-18788  
 pyrophyllite, natural and synthetic, structure rel. to polytypism with mica-like minerals 9-1192  
 pyrophyllite, thermal-chemical props. and applications 9-3459  
 pyroxene deformation in stony meteorites 9-6185  
 pyrrhotite, Fe<sub>9-10</sub>S and Fe<sub>9-10</sub>Se, magnetic phases 9-18821  
 rocks, ring heat source probes for rapid thermal conductivity determ. 9-15018  
 rocks, small magnetic anisotropy by portion pendulum method 9-18818  
 rocks, thermal conductivity rel. to piercing 9-15019  
 rutile, phase changes 9-16516  
 sericite clay, i.r. absorpt. 3800-700 cm<sup>-1</sup> obs. 9-12372  
 serperite, Ca(Cu, Zn)<sub>2</sub>(OH)<sub>2</sub>(AsO<sub>4</sub>)<sub>2</sub>.3H<sub>2</sub>O, crystal structure 9-3286  
 shear strength pressure and temp. dependence 9-5477  
 silicates, adhesion when cleaved in ultra high vacuum 9-7364  
 spectrochemical analysis in d.c. arc, borate fusion method 9-21734  
 stishovite, phase changes 9-16516  
 talc, structure rel. to polytypism with mica-like minerals 9-1192  
 titanomagnetite, natural, susceptibility of fine grain assemblage rel. uniaxial compression 9-21587  
 titanomagnetite, pressure remanent magnetization and related phenomena 9-19953  
 tourmaline, crystal field spectra and dichroism 9-15171  
 tourmaline, X-ray absorpt. detection from pyroelectric props. 9-18973  
 vinogradovite, crystal structure determ. by Fourier-transformation of minimum function 9-11831  
 X-ray fluoresc. analysis with matrix mass absorpt. correction 9-21741  
 zeolite, Linde Y, selective exchange of cation sites from Mn<sup>2+</sup> e.s.r. obs. 9-1889  
 zeolite, synthetic Linde 5-A-water system, permittivity and loss factor 9-17426

**Minerals** continued

- zeolite, synthetic Linde-type-A, dielec. props. with adsorbed water 9-17427  
 zincite, Fe entry during hydrothermal growth 9-18419  
 Ag<sub>3</sub>SnFeS<sub>4</sub>, hocatite, comp., structure and reflectivity 9-19705  
 AlSiO<sub>3</sub>, kyanite, absorpt. and e microprobe obs. 9-10191  
 Ca<sub>2</sub>(Mg, Fe)<sub>2</sub>(PO<sub>4</sub>)<sub>6</sub>, stanfieldite, in meteorites, Mg:Fe ratio obs. 9-12758  
 Cu complex-sulphide-bearing, crystal chemistry 9-13593  
 Fe-Ti; oxides in basalts, composition and paleomagnetism 9-16545  
 Fe<sub>2</sub>O<sub>3</sub> (hematite), antiferromag. with weak ferromagnetism, effect of hydrostatic press. on mag. anisotropy 9-3836  
 $\alpha$ -Fe<sub>2</sub>O<sub>3</sub> polycrystalline, elastic constant rel. to pressure up to 3 Kbar 9-11902  
 K conc. determ., by radioactive analysis 9-1932  
 Na<sub>3</sub>Al<sub>6</sub>, cryolite, liq., complex ion identification 9-1017  
 NaMg<sub>2</sub>CrSiO<sub>10</sub>, krinovite, obs. in meteorites 9-18922  
 Na<sub>2</sub>ZnGeO<sub>4</sub>, synthetic D phase, crystal structure 9-13643  
 U underground leaching from water-bearing deposits 9-20081

**Minor planets** see *Planets***Mirages** see *Atmospheric optics***Mirrors**

- See also *Telescopes/astronomical*  
 circular, with linearly var. thickness, supported at central hole, deflection 9-10696  
 circular parabolic, quality of collecting systems, estimation 9-4529  
 elastic deform. of curved mirrors, dynamic relax. meas. 9-10695  
 ferroelectric ceramic, wideband interference light modulator 9-13051  
 interference reflectors, independ. variable wavelength and reflectance 9-8650  
 laser, transmissivity optimization 9-4455  
 magnetic geometries, plasma trapping and heating, non-adiabatic and stochastic mechanism 9-21076  
 manufacture, with surface of elliptic cylinder 9-274  
 mounting for internal use in laser 9-10859  
 plane inhomogeneous, laser resonator, effect on radiation ang. distrib. 9-2367  
 proximity effect on mol. fluorescence decay time 9-15838  
 sputtered multilayer, dielectric, optical properties 9-4528  
 surface non-uniformity meas. in split confocal resonator 9-8596  
 Au, use in meas. u.v. synchrotron radiation 9-10979

**Mixing** see *Heat of solution; Solubility; Solutions***Moderation** see *Neutrons and antineutrons/moderation***Moderators** see *Nuclear reactors, fission/materials***Modulation of light** see *Light/modulation***Mcire fringes** see *Interference/light***Moisture**

- See also *Atmosphere/humidity; Humidity; Permeability, mechanical*  
 polyurethane films, resistance to degradation improved by high cross-link density, chem. content effect 9-14983  
 transfer in capillary-porous substances 9-18336  
 n gauge, correction for dry bulk density 9-3065

**Molar volume** see *Density***Molecular beams**

- See also *Particle velocity analysis*  
 atom-molecule, very fast reactions, mass spectrometry 9-10334  
 Bayard-Alpert gauge sensitivity meas. appl. 9-4198  
 Detection by surface ionization 9-9396  
 electron beam scatt. 9-2856  
 falling particle molecular beam furnace, temp. corrections 9-19492  
 halogen atom-mol. exchange reactions, short-range attraction 9-10309  
 halogen-alkali reactions, Monte Carlo trajectories 9-1888  
 ionization on striking various surfaces 9-9396  
 jets, containing molecules and crystals, e diff. study 9-17025  
 macroions 9-9298  
 mass spectroscopy, background effect reduction 9-6954  
 N<sub>2</sub>-Na beam interaction, excitation energy transfer, obs. 9-9308  
 reaction kinetics 9-9307  
 reactive scattering, phenomenological anal. 9-10315  
 reactive scattering kinetics 9-7096  
 scattering, transformation relationships from c.-of-m. to lab. obs. 9-2932  
 scattering by metal surfaces, flux and speed distrib. 9-3184  
 Ar, supersonic, intermolecular binding 9-18179  
 Ar, supersonic, production and temp. distribution 9-11454  
 CO<sub>2</sub>, supersonic, intermolecular binding 9-18179  
<sup>13</sup>C<sup>16</sup>O, mag. reson. determ. spin rot. and rot. mag. moment 9-9198  
 H<sub>2</sub>, plasma prod. of 1 × 10<sup>17</sup> ions/cm<sup>2</sup> 9-7170  
 H<sup>35</sup>Cl and H<sup>37</sup>Cl, nuclear mag. hyperfine spectra 9-9206  
 HI+DI→2I+HD, reaction cross-section 9-8068  
 K+Br<sub>2</sub> r collisions, quasiclassical trajectory calc. 9-10323  
 NH<sub>3</sub>, absorptive, superradiative transient obs. 9-15909  
 O<sub>2</sub>, reaction with Na beam 9-909  
 Si film, epitaxial, chemically grown, technique for studying nucleation kinetic meas. on (100) surfaces 9-21298  
 Xe, supersonic, intermolecular binding 9-18179

**Molecular orbitals** see *Molecules/electronic structure; Orbital calculation methods***Molecular relaxation** see *Molecules/relaxation***Molecular spectra** see *Spectra/inorganic molecules; Spectra/molecules; Spectra/organic molecules and substances***Molecular structure** see *Molecules/configuration and dimensions***Molecular weight**

- distribution alterations by u.s. energy, computer analysis 9-17070  
 polymer, fractionation 9-15991  
 polymethyl acrylate in dilute solution 9-15907  
 polymethylmethacrylates, and w.s. absorpt. 9-1008  
 polystyrols, electric strength dependence 9-3704  
 K<sub>2</sub>SiO<sub>3</sub> aq. solns., cryoscopic determ. 9-982

**Molecular weight determination**

- high polymer soln., by e microscopy 9-14836  
 poly(vinyl chloride) soln., by osmometry, light scatt. and sedimentation anal. 9-14837  
 polymer fractionation, mol. wt. distrib. 9-15992

**Molecules**See also *Kinetic theory; Spectra*

- alkali metal vapour, formation and optical pumping 9-15818  
 alkali metals, potential energy functions rel. to electronegativity 9-7027

**Molecules** continued

- benzene, CH stretching anharmonicities of triplet state 9-803  
 benzene, dimerization rel. to quadrupole moment 9-4908  
 carbonyl cpds., conjugated, ioniz. pot., Pariser-Parr-Pople methods 9-9253  
 complexes in excited state, characts. 9-15844  
 conjugated systems, molecular orbital theory, book 9-13370  
 diagrammatic representation of resonances in collision theory 9-7006  
 diamagnetic, quantum theory of electric birefringence 9-745  
 diatomic, resonance light scatt. in external fields, ang. distrib. rel. to excited levels 9-750  
 diazomethyl, trapped radical vibrational absorption 9-20970  
 dimerization, effect of quadrupole moment 9-4908  
 dispersion forces, second- and third order energies 9-13273  
 electron scattering, (e, 2e), quasielastic ejection 9-14669  
 electron spin polarization from unpolarized targets scatt. at low-energy, review 9-18148  
 electronic functions, independ. of translational and rot. co-ords., rel. to nuclear motions 9-739  
 electronic transitions in near adiabatic collisions 9-4979  
 ethylphenylphosphine, geminal coupling const., n.m.r. anal. 9-13546  
 fluoromethane in liq. crystal solvent, NMR spectra obs. 9-7067  
 gas, vel. determ. by gas effusion, intermediate laboratory ext. 9-12823  
 halogen-substituted methanes, 2nd virial coeff. determ. by gas balance method 9-7070  
 high polymer molecules, mechanical entanglements 9-19488  
 ion-molecular mixed system, statistical theory, group decomposition 9-20360  
 Jahn-Teller induced optical transitions 9-7928  
 luminescence theory, book 9-6997  
 methacrylonitrile, photosensitized dimerization obs. 9-16501  
 methane; mechanical, thermodynamic and transport props., 0-300°K bibliography 9-19470  
 optical activity, rel. to dissymmetry 9-9167  
 orientational in liqs., from Rayleigh scatt. 9-1009  
 phosphorescent, short lifetime, EPR in vitreous solid solution 9-8007  
 photoionization cross section calc. by AMO LCAO approx. 9-9165  
 photon absorption effective cross-sections, empirical formulation 9-16998  
 polyatomic, radiative and nonradiative transitions between electronic states 9-9189  
 polychloro-cyclobutanes, NQR study of <sup>35</sup>Cl 9-15906  
 reson. scatt. of electrons by mol., attenuation of ang. distrib. coeffs., rot. effects 9-4903  
 resonant scatt. of electrons, ang. distrib. 9-4895  
 saturated, inductive effect, var.-perturbation theory, geminal method 9-11443  
 spin-coupled wave function Hamiltonians 9-6952  
 structural group anal. from i.r. spectra, using Boolean algebra and computers 9-6998  
 symmetry and optical inactivity 9-19418  
 theory, 1900-66, review 9-9598  
 thermodynamic functions, valence-force calc. 9-4912  
 two centre problem, quantum numbers and commutative operators 9-15842  
 vinyl chloride, wavefunction calc., approx., by semiempirical  $\Pi$ -electron methods 9-13393  
 CN<sup>-</sup> in alkali halides, electric field induced dichroism 9-3857  
 CO<sub>2</sub>, dimerization rel. to quadrupole moment 9-4908  
 CO<sub>2</sub>, spectra, calc. rel. obs. 9-4927  
 Cl<sub>2</sub>, radiative recombination spectrum studied 9-20891  
 DNCO, extreme centrifugal distortion, interpret. rel. to Q-branch freqs. 9-13356  
 DNCS, extreme centrifugal distortion, interpret. rel. to Q-branch freqs. 9-13356  
 H<sub>2</sub>, e.m. interaction theory, nuclear shielding const. calc. 9-7025  
 HNCO, extreme centrifugal distortion, interpret. rel. to Q-branch freqs. 9-13356  
 HNCS, extreme centrifugal distortion, interpret. rel. to Q-branch freqs. 9-13356  
 H<sub>2</sub>O spectra, calc. rel. obs. 9-4927  
 LiH e.m. interaction theory, nuclear shielding const. calc. 9-7025  
 N by scatt. on He atoms, resonances in cross section obs. 9-7034  
 N<sub>2</sub>, D<sub>2</sub> reactions, product energy and ang. distrib. meas., 25-135 eV 9-7035  
 N<sub>2</sub>, D<sub>2</sub> reactions, product energy and ang. distrib. meas., 25-135 eV 9-7035  
 N<sub>2</sub>, dimerization rel. to quadrupole moment 9-4908  
 N<sub>2</sub><sup>+</sup>, H<sub>2</sub> reactions, product energy and ang. distrib. meas., 25-135 eV 9-7035  
 N<sub>2</sub><sup>+</sup>, mass-spectrometric identification in h.f. discharge 9-9223
- configuration and dimensions**  
 See also *Chemical structure; Crystal structure, atomic*  
 benzenes, ortho-disubstituted inter-proton distances 9-7280  
 benzophenones, protonated, isomer obs. and config. in NMR spectrum 9-20953  
 book, specialized topics 9-14903  
 carboxylic acid dimer, planarity 9-7018  
 cation with inert-gas shell, empirical formula for radius 9-19482  
 conformation of minimum potential energy, valence-force calc. 9-4912  
 3 $\beta$ ,17 $\alpha$ -dihydroxy-16 $\beta$ -bromo-5 $\alpha$ -pregnan-11,20-dione, and mol. structure 9-13654  
 electron diffraction camera adapted for study 9-11452  
 geometry and barriers to interval rot. in Hartree-Fock theory 9-2855  
 2,2,4,4,6,6-hexaphenylcyclotriphenylphosphazatriene and crystal structure 9-13657  
 INDO calc. of molec. equilib. geometries 9-15843  
 methods of structure study, book 9-19424  
 NMR in liquid crystals as method 9-18171  
 orbital exponents and wave function goodness calc. 9-7008  
 Cu II complexes, mol., Jahn-Teller eff. 9-18181  
 MgF first excited electronic state, calc. and empirical arguments using matrix Hartree-Fock eqns. 9-4930
- configuration and dimensions, inorganic**  
 bond distance, force const., dipole moments calc. from semi-empirical model 9-9193  
 cyclohexane, configuration from X-ray obs. 9-17055  
 cyclooctane, configuration from X-ray obs. 9-17055  
 symmetric triatomic mol., geometry 9-7031  
 AICN, and possible isomers 9-753



**Molecules continued****configuration and dimensions, inorganic continued**

- AlCl<sub>3</sub>.N(CH<sub>3</sub>)<sub>3</sub>, and mol. structure 9-13625  
 BNH<sub>6</sub>, umbrella vs. bridged geometries 9-756  
 BeH<sub>2</sub>, LCAO-MO-SCF calc. 9-15849  
 CO<sub>2</sub>, Geometry, MO calc. 9-13347  
 Cd complex, bis(hydrazinecarboxylato-N',O) cadmium monohydrate, and crystal structure 9-13630  
 Co complex, bis(1,2,3,4-tetrachlorobenzene-5,6-dithiolato)cobaltate 9-17266  
 CsOH and CsOD 9-761  
 Cu complex, pyridine- $\beta$ -alaninatoaquocopper (II), dihydrate, and crystal structure 9-7437  
 Cu(II) complexes, bis(thiosemicarbazone) Cu(II) and others 9-2861  
 GeH<sub>3</sub>NCO, Ge-N-C angle determ. 9-19430  
 H<sub>2</sub>S<sub>2</sub> and D<sub>2</sub>S<sub>2</sub> 9-9211  
 He<sub>2</sub><sup>+</sup> ion, orbital exponents and wave function goodness calc. 9-7008  
 Mn(II) complexes, e.s.r. obs. 9-18185  
 NCl<sub>3</sub>, i.r. 9-9222  
 NH<sub>3</sub> and ND<sub>3</sub>, electron diffraction determ. 9-7032  
 NiO, geometry, MO calc. 9-7031  
 Ni complex, bis(thioacetamide) nickel (II) thiocyanate, and crystal structure 9-3301  
 Ni complex, diaquobis-(2,2'-biimidazole)nickel(II)dinitrate, and crystal structure 9-21319  
 Ni complex, tetra (thiourea) nickel (II) thiosulphate monohydrate, and crystal structure 9-14920  
 Rh complex, RhCl(C<sub>6</sub>H<sub>6</sub>)<sub>2</sub> and crystal structure 9-13647  
 S<sub>2</sub>Br<sub>2</sub>, Raman and far-i.r. data 9-9234  
 SeO<sub>2</sub>, molecular structure 9-19447  
 Si complex, tetrafluorobispyridinesilicon (IV), and crystal structure 9-13648  
 UNO, gaseous, mass spectrometric obs. 9-790  
 XeO<sub>2</sub>F<sub>2</sub> 9-791

**configuration and dimensions, macromolecules**

- $\alpha$ -methylpentafluorostyrene-styrene copolymer, n.m.r. obs. 9-12518  
 $\alpha$ ,  $\beta$ -trifluorostyrene dimers, n.m.r. obs. 9-12518  
 chain structure, polymer mech. relax. process., quantitative rules 9-14731  
 dilute soln., elec. birefringence, orientation factor tables 9-9541  
 D.N.A., alkali denaturation by p capture 9-8300  
 DNA, double-stranded, possible co-operative phase for electrons 9-7091  
 DNA, excited electronic states 9-18223  
 DNA, sodium salt, elec. conductivity 9-1459  
 DNA periodic models, deform. pot. approximation for conductivity 9-19485  
 electronic state calc. method 9-4973  
 finite chain molecules, configurational distributions 9-17065  
 gelatin, photographic props., bibliography 9-6564  
 helical, helix-coil transitions using Ising theory 9-19486  
 Kirkwood-Riseman theory of intrinsic viscosities, numerical soln. of relevant eqn. 9-16656  
 light scatt. by coiled mols., asymptotic behaviour 9-17209  
 light scatt. by flexible mols., excluded vol. effect 9-17208  
 light scatt. from flexible coils, spectral distrib. 9-3101  
 light scatt. from optically anisotropic mols. 9-1011  
 macroions of rigid core, thermodynamic functions 9-2922  
 $\alpha$ -methylpentafluorostyrene-p methyl- $\alpha$ ,  $\beta$ ,  $\beta$ -trifluorostyrene-styrene copolymer, n.m.r. obs. 9-12518  
 nucleic acids, submolecular structure, quantum chemistry 9-14728  
 nucleic acids, submolecular structure, quantum chemistry 9-14728  
 Overhauser phase and bond alternation, carbon chains 9-4972  
 pentafluorostyrene-styrene copolymer, n.m.r. obs. 9-12518  
 poly(vinyl chloride) soln., dimens. determ. by viscometry 9-14837  
 poly-L-aspartic acid, helical struct. and conformational anal. 9-4974  
 poly-L-glutamic acid, helical struct. and conformational anal. 9-4974  
 polyamino acids, helix-coil transition molecular theory 9-18225  
 polychloroprene uniaxially stretched, length of statistical segment calc. 9-19781  
 polyesters, aliphatic 9-9301  
 polyethylene, orientation rel. to drawing and annealing 9-19738  
 polymethylene liquids, chain shortening 9-13511  
 RNA bacterial transfer, crystallization 9-16059  
 rodlike, viscosity in soln., theory 9-989  
 rubber, uniaxially stretched, length of statistical segment calc. 9-19781  
 self-interacting linear chains, Monte Carlo calc. 9-833  
 sodium humate solns., structure determ. from small-angle X-ray scatt. 9-9480  
 suspension mixture, mass separation method, centrifugal field tests 9-7285  
 suspension mixture, mass separation method, gravitational tests 9-9564  
 suspension mixture, mass separation method, theory 9-7284  
 systems, applic. of correlations in vib. spectra of hydrocarbons 9-20965  
 translational and rotational frictional coefficients calc. 9-17066  
 wool, air-dried, alkali-treated, radii of gyration, low-angle X-ray meas. 9-13400  
 X-ray small angle scatt. investigation of segment shape 9-17064  
 Na polyethylenesulphonate solns., transient elec. birefringence 9-16004  
 DNA, statistical mech., matrix method 9-8432  
 DNA, excitation energy of low-lying collective excited state for different periodic models 9-12064  
 solutions, Kerr consts., table 9-16004

**configuration and dimensions, organic**

- cis-, trans- cyano-1-dimethyl-1,2 oxiranes, n.m.r. determ. 9-13380  
 15,15'-dehydrocanthaxanthin, from crystal structure 9-11863  
 2,2'-dichlorotrimethylene sulphite, and crystal structure 9-19732  
 L(+)-dihydrodesoxystreptose, from NMR and mass spectra 9-18203  
 2-dimethylsulfuranylidenealmononitrile, and crystal structure 9-13655  
 $\alpha$ -methylpentafluorostyrene, n.m.r. obs. 9-12518  
 n-alkane mols., calc. of mean optical anisotropy, in liquid state 9-21208  
 alkanes, acentric factor from critical press and temp, and vapour press 9-18381  
 alkanes, linear, dimensions calc. by computer 9-17046  
 arsenomethane, pseudo-rotation, from n.m.r. data 9-20949  
 arsenoperfluoromethane, pseudo-rotation, from n.m.r. data 9-20949  
 L-aspartic acid, and crystal structure 9-7458  
 azobenzene-2-sulphenyl cyanide, and crystal structure 9-11861  
 benzene, photoexcited triplet-state in benzene crystal. 9-14118  
 benzophenonimines, methyl substituted, config. obs. from proton NMR 9-14705  
 bicyclo (1.1.1) pentane derivative n.m./r. correl. with cryst. and molec. struct. 9-15205

**Molecules continued****configuration and dimensions, organic continued**

- biphenyl, geom. struct. in gas and solid phases 9-9250  
 bond lengths of S, C, O and N rel. to energies 9-798  
 1,2-bromofluoroethane, stable configs. in liq. and vapour phases 9-14706  
 calcium tartrate tetrahydrate, and crystal structure 9-19737  
 canthaxanthin, and crystal structure 9-9686  
 cembrene, and crystal structure 9-13650  
 1-chloro-1,1-difluoroethane 9-13377  
 1,2-chlorofluoroethane, stable configs. in liq. and vapour phases 9-14706  
 coronene negative ion, ground state, influence of ionic assoc. 9-13378  
 cyclobutane cpds., substituent effects on conformation, n.m.r. meas. 9-13544  
 cyclobutanone, ring struct. 9-805  
 cyclohexanes, monohalosubstituted, conform. equilib. and vibratory spectra 9-9262  
 cyclohexene 9-9261  
 cyclophanes, valence-force calc. 9-4912  
 L-cystinediamide dihydrochloride, and crystal structure 9-19731  
 D-deoxyribose, dihedral angles from nucleotide phosphates n.m.r. spectra 9-18220  
 4,4'-diamino 3,3'-dichlorobiphenyl, and crystal structure and mol. structure 9-9687  
 trans-1,4-diiodocyclohexane, rotational isomerism and vibr. spectra 9-17482  
 dimethyl diselenide 9-9264  
 2,6-dimethyl-1,4-phenylpyridine, bond lengths and angles from rot. spectra 9-9273  
 dimethyl-acetylene in nematic solvents, n.m.r. 9-13545  
 dimethylamine, bond lengths, C-N-C angles, and struct. 9-18210  
 dimethyldiazirine 9-9263  
 2,2'-di(1,4-naphthoquinone), and crystal structure 9-13656  
 dioxynolionucleic acid (DNA), X-ray diffraction study 9-7093  
 ethane positive ions, geometries 9-756  
 ethene, and ethene-d<sub>4</sub> struct. deduced from vibronic spectra 9-813  
 hydrazinium hydrazinedithiocarbonylate, and crystal structure 9-13658  
 iminoxy radicals formed from tetranitromethane and 1,3-dicarbonyl cpds., structure from e.s.r. 9-20987  
 1-isopropyl-4,8,12-trimethyl-2,4,7,11-cyclotetradecatetraene, crystal and mol. struct. 9-13650  
 K-D-mannitol and crystal structure 9-19734  
 Meisenheimer salts, 2,4,6-trinitrophenolate-caesium(potassium) ethoxide complexes, and crystal structure 9-7467  
 methanesulfonic acid, and crystal structure 9-14929  
 6-methoxy-8-nitro-5(1H)-quinoline, and crystal structure 9-13660  
 with methyl groups, hindrance pots. 9-17058  
 N-methylbenzophenonimines, methyl substituted, config. obs. from proton NMR 9-14705  
 methylglyoxal bisguanyldiazirone dihydrochloride monohydrate, and crystal structure 9-3319  
 2-methylnaphthalene-1,4-diol, and crystal structure 9-21324  
 1-methylthymine H-addition radical, conformation 9-828  
 3-nitroperchlorylbenzene, and crystal structure 9-3312  
 nitrosomethane 9-817  
 ophiobolin methoxybromide 9-7466  
 perfluorodimethyl-acetylene in nematic solvents, n.m.r. 9-13545  
 9-phenylxanthyl free radical, spatial config. 9-13398  
 phthalocyanine, metal-free, polymorph, spectroscopic characterization 9-19736  
 potassium allantoate, and crystal structure 9-11859  
 rare earth ethyl sulphates, normal coordinates, tables 9-795  
 rauvioxine, absolute config. 9-16086  
 D-ribose, dihedral angles from nucleotide phosphates n.m.r. spectra 9-18220  
 sodium D-tartrate dihydrate and crystal structure 9-7464  
 strontium tartrate trihydrate, and crystal structure 9-19737  
 structure loss, spontaneous and radiation-induced, comparison 9-8302  
 terpenoid, C<sub>25</sub>, ophiobolin methoxybromide 9-7466  
 thioacetanilide S-oxide, and crystal structure 9-13662  
 thiosemicarbazide, and crystal structure 9-13663  
 thunbergene, and crystal structure 9-13650  
 thymine photodimer E, and crystal structure 9-14933  
 1,2,4-triazole, and crystal structure at -160°C refinement 9-13665  
 trifluoromethylfluorophosphorane 9-2916  
 trimelic acid, and crystal structure 9-13664  
 trimethylamine bond lengths, C-N-C angles, and struct. 9-18210  
 2,4,6-trinitrophenolate-caesium (potassium) ethoxide complexes, (Meisenheimer salts), and crystal structure 9-7467  
 urea, interatomic distances and thermal motion 9-13391  
 C<sub>2</sub>H<sub>5</sub>O<sup>+</sup> ion in mass spectra of Z-alkanols, struct. 9-15885  
 CF<sub>3</sub>CCl<sub>3</sub> struct. from microwave spectrum 9-15888  
 CH<sub>3</sub><sup>+</sup> ion, CNDO study of geometry 9-19461

**dissociation***See also Heat of dissociation*

- n-butane, propane, superexcited, decomposition primary modes 9-21723  
 n-butane for bombardment by ionized atoms and molecules 9-7080  
 diatomic, homopolar, collisional, proper choice of final state wave function 9-9288  
 diatomic, thermal dissociation at high temp., gas-kinetic theory 9-19479  
 dissociative attachment and recomb., theory 9-4967  
 iodoheptafluorobutane, effect of laser emission on formation of I<sub>2</sub> 9-15902  
 kinetics of recomb.-dissoc., nonequilibrium effects 9-2919  
 low-kinetic energy collision-induced dissociation 9-9406  
 molar ratio curves, new plotting method 9-17506  
 organic gases, in low-pressure glow discharge, expt. study 9-11630  
 pentane isomer fragments after electron impact, kinetic energy 9-7087  
 photochemical reactions, theory 9-6018  
 photodissociation primary products, energy distrib. in vibr. excitation 9-10350  
 Propane, superexcited, decomposition primary modes 9-21723  
 radiation induced, velocity distrib. func. of products 9-4966  
 Br<sub>2</sub>, shock heated in Ar, rate determ. by two-body emission 9-19480  
 Br<sub>2</sub>, shock heated 9-13395  
 Br<sub>2</sub>, shock heated in Ar, rate determ. by two-body emission 9-13394  
 CH<sub>3</sub>, interstellar, mechanism 9-18880  
 CO by electronic collision in solar photosphere 9-17662  
 CO<sub>2</sub>, electron attachment, O<sup>-</sup> formation and calc. of O electron affinity 9-11614  
 CO<sub>2</sub>, MO calc. 9-13347  
 Cl<sub>2</sub>, radiative recomb. in shockwaves 9-9289

**Molecules continued****dissociation continued**

- CsBr, invented population 9-822  
 $D_2^+$  9-2920  
 $H_2$ , interstellar, mechanism 9-18880  
 $H_2^+$  ions, collision-induced, 0.7→2 keV, non-vertical transitions 9-15901  
 $H_2$ , rates behind shock wave 9-1902  
 $H_2$  and  $D_2$ , in collisions with slow  $K^+$  9-2937  
 $H_2^+$ , by collisions with Ar,  $H_2$  and Xe, energy, distrib. of prod. protons 9-4968  
 $HD^+$ , in collision with inert gases 9-7077  
 $HN_3$ , photodissoc. in vac. u.v. 9-7078  
 $H(2S)$  atom production by mol. dissociative excitation 9-14725  
 $He_2$ , excitation of band spectrum in discharge and recombination 9-5082  
 $I-B(\Pi_{out})$ , direct predissociation 9-9291  
 $N_2$ , in charge-transfer collisions with inert-gas ions 9-15957  
 $N_2$ , in weak r.f. discharge 9-9293  
 $N_2$ , vibr.-dissoc. relax. behind shock wave 9-13483  
 $N_2F_4$ , kinetics of thermal dissoc. in shock waves 9-1903  
 $NOCl$  and  $NO_2$  in vacuum u.v., photodissoc. 9-16492  
 $N_2^+ = N_2^+ + N_2$  equilb.: const. and rates rel. to elec. field strength and press., 0.63-1.24 torr. 9-4969  
 $O_2$ , dissociative recomb., quantum mech. calc. 9-5074  
 $O_2$ , electron collision, 0-200eV, vac.u.v. emission 9-17040  
 $O_2$ , ion-ion dissociative recomb. calc. 9-5075  
 $O_2$ , vibr., dissoc. relax. behind shock wave 9-13483  
 $OD$  chemiluminescent, breaking-off pts. on limiting curve 9-18221  
 $OH$  chemiluminescent, breaking-off pts. on limiting curve 9-18221  
 $UC$ , thermal dissoc. 9-1897  
 $XeF_2$ , by photon impact 9-11617

**dissociation energies**

- alkaline earth hydroxides, gaseous, in fuel-rich  $H_2 + O_2 + N_2$  flames 9-17517  
bond-breaking energy connection from Monte-Carlo calcs. 9-7076  
group III-VI transition- metal nitrides, diatomic 9-824  
Monte-Carlo calcs, connection with bond-breaking energies 9-7076  
organic cpds., C, S, O and N bonds 9-798  
 $BeH_2$ , LCAO-MO-SCF calc. 9-15849  
 $BeO$ , computed values 9-7015  
 $BiBr$  and states from emission spectra 9-2858  
 $CH$  halides, photodissociation 9-17062  
 $C_2N_2$ , photodissociation 9-17062  
 $CaO$ , computed values 9-7015  
 $D_2$ , ground-state, obs. rel. to long-range interaction theory 9-9157  
 $GaP$ , gaseous 9-11504  
 $GeCo$  9-9290  
 $GeCr$  9-9290  
 $GeCu$  9-9290  
 $GeFe$  9-9290  
 $H_2$ , ground-state, obs. rel. to long-range interaction theory 9-9157  
 $HCN$ , photodissociation 9-17062  
 $HCl$ , photoionization efficiency curves, mass spectrometric study, ionization threshold to 600 Å 9-3004  
 $HD$ , ground-state, obs. rel. to long-range interaction theory 9-9157  
 $HeH^+$  and other inert-gas-H cpds. 9-7132  
 $InS$  mass spectrometric determ., also other  $In$  sulphides 9-19481  
 $InSe$ , mass spectrometric determ., also other  $In$  selenides 9-19481  
 $InTe$  mass spectrometric determ., also other  $In$  tellurides 9-19481  
 $IrC$ , gaseous mass spect. determination 9-14726  
 $K_2$ , determ. from heat capacity obs. 9-17161  
 $KF$ , MO calc 9-2872  
 $Li_2$ , diatomic-in-mols. theory of stable mol. 9-9218  
 $MgO$ , computed values 9-7015  
 $Mn_2$  9-9292  
 $PbBr$ , from emission spectrum up to 6100 Å 9-4936  
 $PbCl_2 + AlCl_3$  (A=Na, K, Rb or Cs) electron impact 9-9408  
 $PtB$ , gaseous, mass spect. determination 9-14726  
 $RuC$ , gaseous, mass spect. determination 9-14726  
 $SeD$  diffuse spectra, 3000-3250 Å 9-18193  
 $SeH$  diffuse spectra, 3000-3250 Å 9-18193  
 $SrO$ , computed values 9-7015  
 $ThN$  9-824  
 $VO$  potential energy curves for 3 known states, transitions predicted 9-7079  
 $ZrN$  9-823

**electronic structure****See also Bonds**

- $AB_2$ -type, potential energy surfaces, existence of double minima 9-19423  
atomic electron populations, INDO-MO vs. SCF calc. 9-17020  
bare-nucleus and screened-nucleus perturbation theory 9-20930  
benzyl radical, doublet electronic states 9-9247  
bond orbitals, fully localized, and perturbation theory in correl. energy calc. 9-13332  
bond orders in completely filled MO shells 9-9186  
charge distrib. and force const. 9-2846  
conjugated polymers, LCAO-MO treatment 9-832  
correlated wavefunctions, symmetry props. 9-6950  
correlation energy calc. using fully localized bond orbitals and perturbation theory 9-13332  
 $d$ -orbital energies in weak and strong ligand fields, calc. 9-18167  
diamagnetism of mols. with unpaired electrons 9-20866  
diatomic, electronic energy for small  $R$  9-2854  
diatomic, excited levels, characts. from resonance light scatt. in external fields 9-750  
diatomic homonuclear, potential energy, bond-charge model 9-2853  
diatomic two-electron mol., large  $Z$  asymptotic wavefunction 9-17015  
distinguishable electron method calc. 9-8412  
doubly occupied  $MO$ 's atomic orbital energy matching 9-9180  
eigenvalues of self-adjoint diff. operators, iterative procedure of calc. 9-4928  
electron correlation calcs. 9-4819  
electron density, semiempirical determ. in diatomic mols. 9-13336  
electron density semi-empirical determ., Hellman-Feynman type constraint 9-18170  
electron density semi-empirical determ. differential eqn. for scale factor 9-13337  
electron density semiempirical determ. avoiding occupation no. difficulty 9-18169  
electron-in-box theory of metal-atom clusters 9-748  
electrostatic potential of point charge systems, potential expansion symmetry 9-4910

**Molecules continued****electronic structure continued**

- excited states, electr. symmetries from polarized Raman spectra 9-17021  
excited triplet→singlet intersystem crossing, quantum yields 9-17022  
formulas for molec. integrals over Hermite-Gaussian functions 9-17018  
Gaussian wavefunctions in oscillator strength calc. 9-9187  
Hartree-Fock eqn. for simple open-shell case, soln. and stability conditions 9-20917  
Hartree-Fock geometry and barriers to internal rot. 9-2855  
Hartree-Fock  $\phi_0$ , modified perturbation theory 9-6949  
intergroup config. interaction and nuclear spin-spin coupling 9-9190  
isoelectronic systems, scaling of SCF wavefunctions 9-749  
isotope shift, Born-Oppenheimer approx. breakdown 9-18168  
linear molecules, multiplet states, population analysis applic. to spin-orbit coupling constants calc. 9-15845  
localized orbitals, semiempirical determ. 9-741  
multipolar mol., opt. second harmonic generation, d.c. elec. field-induced 9-13038  
nuclear corrections to expectation values, zero-point vibr-effects 9-9209  
orbitals, localized, for arbitrary wave functions 9-13329  
Pariser-Parr-Pople model, derivation and anal. 9-743  
perturbation theory, self-consistent, finite methods 9-17016  
polar gas, screened, elastic e scatt., eff. of exponential attenuating factor 9-15846  
polar mol., thermal e scatt., mean cross-sections and drift vel. data 9-13335  
polarizability of excited mols. from solvent shift 9-14683  
polyatomic, 'multiple-scatt.' model, inclusion of many-body effects 9-14684  
polyatomic many-electron systems, determ. of allowed multiplets 9-13338  
use of pseudopotentials, validity 9-13360  
quantum number assignment 9-9181  
 $\pi$ -electron energies, localized and delocalized, in MO and VB theory 9-9188  
radiationless transitions of isolated mol. 9-742  
resonance tunnelling reactions 9-6001  
Schrödinger eqn. for any mol. pot., numerical soln. 9-4911  
Schrödinger eqn. for diatomic system, separation of rot. coords. 9-14682  
segmental systems, electronic state calc. method 9-4973  
single-electron syst., molecular transitions calc., applic. of Coulomb approx. 9-13333  
singlet-triplet transitions, spin-orbit-interaction effects 9-17023  
spin-orbit coupling constants, Hartree-Fock calc. for diatomic mols. 9-13328  
statistical two-particle density matrix 9-9112  
ten-electron mols. of type  $MH_x$ , energies, perturbation calc. 9-11450  
three-centre two-electron systems, electron-density and energy anal. 9-17017  
valence electron approximation, theory 9-17035  
wave functions, accurate, without exchange terms, perturbation calc. 9-4832  
 $^{2\Sigma}$ - $^1\Sigma$  transitions, rotational line intensities for linear mols. 9-2880  
 $BeH$  spin orbit coupling constants, Hartree-Fock calc. 9-13328  
 $CH$  spin-orbit coupling constants, Hartree-Fock calc. 9-13328  
 $Co$  II complexes, mol., Jahn-Teller eff. 9-18181  
 $H_2O$  allowed molecular multiplets set up from prescribed atomic states, general method 9-14679  
 $H_2$ , molecular transitions calc., applic. of Coulomb approx. 9-13333  
 $H_2^+$ , equilateral triangle config. localized orbitals for arbitrary wave functions 9-13329  
 $HeH_2^+$ , ground-state energy, perturbation calc. 9-2870  
 $He$  electronic moment depend. on internuclear separation, calc. of Halevi's correction 9-19437  
 $N$  Is electron binding energies correl. with CNDO charges 9-11451  
 $NH(XYZ)$ , where  $X,Y,Z=H$  or  $R$ , anomalous magneto-optical effect 9-780  
 $OH$  spin-orbit coupling constants, Hartree-Fock calc. 9-13328

**electronic structure, inorganic**

- alkali metals, energy level calcs. from force consts. and electronegativity 9-7027  
borazine, orbital energies and charge densities 9-2857  
electronic energies calc. 9-2854  
group IIIA monohalides, potential energy curves 9-20919  
polyethylene, LCAO band calc. for ideal chain 9-2928  
Rydberg and scatt. states 9-766  
 $SCO^+ X^2\Pi$  and  $A^2\Pi$  states, spin-orbit coupling constants calc. 9-15845  
transition metal carbonyls, electronic structure, SCCC-MO calc. method 9-19448  
transition metal complexes, from mol. orbital theory interpretation of X-ray K absorpt. spectral data 9-14065  
transition-metal dichlorides 9-15858  
transition-metal tetrahalide complexes, charge-transfer spectra 9-1764  
water from photoelectron spectroscopy 9-17895  
water vapour, electron collision freq. 9-13352  
 $Al(III)$  halides in  $N,N$ -dimethylformamide solutions, outer-sphere ion-pair formation obs. by NMR 9-19645  
 $AsN$ , rotation structure of band rel. to new transition 9-7011  
 $B_2N_2H_4$ ,  $\sigma$ - and  $\pi$ -electron system, CNDO/2 calc. 9-20922  
 $BH$ , electronic energies calc. 9-2854  
 $BH$ , pair correl. energies and unitary transf., SCF orbital depend. 9-19427  
 $BNH_2$ , SCF and CI calc. of geometries 9-756  
 $BeH$ , theoretical calc. 9-757  
 $BeH_2$ , LCAO-MO-SCF calc. 9-15849  
 $BeO$ , computed ground state props. in orbital approx. 9-7015  
 $BiBr$  bands from emission spectra 9-2858  
 $BiF$ , from rot. analysis of 3050-3250 Å syst. 9-4919  
 $C_2$  electronic transition moment of Swan bands determ. in  $CO_2$ -Ar shock tube 9-19429  
 $C_2$  electronic transition moment of Swan bands determ. in  $CO_2$ -Ar shock tube 9-19429  
 $C_2$ , isoelectronic series, charge distrib. and binding 9-2876  
 $CH$ , valence excited states and transition probabilities 9-2875  
 $CO$ , B-X, C-X and possible  $J^2-X^1$  transitions, from u.v. absorpt. spectra 9-11456  
 $CO$ , mag. props., Hartree-Fock calc. 9-2859  
 $CO^+$ ,  $X^2\Pi$  and  $A^2\Pi$  states, spin-orbit coupling constants calc. 9-15845  
 $CO^+$ , A-X transition, electr. transition moment integrals eval., r-centroid approx. limits 9-20925  
 $CO$  first ioniz., electr. transition moment integrals eval., r-centroid approx. limits 9-20925



## Molecules continued

## electronic structure, inorganic continued

- CO<sub>2</sub>, MO calc. and geometry 9-13347  
 CaO, computed ground state props. in orbital approx. 9-7015  
 ClO<sub>3</sub><sup>-</sup>, from X-ray spectra 9-7019  
 ClO<sub>4</sub><sup>-</sup>, from X-ray spectra 9-7019  
 Co complex, [CoX<sub>2</sub>.2L] and [CoL<sub>4</sub>] (ClO<sub>4</sub>)<sub>2</sub> (X=Cl, Br, I and L=2-thiazolidine) i.r. and electronic spectral studies 9-20926  
 Co(II) complexes, electron delocalization and spin density distrib. 9-13349  
 Cs<sub>2</sub>, energy levels 9-4923  
 DF<sub>2</sub><sup>-</sup>, potential energy constants 9-4838  
 D<sub>2</sub>O from photoelectron spectroscopy 9-17895  
 H<sub>2</sub>, Rydberg and scatt. states 9-766  
 H<sub>2</sub>O, mag. susceptibility calc. 9-744  
 H<sub>2</sub>O<sub>2</sub>, mag. susceptibility calc. 9-744  
 H<sub>3</sub>, energy surface, superposition of configs. calc. 9-768  
 H<sub>4</sub>, ground and excited states, diatomics-in-mols. calc. 9-770  
 H<sub>2</sub>, lowest triplet states, excitation by low-energy electrons 9-17032  
 H<sub>2</sub><sup>+</sup>, energy expectation values and integral Hellmann-Feynman theorem 9-2867  
 H<sub>2</sub><sup>+</sup>, Green function calc., 2nd-order perturbation 9-9106  
 H<sub>2</sub><sup>+</sup>, config.-interaction calc., expanded basis 9-9210  
 H<sub>2</sub><sup>+</sup>, natural orbital, electron-population, and energy anal. 9-17017  
 H<sub>2</sub><sup>+</sup>, wave function expansion, overlap matrix elements, related integrals, correl. functions 9-11462  
 HF<sup>+</sup> mol. X<sup>2</sup>Π<sub>g</sub>, A<sup>2</sup>Σ<sup>+</sup> Hartree-Fock level calc. 9-19434  
 HF chemical bond, minimal basis SCGF calc. 9-13353  
 HF<sub>2</sub><sup>-</sup>, potential energy constants 9-4838  
 H<sub>2</sub>O, approx. Hartree-Fock wavefunctions, one-electron props. 9-9208  
 H<sub>2</sub>O, nuclear corrections to expectation values, zero-point vibr. effects 9-9209  
 He<sub>2</sub>, bare-nucleus and screened-nucleus perturbation theory 9-20930  
 He<sub>2</sub>, (Σ<sub>g</sub><sup>+</sup> and Σ<sub>u</sub><sup>+</sup> states, first six levels 9-4928  
 HeH<sup>+</sup>, bare-nucleus perturbation calc. 9-9214  
 HeH<sup>2+</sup> and HeH<sup>+</sup>, one-centre MO's with variable origin 9-13359  
 K<sub>2</sub>, from laser-induced fluoresc. spectra 9-15856  
 KF, MO calc., and molec. props. 9-2872  
 Li<sub>2</sub>, use of pseudopotentials, validity 9-13360  
 Li<sub>2</sub>, diatomics-in-mols. theory of stable mol. 9-9218  
 LiH, correl. energy calc. and unitary transforms. 9-773  
 LiH, low-lying states, theoretical calc. 9-9219  
 LiH, use of pseudopotentials, validity 9-13360  
 LiH, valence electron calc. 9-17035  
 MgF, r-centroids for B-X and C-X systems 9-11466  
 MgF first excited state, configurations 9-4930  
 MgO, computed ground state props. in orbital approx. 9-7015  
 Mo(IV)Cl<sub>6</sub>, electronic spectra 9-7982  
 N<sub>2</sub>, electronic transition moment of first positive system using published data 9-19438  
 N<sub>2</sub>, second positive system, laser transitions in 0-0 band 9-19422  
 N<sub>2</sub>O, transitions and states rel. to u.v. absorpt. spectrum 9-15863  
 N<sub>2</sub>, C<sup>2</sup>Π<sub>g</sub>-B<sup>2</sup>Π<sub>g</sub>(0,0) simulated transitions, high resolution study 9-2873  
 N<sub>2</sub>, isoelectronic series, charge distrib. and binding 9-2876  
 NH, valence excited states and transition probabilities 9-2875  
 NH<sub>3</sub>, mag. susceptibility calc. 9-744  
 NH singlet triplet intercombination separation, calc. 9-2874  
 NH<sub>3</sub>, non-empirical SCF LCAO MO study 9-13364  
 NO, radiative lifetime of a<sup>2</sup>Π state 9-779  
 NO<sub>2</sub>, nonempirical SCF calc. 9-776  
 Nd<sup>3+</sup> complexes, hypersensitivity, environmental effects on f-f transitions 9-782  
 Ni, complexes with subst. phosphine ligands 9-11470  
 Ni(II) complexes, electron delocalization and spin density distrib. 9-13349  
 O<sub>2</sub>, forbidden electronic transitions 9-9228  
 OH<sup>+</sup> singlet-triplet intercombination separation, calc. 9-2874  
 PH singlet-triplet intercombination separation, calc. 9-2874  
 SH<sup>+</sup> singlet-triplet intercombination separation, calc. 9-2874  
 SO<sub>2</sub>, radiationless transitions 9-2881  
 Sn cpds., correl. with Mossbauer isomer shifts 9-11475  
 SnCl<sub>4</sub>, A<sup>2</sup>Σ<sup>+</sup>-X<sup>2</sup>Π<sub>1/2</sub> transition 9-789  
 SrO, computed ground state props. in orbital approx. 9-7015  
 VOF<sub>3</sub><sup>-</sup> ion complexes 9-14114

## electronic structure, organic

- 4-fluoro-3-chloro aniline, six upper and one ground state ident. 9-814  
 acephaladylene, LCAO calc. 9-800  
 alkoxybenzene radical anions 9-7085  
 allyl radical and ions, e wave function construction method 9-9267  
 18 annulene, spectrum 9-19457  
 anthracene, singlet excited states polarizability, obs. 9-15879  
 aromatic, heteroaromatic mols., perturbations between electronic states 9-2894  
 aromatic, polarizability of excited mols. from solvent shift 9-14683  
 aromatic, triplet-singlet transitions 9-15871  
 aromatic hydrocarbons, extinction coeffs. of triplet-triplet transitions 9-1800  
 aromatic hydrocarbons, overlap integrals, mag. anisotropy and proton screening 9-17048  
 aromatic hydrocarbons, singlet-ground-state transitions 9-11480  
 aromatics, in frozen solns., triplet-state energy transfer 9-17488  
 aryl fluorides, <sup>19</sup>F n.m.r. chem. shifts, MO calc. 9-802  
 1-azatriphenylene, and electronic spectra 9-9243  
 azines, SCF calc. 9-7048  
 azulene, ground and doubly excited states, charge densities, SCF calc. 9-20951  
 benzaldehyde, 3715 Å π\*-n system, allowed and forbidden 9-9245  
 benzene, ab initio SCF MO and CI calc. on electronic spectrum 9-9246  
 benzene, e wave function construction method 9-9267  
 benzene, low-energy photoionization 9-7190  
 benzene, model for elementary excitations 9-804  
 benzene, photoexcited triplet-state in benzene crystal 9-14118  
 benzene, radiationless decay of triplet state 9-803  
 benzene anion, removal of orbital degeneracy at 4.2°K 9-14727  
 benzenes, monosubstituted, CNDO calc. 9-7052  
 benzenes, substituted with electron-donating groups, triplet-triplet absorpt. 9-9248  
 4-bromo-testosterone acetate, excited singlet and triplet state 9-11487  
 butadiene, e wave function construction method 9-9267  
 butadiene, π-electron correl. energy calc. using extended separated pair theory 9-19460

## Molecules continued

## electronic structure, organic continued

- cage amines 9-2918  
 carbazole:pyridine (triethylamine) system, electronic energy relaxation processes 9-7056  
 carbonyl cpds., conjugate, E.S.R. spectra, calc. of π-e spin densities, Pariser-Parr-Pople methods, comparison with p hyperfine coupling consts. 9-9255  
 carbonyl cpds., conjugated, energies and intensities of n→π\* and π→π\* transitions, Pariser-Parr-Pople method 9-9254  
 conjugated hydrocarbons, π-electron screening, MO calc. 9-815  
 conjugated mols., BEEM-π calc. 9-7061  
 diazanaphthalenes, vibronic spin-orbit interactions 9-9281  
 2,6-dimethyl naphthalene, temp. effect on first electronic transition 9-15178  
 enone, cyclic conjugated, excited singlet and triplet states 9-11487  
 ethane, excited state, normal coord. anal. 9-9265  
 ethane positive ions, SCF and CI calc. of geometries 9-756  
 ethylene, e wave function construction method 9-9267  
 ethylene, vibr. struct. of π\*-π transition 9-20963  
 ethylene sulphide, <sup>33</sup>S localized electron distrib. 9-20961  
 ethylenimine, <sup>14</sup>N field gradient tensor and bonding 9-20962  
 ferrimyoglobin complexes 9-3899  
 fluoranthene, LCAO calc. 9-800  
 fluorene and derivs., quantum mech. calc. rel. to absorpt. spectra 9-3107  
 fluorene and derivs., quantum mech. calc. rel. to absorpt. spectra 9-3106  
 fluorene iodo-derivs., quantum mech. calcs. rel. to absorpt. spectra 9-3108  
 fluorenone and derivs., quantum mech. calc. rel. to absorpt. spectra 9-3107  
 fluorenone and derivs., quantum mechan. calc. rel. to absorpt. spectra 9-3106  
 fluorenone iodo derivs., quantum mech. calcs. rel. to absorpt. spectra 9-3108  
 formaldehyde, <sup>3</sup>A<sub>2</sub>→<sup>1</sup>A<sub>1</sub> transition, spin-orbit enhancement 9-17023  
 formaldehyde, one-electron props. on Gaussian basis 9-14713  
 formaldehyde, SCF calc. using Gaussian basis 9-2908  
 formic acid, assoc. types, LCAO-MO-description 9-13385  
 hydrocarbons, alternant, pairing betw. valence bond spin-coupled wave functions for π electrons of +ve and -ve ions 9-17056  
 Hydrocarbons, MO theory of elec. polarizabilities and mag. susceptibilities 9-9238  
 hydrocarbons, polycyclic: ring currents and p shielding 9-11478  
 hydrocarbons, π electron energy states, bond lengths derived 9-4952  
 p-hydroxybenzaldehyde, emission and proton transfer 9-9532  
 intermolecular H-bonded systems, electronic energy relaxation processes 9-7056  
 ionization potentials from photoelectron spectra, SCF MO calc. 9-21109  
 long-chain, Overhauser Phase and bond alternation 9-4972  
 methane, mag. susceptibility calc. 9-744  
 methane, SCF-MO's and molec. props. 9-9270  
 methyl fluoride and CH<sub>3</sub>F<sup>-</sup> ion, mol. orbital calc., significance for adiabatic proc. with bond-breaking 9-17057  
 naphthalene, ground and doubly excited states, charge densities, SCF calc. 9-20951  
 naphthalene, phosphoresc. triplet lifetime, deuterium substitution effects 9-14086  
 naphthalene, SCF MO iteration calc. 9-9109  
 naphthalene, singlet excited states polarizability, obs. 9-15879  
 naphthalene, triplet-states yield from radiolysis in hydrocarbon glass 9-17543  
 nitrobenzene derivs., σ-complexes, LCAO MO calcs. 9-11482  
 octafluorocyclohexa-1,3-dienion tricarboxyl, crystallography and electron distribution 9-1198  
 oxalyl bromide, vapor phase absorption spectra anal. in S-S, T-S systems 9-18212  
 paramagnetic species, spin densities, INDO calc. 9-17044  
 phenyldibiphenyl methyl, calc. of electron spin density by valence bond method 9-830  
 phosphorescent triplet state in mixed crystals, host effects 9-10248  
 phthalocyanines, optical density of states 9-2914  
 polarizability tensors calc. 9-5174  
 polyadenic acid, triplet exciton dynamics 9-14733  
 polyadenic acid, triplet exciton dynamics 9-9300  
 polyene, spin density wave and charge transfer wave 9-20990  
 polyenes, instability of conventional diamagnetic ground state 9-11508  
 polyenic radicals, odd linear, applic. of stability conditions for Hartree-Fock eqn. to π-electron model 9-20917  
 porphyrins, optical density of states 9-2914  
 purines, 2-, 6- and 8-substituted, SCF MO CI calcs. 9-9280  
 pyrazine, triplet-singlet transitions 9-15871  
 pyrazine phosphorescent state, non-bonding orbitals 9-14719  
 pyrene-N,N-dimethylamine Heteroexcimer 9-13389  
 pyridines, monosubstituted, CNDO calc. 9-7052  
 quinoxaline, vibronic spin-orbit interactions 9-9281  
 quinuclidine 9-2918  
 semidiones, long-range e.p.r. coupling consts. calc. 9-14720  
 spin density wave and charge transfer wave in long conjugated mols. 9-20990  
 stilbene, lowest triplet state by absorption spectra 9-19476  
 toluene, electronic energy relax. 9-9283  
 tridibiphenyl methyl, calc. of electron spin density by valence bond method 9-830  
 triethylenediamine 9-2918  
 trinitrene, septet ground state, e.p.r. detect. 9-2917  
 triphenylcyclopropenium cation, charge density meas. from <sup>13</sup>C NMR shifts 9-13388  
 unsaturated mols., Pariser-Parr-Pople model 9-743  
 CH radicals, proton hyperfine splittings, theory 9-827  
<sup>35</sup>Cl in conjugated mols., BEEM-π calc. 9-7061  
 Cu complex, triphenylmethylphosphonium bis((3)-1,2-dicarbolyl)-cuprate(III) 9-19712  
 H<sub>2</sub>O, one-electron props. of near Hartree-Fock wavefunctions 9-9207  
 N penta-atomic heterocyclic cpds., model for π electron spectra 9-4944  
 O penta-atomic heterocyclic cpds., model for π electron spectra 9-4944  
 S penta-atomic heterocyclic cpds., model for π electron spectra 9-4944

## excitation

- 2ν<sub>4</sub> around 6000cm<sup>-1</sup> 9-2911  
 acetone, monomer and excimer emission 9-16011  
 aminonitroolefins, energy levels, Pople's method calc. 9-17047  
 anthracene, electronically excited, charge transfer proc. 9-17076

**Molecules continued  
excitation continued**

anthracene in cyclohexane, elec. field effects from radiation-induced fluorescence obs. 9-18765  
azulene, SCF calc. on doubly excited states, ioniz. pot., bond orders and charge density 9-20951  
benzene, electronic model 9-804  
benzene, quenching of excited singlet state by olefins 9-2896  
benzene and liq. derivatives, excimers from electron-impact 9-9530  
benzene in cyclohexane, aggregation effects 9-2556  
benzene in cyclohexane, quenching by O<sub>2</sub> and CCl<sub>4</sub> 9-3112  
benzophenone, second triplet state obs. 9-15881  
borosilicate glass, Fe<sup>3+</sup> activated, absorpt. bands 9-747  
complexes in excited state, characts. 9-15844  
configurational-interaction calc., computer program 9-17019  
conjugated hydrocarbons, low-lying excitations, MO calc. 9-815  
dimers, vibronic energy calc. of absorpt. and fluoresc. spectra 9-736  
DNA, excited electronic states 9-18223  
doubly excited electronic states, spectroscopic excitation 9-2868  
electronically excited states, symmetries from polarized Raman spectra 9-17021  
by electrons, energy lost, calc. 9-13339  
eosin, dipole moment var. 9-13535  
intersystem crossing rate constant from lowest excited singlet to be lowest triplet state, expl. determ. 9-19452  
lifetime, rel. to absorpt. spectrum 9-2841  
liquid light scatt. spectra, peaks due to coupling of mol. orientations to thermally excited shear waves 9-21211  
methane, laser saturation of absorpt. for 3.39  $\mu$  line press. shift and broaden ing 9-11496  
methyl fluoride, 2 $\nu_4$  band around 6000cm<sup>-1</sup> 9-2911  
modulation excitation of vibronic states, relax. theory 9-20910  
molecular excitation mechanisms in nonequilibrium gases up to 20000°K, classification schemes 9-19407  
naphthalene, photoexcitation of triplet state, ENDOR meas. 9-7073  
naphthalene, SCF calc. on doubly excited states, ioniz. pot., bond orders and charge density 9-20951  
naphthalene liq. derivatives, excimers from electron-impact 9-9530  
1-naphthol, H bond and level reversal 9-9519  
O<sub>2</sub>, electron collision, 0-200eV, vac.u.v. emission 9-17040  
optically excited in soln., electron transfer with SnO<sub>2</sub> electrode, photocurrent obs. 9-16486  
organic liquids, electronic energy migration 9-7246  
Osmium complexes with phenyl and pyridine ligands, exciton interactions between ligands 9-7981  
polarizability of excited mols. from solvent shift 9-14683  
polarization corrections in optical excitation meas., elimination 9-14667  
pyrene cry. and soln., excimer-excimer interac. 9-11479  
pyrene excimer, fluorescence yield and lifetime 9-15897  
pyrene in cyclohexane, elec. field effects from radiation-induced fluorescence obs. 9-18765  
pyrene in soln., excimer formation and saturation obs. 9-11701  
pyrene-h<sub>10</sub> and -d<sub>10</sub>, intersystem crossing, temp. depend. of rate const. 9-14718  
radiationless transitions of isolated mol. 9-742  
rare earth, transition metal, in II-VI compounds, by e impact 9-5975  
resonance transfer of energy between compound mols. 9-9522  
resonant scatt. of electrons, ang. distrib. 9-4895  
resonant states, line-shape from interference of reson. and non-reson. proc. calc. 9-11437  
rotation, resonances in nonreactive collisions 9-837  
rotational, in mol. collisions, transition probabilities, exact eval., vs. variational computation 9-11512  
scintillators in aliphatic solvents, high-energy excitation, ionic processes 9-21218  
short-lives states, obs. by optical r.f. double reson. and fluoresc. 9-8559  
spectra, electronic, eff. due to interaction potential with solvent 9-9249  
in the Galaxy, OH in H I region, 18 cm absorpt. lines obs. 9-14190  
toluene fluorescence, excimer and mol., obs. of lifetimes and quantum yields for eval. of parameters 9-4964  
triplet-singlet intersystem crossing, quantum yields 9-17022  
triplet state of donor and acceptor, demonstration of resonance transfers of type T<sub>0</sub>→T<sub>0</sub>\* 9-17011  
triplet-triplet absorpt., obs., effects of varying strength of spin-orbital perturbations 9-11434  
triplet-triplet energy transfer, diffusion-controlled, conditions for 9-14738  
vibration, in inelastic collisions, coupled eqns. 9-838  
vibrational, in collisions, preferential orientations 9-13401  
p-xylene in cyclohexane, aggregation effects 9-2556  
p-xylene in cyclohexane, quenching by O<sub>2</sub> and CCl<sub>4</sub> 9-3112  
Al<sub>2</sub>O<sub>3</sub>, mean excitation potentials from stopping power data 9-9135  
C<sub>2</sub> radical, rot. distrib. obs. in low-pressure plasma 9-20983  
C<sub>2</sub>H<sub>2</sub>O<sub>2</sub>, mean excitation potentials from stopping power data 9-9135  
CO<sub>2</sub>, electron impact vibration excitation 9-760  
CuH, abs. spectrum in far u.v. new band system, rot. analysis 9-9201  
H<sub>2</sub>, by electron impact, cross-sections calc., semiclassical method 9-19433  
H<sub>2</sub>, rotational levels up to J=15 in collisions with H atoms 9-14227  
H<sub>2</sub>, spectroscopic excitation of doubly excited electronic states 9-2868  
H<sub>2</sub>, vibrational, in central collisions with Li<sup>+</sup> beams 9-7097  
H<sub>2</sub> and D<sub>2</sub>, in collisions with slow K<sup>+</sup>, vibr. excit. 9-2937  
H<sub>2</sub> lowest triplet states, by low-energy electrons, ang. depend. 9-17032  
H(2S) atom production by mol. dissociative excitation 9-14725  
K<sub>2</sub>, laser-induced fluoresc. 9-15856  
methane-Ar mixture, thermalization times of positrons 9-15974  
MgF, configurations for first electronic state 9-4930  
N<sub>2</sub>-Ar mixture, thermalization times of positrons 9-15974  
N<sub>2</sub>, by electron impact, cross-sections calc., semiclassical method 9-19433  
N<sub>2</sub>\* 3914A, in collisions of heavy ions with N<sub>2</sub> 9-18187  
N<sub>2</sub> by pulsed laser, optical gain in C<sup>3</sup>P<sub>1</sub>→B<sup>3</sup>Π transition 9-781  
N<sub>2</sub> charge exchange with Ne<sup>+</sup> below 250 eV, optical excitation 9-7193  
N<sub>2</sub> vibrationally excited, detect. by superelastic e scatt. 9-9224  
N<sub>2</sub>\* in H<sub>2</sub>\*-N<sub>2</sub> collisions, rot. excitation, 0.4-3.0 keV 9-4982  
N<sub>2</sub>\* Meinel band, by e impact, cross-sections 9-13363  
NH, electronic, in vac. u.v. photodissoc. of HN<sub>2</sub> 9-7078  
NO, 3p mol. Rydberg state (π(V=O)), spin-orbit coupling const. 9-15860  
NO, B<sup>2</sup>π state collisional quenching rate const. determ. 9-18186  
NO\*, excited electronic states 9-774  
NOD<sup>2</sup>Σ<sup>+</sup>(V=O) state, e-fluorescence, mean-lifetime obs. 9-17037

**Molecules continued  
excitation continued**

Na, in -N<sub>2</sub>, -H<sub>2</sub>, -HD, -D<sub>2</sub> collisions, 3<sup>2</sup>P<sub>1/2</sub>→3<sup>2</sup>P<sub>3/2</sub> transfer cross sections, obs. 9-9309  
O<sub>2</sub> charge exchange with Ne<sup>+</sup> below 250 eV, optical excitation 9-7193  
O<sub>2</sub>\* ground state, high vibrational excitation, evidence from photoelectron spect. 9-17039  
O<sub>2</sub>(Δg) photochemical prod. in benzene-oxygen mixtures 9-13368  
OH radical, rot. distrib. obs. in low-pressure plasma 9-20983  
OH(A<sup>2</sup>Σ<sup>+</sup>) form. from ground-state atoms, obs. 9-9227  
SF<sub>6</sub>, optical nutation effect on rot.-vib. transition 9-788  
SiO<sub>2</sub>, mean excitation potentials from stopping power data 9-9135

**intermolecular mechanics**  
*See also Association; Collision processes/molecules; Kinetic theory/gases; Liquids/structure; Liquids/theory; Solids/theory*  
alkanes, chlorinated C-H valence freq. intermol. interact. 9-7044  
benzene, cryst., vib. spectral splittings due to intermolec. forces 9-5932  
benzene, quadrupole moment calc. 9-4947  
benzene interact. with graphite, analysis w.r.t. virial treatment of physical ads., errors due to hindered rot. 9-17077  
tert butyl alcohol, determ. from vapour viscosity 30°-200°C 9-13497  
diethyl ether, determ. from vapour viscosity 30°-200°C 9-13497  
dimers, vibronic coupling, displaced oscillator model 9-4901  
dimethylsulfoxide in solns., i.r. Raman obs. 9-18365  
dipolar gases, equilib. and transport props. 9-5110  
dispersion interaction with solvent, effect on electronic spectra 9-9249  
energy parameters for 2 unlike mols. 9-15972  
energy transfer in distorted wave approx. 9-4978  
ethyl acetate, determ. from vapour viscosity 30°-200°C 9-13497  
exchange interactions, perturbation theory 9-9108  
forces, effects of molec. identity 9-2930  
globular mols., intermolec. forces 9-4947  
hard-sphere and square-well mols., free-path distrib. and collision rates 9-8457  
heavy ions, 5-50keV, range in various gases 9-14739  
heterocyclic ring, saturated, medium intermol. force effects, n.m.r. obs. 9-19493  
intermolecular potential functions from state and transport props. taken in pairs, data 9-17072  
ion-dipole system, binary distribution functions 9-4980  
liquids, monatomic, cybotactic group assumed; C<sub>v</sub> eqn. of state determ. 9-7247  
liquids and solns. effect on isotope struct. of Raman bands 9-7266  
long-range interactions, refr. index data fitted 9-9304  
methane, slow neutron scattering rel. to intermolecular interactions 9-11511  
methane, vibr. energy transfer 9-2935  
mixtures of mol. with different sizes, free energy, stat. calc. 9-20993  
molecular spectra, effect on 9-2840  
molecular theory of liquids and mixtures 9-11679  
Morse scatt. in Coulomb field partial wave analysis 9-835  
naphthalene, cryst., vib. spectral splittings due to intermolec. forces 9-5932  
naphthalene in compressed ethane and N<sub>2</sub>O 9-13485  
neutron scattering by gases, infl. of intermol. interactions, quasi-ideal approx. 9-9303  
nonpairwise additivity in intermolec. potential 9-15911  
non-spherical polar mols., statistical mech. 9-20915  
octanol isomers, sterically hindered, intermol. association, dielec. meas. 9-19495  
optical scatt., Einstein's eqn., microscopic theory 9-13330  
optical scatt., Einstein's eqns., microscopic extensions 9-13331  
pair pot. determ. from guessed equilibrium pair distrib. 9-12898  
phenol-quinone system, i.r. spectra and intermol. interaction 9-2912  
polar, graphite surface interaction pot. 9-1090  
potential, two-temp. effect of molec. identity 9-2931  
in protein, globular, heat aggregation process 9-18222  
pyrene cry. and soln., excimer-excimer interac. 9-11479  
quenching of glory undulations by anisotropy in intermolec. potential 9-2934  
relaxation by vibr.-vibr. exchange in binary mixtures 9-7221  
relaxation by vibr.-vibr. exchange in pure gases 9-3048  
scattering of slow neutrons by real gases 9-11511  
scattering of slow neutrons by real gases, non-quasi-ideal correction 9-11510  
in solid, density, equation of state and entropy for hard disks and spheres 9-8459  
spherical and linear mols. interaction, intermol. dispersion pot. 9-20992  
triplet-triplet energy transfer, diffusion-controlled, conditions for 9-14738  
van der Waals interactions, effect on vibr. spectra 9-9177  
van der Waals potentials, two-temp. 9-17079  
vibrational and rotational energy transfer 9-4981  
vibrational-translational energy transfer, Morse potential calc. 9-9306  
Ar<sup>+</sup> in N<sub>2</sub>O<sub>2</sub>:CO:NO, charge transfer proc., drift data 9-15956  
Ar supersonic jet, electron diff. obs. 9-18179  
C atom trio in triangle, nonpairwise additivity in exchange energy 9-15911  
CO<sub>2</sub> supersonic jet, electron diff. obs. 9-18179  
CO<sub>2</sub> reorientation cross-section from depolarized Rayleigh line width meas. 9-13345  
H<sub>2</sub>-H<sub>2</sub> bimolec. exchange reaction 9-770  
H<sub>2</sub> and H<sub>2</sub>-He mixture, u.s. dispersion obs. 9-3055  
H<sub>2</sub> reorientation cross-section from depolarized Rayleigh line width meas. 9-13345  
HCl-Ar interaction, intermol. dispersion pot. 9-20992  
HCl-He interaction, intermol. dispersion pot. 9-20992  
HCl-Ne interaction, intermol. dispersion pot. 9-20992  
H+H<sub>2</sub> reactive scatt., quantum mechanics 9-10317  
He-He potential near van der Waals minimum 9-7098  
He\* in N<sub>2</sub>, charge and dissociative charge transfer proc., drift data 9-15956  
He\*+2He-He\*+He, charge and dissociative charge transfer proc., drift data 9-15956  
He\* atom collisions resonances in cross section obs. 9-7034  
N<sub>2</sub> reorientation cross-section from depolarized Rayleigh line width meas. 9-13345  
N<sub>2</sub>O, vibr.-vibr. energy transfer in gas mixtures 9-4983  
Xe supersonic jet, electron diff. obs. 9-18179

**intermolecular mechanics**

amine-halogen charge-transfer complexes, intramolec. potentials 9-2892



**Molecules continued****internal mechanics continued**

- i- amyl. groups, motion in clathrate hydrate 9-14117  
 n- butyl groups, motion in clathrate hydrate 9-14117  
 centrifugal dilation consts. calc. 9-7007  
 centrifugal distortion consts. for polyat. mols. 9-7001  
 collision states, Born- Oppenheimer approx., accuracy 9-20914  
 Coriolis  $\zeta$  sum roles for planar asymmetric top mols. 9-13327  
 Coriolis coupling consts., formulae and mass depend. 9-7005  
 cyclopropane, density of states calc. 9-12886  
 density of states, steepest descent calc. 9-12886  
 D deoxyribose, coupling consts. from nucleotide phosphates n.m.r. spectra 9-18220  
 diatomic, potential energy, perturbation theory 9-738  
 diatomics-in mols. theory 9-9218  
 diazomethane, Coriolis coupling consts. evaluation 9-20967  
 dielectric absorpt. parameters for various organic cpds. 9-5869  
 electron-nuclear interaction operators 9-739  
 ethylenes, deuterated, coriolis  $\zeta$  sum rules 9-13327  
 force field for XY<sub>3</sub> type, potential const. evaluations 9-7000  
 general internal motion, Hamiltonian 9-2845  
 ketene, Coriolis coupling consts. evaluation 9-20967  
 ketene and ketene-d<sub>2</sub>, force consts. evaluation 9-20967  
 kinematic coeffs. calc. by electronic computer 9-4906  
 methyl groups substitution in o-, m-, p-xylenes, effs. and reorient. 9-14724  
 nuclear screening, effect of mag. anisotropic solvent mols. 9-9552  
 operators representing intert. between different types of motion 9-740  
 pyrene-h<sub>10</sub> and -d<sub>10</sub>, intersystem crossing, temp. depend. of rate const. 9-14718  
 rhodopsin, opsin-chromophore intramol. energy transfer 9-9299  
 D- ribose, coupling consts. from nucleotide phosphates n.m.r. spectra 9-18220  
 rot. effects in electron mol. reson. 9-4903  
 triatomic mol., intramol. vib.-vib. energy transfer 9-11440  
 Urey Bradley force field of XY<sub>2</sub> systems 9-20913  
 X<sub>2</sub>YZW planar type, pot. and Coriolis coupling consts. 9-20967  
 xanthyl radicals, spin densities, unrestricted Hartree-Fock calc. 9-11506  
 o-, m-, p- xylenes, methyl groups substitution, effs. and reorient. 9-14724  
 BCl potential energy curve of  $\Pi$  and  $\Sigma$  states 9-754  
 BrF<sub>3</sub> coriolis coupling coeffs. 9-18177  
 ClF<sub>3</sub> coriolis coupling coeffs. 9-18177  
 H-bond distances in cry., rel. to i.r. stretching freq. 9-11449  
 H<sub>2</sub>, exchange and Coulomb energy, perturbation calc. 9-765  
 H<sub>2</sub>, ground state energy calc. 9-769  
 He-He potential near van der Waals minimum 9-7098  
 IF<sub>3</sub>, force consts., vibration amplitudes, shrinkage effect, Coriolis consts., calcs. 9-9216  
 IOF<sub>3</sub>, force consts., vibration amplitudes, shrinkage effect, Coriolis consts., calcs. 9-9216  
 Li, bonding and correl. energies, germinal calc. 9-4909  
 NSF<sub>3</sub>, Coriolis consts. from i.r. absorpt. and Raman obs. 9-15862  
 OH radical interatomic force in  $\beta^{2+}$  obtained 9-20981  
 XeF<sub>4</sub> force field, Coriolis coupling, vibration and shrinkage props. 9-14696  
 XeOF<sub>4</sub> force field, Coriolis coupling, vibration and shrinkage props. 9-14696

**moments**

- amyl phenyl acetate, dipole moment in benzene and CCl<sub>4</sub> solns., obs. 9-796  
 anisotropic mols. in liqs., dipole moment determ. 9-17185  
 axially symmetric, dipole moment expansion, nonvanishing coeffs. 9-13334  
 azobenzene-2-sulphenyl cyanide, dipole moment, theor. estimation 9-14702  
 benzene, quadrupole, calc. from intermolec. forces 9-4947  
 benzyl phenyl acetate, dipole moment in benzene and CCl<sub>4</sub> solns., obs. 9-796  
 chloroform, dipole moment determ. in liq. 9-17185  
 cyclobutanone, dipole 9-805  
 cyclohexene, dipole 9-9261  
 dimethyl diazirine, dipole 9-9263  
 dimethylsiloxane chains, dipole 9-2927  
 dipole, of eosin from absorption and fluorescence spectra obs. 9-13535  
 dipole derivatives from perturbed Hartree-Fock calc. 9-2847  
 dipole derivatives from perturbed Hartree-Fock calc. 9-2848  
 dyes, elec. field effect on transition moment, electro-optical absorpt. meas. 9-7041  
 dyes, elec. field effect on transition moment and dipole moment 9-7075  
 ethylene episufoxide, dipole moment 9-19464  
 ethyl isocyanide, dipole 9-13383  
 ethyl phenyl acetate, dipole moment in benzene and CCl<sub>4</sub> solns., obs. 9-796  
 excited state mag. moments, from mag. circular dichroism 9-9184  
 excited-state dipole, from elec. field-induced spectra 9-732  
 fluorostyrene, o-, m-, p-, and para-, elec. dipole 9-11490  
 H<sub>2</sub>O, in first hydration shell of monovalent ion, mean dipole moment 9-5077  
 methyl phenyl acetate, dipole moment in benzene and CCl<sub>4</sub> solns., obs. 9-796  
 methylenecyclobutane, dipole 9-11493  
 1- naphthaldehyde, dipole moment in ICl complex and free 9-15894  
 nitrosomethane, dipole 9-817  
 nonpolar liquids, calc. from dielec. relax 9-7268  
 phenyl ethyl acetate, dipole moment in benzene and CCl<sub>4</sub> solns., obs. 9-796  
 polar mol., dipole mom., rel. to scatt. cross-sections and drift vel. of thermal e 9-13335  
 polarizability, calc. considering internal fields 9-9185  
 quadrupole, effect on dimerization const. 9-4908  
 quadrupole, from broadening of microwave lines 9-9195  
 quinol hydrogen cyanide clathrate, dipolar interaction among enclathrated methanol mols. rel. to phase transition 9-1578  
 BeO, elec. dipole and quadrupole moments, computed values 9-7015  
 CF<sub>3</sub>COOH-HCOOH microwave abs. spectrum, dipole moment meas. 9-4941  
 CH bond moments of aromatic hydrocarbons, depend. on bond angle 9-7069  
 CN, dipole moments of X( $\Sigma^+$ ) and B( $\Sigma^+$ ) states 9-15850  
 CO, Hartree-Fock calc. 9-2859

**Molecules continued****moments continued**

- CO\*, A-X transition, electr. transition moment integrals eval., r-centroid approx. limits 9-20925  
 CO first ioniz., electr. transition moment integrals eval., r-centroid approx. limits 9-20925  
<sup>13</sup>C<sup>16</sup>O, rotational 9-9198  
 CS, dipole, in ground and first excited vib. state 9-11458  
 CaO, elec. dipole and quadrupole moments, computed values 9-7015  
 Co(II) thiourea complex, subnormal mag. moment 9-18194  
 H<sub>2</sub>-He mixture, moment relations for force autocorrelation function 9-9203  
 H, adsorbed isotopes, hindered rot. 9-13586  
 o-H<sub>2</sub> in solid, pair interaction from p.m.r. obs. 9-17504  
 HCl, dipole and quadrupole, from vibration-rotation spectrum 9-18182  
 HD, elec. dipole, radial matrix elements  $\zeta$  depend. 9-2863  
 H<sub>2</sub>O, one-electron props. calc. 9-9207  
 MgO, elec. dipole and quadrupole moments, computed values 9-7015  
 N<sub>2</sub>, quadrupole 9-9455  
 NS radical, elec. dipole 9-7082  
 NaSH, dipole-dipole interact. bet. SH<sup>-</sup> ions 9-17038  
 Ni(II) thiourea complex, subnormal mag. moment 9-18194  
 PCl<sub>3</sub>, dipole 9-787  
 POCl<sub>3</sub>, dipole 9-787  
 SeF<sub>4</sub> isotopes, dipole determ. from microwave spectra 9-18191  
 SeOF<sub>2</sub> isotopes, microwave spectra obs., rotn. const. and dipole moment determ. 9-18192  
 SrO, elec. dipole and quadrupole moments, computed values 9-7015
- nuclear coupling**  
 allenic germinal coupling const., sign determ. 9-2891  
 aziridine, 1-substituted, interproton coupling consts. from <sup>13</sup>C-H satellite n.m.r. 9-13543  
 2- butene, cis and trans, allylic and homoallylic coupling from n.m.r. spectra 9-13376  
 1-chloro-1,1-difluoroethane, quadrupole 9-13377  
 1- chloro-1, 2-dibromo-2-iodoethane, internal rot. gauche coupling consts 9-807  
 cyclohexane fragments, long-range coupling 9-17050  
 dichloromethane-d<sub>2</sub>, deuterium quadrupole coupling const. 9-13382  
 dielectric absorpt. parameters for various organic cpds. 9-5869  
 1,1- difluoro-2-chloroethylene, quadrupole coupling 9-2906  
 difluorodichloroethylene, signs of F spin coupling consts. 9-7065  
 dimethyl diazirine, quadrupole 9-9263  
 ethyl formate, temp., solvent depend of <sup>13</sup>C-H spin-spin coupling consts. 9-17054  
 ethyl isocyanide, quadrupole coupling consts. 9-13383  
 ethylene sulphide, <sup>33</sup>S quadrupole coupling consts. 9-20961  
 ethylenimine, <sup>14</sup>N quadrupole coupling const. 9-20962  
 hydrocarbons, saturated, e-coupled p. spin spin interaction interbond correlation effects 9-816  
 linear molecules, spin-orbit coupling constants for multiplet states 9-15845  
 methane, e-coupled p. spin-spin interaction, interbond, correlation effects 9-816  
 2- methyl propene, CH<sub>3</sub>-CH<sub>3</sub> coupling, possibility of 'through-space' contribution 9-13376  
 nitrosomethane, quadrupole coupling consts. 9-817  
 para-dichlorobenzene, singlet-triplet transition spectra, spin-orbit coupling 9-19451  
 perturbation calc. of nuclear-spin coupling consts. 9-11446  
 polycyclic hydrocarbons, spin spin coupling, MO calc. 9-13386  
 proton-proton coupling by  $\pi$  electrons 9-17042  
 SCO<sup>+</sup>  $X^2\Pi$  and  $A'^2\Pi$  states, spin-orbit coupling constants calc. 9-15845  
 spin spin, solvent depend., change in coupling const., empirical correlation 9-7009  
 spin-spin coupling and electron cor. 9-9190  
 [AX]<sub>4</sub> nuclear spin system with tetrahedral symmetry 9-17024  
 B<sub>2</sub>H<sub>4</sub> 9-755  
<sup>13</sup>C-H, substituent effects, MO calc. 9-7042  
<sup>13</sup>C-H spin-spin coupling const., extended Huckel calc. on methyl cpds. 9-20969  
 C<sub>2</sub> electronic moment variation with internuclear separation 9-19429  
 CO<sub>2</sub><sup>+</sup>,  $X^2\Pi$  and  $A'^2\Pi$  states, spin-orbit coupling constants calc. 9-15845  
 C-F spin spin coupling, variation with C substituent bond length 9-4943  
<sup>35</sup>Cl in conjugated mols. 9-7061  
 D<sub>2</sub>S, Coriolis coupling constants, ground state inertia defects 9-9212  
 D<sub>2</sub>Se, Coriolis coupling constants, ground state inertia defects 9-9212  
 F-C, signs of spin coupling consts. 9-7065  
 F, in cpds. with S 9-762  
 HCl, spin spin coupling in liq. 9-9553  
 H<sup>35</sup>Cl and H<sup>37</sup>Cl, nuclear mag. hyperfine spectra 9-9206  
 H<sub>2</sub>O, one electron props. calc. 9-9207  
 H<sub>2</sub>S, coriolis coupling constants, ground state inertia defects 9-9212  
 H<sub>2</sub>Se, Coriolis coupling, constants, ground state inertia defects 9-9212  
 KF, MO calc 9-2872  
 LiAlD<sub>4</sub>, polycrystalline, deuteron quadrupole coupling const. meas. 9-11464  
 N<sub>2</sub> electronic moment depend. on internuclear separation, calc. of Halevi's correction 9-19437  
 NH<sub>3</sub>D, quadrupole coupling consts. 9-17036  
 NS radical, quadrupole coupling constant 9-7082  
 PBr<sub>3</sub>, quadrupole coupling of Br 9-17221  
 PCl<sub>3</sub>, quadrupole coupling consts. 9-787  
 POCl<sub>3</sub>, quadrupole coupling consts. 9-787
- relaxation**  
*See also Acoustic wave propagation; Dielectric phenomena; Liquids/theory; Nuclear magnetic resonance and relaxation; Paramagnetic resonance and relaxation*  
 benzene, ultrasonic relaxation in gas mixture with O<sub>2</sub> 9-2901  
 charge distrib. and vibr. force const. 9-2846  
 2- chlorostyrene - styrene copolymers, mol. motion from dielec. meas. 9-14888  
 cyclohexane, liq. and solid phase, rot. and diff. relax. times, cold-neutron scatt. study 9-14707  
 cyclopentane, liq. and solid phase, rot. and diff. relax. times, cold neutron scatt. study 9-14707  
 cyclopropane, vibrational relaxation, temp. depend 9-4953  
 diatomic, vibr.-dissoc. relax. behind shock wave 9-13483  
 ethylene, vibrational relaxation, temp. depend 9-4953  
 heterocyclic amines in dilute soln. 9-20947  
 hydrocarbon gases, effect of temp. on rot. and vibr. relax. 9-957

## Molecules continued

## relaxation continued

- microwave relaxation of molecules containing librating polar groups 9-21220  
 modulation excitation of vibronic states, theory 9-20910  
 of orientation, discussion 9-17164  
 polar gases, rotational 9-9447  
 polyatomic, of vibrational energy 9-9179  
 solvent-solute relax., resulting spectral shifts, time-resolved nanosec. emission spectroscopy studies 9-13534  
 stochastic model 9-86  
 toluene, electronic energy relax. 9-9283  
 vibration-vibr. exchange in binary mixtures 9-7221  
 vibration-vibr. exchange in pure gases 9-3048  
 vibrational, mechanisms 9-737  
 CO<sub>2</sub>, vibr., shock tube meas. 9-759  
 CO<sub>2</sub>, rotational relax. time, direct meas. 9-2852  
 CO<sub>2</sub>, ultrasonic relaxation in gas mixture with O<sub>2</sub> 9-2901  
 Co(II) complexes, anomalous relax. from isotropic proton mag. reson. shifts 9-13349  
 N<sub>2</sub>O, vibr., shock tube meas. 9-775  
 N<sub>2</sub>, vibr.-dissoc. relax. behind shock wave 9-13483  
 N<sub>2</sub>O, vibr., laser-induced 9-7030  
 N<sub>2</sub>O, vibr. relax. in gas mixtures 9-4983  
 Ni(II) complexes, anomalous relax. from isotropic proton mag. reson. shifts 9-13349  
 O<sub>2</sub>, vibr.-dissoc. relax. behind shock wave 9-13483  
 OH(A<sup>2</sup>Σ<sup>+</sup>, v'=0, K') quenching and rotational relax. 9-7083  
 SF<sub>6</sub>, vibrational relaxation, temp. depend. 9-4953  
 SF<sub>6</sub> oscillation, temp. depend. 10° to 215°C, from acoustic absorpt. obs. 9-2879

## rotation

- acetylenes, substituted, rot. correl. times in liq. 9-9557  
 anisole and monohalogen deriv., torsional barriers 9-14700  
 benzene, rot. const. from near i.r. vibr. band 9-7050  
 2,1,3-benzothiadiazole, band contours in 3280 Å electronic system 9-15884  
 butane, internal rot., Hartree-Fock calc. 9-9251  
 1-chloro-1,1-difluoroethane, internal barrier 9-13377  
 CO<sub>2</sub>, relax. time, direct meas. 9-2852  
 Coriolis interac. const. and centrifugal stretching const. relationship derivation 9-4907  
 cyclohexane, liq. and solid phase, cold-neutron scatt. study of rot. motions 9-14707  
 cyclopentane, pseudorotation 9-9260  
 cyclopropane-D<sub>6</sub>, i.r. vib.-rotn. bands anal. 9-18217  
 diatomic, vibration-rot. bands, emission-absorption intensity ratio temp. meas., thermal non-equl. conditions 9-20906  
 diatomic rotators in liqs. and solids, ang. correl. 9-15841  
 1,1-difluoro-2-chloroethylene 9-2906  
 trans-1,4-diiodocyclohexane, rotational isomerism and vibr. spectra 9-17482  
 2,6-dimethyl-1,4-phenylpyridine, from absorpt. spectra 9-9273  
 dimethyldiazirine 9-9263  
 effects in electron-mol. reson. attenuation of ang. distrib. coeffs. 9-4903  
 energy transfer in collisions 9-4981  
 ethane, barriers, bond-function anal. 9-7063  
 ethyl isocyanide, barrier 9-13383  
 ethyl isocyanide, spectrum analysis, 4000-200 cm<sup>-1</sup> 9-18205  
 ethylene episufoxide, rot. spectrum 9-19464  
 ethylene sulphide 9-20961  
 excitation, resonances in nonreactive collisions 9-837  
 fluoroacetic acid, from microwave spectra, and centrifugal distortion parameters 9-13371  
 geometry and barriers to interval rot. in Hartree-Fock theory 9-2855  
 hydrocarbon gases, effect of temp. on rot. and vibr. relax. 9-957  
 inertial const. of mols. with internal rotor 9-9175  
 i.r. lines, pressure-induced shifts, j-depend., elastic cross-section expansion 9-17012  
 laser scatt. for motion determ. 9-19421  
 mag. double refr. of paramag. complexes, quantum theory for Cotton-Mouton eff. 9-9183  
 methane, compressed, rot. correl. functions, effect of nuclear-spin 9-4940  
 methane, solid, reorientation effects on neutron scatt. 9-9823  
 methyl bromide, vibration-rotation spectrum, interpretation near 6000 cm. 9-18211  
 methyl group, internal rot., Hartree-Fock calc. 9-9251  
 methyl groups in o-, m-, p-xylenes, substitution, effs. and reorient. 9-14724  
 methyl iodide, rotational Zeeman effect 9-2910  
 methyl thiocyanate, torsional fine struct. in rot. spectrum 9-4958  
 methylbenzenes, hindered rotations in solid 9-1882  
 microwave relaxation of molecules containing librating polar groups 9-21220  
 monochloroacetylene HCC<sup>35</sup>Cl and HCC<sup>37</sup>Cl, rot. const. 9-17045  
 nitrosomethane, internal barrier 9-817  
 Osmium complexes with phenyl and pyridine ligands, exciton interactions between ligands 9-7981  
 phenol, rotational band contour of 0-0 band at 2750Å, computer fit 9-18213  
 polar liqs. 9-1016  
 propane, quantum-mech. calc. 9-2915  
 1,3-pseudorotation 9-809  
 pure-rotational absorpt.-line-intensity law, microwave 9-11433  
 rigid rotor energy levels computer program for calc. 9-20911  
 rotor strengths, partial f-sum rules 9-7002  
 rotors, asym., evaluation of (P<sub>2</sub><sup>2</sup>), (P<sub>4</sub><sup>2</sup>) matrix elements 9-11436  
 selection rules of internal rot. and rot., assym. mols. 9-2851  
 separation of rot. coord. from diatomic Schrodinger eqn. 9-14682  
 spin-rot. interac. rel. to <sup>31</sup>P spin-lattice relax. in liq. PAOs 9-9231  
 symmetric rotor, centrifugal distortion eff. on levels 9-4905  
 torsion-vibr.-rot. interaction in rot. spectra 9-7004  
 vibration-rot. bands, emission-absorption intensity ratio temp. meas., thermal non-equl. conditions 9-20906  
 vibration-rotation Hamiltonian, simplification 9-17014  
 XY<sub>2</sub>-type, transformation of vibratory-rotatory Hamiltonian 9-18165  
 XYX nonlinear mols; 4th-order vibr.-rot. Hamiltonian 9-735  
<sup>7</sup>LiD microwave obs. in ground and first excited vibr. states 9-13361  
 AsN, structure of band rel. to new transition 9-7011

## Molecules continued

## rotation continued

- BF<sub>3</sub> isotopes spectra, v<sub>3</sub> bands meas., fine structure determ. 9-17027  
 BiBr spectra, visible A-X system, rotn. const. determ. 9-18176  
 BiCl, analysis of bands of A'-X system 9-4918  
 BiF, struct. of 3050-3250 Å syst., electronic state struct. deduced 9-4919  
 C<sub>2</sub> radical, rot. distrib. obs. in low press. plasma 9-20983  
 C<sub>2</sub>, swan system, additional perturbations in A'<sup>2</sup>Σ<sup>+</sup> state 9-11457  
 CF<sub>3</sub>CCL<sub>3</sub>, internal rot. 9-15888  
 CN<sup>-</sup> in cubic KCN 9-16465  
 CO<sub>2</sub>, self and N<sub>2</sub> broadenings of rot. lines of 15 and 4.3 μ bands, width meas. 9-19494  
 CO<sub>2</sub> laser, rot. level competition 9-13004  
 CO<sub>2</sub> laser rotational competition and Lamb dip study, stabilization and gas absorption coeff. meas. appln. 9-13009  
<sup>12</sup>C<sup>18</sup>O<sub>2</sub>, constants from vib.-rot. bands of i.r. spectrum 9-13348  
<sup>13</sup>C<sup>18</sup>O<sub>2</sub>, constants from vib.-rot. bands of i.r. spectrum 9-13348  
 D<sub>2</sub>, pure rot. absorpt. spectra, analysis 9-20928  
 DCl, higher J rot. struct. of near i.r. bands 9-13357  
 H<sub>2</sub>O, centrifugal-distortion effects 9-15855  
 H<sub>2</sub>O vapour, line shape of rot. transition at 22GHz, dispersion studies, Lorentzian behaviour 9-19432  
 H<sub>2</sub>S, anal. of pure rot. absorpt. spectra 9-20928  
 H<sup>79</sup>Br, dipole matrix elements for 2-0 vib.-rot. band lines 9-15853  
 H halides in cyclohexane solns. 9-9488  
 HCP, intensities of lines in Σ<sup>+</sup>Σ<sup>-</sup> electronic transitions 9-2880  
 HCl, higher J rot. struct. of near i.r. bands 9-13357  
 HCl, vibration-rotation spectrum, density and linewidth 9-18182  
 HF, higher J rot. struct. of near i.r. bands 9-13357  
 HI, h.f.s. of rot. spectrum in sub-mm region 9-9204  
 HN<sub>3</sub>, and D derivs., const. and distortion, study in i.r. spectra 9-13355  
 HNCO, and D derivs., const. and distortion, study in i.r. spectra 9-13355  
 HNCS, and D derivs., const. and distortion, study in i.r. spectra 9-13355  
 H<sub>2</sub>O, from expt. data, const. of centrifugal distortion calc. 9-7024  
 H<sub>2</sub>O vapour, spectrum, vibrational-rotational fine struct. 9-4926  
 H<sub>2</sub>S<sub>2</sub> and D<sub>2</sub>S<sub>2</sub> 9-9211  
 H+H<sub>2</sub>, reaction, two-dimens., energy calc. 9-10318  
 LiCl from microwave meas. 9-18184  
<sup>6</sup>LiD microwave obs. in ground and first excited vibr. states 9-13361  
 LiF, from microwave meas. 9-18184  
 LiH, calc. of mol. constants from microwave obs. of LiD. 9-13361  
 N<sub>2</sub>, abnormal rot. energy distrib. in C<sup>2</sup>Π<sub>u</sub> B'<sup>2</sup>Π<sub>g</sub> bands 9-778  
 N<sub>2</sub>O, c.w. oscillations in rotation-vibration transitions 9-20519  
 ND, 0-0 band or A<sup>1</sup>Π<sub>inv</sub>-X<sup>2</sup>Σ<sup>-</sup> system, rot. analysis 9-19440  
 NH<sub>3</sub>, constants from K splitting in spectrum 9-13367  
 NH<sub>3</sub>, inert-gas collision-induced transitions between rot. levels 9-11469  
 NO, Rydberg state, spin-orbit coupling 9-20935  
 N<sub>2</sub>O, anharmonic and vib.-rot. coupling const., to fourth order 9-13366  
 NO<sub>2</sub>F, centrifugal distortion anal. 9-7033  
 O<sub>2</sub> rotational transition obs. by microwave spectroscopy 9-9229  
 OH radical, rot. distrib. obs. in low press. plasma 9-20983  
 OH(A<sup>2</sup>Σ<sup>+</sup>, v'=0, K') quenching and rotational relax. 9-7083  
<sup>31</sup>P in P<sub>4</sub>O<sub>6</sub> liquid, spin-lattice relax., rel. to spin-rot. interac. 9-9231  
 P<sub>2</sub>, C<sup>2</sup>Σ<sup>+</sup>-X<sup>2</sup>Σ<sup>+</sup> system bands, rot. analysis 9-9230  
 PH<sub>4</sub><sup>+</sup>m barriers to rot., obs. in laser-Raman spectra of PH<sub>4</sub>Cl, Ph<sub>4</sub>Br and Ph<sub>4</sub>I 9-15865  
 PbBr A-X system analysis, obs. 9-4935  
<sup>35</sup>S<sup>16</sup>O<sub>2</sub>, rotation spectra, Herzian, second-order 9-20938  
 SO, intensities of lines in Σ<sup>+</sup>Σ<sup>-</sup> electronic transitions 9-2880  
 SO<sub>2</sub> isotopic molecules, rotation spectra 9-20939  
<sup>33</sup>SO<sub>2</sub> rotation spectra in fundment state 9-19446  
 SeO, blue-green emission system rot. analysis, obs. 9-4937  
 SeF<sub>4</sub> isotopes microwave spectra, isotopes, rotn. const., dipole moment, structure parameter determ. 9-18191  
 SeOF<sub>2</sub> isotopes, microwave spectra obs., rotn. const. and dipole moment determ. 9-18192  
 SiF, rot. analysis of (0,0) band 9-11474  
<sup>28</sup>SiF<sub>2</sub>D centrifugal distortion const. calc. 9-17041  
<sup>29</sup>SiF<sub>2</sub>H centrifugal distortion const. calc. 9-17041  
 SnTe, microwave spectrum, 27 isotopic mols. 9-15873  
 SnTe, microwave spectrum, 27 isotopic mols. 9-2883

## vibration

- acrolein and deuterio derivs., from i.r. and combination scatt. spectra 9-11491  
 9 alkylxanthyl free radicals, torsional oscill. of alkyl groups 9-9295  
 amino-pyridines 9-14699  
 amino-pyrimidines 9-14699  
 amplitude, generalized mean-square, of XY<sub>2</sub>Z<sub>2</sub> type 9-17013  
 anisole and monohalogen deriv., vib. spectra and torsional barriers to rot. 9-14700  
 anthracene, Raman spectra study 9-18196  
 aromatic hydrocarbon bases, H-bonded complexes, i.r. spectra in O-H stretching vibration region 9-4942  
 aromatic hydrocarbons, anharmonicity 9-11480  
 1-azatriphenylene, rel. to electronic spectra 9-9243  
 benzene, energy transfer in excited electronic states 9-15880  
 benzene, self-consistent calc. 9-7049  
 benzene, substituted; freq. assignments from i.r. and Raman spectra obs. 9-7051  
 benzene d<sub>6</sub> in active solvent, integrated intensities of C-D valence vib. 9-4949  
 p-benzoquinone, Fermi reson. params., obs. 9-14681  
 benzoyl chloride, Fermi reson. params., obs. 9-14681  
 biphenyl, rel. to i.r. absorpt. band intensities, temp. depend. 9-18215  
 bond charge model for vibr. in covalent crystals 9-9808  
 boroxol skeleton, vibrational assignment and valence force field 9-18174  
 2-bromo propionitrile, i.r. and Raman spectra freq. assignments 9-20975  
 bromocyclobutane, i.r. and Raman spectra, ring-puckering vib. and potential functions determ. 9-20957  
 bromonitromethane and d<sub>2</sub> analogue, i.r. and Raman obs. 9-15893  
 β-bromostyrene, from i.r. absorption spectrum 9-18201  
 C<sub>3</sub>S<sub>2</sub>, mean amplitudes, and force const. determ. 9-20924  
 carbazole 9-9252  
 carbohydrates, i.r. spectroscopy, review 9-2897  
 carbon tetrabromide, force constant calculation 9-18175  
 carbon tetrachloride, force constant calculation 9-18175  
 centrifugal distortion const. for polyat. mols. 9-7001  
 characteristic vib. in mol. spect., defin. 9-18166  
 chlorinated tetrahedral cpds., matrix-isolated 9-2900



**Molecules continued**  
**vibration continued**

2-chloro propionitrile, i.r. and Raman spectra, freq. assignments 9-20975  
 chlorocyclobutane, i.r. and Raman spectra, ring-puckering vib. and potential functions determ. 9-20957  
 chloroform, effect of molec. interactions on vibr. freqs. 9 808  
 1-(chloromethyl) naphthalene absorption spectra spectrophotometry obs. 250-4000 cm<sup>-1</sup> freq. assignments 9-9258  
 chloronitromethane and d<sub>3</sub> analogue, i.r. and Raman obs. 9 15893  
 collision of two diatomic mols., energy transfer 9-840  
 conformation of minimum potential- energy, valence force calc. 9-4912  
 Coriolis coupling and force consts. for AXYZ linear type 9-7020  
 Coriolis interac. const. and centrifugal stretching const. relationship derivation 9-4907  
 Coriolis coupling const., formulae and mass depend. 9-7005  
 cubic secular eqn., extremal force constants 9-11439  
 cyclobutane, -d<sub>8</sub> vibration mean square amplitude calc. from spectra, 300°K 9 9259  
 cyclobutane, ring-puckering potential and dihedral angle 9-806  
 cyclobutanol, i.r. and Raman spectra, ring-puckering vib. and potential functions determ. 9-20957  
 cyclobutanone, ring-puckering potential function 9-805  
 cyclohexane, least-energetic E<sub>g</sub> vibr. 9-20959  
 cyclohexane d<sub>12</sub> in active solvent, integrated intensities of C-D valence vib. 9-4949  
 cyclohexanes, monohalosubstituted, rel. to gas and liq. phase spectra 9-9262  
 cyclopentadiene and deuterio-derivs., force constants from vibration spectra 9-2904  
 cyclopentane, pseudorotation 9-9260  
 cyclopentanone, Fermi reson. params., obs. 9-14681  
 cyclopropane, relaxation times, -70-150°C 9-4953  
 cyclopropane-D<sub>6</sub>, i.r. vib. rotn. bands anal. 9-18217  
 cyclopropylcarbonyl chloride 9-794  
 deuterovinyl chlorides, seven, fundamental wave number assignment, by normal co ord. treatment 9-13392  
 diacetyl and deuterio-derivs., from i.r. and combination scatt. spectra 9-11491  
 diatomic, freq. and anharmonicity constants 9-2842  
 diatomic, potential energy, perturbation theory 9-738  
 diatomic, rotation-vibration bands, emission-absorption intensity ratio temp. meas., thermal non-equil. conditions 9-20906  
 diatomic mol., vib. eigenvalues calc., non-iterative method, applic. 9-20912  
 diboranes, methyl substituted, sum rules for frequencies and squares of frequencies 9 19428  
 dibromocarbene 9-810  
 dibromomethane, d<sub>0</sub>, d<sub>1</sub> and d<sub>2</sub> 9-15886  
 2,4-, 2,5-, 2,6- dichlorotoluenes, i.r. absorption spectra, assignments of fundamental vib. 9-11485  
 diethyl ether and deuterated analogues, valence force field for conformers 9-14708  
 cis- difluorodiazine mean amplitudes by applic. of theory of X<sub>2</sub>Y<sub>2</sub> mol. with C<sub>2v</sub> symmetry 9-4900  
 2,5- dihydrothiophene, ring puckering 9-820  
 trans-1,4-diiodocyclohexane, vibrational spectra and rotational isomerism 9-17482  
 diketene, i.r. and Raman spectra, ring-puckering vib. and potential functions determ. 9-20957  
 dimers, vibronic coupling, displaced oscillator model 9-4901  
 dimers, vibronic energy calc. of absorpt. and fluoresc. spectra 9-736  
 dimethyl diselenide 9-9264  
 dimethyl ether, valence force field calc. using vib. freq. of (CH<sub>3</sub>)<sub>2</sub>O, (CD<sub>3</sub>)<sub>2</sub>O and CH<sub>3</sub>OC(D<sub>3</sub>) mols. 9-20968  
 N, N- dimethylacetamide, i.r. and Raman spectra, 3100-250 cm.<sup>-1</sup> obs. 9-4957  
 dimethylamine, mean amplitudes 9-7045  
 N,N dimethylformamide, i.r. and Raman spectra, 3100-250 cm.<sup>-1</sup> obs. 9-4957  
 ethanes, 1:1 di-substituted, spectrum, cal. and interpret. 9-15889  
 energy calc., S function selection for polyatomic mols. 9-2849  
 energy transfer in collisions 9-4981  
 energy transfer in inelastic collisions, coupled eqns. 9-838  
 energy transfer in system of radiating oscillators 9-3049  
 ethene, and ethene-d<sub>4</sub>, vibronic spectra 9-813  
 ethyl isocyanide 9-13383  
 ethyl isocyanide, spectrum analysis, 4000-200 cm.<sup>-1</sup> 9-18205  
 ethyl pyridines in liquid phase, explaining i.r. absorpt. spectrum 9-1026  
 ethylene, Green's function analysis 9-11477  
 ethylene, relaxation times, -70-150°C 9-4953  
 ethylene, vibr. struct. of π<sup>-</sup>π transition 9-20963  
 ethylene carbonate, Fermi reson. params., obs. 9-14681  
 ethylene oxide (d<sub>4</sub>), force constants calc. and interpretation of gas and liq. phase spectra 9-9268  
 ethylenimine, barrier to proton tunneling 9-20962  
 excitation in collisions, preferential orientations 9-13401  
 excited vibr. states in adiabatic approx. 9-2844  
 Fermi reson. parameters meas. by solvent variation 9-14681  
 fluorene, vibr. anal. 9-14712  
 4π fluoro-3-chloro aniline, six upper and one ground state ident. 9-814  
 1- fluoro- 2-haloethanes, rot. isomers 9-812  
 p- fluoroaniline, i.r. absorption and near u.v. emission spectra, correl. and comp. of ground state vib. freq. 9-14711  
 fluorobromobenzene, o-, p-, m-, out-of-plane vibrs., normal coordinate analysis 9-13374  
 fluorochlorobenzene, o-, p-, m-, out- of-plane vibrs., normal coordinate analysis 9-13374  
 force constants, determ. from kinematically defined normal coords, new model 9-13326  
 force const., Coriolis coupling const., mean amplitude ZXY<sub>2</sub>(C<sub>2v</sub>) and ZXY<sub>2</sub>(C<sub>3v</sub>) type 9-7010  
 force const., multiplicity in vibr. anal. 9-19419  
 force const., multiplicity in vibr. anal. 9-19420  
 force const., multiplicity in vibr. anal. 9-14680  
 force const., calc. 9-4902  
 force const. from perturbed Hartree-Fock calc. 9-2848  
 force const. from perturbed Hartree-Fock calc. 9-2847  
 force fields determ., validity of approx. 9-2850  
 frequency depend. on electro- negativity of constituent atoms 9-6999  
 glycerol, Raman eff. using 4880 Å Ar laser 9-15890

**Molecules continued**  
**vibration continued**

glyoxal and deuterio-derivs., from i.r. and combination scatt. spectra 9-11491  
 haloethanes, monosubstituted, rel. to gas and liq. phase spectra 9-9269  
 Hg complexes of triphenylphosphine, i.r. spectra, assignments 9-20944  
 hydrocarbon gases, effect of temp. on rot. and vibr. relax. 9-957  
 hydrocarbons, i.r. spectra, correl. in rocking vib., applic. to macromol. syst. 9-20965  
 hydrocarbons, substituted, skeletal deformation freq. and boiling pts., correl. 9-21249  
 inertial const. of mols. with internal rotor 9-9175  
 i.r. lines, pressure-induced shifts, j-depend., elastic cross-section expansion 9-17012  
 Lagrange eqn. with non-vanishing couplings application, comment 9-9178  
 laser scatt. for motion determ. 9-19421  
 liquid, oscillation rel. to Rayleigh line spectrum 9-2888  
 matrix-trapped diatomic mols., effect of localized vibr. on spectra 9-3883  
 mean amplitude of vib. matrix elements, and equiv. conditions in second order secular eqn. 9-13325  
 mean amplitudes for mols. with internal rot. 9-9235  
 methane, vibr. energy transfer 9-2935  
 methyl bromide, vibration-rotation spectrum, interpretation near 6000 cm. 9-18211  
 methyl iodide liq. phase, Raman band width C-I stretching vibrs. 9-4959  
 methyl thiocyanate, torsional fine struct. in rot. spectrum 9-4958  
 methylamine, mean amplitudes 9-7045  
 methylamine, NH<sub>2</sub> twisting vibr. 9-10215  
 methylene, B<sub>2g</sub> wagging mode in polyethylene, laser-Raman obs. 9-14063  
 methylenecyclobutane, ring puckering potential function 9-11493  
 methylethoxymethanes, from i.r. absorpt. spectra 9-11495  
 modulation excitation of vibronic states, relax. theory 9-20910  
 1- naphthaldehyde, free and -ICl complex, C=O stretching freq. solvent depend. 9-15894  
 naphthalene, energy transfer in excited electronic states 9-15880  
 naphthalene phosphoresc., vibr. assignment 9-5967  
 nitriles, freqs., valence force field calc. 9-15874  
 one-dimensional oscillator eigenfunctions, choice of basis set 9-9176  
 organic diat. groups valence freq. var. vap-liq transition 9-7040  
 oxalyl bromide, vapor phase absorption spectra anal. in S-S, T-S systems 9-18212  
 oxide halides of heavy transition metals, metal-oxygen stretching frequencies 9-19425  
 pentaerythritol derivs., vibr. spectra 4000-400 cm.<sup>-1</sup> 9-17053  
 pentafluorobenzyl and pentafluorobenzylidene halides, vib. modes and freq. 9-20974  
 perchlorylamide ion, in cryst. or soln., normal vibrs., effect of bond lengths 9-7046  
 perfluorocyclobutane, vibration mean square amplitude, Coriolis const. calc. from spectra, 300°K 9-9259  
 perfluorotoluene, i.r. and Raman spectra, modes and assignments 9-20973  
 phenanthrene, energy transfer in excited electronic states 9-15880  
 phosphorus pentahalide, pseudo-rotation and intramolecular exchange 9-19445  
 photodissociation primary products, energy distrib. in vibr. excitation 9-10350  
 planar, homonuclear, equilateral, use of group theory to det. normal modes 9-9  
 polyatomic, approx. anharmonic potential function, transition freq. calc. 9-4904  
 polyatomic, inverse population obtainment of levels 9-9179  
 polyatomic, partition function calc. including Fermi- or Darling-Dennison-reson. 9-11438  
 polypropylene, isotactic, dispersion curves and freq. distrib. 9-9302  
 β-propiolactone, i.r. and Raman spectra, ring-puckering vib. and potential functions determ. 9-20957  
 propionitrile, i.r. and Raman spectra, freq. assignments 9-20975  
 1,3-, pseudorotation 9-809  
 pyramidal XY<sub>2</sub>Z and XY<sub>2</sub>Z<sub>2</sub> type, force const. by Green's function analysis 9-11441  
 pyramidal XYZ<sub>2</sub> type mean amplitudes 9-2843  
 relaxation by vibr. vibr. exchange in binary mixtures 9-7221  
 relaxation by vibr.-vibr. exchange in pure gases 9-3048  
 relaxation mechanisms 9-737  
 relaxation of force const. and charge distrib. 9-2846  
 resonant states, line-shape from interference of reson. and non-reson. proc. calc. 9-11437  
 rotation-vibration bands, emission- absorption intensity ratio temp. meas., thermal non equil. conditions 9-20906  
 silacyclopent-3-ene, ring puckering 9-20977  
 symmetry co-ordinates for factorizing G and F matrices, simple non-Wigner construction 9-11442  
 ten-electron mols. of type MH<sub>6</sub>, force const., perturbation calc. 9-11450  
 tetrahalo p-benzoquinone complexes with aromatic amines 9-14721  
 tetrahedral XY<sub>4</sub> type, force const. by Green's function analysis 9-11441  
 s-tetrazine-d<sub>0</sub> and -d<sub>2</sub>, fundamental vibr. freqs. from i.r. and Raman spectra 9-11500  
 thiophere derivatives, vibration deformation frequencies, effect of solvents 9-821  
 o-, m-, p- tolualdehydes in liquid phase, vibrational spectra, assignments of freq. 9-11501  
 toluene, energy transfer in excited electronic states 9-15880  
 torsion-vibr. rot. interaction in rot. spectra 9-7004  
 transition-metal dihalides, bending freqs. and dimer modes 9-15857  
 transition-metal octahedral complexes, vibronic transitions 9-14056  
 triatomic mol. interac. with atom, intramol. vib.-vib. energy transfer 9-11440  
 tribromomethyl radical 9-810  
 tricarboxylatostannates (II), i.r. spectra assignment of skeletal vib. 9-14722  
 triethylphosphine selenide, i.r. and Raman spectra 9-18204  
 triethylphosphine sulfide, i.r. and Raman spectra 9-18204  
 trimethylamine -H<sub>2</sub>, D<sub>3</sub>, Coriolis coupling coeff. for degenerate vib. assignments and amp., valence force field calc. 9-20980  
 trimethylethoxysilane, from i.r. absorpt. spectra 9-11495  
 urea, thermal motion and interatomic distances 9-13391  
 vibration-rotation Hamiltonian, simplification 9-17014  
 vibrational-translational energy transfer, Morse potential calc. 9-9306

**Molecules continued**  
**vibration continued**

- vinyl chloride, fundamental wave number assignment, by normal co-ord. treatment 9-13392
- vinyl esters, spectral freq. and intensities determ. 9-9287
- water of crystallization, optical activity in vibration-transition region 9-7941
- X<sub>2</sub>Y<sub>2</sub> model with C<sub>2v</sub> symmetry, mean amplitudes 9-4900
- XeO<sub>2</sub>F<sub>2</sub> 9-791
- XY<sub>2</sub> type, transformation of vibratory rotatory Hamiltonian 9-18165
- XXX nonlinear mols: 4th-order vibr.-rot. Hamiltonian 9-735
- zero-point vibr.-effects on electronic expectation values 9-9209
- B halides BXY<sub>2</sub>: type, const.,  $\zeta$  element var. determ. 9-7012
- BBr<sub>3</sub>, force constant calculation 9-18175
- BCl<sub>3</sub>, force constant calculation 9-18175
- BeH<sub>2</sub>, LCAO MO-SCF calc. 9-15849
- BiBr ground state constants 9-2858
- BrF<sub>3</sub>, force field 9-20923
- C-Cl and C-Br of organic cpds., gaseous and in soln. 9-14697
- C-H in tetrahedrally hybridized carbons, deuterium substitution eff. on  $\nu_{13A}$  coupling const. 9-17043
- C<sub>4</sub>, C<sub>3</sub> and C<sub>6</sub>, bending and stretching freqs. 9-9199
- CCl<sub>3</sub> group bound to benzene ring, freq. determ. from NQR obs. 9-4951
- $\gamma$ (CH), deformation vibrations, thiophene effect of substituted derivatives 9-7057
- CO, (A<sup>1</sup> $\Pi$ -X<sup>2</sup> $\Sigma^+$ ) syst. in absorption at high resolution in vacuum u.v. 9-18178
- CO<sub>2</sub>, on excitation by electron impact 9-760
- CO<sub>2</sub>, relax., shock tube meas. 9-759
- CO<sub>2</sub> vibration energy transfer mechanism in collision between isotopes 9-18227
- CO<sub>2</sub>+N<sub>2</sub>, near resonant transfer of vibr. energy 9-20996
- CO<sub>2</sub>, level population inversion in laser 9-13008
- CO<sub>2</sub>,  $\nu_3$  vibr., collisional relaxation meas. from fluorescence obs., variation with temp. 9-4922
- Ca(H<sub>2</sub>PO<sub>4</sub>)<sub>2</sub>·H<sub>2</sub>O, H<sub>2</sub>PO<sub>4</sub> and H<sub>2</sub>O vibrs., 4000-200 cm<sup>-1</sup> 9-15872
- Cd complexes of triphenylphosphine, i.r. spectra, assignments 9-20944
- Cdl band spectra, 4130-4800 Å, electronic transition (B)<sup>2</sup>  $\Sigma$ -(X)<sup>2</sup>  $\Sigma$ , spectrographic obs. 9-4920
- C<sub>70</sub>O<sub>2</sub> 9-18705
- CsOH and CsOD 9-761
- CuCl band system,  $\tau$ -centroid, Franck-Condon eff. determ. 9-4925
- D<sub>2</sub> in solid Ar, 77°K, fundamental band 9-14687
- D<sub>2</sub>F(BH<sub>3</sub>)<sub>2</sub>, i.r. and Raman obs. 9-18183
- DF<sub>2</sub>, mean amplitudes 9-4838
- D<sub>2</sub>S, inertia defects at fundamental state, accounting for vib. anharmonicity 9-9212
- D<sub>2</sub>Se, inertia defects at fundamental state, accounting for vib. anharmonicity 9-9212
- GeCl, new band system 9-763
- GeF<sub>2</sub>, bending frequencies, study in u.v. absorpt. spectrum 9-13351
- GeF<sub>4</sub>, force constants, determ. from harmonic freqs., equilb. config. and scaling 9-13326
- H<sub>2</sub> in solid Ne, 4°K, fundamental band 9-14687
- H<sub>2</sub>(BD<sub>3</sub>)<sub>2</sub>, i.r. and Raman obs. 9-18183
- H<sub>2</sub>(BH<sub>3</sub>)<sub>2</sub>, i.r. and Raman obs. 9-18183
- H<sup>79</sup>Br, dipole matrix elements for 2-0 vib. rot. band lines 9-15853
- H<sub>2</sub>, excited vibr. states in adiabatic approx. 9-2844
- H<sub>2</sub>, following collisions with Li<sup>+</sup> 9-7097
- H<sub>2</sub> and D<sub>2</sub>, vibr.-rot effects in Franck-Condon factors for ionization 9-5059
- HBr-HBr collisions, vib. transitions P<sub>1,0</sub> probabilities 9-11514
- HCl-CO<sub>2</sub>, H<sub>2</sub> mixtures, laser-excited vib. fluorescence, energy transfer rates 9-15854
- HCl-HC $\cdot$  and H<sub>2</sub>Cl-H<sub>2</sub>Cl collisions, vib. transitions P<sub>1,0</sub> probabilities 9-11514
- HCl, vibration-rotation spectrum, density and linewidth 9-18182
- HF<sub>2</sub><sup>-</sup>, mean amplitudes 9-4838
- HI Ar, HI<sub>2</sub> collisions, vib. transitions P<sub>1,0</sub> probabilities 9-11514
- HI-CO<sub>2</sub> mixtures, laser-excited vib. fluorescence, energy transfer rates 9-15854
- HNO<sub>3</sub>, NO<sub>2</sub> force consts and  $\langle D^2 \rangle$  in gas and liq. 9-764
- HNO<sub>3</sub>, trans. amplitudes, coriolis coupling coeff. determ. 9-4929
- HNO<sub>3</sub>, from i.r. spectra at 77°K 9-7029
- H<sub>2</sub>O, 030, 041, 131 and 031 states, calc. of Hamiltonian consts. 9-7024
- H<sub>2</sub>O, dynamics in liquid 9-13529
- H<sub>2</sub>O, force constants, determ. from harmonic freqs., equilb. config. and scaling 9-13326
- H<sub>2</sub>O, wave functions 9-9205
- H<sub>2</sub>O vapour, spectrum, vibrational-rotational fine struct. 9-4926
- H<sub>2</sub>S, extremal props. of force consts. 9-7023
- H<sub>2</sub>S, inertia defects at fundamental state, accounting for vib. anharmonicity 9-9212
- H<sub>2</sub>S and D<sub>2</sub>S 9-9211
- H<sub>2</sub>Se, inertia defects at fundamental state, accounting for vib. anharmonicity 9-9212
- Hf H<sub>2</sub>, He, Ar: collisions, vib. transitions P<sub>1,0</sub> probabilities 9-11514
- Li halides 9-9220
- Li, diatomics in mols. theory of stable mol. 9-9218
- LiCl from microwave meas. 9-18184
- LiF, from microwave meas. 9-18184
- MgCl<sub>2</sub> <sup>2</sup>H<sub>1/2</sub> rot. anal. of A<sup>2</sup> $\Pi_{1/2}$ →X<sup>2</sup> $\Sigma^+$  system,  $\lambda\lambda$ 3950-3600LB 9-11465
- MoSe<sub>2</sub><sup>-</sup>, and force consts., i.r. and Raman obs. 9-15859
- N<sub>2</sub>O, c.w. oscillations in rotation-vibration transitions 9-20519
- N<sub>2</sub>O, relax., shock tube meas. 9-775
- N<sub>2</sub>, excited in ion-mol. collisions, Franck-Condon principle violated below a certain projectile vel. 9-13402
- N<sub>2</sub>, forbidden vibr. transitions in electron-impact spectra 9-9228
- NCl<sub>3</sub>, i.r. 9-9222
- NFCl<sub>2</sub> 9-19441
- NH valency vibrations of secondary sulphonamides, temp. depend. 9-797
- NO<sub>2</sub>, force constants, determ. from harmonic freqs., equilb. config. and scaling 9-13326
- NO<sub>3</sub><sup>-</sup>, Raman frequencies from exam. of Na(K)NO<sub>3</sub>-Ca(NO<sub>3</sub>)<sub>2</sub> binary melts 9-9516
- N<sub>2</sub>O, laser-induced vibr. fluoresc. 9-7030
- N<sub>2</sub>O, vibr.-vibr. energy transfer in gas mixtures 9-4983
- N<sub>2</sub>O, vibr. excitation in N+NO<sub>2</sub> reaction, obs. 9-10326
- N<sub>2</sub>O, zero-order freqs., vib. rot. coupling consts. up to fourth order 9-13366

**Molecules continued**  
**vibration continued**

- NOCl, freqs. and force consts., isotopic species 9-777
- NO<sub>2</sub>F, force field 9-7033
- NO<sub>2</sub>, oscillator strength of Schumann-Runge band obs. 9-19444
- O<sub>2</sub><sup>+</sup> cation, frequency 9-15864
- O<sub>2</sub>, forbidden vibr. transitions in electron-impact spectra 9-9228
- O<sub>2</sub><sup>-</sup>, vibr. consts. in alkali halide crystals. 9-1807
- O<sub>2</sub><sup>+</sup> ground state, high vibrational excitation, evidence from photoelectron spect. 9-17039
- O<sub>3</sub>, intervibr. state transitions in microwave spectrum 9-4932
- OCS, potential consts., anharmonic, least squares determ. to fourth order 9-11472
- OH, H-bonded in quartz, i.r. spectra 9-5267
- O<sup>3</sup>P+CS<sub>2</sub>→SO+CS, product vibr. energy, expt. and computation 9-10327
- OS(Se) halides, mean amplitude calc. 9-7037
- (PNCI)<sub>3</sub>, vibrational spectrum, assignment of fundamental freq. 9-14693
- PO<sub>4</sub><sup>3-</sup>, Davydov splitting in Ca<sub>10</sub>(PO<sub>4</sub>)<sub>6</sub>F<sub>2</sub> cryst. 9-16167
- PSF<sub>3</sub>, vibr. anal. 9-15866
- Pd complex, Pd X<sub>2</sub>2RCN (XCl or Br and R=Me or Ph), metal-nitrogen stretching freq. 9-20937
- Pt<sub>2</sub>Cl<sub>2</sub>(AsEt<sub>3</sub>), Pt-Cl and ligand stretching vibrs., far i.r. obs. 9-15869
- Pt<sub>2</sub>Cl<sub>2</sub>(AsPh<sub>3</sub>), Pt-Cl and ligand stretching vibrs., far i.r. obs. 9-15869
- Pt<sub>2</sub>Cl<sub>2</sub>(PEt<sub>3</sub>), Pt-Cl and ligand stretching vibrs., far i.r. obs. 9-15869
- Pt<sub>2</sub>Cl<sub>2</sub>(PPh<sub>3</sub>), Pt-Cl and ligand stretching vibrs., far i.r. obs. 9-15869
- Pt<sub>2</sub>Cl<sub>2</sub>(PPrn)<sub>2</sub>, Pt-Cl and ligand stretching vibrs., far i.r. obs. 9-15869
- Pt complex, Pt X<sub>2</sub>2RCN (X=Cl or Br and R=Me or , metal-nitrogen stretching freq. 9-20937
- Pt(CO)Cl<sub>2</sub>, metal ligand vibr., i.r. and Raman obs. 9-15868
- Pt(NH<sub>3</sub>)Cl<sub>3</sub>, metal-ligand vibr., i.r. and Raman obs. 9-15868
- S<sub>2</sub> in KI cryst. 9-14082
- S<sub>2</sub>O<sub>2</sub> ion, generalised mean square amplitudes 9-20943
- S<sub>2</sub>O<sub>4</sub> ion, generalised mean square amplitudes 9-20943
- S<sub>2</sub>O<sub>6</sub> ion, generalised mean square amplitudes 9-20943
- S<sub>2</sub>-S<sub>8</sub> bond energy diff. and force consts., 9-parameter potential function 9-20941
- S<sub>2</sub>Cl<sub>2</sub>, mean amplitudes 9-9235
- SF<sub>6</sub>, de-excitation by saturable absorption 9-11473
- SF<sub>6</sub>, relaxation times, -70-150°C 9-4953
- SO<sub>2</sub>BrF, Raman and i.r. obs. 9-15870
- SO<sub>4</sub> ion, generalised mean square amplitudes 9-20943
- Se<sub>2</sub> in KI cryst. 9-14082
- SeSe<sup>-</sup> in KI cryst. 9-14082
- SiD<sub>2</sub>Cl<sub>2</sub>, fundamental freq. from i.r. absorpt. spectrum 9-13369
- SiD<sub>2</sub>HCl<sub>2</sub>, fundamental freq. from i.r. absorpt. spectrum 9-13369
- SiF<sub>4</sub>, force field calc. 9-20942
- SiH<sub>2</sub>Cl<sub>2</sub>, fundamental freq. from i.r. absorpt. spectrum 9-13369
- SiO<sub>4</sub>, in fused silica, calc. from model rel. to observed i.r. and Raman spectra 9-14694
- SnF<sub>3</sub><sup>-</sup> ion in pentafluorodistannates (II), i.r. spectra, assignments 9-20985
- SnCl, visible band system 9-789
- SnF<sub>2</sub> 9-9236
- WS<sub>2</sub><sup>2-</sup>, and force consts., i.r. and Raman obs. 9-15859
- XY<sub>3</sub>(C<sub>3v</sub>) type mol., mean vibr. amplitude calc. 9-7003
- Zn complexes of triphenylphosphine, i.r. spectra, assignments 9-20944
- Zn halides, spectra 9-792

**Molecules, mesic and muonic**

- mesomolecules, large 9-14737
- review 9-6607
- (*mu*)<sup>+</sup> ions, L=I ortho bound state h.f.s., calc. 9-4976
- $\mu$ , with momentum 1, fusion reaction rate 9-15908

**Mollier diagrams** see *Thermodynamic properties***Molybdenum**

- adsorption and desorption of O from polycryst. filament, thermionic meas. 9-11787
- adsorption of O<sub>2</sub>, mass spectroscopic investigation 9-5256
- adsorption of O<sub>2</sub> and H<sub>2</sub>, study by field emission retarding potential anal yser 9-11782
- brittleness temp. threshold, gaseous impurity effect 9-1309
- cathodic sputtering with 70 keV Ar ions, eff. of target cooling 9-19871
- crystals, slip bands on surface, study by optical microscopy 9-7546
- deposition, chemical, on Si, rel. to Schottky diode fabrication 9-6010
- dislocation redistribution during annealing and deformation 9-13688
- dislocation structure and multiplication of dislocations during thermal cycling 9-5366
- dislocation velocity temp. dependence 9-7490
- electron emission, secondary on ion bombardment, dependence on ion charge 9-21556
- electron emission and ion reflection on bombardment by rare gas ions 9-12218
- electrotransport and Soret effect, 1650-1900°C 9-16112
- Fermi surface area, exptl. estimation from size effect meas. 9-12062
- foils, deformation under electron microscope, study of slip geometry 9-5460
- impurity distrib. in single crystals obtained by electron beam zone melting 9-5344
- internal friction, dynamic modulus and creep up to 2000°C at low freq. 9-14965
- interstitial impurity content eff. on stresses 9-5452
- K $\alpha$ , emission lines, width meas. with three cryst. spectrometer 9-1820
- lattice parameter changes on defect formation on quenching and  $\gamma$ -irradiation 9-1186
- oxidation zone 9-1911
- replacement of W in alloys 9-19842
- in steel, analysis by vacuum spectrometer 9-20069
- thermionic emission CO<sub>2</sub> laser, induced 9-10079
- thin film, infl. of thickness and substrate temp. on elec. conductivity and structure 9-5238
- u.s. damping, relax. peaks activation energy rel. to prestraining 9-5546
- wines, recrystallization phenomena, investigation using simple electron optics apparatus 9-3247
- n irradiated, E<sub>a</sub>>1 MeV anomalous high temp. recovery 9-12030
- neutron irradiated, effect on yield stress and cold brittleness 9-19808
- Al electrode erosion by impulse accelerator plasmas 9-9411
- C diffusion from UC, 1000-1800°C, layer thickness calc. 9-19764
- in Fe, analysis by vacuum spectrometer 9-20069
- in Ni-Ba<sup>2+</sup>Mo alloys, ionization sign and degree from diffusion and electrotransport processes 9-1253



**Molybdenum compounds**

- carbides, supercond., heat capacities, 1.5-20°K 9-1396  
 Sical F1 n induced swelling, 500 MWd/t 9-16188  
 Sical F2, n induced swelling, 500 MWd/t 9-16188  
 single crystal, mag. susceptibility rel. to temp. 90°-750°K 9-16324  
 U-Mo 1,1 n induced swelling, 500 MWd/t 9-16188  
 CaMoO<sub>4</sub>, refractive index, pressure dependence 9-16393  
 Fe-Mo alloys, ferromagnetic magnetization 9-18679  
 Fe-Mo alloys, wetting with molten Ag 9-13508  
 Mo-Fe alloys, dil., superconductivity and Kondo effect 9-1500  
 Mo-Re alloys, elastic constants, -190 to +100°C 9-11905  
 Mo-Rh alloys, low temp. sp. ht. 9-17354  
 Mo-Ru alloys, low temp. sp. ht. 9-17354  
 Mo(CO)<sub>6</sub>, negative-ion metastable transitions 9-3015  
 MoF<sub>6</sub>, n.m.r. of <sup>19</sup>F, line narrowing indicating diffusion of molecules 9-16468  
 Mo(IV)Cl<sub>6</sub>, vibr. and electronic spectra 9-7982  
 MoNi<sub>3</sub>, close-packed ordered structures 9-19718  
 MoO<sub>3</sub>, growth of plates from vapour 9-1137  
 MoO halide complexes, ligand hyperfine interactions 9-17498  
 MoO<sub>3</sub>, adsorpt. of photosensitized H atoms, suction effect 9-17247  
 MoO<sub>3</sub> thin film detector for H beams 9-6728  
 MoS<sub>2</sub>, Kikuchi lines, intensity anomaly 9-14918  
 MoS<sub>2</sub> film lubricant on steel, pressure effects on friction coefficient 9-16138  
 MoS<sub>2</sub>, angular distribution of evaporated Au nuclei 9-9614  
 MoS<sub>2</sub>, hexagonal and rhombohedral crystals, optical absorption props. 9-1798  
 MoS<sub>2</sub>, Kikuchi lines, intensity anomaly 9-9679  
 MoS<sub>2</sub> films, transmission of electrons, anomalous 9-9680  
 MoS<sub>2</sub> thin crystals, photovoltage, 77°-290°K 9-13934  
 MoSe<sub>2</sub><sup>2-</sup>, vibrs. and force consts., Raman and i.r. obs. 9-15859  
 MoZn<sub>22</sub>, crystal structure from X-ray powder data 9-19719  
 Ni-Fe-Cu-Mo alloy, rolled from sintered compacts, high mag. permeability 9-13965  
 Ni (10 at.%)Mo alloy, K-state formation, activation energy 9-17342  
 Ni-Mo alloys, anodic props., mag. field effects 9-21709  
 Ni-Mo alloys, in H<sub>2</sub>SeO<sub>4</sub>, anodic behaviour, effect of mag. transform 9-21708  
 Ni (8at.%)Mo alloy, Mo ion diffusion and electrotransport process 9-1253  
 Ti-Mo alloys, U diffusion 9-19769  
 U-Mo-Al-Sn, n induced swelling 500 MWd/t 9-16188  
 α-U-Mo alloys, supercond. props. pressure dependence, 0-10 kbar 9-12130  
 U (10 wt.%)Mo alloy, stress-corrosion cracking, effects of heat treatment and ambient atmospheres 9-21384  
 UO<sub>2</sub>-Mo cermets, isothermal Young's modulus 9-19777

**Monitoring** *see Radiation monitoring***Monochromators**

- See also Filters, optical; Light sources; X-ray monochromators*  
 electronic control, for Warsaw flash spectrophotometer 9-10937  
 microwave cavity in far u.v. light intensities absolute calibration 9-17891  
 neutron, Ge monocrystal, temp. and press. effects 9-5307  
 neutron, improvements using Cu crystals doped with Be and distorted Ge 9-19700  
 neutron, unit for crystal spectrometer 9-18032  
 for neutron scatt. and diffr. meas., laminated crysts. 9-17263  
 trochoidal, for e beam, in axial mag. field 9-2340  
 u.v., mass spectrometer, combination for photoionization obs. 600-1000 Å 9-7195  
 wavelength modulation for 9-15557  
 wavelength modulation for 9-6561

**Monolayers** *see Adsorbed layers***Monomers** *see Molecules***Monomolecular layers** *see Adsorbed layers***Monte Carlo method** *see Statistical analysis***Moon**

- altitude var., asymmetry rel. to equator 9-2038  
 brightness in i.r. region as function of phase angle, and albedos 9-6162  
 capture and evolution, rel. to exterior origin of earth's crust, theory 9-10377  
 capture and evolution, rel. to exterior origin of earth's crust, theory 9-10378  
 chemical analysis by Surveyor VI, preliminary obs. 9-21927  
 chemical analysis by Surveyor VII, prelim. obs. 9-17640  
 colour index distribution regularities across the surface 9-4115  
 crater formation, inapplicability of Baldwin's relation for determining causes 9-8274  
 crater formation, inapplicability of Baldwin's relation for determining causes 9-8273  
 craters, geological obs. from lunar precursor probes 9-21921  
 craters, rings, comparative morphology; and volcanic formations in Kamchatka 9-2041  
 crust, Brewster angle of reflections 9-18902  
 crust and crater morphology, and geological history 9-6163  
 crystals on surface 9-18900  
 diamagnetic solar-wind cavity, Explorer obs. 9-10547  
 Earth-Moon system, history, effect of tidal friction 9-6171  
 Earth-Moon system, history, effect of tidal friction, reply to comments 9-8276  
 Earth-Moon system L<sub>4</sub> point, choice of consts. influence on spacecraft motion 9-8216  
 Earth-Moon triangular points, sun disturbed, two stable periodic orbits 9-10449  
 eclipse, calcs. 9-12745  
 eclipse, infrared variation over surface obs. 9-4117  
 during eclipse, thermal conditions of upper cover and integral radio emission 9-4114  
 eclipse, total, 18 Oct 1967, black-body disk temp. obs. 9-20215  
 electrons, 30 KeV, recording in circumlunar space using Luna-11 satellite 9-18899  
 elliptic motion, periodic soln. of plane 3-body problem 9-17637  
 ephemeris inconsistency, radio tracking confirmation 9-20217  
 ephemeris inconsistency, numerical determ. 9-20216  
 ephemeris inconsistent with radar data 9-20218  
 Far side, comparison of American and Soviet co-ord. systems. 9-6164  
 gamma radiation from rocks, composition according to results of Lunar-10 experiment 9-18898

**Moon continued**

- geological results from lunar precursor probes 9-21921  
 geothermal prospects and deposits, evidence, possible recovery and applics. 9-10509  
 gravitating field and lunar figure obs. 9-21920  
 hot and cold, distinction between, method based on solar wind-induced planetary dynamo current system 9-14235  
 infrared obs. 9-4117  
 introductory book 9-14234  
 i.r. spectra, surface thermal emission, balloon-borne obs. 9-2044  
 laser ranging for earth separation determ, test of non-Newtonian gravitational theories 9-8380  
 libration clouds, visual obs. and an observing ephemeris 9-14237  
 light location, use of laser 9-250  
 literal series for integration of eqns. of motion 9-10508  
 luminescence, lab. simulation, powdered rock sample, proton and u.v. irradiation 9-20221  
 luminosity in eclipse, and shape of solar corona 9-15352  
 lunar figure and gravitating field obs. 9-21920  
 lunar hour angle relationship to meteorite falls 9-21951  
 lunar surface layer, thickness determ. 9-6166  
 magnetic material in Sinus Medii, Surveyor 6 obs. 9-21924  
 Marius Hills, geological obs. from lunar precursor probes 9-21921  
 mascons, as iron meteorites, depth calc. 9-18904  
 mascons. due to lava flows into meteor-formed hollows 9-18907  
 mascons and isostasy 9-18906  
 mascons and lunar history 9-18908  
 mascons due to geological structure and fill of maria 9-18905  
 mass and earth orbit determ., Mariner V expt. 9-10532  
 microwave emissivity rel. surface roughness 9-21947  
 orbiting vehicles, meteoroid hazard 9-21950  
 Orientale Basin, geological obs. from lunar precursor probes 9-21921  
 outer layer, determination of elastic limit 9-21922  
 plasma, low energy meas., by Explorer 35 9-21929  
 position, basic scheme revision for Janus (Saturn satellite X) 9-10523  
 profile from occultation of ZC 1137 on 17 Sep 1968 9-18851  
 radar obs. 9-20220  
 radiation intensities in 3.6-4 mm. range, comparison with sun's radiations 9-8288  
 radio waves from distant source, focusing by ionosphere 9-1962  
 regolith thickness variations, genetic implications 9-21923  
 r.f. spectra, influence of temp. depend. of mat. props. 9-2042  
 rotation axis, precession, nutation and selenographic co-ords. 9-2039  
 satellite motion, eff. of rad. press. of solar, lunar e.m. rad. 9-2040  
 satellite orbits classification, secular eff. of earth and moon 9-2045  
 scattering, radio range 9-18901  
 seas, origination mechanism 9-18897  
 seismicity rel. meteoritic impacts 9-17638  
 soil strength rel. relative cleanliness 9-16606  
 soil struct. and surface optical props., Surveyor I and III obs. 9-15336  
 soil structure, inconsistent with chondritic meteorites 9-10517  
 soil-density meter-penetrator of automatic lunar station Luna-13 9-6157  
 space flight trajectories, passing through centre of moon, return to earth 9-18823  
 star map of lunar sky, ecliptic coordinate system 9-18846  
 steady state homogeneous, density dist. 9-10510  
 stratovolcanoes in lunar mesorelief 9-4116  
 surface, brightness, colour index and colour distrib. of areas, multicolour photometry 9-6159  
 surface, e.m. props., Surveyor 5 magnet expt. 9-21925  
 surface, photographs, Lunar Orbiters I-V 9-18896  
 surface, reradiation and thermal emission 9-6167  
 surface bleaching by solar photoreduction 9-21928  
 surface brightness temp. and thermal characts., Surveyor 5 obs. 9-21926  
 surface density meas. by automatic station Luna 13 9-6158  
 surface i.r. absorpt. bands, petrologic significance 9-17639  
 surface materials mechanical props., Surveyor 5 obs. 9-21930  
 surface mechanical props. at Surveyor 3 landing site 9-10514  
 surface navigation, method using struct. of Nautical Ephemeris for the Moon 9-6161  
 surface soil, density 9-6168  
 surface solar wind spectrometer expt. for Apollo astronauts 9-20236  
 surveyor 3, TV observations 9-10513  
 surveyor 3 landing 9-10511  
 Surveyor 3 lunar theory and processes 9-10516  
 surveyor 3 mission, principle scientific results 9-10512  
 surveyor footprints, albedo and photometry comparisons with undisturbed surface 9-8275  
 temp. and thermal characts. Surveyor 3 results 9-10515  
 thermal conditions of upper cover and integral radioemission during the eclipse 9-4114  
 thermal radiation obs. 9-20219  
 thermoluminescence 9-6165  
 three-colour photoelec. scanning, showing colour variations in range 5 to 15% with fluctuation period ≈ 1 sec 9-6160  
 tidal variations in Fe<sub>2</sub> in American zone, geomag. anomaly eff. 9-18816  
 Tsiolkovsky crater, farside, nature and origin 9-18903  
 Tycho crater, radar study 3.8, 70 cm wavelength 9-2043  
 umbra radius during total solar eclipse (12 Nov 1966) 9-17636
- Morse potential** *see Kinetic theory; Molecules; intermolecular mechanics*  
**Mosaic structure** *see Crystal structure; microstructure*  
**Mossbauer effect**  
*See also Gamma-rays/absorption; Nuclear excitation*  
 alkaline earth phosphate glasses, of iron 9-15173  
 γ-optical transitions, laser-stimulated, rel. to hyperfine structure of ions of Mossbauer nuclei 9-18696  
 chalcopyrite, 80-700°K, meas. 9-5889  
 coincidence spectroscopy, inclusion of finite resolution time in anal. 9-441  
 colloid solns., effect of viscosity 9-3138  
 cubic lattice with line defect 9-12354  
 cytochrome c 9-831  
 diffusion in solids, direct obs. method 9-5401  
 diffusion of Fe in Au, measurement 9-3377  
 ferroelectrics, near phase transition 9-1364  
 films, importance of local modes 9-18544  
 films magnetic moment motion detection by spectroscopy, r.f. field eff. 9-15147  
 hemin, pressure effects 9-9202

**Mossbauer effect** continued

- hyperfine interactions for  $I=1/2-3/2$  in electron degenerate system 9-16399
- iron gluconate, quadrupole splitting and isomer shift obs. 9-5894
- line shape, generalized Kubo-Anderson model, a stochastic theory 9-7931
- parity-isospin nonconservation detection 9-497
- phthalocyanine iron (II),  $^{57}\text{Fe}$  Mossbauer spectrum at 4.2 and 100°K 9-10100
- recoilless absorpt. and emission of  $\gamma$ -rays rel. to solid state props. 9-18695
- resonance strength rel. to second-order Doppler shift in zero-point velocity determ. 9-14020
- resonance study, high press.-low temp., clamp cell meas. 9-12355
- self-inversion of  $\gamma$  lines 9-8972
- solid, resonance lines inhomogeneous broadening, review 9-18689
- space parity violation effects in e.m. transitions 9-498
- spectra, smoothing in multichannel analyzer 9-20706
- spectrometer, increased capacity using tape recorder 9-2568
- spectrometer for the meas. of isomer shifts 9-19222
- spectrometer multiscaling module 9-13174
- spectrometry, review 9-3868
- spectroscopy, chemical and biological applics. 9-21608
- spectroscopy, zero point calibration technique 9-19973
- spin broadening of lines of impurities in ferromagnetics, of atoms in antiferromagnetics 9-3869
- steel, phase transition obs. 9-16151
- steel, stainless, infl. of plastic deformation 9-19981
- structure formed by cryst. mag. fields at nuclei having Mossbauer isotopes, direct determ. 9-1747
- T-reversal invariance of nuclear reactors, tests for  $E(L+1)-M(L)$  phase differences 9-500
- temperature depend., correl. of recoilless  $\gamma$  reson. fraction with density 9-8971
- tetraphenyl tin, thermal neutron reactor radiation eff. 9-5582
- transition metals, of  $^{57}\text{Fe}$ , isomer shift 9-12357
- X-ray scattering relationship from Fourier transform of time independent Patterson function 9-7385
- zeolite molecular sieve,  $\text{Fe}^{3+}$  introduction, Mossbauer evidence of superparamagnetism 9-5810
- $\gamma$  ray abs. theory 9-6599
- $^{232}\text{Th}$ , following Coulomb excitation 9-4742
- $^{153}\text{Eu}$  8.34 keV rot. level, mag. moment and charge radius meas. 9-6792
- $^{125}\text{Te}$  cpds., meas. and anal. 9-16405
- $^{237}\text{Np}$ , 77°K 9-13198
- $^{89}\text{Sr}$  69.6 keV  $\gamma$ 's obs. at 4.2°K, half life, mag. moment determ. 9-4739
- $^{119}\text{Sn}$  isomer shifts, correl. with electronic props. 9-11475
- $^{119}\text{mSn}$  23.9 keV g.s. transition total internal conversion coeff. obs. 9-6800
- Ag-Sn solid solns., plastic deform. and annealing effects 9-1750
- Ba $\text{Fe}_{12}\text{-xAl}_x\text{O}_{19}$ , obs. of effects on saturation magnetization of Al substitution 9-16366
- CaSnO<sub>3</sub>, suitable source 9-12358
- $^{57}\text{Co}$ -Pd experimental source production 9-11898
- Co oxides, Fe atoms behaviour, crystal structure interpretation 9-5887
- CoMn<sub>2</sub>Fe<sub>2-x</sub>O<sub>4</sub> charge distrib. 9-1119
- CoO,  $^{57}\text{Fe}$  relaxation rates, limitations 9-1749
- CrI<sub>3</sub>, of  $^{129}\text{I}$ , internal field obs. 9-21609
- CsI, of  $^{129}\text{I}$ , 26.8 keV transition, calc. using Debye model of phonon spectrum 9-12359
- Cs-graphite cpds, lammelar, study of chem. bonding 9-7353
- Cu:Fe, diffusion obs. 9-5401
- Cu:Fe $^{2+}$ , lattice dynamical props 9-7638
- Cu-Sn alloys, isomeric shift of  $^{119}\text{Sn}$  9-5888
- Cu-Sn solid solns., plastic deform. and annealing effects 9-1750
- Cu, of  $^{57}\text{Fe}$ , high pressure effect at room temp. 9-21610
- Cu<sub>0.75</sub>Au<sub>0.25</sub> solid solns., plastic deform. and annealing effects 9-1750
- Cu<sub>0.5</sub>Cd<sub>0.5</sub>Fe<sub>2-x</sub>O<sub>4</sub> $^{57}\text{Fe}$ , 4.2-1000°K, in ext. mag. fields 9-7956
- CuCr<sub>2</sub>Te<sub>2</sub>, of  $^{129}\text{I}$ , internal mag. field in iodine impurities 9-16400
- CuFe<sub>2-x</sub>O<sub>4</sub> $^{57}\text{Fe}$ , 4.2-1000°K, in ext. mag. fields 9-7956
- CuFeS<sub>2</sub>, of Fe $^{3+}$ , obs., discrepancy with previous work 9-10182
- CuFeS<sub>2</sub> (chalcopyrite), 80-700°K, meas. 9-5889
- Cu<sub>0.5</sub>Zn<sub>0.5</sub>Fe<sub>2-x</sub>O<sub>4</sub> $^{57}\text{Fe}$ , 4.2-1000°K, in ext. mag. fields 9-7956
- Dy, conduction e. density at nucleus from isomer shifts 9-16211
- Er: $^{119}\text{Sn}$ , hyperfine mag. fields 9-5890
- Eu-Ba, of  $^{151}\text{Eu}$  21.7 keV line 9-7957
- Eu-Yb, of  $^{151}\text{Eu}$  21.7 keV line 9-7957
- Eu, first order transitions obs. 9-15148
- EuFe garnet, of  $^{151}\text{Eu}$  rel. to hyperfine interac. of 21.7 keV level 9-16401
- Fe-rare earth intermetallics, cubic Laves, hyperfine field study 9-7958
- Fe-Al, alloys, electron transitions from isomeric shift and X-ray emission spectra parameters 9-3871
- Fe-Be solid solution, elec. field gradient variation 9-17477
- Fe-Cr alloys, spectra, use of zero point calibration technique 9-19973
- Fe, of  $^{57}\text{Fe}$ , high pressure eff. at room temp. 9-21610
- Fe $\beta$  ferromagnetic, hyperfine mag. field and quadrupole interaction obs. 9-21670
- Fe $\beta$ Zr ferromagnetic, hyperfine mag. field and quadrupole interaction obs. 9-21670
- Fe $^{3+}$  spectra, hyperfine structure, rel. to spin-lattice relax. study 9-18688
- Fe complex, [Fe(salen)Cl]<sub>2</sub>, {salen=NN'-ethylenbis-(salicylaldiminato) anion} 9-18697
- Fe corrosion prods. analysis by Mossbauer backscatt. spectroscopy 9-10363
- Fe cpds., standard ref. mat. for chemical shift 9-3872
- Fe dimeric compounds, Mossbauer effect, relaxation effects 9-18697
- Fe halides, ferrous, anhydrous, obs. 3d electron delocalization 9-14036
- Fe phthalocyanine, pressure effects 9-9202
- $^{57}\text{Fe}$ , interference of Mossbauer scatt. and Rayleigh scatt. 9-7959
- $^{57}\text{Fe}$ , spectrum of resonance  $\gamma$ -rad., rel. to relax. time in excited state 9-501
- $^{57}\text{Fe}$  narrow-line sources, prep., and investigation of causes of line broadening 9-5891
- $^{57}\text{Fe}$  spectra, nuclear polarisation effects, depend. on hyperfine field magnitude and sign 9-19289
- Fe $^{3+}$  ions in ice and FeCl<sub>3</sub>·6H<sub>2</sub>O 9-14037
- Fe $\beta$ (CO)<sub>5</sub>, effect of high press. 9-10183
- Fe $\beta$ (CO)<sub>12</sub>, effect of high press. 9-10183
- FeCl<sub>3</sub>, thermal shift meas., 83-350°K 9-16402
- FeCl<sub>3</sub>, transition from h.c.p.-f.c.c., evidence 9-5515

**Mossbauer effect** continued

- Fe(ClO<sub>4</sub>)<sub>3</sub> frozen soln., obs. mag. relax. eff. 9-12360
- FeGe, cubic, mag. props. exam. 80-300°K 9-16355
- Fe(III) tetrahedral ions, hyperfine interactions 9-1748
- $\alpha$ -Fe<sub>2</sub>O<sub>3</sub> microcrystals, quadrupole interaction 9-3870
- Fe<sub>2</sub>O<sub>3</sub>, magnetite microcrystals, superparamagnetism obs. 9-10135
- $\beta$ -FeOOH detect. on steel by Mossbauer backscatt. spectroscopy 9-10363
- FePO<sub>4</sub>, antiferromagnet, rel. to anisotropy const. 9-5854
- FeS, near stoichiometric, hyperfine interactions, meas. rel. to temp. depend. 9-5892
- FeS<sub>8</sub>, magnetic structure study 9-10119
- FeSb<sub>2</sub>O<sub>4</sub>, paramagnetic, spectra quadrupole splitting, 50 to 817°K 9-14038
- n-GaP, of  $^{57}\text{Fe}$ , anomalous broadening during cooling 9-5893
- $^{72}\text{Ge}$ , coulomb-recoil implantation expts. rel. to nuclear and solid-state props. 9-6827
- I<sub>2</sub>O<sub>4</sub>, of  $^{129}\text{I}$ , quadrupole splitting at 80°K 9-16403
- n-InAs:Te, of  $^{57}\text{Fe}$  9-5893
- KNO<sub>3</sub> spectra,  $^{57}\text{Co}$  source, isomer shift, Debye-Wallace factor, quadrupole splitting obs. 9-14039
- Kr, solid recoilless fraction 9-12361
- Kr in clathrate, dynamics 9-3513
- $^{57}\text{mFe}$ , nuclear quadrupole moment determ. 9-3976
- Mg<sub>2</sub>SnO<sub>4</sub>, thermal neutron capture, chem. eff. study 9-17549
- Na<sub>2</sub>O-SnO<sub>2</sub>-SiO<sub>2</sub> glass, rel. to Sn valence states 9-1751
- Na<sub>2</sub>[Fe(CH<sub>3</sub>NO)<sub>2</sub>·H<sub>2</sub>O] standard ref. for chemical shift of Fe cpds. 9-3872
- Nb<sub>2</sub>S<sub>6</sub>, of  $^{119}\text{Sn}$  rel. to temp-dependent isomer shift and anharmonic binding of  $^{119}\text{Sn}$  9-7960
- Ni:Fe $^{2+}$  Fe atom state at grain boundaries 9-21611
- Ni, of  $^{57}\text{Fe}$ , magnetocrystalline anisotropy study 9-12279
- NpO<sub>2</sub>, of  $^{237}\text{Np}$  rel. to hyperfine field and antiferromag. ordering obs. 9-1708
- Pd:Fe $^{2+}$ , lattice dynamical props 9-7638
- Pd<sub>2</sub>MnSn Heusler alloy, internal field at  $^{119}\text{Sn}$  site 9-16404
- Pt:Fe $^{2+}$ , lattice dynamical props 9-7638
- Pt-Fe alloy, mag. structure rel. to ordering 9-12362
- Rb<sub>2</sub>FeF<sub>4</sub> antiferromagnetic planar long-range order investigation 9-7922
- Sb-organic cpds., isomeric chem. shift 9-3874
- Sm, conduction e. density at nucleus from isomer shifts 9-16211
- Sm<sub>2</sub>Co<sub>7</sub>,  $^{151}\text{Eu}$ , hyperfine interactions meas. 9-14040
- Sm<sub>2</sub>Ni<sub>7</sub>,  $^{151}\text{Eu}$ , hyperfine interactions meas. 9-14040
- SmFe $^{2+}$ ,  $^{151}\text{Eu}$ , hyperfine interactions meas. 9-14040
- Sn-transition metal bond,  $^{119}\text{mSn}$  data on nature 9-16048
- Sn, resonant  $\gamma$  radiation, diffraction in Bragg scattering by nuclei and electrons 9-21612
- SnCl<sub>2</sub>, thermal neutron reactor radiation eff. 9-5582
- SnI<sub>4</sub>, lattice dynamics 9-1365
- SnM<sub>2</sub>O<sub>4</sub>, (M=Co, Mg, Zn, Mn), oxidic spinels 9-1752
- SnO, resonance line form, microstructure dependence 9-1753
- SnO, thermal neutron reactor radiation eff. 9-5582
- SrFe<sub>12-x</sub>Ga<sub>x</sub>O<sub>19</sub> partial substitution of Fe by Ga, effects obs. 9-16373
- Te, of  $^{57}\text{Fe}$ , high pressure effect at room temp. 9-21610
- UFeO<sub>4</sub>, magnetic ordering study 9-3873
- V, of  $^{57}\text{Fe}$ , high pressure effect at room temp. 9-21610
- V<sub>2</sub>O<sub>5</sub>:Fe $^{3+}$ , Sn $^{4+}$ , of  $^{57}\text{Fe}$  and  $^{119}\text{Sn}$  9-21613
- Xe bromides, formation in  $\beta$ -decay of  $^{129}\text{IBr}_2$  9-4016
- Y<sub>10</sub>Ga<sub>2</sub>Fe<sub>8</sub>O<sub>12</sub> of  $^{57}\text{Fe}$ , 78° and 300°K, mag. sublattices 9-21591
- ZnMn<sub>2</sub>Fe<sub>2-x</sub>O<sub>4</sub> charge distrib. 9-1119
- (Zr<sub>1-x</sub>Nb<sub>x</sub>)Fe<sub>2</sub>, magnetism study 9-16406

**Motors** *see* **Electrical machines****Multiple stars** *see* **Stars****Muonic atoms** *see* **Atoms, mesic and muonic****Muonic molecules** *see* **Molecules, mesic and muonic****Muonium****Muonium** *see* **Acoustics/musical**

in chemical reactions, classification and reaction rate 9-10316

formation in Kr, fractional press. shift of hyperfine structure interval 9-20905

hyperfine splitting and fine struct. const. 9-4870

muonium-antimonium conversion, search 9-6610

review 9-6607

hyperfine structure interval, low mag. field obs. 9-20905

**Muons**

*See also Cosmic rays/muons; Nuclear reactions and scattering due to muons*

depolarization reviewed 9-6607

gravitational coupling, test for equivalence principle 9-4567

heavy, lower bound mass estimated 9-10977

magnetic moment, anomalous, and field current identity 9-20606

magnetic moments, gyromag. ratio with electron, calc. of sixth-order contrib. from fourth-order vacuum polar. 9-16826

polarization in superconductors, rel. to exptl. investigation of periodic structure 9-1493

production in elastic neutrino scatt. interaction, obs. in CERN spark-chamber 9-14469

X-ray spectra, intensity meas. in different targets 9-3909

$\mu^-$  polarization, residual, relative values in water (-196°-+100°C) and hydrocarbons 9-10986

$\mu^+$  from K $\beta$  decay, polarization meas. 9-17974

**capture**

angular correlations in unique capture by spin targets 9-8757

$\mu^-$ , by  $^{12}\text{C}$ , capture rate and wave functions calc. 9-14605

**decay**

$\mu$ -e n sec. time analyser 9-2608

radiative corrections, finiteness generalised to all orders 9-2470

spectrum of polar.  $\mu$  in Fermi interac., parameter meas., radiative correct. 9-6609

**detection, measurement**

absorption obs. from underground laboratory, depth determ. 9-10987

beam, 11 GeV/c momentum meas. method 9-4433

**interactions**

cosmic ray, current model 9-435

e.m. reviewed 9-6607

Fermi, general, polar.  $\mu$  decay spectrum, parameter meas. 9-6609

range in medium with  $Z=10-13$  and ang. distrib. underground 9-10988

X-ray production and calibration of a Ge (Li) detector 9-19234

$\mu$  collisions, calc. of bremsstrahlung 9-15581



**Muons continued****interactions continued**

$\mu^+\mu^- \rightarrow \nu\nu$  diff. and total cross sections formulae determ. 9-10983

**production**

cosmic ray, at high energies, direct prod. rate limit 9-437

electron accelerators, theory and experiment 9-19254

TeV region by  $\pi$ , K in cosmic rays 9-1981

$\mu^+\mu^-p$  from  $\gamma\gamma$  interaction, differential cross section meas., quantum electrodynamics test 9-20583

**scattering**

electron accelerators, theory and experiment 9-19254

$\mu^-$  from electrons at 6 and 11 GeV, obs. 9-6608

$\mu^+$  from electrons at 6 and 11 GeV, obs. 9-6608

$\mu p$ , p-odd correlations calc., Tanikawa-Watanabe renormalizable theory 9-10981

$\mu p$ , polarization-odd effects,  $E_0 \approx 10$  GeV 9-14471

$\mu p$  radiative corrections, review 9-20603

$\mu^2p$ , renormalizable theory of weak interaction 9-335

**Musical instruments**

flute, acoustics when viewed as positive-feedback oscillator 9-6386

flute, fund. freq. shift by tract resonance 9-6387

flute, long tone relative SPL and harmonic struct. 9-10737

flute and organ pipe, sounding mechanism 9-2224

pipe organ, initial delay and rise time meas. 9-4344

violin, electroacoustic meas. techniques 9-20434

violin, parts and mutes 9-6388

violin varnish, acoustical eff., mass, stiffness, and internal friction meas. 9-4345

wood-wind, reed blown, reed motion influence on reson. freq. 9-20433

**Navier-Stokes equations** *see Flow; Hydrodynamics***Nebulae**

*See also Galaxies*

3C 454.3, optical variability 9-12672

Andromeda, dust matter 9-1998

BD+30°3639, planetary, spectra, absolute intensities of i.r. lines 9-21854

Coal Sack, flare star obs. 9-16588

cometary, investigation of Simeiz 129 and 130 9-1996

Crab,  $\gamma$  emission search, X-ray telescope 9-21858

crab,  $\gamma$ -ray detection by digitized spark chamber 9-8232

Crab, polarization distrib., interferometric technique 9-12734

crab, position of radio source of small angula dimens. 9-2036

Crab, special relativity applic. for determ. of nature of radiation 9-4107

Crab, two pulsating radio sources 9-18892

Cygnus Loop, O III temperature for one 'filament' 9-18843

diffuse, high-velocity motions rel. to interaction with stellar wind 9-8229

diffuse, Ly- $\alpha$  radiation transfer 9-6117

diffuse, O, N, Ne abund., mechanism 9-20162

emission, high resolution obs. at 408 MHz 9-20165

extragalactic, orthogonal fan jet in central region 9-4091

gas motions and stellar wind 9-4094

gaseous, eff. of self-absorption and internal dust on H-line intensities 9-20163

glow of reflection near Meropa and Maia 9-1997

He 1-5, planetary, photoelec. obs. of nuclei 9-21853

H II region, radio obs. of NGC 281 and an unnamed nebula 9-10468

H II regions, ionized, temp. struct. and emission props. 9-8233

Horseshoe, helium radioline at 5765.2 Mhz 9-4093

IC 443, radio spectra abs. 9-1999

IC 1396, spectra of  $H_\alpha$ -emissive objects 9-1995

IC 2149, planetary, spectra, absolute intensities of i.r. lines 9-21854

IC 3568, planetary, spectrophotometric studies 9-16560

IC 405, electron temp., high resolution interference method 9-18844

IC 418, H II region photoelectric study, temp., chemical abundance determ. 9-21852

IC 418 spectra discrepancies for expt. obs. and computer model 9-6116

IC 443 supernova relic, spectrophotometry,  $H_\alpha$  and (NII) intensities, rel. meas. 9-21857

IC 4997, planetary, spectra, absolute intensities of i.r. lines 9-21854

M 87, orthogonal fan jet in central region 9-4091

M 17, H II region photoelectric study, temp., chemical abundance determ. 9-21852

M 8, H II region photoelectric study, temp., chemical abundance determ. 9-21852

near Meropa and Maia, glow of reflection 9-1997

Monoceros Nebulosity, rel. to supernova remnant 9-16562

NGC 1499, electron temp., high resolution 9-18844

NGC 1514, planetary, obs. rel. to binary system hypothesis 9-8226

NGC 1514, planetary, photoelec. obs. of nuclei 9-21853

NGC 6572, H II region photoelectric study, temp., chemical abundance determ. 9-21852

NGC 6803, H II region photoelectric study, temp., chemical abundance determ. 9-21852

NGC 6888 supernova relic, spectrophotometry,  $H_\alpha$  and (NII) intensities, vel. meas. 9-21857

NGC 7027, i.r. emission rel. to discrete line emission 9-8230

NGC 7293, mass, dimens. of radial filaments 9-1993

NGC 7293, planetary thin radial filaments, model 9-21855

NGC 7640, planetary, spectra, absolute intensities of i.r. lines 9-21854

NGC 7662, planetary, spectre, absolute intensities of i.r. lines 9-21854

NGC 7662, spectra discrepancies for expt. obs. and computer model 9-6116

NRAO 591/593 radio nebula, struct. and analysis 9-20164

Omega, H56 $\alpha$  recombination radio line detect. 9-16563

Orion, comparative study of variable stars 9-18867

Orion, electron temp., high resolution interference method 9-18844

Orion, electron temp. from 28 hydrogen  $n\alpha$  lines obs. 9-16564

Orion, H II region photoelectric study, temp., chemical abundance determ. 9-21852

Orion, helium radioline at 5765.2 Mhz 9-4093

planetary, absolute intensities of emission lines 9-4090

planetary, at 408 MHz, thermal spectra obs. 9-15279

planetary, distances, masses and space densities 9-4089

planetary, electron temp. in outer regions, 3000-10000°K, radio spectra and isophotes obs. 9-6115

planetary, He I-5 and NGC 1514, photoelec. obs. of nuclei 9-21853

planetary, high excitation, opt. depth due to continuum abs. by N, O and Ne 9-16561

planetary, in magellanic clouds, kinematics 9-12671

planetary, low-density, Lyman-line decrements 9-18841

planetary, model, e temp. and ionization stratification 9-8228

**Nebulae continued**

planetary, population discrimination 9-8227

planetary, radio obs. on 84 at 5000 MHz 9-12670

planetary, reddening curves from comparison of radio obs. with H recombination lines 9-15278

planetary, SMC, kinematics 9-12671

planetary, southern, observations 9-21856

planetary calc. of electron densities from from S II line 9-14195

planetary in LMC, kinematics 9-12671

planetary NGC 3132, magnitude and color of central star HD 87892

determ. 9-14194

planetary stage in stellar evolution using He shell burning model 9-2008

plasma, partial maser effect in recombination lines of H atoms 9-8231

reflection, associations, use to outline Orion spiral arm 9-4092

Rosette, interferometric study of H $_2$ /(NII) ratio 9-18842

Rosetti, electron temp. 9-16562

Simeiz 130, spectra of  $H_\alpha$ -emissive objects 9-1995

Simeiz 129 and 130, cometary, investigation 9-1996

Stromlo 16, optical spectrum of Vela X 9-1994

H56 $\alpha$  recombination radio line detect. in Omega nebula 9-16563

**Neel temperature** *see Magnetic properties of substances***Negatons** *see Electrons***Negatrons** *see Electrons***Nematic phase** *see Liquid crystals***Neodymium**

crystal, d.h.c.p., Fermi surface, rel. to mag. ordering and structure 9-5615

glass laser, 1 GW, design 9-4479

glass laser, continuous shift in emission band 9-15529

glass laser, two channel, single pulse, 180 joule output 9-19160

ions, NdIV 4F free-ion levels from LaCl $_3$ :Nd $^{3+}$  spectra and calc. 9-4831

laser, clearing effect on phthalocyanine soles. 9-1015

laser, dynamic emission under nonuniform broadening conditions 9-4480

laser, pumping efficiency, effect of rare gas spectra 9-15530

lasers, Nd $^{3+}$  glass, passive transverse mode locking by dye technique 9-20524

CaWO $_4$ :Nd $^{3+}$  solid laser, sun-pumped, 130 mW power output 9-13031

Nd:CaWO $_4$  laser, slowly Q-switched, output characts. 9-10867

Nd:glass laser, compression of picosecond light pulses 9-6525

Nd:glass laser, subpicosecond structure in relax. oscills. 9-20525

Nd:glass laser oscillator, spectral control by secondary light sources 9-13032

Nd $^{3+}$ :SeOCl $_2$  liquid laser, operating characts. 9-13023

Nd $^{3+}$ :SeOCl $_2$  liquid lasers, Q-switching and mode-locking 9-8621

Nd:YAl garnet laser, continuously pumped, repetitive Q-switching using Fabry-Perot interferometer 9-13033

Nd-glass laser, two-rod assembly, reln. between output and design parameters 9-8623

Nd $^{3+}$ :POCl $_3$  liquid lasers 9-14430

Nd $^{3+}$ /SeOCl $_2$  soln. prep. 9-14431

Nd $^{3+}$ , e.p.r. and spin-lattice relaxation in LaNbO $_4$  9-20021

Nd $^{3+}$  doped laser resonator, e.m. coupling with glass-fibre waveguide 9-14434

Nd $^{3+}$  in Ca $_2$ (PO $_3$ ) $_4$ F, absorpt., luminescence spectra and stimulated emission 9-18709

Nd $^{3+}$  in CaWO $_4$ , Lande factor of excited state by Cotton-Mouton eff. 9-18698

Nd $^{3+}$  in POCl $_3$ -SnCl $_4$  soln., fluorescence spectra and radiative lifetimes 9-21217

Nd glass laser peak separation and energy characts. rel. to focusing elements in resonator 9-6526

Nd $^{3+}$ ,  $^4I_{9/2} \rightarrow ^4P_{1/2}$  transition in Al-Y garnet, vib. mechanism due to ion-phonon relax. 9-10186

Nd $^{3+}$  in glass, optical absorption spectra obs., structural features determ. 9-10193

Nd $^{3+}$  in SeOCl $_2$  aprotic solvent, laser emission 9-17876

Nd $^{3+}$  in YVO $_4$ , e.p.r. 9-16461

Nd $^{3+}$  ion interaction in CaF $_2$ , SrF $_2$ , and BaF $_2$  crystals 9-15161

Nd $^{3+}$  in Ba $_2$ MgGe $_2$ O $_7$ , laser action and optical spectra 9-5914

$^{16}\text{O}(^3\text{He},p)^{18}\text{F}$ ,  $E_{\text{th}} = 19.8 \text{ MeV}$ , spectrum and ang. distrib. obs. 9-6895

in SeOCl $_2$ , circulating liquid laser system 9-13022

YAl garnet:Nd laser, non-mode-locked, two photon fluorescence displays 9-6527

**Neodymium compounds**

Nd $^{3+}$  complexes, hypersensitivity, environmental effects on f-f transitions 9-782

NdCl $_3$ , cryst. struct. 9-11850

NdCl $_3$ , effective density of phonon states from vibronic spectra and appl. to ion-lattice interactions 9-17350

Nd $_2$ Y $_2$ Sb system, mag. props. of single crystals 9-16380

Nd(IV) weak-field fluoride complexes, electronic spectra 9-16416

Nd $_2$ Mg $_3$ (NO $_3$ ) $_2$ ·24H $_2$ O, spin-phonon relax. field dependence 9-10156

NdMnO $_3$ , crystal and antiferromagnetic structures 9-19717

Nd $_2$ O $_3$  concentration, effect, suppression of parasitic oscillations, inversion population 9-4448

**Neon**

3p $_x$  and 3p $_y$  levels, fine-structure splitting, difference-frequency resonance meas. 9-20881

adsorption on Xe surface 9-9622

atom, 1s metastable states, spatial distribution in auxiliary active discharge 9-20520

atom, collision with oriented metastable He atom, polarization transfer 9-711

atom, correlated wavefunction calc. method 9-20327

atom, energy loss spectra for keV electrons interaction with electron shell 9-18150

atom, energy loss spectra for keV electrons interaction with electron shell 9-11398

atom, metastable ( $^3P_2$ ), optical pumping in elec. discharge 9-688

atom, splitting of 3p $_x$ , 3p $_y$  fine structure levels, study by difference freq. reson. technique 9-2816

atom interaction with laser beam, fluorescence polarization 9-13292

atoms and ion, bibliography of spectra 9-13287

breakdown voltage increase with applied a.c. voltage 9-3032

collision diff. cross section meas., intermolecular potential determ. 9-11412

collision-broadened homogeneous linewidths meas. 9-2824

continuum absorption in high-excitation planetary nebulae 9-16561

crystal, Debye-Waller factors 9-5536

crystal, improved self-consistent phonon approx. 9-5530

**Neon** continued

- crystals, review 9-13567  
 crystals, single, isotope effects in lattice constant and thermal expansion 9-7624  
 discharge, plasma params. in slow-moving striations 9-3031  
 discharge plasma, striated, acoustic waves effects 9-11541  
 discharge tubes used with gas laser for phase-locking 9-6505  
 dissociative recombination and molecular ion formation in decaying plasma 9-13414  
 elastic constants, at absolute zero, effect of long-range three-body forces 9-11906  
 electronic pair-correlation energies of ground states, soln. of Bethe-Goldstone eqns. 9-11383  
 flash-tube hodoscope for cosmic ray showers 9-4561  
 glow discharge, low pressure, p-type striations generated by external excitation 9-19552  
 hollow cathode discharges, obs. 9-922  
 ionization, primary coeff. 9-911  
 ionization equilibrium in low-density plasma 9-15820  
 ionization in low energy Ne-Ne atomic collisions 9-13456  
 ions I, II, III states radiative lifetimes, u.v. obs. 9-4844  
 ions II, III, IV, V, photoionisation cross sections, calc., 39.1-867.9 Å 9-6979  
 laser 3.39  $\mu$ m line width from Lamb-dip 9-17874  
 liquid, quantum deviations from classical behaviour, effs. of using perturbation theory 9-10643  
 nebular abundance 9-20162  
 optical absorption meas. of atom density formed by luminescent discharge 9-6967  
 plasma columns, positive, of discharges at moderate pressure 9-14762  
 polarization bounds 9-8410  
 positive column of low current discharge, influence of distrib. function on microwave emission and r.f. conductivity 9-19561  
 positive column with moving striations, electron thermal relax. length, obs. 9-7199  
 range and  $dE/dx$  in Be and C from 500 keV and 2 MeV 9-9871  
 relaxation length of electron temp. in positive column of glow discharge 9-17139  
 scattering of He<sup>+</sup>, analysis using differential cross-section formulae 9-9149  
 solid thermodynamic props. evaluation using improved self-consistent phonon theory 9-12016  
 streamer breakdown, exptl. investigation of development 9-930  
 Ar-Ne gas mixture, obs. of elec. conductivity 9-929  
 Ar and He mixtures, thermal cond. obs. at 296.8°K 9-19584  
 H-Ne atom collisions, Lyman- $\alpha$  polarization, Born and distortion rot. approx. 9-13313  
 HCl-Ne interaction, intermol. dispersion pot. 9-20992  
 He-Ne discharge, population inversion distrib. rel. to He:Ne ratio, obs. 9-18312  
 He-Ne laser, 3.39  $\mu$ , state mixing effects prod. by optical freq. fields 9-2816  
 He-Ne laser, anomalous circular polarization of 1.523  $\mu$  line 9-6520  
 He-Ne laser, competing-wavelength interaction 9-10862  
 He-Ne laser, emission line intensities modification rel. to population inversion, obs. 9-17873  
 He-Ne laser, mode coupling effects in mode selection expts. 9-4471  
 He-Ne laser, oscil. freq. shift by discharge current increase 9-6518  
 He-Ne laser with 3 mirror resonator, radiation generation at 0.63 and 3.39  $\mu$  9-6519  
 K scatt. in thermal energy range, total cross section meas. 9-11413  
 N<sub>2</sub>-Ne mixture, shock front u.v. radiometry 9-21142  
 Ne-He laser, power saturation at 6328 Å 9-2375  
 Ne<sup>+</sup>, <sup>2</sup>P state, electron scatt., nonrelativistic partial wave analysis 9-18147  
 Ne I, i.r. transition arrays, transition probabilities and oscillator strengths 9-20880  
 Ne II, 3p and 3d levels, lifetime determ. 9-20877  
 Ne<sup>+</sup> collisions with Ar and Kr, optical excitation 9-6996  
 Ne<sup>2+</sup>, excitation cross section for fast e. impact 9-5057  
 NeI 3d-4f lines meas. 2p<sup>2</sup>5f config. derived. 9-15813  
 Ne<sup>+</sup>, ionizing collisions with H<sub>2</sub>, relative cross-sections for prod. of NeH<sup>+</sup>, NeH<sub>2</sub><sup>+</sup> and H<sub>2</sub><sup>+</sup> 9-7188

**Neon compounds**

No entries

**Neptunium**

- <sup>237</sup>Np in NpO<sub>2</sub>, hyperfine field from Mossbauer effect, rel. to antiferromag. ordering 9-1708  
 Np (VII) oxidation state 9-12542

**Neptunium compounds**

- NpCo<sub>0.85</sub> mag. and elec. props. 9-5817  
 NpF<sub>4</sub> fluorination with F<sub>2</sub>, BrF<sub>3</sub>, at 250°-400°C obs. 9-6026  
 NpN mag. and elec. props. 9-5817  
 NpO<sub>2</sub>, <sup>237</sup>Np hyperfine field from Mossbauer effect, rel. to antiferromag. ordering 9-1708  
 NpO<sub>2</sub> film, grain growth and crystallization 9-5251

**Nernst effect** *see Magnetothermal effects***Nernst-Ettinghausen effect** *see Magnetothermal effects***Neutretos** *see Neutrinos and antineutrinos***Neutrinos and antineutrinos**

- See also Cosmic rays/neutrinos; Nuclear reactions and scattering due to neutrinos*  
 in cosmological solutions, anisotropic 9-17605  
 degenerate Fermi sea of  $\nu$ , effect on electromagnetism 9-16825  
 emission from red supergiants 9-20174  
 $\nu$  emission, energy losses during stellar evolution 9-15294  
 Penney's geometric theory, investigation 9-4586  
 review of developments 9-4584  
 solar, convection in core 9-21966  
 solar, flux, upper limit, rel. to initial He abund. 9-2075  
 solar, flux mixing effect 9-4126  
 solar, identification and flux-cross section prod. 9-10544  
 solar, no, decrease at earth surface due to  $\nu e \rightarrow \mu \mu$ , lepton nonconservation 9-14528  
 solar evidence from pp and pe reactions in the sun 9-10475  
 on stars collapsing 9-6124  
 stellar evolution, energy losses due to neutrino emission 9-15294  
 sun, core rotation rel. to neutrino flux 9-10546  
 from sun, detect. 9-18934

**Neutrinos and antineutrinos** continued

- symmetry violation and properties 9-13097  
 third hypothesis and hadron leptonic decay 9-8773  
 viscosity effects in anisotropic cosmological models 9-10462  
 $e^+e^- \rightarrow \nu\bar{\nu}$ , rel. to astrophysics, energy loss rate and  $\nu$  luminosity 9-10477  
 $\gamma$ - $\nu$ , range effect in angular correlation experiment 9-19191  
 $\gamma\gamma \rightarrow \nu\bar{\nu}$ , rel. to astrophysics, energy loss rate and  $\gamma$ - $\nu$  weak coupling theory 9-10477  
 $\nu$ - $e$ ,  $\nu$ - $e$  interact., e.m. renormalization of vector part 9-8750  
 $\nu$ N- $\bar{\nu}$ N interaction cross sections asymptotic equality determ. 9-6600  
 $\nu$ N- $\bar{\nu}$ N<sup>\*</sup>, polarization eff., where N is polarized 9-20601  
 $\nu$ N- $\gamma$ Yl<sup>+</sup> and weak angle, weak boson theory 9-4585  
 $\nu$ n- $\bar{\nu}$ p<sup>+</sup> and weak angle, weak boson theory 9-4585  
 $\nu$ N interaction at 10<sup>9</sup> GeV, Upper limit of cross section 9-8749  
 $\nu$ p- $\bar{\nu}$ n<sup>+</sup> and weak angle, weak boson theory 9-4585  
 rest mass connected with  $\beta^+$  decay of <sup>22</sup>Na 9-9010  
 $\rho$  prod.,  $\beta$ -decay coupling const., meas. by high energy neutrinos 9-11077

**Neutron diffraction**

- diffractometer, computer control, design and alignment method 9-21314  
 powder, time of flight collimator role 9-7397  
 time modulation of beam by quartz crystal vibrated by h.f. pulses 9-21307  
<sup>160</sup>Dy in Dy<sub>2</sub>O<sub>3</sub> sample, coherent scatt. amplitudes determ. 9-4735  
**Neutron diffraction crystallography**  
*See also Crystal structure, atomic*  
 anomalous scatt., location of anomalous scattering atom 9-18436  
 anomalous scattering by centrosymmetric structures 9-11825  
 apparatus for mag. and cryst. struct. determ. 9-5310  
 automatic n diffractometer, 20 zero layer reflections scanned 9-5309  
 Bragg intensity correction for thermal diffuse scatt. 9-19702  
 Bragg peak meas. from resolution function 9-11824  
 centrosymmetric structure analysis using anomalous scatt. 9-11825  
 data assessment from automatic installations 9-19699  
 diffractometer- collected data, least squares weighting schemes, effect of random setting errors 9-13621  
 forbidden reflections simulated by multiple Bragg reflection, intensities 9-9662  
 lattice spacing determ. by successive reflections of n beam from two crystal specimens 9-11826  
 neutron monochromators improvements using Cu crystals doped with Be and distorted Ge 9-19700  
 patterns using pulsed linear accelerator 9-14913  
 powders, intensity and resolution depend. on apparatus geometry, math. reln. 9-18437  
 resolution function in Bragg peak meas. 9-11824  
 resolution function of 'elastic two-crystal' scatt. meas. 9-11823  
 resolution function of conventional two-crystal diffractometer for elastic scatt. 9-5308  
 solid solutions with short range order and size effects, kinematical theory 9-3251  
 stereo plotting of 3-dimens. e. density 9-13622  
 thermal diffuse scatt. corrections in measured integrated intensities from cubic single crystals 9-18543  
 time modulation of beam by quartz crystal vibrated by h.f. pulses 9-21307  
 two-crystal elastic scatt. diffractometer, resolution function 9-11823  
 Be, forbidden reflections simulated by multiple Bragg reflection, intensities 9-9662  
 Fe<sub>3</sub>(CO)<sub>12</sub>/P(C<sub>6</sub>H<sub>5</sub>)<sub>3</sub> crystal structure determ. 9-21314  
 Ge, forbidden reflections simulated by multiple Bragg reflection, intensities 9-9662  
 Ge monocrystal, temp. and press. eff. on mosaic spread, 1.884 Å 9-5307  
 Pb single crystal, coherent extinction of Bragg reflection, temp. depend. 9-21306

**Neutron diffraction examination of materials**

- $\alpha$ -brass, fibre texture, comparison with X-ray diff. method 9-5490  
 L-ascorbic acid, crystal structure 9-19727  
 crystals, cubic, with impurities, effects of force-constant changes on incoherent scatt. 9-9822  
 ferromag. alloys conduction electron spin polarization range depend. on impurity conc. 9-10120  
 ferromagnets, imperfect, temperature dependence 9-10111  
 Heisenberg systems, mag. scatt. phenomenology 9-12254  
 ice Ic 9-16076  
 ice II 9-16075  
 ice IX 9-5321  
 magnetic structure and dynamics 9-19941  
 manganese formate dihydrate, H atom positions 9-7455  
 metal sheets, coarse grain, texture studies 9-19698  
 monochromator laminated crystal applic. 9-17263  
 Perovskite-type crystals, rel. to dielec. props. 9-13910  
 piezoelectric vibrating resonators, lattice mechanics 9-1355  
 quartz, vibrating crystal 9-3516  
 rare earth metals, magnetic structure and form factor meas. 9-13971  
 reactor fuel problems examined 9-11367  
 thiourea, mol. dynamics study 9-4962  
 vitamin C, crystal structure 9-19727  
 white beam apparatus for detect. spin-wave contrib. 9-19701  
<sup>160</sup>Gd crystal, rel. to mag. props. 9-10114  
 Al, fibre texture, comparison with X-ray diff. method 9-5490  
 Al, X-ray Debye temp. determ. 9-7639  
 BaF<sub>2</sub>, anharmonic temp. factors 9-3514  
 BaSc<sub>2</sub>Fe<sub>12</sub>-xO<sub>19</sub>(M), helicoidal antiphase spin ordering, neutron diffraction 9-16367  
 Ba<sub>2</sub>Zn<sub>2</sub>Al<sub>2</sub>SFe<sub>9</sub>O<sub>22</sub>, unit cell parameters, configuration 9-5314  
 BeSO<sub>4</sub>·4H<sub>2</sub>O, crystal structure 9-13628  
 CaSn(OH)<sub>6</sub>, crystal structure 9-19709  
 Cr powder, long range magnetic order 9-14009  
 Cu, fibre texture, comparison with X-ray diff. method 9-5490  
 D, solid struct. above and below  $\lambda$  transition 9-9675  
 Er, form factor meas. 9-13971  
 EuSe, mag. struct. 9-14011  
 Fe-Cr alloy, ageing, at 475°C, rel. to Guinier-Preston zones formation 9-9785  
 Fe-Si sheet, coarse grain, pole figure determ. 9-19698  
 Fe<sub>3</sub>/Ga<sub>2</sub>O<sub>4</sub> ion distribution 9-3828  
 Ga<sub>2</sub>Fe<sub>3</sub>-O<sub>4</sub>, spin wave spectrum from inelastic n. scatt. 9-21581  
 He, liquid, scatt. at large energy and momentum transfers 9-1052  
 KNbO<sub>3</sub>, rel. to dielec. props. 9-13910  
 La-Tb dil. alloys, mag. props. exam 9-17454



**Neutron diffraction examination of materials continued**

- LaErO<sub>3</sub>, antiferromag. struct. 9-12310  
 Li<sub>0.5</sub>Fe<sub>2.5</sub>Al<sub>2</sub>O<sub>4</sub>, lattice structure and cation distrib. 9-21316  
 MnAu<sub>2</sub>, mag. structure 9-10152  
 Nb, X ray Debye temp. determ. 9-7639  
 Pb-Ni alloys, radiation-induced precipitation, small-angle scatt. meas. 9-9805  
 Pb, X-ray Debye temp. determ. 9-7639  
 Si, Pendellösung interf. fringes in Bragg refls., obs. 9-9663  
 (Sr<sub>0.8</sub>Ba<sub>0.2</sub>)Zr<sub>2</sub>Fe<sub>2</sub>O<sub>4</sub>, angular spin ordering 9-10140  
 Ta H(D) solid solns., structure and phase transitions 9-7449  
 Tb, form factor meas. 9-13971  
 UAs, antiferromagnetic ordering 9-3837  
 U<sub>2</sub>O<sub>9</sub>, superlattice reflections 9-7450  
 Y<sub>3</sub>LnGa<sub>2</sub>Fe<sub>2</sub> xO<sub>2</sub> magnetic Fe sublattices, nature 9-21591  
 Zn liquid, struct. 9-14011  
 ZnSn(OH)<sub>6</sub>, crystal structure obs. 9-19709

**Neutron radiography** *see Radiography***Neutron sources** *see Neutrons/production***Neutron spectra**

- absorption rate evaluation by activation rate meas. 9-18115  
 dosimetry application 9-12784  
 epithermal, spatially depend., synthesis 9-14639  
 fast, spectroscopy in reactor media 9-11369  
 flux in multiplying assemblies, Cd and Gd ratios obs. 9-18117  
 group cross-sections for mixtures with resonance-scattering component 9-19314  
 in heterogeneous cells at epithermal energies 9-19333  
 hexagonal lattice, ZrH<sub>1.7</sub> moderated, Monte Carlo calc. of n distribution 9-19365  
 hexagonal lattice, ZrH<sub>1.7</sub> moderated nuc. reactors fiss./theory 9-19365  
 in ice, asymptotic, determ. of diffusion parameters, effect of temp. 9-18573  
 in IRT-2000 reactor test hole, meas. at high energies 9-20840  
 moderators contaminated with resonance absorbers, meas. and calc. 9-19375  
 multigroup, coming from moderator and entering fuel element of reactor 9-11348  
 in multiregion reactors, asymptotic, use of overlapping groups without staggered discontinuities 9-19346  
 in reactor, fast, Na void reactivity effects, calc. 9-15791  
 reactor, fast, scatt. process approach 9-18109  
 reactor, fluctuation spatial effects 9-6245  
 in reactor, large zero-power graphite, fluctuation spectra, edge anomalies, obs. 9-15796  
 reactor flux noise, rel. to  $\beta/\lambda^*$  meas., L-54 Milan obs. 9-19350  
 reactors, time of flight spectroscopy 9-11359  
 resonances, unresolved, in n spectroscopy, missing level probability calc. method 9-16960  
 scintillation counter containing d, analysis 9-11137  
 slabs and cylinders, time of flight meas. of thermal neutron spectra 9-20835  
 spectroscopy, intermediate energy 9-8928  
 square, water-moderated lattice, Monte Carlo calc. 9-19365  
 square, water-moderated lattice Monte Carlo calc. of neutron distribution 9-19365  
 unfolded, from foil activation, explicit error calc. 9-4241  
 water, fast n, and space, angular distrib. 9-19329  
 in  $\gamma$  fluxes, high, using nuclear emulsions 9-20713  
 p synchrocyclotron, 660 MeV, nearby neutron spectra obs. 9-478  
 from <sup>32</sup>S(n,  $\gamma$ ) react., reson. mechanism of  $\mu$  capture obs. 9-18090  
 from <sup>40</sup>Ca( $\mu$ ,  $\gamma$ ) react., reson. mechanism of  $\mu$  capture obs. 9-18090  
<sup>208</sup>Pb, cosmic ray interaction, evaporation n energy spectra obs., detection method 9-20809  
 B,C, fast n, and space, angular distrib. 9-19329  
 Fe-water layer, rel. to transport problem in multilayered shield 9-15788  
 H(n,2n)<sup>3</sup>H, diff. cross section obs., 14.1 MeV 9-598  
<sup>2</sup>H(p,n)2p, n spectra obs., Ep=30, 50 MeV 9-15759  
 LiH, fast n, and space, angular distrib. 9-19329  
<sup>23</sup>Na(d,n)<sup>24</sup>Mg, E<sub>d</sub>=5.5 MeV, obs. 9-19282  
 RaD-Be source, He diffusion cloud chamber obs. 9-8907  
 U, depleted slab between borated polyethylene, spatially depend. resonance n spectra 9-16987  
 W, fast n, and space, angular distrib. 9-19329

**Neutron spectrometers**

- crystal, with new monochromator unit 9-18032  
 digital control system 9-4683  
 double scatt. fast time-of-flight, are of continuous n beam 9-2573  
 graphite prism 9-14523  
 liquid scintillation counter NE214 in n spectrometer with n- $\gamma$  discrimination 9-18029  
 p recoil with time-of-flight system 9-2574  
 scintillator, organic, calibration 9-5860  
 time-of-flight expt. data selection, use of electronic conditioner 9-2565  
 N spectrometry using recoil H tracks, computer analysis of random sampling 9-2617  
<sup>6</sup>Li sandwich, triton energy response function 9-19225

**Neutrons and antineutrons**

- See also Cosmic rays/neutrons; Nucleons and antineutrons*  
 $\beta$ -decay, radiative correction to axial vector coupling constant, divergent parts 9-8904  
 Boltzmann eqn., static eigenvalue problem Monte Carlo technique for soln. 9-20832  
 cylindrical geometry, method for soln. of multigroup P<sub>3</sub> eqns. 9-20836  
 Density control, optimization of main parameters 9-2777  
 density fluctuation spectra in reactor, and subcritical reactivity meas. 9-13267  
 e.m. wave scattering by unpolarized neutrons 9-2280  
 flux distrib. in large reactors, optimal control 9-13254  
 flux in multiplying assemblies, Cd and Gd ratios obs. 9-18117  
 flux ratios in critical systems, calc. by indirect variational method 9-18114  
 flux spatial oscs. in reactor, modal stability anal. 9-9078  
 form factors, e.m., fit in terms of reson. 9-6685  
 form factors, from ed quasielastic scatt. 0.27-4.47 (BeV/c)<sup>2</sup> 9-8752  
 fundamental mode decay const. of transport operator for slabs and spheres with isotropic scatt. 9-9082  
 glassy carbon, total cross-section from 0.001-0.1 eV 9-20824

**Neutrons and antineutrons continued**

- graphite, pyrolytic, hot-worked, prod. of peak in shear modulus 9-7521  
 magnetic moment, anomalous, primary universal interaction theory 9-319  
 magnetic monopole moment, upper limit obs. 9-8751  
 Milne problem, solution by Kofink's method 9-20830  
 monochromator laminated crystals, diff. meas. 9-17263  
 monoenergetic, half-space and slab problems, Case's method 9-20830  
 multiple collision processes, stochastic formulation 9-13259  
 multiplying slab, soln. of transport eqn. by Laplace transformation 9-20831  
 noise in reactor, conditional probability method of analysis 9-20845  
 number probability and counts in multiplying medium 9-18110  
 P<sub>n</sub> blackness theory in plane geometry, boundary conds. generalized in standard matrix formalism 9-16975  
 penetration, calc. and expt. methods and obs. review 9-11104  
 population decay in ice, effect of temp., determ. of diffusion parameters 9-18573  
 radiography, and appls., review 9-17673  
 radiography, results display by direct viewing of scintillating plate 9-10951  
 reactor kinetics, modification of Liapunov's direct method due to Lasalle 9-20839  
 reactor kinetics, two-time doublet Boltzmann eqn. 9-6931  
 Sical F1, swelling, press. effects, 500 MWd/t 9-16188  
 Sical F2, swelling, press. effects, 500 MWd/t 9-16188  
 slab geometry transport anal., new MS<sub>n</sub> and double MS<sub>n</sub> methods 9-11341  
 slowing down from delta-function source, approach to asymptotic density 9-13260  
 source, plane monoenergetic in H<sub>2</sub>, spatially depend. slowing down distrib., anal. of calc. methods 9-19339  
 source using <sup>252</sup>Cf, design data and shielding requirements 9-14634  
 steaming about annular duct, distrib. of flux and dose rate rel. to rad. shields 9-13272  
 superconductor, mixed state, dissipative processes 9-13850  
 synchrocyclotron shielding, concrete, attenuation obs. 9-479  
 total cross section of Cd near  $\lambda=10$  nm, E<sub>n</sub>=8  $\mu$ eV 'Doppler chopper' method meas. 9-4640  
 transport, multigroup system of integral eqns. 9-628  
 transport eqn. soln. in P<sub>n</sub> spherical harmonics approx. for cylindrical geometry 9-9084  
 transport operator in non-uniform media, spectrum 9-11343  
 transport problems, use of reflection and transmission matrices as input instead of cross-sections 9-19340  
 transport problems in bare sphere,  $j_n$  method of anal., time depend. problems 9-14642  
 transport theory, monoenergetic Boltzmann eqn. approx., variational principles 9-18112  
 transport theory in USA, 1967 status 9-6928  
 'trineutron' unbound by 1-1.5 MeV, evidence for existence from <sup>3</sup>H(t,<sup>3</sup>He)3n spectra 9-11321  
 wave propag. in graphite, effects of Bragg cut-off, anal. 9-13255  
 wave propagation in graphite parallelepipeds, interpret. of expt. results 9-9083  
 $\beta$  decay, correl. functions and relativistic corrections to recoil spectrum 9-4642  
 $\beta$  decay time-parity violation search, polarized n 9-4641  
 K $\pi$ -K $\pi$ N, isospin-1/2 K $\pi$  mass enhancement of 1160 MeV obs., M<sub>K</sub>=3.9 GeV/c 9-20638  
 n-p mass difference, contribution by A2 Regge pole 9-15640  
 n- $\rho$ <sup>0</sup> $\gamma$  decay, radiative corrections 9-417  
 p-n mass difference calc. in reciprocal bootstrap model 9-15639  
 resonance meas. with Ce(Li) detector partial and total capture x-sections 9-6878  
<sup>252</sup>Cf as source 9-2692  
<sup>238</sup>U, fission, by 0.8-3.4 MeV neutrons, angular anisotropy 9-13248  
 Ge:Cu, radiation induced defects generation rate, effect of impurities and disloc. 9-5335  
 n-p mass difference, theory using nucleon form factors 9-13139  
 NbC fracture and vol. changes, 0.8-5.4  $\times 10^{21}$  fast n/cm<sup>2</sup> 9-9862  
 source <sup>252</sup>Cf 9-2692  
 TaC fracture and vol. changes, 0.8-5.4  $\times 10^{21}$  fast n/cm<sup>2</sup> 9-9862  
 TiC fracture and vol. changes, 0.8-5.4  $\times 10^{21}$  fast n/cm<sup>2</sup> 9-9862  
 U-MO-Al-Si, swelling, press. effects, 500 MWd/t 9-16188  
 U-Mo 1,1 swelling, press. effects, 500 MWd/t 9-16188  
 WC fracture and vol. changes, 0.8-5.4  $\times 10^{21}$  fast n/cm<sup>2</sup> 9-9862  
 ZrC fracture and vol. changes, 0.8-5.4  $\times 10^{21}$  fast n/cm<sup>2</sup> 9-9862

**absorption**

*See also Nuclear excitation; Nuclear reactions and scattering due to neutrons*

- black, cylindrical absorbers, linear extrapolation distance, endpoint and effective radius 9-14643  
 in block, unresolved resonances energy range 9-16972  
 cross section, pile oscillator meas. 9-20862  
 graphite, thermalized n pulse decay 9-9019  
 grey cylindrical absorbers, linear extrapolation distance, endpoint and effective radius 9-14643  
 iniron of magnet yoke, high energy from extended source 9-422  
 P<sub>n</sub> blackness theory in plane geometry, boundary conds. generalized in standard matrix formalism 9-16975  
 polyethylene, with steel, 14 MeV broad beam attenuation 9-18949  
 rate evaluation from activation rate meas. 9-18115  
 resonance, intermediate param. range 9-15787  
 resonance absorption and flux spectra, epithermal in heterogeneous cells 9-19333  
 resonance parameter determ., known partner selection 9-16905  
 resonances, area anal. using mutual-indication method 9-16904  
 self-shielding in solids of thermal neutrons 9-19328  
 steel, with polyethylene, 14 MeV broad beam attenuation 9-18949  
<sup>123</sup>Sb capture cross section meas., resonant level parameters determ. 9-14567  
<sup>123</sup>Sb capture cross section meas., resonant level parameters determ. 9-14567  
<sup>238</sup>U, capture rate determ. from  $\gamma$ - $\gamma$  coinc. meas. of <sup>237</sup>U decay 9-11339  
 Cd, cross-sections between 0.01 and 10 eV 9-19315  
 Co detector mat., resonance self-shielding factors for  $\Gamma_n \gg \Gamma_\gamma$  9-18123  
 Mn detector mat., resonance self-shielding factors for  $\Gamma_n \gg \Gamma_\gamma$  9-18123  
 UO<sub>2</sub>, effective reson. integral of rad. and cluster, obs. 9-19366

**Neutrons and antineutrons continued angular distributions**

- energy spectrum of photoneutron sources, Monte Carlo program for determ. 9-19303  
flux, discrete  $S_n$  approx., variational selection of directions and weights 9-16976  
Li, and space-energy distrib. 9-19331  
in non-hydrogenous media, exponential coeffs. 9-19330  
water, and space energy distrib., fast neutrons 9-19329  
in np scatt., anal. of data obtained below 10 MeV 9-11102  
 $^{235}\text{U}$ , scatt. obs.  $E_n=14$  MeV 9-15768  
B+C, and space energy distrib., fast neutrons 9-19329  
Bi(n,2n), 14 MeV, ang. correl. obs. 9-20798  
 $^{12}\text{C}(\gamma, n)$ , n ang. distrib. meas. in giant resonance region  $E_\gamma \leq 10$ ; MeV 9-16954  
 $^3\text{H}(\text{p}, n)^3\text{He}$ , 2.5-3.0 MeV, ang. distrib. obs. 9-20783  
LiH, and space energy distrib., fast neutrons 9-19329  
Pb(n,2n), 14 MeV, ang. correl. obs. 9-20798  
W, and space energy distrib., fast neutrons 9-19329

**capture** see *Nuclear reactions and scattering due to neutrons*

**detection, measurement**

- See also *Dosimetry; Neutron spectrometers*  
co-ordination of ZnS(Ag)-plexiglass and Basso detectors 9-659  
detector type A.I.S.C., meas. dispersion, three-section comparison 9-2597  
discriminator, slope of pulse height distrib. 9-2610  
dosimeter, personal, for thermal and fast n,  $3 \times 10^{-2}$ - $10^3$  rem 9-11146  
dosimetry, physical basis 9-453  
in dosimetry, spectroscopy appls. 9-12784  
dosimetry in Triga II reactor, fast flux from  $^{235}\text{U}(\text{n}, 2\text{n})$  thermal from  $^{238}\text{U}(\text{n}, \gamma)$  reactions 9-6934  
energy, angle distrib. from Fe slab after n bombardment 9-6702  
fast flux densities, paired detector techniques 9-19247  
fast n spectrum at edge of reactor core, meas. by threshold activation detectors 9-11356  
flux detector, low intensity 9-20861  
graphite prism for determ. of flux and spectrum 9-14523  
ion-chamber dosimeters for excessive fluxes of fast n. 9-454  
moisture gauge, correction for dry bulk density 9-3065  
multiplication determ., expt. and analysis 9-6929  
polarimeter using liquid He 9-4645  
prompt decay constant meas., dead-time method 9-11129  
in reactor media, fast n spectroscopy 9-11369  
reactor transmission through shield 9-636  
in reactor vertical channels, use of cellulose diacetate for  $\gamma$ , n meas., determ. of n volumetric field 9-660  
in reactors, time-of-flight spectroscopy 9-11359  
semiconductor counters for detect. of n with  $\gamma$  9-19238  
spectrometer, double scatt. fast time-of-flight, are of continuous n beam 9-2573  
spectroscopy, intermediate energy 9-8928  
standards, role of N.B.S. 9-9102  
in thermonuclear plasma produced by laser beam focussing on LiD surface 9-7171  
time analyzer using binary scalars 9-4687  
transport systems, expansion of system to allow meas. 9-2778  
zero probability method in reactors to obtain information on materials 9-2799  
 $\beta$ -emitting self-powered detectors, characts. and appls. 9-8938  
 $^{235}\text{U}$  fission, mass and time depend. of delayed n 9-18108  
 $^{237}\text{Np}$  thin layer prep. methods 9-13158  
Ag foil Geiger counter 9-444  
 $^{10}\text{BF}_3$  graphite moderated counter, design and efficiency 9-2575  
Co detector mat., resonance self-shielding factors for  $\Gamma_n \gg \Gamma_\gamma$  9-18123  
Cu, natural, photoneutron cross section 9-7691  
Gd target secondary emission of electrons 9-2562  
In activation detectors for neutron flux, some corrections 9-658  
In foils in light water, interaction 9-4814  
Li detector with B-10 or Li-6 shield, patent 9-20700  
Li glass scintillation characts. 9-449  
 $^6\text{Li}$  glass scintillator, effect of  $^{23}\text{Na}$  impurity 9-2583  
 $^6\text{LiF-ZnS(Ag)}$ -polyethylene scintillation detector for subcritical thermal n flux 9-6723  
Mn detector mat., resonance self-shielding factors for  $\Gamma_n \gg \Gamma_\gamma$  9-18123  
 $\text{MnSO}_4 \cdot \text{D}_2\text{O}$  liquid foils, non-perturbing, for thermal flux meas. in graphite 9-9099  
NaI(Tl) crystal detector in time-of-flight app., characts. and efficiency 9-13170  
 $^{90}\text{Nb}$  fast n fluence detection 9-11340  
Pb, natural, photoneutron cross section 9-7691  
in reactor core, flux meas. with semiconductor detectors 9-662

**diffusion**

- cylindrical geometry and multiple diffusion 9-20822  
n dense lattice, pulse determ. of parameters 9-629  
discrete  $S_n$  approx. for flux, variational selection of directions and weights 9-16976  
energy depend. diff. and transport eqn., infinite medium 9-19342  
flux distrib. with alternating slabs of non-fissile material 9-19335  
graphite slabs, diff. length problem as a function of absorption and transverse dimension 9-20833  
in ice, from pulsed decay data, effect of temp. 9-18573  
in lattice, axial coeff. and Benoist's formula direct derivation 9-16973  
in lattices, streaming effects and collision probabilities, applic. to fueled channels 9-18113  
length and criticality in cylinder two- and three-dimensional 9-14641  
length and criticality in slab, two-, three-dimensional 9-14640  
mean-square-displacement function 9-985  
method for determ. parameters for small amounts 9-11342  
Milne problem in non-grey radiative transfer 9-10679  
multigroup benchmark calc. by soln. of Boltzmann integral eqn. 9-16978  
multigroup theory, reality of eigenvalues for bare reactors 9-20834  
 $P_n$  approximation, numerical integration 9-15790  
 $P_n$  blackness theory in plane geometry, boundary conds. generalized in standard matrix formalism 9-16975  
parameters, improved, Pomraning's method 9-20825  
Perfluorodimethylcyclohexane, neutron diffusion parameters, method for determ. 9-11342  
reaction kinetics in one-group diffusion eqn., equilibrium state stability 9-630

**Neutrons and antineutrons continued diffusion continued**

- in reactors, possible stationary distribs. 9-11354  
Rossi- $\alpha$  expts., space depend. eff. 9-19338  
slab, finite, diff. length problem as a function of absorption and transverse dimension 9-20833  
in slab geometry, discrete ordinates numerical integration method 9-15788  
solar, transport in Earth's atmosphere 9-10396  
space depend. problem, one neutron-energy group model 9-15789  
steady state multigroup diff. eqns, positivity theorems for discrete form 9-13262  
thermal fluxes dosimetry 9-6732  
time-depend., combined space-time numerical synthesis 9-14647  
transport, space-angle energy-time depend., in homogeneous slab,  $j_n$  calc. 9-14645  
transport eqn. 2-group, numerical solns to Milne and constant source problems 9-20827  
transport eqn., explicit behaviour of quantum correction terms at very low energy 9-13264  
transport eqn., one vel., for infinite cylinder, soln. by Fourier series 9-14646  
transport eqn. in plane geometry, multigroups, eigensolutions by case's method 9-20826  
transport equation, solution for heterogeneous reactors, matrix form 9-632  
transport equations, numerical methods of solution using  $P_n$  approximation 9-11344  
transport in medium with free surface, extrapolation distance 9-19343  
water, diffusion and extrapolation lengths, stationary meas. 9-9079  
in water, thermal diff. parameters obtained using pulsed method 9-19341  
Be, n thermalization in large buckling range 9-19334  
Be slabs, diff. length problem as a function of absorption and transverse dimension 9-20833  
 $^{12}\text{C}$ , cylindrical geometry 9-20822  
in ZrH $_2$ , temp. depend. 9-19326

**effects**

- See also *Nuclear reactions and scattering due to neutrons*  
binary  $\alpha$  phases, radiation damage from X-ray diff. obs. 9-11868  
bone-tissue interface, recoil p dose determ. 9-15379  
 $\gamma$  production, 4-10 MeV, IEAR-1 swimming pool reactor and targets 9-20841  
carbon blacks, P33 and Thermax, e.s.r. 9-8018  
embrittlement of austenitic iron-base alloys at elevated temps. 9-19369  
Fe, work hardening characts. 9-3468  
ferrites, on ferromagnetic resonance 9-14105  
graphite, contraction, effect of process temps. and binder graphitization 9-411  
graphite, contraction rel. to processing temp. and binder graphitization, obs. 9-7679  
graphite, decrease in linear thermal expansion coeffs. 9-7660  
graphite, from diffuse X-ray diff. obs. 9-7404  
graphite, dimensional effects of long-term radiation 9-6945  
graphite, dose effect on dilation due to liq. Na 9-7661  
graphite, effect of B on nucleation pattern of rad. damage 9-7477  
graphite, from uncalcined coke pitch-binder content influence on changes 9-7432  
graphite, impregnated, thermal cond. and elec. resistivity changes 9-7667  
graphite, induced creep under const. tensile and compressive stresses 9-7553  
graphite, isotropic, thermal expansion and bulk dimensional changes 9-7410  
graphite, lattice parameter and dimensional changes 9-7471  
graphite, low temp., released energy profile and elec. resistivity changes 9-7741  
graphite, natural, shear modulus variation 9-7513  
graphite, on Vickers hardness 9-7578  
graphite, purified, pre-irrad. effects on thermal oxidation rate 9-8086  
graphite, pyrolytic, compression-annealed, shear modulus variation 9-7513  
graphite, pyrolytic, vacancy and interstitial loop prod. 9-7472  
graphite and evaporated carbon films, change in e.s.r. 9-8017  
metals, mechanical props., long-term, under stress at elevated temps and on irrad. 9-21380  
m.o.s.f.e.t.'s in pure neutron environment, theory and experiment 9-17419  
polyethylene, n- $\gamma$  reactor radiation effect on e.p.r. and spin-lattice relax. 9-21669  
reactor fuels, ceramic, high burn up behaviour 9-2787  
semiconductors, n bombarded, carrier scattering from defects 9-17389  
solids, organic and inorganic, effect of n irrad. on annealing behaviour 9-21388  
steel, austenitic, Cr-Ni, eff. on corrosion chemistry 9-21701  
structure materials, irradiated, corrosion and electrochem. props. 9-1912  
superconductor, mixed state, dissipative processes 9-3587  
tetraphenyl tin, thermal neutron reactor radiation Mossbauer study 9-5582  
thermocouple calibration, influence of dose rate 9-4377  
U irradiated, length and electrical resistivity changes 9-3574  
Zr (2.7 wt.%)Nb, irradiation strengthening, effect of Nb 9-5479  
 $^{181}\text{Os}$  radiative n capture, transformation and annealing in crystal 9-21724  
Ag, irradiated, black-spot damage, nature 9-18459  
Ag, thin films, resistivity change 9-17378  
Al thin films, resistivity change 9-17378  
Au thin films, resistivity change 9-17378  
BaS, radiation-damage centres, e.s.r. obs. 9-13697  
Be, defect prod. and recovery, study by elec. resistivity and stored energy meas. 9-16091  
Be, irradiated at 4.2°K, damage and recovery up to 350°K from elec. resist. meas. 9-5578  
C, pyrolytic, changes in linear dimensions, density, layer spacing and anisotropy 9-7409  
C, pyrolytic, dimensional changes, descriptive model 9-7651  
C blacks, on e.s.r. 9-8012  
CdS evaporated films, on acoustic performance 9-15002  
Cr irradiation effects on ductility 9-1310  
Cu-Al alloy irradiated, Brinell hardness, comparison with Cu, peak annealing temp. determ. 9-21401  
Cu-Si alloy irradiated, Brinell hardness, comparison with Cu, peak annealing temp. determ. 9-21401  
 $\beta_1$ -Cu-Zn, irradiation effects on martensitic transformations 9-5512



**Neutrons and antineutrons continued**

- effects continued  
 Cu, deformed rel. to dislocation pinning at 4.2°K or 20°K 9-14946  
 Cu, irradiated, hardening, thermally activated obstacles 9-11943  
 Cu fatigue-hardened foils, irradiation effect on dislocation loss and rearrangement 9-11882  
 Cu irradiated, Brinell hardness, peak annealing temp. determ. 9-21401  
 Fe-Al solid solns., heterogeneous, resistivity changes rel. to ordering changes 9-1465  
 Fe-6.5%Si alloy, zero magnetostriction, induced mag. viscosity, obs. 9-19952  
 Fe, irradiated, yield stress, saturation and exposure depend. 9-11929  
 Fe, slip activation parameters 9-1296  
<sup>56</sup>Fe, 0.85 MeV level excitation by 14 MeV neutrons 9-6825  
 GaAs devices 9-17403  
 Gd, point defect production and recovery 9-11870  
 Ge-Si alloys, on thermoelec. props. 9-7849  
 Ge, irradiated, electron microscopic obs. of defects 9-16090  
 n-Ge, irradiated, impurity photoconductivity kinetics 9-10072  
 Ge, partition of energy deposited as a function of incident energy 9-7684  
 Ge, radiation-induced defects, small-angle X-ray scatt. exam. 9-5331  
 Ge, thermal cond. changes, 5-300°K 9-1402  
 n-Ge, transient processes after pulsed irradiation 9-3654  
 Ge crystals irradiated, lattice parameter expansion calc.  $E_n > 0.6$  MeV 9-1189  
 LiF, dislocation mobility and microhardness 9-11885  
 LiF, irradiated, thermoluminescence charact. rel. to dose 9-17492  
 Li<sub>2</sub>O-SiO<sub>2</sub>, glasses, heat treated, rel. to dielec. and d.c. props. 9-7833  
 MgF<sub>2</sub>, induced vacuum u.v. absorpt. 9-1787  
 Mo,  $E_n \geq 1$  MeV anomalous high temp. recovery 9-12030  
 Mo, tensile strength and hardness changes following irradiation 9-19808  
 Ni, causing magnetic after-effect 9-3802  
 Ni, voids prod. by fast n,  $5 \times 10^{19}$  n/cm<sup>2</sup> 9-7499  
 Ni foils, interstitial Frank dislocation loops and tetrahedral voids 9-3326  
 NiCr thin films, resistivity change 9-17378  
 Pb-Ni alloys, radiation induced precipitation, small angle scatt. meas. 9-9805  
 Pb, natural, photoneutron cross section 9-7691  
 Si-Cu, radiation induced defects generation rate, effect of impurities and disloc. 9-5335  
 Si-P, A and E centres, influence on minority-carrier density dependence on neutron dose 9-1549  
 p-Si, P, radiation damage dependence on energy spectrum 9-3660  
 Si, irradiation, recombination luminescence 9-7989  
 Si, radiation defects, i.r. spectral obs. 9-15177  
 Si, thermal cond. changes, 5-300°K 9-1402  
 Si crystals irradiated, lattice parameter expansion calc.  $E_n > 0.6$  MeV 9-1189  
 Si defect activation energy 1.2±0.1 eV obs. 100-156°C by annealing studies 9-17275  
 Si diodes, n irradiated, majority and minority carrier trapping by capacitance recovery 9-17408  
 Si diodes, on I-V charact. 9-10018  
 Si IMPATT X-band diodes, fast n, d.c. and microwave charact. 9-17409  
 Si n-p-n planar transistors, n-pulse irradiated, rapid annealing data 9-17413  
 p-Si n irradiation-induced defect clusters from Hall effect and conductivity meas. at 76°K 9-17401  
 Si resistivity changes at room temp., design curves for predicting 9-1550  
 Si transistors, n bombarded, radiation and annealing charact. 9-17415  
 Si transistors, n induced base current, recombination statistical model 9-17414  
 Si traristors, second breakdown and thermal behaviour 9-17416  
 SnCl<sub>2</sub>, thermal neutron reactor radiation, Mossbauer study 9-5582  
 SnO, thermal neutron reactor radiation, Mossbauer study 9-5582  
 $\alpha$ -U, defects, deviations from Matthiessen's rule 9-16089  
 $\alpha$ -U induced growth at low doses, mechanism 9-19870  
 UO<sub>2</sub>-SiO<sub>2</sub> system, elec. props., effect of fission fragments 9-7743  
 UO<sub>2</sub>, elec. conductivity flux dependence 9-1457  
 UO<sub>2</sub>, n irradiation, behaviour rel. to initial structure and props. 9-2787  
 UO<sub>2</sub>, swaged, microstruct. changes 9-11358  
 W, recovery at high temps. post-irradiation 9-13812  
 W irradiated and annealed, vacancy dislocation loops 9-7491  
 YFe garnet, on ferromag. resonance 9-14105  
 Zr alloys oxidation in high temp. H<sub>2</sub>O, review 9-10343  
<sup>90</sup>Zr irradiated, damage rate and distrib. determ., depend on lattice energy 9-17365

**interactions**

- graphite in reactor, stress, creep and crystal dimension changes 9-20851  
 nuclear orientation expts. using low energy n 9-19270  
 (n, xy), 14.1 MeV n interaction with Na, Mg, S, Si, Mn, Fe 9-600  
 nd- $\gamma$ -H, and parity nonconservation 9-4643  
 nd-nnp, 14 MeV 9-19210  
 np-dy weak parity-nonconserving potentials 9-16835  
 pn data compilation 1.27 GeV/c 9-6695  
 Bi as low-pass vel. filter, transparency determ.,  $\lambda_n = 1.5 \text{ \AA}$  9-11105  
 MgO as low-pass vel. filter at 83°K, transparency determ.,  $\lambda_n = 1.5 \text{ \AA}$  9-11105  
 PbF<sub>2</sub>, as low-pass vel. filter, high transmission,  $\lambda_n = 1.35 \text{ \AA}$  9-11105  
 SiO<sub>2</sub>, as low-pass vel. filter, transparency determ.,  $\lambda_n = 1.5 \text{ \AA}$  9-11105

**moderation**

- benzene, neutron thermalization, computed 9-20855  
 Boltzmann eqn., quantum-mechanical description, avoidance of singular and non-physical terms 9-19336  
 bycylindrical absorbers, grey and black, extrapolation distance and boundary cond. 9-14643  
 distribution in moderators, derivation of formulae 9-649  
 fast reactor, effect on damage flux 9-20829  
 filter, Be slow-neutron, intrachannel cooling, cryostat 9-4189  
 graphite, equilib. energy spectra, expt. installation and results 9-19378  
 graphite, thermalization calc. 9-9094  
 in graphite, wave propag., fundamental mode eigenvalue 9-13261  
 graphite systems, finite, resonance-filter meas. 9-6930  
 inelastic scattering in moderator 9-19327  
 in infinite medium, asymptotic props. of energy distrib. 9-11345  
 moderators contaminated with resonance absorbers, meas. and calc. of neutron spectra 9-19375  
 multi-group calcs., slowing down interval curtailment 9-15646  
 multiple collision method fundamental recurrence relation 9-13259  
 by paraffin wax, spectra obs. 9-18574

**Neutrons and antineutrons continued**

- moderation continued**  
 polyethylene round <sup>252</sup>Cf source, and shielding of concrete or water 9-14634  
 reactor, fast, Na void reactivity effects, calc. 9-15791  
 resonance intermediate param. range 9-15787  
 rethermalization in heavy gas, angle-depend. flux calc. 9-9080  
 slowing down from delta-function source, approach to asymptotic density 9-13260  
 spatially depend. slowing down distrib., anal. of calc. methods 9-19339  
 spherical light water assemblies, fundamental mode discrete time-decay const. 9-9077  
 time-dependent thermalization, applic. of Horowitz operators 9-19359  
 water, light, n thermalization, modified Nelkin model 9-20856  
 wave propag., neutron, convergence of eigenfunction analysis 9-20854  
 N behaviour in transport and diff. regions of D-lattice, cruciform control rod worth calc. 9-19354  
 N wave propag. in heterogeneous multiplying medium, solns., behaviour 9-19332  
 n wave propagation in polycryst. moderators, anal. by modeled vel. depend. transport theory 9-9083  
 Be, equilib. energy spectra, expt. installation and results 9-19378  
 H<sub>2</sub>O, B poisoned, decay of thermal n 9-14644  
 H<sub>2</sub>O, Cd poisoned, non-1/v absorber, decay of thermal n 9-14644  
 H compounds of transition metals as moderator material 9-14655  
 H<sub>2</sub>O, total cross section 9-16988  
 H<sub>2</sub>O light, thermalization params., obs. 9-6701  
 in U-D<sub>2</sub>O lattice with Pu in fuel, thermalization, model 9-16974  
 U, enriched, water-graphite moderated critical assembly, buckling, obs. 9-19348  
**polarization**  
 P from <sup>28</sup>Si (d,n)<sup>29</sup>P at 5.0 MeV ang. distrib., spin-depend. eff. 9-6902  
 $\beta$  decay, search for T-violation 9-418  
 in <sup>3</sup>H(d,n)<sup>3</sup>He reaction, for  $E_d = 80$  to 150 keV 9-4801  
 K<sup>+</sup>p→K<sup>0</sup>n near-maximal near  $t=0$  9-6638  
 n polarimeter, resolution for 14 MeV 9-2779  
 in  $\pi$  p→ $\eta$ n rel. to  $\pi$  conspirator, calc. 9-8838  
 $\pi$  p→ $\pi^0$ n at intermediate energies 9-6638  
 in <sup>13</sup>C( $\alpha$ ,n)<sup>16</sup>O reaction 9-20805  
<sup>13</sup>C(<sup>3</sup>He,n)<sup>15</sup>O<sub>g.s.</sub>, n polarization ang. distrib. obs., 2.9-3.9 MeV 9-6896  
<sup>12</sup>C(d,n)<sup>13</sup>N, 5.2-6.2 MeV obs. 9-2756  
<sup>55</sup>Co(d,n) at 11.7 MeV, obs. 9-613  
<sup>56</sup>Fe(d,n) at 11.7 MeV, obs. 9-613  
<sup>3</sup>H(d,n)<sup>3</sup>He, 0.3-1.83 MeV, n polarization deduced, d-s-wave 9-9065  
<sup>3</sup>H(d,n)<sup>3</sup>He, 70°(lab), d energies below 2 MeV 9-4803  
<sup>3</sup>H(d,n)<sup>3</sup>He, n polarization obs., parity conservation concluded in strong reaction 9-6900  
 from <sup>3</sup>H(d,n)<sup>3</sup>He react., 90-175 keV 9-13242  
<sup>60</sup>Ni(d,n) and isotopes, at 11.7 MeV, obs. 9-613  
<sup>64</sup>Zn(d,n) and isotopes, at 11.7 MeV, obs. 9-613

**production**

No entries

**production**

- 14 MeV pulse generator, utilizing d beam and d-d interaction 9-11101  
 auto ionic emission and surface ionization of deuterium in strong elec. fields 9-16322  
 energy spectrum of photoneutron sources, Monte Carlo program for determ. 9-19303  
 greater, technique for beam centering 9-16766  
 neutron wave production from positive-ion, electrostatic accelerator 9-19259  
 in reactors, transport equation solution functionals, differentiation by Monte Carlo method 9-11346  
 source, monoenergetic, nuclear design parameters 9-19205  
 source, pulsed, and bore-hole fast generator 9-4646  
 sources, improvement in absolute calibration 9-11106  
 thermal neutron-beams, need for greater intensity flexes 9-16906  
<sup>241</sup>Am/<sup>241</sup>Be source, used in moderation effects of paraffin wax meas. 9-18574  
<sup>208</sup>Pb( $\mu$ ,n) photonuclear total cross section determ. 9-15645  
 Li following  $\alpha$ ,d,p, bombard., yield obs 9-616  
 LiD surface, thermoneuclear neutron emission at Nd-glass laser beam focus 9-13245  
 Pb-H<sub>2</sub>O system n yield under bombard. by 400, 500 and 660 MeV p 9-19364

**reflection**

- by steel rods in water 9-18125

**scattering**

- albedo problem, inverse thin-slab, iterative proc. for scatt. kernel, applic. to one-speed isotropic scatt. 9-11103  
 anisotropic, in infinite medium, effective source strength 9-13256  
 anomalous, in ferromagnets with small mag. anisotropy 9-13972  
 beam extraction, by tangential channel, from reactor, target material depend. on intensity 9-20823  
 benzene, neutron thermalization, computed 9-20855  
 cold n-scatt. study of mol. motions in cyclohexane and cyclopentane 9-14707  
 crystal structure analysis, anomalous scatt. by centrosymmetric structures 9-11825  
 crystals, cubic, with impurities, effects of force-constant changes 9-9822  
 cyclohexane, least-energetic E<sub>m</sub> vib. 9-20959  
 ferromagnets, temp. shift of maximum,  $|\sin \kappa r|/r$  spin correlation discussion 9-12258  
 ferromagnets with weak magnetic anisotropy 9-18677  
 by gases, real, quasi-ideal approximation and total cross-section 9-9303  
 glycerine, partially deuterated, quasi-elastic cold, at various temps. 9-7250  
 Heisenberg systems, mag. scatt. phenomenology 9-12254  
 inelastic, by spin waves in ferromagnetic metals with multiple bands 9-7892  
 length from  $\pi$ -d-2 $\pi$  obs. 9-2507  
 liquid studies 9-11676  
 from liquids, classical, continued fraction representation for autocorrel. function calcs. 9-13510  
 low energy in various substances, book 9-13258  
 magnetic structure and dynamics 9-19941  
 methane, slow neutron scattering rel. to intermolecular interactions 9-11511  
 methane, solid, molec. reorientation effects 9-9823

**Neutrons and antineutrons continued****scattering continued**

- Milne problem in infinite slab geometry, depend. of asymptotic characteristics on scatt. operation 9-54  
 molecular crystals, single phonon scattering, peak width 9-14997  
 monochromator laminated crystals, scatt. meas. 9-17263  
 multiple, quantum-mechanical approach, diagram tech. 9-6699  
 optical potential derived, particle-hole states and intermediate structure discussed 9-6847  
 paramagnets, rel. to time-depend, two-spin autocorrelation function 9-12245  
 paramagnets in strong mag. field 9-21568  
 in paramagnets subjected to strong mag. fields, cross section 9-12028  
 pentanol, angular and energy distrib. obs. 9-5141  
 point defect cross-section in a relaxed lattice calc. method 9-19741  
 polycrystals, inelastic n. scatt. cross section calc. in one-phonon approx 9-11991  
 by polyethylene 9-19491  
 polyethylene, l.f. vibr. determ. 9-1366  
 polypropylene, isotactic, dispersion curves and freq. distrib. 9-9302  
 by real gas, rel. to intermolecular interactions 9-11511  
 by real gases, non-quasi-ideal correction 9-11510  
 semiconductor, mag., by anomalous fluctuations of spin waves in elec. field 9-5814  
 spectrum in fast reactor 9-18109  
 by spin waves in twin films, angular distrib. rel. to freq. 9-16349  
 thiourea, spectrum, mol. dynamics study 9-4962  
 transport calcs., sensitivity to cross-section detail, applic. to fission n in O<sub>2</sub> 9-18116  
 transport eqn., two-group, with isotropic scatt. 9-19337  
 transport theory algorithm for speeding up Monte Carlo calcs. 9-13257  
 molecular, from point group C<sub>3v</sub> 9-4892  
 water, light, modified Nelkin model 9-20856  
 in water, mixed heavy and light 9-19377  
 waves in polycrystalline medium with assumption of anisotropic scatt. 9-2780  
 (n,r) as polar. analyzer for n polarimeter, resolution for 14 MeV 9-2779  
 KN generalized superconvergence relations 9-4620  
 KN generalized superconvergence relations 9-4620  
 nd. differential cross sections, elastic and inelastic at 14.1 MeV 9-8906  
 nd. scatt. length calc. using separable representation of two-nucleon t-matrices 9-13151  
 nd cross section obs., 14 MeV, charge symmetry comparison with np results 9-6700  
 nd total cross sections, 10 GeV/c 9-4644  
 np singlet effective range from total cross-section meas. 9-6871  
 np total cross sections, 10 GeV/c 9-4644  
 ν-n-ρπ<sup>0</sup>, time-reversal apparent violation 9-4573  
 π<sup>+</sup>n-ωp Regge pole model, cuts generated by absorpt. 9-15627  
 by ρ, interference effects in double minimum potential 9-2538  
 Al slab 9-591  
 Ar, liq., continued fraction representation for autocorrel. function calcs. 9-13510  
 Ar, liquid thermal n. scatt., new model 9-11682  
 Ar, liquid zero sound in classical liquids theory explanation 9-100  
 Bi-Zn binary liquid metal mixture, critical inelastic slow neutron scatt. 9-19607  
 Cu, deformed polycrystalline, small angle scatt. of subthermal neutrons 9-3346  
 Cu-<sup>62</sup>Ni alloy, cluster diffuse scatt. 9-9673  
 D<sub>2</sub>O, spectral density of modes of motion determ. 9-13500  
 Fe, Curie point, temp. depend. obs. in critical scatt. 9-12269  
 Fe slab 9-591  
 Ga<sub>2</sub>Fe<sub>3-x</sub>O<sub>4</sub>, spin wave spectrum from inelastic n. scatt. 9-21581  
 by HCl liq. at 183°K, intensity meas. 9-15987  
 Li, angular and space-energy distrib. 9-19331  
 MgO, obs. and calcs. from lattice-dynamical model 9-9821  
 Na liquid, analysis in terms of atomic displacement 9-21185  
 n-r forward dispersion relations and exchange effects 9-4782  
 O<sub>2</sub>, gaseous, inelastic scatt. 9-785  
 Pb liquid, analysis in terms of atomic displacement 9-21185  
 Pb single crystal, coherent extinction of Bragg reflection, temp. depend. 9-21306

**scattering, neutron-proton**

- angular distrib. data anal. below 10 MeV 9-11102  
 chemically coupled; corrections to Fermi approximation found negligible for all energies 9-421  
 cross section, rel. part of amplitude calc. from Glauber model, I 10 GeV 9-2535  
 elastic, 3.0 to 6.8 GeV/c, cross-sections 9-419  
 momentum and angular spectra of sec. parts in c.m.s., obs., 20 GeV 9-2539  
 N-N potential, vel. depend. term, phase shift anal. 9-13144  
<sup>3</sup>H triple scatt. parameters calc. target of polarised p, 425 MeV 9-11095

**Newtonian fluids see Fluids****Nickel**

- adsorption of bromide, <sup>80</sup>Bu nucl. isomers separation 9-18769  
 adsorptive behaviour in H<sub>2</sub>SeO<sub>4</sub>, effect of mag. transform 9-21708  
 anodic props., mag. field effects 9-21709  
 atom. core-e energy levels and density of states, X-ray photoelectron spectrum 9-1813  
 atomic scatt. factor for low-energy e 9-9660  
 Barkhausen discontinuities due to mech. stresses 9-5827  
 bolometers, production and properties 9-10750  
 cathode protrusion formation during pre-breakdown conditioning 9-11633  
 with chemisorbed H, surface diffusion 9-1086  
 conductivity, elec. and thermal, near Curie point 9-7755  
 conductivity, thermal, and diffusivity at 900-1670°K 9-5574  
 contact resistance of electrodeless nickel on silicon 9-19892  
 in corundum, comp. and absorpt. spectra rel. to growth conditions 9-1132  
 cylindrical crystal, stray mag. field above Bloch walls, electron-optical invest. 9-13974  
 d-band optical density of states, photoemission study 9-1629  
 d-band structure in ls coupling 9-9896  
 defect network, deformation-produced, in high-purity mat., elimination 9-9697  
 defect structure, loading rate effects, e. microscope exam. 9-3352  
 deposited on SiO<sub>2</sub>-Al<sub>2</sub>O<sub>3</sub> catalysts, particle size 9-1909  
 desorption of H<sub>2</sub> mol., angular distrib. 9-7349

**Nickel continued**

- diffusion in Ni<sub>3</sub>Zn<sub>(1-x)</sub>Fe<sub>2</sub>O<sub>4</sub> 9-1252  
 diffusion in p-PbTe, 700°C, junction formation 9-19767  
 diffusion in ZnSb-constantan semiconductor thermoelements, X-ray microprobe analysis 9-10062  
 diffusion of Be, 1020 1400°C 9-5403  
 diffusion of Fe and Co and diffusion in Fe and Co, heterodiffusion coeff., 1136-1370°C 9-19763  
 elastic consts. and sp. hts., 4.2°K 9-5421  
 electrical resistance, magnetic component at low temp. 9-13845  
 electrodes, anodic dissolution and pitting in NiCl<sub>2</sub> soln. 9-21713  
 electronic specific heat calcs., 0-300°K 9-16177  
 electroplated, magnetocrystalline anisotropy, effect of electrolytic charging with H 9-15152  
 emission, thermionic of Na<sup>+</sup>+K<sup>+</sup> from ribbons, effect of deformation 9-21554  
 epitaxial films, secondary twinning in e. diff. patterns 9-9618  
 epitaxial growth on KCl, KBr and KI crystals 9-7377  
 f.c.c., ferromagnetic and paramagnetic props., comparison from theoretical eqns. 9-3787  
 Fermi surface anisotropy in de Haas-van Alphen effect data 9-12063  
 ferrite, u.s. vel. minimum, depend. on temp. and mag. polarization 9-9827  
 ferromagnetic, Kerr effect rel. to spin-orbit splitting of 0.7-eV transition and electron structure 9-7948  
 ferromagnetic reson. line width var. rel. to lattice microdistortions during plastic deform. and annealing 9-14103  
 ferromagnetic resonance in polycrystals as function of angle between static mag. field and sample surface 9-14104  
 film, epitaxially grown, polycryst., double diffraction 9-5244  
 film, negative magnetoresistance anisotropy 9-18682  
 film, produced by chem. reduction method, mag. anisotropy 9-16358  
 film, transverse phonon generation at zero field by mech. stresses. 9-10126  
 film, vacuum deposited, elec. props. and mean free paths of electrons 9-17369  
 film on Fe-Si alloys, effect on mag. props. 9-13990  
 films, electrodeposited, magnetocrystalline and uniaxial anisotropies 9-1678  
 films, mean free paths of 4s electrons 9-17370  
 films, thin, electrodeposited uniaxial mag. anisotropy due to lattice distortion 9-9611  
 films epitaxed on NaCl, Xe ads., comparison with data for films on pyrex 9-17248  
 films evap. on glass, X-ray texture investigation 9-7336  
 films evap. on glass struct. depend. on thickness 9-7337  
 foil, agglomerated defects after n and e irradi. 9-3326  
 growth of Co film, f.c.c. structure 9-7341  
 Hall effect, magnetic resistivity and mag. susceptibility 9-21485  
 Hall effect, magnetoresistance, resistivity and size effect 9-1468  
 hole-hole interaction, magnetization dependence 9-21461  
 induction of Si(111) surface structure LEED study 9-21261  
 induction of Si(111) surface structure, LEED study 9-21262  
 internal friction during creep, 823-1023°K 9-13721  
 ions, optical absorpt. spectra in three Tutton salt crystals 9-12369  
 in MnF<sub>2</sub>, Raman scattering from localized magnons 9-12426  
 lattice atoms, mean square displacement determ. 9-7403  
 lattice parameter changes on defect formation on quenching and γ-irradiation 9-1186  
 loading rate effects on defect structure, e. microscope exam 9-3352  
 magnetic, anisotropy constants temp. dependence at low temps. 9-12285  
 magnetic anisotropy, uniaxial, formation by plastic deformation 9-12295  
 magnetic anisotropy energy in (111) plane 9-12283  
 magnetic domain patterns rel. to magnetization process 9-16353  
 magnetic domain structure, plastic deformation effects 9-12280  
 magnetic remanence, strain induced 9-7905  
 magnetization, stress control, implications for rock magnetism 9-21586  
 magnetocrystalline anisotropy, Mossbauer study 9-12279  
 magnetocrystalline anisotropy energy, 4.2-296°K 9-1668  
 magnetomechanical behaviour associated with dislocation slip during fatigue deformation 9-17308  
 memory, coercive force, isothermal remanent magnetization, variation with internal stress 9-5828  
 neutron irradi., voids, 5×10<sup>19</sup> fast n/cm<sup>2</sup> 9-7499  
 normal oscillation frequencies, 300-700°K 9-3507  
 oxidation, monolayer of O on (110), and diffusion of O to and from interior 9-12544  
 partial substitution in AuCu or AuCu<sub>3</sub> alloys, effect on order-disorder transforms 9-5522  
 plastic deformation of a single crystal in an alternating magnetic field 9-5461  
 plating Ti alloys, effect on fatigue strength 9-3442  
 powder, particle size from X-ray powder diffraction line broadening 9-3303  
 preparation, properties and uses of high-purity and commercial material, review 9-7581  
 recovery after low temp. deformation 9-3419  
 resistivity, elec., meas. and interpret., 1°-120°K 9-7754  
 in rock, spectrophotometric estimation 9-16525  
 specific heat, mag. fields effects near Curie temp. 9-13802  
 spectrum, IV, by vacuum spectrograph 9-4845  
 spectrum, IV, sextet and quartet system, intercombination 9-4846  
 susceptibility of fine grain assemblage rel. uniaxial compression 9-21587  
 texture, axial, X-ray diff. exam. 9-3289  
 thermionic parameters of (111), (100) and (110) faces 9-1625  
 thermoelectric power, effect of high pressure 9-16306  
 thermoelectromotive forces and structure of 3d-zone 9-16310  
 thermopower and structure of 3d zone 9-12207  
 thin films, prep. and study of elec. props. 9-1109  
 u.s. attenuation and vel. anomalies at high temp. 9-5547  
 vacancy, formation energy after liquid He-II quenching 9-5338  
 X-ray emission L<sub>23</sub>-bands in Ni, Ni-V, Ni<sub>3</sub>Ti and Ni-Ti alloys, structure 9-12456  
 X-ray scatt., small-angle, by n irradi. induced voids, obs. 9-9718  
 X-ray spectra and electronic structure 9-14067  
 in Al-10 wt.%Si composites containing Ni-coated sapphire whiskers, role and eff. on hardness 9-21385  
 Al X-ray atom form factor determ. from vanishing second order reflection in high-voltage electron diff. 9-9676  
 films, ultra-thin, elec. props. rel. to structure and tunneling mechanism of conduction 9-5644



**Nickel** continued

- H diffusion at 78°K following 35 KeV implantation 9-21352  
<sup>14</sup>N ions passing thro., range-energy relations 9-9869  
 Ni-<sup>57</sup>Fe, Fe atom state at grain boundaries 9-21611  
 Ni-S, embrittlement mechanism during annealing at 600°C 9-3443  
 Ni/NiF<sub>2</sub> anode in pulsed electrolysis of wet HF, electrochem. behaviour 9-21716  
 Ni-Al powder mixtures, sintering, exothermal effs. on Al content and porosity 9-17325  
 Ni-Al powder mixtures, sintering, exothermic effs. 9-17324  
 Ni-on-Si catalysts, finely divided in direct and alternating fields, superparamagnetism 9-21569  
 Ni, X-ray interferences in the Curie point neighbourhood, temperature dependence 9-5816  
 Ni<sup>2+</sup> in benzene amino-nickel cyanide clathrate, magnetic states 9-1710  
 Ni<sup>2+</sup> in CaO, electronic absorption spectrum 9-10195  
 Ni<sup>2+</sup> in MgO, spin lattice relax. anisotropy theory 9-12318  
 Ni<sup>2+</sup> in MgO, u.s. wave propagation, rotation of polarization plane 9-1380  
 Ni(II) ion solutions in methanol, p.m.r. 9-9554  
 Pu diffusion and solubility 9-19768  
 UO<sub>2</sub>, 90% enriched, -Ni fuel element plates, irradi. stability, 1.9-30% burn-up 9-19362

**Nickel alloys***See also Nickel compounds*

- alnico structural states, X-ray diff. exam. 9-1179  
 $\gamma$  precipitation hardened, slip and climb processes 9-7579  
 constantan-ZnSb semiconductor thermoelements, diffusion phenomena and phase transitions, X-ray microprobe analysis 9-10062  
 creep behaviour, stress cycling effect at 955°C on wrought specimens 9-18511  
 disilicide cobalt disilicide solid solns., lattice parameters, densities, thermal expansion and elec. conductivity 9-3480  
 f.c.c., ferromag. quantities, calc. in band model 9-1662  
 heat treatment, patent 9-13756  
 Invar, magnetism 9-3793  
 Invar alloys, mag. contrib. to low temp. thermal expansion and Curie temp. pressure dependence 9-21580  
 Invar lattice constants and anomalous, low, expansion coefficient 9-3243  
 magnetostatic and exchange interactions between particles 9-18676  
 Ni-Cr-Ti, internal friction temp. dependence b// 9-14966  
 Nimonic 80A, tertiary-creep behaviour, 750°C 9-18510  
 Nimonic alloy, precip. hardening mechanism 9-3469  
 Nimonic type, recovery after ageing, dissolution of precipitated  $\gamma'$ -phase 9-13765  
 permalloy, Barkhausen discontinuities due to mech. stresses 9-5827  
 Permalloy, magnetic analysis by electron diffraction 9-12277  
 Permalloy, thin-films, hysteresis loop meas. 9-12296  
 Permalloy film, coercive force and anisotropy field, eff. of crystallite size 9-13996  
 Permalloy film, magnetoresist. rel. to torque 9-7906  
 permalloy film, supercritical, thickness effects on mag. props. 9-1677  
 permalloy films, He irradi. effects on anisotropy field inhomogeneity and coercive force 9-7908  
 Permalloy films, ferromag. reson. linewidth thickness depend. 9-8005  
 permalloy films, ferromag. resonance, X-band obs. by reflecto-polarimetric exam. 9-10270  
 Permalloy films, optimization of props. for computer memories 9-13995  
 permalloy films, rotational hysteresis 9-10134  
 permalloy films, stresses, annealing and substrate temp. effects 9-13724  
 permalloy films, vacuum-deposited elastic limit and tensile strength 9-3412  
 permalloy fine wires, Nb addition, materials parameters affecting reentrancy 9-5824  
 permalloy thin film pairs with large separations, domain wall coupling 9-10132  
 permalloy thin films, ageing and stabilization 9-3471  
 permalloy thin films, angular dependence of magnetic annealing effects 9-10131  
 permalloy thin films, anisotropy inhomogeneity, origin 9-5838  
 permalloy thin films, uniaxial anisotropy, origin 9-3815  
 permalloy thin tapes annealed below recrystallization temp., mag. props. 9-3814  
 permalloy/Mn double layer films with exchange anisotropy, stabilisation of ferromag. domain structures 9-10130  
 properties and uses, review 9-7581  
 for reactor melting pot, corrosion resistance 9-651  
 resistivity, elec. meas. and interpret, 1°-120°K 9-7754  
 thermal expansion, low temp. 9-19864  
 thermoelectromotive forces and structure of 3d-zone 9-16310  
 thermopower and structure of 3d zone 9-12207  
 Ticonal 2000, sintered, in high coercivity state, structure 9-3302  
 wrought, creep behaviour, stress cycling effect at 955°C 9-18511  
 alloy, polymorphic transform., effect on kinetics and phase equilb. temp. 9-5513  
 CdSb-Ni, mag. susceptibility 9-16328  
 Co-Ni-Fe films, vapour deposited nonmagnetic mag. props. 9-5837  
 Cr-Ni, thermoelectric power and resistivity, max. due to ordering for low Ni content 9-3721  
 Cu-(20at.%)Ni-(20at.%)Mn ordering process 400-450°C 9-1342  
 Cu-Ni-Zn, yield point and plastic deformation rel. to degree of ordering 9-19794  
 Cu-Ni, corrosion rate, effect of Fe 9-4000  
 Cu-Ni, damping behaviour, miscibility gap existence 9-3400  
 Cu-Ni, electrical resistivity change due to cyclic deformation 9-3579  
 Cu-Ni, electron band structure 9-12058  
 Cu-Ni, lattice constant temp. dependence over conc. range 9-19955  
 Cu-Ni, plastically deformed, internal friction 9-13720  
 Cu-Ni oxidation kinetics, scale formation 9-21693  
 Cu-Ni resistance alloys for high temp. strain gauges 9-3409  
 Cu-<sup>62</sup>Ni, clustering, n. scatt. meas. 9-9673  
 Fe-Cr-Ni, austenitic, in oxidizing acids, effect of Si content on corrosion resistance 9-17535  
 Fe-Ni-Co, monocrystalline thin films, epitaxial growth and coercive force 9-12298  
 Fe-Ni-Cr, magnetization intensity and susceptibility rel. to heat treatment 9-12288  
 Fe-Ni-Mn, isothermal martensitic transformation nucleation rate 9-14990  
 Fe-Ni-Mn, uniaxial mag. anisotropy in martensitic transform 9-1667

**Nickel alloys continued**

- Fe-Ni-Ti, mechanical props. improvement by ageing 9-11928  
 Fe-30wt.%Ni-5wt.%Nb austenitic, structure and hardening on heat treatment and cold working 9-9802  
 Fe-Ni, f.c.c. Curie temp. pressure dependence 9-12289  
 Fe-Ni, hysteresis loops, constant field, effect of anisotropy and atomic arrangement, X-ray exam. of textures 9-5825  
 Fe-Ni, Invar effect 9-1662  
 Fe-Ni, magnetic anisotropy and ordering 9-3792  
 Fe-Ni, martensitic transform., effect of additions 9-9799  
 Fe-Ni, martensitic transform. rel. to change in mech. of transform. 9-5514  
 Fe-Ni, uniaxial mag. anisotropy in martensitic transform 9-1667  
 Fe-Ni invar., Curie point, effect of third component 9-10113  
 Fe-Ni thin films, grain size variation, X-ray diff. study 9-13577  
 Fe-30at.%Ni, martensitic transformation, mag. fields effect 9-3491  
 (19wt.%)Fe-(81wt.%)Ni films, anhysteretic behaviour, 20°C 9-13992  
 Fe-28 wt.% Ni-0.04 wt.% C, martensite grain substructure (fragmented structure) 9-1187  
 Fe-30 wt.% Ni, elastic moduli, rel. to martensitic transformations 9-7516  
 Fe-Ni-C, ferromagnetic f.c.c., plastic deform. 9-13727  
 Mg (9 wt.%) Ni, age hardening precipitation 9-3472  
 Mn-Ni,  $\gamma$ -phase, antiferromagnetism 9-12311  
 (48.2-57.0 at.%)Ni-(51.8-43.0 at.%)Cu, short-range dissoc. 9-17344  
 Ni-Al-Ti, coherency hardening 9-11945  
 Ni-Al-Ti, coherency hardening, comments 9-11946  
 Ni-Al, coherency hardening 9-11945  
 Ni-Al, critical shear stress, conc. depend. 9-9756  
 $\beta$ -Ni-Al, Hall coeff. and magnetoresistance at liq. He temps. 9-5639  
 Ni-Al, phase structure rel. to Hall coeff. 9-3582  
 Ni-Al precip. hardening mechanism 9-3469  
 Ni-Al<sub>2</sub>O<sub>3</sub> system, grain boundary grooving at interface, kinetics const. 9-1251  
 Ni-Co-Si, 'Nicosi', magnetostrictive, anisotropy, static and dynamic props. 9-5830  
 Ni-Co, absolute thermo e.m.f., eff. of plastic deformation 9-21543  
 Ni-Co, deformed, positron annihilation 9-21477  
 Ni-Co, dil. ferromag., elec. resistivity and screening 9-5645  
 Ni-Co thin films, strain insensitive, 17 to 50 at.%Ni 9-5843  
 Ni-Cr-Al, internal friction temp. dependence 9-14966  
 Ni-Cr-Cu-Al alloy, vacuum fractionation model. 9-7342  
 Ni-Cr-W-Co-Al-Ti, with horophilic addition, mech. props., effect of grain boundary composition 9-5475  
 Ni-Cr, dilute, oxidation mechanism 9-20047  
 Ni-Cr, X-ray study of thermal expansion up to 900°C 9-21438  
 Ni-Cr electrodeposition from aq. electrolytes 9-4007  
 Ni-Cr films, bias-sputtered, preferred orientation 9-21265  
 Ni-Cr white castiron, heat treatment for improving mech. props., patent 9-13757  
 Ni-(20wt.%)Cr wires of different lifetimes, oxidation 9-21695  
 Ni-(30wt.%)Cu, with interstitial occluded hydrogen, spontaneous magnetization temp. dependence 9-16361  
 Ni-Cu, conductivity, elec. and thermal, near Curie point 9-7755  
 Ni-Cu, Hall effect, magnetic resistivity and mag. susceptibility 9-21485  
 Ni-Cu alloys, interstitial H occlusion 9-17278  
 Ni (17 wt.%)Fe/EuS double layers, mag. hysteresis, thickness dependence 9-18678  
 Ni-Fe-Cu-Mo rolled from sintered compacts, high mag. permeability 9-13965  
 Ni-Fe-Cu layers, mag. and struct. props., influence of annealing 9-3821  
 Ni-Fe-Pd, films, composition and deposition for use as magnetic storage elements, patent 9-13998  
 Ni-(35 wt.%)Fe, ferromagnetic domain structures 9-13973  
 Ni-(19 wt.%)Fe ferromagnetic thin films, mag. birefringence 9-14034  
 Ni-Fe, absolute thermo e.m.f., eff. of plastic deformation 9-21543  
 Ni-Fe, dil. ferromag., elec. resistivity and screening 9-5645  
 Ni-Fe, effects of radiation on magnetic props. 9-1661  
 Ni-Fe, evaporated film, lattice parameter composition dependence 9-14986  
 Ni-Fe, f.c.c., elastic const. and sp. hts., 4.2°K 9-5421  
 Ni-Fe, Kerr magneto-optic effect, longit., and optical const. 9-10175  
 Ni-Fe, solute C effects on Curie pt. and spontaneous magnetization 9-13984  
 Ni-(19 wt.%)Fe ferromagnetic film, domain walls, low angle electron diffraction invest. 9-13997  
 Ni-Fe ferrite single crystal, mag. anisotropy, effect on ferromag. resonance line breadth 9-12494  
 Ni-Fe films, electrodeposited, coercive force rel. to crystallite size 9-7909  
 Ni-Fe films, magnetization-ripple, crystallite-size and film-thickness dependence 9-7907  
 Ni-Fe films, magnetostriction meas. method 9-13985  
 Ni-Fe films, uniaxial, analog, storage using non-uniform fields 9-5844  
 Ni-Fe films coupled with stripe domain films, mag. props. 9-10133  
 Ni-Fe with 50 to 60%Ni after isothermal treatment with mag. field, permeability obs. 9-5831  
 Ni-(19wt.%)Fe magnetic films, energy of combined Bloch and Neel type domain wall 9-18683  
 Ni-Mn, NMR study of <sup>55</sup>Mn 9-8042  
 Ni-(10 at.%)Mo, K-state formation, activation energy 9-17342  
 Ni-Mo, anodic props., mag. field effects 9-21709  
 Ni-Mo in H<sub>2</sub>SeO<sub>4</sub>, anodic behaviour, effect of mag. transform 9-21708  
 Ni-(8at.%)Mo alloy, Mo ion diffusion and electrotransport process 9-1253  
 Ni-(14.9wt.%)P, electrodeposited, amorphous structure 9-19839  
 2a/oNi-Pt short-range order field ion microscope investigation 9-3305  
 Ni-Rh, ferromagnetic behaviour 9-5821  
 Ni-Rh, mag. behaviour 9-16351  
 Ni-Ti, equi-atomic, martensite transform. 9-7615  
 Ni-Ti, X-ray emission L<sub>III</sub>-bands of Ni, structure 9-12456  
 Ni-V, X-ray emission L<sub>III</sub>-bands of Ni, structure 9-12456  
 Ni-Zn-Co, Procopiiu effect in bar sample 9-3832  
 (63wt.%)Ni (37wt.%)Rh anomalous low temp. sp. ht. near crit. conc. for ferromag. 9-16176  
 82.5 wt.% Ni-17.5 wt.% Fe permalloy film, Faraday and Kerr effect 9-16364  
 NiAl, conduction electron scatt. by paramagnons 9-21462  
 NiFe(Mn)-based ternary alloys with transition metal, electronic structure and ordering processes 9-19834

**Nickel alloys continued**

- Ni<sub>3</sub>Mn, electronmicroscope obs. of antiphase boundaries and dynamic effects under high voltage 9-14921  
 Ni dilute, resistivity, low-temp., two-current conduction, spin-electrons 9-3583  
 Ni<sub>3</sub>Al, strain hardening 9-13761  
 NiCr, thin films, resistivity change due to neutrons and  $\gamma$  rays 9-17378  
 Ni<sub>3</sub>Fe-based, isothermal ordering effects on elastic constants and deformational hardening 9-9741  
 NiSi<sub>x</sub>, ( $x=1,2$ ), X-ray spectral determ. of Ni 3d-band structure 9-3911  
 Ni<sub>3</sub>V, ordering transition 9-13781  
 Ni-Fe, deformed, positron annihilation 9-21477  
 Ni-(12 at. wt%)/Ti, precipitation behaviour 9-11959  
 Pb-Ni, radiation-induced scatt., small angle X-ray and n. scatt. meas. 9-9805  
 Pd-Ni paramagnetic, magnetostriction, thermal expansion, Pd contrast 9-1642  
 Pd-Ni dilute specific heat of nearly magnetic centres 9-1398  
 Sn-Ni, electrodeposited, structure composition and thermal stability rel. to acid bath conditions 9-14926  
 Zr-Ni spot-cooled, new non-crystalline phases 9-5523

**Nickel compounds**

- See also *Nickel alloys*  
 complexes with subst. phosphine ligands, electronic structure determ. 9-11470  
 complexes with subst. phosphine ligands, SCCC-MO calc. 9-11470  
 ferrite, alignment and microwave props. 9-1685  
 hydrated salts, paramag. spin relax. 9-18741  
 permalloy, domain tip motion control 9-5841  
 permalloy film, creeping mechanism of magnetization 9-5842  
 X-ray spectrum, Ni K $\beta$ / $\beta'$  lines, effect of chem. bonding 9-19998  
 Ni-Al intermetallic, mag. susceptibility and n.m.r. study 9-7888  
 Ni-Alumina powdered mixture, 20-320°C in atm. of H, He, O, N or p-type depend. on Ni content 9-13887  
 Ni-Cd batteries, state of charge meas. 9-17844  
 Ni-Co ferrite, alignment and microwave props. 9-1685  
 Ni-Cr<sub>2</sub>O<sub>3</sub> catalyst, H desorpt. rel. to H<sub>2</sub>O-H ISOTOPIC EXCHANGE, obs. 9-16046  
 Ni-Fe double films, coupling between 9-3816  
 Ni-Fe ferrite single crystals containing Co, stabilized-domain walls, effect on hysteresis loop shape 9-5849  
 Ni-Fe ferrites, rotational losses 9-3831  
 Ni-Fe film, domain boundary propag., slow to intermediate speed, Kerr magneto optical obs. 9-3819  
 Ni-Fe film, domain wall streaming, creeping and parade motion, hard axis pulse excitation 9-3820  
 Ni-Fe films, transverse Kerr effect, 0.3 to 3  $\mu$  9-5840  
 Ni-20%Fe film, annealing in rotating mag. field 9-3817  
 Ni-Fe films susceptibility, effect of strain, polycrystalline 9-3818  
 Ni-W solid solutions, impurity atom causing distortion of matrix lattice 9-5345  
 Ni-Zn ferrite, elastic moduli, 80-303°K, meas. 9-1260  
 Ni-Zn ferrites, magnetic transition parameters, chemical homogeneity eff. 9-7911  
 Ni-Zn polycrystalline ferrite spinel, ferrimag. reson. line broadening mechanism and temp. dependence 9-1852  
 Ni-chromium oxide mixture, semicond. obs. 9-13887  
 Ni, hexagonal form, metal-to-semicond. transition 9-12084  
 Ni<sub>0.5</sub>Zn<sub>0.5</sub>Fe<sub>2</sub>O<sub>4</sub>, magnetic resonance spectrum 9-21662  
 Ni<sub>3</sub>Mo, ordered, contrast variation, in field-ion images 9-16077  
 Ni<sub>3</sub>Mo, ordered, field ion images 9-14922  
 Ni<sub>3</sub>Fe<sub>1-x</sub><sup>2+</sup>Fe<sub>2</sub>O<sub>4</sub> 9-21640  
 Ni(II) thiourea complex, subnormal mag. moment 9-18194  
 Ni complex, benzene amino-nickel cyanide clathrate, magnetic props. 9-1710  
 Ni complex, bis(thiocetamide) nickel(II) thiocyanate, crystal and mol. structure 9-3301  
 Ni complex, diaquobis(2,2'-biimidazole) nickel(II)dinitrate, crystal and mol. structure 9-21319  
 Ni complex, tetra (thiourea) nickel(II) thiosulphate onohydrate, crystal and mol. structure 9-14920  
 Ni-Fe, conductivity mechanism 9-3632  
 Ni-Fe ferrite, optical props. and conduction mechanism 9-10171  
 Ni-Zn-Fe ferrite, optical props. and conduction mechanism 9-10171  
 NiAl, deformation modes of intermediate phase 9-5462  
 NiAl<sub>3</sub>, applic. of powder pattern indexing procedure 9-11813  
 Ni<sub>3</sub>Al, sheet solid solns., yield stress,  $\epsilon$  irradi. eff. 9-5502  
 Ni<sub>3</sub>Al particles in foils, visibility criteria from electron transmission contrast 9-7334  
 Ni<sub>3</sub>B<sub>2</sub>O<sub>7</sub>, ferromagnetolectric, spin arrangements 9-17455  
 Ni(CH<sub>3</sub>COO)<sub>2</sub>4H<sub>2</sub>O, electronic abs. spectrum 9-783  
 Ni(CN)<sub>2</sub>4H<sub>2</sub>O, fine structure of Ni K X-ray absorption obs. 9-17484  
 NiCl<sub>2</sub>, paramag. impurity in phthalimide/boric acid soln., phosphoresc. 9-7994  
 NiCl<sub>2</sub>6H<sub>2</sub>O, fine structure of Ni K X-ray absorption obs. 9-17484  
 NiCr, thin film resistors, flash evaporation 9-15393  
 NiCr<sub>2</sub>Se<sub>4</sub>, physical props., effect of interactions between d shells of transition element 9-16253  
 NiF<sub>2</sub>, specific heat, spin-wave contrib., 0.36-50°K 9-15006  
 NiF<sub>2</sub>, space group corepresentations and magnon dispersion relations 9-16381  
 NiF<sub>2</sub>5HF.6H<sub>2</sub>O, magnetic anisotropy and susceptibility 9-7878  
 NiF<sub>2</sub>Fe, work hardening rel. to superlattice structure 9-13758  
 Ni<sub>1-x</sub><sup>2+</sup>Fe<sub>x</sub><sup>2+</sup>Fe<sub>2</sub>O<sub>4</sub>, resistivity vs. Fe<sup>2+</sup> concentration (x) curves 77-373°K 9-12090  
 Ni<sub>1-x</sub>Fe<sub>x</sub><sup>2+</sup>Fe<sub>2</sub>O<sub>4</sub>, elec. conductivity in strong microwave fields 9-12092  
 Ni<sub>1-x</sub>Ge<sub>x</sub>Fe<sub>2-x</sub>O<sub>4</sub>, anisotropy field, effect of heat treatment 9-5850  
 Ni(II) complexes, isotropic proton mag. reson. shifts 9-13349  
 Ni(II) ions in dimethyl sulphoxide solns. 9-9555  
 Ni<sub>3</sub>Mn alloy, effect of Fe and Co additions on props. 9-12278  
 [Ni(NH<sub>3</sub>)<sub>6</sub>]Cl<sub>2</sub>, fine structure of Ni K X-ray absorption 9-17484  
 NiO-Li, elec. conductivity and thermolec. power rel. press. and temp. 9-21506  
 NiO, antiferromag., coherent exchange scatt. in electron diffraction 9-1698  
 NiO, antiferromag., low-lying surface-spin-wave band prediction 9-21595  
 NiO, band structure and elec. conductivity due to holes in O: 2p band 9-1469

**Nickel compounds continued**

- NiO, fine structure of Ni K X-ray absorpt. obs. 9-17484  
 NiO, heats of formation of point defects 9-17276  
 NiO, hightemp. defect struct. and elec. props 9-3571  
 NiO, microhardness anisotropy rel. to dislocations motion, obs. 9-3454  
 NiO, self diffusion of O, condensation coeff. 9-3387  
 NiO, semiconducting, optical absorpt. of small polarons in near and far i.r. 9-5929  
 NiO crystals, growth by solar furnace fusion 9-13608  
 NiO films, growth, eff. of structural defects 9-9621  
 Ni<sub>2</sub>P<sub>2</sub>O<sub>4</sub>, monoclinic, crystallographic data 9-5324  
 NiSO<sub>4</sub>(NH<sub>4</sub>)<sub>2</sub>SO<sub>4</sub> soln., H gas reduction, effect of surface active agent 9-18757  
 $\alpha$ -NiSO<sub>4</sub>6H<sub>2</sub>O low-temp. magnetothermodynamics 9-19862  
 NiSO<sub>4</sub>6H<sub>2</sub>O, fine structure of Ni K X-ray absorpt. obs. 9-17484  
 NiTi, tensile properties, 150° to 370°C, effect of room-temp. prestrain 9-18491  
 NiZn ferrite, magnetization at near saturation 9-15155  
 (Ni<sub>1-x</sub>Zn<sub>x</sub>)<sub>1-y</sub>Fe<sub>2-y</sub>Fe<sub>2</sub>O<sub>4</sub>, elec. conductivity in strong microwave fields 9-12092  
 Ni<sub>1-x</sub>Zn<sub>x</sub>Fe<sub>2</sub>O<sub>4</sub>, diffusion of Ni 9-1252  
 Ni<sub>2</sub>(OR)<sub>3</sub>Cl<sub>2</sub> liq., mag. susceptibilities, effect of progressive substitutions 9-1042  
 Ni-Fe film annealing, cylindrical 9-5839

**Night sky** see *Airglow***Nightglow** see *Airglow***Nilsson's model** see *Nucleus/models***Niobium**

- See also *Superconducting materials/niobium*  
 chemisorption of hydrogen on (110) surface from LEED 9-15215  
 de Haas-van Alphen oscills., Fermi surface model 9-7727  
 diffusion of <sup>51</sup>Cr, 953°-1435°C 9-13706  
 dislocation relaxations in single crystals 9-3351  
 electrolytic charging with H in prep. of pure Nb-H 9-13750  
 galvanomagnetic high field properties 9-3770  
 hysteresis in u.s. attenuation near H<sub>c1</sub> 9-9831  
 superconductor, type II magnetic flux penetration depend. on surface condition 9-13861  
 surface impedance near H<sub>c2</sub>, mag. field and ang. depend. 9-1479  
 thermal conductivity, lattice component 9-9855  
 u.s. attenuation anisotropy and temp. dependence in mixed state 9-7645  
 X-ray Debye temp. from n. scatt. obs. 9-7639  
 Au on Ba, double film on Nb contact potential difference 9-1093

**Niobium compounds**

- alloy, conc. of Zr by photoactivation 9-1933  
 alloys with elevated-temp. strengths, improved oxidation-resistance and fabrication ease 9-13770  
 niobates, thermal expansion of interatomic bonds 9-7659  
 Co-Nb alloy, precip. of new phase after ageing 9-9796  
 Fe-30wt.%Ni-5wt.%Nb austenitic alloy, structure and hardening on heat treatment and cold working 9-9802  
 Nb-C system, supercond., heat capacities, 1.5 18°K 9-1397  
 Nb-H, pure, prep. by electrolytic charging of Nb with H 9-13750  
 Nb-Ta alloys, superconducting props. and electronic spec. heat 9-13866  
 Nb-Ti alloy, deform effects, X-ray powder diffraction studies 9-11930  
 Nb-Ti alloy, dislocation structure after annealing at 1250-1500°C 9-5368  
 Nb-Ti alloys, supercond., T<sub>c</sub> and H<sub>c</sub> meas. 9-1504  
 Nb-Ti alloys, superconductivity, influence of structure 9-12125  
 Nb(44wt.%)Ti superconducting wire, microstructure obs. 9-18450  
 Nb-V alloy, deform effects, X-ray powder diffraction studies 9-11930  
 Nb-W alloys, solution-hardening and deformation 9-3411  
 Nb-X-Al alloys, (X=Fe, Co, Ni, Cu, Cr, Mo),  $\mu$ -phase extension and  $\mu$ -phase occurrence 9-19844  
 Nb-Zr-Ti alloy, thermal expansion, 10-300°K 9-21437  
 Nb-Zr-Ti alloys, supercond., T<sub>c</sub> and H<sub>c</sub> meas. 9-1504  
 Nb-Zr alloy, deform effects, X-ray powder diffraction studies 9-11930  
 Nb-Zr alloys, superconducting, eff. of hydrostatic pressure on critical current 9-15074  
 Nb-Zr and Lipowitz alloy plates, type-II superconductors, mag. flux penetration 9-9952  
 Nb-Zr superconducting tube, flux penetration 9-7774  
 Nb-(25 at.%)Zr wire, defn. of critical surface between normal and supercond. state 9-13867  
 Nb-base alloy, creep-rupture props., eff. of ht. treatment 9-14975  
 Nb-base alloys, creep-rupture props., response to ht. treatment 9-14976  
 Nb<sub>3</sub>Al, with V partial substitution, supercond. props. 9-7778  
 Nb<sub>3</sub>Al sintered, Ginzburg-Landau parameter and mag. field penetration depth calc. 9-18611  
 Nb<sub>3</sub>Ga, with V partial substitution, supercond. props. 9-7778  
 Nb<sub>3</sub>Sn sintered, Ginzburg-Landau parameter and mag. field penetration depth calc. 9-18611  
 Nb V hydrated oxide u.v. absorption bands obs. 9-21616  
 Nb<sub>3</sub>(Al,Ge) system, superconductivity above 20.5°K, obs. 9-12128  
 NbC C composite, effect of particle size and C source powders on properties 9-3391  
 NbC graphite composite system, effect of processing parameters 9-3161  
 NbC, fast n. irradi., fracture and vol. changes, 10<sup>21</sup> n/cm<sup>2</sup> 9-9862  
 Nb<sub>3</sub>CoSi, crystal structure 9-13645  
 Nb<sub>3</sub>(M<sub>1-x</sub>N<sub>x</sub>) solid solns. (M,N=Al, Ga, Ge, In, Sn), supercond. transition temp., reln. with microhardness 9-5664  
 NbN, superconducting, energy gap meas. 9-12127  
 Nb<sub>3</sub>Nb, crystal structure 9-1193  
 Nb<sub>2</sub>O<sub>3</sub>, B-modification, dielec. props. depend. on impurity conc. 9-3694  
 Nb<sub>2</sub>O<sub>3</sub>, lattice dielec. const. rel. to atom polarisability 9-3695  
 Nb<sub>2</sub>O<sub>3</sub> thin films, voltage controlled negative resistance 9-12089  
 Nb<sub>2</sub>O<sub>3</sub>-Cl<sub>2</sub>, dielec. constants, refractive index and optical band gaps for principal crystal axes 9-10030  
 Nb<sub>3</sub>S<sub>4</sub>, prep., props. and structure 9-9681  
 Nb<sub>3</sub>Sn, temp.-dependent isomer shift and anharmonic binding of <sup>119</sup>Sn from Mossbauer effect meas. 9-7960  
 Nb<sub>3</sub>Sn and Nb-Ti plates, type-II superconductors, mag. flux penetration 9-9952  
 Nb<sub>3</sub>Sn composite tapes, superconducting props. and appl. mag. field production 9-5663  
 Nb<sub>3</sub>Sn ribbon, definition of critical surface between normal and superconducting state 9-13867  
 NbTi, Superconducting, effective resistivity during mag. field step transition 9-9957



**Niobium compounds continued**

- NbTi wire, superconducting, type II, pinning force depend. on mag. fields 9-12118  
 NbZr wire, superconducting, type II, pinning force depend. on mag. fields 9-12118  
 Nb-Ti alloy, superconducting props. and appl. mag. field production 9-5663  
 Ni-Nb alloy system galvanomagnetic eff. 9-3790  
 Ti-(47 wt.%)Nb alloy, superconducting props., dependence on structure 9-13865  
 V-Ti Nb alloys, creep and stress-rupture behaviour 9-19801  
 Zr-(2.5 wt.%)Nb corrosion resistance, cold deformation effect 9-647  
 Zr-Nb alloys, oxidation by CO<sub>2</sub>, resistance behaviour 9-20050  
 Zr-Nb alloys, superconducting transition temp., critical field and resistivity 9-18606  
 Zr-(2.7 wt.%)Nb, irradiation strengthening, effect of Nb 9-5479

**Nitrogen**

- afterglow, prod. and loss of N<sub>2</sub><sup>+</sup> 9-13465  
 in air, fluorescence efficiency under e bombardment, 65 km, Ee=700 eV 9-14158  
 arc, cylindrical with whirl round axis, stabilization effects 9-5095  
 arc column, decay, effects of temp.-depend. thermal diffusivity and rad. losses 9-9423  
 arc plasma, transparent and non-transparent rad., share in total energy flux 9-7140  
 atom, excitation of second positive bands by electron impact, cross sections 9-13300  
 atom, hyperfine constant in <sup>4</sup>S<sub>3/2</sub> ground state, applic. of Brueckner-Goldstone many-body problem 9-18141  
 atom atmosphere, spectral line formation and radiative transfer 9-19391  
 atom in He atm., hyperfine const. press. shift, short range effects 9-4864  
 atom, upper atmosphere day time production and loss mechanism 9-16534  
 atoms and ion, bibliography of spectra 9-13287  
 C<sup>3</sup>Π<sub>u</sub>-B<sup>3</sup>Π<sub>g</sub>(0,0) stimulated transitions, high resolution study 9-2873  
 3β- cholestanol multilayers permeability, obs. 9-5415  
 continuum absorption in high-excitation planetary nebulae 9-16561  
 crystals, sound velocity meas. elastic and thermal prop. calcs. 9-3519  
 in diamond, as disperse impurity, effect on thermoluminescence 9-3935  
 diethyl ether-nitrogen gas mixtures, thermal conductivity 9-14818  
 differential cross section for 25-60eV e scatt. 9-9142  
 dimerization rel. to quadrupole moment 9-4908  
 discharge and afterglow, intensity of first neg. bands reduced by O<sub>2</sub> traces 9-5111  
 discharge used for CO<sub>2</sub> laser, e. energy distrib. 9-18298  
 dissociative excitation transfer, laser action obs. 9-4851  
 donors in SiC, exchange interactions 9-19972  
 electronic pair-correlation energies of ground states, soln. of Bethe-Goldstone eqns. 9-11383  
 enthalpy, eff. of pressure 9-17163  
 e.s.r. of atoms trapped in inert matrices at 4.2°K, matrix perturbing effects 9-12501  
 flames, active, determ. of ground-state CN conc. 9-826  
 freezing apparatus, Dewar modification 9-5  
 gas mixture H<sub>2</sub>/N<sub>2</sub> separation in supersonic jet 9-21145  
 gas Ar mixture, thermalization times of positrons 9-15974  
 glow in throat region of sonic nozzle, effects of changes in downstream geometry 9-9429  
 ion implantation on p type Si monocrystal, 20≤E≤215 keV 9-15107  
 ionization, yields, X-sections and loss functions 9-5054  
 ionization and fragmentation by 5-45 keV protons, mass spect. investigation, X-section meas. 9-5060  
 ionized, Boltzmann eqn. suitability for thermal conductivity calc. 9-14814  
 ions, N<sub>2</sub><sup>+</sup> rot. excitation in H<sub>2</sub><sup>+</sup>-N<sub>2</sub> collisions, 0.4-3.0 keV 9-4982  
 ions, N<sub>4</sub><sup>+</sup>-N<sub>2</sub><sup>+</sup>+N<sub>2</sub> equilib: const. and rates rel. to elec. field strength and press., 0.63-1.24 torr. 9-4969  
 ions III, IV, V, photoionisation cross sections, calc., 39.1-867.9 Å 9-6979  
 laser, high power, design considerations 9-10863  
 liquid, level control in dewar, instrument description 9-12804  
 liquid, stimulated combinational scattering, energy and time characts. 9-1013  
 liquid N<sub>2</sub>, stimulated Raman emission obs. with laser beam 9-21216  
 migration of second layer in W, with trapping on first layer sites 9-11900  
 molecule, absorption spectra obs., b<sup>1</sup>Π<sub>u</sub>-X<sup>1</sup>Σ<sub>g</sub><sup>+</sup> syst. high resolution, 795-1015 Å 9-14690  
 molecule as ligand in nitrogenpentammineruthenium (II) dichloride and related salts 9-7448  
 N<sub>2</sub>-Na beam interaction, excitation energy transfer, obs. 9-9308  
 nebular abundance 9-20162  
 negative ion, metastability of <sup>1</sup>D state 9-9138  
 nitridation of Si substrate in Si<sub>3</sub>N<sub>4</sub> film preparation 9-21281  
 oleic acid multilayers permeability, obs. 9-5415  
 plasma, K-seeded, elec. conductivity for conds. of MHD accelerator 9-7151  
 plasma, nonequilibrium, spectral line intensities 9-19528  
 plasma diagnostics, electrostatic Langmuir probe design characteristic 9-5045  
 plasma discharge, ionization waves dispersion curves 9-13418  
 radiative lifetimes, ultraviolet multiplets, phase shift measurement technique 9-11386  
 relaxation, thermal, of mixture with wet CO<sub>2</sub>, Kundt's tube obs. 9-13492  
 relaxation, vibr. dissoci., behind shock wave 9-13483  
 reorientation cross-section from depolarized Rayleigh line width meas. 9-13345  
 sorption on silica gel 9-21288  
 spark prod. by focused subnanosec. laser pulse 9-891  
 stearate multilayers permeability, obs. 9-5415  
 steel foils X25T, H41XT, X25Yu5 and Cr-Ni spectrochem. analysis, obs. 9-18778  
 stream with C particles, transmittances and absorption cross sections 9-11726  
 in transition metals, high-melting, gaseous impurity effect on brittleness temp. dependence 9-1309  
 Ar+N<sub>2</sub> liquid-vapour equil., 10 atm. 9-17228  
 CO<sub>2</sub>-N<sub>2</sub> laser, vibrational relax. data, kinetic model, review 9-15509  
 CO<sub>2</sub>-N<sub>2</sub>-He laser, output 80W 9-17869  
 in Cr, reaction with spinel in Cr 9-20032  
 in α-Fe dipole strength 9-9739  
 in GaP, isoelectronic impurities theory 9-7801

**Nitrogen continued**

- H<sub>2</sub>-N<sub>2</sub>-O<sub>2</sub> flame, temp. profile at atm. press. 9-15480  
 He-N<sub>2</sub> mixture, coeff. of thermal diffusion determ. 9-19590  
 in He, hyperfine press. shift rel. to van der Waals interaction 9-6989  
 N<sub>2</sub>-CO<sub>2</sub>, thermal conductivity from 0° to 200°C 9-3094  
 N<sub>2</sub>-CO<sub>2</sub> gas laser system, simultaneous laser action of CO<sub>2</sub> and N<sub>2</sub>O mols. 9-8608  
 N<sub>2</sub>-CO<sub>2</sub> gaseous mixtures, u.s. wave propag. at 95 atm., 31-100°C 9-9451  
 N<sub>2</sub>-O<sub>2</sub> mixtures adsorbed on anatase, activity coeffs. 9-7350  
 N<sub>2</sub>-Ne mixture, shock front u.v. radiometry 9-21142  
 N<sub>2</sub>-methane mixture, fission fragment prod. of H<sup>14</sup>CN 9-18770  
 N<sub>2</sub>, abnormal rot. energy distrib. in C<sup>3</sup>Π<sub>u</sub>-B<sup>3</sup>Π<sub>g</sub> bands 9-778  
 N<sub>2</sub>, absorption structure near K edge 9-20932  
 N<sub>2</sub>, adsorbed on silica-supported Ir, i.r. spectra 9-20934  
 N<sub>2</sub>, band strengths calc. of Halevi's correction 9-19437  
 N<sub>2</sub>, C<sup>3</sup>Π<sub>u</sub>-B<sup>3</sup>Π<sub>g</sub> transition on pulsed laser action, optical gain meas. 9-781  
 N<sub>2</sub>, collision with electron rel. to formation of highly excited atoms 9-685  
 N<sub>2</sub>, dissoci. and charge-transfer in collisions with inert-gas ions 9-15957  
 N<sub>2</sub>, dissociative ionization, due to vibrational mode excitation 9-14799  
 N<sub>2</sub>, electronic transition moment of first positive system using published data 9-19438  
 N<sub>2</sub>, ioniz. and excitation by electron impact, cross-section calc., semiclassical method 9-19433  
 N<sub>2</sub>, second positive system, laser transitions in 0-0 band 9-19422  
 N<sub>2</sub><sup>+</sup>, charge transfer with H<sub>2</sub> and D<sub>2</sub> at 20 and 1000 eV 9-15958  
 N<sub>2</sub><sup>+</sup> 3914Å, collision-induced excitation 9-18187  
 N<sub>2</sub><sup>+</sup> band 4278 Å in aurora, intensity ratio 5577 Å O line 9-20105  
 N<sub>2</sub> plasma, thermal rad. 0.5-1.1 μ, intensity meas. 9-19524  
 N<sub>2</sub> reaction with O<sup>1</sup>D atom, ozone quantum yield 9-21719  
 N<sup>+</sup>, formation by dissociative ionization of N<sub>2</sub> 9-14799  
 N<sup>+</sup>, N<sub>2</sub><sup>+</sup> in N, longitudinal and transverse diffusion coeff., 12-300×10<sup>-27</sup> Vcm<sup>2</sup> 9-918  
 N<sup>24</sup>, ion, probability of 1<sup>1</sup>S<sub>0</sub>-2<sup>3</sup>P<sub>1</sub> transition 9-916  
 N I multiplex, transition probabilities meas. in far u.v. 9-16995  
 N IV, 2p<sup>2</sup> <sup>1</sup>D level mean lifetime 9-9137  
 N V, absolute oscillator strengths for important transitions 9-15808  
 N V, semiempirical atomic core potentials, coeffs. 9-19397  
<sup>14</sup>N<sub>2</sub> mol., spectra, intensity alternations in second positive bands (C<sup>3</sup>Π<sub>u</sub>-B<sup>3</sup>Π<sub>g</sub>) 9-18188  
<sup>14</sup>N ions passing thro. Al, Ni, Ag and Au, energy-loss curves, range-energy relations 9-9869  
<sup>14</sup>N n.m.r. in THN 9-10295  
<sup>14</sup>N n.q.r. in benzene sulphonamide 9-14099  
<sup>15</sup>N<sub>2</sub> mol., spectra, intensity alternations in second positive bands (C<sup>3</sup>Π<sub>u</sub>-B<sup>3</sup>Π<sub>g</sub>) 9-18188  
 N<sub>2</sub>, dissoci. in weak r.f. discharge 9-9293  
 N<sub>2</sub>, hidden vibr. transitions in electron-impact spectra 9-9228  
 N<sub>2</sub>, molec. charge distribts. and chem. binding 9-2876  
 N<sub>2</sub>, solid, sp. ht. anomaly due to O<sub>2</sub> impurity 9-1392  
 N<sub>2</sub> adsorbed layers, heat of adsorp., two-dimens. condensation 9-9594  
 N<sub>2</sub> and e vibrational temp. in ionospheric E-region b// c// 9-1971  
 N<sub>2</sub> first positive system in type-B red aurora 9-4071  
 N<sub>2</sub> microwave absorpt., press.-induced 9-9455  
 N<sub>2</sub> mixtures with inert gases, H<sub>2</sub>, methane, refr. index rel. to long-range atom-mol. interactions 9-9304  
 N<sub>2</sub> multilayer adsorp. on C surface, two-dimens. van der Waals eqn. 9-9593  
 N<sub>2</sub> scatt. on He atoms resonances in cross section obs. 9-7034  
 N<sub>2</sub> solubility in alloyed ferrites 9-5395  
 N<sub>2</sub> sorption on Ti film, all-metal meas. apparatus 9-13588  
 N<sub>2</sub> vibr. excited mol., superelastic e scatt. 9-9224  
 N<sub>2</sub><sup>+</sup>, D<sub>2</sub> reactions, product energy and ang. distrib. meas., 25-135 eV 9-7035  
 N<sub>2</sub><sup>+</sup>, H<sub>2</sub> reactions, product energy ang. distrib. meas., 25-135 eV 9-7035  
 N<sub>2</sub><sup>+</sup>, HD reactions, product energy and ang. distrib. meas., 25-135 eV 9-7035  
 N<sub>2</sub><sup>+</sup> Meinel band, excitation by e impact, cross-sections 9-13363  
 N<sub>2</sub><sup>+</sup>, mass-spectrometric identification in h.f. discharge 9-9223  
 N<sub>2</sub><sup>+</sup> air jets, turbulent, similarities at temps. 4000 to 6000°K 9-9433  
 N<sub>2</sub><sup>+</sup>+D<sub>2</sub>, product energy and ang. distrib. obs. 2.3 to 11.6 eV 9-10325  
 N<sub>2</sub><sup>+</sup>+D<sub>2</sub>-N<sub>2</sub><sup>+</sup>+D, reaction cross sections, 1-100eV 9-17075  
 N<sub>2</sub><sup>+</sup>+H<sub>2</sub>, product energy and ang. distrib. obs. 2.3 to 11.6 eV 9-10325  
 N<sub>2</sub><sup>+</sup>+HD, product energy and ang. distrib. obs. 2.3 to 11.6 eV 9-10325  
 Pt surface accommodation coeff., press. depend. 9-16039  
 Th-U-N system phases, ≥50 at.% N, 1000°C 9-16157

**Nitrogen compounds**

- 1.s electron binding energies correl. with CNDO charges 9-11451  
 absorptive beam, superradiative transient obs. 9-15909  
 hydrazine diborene, i.r. spectra for struct. 9-11463  
 N<sub>2</sub>H<sub>2</sub>UF<sub>6</sub> unit cell dimens. from powder pattern 9-9682  
 nitrides, refractory, crystal structure high temp. 9-7433  
 nitrides of transition metals, physical and mechanical props. 9-7510  
 penta-atomic heterocyclic cpds., model for π electron spectra 9-4944  
 (90wt.%)Ar-(10wt.%)N<sub>2</sub> proportional counter gas, pulse shape calcs. 9-19228  
 Fe-N alloys, phase transformations during tempering, eff. of prior plastic deform. 9-13777  
 HNO<sub>3</sub>, vibration spectra at 77°K 9-7029  
 N<sub>2</sub>-CO solid solns., equilibrium vapour press. meas. 9-21253  
 N<sub>2</sub>H<sub>4</sub>, decom. in glow discharge 9-14125  
 N<sub>2</sub>O, c.w. oscillations in rotation-vibration transitions 9-20519  
 N<sub>2</sub>O, three-body electron capture 9-15953  
 N<sub>2</sub>O, u.v. absorption spectrum, interpretation 9-15863  
 N<sub>2</sub>O, vibr. relax. in shock tube 9-775  
 N<sub>2</sub>O<sub>4</sub>, e.s.r. in liquid and solid states, 77-300°K 9-19643  
 N<sub>2</sub>O i.r. spectra, adsorbed on NaCl, NaBr, NaI films 9-19443  
 N<sub>2</sub>O reaction with O<sup>1</sup>D atom, ozone quantum yield 9-21719  
 NCO gaseous free-radical, electron reson. spectrum 9-17063  
 NCl<sub>3</sub>, struct. and vibr. spectra 9-9222  
 ND, 0-0 band or A <sup>3</sup>Π<sub>u</sub>-X <sup>1</sup>Σ<sup>+</sup> system, rot. analysis 9-19440  
 ND, C<sup>3</sup>Π<sub>u</sub>-B<sup>3</sup>Σ<sup>+</sup> band system, characts. 9-4931  
 N<sub>2</sub>F<sub>4</sub>, kinetics of thermal dissociation, in shock waves 9-1903  
 NFCl<sub>2</sub>, i.r. spectrum 9-19441  
 NH, C<sup>3</sup>Π<sub>u</sub>-B<sup>3</sup>Σ<sup>+</sup> band system, characts. 9-4931  
 NH, valence excited states and transition probabilities 9-2875  
 NH<sub>3</sub> viscosity coeff. depend. on N isotopic composition and temp. 9-21146  
 NH singlet triplet intercombination separation, calc. 9-2874

**Nitrogen compounds continued**

- NH valency vibrations of secondary sulphonamides, temp. depend. 9-797  
 $N_2H_4$ , abs. coeff., 1200-2000Å 9-7022  
 $N_2H_4^+$  in p-irrad. hydrazinium hydrogen oxalate cryst. 9-1927  
 $NH_4H_2PO_4$ , refractive index, pressure dependence 9-16393  
 $NH_4^+IO_3^-$ , electro-optical and nonlinear optical props. 9-3867  
 $N_2H_4^{15}N$ , vac. u.v. photolysis 9-1918  
 $N_2O$ -Acetylene, flame for atomic absorption spectroscopy interference 9-6030  
 $N_2O$ -acetylene flame appl. in atomic absorpt. spectrochem. analysis 9-10366  
 $N_2O$ -acetylene flames, temp. distrib. obs. 9-15562  
 $NO$ ,  $^2\Pi_{3/2}$ ,  $v=0$ ,  $J=7/2$  state hyperfine perturbations, magnetic resonance 9-11468  
 $NO$ , 1-0 vib.-rot. bands; absorption, Zeeman and mag. rot. spectra obs. 9-9225  
 $NO$ , 3p mol. Rydberg state ( $^2\Pi(\tilde{V}=\tilde{O})$ ), spin-orbit coupling const. 9-15860  
 $NO$ , expanding jets, cluster formation 9-20031  
 $NO$ , interstellar mol., radiolines obs. 9-17626  
 $NO$ , ionization, higher potentials 9-11467  
 $NO$ ,  $\gamma$  and  $\beta$  band syst., RKR Franck-Condon factors 9-20933  
 $NO$ , mag.-rot. spectra of 1-0 vib.-rot. band 9-9221  
 $NO$ , near i.r. mag. rot. spectrum calc. 9-2877  
 $NO$ , near i.r. spectrum, transitions betw. Rydberg states, oscillator strengths 9-19439  
 $NO$ , radiative lifetime of  $a^4\Pi$  state 9-779  
 $NO$ , Rydberg state, spin-orbit coupling 9-20935  
 $NO$ ,  $B^2\Pi$  state collisional quenching rate const. determ. 9-18186  
 $NO_2$ , electronic struct. and spectrum, nonempirical SCF calc. 9-776  
 $NO_2^-$  in KCl, impurity local vibration quantum decomposition into phonons 9-15000  
 $NO_2$  fluorescence, radiative lifetime and collisional quenching, nature of air afterglow 9-15861  
 $NO_2$  in  $SiO_2$  film deposition at low temps. 9-18403  
 $NO_2$ , vibr. spectra rel. to H bond form. in substituted phenols, obs. 9-15896  
 $NO_2+O \rightarrow NO+O_2$  reaction kinetics 9-21681  
 $NO^+$ , excited electronic states 9-774  
 $NO$ ,  $D^2\Sigma^+(V=0)$  state,  $\epsilon$ -fluorescence, mean-lifetime obs. 9-17037  
 $NO$  ioniz. transitions, use of Franck-Condon factors 9-4934  
 $NO$  many quanta transitions between components of  $\Lambda$  doublets 9-14691  
 $NO$  mixed with Ne, afterglow, microwave and mass spectrometric study of recombination, diffusion 9-9341  
 $NO$  photolysis,  $^{15}N$ -enriched  $N_2$  formation 9-16491  
 $NO$  upper atmosphere day time production and loss mechanism 9-16534  
 $NO$  viscosity coeff. depend. on N isotopic composition and temp. 9-21146  
 $NO^+$ , ioniz. transitions of  $(A^1\Sigma^+X^1\Sigma)$  band system, use of Franck-Condon factors 9-4934  
 $NO^+$  abundances in E-region, analysis of rocket-measured profiles 9-10436  
 $NO^+$  ion beam, abundance of excited ions 9-8589  
 $NO_2$ , vib. force constants determ. 9-13326  
 $NO_2^-$ , polarizability, anisotropic and refractive index of  $NaNO_2$  9-3855  
 $NO_2$  in alkali halides, Raman spectra 9-12407  
 $NO_2$  in potassium halides, vibration structure in absorpt. and luminescence spectra at 4.2°K 9-16432  
 $NO_2^+$ , Raman frequencies from exam. of  $Na(K)NO_3 \cdot Ca(NO_3)_2$  binary melts 9-9516  
 $N_2O$ , geometry and spectrum, MO calc. 9-7031  
 $N_2O$ , laser induced vibr. fluoresc. 9-7030  
 $N_2O$ , rotational line  $J=5 \rightarrow 6$ , broadening by foreign gases 9-13365  
 $N_2O$ , vibr.-vibr. energy transfer in gas mixtures 9-4983  
 $N_2O$ , vibr. excitation in  $N+NO_2$  reaction, obs. 9-10326  
 $N_2O$ , zero-order freqs., anharmonic and vib.-rot. coupling const., to fourth order 9-13366  
 $N_2O$  molecular laser, comparison with  $CO_2$  9-13019  
 $N_2O$  mols., simultaneous laser action with  $CO_2$  in  $CO_2:N_2$  gas laser system 9-8608  
 $N_2O_4$ , iron content determ. by atomic absorption spectroscopy 9-4028  
 $NOCl$ , reaction with hydrogen, laser effect prod. 9-6521  
 $NOCl$ , vibr. spectra and force const., isotopic species 9-777  
 $NOCl$  and  $NO_2$  in vacuum u.v., photodissoc. 9-16492  
 $NO_2F$ , mm. wave spectrum, force field 9-7033  
 $NO+N \rightarrow N_2+O$  reaction kinetics 9-21681  
 $NO^+ + NO_2^- \rightarrow N_2O_2$  rate determ. in various gases 9-7194  
 $NO+O$  chemiluminesc. in expanding flow, effect of molec. clusters 9-20031  
 $NO+O+(M) \rightarrow NO_2^+(M)$ , chemiluminescent reaction, three-body mechanism 9-16478  
 $NS$ , gas phase e.s.r. 9-7082  
 $NSF_3$ , i.r. and Raman spectra, Coriolis const., thermodynamic functions and bonds, obs. 9-15862  
 $N(XYZ)$ , where  $X,Y,Z=H$  or  $R$ , anomalous magneto-optical effect 9-780  
 $Na_2Fe(CN)_6$  affect on NaCl crystal growth and characteristics 9-18415

**ammonia**

- adsorption and decomp. on W(100) surface 9-1114  
 adsorption and decomposition on W(211) surface 9-19679  
 collision-induced transitions between rot. levels 9-11469  
 electronic struct., non-empirical SCF LCAO MO study 9-13364  
 impurity in ice, effect on mechanical props. 9-13711  
 $n$  interstellar molecular detection 9-8266  
 metal- $NH_3$  solns., Hall effect 9-1041  
 microwave echoes 9-13362  
 molecule, mag. susceptibility calc. 9-744  
 MPD arc thruster, efficiency rel. to ionization and mass flow rate at low press. 9-9376  
 rotation-inversion spectrum, K splitting and rot. const., 9-13367  
 solutions in  $H_2O$ , X-ray diffraction and struct. 9-3078  
 thermal cond. and rotational relax. 9-9447  
 $NH_3$  and  $ND_3$ , electron, diff. and molec. struct. 9-7032  
 $NH_3D$ , h.f.s. of rotation-inversion transition 9-17036  
 $Na-NH_3$  solns., microwave dielec. const., temp.-variation studies, nonmetal-to-metal transition 9-14854  
 $Na-NH_3$  conc. solns.,  $^{23}Na$  and  $^{14}N$  Knight shifts 9-3125  
 soln., aq., u.s. vel. depend. on conc., 1.48-10.37 MHz 9-5162

**ammonium compounds**

- $ND_4Br$  modifications III and IV, -56° to -192°C 9-16153  
 $NH_4Br$ , modifications III and IV, -56° to -192°C 9-16153

**Nitrogen compounds continued****ammonium compounds continued**

- $NH_4Cl$  dendrites, ageing by dissolution of side arms 9-3473  
 $NH_4ClO_4$ , thermal decomposition, role of point defects. 9-20033  
 $NH_4NO_3$ , phase transformation, I=II, II=III and III=IV effect of deuteration on transform. temps. 9-7614  
 $NH_4NO_3$ , phase transformations, formation obs. 9-16154  
 $(NH_4)_2H_2IO_6$ , antiferroelec. props. 9-16302  
 $(NH_4)_2MoO_4S_2$ , laser Raman spectrum, obs. 9-15859  
 $(NH_4)_2MoS_4$ , laser Raman spectrum, obs. 9-15859  
 $(NH_4)_2WO_4S_2$ , laser Raman spectrum, obs. 9-15859  
 $NH_4n.m.r.$  isotope chem. shifts 9-7013  
 $NH_4$  CL vibrational Raman spectra of order-disorder transition 9-11973  
 $(NH_4)_2PO_4$  soln., aq., u.s. vel. depend. on conc., 1.48-10.37 MHz 9-5162  
 $NH_4Br$ , Raman spectra for order evolution at  $\lambda$  transition 9-11972  
 $NH_4Br$ , radiation-induced paramagnetic  $NH_4Cl$  colour centre, e.p.r. 9-9723  
 $NH_4Br$ , vibrational Raman spectra of order-disorder transition 9-11973  
 $NH_4Cl$ , optical harmonic scattering 9-12444  
 $NH_4Cl$ , radiation-induced paramagnetic  $NH_4Cl$  colour centre, e.p.r. 9-9723  
 $NH_4Cl$ , Rayleigh Brillouin spectra 9-16426  
 $NH_4Cl$  fog, appl. to elec. field visualization 9-202  
 $NH_4ClO_4$ , deflagration, surface temp. meas. from orthorhombic-cubic transition thickness 9-10755  
 $NH_4ClO_4$ , thermal decomp., effects of X- and p-irrad. 9-4011  
 $NH_4ClO_4$ , thermal decomp., effects of X- and p-irrad. 9-4012  
 $NH_4ClO_4$ , thermal decomposition, reaction mech., effect of Cu chromite catalysis 9-12528  
 $(NH_4)_2CrO_4$ , absorption spectra, effect of uniaxial compression, 20°K 9-10206  
 $NH_4F$  impurity in ice, effect on mechanical props. 9-13711  
 $NH_4Fe(OH)(SO_4)_2$  9-5800  
 $NH_4H_2PO_4$ , dielectric phase transitions from l.f. Raman spectra and lattice modes 9-12422  
 $NH_4H_2PO_4$ , growth, impurity effects, reln. to pH of soln. 9-13601  
 $NH_4H_2PO_4$ , i.r. spectral meas. 9-5896  
 $NH_4H_2PO_4$  crystals, shape, effects of pH 9-13604  
 $(NH_4)_4Mo_2O_{10} \cdot 4H_2O$  e.s.r. of X irrad. crystals. 9-10288  
 $(NH_4)_2SO_4 \cdot CaSO_4 \cdot H_2O$  system, phase equilibria in solid and solution states 9-3147  
 $nHhSO_4$ , ferroelectric p-T diag. 9-3710

**Nobelium**

- No (II) oxidation state 9-12542

**Nobelium compounds**

- No entries

**Noble gases see Inert gases****Noctilucent clouds see Atmosphere/upper; Clouds****Noise**

- ambient, in shallow bay, particle vel. and press. meas. 9-12574  
 atmospheric, intensity, frequency dependence, 1 to 1000 kHz at low and medium latitudes 9-10390  
 in Fourier spectroscopy, rel. resolution 9-19171  
 galactic, radio, freq. spectrum rel. to cosmic ray energy spectrum 9-12730  
 Johnson, from conducting environment, quantum interference magnetometry 9-7783  
 magnetic tape stat. fluct. and stochastic approach, information capacity meas. 9-4352  
 MOS transistors, 1/f noise 9-7816  
 in nuclear reactors, analysis 9-16979  
 in nuclear reactors, conditional probability analysis 9-20845  
 optical parametric, theory 9-5865  
 random, X-ray fluorescent screens 9-12817  
 seismic, stationarity 9-6044  
 sources in separated flow region, press. fluct. investig. 9-5104  
 speckle, in holograms with redundancy, elimination 9-4490  
 from submobile, self-noise during bioacoustic investig. 9-15239  
 temperature, out-of-pile heat transfer loop, measurement 9-20863  
 under-ice, oceanic, a review 9-6390  
 v.l.f. radio, spectral charact. 9-10394  
 Si avalanche diodes, multiplication effect, measurement 9-5730
- acoustic**  
 analysis by analogue computer techniques from critical, subcritical zero power reactor 9-6935  
 annoyance of noise of different bandwidths 9-17810  
 boundary-layer section of fluid, analysis of radiation 9-18229  
 cancellation at receiving arrays using DICANNE digital processor 9-19072  
 cavitation, hydrodynamic, acoustic noise rel. to erosion 9-7100  
 cavitation noise spectra, statistical characts. 9-5134  
 detection of known and random signals in noise, optimum arrays 9-12940  
 from dome plate, arbitrarily reinforced, signal reception 9-19071  
 ear readaptation after interrupted traffic noise 9-6216  
 in electric discharges, spectra 9-5078  
 flow, spoiler generated, obs. and analytical model 9-15471  
 from cavitation, liquid, caused by cylinder 9-5157  
 graphite, emission when stressed in compression 9-7641  
 eff. on hearing, induction of tinnitus 9-12787  
 hearing loss due to steady-state noise 9-4164  
 helicopters, Mi 8, Mi 4, characts. 9-4359  
 impact noise, transmission by single layer floors 9-4357  
 impulse, resultant deafness 9-2095  
 impulsive, eff. on hearing, duration and temporary threshold shift 9-15387  
 jet airliner, relations for calc. total and perceived levels 9-16735  
 loudness evaluation 9-19070  
 multisource averaging technique for airborne sound insulation meas. 9-2230  
 non ergodic signals meas. by synchronous filtration 9-15470  
 optimum arrays and use of Schwartz inequality for signal detection 9-12940  
 piezoelectric semiconductors, fluctuations, nature and exptl. methods for investigation, review 9-13793  
 piezoelectric semiconductors, fluctuations, nature and exptl. methods for investigation, review 9-13793  
 pitch determ. by noise bands 9-18954  
 pitch matching in interrupted white noise, periodicity theory substantiated? 9-16642



**Noise continued****acoustic continued**

- plane wave, rejection at acoustic arrays, anal. 9-16736
- pressure field on recessed plane baffle 9-4315
- pressure above infinite plane baffle, cross-spectral density 9-4314
- reducing materials in construct. industry, performance and economics 9-17782
- reverberant, response of supersonic transport fuselage 9-20435
- rocket exhaust, meas. of high alt. wind profiles 9-4054
- shake tables, generation, radiation characts. 9-4358
- sound produced in breaking ice 9-17556
- speech interfering aspects and freq. weighting contours 9-8304
- statistical relationship to cavitation noise 9-5152
- turbulent boundary layer noise, response of supersonic transport fuselage 9-20435
- underwater, due to rain, obs. in shallow lake 9-12939
- white, bandwidth influence on pitch perception 9-19069
- PbZrO<sub>3</sub>-PbTiO<sub>3</sub> piezoelec. transducers for broad-band meas. 9-2228

**electrical**

*See also Cosmic radiation, radiofrequency; Sun/radiation, radiofrequency*

- 1/f spectrum extent 9-15491
- in acoustoelectric steady state in piezoelec. semiconductors 9-5559
- diodes, thermodynamics rel. to nonlinearities 9-12165
- double injection, and equivalent circuit 9-15115
- in i.r. quantum counters, thermal 9-6499
- in Josephson oscillator, quantum mechanical theory 9-12119
- lower hybrid reson., in ionosphere, electrostatic wave origin 9-14174
- probe noise in quiescent plasma 9-9379
- semiconductors, excess, rel to anisotropic current instability 9-21497
- signal-to-noise ratio amelioration, integrated cct. soln., applic. in boron lined neutron detect. 9-19216
- transient response to disturbances in MGD generators 9-19122
- transport, decomp. under space charge conditions, anal. 9-4411
- voltage, extra high, transmission lines, charact. and meas. 9-6446
- CdS, current noise induced by electron-phonon interaction 9-5686
- CdS photoconductors, g-r noise dependence on light penetration depth 9-12211
- GaAs, c.w. laser diode 9-247
- Ge: Au, properties, 80° 300°K, n- and p-type 9-9996
- n Ge, high field current fluctuations, n-type 9-16272
- n-InSb, 4.2°K, hot electrons 9-16252
- n-SiSb, props. 80-300°K 9-9996
- Si:SiO<sub>2</sub> interface states 1/f type noise, quantitative theory 9-5738

**Noise abatement**

*See also Absorption/acoustic waves*

- of loudness analyser 9-19068
- loudness evaluation 9-19070

**Nomenclature and symbols**

*See also Units*

No entries

**Nomograms**

*See also Graphs*

- Grover, for plane bilayer wall, appl. to temp. calc. of heat-insulated cylindrical wall 9-14396

**Non-crystalline state** *see Amorphous state; Vitreous state***Non-Newtonian fluids** *see Fluids***Nonlinear optics**

- acoustic—i.r. e.m. wave interaction 9-16389
- alkali halide crystals, light amplification, possible use 9-10164
- amplifier laser, high power 9-16775
- bleach-out effect, nonlinear wave equations description 9-10840
- coherence props. of dielectric media 9-10846
- crystals, light scatt. by light, cross-section rel. to nonlinear polarizability 9-1720
- crystals, parametric amplification and light generation 9-1722
- diffraction theory and expt. verification 9-4519
- homodyne expts., angular alignment sensitivity 9-19134
- iodates, noncentric (MIOs where M=H<sup>+</sup>, Li, Ti<sup>+</sup>, K<sup>+</sup> and NH<sub>4</sub><sup>+</sup>), nonlinear and electro opt. props. 9-3867
- laser light statistics 9-15534
- liquid, contributions of molecular interactions 9-13524
- liquid, third-harmonic generation by anomalous dispersion 9-21205
- liquid, third harmonic nonlinear reflection rel. to adjustable momentum matching 9-9513
- liquid cry., second harmonic generation, origin, applic. to struct. study 9-21207
- liquids, intense laser light propagation, molecular angular correlations and strong optical nonlinearities 9-11695
- non stationary phenomena and space-time analogy 9-8639
- nonstationary effects occurring in the field of ultrashort high-intensity light pulses, theory 9-12995
- parametric interactions and tunable oscillators 9-14025
- parametric noise, theory 9-5865
- polaritons, coherent excitation in III-V semiconductor 9-12326
- pulse propagation in inhomogeneously broadened medium 9-16774
- pulses, picosecond, shape asymmetry meas. method 9-8641
- quadratic Compton effect, mixed-freq. incident wave 9-8739
- quadratic Compton effect, scatt. cross-section for arbitrarily polarized monochromatic radiation 9-8738
- resonance variation of coherent props. of light scattered in many-level system, possibility 9-8638
- ruby, interaction of ruby laser radiation from double-resonance meas. 9-10163
- scattering medium, laser beam absorpt. anomalies 9-3128
- second harmonic generation, amplitude and susceptibility rel. to fundamental wave 9-4501
- second order susceptibilities of III-V and II-VI cpds., Phillips model 9-3845
- second-harmonic generation in reflection from media with inversion symmetry 9-5864
- self-induced transparency, consequences of different phase and signal velocities 9-15541
- stimulated scatt., saturation and depletion 9-14420
- triglycine sulphate, second harmonic generation and nonlinear polarizabilities 9-1724
- u.s. generation by stimulated Brillouin effect 9-10836
- Ag films, second harmonic excitation, eff. of thickness 9-19974
- CO<sub>2</sub>, Q-switched laser, non-linear amplification characts. 9-10860
- CuCl light output analysis when laser irradiated 9-10160

**Nonlinear optics continued**

- GaP, coherent excitation of polaritons by nonlinear parametric process 9-12326
- HgS light output analysis when laser irradiated 9-10160
- KCl crystals, possible use in light amplification 9-10164
- LiNbO<sub>3</sub>, d<sub>31</sub> and d<sub>32</sub> coeffs. opposite signs, obs. 9-10165
- LiNbO<sub>3</sub>, pumped by c.w. Ar laser forming optical parametric oscillator 9-10161
- Se-Te alloy, light output analysis when laser irradiated 9-10160

**Novae**

*See also Stars*

- Cen XR-2, high temp. component rel. to model 9-20212
- Delphini 1967, H and He absorption lines velocities 9-4100
- Delphini 1967, permitted and forbidden lines velocities 9-4100
- Delphini 1967, spectra, radial vels. of emission and absorpt. features 9-10491
- Delphini 1967, spectrum since Oct. 1967, nebular lines 9-10490
- HB 9, supernova remnant, 610.5 MHz contour map., spectra obs. of rad. 9-18866
- IC 4182 supernova spectrum, electr. density and mass obs. 9-17617
- IC 443, supernova remnant, 610.5 MHz contour map., spectra obs. of rad. 9-18866
- IC 443 supernova remnant, polarized brightness distrib., 6 cm wavelength 9-16580
- IC 443 supernovae relic, spectrophotometry 9-21857
- light scatt. in medium with moving boundary, results applic. 9-19165
- models, instantaneous eye and continued ejections, possibility 9-10489
- NGC 2276, second supernova obs. 9-20184
- NGC 6888 supernova relic, spectrophotometry 9-21857
- Simeis 147, supernova remnant, 610.5 MHz contour map., spectra obs. of rad. 9-18866
- supernova, enormously energetic, explosions, eruption in M82 galaxy, book 9-8220
- supernova explosion freq. in galaxy clusters 9-12705
- supernova in NGC 3198, and photometric obs. 9-14219
- supernova NGC 4254, spectrographic obs. 9-12708
- supernova remnant in Centaurus as radio source 9-15328
- supernova remnants as radio sources 9-12704
- supernova shell, ejected, brightness increase obs., mass and electr. density meas. 9-17617
- supernovae, 1967 Palomar obs. 9-18873
- supernovae, book 9-8254
- supernovae, prod. of 4N nuclei due to triple-alpha reaction 9-6125
- supernovae, type I, identification of absorption of the spectrum 9-4101
- supernovae, type II, explosion rel. to formation of peculiar A stars 9-16572
- supernovae absolute magnitudes, 33 results 9-10488
- supernovae remnants, young, γ-ray lines due to radioactive decay of Ni<sup>56</sup> 9-16579
- supernovae remnants as radio sources, polar. distrib. 9-15329
- T Pyxidis, nine spectra, comparison with previous outbursts 9-12706
- Vulpeculae 1968, spectrum 9-15310
- W 44 supernova remnant, polarized brightness distrib., 6 cm wavelength 9-16580

**Novoids** *see Novae***Novolac acoustic resonance** *see Absorption/acoustic waves, ultrasonic;***Nuclear magnetic resonance and relaxation****Nuclear alignment** *see Nuclear polarization***Nuclear bombardment targets**

- neutron wave production from positive-ion, electrostatic accelerator 9-19259
- radioactive gases for medical use, preparation 9-21990
- reactor materials, γ spectra from 14 MeV n 9-652
- thickness meas. by α energy loss 9-2560
- thickness monitor 9-19218
- Ag, e pair prod due to γ-ray of 2.62 MeV, obs. 9-10976
- Al, e pair prod due to γ rays, 2.62, 13 MeV obs. 9-10976
- Al foils, electron energy loss 0.3-1 MeV Monte Carlo calc. 9-5587
- Al neutron scatt. 9-591
- Au, e pair prod. due to γ rays of 2.62, 13 MeV obs. 9-10976
- Au, Mott scatt. asymm. obs. depend on foil thickness 9-15582
- <sup>68</sup>Cu direct pair prod. by 5.5 and 32 MeV electrons, diff. cross-sections 9-6857
- Fe neutron scatt. 9-591
- Gd secondary emission of electrons as n detector 9-2562
- Ti, 660 MeV p bombardment, N yield obs. 9-587
- UO<sub>2</sub>, large-surface, prep. technique 9-13157

**Nuclear decay schemes** *see Radioactivity/decay schemes***Nuclear decay theory**

*See also Beta decay theory; Nucleus/theory*

- rare-earth region, N forbidden β transitions 9-2694
- super heavy prolate spheroid nuclei with Z>104 9-551

**Nuclear emulsions** *see Nuclear track emulsions***Nuclear energy level lifetimes** *see Nucleus/energy level transitions***Nuclear excitation**

*See also Mossbauer effect; Nucleus/energy levels*

- <sup>45</sup>Sc, isobaric analogue resonances of 6th state, obs. in (p,p) react., spins, parities and widths 9-8995
- Adler-Weisberger sum rule, Goldberger-Treiman rel. 9-8960
- analog state resonances, K-matrix formulation of shell-model theory 9-11192
- analogue resonances fine structure 9-6775
- analogue resonances fine structure, phenomenological theory 9-13183
- analogue states in s-d shell 9-15706
- BCS method extension for weakly deformed nuclei 9-11190
- cluster states at high excitation, props. 9-18062
- coherence radiation in ext. mag. and elec. fields 9-15815
- collective, ground state correlations, quasi-boson approx. queried 9-8963
- collective charge oscillations in deformed nuclei 9-8970
- collective motion theory in pairing-plus-quadrupole model 9-15702
- Coulomb, multiple excitation correction, even spherical nuclei 9-13189
- Coulomb, reorientation effect 9-13187
- deformation, pear-shaped, in oscillator model, perturbation oscillations 9-15707
- deformation eff., 152≤A on fast n total cross section 9-11291
- dipole, of nuclei with n excess, isospin fragmentation 9-15705
- E1(K=1) anomalous transitions absolute intensity obs. 9-6786
- electron pair prod. in spherical static nuclear charge, second Born correction 9-484

**Nuclear excitation continued**

- electronic shell effect on  $\gamma$ -rad. 9-13186  
 equilibrium deformations, g.s. energy depend., even-even nuclei,  $50 < Z < 82$ ,  $50 < N < 82$  9-11196  
 even-even nuclei, axially symmetric non-spherical, excitation of rotational-vibrational state, influence of change of configuration 9-16933  
 excitation and n-p exchange energy vary regularly 9-2632  
 giant dipole resonance,  $A^{-1/6}$  depend in hydrodynamic model 9-2638  
 giant resonance nuclei, photodisintegration 9-4766  
 giant resonant states, shell model description 9-6256  
 group constants, calculation in resonance region 9-627  
 highly-excited resonant states, shell models 9-6777  
 identification with part.- $\alpha$  coincidences, lifetimes meas. using twin-target technique for Doppler shift attenuation meas. 9-2640  
 intermediate structure observability calc. using Brueckner K-matrix methods 9-6778  
 internal conversion spectra, partial decay schemes deduced,  $173 \leq A \leq 185$  9-15721  
 isobaric analogue states 9-14553  
 isobaric analogue states, Coulomb displacement energies 9-6788  
 isobaric analogue states formed in (d, n) reaction, p decay. 9-2754  
 mass-18, SU(3) group to classify singly excited states 9-2654  
 medium and heavy nuclei, (p,p') react. through interfering isobaric analogue and giant dipole reson. 9-14608  
 particle emission following ion bombard., Monte Carlo calc. 9-20819  
 particle-hole, on spherical shells, sum of separable interact. 9-8961  
 resonance parameter distrib., Monte Carlo calc. 9-18061  
 resonances in stripping and pickup reacts., Pb region 9-6862  
 rotational, changes in mean square nuclear charge radii 9-4721  
 rotational and intrinsic motion of deformed nuclei 9-8966  
 rotational motion of deformed nuclei 9-8965  
 rotational spectra in odd-A nuclei,  $I(1+1)^2$  corrections, B parameter calc. 9-20729  
 rotational states, by p,d scatt., 2nd order Born approx. 9-15710  
 rotational states, modifications to rigid rotator law  $(I+1)$  9-11198  
 shell correction model, nucleon shells eff. 9-15708  
 spectra of pair nuclei, influence of excitation of core 9-491  
 spin polarization eff. in odd-mass nuclei 9-14554  
 Xe excited levels, from ( $\alpha$ ,2n) react., Te and Sn targets 9-16940  
 n and p distrib. in deformed nuclei 9-6776  
 N escape widths from giant dipole resonances 9-19287  
<sup>140</sup>Ce, isobaric analogue resonances in photoproton react. 9-11246  
<sup>150</sup>Nd (<sup>16</sup>O,<sup>16</sup>O $\gamma$ ), g meas. for 2<sup>+</sup> state 9-15723  
<sup>141</sup>Pr, isobaric analogue resonances in photoproton react. 9-11246  
<sup>171</sup>Yb, isobaric analogue states, Coulomb displacement energies 9-6807  
<sup>232</sup>Th Coulomb excitation obs. of Mossbauer effect 9-4742  
<sup>238</sup>Eu nuclear rotation and single particle excitation effects on X-ray spectr. 9-11432  
<sup>171</sup>Yb, isobaric analogue states, Coulomb displacement energies 9-6807  
<sup>167</sup>Dy, by radiative neutron capture, spectrum of conversion electrons emitted 9-522  
<sup>115</sup>In by threshold-energy e, M1/E2 mixing ratios determ. 9-6798  
<sup>152</sup>Yb, isobaric analogue states, Coulomb displacement energies 9-6807  
<sup>196</sup>Pt giant-dipole-resonance abs., radiative strength function at n binding energy 9-2671  
<sup>148</sup>Sn, by inelastic p, scatt. at 14.695 MeV and collective states 9-512  
<sup>127</sup>(n,n') 59 keV level excited, cross section meas.,  $E_n=50-500$  keV 9-19277  
<sup>127</sup>(p,p') Coulomb excitation, E2 transition prob. determ.,  $E_p=3.5-5$  MeV 9-20737  
<sup>127</sup>( $\alpha,\alpha'$ ) Coulomb excitation, E2 transition prob. determ.,  $E_\alpha=3.5-5$  MeV 9-20737  
<sup>207</sup>Pb, excitation curves measured to the  $7/2^+$ ,  $5/2^+$  doublet 9-8991  
<sup>207</sup>Pb, single n hole states, by inelastic scatt.  $E_p=20.2$  MeV 9-530  
<sup>171</sup>Te from <sup>148</sup>Sn( $\alpha$ ,n), search for isomeric transition,  $E_\alpha=17.27$  MeV 9-15716  
<sup>171</sup>Te from <sup>148</sup>Sn( $\alpha$ ,2n), search for isomeric transition,  $E_\alpha=17.27$  MeV 9-15716  
<sup>171</sup>Yb, isobaric analogue states, Coulomb displacement energies 9-6807  
<sup>209</sup>Bi isobaric analogue resonance 0<sup>+</sup> state, calc. of p decay width 9-11231  
<sup>209</sup>Pb, particle-hole, RPA calc. on collective 3<sup>-</sup> state, sum of separable interact. tech. 9-8961  
<sup>209</sup>Pb, single-particle analog reson., total widths and reson. energies, analog in <sup>209</sup>Bi 9-14577  
<sup>209</sup>Bi, single-particle analog reson., total widths and reson. energies obs. 9-14577  
<sup>129</sup>I, excited states following <sup>129m</sup>Te decay 9-15717  
<sup>139</sup>La, isobaric analogue resonances in photoproton react. 9-11246  
<sup>239</sup>Pu resons., fission-neutron multiplicity obs., 20-100 eV 9-20746  
<sup>118</sup>Sn, to 23.8keV level,  $\Delta R/R$  sign magnitude 9-11221  
<sup>27</sup>Al, by n inelastic scatt., cross section, modified optical model transmission coeff. 9-20791  
<sup>12</sup>B even-parity T=1 levels, particle hole description 9-14562  
<sup>7</sup>Be, isobaric analogue state excited in <sup>7</sup>Li(p,n)<sup>7</sup>Be, impulse approx. calc. 9-9029  
<sup>11</sup>C in <sup>12</sup>C(p,n)<sup>11</sup>C 9-15749  
<sup>12</sup>C, form factor for electron scatt. excitation Coulomb distortion correction calc. 9-11210  
<sup>14</sup>C part.  $\gamma$  correlation experiments e.m. multiple mixing ratios, spring, branching ratios, calc. 9-2643  
<sup>12</sup>C(<sup>12</sup>C, $\alpha$ )<sup>20</sup>Ne excitation functions obs. and compared with theory 9-6917  
<sup>12</sup>C(<sup>6</sup>Li,p)<sup>13</sup>O excitation functions obs. and compared with theory 9-6917  
<sup>12</sup>C(<sup>16</sup>O, $\alpha$ )<sup>24</sup>Mg excitation functions obs. and compared with theory 9-6917  
<sup>40</sup>Ca, 4p-4h excitations, J=T=0 levels calc. 9-14585  
<sup>40</sup>Ca, particle-hole, odd-parity levels, correlations in ground-state 9-8996  
<sup>48</sup>Ca(p,p) analogue resonances fine structure 9-4777  
<sup>12</sup>C(p,p') levels obs., distorted wave impulse approx. calc.,  $E_p=100$  MeV 9-18091  
<sup>63</sup>Cu, excited states from  $\alpha$ -part. inelastic scatt. at 29 MeV. 9-543  
<sup>18</sup>F, wave functions and spectroscopy study from (<sup>2</sup>He,p) and ( $\alpha$ , d) react 9-6808  
<sup>56</sup>Fe, by n inelastic scatt., cross section, modified optical model transmission coeff. 9-20791  
<sup>3</sup>He, search for unbound states from <sup>6</sup>Li(p, $\alpha$ ) react. 9-11211  
<sup>4</sup>He states obs. in <sup>4</sup>He(p,p')H expt. 9-16937  
<sup>4</sup>He lifetimes of 1.37 and 4.23 MeV states, twin-target technique with Doppler shift attenuation meas. 9-2640  
<sup>24</sup>Mg static quadrupole moment of first excited J $\pi=2^+$  state 9-8994

**Nuclear excitation continued**

- <sup>26</sup>Mg form factor for electron scatt. excitation Coulomb distortion correction calc. 9-11210  
<sup>89m</sup>Y, cross section for inelastic n. scatt. 9-13226  
<sup>23</sup>Na, isobaric analog reson. obs., high-resolution study 9-14580  
<sup>19</sup>Ne first excited state, g-factor 9-16936  
<sup>12</sup>Ni collective 2<sup>+</sup>, 3<sup>-</sup> states from inelastic d scatt 9-16967  
<sup>12</sup>O part.-hole states, e excitation 9-504  
<sup>16</sup>O, of particle-hole intermediate states in <sup>15</sup>O(n,p) <sup>16</sup>O at 0-10 MeV 9-20796  
<sup>17</sup>O, <sup>17</sup>F doublet, particle-core coupling, low-lying parity states calc. 9-6791  
<sup>31</sup>P, 1st and 2nd levels mean life determ. by Doppler shift attenuation method 9-14584  
<sup>31</sup>P, 1st and 2nd levels mean life determ. by Doppler shift attenuation method 9-14584  
<sup>125</sup>Sc, Coulomb reorientation effect to deduce static quadrupole moment of <sup>125</sup>Mg 9-8994  
<sup>43</sup>Sc, isobaric analogue resonances of 10<sup>th</sup> and 19<sup>th</sup> states, obs. in (p,p) react., spins, parities and widths 9-8995  
<sup>49</sup>Sc from <sup>48</sup>Ca(p,n), g.s. isobaric analogue resonance obs.,  $\gamma$  spectra meas.,  $E_p=1.2-4$  MeV 9-19284  
<sup>28</sup>Si form factor for electron scatt. excitation, Coulomb distortion correction calc. 9-11210  
<sup>84</sup>Sr, particle-hole, finite range force calc. 9-11245  
<sup>92</sup>Tc isobaric analog resonance, 11.80 MeV decay 9-4752  
<sup>48</sup>Tl, spin 1 states, from particle- $\gamma$  correlations, mixing ratios of transitions 9-8997  
<sup>50</sup>Ti(p,p) analogue resonances fine structure 9-4777  
<sup>89</sup>Y, isobaric analogue resonances in photoproton reaction 9-11246  
<sup>70</sup>Zn collective 2<sup>+</sup>, 3<sup>-</sup> states from inelastic d scatt 9-16967  
<sup>86</sup>Zn resonant scatt. meas. on 7368 keV level by Pb capture  $\gamma$  9-2689  
<sup>89</sup>Zr, excited states due to 2<sup>-</sup> isobaric analog reson. in <sup>89</sup>Y(p,n)<sup>89</sup>Zr react. 9-14610  
<sup>90</sup>Zr, by n inelastic scatt., cross section, modified optical model transmission coeff. 9-20791  
<sup>90</sup>Zr, dipole excitation, isospin fragmentation 9-15705  
<sup>90</sup>Zr, energies of low-lying excited levels from meas. on <sup>90</sup>Nb decay 9-13205  
<sup>90</sup>Zr, isobaric analogue resonances in photoproton react. 9-11246  
<sup>91</sup>Zr, energies of low-lying excited levels from meas. on <sup>91</sup>Nb decay 9-13205  
<sup>92</sup>Zr, energies of low-lying excited levels from meas. on <sup>92</sup>Nb decay 9-13205  
**Nuclear explosions** see *Explosions/nuclear*  
**Nuclear field theory** see *Field theory, quantum*  
**Nuclear fission**  
 See also *Explosions/nuclear; Nuclear reactors, fission*  
 absolute fission rate meas. with solid state track recorders 9-11142  
 asymmetric, dynamic model calc. 9-6921  
 concentration of fissionable mats. in solid bodies, determ. method 9-11328  
 density of one-nucleon states, deviation from uniform at Fermi energy and shell corrections at deformation 9-15782  
 dynamic model, Th-Fm ground state props., saddle pt. props., comparison with quadrupole moments and barrier energies 9-2676  
 heavy nuclei, stat. model and repulsive nucleus-nucleus forces 9-20811  
 isomers in transuranic elements region, optical anisotropy 9-2767  
 with light particle emission, deformed nuclear model 9-13182  
 mass ratios for rapid deform. leading to scission, reflection symmetry 9-618  
 neutron induced, optical model parameters effect on channel analysis 9-11331  
 nuclei with  $158 \leq N$ , spontaneous fission instability 9-4805  
 nucleus excited following bombard. by ion, Monte Carlo calc. 9-20819  
 products fission gas escape from reactor fuel during irradiation 9-20848  
 in reactor core, obs. 9-645  
 review 9-16968  
 separation of U from fission product, by eutectic freezing 9-18749  
 spherical nuclei model for fission with light particle emission 9-11326  
 statistical model for heavy nuclei and repulsive nucleus-nucleus forces 9-20811  
 superheavy nuclei,  $A \approx 298$ ,  $\alpha$  and spontaneous fission half life theoretical estimate 9-14590  
 superheavy nuclei, fission barriers from single particle levels calc., stability 9-18107  
 ternary, three-point-charge model 9-13246  
 (n, 2n) cross section averaged over fission n spectrum 9-20794  
 (n,  $\alpha$ ) cross-section averaged over fission n spectrum 9-20794  
 (n, p) cross-section averaged over fission n spectrum 9-20794  
<sup>252</sup>Bk, n cross section obs. 9-9072  
<sup>240</sup>Pu, nuclear pairing energy of transition nucleus calc. 9-6920  
<sup>240</sup>Pu, sub threshold, rel. to resons. radiative widths, 38 820eV 9-9040  
<sup>252</sup>Cf,  $\gamma$  radiation analysis, spectra meas. 9-6923  
<sup>252</sup>Cf, spontaneous, available n fluxes and shielding requirements for use as n source 9-14634  
<sup>252</sup>Cf, ternary, three-point-charge model 9-13246  
<sup>252</sup>Cf spontaneous, n energy calc. using statistical model 9-621  
<sup>240</sup>Pu(n,f), resonances and parameters, fis. components 9-16969  
<sup>237</sup>Th cumulative fission yield, fine structure in symmetric mass region 9-11333  
<sup>232</sup>Th(n,f), fragment distribution near threshold 9-2769  
<sup>232</sup>Th(p,f) fragments mass and energy distrib. meas.,  $E_p=13.53$  MeV 9-16970  
<sup>243</sup>Pu, n cross-section obs. 9-9072  
<sup>233</sup>Th induced, ang. distrib. and cross section of fragments 9-2772  
<sup>233</sup>U, fast n cross-section ratio 0.3-2.5 MeV 9-623  
<sup>233</sup>U, n fission cross-section measurements 9-20814  
<sup>135</sup>Xe direct yield 9-4811  
<sup>24</sup>Cm, spontaneous, for absolute calibration of solid state track recorders 9-11142  
<sup>254</sup>Es, n cross-section obs. 9-9072  
<sup>248m</sup>Es, n cross-section obs. 9-9072  
<sup>238</sup>U resonances, fission components. 9-2768  
<sup>248</sup>Cm, n cross-section obs. 9-9072  
<sup>239</sup>Pu, fission cross-section measurements 9-20814  
<sup>233</sup>U, fast n cross-section ratio 0.3-2.5 MeV 9-623  
<sup>233</sup>U, n fission cross-section measurements 9-20814  
<sup>235</sup>U spontaneous n energy calc. using statistical model 9-621  
<sup>246</sup>Cf, half life meas. 9-620



**Nuclear fission continued**

- <sup>246</sup>Cf, half life meas. 9-620  
<sup>247</sup>Cm, n cross-section obs. 9-9072  
<sup>238</sup>Pu, neutron-induced angular anisotropy 9-20817  
<sup>209</sup>Bi, photofission, total cross-section and mass yield curve 9-13249  
<sup>239</sup>Pu, fast n cross-section ratio 0.3-2.5 MeV 9-623  
<sup>239</sup>Pu, resonance neutron-induced, effective cross-section meas. at high resolution 9-9075  
<sup>239</sup>Pu, ternary thermal neutron induced emission of Li, Be, B, C obs. 9-15783  
Ag<sub>2</sub> emulsion nuclei, 13.8 GeV p fragmentation 9-4808  
Br emulsion nuclei, 13.8 GeV p fragmentation 9-4808  
UO<sub>2</sub> irradiated, gas determ. by heating, 2300°C, evaporation 9-4815

**products**

- <sup>235</sup>U thermal n-induced, fragment energy-correlation meas. 9-4812  
<sup>235</sup>U, energy and time of flight correl. expts. for fragment mass distrib. 9-16971  
of <sup>235</sup>U by 14.8 MeV n, fragment mass spectra 9-15786  
atmosphere, precipitation,  $\beta$  activity meas., Debrecen, Hungary, (1966-7) 9-16533  
Chinese test 28 Dec, 1966, quantitative investigation of fallout sample 9-6082  
concentration measurement, by recording delayed neutrons 9-2771  
fission-gas release from UO<sub>2</sub> at around 2000°C 9-13250  
fragment mass distrib. in <sup>238</sup>U(<sup>20</sup>Ne, f) <sup>238</sup>U(<sup>40</sup>Ar, f) and <sup>209</sup>Bi(<sup>20</sup>Ne, f) 9-11332  
fragment temp. determ. after <sup>238</sup>U bombard, with 6.1 MeV n 9-11329  
interdependence of point mass, velocity and energy distrib. 9-11334  
parameter determ. from fission fragment energy spectrum 9-2773  
plastic foil tracks, spark scanning 9-18044  
reactor fuel particles, spherical, with multilayer coatings, release of fission prod. 9-18126  
release and fuel evaporation in loss-of-coolant accident, boundary-layer diffusion model 9-16989  
system for rapid chemical separation and spectroscopic examination 9-4811  
yield decrease of gaseous and increase of solid products on increasing thermal neutron flux 9-11337  
 $\gamma$  radiation analysis from <sup>252</sup>Cf, spectra meas. 9-6923  
<sup>140</sup>Ba from <sup>238</sup>U, ang. distrib. and range determ. 9-4810  
<sup>240</sup>Pu, spontaneous, average number of prompt n per fission, relative to <sup>252</sup>Cf 9-14635  
<sup>240</sup>Pu fission-fragment ang. distrib. after n radiation, 150-1500 keV 9-6920  
<sup>241</sup>Am,  $n_{th}$  induced, long-range  $\alpha$  energy spectra meas. 9-9074  
<sup>231</sup>Ba from <sup>238</sup>U, ang. distrib. and range determ. 9-4810  
<sup>231</sup>Pa, n fission fragment mass distrib. 9-6924  
<sup>241</sup>Pu,  $n_{th}$  induced, long-range  $\alpha$  energy spectra meas. 9-9074  
<sup>252</sup>Cf, number of n per fission, absolute determ. 9-14637  
<sup>252</sup>Cf, prompt n, average number per fission 9-14636  
<sup>242</sup>Pu, spontaneous, average number of prompt n per fission, relative to <sup>252</sup>Cf 9-14635  
<sup>242</sup>Pu, spontaneous, I isotope yield obs. 9-6925  
<sup>232</sup>Th, n induced, prob. of long-range  $\alpha$  prod. meas. 9-9073  
<sup>232</sup>Th 9-6925  
<sup>101</sup>Pd from <sup>238</sup>U, ang. distrib. and range determ. 9-4810  
<sup>233</sup>U, neutron emission rel. to fragment mass 9-4813  
<sup>233</sup>U, thermal n fission yield obs. 9-6925  
<sup>233</sup>U thermal fission, time var. of mean  $\beta$  activity 9-11338  
<sup>134</sup>Sb, from <sup>235</sup>U, cumulative yield and half life 9-622  
<sup>235</sup>U,  $\gamma$  anisotropy depend. on total fragment mass ratio and kinetic energy 9-2775  
<sup>235</sup>U,  $\gamma$  quanta, two dimens. depend. of anisotropy on kinetic energy 9-626  
<sup>235</sup>U, mass and energy distrib. of fragments up to 15.5 MeV 9-2774  
<sup>235</sup>U fragments, range determ. in Lexan detector 9-20820  
<sup>235</sup>U thermal fission, time var. of mean  $\beta$  activity 9-11338  
<sup>236</sup>U, light nuclei energy distrib. calc. 9-15785  
<sup>236</sup>U, statistical description of product yields 9-20821  
<sup>237</sup>Np, n fission fragment mass distrib. 9-6924  
<sup>238</sup>Pb, p radiation at 450 MeV, cross sections, recoil props., charge distrib. for A=111 products 9-20818  
<sup>238</sup>U, charge distribution in symmetric fission by 450 MeV p 9-13252  
<sup>238</sup>U, isobaric products with A=103 and 111 in symmetric p fission 9-13253  
<sup>238</sup>U( $\gamma$ , f), f ang. distrib. meas., K-level energy determ.,  $E_p=5.4-9$  MeV 9-15784  
<sup>209</sup>Bi, 14.8 MeV n fission yield obs. 9-6925  
<sup>209</sup>Bi, fragment yields for photofission, mass yield curve 9-13249  
<sup>239</sup>Pu thermal fission, time var. of mean  $\beta$  activity 9-11338  
<sup>239</sup>Th, yield of 46 isotopes, fine structure in A=134, 140 and 144 obs. 9-11330  
Ag in 20 GeV/c proton interac., range and vel. space angle 9-9076  
<sup>83</sup>As from <sup>235</sup>U,  $n_{th}$  irradiation, identification and half-life determ. 9-20813  
<sup>84</sup>As from <sup>235</sup>U,  $n_{th}$  irradiation, identification and half-life determ. 9-20813  
Br in 20 GeV/c proton interac., range and vel. space angle 9-9076  
Kr gas bubbles, nucleation and behaviour in non-uniform temp. 9-624  
<sup>83</sup>Kr from treated, evaporated, irradiated UO<sub>2</sub>, spectrometry 9-4815  
<sup>99</sup>Mo from <sup>238</sup>U, ang. distrib. and range determ. 9-4810  
<sup>84</sup>Se from <sup>235</sup>U, decay characteristics determ. by  $\beta$ ,  $\gamma$  spectra meas. 9-19300  
<sup>87</sup>Se, delayed n precursor study, half-life and fission yield 9-13251  
Sn isotopes, separation and half-life determ. 9-11335  
<sup>91</sup>Sr from <sup>238</sup>U, ang. distrib. and range determ. 9-4810  
U, fission gas bubble distrib., rel. to stress annealing and irradi. dose 9-11336  
<sup>U</sup><sup>235</sup>, triple fission induced by thermal neutrons, Z>2 long range particles obs. 9-625  
Xe gas bubbles, nucleation and behaviour in non-uniform temp. 9-624  
Xe in Al, bubble distrib. rel. to grain-boundary migration 9-657

**uranium**

- <sup>235</sup>U thermal-n-induced, fragment energy-correlation meas. 9-4812  
depleted slab between borated polyethylene, spatially depend. resonance neutron spectra 9-16987  
fission gas bubble distrib. rel. to post-irrad. annealing and stress 9-11336  
photofission, fragment ang. distrib. 9-2506  
reserves, long term optimal utilization, linear programming model 9-6927

**Nuclear fission continued****uranium continued**

- solid product decrease with increase of fission gas, rel. to thermal n flux 9-11337  
<sup>235</sup>U, autocorrelation effects in n induced fission cross section 9-2770  
<sup>233</sup>U, n-induced, prob. of long-range  $\alpha$  prod. meas. 9-9073  
<sup>233</sup>U, and n captive, cross-sections in region 0.4 to 2000 eV 9-13247  
<sup>233</sup>U, neutron emission rel. to fission fragment mass 9-4813  
<sup>233</sup>U, thermal n fission yield obs. 9-6925  
<sup>233</sup>U, thermal neutron induced, K emission obs. 9-20816  
<sup>233</sup>U thermal fission products, time var. of mean  $\beta$  activity 9-11338  
<sup>235</sup>U, 2.5 or 14 MeV n bombard, ternary fission obs. 9-20815  
<sup>235</sup>U, by  $n_{th}$ , motion from saddle to scission pts., mass, kinetic energy and fis. fragment kinetic energy distrib. 9-6921  
<sup>235</sup>U, cumulative yield and half-life of <sup>134</sup>Sb, obs. 9-622  
<sup>235</sup>U, fragment mass distrib., expts. with two solid state detectors 9-16971  
<sup>235</sup>U, induced by 14.8 MeV n, mass spectra of fragments meas. 9-15786  
<sup>235</sup>U,  $\gamma$  anisotropy depend. on total fragment mass ratio and kinetic energy 9-2775  
<sup>235</sup>U, mass and energy distrib. of fragments up to 15.5 MeV 9-2774  
<sup>235</sup>U, n-induced, prob. of long-range prod. meas. 9-9073  
<sup>235</sup>U,  $n_{th}$  irradiated, <sup>83,84</sup>As identification and half-life determ. 9-20813  
<sup>235</sup>U delayed n emission, mass and time depend. obs. 9-18108  
<sup>235</sup>U fission resonance in homogeneous system, temp. depend. 9-19324  
<sup>235</sup>U fragments, range determ. in Lexan detector 9-20820  
<sup>235</sup>U thermal fission products, time var. of mean  $\beta$  activity 9-11338  
<sup>235</sup>U-<sup>84</sup>Se, decay characteristics determ. by  $\beta$ ,  $\gamma$  spectra meas. 9-19300  
<sup>236</sup>U, intermediate structure dependence of fission probability on excitation energy 9-619  
<sup>236</sup>U, light nuclei energy distrib. calc. 9-15785  
<sup>236</sup>U, moment of inertia at saddle point, calc. in cranking approx. 9-4807  
<sup>236</sup>U, statistical description of product yields 9-20821  
<sup>236</sup>U, ternary, three-point charge model 9-13246  
<sup>238</sup>U, <sup>20</sup>Ne- $\alpha$ -Po, At isotopes, yields meas. 9-6922  
<sup>238</sup>U, 14 MeV n bombard, ternary fission obs. 9-20815  
<sup>238</sup>U, <sup>41</sup>Ar- $\alpha$ -Po, At isotopes, yields meas. 9-6922  
<sup>238</sup>U, by 0.8-3.4 MeV neutrons, angular anisotropy 9-13248  
<sup>238</sup>U, e induced, cross section calc. 9-14638  
<sup>238</sup>U, n-induced, prob. of long-range  $\alpha$  prod. meas. 9-9073  
<sup>238</sup>U, by p, symmetric, nuclear charge distrib. 9-13252  
<sup>238</sup>U, p 2.2 GeV irradiation, products ang. distrib. and range determ. 9-4810  
<sup>238</sup>U, symmetric by p, isobaric products with A=103 and 111, recoil study 9-13253  
<sup>238</sup>U cumulative fission yield, fine structure in symmetric mass region 9-11333  
<sup>238</sup>U fission in isolated low-enriched rods, calc. 9-11364  
<sup>238</sup>U spontaneous decay const. determ. 9-4806  
<sup>238</sup>U spontaneous decay rate from accumulation of Xe in U materials 9-20812  
<sup>238</sup>U( $\gamma$ , f), f ang. distrib. meas., K-level energy determ.,  $E_p=5.4-9$  MeV 9-15784  
Ba isotope prod. cross-sections for 1-2.9 GeV p 9-4809  
Cs isotope prod. cross-sections for 1-2.9 GeV p 9-4809  
I isotope prod. cross-sections for 1-2.9 GeV p 9-4809  
Te isotope prod. cross-sections for 1-2.9 GeV p 9-4809  
UO<sub>2</sub> D<sub>2</sub>O lattices, fast fission ratio, obs. 9-19349
- Nuclear fission reactors** see *Nuclear reactors, fission*
- Nuclear forces**
- See also *Field theory, quantum/meson field*
- B<sub>A</sub> binding energy, Green function formulae 9-8973  
binding energies and two-particle spectra 9-8957  
binding energy and isotope mass from mass spectroscopy 9-2635  
binding energy for finite nuclei with tensor forces, calc. 9-6771  
central, residual interaction and range 9-11181  
central, Slater integrals estimated 9-15701  
charge dependence, evidence from  $\beta$  decay higher order effects 9-13207  
collective potential-energy: surface, structure 9-4711  
Coulomb interaction between states of definite isospin, average value of Coulomb interaction in nuclei 9-11180  
Coulomb energy radii from mass parabolas 9-9103  
dispersion theory, partial wave, applied to N-N scatt. 9-6759  
effective interaction rel. to free nucleon-nucleon interact. 9-4712  
four-body, virtual pion interaction in nuclear matter 9-489  
hard-core potential and two-body t matrix expansion 9-4706  
Hartree-Fock Coulomb and c.m. corrections 9-2629  
for Hartree-Fock interactions, binding energy and radius depend on phenomenological short-range n-n interaction 9-2633  
Hartree-Fock methods applied 9-20725  
interaction between nucleons in triplet states, effective nuclear potential 9-8950  
many particle, orbital and spin - isospin contrib. to fractional parentage coeff. 9-6760  
N-N potential, realistic, core polar, correct by self-consistent method 9-6755  
nonstatic nuclear potential, one and two pion exchange potentials reviewed 9-6757  
nuclear matter, exchange diagrams 9-16931  
nuclear matter, properties, two-body reactions reviewed 9-4719  
nucleon-nucleon field theor. pot. 9-19265  
nucleon-nucleon S-wave phase shifts rel. to solvable S-wave potentials 9-4710  
nucleon-nucleon scatt. obs., 25-310 MeV, meson interactions 9-4707  
one boson-exchange model reviewed 9-6758  
parity-nonconserving nucleon-nucleon pot. from Oakes weak interaction theory 9-8952  
potential, axi-symmetric, calc. of one-particle energy spectrum, bound and quasi-stationary states 9-15709  
potential barrier penetration for diffuse Woods-Saxon potential of strong interaction 9-486  
potential depend. on isospin, determ. 9-14547  
potential model review 9-6756  
potentials, pathological separable, deriv. and study using positive-model phase shifts 9-6753  
primary universal interaction theory 9-319  
Q.Q., acting on part. in N=2, 3 shells, Hartree-Fock calc., ang. momentum projection 9-14544  
residual interaction, range 9-13181  
rotational energies calc. from Coriolis pair field decoupling 9-11191  
shell potential, isospin term determ. from N binding energies 9-15703  
surface delta interaction, props 9-20726

**Nuclear forces continued**

- Tabakin realistic N-N potential, core polar correct by self-consistent method 9-6755  
 tensor and central force matrix elements computation method for shell model states 9-11176  
 tritium, e.m. radii calc. in a theory of zero-range forces 9-11213  
 two body potential, transform into hermitian Brueckner matrix 9-4708  
 Woods-Saxon potentials, analytical soln. for n bound s-states energy eqn. 9-8956  
 N-N bremsstrahlung of potential model, anal. 9-18057  
 N-N potential, matrix elements for nuclear structure structure calc. 9-11178  
 N-N potential, soft-core, finite square wells 9-20724  
 n-p exchange energy, regular variation with excitation energy 9-2632  
 NN scatt. in 50 MeV region, expts. 9-6689  
 NN weak interaction for p polarization and ang. distrib. asymm. in  $^2\text{H}(n,p)^3\text{H}$  9-15767  
 nn interaction, short-range, phenomenological to fit Hartree-Fock calcs. 9-2633  
 p-p, p-n effective range difference due to p-n exchange process in N-N interaction 9-15637  
 p, n coupled vibrations, phenomenological model, pot. cubic terms consideration 9-14546  
 $^{210}\text{Bi}$  Slater integral of central forces, calc. 9-15701  
 $^{112}\text{Sn}$ , form factor of real symmetry potential, depend. on n-p interaction strength 9-6822  
 $^{116}\text{Sn}$ , and energy spectrum 9-19275  
 $^{207}\text{Pb}$ , particle vibration coupling 9-6810  
 $^{208}\text{Pb}$  form factor of real symmetry potential depend. on n-p interaction strength 9-6822  
 $^{12}\text{C}$  surface absorptive pot. and optical parameters calcs. from  $^{12}\text{C}(\text{p},\text{He})$   $^{12}\text{C}$ , 12-18 MeV 9-607  
 $^{48}\text{Ca}$ , form factor of real symmetry potential, depend. on n-p interaction strength 9-6822  
 $^3\text{H}$ , binding energy and R.M.S. charge radii of tri-nucleons 9-2657  
 $^3\text{H}$ , binding energy and wave function calc. 9-2658  
 $^3\text{H}$ , wave func. and weak interaction determ. 9-11214  
 $^3\text{H}$  binding energy, with tensor forces and hard shell repulsion 9-8979  
 $^3\text{H}$  binding energy and Coulomb energy 9-11212  
 $^3\text{He}$ , binding energy and wave function calc. 9-2658  
 $^3\text{He}$ , Coulomb effects and Faddeev equations 9-19272  
 $^3\text{He}$  binding energy and Coulomb energy 9-11212  
 $^{92}\text{Nb}$  Slater integral of central forces, calc. 9-15701  
 $^{14}\text{Ne}$  Coulomb energies of valence particles calc. 2-particle wave function 9-4728  
 $^{16}\text{O}$  binding energy, using Hamada-Johnson potential calc. 9-6771

**Nuclear fusion**

- See also *Explosions/nuclear; Nuclear reactors, fusion; Thermonuclear reactions*  
 light element energy sources, survey 9-2765  
 power generation feasibility 9-19121  
 power research 9-2766  
 reactor, review of progress 9-11327  
 in stars, astronomical evidence 9-21878  
 stellar shell burning, thermal instability evolution 9-4098

**Nuclear induction** see *Nuclear magnetic resonance and relaxation***Nuclear interactions** see *Collision processes; Field theory, quantum/interactions; Elementary particles; Nuclear reactions and scattering***Nuclear isomerism**

- See also *Nucleus/energy levels*  
 cross section ratios for (n,2n) reactions 9-15761  
 Mossbauer spectrometer for small shifts 9-19222  
 production by (n,n') reactions, appl. to flux density meas. 9-11293  
 transuranic elements, optical anisotropy 9-2767  
 $^{170}\text{Ho}$  isomer, 2.9 min., from  $^{170}\text{Er}(n,p)$  obs., decay scheme 9-14594  
 $^{190}\text{Os}$  muonic isomer shifts rel. to nuclear charge distrib. 9-2836  
 $^{101m}\text{Te}$  from (p,n) reaction, half life and energy meas. 9-11217  
 $^{192}\text{Os}$  muonic isomer shifts rel. to nuclear charge distrib. 9-2836  
 $^{142}\text{Pr}$ , 5- isomeric state at 3.683 keV, half life meas. 9-2667  
 $^{152}\text{Sm}$  muonic isomer shifts rel. to nuclear charge distrib. 9-2836  
 $^{182}\text{W}$  muonic isomer shifts rel. to nuclear charge distrib. 9-2836  
 $^{193}\text{Os}^{9/2-}$  [505] isomeric state found 9-19280  
 $^{103m}\text{Ru}$  from (p,n) reaction, half life and energy meas. 9-11217  
 $^{133}\text{Xe}$  transition, K internal. conversion coeff. determ. 9-15718  
 $^{214}\text{Fr}$ - $^{210}\text{At}$ , energy levels and lifetimes determ. 9-4758  
 $^{14}\text{Sb}$  and its fission yield 9-622  
 $^{114}\text{Sn}(\alpha,n)^{117}\text{Te}$ , search for isomeric transition,  $E_\alpha=17.27$  MeV 9-15716  
 $^{184}\text{W}$  muonic isomer shifts rel. to nuclear charge distrib. 9-2836  
 $^{115}\text{Sn}(\alpha,2n)^{117}\text{Te}$ , search for isomeric transition,  $E_\alpha=17.27$  MeV 9-15716  
 $^{185}\text{W}$ , 1.7 min. isomer identification and obs. from decay studies 9-16941  
 $^{125m}\text{Xe}$ , half-life and decay scheme 9-4755  
 $^{186}\text{W}$  muonic isomer shifts rel. to nuclear charge distrib. 9-2836  
 $^{137}\text{Ce}$  high and low-spin isomer ratio, formed in reactions due to  $^3\text{He}$ ,  $^4\text{He}$ ,  $^4\text{Li}$ ,  $^{12}\text{C}$  9-2665  
 $^{117}\text{Te}$  from  $^{114}\text{Sn}(\alpha,n)$ , search for isomeric transition,  $E_\alpha=17.27$  MeV 9-15716  
 $^{117}\text{Te}$  from  $^{115}\text{Sn}(\alpha,2n)$ , search for isomeric transition,  $E_\alpha=17.27$  MeV 9-15716  
 $^{127m}\text{Xe}$ , half-life and decay scheme 9-4755  
 $^{208m}\text{Bi}$  from (p,n) reaction, half life and energy meas. 9-11217  
 $^{118}\text{In}$  7- or 8- isomeric state found, decay obs., levels, spin and parity determ. 9-19276  
 $^{188}\text{Os}$  muonic isomer shifts rel. to nuclear charge distrib. 9-2836  
 $^{158m}\text{Tb}$  from (p,n) reaction, half life and energy meas. 9-11217  
 $^{80}\text{Br}$  nuclear isomers separation at metal surfaces 9-18769  
 $^{67}\text{Co}$  decays,  $\beta$ ,  $\gamma$  spectra obs., decay schemes determ. 9-14589

**Nuclear magnetic resonance and relaxation**

- See also *Molecules/nuclear coupling*  
 3,4,5-trichloro-2,6-difluoropyridine fluorine spectrum, band-shape, coupling const. 9-9239  
 $\alpha$  in Hparaelectric phase of  $^{87}\text{Rb}$  9-16469  
 $\alpha$ -methylpentafluorostyrene - p-methyl -  $\alpha$ ,  $\beta$ ,  $\beta$ -trifluorostyrene - styrene copolymer:  $^{19}\text{F}$  19 and 37.6 MHz 9-12518  
 $\text{A}_2\text{BX}_4$  systems, spin-echo formulas 9-13340  
 $\text{AA}'\text{BB}'$  system, oriented 4-spin with  $\text{C}_2$  symmetry 9-20979  
 acetanilides, ortho-substituted, selective deshielding of aromatic protons 9-19454  
 acetylenes, substituted, molec. motion in liq. 9-9557  
 acoustical excitation of nuclear spin system with  $l=3/2$  9-1711

**Nuclear magnetic resonance and relaxation continued**

- aliphatic secondary amines, H-bonding from p.m.r. obs. 9-19455  
 alkali metals, spin-lattice relax. rates and Knight shifts, electron-electron interaction effects 9-17501  
 alkyl radical reactions in soln., dyn. nucl. polarization 9-17222  
 alkyl radicals, chem. induced dynamic nuclear polarization 9-2921  
 alloys, liq., Knight shift rel. to composition 9-5190  
 amines, aromatic, and derived amides, p.m.r. spectra 9-19456  
 p-anisaldazine, liq. crystal transition, proton spin-lattice relaxation study 9-11723  
 in antiferromagnets, nuclear spin-wave relaxation 9-8037  
 arsenomethane, rel. to pseudo-rotation 9-20949  
 arsenoperfluoromethane, rel. to pseudo-rotation 9-20949  
 aryl fluorides,  $^{19}\text{F}$  chem. shifts 9-802  
 averaging effects, coherent, theory and appl. to high-resolution technique analysis 9-17502  
 aziridine, 1-substituted,  $^{13}\text{C}$ -H satellite resonances, coupling parameters 9-13543  
 $\text{B}_3\text{AA}'\text{B}_3'$  type spectra, 2-butene and related cpds. as examples 9-13376  
 benzene anion,  $\text{T}_1/\text{T}_2$  and spin relax. 9-15904  
 benzene derivatives, para deuterated,  $\text{DC}_6\text{H}_4\text{X}$ , proton  $\delta$  effect in o- and m-positions 9-7279  
 benzene- $d_6$  cryst., ENDOR of photoexcited triplet-state benzene- $h_\alpha$  9-14118  
 benzene-polymethylmethacrylate solns., nuclear relax. 9-9558  
 benzenes, ortho-disubstituted, dissolved in nematic phase 9-7280  
 benzo-2,1,3-oxadiazole and derivatives, p spectra rel. to bond order, obs. 9-15882  
 benzo-2,1,3-selenadiazole and derivatives, p spectra rel. to bond order, obs. 9-15882  
 benzo-2,1,3-thiadiazole and derivatives, p spectra rel. to bond order, obs. 9-15882  
 benzophenones, protonated, spectra, isomer obs. and config. 9-20953  
 benzophenonimines, methyl substituted, proton NMR 9-14705  
 bicyclo (1.1.1) pentane derivative, correl. with cryst. and molec. struct. 9-15205  
 2-butene, cis and trans,  $\text{B}_3\text{AA}'\text{B}_3'$  spectral analysis, allylic and homoallylic coupling 9-13376  
 2-butene, trans-1,4-disubstituted cpds., rotational isomerism about single bond joining trigonal to tetrahedral carbon 9-13376  
 calculation of high-resolution spectra 9-16756  
 carboxylic acid-water mixture, var. in p relaxation time 9-3126  
 carboxypeptidase A 9-17067  
 chemical exchange kinetics application 9-8344  
 chemical exchange rates determ. 9-5996  
 1-chloro-1,2-dibromo-2-iodoethane, internal rot. 9-807  
 chloroform, proton double reson. 9-9256  
 $\alpha$  chlorovinyltrichlorosilane, chemical shifts and coupling const., solvent and conc. effects 9-11503  
 $\alpha$ -chlorovinyltrimethylsilane, chemical shifts and coupling const., solvent and conc. effects 9-11503  
 coherence resonances and O freq. transitions 9-8562  
 colloidal systems, proton self-diffusion, by spin echo 9-3127  
 copper acetate monohydrate, low-temp., T, anisotropy of  $\text{CH}_3$  group 9-5994  
 cross-relaxation of protons in pure liqs. 9-3121  
 cis-, trans-cyano-1-dimethyl-1,2-oxiranes, determ. of mol. configurations 9-13380  
 2-cyanoethylsilanes, spectra analyses and parameter predictions 9-20960  
 cyclobutane cpds., rel. to substituent effects on conformation 9-13544  
 L-cysteic acid monohydrate p-p vector of water of hydration 9-13652  
 4,4'-diaminodiphenylmethane, direct anal. 9-17052  
 diaryl carbonium ions, PMR spectra 9-14709  
 dibarium zinc formate tetrahydrate,  $\text{H}_2$  bonding scheme proposed 9-8043  
 o-dichlorobenzene, direct anal. 9-17052  
 for diffusion of water molecules in hydrates 9-13704  
 for diffusion of water molecules in hydrates 9-1242  
 1,4-difluoro-2,6-bis(trifluoromethyl)benzene 9-14717  
 L(+)-dihydrodesoxytreptose, structure obs. 9-18203  
 dimethyl sulphoxide, proton motion  $\text{CH}_3$  group frozen at  $-123^\circ\text{C}$  9-5993  
 dimethyl sulphoxide, proton obs. in  $\text{CH}_3$  group frozen at  $-123^\circ\text{C}$  9-5993  
 dimethyl-acetylene in nematic solvents 9-13545  
 1,4-dioxane, spectra temp. depend. rel. to molecular mobility 9-11901  
 double, single spin  $1/2$  system 9-9256  
 double resonance, weak perturbing r.f. field effects, meas. method 9-12964  
 5-endo-1,2,3,4,7,7'-hexachlorobicyclo[2.2.1] hept-2-ene, triple reson. tickling, obs. 9-18207  
 ENDOR high press. cavity design 9-10785  
 ENDOR in randomly oriented paramag. mols. 9-5995  
 error bounds, upper and lower, from equilibrium moments of spectral density 9-8435  
 ethyl formate, temp., solvent depend. of  $^{13}\text{C}$  H coupling const. and chem. shift 9-17054  
 ethylenes interac. with OH-containing cpds., bond obs. 9-18751  
 di-(2-ethylhexyl) Na sulfosuccinate in n-octane solns, p.m.r. study of phases formed by  $\text{H}_2\text{O}$  addition 9-9559  
 ethylphenylphosphine, geminal coupling const. anal. 9-13546  
 ferrocene,  $^{57}\text{Fe}$  nuclear quadrupole moment 9-3976  
 in ferromagnets, nuclear spin-wave relaxation 9-8037  
 flowmeter, n.m.r., optimum detectors, discussion 9-19592  
 fluorocarbons, intermolec. radical-solvent hyperfine coupling 9-21226  
 fluoromethane mols. in liq. crystal solvent, spectra obs. 9-7067  
 p-fluorophenyl labelled acids with organic bases, H bonding determ. 9-7068  
 fluorostyrenes, spin-spin interactions of F nuclei 9-19466  
 four-spin systems, oriented, with  $\text{C}_2$  symmetry, spectra 9-20979  
 free induction decay in system of several species 9-7924  
 frequency sweep circuit, uniform 9-4408  
 furnace for expts. 20-1300°C 9-2293  
 group IVB elements, tetraaryl and triphenylvinyl derivatives 9-20945  
 hen egg-white lysozyme, NMR studies 9-17068  
 heterocyclic ring, saturated, medium intermolec. force effect obs. 9-19493  
 hexachloride ions, spin-rot. relax. rate, observability 9-15207  
 histidine residue, struct. and binding sites, obs. 9-7092  
 hydrated crystals, diffusion of water mol. effects 9-1241  
 hydration, negative, nucl. mag. relax. study 9-17190  
 hydroquinone,  $^{13}\text{C}$ -H satellite patterns, rel. to couplings 9-13373  
 ice, hexagonal, proton relaxation time, 0.125-6.57 kOe, -10 to  $-80^\circ\text{C}$  9-16384



**Nuclear magnetic resonance and relaxation continued**

ice polymorphs, p.m.r. and d.m.r. 9-16463  
 impurity states detection in relaxation 9-10297  
 indirect spin saturation, solns. of spin-density matrix 9-16755  
 ionic solids, spin-rot. relax. rate, observability 9-15207  
 ions, free atomic, nuclear moment meas. technique 9-11399  
 Knight shift rel. to mag. field 9-20026  
 line broadening, due to ferromagnetic quasi-local spin states 9-3786  
 line shape, generalized Kubo-Anderson model, a stochastic theory 9-7931  
 liquid crystals, as method for determ. mol. struct. 9-18171  
 liquid crystals, nematic, spectroscopy of dissolved mols. 9-19609  
 in magnetic structure determ. 9-5787  
 methyl n alkylphenylphosphinates, spectra 9-19471  
 metals, liquid, spin relaxation, quadrupole mechanism 9-16023  
 metals line shape field dependence rel. to Ruderman-Kittel-Kasuya-Yosida (RKKY) exchange interaction mag. field dependence 9-5792  
 methane, isotope chem. shifts 9-7013  
 methane, solid, ground state conversion obs. 9-16471  
 methanol system, Overhauser effect 9-9560  
 methyl ammonium aluminium sulphate of  $^{27}\text{Al}$  rel. to ferroelectric phase transition 9-3968  
 methyl methacrylate, cryst. and in  $\text{CS}_2$  soln., Overhauser enhancement parameters 9-14119  
 2-methyl propene,  $\text{CH}_3\text{-CH}_3$  coupling, possibility of 'through-space' contribution 9-13376  
 methylbenzenes, hindered rotations in solid 9-1882  
 N-methylbenzophenonimines, methyl substituted, proton NMR 9-14705  
 4,5-methylenephenanthrene react. with alkali metal, spect. investig. of carbanions  $\text{MH}^-$  and  $\text{H}_2\text{MH}^-$  9-19468  
 $\alpha$ -methylpentafluorostyrene,  $^{19}\text{F}$ , 19 and 376 MHz 9-12518  
 $\alpha$ -methylpentafluorostyrene-styrene copolymer:  $^{19}\text{F}$ , 19 and 376 MHz 9-12518  
 molecular line shapes, theory 9-9168  
 molecule containing quadrupolar nuclei, band-shape, coupling const. 9-9239  
 molecules containing  $\text{CF}_2$  groups, spin syst. study, use of composite part. basis functions 9-20908  
 monoorganosilanes, Si-H bond props., n.m.r. obs. 9-19475  
 N chemical shifts, theoretical calc. 9-2886  
 nematic liquid crystals, relaxation times, striking depend. on resonance freq. 9-18370  
 Ni-Mn, of  $^{55}\text{Mn}$  investigation 9-8042  
 nitrobenzene in  $\text{CCl}_4$ , effect of addition of tetra-n-butylammonium salts 9-7281  
 noble metals, spin-lattice relax. rates and Knight shifts, electron-electron interaction effects 9-17501  
 nucleotide 3',5' cyclic phosphates and acetylated derivatives rel. to sugars struct. 9-18220  
 organic cpd. purity determ. 9-21733  
 organic four spin systems, analysis of complex spectra 9-20918  
 p-deuterated benzene derivatives,  $\text{DC}_6\text{H}_4\text{X}$ , proton  $\delta$  effect in o- and m-positions 9-7279  
 p-dimethoxybenzene,  $^{13}\text{C}$ -H satellite patterns, rel. to couplings 9-13373  
 paramagnetic centres influence, e.s.r. thermal correlation time, structure parameters determ. 9-6437  
 paramagnetic ion nuclei in solid, line profile by Green's function method 9-20027  
 paramagnetic solutions, relaxation 9-14859  
 pentaerythritol, cry. struct. determ. 9-9690  
 pentafluorobenzene, heteronuclear double reson. 9-9278  
 pentafluorobenzene, spectrosc. anal. 9-15895  
 pentafluorophenyl cpds. of group IV elements,  $^{19}\text{F}$  n.m.r. 9-14716  
 pentafluorostyrene-styrene copolymer:  $^{19}\text{F}$  19 and 376 MHz 9-12518  
 perfluoro-m-xylene 9-14717  
 perfluorobutane, of F, rel. to (F, group coupling, and  $^{13}\text{C}$  satellites 9-13375  
 perfluorocyclobutene, spectra, spin syst. study, use of composite part. basis functions 9-20908  
 perfluorodimethyl-acetylene in nematic solvents 9-13545  
 phenyl radical reactions in soln., dyn. nucl. polarization 9-17222  
 polyarylates,  $\text{CH}_2$ -group motion and glass transition on heating 9-21415  
 polycyclic hydrocarbons, high-resolution 9-13386  
 polyethylene, drawn, broad line, rel. to orientation distrib. functions 9-12517  
 polyhalobenzenes in cyclohexane and carbon tetrachloride, chemical shift, additivity scheme 9-19646  
 polymethylmethacrylate, solvent eff. on spectra 9-18372  
 polypropylenes, deuterated, of highest sterical purity, meas. 9-14736  
 preamplifier using MOSFETs at liquid He temps. 9-6439  
 proton, in dibarium zinc formate tetrahydrate,  $\text{H}_2$  bonding scheme proposed 9-8043  
 pulse expts. in solids, n.m.r. signal form approx. solns 9-3967  
 pyridazine oriented in a nematic phase 9-18371  
 pyridine, oriented in nematic phase, spectrum analysis, inter-p distance ratios obs. 9-9277  
 pyridine oriented in a nematic phase 9-18371  
 quadrupole shift, effect of lattice defects 9-12506  
 quadrupole spin-lattice relax., anharmonic crystals, in terms of perturb. theory and phonon Green functions 9-5857  
 quantum transitions, single and double, eff. of spin tickling 9-9192  
 rare earth intermetallic cpds., Knight shift meas. rel. to interband mixing 9-14116  
 rigid-lattice moments and line shapes with chem. shift anisotropy 9-1869  
 rochelle salt, of  $^{23}\text{Na}$  and  $^{2}\text{D}$ , spin-lattice relaxation 9-10155  
 rotating solid, effect on bilinear spin interactions 9-8036  
 ruby, saturation effects in e.p.r. homogeneous broadening 9-1853  
 ruby, spin relax. rel. to electron spin-spin interactions and polarization 9-15160  
 ruby doped with  $^{27}\text{Al}$ , dynamic nuclear polarization 9-5991  
 saturation effects in e.p.r. homogeneous broadening 9-1853  
 Sc, metallic, relax. anisotropy 9-12514  
 sodium caprylate-decanol-water system, relax. of  $^{23}\text{Na}$  in different phases 9-5191  
 solid, resonance lines inhomogeneous broadening, review 9-18689  
 solutions, effect of mag. anisotropic solvent mols. on nuclear screening 9-9552  
 spectrometer, field-locked, appl. to r.f. mag. field meas. 9-218  
 spectrometer, high resolution 9-16757

**Nuclear magnetic resonance and relaxation continued**

spectrometer, using superconducting magnet, description, performance 9-12962  
 spectrometers, cryostat, liquid cell with thermistor amplifier feedback control 9-6438  
 spectrometry review 9-2291  
 spin echoes in multi-half-spin systems 9-13340  
 spin-diffusion to a finite density of paramagnetic impurity ions 9-1870  
 superconductors, small size, spin relax 9-1712  
 superconductors, type-II, relax. rate near upper critical field 9-7923  
 symmetrical three-spin syst., NMR spectra, relaxation eff. 9-9191  
 temperature meas., within spinning thermistor 9-17841  
 tetra-n-amy ammonium fluoride clathrate hydrate 9-14117  
 tetra-n-butyl ammonium fluoride clathrate hydrate 9-14117  
 tetrahydroprotoberberine alkaloids 9-19477  
 tetraiodomethane,  $^{13}\text{C}$  chemical shift 9-9282  
 tetrakis (2-fluoro-1,3,2-benzodioxaphosphole) Ni(0), theory 9-17024  
 thiodiglycolic acid, X-irrad., ion formation, ENDOR 9-15202  
 thiophene, spectra 9-20979  
 thulium ethyl sulphate, of  $^{169}\text{Tm}$  9-1879  
 thulium ethyl sulphate, p.n.r. spectra 9-15206  
 toluene, proton n.m.r. anal. 9-9284  
 transport approx.  $\text{SP}$  and  $\text{MP}_2$ , diffusion-like, numerical comparisons for very fast n 9-13263  
 $\alpha,\beta,\beta$ -trifluorostyrene dimers:  $^{19}\text{F}$ , 19 and 376 MHz 9-12518  
 triphenylcarbonium ions, of  $^{19}\text{F}$ , conformational equilibria and interconversion 9-19473  
 triphenylcyclopropenium cation,  $^{13}\text{C}$  NMR shifts, charge densities deriv. 9-13388  
 triple resonance spectra in weak r.f. fields, theory 9-12965  
 tropolone derivatives 9-19478  
 o-, m-, p-xylenes, proton reson. study of methyl groups substitutions, effs. and reorient. 9-17424  
 Y, metal, relax. times and Knight shift meas.,  $2,2^{\circ}\text{-300}^{\circ}\text{K}$  9-12516  
 zinc acetate dihydrate, H bonding scheme investigating by PMR 9-1121  
 [X] nuclear spin system with tetrahedral symmetry 9-17024  
 $^{113}\text{Cd}$  crystal, Knight shift parameters obs., temp. depend.,  $1^{\circ}\text{K}$ -m.p. 9-12515  
 $^{119}\text{Sn}$  crystal, Knight shift parameters obs., temp. depend.,  $1^{\circ}\text{K}$ -m.p. 9-12515  
 $\beta$ -AgI, powders and single crystals, quadrupole coupling constant of  $^{127}\text{I}$  9-18745  
 Al-Mn alloys, dil., of  $^{55}\text{Mn}$  rel. to electronic state 9-1871  
 Al-Zn alloy, dilute of  $^{27}\text{Al}$ , nuclear quadrupole structure 9-12508  
 Al, dipolar relax. time meas. rel. to e. spin correlations 9-7925  
 Al salts in  $\text{H}_2\text{O}$  and  $\text{D}_2\text{O}$ :  $^{27}\text{Al}$ , Larmor freq. ratio 9-16024  
 Al salts in  $\text{H}_2\text{O}$  and  $\text{D}_2\text{O}$ :  $^1\text{H}$ , Larmor freq. ratio 9-16024  
 $^{27}\text{Al}$  in ruby, paramagnetic mag. nuclear spin saturation, obs. 9-10300  
 $^{27}\text{Al}$  in ruby at center of  $\text{Cr}^{3+}$  ESR line, nuclear quadrupole coupling constant not obs. 9-10301  
 $\text{AlCl}_3$ -acetonitrile solns., complexes 9-5189  
 Al(III) halides in N,N-dimethylformamide solutions, outer-sphere ion-pair formation obs. 9-19645  
 $\text{Al}_2\text{O}_3$ : $^{51}\text{Cr}$ , ENDOR determ. of hyperfine splittings 9-8044  
 $\text{AuGa}_2$ , Knight shift, spin-lattice relax., susceptibility, temp. depend. and relationship 9-10292  
 $\text{B}_2\text{H}_6$ , high resolution and mag. nonequivalence 9-755  
 $\text{BH}_4^-$ , isotope chem. shifts 9-7013  
 $\text{BaFe}_2\text{O}_8$ , of  $^{57}\text{Fe}$ , powdered crystals, spin-echo 9-1872  
 Be metal, quadrupole-split system 9-3971  
 p-benzoquinone,  $^{13}\text{C}$ -H satellite patterns, rel. to couplings 9-13373  
 $^{13}\text{C}$  in medium mol.-wt. organic compounds 9-18746  
 $\text{CaAl}_2\text{Si}_2\text{O}_{10}$ :  $^{27}\text{Al}$ , obs. at high temp. 9-10293  
 $\text{Ca}_3\text{Al}_2(\text{SiO}_4)_3$  garnet, grossularite,  $^{27}\text{Al}$  quadrupole coupling constant 9-12509  
 $\text{CaB}_2\text{O}_4$ , polycryst.,  $^{11}\text{B}$  n.m.r. 9-1873  
 $\text{Ca}^{19}\text{F}_2$ :  $^{19}\text{F}$ ,  $^{13}\text{C}$ ,  $^{15}\text{N}$ , ENDOR, interstitial F- obs. 9-8045  
 $\text{CaF}_2$ :  $\text{U}^{3+}$ , spin diffusion coeff. meas. 9-17467  
 $\text{CaF}_2$ :  $\text{V}^{3+}$ , electron-nuclear double resonance 9-16472  
 $\text{CaF}_2$  free induction decay, theory and experiment, comparison 9-5982  
 $\text{CaHPO}_4$ :  $^{31}\text{P}$ -H nucl. double reson. expts. 9-3966  
 $\text{Ca}(\text{OH})_2$ , crystal structure obs. 9-19709  
 Cd, metal, spin-lattice relax. temp. dependence rel. to Knight shifts 9-12510  
 CdFe garnet, of  $^{57}\text{Fe}$  for sublattice magnetization 9-21671  
 Co-Al intermetallic cpds. 9-7888  
 Co-V alloys, of  $^{59}\text{Co}$  9-15204  
 $\text{CoCl}_2 \cdot 2\text{H}_2\text{O}$ , proton spin lattice relaxation time, anomaly in angular dependence 9-3840  
 $\text{Co}(\text{NH}_4)_2(\text{SO}_4)_6 \cdot 6\text{H}_2\text{O}$ , of  $^{59}\text{Co}$  rel. to hyperfine interactions of paramag.  $\text{Co}^{2+}$  9-8038  
 Cs, electron-spin susceptibilities from Knight shift meas. in liquid binary alkali metal alloys 9-13542  
 $^{133}\text{Cs}$  in aq. soln. 9-3122  
 $\text{Cs}_2\text{MX}_4$ :  $^{133}\text{Cs}$ ,  $\text{M}=\text{Cu}$ ,  $\text{Co}$ ,  $\text{Zn}$ ;  $\text{X}=\text{Cl}$ ,  $\text{Br}$  9-17503  
 Cu-Mn alloy,  $^{63}\text{Cu}$  spin lattice relax. meas. 9-14015  
 Cu-8-hydroxyquinolate substituted in phthalimide, ligand ENDOR 9-10302  
 Cu, Knight's ratio predicted from hyperfine fields rel. to Fermi-surface electron 9-9894  
 CuI, of Cu up to  $465^{\circ}\text{C}$  rel. to  $\alpha$ ,  $\beta$  and  $\gamma$  phases 9-8039  
 $\text{Cu}_2\text{S}$  of Cu, up to  $465^{\circ}\text{C}$  rel. to  $\alpha$  and  $\beta$  phases 9-8039  
 $\text{Cu}_2\text{Sb}$ , of  $^{63}\text{Cu}$  and  $^{65}\text{Cu}$ , evidence for absence of antiferromagnetism 9-16376  
 $\text{D}(\text{P}(\text{BH}_3)_2)$ :  $^{11}\text{B}$  and P reson. spectra assignments, obs. 9-18183  
 DyAl, of  $^{27}\text{Al}$ , Knight shift and susceptibilities, temp. depend. 9-3969  
 ErAl, of  $^{27}\text{Al}$ , Knight shift and susceptibilities, temp. depend. 9-3969  
 F, in cpds. with S 9-762  
 $^{19}\text{F}$  chem. shift of alkali fluorides in  $\text{H}_2\text{O}$ - $\text{D}_2\text{O}$  solns. 9-3124  
 Fe-Al alloys, dilute, of  $^{57}\text{Fe}$  and  $^{27}\text{Al}$ , rel. intensities 9-1874  
 Fe-Al intermetallic cpds. 9-7888  
 Fe:B ferromagnetic, hyperfine mag. field and quadrupole interaction obs. 9-21670  
 $\alpha$ - $\text{Fe}_2\text{O}_3$  (hematite) of  $^{57}\text{Fe}$ , freq. and signal intensity rel. to temp. 9-14115  
 $\text{Fe}_2\text{Zr}$  ferromagnetic, hyperfine mag. field and quadrupole interaction obs. 9-21670  
 $^{57}\text{Fe}$  spin relax. in domain walls via magnon interactions 9-7926  
 GdAl, of  $^{27}\text{Al}$ , Knight shift and susceptibilities, temp. depend. 9-3969  
 $\text{GdAlO}_3$ :  $^{27}\text{Al}$  obs. 9-5992  
 H $_2$  solid below  $4,2^{\circ}\text{K}$ , mols. rearrangement obs. 9-1118

**Nuclear magnetic resonance and relaxation continued**

- H<sub>2</sub>O+D<sub>2</sub>O solns. with paramagnetic ions. 9-1045  
 H<sub>2</sub>P(BD)<sub>2</sub><sup>2-</sup> and P reson. spectra assignments, obs. 9-18183  
 H<sub>2</sub>P(BH)<sub>2</sub><sup>2-</sup> and P reson. spectra assignments, obs. 9-18183  
 H adsorbed on Pd, Knight shift 9-17505  
<sup>2</sup>H, solid, rot. ordering above and below  $\lambda$ -transition, spin-lattice relax. obs. 9-12511  
 H<sub>2</sub> solid, pair interaction between ortho- molecules, p.m.r. obs. 9-17504  
 HCl dimethyl ether, vapour-phase determ. of H bonding 9-7021  
 HCl aq. solns., hydration determ. 9-17220  
 HCl liq., proton relax. and scalar spin-spin coupling 9-9553  
 HClO<sub>4</sub>·H<sub>2</sub>O, ionization and molec. states 9-11721  
 HClO<sub>4</sub> aq. solns., hydration determ. 9-17220  
 HD-O-H solid solution, spin relax. time calc. 9-21596  
 HNO<sub>3</sub>·H<sub>2</sub>O, ionization and molec. states 9-11721  
 H<sub>2</sub>O adsorbed on sugar carbon p.m.r. relaxation times 9-5257  
<sup>3</sup>He crystals, nuclear relax., exchange and spin Hamiltonian calcs. 9-21240  
 Ho-Gd alloy, ferromag. of <sup>165</sup>Ho 9-16464  
 HoAl, of <sup>27</sup>Al, Knight shift and susceptibilities, temp. depend. 9-3969  
<sup>2</sup> in aq. soln. 9-3122  
 InSb, impurity states detection in relaxation 9-10297  
 K-Cs liquid binary alloy, electron-spin susceptibilities from Knight shift meas. 9-13542  
 K-Rb liquid binary alloy, electron-spin susceptibilities from Knight shift meas. 9-13542  
 K, electron-spin susceptibilities from Knight shift meas. in liquid binary alkali metal alloys 9-13542  
 K<sub>2</sub>BeF<sub>4</sub>, of <sup>19</sup>F rel. to hindered movement in structure 9-16466  
 KBr, ENDOR obs. in F centres, optical pumping and monitoring 9-21673  
 KCN, cubic cryst., hindered rot. 9-16465  
 KCl-LiCl mixed crystal, ENDOR of A-centres 9-12519  
 KCl, ENDOR obs. in F centres, optical pumping and monitoring 9-21673  
 KCl, F-centre, ENDOR determ. of hyperfine and quadrupole interactions 9-5385  
 KCl(Br), ENDOR spectrum, second-order effects 9-15208  
 KF:Na, field grads. at <sup>39</sup>K nuclei surrounding Na<sup>+</sup> ion 9-1884  
 KH<sub>2</sub>AsO<sub>4</sub>, electric-field-gradient tensor at As site from p. relax. meas. 9-17469  
 KH<sub>2</sub>AsO<sub>4</sub>, <sup>75</sup>As level crossing, asymmetric, and Stark effect of <sup>75</sup>As NQR 9-12521  
 K<sub>2</sub>HPO<sub>4</sub>·<sup>23</sup>Na·<sup>1</sup>H nucl. double reson. expts. 9-3966  
 KH<sub>2</sub>PO<sub>4</sub>, of <sup>39</sup>K, rotary saturation of spin calorimetry 9-10294  
 K<sub>2</sub>MnF<sub>4</sub>, of <sup>19</sup>F rel. to zero-point spin deviations 9-10151  
 LaAl, of <sup>27</sup>Al, Knight shift and susceptibilities, temp. depend. 9-3969  
 La<sub>2</sub>Mg<sub>3</sub>(NO<sub>3</sub>)<sub>12</sub>·Dy<sup>3+</sup>, electronic and nuclear relaxation and polarization 9-10298  
<sup>6</sup>Li and <sup>7</sup>Li in aq. soln. 9-3122  
 LiAlD<sub>4</sub>, polycrystalline, deuteron quadrupole coupling const. 9-11464  
 LiCl solns., spin-lattice relax. 9-1046  
 LiF, ENDOR meas. of self-trapped hole 9-10284  
 LiF, ENDOR spectrum, second-order effects 9-15208  
 LiNbO<sub>3</sub>, of <sup>7</sup>Li, acoustic saturation 9-8040  
 LiSb, powder 9-1875  
 LuFe garnet, of <sup>57</sup>Fe for sublattice magnetization 9-21671  
 MgO·<sup>51</sup>V<sup>2+</sup>, spin Hamiltonian of <sup>51</sup>V<sup>2+</sup> from ENDOR 9-12520  
 MgO, ENDOR spectra for V<sub>ok</sub> centre 9-8046  
 MnCO<sub>3</sub>, antiferromagnetic, hyperfine interaction 9-14106  
 MnCO<sub>3</sub>, antiferromagnetic, hyperfine interaction 9-3950  
 MnCO<sub>3</sub>, uniaxial pressure depend., rel. to magneto-elastic anisotropy, 4.12°K and 20.0°K 9-8028  
 Mn(II) complexes in methanol 9-9551  
 MnO, of O<sup>15</sup>, shift due to hyperfine interaction 9-1876  
 Mn<sub>2</sub>P, of <sup>31</sup>P, Knight shift and paramagnetic susceptibility meas. of hyperfine fields at P sites 9-16379  
 MnSi, study at 4.2°K 9-16467  
 MoFe<sub>6</sub>, of <sup>19</sup>F, diff. of molecules rel. to line narrowing 9-16468  
 NH<sub>4</sub><sup>+</sup>, isotope chem. shifts 9-7013  
 Na-Cs liquid binary alloy, electron-spin susceptibilities from Knight shift meas. 9-13542  
 Na-NH<sub>3</sub> conc. solns., <sup>23</sup>Na and <sup>14</sup>N Knight shifts 9-3125  
<sup>23</sup>Na in aq. soln. 9-3122  
 Na salts, aqueous soln., <sup>23</sup>Na resonance, amps. and half-widths rel. to conc. 9-11722  
 Na<sub>3</sub>As, powder 9-1875  
 Na<sub>2</sub>BeF<sub>4</sub>, of <sup>19</sup>F rel. to hindered movement in structure 9-16466  
 NaClO<sub>4</sub> aq. solns., hydration determ. 9-17220  
 NaD<sub>2</sub>(SeO<sub>3</sub>), temp. dependence rel. to ferroelectric transitions 9-17435  
 NaF·Li, ENDOR spectrum of self-trapped hole associated with Li<sup>+</sup> impurity 9-10286  
 NaF, ENDOR spectrum of V<sub>k</sub> centre 9-10285  
 NaH<sub>2</sub>(SeO<sub>3</sub>), temp. dependence rel. to ferroelectric transitions 9-17435  
 Na<sub>2</sub>Sb, powder 9-1875  
 Ni-Al intermetallic cpds. 9-7888  
 Ni(II) in methanol, p.m.r. and solvation 9-9554  
 Ni(II) ions in dimethyl sulphoxide solns., proton relax. 9-9555  
<sup>17</sup>O, solvation determ. of Co(II) ion 9-3123  
 P<sub>2</sub>O<sub>10</sub>, <sup>31</sup>P NMR spectra, chemical shift anisotropies 9-20936  
 P<sub>2</sub>Si<sub>6</sub>, <sup>31</sup>P NMR spectra, chemical shift anisotropies 9-20936  
<sup>31</sup>P, low-field dynamic polarization in solns. 9-9556  
 PBr<sub>3</sub>, liq., spin-lattice relax. 9-17221  
 P(CN)<sub>3</sub>, <sup>31</sup>P NMR spectra, chemical shift anisotropies 9-20936  
 PbZrO<sub>3</sub>, of <sup>207</sup>Pb, rel. to soft lattice mode and chemical bonding aspects 9-7625  
 Pd-H system, Knight shift for adsorbed H 9-17505  
 Pd(1at.%)MnH system, Knight shift for adsorbed H 9-17505  
 PrF<sub>3</sub>, paramag. single cryst., of <sup>19</sup>F, temp. depend. of component shift 9-1877  
 R<sup>24</sup>Mg impurity in Li, Na, Sr, Sn, Pb, Bi melts, nucl. reson. fluoresc. 9-7278  
 Rb-Cs liquid binary alloy, electron-spin susceptibilities from Knight shift meas. 9-13542  
 Rb, electron-spin susceptibilities from Knight shift meas. in liquid binary alkali metal alloys 9-13542  
 Rb<sub>2</sub>MnCl<sub>4</sub>·2H<sub>2</sub>O, antiferromag., spin lattice relax of <sup>87</sup>Rb, <sup>35</sup>Cl and <sup>1</sup>H 9-21597  
<sup>87</sup>Rb in aq. soln. 9-3122

**Nuclear magnetic resonance and relaxation continued**

- <sup>87</sup>Rb, zero-field level crossing resonances and very weak magnetic field detection 9-15822  
 Rb<sub>2</sub>BeF<sub>4</sub> of <sup>19</sup>F rel. to hindered movement in structure 9-16466  
 RbMnF<sub>2</sub>, ENDOR obs. 9-21674  
 ReO<sub>3</sub>, of <sup>185</sup>Re, Knight shifts and spin relax. rates 9-12512  
 RnNO<sub>3</sub>, of <sup>87</sup>Rb, linewidth rel. to temp. for ionic diffusion 9-19770  
 Sc-Gd alloys, rel. to conduction-electron polarization 9-12513  
 ScAl<sub>3</sub> and ScAl<sub>5</sub>, Knight shift mechanism and structure of Sc 9-1878  
 Si:As(Sb), irradi., endor and e.p.r. meas. of impurity-vacancy pairs 9-5341  
 Si phenyl cpds., bonding studied 9-11499  
 SiP, <sup>29</sup>Si w.r.t. metal-nonmetal transition 9-15109  
 Sn-transition metal bond, p.m.r. data on nature 9-16048  
 TbAl, of <sup>27</sup>Al, Knight shift and susceptibilities, temp. depend. 9-3969  
 Te crystal, <sup>125</sup>Te relax. obs. and mechanism 9-10299  
 ThN, <sup>14</sup>N n.m.r. 9-10295  
 ThP, <sup>31</sup>P n.m.r. 9-10295  
 Tl borate glasses, <sup>205</sup>Tl chem. shift 9-8041  
 TiNO<sub>3</sub>, of <sup>205</sup>Tl, linewidth rel. to temp. for ionic diffusion 9-19770  
 Tm Ga garnet, of <sup>169</sup>Tm at 4°K 9-1880  
 TmFe garnet, of <sup>57</sup>Fe for sublattice magnetization 9-21671  
 U<sup>4+</sup> in CaF<sub>2</sub>, ultrasonic endor, absorption line broadening by superhyperfine interaction 9-15209  
 UO<sub>2</sub>·H<sub>2</sub>O obs., motion of OH and H<sub>2</sub>O mols. in lattice 9-1881  
 UP-US solid solns. in paramagnetic state, <sup>31</sup>P Knight shifts 9-10296  
 V-Mn alloys, <sup>51</sup>V and <sup>53</sup>Mn Knight shift 9-21672  
 VHS(x<2), of <sup>51</sup>V and proton 9-3970  
 VO<sup>2+</sup> complexes,  $\pi$ -bonding by equatorial O, proved by proton n.m.r. 9-13590  
 YFe garnet, of <sup>57</sup>Fe for sublattice magnetization 9-21671  
 ZnSn(OH)<sub>4</sub>, crystal structure obs. 9-19709
- measurement**  
 AA'/BB' spectra, direct anal. 9-17052  
 analytical probe into flowing liquid mixture 9-20065  
 apparatus, patent 9-20476  
 apparatus, patent 9-20475  
 distortion of low frequency modulation 9-2292  
 electromagnet for use, design and construction 9-17840  
 fine-structure lines, with mutually depend. broadening, use of diagonal sum methods 9-20477  
 high-resolution techniques, theoretical analysis and comparison based on coherent averaging effects 9-17502  
 microwave spectroscopic signals, mechanical resonance simulator 9-192  
 signal-to-noise ratio improved by making meas. on flowing liquid 9-20065  
 spectrometer, high-resolution, adaptation for heteronuc. double and multiple reson. expts. 9-8669  
 spectrometer twin-T bridge, automatically stabilized 9-15488  
 spectrometers, double reson., mag. field fluctuations and resonance condition stabilization 9-17842  
 spin-echo apparatus for ferro- and ferrimag. mats. 9-2294  
 spin-lattice relax., methods for very weak fields 9-10153  
 structure resolution by nuclear polarization techniques 9-12507  
<sup>12</sup>B relax. time of nuclear polarization 9-2648
- Nuclear matter** see *Nucleus/theory*  
**Nuclear orientation** see *Nuclear polarization*  
**Nuclear photoeffect** see *Gamma-rays/effects; Nuclear reactions and scattering due to photons*  
**Nuclear physics**  
 atomic and nuclear physics, introduction in SI units, book 9-8345  
 chemistry of nuclei reactions, disintegrations, fission, applic., book 9-8948  
 computer usage in laboratories 9-22014  
 engineering courses, Univ. Rio de Janeiro (1966) 9-10599  
 experimental design technique 9-8310  
 Nimrod applications, conference (Rhel, 1968) 9-14541  
 and particle physics, two different subjects? 9-8947  
 quasi-particle, transcription into ideal space, canonical transf., boson method 9-14542
- Nuclear polarization**  
 alkyl radical reactions, chem. induced dyn. nucl. polarization 9-17222  
 alkyl radicals, dynamic chem. induced 9-2921  
 experiments using low energy neutrons 9-19270  
 free radicals in fluorocarbon solns. 9-21226  
 muonic atom levels corrected from information about e.m. transition vertex 9-13319  
 non-paramagnetic materials, orientation at low-temp., static methods 9-15162  
 phenyl radical reactions, chem. induced dyn. nucl. polarization 9-17222  
 population of a ground state sublevel following exposure to polarized  $\gamma$  radiation 9-15711  
 radiative transitions from aligned nuclei, ang. correl. coeff. tables 9-6782  
 ruby, rel. to electron spin-spin interactions and nuclear spin relax. 9-15160  
 semiconductors, by hot carrier flow in crossed static and mag. fields 9-15042  
 in solid, dynamic, nuclear spin. exchange effects 9-1719  
 spin dynamic polarization in liquids and solids, unitary theory 9-17471  
 spin eff. in odd-mass deformed nuclei 9-14554  
 techniques for resolving solid n.m.r. structures 9-12507  
 $\gamma$  ang. distrib. from aligned nuclei, coeff. tables 9-6781  
 n spin flip probability in scatt. on polarized nuclei 9-19313  
<sup>210</sup>Po, E<sub>2</sub> core by h<sub>2</sub> proton 9-8992  
<sup>113</sup>Cd optical pumping method 9-4447  
<sup>113</sup>Cd optical pumping with <sup>51</sup>Se-<sup>51</sup>Pi, resonance line 9-20384  
<sup>113</sup>Cd optical pumping method 9-4447  
<sup>27</sup>Al NMR structure in ruby 9-10301  
<sup>57</sup>Fe Mossbauer spectra obs., depend., on hyperfine field magnitude and sign 9-19289  
 HD mols. at 20°K in contact with charcoal, dynamic polarization of nuclei 9-7270  
<sup>3</sup>He, solid, spin exchange interaction effect 9-1719  
<sup>3</sup>He gas, electric discharge in mag. field 9-9417  
<sup>31</sup>P, low-field dynamic, in solus. 9-9556  
 Pb, orientation by optical pumping, attempt 9-9139
- Nuclear power** see *Nuclear reactors, fission*  
**Nuclear quadrupole resonance**  
 p-dichlorobenzene, librational amplitudes 9-10224



**Nuclear quadrupole resonance continued**

- $\alpha$ -Al<sub>2</sub>O<sub>3</sub>, computed field gradient 9-10158  
 chlorobenzene, <sup>35</sup>Cl Zeeman effect 9-8049  
 chlorobenzene derivatives, <sup>35</sup>Cl correlations 9-14120  
 chlorodiazines, <sup>35</sup>Cl reson. 9-9237  
 crystalline elec.-field-gradient determ. 9-8047  
 malononitrile, pure n.q.r., phase transitions determ. 9-13780  
 metal cyano complexes, <sup>14</sup>N resonance 9-19436  
 microwave spectroscopic signals, mechanical resonance simulator 9-192  
 quaternary ammonium bromide aq. solns., <sup>79</sup>Br relax. obs. 9-19647  
 spectral analysis, setup for visual recording 9-15490  
 spectrometers super regenerative, reduction of distortion 9-6440  
 spectroscopy, Zeeman modulator circuit with thyristors 9-6441  
 spin echo slow beats rel. to asymmetry parameter of crystal elec. field gradient 9-3973  
 spin lattice relax., anharmonic crystals, in terms of perturb. theory and phonon Green functions 9-5857  
 spin-spin interactions via electron shell obs. 9-15210  
<sup>197</sup>Au chemical bond obs. 9-4916  
 AsI<sub>3</sub>, freq. calc. from electric field gradient tensor 9-20920  
 Ba(NO<sub>3</sub>)<sub>2</sub>·H<sub>2</sub>O, of <sup>14</sup>N, temp. depend. between 77°K and 300°K 9-10303  
 CCl<sub>4</sub> group bound to benzene ring, torsional vib. freq. determ. from NQR obs. 9-4951  
 CCl<sub>3</sub>CCl<sub>2</sub>CCl<sub>3</sub>, liq. air temp. 9-3977  
 chalcogens, inorganic, of <sup>75</sup>As, for piezoelec. and ferroelec. props. 9-18747  
 p-Cl<sub>2</sub>- $\phi$  mono- and polycrystals, effect of elastic actions and mag. field 9-15211  
<sup>35</sup>Cl, spin 3/2 in a series of polychlorous compounds of cyclobutane type 9-15906  
<sup>35</sup>Cl in conjugated mols., quadrupole freqs. 9-7061  
 Cs<sub>2</sub>MnCl<sub>4</sub>·2H<sub>2</sub>O, elec. field-gradient tensors determ. 9-8047  
<sup>63</sup>Cu, spin-lattice relax. time, press. depend. at two temps. 9-18687  
 Cu<sub>2</sub>O mono- and polycrystals, effect of elastic actions and mag. field 9-15211  
 KBrO<sub>3</sub>, temp. depend. of <sup>79</sup>Br freq. 9-10304  
 KH<sub>2</sub>AsO<sub>4</sub>, of <sup>75</sup>As, Stark effect 9-12521  
 K<sub>2</sub>PtCl<sub>6</sub>, lattice dynamics exam. 9-11987  
 KReO<sub>4</sub>, pure n.q.r. of Re 9-3974  
 La<sub>2</sub>Mg<sub>3</sub>(NO<sub>3</sub>)<sub>12</sub>·24H<sub>2</sub>O:Mn<sup>2+</sup>, ENDOR study of quadrupole splitting 9-1883  
<sup>14</sup>N in benzene sulphonamide 9-14099  
 NaBrO<sub>3</sub>, temp. depend. of <sup>79</sup>Br freq. 9-10304  
 NaCl-NaBr:<sup>23</sup>Na, elec. field gradient at <sup>23</sup>Na 9-8048  
 NaClO<sub>3</sub> mono- and polycrystals, effect of elastic actions and mag. field 9-15211  
 Re, in KReO<sub>4</sub>, pure n.q.r. 9-3974  
 Re<sub>2</sub>[Co]<sub>10</sub> 9-3975  
 UI<sub>3</sub>, antiferromagnetic, of <sup>127</sup>I 9-1885
- Nuclear radius** *see* Nucleus/size
- Nuclear reactions and scattering**  
*See also* Chemical analysis/by nuclear reactions; Fallout; Nuclear bombardment targets; Nuclear excitation; Nuclear fission; Nuclear fusion; Nuclear spallation; Radioactivity; Thermonuclear reactions  
 1+1→0+0 type, spin structure anal. 9-6914  
 5-15 GeV/c, shadow effects 9-9020  
<sup>198</sup>Au(p, <sup>19</sup>N) new isotope identified, 3 GeV 9-506  
 binary direct reactions, mechanism, identification rel. to internal bremsstrahlung 9-13214  
 complex angular-momentum formulation, validity and use in scatt. by analysis of  $\alpha$ -part. scatt. using Regge poles 9-14623  
 compound-nuclear, isotopic spin mixing 9-573  
 Coulomb distortion analysis disagreeing with plane wave Born approx. 9-11210  
 Coulomb-nuclear S-matrix study, asymptotic behaviour in left-half  $\lambda$ -plane 9-13215  
 crossover angles, nonrelativistic kinematics expression derived 9-11260  
 direct, isotopic spin mixing 9-573  
 energy depend on short-distance scatter 9-20770  
 Euclidean expansion of non-relativistic and energy-averaged scatt. amplitude 9-9013  
 exclusion principle and equivalent potential, neutral complex particles 9-568  
 Faddeev eqns. for transfer processes 9-11259  
 Feynman diagram dispersion theory 9-4795  
 Feynman method for tunnelling, binding energy and recoil corrections 9-11263  
 five particle kinematics, physical regions in invariant variables 9-6846  
 giant resonances, fine structure 9-6845  
 Glauber approx. and Watson multiple-scatt. eqn. relationship determ. 9-18088  
 graphs and tables which are useful 9-13216  
 Griffin's statistical model, extension to include charged-particle emission 9-4765  
 heavy ion collisions new pot. based on statistical theory of nuclear matter. 9-2763  
 inelastic cross section calcs for reactors 9-571  
 kinematics, book 9-2710  
 knock-out processes, finite range, duster model 9-14603  
 localization of react. proc. for investig. of nuc. surface 9-14543  
 low and high energy, book 9-4719  
 many-body theory in single-particle shell model with configuration mixing 9-4764  
 math scatt. asymmetry, scatterer thickness effect 9-15582  
 matrix elements calc., phase shifts in singlet S channel and Scott-Moszkowski separation 9-18087  
 microscopic approach 9-14600  
 multiparticle products, quasi-free reactions and new expt. techniques 9-14601  
 nuclear potential depend. on isospin, determ. 9-14547  
 overlapping compound nucleus resonances in scatt. 9-572  
 particle exchange reactions, amplitude calc. 9-15745  
 particle-hole states and intermediate structure 9-6847  
 polarization of residual nucleus after 3 particle reaction 9-11261  
 R-matrix theory, extension 9-570  
 reactor neutron flux, activation analysis method 9-6036  
 resonance scatt., time depend. of prompt pot. and delayed resonance scatt. 9-4763  
 resonance scatt. test by exactly soluble model 9-15698  
 review, E>10 MeV 9-16951

**Nuclear reactions and scattering continued**

- shell potential, isospin term determ. from N binding energies 9-15703  
 small angle scattering and peak formation 9-19301  
 statistical theory 9-13217  
 stripping reaction, diffraction theory using partial wave expansion 9-11262  
 stripping reactions, 3 particles, coupled channel anal. formalism 9-20769  
 transfer reactions induced by heavy ions 9-6915  
 tunnelling, Feynman method, binding energy and recoil corrections 9-11263  
 unified theory and the singular Lippmann-Schwinger equations 9-569  
 unitary statistical model 9-15746  
 D(<sup>3</sup>He,  $\gamma$ )<sup>7</sup>Li, 90° yield, from 2 to 11 MeV energy range 9-4799  
 $\pi^-$ , scatt., diffraction and absorption cross section meas., E<sub>π</sub>=600-1600 MeV 9-9047  
<sup>24</sup>Mg(<sup>3</sup>He, p)<sup>26</sup>Al 1<sup>+</sup> state obs. 9-2679  
<sup>141</sup>Pr(n,  $\gamma$ )<sup>142</sup>Pr, for study of levels of <sup>142</sup>Pr 9-2667  
<sup>116</sup>Sn-<sup>121</sup>Sn, neutron stripping and pick-up 9-513  
 Au(p,  $\gamma$ ), atomic, incoherent scatt. of 662 keV  $\gamma$  by K-shell electrons, differential cross-section 9-9120  
<sup>12</sup>C(<sup>3</sup>He, <sup>3</sup>He)<sup>12</sup>C 12-18 MeV surface absorptive pot. and optical parameters calc. 9-607  
<sup>12</sup>C(p, p)<sup>12</sup>C level assignments to <sup>13</sup>N 9-2727  
<sup>56</sup>Fe, resonance peaks of total cross-sections, 0.5 to 1.5 MeV, quantum states of compound nucleus 9-9043  
 Ge isotopes, neutron cross sections and strength functions 9-592  
 Ge (d, p)<sup>73</sup>Ge, 8 MeV parities, transitions strengths for levels up to 3 MeV 9-8998  
<sup>4</sup>He, cross sections compared with e scatt. meas., light nuclei structure determ. 9-4774  
<sup>3</sup>He(t, p)<sup>3</sup>He, 22.25 MeV, obs. 9-2659  
<sup>3</sup>H(t, p)<sup>3</sup>H, 22.25 MeV, obs. consistent with <sup>3</sup>H ground state 9-2659  
 N isotope cross-sections, tables and graphs 9-11264  
 N(<sup>3</sup>He,  $\gamma$ , n) cross-section obs. to 25 MeV 9-11276  
 N(<sup>3</sup>He,  $\gamma$ , n) cross-section obs. to 25 MeV 9-11276  
 O isotope cross-sections, tables and graphs 9-11264  
<sup>48</sup>Sc (p, p' $\gamma$ )<sup>48</sup>Sc, 2.8, 3.2 and 3.6 MeV,  $\gamma$  decays of levels, some spin assignments 9-2729  
 Si, E<sub>p</sub>=0.5 to 2.9 GeV, formation cross-sections for <sup>24</sup>Na and <sup>22</sup>Na 9-19310  
<sup>64</sup>Zn(p,  $\gamma$ )<sup>64</sup>Zn ang. distrib. meas., levels determ., E<sub>p</sub>=26 MeV 9-20785  
<sup>64</sup>Zn(p, p' $\gamma$ )<sup>64</sup>Zn, ang. distrib. meas., levels determ., E<sub>p</sub>=26 MeV 9-20785
- chemical effects**  
*See also* Chemical effects of radiations/ionizing radiations  
 alkyl chloride syst. bombarded by Cl atoms 9-10362  
 methyl isocyanide, <sup>13</sup>C bombardment, thermal isomerization 9-8112  
 propylene bombarded by <sup>3</sup>H, H ejected, C-H bond dissociation energy calc. 9-20064  
 thermal neutron capture in Mg<sub>2</sub>SO<sub>4</sub>, chem. and Mossbauer study 9-17549  
<sup>191m</sup>Os radiative n capture, transformation and annealing in crystal 9-21724  
<sup>193</sup>Os radiative n capture, transformation and annealing in crystal 9-21724  
<sup>10</sup>B(n,  $\alpha$ )<sup>7</sup>Li, in CeIV-H<sub>2</sub>SO<sub>4</sub> solns. 9-15229  
<sup>67</sup>Cu, prep. by <sup>67</sup>Zn(n, p) <sup>69</sup>Cu in reactor 9-16502  
 K<sub>4</sub>Fe(CN)<sub>6</sub>, thermal n capture, <sup>59</sup>Fe species obs. 9-6022  
<sup>79</sup>Br in emulsion, E<sub>p</sub>=13.8 GeV 9-19308
- high energy ≥1 GeV**  
 cross-section depend. on mass number investigated in cosmic ray expts. at Nor-Amberd 9-15683  
 10<sup>6</sup> GeV study and cosmic rad. obs. 9-20771  
 cosmic rad. composition obs., ~10<sup>6</sup> GeV 9-20771  
 cosmic ray Wilson cloud chamber obs. at Tskhra-Tskaro 9-20679  
 hydrodynamic model modified 9-15679  
 light nuclei, 22.8 GeV/c protons, multiparticle prod. 9-6693  
 many-particle interaction model 9-15681  
 multiple Coulomb scatt. in nuc. emulsions, primary p beam exposure 5-24 GeV/c 9-4637  
 $\pi$ -nuclei at 200 GeV 9-6662  
 shadow effects 9-9020  
 unitary statistical model of multiple particle production 9-15746  
 p on nucleus, 1-21 GeV, and composite model of elementary particles 9-2725  
 p fragmentation of emulsion nuclei at 13.8 GeV 9-4808  
 $\pi$ , 200 GeV, interactions with emulsion nuclei, four-momentum transfer and effective mass estimation 9-4626  
 $\pi^-$ , scatt., diffraction and absorption cross section meas., E<sub>π</sub>=600-1600 MeV 9-9047  
 $\pi^-$ N in emulsion, 7.2 GeV, secondary particle analysis 9-15623  
 scattering at moderately large angles, amp. obs., eikonal approx. 9-14602  
 Fe cosmic rays, 5×10<sup>10</sup>-10<sup>12</sup>eV cross-sections obs. at Tskhra-Tskaro 9-15682  
 Mg, E<sub>p</sub>=1.5 to 2.9 GeV, formation cross-sections for radionuclides 9-19310  
 10<sup>11</sup>eV particles with Pb, cross section and interaction free path 9-18025  
<sup>107</sup>Ag in emulsion, E<sub>p</sub>=13.8 GeV 9-19308  
<sup>198</sup>Au(p, <sup>19</sup>N) new isotope identified, 3 GeV 9-506  
<sup>198</sup>Au(p, <sup>21</sup>O) new isotope identified, 3 GeV 9-506  
 Ag disintegration by 20 GeV/c protons, analysis of stars 9-9076  
 C 100 GeV cosmic ray obs. at Nor-Amberd 9-15684  
 C(n, p), 10<sup>10</sup>-10<sup>12</sup>eV, cross-section obs. on satellites Proton 1 and 2 9-18024  
 Fe, E<sub>p</sub>=1.5 to 2.9 GeV, formation cross-sections for radionuclides 9-19310  
<sup>2</sup>H, cross sections compared with e scatt. meas., light nuclei structure determ. 9-4774  
<sup>4</sup>He, cross sections compared with e scatt. meas., light nuclei structure determ. 9-4774  
 Ni, E<sub>p</sub>=1.5 to 2.9 GeV, formation cross-sections for radionuclides 9-19310  
 Pb cross-section obs. in cosmic-ray expts. at Nor-Amberd 9-15683  
 Si, E<sub>p</sub>=1.5 to 2.9 GeV, formation cross-sections for radionuclides 9-19310  
 Xe( $\pi^+$ ,  $\pi^0$ ) 2.34 GeV/c, in Xe bubble chamber,  $\gamma$  spectrum, obs. 9-20645  
<sup>16</sup>O cross sections compared with e scatt. meas., light nuclei structure determ. 9-4774  
 He total n cross-section at 10 GeV/c, interaction radii calc. 9-9036  
 Li total n cross-section at 10 GeV/c, interaction radii calc. 9-9036

### Nuclear reactions and scattering due to continued deuterons

**cosmic rays**  
See also *Cosmic rays/effects and interactions*  
<sup>208</sup>Pb, evaporation n energy spectra obs., detection method 9-20809

(d,n) linked-cluster expansion for transition amplitude 9-19320  
collective states excitation, eff. on internal d structure 9-11309  
coupling potential, effects of finite size and target charge density diffuseness, inelastic 9-11313  
Feynman diagram method, building energy and recoil corrections 9-11263  
nuclei, N=50; differential cross sections obs., increase in filled n shell region, 13.6 MeV 9-608  
optical potential 9-2656  
optical potential calc., improved method 9-9069  
optical potential rel to nucleon optical potential 9-14606  
polarization in (d,p)  $\ell=0$  stripping reaction, formula determ. 9-20802  
polarizations and asymmetries in stripping reactions 9-20803  
quadrangle graph method at 5-10 MeV 9-20778  
rotational states excitation, 2nd order Born approx. 9-15710  
spectroscopic multipliers of 2p transition in (d, p) reaction 9-11315  
stripping anal., BHMM, model including core degrees of freedom 9-13239  
three-body models, use of eff. interac. 9-2750  
three-body reacts, resulting from  $^6\text{Li} + d$ , investigation 9-6911  
time, collision for 13.6 MeV, on various nuclei calc. by Wigner's method 9-15748  
(d, n) reactions, p decay of analogue states is formed 9-2754  
(d, t) on N=Z nuclei, compared with (d, t), differential cross sections 9-9059  
(d,d'), rectangle diagrams in nuclei p-shell, for calc. of ang. distrib. 9-585  
(d,He) on N=Z nuclei, compared with (d,t), differential cross sections 9-9059  
(d,p), (d,n) DWBA stripping amplitudes near Butler pole 9-609  
(d,p) and (d,t) stripping studies near  $A=110_{g7/2-111/2}$  anomaly 9-14624  
(d,p) reson. structs. in Pb region 9-6862  
(d,p) spectroscopic factors 9-4794  
 $\alpha$  14.2 MeV, obs., phenomenological pot. analysis 9-4789  
dd, 14.2 MeV, obs., phenomenological pot. analysis 9-4789  
 $^2\text{H}(d,n)^3\text{He}$ , polarization at  $E_d=80$  to 150 deV 9-4801  
Li 21 MeV, neutron yield 9-616  
(Od,p) absolute values of stripping cross section calc. method 9-11314  
 $^{240}\text{Am}$  spontaneously fission isomeric state production, cross sections meas.,  $E_d=9-13$  MeV 9-9056  
13.6 MeV, various nuclei N=82, elastic scatt., anomalies in ang. distrib., obs. 9-13237  
 $\text{I}_{f7/2}$  nuclei, inelastic scatt. 9-2751  
 $^{141}\text{Pr}(d, p)^{142}\text{Pr}$ , for study of levels of  $^{142}\text{Pr}$  9-2667  
 $^{241}\text{Am}$  spontaneously fission isomeric state production, cross sections meas.,  $E_d=9-13$  MeV 9-9056  
 $^{231}\text{U}(d, p)$  and  $^{234}\text{U}(d, t)$  energy levels 9-2677  
 $^{14}\text{C}(d, d')$ , inelastic scattering near Coulomb barrier 9-9053  
 $^{14}\text{Sm}(d, p)^{137}\text{Cs}$ ,  $^{139}\text{La}$ ,  $^{143}\text{Pm}$  and  $^{145}\text{Eu}$  level structure 9-6802  
 $^{132}\text{Te}(d, p)^{132}\text{Te}$  levels and spectroscopic factors determ.,  $E_d=7.5$  MeV 9-11223  
 $^{197}\text{Au}(d, p)^{198}\text{Au}$ , evidence for a 130ns isomeric state 9-2672  
 $^{208}\text{Pb}(d, \alpha)^{206}\text{Bi}$ , rel. to n and p hole states in  $^{206}\text{Bi}$  9-19281  
 $^{139}\text{Ba}(d, p)^{139}\text{Ba}$  at 5-7.5 MeV, differential cross-sections of proton groups, stripping analysis for transitions, reduced normalization and spectroscopic factors 9-9061  
 $^{80}\text{Ba}(d, p)^{79}\text{Cs}$ ,  $^{139}\text{La}$ ,  $^{143}\text{Pm}$  and  $^{145}\text{Eu}$  level structure 9-6802  
 $^{208}\text{Pb}(d, \alpha)^{206}\text{Bi}$  at energies above and below Coulomb barrier 9-18100  
 $^{208}\text{Pb}(d, p)^{209}\text{Bi}$  at energies above and below Coulomb barrier 9-18100  
 $^{139}\text{La}(d, p)$  at 6-18 MeV, radiative capture cross sections, induced radioact. methods 9-9062  
 $^{10}\text{B}$ , at 270 KeV Feynman diagram dispersion theory 9-4795  
 $^{10}\text{B}$  target, elastic scatt. from 1.0 to 2.0 MeV 9-13236  
 $^{11}\text{B}(d, p)^{12}\text{B}$  700 keV, p $\ell$  ang. distrib., p $\ell$ -p $\ell$  ang. correlations, 955 keV p comparison 9-2755  
 $^{10}\text{B}(d, p)^{11}\text{B}$ , p ang. distrib. and differential cross sections meas., comparison with theory 9-9060  
 $^{10}\text{B}(d, \alpha)^{7}\text{Be}$ , 0.8-2.5 MeV ang. distrib. obs., 2N pickup and heavy particle stripping analysis 9-11316  
 $^{10}\text{B}(d, \alpha)^{7}\text{Be}$ , width variations of short-lived states 9-13222  
 $^{11}\text{B}(d, \alpha)^{7}\text{Be}$ , 0.8-2.5 MeV ang. distrib. obs., agreement with two-particle pick-up 9-11316  
 $^{10}\text{B}(d, d)$ ,  $^{10}\text{B}$ , quadrangle graph calc. 9-20778  
 $^{10}\text{B}(d, n)^{11}\text{B}$ , low-Q stripping react., charact., DWBA fits and optical-model parameters 9-16966  
 $^{40}\text{Ca}(d, d)^4\text{E}_x$  (polarised)=5.11 MeV, opt. model analysis, cross-section meas., 5-34 MeV 9-18101  
 $^{40}\text{Ca}(d, p)^{39}\text{Ca}$ ,  $\alpha$ ,  $\alpha$ ,  $\alpha$  (p) $^{40}\text{Ca}$  p-n correlation due to proximity scatt. obs.,  $E_d=5.8$  MeV 9-11311  
 $^{40}\text{Ca}(d, p)$  ang. distrib., spectroscopic strength of  $^{41}\text{Ca}$  9-9067  
 $^{40}\text{Ca}(d, p)$  cross section and spectroscopic factors of  $^{41}\text{Ca}$ , 7.0 and 7.2 MeV 9-9066  
 $^{42}\text{Ca}(d, p)$  ang. distrib., spectroscopic strength of  $^{43}\text{Ca}$  9-9067  
 $^{42}\text{Ca}(d, p)$  cross section and spectroscopic factors of  $^{43}\text{Ca}$ , 7.0 and 7.2 MeV 9-9066  
 $^{44}\text{Ca}(d, p)$  ang. distrib., spectroscopic strength of  $^{45}\text{Ca}$  9-9067  
 $^{44}\text{Ca}(d, p)$  cross section and spectroscopic factors of  $^{45}\text{Ca}$ , 7.0 and 7.2 MeV 9-9066  
 $^{46}\text{Ca}(d, p)$  ang. distrib., spectroscopic strength of  $^{47}\text{Ca}$  9-9067  
 $^{46}\text{Ca}(d, p)$  cross section and spectroscopic factors of  $^{47}\text{Ca}$ , 7.0 and 7.2 MeV 9-9066  
 $^{48}\text{Ca}(d, p)$  ang. distrib., spectroscopic strength of  $^{49}\text{Ca}$  9-9067  
 $^{48}\text{Ca}(d, p)$  cross section and spectroscopic factors of  $^{49}\text{Ca}$ , 7.0 and 7.2 MeV 9-9066  
 $^{13}\text{C}(d, \alpha)^{11}\text{B}$ ,  $\alpha$ , ang. distrib. obs., 6.3 MeV 9-2757  
 $^{13}\text{C}(d, n)^{12}\text{C}$ , n polarization obs. 9-2756  
 $^{12}\text{C}(d, \alpha)^{10}\text{B}$  ( $T=1$ ) isospin-nonconserving, cross section meas. 9-20804  
 $^{13}\text{C}(d, n)^{13}\text{N}$ , low-Q stripping react., charact., DWBA fits and optical-model parameters 9-16966  
 $^{13}\text{C}(d, n)^{14}\text{N}$  first three states ratios of spectroscopic factors 9-6897  
 $^{13}\text{C}(d, n)^{14}\text{N}$ , low-Q stripping react., charact., DWBA fits and optical-model parameters 9-16966  
 $^{13}\text{C}(d, p)^{13}\text{C}$ , with polarized d 9-4797  
 $^{37}\text{Cl}(d, p)^{37}\text{Cl}$ , shell-model calc. for meas.  $\beta$  branching ratios, mean lines, ft values, spectroscopic factors 9-16946  
 $^{59}\text{Co}(d, n)$ , neutron polarization obs. 11.7 MeV 9-613  
 $^{59}\text{Co}(d, n)^{58}\text{Ni}$  particle-hole configuration of highly excited state 9-18106  
 $^{65}\text{Cu}$ , optical potential calc., comparison with, 3 body model theory 9-9055  
 $^{63}\text{Cu}(d, n)^{64}\text{Zn}$  particle-hole configuration of highly excited state 9-18106



# Nuclear reactions and scattering continued

## deuterons continued

- <sup>65</sup>Cu(d,n)<sup>66</sup>Zn particle-hole configuration of highly excited state 9-18106  
<sup>11</sup>(d,p)<sup>12</sup>B, 995 keV, p, ang. distrib., plane polar., e.m. transitions 9-2646  
<sup>19</sup>F(d,α)<sup>17</sup>O excitation energy and ang. distrib., 2.4-3.95 MeV 9-18103  
<sup>19</sup>F(d,α)<sup>17</sup>O, 2.0 and 2.2 MeV, meas. of eight α groups 9-16965  
<sup>19</sup>F(d,α)<sup>17</sup>O ang. distrib. of α part., use of solid-state track detect. 9-2611  
<sup>19</sup>F(d,d)<sup>19</sup>F, 2.0 and 2.2 MeV, cross sections 9-16965  
<sup>19</sup>F(d,p)<sup>19</sup>F, 2.0 MeV, meas. of two p groups 9-16965  
<sup>55</sup>Fe, optical potential calc., comparison with, 3 body model theory 9-9055  
<sup>56</sup>Fe levels by inelastic scatt., angular distrib. meas. and anal. 9-2753  
<sup>56</sup>Fe(d,n), neutron polarization obs. 11.7 MeV 9-613  
Gd even isotopes (d,p), (d,t) reactions, odd isotopes energy level determ. 9-6803  
<sup>2</sup>H(d,n)<sup>3</sup>He, 27.5 MeV, time of flight method 9-20801  
<sup>2</sup>H(d,n)<sup>3</sup>He, with polarized d above 107 keV resonance 9-6906  
<sup>2</sup>H(d,p,n), two dimensional meas. of deuteron break-up at E<sub>d</sub>=14 MeV 9-6893  
<sup>2</sup>H(d,n)<sup>3</sup>He, 90-175 keV neutron polar. 9-13242  
<sup>2</sup>H(d,n)<sup>3</sup>He, 0.3-1.83 MeV, n polarization deduced, d s-wave 9-9065  
<sup>2</sup>H(d,n)<sup>3</sup>He, 70<sup>3</sup>(lab) d energies below 2 MeV n polar 9-4803  
<sup>2</sup>H(d,n)<sup>3</sup>He, n polarization obs., parity conservation concluded in strong reaction 9-6900  
<sup>2</sup>H(d,p)<sup>3</sup>He, p ang. distrib. meas., 80<E<sub>d</sub><150 keV 9-13241  
<sup>2</sup>H(d,d') double scatt. at 11.5 MeV, d polarization obs. 9-11312  
<sup>2</sup>H(d,p)<sup>3</sup>He, input channel with angular momentum 1.0, partial wave investigation 9-19321  
<sup>2</sup>He(d,p)<sup>3</sup>He, polarized targets, 430 keV 9-4802  
<sup>2</sup>He(d,t)<sup>3</sup>He, energy spectra obs. 9-6908  
<sup>39</sup>K(d,t)<sup>38</sup>Ar and the s-d shell structure of <sup>38</sup>Ar 9-2684  
<sup>6</sup>Li three-body reacts, investigation, 10 MeV 9-6911  
<sup>6</sup>Li(d,α)<sup>4</sup>He, possible level schemes examination 9-20808  
<sup>6</sup>Li(d,α)<sup>4</sup>He, d polarization analyser method below 3.5 MeV 9-6913  
<sup>6</sup>Li(d,α)<sup>4</sup>He, study of spin structure 9-6914  
<sup>6</sup>Li(d,α)<sup>4</sup>He, polarization effects, 4-12 MeV 9-6912  
<sup>6</sup>Li(d,p)<sup>7</sup>Li, p ang. distrib. j-depend., l=1 transitions vector analysing power, E<sub>d</sub>=2.7-10.9 MeV 9-15778  
<sup>246</sup>Am A spontaneously fissile isomeric state production, cross sections meas., E<sub>d</sub>=9-13 MeV 9-9056  
<sup>25</sup>Mg(d,α)<sup>23</sup>Na, K=3/2 states prod. depend. on <sup>23</sup>Na rotational states, 21 MeV 9-612  
<sup>25</sup>Mg(d,α)<sup>23</sup>Na, cross-section fluctuations, E<sub>d</sub>=1.5 to 2.5 MeV, obs. 9-9064  
<sup>24</sup>Mg(d,α)<sup>22</sup>Na fluctuation anal., E<sub>d</sub>=1.83 to 3.05 MeV 9-11319  
<sup>14</sup>Mg(d,p)<sup>25</sup>Mg energy levels, spectroscopic factors determ., E<sub>d</sub>=2.02-4.22 MeV 9-11318  
<sup>25</sup>Mg(d,p)<sup>26</sup>Mg excitation functions meas. 9-11235  
<sup>26</sup>Mg(d,p)<sup>27</sup>Mg excitation functions meas. 9-11235  
<sup>26</sup>Mg(d,p)<sup>27</sup>Mg, ang. correl. obs. and spin assignment of <sup>27</sup>Mg levels 9-13199  
<sup>24</sup>Mg(d,<sup>3</sup>He)<sup>24</sup>Mg optical pot., bound state, DWBA calc. 9-4790  
<sup>27</sup>Mo(d,<sup>3</sup>He), experimental ang. distrib. and strengths of components, analysis 9-14630  
<sup>94</sup>Mo(d,<sup>3</sup>He), experimental ang. distrib. and strengths of components, analysis 9-14630  
<sup>94</sup>Mo(d,<sup>3</sup>He), experimental ang. distrib. and strengths of components, analysis 9-14630  
<sup>23</sup>Na(d,n)<sup>24</sup>Mg, energy levels determ., ang. and energy distrib. meas., E<sub>d</sub>=6 MeV 9-15727  
<sup>23</sup>Na(d,n)<sup>24</sup>Mg, n spectra meas., levels, spin and parity determ., E<sub>d</sub>=5.5 MeV 9-19282  
<sup>20</sup>Ne(d,n)<sup>21</sup>Na, n spectra for <sup>21</sup>Na bound states, differential X-sections and spectroscopic factors deduced 9-4800  
<sup>22</sup>Ne(d,p)<sup>23</sup>Ne 4-6 MeV rel. to levels of Ne<sup>23</sup> 9-6814  
Ni, 9, 11 MeV, d disintegration obs. 9-6909  
<sup>58</sup>Ni, elastic, polarized, asymmetry of angular distribution 9-4791  
<sup>58</sup>Ni(d,α)<sup>56</sup>Co, energy levels determ., E<sub>d</sub>=12 MeV 9-15730  
Ni(d,d'), collective 2<sup>+</sup>, 3<sup>-</sup> excitations 9-16967  
<sup>60</sup>Ni(d,n)<sup>61</sup>Cu, proton states obs. 9-18105  
<sup>58</sup>Ni(d,n)<sup>59</sup>Cu, proton states obs. 9-18105  
<sup>60</sup>Ni(d,n), and isotopes; neutron polarization obs. 11.7 MeV 9-613  
<sup>62</sup>Ni(d,n)<sup>63</sup>Cu, proton states obs. 9-18105  
<sup>64</sup>Ni(d,n)<sup>65</sup>Cu, proton states obs. 9-18105  
<sup>16</sup>O(d,α)<sup>14</sup>N detailed balance obs., time reversal invariance test 9-6898  
<sup>16</sup>O(d,p)<sup>17</sup>O spectroscopic factors calc. 9-6789  
<sup>16</sup>O(d,α)<sup>14</sup>N(0<sup>+</sup>, T=1) isospin-nonconserving, cross section meas. 9-20804  
<sup>16</sup>O(d,n)<sup>17</sup>F effective cross-section 9-15776  
<sup>37</sup>P(d,α)<sup>35</sup>Si, date analysis using Ericson fluctuation theory, coherence width and fraction of direct react. meas., E<sub>d</sub>=7.3-12.02 MeV 9-14626  
<sup>32</sup>S, elastic, polarized, asymmetry of angular distribution 9-4791  
<sup>32</sup>S(d,pα)<sup>30</sup>Si energy ground state, ang. distrib. meas., reaction mechanism determ., E<sub>d</sub>=12-17 MeV 9-15777  
<sup>28</sup>Si(d,n)<sup>29</sup>P at 5.0 MeV, polar, ang. distrib. of neutrons 9-6902  
<sup>28</sup>Si(d,d) absolute cross sections, E<sub>d</sub>=4.74-5.26 MeV 9-6903  
<sup>30</sup>Si(d,p)<sup>29</sup>P at 6-18 MeV, radiative capture cross sections, induced radioact. methods 9-9062  
<sup>28</sup>Si(d,p)<sup>29</sup>Si levels spectroscopic factors, absolute cross sections, E<sub>d</sub>=4.74-5.26 MeV 9-6903  
<sup>28</sup>Si(d,p)<sup>29</sup>Si, applic of Faddeev eqns. 9-11259  
<sup>29</sup>Si(d,p)<sup>30</sup>Si, E<sub>d</sub>=1-2 MeV, excitation functions and angular distrib. for p groups 9-6904  
<sup>86</sup>Sr, differential cross sections obs., increase in filled n shell region, 13.6 MeV 9-608  
<sup>48</sup>Ti(d,p)<sup>49</sup>Ti, 12.9 MeV, proton spectra 9-9068  
<sup>48</sup>Ti(d,p)<sup>49</sup>Ti, 12.9 MeV, proton spectra 9-9068  
Yb stable isotopes, (d,p), (d,t), (d,d') reaction even-even nuclei energy levels determ. 9-6806  
Zn(d,d'), collective 2<sup>+</sup>, 3<sup>-</sup> excitations 9-16967  
<sup>64</sup>Zn(d,n), and isotopes; neutron polarization obs. 11.7 MeV 9-613  
<sup>64</sup>Zn(d,n)<sup>65</sup>Ga, proton states obs. 9-18105  
<sup>66</sup>Zn(d,n)<sup>67</sup>Ga, proton states obs. 9-18105  
<sup>68</sup>Zn(d,n)<sup>69</sup>Ga, proton states obs. 9-18105

## electrons

- <sup>2</sup>He(e<sup>+</sup>)N<sup>(1470)</sup> search for N<sup>(1470)</sup> resonance, M<sub>π</sub>=1578 MeV 9-18089  
cross-section with arbitrary Fermi charge distribution, calc. method 9-20773  
cross-sections by activation method 9-14604

# Nuclear reactions and scattering continued

## electrons continued

- deuteron electrodisintegration near threshold, at low momentum transfer 9-13191  
e<sup>+</sup>He scatt., influence of nucleon-nucleon correls. 9-4772  
elastic and inelastic scattering corrections, high energy 9-2722  
electroproduction cross sections asymptotic behaviour, electric current constitution 9-11279  
electroproduction structure functions asymptotic props. 9-20774  
mixing parameters of rotation states determ. 9-20730  
Pb. backscatt. coeffs., 10 and 20 MeV 9-6855  
positron scattering in thin films 9-2714  
quasi-elastic, independent-particle model, axial-vector form factor 9-9017  
scattering, inelastic, by nuclei with nucleon knockout 9-579  
<sup>115</sup>Sn, differential cross section, elastic 9-13219  
<sup>115</sup>In M1/E2 mixing ratios determ., expt. and theory comparison 9-6798  
<sup>115</sup>Sn, differential cross section, elastic 9-13219  
Al backscatt. coeffs. 10 and 20 MeV 9-6855  
Al foils, energy loss, 0.3-MeV Monte Carlo calc. 9-5587  
Au, Mott scatt. asym. obs. depend on foil thickness 9-15582  
<sup>9</sup>Be(e,e'), levels obs., 25-58 MeV e scatt on nucleons obs. 9-20775  
<sup>7</sup>Be(e,e')<sup>7</sup>Li, in stars 9-15293  
<sup>12</sup>C, 580, 805, 968 MeV e scatt on nucleons obs. 9-20775  
<sup>12</sup>C, cross section, inelastic N-N correlation, N reabsorption considered 9-15754  
<sup>12</sup>C, elastic scatt. insensitivity to parity mixing in Hartree-Fock orbitals 9-11280  
<sup>12</sup>C, inelastic from giant M1 state, Coulomb distortion correction calc. 9-11210  
<sup>12</sup>C, quasi-elastic region, 500-1000 MeV, e.m. form factors meas. 9-8976  
<sup>12</sup>C and projected Hartree-Fock wave functions 9-6852  
<sup>12</sup>C part.-hole states, excitation, scatt. 9-504  
<sup>(40)</sup>Ca(e) scatt., charge distrib. calc. at 250, 500 MeV 9-4771  
<sup>(40)</sup>Ca(e) scatt., charge distrib. calc. at 250, 500 MeV 9-4771  
<sup>(40)</sup>Ca(e) scatt., charge distrib. calc. at 250, 500 MeV 9-4771  
<sup>(40)</sup>Ca(e) scatt., charge distrib. calc. at 250, 500 MeV 9-4771  
<sup>40</sup>Ca, inelastic scatt. obs. 9-9018  
<sup>40</sup>Ca inelastic scatt. obs. 9-9018  
<sup>42</sup>Ca(e,e'<sup>+</sup>)<sup>42</sup>Sc theoretical prediction 9-6658  
Cd, backscatt. coeffs., 10 and 20 MeV 9-6855  
<sup>12</sup>C(e, e') giant resonance, mag. quadrupole strength calc., comparison with theory 9-2721  
<sup>12</sup>C(e,e'<sup>+</sup>) form factor, ang. and energy distrib. 9-6852  
<sup>12</sup>C(e,e'<sup>+</sup>) insensitivity to parity mixing in Hartree-Fock orbitals 9-11280  
Cu, backscatt. coeffs., 10 and 20 MeV 9-6855  
Cu, direct pair prod. at 5.5 and 32 MeV diff. cross-sections 9-6857  
H, super perturbation theory and bounds in s-wave scatt., triplet state 9-11278  
<sup>4</sup>He, cross section, inelastic N-N correlation, N reabsorption considered 9-15754  
<sup>6</sup>Li, 2.18 and 3.56 MeV levels 9-6856  
<sup>6</sup>Li scatt. and disintegration cross-section obs. 9-6854  
<sup>7</sup>Li scatt. and disintegration cross-section obs. 9-6854  
<sup>24</sup>Mg, g.s. radiation widths, matrix elements determ., up to 11.5 MeV excitation energy 9-20776  
<sup>26</sup>Mg, inelastic 39.56 MeV, magnetic dipole transitions obs. 9-578  
<sup>26</sup>Mg inelastic from giant M1 state, Coulomb distortion correction calc. 9-11210  
<sup>23</sup>Na, 225 MeV, coeffs. of mixing of two states with I=5/2, and K=3/2, 1/2 determ. 9-20730  
<sup>23</sup>Na, elastic and inelastic, absolute cross-sections at 225 MeV 9-4770  
<sup>56</sup>Ni differential cross section, elastic 9-13219  
<sup>56</sup>Ni differential cross section, elastic 9-13219  
<sup>56</sup>Ni differential cross section, elastic 9-13219  
<sup>16</sup>O, cross section, inelastic N-N correlation, N reabsorption considered 9-15754  
<sup>16</sup>O(e, e') giant resonance, mag. quadrupole strength calc., comparison with theory 9-2721  
<sup>16</sup>O(e, e'<sup>+</sup>)<sup>16</sup>N 9-6658  
<sup>Si</sup> natural, differential cross sections 9-11277  
<sup>Si</sup>, deformation and oscillation parameters, internal quadrupole moment, 110-260 MeV 9-11277  
<sup>28</sup>Si, inelastic from giant M1 state, Coulomb distortion correction calc. 9-11210  
<sup>28</sup>Si giant resonance excitation, 150-225 MeV expt. data compared with prediction 9-2681  
<sup>28</sup>Si(e, e') giant resonance, mag. quadrupole strength calc., comparison with theory 9-2721  
<sup>88</sup>Sr(e, e'<sup>+</sup>)<sup>88</sup>Y theoretical prediction 9-6658  
<sup>(87)</sup>Ti(e) scatt., charge distrib. calc. at 250, 500 MeV 9-4771

gamma rays see Nuclear reactions and scattering due to photons

heavy ions see Nuclear reactions and scattering due to nuclei of Z>2

## helium-3

- <sup>18</sup>O(<sup>3</sup>He,t)<sup>18</sup>F ang distrib. obs. and DWBA analysis 17.3 MeV 9-6899  
on heavy target nuclei at 10-33 MeV, comparison with 10-44 MeV <sup>4</sup>He 9-9058  
(<sup>3</sup>He,p) rectangle diagrams in nuclei p-shell, for calc. of ang. distrib. 9-585  
<sup>3</sup>H(<sup>3</sup>He,<sup>3</sup>He) cross section, comparison with resonating group, 11.9-18.9 MeV 9-6907  
<sup>40</sup>Ca(<sup>3</sup>He,d)<sup>44</sup>Pr, rel. to nuclear structure study of <sup>141</sup>Pr 9-15719  
<sup>115</sup>Sn(<sup>3</sup>He,d)<sup>115</sup>Sb Sb isotopes, levels determ. from d ang. distrib. 18 MeV 9-610  
<sup>144</sup>Sm(<sup>3</sup>He,d)<sup>137</sup>Cs, <sup>139</sup>La, <sup>143</sup>Pm and <sup>145</sup>Eu, level structure 9-6802  
<sup>137</sup>Ba(<sup>3</sup>He, 3n) <sup>137</sup>Ce ratio of high and low-spin isomers obs. 9-2665  
<sup>138</sup>Ba(<sup>3</sup>He,d)<sup>135</sup>Cs, <sup>139</sup>La, <sup>143</sup>Pm and <sup>145</sup>Eu level structure 9-6802  
<sup>115</sup>Sn(<sup>3</sup>He,d)<sup>115</sup>Sb, for energy level study in <sup>115</sup>Sb 9-4754  
B scattering, elastic and inelastic at 32 MeV 9-2752  
<sup>13</sup>B(<sup>3</sup>He,α)<sup>10</sup>B, e.m. branching ratio determ. 9-14559  
<sup>10</sup>B(<sup>3</sup>He,t)<sup>6</sup>C, mass excess and 1st excited state energy meas. 9-4796  
<sup>9</sup>Be(<sup>3</sup>He,<sup>3</sup>He) elastic scatt., optical model calc., 6 and 8 MeV 9-4792  
<sup>12</sup>C, polarization of 40 MeV ions, obs. 9-6892  
<sup>12</sup>C(<sup>3</sup>He,<sup>3</sup>He) diff. cross-sections meas. E<sub>He</sub>=5.29-5.5 MeV 9-15775  
<sup>12</sup>C(<sup>3</sup>He,p)<sup>14</sup>N diff. cross-sections meas. E<sub>He</sub>=5.29-5.5 MeV 9-15775  
<sup>12</sup>C(<sup>3</sup>He,<sup>3</sup>He)<sup>12</sup>C, E<sub>He</sub>=20.13 MeV, spectrum and ang. distrib. obs. 9-6895  
<sup>12</sup>C(<sup>3</sup>He, n), <sup>16</sup>O energy levels, 9 and 10.6 MeV, ang. distributions, excitation functions, calc. spins and parities. 9-2649  
<sup>12</sup>C(<sup>3</sup>He, p)<sup>14</sup>N; E<sub>He</sub>=20.1 MeV, spectrum and ang. distrib. obs. 9-6895

**Nuclear reactions and scattering due to continued****helium-3 continued**

- <sup>12</sup>C(<sup>3</sup>He,<sup>3</sup>He) ang. distrib. meas., optical model parameters determ. E=18-24 MeV 9-11310
- <sup>12</sup>C(<sup>3</sup>He,n)<sup>15</sup>O<sub>g</sub>, n polarization ang. distrib. obs., 2.9-3.9 MeV 9-6896
- <sup>40</sup>Ca(<sup>3</sup>He, $\alpha$ )<sup>39</sup>Ca, DWBA analysis, spectroscopic factors, ang. distrib. 9-14627
- <sup>63</sup>Ca(<sup>3</sup>He,n), 17-32 MeV obs. in agreement with distorted wave calc. for 2p process 9-615
- <sup>54</sup>Cr(<sup>3</sup>He,d)<sup>52</sup>Mn, d ang. distrib. meas., transition strengths, I<sub>p</sub> determ., E<sub>tr</sub>=10 MeV 9-13243
- <sup>54</sup>Fe(<sup>3</sup>He,p)<sup>52</sup>Co, energy levels determ., E<sub>tr</sub>=18 MeV 9-15730
- <sup>1</sup>H(<sup>3</sup>He,d)<sup>3</sup>He, energy spectra obs. 9-6908
- <sup>3</sup>H(<sup>3</sup>He,p)<sup>3</sup>Li, 0.5-11 MeV, p spectra, obs. of transitions in <sup>6</sup>Li 9-11320
- <sup>3</sup>H(<sup>3</sup>He,t)<sup>3</sup>He, energy spectra obs. 9-6908
- <sup>3</sup>He(<sup>3</sup>He,<sup>3</sup>He) cross section, comparison with resonating-group calc., 4.3-21.4 MeV 9-6907
- <sup>3</sup>He(<sup>3</sup>He,2p), n tunneling, 10-20 keV 9-6905
- <sup>3</sup>He(<sup>3</sup>He, $\alpha$ )<sup>3</sup>He, energy spectra obs. 9-6908
- <sup>86</sup>Kr(<sup>3</sup>He, $\alpha$ ), neutron-hole states study of N-49 nuclei, spectroscopic information 9-14629
- <sup>6</sup>Li, ang. distrib. of resultant particles meas. E<sub>tr</sub>=21.2, 24.5, 26.8 MeV 9-11323
- <sup>7</sup>Li, ang. distrib. of resultant particles meas. E<sub>tr</sub>=21.2, 24.5, 26.8 MeV 9-11323
- <sup>7</sup>Li(<sup>3</sup>He,<sup>6</sup>He)<sup>3</sup>Li, unsuccessful search for T=2 state in <sup>6</sup>Li 9-15713
- <sup>6</sup>Li(<sup>3</sup>He, $\alpha$ p)<sup>3</sup>He at 1-1.5 MeV eff. of lifetime of intermediate <sup>3</sup>Li state, assoc. with cylindrical asymmetry obs. 9-6910
- <sup>7</sup>Li(<sup>3</sup>He,d)<sup>6</sup>Be, width variations of short-lived states 9-13222
- <sup>6</sup>Li(<sup>3</sup>He,p)<sup>6</sup>Be, width variations of short-lived states 9-13222
- <sup>24</sup>Mg(<sup>3</sup>He,<sup>3</sup>He)<sup>24</sup>Mg optical pot., bound state, DWBA calc. 9-4790
- <sup>24</sup>Mg(<sup>3</sup>He, $\alpha$ )<sup>23</sup>Mg, 15 MeV 9-6901
- <sup>24</sup>Mg(<sup>3</sup>He,<sup>3</sup>He,<sup>3</sup>He), at 18-20 MeV, ang. distrib., opt. model analysis, eff. of spin-orbit term 9-9063
- <sup>22</sup>Ne(<sup>3</sup>He, $\alpha$ )<sup>21</sup>Ne, E<sub>tr</sub>=15 MeV, obs. 9-6901
- <sup>22</sup>Ne(<sup>3</sup>He, $\alpha$ )<T=1/2 states in <sup>21</sup>Ne obs. 9-11233
- <sup>16</sup>O(<sup>3</sup>He, n), <sup>14</sup>Ne energy levels, ang. distrib. at 9 and 10.6 MeV 9-2649
- <sup>17</sup>O(<sup>3</sup>He,d)<sup>17</sup>F, ang. distrib. obs. and DWBA analysis 17.3 MeV 9-6899
- <sup>19</sup>F(<sup>3</sup>He,d)<sup>18</sup>S, energy levels determ. up to 9.5 MeV excitation energy 9-11236
- <sup>35</sup>S(<sup>3</sup>He, $\alpha$ p)<sup>33</sup>S, levels determ. and lowest T=1/2 states found, 7,12 MeV 9-537
- <sup>32</sup>S(<sup>3</sup>He,<sup>3</sup>He), at 18-20 MeV, and distrib., opt. model analysis, eff. of spin-orbit term 9-9063
- <sup>46</sup>Sc(<sup>3</sup>He,d)<sup>46</sup>Ti, for nuclear structure of <sup>46</sup>Ti 9-6819
- <sup>31</sup>Si(<sup>3</sup>He,p)<sup>31</sup>P, p distrib. meas., excitation energies determ., E=9 MeV 9-14582
- <sup>30</sup>Si(<sup>3</sup>He,d)<sup>31</sup>P, p distrib. meas., excitation energies determ., E=10 MeV 9-14582
- <sup>31</sup>Si(<sup>3</sup>He,<sup>3</sup>He), at 18-20 MeV, ang. distrib., opt. model analysis, eff. of spin-orbit term 9-9063
- <sup>30</sup>Si(<sup>3</sup>He,<sup>3</sup>He), at 18-20 MeV, ang. distrib., opt. model analysis, eff. of spin-orbit term 9-9063
- <sup>89</sup>Y(<sup>3</sup>He, $\alpha$ ), neutron-hole states study of N-49 nuclei, spectroscopic information 9-14629

**hyperons**

No entries

**mesons***See also Cosmic rays/effects and interactions*

- cross-section high energy, quasi classical approx. calc. with optical model 9-15755
- ( $\pi^+$ , 2p) on 1p shell of light nuclei, 200 MeV 9-2749
- N( $\pi^+$ ,  $\pi^-$ )X, cross section obs., double charge exchange studied, 200 MeV 9-4786
- K<sup>-</sup>, <sup>8</sup>Li fragment production 9-15772
- K<sup>-</sup> absorption, and branching ratios, kaonic X-rays obs. 9-11307
- $\pi^-$  complex nuclei; single scatt., single and double charge exchange obs. 9-11304
- $\pi^-$ , p,n. scatt. lengths determ., resonance production obs. 9-11306
- $\pi^-$  single and double charge exchange, radiative capture and absorption En200 MeV 9-11305
- $\pi^-$  transfer in mixture of H<sub>2</sub> and other gases 9-14620
- $\pi^+$  charge exchange scatt. on freon or Xe, nuclear form factor eff. 9-15771
- $\pi^-$  radiative capture and nucleon interac., cross section from Fermi-liq. model 9-11303
- $\pi^-$  absorption, radiative, and U<sup>-</sup> capture in nuclei 9-13234
- $\pi^-$  capture in light elements, calcs. and comparison with cancer radiotherapy expts. 9-13233
- $\pi$ dd, cross sections meas., 500-2500 MeV/c 9-14621
- $\pi$ -Li( $\pi$ ,np)<sup>6</sup>He ang. and energy distrib., excitation spectrum calc. 9-20800
- <sup>208</sup>Pb,  $\pi^+$  absorption and diffraction cross sections meas., E<sub>tr</sub>=3.5 GeV/c 9-9051
- <sup>27</sup>Al, K<sup>+</sup> absorption and diffraction cross sections meas., E<sub>tr</sub>=3.5 GeV/c 9-9051
- <sup>27</sup>Al,  $\pi^+$  absorption and diffraction cross sections meas., E<sub>tr</sub>=3.5 GeV/c 9-9051
- <sup>1</sup>B,  $\pi^-$ -mesic atom, 2p-1s transition natural line width meas. 9-9050
- <sup>1</sup>B,  $\pi^-$ -mesic atom, 2p-1s transition natural line width meas. 9-9050
- Be, K<sup>+</sup>n $\rightarrow$ K<sup>+</sup>p charge-exchange scatt., 0.97 BeV/c 9-8802
- Be, K<sup>+</sup> absorption and diffraction cross sections meas., E<sub>tr</sub>=3.5 GeV/c 9-9051
- Be,  $\pi^-$ -mesic atom, 2p-1s transition natural line width meas. 9-9050
- Be,  $\pi^+$  absorption and diffraction cross sections meas., E<sub>tr</sub>=3.5 GeV/c 9-9051
- <sup>12</sup>C, K<sup>+</sup> absorption and diffraction cross sections meas., E<sub>tr</sub>=3.5 GeV/c 9-9051
- <sup>12</sup>C, pion charge exchange scatt., differential cross section calc. 9-11302
- <sup>12</sup>C,  $\pi^-$ -mesic atom, 2p-1s transition natural line width meas. 9-9050
- <sup>12</sup>C,  $\pi^+$  absorption and diffraction cross sections meas., E<sub>tr</sub>=3.5 GeV/c 9-9051
- <sup>12</sup>C radiative capture, neutron emissio 9-2645
- <sup>12</sup>C( $\pi^+$ ,p)<sup>13</sup>C low-energy  $\pi$ N interactions perturbation theory test, 68 MeV 9-4787
- <sup>12</sup>C( $\pi$ , $\pi^+$ )<sup>3</sup>He, pole approx. validity testing, 117 MeV 9-11308
- <sup>12</sup>C( $\pi^-$ , $\pi^-$ p) <sup>11</sup>B mechanism, characteristic identification conditions, p<sub>tr</sub>=1.04 GeV/c 9-4788
- <sup>12</sup>C( $\pi^-$ , $\pi^-$ p)<sup>11</sup>B at 1.04 GeV/c momentum, mechanism 9-18099
- <sup>12</sup>C( $\pi^+$ , 2p)d $\alpha$ , cross section and products angular and energy distributions obs. 117 MeV 9-605

**Nuclear reactions and scattering due to continued****mesons continued**

- <sup>60</sup>Cu, K<sup>+</sup> absorption and diffraction cross sections meas., E<sub>tr</sub>=3.5 GeV/c 9-9051
- <sup>60</sup>Cu,  $\pi^+$  absorption and diffraction cross sections meas., E<sub>tr</sub>=3.5 GeV/c 9-9051
- <sup>3</sup>He  $\pi^+$  charge-exchange scatt., cross-section calc. 9-604
- <sup>3</sup>He  $\pi^-$ -s-wave radiative capture and  $\pi^+$ He<sup>+</sup>H vertex function 9-9048
- <sup>2</sup>H( $\pi$ , $\pi^+$ )<sup>2</sup>H, corrections to Weinberg formula 9-18098
- <sup>7</sup>Li( $\pi^-$ , $\pi^-$ ) cross section,  $\pi$  charge, moment and range determ. 9-6891
- <sup>6</sup>Li,  $\pi^-$  absorpt. at rest, capture rate calc. 9-9049
- <sup>6</sup>Li,  $\pi^-$ -mesic atom, 2p-1s transition natural line width meas. 9-9050
- <sup>7</sup>Li,  $\pi^-$ -mesic atom, 2p-1s transition natural line width meas. 9-9050
- <sup>7</sup>Li,  $\pi^-$  cross section obs., double charge exchange studied, 200 MeV 9-4786
- <sup>7</sup>Li( $\pi^-$ ,pn)<sup>3</sup>H, search for <sup>3</sup>H activity 9-6918
- <sup>6</sup>Li( $\pi^-$ ,2n)<sup>4</sup>He rescattering eff. due to  $\pi$  low energy absorption by d 9-20799
- <sup>6</sup>Li( $\pi^-$ ,nn)<sup>3</sup>Li ang. and energy distrib., excitation spectrum calc. 9-20800
- <sup>6</sup>Li( $\pi^-$ ,pp)<sup>3</sup>He cross section and transition operator 9-15774
- <sup>7</sup>Li( $\pi^-$ ,nn)<sup>3</sup>Li ang. and energy distrib., excitation spectrum calc. 9-20800
- <sup>7</sup>Li( $\pi^-$ ,np)<sup>3</sup>He ang. and energy distrib., excitation spectrum calc. 9-20800
- <sup>56</sup>Ni,  $\pi^-$  double charge exchange and capture at 15 MeV 9-15773
- <sup>10</sup>O( $\pi^-$ , $\pi^-$ ) $\alpha\alpha\alpha\alpha$ , 117 MeV 9-13235
- <sup>15</sup>V( $\pi^-$ , $\pi^-$ ) cross section,  $\pi$  charge, momenta and range determ. 9-6891
- <sup>15</sup>V( $\pi^-$ , cross section obs., double charge exchange studied, 200 MeV 9-4786
- <sup>90</sup>Zr,  $\pi^-$ , cross section obs., double charge exchange studied, 200 MeV 9-4786

**muons**

- capture rates rel. to shell and Nilsson models 9-2723
- cosmic ray, calc. of probable upward backscatter at sea-level 9-15689
- cosmic rays, underground scatt. from emulsion 9-6718
- $\mu^-$  capture and radiative  $\pi^-$  absorption in nuclei 9-13234
- <sup>208</sup>Pb( $\mu$ ,n) photonuclear total cross section determ. 9-15645
- <sup>12</sup>C capture, neutron emission 9-2645
- <sup>40</sup>Ca spectrum and asymmetry of emitted neutrons, calc. 9-11281
- <sup>40</sup>Ca( $\mu$ , $\nu$ n), n energy spectra, obs. of  $\mu$  capture reson. mechanism 9-18090
- <sup>12</sup>C( $\mu^-$ , $\pi^-$ )<sup>12</sup>B,  $\mu^-$  capture rate and wave functions calc. 9-14605
- <sup>16</sup>O capture calc. in configuration mixing model 9-6790
- <sup>32</sup>S( $\mu$ , $\nu$ n), n energy spectra, obs. of  $\mu$  capture reson. mechanism 9-18090

**neutrinos**

No entries

**neutrons***See also Nuclear fission*

- 1.5-8.1 MeV off Al, S, Ca, Cr, Mn, Fe, Co, Ni, Cu, Zn, In and Bi elastic scatt. obs. 9-20787
- 55<A<141 nuclei targets, levels and spins from  $\gamma$ -ray obs. 9-4747
- <sup>123</sup>Sb(n, $\gamma$ )<sup>122</sup>Sb, cross-section obs. 9-596
- <sup>147</sup>Gm thermal n capture, study of following  $\gamma$  spectra 9-18066
- <sup>149</sup>Gm thermal n capture, study of following  $\gamma$  spectra 9-18066
- <sup>152</sup>Gm thermal n capture, study of following  $\gamma$  spectra 9-18066
- <sup>68</sup>Zn(n, $\alpha$ )<sup>66</sup>Zn 9-18075
- <sup>82</sup>Se(n,p), <sup>82</sup>As formation 9-11243
- (n,p) singlet effective range, from total cross section meas. below 5 MeV 9-6871
- Am<sup>241</sup>(n,p)<sup>242</sup>Cm, <sup>244</sup>Cm, <sup>242</sup>Cm yield 9-2747
- capture  $\mu$  meas. chem. analysis, sensitivity 9-21744
- capture  $\gamma$ -ray activation analysis with Ge(Li) detectors 9-4682
- capture cross sections, 8 nuclei 52<A<197, 8-120 keV 9-15763
- capture cross sections, obs. rel. to statistical model, 5 keV-3 MeV 9-9042
- capture cross-section for thermal n capture by nuclei with A<50 9-15762
- cross sections, nuclear polarizing power determ., E<sub>tr</sub>=4MeV 9-14612
- cross sections multilevel description, statistical treatment 9-19311
- deformation eff., 152<A on fast n total cross section 9-11291
- deuteron, cross section obs., 14 MeV, charge symmetry comparison with np results 9-6700
- doorway state theory and decay prob. for reaction 9-11295
- elastic and inelastic scatt. of n from Be to Pb nuclei, use of strong abs. model 9-2736
- even-even nuclei, inelastic, collective effects 9-4780
- graphite, reactor-grade scatt. for energies to 0.611 eV, energy transfer and plural scatt. eff. 9-13225
- graphite, thermal n scatt., inelastic, rel. to lattice model and phonon freq. 9-19855
- group cross-sections for mixtures with resonance-scattering component 9-19314
- inelastic, slow neutrons in moderator 9-19327
- inelastic by even-even nuclei, collective effects 9-4780
- inelastic scatt. of fast n, model 9-6872
- intermediate resonances, observability of two-particle-one-hole states 9-6778
- iniron of magnet yoke, high energy from extended source 9-422
- isomeric cross section ratios for (n,2n) reactions 9-15761
- isotope generator fuel prod. by n irradi., self-shielding and reactor flux depression 9-19316
- light nuclei, forward dispersion relations and exchange effects 9-4782
- low-energy in various substances, book 9-13258
- optical model analysis of elastic scatt., nuclear mass distrib. radii obs. 9-2634
- radiative capture, direct and collective, interference 9-581
- reaction rates from nuclear reactor neutrons 9-18095
- reactor materials subject to 14 MeV n, resulting  $\gamma$  obs. 9-652
- resonance cross sections, statistical calc. 9-14614
- resonance meas. with Ge(Li) detector partial and total capture x-sections E<sub>tr</sub>>5 KeV 9-6878
- resonance parameters, strength functions from cross section meas. and multi-level formula 9-13227
- resonance-integral ratio to thermal activation, meas. using Cd ratios or Au standard 9-6877
- shielding materials, total cross sections minima, 1-11 MeV 9-15760
- spectroscopy, slow n, missing level probability calc. method 9-16960
- spin flip probability in scatt. on polarized nuclei 9-19313
- theory contrib., allowance for radiative channels 9-2741
- thermal (n,p) energy and intensity obs., compendium 9-9033
- thermal n capture in Mg<sub>2</sub>SnO<sub>4</sub>, chem. and Mossbauer study 9-17549
- time, collision, for 6.8 MeV on various nuclei calc. by Wigner's method 9-15748
- total cross sections between 3.2 MeV and 5.2 MeV, fluctuation 9-593



**Nuclear reactions and scattering due to continued****neutrons continued**

- (n, 2n) reaction, role of isospin 9-11294  
 (n, 2n) processes, cross sections for various heavy nuclei, 14.7 MeV 9-2737  
 (n,  $\alpha$ ) cross-section averaged over fission n spectrum 9-20794  
 (n, p) knock-out, distorted wave theory 9-11284  
 (n,  $\gamma$ ), 14.1 MeV n interaction with Na, Mg, S, Si, Mn, Fe 9-600  
 (n, 2n), isomeric cross section ratio at 14.7 MeV 9-2740  
 (n, 2n) cross section a function of (N-Z)/A only if shell effect is taken into account 9-20795  
 (n, 3n) and statistical theory 9-2739  
 (n,  $\nu$ ) as polar, analyser for n polarimeter, resolution for 14 MeV 9-2779  
 (n,  $\alpha$ ) telescope involving two proportional and one scintillation counter 9-11131  
 (n, n') production of isomers, appl. to reactor flux density meas. 9-11293  
 (n, n') on low atomic no. foils, obs. of  $\gamma$ -spectra 9-9035  
 (n, n') on low atomic no. foils, obs. of  $\gamma$ -spectra 9-16961  
 (n, n') (p, n'), theory contrib., allowance for radiative channels 9-2741  
 (n, p), phase-shift analyses rel. to NN scatt. matrix determ., 7-750 MeV 9-9034  
 (n, 2n) cross-section averaged over fission n spectrum 9-20794  
 (n, p) cross-section averaged over fission n spectrum 9-20794  
 n resonance analysis, apparatus 9-17548  
 NN scatt. matrix from (n, p) phase-shift analyses, 7-750 MeV 9-9034  
<sup>41</sup>(n, p) cross section meas.,  $E_n=6.7-13.4$  MeV 9-14617  
<sup>62</sup> Ni(n, p)<sup>63</sup> Ni, intensities and energies of  $\gamma$  lines 9-603  
<sup>62</sup> Ce(n, 2n)<sup>139</sup> Ce, absolute activation cross-section for  $E_n=14.8$  MeV, obs. 9-14615  
<sup>170</sup> Er(n, p), existence of 2.9 min <sup>170</sup> Ho isomer 9-14594  
<sup>240</sup> Pu rel. to reson. n widths, total cross section, 20 eV-5.7 keV 9-14616  
<sup>240</sup> Pu rel. to reson. radiative widths, radiative, 38-820 eV 9-9040  
<sup>150</sup> Sm polarised thermal capture,  $\gamma$  circular polarisation obs. 9-13230  
<sup>130</sup> Te radiative capture, direct and collective proc. interference 9-581  
<sup>130</sup> Te(n,  $\gamma$ ) isomeric cross section ratios, spin-cutoff parameter deduced, 24 keV 9-544  
<sup>230</sup> Th, neutron reson. obs. 9-11299  
<sup>230</sup> Th, total neutron cross-section below 1 eV, time of flight method 9-599  
<sup>190</sup> Yb and isotopes, cross section, level density and s-wave strength function obs. 9-4736  
<sup>161</sup> Pr, n energy and ang. distrib. meas., energy levels determ.  $E_n=230-2580$  keV 9-18094  
<sup>241</sup> Am(n,  $\gamma$ ) <sup>242m</sup> Am, excitation function distortion by <sup>7</sup>Li(p, n) soft-n 'impurities', 0.25-7 MeV 9-18097  
<sup>141</sup> Pr(n, p)<sup>141</sup> Ce, absolute activation cross-section for  $E_n=14.8$  MeV, obs. 9-14615  
<sup>141</sup> Pr(n, t)<sup>139</sup> Ce, absolute activation cross-section for  $E_n=14.8$  MeV, obs. 9-14615  
<sup>141</sup> Pr(n, n')  $\gamma$  spectra meas., energy levels determ.,  $E_n=0.5-2.3$  MeV 9-14613  
<sup>241</sup> Pu cross section meas. 1-30 eV spin assignments for 2-32 eV resonances 9-4781  
<sup>154</sup> Sm(n,  $\gamma$ ) <sup>155</sup> Sm  $\beta$  decay and <sup>155</sup> Eu deduced levels 9-16949  
<sup>181</sup> Ta(n, 2n)<sup>180m</sup> Ta,  $E_n=12.2-17.9$  MeV 9-15765  
<sup>181</sup> Ta(n,  $\gamma$ ) <sup>182</sup> Ta, excitation curves meas.,  $E_n=0.03-5.1$  MeV 9-15765  
<sup>181</sup> Ta(n, p)<sup>181</sup> Hf,  $E_n=13.2-17.5$  MeV 9-15765  
<sup>181</sup> Ta(n, p)<sup>181</sup> Hf, excitation curve, 13-17.5 MeV 9-20797  
<sup>232</sup> fission, ang. distrib. and cross section of fragments rel. to energies 9-2772  
<sup>142</sup> Ce radiative capture, direct and collective proc. interference 9-581  
<sup>142</sup> Ce(n, 2n)<sup>141</sup> Ce, absolute activation cross-section for  $E_n=14.8$  MeV, obs. 9-14615  
<sup>2</sup> H(n, p)2n, <sup>3</sup> So n-n scatt. length compared with that obtained from <sup>2</sup>H(p, n)2n Nuclei with  $A \leq 5$  (<sup>2</sup> cc <sup>2</sup> H, <sup>3</sup> So n-n scatt. length from <sup>2</sup>H(n, p)2n and <sup>2</sup>H(n, p)2p compared 9-2733  
<sup>142</sup> Nd(n,  $\gamma$ ) spectra obs., transition schemes determ. 9-14569  
<sup>122</sup> Sn(n,  $\gamma$ ) <sup>123</sup> Sn, cross-section defined, 0.3-2.7 MeV 9-596  
<sup>182</sup> Ta, total cross-section, 0.01 to 1000 eV, resonance parameters for levels <30 eV 9-19312  
<sup>133</sup> In(n, 2n)<sup>132</sup> In,  $E_n=14.7$  MeV, cross-section and spin distrib. obs. 9-11296  
<sup>143</sup> Nd(n,  $\gamma$ ) spectra obs., transition schemes determ. 9-14569  
<sup>123</sup> Sb(n,  $\gamma$ ) <sup>124</sup> Sb cross-section obs. 9-596  
<sup>131</sup> Sn (n,  $\gamma$ ),  $\gamma$  spectra obs., E1, M1 transitions meas. 9-13228  
<sup>233</sup> U, capture and fission cross-sections, energy region 0.4 to 2000 eV 9-13247  
<sup>233</sup> U cross section meas. 1-30 eV 9-4781  
<sup>183</sup> W energy levels determ. from radiative n capture meas. 9-18096  
<sup>164</sup> Dy(n,  $\gamma$ ) isomeric cross section ratios, spin-cutoff parameter deduced, 24 keV 9-544  
<sup>144</sup> Nd(n,  $\gamma$ ) spectra obs., transition schemes determ. 9-14569  
<sup>124</sup> Sn(n,  $\gamma$ ) <sup>125</sup> Sn cross-section obs. 9-596  
<sup>184</sup> W(n,  $\gamma$ ), 1 resonances spectra anal., level schemes determ.,  $E_n=7-360$  eV 9-18096  
<sup>115</sup> In, inelastic cross sections rel. to spin assignments, calc. 9-541  
<sup>115</sup> In, (n, 2n)<sup>114</sup> In,  $E_n=14.7$  MeV, cross-section and spin distrib. obs. 9-11296  
<sup>145</sup> Nd(n,  $\gamma$ ) spectra obs., transition schemes determ. 9-14569  
<sup>105</sup> Pd(n,  $\gamma$ ) <sup>106</sup> Pd, spin assignment of n resonances, from captured  $\gamma$  data 9-2662  
<sup>235</sup> U cross section meas. 1-30 eV 9-4781  
<sup>185</sup> W energy levels determ. from radiative n capture meas. 9-18096  
<sup>176</sup> Lu(n,  $\gamma$ ) <sup>177</sup> Lu, internal conversion electron spectrum 9-2745  
<sup>146</sup> Nd(n,  $\gamma$ ) spectra obs., transition schemes determ. 9-14569  
<sup>197</sup> Au, capture cross-section in keV energy region 9-20789  
<sup>197</sup> Au(n,  $\gamma$ ) <sup>198</sup> Au, obs. on  $\gamma$  9-2746  
<sup>137</sup> Ba(n,  $\gamma$ ) <sup>138</sup> Ba, energy level determ. from  $\gamma$  spectra 9-6881  
<sup>157</sup> Gd(n,  $\gamma$ ) <sup>158</sup> Gd, conversion electron spectrum 9-15764  
<sup>177</sup> Hf(n, e)<sup>178</sup> Hf  $\gamma$  transitions in range 70-2000 keV 9-16939  
<sup>177</sup> Hf(n,  $\gamma$ ) <sup>178</sup> Hf, levels determ. from  $\gamma$  spectra meas.  $E_n=0.06-8.8$  eV 9-13195  
<sup>127</sup> I, 59 keV level excited, cross section meas.,  $E_n=50-500$  keV 9-19277  
<sup>127</sup> (n, p)<sup>127</sup> Te, at  $E_n=14.7$  MeV, <sup>127</sup> Te lifetime and activation cross-section obs. 9-9038  
<sup>127</sup> (n, 2n)<sup>126</sup> I, at  $E_n=14.7$  MeV, <sup>126</sup> I lifetime and activation cross-section obs. 9-9038  
<sup>127</sup> (n, 3n)<sup>125</sup> I, at  $E_n=14.7$  MeV, <sup>125</sup> I lifetime and activation cross-section obs. 9-9038  
<sup>127</sup> (n,  $\gamma$ ) <sup>128</sup> I, at  $E_n=14.7$  MeV, <sup>128</sup> I lifetime and activation cross-section obs. 9-9038

**Nuclear reactions and scattering due to continued****neutrons continued**

- <sup>127</sup>(n,  $\alpha$ ) <sup>124m</sup> Sb, at  $E_n=14.7$  MeV <sup>124m</sup> Sb, lifetime and activation cross-section obs. 9-9038  
<sup>207</sup> Pb(n,  $\gamma$ ) + <sup>208</sup> Pb levels determ.,  $E_n=15-60$  keV 9-18068  
<sup>207</sup> Pb(n,  $\gamma$ ) n capture, asymmetry in 43 keV resonance,  $E_n=15-60$  keV 9-18068  
<sup>237</sup> Th(n, f), fission fragment distribution, near threshold 9-2769  
<sup>187</sup> W energy levels determ. from radiative n capture meas. 9-18096  
<sup>198</sup> Au, capture,  $\gamma$  intensity obs., 10-60 keV 9-529  
<sup>208</sup> Pb radiative capture, direct and collective proc. interference 9-581  
<sup>148</sup> Pd(n,  $\gamma$ ) isomeric cross section ratios, spin-cutoff parameter deduced, 24 keV 9-544  
<sup>238</sup> U, ang. distrib. obs.,  $E_n=14$  MeV 9-15768  
<sup>238</sup> U capture cross section, calc. from statistical reson., 4-80 keV 9-14614  
<sup>238</sup> U(n,  $\gamma$ ) in U<sub>2</sub>O<sub>8</sub>, Doppler effect 300°-2000°K, obs 9-654  
<sup>238</sup> U(n, 2n)<sup>237</sup> U, as fast n flux monitor in TRIGA-II reactor 9-6934  
<sup>238</sup> U(n,  $\gamma$ ),  $\gamma$  spectra obs., decay scheme determ. 9-15769  
<sup>238</sup> U(n,  $\gamma$ ) <sup>239</sup> Np, as thermal n flux monitor in TRIGA-II reactor 9-6934  
<sup>238</sup> U(n,  $\gamma$ ) <sup>239</sup> U, cross-sections 25 to 500 keV, absolute at 30 keV 9-11300  
<sup>238</sup> U(n, n) differential cross section meas., analysis and comparison with optical model,  $E_n=14.7$  MeV 9-6876  
<sup>209</sup> Bi(n,  $\gamma$ ) cross sections 9-6886  
<sup>199</sup> Hg(n,  $\gamma$ ) <sup>200</sup> Hg, conversion spectrum, branching and mixing ratios, expt. and theory 9-4784  
<sup>139</sup> La, n energy and ang. distrib. meas., energy levels determ.  $E_n=230-2580$  keV 9-18094  
<sup>139</sup> La(d, Zn), <sup>139</sup> Ce production, energy dependence 9-586  
<sup>139</sup> La(n, n')  $\gamma$  spectra meas., energy levels determ.,  $E_n=0.5-2.3$  MeV 9-14613  
<sup>167</sup> Tm(n,  $\gamma$ ) <sup>170</sup> Tm radiative transitions intensities and resonance widths obs. up to 136 eV 9-4783  
 Al optical model analysis, 100-150 MeV 9-9046  
 Al slab 9-591  
<sup>27</sup> Al, inelastic scatt. cross section, modified optical model transmission coeff. 9-20791  
<sup>28</sup> Al polarised thermal n capture,  $\gamma$  circular polarisation obs. 9-13230  
<sup>27</sup> Al(n,  $\alpha$ ) <sup>24</sup> Na, absolute activation cross-sections for 14.7-14.8 n 9-13231  
 Be neutron cross-sections for  $E=13.7-14.6$  MeV 9-9041  
 Bi cross-section determ. with slow neutrons and He-cooled target 9-20790  
 Bi(n, 2n), 14 MeV ang. correl. obs. 9-20798  
<sup>138</sup> B(n, d) <sup>140</sup> Be d ang. distrib. and Be ground state 9-594  
<sup>10</sup> B(n,  $\gamma$ ) <sup>10</sup> B, 14 MeV, cross-sections 9-9032  
<sup>11</sup> B(n,  $\gamma$ ) <sup>11</sup> B, 15 MeV, cross-sections, elastic and inelastic 9-9032  
<sup>11</sup> B(n, p) <sup>11</sup> Be cross section for  $E_n=14.7$  MeV, obs. 9-6883  
 Br isomers (n,  $\gamma$ ) process, active Br collection on electrodes 9-4785  
<sup>79</sup> Br(n, n') <sup>79</sup> Br, rel. to (n, 2n) reaction mechanism 9-9045  
<sup>79</sup> Br energy transfer from neutrons up to 18 MeV, obs. 9-20786  
<sup>10</sup> B(n,  $\alpha$ ) <sup>7</sup> Li, <sup>7</sup> Li relative cross sections determ.,  $E_n=30-800$  keV 9-19318  
 C 100 GeV cosmic ray obs. at Nor-Amberd 9-15684  
 C neutron cross-sections for  $E=13.7-14.6$  MeV 9-9041  
<sup>14</sup> C, s- and p-wave elastic, through <sup>15</sup> N compound state, Regge trajectory 9-20777  
<sup>40</sup> Ca(n, t) <sup>39</sup> K, search with 14.7 MeV n 9-11301  
 Cd, cross-sections between 0.01 and 10 eV 9-19315  
 Cd, cross section meas., 10  $\mu$ eV range 9-6873  
 Cd optical model analysis, 100-150 MeV 9-9046  
<sup>33</sup> Cl(n,  $\gamma$ ),  $\gamma$ - $\gamma$  coincidence meas., time non-invariant amplitude determ. 9-11238  
<sup>12</sup> C(n,  $\alpha$ ) <sup>9</sup> Be, 13.9 and 15.6 MeV 9-2743  
<sup>12</sup> C(n, n) scatt., coupled channel calc., comparison with other treatments, 0-5 MeV 9-11292  
<sup>12</sup> C(n, n) polarization meas.,  $E_n=3.2-4.2$  MeV 9-20788  
<sup>12</sup> Cn cross section obs., peak widths meas. 14-25 MeV 9-6880  
<sup>60</sup> Co polarised thermal n capture,  $\gamma$  circular polarisation obs. 9-13230  
<sup>59</sup> Co(n,  $\gamma$ ) <sup>60</sup> Co, direct n capture, cross-section, intensity var. of  $\gamma$  produced 9-14618  
<sup>53</sup> Cr(n,  $\gamma$ ) <sup>54</sup> Cr  $\gamma$ -ray obs. using second-escape peak method 9-13202  
 Cu optical model analysis, 100-150 MeV 9-9046  
<sup>64</sup> Cu capture cross section rel. to reactor poisoning, obs. 9-19317  
<sup>67</sup> Cu, prep. by <sup>67</sup> Zn(n, p) <sup>69</sup> Cu in reactor 9-16502  
<sup>65</sup> Cu(n, 2n) <sup>64</sup> Cu, absolute activation cross-sections for 14.7-14.8 n 9-13231  
<sup>63</sup> Cu(n, 2n) <sup>62</sup> Cu, absolute activation cross-sections for 14.7-14.8 n 9-13231  
 D, bound atoms, coherent scatt. amplitude, mirror-refl. obs. 9-6875  
 in D<sub>2</sub>O gas, P1-moment of total scattering probability 9-20792  
 D capture cross section, 2200 m/sec 9-15766  
 F, bound atoms, coherent scatt. amplitude, mirror-refl. obs. 9-6875  
 F neutron cross-sections for  $E=13.7-14.6$  MeV 9-9041  
 Fe fast, high-resolution cross-sections 9-2742  
 Fe slab 9-591  
<sup>56</sup> Fe, inelastic scatt. cross section, modified optical model transmission coeff. 9-20791  
<sup>54</sup> Fe(n,  $\gamma$ ), overlap of configuration of capture and final states rel. to  $\gamma$ -ray intensities, 15-80 keV 9-6885  
<sup>56</sup> Fe(n,  $\gamma$ ), overlap of configuration of capture and final states rel. to  $\gamma$ -ray intensities, 15-80 keV 9-6885  
<sup>56</sup> Fe(n, n), 150 keV wide struct. analysis, doorway-state hypothesis 9-16964  
<sup>56</sup> Fe(n,  $\gamma$ ) <sup>56</sup> Mn cross section meas.,  $E_n=14.4$  MeV 9-13229  
 Fe(n, x) total cross sections meas., 1.8-2.6 MeV 9-601  
<sup>19</sup> F(n,  $\gamma$ ), thermal n capture  $\gamma$  obs. and <sup>20</sup> deduced levels 9-16962  
<sup>69</sup> Ga(n,  $\gamma$ ) <sup>69m</sup> Zn 9-18075  
<sup>76</sup> Ge(n,  $\gamma$ ) isomeric cross section ratios, spin-cutoff parameter, deduced 24 keV 9-544  
 H, energy transfer from neutrons up to 18 MeV, obs. 9-20786  
<sup>1</sup> H, 2n spectra cross section obs., 14.1 MeV 9-598  
<sup>2</sup> H, amplitude determ. in 1st order in N weak interac. 9-11214  
 H<sub>2</sub>O, total cross-section 9-16988  
 Hg, bound atoms, coherent scatt. amplitude, mirror-refl. obs. 9-6875  
<sup>2</sup> H(n, n') <sup>2</sup> H, 14 MeV, elastic 9-6874  
<sup>2</sup> H(n, p) <sup>2</sup> H cross section, theoretical analysis 9-2748  
<sup>2</sup> H(n,  $\gamma$ ) <sup>2</sup> H  $\gamma$  polarization and ang. distrib. asymm. expressed in terms of NN interac. 9-15767  
<sup>2</sup> H(n, 2n) p spectra and n-n scatt. length, 8-28 MeV 9-6882  
 In(n, 2n), isomeric cross-section ratios for 14.7 MeV n 9-6879  
 Kr(n, 2n), cross sections at 14.4 MeV 9-6889  
<sup>86</sup> Kr(n,  $\alpha$ ), cross sections at 14.4 MeV 9-6889

# Nuclear reactions and scattering due to continued neutrons continued

- Kr( $n, \alpha, \gamma$ ) cross sections meas. 9-6888  
 Kr( $n, p$ ), cross sections at 14.4 MeV 9-6889  
<sup>6</sup>Li( $n, t$ )<sup>4</sup>He, rel. to Li semiconductor neutron sandwich spectrometers 9-19225  
<sup>58m</sup>Co capture cross section, thermal, and reson. integral, rel. to reactor poisoning, obs. 9-19317  
<sup>55</sup>Mn, activation resonance integral using bath technique 9-20793  
<sup>92</sup>Mo( $n, 2n$ )<sup>91</sup>Mo, absolute activation cross-sections for 14.7-14.8 n 9-13231  
<sup>89m</sup>Y, excitation cross section for inelastic n. scatt. 9-13226  
 N, energy transfer from neutrons up to 18 MeV, obs. 9-20786  
<sup>14</sup>N, s- and p-wave elastic, through <sup>15</sup>N compound state, Regge trajectory 9-20777  
<sup>14</sup>N, search for resonance in inelastic channel 9-4773  
<sup>15</sup>N part-hole states, scatt. amp. and reson., spectroscopic TD calc. 9-6870  
<sup>23</sup>Na( $n, \alpha$ )<sup>20</sup>F cross-section for  $E_n=14.7$  MeV, obs. 9-6883  
<sup>23</sup>Na( $n, p$ )<sup>23</sup>Ne cross-section for  $E_n=14.7$  MeV, obs. 9-6883  
<sup>23</sup>Na( $n, p\gamma$ )<sup>23</sup>Ne 8-9 MeV rel. to levels of Ne<sup>23</sup> 9-6814  
<sup>91</sup>Nb( $nn\gamma$ )<sup>90</sup>Nb,  $\gamma$  spectra obs., energy levels determ. and resonances spin assignments 9-6890  
 Nd, natural and enriched with Nd isotopes, penetration and yield of  $\gamma$  rays from n capture 9-11298  
<sup>60</sup>Ni( $n, \gamma$ )<sup>61</sup>Ni, intensities and energies of  $\gamma$  lines 9-603  
<sup>58</sup>Ni( $n, \gamma$ ),  $\gamma$  transitions, energy distrib. obs.  $E_n=10-90$  keV 9-15770  
<sup>58</sup>Ni( $n, p$ ) cross sections 9-6886  
<sup>14</sup>N( $n, \alpha$ )<sup>11</sup>B, energy and ang. distrib. of  $\alpha$ -particles rel. to reaction mechanism 9-9039  
<sup>14</sup>N( $n, \alpha$ )<sup>11</sup>B, energy and ang. distrib. for  $E_n=14.1$  MeV 9-11297  
 O, energy transfer from neutrons up to 18 MeV, obs. 9-20786  
 O, fission n transport calcs., sensitivity to cross-section detail 9-18116  
<sup>16</sup>O( $n, \alpha$ )<sup>12</sup>C cross section obs., 8-12 MeV 9-597  
<sup>16</sup>O( $n, \alpha$ )<sup>12</sup>C, 14.8-18.8 MeV, differential cross-section 9-2744  
<sup>15</sup>O( $n, p$ )<sup>14</sup>O,  $E_n=0-10$  MeV n widths and total capture cross-section calc. 9-20796  
 Pb, cross-section determ with slow neutrons and He-cooled target 9-20790  
 Pb, natural, elastic cross-section, 10-40°, 4.56 MeV 9-2738  
 Pb optical model analysis, 100-150 MeV 9-9046  
 Pb( $n, 2n$ ), 14 MeV, ang. correl. obs. 9-20798  
 Rb( $n, p$ )<sup>86</sup>Rb,  $\gamma$ -ray intensity and energy meas. 9-13232  
 Sb, total cross-sections in energy-range 0.002 to 0.4 eV 9-11290  
 Sb( $n, 2n$ ), isomeric cross-section ratios for 14.7 MeV n 9-6879  
<sup>46</sup>Sc capture cross section and burn-up in <sup>46</sup>Ti( $n, p$ ), obs. 9-19317  
<sup>28</sup>Si( $n, \alpha$ ) cross section meas.,  $E_n=6.7-13.4$  MeV 9-14617  
<sup>28</sup>Si( $n, n$ ) cross section meas.,  $E_n=6.7-13.4$  MeV 9-14617  
<sup>28</sup>Si( $n, p$ )<sup>28</sup>Al, cross section meas.,  $E_n=14.4$  MeV 9-13229  
<sup>30</sup>Si( $n, p$ )<sup>30m</sup>Al cross section meas.,  $E_n=14.4$  MeV 9-13229  
<sup>32</sup>S( $n, \alpha$ ) absolute cross section obs. of isotopes, 14.8 MeV 9-602  
<sup>32</sup>S( $n, p$ )<sup>32</sup>P contamination determ 9-15836  
<sup>32</sup>S( $n, p$ ) absolute cross section obs. of isotopes, 14.8 MeV 9-602  
<sup>32</sup>S( $n, t$ )<sup>30</sup>P, search with 14.7 MeV n 9-11301  
 S( $n, x$ ) total cross sections meas., 1.8-2.6 MeV 9-601  
 Sn( $n, 2n$ ),  $(n, p)$ , activation cross-sections, isomeric ratios 9-9037  
<sup>46</sup>Ti( $n, p$ ) <sup>46</sup>Sc burn-up rel. to fast-n monitoring 9-19317  
<sup>49</sup>Ti( $nn, p$ ) time-reversal non-invariance search 9-6884  
 U isotopes, 14 MeVn, Pa heavy isotope prod. 9-16963  
 U optical model analysis, 100-150 MeV 9-9046  
<sup>51</sup>V( $n, n'$ ) excitation derived for levels, ang. distrib. obs. 9-542  
 Xe( $n, 2n$ ), cross sections at 14.4 MeV 9-6889  
 Xe( $n, \alpha, \gamma$ ) cross sections, spin cut-off parameters 9-6888  
 Xe( $n, p$ ), cross sections at 14.4 MeV 9-6889  
 Zn, total cross-sections in energy-range 0.002 to 0.4 eV 9-11290  
<sup>64</sup>Zn( $n, p$ )<sup>64</sup>Cu, energy spectra and angular distribution of protons 9-6887  
<sup>66</sup>Zn( $n, p$ )<sup>66</sup>Cu, energy spectra and angular distribution of protons 9-6887  
<sup>64</sup>Zn( $n, t$ )<sup>62</sup>Cu, cross-section for  $E_n=14.7$  MeV, obs. 9-14619  
<sup>70</sup>Zn( $n, 2n$ )<sup>69m</sup>Zn cross section meas.,  $E_n=14.4$  MeV 9-13229  
<sup>90</sup>Zr, inelastic scatt. cross section, modified optical model transmission coeff. 9-20791  
 5-13230

## nuclei of Z>2

### See also Ions/scattering

- <sup>10</sup>B scatt. of <sup>16</sup>O ions, elastic, obs. and anal. of results 9-15503  
<sup>12</sup>Sn(<sup>16</sup>O,  $4n\gamma$ )<sup>124</sup>Ce, collective levels deduced, 4-5 MeV/nucleon 9-516  
<sup>124</sup>Sn(<sup>16</sup>O,  $4n\gamma$ )<sup>124</sup>Ce, collective levels deduced 4-5 MeV/nucleon 9-516  
 elastic scatt. of strongly absorbed projectiles 9-6916  
 heavy ion reactions 9-19323  
 nucleus transfer in (<sup>18</sup>F, <sup>16</sup>O), final nucleus level excitation calc. 9-13244  
 nucleus transfer in (<sup>6</sup>Li,  $\alpha$ ) final nucleus level excitation calc. 9-13244  
<sup>120</sup>Cd(<sup>20</sup>Ne,  $4n\gamma$ )<sup>128</sup>Ce, collective levels deduced, 4.5 MeV/nucleon 9-516  
<sup>150</sup>Nd(<sup>16</sup>O, <sup>16</sup>O $\gamma$ ) 2<sup>+</sup> states  $\gamma$  emission ang. distrib., hyperfine interactions 9-15781  
<sup>150</sup>Nd(<sup>16</sup>O, <sup>16</sup>O $\gamma$ ), g meas. for 2<sup>+</sup> state 9-15723  
<sup>151</sup>Sm(<sup>16</sup>O, <sup>16</sup>O $\gamma$ ) 2<sup>+</sup> states  $\gamma$  emission ang. distrib., hyperfine interactions 9-15781  
<sup>120</sup>Sn(<sup>16</sup>O,  $4n\gamma$ )<sup>122</sup>Ce, collective levels deduced, 4-5 MeV/nucleon 9-516  
<sup>112</sup>Cd(<sup>20</sup>Ne, 3n $\gamma$ )<sup>128</sup>Ce, collective levels deduced, 4.5 MeV/nucleon 9-516  
<sup>120</sup>Cd(<sup>20</sup>Ne,  $4n\gamma$ )<sup>128</sup>Ce, collective levels deduced, 4.5 MeV/nucleon 9-516  
<sup>151</sup>Sm(<sup>16</sup>O, <sup>16</sup>O $\gamma$ ) 2<sup>+</sup> states  $\gamma$  emission ang. distrib., hyperfine interactions 9-15781  
<sup>150</sup>Nd(<sup>16</sup>O, <sup>16</sup>O $\gamma$ ) 2<sup>+</sup> states  $\gamma$  emission ang. distrib., hyperfine interactions 9-15781  
<sup>151</sup>Sm(<sup>16</sup>O, <sup>16</sup>O $\gamma$ ) 2<sup>+</sup> states  $\gamma$  emission ang. distrib., hyperfine interactions 9-15781  
<sup>16</sup>Ho, nitrogen ions bombardment,  $\gamma$  spectrum obs. magnetic dipole transitions, reduced probabilities 9-523  
<sup>163</sup>Ho(<sup>16</sup>O, 5n)<sup>178</sup>Re, new isotope prod. 9-14633  
<sup>133</sup>Cs(<sup>17</sup>Li, 3n)<sup>133</sup>Ce ratio of high and low-spin isomers obs. 9-2665  
<sup>120</sup>Cd(<sup>20</sup>Ne,  $4n\gamma$ )<sup>128</sup>Ce, collective levels deduced, 4.5 MeV/nucleon 9-516  
<sup>150</sup>Nd(<sup>16</sup>O,  $4n\gamma$ )<sup>128</sup>Ce, collective levels deduced, 4.5 MeV/nucleon 9-516  
<sup>150</sup>Nd(<sup>16</sup>O, <sup>16</sup>O $\gamma$ ) 2<sup>+</sup> states  $\gamma$  emission ang. distrib., hyperfine interactions 9-15781  
<sup>151</sup>Sm(<sup>16</sup>O,  $4n\gamma$ )<sup>130</sup>Ce, collective levels deduced, 4-5 MeV/nucleon 9-516  
<sup>128</sup>Te(<sup>12</sup>C, 3n)<sup>137</sup>Ce ratio of high and low-spin isomers obs. 9-2665  
<sup>232</sup>U(<sup>20</sup>Ne, f) fragment mass distrib. 9-11332  
<sup>208</sup>Bi(<sup>20</sup>Ni, f) fragment mass distrib. 9-11332  
 Al neutron scatt., total cross-sections, interaction radii inferred, at 10 GeV/c 9-9036  
<sup>10</sup>B(<sup>14</sup>N, <sup>12</sup>C)<sup>12</sup>C cross section, ang. distrib. meas.,  $E=22.5-32.5$  MeV 9-15780

# Nuclear reactions and scattering due to continued nuclei of Z>2 continued

- <sup>10</sup>B(<sup>16</sup>O, <sup>14</sup>N)<sup>12</sup>C cross section, ang. distrib. meas.,  $E=22.5-32.5$  MeV 9-15780  
<sup>9</sup>Be (<sup>18</sup>O, <sup>18</sup>O)<sup>9</sup>Be, excitation curves from  $\gamma$  yield meas., 12-30 MeV 9-617  
 Be neutron scatt., total cross-sections, interaction radii inferred, at 10 GeV/c 9-9036  
<sup>9</sup>Be scatt. of <sup>16</sup>O ions, elastic, obs. and anal. of results 9-15503  
 C neutron scatt., total cross-sections, interaction radii inferred, at 10 GeV/c 9-9036  
<sup>12</sup>C scatt. of <sup>16</sup>O ions, elastic, obs. and anal. of results 9-15503  
<sup>12</sup>C(<sup>13</sup>C,  $\alpha$ )<sup>20</sup>Ne excitation functions obs. and compared with theory 9-6917  
<sup>12</sup>C(<sup>6</sup>Li, p)<sup>17</sup>O excitation functions obs. and compared with theory 9-6917  
<sup>12</sup>C(<sup>16</sup>O,  $\alpha$ )<sup>24</sup>Mg excitation functions obs. and compared with theory 9-6917  
<sup>30</sup>CO (<sup>14</sup>N, 3n)<sup>70</sup>Se, lifetime and  $\gamma$  decay of <sup>70</sup>Se, obs. 9-9012  
 Cu neutron scatt., total cross-sections, interaction radii inferred, at 10 GeV/c 9-9036  
 Fe neutron scatt., cross-sections, interaction radii inferred, at 10 GeV/c 9-9036  
 He, neutron scatt., total cross-sections, interaction radii inferred, at 10 GeV/c 9-9036  
 Li neutron scatt., total cross-sections, interaction radii inferred, at 10 GeV/c 9-9036  
<sup>6</sup>Li ang. distrib. meas., optical-model parameters determ.,  $E=20$  MeV, various nuclei ( $12 \leq A \leq 40$ ) 9-15779  
<sup>7</sup>Li, ang. distrib. meas., optical-model parameters determ.,  $E=20$  MeV, various nuclei ( $12 \leq A \leq 40$ ) 9-15779  
<sup>24</sup>Mg, optical pot. ambiguities for <sup>16</sup>O elastic scatt. near Coulomb barrier 9-2764  
<sup>14</sup>N(<sup>6</sup>Li,  $\alpha$ )<sup>16</sup>O levels obs.,  $E_{rel}=5.3, 5.64, 6.0$  MeV 9-11324  
<sup>14</sup>N(<sup>6</sup>Li, d)<sup>18</sup>F levels obs.,  $E_{rel}=5.3, 5.64, 6.0$  MeV 9-11324  
<sup>14</sup>N(<sup>6</sup>Li, p)<sup>19</sup>F levels obs.,  $E_{rel}=5.3, 5.64, 6.0$  MeV 9-11324  
<sup>14</sup>N(<sup>6</sup>Li,  $\alpha$ )<sup>18</sup>F,  $\alpha$ -part. yields and ang. distrib., analysis, 4.8-13.8 MeV 9-11325  
<sup>16</sup>O <sup>16</sup>O elastic scatt. pot., compressibility of nuc. matter 9-9070  
<sup>16</sup>O( $t, p$ )<sup>18</sup>O(g.s.), cross section determ. by DWBA 9-14632  
 Pb, neutron scatt., total cross-sections, interaction radii inferred, at 10 GeV/c 9-9036
- nucleons**  
 cross-section high energy, quasi classical approx. calc. with optical model 9-15755  
 optical pot. calc., 90-310 MeV with second order corrections to impulse approx. 9-580  
 optical potential, rel. to deuteron optical potential 9-14606  
 Regge trajectory for scattering 9-20777  
<sup>3</sup>Ni(p, d), transfer reactions, realistic form factors 9-2724
- photons**  
 $23 \leq Z \leq 82$  elements, photo-n angular distrib. anisotropy rel. to subshells occupation, >5 MeV 9-4767  
<sup>63</sup>Cu( $\gamma, 2n$ ) cross section obs.,  $E_\gamma \leq 25$  MeV 9-19304  
<sup>63</sup>Cu( $\gamma, p$ ) cross-section obs.,  $E_\gamma \leq 25$  MeV 9-19304  
 C( $\gamma, e^+e^-$ ) $\gamma$ C meas., use as validity test of quantum electrodynamics at small distances 9-6575  
 concrete slabs, penetration and backscatter obs. 9-2712  
 cross-sections by activation method 9-14604  
 energy spectrum of photonuclear sources, Monte Carlo program for determ. 9-19303  
 giant dipole resonance, hydrodynamic model with  $A^{-1/6}$  depend 9-2638  
 magnetic internal Compton effect, transition rate calc. 9-6848  
 nucleon pairs yield from ( $\gamma, np$ ) reaction 9-11269  
 photodisintegration cross-sections for three-nucleon syst., sum rule calc. with Hamada-Johnston pot. 9-16953  
 photodisintegration reactions, 15-25 MeV 9-4766  
 photomesic and photonuclear processes, book 9-2506  
 polarized, prod. predominant population of one of the ground state sublevels 9-15711  
 scattering, polarizabilities and nuclear orientation effects 9-2713  
 single particle wave function method tested 9-11268  
 e pair prod on Al Ag Au targets obs. due to 2.62 13 MeV photons 9-10976  
 e pair prod. in nuclear field 2-20 MeV 9-11265  
 $\pi$  pair prod. below 850 MeV 9-4624  
 W meson pair production, cross section analytical expression, mass=2, 2.5, 3 MeV 9-11073  
<sup>181</sup>Ta( $\gamma, xn$ )  $x=1-4$ , cross sections meas.,  $E_\gamma \leq 36$  MeV 9-11271  
<sup>181</sup>Mo( $\gamma, xn$ )  $x=1-3$ , cross sections meas.,  $E_\gamma \leq 30$  MeV 9-11271  
<sup>218</sup>U( $\gamma, f$ ), ang. distrib. meas., K-level energy determ.,  $E_\gamma=5.4-9$  MeV 9-15784  
<sup>209</sup>Bi( $\gamma, n$ ), ang. and energy distrib. meas., symmetry search,  $E_n \geq 5$  MeV for  $E_{\gamma max}=20$  MeV 9-6849  
<sup>139</sup>La( $\gamma, xn$ )  $x=1-3$ , cross sections meas.,  $E_\gamma \leq 30$  MeV 9-11271  
<sup>159</sup>Tb( $\gamma, xn$ )  $x=1-3$ , cross sections meas.,  $E_\gamma \leq 30$  MeV 9-11271  
 Ag e pair prod. 2.62 MeV  $\gamma$  9-10976  
 Al e pair prod. 2.62, 13 MeV  $\gamma$  9-10976  
<sup>27</sup>Al( $\gamma, \pi^+$ )<sup>27</sup>Mg, yield and cross section meas. 9-575  
 Au e pair prod. 2.62 MeV  $\gamma$  9-10976  
 Be, incoherent scatt. cross-section for  $E_\gamma=30$  to 130 keV 9-11266  
<sup>7</sup>Be, absorption spectra calc., 35 MeV 9-577  
<sup>118</sup>Bi( $\gamma, \pi^-$ )<sup>118</sup>C, yield and cross section meas. 9-575  
<sup>10</sup>B( $\gamma, p$ )<sup>9</sup>Be, energy distrib. meas., quantum numbers assigned to levels,  $E_\gamma \leq 12.5$  MeV 9-9015  
 C, incoherent scatt. cross-section for  $E_\gamma=30$  to 130 keV 9-11266  
<sup>40</sup>Ca, photoproton energy and ang. distrib. 9-2716  
<sup>40</sup>Ca( $\gamma, n\gamma$ ) cross section meas.,  $\gamma$  obs.,  $E_\gamma \leq 32$  MeV 9-13218  
<sup>40</sup>Ca( $\gamma, p\gamma$ ) cross section meas.,  $\gamma$  obs.,  $E_\gamma \leq 32$  MeV 9-13218  
<sup>12</sup>C( $\gamma, p$ )<sup>11</sup>B, photoproton spectrum 9-2715  
<sup>12</sup>C( $\gamma, n$ ), ang. distrib. meas. in giant resonance region  $E_\gamma \leq 10$  MeV 9-16954  
<sup>12</sup>C( $\gamma, n$ )<sup>12</sup>C up to 260 MeV anomaly in recoil nuclei with energy >2.27 MeV 9-15749  
 C( $\gamma, p, p$ )<sup>11</sup>B, energy and ang. distrib. of photoprotons, obs. in giant reson. region, anisotropy and particle-hole states deductions 9-11270  
 Cr( $\gamma, n$ ), >5 MeV photon n anisotropy,  $E_\gamma=22-32$  MeV 9-4769  
 Cu, photonuclear cross-section and absolute measurement of X-ray beam energy 9-2717  
<sup>63</sup>Cu( $\gamma, n$ ) cross-section obs.,  $E_\gamma \leq 25$  MeV 9-19304  
<sup>63</sup>Cu( $\gamma, p$ )<sup>62</sup>Ni, photoproton spectra from 26.6 MeV bremsstrahlung 9-15752



**Nuclear reactions and scattering due to continued****photons continued**

- <sup>65</sup>Cu(p,p)<sup>64</sup>Ni, photoproton spectra from 26.6 MeV bremsstrahlung 9-15752
- <sup>56</sup>Fe, photoproton measurement 9-2716
- <sup>19</sup>F( $\gamma$ ,2p)<sup>17</sup>N+<sup>16</sup>O+n, use in high sensitivity chemical analysis 9-4029
- <sup>74</sup>Ge( $\gamma$ , $\alpha$ ), energy spectra  $\alpha$ , meas. and interpretation 9-2720
- <sup>4</sup>He photodisintegration cross-section appl. of particle hole states 9-6764
- <sup>4</sup>He(p, n)<sup>3</sup>He, effective cross section and angular distrib. meas. 9-6850
- <sup>4</sup>He(p, p)<sup>3</sup>H, energy spectrum of photo protons for 28 and 32.5 MeV  $\gamma$  9-4768
- <sup>4</sup>He(p, pn)D multipolarity investigation 9-11274
- <sup>4</sup>He(p,n)<sup>3</sup>He cross sections and ang. distrib. 9-2719
- <sup>4</sup>He(p,p), total cross-section, effect of vel. depend. nuclear forces 9-2718
- <sup>4</sup>He(p,p)<sup>3</sup>H, effective cross section and angular distrib. meas. 9-6850
- <sup>4</sup>He(p,p)<sup>3</sup>H, p spectra meas., <sup>4</sup>He excited states determ. 9-16937
- <sup>4</sup>He(p,p)<sup>3</sup>H cross sections and ang. distrib. 9-2719
- <sup>4</sup>He(p, $\pi^0$ ), diff. cross section meas.,  $E_\gamma=160-450$  MeV 9-11275
- <sup>7</sup>Li( $\gamma$ ,p)<sup>6</sup>He, integrated cross-section obs. 9-11320
- Mg, incoherent scatt. cross-section for  $E_\gamma=30$  to 130 keV 9-11266
- <sup>55</sup>Mn, photoproton energy and ang. distrib. 9-2716
- Mo( $\gamma$ ,p) and ( $\gamma$ , n), cross-section obs. 9-9016
- <sup>23</sup>Na, photoproton energy and ang. distrib. 9-2716
- <sup>93</sup>Nb( $\gamma$ , $\alpha$ ), energy spectra  $\alpha$ , meas. and interpretation 9-2720
- <sup>58</sup>Ni(p,n), cross sections 9-6851
- <sup>60</sup>Ni(p,n), cross sections 9-6851
- O photo disintegration electric quadrupole contribution 9-11272
- <sup>16</sup>O(p,n) yield and cross section meas.,  $E_p=20-300$  MeV [cc <sup>19</sup>F(p,2pn) yield and cross section meas.,  $E_p=20-300$  MeV] [cc <sup>27</sup>Al(p,2pn) yield and cross section meas.,  $E_p=20-300$  MeV] [cc <sup>51</sup>V( $\gamma$ , $\alpha$ ) yield and cross section meas.,  $E_p=20-300$  MeV 9-20772
- <sup>16</sup>O(p,n $\gamma$ ) cross section meas.,  $\gamma$  obs.,  $E_p \leq 32$  MeV 9-13218
- <sup>16</sup>O(p, $\pi^+$ )<sup>15</sup>N angular distrib. of photoproton 9-11273
- <sup>16</sup>O( $\gamma$ ,p $\gamma$ ) cross section meas.,  $\gamma$  obs.,  $E_p \leq 32$  MeV 9-13218
- <sup>31</sup>P, photoproton energy and ang. distrib. 9-2716
- Pb, photoneutron cross-section and X-ray beam energy, absolute meas. 9-2717
- Pb( $\gamma$ ,n),  $>5$  MeV photon-n anisotropy  $E_\gamma=22-32$  MeV 9-4769
- <sup>31</sup>P(p,p)<sup>30</sup>Si, photoproton spectra from 26.6 MeV bremsstrahlung 9-15750
- S, incoherent scatt. cross-section for  $E_\gamma=30$  to 130 keV 9-11266
- <sup>32</sup>S, photoproton energy and ang. distrib. 9-2716
- <sup>32</sup>S( $\gamma$ ,N), absorpt. cross section in giant dipole resonance region meas., 10-30 MeV 9-14583
- Sn-Al,  $\gamma$  backscatt. by stratified slab, <sup>90</sup>Co, <sup>137</sup>Cs sources 9-9014
- <sup>88</sup>Sr( $\gamma$ , $\pi^-$ )<sup>88</sup>Y theoretical prediction 9-6658
- U isotopes, 100 MeV bremsstrahlung irradi., Pa heavy isotope prod. 9-16963
- <sup>9</sup>Be(p, n)<sup>8</sup>Be cross-section, R-matrix fit. 9-576
- <sup>51</sup>V(p,  $\pi^-$ )<sup>50</sup>Cr, yield and cross section meas. 9-575
- <sup>51</sup>V(p,  $\pi^+$ )<sup>51</sup>Ti, yield and cross section meas. 9-575
- <sup>51</sup>V( $\gamma$ , $\alpha$ 3n) yield and cross section meas.,  $E_p=20-300$  MeV 9-20772
- <sup>69</sup>Zn resonant scatt. meas. on 7368 keV level by Pb capture  $\gamma$  9-2689
- <sup>63</sup>Zn(p,n) cross sections meas., giant resonance structure studied,  $E_p=11-23$  MeV 9-15753
- <sup>64</sup>Zn(p,n) cross sections meas., giant resonance structure studied,  $E_p=11-23$  MeV 9-15753
- protons**
- 2H(p,p) ang. distrib. of p polarization, 12.0 MeV 9-9021
- 20 and 24 GeV/c with emulsion stacks, dbl. emission of heavy fragments 9-583
- <sup>112</sup>Cd(p,p)(p,p)<sup>110</sup>DWBA and coupled-channel calc., meas. of differential X-sections and deformation parameters of two-phonon-states 9-6864
- <sup>27</sup>Al(p, $\alpha$ )<sup>24</sup>Mg, 2.3-3.4 MeV proton energies 9-9027
- <sup>7</sup>H(p,p)<sup>6</sup>H cross section calc., separable S-interaction, E=100 MeV 9-13223
- <sup>34</sup>S(p,p' $\gamma$ )<sup>34</sup>S,  $\gamma$  spectra and reaction excitation function obs. 9-567
- A(p,pd)A-2, function of uncorrelated nucleons 9-9023
- analog state resonances, K-matrix formulation of shell-model theory 9-11192
- cosmotron expt. at Brookhaven 9-9025
- high-energy, calc. using Cabibbo-Horowitz-Ne'eman model of factorized residues 9-15756
- ionographic emulsion nuclei, 5 GeV/c  $\bar{p}$  interact., study of hyperfragments prod. 9-20781
- isobaric analogue resonance for determ. of neutron spectroscopic factors 9-494
- isobaric analogue resonances in photoproton reaction 9-11246
- level formation by p capture, tables 9-6861
- multiparticle prod. in interact with light emulsion nuclei at 22.8 GeV/c, characts. of secondary particles 9-6693
- optical potential and asymmetry spin-dependent Thomas form, 20 MeV 9-13221
- radiative capture, giant dipole resonance meas. 9-8968
- rotational states excitation, 2nd order Born approx. 9-15710
- spin independent forward scatt. amplitude; pp, pd; 1.3-1.7 GeV/c 9-14609
- time, collision, for 6.8 MeV on various nuclei calc. by Wigner's method 9-15748
- two-particle transfer, transition-matrix element 9-584
- (p, n) knock-out, distorted wave theory 9-11284
- (p,2p) ang. distrib. calc. for light nuclei, 160-1000 MeV 9-11285
- (p,2p) cross-section calc., nonlocal model t-matrix 9-6863
- (p,d), reson. structs. in Pb region 9-6862
- (p, $\gamma$ ) through interfering isobaric analogue and giant dipole reson. in medium and heavy nuclei 9-14608
- (p,n) charge exchange reacts. on light nuclei, compound nucleus effects 9-9024
- (p,p'), rectangle diagrams in nuclei p-shell. for calc. of ang. distrib. 9-585
- (p,p') and (pn)-resonance react. with excitation of analogue states, fine struct. and cross sections 9-6775
- d singlet and triplet final state, DWBA anal. 9-14607
- <sup>7</sup>H target, spin and isospin-depend. anal. 9-4775
- <sup>3</sup>H(<sup>3</sup>He,p)<sup>4</sup>He, 15.8 MeV proton total react. cross section using associated particle method 9-16957
- n, thermal, prod. by thick targets in water, Ep 540-2000 MeV 9-15757
- <sup>140</sup>Ce isobaric analogue resonances in photoproton reaction 9-11246
- <sup>160</sup>Mo(p,p') at 5-20 MeV, radiative capture cross sections, induced radioact. methods 9-9062
- <sup>120</sup>Sn, nuclear-matter size from opt.-model analysis of 39.6 MeV p scatt. 9-11219

**Nuclear reactions and scattering due to continued****protons continued**

- <sup>120</sup>Sn (p,p) nuclear matter radii and charge distrib. calc. from cross sections 9-11220
- <sup>141</sup>Pr isobaric analogue resonances in photoproton reaction 9-11246
- <sup>122</sup>Sn, nuclear-matter size from opt.-model analysis of 39.6 MeV p scatt. 9-11219
- <sup>122</sup>Sn(p, p) nuclear matter radii and charge distrib. calc. from cross sections 9-11220
- <sup>143</sup>Nd(p,n)<sup>143</sup>Pm, evidence for 273 k3V level of <sup>142</sup>Pm with spin  $7/2^+$  9-8983
- <sup>231</sup>U fission, n emission rel. to fragment mass 9-4813
- <sup>114</sup>Cd(p,p)(p,p)<sup>112</sup>DWBA and coupled-channel calc., meas. of differential X-sections and deformation parameters of two-phonon states 9-6864
- <sup>114</sup>Cd(p,p') diff. cross sections and asymmetries anal., 24 $\gamma$ , 3 $\gamma$  single phonon states, 50 MeV 9-2731
- <sup>120</sup>Sn(p,p) nuclear matter radii and charge distrib. calc. from cross section 9-11220
- <sup>124</sup>Sn, nuclear-matter size from opt.-model analysis of 39.6 MeV p scatt. 9-11219
- <sup>163</sup>Ho (p,2n)<sup>164</sup>Er, 4 $\gamma$  ground state levels, mean lifetimes obs. 9-519
- <sup>145</sup>Nd(p,2n), <sup>144</sup>Pm e capture decay scheme 9-6836
- <sup>118</sup>Sn, inelastic scatt. at 14.695 MeV, rel. to nuclear excited states 9-512
- <sup>118</sup>Sn, nuclear-matter size from opt.-model analysis of 39.6 MeV p scatt. 9-11219
- <sup>118</sup>Sn(p, p) nuclear matter radii and charge distrib. calc. from cross sections 9-11220
- <sup>136</sup>Xe, neutron particle-hole states observed by inelastic scatt. 9-20779
- <sup>209</sup>Bi (p,2n)<sup>208</sup>Po,  $\gamma$  energy, ang. distrib. and lifetimes obs. 9-531
- <sup>107</sup>Ag in emulsion,  $E_p=13.8$  GeV 9-19308
- <sup>127</sup>(p,p' $\gamma$ ),  $\gamma$  spectra meas., Coulomb excitation, E2 transition prob. determ.  $E_p=3.5-5$  MeV 9-20737
- <sup>207</sup>Pb, differential cross sections of neutron hole excitation obs., 20.2 MeV 9-530
- <sup>207</sup>Pb(p,p'), Robson analogue theory, appl. to ground state of <sup>208</sup>Pb 9-18092
- <sup>198</sup>Au(p, <sup>210</sup>O) new isotope identified, 3 GeV 9-506
- <sup>208</sup>Pb(p,p), elastic and inelastic, cross sections and polarization, 155 MeV 9-20780
- <sup>118</sup>Sn, nuclear-matter size from opt.-model analysis of 39.6 MeV p scatt. 9-11219
- <sup>118</sup>Sn (p,p) nuclear matter radii and charge distrib. calc. from cross sections 9-11220
- <sup>139</sup>La isobaric analogue resonances in photoproton reaction 9-11246
- <sup>139</sup>La(p,n), <sup>139</sup>Ce production, energy dependence 9-586
- <sup>159</sup>Tb(p,2n)<sup>158</sup>Dy, 4 $\gamma$  ground state levels, mean lifetimes obs. 9-519
- <sup>27</sup>Al-<sup>28</sup>Si, lowest T=2 level unobs. as compound nucleus resonance 9-16944
- <sup>27</sup>Al(p, p')<sup>27</sup>Al excitation function meas., 3 MeV investigation 9-2680
- <sup>27</sup>Al(p, $\alpha$ )<sup>24</sup>Mg, resonances meas.,  $\alpha$  ang. distrib. meas.,  $E_p=1180-1920$  keV 9-20782
- <sup>27</sup>Al(p, $\gamma$ )<sup>28</sup>Si, resonances meas.,  $E_p=1180-1920$  keV 9-20782
- <sup>36</sup>Ar(p,p') energy levels deduced from scatt. cross sections, 24.85 MeV 9-539
- <sup>40</sup>Ar(p,p') energy levels deduced from scatt. cross sections, 24.85 MeV 9-539
- <sup>8</sup>Be prod. in 20 GeV/c interactions with heavy nuclei of emulsion 9-16955
- <sup>9</sup>Be(p,d), deuteron vector polarization, 185 MeV 9-2735
- <sup>9</sup>Be(p,d) energy spectra analyzed diff. cross section meas., 185 MeV 9-11289
- <sup>9</sup>Be(p,d)<sup>8</sup>Be tensor polar. of d, 1.6-3.8 MeV 9-9031
- <sup>9</sup>Be(p,p')<sup>8</sup>Be quadrangle graph calc. 9-20778
- <sup>9</sup>Be(p, $\alpha$ )<sup>7</sup>He, 57 MeV, analysis and extent of quasifree p- $\alpha$  scatt. 9-14611
- <sup>11</sup>B( $\alpha$ ,p)<sup>8</sup>Be, coincidence spectra study,  $E_p=1.4$  MeV 9-9026
- <sup>10</sup>B( $\alpha$ , $\alpha'$ )<sup>8</sup>Be,  $\alpha$  part. identification and nonexistence of 14.6 MeV state in <sup>7</sup>Be 9-11216
- <sup>11</sup>B( $\alpha$ , $\alpha'$ )<sup>8</sup>Be, width variations of short-lived states 9-13222
- <sup>11</sup>B(p, $\gamma$ ), peak of giant dipole reson. 9-16956
- <sup>7</sup>Br in emulsion,  $E_p=13.8$  GeV 9-19308
- C,  $E_p=0.5$  to 2.9 GeV, formation cross-section for <sup>7</sup>Be 9-19310
- <sup>12</sup>C, cross sections compared with e scatt. meas., light nuclei structure determ. 9-4774
- <sup>12</sup>C, level excitation distorted wave, impulse approx. calc.  $E_p=100$  MeV 9-18091
- <sup>12</sup>C, Regge model application 9-348
- <sup>13</sup>C time reversal invariance, polarization-asymmetry test 9-6859
- <sup>14</sup>C, s- and p-wave elastic, through <sup>13</sup>N compound state, Regge trajectory 9-20777
- <sup>40</sup>Ca, ang. distrib. meas., optical model anal., r.m.s. radius of n, p determ.,  $E_p=30, 40$  MeV 9-14586
- <sup>40</sup>Ca, p extent from nucleus centre optical model reformulated, 9.6 MeV 9-582
- <sup>48</sup>Ca(p,n)<sup>48</sup>Sc levels determ. from  $\gamma$  spectra meas.,  $E_p=1.2-4$  MeV 9-19284
- <sup>44</sup>Ca(p,p)<sup>44</sup>Ca, obs. of isobaric analogue resonances in <sup>43</sup>Sc and <sup>45</sup>Sc, fine struct., comparison with (d,p) stripping 9-8995
- <sup>42</sup>Ca(p,p)<sup>42</sup>Ca, obs. of isobaric analogue resonances in <sup>43</sup>Sc and <sup>45</sup>Sc, fine struct., comparison with (d,p) stripping 9-8995
- <sup>44</sup>Ca(p,p) analogue resonances fine structure 9-4777
- <sup>44</sup>Ca(p,t)<sup>42</sup>Ca, t spectra, cross sections meas., levels, spin and parity determ.,  $E_p=26.5$  MeV 9-19309
- <sup>42</sup>Ca(p,t)<sup>40</sup>Ca, t spectra, cross sections meas., levels, spin and parity determ.,  $E_p=26.5$  MeV 9-19309
- Cd even isotopes, cross sections and ang. distrib. meas. for 0 $\gamma$ , 2 $\gamma$ , 3 $\gamma$  states 9-6858
- <sup>51</sup>Cl(p,n)<sup>51</sup>Ar reaction threshold meas., vector coupling const. calc. 9-564
- C(n,p),  $10^{10}-10^{12}$  eV, cross-section obs. on satellites Proton 1 and 2 9-18024
- <sup>59</sup>Co-<sup>60</sup>Ni compound nucleus decay depend on ang. momentum 9-4748
- <sup>12</sup>C(p, <sup>3</sup>He) energy spectra analyzed, diff. cross section meas., 185 MeV 9-11289
- <sup>12</sup>C(p, <sup>3</sup>He)<sup>10</sup>B cross section, calc. 9-584
- <sup>12</sup>C(p, <sup>3</sup>He)<sup>11</sup>B, obs. lowest p-shell T=3/2 states of <sup>11</sup>B 9-14561
- <sup>12</sup>C(p, <sup>3</sup>He)<sup>11</sup>B spin and parity assignments 9-6866
- <sup>12</sup>C( $\alpha$ ,p)<sup>9</sup>B DWBA theory fit examined, exchange process possibility, 44.5 MeV 9-4779
- <sup>12</sup>C(p,d) deuteron vector polarization, 185 MeV 9-2735
- <sup>12</sup>C(p,d) energy spectra analyzed, diff. cross section meas., 185 MeV 9-11289
- <sup>12</sup>C(p,d)<sup>11</sup>C, distorted wave Born approx. anal.,  $E_p=100$  MeV 9-11286

# Nuclear reactions and scattering due to continued protons continued

- <sup>13</sup>C(p,d)<sup>12</sup>C, 1p neutron pick-up strengths, DWBA analysis and spectroscopic factors for assoc. states 9-6865
- <sup>12</sup>C(p,p)<sup>11</sup>C, radiative width meas. for 2.37 MeV state of <sup>12</sup>C 9-11209
- <sup>12</sup>C(p,p) polarization meas.,  $E_p=1.3$  MeV 9-11282
- <sup>12</sup>C(p,p)<sup>12</sup>C, p polarization obs. 4.6-72 MeV 9-2726
- <sup>13</sup>C(p,i)<sup>11</sup>C, obs. lowest p-shell  $T=3/2$  states of <sup>11</sup>C 9-14561
- <sup>13</sup>C(p,i)<sup>11</sup>C spin and parity assignments 9-6866
- <sup>50</sup>Cr, study of resonant state 9-19305
- <sup>52</sup>Cr(p,p)<sup>52</sup>Cr, 5.7-6.0 MeV, p polarization 9-4776
- <sup>54</sup>Cr(p,n)<sup>54</sup>Mn, rel. to low energy excited states of <sup>54</sup>Mn 9-19286
- <sup>63</sup>Cu(p,n)<sup>63</sup>Zn, excitation function, yield 9-590
- <sup>63</sup>Cu(p,n)<sup>63</sup>Zn, production yield by recoil p in reactors 9-589
- <sup>63</sup>Cu(p,n)<sup>63</sup>Cu, recoil nuclei ang. distrib. obs. 0.37-2.8 GeV 9-6869
- Fe,  $E_p=0.5$  to 2.9 GeV, formation cross-sections for Co, Mn, Cr, V, Sc radionuclides 9-19310
- <sup>54</sup>Fe, study of resonant state 9-19305
- <sup>56</sup>Fe, proton and neutron distributions calc. 9.6 MeV 9-582
- <sup>56</sup>Fe, study of resonant state 9-19305
- <sup>56</sup>Fe(p,p)<sup>56</sup>Fe, levels investigated by  $\gamma$ - $\gamma$  ang. correl. dis. 9-14588
- <sup>56</sup>Fe(p,n)<sup>Co</sup>, cross-sections at 370 MeV 9-13224
- <sup>56</sup>Fe(p,n)<sup>Co</sup>, cross-sections at 370 MeV 9-13224
- <sup>58</sup>Fe(p,n)<sup>Co</sup>, cross-sections at 370 MeV 9-13224
- <sup>19</sup>F(p,n), <sup>19</sup>F excited states obs., g-factor 9-16936
- <sup>64</sup>Ga, proton and neutron distributions calc. 9.6 MeV 9-582
- <sup>73</sup>Ge(p,p)<sup>73</sup>Ge, 12 MeV obs. parities, transitions strengths for levels up to 3 MeV 9-8998
- <sup>2</sup>H, cross sections compared with e scatt. meas., light nuclei structure determ. 9-4774
- <sup>2</sup>H triple scatt. parameters calc., polarization meas. 425 MeV 9-11095
- <sup>4</sup>He, p multiple scatt., large-angle theory, 1 BeV/c 9-9028
- <sup>4</sup>He, p polarization obs. at 540 MeV 9-9022
- <sup>4</sup>He target, spin and isospin depend. anal. 9-4775
- He nuclei ejected from nuclear emulsions by 2.26, 9 and 19.5 GeV p and 2.23 GeV p, importance of cascade N 9-15758
- <sup>4</sup>He(p,p) cross section, excitation function obs.,  $E_p=20-28$  MeV 9-6867
- <sup>3</sup>He(p,pd)<sup>3</sup>He, final state p-p interaction 9-11287
- <sup>3</sup>He(p,n)<sup>3</sup>He, 2.5-3.0 MeV, ang. distrib. obs. 9-20783
- <sup>3</sup>He(n,p)2p, <sup>15</sup>O n-n scatt. length compared with that obtained from <sup>3</sup>H(n,p)2n 9-2733
- <sup>3</sup>H(n,p)2p, n spectra obs.,  $E_p=30, 50$  MeV 9-15759
- <sup>3</sup>H(p,p)<sup>3</sup>H, phase shift anal., <sup>4</sup>He low levels studied,  $E_p=3.11-4.6$  MeV 9-14564
- <sup>41</sup>K(p, $\alpha$ )<sup>38</sup>Ar, excitation function and  $\alpha$ -part. ang. distrib. obs.,  $E_p=1550-2000$  keV 9-20784
- <sup>39</sup>K(p, $\gamma$ )<sup>39</sup>Ca, energy levels, lifetimes and  $\gamma$ -ray branching determ.,  $E_p=1.1-2.5$  MeV 9-15729
- Li 22 MeV, neutron yield 9-616
- <sup>6</sup>Li, (<sup>3</sup>He)<sup>4</sup>He, particles ang. distrib. from polarized beam obs., 0.4-3.2 MeV 9-588
- <sup>6</sup>Li spin-isospin dependent,  $E_p=24.4$  MeV 9-4778
- <sup>7</sup>Li (p,d)<sup>4</sup>He, student exercise 9-9030
- <sup>7</sup>Li (p, $\gamma$ )<sup>7</sup>Be, for Li concentration determ. 9-12553
- <sup>6</sup>Li(p, $\alpha$ ), search for unbound states in He<sup>3</sup> 9-11211
- <sup>6</sup>Li(p,d)<sup>3</sup>Li, DWBA analysis, 100 MeV 9-16958
- <sup>6</sup>Li(p,d)<sup>3</sup>Li, DWBA analysis, 100 MeV 9-16958
- <sup>6</sup>Li(p,n), <sup>6</sup>Be levels obs.,  $E_p=30, 50$  MeV,  $0^\circ \leq \theta_{lab} \leq 60^\circ$  9-6868
- <sup>6</sup>Li(p,n), <sup>6</sup>Be levels obs.,  $E_p=30, 50$  MeV,  $0^\circ \leq \theta_{lab} \leq 60^\circ$  9-6868
- <sup>7</sup>Li(p,n)<sup>7</sup>Be 94 MeV, excitation of isobaric analogue state and 0.431 MeV state, calc. 9-9029
- <sup>7</sup>Li(p,p)<sup>7</sup>Li\* to 0.478 MeV state, impulse approx. calc. 9-9029
- <sup>7</sup>Li(p,p)<sup>7</sup>Li,  $E_p=3.56$  MeV, var. of total cross-section with energy, microscopic model and effective interaction. 9-11283
- <sup>6</sup>Li(p, $\alpha$ )d, cross section meas., ang. distrib. comparison with free p- $\alpha$  elastic scatt.,  $E_p=61.5$  MeV 9-16959
- <sup>7</sup>Li(p, $\gamma$ )<sup>7</sup>Be  $\rightarrow 2\alpha$  magnetic dipole transitions and isospin mixing in Be 9-2660
- Mg,  $E_p=0.5$  to 2.9 GeV, formation cross-sections for <sup>24</sup>Na and <sup>22</sup>Na 9-19310
- <sup>24</sup>Mg, polarization at 185 MeV 9-2728
- <sup>24</sup>Mg elastic scatt.,  $E_p=0.85$  to 4.58 MeV, differential cross-section obs. 9-6860
- <sup>24</sup>Mg(p,<sup>3</sup>He)<sup>24</sup>Na levels determ. from  $\gamma$  transitions,  $E_p=50$  MeV 9-18093
- <sup>24</sup>Mg(p, $\gamma$ ) to study 4.509 MeV state of <sup>27</sup>Al. 9-507
- <sup>24</sup>Mg(p,p)<sup>24</sup>Mg, 5.7-6.0 MeV, p polarization 9-4776
- <sup>24</sup>Mg(p,p)<sup>24</sup>Al,  $\gamma$  and coincidence spectra obs. 2322 keV 9-533
- <sup>24</sup>Mg(p,p)<sup>24</sup>Al resonances located,  $\gamma$  decay of  $T=3/2$  states obs. 9-4743
- <sup>24</sup>Mg(p,i)<sup>24</sup>Mg, levels determ. from  $\gamma$  transitions,  $E_p=50$  MeV 9-18093
- <sup>55</sup>Mn octupole weak coupling obs., 17.5 MeV 9-2688
- <sup>52</sup>Mo, 5- and 3- states from decay of <sup>13</sup>Tc 11.80 MeV isobaric analog resonance 9-4752
- <sup>14</sup>N, s- and p-wave elastic, through <sup>15</sup>N compound state, Regge trajectory 9-20777
- <sup>14</sup>N, search for resonance in inelastic channel 9-4773
- <sup>20</sup>Ne(p, $\gamma$ )<sup>21</sup>Na states study 9-16943
- <sup>20</sup>Ne(p,p), <sup>21</sup>Na states study 9-16943
- <sup>22</sup>Ne(p,p) $\gamma$  p- $\gamma$  ang. correlation meas.,  $E_p=4.8-5.5$  MeV 9-13220
- <sup>20</sup>Ne(p, $\pi^+\pi^-$ ) coherent production of mass enhancement at 1470 MeV 9-15619
- Ni,  $E_p=0.5$  to 2.9 GeV, formation cross-sections for <sup>46</sup>Co, <sup>54</sup>Mn, <sup>51</sup>Cr and <sup>48</sup>V 9-19310
- <sup>58</sup>Ni(p,p)<sup>58</sup>Ni, 5.7-6.0 MeV, p polarization 9-4776
- <sup>58</sup>Ni(p,d)<sup>57</sup>Ni form. factor calc. 9-11288
- <sup>15</sup>N(p,<sup>3</sup>He)<sup>15</sup>C spin and parity assignments 9-6866
- <sup>15</sup>N(p,p)<sup>15</sup>O, eff. on CN cycle products abundance, stellar conditions 9-2732
- <sup>15</sup>N(p,n)<sup>15</sup>O, <sup>16</sup>O analogue states obs. 9-8977
- <sup>15</sup>N(p,i)<sup>13</sup>N spin and parity assignments 9-6866
- <sup>16</sup>O, cross sections compared with e scatt. meas., light nuclei structure determ. 9-4774
- <sup>16</sup>O(p,d)<sup>15</sup>O spectroscopic factors calc. 9-6789
- <sup>16</sup>O(p,n)<sup>15</sup>O rel. to <sup>15</sup>F excited states isobaric spin determ. 9-505
- <sup>16</sup>O(p,n)<sup>15</sup>F, prod. of <sup>15</sup>F in cooling water of reactor 9-16985
- <sup>16</sup>O(p,p)<sup>16</sup>O levels excitation energy, 6.20-6.54 MeV 9-6824
- <sup>7</sup>P,  $\gamma$  decay of  $T=3/2$  states obs. 9-4743
- <sup>8</sup>Pb, excitation functions, single-particle analog reson. 9-14577
- <sup>31</sup>P( $\alpha$ )<sup>28</sup>Si,  $\alpha$  ang. distrib. for spin mixing coeff. determ. 9-2734
- <sup>31</sup>P( $\alpha$ ), <sup>32</sup>S compound states average widths determ., excitation energy, 18-21 MeV 9-15728
- quadrangle graph method at 5-10 MeV 9-20778

# Nuclear reactions and scattering due to continued protons continued

- <sup>45</sup>Sc, proton and neutron distributions calc. 9.6 MeV 9-582
- <sup>45</sup>Sc(p,p)<sup>45</sup>Ti, rel. to energy and decay of <sup>46</sup>Ti levels 9-6821
- <sup>45</sup>Sc(p,n), <sup>45</sup>Ti ground state triplet at 0, 36.7 and 40.2 KeV obs. 9-19283
- <sup>32</sup>S(p,p) at 5-50 MeV, radiative capture cross sections, induced radioact. methods 9-9062
- <sup>32</sup>Si(p,d)<sup>32</sup>Si, DWBA anal. of polarization and power 30.5 MeV 9-534
- <sup>252</sup>S(p,d) deuteron vector polarization, 185 MeV 9-2735
- <sup>252</sup>S(p,d) energy spectra analyzed, diff. cross section meas., 185 MeV 9-11289
- <sup>30</sup>Si(p,p)<sup>30</sup>P,  $\gamma$  spectra meas., resonance levels, spin and parity determ.,  $E_p=0.8-2.2$  MeV 9-18069
- Sn even isotopes, cross sections and ang. distrib. meas. for 0<sup>+</sup>, 2<sup>+</sup>, 3<sup>-</sup> states 9-6858
- <sup>36</sup>S(p,p)<sup>36</sup>Cl, radiative capture;  $\gamma$  spectrum recorded, <sup>37</sup>Cl levels determ. 1147 keV 9-540
- <sup>32</sup>S(p,p)<sup>32</sup>S, energy levels deduced,  $E_p=12$  MeV 9-11237
- <sup>88</sup>Sr(p,n)<sup>88</sup>Y, <sup>88</sup>Y production yield by recoil p in reactors 9-589
- T even isotopes cross sections and ang. distrib. meas. for 0<sup>+</sup>, 2<sup>+</sup>, 3<sup>-</sup> states 9-6858
- Ti, nucleon yield of target following 660 MeV bombardment 9-587
- <sup>46</sup>Ti, 2.5-3 MeV, study of resonant state 9-19305
- <sup>46</sup>Ti, study of resonant state 9-19305
- <sup>46</sup>Ti (p,p'<sup>46</sup>Ti ang. correlation meas. to det. spins and  $\gamma$  branching ratios 9-2730
- <sup>30</sup>Ti(p,n)<sup>30</sup>V, <sup>30</sup>V low-lying level transitions obs. 9-18074
- <sup>46</sup>Ti(p,p') 9-19306
- <sup>30</sup>Ti(p,p) analogue resonances fine structure 9-4777
- <sup>51</sup>V, proton and neutron distributions calc. 9.6 MeV 9-582
- <sup>89</sup>Y, inelastic scatt. 24.5 MeV p, ang. distrib. and microscopic model study 9-19307
- <sup>89</sup>Y isobaric analogue resonances in photoproton reaction 9-11246
- <sup>89</sup>(p,n)<sup>89</sup>Zr, 78.4h <sup>89</sup>Zr sources prod., decay props., energies  $\gamma$  transitions meas. 9-2708
- <sup>89</sup>(p,n)<sup>89</sup>Zr, 2- isobaric analog reson.  $E_p=4.807$  MeV, excited states of <sup>89</sup>Zr, cross-sections and ang. distrib. of n groups 9-14610
- <sup>89</sup>(p,p)<sup>89</sup>Y polarization and diff. cross sections meas., spin and parity assignments 9-20751
- <sup>66</sup>Zn(p,p') diff. cross sections and asymmetries anal., 2<sup>+</sup>, 3<sup>-</sup> single phonon states, 50 MeV 9-2731
- <sup>68</sup>Zn(p,p') diff. cross sections and asymmetries anal., 2<sup>+</sup>, 3<sup>-</sup> single phonon states 50 MeV 9-2731
- <sup>70</sup>Zn(p,p') diff. cross sections and asymmetries anal., 2<sup>+</sup>, 3<sup>-</sup> single phonon states 50 MeV 9-2731
- <sup>64</sup>Zn(p,p') diff. cross sections and asymmetries anal., 2<sup>+</sup>, 3<sup>-</sup> single phonon states, 50 MeV 9-2731
- <sup>90</sup>Zr isobaric analogue resonances in photoproton reaction 9-11246
- <sup>90</sup>Zr(p, $\gamma$ ), <sup>91</sup>Nb d<sub>1/2</sub> analog state E1  $\gamma$  decay 9-4751
- <sup>90</sup>Zr(p,p)<sup>90</sup>Zr isobaric analogue resonance spectroscopic factors 9-494
- <sup>90</sup>Zr(p,d)<sup>89</sup>Zr, excited levels structure obs. up to 13 MeV 9-545

## tritons

- Feynman diagram method, building energy and recoil corrections 9-11263
- optical t parameter from fit of (t,p) ang. distrib. meas., 12 MeV 9-13240
- (t,d) zero range DWBA cross section normalisation coeff.,  $E_t=8.85$  MeV 9-2760
- (t,p) rectangle diagrams in nuclei p-shell, for calc. of ang. distrib. 9-585
- (t,d) normalisation factor calc. 9-14625
- <sup>210</sup>Pb(p,d)<sup>209</sup>Pb 2p-1h state obs., levels below 3561 keV 9-20745
- <sup>207</sup>Pb(p,d)<sup>206</sup>Pb 2p-1h state obs., levels below 3561 keV 9-20745
- <sup>18</sup>Ba(t,p) at 6-13 MeV, radiative capture cross sections, induced radioact. methods 9-9062
- <sup>208</sup>Pb(t,d)<sup>207</sup>Pb zero range DWBA cross section normalisation coeff.,  $E_t=8.85$  MeV 9-2760
- <sup>11</sup>B(t, $\alpha$ )<sup>11</sup>B, delayed n emission in  $\beta$  decay of <sup>13</sup>B 9-11250
- Ca(t, $\alpha$ ) even isotopes 9-2761
- <sup>32</sup>Cr(t,p), energy levels in final nuclei 9-4746
- <sup>32</sup>Cr(t,p), energy levels in final nuclei 9-4746
- <sup>36</sup>Cr(t,p), energy levels in final nuclei 9-4746
- <sup>4</sup>He(t,i) scatt., elastic, resonating-group method calc. of phase shift 9-14622
- <sup>3</sup>H(t,<sup>3</sup>He)3n, search for new states in <sup>3</sup>He spectra, evidence of existence of "trineutron" unbound by 1-1.5 MeV 9-11321
- <sup>210</sup>Ne(p,t)<sup>209</sup>Ne, angular correl. study, <sup>210</sup>Ne decay modes and spins of levels below ~5 MeV 9-11234
- <sup>16</sup>O(t,n)<sup>15</sup>F, excitation function at 0.5-3.0 MeV triton energies 9-2758
- <sup>40</sup>Ti(t,p), <sup>41</sup>Ti low-lying states rel. to 2p-1h configurations 9-2687
- <sup>96</sup>Zr (t,p) <sup>96</sup>Zr, p, ang. distrib. meas., spin, parity, n configurations determ. 9-20752

# X-rays see Nuclear reactions and scattering due to photons nuclear reactors, fission

- asymptotic reflector savings, meas. in water-moderated and reflected exponential cores 9-19371
- Calder Hall type, n-flux spatial osc., modal stability anal. 9-9078
- chemistry of reactors 9-21729
- critical assembly at Academy of Sciences, Latvian SSR 9-16981
- design, description of concrete container vessels, patent 9-13268
- design, power flattening and total output, comments on criticism 9-15794
- design, reply to comments of Judge and Bohl 9-9088
- Enrico Fermi fast breeder, fuel damage incident 9-9089
- fission rate fluctuations at low power rel. to kinetic parameters, from photon obs. 9-14651
- fission-product release and fuel evaporation in accident, boundary-layer diffusion model 9-16989
- fluctuation spectra of n density, and subcritical reactivity, meas. 9-13267
- flux density meas. by (n,n') isomer prod. 9-11293
- fuel element fault, in multichannel irr. rigs 9-9100
- fuel elements, moulding, patent 9-20858
- fuel elements state comparison by U equiv. contents calc. 9-16983
- fuel elements with thermocouples, patent 9-11366
- fuel handling mechanism construction, patent 9-13270
- fuel handling system construction, patent 9-11365
- fuel rod array, heat transfer to turbulent coolant flow 9-639
- fuel rod bundles, departure from nucleate boiling, uncertainties of heat fluxes 9-9092
- fuel rod parer distrib. meas. 9-11368
- heat transfer and water mixing between semiopen channels in square lattice, obs. 9-15795
- intermediate structure 9-9071



**nuclear reactors, fission continued**

- low reactivity meas. using reactor oscillator 9-6947  
 noise analysis 9-16979  
 noise analysis by analogue computer techniques from critical, subcritical zero 9-6935  
 reactions in reactor core obs. 9-645  
 reactivity, analogue on-line computation using integrating syst. 9-9101  
 reactivity meas. by n multiplication, validity 9-14659  
 safety of reactors in France 9-15797  
 shape isomers 9-6919  
 spatial effects on n fluctuation spectra 9-6245  
 swimming pool type, IEAR-1, for  $\gamma$  prod. by n capture 9-20841  
 teaching aids and literature review 9-2272  
 two-component reactor thermal eqns., inversion soln. 9-16977  
 UA-RR-I core, fast n spectrum at edge, meas. by threshold activation detectors 9-11356  
 flux distrib. controllability rel. to numbers of modes and control rods 9-13254  
 n absorpt. cross sections, pile oscillator meas. 9-20862  
 N absorption rates in assembly, eval. by activation rate meas. 9-18115  
 n fluctuation spectra, edge anomalies in large zero-power graphite reactor, obs. 9-15796  
 n flux noise spectra and  $\beta/\Gamma$ , L-54 Milan obs. 9-19350  
 n multiplication determ., expt. and analysis 9-6929  
 n spectroscopy, fast, in reactor media 9-11369  
 n time-of-flight spectroscopy in reactors 9-11359  
 $^{235}\text{U}(n,2n)^{235}\text{U}$ , as fast n flux monitor in TRIGA-II reactor 9-6934  
 $^{238}\text{U}(n,p)^{239}\text{Np}$ , as thermal n flux monitor in TRIGA-II reactor 9-6934  
 Fe, nucleon-meson cascade initiated by 1.3 GeV p 9-20853  
 In activation detectors for neutron flux, some corrections 9-658  
 LiOH reactor shield, fast neutron transmission through partially penetrating channel 9-636  
 $\text{MnSO}_4\cdot\text{D}_2\text{O}$  liquid foils, non-perturbing, for thermal flux meas. in graphite 9-9099  
 stripping and pickup, isobaric analog resons. 9-6862  
 THTR reactor, behaviour at partial power 9-14652  
 U-H<sub>2</sub>O assembly, fuel loading and critical mass expt. 9-18120  
 U-H<sub>2</sub>O subcritical assembly with n source, params, obs. 9-11347  
 U, enriched, water-graphite moderated critical assembly, buckling, obs. 9-19348  
 UC-D<sub>2</sub>O lattice fast fission ratio, ECO reactor obs. 9-11355  
 $\text{UO}_2\text{-D}_2\text{O}$  lattices, fast fission ratio, obs. 9-19349

**Nuclear reactors, fission materials**

- benzene, neutron thermalization, computed 9-20855  
 carbide fuel, spherical particles, and their mixtures with diluent ceramics prod., patent 9-13271  
 carbon blacks, P33 and Thermax, temp. depend. and n irradi. effects on e.s.r. 9-8018  
 corrosion chemistry of austenitic Cr-Ni steel following neutron irradiation 9-21701  
 critical assembly parameters, integral method for absolute meas. 9-644  
 electron probe microanalysis, expts. and shielded facility plans 9-20860  
 fast-breeder, review of technology 9-635  
 fission gas escape from reactor fuel during irradiation 9-20848  
 fuel, fission-product release in loss-of-coolant accident, boundary-layer diffusion model 9-16989  
 fuel element exam. by n radiography 9-11367  
 fuel element temp. distrib., use of electrolytic tank model for determ. 9-14654  
 fuel elements, swelling, relation to burn-up 9-6936  
 fuel irradiation in multipurpose research reactor 9-14657  
 fuel irradiation in multipurpose research reactor 9-14656  
 fuel particles, spherical with multilayer coatings, release of fission prod. 9-18126  
 fuel pin design to allow for sintering of fast oxide fuels 9-11363  
 fuel reprocessing in France 9-20850  
 fuels, ceramic, evolution and high burn up behaviour 9-2787  
 graphite, artificial, e.s.r. change annealing to 1000°C after n-irrad. 9-8017  
 graphite, densified by natural gas thermal cracking, pore size distrib. meas. 9-7416  
 graphite, diffusion-convective corrosion due to water vapour, soln. 9-9095  
 graphite, dilation on exposure to liq. Na rel. to irradi. dose 9-6003  
 graphite, dimensional effects of long-term radiation 9-6945  
 graphite, fracture behaviour under torsional and biaxial stresses 9-7565  
 graphite, from uncalcined coke, microstruct. and expansion changes under high-temp. irradi. 9-7432  
 graphite, I arpt. and desorpt. in vacuum and Ar, 27-1100°C 9-9626  
 graphite, n scatt. characts. for initial energies to 0.611 eV 9-13225  
 graphite, n thermalization calc. 9-9094  
 graphite, n-irrad., dilation on exposure to liq. Na 9-7661  
 graphite, neutron irradiation, stress, creep and crystal dimension changes 9-20851  
 graphite, neutron wave propag., effects of Bragg cut-off, anal. 9-13255  
 graphite, noise emission under compressive stress 9-7641  
 graphite, nucleation pattern of rad. damage, effect of B addition 9-7477  
 graphite, pile-irrad., electronic props. rel. to annealing temp. 9-7587  
 graphite, porous texture changes due to thermal and radiolytic oxidations 9-7408  
 graphite, purified, pre-irrad. effects on thermal oxidation rate 9-8086  
 graphite, pyrolytic, effect of B content on mech. and physical props. 9-7515  
 graphite, pyrolytic, interstitial and vacancy loop prod. on neutron irradi. 9-7472  
 graphite, pyrolytic, shear modulus rel. to short-term n-irrad. 9-7521  
 graphite, relax. of tensile stress, 2000° to 2700°C 9-7532  
 graphite, self-diffusion in single crystals, 2000-2600°C 9-16110  
 graphite, spherical fuel elements for pebble bed reactors, fabrication 9-6940  
 graphite, stability of surface complexes after radiolytic oxidation and thermal degassing 9-8087  
 graphite, tensile stress relax. in across-grain specimens, 2000-2700°C 9-7533  
 graphite, thermal n scatt. rel. to lattice model parameters and phonon freq. 9-19855  
 graphite, thermalized n pulse decay 9-9019  
 graphite, Vickers hardness before and after n-irrad., annealing effects 9-7578

**Nuclear reactors, fission continued materials continued**

- graphite anisotropic and near-isotropic, thermal expansion and cond. rel. to high-temp. irradi. 9-7663  
 graphite moderator, n wave propag. fundamental mode eigenvalue 9-13261  
 graphite moderators, equilib. neutron energy spectra, meas. and results 9-19378  
 graphite powders, compactibility 9-2797  
 graphite reflector, after 112,550 MWD of op., stored energy, Co space change and weight loss 9-6946  
 graphite slabs, neutron diffusion length 9-20833  
 graphite systems, finite, n moderation meas. by resonance filters 9-6930  
 graphite-pyrocabon composite bodies obtained by thermal cracking of natural gas, nuclear radiation effects 9-9861  
 light water assemblies, spherical, pulsed-n, fundamental mode discrete time-decay const. 9-9077  
 methyl iodide detection upon heating irradiated fuels 9-19367  
 moderators, freq. distrib. at various temps., obs. 9-19376  
 moderators contaminated with resonance absorbers, meas. and calc. of neutron spectra 9-19375  
 nuclear reactor containers, spray cooling 9-20849  
 organic coolants for heat transfer 9-643  
 oxalic acid in light and heavy water as in-pile chemical dosimeter 9-20864  
 oxide fuel, spherical particles, and their mixtures with diluent ceramics, prod., patent 9-13271  
 oxide fuels, identification of unknown constituent in electron-probe microanal. 9-17546  
 perfluorodimethylcyclohexane, neutron diffusion parameters, method for determ. 9-11342  
 point defect, neutron scatt. cross-section in a relaxed lattice calc. method 9-19741  
 radiation shielding, flexible alloy-elastomer, patent 9-9098  
 released energy profile on neutron or electron irradi., resistivity changes 9-7741  
 resins to minimize radiation damage on electrical insulation 9-19379  
 shielding technique, development 9-6943  
 Sical F1, n induced swelling, 500 MWD/t 9-16188  
 Sical F2, n induced swelling, 500 MWD/t 9-16188  
 stainless-steel tubes, vented, corrosion to CO<sub>2</sub>-CO mixture 9-15221  
 steel, stainless, fuel cladding, burst strength rel. to thickness and defects obs. 9-15799  
 steels and Ni alloys as melting pot materials, corrosion resistance 9-651  
 temperature distrib. in fuel elements with defects using heat transfer eqns. 9-19363  
 water, light, neutron thermalization Nelkin model modification 9-20856  
 water, mixed heavy and light, neutron scatt. 9-19377  
 water reactor high flux, effect of water density on reactivity 9-646  
 zero probability method in neutron counts to obtain meas.  $\alpha$  9-2799  
 Zircaloy-2, annealed, effect of irradi. on strain ageing 9-17330  
 Zircaloy-2 fuel cladding, burst strength rel. to thickness and defects obs. 9-15799  
 Zircaloy-4, dissolution kinetics of dispersed hydride platelets 9-17336  
 n beam quality improvement, core element rearrangement 9-4817  
 n bombard., 14 MeV, prod. of  $\gamma$  obs. 9-652  
 n diffusion mats., expt. method of determ. 9-11342  
 n shielding materials, total cross sections minima, 1-11 MeV 9-15760  
 $^{232}\text{Th}$  resonance absorpt., influence of scatt. interference 9-9093  
 $^{233}\text{UO}_2$  97 wt.% ThO<sub>2</sub>, calc. differences between thermal flux shape and reflector savings 9-19371  
 $^{235}\text{U}$ , graphite critical assemblies, leakage anal. and cross-sections 9-18122  
 $^{235}\text{U}$ -enriched assemblies, statistical wt. determ. 9-642  
 $^{235}\text{U}$  fission resonance in homogeneous system, temp. depend. 9-19324  
 $^{235}\text{U}$  reactor cores, moderated or unmoderated, criticality data 9-14650  
 $^{135}\text{Xe}$ , concentration calc. 9-14652  
 $^{147}\text{Pm}$ ;  $\text{O}_2$  microspheres, high density, production by r.f. induction plasma heating 9-2795  
 $^{238}\text{PuO}_2$  particles, pyrolytic coated 9-2793  
 $^{238}\text{U}$  absorption near Na resonance, self-shielding factor 9-2798  
 $^{238}\text{U}$  fuel lattice, resonance absorpt. rel. to cladding of Al, Zr or Fe 9-11362  
 $^{238}\text{U}$  resonance absorpt., influence of scatt. interference 9-9093  
 $^{238}\text{U}$  isolated low-enriched rods, fission calc. 9-11364  
 $^{239}\text{Pu}$  bare critical assembly, central reactivity contribs. of gram-sized samples of  $^{244}\text{Cm}$ ,  $^{239}\text{Pu}$  and  $^{235}\text{U}$  9-19370  
 $^{149}\text{Sm}$  concentration calc. 9-14652  
 Al, Xe, bubble distrib. rel. to grain-boundary migration 9-657  
 $\alpha$ -U, dislocation energies and easy glide parameters rel. to slip systems 9-1226  
 B pyrolytic graphite, effect of B content on mech. and physical props. 9-7515  
 Be, n thermalization in large buckling range 9-19334  
 Be, oxidation by water vapour obs., 600-800°C 9-6011  
 Be moderators, equil. neutron energy spectra, meas. and results 9-19378  
 Be slabs, diff. length problem as a function of absorption and transverse dimension 9-20833  
 Bi cross-section determ. with slow neutrons and He-cooled target 9-20790  
 CO<sub>2</sub> with organic impurities as gas coolant mixture, patent 9-20859  
 CaF<sub>2</sub> X-ray powder diffraction investigation of structure 9-11838  
 Cl trace determination in uranyl salts 9-8113  
 Co detector mat. in moderator, resonance self-shielding factors for  $\Gamma_n \gg \Gamma_\gamma$  9-18123  
 Cs metal, oxygen concentration by vacuum distillation 9-648  
 D<sub>2</sub>O, modes of motion spectral density from inelastic neutron scatt. meas. 9-13500  
 $^{18}\text{F}$  in cooling water due to  $^{18}\text{O}(p,n)^{18}\text{F}$  9-16985  
 Fe-base-alloys, neutron embrittlement in superheat reactors 9-19369  
 H contamination of sodium coolant by thermal dissociation of hydride 9-650  
 H transition metal cpds. as moderators 9-14655  
 H<sub>2</sub>O, total n cross-section, precision meas. 9-16988  
 He coolant, removal of CO<sub>2</sub> and water contaminants by cosorption by molec. sieves 9-19373  
 Hf, infinite dilution resonance absorption integrals 9-19372  
 K<sub>2</sub>Cl<sub>4</sub>-NaCl eutectic diagram predicted and confirmed by X-ray diffraction 9-11969  
 Mg coated fuel elements, electrophoretic deposition, patent 9-9097

**Nuclear reactors, fission continued**  
**materials continued**

- Mn, detector mat. in moderator, resonance self-shielding factors for  $\Gamma_{\alpha} \gg \Gamma_{\gamma}$  9-18123
- NbC, fast n irradi., fracture and vol. changes,  $10^{21}$  n/cm<sup>2</sup> 9-9862
- Pb-H<sub>2</sub>O system n yield under bombard. by 400, 500 and 660 MeV p 9-19364
- Pb, cross section determ. with slow neutrons and He-cooled target 9-20790
- Pm<sub>2</sub>O<sub>3</sub>-Sm<sub>2</sub>O<sub>3</sub>, prop. meas. rel. to <sup>147</sup>Pm as power source 9-2790
- Pu-based fuels, nucleation and behaviour of inert gas bubbles in non-uniform temp. 9-624
- Pu, diffusion and solubility in Al 9-11957
- Pu, distribution in fuels, determ. by  $\alpha$  autoradiography, improved resolution 9-19374
- Pu, liquid, solubilities of Ti, V, Cr, Mn, Zr, Nb and Mo, 700 to 1000°C 9-11685
- Pu and U, separation by fractional sublimation 9-20857
- Pu core moderated or unmoderated, criticality data 9-14650
- Pu in organic solns., chemical analysis 9-1929
- Pu inclusions analysis using laser microprobe 9-4023
- PuF<sub>6</sub>, recovery and purification by sorption and desorption using LiF 9-5254
- Pu(1.5at%)Hf,  $\beta \rightarrow \alpha$  transform. kinetics 9-11977
- PuO<sub>2</sub>, pyrolytic C-coated, high-temp. compatibility 9-2792
- Th-U-N system phases,  $\geq 50$  at.% N, 1000°C 9-16157
- Th hydrolysis in NaNO<sub>3</sub> and NaClO<sub>4</sub> solns., obs. 9-12529
- ThO<sub>2</sub>-PuO<sub>2</sub> sintering in Ar at 1600°C, in air and in wet and dry H<sub>2</sub> 9-19822
- ThO<sub>2</sub>-(1.3 wt.%)UO<sub>2</sub>, thermal cond. changes, irradi. induced, annealing 9-7676
- Ti-Mo alloys, U diffusion 9-19769
- U-(Fe,Al),  $\beta$ -quenched, recrystallization kinetics on annealing 9-3466
- U-H<sub>2</sub>O assembly, fuel loading and critical mass expt. 9-18120
- U-H<sub>2</sub>O lattice, angular n spectra meas. 9-9086
- U-H<sub>2</sub>O subcritical syst., pulsed neutron determ. of 2 group reactor-physical parameters 9-16984
- U-MO-Al-Sn, n induced swelling, 500 MWD/t 9-16188
- U-MO 1,1, n induced swelling, 500 MWD/t 9-16188
- U-Nb alloys, electrolytic etching in conc. aqueous citric acid, potentiostatic method 9-1129
- U-Mn<sub>2</sub>-UF<sub>6</sub> system, phase equilibrium 9-1353
- U-Zr-C phase diagram and (U, Zr)C lattice params., 1700-2000°C 9-11976
- U-based fuels, nucleation and behaviour of inert gas bubbles in non-uniform temp. 9-624
- U-bearing fuels, heat contents and specific heats 9-17356
- U-graphite assemblies, enriched, accurate criticality meas. 9-18121
- (U, Pu)C, synthesis from U-Pu alloy and fabrication of pellets 9-2791
- (U, Pu)C fuels, prep. by coprecipitation 9-6939
- (U,Ce)N solid solns. prep. and UN-CeN miscibility, 1800°C 9-9791
- (U,Nd)N solid solns. prep. and UN-NdN miscibility, 1800°C 9-9791
- (U,Pu)O<sub>2</sub> microspheres, techniques for ceramography and alpha autoradiography 9-3309
- U, 20% enriched, ignition in O<sub>2</sub> and air, irradi. effects, obs. 9-10332
- U, depleted slab between borated polyethylene, spatially depend. resonance n spectra 9-16987
- $\alpha$ -U, growth under irradi. at 25°C 9-7371
- $\alpha$ -U, n-induced growth at low doses, mechanism 9-19870
- $\alpha$ -U, precipitation kinetics of UAl<sub>2</sub> 9-11960
- U, prospecting, use of isotopic composition of Pb 9-20079
- U, separation from fission product, by eutectic freezing 9-18749
- $\alpha$ -U, slip in range 400-600°C 9-1298
- $\alpha$ -U, slip modes rel. to dislocation parameters and elastic consts. 9-1228
- U<sub>3</sub>O<sub>8</sub>, <sup>238</sup>U (n,  $\gamma$ ) reaction, Doppler effect 300°-200°K obs. 9-654
- U<sub>3</sub>P<sub>4</sub>, enthalpies of formation, qualitative method of differential thermal analysis 9-19368
- U<sub>3</sub>Si alloys, approx., effect of C on  $\delta$ -peritectoid reaction 9-16158
- U bearing liquid metal-immiscible solvent metal system, mass transfer meas. rel. to extraction processes 9-16473
- U cylinders, with min. <sup>235</sup>U enrichment, criticality study 9-9096
- U diffusion in Al at infinite dilution 9-17282
- U fuel element with defective Zircalloy-2 cladding, corrosion in steam - H<sub>2</sub>O, 285°C 9-11361
- U fuel in contact with can, thermal resistance 9-1408
- U graphite lattice, meas. d infinite multiplication factor by null reactivity method 9-13266
- U in organic solns., chemical analysis 9-1929
- U metal turnings, detection of methyl iodide when heated 9-19367
- UAl<sub>2</sub>-UMn<sub>2</sub>-UF<sub>6</sub> system, phase equilibrium 9-1353
- UC, arc cast and sintered, thermal conductivity, irradiation eff., 150-1600°C 9-15034
- UC, diffusion of U and C, and mechanisms, 1266-1863°C 9-11899
- UC, dihedral angles of U inclusions 9-11855
- UC, fabrication of stabilized compacts 9-20847
- UC, Kr sorption, fission induced, mechanism 9-16047
- UC, reactions with aqueous NaOH soln. 9-16482
- UC diffusion of C into Mb and W, 1000-1800°C 9-19764
- U<sub>2</sub>C<sub>3</sub> form. in UC-UC<sub>2</sub> melt, reactions rel. to grain orientation, 1350°C 9-12530
- UCl<sub>4</sub>-KCl-NaCl eutectic diagram, predicted and confirmed by X-ray diffraction 9-11969
- UCl<sub>4</sub>-NaCl eutectic diagram predicted and confirmed by X-ray diffraction 9-11969
- UF<sub>6</sub> thermodynamic properties evaluated from analysis of available experimental data. 9-2786
- UN, thermal diffusivity from 20 to 1000°C, by laser pulse method 9-13269
- UN microspheres, prep. by carbothermic reduction of UO<sub>2</sub> in N atm. 9-2794
- UO<sub>2</sub>-(20 wt.%) PuO<sub>2</sub> fuel, stoichiometry rel. to temp. gradient 9-2788
- UO<sub>2</sub>-Nb-H system compatibility 9-6941
- UO<sub>2</sub>-Ta-H system compatibility 9-6941
- UO<sub>2</sub>-UCl<sub>4</sub>-KCl, X-ray examination 9-16986
- UO<sub>2</sub>-PuO<sub>2</sub> fuels, stoichiometry, effect of external O sink 9-2789
- UO<sub>2</sub>-H<sub>2</sub>O lattice, subcritical multiplying medium, diffusion constants determ. 9-18127
- UO<sub>2</sub>-Nb cermet, high-loaded, rel. to fabrication 9-3475
- UO<sub>2</sub>-SiO<sub>2</sub> system, thermal cond. and resist., 100-800°C 9-16186
- UO<sub>2</sub>, 90% enriched, -Ni fuel element plates, irradi. stability, 1.9-30% burn-up 9-19362

**Nuclear reactors, fission continued**  
**materials continued**

- UO<sub>2</sub>, effective reson. integral of rad. and cluster, obs. 9-19366
- UO<sub>2</sub>, n space energetic distrib. 9-653
- UO<sub>2</sub>, sintered, thermal conductivity, irradiation eff., 150-1600°C 9-15034
- UO<sub>2</sub>, sintered irradiated, detection of methyl iodide when heated 9-19367
- UO<sub>2</sub>, with cracks, thermal diffusivity, flash method suitability 9-15033
- UO<sub>2</sub> base elements, influence of filling gas and radial distance between fuel and can 9-656
- UO<sub>2</sub> crystallization from melt by electrolysis 9-19690
- UO<sub>2</sub> pellets, sintered, powder morphology and energy effects on densification 9-3465
- UO<sub>2</sub> unenriched barrier beneath core, as safety device against melt-through 9-18124
- UO<sub>2</sub>, fission-gas release around 2000°C 9-13250
- UO<sub>2</sub>, flow of single crystals, slip planes rel. to orientation, 600-1800°C 9-9762
- UO<sub>2</sub>, n irradi. behaviour rel. to initial structure and props. 9-2787
- UO<sub>2</sub>, reprocessing of irradiated fuels, by fluorinating with BrF<sub>3</sub> and F<sub>2</sub> 9-6944
- UO<sub>2</sub>, sintered, exaggerated grains and growth mechanism, obs. 9-11798
- UO<sub>2</sub>, sintered, stainless steel inclusion, laser microprobe analysis obs. 9-12552
- UO<sub>2</sub>, swaged, microstruct. changes on irradi. 9-11358
- UO<sub>2</sub>, W microdiffusion, laser microprobe analysis obs. 9-12552
- UO<sub>2</sub>, yield and flow in compression, 600-2000°C 9-11931
- UO<sub>2</sub> fuel pellets, microstruct. after irradi., defects, gas bubbles and grain growth 9-11856
- UO<sub>2</sub> fuel rod fabrication by vibratory compaction 9-6942
- UO<sub>2</sub> fuels, oxygen redistrib. 9-11360
- UO<sub>2</sub> sintered pellets, quality control rel. to stoichiometry, density and struct. 9-2796
- UO<sub>2.14</sub>-Y<sub>2</sub>ThO<sub>2</sub>, magnetic susceptibilities of nonstoichiometric samples 9-13950
- UP<sub>2</sub>, enthalpies of formation, qualitative method of differential thermal analysis 9-19368
- (U<sub>0.85</sub>Pu<sub>0.15</sub>)C pellets, low density, prep. by reproducible process 9-6938
- US<sub>1</sub>.stoUS<sub>3</sub>, cryst. structs., phases and mag. props. 9-16081
- US<sub>3</sub>, heat capacity and thermodynamic props., 5 to 350°K 9-16082
- US<sub>3</sub>, heat capacity and thermodynamic props., 5 to 350°K 9-16082
- US<sub>1</sub>.stoUS<sub>3</sub>, cryst. struct., phases and mag. props. 9-16081
- Xe-power spatial transients, optimal control by computing algorithm 9-16982
- Zr-(2.5 wt.%)Nb corrosion resistance, cold deformation effect 9-647
- Zr-Cu alloys, effect of O<sub>2</sub> on ductile-brittle transition 9-11940
- Zr-Cu alloys (<5wt%Cu), phase transforms after quenching and tempering from  $\beta$  phase 9-11970
- Zr-1% Nb alloy, radiation resistance, suitability for high flux reactors 9-6937
- Zr, with hydride precipitates, crack nucleation and propag. 9-3452
- Zr alloys oxidation in high temp. H<sub>2</sub>O, irradi. effects, review 9-10343
- ZrC, fast n irradi., fracture and vol. changes,  $10^{21}$  n/cm<sup>2</sup> 9-9862
- ZrCl<sub>4</sub>, reaction kinetics with Zr 9-1898
- ZrH<sub>2</sub>, temp. depend. of neutron diffusion 9-19326
- Zr1wt%Nb, tensile strength and ductility, effect of H<sub>2</sub> and extension rates 9-17313
- ZrO<sub>2</sub>, O<sub>2</sub> diffusion in growing films, 400-500°C 9-9735
- ZrO<sub>2</sub> films on Zr in O<sub>2</sub> atm., struct. and epitaxy, 300°C 9-9619
- Zr-H phase boundaries and lattice params., 0.61-0.66 wt.% H 9-16160

**operation**

- cavity reactor critical experiments 9-19325
- cellulose diacetate meas. of  $\gamma$ , n volumetric field 9-660
- control rods, interrupted efficiency 9-638
- direct analog reactivity meter meas. of small reactivities 0.01 pcm. 9-2800
- fast fission factor, calc. of backscatter and interaction effects 9-20844
- fast-breeder, review of technology 9-635
- flux stability in slab reactors, applications of differential equations theory 9-9090
- fuel composition in fast power reactor, calc. 9-19352
- fuel tubes, apparatus for providing artificial defects for pressure burst tests 9-2785
- fuel-temp. coeff. in water moderated lattices 9-19360
- gas-cooled fast reactors with artificially roughened fuel elements, performance 9-19355
- irradiation facility with heavy water circulation 9-14656
- irradiation facility with pressurized water and boiling water circulation 9-14657
- IRT-2000, fast n. spectra meas. in test hole 9-20840
- kinetics, spatially dependent, with positive and varying feedback 9-19357
- L-54, Milan, pile oscillator, meas. of transfer functions 9-2783
- liquid N<sub>2</sub> lines, poor thermal insulation 9-19361
- neutron cross-section analysis, research programmes 9-20846
- neutron density control, optimization of main parameters 9-2777
- PHENIX fast reactor described 9-4816
- polyethylene meas. of  $\gamma$  volumetric absorpt. 9-661
- power control by discrimination of gamma-ray background 9-637
- pressure tubes, strain gauge for creep meas. 9-4818
- Pulse reactor transient behaviour immediately following pulse 9-20843
- RAPSODIE fast reactor described 9-4816
- reactivity meas. by rod drive method 9-655
- reactivity measurements, pulsed neutron source with and without boric acid poisoning 9-9091
- resonance absorption in lump surrounded by homogeneous medium containing same absorber 9-15798
- Rossi- $\alpha$  expt., time-dependence of uncorrelated term 9-19382
- shielding, Monte Carlo integration of adjoint  $\gamma$ -ray transport eqn 9-19356
- SPERT transient calc. rel. to accident studies in water moderated reactors 9-16980
- steam fraction dynamics eqn. with surface boiling in steam generator 9-19353
- steel rods in water reflector, fast n reflection 9-18125
- temperature and fuel element gas pressure monitoring by acoustic transducers, patent 9-6948
- thermal reactor, optimum strategy for power reduction 9-2784
- thermionic diodes outside reactor, with heat pipes, as space power supply 9-11357
- $\gamma$  penetration through heterogeneous barriers, perturbation calc. 9-20842
- n counts, reactor noise analysis 9-20845
- n flux density meas. with activation detectors. 9-641



**Nuclear reactors, fission continued****operation continued**

- n flux density meas. with semiconductor detectors 9-662  
 n flux meas. in FDR, zero power comparison of theory with expt. 9-640  
 n resonance absorption and flux spectra, epithelial in heterogeneous cells 9-19333  
 n thermalization, time-dependent 9-19359  
<sup>235</sup>U cores, moderated or unmoderated, criticality data 9-14650  
 P cores, moderated or unmoderated, criticality data 9-14650  
 X-power spatial transients, control problem in terms of dynamic programming formalism 9-16982

**theory**

- blanket optimization calcs. for steam cooled fast breeder reactor 9-20837  
 buckling, substitution meas., perturbation analysis 9-11351  
 coherence function in two-node reactor models 9-18111  
 cone optimization, max. power rel. to n flux distribution 9-15793  
 coupled core kinetics, delay-time distrib. function 9-11352  
 critical assembly, arbitrary ratio of processes, comparison of two variational principles of calc. 9-14648  
 critical reactor eqn. soln. 9-634  
 critical system, n flux ratios calc. by indirect variational method 9-18114  
 criticality problems in secant shaped reactor 9-20838  
 cruciform control rods in D-lattice, worth calc., n behaviour in transport and diff. regions method 9-19354  
 energy distribution, analysis and instrumentation 9-11370  
 equilibrium state stability in one-group diffusion approx. 9-630  
 fast, Na void reactivity effects calc. 9-15791  
 fast fission factor calc. and study, multigroup procedure for thermal reactor lattice 9-11348  
 fuel, cylindrical clad in compress. coolant, transient temps. 9-14649  
 fuel and coolant axial temp. distrib. in coolant channel 9-19344  
 GODIVA benchmark problem, soln. by solving Boltzmann integral eqn. 9-16978  
 group constants, calculation in resonance region 9-627  
 inelastic cross-section calcs for reactors 9-571  
 withintrinsic n source, iterative method for evaluation of period meas. 9-14658  
 KFZ Argonaut, coherence function determ. 9-19351  
 kinetics, modification of Liapunov's direct method due to Lasalle 9-20839  
 moderation effect on damage flux 9-20829  
 multigroup diffusion problem, steady-state, positivity theorems for discrete form 9-13262  
 multigroup diffusion theory, eigenvalue reality 9-20834  
 multiregion, asymptotic spectra, use of discontinuous overlapping groups without staggered discontinuities 9-19346  
 neutron stationary distrib. possibility 9-11354  
 nonseparable transients, calc. by variational multichannel space-time synthesis 9-11349  
 perturbation theory used to minimize fuel loading of reactors 9-631  
 point reactor prompt kinetics eqn., exact soln. 9-18119  
 ratio calc. in critical systems 9-9087  
 reactivity, negative, multiplication meas. method 9-11350  
 reactivity determ. from reactor kinetic phenomena 9-18118  
 reactivity introduced by ramp insertion including effect of delayed neutrons 9-19358  
 Schwarz-Christoffel conformal mapping of hexagon on circle, integration 9-19345  
 stability and critical case relating to reactor kinetics eqns. 9-19347  
 subcritical, n balance eqn. and const. 9-11347  
 thermal flux, distribution at channel exits, dependence on reflector arrangement 9-6933  
 three-region lattices, cladding effect on resonance absorpt. 9-11362  
 transport approximations SP<sub>i</sub> and MP<sub>2</sub>, numerical comparisons for very fast n 9-13263  
 transport eqn. solution functionals, differentiation by Monte Carlo method 9-11346  
 transport equation, solution for heterogeneous reactors, matrix form 9-632  
 two-region sphere, critical problem 9-9085  
 n diffusion in dense lattice using pulsed method 9-629  
 n flux distrib. optimization for max. power generation 9-14653  
 n spectra, epithelial, synthesis 9-14639  
 n transport systems, expansion of system to allow meas. 9-2778  
 n transport, multigroup system of integral eqns. 9-628  
 U-D<sub>2</sub>O lattice with Pu in fuel, n thermalization 9-16974  
 U-D<sub>2</sub>O lattice with Pu in fuel, n thermalization, model 9-16974

**Nuclear reactors, fusion**

- open ended high-β reactors, applic. of cusp containment theory 9-11568  
 plasma physics at Kurchatov Institute 9-21047  
 pulsed, power production study 9-11353  
 review 9-11327  
 screening of a high density plasma from neutral gas penetration 9-11569

**Nuclear relaxation** *see Nuclear magnetic resonance and relaxation***Nuclear scattering** *see Nuclear reactions and scattering***Nuclear spallation**

- hyperfragment decay lifetime meas. 9-11206  
 Fe nucleon-meson cascade initiated by 3 GeV p 9-20853  
<sup>4</sup>He emission at high energy, fluctuation mech. for cross section determ. 9-11173

**Nuclear structure** *see Nucleus/energy levels; Nucleus/theory***Nuclear track emulsions**

- cascade theory test, e obs., 180-2000 BeV 9-17946  
 energy loss by ionization, 5-24 GeV/c p and 5 GeV/c π, comparison 9-18047  
 fast neutron spectrum measurement in high gamma fluxes 9-20713  
 grain noise distrib. on relativistic tracks, obs. 9-19251  
 Ilford G-5, primary p beam exposure, scatt. const. and multiple coulomb scatt. 9-4637  
 ilford K-5, polarized p analysing power, 10-50 MeV 9-467  
 ionographic, hyperfragment prod. by 5 GeV/c antiprotons 9-20781  
 L4, charge identification of stopping part., rel. to track-width 9-2616  
 latent image destruction in electric field 9-4694  
 latent image formation by atomic H evolved from Si, Ge and other metal surfaces 9-18045  
 light nuclei, p interaction multiparticle prod. at 22.8 GeV/c 9-6693  
 multiple Coulomb scatt. of high-energy part. 9-4637  
 nuclei coherent interactions with 200 GeV pions, four momentum transfer and effective mass estimation 9-4626

**Nuclear track emulsions continued**

- optical meas. using digitized and telecontrolled cross-wire eye-piece 9-2416  
 plate, electron sensitive, prep. in lab. 9-4695  
 proton interactions at 13.8 GeV 9-19308  
 scattering factor determ. by 'angular dispersion' and 'tangent angle' methods for different cell lengths 9-20712  
 shrinkage factor, α track meas. 9-18046  
 trident detection, e<sup>+</sup>e<sup>-</sup> creation, automatic scanning device 9-18048  
 X-ray, p-ray spectrograph component, processing method 9-11161  
 α track autoradiography of submicron aerosol particles with electron microscope 9-15693  
 γ response of commercial photographic films, 0.667 to 1.25 MeV 9-15694  
 K<sup>-</sup> star charact., 3.0 GeV/c, prod. of hyperfragments and nuc. fragments 9-20639  
 N spectrometry using recoil H tracks, computer analysis of random sampling 9-2617  
 P scattering, multiple coulomb scatt. at 19.8 GeV/c 9-14537  
 Ag disintegration, by 20 GeV/c protons, analysis of stars 9-9076  
 Br disintegration in 20 GeV/c proton interac. analysis of products 9-9076

**Nuclear-solid interactions** *see Mossbauer effect; Solids***Nucleation** *see Clouds; Crystallization; Freezing***Nuclei with 150≤A**

- <sup>152</sup>Sm, γ spectra following thermal n capture 9-18066  
<sup>164</sup>Dy(n, γ) isomeric cross-section ratios, spin cut-off parameter deduced, 4 keV 9-544  
<sup>173</sup>Re, first prod. from <sup>165</sup>Ho(<sup>16</sup>O,6n) and <sup>159</sup>Tb(<sup>22</sup>Ne,6n) 9-14633  
<sup>176</sup>Re, first prod. from <sup>165</sup>Ho(<sup>16</sup>O,5n) and <sup>159</sup>Tb(<sup>22</sup>Ne,5n) 9-14633  
<sup>171</sup>Hf energy level transitions 321, 113 kev lifetimes, E1 transition prob. determ. 9-8989  
<sup>194</sup>Hg from <sup>194</sup>Tl decay, energy levels determ. from γ and conversion e spectra meas. 9-4740  
<sup>194</sup>Tl-<sup>194</sup>Hg, energy levels determ. from γ and conversion e spectra meas. 9-4740  
<sup>198</sup>Au half-life obs. 9-18083  
<sup>207</sup>Pb(t,p)<sup>209</sup>Pb 2p-1h state obs., levels below 3561 keV 9-20745  
<sup>218</sup>Po, conc. in atm., α-spectrometry meas. method 9-20092  
<sup>240</sup>Pu, reson. params. and n widths, 20-1500 eV 9-14616  
 deformed even, ground-state rot. bands, formula 9-496  
 electron shells, binding energies and vacuum polarization corrections tabulators 9-6793  
 fission thermal-n induced, fragment energy-correlation meas. 9-4812  
 low-lying level calc. using Tamm-Dancoff theories with Tabakin's realistic 2N potential 9-513  
 mass numbers 152 to 198, internal conversion K/L<sub>1</sub> ratio for E2 transitions 9-4757  
 neutron elastic scatt., cross-section for natural Pb, 10-40°, 4.56 MeV 9-2738  
 nuclei with 158≤N, spontaneous fission instability 9-4805  
 photoneutron angular distrib. anisotropy from Pa, Pt and Pb, rel. to sub-shell occupation 9-4767  
 rare-earths, rotational bands calc. model from Coriolis pair field decoupling 9-11191  
 spectroscopic factors of non rotational states, odd-A 155-181, ≤1 MeV 9-510  
 super heavy nuclei with Z>104, instability 9-551  
 superheavy nuclei, A≈298, α and spontaneous fission half-life theoretical estimate 9-14590  
 superheavy nuclei, shell corrections and deformation 9-15732  
 transuranic elements, optical anisotropy of isomers 9-2767  
 (n, 2n) cross-sections at 14.7 MeV, obs. 9-2737  
 γ internal conversion coeffs. at threshold energy for Z≤95 9-6783  
<sup>215</sup>Pu, fission cross-section measurements 9-20814  
<sup>200m</sup>Au decay of a new 18.7h isomer 9-2673  
<sup>240</sup>Am from (d,p), (d,t) reactions, cross sections meas., Ed-9-13 MeV 9-9056  
<sup>210</sup>At e p pair formation, competition between decay and K-capture 9-6833  
<sup>210</sup>At from <sup>214</sup>Fr α decay, levels determ. 9-4758  
<sup>190</sup>Au intensities, α conversion coefficient and multipolarities 9-528  
<sup>210</sup>Bi, low-lying levels and reaction matrix theory 9-11232  
<sup>210</sup>Bi, pure M1(1±) transitions, L-subshell conversion line intensity ratios 9-14570  
<sup>250</sup>Bk, n fission cross-section obs. 9-9072  
<sup>160</sup>Dy, -ve parity states, rotational band-mixing parameters determ. 9-15724  
<sup>160</sup>Dy, n diffraction meas. on Dy<sub>2</sub>O<sub>3</sub> 9-4735  
<sup>170</sup>Er, n capture, 5 keV-3 MeV 9-9042  
<sup>180</sup>Hf energy levels and internal conversion coeffs. for γ transition obs. 9-525  
<sup>208</sup>Hg, low-lying states and transitions, study by slow n capture of <sup>199</sup>Hg 9-4784  
<sup>200</sup>Hg internal conversion coeffs., high energy calc. 9-11200  
<sup>170</sup>Ho isomer, 2.9 min., from <sup>170</sup>Er(n,p) obs. decay scheme 9-14594  
<sup>150</sup>Nd(<sup>16</sup>O, <sup>16</sup>O<sup>+</sup>)<sup>2+</sup> states γ-emission ang. distrib., hyperfine interactions 9-15781  
<sup>150</sup>Nd(<sup>16</sup>O, <sup>16</sup>O<sup>+</sup>)<sup>2+</sup> g. meas. for 2<sup>+</sup> state 9-15723  
<sup>150</sup>Nd n resonances, level spacing 9-11298  
<sup>180</sup>Os, neutron deficient, decay by e capture, charact. 9-13196  
<sup>190</sup>Os muonic isomer shifts rel. to nuclear charge distrib. 9-2836  
<sup>210</sup>Pb(p,d)<sup>209</sup>Pb 2p-1h state obs., levels below 3561 keV 9-20745  
<sup>210</sup>Po, half life of 8<sup>+</sup> state and E2 core polarization 9-8992  
<sup>210</sup>Po α source, ion pair prod. energy for various gases 9-15951  
<sup>190</sup>Pt from (α, 2nγ) reaction, g.s. rotational levels rel. intensity determ., E<sub>g</sub>=19.2-31.7 MeV 9-20740  
<sup>240</sup>Pu, reons. radiative widths, n capture obs., 38-820 eV 9-9040  
<sup>240</sup>Pu, spontaneous fission, average number of prompt n per fission, rel. to <sup>252</sup>Cf 9-14635  
<sup>240</sup>Pu fission-fragment ang. distrib. after n radiation, 150-1500 keV 9-6920  
<sup>240</sup>Pu total internal conversion coeff. for E2 transitions obs. 9-2675  
<sup>150</sup>Sm polarised thermal n capture, γ circular polarisation obs. 9-13230  
<sup>160</sup>Tb, decay to levels in <sup>160</sup>Dy 9-2701  
<sup>160</sup>Tb, from <sup>159</sup>Tb(n,γ), relative K,L,M, (N+O+P) line intensities of pure E2 transitions 9-11253  
<sup>210</sup>Th, neutron reson. obs. 9-11299  
<sup>210</sup>Th total n cross section below 1 eV 9-599  
<sup>170</sup>Tm, β-γ correl. in first forbidden decay 9-15738  
<sup>170</sup>Tm, decay, form of β spectra of transitions 1<sup>-</sup>→0<sup>+</sup> 9-16948

Nuclei with  $150 \leq A$  continued

- <sup>170</sup>Tm, from <sup>169</sup>Tm( $n, \gamma$ ), relative K.L.M.(N+O) <sup>169</sup>T, (relative K.L.M.(N+O+P) line intensities of pure E2 transitions 9-11253
- <sup>180</sup>W from ( $\alpha, 2n\gamma$ ) reaction, g.s. rotational levels rel. intensity determ.,  $E_\alpha = 19.2-31.7$  MeV 9-20740
- <sup>191</sup>Os radiative n capture, transformation and annealing in crystal 9-21724
- <sup>241</sup>Am,  $\alpha$  half-life determ. from specific activity of metal solns. 9-15741
- <sup>241</sup>Am fission,  $n_{th}$  induced, long-range energy spectra meas. 9-9074
- <sup>241</sup>Am( $n, \gamma$ ) <sup>242m</sup>Am, excitation function distortion by <sup>7</sup>Li(p,n) soft-n 'impurities', 0.25-7 MeV 9-18097
- <sup>151</sup>Eu in EuFe garnet, hyperfine field interac. of 21.7 keV level from Mossbauer meas. 9-16401
- <sup>151</sup>Eu<sup>2+</sup> in BaF<sub>2</sub> and SrF<sub>2</sub>, e.p.r., hyperfine coupling constant of <sup>151</sup>Eu<sup>2+</sup>, temp. depend. 9-12502
- <sup>223</sup>Fr  $\alpha$ -decay; classification of nuclei as spherical or deformed 9-563
- <sup>161</sup>Gd  $\rightarrow$  <sup>161</sup>Tb,  $\beta$ -decay obs. 9-19297
- <sup>161</sup>Gd  $\rightarrow$  <sup>161</sup>Tb,  $\beta^-$ , 3.6 min. obs. 9-9006
- <sup>181</sup>Os, neutron deficient, decay by e capture, charact. 9-13196
- <sup>213</sup>Pa  $\rightarrow$  <sup>212</sup>Ac, levels, transitions, rotational structure determ. from  $\gamma$  spectra 9-14579
- <sup>151</sup>Pm, from <sup>151</sup>Nd  $\gamma$ -decay, energy levels obs. 9-518
- <sup>241</sup>Pu, fission,  $n_{th}$  induced, long-range  $\alpha$  energy spectra meas. 9-9074
- <sup>241</sup>Pu, lifetime mass-spectrometric obs. 9-4759
- <sup>241</sup>Pu, monitoring, liq. scintillation technique 9-18082
- <sup>241</sup>Pu, number of n per fission, recommended value 9-14637
- <sup>241</sup>Pu cross section meas. 1-30 eV spin assignments for 2-32eV resonances 9-4781
- <sup>241</sup>Pu cross section meas. 1-30 eV, spin assignments for 2-32 eV resonances 9-4781
- <sup>241</sup>Pu  $\alpha$ -decay,  $\gamma$  and  $\alpha$ -part. transition energies and intensities, applic. to <sup>237</sup>U energy levels and half-life meas. 9-6815
- <sup>121</sup>Sn fission product, separation and half-life determ. 9-11335
- <sup>181</sup>Ta, search for parity mixing in 482 keV state 9-19279
- <sup>181</sup>Ta recoilless resonance absorpt. and hyperfine struct. 62 keV Mossbauer effect 9-526
- <sup>181</sup>Ta( $\alpha, \alpha'$ ), ang. and energy distrib. meas., spectra evaporation component,  $E_\alpha = 50-90$  MeV 9-13238
- <sup>181</sup>Ta( $\gamma, xn$ )  $x=1-4$ , cross sections meas.,  $E_\gamma \leq 30$  MeV 9-11271
- <sup>181</sup>Ta( $n, 2n$ ) <sup>180m</sup>Ta,  $E_n = 12.2-17.9$  MeV 9-15765
- <sup>181</sup>Ta( $n, \gamma$ ) <sup>182</sup>Ta, excitation curves meas.,  $E_n = 0.03-5.1$  MeV 9-15765
- <sup>181</sup>Ta( $n, p$ ) <sup>181</sup>Hf,  $E_n = 13.2-17.5$  MeV 9-15765
- <sup>181</sup>Ta( $n, p$ ) <sup>181</sup>Hf, excitation curve, 13-17.5 MeV 9-20797
- <sup>161</sup>Tb, obs. in <sup>161</sup>Gd  $\rightarrow$  <sup>161</sup>Tb,  $\beta$  decay 9-19297
- <sup>161</sup>Tb  $\rightarrow$  <sup>161</sup>Dy,  $\beta^-$ , 6.9 days obs. 9-9006
- <sup>171</sup>Tm, ground state,  $K=1/2$ , rotational bands 9-2670
- <sup>171</sup>Yb, half lives of intrinsic states, transition probability to ground state 9-8985
- <sup>171</sup>Yb, isobaric analogue states, Coulomb displacement energies 9-6807
- <sup>232</sup>Th fission, n induced, prob. of long-range  $\alpha$  prod. meas. 9-9073
- <sup>242</sup>Am from (d,p), (d,t) reactions, cross sections meas.,  $E_d = 9-13$  MeV 9-9056
- <sup>192</sup>Au intensities,  $\alpha$ , conversion coefficient and multipolarities 9-528
- <sup>212</sup>Bi, pure M1( $l=0$ ) transitions, L-subshell conversion line intensity ratios 9-14570
- <sup>212</sup>Bi decay, high energy  $\gamma$ -radiation 9-11254
- <sup>252</sup>Cf, fission, average number of n per fission 9-14636
- <sup>252</sup>Cf, n source, design data for available flux and shielding requirements 9-14634
- <sup>252</sup>Cf, number of n per fission, absolute determ. 9-14637
- <sup>252</sup>Cf, ternary fission, three-point-charge model 9-13246
- <sup>252</sup>Cf as neutron source 9-2692
- <sup>252</sup>Cf fission, spontaneous, statistical model, n energy calc. 9-621
- <sup>252</sup>Cf nuclear fission,  $\gamma$  radiation analysis, spectra meas. 9-6923
- <sup>242</sup>Cm and <sup>244</sup>Cm prod. in <sup>241</sup>Am( $n, \gamma$ ) 9-2747
- <sup>192</sup>Hg from <sup>191</sup>Tl decay, energy levels determ. from  $\gamma$  and conversion e spectra meas. 9-4740
- <sup>182</sup>Os, neutron deficient, decay by e capture charact. assoc. with positron group 9-13196
- <sup>192</sup>Os energy levels, e.m. moment calc. from pairing-plus-quadrupole model 9-15702
- <sup>192</sup>Os muonic isomer shifts rel. to nuclear charge distrib. 9-2836
- <sup>212</sup>Po, multipolar character. of transitions rel. to low energy  $\gamma$ -radiation of <sup>232</sup>Th decay. 9-13212
- <sup>242</sup>Pu, spontaneous fission, average number of prompt n per fission, rel. to <sup>252</sup>Cf 9-14635
- <sup>242</sup>Pu resonances, fission components 9-16969
- <sup>252</sup>Sm, K-conversion particle parameters for E2 transitions 9-14572
- <sup>252</sup>Sm muonic isomer shifts rel. to nuclear charge distrib. 9-2836
- <sup>182</sup>Ta, from <sup>181</sup>Ta( $n, \gamma$ ), relative K.L.M.(N+O+P) line intensities 9-11253
- <sup>182</sup>Ta, total n cross-section, 0.01 to 1000 eV, resonance parameters 9-19312
- <sup>182</sup>Ta 0.3 sec. isomeric transition multipolarity, M2 determ. by L X-ray pattern 9-527
- <sup>162</sup>Tb decay, investigation of  $\beta$  and  $\gamma$  radiations 9-2702
- <sup>212</sup>Th,  $\beta$  spectrum conversion line energies, obs. 9-2696
- <sup>212</sup>Th cumulative fission yield, fine structure in symmetric mass region 9-11333
- <sup>232</sup>Th Mossbauer effect following Coulomb excitation 9-4742
- <sup>232</sup>Th resonance absorpt., influence of scatt. interference 9-9093
- <sup>232</sup>Th study of induced fission fragments 9-2772
- <sup>232</sup>Th(p,f) fragments mass and energy distrib. meas.,  $E_p = 13.53$  MeV 9-16970
- <sup>192</sup>Tl  $\rightarrow$  <sup>192</sup>Hg energy levels determ. from  $\gamma$  and conversion e spectra meas. 9-4740
- <sup>182</sup>W, 1694.5 keV level, from <sup>182</sup>Ta decay obs. 9-6834
- <sup>182</sup>W from ( $\alpha, 2n\gamma$ ) reaction, g.s. rotational levels rel. intensity determ.,  $E_\alpha = 19.2-31.7$  MeV 9-20740
- <sup>182</sup>W muonic isomer shifts rel. to nuclear charge distrib. 9-2836
- <sup>172</sup>Yb, vib. levels and two-quasi-particle levels, exp. study 9-4737
- <sup>172</sup>Yb cascade decay, levels determ., ang. correlation meas. computer program and automatic control 9-20743
- <sup>172</sup>Yb from <sup>172</sup>Lu decay, sign of  $\delta$  for E2+M1 multipole mixture 9-561
- <sup>243</sup>Am lifetime, comparison of coulombic and mass-spectrometric obs. 9-4760
- <sup>253</sup>Cf  $\rightarrow$  <sup>249</sup>Cm,  $\alpha$ -decay spectra, energy and intensity meas. 9-11251
- <sup>193</sup>Eu, rotational level, 83.4 keV, magnetic moment and charge radius 9-6792
- <sup>151</sup>Eu in SmFe<sub>2</sub>, Sm<sub>2</sub>Co<sub>17</sub>, Sm<sub>2</sub>Ni<sub>17</sub>, hyperfine interac. 9-14040

Nuclei with  $150 \leq A$  continued

- <sup>153</sup>Eu nuclear rotation and single particle excitation effects on X-ray spectrum 9-11432
- <sup>163</sup>Fr, from <sup>163</sup>Tm decay, three quasiparticle levels search 9-520
- <sup>193</sup>Ir from <sup>193</sup>Os, energy levels deduced from  $\gamma$ - $\gamma$  coinc. meas. 9-11229
- <sup>193</sup>Os  $\gamma_2$ -[505] isomeric state found 9-19280
- <sup>193</sup>Os  $\rightarrow$  <sup>193</sup>Ir energy levels deduced from  $\gamma$ - $\gamma$  coinc. meas. 9-11229
- <sup>233</sup>Pa, K.L.L. Auger spectra, obs. in  $\beta$ -decay 9-2817
- <sup>233</sup>Pa, rapid determ. and chem. yield 9-21742
- <sup>203m</sup>Pb  $\rightarrow$  <sup>203</sup>Pb decay spectra and M4 transition obs. 9-6809
- <sup>233</sup>Pu, n fission cross-section obs. 9-9072
- <sup>223</sup>Ra, energy level transitions from internal conversion obs. in  $\alpha$ -decay of <sup>223</sup>Th 9-6812
- <sup>123m</sup>Sn fission product, separation and half-life determ. 9-11335
- <sup>203</sup>Tl, 279, 404 keV transitions,  $\alpha$  obs. 9-15726
- <sup>203</sup>Tl, K-conversion coeff. of 279 keV level, obs. 9-20744
- <sup>203</sup>Tl, single-hole collective model, energy spectra, e.m. transition probs. calc. 9-18067
- <sup>203</sup>Tl 279 keV level lifetime meas. by delayed e-c coincidence spectrometer 9-2563
- <sup>203</sup>Tl muonic, nuclear  $\gamma$  ray mag. hyperfine splitting 9-2837
- <sup>233</sup>U, fission cross-section measurements 9-20814
- <sup>233</sup>U, half-life by specific activity methods 9-20759
- <sup>233</sup>U, neutron fission and capture cross-sections, 0.4 to 2000eV 9-13247
- <sup>233</sup>U, number of n per fission, recommended value 9-14637
- <sup>233</sup>U, thermal neutron induced, K emission obs. 9-20816
- <sup>233</sup>U cross section meas. 1-30 eV 9-4781
- <sup>233</sup>U fission, n-induced, prob. of long-range  $\alpha$  prod. meas. 9-9073
- <sup>233</sup>U thermal fission products, time var. of mean  $\beta$  activity 9-11338
- <sup>172</sup>Yb, isobaric analogue states, Coulomb displacement energies 9-6807
- <sup>194</sup>Ir  $\rightarrow$  <sup>194</sup>Pt,  $\gamma$  spectra obs., intensity meas.,  $E_\gamma \leq 1.4$  MeV 9-15739
- <sup>244</sup>Am from (d,p), (d,t) reactions, cross sections meas.,  $E_d = 9-13$  MeV 9-9056
- <sup>244</sup>Bi conc. in atm.,  $\alpha$ -spectrometry meas. method 9-20092
- <sup>244</sup>Cf  $\alpha$ -decay spectra, energy and intensity meas. 9-11251
- <sup>244</sup>Cm,  $\alpha$  half-life 9-15742
- <sup>244</sup>Cm, central reactivity contrib. of gram-sized sample to bare Pu critical assembly 9-19370
- <sup>164</sup>Er, 4<sup>+</sup> ground state levels, mean lifetimes obs. 9-519
- <sup>164</sup>Er from <sup>164</sup>Tm  $\gamma$  transition;  $I^\pi = 0^+$ ,  $K=0$  levels determ. 9-521
- <sup>164</sup>Er from ( $\alpha, 2n\gamma$ ) reaction, g.s. rotational levels rel. intensity determ.,  $E_\alpha = 19.2-31.7$  MeV 9-20740
- <sup>244</sup>Es, n fission cross-section obs. 9-9072
- <sup>244</sup>Es, n fission cross-section obs. 9-9072
- <sup>154</sup>Eu decay, e spectroscopy studies 9-2700
- <sup>154</sup>Eu  $\rightarrow$  <sup>154</sup>Gd, E0 transitions, conversion coeff. determ. from  $\gamma$  spectra meas. 9-13210
- <sup>244</sup>Er  $\alpha$  decay from ground and isomeric states lifetimes determ. 9-4758
- <sup>144</sup>Gd, 692KeV level  $2^{1+} \rightarrow 2^{1+} \rightarrow 0^+$  cascade obs., transition pure E2 9-11226
- <sup>144</sup>Gd, K-conversion particle parameters for E2 transitions 9-14572
- <sup>144</sup>Gd from <sup>154</sup>Eu decay, E0 transitions, conversion coeff. determ. from  $\gamma$  spectra meas. 9-13210
- <sup>144</sup>Gd from ( $\alpha, 2n\gamma$ ) reaction, g.s. rotational levels rel. intensity determ.,  $E_\alpha = 19.2-31.7$  MeV 9-20740
- <sup>144</sup>Gd from Eu isotopes decay,  $\gamma$  spectra obs., energy levels determ. 9-4734
- <sup>144</sup>Gd Ke intensities, evidence for new  $O^+$  9-2668
- <sup>214</sup>Pb conc. in atm.,  $\alpha$ -spectrometry meas. method 9-20092
- <sup>214</sup>Pc,  $\gamma$  spectra, 1.1 to 3.3 MeV, 4.5 keV resolution 9-13211
- <sup>214</sup>Pr, pure M1( $l=0$ ) transitions, L-subshell conversion line intensity ratios 9-14570
- <sup>194</sup>Pt from <sup>194</sup>Ir,  $\gamma$  spectra obs., intensity meas.,  $E_\gamma \leq 1.4$  MeV 9-15739
- <sup>244</sup>Pu <sup>135</sup>Xe decay intervals of chondrite dark phases 9-2061
- <sup>234</sup>Ra total internal conversion coeff. for E2 transitions obs. 9-2675
- <sup>153</sup>Sm ( $^{146}, ^{161} \text{O}^+$ )  $\gamma$   $2^+$  states  $\gamma$  emission ang. distrib., hyperfine interactions 9-15781
- <sup>234</sup>U Energy levels from  $\beta$ -decay of <sup>234</sup>Pa (UZ) 9-2678
- <sup>234</sup>U fission components for resonances 9-2768
- <sup>234</sup>U total internal conversion coeff. for E2 transitions obs. 9-2675
- <sup>184</sup>W, energy levels, e.m. moment calc. from pairing-plus-quadrupole model 9-15702
- <sup>184</sup>W energy levels determ. from radiative n capture meas. 9-18096
- <sup>184</sup>W muonic isomer shifts rel. to nuclear charge distrib. 9-2836
- <sup>184</sup>W( $n, p$ ), l-resonances spectra anal., level schemes determ.,  $E_n = 7-360$  eV 9-18096
- <sup>225</sup>Ac  $\alpha$ -decay; classification of nuclei as spherical or deformed 9-563
- <sup>245</sup>Cm, n fission cross-section obs. 9-9072
- <sup>165</sup>Dy, energy levels calc. from decay scheme after radiative capture 9-522
- <sup>165</sup>Er 242.8 keV energy level lifetime meas. from <sup>165</sup>Im decay 9-11227
- <sup>173</sup>Gd<sup>4+</sup> in ThO<sub>2</sub>, hyperfine coupling constant, temp. dependence 9-8031
- <sup>173</sup>Hf  $\rightarrow$  <sup>173</sup>Lu decay, L-Auger spectrum, line energy and intensities, fluorescence yields 9-9007
- <sup>165</sup>Ho, 1/2 + [411 spin down] and 3/2 + [411 spin up] bands 9-20742
- <sup>165</sup>Ho, magnetic dipole transitions, reduced probabilities 9-523
- <sup>173</sup>Lu,  $\gamma$ - $\gamma$  angular correlations in 89-343, 161-343 KeV 9-4738
- <sup>173</sup>Lu, n capture cross section, 5 keV, 3 MeV 9-9042
- <sup>165</sup>Mo( $\gamma, xn$ )  $x=1-3$ , cross sections meas.,  $E_\gamma \leq 30$  MeV 9-11271
- <sup>235</sup>Pa, prod. and decay props. 9-16963
- <sup>185</sup>Re and <sup>187</sup>Re in ReO<sub>3</sub>, NMR, Knight shift and spin relax. rates 9-12512
- <sup>155</sup>Sm,  $\beta$  decay, half-life,  $\gamma$  energies and intensities, <sup>155</sup>Eu deduced levels 9-16949
- <sup>125</sup>Sn fission product, separation and half-life determ. 9-11335
- <sup>205</sup>Tl, single-hole collective model, energy spectra, e.m. transition probs. calc. 9-18067
- <sup>205</sup>Tl muonic, nuclear  $\gamma$  ray mag. hyperfine splitting 9-2837
- <sup>235</sup>U, graphite critical assemblies, leakage anal. and cross-sections 9-18122
- <sup>235</sup>U, central reactivity contrib. of gram-sized sample to bare Pu critical assembly 9-19370
- <sup>235</sup>U, fission cross-section measurements 9-20814
- <sup>235</sup>U, induced by 14.8 MeV n, mass spectra of fragments meas. 9-15786
- <sup>235</sup>U,  $\gamma$  anisotropy obs., slow in fission 9-2775
- <sup>235</sup>U, mass and energy distrib. of fission fragments up to 15.5 MeV 9-2774
- <sup>235</sup>U, minimum enrichment of U cylinders, rel. to criticality 9-9096
- <sup>235</sup>U, number of n per fission, recommended value 9-14637
- <sup>235</sup>U asymmetric fis. by  $n_{th}$ , dynamic 9-6921



Nuclei with  $150 \leq A$  continued

- <sup>235</sup>U cross section meas. 1-30 9-4781  
<sup>235</sup>U fission, <sup>84</sup>Se decay characteristics determ. by  $\beta$ ,  $\gamma$  spectra meas. 9-19300  
<sup>235</sup>U fission, n induced, prob. of long-range  $\alpha$  prod. meas. 9-9073  
<sup>235</sup>U fission, spontaneous, statistical model, n energy calc. 9-621  
<sup>235</sup>U fission cross section, n induced, autocorrelation effects 9-2770  
<sup>235</sup>U fission two dims. of  $p$  quantita anisotropy on kinetic energy 9-626  
<sup>235</sup>U fission,  $n_{th}$  irradiated, <sup>83,84</sup>As identification and half-life determ. 9-20813  
<sup>235</sup>U thermal fission products, time var. of mean  $\beta$  activity 9-11338  
<sup>185</sup>W, 1.7 min. isomer identification and obs. from decay studies 9-16941  
<sup>185</sup>W energy levels determ. from radiative n capture meas. 9-18096  
<sup>175</sup>Yb, isobaric analogue states, Coulomb displacement energies 9-6807  
<sup>186</sup>Pt energy levels, e.m. moment calc. from pairing-plus-quadrupole model 9-15702  
<sup>166</sup>Er, E1 transition  $\gamma$  polarization meas., level parity determ. 9-14573  
<sup>166</sup>Er from <sup>166</sup>Tm decay, energy levels, spin and parity assigned 9-2704  
<sup>156</sup>Eu from <sup>156</sup>Sm decay, lifetimes of excited states determ. 9-559  
<sup>156</sup>Gd,  $g$ -factors and multipole mixing ratios 9-6804  
<sup>156</sup>Hg from <sup>196</sup>Tl decay, energy levels determ. from  $\gamma$  and conversion e spectra meas. 9-4740  
<sup>166</sup>Ho,  $\beta$ ,  $\gamma$  ang. correl.  $P_1(\cos \theta)$  depend. 9-6844  
<sup>166</sup>Ho,  $\beta$ ,  $\gamma$  ang. correlation obs., attenuation for solid, liquid HoCl<sub>3</sub> compared 9-560  
<sup>166</sup>Ho, from <sup>165</sup>Ho(n, $\gamma$ ), relative K,L,M,(N+O+P) line intensities of pure E2 transitions 9-11253  
<sup>166</sup>Ho, from <sup>165</sup>Ho(n, $\gamma$ ), relative M line intensities in pure E2 transitions 9-6838  
<sup>166</sup>Ho,  $\gamma$ ,  $\gamma$  correlation, temp. effect obs. in crystals of lanthanum ethyl sulfate 9-19298  
<sup>166</sup>Ho, pure M1(1 $\pm$ 0) transitions, L-subshell conversion line intensity ratios 9-14570  
<sup>166</sup>Ho-<sup>166</sup>Er, E1 transition  $\gamma$  polarization meas., level parity determ. 9-14573  
<sup>176</sup>Lu-<sup>176</sup>Hf, half life determ. by  $\beta$ ,  $\gamma$  coincidence methods 9-9008  
<sup>176</sup>Lu(n, $\gamma$ )/<sup>176</sup>Lu, internal conversion electron spect. 9-2745  
<sup>186</sup>Os from <sup>186</sup>Re decay,  $\beta$  spectra of 1 $\rightarrow$ 2 $^{+}$  transition obs. 9-14575  
<sup>238</sup>Pa, prod. and decay props. 9-16963  
<sup>206</sup>Pb, muonic X-rays, weak transitions, meas., nuc. polarization by  $\mu$  9-17009  
<sup>198</sup>Pt giant, dipole-resonance abs., radiative strength function at n binding energy 9-2671  
<sup>186</sup>Re  $\beta$ -decay, use of CVC theory, superfluid corrections 9-6839  
<sup>186</sup>Re decay, form of  $\beta$  spectra of transitions 1 $\rightarrow$ 0 $^{+}$  9-16948  
<sup>186</sup>Re-<sup>186</sup>Os,  $\beta$  spectra of 1 $\rightarrow$ 2 $^{+}$  transition obs. 9-14575  
<sup>238</sup>Ru low activity source in monitor film badges calibration apparatus 9-20756  
<sup>156</sup>Sm-<sup>156</sup>Eu, lifetimes of excited states determ. 9-559  
<sup>196</sup>Tl-<sup>196</sup>Hg energy levels determ. from  $\gamma$  and conversion e spectra meas. 9-4740  
<sup>206</sup>Tl, na and p-hole states investigated by <sup>208</sup>Pb (d, $\alpha$ )/<sup>206</sup>Tl 9-19281  
<sup>166</sup>Tm-<sup>166</sup>Er decay scheme obs., energy levels, spin and parity assigned 9-2704  
<sup>236</sup>U, fission, low-energy, moment of inertia at saddle point 9-4807  
<sup>236</sup>U, intermediate structure dependence of fission probability on excitation energy 9-619  
<sup>236</sup>U, n capture rate determ. from  $p$ - $\gamma$  coinc. meas. of <sup>237</sup>U decay 9-11339  
<sup>236</sup>U, ternary fission, three-point-charge model 9-13246  
<sup>236</sup>U fission, light nuclei energy distrib. calc. 9-15785  
<sup>236</sup>U total internal conversion coeff. for E2 transitions obs. 9-2675  
<sup>186</sup>W muonic isomer shifts rel. to nuclear charge distrib. 9-2836  
<sup>175</sup>Yb, n capture cross section, 5 keV-3 MeV 9-9042  
<sup>207</sup>Pb, p, inelastic scatt. and neutron hole excitation at 20.2 MeV 9-530  
<sup>227</sup>Ac from <sup>231</sup>Pa decay; levels, transitions, rotational structure from  $\gamma$  spectra meas. 9-14579  
<sup>197</sup>Au, capture cross-section in keV energy region 9-20789  
<sup>197</sup>Am lifetime and cross-section for reactor n scatt. 9-9009  
<sup>197</sup>Au( $\alpha$ ,  $\alpha'$ ), ang. and energy distrib. meas., spectra evaporation component,  $E_a=50-90$  MeV 9-13238  
<sup>197</sup>Au(n, $\gamma$ )/<sup>198</sup>Au, obs. on  $p$  9-2746  
<sup>247</sup>Cm, n fission cross-section obs. 9-9072  
<sup>177</sup>Hf from <sup>177</sup>Lu decay, internal conversion studies of 113 keV transition 9-524  
<sup>177</sup>Hf(n,e)-<sup>178</sup>Hf,  $\gamma$  transitions in range 70-200 keV 9-16939  
<sup>177</sup>Hf(n, $\gamma$ )/<sup>178</sup>Hf, levels determ. from  $\gamma$  spectra meas.  $E_n=0.06-8.8$  eV 9-13195  
<sup>177</sup>Lu,  $\beta$ ,  $\gamma$  transitions obs. 9-15725  
<sup>237</sup>Np, Mossbauer effect, 77°K 9-13198  
<sup>237</sup>Np thin layer prep. methods for neutron detectors and  $\alpha$ -counters 9-13158  
<sup>207</sup>(p,p'), Robson analogue theory, appl. to ground state of <sup>208</sup>Pb 9-18092  
<sup>237</sup>Pa, prod. and decay props. 9-16963  
<sup>207</sup>Pb, excitation curves measured to the 7/2 $^{+}$ , 5/2 $^{+}$  doublet 9-8991  
<sup>207</sup>Pb angular correl. data meas. with Ge(Li) detector 9-16922  
<sup>207</sup>Pb particle vibration coupling 9-6810  
<sup>207</sup>Pb(n,p), <sup>208</sup>Pb levels determ.,  $E_n=15-60$  keV 9-18068  
<sup>207</sup>Pb(n,p), n capture, asymmetry in 43 keV resonance,  $E_n=15-60$  keV 9-18068  
<sup>177</sup>Re, neutron deficient, decay charact., positron emitter 9-13196  
<sup>187</sup>Re-<sup>187</sup>W,  $\gamma$  angular correlation meas., spin values determ. 9-20766  
<sup>227</sup>Th-<sup>223</sup>Ra, internal conversion obs. rel. to <sup>223</sup>Ra energy level transitions 9-6812  
<sup>237</sup>Th(n,f), fission fragment distribution, near threshold 9-2769  
<sup>237</sup>U, quantitative determ. of fallout sample, Chinese nuc. test 28 Dec 1966 9-6082  
<sup>237</sup>U energy levels, half-life meas. from coincidence studies 9-6815  
<sup>187</sup>W energy levels determ. from radiative n capture meas. 9-18096  
<sup>187</sup>W from <sup>187</sup>Re decay,  $\gamma$  angular correlation meas. 9-20766  
<sup>175</sup>Yb, isobaric analogue states, Coulomb displacement energies 9-6807  
<sup>208</sup>Pb, cosmic ray interaction, evaporation n energy spectra obs., detection method 9-20809  
<sup>208</sup>At decay scheme calc. from spectroscopy 9-531  
<sup>198</sup>Au, longitudinal depolarization of  $\beta$ -particles in source 9-15740  
<sup>198</sup>Au electron flux spectra in Al 9-18571  
<sup>198</sup>Au evidence for a 130ns isomeric state 9-2672  
<sup>198</sup>Au first-forbidden  $\beta$  transitions, nuc. matrix elements parameters, agree with single part. predictions 9-2705  
<sup>198</sup>Au in activated Au-Pb alloy,  $\beta$ -decay angular spectra rel. to interstitial sites 9-3332

Nuclei with  $150 \leq A$  continued

- <sup>198</sup>Au(n,  $\gamma$ ) transition strengths to final states, 0.2-1.2 MeV obs., 10-60 keV 9-529  
<sup>198</sup>Au(p, <sup>198</sup>N) new isotope identified, 3 GeV 9-506  
<sup>198</sup>Au(p, <sup>210</sup>N) new isotope identified, 3 GeV 9-506  
<sup>138</sup>Ba from <sup>137</sup>Ba(n, $\gamma$ ), energy level determ. from  $\gamma$  spectra obs. 9-6881  
<sup>206</sup>Bi isobaric analogue resonance 0 $^{+}$  state, cac. of  $p$  decay width 9-11231  
<sup>152</sup>Dy, 4 $^{+}$  ground state levels, mean lifetimes obs. 9-519  
<sup>158</sup>Er decay scheme 9-11252  
<sup>158</sup>Gd, n capture cross section, 5 keV-3 MeV 9-9042  
<sup>178</sup>Hf, spin assignment of n resonances, from captured  $\gamma$  data 9-2662  
<sup>178</sup>Hf from <sup>177</sup>Hf(n, $\gamma$ ), levels determ. from  $\gamma$  spectra meas.,  $E_n=0.06-8.8$  eV 9-13195  
<sup>178</sup>Hf subjected to excitation at (n,e-) reaction, 70-2000 keV 9-16939  
<sup>178</sup>Hg 411 keV. level lifetime meas. by delayed e-e coincidence spectrometer 9-2563  
<sup>198</sup>Hg E2 transitions, 2' $\rightarrow$ 0, 2' $\rightarrow$ 2 obs. 9-20684  
<sup>198</sup>Hg from <sup>198</sup>Tl decay, energy levels determ. from  $\gamma$  and conversion e spectra meas. 9-4740  
<sup>198</sup>Hg low-pressure discharge, photon correlation meas. 9-9339  
<sup>158</sup>Ho energy levels from <sup>158</sup>Er decay 9-11252  
<sup>188</sup>Os muonic isomer shifts rel. to nuclear charge distrib. 9-2836  
<sup>238</sup>Pa, prod. and decay props. 9-16963  
<sup>208</sup>Pb, form factor of real symmetry potential, depend. on n-p interaction strength 9-6822  
<sup>208</sup>Pb, particle-hole excitations, RPA calc. on collective 3 $^{-}$  state, sum of searable interac. tech. 9-8961  
<sup>208</sup>Pb,  $\pi$ ,  $\pi$  absorption and diffraction cross section meas.,  $E_n=3.5$  GeV/c 9-9051  
<sup>208</sup>Pb, single-particle analog reson., total widths and reson. energies, analog in <sup>209</sup>Bi 9-14577  
<sup>208</sup>Pb and neighbouring nuclei, single-particle core-excitation coupling calc. 9-16942  
<sup>208</sup>Pb fast calc. using spherical Hartree-Fock technique 9-11230  
<sup>208</sup>Pb fission,  $p$  radiation at 450 MeV, cross section, recoil props., charge distrib. for A=111 products 9-20818  
<sup>208</sup>Pb ground state analogue using Robson theory on <sup>207</sup>Pb(p,p') reaction 9-18092  
<sup>208</sup>Pb levels populated in decay of <sup>208</sup>Tl 9-13197  
<sup>208</sup>Pb shell model 9-6811  
<sup>208</sup>Pb( $\alpha$ ,  $\alpha'$ ), ang. and energy distrib. meas., spectra evaporation component,  $E_a=50-90$  MeV 9-13238  
<sup>208</sup>Pb(d,d), <sup>208</sup>Pb study at energies above and below Coulomb barrier 9-18100  
<sup>208</sup>Pb(d,p), <sup>209</sup>Pb study at energies above and below Coulomb barrier 9-18100  
<sup>208</sup>Pb(u,n) photonuclear total cross section determ. 9-15645  
<sup>208</sup>Pb(p,p), elastic and inelastic, cross sections and polarization, 155 MeV 9-20780  
<sup>208</sup>Po, energy levels determ. from  $\gamma$  spectroscopy 9-531  
<sup>238</sup>Pu, neutron-induced fission, angular anisotropy 9-20817  
<sup>178</sup>Re, neutron deficient, decay charact., positron emitter 9-13196  
<sup>186</sup>Re decay, form of  $\beta$  spectra of transitions 1 $\rightarrow$ 0 $^{+}$  9-16948  
<sup>186</sup>Re-<sup>186</sup>Os,  $\beta$  spectra of 1 $\rightarrow$ 2 $^{+}$  transition obs. 9-14575  
<sup>186</sup>Re  $\beta$ -decay, use of CVC theory, superfluid corrections 9-6839  
<sup>128</sup>Sn fission product, separation, half-life determ. and  $\gamma$ -ray energies 9-11335  
<sup>228</sup>Th and <sup>226</sup>Ra,  $\alpha$ ,  $\alpha$  ang. correl of serial decay 9-6840  
<sup>228</sup>Th-<sup>232</sup>Po decay, low energy  $\gamma$ -radiation rel. to multipolar character of <sup>212</sup>Po 9-13212  
<sup>228</sup>Th total internal conversion coeff. for E2 transitions obs. 9-2675  
<sup>198</sup>Tl-<sup>198</sup>Hg energy levels determ. from  $\gamma$  and conversion e spectra meas. 9-4740  
<sup>238</sup>U, <sup>20</sup>Ne  $\rightarrow$  Po, At isotopes in fission fragments, yields meas. 9-6922  
<sup>238</sup>U, <sup>40</sup>Ar  $\rightarrow$  Po, At isotopes in fission fragments, yields meas. 9-6922  
<sup>238</sup>U, absolute radiative capture cross-sections for n energies 25 to 500 keV 9-11300  
<sup>238</sup>U, charge distribution in symmetric fission by 450 MeV  $p$  9-13252  
<sup>238</sup>U, fission, by 0.8-3.4 MeV neutrons, angular anisotropy 9-13248  
<sup>238</sup>U, fragment temp. determ. after bombard. with 6.1 MeV n 9-11329  
<sup>238</sup>U, n scatt., ang. distrib. obs.,  $E_n=14$  MeV 9-15768  
<sup>238</sup>U, spontaneous-fission decay const. determ. 9-4806  
<sup>238</sup>U, symmetric fission by  $p$ , recoil study of isobaric products with A=103 and 111 9-13253  
<sup>238</sup>U cumulative fission yield, fine structure in symmetric mass region 9-11333  
<sup>238</sup>U electrofission cross section calc. 9-14638  
<sup>238</sup>U fission, n induced, prob. of long-range  $\alpha$  prod. meas. 9-9073  
<sup>238</sup>U fission after  $p$  2.2 GeV irradiation products ang. distrib. and range determ. 9-4810  
<sup>238</sup>U fission in isolated low-enriched rods, calc. 9-11364  
<sup>238</sup>U fuel lattice, resonance absorpt. rel. to cladding of Al, Zr or Fe 9-11362  
<sup>238</sup>U in UC, fabrication of stabilized compacts 9-20847  
<sup>238</sup>U n capture cross section, calc. from statistical reons., 4-80 keV 9-14614  
<sup>238</sup>U resonance absorpt., influence of scatt. interference 9-9093  
<sup>238</sup>U $^{4+}$  in CaF<sub>2</sub>, ultrasonic endor, absorption line broadening by superhyperfine interaction 9-15209  
<sup>238</sup>U( $\gamma$ ,f), f ang. distrib. meas., K-level energy determ.,  $E_\gamma=5.4-9$  MeV 9-15784  
<sup>238</sup>u(n,Zn)<sup>237</sup>u, as fast n flux monitor in TRIGA-II reactor 9-6934  
<sup>238</sup>U(n,p),  $\gamma$  spectra obs., decay scheme determ. 9-15769  
<sup>238</sup>u(n,p)-<sup>239</sup>Np, as thermal n flux monitor in TRIGA-II reactor 9-6934  
<sup>238</sup>U(n,n) differential cross section meas., analysis and comparison with optical model,  $E_n=14.7$  MeV 9-6876  
<sup>178</sup>W from ( $\alpha$ ,2np) reaction, g.s. rotational levels rel. intensity determ.,  $E_n=19.2-31.7$  MeV 9-20740  
<sup>199</sup>Au, decay obs. with 4 $\pi$  spectrometer 9-562  
<sup>209</sup>Bi, photofission, fragment yields and mass yield curve 9-13249  
<sup>209</sup>Bi, single-particle analog reson., total widths and reson. energies obs. 9-14577  
<sup>209</sup>Bi radiative neutron capture cross sections 9-6886  
<sup>199</sup>Hg, slow n capture and conversion e spectrum, comparison with theory 9-4784  
<sup>237</sup>Np, quantitative determ. of fallout sample, Chinese nuc. test 28 Dec, 1966 9-6082  
<sup>189</sup>Os, 36.2 keV level, lifetime and mag. moment 9-14576  
<sup>189</sup>Os, 69.6 keV level, spin 5/2 $^{-}$ , mag. and quadrupole moments 9-8990  
<sup>189</sup>Os 69.6 keV  $\gamma$ 's obs. at 4.2°K, half life, mag. moment determ. 9-4739

Nuclei with  $150 \leq A$  continued

- <sup>209</sup>Pb, <sup>208</sup>Pb(t,d) zero range DWBA cross section normalisation coeff.,  $E_t=8.85$  MeV 9-2760  
<sup>219</sup>Pu, fission by resonance neutrons, effective cross-section meas. at high resolution 9-9075  
<sup>219</sup>Pu, in urine, a year's sampling 9-20073  
<sup>239</sup>Pu, number of n per fission, recommended value 9-14637  
<sup>239</sup>Pu, ternary thermal neutron induced emission of Li, Be, B, C obs. 9-15783  
<sup>239</sup>Pu bare critical assembly, central reactivity contribs. of gram-sized samples of <sup>241</sup>Cm, <sup>239</sup>Pu and <sup>235</sup>U 9-19370  
<sup>239</sup>Pu thermal fission products, time var. of mean  $\beta$  activity 9-11338  
<sup>239</sup>Re neutron deficient, decay be e capture, character. 9-13196  
<sup>239</sup>Th fission prod. yield of 46 isotopes, fine structure in A=134, 140 and 144 obs. 9-11330  
<sup>169</sup>Tm, ground state,  $K=1/2$ , rotational bands 9-2670  
<sup>169</sup>Tm,  $K=1/2$  rotational band, e.m. props. 9-14574  
<sup>169</sup>Tm(n,p), <sup>170</sup>Tm radiative transitions intensities and resonance widths obs. up to 136 eV 9-4783  
<sup>219</sup>U from <sup>238</sup>U(n,p), energy levels determ. from  $\gamma$  spectra obs. 9-15769  
<sup>169</sup>Yb, half lives of intrinsic states, transition probability to ground state 9-8985  
<sup>169</sup>Yb level struct., configuration mixings 9-8988  
<sup>179</sup>Yb and isotopes, n transmission cross section and s-wave strength function obs. 9-4736  
Au, Mott scatt. asym. obs. depend on foil thickness 9-15582  
Bi cross-section determ. with slow neutrons and He-cooled target 9-20790  
Bi(n,2n), 14 MeV, ang. correl. obs. 9-20798  
<sup>40</sup>Ca(p,p) protons extent from nucleus centre, 9.6MeV 9-582  
<sup>181</sup>F-<sup>140</sup>Ta, p- $\gamma$  ang. correl. and quadrupole interaction 9-3972  
<sup>56</sup>Fe, proton and neutron distributions calc. 9.6MeV 9-582  
<sup>64</sup>Ga, proton and neutron distributions calc. 9.6MeV 9-582  
Hf, infinite dilution resonance absorption integrals 9-19372  
Hg, bound atoms, n coherent scatt. amplitudes, obs. 9-6875  
<sup>135</sup>Bd, half lives of intrinsic states, transition probability to ground state 9-8985  
No, synthesis and investigation of props. 9-532  
Pb, cross section and interaction free path for 10<sup>11</sup>ev cosmic particles, obs. 9-18025  
Pb, orientation attempt by optical pumping 9-9139  
Pb, photoneutron cross section and X-ray beam energy, absolute meas. 9-2717  
Pb backscatt. coeffs., 10 and 20 MeV 9-6855  
Pb cross-section determ. with slow neutrons and He-cooled target 9-20790  
Pb( $\gamma$ ,n), >5 MeV photo-n anisotropy,  $E_\gamma=22-32$  MeV 9-4769  
Pb(n,2n), 14 MeV, ang. correl. obs. 9-20798  
<sup>43</sup>Sc, proton and neutron distribution calc. 9.6MeV 9-582  
<sup>87</sup>Se, fission product, half-life and yield, rel. to delayed n precursor 9-13251  
Sm-La L-subshell internal conversion calcs. including deformation due to quadrupole moment 9-2641  
Th, new isotopes obs. with assignments A=213 to 217 9-14578  
<sup>U</sup><sup>235</sup>, triple fission induced by thermal neutrons, Z>2 long range particles obs. 9-625  
<sup>51</sup>V, proton and neutron distributions calc. 9.6MeV 9-582

Nuclei with  $20 \leq A \leq 49$ 

- <sup>113</sup>In spin of 935 and 1129 keV levels 9-541  
<sup>26</sup>Mg, inelastic e scatt., 39-56 MeV, magnetic dipole transitions obs. 9-578  
<sup>26</sup>Mg(p,t)<sup>24</sup>Mg levels determ. from  $\gamma$  transitions,  $E_p=50$  MeV 9-18093  
<sup>27</sup>Al(p,t)<sup>24</sup>Mg reaction, study for proton energies 2.3-3.4 MeV 9-9027  
<sup>32</sup>( $\mu^-$ , $\nu$ ) n energy spectra obs. of  $\mu$  capture reson. mechanism 9-18090  
<sup>42</sup>Ti Coulomb energies of valence particles calc. 2-particle wave function 9-4728  
<sup>44</sup>Ca high-spin levels at 3660 and 2824 keV, evidence against 9-2686  
A=38 nuclei, shell-model calc. 9-16946  
ground state structure and binding energy calc. for A $\leq$ 40 9-11189  
photoproton production, energy and ang. distrib. 9-2716  
ruby doped with <sup>27</sup>Al, dynamic nuclear polarization 9-5991  
 $\gamma$  internal conversion coeffs. at threshold energy 9-6783  
Ca, spin-orbit splitting in Hartree-Fock calc. 9-20741  
<sup>43</sup>Sc, isobaric analogue resonances, obs. in (p,p) react., spins, parities and widths 9-8995  
<sup>28</sup>Si deuteron vector polarization in (p,d) at 185 MeV 9-2735  
<sup>28</sup>Si(n, $\alpha$ ) cross section meas.,  $E_n=6.7-13.4$  MeV 9-14617  
<sup>28</sup>Al mean energy level width at high energies 9-1235  
Al-Sn,  $\gamma$  backscatt. by stratified slab, <sup>40</sup>Co, <sup>137</sup>Cs sources 9-9014  
<sup>27</sup>Al, 4.509MeV state, study by <sup>26</sup>Mg(p, $\gamma$ ) reaction 9-507  
Al e backscatt. coeffs., 10 and 20 keV 9-6855  
Al, ground states, 5/2<sup>+</sup> spins, as evidence for hexadipole deform. in Nils-son model 9-8993  
<sup>25</sup>Al  $\gamma$  decay of T=3/2 states obs. 9-4743  
<sup>26</sup>Al, lifetimes and decay of 2.07 MeV  $\gamma$  triplet 9-20736  
<sup>26</sup>Al new 1<sup>+</sup> state from <sup>24</sup>Mg(<sup>4</sup>He,p) obs. 9-2679  
<sup>26</sup>Al radioactivity in Greenland ice, obs. 9-10380  
<sup>27</sup>Al, 3.00 MeV level  $\gamma$ -width calc. from bremsstrahlung resonant scatt. 9-4744  
<sup>27</sup>Al, from <sup>26</sup>Mg(p, $\gamma$ ),  $\gamma$  and coincidence spectra at 2322 keV obs. 9-533  
<sup>27</sup>Al, K<sup>+</sup> absorption and diffraction cross section meas.,  $E_x=3.5$  GeV/c 9-9051  
<sup>27</sup>Al, n inelastic scatt., cross section, modified optical model transmission coeff. 9-20791  
<sup>27</sup>Al, NMR in CaAl<sub>2</sub>Si<sub>2</sub>O<sub>8</sub> at high temp. 9-10293  
<sup>27</sup>Al, n.m.r. from Al salts in H<sub>2</sub>O and D<sub>2</sub>O 9-16024  
<sup>27</sup>Al,  $\pi^+$  absorption and diffraction cross section meas.,  $E_x=3.5$  GeV/c 9-9051  
<sup>27</sup>Al, NMR in GdAlO<sub>3</sub> obs. 9-5992  
<sup>27</sup>Al 3Me excitation, investigation 9-2680  
<sup>27</sup>Al energy levels using resolution surface barrier counter 9-14581  
<sup>27</sup>Al in Ca<sub>3</sub>Al<sub>2</sub>(SiO<sub>4</sub>)<sub>2</sub> garnet, grossularite, NMR 9-12509  
<sup>27</sup>Al in ruby, parametric mag. nuclear spin saturation, obs. 9-10300  
<sup>27</sup>Al mean energy level width at high energies 9-1235  
<sup>27</sup>Al NMR in ruby at center of C<sup>2+</sup> ESR line, nuclear quadrupole coupling constant not obs. 9-10301  
<sup>27</sup>Al n.m.r. in dilute Al-Zn alloys, quadrupole structure 9-12508  
<sup>27</sup>Al  $\pi^-$  capture, calc. of resulting reacts. and comparison with cancer radiotherapy expts. 9-13233  
<sup>28</sup>Al, applic. of symmetric-core collective model 9-19267

Nuclei with  $20 \leq A \leq 49$  continued

- <sup>28</sup>Al polarised thermal n capture,  $\gamma$  circular polarisation obs. 9-13230  
<sup>29</sup>Al low-lying levels,  $\gamma$  branching ratios 9-13200  
<sup>27</sup>Al( $\gamma$ ,  $\pi^+$ )<sup>27</sup>Mg, yield and cross sections meas. 9-575  
<sup>27</sup>Al( $\gamma$ , 2pn) yield and cross section meas.  $E_\gamma=20-300$  MeV 9-20772  
<sup>27</sup>Al(p, $\alpha$ )<sup>24</sup>Mg, resonances meas.,  $\alpha$  ang. distrib. meas.,  $E_p=1180-1920$  keV 9-20782  
<sup>27</sup>Al(p, $\gamma$ )<sup>28</sup>Si, resonances meas.,  $E_p=1180-1920$  keV 9-20782  
<sup>37</sup>Ar, positron decay, vector coupling coeff. calc. 9-564  
<sup>37</sup>Ar, energy levels deduced from  $\alpha$  scatt. cross section, 24-85 MeV 9-539  
<sup>37</sup>Ar, shell model, intermediate coupling states structure 9-487  
<sup>37</sup>Ar, energy levels deduced from  $\alpha$  scatt. cross section, 24-85 MeV 9-539  
<sup>37</sup>Ar diffusion from KCl and microcline feldspar, elec. field effects 9-11897  
<sup>41</sup>Ar,  $\gamma$  energy precision obs. 9-13202  
<sup>38</sup>Ar <sup>39</sup>K(d,<sup>3</sup>He)<sup>38</sup>Ar and the s-d shell structure 9-2684  
<sup>11</sup>Be, from <sup>11</sup>B(n,p) at 14.7 MeV, lifetime obs. 9-6883  
<sup>(40</sup>Ca e scatt., charge distrib. calc. at 250, 500 MeV 9-4771  
<sup>(42</sup>Ca e scatt., charge distrib. calc. at 250, 500 MeV 9-4771  
<sup>(44</sup>Ca e scatt., charge distrib. calc. at 250, 500 MeV 9-4771  
<sup>(42</sup>Ca e scatt., charge distrib. calc. at 250, 500 MeV 9-4771  
Ca even isotopes, even, proton pick-up reactions 9-2761  
<sup>37</sup>Ca mass excess and 1st excited state energy from <sup>10</sup>C values 9-4796  
<sup>40</sup>Ca, 4p-4h excitations, J=T=0 levels calc. 9-14585  
<sup>40</sup>Ca,  $\alpha$  scatt., ang. distrib. meas., 12-18 MeV 9-9054  
<sup>40</sup>Ca, K-band mixing and 8p-8h states 9-18072  
<sup>40</sup>Ca,  $\mu$  capture, spectrum and asymmetry of emitted neutrons, calc. 9-11281  
<sup>40</sup>Ca, p, n distrib. r.m.s. radii determ. from p scatt. data,  $E_p=30, 40$  MeV 9-14586  
<sup>40</sup>Ca,  $\tau=0$ , 1 1p<sup>1</sup>h monopole state calc., Migdal theory 9-20748  
<sup>40</sup>Ca(<sup>4</sup>He, $\alpha$ )<sup>36</sup>Ca, DWBA analysis, spectroscopic factors, ang. distrib. 9-14627  
<sup>40</sup>Ca elec. monopole transitions by inelastic e scatt. matrix elements and transitions radii, comparison with E2 excitations 9-6816  
<sup>40</sup>Ca from <sup>39</sup>K(p,p), energy levels, lifetimes and  $\gamma$ -ray branching determ.,  $E_p=1.1-2.5$  MeV 9-15729  
<sup>40</sup>Ca from <sup>42</sup>Ca(p,t), t spectra, cross sections meas., levels, spin and parity determ.,  $E_p=26.5$  MeV 9-19309  
<sup>40</sup>Ca inelastic e scatt. obs. 9-9018  
<sup>40</sup>Ca rms charge and mass radii, total binding energies, densities and single-particle wave functions 9-11230  
<sup>41</sup>Ca spectroscopic factors 9-9066  
<sup>41</sup>Ca spectroscopic strength 9-9067  
<sup>42</sup>Ca, elec. quadrupole transitions, lifetimes 9-13203  
<sup>42</sup>Ca spectroscopic factors 9-9066  
<sup>42</sup>Ca spectroscopic strength 9-9067  
<sup>42</sup>Ca from <sup>44</sup>K decay,  $\gamma$  spectra meas., levels determ. 9-19299  
<sup>42</sup>Ca spectroscopic factors 9-9066  
<sup>42</sup>Ca spectroscopic strength 9-9067  
<sup>42</sup>Ca, intensities of inner  $\beta$  groups 9-565  
<sup>42</sup>Ca spectroscopic factors 9-9066  
<sup>42</sup>Ca spectroscopic strength 9-9067  
<sup>42</sup>Ca-<sup>43</sup>Sc,  $\gamma$  spectra meas. 9-20767  
<sup>42</sup>Ca, form factor of real symmetry potential, depend. on n-p interaction strength 9-6822  
<sup>42</sup>Ca, particle-hole, excitations, odd-parity levels, correlations in ground-state 9-8996  
<sup>42</sup>Ca inelastic e scatt. obs. 9-9018  
<sup>42</sup>Ca rms charge and mass radii, total binding energies, densities and single-particle wave functions 9-11230  
<sup>42</sup>Ca spectroscopic factors 9-9066  
<sup>42</sup>Ca spectroscopic strength 9-9067  
<sup>40</sup>Ca, mag. moments deviation from Schmidt lines induced by non-local two-body pot. 9-6785  
<sup>42</sup>Ca from <sup>41</sup>Ca(p,t), t spectra, cross sections meas., levels, spin and parity determ.,  $E_p=26.5$  MeV 9-19309  
<sup>10</sup>Ca( $\alpha$ , $\alpha'$ ) deformation parameters and ns cross sections meas., 9-536  
<sup>40</sup>Ca(d,d)  $E_d$  (polarised)=5-11 MeV, opt.-model analysis, cross-section meas. 5-34 MeV 9-18101  
<sup>40</sup>Ca( $\gamma$ ,n $\gamma$ ) cross section meas.,  $\gamma$  obs.,  $E_\gamma \leq 32$  MeV 9-13218  
<sup>40</sup>Ca( $\gamma$ ,p $\gamma$ ) cross section meas.,  $\gamma$  obs.,  $E_\gamma \leq 32$  MeV 9-13218  
<sup>40</sup>Ca( $\mu$ , $\nu$ ), n energy spectra, obs. of  $\mu$  capture reson. mechanism 9-18090  
<sup>40</sup>Ca(n,t)<sup>38</sup>K, search with 14.7MeV n 9-11301  
<sup>40</sup>Ca(p,d)<sup>39</sup>Ca, DWBA anal. of polarisation and power, 30.5 MeV 9-534  
<sup>48</sup>Ca(p,n)<sup>48</sup>Sc levels determ. from  $\gamma$  spectra meas.,  $E_p=1.2-4$  MeV 9-19284  
<sup>42</sup>Ca(p,t)<sup>40</sup>Ca, t spectra, cross sections meas., levels, spin and parity determ.,  $E_p=26.5$  MeV 9-19309  
<sup>42</sup>Ca(p,t)<sup>42</sup>Ca, t spectra, cross sections meas., levels, spin and parity determ.,  $E_p=26.5$  MeV 9-19309  
<sup>35</sup>Cl, nuclear spin lattice relax. in antiferromag. Rb; MnCl<sub>2</sub>.2H<sub>2</sub>O 9-21597  
<sup>35</sup>Cl, spin 3/2, NQR study in a series of polychlorous cpds. of cyclobutane type 9-15906  
<sup>35</sup>Cl, spin and parity assigned to 3.01, 2.65 MeV levels 9-538  
<sup>35</sup>Cl from <sup>34</sup>S(p, $\gamma$ ), angular distributions of 2.13 MeV  $\gamma$  rays obs. 9-567  
<sup>35</sup>Cl, applic. of symmetric-core collective model 9-19267  
<sup>35</sup>Cl, from <sup>35</sup>Cl(n, $\gamma$ ), time reversal invariance expt. 9-11238  
<sup>35</sup>Cl, from <sup>35</sup>S(p, $\gamma$ ),  $\gamma$  spectrum recorded and levels determ. 1147 keV 9-540  
<sup>20</sup>F, from <sup>23</sup>Na(n, $\alpha$ ) at 14.7 MeV, lifetime obs. 9-6883  
<sup>20</sup>F new values for levels from <sup>19</sup>F thermal n capture obs., spin assignments of low-lying levels 9-16962  
<sup>38</sup>K, e.m. props. of levels, shell-model interac. calc. 9-18071  
<sup>39</sup>K in KH<sub>2</sub>PO<sub>4</sub>, n.m.r., rotary saturation and spin calorimetry 9-10294  
<sup>40</sup>K,  $\gamma$ -ray energy meas. 9-20747  
<sup>40</sup>K radioactivity, tracer expt. 9-2108  
<sup>41</sup>K, n capture cross section, 5 keV-3 MeV 9-9042  
<sup>42</sup>K  $\beta$ -spectra meas.  $E_\beta$  and  $\beta$ -CP, deduced  $\beta$ -shape factor, matrix elements best values 9-2685  
<sup>44</sup>K-<sup>44</sup>Ca,  $\gamma$  spectra meas., levels determ. 9-19299  
<sup>45</sup>K, (Si and Ag), exc. dipole moment determ. 9-6820  
<sup>36</sup>K(p, $\gamma$ )<sup>36</sup>Ar, excitation function and  $\alpha$ -part. ang. distrib. obs.,  $E_p=1550-2000$  keV 9-20784  
<sup>39</sup>K(p, $\gamma$ )<sup>39</sup>Ca, energy levels, lifetimes and  $\gamma$ -ray branching determ.,  $E_p=1.1-2.5$  MeV 9-15729  
Mg, incoherent scatt. cross-section for  $E_\gamma=30$  to 130 keV 9-11266  
Mg (n,  $\gamma$ ), 14.1 MeV 9-600  
Mg region, scatt. and bound state pot. for composite part., DWBA calc. 9-4790



Nuclei with  $20 \leq A \leq 49$  continued

- <sup>22</sup>Mg, mass and mass excess, energy of low levels, from (<sup>3</sup>He, n) reaction 9-2644
- <sup>23</sup>Mg, from <sup>24</sup>Mg(<sup>3</sup>He,  $\alpha$ ) at 15 MeV, excited states obs. 9-6901
- <sup>24</sup>Mg,  $\alpha$  (42 MeV) inelastic scatt., ang. correl. with subsequent  $\gamma$ -rays 9-19319
- <sup>24</sup>Mg, optical pot. ambiguities for <sup>16</sup>O elastic scatt. near Coulomb barrier 9-2764
- <sup>24</sup>Mg, proton polarization in scattering at 185 MeV 9-2728
- <sup>24</sup>Mg (p, p') <sup>24</sup>Mg, 5.7-6.0 MeV, p polarization 9-4776
- <sup>24</sup>Mg e scatt. g.s. radiation widths, matrix elements determ., up to 11.5 MeV excitation energy 9-20776
- <sup>24</sup>Mg elec. monopole transitions by inelastic e scatt., matrix elements radii, comparison with E2 excitations 9-6816
- <sup>24</sup>Mg from <sup>23</sup>Na(d, n), levels, spin and parity calc. from n spectra 9-19282
- <sup>24</sup>Mg from <sup>23</sup>Na(d, n) energy levels determ., ang. and energy distrib. meas., Ed=6 MeV 9-15727
- <sup>24</sup>Mg from <sup>26</sup>Mg(p, t), levels determ. from  $\gamma$  transitions,  $E_p=50$  MeV 9-18093
- <sup>24</sup>Mg impurity in Li, Na, Sr, Sn, Pb, Bi melts, nucl. reson. fluoresc. 9-7278
- <sup>24</sup>Mg spectra, Tamm-Dancoff approx. wave functions 9-4741
- <sup>24</sup>Mg static quadrupole moment of first excited  $J^\pi=2^+$  state 9-8994
- <sup>25</sup>Mg, from <sup>26</sup>Mg(<sup>3</sup>He,  $\alpha$ ) at 15 MeV, excited states obs. 9-6901
- <sup>25</sup>Mg, ground states,  $5/2^+$  spins, as evidence for hexadipole deform. in Nilsson model 9-8993
- <sup>25</sup>Mg from <sup>24</sup>Mg (d, p), energy levels, spectroscopic factors determ., Ed=2.02-4.22 MeV 9-11318
- <sup>26</sup>Mg elastic scatt.,  $E_p=0.85$  to 4.58 MeV, differential cross-section obs. 9-6860
- <sup>26</sup>Mg electron scatt., inelastic from giant M1 states Coulomb distortion correction calc. 9-11210
- <sup>27</sup>Mg, first two excited states, spin assignments from ang. correl. in <sup>26</sup>Mg(d, p $\gamma$ ) reaction 9-13199
- <sup>27</sup>Mg decay  $\gamma$  spectrum obs. 9-14595
- <sup>28</sup>Mg (d,  $\alpha$ ) <sup>23</sup>Na fluctuation anal.,  $E_d=1.83$  to 3.05 MeV 9-11319
- <sup>28</sup>Mg (d,  $\alpha$ ) <sup>23</sup>Na,  $K=7/2$  states prod. depend. on <sup>23</sup>Na rotational states, 21 MeV 9-612
- <sup>28</sup>Mg (d, p) <sup>25</sup>Mg energy levels, spectroscopic factors determ., Ed=2.02-4.22 MeV 9-11318
- <sup>28</sup>Mg (p, <sup>3</sup>He) <sup>23</sup>Na levels determ. from  $\gamma$  transitions,  $E_p=50$  MeV 9-18093
- <sup>28</sup>Mn  $\gamma$  decay meas. using  $4\pi$  coincidence counter, sensitivity corrections 9-20708
- <sup>29</sup>Na in aq. soln. n.m.r. signals 9-3122
- <sup>29</sup>Na, resonance states from <sup>28</sup>Ne(p, p'), (p, p') react., comparison with <sup>21</sup>Ne 9-16943
- <sup>29</sup>Na struct. from <sup>28</sup>Ne(d, n) <sup>21</sup>Na, differential X-sections and spectroscopic factors deduced, rel. to Nilsson and shell-model predictions 9-4800
- <sup>29</sup>Na,  $\beta^+$  spectrum, rest mass of  $\nu$  from  $\beta$ -decay 9-9010
- <sup>29</sup>Na, mixing ratios from 2.572 MeV level 9-2674
- <sup>29</sup>Na K capture peak detection by NaI(Tl), 0.87 keV 9-4676
- <sup>29</sup>Na, 225 MeV, coeffs. of mixing of two states with  $I^\pi=5/2$ , and  $K=3/2$ ,  $5/2$  determ. 9-20730
- <sup>29</sup>Na, electron scattering, elastic and inelastic, absolute cross sections at 225 MeV 9-4770
- <sup>29</sup>Na, excited, obs. of isobaric analog resons., high-resolution study 9-14580
- <sup>29</sup>Na, from <sup>25</sup>Mg(d,  $\alpha$ ),  $K=3/2$  state depend. on rotational state, 21 MeV 9-612
- <sup>29</sup>Na, in NaCl-NaBr, nuclear quadrupole resonance and electric field interaction 9-8048
- <sup>29</sup>Na, n.m.r. relax. in sodium caprylate-decanol-water system 9-5191
- <sup>29</sup>Na, n.m.r. study of aqueous Na salts, conc. depend. of amplitudes and half-widths 9-11722
- <sup>29</sup>Na, pionic and muonic 2p-1s X-ray transitions, energy and natural line-width 9-6813
- <sup>29</sup>Na, spin-lattice relax. in rochelle salt 9-10155
- <sup>29</sup>Na(<sup>18</sup>O, <sup>17</sup>O) <sup>24</sup>Na, excitation curves from  $\gamma$  yield meas., 12-30 MeV 9-617
- <sup>29</sup>Na(<sup>18</sup>O, <sup>16</sup>O) <sup>23</sup>Na, excitation curves from  $\gamma$  yield meas., 12-30 MeV 9-617
- <sup>29</sup>Na from <sup>26</sup>Mg(p, <sup>3</sup>He) levels determ. from  $\gamma$  transitions,  $E_p=50$  MeV 9-18093
- <sup>29</sup>Na(d, n) <sup>28</sup>Mg, energy levels determ., ang. and energy distrib. meas., Ed=6 MeV 9-15727
- <sup>29</sup>Na(d, n) <sup>28</sup>Mg, n spectra meas., levels, spin and parity determ.,  $E_d=5.5$  MeV 9-19282
- Na(n,  $\gamma$ ), 14.1 MeV n 9-600
- <sup>29</sup>Ne alpha-particle model, generator coordinate theory appl. 9-6766
- <sup>29</sup>Ne spectra, Tamm-Dancoff approx. wave functions 9-4741
- <sup>29</sup>Ne, exclusion of spin as explanation for anomalous circular polarization of 1.523  $\mu$  He-Ne laser line 9-6520
- <sup>29</sup>Ne, from <sup>28</sup>Ne(<sup>3</sup>He,  $\alpha$ ) at 15 MeV, excited states obs. 9-6901
- <sup>29</sup>Ne, resonance states, comparison with <sup>21</sup>Na 9-16943
- <sup>29</sup>Ne, spectroscopic information 9-18103
- <sup>29</sup>Ne structure studied by (d, p) 4-6 MeV and (n, p $\gamma$ ), 8-9 MeV reactions 9-6814
- <sup>29</sup>Ne, spins and decay modes of levels below  $\sim 5$  MeV, from <sup>29</sup>Ne(t, p $\gamma$ ) <sup>24</sup>Ne ang. correl. study 9-11234
- <sup>29</sup>Ne  $T=3/2$  states, obs. in <sup>28</sup>Ne(<sup>3</sup>He, d)  $I_n$  values and ang. distrib. 9-11233
- <sup>29</sup>Ne(p, p $\gamma$ ) p $\gamma$ -ang. correlation meas.,  $E_p=4.8-5.5$  MeV 9-13220
- <sup>29</sup>Ne(p,  $\pi^+\pi^-$ ) coherent production of mass enhancement at 1470 MeV 9-15619
- <sup>29</sup>O, new isotope identified from p. scatt. off <sup>18</sup>Au, 3 GeV 9-506
- P, shell-model calc., level energies, spectroscopic factors 9-6818
- P isotopes, shell-model calc., level energies spectroscopic factors 9-6818
- <sup>29</sup>P,  $\gamma$  decay of  $T=3/2$  states obs. 9-4743
- <sup>29</sup>P, applic. of symmetric-core collective model 9-19267
- <sup>29</sup>P, 1st and 2nd excited levels mean life determ. by Doppler shift attenuation method 9-14584
- <sup>31</sup>P, 3.13 MeV level  $\gamma$  width calc. from bremsstrahlung resonant scatt. 9-4744
- <sup>31</sup>P from <sup>29</sup>Si(<sup>3</sup>He, p), p distrib. meas., excitation energies determ.,  $E=9$  MeV 9-14582
- <sup>31</sup>P from <sup>30</sup>Si(<sup>3</sup>He, d), d distrib. meas., excitation energies determ.,  $E=10$  MeV 9-14582
- <sup>31</sup>P from <sup>30</sup>Si(p,  $\gamma$ )  $\gamma$  spectra meas., resonance levels, spin and parity determ.,  $E_p=0.8-2.2$  MeV 9-18069
- <sup>31</sup>P in Mn<sub>2</sub>P, n.m.r. obs. of hyperfine fields at P sites 9-16379
- <sup>31</sup>P in UP-US solid solns. in paramagnetic state, Knight shifts 9-10296

Nuclei with  $20 \leq A \leq 49$  continued

- <sup>32</sup>P, applic. of symmetric-core collective model 9-19267
- <sup>32</sup>P prod. by <sup>32</sup>S(n, p) <sup>32</sup>P, <sup>32</sup>P contamination determ. 9-15836
- <sup>32</sup>P, 1st and 2nd excited levels mean life determ. by Doppler shift attenuation method 9-14584
- <sup>32</sup>P from <sup>30</sup>Si( $\alpha$ , p $\gamma$ ), spin and parity assignments 9-4745
- <sup>32</sup>P isobaric analogue states, M1 transition probabilities, shell-model calc. 9-14555
- <sup>32</sup>P obs. by Siegbahn-Slater intermediate image spectrometer 9-15690
- <sup>32</sup>P( $\alpha$ ,  $\alpha'$ ) <sup>28</sup>Si,  $\alpha$  ang. distrib. for spin mixing coeff. determ. 9-2734
- <sup>32</sup>P( $\alpha$ ,  $\alpha'$ ), <sup>32</sup>S compound states average widths determ., excitation energy, 18-21 MeV 9-15728
- S, incoherent scatt. cross-section for  $E_\gamma=30$  to 130 keV 9-11266
- S isotopes, shell-model calc., level energies, spectroscopic factors 9-6818
- S shell-model calc., level energies spectroscopic factors 9-6818
- <sup>32</sup>S, d scattering, elastic, polarized, asymmetry of angular distribution 9-4791
- <sup>32</sup>S elec. monopole transitions, by inelastic e scatt., matrix elements and transition radii, comparison with E2 excitations 9-6816
- <sup>32</sup>S from <sup>48</sup>Si( $\alpha$ ,  $\gamma$ ), levels, spin determ. from  $\gamma$  spectra,  $E_\alpha=3.7-3.9$  MeV 9-18070
- <sup>32</sup>S from <sup>31</sup>P(<sup>3</sup>He, d), energy levels determ. up to 9.5 MeV excitation energy 9-11236
- <sup>32</sup>S(<sup>3</sup>He,  $\alpha$ ) <sup>33</sup>S, levels determ. and lowest  $T=3/2$  states found, 7, 12 MeV 9-537
- <sup>33</sup>S unreported level at 1.56 MeV 9-2683
- <sup>33</sup>S from <sup>34</sup>S(<sup>3</sup>He,  $\alpha$ ), levels rm. 7, 12 MeV 9-537
- <sup>34</sup>Sc, low  $3/2^-$  rotational band mixing with (fp)<sup>3</sup> states 9-18073
- <sup>34</sup>Sc, isobaric analogue resonances, obs. in (p, p) react., spins, parities and widths 9-8995
- <sup>34</sup>Sc, (357 keV,  $4^+ \rightarrow 4^+; \beta^-$ ) (1.121+0.889 MeV,  $\gamma$ ),  $\beta$ - $\gamma$  circular polarization meas. 9-15743
- <sup>34</sup>Sc, n capture cross section and burn-up in <sup>46</sup>Ti(n, p), obs. 9-19317
- <sup>34</sup>Sc from <sup>48</sup>Ca(p, n $\gamma$ ), levels determ. from  $\gamma$  spectra meas.,  $E_p=1.2-4$  MeV 9-19284
- <sup>46</sup>Sc from <sup>48</sup>Ca(p, n $\gamma$ ), g.s. isobaric analogue resonance obs.,  $\gamma$  spectra meas.,  $E_p=1.2-4$  MeV 9-19284
- <sup>46</sup>Sc(<sup>3</sup>He, d) <sup>46</sup>Ti, for nuclear struct. of <sup>46</sup>Ti 9-6819
- <sup>46</sup>Sc(p,  $\gamma$ ) <sup>46</sup>Sc, 2.8, 3.2 and 3.6 MeV,  $\gamma$  decays and some spin assignments 9-2729
- <sup>35</sup>S(d, p $\alpha$ ) <sup>29</sup>Si energy ground state, ang. distrib. meas., reaction mechanism determ.,  $E_d=12-17$  MeV 9-15777
- Si-Ti charge radius based on muonic K $\alpha$  isotope shifts 9-535
- Si isotopes, shell-model calc., level energies, spectroscopic factors 9-6818
- Si shell-model calc., level energies, spectroscopic factors 9-6818
- <sup>28</sup>Si, mass and mass excess, energy of low levels, from (<sup>3</sup>He, n) reaction 9-2644
- <sup>28</sup>Si, deformation and oscillation parameters, internal quadrupole moment 9-11277
- <sup>28</sup>Si, form factor of 17.5 MeV level 9-16945
- <sup>28</sup>Si, O<sup>+</sup>  $T=2$  state isospin-forbidden alpha decay, excitation energy 9-2682
- <sup>28</sup>Si, spin assignment of 8.555 MeV state  $J^\pi=6^+$  9-6817
- <sup>28</sup>Si elec. monopole transitions by inelastic e scatt., matrix elements radii, comparison with E2 excitations 9-6816
- <sup>28</sup>Si electron scatt., inelastic from giant M1 states Coulomb distortion correction calc. 9-11210
- <sup>28</sup>Si from ( $\alpha$ , <sup>24</sup>MG), lowest  $T=2$  level obs., compound nucleus resonance 9-16944
- <sup>28</sup>Si from (p, <sup>27</sup>Al), lowest  $T=2$  level unobs. as compound nucleus resonance 9-16944
- <sup>28</sup>Si giant resonance, excitation of strong transitions by inelastic e scatt. 9-2721
- <sup>28</sup>Si giant resonance electroexcitation, 150-225 MeV expt. data compared with prediction 9-2681
- <sup>29</sup>Si(<sup>3</sup>He, p) <sup>31</sup>P, p distrib. meas., excitation energies determ.,  $E=9$  MeV 9-14582
- <sup>29</sup>Si spectroscopic factors 9-6903
- <sup>30</sup>Si, 3<sup>+</sup> level at 5.22 MeV 9-13201
- <sup>30</sup>Si(<sup>3</sup>He, d) <sup>31</sup>P, p distrib. meas., excitation energies determ.,  $E=10$  MeV 9-14582
- <sup>30</sup>Si radiative capture cross-sections of d 9-9062
- <sup>32</sup>Si, atmos. conc. unexpectedly high 9-21781
- <sup>32</sup>Si( $\alpha$ ,  $\gamma$ ) <sup>32</sup>S, levels determ. from  $\gamma$  spectra,  $E_\alpha=3.7-3.9$  MeV 9-18070
- <sup>28</sup>Si(d, p) <sup>29</sup>Si, applic. of Faddeev eqns. 9-11259
- <sup>28</sup>Si(d, p) <sup>29</sup>Si,  $E_d=1-2$  MeV, excitation functions and angular distrib. for p groups 9-6904
- <sup>28</sup>Si(n, n) cross section meas.,  $E_n=6.7-13.4$  MeV 9-14617
- <sup>28</sup>Si(n, p) cross section meas.,  $E_n=6.7-13.4$  MeV 9-14617
- <sup>28</sup>Si(n, p) <sup>28</sup>Al, cross section meas.,  $E_n=14.4$  MeV 9-13229
- <sup>28</sup>Si(n, p) <sup>28</sup>Al cross section meas.,  $E_n=14.4$  MeV 9-13229
- <sup>28</sup>Si(p, d) <sup>27</sup>Si, DWBA anal. of polarization and power, 30.5 MeV 9-534
- <sup>30</sup>Si(p,  $\gamma$ ) <sup>31</sup>p,  $\gamma$  spectra meas., resonance levels, spin and parity determ.,  $E_p=0.8-2.2$  MeV 9-18069
- <sup>32</sup>( $\gamma$ , N) absorpt. cross section in giant dipole resonance region meas., 10-30 MeV 9-14583
- <sup>32</sup>S(n,  $\alpha$ ) absolute cross section obs. of isotopes, 14.8 MeV 9-602
- <sup>32</sup>S(n, p) absolute cross section obs. of isotopes, 14.8 MeV 9-602
- <sup>32</sup>(n, t) <sup>30</sup>P, search with 14.7 MeV n 9-11301
- <sup>32</sup>(n, x) total cross sections meas., 1.8-2.6 MeV 9-601
- <sup>32</sup>(p, n) <sup>34</sup>S, energy levels deduced,  $E_p=12$  MeV 9-11237
- Ti, 660 MeV p bombardment, N yield obs. 9-587
- <sup>46</sup>Ti from <sup>44</sup>Ca,  $\alpha$  bound  $\alpha$ -s state, well depth of 136 MeV calc. 9-9054
- <sup>46</sup>Ti, ground state triplet at 0, 36.7 and 40.2 MeV, from <sup>46</sup>Sc(p, n) 9-19283
- <sup>46</sup>Ti, nuclear structure by <sup>45</sup>Sc(<sup>3</sup>He, d) <sup>46</sup>Ti reaction 9-6819
- <sup>46</sup>Ti, p scatt. 2.5-3 MeV study of resonant state 9-19305
- <sup>46</sup>Ti from <sup>45</sup>Sc (p,  $\gamma$ ) <sup>46</sup>Ti reaction decay and energy of excited levels 9-6821
- <sup>46</sup>Ti, p scatt. 2.5-3 MeV study of resonant states 9-19305
- <sup>46</sup>Ti, spin-1 states, from particle- $\gamma$ -ray correlations, mixing ratios, rel. to shell model 9-8997
- <sup>49</sup>Ti levels from <sup>48</sup>Ti(d, p) <sup>49</sup>Ti reaction 9-9068
- <sup>48</sup>Ti(d, p) <sup>49</sup>Ti, 12.9 MeV, proton spectra 9-9068
- <sup>46</sup>Ti(n, p), <sup>46</sup>Sc burn-up rel. to fast-n monitoring 9-19317
- <sup>49</sup>Ti(nu, p) time-resolved non-invariance search 9-6884
- <sup>48</sup>Ti(p, p') 9-19306

Nuclei with  $50 \leq A \leq 89$ 

- <sup>50</sup>Mn half life obs. 9-18083
- <sup>58</sup>Ni, electron elastic scatt. differential cross section 9-13219
- <sup>72</sup>Ga  $\rightarrow$  <sup>72</sup>Ge,  $\gamma$  spectra, energy levels determ. 9-20750

**Nuclei with  $50 \leq A \leq 89$  continued**

- <sup>83</sup>As from <sup>235</sup>U, n<sub>th</sub> irradiation identification and half-life determ. 9-20813  
N=50 isotones, vib. props. and core-coupling considered 9-511  
neutron-hole states and spectroscopic information from (<sup>2</sup>He,  $\alpha$ ) react. on <sup>89</sup>Y and <sup>86</sup>Kr 9-14629  
photoneutron angular distrib. anisotropy from V, Cr, Mn and Br, rel. to subshell occupation 9-4767  
single particle strength of collective 3<sup>+</sup> state 9-2636  
 $\gamma$  internal conversion coeffs. at threshold energy 9-6783  
<sup>70</sup>Zn(p,p') diff. cross sections, asymmetries anal., 2<sup>+</sup>, 3<sup>-</sup> somg-e/ $\mu$ m states 50 MeV, 50 MeV 9-2731  
<sup>84</sup>Se from <sup>235</sup>U fission, decay characteristics determ. by  $\beta$ ,  $\gamma$  spectra meas. 9-19300  
<sup>163</sup>Ho in Ho-Gd alloy, ferromag., n.m.r. 9-16464  
<sup>112</sup>Sn, electron elastic scatt. differential cross section 9-13219  
<sup>114</sup>Cd(p,p') diff. cross sections, asymmetries anal., 2<sup>+</sup>, 3<sup>-</sup> single phonon states 50 MeV 9-2731  
<sup>56</sup>Ni, structure studied using Shell model 9-13204  
<sup>118</sup>Sn, electron elastic scatt. differential cross section 9-13219  
<sup>72</sup>As-<sup>72</sup>Ge spectra, energy levels determ. 9-20750  
<sup>72</sup>As in inorg. chalcogens, n.g.r. for piezo- and ferroelectric props. 9-18747  
<sup>72</sup>As in KH<sub>2</sub>AsO<sub>4</sub>, Stark effect in NQR and asymmetric <sup>1</sup>H-<sup>75</sup>As level crossing 9-12521  
<sup>72</sup>As low-lying levels, assignment of transitions of <sup>72</sup>Ge decay 9-11256  
<sup>72</sup>As, new  $\gamma$ 's in decay, obs. 9-566  
<sup>72</sup>As low-lying levels, assignment of transitions of <sup>72</sup>Ge decay 9-11256  
<sup>82</sup>As, formation in <sup>75</sup>Se(n,p) 9-11243  
<sup>82</sup>As from <sup>235</sup>U, n<sub>th</sub> irradiation, identification and half-life determ. 9-20813  
<sup>76</sup>As 46-keV state, lifetime and population, depopulation schemes, obs. 9-4750  
<sup>78</sup>Br compound nuclei from <sup>12</sup>C+<sup>63</sup>Cu, p and  $\alpha$  emission energy comparison 9-6828  
<sup>78</sup>Br compound nuclei from <sup>26</sup>O+<sup>58</sup>Co, p and  $\alpha$  emission energy comparison 9-6828  
<sup>78</sup>Br in aq. quaternary ammonium bromide solns., NQR 9-19647  
<sup>78</sup>Br in emulsion, interaction with 13.8 GeV protons 9-19308  
<sup>80</sup>Br nucl. isomers separation at metal surfaces 9-18769  
<sup>82</sup>Br, 3h $\beta$  decay,  $\gamma$  directional corrs. 9-11257  
<sup>82</sup>Ca, half-life obs. 9-6842  
<sup>56</sup>Co from <sup>54</sup>Fe(<sup>2</sup>He,p), energy levels determ., E<sub>h</sub>=18 MeV 9-15730  
<sup>56</sup>Co from <sup>59</sup>Ni(d, $\alpha$ ), energy levels determ., E<sub>h</sub>=12 MeV 9-15730  
<sup>57</sup>Co, Moseley's law demonstration apparatus 9-3  
<sup>57</sup>Co, NMR in PbZrO<sub>3</sub> meas. rel. to soft lattice mode and chemical bonding aspects 9-7625  
<sup>58</sup>Co, 485 keV allowed  $\beta$  transition,  $\beta$ - $\gamma$  correl. obs. 9-6841  
<sup>58</sup>Co, (475 keV, 2<sup>+</sup>+2<sup>+</sup>,  $\beta^+$ ) (0.810 MeV,  $\gamma$ ),  $\beta$ - $\gamma$  circular polarization meas. 9-15743  
<sup>59</sup>Co, energy levels and spins from n inelastic scatt., 2.9 MeV 9-4747  
<sup>59</sup>Co, n.m.r. in Co-V alloys 9-15204  
<sup>59</sup>Co, thermal neutron activation cross section w.r.t. <sup>197</sup>Au 9-9044  
<sup>59</sup>Co in Co(NH<sub>4</sub>)<sub>2</sub>(SO<sub>4</sub>)<sub>6</sub>H<sub>2</sub>O, NMR rel. to hyperfine interactions of paramag. Co<sup>2+</sup> 9-8038  
<sup>60</sup>Co,  $\gamma$  energy precision obs. 9-13202  
<sup>60</sup>Co cylindrical source with shell-shaped shield, dose buildup factor 9-19380  
<sup>60</sup>Co in Pt-Co dil. alloys, nuclear orientation meas. of hyperfine field 9-13966  
<sup>60</sup>Co polarised thermal n capture,  $\gamma$  circular polarisation obs. 9-13230  
<sup>62</sup>Co isomer decays,  $\beta$ ,  $\gamma$  spectra obs., decay schemes determ. 9-14589  
<sup>62</sup>Co-<sup>62</sup>Ni,  $\gamma$  spectra obs., decay scheme determ. 9-16950  
<sup>62</sup>Co(d,n), neutron polarization obs. 11.7 MeV 9-613  
<sup>62</sup>Co(d,n)<sup>60</sup>Ni particle-hole configuration of highly excited state 9-18106  
<sup>59</sup>Co( $\gamma$ ,n) energy distrib., polarization meas. E<sub>h</sub>≥85 MeV 9-15751  
<sup>56</sup>Cr, p scatt. 2.5-3 MeV study of resonant states 9-19305  
<sup>51</sup>Cr, decay obs. 9-9011  
<sup>51</sup>Cr species in n irradi. Cr(III) tris-acetylacetonate, thermally annealed, obs. 9-16504  
<sup>52</sup>Cr (p,p')<sup>52</sup>Cr, 5.7-6.0 MeV, p polarization 9-4776  
<sup>52</sup>Cr from <sup>51</sup>V( $\alpha$ ,t) levels and spectroscopic factors deduced 9-2762  
<sup>53</sup>Cr levels excitation energy and branching ratios 9-6824  
<sup>53</sup>Cr in Al<sub>2</sub>O<sub>3</sub>, ENDOR determ. of hyperfine splittings 9-8044  
<sup>54</sup>Cr, neutron binding energy, from <sup>53</sup>Cr(n, $\alpha$ )<sup>54</sup>Cr react. obs. 9-13202  
<sup>54</sup>Cr(<sup>2</sup>He,d)<sup>54</sup>Mn, d ang. distrib. meas., transition strengths, I<sub>p</sub> determ., E<sub>h</sub>=10 MeV 9-13243  
Cr( $\gamma$ ,n), >5 MeV photo n anisotropy, E<sub>h</sub>=22.32 MeV 9-4769  
<sup>53</sup>Cr(n,p)<sup>54</sup>Cr p-rays obs. using second-escape peak method 9-13202  
<sup>54</sup>Cr(p,n)<sup>54</sup>Mn, rel. to low energy excited states of <sup>54</sup>Mn 9-19286  
<sup>52</sup>Cr(t,p), energy levels in final nuclei 9-4746  
<sup>52</sup>Cr(t,p), energy levels in final nuclei 9-4746  
<sup>52</sup>Cr(t,p), energy levels in final nuclei 9-4746  
Cu, photoneutron cross section and X-ray beam energy, absolute meas. 9-2717  
Cu in CuI, NMR up to 465°C rel to  $\alpha$ ,  $\beta$ , and  $\alpha$  phases 9-8039  
Cu e backscatt. coeffs., 10 and 20 MeV 9-6855  
<sup>59</sup>Cu, 81<sup>+</sup> decay,  $\gamma$  spectra obs. 9-20768  
<sup>59</sup>Cu, low energy spectrum, shell model approach 9-19290  
<sup>59</sup>Cu proton states, orbital momentum of capture proton and one-particle transition strength 9-18105  
<sup>61</sup>Cu proton states, orbital momentum of capture proton and one-particle transition strength 9-18105  
<sup>62</sup>Cu, from <sup>64</sup>Zn(n,t), weak activity and yield obs. 9-14619  
<sup>61</sup>Cu, energy levels and spins from n inelastic scatt., 2.9 MeV 9-4747  
<sup>61</sup>Cu, photoproton spectra from 26.6 MeV bremsstrahlung 9-15752  
<sup>61</sup>Cu in Cu-Mn alloy, spin lattice relax. meas. 9-14015  
<sup>61</sup>Cu in Cu<sub>2</sub>Sb, n.m.r. evidence for absence of antiferromagnetism 9-16376  
<sup>61</sup>Cu nucleus, in Cu<sub>2</sub>O, spin-lattice relax. time, press. depend. at two temps. 9-18687  
<sup>61</sup>Cu proton states, orbital momentum of capture proton and one-particle transition strength 9-18105  
<sup>64</sup>Cu, n capture cross section rel. to reactor poisoning, obs. 9-19317  
<sup>64</sup>Cu electron flux spectra in Al 9-18571  
<sup>64</sup>Cu prod. by (n,p) reaction purity investigated 9-18159  
<sup>64</sup>Cu radioactivity in biological material determ. simul. with <sup>56</sup>Mn meas., n activation 9-18783  
<sup>64</sup>Cu, energy levels and spins from n inelastic scatt., 2.9 MeV 9-4747  
<sup>64</sup>Cu, excited states from  $\alpha$ -part. inelastic scatt. at 29 MeV 9-543  
<sup>64</sup>Cu, photoproton spectra from 26.6 MeV bremsstrahlung 9-15752

**Nuclei with  $50 \leq A \leq 89$  continued**

- <sup>65</sup>Cu 1114 MeV level from <sup>65</sup>Zn decay, L/K e capture ratio determ. 9-6826  
<sup>65</sup>Cu in Cu<sub>2</sub>Sb, n.m.r. evidence for absence of antiferromagnetism 9-16376  
<sup>65</sup>Cu proton states, orbital momentum of capture proton and one-particle transition strength 9-18105  
<sup>67</sup>Cu, 1.13, 1.62 MeV levels J<sup>+</sup> assignments, from <sup>64</sup>Ni( $\alpha$ ,p) 9-18104  
<sup>69</sup>Cu, K<sup>+</sup> absorption and diffraction cross section meas., E<sub>h</sub>=3.5 GeV/c 9-9051  
<sup>69</sup>Cu,  $\pi^+$  absorption and diffraction cross section meas., E<sub>h</sub>=3.5 GeV/c 9-9051  
Cuin Cu<sub>2</sub>S, NMR up to 465°C rel. to  $\alpha$  and  $\beta$  phases 9-8039  
Cu( $\gamma$ ,n) cross sections meas., giant resonance structure studied, E<sub>h</sub>=11-23 MeV 9-15753  
<sup>61</sup>Cu(p,n)<sup>62</sup>Zn, <sup>62</sup>Zn production yield by recoil p in reactors 9-589  
<sup>61</sup>Cu(p,n)<sup>62</sup>Zn, excitation function yield 9-590  
<sup>61</sup>Cu(p,p)n<sup>60</sup>Cu, recoil nuclei ang. distrib. obs. 0.37-2.8 GeV 9-6869  
<sup>57</sup>Fe, Mossbauer spectrum 9-501  
Fe, n scatt. by slab 9-591  
Fe<sup>3+</sup>,  $\gamma$ -ray spectra after  $\beta$ -decay 9-19285  
Fe<sup>3+</sup>m,  $\gamma$ -transitions in decay, and level scheme 9-19285  
Fe high-resolution fast-neutron cross sections 9-2742  
<sup>54</sup>Fe, p scatt. 2.5-3 MeV study of resonant states 9-19305  
<sup>54</sup>Fe(<sup>2</sup>He,p)<sup>56</sup>Co, energy levels determ., E<sub>h</sub>=18 MeV 9-15730  
<sup>54</sup>Fe, d scatt. optical potential calc., comparison with 3 body model theory 9-9055  
<sup>57</sup>Fe resonance, from neutron capture 9-6885  
<sup>56</sup>Fe, 0.85 MeV level excitation by 14 MeV neutrons 9-6825  
<sup>56</sup>Fe, cross-sections for (p,xn) reactions at 370 MeV 9-13224  
<sup>56</sup>Fe, n inelastic scatt., cross section, modified optical model transmission coeff. 9-20791  
<sup>56</sup>Fe, orbital momentum of resonant induced by neutrons 9-19288  
<sup>56</sup>Fe, p scatt. 2.5-3 MeV study of resonant states 9-19305  
<sup>56</sup>Fe, photoproton production, energy and ang. distrib. 9-2716  
<sup>56</sup>Fe, resonance peaks for n cross-sections 0.5 to 1.5 MeV, quantum states of compound nucleus 9-9043  
<sup>56</sup>Fe from <sup>55</sup>Mn( $\alpha$ ,t), levels and spectroscopic factors deduced 9-2762  
<sup>56</sup>Fe levels by inelastic scatt., angular distrib. meas. and anal. 9-2753  
<sup>56</sup>Fe levels investigated by  $\gamma\gamma$  ang. correlation meas., following p scatt. 9-14588  
<sup>57</sup>Fe, cross-sections for (p,xn) reactions at 370 MeV 9-13224  
<sup>57</sup>Fe, Mossbauer eff. in Fe, Cu, V and Ti, high pressure eff. at room temp. 9-21610  
<sup>57</sup>Fe, Mossbauer effect in cubic Laves Fe-rare earth intermetallics 9-7958  
<sup>57</sup>Fe, Mossbauer effect in Ni, magnetocrystalline anisotropy study 9-12279  
<sup>57</sup>Fe, Mossbauer meas. in near stoichiometric FeS, rel. to temp. depend. of hyperfine interactions 9-5892  
<sup>57</sup>Fe, Mossbauer scatt. interference with Rayleigh scatt. 9-7959  
<sup>57</sup>Fe, Mossbauer spectra in n-InAs:Te and n-GaP 9-5893  
<sup>57</sup>Fe, n.m.r. in YFe garnet for sublattice magnetization 9-21671  
<sup>57</sup>Fe in  $\alpha$ -Fe<sub>2</sub>O<sub>3</sub> (hematite), n.m.r., freq. and signal intensity rel. to temp. 9-14115  
<sup>57</sup>Fe in Ni, Mossbauer study of Fe atom state at grain boundaries 9-21611  
<sup>57</sup>Fe in transition metals, isomer shift in Mossbauer spectra 9-12357  
<sup>57</sup>Fe in V<sub>2</sub>O<sub>5</sub>:Fe<sup>3+</sup>, Sn<sup>4+</sup>, Mossbauer effect 9-21613  
<sup>57</sup>Fe K-conversion e meas., by Si detector and parallel FET preamp. 9-20703  
<sup>57</sup>Fe Mossbauer narrow-line sources, prep., and investigation of causes of line broadening 9-5891  
<sup>57</sup>Fe Mossbauer spectra, nuclear polarisation effects, depend. on hyperfine field 9-19289  
<sup>57</sup>Fe resonance, from neutron capture 9-6885  
<sup>57</sup>Fe spin relax. in domain walls via magnon interactions 9-7926  
<sup>56</sup>Fe, cross-sections for (p,xn) reactions at 370 MeV 9-13224  
<sup>56</sup>Fe, diffusion in b.c.c. Fe-Cr alloys, rel. to solvent atom diffusion mechanism 9-7507  
<sup>56</sup>Fein FePO<sub>4</sub> antiferromag. Mossbauer effect rel. to anisotropy const. meas. 9-5854  
<sup>56</sup>Fe(d,n), neutron polarization obs. 11.7 MeV 9-613  
<sup>56</sup>Fe(n,p)<sup>56</sup>Mn cross section meas., E<sub>h</sub>=14.4 MeV 9-13229  
<sup>56</sup>Fe(n,x) total cross sections meas., 1.8-2.6 MeV 9-601  
<sup>63</sup>Ga decay, for low energy excited states of <sup>63</sup>Zn 9-19291  
<sup>63</sup>Ga proton states, orbital momentum of capture proton and one-particle transition strength 9-18105  
<sup>66</sup>Ga gaseous source preparation method 9-18084  
<sup>63</sup>Ga proton states, orbital momentum of capture proton and one-particle transition strength 9-18105  
<sup>63</sup>Ga from <sup>69m</sup>Zn, <sup>69</sup>Ge decay; energy levels, spin, parity determ. 9-18085  
<sup>63</sup>Ga proton states, orbital momentum of capture proton and one-particle transition strength 9-18105  
<sup>69</sup>Ge-<sup>69</sup>Ga,  $\gamma$  spectra,  $\beta$  meas., half life determ. 9-18085  
<sup>72</sup>Ge, 0<sup>+</sup> excited state half life meas. 9-11242  
<sup>72</sup>Ge (d,p)<sup>72</sup>Ge, 8 MeV parities, transition strengths for levels up to 3 MeV 9-8998  
<sup>72</sup>Ge from <sup>71</sup>As,  $\gamma$  spectra energy levels determ. 9-20750  
<sup>72</sup>Ge from <sup>71</sup>As,  $\gamma$  spectra energy levels determ. 9-20750  
<sup>72</sup>Ge, coulomb-recoil: implantation Mossbauer expts. rel. to nuclear and solid-state props. 9-6827  
<sup>72</sup>Ge irradiated, anal. of  $\alpha$  energy spectra 9-2720  
<sup>72</sup>Ge decay,  $\gamma$  spectra study, assignment of transitions in <sup>72</sup>As level scheme 9-11256  
<sup>72</sup>Ge,  $\gamma$  spectra obs. and energy levels determ. 9-8981  
<sup>72</sup>Ge decay,  $\gamma$  spectra study, assignment of transitions in <sup>72</sup>As level scheme 9-11256  
<sup>72</sup>Ge(n, $\gamma$ ) isomeric cross section ratios, spin-cutoff parameter deduced, 24 keV 9-544  
<sup>72</sup>Ge(p,p')<sup>72</sup>Ge, 12 MeV obs. parities, transition strengths for levels up to 3 MeV 9-8998  
<sup>68</sup>Zn-<sup>68</sup>Ga,  $\gamma$  spectra,  $\beta$  meas., half life determ. 9-18085  
<sup>82</sup>Kr levels from <sup>82</sup>Br decay,  $\gamma$  directional corrs. 9-11257  
<sup>82</sup>Kr, Mossbauer recoilless fraction in solid Kr 9-12361  
<sup>82</sup>Kr, leak detection in high press. gas system 9-12806  
<sup>82</sup>Kr, radioactivity meas. with charcoal trap, calibration 9-2711  
<sup>82</sup>Kr from treated, evaporated, irradiated UO<sub>2</sub>; spectrometry 9-4815  
<sup>82</sup>Kr,  $\beta$  decay, 1.3 h., to <sup>82</sup>Rb, isotope sep., level schemes 9-13213  
<sup>82</sup>Kr,  $\beta$  decay, 2.8 h., to <sup>82</sup>Rb, isotope sep., level schemes 9-13213



Nuclei with  $50 \leq A \leq 89$  continued

- <sup>58m</sup>Co, n capture cross section, thermal, and reson. integral rel. to reactor poisoning, obs. 9-19317
- <sup>52</sup>Mn, g and m states from <sup>51</sup>V( $\alpha$ ,3n), isomeric cross-section ratio meas., 32-51 MeV 9-20807
- <sup>53</sup>Mn, activation resonance integral using bath technique 9-20793
- <sup>54</sup>Mn, electron capture decay, rates and half-lives 9-4761
- <sup>54</sup>Mn, low energy excited states by <sup>54</sup>Cr(p,n)<sup>54</sup>Mn reaction 9-19286
- <sup>55</sup>Mn, energy levels and spins from n inelastic scatt., 2.9 MeV 9-4747
- <sup>55</sup>Mn, n capture ion, 5 keV-3 MeV 9-9042
- <sup>55</sup>Mn, photoproton production, energy and ang. distrib. 9-2716
- <sup>55</sup>Mn from <sup>53</sup>Cr(He,d), d ang. distrib. meas., transition strengths, *I<sub>p</sub>* determ., *E<sub>th</sub>*=10 MeV 9-13243
- <sup>55</sup>Mn in Mn<sub>2</sub>P, n.m.r. obs. 9-16379
- <sup>55</sup>Mn in V-Mn alloys, Knight shift 9-21672
- <sup>55</sup>Mn octupole weak coupling states obs. in 17.5 MeV p inelastic scatt. 9-2688
- <sup>56</sup>Mn radioactivity in biological material determ. simul. with <sup>64</sup>Cu meas., in activation 9-18783
- <sup>60</sup>Mn  $\gamma$  decay meas. using 4 $\pi$  coincidence count, sensitivity corrections 9-20708
- <sup>55</sup>Mn(p,n) energy distrib., polarization meas. *E<sub>p</sub>*≥85 MeV 9-15751
- <sup>86m</sup>Rb conversion coeffs., half-life, multipolarity of E4 transition, spin obs. 9-9000
- <sup>89m</sup>Y, excitation cross section for inelastic n. scatt. 9-13226
- <sup>89m</sup>Y lifetime and cross-section for reactor n. scatt. 9-9009
- <sup>69m</sup>Zn prod. by two nuclear reactions 9-18075
- <sup>69m</sup>Zn→<sup>69</sup>Ga,  $\gamma$  spectra,  $\beta$  meas., half life determ. 9-18085
- <sup>58</sup>Ni  $\alpha$  particles scattering, elastic and inelastic, at 34.4 MeV 9-4804
- Ni, collective 2<sup>+</sup>, 3<sup>-</sup> excitations from inelastic d scatt. 9-16967
- Ni isotope multipole collective states excitation by  $\alpha$  scatt. at 40 MeV 9-11240
- <sup>56</sup>Ni rms charge and mass radii, total binding energies, densities and single-particle wave functions 9-11230
- <sup>58</sup>Ni, d scattering, elastic, polarized, asymmetry of angular distribution 9-4791
- <sup>58</sup>Ni,  $\pi^-$  double charge exchange and capture at 15 MeV 9-15773
- <sup>58</sup>Ni radiative neutron capture cross section 9-6886
- <sup>59</sup>Ni, calc. from reaction matrix elements 9-14587
- <sup>59</sup>Ni from <sup>58m</sup>(n,p),  $\gamma$  transition strengths energy depend. determ., *E<sub>n</sub>*=10-90 keV 9-15770
- <sup>60</sup>Ni, 3.12 MeV state, DWBA anal. of (d,d') and (t,p) meas., recal. 9-20749
- <sup>60</sup>Ni, electron elastic scatt. differential cross section 9-13219
- <sup>60</sup>Ni  $\alpha$  particles scattering, elastic and inelastic, at 34.4 MeV 9-4804
- <sup>60</sup>Ni compound nucleus decay depend. on ang. momentum 9-4748
- <sup>60</sup>Ni particle-hole configuration of highly excited state 9-18106
- <sup>60</sup>Ni from <sup>62</sup>Co decay,  $\gamma$  spectra obs., scheme determ. 9-16950
- <sup>64</sup>Ni, electron elastic scatt. differential cross section 9-13219
- <sup>60</sup>Ni<sup>90</sup> photodisintegration, giant-dipole resonance region, shell effect 9-11276
- <sup>60</sup>Ni<sup>78</sup> photodisintegration, giant-dipole resonance region, shell effects 9-11276
- <sup>58</sup>Ni( $\alpha$ ,p)<sup>61</sup>Cu angular distrib. rel. to total J transfer, 19.3 and 20.1 MeV 9-18104
- <sup>60</sup>Ni( $\alpha$ ,p)<sup>63</sup>Cu angular distrib. rel. to total J transfer, 19.3 and 20.1 MeV 9-18104
- <sup>62</sup>Ni( $\alpha$ ,p)<sup>65</sup>Cu angular distrib. rel. to J transfer, 19.3 and 20.1 MeV 9-18104
- <sup>64</sup>Ni( $\alpha$ ,p)<sup>67</sup>Cu angular distrib. rel. to total J transfer, 19.3 and 20.1 MeV 9-18104
- <sup>58</sup>Ni(d, $\alpha$ )<sup>56</sup>Co, energy levels determ., *E<sub>x</sub>*=12 MeV 9-15730
- <sup>60</sup>Ni(d,n), and isotopes; neutron polarization obs. 11.7 MeV 9-613
- <sup>58</sup>Ni( $\gamma$ ,n), cross sections 9-6851
- <sup>58</sup>Ni( $\gamma$ ,n) energy distrib., polarization meas. *E<sub>p</sub>*≥85 MeV 9-15751
- <sup>60</sup>Ni( $\gamma$ ,n), cross sections 9-6851
- <sup>58</sup>Ni(n,p),  $\gamma$  transitions, energy distrib. obs. *E<sub>n</sub>*=10-90 keV 9-15770
- <sup>58</sup>Ni(p,d), nucleon-transfer reactions, realistic form factors 9-2724
- <sup>87</sup>Rb in aq. soln., n.m.r. signals 9-3122
- <sup>87</sup>Rb, excitation levels from  $\gamma$ -ray meas. in Rb(n,p)Rb reaction 9-13232
- <sup>87</sup>Rb, n capture cross section, 5 keV-3 MeV 9-9042
- <sup>87</sup>Rb regenerative mass oscillator, freq. stability 9-15505
- <sup>87</sup>Rb, nuclear spin-lattice relax. in antiferromag. Rb<sub>2</sub>MnCl<sub>4</sub>·2H<sub>2</sub>O 9-21597
- <sup>87</sup>Rb, zero-field level crossing resonances and very weak magnetic field detection 9-15822
- <sup>87</sup>Rb 3rd forbidden  $\beta$ -decay, shape explanation 9-14597
- <sup>87</sup>Rb in RbH<sub>2</sub>PO<sub>4</sub> in paraelectric phase, n.m.r. obs. 9-16469
- <sup>87</sup>Rb,  $\beta$  decay, 15 min., to <sup>86</sup>Sr, isotope sep., level schemes 9-13213
- Rb(n,p)Rb,  $\gamma$ -ray intensity and energy meas. 9-13232
- <sup>70</sup>Se, from <sup>70</sup>Co (<sup>14</sup>N, 3n) at *E<sub>14N</sub>*=140 MeV, lifetime obs. 9-9012
- <sup>73</sup>Se,  $\beta$  spectra obs., isomer state life times calc. 9-2690
- <sup>73</sup>Se, spin, anomalous coupling  $7/2^+$  and  $1/2^-$  states 9-8999
- <sup>75</sup>Se, half-life of 287keV level 9-6829
- <sup>82</sup>Se radiative capture cross sections of p 9-9062
- <sup>88</sup>Sr (d,d) differential cross sections obs., increase in filled n shell region, 13.6 MeV 9-608
- <sup>88</sup>Sr, particle-hole excitation, finite range force calc. 9-11245
- <sup>88</sup>Sr and neighbouring nuclei, single-particle core-excitation coupling calc. 9-16942
- <sup>88</sup>Sr dipole states, struct. and analysis 9-11244
- <sup>88</sup>Sr rms charge and mass radii, total binding energies, densities and single-particle wave functions 9-11230
- <sup>89</sup>Sr, activity in air and surface deposition 9-21783
- <sup>88</sup>Sr(p,n)<sup>88</sup>Y, <sup>88</sup>Y production yield by recoil p in reactors 9-589
- <sup>51</sup>Ti levels from <sup>50</sup>Ti(d,p)<sup>51</sup>Ti reaction 9-9068
- <sup>51</sup>Ti low-lying states rel. to 2p-1h configurations 9-2687
- <sup>50</sup>Ti(d,p)<sup>51</sup>Ti, 12.9 MeV, proton spectra 9-9068
- <sup>50</sup>Ti(p,n)<sup>50</sup>V, <sup>50</sup>V low-lying level transitions obs. 9-18074
- V-Y charge radius based on muonic K $\alpha$  isotope shifts 9-535
- <sup>50</sup>V, low-lying levels, <sup>50</sup>Ti(p,n)<sup>50</sup>V obs., multiplicities of transitions and spins 9-18074
- <sup>51</sup>V, 320 keV transition, internal conversion of s-electrons 9-6823
- <sup>51</sup>V, calc. from reaction matrix elements 9-14587
- <sup>51</sup>V, g-factor of 320 keV state meas. in Fe-V alloy by Coulomb excitation 9-11239
- <sup>51</sup>V, s-electrons internal conversion coeff. meas. 9-14596
- <sup>51</sup>V in V-Mn alloys, Knight shift 9-21672
- <sup>51</sup>V( $\alpha$ ,3n)<sup>52m</sup>Mn isomeric cross-section ratio meas., 32-51 MeV 9-20807
- <sup>51</sup>V( $\gamma$ ,  $\pi^-$  2n)<sup>49</sup>Cr, yield and cross sections meas. 9-575

Nuclei with  $50 \leq A \leq 89$  continued

- <sup>51</sup>V( $\gamma$ ,  $\pi^+$ )<sup>51</sup>Ti, yield and cross sections meas. 9-575
- <sup>51</sup>V( $\gamma$ ,  $\alpha$ ) yield and cross section meas. *E<sub>p</sub>*=20-300 MeV 9-20772
- <sup>51</sup>V( $\gamma$ ,  $\alpha$ 3n) yield and cross section meas. *E<sub>p</sub>*=20-300 MeV 9-20772
- <sup>51</sup>V( $\gamma$ , n), n energy distrib., polarization meas. *E<sub>p</sub>*≥85 MeV 9-15751
- <sup>51</sup>V(n,n') excitation curves and ang. distrib. obs., level spins meas. 9-542
- <sup>51</sup>V( $\pi^+$ ,  $\pi^-$ ) cross section  $\pi$  charge, moment and range determ. 9-6891
- <sup>58</sup>W(p,p)<sup>58</sup>Ni 5.7-6.0 MeV, p polarization 9-4776
- <sup>88</sup>Y yield in <sup>88</sup>Sr(p,n)<sup>88</sup>Y by recoil p in reactors 9-589
- <sup>89</sup>Y, inelastic scatt. of 24.5 MeV p, analysis 9-19307
- <sup>89</sup>Y energy levels using high resolution surface barrier counter 9-14581
- <sup>89</sup>Y N CAPTURE CROSS SECTION, KEV-3 MeV 9-9042
- <sup>89</sup>Y(p,p)<sup>89</sup>Y polarization and diff. cross sections meas., spin and parity assignments 9-20751
- Zn, collective 2<sup>+</sup>, 3<sup>-</sup> excitations from inelastic d scatt. 9-16967
- Zn isotope multipole collective states excitation by  $\alpha$  scatt. at 40 MeV 9-11240
- <sup>64</sup>Zn, total n cross-sections for energy range 0.002 to 0.4 eV. 9-11290
- <sup>64</sup>Zn particle-hole configuration of highly excited state 9-18106
- <sup>64</sup>Zn, K-electron capture rates, branching ratio, positron rate and decay half-lives 9-4761
- <sup>65</sup>Zn, low energy excited states from decay of <sup>64</sup>Ga 9-19291
- <sup>65</sup>Zn L K capture peak detection by NaI(Tl), 1 keV 9-4676
- <sup>65</sup>Zn yield in <sup>64</sup>Cu(p,n)<sup>65</sup>Zn by recoil p in reactors 9-589
- <sup>65</sup>Zn→<sup>65</sup>Cu, 1114 MeV level L/K e capture ratio determ. 9-6826
- <sup>65</sup>Zn particle-hole configuration of highly excited state 9-18106
- <sup>67</sup>Zn after <sup>41</sup>Se-<sup>41</sup>Pi, optical pumping 9-4447
- <sup>68</sup>Zn from <sup>68</sup>Ga decay,  $\gamma$  conversion levels determ., evidence for 0<sup>+</sup> state 9-4749
- <sup>68</sup>Zn from <sup>68</sup>Ga  $\gamma$  internal conversion, levels determ., evidence for 0<sup>+</sup> state 9-4749
- <sup>64</sup>Zn(d,n), and isotopes; neutron polarization obs. 11.7 MeV 9-613
- <sup>64</sup>Zn(p,n) cross sections meas., giant resonance structure studied, *E<sub>p</sub>*=11-23 MeV 9-15753
- <sup>64</sup>Zn(n,p)<sup>64</sup>Cu, energy spectra and angular distribution of protons 9-6887
- <sup>66</sup>Zn(n,p)<sup>66</sup>Cu, energy spectra and angular distribution of protons 9-6887
- <sup>70</sup>Zn(n,n)<sup>69m</sup>Zn cross section meas., *E<sub>n</sub>*=14.4 MeV 9-13229
- <sup>64</sup>Zn(p,d)<sup>63</sup>Zn, ang. distrib. meas., levels determ., *E<sub>p</sub>*=26 MeV 9-20785
- <sup>64</sup>Zn(p,p)<sup>64</sup>Zn, ang. distrib. meas., levels determ., *E<sub>p</sub>*=26 MeV 9-20785
- <sup>64</sup>Zn(p,p') diff. cross sections, asymmetries anal., 2<sup>+</sup>, 3<sup>-</sup> single phonon states, 50 MeV 9-2731
- <sup>66</sup>Zn(p,p') diff. cross sections, asymmetries anal., 2<sup>+</sup>, 3<sup>-</sup> single phonon states, 50 MeV 9-2731
- <sup>68</sup>Zn(p,p') diff. cross sections, asymmetries anal., 2<sup>+</sup>, 3<sup>-</sup> single phonon states, 50 MeV 9-2731
- <sup>89</sup>Zr 78.4h, decay props., energies  $\gamma$  transitions meas. 9-2708
- <sup>89</sup>Zr excited states due to 2<sup>-</sup> isobaric analog reson. in <sup>89</sup>Y(p,n)<sub>2</sub><sup>89</sup>Zr react. 9-14610
- <sup>89</sup>Zr from <sup>90</sup>Zr(p,d), excited energy levels obs. up to 13MeV 9-545
- <sup>89</sup>Zr isomers, decay,  $\gamma$  energies and intensities, <sup>89</sup>Y levels deduced 9-14598

Nuclei with  $6 \leq A \leq 19$ 

- <sup>14</sup>C, anal., using  $\Lambda$ - $\Lambda$  interactions determined from <sup>14</sup>He anal. 9-19273
- <sup>12</sup>C spallation with 3 $\alpha$  in final state induced by  $\pi$  reaction at 117 MeV 9-11308
- <sup>12</sup>C( $\alpha$ ,n)<sup>15</sup>O, for nuclear design parameters of monoenergetic neutron source 9-19205
- <sup>14</sup>C activity in <sup>14</sup>CO<sub>2</sub>, direct meas. in liq. scintillation counter 9-20764
- <sup>16</sup>O  $\gamma$ -ray branching in decay of 6.92, 7.12, 8.88 and 13.10 MeV states 9-2651
- <sup>18</sup>F  $\Delta$ =1,  $\Delta$ Y=0 nonleptonic weak interaction testing 9-8967
- <sup>18</sup>O(<sup>18</sup>He, $\gamma$ )<sup>18</sup>F ang distrib. obs. and DWBA analysis 17.3 MeV 9-6899
- <sup>19</sup>F(d,d)<sup>19</sup>F, 2.0 and 2.2 MeV bombarding energies, cross sections 9-16965
- <sup>19</sup>F(d,p)<sup>18</sup>F, 2.0 MeV bombarding energies, meas. of two p groups 9-16965
- <sup>7</sup>Li(p,n)<sup>6</sup>He 94 MeV, excitation of isobaric analogue state and 0.431 MeV state, calc. 9-9029
- A=18 core polarization contrib. to effective interactions, higher-order 9-4717
- emission from <sup>239</sup>Pu(n,f) ternary fission, obs. 9-15783
- ground state structure and binding energy calc. 9-11189
- magnetic moments deviation from Schmidt lines induced by non-local two-body pot. 9-6785
- mass-18, SU(3) group to classify singly excited states 9-2654
- ( $\pi^+$ , 2p) on reactions on 1p shell, 200 MeV 9-2749
- <sup>14</sup>C, e.m. transition strengths, lifetime of 6.72 MeV level 9-4727
- $\gamma$  internal conversion coeffs. at threshold energy for  $6\leq Z$  9-6783
- <sup>14</sup>N, e.m. transition strengths, lifetimes of 5.10 and 5.83 MeV levels 9-4727
- <sup>10</sup>B from <sup>10</sup>C positron decay,  $\gamma$  spectra meas., ft values and branching ratios determ. 9-18086
- <sup>10</sup>C→<sup>10</sup>B,  $\gamma$  spectra meas., ft values and branching ratios determ. 9-18086
- <sup>8</sup>B part,  $\gamma$  correlation experiments, e.m. multipole mixing ratios, spins, branching ratios 9-2643
- <sup>12</sup>C excitation in <sup>12</sup>C( $\gamma$ , n)<sup>11</sup>C 9-15749
- Al, n scatt. by slab 9-591
- <sup>8</sup>B hypernucleus,  $\pi^+$  decay 9-15715
- <sup>10</sup>B, at 270 KeV Feynman diagram dispersion theory 9-4795
- <sup>10</sup>B, lifetimes of 3.59 and 2.15 MeV levels, transition strengths 9-14560
- <sup>10</sup>B(<sup>14</sup>N, <sup>12</sup>C)<sup>12</sup>C cross section, ang. distrib. meas., *E*=22.5-32.5 MeV 9-15780
- <sup>10</sup>B(<sup>16</sup>O, <sup>4</sup>N)<sup>12</sup>C cross section, ang. distrib. meas., *E*=22.5-32.5 MeV 9-15780
- <sup>10</sup>B deuteron elastic scatt. from 1.0 to 2.0 MeV 9-13236
- <sup>10</sup>B  $\Delta$ =1,  $\Delta$ Y=0 nonleptonic weak interaction testing 9-8967
- <sup>10</sup>B from <sup>11</sup>B(<sup>2</sup>He, $\alpha$ ), e.m. branching ratio determ. 9-14559
- <sup>10</sup>B scatt. of <sup>16</sup>O ions, elastic, obs. and anal. of results 9-15503
- <sup>10</sup>B scattering, elastic and inelastic at 32 MeV 9-2752
- <sup>11</sup>B, from <sup>12</sup>C(p,<sup>3</sup>He), spin and parity assignments 9-6866
- <sup>11</sup>B(<sup>2</sup>He, $\alpha$ )<sup>10</sup>B, e.m. branching ratio determ. 9-14559
- <sup>11</sup>B excited, e.m. multipole mixing ratios, spins, branching ratios, calc. 9-2643
- <sup>11</sup>B in <sup>12</sup>C( $\pi^-$ ,  $\pi^-$ ), reaction mechanism, characteristic identification conditions, *p<sub>n</sub>*=1.04 GeV/c 9-4788
- <sup>11</sup>B lowest p-shell  $\pi$ = $\pi/2$  states, obs., spins, parities, isospin purity 9-14561
- <sup>12</sup>B from <sup>12</sup>C( $\mu^-$ ,  $\nu$ ), ft value meas. 9-14605
- <sup>12</sup>B 995 keV,  $\gamma$ , ang. distrib., plane polar., e.m. transitions 9-2646
- <sup>12</sup>B even-parity T=1 levels, particle-hole description 9-14562

Nuclei with  $6 \leq A \leq 19$  continued

- $^{12}\text{B}$  p<sub>1</sub> ang. distrib. and p<sub>1</sub>- $\gamma$  ang. correlations 9-2755  
 $^{12}\text{B}$  relax. time of nuclear polarization 9-2648  
 $^{12}\text{B}$ , delayed neutrons in  $\beta$ -decay 9-11250  
 $^{10}\text{Be}$ , lifetime of 3.37 MeV level, transition strengths 9-14560  
 $^{10}\text{Be}(\text{d},\alpha)^8\text{Be}$ , 0.8-2.5 MeV ang. distrib. obs., 2N pickup and heavy particle stripping analysis 9-11316  
 $^{11}\text{Be}(\text{d},\alpha)^9\text{Be}$ , 0.8-2.5 MeV ang. distrib. obs., agreement with two-particle pickup  $\alpha$  9-11316  
 $^{10}\text{Be}(\text{d},\text{d})^{10}\text{Be}$ , quadrangle graph calc. 9-20778  
 $\text{Be}$ , incoherent scatt. cross-section for  $\text{E}_\text{p}=30$  to 130 keV 9-11266  
 $^6\text{Be}$  levels obs. from  $^4\text{Li}(\text{p},\text{n})$  at  $\text{E}_\text{p}=30$ , 50 MeV 9-6868  
 $^6\text{Be}$ , 14.6 MeV state, nonexistence 9-11216  
 $^6\text{Be}$ , ocean surface interac. and mixing obs. 9-18789  
 $^6\text{Be}$  levels obs. from  $^7\text{Li}(\text{p},\text{n})$  at  $\text{E}_\text{p}=30$ , 50 MeV 9-6868  
 $^7\text{Be}$  hypernucleus,  $\pi^+$  decay 9-15715  
 $^7\text{Be}$ , energy levels from  $\alpha\alpha$  interaction data, review 9-15649  
 $^6\text{Be}$  magnetic dipole transitions and isospin mixing 9-2660  
 $^6\text{Be}$  prod. in 20GeV/c proton interactions with heavy nuclei of emulsion 9-16955  
 $^6\text{Be}$  T=0 levels with even spin and parity determ. from  $^4\text{Li}(\text{d},\alpha)^4\text{He}$  9-6913  
 $^6\text{Be}$  three-body react., width variations of short-lived states 9-13222  
 $^6\text{Be}$ , absorpt. spectra for dipole  $\gamma$ , 35MeV 9-577  
 $^6\text{Be}$ , K $\pi^+$  absorption and diffraction cross section meas.,  $\text{E}_\text{e}=3.5$  GeV/c 9-9051  
 $^6\text{Be}$ ,  $\pi^+$  absorption and diffraction cross section meas.,  $\text{E}_\text{e}=3.5$  GeV/c 9-9051  
 $^6\text{Be}(^{16}\text{O},^{16}\text{O})^6\text{Be}$ , excitation curves from  $\gamma$  yield meas., 12-30 MeV 9-617  
 $^6\text{Be}(^{19}\text{F},^{19}\text{F})^6\text{Be}$ , excitation curves from  $\gamma$  yield meas., 12-30 MeV 9-617  
 $^6\text{Be}$  deuteron vector polarization in (p,d) at 185 MeV 9-2735  
 $^6\text{Be}$  levels obs. 9-6853  
 $^6\text{Be}$  scatt. of  $^{16}\text{O}$  ions, elastic, obs. and anal. of results 9-15503  
 $^{10}\text{Be}$  radioactivity in Greenland ice, obs. 9-10380  
 $^6\text{Be}$ , from  $^{11}\text{B}(\text{n},\text{p})$  at 14.7 MeV, lifetime obs. 9-6883  
 $^6\text{Be}$ , information from  $\mu$  capture by  $^{11}\text{B}$  9-11208  
 $^6\text{Be}(\text{p},\text{p})^6\text{Be}$  quadrangle graph calc. 9-20778  
 $^{10}\text{Be}(\gamma, \pi^-)^{11}\text{C}$ , yield and cross section meas. 9-575  
 $^{10}\text{Be}(\text{p},\text{p})^6\text{Be}$ , energy distrib. meas., quantum numbers assigned to levels,  $\text{E}_\text{p} \leq 12.5$  MeV 9-9015  
 $^{11}\text{B}(\text{n},\text{d})^{10}\text{Be}$  d ang. distrib. and  $\text{Be}$  ground state 9-594  
 $^{10}\text{B}(\text{n},\text{n})^{10}\text{B}$ , 14 MeV, cross-sections 9-9032  
 $^{11}\text{B}(\text{n},\text{n})^{11}\text{B}$ , 15 MeV, cross-sections, elastic and inelastic 9-9032  
 $^{10}\text{B}(\alpha^+, \text{T}=1)$  from  $^{12}\text{C}(\text{d},\alpha)$  isospin-nonconserving, cross section meas. 9-20804  
 $^{11}\text{B}(\text{p}, \alpha)^8\text{Be}^*$ , coincidence spectra study,  $\text{E}_\text{p}=1.4$  MeV 9-9026  
 $^3\text{C}$ -H satellite resonances of 1-substituted aziridines, coupling parameters 9-13543  
 $^3\text{C}$ -H spin-spin coupling const., extended Huckel calc. on methyl cpds. 9-20969  
 $\text{C}$ , cosmic ray high energy interac., distrib. of shower particles 9-15673  
 $\text{C}$ , energy transfer from neutrons up to 18 MeV obs. 9-20786  
 $\text{C}$ , incoherent scatt. cross-section for  $\text{E}_\text{p}=30$  to 130 keV 9-11266  
 $^{10}\text{B}(\text{n},\alpha)^7\text{Li}$ ,  $^7\text{Li}^*$  relative cross sections determ.,  $\text{E}_\text{e}=30$ -800 keV 9-19318  
 $\text{C}$  neutron cross-sections  $\text{E}=13.7$ -14.6 MeV 9-9041  
 $\text{C}$ , lifetime of 3.36 MeV level, transition strengths 9-14560  
 $\text{C}$  from  $^{10}\text{B}(\text{He},\text{t})$ , mass excess and 1st excited state energy meas. 9-4796  
 $^{11}\text{C}$ , from  $^{13}\text{C}(\text{p},\text{t})$ , spin and parity assignments 9-6866  
 $^3\text{C}$ , spin and parity assigned from  $\gamma$  spectrum determ. 9-11218  
 $^3\text{C}$  lowest p-shell  $\text{T}=\frac{1}{2}$  states, obs., spins, parities, isospin purity 9-14561  
 $^{11}\text{C}$  radioisotope prod. from Van de Graaff 3 MeV d beam 9-6745  
 $^{11}\text{C}$  superallowed positron decay, internal bremsstrahlung meas. 9-20733  
 $^3\text{C}$ , 580, 805, 968 MeV e scatt on nucleons obs. 9-20775  
 $^{12}\text{C}$ , e scatt. cross section, inelastic N-N correlation, N reabsorption considered 9-15754  
 $^{12}\text{C}$ , electron scatt., inelastic from giant Mi states Coulomb distortion correction calc. 9-11210  
 $^{12}\text{C}$ , glassy carbon, total cross-section from 0.001-0.1 eV 9-20824  
 $^{12}\text{C}$ , inelastic e.m. form factors meas. in e quasi-elastic scatt. region, 500-1000 MeV 9-8976  
 $^{12}\text{C}$ , lifetime of 4.43 MeV level 9-11209  
 $^{12}\text{C}$ , low-lying 0 $^+$  states in three alpha model 9-19271  
 $^{12}\text{C}$ ,  $\mu^-$  capture rate and  $^{12}\text{B}$  f value meas. 9-14605  
 $^{12}\text{C}(\text{He}, ^7\text{He})^{12}\text{C}$ , 12-18 MeV surface absorptive pot. and optical parameters calc. 9-607  
 $^{12}\text{C}(\text{He}, ^7\text{He})^{12}\text{C}$  diff. cross-sections meas.  $\text{E}_\text{e}=5.29$ -5.5 MeV 9-15775  
 $^{12}\text{C}(\text{He}, \text{p})^{11}\text{C}$  diff. cross-sections meas.  $\text{E}_\text{e}=5.29$ -5.5 MeV 9-15775  
 $^{12}\text{C}$  and projected Hartree-Fock wave functions 9-6852  
 $^{12}\text{C}$  compound nucleus resons. in  $^{10}\text{B}$  deuteron elastic scatt. at low energies 9-13236  
 $^{12}\text{C}$  cross sections compared with e scatt. meas., light nuclei structure determ. 9-4774  
 $^{12}\text{C}$  deuteron vector polarization in (p,d) at 185 MeV 9-2735  
 $^{12}\text{C}$  elec. monopole transitions, by inelastic e scatt., matrix elements and transitions radii, comparison with E2 excitations 9-6816  
 $^{12}\text{C}$  energy spectra of fast photoprotons for bremsstrahlung 50 to 80 MeV 9-2647  
 $^{12}\text{C}$  giant resonance, excitation of strong transitions by inelastic e scatt. 9-2721  
 $^{12}\text{C}$  part.-hole states, e excitation 9-504  
 $^{12}\text{C}$   $\pi^-$  capture, calc. of resulting reacts. and comparison with cancer radiotherapy expts. 9-13233  
 $^{12}\text{C}$  wave functions for ground state and  $2^+$  at 4.43 MeV 9-503  
 $^3\text{C}$ , from  $^{11}\text{N}(\text{p},\text{He})$ , spin and parity assignments 9-6866  
 $^3\text{C}$ , lifetime limits for 3.09 and 3.68 MeV levels and lifetime of 3.86 MeV level 9-11209  
 $^{13}\text{C}$  and  $^{13}\text{N}$  mirror nuclei prod. in isospin multiplet from  $^{14}\text{N}$ ,  $^{12}\text{C}$  interac. 9-14568  
 $^{13}\text{C}$  n.m.r. of medium mol.-wt. organic compounds 9-18746  
 $^{13}\text{C}$  satellite n.m.r. in perfluorobutane, rel. to  $\text{CF}_2$  group couplings 9-13375  
 $^{13}\text{C}$  time reversal invariance, polarization-asymmetry test 9-6859  
 $^{14}\text{C}$ , s- and p-wave elastic proton and neutron scatt., Regge trajectory 9-20777  
 $^{14}\text{C}$  and  $^{14}\text{N}$  autoradiography, simultaneous, correlation with gas counting 9-21995  
 $^{14}\text{C}$  in atmospheric  $\text{CO}_2$ , measuring technique and results 9-15248  
 $^{14}\text{C}$ , combined time-of-flight particle-identification technique obs. 9-2653

Nuclei with  $6 \leq A \leq 19$  continued

- $^{12}\text{C}(\text{C},\alpha)^{10}\text{Ne}$  excitation functions obs. and compared with theory 9-6917  
 $^{12}\text{C}(\text{He}, ^7\text{He})$  ang. distrib. meas., optical model parameters determ.  $\text{E}=18$ -24 MeV 9-11310  
 $^{12}\text{C}(\text{He}, \text{n})^{15}\text{O}_{\text{g.s.}}$ , n polarization ang. distrib. obs., 2.9-3.9 MeV 9-6896  
 $^{12}\text{C}(\text{He}, \text{Li})^{17}\text{O}$  excitation functions obs. and compared with theory 9-6917  
 $^{12}\text{C}(\text{O},\alpha)^{14}\text{Mg}$  excitation functions obs. and compared with theory 9-6917  
 $^{12}\text{C}$ -H satellite nmr spectra in p-benzoquinone, hydroquinone and p dimethoxybenzene 9-13373  
 $^{12}\text{C}(\alpha, \text{n})^{15}\text{O}$ , neutron polarization obs. 9-20805  
 $^{12}\text{C}(\alpha, \text{n})^{15}\text{O}$ ,  $\alpha$ - $\gamma$  correlation meas., depend. on  $\text{E}_\alpha=18$ -24 MeV 9-11317  
 $^{12}\text{C}(\text{d}, \alpha)^{11}\text{B}$ ,  $\alpha$ 's ang. distrib. obs., 6.3 MeV 9-2757  
 $^{12}\text{C}(\text{d}, \text{n})^{13}\text{N}$ , n polarization obs. 9-2756  
 $^{12}\text{C}(\text{d}, \alpha)^{10}\text{B}(\alpha^+, \text{T}=1)$  isospin-nonconserving, cross section meas. 9-20804  
 $^{12}\text{C}(\text{p}, \alpha)^{13}\text{C}$ , with polarized d 9-4797  
 $^{12}\text{C}$ , e $\pi$  and elastic e scatt. parity mixing in nuclear Hartree-Fock orbitals 9-11280  
 $^{12}\text{C}$  neutron emission following  $\mu$  capture and radiative  $\pi$  capture 9-2645  
 $^{12}\text{C}(\gamma, \text{p})^{11}\text{B}$ , photoproton spectrum 9-2715  
 $^{12}\text{C}(\gamma, \text{n})$ , n ang. distrib. meas. in giant resonance region  $\text{E}_\text{p} \leq 10$ ; MeV 9-16954  
 $^{12}\text{C}(\gamma, \text{n})^{11}\text{C}$  up to 260 MeV anomaly in recoil nuclei with energy  $>2.27$  MeV 9-15749  
 $^{12}\text{C}(\text{n}, \alpha)^9\text{Be}$ , 13.9 and 15.6 MeV 9-2743  
 $^{12}\text{C}(\text{n}, \text{n})$  scatt., coupled channel calc., comparison with other treatments, 0-5 MeV 9-11292  
 $^{12}\text{C}(\text{n}, \text{n})$  polarization meas.,  $\text{E}_\text{e}=3.2$ -4.2 MeV 9-20788  
 $^{12}\text{C}$  n cross section obs., peak widths meas. 14-25 MeV 9-6880  
 $^{12}\text{C}(\text{p}, \text{He})^{10}\text{B}$  cross section, calc. 9-584  
 $^{12}\text{C}(\text{p}, \alpha)^9\text{Be}$  DWBA theory fit examined, exchange process possibility, 44.5 MeV 9-4779  
 $^{12}\text{C}(\text{p}, \text{d})^{11}\text{C}$ , distorted wave Born approx. anal.,  $\text{E}_\text{p}=100$  MeV 9-11286  
 $^{12}\text{C}(\text{p}, \text{p})$  polarization meas.,  $\text{E}_\text{p}=1.3$  MeV 9-11282  
 $^{12}\text{C}(\text{p}, \text{p})^{11}\text{C}$ , p polarization obs., 4.6-72 MeV 9-2726  
 $^{12}\text{C}(\text{p}, \text{p})$  level excitation, distorted wave, impulse approx. calc.,  $\text{E}_\text{p}=100$  MeV 9-18091  
 $^{12}\text{C}(\pi^+, \text{p})^{13}\text{C}$  low-energy  $\pi\text{N}$  interactions perturbation theory test, 68 MeV 9-4787  
 $^{12}\text{C}(\pi^-, \pi^+)^{11}\text{B}$  at 1.04 GeV/c momentum, reaction mechanism 9-18099  
 $^{12}\text{C}(\pi^+, 2\text{p})\text{d}^{10}\text{C}$ , cross section and products angular and energy distributions obs. 117 MeV 9-605  
 $\text{F}$ , bound atoms, n coherent scatt. amplitude, obs. 9-6875  
 $\text{F}$ , spin-spin interactions in fluorostyrene n.m.r. 9-19466  
 $\text{F}$  neutron cross-sections for  $\text{E}=13.7$ -14.6 MeV 9-9041  
 $^4\text{F}$ , mass and mass excess, energy of low levels, from  $(^3\text{He}, \text{n})$  reaction 9-2644  
 $^4\text{F}$ , isobaric spin of excited states determ. from  $^{18}\text{O}(\text{p}, \text{n}, \text{t}, \text{d})^4\text{F}$  9-505  
 $^4\text{F}$  hole-particle states assigned from  $^{14}\text{N}(\text{Li}, \text{t})$  reaction 9-8978  
 $^4\text{F}$  in cooling water due to  $^{18}\text{O}(\text{p}, \text{n})^4\text{F}$  9-16985  
 $^4\text{F}$  levels excited by  $^{14}\text{N}(\text{Li}, \text{d})$  9-11324  
 $^4\text{F}$  low energy levels calc. in harmonic oscillator shell model 9-11228  
 $^4\text{F}$ , in triphenylcarbonium ions, n.m.r. study of conformational equilibrium and interconversion 9-19473  
 $^4\text{F}$ , levels excited by  $^{14}\text{N}(\text{Li}, \text{p})$  9-11324  
 $^4\text{F}$ , n.m.r. in  $\text{Me}_2\text{F}_6$ , line narrowing rel. to molecular diffusion 9-16468  
 $^4\text{F}$ , n.m.r. in perfluorobutane, including  $^{12}\text{C}$  satellites 9-13375  
 $^4\text{F}$ , static nuclear quadrupole- interact. parameters, meas. in polycryst. targets 9-4730  
 $^4\text{F}$  in  $\text{K}_2\text{MnF}_4$ , n.m.r. obs. of zero-point spin deviations 9-10151  
 $^4\text{F}$  in  $\text{M}_2\text{BeF}_4$  ( $\text{M}=\text{Na}, \text{K}, \text{Rb}$ ), NMR temp. dependence rel. to crystal structure 9-16466  
 $^4\text{F}$  n.m.r. in  $\alpha$ -methylpentafluorostyrene,  $\alpha$ ,  $\beta$ ,  $\beta$ -trifluorostyrene and copolymers, obs. 9-12518  
 $^4\text{F}$ , shell model, intermediate coupling states structure 9-487  
 $^{17}\text{F}(\text{d}, \alpha)^{17}\text{O}$  excitation energy and ang. distrib., 2.4-3.95 MeV 9-18103  
 $^{17}\text{F}(\text{d}, \alpha)^{17}\text{O}$ , 2.0 and 2.2 MeV bombarding energies, meas. of eight  $\alpha$  groups 9-16965  
 $^{17}\text{F}(\gamma, 2\text{pn})$  yield and cross section meas.  $\text{E}_\text{p}=20$ -300 MeV 9-20772  
 $^4\text{He}$  from  $^4\text{Li}(\text{d}, \alpha)$ , possible level schemes examination 9-20808  
 $^4\text{He}$ , ground state 9-509  
 $^7\text{Li}(\pi^-, \pi^-)$  cross section,  $\pi$  charge, moment and range determ. 9-6891  
 $^7\text{Li}$ , neutron yield following bombard. by  $\alpha$ , d, p, 21-42 MeV 9-616  
 $^7\text{Li}$ , structure from calc. in reactions  $\text{Li}(\pi^-, \text{n})$  and  $\text{Li}(\pi^-, \text{np})$  9-20800  
 $^7\text{Li}$  and  $^7\text{Li}$  in aq. soln., n.m.r. signals 9-3122  
 $^7\text{Li}$ ,  $^7\text{He}$ -induced ang. distrib. of resultant articles meas.  $\text{E}_\text{e}=21.2$ , 24.5, 26.8 MeV 9-11323  
 $^7\text{Li}$ , (p,  $^7\text{He}$ ) $^4\text{He}$ , particles ang. distrib. from polarized beam obs., 0.4-3.2 MeV 9-588  
 $^7\text{Li}$ , e scatt. from 2.18 and 3.56 MeV levels 9-6856  
 $^7\text{Li}$ , obs. of transitions in ground and 1st. two excited states and ang. distrib., from  $^{10}\text{B}(\text{He}, \text{p})^7\text{Li}$  reaction 9-11320  
 $^7\text{Li}$ ,  $\pi^-$  absorpt. at rest, capture rate calc. 9-9049  
 $^7\text{Li}$ ,  $\pi^-$  to mesic atom, 2p-1s transition natural line width meas. 9-9050  
 $^7\text{Li}$ , shell model wave function residual N-N interaction 9-15714  
 $^7\text{Li}$ , width of low-lying states 9-11215  
 $^7\text{Li}$  elastic charge form factor var. calc. 9-13192  
 $^7\text{Li}$   $\pi$ -s-wave radiative capture and  $^7\text{LiHe}^7\text{H}$  vertex junction 9-9048  
 $^7\text{Li}$  scatt. by nuclei, ang. distrib. meas., optical-model parameters determ.,  $\text{E}=20$  MeV, various nuclei ( $12 \leq A \leq 40$ ) 9-15779  
 $^7\text{Li}$  spin-isospin dependent interaction from inelastic p scatt. at 24.4 MeV 9-4778  
 $^4\text{Li}$  mesonic decay to  $\geq 4$  particles obs. 9-20735  
 $^4\text{Li}$ ,  $^7\text{He}$ -induced, ang. distrib. of resultant particles meas.  $\text{E}_\text{e}=21.2$ , 24.2, 24.5, 26.8 MeV 9-11323  
 $^7\text{Li}$ ,  $^7\text{Li}$  from  $^{10}\text{B}(\text{n}, \alpha)$ , relative cross sections determ.,  $\text{E}_\text{e}=30$ -800 keV 9-19318  
 $^7\text{Li}$  scatt. by nuclei, ang. distrib. meas., optical-model parameters determ.,  $\text{E}=20$  MeV, various nuclei ( $12 \leq A \leq 40$ ) 9-15779  
 $^7\text{Li}$  decay, meas.  $\text{T}_{1/2}$  9-2685  
 $^7\text{Li}$  fragments from  $\text{K}^-$  meson interaction 9-15772  
 $^7\text{Li}(\alpha, 2\alpha)$ , two stage channel investigation; 2.5 MeV 9-614  
 $^7\text{Li}(\alpha, 2\alpha)^7\text{H}$  cluster knockout reaction, peripheral model tests 9-19322  
 $^7\text{Li}(\text{d}, \alpha)^4\text{He}$ , possible level schemes examination 9-20808  
 $^7\text{Li}(\text{d}, \alpha)^4\text{He}$  reaction, spin struct. study 9-6914  
 $^7\text{Li}(\text{d}, \alpha)^4\text{He}$ , polarization effects, 4-12 MeV 9-6912  
 $^7\text{Li}(\text{d}, \text{p})^7\text{Li}$ , p ang. distrib. j-depend.,  $l_\text{e}=1$  transitions vector analysing power,  $\text{E}_\text{d}=2.7$ -10.9 MeV 9-15778



Nuclei with  $6 \leq A \leq 19$  continued

- <sup>6</sup>Li(n, $\alpha$ )<sup>3</sup>He. rel. to Li semiconductor neutron sandwich spectrometers 9-19225  
<sup>6</sup>Li(p,d)<sup>3</sup>Li. DWBA analysis, 100 MeV 9-16958  
<sup>7</sup>Li(p,d)<sup>6</sup>Li. DWBA analysis, 100 MeV 9-16958  
<sup>7</sup>Li(p, $\alpha$ ,d), cross section meas., ang. distrib. comparison with free p- $\alpha$  elastic scatt.,  $E_p=61.5$  MeV 9-16959  
<sup>7</sup>Li( $\pi$ ,nn), structure of Li, calc. 9-20800  
<sup>7</sup>Li( $\pi$ ,np)He, structure of Li, calc. 9-20800  
<sup>6</sup>Li( $\pi$ ,2n)<sup>3</sup>He rescattering eff. due to  $\pi$  low energy absorption by d 9-20799  
<sup>6</sup>Li( $\pi$ , $\pi$ )pp<sup>3</sup>He cross section and transition operator 9-15774  
<sup>7</sup>N, energy transfer from neutrons up to 18 MeV obs. 9-20786  
<sup>7</sup>N isotopes, charged-particle reaction cross-sections 9-11264  
<sup>7</sup>N, mass and mass excess, energy of low levels, from (<sup>3</sup>He, n) reaction 9-2644  
<sup>7</sup>N, from <sup>15</sup>N(p,t), spin and parity assignments 9-6866  
<sup>7</sup>N, radiative width for 2.37 MeV state and lifetime 9-11209  
<sup>7</sup>N and <sup>13</sup>C mirror nuclei prod. in isospin multiplet from <sup>14</sup>N, <sup>12</sup>C interac. 9-14568  
<sup>7</sup>N parameters from <sup>13</sup>C(p,p)<sup>12</sup>C. 9-2727  
<sup>7</sup>N radioisotope prod. from Van de Graaff 3 MeV d beam 9-6745  
<sup>7</sup>N, from <sup>12</sup>C(<sup>3</sup>He,p) at 20.1 MeV spin and parity assignment 9-6895  
<sup>7</sup>N, s- and p-wave elastic proton and neutron scatt., Regge trajectory 9-20777  
<sup>7</sup>N, search for resonance in inelastic channel 9-4773  
<sup>7</sup>N, search for resonance in inelastic channel 9-4773  
<sup>7</sup>N(<sup>12</sup>C,<sup>13</sup>C)<sup>13</sup>N, A=13 mirror nuclei prod. in isospin multiplet 9-14568  
<sup>7</sup>N(<sup>12</sup>C,<sup>13</sup>C)<sup>13</sup>N, A=13 mirror nuclei prod. in isospin multiplet 9-14568  
<sup>7</sup>N in Ba(NO<sub>3</sub>)<sub>2</sub>·H<sub>2</sub>O, n.q.r. temp. depend. between 77°K and 300°K 9-10303  
<sup>7</sup>N in metal cyano complexes, n.q.r. 9-19436  
<sup>7</sup>N  $\pi^-$  capture, calc. of resulting reacts. and comparison with cancer radiotherapy expts. 9-13233  
<sup>7</sup>N from <sup>2</sup>H, <sup>14</sup>N; e.m. decay rates of 7.563 MeV bound level calc. 9-6837  
<sup>7</sup>N, e pair emission in decay competition from internal formation 9-6833  
<sup>7</sup>N, from <sup>198</sup>Au, p scatt. at 3 GeV new isotope identified 9-506  
<sup>7</sup>N(O<sup>+</sup>,T=1) from <sup>16</sup>O(d, $\alpha$ ) isospin-nonconserving, cross section meas. 9-20804  
<sup>7</sup>N( $\alpha$ , $\gamma$ )<sup>10</sup>F, 1.00-1.70 MeV, new resonances discovered. 9-611  
<sup>7</sup>N( $\alpha$ ,p)<sup>10</sup>O\*, cross sections meas., levels determ.,  $E_\alpha=13-18$  MeV 9-20806  
<sup>7</sup>Ne Coulomb energies of valence particles calc. 2-particle wave function 9-4728  
<sup>7</sup>Ne energy level spins and parities data, ang. distribution excitation functions, DWBA double stripping calc. 9-2649  
<sup>7</sup>Ne levels lifetime, new level found at  $E_x=3576$  KeV 9-13190  
<sup>7</sup>Ne first excited state, g-factor 9-16936  
<sup>7</sup>NeK $\gamma$  interac. hyper-fragment prod., decay and non-mesic absorpt., bubble chamber obs. 9-364  
<sup>7</sup>N(n, $\alpha$ )<sup>11</sup>B, reaction mech. from energy and ang. distrib. of  $\alpha$ -particles, 14.1 MeV n energy 9-9039  
<sup>7</sup>O, energy transfer from neutrons up to 18 MeV, obs. 9-20786  
<sup>7</sup>O isotopes, charged-particle reaction cross-sections 9-11264  
<sup>7</sup>O energy level spins and parities data, ang. distribution excitation functions, DWBA double stripping calc. 9-2649  
<sup>7</sup>O, 7/2<sup>+</sup> 7.28 MeV g.s. transition meas., B(E3) determ. 9-20739  
<sup>7</sup>O core polarization effects 9-6789  
<sup>7</sup>O from <sup>2</sup>H, <sup>14</sup>N; e.m. decay rates of 7.276 MeV bound level calc. 9-6837  
<sup>7</sup>O radioisotope prod. from Van de Graaff 3 MeV d beam 9-6745  
<sup>7</sup>O, 6.92(2<sup>+</sup>) and 7.12(1<sup>-</sup>) MeV levels widths 9-2652  
<sup>7</sup>O, cross sections compared with e scatt. meas., light nuclei structure determ. 9-4774  
<sup>7</sup>O, electric quadrupole contrib. to photodisintegration 9-11272  
<sup>7</sup>O, of particle-hole intermediate states in <sup>15</sup>O(n, $\gamma$ ) <sup>16</sup>O at 0-10 MeV 9-20796  
<sup>7</sup>O, reaction matrix elements calc. method for <sup>15</sup>So, <sup>15</sup>Si states 9-8987  
<sup>7</sup>O, spin-orbit splitting in Hartree-Fock calc. 9-20741  
<sup>7</sup>O, 1<sup>-</sup>→0<sup>+</sup> E 1 transition, deformed admixtures obs. 9-8986  
<sup>7</sup>O 0<sup>+</sup> state from <sup>16</sup>N g.s. decay, deformed admixtures obs. 9-8986  
<sup>7</sup>O analogue states in <sup>15</sup>N(p,n)<sup>15</sup>O, excitation function and cross sections 9-8977  
<sup>7</sup>O energetics calc. from Brueckner theory in oscillator basis 9-4716  
<sup>7</sup>O giant resonance, excitation of strong transitions by inelastic e scatt. 9-2721  
<sup>7</sup>O levels excited by <sup>14</sup>N( $\alpha$ ,Li $\alpha$ ) obs. 9-11324  
<sup>7</sup>O  $\mu$ -capture and photon-absorption calc. in configuration-mixing model 9-6790  
<sup>7</sup>O  $\pi^-$  capture, calc. of resulting reacts. and comparison with cancer radiotherapy expts. 9-13233  
<sup>7</sup>O rms charge and mass radii, total binding energies, densities and single-particle wave functions 9-11230  
<sup>7</sup>O structure understanding from 0<sup>+</sup> state position, incalculable by Hartree-Fock or related methods 9-20734  
<sup>7</sup>O target, centroids and sums of one-nucleon transfer strengths 9-6805  
<sup>7</sup>O, <sup>17</sup>F doublet, particle-core coupling, low-lying parity states calc. 9-6791  
<sup>7</sup>O, 5.70 and 5.73 MeV levels, from <sup>19</sup>F(d, $\alpha$ )<sup>17</sup>O reaction 9-16965  
<sup>7</sup>O, shell model, harmonic oscillator eigenvalue problem modified 9-14549  
<sup>7</sup>O compound nucleus, spectroscopic data from <sup>13</sup>C( $\alpha$ ,n)<sup>16</sup>O reaction 9-20805  
<sup>7</sup>O, energy levels, shell model new assignments 9-19278  
<sup>7</sup>O low energy levels calc. in harmonic oscillator shell model 9-11228  
<sup>7</sup>O(<sup>3</sup>He,t)<sup>17</sup>F ang. distrib. obs. and DWBA analysis 17.3 MeV 9-6899  
<sup>7</sup>O(<sup>16</sup>O, <sup>16</sup>O)<sup>16</sup>O, new pot. based on statistical theory of nuclear matter. 9-2763  
<sup>7</sup>O\* from <sup>14</sup>N( $\alpha$ ,p), levels, spin, cross sections determ.,  $E_\alpha=13-18$  MeV 9-20806  
<sup>7</sup>O( $\alpha$ ,2 $\alpha$ )<sup>12</sup>C $\gamma$  angular correlation of 2 $\alpha$ 's, reaction mechanisms proposed, 25 MeV 9-4798  
<sup>7</sup>O(d, $\alpha$ ) <sup>14</sup>N(0<sup>+</sup>,T=1) isospin-nonconserving, cross section meas. 9-20804  
<sup>7</sup>O(d,n)<sup>17</sup>F effective cross-section 9-15776  
<sup>7</sup>O( $\gamma$ ,2n) yield and cross section meas.,  $E_\gamma=20-300$  MeV 9-20772  
<sup>7</sup>O( $\gamma$ ,n $\gamma$ ) cross section meas.,  $\gamma$  obs.,  $E_\gamma \leq 32$  MeV 9-13218  
<sup>7</sup>O( $\gamma$ ,p)<sup>15</sup>N angular distrib. of photoproton 9-11273  
<sup>7</sup>O( $\gamma$ ,p $\gamma$ ) cross section meas.,  $\gamma$  obs.,  $E_\gamma \leq 32$  MeV 9-13218  
<sup>7</sup>O(n, $\alpha$ )<sup>13</sup>C cross section obs., 8-12 MeV 9-597

Nuclei with  $6 \leq A \leq 19$  continued

- <sup>16</sup>O(n, $\alpha$ )<sup>13</sup>C, 14.8-18.8 MeV, differential cross-section 9-2744  
<sup>16</sup>O(n, $\gamma$ )<sup>16</sup>O,  $E_n=0-10$  MeV n widths and total capture cross-section calc. 9-20796  
<sup>16</sup>O( $\pi$ , $\pi$ ) $\alpha\alpha\alpha$ , 117 MeV 9-13235  
<sup>16</sup>O(n, $\gamma$ )<sup>16</sup>F, excitation function at 0.5-3.0 MeV triton energies 9-2758  
<sup>16</sup>O(t,p)<sup>16</sup>O(g.s.), cross section determ. by DWBA 9-14632  
<sup>9</sup>Be(p,n)<sup>9</sup>Be cross-section, R-matrix fit. 9-576
- Nuclei with  $90 \leq A \leq 149$
- 110 region, stripping studies  $G_{7/2}-H_{11/2}$  9-14624  
<sup>120</sup>Sn(p, $\gamma$ ) nuclear matter radii and charge distrib. calc. from cross sections 9-11220  
<sup>121</sup>Sb(n, $\gamma$ )<sup>122</sup>Sb, cross-section obs. 9-596  
<sup>121</sup>Pd(n, $\gamma$ ) isomeric cross-sections ratios, spin-cutoff parameter, deduced 24 keV 9-544  
<sup>133</sup>Xe-<sup>133</sup>Cs,  $\gamma$  spectra obs., Cs energy levels determ. 9-15718  
<sup>139</sup>La(n,n'), n energy and ang. distrib. meas., energy levels determ.  $E_n=230-2580$  keV 9-18094  
<sup>99</sup>Tc energy level transitions 181 keV half-life,  $\gamma$  E2 transition prob. determ. 9-9002  
<sup>99</sup>Tc 50 isotones, vib. props. and core-coupling considered 9-511  
<sup>99</sup>Tc photoneutron angular distribution anisotropy from Mo, Ru, Rh, Sb, La and Pr. rel. to subshell occupation 9-4767  
<sup>99</sup>Tc Sn-Al,  $\gamma$  backscatt. by stratified slab, <sup>60</sup>Co, <sup>137</sup>Cs sources 9-9014  
<sup>99</sup>Tc transplutonium elements, bibliography 9-16938  
<sup>99</sup>Tc internal conversion coeffs. at threshold energy 9-6783  
<sup>99</sup>Tc, ratio to <sup>95</sup>Zr in over-ocean fallout 9-18806  
<sup>110m</sup>Ag decay,  $\gamma$  energy obs. 9-6834  
<sup>210</sup>Bi Slater integral of central forces, calc. 9-15701  
<sup>110</sup>Cd and even isotopes, p scatt. cross sections and ang. distrib. meas. 9-6858  
<sup>140</sup>Ce, (n, 2n) cross-sections at 14.7 MeV, obs. 9-2737  
<sup>140</sup>Ce, energy levels, spin and parity assigned from La<sup>140</sup> pair-conversion positrons 9-2666  
<sup>140</sup>Ce(<sup>3</sup>He,d)<sup>141</sup>Pr, rel. to nuclear structure study of <sup>141</sup>Pr 9-15719  
<sup>140</sup>Ce(n, 2n)<sup>139</sup>Ce, absolute activation cross-section for  $E_n=14.8$  MeV, obs. 9-14615  
<sup>140</sup>La  $\beta$  decay,  $\beta$ - $\gamma$  directional correlation from outer group, matrix elements determ. 9-20765  
<sup>100</sup>Mo radiative capture cross sections of p 9-9062  
<sup>100</sup>Ru, spin assignment of n resonances, from captured  $\gamma$  data 9-2662  
<sup>120</sup>Sb, spin and mag. dipole moment determ. 9-6820  
<sup>120</sup>Sb, spins, hyperfine struct., magnetic moments 9-14566  
<sup>120</sup>Sn, nuclear-matter size from opt.-model analysis of 39.6 MeV p scatt. 9-11219  
<sup>130</sup>Te nuclear radiative capture, direct and collective proc. interference 9-581  
<sup>130</sup>Te( $\alpha$ ,n)<sup>133</sup>, <sup>133m</sup>Xe, cross-section meas. 9-15718  
<sup>111m</sup>Pd-<sup>111</sup>Ag,  $\gamma$  spectra meas., energy levels, spin and parity determ. 9-20760  
<sup>111</sup>Ag from <sup>111</sup>Pd, <sup>111m</sup>Pd decay,  $\gamma$  spectra meas., energy levels, spin and parity determ. 9-20760  
<sup>111</sup>Cd, nuclear orientation by optical pumping 9-4447  
<sup>141</sup>Ce, 435 keV first forbidden  $\beta$  transition,  $\beta$ - $\gamma$  correl. obs. 9-6841  
<sup>141</sup>Ce meas. By-CP, deduced  $\beta$ -decay matrix element ratio 9-2685  
<sup>131</sup>I, intermediate-coupling unified nuclear model application, low-lying levels determ. 9-515  
<sup>131</sup>I decay scheme investigation 9-2697  
<sup>111</sup>Pd and <sup>111m</sup>Pd decay scheme, using scintillation spectrometer 9-9004  
<sup>111</sup>Pd-<sup>111</sup>Ag,  $\gamma$  spectra meas., energy levels, spin and parity determ. 9-20760  
<sup>141</sup>Pr, energy levels and spins from n inelastic scatt., 2.9 MeV 9-4747  
<sup>141</sup>Pr,  $\gamma$  spectra obs. 9-11224  
<sup>141</sup>Pr, n capture cross section, 5 keV-3 MeV 9-9042  
<sup>141</sup>Pr, structure study from <sup>140</sup>Ce(<sup>3</sup>He,d)<sup>141</sup>Pr reaction, 0-4 MeV 9-15719  
<sup>141</sup>Pr(n,p)<sup>141</sup>Ce, absolute activation cross-section for  $E_n=14.8$  MeV, obs. 9-14615  
<sup>141</sup>Pr(n,t)<sup>139</sup>Ce, absolute activation cross-section for  $E_n=14.8$  MeV, obs. 9-14615  
<sup>141</sup>Pr(n,n'), n energy and ang. distrib. meas., energy levels determ.  $E_n=230-2580$  keV 9-18094  
<sup>141</sup>Pr(n,n'),  $\gamma$  spectra meas., energy levels determ.,  $E_n=0.5-2.3$  MeV 9-14613  
<sup>123</sup>Sb, n and radiative capture total cross sections meas. 9-14567  
<sup>123</sup>Sb total n cross-sections for energy range 0.002 to 0.4 eV 9-11290  
<sup>111</sup>Sn-<sup>111</sup>In decay, <sup>111</sup>In de-excitation, <sup>111</sup>Sn capture 9-19293  
<sup>127</sup>Sn(p, p) nuclear matter radii and charge distrib. calc. from cross sections 9-11220  
<sup>101m</sup>Tc from (p,n) reaction, half life and energy meas. 9-11217  
<sup>132</sup>Ce, collective levels from (<sup>16</sup>O, 4n) (<sup>18</sup>Ne, 4n) reactions, 4-5 MeV/nucleon 9-516  
<sup>112</sup>Ag-<sup>112</sup>Cd, energy levels, spin and parity determ. 9-13208  
<sup>112</sup>Cd from <sup>112</sup>Ag decay, energy levels, spin and parity determ. from  $\gamma$  spectra 9-13208  
<sup>142</sup>Ce, (n, 2n) cross-sections at 14.7 MeV, obs. 9-2737  
<sup>142</sup>Ce nuclear radiative capture, direct and collective proc. interference 9-581  
<sup>142</sup>Ce(n, 2n)<sup>141</sup>Ce, absolute activation cross-section for  $E_n=14.8$  MeV, obs. 9-14615  
<sup>122</sup>I, decay scheme from  $\gamma$ -ray study 9-11222  
<sup>132</sup>I, new high energy gammas, obs. 9-18081  
<sup>132</sup>I, standardized soln. used in calibration of 1383A ionization chamber 9-19230  
<sup>132</sup>I soln. activity meas. by 4 $\pi$  $\gamma$ -coincidence technique 9-19230  
<sup>142</sup>Nd, (n, 2n) cross-sections at 14.7 MeV, obs. 9-2737  
<sup>142</sup>Nd,  $\gamma$  spectra obs. 9-11224  
<sup>142</sup>Nd, thermal-n capture,  $\gamma$  spectra obs., transition schemes determ. 9-14569  
<sup>142</sup>Nd n resonances, level spacing 9-11298  
<sup>142</sup>Pr, energy levels from (d, p) reaction 9-2667  
<sup>102</sup>Ru, spin assignment of n resonances, from captured  $\gamma$  data 9-2662  
<sup>122</sup>Sb, radioactive decay, negaton spectrum obs. 9-556  
<sup>122</sup>Sb first-forbidden  $\beta$  transitions, nuc. matrix elements parameters, agree with single-part. predictions 9-2705  
<sup>112</sup>Sn and even isotopes, p scatt. cross sections and ang. distrib. meas. 9-6858  
<sup>122</sup>Sn, nuclear-matter size from opt.-model analysis of 39.6 MeV p scatt. 9-11219  
<sup>132</sup>Sn, form factor of real symmetry potential, depend. on n-p interaction strength 9-6822

Nuclei with  $90 \leq A \leq 149$  continuedNuclei with  $90 \leq A \leq 149$  continued

- <sup>122</sup>Sn(0, p) nuclear matter radii and charge distrib. calc. from cross sections 9-11220
- <sup>122</sup>Sn(n,  $\gamma$ )<sup>123</sup>Sn, cross-section defined, 0.3-2.7 MeV 9-596
- <sup>122</sup>Te E2 transitions,  $2^+ \rightarrow 0$ ,  $2^+ \rightarrow 2^+$  obs. 9-20684
- <sup>102</sup>Ag decay,  $\beta$  and  $\gamma$  half-lives, levels and transitions 9-18078
- <sup>113</sup>Cd nuclear orientation by optical pumping 9-4447
- <sup>113</sup>Ba decay, energy of  $\gamma$  emitted meas. with Ge(Li) detect. 9-2695
- <sup>113</sup>Ba-<sup>137</sup>Cs, 437 KeV level, (L+M+...)/K capture ratio obs. 9-14593
- <sup>113</sup>Ba e. capture decay, 222 keV  $\gamma$  obs. 9-15737
- <sup>113</sup>Cd, n.m.r. in cadmium metal, spin-lattice relax. temp. dependence 9-12510
- <sup>143</sup>Ce decay to <sup>143</sup>Pr, role of weak transitions 9-15720
- <sup>137</sup>Cs, ang. correlation of 223-161 keV cascade, spin of 384 keV state 9-20738
- <sup>137</sup>Cs, Debye-Waller factors in Cs halides 9-11986
- <sup>137</sup>Cs from <sup>137</sup>Ba decay, spin assignments for  $\gamma$  spectra 9-8981
- <sup>137</sup>Cs from <sup>137</sup>Xe  $\gamma$  decay, energy levels determ. 9-15718
- <sup>137</sup>Cs n.m.r. in Cs<sub>2</sub>MX<sub>4</sub> 9-17503
- <sup>113m</sup>In, e.m. decay, search for double electron ejection 9-6796
- <sup>113</sup>In(n,  $2n$ )<sup>112</sup>In,  $E_n=14.7$  MeV, cross-section and spin distrib. obs. 9-11296
- <sup>143</sup>Nd, thermal-n capture,  $\gamma$  spectra obs., transition schemes determ. 9-14569
- <sup>143</sup>Nd n resonances, level spacing 9-11298
- <sup>143</sup>Pm level structure obs. 9-6802
- <sup>143</sup>Pm log ft values, levels, spins from <sup>143</sup>Sm decay 9-8983
- <sup>103m</sup>Ru from ( $\gamma$ , n) reaction, half life and energy meas. 9-11217
- <sup>127</sup>Sb, n and radiative capture total cross sections meas. 9-14567
- <sup>127</sup>Sb(n,  $\gamma$ )<sup>128</sup>Sb cross-section obs. 9-596
- <sup>127</sup>Sn(n,  $\gamma$ ),  $\gamma$  spectra obs., E1, M1 transitions meas. 9-13228
- <sup>127</sup>Sn decay, energy of  $\gamma$  emitted meas. with Ge(Li) detect. 9-2695
- <sup>127</sup>Xe isomeric transition, K internal conversion coeff. determ. 9-15718
- <sup>127</sup>Ce, collective levels from (<sup>16</sup>O, 4n) (<sup>20</sup>Ne, 4n) reactions, 4-5 MeV/nucleon 9-516
- <sup>114</sup>Cd, quadrupole moment, from reorientation eff. 9-6797
- <sup>114</sup>Cd K conversion coeffs., 1.9 MeV 9-2663
- <sup>144</sup>Cd(d, d'), inelastic scattering near Coulomb barrier 9-9053
- <sup>124</sup>I, decay scheme 9-13209
- <sup>114</sup>In obs. by Siegbahn-Slater intermediate image spectrometer 9-15690
- <sup>144</sup>Nd, energy levels determ. from <sup>144</sup>Pm  $\gamma$  decay 9-517
- <sup>144</sup>Nd, thermal-n capture,  $\gamma$  spectra obs., transition schemes determ. 9-14569
- <sup>144</sup>Nd high energy levels excited in <sup>144</sup>Pm decay 9-8984
- <sup>144</sup>Nd n resonances, level spacing 9-11298
- <sup>144</sup>Pm, e capture decay scheme 9-6836
- <sup>144</sup>Pm-<sup>144</sup>Nd,  $\gamma$  decay scheme obs. Nd levels determ. 9-517
- <sup>144</sup>Pr, decay scheme using scintillation spectrometer 9-9005
- <sup>127</sup>Sb-<sup>124</sup>Te,  $\gamma$  spectra meas., partial decay scheme proposal, levels determ. 9-18079
- <sup>118</sup>Sb, fission yield and half life, isomeric states 9-622
- <sup>125</sup>Sn, nuclear-matter size from opt.-model analysis of 39.6 MeV p scatt. 9-11219
- <sup>114</sup>Sn( $\alpha$ , n)<sup>117</sup>Te, search for isomeric transition,  $E_\alpha=17.27$  MeV 9-15716
- <sup>124</sup>Sn(n,  $\gamma$ )<sup>125</sup>Sn cross-section obs. 9-596
- <sup>124</sup>Te, 1103.5 keV level, from <sup>124</sup>Sb decay obs. 9-6834
- <sup>124</sup>Te, excited levels, from <sup>124</sup>I decay 9-13209
- <sup>124</sup>Te from <sup>124</sup>Sb decay,  $\gamma$  spectra meas. partial decay scheme proposal, levels determ. 9-18079
- <sup>125m</sup>Te as X-ray source 9-22023
- <sup>115</sup>Cs, 662 keV allowed  $\beta$  transition,  $\beta$ - $\gamma$  correl. obs. 9-6841
- <sup>115</sup>Cs from <sup>135</sup>Xe decay, levels and spin determ. from  $\gamma$  meas. 9-19296
- <sup>115</sup>Cs from <sup>135</sup>Xe  $\gamma$  decay, energy levels determ. 9-15718
- <sup>145</sup>Eu level structure obs. 9-6802
- <sup>145</sup>Eu-<sup>145</sup>Sm energy levels, spin and parity assignments 9-14571
- <sup>115</sup>Gd in GdFe<sub>2</sub>, absence of induced mag. field at nuclei 9-17470
- <sup>121</sup>I, from <sup>127</sup>In,  $3n$  at  $E_n=14.7$  MeV, lifetime and activation cross-section obs. 9-9038
- <sup>115</sup>In, e excitation, comparison of expt. and theory 9-6798
- <sup>115</sup>In(n,  $2n$ )<sup>114</sup>In,  $E_n=14.7$  MeV, cross-section and spin distrib. obs. 9-11296
- <sup>145</sup>Nd, thermal-n capture,  $\gamma$  spectra obs., transition schemes determ. 9-14569
- <sup>145</sup>Nd n resonances, level spacing 9-11298
- <sup>145</sup>Nd(p,  $2n$ ), <sup>145</sup>Pm e capture decay scheme 9-6836
- <sup>115</sup>Sb, spins, hyperfine struct., magnetic moments 9-14566
- <sup>115</sup>Sb-<sup>115</sup>Sn,  $\gamma$  spectra obs., energy levels determ. 9-14592
- <sup>125</sup>Sb decay,  $\gamma$ -ray study for <sup>125</sup>Te level scheme 9-15736
- <sup>145</sup>Sm from <sup>145</sup>Eu decay; energy levels, spin and parity assignments 9-14571
- <sup>115</sup>Sn from <sup>115</sup>Sb decay,  $\gamma$  spectra obs., energy levels determ. 9-14592
- <sup>115</sup>Sn( $\alpha$ ,  $2n$ )<sup>117</sup>Te, search for isomeric transition,  $E_\alpha=17.27$  MeV 9-15716
- <sup>125</sup>Te, level scheme from <sup>125</sup>Sb decay 9-15736
- <sup>125</sup>Te, mag. relax. in Te crystal, obs. and mechanism 9-10299
- <sup>125m</sup>Xe, half-life and decay scheme 9-4755
- <sup>135</sup>Xe-<sup>135</sup>Cs,  $\gamma$  half-life determ. 9-15718
- <sup>135</sup>Xe-<sup>135</sup>Cs, levels and spin determ. from  $\gamma$  meas. 9-19296
- <sup>126</sup>I, from <sup>127</sup>In,  $2n$  at  $E_n=14.7$  MeV, lifetime and activation cross-section obs. 9-9038
- <sup>136</sup>I  $\beta$  decay,  $\gamma$  spectra obs., energy levels, lifetime determ. 9-20762
- <sup>146</sup>Nd, thermal-n capture,  $\gamma$  spectra obs., transition schemes determ. 9-14569
- <sup>146</sup>Nd n resonances, level spacing 9-11298
- <sup>106</sup>Pd, spin assignment of n resonances, from captured  $\gamma$  data 9-2662
- <sup>106</sup>Pd  $\gamma$  spectra obs., energy levels, spin and parity determ. 9-13193
- <sup>106</sup>Pd levels from decay of <sup>106a</sup>Rh 9-4753
- <sup>146</sup>Pr 24 min,  $\beta$ -decay 9-2698
- <sup>106</sup>Rh, decay, conversion electrons and  $\gamma$ -spectrum obs. 9-555
- <sup>106</sup>Rh-<sup>106</sup>Pd,  $\beta$ - $\gamma$  ang. correlation, test of time-reversal 9-4732
- <sup>106</sup>Rh, decay scheme of 19 levels 9-4753
- <sup>116</sup>Sb, 103.2 keV transition from conversion electron obs. 9-6799
- <sup>116</sup>Sb from <sup>116</sup>Te,  $\beta$ - $\gamma$  spectra obs., decay scheme determ. 9-11249
- <sup>116</sup>Sb-<sup>116</sup>Sn,  $\beta$ - $\gamma$  spectra obs., decay scheme determ. 9-11249
- <sup>146</sup>Sm energy levels determ. from conversion e meas. 9-15721
- <sup>116</sup>Sn, 134.5 keV transition from conversion electron obs. 9-6799
- <sup>116</sup>Sn, energy spectrum and effective nuclear forces 9-19275
- <sup>116</sup>Sn, excitation by inelastic p. scatt. at 14.695 MeV and collective states 9-512
- <sup>116</sup>Sn, nuclear-matter size from opt.-model analysis of p scatt. 9-11219
- <sup>116</sup>Sn from <sup>116</sup>Sb,  $\beta$ - $\gamma$  spectra obs., decay scheme determ. 9-11249
- <sup>116</sup>Sn(p, p) nuclear matter radii and charge distrib. calc. from cross sections 9-11220
- <sup>116</sup>Te-<sup>116</sup>Sb,  $\beta$ ,  $\gamma$  spectra obs., decay scheme determ. 9-11249
- <sup>126</sup>Te and even isotopes, p scatt. cross sections and ang. distrib. meas. 9-6858
- <sup>136</sup>Xe, neutron particle-hole states observed by inelastic scatt. 9-20779
- <sup>137m</sup>Ce and <sup>137g</sup>Ce, isomer ratios formed in reactions due to <sup>3</sup>He, <sup>4</sup>He, <sup>7</sup>Li and <sup>12</sup>C 9-2665
- <sup>107</sup>Ag in emulsion, interaction with 13.8 GeV protons 9-19308
- <sup>107</sup>Ag muonic X-ray spectra, isotope shift of K lines and RMS radius, comparison with opt. spect. 9-6794
- <sup>107</sup>Ag( $\alpha$ ,  $2n$ )<sup>109m</sup>In isomeric cross-section ratios with <sup>107</sup>Ag reaction 9-6894
- <sup>137</sup>Ba, metastable state, M4 decay obs. 9-6848
- <sup>117</sup>Cd-<sup>117</sup>In,  $\beta$  decay periods and charactrs. 9-20761
- <sup>137</sup>Cs,  $\beta$ -branching ratio, and internal K-conversion coeffs. 9-4762
- <sup>137</sup>Cs in fallout annual variation at Vilnius (1966) 9-12590
- <sup>137</sup>Cs level structure obs. 9-6802
- <sup>137</sup>Cs low activity source in monitor film badges calibration apparatus 9-20756
- <sup>157</sup>Gd(n,  $\gamma$ )<sup>158</sup>Gd, conversion electron spectrum 9-15764
- <sup>127</sup>I, intermediate-coupling unified nuclear model application, low-lying levels determ. 9-515
- <sup>127</sup>I, quadrupole coupling constant in  $\beta$ -AgI powders and single crystals 9-18745
- <sup>127</sup>I( $\alpha$ ,  $\alpha'$ ),  $\gamma$  spectra meas., Coulomb excitation, E2 transition prob. determ.,  $E_\alpha=3.5$ -5 MeV 9-20737
- <sup>127</sup>I(n, n') 59 keV level excited, cross section meas.,  $E_n=50$ -500 keV 9-19277
- <sup>127</sup>In excited states life-times and  $\gamma$  meas. 9-2664
- <sup>127</sup>I(p, p'),  $\gamma$  spectra meas., Coulomb excitation, E2 transition prob. determ.,  $E_p=3.5$ -5 MeV 9-20737
- <sup>147</sup>Pm, spin assignment of 413 keV state 9-11225
- <sup>117</sup>Sb, spins, hyperfine struct., magnetic moments 9-14566
- <sup>117</sup>Sb-<sup>117</sup>Sn,  $\gamma$  spectra meas., energy levels, spin and parity determ. 9-13194
- <sup>127m</sup>Sb, from <sup>127</sup>I(n,  $\alpha$ ) at  $E_n=14.7$  MeV, lifetime and activation cross-section obs. 9-9038
- <sup>147</sup>Sm,  $\alpha$  emission, half-life and energy determ. 9-2699
- <sup>147</sup>Sm,  $\gamma$  spectra following thermal n capture 9-18066
- <sup>147</sup>Sm energy levels determ. from  $\gamma$ - $\gamma$  coinc. method 9-15722
- <sup>117</sup>Sn from <sup>117</sup>Sb decay,  $\gamma$  spectra meas., energy levels, spin and parity determ. 9-13194
- <sup>127</sup>Te, from <sup>127</sup>In, p at 14.7 MeV, lifetime and activation cross-section obs. 9-9038
- <sup>127</sup>Te, lifetime of 341 keV level 9-6801
- <sup>127</sup>Te from <sup>126</sup>Te(d, p); energy levels and spectroscopic factors determ.,  $E_d=7.5$  MeV 9-11223
- <sup>127m</sup>Xe half-life and decay scheme 9-4755
- <sup>108</sup>Pd(n,  $\gamma$ ) isomeric cross section ratios, spin-cutoff parameter deduced, 24 keV 9-544
- <sup>138</sup>Ba radiative capture cross sections of triton 9-9062
- <sup>208m</sup>Bi from ( $\gamma$ , n) reaction, half life and energy meas. 9-11217
- <sup>128</sup>Ce, collective levels from (<sup>16</sup>O, 4n) (<sup>20</sup>Ne, 4n) reactions 4-5 MeV/nucleon 9-516
- <sup>128</sup>I, from <sup>127</sup>In,  $\gamma$  at  $E_n=14.7$  MeV, lifetime and activation cross-section obs. 9-9038
- <sup>128</sup>I decay 9-19294
- <sup>118</sup>In 7- or 8- isomeric state found, decay obs., levels, spin and parity determ. 9-19276
- <sup>148</sup>Nd (<sup>16</sup>O, <sup>16</sup>O $\gamma$ )  $2^+$  states  $\gamma$  emission ang. distrib., hyperfine interactions 9-15781
- <sup>148</sup>Nd n resonances, level spacing 9-11298
- <sup>148</sup>Pm decay,  $\beta$ - $\gamma$  directional correlation 9-558
- <sup>118</sup>Sb, spins, hyperfine struct., magnetic moments 9-14566
- <sup>148</sup>Sm,  $\alpha$  emission, half-life and energy determ. 9-2699
- <sup>148</sup>Sm energy levels determ. from conversion e meas. 9-15721
- <sup>118</sup>Sn nuclear-matter size from opt.-model analysis of 39.6 MeV p scatt. 9-11219
- <sup>118</sup>Sn(p, p) nuclear matter radii and charge distrib. calc. from cross sections 9-11220
- <sup>158m</sup>Tb from ( $\gamma$ , n) reaction, half life and energy meas. 9-11217
- <sup>128</sup>Te-<sup>129</sup>I,  $\gamma$  spectra obs., energy levels, spin and parity determ. 9-18080
- <sup>129m</sup>Te-<sup>129</sup>I,  $\gamma$  spectra obs., energy levels, spin and parity determ. 9-18080
- <sup>109</sup>Ag, muonic X-ray spectra, isotope shift of K lines and RMS radius, comparison with opt. spect. 9-6794
- <sup>109</sup>Ag levels from <sup>109</sup>Pd decay 9-19274
- <sup>109</sup>Ag( $\alpha$ ,  $2n$ )<sup>111g</sup>In reaction, isomeric cross-section ratios with <sup>107</sup>Ag reaction 9-6894
- <sup>139</sup>Ba, reduced normalization and spectroscopic factors 9-9061
- <sup>139</sup>Ba decay to levels in <sup>139</sup>La to study struct. of N=82 isotones 9-8982
- <sup>139</sup>Ba first-forbidden  $\beta$  decay, spectral shape factor, directional correlation meas. 9-20763
- <sup>139</sup>Ce, decay, probability of K-capture 9-4756
- <sup>139</sup>Ce production in <sup>139</sup>La (p, n) and (d,  $2n$ ) reactions 9-586
- <sup>140</sup>Ce from <sup>140</sup>La decay,  $\gamma$  spectra obs., spin and parity assigned 9-11224
- <sup>119</sup>I in CsI, recoilless fraction of 26.8 keV transition, calc. using Debye model of phonon spectrum 9-12359
- <sup>129</sup>I, Debye-Waller factors in CsI 9-11986
- <sup>129</sup>I, excited states following <sup>129m</sup>Te decay 9-15717
- <sup>129</sup>I, Mossbauer effect in CuCr<sub>2</sub>Te ferromag. spinel, internal mag. field determ. 9-16400
- <sup>129</sup>I from <sup>129m</sup>Te decay, energy levels, spin and parity determ. from  $\gamma$  spectra 9-18080
- <sup>129</sup>I in CrI<sub>3</sub>, Mossbauer effect obs. of internal fields 9-21609
- <sup>129</sup>I in I<sub>2</sub>O<sub>4</sub>, quadrupole splitting of Mossbauer level at 80°K 9-16403
- <sup>129</sup>I/<sup>129</sup>Xe decay intervals of chondrite dark phases 9-2061
- <sup>139</sup>La, energy levels and spins from n inelastic scatt., 2.9 MeV 9-4747
- <sup>139</sup>La, n capture struct. of N=82 isotones from <sup>139</sup>Ba decay 9-8982
- <sup>139</sup>La, n capture cross section, 5 keV-3 MeV 9-9042
- <sup>139</sup>La  $\gamma$  spectra obs. 9-11224
- <sup>139</sup>La level structure obs. 9-6802
- <sup>139</sup>La radiative capture cross sections of  $\alpha$  and d 9-9062
- <sup>139</sup>La( $\gamma$ ,  $\pi$ )  $\pi=1, 3$ , cross sections meas.,  $E_\pi \leq 30$  MeV 9-11271
- <sup>139</sup>La(n, n'),  $\gamma$  spectra meas., energy levels determ.,  $E_n=0.5$ -2.3 MeV 9-14613
- <sup>139</sup>La(p, n), and (d,  $2n$ ) <sup>139</sup>Ce production, energy dependence 9-586
- <sup>139m</sup>Nd,  $\beta$ -decay 9-6835



Nuclei with  $90 \leq A \leq 149$  continued

- <sup>149</sup>Pm, numerical estimate of existence of probable levels 9-2637  
<sup>139</sup>Pr, level scheme 9-6835  
<sup>119</sup>Sb, energy level determ., nuclear model discussion 9-4754  
<sup>119</sup>Sb, spins, hyperfine struct., magnetic moments 9-14566  
<sup>149</sup>Sm,  $\alpha$  emission, half-life and energy determ. 9-2699  
<sup>149</sup>Sm,  $\gamma$  spectra following thermal n capture 9-18066  
<sup>119</sup>Sn,  $\Delta R/R$  sign and magnitude for excitation to 23.8 keV level 9-11221  
<sup>119</sup>Sn, isomeric shift in Cu-Sn alloy Mossbauer spectrum 9-5888  
<sup>119</sup>Sn crystal, Knight shift parameters obs., temp. depend., <sup>139</sup>K-m.p. 9-12515  
<sup>119</sup>Sn in Er, Mossbauer spectra, hyperfine mag. fields 9-5890  
<sup>119</sup>Sn in Gd, mag. field 9-12282
- <sup>119</sup>Sn in Pd<sub>2</sub>MnSn Heusler alloy, internal field at site 9-16404  
<sup>119</sup>Sn in V<sub>2</sub>O<sub>5</sub>:Fe<sup>3+</sup>, Sn<sup>4+</sup> Mossbauer effect 9-21613  
<sup>119</sup>Sn in Nb<sub>2</sub>Sn, temp.-dependent isomer shift and anharmonic binding from Mossbauer effect meas. 9-7960  
<sup>119</sup>Sn source,  $\gamma$ -quanta correlation in X-ray band 9-20598  
<sup>119m</sup>Sn 23.9 keV-g.s. transition total internal conversion coeff. obs. 9-6800  
<sup>119m</sup>Sn in CaSnO<sub>3</sub>, suitable source for Mossbauer studies 9-12358  
<sup>159</sup>Tb( $\gamma$ ,xn) x=1-3, cross sections meas., E <sub>$\gamma$</sub>  < 30 MeV 9-11271  
<sup>119</sup>Tb, decay analysis by  $\gamma$ - $\gamma$  coincidence spectra 9-4754  
Ba, even-even isotopes, high-spin rotational levels 9-514  
Ba isotope prod. cross-sections for U fission by 1-2.9 GeV p 9-4809  
Cd, cross section meas. for neutrons, 10  $\mu$ eV range 9-6873  
Cd, e backscatt. coeffs. 10 and 20 MeV 9-6855  
Cd, neutron cross-sections between 0.01 and 10 eV 9-19315  
Ce, even-even isotopes, high-spin rotational levels 9-514  
<sup>133</sup>Cs in aq. soln., n.m.r. signals 9-3122  
Cs isotope prod. cross-sections for U fission by 1-2/9 GeV p 9-4809  
decay,  $\gamma$ - $\gamma$  directional correlation 9-19295  
I isotope prod. cross-sections for U fission by 1-2.9 GeV p 9-4809  
In, isomeric cross section ratios for (n,2n) reactions induced by 14.7 MeV n 9-6879  
La-Pm L-subshell internal conversion calcs. including deformation due to quadrupole moment 9-2641  
<sup>91</sup>Mo, 5<sup>-</sup> and 3<sup>-</sup> states, study via decay of 11.80 MeV isobaric analog reson. of <sup>91</sup>Tc 9-4752  
<sup>91</sup>Mo, energy levels, spin, parity assigned from cross sections, 31 MeV of  $\alpha$  scatt. 9-546  
<sup>91</sup>Mo, ground state, exptl. strengths of g<sub>9/2</sub> and p<sub>1/2</sub> components 9-14630  
<sup>96</sup>Mo, energy levels excited in decay of <sup>96m</sup>Tc isomeric pair, and <sup>96</sup>Nb 9-6831  
<sup>96</sup>Mo, spin assignment of n resonances, from captured  $\gamma$  data 9-2662  
<sup>96</sup>Mo polarised thermal n capture,  $\gamma$  circular polarisation obs. 9-13230  
<sup>96</sup>Mo, n capture crn, 5 keV-3 MeV 9-9042  
<sup>96</sup>Mo, spin assignment of a n resonances, from captured  $\gamma$  data 9-2662  
<sup>96</sup>Mo, forbidden beta transition  $1/2^+ \rightarrow 3/2^+$ , ang. correl. 9-6843  
<sup>96</sup>Mo-<sup>99</sup>Tc, energy levels determ. from  $\gamma$  internal conversion spectra 9-11258  
<sup>96</sup>Mo-<sup>99</sup>Tc,  $\gamma$  spectra meas., decay scheme determ. 9-15731  
<sup>96</sup>Mo( $\gamma$ , p) and ( $\gamma$ , n) cross-section obs. 9-9016  
<sup>91m</sup>Tc isolation from worn-out parts of U-120 cyclotrons 9-19258  
<sup>96m</sup>Tc isomeric pair, decay rel. to levels of <sup>96</sup>Mo 9-6831  
<sup>96m</sup>Tc labeling of cystine and methionine 9-21989  
<sup>91</sup>Nb d<sub>3/2</sub> analog state E1  $\gamma$  decay from <sup>90</sup>Zr(p,  $\gamma$ ) obs. 9-4751  
<sup>91</sup>Nb Slater integral of central forces, calc. 9-15701  
<sup>91</sup>Nb detection of fast n fluence 9-11340  
<sup>91</sup>Nb, isolation from worn-out parts of U-120 cyclotrons 9-19258  
<sup>91</sup>Nb from <sup>95</sup>Zr decay, lifetime, energy levels, spin and parity from  $\beta$ ,  $\gamma$  spectra 9-15744  
<sup>96</sup>Nb, decay rel. to levels of <sup>96</sup>Mo 9-6831  
<sup>91</sup>Nb  $\gamma$  irradiated, anal. of  $\alpha$  energy spectra 9-2720  
<sup>93</sup>Nb(d,d) differential cross sections obs., increase in filled n shell region, 13.6 MeV 9-608  
Sb, isomeric cross-section ratios for (n, 2n) reactions induced by 14.7 MeV n 9-6879  
Sn, applic. of Tamm-Dancoff theories of vibrational states 9-2639  
Sn even-mass isotopes including hard core excitation, shell-model calc. 9-6795  
Sn isotopes, activation cross-sections for (n,2n) and (n,p) react., comparison with compound-nucleus theory, isomeric ratios meas. 9-9037  
<sup>90</sup>Sr, activity in air and surface deposition 9-21783  
<sup>90</sup>Sr on Earth's surface, rel. to fallout rate 9-17555  
<sup>91</sup>Tc, isobaric analog reson. at 11.80 MeV, decay rel. to 5<sup>-</sup> and 3<sup>-</sup> states of <sup>91</sup>Mo 9-4752  
<sup>95</sup>Tc isomers, decay to levels in <sup>95</sup>Mo,  $\gamma$  energies and intensities 9-14599  
<sup>95</sup>Tc from <sup>99</sup>Mo decay, levels, spin, parity determ. from  $\gamma$  spectra 9-15731  
<sup>95</sup>Tc from <sup>99</sup>Mo decay, energy levels determ. from  $\gamma$  internal conversion spectra 9-11258  
Te isotope prod. cross-sections for U fission by 1-2.9 GeV p 9-4809  
Xe, even-even isotopes, high-spin rotational levels 9-514  
Xe excited levels from ( $\alpha$ ,2n) react., Te and Sn targets 9-16940  
<sup>90</sup>Y, e pair emission in decay competition from internal formation 9-6833  
<sup>90</sup>Y, spin, orb. ang. mom. config. from isobaric analog, comparison, <sup>89</sup>Y(p,p) meas. 9-20751  
Zr-Sn charge radius based on muonic K $\alpha$  isotope shifts 9-535  
<sup>90</sup>Zr, energies of low-lying excited levels 9-13205  
<sup>90</sup>Zr, energy levels, spin, parity assigned from cross sections, 31 MeV of  $\alpha$  scatt. 9-546  
<sup>90</sup>Zr, isobaric splitting of 1<sup>-</sup> levels 9-15705  
<sup>90</sup>Zr, n inelastic scatt. cross section, modified optical model transmission coeff. 9-20791  
<sup>90</sup>Zr rms charge and mass radii, total binding energies, densities and single-particle wave functions 9-11230  
<sup>91</sup>Zr, energies of low-lying excited levels 9-13205  
<sup>91</sup>Zr, energies of low-lying excited levels 9-13205  
<sup>91</sup>Zr, lifetime of 267 keV state scintillation methods 9-9001  
<sup>91</sup>Zr, ratio to <sup>95</sup>Nb in over-ocean fallout 9-18806  
<sup>95</sup>Zr-<sup>99</sup>Nb, decay scheme, lifetime, energy levels, spin and parity from  $\beta$ ,  $\gamma$  spectra 9-15744  
<sup>96</sup>Zr (t,p) <sup>98</sup>Zr, p ang. distrib. meas., spin, parity, n configurations determ. 9-20752  
<sup>98</sup>Zr from <sup>96</sup>Zr(t,p), p ang. distrib. meas., spin, parity, n configurations determ. 9-20752  
<sup>96</sup>Zr(p,p) <sup>90</sup>Zr isobaric analogue resonance spectroscopic factors 9-494

Nuclei with  $A \leq 5$ 

- <sup>3</sup>H polarised proton ang. distrib., scatt. at 12.0 MeV 9-9021

Nuclei with  $A \leq 5$  continued

- binding energy and wave function calc., absence of three neutron and <sup>3</sup>H excited state 9-2658  
deuteron electrodisintegration near threshold, at low momentum transfer 9-13191  
deuterons, photodisintegration, 100-320 MeV 9-2655  
energy levels from translation-invariant shell model calc. for A=4,5 9-14565  
ground state structure and binding energy calc. 9-11189  
three-particle, nuclear photoeffect 9-2506  
tritium, e.m. radii calc. in a theory of zero-range forces 9-11213  
triton binding energy calc., realistic local potentials 9-13150  
triton binding energy calc. from N-N interaction potential 9-13140  
d optical potential 9-2656  
<sup>3</sup>H, p scatt. spin and isospin-depend. anal. 9-4775  
<sup>3</sup>H elastic scatt. cross section from <sup>3</sup>He, 11.9-18.9 MeV 9-6907  
<sup>3</sup>H(<sup>2</sup>He,p)<sup>4</sup>He, 15.8 MeV proton total react. cross section using associated particle method 9-16957  
<sup>3</sup>He elastic scatt. cross section from <sup>3</sup>He, 4.3-21.4 MeV 9-6907  
<sup>3</sup>Li, level struct. from D(<sup>2</sup>He,p)<sup>3</sup>Li reaction, 2.3-12.2 MeV <sup>3</sup>He energy 9-4799  
<sup>4</sup>He, cross sections compared with e scatt. meas., light nuclei structure determ. 9-4774  
Be neutron cross-sections for E=13.7-14.6 MeV 9-9041  
D, bound atoms, n coherent scatt. amplitude, obs. 9-6875  
D, n capture cross section, 2200 m/sec 9-15766  
<sup>2</sup>D, spin lattice relax. in rochelle salt 9-10155  
H, energy transfer from neutrons up to 18 MeV, obs. 9-20786  
<sup>3</sup>H in aq. soln. n.m.r. signals 9-3122  
<sup>3</sup>H, e scatt. super perturbation theory and bounds in s-wave triplet state 9-11278  
<sup>3</sup>H, nuclear spin-lattice relax. in antiferromag. Rb<sub>2</sub>MnCl<sub>4</sub>·2H<sub>2</sub>O 9-21597  
<sup>3</sup>H, n) spectra cross section obs., 14.1 MeV 9-598  
<sup>3</sup>H, cross sections compared with e scatt. meas., light nuclei structure determ. 9-4774  
<sup>3</sup>H, n scatt. amplitude determ. in 1st order in N weak interac. 9-11214  
<sup>3</sup>H, n.m.r. from Al salts in H<sub>2</sub>O and D<sub>2</sub>O 9-16024  
<sup>3</sup>H deuteron break-up by proton obs. 9-6893  
<sup>3</sup>H disintegration by 8-28 MeV neutron, p spectra and n-n scatt. length obs. 9-6882  
<sup>3</sup>H transient n.m.r., spin-lattice relax. times determ. near  $\lambda$ -transition 9-12511  
<sup>3</sup>H, binding energy and wave function calc., no excited state 9-2658  
<sup>3</sup>H, mag. moment anomaly, baryon reson. admixtures description 9-14563  
<sup>3</sup>H, wave func. and weak interaction determ. 9-11214  
<sup>3</sup>H and <sup>14</sup>C autoradiography, simultaneous, correlation with gas counting 9-21995  
<sup>3</sup>H binding energy, with tensor forces and hard shell repulsion 9-8979  
<sup>3</sup>H binding energy and Coulomb energy 9-11212  
<sup>3</sup>H binding energy and R.M.S. charge radii of tri-nucleons 9-2657  
<sup>3</sup>H total energy lower bound in Schrodinger eqn. framework 9-11117  
<sup>4</sup>He-<sup>3</sup>H $\pi^-$ , energy spectra and particle angular correlations obs. 9-2661  
<sup>3</sup>H, search for ground state <sup>3</sup>H(t, p), 22.25 MeV 9-2659  
<sup>3</sup>H e.m. formfactor, wave functions determ. 9-18064  
<sup>3</sup>H-<sup>75</sup>As asymmetric level crossing in paraelectric KH<sub>2</sub>AsO<sub>4</sub> 9-12521  
<sup>2</sup>H( $\alpha$ , p)<sup>3</sup>H tensor polarization obs., 160-470 keV 9-2759  
<sup>2</sup>H(d, n)<sup>3</sup>He, 27.5 MeV, time of flight method 9-20801  
<sup>3</sup>H(d,n)<sup>3</sup>He, 0.3-1.83 MeV, n polarization deduced, d-s-wave 9-9065  
<sup>3</sup>H(d,n)<sup>3</sup>He, 70<sup>o</sup>(lab) d energies below 2 MeV n polar 9-4803  
<sup>3</sup>H(d,n)<sup>3</sup>He, n polarization obs., parity conservation concluded in strong reaction 9-6900  
<sup>2</sup>H(d,p)<sup>3</sup>H, p ang. distrib. meas., 80  $\leq$  E<sub>d</sub>  $\leq$  150 keV 9-13241  
<sup>3</sup>He, binding energy and wave function calc. 9-2658  
<sup>3</sup>He, mag. moment anomaly, baryon reson. admixtures description 9-14563  
<sup>3</sup>He, search for unbound states from <sup>6</sup>Li(p, $\alpha$ ) react. 9-11211  
<sup>3</sup>He binding energy and Coulomb energy 9-11212  
<sup>3</sup>He e.m. formfactor, wave functions determ. 9-18064  
<sup>3</sup>He, e elastic scatt., influence of nucleon-nucleon correl. 9-4772  
<sup>3</sup>He, in <sup>3</sup>H(p,p)<sup>3</sup>H, low levels studied, Ep=3.11-4.6 MeV 9-14564  
<sup>3</sup>He, p scatt., polarization obs. at 540 MeV 9-9022  
<sup>3</sup>He, properties by Slater variational calculations 9-508  
<sup>3</sup>He, velocity depend. nuclear forces effect on total cross-section 9-2718  
<sup>3</sup>He(<sup>3</sup>He,<sup>3</sup>He) scatt., elastic, resonating-group method calc. of phase shift 9-14622  
<sup>3</sup>He charge distrib. calc. 9-4731  
<sup>3</sup>He cross sections and ang. distrib. of ( $\gamma$ ,p) and ( $\gamma$ ,n) reaction 9-2719  
<sup>3</sup>He emission at high energy from nuclear spallation process, fluctuation mech. description 9-11173  
<sup>3</sup>He optical potential analytical expressions construction for scatt., E $\alpha$  < 400 MeV 9-9057  
<sup>3</sup>He p scatt. spin and isospin-depend. anal. 9-4775  
<sup>3</sup>He particle-hole states and photodisintegration cross-section 9-6764  
<sup>3</sup>He target in deuteron scatt., polarization obs. 9-11312  
<sup>3</sup>He total energy lower bound in Schrodinger eqn. framework 9-11117  
<sup>4</sup>He-<sup>3</sup>H $\pi^-$ , energy spectra and particle angular correlations obs. 9-2661  
<sup>3</sup>He- $\pi^-$ , energy spectra and particle angular correlations obs. 9-2661  
<sup>3</sup>He  $\pi$ -s-wave radiative capture and  $\pi^+$ He<sup>+</sup>H vertex function 9-9048  
<sup>3</sup>He(d,p)<sup>4</sup>He reaction, polarized targets, 430 keV 9-4802  
<sup>4</sup>He( $\gamma$ , n)<sup>3</sup>He, effective cross section and angular distrib. meas. 9-6850  
<sup>4</sup>He( $\gamma$ , p)<sup>3</sup>He, effective cross section and angular distrib. meas. 9-6850  
<sup>4</sup>He( $\gamma$ , p)<sup>3</sup>He, energy spectrum of photoprotons, and ( $\gamma$ , p) cross-section 9-4768  
<sup>4</sup>He( $\gamma$ , pn)D multipolarity investigation 9-11274  
<sup>4</sup>He( $\gamma$ , p)<sup>3</sup>H, p spectra meas., <sup>3</sup>He excited states determ. 9-16937  
<sup>4</sup>He( $\gamma$ ,  $\pi^+$ ), diff. cross section meas., Ep=160-450 MeV 9-11275  
<sup>4</sup>He(p,p) cross section, excitation function obs., Ep=20-28 MeV 9-6867  
<sup>3</sup>He(p,pd)<sup>3</sup>H, final state p-p interaction 9-11287  
<sup>3</sup>He(t, p)<sup>3</sup>He, 22.25 MeV, obs. 9-2659  
<sup>4</sup>He(t,t) scatt., elastic, resonating-group method calc. of phase shift 9-14622  
<sup>3</sup>H(n, n)<sup>3</sup>H, 14 MeV, elastic 9-6874  
<sup>3</sup>H(n, p)<sup>3</sup>n cross section, theoretical analysis 9-2748  
<sup>3</sup>H(p,n)2p, n spectra obs., Ep=30, 50 MeV 9-15759  
<sup>3</sup>H(p,p)<sup>3</sup>H, phase shift anal., <sup>4</sup>He low levels studied, Ep=3.11-4.6 MeV 9-14564  
<sup>3</sup>H(t, p)<sup>3</sup>H, 22.25 MeV obs. consistent with <sup>3</sup>H ground state 9-2659

**Nuclei with  $A \leq 5$  continued**

- $^3\text{H}$ , search for activity negative in  $^7\text{Li}(\pi^-, \text{pn})^3\text{H}$  9-6918  
 $^4\text{Li}$  unsuccessful search for  $T=2$  state 9-15713  
 $^5\text{Li}$ , cylindrical asymmetry in  $^4\text{Li}(\text{He}, \alpha \text{p})^4\text{He}$  react. eff. of lifetime of intermediate state 9-6910  
 $^6\text{Li}$   $\pi$  s-wave radiative capture and  $\pi^3\text{He}^3\text{H}$  vertex junction 9-9048

**Nucleic acids** see *Macromolecules***Nucleons and antinucleons**

- See also *Cosmic rays/nucleons; Neutrons and antineutrons; Nuclear reactions and scattering due to nucleons; Protons and antiprotons*  
 e.m. form factors predicted by group theory 9-6586  
 electric dipole moment, upper limits from  $K \rightarrow 2\pi$  decay obs. 9-2528  
 e.m. form factor rel. to Nu-Nu scatt. and  $O(4,2)$  model with simple scalar interaction 9-2533  
 e.m. radii, field current identities calc. 9-8888  
 form factor, domination by monopole  $\omega \rho$  and dipole  $\rho$  mesons 9-8887  
 form factor, isovector struct., dipole parametrization, rel. to  $\pi$  form factor zero 9-16900  
 form factor  $1/q^4$  behaviour explanation by  $\rho$  meson dipole model 9-8886  
 form factors, e.m., from sidewise dispersion relation calc. 9-6686  
 form factors, in terms of reson. 9-6685  
 form factors and n-p mass difference 9-13139  
 form factors calc. from Fermi statistics 9-8763  
 nucleon-nucleon field theor. pot. 9-19265  
 pair production yield from  $(\text{p}, \text{np})$  reaction 9-11269  
 radius, axial mean square from photoproduction sum rules 9-2527  
 reactions, independent-particle model, axial-vector form factor 9-9017  
 resonances, of spin  $3/2$  and isos.,  $1/2$  off-mass-shell self-consistency approach 9-16890  
 surface location and depend. on p.n. density distrib. 9-14551  
 three point functions, Ward identities calc. 9-19203  
 $\beta$ -decay, relativistic quark model 9-17969  
 $\mu$  prod., studied in CERN spark-chamber 9-14469  
 n and p density distrib., variational calc. 9-11188  
 $\text{N}^*(1400)$  phenomenon, suitability of one-pion exchange process explanation 9-17985  
 p-n mass difference calc. in reciprocal bootstrap model 9-15639

**antinucleons**

- NN collision, polarization calc. using optical potential 9-11088

**interactions**

- cosmic ray above  $10^{12}\text{eV}$ , emulsion stack obs. 9-15671  
 e.m. effects 9-8889  
 $g_{\pi\pi}$  coupling constant determ. 9-4613  
 nucleon-meson cascade, accelerator and spacecraft shielding 9-8890  
 $\text{pN} \rightarrow \text{N}\pi$  photoprod., modified PCAC hypothesis 9-6661  
 $\text{pN} \rightarrow \pi^2\text{N}$ , interaction const. and s-lengths determ.,  $E_{\pi}=210, 225\text{ MeV}$  9-14504  
 KN inelastic processes above  $1.4\text{ GeV}/c$  with more than two particles in final or intermediate state, reviews 9-11042  
 $\text{KN} \rightarrow \text{K}^*\text{N}$ ,  $\text{K}^*\pi$  mass spectra low-mass enhancement, Deck-model calc. of double charged syst. 9-20636  
 $\text{K} \rightarrow \text{N} \rightarrow 2\pi$ , total cross sections meas.,  $M_K=0.6-1.2\text{ GeV}/c$  9-11043  
 $\Delta\text{N} \rightarrow \text{NN}$ , structure of weak interaction and SU(6) symmetry 9-425  
 NN annihilation, multiple particle prod. unitary-symmetrical statistical model 9-16833  
 $\text{NN} \rightarrow \text{PV}$ , t channel, residue functions soln. for zero  $\bar{\text{N}}\text{N}$  channel spin 9-8784  
 $\text{pN} \rightarrow \text{N}^*\pi$ , polarization eff., where N is polarized 9-20601  
 pN,  $24\text{ GeV}/c$ , velocity space transform method of analysis 9-15654  
 $\pi^+\text{N}$ ,  $2.34\text{ GeV}/c$  in Xe bubble chamber,  $\pi^0$  prod.  $\gamma$  spectrum 9-20645  
 $\pi\text{N}$ ,  $17\text{ GeV}/c$  CERN experiment 9-15622  
 $\pi\text{N}$  review of inelastic processes 9-6664  
 $\pi\text{N}$  using  $\pi d$  9-2511  
 $\pi\text{N}$ ,  $17\text{ GeV}/c$  velocity space transform method of analysis 9-15654  
 $\pi\text{N}$  in emulsion,  $7.2\text{ GeV}$ , secondary particle analysis 9-15623  
 $\pi\text{N} \rightarrow$  axial vector meson, Regge model 9-11072  
 $\pi\text{N} \rightarrow \rho\text{N}^*(1238)$ , OPE contrib. verified 9-2530  
 $\Xi\text{N}$ , potential 9-6687  
 Nd cross section spin depend., Glauber approx. 9-11118  
 circuit binding energy calc. from potential 9-13140

**interactions, nucleon-nucleon**

- bremsstrahlung of nuclear potential model, anal. 9-18057  
 diff. cross section calc., sum rules obtained 9-11050  
 fireball model for very high energy 9-2529  
 Lennard-Jones N-N pots. in Bethe-Weizsacker mass formula derivation 9-6769  
 Oakes theory and parity-nonconserving nuclear forces 9-8952  
 one-boson-exchange potential description 9-6754  
 one-boson-exchange potentials for exam. of low-energy props. 9-11086  
 parity-violating weak interaction pot. 9-6623  
 phase shift calc. from multi-channel theory 9-19204  
 phase shift matrix elements determ., t,  $\alpha$  props. calc. 9-16911  
 potential made up from OPE vector meson exchange and contribs. from inelastic N-N interactions 9-6687  
 potential, soft-core, finite square wells 9-20724  
 potential matrix elements for nuclear structure calc. 9-11178  
 resonant reaction with pion, Faddeev eqn. study, 2 resonances at  $350\text{ MeV}$  9-11085  
 scattering matrix determ., from (n,p) phase-shift analyses,  $7-750\text{ MeV}$  9-9034  
 strong, applic. of unitary Pade approximants 9-20667  
 NN collision, polarization calc. using optical potential 9-11088  
 $\text{NN} \rightarrow \text{NN}$  analyticity constraint and daughter structure of conspiring Regge-pole families 9-8841  
 $\text{NN} \rightarrow \text{NN}\pi$  bremsstrahlung amp. determ. 9-11087  
 $\pi$  M-function expansion in  $O(4)$  from Bethe-Salpeter eqn. 9-17980  
 $\pi$  threshold prod. in soft-pion approx. 9-11051  
 $\text{NN} \rightarrow \text{m}\pi$  ( $m \geq 2$ ) with intermediate states, review of data 9-6690  
 NN, strong short-range absorption and rel. to nearby-singularity approx. in NN syst. 9-15636  
 $\text{NN} \rightarrow \text{KK} + \text{m}\pi$   $m \geq 0$ , review of data 9-6690  
 $\text{NN} \rightarrow \text{NN} + \text{m}\pi$   $m \geq 1$ , review of data 9-6690  
 $\text{NN} \rightarrow \text{NN}\pi$  near threshold, soft- $\pi$  calc. 9-406  
 $\text{NN} \rightarrow \text{YY}$ , conspiracy relation 9-424  
 $\text{NN} \rightarrow \text{YY} + \text{m}\pi$   $m \geq 0$ , review of data 9-6690  
 $\phi\pi$  exchange process, charge dependent effects on low-energy parameters 9-15637  
 $^6\text{Li}$  shell model wave function, residual interaction 9-15714

**In teractions, pion-nucleon** see *Pions/interactions, pion-nucleon***Nucleons and antinucleons****scattering**

- charge symmetry and charge independence, low-energy 9-6688  
 form factor at asymptotically great transferred momentum 9-8885  
 meson-nucleon, SU(3) crossing relation and Regge pole theory rel. to obs.,  $6-18\text{ GeV}/c$  9-11029  
 meson-nucleon, Regge-pole model for invariant functions 9-15638  
 nucleon-meson, SU(3) crossing reln. and Regge pole theory 9-16859  
 vector, tensor trajectory hypothesis rel. to  $\pi\text{N}$ , KN, NN 9-15604  
 KN, low energy, effective Lagrangian 9-366  
 KN complex scatt. length calc. from soft-meson current algebra 9-17979  
 KN forward crossing-even amplitudes, applic. of modified dispersion relations 9-16868  
 KN including symmetry breaking of chiral SU(3) SU(3) 9-14498  
 KN Pomeranchuk parameters using modified dispersion relations 9-14502  
 K $\bar{\text{N}}$ , Regge-pole parameters from total cross sections 9-11044  
 N-d, elastic in GeV region, first-order dispersive impulse approx. 9-4634  
 NN, quark model multiple-scatt. contributions 9-8787  
 $\pi\text{N}$  interference model, modifications data analysis  $2-6\text{ GeV}/c$  9-4628  
 $\pi\text{N}$ , causality violation obs. 9-2443  
 $\pi\text{N}$ ,  $\text{D}_{13}$  amplitude below  $700\text{ MeV}$  predicted by  $\rho\text{N} \rightarrow \pi\text{N} \rightarrow \pi\Delta$  system 9-8848  
 $\pi\text{N}$ , daughter and conspiracy constraint phenomena derivation 9-15600  
 $\pi\text{N}$ , pseudoscalar-pseudoscalar coupling model calc. of p, s-wave scatt. lengths 9-16879  
 $\pi\text{N}$ , Regge pole parameters, new determ. 9-4629  
 $\pi\text{N}$ , S-matrix evaluation, appl. of approx. method 9-8843  
 $\pi\text{N}$  charge exchange and cross-over, Regge-pole absorption model 9-15626  
 $\pi\text{N}$  Coulomb interference 9-2518  
 $\pi\text{N}$  Harari model and forward scatt. 9-11061  
 $\pi\text{N}$  impact parameter representation, spin flip amplitude determ. 9-4630  
 $\pi\text{N}$  radiative, use of current algebra in off-mass-shell limit 9-13129  
 $\pi\text{N}$  Regge-pole residue function determ. from fixed- $t$  dispersion reln. 9-14510  
 $\pi\text{N}$  vector dominance sum rules for invariant amplitudes 9-6672  
 $\pi\text{N}$  eight low-energy scatt. parameters 9-19203

**scattering, nucleon-nucleon**

- 50 MeV expts. reviewed 9-6689  
 amplitude relations, assuming  $\text{SU}(2) \times \text{SU}(2)$  symmetry 9-2531  
 bootstrap multiperipheral model, Pomeranchuk trajectory studied  $E \leq 30\text{ GeV}$  9-18008  
 effective range theory based on N-S-B equation 9-20668  
 and e.m. form factors,  $O(4,2)$  model of baryons 9-2533  
 left-hand-cut contributions, obs. 9-4635  
 phase shift anal.,  $^1\text{S}_0$  state charge splitting,  $210\text{ MeV}$  9-18006  
 potential, local phenomenological, model 9-13141  
 quark model multiple-scatt. contributions 9-8787  
 Regge-pole model for invariant functions 9-15638  
 S-wave phase shifts, rel. to solvable S-wave potentials 9-4710  
 S-wave lengths, applic. of pion-nucleon Lagrangian and addition of 2 four-fermion interac. 9-16852  
 triple scattering parameters for recoil particles 9-405  
 two-pion-exchange contrib. at  $2.6\text{ GeV}/c$  9-2530  
 $\pi\pi$  exchange contrib. obs.,  $E_{\pi}=95, 310\text{ MeV}$  9-18007  
 NN,  $O(4)$  off-shell formalism, six types of Lorentz pole found 9-6691

**scattering, pion-nucleon** see *Pions/scattering, pion-nucleon***Nucleus**

- See also *Elements/origin; Hypernuclei; Radioactivity; Scattering, particles*  
 coulomb displacement energies of isobaric analogue states 9-6788  
 deformed, collective charge oscills. 9-8970  
 deformed, energy expectation values and cranking eqns. 9-4709  
 deformed, mean square nuclear charge radii, changes in rotational excitation 9-4721  
 empirical abundance distrib. rel. to formation and conds. of physical environment of heavy nuclei 9-6770  
 heavy, formation processes and conds. of physical environment based on empirical abundance distrib. 9-6770  
 reorientation effect in Coulomb excitation 9-13187  
 shape isomers 9-6919  
 spherical, particle-hole amplitudes of excited states, calc. 9-4720  
 n and p density distrib., variational calc. 9-11188  
 $^{16}\text{F}$ , atomic mass and mass excesses, determ. using  $(^3\text{He}, \text{n})$  reaction 9-2644  
 $^{181}\text{F}$ ,  $^{181}\text{Ta}$ ,  $\gamma$ - $\gamma$  ang. correl. and quadrupole interaction 9-3972  
 $^{56}\text{Fe}$ , orbital moment of resonant induced by neutrons 9-19288  
 $^4\text{He}$  charge distrib. calc. 9-4731  
 $^{212}\text{Hg}$ , atomic mass and mass excesses, determ. using  $(^3\text{He}, \text{n})$  reaction 9-2644  
 $^{24}\text{Mg}$  static quadrupole moment of first excited  $J^\pi=2^+$  state 9-8994  
 $^{131}\text{N}$ , atomic mass and mass excesses, determ. using  $(^3\text{He}, \text{n})$  reaction 9-2644  
 $^{26}\text{Si}$ , atomic mass and mass excesses, determ. using  $(^3\text{He}, \text{n})$  reaction 9-2644

**electric moment**

- See also *Molecules/nuclear coupling*  
 deformed odd-mass nuclei, anomalous  $E1(\Delta K=1)$  transition intensities obs. 9-6786  
 dipole states in deformed nuclei, energy calc. using finite Fermi-syst. theory, influence of superfluid pairing correlations 9-4726  
 e.m. transitions effective charge depend. on multipolarity, 1st order perturbation theory 9-14557  
 e.m. transitions effective charge depend. on multipolarity, RPA applic. 9-14558  
 polar, quadrupole, effect on elastic scatt. of charged part. 9-2642  
 quadrupole effect on atomic electrons and internal conversions coefficients 9-2641  
 quadrupole variation due to rotation of deformed nuclei 9-11203  
 n closed shell, BCS theory applied 9-483  
 $^{192}\text{Os}$ , monopole transitions and quadrupole moments calc. from pairing-plus-quadrupole model 9-15702  
 $^{152}\text{Sm}$ , K-conversion particle parameters for E2 transitions 9-14572  
 $^{113}\text{Sn}(\text{n}, \gamma)$ , E1 transitions evaluation from  $\gamma$  spectra 9-13228  
 $^{114}\text{Cd}$ , quadrupole, zero static from reorientation eff. 9-6797  
 $^{154}\text{Gd}$ , K-conversion e intensities of transitions of strong E0 components meas. 9-13210  
 $^{154}\text{Gd}$ , K-conversion particle parameters for E2 transitions 9-14572



**Nucleus continued****electric moment continued**

- <sup>184</sup>W, monopole transitions and quadrupole moments calc. from pairing-plus-quadrupole model 9-15702  
<sup>115</sup>In excitation by threshold- energy  $e$ , M1/E2 mixing ratios determ. 9-6798  
<sup>196</sup>Pt monopole transitions and quadrupole moments calc. from pairing-plus-quadrupole model 9-15702  
<sup>166</sup>Er, E1 transition  $\gamma$  polarization meas., level parity determ. 9-14573  
<sup>238</sup>U(n, $\gamma$ ), E1 transition strengths distribution 9-15769  
<sup>169</sup>Tm,  $K=1/2$  rotational band, E2/M1 mixing ratios 9-14574  
<sup>42</sup>Ca, quadrupole transitions, lifetimes 9-13203  
<sup>19</sup>F, static nuclear quadrupole-interact. parameters in polycryst. targets 9-4730  
<sup>Fe</sup><sup>57m</sup>, nuclear quadrupole moment from  $\alpha$ -Fe<sub>2</sub>O<sub>3</sub> data 9-7930  
<sup>57m</sup>Fe, quadrupole, from Mossbauer spectra 9-3976  
<sup>15</sup>N E1 transitions sum rules and single-part. amplitude 9-2650  
<sup>16</sup>O,  $1^{-} \rightarrow 0^{-}$  E1 transition, deformed admixtures obs. 9-8986  
<sup>16</sup>O E1 transitions sum rules and single-part. amplitude 9-2650  
<sup>88</sup>Sr dipole states, struct. and analysis 9-11244

**energy level transitions**

- <sup>153</sup>Gd, half lives of intrinsic states, and transition probability to ground state 9-8985  
<sup>16</sup>O  $\gamma$ -ray branching in decay of 6.92, 7.12, 8.88 and 13.10 MeV states 9-2651  
<sup>236</sup>U E2 transitions meas. of total internal conversion coeffs. 9-2675  
 $\Delta I=1, \Delta Y=0$  nonleptonic weak interaction testing 9-8967  
E2 transitions rel. to intrinsic structure of  $1f_{7/2}$  shell 9-11194  
e.m. transitions effective charge depend. on multipolarity, 1st order perturbation theory 9-14557  
e.m. transitions effective charge depend. on multipolarity, RPA applic. 9-14558  
internal conversion coeff., high energy calc. 9-11200  
intranuclear cascades, Monte-Carlo simulation, eff. of using vel.-depend. pot. 9-11193  
isobaric analogue states, M1 transition probabilities, shell-model calc. 9-14555  
L-shell internal conversion E and M coeffs. calc. including distortion due to nuclear quadrupole moment 9-2641  
lifetime spectroscopy, meas. circuit 9-4417  
metastable system lifetime calc. methods compared 9-4724  
population of a ground state sublevel following exposure to polarized  $\gamma$  radiation 9-15711  
radiative, from aligned nuclei, ang. correl. coeff. tables 9-6782  
rotational, in g.s. bands, intensities and ang. distrib. meas. 9-4793  
space parity violation effects rel. to  $\gamma$ -ray polarization and resonance absorpt. 9-498  
spurious states, random phase approximation corrections and extension 9-8962  
sum-coincidence methods for use in determ. branching ratios 9-20684  
<sup>14</sup>C, e.m., lifetime of 6.72 MeV level 9-4727  
 $\gamma$ - $\nu$ , range effect in angular correlation experiment 9-19191  
<sup>14</sup>N, e.m., lifetimes of 5.10 and 5.83 MeV levels 9-4727  
<sup>15</sup>N, E1, sum rules and single-part amplitude 9-2650  
<sup>210</sup>Bi, pure M1( $l=0$ ) transitions, L-subshell conversion line intensity ratios 9-14570  
<sup>140</sup>Ce from <sup>140</sup>La decay,  $\gamma$  spectra obs., spin and parity assigned 9-11224  
<sup>180</sup>Hf, internal conversion coeffs. for  $\gamma$  transition obs. 9-525  
<sup>200</sup>Hg, study by slow n capture of <sup>199</sup>Hg 9-4784  
<sup>200</sup>Hg internal conversion coeffs., high energy calc. 9-11200  
<sup>110</sup>Mg, 530 keV allowed  $\beta$  transition,  $\beta$ - $\gamma$  correl. obs. 9-6841  
<sup>240</sup>Pu E2 transitions, meas. total internal conversion coeffs. 9-2675  
<sup>141</sup>Ce, 435 keV first forbidden  $\beta$  transition,  $\beta$ - $\gamma$  correl. obs. 9-6841  
<sup>181</sup>Ta, parity mixing in 482 keV level from g.s. transition circular polarization meas. 9-19279  
<sup>171</sup>Yb, half lives of intrinsic states, transition probability to ground state 9-8985  
<sup>212</sup>Bi, pure M1( $l=0$ ) transitions, L-subshell conversion line intensity ratios 9-14570  
<sup>122</sup>I, decay scheme from  $\gamma$ -ray study 9-11222  
<sup>142</sup>Nd, thermal-n capture,  $\gamma$  emission, transition schemes determ. 9-14569  
<sup>238</sup>Po, multipolar charact. of transitions rel. to low energy  $\gamma$ -radiation of <sup>238</sup>Th decay. 9-13212  
<sup>152</sup>Sm, K-conversion particle parameters for E2 transitions 9-14572  
<sup>182</sup>Ta 0.3 sec. isomeric transition multipolarity, M2, determ. 9-527  
<sup>128</sup>Te E2 transitions,  $2^{-} \rightarrow 0$ ,  $2^{-} \rightarrow 2$  obs. 9-20684  
<sup>103</sup>Ag decay,  $\beta$  and  $\gamma$  half-lives, levels and transitions 9-18078  
<sup>133</sup>Ba c, capture decay, 222 keV  $\gamma$  obs. 9-15737  
<sup>143</sup>Ce decay to <sup>143</sup>Pr, role of weak transitions 9-15720  
<sup>133</sup>Cs, 223-161 keV cascade rel. to spin of 384 keV cascade 9-20738  
<sup>119m</sup>In, e.m. decay, search for double electron ejection 9-6796  
<sup>193</sup>Ir from <sup>193</sup>Os decay, energy levels determ. from  $\gamma$ - $\gamma$  coinc. meas. 9-11229  
<sup>142</sup>Nd, thermal-n capture,  $\gamma$  emission, transition schemes determ. 9-14569  
<sup>Os</sup><sup>193</sup>,  $\gamma$  energy levels determ. from  $\gamma$ - $\gamma$  coinc. meas. 9-11229  
<sup>203m</sup>Pb-<sup>203</sup>Pb decay spectra and M4 transition obs. 9-6809  
<sup>141</sup>Pr, populated in <sup>141</sup>Ce decay, role of weak transitions 9-15720  
<sup>227</sup>Ra, from internal conversion obs. in  $\alpha$ -decay of <sup>227</sup>Th 9-6812  
<sup>207</sup>Tl, 279, 404 keV,  $\alpha$  obs. 9-15726  
<sup>207</sup>Tl, e.m. transition prob. calc., single-hole collective model 9-18067  
<sup>141</sup>Cd K conversion coeffs.,  $1^{-} \rightarrow 9$  MeV 9-2663  
<sup>134</sup>Cs, 662 keV allowed  $\beta$  transition,  $\beta$ - $\gamma$  correl. obs. 9-6841  
<sup>154</sup>Gd K intensities, evidence for new  $O^{+}$  level 9-2668  
<sup>154</sup>Gd, 692 keV level  $2^{+} \rightarrow 2^{+} \rightarrow 0^{+}$  cascade obs., transition pure E2 9-11226  
<sup>154</sup>Gd, K-conversion particle parameters for E2 transitions 9-14572  
<sup>164</sup>Ho-<sup>164</sup>Er 91.5 keV E2 transition,  $\alpha$  obs. 9-2669  
<sup>142</sup>Nd, thermal-n capture,  $\gamma$  emission, transition schemes determ. 9-14569  
<sup>144</sup>Pr, pure M1( $l=0$ ) transitions, L-subshell conversion line intensity ratios 9-14570  
<sup>224</sup>Ra E2 transitions, meas. of total internal conversion coeffs. 9-2675  
<sup>234</sup>U E2 transitions, meas. of total internal conversion coeffs. 9-2675  
<sup>145</sup>Eu-<sup>145</sup>Sm energy levels, spin and parity assignments 9-14571  
<sup>175</sup>Lu,  $\gamma$ - $\gamma$  angular correlations in 89-343, 161-343 KeV 9-4738  
<sup>142</sup>Nd, thermal-n capture,  $\gamma$  emission, transition schemes determ. 9-14569  
<sup>145</sup>Sm from <sup>145</sup>Eu decay; energy levels, spin and parity assignments 9-14571  
<sup>205</sup>Tl, e.m. transition prob. calc., single-hole collective model 9-18067  
<sup>165</sup>Tm-<sup>165</sup>Er, 242.8 keV energy level lifetime meas. 9-11227  
<sup>125m</sup>Xe, half-life and decay scheme 9-4755  
<sup>16</sup>Er, E1 transition  $\gamma$  polarization meas., level parity determ. 9-14573

**Nucleus continued****energy level transitions continued**

- <sup>166</sup>Ho, pure M1( $l=0$ ) transitions, L-subshell conversion line intensity ratios 9-14570  
<sup>146</sup>Nd, thermal-n capture,  $\gamma$  emission, transition schemes determ. 9-14569  
<sup>106</sup>Pd, energy levels, spin and parity determ. from  $\gamma$  spectra 9-13193  
<sup>116</sup>Sb, 103.2 keV transition from conversion electron obs. 9-6799  
<sup>116</sup>Sn, 134.5 keV transition from conversion electron obs. 9-6799  
<sup>137</sup>Ba, metastable state, M4 decay obs. 9-6848  
<sup>171</sup>Hf 321, 113 keV lifetimes, E1 transition prob. determ. 9-8989  
<sup>127</sup>( $\alpha$ , $\alpha'$ ) Coulomb excitation, E2 transition prob. determ.,  $E_{\alpha}=3.5$  MeV 9-20737  
<sup>117</sup>In life-times from  $\gamma$  emission from excited state 9-2664  
<sup>127</sup>(p,p') Coulomb excitation, E2 transition prob. determ.,  $E_{\alpha}=3.5$  MeV 9-20737  
<sup>177</sup>Lu,  $\beta$ ,  $\gamma$  transitions obs. 9-15725  
<sup>187</sup>Re-<sup>187</sup>W,  $\gamma$  angular correlation meas., E1, E2 transitions determ. 9-20766  
<sup>117</sup>Te from <sup>114</sup>Sn( $\alpha$ ,n), search for isomeric transition,  $E_{\alpha}=17$ -27 MeV 9-15716  
<sup>117</sup>Te from <sup>115</sup>Sn( $\alpha$ ,n), search for isomeric transition,  $E_{\alpha}=17$ -27 MeV 9-15716  
<sup>127</sup>Te, lifetime of 341 keV level 9-6801  
<sup>237</sup>U half-life, coincidence obs. 9-6815  
<sup>127m</sup>Xe, half-life and decay scheme 9-4755  
<sup>198</sup>Au(n,  $\gamma$ ) transition strengths to final states, 0.2-1.2 MeV obs., 10-60 keV 9-529  
<sup>198</sup>Hg, E2 transitions,  $2^{-} \rightarrow 0$ ,  $2^{-} \rightarrow 2$  obs. 9-20684  
<sup>228</sup>Th E2 transitions, meas. total internal conversion coeffs. 9-2675  
<sup>238</sup>U(n, $\gamma$ ),  $\gamma$  spectra obs., decay scheme determ. 9-15769  
<sup>199</sup>Au, ( $E_{\gamma}$ )<sub>208</sub>(M<sub>1</sub>)<sub>300</sub> obs. in agreement with core excitation model 9-562  
<sup>139</sup>Ce, decay, probability of K-capture 9-4756  
<sup>189</sup>Os, lifetime of 36.2 keV level 9-14576  
<sup>189</sup>Os 69.6 keV  $\gamma$ -g.s. half life determ. from  $\gamma$  meas. 9-4739  
<sup>119</sup>Sb, half-lives of 270 and 1366 keV levels 9-4754  
<sup>119m</sup>Sn 23.9 keV-g.s. transition total internal conversion coeff. obs. 9-6800  
<sup>169</sup>Yb, half lives of intrinsic states, transition probability to ground state 9-8985  
<sup>25</sup>Al  $\gamma$  decay of  $T=3/2$  states obs. 9-4743  
<sup>26</sup>Al, lifetimes and decay of 2.07 MeV triplet 9-20736  
<sup>76</sup>As 46-keV state, lifetime and population, depopulation schemes, obs. 9-4750  
<sup>103</sup>B, lifetimes of 3.59 and 2.15 MeV levels, transition strengths 9-14560  
<sup>8</sup>B  $\Delta I=1, \Delta Y=0$  nonleptonic weak interaction testing 9-8967  
<sup>8</sup>Be resonant cross-sections and branching ratios obs. following <sup>7</sup>Li( $p$ , $\gamma$ )\*<sup>8</sup>Be 9-2660  
<sup>10</sup>Be, lifetime of 3.37 MeV level, transition strengths 9-14560  
<sup>11</sup>Be, information from  $\mu$  capture by <sup>11</sup>B 9-11208  
<sup>10</sup>C, lifetime of 3.36 MeV level, transition strengths 9-14560  
<sup>12</sup>C, lifetime of 4.43 MeV level 9-11209  
<sup>12</sup>C, lifetime limits for 3.09 and 3.68 MeV levels and lifetime of 3.86 MeV level 9-11209  
Ca even isotopes, in proton pick-up reactions 9-2761  
<sup>40</sup>Ca from <sup>39</sup>K (p, $\gamma$ ), level lifetimes and  $\gamma$ -ray branching determ.,  $E_{\alpha}=1.1$ -2.5 MeV 9-15729  
<sup>40</sup>Ca monopole, by inelastic e scatt., matrix elements and transition radii, comparison with E2 excitations 9-6816  
<sup>42</sup>Ca, elec. quadrupole transitions, lifetimes 9-13203  
<sup>37</sup>Cl, following  $\beta$  decay of <sup>37</sup>S meas. with Ge(Li) detector 9-2707  
<sup>58</sup>Co, 485 keV allowed  $\beta$  transition,  $\beta$ - $\gamma$  correl. obs. 9-6841  
<sup>12</sup>C monopole, by inelastic e scatt., matrix elements and transition radii, comparison with E2 excitations 9-6816  
<sup>63</sup>Cu, strengths for six quadrupole and eight octupole states using DWBA method 9-543  
<sup>18</sup>F branching ratios for e.m. decays of resonances. 9-611  
<sup>18</sup>F  $\Delta I=1, \Delta Y=0$  nonleptonic weak interaction testing 9-8967  
<sup>18</sup>F, 2797 keV, spin and lifetime 9-4729  
<sup>56</sup>Fe, third  $\rightarrow$  first excited, E2/M1 mixing ratio 9-14588  
<sup>75</sup>Ge decay,  $\gamma$  spectra study, assignment of transitions in level scheme of <sup>75</sup>As 9-11256  
<sup>75</sup>Ge decay,  $\gamma$  spectra study, assignment of transitions in level scheme of <sup>75</sup>As 9-11256  
<sup>38</sup>K, e.m. props., shell-model interac. calc. 9-18071  
<sup>40</sup>K,  $\gamma$ -ray energy meas. 9-20747  
<sup>82</sup>Kr from <sup>82</sup>Bv decay,  $\gamma$  directional corrs. 9-11257  
<sup>5</sup>Li cylindrical asymmetry in <sup>4</sup>Li(<sup>4</sup>He,  $\alpha$ p)<sup>4</sup>He react. eff. of lifetime of intermediate state 9-6910  
<sup>6</sup>Li, obs. in ground and 1st. two excited states and ang. distrib., from <sup>4</sup>H(<sup>4</sup>He, $\gamma$ )<sup>6</sup>Li reaction 9-11320  
<sup>6</sup>Li  $T_{1/2}$  meas. 9-2685  
<sup>24</sup>Mg monopole, by inelastic e scatt., matrix elements and transition radii, comparison with E2 excitations 9-6816  
<sup>24</sup>Mg spectra, Tamm-Dancoff approx. wave functions 9-4741  
<sup>26</sup>Mg, magnetic dipole from various  $1^{+}$  states 9-578  
<sup>18</sup>N, radiative width for 2.37 MeV state and lifetime 9-11209  
<sup>15</sup>N  $1/2^{-} \rightarrow 1/2^{-}$ , E2/M1 mixing ratio 9-6789  
<sup>22</sup>Nb, M2/E1 mixing ratios from 2.572 MeV level 9-2674  
<sup>91</sup>Nb  $d_{3/2}$  analog state E1  $\gamma$  decay 9-4751  
<sup>91</sup>Nb, M4 transition prob. calc. from  $\gamma$  internal conversion meas. 9-15744  
<sup>18</sup>Ne, lifetime, new level found at  $E_{\alpha}=3576$  KeV 9-13190  
<sup>20</sup>Ne spectra, Tamm-Dancoff approx. wave functions 9-4741  
<sup>24</sup>Ne, decay modes of levels below  $\sim 5$  MeV, from <sup>22</sup>Ne( $t$ ,pp)<sup>24</sup>Ne ang. correl. study 9-11234  
<sup>10</sup>O, 6.79, 8.29, 8.74 MeV level decay calcs. 9-6789  
<sup>10</sup>O,  $7/2^{+}$  7.28 MeV g.s. transition meas., B(E3) determ. 9-20739  
<sup>10</sup>O, E2, between odd parity states, effective charge 9-6789  
<sup>10</sup>O, electric quadrupole contrib. to photodisintegration 9-11272  
<sup>16</sup>O,  $1^{-} \rightarrow 0^{+}$  E1 transition, deformed admixtures obs. 9-8986  
<sup>10</sup>O E1, sum rules and single-part amplitude 9-2650  
<sup>29</sup>P,  $\gamma$  decay of  $T=3/2$  states obs. 9-4743  
<sup>31</sup>P, 1st and 2nd excited levels mean life determ. by Doppler shift attenuation method 9-14584  
<sup>31</sup>P isobaric analogue states, M1 transition probabilities, shell-model calc. 9-14555  
<sup>31</sup>P, 1st and 2nd excited levels mean life determ. by Doppler shift attenuation method 9-14584  
<sup>86</sup>Rb, E4 transition multipolarity 9-9000  
<sup>33</sup>S monopole by inelastic e scatt., matrix elements and transition radii, comparison with E2 excitations 9-6816

## Nucleus continued

## energy level transitions continued

- <sup>43</sup>Sc, e.m. transition explanation by (fp)<sup>3</sup> states mixing with low  $3/2^-$  rot. band 9-18073  
<sup>45</sup>Sc  $\gamma$  decays of 14 levels obs. 9-2729  
<sup>73</sup>Se, E5 25.9±0.3 KeV transitions rel. to spins calc. 9-8999  
<sup>75</sup>Se, half-life of 287keV level 9-6829  
<sup>78</sup>Si monopole, by inelastic e scatt., matrix elements and transition radii, comparison with E2 excitations 9-6816  
<sup>93</sup>Tc, decay of 11.80 MeV isobaric analog resonance rel. to 5<sup>-</sup> and 3<sup>-</sup> states in <sup>92</sup>Mo 9-4752  
<sup>98</sup>Ti, spin-1 states, from particle- $\gamma$  ray correlations, mixing ratios, rel. to shell model 9-8997  
<sup>98</sup>V, low-lying levels, <sup>90</sup>Ti(p,n)<sup>99</sup>V obs., multiplicities of transitions and spins 9-18074  
<sup>91</sup>V, 320 keV, internal conversion s-electrons 9-6823  
<sup>91</sup>Zr lifetime of 267 keV state scintillation methods 9-9001  
<sup>96</sup>Tc, 181 keV half-life,  $\gamma$  E2 transition prob. determ 9-9002

## energy levels

## See also Radioactivity/decay schemes

- 0<sup>+</sup> collective states, associated intrinsic deform. 9-13185  
 2<sup>+</sup>, in even spherical nuclei, sign of Q<sub>2</sub> 9-13189  
 23<Z≤82 elements, photo-n angular distrib. anisotropy rel. to subshells occupation, >5MeV 9-4767  
 55≤A≤141, from n inelastic scatt., 2.9 MeV 9-4747  
<sup>144</sup>Pr(n,n'),  $\gamma$  spectra meas., E<sub>0</sub>=0.5-2.3 MeV 9-14613  
<sup>142</sup>Gd from ( $\alpha$ , 2n) $\gamma$  reaction, g.s. rotational levels rel. intensity determ., E<sub>0</sub>=19.2-31.7 MeV 9-20740  
<sup>240</sup>Pu, reson. params. and n widths, 20-1500 eV 9-14616  
<sup>67</sup>Cu 1.13, 1.62 MeV levels J<sup>π</sup> assignments, from <sup>64</sup>Ni( $\alpha$ ,p) 9-18104  
 A=38 nuclei, shell-model calc. 9-16946  
 blocking eff. in K=2 and  $\beta$  vib. bands, comparison 9-8964  
 bound states calc. in strong coupling approx. 9-20722  
<sup>95</sup>Nb from <sup>95</sup>Zr decay,  $\beta$ ,  $\gamma$  spectra meas. 9-15744  
 cascading, population calc., diagrammatic mnemonic 9-6258  
 cluster states at high excitation, props. 9-18062  
 collective Hamiltonian, self-consistent microscopic theory 9-6779  
 deformed, pairing correl. appl. of Green's function method, compared with BCS-theory 9-4713  
 deformed, quadrupole moment var. due to rotation 9-11203  
 deformed light nuclei, Hartree-Fock theory 9-13184  
 density formula in Fermi-gas model, study of factor U<sup>-n</sup> 9-4715  
 dipole states in deformed nuclei 9-4726  
 doorway state theory and decay prob. for n-nuclear reaction 9-11295  
 doorway states, statistical density calc. and expl. detection 9-11195  
 energy-loss analyser for inelastic e scatt. obs. of excited states 9-11197  
 ensembles of random matrices, method of predicting nuclear energy levels, calc. of nearest neighbour spacing distrib. 9-8949  
 even nuclei, collective parameter behaviour 9-6773  
 even-even nuclei, axially symmetric non-spherical, excitation of rotational-vibrational state, influence of change of configuration 9-16933  
 even-even nuclei, semi-empirical formula 9-20728  
 even-even spherical, anharmonic vibr., phonon Hamiltonian 9-4722  
 giant resonant states, shell model description 9-6256  
 highly-excited resonant states, shell models 9-6777  
 $j/\pi$  nuclei, low lying level calc. using rotor vibrator model 9-11182  
 intermediate structure observability calc. using Brueckner K-matrix methods 9-6778  
 isobaric splitting of 1<sup>-</sup> levels of nuclei with n excess, energy splitting calc. 9-15705  
 lifetime meas., photon pile-up correction 9-10845  
 mixed-parity configurations spectroscopy 9-6772  
 numerical calc. of possible existence 9-2637  
 one-particle and wave functions of nuclear coupled states 9-14550  
 one-particle spectrum of finite axi-symmetrical potential 9-15709  
 pairing and deformation in solvable model, validity of different approx. methods 9-8953  
 pairing calculations, influence of self-energy term 9-492  
 rare-earths, rotational bands calc. model from Coriolis pair field decoupling 9-11191  
 rotational, double excitation by p,d; 2nd order Born approx. 9-15710  
 rotational, many-body nuclear wave functions, centre of mass and rotational motion, applications 9-495  
 rotational bands, ground state of deformed even nuclei, formula 9-496  
 rotational bands calc. model from Coriolis pair field decoupling 9-11191  
 rotational spectra in odd-A nuclei, I<sup>2</sup>(I+1)<sup>2</sup> corrections, B parameter calc. 9-20729  
 rotational states, mixing parameters determ. by high energy e scatt. 9-20730  
 seniority-zero and intermediate states 9-493  
 shell model, low-lying states belonging to each spin, calc. method 9-19266  
 shell model, translation-invariant, calc. for A=4,5 9-14565  
 single particle strength of collective 3<sup>-</sup> in medium mass nuclei 9-2636  
 spectroscopic factors of non rotational states, odd-A 155-181, ≤1 MeV 9-510  
 spectroscopic information for light nuclei from  $\pi^{\pm}$  charge exchange scatt. 9-11207  
 spherical, particle-hole amplitudes, calc. 9-4720  
 spin-quadrupole forces and collective states, 0<sup>+</sup>, 2<sup>+</sup> 9-499  
 spins of isolated resonances, calc. by coincidence meas. 9-11199  
 structure of g.s., and binding energy, calc. for light nuclei, A≤40 9-11189  
 superheavy nuclei, fission barriers from single-particle levels calc., stability 9-18107  
 superheavy nuclei, shell corrections and deformation 9-15732  
 two-mode monopole model, RPA validity 9-6762  
 vibrational, medium and heavy nuclei, 2- and 4-quasiparticle Tamm-Dancoff theories 9-19269  
<sup>5</sup>Li, study via D(<sup>3</sup>He,p)<sup>3</sup>Li reaction for the energy 2.3-12.2 MeV 9-4799  
 n spectroscopic factors from isobaric analogue states, depend on matching radius. 9-494  
 p capture formation tables 9-6861  
<sup>210</sup>At from <sup>214</sup>Fr isomers  $\alpha$  decay obs. 9-4758  
<sup>190</sup>Au intensities,  $\alpha$ ,  $\gamma$  conversion coefficients and multiplicities 9-528  
<sup>210</sup>Bi, low-lying, and reaction matrix theory 9-11232  
<sup>136</sup>Ce, collective levels from (<sup>16</sup>O, 4n) (<sup>20</sup>Ne, 4n) reactions, 4-5 MeV/nucleon 9-516  
<sup>140</sup>Ce, transitions determ. from La<sup>140</sup> pair-conversion positrons 9-2666  
<sup>160</sup>Dy, -ve parity states, rotational band-mixing parameters determ. 9-15724  
<sup>140</sup>La, principal  $\gamma$ -rays obs. 9-4680

## Nucleus continued

## energy levels continued

- <sup>150</sup>Nd n resonances, level spacing 9-11298  
<sup>150</sup>Po, half life of 8<sup>+</sup> state and E2 core polarization 9-8992  
<sup>190</sup>Pt from ( $\alpha$ , 2n) $\gamma$  reaction, g.s. rotational levels rel. intensity determ., E<sub>0</sub>=19.2-31.7 MeV 9-20740  
<sup>240</sup>Pu, reons. radiative widths, n capture obs., 38-820eV 9-9040  
<sup>160</sup>Tb, from <sup>157</sup>Tb(n,p), relative K,L,M,(N+O+P) line intensities of pure E2 transitions 9-11253  
<sup>170</sup>Tm, from <sup>169</sup>Tm(n,p), relative K,L,M,(N+O+P) line intensities of pure E2 transitions 9-11253  
<sup>180</sup>W from ( $\alpha$ , 2n) $\gamma$  reaction, g.s. rotational levels rel. intensity determ., E<sub>0</sub>=19.2-31.7 MeV 9-20740  
<sup>130</sup>Xe from <sup>130</sup>Ce  $\beta$  decay,  $\gamma$  spectra obs. 9-4733  
<sup>130</sup>Xe from  $\gamma$ - $\gamma$  angular correlation meas. 9-8980  
<sup>131</sup>I, intermediate-coupling unified model for determ. 9-515  
<sup>141</sup>Pr, from n scatt. ang. and energy distrib. meas., E<sub>0</sub>=230-2580 keV 9-18094  
<sup>111</sup>Ag from <sup>111</sup>Pd decay,  $\gamma$  spectra meas. 9-20760  
<sup>151</sup>Pm, from <sup>151</sup>Nd  $\gamma$  decay, levels obs. 9-518  
<sup>141</sup>Pr, structure study from <sup>140</sup>Ce(<sup>3</sup>He,d)<sup>141</sup>Pr reaction, 0-4 MeV 9-15719  
<sup>161</sup>Tb, obs. in <sup>161</sup>Gd+<sup>161</sup>Tb,  $\beta$  decay 9-19297  
<sup>171</sup>Tm, ground state, K=1/2, rotational bands 9-2670  
<sup>192</sup>Au intensities, A<sub>K</sub> conversion coefficient and multiplicities 9-528  
<sup>112</sup>Cd from <sup>112</sup>Ag decay,  $\gamma$  spectra meas. 9-13208  
<sup>137</sup>Ce, collective levels from (<sup>16</sup>O, 4n) (<sup>20</sup>Ne, 4n) reactions, 4-5 MeV/nucleon 9-516  
<sup>192</sup>Hg from <sup>192</sup>Tl decay,  $\gamma$  and conversion e spectra meas. 9-4740  
<sup>122</sup>I, decay scheme from  $\gamma$ -ray study 9-11222  
<sup>142</sup>Nd, n resonances, level spacing 9-11298  
<sup>195</sup>Os, calc. from pairing-plus-quadrupole model 9-15702  
<sup>142</sup>Pr using (d,p) reaction thermal neutron capture 9-2667  
<sup>182</sup>Ta, from <sup>181</sup>Ta(n,p), relative K,L,M,(N+O+P) line intensities of pure E2 transitions 9-11253  
<sup>182</sup>Ta, n resonance parameters for levels below 30 eV, for 0.01 to 1000 eV n 9-19312  
<sup>182</sup>W, 1694.5 keV level, from <sup>182</sup>Ta decay obs. 9-6834  
<sup>182</sup>W from ( $\alpha$ , 2n) $\gamma$  reaction, g.s. rotational levels rel. intensity determ., E<sub>0</sub>=19.2-31.7 MeV 9-20740  
<sup>172</sup>Yb, vibrational and two-quasi-particle levels, expt. study 9-4737  
<sup>172</sup>Yb cascade decay, levels determ., ang. correlation meas. computer program and automatic calc. 9-20743  
<sup>172</sup>Yb from <sup>172</sup>Lu decay, sign of  $\delta$  for E2+M1 multipole mixture 9-561  
<sup>152</sup>Eu, rotational level, 83.4 keV, magnetic moment and charge radius 9-6792  
<sup>163</sup>Fr from <sup>163</sup>Tm decay, three quasi-particle levels search 9-520  
<sup>193</sup>Ir from <sup>193</sup>Os decay,  $\gamma$ - $\gamma$  coinc. meas. 9-11229  
<sup>142</sup>Nd n resonances, level spacing 9-11298  
<sup>142</sup>Pm, from (d,<sup>3</sup>He) and (<sup>3</sup>He,d) at 40 MeV 9-6802  
<sup>142</sup>Pm log ft values, levels, spins from <sup>143</sup>Sm decay 9-8983  
<sup>113</sup>Sb-<sup>125</sup>Sb, odd, calc. from d ang. distrib. from Sn(<sup>3</sup>He,d) reaction, 18 MeV 9-610  
<sup>201</sup>Tl, K-conversion coeff. of 279 keV level, obs. 9-20744  
<sup>201</sup>Tl 279 keV, lifetime meas. by delayed e-e coincidence spectrometer 9-2563  
<sup>133</sup>Xe structure obs. 9-4811  
<sup>136</sup>Ce, collective levels from (<sup>16</sup>O, 4n) (<sup>20</sup>Ne, 4n) reactions, 4-5 MeV/nucleon 9-516  
<sup>164</sup>Er, 4<sup>+</sup> ground state levels, mean lifetimes obs. 9-519  
<sup>164</sup>Er from <sup>164</sup>Tm  $\gamma$  transition: I<sup>0</sup>=0<sup>+</sup>, K=0 levels determ. 9-521  
<sup>164</sup>Er from ( $\alpha$ , 2n) $\gamma$  reaction, g.s. rotational levels rel. intensity determ., E<sub>0</sub>=19.2-31.7 MeV 9-20740  
<sup>154</sup>Gd from Eu isotopes decay,  $\gamma$  spectra obs. 9-4734  
<sup>194</sup>Hg from <sup>194</sup>Tl decay,  $\gamma$  and conversion e spectra meas. 9-4740  
<sup>146</sup>Nd, excited in <sup>144</sup>Pm decay 9-8984  
<sup>144</sup>Nd, from <sup>144</sup>Pm decay 9-517  
<sup>144</sup>Nd n resonances, level spacing 9-11298  
<sup>126</sup>Sb, principal  $\gamma$ -rays obs. 9-4680  
<sup>126</sup>Sb, including isomeric states 9-622  
<sup>126</sup>Te, 1103.5 keV level, from <sup>124</sup>Sb decay obs. 9-6834  
<sup>124</sup>Te, excited, from <sup>124</sup>I decay 9-13209  
<sup>124</sup>Te from <sup>124</sup>Sb decay,  $\gamma$  spectra meas. 9-18079  
<sup>234</sup>U, populated by <sup>234</sup>U(d,p) and <sup>234</sup>U(d,t) processes 9-2677  
<sup>234</sup>U in the  $\beta$ -decay of <sup>234</sup>Pa (UZ) 9-2678  
<sup>234</sup>U resonances, fission components 9-2768  
<sup>184</sup>W, calc. from pairing-plus-quadrupole model 9-15702  
<sup>163</sup>Cs from <sup>152</sup>Xe decay,  $\gamma$  spectra meas. 9-19296  
<sup>163</sup>Dy, from decay scheme after radiative n capture 9-522  
<sup>163</sup>Eu 242.8 keV lifetime meas. from <sup>165</sup>Tm decay 9-11227  
<sup>163</sup>Eu, from (d,<sup>3</sup>He) and (<sup>3</sup>He,d) at 40 MeV 9-6802  
<sup>155</sup>Eu, levels deduced from <sup>152</sup>Sm  $\beta$  decay in <sup>154</sup>Sm(n,p) 9-16949  
<sup>155</sup>Ho, 1/2 + [411 spin down] and 3/2 + [411 spin up] bands 9-20742  
<sup>145</sup>Nd n resonances, level spacing 9-11298  
<sup>145</sup>Sm spin and parity assignments from <sup>145</sup>Eu decay obs. 9-14571  
<sup>145</sup>Sm from <sup>145</sup>Sb decay,  $\gamma$  spectra meas. 9-14592  
<sup>122</sup>Te, from  $\gamma$ -ray study of <sup>122</sup>Te decay 9-15736  
<sup>136</sup>W, isomeric level obs., 1.7 min 9-16941  
<sup>136</sup>Ce, collective levels from (<sup>16</sup>O, 4n) (<sup>20</sup>Ne, 4n) reactions, 4-5 MeV/nucleon 9-516  
<sup>166</sup>Er from <sup>166</sup>Tm decay,  $\gamma$  energy obs. 9-2704  
<sup>166</sup>Hg from <sup>166</sup>Tl decay,  $\gamma$  and conversion e spectra meas. 9-4740  
<sup>166</sup>Ho, from <sup>165</sup>Ho, from <sup>165</sup>Ho(n,p), relative K,L,M,(N+O+P) line intensities of pure E2 transitions 9-11253  
<sup>140</sup>Nd n resonances, level spacing 9-11298  
<sup>166</sup>Pd, from decay of <sup>166</sup>Rh 9-4753  
<sup>166</sup>Pd,  $\gamma$  spectra obs. of level transitions 9-13193  
<sup>196</sup>Pt, calc. from pairing-plus-quadrupole model 9-15702  
<sup>146</sup>Sm, from conversion e meas. by nuclear spectroscopy 9-15721  
<sup>116</sup>Sn-<sup>121</sup>Sn, low-lying level calc. using Tamm-Dancoff theories with Tabakin's realistic 2N potential 9-513  
<sup>116</sup>Sn, excited by inelastic p. scatt. at 14.695 MeV 9-512  
<sup>206</sup>Tl n and p-hole states investigated by <sup>208</sup>Pb(d, $\alpha$ )<sup>206</sup>Tl 9-19281  
<sup>136</sup>Xe, neutron particle-hole states observed by inelastic scatt. 9-20779  
<sup>227</sup>Np, Mossbauer effect, 77°K 9-13198  
<sup>227</sup>Ac from <sup>227</sup>Pa decay,  $\gamma$  spectra meas. 9-14579  
<sup>137</sup>Cs, from (d,<sup>3</sup>He) and (<sup>3</sup>He,d) at 40 MeV 9-6802  
<sup>137</sup>Cs, principal  $\gamma$ -rays obs. 9-4680  
<sup>127</sup>I, intermediate-coupling unified model for determ. 9-515  
<sup>207</sup>Pb(n,p), <sup>208</sup>Pb levels determ., E<sub>0</sub>=15-60 keV 9-18068  
<sup>147</sup>Pm, spin assignment of 413 keV state 9-11225  
<sup>147</sup>Sm, from  $\gamma$ - $\gamma$  coinc. methods 9-15722



## Nucleus continued

## energy levels continued

- <sup>117</sup>Sn from <sup>117</sup>Sb decay,  $\gamma$  spectra meas. 9-13194  
<sup>127</sup>Te from <sup>126</sup>Te(d,p); ang. distrib. of  $p$  obs., Ed=7.5 MeV 9-11223  
<sup>148</sup>Sm, from conversion  $e$  meas. by nuclear spectroscopy 9-15721  
<sup>198</sup>Au, 130ns isomeric state from <sup>197</sup>Au(d,p)<sup>198</sup>Au 9-2672  
<sup>128</sup>Ba from <sup>137</sup>Ba(n,p),  $\gamma$  spectra obs. 9-6881  
<sup>128</sup>Ce, collective levels from (<sup>16</sup>O, 4n) (<sup>20</sup>Ne, 4n) reactions, 4-5 MeV/nucleon 9-516  
<sup>158</sup>Dy, 4<sup>+</sup> ground state levels, mean lifetimes obs. 9-519  
<sup>178</sup>Hf from <sup>177</sup>Hf(n,p),  $\gamma$  spectra meas., E<sub>0</sub>=0.06-8.8 eV 9-13195  
<sup>178</sup>Hf subjected to excitation at (n,e-) reaction, 70-2000 keV 9-16939  
<sup>198</sup>Hg 411 keV. lifetime meas. by delayed e- coincidence spectrometer 9-2563  
<sup>198</sup>Hg from <sup>198</sup>Tl decay,  $\gamma$  and conversion  $e$  spectra meas. 9-4740  
<sup>158</sup>Ho, from <sup>157</sup>Er decay, multipolarities transition 9-11252  
<sup>118</sup>In, 7<sup>+</sup> or 8<sup>+</sup> isomeric state decay  $\gamma$  spectra meas. 9-19276  
<sup>148</sup>Nd n resonances, level spacing 9-11298  
<sup>208</sup>Pb levels populated in decay of <sup>208</sup>Tl 9-13197  
<sup>208</sup>Po, from <sup>209</sup>Bi(p, 2n),  $\gamma$  obs. 9-531  
<sup>208</sup>Tl, principal  $\gamma$ -rays obs. 9-4680  
<sup>178</sup>W from ( $\alpha$ , 2np) reaction, g.s. rotational levels rel. intensity determ., E<sub>0</sub>=19.2-31.7 MeV 9-20740  
<sup>199</sup>Ag, from <sup>199</sup>Pd decay, and K conversion coeffs. 9-19274  
<sup>139</sup>Ba from <sup>138</sup>Ba(d,p), reduced normalization and spectroscopic factors 9-9061  
<sup>139</sup>Ba to levels in <sup>139</sup>La to study struct. of radioact., decay schemes 9-8982  
<sup>129</sup>I, excited states following <sup>129m</sup>Te decay 9-15717  
<sup>129</sup>I, intermediate- coupling unified model for determ. 9-515  
<sup>129</sup>I from <sup>129m</sup>Te decay,  $\gamma$  spectra obs. 9-18080  
<sup>139</sup>La, from (d,He) and (<sup>3</sup>He,d) at 40 MeV 9-6802  
<sup>139</sup>La, from n scatt. ang. and energy distrib. meas., E<sub>0</sub>=230-2580 MeV 9-18094  
<sup>139</sup>La(n,n'),  $\gamma$  spectra meas., E<sub>0</sub>=0.5-2.3 MeV 9-14613  
<sup>189</sup>Os, 36.6 keV level, lifetime and mag. moment 9-14576  
<sup>189</sup>Os, 69.6 keV level, spin 5/2- mag. and quadrupole moments 9-8990  
<sup>149</sup>Pm numerical calc. of possible existence 9-2637  
<sup>139</sup>Pr 9-6835  
<sup>195</sup>Sb, from <sup>118</sup>Sn(<sup>3</sup>He,d)<sup>195</sup>Sb reaction, and <sup>118</sup>Te decay, nuclear model discussion 9-4754  
<sup>195</sup>Sn, 23.8 keV level,  $\Delta R/R$  sign and magnitude for excitation 9-11221  
<sup>169</sup>Tm, ground state, K=1/2, rotational bands 9-2670  
<sup>239</sup>U from <sup>238</sup>U(n,p),  $\gamma$  spectra obs. 9-15769  
<sup>169</sup>Yb, struct., configuration mixings 9-8988  
<sup>27</sup>Al, 4.509MeV state, study by <sup>3</sup>Mg(p,  $\gamma$ ) reaction 9-507  
<sup>26</sup>Al new 1<sup>+</sup> state from <sup>26</sup>Mg(He,p) obs. 9-2679  
<sup>27</sup>Al, 3.00 MeV,  $\gamma$  width calc. from bremsstrahlung resonant scatt. 9-4744  
<sup>27</sup>Al, from <sup>26</sup>Mg(p,p),  $\gamma$  and coincidence spectra at 2322 keV obs. 9-533  
<sup>27</sup>Al, using high resolution surface barrier counter 9-14581  
<sup>27</sup>Al 3 MeV excitation, investigation 9-2680  
<sup>27</sup>Al mean energy level width at high energies 9-11235  
<sup>27</sup>Al mean energy level width at high energies 9-11235  
<sup>27</sup>Al low-lying levels,  $\gamma$  branching ratios 9-13200  
<sup>39</sup>Ar from  $p$  scatt. cross sections, 24.85 MeV 9-539  
<sup>40</sup>Ar from  $p$  scatt. cross sections, 24.85 MeV 9-539  
<sup>40</sup>Ar odd isotopes, level spectra in Coriolis coupling model with residual interac. of pairing type 9-11241  
<sup>75</sup>As low-lying levels, assignment of transitions of <sup>75</sup>Ge decay 9-11256  
<sup>75</sup>As low-lying levels, assignment of transitions of <sup>75</sup>Ge decay 9-11256  
<sup>17</sup>B lowest  $p$ -shell T=3/2 states, obs. and levels, spins and parities 9-14561  
<sup>17</sup>B even-parity T=1 levels, particle-hole description 9-14562  
<sup>17</sup>B  $p$  ang. distrib. and  $p$ ;  $\gamma$  ang. correlations 9-2755  
<sup>17</sup>Ba, even-even isotopes, high-spin rotational levels 9-514  
<sup>6</sup>Be, from <sup>6</sup>Li(p,n) at E<sub>p</sub>=30, 50 MeV 9-6868  
<sup>6</sup>Be, ground state anal. from  $\alpha$ +2 model approx. 9-509  
<sup>7</sup>Be, 14.6 MeV state, nonexistence 9-11216  
<sup>7</sup>Be from <sup>7</sup>Li(p,n) at E<sub>p</sub>=30, 50 MeV 9-6868  
<sup>7</sup>Be from  $\alpha$  interaction data, review 9-15649  
<sup>8</sup>Be isospin mixing in highly excited states 9-2660  
<sup>8</sup>Be resonance width of short-lived states from three-body react. 9-13222  
<sup>9</sup>Be, from <sup>9</sup>Be(e,e') 9-6853  
<sup>10</sup>Be, ground state from <sup>11</sup>B(n, d)<sup>10</sup>Be 9-594  
<sup>Br</sup> odd isotopes, level spectra in Coriolis coupling model with residual interac. of pairing type 9-11241  
<sup>12</sup>C lowest  $p$ -shell T=3/2 states, obs. and levels, spins and parities 9-14561  
<sup>12</sup>C, 0<sup>+</sup> states in three-alpha model 9-19271  
<sup>12</sup>C, from <sup>13</sup>C(p,d) 1p neutron pick-up strengths DWBA analysis and spectroscopic factors for assoc. states. 9-6865  
<sup>12</sup>C neutron emission following  $\mu$  capture and radiative  $\pi$  capture 9-2645  
<sup>12</sup>C part.-hole states,  $e$  excitation 9-504  
<sup>12</sup>C wave functions for ground state and 2<sup>+</sup> at 4.43 MeV 9-503  
<sup>40</sup>Ca, 4p-4h excitations, J=T=0 levels calc. 9-14585  
<sup>40</sup>Ca, K-band mixing and 8p-8h states 9-18072  
<sup>40</sup>Ca from <sup>39</sup>K(p,p'), resonance decay obs. E<sub>p</sub>=1.1-2.5 MeV 9-15729  
<sup>40</sup>Ca from <sup>42</sup>Ca(p,t), t spectra, cross sections meas. 9-19309  
<sup>40</sup>Ca, from <sup>40</sup>Ca(d,p), spectroscopic strength 9-9067  
<sup>40</sup>Ca, from <sup>40</sup>Ca(d,p), spectroscopic factors 9-9066  
<sup>42</sup>Ca from <sup>42</sup>Ca(p,t), t spectra, cross sections meas. 9-19309  
<sup>42</sup>Ca, from <sup>42</sup>Ca(d,p), spectroscopic factors 9-9066  
<sup>42</sup>Ca, from <sup>42</sup>Ca(d,p), spectroscopic strength 9-9067  
<sup>42</sup>Ca from <sup>44</sup>K decay,  $\gamma$  spectra meas. 9-19299  
<sup>44</sup>Ca high-spin levels at 3660 and 2824 keV, evidence against 9-2686  
<sup>44</sup>Ca, from <sup>44</sup>Ca(d,p), spectroscopic strength 9-9067  
<sup>44</sup>Ca, from <sup>44</sup>Ca(d,p), spectroscopic factors 9-9066  
<sup>44</sup>Ca, from <sup>44</sup>Ca(d,p), spectroscopic strength 9-9067  
<sup>44</sup>Ca, from <sup>46</sup>Ca(d,p), spectroscopic factors 9-9066  
<sup>44</sup>Ca, from <sup>46</sup>Ca(d,p), spectroscopic strength 9-9067  
<sup>46</sup>Ca, from <sup>48</sup>Ca(d,p), spectroscopic factors 9-9066  
<sup>Ce</sup>, even-even isotopes, high-spin rotational levels 9-514  
<sup>31</sup>Cl, spin and parity assigned to 3.01, 2.65 MeV levels 9-538  
<sup>31</sup>Cl from <sup>34</sup>S(p,p); angular distributions of 2.13 MeV  $\gamma$  rays obs. 9-567  
<sup>31</sup>Cl, from <sup>36</sup>S(p,p);  $\gamma$  spectrum recorded and levels determ. 1147 keV 9-540  
<sup>56</sup>Co, principal  $\gamma$ -rays obs. 9-4680  
<sup>52</sup>Cr from <sup>51</sup>V( $\alpha$ , t) levels and spectroscopic factors deduced 9-2762  
<sup>52</sup>Cr from <sup>52</sup>(p,p'), excitation energy and branching ratios 9-6824  
<sup>52</sup>Cr from Cr(t, p) 9-4746  
<sup>52</sup>Cr from Cr(t, p) 9-4746  
<sup>52</sup>Cr from Cr(t, p) 9-4746

## Nucleus continued

## energy levels continued

- <sup>59</sup>Cu, low energy spectrum, shell model approach 9-19290  
<sup>59</sup>Cu proton states obs., orbital momentum of captured proton and one-particle transition strength 9-18105  
<sup>61</sup>Cu proton states obs., orbital momentum of captured proton and one-particle transition strength 9-18105  
<sup>63</sup>Cu proton states obs., orbital momentum of captured proton and one-particle transition strength 9-18105  
<sup>65</sup>Cu, excited states from  $\alpha$ -part. inelastic scatt. at 29 MeV. 9-543  
<sup>65</sup>Cu proton states obs., orbital momentum of captured proton and one-particle transition strength 9-18105  
<sup>18</sup>F, calc. for harmonic oscillator shell model 9-11228  
<sup>18</sup>F, from <sup>14</sup>N(<sup>4</sup>Li,d) obs. 9-11324  
<sup>18</sup>F, from <sup>16</sup>O(e,p) at 19.8MeV, 8.596MeV level obs. 9-6895  
<sup>18</sup>F, hole-particle states using <sup>14</sup>N(<sup>4</sup>Li,t)<sup>18</sup>F reaction 9-8978  
<sup>19</sup>F, from <sup>14</sup>N(<sup>4</sup>Li,p) obs. 9-11324  
<sup>19</sup>F lifetime measurements 9-2674  
<sup>20</sup>F, new values for levels from <sup>19</sup>F thermal n capture obs., spin assignments of low-lying levels 9-16962  
<sup>Fe</sup><sup>53</sup>, scheme from decays of Fe<sup>53g</sup> and Fe<sup>53m</sup> 9-19285  
<sup>55</sup>Fe resonance, from neutron capture 9-6885  
<sup>56</sup>Fe, 0.85 MeV level by 14 MeV neutrons 9-6825  
<sup>56</sup>Fe, 0.85 MeV level excitation by 14 MeV neutrons 9-6825  
<sup>56</sup>Fe doorway state struct. 9-16964  
<sup>56</sup>Fe from <sup>55</sup>Mn( $\alpha$ , t), levels and spectroscopic factors deduced 9-2762  
<sup>56</sup>Fe by inelastic scattering 9-2753  
<sup>57</sup>Fe resonance, from neutron capture 9-6885  
<sup>Ga</sup> odd isotopes, level spectra in Coriolis coupling model with residual interac. of pairing type 9-11241  
<sup>63</sup>Ga proton states obs., orbital momentum of captured proton and one-particle transition strength 9-18105  
<sup>67</sup>Ga proton states obs., orbital momentum of captured proton and one-particle transition strength 9-18105  
<sup>69</sup>Ga from <sup>68</sup>mZn, <sup>69</sup>Ge decay,  $\beta$  and  $\gamma$  spectra meas. 9-18085  
<sup>69</sup>Ga proton states obs., orbital momentum of captured proton and one-particle transition strength 9-18105  
<sup>Gd</sup> odd isotopes, from (d, p), (d,t) reactions on even isotopes 9-6803  
<sup>Gd</sup>, 0<sup>+</sup> excited state half life meas. 9-11242  
<sup>72</sup>Ge from <sup>71</sup>As decay,  $\gamma$  spectra meas. 9-20750  
<sup>72</sup>Ge from <sup>71</sup>As decay,  $\gamma$  spectra meas. 9-20750  
<sup>72</sup>Ge excited by scatt. of 12 MeV  $p$  and 8 MeV  $d$ . 9-8998  
<sup>72</sup>Ge  $\gamma$  spectra obs. and level scheme determ. 9-8981  
<sup>7</sup>He, search for unbound states from <sup>6</sup>Li(p, $\alpha$ ) react. 9-11211  
<sup>7</sup>He from <sup>6</sup>Li(d, $\alpha$ ), possible level schemes examination 9-20808  
<sup>7</sup>He in <sup>7</sup>H(p,p)<sup>7</sup>H, phase shift anal., Ep=3.11-4.6 MeV 9-14564  
<sup>7</sup>He ground state and anal. from  $\alpha$ +2 model approx. 9-509  
<sup>8</sup>K, e.m. props., shell-model interac. calc. 9-18071  
<sup>Li</sup>, from ( $\pi$ ,nn), ( $\pi$ ,np) reactions, calc. 9-20800  
<sup>Li</sup> unsuccessful search for T=2 state 9-15713  
<sup>6</sup>Li, 2.18 and 3.56 MeV,  $e$  scatt. 9-6856  
<sup>6</sup>Li, width of low-lying states 9-11215  
<sup>23</sup>Mg, from <sup>24</sup>Mg(<sup>3</sup>He, $\alpha$ ) reaction at 15 MeV, obs. 9-6901  
<sup>23</sup>Mg from <sup>23</sup>Na(d,n), n spectra meas. 9-19282  
<sup>23</sup>Mg from <sup>23</sup>Na(d,n) ang. and energy distrib. meas., Ed=6 MeV 9-15727  
<sup>24</sup>Mg from <sup>26</sup>Mg from <sup>26</sup>Mg(p,t),  $\gamma$  transitions meas., E<sub>p</sub>=50MeV 9-18093  
<sup>24</sup>Mg, from <sup>24</sup>Mg(d,p), spectroscopic factors determ., Ed=2.02-4.22 MeV 9-11318  
<sup>25</sup>Mg, from <sup>26</sup>Mg(<sup>3</sup>He, $\alpha$ ) reaction at 15 MeV, obs. 9-6901  
<sup>26</sup>Mg, excited by 0.85 to 4.58MeV  $p$ , obs. 9-6860  
<sup>26</sup>Mg, first two excited states, spin assignments from ang. correl. in <sup>26</sup>Mg(d,pp) reaction 9-13199  
<sup>Mn</sup><sup>53</sup>, scheme from decays of Fe<sup>53g</sup> and Fe<sup>53m</sup> 9-19285  
<sup>54</sup>Mn, low energy excited states by <sup>54</sup>Cr(p,n)<sup>54</sup>Mn reaction 9-19286  
<sup>55</sup>Mn from <sup>54</sup>Cr(<sup>3</sup>He,d) ang. distrib. meas., E<sub>0</sub>=10 MeV 9-13243  
<sup>55</sup>Mn octupole weak coupling obs. in 17.5 MeV  $p$  inelastic scatt. 9-2688  
<sup>92</sup>Mo, from  $\alpha$  scatt. differential cross section, 31 MeV 9-546  
<sup>92</sup>Mo, negative parity states, excited by  $p$  scatt. going through 11.80 MeV isobaric analog reson. in <sup>92</sup>Tc 9-4752  
<sup>92</sup>Mo level scheme deduced from decay of <sup>92</sup>Tc isomers 9-14599  
<sup>96</sup>Mo, from decay of <sup>96</sup>Tc isomeric pair and <sup>96</sup>Nb 9-6831  
<sup>14</sup>N first three states, 7-12 MeV, from <sup>13</sup>C(d,n) ratios of spectroscopic factors 9-6897  
<sup>14</sup>N, 5.563 MeV level e.m. decay rate calc. 9-6837  
<sup>15</sup>N wave functions constructed for 1/2-, 3/2 states by mixing spherical and deformed configurations 9-6789  
<sup>21</sup>Na, resonance states from <sup>20</sup>Ne(p,p), (p,p') react., comparison with <sup>21</sup>Ne and Nilsson model predictions 9-16943  
<sup>22</sup>Na, lifetime measurements 9-2674  
<sup>23</sup>Na, 225 MeV, coeffs. of mixing of two states with I=3/2, K=3/2, 3/2 determ. 9-20730  
<sup>24</sup>Na from <sup>26</sup>Mg(p,<sup>3</sup>He),  $\gamma$  transitions meas., E<sub>p</sub>=50MeV 9-18093  
<sup>91</sup>Nb d<sub>3/2</sub> analog state E1  $\gamma$  decay, from <sup>92</sup>Zr(p,p') obs. 9-4751  
<sup>91</sup>Nb from <sup>93</sup>Nb (n<sub>res</sub>,  $\gamma$ ), determ. from spectra 9-6890  
<sup>91</sup>Ne, (<sup>3</sup>He, n) reactions ang. distribution, excitation functions, energy-level spins and parity data 9-2649  
<sup>19</sup>Ne first-excited state, g-factor 9-16936  
<sup>21</sup>Ne, from <sup>22</sup>Ne(<sup>3</sup>He, $\alpha$ ) reaction at 15 MeV, obs. 9-6901  
<sup>21</sup>Ne, resonance states, comparison with <sup>21</sup>Na 9-16943  
<sup>21</sup>Ne structure studied by <sup>22</sup>Ne(d,<sup>3</sup>He)<sup>21</sup>Ne and <sup>23</sup>Na(n,p)<sup>21</sup>Ne 9-6814  
<sup>Ni</sup> isotope multipole collective states excitation by  $\alpha$  at 40 MeV 9-11240  
<sup>59</sup>Ni, calc. from reaction matrix elements 9-14587  
<sup>60</sup>Ni, 3.12 MeV state, DWBA anal. of (d,d') and (t,p) meas., recalc. 9-20749  
<sup>10</sup>O, (<sup>3</sup>He, n) reactions, ang. distribution, excitation functions, energy-level spins and parity data 9-2649  
<sup>10</sup>O, 7.276 MeV level e.m. decay rate calc. 9-6837  
<sup>10</sup>O, wave functions constructed for 1/2-, 3/2 states by mixing spherical and deformed configurations 9-6789  
<sup>16</sup>O, 6.92(2<sup>+</sup>) and 7.12(1<sup>-</sup>) MeV, widths 9-2652  
<sup>16</sup>O, from <sup>14</sup>N(<sup>4</sup>Li, $\alpha$ ) obs. 9-11324  
<sup>16</sup>O analogue states in <sup>15</sup>N(p,n)<sup>16</sup>O, excitation function and cross sections 9-8977  
<sup>17</sup>O, 5.70 and 5.73 MeV levels, from <sup>19</sup>F(d, $\alpha$ )<sup>17</sup>O reaction 9-16965  
<sup>18</sup>O, calc. for harmonic oscillator shell model 9-11228  
<sup>18</sup>O, shell model new assignments 9-19278  
<sup>20</sup>O\* from <sup>14</sup>N( $\alpha$ ,p), cross sections determ., E<sub>0</sub>=13-18 MeV 9-20806  
<sup>21</sup>P from <sup>28</sup>Si(d,n) at 5.0 MeV 9-6902  
<sup>31</sup>P 3.13 MeV  $\gamma$  width calc. from bremsstrahlung resonant scatt. 9-4744  
<sup>31</sup>P from <sup>29</sup>Si(<sup>3</sup>He,p),  $p$  energy, ang. distrib. meas., E=9 MeV 9-14582  
<sup>31</sup>P from <sup>30</sup>Si(<sup>3</sup>He,d),  $d$  energy, ang. distrib. meas., E=10 MeV 9-14582

**Nucleus continued****energy levels continued**

- <sup>31</sup>P from <sup>30</sup>Si(p,p),  $\gamma$  spectra meas.,  $E_p=0.8\text{--}2.2$  MeV 9-18069  
 Rb odd isotopes, level spectra in Coriolis coupling model with residual interac. of pairing type 9-11241  
<sup>32</sup>S from <sup>28</sup>Si( $\alpha$ ,p),  $\gamma$  spectra meas.,  $E_\alpha=3.7\text{--}3.9$  MeV 9-18070  
<sup>32</sup>S from <sup>31</sup>P(<sup>3</sup>He,d), excitation energy  $\leq 9.5$  MeV 9-11236  
<sup>33</sup>S from <sup>32</sup>S(<sup>3</sup>He, $\alpha$ p), at 7.12 MeV 9-537  
<sup>34</sup>S unreported level at 1.56 MeV 9-2683  
<sup>43</sup>Sc, isobaric analogue resonances fine struct. 9-8995  
<sup>45</sup>Sc isobaric analogue resonances fine struct. 9-8995  
<sup>48</sup>Sc from <sup>48</sup>Ca(p,n $\gamma$ ),  $\gamma$  spectra meas.,  $E_p=1.2\text{--}4$  MeV 9-19284  
<sup>28</sup>Si, form factor of 17.5 MeV level 9-16945  
<sup>28</sup>Si, from e scatt, deformation and oscillation parameters, internal quadrupole moment 9-11277  
<sup>26</sup>Si, O<sup>+</sup> T=2 state isospin-forbidden alpha decay, excitation energy 9-2682  
<sup>28</sup>Si giant resonance electroexcitation, 150-225 MeV expt. data compared with prediction 9-2681  
<sup>28</sup>Si spin of 8.555 MeV state,  $J^\pi=6^+$  9-6817  
<sup>28</sup>Si spectroscopic factors 9-6903  
<sup>30</sup>Si,  $J^\pi=3^+$ , at 5.22 MeV 9-13201  
 Sn, Tamm-Dancoff theory of vibrational states 9-2639  
 Sn, Tamm-Dancoff theory of vibrational states 9-2639  
<sup>34</sup>S(p,p)<sup>32</sup>S,  $E_p=12$  MeV 9-11237  
<sup>88</sup>Sr dipole states, struct. and analysis 9-11244  
<sup>99</sup>Tc from <sup>99</sup>Mo decay,  $\gamma$  spectra meas. 9-15731  
<sup>45</sup>Ti, ground state triplet at 0, 36.7 and 40.2 KeV, from <sup>45</sup>Sc(p,n) 9-19283  
<sup>46</sup>Ti, structure by <sup>45</sup>Sc(<sup>3</sup>He,d)<sup>46</sup>Ti reaction 9-6819  
<sup>46</sup>Ti from <sup>45</sup>Sc(p,p)<sup>46</sup>Ti react. 9-6821  
<sup>46</sup>Ti spins, ang. correlation meas. 9-2730  
<sup>49</sup>Ti, from <sup>46</sup>Ti(d,p)<sup>49</sup>Ti reaction study 9-9068  
<sup>51</sup>Ti, 2p-1h configurations effect, from <sup>49</sup>Ti(t,p) 9-2687  
<sup>51</sup>Ti, from <sup>50</sup>Ti(d,p)<sup>51</sup>Ti reaction study 9-9068  
<sup>50</sup>V, low-lying levels, <sup>50</sup>Ti(p,n)<sup>50</sup>V obs., multipolarities of transitions and spins 9-18074  
<sup>51</sup>V, calc. from reaction matrix elements 9-14587  
<sup>51</sup>V(n,n') level scheme and spins derived for levels, excitation curves obs. 9-542  
 Xe, even-even isotopes, high-spin rotational levels 9-514  
 Xe excited levels, from ( $\alpha$ ,2n) react., Te and Sn targets 9-16940  
<sup>88</sup>Y, principal p-rays obs. 9-4680  
<sup>89</sup>Y, deduced from <sup>89</sup>Zr isomers decay study 9-14598  
<sup>89</sup>Y, using high resolution surface barrier counter 9-14581  
<sup>89</sup>Y, scheme, from <sup>89</sup>Zr decay 9-6830  
 Yb, from (d,p), (d,t), (d,d') reactions on stable isotopes 9-6806  
 Zn multiple collective states excitation 9-11240  
<sup>62</sup>Zn, low energy excited states from decay of <sup>62</sup>Ga 9-19291  
<sup>68</sup>Zn from <sup>68</sup>Ga decay,  $\gamma$  conversion levels determ., evidence for O<sup>+</sup> state 9-4749  
<sup>64</sup>Zn(p,p)<sup>63</sup>Zn, ang. distrib. meas., levels determ.,  $E_p=26$  MeV 9-20785  
<sup>64</sup>Zn(p,p)<sup>64</sup>Zn, ang. distrib. meas., levels determ.,  $E_p=26$  MeV 9-20785  
<sup>90</sup>Zr from <sup>90</sup>Zr(p,d), excited levels structure obs., up to 13 MeV 9-545  
<sup>90</sup>Zr, energies of low-lying excited levels from meas. on <sup>90</sup>Nb decay 9-13205  
<sup>90</sup>Zr, from  $\alpha$  scatt. differential cross section, 31 MeV 9-546  
<sup>90</sup>Zr, isobaric splitting of 1-levels, energy splitting calc. 9-15705  
<sup>91</sup>Zr, energies of low-lying excited levels from meas. on <sup>91</sup>Nb decay 9-13205  
<sup>92</sup>Zr energies of low-lying excited levels from meas. on <sup>92</sup>Nb decay 9-13205  
<sup>96</sup>Zr from <sup>96</sup>Zr(t, p), p ang. distrib. meas., n configurations determ. 9-20752  
 9-11207

**excitation see Nuclear excitation****magnetic moment**

See also *Gyromagnetic ratio; Molecules/nuclear coupling; Nuclear magnetic resonance and relaxation*

- Brueckner correlations 9-13188  
 deviation from Schmidt lines induced by non-local two-body pot., up to <sup>41</sup>Ca 9-6785  
 dipole calc. in Wigner supermultiplet approx. 9-11202  
 M1 transition probabilities from isobaric analogue states 9-14555  
 odd-mass nuclei, eff. of two-body interaction currents 9-14556  
 reorientation effect in Coulomb excitation 9-13187  
 short-range correlations 9-13188  
 n closed shell, BCS theory applied 9-483  
<sup>210</sup>Bi, pure M1(1=0) transitions, L-subshell conversion line intensity ratios 9-14570  
<sup>120</sup>Sb, spin and dipole moment determ. 9-6820  
<sup>212</sup>Bi, pure M1(1=0) transitions, L-subshell conversion line intensity ratios 9-14570  
<sup>192</sup>Os, calc. from pairing plus-quadrupole model 9-15702  
<sup>153</sup>Eu, of 83.4 KeV rot. state from Mossbauer effect meas. 9-6792  
<sup>131</sup>Sn(n,p), M1 transitions evaluation from  $\gamma$  spectra 9-13228  
<sup>144</sup>Pr, pure M1(1=0) transitions, L-subshell conversion line intensity ratios 9-14570  
<sup>184</sup>W, calc. from pairing- plus-quadrupole model 9-15702  
<sup>165</sup>Ho, magnetic dipole transitions, reduced probabilities 9-523  
<sup>115</sup>In excitation by threshold- energy e, M1/E2 mixing ratios determ. 9-6798  
<sup>115</sup>Sb, in terms of configuration-mixing calc. 9-14566  
<sup>196</sup>Pt, calc. from pairing-plus-quadrupole model 9-15702  
<sup>156</sup>Gd, g-factors and multipole mixing ratios 9-6804  
<sup>166</sup>Ho, pure M1(1=0) transitions, L-subshell conversion line intensity ratios 9-14570  
<sup>117</sup>Sb, in terms of configuration-mixing calc. 9-14566  
<sup>147</sup>Sm g-factor determ. from internal rotation obs. 9-15722  
<sup>118</sup>Sb, in terms of configuration-mixing calc. 9-14566  
<sup>199</sup>Os, 36.2 keV level 9-14576  
<sup>199</sup>Os, 69.6 keV level, determ. from  $\gamma$  meas. 9-4739  
<sup>199</sup>Os, of 69.9 keV level, and quadrupole moment 9-8990  
<sup>169</sup>Tm, K=1/2 rotational band, E2/M1 mixing ratios 9-14574  
<sup>12</sup>B relax. time of nuclear polarization 9-2648  
<sup>3</sup>H anomaly, baryon reson. admixtures description 9-14563  
<sup>3</sup>He anomaly, baryon reson. admixtures description 9-14563  
<sup>45</sup>K spin and dipole moment determ. 9-6820  
<sup>95</sup>Nb, M4 assignment theor. calc. from  $\gamma$  internal conversion meas. 9-15744

**Nucleus continued****magnetic moment continued**

- <sup>51</sup>V, first excited state 320 keV, g-factor meas. by Coulomb excitation in Fe-V alloy 9-11239

**magnetic resonance see Nuclear magnetic resonance and relaxation models**

- Bethe-Weizsacker mass formula, derivation assuming Lennard-Jones N-N pots. 9-6769  
 boson expansion methods in soluble two-level shell, reformulation, rel. to vibr. 9-6780  
 closed formula for 3nj coefficients of R3 (Racah coefficient) 9-20865  
 cluster, matrix elements in super multiplet scheme 9-16932  
 cluster knockout test by <sup>6</sup>Li (p,p $\alpha$ d),  $E_p=61.5$  MeV 9-16959  
 collective potential-energy-surface, structure 9-4711  
 compound, <sup>99</sup>Ni decay depend. on ang. momentum 9-4748  
 compound, applic. to (n,3n) and statistical theory 9-2739  
 configuration mixing in shell calc., concealing of 9-6763  
 Coriolis coupling with residual interact of pairing type, for calc. of level spectra of Ga, As, Br, Rb odd isotopes 9-11241  
 deformed, for fission with light particle emission 9-13182  
 deformed, rot. and intrinsic motion 9-8966  
 deformed n, rot. motion 9-8965  
 duster for finite range knock-out reactions 9-14603  
 effective interaction rel. to free nucleon- nucleon interact. 9-4712  
 excitation and n-p exchange energy vary regularly 9-2632  
 excited-core, reducing to shell and quasi-particle models 9-2631  
 Fermi-gas type, study of U<sup>-1/2</sup> factor in level density formulae 9-4715  
 Griffin's statistical model, extension to include charged-particle emission 9-4765  
 hydrodynamic, for giant dipole resonance, A<sup>-1/6</sup> depend 9-2638  
 light nuclei, evidence for cluster props. 9-15712  
 liquid-drop, instability of super-heavy nuclei 9-551  
 monopole, two-vibrational-mode, RPA and 2nd-order perturbation theory, validity 9-6762  
 Nilsson's,  $\mu$  capture theory 9-2723  
 Nilsson, 2s-1d shell, hexadipole deform., evidence 9-8993  
 Nilsson, applicability to <sup>23</sup>Ne 9-6814  
 nuclear matter, pairing correlations, calc. 9-490  
 optical, analysis of d and  $\alpha$  scatt. 9-606  
 optical, deuteron-nucleus syst., three-body effective interaction 9-2750  
 optical, in <sup>3</sup>He scatt. analysis 9-9063  
 optical, meas. of neutron total X-sections from 100 - 150 MeV 9-9046  
 optical, parameters correl. with d scatt. ang. distrib. anomalies for N=50, obs. 9-608  
 optical, pot. ambiguities in <sup>16</sup>O-<sup>24</sup>Mg elastic scatt. near Coulomb barrier 9-2764  
 optical, rel. to collision time calcs. for scatt. of n, p, and d 9-15748  
 optical, s-wave n strength function and pot. scatt. radius appl. 9-11204  
 optical, study using n scatt. off several elements 9-20787  
 Optical in Mg region, composite part., scatt. and bound state pot., DWBA calc. 9-4790  
 optical potential and asymmetry of 20 MeV polarized p, spin-dependent Thomas form 9-13221  
 optical potential for deuterons 9-9069  
 optical proton neutron distributions calc. 9.6 MeV 9-582  
 pairing correlations of deformed nuclei, appl. of Green's function method 9-4713  
 pairing-plus-quadrupole, nuclear deformations, collective motion theory 9-15702  
 parameters effect on channel analysis of neutron induced nuclear fission 9-11331  
 parity mixed configurations 9-2630  
 perturbed symmetric, study of relative blocking eff. in K=2 and  $\beta$  vib. bands, in deformed nuclei 9-8964  
 potential, N-N bremsstrahlung anal. 9-18057  
 potential model review 9-6756  
 pseudonium, configuration mixing, concealing of 9-6763  
 quantized liquid drop, skin thickness, elec. form factor for elastic scatt., nuc. radius rel. to atomic no. 9-11184  
 rotor-vibrator used successfully to calc. low-lying excited states of  $if_{7/2}$  even-even nuclei 9-11182  
 shell, 2s-1d, Nilsson, hexadipole deform. evidence 9-8993  
 shell, applic. of transcription of quasiparticle into ideal space 9-14542  
 shell, calc. for 30<A<33 9-6818  
 shell, C.M. motion Hamiltonian depend. and RPA, arbitrary central potential 9-20727  
 Shell, for <sup>36</sup>Ni structure study 9-13204  
 shell, harmonic oscillator eigenvalue problem modified 9-14549  
 shell, intermediate coupling states structure 9-487  
 shell, low-lying states belonging to each spin calc. method. 9-19266  
 shell, mixed-parity configurations spectroscopy 9-6772  
 shell, N=2, 3, Q,Q force acting on particles, Hartree-Fock calc. and ang. momentum projection 9-14544  
 shell,  $\mu$  capture theory 9-2723  
 Shell, of <sup>208</sup>Pb 9-6811  
 shell, of highly-excited resonant states 9-6777  
 shell, pseudonium nuclei, configuration mixing, concealing of 9-6763  
 shell, soluble two-level, for boson expansion methods, vibrational nuclei anal. 9-4723  
 shell, soluble two-level, for boson expansion methods reformulation and rel. to vibr., time-depend. Hartree-Fock theory and equivalence 9-6780  
 shell, spherical, particle-hole excitations with a sum of separable interac. 9-8961  
 shell, wave function of <sup>6</sup>Li, residual N-N interaction 9-15714  
 shell and cluster configs, recoupling coeffs. of symmetric group 9-4714  
 shell and translationally invariant model 9-6764  
 shell calc. of even-mass tin isotopes including hard core excitation 9-6795  
 shell description of nuc. reac., part.-hole excitation, scatt. ampl. and reson., spectroscopic TD calc. 9-6870  
 shell effect in (n,2n) reactions 9-20795  
 shell potential, isospin term determ. from N binding energies 9-15703  
 shell-model calc. on A=38 nuclei 9-16946  
 shell-model interac. calc. of states in <sup>18</sup>K 9-18071  
 solvable, pairing and deformation, validity of different approx. methods 9-8953  
 spherical, for fission with light particle emission 9-11326  
 spherical potential, coupled one-particle states of nucleons 9-14550  
 SU(3), review 9-19268  
 SU(3), rotational bands assignment validity 9-18059  
 superfluid, approx. methods accuracy 9-11185



**Nucleus continued**  
**models continued**

- superfluid, nucleons form  $\alpha$ , effective mass calc. 9-6713  
symmetric-core collective model for odd-odd nuclei; formulation and applic. in 2s-1d shell 9-19267  
three-body of the deuteron-nucleus syst., eff. interac. deriv. in terms of nucleon-nucleon opt. pot. 9-2750  
time depend. Hartree-Fock theory in two-level shell, equivalence and rel. to boson expansion methods 9-6780  
translationally invariant model for calc. of particle hole states. 9-6764  
two-body potential, transform into Hermitian Brueckner matrix 9-4708  
unified intermediate coupling; odd-mass I isotopes low levels determ. 9-515  
( $\alpha, n$ ) temps. rel. to Fermi-gas and const. temp. models, 4-7 MeV 9-18102  
d optical potential 9-2656  
<sup>40</sup>Ca multiparticle-multihole model, introduction of K-band mixing and higher order deformed states 9-18072  
<sup>208</sup>Pb. Shell model 9-6811  
Al, opt., mes. of n total X-sections from 100 - 150 MeV 9-9046  
<sup>38</sup>Ar s-d shell structure, <sup>39</sup>K(d,<sup>3</sup>He)<sup>38</sup>Ar 9-2684  
<sup>12</sup>C, three-alpha, low-lying 0<sup>+</sup> states 9-19271  
<sup>48</sup>Ca, particle-hole excitations, odd-parity levels, correlations in ground-state 9-8996  
Cd, opt., meas. of n total X-sections from 100 - 150 MeV 9-9046  
Cu, opt., meas. of n total X-sections from 100 - 150 MeV 9-9046  
<sup>90</sup>Y shell model approach to low energy spectrum 9-19290  
<sup>14</sup>N shell-model calc., E1 transitions, giant resonance 9-2650  
<sup>21</sup>Na, Nilsson and shell descriptions, comparison with absolute spectroscopic factors deduced from <sup>20</sup>Ne(d,n)<sup>21</sup>Na react. 9-4800  
<sup>16</sup>O opt. shell ground state, part.-hole states, scatt. amp. and reson., spectroscopic TD calc. 9-6870  
<sup>17</sup>O, shell model, harmonic oscillator eigenvalue problem modified 9-14549  
P isotopes shell calc., level energies spectroscopic factors 9-6818  
Pb, opt., meas. of n total X-sections from 100 - 150 MeV 9-9046  
S isotopes shell calc., level energies, spectroscopic factors 9-6818  
Si isotopes, shell calc., level energies, spectroscopic factors 9-6818  
<sup>48</sup>Ti, shell, spin-1 states 9-8997  
U, opt., meas. of n total X-sections from 100 - 150 MeV 9-9046

**size**

- <sup>3</sup>H. R.M.S. charge radii 9-2657  
Coulomb-energy radii from mass parabolas 9-9103  
deformation, intrinsic, associated with collective 0<sup>+</sup> states 9-13185  
form factor rel. to  $\pi^+$  charge exchange scatt. 9-15771  
mass distrib. radii from optical model analysis of n elastic scatt. 9-2634  
 $R=r_0A^{1/3}$  not followed, slow increase of  $r_0$  with mass number 9-20787  
radial depend on phenomenological form of n interaction 9-2633  
radius of charge, mass distrib. from e, p scatt. 9-11205  
S-wave n strength function and pot. scatt. radius, optical model 9-11204  
tritium, e.m. radii calc. in a theory of zero-range forces 9-11213  
<sup>150</sup>Sn, nuclear-matter size from opt.-model analysis of 39.6 MeV p scatt. 9-11219  
<sup>150</sup>Sn(p, p) nuclear matter radii and charge distrib. calc. from cross sections 9-11220  
<sup>152</sup>Sn, nuclear-matter size from opt.-model analysis of 39.6 MeV p scatt. 9-11219  
<sup>152</sup>Sn(p, p) nuclear matter radii and charge distrib. calc. from cross sections 9-11220  
<sup>153</sup>Eu mean square charge radius of 83.4 keV rotational level 9-6792  
<sup>152</sup>Sn, nuclear matter size from opt.-model analysis of 39.6 MeV p scatt. 9-11219  
<sup>154</sup>Sn(p, p) nuclear matter radii and charge distrib. calc. from cross sections 9-11220  
<sup>156</sup>Sn, nuclear-matter size from opt.-model analysis of 39.6 MeV p scatt. 9-11219  
<sup>156</sup>Sn(p,p) nuclear matter radii and charge distrib. calc. from cross sections 9-11220  
<sup>158</sup>Sn, nuclear-matter size from opt.-model analysis of 39.6 MeV p scatt. 9-11219  
<sup>158</sup>Sn(p, p) nuclear matter radii and charge distrib. calc. from cross sections 9-11220  
<sup>159</sup>Sn,  $\Delta R/R$ , sign and magnitude for excitation to 23.8 keV level 9-11221  
Si-Sn, 29 nuclei, based on muonic K $\alpha$  isotope shifts 9-535

**spin and parity**

- See also *Gyromagnetic ratio; Molecules/nuclear coupling*  
<sup>55</sup>Co  $\leq 141$  nuclei, n inelastic scatt. obs. at 2.9 MeV 9-4747  
<sup>16</sup>C, from <sup>14</sup>N(p,<sup>3</sup>He) reaction obs. 9-6866  
<sup>9</sup>Mo, from  $\alpha$  scatt. differential cross section, 31 MeV 9-546  
<sup>c</sup><sup>95</sup>Nb from <sup>95</sup>Zr decay,  $\beta$ ,  $\gamma$  spectra meas. 9-15744  
configurations using a simple model 9-2630  
Elliott ang. momentum states, projection from Gel'fand U(3) basis 9-8954  
isobaric spin existence rel. to nuclear spectroscopy and structure determ. 9-20732  
isospin fragmentation of dipole excitations of nuclei with n excess, 1<sup>-</sup> levels 9-15705  
p 9-6784  
resonance states, spin calc. by coincidence meas. 9-11199  
rotation and vibration bands, deformed even nuclei, blocking eff. 9-8964  
seniority, 0, 1, sharp wave func. and BCS approx. comparison heavy spherical nucleus 9-11172  
shell model for p, n system stretch scheme vs. seniority scheme 9-15699  
in solids, exchange interaction effect on dynamic nuclear polarization 9-1719  
space parity violation effects in e.m. transitions 9-498  
spin polarization eff. in odd-mass deformed nuclei 9-14554  
spin systems at negative absolute temp., thermodynamics 9-11201  
spin-quadrupole forces and collective states, 0<sup>+</sup>, 2<sup>+</sup> 9-499  
K<sup>0</sup>-nucleus interaction amplitudes, spin dependence of regeneration amplitude 9-361  
<sup>90</sup>Zr, isospin fragmentation of dipole excitations, 1<sup>-</sup> levels 9-15705  
<sup>140</sup>Co, levels determ. from La<sup>140</sup> pair-conversion positrons 9-2666  
<sup>140</sup>Ce from <sup>140</sup>La decay,  $\gamma$  spectra obs. 9-11224  
<sup>160</sup>Nd(<sup>16</sup>O, <sup>16</sup>O' $\gamma$ ), g. meas. for 2<sup>+</sup> state 9-15723  
<sup>120</sup>Sb, spin and h.f.s. determ. 9-6820  
<sup>120</sup>Sb, spins, hyperfine struct., magnetic moments 9-14566  
<sup>120</sup>Sn spin assignments rel. to  $\gamma$ - $\gamma$  angular correlation meas. 9-8980  
<sup>114</sup>Ag from <sup>113</sup>Pd decay,  $\gamma$  spectra meas. 9-20760  
<sup>241</sup>Pu cross section meas. 1-30 eV spin assignments for 2-32eV resonances 9-4781  
<sup>181</sup>Ta, search for parity mixing in 482 keV state 9-19279

**Nucleus continued**  
**spin and parity continued**

- <sup>112</sup>Cd from <sup>112</sup>Ag decay,  $\gamma$  spectra meas. 9-13208  
<sup>142</sup>Pr, assignments 9-2667  
<sup>137</sup>Cs, 384 keV level,  $\gamma/2$  from  $\gamma$  ang. correl. 9-20738  
<sup>133</sup>Cs from <sup>133</sup>Ba decay, spin assignments from  $\gamma$  spectra 9-8981  
<sup>153</sup>Eu nuclear rotation and single particle excitation effects on X-ray spectrum 9-11432  
<sup>143</sup>Pm, evidence for  $7/2^+$  level at 273 keV predicted by Kissinger-Sorensen theory 9-8983  
<sup>135</sup>Cs from <sup>135</sup>Xe decay,  $\gamma$  spectra meas. 9-19296  
<sup>163</sup>Ho, 1/2 + [411 spin down] and 3/2 + [411 spin up] bands 9-20742  
<sup>115</sup>In 935 and 1129 keV levels 9-541  
<sup>115</sup>Sb, spins, hyperfine struct., magnetic moments 9-14566  
<sup>145</sup>Sm level assignments from <sup>145</sup>Eu decay obs. 9-14571  
<sup>166</sup>Er from <sup>166</sup>Ho decay, E1 transition  $\gamma$  polarization meas. 9-14573  
<sup>166</sup>Er from <sup>166</sup>Tm decay,  $\gamma$  energy obs. 9-2704  
<sup>106</sup>Pd,  $\gamma$  spectra obs. of level transitions 9-13193  
<sup>147</sup>Pm, spin assignment of 413 keV state 9-11225  
<sup>187</sup>Re-<sup>187</sup>W,  $\gamma$  angular correlation meas., parity and E1, E2 transitions determ. 9-20766  
<sup>117</sup>Sb, spins, hyperfine struct., magnetic moments 9-14566  
<sup>117</sup>Sn from <sup>117</sup>Sb decay,  $\gamma$  spectra meas. 9-13194  
<sup>178</sup>Hf from <sup>177</sup>Hf(n, $\gamma$ ),  $\gamma$  spectra meas.,  $E_\alpha=0.06-8.8$  eV 9-13195  
<sup>118</sup>In, 7<sup>-</sup> or 8<sup>-</sup> isomeric state decay  $\gamma$  spectra meas. 9-19276  
<sup>118</sup>Sb, spins, hyperfine struct., magnetic moments 9-14566  
<sup>109</sup>Ag, levels 9-19274  
<sup>129</sup>I from <sup>129m</sup>Te decay,  $\gamma$  spectra obs. 9-18080  
<sup>119</sup>Sb, spins, hyperfine struct., magnetic moments 9-14566  
<sup>25</sup>Al, 5/2<sup>+</sup> spins of ground states as evidence for hexadipole deform. in Nilsson model 9-8993  
<sup>36</sup>Ar, assigned from p scatt. cross sections, 24.85 MeV 9-539  
<sup>40</sup>Ar, assigned from p scatt. cross sections, 24.85 MeV 9-539  
<sup>11</sup>B, from <sup>13</sup>C(p,<sup>3</sup>He) reaction obs. 9-6866  
<sup>11</sup>B lowest p-shell T=3/2 states, obs., spins, parities, isospin purity 9-14561  
<sup>12</sup>B even-parity T=1 levels, particle-hole description 9-14562  
Ba, even-even isotopes, high-spin rotational levels 9-514  
<sup>11</sup>C, from <sup>13</sup>C(p,t) reaction obs. 9-6866  
<sup>11</sup>C, spin and  $\gamma$  spectra determ. 9-11218  
<sup>11</sup>C lowest p-shell T=3/2 states, obs., spins, parities, isospin purity 9-14561  
<sup>40</sup>Ca from <sup>42</sup>Ca(p,t), t spectra, cross sections, meas. 9-19309  
<sup>42</sup>Ca from <sup>44</sup>Ca(p,t), t spectra, cross sections, meas. 9-19309  
<sup>42</sup>Ca high-spin levels at 3660 and 2824 keV, evidence against 9-2686  
<sup>48</sup>Ca, odd-parity levels, by particle-hole excitations, correlations in ground-state 9-8996  
Ce, even-even isotopes, high-spin rotational levels 9-514  
<sup>53</sup>Cl,  $\gamma$ -ray ang. distrib. obs. for 3.01, 2.65 MeV levels 9-538  
<sup>50</sup>Cr, first excited state with spin 2 9-19305  
<sup>18</sup>F, isobaric spin of excited states determ. from <sup>18</sup>O(p, n<sub>1,2</sub>)<sup>18</sup>F 9-505  
<sup>19</sup>F 2797 keV level, spin and lifetime 9-4729  
<sup>56</sup>Fe, of resonant state obs. by means of 2.5-3 MeV p scatt. 9-19305  
<sup>56</sup>Fe, of resonant state obs. by means of 2.5-3 MeV p scatt. 9-19305  
<sup>56</sup>Fe, of second and third excited levels 9-14588  
<sup>69</sup>Ga from <sup>68</sup>mZn, <sup>69</sup>Ge decay,  $\beta$  and  $\gamma$  spectra meas. 9-18085  
He<sup>3</sup>, solid, exchange interaction effect on dynamic nuclear polarization 9-1719  
<sup>3</sup>H(n,p)<sup>3</sup>H parity nonconservation eff. 9-15767  
<sup>4</sup>K spin and h.f.s. determ. 9-6820  
<sup>4</sup>Li unsuccessful search for T=2 state 9-15713  
<sup>2</sup>Mg from <sup>23</sup>Na(d,n), n spectra meas. 9-19282  
<sup>2</sup>Mg, 5/2<sup>+</sup> spins of ground states as evidence for hexadipole deform. in Nilsson model 9-8993  
<sup>2</sup>Mg, first two excited states, spin assignments from ang. correl. in <sup>26</sup>Mg(d,pp) reaction 9-13199  
<sup>86m</sup>Rb, spin 6<sup>-</sup> assigned 9-9000  
<sup>13</sup>N 3/2<sup>-</sup>, 1/2<sup>-</sup> level assignments 9-2727  
<sup>13</sup>N, from <sup>15</sup>N(p,t) reaction obs. 9-6866  
<sup>14</sup>N, from <sup>12</sup>C(<sup>3</sup>He,p) at 20.1 MeV, obs. 9-6895  
<sup>22</sup>Na, evidence for K=1, odd-parity rotational band 9-2674  
<sup>90</sup>Nb from <sup>91</sup>Nb(n<sub>res</sub>,p) resonances spin assignments 9-6890  
<sup>18</sup>Ne (<sup>3</sup>He, n) reactions, ang. distribution, excitation functions, energy-level spins and parity data 9-2649  
<sup>21</sup>Ne, exclusion of spin as explanation for anomalous circular polarization of I.523 $\mu$  He-Ne laser line 9-6520  
<sup>24</sup>Ne, spins of levels below ~5 MeV, from <sup>22</sup>Ne(t,p)<sup>24</sup>Ne ang. correl. study 9-11234  
<sup>21</sup>Ne T=3/2 states, obs. in <sup>22</sup>Ne(<sup>3</sup>He,d)<sub>n</sub> values and ang. distrib. 9-11233  
<sup>16</sup>O, (<sup>3</sup>He, n) reactions, ang. distribution, excitation functions, energy-level spins and parity data 9-2649  
<sup>17</sup>O, <sup>17</sup>F doublet, particle-core coupling, low-lying parity states calc. 9-6791  
<sup>170</sup>\* from <sup>14</sup>N( $\alpha$ ,p), spin, cross sections determ.,  $E_\alpha=13-18$  MeV 9-20806  
<sup>31</sup>P from <sup>30</sup>Si(p,p),  $\gamma$  spectra meas.,  $E_\alpha=0.8-2.2$  MeV 9-18069  
<sup>31</sup>P from <sup>30</sup>Si( $\alpha$ , pp), method II- angular correlation calc. 9-4745  
<sup>19</sup>Sc from <sup>18</sup>Si( $\alpha$ ,p), spin determ. from  $\gamma$  spectra,  $E_\alpha=3.7-3.9$  MeV 9-18070  
<sup>9</sup>Sc, some assignments, 9-2729  
<sup>48</sup>Sc from <sup>48</sup>Ca(p,n),  $\gamma$  spectra meas.,  $E_\alpha=1.2-4$  MeV 9-19284  
<sup>72</sup>Se, anomalous coupling 1/2<sup>+</sup> and 1/2<sup>-</sup> states 9-8999  
<sup>2</sup>Si spin of 8.555 MeV state, J<sup>+</sup>=6<sup>+</sup> 9-6817  
<sup>97</sup>Tc from <sup>99</sup>Mo decay,  $\gamma$  spectra meas. 9-15731  
<sup>46</sup>Ti, resonance state induced by 2.5-3 MeV p scatt. obs. 9-19305  
<sup>46</sup>Ti, of resonant state obs. by means of 2.5-3 MeV p scatt. 9-19305  
<sup>48</sup>Ti, spin-1 states, from particle- $\gamma$  ray correlations, mixing ratios of transitions, rel. to shell model 9-8997  
<sup>46</sup>Ti(p,p')<sup>46</sup>Ti ang. correlation meas. 9-2730  
<sup>50</sup>V, spins of low-lying levels, <sup>50</sup>Ti(p,n)<sup>50</sup>V obs. 9-18074  
<sup>51</sup>V, spin Hamiltonian from ENDOR in MgO 9-12520  
<sup>51</sup>V(n,n') excitation derived from levels, ang. distrib. obs. 9-542  
Xe, even-even isotopes, high-spin rotational levels 9-514  
<sup>90</sup>Y, spin, orb. ang. mom. config. from isobaric analog. comparison, <sup>89</sup>Y(p,p) meas. 9-20751  
<sup>90</sup>Zr, from  $\alpha$  scatt. differential cross section, 31 MeV 9-546  
<sup>98</sup>Zr from <sup>96</sup>Zr(t,p), p ang. distrib. meas. and DW calc. 9-20752

**theory**See also *Nuclear forces*

- 2p-1f shell, structure of self-consistent soln. 9-4705  
Adler-Weisberger sum rule and Goldberger-Treiman rel. 9-8960  
angular momentum projection from Hartree-Fock soln. of Q.Q force in N=2,3 shells 9-14544

**Nucleus continued**  
**theory continued**

BCS approx. and sharp wave func., seniority of 0, 1, comparison, heavy spherical nucleus 9-11172  
 BCS method extension for weakly deformed nuclei 9-11190  
 BCS-spin model, thermodynamic representations, time evolution and vacuum props. 9-7762  
 Beliaev-Zelevinsky expansion, convergence 9-13177  
 Bethe-Goldstone eqn., soln. method comparison 9-18056  
 binding energy for finite nuclei with tensor forces, calc. 9-6771  
 Born approx., 2nd order, for rotational states excitation by p,d scatt. 9-15710  
 boson expansion methods insoluble two-level shell 9-4723  
 boson expansion of fermion pair operators, degenerate model, interpretation of parameter  $\gamma^0$  and its applic. to quadrupole interac. 9-8448  
 bound states calc. in strong coupling approx. 9-20722  
 Brueckner 9-4716  
 Brueckner reaction matrix in oscillator rep., calc. and applic. 9-18054  
 Brueckner theory in oscillator basis 9-4716  
 centroids and sums of one-nucleon transfer strengths, calc. for  $^{16}\text{O}$  target 9-6805  
 charge symmetrical pairing correlation, Bogoliubov transformation for  $N=Z$  even-even nuclei 9-6787  
 composite systems, loosely-bound, e.m. interac. 9-16910  
 core polarization contrib. to effective interactions, higher-order 9-4717  
 Coulomb-nuclear S-matrix along imaginary  $\lambda$ -axis, asymptotic behaviour 9-8951  
 coupled state of three particle, allowance for Coulomb interaction 9-8975  
 deformation, pear-shaped, in oscillator model, perturbation oscillations 9-15707  
 Elliott ang. momentum states, projection from Gelfand U(3) basis 9-8954  
 energy per particle in Hartree-Fock approx., use of unitary transforms 9-4718  
 form factor calc. for pick-up reactions 9-11288  
 Gaussian potential, modified, study of scattering 9-11175  
 generator coordinate theory of collective motion in many-particle systems 9-6766  
 Goldstone diagram in nuclear matter, second-order, calc. 9-8955  
 ground state rotational motion and non-adiabaticity, effective internal Hamiltonian 9-16934  
 Hartree-Bogoliubov, applic. of Ripka's theorem on self-consistent symmetries 9-11183  
 Hartree-Fock, Coulomb and c.m. corrections 9-2629  
 Hartree-Fock, of deformed light nuclei 9-13184  
 Hartree-Fock approx. in finite nuclei, includes relative  $l$ -value 9-11230  
 Hartree-Fock methods applied 9-20725  
 Hartree-Fock multi-configuration theory for 2-body force coupling const. 9-6761  
 Hartree-Fock multi-configuration theory 9-20723  
 Hartree-Fock orbitals, parity mixing 9-11280  
 Hartree-Fock spectra, ang. mom. and isospin states calc. by projection method 9-11177  
 hypernuclear struct calc., rel. to Talmi transformation for different part. 9-4236  
 independent-pair wave functions for 3-, 4-body nuclei, g.s. energy bounds calc. 9-15700  
 inverse gap equation procedure for quasi-particle calc. 9-6750  
 K-matrix methods used to develop condns. for observability of intermediate structure in resonances 9-6778  
 light and intermediate nuclei, effective interac. deriv. from Yale pot. matrix elements 9-11179  
 many-body nuclear wave functions, center of mass and rotational state projection, applications 9-495  
 many-body problem, wave functions formation methods, review 9-14548  
 mass distrib. radii from optical model analysis of  $n$  elastic scatt. 9-2634  
 mass formulae based on different models, comparison 9-18060  
 mass-18, SU(3) group to classify singly excited states 9-2654  
 matter, compressibility from elastic  $^{16}\text{O}$ - $^{16}\text{O}$  scatt. pot. data 9-9070  
 matter, pathological separable potentials 9-6753  
 matter, perturbation theory, eval. of terms, applic. to Pauli correction 9-11186  
 matter saturation props. determ. by separable potentials 9-11187  
 Migdal; nuclear compressibility, effective mass and symmetry energy calc. 9-6751  
 moment of inertia for g.s. bands, comparison of calc. methods 9-4725  
 moments of inertia, a new method of calc. 9-6784  
 $N=50$  isotones, vib. props. and core-coupling considered 9-511  
 non-relativistic crossed partial-wave expansion, physical meaning 9-16930  
 nuclear matter, exchange diagrams 9-16931  
 nuclear matter, superfluid transition critical temp. 9-488  
 odd-mass nuclei, eff. of two-body interac. currents on dipole mag. moment 9-14556  
 odd-nucleus collective Hamiltonian rel. to particle-phonon interaction and conservation laws 9-13178  
 one-boson-exchange potentials, realistic N-N 9-6754  
 one-particle states and wave functions of nucleon coupled states 9-14550  
 pairing interact., number-conserving treatment iteration soln. 9-485  
 pairing calculations, influence of self-energy term 9-492  
 particle number conserving ground state wave functions developed with Thouless-Peierls formalism 9-6752  
 particle-hole Gilet interact. in 2s-1d shell, space scalar approx. 9-502  
 potential barrier penetration for diffuse Woods-Saxon potential of strong interaction 9-486  
 quadrupole surface vibrations, applic. of traceless symm. tensors of  $R(5)$  9-6289  
 quasi-boson approx., rel. to generator coordinate method 9-6767  
 quasi-boson approx. and collective nuclear excitation 9-8963  
 random phase approx. and ground state correlations for N scatt. 9-6765  
 reorientation effect in Coulomb excitation 9-13187  
 resonance scatt. test by exactly soluble model 9-15698  
 restricted quasi-particle transformation investigated 9-11183  
 scattering amplitude matrix, parity and time reversal invariant form, spin  $1/2$ -spin-1 scatt. 9-18055  
 seniority-zero and intermediate states 9-493  
 shell correction model of deformed and spherical nuclei, nucleon shells eff. 9-15708  
 shell model for p, n system stretch scheme vs. seniority scheme 9-15699  
 single particle wave function method tested 9-11268  
 single-particle motion change due to collective states 9-13180

**Nucleus continued**  
**theory continued**

spectra, optimization of phenomenological parameters characterizing effective interaction 9-482  
 spherical or deformed; classification by spectra of  $\alpha$ -decay schemes 9-563  
 stripping reaction, diffraction theory using partial wave expansion 9-11262  
 structure, ground-state, description using differential forms and appropriate manifolds 9-18058  
 superfluid nuclei, effective external field acting on quasiparticle, calc. 9-481  
 superheavy nuclei, shell corrections and deformation 9-15732  
 surface, investig. proc. using localization of react. 9-14543  
 tensor and central force matrix elements computation method for shell model states 9-11176  
 thermodynamical functions depend. of 1-part. spectrum discrete structure 9-11174  
 three-particle correl. effects, calc. 9-6768  
 wave functions for arbitrary numbers of nucleons, orthonormalization props. and matrix element calc. for one- and two-particle operators 9-15704  
 Wigner 9j symbols, relationships and identities 9-292  
 WKB modified approx. for bound-state problem 9-11171  
 Woods-Saxon potentials, analytical soln. for  $n$  bound s-states energy eqn. 9-8956  
 ZeZ' system, configurational interaction of terms 9-13179  
 $\alpha$  decay from even-even nuclei,  $\alpha$  surface distrib. determ. 9-19292  
 $\eta$  generation of 3-body forces 9-14545  
 $n$  and  $p$  distrib. in deformed nuclei 9-6776  
 $n$  closed shell, BCS theory applied to valence nucleons 9-483  
 $^{19}\text{O}$  s.m. moment 9-15702  
 $^{184}\text{W}$  e.m. moment calc. from pairing-plus-quadrupole model 9-15702  
 $^{196}\text{Pt}$  e.m. moment 9-15702  
 $^{208}\text{Pb}$  and neighbouring nuclei, single-particle core-excitation coupling calc. 9-16942  
 $^{208}\text{Pb}$  fast calc. using spherical Hartree-Fock technique 9-11230  
 $^{40}\text{Ca}$ ,  $r=0$ , 1  $1p^h$  monopole state calc. Migdal theory 9-20748  
 $^3\text{H}$  e.m. formfactor, wave functions determ. 9-18064  
 $^3\text{H}$  e.m. formfactor, wave functions determ. 9-18064  
 $^4\text{He}$  Hartree-Fock and limited Hartree-Fock calculators compared 9-508  
 $^6\text{Li}$  elastic charge form factor var. calc. 9-13192  
 $^6\text{Li}$  shell model wave function, residual N-N interaction 9-15714  
 $^{16}\text{O}$ , reaction matrix elements calc. method for  $^3\text{S}_1$ ,  $^3\text{S}_1$  states 9-8987  
 $^{16}\text{O}$   $0^+$  state position, incalculable by Hartree-Fock or related methods 9-20734  
 $^{16}\text{O}$  energetics calc. from Brueckner theory in oscillator basis 9-4716  
 $^{88}\text{Sr}$  and neighbouring nuclei, single-particle core-excitation coupling calc. 9-16942

**Oceanography**  
*See also Liquid waves; Seawater*  
 acoustic signals, optimum array detection tech. 9-8161  
 acoustic wave reflection at ocean bottom-sea water boundary 9-16731  
 acoustics, underwater, ray and modal interference theory, eff. of shear flow 9-16526  
 air temp. field adaptation to case of sea 9-6060  
 air-sea interaction 9-12578  
 ambient noise in shallow bay, particle vel. and press. meas. 9-12574  
 bioacoustic investig. from submersible, masking of biol. signals with vehicles self-noise 9-15239  
 bottom current measuring device employing thermistor 9-8164  
 cnoidal waves, mass transport 9-8163  
 coastal streams, sediment content due to erosion 9-21753  
 cold water upwelling and convergence at equator in eastern Pacific 9-14152  
 course for nonscience major 9-8158  
 earthquake, submarine, resulting bottom and surface waves 9-6059  
 electronics, limitations and amelioration 9-4041  
 explosion, underwater, near surface calc. of cavitation propag. 9-17178  
 forecasting for advective region, numerical modelling 9-6063  
 forecasting for advective region, numerical modelling 9-8162  
 global scale parameters, synoptic analysis 9-4033  
 hydroscience advances, book 9-15241  
 IEEE region six conf. Portland (1968) 9-6247  
 IEEE region six conf. Portland (1968) 9-2106  
 long waves on oceanic ridges 9-6068  
 magnetic field, anomalous 9-21830  
 microscale phenomena in ocean and atmospheric boundary layer 9-4042  
 models and deterministic operators, seismic marine reverberations 9-6043  
 noise, under ice, a review 9-6390  
 ocean bottom microseisms, rel. waves and weather 9-10383  
 ocean motions, mesoscale, meas. for numerical simulation 9-4043  
 optics of the sea, underwater radiant energy, meas., techniques, book 9-15240  
 resistance thermometer, in stagnation region following ship 9-6062  
 review 9-4032  
 role of electronics 9-8165  
 sea floor spreading and continental drift 9-12565  
 sea-floor mineral deposits, location and exam., phys. techs. involved 9-18788  
 sediment cores, mag. susceptibility stratigraphy 9-12648  
 sedimentation velocity of abyssal plain of Western Mediterranean since end of Wurm period 9-14159  
 seismic energy prod. by non-explosive methods, advantages 9-6048  
 shallow water, bottom backscatt. near grazing incidence 9-15237  
 shallow-water, Wood's model, sound focusing and beaming in the interference field 9-15236  
 sound channel, with parabolic profile, range focusing 9-6061  
 sound scatt. layer due to Myctophid fish schools 9-4040  
 stratified fluid, wake collapse scaling characts. 9-4988  
 submarine topographic echoes from Chase V 9-12575  
 surface gravity waves, measurement of directional spectra and wave height 9-14157  
 temperature vars. resulting from hurricanes 9-6064  
 thermocline oscillations having inertia period at Laboratory-Bouy 9-4039  
 tidal waves, shallow, intensive harmonic analysis 9-20083  
 tidal waves near shore, asymptotic analysis 9-20082  
 turbid water, under water acoustic imaging 9-15238  
 two-dimensional flows, boundary layer eqn. 9-8159  
 underwater sound meas., international standardization 9-2227



**Oceanography** continued

- underwater sound propagation, effect of near source bottom conditions 9-12554
- wave refraction, grid and projection problems in numerical calc. 9-21754
- waves, breaker type classification on 3 lab. beaches 9-10382
- waves in shallow water, velocity pot. and surface elevation for arbitrary surface disturbances 9-11672
- <sup>7</sup>Be tracing of surface interac. and mixing processes 9-18789

**Octet theory** see *Elementary particles/symmetry; Field theory, quantum*

**Omegatrons** see *Leak detection; Mass spectrometers; Vacuum technique*

**Onsager relations** see *Statistical mechanics; Thermodynamics*

**Optical activity** see *Optical rotation*

**Optical communication** see *Laser beams/applications*

**Optical constants**

- See also *Absorption/light; Reflectivity*
- metals, theory including effects of surface layer struct. 9-21433
- electro-optical effects rel. to interband transitions at critical points 9-1741
- AlTe 9-7933
- fibrous thin-layer mats, total solar spectrum coeffs 9-1726
- liquid metals, apparatus for meas. 9-5168
- measuring accuracy determ. using special eqns. in metal optics 9-6546
- metal film in island form, effective 9-12327
- of metal films, ellipsometric determ. using transmitted light 9-3849
- phthalocyanines, opt. density of states 9-2914
- plasma, laser-produced, measurement 9-18294
- porphyrins, opt. density of states 9-2914
- Ag<sub>3</sub>AsS<sub>3</sub>, i.r. 9-1727
- Ag<sub>3</sub>SbS<sub>3</sub>, i.r. 9-1727
- Ba ferrite, hexagonal, and magneto-optical effects 9-12343
- CdO, freq. depend. rel. to band struct. 9-3886
- Eu chalcogenides, room temp. 9-12328
- Eu chalcogenides, room temp. 9-16391
- EuSe 9-7933
- Ga films, solid and liquid 9-3192
- Gd, ferromagnetic and paramagnetic states, internal reflection meas. 9-16412
- of Ge, polarized light meas., 310 and 550 Å 9-12334
- Hg-In amalgam, optical constants obs. 9-16392
- KBr, plasmon struct., from energy loss spectrum of electrons 9-5591
- Ni-Fe, and Kerr magneto-optic effect 9-10175
- PbCrO<sub>4</sub>, natural and artificial single crystals. 9-17473
- Se, amorphous, reflectance, refractive index and absorption in vacuum u.v. 9-12335
- Te, calc. from reflectivity spectrum in fundamental absorpt. region 9-21630
- VO<sub>2</sub>, mea. above and below semicond.-metal transition temp. 9-12329
- Xe, solid, from energy loss meas. of 51 keV electrons 9-7694
- ZnSnP<sub>2</sub>, calc. from i.r. reflection spectra of chalcopyrite and sphalerite structures 9-5904

**Optical dispersion** see *Dispersion, optical*

**Optical fibres** see *Fibres/optical*

**Optical films** see *Films/liquid; Films, solid/optical properties*

**Optical filters** see *Filters, optical*

**Optical images**

- See also *Aberrations, optical; Holography; Resolving power, optics*
- coherent light images improvement using pseudo-random coded diffuser 9-8652
- enhancement by prolate spheroidal functions, truncation effect 9-20543
- formation and evaluation 9-6544
- Fresnel, optical correl. by collinear heterodyning 9-10887
- hologram microscopy, carrier suppression and restoration 9-20537
- holographic, brightness increase by using density relief of photographic emulsion 9-10877
- holographic deconvolution 9-8632
- laser-produced, quality improvement 9-10890
- mirage, induced, the self-isolation of the surface of a body in a medium against intense light flux 9-4509
- noisy, optimum nonlinear processing 9-14450
- photographic, optical integration 9-287
- photographic, quality rel. to aberration state 9-6543
- quality in terms of optical transfer functions, significance of phase 9-10892
- radioisotope imaging systems, image restoration 9-14535
- scanning trajectories, classification of scan patterns 9-13046
- star, visual and photographic, radial lines due to diffraction 9-8653
- virtual, orthoscopic, reconstruction by integral photography, single step process 9-10945

**Optical instrument testing**

- autocollimator errors, interferometry 9-2401

**Optical instruments**

- Some instruments are listed separately, e.g. *Refractometers*
- analyzer, description and components, patent 9-17892
- autocollimating technique, increased angular range, measurement of large rotations of a body 9-12847
- beam splitters, optomechanical considerations, in operational environment problems 9-4523
- cell, low temp., for u.v. and visible region absorpt. spectroscopy 9-15558
- cell for temp. depend. of refr. index of fluids 9-13060
- Dewar for two-beam expts. 9-2411
- digital reader of oscilloscope trace photographs 9-286
- electroscopie type dosimeter, patent 9-10583
- ellipsometer, photoelec., for visible and u.v. 9-10919
- field-widened long retardation plates, design 9-10920
- goniometer to aid have X-ray orientation of single crystals 9-3261
- goniophotometer, measurement of scattering characteristics of various objects 9-13054
- image storage, tube, for optoelectronic computing 9-14287
- interferometer, confocal for pointing at coherent source, alternative to tele-dolite 9-4518
- for laser incoherent wide-angle beam prod., 10.6  $\mu$  9-10917
- laser wavelength selection device 9-10857
- light modulator, using multi-beam interferometer 9-2395
- optico-acoustic radiation detectors, desiems 9-6555
- pattern recognizer 9-2409
- photoelectric autocollimators with half-disk modulators, sensitivity 9-13062
- Physics Exhibition, London, 1968 review 9-273

**Optical instruments continued**

- range-finder, stadimetric, sighting errors reduction for moving targets 9-10918
- reflectance, diffuse, simple apparatus for meas. at low temps. 9-4525
- shutter, fast using Kerr effect 9-8672
- Sofica and Brice-Phoenix light scatt. photometers, comparison of reflection effects 9-14832
- timing mark counter for film record scanning 9-275
- vertex power meas. of nonastigmatic spectacle lenses 9-4526
- Wadsworth mounting inversion 9-16796
- SiO<sub>2</sub> optical waveguide, formed by proton channeling changing refractive index 9-20556

**Optical materials**

- See also *Filters, optical*
- carbon blacks, book 9-12324
- chalcogenide i.r. optical mats., elastic constants 9-14962
- crown glass, high relative dispersion in blue spectrum 9-4527
- glass, reduced dispersion with unaltered refractive index, patent 9-8663
- glass, spectrophotometer for meas. of attenuation coeffs. 9-2422
- glass, TeO<sub>2</sub>-MgO mixture with low i.r. absorpt., patent 9-8662
- glass in the softening and annealing range, viscosity 9-5147
- glass surface damage by laser radiation rel. to optical quality and adsorption props. 9-3176
- i.r., refl. and transmission spectra, 2-50  $\mu$  9-12366
- for i.r. interference filters 9-4532
- i.r. transmission, image-spoiling props. 9-4510
- Irtran 1, i.r. scatt. angular distrib., obs. 9-12325
- metal blacks, book 9-12324
- refractive index, gradual variation using multilayer anti-reflection coatings 9-5874
- BaF<sub>2</sub>, spectrochem. meas. of metal impurities 9-16513
- SrF<sub>2</sub>, spectrochem. meas. of metal impurities 9-16513

**Optical mode, crystals** see *Crystals/lattice mechanics*

**Optical model** see *Nucleus/models*

**Optical properties of substances**

- See also *Optical constants; Optical materials*
- alkali halide crystals, optical strength and laser-induced damage 9-16390
- n-alkane molcs., calc. of mean optical anisotropy 9-21208
- n-alkanes, molecular anisotropy, from depolarized light scatt. 9-14830
- BaTiO<sub>3</sub> thin film, vacuum deposited, presentation of properties and formulations of thermodynamic model 9-12197
- carbon blacks, book 9-12324
- $\alpha$ -chloronaphthalene, mode locking and ultrashort pulse induction in ruby laser 9-6523
- cholesteric liquid crystals, reflective optical storage, electric field control 9-3099
- crystalline solids exhibiting nonlinear optical effects, systematic approach for finding new materials 9-18690
- crystals, uniaxial, with electron plasma 9-21602
- dielectrics, condensed, shock-compressed, review 9-16285
- dyes, organic liquid solns., light generation mechanisms 9-5169
- electrolyte-conductor interface, eff. of elec. double layer on reflectance and ellipsometry 9-14136
- exciton-phonon bound state, new quasiparticle 9-12319
- films, granular metallic, parameters  $\nu$ ,  $\chi$  and  $d$  9-16398
- fluids, optical cell for temp. depend. of refr. index 9-13060
- free-electron-like foils 9-14022
- gas, non-equilibrium plane-parallel layers, finite continuous opacity 9-19586
- gases fully ionized radiation spectrum from Planck's law 9-13459
- gelatin, dichromated, phase hologram recording appls. 9-10873
- graphite, book 9-13566
- igneous rocks, light scatt., spectral obs., Stokes parameters 9-17476
- insulations, ferromagnetic, phonon wavelength shift, temp. depend. 9-7946
- iodates, noncentric (MIO<sub>3</sub> where M=H<sup>+</sup>, Li, Ti<sup>4+</sup>, K<sup>+</sup> and NH<sub>4</sub><sup>+</sup>), nonlinear and electro-opt. props. 9-3867
- i.r. materials, refl., transmission, and refr. index, bibliography 9-12332
- liquid, Kramers-Kronig dispersion eqns., validity test 9-3104
- liquid, self-focusing and nonlinear scatt., mol. interac. contrib. 9-13524
- liquid cry., second harmonic generation, origin, applic. to struct. study 9-21207
- liquid crystals, cholesteric phase, relevance to thermal mapping 9-3098
- liquid metals, apparatus for meas. 9-5168
- liquids, opt. permittivity, molecular angular correlations 9-11695
- liquids, stimulated thermal Rayleigh scatt., critical abs. coeff., nonlinear attenuation meas. 9-9512
- metal blacks, book 9-12324
- nematic liquid crystals, reflective optical storage, electric field control 9-3099
- nitrobenzene, mode locking and ultrashort pulse induction in ruby laser 9-6523
- photochromic materials, idealized, characts. defined 9-19978
- pigment organic pigment solns. generation intensity, calc., monochromatic excitation, calc. 9-18366
- poly(vinyl chloride) solns., anisotropy determ. by streaming birefringence evaluation 9-14837
- polymethine dye soln., generation, excited by Nd-glass laser emission ( $\lambda=1.06\mu$ ) 9-1014
- quartz, critical, opalescence, obs. and interpretation 9-10181
- quartz, i.r. generation on stimulated Raman scatt. at 10°K 9-7983
- quartz, optical perfection in crystals grown hydrothermally in Fe-lined vessel 9-13605
- Rayleigh scattering in liquids, stimulated thermal, critical abs. coeff. and nonlinear attenuation meas. 9-9512
- rocks and minerals, measurement at high static pressure 9-12572
- ruby, optical homogeneity rel. to laser radiation divergence 9-5885
- solids, theory, book 9-14023
- solids and liquids, interference due to low-power heating 9-12323
- thermopaper, temp. dependence, 50-150°C 9-21607
- triglycine sulphate type, indicatrix tensor orientation, high temp. 9-21540
- twisted C-C double bond, optical activity meas., electronic structure proposal 9-9274
- Ag granular film, parameters  $\nu$ ,  $\chi$  and  $d$  9-16398
- Al, e energy losses and optical data 9-16191
- Al, layers, influence of dielectric films 9-5886
- Al<sub>2</sub>O<sub>3</sub>, AlO<sub>3</sub><sup>2+</sup>, radiation-induced, rel. to electronic and crystal field interactions 9-12322
- As<sub>2</sub>S<sub>3</sub> glasses, development since 1950, review 9-3175

**Optical properties of substances continued**

- Au, films, grown on rough surfaces, meas. technique 9-5236  
 BaTiO<sub>3</sub>, melt-grown, dielectric props. 9-5745  
 BaWO<sub>4</sub>, phototropy, pink after irradi., by u.v. light 9-3866  
 Bi<sub>2</sub>TiO<sub>5</sub> crystals, optically induced refractive index changes, obs. with internally formed holograms 9-19976  
 CaF<sub>2</sub>, rare-earth doped, photochromic parameters for electro-optic applications 9-19978  
 CaWO<sub>4</sub>, phototropy, reddish-green after irradi. by u.v. light 9-3866  
 CdGe(As<sub>2</sub>P<sub>1-x</sub>)<sub>2</sub> glasses, activation energies 9-17394  
 Cu, consistency with direct wave vector conserving transitions between one-electron states 9-18585  
 CuSO<sub>4</sub> cry. as, u.v. transmitting filters 9-20558  
 Eu-chalcogenide alloys, anomalous, explanation by mag. exciton 9-9878  
 EuO phonon wavelength shift, temp. depend. 9-7946  
 Fe<sub>2</sub>O<sub>4</sub>, explanation of results in framework of small radius polaron theory 9-10171  
 Ga-Al-As system, treatment of phase diagram 9-17346  
 GaP, e energy losses and optical data 9-16191  
 Ge, e energy losses and optical data 9-16191  
 Ge cleaved (111) surface, surface states, abs., excitation, conduction and valence band 9-1544  
 H atom, polarisability, magnitude 9-2825  
 In, layers, influence of dielectric films 9-5886  
 KBr, e energy losses and optical data 9-16191  
 KBr cry. with H<sup>+</sup> ions, far-infrared abs. 9-10184  
 KI cry. with H<sup>+</sup> ions, far-infrared abs. 9-10184  
 LiNbO<sub>3</sub> holographic storage 9-15536  
 LiF thin cry, i.r. reflect. characts., nonuniform e.m. field treatment 9-17352  
 LiTaO<sub>3</sub>, light modulation rel. to light extinction ratios 9-10178  
 Mg Mn ferrite, explanation of results in framework of small radius polaron theory 9-10171  
 N<sub>2</sub>-Ne mixture, shock front u.v. radiometry 9-21142  
 Na<sub>2</sub>ZrO<sub>3</sub>, crystallographic data 9-19721  
 NaCl:Pb, luminous flux scattered at ambient temp. after thermal annealing 9-19979  
 NaD<sub>2</sub>(SeO<sub>3</sub>), for low temp. ferroelec. phase transition study 9-17434  
 Nb<sub>2</sub>O<sub>5</sub>Cl, band gap, meas. and dielec. constants for principal crystal axes 9-10030  
 Ni Fe ferrite, explanation of results in framework of small radius polaron theory 9-10171  
 Ni Zn Fe ferrite, explanation of results in framework of small radius polaron theory 9-10171  
 PbCrO<sub>4</sub>, natural and artificial single crystals. 9-17473  
 PbS and PbSe, thin films, spectral absorption, structure and phase composition 9-14021  
 SrTiO<sub>3</sub>:Mo(Fe or Ni), reversible photochromic changes, observations and model 9-19980  
 SrTiO<sub>3</sub>, transition-metal doped, photochromic parameters for electro-optic applications 9-19978  
 SrWO<sub>4</sub>, phototropy, green after irradi. by u.v. light 9-3866  
 TiO<sub>2</sub>, opacified porcelain enamels, role of P<sub>2</sub>O<sub>5</sub> on colour and reflectance 9-3854  
 VO<sub>2</sub>, reflectivity and transmission spectra, for both sides of semicond. metal transition 9-12329  
 Y<sub>3</sub>Al<sub>5</sub>O<sub>12</sub>:Nd<sup>3+</sup>, laser emission threshold, temp. depend. 9-5955

**Optical pumping**

- alkali metal vapour, molecule formation 9-15818  
 chambers for solid-state lasers, spherical 9-10865  
 laser threshold, inhomogeneously widened at lines 9-13295  
 magneto-optical props. of pumped medium with near-reson. r.f. irradi. 9-2407  
 modulation excitation of vibronic states, relax. theory 9-20910  
 organic dye lasers, flashlamp pumped, theoretical and experimental studies 9-13021  
 polarization filter, for alkali metals, Zeeman sublevels population obs. 9-4830  
 quinoxaline in durene cryst. 9-5968  
 ruby maser, generated power rel. to pumping intensity 9-4451  
 superposition of states, technique and Raman echo theory 9-12990  
 and temperature definition 9-168  
 vapour, very high optical density, and mag. resonance obs. 9-9452  
<sup>201</sup>Hg, transients of mag. and subharmonic resons. 9-9145  
<sup>111</sup>Cd, resonance line 5'S<sub>1/2</sub> 5'P<sub>1/2</sub>, nuclear orientation depend. on mag. field 9-20884  
 Al<sub>2</sub>O<sub>3</sub>:Cr<sup>3+</sup>, absorption spectrum 9-7967  
 CO<sub>2</sub> laser, effect on generation intensity along rot. lines 9-8610  
 Cd, nuclear orientation of stable odd isotopes 9-4447  
 Cs, population inversion of 7<sup>2</sup>P<sub>1/2</sub> level 9-686  
 Cs vapour cells as hyperfine filters 9-19406  
 He atoms, excitation of n<sup>2</sup>P states, transfer mechanism 9-4880  
 LiNbO<sub>3</sub>, by c.w. Ar laser, as tunable optical parametric oscillator 9-10161  
 Nd:glass laser giant pulse production using harmonic pumping 9-19149  
 Nd<sub>2</sub>O<sub>3</sub> concentration, effect, suppression of parasitic oscillations, inversion population 9-4448  
 Ne atoms, metastable (<sup>3</sup>P) in He-Ne discharge, g-factor 9-688  
 Pb atom, nuclear orientation attempt 9-9139  
 Rb, spin exchange signals with Ag, Li, H, N and electrons 9-14422  
<sup>85</sup>Rb maser, 0-0 transition theory and expt. arrangement 9-4449  
<sup>87</sup>Rb vapour, microwave light modulation 9-679  
 SrCl<sub>2</sub>:Sm<sup>2+</sup>, absorpt. spectra 9-10210  
 SrF<sub>2</sub>:Sm<sup>2+</sup>, absorpt. spectra 9-10210  
 YAl garnet:Nd<sup>3+</sup>, efficiency, influence of pump-power level and pump light spectral filtering 9-20526  
<sup>67</sup>Zn nuclear orientation unobtainable in diamagnetic g.s. 9-4447

**Optical quantum generators see Lasers****Optical rotation**

- See also *Magneto-optical effects; Optical constants; Polarimeters; Polarized light*  
 activity meas. spectropolarimeter for 8-0.23μ 9-269  
 birefringence, quantum field theory 9-268  
 trans-cyclo-octene, optical activity of twisted C-C double bond 9-9274  
 1,8-dimethyl-5,12-dimethylene-biphenyl, optical activity of twisted C-C double bond 9-9274  
 ellipsometric determ. of metal films using transmitted light 9-3849  
 n-GaSb:TI Faraday rot. of free carrier obs., GaSb cond. bands calc. 9-13889  
 molecules, circular dichroism rel. to dissymmetry 9-9167

**Optical rotation continued**

- molecules and symmetry 9-19418  
 photoelectric measurement, errors 9-13057  
 of polarisation plane, angle meas. by photoelec. method 9-8659  
 polymer, long helical, and Umklapp process effects, microscopic theory 9-5879  
 quarter wave, visible achromatic comprising 6 sapphire plates 9-10925  
 α-quartz, variation of rotary power due to press. and temp. 9-12341  
 rotatory dispersion in transparent media demonstration expt. 9-20287  
 wave of crystalization, in vibration transition region 9-7941  
 AgGaS<sub>2</sub>, non-enantiomorphic, optical activity obs. 9-12339  
 CaS<sub>2</sub>O<sub>4</sub>.4H<sub>2</sub>O, in vibration transition region 9-7941  
 Eu chalcogenides, Faraday effect 9-5878  
 K<sub>2</sub>S<sub>2</sub>O<sub>8</sub>, in vibration transition region 9-7941  
 NO, mag.-rot. spectra of 1-0 vibr.-rot. band 9-9221  
 SiBi<sub>2</sub>O<sub>6</sub>, of plane of polarized light 9-18648  
 SrS<sub>2</sub>O<sub>4</sub>.4H<sub>2</sub>O, in vibration transition region 9-7941

**Optical systems**

- See also *Aberrations, optical; Lenses; Optical images; Optical instruments; Optical materials; Resolving power, optics*  
 aberration dependent coeffs. of optical transfer func. calc. 9-4531  
 basic parameters, relationship with component parameters 9-4507  
 Cassegrain telescope correction 9-6199  
 caustics, random, and fluctuations of light wave amplitude 9-13040  
 caustics, random, and fluctuations of light wave amplitude 9-2396  
 chromatic aberration correction with single element lenses 9-2397  
 collecting, estimation of quality using circular parabolic reflectors 9-4529  
 communication, coherent and noncoherent detect., 0.6328 μ and 10.6 μ 9-10882  
 correction for higher orders of spherical and spherochromatic aberrations 9-6542  
 correlator, real time, collinear heterodyning of Fresnel images 9-10887  
 damping factor for the least squares method of optical design 9-19161  
 data processors, design and specification criteria 9-12803  
 electric signal traces formation/analogy 9-258  
 electrooptic sensing methods for agricultural application 9-4524  
 fibre assembly, frequency contrast characteristic, energy distribution function 9-15548  
 fixed store, random access 9-2408  
 focussing error detection in optical paths 9-8645  
 fundamental, optical random process, math. description 9-14444  
 heterodyne, with pyroelectric detectors 9-14443  
 hologram chromatism corrector, two-lens 9-17884  
 imaging, achieving aperture synthesis from non-conventional optics by a posteriori lensless Fourier-transform holography 9-15539  
 imaging, resolution, optical-channel capacity and information theory 9-20541  
 incoherent objects detection and resolution 9-20542  
 infinitesimally thin lenses, spherical aberration, analysis 9-4506  
 information storage, Lippman emulsion three-dims. memory 9-10916  
 infrared imaging, design and theory 9-13059  
 kaleidoscope for point group symmetry demonstration 9-13048  
 modulation transfer function, transverse geometrical aberrations, evaluation 9-10885  
 phase difference measurement using Babinet compensator, effect of reorientation of components 9-13061  
 with photodetector, response using optical reciprocity 9-4508  
 Physics Exhibition, London, 1968 review 9-273  
 polarized light, Mueller matrices, Operational notation 9-20551  
 ray tracing, transition formulae 9-13045  
 ray-tracing equations, differentiation w.r.t. optical system construction parameters 9-10891  
 reciprocal, for meas. reflected image state of focus 9-10894  
 rectangular prism, total reflection, for smoothly rotating light source image 9-16793  
 reflectors, interference, with indep. variable wavelength and reflectance 9-8650  
 shadowless beams for operating table patent 9-10567  
 Soller, use as collimators and diffraction filters 9-6545  
 for still stroboscopic viewing of cine films 9-2431  
 variable magnification systems, linear relationships between components 9-13047  
 e microscope-Quantimet combination for direct image anal. 9-12982  
 CaF<sub>2</sub>:Tm<sup>3+</sup> acoustical phonon detector, tunable, sensitivity and versatility 9-5524  
 SiO<sub>2</sub>, waveguide, formed by proton channeling changing refractive index 9-20556

**Optical waveguides see Electromagnetic wave propagation/guided waves****Optics**

- See also *Aberrations, optical; Atmospheric optics; Lenses; Mirrors, etc.; Optical images; Quantum optics*  
 in Czechoslovakia, review 9-10883  
 difference frequency in far i.r., prod. by solid lasers and external photoeffect 9-6532  
 fibre, faceplates for c.r.t., extended m.v. transmission 9-20557  
 fundamental systems, optical random process, math. description 9-14444  
 harmonic generation, second, by multipolar mol., d.c. elec. field induced 9-13038  
 Hertzian resonance obs., optical methods 9-9144  
 metal, special eqns to determine measuring accuracy of optical constants 9-6546  
 noisy images, optimum nonlinear processing 9-14450  
 quasi optical lines with finite nonequidistant correctors 9-17885  
 U.S. waves, interaction with rel. to use as optical signal processor. 9-6389  
 Ag<sub>3</sub>As<sub>2</sub> (proustite), second harmonic generation 9-6540

**geometrical**

- approximation in general case of inhomogeneous and nonstationary media with freq. and space dispersion 9-8543  
 glare impression, influence of geometry and high luminance light 9-12798  
 glass prism, linear heterogeneity, effect on ray path 9-10889  
 limit, inverse scattering 9-10893  
 modulation transfer function, transverse geometrical aberrations, evaluation 9-10885  
 ray tracing in arbitrary system 9-13045  
 ray tracing in inhomogeneous media 9-10886  
 ray tracing equations differentiation w.r.t. construction parameters of optical system 9-10891

**nonlinear see Nonlinear optics**



**Orbital calculation methods**

- AB<sub>2</sub>-type molecules rel. to double minima in potential energy surfaces 9-19423
- alkyl acetates, scission probabilities of skeletal bonds in mass spectra, applic. of MO theory 9-14698
- allyl radical and ions, e wave function construction, method 9-9267
- alternant, formalism of separated pair theory 9-11445
- arsenomethane, pseudo-rotation, from n.m.r. data 9-20949
- atomic orbitals, computer method 9-9131
- atomic SCF functions with minimal basis sets 9-2802
- atoms field calc. on 3rd row periodic syst., Hartree-Fock pot. comparison 9-4826
- benzene, e wave function construction method 9-9267
- butadiene, e wave function construction method 9-9267
- CNDO charges correl. with N1.s electron binding energies 9-11451
- complex wavefunctions and conservation of total momentum in Hartree-Fock theory 9-13275
- conjugated systems, molecular orbital theory, book 9-13370
- correlated pair functions, pseudopotential transform. of orthogonality projection operator 9-663
- Coulomb and hybrid integrals expressed by overlap integrals 9-6276
- Coulomb integrals over Slater-type AO's 9-15802
- Coulomb-Born approx. for s-s transitions 9-700
- discrete and continuum orbitals of model eigenvalues, for calc. of photoioniz. cross-sections of He to Xe 9-9124
- doubly occupied MO's atomic orbital energy matching 9-9180
- electron correlation calcs. 9-4819
- ethylene, e wave function construction method 9-9267
- formulas for molec. integrals over Hermite-Gaussian functions 9-17018
- Hartree-Fock applied to calc. spin-orbit coupling constants of diatomic mols. 9-13328
- Hartree-Fock approx. for 2p<sup>2</sup>3p atomic configurations, orthogonality assumption 9-4824
- Huckel method, general perturbation theory 9-9182
- hybrid integrals over Slater-type AO's 9-15800
- INDO calc. of molec. equilib. geometries 9-15843
- INDO-MO, for ioniz. pot. of CF<sub>4</sub>, comp. with photoelectron spectroscopy calc. 9-13457
- INDO MS vs. SCF calc. of atomic electron populations in mols. 9-17020
- inorganic mols. semi-empirical model; energy levels, dipole moments and force consts. calc. 9-9193
- LCAO approx in theor. estimation of dipole moment of azobenzene-2-sulphenyl cyanide 9-14702
- LCAO-MO calc. of spin densities for radical ions of conjugated hydrocarbons 9-13396
- LCAO-MO treatment of conjugated polymers 9-832
- localized in mols., semiempirical method 9-741
- nitrobenzene derivs.,  $\sigma$ -complexes, LCAO MO calcs. 9-11482
- octahedral field theory, extension to general complexes 9-18167
- one electron, less than half electron pair 9-9110
- one-centre MO's with variable origin 9-13359
- organic epds., MOLKAO method applic. 9-20946
- overlap integrals, effect on diamag. calc. 9-17048
- overlap integrals over Slater-type AO's 9-15801
- Pariser-Parr-Pople model, derivation and anal. 9-743
- perturbation theory, finite methods 9-17016
- perturbation theory, self-consistent 9-11446
- perturbed Hartree-Fock calc. 9-2848
- perturbed Hartree-Fock calc. 9-2847
- pseudonatural orbitals as basis for superposition of configs. 9-768
- pseudopotentials in atomic struct. calc. 9-6958
- quadratically convergent iteration for self-consistent calcs. 9-9109
- SCF LCAO MO study of NH<sub>3</sub> electr. struct. 9-13364
- SCF MO calc. of electr. struct. of methyl fluoride, significance for adiabatic proc. with bond-breaking 9-17057
- segmental systems, electronic state calc. method 9-4973
- spin-coupled wave functions 9-6952
- spin-orbit interaction of <sup>1</sup>h-<sup>1</sup>l<sup>1</sup> configuration in L-S coupling 9-13274
- transition metal complexes, unrestricted Hartree-Fock molecular-orbital treatment 9-12232
- two-centre integrals,  $\alpha$ -function technique 9-2132
- valence electron approximation, theory 9-17035
- vinyl chloride, wavefunction calc., approx., by semiempirical *II*-electron methods 9-13393
- wave function for 2N<sup>-</sup> electron system, strongly orthogonal geminal product, refinement 9-11444
- X-ray K absorption spectral data, use of molecular orbital theory in interpretation 9-14065
- B<sub>2</sub>N<sub>2</sub>H<sub>4</sub>,  $\sigma$ - and  $\pi$ -electron system, CNDO/2 calc. 9-20922
- He ground state, Slater transform functions appl. 9-20900
- He multiplets with non-orthogonal orb., Hartree Fock eqn. 9-4875
- He SCF eigenvalue rel. to ionization pot. 9-4874
- KNiF<sub>3</sub>, unrestricted Hartree-Fock molecular-orbital treatment 9-12232
- Li ground state, Hartree-Fock eqn., Z<sup>-1/2</sup> expansion 9-4828
- Ni complexes with subst. phosphine ligands, SCCMO calc. 9-11470

**Orbitals** see *Molecules/electronic structure*

**Order-disorder transformations** see *Phase transformations/solid-state*

**Ordered structure** see *Crystal/structure; Solids/structure*

**Organic compounds**

- See also *Free radicals; Macromolecules; Plastics; Polymers; Waxes*
- arsenoperfluoromethane, pseudo-rotation, from n.m.r. data 9-20949
- 4-4'-nitrodiphenyl + propyl alcohol in frozen decaline soln., fluorescence obs. 9-7071
- ,dimethyl-1,4-phenyl pyridine, absorpt. spectra rel. to rotation and bonding 9-9273
- 2,6-dichlorotoluene, infrared spectrum 9-17049
- N,N'-dimethylaniline, irradi., +benzene halogen derivs., electron affinity of acceptor 9-4010
- di-(2-ethylhexyl) Na sulfosuccinate- n-octane solns, p.m.r. study of phases formed on H<sub>2</sub>O addition 9-9559
- acenaphthene triplet state e.p.r. obs. 9-19458
- acenaphthylene, pyrolysis, chem. mechanism and residues 9-10330
- acepleadiene, electronic struct. 9-800
- acetaldehyde, entropy and enthalpy 9-18325
- acetaldehyde-2,2,2-d<sub>3</sub>, i.r. and Raman spectra 9-2889
- acetanilide and deuterio derivatives, absorpt. spectra, 50-300 cm<sup>-1</sup> 9-18195
- acetanilides, ortho-substituted, selective deshielding of aromatic protons 9-19454
- acetone, monomer and excimer emission 9-16011

**Organic compounds continued**

- acetone, photolysis at 185nm, quantum yields 9-16494
- acetone-carbon tetrachloride binary system, superheat temp. 9-18388
- acetone-chloroform mixtures, dielec. props., x-band microwave obs. 9-3116
- acetonitrile, ion-mol. reactions, ion cyclotron reson. 9-20034
- acetyl chloride, Raman spectra, absolute intensities and depolarizations 9-2890
- 4-acetyl-2'-chlorobiphenyl, crystal structure 9-3313
- acetylene, burning in O<sub>2</sub> and N<sub>2</sub>O, comparative soot yields 9-12535
- acetylene, fine struct. in ioniz.-efficiency curves 9-9395
- acetylene, gas, electron drift velocities 9-17166
- acetylene, ion formation energy for  $\gamma$  radiation of Cs<sup>137</sup> 9-9409
- acetylene, ioniz. by electron impact, Franck-Condon principle validity 9-19453
- acetylene, mol., emission spectra, two new band systems of CH<sup>+</sup> 9-18208
- Acetylene in NO<sub>2</sub>-Acetylene, flame for atomic absorption spectroscopy ~ interference 9-6030
- acetylene prod. in flame reaction, patent 9-12533
- acetylene-N<sub>2</sub>O+air flame for atomic absorpt. spectroscopy 9-10944
- acetylenes, 584A photoelectron spectra, obs. 9-4945
- acetylenes, substituted, molec. motion in liq. 9-9557
- acids, corrosion of steel 9-20056
- acrolein and deuterio-derivs., vibratory spectra 9-11491
- afatoxins B<sub>1</sub> and G<sub>1</sub>, fluorescence and phosphorescence for presence determ. 9-6201
- agarose as constituent of electrophoretic medium 9-10566
- alcohol, chlorosubstituted; monomeric mols. in CCl<sub>4</sub>, i.r. absorption spectra fine structure obs. 9-9242
- alcohols, 1- and 2-, films dissolution rate on water surface 9-5144
- alcohols, eff. on  $\gamma$ -ray induced polymerization, of ethylene 9-20039
- alcohols, gas diffusion at low temps. 9-21194
- alcohols, primary aliphatic, velocity of sound, along saturation line 9-16001
- alcohols, quenching props. in toluene and dioxane base scintillation solns., rel. to molec. weight 9-9528
- alcohols, rotation and magnetic rotary dispersion 9-15878
- alcohols, semicond., cond., 20°C 9-13538
- alcohols, spreading press. on water, rel. to interfacial tension, work of adhesion and solubility 9-9494
- alcohols, thermal conductivity data considerations for standard reference materials 9-14847
- alcohols of common purity, characteristics of ions 9-19642
- aliphatic secondary amines, H-bonding from p.m.r. obs. 9-19455
- n-alkane mols., calc. of mean optical anisotropy, in liquid state 9-21208
- alkanes, critical pressures and temps. correl with molec. struct. 9-18381
- n-alkanes, liq. flow birefringence, var. with temp. 9-17207
- n-alkanes, molecular optical anisotropies, from depolarized light scatt. 9-14830
- alkanes, n-butane to n-nonane, ads. on  $\gamma$ -Al<sub>2</sub>O<sub>3</sub>, ads. energy 9-7344
- alkanethiols, torsional bands in far i.r. spectra 9-11488
- alkoxybenzoic acids, liq. crystals, H-D isotope effect 9-3982
- alkyl acetates, mass spectra, skeletal bonds, scission probabilities 9-14698
- alkyl chloride syst. bombarded by Cl atoms 9-10362
- alkyl fluorides, activated, decomposition obs. 9-10331
- alkyl radical reactions, chem. induced dyn. nucl. polarization 9-17222
- alkylanines, torsional bands in far i.r. spectra 9-11488
- alkylbenzenes, proton affinity and basicity 9-8071
- allene, photoionization 9-9403
- allenic geminal coupling const., sign determ. 9-2891
- allyl radical and ions, e wave function construction method 9-9267
- amide ions in K halides, paraelec. and paraelastic orientation 9-5747
- amide-halogen charge-transfer complexes, vibr. spectra and intramolec. potentials 9-2892
- 4 amine-p-terphenyl, monolayer, intermediate state 9-3208
- amines, aromatic, and derived amides, p.m.r. spectra 9-19456
- amines of common purity, characteristics of ions 9-19642
- DL- $\alpha$ -amino-n-butiric acid, A and B modifications, crystal structures 9-19728
- 1-amino cyclopentane carboxylic acid hydrobromide, X-ray diff. obs. of crystal structure 9-18454
- amino-pyridines, vapour-phase u.v. absorpt. 9-14699
- amino-pyrimidines, vapour-phase u.v. absorpt. 9-14699
- aminoacids, single cry. and polycrystalline, protein semicond. study 9-21510
- e*-aminocaproic acid soln. dielec. dispersion obs. 70-2000 MHz 9-19638
- aminonitroolefins, energy levels, Pople's method calc. 9-17047
- 2-aminopyridine, fluoresc. sensitization of biacetyl 9-1031
- ammonium uranyl sulphate, electronic and infrared absorpt. spectra 9-1790
- amyl phenyl acetate, dipole moment in benzene and CCl<sub>4</sub> solns., obs. 9-796
- aniline binary liquid mixtures, vel., absorption, compressibility meas. of u.s. waves 9-3097
- aniline-cyclohexane binary mixture, long range correlation effects 9-3105
- anilines, substituted, molar polarization and assoc. 9-934
- anils, photochromism and thermal reactions 9-10353
- p-anisaldehyde, liq. crystal transition, proton spin-lattice relaxation study 9-11723
- anisaldehyde azine, crystal structure 9-19729
- o-m-p-anisaldehyde mol. in liquid state, i.r. Spectrophotometer, spectra vib./study 9-7047
- anisol p-aminoazobenzene liq. cry. phase, static dielec. const., influence of mag. and elec. fields 9-11684
- anisole and monohalogen deriv., vibrational spectra, torsional barriers calc. 9-14700
- 18 annulene, electronic spectrum 9-19457
- anthracene, absorpt. spectra, in frozen soln. 9-2893
- anthracene, broad band existence, confirmation by photoemission of electrons from alkaline-earth contacts 9-5616
- anthracene,  $\gamma$ -irradiated, e.s.r. and optical spectra of paramag. centres 9-3963
- anthracene, carrier prod. and transport 9-17445
- anthracene, chem. effects of X-rays, compared with  $\gamma$ -rays 9-6020
- anthracene, dark conductivity electrode dependence 9-15094
- anthracene, dark injection of electrons from alkali metals, photoelectric effect 9-1618
- anthracene, eff. of surface purity on photo-generation of charge carriers 9-15049

**Organic compounds continued**

- anthracene, electrogenerated chemiluminesc. in soln. 9-21219  
 anthracene, electronically excited, charge transfer proc. 9-17076  
 anthracene, emission decay time and singlet exciton diffusion 9-1847  
 anthracene, hole and electron photogeneration mechanisms 9-1617  
 anthracene, lattice vibr. intensities, Raman obs. 9-18551  
 anthracene, oriented nucleation in elec. field 9-21299  
 anthracene, photocond., elec.-field and temp. depend. 9-3738  
 anthracene, polarized Raman spectra of single cryst. 9-15180  
 anthracene, singlet excited states polarizability obs. 9-15879  
 anthracene, singlet excitons, diffusion and surface reactions 9-13835  
 anthracene, surface states existence 9-1540  
 anthracene, thermal expansion tensor, 78-440°K 9-13805  
 anthracene, triplet exciton quenching by paramag. impurities, field depend. 9-1832  
 anthracene, triplet excitons review 9-5623  
 anthracene, triplet-triplet annihilation emission as indicator of low-level  $\gamma$ -dose 9-12472  
 anthracene, vibrational study by Raman spectra 9-18196  
 anthracene, X-ray induced photoconductivity 9-3739  
 anthracene, zone refining, use of triplet lifetime as monitor 9-5282  
 anthracene complexes with tetra halo p-benzoquinone, cryst., spectra 9-1799  
 anthracene crystal doped with tetracene as a hole trap 9-7376  
 anthracene crystals, hole injection from electronically excited iodine mols. 9-16313  
 anthracene crystals, optical activation of traps. 9-19934  
 anthracene crystals, spin-lattice relax. of protons 9-16470  
 anthracene in cyclohexane, radiation-induced fluorescence, elec. field effects 9-18765  
 anthracene in naphthalene, solid soln., fluorescence decay pattern 9-12471  
 anthracene and mesoderivs. in soln, fluoresc. quenching by 'heavy atom quenchers' 9-9529  
 anthracene mol. cry., electr. abs. spectra, exciton config. construct. from orbitals 9-21617  
 anthracene singlet-triplet interactions 9-1418  
 anthracene soln. in polyethylene matrices, luminesc. spectra for various concs. at 77°K 9-17211  
 9,10-anthraquinone, polarization of absorpt. and emission spectra 9-19991  
 aromatic, heteroaromatic mols., perturbations between electronic states 9-2894  
 aromatic, polarizability of excited mols. from solvent shift 9-14683  
 aromatic, triplet-singlet transitions 9-15871  
 aromatic anhydrides mixtures, graphitization by coprolysis with benzene precursors 9-8055  
 aromatic crystals, internal polarization as function of temp. and elec. field 9-17425  
 aromatic hydrocarbon bases, H-bonded complexes 9-4942  
 aromatic hydrocarbons, electrochemilum., cation-anion annihilation study 9-14701  
 aromatic hydrocarbons, extinction coeffs. of triplet-triplet transitions 9-1800  
 aromatic hydrocarbons, overlap integrals, mag. anisotropy and proton screening 9-17048  
 aromatic hydrocarbons, phosphoresc. growth and decay 9-10249  
 aromatic hydrocarbons, press. effect on fluoresc. lifetimes 9-14084  
 aromatic hydrocarbons, singlet→ground-state transitions 9-11480  
 aromatic hydrocarbons, thermoluminesc. in boric acid glass 9-17493  
 aromatic hydrocarbons in soln., bimolec. ionization of triplet state 9-3120  
 aromatic liqs., fluoresc. excitation spectra, yield rel. to wavelength, conc. and excimer states 9-5176  
 aromatic mol. in sol., electron exchange rate const., NMR meas. 9-20950  
 aromatic molecules, fluorescence lifetime short, relevant factors 9-9240  
 aromatic nitrogen heterocycles, triplet states, e.p.r. obs. 9-19458  
 aromatic semiconductors, electrode injection of charge carriers 9-21509  
 aromatic solvents with low solute concs. down to 0.005g/lg radiative transfer rel. to luminesc. yield 9-9525  
 aromatic structs. in coals and chars rel. to 1600 cm<sup>-1</sup> absorpt. band 9-7964  
 aromatics, in frozen solns., triplet-state energy transfer 9-17488  
 aryl fluorides, <sup>19</sup>F n.m.r. chem. shifts 9-802  
 arylethylenes, sterically hindered, fluorescence rel. to viscosity of soln. 9-20948  
 L-ascorbic acid, crystal structure from n. diff. analysis 9-19727  
 L-aspartic acid, crystal and mol. structure 9-7458  
 atrachene, delayed fluoresc., ionic energy levels and charge-transfer exciton state 9-16437  
 8,16-axido-cis-[2,2]metacyclophane, crystal structure 9-14931  
 aza-acetylenes, 584Å photoelectron spectra, obs. 9-4945  
 8-azaguanine monohydrate, crystal structure refinement 9-11860  
 1-azatriphenylene, electronic states and quasilinear electronic spectra 9-9243  
 azines, SCF calc. 9-7048  
 aziridine, 1-substituted, <sup>13</sup>C-H n.m.r. spectra, coupling parameters 9-13543  
 azobenzene -2- sulphenyl cyanide, crystal and mol. structure 9-11861  
 azobenzene-2-sulphenyl cyanide, dipole moment, theor. estimation 9-14702  
 p-oxoyanisole liq. crystals, e.p.r. study of radicals 9-7086  
 azulene, ground and doubly excited states, ab initio SCF calc. 9-20951  
 benzaldehyde, 3715 Å  $\pi^* \leftarrow n$  system, allowed and forbidden 9-9245  
 1,2-benzanthracene, excited singlet absorpt., laser photolysis and spectroscopy 9-20952  
 1,2-benzanthracene, triplet formation, quantum yield, fluoresc. and phosphoresc. 9-16438  
 benzen-d<sub>6</sub> in active solvent, C-D valence vib. integrated intensities 9-4949  
 benzene, ab initio SCF MO and CI calc. on electronic spectrum 9-9246  
 benzene, adsorption on carbon, rel. to Dubinin theory of pore filling 9-7346  
 benzene, CH stretching anharmonicities of triplet state 9-803  
 benzene, criticism of existing photochem. data 9-16496  
 benzene, cryst., vib. spectral transitions, splittings due to intermolec. forces 9-5932  
 benzene, doubled thermo-spectrum of 8050 Å stimulated Raman line 9-14703  
 benzene, e wave function construction method 9-9267  
 benzene, electron distrib. in ground state, calc. 9-4952  
 benzene, elementary excitations model 9-804

**Organic compounds continued**

- benzene, energy transfer in excited electronic states 9-15880  
 benzene, fluoresc., solvent and temp. effects 9-16012  
 benzene, fluoresc. in cyclohexane, aggregation effects 9-2556  
 benzene, fluoresc. in cyclohexane quenching by O<sub>2</sub> and CCl<sub>4</sub> 9-3112  
 benzene, gas, effect of quadrupole moment on dimerization 9-4908  
 benzene, gas, ion-mol. react. 9-17078  
 benzene, i.r. spectrum in Ar matrix, multiplet structure analysis 9-18199  
 benzene, laser-stimulated Raman scatt., instability growth rates 9-11699  
 benzene, lig. and cryst., combination light scatt., absolute cross-sections 9-1732  
 benzene, liq., course of electrostatic pot., meas. 9-7275  
 benzene, liq., radiolysis by low-energy <sup>4</sup>He ions 9-17542  
 benzene, liq., X-ray structural anal. 9-5142  
 benzene, liquid, injected charge-carrier drift mobility 9-11713  
 benzene, low-energy photoionization, theory 9-7190  
 benzene, luminescence quenching by carbon tetrachloride, solvent excimers 9-7267  
 benzene, neutron thermalization 9-20855  
 benzene, nonexponential phosphoresc. decay 9-1835  
 benzene, phosphoresc. lifetime, solvent and temp. effects 9-10250  
 benzene, phosphorescence polarization and triplet level energy transfer 9-1836  
 benzene, quadrupole moment calc. from intermolec. forces 9-4947  
 benzene, quenching of excited singlet state by olefins 9-2896  
 benzene, Raman scatt., stimulated by focused low power ruby laser beam 9-5171  
 benzene, Raman spectra cross sections, temp. depend. 9-12428  
 benzene, rot. const. from near i.r. vibr. band 9-7050  
 benzene, singlet, quenching by O 9-13368  
 benzene, sorption and dielec. behaviour on silica gel 9-21288  
 benzene, substituted; vib. freq. assignments from i.r. and Raman spectra obs. 9-7051  
 benzene, thermo-spectrum of stimulated Raman 8050 Å line, fine structure period 9-1022  
 benzene, triplet formation, quantum yields, fluoresc. and phosphoresc. 9-16438  
 benzene, ultrasonic absorption 9-153  
 benzene, ultrasonic relaxation in gas mixture with O<sub>2</sub> 9-2901  
 benzene, u.s. velocity along saturation line 9-9509  
 benzene, vibr. spectra, test of Kromers-Kronig eqns. 9-3104  
 benzene, molec. vibrs., self consistent calc. 9-7049  
 benzene and derivatives, luminesc. quenching mechanism 9-1030  
 benzene and derivatives, luminesc. quenching mechanism 9-1029  
 benzene and liq. derivatives, emission excited by electron-impact 9-9530  
 benzene anion, removal of orbital degeneracy at 4.2°K 9-14727  
 benzene derivatives, para-deuterated, DC<sub>6</sub>H<sub>4</sub>X, NMR 9-7279  
 benzene in dosimetry of high intensity electron pulses, possible space charge effects 9-1925  
 benzene in hexane and cyclohexane, fluoresc. quenching by biacetyl at 28° rel. to dilution 9-16014  
 benzene interact. with graphite, analysis w.r.t. virial treatment of physical ads., errors due to hindered rot. 9-17077  
 benzene luminescence in cyclohexane, mol. symmetry determ., 77°K 9-4948  
 benzene negative ion, e.s.r. 9-2895  
 benzene plus p-terphenyl solns., scintillation efficiency 9-16013  
 benzene precursors, effect on graphitization by coprolysis of org. cpd. mixtures 9-8055  
 benzene single cryst., temp. depend. of elec. current 9-16227  
 benzene single cryst., temp. depend. of elec. current 9-3575  
 benzene solns with trans-stilbene and diphenyloxazole, luminesc. and quenching 9-3113  
 benzene sulphonamide, n.q.r. of <sup>14</sup>N 9-14099  
 benzene sulphonylchloride, i.r. spectra, optical density of absorpt. bands, eff. of substitutions 9-7053  
 benzene synthesis for sensitivity enhancement in liq. scintillator for <sup>14</sup>C and tritium dating 9-11247  
 benzene vapour, <sup>13</sup>B<sub>2</sub>→<sup>1</sup>A<sub>1g</sub> transition, fluorescence obs. 9-19450  
 benzene vapour photolysis at 1849Å, cis-1, 3-hexadien-5-yne form 9-10354  
 benzen-d<sub>6</sub> cryst., ENDOR of photoexcited triplet-state benzene-h<sub>6</sub> 9-14118  
 benzenedinitrogen tetroxide equimolec. complex crystal structure 9-11862  
 benzene-polyisobutylene soln., thermodynamics 9-21201  
 benzene-rubber soln., thermodynamics 9-21200  
 benzenes, alkyl substituted, proton-donor effects 9-11698  
 benzenes, monosubstituted, CNDO calc. 9-7052  
 benzenes, ortho-disubstituted, dissolved in nematic phase, n.m.r. 9-7280  
 benzenes, substituted with electron-donating groups, triplet-triplet absorpt. 9-9248  
 benzenes containing OH and NH<sub>2</sub> groups, substituted, singlet-triplet transitions 9-9244  
 benzenesulphonamide and benzen-d<sub>6</sub> analogue, spectra, 4000-400 cm<sup>-1</sup> 9-14704  
 benzenesulphonanilide and benzen-d<sub>6</sub> analogue, spectra, 4000-400 cm<sup>-1</sup> 9-14704  
 benzenesulphonyl chloride and benzen-d<sub>6</sub> analogue, spectra, 4000-400 cm<sup>-1</sup> 9-14704  
 benzil crystal, Raman spectrum 9-5939  
 benzo-2,1,2-oxadiazole and derivatives, p mag. reson. rel. to bond order, obs. 9-15882  
 benzo-2,1,3-selenodiazole and derivatives, p mag. reson. rel. to bond order, obs. 9-15882  
 benzo-2,1,3-thiadiazole and derivatives, p mag. reson. rel. to bond order, obs. 9-15882  
 benzoic acid, absorption spectra in polarized light 9-10214  
 benzophenone, absorpt. spectrum, second triplet state obs. 9-15881  
 benzophenone, collision breeding from melt 9-18421  
 benzophenone, fluorinated, anion radicals, e.s.r. 9-4970  
 benzophenone, phosphoresc. and triplet-singlet absorpt. at 4.2°K 9-10251  
 benzophenone, phosphoresc. in mixed crystals 9-10248  
 benzophenone, phosphoresc. rel. to phenanthrene and phenazine additive concs. 9-3931  
 benzophenone crystals, pure and impure, phosphorescence, temp. depend 9-16441  
 benzophenone ion, radical high resolution transient e.s.r. spectra 9-20954



## Organic compounds continued

- benzophenone-naphthalene solid soln., phosphorescence decay at 7  
9-12476  
benzophenones, protonated, NMR spectra, isomer obs. and config.  
9-20953  
benzophenonimines, methyl substituted, proton NMR 9-14705  
3,4-benzopyrene, i.r. spectrum, anthracene vibr. rel. to mol. struct., obs.  
9-15883  
5,6-benzoquinoline, phosphoresc. rel. to  $\pi$  transitions and N effects on mol.  
levels, 77°K 9-15899  
5,6-benzoquinoline boronic acid phosphor, luminesc. props. 9-1827  
p-benzoquinone,  $^{13}\text{C}$ -H satellite NMR Patterns, rel. to couplings  
9-13373  
p-benzoquinone, Fermi reson. params., obs. 9-14681  
p-benzoquinone chemisorption on NaF and BaF<sub>2</sub> films, i.r. spectra  
9-8084  
p-benzoquinone-p-benzoquinone radical anion in sol., electron exchange  
rate const., NMR meas. 9-20950  
p-benzosemiquinone-potassium, e.s.r. and ion pair assoc. 9-19644  
benzotrifluoride, crystal structure, phase refinement 9-3314  
benzoxazole derivatives, fluoresc. solutes for liq. scintillators, performance  
and phys. props. 9-16009  
benzoxazolyl-thiophene, fluoresc. solute for liq. scintillators, performance  
and phys. props. 9-16009  
benzoyl chloride, Fermi reson. params., obs. 9-14681  
benzoyl chloride, Raman and i.r. spectra in liq., solid and gaseous states  
9-11481  
benz-2,1,3-thiadiazoles, monosubstituted, i.r. absorpt. spectra 9-18200  
benzyl acetate, u.v. absorpt. spectra in gaseous liq. and solid states  
9-18198  
benzyl phenyl acetate, dipole moment in benzene and CCl<sub>4</sub> solns., obs.  
9-796  
benzyl radical, doublet electronic states 9-9247  
biacetyl, fluoresc. sensitization with 2-aminopyridine 9-1031  
biacetyl, quenching of benzene fluoresc. in hexane and cyclohexane  
9-16014  
biacetyl in vapour phase, photoluminescence and phosphorescence spec-  
trum 9-793  
binary liquid mixtures, surface tension 9-19623  
biphenyl, i.r. absorpt. bands, temp. depend. 9-18215  
biphenyl, working fluid for Rankine cycle power conversion, thermal stabil-  
ity 9-3092  
biphenyl triplet state e.p.r. obs. 9-19458  
biphenyls, phosphorescence, eff. of partial deuteration 9-17489  
bismuth tritellurides, quadrupole spin echo slow beats 9-3973  
2-bromo propionitrile, vibrational spectra 9-20975  
5-bromo veratric acid, cry. struct. determ. 9-18455  
4-bromo-testosterone acetate, excited singlet and triplet state 9-11487  
p-bromoacetanilide, crystal structure 9-3316  
o-bromoaniline, vapour absorpt. spectra, 3023-2827 Å 9-4946  
m-bromoaniline, vapour absorpt. spectra, 3032-2873 Å 9-4946  
bromobenzene, vapour press. meas., 16 torr-atmospheric press. 9-3157  
bromobenzene use in tail quenching and decay time shortening of org. liq.  
scintillators 9-9526  
bromocyclobutane, i.r. and Raman spectra, ring-puckering vib. and poten-  
tial functions determ. 9-20957  
1,2-bromofluoroethane, stable configs. in liq. and vapour phases 9-14706  
bromonitromethane and d<sub>2</sub> analogue, vibr., i.r. and Raman obs. 9-15893  
bromophthalocyanine solns., clearing effect of Nd laser beam 9-1015  
 $\beta$ -bromopicrotoxinin, crystal structure, direct determ. 9-3315  
 $\beta$ -bromostyrene, i.r. abs. spectrum 9-18201  
bromostyrene, o-, p-, m-, spectra, near u.v. and i.r. 9-819  
butadiene, e wave function construction method 9-9267  
cis-1, 3-butadiene, ionization potential 9-9402  
butadiene, photoionization 9-9403  
butadiene,  $\pi$ -electron correl. energy calc. using extended separated pair  
theory 9-19460  
butane, electron impact spectrum 9-9265  
n-butane, electrooptical parameters calc. from i.r. spectra absolute intensi-  
ties 9-4960  
n-butane, H formation in liq. radiolysis 9-16503  
butane, internal rot., Hartree-Fock calc. 9-9251  
n-butane, propane, superexcited, decomposition primary modes 9-21723  
n-butane for bombardment by ionized atoms and molecules 9-7080  
2-butene, cis and trans, n.m.r., allylic and homoallylic coupling 9-13376  
2-butene, trans-1,4-disubstituted cpds., n.m.r., rel. to rotational isomerism  
about single bond joining trigonal to tetrahedral carbon 9-13376  
ter-butyl alcohol, vapour viscosity, 30°-200°C obs. for intermol. force  
determ. 9-13497  
t-butyl alcohol-water mixtures, u.s. absorpt. props. relax. curves anal.  
9-19630  
1',4'-bis(2-butyloxyloxy)-p-quater phenyl in toluene, fast response and  
high efficiency scintillator 9-16007  
n-butyramide,  $\gamma$ -irrad., free radical reactions with O<sub>2</sub> and SO<sub>2</sub> 9-12538  
calcium tartrate tetrahydrate, crystal and mol. structure 9-19737  
D-camphor, liquid-solid phase transition, change in dielectric constant  
obs. 9-3148  
camphor saturated vapour, rel. to melting of orthonitrophenol crystals,  
anisotropy 9-18384  
canthaxanthin, crystal and mol. structure 9-9686  
carba, spectra and vibr. assignment 9-9252  
carbanions MH<sup>-</sup> and H<sub>2</sub>MH<sup>-</sup> of 4,5-methylenepheneanthrene and related  
cpds., spect. investig. 9-19468  
carbazole, crystal structure 9-16083  
carbazole, vapour, spectrum and electronic transitions 9-13384  
carbazole-pyridine (triethylamine) system, electronic energy relaxation  
processes 9-7056  
carbohydrates, i.r. spectroscopy, review 9-2897  
carbohydrates and O derivs., ionization cross-sections 9-7191  
carbon tetrabromide, force constant calculation 9-18175  
carbon tetrachloride, aniline liquid mixture, u.s. vel., absorption, compressi-  
bility meas. 9-3097  
carbon tetrachloride, force constant calculation 9-18175  
carbon tetrachloride, Raman spectrum and i.f. motions in liq. 9-9518  
carbon tetrachloride, u.s. and light scatt. 9-3100  
carbon tetrachloride quenching of benzene luminescence 9-7267  
carbon tetrachloride vapour, thermal cond. rel. to temp. 9-21135  
carbon tetrafluoride, ionization potential 9-13457  
carbon tetrafluoride, photoelec. spectrum, band assignments from orbital  
obs. 9-19462  
carbon tetrafluoride, vibr. spectra, liq. and cryst. 9-1023  
carboxylic acid dimer configuration, planarity 9-7018  
carboxylic acid-water mixture, dielectric const. and loss anomalous var.  
9-7271  
carboxylic acid-water mixture, var. in p relaxation time 9-3126  
carboxymethyl cellulose, viscoelastic, turbulent heat transfer coeff. determ.  
9-19628  
carboxymethylcellulose-water soln., non-Newtonian film flow on rotating  
disc, surface 9-21181  
 $\beta$ -carotene, solns., fluorescence and phosphorescence 9-17212  
carrageenan, as constituent of electrophoretic medium 9-10566  
catecholamine, dopamine hydrochloride, crystal structure 9-19730  
cellulose, adhesion of Auspheres, effect of immersion in water or aqueous  
solns. 9-9605  
cellulose diacetate for neutron volumetric determ. in vertical reactor chan-  
nels 9-660  
cellulose fibres, thermal decomp. effect on preferred orientation 9-8072  
cellulose gel, wet, coating of Ca stearate and polymer monolayers by  
transfer from aqueous sub-phase 9-9573  
cellulose acetate membrane in saline soln., effect of surfactant layer on  
reverse osmosis 9-9502  
cembrene, crystal and mol. structure 9-13650  
cerium ethyl sulphate, anomalous phonon effects on sp. ht., spin-lattice  
relax. 9-7658  
cetane films in O<sub>2</sub> or air, ignition by reflected shock waves 9-14127  
CH<sub>4</sub> gas, i.r. spectral transmission function 9-17031  
charcoal trap for Kr, Xe radioact. meas., calibration 9-2711  
chelate carbonyls, conjugated, in coals and chars, rel. to 1600 cm<sup>-1</sup>  
absorpt. band 9-7964  
chelates of ammonium aurintricarboxylate with U(VI), Th(IV), stepwise  
stability const. 9-16481  
chloral hydrate, aqueous solutions, dosimetry studies and radiolysis  
9-21224  
chloranil radical anion, optical spectrum 9-5173  
chloranil-p-phenylenediamine, e.p.r. absorption rel. to temp. 9-3964  
n-chlorodiazoaminobenzene, crystal structure and tautomerism 9-3320  
chlorinated tetrahedral cpds., matrix-isolated i.r. spectra 9-2900  
2-chloro propionitrile, vibrational spectra 9-20975  
1-chloro-1,1-difluoroethane, microwave spectrum, molec. props. 9-13377  
1-chloro-1, 2-dibromo-2-iodoethane, internal rot., n.m.r. and rotational  
isomerism 9-807  
1-chloro-2,3,5,6-tetramethyl benzene, orientational disorder 9-17273  
1-chloro-9, 10-anthraquinone vapour, near u.v. absorption spectra, 90-  
150°C 9-18202  
chloroanthraquinone derivatives in solid phase 650-4000 cm<sup>-1</sup> i.r. spectra  
9-7060  
chlorobenzene,  $^{35}\text{Cl}$  n.q.r. Zeeman effect 9-8049  
chlorobenzene, vapour press. meas., 16 torr-atmospheric press. 9-3157  
chlorobenzene derivatives,  $^{35}\text{Cl}$  n.q.r. correlations 9-14120  
chlorobenzene-iodobenzene-n-hexane, microwave abs., 6.32 to 0.75 cm,  
30 to -40°C 9-19635  
2'-chlorobiphenyl 4-carboxylic acid, crystal structure 9-13651  
chlorobiphenyls, viscosity, thermal variation 9-13514  
chlorocyclobutane, i.r. and Raman spectra, ring-puckering vib. and poten-  
tial functions determ. 9-20957  
chlorodiazines,  $^{35}\text{Cl}$  n.q.r. 9-9237  
chloroethane-d<sub>2</sub> and -d<sub>3</sub>, chem. activated isotope effects in unimolec. reac-  
tions 9-3990  
chloroethylenes, substituted, C-Cl bonds 9-2906  
1,2-chlorofluoroethane, stable configs. in liq. and vapour phases 9-14706  
chlorofluorohydrocarbons, FC-78 and Freons, C51-12 and 113, thermal  
conductivity 9-14848  
chloroform, dielec. relax. 9-9542  
chloroform, dipole moment determ. in liq. 9-17185  
chloroform, double n.m.r. 9-9256  
chloroform, effect of molec. interactions on vibr. freqs. 9-808  
chloroform, intermolec. interactions and isotope struct. of Raman bands  
9-7266  
chloroform, thermodynamic props. up to 750°K and 200 atm. 9-7231  
chloroform-triethylamine system, dielec. props. 9-1039  
Chloroform-carbon tetrachloride binary system, superheat temp.  
9-18388  
1-(4-chloromethyl) naphthalene absorption spectra spectrophotometry obs.  
250-4000 cm<sup>-1</sup> freq. assignments 9-9258  
 $\alpha$ -chloronaphthalene, induction of mode locking and ultrashort pulses in  
ruby laser 9-6523  
p-chloronitrobenzene diamagnetic susceptibilities and anisotropies  
9-18668  
chloronitromethane and d<sub>2</sub> analogue, vibr., i.r. and Raman obs. 9-15893  
p-chlorophenol u.v. emission and absorption spectra obs. 9-2898  
p- and m-chlorophenols, assoc. effects on i.r. spectra 9-1024  
chlorophyll b, two phase system, spectral props. 9-16418

## Organic compounds continued

- coal-tar pitch, microstrains in coalesced mesophase during carbonization 9-7418  
 colloid, adsorption of Sb and Sb migration path e. microscope determ. 9-1111  
 conjugated hydrocarbons,  $\pi$ -electron screening, MO calc. 9-815  
 conjugated systems, molecular orbital theory, book 9-13370  
 coolants for reactors 9-643  
 copper acetate monohydrate, anomalous magnetic susceptibility and optical behaviour interpretation 9-7043  
 copper acetate monohydrate, low-temp., T, anisotropy of  $\text{CH}_3$  group 9-5994  
 copper acetate-quinoline cpd., crystal structure 9-1197  
 copper calcium acetate hexahydrate, magnetic susceptibility obs., 90-300°K 9-7891  
 copper formate dihydrate, crystal structure re-refinement 9-7455  
 copper formate tetrahydrate, antiferroelec. props. 9-12200  
 copper phthalocyanine, c. drift mobilities 9-17393  
 copper phthalocyanine, semiconducting, hopping and band conduction mechanisms 9-19915  
 copper phthalocyanine, single crystal, dark conduct. and photocond. meas. 9-1619  
 copper (II) salicylate adducts, e.p.r. and mag. susceptibility 9-17500  
 coronene, e.s.r. of dimer cation 9-2902  
 coronene negative ion, ground state, influence of ionic assoc. 9-13378  
 corrosion inhibitors for Fe in  $\text{HClO}_4$  conc. vs. surface coverage, transition 9-15223  
 Coumarin, solid and molten, relative Raman intensities 9-11483  
 m-cresol, u.s. vel. and absorpt. variation along state isotherms, isobars and isochors 9-5164  
 o-cresol, viscosity, rel. to glass transition,  $10^1$ - $10^{14}$  poise 9-3084  
 crystal phosphates, spectra, P=0 band splitting, 400-3600  $\text{cm}^{-1}$  9-18364  
 cryptocyanine dyes, polarized emission of laser radiation 9-4473  
 crystal growth and mechanism for melt grown single crystals 9-13600  
 cumene hydroperoxide, intermolecular H bond 9-2903  
 cupric halide: dialkylamine complexes, prep., props., i.r. spectra 9-13379  
 cis-, trans-cyano-1-dimethyl-1,2-oxiranes, n.m.r. determ. of mol. configurations 9-13380  
 2-cyanoethylsilanes, NMR spectra, analyses 9-20960  
 cyclobutane, -d<sub>8</sub>, vibration mean square amplitude calc. from spectra, 300°K 9-9259  
 cyclobutane, ring-puckering potential and dihedral angle 9-806  
 cyclobutane cpds., conformation, substituent effects, n.m.r. meas. 9-13544  
 cyclobutanol, i.r. and Raman spectra, ring-puckering vib. and potential functions determ. 9-20957  
 cyclobutanone, microwave spectrum, molec. struct. 9-805  
 cycloheptaamylose complexes with small organic molcs., interrelated space groups 9-7456  
 cyclohexane, least-energetic  $E_a$  vibr. 9-20959  
 cyclohexane, liq. and solid phase, study of molecular motions by cold-neut-ron scatt. 9-14707  
 cyclohexane, new components of stimulated Raman scatt. 9-1809  
 cyclohexane, vibr. spectra of cryst. phases 9-1801  
 cyclohexane containing H halides, molecular rotation 9-9488  
 cyclohexane fragments, long-range coupling 9-17050  
 cyclohexane molecule, configuration from X-ray obs. 9-17055  
 cyclohexane scintillator systems, luminesc. decay curves after high-energy excitation 9-11703  
 cyclohexane system, energy transfer in luminesc. processes 9-9531  
 cyclohexane-methyl alcohol critical mixture, acoustic absorpt., freq. and temp. depend. 9-11604  
 cyclohexane-aniline binary mixture, long range correlation effects 9-3105  
 cyclohexane-d<sub>12</sub> in active solvent, C-D valence vib. integrated intensities 9-4949  
 cyclohexane-polyisobutylene soln., thermodynamics 9-21202  
 cyclohexanes, monohalosubstituted, vibratory spectra and conformational equilb 9-9262  
 cyclohexanol cleavage by u.s. to prod. acetylene 9-5166  
 cyclohexene, microwave spectrum and struct. 9-9261  
 cyclohexylbromide, mol. dielectric absorpt. parameters 9-5869  
 cyclohexylchloride, mol. dielectric absorpt. parameters 9-5869  
 cyclopentadiene: intensity, depolarization, width of Raman line obs. in liquid, 30±5°C 9-4963  
 cyclopentadiene and deuterio-derivs., force constants from vibration spectra 9-2904  
 cyclopentane, i.r. spectrum, Pseudorotation 9-9260  
 cyclopentane, i.r. spectrum in Ar matrix, multiplet structure analysis 9-18199  
 cyclopentane, liq. and solid phase, study of molecular motions by cold-neut-ron scatt. 9-14707  
 cyclopentanone, Fermi reson. params., obs. 9-14681  
 cyclophanes, molec. props., valence-force calc. 9-4912  
 cyclopropane, gas-phase photolysis and radiolysis 9-10355  
 cyclopropane, mol., density of states calc. 9-12886  
 cyclopropane, vibrational relax. times, temp. depend 9-4953  
 cyclopropane carboxaldehyde, vapour-phase photolysis, products 9-16497  
 cyclopropane-D<sub>8</sub>, i.r. vib.-rotn. bands anal. 9-18217  
 cyclopropyl bromide, microwave spectrum 9-2905  
 cyclopropylcarboranyl chloride, vibr. spectra and conformational isomerism 9-794  
 cyclotrimethylene trinitramine, solution growth and dislocation etching for habit faces 9-18475  
 cyclohexyl amine + o-cresol molecular complex formation due to H.bonding dielec. const. var. 9-5744  
 cyclooctane molecule, configuration from X-ray obs. 9-17055  
 L-cysteic acid monohydrate, p.m.r. and crystallographic data 9-13652  
 cystine,  $^{99m}\text{Tc}$ -labeled, prep. and distrib. in mice 9-21989  
 L-cystinamide dihydrochloride, crystal and mol. structure 9-19731  
 3'-cytidylic acid single cry.  $\gamma$  irr., e.s.r. absorption at room temp. 9-18743  
 cytosine-5- $^3\text{H}$ , free radicals formed by decay of constituent T atom 9-1928  
 decacyclene, triplet dianions, e.s.r. 9-4965  
 15,15'-dehydrocanthaxanthin, crystal structure 9-11863  
 D-deoxyribose, dihedral angles and coupling consts. 9-18220  
 deuterovinyl chlorides, seven, fundamental wave number assignment, by normal co-ord. treatment 9-13392

## Organic compounds continued

- dextran solution, light scatt. meas. in Brice-Phoenix and Sofica photomet-ers, comparison of refl. effects 9-14832  
 di(benzol[anthracene]) photodimer, electronic spectrum 9-13381  
 diacetyl and deuterio-derivs., vibratory spectra 9-11491  
 diacetyl excitation by methylethylketone oxidation, liquid-phase chemilu-minescence obs. 9-9527  
 dialkylthallium III ions interaction with dibenzoylmethanate ion, enthalpy and entropy determ. 9-19859  
 4,4'-diamino-3,3'-diamethylbiphenyl, crystal structure 9-3317  
 4,4'-diamino-3,3'-dichlorobiphenyl, crystal and mol. structure 9-9687  
 or-diaminobenzene, crystal structure 9-13653  
 4,4'-diaminodiphenylmethane, n.m.r. spectrum anal. 9-17052  
 diaryl carbonium ions, u.v. and PMR spectra 9-14709  
 diaryl glycol acid amides, basic, i.r. absorpt. spectra, obs. 9-18197  
 trans-1, 2-diarylethenes, synthesis and test as scintillator solutes in tolu-ene, effects of methyl group 9-11704  
 1,1-diarylpropenes, methyl substituted, electr. spectra, config. assign-ments 9-11486  
 1,8-diazacyclotetradecane-2,7-dione, crystal structure 9-16084  
 diazanaphthalenes, vibronic spin-orbit interactions 9-9281  
 diazomethyl, trapped radical, vibrational absorption spectrum 9-20970  
 dibarium zinc formate tetrahydrate PMR, H<sub>2</sub> bonding scheme proposed 9-8043  
 1,2,5,6-dibenzanthracene, phosphoresc. spectra and decay times in polymeric matrices, compared with glass 9-21654  
 dibenzenechromium cation, liq. and solid solns., ESR spectra meas. 9-19459  
 dibenzofuran, vapour, spectrum and electronic transitions 9-13384  
 dibenzyl amine+phenol, molecular complex formation due to H-bonding dielec. const. var. 9-5744  
 o-m-dibromobenzene, dielec. relax. 9-9543  
 1,4-dibromobutane in benzene-paraffin mixtures, dielec. relax. times, viscosity depend. 9-11712  
 dibromocarbene, i.r. spectrum in solid Ar 9-810  
 dibromomethane, d<sub>0</sub>, d<sub>1</sub> and d<sub>2</sub>, Raman and i.r. spectra 9-15886  
 1,3-dibromopropane in benzene-paraffin mixtures, dielec. relax. times, viscosity depend. 9-11712  
 is-1,2-dichloroethylene, absorpt. coeff. rel. to press., 0.1  $\text{cm}^{-1}$  9-811  
 9,10-dichloroanthracene dimer, fluorescence, temp. depend. 9-13322  
 o-m-dichlorobenzene, dielec. relax. 9-9543  
 p-dichlorobenzene, librational amplitudes, Raman and n.q.r. spectra 9-10224  
 dichlorobenzene, mol. dielectric absorpt. parameters 9-5869  
 o-dichlorobenzene, n.m.r. spectrum anal. 9-17052  
 p-dichlorobenzene, singlet-triplet transition spectra obs. 9-19451  
 4, 8-dichloro-2, 6-diethylbenzo (1-2,4-5, bisoxazole, unit cell and space group 9-7459  
 1,2-dichloroethane-d<sub>6</sub> and -d<sub>4</sub> chem. activated, isotope effects in unimolec. reactions 9-3990  
 dichloroethylene +  $\text{C}_2\text{H}_2\text{Cl}_2$  (or  $\text{CH}_2=\text{CH}_2 + \text{Cl}_2$ ) + neutral prods., direct processes 9-4984  
 cis-1,2-dichloroethylene vapor, elec. susceptibility rel. to press. at 9231 MHz 9-11660  
 dichloromethane-d<sub>3</sub>, deuterium quadrupole coupling const. 9-13382  
 2,4-dichlorotoluene, near u.v. absorption, spectra, -10° to 80°C 9-20955  
 2,4-, 2,5-, 2,6-dichlorotoluenes, i.r. absorption spectra, assignments of fundamental vib. 9-11485  
 2,2'-dichlorotrimethylene sulphate, crystal and mol. structure 9-19732  
 dideuteroacetylene, mol. spectrum, 4.1  $\mu$  bands analysis, obs. 9-13372  
 dielectrics, transparent, laser light absorpt. and opacity production 9-1721  
 diethyl ether, vapour viscosity, 30°-200°C obs. for intermol. force determ. 9-13497  
 diethyl ether and deuterated analogues, vibr. spectra of conformers 9-14708  
 diethyl ether-nonpolar gas mixtures, thermal conductivity 9-14818  
 1, 1'-diethyl-p-cyano-2, 2'-di- carbocyanine-tetrafluoroborate laser dye props. 9-20562  
 1, 1'-diethyl-p-nitro-4, 4'-di-carbocyanine- tetrafluoroborate laser dye props. 9-20562  
 diethylether-chloroform mixtures, dielec. props., x-band microwave obs. 9-3116  
 1,4-difluoro-2,6-bistrifluoromethylbenzene, n.m.r. 9-14717  
 1, 1-difluoro-2-chloroethylene, principal field gradient tensor 9-2906  
 m-difluorobenzene, u.v. emission spectra obs., 2500-3000 Å 9-7066  
 cis-difluorodiazine, vibration, mean amplitudes, applic. of  $\text{X}_2\text{Y}_2$  mol. with  $\text{C}_2$  symmetry theory 9-4900  
 difluorodichloroethylene, signs of F spin coupling consts. 9-7065  
 L(+)-dihydrodesoxyxystreptose, structure from NMR and mass spectra 9-18203  
 2,5-dihydrothiophene, ring. puckering vibr. 9-820  
 dihydroxyanthracenemiquinones, H bond and hyperfine splitting obs. 9-20966  
 7, 8-dihydroxybenzopyrylium chloride derivatives, photographic develop-ers 9-13077  
 3 $\beta$ ,17 $\alpha$ -dihydroxy-16 $\beta$ -bromo-5 $\alpha$  pregnan-11,20-dione, crystal and mol. structure 9-13654  
 7, 8-dihydroxycoumarin derivatives, photographic developers 9-13077  
 o-, m-diiodobenzene, dielec. relax. 9-9543  
 4,4'-diiodobenzophenone, absorpt. spectrum 9-15881  
 trans-1,4-diiodocyclohexane, vibrational spectra and rotational isomerism 9-17482  
 1,2-diiodotetrafluoroethane, rot. isomers, i.r. obs. 9-15887  
 diketene, i.r. and Raman spectra, ring-puckering vib. and potential func-tions determ. 9-20957  
 $\beta$ -diketones, absorpt. under strong optical excitation 9-17051  
 dimethacrylate-bis-diethyleneglycolphthalate, polymerization studies by elec. conductivity meas. 9-15219  
 dimethacrylate-bis-ethyleneglycolphthalate, polymerization studies by elec. conductivity meas. 9-15219  
 dimethacrylate-bis-triethyleneglycolphthalate, polymerization studies by elec. conductivity meas. 9-15219  
 3,4-dimethoxyacetophenone and substituted acetophenones (II; n=1-3), u.v. absorption spectrum 9-14714  
 dimethyl carbonate, vapour-phase photolysis, 30°-103°C obs. 9-16500  
 dimethyl diselenide, vibr. spectra and struct. 9-9264  
 dimethyl ether, gas, electron drift velocities 9-17166  
 dimethyl ether, valence force field calc. using vib. freq. of  $(\text{CH}_3)_2\text{O}$ ,  $(\text{CD}_3)_2\text{O}$  and  $\text{CH}_3\text{OCD}_3$  molcs. 9-20968



## Organic compounds continued

- 2,6-dimethyl naphthalene, temp. effect on first electronic transition 9-15178
- N, N-dimethyl p-phenylenediamine bromide, Wurster's red bromide, crystal structure 9-7460
- dimethyl sulphoxide, proton magnetic resonance study, CH<sub>3</sub> group frozen at -123°C 9-5993
- 4,4'-bis dimethyl-aminodiphenylamine radical iodide, growth from solution 9-11801
- dimethyl-acetylene in nematic solvents, n.m.r. 9-13545
- 1,8-dimethyl-5,12-dimethylene biphenyl, twisted C-C double bond, optical activity meas., electronic structure proposal 9-9274
- N, N-dimethylacetamide, i.r. and Raman spectra, 3100-250 cm<sup>-1</sup> obs. 9-4957
- dimethylamine, molec. structs. bond lengths and angles, electron diff. study 9-18210
- dimethylamine, vibr. mean amplitudes 9-7045
- 4-dimethylamino-4'-nitrophenyl + acetone in frozen decaline soln., fluorescence obs. 9-7071
- 4-dimethylamino-prop-2-en. 1-al, solvent shifts of electronic spectra 9-5174
- dimethylaniline, u.v. spectrum C band assignment 9-15892
- N,N-dimethylaniline in acetonitrile soln., h.f. splitting const. from e.s.r. spectra 9-11494
- 1,1'-dimethylchromocene, -ve methyl contact shifts,  $\Sigma$  and  $\pi$  e delocalisation model consideration 9-7072
- dimethyldiazirine, rotational spectra 9-9263
- dimethyldodecylamine oxide micelle surface pot., long-chain alkyl and small ions effects 9-7289
- N, N-dimethylformamide, i.r. and Raman spectra, 3100-250 cm<sup>-1</sup> obs. 9-4957
- dimethylformamide in polar solvent, large viscosity range dielec. relax. obs. 9-5183
- 2,3-dimethylnaphthalene single crystals, near i.r. absorption spectra 9-5933
- dimethylsulfoxide intermol. interaction in solns., i.r. Raman obs. 9-18365
- 2-dimethylsulfonylidenemalononitrile, crystal and mol. structure 9-13655
- 1,1'-dimethylvanadocene, -ve methyl contact shifts,  $\Sigma$  and  $\pi$  delocalisation model consideration 9-7072
- 2,2'-di(1,4-naphthoquinone, crystal and mol. structure 9-13656
- m-dinitrobenzene, diamagnetic susceptibilities and anisotropies 9-18668
- m-dinitrobenzene soln. in tetrahydrofuran, e.s.r. photoinduced spectra 9-11497
- o-dinitrobenzene soln. in tetrahydrofuran, e.s.r. photoinduced spectra 9-11497
- p-dinitrobenzene soln. in tetrahydrofuran, e.s.r. photoinduced spectra 9-11497
- o-, m-, p-dinitrobenzene soln. in tetrahydrofuran, e.s.r. photoinduced spectra 9-9276
- 1,4-dioxane, molecular mobility, n.m.r. study 9-11901
- dioxane base scintillator solns., quenching props. of alcohols 9-9528
- dioxycoumarins, (6,7 and 7,8), u.v. spectra in alcohol solns. 9-7062
- dioxynolionic acid, (DNA), X-ray diffraction study 9-7093
- diphenyl, single cry., polarized i.r. abs. spectra 9-19992
- diphenyl - $\Delta^2$  pyrazoline, crystal structure 9-3318
- diphenyl sulphone and benzene-d<sub>3</sub> analogue, spectra, 4000-400 cm<sup>-1</sup> 9-14704
- diphenyl vapour, thermal cond. rel. to temp. 9-21135
- 4,4-diphenylcyclohexene and derivatives, photochemistry 9-8110
- 9, 10-diphenylanthracene, lowest triplet state obs., eff. of phenyl substitution 9-11484
- 9, 10-diphenylanthracene in polystyrene, fluoresc. quenching and energy transfer 9-10247
- diphenylene oxide, frozen paraffin solns., conc., effect on absorption spectra 9-2913
- diphenylene oxide, in paraffins absorpt. spectra and conds. for Shopolskii effect 9-1802
- diphenylene oxide soln., fluorescence spectra conc. depend. 9-9279
- diphenylmethene, fluoresc. lifetime 9-1833
- diphenylstilbene, absorpt. and fluorescence spectra 9-4961
- N, N-diphonylacetamide, crystal structure 9-7461
- divinylbenzene soln, absorpt. and luminesc. spectra 9-801
- 1,4-di(2-(5-toloxylazoly))benzene, improvement of  $\beta$  scintillation counter 9-18035
- docosyl triethylammonium bromide, ionized monolayers, at air/water and oil/water interface, eqns. of state 9-9500
- dopamine hydrochloride, catecholamine, crystal structure 9-19730
- DPPH, EPR obs. used as device for meas. nonuniform magnetic fields 9-10808
- DPPH iodine complex, magnetic and electrical props. 9-5797
- durene, thermoluminesc. after photoioniz. in methylcyclohexane glass 9-17494
- durene in rigid glass, thermoluminescence following photoionization 9-21655
- durene radiolysis, production of radical with 13 equiv. protons 9-8078
- duroquinone, flash photolysis and triplet state reactions 9-21720
- duroquinone-duroquinone radical anion in sol., electron exchange rate const., NMR meas. 9-20950
- dye fluorescence quenching by inorganic salt, soln. structure depend. 9-9174
- dye mols., solvent depend of position and intensity of absorpt. bands 9-7075
- dye solns., liquid, light generation mechanisms 9-5169
- dyes, elec. field effect on optical absorpt. of mols. 9-7041
- dyes, liq. laser applications 9-15523
- dyes, wide-angle interference and multipole fluorescence 9-15839
- dysprosium ethyl sulphate, anisotropic mag. dipole interacts. below Curie point 9-1670
- dysprosium ethyl sulphate, mag. props. and specific heat, 1°K to 0.13°K 9-1669
- ebonite, reflection coeff. diminution for laser light 9-21603
- electrophotoluminescence of rigid org. solns. 9-16447
- ellagic acid, crystal structure 9-19733
- 5-endo-1,2,3,4,7,7'-hexachlorobicyclo[2,2,1] hept-2-ene, nuclear triple reson. tickling, obs. 9-18207
- erbium tricyclopentadienide, absorpt. spectra 9-3898
- ethane, electron impact spectrum 9-9265
- ethane, gas, electron drift velocities 9-17166
- ethane, Kerr constant determ. from quantum theory 9-746

## Organic compounds continued

- ethane, liquid solns.,  $\gamma$ -radiolysis at -78°C, products obs. 9-21726
- ethane, photolysis at 1470 and 1577 Å, pressure effects 9-16498
- ethane, rotational barriers, bond-function anal. 9-7063
- ethane positive ions, geometries 9-756
- ethanes, 1:1 di-substituted, vibratory spectrum, calc. and interpret. 9-15889
- ethanol, adsorpt. on MgO, i.r. spectra 9-3215
- ethanol soln. of pyrene, ratio of excimer to molec. fluoresc. intensities, rel. to triplet-triplet annihilation 9-11705
- ethanol-water, methanol mixtures, light scatt. 9-21209
- ethene, and ethene-d<sub>4</sub>, struct. deduced from vibronic spectra 9-813
- ethyl acetate, vapour viscosity, 30°-200°C obs. for intermol. force determ. 9-13497
- ethyl alcohol, ultrasonic absorption 9-153
- ethyl alcohol, Townsend coeff. and excitation potential 9-18308
- ethyl bromide (n,p): active Br collection on electrodes 9-4785
- ethyl chloride, dielec. consts. in liq., solid and absorbed states 9-12186
- ethyl chloride, entropy and enthalpy 9-18326
- ethyl chloride adsorbed layers, heat of adsorpt. two-dimens. condensation 9-9594
- ethyl formate in CCl<sub>4</sub>, CS<sub>2</sub> and CH<sub>3</sub>OH, temp., solvent depend. of coupling const. and chem. shift 9-17054
- ethyl isocyanide, microwave spectrum 9-13383
- ethyl isocyanide, vibr. and rot. spectra, 4000-200 cm<sup>-1</sup> 9-18205
- ethyl phenyl acetate, dipole moment in benzene and CCl<sub>4</sub> solns., obs. 9-796
- ethyl pyridines, m liquid phase, i.r. adsorption spectra 9-1026
- ethylene, burning in O<sub>2</sub> and N<sub>2</sub>O, comparative soot yields 9-12535
- ethylene,  $\gamma$ -ray induced polymerization, eff. of alcohols 9-20039
- ethylene, diffusion flame in O<sub>2</sub>-Ar and O<sub>2</sub>-N<sub>2</sub>, polycyclic aromatic hydrocarbon prod. in soot, rel. to O<sub>2</sub> conc. 9-12536
- ethylene, e wave function construction method 9-9267
- ethylene, gas, electron drift velocities 9-17166
- ethylene, hydrogenation on metal catalysts 9-10336
- ethylene, ion formation energy for  $\gamma$  radiation of Cs<sup>137</sup> 9-9409
- ethylene, laminar diffusion flames, effects of diluents on soot production 9-15214
- ethylene, molecular vibrations, Green's function analysis 9-11477
- ethylene, Rydberg states obs. in Kr matrix 9-14710
- ethylene, vibr. struct. of  $\pi^*-\pi$  transition 9-20963
- ethylene, vibrational relax. times, temp. depend. 9-4953
- ethylene carbonate, Fermi reson. params., obs. 9-14681
- ethylene episulfoxide, rot. spectrum 9-19464
- ethylene glycol, u.s. vel. and absorpt. variation along state isotherms, iso-bars and isochors 9-5164
- ethylene in aq. soln., radiolysis products 9-21725
- ethylene oxide (-d<sub>4</sub>), force constants calc. and vibratory spectra interpretation 9-9268
- ethylene sulphide, <sup>33</sup>S nuclear quadrupole coupling and localized electron distrib. 9-20961
- ethylene-air diffusion flame, addition of H<sub>2</sub> to ethylene rel. to polycyclic aromatic hydrocarbon prod. 9-12537
- ethylene-d<sub>3</sub> and -d<sub>4</sub>, vapour press. 9-17232
- ethylenes, deuterated, coriolis  $\zeta$  sum rules 9-13327
- ethylenes, unsymmetrically substituted, cis-trans effect on <sup>13</sup>C chem. shifts 9-9266
- ethylenes interact. with OH-containing cpds., NMR and i.r. study 9-18751
- ethylenimine, microwave spectra and molec. props. 9-20962
- ethylmagnesium bromide dietherate, crystal, struct. obs. 9-9688
- ethylphenylphosphine, n.m.r. anal. of geminal coupling const. 9-13546
- europium theonyltrifluoroacetate, luminescence props. 9-16016
- ferricytochrome C single cryst., spectra in polarized light, 3700-7500 Å 9-11489
- ferrimyoglobin complexes single cryst., spectra in polarized light, 3700-7500 Å 9-11489
- ferrocene, <sup>57</sup>Fe nuclear quadrupole moment 9-3976
- ferrocenes, substituted, electronic absorpt. spectra and photodecomposition 9-20964
- ferrocenium triiodide, crystal structure 9-9689
- films, diffraction patterns produced by nuclear reactions 9-15039
- fluoranthene, electronic struct. 9-800
- fluorene, vapour, spectrum and electronic transitions 9-13384
- fluorene, vibr. anal. 9-14712
- fluorene and derivs., u.v. absorpt. spectra in soln. rel. to electronic structure 9-3106
- fluorene and derivs., u.v. absorpt. spectra in soln. rel. to electronic structure 9-3107
- fluorene iodo-derivs., electronic structure quantum mech. calcs. rel. to absorpt. spectra 9-3108
- fluorenone and derivs., u.v. absorpt. spectra in soln. rel. to electronic structure 9-3106
- fluorenone and derivs., u.v. absorpt. spectra in soln. rel. to electronic structure 9-3107
- fluorenone iodo-derivs., electronic structure quantum mech. calcs. rel. to absorpt. spectra 9-3108
- 9-fluorenone mol. dielectric absorpt. parameters 9-5869
- fluorescein, emission and absorpt. spectra rel. to species, 80 and 300°K 9-1034
- fluorescein in boric acid glass, photoconductivity and thermoluminescence 9-16314
- 4 $\pi$  fluoro-3-chloro aniline, six upper and one ground state ident. 9-814
- 1-fluoro-2-haloethanes, rot. isomers 9-812
- fluoroacetic acid, microwave spectrum, rot. consts. and centrifugal distortion parameters 9-13371
- p-fluoroaniline, i.r. absorption and near u.v. emission spectra, correl. and comp. of ground state vib. freq. 9-14711
- fluorobenzenes, criticism of existing photochem. data 9-16496
- fluorobromobenzene, o-, p-, m-, mols. out-of-plane vibrs., normal coordinate analysis 9-13374
- fluorocarbons, alicyclic and aromatic, transient negative-ion states 9-7192
- fluorocarbons,  $\gamma$ -dosimetry 9-19242
- fluorocarbons, chem. eff. of reactor  $\gamma$  rays 9-20061
- fluorocarbons, intermolec. radical-solvent hyperfine coupling 9-21226
- fluorocarbons, photoioniz., mass spect. study 9-18206
- fluorochlorobenzene, o-, p-, m-, mols. out-of-plane vibrs., normal coordinate analysis 9-13374
- fluoromethane mols. in liq. crystal solvent, NMR spectra obs. 9-7067

## Organic compounds continued

- fluoromethanes, variation of C-F spin-spin coupling with substituent 9-4943
- $\beta$ -fluoronaphthalene vapour, absorption and emission spectra obs. 9-4954
- $\beta$ -fluoronaphthalene-naphthalene, block structure 9-1334
- p-fluorophenyl labelled acids with organic bases, H bonding determ. from F NMR shift 9-7068
- p-fluorostyrene, i.r. spectra, 250-4000  $\text{cm}^{-1}$ , liq. phase, spectrophotometer obs. 9-4955
- fluorostyrene, o-, m-, p-, and para- elec. dipole moments 9-11490
- fluorostyrenes, spin-spin interactions of F nuclei 9-19466
- foamed polystyrene, use for i.r. laser beam profile recording 9-13010
- formaldehyde,  $^3A_2 \rightarrow ^1A_1$  transition, spin-orbit enhancement 9-17023
- formaldehyde, one-electron props on Gaussian basis 9-14713
- formaldehyde, SCF calc. using Gaussian basis 9-2908
- formic acid, LCAO-MO-description of assoc. types 9-13385
- Freon-12, thermodynamic props., tables 9-3053
- Freons, heat transfer estimation 9-1004
- furan; intensity, depolarization, width of Raman line obs. in liquid, 30 $\pm$ 5°C 9-4963
- furfurylalcohol resin, pyrolysis, study of carbon residue 9-7319
- gas, ideal, entropy estimation 9-3050
- gases, analysis, gas chromatograph-mass-spectrometer combination 9-1887
- gelatin, dichromated, phase hologram recording appls. 9-10873
- glass, photo- and p-ionization compared by e.p.r. spectroscopy 9-10082
- glass, thermal expansion, 10-300°K 9-21437
- glucose kinetics of human body, analog. computer study 9-20254
- glycerine, partially deuterated, quasi-elastic cold neutron scattering at various temps. 9-7250
- glycerine, viscosity rel. to glass transition, 10 $^1$ -10 $^{14}$  poise 9-3084
- glycerol, Raman eff. using 4880 Å Ar laser 9-15890
- glycerol mixtures, u.s. absorption, temp. and freq. depend. 9-11693
- glycine silver nitrate, cry. struct., obs. 9-1199
- glyoxal and deuterio-derivs., vibratory spectra 9-11491
- guanidium aluminium sulphate hexahydrate, e.p.r. of Mn $^{2+}$  9-18744
- guanine hydrochloride dihydrate, irrad. single crystal, e.p.r. obs. 9-8038
- haloethanes, monosubstituted, vibratory spectra interpretation 9-9269
- halogen-substituted methanes, 2nd virial coeff. determ. by gas balance method 9-7070
- halogenated aliphatic hydrocarbons, electron attachment 9-3010
- halonaphthalenes, phosphoresc. triplet decay in compressed polymethylmethacrylate 9-17491
- heat capacity meas. at low temps., new method 9-5564
- hemin, h.p. Mossbauer effect 9-9202
- n-heptane, thermodynamic props. from sound vel. obs. 9-17204
- heterocyclic amines, molecular relaxation 9-20947
- heterocyclic ring, saturated, medium intermol. force effects, n.m.r. obs. 9-19493
- hexachlorobiphenyl, viscoelastic liq. with inert-gas infusion 9-15996
- hexachloroethane, polymorphous transition from crystalline to rotational state 9-21414
- n-hexadecane, vapour pressure meas., 0.02-200 torr 9-3157
- hexadecane-diol-1,16-urea, phase and dielec. abs. changes 9-16288
- hexadecanol-1-urea, phase and dielec. abs. changes 9-16288
- hexafluoroacetone, luminesc. quenching by O $_2$ , NO and hydrocarbons 9-799
- hexafluoroacetone, photolysis, identification of quenching addends 9-1922
- hexafluoroacetone, with diborane, gas-phase photolysis 9-16495
- hexafluoroacetone vapour, photodecomp., effect of temp., ketone conc. and wavelength 9-1920
- hexafluoroacetone vapour, photolysis, intersystem crossing 9-1919
- hexafluoroacetone vapour, photolysis, mechanics for primary process. 9-1923
- hexafluoroacetone vapour photo-excited, fluoresc. and phosphoresc. rel. to ketone press. 9-1921
- hexafluorobenzene, thermal properties, liquid vapour transformation 9-1000
- hexahelicene, low-temp. circular dichroism 9-15165
- hexahydroxyanthracenemiquinones, H bond and hyperfine splitting obs. 9-19467
- hexane, combustion, effect of olefins at different oxidation stages leading to ignition 9-14126
- n-hexane, electrooptical parameters calc. from i.r. spectra absolute intensities 9-4960
- hexane, ionization currents induced by  $\alpha$  or  $\beta$  particles 9-9549
- hexane, liq., ion mobility, effect of motion 9-13536
- n-hexane liquid with series of dielectric admixtures, breakdown 9-5185
- n-hexane-chlorobenzene-iodobenzene, microwave abs., 6.32 to 0.75 cm, 30 to -100°C 9-19635
- hexaphenylbenzene modification, crystal structure 9-7462
- 2,2,4,4,6,6-hexaphenylcyclotriphenylphosphazatriene crystal structure 9-13657
- hexatriene substituted in heptane, toluene; fluorescent props. comparison, temp. depend. 200-350°K 9-4956
- hydrazinium hydrazinedithiocarboxylate, crystal and mol. crystal structure 9-13658
- hydrazinium hydrogenoxalate, N $_2$ H $_4^+$  in  $\gamma$ -irrad. cryst. 9-1927
- hydrocarbon, elementary steps in gas-phase oxidation 9-21692
- hydrocarbon gases, effect of temp. on rot. and vibr. relax. 9-957
- hydrocarbon liquid-water interfacial interaction energy rel. to hydrocarbon orientation 9-7260
- hydrocarbon mixtures, light, liq. density and excess vol., -165°C 9-17195
- hydrocarbon systems, diffusion, press. change meas. 9-964
- hydrocarbon type analysis by chromatography, fluorescent indicators 9-6031
- hydrocarbons,  $^{13}\text{C}$ -H coupling constants, MO calc. 9-7042
- hydrocarbons, alternant, pairing betw. valence bond spin-coupled wave functions for  $\pi$ -electrons of +ve and -ve ions 9-17056
- hydrocarbons, condensed aromatic, monochromatic e energy loss 9-13539
- hydrocarbons, conjugated, spin densities for radical ions, LCAO-MO calc. 9-13396
- hydrocarbons, correlations in vib. spectra 9-20965
- hydrocarbons, electron cyclotron reson. during chem-ionization 9-3999
- hydrocarbons, electron distrib. in ground state, calc. 9-4952
- hydrocarbons, irrad. liq., chem. determ. of free-ion yields 9-6024
- hydrocarbons, liq., radiation-induced cond. and molec. struct. 9-16022

## Organic compounds continued

- hydrocarbons, liq. aromatic criteria necessary for photocond. in electrode-liq. syst. 9-17219
- hydrocarbons, liq. radiolysis, ion yield and molec. struct. 9-1926
- Hydrocarbons, MO theory of elec. polarizabilities and mag. susceptibilities 9-9238
- hydrocarbons, nanosecond absorption spectroscopy using laser beam photolysis 9-19170
- hydrocarbons, polycyclic; ring currents and p shielding 9-11478
- hydrocarbons, polycyclic, analysis by quasi-line fluoresc., obs. 9-18780
- hydrocarbons, proton-proton coupling by  $\pi$  electrons 9-17042
- hydrocarbons, saturated, e-coupled p. spin-spin interaction, interbond correlation effects 9-816
- hydrocarbons, saturated liquid entropy, prediction 9-19629
- hydrocarbons, substituted, skeletal deformation freq. and boiling pts., correl. 9-21249
- hydrocarbons adsorbed on silica gel, mechanism of radiolysis 9-20063
- hydroquinone,  $^{13}\text{C}$ -H satellite NMR Patterns, rel. to couplings 9-13373
- O-, M- hydroxy anilines, dielectric const., and loss determ. r.f. - microwave region 9-7835
- 3-hydroxy-1-(p-nitrobenzyl) pyridinium hydroxide anhydro salt, absorption spectra, intensity and solvent eff. 9-11492
- 8-hydroxy-1-methylquinolinium hydroxide anhydro salt, absorption spectra, intensity and solvent eff. 9-11492
- p-hydroxybenzaldehyde, emission and proton transfer 9-9532
- imidazole, l.f. Raman spectrum of cryst. 9-16424
- iminoxy radicals formed from tetranitromethane and 1,3-dicarbonyl cpds., structure from e.s.r. 9-20987
- indazole, vapour phase luminescence 9-15898
- indole, crystal structure 9-16083
- intermolecular H-bonded systems, electronics energy relaxation processes 9-7056
- iodobenzene-chlorobenzene-n-hexane, microwave abs., 6.32 to 0.75 cm, 30 to -40°C 9-19635
- $\pi$ -iodocyclopentadienyltetraphenylcyclobutadienylcobalt, lattice constants and space group 9-7463
- iodeheptafluorobutane, photodissociation in laser rel. to formation of I $_2$ , effect of stimulated emission 9-15902
- ionization potentials meas. in mass spectrometer 9-15950
- 1, 3-, i.r. spectra and pseudorotation 9-809
- iron gluconate, Mossbauer quadrupole splitting and isomer shift obs. 9-5894
- iso-octane-water emulsion, u.s. attenuation obs. 9-3139
- isobutene, -d $_8$ , i.r. and Raman spectra obs. 9-7055
- isobutyramide,  $\gamma$ -irrad., free radical reactions with O $_2$  and SO $_2$  9-12538
- isooctane-nitroethane solutions, conc. fluctuation kinetics near critical stratification pt., from acoustic dispersion obs. 9-984
- isopentane, refractive index at high press. 9-5170
- isopropyl alcohol, aniline liquid mixture, u.s. vel., absorption, compressibility meas. 9-3097
- 1-isopropyl-4, 8, 12-trimethyl-2, 4, 7, 11-cyclotetradecatetraene, crystal and mol. structure 9-13650
- isoquinoline, vapour phase luminescence 9-15898
- ketene, reaction with atomic H and O 9-1899
- ketene-NO-H $_2$  system, photochem. products 9-21721
- krypton-ethylchloride, binary diffusion and unlike interactions, non-polar mixtures 9-21147
- krypton-methylene chloride, binary diffusion and unlike interactions, non-polar mixtures 9-21147
- labelled, for radioactive analysis, stability 9-14145
- in laser reson., pigment solns. generation intensity, calc. 9-15524
- LCAO-MO description of assoc. types of formic acid 9-13385
- lipid films, semiconducting depend. on electrical conductivity 9-12138
- liquid systems, high-energy-induced luminescence, ionic processes 9-1028
- liquids, pure, thermal conductivity, 15-130°C 9-14846
- lithium, acetate dehydrate, Raman effect meas. in polarized light 9-10225
- lithium methanesulphonate, vibr. spectra 9-18218
- long-chain semiconductor, Overhauser phase and bond alternation 9-4972
- Lysozyme, Raman spectrum, laser induced 9-5940
- magnesium, phthalocyanine, semiconducting, hopping and band conduction mechanisms 9-19915
- magnesium bromide tetrahydrofuran complex, crystal structure 9-19716
- maleic anhydride,  $\gamma$ -irrad. cryst., e.s.r. of ion radical pairs 9-10291
- maleimides and maleamic acid,  $\gamma$ -irrad., e.p.r. spectra study 9-21323
- malononitrile, dispersive phase transitions 9-13780
- manganese acetate tetrahydrate, heat capacity, 0.4-20°K 9-12020
- manganous formate dihydrate, H atom positions from n. diff. data 9-7455
- manganous formate dihydrate, kinetic parameters from thermogravimetric analysis 9-16506
- K-D-mannitol crystal structure 9-19734
- Meisenheimer salts, 2,4, 6-trinitrophenolate- caesium(potassium) ethoxide complexes, crystal and mol. structure 9-7467
- menthyl n-alkylphenylphosphinates, p.m.r. spectra 9-19471
- mercaptals in n-hexane and propan-2-ol soln., electr. spectra, absorpt. study 9-14715
- 2-mercaptop-6-methyl-purine monohydrate, crystal structure 9-11864
- mesitylene, refractive index at high press. 9-5170
- with metallic conduction props. 9-7756
- metalloporphyrins, mag. susceptibility and moments 9-16325
- metalorganic phenyls, lum. and spectra, 77 and 290°K 9-15848
- methacrylonitrile, photosensitized dimerization obs. 9-16501
- methane; mechanical, thermodynamic and transport props., 0-300°K bibliography 9-19470
- methane, 3.39  $\mu$  line, press. shift and broadening, laser-saturated mol. absorpt. study 9-11496
- methane, 9050  $\text{cm}^{-1}$  absorpt. band 9-9271
- methane, collision-induced mixing of Cs  $6^3P_{1/2}$ - $6^3P_{3/2}$  9-13298
- methane, compressed, rot. correl. functions, effect of nuclear-spin 9-4940
- methane, corresponding states with Ar 9-9440
- methane, e-coupled p. spin-spin interaction, interbond correlation effects 9-816
- methane, electron impact spectrum 9-9265
- methane, halogen substituted, Raman intensities calc. by bond polarizability theory 9-13387
- methane, ioniz. pot. and X-ray abs. spectra in 10-50 Å range 9-15955
- methane, ionization and fragmentation by 5-45 keV protons, mass spect. investigation, X-section meas. 9-5060
- methane, ionizing photolysis 9-6019



## Organic compounds continued

- methane, Kerr constant determ. from quantum theory 9-746  
 methane, liquid, props. obs. review 9-13509  
 methane, mixtures with inert gases, H<sub>2</sub>, N<sub>2</sub>, refr. index rel. to long-range atom-mol. interactions 9-9304  
 methane, mol., emission spectra, two new band systems of CH<sup>+</sup> 9-18208  
 methane, mol., mag. susceptibility calc. 9-744  
 methane, n.m.r. isotope chem. shifts 9-7013  
 methane, photolysis at 1236 Å 9-10356  
 methane, press. broadening and shift of 3.39 μ line perturbed by inert gases 9-15891  
 methane, pyrolysis, spiral and whisker growth of C 9-8073  
 methane, scattering of slow neutrons, rel. to intermolecular interactions 9-11511  
 methane, SCF MO's and molec. props. 9-9270  
 methane, solid, ground state conversion, NMR obs. 9-16471  
 methane, solid, molec. reorientation effects on neutron scatt. 9-9823  
 methane, solid, u.s. wave velocity, temp. depend. rel. to disorder 9-1370  
 methane, synthesis and purification using Cu on SiO<sub>2</sub>-MgO support 9-12526  
 methane, vibr. energy transfer 9-2935  
 methane and methane-d<sub>4</sub>, ioniz. by 2'S and 2'S He atoms 9-912  
 methane and mixture, virial coeff., second, from boiling point to room temp., from value at one temp., calc. method 9-15972  
 methane gas, i.r. rad., large path length limit 9-19585  
 methane gas, u.s. absorpt. 50-600 kHz and -30+120°C 9-5117  
 methane 68.7% F1 flame, temp., calc. and obs. 9-15561  
 methane-Ar, gaseous, heat of mixing, 170-2930°K 9-954  
 methane-Ar gaseous mixtures, excess enthalpy at high densities 9-955  
 methane-d<sub>4</sub>, collision-induced mixing of Cs 6<sup>2</sup>P<sub>1/2</sub>-6<sup>2</sup>P<sub>3/2</sub> 9-13298  
 methane N<sub>2</sub>, gaseous, heat of mixing, 170-2930°K 9-954  
 methane-N<sub>2</sub> gaseous mixtures, excess enthalpy at high densities 9-955  
 methane-N<sub>2</sub> mixture, fission fragment prod. of H<sup>14</sup>CN 9-18770  
 methane-oxygen mixtures, acoustic wave absorpt., O<sub>2</sub> vibr. relax. obs. 9-21137  
 methanesulfenylchloride, microwave spectra, quadrupole coupling consts., dipole moment 9-11700  
 methanesulfonic acid, crystal and mol. structure 9-14929  
 methanol, adsorp. on MgO, i.r. spectra 9-3215  
 methanol, adsorption by wood charcoal, expansion meas. 9-11781  
 methanol, and water, simultaneous condensation from turbulent air flow 9-1070  
 methanol, collision induced predissoc., quantum yields 9-16499  
 methanol, effect on load relaxation of fatigue-cracked Ti-(6 wt.%)Al-(4 wt.%)V alloys 9-19786  
 methanol, gas, electron drift velocities 9-17166  
 methanol adsorp. on Na bentonite amine complexes rel. to hydrophilic-hydrophobic props., obs. 9-5261  
 methanol glasses, p-irrad., spatial distrib. of trapped electrons 9-4014  
 methanol system, Overhauser effect 9-9560  
 methanol-water, ethanol mixtures, light scatt. 9-21209  
 methanol-water system, mass transfer from single bubbles under distillation conditions 9-18329  
 methionine, prep., and distrib. in mice 9-21989  
 3,4-methoxyacaphenone, u.v. absorption spectrum 9-14714  
 6-methoxy 8-nitro-5(1*H*)-quinoline, crystal and mol. structure 9-13660  
 methyl alcohol-cyclohexane critical mixture, acoustic absorpt., freq. and temp. depend. 9-11694  
 methyl bromide, vibration-rotation spectrum, interpretation near 6000 cm. 9-18211  
 methyl chloride, dielec. consts. in liq. solid and adsorbed states 9-12186  
 Methyl chloride, gas electron drift velocities 9-17166  
 methyl chloride, parallel component of 2ν<sub>3</sub> band near 6015 cm<sup>-1</sup> 9-20971  
 methyl fluoride and CH<sub>3</sub>F<sup>+</sup> ion, electr. struct., SCF MO calc. 9-17057  
 methyl formate, vapour-phase photolysis, 30°-103° C obs. 9-16500  
 methyl group, stern effects on luminesc. of liq. trans-1, 2-diarylethylenes 9-11704  
 methyl group in copper acetate monohydrate, T, anisotropy 9-5994  
 methyl halides, photoionization efficiency curves, mass spectrometric study, ionization threshold to 6001b 9-3004  
 methyl iodide, detection after heating of irradiated nuc. fuels 9-19367  
 methyl iodide, reaction with electronically excited I atoms 9-1924  
 methyl iodide, rotational Zeeman effect 9-2910  
 methyl iodide + K system, complex optical pot. calc. 9-10322  
 methyl iodide (-d<sub>3</sub>), i.r. absorption intensities, solvent eff. 9-18209  
 methyl iodide aqueous solutions, effect of ultrasound 9-3096  
 methyl iodide liq. phase, Raman band width C-I stretching vibrs. 9-4959  
 methyl isocyanide, <sup>13</sup>C bombardment, thermal isomerization 9-8112  
 methyl methacrylate, cryst. and in CS<sub>2</sub> soln., Overhauser enhancement parameters 9-14119  
 DL-2 methyl -7- oxododecanoic acid, crystal structure 9-19735  
 methyl phenyl acetate, dipole moment in benzene and CCl<sub>4</sub> solns., obs. 9-796  
 2-methyl propene, n.m.r., CH<sub>3</sub>-CH<sub>3</sub> coupling, possibility of 'through-space' contribution 9-13376  
 methyl red dye interaction with solid polymer, study by electrochromic effect (Stark effect) 9-16419  
 methyl thiocyanate, torsional fine struct. in rot. spectrum 9-4958  
 2-methyl triethylenediamine (II), u.v. spectra 9-11476  
 2-methyl-9,10-anthraquinone, polarized absorption 9-19991  
 methyl-group-containing mols., hindrance pot. 9-17058  
 methylamine, condensed phases, i.r. and Raman spectra 9-10215  
 methylamine, vibr. mean amplitudes 9-7045  
 methylamine alum: Fe<sup>3+</sup>, e.p.r. rel. to spin-Hamiltonian coeffs. determ., 77°K 9-5990  
 methylbenzenes, n.m.r. and hindered rotations in solid 9-1882  
 N-methylbenzophenonimines, methyl substituted, proton NMR 9-14705  
 methylchloromethane cpds., polymorphism, and disorder of high temp. phases 9-5269  
 3-methylcholanthrene, quasi-line luminesc. and i.r. absorpt., 77°K 9-16434  
 n-methyldiazabenzene, crystal struct. 9-3320  
 methylene, B<sub>2g</sub> wagging mode in polyethylene, laser-Raman obs. 9-14063  
 methylene bromide, polarized i.r. spectrum and cryst. struct. 9-17480  
 methylene violet, anomalies in high-resolution e.p.r. 9-9272  
 methylenecyclobutane, microwave spectrum, molec. consts. 9-11493  
 4,5-methylenephenanthrene and related cpds., spect. investig. of carbanions 9-19468  
 methylethoxymethanes, vibratory spectra from i.r. absorpt. 9-11495

## Organic compounds continued

- methylglyoxal bisguanylylhydrazone dihydrochloride monohydrate, crystal and mol. structure 9-3319  
 2-methylnaphthalene-1,4-diol, crystal and mol. structure 9-21324  
 α-methylpentafluorostyrene, <sup>19</sup>F n.m.r. and mol. struct., obs. 9-12518  
 N-methylpropionamide solutions, relative viscosity and apparent molal volume 9-19620  
 methyls, <sup>13</sup>C-H spin-spin coupling const., extended Huckel calc. 9-20969  
 α-methylstyrene in glasses, radical ion and intermediates, form and assignments 9-20988  
 methyltetrahydrofuran glasses, p-irrad., spatial distrib. of trapped electrons 9-4014  
 molecules, finite chain, i.r. band freqs. rel. to length and end groups 9-15875  
 monochloroacetylene HCC<sup>35</sup>Cl and HCC<sup>37</sup>Cl, ν, band struct. and rot. 9-17045  
 monoorganosilanes, Si-H bond props., n.m.r. obs. 9-19475  
 N-methylacetamide, absorpt. spectrum, 50-300 cm<sup>-1</sup> 9-18195  
 1-naphthaldehyde, in ICl complex and free, C=O stretching freq. solvent depend. 9-15894  
 2-naphthaldehyde, phosphorescence radiationless decay proc., deuteration eff. 9-19472  
 naphthalene, cryst., vib. spectral transitions, splittings due to intermolec. forces 9-5932  
 naphthalene, current flow characts. 9-18621  
 naphthalene, elastic constants, +20 to -180°C 9-16115  
 naphthalene, energy transfer in excited electronic states 9-15880  
 naphthalene, fluoresc. decay rel. to temp and thickness, lifetimes of two Davydov-components 9-10246  
 naphthalene, ground and doubly excited states, ab initio SCF calc. 9-20951  
 naphthalene, lattice vibr. intensities, Raman obs. 9-18551  
 naphthalene, low freq. phonons near Brillouin zone boundaries 9-19854  
 naphthalene, mass transfer to air, eff. of transverse vibrations 9-21250  
 naphthalene, mltin, migration of triplet excitons from excitation region to anode 9-9533  
 naphthalene, phonon structure in emission spectra 9-18714  
 naphthalene, phosphoresc. of pure cryst. 9-1838  
 naphthalene, phosphoresc. triplet lifetime, deuterium substitution effects 9-14086  
 naphthalene, photoexcitation of triplet state, ENDOR meas. 9-7073  
 naphthalene, polarized Raman spectra of single cryst. 9-15180  
 naphthalene, SCF MO iteration calc. 9-9109  
 naphthalene, singlet excited states polarizability, obs. 9-15879  
 naphthalene, solubility in compressed ethane and N<sub>2</sub>O 9-13485  
 naphthalene, triplet formation, quantum yield, fluoresc. and phosphoresc. 9-16438  
 naphthalene cr sensitized fluoresc., temp. depend. rel. to energy transfer mechanism 9-10245  
 naphthalene derivatives, substituted, intermol. fluorescence quenching 9-20972  
 naphthalene evap. films, exciton diff. 9-7718  
 naphthalene fluoresc. in compressed polymethylmethacrylate 9-12477  
 naphthalene in anthracene, solid soln., fluorescence decay pattern 9-12471  
 naphthalene in ether. solns., pulse radiolysis, solute excited states and radicals formation 9-21728  
 naphthalene in hydrocarbon glass pulse radiolysis triplet-states yield 9-17543  
 naphthalene liq. derivatives, emission excited by electron-impact 9-9530  
 naphthalene phosphoresc., vibr. assignment 9-5967  
 naphthalene strained crystals, spectral change due to thermal deformation 9-5349  
 naphthalene bipl mixed crystals triplet-triplet annihilation kinetics, from fluoresc. and phosphoresc. obs. 9-16439  
 naphthene oil, upward and downward motion in filter paper 9-5131  
 1-naphthol, excited, H bond and level reversal 9-9519  
 naphthols, fluoresc. and π-H bonding 9-17059  
 naphthalene, phosphoresc., rel. to quinoline and 5,6-benzoquinoline, 77°K 9-15899  
 naphthalene in benzophenone crystal, triplet-triplet absorption spectra 9-9275  
 neopentylalcohol, unit cell and space group 9-16085  
 nickelocene, bonding 9-15900  
 ninhydrin, crystal structure 9-14930  
 nitriles, vibr. freqs., valence force field calc. 9-15874  
 n- nitroaniline, proton-donor effects, obs. from spectra in o-xylol 9-11698  
 o-, m- and p- nitroaniline, spectroscopic study of chelation and complex formation 9-17060  
 nitrobenzene, electro-optical Kerr effect used for fast light shutter 9-8672  
 nitrobenzene, induction of mode locking and ultrashort pulses in ruby laser 9-6523  
 nitrobenzene, laser pulse shape distortion by self-focusing 9-10871  
 nitrobenzene, pure, and in solution, dipolar interactions from elec. birefringence meas. 9-9544  
 nitrobenzene, Raman scatt., stimulated by focused low power ruby laser beam 9-5171  
 nitrobenzene derivs., σ-complexes, LCAO MO calcs. 9-11482  
 nitrobenzene in CCl<sub>4</sub>, n.m.r., effect of addition of tetra n-butylammonium salts 9-7281  
 nitrobenzene liquid, electrical conduction mechanism and electrochemical props. 9-21221  
 nitrobenzene soln. in tetrahydrofuran, e.s.r. photoinduced spectra 9-9276  
 nitrobenzene soln. in tetrahydrofuran, e.s.r. photoinduced spectra 9-11497  
 nitrobenzene-aniline complex, absorption spectra 9-17061  
 nitrobenzene-phenol complex, absorption spectra 9-17061  
 nitrogen cpds., N 1s electron binding energies correl. with CNDO charges 9-11451  
 nitromethane-hydrocarbon binary systems, demixing curves, obs. 9-10308  
 3-nitroperchlorylbenzene, crystal and mol. structure 9-3312  
 nitrosomethane, microwave spectrum, molec. struct. 9-817  
 m-nitrotoluene and its solns. in benzene, dielec. saturation, effect of hydrostatic pressure 9-5180  
 n.m.r. of four-spin systems, analysis of complex spectra 9-20918  
 non-polar liquids, Kerr eff. hyperpolarizability contrib. 9-17218  
 nucleotide 3', 5' cyclic phosphates and acetylated derivatives, n.m.r. spectra rel. to sugar struct. 9-18220  
 Nujol/water emulsions, rheological changes in aging 9-5201

**Organic compounds continued**

- octafluorocyclohexa-1,3- diene tricarbonyl crystallography and electron distribution 9-1198  
 n-octanethiol liq. dielec. props. 9-16019  
 octanol isomers, sterically hindered, intermol. association, dielec. meas. 9-19495  
 oil in diffusion pump vapour jet, mol. velocity distrib. after impact 9-20994  
 oil-in-water emulsions, globule-size distrib., by spectroturbidimetry 9-14869  
 olefin reactions with H atoms, rate const. determ. from Lyman- $\alpha$  re-emission 9-12527  
 olefins, pre-flame and ignition behaviours, effect on hexane combustion 9-14126  
 oleic acid multilayers, CO<sub>2</sub>, N<sub>2</sub> and He permeabilities, obs. 9-5415  
 p-oligophenylene series, scintillator solute, correl. between molec. struct. and luminesc. props. 9-9534  
 ophiobolin methoxybromide, crystal structure 9-7466  
 orbital calc. method, MOLKAO, applic. to reaction mechanisms and spectral obs. 9-20946  
 organic semiconductors, conductivity mechanism 9-9982  
 organotin cpds., X-ray irradi., e.s.r. investigation of radicals formed 9-7592  
 oric scintillators, fluoresc. and energy transfer rel. to high temp. 9-11702  
 orthonitrophenol crystals, melting in saturated vapour of camphor, anisotropy 9-18384  
 Osmium complexes with phenyl and pyridine ligands, exciton splittings of ligand u.v. bands 9-7981  
 oxadiazole derivatives fluoresc. solute for liq. scintillation characts. 9-16009  
 oxadiazoles fluoresc. and scintillation props. rel. to use as secondary solute 9-9535  
 oxalic acid in light and heavy water as in-pile chemical dosimeter 9-20864  
 oxalyl bromide, vapor phase absorption spectra meas., 3200-4400 9-18212  
 oxazoles, fluoresc. and scintillation props. rel. to use as secondary solute 9-9535  
 p-dimethoxybenzene, <sup>13</sup>C-H satellite NMR Patterns. rel. to couplings 9-13373  
 palladium n-propyl mercaptide, crystal structure 9-11865  
 para-azoxyanisole twist elastic const. determ. from magnetically induced liq. crystal phase transition 9-14831  
 para-bromobenzonitrile vapour, u.v. absorption, i.r., spectra obs., fundamentals assigned 9-7054  
 para-dichlorobenzene spin-orbit coupling 9-19451  
 paraffin, upward and downward motion in Filter paper 9-5131  
 paraffin channel placed against reactor shielding for det. of fast neutron flux. 9-636  
 paraffin crystals, rotational phase transition 9-3497  
 paraffin film lubricant, pressure effects on friction coeff. 9-16138  
 paraffin-water syst., mass spectrometric study of ion-mol. reaction 9-18228  
 paraffins, rheological props. 9-5416  
 pentaerythritol, crystal struct. from n.m.r. obs. 9-9690  
 pentaerythritol derivs., vibr. spectra 4000 400 cm<sup>-1</sup> 9-17053  
 pentafluorobenzene, heteronuclear double reson. 9-9278  
 pentafluorobenzene, microwave spectra, rot. const. and bond distances obtained 9-2907  
 pentafluorobenzene, n.m.r. subspectral anal. 9-15895  
 pentafluorobenzyl and pentafluorobenzylidene halides, vib. modes and freq. 9-20974  
 pentafluorophenyl cpds. of group IV elements, <sup>19</sup>F n.m.r. 9-14716  
 pentafluorotoluene, vib. spectra, assignments 9-11498  
 n-pentane, electrooptical parameters calc. from i.r. spectra absolute intensities 9-4960  
 pentane isomer fragments after electron impact, kinetic energy 9-7087  
 n-pentane-polyisobutylene soln., thermodynamics 9-21203  
 1,5-pentadienol, liquid, products produced under  $\gamma$ -radiation 9-4015  
 pentanol, angular and energy distrib. of slow neutrons 9-5141  
 1-pentene-AgBr<sub>2</sub> phase equilibria 9-21242  
 pentenoic acid, mean excitation potentials from stopping power data 9-9135  
 Pepsin, Raman Spectrum, laser induced 9-5940  
 perchlorylamide ion, normal vib. rel. to cryst. or soln. state, and effect of bond lengths 9-7046  
 perfluoro-m-xylene, n.m.r. 9-14717  
 perfluorobutane, F n.m.r. spectrum, inc. <sup>13</sup>C satellites, ref. to CF<sub>2</sub> group couplings 9-13375  
 perfluorobutane, ionization and attachment coeffs. 9-913  
 perfluorocyclobutane, vibration mean square amplitude, Coriolis const. calc. from spectra, 300°K. 9-9259  
 perfluorocyclobutene, NMR spectrum, coupling const. 9-20908  
 perfluorodimethyl-acetylene in nematic solvents, n.m.r. 9-13545  
 perfluorodimethylcyclohexane, neutron diffusion parameters, method for determ. 9-11342  
 perfluoromethylcyclohexane, gas, thermal electron attachment rates 9-3007  
 perfluorotoluene, vibrational spectra 9-20973  
 trans-perhydrotriphenylene, adducts with cyclohexane and dioxane, crystal structure 9-7465  
 trans-perhydrotriphenylene, crystal structure 9-9691  
 petroleum coke, desulphurization and struct. changes 9-7611  
 petroleum cokes, 'doublet' (001) X-ray diff. peaks rel. to closed pore vol. 9-7457  
 petroleum products, radiolysis with <sup>60</sup>Co  $\gamma$  and 19 MeV e, G values for H<sub>2</sub> and methane 9-8111  
 phenanthrene, capacitance temp. dependence, 25-79°C 9-10031  
 phenanthrene, energy transfer in excited electronic states 9-15880  
 phenanthrene, fluoresc. decay, effect of diffusion in presence of acridine 9-5178  
 phenanthrene, triplet formation, quantum yield, fluoresc. and phosphoresc. 9-16438  
 phenanthrene-biphenyl mixed crystals, triplet-triplet annihilation kinetics, from fluoresc. and phosphoresc. obs. 9-16439  
 phenanthrene in EPA, phosphoresc. rise and decay curves at 77°K 9-14087  
 phenanthrene in benzophenone crystal, triplet-triplet absorption spectra 9-9275  
 phenanthridine, crystal structure 9-16083

**Organic compounds continued**

- 2,3-phenanthro, 4,5-naphtho furan, X-ray diffraction data 9-18456  
 phenanthrene, phosphoresc., rel. to quinoline and 5,6-benzoquinoline, 77°K 9-15899  
 phenazine single crystals, photoconduction carrier generation 9-7860  
 phenidone-hydroquinone developers for astronomical use, evaluation 9-12771  
 phenol, rotational band contour of O-O band at 2750Å, computer fit 9-18213  
 phenol blue dye interaction with solid polymer study by electrochromic effect (Stark effect) 9-16419  
 phenol-benzene liq. mixture, viscosity calc. from Eyring's theory model 9-993  
 phenol-formaldehyde resin, pyrolysis, study of carbon residue 9-7319  
 phenol-formaldehyde resin carbons, contact pot. difference rel. to heat treatment temp. 9-7324  
 phenol-quinone system, i.r. spectra and intermol. interaction 9-2912  
 phenol-sulfonic cation-exchange membrane, transport numbers and ratios of tracer fluxes 9-9501  
 phenol-water system, diff. const. temp. depend., photon correlation method 9-9497  
 phenols, two-substituted, NO<sub>2</sub> group vibrs. rel. to H bond form., i.r. obs. 9-15896  
 phenon, mass transfer to air, eff. of transverse vibrations 9-21250  
 phenoxanthin mol. dielectric absorpt. parameters 9-5869  
 phenoxyl radicals in solid ion-exchange resins, inhomogeneous c.p.r. line broadening 9-829  
 phenoxyl-nitroxide biradical, ESR 9-13397  
 $\alpha$ -phenyl, viscosity, rel. to glass transition, 10<sup>1</sup>-10<sup>14</sup> poise 9-3084  
 phenyl ether-biphenyl eutectic, working fluid for Rankine cycle power conversion, thermal stability 9-3092  
 phenyl ethyl acetate, dipole moment in benzene and CCl<sub>4</sub> solns., obs. 9-796  
 2-phenyl indole solns., fluoresc., u.v. excitation 9-17214  
 2-phenyl indole solns., fluoresc. excited by fast electrons 9-17213  
 phenyl radical reactions, chem. induced dyn. nucl. polarizations 9-17222  
 phenyl salicylate, viscosity rel. to glass transition, 10<sup>1</sup>-10<sup>14</sup> poise 9-3084  
 phenyldibiphenyl methyl, calc. of electron spin density by valence bond method 9-830  
 o-phenylenediamine, for spectrophotometric determ. of Au(III) 9-12551  
 p-phenylenediamine dihydrochloride crystal structure 9-13659  
 p-phenylenediamine-chloranil, temp.-depend. g-tensor splittings 9-8035  
 phenylthiourea, inhibition of acid corrosion of Fe 9-12545  
 phospholipids, activation energy meas., 4.8 to 6.3 eV 9-12138  
 phosphor solns.  $\alpha$ -phosphoresc. rel. to activator conc. and excitation wavelength, obs. 9-16010  
 photochromic spiropyran layers, coloration by u.v. laser radiation 9-18219  
 photochromic props. of solids, applic. of apparatus for diffuse reflectance meas. 9-4525  
 phthalates, electron affinities and ioniz. potential 9-17135  
 phthalic acid diester dispersions for photographic prints, patent 9-6565  
 phthalimide in soln., fluorescence polarisation 9-3114  
 phthalimide in vitrifying solvent, limit fluorescence polarization determ. 9-16015  
 phthalimide solns., luminesc. and absorpt. rad. 9-9536  
 phthalimide unboric acid, solid soln., phosphoresc. with foreign NiCl<sub>2</sub>, KBr or KI mols. 9-7994  
 phthalocyanine, metal-free, polymorph, spectroscopic characterization 9-19736  
 phthalocyanine, metal-free single cry., transfer integrals 9-12048  
 phthalocyanine aluminium chloride solns., dimeric, decrease of transmittance in intense light flux 9-1025  
 phthalocyanine Fe(II), Mossbauer effect 9-10100  
 phthalocyanines, optical density of states 9-2914  
 picolines, combination scattering spectrum, freq. shift and line widening 9-18216  
 pigment organic pigment solns. generation intensity, calc., monochromatic excitation, calc. 9-18366  
 pitch mats. suitable for prod. of MP carbon fibres 9-8054  
 polyamino acids, helix-coil transition molecular theory 9-18225  
 polybutene, creeping flow in rectangular duct with partition 9-21158  
 polycyclic aromatic hydrocarbons, prod. in ethylene diffusion flames rel. to O<sub>2</sub> conc. in burning mixture 9-12536  
 polycyclic aromatic mols. in interstellar space, extinction curves 9-15323  
 polycyclic hydrocarbons, high-resolution n.m.r. 9-13386  
 polyethylene, B<sub>2</sub>g methylene wagging freq., laser-Raman obs. 9-14063  
 polymethine dye solns., generation, excited by Nd glass laser emission ( $\lambda$ =1.06 $\mu$ ) 9-1014  
 polypeptide, prep. and distrib. in mice 9-21989  
 p-polyphenyl and oligomers, electrical conductivity 9-9924  
 polystyrene, proton-donor effects, obs. from spectra in benzene 9-11698  
 polystyrene, cyclic foamed, for radioactive transport packaging 9-21993  
 polystyrene in cyclohexane, macromolecular solutions, critical opalescence 9-16027  
 porphyrin, degree of polarization of fluorescence depend. on emission wavelength 9-5965  
 porphyrins, intercombination transitions quantum output meas. using heavy atom effect, obs. 9-15877  
 porphyrins, optical density of states 9-2914  
 potassium alantoinate, crystal and mol. structure 9-11859  
 potassium citrates, crystallized from aqueous soln. at 25°C, crystal structure 9-19720  
 praseodymium ethyl sulphate, high resolution of crystal field lines in far i.r. 9-5862  
 praseodymium ethylsulphate, thermal resistivity mag. field dependence, 0.4-4°K, anomalies 9-13811  
 proline, aqueous, and hydroxyproline solns., dielec. dispersion obs., 80-2000 MHz 9-19639  
 propaga, gas, electron drift velocities 9-17166  
 propane, electron impact spectrum 9-9265  
 propane, electrooptical parameters calc. from i.r. spectra absolute intensities 9-4960  
 propane, internal rotation, quantum-mech. calc. 9-2915  
 propane, photolysis at 1470 Å, pressure effects 9-16498  
 propane, pyrolysis below 500°C, propyl radical isomerization 9-1900  
 propane, superexcited, decomposition primary modes 9-21723  
 propane-butane-N<sub>2</sub>O flame for atomic absorpt. spectroscopy 9-10944  
 propane-oxygen flames, electric breakdown 9-933



**Organic compounds continued**

- $\beta$ -propiolactone, i.r. and Raman spectra, ring-puckering vib. and potential functions determ. 9-20957
- propionaldehyde, gas phase slow combustion 155° to 220°C, study of rate and products 9-10333
- propionaldehyde, liq.,  $\gamma$  radiolysis 9-14139
- propionamide,  $\gamma$ -irrad., free radical reactions with O<sub>2</sub> and SO<sub>2</sub> 9-12538
- propionamide, X-irradiated, e.s.r. spectra of free radicals 9-9294
- propionitrile, vibrational spectra 9-20975
- propylene bombarded by <sup>1</sup>H, H ejected, C-H bond dissociation energy calc. 9-20064
- propyne, photoionization 9-9403
- purine nucleotides,  $\gamma$  irrads. effects 9-11718
- purines, 2-, 6- and 8-substituted, electronic structure and spectra, SCF MO CI calcs. 9-9280
- purity determination by n.m.r. 9-21733
- pyrazine, far-i.r. lattice vibr. 9-1363
- pyrazine, radical anion in liq. NH<sub>3</sub>, e.p.r. spectrum obs. 9-7276
- pyrazine, triplet-singlet transitions 9-15871
- pyrazine, vapour phase luminescence 9-15898
- pyrazine phosphorescent state, ESR and non-bonding orbitals 9-14719
- pyrazolines, fluoresce. and scintillation props. rel. to use as secondary solute 9-9535
- pyrene, excimer, fluorescence yield and lifetime in solution and crystalline form 9-15897
- pyrene cry. and soln., excimer-excimer interac. 9-11479
- pyrene crystals, excimer interaction potential from fluorescence spectra, 4-353°K 9-1834
- pyrene crystals., intrinsic photocond. 9-5771
- pyrene in cyclohexane, radiation-induced fluorescence, elec. field effects 9-18765
- pyrene in soln., excimer formation and saturation obs. 9-11701
- pyrene trapped in methylcyclopentane, fluorescence spectrum at 88°K 9-17490
- pyrene-*h*<sub>10</sub> and -*d*<sub>10</sub>, intersystem crossing, temp. depend. of rate const. 9-14718
- pyrene-N,N-dimethylaniline Heteroexcimer, mol. electronic structure 9-13389
- pyridazine oriented in a nematic phase, NMR studies 9-18371
- pyridine\* o-cresol, molecular complex formation due to H-bonding dielec. const var. 9-5744
- pyridine, criticism of existing photochem. data 9-16496
- pyridine, induced Raman scatt., effects of dissolved subst. 9-3109
- pyridine, radical anion in liq. NH<sub>3</sub>, e.p.r. spectrum obs. 9-7276
- pyridine and water in CCl<sub>4</sub>, i.r. spectra obs. 9-20976
- pyridine oriented in a nematic phase, NMR studies 9-18371
- pyridines, monosubstituted, CNDO calc. 9-7052
- pyrimidine, radical anion in liq. NH<sub>3</sub>, e.p.r. spectrum obs. 9-7276
- pyrimidine, vapour phase luminescence 9-15898
- pyrimidine nucleotides,  $\gamma$  irrads. effects 9-11718
- pyrrole; intensity, depolarization, width of Raman line obs. in liquid, 30±5°C 9-4963
- pyrrole between polyethylene supports, surface forces and i.r. determ of interfacial region thickness 9-13515
- quaternary ammonium bromide aq. solns., <sup>79</sup>Br NQR 9-19647
- p-quaterphenyl, single crystal, polarized i.r. absorpt. spectra, comparison with spectra of soln. 9-19992
- quinol hydrogen cyanide clathrate, phase transition 9-1578
- quinoline, phosphoresc. rel. to  $\pi$  transitions and N effects on mol. levels, 77°K 9-15899
- quinoxaline, optical pumping in durenne cryst. 9-5968
- quinoxaline, vibronic spin-orbit interactions 9-9281
- quinuclidine, electronic struct. and spectra 9-2918
- quinuclidine (III), u.v. spectra 9-11476
- R-ethyl and normal propyl, polynuclear metal complex vib. spectra obs. 9-11455
- rare earth ethyl sulphates, mol. normal coordinates, tables 9-795
- rauvoxinine, absolute config. 9-16086
- resin, ion-exchange, heat and  $\gamma$  irrads. effects 9-6021
- resin, low-temp. fatigue characteristics 9-11939
- rhenium thiocyanate complexes and exchanges, activation energy determ. 9-8052
- rhodamine, cooled alcohol solns. laser action 9-2378
- rhodamine-B films, semicond., linear and quadratic recombination of photo-carriers 9-12213
- D-ribose, dihedral angles and coupling consts. 9-18220
- rubber cylinders, surface strain distrib. under shear 9-7538
- rubrene, triplet-triplet fluoresc. in soln. 9-3115
- ruthenium triacetylacetonate, mag. anisotropy 9-21566
- salal, crystal surface temp. under unidirectional cooling 9-18424
- salicylic acid, phosphoresc. polarization and triplet level energy transfer 9-1836
- salicylic acid, epitaxy on muscovite 9-1159
- salicylic acids, substituted, intramol. H-bonding in lowest excited singlet states 9-19474
- salol films, structure control during growth process from supersaturated condensate current 9-1103
- samarium dibenzoylmetanate, luminescence props. 9-16016
- sarcosine hydrochloride, crystal structure 9-11866
- scintillators with an impurity for measuring the power of  $\gamma$ -radiation dose 9-8935
- semiconductor dye films, photoconductivity spectra, polarization changes and external field effects 9-1616
- semiconductors, kinetic transport coeff. theory, weak-field magnetoresistance approximation 9-21508
- semiconductors, pre-exponential factor 9-13888
- semicond., long-range e.p.r. coupling consts. calc. 9-14720
- semiquinones, fluorinated, anion radicals, e.s.r. spectra 9-4971
- silacyclopent-3-ene, far i.r. spectra and ring puckering 9-20977
- silicate decomposition in low-temp SiO<sub>2</sub> film deposition 9-18405
- sodium caprylate-decanol-water system, n.m.r. relax. of <sup>23</sup>Na in different phases 9-5191
- sodium carboxymethylcellulose, aqueous soln., thermal cond. rel. to displacement vel. 9-9506
- sodium citrates, crystallized from aqueous soln. at 25°C, crystal structure 9-19720
- sodium D-tartrate dihydrate, crystal and molecular structure 9-7464
- sodium humate solns., structure determ. from small angle X-ray scatt. 9-9480
- sodium hydrogen fumarate, crystal structure determ. 9-18457

**Organic compounds continued**

- sodium lauryl sulphate, black film, contact angles with bulk liq., and expansion kinetics 9-19602
- sodium methanesulphonate, vibr. spectra 9-18218
- sodium 2-oxalate, polytypism 9-3226
- soils, removal by oxidation, effect of catalyst bearing porcelain enamels 9-1910
- solvent binary mixture, dielec. constant rel. to solubility of alkali halide 9-14834
- spiropyran layers, photochromic, coloration by u.v. laser radiation 9-18219
- starch granules, light scatt. rel. to fluctuations in anisotropy 9-15167
- stearate multilayers, CO<sub>2</sub>, N<sub>2</sub> and He permeabilities, obs. 9-5415
- stilbene, absorpt. and fluorescence spectra 9-4961
- stilbene, lowest triplet state by absorption spectrum 9-19476
- stilbene, Raman spectra cross sections, temp. depend. 9-12428
- strontium tartrate trihydrate, crystal and mol. structure 9-19737
- styrene, rad.-induced graft copolymerization on to poly(vinyl alcohol) 9-14130
- styrylstilbene, absorpt. and fluorescence spectra 9-4961
- sugar, e.s.r. intensity and temp. studies rel. to heat treatment and A centres 9-8022
- sugar coke, heat treated from 400 to 3000°C, pore development, graphite and turbostratic C 9-7358
- sulphonamides, NH valency vibrations, temp. depend. 9-797
- sulphonyl chlorides, aromatic, substituted, SO<sub>2</sub> antisymmetric stretching vibr. band, i.r. obs. 9-15876
- tarrates, i.r. absorpt. spectra in thin crystal textures, temp. dependence, -195 to 51°C 9-1803
- TCNQ complex salts, energy levels of triplet excitons by ESR 9-19883
- terephthalic acid, aldehyde and acid chloride, absorpt. and luminesc. spectra 9-801
- terpenoid, C<sub>25</sub>, ophiobolin methoxybromide, crystal structure 9-7466
- o-, m- and p-terphenyl, far u.v. spectra 9-818
- p-terphenyl, single crystal, polarized i.r. absorpt. spectra, comparison with spectra of soln. 9-19992
- tetra  $\alpha$ -pico M-fluoborates, (M=Ni, Co, Zn or Cd), X-ray diffraction data 9-18456
- tetra-n-butylammonium salts, addition to nitrobenzene, effect on n.m.r. 9-7281
- tetra cyanoquinodimethane derivatives, e.p.r. and thermal conductivity rel. to moving excited states 9-12505
- tetra-n-butyl ammonium fluoride clathrate hydrate, n.m.r. 9-14117
- tetra-n-butyl ammonium fluoride clathrate hydrate n.m.r. 9-14117
- tetra-n-butyl ammonium picrate soln., dielec. dispersion 9-1038
- tetrabromoethane-tetrachloroethane solns. thermal diffusion 9-9498
- tetrabromomethane, polymorphous transition from crystalline to rotational state 9-21414
- tetracene, bimolecular radiationless transitions of excitons as fluorescence quenching channel 9-14085
- tetrachloroethylene, bond length changes on ioniz., mechanisms 9-20916
- tetracyanoquinodimethane-phenazine complex, conduction mechanism 9-18599
- tetraethylammonium iodide,  $\gamma$ -irradiated, e.s.r. study 9-20978
- tetrahalo p-benzoquinone complexes with aromatic amines, vibr. struct. 9-14721
- tetrahydronaphthalene frozen soln., EPR spectra temp. depend after  $\gamma$  rad. 9-8034
- tetrahydroprotoberberine alkaloids, mass spectra and n.m.r. 9-19477
- tetrakis (2-fluoro-1,3,2-benzodioxaphosphole) Ni(0), theory of n.m.r. spectrum 9-17024
- tetramethylammonium sulphate tetrahydrate, cryst. struct. 9-16087
- tetramethylbenzene, phase transition 9-1882
- tetramethylbenzenes, solid-state photolysis, radical form. 9-21722
- 2,2,6,6-tetramethyl-4-hydroxypiperidine-1-oxyl, mag. props., 1.8°K to 300°K 9-10115
- tetraphenyl tin, Mossbauer study of reactor radiation eff. 9-5582
- tetravinyl derivatives of group IVB elements, proton magnetic resonance spectra 9-20945
- s-tetrazine, 5515 Å band, high resolution study 9-13390
- S-tetrazine (d<sub>0</sub> and d<sub>2</sub>), i.r. and Raman spectra rel. to vib. freqs. 9-11500
- thianthren mol. dielectric absorpt. parameters 9-5869
- thioacetanilide-S-oxide, crystal and mol. structure 9-13662
- thioglycolic acid, ion formation in X-irrad. cryst., e.s.r. 9-15202
- 2-thiohydantoin, crystal structure 9-13661
- thiophene; intensity, depolarization, width of Raman line obs. in liquid, 30±5°C 9-4963
- thiophene, n.m.r. spectra 9-20979
- thiophene liq. phase, Raman spectra 9-3110
- thiophene derivatives, vibration deformation frequencies, effect of solvents 9-821
- thiosemicarbazide, crystal and mol. structure 9-13663
- thiourea aq. solns., surface reaction with Sn 9-21702
- thiourea ionic complexes, Madelung energy 9-9633
- thiourea nitrate, crystal structure 9-7454
- thorium acetate, cryst. struct. and isomorphism 9-14932
- thulium ethyl sulphate, <sup>199</sup>Tm 9-1879
- thulium ethyl sulphate, p.n.r. spectra 9-15206
- thunbergene, crystal and mol. structure 9-13650
- thymine frozen soln., dimer formation 9-9297
- thymine photodimer E, crystal and mol. structure 9-14933
- titanium-aluminium acetylacetonate, mixed cryst., spin-lattice relax. 9-16386
- tolan phase in tolan-diphenylmercury system, mol. packing from X-ray structural analysis 9-1200
- O-tolidine, crystal structure 9-3317
- tolualdehydes, isomeric, liq. i.r. absorpt. spectra 9-9520
- o-, m-, p-tolualdehydes in liquid phase, vibrational spectra, assignments of freq. 9-11501
- toluene, Brillouin line widths, using laser and interferometer 9-9521
- toluene, criticism of existing photochem. data 9-16496
- toluene, energy transfer in excited electronic states 9-15880
- toluene, gas, ion-mol. react 9-17078
- toluene, proton n.m.r. anal. 9-9284
- toluene, ultrasonic absorption 9-153
- toluene base scintillator solns, quenching props. of alcohols 9-9528
- toluene solns., luminesc. and triplet-triplet transfer to chelates through an intermediary 9-1032
- toluene vapour, electronic energy relax. 9-9283
- toluene vapour, thermal cond. at various temp. 9-21135

**Organic compounds continued**

- triacylbenzene soln., absorpt. and luminesc. spectra 9-801  
 s- triazine, mol. bonds, X-ray and n. diff. obs. 9-11502  
 1,2,4-triazole, crystal and mol. structure at  $-160^{\circ}\text{C}$ , refinement 9-13665  
 triphenyl methyl, calc. of electron spin density by valence bond method 9-830  
 tricarboxylatostannates (II), i.r. spectra assignment of skeletal vib. 9-14722  
 1,2,4-trichlorobenzene, crystal surface temp. under unidirectional cooling 9-18424  
 trichloroethylene, u.v. absorption spectrum, nature of transitions 9-20956  
 trichloromethyl cyanide, intermolec. interactions and isotope struct. of Raman bands 9-7266  
 trichloromethyl fluoride, intermolec. interactions and isotope struct. of Raman bands 9-7266  
 triethylenediamine, electronic struct. and spectra 9-2918  
 triethylenediamine (I), u.v. spectra 9-11476  
 triethylphosphine selenide, i.r. and Raman spectra, fundamental vibrations assignment 9-18204  
 triethylphosphine sulfide, i.r. and Raman spectra, fundamental vibrations assignment 9-18204  
 trifluoromethyl halides, photoioniz., mass spect. study 9-18206  
 trifluoromethylfluorophosphorane, i.r. spectrum and molec. struct. 9-2916  
 $\alpha$ ,  $\beta$ ,  $\gamma$ -trifluorostyrene dimers,  $^{19}\text{F}$  N.M.R. and mol. struct. obs. 9-12518  
 triglycine selenate, deuterated, dielectric properties 9-1136  
 triglycine selenate, high temp. structural transitions 9-13920  
 triglycine selenate, pyroelec. props. 9-13923  
 triglycine sulphate: vandy, switching effect obs. by e.p.r. 9-3713  
 triglycine sulphate,  $180^{\circ}$  domains, topography of deformation, nucleation and growth 9-16301  
 triglycine sulphate, domain structure, e. microscope exam. of elec. decorated surfaces 9-1599  
 triglycine sulphate, ferroelec. phase transition, high pressure and elec. fields effects 9-1598  
 triglycine sulphate, ferroelectric domain switching induced temp. instabilities 9-21541  
 triglycine sulphate, high temp. structural transitions 9-13920  
 triglycine sulphate, i.f. Raman spectra near Curie point 9-1808  
 triglycine sulphate, second harmonic generation and nonlinear polarizabilities 9-1724  
 triglycine sulphate, u.s. relax., absorpt., anisotropy 9-3524  
 triglycine sulphate cryst., dielec. const., role of surface layers 9-5753  
 triglycine sulphate crystals, dielec. props., effect of growth conditions 9-10050  
 triglycine sulphate crystals, permittivity, temp. hysteresis 9-10052  
 triglycine sulphate type, optical indicatrix tensor orientation, high temp. 9-21540  
 trimelic acid crystal structure 9-13664  
 trimethylamine, molec. struct. bond lengths and angles, electron diff. study 9-18210  
 trimethylamine -  $\text{H}_2$ ,  $\text{D}_3$ , Coriolis coupling coeff. for degenerate vib. assignments and amp., valence force field calc. 9-20980  
 trimethylene oxide, i.r. abs. and Raman scattering spectra 9-17483  
 trimethylethoxysilane, vibratory spectra from i.r. absorpt. 9-11495  
 2, 2, 4-trimethylpentane, ads. on  $p\text{-Al}_2\text{O}_3$ , ads. energy 9-7344  
 trimethylphosphinoallylnickel (II) chloride, bonding, phys. and chem. predictions 9-19469  
 trinitrene, septet ground state, e.p.r. detect. 9-2917  
 trinitrobenzene soln. in tetrahydrofuran, e.s.r. photoinduced spectra 9-11497  
 trinitrobenzene soln. in tetrahydrofuran, e.s.r. photoinduced spectra 9-9276  
 2,4,6-trinitrophenolate-caesium (potassium) ethoxide complexes, (Meisenheimer salts), crystal and mil. structure 9-7467  
 8m59/15/1 9-4965  
 triphenylcarbonium ions, n.m.r. of  $^{19}\text{F}$ , conformational equilibrium and interconversion 9-19473  
 triphenylcyclopropenium cation, charge densitiw meas. from  $^{13}\text{C}$  NMR shifts 9-13388  
 triphenylene, electronic spectra using 'mol. in mol.' method 9-18214  
 triphenylvinyl derivatives of group IVB elements, proton magnetic resonance spectra 9-20945  
 Tropolone derivatives, N.M.R. spectra 9-19478  
 tryptaflavine radical in soln. absorption band spectra detection, 380 nm 9-9285  
 twisted C-C double bond, optical activity meas., electronic structure proposal 9-9274  
 unsaturated mols., Pariser-Par-Pople model 9-743  
 Uranin, aggregate fluorescence obs. 9-1033  
 uranin, emission and absorpt. spectra rel. to species, 80 and  $300^{\circ}\text{K}$  9-1034  
 uranin soln. containing KI, polarization of fluorescence 9-9537  
 uranium(IV) acetate, cryst. struct. and isomorphism 9-14932  
 uranyl-EDTA complex, emission spectra obs. 9-14723  
 urea, crystal lattice vibrations 9-17351  
 urea, interatomic distances and thermal motion 9-13391  
 ureas, symmetric substituted, unit cells and space groups 9-7468  
 valence freq. var. in vap. liq. transition of diat. groups 9-7040  
 D,L-valine, crystal structure 9-13666  
 vanadocene, bonding 9-15900  
 vanadocene molecular orbital calc. of e.s.r. spectrum,  $\Sigma$  and  $\pi$  e delocalisation mdel consideration 9-7072  
 vinyl chloride, fundamental wave number assignment, by normal co-ord. treatment 9-13392  
 vinyl chloride, wavefunction calc., approx., by semiempirical  $\Pi$ -electron methods 9-13393  
 vinyl esters vibrational spectra, freq. and intensities determ. 9-9287  
 vinyl oleate, radiation-induced polymerization, phase transition in liq. cry. or cry. state 9-14734  
 9-vinylanthracene, free radical copolymerization 9-20038  
 viscose, and stable derivatives, ultraviolet spectra 9-14852  
 viscosity at constant pressure, temp. depend. 9-14839  
 vitamin C, crystal structure from n. diff. analysis 9-19727  
 Wursters red bromide, crystal structure 9-7460  
 xanthyl radicals, spin densities, unrestricted Hartree-Fock calc. 9-11506  
 xylene, aniline liquid mixture, u.s. vel., absorption, compressibility meas. 9-3097  
 p-(o)-xylene, Brillouin line widths, using laser and interferometer 9-9521  
 o-xylene, criticism of existing photochem. data 9-16496

**Organic compounds continued**

- para-xylene, crystal surface temp. under unidirectional cooling 9-18424  
 p-xylene, fluoresc. in cyclohexane, aggregation effects 9-2556  
 p-xylene, fluoresc. in cyclohexane, quenching by  $\text{O}_2$  and  $\text{CCl}_4$  9-3112  
 xylenes, gas, ion-mol. react. 9-17078  
 o-, m-, p- xylenes, proton reson. study of methyl groups substitutions, effs. and reorient. 9-14724  
 p-xytol solns., with trans-stilbene and diphenyloxazole, luminesc. and quenching 9-3113  
 zinc acetate dihydrate, H bonding scheme investing by PMR 9-1121  
 zinc methacrylate, postirradiation polymerization 9-21691  
 acetone-water mixture, rel. to relax. of conc. fluctuations 9-5167  
 (90wt.%)Ar-(10wt.%) $\text{C}_4\text{H}_{10}$  proportional counter gas, pulse shape calcs. 9-19228  
 C-H in tetrahedrally hybridized carbons, deuterium substition eff. on  $^{13}\text{C}$  coupling const. 9-17043  
 $\text{C}_2\text{H}_2$  ionization by low-energy heavy ions 9-904  
 $\text{C}_2\text{H}_4$  ionization by low-energy heavy ions 9-904  
 $\text{C}_2\text{H}_5\text{O}^+$  ion in mass spectra of Z-alkanols, struct. 9-15885  
 $^{13}\text{C}$  n.m.r. obs. 9-18746  
 CBR- reaction with alkali-metal atoms 9-810  
 $\text{CCl}_4$ - cyclohexane liq. mixture, viscosity calc. from Eyring's theory model 9-993  
 $\text{CCl}_4$ , He-Ne laser beam induced index change associated with thermal blooming, interferometric observation 9-18361  
 $\text{CCl}_3$  group bound to benzene ring, torsional vib. freq. determ. from NQR obs. 9-4951  
 $\text{CCl}_4$ , Jahn-Teller eff. and Raman spectra obs., mol. symmetry calc. 9-4950  
 $\text{CCl}_3\text{CCl}_2\text{CCl}_3$ , n.q.r. spectrum, liq. air temp. 9-3977  
 $\text{CF}_3\text{CCl}_3$ , microwave spectrum, struct. and internal rot. 9-15888  
 $\text{CF}_3\text{COOH}$ - $\text{HCOOH}$ , K splitting obs. linewidth determ. 9-19463  
 $\text{CF}_3\text{OF}$ , i.r. and Raman spectra obs., freq. assignments, thermodynamic props. calc. 9-19465  
 $\text{CH}_3^+$  ion, geometry investig., CNDO method 9-19461  
 CH bond moments of aromatic hydrocarbons, depend. on bond angle 9-7069  
 CH mol., interstellar, photodissociation mechanism 9-18880  
 $^{12}\text{CH}$  molecule, Franck-Condon factor and r-centroids for C-X band system 9-7058  
 $\text{C}_2\text{H}_4$ , slow electron drift velocity 9-3011  
 carbon tetrachloride, Cl KLL Auger spectrum obs. 9-14668  
 Cu-8-hydroxyquinolate substituted in phthalimide, ligand ENDOR 9-10302  
 I<sub>2</sub>-gasoline vapour mixture, ice nuclei prod. 9-9595  
 K ferrioxalate reduction, oxidation processes, u.s. wave instigated 9-6025  
 methane-Ar mixture, thermalization times of positrons 9-15974  
 methyltribromosilane, microwave spectra, 30-40 GHz 9-10230  
 Na bentonite amine complexes,  $\text{H}_2\text{O}$  vapour and methanol adsorpt., hydrophilic hydrophobic props., obs. 9-5261  
 Na stearate -19.7 to 35.7%  $\text{H}_2\text{O}$ , creep rel. to struct.,  $5-60^{\circ}\text{C}$  9-5470  
 $\text{O}(\text{P})+\text{CS}_2\rightarrow\text{SO}+\text{CS}$ , product vibr. energy, expt. and computation 9-10327  
 Sb, Mossbauer eff., isomeric chem. shift 9-3874  
 Si phenyls, n.m.r. spectra obs., bonding studied 9-11499  
 stilbene, liq. and cryst., combination light scatt., absolute cross-sections 9-1732  
 VO tartrate chelates, triplet state e.s.r. in aq. soln. 9-7277
- Organometallic compounds** see Under appropriate metal compound heading
- Orthicons** see Electron tubes
- Oscillations**  
 See also Electromagnetic oscillations; Liquid oscillations; Piezoelectric oscillations; Vibrations  
 acoustic, review 9-13793  
 atomic oscillator strengths, systematic trends in isoelectronic sequences 9-19388  
 axisymmetrical flutter of circular cylindrical shells of finite length 9-17785  
 conservative syst., dissipative, time-translational invar., lagrangian eqn. 9-2187  
 crystals, impurity spectra, and broadening of phonon-free lines 9-7961  
 damping, necessary and sufficient, for second-order oscillator 9-20375  
 elastomer, stress due to sinusoidal oscillations superposed on finite strain 9-19052  
 excitation in non-linear medium by modulated current 9-7148  
 finite, in curvilinearly aeolotropic elastic cylinders 9-8489  
 fluid in spherical cavity, non-linear acoustic oscill., soln. 9-18247  
 flute, long-tone relative SPL and harmonic struct. 9-10737  
 due to friction, dry, anal. 9-14382  
 Gunn effect, explanatory account 9-5683  
 high-order sub-harmonics in optical range, generation 9-4385  
 impacting devices, general characts. by study of two-rod device 9-12926  
 n-InSb, current, highly sensitive to magnetic field 9-15092  
 ion-sound, from decay of longit. plasma oscillations 9-3000  
 l.f., in n-GaAs Gunn diodes, mag. field effect 9-5737  
 linearly damped harmonic, time-translational invar., Lagrangian eqn. 9-2187  
 liquid film, thick, viscous, undergravity 9-21002  
 LSA mode 9-5684  
 magnetic, transformation into elastic waves in antiferromagnets 9-1693  
 magnetostriictively induced longit., e.m. aspect 9-13958  
 mechanical, excitation, resonant and nonresonant case 9-146  
 mechanical, thin sheets, decay time constants 9-19044  
 mechanical, third-order, oscillator motion and solns. 9-19048  
 mechanics, from any constant of the motion, an invariance generator may be obtained from its first derivatives 9-8466  
 nonlinear, general systems 9-6352  
 optical third, phase-matched, generation in anomalously dispersive liq. 9-21205  
 perpendicular motions, compounding 9-15446  
 of polytropes, non radial adiabatic pulsations, mode obs. 9-15287  
 polytropic compressible cylinder stellar models, eff. of rot. 9-18847  
 quartz crystal, of 285.7 kHz, detection methods 9-15459  
 reflex klystron, study of initiation 9-2350  
 resonant forced non-linear oscillatory and rotary motions 9-2188  
 resonators, parametrically-coupled, self-excitation in optical range 9-4457  
 of self-gravitating masses, oscill. and stability in axial mag. field 9-17624  
 simple harmonic, forced and coupled, book 9-10716  
 sphere, gravitating, and vel. field, soln. 9-18235



**Oscillances continued**

- stability of time-periodic azimuthal flows between coaxial, circular cylinders 9-17087  
 of stars, eff. of rot., polytropic compressible cylinders 9-18847  
 string, nonlinear vib., equivalence to gas motion 9-17786  
 of undamped non-linear spring mass syst. subjected to const. force excitation, transient response 9-19049  
 uniform distribution theory application and its modification 9-145  
 Al, Sondheimer, in elec. resistivity, meas. and interpret. 9-7745  
 Cd (II), efficient CW laser, at 4416 Å 9-6530  
 CdS, rippled, in transient of first current saturation, round trip period 9-11995  
 GaAs, photoexcited high-resistivity, current, and high-field domains 9-12210  
 Si p-i-n junction diodes, relaxation, avalanche induced, computer calcs. 9-16281

**Oscillators**

- cantilever beam, visco-elastic, transverse oscs. rel. to solid viscosities and dynamic load factors 9-4280  
 fluids, viscous, non-homogeneous, in container, decay 9-18248  
 Gunn effect, two domain transit 9-1560  
 Josephson, quantum mechanical theory including noise 9-12119  
 lightly damped, applic. of series soln. of first-passage problem in random vib. 9-17731  
 multivibrator for optoelectrical oscillations based on semiconductor laser and photodiode 9-3669  
 optical, parametric, tunable 9-14025  
 oscillator-detector circuit for programmed laboratory sequencers 9-10790  
 parametric resonance apparatus for teaching demonstrations 9-10715  
 pulsed, interrupted wave synchronization 9-2302  
 quantum statistics of reservoir coupled driven oscillators 9-10656  
 quartz crystal, appl. to cathode sublimation meas. 9-3755  
 quartz crystal as film thickness monitor during deposition 9-11764  
 semiconductor microwave, generalization of theory 9-5715  
 GaAs, microwave instabilities 9-10006  
 n-GaAs Gunn, sheet-type, reduced domain build-up 9-10023  
<sup>85</sup>Rb regenerative maser, freq. stability 9-15505

**Oscillator effect** *see Semiconductors*

**Oscillators** *see Semiconducting devices*

**Oscillographs** *see Electrical measurement*

**Oseen method** *see Flow; Hydrodynamics*

**Osmium**

- Os<sup>4+</sup>, optical spectra in cubic crystals at 4.2°K 9-14055

**Osmium compounds**

- No entries

**Osmosis**

- bacteria in salt soln., vol. changes, study by light scatt. 9-14867  
 binary soln., thermodynamic eqns. 9-9499  
 cellulose acetate membrane-saline soln., reverse effect of surfactant layer at interface 9-9502  
 molal and isopiestic coeff., salting out capacity of soln. 9-17202  
 osmotic jump phenom., membrane swelling 9-17203  
 reverse osmosis, mass transfer coeffs. for process design 9-18356  
 transient electro-osmosis in capillary tubes 9-13517  
 H<sub>2</sub>O-KCl-CaCl<sub>2</sub> soln., osmotic coeffs. 9-21187  
<sup>3</sup>He in <sup>4</sup>He, dil. solns., osmotic pressure, theory 9-9574  
<sup>3</sup>He in <sup>4</sup>He, dilute solns., pressure, effect of mag. field 9-11730

**Overhauser effect** *see Nuclear magnetic resonance and relaxation*

**Oxidation**

- catalysts for waste gas purification, patent 9-20043  
 chlorophyll-a and I<sub>2</sub> in methanol soln., photochemistry 9-18974  
 ethylene-propylene copolymers, oxidation with hexavalent Cr cpds. 9-17531  
 graphite, boronated, effect of B<sub>2</sub>O<sub>3</sub> formation on rate 9-8093  
 graphite, boronated, influence of struct. faults 9-8094  
 graphite, by high temp. water vapour, initial stages and activation energy 9-8095  
 graphite, catalytic, showing mosaic characts. 9-7497  
 graphite, in CO<sub>2</sub> and O<sub>2</sub>/Ar mixtures, at 1500-3000°K, compared with vitreous C 9-8091  
 graphite, mass transfer due to unsteady state conditions 9-8089  
 graphite, nuclear, porosity changes under thermal and radiolytic oxidations 9-7408  
 graphite, purified, influence of pre-irrad. on rates 9-8086  
 graphite, radiolytic oxidation resistance by surface complexes formed during irradi. in CO<sub>2</sub>/CH<sub>4</sub> mixtures 9-8065  
 graphite, radiolytically, stability of surface complexes compared with thermal oxidation 9-8087  
 graphite, resistance increased by transpiration cooling, composite tech. and coating 9-10339  
 graphite, resistance rel. to B content and heat-treatment temp. 9-7608  
 graphite, vertical channel, along bore, effect of in-pore mass transport 9-8090  
 graphite spheron 6, surface complexes formed by contact with air at high temp. 9-8088  
 hematite, reduction rate of dense sphere by hydrogen, mathematical model 9-20046  
 hydrocarbons, chemi-ionization, electron cyclotron reson. 9-3999  
 hydrogen, gas-phase, elementary reaction steps 9-21692  
 kinetics, rel. to vacancy generation 9-12541  
 magnetites, low temp. mechanism 9-15220  
 metal, controlled by surface reaction, logarithmic law 9-14131  
 metals, kinetics investigation 9-10338  
 metals, kinetics rel. to electronic and ionic diffusion in large surface-charge and space-charge fields 9-9620  
 mica oxidation zone 9-1911  
 oxydo-reduction reactions and homogeneous electron transfer 9-20042  
 photoelectric metallic surface properties change 9-5760  
 refractory metals and alloys, retardation by Li<sub>2</sub>O presence 9-3994  
 soil removal, effect of catalyst bearing porcelain enamels 9-1910  
 state in rocks rel. polarity reversal 9-18819  
 steel, austenitic, in CO<sub>2</sub>, thermal cycling effects 9-17528  
 steel, mild, effect of air speed 9-21694  
 steels, hot-rolled electro-technical, structures of reduced oxide films 9-6012  
 trans-Uranium elements, unexpected oxid. state, relative stability, rel. to spectroscopic factors and phenom. baricenter pot. 9-12542

**Oxidation continued**

- water, light and heavy, by peroxydisulphate, rate const. and kinetic isotope eff. obs. 9-18756  
 Z=126(IV) state, relative stability, rel. to spectroscopic factors and phenom. baricenter pot. 9-12542  
 Al-CuO, on sintering 9-3463  
 Al, anodic, and growth and struct. of Al<sub>2</sub>O<sub>3</sub> layers formed 9-4004  
 Al films, effect of oxide thickness 9-18754  
 BN and BN composite, and compatibility, ≤2000°C 9-3995  
 Be in water vapour, 600-800°C blistering and film break away obs. 9-6011  
 C, by atomic O, amounts of surface oxide formed from 0-400°C, temp. depend. 9-8097  
 C, by chemisorpt. of dry O<sub>2</sub> and acidic, basic surface complexes 9-8080  
 C, in CO<sub>2</sub>, rate effects of C struct, temp. impurities etc. on oxide 9-8096  
 C, vitreous, in CO<sub>2</sub> and O<sub>2</sub>/Ar mixtures, at 1500 to 3000°K, compared with graphite 9-8091  
 C black, effect on metallic salts on surface 9-8092  
 C spheres, extent and depth of internal burning, expt. tech. 9-8075  
 Ca, reaction mechanisms 9-10340  
 Cu-Ni alloys and scale formation 9-21693  
 Cu-Zr alloys by CO<sub>2</sub>, resistance behaviour 9-20049  
 Cu, effect of small Li addition on rate at room temp. 9-3996  
 Cu, influence of cryst. orientation 9-12543  
 Cu, rate at room temp., eff. of applied elec. current 9-15224  
 Fe-Al alloys, in CO<sub>2</sub>, composition and temp. dependence 9-14132  
 Fe-Cr-Al-Y alloys, struct. and composition of oxide film formed in CO<sub>2</sub> 9-11779  
 Fe-Cr-Mn alloy, structure effect 9-5503  
 Fe-(18 wt.%)Cr, alloy, increased due to Ni additions, 1123°K 9-20045  
 Fe-Cr alloys, and spalling, hot stage microscope obs. 9-18755  
 Fe-Cr alloys, kinetics 9-20044  
 Fe-Ge alloy, high-temp. study 9-6013  
 Fe-Si alloy crystals, kinetics, optical exam. 9-21277  
 Fe-Si alloy crystals, oxide film structure 9-21278  
 Fe, high temp. electron diffraction studies 9-10823  
 Fe<sub>2</sub>O<sub>3</sub>-Cr<sub>2</sub>O<sub>3</sub> solid solutions, reduction behaviour at high temp. 9-17332  
 Fe(OH)<sub>2</sub> colloid, Cu(II) effects, obs. 9-6014  
 HCl gas, in microwave discharge 9-3035  
 Ir, field ion specimens, structure of oxide film 9-21280  
 K<sub>2</sub>[Fe(C<sub>2</sub>O<sub>4</sub>)<sub>2</sub>] u.s. wave instigated 9-6025  
 Mg foil, growth of dislocation loops 9-18471  
 Mn<sub>2</sub>O<sub>7</sub>, value as oxidizing agent 9-6006  
 Mo oxidation zone 9-1911  
 Nb-Zr alloys by CO<sub>2</sub>, resistance behaviour 9-20050  
 Nb alloys with improved oxidation-resistance 9-13770  
 Ni-Cr dilute alloy, mechanism 9-20047  
 Ni (110) surface, with O monolayer, incipient oxidation on further exposure to O<sub>2</sub> 9-12544  
 Ni(20wt.%)Cr wires of different lifetimes 9-21695  
 NiSO<sub>4</sub>/(NH<sub>4</sub>)<sub>2</sub>SO<sub>4</sub> soln., H gas reduction, effect of surface active agent 9-18757  
 No (II) state, relative stability, rel. to spectroscopic factors and phenom. baricenter pot. 9-12542  
 Np (VII) state, relative stability, rel. to spectroscopic factors and phenom. baricenter pot. 9-12542  
 O- low-energy reactions with H<sub>2</sub> and D<sub>2</sub> 9-9401  
 O<sub>2</sub> reduction mechanism on noble metal cathodes 9-18758  
 Pb film, vacuum deposited, 227-307°C 9-20048  
 Pu, by AgO, Fe reduction, end points amperometric determ. 9-17544  
 Re, by O and O<sub>2</sub> at high temp. 9-17529  
 Si, thermal, and interdepend. between thickness of layer and exptl. conditions 9-3993  
 Si, thermal, effect of oxidation conditions 9-10341  
 SiO<sub>2</sub> film passivation of Si surfaces 9-18404  
 Ti, early stage mechanism 9-14133  
 Tm<sup>3+</sup>→Tm<sup>2+</sup> in SrCl<sub>2</sub> and CaO on γ- and e-irrad. e.s.r. obs. 9-10277  
 α-U, rel. to creep and internal stresses, obs. 9-9765  
 U metal production by C reduction of UO<sub>3</sub> in vacuum 9-14134  
 UO<sub>2</sub>, by steam, 885-1835°C 9-3997  
 UO<sub>2</sub> in CO<sub>2</sub> CO mixtures, and reduction, surface controlled 977-1400C 9-3998  
 W, room temp. 9-10342  
 Zn, ht. of chemisorption of O<sub>2</sub> 9-17530  
 Zr-Cu alloy, resistant for reactor coolant 9-20852  
 Zr-Cu alloys by CO<sub>2</sub>, resistance behaviour 9-20049  
 Zr-Nb alloys by CO<sub>2</sub>, resistance behaviour 9-20050  
 Zr alloys, eff. of alloying mat. on struct. and morphology of thin oxide films formed 9-20051  
 Zr alloys in high temp. H<sub>2</sub>O, irradi. effects, review 9-10343

**Oxide cathodes** *see Cathodes/oxide*

**Oxygen**

- <sup>18</sup>O atom reactions with N<sub>2</sub>O, N<sub>2</sub> and CO<sub>2</sub>, ozone quantum yields 9-21719  
 absorption spectrum, 1750 to 2020 Å at 300, 600 and 900°K 9-14692  
 acoustic wave absorpt. in O<sub>2</sub>-CH<sub>4</sub> mixture, vibr. relax. obs. 9-21137  
 adsorbed layer partially covering W(110) and (111) faces, effect on CO<sub>2</sub> adsorpt. 9-3217  
 adsorbed on partially reduced TiO<sub>2</sub>, e.s.r. 9-17249  
 adsorption and desorption by polycryst. W, Re and Mo, thermionic meas. 9-11787  
 adsorption and desorption by W, meas. via work function the thermionic emission changes 9-11786  
 adsorption on C films, rel. to elec. resist., -196 to 450°C 9-7795  
 adsorption on Fe, effect on surface energy 9-9603  
 adsorption on Mo, study by field emission retarding potential analyser 9-11782  
 adsorption on W (100) face. Two layer process at room temp. 9-21286  
 atmospheric emission at 6300 Å, effect of mag. storms 9-21788  
 atom, magnetic moment of (sp<sup>3</sup>)<sup>2</sup>P<sub>1</sub> and (2p<sup>3</sup>)<sup>2</sup>P<sub>1</sub> terms. 9-18143  
 atom atmosphere, spectral line formation and radiative transfer 9-19391  
 atomic, absorption cross section, effect of autoionization 9-6980  
 atoms and ion, bibliography of spectra 9-13287  
 atoms near 100 km. seasonal vars. 9-10398  
 chemisorption on activated Graphon, kinetics rel. to temp. 9-8079  
 chemisorption on diamond, heat of wetting, e.s.r. and i.r. spectrum 9-8083  
 chemisorption on Graphon, cleaned activated surface, 25 to 400°C 9-10335  
 chemisorption on Graphon at room-temp. 9-8082

## Oxygen continued

- chemisorption on W ribbons 9-12539  
 continuum absorption in high-excitation planetary nebulae 9-16561  
 crystals, sound velocity meas. elastic and thermal prop. calcs. 9-3519  
 current-growth expts., rel. to determ. of ionization and attachment coeffs., detachment and ion-mol. reactions effects 9-11612  
 diffusion in liquid Ag and Cu, electrochem. meas. 9-11690  
 diffusion in n-Si:P,  $\gamma$ -irradiated, rel. to thermal donor formation 9-21333  
 diffusion in  $\text{ZrO}_2$  growing films, 400-500°C 9-9735  
 diffusion through Ag membrane, mass spectra comparison of evolved and diffused gas 9-11663  
 discharges, positive columns, Gunn-instabilities, generation of T-layers 9-19560  
 electronic pair-correlation energies of ground states, soln. of Bethe-Goldstone eqns. 9-11383  
 gas analyser, patent 9-21730  
 heat of chemisorption on Zn 9-17530  
 ion-ion dissociative recomb. calc. 9-5075  
 ioniz. transitions, use of Franck-Condon factors 9-4934  
 ionization, yields, X-sections and loss functions 9-5054  
 ionization and fragmentation by 5-45 keV protons, mass spect. investigation, X-section meas. 9-5060  
 ionization equilibrium in low-density plasma 9-15820  
 in ionosphere, fine structure levels excitation, e temp. cooling 9-12607  
 ions, diffusion in hypostoichiometric  $\text{ZrO}_2$  9-17292  
 ions,  $\text{O}_1^+$ -electron recomb. in  $\text{O}_2$ -rare gas mixtures, temp. depend., 205-690°K 9-5076  
 ions III, IV, V, photoionisation cross sections, calc., 39.1-867.9 Å 9-6979  
 isotope behaviour in the sulphate water system 9-8156  
 isotopes, abundances in  $\text{CO}_2$ , calc. from mass spectrometric meas. 9-11429  
 laser, 8446 Å 9-8619  
 line 5577 Å in aurora, intensity ratio with  $\text{N}_2^+$  4278 Å band 9-20105  
 liquid  $\text{O}_2$ , stimulated Raman emission obs. with laser beam 9-21216  
 Mars atm. abundance, obs. 9-8277  
 microcathode currents, meas. by f.e.t. amplifier 9-17843  
 mixture with H and D, lower explosion limits and kinetics of branching step 9-14129  
 molecular, rotational transition obs. by microwave spectroscopy 9-9229  
 molecules, sub-mm transitions 9-17164  
 monolayer on Ni (110), oxidation process, and diffusion at high temp. 9-12544  
 nebular abundance 9-20162  
 $\text{O}_2$  model from orbital theory 9-14301  
 organic-foil particle detector sensitivity effect 9-20710  
 range and  $dE/dx$  in Be and C from 500 keV and 2 MeV 9-9871  
 reaction kinetics for various reactions involving  $\text{O}_2$ ,  $\text{O}_2$  and  $\text{O}_3$  9-15212  
 redistribution mechanism in  $\text{UO}_2$  fuels 9-11360  
 reduction mechanism on noble metal cathodes 9-18758  
 relaxation, vibr.-dissoc., behind shock wave 9-13483  
 seawater saturation, NE Pacific 9-6067  
 self diffusion in  $\text{NiO}$ , condensation coeff. 9-3387  
 solar photospheric, spectra, equivalent widths analysis, new method, applic. 9-16621  
 in solar wind, ioniz. stages 9-14255  
 solubility in liquid sodium 9-19610  
 sorption by polyolefins, automatic recording apparatus 9-1116  
 sorption on anthracite, influence on e.p.r. 9-10273  
 spectra, emission mechanism suggested for tropical night airglow 9-8191  
 spectrum with new photoelectron spectroscopy 9-17898  
 supersonic jet flow through non-symmetric nozzle 9-13480  
 tail quenching and decay time shortening by addition to org. liq. scintillators 9-9526  
 traces in Ag, influence on self-diffusion 9-3376  
 traces in  $\text{N}_2$  discharges, reduction effect on intensity of first neg. bands 9-5111  
 in transition metals, high-melting, gaseous impurity effect on brittleness temp. dependence 9-1309  
 vapour trapping in vacuum device by Cs injection 9-10585  
 Venus atm. abundance, obs. 9-8277  
 [OI]  $\lambda 5577$ , 46300 auroral emissions, Antarctic night sky photometry 9-1955  
 Ag compacts, effects on sintering rate 9-5498  
 Ar-O system, liquefied, sound vel. in solns. 9-9508  
 Cu spherical single crystals,  $\text{O}_2$  ads., surface struct. 9-5259  
 Ge surface elec. props. after exposure to  $\text{O}_2$  after heating in vacuo 9-3651  
 $\text{H}_2$ - $\text{N}_2$ - $\text{O}_2$  flame, temp. profile at atm. press. 9-15480  
 H-O, explosive mixture, transverse flame-shock interactions 9-1901  
 H-O mixtures, speed of products of detonations 9-10743  
 $\text{H}_2$ - $\text{O}_2$ -Ar mixtures, detonation initiation by incident shock waves, reaction mech. 9-14128  
 $\text{H}_2$ - $\text{O}_2$  diffusion flame structure 9-19098  
 $\text{N}_2$ - $\text{O}_2$  mixtures adsorbed on anatase, activity coeffs. 9-7350  
 O-H mixtures, detonation propagation in supersonic flow 9-19582  
 O- low energy reactions with  $\text{H}_2$  and  $\text{D}_2$  9-9401  
 $\text{O}_2$ , adsorption and interac. on Cu, 77°K 9-12185  
 $\text{O}_2$ , collision with electron rel. to formation of highly excited atoms 9-685  
 $\text{O}_2$ , high resolution electron-energy-loss spectrum 9-784  
 $\text{O}_2$ , neutron scatt., inelastic 9-785  
 $\text{O}_2$ , oscillator strength of Schumann-Runge band obs. 9-19444  
 $\text{O}_2$ , specific ht. at 4.2°K  $\rightarrow$  0.8°K, study of results w.r.t. residual entropies of CO and NO 9-15007  
 $\text{O}_2^+$  cation, vibrational frequency 9-15864  
 $\alpha$ - $\text{O}_2$  crystalline, light absorption peculiarities in range 700-1150  $\text{cm}^{-1}$  9-21629  
 $\text{O}_2$  e.p.r. abs., using HCN laser 9-786  
 $\text{O}_2$  first ionization potential determ. 9-15954  
 $\text{O}_2(^1\Delta_g^+ - ^3\Sigma_g^-)$  band obs. in day airglow 9-14167  
 $\text{O}_2^+$   $^2\P$  state, electron scatt., nonrelativistic partial wave analysis 9-18147  
 $^{15}\text{O}$  preparation of gas for medical use 9-21990  
 $\text{O}^{4+}$  ion, probability of  $1^1\text{S}_0$ ,  $2^1\P_1$ , transition 9-916  
 O I-lines stark eff., displacement and splitting obs. 9-2821  
 O VI, absolute oscillator strengths for important transitions 9-15808  
 O VI, semiempirical atomic core potentials, coeffs. 9-19397  
 O VI solar emission 9-2081  
 O VIII in solar corona, Ly- $\alpha$  and Ly- $\beta$  rad. ratio, temp. depend. 9-16630  
 O-, electron affinity calc. using mol. dissoci. of  $\text{CO}_2$  9-11614  
 O- trapped in alkali iodide crystals, e.s.r. 9-10289  
 $^{16}\text{O}$ , at. mass using high resolution spectrometer 9-11414  
 $^{17}\text{O}$  in  $\text{MnO}$ , NMR shift due to hyperfine interactions 9-1876

## Oxygen continued

- $\text{O}^+$  in O, drift vel. meas., diff. coeff. data, X-section and binding energy meas. 9-5068  
 $\text{O}_2$ , atomization on Pt 9-1908  
 $\text{O}_2$ , electron collision, 0-200eV, vac.u.v. emission 9-17040  
 $\text{O}_2$ , forbidden vibr. transitions in electron-impact spectra 9-9228  
 $\text{O}_2$ , Stark-broadening in Schumann-Runge system, relax. treatment 9-11471  
 $\text{O}_2$ , adsorption in Mo single crystal, mass spectroscopic investigation 9-5256  
 $\text{O}_2$  impurity in Ar, effect on  $\text{SiO}_2$  r.f. sputtering 9-7332  
 $\text{O}_2$  impurity in solidified gases, sp. ht. anomaly obs. 9-1392  
 $\text{O}_2$  reaction with free radicals in  $\gamma$ -irrad. propionamide, n-butyramide and isobutyramide 9-12538  
 $\text{O}_2^-$  in alkali halides, Raman spectra 9-10220  
 $\text{O}_2^-$ , E.S.R. in alkali halides 9-8010  
 $\text{O}_2^-$ , Raman spectra in alkali halide crystals 9-1807  
 $\text{O}_2^-$  in KBr, luminescence decay time, pressure effects 9-15184  
 $\text{O}_2^-$ , electron-ion recomb., quantum mech. calc. 9-5074  
 $\text{O}_2^+$ , high vibrational excitation in ground state, evidence from photoelectron spect. 9-17039  
 $\text{O}_2^+$  abundances in E-region, analysis of rocket-measured profiles 9-10436  
 $\text{O}_2^+$  dissociative recombination coefficient with electrons, 180°-630°K 9-1959  
 $\text{O}_2^+$  first negative system in type-B red aurora 9-4071  
 $\text{O}(^3\Sigma_g^- - ^3\Sigma_g^-)$  Herzberg I band system, source in Ar-4% $\text{O}_2$  afterglow 9-4933  
 $\text{O}_2(^1\Delta_g^+ - ^3\Sigma_g^-)$  band in evening twilight, interpret rel. to ozone dissociation 9-4069  
 $\text{O}_2(^1\Delta_g)$  photochem. prod. in benzene oxygen mixtures 9-13368  
 OI green emission spectra at mid-latitude in ionosphere 9-12600  
 OI nightglow, 6300 Å and 5577 Å, intensity profiles 9-8192  
 $\text{O}(\text{P}) + \text{CS}_2 \rightarrow \text{SO} + \text{CS}$ , product vibr. energy, expt. and computation 9-10327  
 $\text{O}_2(^3\Sigma_g^-)$  formation, reaction and deactivation obs. 9-8069  
 $\text{O}_4^+$  +  $\text{O}_2^- \rightarrow \text{O}_6$ , rate determ. in  $\text{O}_2$  9-7194  
 Pt surface accommodation coeff., press. depend. 9-16039  
 in W, influence on intergranular fracture 9-16134  
 W field emission tip, heated, effect on electron current 9-12220  
 W ribbon interaction, obs. by flash method 9-9600

## Oxygen compounds

- hydroxyl ion in alkali halides, concn. from u.v. absorpt. spectra 9-7374  
 ionic oxides, binary solid solns., interaction and substitutional disorder 9-17333  
 ionic oxides, binary solid solns., pair interactions 9-17334  
 metal oxide crystals sorption of orthophosphate 9-21689  
 OH mol. in interstellar space, r.f. spectra 9-18879  
 oxide film growth on metals, kinetics rel. to electronic and ionic diffusion in large surface-charge and space charge fields 9-9620  
 oxide films on metals, growth kinetics 9-10338  
 oxide surface-density meas. based on charact. X-ray production by 100-keV protons 9-13575  
 oxides, bonding from X-ray K-emission spectroscopy 9-13589  
 oxides, orthopositronium lifetimes and nature of  $10^{-8}$  sec. lifetime 9-12080  
 penta-atomic heterocyclic cpds., model for  $\pi$  electron spectra 9-4944  
 $\text{CaMoO}_4$ , refractive index, pressure dependence 9-16393  
 $\text{CaWO}_4$ ,  $\text{Nd}^{3+}$  solid laser, pump-pumped, 130 mW power output 9-13031  
 $\text{CaWO}_4$ , refractive index, pressure dependence 9-16393  
 $\text{KH}_2\text{PO}_4$ , refractive index, pressure dependence 9-16393  
 $\text{NH}_4\text{H}_2\text{PO}_4$ , refractive index, pressure dependence 9-16393  
 OCS, anharmonic pot. consts., least squares determ. to fourth order 9-11472  
 OH-emission sources, positions and Stokes parameters 9-16593  
 OH, H bonded in quartz, i.r. spectra 9-5267  
 OH $^+$  mol., fine structure obs. 9-18189  
 OH 1665 MHz wideband emission, new type Carina region of Galaxy 9-16596  
 OH mol., (4-1) and (5-2) bands in night airglow spectrum 9-20101  
 OH radical, collision broadening of (0,0) (A-X) u.v. transition, linewidths, low temp. 9-19484  
 OH radical, Hanle eff. in  $2^1\Sigma^+(\nu=0)$  state obs., g-factor-lifetime product determ. 9-20984  
 OH radical, rot. distrib. obs. in low-press. plasma 9-20983  
 OH radical in  $\text{BaTiO}_3$ , effect on ferroelec. transition 9-10048  
 OH radical interatomic force in  $\beta^2\Sigma^+$  obtained 9-20981  
 OH radio emission from infrared stars, obs. 9-21892  
 OH adsorption at  $\text{TiO}_2$ -aqueous soln. interface, obs. 9-7351  
 OH $^-$  in alkali halide cryst., one-phonon relax. 9-5534  
 OH $^-$  in alkali halides, Raman spectra 9-12407  
 OH $^-$  in alkali halides, Raman scattering 9-12432  
 OH $^-$  in NaCl, i.r. absorpt. 0.6-4.2°K 9-16415  
 OH $^+$  singlet-triplet intercombination separation, calc. 9-2874  
 $\text{OH}(\text{A}^2\Sigma^+ - \nu=0, \text{K}')$  quenching and rotational relax. 9-7083  
 $\text{OH}(\text{A}^2\Sigma^+)$  form. from ground-state atoms, obs. 9-9227  
 oxides, wetting promotion by addition of Ti to brazes 9-3180  
 $\text{TiO}_2$ , rutile, refractive index, pressure dependence 9-16393

## Ozone

- absorption coeffs., u.v. and visible 9-960  
 atmospheric, electrochem. ozonodeson 9-4047  
 atmospheric concn. near sunrise, absorption spectroscopy, rocket obs. 9-1946  
 atmospheric vert. dist., San Francisco 9-8168  
 atmospheric vert. dist., rel. to thermal structure of atmos. 9-6071  
 microwave spectrum, intervir.-state transitions 9-4932  
 photolysis, l.p. quantum yield meas. 9-16493  
 quantum yields of O'D atom reactions with  $\text{N}_2\text{O}$ ,  $\text{N}_2$  and  $\text{CO}_2$  9-21719  
 reaction kinetics for various reactions involving  $\text{O}_2$  and  $\text{O}_3$  9-15212  
 thermal decomposition, heat transfer study 9-3051  
 preparation by electric discharge 9-3018

## Ozonosphere see Atmosphere

## p-n junctions see Semiconducting devices/junctions

## P-V-T relations see Equations of state

## Pair creation see Electron pairs; and under individual particles, e.g. Mesons

## Palaeomagnetism see Rock magnetism

## Palladium

- d-band structure in Is coupling 9-9896  
 desorption of  $\text{H}_2$  mol., angular distrib. 9-7349



**Palladium continued**

- electrodeposition of ductile Pd 9-15228  
 electron-phonon interband scatt. 9-21463  
 epitaxial growth on cleavage face of mica 9-5242  
 epitaxial growth on KCl, KBr and KI crystals 9-7377  
 magnetic spin susceptibility field dependence 9-16333  
 magnetostriction, thermal expansion, Pd:Ni alloy contrast 9-1642  
 membrane, pumping out H impurities in He discharge tube 9-3021  
 self-diffusion, infl. of bound vacancies on isotope eff. 9-18487  
 surface, specular low-energy electron beam scatt 9-11760  
 thermal expansion interferometric meas., Gruneisen parameters calc. 9-19863  
 Young's modulus, 0-600°C 9-14964  
 in Cu, high speed dislocations, effect of impurity atoms on frictional force 9-3397  
 Pd:Fe<sup>57</sup>, lattice dynamics using Mossbauer effect 9-7638  
 Ti-Pd system, crystal structures of Ti<sub>3</sub>Pd<sub>3</sub>, Ti<sub>3</sub>Pd<sub>2</sub>, TiPd<sub>2</sub>, TiPd<sub>2</sub> 9-19725

**Palladium compounds**

- diethylammonium palladium cyanide, 001 Fourier synthesis 9-21320  
 Pd-Fe alloys, ferromag. ordering temp. by resist. obs. 9-5818  
 velocity of sound in transition metal doped alloys 9-7642  
 Ag-Pd alloy film, transmission, reflection and absorpt. coeffs., rel. to resonant states 9-7937  
 Ag-Pd alloys, faulting in severely cold-worked filings, X-ray meas. 9-7493  
 Au-Pd alloy film, transmission, reflection and absorpt. coeffs., rel. to resonant states 9-7937  
 Au-Pd film, diffusion coeff., 400-600°C, electron diffraction study 9-5399  
<sup>57</sup>Co-Pd experimental Mossbauer source prod 9-11898  
 Cu-75 wt.%Pd alloys, residual resistivity rel. to short-range-order 9-12100  
 Cu-Pd alloy film, transmission, reflection and absorpt. coeffs., rel. to resonant states 9-7937  
 Cu-Pd alloys, specific heat changes at low temps. from changes in short-range order 9-9844  
 Cu-Pd solid solns., ordered and disordered, magnetoresistance variation 9-21483  
 Fe-Pd, alloy, coercive force rel. to ferromag. domain ordering 9-12275  
 Fe-Pd alloy, dil. mag. magnetization distrib. 9-7900  
 Fe-Pd alloy, dilute, spin-wave stiffness by neutron scattering technique 9-12268  
 H-Pd electrical resistivity, 2/300°K 9-3580  
 Mn-Pd alloys,  $\rho$ -phase, antiferromagnetism 9-12311  
 Ni-Fe-Pd alloy, films, composition and deposition for use as magnetic storage elements, patent 9-13998  
 PbO(Fe<sub>2</sub>O<sub>3</sub>), magnetic stiffness field dependence rel. to domain behaviour 9-13991  
 p-PbSe, band structure from temp. dependence of elec. props. 9-3643  
 p-PbTe:Fe,Mn, thermoelec. power, thermal and elec. cond. temp. depend. obs. 9-13876  
 n-PbTe:Gd,Mn, thermoelec. power, thermal and elec. cond. temp. depend. obs. 9-13876  
 PbTe, magneto-reflection spectra of coupled plasmon-phonon modes 9-18699  
 Pd:Ni paramagnetic, magnetostriction, thermal expansion, Pd contrast 9-1642  
 Pd-Ag alloy tube for ion sources, H<sub>2</sub> permeation rate meas. 9-21353  
 Pd-Ag alloys, low-temp. Hall effect 9-12102  
 Pd-Ag alloys dil., mag. susceptibility meas. rel. to impurity scatt. and electron density states 9-13986  
 Pd-Au alloys, high temp. transport props. 9-15027  
 Pd-B alloys, mag. susceptibility and H<sub>2</sub> diff. 9-7889  
 Pd-Co alloy, dil., microwave ferromag. resonance 9-3948  
 Pd-Co alloys, ferromag., specific heat, 1.4 to 4.2°K 9-16178  
 Pd-Cr alloy films, e. diff. obs. rel. to elec. characts. 9-17242  
 Pd-Fe alloy, dil., microwave ferromag. resonance 9-3948  
 Pd-H system, Knight shift for adsorbed H 9-17505  
 (Pd-H) electrodes oxidation in H<sub>2</sub>SO<sub>4</sub>, mass transport, obs. 9-16485  
 Pd (1at.%Mn)H system, Knight shift for adsorbed H 9-17505  
 Pd-Ni dilute specific heat of nearly magnetic centres 9-1398  
 Pd-Rh alloys, dil., mag. susceptibility meas. rel. to impurity scatt. and electron density states 9-13986  
 Pd complex, Pd X<sub>2</sub>ZRCN (X=Cl or Br and R=Me or Ph), vibrational spectra 9-20937  
 PdCl<sub>2</sub> whiskers, prep. and props. 9-17259  
 PdF<sub>2</sub>, weak ferromagnetism 9-10124  
 PdFe conduction electron spin polarization range, depend. on impurity conc. determ. by neutron scatt. 9-10120  
 Pd(II) selenourea complexes, i.r. and laser Raman spectra and prep., obs. 9-15867  
 Pd(II) thiourea complexes, i.r. and laser Raman spectra and prep., obs. 9-15867  
 Pd<sub>3</sub>MnSn Heusler alloy, internal field at <sup>119</sup>Sn site 9-16404  
 Pd<sub>3</sub>O<sub>7</sub><sup>4-</sup>, ternary oxide, (a<sub>2</sub>PdO<sub>4</sub>, A=rare earth or In), pyrochlore struct., prep. at 3 kbar 9-5274  
 Pt-Pd-Au alloys, high temp. transport props. 9-15027  
 Pu-Pd alloys, mag. susceptibility as function of relative composition 9-19944  
 Rh-Pd-Ag, alloy, electron reflection, 200-800eV, energy loss spectra obs. 9-16194  
 Rh-Pd, Fe impurities, magnetic and transport processes 9-3766  
 Zr-Pd alloy, spot-cooled, new non-crystalline phases 9-5523

**Paper**

- thermopaper, optical props. 9-21607

**Paraelectric materials see Dielectric properties of substances****Paramagnetic resonance and relaxation**

See also Lasers; Masers

- acenaphthene triplet state obs. 9-19458  
 alkali halide crystals, of S<sup>-</sup> trapped impurity 9-3954  
 alkali halide crystals, reson. of stabilized Ag atoms 9-14108  
 alkali halides, of O<sub>2</sub><sup>-</sup> 9-8010  
 alkali iodide crystals, trapped O<sup>-</sup> 9-10289  
 alkali-silicate glasses,  $\rho$ -irrad., spectral form 9-15200  
 alkaline earth oxides, defect studies, review 9-9693  
 alkaline earth phosphate glasses, of iron 9-15173  
 alkoxybenzene radical anions 9-7085  
 9-alkylxanthyl free radicals 9-9295  
 alloys, dil., theory 9-12497  
 anthracene, single, paramagnetic centres when  $\rho$ -irradiated 9-3963

**Paramagnetic resonance and relaxation continued**

- anthracite, influence of oxygen sorption 9-10273  
 applications to organic chemistry 9-17507  
 aromatic free radical intermediates in carbonization 9-7088  
 aromatic hydrocarbons, triplet-triplet transitions 9-1800  
 aromatic nitrogen heterocycles, triplet states obs. 9-19458  
 p-azoxyanisole liq. crystals, study of radicals 9-7086  
 benzene negative ion, effects of deuterium substitution 9-2895  
 benzophenone, fluorinated, anion radicals 9-4970  
 benzophenone ion, radical high resolution transient e.s.r. spectra 9-20954  
 p-benzosemiquinone-potassium, ion pair assoc. and <sup>13</sup>C hyperfine splitting 9-19644  
 1,1' and 2,2'-biazulenyl anion radicals, spectra 9-20986  
 bibliography 9-2285  
 biphenyl triplet state obs. 9-19458  
 n-butyramide, X-irradiated, e.s.r. spectra of free radicals 9-9294  
 n-butyramide single crystals, X-irradiated, spectra of free radicals 9-9294  
 calcite:Mn<sup>2+</sup>, origin of forbidden transitions 9-15199  
 carbon blacks, P33 and Thermax, temp. depend. and n irrad. effects 9-8018  
 CdF<sub>2</sub>:Yb<sup>3+</sup>, interpretation of optical spectrum 9-1771  
 chars with A-centres from sugar and PVC, temp. depend. 9-8022  
 chloral hydrate, aqueous solutions, dosimetry studies and radiolysis 9-21224  
 chloranil charge transfer complexes, liquid and solid 9-20025  
 chloranil-p-phenylenediamine, absorption rel. to temp. 9-3964  
 chlorophyll water aggregates 9-15377  
 chromium dibutylthiocarbamate, EPR obs. 9-20024  
 copper (II) salicylate adducts, and mag. susceptibility 9-17500  
 coronene, dimer cation 9-2902  
 crystals with impurity centres, structure of centres rel. to role in luminescence 9-20001  
 3'-cytidylic acid single cry.  $\rho$  irrad. 9-18743  
 cytosine-5<sup>2</sup>H, free radicals formed by decay of constituent T atom 9-1928  
 decacyclene, triplet dianions 9-4965  
 diamond with chemisorbed H, F, Cl, Br and O, obs. 9-8083  
 dibenzenechromium cation, liq. and solid solns., hyperfine struct. and coupling const. 9-19459  
 dihydroxyanthrasemiquinones, H bond and hyperfine splitting obs. 9-20966  
 N,N-dimethylaniline in acetonitrile soln., h.f. splitting const. from spectra 9-11494  
 1,1'-dimethylchromocene, -ve methyl contact shifts,  $\Sigma$  and  $\pi$  delocalisation model consideration 9-7072  
 1,1'-dimethylvanadocene, -ve methyl contact shifts,  $\Sigma$  and  $\pi$  delocalisation model consideration 9-7072  
 dipole line width, temp. depend. 9-20013  
 discrete saturation in inhomogeneously broadened spectral lines 9-17839  
 dispersion characterization by line shape params. 9-10784  
 donor clusters 9-8008  
 DPPH, used as device for meas. nonuniform magnetic fields 9-10808  
 durene radical, production of radical with 13 equiv. protons 9-8078  
 elbaite, rel. to colour centre obs. 9-1236  
 electron spin echo envelope modulation by very small alternating mag. field 9-10282  
 electron spin-lattice relaxation time, determ. 9-3839  
 ENDOR high press. cavity design 9-10785  
 fluorocarbon radicals in  $\rho$ -irrad. tetrafluoroethylene 9-21727  
 forbidden transitions, origin 9-15199  
 free radicals formed from Group-IV and Group V hydrides in inert matrices at low temps. 9-12498  
 glass:Co<sup>2+</sup>, spectra obs., structural features determ. 9-10193  
 glass:Mn<sup>2+</sup>, spectra obs., structural features determ. 9-10193  
 glass, borate, silicate and phosphate, of Cu<sup>2+</sup> 9-14111  
 glass, of Cu<sup>2+</sup>, eff. of Co addition 9-18736  
 glass, organic, photo- and  $\rho$ -ionization compared by e.p.r. spectroscopy 9-10082  
 glasses containing Pb,  $\rho$ -irrad. 9-3958  
 graphite, linewidth and spin-lattice relax. time, temp. depend. at 335 MHz and 9.3 GHz 9-8015  
 graphite,  $\rho$ -irrad., behaviour rel. to annealing temp. 9-7587  
 graphite, powdered, e.p.r. line at  $\nu \approx 10$  GHz, width, shape and position 9-8013  
 graphite, two-dimens. g-factor, theory and calc. 9-8016  
 graphitic carbons, powdered, determ. of g-factor anisotropy 9-8014  
 guanidium aluminium sulphate hexahydrate, of Mn<sup>2+</sup> 9-18744  
 guanine hydrochloride dihydrate, irrad. single crystal, obs. 9-8033  
 helices, resonant as probes, high sensitivity and intense microwave field 9-3951  
 hexahydroxyanthrasemiquinones, H bond and hyperfine splitting obs. 9-19467  
 hydrazinium hydrogenoxalate, N<sub>2</sub>H<sub>4</sub><sup>+</sup> in  $\rho$ -irrad. cryst. 9-1927  
 iminoxy radicals formed from tetranitromethane and 1,3-dicarbonyl cpds., structure obs. 9-20987  
 isobutyramide, X-irradiated, e.s.r. spectra of free radicals 9-9294  
 isobutyramide single crystals, X-irradiated, e.s.r. spectra of free radicals 9-9294  
 KClO<sub>4</sub>, of ClO<sub>3</sub> radical created by X-irrad. 9-18737  
 Linde Y zeolite, of Mn<sup>2+</sup> rel. to cation distrib. and selective exchanges 9-1889  
 line, inhomogeneously broadened, dynamic distortion 9-1855  
 line form in zero field 9-8009  
 lines, inhomogeneously broadened, discrete saturation 9-8561  
 magnetic field modulator with amplitude stabilizer, g shift of metal impurities meas. 9-2324  
 maleic anhydride,  $\rho$ -irrad. cryst., ion radical pairs 9-10291  
 measurement autodyne for e.p.r. observation in weak fields 9-2295  
 metals, impurity spin resonance theory 9-12497  
 methanol glasses,  $\rho$ -irrad., spatial distrib. of trapped electrons 9-4014  
 methylamine alum: Fe<sup>3+</sup>, rel. to spin-Hamiltonian coeffs. determ., 77°K 9-5990  
 methylene violet, high resolution, anomalies 9-9272  
 4,5-methylenepheneanthrene react. with alkali metal, spect. investig. of carbanions MH and H<sub>2</sub>MH<sup>-</sup> 9-19468  
 methyltetrahydrofuran glasses,  $\rho$ -irrad., spatial distrib. of trapped electrons 9-4014  
 molecular line shapes, theory 9-9168  
 nickelocene, bonding determ. 9-15900

## Paramagnetic resonance and relaxation continued

- n.m.r. saturation effects in case of homogeneous broadening 9-1853  
 oxidized carbons, characterization by e.s.r. 9-8096  
 paramagnetic centre distrib. statistics from relax. parameters of inhomogeneously broadened e.p.r. lines 9-1754  
 paramagnetic centres in  $\gamma$ -irradiated Anthracene 9-3963  
 paramagnetic centres influence on spectra thermal correlation time, structure parameters determ. 9-6437  
 phenoxyl radicals in solid ion-exchange resins, inhomogeneous line broadening 9-829  
 phenoxyl-nitroxide biradical 9-13397  
 p-phenylenediamine-chloranil, temp. depend. g-tensor splittings 9-8035  
 9-phenylxanthyl free radical 9-13398  
 phosphorescent molecules of short lifetime in vitreous solid solution 9-8007  
 poly(tetrafluoroethylene)-styrene, decay of peroxy radicals obs. rel. to graft copolymerization 9-20040  
 poly 4-vinylpyridine,  $\gamma$ -irrad., structure obs. 9-18226  
 poly 2-vinylpyridine,  $\gamma$ -irrad., structure obs. 9-18226  
 polyethylene, irrad., and spin-lattice relax. mechanism 9-21669  
 polyethylene, irradiated, spectra of  $\text{CH}_2\text{-CH}(\alpha)\text{-CH}_2$  free radical, anisotropic hyperfine constant 9-15203  
 polyethylene terephthalate, photo-induced post-irrad. radical conversions 9-10357  
 polymers, carbazole-ring based, x-irrad., rel. to cross linking 9-3965  
 in polytetrafluoroethylene, of free radicals produced during irradiation 9-2558  
 propionamide single crystals, X-irradiated, spectra of free radicals 9-9294  
 proteins, free radical formation under x-irradiation 9-4013  
 PVC irrad. in air, resolution of spectrum 9-17496  
 pyrazine phosphorescent state 9-14719  
 pyrazine radical anion in Liq.  $\text{NH}_3$ , spectrum obs. 9-7276  
 pyridine radical anion in Liq.  $\text{NH}_3$ , spectrum obs. 9-7276  
 pyrimidine radical anion in Liq.  $\text{NH}_3$ , spectrum obs. 9-7276  
 pyrocarbons 9-8020  
 quartz glass, of  $\text{Ti}^{3+}$  9-21664  
 radical ion and intermediates from  $\alpha$ -methylstyrene in org. glasses, formation and assignments 9-20988  
 radical solutions, hyperfine structure by weak field e.p.r. 9-9550  
 radicals in solid phase, applicability of inhomogeneous line-broadening theory 9-829  
 rare-earth ethyl sulphates, zero-field splitting of  $\text{Gd}^{3+}$  9-1859  
 rare-earth halides, of pairs of coupled ions for energy transport mechanisms 9-7697  
 rare-earth impurities in II-VI compounds 9-1854  
 resolution of superimposed spectra, method 9-17496  
 Rochelle salt single crystal,  $\gamma$  irradiated, analysis of centre no.1 9-3953  
 ruby, electron spin-spin interactions, connection with polarization and nuclear spin relax. 9-15160  
 ruby, investigation of lattice defects 9-9694  
 ruby, laser-beam irradiated, double-resonance meas. of radiation interaction 9-10163  
 ruby, line broadening, n.m.r. saturation eff 9-1853  
 ruby, of Cr ion pair 9-18734  
 ruby spin-relaxation conc. depend. He temp. 9-18686  
 rutile, of ions with d' shells rel. to internal crystal field 9-16460  
 rutile, reduced, paramag. centre-charge carrier interaction 9-1864  
 s-f coupling, effect of range on 1/T 9-5858  
 semidiones, long-range coupling consts. calc. 9-14720  
 semiquinones, fluorinated, anion radical, spectra 9-4971  
 simple Dewar system for meas. at 4.2°K 9-6436  
 solid, resonance lines inhomogeneous broadening, review 9-18689  
 spectra of broad and narrow absorpt. lines, theoretical treatment 9-16754  
 spectra in solution, least squares curve fitting for computer anal. 9-11720  
 spectrometer and  $^2\text{He}$  cryostat, relax. times 1  $\mu$  sec. meas. 0.24-4.2°K 9-4190  
 spin coords transformation, soln. of Hamiltonian for orthorhombic paramag. center in rigid lattice 9-10274  
 spin Hamilton of two equivalent nuclei, appl. to  $\text{I}_2^-$  centres 9-5986  
 succinic acid,  $\gamma$ -irrad. crystals 9-16462  
 TCNQ complex salts, energy levels of triplet excitons by ESR 9-19883  
 tetra cyanoquinodimethane derivatives, rel. to moving excited states 9-12505  
 tetraethylammonium iodide,  $\gamma$ -irradiated 9-20978  
 tetrahydronaphthalene frozen soln,  $\gamma$  irradiation eff. and temp. depend. 9-8034  
 tetramethyl- 2, 2, 6, 6-piperidinol-4-oxyl-1 solid soln. in polyisoprene and polybutadiene, paramagnetic analysis 9-9296  
 2,2,6,6-tetramethyl-4-hydroxypiperidine-1-oxyl, absorption spectra, 1.8°K to 300°K 9-10115  
 thienyl-phenyl ketones, radical anions, hyperfine splitting consts. 9-20989  
 thioglycolic acid, X-irrad., ion formation 9-15202  
 titanium-aluminium acetylacetonate, mixed cryst., spin-lattice relax. 9-16386  
 triglycine sulphate: vandyli, switching effect obs. by e.p.r. 9-3713  
 trinitrene, septet ground state 9-2917  
 1,3,5 triphenylbenzene triplet dianions 9-4965  
 undiluted salts in the parallel configuration 9-1755  
 vanadocene, bonding determ. 9-15900  
 vandyli acetylacetonate dissolved in p-azoxyanisole, alignment by elec. field, eff. on spectrum 9-21225  
 wave, detect. of hydrated electrons 9-1044  
 waveguide window and nonconducting vacuum can for low. temp. meas. 9-17838  
 xanthyl free radicals 9-7089  
 zeolite, Linde Y, of  $\text{Mn}^{2+}$  rel. to cation distrib. and selective exchanges 9-1889  
 $(\text{OCu}_2\text{Mn}_{1-x})_2\text{S}_2\text{O}_{10}$  mixed crystal 9-5984  
 $\text{AgCl:Fe}^{3+}$ , study 9-5980  
 $\text{AgCl:Mn}^{2+}$ , temp. depend. 9-21642  
 Al, e. spin correlations from nuclear dipole relax. time meas. 9-7925  
 $\text{Al}_2\text{SiO}_5\text{:Fe}^{3+}$  spin-lattice relaxation and cross-relaxation times and inversion ratio 9-14069  
 $\text{AlCl}_3\text{:Ti}^{3+}(\text{Cr}^{3+})$ , spectra 9-12499  
 $\text{Al}_2\text{O}_3\text{:Cr}^{3+}$ , elec. field effect 9-10275  
 $\text{Al}_2\text{O}_3\text{:Cr}^{3+}$ , two-photon transitions in e.p.r. spectrum 9-16453  
 $\text{Al}_2\text{O}_3\text{:}^3\text{Cr}$ , ENDOR determ. of hyperfine splittings 9-8044  
 $\text{Al}_2\text{O}_3$ , of  $\text{AlO}^+$ , radiation-induced, crystal field interactions 9-12322  
 $\text{Al}_2\text{O}_3$  spin-lattice relax. calcs. from ground state of ferrons ion 9-12315

## Paramagnetic resonance and relaxation continued

- $\text{Al}_2\text{O}_3\text{:H}_2\text{O:Fe}^{3+}$  9-5981  
 As atoms trapped in inert matrices at 4.2°K, matrix perturbing effects 9-12501  
 Au(ii) diethyldithiocarbamate, single cry., quadrupole eff. on hyperfine struct. 9-14109  
 Ba  $\text{Cl}_2$ , electrolytically coloured, rel. to F centre existence 9-17279  
 $\text{BaF}_2\text{:Eu}^{2+}$ , hyperfine coupling constant of  $^{151}\text{Eu}^{2+}$ , temp. depend. 9-12502  
 $\text{BaF}_2$ , of  $\text{Tb}^{3+}$  9-20014  
 BaO films, evaporated, abs., band I 9-8011  
 BaS, neutron radiation-damage centres, obs. 9-13697  
 $\text{BeO:Li}$ , radiation-induced paramagnetic centre structure 9-1868  
 C, amorphous, before and after air admission, linewidth and spin conc. 9-8021  
 C, amorphous, g-anisotropy rel. to air adsorbed 9-8023  
 C blacks, P33 and Therman, temp. depend. and neutron irrad. effects 9-8012  
 C deposits on  $\text{Al}_2\text{O}_3$ , rel. to phases produced on deposition 9-20015  
 C films, change on annealing to 1000°K after n-irrad. 9-8017  
 CH radicals, proton hyperfine splittings, theory 9-827  
 $\text{CH}_3$ , ESR studies during redox polymerization 9-15217  
 $\text{CaCO}_3\text{:Mn}^{2+}$ , superhyperfine interaction of  $\text{Mn}^{2+}$  with  $^{13}\text{C}$  9-5987  
 $\text{CaF}_2\text{:Ce}^{3+}\text{-H}^+(\text{D}^-)$ , spectra, interstitial location of ions, charge compensators 9-1857  
 $\text{CaF}_2\text{:Eu}^{2+}$ , relaxation eff. from e.s.r. signals using opt. Faraday rotation 9-7945  
 $\text{CaF}_2\text{:Nd}^{3+}(\text{H}^-)$ , spectra, interstitial location of ions charge, compensators 9-1857  
 $\text{CaF}_2\text{:}^{47}\text{Ti}$ , valency determ. 9-10276  
 $\text{CaF}_2\text{:V}^{3+}$ , electron-nuclear double resonance 9-16472  
 $\text{CaO:Ti}^{4+}$ , of  $\text{Ti}^{4+}$  produced by  $\gamma$ - and e-irrad. 9-10277  
 CaO, Faraday rotation-e.s.r. double resonance technique 9-21342  
 $\text{Ca}(\text{S:Se})\text{:Mn}^{2+}$ , phosphors 9-3957  
 $\text{CaWO}_4\text{:Ce}^{3+}$ , e spin echo envelope modulation by very small alternating mag. field 9-10282  
 $\text{CaWO}_4$ , of  $\text{Er}^{3+}$  spin-Hamiltonian parameters determ. 9-12500  
 $\text{CaWO}_4$ , thermoluminescent colour centres 9-19757  
 carbon black, P33, effect of B acceptors and Na donors, 1800°-2400°K 9-8019  
 CdS, photo-induced of  $^{251}\text{In}$ -state impurity centres 9-20017  
 CdS, undoped, meas. 9-5983  
 $\text{CdS:Se}_x$ , of  $\text{Mn}^{2+}$  9-3955  
 $\text{CdS:Se}_x$ , photo-induced, of trapped electrons 9-16454  
 CdSe, photo-induced of  $^{251}\text{In}$ -state impurity centres 9-20017  
 $\text{CdTe:Ti}^{2+}$ , and optical absorption 9-1772  
 CdWO<sub>4</sub>, of  $\text{Co}^{2+}$ , elec-field eff. and angular dependence of line half-width 9-20016  
 $\text{Cl}^-$  in polycryst. matrix 9-8024  
 $\text{CoCl}_2\text{H}_2\text{O:Mn}^{2+}$  antiferromagnetic, exchange interactions 9-3834  
 $\text{Co}(\text{NH}_4)(\text{SO}_4)_2\cdot 6\text{H}_2\text{O}$ , of  $^{59}\text{Co}$  rel. to hyperfine interactions 9-8038  
 Cr-Fe alloys, dil., rel. to mag. props. 9-1858  
 $\text{Cr}^{3+}$  in ruby, opt. detection of reson. in excited state  $\bar{E}(^4\text{E})$  and ground state  $^4\text{A}_2$  9-20018  
 $\text{Cr}^{3+}$  in  $\text{NaInS}_2$  obs. 9-8029  
 $\text{CrO}_4\text{K}_2$ ,  $\gamma$  and n irrad.,  $\text{CrO}_3$  form., obs. 9-20062  
 $\text{CrO}_4(\text{NH}_4)_2$ ,  $\gamma$  and n irrad.,  $\text{Cr}(\text{V})$ ,  $\text{Cr}(\text{III})$  form., obs. 9-20062  
 $\text{Cr}^{3+}$  halide complexes, ligand hyperfine interactions 9-17498  
 $\text{CsI:Mn}^{2+}(\text{Eu}^{2+})$ , thermal treatment, spectra comparison with luminescence of  $\text{LCSl}$  9-20028  
 $\text{CsI}(\text{Ti}^{3+})$  spectra obs., trapped holes determ. in  $\text{CsI}$  luminescence 9-20028  
 $\text{CsMnF}_3$ , antiferromagnet, critical fluctuations study 9-18735  
 $\text{CsNO}_3\text{:VO}^{2+}$  9-3961  
 $\text{Cs}_2\text{ZnCl}_4\text{:Fe}^{2+}$ , rel. to interstitial dopant sites 9-8025  
 Cu-Cr, dilute, transmission conduction 9-8030  
 Cu-Gd dilute alloy, of Gd 9-14110  
 Cu-8-hydroxyquinolate, effect of lost lattice 9-10279  
 $\text{Cu}(\text{C}_2\text{SO}_4)_2\cdot 6\text{H}_2\text{O}$ , orthorhombic g-tensors and orientations, e.p.r. determ. 9-12240  
 Cu(II) complexes, bis(thiosemicarbazone) Cu(II) and others 9-2861  
 $\text{Cu}(\text{RbSO}_4)_2\cdot 6\text{H}_2\text{O}$ , orthorhombic g-tensors and orientations, e.p.r. determ. 9-12240  
 $\text{Cu}(\text{TlSO}_4)_2\cdot 6\text{H}_2\text{O}$  orthorhombic g-tensors and orientations, e.p.r. determ. 9-12240  
 $(\text{Cu+Zn})\text{K}(\text{SO}_4)_2\cdot 6\text{H}_2\text{O}$  crystal, magnetically dilute, e.p.r. line width expt. and theory 9-15201  
 EuO resonance linewidth temp. dependence, 2-300°K 9-10269  
 Fe-Rh alloy, meas. rel. to antiferromag.-ferromag. transition 9-16455  
 $\text{Fe}^{3+}$  ions in ice and  $\text{FeCl}_3\cdot 6\text{H}_2\text{O}$ , h.f.s., Mossbauer determ. 9-14037  
 $\alpha\text{-Fe}_2\text{O}_3$ , piezomagnetism, microscopic origin, rel. to e.p.r. meas. 9-1704  
 Gd in  $\text{LaNi}_5$ , dynamic effects, g shift 9-10280  
 Ge:As, acoustic paramag. resonances 9-10281  
 Ge:Mn, rel. to state of Mn in single crystals 9-3658  
 graphite, artificial, n-irrad., change on annealing to 1000°K 9-8017  
 H atoms trapped in inert matrices at 4.2°K, matrix perturbing effects 9-12501  
 H in Ar, hyperfine splitting press. shift, obs. 9-4870  
 H in He, hyperfine press. shift rel. to van der Waals interaction 9-4873  
 $^3\text{H}$  in Ar, hyperfine splitting press. shift, obs. 9-4870  
 HCN- in KCl magnetic parameters completely determ. 9-13358  
 $\text{HO}_2$ , in solns. of  $\text{H}_2\text{O}_2$  in  $\text{H}_2\text{O}$  at 77°K 9-7081  
 $\text{H}_2\text{O}_2$  decomposition, study of intermediates formed after u.v. irradiation 9-17034  
 $\text{H}_2\text{O}_2$  decomposition, study of intermediates formed after u.v. irradiation 9-9213  
 $^3\text{He}$ , hyperfine struct. of  $2^1\text{P}$  level 9-9159  
 $\text{I}_2$  single crystals, p-phenylenediamine-doped 9-10039  
 $\text{I}_2^-$  centre, derivation of spin Hamiltonian of two equivalent nuclei 9-5986  
 n-InSb, rel. to impurity 9-8027  
 KBr, additively coloured, pure and doped, and elec. studies of K colloids 9-16414  
 KCl, of Mn-S complexes 9-20019  
 KCl: Cd, coloured, studies 9-5925  
 KCl:Mn $^{2+}$  at cation vacancies, super hyperfine struct. 9-5988  
 KCl:LiCl mixed crystal, ENDOR of A-centres 9-12519  
 KCl, F-centre, ENDOR determ. of hyperfine and quadrupole interactions 9-5385  
 KCl, F centres, EPR obs. 9-20020  
 KCl(Br), ENDOR spectrum, second-order effects 9-15208  
 $\text{KClO}_3$ , of  $\text{ClO}_2$  radical created by X-irrad. 9-18737



## Paramagnetic resonance and relaxation continued

- KClO<sub>4</sub> of Cl<sup>2+</sup> molecular ion, X-irradiated crystal 9-21625  
 K<sub>2</sub>Co(CN)<sub>6</sub>:Cr<sup>3+</sup>, e. spin echo envelope modulation by very small alternating mag. field 9-10282  
 K<sub>2</sub>Co(CN)<sub>6</sub>, X-irrad. crystals. 9-10278  
 KH<sub>2</sub>PO<sub>4</sub>:Cu<sup>2+</sup>, chem. structure from spectra 9-1860  
 KH<sub>2</sub>PO<sub>4</sub>:KH<sub>2</sub>AsO<sub>4</sub> mixed crystals, proton dynamics study 9-3956  
 K<sup>+</sup>:Mn<sup>2+</sup>(Eu<sup>2+</sup>), thermal treatment, spectra comparison with luminescence of LCsT 9-20028  
 K<sup>+</sup>(Ti<sup>3+</sup>) crystals, X-ray treated, V<sub>k</sub> centre spectra obs. 9-20028  
 K<sub>2</sub>MnCl<sub>6</sub>, 1.4°-300°K 9-16456  
 K<sub>2</sub>MnF<sub>4</sub>:Mn<sup>2+</sup>, zero-point spin deviations obs. 9-10151  
 KMnF<sub>3</sub>, antiferromagnet, critical fluctuations study 9-18735  
 KNO<sub>3</sub>:VO<sup>2+</sup> 9-3961  
 La<sub>2</sub>Mg<sub>3</sub>(NO<sub>3</sub>)<sub>12</sub>:Ce<sup>3+</sup>, Pr<sup>3+</sup>, coupling of two spin species by resonant phonons 9-18738  
 LaBr<sub>3</sub> of pairs of Ce<sup>3+</sup> and Nd<sup>3+</sup> ions, obs. of superexchange interacts. 9-1697  
 La(ClBr)<sub>3</sub>:Ce(Er)<sup>3+</sup>, modified Orbach relax. process 9-12317  
 LaCl<sub>3</sub>, Ce<sup>3+</sup> pair-interaction meas. 9-10283  
 LaCl<sub>3</sub>, of pairs of Ce<sup>3+</sup> and Nd<sup>3+</sup> ions, obs. of superexchange interacts. 9-1697  
 La<sub>2</sub>Mg<sub>3</sub>(NO<sub>3</sub>)<sub>12</sub>:24H<sub>2</sub>O:Mn<sup>2+</sup>, ENDOR study of quadrupole splitting 9-1883  
 LaNbO<sub>4</sub> of Nd<sup>3+</sup>, g-factor, hyperconst. 9-20021  
 LaNi<sub>3</sub> of Gd, dynamic effects, g shift 9-10280  
 Li, hyperfine coupling const., many-body calc. 9-4841  
 LiF, ENDOR meas. of self-trapped hole 9-10284  
 LiF, ENDOR spectrum, second-order effects 9-15208  
 LiF conduction electrons, spin reson. 9-1861  
 Mg, conduction e.s.r. obs. 9-16457  
 α-MgMoO<sub>4</sub>:Cr<sup>3+</sup>, pseudo-Stark line splitting 9-18739  
 MgO:Cr<sup>3+</sup>, acoustic paramag. reson. 9-21666  
 MgO:F<sup>2+</sup>, spin-lattice coupling constants 9-14016  
 MgO:M<sup>2+</sup>, (M=Co, Ni, Cr paramag. ions), spin lattice relax. anisotropy, theory 9-12318  
 MgO, ENDOR spectra for V<sub>oh</sub> centre 9-8046  
 MgO, of Fe<sup>2+</sup>, by saturation by u.s. waves 9-21665  
 MgO, plastic deformation eff. 9-18740  
 MgScO<sub>4</sub>:6H<sub>2</sub>O:Co<sup>2+</sup> 9-1856  
 Mn<sup>2+</sup>:Ge, effect of heat treatment on struct. state 9-16459  
 Mn<sup>2+</sup> in CdF<sub>2</sub>, meas. Mn<sup>2+</sup>-F<sup>-</sup> interac. parameters 9-14112  
 Mn<sup>2+</sup>, ESR spectrum in ferroelec. LiTaO<sub>3</sub> and LiNbO<sub>3</sub> single cry. 9-16458  
 Mn<sup>2+</sup> in ferroelec. LiTaO<sub>3</sub> and LiNbO<sub>3</sub> single crystals 9-16458  
 MnCO<sub>3</sub>, uniaxial pressure depend., rel. to magneto-elastic anisotropy, 4.12°K and 20.0°K 9-8028  
 MnCl<sub>2</sub>-alkali chloride fused mixtures, rel. to mag. props. 9-13948  
 Mn<sub>2</sub>Fe<sub>3</sub>O<sub>8</sub>, 20-500 K/s, 80-350°K 9-14017  
 Mn(II) complexes, stereochemistry 9-18185  
 Mn(II) complexes in methanol 9-9551  
 MoO halide complexes, ligand hyperfine interactions 9-17498  
 N<sub>2</sub>O<sub>2</sub> in liquid and solid states, 77-300°K 9-19643  
 N atoms trapped in inert matrices at 4.2°K, matrix perturbing effects 9-12501  
 N in He, hyperfine press. shift rel. to van der Waals interaction 9-6989  
 N in He atm., hyperfine const. press. shift, short-range effects 9-4864  
 NH<sub>4</sub>Br, of radiation-induced NH<sub>3</sub>Br defect centre 9-9723  
 NH<sub>4</sub>Cl, of radiation-induced NH<sub>3</sub>Cl defect centre 9-9723  
 (NH<sub>4</sub>)<sub>2</sub>MoO<sub>4</sub>:4H<sub>2</sub>O, X-irrad. crystals. 9-10288  
 NS radical, gas phase 9-7082  
 Na, fine particles, 1.6-300°K 9-20022  
 Na, liquid, eff. of Rb, Tl and Cs additions 9-13541  
 Na<sub>2</sub>HPO<sub>4</sub>:5H<sub>2</sub>O-X-irrad. crystals. 9-14113  
 Na<sub>2</sub>O-Al<sub>2</sub>O<sub>3</sub>-GeO<sub>2</sub> glass, study of p-induced colour centres 9-18482  
 NaCl:Mn<sup>2+</sup>, X-irrad., spectral analysis 9-21667  
 NaCl-Fe system, complex spectra after X-irrad. 9-20023  
 NaF:Li, ENDOR spectrum of self-trapped hole associated with Li<sup>+</sup> impurity 9-10286  
 NaF, ENDOR spectrum of V<sub>k</sub> centre 9-10285  
 NaInS<sub>2</sub>:Cr<sup>3+</sup>, of Cr<sup>3+</sup> in layer structure 9-10287  
 Nd<sub>2</sub>Mg<sub>3</sub>(NO<sub>3</sub>)<sub>12</sub>:24H<sub>2</sub>O, spin phonon relax. field dependence 9-10156  
 Ni salts, hydrated 9-18741  
 O<sub>2</sub>, HCN laser absorption 9-786  
 O<sup>-</sup> trapped in alkali iodide crystals. 9-10289  
 α-OMNS, absorption in single crystals 9-3875  
 P atoms trapped in inert matrices at 4.2°K, matrix perturbing effects 9-12501  
 PO<sub>2</sub><sup>2-</sup> radicals trapped in Na<sub>2</sub>HPO<sub>4</sub>:5H<sub>2</sub>O, <sup>17</sup>O hyperfine splitting 9-14113  
 Pb glasses, p-irrad. 9-3958  
 Rb<sup>+</sup>(Ti<sup>3+</sup>) crystals, X-ray treated, V<sub>k</sub> centre, spectra obs. 9-20028  
 RbMnF<sub>3</sub>, antiferromagnet, critical fluctuations study 9-18735  
<sup>6</sup>Se<sup>2+</sup> ions in trigonal crystal fields, spin Hamiltonian description 9-3952  
 Si:As(Sb), irrad. of impurity-vacancy pairs, and endor meas. 9-5341  
 Si:P, line shift 9-3959  
 Si, single line due to paramagnetic stacking faults 9-1862  
 Sn-organic cpds., X-ray irrad., e.s.r. investigation of radicals formed 9-7592  
 SnO<sub>2</sub>:Fe<sup>3+</sup>, spectrum 9-17497  
 SrCl<sub>2</sub>:Er<sup>3+</sup> 9-1863  
 SrCl<sub>2</sub>:Tm<sup>3+</sup>, of Tm<sup>3+</sup> produced by p- and e-irrad. 9-10277  
 SrCl<sub>2</sub>:Yb<sup>3+</sup> 9-1863  
 SrF<sub>2</sub>:Eu<sup>2+</sup>, hyperfine coupling constant of <sup>151</sup>Eu<sup>2+</sup>, temp. depend. 9-12502  
 SrF<sub>2</sub>:Tm<sup>3+</sup>, diffusion of warm band, spin temp. spatial distrib. 9-1714  
 SrTiO<sub>3</sub>:Fe<sup>3+</sup>, cubic splitting temp. dependence, 123-773°K 9-18742  
 SrTiO<sub>3</sub>:Mo(Fe or Ni), reversible photochromic changes, model verification 9-19980  
 ThO<sub>2</sub>:<sup>153</sup>Gd<sup>3+</sup>, hyperfine coupling, temp. dependence 9-8031  
 ThO<sub>2</sub> of Gd<sup>3+</sup>, low field spectrum 9-12503  
 n-TiO<sub>2</sub>, interstitially doped, defects exam. 9-9704  
 TiO<sub>2</sub>, partially reduced, e.s.r. of adsorbed O<sub>2</sub> 9-17249  
 UF<sub>6</sub>X (X=Li, Na or Cs), absorpt. study 9-3960  
 V<sup>2+</sup> in cubic fields, hyperfine fields, effect of dynamic phonon interaction 9-5531  
 VO tartrate chelates, triplet state in aq. soln. 9-7277  
 VO<sup>2+</sup> in KNO<sub>3</sub> and CsNO<sub>3</sub> crystals. 9-3961  
 VO<sub>2</sub><sup>3+</sup>-ion complexes 9-14114  
 Y Ga garnet:Cr<sup>3+</sup> 9-1865

## Paramagnetic resonance and relaxation continued

- YAsO<sub>4</sub>:Gd<sup>3+</sup>, rel. to crystal field parameters 9-21668  
 YPO<sub>4</sub>:Gd<sup>3+</sup>, cryst.-field determ. by variable freq. 9-5985  
 YPO<sub>4</sub>:Gd<sup>3+</sup>, zero-field reson. of Gd<sup>3+</sup> 9-8026  
 YPO<sub>4</sub>:Gd<sup>3+</sup>, rel. to crystal field parameters 9-21668  
 YVO<sub>4</sub>:Gd<sup>3+</sup>, cryst.-field determ. by variable freq. 9-5985  
 YVO<sub>4</sub>:Gd<sup>3+</sup>, zero-field reson. of Gd<sup>3+</sup> 9-8026  
 YVO<sub>4</sub>:Nd<sup>3+</sup>(Dy<sup>3+</sup>) (Er<sup>3+</sup>) (Yb<sup>3+</sup>), at X and Ka bands and at 4.2 and 1.8°K. 9-16461  
 YVO<sub>4</sub>:Gd<sup>3+</sup>, rel. to crystal field parameters 9-21668  
 Yb, of dissolved Eu<sup>2+</sup>, g-shift and exchange integral calc. 9-12504  
 Zn(ClO<sub>4</sub>)<sub>2</sub>:6H<sub>2</sub>O:Mn<sup>2+</sup>, in a parallel and perpendicular configuration 9-8032  
 ZnO:Mn<sup>2+</sup>, at 9.5 and 35 kMc/s 9-1867  
 ZnO:Li, radiation-induced paramagnetic centre structure 9-1868  
 ZnO, red. characterization 9-3962  
 ZnS:Cr<sup>3+</sup>, photo-induced, decay behaviour 9-10290  
 ZnS:Mn<sup>2+</sup>, effect of elec. field 9-17499  
 ZnWO<sub>4</sub>:Cu<sup>2+</sup>, line half width angular, dependence 9-1866  
 ZnWO<sub>4</sub>-MnWO<sub>4</sub>, of Mn<sup>2+</sup>, 1.5° to 300°K 9-5989
- measurement**  
 areas under absorpt. curves 9-9272  
 crystal (single) transfer device and rot. system 9-20012  
 crystal-field parameters, variable-freq. method 9-5985  
 h.f.s.-zero-field method 9-11505  
 high pressure spectrometer for meas. to 10<sup>4</sup> kg/cm<sup>2</sup> 9-10783  
 line shapes, Gaussian and Lorentzian, comparison 9-4407  
 maleimides and maleamic acid, p-irrad., e.p.r. spectra study 9-21323  
 Q-band spectrometer with improved sensitivity and resolution 9-6433  
 relation time, using field modulation with boxcar integrator 9-190  
 relaxation time meas., very short, goniometric method 9-2287  
 relaxation time precise meas. using spectrometer modified to tone-burst modulation scheme 9-14409  
 sample probe, optical-c.p.r., with tunable coaxial coupling, low temp. 9-17837  
 spectrometer, frequency-variation 9-8026  
 spectrometer sensitivity using parametric and maser preamplifiers 9-10781  
 spectrometer sensitivity using parametric and maser preamplifiers 9-10782  
 τ<sub>r</sub>, from observed lineshape 9-2286  
 ultrasonic, techniques for derivative line shapes and spin relaxation 9-191
- Paramagnetism**  
*See also Magnetic properties of substances/paramagnetic*  
 alloys, dilute, "non-magnetic", mag. behaviour due to localized spin fluctuations 9-12234  
 cooling, mag., reversibility 9-14293  
 Fermi gas, magnetized, mag. moment 9-8450  
 ferromagnetic spin correlation function in paramag. temp. range 9-3780  
 Heisenberg paramagnet, diffuse and propagating modes 9-7887  
 Hersenberg model, time depend. correl. functions, appl. at critical point 9-5671  
 Joule Thomson effect 9-12244  
 neutron scattering, rel. to time-depend. two-spin autocorrelation function 9-12245  
 paramagnetic system, steady-state thermodynamics 9-14353  
 paramagnons, existence in strongly anisotropic ferromag. crystals 9-10101  
 spin susceptibility, generalized, in correlated narrow energy-band model 9-12051  
 spin-operators, fermion presentation, non-reduction of unbonded diagrams 9-16329  
 strong, statistical model for atoms and ions 9-12243  
 susceptibility in random dilute systems, molec. field theory extension 9-12246  
 time-correlation of spins, long-time behaviour, Halperin-Hohenberg law with 0=(5+η)/2 9-12235
- Parametric amplifiers** *see Amplifiers*  
**Parent** *see Nucleus; Radioactivity*  
**Parity**  
*See also individual particles, e.g. Mesons/spin and parity*  
 bosons, non-dynamical tests using decay mechanisms 9-4562  
 doubling rel. to sum rule constraints for baryon Regge trajectories 9-2525  
 fermion, assignment of definite number 9-6583  
 fermions, non-dynamical tests using decay mechanisms 9-4562  
 and isospin nonconservation detection by Mossbauer effect 9-497  
 nonconservation, broken mirror symmetry treatment 9-13097  
 nonconserving nuclear forces, calc. from Oakes weak interaction theory 9-8952  
 particles, unstable; non-dynamical test by meas. momentum ang. distrib. in <sup>1</sup>/<sub>2</sub>+0→S<sub>1</sub>+S<sub>4</sub> 9-15575  
 quasi-two-body react., natural or unnatural exchange, splitting of cross-section 9-4569  
 Regge trajectories, boson, parity doubling 9-2493  
<sup>3</sup>H(d,n)<sup>4</sup>He, n polarization obs., parity conservation concluded in strong reaction 9-6900
- Particle accelerators**  
*See also Ion beams*  
 beam vacancies as timing markers, high currents 9-6741  
 chemical: high intensity, low energy spread ion source 9-10829  
 circular, equilibrium orbit correction effectiveness 9-473  
 cyclic, particles losses at nonlinear resonance and fine parametric resonance 9-471  
 direct action pulse, charging units built on Tesla transformer principle 9-11163  
 disc-constrained beam, electrode design 9-8944  
 driving and focussing systems, variants of parameter choice 9-6747  
 electron, max. bremsstrahlung energies calibration with photoproton spectrometer 9-2628  
 electron output beam, radial-angular characteristics determination 9-2618  
 electron ring, method of forming compressed ring in static mag. field 9-19263  
 electron ring trapping in pulsed mag. mirror field 9-4430  
 heavy ion, two models using new principles, and general theory 9-11164  
 influence on society, Richtmyer memorial lecture 9-2114  
 instabilities due to magnetic field spatial variations 9-216  
 isochronous sector ring for heavy ions, design and pre-stripper choice 9-18051

**Particle accelerators continued**

- microtron, 10 MeV, beam emittance meas. 9-4700
- microtron, 30 MeV, SHF waveguide channel 9-2623
- muons, shielding, theory and meas. 9-19254
- Nimrod, applications to nuclear structure physics, conference (Rhel, 1968) 9-14541
- operation and principles, book 9-6742
- principles explained, book 9-20715
- shielding against nucleon-meson cascade 9-8890
- stability with resonance perturbation due to beam feedback 9-11162
- toroidal resonator, voltage meas. in gap in metre range 9-2625
- trajectory envelope of particles in strong focussing accelerator with straight sections, calc. 9-14538
- transportation channel design 9-225
- e ring using rings of electrons to sweep along heavy ions 9-20714
- P, rad. shielding from high energy  $\mu$ , cylindrically sym. shield, no mag. field 9-4696

**accessories**

- accelerating cavity, power transmission from amplifier, wideband channel 9-472
- beam transport system, analogue control method 9-16929
- betatron bremsstrahlung targets, comparison, obs. 9-15697
- charging units built on Tesla transformer principle for direct action pulse accelerator 9-11163
- magnetic lenses focusing system design 9-224
- magnetic quadrupole lens, circular aperture, excitation winding effect on mag. field nonlinearity 9-2328
- magnets, calc. of minor components of field 9-2322
- magnets, gradient, for strong focusing synchrotrons, pole shape study 9-16928
- proton sputtering apparatus 9-19252
- resonator buncher, harmonic composition of current, allowing for space charge 9-4704
- storage elements particle losses at nonlinear resonance and fine parametric resonance 9-471
- storage ring expts. to determine electron transverse polarization 9-20604
- storage rings, relativistic cluster stability 9-20720
- storage rings, scatt. eff. with polarized electron bunches 9-19264
- synchrotron equilb. orbits automatic meas. apparatus 9-18052
- e storage and accumulation ring, CERN 9-20721

**betatrons**

- bremsstrahlung targets, comparison, obs. 9-15697
- CERN work reviewed 9-2626
- collimation of internal electron beam 9-6748
- flux forced, field biased construction, 35 MeV, as compared with conventional types 9-11167
- influence of 200 BeV on society, Richtmyer memorial lecture 9-2114

**cyclotrons**

- focussing force near centre 9-2621
- heavy ions, subharmonic acceleration 9-20719
- Institute of Physical and Chemical Research, Saitama-ken, Japan 9-6746
- ion beam extraction by magnetic shielding 9-19260
- ion source, heavy, multicharged 9-19130
- ion vertical motion and space charge near centre 9-4699
- isochronous, at Julich, multi particle variable energy machine 9-14540
- isochronous, with axially-symmetric elec. and mag. fields 9-4703
- MSU external beam syst., remote controlled slits design 9-2627
- NRL isochronous, magnetic coils, computer programme to determine settings 9-2622
- radial oscillations meas. 9-11166
- ring, isochronous, with radial sectors, orbital props. 9-13176
- scattered neutrons, attenuation by concrete shielding 9-479
- target, radioactive elements rapid separation, vacuum evaporation 9-18392
- U-120, utilization possibilities replaced worn-out parts 9-19258
- variable-energy multiparticle, focusing mag. channel 9-8946
- $\beta$ -spectrometers, iron toroidal, for on-line work 9-19220
- p synchrocyclotron, 660 MeV, nearby neutron spectra obs. 9-478

**linear**

- 35 MeV electron, for medical applic. 9-2093
- cavity, design parameters and e.m. field, numerical calc. 9-20717
- Cockcroft-Walton voltage multipliers with arbitrary number of stages, anal. 9-17850
- electron, 10 MeV, of U-27 series 9-469
- electron, 2 GeV travelling-wave, Ukrainian Academy Science 9-16925
- electron, accelerating structure r.f. meas. 9-15696
- electron, general mode propag. and pulse-shortening phen. analysis 9-14539
- electron injection system with waveguide prebuncher, focusing problems 9-4697
- electron instabilities effect on resolution 9-470
- electrostatic, positive-ion, high frequency neutron wave production 9-19259
- fast pulse-d.c. integrator for use in e linac 9-2601
- inclined-field tubes, particle trajectories 9-19253
- light ion beam, target chamber vacuum system 9-11165
- pulsed, rel. to obtaining neutron diff. patterns from polycrysts. 9-14913
- pumping systems, effect on conductance and pressure 9-6743
- spectrometer, charged particle facility at Stanford USA 9-19219
- Stanford, 2 miles, history and construction, book 9-19256
- Stanford, project, review 9-20716
- with superconducting resonance cavities utilizing liquid He 9-8318
- Van de Graaff, modifications for at. displacement threshold energy meas., beam energy calib. 9-2620
- van de Graaff, UAR, isodose curves for main hall 9-15695
- Van de Graaff PIG ion source of  $^3\text{He}^+$  9-2355
- Van de Graaff, vacuum system 9-6749
- d beam from Van de Graaff, 3 MeV;  $^{11}\text{C}$ ,  $^{11}\text{N}$ ,  $^{15}\text{O}$  radio isotopes production 9-6745
- e 20 MeV prototype development 9-19257
- p, high energy, cylindrical resonator accelerating structure 9-6744
- p, Univ. Minnesota, new polar, p source. 9-2619
- Au-W thick target bremsstrahlung spectra meas. with large NaI scintillation spectrometer 9-16926
- e beam instability due to nonsymmetrical e.m. field 9-19255

**synchrotrons**

- 1.5 GeV, Tomsk, construction and operation 9-19261
- 6 GeV electron, at Erevan 9-474
- 10 GeV at Cornell 9-19262

**Particle accelerators continued****synchrotrons continued**

- 10 MeV, based on smooth curved waveguide 9-4701
- 70 GeV p Serpukhov 9-477
- 1000 GeV, p design study 9-476
- betatron oscillations theory 9-20718
- electron beam, 1.5 GeV, var. in transverse dimensions 9-475
- ignition converter control system 9-11169
- INS-AG e synchrotron, one-third resonance extraction 9-4702
- numerical control of orbit, display system 9-4698
- power transmission from amplifier to accelerating cavity, wideband channel 9-472
- proton, nonlinear resonance at fluctuations of square nonlinearity of mag. field 9-480
- space charge effects on frequency 9-2624
- strong focusing, pole shape of gradient magnets, study 9-16928
- synchrospasotron, particle injector, achromatic rotation-focusing system 9-11168
- wave-guide, sectionalization of accelerating system 9-16927
- waveguide, with pin comb structures, accelerating system production accuracy 9-8945

**Particle beams**

- collimation from accelerator, surface microanalysis by scanning 9-18435
- deuteron, time structure study by electronic method 9-13149
- disc-constrained, accelerating electrode design 9-8944
- line design, high resolving power 9-18049
- multicomponent, invariant solns. of eqns. 9-2334
- solids, interaction with high-energy particles 9-16189
- source, nozzle, pumping requirements 9-6475
- time-of-flight meas. method, accelerator with high energy burst rate 9-18050
- trajectory envelope of particles in strong focussing accelerator with straight sections, calc. 9-14538
- $\mu$ , with large angular divergence and spatial extent, momentum meas. 9-4433
- n generator, technique for beam centering 9-16766

**Particle detectors**

- See also Bubble chambers; Cloud chambers; Counters; Ionization chambers; Nuclear track emulsions; Particle track visualization*
- activation for n flux meas. in reactors 9-641
- channeltron: e.p. efficiency comparison at  $10^{-6}$  torr 9-11124
- computer aided data analysis 9-13154
- correlation amplitude, basic studies on the Rossi- $\alpha$  experiment 9-20687
- discriminator, fast leading-edge, 20 mV-1 V threshold, 0.5 ns resolution 9-18041
- discriminator of amplitude, zero crossing detector, tunnel diode circuit 9-18040
- dispersed detector filler, light absorption effect on characteristics 9-262
- dispersion double system, analysing high-resolution for reaction-product 9-20685
- gas discharge, for digital reproduction of ionizing particle distrib. 9-13165
- gas target angular correlation expt. effective solid angle computation 9-4662
- guard, plastic scintillator, for low activity  $\beta$  meas. 9-13168
- identifier with  $\Delta E \times E$  solid state detector telescope 9-8936
- ionization of KCl coating on foils used to meas. energy of ultrarelativistic part. 9-11143
- n activation analysis, spectrum stripping technique using comp. prog. 9-4170
- neutron, boron lined, integrated circuit solution for amelioration of signal-to-noise ratio 9-19216
- neutron, directional, flat response, const. sensitivity in range 5 eV to 5 MeV 9-2598
- neutron scintillation detector using time-of-flight method 9-18036
- photons from atomic cascade, signal-to noise ratio calc., Monte-Carlo method 9-4653
- Physics Exhibition, London, 1968, review 9-439
- positron annihilation apparatus, resolution functions for cylindrical geometry 9-13155
- pulse shape meas. device circuit 9-4420
- range telescope, remote controlled absorber system 9-4669
- scanning efficiency, detection of inhomogeneity, statistical study 9-20688
- scattering chamber, inverted, for angular correlation study 9-6735
- scintillator photodiode, high energy charged particles 9-20697
- solid state for  $^{235}\text{U}$  fission fragment mass distrib. expts. 9-16971
- streamer chamber, He filled 9-11155
- triparametric device and associated electronics for nuclear physics 9-18037
- window discriminator with integrated circuits, design criteria, 10 mv-10v 9-4690
- X-ray beam energy, Cu and Pb photoneutron cross sections 9-7691
- $\beta$ - $\gamma$  (circularly polarized) correlations energy depend. meas. method 9-18077
- e, channeltron fatigue and efficiency in  $10^{-6}$  torr 9-11124
- e dynode multiplier arrays, ratio of incident secondary calc. 9-18038
- $\gamma$  polarization meas. 9-19241
- $\gamma$  time resolved exposure rates, paired detector techniques 9-19247
- n epithermal, and  $\gamma$ , patent 9-20700
- N fast flux densities, paired detector technique 9-19247
- n type A.I.S.C., meas. dispersion, three section comparison 9-2597
- p, channeltron fatigue and efficiency in  $10^{-6}$  torr 9-11124
- $^{239}\text{Np}$  thin layer prep. methods for neutron detectors and  $\alpha$ -counters 9-13158
- Ge(Li), characts. and basic expts. with them for undergraduates 9-12824
- Ge(Li)  $\gamma$ -ray detector, directional-correlation attenuation factors 9-16922
- Li with B 10 or Li-6 shield, for n and  $\gamma$ , patent 9-20700
- MoO<sub>3</sub> thin film, for H beams 9-6728
- Si(Li) drifted p.i.n. types, fabrication and testing 9-14531

**Particle focusing see Particle optics****Particle optics**

- See also Electron optics; Ion optics*
- aberrations, matrix representation for calc. in homogeneous and inhomogeneous ( $n=1$ ) mag. fields 9-17858
- achromatic rotation-focusing system for injector to synchrospasotron 9-11168
- beam transport system, analogue control method 9-16929
- focusing, magnetic lense system design 9-224
- focusing props. of a toroidal electrostatic field 9-4432
- in inclined field acceleration tubes of minimum section length 9-19253



**Particle optics continued**

- mag. focusing prisms with  $r^{-1}$  fields, invest. of image parameters 9-4431  
 magnet with sloping circular edges, influence of vertical motion on horiz. 2nd order aberrations 9-6474  
 magnetic prisms with  $r^{-1}$  field for focusing wide angle beams 9-6473  
 positron beam handling system for photon resolution improvement in annihilation expts. 9-16821  
 prism spectrometer with quadrupole lenses, optical diagrams 9-2566  
 quadruplet, antisymmetric, formed by quadrupolar lenses, acceptance in phase plane 9-6472  
 relativistic, transition rad. from Al and Ag foils 9-9860  
 transportation channel calc., periodically arranged lenses, stability diagram 9-225  
 triplet, quadrupolar symmetric, phase acceptance 9-10817  
 uniform density particle beam, scatt. perpendicular to rectangular edge of slit 9-20493  
 $e$  relativistic, transition rad. from Al and Ag foils 9-9860  
 $p$  relativistic, transition rad. from Al and Ag foils 9-9860  
 $\pi$  relativistic, transition rad. from Al and Ag foils 9-9860

**Particle range** *see Energy loss of particles***Particle size**

- See also Surface measurement*  
 bacteria in salt solution, osmotic vol. changes, study by light scatt. 9-14867  
 coarsening theory, further applic. 9-11954  
 coarsening theory, further applic., comments 9-11955  
 colloidal suspensions, rel. to light absorpt. and scatt. 9-14865  
 colloidal systems, and shape, from nonlinear scatt. of laser light 9-14866  
 distribution in mixed monodisperse systems, Coulter counter meas. rel. to coagulation kinetics 9-9562  
 in foils, statistics determ. 9-7334  
 glass, shape effects on sintering kinetics 9-19820  
 graphite powder mixtures, distrib., computing and comparing statistics 9-7427  
 hectorite solutions, rod-like struct. study by light scatt. in elec. fields 9-14861  
 Mars surface albedo effects 9-18911  
 measurement using laser homodyne spectrometer 9-17224  
 measurement with laser 9-7283  
 oil-in-water emulsions, globule-size distrib., by spectroturbidimetry 9-14869  
 photometry, light extinction method in polydispersions 9-3135  
 starch granules, average diameter from light scatt. pattern 9-15167  
 suspension, separation by electronically sensed vol. 9-11728  
 X-ray powder diffractometry, determ. of size from line broadening 9-3303  
 yeast cells in water, rel. to small ang. depend. of light scatt. 9-14868  
 Al<sub>2</sub>O<sub>3</sub> alloys, of oxide, effect on ductility 9-17305  
 Au sol., particle diameter distrib., for  $d < 1000$  Å, X-ray scatt. determ. 9-14873  
 BaTiO<sub>3</sub> powders, effect on discoloration 9-21619  
 Fe<sub>3</sub>O<sub>4</sub> colloidal soln. in mag. field, 74 Å radius from magneto-optical meas. 9-5200  
 MgO single cryst. with magnesioferrite precipitates, rel. to fracture 9-7573  
 Ni on SiO<sub>2</sub> - Al<sub>2</sub>O<sub>3</sub> catalyst 9-1909  
 Ni powder, from X-ray powder diffraction line broadening 9-3303  
 Pt black samples, average, rel. to catalytic activity 9-5325  
 Pt catalyst, distrib. meas. by electron microscopy 9-5326  
 S, La Mer sols, time depend. of distrib. and number conc. 9-14871  
 Sb<sub>2</sub>Te<sub>3</sub>-Bi<sub>2</sub>Te<sub>3</sub> powders, grain size effect on thermal conductivity 9-19867  
 Se sols, distribution anal. by comparison of expt. and theor. spectra 9-14872  
 SiO<sub>2</sub> suspension, particle-diameter distrib., for  $d < 1000$  Å, X-ray scatt. determ. 9-14873

**Particle spectrometers**

- See also Alpha-particle spectrometers, etc.*  
 1.6 GeV/c at linear accelerator centre, Stanford, USA 9-19219  
 auroral electron and proton fluxes, satellite instrument, calibration 9-8219  
 cosmic ray  $\mu$  component intensity at 80° to zenith spectrographic meas. 4-500 GeV 9-19213  
 discrimination  $\alpha$ - $p$  9-19226  
 double focussing, for nuclear reactions products at 180° to beam direction 9-16917  
 magnetic, absolute spectrograph for precise nuclear energy measurements 9-19221  
 magnetic, for analysis up to 6 GeV/c 9-11130  
 magnetic, for investigating nuclear reactions 9-4663  
 magnetic, luminosity increase by azimuthally variable field 9-2564  
 neutron, single crystal used will detector to estimate flux, below spectroscopic threshold 9-2598  
 photoproton, electron accelerator max. bremsstrahlung energies calibration 9-2628  
 prism, quadrupole lens syst., opt. diagrams, parameter calc. 9-2566  
 prism with quadrupole lenses, opt. diagrams, parameter calc. 9-2566  
 semiconductor, review 9-13161  
 solar wind, expt. for Apollo astronauts on lunar surface 9-20236  
 in space, ATS-1 omnidirectional for solar proton and electron fluxes 9-21968  
 spectra, measured; unfolding method 9-4219  
 $e$  energy spectra in earth radiation belt, rocket probe meas. 9-12604  
 $\pi^-$ , momentum anal., construction 1 GeV/c 9-20694  
<sup>203</sup>Tl energy level lifetime meas., delayed  $e$ - $e$  coincidence 9-2563  
<sup>198</sup>Hg energy level lifetime meas., delayed  $e$ - $e$  coincidence 9-2563

**Particle symmetry** *see Elementary particles/symmetry***Particle track visualization**

- See also Bubble chambers; Cloud chambers; Luminescence chambers; Nuclear track emulsions; Spark chambers*  
 atomic scatt. chamber, large angle collision ions detect., 0.5-10 MeV 9-11151  
 camera, stereoscopic, six-objective, for one-meter bubble chamber 9-2612  
 diffusion chamber filled with H<sub>2</sub>, 0.1 atm., working conditions 9-11149  
 emulsions, diluted, with reduced shrinkage factor 9-465  
 emulsions, nuclear, type-R, estimation of microdistortions 9-466  
 energy-range relations of low velocity heavy ions in visual plastic detectors 9-20709  
 foil, organic, sensitivity effects of O<sub>2</sub> and humidity 9-20710

**Particle track visualization continued**

- hyperfragment and nuc. fragment prod. from 3.0 FeV/c K<sup>-</sup> interact. in nuc. emulsion 9-20639  
 plastic foils, spark scanning for fission fragments 9-18044  
 radioisotope imaging systems, image restoration 9-14535  
 solid-state elect., ang. distrib. of  $\alpha$  part. from nuc. react. 9-2611  
 spatial co-ordinates calc. from stereo projections 9-11150  
 streamer chamber, He filled 9-11155  
 $\alpha$  track autoradiography of submicron aerosol particles with electron microscope 9-15693  
 K<sup>-</sup> star character., obs. of hyperfragment and nuc. fragment prod. in emulsion 9-20639

**Particle tracks**

- See also Energy loss of particles*  
 dielectric detectors, density meas. fusing scatt. light 9-6736  
 direction measurement variance determination, in bubble chambers 9-459  
 fission track counting with solid state recorders, for absolute rate meas. 9-11142  
 hammer, energy spectra obs.,  $p$ - $\pi^-$  interact. with Li emulsions 9-4636  
 in nuclear emulsion, grain noise distrib. on relativistic tracks, obs. 9-19251  
 propane, allowing for Coulomb scatt. and bremsstrahlung in track analysis bubble chamber 9-11153  
 range-energy reln. for heavy particles in dielectric 9-18042  
 width meas. in L<sub>4</sub> emulsions, rel. to charge 9-2616  
 N spectrometry using recoil H tracks, computer analysis of random sampling 9-2617

**Particle velocity analysis**

- See also Alpha-particle spectrometers; Beta-ray spectrometers; Energy loss of particles; Ion velocity; Mass spectrometers*  
 fluidised beds, liq., distrib. 9-19648  
 $\mu$ - $e$  decay, nanosecond time analyser 9-2608

**Particles** *see Elementary particles; Energy loss of particles; Scattering, particles; and under individual particles, e.g. Protons and antiprotons***Paschen-Back effect** *see Spectra***Patterson diagrams** *see X-ray crystallography/calculation methods***Pierls-Nabarro force** *see Crystal imperfections/dislocations; Internal friction***Peltier effect** *see Thermoelectricity***Pendellosung fringes** *see X-ray crystallography***Pendulums**

- ball 9-4210  
 ball, using spring gun 9-15402  
 ballistic, use of blowgun 9-14  
 centripetal force demonstration design 9-6351  
 conical, lab. expt. 9-12  
 coupled simple with periodic disturbances, periodic motion 9-6352  
 elastic, asymptotic and analog computer solns. 9-16727  
 horizontal, mag. suspended, gravity-induced energy losses 9-120  
 Kater, theory 9-8470  
 nonlinear, for subharmonics, frequency-demultiplication exhibited in physical system 9-6353  
 single-wire torsional, use in moments of inertia measurements 9-10687  
 swings, pumping, theory 9-6261  
 torsional, crystal structure effects on peaks 9-5291

**Periodic system***See also Elements*

- 3rd row, field calc., Hartree-Fock pot. comparison 9-4826  
 and ionization potentials 9-5056

**Permalloy** *see Iron alloys; Nickel alloys***Permeability, magnetic** *see Magnetic properties of substances; Magnetization process***Permeability, mechanical***See also Diffusion in solids*

- albumin, bovine serum, adsorbed monolayers to water, obs. 9-7262  
 $3\beta$ -cholestanol multilayers to CO<sub>2</sub>, N<sub>2</sub> and He, obs. 9-5415  
 oleic acid multilayers to CO<sub>2</sub>, N<sub>2</sub> and He, obs. 9-5415  
 phase permeabilities of displacing and displaced liquids 9-18354  
 protein adsorbed monolayers to water, obs. 9-7262  
 stearate multilayers to CO<sub>2</sub>, N<sub>2</sub> and He, obs. 9-5415  
 Na dodecyl sulphate adsorbed monolayers to water, obs. 9-7262  
 Pd-Ag tube, of H<sub>2</sub>, rate meas. 9-21353

**Permittivity** *see Dielectric properties of substances***Perturbation theory** *see Field theory, quantum; Quantum theory***pH** *see Electrochemistry***Phase diagrams** *see Phase equilibrium; Phase transformations***Phase equilibrium***See also Solubility; Solutions*

- akermite-gelenite-merwinite system, X-ray analysis 9-18541  
 binary B-metal alloys, new metastable electron phases 9-9794  
 biphenyl, working fluid for Rankine cycle power conversion, thermal stability 9-3092  
 density gradient in one-component system near critical point 9-18387  
 diagrams, high-temp., recent developments in equipment and techniques 9-7618  
 dissolution studies, use of phase diagrams 9-17226  
 di-(2-ethylhexyl) na sulfosuccinate-n-octane solns., clear and turbid phases due to H<sub>2</sub>O addition 9-9559  
 eutectic crystal behaviour below eutectic pts. 9-5213  
 eutectic growth front stability 9-3149  
 graphite fibres, co-existence of cryst. graphite and turbostratic C 9-7363  
 liquid binary systems, separation, microcalorimetry 9-17191  
 liquid-liquid immiscibility in aq. salt solns. at low temp. 9-15988  
 permeabilities of displacing and displaced liquids 9-18354  
 phenyl ether-biphenyl eutectic, working fluid for Rankine cycle power conversion, thermal stability 9-3092  
 phosphoric acid organic solvent-water, rel. to selectivity of phosphoric acid 9-15989  
 polymer solns., multicomponent, liq-liq. phase separation 9-11686  
 polymer solns., multicomponent, liq-liq. phase separation 9-15990  
 polymer solns., multicomponent, liq-liq. phase separation 9-7256  
 Pu,  $\epsilon$  phase, elastic constants 9-21359  
 refractory binary and ternary systems, phase boundary relationships 9-7603  
 refractory materials, phase diagrams 9-7619  
 steel, tempered, alloyed with W, orientation of carbide phases 9-5504  
 substances at critical point, properties 9-9586

**Phase equilibrium** continued

- transition metal compounds, phase stability rel. to point defects 9-5332  
 vapour-liquid, rapid determ. 9-14882  
 water-nonionic detergent system, temp.- comp. diagrams 9-9485  
 zirconia, phase comp. effect on thermal shock resistance 9-13742  
 Ag-Al system, hexagonal  $\zeta$ -phase, stacking-fault energy calc. from thermodynamic data 9-19750  
 Ag-Al system, hexagonal  $\zeta$ -phase, stacking-fault energy, exptl. determ. 9-19751  
 Ag, Cs/Cl, NO<sub>3</sub> liquid-liquid and solid-liquid equilibria 9-18380  
 AgBF<sub>4</sub>-1-pentene system 9-21242  
 Ag<sub>2</sub>S-As<sub>2</sub>S<sub>3</sub> system, phase diagram for proustite, smithite and pyrrargyrite growth 9-17255  
 Al<sub>2</sub>O<sub>3</sub>-Cr<sub>2</sub>O<sub>3</sub>-SiO<sub>2</sub> system, diagrams 9-19655  
 Al<sub>2</sub>O<sub>3</sub>-Al system, curve, condensed phases, obs. 9-1341  
 Ar-N<sub>2</sub> liquid-vapour equil., vapour press. and compositions up to 10 atm., rel. volatility, condensation press. 9-17228  
 Au-Sb alloys, metastability of phases prepared by splat cooling 9-3478  
 Au-Se system, relationships 9-21411  
 BaO-Al<sub>2</sub>O<sub>3</sub>-SiO<sub>2</sub> system, new BaAl<sub>2</sub>SiO<sub>6</sub> phase, crystal structure 9-14987  
 Ca(NO<sub>3</sub>)<sub>2</sub>-Ba(NO<sub>3</sub>)<sub>2</sub>-Sr(NO<sub>3</sub>)<sub>2</sub> binary fused systems, from Raman scatt. 9-17186  
 CaO-Nb<sub>2</sub>O<sub>5</sub>-TiO<sub>2</sub> system 9-3496  
 CaO-Ta<sub>2</sub>O<sub>5</sub>-SiO<sub>2</sub> system, diagram for melting relations 9-7300  
 CdAs<sub>2</sub>-Zn<sub>3</sub>As<sub>2</sub> system, rel. to solid soln. growth and props. 9-13882  
 CdS-MnS, diagrams construction 9-19656  
 CdSe-MnSe, diagrams construction 9-19656  
 Ce, P-T diagram, rel. to theory of isomorphism 9-5268  
 Co-In system, liquid immiscible behaviour 9-21241  
 Cr-O systems, phase diagrams, high temp. 9-1351  
 Cr-SiC system 9-1328  
 Cr-O system, diagram 9-18382  
 Cs-C black system, Cs content rel. to press. compared with Cs-graphite system 9-7620  
 Cu-Ag-Se system 9-18562  
 Cu-Al alloys, phase transformations and equilibria under high pressure 9-19837  
 Fe-Si-Zn system, constitution anal. using mag. and X-ray techs. 9-11975  
 Fe-Si, constitutional diagram, 900-1200°C, for 30 to 40 at.% Si 9-11974  
 Fe-Si, eutectic crystal behaviour below eutectic pts. 9-5213  
 $\alpha$ -Fe-Si, superlattice phases, Fe rich portion 9-11965  
 $\alpha$ -Fe<sub>2</sub>O<sub>3</sub>-La<sub>2</sub>O<sub>3</sub>-Cr<sub>2</sub>O<sub>3</sub>, ternary diagram 9-13774  
 FeS, miscibility gap with Fe<sub>1-x</sub>S 9-21408  
 Ga-Al-As system, thermodynamic and optical treatment 9-17346  
 H<sub>2</sub>O-KCl-CaCl<sub>2</sub> soln., isopiestic vapour press. meas., osmotic and activity coeffs. 9-21187  
 He-H<sub>2</sub> liq. vapour equil. at 100 atm. 9-9590  
<sup>3</sup>He-<sup>4</sup>He solns., liq. vapour diagram by NMR method 9-9576  
 Hf-Cr system, phase diagram based on microscopic, X-ray and thermal analysis 9-14996  
 K-graphite lamellar cpds., from solid-state e.m.f. meas. 9-1391  
 K<sub>2</sub>Cr<sub>2</sub>O<sub>4</sub>, differential thermal analysis study to 30-40 kbar 9-14905  
 K<sub>2</sub>SO<sub>4</sub>, differential thermal analysis study to 30-40 kbar 9-14905  
 K<sub>2</sub>SeO<sub>4</sub>, differential thermal analysis study to 30-40 kbar 9-14905  
 La<sub>2</sub>O<sub>3</sub>-Cr<sub>2</sub>O<sub>3</sub>, diagram up to 1,700°C 9-16152  
 Li-C system, compound formation 9-14992  
 LiCl-H<sub>2</sub>O system, liq.-liq. immiscibility at low temp. 9-15988  
 LiF-BeF<sub>2</sub>-ZrF<sub>4</sub> phase diagram 350-1000°C 9-16031  
 Li<sub>2</sub>O-SiO<sub>2</sub>-P<sub>2</sub>O<sub>5</sub> glass film, prep. and phase separation study 9-5226  
 LiO<sub>2</sub>-SiO<sub>2</sub>-Li<sub>2</sub>O-Al<sub>2</sub>O<sub>3</sub>-4SiO<sub>2</sub>, glasses, isostructure and correlation 9-21254  
 LiO<sub>2</sub>-SiO<sub>2</sub>-Li<sub>2</sub>O-Al<sub>2</sub>O<sub>3</sub>-4SiO<sub>2</sub>, glasses, isostructure and correlation 9-3177  
 Mg-Te system, MgTe: phase formation 9-17341  
 MgCr<sub>2</sub>O<sub>4</sub>-MgFe<sub>2</sub>O<sub>4</sub> system, spinel characteristics 9-19843  
 MgO-FeO-Fe<sub>2</sub>O<sub>3</sub>, thermogravimetric study 9-21412  
 (NH<sub>4</sub>)<sub>2</sub>CaSO<sub>4</sub>-H<sub>2</sub>O system, solid and solution states 9-3147  
 N<sub>2</sub>-Ar liquid-vapour equil., vapour press. and compositions up to 10 atm., rel. volatility, condensation press. 9-17228  
 Na<sub>2</sub>BaO<sub>3</sub>-SiO<sub>2</sub> glasses, phase separation rel. to thermal expansion 9-1083  
 NaNbO<sub>3</sub>-KNbO<sub>3</sub> system, thermal and X-ray diff. meas. 9-7621  
 Nb-X-Al alloys, (X=Fe, Co, Ni, Cu, Cr, Mo),  $\mu$ -phase extension and  $\mu'$  phase occurrence 9-19844  
 Ni-Al alloy, phase structure rel. to Hall coeff. 9-3582  
 Ni-Fe alloy evaporated films, rel. to lattice parameter composition dependence 9-14986  
 SbSi, interphase boundary formation, eff. of non-equilibrium carriers 9-5752  
 Si-O systems, phase diagrams, high temp. 9-1351  
 SiO<sub>2</sub>-ZrO<sub>2</sub>-Al<sub>2</sub>O<sub>3</sub> system, for Corhart-ZAC type refractories 9-13784  
 Si-O system, diagram 9-18382  
 Si<sub>3-x</sub>Mg<sub>x</sub>P<sub>2</sub>O<sub>7</sub> system, crystallographic character 9-18453  
 SrO-ZrO<sub>2</sub> system, phase diagram, eutectics, solid solubility 9-1352  
 Ta-X-Al alloys, (X=Fe, Co, Ni, Cu, Cr, Mo),  $\mu$ -phase extension and  $\mu'$  phase occurrence 9-19844  
 Ta films, deposited in reactive cathodic pulverisation, three-dimens. diag. 9-3197  
 Ta<sub>2</sub>O<sub>5</sub> films, deposited in reactive cathodic pulverisation, three-dimens. diag. 9-3197  
 Th-U-N system,  $\geq 50$  at.% N, 1000°C 9-16157  
 Ti-Cu alloys, spot-cooled, new non-crystalline phases 9-5523  
 Ti<sub>3</sub>Au-Ti<sub>3</sub>Pt system, relationships and ordering 9-5521  
 TiO<sub>2</sub>-SnO<sub>2</sub> crystalline soln., annealed at 850°C and 1000°C, mech. of separation and modulated struct. 9-7602  
 U-UMn<sub>2</sub>-UF<sub>6</sub> system 9-1353  
 U-Zr-C phase diagram, 1700-2000°C 9-11976  
 U<sub>2</sub>N<sub>3</sub>, relations between  $\alpha$  and  $\beta$  types 9-16159  
 U<sub>2</sub>Si alloy, approx.,  $\delta$ -peritectoid reaction, effect of C content 9-16158  
 UAl<sub>3</sub>-UMn<sub>2</sub>-UF<sub>6</sub> system 9-1353  
 UO<sub>2</sub>-GdO<sub>2</sub> phase diagram 9-3979  
 US<sub>1-x</sub>toUS<sub>1</sub> range, structures and homogeneity 9-16081  
 USe<sub>1-x</sub>toUS<sub>1</sub> range, structures and homogeneity 9-16081  
 WC-NbC-(10 wt. %)Go sintered alloy, eff. of C content 9-13779  
 W-Cr phase boundaries, 0.61-0.66 wt.% H 9-16160  
 Zr-Ni(Pd, Cu, Co) alloys, spot-cooled, new non-crystalline phases 9-5523  
 Zr-U-H system, phase boundaries by elec. resistivity and thermal expansion meas. 9-14995  
 ZrO<sub>2</sub>-CaO-P<sub>2</sub>O<sub>5</sub> systems, phase identification in high ZrO<sub>2</sub> portion 9-3989

**Phase equilibrium** continued

- ZrO<sub>2</sub>-Y<sub>2</sub>O<sub>3</sub> system, phase diagram 9-1354  
**Phase flow** *see* Flow/two-phase  
**Phase meters** *see* Electrical measurement  
**Phase transformations**  
 acoustic absorpt. near critical point 9-4326  
 alkoxybenzoic acids, liq. crystals, H-D isotope effect 9-3982  
 alloys, binary, liquidus solidus curves 9-3150  
 p-anisaldazine, liq. crystal transition, proton spin-lattice relaxation study 9-11723  
 Birch's eqn. state rel. seismology 9-16516  
 boson gas, with falling temp. 9-16697  
 D-Camphor, absorption bands and variations in dielectric constant 9-3148  
 cholesteric-nec. field strength rel. to helix pitch 9-9483  
 continuous, generalized Landau theory 9-95  
 correlation functions, asymptotic forms 9-13556  
 critical behaviour of singular quantities near second-order transition line 9-16195  
 critical phenomena, microscopic analysis 9-12888  
 critical phenomena, microscopic analysis 9-83  
 critical point, fluctuation theory 9-9587  
 critical points, unified thermodynamic theory 9-11741  
 crystallization, nonequib. distrib. coeffs. 9-16054  
 Ehrenfest relations, for second order, new deriv. 9-8441  
 eutectic growth front stability 9-3149  
 experimental data in critical region 9-11676  
 fog formation conds. near cool surfaces during condensation 9-9591  
 graphite, triple point press. and temp., solidus-liquidus interface 9-1092  
 hexafluorobenzene, thermal properties, liquid vapour transformation 9-1000  
 hydrocarbon at low temperatures new phase origin 9-3235  
 investigation using laser beam interaction 9-20531  
 Ising lattice membranes, steady-state props. 9-88  
 lattice gas, hard-square, statistical mechanics 9-20369  
 lattice models of hard-core mols. 9-8458  
 liquid metals, second order suggested 9-21183  
 liquid-gas transition, dynamics of associated critical fluctuations 9-21244  
 liquid-vapour, use in immersion cooler 9-18966  
 liquid-vapour interface, transient movement, u.s. meas. technique 9-11746  
 metastable phase decay rate, nucleation theory 9-101  
 nucleation theory, reconsideration 9-7303  
 one-dimensional systems, statistical mechanics analysis 9-1065  
 polyarylates, CH<sub>3</sub> group motion and glass transition on healing 9-21415  
 polymer melts, glass transition 9-3085  
 polystyrene, melt viscosity and glass transition, analysis 9-18385  
 of second kind, eff. of sample nonuniformity 9-15005  
 second order, phenomenological theory 9-10655  
 second-order, Abelian group violation 9-10657  
 second-order Ehrenfest relations, new deriv. 9-8441  
 second-order transition line, critical behaviour of singular quantities in its neighbourhood 9-16195  
 semiconductor, metal-nonmetal transition, impurity states model 9-15098  
 separation due to cross-linking, 3-dimens. polymer formation 9-15216  
 solid fluid, statistical mechanics 9-20355  
 solid-liquid interface position, and temp. distrib. as function of time 9-9588  
 specific heat, singularities at transition points of second kind, qualitative characts. 9-9837  
 spectrum of scattered light near critical point by fluctuations 9-11742  
 spherical model as an instance of eigenvalue degeneracy 9-8434  
 struct. transitions perovskite-type cry. temp. depend. of rot. angle and soft-mode freq. below T<sub>0</sub> 9-3281  
 triangular lattice gas of hard-core mols. 9-107  
 two-dimensional, in grain boundaries 9-11780  
 vapour-liquid, of organic diatomic groups, valence freq. var. 9-7040  
 vinyl oleate, liq. cryst. state, radiation induced polymerization 9-14734  
 zeros in complex temperature plane 9-9585  
 zeros in several physical variables 9-9584  
 Au-Sb alloys, metastability of phases prepared by splat cooling 9-3478  
 Be, thermoelec. props., eff. of metallic impurities 9-18368  
 H<sub>2</sub>O, at critical temp. 9-11681  
<sup>3</sup>He-<sup>4</sup>He mixtures at critical pt., hydrodynamic modes and damping 9-11729  
 KCNS and alkali halides, molten mixture, eutectic coms. 9-17193  
 KNO<sub>3</sub>, Mossbauer spectra investigation, <sup>57</sup>Co source, 170-25°C 9-14039  
 NiS, hexagonal form, metal-to-semicond. transition 9-12084  
 Pu-Hf alloys, constitution 9-21410  
 S, liquid, density discontinuity near 160°C  $\lambda$ -transition 9-9479  
 Se, crystalline-liquid, rel. to metallic impurities effects on conductivity 9-12103  
 Se thermoelec. props., eff. of metallic impurities 9-18368  
 SrTiO<sub>3</sub>, 110°K, soft phonon modes and interactions 9-11968  
 Te, thermoelec. props., eff. of metallic impurities 9-18368  
 Ti<sub>2</sub>O<sub>3</sub> elec. transition, semiconductor-semimetal model 9-15060  
 V carbide melt, C saturated, reaction with disordered carbons, rel. to catalytic graphitization 9-12531  
 VO<sub>2</sub>, electronic phase transitions and nature of 'metallic' state 9-15048  
**solid-state**  
*See also* Ageing  
 apparatus for high press. and temp. expts. 9-17338  
 austenite to martensite, dilation coeff. variation 9-5507  
 austenitic-martensitic phase transformation in steel, obs. by transmission electron microscopy 9-5516  
 austenitic, C redistrib. laws 9-3490  
 austenitic stainless steel, ferrite and sigma-phase formation 9-14989  
 Bose fluid, transition of second kind and diagram technique near Curie pt. 9-12900  
 carbon tetrafluoride, vibr. spectra 9-1023  
 cellulose films, regenerated,  $\sim 25^\circ\text{C}$ , drying and temp. effects on i.r. spectra 9-11509  
 cements, composition and hydration from differential thermal analysis and other analyses 9-14123  
 $\beta$ -cristobalite, metastability rel. to internal stresses developed during cooling 9-1348  
 critical indices, restriction of values by thermodynamic stability condition 9-21413  
 crystalline  $\rightarrow$  amorphous, consequences for electron states 9-9599



# Phase transformations continued

## solid-state continued

- $\beta$ -Cu-Sn alloys, martensitic 9-1338  
cyclohexane, phases I and II 9-1801  
domain formation and structure on transf. with spontaneous decomposition 9-16062  
ferroelectric and ferromagn., Ising model with two and three transitions 9-5754  
first-order, in non Mossbauer substs.,  $\rho$  resonance absorpt. obs. 9-11961  
glass, structural changes rel. to ionic conductivity 9-18649  
graphite, pyrolytic B, graphitization study via Co lattice spacing 9-8059  
graphite nitrates,  $\lambda$  transform. at  $\sim -21^\circ\text{C}$ , struct. elec. and thermal props. 9-7607  
graphite to hexagonal diamond, by heat and press. treatment 9-7612  
hardening dilatometry, study of alloys 9-3484  
hexachloroethane, crystalline to rotational, mechanism 9-21414  
ice Ic formation 9-16076  
ice V to ice II 9-16075  
in Ising one-dimens. ferromagnet 9-21572  
limestone, 15 kb, rate 9-8153  
magnetization of superconducting films 9-12231  
malononitrile, displacive phase transitions 9-13780  
metal single crystals, bicrystals and tricrystals, growth 9-21300  
metals, isomorphous phase transitions, T-P diag. 9-9793  
metals and alloys, ordering processes rel. to positron annihilation 9-12078  
methane, mole. reorientation effects on neutron scatt. 9-9823  
methylchloromethane cpds., disorder of high temp. phases 9-5269  
new-phase formation kinetics under ion bombardment 9-3483  
nucleation and condensing in binary condensed phases, computer simulation 9-5283  
paraffin crysts., rotational transition 9-3497  
perovskite type cpds, charact. by normalized rot. angles of octahedra 9-1349  
petroleum coke, fraction to graphite during desulphurization 9-7611  
polyacrylate, glass transition temp. calc., 202-398°K 9-20991  
polychloroacrylate, glass transition temp. calc. 202-398 K 9-20991  
polyethylene, crystalline-amorphous using theory of helix-coil transition 9-19486  
polymeric solids, relaxational structure transitions and Erilouin spectra 9-12450  
polymethacrylate, glass transition temp. calc. 202-398°K 9-20991  
polypropylene, crystalline-amorphous using theory of helix-coil transitions 9-19486  
polyvinylchloride, glass transition and elec. conduction 9-16294  
precipitate morphology theory application to massive transformation 9-3485  
PVC, structural changes due to mechanical and heat treatments 9-21416  
quartz,  $\alpha$ - $\beta$ , rel. to Raman, Erilouin and Rayleigh scatt. 9-12445  
quinol hydrogen cyanide clathrate, mechanism 9-1578  
Se, amorphous to polycrystalline hexagonal, nonthermal methods 9-9806  
steel, 12% Mn, austenitic-martensitic due to cold working 9-5516  
steel, austenitic stainless,  $\gamma$  to  $\text{Ni}_3\text{Ti}$  phase 9-5517  
steel, austenitic stainless, rel. to strain hardening and strengthening 9-5499  
steel, Cr-Mn-N, cold-worked, changes during annealing 9-13776  
steel, Cr-Ni, nitride layer formation in intermediate stages of  $\gamma$ - $\alpha$  transformation 9-13775  
steel, decarburization and graphitization on contact with Na at 600°C 9-16150  
steel, Mossbauer effect obs. 9-16151  
steel, pearlite to austenite, edgewise growth rate 9-11964  
steel, Re,  $\gamma$ -martensite formation at  $-180^\circ\text{C}$  9-9800  
steel, var. residual austenite content, residual stress 9-3415  
steel OKH 32N8, quench-hardened,  $\delta$ -ferrite decomp. during tempering 9-1343  
strain-induced, effect on strain-ratio values 9-16149  
supercond., second order, Ehrenfest relations, new deriv. 9-8441  
tetrabromomethane, crystalline to rotational, mechanism 9-21414  
tetramethylbenzene 9-1882  
thalous halides, pressure effect and melting points 9-7622  
thermodynamics of structure transforms. 9-5508  
tracing by means of h.f. a.c. meas. using Q-meter 9-5506  
triglycine selenate, high temp. structural transitions 9-13920  
triglycine sulphate, high temp. structural transitions 9-13920  
ZnSb-constantan semiconductor thermoelements, X-ray microprobe analysis 9-10062  
Ag-Cu solid solns, supersaturated, substructure changes during decomposition 9-1339  
Ag-(10 wt.%) Mn-(1.5 wt.%) Sb alloys, solid soln. decomposition, work hardening effects 9-1326  
Ag<sub>3</sub>AsS<sub>3</sub>, suspected at high temp., and by dilatometry and calorimetry 9-13782  
Al-Zn-Mg alloy, kinetics of clustering 9-7600  
Al-Zn alloys, rhombohedral distortion of transition phase, Zn content effect 9-7604  
 $\gamma$ -AlOOH, in electron beams 9-13773  
alloy, rel. to ageing 9-9782  
As<sub>2</sub>S<sub>3</sub>(Se<sub>2</sub>), optical props. during transition from crystalline to glassy state 9-10192  
Au-(47.5 wt.%)Cd, b.c.c. to orthorhombic martensitic, mechanism 9-5509  
 $\beta$ -Au-Cd alloys, and structures 9-11835  
Au-Cu alloys, order-disorder props. rel. to Ni or Ga partial substitution 9-5522  
Au-Cu<sub>3</sub> alloys, order-disorder props. rel. to Ni or Ga partial substitution 9-5522  
Au, cold worked, phase V restoration 9-19827  
AuMn,  $\beta$ -martensitic f.c.c., caused by cold work and subsequent heating 9-3486  
B pyrolytic graphite, graphitization study via C<sub>60</sub> lattice spacing 9-8059  
Ba<sub>1-x</sub>Sr<sub>x</sub>RuO<sub>3</sub>, rel. to pressure and composition x 9-5510  
BaTiO<sub>3</sub>, tetragonal-orthorhombic transformation, lattice parameters rel. to temp. 9-1183  
BiCrO<sub>3</sub>, at 410°K, crystal distortion of each phase 9-10112  
BiMnO<sub>3</sub>, at 500°K, crystal distortion of each phase 9-10112  
C, disordered, transition to ordered graphite on reaction with V carbide melt 9-7617  
C, graphitization acceleration under high press. 9-7606  
C membranes, graphitization during annealing, charact. variation 9-7609  
C powders, sintering and graphitization by elec. discharge 9-7610

# Phase transformations continued

## solid-state continued

- CaCO<sub>3</sub>, u.s. study to 20 kb and 180°C 9-9825  
CdMg<sub>2</sub> alloy, order-disorder, 10° to 185°C, obs. 9-11971  
Ce, f.c.c. = d.h.c.p. martensitic, effect of plastic deform. 9-3487  
Co-Nb alloy, precip. of new phase after ageing 9-9796  
Co, martensite platelets, shear-induced during  $\alpha$ - $\beta$  transform., geometrical form 9-9795  
Co cast,  $\epsilon$ - $\gamma$ , rel. to galvanomagn. effect 9-3578  
CoF<sub>2</sub>·5HF<sub>6</sub>H<sub>2</sub>O, reversible, at T $\sim$ 246°K, rel. to mag. props. 9-7878  
(8.2 wt.%)Cr-Fe alloy, polymorphic, effect of high pressure on kinetics and phase equilib. temp. 9-5513  
Cr-Mn-N steel, cold worked, structural changes during annealing 9-13776  
(8.85 wt.%) Cr-(1.0 wt.%) Ni-Fe alloy, polymorphic, effect of high pressure on kinetics and phase equilib. temp. 9-5513  
Cr-Ni steel, formation of nitride layers in intermediate states of  $\gamma$ - $\alpha$  transformation 9-13775  
Cr<sub>1-x</sub>S with x $\leq$ 0.12, structural and mag. phase transitions 9-13783  
Cr<sub>2</sub>S<sub>3</sub>, structural and mag. phase transitions, vacancy ordering, obs. of trigonal superstructure 9-13783  
CsCl, kinetics, from elec. cond. obs. 9-11963  
CsPbCl<sub>3</sub>, superstructure at  $-40^\circ\text{C}$  9-21407  
CsSb, films, phase transition and photoemissive quantum yield 9-3756  
Cu-Al, phase transformations and equilibria under high pressure 9-19837  
Cu-Al alloy,  $\beta$  martensite, new ordered phase structure 9-1350  
Cu-Al alloys, and equilibria under high pressure 9-19837  
Cu Sn  $\gamma$  solid solns., eutectoid decomposition structural changes 9-7613  
 $\beta$ -Cu-Zn, martensitic, effect of n irradiation, heat treatment and deform. 9-5512  
Cu-20 at.% Ni-20 at.% Mn ordering process, 400-500°C 9-1342  
Cu<sub>2</sub>Se, rel. to electrical conductivity 9-17390  
D, cryst. struct. above and below  $\lambda$  transition 9-9675  
DyP, lattice deformation at Neel pt. 9-12309  
Fe-(23 at.%)Be, structure changes during ageing, study by transmission e. microscopy 9-17343  
Fe-C alloys, deformed during annealing above room temp. rel. to effect of C 9-13754  
Fe-C alloys, during tempering, eff. of prior plastic deformation 9-13777  
Fe-Co alloys, order-disorder rel. to ferromagnetism 9-3788  
Fe-N alloys, during tempering, eff. of prior plastic deformation 9-13777  
Fe-30wt.%Ni-5wt.%Nb austenitic alloy, structure and hardening on heat treatment and cold working 9-9802  
Fe-Ni-Mn alloys, isothermal martensitic nucleation rate 9-14990  
Fe-Ni-Mn alloys, martensitic, uniaxial mag. anisotropy appearance 9-1667  
Fe-Ni alloy, martensitic transform. rel. to change in mech. of transform. 9-5514  
Fe-Ni alloys, martensitic, uniaxial mag. anisotropy appearance 9-1667  
Fe-Ni alloys, martensitic, effect of additions 9-9799  
Fe-30at.%Ni alloy, martensitic, mag. fields effect 9-3491  
 $\alpha$ -Fe-Si, of superlattice phases, electron microscope study 9-11965  
Fe-Si, constitutional diagram, 900-1200°C, for 30 to 40 at.% Si 9-11974  
Fe- wt.%)Ni, elastic moduli, rel. to elastic moduli 9-7516  
Fe,  $\alpha$ - $\gamma$  phase transition revealed by hysteresis in thermoelectric e.m.f. 9-17340  
Fe, high-pressure, dynamic elec. resistivity obs. 9-14991  
Fe<sub>2</sub>Al alloy, order-disorder relationships, eff. on change kinetics of magnetic parameters 9-21584  
Fe- $\gamma$ - $\alpha$ , anisotropic and heterogeneous 9-3489  
Fe<sub>2</sub>Al, rel. to ordering 9-9801  
FeCl<sub>3</sub>, h.c.p.-f.c.c., Mossbauer evidence 9-5515  
FeS near stoichiometric, rel. to Mossbauer meas. 9-5892  
Ga, pressure induced, from pseudopotential and second-order perturbation theory 9-5319  
Gd, high order, near T<sub>c</sub>, effect of impurities from thermal expansion data 9-1399  
H, intermolecular interactions, Ising model 9-3492  
H, para-ortho transitions 9-1345  
Hg, crystalline,  $\alpha$  to  $\gamma$  martensitic, and crystallography 9-5519  
Hg<sub>1-x</sub>Cd<sub>x</sub>Te phase diagrams, (P,T) for x=0.2 and segregation coeff. data given 9-5518  
HgTe, h.p., effect of Ga impurities 9-11966  
KCl, polymorphic transition at high pressure, martensite character 9-9804  
KNO<sub>3</sub>, III-II, press depend 9-9803  
KNO<sub>3</sub>, between phases I, II and III, Raman scattering 9-12424  
K<sub>2</sub>UCl<sub>6</sub>-NaCl eutectic diagram predicted and confirmed by X-ray diffraction 9-11969  
LaAlO<sub>3</sub>, x-ray study 9-3504  
LaAlO<sub>3</sub>, charact. by normalized rot. angles of octahedra 9-1349  
LiF-BaF<sub>2</sub>-ZrF<sub>4</sub> system, solid-liquid transition temp. 9-16031  
Mg-Cd alloy, order-disorder, change in props. 9-16155  
Mg-Cd alloy, ordering speed, effect on props. 9-16156  
MgO-Al<sub>2</sub>O<sub>3</sub>-SiO<sub>2</sub> ceramic, phase composition and cordierite formation, 800-1400°C 9-21409  
 $\alpha$ -Mn<sub>2</sub>O<sub>3</sub>-Fe<sub>2</sub>O<sub>3</sub> system, crystallographic and mag. transitions 9-17464  
NH<sub>4</sub>Br and Nd<sub>2</sub>Br, modifications III and IV,  $-56^\circ$  to  $-192^\circ\text{C}$  9-16153  
NH<sub>4</sub>NO<sub>3</sub>, formation obs. through polarizing microscope 9-16154  
NH<sub>4</sub>NO<sub>3</sub>, I=II, II=III and III=IV effect of deuteration on transform. temps. 9-7614  
NH<sub>4</sub>Br,  $\lambda$  transition order evolution Raman spectra evidence 9-11972  
NH<sub>4</sub>Br, order-disorder, vibrational Raman spectra 9-11973  
NH<sub>4</sub>Cl, order-disorder, vibrational Raman spectra 9-11973  
NH<sub>4</sub>ClO<sub>4</sub>, deflagration, surface temp. meas. from orthorhombic-cubic transition thickness 9-10755  
Na martensitic transform 9-1346  
NaNO<sub>3</sub>,  $\lambda$  transition, u.s. and i.r. meas. 9-1369  
NaNbO<sub>3</sub>, heat of transition at 372, 527, 576 and 640°C 9-14993  
(48.2-57.0 at.%)Ni<sub>2</sub>-(51.8-43.0 at.%)Cu, short-range dissoc. 9-17344  
Ni-Al powder mixtures, exothermic effs. during sintering 9-17324  
Ni-(10 at.%)Mo alloy, K-state formation, activation energy 9-17342  
Ni-(14.9wt.%)P alloy, amorphous electrodeposit 9-19839  
Ni-Ti, equi-atomic, martensite behaviour 9-7615  
NiCr<sub>2</sub>O<sub>4</sub>, tetragonal-cubic, X-ray exam. 9-1347  
NiTi, martensitic, by room-temp. deform., rel. to tensile props., 150° to 370°C 9-18491  
Ni<sub>2</sub>V, ordering transition 9-13781  
Pb(Mg<sub>1/3</sub>Nb<sub>2/3</sub>)O<sub>3</sub>-PbTiO<sub>3</sub>-PbZrO<sub>3</sub> system, antiferro-ferroelec. and ferroelec. 1-2 phase boundaries, obs. 9-7844  
Pu(1.5 at.%)Hf,  $\beta$ - $\alpha$ , kinetics 9-11977

**Phase transformations continued****solid-state continued**

- RbNO<sub>3</sub>, rel. to electrical conductance 9-16254  
 RbNO<sub>3</sub>, polymorphic forms 9-5520  
 Re<sub>2</sub>(CO)<sub>10</sub>, n.q.r. obs. 9-3975  
 SrTiO<sub>3</sub>, charact. by normalized rot. angles of octahedra 9-1349  
 Ta H(D) solid solns., n scatt. study 9-7449  
 TbP, lattice deformation at Neel pt. 9-12309  
 Ti-Nb alloys, superconducting 9-1507  
 Ti<sub>3</sub>Au-Ti<sub>3</sub>Pt system, relationships and ordering 9-5521  
 TiO<sub>2</sub>-SnO system separation kinetics, 850-1200°C 9-3494  
 Ti<sub>3</sub>Sn(Se)<sub>2</sub><sup>2-</sup> cpds, MTi<sub>3</sub>X<sub>4</sub> (M=Fe, Co, Ni), rel. to elec. props. 9-9934  
 TlI, pressure induced, results from pressure depend. of Raman spectra 9-18716  
 U-Ti alloys, orthorhombic, metastable phases 9-19823  
 U<sub>2</sub>N<sub>3</sub>, phase relations betw.  $\alpha$  and  $\beta$  types, equil. diagram construct. 9-16159  
 U<sub>3</sub>Si alloy, approx.,  $\delta$ -peritectoid reaction, effect of C content 9-16158  
 U<sub>3</sub>O<sub>8</sub>, mechanism obs. in sp. ht. meas. 9-3495  
 UCl<sub>4</sub>-KCl-NaCl eutectic diagram predicted and confirmed by X-ray diffraction 9-11969  
 UCl<sub>4</sub>-NaCl, eutectic diagram predicted and confirmed by X-ray diffraction 9-11969  
 U<sub>3</sub>O<sub>8</sub>, e. microscope obs., 300°-1000°C 9-11854  
 VO<sub>2</sub>, semicond. to metal, resist. jump 9-16255  
 VS, 2nd-order, in one-phase region 9-9807  
 YbH<sub>2</sub>, orthorhombic to cubic, X-ray diff. study 9-18542  
 YnbTiO<sub>6</sub> 9-18538  
 ZnS, hexagonal-cubic, kinetics 9-14994  
 ZnS, hexagonal-cubic, kinetics 9-7616  
 Zr-Cu alloys (<5wt%Cu), after quenching from  $\beta$  phase and tempering 9-11970  
 ZrO<sub>2</sub>, high-pressure induced 9-19840

**Phase transitions** *see* **Phase transformations**

**Phase-contrast microscopy** *see* **Microscopy**

**Phonographs** *see* **Sound reproduction**

**Phonon bottleneck** *see* **Crystals/lattice mechanics**

**Phonon drag** *see* **Crystal electron states/transport processes; Crystals/lattice mechanics**

**Phonon-electron interactions** *see* **Crystal electron states/transport processes; Crystals/lattice mechanics**

**Phonons** *see* **Crystals/lattice mechanics**

**Phosphorescence** *see* **Luminescence**

**Phosphors** *see* **Luminescence; Luminescent devices**

**Phosphorus**

- atom, d orbitals in sp<sup>3</sup>d, sp<sup>2</sup>d<sup>2</sup> and p<sup>3/2</sup> configs. 9-9131  
 atoms, hyperfine structure, Brueckner-Goldstone many-body theory, core-polarization effect 9-678  
 atoms and ions, bibliography of spectra 9-13287  
 diffusion and solubility in CdTe and CdSe rel. to temp. and Cd partial pressure 9-11895  
 donor in Si, ground state energy, corrected 9-12160  
 e.s.r. of atoms trapped in inert matrices at 4.2°K, matrix perturbing effects 9-12501  
 Hittorf's, atomic crystal structure 9-13646  
 ion beam bombardment of p-Si at 30keV and effects on elec. props. 9-9999  
 ions, channelling in Si, effect of defects 9-9708  
 red and black, X-ray L<sub>2,3</sub> emission bands rel. to energy struct. 9-5944  
 superconductivity at 170-260 kbar 9-1505  
<sup>31</sup>P, low-field dynamic polarization in solns., 9-9556  
<sup>31</sup>P n.m.r. in THF 9-10295  
 P<sub>2</sub>, C<sup>1</sup>S<sub>2</sub><sup>+</sup>, X<sup>1</sup>S<sub>2</sub><sup>+</sup> system bands, rot. analysis 9-9230  
 P<sup>31</sup> in KH<sub>2</sub>PO<sub>4</sub> spin-lattice relax. time anomalous decrease near Curie point 9-1713

**Phosphorus compounds**

- III-V type phosphides, semicond., X-ray L<sub>2,3</sub> emission bands and energy struct. 9-5944  
 orthophosphate sorption on metal oxide crystals 9-21689  
 peatahalide molecules, intramolecular exchange 9-19445  
 phosphine, gas, electron drift velocities 9-17166  
 phosphoric acid-organic solvent-water, liquid-liquid equilibria rel. to selectivity of phosphoric acid 9-15989  
 POCl<sub>3</sub>-SnCl<sub>4</sub> mixture, Nd<sup>3+</sup>, Eu<sup>3+</sup>, Tb<sup>3+</sup> in soln., fluorescence spectra and radiative lifetimes of ions 9-12117  
 CaHPO<sub>4</sub>, <sup>31</sup>P-<sup>1</sup>H nucl. double reson. expts. 9-3966  
 KH<sub>2</sub>PO<sub>4</sub>, refractive index, pressure dependence 9-16393  
 K<sub>2</sub>HPO<sub>4</sub>, <sup>31</sup>P-<sup>1</sup>H nucl. double reson. expts. 9-3966  
 Ni(14.9wt.%P) alloy, electrodeposited, amorphous structure 9-19839  
 P<sub>2</sub>O<sub>5</sub>, <sup>31</sup>P NMR spectra, chemical shift anisotropies 9-20936  
 P<sub>2</sub>S<sub>10</sub>, <sup>31</sup>P NMR spectra, chemical shift anisotropies 9-20936  
 P<sup>16</sup>O, isotope shift studies of u.v. and visible bands 9-18190  
 P<sup>18</sup>O, isotope shift studies of u.v. and visible bands 9-18190  
 PBr<sub>3</sub>, liq., spin-lattice relax. 9-17221  
 P(CN)<sub>3</sub>, <sup>31</sup>P NMR spectra, chemical shift anisotropies 9-20936  
 PCl<sub>3</sub>, microwave spectra, quadrupole h.f.s. 9-787  
 PCl<sub>3</sub>, diffusion in Si rel. to prod. of highly alloyed n<sup>+</sup>-type layer 9-17245  
 PD<sub>4</sub>I, proton and deuteron spin-lattice relax. times 9-16385  
 PH<sub>4</sub>Br, laser-Raman spectra, barriers to PH<sub>4</sub><sup>+</sup> rot. obs. 9-15865  
 PH<sub>4</sub>Cl, laser-Raman spectra, barriers to PH<sub>4</sub><sup>+</sup> rot. obs. 9-15865  
 PH<sub>4</sub>I, laser-Raman spectra, barriers to PH<sub>4</sub><sup>+</sup> rot. obs. 9-15865  
 PH<sub>4</sub>I, proton and deuteron spin-lattice relax. times 9-16385  
 PH<sub>4</sub>I and PD<sub>4</sub>I, far-i.r. and Raman spectra 9-1794  
 (PNCl<sub>2</sub>)<sub>4</sub>, vibrational spectrum, assignment of fundamental freq. 9-14693  
 PO<sub>2</sub><sup>2-</sup>, Davydov splitting in Ca<sub>10</sub>(PO<sub>4</sub>)<sub>6</sub>F<sub>2</sub> cryst. 9-16167  
 PO<sub>3</sub><sup>3-</sup>, e.p.r. in X-irrad. Na<sub>2</sub>HPO<sub>4</sub>·5H<sub>2</sub>O crystals 9-14113  
 PO spectra, D and D' states, rotational analysis 9-2878  
 P<sub>2</sub>O<sub>5</sub>, effect on colour and reflectance of TiO<sub>2</sub>: opacified porcelain enamels 9-3854  
 POCl<sub>3</sub>, microwave spectra, quadrupole h.f.s. 9-787  
 POCl<sub>3</sub>, solvent for Nd<sup>3+</sup> salts in liquid lasers 9-14430  
 PSF<sub>3</sub>, vibr. anal. 9-15866  
 Ph singlet-triplet intercombination separation, calc. 9-2874

**Photochemistry**

*See also* **Photographic process**

- N,N-dimethylaniline, irrad., +benzene halogen derivs., electron affinity of acceptor 9-4010  
 acetone, photolysis at 185nm, quantum yields 9-16494  
 anils. photochromic, spectra and mechanisms 9-10353

**Photochemistry continued**

- benzene, criticism of existing data 9-16496  
 benzene vapour photolysis at 1849Å, cis-1, 3-hexadien-5-yne form 9-10354  
 n-butane, propane, superexcited, decomposition primary modes 9-21723  
 chlorophyll-a and l: methanol soln., reversible oxidation 9-18974  
 cyclopropane, gas-phase photolysis 9-10355  
 cyclopropane carboxaldehyde, vapour-phase photolysis, products 9-16497  
 dimethyl carbonate, vapour-phase photolysis, 30°-103°C obs. 9-16500  
 4,4-diphenyl-cyclohexenone and derivatives 9-8110  
 dissociation reactions, theory 9-6018  
 duroquinone, flash photolysis and triplet state reactions 9-21720  
 ethane, photolysis at 1470 and 1577Å, pressure effects 9-16498  
 ferrocenes, substituted, photodecomposition and electronic absorpt. spectra 9-20964  
 flash photolysis, apparatus and applications 9-17540  
 fluorobenzenes, criticism of existing data 9-16496  
 hexafluoroacetone, fluoresc. and phosphoresc. rel. to ketone press. 9-1921  
 hexafluoroacetone, photodecomp. 9-1920  
 hexafluoroacetone, quenching addends during photolysis, identification 9-1922  
 hexafluoroacetone, with diborane, gas-phase photolysis 9-16495  
 hexafluoroacetone photolysis, intersystem crossing efficiency 9-1919  
 hexafluoroacetone vapour, photolysis, mechanics for primary process 9-1923  
 investigations at Institute for Radium Research and Nuclear Physics, Austria 9-12549  
 ketene-NO H<sub>2</sub> system, products 9-21721  
 laser photolysis and spectroscopy for nanosecond reactions 9-6559  
 light sources, vacuum u.v., microwave excited gas flow lamps 9-8665  
 methacrylonitrile, photosensitized dimerization obs. 9-16501  
 methane, ionizing photolysis 9-6019  
 methane, photolysis at 1236 Å 9-10356  
 methanol, collision-induced predissoc., quantum yields 9-16499  
 methyl formate, vapour-phase photolysis, 30°-103°C obs. 9-16500  
 methyl iodide, photolysis, reaction of excited I atoms 9-1924  
 molecule, photoexcited, rate constant direct meas. 9-16489  
 ozone photolysis, l.p. quantum yield meas. 9-16493  
 photocurrent in electrodes immersed in solns. 9-1916  
 photodissociation primary products, energy distrib. in vibr. excitation 9-10350  
 photolysis, flash; and time resolved mass spectrometry, reaction vessel 9-4009  
 photolysis demountable flash lamp 9-13067  
 photosynthesis, e transfer mechanisms, obs. 9-16490  
 photosynthesis, entropy balance 9-16632  
 polyethylene terephthalate, radical conversions, e.s.r. study 9-10357  
 propane, photolysis at 1470 Å, pressure effects 9-16498  
 propane, superexcited, decomposition primary modes 9-21723  
 pyridine, criticism of existing data 9-16496  
 reactions, conference, Munich (1967) 9-16488  
 tetramethylbenzenes, solid-state photolysis, radical form. 9-21722  
 toluene, criticism of existing data 9-16496  
 o-xylene, criticism of existing data 9-16496  
<sup>131</sup>I scavenger, for free radical conc. in polymers, estimation 9-18764  
 Ag photolytic reduction on oxide semicond. surface, u.v. irrad. 9-6017  
 Br reaction with H<sub>2</sub> at room temp. 9-1917  
 CO<sub>2</sub>, photolysis in far u.v. 9-10351  
 CdS, interpretation of slow (opto-electronic) phenomena 9-21547  
 HI, flash photolysis with deuterated hydrocarbons 9-8109  
 HN<sub>3</sub>, photodissoc. in vac. u.v., prod. of electronically excited NH 9-7078  
 HO<sub>2</sub>, in irrad. H<sub>2</sub>O<sub>2</sub>-H<sub>2</sub>O solns., e.s.r. 9-7081  
 KBr·OH<sup>-</sup>, dissociation 9-18480  
 KBr, with NO<sub>2</sub>, NO<sub>2</sub> impurities, reactions due to u.v. exposure 9-5581  
 KCl·OH<sup>-</sup>, dissociation 9-18480  
 KI, with NO<sub>2</sub>, NO<sub>2</sub> impurities, reactions due to u.v. exposure 9-5581  
 N<sub>2</sub>H<sub>4</sub>, <sup>15</sup>N, vac. u.v., photolysis 9-1918  
 NO photolysis, <sup>15</sup>N-enriched N<sub>2</sub> formation 9-16491  
 NOCl and NO<sub>2</sub> in vacuum u.v., photodissoc. 9-16492  
 O <sup>1</sup>D atom reactions with N<sub>2</sub>O, N<sub>2</sub> and CO<sub>2</sub>, ozone quantum yields 9-21719  
 O<sub>2</sub>(<sup>1</sup>Δg) prod. in benzene-oxygen mixtures 9-13368  
 O<sup>3</sup>P(=CS)<sub>2</sub>→SO+CS, product vibr. energy, expt. and computation 9-10327  
 SiH<sub>2</sub>F<sub>2</sub> vac. u.v. photolysis, matrix isolation of SiF<sub>2</sub> 9-15903  
 SiH<sub>3</sub>Cl<sub>2</sub>, matrix-isolation vac. u.v. photolysis 9-10352

**Photoconducting devices**

- a.c. biased, photocurrent gain 9-7852  
 Lewis acid with polyurethane as material for electrophotographic plates, patent 9-20574  
 p<sup>+</sup>-n junction, non-uniformly illuminated, time-depend. photovoltage distrib. 9-3672  
 photodiode circuit for meas. of variable component of luminous flux 9-10912  
 photodiodes, eff. of r.f. bias on microplasma 9-10076  
 Schottky diodes, barium titanate, photocurrents generation 9-18660  
 semiconductor, design introduction, book 9-15142  
 BaTiO<sub>3</sub>, Schottky diode, photosensitive 9-18660  
 CdS-n:Ge, photosensitive cells, temp. depend. of elec. props. 9-5723  
 CdSe-n:Ge, photosensitive cells, temp. depend. of elec. props. 9-5723  
 Cu<sub>2</sub>O photoresistors, characts. 9-16316  
 Ge:Ga detector, spectral response 9-3745  
 Hg<sub>1-x</sub>Cd<sub>x</sub>Te alloy, photoconductive i.r. detector 9-8522  
 InSb far i.r. detector, response enhancement by near i.r. irrad. 9-3746  
 PbS polycrystalline photoresistors, V-I, luminous charac. and absolute spectral sensitivity 9-13935  
 Se cell solar u.v. sensor 9-10075  
 Si photodiode, p-i-n, u.v. response obs. 9-12217

**Photoconductivity**

*See also* **Photoconducting devices**

- alkali halide crystals, multiphoton excitation by laser emission 9-13941  
 alkali halides, additively-coloured 9-13930  
 anthracene, carrier prod. and transport 9-17445  
 anthracene, rel. to diffusion and surface reactions of singlet excitons 9-13835  
 anthracene, elec. field and temp. depend. 9-3738  
 anthracene, hole and electron photogeneration mechanisms 9-1617  
 anthracene, X-ray induced, temp. dependence 9-3739



**Photoconductivity** continued

- anthracene crystals, hole injection from electronically excited iodine mols. 9-16313
- copper phthalocyanine, single crystal, dark conduct. and photocond. meas. 9-1619
- decay phenomenon of II-VI compound semiconductors 9-1622
- electric-field and temp. depend. 9-3738
- excitation by optical lasers, generation of difference freqs. in far i.r. 9-6532
- fluorescein in boric acid glass, and thermoluminescence 9-16314
- glasses, chalcogenide, rel. to energy levels and progressive crystn. model 9-3611
- hydrocarbons, liq. aromatic, criteria necessary for photocond. in electrode-liq. syst. 9-17219
- inhomogeneity effects, non-uniform illumination 9-13928
- inhomogeneous materials, Hall and photo-Hall effect 9-3730
- lamellar structure on illumination near phase transition temp. 9-15135
- metal-photocond. contact investigation 9-16312
- naphthalene, molten, photocurrent from triplet state generation by light 9-9533
- organic dye films, polarization changes and external field effects on spectra 9-1616
- p<sup>+</sup>-n junction, non-uniformly illuminated, time-depend. photovoltage distrib. 9-3672
- phenazine single crystals, carrier generation 9-7860
- photoconductors, a.c. biased, current gain 9-7852
- photoconductors, gain meas., steady state and pulse 9-7854
- polymer compositions for xerography, patent 9-8674
- polystyrene, delayed effects 9-1620
- pyrene crystals., intrinsic 9-5771
- relaxation phenomena rel. to semiconductor field effect 9-10064
- rhodamine B films, semicond., linear and quadratic recombination of photocarriers 9-12213
- semiconductor, anisotropic, photosensitivity from I-V characts. 9-15134
- semiconductor surface potential dependence rel. to surface recombination rates 9-5698
- semiconductors, subject to high illumination intensities 9-1609
- superconductivity, photo-induced, theoretical exam. 9-5656
- transverse photo-e.m.f., appearance during observation 9-13933
- works in. review 9-10065
- AgBr film, maxima and their origin 9-21545
- AgCl film, maxima and their origin 9-21545
- AgI film, maxima and their origin 9-21545
- CaS:Ce phosphor, thermally stimulated currents and trap depths 9-21546
- Cd<sub>0.98</sub>Hg<sub>0.02</sub>Te graded gap structure, rel. to photocarrier transport 9-18619
- CdIn<sub>2</sub>S<sub>4</sub> crystal, spectra 9-3733
- CdIn<sub>2</sub>S<sub>4</sub> 9-3732
- CdO:B<sub>2</sub>O<sub>3</sub> SiO<sub>2</sub> glasses, optimization of props. 9-7853
- CdS, acoustic flux distrib., Brillouin scatt. meas. 9-3907
- CdS, conductivity storage, model 9-13929
- CdS, decay, oscillatory lifetime obs. 9-3734
- CdS, depolarization field eff. on electro-elastic props. 9-17439
- CdS, field-effect 9-10067
- CdS, field effect photocurrent rel. to hole mobility, obs. 9-1612
- CdS, g r noise dependence on light penetration depth 9-12211
- CdS, in vicinity of absorption edge 9-1611
- CdS, isothermal decay, trap mechanism 9-18655
- CdS, oscillatory phase 9-1613
- CdS, photoelectrons, Hall mobility 9-5761
- CdS, resistance, negative, and relax. effect of conductivity at low temp. 9-5764
- CdS, surface states and photocurrent pinch-off effect 9-7855
- CdS, trap depth and density determ. by space-charge-limited currents 9-10070
- CdS crystals with edge emission, i.r. effects and temp. depend. 9-21644
- CdS films, high photovoltage generation and decay, light intensity and temp. effects, mechanism 9-15136
- CdS films, recombination centres 9-10068
- CdS platelets, h.f. acoustoelec. currents, departure from Ohm's Law 9-13798
- CdS single crystal, trap distrib. obs. 9-16440
- CdS slow phenomena, photochemical interpretation 9-21547
- Cd(S<sub>0.98</sub>Se<sub>0.02</sub>) crystal, steady-state and pulse gain meas. at 300°K 9-7854
- CdS<sub>0.98</sub>Se<sub>0.02</sub> graded films 9-3735
- CdSe, function of temp. and excitation intensity 9-10234
- CdSe, photocurrent saturation mechanism 9-5762
- CdSe surface u.s. wave amplification using photostimulation 9-7647
- n-CdTe, high-resistivity, spectra and kinetics rel. to impurity eff. 9-3621
- p-CdTe, interaction of excitons with opt. phonons 9-10069
- n-CdTe, oscillatory, from shallow donors 9-5763
- CuCl single crystals, 10 to 150°K 9-10071
- Cu<sub>2</sub>O, at 110°K rel. to bound states 9-12375
- Cu<sub>2</sub>O, polycrystalline, high-resistivity, combined prep. and low temp. meas. device 9-3742
- Eu chalcogenides 9-12328
- EuO, low-temp., magnetic effects 9-12212
- EuO magnetic effects 9-19935
- EuO 9-7856
- EuS, low-temp., magnetic effects 9-12212
- EuS 9-7856
- EuSe 9-7856
- GaAs, epitaxial, extrinsic far i.r. photocond. 9-7857
- n-GaAs, h.f. phase shift meas. 9-18656
- n-GaAs, interaction of excitons with opt. phonons 9-10069
- GaAs, semi-insulating, elec. and optical enhancement 9-5766
- GaAs, shallow donor interpretation 9-12377
- n-GaAs diffused with Cu, electron lifetime, temp. depend. 9-5765
- GaS, n- and p-type, room temp. 9-1614
- n-Ge:Cu, decay kinetics rel. to electron lifetime 9-21549
- Ge:Sb, far i.r., two types 9-18657
- Ge, exciton states in photocurrent formation 9-7858
- n-Ge, neutron irradiated, impurity kinetics 9-10072
- Ge, plastically deformed and irradiated, spectra 9-15137
- Ge, uniaxially compressed, photoionization of acceptor impurities 9-1610
- Ge layers, voltage sensitivity meas. 9-10074
- Ge radiation detectors, optimal thickness of sensitive layers 9-10073
- Ge surface recombination centres, nature 9-17443
- n-In<sub>2</sub>O<sub>3</sub> film 9-15138
- n-InSb, due to cyclotron resonance absorpt. 9-5767

**Photoconductivity** continued

- n-InSb, electron heating effects 9-10063
- n-InSb, far i.r. resonant props. due to cyclotron resonance 9-17440
- n-InSb, resonant, rel. to transport props. 9-17444
- InSe, kinetic and stationary characts. 9-18658
- KCl, coloured, sensitivity changes during bleaching 9-5768
- KCl, photomobility of dislocations in irradiated crystals 9-21548
- PbSe, evaporated film, O<sub>2</sub> effect on photosensitivity 9-5770
- Pb<sub>1-x</sub>Sn<sub>x</sub>Te single crystal, 77°K-4.2°K 9-5769
- SbSI, Curie temp. shift due to illumination and nonequilibrium carriers 9-16300
- SbSI, eff. on ferroelec. phase transition 9-7845
- Sb<sub>2</sub>Se<sub>3</sub>:I, needle-like crystals 9-1194
- Se:Br polycrystal, obs. and theory 9-13931
- Se crystallized nonthermally, temp. depend. 9-9806
- Si:In acceptors 9-7859
- Si-Au alloys, i.r. impurity photocond. of Si surface 9-15140
- Si, defects; divacancy-associated energy levels 9-3327
- n-Si, e. irradi., after stress-induced reorientation of defects rel. to defect obs. 9-21340
- p-Si, e. irradi., oscillations in spectrum rel. to A-centres 9-18659
- SiC-CdSe p-n junctions, photosensitivity 9-10013
- n-SiC, 77°K 9-13932
- TlSe, meas. for optical energy gap 9-3556
- WSe<sub>2</sub>, n and p type, 77° to 295°K 9-5692
- ZnIn<sub>2</sub>Te 9-3732
- ZnS:Cu, Cl photodielectric effect due to photoconduction in grains 9-1570
- ZnSe, interaction of excitons with opt. phonons 9-10069
- Photodisintegration** *see Deuterons/photodisintegration; Nuclear reactions and scattering due to photons*
- Photodissociation** *see Photochemistry*
- Photoeffect, nuclear** *see Gamma-rays/effects; Nuclear reactions and scattering due to photons*
- Photoelasticity**  
*See also Double refraction/mechanical*
- bar, h.f. elastic stress waves anal. 9-19058
- bar, interference fringes behaviour on bending 9-20397
- cylindrical bar under band-press., 3D photoelastic stress anal. 9-20401
- dynamic, use of multiple-spark-gap camera 9-6363
- elastoopic constant meas. methods, sensitivity improvement 9-15450
- holographic interferometer for isopachic analysis 9-6365
- hyperstatic systems appl. 9-20396
- polycaprolactam, degradation and lifetime 9-11937
- polyethylene networks, stress-optical coeff. 9-14969
- polyethylene terephthalate, change in extinction direction in deform. bands 9-5463
- rheo-optical behaviour of polymer solids obs. by X-ray diffraction 9-7536
- silk, degradation and lifetime 9-11937
- stress analysis, 'freezing' deformation method 9-14378
- stress analysis of plate with reinforced circular hole 9-10691
- stress wave diffraction by solids, expt. representation 9-6380
- three-dimensional photoelastic anal., design of stress-freezing oven, applic. 9-20401
- Ag<sub>3</sub>GeS<sub>4</sub>, photochemical effect 9-14982
- CaMoO<sub>4</sub> refractive index pressure dependence 9-16393
- CaWO<sub>4</sub> refractive index pressure dependence 9-16393
- CsX, (X=Cl, I), stress-optical dispersion meas. 9-5873
- $\alpha$ -HIO<sub>3</sub> solution-grown crystal, high figure of merit, applications 9-3865
- KH<sub>2</sub>PO<sub>4</sub> refractive index pressure dependence 9-16393
- NH<sub>4</sub>H<sub>2</sub>PO<sub>4</sub> refractive index pressure dependence 9-16393
- RbX, (X=Br, I), stress-optical dispersion meas. 9-5873
- TiO<sub>2</sub> rutile, refractive index pressure dependence 9-16393
- Photoelectrets** *see Electrets; Photography*
- Photoelectric cells** *see Photoconducting devices; Photoconductivity; Photoelectricity; Photovoltaic effects*
- Photoelectric effect, atomic** *see Atoms*
- Photoelectric emission** *see Electron emission/photoelectric*
- Photoelectricity**  
*See also Electron emission/photoelectric; Photoconductivity; Photovoltaic effects*
- anthracene, dark injection of electrons from alkali metals 9-1618
- anthracene crystals, optical activation of traps. 9-19934
- ellipsometer, visible and u.v. 9-10919
- junction photoelec. response rel. to narrow light beam displacement 9-7850
- metallic surface properties change in the oxidation process 9-5760
- optical rotation meas. applic., errors 9-13057
- p-n junctions, testing of inhomogeneities 9-13900
- photodielectric effect in thin phosphor film, due to photoconduction in grains 9-1570
- photon counting techniques and applications 9-6498
- plasma temp. meas. by relative intensity of spectral lines, photoelectronic technique 9-9377
- Se, films, amorphous, field controlled and free-carrier transport 9-3729
- semiconductor photoelectric devices, design introduction, book 9-15142
- semiconductors, degenerate phenom. with e heated by light 9-12209
- AgN<sub>3</sub>, photo e.m.f. meas. 9-10066
- As<sub>2</sub>S<sub>3</sub>(Se<sub>2</sub>) films, photosensitivity rel. to frequency of incident radiation 9-3731
- Au thin film, infl. of elec. field 9-17442
- Au thin film on Ag, photoelec. eff. 9-17441
- CdO-p-Si diode, photocurrent and photo-e.m.f. characts. 9-5728
- CdSe, sensitization as result of etching, investigation 9-3917
- n-CdTe, surface props. in contact with electrolytes 9-3727
- Cu<sub>2</sub>HgI<sub>4</sub>, properties 9-12216
- Cu<sub>2</sub>O, photocurrent amplification by mag. field 9-5759
- GaAs, high-resistivity, current oscillations and high-field domains 9-12210
- Ge, photoelectron mobility, variation with photon energy 9-13927
- n-Ge films, props 9-3736
- InP clean surface, yield near threshold 9-16319
- MoS<sub>3</sub> thin crystals, photovoltage, 77°-290°K 9-13934
- Na film, props. and optical props. rel. to electronic structure 9-17472
- PbN<sub>6</sub>, photo e.m.f. meas. 9-10066
- PbO, red, vapour-deposited layers, space-charge-limited photocurrent 9-15139

**Photoelectricity** continued

- PbO, two-phase crystals, photoelec. sensitivity spectra temp. dependence 9-3737  
 PbS films, photo e.m.f., angular dependence 9-1615  
 photocurrent amplification by mag. field 9-5759  
 Pt-Rh alloys, photoelectric  $\gamma$  cross-sect. by dis. and calc. 9-18654  
 Sb<sub>2</sub>Se<sub>3</sub>-x mixed crystals, spectral distribution of internal photoelec. eff. 9-12385  
 SbTeI, internal photoeffect 9-3728  
 Se vitreous, generation of carriers 9-7851  
 Si, photoelectron mobility, variation with photon energy 9-13927  
 ZnS-Cu, Cl photoelectric effect due to photoconduction in grains 9-1570

**Photoelectromagnetic effects**

- Dember voltage short-circuiting, effects 9-5772  
 open-circuit voltage, for semiconducting materials and allied devices with quadratic volume recombination 9-1608  
 P.V.K., hole photoemission from metals 9-5739  
 in quantizing mag. fields during electron electron heating by light 9-3744  
 semiconductor, photomagnetic effect increase rel. to pair generation rate 9-1621  
 n-Bi<sub>2</sub>Te<sub>3</sub>, photomag. eff., quantum oscillations 9-12144  
 Cd<sub>2</sub>Hg<sub>1-x</sub>Te graded gap structure, rel. to photocarrier transport 9-18619  
 CdCr<sub>2</sub>Se<sub>4</sub>:Ga initial permeability, photomag. change 9-12215  
 Cu<sub>2</sub>O, polycrystalline, high-resistivity, combined prep. and low temp. meas. device 9-3742  
 Cu<sub>2</sub>O, single crystals, even eff. mag. field orientation dependence 9-1623  
 Fe garnet 9-16315  
 Ge radiation detectors, optimal thickness of sensitive layers 9-10073  
 InAs(Sb), Gurevich-Firsov oscillations rel. to photomagnetic eff. 9-3743  
 InSb-NiSb, anisotropic, as i.r. detector 9-6396  
 n-InSb, in quantizing mag. fields during electron heating by light 9-3744

**Photoionisation** see *Nuclear fission***Photographic light sources** see *Light sources; Photography***Photographic materials**

- See also *Nuclear track emulsions*  
 7,8-dihydroxybenzoyl chloride derivatives, developers 9-13077  
 7,8-dihydroxycoumarin derivatives, developers 9-13077  
 electrophotographic plates, material comprising Lewis acid and polyurethane, patent 9-20574  
 emulsion, holographic, movement reduction method 9-13037  
 emulsion, thick, holographic props. 9-253  
 emulsion as a 3d recording medium 9-20569  
 emulsion layers, modulation transfer function, determ. from physical meas. 9-10946  
 emulsion plate, electron sensitive, prep. in lab. 9-4695  
 emulsions, diluted, with reduced shrinkage factor, for particle track visualization 9-465  
 emulsions, Eastman Kodak IIa, performance data 9-4543  
 emulsions, nuclear, type-R, estimation of microdistortions, for particle track visualization 9-466  
 film nonlinearities, effects on wavefront-reconstruction images of diffuse objects 9-10875  
 films for examination of highly radioactive samples 9-2691  
 gelatin, macromolecule, bibliography 9-6564  
 gelatin, residual thiosulphate analysis, colorimetry 9-6563  
 granularity, stat. model, rel. to Weiner spectrum 9-19173  
 Ilford S4071 plate as ion detect. in mass spectrography, plate-to-plate eff. on darkening 9-14660  
 i.r. sensitive emulsions, hypersensitization, rel. to astron. photo., photometric usefulness 9-4544  
 Lippmann film recording by transmission and reflection, patent 9-8678  
 photochromic dispersion in thermoplastic resin, patent 9-8676  
 photochromic film, hologram storage 9-13036  
 photochromic film on polyester, patent 9-8675  
 photoconductive insulating material for electro-photography, patent 9-13076  
 photoconductive polymers for xerography, patent 9-8674  
 phthalic acid diester dispersions, fluorescent, patent 9-6565  
 polyethylene oxides, physical and photographic props. 9-7095  
 silver halide emulsions, optically sensitized method, patent 9-8680  
 Ag, thin metallic layers and halides, abs. spectra, fine struct. obs. 9-19172  
 Ag halide emulsion, open-cell cellular form, 10-95 vol.% void, support method, patent 9-20571  
 Ag halide layer litho development, patent 9-20572  
 Ag halides, role of holes 9-17901  
 AgBr, adsorption of gelatin 9-7343  
 AgBr suspension, surface area meas. from cyanine dye ads. obs. 9-20566  
 AgI suspension, surface area meas. from cyanine dye ads. obs. 9-20566  
 KBr layers, fine grain, modulation transfer function, determ. from physical meas. 9-10946

**sensitivity**

- absolute determination in vacuum ultraviolet 9-20570  
 emulsion, effect on radiance of holographic image 9-10876  
 films, commercial,  $\gamma$  response 0.667 to 1.25 MeV 9-15694  
 grains, rel. below surface and internal sensitivity 9-20568  
 holographic film (Aga-Gevaert type 10E70), characts. 9-4545  
 sensitometry, 3-aminophthalhydrazide chemiluminescence applic. 9-20565  
 X-ray film, industrial, detail visibility 9-4546  
 Ag halide emulsions, dye-sensitized, patent 9-8677

**Photographic process**

- See also *Photochemistry*  
 electrophotography, latent image formation, patent 9-13080  
 electrophotography, photoconductive insulating material, patent 9-13076  
 holes, role 9-17901  
 Fe ions eff. on devel. and latent image formation 9-20567  
 Pb ions eff. on devel. and latent image formation 9-20567
- development**  
 accelerator for silver halide emulsion, patent 9-13078  
 electrolytic electrophotographic process, patent 9-20059  
 electrostatographic method, patent 9-8679  
 latent image structure 9-16800  
 phenidone-hydroquinone developers for astronomical use, evaluation 9-12771  
 residual thiosulphate in gelatin, colorimetric analysis 9-6563  
 spectral lines, double intensification of blackening 9-8673  
 SWR film, optimum temp. and conc. conditions 9-10947  
 Ag halide layer litho development, patent 9-20572

**Photographic process continued**  
**development** continued

- Ag halides, limiting factor for Ag, water and colloid binders 9-17902  
 Fe ions eff. on devel. and latent image formation 9-20567  
 Pb ions eff. on devel. and latent image formation 9-20567

**Photography**

- See also *Cameras; Cinematography; Lenses/photographic; Radiography*  
 at diffraction limit, props. and problems 9-20564  
 digital reader of oscilloscope trace photographs 9-286  
 flash fluorescence, taking colour micrographs 9-10921  
 holographic image of diffuser, radiance, comparison of expt. and theoretical values 9-10876  
 image, effect of fluctuations in density of medium 9-4547  
 image quality rel. to aberration state 9-6543  
 images, optical integration 9-287  
 integral, virtual orthoscopic image reconstruction by single step process 9-10945  
 laser illuminated objects 9-4548  
 noisy images, optimum nonlinear processing 9-14450  
 resolving power computation, periodic bar pattern reproduction 9-15563  
 spectrographic calibration data, processing method 9-12802  
 still stroboscopic viewing of cine film 9-2431  
 X-ray fluorescent screens, random noise 9-12817  
 ZnO:Si resin electrophotographic films, characts. 9-15564

**applications**

- astronomical negative reduction by local error method 9-12773  
 astrophotometry, Vienna Univ. refractor and accessories 9-8297  
 emulsions, automatic data handling of film records 9-2430  
 films, physics, selected bib. 9-285  
 high speed process, recording, problems, choice of equipment, etc., book 9-17903  
 holograms, storing on photochromic films 9-13036  
 integral, and holography 9-20534  
 optical information storage, Lippman emulsion three-dimens. memory 9-10916  
 photoelasticity, dynamic, multiple-spark-gap camera use 9-6363  
 photolithography for etching masks, rel. to ion-implantation doping 9-19918  
 recorded profile of spectral line, and effective line breadth 9-16508  
 solar flare fine structure, exposure series 9-21976  
 solar mag. field meas., comparison with photoelec. magnetograph 9-2066  
 solar spicule investigation by three dimen. H $\alpha$  pictures 9-16626  
 stat images, visibility in perfect records and photographs 9-19175  
 stellar position reduction errors 9-16631  
 stereophotography with light and electron microscopes 9-15198  
 in velocity meas. of liquid droplets in air stream 9-18346  
 X-ray diffraction crystallography, meas. accuracy 9-19694  
 e, relativistic in magnetic field, radiation polarization obs. 9-4587

**colour**

No entries

**high-speed**

- camera, multiple-spark-gap, for dynamic photoelasticity 9-6363  
 for high speed processes, basic problems, choice of equipment and applic., book 9-17903  
 shutter, electromech. uncapping 9-288

**Photoionization**

No entries

**gases**

- allene 9-9403  
 butadiene 9-9403  
 efficiencies of mol., 1067Å, and 1067Å cornel. with 'Jesse' eff. in irradiat. Ar 9-13447  
 propyne 9-9403  
 u.v. monochromator - mass spectrometer combination for obs. in 600-1000 Å region 9-7195  
 Ar, simple- and cluster-ion mobility at h.p. 9-18310  
 C<sub>2</sub>N<sub>2</sub> 9-9398  
 H<sub>2</sub>S, mass spectra 9-905  
 H<sub>2</sub> + inert gases, ion-mol. reactions 9-17132  
 SO<sub>2</sub>, mass spectra 9-905  
 XeF<sub>2</sub> 9-11617  
 Zn vapour vacuum u.v. spectrum, abs. cross-section meas. 9-13453

**Photolysis** see *Photochemistry***Photoelectromagnetic effects** see *Photoelectromagnetic effects***Photoelectroelectric effects** see *Photoelectromagnetic effects***Photometers**

- See also *Spectrophotometers*  
 calibration of light-scattering photometer 9-271  
 calorimeter for short low-energy light pulse meas. 9-255  
 iris, new design for measurement of stellar atmospheres 9-21988  
 light-scattering, for use with dil. polymer solns. 9-16003  
 microphotometer, integrating 9-10564  
 precision, using mW light sources and photon counting 9-20552  
 Sofica and Brice-type, reflection effects comparison, anal. of ang. scatt. data 9-14832

**Photometry**

- See also *Brightness; Densitometry; Illumination; Spectrophotometry*  
 640 phosphor use as optical converter 9-15547  
 astrophotometry, Vienna Univ. refractor and accessories 9-8297  
 basic laws, deriv. from partial coherence theory 9-10910  
 BV357 eclipsing binary star, study 9-14203  
 calibration of photometric systems without optical standard 9-19167  
 Ru Camelopardalis UVB study (Feb. 1966-June 1968) 9-21902  
 candela, (cd), definition 9-10606  
 comets, book 9-4123  
 crystals, single, melting values recording 9-11744  
 detector responsivity, source-detector spectral matching factors 9-10909  
 device for measuring stones and seeds in glass discs 9-3173  
 dwarf stars, red, narrow and broad-band study 9-16576  
 equivalent luminance of any light, as function of scotopic and photopic luminances 9-14446  
 flame book 9-4374  
 intensity calibrations in far u.v., new developments 9-17891  
 interference fringe strengths meas. 9-10908  
 irradiance, international comparison of measurements 9-13058  
 K-giants, metal abundances and temp. calibration determ. 9-16567  
 measurements, book 9-6267



**Photometry continued**

- Metcalf refractor at Boyden observatory, photometric centre correction 9-10562  
 NEC 7261, galactic cluster, distance age, physical members 9-14224  
 particle size meas. in polydispersions 9-3135  
 photoelectric UVB obs. of CM Lacertae, eclipsing binary 9-21903  
 photoelectric UVB obs. of  $\delta$  Scuti star 4 Canum Venaticorum 9-14220  
 photographic, suitability of 84" reflector and its photometer for stellar obs. 9-21906  
 photon counting system for Raman spectroscopy 9-10818  
 planets, brighter, photometric obs. (1963 1965) 9-14236  
 Puppis UVB study 9-17619  
 Puppis Vela stars, no colour excess in 1 kpc 9-6119  
 radiometric scales, international comparison 9-10911  
 and radiometry units, definitions and conversion factors 9-10749  
 Scorpio Centaurus assoc., intrinsic colours and magnitude correction for interstellar absorpt. 9-14201  
 several-colour, in stellar rot. study 9-21866  
 of star number 1 in NGC 2024, comparison with  $\theta^2$  Ori B 9-14210  
 stars, blue faint and white dwarfs, spectra obs. and space distrib. estimation 9-14202  
 stellar associations in Large Magellanic cloud, UVB obs. 9-14223  
 stellar radii, photometric computations for 46 stars 9-12673  
 sunspot, pinhole device reducing diffracted light 9-8291  
 telescope, photometric, computer controlled 9-14277  
 UVB, of Puppis Vela stars, no colour excess in 1 kpc 9-6119  
 variable component of luminous flux, photodiode circuit for meas. 9-10912

**light sources**

- exploding wire lamp with monochromator 9-277  
 linear, effect of gonio-photometer arm length on error in luminous intensity meas. 9-6552  
 linear, illumination meas. 9-6553  
 tungsten-filament lamps for comparison of irradiance measurements 9-13058  
 tungsten-filament lamps for international comparison of radiometric scales 9-10911

**Photomultipliers**

- hunching factor in primary segment 9-10826  
 dark current props., rel. to ght flux meas. 9-10844  
 extreme u.v., quantum efficiency and dynamic range 9-19135  
 fast response, high current, patent 9-8585  
 gain shift due to extraneous mag. field in  $\gamma$ -rays polarisation meas., elimination 9-19192  
 Light signal analysis after propag. through turbulent atmos. 9-8646  
 logarithmic props., investigation 9-17861  
 low resistance voltage-divider for high counting rates stability 9-4442  
 organic scintillator response meas. appl. 9-6722  
 photodetector time response 9-2351  
 photoelectron transit time spread when operating in time mode 9-16771  
 pulse linear subtraction method for accidental counts elimination 9-4656  
 single electron response and afterpulsing 9-4443  
 voltage diodes, low-resistance 9-4441  
 XP 1210 high speed tube, light-pulsar obs. 9-19128  
 Ag-Cs-O photocathode, increased sensitivity using optical effects 9-19938  
 CsI photocathode tube containing channel electron multiplier 9-17894  
 NaI crystal, tube combinations, packaging techniques 9-19129

**Photons**

- See also Cosmic rays/photons; Gamma rays; Nuclear reactions and scattering due to photons; X-rays*  
 'whirls' in protogalaxy formation 9-17610  
 absorption and light fluctuations from quasi-monochromatic beam 9-4446  
 coherent emission by many atoms 9-6497  
 counter, extreme u.v., quantum efficiency and dynamic range 9-19135  
 counting, 'pile-up' correction in radiative lifetimes meas. 9-10845  
 counting, low light flux meas. 9-10844  
 dosimetry, physical basis 9-453  
 electric and magnetic structure, tested in collisions with mols. 9-13101  
 field in vacuum with multiple mirror reflections on boundary 9-12989  
 graviton production in e.m. field 9-61  
 intense light interact. with atoms, effective electronic binding pot. 9-684  
 i.r. quantum counter using rare earths 9-10927  
 i.r. quantum counters, thermal noise 9-6499  
 isolated, collision with plane e.m. wave, rel. to electron-positron pair creation 9-15583  
 momentum distrib. in ionized gases 9-13458  
 momentum distrib. rel. to e.m. waves in fully ionized gas 9-13459  
 photon cascades in  $(\alpha, 2n)$ ,  $(\alpha, 3n)$  on rare-earth nuclei 9-14631  
 polarized, Compton scattering by polarized particle with spin  $1/2$ , theory 9-15579  
 production in universal 3°K region 9-18886  
 radiative decay of tangential surface plasmons 9-7720  
 time correlation, emitted during Xe excitation 9-13301  
 wave+particle model and laser interference expts. 9-6500

**interactions**

- atomic photoeffect relativistic, from K shell near threshold 9-690  
 Coulomb field e pair prod., total Born approximation cross-section 9-13104  
 deuteron photodisintegration, proton polarization obs.  $E_p=282$  to 405 MeV 9-17938  
 electron pair prod. in nuclear field 2-20MeV 9-11265  
 fermions, meson photoprod. amplitudes asymptotic props. 9-8801  
 $\eta^0$  photoprod. at 4 GeV 9-351  
 in liquid Xe, e pair production, 100, 200, 500, 2000 MeV obs. 9-15584  
 meson photoproduction by polarized photons, Primakoff effect, coherent and incoherent 9-11027  
 meson resonance production, modified coherent-droplet model 9-20656  
 mesons, pseudoscalar and neutral vector; production on nucleons; Regge-pole model 9-391  
 new non strongly interacting particles prod. by  $<18$  GeV  $\gamma$ -rays, search 9-8743  
 with nucleons at high energy, meson-baryon prod. and decay distrib. obs. 9-8736  
 $p$ - $p\omega$  via diffraction and elementary  $\pi$  exchange, analysis 9-15635  
 photoprod. of  $\pi^-$  from H target 9-8829  
 photoproduction sum rules and N axial mean square radius 9-2527  
 $\pi$  prod., charged, Regge trajectory slope and conspiracy theory 9-6657

**Photons continued****interactions continued**

- Si. Collimation tests on coherent beam 9-13103  
 vector-meson prod. cross section calc., vertex-strength - algebra treatment 9-11075  
 $ap \rightarrow p\pi^0$ , recoil p polarization 9-415  
 e pairs prod. in liquid Xe, 100, 200, 500, 2000 MeV 9-15584  
 $\gamma D \pi^+$  prod., low momentum transfer 9-15616  
 $\gamma d \rightarrow \pi^+ p p, \gamma d \rightarrow \pi^+ n n$ , ratio of  $\pi$  production for varying momentum transfers, 8 and 16 GeV 9-15620  
 $\gamma\gamma \rightarrow \nu\bar{\nu}$ , rel. to astrophysics, energy loss rate and  $\gamma$ - $\nu$  weak coupling theory 9-10477  
 $\gamma N \rightarrow \Delta N$  cross-section, hard-pion current algebra predictions 9-16893  
 $\gamma N \rightarrow \Delta(1920) \rightarrow \rho^0 N$  cross section, vector-meson dominance model 9-18013  
 $\gamma N \rightarrow \Delta(2420) \rightarrow \rho^0 N$  cross section, vector-meson dominance model 9-18013  
 $\gamma n \rightarrow p\pi^-$  differential asymmetry ratios 9-2505  
 $\gamma N \rightarrow \pi^+ N$ , interaction const. and s-lengths determ.,  $E_p=210, 225$  MeV 9-14504  
 $\gamma p$ , cross section at high energy, sum rules and vector dominance model 9-6596  
 $\gamma p$  hadrons prod. total cross section, up to 5 GeV 9-2472  
 $\gamma p$  interactions in H<sub>2</sub> bubble chamber, 0.3-5.8 GeV, meson and baryon resonance obs. 9-11071  
 $\gamma p$  partial photoprod. cross sections up to 12 GeV 9-4580  
 $\gamma p$  total hadronic cross sections at 75 GeV 9-4581  
 $\gamma p \rightarrow \Delta^{++}(1236)\pi^-$ , theory discussed, low energies 9-11049  
 $\gamma p \rightarrow \Delta^{++}\pi^-$ , expt. comparison with intermediate isobar model  $E_p \leq 1.8$  GeV 9-19207  
 $\gamma p \rightarrow K^+ \Lambda$ , forward cross section prediction by SU(6)<sub>w</sub>,  $E_p=5-16$  GeV 9-8894  
 $\gamma p \rightarrow K^+ \Sigma^0$ , forward cross section prediction by SU(6)<sub>w</sub>,  $E_p=5-16$  GeV 9-8894  
 $\gamma p \rightarrow \Lambda^0 K^+$  near threshold in Born approx. 9-8908  
 $\gamma p \rightarrow \Sigma^0 K^+$  near threshold in Born approx. 9-8908  
 $\gamma p \rightarrow p' p'$  by polarised photons, in c.m. system and first reson. region, differential cross sections, comparison with isobaric model 9-16822  
 $\gamma p \rightarrow \mu^+ \mu^- p$  differential cross section meas., quantum electrodynamics test 9-20583  
 $\gamma p \rightarrow n\nu^+$ , cross-section for  $w^+$  mag. and T-violating elec. dipole moment 9-16887  
 $\gamma p \rightarrow p\eta$ , differential cross section 0.8 to 1.45 GeV 9-352  
 $\gamma p \rightarrow p\pi^+ \pi^-$  below 1 GeV, isobar excitation 9-2502  
 $\gamma p \rightarrow \rho^0$ , multiplicity prod. with 16 GeV bremsstrahlung 9-401  
 $\gamma p \rightarrow \pi^- \Delta^{++}$ , vector dominance assumption for hadron e.m. current 9-16909  
 $\gamma p \rightarrow \pi^0 p$ , test for current algebra 9-2504  
 $\gamma p \rightarrow \pi^+ n$  at 300-750 MeV, absence of  $P_{11}$  resonance at 1466 MeV 9-2503  
 $\gamma p \rightarrow \pi^+ \pi^- p$ , H bubble chamber photographs, 1000 MeV  $< E$  9-20644  
 $\gamma p \rightarrow \eta p$ , validity in Chou-Yang high-energy scatt. model 9-14520  
 $\gamma p \rightarrow \rho^0 p$ ,  $2\pi$  exchange model, cross section and  $\rho^0$  decay ang. distrib. calc.,  $E_p=4.4$  GeV 9-14468  
 $\gamma p \rightarrow \pi^- \Delta^{++}(1236)$  cross section meas.,  $t$  depend. determ., 5-16 GeV 9-20642  
 $K^0(890)$  prod., Regge pole model, conspiracy reln., factorization and kinematic constraints 9-18000  
 $\pi\gamma \rightarrow$  neutral vector mesons, Regge pole model, high-energy 9-11074  
 $\pi$  photoprod. and  $\pi, N$  Compton scatt. invariant amplitudes 9-8735  
 $\pi$  production from nucleons with fixed  $u$ , dispersion sum rules 9-2501  
 $\pi$  production in  $\Delta(1236)$  resonance region, fixed- $t$  dispersion relations discussion 9-8831  
 $\pi^0$  photoprod., vector dominance and Regge parametrization 9-371  
 $\rho^0$ , high energy, prod. from  $^1H$  and  $^2H$  9-20664  
 $\rho^0$ , prod. from complex nuclei 9-20665  
 $\rho^0$  photoprod. from complex nuclei,  $p$   $\gamma$  coupling calc.,  $E_p=8.8$  BeV 9-20662  
 $\rho^0$  photoproduction, non-forward coherent, from complex nuclei 9-396  
 $\gamma p \rightarrow \pi^+ n$  photoprod. cross sections at backward angles obs. 9-375  
 $^{16}O$ , absorption calc. in configuration mixing model 9-6790

**polarization**

- $^{150}Sm$  polarised thermal n capture,  $\gamma$  obs. 9-13230  
 $^{60}Co$  polarised thermal n capture,  $\gamma$  obs. 9-13230  
 bremsstrahlung induced emission, rel. to intensity 9-8747  
 photomultiplier-scintillator meas., elimination of photomultiplier gain shift 9-19192  
 $^{28}Al$  polarised thermal n capture,  $\gamma$  obs. 9-13230  
 $^{96}Mo$  polarised thermal n capture,  $\gamma$  obs. 9-13230

**scattering**

- ang. distrib. meas., from  $p$ - $p$  bremsstrahlung 9-8900  
 atomic bound syst., infinitely high energy, amplitude determ. 9-17940  
 by atoms, quantum interpretation of resonances 9-20869  
 boson targets, non-abelian Compton effect obs. 9-10970  
 Compton, possible subtraction const. in sum rules at high energy 9-16819  
 Compton, subtraction const. and vector-meson dominance 9-8741  
 Compton effect., amplitude theorem derivation 9-17941  
 Compton effect on relativistic electrons 9-6598  
 Compton type, low energy theorems to fourth order in  $e$  9-326  
 molecules with permanent moments, rel. to possibility of photon structure 9-13101  
 non-coherent, non-correlated, in spectral lines, redistrib. functions 9-19392  
 from point source near air-ground interface, spectral obs. 9-19189  
 spin-zero systems, Feynman graphs for calc. of low energy theorems 9-6597  
 e gas, Compton eff. 9-20597  
 N Compton scatt., low-energy, invariant amplitude calc. 9-13102  
 $\pi$  Compton scatt., low-energy, invariant amplitude calc. 9-13102  
 H atoms, retardation in elastic scatt. 9-15831

**Photonuclear reactions** *see Nuclear reactions and scattering due to photons***Photophoresis**

No entries

**Photoproduction** *see Gamma-rays/effects; Nuclear reactions and scattering due to photons; Photons/interactions***Photoresistors** *see Photoconducting devices; Semiconducting devices***Photosphere** *see Sun***Photovoltaic effects**

energy converter, photovoltaic-type change in collection efficiency 9-1608

**Photovoltaic effects continued**

- semiconductor diode, in impurity absorpt. region 9-3740
- transverse photo- e.m.f., appearance during obs. of photoconductivity 9-13933
- Al-Al<sub>2</sub>O<sub>3</sub>-Au tunnel structures, annealing effect 9-7861
- GaP films, anomalous 9-3741
- Ge film, high-voltage, study 9-15141
- Ge film, mechanism 9-12214
- MoS<sub>2</sub> thin crystals, photovoltage, 77°-290°K 9-13934
- Te thin film-lead contact 9-17446

**Physical chemistry**

- dictionary of chemistry 9-4212
- methanol-water system, mass transfer from single bubbles under distillation conditions 9-18329
- microwave spectroscopy, applications 9-17508
- molar ratio curves, new plotting method 9-17506
- radiant heat transfer in adiabatic tubular reactor containing gray gas 9-12945

**Physical effects of radiations**

- See also Under individual radiations. e.g. Neutrons and antineutrons/ effects*
- alkali-halide crystals, laser-induced damage 9-16390
- alkaline earth oxides, defect and colour centre production, review 9-9693
- b.c.c. crystals, mathematical modelling of radiation damage 9-13669
- bipolar planar transistors, prediction and selection techniques for radiation effects 9-17410
- channeling of particles in crystals, classical theory and review of types of expts. 9-7685
- crystal, creep, system of eqns. with allowance for formation of gas atoms 9-5466
- depletion zone growth, conversion into dislocation zones at pores 9-7480
- dynamic response of solids induced by charged particle interaction, laser interferometric determination 9-17348
- electron ejection probability distribns. 9-7868
- electron-photon cascade, due to bremsstrahlung from cosmic rays 9-20683
- f.c.c. crystals, mathematical modelling of radiation damage 9-13669
- fission gas escape from reactor fuel during irradiation 9-20848
- glass fibre, strength 9-11934
- graphite, irradiation defects and self-diffusion mechanism, thermal annealing studies 9-5337
- graphite-pyroc carbon composite bodies obtained by thermal cracking of natural gas, nuclear radiation effects 9-9861
- hardening, saturation, model 9-16143
- high-energy, resistance of plastics 9-3544
- metals, resistivity changes during and after irradiation, meas. method 9-19888
- metamictization, not removed by heat treatment 9-3280
- m.i.s. structures, process techniques and space radiation effects, interrelation 9-19924
- molecule, photodissoc., velocity distrib. function 9-4966
- Moon, surface bleaching by solar photo reduction 9-21928
- m.o.s. devices, ionizing radiation effects 9-18643
- m.o.s. structures, in modified oxide insulators 9-17420
- neutron irradiat., voids,  $5 \times 10^{19}$  fast n/cm<sup>2</sup> 9-7499
- Ovonic threshold switches, radiation hardness 9-17402
- particle cloud, hypervel. impingement on metals, micron sized, damaging effects 9-9859
- particulate, expt. for eval. of props. 9-6255
- polytetrafluoroethylene, free radical formation 9-2558
- polyurethane films, u.v. resistance, chemical prep. eff. 9-14983
- purine nucleotides,  $\gamma$  irradiat. effects 9-11718
- pyrimidine nucleotides,  $\gamma$  irradiat. effects 9-11718
- semiconductors, Frenkel pairs formation 9-3328
- semiconductors, induced defects, factors influencing stability 9-17388
- semiconductors, ion implantation and radiation damage, correlations 9-17395
- silica, vitreous, ionizing-radiation-induced dilatation, impurity effect 9-14961
- solar cells on near-sun missions 9-4424
- solar intensity rel. Si cell charactrs. 9-4423
- steel, laser irradiat., surface hardening causing structural changes 9-5418
- stopping cross-sections showing Z<sub>1</sub> oses., and size effect 9-5583
- thermocouple calibration, influence of n dose rate 9-4377
- on thermocouple materials 9-17359
- transition radiation, in opt. and relativistic energy region, from passing Ag and Al foils 9-9860
- Zircaloy-2, annealed, strain ageing 9-17330
- $\alpha$ , expt. for eval. of props 9-6255
- $\beta$ , expt. for eval. of props. 9-6255
- Ag, Au films, epitaxial and polycrystalline, elec. resistance and struct.,  $\alpha$ -irrad. 9-5240
- Al,  $\alpha$ - and  $\beta$ -irradiated, elec. resistance meas. rel. to strain and temp. 9-7746
- Au, internal friction, cold-worked and irradiated at low temp. 9-5430
- Be, recovery data of mechanical and physical props. from kinetics of He evolution temp. depend. 9-13710
- Cu damage rate at 80°K, infl. of interstitials 9-3329
- Fe, electron-photon cascade, due to bremsstrahlung from cosmic rays 9-20683
- GaAs diffusion improved by defect form., patent 9-21354
- Ga<sub>1-x</sub>In<sub>x</sub>As, i.r. reflection spectra, mixed cry. behaviour 9-1760
- Ge crystal lattice parameter expansion due to fast n 9-1189
- Ge diffusion improved by defect form., patent 9-21354
- InAs diffusion improved by defect form., patent 9-21354
- InSb diffusion improved by defect form., patent 9-21354
- KBr, with NO<sub>2</sub><sup>-</sup>, NO<sub>3</sub><sup>-</sup> impurities photochemical reactions due to u.v. light 9-5581
- KCl, u.v., F-centre production 9-1235
- Kl, with NO<sub>2</sub><sup>-</sup>, NO<sub>3</sub><sup>-</sup> impurities, photochemical reactions due to u.v. light 9-5581
- MgO:Cr X-irrad., Cr<sup>3+</sup> phonon scatt., thermal cond. meas. 9-5535
- NaCl, u.v., F-centre production 9-1235
- Ni-Fe alloys, order-disorder, mag. props. 9-1661
- Si diffusion improved by defect formation, patent 9-21354
- n-Si electron damage, thin specimen prep. 9-13815
- SiO<sub>2</sub>, vitreous silica, compaction 9-11921
- SiO<sub>2</sub> films, evaporated, u.v. irradiat. effects on optical and dielec. props. 9-5868
- TiB<sub>2</sub> irradiated by thermal neutrons, investigation of stability 9-1409

**Physical effects of radiations continued**

- $\alpha$ -U, growth under irradiat. at 25°C 9-7371
- UO<sub>2</sub>, arc cast and sintered, on thermal conductivity, 150-1600°C 9-15034
- UO<sub>2</sub>, sintered, on thermal conductivity, 150-1600°C 9-15034
- W, thin, heating due to  $\gamma$  9-12038
- Xe trapping in oxides and halides 9-19746
- YFe garnet:Si i.r. irradiat., photomag. anneal props. by torque meas. 9-10137
- ZnO diffusion improved by defect form., patent 9-21354
- <sup>90</sup>Zr, neutron irradiated, damage rate and distrib. determ., depend on lattice energy 9-17365

**Physics**

- See also Biographies; History; Nuclear physics; Teaching*
- A-level physics textbook with modern approach 9-20289
- accomplishments of six scientists having anniversaries in 1969 9-12821
- artistic invitations to its study, lecture 9-6254
- atomic, experiments and projects 9-2120
- career aspects, stat. on choice of degree, declining interest 9-2111
- conference, (1968), Oaxtepec, Mexico 9-12819
- elementary teaching, individual work approach 9-6250
- examinations, objective testing methods 9-4205
- human intervention, effect on physical laws 9-6246
- plasma, computer based selective dissemination of information 9-857
- pocket-book of useful formulae, derivations and data 9-4203
- Swiss physicists in industry 9-15401

**Physics fundamentals**

- See also Cosmology; Elementary particles; Field theory, classical; Field theory, quantum; Indeterminacy; Mechanics; Parity; Probability; Quantum theory; Relativity; Thermodynamics; Units*
- bootstrap concept, scientific status 9-20596
- causality, stable, necessary and sufficient for cosmic time functions 9-6104
- causality and determ. within physical reasoning 9-15398
- constants, cosmological, numerical relations 9-6268
- continuity, passage to discontinuity, application of current theory 9-18987
- elementary particle interactions and cosmological quantities, interrelation 9-6585
- energy-field strength in electrostatic field, simple proof 9-18
- magnetic charge, photon source model 9-10597
- metrology methods comparison, for length and time standards 9-10605
- quantum mechanical description using Jaynes' irreversible statistical mech. 9-20323
- symmetry, Amer. J. Phys. resource letter 9-6584
- time invariant in Hamiltonian formalism for nonrelativistic quantum field theory 9-16801

**Physiology**

- See also Biological technique and instruments; Blood; Hearing; Vision*
- primates, colour vision 9-18962
- renograms, radioisotope, quantitative evaluation method 9-20255

**Piezo-optical effects *see Photoelasticity*****Piezoelectric oscillations**

- acoustic second-harmonic generation crystals 9-2200
- crystal plates, mechanical coupling between bending and contour shear vibrations 9-152
- neutron diffraction examination 9-1355
- resonator, self excited, perfect for amplification of ultra and hypersound 9-12201
- transducer, piezo-ceramic, mech. response calc. 9-13921
- wurtzite type crystals, ultrasonic surface waves 9-7646

**Piezoelectricity**

- See also Electrostriction; Piezoresistance*
- acoustic second-harmonic generation crystals 9-2200
- acoustic wave amplification by semiconducting plate in liquid 9-18556
- acoustic waves, anomalous fluctuations in semiconductors in external electric field 9-5670
- chalcogens, new materials <sup>75</sup>As n.q.r. study 9-18747
- compound vibrator, for internal friction meas. in absorbent mats. 9-7523
- crystals adjacent to semiconds., acoustic surface wave amplification 9-9833
- lattice, X-ray strainmeter 9-3262
- piezo-semiconductors, sonic waves, theory of fluctuations 9-18552
- polymer transducer, due to uniaxial crystallites orientation 9-2926
- semiconductor, acoustic wave amplification and acoustoelect. effects 9-5549
- semiconductor, acoustoelectric domains, sound reflection 9-18559
- semiconductor, acoustoelectric gain and current non-linear theory 9-5558
- semiconductor, depolarization field eff. on electromechanical props. 9-17438
- semiconductor, free-carrier Faraday effect at microwave freq. 9-14030
- semiconductors, acoustoelectric effect theory accounting for anisotropic dielec. and piezoelec. props. 9-12009
- semiconductors, minority carriers in u.s. amplification 9-11999
- semiconductors, nonlinear amplification and automodulation of sound 9-12141
- surface elastic wave dispersion produced by conducting grating on piezoelec. crystal 9-15126
- transducer for stress on bolted joint 9-8352
- ultra and hypersound generation in cubic piezoelectric crystals using Cherenkov waves 9-10053
- ultra and hypersound generation in piezoquartz using Cherenkov effect 9-10054
- uniaxial stress effect meas., high compression vice 9-1165
- wood, complex modulus, temp. dispersion 9-15127
- BaMgF<sub>6</sub> (M=Mn, Fe, Co and Ni) antiferromagnetic crystals 9-12308
- BaTiO<sub>3</sub>:PbTiO<sub>3</sub> single cryst. solid solns., modulus 9-12196
- CdS, depolarization field eff. on electro-elastic props. 9-17439
- CdS multilayer transducers, method of c axes flipping 9-10055
- CdS semiconducting, acoustoelect. effect rel. to anisotropic dielec. and piezoelec. props. 9-12009
- CdS surface waves with allowance for piezoelectric effect 9-18555
- DIO<sub>2</sub>, and elastic props. rel. to bonding 9-12202
- HfO<sub>2</sub>, and elastic props. rel. to bonding 9-12202
- KH<sub>2</sub>PO<sub>4</sub>, paraelec. phase analysis in terms of coupling of Brillouin-scatt. spectrum 9-5750
- LiNbO<sub>3</sub>, acoustic surface wave transducers and delay lines 9-10057
- NaCl crystal, p.d. meas., temp. depend. determ. 9-15128



**Piezoelectricity continued**

- PbZrO<sub>3</sub>-PbTiO<sub>3</sub> transducers for broad-band acoustic noise meas. 10-100 kHz 9-2228  
 SiBi<sub>2</sub>O<sub>7</sub> of plane of polarized light 9-18648  
 Te,  $D_{31}$  coeff. determ. 9-16303  
 Te films, orientation from X-ray analysis rel. to coeff. 9-14894  
 p-TeO<sub>2</sub>, a new piezoelectric material 9-7846  
 ZnS multilayer transducer, method of c axes flipping 9-10055

**Piezomagneto-optical effects** *see Magneto-optical effects***Piezoresistance***See also Piezoelectricity*

- n-GaSb InSb mixed crystal, rel. to conduction bands 9-5690  
 Si:P, 1.5 to 500°K 9-10000  
 n-Si:P, and mag. susceptibility 9-16276  
 Te, coeff., pressures lowering symmetry 9-3716  
 n ZnSe, and piezo-Hall effects 9-5693

**Piles, nuclear fission** *see Nuclear reactors, fission***Pinch effect** *see Discharges, electric; Plasma confinement; Semiconducting materials***Pions**

- amp., low-energy theorem 9-8844  
 beam, plexiglas radiator for seapration of electrons in Cherenkov counter 9-11140  
 beam momentum,  $\mu$  and e contamination, meas. with Cher. counter 9-2584  
 Brewster angle for lunar surface 9-18902  
 bubble chamber range energy relation 9-458  
 charge form-factor and SL(N,C) D-functions 9-8370  
 e.m. form factor, space and timelike 9-6663  
 e.m. form factor determ. from electroproduction data, cross sections meas 9-8827  
 $f_0/f_\pi$  sum rules and  $m_\pi$  and  $\kappa$  width 9-14500  
 form factor, determ. from Chou-Yang high-energy scatt. model 9-14520  
 form factor, domination by monopole  $\omega$ ,  $\rho$  and dipole  $\rho$  mesons 9-8887  
 form factor zero, from rise of phase shift 9-16900  
 hard-pion, calc. of meson processes, N-point functions 9-8858  
 leptonic interactions intermediate boson 9-20600  
 PCAC, integral form between  $\pi$  and A<sub>1</sub> mesons 9-4622  
 physical, dispersion treatment of mass extrapolation and vertex functions 9-6630  
 radius, sum rule for upper bound 9-6663  
 scalar Goldstone, absence 9-6656  
 three point functions, hard-pion calc. of meson vertex functions 9-16892  
 X-ray spectra, intensity meas. in different targets 9-3909  
 X-rays, 4f-3d and 5g-4f  $\pi$  mesic, for nucleus energy, width determ. 9-373  
 zero mass, O(4) quantum numbers 9-6691  
 in NN syst., M-function expansion in O(4) from Bethe-Salpeter eqn. 9-17980  
 $\pi^+\pi^0$  mass difference, calc. from spectral function sum rules 9-4623  
 $\pi^-$  beam in water, LET spectrum and Bragg curve calc. 9-21223  
 $\pi^-$  beam transport system and momentum spectrometer 9-20694  
 $\pi^-$  capture by H in chem. cpds. 9-14505  
 $\pi^-$ , zero spin assignment, direct evidence 9-11047  
 $\pi^-$  beam therapy in cancer treatment 9-12779  
 $\pi^0$  energy transfer from cosmic rays, meas. 9-18023  
 $\pi\pi$  exchange contrib. obs. for NN scatt.,  $E_\pi=95, 310$  MeV 9-18007

**decay**

- muonic, reviewed 9-6607  
 $f_0/f_\pi$  determ. in terms of pseudoscalar nonet masses, sum rules 9-6637  
 $\pi^0 \rightarrow \gamma\gamma$  in  $\sigma$ -model, PCAC puzzle, resolution 9-20641  
 $\pi^+$ , of light hyperfragments 9-18065  
 $\pi^0$ , photon hard mes. analysis PCAC breakdown 9-6640  
 $\pi^0 \rightarrow 2\gamma$ , rate rel. to integrally charged quarks 9-2500  
 $\pi^0 \rightarrow 2\gamma$ , vertex function, current algebra tech. 9-16894  
 $\pi^0 \rightarrow \gamma\gamma$ , use of Lehmann-Kallen representation for 3-point functions 9-17949  
 $\pi^+ \rightarrow \mu^+ \nu$ , struct.-depend. axial-vector form factor, hard- $\pi$  calc. 9-8828  
 $\pi^- \rightarrow e\bar{\nu}$ , decay prob. determ. from current algebra 9-11046  
 $\pi^0 \rightarrow e^+e^-$  radiative corrections from asymptotic behaviour on n-point function 9-8826  
 $\pi^- \rightarrow \gamma\gamma$ , vector gauge field anal., current mixing and octet breaking 9-392  
 $\pi^- \rightarrow \nu l$  radiative rel. to universality concept in weak interactions 9-16870

**interactions**

- with emulsion nuclei, 200 GeV, four-momentum transfer and effective mass estimation 9-4626  
 $\pi^+d \rightarrow pp$  in Regge-pole theory, residue functions, rel. to low-energy models 9-16874  
 $\pi^+d \rightarrow \pi^+ \pi^- d$  at  $E_\pi^+=8$  GeV/c 9-13133  
 2 body interact with meson resonance production use of Pade approximants. 9-2522  
 $\pi d$  rel to  $\pi N$  interact. 9-2511  
 $\pi d$  total cross section depend. on d alignment, Glauber approx. 9-17981  
 $\pi^+d \rightarrow p p \pi^+ \pi^-$ ,  $\rho^+ \Delta^0$  associated prod., 5 GeV/c 9-17998  
 $\pi^+d \rightarrow p n \pi^+ \pi^-$ ,  $\rho^+ \Delta^0$  associated prod., 5 GeV/c 9-17998  
 $\pi^+d \rightarrow p p p$ , Glauber corrections, spin and isospin at 5.1 GeV/c 9-2546  
 $\pi e \rightarrow NN$  equal-mass conspiracy relations as unequal-mass case limit 9-8728  
 $\pi^+He^+H$  vertex junction 9-9048  
 $\pi N \rightarrow N \pi^+ \pi^+$ ,  $\pi^+$  enhancement at  $M=1.05$  GeV 9-11083  
 $\pi \Sigma A$  and  $\pi \Sigma \Sigma$  coupling constants determ. 9-13126  
 $\pi X \rightarrow \pi \pi X$  for study of  $\pi\pi$  interactions 9-2508  
 $\rho^-$  backward prod.; Regge-pole anal. 9-20663  
 He s-wave radiative capture and  $\pi^+He^+H$  vertex function 9-9048  
 Li emulsion, hammer track emission, energy spectra obs., 3.5 GeV/c 9-4636  
 $^6Li$  s-wave radiative capture and  $\pi^+He^+H$  vertex function 9-9048

**interactions, pion-nucleon**

- 17 GeV/c, CERN expt. 9-15622  
 axial vector meson production, Regge model 9-11072  
 charge-exchange, single  $\rho$  residue, Regge dips formalism reviewed 9-8837  
 coupling constants, e.m. correction calc. 9-6666  
 coupling consts. e.m. corrections calc. by sum rules, Feynman graphs 9-15621  
 reaction matrix theory appl. 9-16876  
 Regge-pole residue function determ. from fixed- $t$  dispersion reln. 9-14510  
 resonant reaction with 2-nucleon bound state, 350 MeV broad resonances 9-11085  
 review of inelastic expts. 9-6664  
 strange particle creation at high energy 9-11053

**Pions continued****interactions, pion-nucleon continued**

- strong interaction amplitudes, constraints imposed by PCAC and current algebra 9-6665  
 charge exchange process, single  $\rho$  Regge-pole exchange model 9-2510  
 $\pi^+N$ , 2.34 GeV/c in Xe bubble chamber,  $\pi^0$  prod.  $\gamma$  spectrum 9-20645  
 using  $\pi d$  interaction 9-2511  
 $\pi^-N$ , 17 GeV/c velocity space transform method of analysis 9-15654  
 $\pi^-N$  in emulsion, 7.2 GeV, secondary particle analysis 9-15623  
 $\pi^-n \rightarrow p \chi^-$ , search for  $\chi^-$  9-388  
 $\pi N \rightarrow VN$ , analyticity constraint and daughter structure of conspiring Regge-pole families 9-8841  
 $\pi N \rightarrow \eta^0 N^*(1238)$ , OPE contrib. verified 9-2530  
 $\pi N \rightarrow \pi N^*5$ , PCAC predictions of threshold amplitude 9-11054  
 $\pi N \rightarrow \pi \pi N$ ,  $\pi$  scatt. length determ.,  $E_\pi=350-600$  MeV 9-8849  
 $\pi N \rightarrow \rho N$ , hard-pion current algebra calc., use as test of mes.-vertex functions for spacelike momentum transfers 9-16893  
 rel. to  $\pi\pi$   $t=0$ , J=0 phase shift turnover, partial-wave discrepancy 9-8840  
 $^{12}C(\pi^+, p)^{11}C$ , perturbation theory test, 68 MeV 9-4787

**interactions, pion-pion**

- multiple particle prod., unitary-symmetrical statistical model, 10 GeV/c 9-16833  
 S-wave in isospin-zero channel,  $\pi$  pole dominance model, information on  $\delta$  meson 9-6670  
 scattering amplitudes rel. to isospin, I=2 states 9-383  
 A<sub>3</sub>  $\pi\pi$  1660 MeV resonance production from  $\pi^+\pi^-$  parity, spin, isospin assignment;  $E_\pi=8$  GeV/c 9-8876  
 $\pi^+\pi^-$  at 17 GeV,  $\omega^-$  and heavy resonance prod. obs. in nuclear emulsion stars 9-20648  
 $\pi^+p \rightarrow A_2^+ p \rightarrow \eta \pi p$ , 2.26 GeV/c evidence for intermediate prod. of  $A_2^+$  and  $J^P=2^-$  for it. 9-14509  
 $\pi^+p \rightarrow \pi^+ \pi^- n$ , 360 780 MeV, amplitudes of  $N^*$  production 9-20676  
 $\pi^+p \rightarrow \rho^+ p$ , ang. distrib. meas.,  $E_\pi=2.7, 3$  GeV/c 9-14508  
 $\pi^+p \rightarrow \rho^0$ , density matrix elements calc.,  $M_\pi=4$  GeV/c 9-20646  
 $\pi^+\pi^-$ , peripheral and central collisions distinction, 8 GeV/c 9-14480  
 $\pi^+\pi^-$ , 1.4-4.0 GeV/c, partial cross-sections for  $\eta^0$  and  $\eta^0$  prod. 9-378  
 $\pi^+$ , reson prod. at 6 BeV/c 9-8839  
 $\pi^+p \rightarrow \Lambda K^0$ , pole-reson. model, <1200 MeV 9-8355  
 $\pi^+p \rightarrow \eta^0 n$  charge-exchange, multiple-Regge-pole model 9-8852  
 $\pi^+p \rightarrow \eta n$ , double-pole A<sub>2</sub> Regge analysis and n polarization rel. to  $\pi$  conspirator 9-8838  
 $\pi^+p \rightarrow \eta^0 n \rightarrow \pi^+ \pi^+ \pi^- n$ , obs. at 5 GeV/c 9-8871  
 $\pi^+p \rightarrow \pi X^0 \rightarrow n \eta \gamma$ , evidence for new decay mode,  $E_\pi=1.93$  GeV/c 9-15634  
 $\pi^+p \rightarrow \eta \eta \rightarrow \pi \pi^+ \pi^0$ , charge asymmetry assuming C invariance for  $\eta$  delay 9-377  
 $\pi^+p \rightarrow \rho^+ \pi^+ \pi^- \pi^-$ , A<sub>2</sub> prod. cross sections and decay ang. distrib. 9-398  
 $\pi^+p \rightarrow \pi^+ \pi^+ \pi^- \pi^-$  13 and 20 GeV/c,  $3\pi$  mass spectrum observations 9-2513  
 $\pi^+p \rightarrow \pi^+ \pi^+ \pi^- \pi^- \pi^-$ , 16 GeV/c cross-sections, resonance production, momentum distrib. obs. ang. 9-11056  
 $\pi^+p \rightarrow \pi^+ \pi^+ \pi^- \pi^- \pi^-$ , 16 GeV/c, cross sections, reson. prod., momentum distrib. obs., ang. correl. of  $\pi$  pairs 9-11056  
 $\pi^+p \rightarrow \rho^+ p$ , spin and parity determ. of A<sub>2</sub> 9-6679  
 $\pi^+p \rightarrow \pi^0 n$  charge-exchange, multiple Regge-pole model 9-8852  
 $\pi^+p \rightarrow \rho^+ n$ , vector-dominance model test 9-4627  
 $\pi^+\pi^-$ , two prong interactions, 2.77 BeV/c 9-8354  
 $\pi^+\pi^- \rightarrow \pi^+ \pi^0 \pi^0$ , 2.34 GeV/c,  $\pi^+$  and  $N^{*++}$  prod. 9-15624  
 $\pi^+p \rightarrow \pi^+ \pi^+ \pi^-$  background eff. on I=2  $\pi\pi$  scatt. phase shift,  $E_\pi=3.9$  GeV/c 9-16877  
 $\pi p \rightarrow \Lambda \Lambda n$ , at 7 and 12 GeV/c 9-6667  
 $\pi\pi$  S-wave phase shift model, extension to  $K\pi$  9-6671  
 $\pi\pi \rightarrow NN$  vertex function  $\pi\pi$ -meson resonance, form factors 9-15630  
 $\pi\pi \rightarrow VV$ , analyticity constraint and daughter structure of conspiring Regge-pole families 9-8841  
 $\pi\pi \rightarrow \eta\rho$ ,  $\rho$  bootstraps inconsistency with daughter Regge pole residues factorization constraints 9-14507  
 $\pi\pi \rightarrow \pi\omega$ ,  $\rho$  bootstraps inconsistency with daughter Regge pole residues factorization constraints 9-14507  
 $\pi^+\pi^-\pi^-$  from  $K^+$  decay, weak interac. in final state decay rates ratio determ. 9-8817  
 $\pi X \rightarrow \pi \pi \pi X$  as source of information 9-2508  
 $\pi N \rightarrow \pi \pi B$  s wave low energy phase shifts, nuclear and Coulomb amplitudes interference 9-382

**interactions, pion-proton**

No entries

**production**

- charged, photoprod., Regge trajectory slope and conspiracy theory 9-6657  
 double  $\pi$  photoprod. on p below 1 GeV, Isobar excitation invest 9-2502  
 electroproduction near  $\Delta(1236)$  isobar transverse and longitudinal cross sections 9-6659  
 e.m. prod. from complex nuclei, theory 9-6658  
 pairs, photoprod. below 850 MeV 9-4624  
 by photons, diff. cross section calc., sum rules obtained 9-11050  
 by photons, in  $\Delta(1236)$  resonance region, fixed- $t$  dispersion relations discussion 9-8831  
 by photons, isotensor e.m. current determ. 9-8832  
 by photons, unpolarized and linearly polarized, vector meson dominance model application 9-15617  
 photoproduction, at high energy O(3,1) symmetry and conspiracy 9-16871  
 photoproduction, B- $\rho'$  conspiracy, evidence from sum rules 9-20660  
 photoproduction, invariant amplitudes 9-8735  
 photoproduction, Kroll Rudermann theorem, invariant amplitude derivation 9-13102  
 photoproduction, pion-conspiracy hypothesis studied by continuous-moment sum rules 9-8833  
 photoproduction from nucleons with fixed  $u$ , dispersion sum rules 9-2501  
 $\pi^-$ , with 3.4 GeV polarized photons, test of vector dominance model 9-11052  
 Regge trajectories of opposite normality connected by  $\pi$  emission must have same slope 9-11015  
 ss in pp single- $\pi$  channels and interactions, cross sections, 6.92 BeV/c 9-8892  
 sum rules for photoprod. amp., with fixed poles 9-11048  
 threshold prod. in N-N collisions soft-pion approx. 9-11051  
 $\alpha p \rightarrow \pi^+ p$ , recoil  $p$  polarization 9-415  
 $e^+e^- \rightarrow \pi^+ \pi^-$ , pion e.m. form factor compared with vector meson decay data 9-393  
 $e^+e^- \rightarrow \pi\pi$ , in  $\rho$  resonance region, max. cross-section calc. 9-15585

**Pions continued****interactions, pion-pion continued**

- eN $\rightarrow$ eN $\pi$  threshold prod., current algebra calc. with PCAC 9-8830  
 $\eta\rightarrow\pi^+\pi^-\pi^0$ , Dalitz diagram 9-4611  
 $\rho\text{d}\rightarrow\pi^+\rho\text{p}, \rho\text{d}\rightarrow\pi^-\rho\text{n}$  at 8 and 16 GeV, ratio for momentum transfers 0.001-1.3 GeV<sup>2</sup> 9-15620  
 $j^4\text{He}\rightarrow^4\text{He}\pi^0$ , differential cross-sections calc. using impulse approx. 9-6660  
 $\gamma\text{N}\rightarrow\text{N}\pi$  photoprod., modified PCAC hypothesis 9-6661  
 $\gamma\text{p}\rightarrow\pi^+\Delta^+$ , vector dominance assumption for hadron e.m. current 9-16909  
 $\gamma\text{p}\rightarrow\pi^0\text{p}$  differential cross section at 180°, 650-1750 MeV 9-372  
 $\Delta\pi\pi$  in K $\pi$ n, structure from 1600 to 1740 MeV 9-369  
NN processes, review of data 9-6690  
 $\text{pd}\rightarrow^3\text{He}\pi^0$  diff. cross section,  $\text{pd}^3\text{He}$  vertex form factor meas.  $E_{\text{p}}=1.515$  BeV 9-8895  
 $\text{pp}\rightarrow\pi\pi$  interactions, 6.94 GeV/c 9-8903  
 $\text{pp}\rightarrow\pi^+\pi^-\pi^+\pi^0$  phase space distrib., spin and parity of resonance 9-2521  
 $\text{pp}\pi^+\pi^-$  mass enhancement, 1470 MeV, from 28 GeV/c p on Ne 9-15619  
 $\pi^-$  photoprod. from H at 60° for 0.85-1.21 GeV 9-8829  
 $\pi^-$ , from  $\text{pp}\rightarrow\Delta^+(1236)$  9-20642  
 $\pi^0$  in  $\pi^+$  bombard of Xe bubble chamber at 2.34 GeV/c 9-20645  
 $\pi^+\pi^-\text{p}$  from  $\gamma\text{p}$  interaction, H bubble chamber photographs, 1000 MeV < E 9-20644  
 $\pi^+\pi^-\pi^+\pi^0$  from  $\pi\text{n}$  annihilation in D<sub>2</sub> bubble chamber 9-20671  
 $\pi^+$  photoprod. amplitudes,  $E_{\text{p}}=3.4$  GeV 9-20643  
 $\pi^+$ , from  $\gamma\text{N}$ , interaction const. and s-lengths determ.,  $E_{\text{p}}=210, 225$  MeV 9-14504  
 $\pi^-$ , in 12.5 GeV/c p-p collisions, differential cross section 9-370  
 $\pi^-$  from  $\gamma\text{n}$  asymmetry ratio obs. 9-2505  
 $\pi^-$  from  $\gamma\text{p}$ , theory discussed, low energies 9-11049  
 $\pi^0$ , from  $\text{pp}\rightarrow\pi^+\pi^0\text{p}$ , test for current algebra 9-2504  
 $\pi^0$  photoprod., vector dominance and Regge parametrization 9-371  
 $\pi^0$  photoprod. from  $^4\text{He}$ , diff. cross section meas.,  $E_{\text{p}}=160-450$  MeV 9-11275  
 $\pi^+$ , from  $\text{pp}\rightarrow\pi^+\text{n}$ , at 300-750 MeV, absence of P<sub>11</sub> resonance at 1466 MeV 9-2503  
 $\pi^+$ , in 12.5 GeV/c p-p collisions, differential cross section 9-370  
 $\pi^+$ , with 3.4 GeV polarized photons, test of vector dominance model 9-11052  
 $\pi^+$ , in e $^+e^-\rightarrow\pi^+\pi^+$ , asymmetry calc. by  $\pi$  e.m. form factor 9-11000  
 $\pi^+$  in  $\gamma\text{p}$  photoprod. cross-sections at backward angles obs. 9-375  
 $\pi^+$  photoproduction off nucleons, radiative corrections 9-16873  
 $\pi^+$  photoprod. by  $\gamma$  on D, low momentum transfer 9-15616  
 $\pi^0$  photoproduction by D close to threshold 9-2506  
 $\pi(1640)$  meson 9-2513  
 $\pi\pi$  in  $\chi\rightarrow\pi\pi\chi$  for study of  $\pi\pi$  interactions 9-2508  
 $\pi\pi$  photoprod., current algebra in off-mass shell limit 9-16872  
 $\pi\pi\pi\pi$  from decay of isosinglet resonance spin, symmetry and polarization effects 9-6676  
 $\pi\pi\pi\pi$  from decay of isosinglet resonance spin, symmetry and polarization effects 9-13131  
 $\chi\text{p}\rightarrow\text{Nn}\pi, \chi\text{p}\rightarrow\pi, \text{K}, \text{p}$ : cross sections meas., isospin independence and quark sum rules application 9-15618

**scattering**

- amplitude calc. method by bound state and resonance poles 9-8834  
emulsion nuclei at 200 GeV 9-6662  
low energy zero mass, forward off any target 9-8844  
nuclear charge exchange, form factor eff. 9-15771  
photoproduction, at high energy O(3,1) symmetry and conspiracy 9-16871  
Regge trajectories of opposite normality connected by  $\pi$  emission must have same slope 9-11015  
Regge trajectory, current algebra and Toller quantum number M=0 9-374  
Regge trajectory, rel. to large angle p-p scatt. at high energies 9-4638  
Regge trajectory analysis, O(4) symmetry method 9-16875  
 $\pi\text{K}^*$  finite-energy sum rules, boson states, Regge  $p$ -trajectories couplings 9-4625  
 $\pi\text{K}$  finite energy sum rules, boson states, Regge  $p$ -trajectories couplings 9-4625  
 $\pi\rho$ , off-mass-shell extensions, four-point functions Bjorken limit and pole dominance approx. 9-16895  
virtual photon, hard- $\pi$  current algebra and dispersion soln. 9-17987  
K $\pi$  phase shift calc. using  $\pi$ -pole dominance model 9-6671  
K $\pi$  s-wave scatt. lengths estimation, scalar density term and sym.-breaking parameter 9-16869  
 $\text{Pd}\rightarrow\text{Pd}$  cross section and d final state polarization meas., scatt. amplitude determ. 9-8836  
 $\pi$ -baryon, backward, dispersion sum rules at  $\mu=0$  9-17983  
 $\pi^+\text{He}$ , charge-exchange, cross section, calc. 9-604  
 $\pi^+$  d Fermi motion at high energies, expt. and Glauber theory comparison 9-8842  
 $\pi\text{d}$ , 895 MeV/c, cross section diff. 9-8835  
 $\pi\text{d}$ , Glauber formula and obs. comparison for  $\pi\text{p}$ ,  $\pi\text{n}$  amplitudes phase determ. 9-8851  
 $\pi^+\text{d}\rightarrow 2\text{n}, \pi^-\text{d}$  scatt. length calc. 9-2507  
 $\pi\text{d}\rightarrow\pi\text{d}$  cross section and d final state polarization meas., scatt. amplitude determ. 9-17982  
 $\pi\text{K}$ , superconvergent sum rule 9-11007  
 $\pi\text{K}$  amplitude calc. method by bound state and resonance poles 9-8834  
 $\pi\text{n}$  amplitudes phase, from  $\pi\text{d}$  scatt. obs. and Glauber formula comparison 9-8851  
 $\pi\rho$ , differential cross-section, ang. distrib., elastic at 9.8 and 13.6 GeV/c 9-11066  
 $\pi\rho$  finite-energy sum rules, boson states, Regge  $p$ -trajectories couplings 9-4625  
 $\pi\Sigma$ , (0,  $\frac{1}{2}^+$ ), (2,  $\frac{1}{2}^+$ ) possible resonance search, amplitude superconvergence reln. 9-17988  
 $\pi\Sigma$ , S-wave length, current algebra tech., consistency with forward dispersion rel. 9-4599  
 $\pi\Sigma$  vector dominance sum rules for invariant amplitudes 9-6672

**scattering, pion-nucleon**

- causality violation obs. 9-2443  
charge exchange and cross-over, Regge-pole absorption model 9-15626  
charge-exchange, high-energy, model 9-13115  
Chew-Low model, e.m. perturbations of  $\pi\text{NN}$ ,  $\pi\text{NN}^*$  couplings calc. 9-2517  
Chew-Low model, e.m. perturbations of  $\pi\text{NN}$ ,  $\pi\text{NN}^*$  couplings, general features 9-2516

**Pions continued****scattering, pion-nucleon continued**

- diffraction part description by Dirac eqn., cross section and polarization determ., 1.7-18.4 GeV/c 9-8847  
eight low-energy scatt. parameters 9-19203  
elastic unitarity and amplitudes phase equality 9-8845  
e.m. corrections in dispersion relations 9-11063  
finite energy sum rules for backward scatt. 9-6673  
finite-energy sum rules for (1236 MeV)<sup>2</sup> 9-386  
forward, invariant amplitudes, study of superconvergence 9-19201  
Harari model and forward scatt. 9-11061  
high energy, Coulomb interference 9-2518  
impact parameter representation, spin flip amplitude determ. 9-4630  
inelastic effects in P<sub>11</sub>-state 9-16882  
low-energy, theory of composite part connection 9-8844  
low-energy phase shift analyses giving quantitative high-energy  $\pi$ -p scatt. predictions 9-14499  
multi-resonance structure in  $\text{p}_{11}$  state, 2 GeV 9-20651  
 $\text{p}_{11}$ ,  $\text{p}_{13}$  partial waves dispersion reln. reson. solns. 9-11064  
 $\text{p}_{11}$ -state inelastic effects using two-channel model, multichannel ND<sup>1</sup> formalisms 9-16882  
polarization and amplitudes for asymptotically large energies and transferred momenta or possible relation 9-4572  
pseudoscalar-pseudoscalar coupling model calc. of p, s-wave scatt. lengths 9-16879  
quark model multiple-scatt. contributions 9-8787  
radiative, use of current algebra in off-mass-shell limit 9-13129  
Regge behaved amplitude, crossing symmetric, construct. 9-13130  
Regge pole parameters, P, P', new determ. 9-4629  
Regge poles P and P', parameters in elastic scatt. 9-384  
Regge trajectories mass depend. constraints, analyticity and broken SL(2, c) symmetry 9-8846  
reviewed up to 30 GeV/c 9-11030  
S-matrix evaluation, appl. of approx. method 9-8843  
S-wave lengths, even-crossing, current algebra calc., off-mass-shell correct. 9-16881  
scattering lengths, chief Lagrangian calc. 9-17989  
superconvergent sum rule 9-11007  
three-body eqns., relativistic, applic. 9-16842  
unitarity-analyticity eqns., numerical anal. 9-20650  
vector, tensor trajectory hypothesis 9-15604  
vector dominance sum rules for invariant amplitudes 9-6672  
interference model, modifications data analysis 2-6 GeV/c 9-4628  
 $\pi\text{d}$  Glauber theory extended to include spin variables 9-11062  
 $\pi\text{n}$  amplitude calc. method by bound state and resonance poles 9-8834  
 $\text{P}_{11}\pi\text{N}$  phase shift and abs. coeff., matrix N<sup>1</sup> method using coupled  $\pi\text{N}$ ,  $\sigma\text{N}$ , and  $\pi\text{N}$  channels 9-16880  
 $\pi\text{N}$  symmetric amplitude, constraints on asymptotic behaviour 9-385  
 $\pi^+\text{n}\rightarrow\omega\text{p}$  Regge pole model, cuts generated by absorpt. 9-15627  
 $\pi\text{N}$ , N<sup>1</sup>(1236) as resonance generating mechanism possibility 9-11065  
Regge struct. of B<sup>+</sup> at large momentum transfer 9-11079  
 $\rho\text{N}\rightarrow\pi\text{N}\rightarrow\pi\text{d}$  system giving good representation of D<sub>13</sub> amplitude below 700 MeV 9-8848  
 $^3\text{H}(\pi, \pi^+)\text{H}$ , corrections to Weinberg formula 9-18098  
Su(6) invariance in s-wave meson-baryon scatt. 9-8791

**scattering, pion-pion**

- amplitude, construct. from superconvergence relations 9-14514  
amplitude in Mandelstam representation, existence determ. from fixed point theorem 9-8859  
amplitudes phase, from  $\pi\text{d}$  scatt. obs. and Glauber formula comparison 9-8851  
amplitudes rel. to isospin, I=2 states 9-383  
coupling constant, upper bounds, comparison to other estimates 9-8865  
direct-channel strips, partial wave amp. study, potential in Born approx. correct. 9-6675  
final state resonances with I=0, obs. at mass 1.06 GeV/c 9-8877  
finite-energy sum rules, boson states, Regge  $p$ -trajectories, couplings 9-4625  
hard-pion four-point func. applic., Weinberg scatt. length, ranges determ. 9-8857  
inelasticity effects on p-wave amplitude, N/D formalism based on modified phase representation 9-16885  
isospin 0, 2 s-waves low energy behaviour, scatt. length and phase shift calc. 9-11069  
lengths calc. using theory and current algebra 9-16884  
low-energy, partial-wave eqns. soln. 9-14513  
Mandelstam rel. amplitudes, full crossing sym., elastic unitarity 9-15629  
N/D formalism for p-wave amplitude 9-16885  
nuclear matter, four-body force, virtual pion interaction 9-489  
p-wave amplitude, inelasticity eff. N/D formalism based on modified phase representation 9-16885  
partial-wave dispersion relation and short-range force; threshold behavior 9-8862  
phase shifts calc. for p- and s-wave, 753 MeV 9-8866  
polarization in high-energy charge exchange, Lorentz-pole model 9-11060  
potential in Born approx., arising from direct-channel strips., correction, low-energy applic. 9-6675  
 $\pi^+\text{p}$ , on- and off-mass-shell inelasticities, comparison 9-4631  
 $\pi^+\pi^+$ , elastic scatt. obs. using Chew-Low extrapolation method 9-8863  
Regge trajectories bootstrap models 9-11021  
Reggeized absorption model, effective trajectory calc. 9-15601  
S wave, low-energy, model with rigorous constraints 9-8864  
S-wave scatt. length predictions Weinberg tested with modified dispersion rules. 9-2519  
s-wave scatt. lengths and phase shifts, current algebra calc. 9-8860  
scattering length from K,  $\eta$  decay 9-17991  
scattering phases to T=0.2 states 9-387  
strong-interaction dynamics, long-range potential in Regge-pole - resonance interference model 9-8861  
sum rules at sym. pt., high-spin resonances contrib. 9-20654  
superconvergent sum rule 9-11007  
vertex function  $\pi\pi$ -meson resonance, form factors 9-15630  
 $\eta\rightarrow\pi^+\pi^0$  s-wave  $\pi\pi$  phase shift obs. 9-20632  
 $\pi^+\pi^-$  ang. distrib. study from  $\pi^+\pi^-\pi^+\pi^0$ , T=2 D-wave phase shift 9-20653  
 $\text{III}\rightarrow\text{IV}$ , Veneziano representation extension of  $\text{III}\rightarrow\text{II}\omega$ ,  $\text{II}(\text{V})=\text{vector}$  SU(3) octuplet 9-20649  
 $\pi^+\text{p}$  backward elastic and inelastic scatt. at  $E_{\text{p}}=2.15$  GeV/c 9-8855  
 $\pi^+\text{p}$  elastic, optical strong-absorpt. and two slope models, 2.26 GeV/c 9-8850



## Pions continued

## scattering, pion-pion continued

- $\pi^+p$  elastic scatt. at 1.7 GeV/c, differential cross section, analysis 9-8856
- $\pi^+p$ , polarisation obs. for elastic scatt. at 5.15 GeV/c 9-8854
- $\pi^+p$  elastic, multiple-Regge-pole model 9-8852
- $\pi^+p$  with single-meson prod.,  $SU(6) \times O(3)$  quark model 9-8762
- $\pi^+\pi^-$ , elastic scatt. obs. using Chew-Low extrapolation method 9-8863
- $\pi^0\pi^0 \rightarrow \pi^0\pi^0$  s-wave amp. rigorous inequality 9-11068
- $\pi^+\pi^- \rightarrow \pi^+\pi^- A_1$ , Weinberg mass relation for  $A_1$  mes. from Veneziana formula calc. 9-17997
- $\pi^+\pi^- N$  from  $\pi^+p$ , S-wave phase shift calc.,  $M_{\pi^+} = 4$  GeV/c 9-20646

## scattering, pion-proton

No entries

Pitch detection *see Acoustical measurement; Hearing*Plages *see Sun*Planetary nebulae *see Nebulae; Stars*

## Planets

*See also Solar system*

- Atmosphere, CO<sub>2</sub>, Monte Carlo calc. of H<sub>2</sub> escape rate 9-12747
- atmospheres, gray optically thick, in radiative-convective equil., investig. 9-15337
- atmospheres, models for evolution of general circulation 9-20223
- atmospheres, rotational Raman scatt. 9-15335
- atmospheres, solution of radiative transfer problems 9-21933
- atmospheric properties by inversion of occultation data 9-2047
- brighter, photolec. photometry obs., (1963-1965) 9-14236
- diffuse reflection from a plane-parallel atmosphere, method of doubling thin layers 9-15338
- Earth, effective height of shadow for glow cloud experiments 9-2048
- Earth Moon system, effect of tidal friction on history, reply to comments 9-8276
- Earth Moon system, particle motion near L4 libration point, stability anal. 9-10447
- Earth-Moon system L<sub>4</sub> point, choice of consts. influence on spacecraft motion 9-8216
- Earth Moon triangular points, sun disturbed, two stable periodic orbits 9-10449
- fluid mass. calc. of secularly stable equilibria, formation of satellites 9-12749
- Hilda group of asteroids, motion rel. to Hecuba gap 9-15339
- Icarus, photographic position obs. (June-July 1968) 9-15340
- Icarus, radius and rot. period, Doppler radar obs. 9-21936
- inner, atmospheric circulation 9-6169
- interiors, convection, thermal and nonthermal, combined effects 9-21934
- introductory book 9-14234
- i.r. Fourier spectroscopy 9-8298
- Jupiter, asymmetry of radiation belts in polarized light 9-6174
- Jupiter, decameter radio emission rel. to solar activity 9-2050
- Jupiter, drift pattern in dynamic spectra of decametric radiation 9-6173
- Jupiter, equatorial acceleration, mechanism 9-21937
- Jupiter, great red spot brightness rel. to solar activity 9-15343
- Jupiter, narrow band decasecond emissions, independent of terrestrial ionosphere scintillation effects 9-4118
- Jupiter, obs. near 1 cm. wavelength, brightness temp. 9-15346
- Jupiter, orbit, planets and appearance 9-15342
- Jupiter, outer satellites, trajectory integration by modified Cowell's method 9-15341
- Jupiter, radii emission, and e.m. wave prod. by plasma 9-11558
- Jupiter, Red Spot, nature and depend. on atm. flow 9-18909
- Jupiter, Red Spot obs. 1966-67, three-month osc. of longitude, and fading 9-6175
- Jupiter, search for limb aurorae 9-21938
- Jupiter, South Equatorial Belt disturbances, test of uniformly rotating source hypothesis 9-6172
- Jupiter, spots on North equatorial belt, obs. (1966-67) 9-2049
- Jupiter, struct. of disk in  $\nu_2$ -band of ammonia at 100,000 Å. new brightness-temp. maps 9-10524
- Jupiter, thermal model calc. 9-16609
- Jupiter, u.v. spectra study 9-21945
- Jupiter and Saturn, stationary and near-conjunctions 9-21939
- Jupiter polarization, 9.55 mm 9-20205
- Jupiter-sun system, stability characts. of short-period Trojan librations 9-17642
- Mars, annular and linear structures 9-4119
- Mars, atmosphere, CO<sub>2</sub> abund. 9-18910
- Mars, atmosphere analysis, Mariner IV 9-2053
- Mars, atmospheric circulation 9-6169
- Mars, CO<sub>2</sub> abundance and temp. 9-4120
- Mars, CO<sub>2</sub> spect. obs., approx. lab. simulation for surface press. estimation 9-20225
- Mars, craters, surface erosion due to wind and thermal creep 9-2051
- Mars, fossil weathering, surface coloration due to limonite 9-2052
- Mars, ice retention 9-21943
- Mars, nature of violet layer 9-21942
- Mars, number density  $\propto$  craters 9-20226
- Mars, O<sub>2</sub> atm. abundance, obs. 9-8277
- Mars, opposition effect 9-21941
- Mars, permanently frozen ground possibility, topographic features possibility, topographic features 9-6177
- Mars, polar cap 9-21940
- Mars, radiation at 1.55 and 0.95 cm, rel. to average disk temp. 9-8278
- Mars, structure theory, reply to criticism 9-16610
- Mars, surface i.r. absorpt. bands, petrologic significance 9-17639
- Mars, surface particle size effects on albedo 9-18911
- Mars, surface relief and photoelectric obs. 9-10525
- Mars, visible and near i.r. study, surface composition proposal 9-8279
- Mars contaminability from spacecraft 9-17643
- Mars dust storm, V groove thermal control surface for Lander 9-1386
- Martian ionosphere 9-20224
- Martian surface, mineral stability 9-6176
- mean motions, tidal evolution in satellite systems and commensurability 9-16607
- Mercury, orbit calc., geometric expt. for students 9-12834
- Mercury, rotation determined 9-10526
- Mercury perihelion advance rel. to solar rotating core 9-2064
- minor, 9, photographic positions 9-14238
- minor, motion close to commensurabilities with Jupiter 9-20222
- minor, precise photographic positions, catalogue 9-10522
- natural satellites, use of intermediate orbits 9-10519
- navigation Earth-Mars, influence of uncertainty in Mars mass 9-20126
- Neptune, atmosphere 9-14240
- Neptune, comet belt beyond, influence on periodic comets 9-15347
- Neptune, diameter determ. 9-6178
- Neptune, diameter estimation 9-18912
- Neptune,  $\lambda = 3.12$  cm obs., unresolved meas. results, no polarization 9-10527
- Neptune, orbit obs. and inferred mass of Plato 9-14239
- Neptune, radius determ. from BD-17°4388 occultation obs. 9-8280
- Neptune, upper atm. scale height determ. from BD-17° 4388 occultation obs. 9-15344
- Neptune, upper atm. scale height determ. from BD-17° 4388 occultation obs. 9-15345
- oblate, satellite motion calc. 9-12748
- Pluto, mass, deduced from Neptune orbit obs. 9-14239
- Pluto, mass determ. from Neptune perturb. obs. 9-18913
- radiation diffusion in atmospheres with nonisotropic scattering 9-4261
- radiative transfer in atmosphere, solns. to eqns. 9-12746
- rotational motion and general relativity 9-10518
- satellite motion, canonical eqns. for intermediate orbits 9-17641
- satellite systems, orbital period relns. 9-16608
- Saturn, features, latitude meas. 9-21944
- Saturn, filter photometry,  $\lambda\lambda 2950-2450$ , H<sub>2</sub> layer obs. 9-14241
- Saturn,  $\lambda = 3.12$  cm obs., unresolved meas. results, no polarization 9-10527
- Saturn, magnitude of satellites 9-14242
- Saturn, magnitude variations of satellites 9-12750
- Saturn, orbit, rot., satellites and rings 9-18914
- Saturn, rings, formation by satellite disintegration 9-8281
- Saturn, rings, optical props. and thickness, 1966 9-20227
- Saturn, satellite X (Janus), revision of universal satellites scheme 9-10523
- Saturn, thermal model calc. 9-16609
- Saturn and Jupiter, stationary and near-conjunctions 9-21939
- self-gravitating globes, thermoelastic deforms., explicit form of governing eqns. 9-6170
- spectra, multiplex analysis method 9-4539
- surface reflection factor from radar obs., eff. of diffuse scatt. 9-2085
- terrestrial, atm. origin by degassing 9-21935
- terrestrial and Cytherean atmospheres, energetic study of evolution 9-21932
- thermal models of surfaces, appl. of reflectance data of CO<sub>2</sub> and H<sub>2</sub>O cryodeposits 9-10188
- thermosphere diurnal temp. variations 9-8185
- Uranus, an observation of Flamsteed in 1714 discovered 9-12751
- Uranus,  $\lambda = 3.12$  cm obs., unresolved meas. results, no polarization 9-10527
- Venus, 8.6 mm brightness temp., phase depend. 9-12752
- Venus, airglow search, differential photometric scan of dark limb 9-2057
- Venus, albedo, depend. on u.v. wavelength 9-21946
- Venus, Ashen Light obs. 9-14243
- Venus, atmosphere development by outgassing of volatile mats. from heated interior, model 9-6181
- Venus, atmospheric evidence from Venera 4 probe 9-17644
- Venus, cloud composition 9-10528
- Venus, high-dispersion spectroscopic studies, CO<sub>2</sub> band near  $1\mu$  9-2054
- Venus, ice clouds, consistent with polarimetric obs. 9-8282
- Venus, ionosphere and atm., radio occultation obs. 9-12754
- Venus, ionosphere and atm., S-band occultation obs. 9-12755
- Venus, lower atm., criticism of Venera 4 and Mariner V obs. 9-18916
- Venus, mag. dipole moment, upper limit, absence of rad. belt 9-16612
- Venus, Mariner V and Venera 4 obs., comparison 9-20228
- Venus, Mariner V observations 9-10531
- Venus, mass and orbit determ., Mariner V expt. 9-10532
- Venus, microwave emissivity rel. surface roughness 9-21947
- Venus, O<sub>2</sub> atm. abundance obs. 9-8277
- Venus, obs. near 1 cm. wavelength, brightness temp. 9-15346
- Venus, plasma and mag. field, Mariner V obs. 9-16611
- Venus, radar obs. rel. to pole cap size 9-18917
- Venus, radius, determined by planetary radar and Mariner 5 radio tracking data 9-18915
- Venus, radius obs. by radar 9-4122
- Venus, radius obs. by space probes or radar, comparison 9-4121
- Venus, surface dielec. permeability from radar data 9-2085
- Venus, surface press. upper limit, and CO<sub>2</sub> abundance 9-6179
- Venus, surface temp. and press., radio and radar obs. 9-17645
- Venus, temp., press., density and comp. of atmosphere, 'Venus-4' study 9-6180
- Venus, temp. and press. var. over surface from spectral obs. 9-2055
- Venus, u.v. emission of outer atm. 9-12753
- Venus, u.v. spectra study 9-21945
- Venus, variation in radar cross-section due to terrain at point of obs. 9-10529
- Venus atmosphere, CO<sub>2</sub> content 9-2056
- Venus atmosphere composition, Venus-4 space probe study 9-10530
- CO<sub>2</sub> atmosphere, Monte Carlo calc. of H<sub>2</sub> escape rate 9-12747
- CO<sub>2</sub> content in Venus atmosphere 9-2056

## Plasma

*See also Discharges, electric; Electrons; Ions; Space charge; Thermonuclear reactions*

- acceleration on scatt. strong beam of electrons rel. to production of high-energy particles 9-15925
- acoustic wave interaction, theory 9-876
- acoustic wave interaction, theory 9-2967
- admittance, r.f. of plane grid capacitor 9-5015
- air, shock-heated, breakdown on interaction of intense r.f. fields with shock heated air 9-9397
- alkali, e. cyclotron resonance heating 9-17109
- arc discharge, low-current, effect of electrode vapour on electron concentration 9-9353
- atomic line broadening calc., Green's function theory 9-19523
- beam-plasma turbulence-like spectrum 9-3003
- Boltzman's eqn. for e. component, transformation, applic. to hard inactive sphere model of weakly ionized gas in a.c. field 9-15921
- Boltzmann's eqn. for e. component, transformation, applic. to Lorentz gas 9-13412
- Bostick plasmod, conventional toroidal model, extension 9-11535
- Bostick plasmods, forward motion, theory 9-9373
- Bostwick plasmod, forward velocity controlling parameters 9-11570
- boundary interactions, transverse plasma flow outside sheath region 9-11574

## Plasma continued

- bounded, magnetised, non-linear wave processes 9-17108  
 bremsstrahlung rad. by plasma, statistical props. 9-7133  
 capacitor, cylindrical, impedance expression derived 9-5014  
 cavity formed by corpuscular flux incident on mag. field of  $n$  line currents, time-depend. motions 9-14754  
 charged particles transport 9-19588  
 cold, antenna impedance with perpendicular static magnetic field 9-7152  
 cold flow, non-equilibrium, charged particle concentration variation 9-14757  
 collisionless, absorption of light in reflecting skin 9-15935  
 collisionless flow over wedge, ion saturation current predictions 9-21054  
 column, density gradient meas. 9-7143  
 of combustion gas, thermodynamic and elec. props. 9-19095  
 conductivity calc. 9-19522  
 conductivity theory in crossed elec. and mag. fields 9-13416  
 convolution eqn., linear response theory of longitudinal excitations 9-7134  
 cosmic, nonlinear ion waves with rot. mag. vector 9-2022  
 cyclotron resonance generalized electron, in weakly ionized plasma 9-2963  
 cylindrical, electron number density, meas. in  $TM_{010}$  cavity, importance of end holes and glass tube 9-9352  
 cylindrical, radial penetration of axially-directed mag. fields 9-19531  
 cylindrical arc, with whirl round axis, stabilization effects 9-5095  
 decay and phenomena in He and A at an elevated pressure with a Cs vapour and impurity 9-4998  
 decaying, diffusion, transition from ambipolar to free due to charge density grads. 9-13419  
 dense, production from exploding Hg wires and meas. 9-9381  
 dense, relaxation processes and amplification of radiation 9-2966  
 dense, relaxation processes and amplification of radiation 9-14761  
 density, high resolution meas. and temp. distrib. 9-13436  
 density distribution, e.m. field eff. created by external currents 9-21058  
 deuterium, laser-produced, X radiation 9-18293  
 dielectric tensor characterization, wave generation theory 9-21063  
 discharges, acoustic wave generation and detection 9-14764  
 dispersion function computation 9-7156  
 dispersion relation, correlational contrib. to h.f. branch 9-11549  
 drift in mag. field, occurrence of strong discontinuities 9-13423  
 electric field transverse fluctuations, nonlinear generation 9-871  
 electric wire explosion later stages, temp. and e. density distrib. 9-9346  
 electrical conductivity of fully ionized magnetoplasma, calc. 9-15930  
 electromagnetokinetic disturbances propag. in mag. field, sheet model 9-11596  
 electron, kinetic model equation 9-18267  
 electron, near cyclotron reson., relativistic influence on permittivity 9-11563  
 electron concentration in low-current arc discharge, effect of electrode vapour 9-9353  
 electron decay, controlled afterglows diff. and recomb. 9-923  
 electron density, 35GHz microwave reflection probe rel. to 150 GHz interferometry 9-17117  
 electron density, method using Stark-broadened line profiles 9-17110  
 electron density and temp., effect of plasma oscillations 9-15926  
 electron density determ. by cylindrical  $TM_{010}$  microwave cavity 9-11552  
 electron density determ. from microwave reflection, boundary effect 9-17114  
 electron density free, upper limit due to negative ion formation 9-19529  
 electron density using swept microwave interferometer 9-865  
 electron distrib. function determ. from bremsstrahlung radiation spectrum 9-13422  
 electron energy distrib. in presence of moving striations 9-866  
 electron heating by beam-plasma interaction in uniform mag. field 9-11543  
 electron plasma waves, dispersion and damping 9-17104  
 electron velocity in gyrotropic warm magnetoplasma 9-5019  
 electron waves and ion wave, three-wave interaction, kinetic equations 9-7135  
 electron-ion, two component, statistical polarization 9-9342  
 electronegative, with moving striations, radial ambipolar field reversal 9-21062  
 energy dissipation in collective effects 9-861  
 equilibrium theory with Debye pot. in partially ionized H plasma 9-13413  
 excited species, radial distrib. meas. technique 9-13461  
 expansion from inductive high frequency discharges 9-13463  
 fire ball inside shock wave, nonadiabatic expansion 9-14812  
 flow in magnetosphere 9-10400  
 generation, containment, diagnostics, review of research 9-7132  
 heat transfer advances, book 9-6399  
 heating, turbulent, anomalously rapid, rel. to ion-ion instabilities 9-21105  
 heating by magnetic pumping of inhomogeneous collisional plasma 9-15922  
 helicon propagation, effect of electron cyclotron resonance 9-15929  
 helicon wave dispersion when e density has particular radical variation 9-7155  
 h.f. conductivity from particle-wave interacts in multi-species turbulent plasma 9-5016  
 hollow-cathode negative glow, current and radiation intensities mag. field influence 9-14804  
 hydrogenous, in equil., radial distrib. functions 9-18269  
 impedance, effect on time variation of inverse pinch 9-9374  
 impedance effect on time variation of inverse pinch 9-13430  
 inhomogeneous, e. distrib. function calc. 9-863  
 in inhomogeneous, external, e.m. field, kinetic description 9-10654  
 inhomogeneous, interaction with relativistic electron beam 9-18273  
 inhomogeneous, one-component, kinetic description in ring approx. 9-14755  
 interplanetary, ionization processes in expanding solar corona 9-8290  
 ion component outflow from discharge in 100kOe mag. field 9-9348  
 ion cyclotron resonance acceleration in a non-uniformly magnetized plasma 9-15920  
 ion recombination in a plasma in which the electron temp. exceeds the gas temp. 9-13421  
 ion-acoustic wave excitation in plasma containing neg. ions 9-17582  
 ionization equilibrium for elements C-Ni in conditions simulating solar corona and chromosphere 9-20238  
 ionized, bose condensation and shock waves in photon spectra 9-14766  
 ionospheric elec. conductivity 105-125 km from solar daily quiet geomag. var. 9-1957

## Plasma continued

- jet, ultraviolet emission, study using spectrograph 9-5030  
 kinetic eqn. developed and solved for fully ionised case 9-19522  
 kinetic eqn. in Vlasov approx. in presence of external e.m. field 9-10654  
 kinetic eqn. with e.m. interaction 9-11542  
 kinetic theory, elec. cond. and supersonic states of highly nonequilibrium plasma 9-11537  
 kinetic theory, eqn. formed from g soln. 9-858  
 Klein's theorem for thermodynamic functions, correction 9-21049  
 laser light absorption increase in partially ionized gas at high intensities 9-7161  
 laser-produced, dynamics, numerical calcs. 9-9347  
 laser-produced, expansion in mag. field 9-9355  
 lifetimes of charged particles in toroidal assembly 9-11534  
 light scatt. in mag. field 9-2975  
 line broadening theory, ion microfield distrib. 9-18292  
 Lorentz, electron distribution function calc. 9-864  
 magnetic field, quantum mechanical treatment of nonlinear phenomena 9-9345  
 magnetic field, quantum mechanical treatment of nonlinear phenomena 9-11539  
 magnetic field generation by viscous forces in non-uniformly rotating plasma 9-6114  
 magnetic interactions in warm plasma 9-13427  
 magnetized, rotation rel. to space variations of mag. field 9-5008  
 magneto-active quasilinear approx. with allowance for collisions, Cherenkov effect 9-18270  
 magnetoacoustic resonance, nonlinear excitation eff., theory and expt. 9-19521  
 magnetoactive, chemical rate equation for reactive nonequilibrium. 9-13411  
 magnetoactive, e. beam relax., quasi-linear theory 9-874  
 magnetoactive, penetration of longit. elec. field 9-872  
 magnetoactive, radiative transfer eqn. 9-15923  
 magnetodynamic approx., criteria of validity and existence of toroidal mode 9-19549  
 metal, ferromagnetic resonance, review 9-21661  
 microfield, collective part and distrib. 9-7149  
 modelling, atomistic and computerized 9-18268  
 molecular spectral anal. of atom groups forming stable radicals 9-9370  
 multicomponent charged-particle beam, invariant solns. of eqns. 9-2334  
 $N_2^+$  ion density, time depend. obs. 0.1 to 1.7 torr 9-13465  
 nebular, partial maser effect in recombination lines of H atoms 9-8231  
 non acoustic waves, e. temp. variation induced effects and Landau damping 9-14791  
 non-isothermal, collisional drift instability 9-17128  
 non-isothermal, under skin effect conditions, excitation of ion-acoustic waves 9-5033  
 nonlinear Poisson-Boltzmann boundary-value problems, variational solns. 9-21048  
 nonuniform, spectral temp., Boltzmann plot investig. 9-17099  
 partially degenerate transport coeffs., calc. 9-5004  
 physics, selective dissemination of information, computer based 9-857  
 plasmoids on spatially periodic mag. fields, influence of Hall currents 9-5013  
 in plexiglass capillary discharge, reduction of glass transparency 9-10179  
 positive column instabilities 9-19550  
 production by laser irradiation of gases 9-11578  
 production by laser irradiation of solids 9-11578  
 properties and obtainment of densities above crit. density in r.f. plasma 9-9386  
 pulsed streams from Sun, radio propag. meas. 9-10535  
 quantum, fully ionized, eqn. of state 9-860  
 quantum, low density free energy 9-13415  
 quantum levels occupancy, rapidly changing plasmas 9-7136  
 quantum low density, free energy derivation from exact scatt. phase 9-7138  
 quantum mech. radial distrib. function 9-9354  
 quantum statistics theory 9-11536  
 quiescent, bounded, e. velocity dist. theory 9-17100  
 quiescent, destruction of coherent motion 9-17129  
 radiative effect influence on stability and oscils. of mag. gaseous mass 9-21091  
 radiative transfer in reson. lines and recomb. continuum, solns. 9-19527  
 rarefied, kinetic theory, book 9-7223  
 rarefied cold, nonstationary cylindrical waves of finite amplitude, propag. in strong mag. field 9-3001  
 relativistic, Alfvén waves properties 9-18301  
 relativistic, phase-space symmetries in Minkowski space 9-859  
 relaxation with dynamic shielding, using Balescu-Lenard eqn. 9-5002  
 saturation electron current in mag. field 9-11557  
 seeded, multispecies ionization effect on elec. cond. calcs. 9-17106  
 s.h.f. field produced, particle concentration and electron temp. 9-21052  
 s.h.f. power impulse, effect 9-21053  
 short emissions in extreme u.v., gas-flow counter 9-5043  
 solar, magnetoactive, origin of type IV meter-wave storms 9-17656  
 solar flares, transport to earth 9-2078  
 space charge waves dispersion, rel. to ionospheric irregularities 9-12616  
 spectra structure using theory of weak turbulence 9-11551  
 spectral line intensities and contours, changes on disturbance of e. energy Maxwellian distrib. 9-9368  
 spectral line profile var., resonance broadening and reabsorption, optical thickness var. 9-9121  
 spectroscopy, rel. to atomic and molec. spectra and applics. book 9-15936  
 Stark broadening of emitted H Balmer lines in strong mag. field, applic. to electron density calc. 9-17110  
 stationary electrostatic configurations due to presence of negative ions 9-17098  
 stationary rarefied, periodic structure 9-2961  
 stresses, time-averaged tensor with an oscillating field 9-2992  
 striations, phase velocity influenced by an H.f. disturbance 9-2973  
 structure near electrode in coaxial gun using striograms 9-17138  
 thermal, elec. breakdown 9-9358  
 thermal quantities, non-thermal equilibrium plasmas, temperature meas. 9-2962  
 thermalization of kinetic energy of a plasma flow by mag. mirror field in BSG-1 expt. 9-15924  
 transport properties study using semi-classical quantum potential 9-19525  
 turbulence effect on h.f. elec. cond. rel. to particle-wave interacts 9-5016



**Plasma continued**

- turbulence fluctuations spectrum, calc. 9-5001  
 turbulence space-correl. and wave-number spectrum-function pairs 9-4999  
 turbulence spectra and acceleration of sub. cosmic rays 9-14775  
 turbulence spectra and acceleration of sub-cosmic rays 9-2976  
 turbulent, diffusion coeffs., elec. field fluctuations and particle orbits 9-11548  
 turbulent, many-particle quasilinear distrib. functions 9-5000  
 turbulent heating in bumpy torus, for afterglow confinement obs. 9-862  
 two-dimensional, partition function 9-9343  
 two-particle density matrix for Coulomb interact., and Slater sum 9-7137  
 u.h.f. discharge in atmospheric-pressure gas, characteristics 9-9338  
 unstable, finite amplitude drift waves 9-13446  
 u.s. wave amplification 9-17097  
 vacuum gap arc, decay after forced extinction 9-11638  
 virial coeff., second, general expression 9-9344  
 Vlasov eqn., stationary solns. with external elec. field and BGK collision terms 9-11550  
 Vlasov eqn. solved, generalized kinetic eqn. derived 9-14756  
 volume and surface wave nonlinear interaction 9-5010  
 waves, ion acoustic, excitation in non-isothermal plasma under skin effect cond. 9-5033  
 weakly ionised, in external field, time depend. phenomena 9-18274  
 weakly ionized, electric field affected by permanent flux, eqn. soln. 9-2960  
 weakly ionized, generalized electron cyclotron resonance 9-2963  
 weakly turbulent, test particle propagator and wave echoes decay appl. 9-11538  
 whistle mode and acoustic waves, coupling 9-2970  
 zeta discharge, energy flow model 9-18272  
 $\epsilon$  quasi oscillation near boundary studied 9-10479  
 Ar-K, electrical conductivity at low current densities as function of gas temp. 9-19532  
 Ar-SF<sub>6</sub> mixture, absorpt. oscillator strengths of 44SI and 9SII lines, 1100-2000 Å 9-7160  
 Ar, dense, recombination coeff. obs. 9000°K 9-5007  
 Ar, discharge, low temp., radial particle distrib. profile, rel. to volume recomb. 9-11553  
 Ar, electron temp. and density eff. on width and shift of Ar II line 9-5031  
 Ar, electron temp. depend. on atom temp. 9-13414  
 Ar, heat transfer to Cu pipe under influence of elec. field 9-21050  
 Ar, K-seeded, tensor conductivity, electron temps., meas. under MHD generator conditions 9-13425  
 Ar, K and Cs seeded, elec. cond. calcs., effect of multispecies ionization 9-17106  
 Ar, radial distrib. of excited species in capillary discharge 9-13461  
 Ar, radial temp. distrib. by photoelec. spectroscopy in visible region 9-21051  
 Ar, shock heated flows, laminar boundary layers, anal. for equilib. ionization 9-14759  
 Ar, turbulent, elec. conductivity in  $e$  density range  $10^{10}$ - $10^{13}$  cm<sup>-3</sup> 9-875  
 Ar are, cylindrical, radiative energy transport with absorption 9-7140  
 Ar discharge positive column, unstable radial density distribution for long. mag. field 9-11628  
 Ar excited states, spect. studies on decaying plasmajet, electron-ion recomb. coeff. 9-21057  
 Ar prod. by azimuthal discharge, light radiation study 9-19539  
 Ar spark broadening and shift of Ar I, Ar II, lines 9-5093  
 Ar  $\theta$ -pinch, coronal 4412Å emission line obs. 9-7162  
 CO<sub>2</sub>-N<sub>2</sub>-He laser, dominant emission spectral lines obs. 9-9200  
 CO<sup>+</sup> envelope of major comets, fountain model of dynamics 9-21949  
 CO<sub>2</sub> mixed with Ne, afterglow, microwave and mass spectrometric study of recombination diffusion 9-9341  
 Cs, current carrying, ion wave propagation 9-11546  
 Cs, drift waves 9-11600  
 Cs, magnetically confined, radial diffusion electric field effect 9-14758  
 Cs, vapour with impurity and inert gases, phenomena during decay 9-4998  
 Cu/Mg electric exploded wire, temp. and  $e$  density meas. in later stages 9-9346  
 D plasmoids from coaxial injector, struct. and impurities obs. 9-13417  
 D<sub>2</sub> laser-produced, theoretical exam. 9-9383  
 H, diamagnetic eff. due to ion press. 9-19551  
 H, glow discharge, atomic transitions and self-absorpt. of line rad. after perturb. 9-5032  
 H, infinite column, press. increase and total thermal cond., calc. 9-11540  
 H, radial temp. distrib. by photoelec. spectroscopy in visible region 9-21051  
 H, thermal conductivity meas. in transverse mag. field, 10,000-50,000°K 9-7139  
 H, turbulent, elec. conductivity in  $e$  density range  $10^{10}$ - $10^{13}$  cm<sup>-3</sup> 9-875  
 H<sub>2</sub><sup>+</sup>-H<sub>3</sub><sup>+</sup> partition functions of ground electronic states 9-867  
 H<sub>2</sub> test of Stark-broadening theory 9-714  
 H<sub>2</sub> test of Stark-broadening theory 9-715  
 H atom conc. in plasma pinch in Tokamak TM-3 machine, meas. method 9-7144  
 H spectral line widening by  $e$  9-2010  
 He, electron temp. depend. on atom temp. 9-13414  
 He, electron vel. generated by  $e$  beam, analysis using Boltzmann eqn. 9-13420  
 He, K-seeded, tensor conductivity, electron temp., meas. under MHD generator conditions 9-13425  
 He, K and Cs seeded, elec. cond. calcs., effect of multispecies ionization 9-17106  
 He, laser-produced, collision processes in post-discharge 9-7141  
 He, low temperature, recombination, study of afterglows 9-11547  
 He atoms excited state population meas., mechanism discussed 9-9340  
 He I line broadening by electron impact, theory 9-21073  
 He metastable molecules (<sup>2</sup>S<sub>u</sub>) and atoms (<sup>2</sup>S) in afterglow, decay 9-15832  
 He plasma expansion from inductive high frequency discharges 9-13463  
 K, current instabilities 9-11610  
 K magneto-plasma, diffusion 9-17102  
 LiD surface, thermonuclear neutron emission at Nd glass laser beam focus 9-13245  
 N, are, cylindrical, radiative energy transport with absorption 9-7140  
 N, discharge, ionization waves dispersion curves 9-13418  
 N<sub>2</sub>, thermal rad. 0.5-1.1  $\mu$ , intensity meas., role of heterogeneities 9-19524

**Plasma continued**

- N spectral line intensities of non-equilibrium plasma calc. 9-19528  
 N<sub>2</sub>, K-seeded, elec. cond. for conditions of MHD accelerator 9-7151  
 NO mixed with Ne, afterglow, microwave and mass spectrometric study of recombination, diffusion 9-9341  
 Na-seeded, emission spectra, series lines investig. 9-19537  
 Ne, electron temp. depend. on atom temp. 9-13414  
 Ne, positive columns of discharges at moderate pressure 9-14762  
 Ne, striated discharge, acoustic waves effect 9-11541  
 Xe, turbulent, elec. conductivity in  $e$  density range  $10^{10}$ - $10^{13}$  cm<sup>-3</sup> 9-875
- collision processes**  
 backscattering of electrons in gas discharge tubes 9-19526  
 BGK collision terms and external elec. fields in stationary solutions of Vlasov eqn. 9-11550  
 binary losses in stellarators, calc. 9-21056  
 charged particle beams, instability 9-901  
 dense, relaxation and amplification of radiation 9-2966  
 dense, relaxation and amplification of radiation 9-14761  
 diffusion of particles across magnetic lines 9-17101  
 drift instability in non isothermal plasma 9-17128  
 drift modes, determination of freq., amp. and azimuthal mode number 9-14795  
 drifted electron type, instabilities by anisotropy in vel. space 9-7142  
 electron impact broadening of spectral lines, improvements 9-21055  
 electron transport coeffs., partially ionized plasma in mag. field 9-18276  
 inelastic, effect on relax. of level population 9-5005  
 inelastic electron-neutral collisions, effects on electrons energy distribution 9-18275  
 interaction with laser radiation, Compton effect induced 9-9351  
 ion-ion collisions, effect on resistive drift modes 9-17122  
 ion-molecule reactions in 50MHz discharge 9-9350  
 measurement 9-19550  
 N<sub>2</sub><sup>+</sup> ion prod. in afterglow by collision with metastable N<sub>2</sub> mol. 9-13465  
 non correlation of anomalous transport and oscillations in Q-devices 9-17112  
 quantum theory of pressure broadening 9-2965  
 radiation scatt. by  $e$ , Brownian motion studied 9-8427  
 in sheath, transition domain between collisionless and collision dominated flows 9-14776  
 stationary waves in ion-electron collision plasma with const. electric field 9-5017  
 two streams 9-2964  
 two-particle density matrix for Coulomb interact., and Slater sum 9-7137  
 velocity depend., freqs., under relax. conditions, weakly ionised plasma in external field 9-18274  
 zeta discharge, energy flow model 9-18272
- confinement**  
 $\epsilon$ -pinch in transverse mag. field, plasma rot., two-dimens. calc. 9-11576  
 adiabatic trap, instability obs. after electron cyclotron resonance heating 9-7181  
 afterglow, after turbulent heating in bumpy torus 9-862  
 boundary interactions, transverse plasma flow outside sheath region 9-11574  
 bounded quiescent plasma,  $e$  velocity distribution theory 9-17100  
 circular cylindrical column, monochromator data reduction, computer program 9-19538  
 cusp containment, applic. to thermonuclear reactors 9-11568  
 cusped magnetic field, high- $\beta$  reflected wave 9-5036  
 cylindrical column, current-induced anomalous behaviour 9-21075  
 in divertor mag. field, interaction of plasma fluxes with cylinder 9-17111  
 expansion of isolated column 9-5035  
 fluctuations, based on new soln. of general integral eqn. 9-11598  
 high speed value for  $\theta$ -pinch dev. 9-883  
 $\theta$ -pinch, slow,  $e$  acceleration, radial space charge field effects 9-881  
 $\theta$ -pinch, slow, local motion obs. 9-882  
 $\theta$ -pinch, slow, meas. by Mach-Zehnder interferometer with giant pulse ruby laser 9-14781  
 inverse pinch, time variation, effect of plasma impedance 9-13430  
 inverse pinch time variation, eff. of plasma impedance 9-9374  
 isotropic, half-confined, surface impedance for interaction between plasma particle and surface 9-5034  
 magnetic bottle, patent 9-7164  
 magnetic configuration, three-turn helical, with shear and minimum  $B$  9-11573  
 magnetic field compression by conducting cylindrical sheath 9-18295  
 magnetic mirror,  $e$  ring trapping in pulsed field 9-4430  
 magnetic mirror compression experiment, electron cyclotron interaction 9-21077  
 magnetic mirror system, stochastic heating of particles, theory 9-13432  
 magnetic traps, l.f., h.f. instabilities and suppression 9-884  
 magnetic-mirror geometries, cyclotron resonance trapping and healing, non-adiabatic and stochastic mechanism 9-21076  
 mirror field, heated by linear turbulent heating, X-rays 9-2978  
 mirror magnetic wells, ion cyclotron drift instability 9-15937  
 negative  $V^*$  system and its equilibrium 9-9371  
 Rayleigh-Taylor Z-pinch instability in constriction process, soln. 9-2977  
 screening of a high density plasma from neutral gas penetration 9-11569  
 sheath, one-dimensional, nonlinear Vlasov equation, stationary solutions, variational method 9-18296  
 sheath, transition between collisionless and collision dominated flows, and ionization effects 9-14776  
 sheath capacitance of glow discharge plasma, freq. conversion 9-11572  
 shock wave, collisionless, and mag. field capture, expts. 9-15932  
 in SM magnetic trap, containment time 9-15938  
 in stellarators, new model 9-11571  
 thermonuclear fusion at Kurchatov Institute 9-21047  
 theta-pinch, switching device using exploding foil 9-19540  
 theta-pinch discharges, meas. methods and analysis 9-11575  
 toroidal, new system 9-9372  
 toroidal mag. field, trapping of transversely injected plasma 9-11577  
 toroidal octopole, fluctuations and transmitted waves 9-11605  
 two-dimensional flow in coaxial channels 9-13431  
 uniform guide field, expansion and shock wave formation due to mag. barrier 9-2979  
 X-rays, mirror field heated by linear turbulent heating 9-2978  
 Z- $\theta$  discharge config. with mag. field of supercond. solenoid 9-7163  
 Ar, azimuthal pinch, emitted light study 9-19539  
 Cs, magnetically confined, radial diffusion, effect of radial electric field 9-14758  
 Cs in Q machine, confinement time meas. 9-14782

**Plasma continued****confinement continued**

- arc torch with mixing nozzle, patent 9-13435
- d.c. jet, two-step model, source of nonequilibrium chemical species 9-13434
- d.c. nitrogen jet for solid-gas heat transfer studies 9-2982
- diode, electron temperature distribution, transport properties 9-21084
- duoplasmatron operation, pulsed ion beam composition meas., for continuous and pulsed gas feed 9-6494
- duoplasmatron operation, pulsed ion beam composition meas., for continuous and pulsed gas feed 9-234
- generator, vortex-stabilized, potential distrib. along arc 9-2990
- generator coaxial sectional, heat transfer in near-electrode region of electric arc 9-19565
- gun, coaxial, rel. to prod. of impulsive plasma 9-11590
- gun, coaxial, simple model with positive central electrode 9-7165
- gun, coaxial single-electrode, operation 9-885
- gun, e.m. as ion emitter 9-10828
- Hall accelerator, design 9-19541
- injector, coaxial; gas composition and partial press var. due to discharge 9-18266
- injector, coaxial quasi-stationary, pot. distrib., obs. 9-13433
- jet for impurity inorganic analysis 9-6028
- magnetic bottle, patent 9-7164
- magnetic Laval nozzle, modification of B field config. of Q-device 9-2980
- magnetic mirror system, stochastic heating of particles, theory 9-13432
- MHD power generation 9-2316
- microwave beam-plasma devices, input and output coupling 9-13438
- Q devices, Langmuir probes compared to other diagnostic techniques 9-11586
- Q machine, ion wave propagation 9-11546
- Q-device, single-ended, equilb. theory 9-11580
- Q-device, single-ended operation 9-11581
- Q-devices, ion cooling effects 9-14779
- Q-devices, non correlation of anomalous transport and oscillations 9-17112
- Q-machine, Cs plasma, confinement time meas. 9-14782
- Q-machine, shear stabilized, oscillations and diffusion 9-14790
- Q-machines, effects related to radial elec. field 9-14778
- Q-machines, electric field effects 9-14777
- reactor, r.f., for polymer surface treatment 9-11579
- single emitter diodes, static potential dist. 9-16760
- sources of ions of high-melting elements, survey 9-2981
- spectroscopic light source jet, interelement effects, obs. 9-20563
- stellarators, confinement times, new model 9-11571
- stellarator containment of single particles 9-886
- subsonic tunnel for evaluating re-entry flight instrumentation 9-21074
- thermionic diode, semiconductor thermocouple analogy 9-17856
- torch, d.c. arc, non-uniformity of flame, operating characteristics 9-21078
- torch, production by laser, characts. 9-887
- torch, r.f. induction-coupled, atomic spectrometry appls. evaluation 9-21735
- torch, sustained at h.f., Stark effect of i.r. Ar I lines 9-9375
- toroidal octopole, plasma fluctuations and transmitted waves 9-11605
- zeta, turbulent fluctuations meas. 9-21060
- Ar jet, radial temperature distribution, analogic analysis 9-21079
- Ar jet, temp. distrib., spectroscopy 9-11582
- D injector, coaxial, plasmods struct. and impurities obs. 9-13417
- H electron torch, h.f., ionization mechanism, obs. 9-15959
- Li, MPD arc thrusters, efficiency for low environmental press. 9-9376
- N<sub>2</sub>, K-seeded, MHD accelerator, elec. cond. meas. 9-7151
- NH<sub>3</sub>, MPD arc thrusters, efficiency for low environmental press. 9-9376

**diagnostics**

- from admittance, r.f., of plane grid capacitor 9-5015
- charge concentration determination, double probe, Druyvesteyn distribution of electron component 9-17105
- charged particles energy spectra, velocity distribution with gridded electrostatic analyzers 9-21082
- collisionless absorption of r.f. electrostatic plasma waves 9-17118
- column excitation by ring source, coupling coefficient and excitation impedance 9-17116
- complex conductivity in low-frequency region 9-5038
- critical aperture, by method of scattering of laser emission 9-889
- current meas. using directional twin probe 9-2983
- decay study using laser interferometry 9-7166
- density, high-resolution meas. and temp. distrib. 9-13436
- density meas. using CO<sub>2</sub> laser interferometer 9-5006
- diagnostics, anisotropic, using microwave Fabry-Perot resonator 9-7167
- dielectric film, applic. of complex transmission and reflection coeffs. 9-19116
- Doppler broadening, relativistic effects 9-17115
- double probe characts. in flame injected with electronegative gas 9-5037
- double-probe systems, asymmetrical 9-13437
- dynamics parameters of laser created plasma expanding in magnetic field 9-21086
- electron density, feedback oscillator meas. 9-5044
- electron density determ. by cylindrical TM<sub>010</sub> microwave cavity 9-11552
- electron density determ. from microwave reflection, boundary effect 9-17114
- electron density in arc plasma, applic. of CO<sub>2</sub> laser interferometer 9-18297
- electron density meas., Mach Zehnder interferometer 9-19543
- electron density meas. by propagation of electron plasma waves in presence of strong mag. field 9-17113
- electron density using swept microwave interferometer 9-865
- electron number density, meas. in TM<sub>010</sub> cavity, importance of end holes and glass tube 9-9352
- electron temp., direct display, magnetised and time varying plasmas 9-2986
- electron temp. determ. using floating double probe 9-2985
- electron temperature distribution in plasma diode, transport properties 9-21084
- electron temps., by admittance probe, time resolved plasmas 9-2987
- electron-density meas. using far i.r. laser interferometry 9-14780
- Fabry-Perot resonator measurements of density 9-888
- $\theta$ -pinch, slow, meas. by Mach-Zehnder interferometer with giant pulse ruby laser 9-14781
- Langmuir probe, elastostatic, for nitrogen plasma, design characts. 9-5045
- Langmuir probe, ion current extrapolation 9-18313

**Plasma continued****diagnostics continued**

- Langmuir probes, comp. to other diagnostic techniques in a Q-device 9-11586
  - laser produced, density meas. by laser light scatt. 9-2989
  - loaded waveguide, complex reflection coeff. as tool 9-7169
  - lunar low energy plasma, E<500 eV, Explorer 35 meas. 9-21929
  - microwave meas. of plasma temp. 9-11587
  - microwave methods 9-11589
  - microwave reflection probe, 35 GHz, comparison with 150 GHz interferometry 9-17117
  - microwave reflection to determ. electron density, boundary effect 9-17114
  - polychromator, eight-channel, continuous spectral line profiles 9-2988
  - probe, characteristics depend. on e emission, low density 9-13936
  - probe at medium press., ionic current rel. photo effect for inert gas discharge 9-21083
  - probe meas. on flowing partially-ionized high-density gases 9-19542
  - probe noise in quiescent plasma 9-9379
  - quantitative schlieren tech. for anal. of boundary-layer flows 9-14760
  - quantitative spectroscopic meas. on plasma prod. by laser from polyethylene 9-5048
  - quasi-optic imaging resonator 9-21080
  - resonance probe, computer simulation with one-dimens. model 9-5040
  - r.f. characts. of electrode in magnetoplasma applic. 9-5041
  - saturation electron current of cylindrical probe in mag. field, quantitative, theoretical treatment 9-2984
  - shutter for obs., utilizing Kerr effect in nitrobenzene 9-8672
  - space charge layer thickness, plasma capacitor method 9-9378
  - spectrometers, rapid scan, for transient plasmas 9-11583
  - spectroscopic analysts, book 9-15936
  - spectroscopic and interferometric methods 9-14784
  - temperature meas. by photoelectronic tech., using relative intensity of spectral lines 9-9377
  - theta-pinch discharges, meas. methods and analysis 9-11575
  - time resolved spectroscopic, laser produced 9-1494
  - weakly, ionized gas, dielectric meas. in v.h.f. range 9-11584
  - zeta, turbulent density fluctuations, theory and experimental observations 9-21081
  - e density in e.m. driven shock-wave plasma, microwave refl. meas. 9-11585
  - Ar, 8 mm. interferometric results, interpretation 9-19544
  - Ar, electron density, feedback oscillator meas. 9-5044
  - Ar, shock-tube wall boundary layer, study by a quantitative schlieren tech. 9-14760
  - Ar,NaK seeded, elastostatic probe meas. of I-V characts. 9-20487
  - Ba Q-plasma, optical study 9-14783
  - CO<sub>2</sub> discharge, electron energy distrib. and effect of He 9-18298
  - Cs, grid probe operation 9-5039
  - Cs in Q machine, confinement time meas. 9-14782
  - Cs low temp., optical and probe obs. comparison 9-11588
  - H atom conc. in plasma pinch in Tokamak TM-3 machine, meas. method 9-7144
  - H decay parameters meas. 9-7168
  - He I line intensity meas. of electronic temp. 9-5042
  - K magneto-plasma, diffusion meas. 9-17102
  - N<sub>2</sub> discharge, electron energy distrib. 9-18298
  - N<sub>2</sub>, Langmuir probe, elastostatic, design characteristics 9-5045
- electromagnetic waves**
- anisotropic, normal to mag. field, dispersion relations 9-18290
  - book 9-2972
  - bremsstrahlung calculation in the region of plasma frequency 9-2993
  - bremsstrahlung from  $\theta$ -pinch, 0.25-25  $\mu$  9-11565
  - cold stream over vacuum and dielec. half spaces, reflection at interface 9-5025
  - collision-induced instability at cyclotron harmonics 9-9391
  - collisional plasma in mag. field, conductivity tensor calc. 9-18282
  - compressible anisotropic medium, potential functions 9-11564
  - continuum radiation, rare gas, positive column, deceleration of electrons by atoms 9-17096
  - conversion of plasma into e.m. waves in strong mag. field 9-11558
  - cyclotron damping 9-14771
  - cyclotron echo phenomena, cooperative effects 9-14774
  - cyclotron echo phenomena, density  $10^{18} \leq n_0 \leq 10^{21}/\text{cm}^3$ , expt. and theoretical investigation 9-9367
  - cyclotron harmonic resonances, higher order, obs in lab and ionosphere 9-9364
  - cyclotron-harmonic wave echoes 9-2998
  - cylindrical electron beam 9-15484
  - diffraction of cylindrical waves at an impedance wedge in anisotropic plasma 9-19535
  - dipole radiated power 9-5027
  - dyadic in theory of waves in inhomogeneous warm magnetoplasma 9-878
  - e. cyclotron resonance heating of alkali plasmas 9-17109
  - electric dipole oscs with no mag. field, elec. fields, radiation resistance and resonance 9-5026
  - electric field in gyrotropic warm magnetoplasma, wave eqn. 9-5019
  - e.m. gain mechanism 9-19536
  - energy total wave in plasma 9-7157
  - fluctuations and scattering in strong fields 9-14773
  - Fresnel dragging of 3 cm. microwaves by low-pressure discharge 9-9365
  - helicon waves in cylindrical waveguide, dispersion and attenuation 9-14768
  - hot, absorption coeff. for intense light, allowing for stimulated emission 9-2974
  - hydrodynamics and drifts of particles in a high frequency component field 9-2950
  - hyperfrequency signal amplification through e. beam interaction 9-19534
  - impedance element in active Fabry-perot microwave resonator 9-8545
  - inhomogeneous column, axially symmetric and dipolar surface modes, quasistatic theory 9-7154
  - instabilities, ion-cyclotron, in thermally anisotropic plasma 9-21103
  - ion cyclotron oscs, excitation 9-7174
  - ion waves, generalized Bernstein modes, struct. from e.m. dispersion relns. 9-5024
  - layer, diffusion of large amplitude waves 9-21072
  - l.f. perturbation spectrum, dispersion equation 9-13429
  - longitudinal, in half-space, BGK particle-conserving collision model 9-14769
  - magnetized columns surrounded by dielectric medium, non-quasistatic analysis 9-17107



**Plasma continued****electromagnetic waves continued**

- magneto-active waveguide excitation 9-21069
- magnetoactive, reflection and absorpt. coeff., inclined incidence 9-879
- magnetoactive anisotropic medium, relativistic electrons generation and radiation transfer, polarization effects 9-5003
- magnetoactive inhomogeneous plasma, nonlinear effects near resonance 9-21071
- magnetoplasma, longitudinally drifting semi-infinite, normally incident waves reflection and transmission 9-14770
- magnetoplasma cylinder, trapped modes, dipole modes and one-wave approx. 9-14763
- microwave excitation of ion acoustic waves 9-15941
- microwave wave, interaction with initially heated air 9-7158
- microwave radiation from Penning discharge plasma in inhomogeneous mag. field 9-5028
- microwave scatt. by turbulent plasma 9-9369
- microwave scattering by plasma instability in mag. field, enhanced 9-9362
- microwaves scatt. by anisotropic turbulence, obs. 9-9361
- mixing interaction in bounded plasmas, second-order a.m. fields solution 9-11561
- mixing interaction in bounded plasmas, second-order e.m. fields solution 9-5021
- moving compressible plasma, refl. and trans. of plane e.m. waves, solns. for E and H waves 9-11559
- non linear wave processes in a bounded magnetised plasma 9-17108
- nonlinear media, theory 9-4389
- oscillations, localized 9-9366
- p-polarized, reflection from moving layers, kinetic theory 9-21070
- plane grid capacitor, r.f. complex admittance and excited elec. field 9-5022
- polarized, reflection in column density gradient meas. 9-7143
- polarized waves, non-linear scatt. near ion cyclotron freq. and damping 9-5023
- propagation in non-homogeneous plasma 9-2969
- pulsars, radiation dispersion 9-6148
- pulse-modulated carrier, Gaussian, amplitude and phase distortion 9-877
- radiation in compressible and anisotropic medium 9-5029
- ray trajectories in anisotropic plasma near resonance 9-10421
- reflection and transmission coeffs. before and after cut-off, formulae assuming trapezoidal electron density distrib. 9-11560
- reflection at interface between vacuum and dielec. half spaces, for cold stream 9-5025
- refractive index, complex, behaviour in isotropic plasma 9-15408
- relative streaming, allowing propag. below plasma freq. 9-11567
- relativistic plasma, nonlinear wave interaction 9-5020
- resonance, hybrid, region of weakly, non-uniform plasma, absorpt. of extraordinary wave 9-2971
- resonance transmission through opaque boundary by cyclotron wave 9-15934
- scattering and transformation, plasma located in ext. fields 9-14772
- scattering by turbulent pulsations in inhomogeneous magnetoactive plasma 9-11562
- scattering calc. indep. of turbulent fluctuations, transport eqn. 9-9363
- self focusing, along magnetic field, of whistler mode 9-21068
- semiconductor-vacuum interface heated by h.f. field, boundary condition effects 9-880
- semiconductor-vacuum interface heated by h.f. field, boundary condition effects 9-13428
- spectra structure using theory of weak turbulence 9-11551
- spectral resolution and solution of field problems 9-7153
- synchrotron polarization Stokes params. 9-2276
- synchrotron radiation from hot e plasma, spectrum, 0.2-4 mm 9-11566
- TEM waves at micro-wave frequencies, non-linear interaction with electro-acoustic waves 9-15933
- transmission, absorption and reflection at moving layer 9-21070
- transverse in relativistic plasma, instability unless isotropic 9-18291
- wave eqns., coupled, for homogeneous gyrotropic compressible warm plasma 9-18289
- wave eqns. for stratified, gyrotropic warm plasma 9-18288
- in waveguide, propagation, phase vel. meas. 9-21067
- waveguides, plasma-filled, power flow 9-14405
- whistler mode, coupling with acoustic waves in high pressure plasma 9-2970
- whistler mode propagations, presence of electrostatic field 9-10423
- Cs, thermally generated, non-linear interactions 9-7159
- H, perturbed, atomic transitions and self-absorpt. of line rad. 9-5032

**magnetohydrodynamics**

- accelerator with progressive e.m. waves, bidimensional flow 9-9356
- Alfven and magnetoacoustic wave propagation in non-homogeneous plasma with axial symmetry 9-15928
- Alfven wave generation, radiation loss effects 9-18279
- Alfven waves, compressional, propagation below ion cyclotron frequency, meas. 9-21097
- Alfven waves, compressional and torsional, propagation under identical plasma conditions 9-21098
- axisymmetric equilibria stability without stagnation point 9-11554
- boundary layer eqns. with perpendicular mag. field 9-9357
- cavity formed by corpuscular flux incident on mag. field of n line currents, time-depend. motions 9-14754
- charged plasma, conductivity, in magnetic field 9-18283
- cold, boundary layer with confined mag. field, effect of transverse plasma vel. component 9-21829
- collisional plasma in mag. field, conductivity tensor calc. 9-18282
- collisional plasma in mag. field, elec. conductivity tensor, relativistic correct. 9-18281
- collisionless, viscous stress tensor expression 9-21061
- cyclotron harmonic wave propagation and instabilities, theory 9-21099
- expansion and thermalization in non-uniform mag. channel 9-869
- flow around magnetic dipole, interaction study 9-21066
- flow assoc. with shock wave evolution in mag. fields and instabilities 9-5018
- flow in shock tube boundary layer 9-19517
- gravitational instability, rotating anisotropic plasma, finite Larmor radius eff. inclusion 9-14189
- Hall current influence on dynamics of plasmoids in spatially periodic mag. fields 9-5013
- Hartmann's flow, non-stationary mass-exchange 9-15927
- interchange instabilities in ideal theory, and driving energy forces 9-5052
- aminar flow along parallel magnetic field, stability 9-18277

**Plasma continued****magnetohydrodynamics continued**

- longitudinal polarisation of flowing plasma in transverse mag. field 9-5012
  - magnetoactive inhomogeneous plasma, nonlinear effects near resonance 9-21071
  - MGD viscous channel flow, boundary layer approx. with heat conduction 9-21059
  - motion and polarization interaction of a plasma in field of a multipole 9-5011
  - Rayleigh Taylor problem with Hall effect, hydromagnetic analogues calc., comparison 9-18278
  - rotating layer in vertical mag. field, effects of Hall currents on thermal instability 9-7145
  - sheets, imploding axisymmetric slug-type, mag. driven 9-11555
  - shock waves, transverse ionizing, jump conditions 9-18285
  - slipping stream instability, effect of mag. field 9-13444
  - space-charge acceleration, in nonuniform axial mag. field 9-7146
  - supersonic MGD generator, transient acoustical response to natural disturbances 9-19122
  - T-layer, solution by finite-difference method 9-13424
  - transverse shocks, critical Alfven-Mach numbers 9-18280
  - turbulent, collisionless plasma, theory 9-5009
  - turbulent, energy partition between mechanical and magnetic modes, theory 9-21060
  - turbulent heating of ions 9-870
  - velocity vorticity depend. on fields and forces, rel. to rotation 9-5008
  - Vlasov low  $\beta$  nonuniform plasma, finite Larmor radius eqns. 9-11556
  - wave motions rel. to solar corona heating 9-21981
  - zeta, turbulent density, fluctuations, theory and experimental observations 9-21081
  - Ar, NaK seeded, electrostatic probe meas. of I-V characts. 9-20487
  - C<sup>+</sup>, excitation-heating of ions, magnetically confined vacuum arcs 9-18271
  - He, diffusion in a mag. field, obs. 9-9349
  - He discharge, mag. enhancement of He I lines, spectral series depend. 9-19530
  - $\theta$  plasmaoid, infected across octupole mag. field, impurity removal 9-7147
- measurement technique** *see Plasma/diagnostics*
- oscillations**
- acoustic modes in high magnetic fields, conduction e splitting into Landau levels 9-897
  - Alfven type waves, stability in anisotropic relativistic plasma 9-14552
  - Alfven waves, compressional, propagation below ion cyclotron frequency, meas. 9-21097
  - Alfven waves, compressional and torsional, propagation under identical plasma conditions 9-21098
  - Alfven waves, polarization 9-15942
  - Alfven waves in magnetosphere, excitation of Pi2 mag. pulsations 9-17590
  - Bernstein modes, dispersion curves for hybrid cases for large plasma parameters 9-14788
  - bremstrahlung calculation in the region of plasma frequency 9-2993
  - charged particles, motion in slightly damped sinusoidal pot. wave 9-6470
  - clusters, mutual quasistatic vibrations 9-21094
  - in confined plasma, from new soln. of integral eqns. 9-11598
  - conversion of plasma into e.m. waves in strong mag. field 9-11558
  - current instability effect in turbulent heating of ions by MHD waves 9-870
  - cyclotron harmonic wave nonlinear interaction 9-14786
  - cyclotron instability suppression of rarefied plasma with and of feedback system 9-7177
  - cyclotron waves, interaction with e.m. waves 9-15934
  - cyclotron-harmonic wave echoes 9-2998
  - cylindrical wave diffraction at an ideally conducting wedge in anisotropic plasma 9-2995
  - cylindrical waves, nonstationary, of finite amplitude, propag. in strong mag. field 9-3001
  - decay to ion sound oscillations 9-3000
  - density waves at or close to equilibrium, mag. interaction effect. 9-13427
  - dipolar surface waves along magnetoplasma column, dispersion eqn., numerical and asymptotic solns. 9-14787
  - drift waves, excitation and damping 9-17123
  - drift waves, finite amplitude 9-13446
  - electron, resonant four-wave interaction 9-21096
  - electron, waves, dispersion 9-18304
  - electron beam in external elec. field 9-2999
  - electron cyclotron waves, harmonic excitation 9-2996
  - electron liquid, magnetoplasma mode determ. 9-20367
  - electron liquid degenerated, spin-wave and plasma-wave propag. ang. depend. 9-4254
  - electron waves diffusion in large-amplitude ion wave background 9-7175
  - electrostatic, excitation near ion cyclotron freq. 9-14792
  - electrostatic, interaction with electrons for 'bump in tail' distribution 9-21090
  - electrostatic I.F. drift-acoustic and gravitational flute modes in periodic 1-dimens. slab 9-21095
  - electrostatic waves in inhomogeneous and magnetized plasmas 9-14785
  - energy dissipation in collective effects 9-861
  - excitation in non-linear medium by modulated current 9-7148
  - gas-discharge tube, effect on electron density and temp. 9-15926
  - helicon waves, dispersion and attenuation in plasma waveguide 9-14768
  - $\theta$ -pinch in static magnetic field, incoherent microwave scatt. 9-21087
  - impure plasma, and drift instability 9-18307
  - inhomogeneous, anisotropic, wave packet, dispersion relation and energy transfer 9-18305
  - inhomogeneous plasma, WKB approx. of linearized Vlasov equation 9-17125
  - instabilities, ion-cyclotron, in thermally anisotropic plasma 9-21103
  - internal resonances in plasma column, observation, comparison of frequency and current modulation 9-21089
  - ion, harmonics, in neutralized ion beam plasma 9-11601
  - ion, quenching at sheath-plasma resonance 9-15943
  - ion, suppression by electron oscils. 9-9388
  - ion acoustic waves, apparent nonlinear damping 9-9389
  - ion acoustic waves, excitation by microwaves 9-15941
  - ion cyclotron, in strong e.m. wave 9-7174
  - ion cyclotron heating, numerical expt. with sheet current model 9-11544
  - ion wave propagation 9-19550
  - ion waves, electrostatic, propag. near ion cyclotron freq. 9-13441

**Plasma continued****oscillations continued**

- ion waves in partially ionized gas in ext. elec. field 9-15940
- ion-acoustic waves, dispersion 9-18303
- ion-acoustic waves, non-linear 9-898
- ionization waves in fast moving type 'r' striations, freq. depend. on electron mean energy 9-7173
- ionosphere, ion-acoustic wave excitation effect on fine structure 9-17583
- kinetics, non-linear, fundamental eqns. rel. to ion wave 9-893
- Langmuir wave decay, instability criteria and growth rate 9-9384
- Langmuir wave decay, resonance conditions, parametric amplification 9-11593
- l.f., in plasma with negative ions 9-11599
- longitudinal, in constant electric field, dispersion relation 9-17121
- magnetized plasma, degenerate ion acoustic mode shown to exist 9-13445
- magnetodynamic toroidal waves, possible existence 9-19549
- magnetoplasma, fully ionized, drift waves effect on transverse diffusion 9-17103
- magnetoplasma, non-uniform, l.f. electrostatic instabilities, Nyquist diag. rams 9-13443
- metal particle, fast incident electron induced 9-13439
- metallic particles, excited by fast electrons 9-9906
- in MGD generators, transient wave growth 9-19122
- in microwave cavity, resonance freq. and field 9-14406
- microwave radiation parameters and plasma behaviour correlated for concs. around  $10^{13} \text{ cm}^{-3}$  9-892
- moving column, surface wave propag. 9-9385
- non acoustic waves, e temp. variation induced effects and Landau damping 9-14791
- non correlation of anomalous transport and oscillations in Q-devices 9-17112
- non-uniform, non-linear one-dimens. electrostatic waves, relativistic treatment 9-18300
- nonlinear, near electron cyclotron harmonics, resonant struct. obs. 9-19547
- nonlinear electron: 'water bag model' 9-9387
- nonlinear oscillations in a cold plasma 9-11594
- nonuniform, ion wave damping 9-894
- partially ionized plasma, fluctuations in external fields 9-14789
- potential vibrations in mag. and h.f. elec. field 9-21092
- pseudowave excitation on grid, wavelength rel. to Debye radius 9-896
- Q-machine, shear stabilized 9-14790
- quantum electrodynamics theory 9-18302
- relativistic, without external field, covariant theory 9-5049
- resonance, l.f., current in non-isothermal plasma-jet 9-21093
- resonance spectrum, electron-density fluctuations effects 9-5050
- r.f. electrostatic plasma waves, meas. of collisionless absorption 9-17118
- solid state, fluctuations 9-5626
- stresses, time-averaged tensor 9-2992
- striation, h.f., high-pressure discharge 9-2994
- striations in discharge, review 9-15945
- Tonks-Dattner resonances in self-sustained plasma, ionic modulation 9-895
- in toroidal octopole, plasma fluctuations and transmitted waves 9-11605
- transverse wave generation, non-linear wave-wave interaction 9-18306
- trapped-particle modes in low- $\beta$  plasmas 9-11595
- turbulent, spontaneous excitation of mag. fields 9-21088
- in warm, inhomogeneous plasma, soln. of Maxwell-Vlasov eqns. 9-13440
- wave echoes decay, test particle propagator appl. 9-11538
- wave propag., high freq., in unbounded electron-plasma system 9-11592
- wave props. rel. to, obtainment of densities above crit. density 9-9386
- waves, extraordinary, propag. in cold plasma, nonlinear effects 9-11597
- waves, harmonic electron cyclotron, excitation 9-2996
- waves, solitary, propagating at an angle to a magnetic field in a collisionless, warm plasma 9-2997
- waves on fluctuations, conversion long. to transverse 9-7172
- Ar, electrostatic waves in GHz freq. range, transmission meas. and dispersion relns. 9-7150
- CO<sub>2</sub> discharge, slight dispersion forward waves, 4.7 to 10 torr 9-18311
- Cs, drift waves 9-11600
- Cs, ion acoustic waves 9-17124
- H, magneto-acoustic resonance obs. 9-19551
- He, <sup>2</sup>P<sub>4</sub>-D and <sup>2</sup>P<sub>4</sub>-D lines, observations 9-725
- He, highly-ionized, in mag. field, l.f. oscils. 9-902
- He, l.f. intensity, in radiation at low temps. 9-7176
- He neutralized ion beam plasma, harmonics of ion oscillations 9-11601
- K, strongly non-uniform, rel. to instabilities diffusion 9-11609
- Ne glow discharge, low pressure, p-type striations generated by external excitation 9-19552

**production**

- deuterium specks targets for laser pulse 9-19545
- field emission discharge high intensity and pulsed 9-5046
- by focussed CO<sub>2</sub> laser radiation 9-890
- generator coaxial sectional, heat transfer in near-electrode region of electric arc 9-19565
- gun, coaxial single-electrode, operation 9-885
- and heating by laser radiation, theory and experiments, review 9-19546
- high density and temp., by large power laser 9-17119
- impulsive, by coaxial plasma gun 9-11590
- injector, coaxial; gas composition and partial press var. due to discharge 9-18266
- ionized, production by heating substance in laser beam focus 9-7185
- by laser, optical measurements 9-18294
- by laser, prebreakdown bubble phenomena 9-9382
- laser beam created, dynamic parameters of plasma expanding in mag. field 9-21086
- laser beam interaction with substances 9-20531
- laser produced, density meas. by laser light scatt. 9-2989
- laser produced, high density and temp. 9-17119
- laser rad. interaction with solids, mass spectrometric investigation 9-9380
- laser-, and numerical calcs. of dynamics 9-9347
- laser-irradiation of solids and expansion in mag. field 9-9355
- laser-produced, laser beam radiation pressure effects 9-18299
- lasers, Q-switched beam focused on single solid target 9-2365
- from polyethylene, by laser, quantitative spectroscopic meas., obs. of new lines 9-5048
- s.h.f. power, impulse effect 9-21053
- s.h.f. power, particle conc. and electron temp. 9-21052
- thermonuclear, by laser beam focussing on LID surface and n. obs. 9-7171

**Plasma continued****production continued**

- torch, by laser beam on solid 9-887
  - by u.v. radiation, for highly ionized, low density plasmas 9-15939
  - vacuum system of toroidal plasma machine 9-8328
  - vortex-stabilized generator, potential distrib. along arc 9-2990
  - Ar, breakdown threshold for focused laser beam 9-891
  - Ar, by shock waves, equilb. ionization in laminar boundary layers 9-14759
  - Ar in shock-tube, quantitative schlieren tech. for study of boundary layers 9-14760
  - Cs, from cylindrical Ta cavity, 1400°K 9-11591
  - D seed targets for laser irradi. 9-2991
  - D<sub>2</sub> by laser, theoretical exam. 9-9383
  - H,  $1 \times 10^{17}$  ions/cm<sup>2</sup>, using condensed mol. beams. 9-7170
  - H, thermonuclear, by field emission discharge irradi. of D-T target 9-5047
  - N, breakdown threshold for focused laser beam 9-891
  - O, by electron beam in adiabatic trap 9-873
- shock waves**
- Alfven wave growth in nonlinear medium quasi linear theory 9-9359
  - collision ion-electron plasma with constant electric field, stationary waves 9-5017
  - converging, cylindrical ionizing shock in applied axial mag. field, theory 9-18284
  - evolution conds, fire-hose and mirror instabilities of assoc. flow 9-5018
  - exploding wires, confined, optical and elec. meas. 9-18287
  - flow around magnetic dipole, interaction study 9-21066
  - flow in e.m. shock tube 9-14765
  - formation by flow interaction with mag. barrier 9-21064
  - formation due to mag. barrier rel. to plasma expansion in uniform field 9-2979
  - hydromagnetic, resistivity-controlled, structure 9-18286
  - ionization processes 9-19517
  - magnetohydrodynamic reduced shock relations for 'jump conditions' 9-15931
  - MHD, transverse ionizing, jump conditions 9-18285
  - precursor effects in e.m. shock tube 9-9360
  - self focussing of an ion-sound wave 9-2968
  - self focussing of an ion-sound wave 9-13426
  - shock tube, magnetically driven, performance effect of impurities during breakdown 9-21065
  - stellar atmosphere, structure and press. depend., nomogram calc. 9-19533
- stability**
- anisotropic, relativistic, of Alfven type waves in mag. field. 9-14552
  - beam instability, h.f. oscillations obs. 9-21100
  - beam instability, influences on system 9-11606
  - beam-plasma discharge generated in mirror magnetic trap 9-7183
  - beam-plasma syst., instability near electron cyclotron harmonics 9-19554
  - Bessel function model, tearing mode instability 9-17126
  - charged particle beams, instability 9-901
  - cold, traversed by two e beams, in external mag. field 9-11602
  - collision-dominated, effect of magnetic shear, hollow column applic. 9-9393
  - collision-induced instability at cyclotron harmonics 9-9391
  - collision-induced instability of partially ionized gases in ext. mag. field 9-9392
  - collisional drift instability in non-isothermal plasmas 9-17128
  - collisional drift modes, determination of freq., amp. and azimuthal mode number 9-14795
  - collisionless fluidlike electron and ion modes 9-900
  - collisionless plasma in h.f. E-wave field, drift instability 9-14793
  - column, bumpy, unstable transverse-displacement mode and stabilization 9-11604
  - cusp curvature stabilisation of universal mode 9-15948
  - cyclotron harmonic wave parametric excitation 9-15944
  - cyclotron harmonic wave propagation and instabilities, theory 9-21099
  - cyclotron instability suppression of rarefied plasma with and of feedback system 9-7177
  - destruction of coherent motion in a quiescent plasma 9-17129
  - diocotron instability of cylindrical layer with gyro-radius of order of mean radius 9-5051
  - drift instability of impure plasma, due to Cherenkov effects 9-18307
  - drift waves, finite amplitude 9-13446
  - drift-dissipative instability in Penning discharge 9-5053
  - drifted electron collision induced instabilities not caused by vel.-space anisotropy 9-7142
  - dynamic, magnetically driven slug-type sheets, axisymmetric 9-11555
  - electron stream, relativistic, helical, interaction with cold magnetoactive plasma 9-13442
  - electrostatic instabilities in synthesised plasma beams 9-14796
  - fire-hose and mirror instabilities of flow assoc. with shock wave evolution 9-5018
  - flute instability in a rarefied noncompensated plasma 9-7184
  - flute instability of a current carrying curved plasma column 9-15947
  - gravitational, rotating anisotropic plasma, finite Larmor radius eff. inclusion 9-14189
  - gravitational instability with Hall effect 9-7178
  - high and low freq. instability in beam plasma expt. parameter dependence 9-17130
  - hot electron in adiabatic trap, instability leading to rapid loss of energy 9-7181
  - hot-cathode discharge, h.f. instability in mag. field 9-21104
  - hydromagnetic waves cyclotron instability 9-3002
  - inhomogeneous plasma in sheared magnetic fields 9-15946
  - instability of plasma drifting across mag. field 9-7179
  - interchange instabilities in ideal hydromag. theory, and during energy forces 9-5052
  - ion cyclotron drift instability in mirror magnetic wells 9-15937
  - ion cyclotron instabilities effect 9-17127
  - ion cyclotron instability in strong e.m. wave 9-7174
  - ion waves, electrostatic, propag. near ion cyclotron freq. 9-13441
  - ion-ion, rel. to anomalously rapid turbulent heating 9-21105
  - Kelvin-Helmholtz problem, new unstable mode due to Hall effect 9-9390
  - l.f. in toroidal traps for long-term containment 9-884
  - l.f. microinstabilities, dynamical stabilization 9-7180
  - magnetic interactions, role 9-13427
  - magnetic shear, eff. of on collision-dominated plasma, hollow column applic. 9-9393
  - magnetized, instability condition electric field fluctuation enhancement 9-13445



**Plasma continued****stability continued**

- magneto plasma, Nyquist diagrams for l.f. electrostatic instabilities 9-13443
- magnetoactive plasma with monoenergetic component 9-14794
- microwave scattering in mag. field, enhanced 9-9362
- non correlation of anomalous transport and oscillations in Q-devices 9-17112
- plane vortex sheet, rel. to compressibility and mag. field applic. 9-21101
- positive column 9-21106
- Q-machine, shear stabilized, universal collisionless instabilities 9-14790
- Rayleigh-Taylor Z pinch instability in constriction process, soln. 9-2977
- relativistic, transverse e.m. waves, unstable unless isotropic 9-18291
- resistive drift modes, effects of ion-ion collisions and shear 9-17122
- resonance spectrum, electron-density fluctuations effects 9-5050
- screw-type instability stabilization by h.f. field 9-899
- shear instability in cold plasmas with external mag. field 9-11603
- slipping stream instability, effect of mag. field 9-13444
- solid state, fluctuations 9-5626
- thermodynamic stability of plasma with strong interaction 9-9394
- in toroidal, axially symmetric 'Tokamak' systems, equilb. and stability 9-19553
- turbulence and diffusion across mag. field by two inhomogeneous plasma instabilities 9-11607
- turbulence expts., generation of suitable electron beams 9-7182
- turbulent, investigation method 9-21088
- universal instabilities, mode synchronization phenomena 9-11608
- vortex flow, jet driven, stationary velocity profile under axial mag. field, hydromagnetic stability 9-21102
- He, highly-ionized, in mag. field, l.f. instabilities 9-902
- K, current instability 9-11610
- K, instabilities diffusion in strongly non-uniform plasma, obs. 9-11609
- N nonequilibrium, relative populations of excited atoms 9-19528
- Ne glow discharge, low pressure, p-type striations generated by external excitation 9-19552
- O discharges, positive columns, Gunn-instabilities, generation of T-layers 9-19560

**Plasma diodes** see *Electricity/direct conversion; Electron tubes;*

*Plasma/devices*

**Plasma guns** see *Plasma/devices*

**Plasma in solids** see *Crystal electron states/plasma; Electron gas; Semiconductor; Solids*

**Plasma jets** see *Plasma/devices*

**Plasma sheath** see *Plasma confinement*

**Plasma thermocouples** see *Electricity/direct conversion; Plasma/devices*

**Plasma torches** see *Plasma/devices*

**Plasma waves** see *Plasma oscillations*

**Plasmoids** see *Plasma*

**Plasmons** see *Crystal electron states/plasma*

**Plastic deformation**

See also *Slip*

- alkali halides, pressure effect, c compatibility of dislocation presence with dissociated cores 9-18503
- alloys, rel. to surface energy formed on fracture 9-11922
- bar, twisted with discontinuous inhomogeneity, kinematics 9-8492
- Bauschinger effect, yield strength rel. to cold-forming state-of-stress 9-5457
- beams of unequal angle section, bending 9-10707
- bland under central impulsive loading 9-17780
- buckling, dynamic, of short cylindrical shells due to impulsive loading 9-17774
- clamped plate, due to projectile impact anal. rel. to mass and vel. 9-1279
- constant true strain rate apparatus 9-4177
- cratering, high-speed in wax and plasticine 9-20410
- crystal, stress-strain relation 9-14968
- ductile creep failure under complex stress 9-8495
- ductility, pressure effect 9-7542
- dynamics, review 9-10706
- glass, under point loading, role of densification 9-19790
- glass polymers, yield 9-14974
- graphite, by high-temp. creep strain, microstruct. changes 9-7545
- group IV B and V B carbides, yield stress stoichiometry depend. 9-21374
- ice, strain relaxation, exptl. investigation 9-16129
- instability of thick-walled tubes with closed ends 9-20411
- martensite, defect production and interaction with C from meas. of thermal effects of ageing 9-7595
- metal, h.c.p., hydrostatic press. and temp. eff. on strength and ductility 9-5478
- metal, rel. to elec. resistivity 9-12093
- metal f.c.c. crystal, rel. to secondary dislocations, sources 9-11879
- metal microcontacts, real area and number of contact points 9-17303
- metals, on cutting at high velocities, specific work consumed 9-9758
- metals, effect on self-diffusion under high pressure 9-3384
- metals tending to brittle fracture, adhesion under combined plastic deformation without heating 9-5492
- naphthalene strained crystals, spectral change due to thermal deformation 9-5349
- notched bars of intermediate thickness with small shoulder ratio, yield point 9-2195
- olivine, mechanisms 9-5456
- plane frames, failure loads evaluation 9-126
- plane surface of plastic body by rolling contact with rigid circular cylinder 9-17776
- plastic shear waves 9-17779
- polycrystalline h.c.p. metals, crystallographic studies 9-21367
- polyethylene, drawn, orientation distrib. functions by broad line n.m.r. 9-12517
- polymethylmethacrylate, yield and fracture, 78°-350°K 9-13729
- pressure vessels with edge zone yielding 9-17775
- rigid body under loads, yield-point load surfaces props. 9-139
- sandwich shell, buckling, optimum thicknesses 9-19034
- shell, cylindrical, dynamic buckling in sustained axial compressive flow 9-138
- steel, 60Kh3G8N8V, hot working effects on stress-corrosion cracking susceptibility 9-3449
- steel, 0.16-0.2C, 0.65-0.75Mn, yield, Al-killing effect 9-19795
- steel, carbon, hydrostatic press. and temp. eff. on strength and ductility 9-5478

**Plastic deformation continued**

- steel, E1702, aged and quenched, effect of grain size on resistance to deform. 9-9760
- steel, Poisson's ratio 9-21373
- steel, rolling effects on Mossbauer spectra 9-16151
- steel, stainless, infl. on Mossbauer eff. 9-19981
- steel, stainless, localized obs., during ductile fracture 9-17315
- steel, strain-aged, yield point directionality 9-17307
- steel, under alternate tension and shear above plastic limit, def. props., qualitative characteristics change 9-11927
- strain measurements, special techniques, review 9-17304
- strain induced phase transformation, effect on strain-ratio values 9-16149
- stress discontinuity surface relations in 3D rigid-plastic bodies 9-17778
- stress-strain relations for plastic materials in compression at medium strain rates 9-17300
- tensile and creep tests, double resonator tech. for continuous meas. of Young's mod. 9-11911
- tensile instability in uniaxial compression tests 9-20412
- transition metal carbides, yield stress stoichiometry dependence 9-21374
- u.s. probing of plastic waves 9-11923
- in visco-elasto-plastic half space, with spherical shock wave 9-12932
- yield point behaviour in Fe single crystals 9-3418
- Ag-Sn solid solns., effect on Mossbauer spectrum 9-1750
- Al-4wt.%Au alloy, effect on sp. elec. resistance 9-12098
- Al-(78 wt.%)Zn alloy, superplastic, rel. to grain boundary sliding, diffusional creep and dislocation interaction 9-21370
- Al, on cutting at high velocities, specific work consumed 9-9758
- Al, effect on positron lifetimes 9-16220
- Al, internal friction, low temp. 9-7524
- Al, quenched hardened, mechanism 9-11924
- Al, shell, cylindrical under axial compression; free edge buckling 9-1280
- Al, single cryst., damping and modulus defects in creep and tensile tests 9-9744
- Al, yield curves in tension, effect of cyclic work softening 9-18504
- Al<sub>2</sub>O<sub>3</sub>, forging 9-3482
- Al alloy, commercial, repeated yielding (Portevin-Le Chatelier effect) rel. to impurity-dislocation interaction 9-11925
- Al alloy, rel. to fatigue crack growth rate 9-21381
- Al as model for steel in study of compression induced fracture 9-18516
- Al crystallites, inhomogeneity after uniaxial compression, and lattice residual deformation distrib., direct obs. 9-1182
- Al crystallites, under uniaxial compression 9-1182
- Al notched bars of intermediate thickness with small shoulder ratio, yield point 9-2195
- Be, compressive, investig. 9-11926
- Be, high-purity, 4.2-300°K 9-1282
- CaCO<sub>3</sub> calcite, colour centre form by X-rad. 9-16105
- CaCO<sub>3</sub> calcite, colour centre form by X-rad. 9-3364
- CaO ceramic crystals, forging and recrystn. 9-3482
- CaSO<sub>4</sub>·2H<sub>2</sub>O, dispersed porous mat., microstresses on pressing, X-ray analysis 9-1276
- Ce, effect on f.c.c. = d.h.c.p. martensitic transform. 9-3487
- Co, production of stable strain-induced magnetic remanence 9-7905
- Cu-Al alloy, martensite, cubic type stacking faults 9-16103
- Cu-Ni alloys, and yield point rel. to degree of ordering 9-19794
- Cu-Ni alloys, rel. to internal friction 9-13720
- Cu-Sn solid solns., effect on Mossbauer spectrum 9-1750
- Cu, dynamic yield strength value at high temp. 9-21371
- Cu, effect on positron lifetimes 9-16220
- Cu, fatigue, magnetomechanical behaviour associated with dislocation slip 9-17308
- Cu, polycrystalline wires, resistivity under tension 9-7753
- Cu, rel. to Young's modulus variation 9-16117
- Cu polycrystalline, at 373-573°K, obs. and mechanism 9-1284
- Cu<sub>75</sub>Al<sub>25</sub> solid solns., effect on Mossbauer spectrum 9-1750
- Cu Fe alloys, eff. on phase transformations during tempering 9-13777
- Fe-(30 wt.%)Cr alloy aged at 475°C, rel. to activation parameters 9-1286
- Fe-N alloys, eff. on phase transformations during tempering 9-13777
- Fe-Ni-Ti, mechanical props. improvement by ageing effect on structure and props 9-11928
- Fe-Si, eff. of dislocation network on plastic strain 9-16098
- Fe, Ferovac-E, strain rate variation with stress in pre-macro yield region 9-17347
- Fe, irradiated, yield stress, saturation and exposure depend. 9-11929
- Fe, resistance, effect of strain rate 9-9759
- Fe, single crystals, behaviour at upper yield point 9-3418
- Fe, stress-strain distrib. in Luders front propag. accompanying yield-point phenomena 9-19785
- Fe whiskers, and recovery 9-1269
- Fe-Ni-C alloys, ferromagnetic f.c.c. 9-13727
- GaP single crystal rel. elec. erosion 9-5350
- Ge, and irradiated, photoconductivity spectra 9-15137
- Ge, dislocation band model for carrier mobility 9-18628
- Ge, infl. of electrically active impurities 9-18505
- Ge epitaxial layers on GaAs 9-19796
- Ge single crystal rel. elec. erosion 9-5350
- p-InSb, effect on elec. props. 9-3631
- KCl:Ba<sup>2+</sup>, yield point, temp. depend. 9-5363
- LiF, p-irrad., effects on F-band thermal bleaching 9-7503
- LiF, u.s. radiation effect 9-9764
- Mg, generation and recovery of lattice defects, from elec. resist. meas. 9-7478
- Mg alloy, hydrostatic press. and temp. eff. on strength and ductility 9-5478
- MgAl<sub>2</sub>O<sub>4</sub> ceramic crystals, forging and recrystn. 9-3482
- MgO, eff. on optical absorption, e.s.r. and thermoluminescence, eff. of plastic deformation 9-18740
- MgO ceramic crystals, forging and recrystn. 9-3482
- Mo crystals, at 293 and 400°K, study of slip bands by optical microscopy 9-5466
- Mo foils, under electron microscope, study of slip geometry 9-5460
- Ni-Co alloys, eff. on absolute thermo e.m.f. 9-21543
- Ni-Fe alloys, eff. on absolute thermo e.m.f. 9-21543
- Ni, causing magnetic after effect 9-3802
- Ni, effect on mag. domain structure 9-12280
- Ni, fatigue, magnetomechanical behaviour associated with dislocation slip 9-17308
- Ni, ferromag. reson. line width variation rel. to lattice microdistortions 9-14103
- Ni, low temps., recovery 9-3419

**Plastic deformation continued**

- Ni, production of stable strain-induced magnetic remanence 9-7905
- Ni, single crystal in an alternating magnetic field 9-5461
- Ni, uniaxial mag. anisotropy, formation 9-12295
- Ni-Co alloys, effect on positron annihilation 9-21477
- Ni-Fe alloys, effect on positron annihilation 9-21477
- Si, edge dislocation prod., effect of contamination on their elec. props. 9-5712
- Si single crystal rel. elec. erosion 9-5350
- Ti, hydrostatic press. and temp. eff. on strength and ductility 9-5478
- TiC ceramic crystals, forging and recryst. 9-3482
- UO<sub>2</sub>, polycryst., yield and flow in compression, 600 to 2000°C 9-11931
- Zn-Al alloy, superplastic, mechanism rel. to slip and grain boundary migration 9-11858
- Zn, and rupture for forbidden basal slip 9-11932
- Zn, hydrostatic press. and temp. eff. on strength and ductility 9-5478
- ZnS, critical shear stress determ., 21°C 9-5348

**Plastic flow***See also Rheology*

- Armco iron, yield and flow stresses, temp. and strain-rate dependence at low temps. 9-1285
- b.c.c. metals, flow stress, inherent lattice or solution hardening 9-3429
- b.c.c. metals, flow stress, inherent lattice or solution hardening 9-3430
- b.c.c. metals, limiting strength produced by solution hardening 9-7562
- b.c.c. metals, limiting strength produced by solution hardening 9-7561
- ductile fracture initiated pressurized penny-shaped crack 9-17314
- metals, b.c.c., stress, 10-300°K 9-13732
- plane polar like rapid flow problems solved 9-20413
- rock, isotropic, homogeneous: analysis under lubricated punch 9-1288
- rock, under pointed punch, plane-strain problem 9-1289
- tunneling mechanism involving escape of dislocations from bound states 9-14943
- unloading yield point effect 9-7543
- velocity from creep eqns. with allowance for formation of gas atoms 9-5466
- yielding serrated, apparent activation energy 9-11917
- Zr-Se alloys, hydried, effects of Se and H contents 9-19805
- Ag, stress theories, rel. to double coplanar slip 9-5471
- Fe, stress, 10-300°K 9-13732
- Mg-Cd alloy, order-disorder phase transition, changes 9-16155
- Mg-Cd alloy, ordering speed, effect 9-16156
- Mg-Cd single crystal, flow stress, conc. and temp. depend. 9-21378
- Nb alloys with improved workability 9-13770
- UO<sub>2</sub>, polycryst., in compression, 600 to 2000°C 9-11931
- UO<sub>2</sub> single crystals, slip planes rel. to orientation, 600-1800°C 9-9762
- Zn-Al alloy, superplastic, microstructure and mech. behaviour 9-11858

**Plasticity***See also Viscoelasticity*

- anisotropic plate, uniform bending, anal. using max. shear stress yield conds 9-4279
- bar with jump inhomogeneity, torsion, sand hill analogue 9-14372
- ceramics, superplasticity 9-7541
- clay-liq. mixtures, characterization using torque meas. rheometer 9-3425
- cylindrical shell, collapse under radial press. difference, elastic-plastic anal. 9-17771
- dynamics of rapid deformation, review 9-10706
- elastic-plastic behaviour of plates 9-17772
- elastic-plastic Prandtl-Reuss solids, stability conditions 9-10705
- elastic-plastic stress waves in semi-infinite bar 9-8506
- elastic-plastic torsion, numerical methods 9-19033
- elastic plastic waves longitudinal, resonance in finite bar 9-8507
- elastic-visco-plastic medium, propag. of loading and unloading waves 9-6379
- elasto-plastic matrix, formulation using 'initial stress' finite element approach 9-8484
- elasto-plastic medium during filtration 9-136
- elastoplastic bodies, nonuniformly heated, shakedown theory analysis 9-2194
- elastoplastic propag. along bar heated at one end 9-19057
- elastoplasticity, nonlinear problems, soln. by finite element method 9-20409
- kinematic hardening, generalization for nonlinear stress/strain law 9-20408
- metal close-packed crystals, factors affecting initial plastic behaviour 9-21368
- metals, expt. approach to theory at elevated temps. 9-14972
- metals, plasticity modulus 9-17293
- metals, superplasticity 9-7541
- of plastics, fibre-reinforced 9-1278
- plates, dynamically loaded; bending moments and membrane forces obs. 9-137
- PVC grains, in suspension, effect of porosity on interaction with plasticizer 9-21231
- quadratic yield condition in elastoviscoplastic materials 9-8496
- rigid body under loads, yield-point load surfaces props. 9-139
- shear waves 9-17779
- sheet metal drawing, plastic anisotropy eff. 9-19830
- slipline fields, mass flux method for dimensions deduction 9-17777
- stress discontinuity surface relations in 3D rigid-plastic bodies 9-17778
- tube thin, subject to internal press., torsion and axial tension 9-17773
- viscoplasticity, thermodynamic restrictions in continuous media 9-19037
- wave propagation, combined torsional and longit. speeds of elastic-plastic boundaries 9-19059
- Al/Al<sub>2</sub>O<sub>3</sub> alloys, ductility rel. to oxide particle size 9-17305
- Al (78 wt.%)Zn alloy, superplasticity, mechanism 9-21370
- Al Zn alloy, superplastic state 9-21369
- Cr ductility, n irradiation effects 9-1310
- HfC and HfC- (10vol%)HfB<sub>2</sub>, hot-pressed, and fracture strength  $\leq 2635^\circ\text{C}$  9-1301
- Sn, in contact with binary alloy, temp. and alloy comp. dependence 9-9761
- U, viscous displacement at grain boundaries during creep, conditions and study 9-19806
- W Re alloys, superplasticity 9-18507
- Zr-Cu alloys, effect of O<sub>2</sub> and temp. on ductility 9-11940
- Zr (1wt%)Nb, ductility, effect of H<sub>2</sub> and extension rates 9-17313
- Zu-Al alloys, superplasticity 9-3428

**Plastics***See also Polymers*

- binary solns., scintillation pulse shapes 9-5177

**Plastics continued**

- crystalline, wear resistance tests 9-11947
- fibre reinforced, model for plastic behaviour 9-1278
- glass reinforced, elastic and viscoelastic behaviour, role of adhesion 9-17237
- matrix for 1,2,5,6-dibenzanthracene, phosphoresc. 9-21654
- metal-plastic surface stick-slip threshold velocity investigation 9-5489
- plexiglass, transparency reduction due to contact with dense plasma 9-10179
- polyacrylonitrile, new, transparent, bulk polymerization method, conventional initiator 9-14735
- polystyrene, kinetics of cracking and major crack growth obs., mass spectrometric investigation 9-18522
- resistance to high energy rays 9-3544
- scintillators, polymer bases 9-11135
- scintillators based on cross-linked epoxy resins, production and advantages 9-10256
- thermal conductivity, apparatus, 90 to 200°K 9-15016
- C<sub>10</sub>H<sub>21</sub>, with pt. source of  $\beta$  rad., distrib. of abs. dose 9-12034

**Platinum**

- atom, p-ray total cross sections, 280 keV 9-16999
- atom, core-e energy levels and density of states, X ray photoelectron spectrum 9-1813
- atoms spectrum, hollow cathode discharge obs. 9-18134
- black, catalyst, activity rel. to particle size, defects and stored energy 9-5325
- catalyst, alumina-supported, ave. crystallite size and crystalline content 9-17271
- catalyst, particle size distrib. and X-ray characts. using Warren-Averbach tech. 9-5326
- conduction-electron g factor, anisotropy 9-1445
- d-band structure in ls coupling 9-9896
- defects injected by quenching and radiation doping by deuterons 9-7479
- desorption of O atoms 9-1908
- electrode, dynamic behaviour of oxygen-periodic couple 9-8104
- electron emission, secondary, multiple distrib. 9-5782
- electron-phonon interband scatt. 9-21463
- emission, thermionic of Na<sup>+</sup>+K<sup>+</sup> from ribbons, effect of deformation 9-21554
- films on W (110), structure from LEED 9-1135
- fusion curves up to 40 kbars, meas. by optical melting 9-7299
- heat capacity, low temp. 9-17355
- Pt+PtRh thermocouples, 300°K-400°K mass., increased sensitivity 9-171
- PtRh thermocouples, 300°K-400°K mass., increased sensitivity 9-6406
- resistance thermometers calibration tables 2-273.15°K 9-2264
- surface, accommodation coeffs. of air, N<sub>2</sub>, O<sub>2</sub>, press. depend. 9-16039
- surface, specular low-energy electron beam scatt 9-11760
- surface ionization coeff. for Rb atoms 9-5786
- thermal conductivity and diffusivity at high temps. 9-5575
- thermal conductivity by Jain and Krishnan method, 1200-1700°K 9-18569
- thermoelectric power, effect of high pressure 9-16306
- thermometers, reduced resist., comparison with standard, 63°K to 373.15°K 9-4379
- thermometers, resist., comparison with standard, 63°K to 373.15°K 9-4378
- wires, quenching methods and rate meas., review 9-11949
- wires, vacancy recovery after quenching in Ar and water 9-19745
- $\gamma$  scatt., photoelectric cross sections, theor., expt. comparison, 50-412 keV 9-5579
- in Cu, high speed dislocations, effect of impurity atoms on frictional force 9-3397
- Pt-Cu crystal, n scatt. for defect mode detection at 300, 570, 930°K 9-7476
- Pt-Fe<sup>2+</sup>, lattice dynamics using Mossbauer effect 9-7638
- Pt-Al discharge, Pt excitatin inhibition, obs. 9-18134
- Pt-Pb discharge, atoms reson. interaction, obs. 9-18134
- Pt/Pt-(13 at. wt.%)Rh thermocouple, stress effect in thermal e.m.f. 9-12208
- Pt and Re, thermal desorption spectra, high resolution, of He 9-11783
- Zr-Pt system, crystal structure of Ti<sub>3</sub>Pt<sub>3</sub> 9-19725

**Platinum compounds**

- alloys, field ion microscope imaging 9-14924
- 2a/OAu-Pt short-range order field ion microscope investigation 9-3305
- Co-Pt alloy, ordered, nature of coercive force 9-10118
- Co-Pt alloys, magnetic ordering, effect of thermomagnetic treatment 9-3767
- Fe-Pt alloys, f.c.c. Curie temp. pressure dependence 9-12289
- 2a/NiPt, short range order, field ion microscope investigation 9-3305
- PT(CN<sub>4</sub>) group, Van Vleck paramag. calc. 9-19946
- Pt-Co alloys, ferromagnetic, specific heat, 1.4 to 4.2°K 9-16178
- Pt-Co alloys, low temp. susceptibility, anomalous 9-13966
- Pt-Co permanent magnetic alloy, improvement of mag. props. by replacement of Pt by Pt group metals 9-12294
- Pt-Fe alloy, Mossbauer effect, mag. structure rel. to ordering 9-12362
- Pt-Fe permanent magnetic alloy, improvement of mag. props. by replacement of Pt by Pt group metals 9-12294
- Pt-Pd Au alloys, high temp. transport props. 9-15027
- Pt-Rh alloys, photoelectric  $\gamma$  cross-section by dis. and calc. 9-18654
- Pt-Cl<sub>2</sub>(AsEt<sub>3</sub>), Pt-Cl and ligand stretching vibrs., far i.r. obs. 9-15869
- Pt-Cl<sub>2</sub>(AsPh<sub>3</sub>), Pt-Cl and ligand stretching vibrs., far i.r. obs. 9-15869
- Pt-Cl<sub>2</sub>(PEt<sub>3</sub>), Pt-Cl and ligand stretching vibrs., far i.r. obs. 9-15869
- Pt-Cl<sub>2</sub>(PPh<sub>3</sub>), Pt-Cl and ligand stretching vibrs., far i.r. obs. 9-15869
- Pt-Cl<sub>2</sub>(PPr<sub>3</sub>), Pt-Cl and ligand stretching vibrs., far i.r. obs. 9-15869
- Pt complex, Pt X<sub>2</sub>2RCN (X=Cl or Br and R=Me or Ph), vibrational spectra 9-20937
- PtB, gaseous, dissociation energies, mass spect. determination 9-14726
- Pt(CO)Cl<sub>2</sub>, vibr. and Pt-Cl bands, i.r. and Raman obs. 9-15868
- PtCo alloys, superlattice formation, field-ion microscope obs. 9-7402
- Pt(II) selenourea complexes, i.r. and laser Raman spectra and prep., obs. 9-15867
- Pt(II) thiourea complexes, i.r. and laser Raman spectra and prep., obs. 9-15867
- Pt(NH<sub>3</sub>)Cl<sub>3</sub>, vibr. and Pt-Cl bands, i.r. and Raman obs. 9-15868
- PtO<sub>2</sub>, ternary oxide, (A<sub>2</sub>PtO<sub>3</sub>, A=rare earth or In), pyrochlore struct., prep. at 3 kbar 9-5274
- Pt/Pt (13 at. wt.%)Rh thermocouple, stress effect on thermal e.m.f. 9-12208
- Pt-(52 wt.%)Co alloy, ordered, magnetic anisotropy, 298° and 77°K 9-21583



**Platinum compounds** continuedTi-Pt system, crystal structure of  $\text{Ti}_3\text{Pt}_5$  9-19725**Pleochroism**

dichroic dye mols. in nematic liq. cry., orientation by elec. field 9-9481  
 fluorene, dichroism of cryst. bands 9-14712  
 hexahelicene, low-temp. circular dichroism 9-15165  
 molecules, circular dichroism rel. to dissymmetry 9-9167  
 molecules, mag. moments from mag. circular dichroism 9-9184  
 photodichroism in frog retina, absence 9-20276  
 tourmaline, dichroism, colour origin and change on heating 9-15171  
 CN in alkali halides, electric field induced dichroism 9-3857  
 $\text{CaF}_2\cdot\text{H}_2\text{O}^{(2/3)}$ , mag. circular dichroism in absorpt. bands 9-1737  
 $\text{CaPd}(\text{CN})_4$  crystals, dichroism 9-16396  
 $\text{KCl}\cdot\text{Sr}$ , circular dichroism of  $\text{Zr}$ -centres 9-18692  
 $\text{KCl}$ , circular dichroism of R-centres 9-7975  
 RbI magnetoreflection dichroism, Zeeman effect irregularity 9-7949  
 n-Si, near ferroelectric phase transition 9-14029  
 n-Si, e. irradi., stress-induced dichroism and photoconductivity meas. rel. to defect obs. 9-21340  
 $\text{SrTiO}_3$ , stress induced dichroism at absorption edge 9-3858

**Plexiglas** *see* **Plastics****Plutonium**

amperometric titration, AgO oxidation, Fe reduction, for determ. 9-17544  
 bare critical assembly, central reactivity contribs. of gram-sized samples of  $^{244}\text{Cm}$ ,  $^{239}\text{Pu}$  and  $^{235}\text{U}$  9-19370  
 diffusion and solubility in Al 9-11957  
 diffusion and solubility in Ni 9-19768  
 distribution in fuels, alpha autoradiography determ., improved resolution 9-19374  
 elastic constants, polycrystalline case, cubic centred  $\epsilon$  phase 9-21359  
 energy release of radioactive decay, also for other other transuranium isotopes 9-547  
 inclusions, laser microprobe analysis 9-4023  
 ions, equilibrium potn. depend. on temp. and conc. in  $\text{PuCl}_3\text{-NaCl}$  9-20892  
 liquid, solubilities of Ti, V, Cr, Mn, Zr, Nb and Mo, 700 to 1000°C 9-11685  
 in organic solns., chemical analysis 9-1929  
 $p_{1/2}$  level splitting by internal elec. field 9-670  
 radioactive, replica preparation 9-7396  
 reactor core moderated or unmoderated, criticality data 9-14650  
 separation from U by fractional sublimation in reactor fuel 9-20857

**Plutonium compounds**

$^{238}\text{PuO}_2$  particles, pyrolytic coated 9-2793  
 $^{239}\text{Pu}$  fast n fission cross-section ratio n energy range 0.3-2.5 MeV 9-623  
 Ph-Hf alloys, phases and constitution 9-21410  
 Pu-Pd alloys, mag. susceptibility as function of relative composition 9-19944  
 $\text{Pu}_3\text{Pd}_4$ , X-ray crystallography 9-19723  
 Pu (1.5at% Hf,  $\beta\rightarrow\alpha$  transformation kinetics 9-11977  
 PuC, thermal diffusivity, USNRDL flash technique 9-15032  
 $\text{PuF}_6$ , gas sorption and desorption for recovery and purification with LiF 9-5254  
 $\text{Pu}(\text{IV})\text{WO}_4$  precip. from aqueous solns. 9-16474  
 $\text{PuO}_2\cdot\text{ThO}_2$ , sintering in Ar at 1600°C, in air and in wet and dry  $\text{H}_2$  9-19822  
 $\text{PuO}_2$ , ht. capacity and thermodynamic props. 9-16179  
 $\text{PuO}_2$ , pyrolytic C-coated, high-temp. compatibility 9-2792  
 $\text{PuO}_2$ , volatilization behaviour, mass spectrometric study, 1980-2350°K 9-3160  
 $\text{PuO}_2$  film, grain growth and crystallization 9-5251

**Pockels effect** *see* **Electro-optical effects****Point defects** *see* **Crystal imperfections****Point groups** *see* **Crystal structure, atomic****Poiseuille flow** *see* **Flow; Hydrodynamics****Poisson ratio** *see* **Elastic constants****Polar cap absorption** *see* **Electromagnetic wave propagation/ionosphere****Polar cap flow** *see* **Airglow****Polarimeters**

airborne, for atm. visible reduction studies 9-13056  
 reflecting, for extreme u.v., using Au mirrors 9-10979  
 spectropolarimeter for 8.023 $\mu$ , optical activity Faraday effect meas. 9-269  
 n, use of (n,  $\alpha$ ) scatt. as polar. analyser, resolution for 14 MeV 9-2779  
 n using liquid He 9-4645

**Polarized light***See also* **Double refraction; Optical rotation; Photoelasticity; Polarimeters**

circularly, in Nd glass laser 9-2380  
 corrections in optical excitation- function meas., elimination 9-14667  
 c.m. waves in nonlinear isotropic dielectric tendency to linear and circular 9-12337  
 far i.r. from water vapour laser 9-19144  
 ferricytochrome C single cryst., spectra obs., 3700 7500 Å 9-11489  
 ferrimyoglobin complexes single cryst., spectra obs., 3700-7500 Å 9-11489  
 fundamentals, short-cut theory, and applications, book 9-8658  
 gas laser, rel. to reflector anisotropy 9-8601  
 Glan-Thompson and Rochon prisms, modified forms, polarizers and polarizing beam splitters 9-10905  
 from helium excitation by proton beam 9-9160  
 h.f. effects in semiconductors with carriers inelastically scattered on optical phonons 9-13879  
 h.f. effects in semiconductors with carriers inelastically scattered on optical phonons 9-1528  
 inverse Faraday effect, quantum field theory 9-17206  
 i.r. abs. for biaxially oriented polymers, graphical representation of data 9-21606  
 Jupiter's radiation, observation at 6.6 cm wavelength 9-6174  
 Malus' law, derivation from Mueller matrix calculus 9-4521  
 Malus law demonstration 9-15406  
 in optical systems, Mueller matrices, operational rotation 9-20551  
 partial polarization by quartz crystal 9-7938  
 pattern copying method, patent 9-10906  
 photons scatt. by mols., possibility of photon structure 9-13101  
 plane rotation on scatt. by rough surface, rel. to radial angle of obs. 9-8656

**Polarized light** continued

porphyrin, degree of polarization of fluorescence depend. on emission wavelength 9-5965  
 quadratic Compton effect, scatt. cross-section, arbitrary polarization 9-8738  
 in quartz, optically active, Rayleigh scatt. by defects, obs. 9-12340  
 $\alpha$ -quartz rotary power, variation due to pressure and temperature 9-12341  
 quartz-2, W filament lamp, polarization anisotropy, obs. 9-276  
 reflected by natural surfaces (soil, desert sand, white sand and water) 9-1939  
 refraction in n dielectric films with different optical properties, theory 9-7939  
 ruby, depolarization of light scattered through small angles 9-5877  
 ruby, Rayleigh scatt. from neutral gas, depolarization ratio determ. 9-9453  
 ruby laser, depolarization ratios in Rayleigh scatt. by neutral gases 9-14435  
 scattering by polymer films, anal. using annular spherulite model 9-7940  
 self-focusing of beam, sensitivity of length to departures from circular polar., paraxial ray approx. 9-10895  
 sky radiation, degree of polarization 9-20091  
 solar magnetographs, effects of polar. in line 9-2067  
 starlight, isolation of non-interstellar component 9-18942  
 starlight, variability, explanation by interstellar dust distrib. 9-15322  
 uranin soln. containing KI, polarization of fluorescence 9-9537  
 zodiacal, comparison with tropospheric scatt. 9-1938  
 $\text{CO}_2$ , depolarization in scatt. including Krishnan effect near crit. point 9-961  
 $\text{CdS}$ , spontaneous polarization, estimation 9-7936  
 for Ge optical constants measurements 9-12334  
 H radiation on quenching from 25 metastable state, calc. including hyperfine effects 9-20896  
 Ne fluorescence polarization, laser beam interaction 9-13292  
 RbI magnetoreflection dichroism, Zeeman effect irregularity 9-7949  
 Sfs depolarization in scatt. inc. Krishnan effect near critical point 9-961  
 synchrotron radiation, polarization, 500-1000Å, 6 GeV electrons 9-10979  
 $\text{ZnO}$ , spontaneous polarization, estimation 9-7936  
 $\text{ZnS}$ , orientation rel. to crystallographic axes, depend. of two-photon absorpt. 9-21631  
 $\text{ZnS}$ , spontaneous polarization, estimation 9-7936

**Polarography** *see* **Chemical analysis/electrochemical****Polarons** *see* **Crystal electron states/polarons****Polishing** *see* **Surface structure****Polonium**

No entries

**Polonium compounds**

No entries

**Polyelectrolytes** *see* **Electrochemistry; Polymers; Solutions****Polymerization**

binary and ternary behaviour, computer calc. 9-17522  
 $p$ -induced, of styrene 9-20037  
 condensation, effect of rate const. 9-2923  
 copolymerization and terpolymerization, computer calculations 9-10337  
 di(t-butylperoxy) fumarate, copolymerization 9-17525  
 dimethacrylate bis-diethyleneglycolphthalate, elec. conductivity meas. 9-15219  
 dimethacrylate bis-ethyleneglycolphthalate, elec. conductivity meas. 9-15219  
 dimethacrylate bis-triethyleneglycolphthalate, elec. conductivity meas. 9-15219  
 ethylene,  $p$ -ray induced, eff. of alcohols 9-20039  
 ethylene polymerization, induced by  $p$ -irradiation 9-17541  
 methylate Xylan, preparation and characterization 9-17526  
 monomers, multifunctional, phase separation, applic. of thermodynamic equilib. Flory theory 9-15216  
 poly(tetrafluoroethylene)- styrene, graft copolymerization, ESR investigations 9-20040  
 polyacrylamide, solid, shock wave polymerization obs. 9-15218  
 polyacrylonitrile, pure, transparent, rigid, plastic; bulk method, conventional initiator 9-14735  
 polymer chemical reactions, symposium 9-17509  
 polystyrene, preparation and characterization 9-17526  
 polystyrene in emulsion due to  $p$  irradiation 9-21686  
 polyvinyl chloroformate, preparation 9-17527  
 propylene, radical, under high press., kinetics 9-17521  
 redox polymerization, ESR studies of  $\text{CH}_3$  radical 9-15217  
 relative reactivity ratios from composition conversion data, computer calc. 9-17524  
 in solid state, formal kinetics 9-18753  
 styrene, cationic, under high press., kinetics 9-17521  
 styrene, rad. induced graft copolymerization on to poly(vinyl alcohol) 9-14130  
 trioxane, in solid state, cationic and radiation induced post-polymerization, kinetics 9-18753  
 trioxane, in solid state, under high press., kinetics 9-17521  
 vinyl oleate, radiation-induced, phase transition in liq. cry. or cry. state 9-14734  
 vinyl terpolymerization patterns, composition calc. 9-17523  
 9-vinylanthracene, free radical copolymerization 9-20038  
 zinc methacrylate, postirradiation polymerization 9-21691  
 $\text{CH}_3$  radical, ESR spectrum, coupling constant 9-15217  
 $\text{K}_2\text{SiO}_3$  aq. solns., cryoscopic determ. 9-982

**Polymers***See also* **Plastics**

aliphatic polyesters, far-i.r. spectra and struct. 9-9301  
 alkylated dicarboxylic acids, mol. struct. by X-ray analysis, non-equivalence of valence angles 9-19489  
 amorphous, glass forming, high-pressure treatment effects, 40 kbar and 300°C 9-3178  
 amorphous, thermodynamic and mol. props. theoretical eqn. of state determ. 9-14729  
 anisotropic discs, light scatt., applic. to growth kinetics of single crystals. from soln. 9-15168  
 bases for plastic scintillators, props. 9-11135  
 bead-and-spring model for soln. dynamics 9-7255  
 biaxially oriented, polarized i.r. abs. data graphical representation 9-21606

## Polymers continued

- biopolymers, collective proton tunneling mode coupling 9-7090  
 biopolymers, statistical-thermodynamic theory 9-14732  
 butadiene-based glow-discharge polymer films, photoionization potential 9-12228  
 carbazole-ring based, x-irrad., e.p.r. rel. to cross linking 9-3965  
 cellulose, natural crystalline, elastic consts. 9-1261  
 chain, excluded volume problem 9-11507  
 chain, intrinsic viscosity theories 9-4975  
 chain in soln., mean-square-displacement function 9-985  
 chains, X-ray small angle scatt. investigation of segment shape 9-17064  
 chemical reactions, symposium 9-17509  
 chemical reactions between, critical factors 9-17511  
 chloranil-ethylmethylamine, ESR in liquid and solid states 9-20025  
 chloranil polydimethylaminostyrene, ESR in liquid and solid states 9-20025  
 chloroacetamide, for finishing cotton 9-17515  
 2-chlorostyrene-styrene copolymers, mol. motion from dielec. meas. 9-14888  
 cholesteryl myristate mesophases, photographic scattering 9-19633  
 coiled, light scatt., asymptotic behaviour 9-17209  
 computer applications, symposium, Atlantic City, USA (1967) 9-11754  
 conjugated, LCAO MO treatment 9-832  
 copolymers and terpolymers, chem. reactions, computer calcs. 9-10337  
 creep, vibrational, in polymer materials 9-3424  
 cross-linked, statistical thermodynamics 9-11755  
 crystalline, structure and properties 9-21325  
 crystallization of thin films, spherulite size depend. on film thickness 9-12171  
 crystals, deformed, morphology of fibres pulled from them 9-18395  
 cyclohexane, F depend on mol. wt. 9-14838  
 dielectric, breakdown, multistage mechanism 9-7841  
 dielectric consts. 8-140 GHz meas. accuracy of impedance method 9-3696  
 dielectric props., eff. of glass transition temp., m.p., impurities and at. struct., review 9-19925  
 dielectric solns., electroconductivity 9-21222  
 dimethylsiloxane chains, dipole moments 9-2927  
 dye molecule-polymer interaction study by electrochromic effect (Størk effect) 9-16419  
 elastic and viscoelastic, relax., thermodynamic description 9-9754  
 elastomer, stress due to sinusoidal oscillations superposed on finite strain 9-19052  
 elastomers, crystallization, device for dilatometric meas. 9-21293  
 electric strength, volume dependence 9-12190  
 electrical cond., p-type 9-1451  
 electrical conductivity when subject to gas doping 9-15065  
 electron-microscope images of ultrathin sections, beam-induced contrast 9-11867  
 ethylene polymerization, induced by  $\gamma$ -irradiation 9-17541  
 ethylene-propylene copolymers, 998  $\text{cm}^{-1}$  band rel. to comp. 9-12389  
 ethylene-propylene copolymers, oxidation with hexavalent Cr cpds. 9-17531  
 exciton theory of vac.-u.v. absorpt. spectra 9-10216  
 excluded vol. theory, contacts density in chains 9-2924  
 fibres, sound wave velocity and coefficient of absorption by travelling wave method in a wide range of temps. 9-5540  
 film, photoresist., scattering effects in ion beam exposure 9-13813  
 film, polarized light scatt., model of annular spherulites 9-7940  
 finite chain molecules, configurational distributions 9-17065  
 flow, unstable, mechanism involving crystallization of molten polymers under shear stress 9-17236  
 formation, 3-dimens. in inert diluents, phase separation due to cross-linking 9-15216  
 fractionation 9-15991  
 fractionation, mol. wt. distrib. determ. 9-15992  
 free positron annihilation, effective number of e per atom 9-5637  
 glassy, with aromatic groups in side chain or backbone, molecular motions 9-19666  
 H $\alpha$  diff. patterns in systems containing spherulites, deformation sensitive control spot 9-12336  
 high polymer molecules, mechanical entanglements 9-19488  
 high-coking, from mixtures of diamino and dihydroxy-aromatic cpds. 9-8070  
 holy (4-methyl pentene-1), dielectric loss at cryogenic temps. 9-12189  
 homopolymers, linear, physical constants, book 9-11756  
 Kirkwood Riseman theory of intrinsic viscosities, numerical soln. of relevant eqn. 9-16656  
 long helical, optical rotation and Umklapp process effects, theory 9-5879  
 macroreticular ion exchange resins, pore structure determ. 9-14892  
 matrices for 1,2,5,6-dibenzanthracene, influence on phosphoresc., compared with glass 9-21654  
 mechanical relaxation processes, chain structure of macromols. quantitative rules 9-14731  
 melt, viscosity and glass transition, theories 9-3085  
 melts, viscoelasticity meas. 9-3069  
 $\alpha$ -methylpentafluorostyrene-p-methyl- $\alpha$ ,  $\beta$ ,  $\beta$ -trifluorostyrene-styrene copolymer,  $^{19}\text{F}$  n.m.r. and mol. struct., obs. 9-12518  
 $\alpha$ -methylpentafluorostyrene-styrene copolymer,  $^{19}\text{F}$  n.m.r. and mol. struct., obs. 9-12518  
 microcrystal gels, rheological props. rel. to particle size distrib., high yield values 9-9571  
 molecular weight distribution alterations by u.s. energy, computer analysis 9-17070  
 monodisperse system, intrinsic viscosity shear rate dependence 9-19621  
 multicomponent solns., liq.-liq. phase separation 9-7256  
 multicomponent solns., liq.-liq. phase separation 9-11686  
 multicomponent solns., liq.-liq. phase separation 9-15990  
 naphthalene based glow-discharge polymer films, photoionization potential 9-12228  
 Naphthazarine-Cu.Chelate elec. conductivity 9-3636  
 neoprene, Si inclusions, laser microprobe analysis obs. 9-12552  
 non-athermal solutions, adsorpt. at solid surface, numerical solns in parallel layer model 9-18400  
 olefin oxides, elec. cond. 9-16293  
 pentafluorostyrene-styrene copolymer,  $^{19}\text{F}$  n.m.r. and mol. struct., obs. 9-12518  
 peroxy, ESR obs. of decay during grafting of styrene on to poly(tetrafluorethylene) 9-20040  
 phenolic-nylon, ablation study 9-20125

## Polymers continued

- photochromic film on polyester, patent 9-8675  
 photoconductive compositions for xerography, patent 9-8674  
 piezoelectric transducer possibility 9-2926  
 poly(dimethyl Ketene), chain structure of two forms from calc. and X-ray analysis 9-19490  
 poly(dimethyl siloxane), adsorption on various surfaces, macromol. size 9-17251  
 poly(ethylene oxide), elec. cond. 9-16293  
 poly(methyl methacrylate), adsorption on various surfaces, macromol. size 9-17251  
 poly(methyl methacrylate), dynamic birefringence obs. 9-18693  
 poly(methyl methacrylate), X-ray small angle scatt. investigation of segment shape 9-17064  
 poly(n-alkyl methacrylate), rubbery state, stress-strain-time relation 9-18396  
 poly(vinyl alcohol), rad.-induced graft copolymerization of styrene 9-14130  
 poly(vinyl alcohol) network in swelling equil., thermoelastic props. 9-21356  
 poly(vinyl chloride) soln., mol. wt., macromol. dimens. and segments optical anisotropy determ. 9-14837  
 poly 3,3-bis(chloromethyl) oxacyclobutane, i.r. spectra and structure 9-17071  
 poly (L-glutamic acid) helix-coil transitions predicted and obs. 9-19486  
 poly-4-vinylpyridine, effect of  $\gamma$ -irrad. 9-18226  
 poly-2-vinylpyridine, effect of  $\gamma$ -irrad. 9-18226  
 poly-L-aspartic acid, helical struct. and conformational anal. 9-4974  
 poly-L-glutamic acid, helical struct. and conformational anal. 9-4974  
 poly-L-lysine, helix coil transitions, predicted and obs. 9-19486  
 polyacrylamide, solid, shock wave polymerization obs. 9-15218  
 polyacrylamide, viscoelastic, turbulent heat transfer coeff. determ. 9-19628  
 polyacrylate, glass transition temp. calc., 202-398°K 9-20991  
 polyacrylonitrile, non-graphitizing, anal. of random layer line profiles 9-7401  
 polyacrylonitrile, pure, transparent, rigid, plastic; bulk polymerization method, conventional initiator 9-14735  
 polyadenic acid, triplet exciton dynamics 9-9300  
 polyadenic acid, triplet exciton dynamics 9-14733  
 polyamide fibres, arranged contribution of macromolecules by magnetic susceptibility and anisotropy 9-21557  
 polyamides, aromatic; electrical props. depend. on vapour sorption 9-7094  
 polyamides, epitaxy on quartz 9-1158  
 polyamides, N-substituted, elec. conductivity 9-18600  
 polyanilines, oligomeric, electronic conductivity and chemical props. 9-19641  
 polyarylates, CH $_3$ -group motion and glass transition on heating 9-21415  
 polycapraome, cranked fibre annealing, long period temp. changes 9-17240  
 polycapraamide films, long period temp. depend. 9-17240  
 polycaprolactam fibres, photomechanical degradation and lifetime 9-11937  
 polycarbonate of bisphenol A, vapour induced crystallization 9-18420  
 polycarbonate resin, use in track recorder for absolute fission rate meas. 9-11142  
 polychloro-cyclobutane, NQR study of  $^{35}\text{Cl}$  9-15906  
 polychloroacrylate, glass transition temp. calc. 202-398°K 9-20991  
 polychloroprene uniaxially stretched, length of statistical segment calc. 9-19781  
 polychlorotrifluoroethylene, relaxation mechanisms, e microscope obs. 9-7535  
 polydimethylsiloxane melts, elasticity 9-15981  
 polydiphenylpropene-polystyrene graft copolymers, viscosity and birefringence 9-994  
 polyelectrolyte solns., dielectric dispersion props. at 25°C and 40 100 kHz 9-16018  
 polycene, spin density wave and charge transfer wave 9-20990  
 polyene mol., instability of conventional diamagnetic ground state 9-11508  
 polyethylene, 14 MeV neutron attenuation, with steel as radiation shield 9-18499  
 polyethylene, as reactor radiation detector, volumetric absorption 9-661  
 polyethylene, biaxially oriented crystallite orient. distrib. 9-3221  
 polyethylene, cranked fibre annealing, long period temp. changes 9-17240  
 polyethylene, crystalline-amorphous transition using theory of helix-coil transition 9-19486  
 polyethylene, drawn, orientation distrib. functions by broad line n.m.r. 9-12517  
 polyethylene, drawn and annealed lamellar structure and molecular orientation 9-19738  
 polyethylene, electron-microscope images of ultrathin sections, beam-induced contrast 9-11867  
 polyethylene, e.s.r. spectra of CH $_2$ -CH( $\alpha$ )-CH $_2$  free radical, anisotropic hyperfine constant 9-15203  
 polyethylene, irrad., e.p.r. and spin-lattice relax. mechanism 9-21669  
 polyethylene, LCAO band calc. for ideal chain 9-2928  
 polyethylene, i.f. vibrs. 9-1366  
 polyethylene, molecular motion 9-5537  
 polyethylene, neutron scatt. 9-19491  
 polyethylene, oriented, dynamic and frictional props. 9-21361  
 polyethylene, P. v. T. eqn of state 9-17239  
 polyethylene, Phillips-type, reactions at terminal vinyl group, mech. props. 9-17516  
 polyethylene, Raman spectrum of cryst. 9-10226  
 polyethylene, relaxation mechanisms, e microscope obs. 9-7535  
 polyethylene, structure change due to redrawing 9-17238  
 polyethylene deformed crystals, morphology of fibres pulled from them 9-18395  
 polyethylene film chlorination by gas and liquid, effects on film 9-17520  
 polyethylene films, containing spherulitic structures, stretching and contraction processes 9-17240  
 polyethylene films, long period temp. depend. 9-17240  
 polyethylene matrix containing anthracene, luminesc. spectra for various concs. at 77°K 9-17211  
 polyethylene networks, stress-optical coeff. 9-14969  
 polyethylene oxides, physical and photographic props. 9-7095  
 polyethylene terephthalate, molecular motion 9-5537



**Polymers continued**

- polyethylene terephthalate monofibres, effect of orientation of visco-elastic properties 9-9750
- polyethylene terephthalate, deform. bands prod. by tensile and shear tests 9-5463
- polyethylene terephthalate, deformation and yield 9-1287
- polyethylene terephthalate, photo-induced post-irrad. radical conversions, e.s.r. study 9-10357
- polyethyleneterephthalate fibres, oriented, supermol. struct. rel. to thermoplasticizing elongation, obs. 9-11757
- polyethylmethacrylate, laser-induced damage temp. dependence meas. Q-switching dye 9-9863
- polyhalobenzenes in cyclohexane and carbon tetrachloride, proton chemical shift, additivity scheme 9-19646
- polyimide seals for u.h. vacuum 9-16651
- polyisobutylene, F depend on mol. wt. 9-14838
- polyisobutylene-benzene soln., thermodynamics 9-21201
- polyisobutylene-cyclohexane soln., thermodynamics 9-21202
- polyisobutylene-n-pentane soln., thermodynamics 9-21203
- polymers, adhesion of Au spheres, effect of immersion in water or aqueous solns. 9-9605
- polymethacrylate, glass transition temp. calc. 202-398 °K 9-20991
- polymethacrylate in acetone, diffusion coeff. determ. in cell 9-14840
- polymethacrylate in benzene, diffusion coeff. determ. in cell 9-14840
- polymethacrylate in toluene, diffusion coeff. determ. in cell 9-14840
- polymethyl acrylate, molecular characterization in dilute solution 9-15907
- polymethylene liquids, chain shortening 9-13511
- polymethylmethacrylate, damage under extreme loads during laser-illumination 9-16137
- polymethylmethacrylate, light absorpt. during short-interval excitation 9-10217
- polymethylmethacrylate, non Newtonian viscosity in dilute solns. 9-17198
- polymethylmethacrylate, solvent eff. on n.m.r. spectra 9-18372
- polymethylmethacrylate, thermoelectric destruction by laser beam 9-19869
- polymethylmethacrylate, yield and fracture, temp. depend. 9-13729
- polymethylmethacrylate - polystyrene graft copolymers, viscosity and birefringence 9-994
- polymethylmethacrylate solns, u.s. absorpt. stereo and mol. wt. effects 9-1008
- polymethylmethacrylate-benzene solns., n.m.r. relax. 9-9558
- poly- $\alpha$ -methylstyrene monodisperse solns., light scatt. rel. to radius of gyration 9-14874
- polyoxymethylene, dynamic mech. props. 9-17321
- polyoxymethylene, hexagonal and orthorhombic, Raman spectra and vib. assignments 9-14064
- polyoxymethylene, morphology of crystallization 9-9645
- polyoxymethylene deformed crystals, morphology of fibres pulled from them 9-18395
- trans- poly(pentenamer), crystal structure from X-ray fiber spectra 9-14934
- polypeptides, synthetic, monolayers, mol. structure and deuterium exchange 9-834
- p-polyphenyl and oligomers, electrical conductivity 9-9924
- p- polyphenylene, compressed, pyrolysis yielding laminated struct. 9-8074
- polypropylene, 998 cm<sup>-1</sup> band rel. to isotacticity and disappearance on melting 9-12389
- polypropylene, cranked fibre annealing, long period temp. changes 9-17240
- polypropylene, crystalline-amorphous transition using theory of helix-coil transition 9-19486
- polypropylene, isotactic, dispersion curves and freq. distribns. 9-9302
- polypropylene, radiolytic cross-linking 9-18767
- polypropylene, syndiotactic, cell constants determ. from fiber spectra 9-14935
- polypropylene, uniaxially drawn isotactic films, quantitative characterization of deform. 9-21375
- polypropylene films, long period temp. depend. 9-17240
- polypropylenes, deuterated, of highest steric purity, NMR meas. 9-14736
- polyradicals, C and N, preparation 9-17518
- polystyrene+9, 10-diphenylanthracene+quencher, fluoresc. quenching and energy transfer 9-10247
- polystyrene+quencher, fluoresc. quenching and energy transfer 9-10247
- polystyrene, adsorption on various surfaces, macromol. size 9-17251
- polystyrene, damage under extreme loads during laser-illumination 9-16137
- polystyrene, kinetics of cracking and major crack growth obs., mass spectrometric investigation 9-18522
- polystyrene, melt viscosity and glass transition, analysis 9-18385
- polystyrene, non-Newtonian viscosity in dilute solns. 9-17198
- polystyrene, photocond., delayed effects 9-1620
- polystyrene, polymerization in emulsion 9-21686
- polystyrene, solid and in soln., fluoresc. yield and spectrum 9-12473
- polystyrene aerosols, adsorption of radon as size meas. method 9-7287
- polystyrene in benzene, F depend. on mol. wt. 9-14838
- polystyrene latex aerosol, attachment coeffs. of charged and neutral <sup>212</sup>Pb 9-9565
- polystyrene latex sphere suspensions, power spectrum of scatt. laser light 9-14875
- polystyrene latices particle size distrib. from Coulter counter, rel. to coagulation kinetics 9-9562
- polystyrene in soln., angular light scatt. of precipitated particles rel. to conc. determ. 9-14870
- polystyrene solution, light scatt. meas. in Brice-Phoenix and Sofica photometers, comparison of refl. effects 9-14832
- polystyrol film, mech. and dielec. effects of discharges 9-10032
- polystyrols, electric strength dependence on mol. wt. 9-3704
- polytetrafluoroethylene, free radical formation on irradi., possible dosimeter base 9-2558
- polytetrafluoroethylene, friction and wear 9-5488
- polytetrafluoroethylene, relaxation mechanisms, e microscopic obs. 9-7535
- polytetrafluoroethylene, transitions and relaxations pressure dependence from u.s. absorpt. and thermal expansion meas. 9-3406
- polytetrafluoroethylene (Teflon), positron lifetime meas. study rel. to  $\gamma$  radiation 9-13841

**Polymers continued**

- polythene, dielectric, breakdown time, meas. 9-12178
- polyurethane, chem. struct. eff. on resistance to various forms of degradation 9-14983
- polyurethane, p-type cond. 9-1451
- polyurethane in material for electrophotographic plate, patent 9-20574
- polyvinyl alcohol aqueous soln., rheological props. by flow birefringence 9-17172
- polyvinyl tolulene latices, particle size distrib. from Coulter counter, rel. to coagulation 9-9562
- polyvinylalcohol fibres, oriented, supermol. struct., rel. to thermoplasticizing elongation, obs. 9-11757
- polyvinylchloride, and glass transition 9-16294
- polyvinylchloride, elec. conduction and glass transition 9-16294
- polyvinylidene chloride, e.s.r. intensity and temp. studies rel. to heat treatment and A centres 9-8022
- PVC, plate-like, twisted to fibrillar structure 9-16088
- PVC, stretched uniaxially, thermal and mechanical props. anisotropy 9-19781
- PVC, structural changes due to mechanical and heat treatments 9-21416
- PVC grains, in suspension, effect of porosity on interaction with plasticizer 9-21231
- PVC irradi. in air, resolution of e.p.r. spectrum 9-17496
- P.V.K., hole photoemission from metals 9-5739
- relaxation processes, activation energies temp. depend. 9-9753
- rheo-optical behaviour obs. by X-ray diffraction 9-7536
- rubber-benzene soln., thermodynamics 9-21200
- rubber-like, non-linear deformation, evaluation of Rivlin's strain energy function 9-19784
- rubbers, chloroprene, crystallization kinetics, obs. 9-11796
- self-interacting chains, config. and thermodynamic props., Monte Carlo calc. 9-833
- semiconductor, organic, film-forming, props. description 9-14730
- sequence distribution calc., Fortran II program 9-17069
- siloxane elastomers, mech. strength -80 to +20°C. rel. to submolecular structure 9-9770
- sodium polyethylenesulphonate solns., transient elec. birefringence 9-16004
- sodium polystyrenesulfonate, counterion binding in aqueous solutions, tracer diffusion coeffs. 9-18355
- solid organic behaviour under high pressure 9-21366
- soln. dilute, showing drag reduction, turbulent heat transfer 9-1006
- soluble, added to water, mechanism to account for turbulence damping effect 9-7242
- in solution, electron microscope study 9-14836
- in solution, spherical suspension model rel. to dielectric props. 9-14855
- solution in good solvent, polydispersity index from light scatt. 9-14862
- solutions, damped torsional oscillator model, applic. to dielec. loss data 9-21188
- solutions, dilute, Huggins const. from relax. spectrum 9-15993
- solutions, excluded-vol. effects on limiting viscosity number 9-9489
- solutions, flexible mols., excluded vol. effects on light scatt. 9-17208
- solutions and melts, nonlinear viscoelastic model 9-21168
- solutions electroconductivity and ion mobility, molecular theory 9-18369
- solutions with general velocity field, orientation of macromols. 9-14835
- specific heat, crystal component, 1.7-4°K 9-2925
- spin density wave and charge transfer wave in long conjugated mols. 9-20990
- statistical copolymers, heterogeneity parameters by light scattering 9-19487
- statistics of condensation polymers 9-2923
- styrene,  $\gamma$ -induced polymerization 9-20037
- surface tension, critical values derived from molecular constitution by modified Hildebrand-Scott equation 9-16041
- surface treatment by r.f. plasma reactor 9-11579
- Teflon, ablation study 9-20125
- vanadyl phthalocyanine, laser-induced damage temp. dependence meas. in Q-switching dye 9-9863
- vinyl terpolymers, composition calc. program. 9-17523
- Viton 'A' elastomer seals for high vacuum 9-16652
- Young's modulus deformation and stress relaxation dependence, mechanism 9-16116
- $\gamma$  irradiation heating 9-19874
- $\gamma$  transmission (from <sup>60</sup>Co source) in polyethylene 9-21447
- $\gamma$ -radiolical prep. 9-17518
- <sup>6</sup>LiF-ZnS(Ag)-polyethylene scintillation detector for subcritical thermal n flux 9-6723
- N polyradical, a polyhydrazyl, preparation 9-17518
- polystyrene, photolysis investigation using radioactive iodine scavenger 9-18764
- Si<sub>3</sub>O<sub>4</sub><sup>2-</sup> polymerized, distrib. in binary silicate melts 9-19612

**Polymorphism***See also Crystal structure*

- n-chlorodiazoaminobenzene, tautomerism and crystal structure 9-3320
- methylchloromethane cpds., cryst. 9-5269
- n-methyldiazooaminobenzene, tautomerism and crystal structure 9-3320
- phthalocyanine, metal-free, spectroscopic characterization 9-19736
- pyrophyllite, natural and synthetic, structure rel. to polytypism with mica-like minerals 9-1192
- sodium 2-oxalate, polytypism 9-3226
- talc, structure rel. to polytypism with mica-like minerals 9-1192
- CS, pressure-induced transitions and electronic structure calcs. using Wigner-Seitz cell method 9-5614
- CuI, temp. depend. at high pressures 9-3488
- Fe, eff. of alloying elements 9-16049
- K, pressure-induced transitions, and electronic structure calcs. using Wigner-Seitz cell method 9-5614
- K<sub>2</sub>Cr<sub>2</sub>SO<sub>4</sub>, differential thermal analysis study to 30-40 kbar 9-14905
- K<sub>2</sub>SO<sub>4</sub>, differential thermal analysis study to 30-40 kbar 9-14905
- K<sub>2</sub>SeO<sub>4</sub>, differential thermal analysis study to 30-40 kbar 9-14905
- KCl polymorphic transition at high pressure, martensite character 9-9804
- LiAlSi<sub>2</sub>O<sub>4</sub> (eucriptite) high temp. form 9-1134
- NaAlSi<sub>3</sub>O<sub>8</sub>-KAlSi<sub>3</sub>O<sub>8</sub> system, inversion phenomena and incipient exsolution, electron optical study 9-21318
- Rb, pressure-induced transitions, and electronic structure calcs. using Wigner-Seitz cell method 9-5614
- RbNO<sub>3</sub> in solid state 9-5520
- SiC, type 120R, direct structure determ. 9-19724
- Zn<sub>2</sub>P<sub>2</sub>O<sub>4</sub> 9-5324

**Polynomials** *see Algebra; Functions*

**Polytypism** *see Polymorphism*

**Pomeranchuk rule** *see Elementary particles/scattering*

**Population inversion** *see Lasers; Masers; Optical pumping*

**Porosity** *see Porous materials*

### Porous materials

- See also Permeability, mechanical; Surface measurement*  
 aggregates, porosity and permittivity 9-7282  
 capillary models: two phase flow in serial model 9-5223  
 capillary porous, moisture diffusion coeff. at all drying temps. 9-21243  
 ceramic fuel elements, pore migration in thermal grad., shape change 9-18483  
 ceramics, sintered, microporosity effects on mech. and elec. props. 9-3431  
 coal, carbonized and activated, microporous struct. from X-ray scatt. and adsorption methods 9-7406  
 concrete, depend. of porous structure on solidification method 9-17345  
 deformation, large static, superimposed small motions of fluid 9-11665  
 diffusion-controlled chem. reactions 9-1904  
 elastic modulus-porosity relation 9-17295  
 flow of liq. in 3D channels, non-Newtonian 9-3067  
 fluid displacement processes, stability conditions 9-11666  
 gas flow, permeability obs. 9-7213  
 gaseous expansion kinetics 9-3167  
 grain growth theory, effect of pores on boundary mobility 9-18397  
 graphite, nuclear, texture changes under thermal and radiolytic oxidation 9-7408  
 graphite, open porosity and bulk density, nondestructive quality control for rocket motors 9-11936  
 graphite, pore size distrib. using Hg porosimeter with  $\gamma$  ray absorpt. 9-7416  
 graphite, pore size distrib. from stat. anal. of Hg porosimetry data 9-7415  
 graphite, pore struct. accessibility rel. to compressibility 9-5455  
 graphite, transmitted light study of pore systems and constituents 9-7423  
 graphitic carbons, pore struct 9-1077  
 laminar source flow, between two parallel coaxial rotating porous discs 9-17174  
 macroreticular ion exchange resins, pore structure determ. 9-14892  
 Mg(OH)<sub>2</sub>, dispersed, microstresses on pressing giving reversible elastic deform., X-ray analysis 9-1276  
 MHD, Rayleigh flow past an infinite porous plate 9-21165  
 parallel plates, moving, two, flow of two conducting immiscible liqs. between 9-17173  
 with perforated facing, design calc. for max. sound absorpt. in given freq. range 9-4325  
 petroleum cokes, closed pore vol. rel. to 'doublet' (001) X-ray diff. peaks 9-7457  
 petroliferous grit, dielec. constant meas. for porosity determ. 9-17422  
 porosimeter, Hg, for meas. of pore size distrib. heterogeneities 9-7416  
 PVC grains, in suspension, effect of porosity on interaction with plasticizer 9-21231  
 saturated, effective thermal conductivity in presence of percolation 9-7666  
 structures, effect of gas diffusion in transition region 9-9666  
 vapour migration in capillary-porous bodies 9-962  
 wall, spreading of incompressible jet 9-973  
 wet, sound propag. 9-5541  
 X-ray scattering curves 9-1168  
 Al, shock response on compaction, computer simulation 9-5437  
 C, adsorpt. of I from aqueous soln. with micropore filling 9-9625  
 C, microporosity, Dubinin theory of pore filling on adsorpt. 9-7346  
 C, molecular sieve, adsorpt. of Kr 9-7345  
 C black aggregates, shape and bulkiness factors 9-7421  
 C blacks, closed porosity in external layer of particles 9-7419  
 C blacks, porosity determ. from gas adsorpt. isotherms 9-7348  
 CaSO<sub>4</sub>·2H<sub>2</sub>O, dispersed, microstresses on pressing giving plastic deform., X-ray analysis 9-1276  
 Cu, shock compression 9-11920  
 Fe, shock compression in region of incomplete compaction 9-11948  
 Fe(CO)<sub>5</sub> powder, porosity effects on X-ray integrated intensities 9-11845  
 He superfluid flow through narrow pores 9-11737  
 MgO, polycrystalline, porosity dependence of sound velocity and Poisson's ratio 9-18494  
 Na-P zeolite, self diffusion of water 9-5130  
 SiO<sub>2</sub> gels, pore size anal. via diffusion coeffs. 9-9572  
 Ti welds, pore formation, surface impurity effects 9-16146  
 Y<sub>2</sub>O<sub>3</sub>, polycrystalline, porosity dependence of Young's and shear moduli 9-17298  
 ZrO<sub>2</sub>, insulating films, pore size determ., porosimeter design 9-9684

**Porter-LeChatelier effect** *see Stress/strain relations*

**Positive column** *see Discharges, electric*

**Positive ray sources** *see Ion sources*

**Positive rays** *see Chemical analysis/by mass spectrometry; Ion beams*

**Positons** *see Positrons*

### Positronium

- decay- $\beta^+$ , <sup>18</sup>O C-forbidden and <sup>18</sup>Si C allowed, obs. separation 9-10985  
 decay, Carruthers theorem rel. to local field theory 9-10984  
 formation in matter, elec. field dependence 9-6606  
 formation positronium in ionic cpds. 9-9916  
 hyperfine energy splitting 9-2807  
 in ice-water system, <sup>35</sup>S-<sup>35</sup>S conversion rel. to positron annihilation mechanism in ice 9-12079  
 in ionic cpds., formation positron bombardment 9-9916  
 orthopositronium scatt. and pick-off quenching in He 9-4886  
 orthopositronium-He atom syst., quenching rate of orthopositronium, parameter  $Z_{eff}$  meas. 9-4888  
 oxides, orthopositronium lifetimes and nature of 10<sup>-8</sup> sec. lifetime 9-12080  
 singularities in quantum electrodynamics, rel. to e. mass and polarization 9-336

### Positrons

*See also Electron pairs; and Electrons, which include both negative and positive electrons when the differences between them are of no special significance*

annihilation, meas. for Fermi surface of metals study 9-18596

annihilation in flight, photon spectra, 80-300 MeV 9-16821

### Positrons continued

- annihilation in metals and alloys, rel. to physical conditions 9-12078  
 annihilation radiation, angular correlation calc. from Hartree-Fock orbitals 9-5638  
 in carbon, penetration range at 1.88 MeV 9-12036  
 in cosmic rays, interplanetary, spectra 12-220 MeV, balloon obs. 9-20141  
 effective mass, in real metals 9-16207  
 ice-water system, <sup>35</sup>S-<sup>35</sup>S conversion of positronium in positron annihilation mechanism 9-12079  
 lifetimes in cholesteryl propionate 9-3079  
 in metals, effective mass, calcs. 9-1424  
 in metals, penetration range at 1.88 MeV 9-12036  
 in polyatomic gases, thermalization times 9-15974  
 polytetrafluoroethylene (Teflon), lifetime meas. study rel. to  $\gamma$  radiation 9-13841  
 in rare earth metals, penetration range at 1.88 MeV 9-12036  
 semiconductors, Annihilation 9-17374  
 e<sup>+</sup>e<sup>-</sup> scatt., and Bhabha exchange effects 9-6603  
 Al, annihilation radiation, angular correlation calc. from Hartree-Fock orbitals 9-5638  
 Al, lifetimes, cyclic deformation effects 9-16220  
 Ar, annihilation rate temp. dependence 9-6604  
 Cu, annihilation meas. of Fermi surface 9-21465  
 Cu, annihilation rel. to Fermi surface 9-7730  
 Cu, lifetimes, cyclic deformation effects 9-16220  
 Ga, lifetimes in solid and liquid 9-7731  
 Gd, ferromagnetic, polarized annihilation 9-9917  
 Ge, annihilation radiation, angular correlation calc. from Hartree-Fock orbitals 9-5638  
 H atom scatt. collisions 9-720  
 Na, lifetimes in solid and liquid 9-7731  
 Ni-Co alloy, annihilation rel. to plastic deformation 9-21477  
 Ni-Fe alloy, annihilation rel. to plastic deformation 9-21477  
 Se, annihilation radiation, angular correlation calc. from Hartree-Fock orbitals 9-5638  
 Si, annihilation radiation, angular correlation calc. from Hartree-Fock orbitals 9-5638  
 Y, annihilation rel. to electronic structure 9-18597  
 Zr, annihilation rel. to electronic structure 9-18597

### Potassium

- atom, enhanced 2 photon emission between 6S and 4S levels 9-20886  
 atoms and ions, bibliography of spectra 9-13287  
 boiling, voids, X ray meas. obs. 9-9468  
 bubble chamber range energy relation 9-458  
 collisions with mols., resonance radiation trapping and quenching, 4<sup>2</sup>P state lifetime meas. 9-14670  
 concentration in Vosges rocks by gamma spectrometry 9-20080  
 conductivity, electrical, temp. var. calc., comparison with expt. 9-16231  
 content in iron meteorites 9-6184  
 de Haas-van Alphen freq. meas. 9-18593  
 deformation and fracture 9-1308  
 e-e scatt. and resistivity low temp. depend. 9-1463  
 electron impact, and electric octupole 4<sup>2</sup>S-4<sup>2</sup>F transition 9-4839  
 electron-spin susceptibility from Knight shift meas. in liquid binary alkali metal alloys 9-13542  
 Fermi surface calc. from de Haas-van Alphen osc. 9-1443  
 Fermi surface from helicon Doppler-shifted cyclotron resonance meas. 9-12060  
 in human body, <sup>40</sup>K  $\gamma$  emission meas. 9-10568  
 Landau Fermi-liquid parameters 9-9912  
 liquid, isotope thermotransport, temp. depend. 9-9491  
 magneto-plasma, diffusion meas. 9-17102  
 magnetoacoustic effects and free electron theory 9-7649  
 in minerals, radioactive determ. of conc. 9-1932  
 molecular beam reaction with RbCl 9-10310  
 optical plasma resonance emission and transmission of thin film 9-12382  
 plasma, current instabilities 9-11610  
 plasma, strongly non-uniform, instabilities diffusion 9-11609  
 Stark effect obs. on 4<sup>2</sup> level 9-13290  
 thermal expansion coeff. calc. from pseudopotential theory 9-12023  
 thin film, ultraviolet transmittance 9-5867  
 transmitted light intensity modulation at 462 MHz, at g.s. h.f. freq. 9-9130  
 upper atmospheric, twilight obs., seasonal var. of abund. 9-12595  
 vacancy-produced lattice distortion, calc. by method of lattice statics 9-21332  
 vapour, heat capacity obs. by calorimetry 9-17161  
 vapour, resonance radiation trapping and quenching, 4<sup>2</sup>P state lifetime meas. 9-14670  
 whiskers, growth rate in critical saturation region 9-16061  
 X-ray emission spectra, anomalies in edges of K-spectrum 9-1817  
 Ar-K plasma, electrical conductivity 9-19532  
 K-Ar rock dating method, source of air Ar contamination 9-12571  
 K-Li ion exchange syst., diff. and reaction coupling 9-17510  
 K<sub>2</sub> vapour, laser-induced fluores. spectra 9-15856  
 K<sup>+</sup>·F<sup>-</sup>, ion pair, overlapping hydration shells, interact., spheroidal cavity model 9-14858  
 K<sup>+</sup> emission from Ni and Pt ribbons, thermionic, effect of deformation on 9-21554  
 K<sup>+</sup> ion scatt. from Ar atoms, 150 4000 eV 9-18152  
 K<sup>+</sup>-He collisions, KII resonance line excitation 9-14676  
 K XI-XIV, u.v. spectrum obs. 9-6972  
<sup>39</sup>K atom collisions, spin-exchange cross-section obs. 9-9152  
<sup>41</sup>K, diffusion in K<sub>2</sub>O-SrO-SiO<sub>2</sub> glass 9-1249  
 K<sup>+</sup>, collisions with H<sub>2</sub> and D<sub>2</sub> 9-2937  
 K<sup>+</sup>, exchange energy of electrons 9-4834  
 K<sup>+</sup>-He collisions, KII resonance line excitation 9-2834  
 K-Na-KCl-NaCl system, light absorpt. by colloidal particles 9-1725  
 K·Br<sub>2</sub>, molec. beams, reactive collisions 9-10323  
 liquid, isothermal compressibility 9-19596

### Potassium compounds

- citrate, crystallized from aqueous soln. at 25°C, crystal structure 9-19720  
 periodates, crystallized from aqueous soln. at 25°C, crystal structure 9-19720  
 selenites, crystallized from aqueous soln. at 25°C, crystal structure 9-19720  
 K·graphite lamellar cpds., thermodynamics, from solid-state e.m.f. 9-1391



**Potassium compounds continued**

- K-Cs liquid binary alloy, electron-spin susceptibility from Knight shift meas. 9-13542  
 K-Rb liquid binary alloy, electron spin susceptibility from Knight shift meas. 9-13542  
 K<sub>2</sub>CrO<sub>4</sub>, phase transitions to 30-40 kbar, differential thermal analysis 9-14905  
 K<sub>2</sub>PO<sub>3</sub>-V<sub>2</sub>O<sub>5</sub> semicond. glass, effect of thermal treatment on a.c. props. 9-3612  
 K<sub>2</sub>PtCl<sub>6</sub>·Os<sup>4+</sup>, optical spectra at 4.2°K 9-14055  
 K<sub>2</sub>SO<sub>4</sub>, phase transitions to 30-40 kbar, differential thermal analysis 9-14905  
 K<sub>2</sub>SeO<sub>4</sub>, phase transitions to 30-40 kbar, differential thermal analysis 9-14905  
 K<sub>2</sub>SiO<sub>3</sub> aq. solns., cryoscopic determ. 9-982  
 K<sub>2</sub>[Ni(CS<sub>2</sub>)<sub>4</sub>], magnetic susceptibility and config. 9-18667  
 K<sub>2</sub>Fe(CN)<sub>6</sub>, crystallography and paramag. anisotropy, 95° and 300°K 9-21343  
 K<sub>3</sub>Fe(CN)<sub>6</sub>, crystallography and paramag. anisotropy, 95° and 300°K 9-21315  
 KAg(CN)<sub>2</sub>, lattice vibrs. and Ag(CN)<sub>2</sub><sup>+</sup>; Raman and i.r. obs. 9-16166  
 K<sub>2</sub>Al<sub>2</sub>(SO<sub>4</sub>)<sub>3</sub>·24H<sub>2</sub>O (potash alum.), dislocations, direct obs. 9-11883  
 KAlSi<sub>3</sub>O<sub>8</sub>-NaAlSi<sub>3</sub>O<sub>8</sub> system, incipient exsolution and inversion phenomena, electron optical study 9-21318  
 K<sub>2</sub>BeF<sub>4</sub>, <sup>19</sup>F NMR rel. to hindered motion in structure 9-16466  
 KBr·O<sub>2</sub><sup>+</sup> dielectric loss meas. and dipole moment found 9-3698  
 KBr cry. with H<sup>+</sup> ions, far-infrared abs. 9-10184  
 KBr decoration and dislocation conduction 9-3355  
 KBrO<sub>3</sub>, n.q.r., temp. depend. of <sup>79</sup>Br freq. 9-10304  
 KCN, n.m.r. of cubic cryst., hindered rot. 9-16465  
 KCNS and alkali halides, molten, eutectic comps. 9-17193  
 KCl:Mn crystal, absorption spectra obs., electrical conductivity meas. 9-3893  
 KCl:O<sub>2</sub><sup>+</sup> dielectric loss meas. and dipole moment found 9-3698  
 KCl, luminescent excitation spectra of F and M centres 9-7988  
 KClO<sub>3</sub>, e.p.r. and optical absorption of ClO<sub>3</sub> radical created by X-irrad. 9-18737  
 KClO<sub>4</sub>, e.p.r. and optical absorption of ClO<sub>3</sub> radical created by X-irrad. 9-18737  
 KClO<sub>4</sub>, X-irradiated, e.p.r. and optical absorption of Cl<sub>2</sub><sup>-</sup> molecular ion 9-21625  
 KClO<sub>3</sub>, quadrupole spin echo, 'slow beats' 9-3973  
 KClO<sub>4</sub> elec. cond. in dioxane-water mixtures at 25°C, ion-solvent interactions 9-11717  
 K<sub>3</sub>Co(CN)<sub>6</sub>·Cr<sup>3+</sup>, e. spin echo envelope modulation by very small alternating mag. field 9-10282  
 K<sub>3</sub>Co(CN)<sub>6</sub>, e.p.r. of X-irrad. crystals 9-10278  
 K<sub>2</sub>CrO<sub>4</sub>, absorption spectra, effect of uniaxial compression, 20°K 9-10206  
 K<sub>2</sub>Cr<sub>2</sub>O<sub>7</sub> crystn., u.s. removal from heat transfer surfaces 9-4347  
 KD<sub>2</sub>PO<sub>4</sub>, ferroelec. region, polarization relax. time and dielec. susceptibility 9-1595  
 K<sub>2</sub>F, field grads. at <sup>39</sup>K nuclei 9-1884  
 K<sub>2</sub>F, field grads. at <sup>39</sup>K nuclei 9-1884  
 K<sub>2</sub>F, photoemission spectra, evidence for L-bands 9-3757  
 KF, second-order Raman spectra calc. for vibration spectra computation 9-12429  
 KFe<sub>3</sub>(OH)<sub>2</sub>(SO<sub>4</sub>)<sub>2</sub>, magnetic properties of Jarosites 9-5800  
 KH<sub>2</sub>PO<sub>4</sub>, H<sub>2</sub>PO<sub>4</sub><sup>-</sup> ion structure from Raman scatt. spectra in ferroelec. and paraelec. states 9-18652  
 KH<sub>2</sub>PO<sub>4</sub>, hyperbroad generation at 10<sup>4</sup> Mc/s frequency at 4.2°K 9-18561  
 KH<sub>2</sub>PO<sub>4</sub>, u.s. velocity and attenuation meas. 9-21430  
 KH<sub>2</sub>AsO<sub>4</sub>, electric-field-gradient tensor at As site from p. relax. meas. 9-17469  
 KH<sub>2</sub>PO<sub>4</sub>·Cu<sup>2+</sup>, chem. structure from e.p.r. spectra 9-1860  
 KH<sub>2</sub>PO<sub>4</sub>·K<sub>2</sub>H<sub>2</sub>AsO<sub>4</sub> mixed crystals, e.p.r. study of proton dynamics 9-3956  
 KH<sub>2</sub>PO<sub>4</sub>, 45°Z cut, light modulation, temp depend. of modulation degree 9-12338  
 KH<sub>2</sub>PO<sub>4</sub>, dielectric phase transitions from l.f. Raman spectra and lattice modes 9-12422  
 KH<sub>2</sub>PO<sub>4</sub>, ferroelectric phase transition, Brillouin scattering study 9-12198  
 KH<sub>2</sub>PO<sub>4</sub>, i.r. spectral meas. 9-5896  
 KH<sub>2</sub>PO<sub>4</sub>, modified Slater model for Kagome lattice 9-5265  
 KH<sub>2</sub>PO<sub>4</sub>, n.m.r. of <sup>39</sup>K, rotary saturation and spin calorimetry 9-10294  
 KH<sub>2</sub>PO<sub>4</sub>, Raman scattering by polarization fluctuations 9-12423  
 KH<sub>2</sub>PO<sub>4</sub>, refractive index, pressure dependence 9-16393  
 KH<sub>2</sub>PO<sub>4</sub>·KD<sub>2</sub>PO<sub>4</sub> press. depend. of ferroelec. props. 9-13919  
 KH<sub>2</sub>PO<sub>4</sub> Brillouin-scatt. study of ferroelec. transitions 9-5750  
 KH<sub>2</sub>PO<sub>4</sub> crystal, absorpt. of ultrasound near phase transition temp. 9-1378  
 KH<sub>2</sub>PO<sub>4</sub> crystal, rel. to interference effects in n scattering on p in double minimum potential well 9-2538  
 KH<sub>2</sub>PO<sub>4</sub> crystal close to Curie temp. in electric field as laser beam deflector 9-10854  
 KH<sub>2</sub>PO<sub>4</sub> Slater model, one-dimens. analogue 9-6257  
 KI: amide ion doped, paraelec. and paraelectric orientation of ions from u.v. absorpt. 9-5747  
 KI:Ag<sup>+</sup>, far i.r. resonant-mode freq. shifts on uniaxial stress 9-5922  
 KI:(Br<sup>-</sup>,Cl<sup>-</sup>), frequency spectrum, statistical calc. 9-5312  
 KI:Mn<sup>2+</sup>(Eu<sup>2+</sup>), thermal treatment, e.p.r. spectra comparison with luminescence of CsI 9-20028  
 KI:NO<sub>2</sub><sup>-</sup>, vibration structure in absorpt. spectra at 4.2°K 9-16432  
 KI:S<sup>-</sup>, luminesc. emission spectra 9-14082  
 KI:Se<sup>-</sup>, luminesc. emission spectra 9-14082  
 KI:Se<sup>-</sup>, luminesc. emission spectra 9-14082  
 KI:Ti, scintillations, electron-hole and exciton mechanisms, photomodeling 9-20008  
 KI-Tl<sup>+</sup>, lattice distortion and binding energy of Tl<sup>+</sup> with light foreign anions 9-3297  
 KI, diamag. impurity in phthalimide/boric acid soln., phosphoresc. 9-7994  
 KI, epitaxial Au film in u.h. vacuum 9-7310  
 KI, epitaxial growth of f.c.c. metals 9-7377  
 KI, fundamental absorption band, elec. field effects 9-1783  
 KI, ionic conductivity, 200-700K 9-16292  
 KI, paraelectric relaxation, mass depend. 9-9752  
 KI, photoemission spectra, L-bands and exciton bands 9-3759  
 KI, second order Raman-laser spectrum 9-12421

**Potassium compounds continued**

- KI, U<sub>1</sub>-centres, vibrational spectra 9-5388  
 KI, u.v. exposure of crystal, with impurities photochemical reaction 9-5581  
 KI, u.v. irradi., defect formation 9-14952  
 KI, X-ray L<sub>III</sub> absorpt. of I, spectrograms 9-12455  
 KI containing CN<sup>-</sup>, u.s. velocity and attenuation 9-11996  
 KI cry. with H<sup>+</sup> ions, far-infrared abs. 9-10184  
 KI in uranin soln., polarization of fluorescence 9-9537  
 KI monocrystal, removal of NO<sub>2</sub><sup>-</sup>, NO<sub>2</sub><sup>-</sup>, SO<sub>4</sub><sup>2-</sup> impurities 9-3240  
 KIO<sub>3</sub>, p irradiated, thermal annealing of radioiodine recoils 9-16193  
 KIO<sub>3</sub>, X-ray L<sub>III</sub> absorpt. of I, spectrograms 9-12455  
 KIO<sub>4</sub>, X-ray L<sub>III</sub> absorpt. of I, spectrograms 9-12455  
 K<sup>+</sup>IO<sub>3</sub>, electro-optical and nonlinear optical props. 9-3867  
 K(Tl<sup>+</sup>) crystals, X-ray treated, V<sub>K</sub> centre spectra obs. 9-20028  
 K<sub>3</sub>LiNb<sub>3</sub>O<sub>10</sub> single cryst., growth and crystallographic characs. 9-11803  
 KMgF<sub>3</sub>·K<sup>+</sup>·K<sup>+</sup> mixed crystals, long-wavelength optical lattice vibrations 9-13789  
 KMrCl<sub>3</sub>, antiferromagnetic, from e.s.r. studies of MnCl<sub>2</sub>-alkali chloride fused mixtures 9-13948  
 K<sub>2</sub>MnCl<sub>6</sub>, e.p.r. and mag. susceptibility, 1.4°-300°K 9-16456  
 KMnCl<sub>2</sub>·2H<sub>2</sub>O, transition to antiferromag. state at 2.70°K, from sp. ht. meas. 9-1395  
 KMnF<sub>3</sub>, antiferromagnet, critical fluctuations, e.p.r. studies 9-18735  
 KMnF<sub>3</sub> near phase transition, temp. behaviour of 2-phonon transition 9-7919  
 K<sub>2</sub>MnF<sub>4</sub>, zero point spin deviation from n.m.r. and e.s.r. obs. 9-10151  
 KMn<sub>1-x</sub>Ni<sub>x</sub>F<sub>3</sub> single cryst., electron-magnon transitions in absorpt. spectra 9-1785  
 K<sub>2</sub>Mn(SO<sub>4</sub>)<sub>2</sub>·4H<sub>2</sub>O, space group and structure refinement using n. diff. 9-3277  
 KNO<sub>3</sub>·VO<sub>2</sub><sup>+</sup>, e.p.r. 9-3961  
 KNO<sub>3</sub>·M(NO<sub>2</sub>)<sub>2</sub>, (M=Ba, Sr, Ca) liq. mixture, composition depend. of light absorpt. 9-1018  
 KNO<sub>3</sub>, III-II transition, press. depend. 9-9803  
 KNO<sub>3</sub>·AgNO<sub>3</sub>, molten mixtures, vibr. spectra and struct. 9-1019  
 KNO<sub>3</sub>·LiNO<sub>3</sub> liquid, dis. of u.s. vel. 9-1007  
 KNO<sub>3</sub>·NaNO<sub>3</sub> liquid, obs. of u.s. vel. 9-1007  
 KNO<sub>3</sub>, Raman scatt. in phases I, II and III 9-14061  
 KNO<sub>3</sub>, dielectric phase transitions from l.f. Raman spectra and lattice modes 9-12422  
 KNO<sub>3</sub>, interdiffusion in dilute solns., of AgNO<sub>3</sub> 9-7261  
 KNO<sub>3</sub>, molten, electromigration of K ions, temp. depend. of isotope effect 9-11716  
 KNO<sub>3</sub>, Mossbauer spectra, <sup>57</sup>Co source, phase transition obs. 170-25°C 9-14039  
 KNO<sub>3</sub>, orthorhombic, principal refractive indices, temp. depend. 9-5871  
 KNO<sub>3</sub>, Raman scattering in phases I, II, and III 9-12424  
 KNbO<sub>3</sub>, chain structure 9-11818  
 KNiF<sub>3</sub>, antiferromagnet, optical absorpt. temp. dependence, 77-620°K 9-1782  
 KNiF<sub>3</sub>, optical absorption, comparison with K<sub>2</sub>NiF<sub>4</sub> 9-7976  
 KNiF<sub>3</sub>, superexchange interactions 9-14012  
 KNiF<sub>3</sub>, unexcited Hartree-Fock molecular-orbital treatment 9-12232  
 K<sub>2</sub>NiF<sub>4</sub>, optical absorption, comparison with KNiF<sub>3</sub> 9-7976  
 K<sub>2</sub>NiF<sub>4</sub> single crystals, charge transfer and dielec. behaviour at room temp. 9-12184  
 xK<sub>2</sub>O·(1-x)Na<sub>2</sub>O·4SiO<sub>2</sub> glasses, elec. resist. and structure rel. to composition 9-3693  
 KPO<sub>3</sub> surface tension of molten mixture obs., surface heat of mixing estimated 9-21191  
 KPB<sub>2</sub>Cl<sub>3</sub>, formation in vaporization of PbCl<sub>2</sub>+KCl mixtures, thermodynamic props. from mass spectra 9-19442  
 (KPB<sub>2</sub>)-(K<sub>2</sub>Sr<sub>2</sub>, NaBa<sub>2</sub>)Nb<sub>5</sub>O<sub>15</sub> ferroelec. transition temp. rel. to lattice structure 9-1594  
 K<sub>2</sub>PtCl<sub>6</sub>, lattice dynamics NQR exam. 9-11987  
 KReO<sub>4</sub>, pure n.q.r. of Re 9-3974  
 K<sub>2</sub>SO<sub>4</sub>·Li<sub>2</sub>SO<sub>4</sub>(41-90 equiv. %), molten isotope effects of electro-migration 9-8102  
 K<sub>2</sub>SO<sub>4</sub>, optical activity in vibration-transition region 9-7941  
 K<sub>2</sub>Sb, three-photon photoelec. eff. 9-10080  
 KSr<sub>2</sub>Nb<sub>5</sub>O<sub>15</sub>, ferroelec. transition temp. rel. to lattice structure 9-1594  
 KTa<sub>2</sub>Nb<sub>1-x</sub>O<sub>7</sub>·Eu<sup>3+</sup>(Sm<sup>3+</sup>), fluorescence 9-10242  
 KTaO<sub>3</sub>:Eu<sup>3+</sup>(Sm<sup>3+</sup>), fluorescence 9-10242  
 KTaO<sub>3</sub>, Raman scatt., elec.-field-induced 9-5938  
 KTaO<sub>3</sub>-KNbO<sub>3</sub> solid solutions, Raman spectra 9-12433  
 K<sub>2</sub>UCl<sub>6</sub>-NaCl eutectic diagram predicted, confirmed by X-ray diffraction 9-11969  
 K<sub>2</sub>UO<sub>2</sub>·SO<sub>4</sub>·2H<sub>2</sub>O effect of D<sub>2</sub>O substitution on fluorescence lifetime 9-1830  
 α-KZnBr<sub>2</sub>·2H<sub>2</sub>O crystal structure 9-7442  
 K+CH<sub>3</sub>I system, complex optical potential calc. 9-10322  
 [K[Au(CN)<sub>2</sub>]]<sub>2</sub>H<sub>2</sub>O, solid soln., crystal structure by X-ray diff. 9-13636  
 K<sub>2</sub>[Ni(CN)<sub>4</sub>], H<sub>2</sub>O, fine structure of Ni K X-ray absorption obs. 9-17484  
 K<sub>2</sub>Fe(CN)<sub>6</sub>, thermal n. capture, <sup>59</sup>Fe spectra obs. 9-6022  
 KMgF<sub>3</sub>, elastic props. 9-1258  
 Li<sub>2</sub>SO<sub>4</sub>·K<sub>2</sub>SO<sub>4</sub> eutectic, corrosion of Fe, thermodynamics 9-15222  
 NaNbO<sub>3</sub>-K<sub>2</sub>NbO<sub>3</sub> system, thermal phase composition and boundaries, thermal and X-ray diff. meas. 9-7621  
 ZnCl<sub>2</sub>-KCl liquid, u.s. vel. obs. 9-986

**potassium bromide**

- absorption spectral, colour centres representation 9-5920  
 breakdown time, meas. 9-12178  
 Brillouin scattering component, linewidth 9-12451  
 channelling of high-energy protons 9-7680  
 diamag. impurity in phthalimide/boric acid soln., phosphoresc. 9-7994  
 electron energy losses and optical data 9-16191  
 ENDOR obs. in F centres, optical pumping and monitoring 9-21673  
 ENDOR spectrum, F-centre experimental explanation 9-15208  
 epitaxial growth of f.c.c. metals 9-7377  
 F-centre absorpt., temp. depend. 9-17820  
 F-to-M colour centre photochem. conversion mechanism 9-5384  
 film, emission in far i.r. 9-15175  
 Frankel defect production and volume expansion obs. in coloration process on X-irradiation 9-21331  
 impurity distrib. coeff. during zone melting 9-3239  
 i.r. eigenfrequency pressure dependence, 1-35 kbar 9-5897  
 luminescence, decay time of O<sub>2</sub><sup>-</sup> centres, effect of pressure 9-15184  
 M<sup>+</sup>-centre electronic states theory, F<sub>2</sub><sup>+</sup>-model 9-19758  
 nucleation centres of condensed phase 9-18425

**Potassium compounds continued**  
**potassium bromide continued**

- optical, c.s.r. and elec. studies of K colloids in additively coloured, pure and doped crystals 9-16414  
optical constns. and band struct. from energy loss meas. of electrons 9-5591  
paraelectric and paraelec. orientation of amide ions, from u.v. absorpt. 9-5747  
photographic layers, modulation transfer function, determ. from physical meas. 9-10946  
proton tunnelling, 6.72 MeV 9-21448  
Raman-laser spectrum, second order 9-12421  
u.s. velocity and attenuation in crystals containing CN<sup>-</sup> 9-11996  
u.v. exposure of crystal, with impurities photochemical reaction 9-5581  
vacancy breakdown under self-diffusion 9-18461  
volume change due to point defects after X-irrad. 9-18460  
Au epitaxial film in u.h. vacuum 9-7310  
KBr: impurity defects, far i.r. absorpt., discontinuities obs. 9-19990  
KBr:Ba<sup>2+</sup>, thermoelec. power and ionic conductivity 9-1607  
KBr:Li<sup>+</sup>, far i.r. resonance line shift induced by electric field 9-1784  
KBr:Li<sup>+</sup>, far i.r. resonant-mode freq. shifts on uniaxial stress 9-5922  
KBr:NO<sub>2</sub><sup>-</sup>, vibration structure in absorpt. and luminescence spectra at 4.2°K 9-16432  
KBr:S<sub>2</sub><sup>-</sup>, luminescence at 4.2°K 9-14078  
KBr:Ti<sup>4+</sup>, lattice distortion and binding energy of Ti<sup>4+</sup> with foreign anions 9-3296  
KBr:Ti<sup>4+</sup> lattice distortion and binding energy of Ti<sup>4+</sup> with light foreign anions 9-3297  
KBr-KCl solid solns., removal of divalent cations by introduction of anion-replacing impurities 9-16053  
KBr-KI:Ti type phosphors, absorption spectra of isostructures, interpretation 9-15176  
KBr-RbBr(NaBr,KCl) solid solutions, evap. films, intrinsic absorption spectra 9-10204  
KBr-TlBr solid solutions, lattice parameter composition dependence 9-13637  
KBrOH<sup>-</sup>, dissociation and U<sub>2</sub> decomposition 9-18480  
KBr-KCl mixed crystals Frenkel defect production and volume expansion obs. in coloration process on X-irradiation 9-21331  
KCl-KBr system, interdiffusion process, role of anion-cation pair vacancies 9-5411  
KOH-doped, dielectric relaxation pressure depend. 9-5746  
OH doped, paraelec dipole equilibrium directions and elec. moment by electro-caloric eff. 9-21532

**potassium chloride**

- channelling of high energy protons 9-7680  
circular dichroism of R centres 9-7975  
colour centre obs. using chemical method 9-16109  
colour centres, F, M and R, electric field eff. at liquid N<sub>2</sub> temp. 9-3367  
contact electrification by metals 9-10029  
crystal dislocations, etching soln. for revealing 9-1221  
crystal growth by heat treatment followed by zone melting 9-18423  
crystals, possible use in light amplification 9-10164  
diffusion of Cu ions, temp. dependence, 350°C 650°C, rel. to ion size effects 9-1250  
elastic constns., meas. by audio freq. reson. method, 20-700°C 9-5423  
elastic constns., meas. by static, reson. and u.s. techniques 9-5422  
electron drift mobility 9-19878  
electrophotoluminescence at room temp. 9-12485  
ENDOR obs. in F centres, optical pumping and monitoring 9-21673  
ENDOR spectrum, F-centre experimental explanation 9-15208  
epitaxial growth of f.c.c. metals 9-7377  
e.p.r. of Mn-S complexes 9-20019  
e.p.r. of stabilized Ag atoms 9-14108  
F<sub>2</sub> band and two new bands 9-9722  
F centres, EPR obs. 9-20020  
F centres, hyperfine and quadrupole interactions, ENDOR determ. 9-5385  
F centre production by u.v. irrad. 9-1235  
F centres, surface, state of localized electrons 9-16108  
F-to-M colour centre photochem. conversion mechanism 9-5384  
growth from melt, free of grain boundaries and with low density dislocations 9-16101  
impurity distrib. coeff. during zone melting 9-3239  
ionic transport, five-defect model 9-13914  
i.r. absorption of small crystals and films, size- and shape-dependence 9-21626  
i.r. eigenfrequency pressure dependence, 1-35 kbar 9-5897  
lattice distortion and binding energy of (I)<sup>1</sup> centre 9-3333  
luminescence in crystal with quasi-colloidal K centres 9-18721  
M' centre electronic states, F<sub>2</sub> theoretical model 9-19758  
microcrystal, lattice const. and energies study 9-17270  
N<sub>2</sub> centre 9-7502  
nucleation centres of condensed phase 9-18425  
optical extinction coeff. of colloidal Ag impurities, rel. to annealing 9-5924  
orthogonalized-plane-waves calcs. 9-13832  
paraelectric and paraelastic orientation of amide ions, from u.v. absorpt. 9-5747  
paraelectric resonance spectroscopy, theory and expt. 9-13916  
permittivity and conductivity meas., freq. limit by 'electrodeless' method 9-14853  
photoconductive sensitivity changes on colour centre bleaching 9-5768  
photoemission spectra, evidence for L-bands 9-3757  
photomobility of dislocations in irrad. crystals 9-21548  
polymorphic transition at high pressure, martensite character 9-9804  
proton tunnelling, 6.72 MeV 9-21448  
relaxation, one-phonon, of OH<sup>-</sup> 9-5534  
relaxation effects with Ni<sup>2+</sup> and Cu<sup>2+</sup> 9-1577  
substrate for epitaxial growth of PbTe 9-1106  
substrate for growth of Au films in high vacuum 9-21274  
surface, dissociation on c. irrad. at low temps. 9-7327  
thermal lattice vibrations 9-21425  
thermoluminescence of Z<sub>1</sub>-centres, Ca-doped crystals, after X-irradiation 9-14088  
thermoluminescence rel. to colour centres and d.c. resistivity in irradiated crystals 9-14092  
transformation of ultrasonic into electrical oscillations 9-12012  
u.s. velocity and attenuation in crystals containing CN<sup>-</sup> 9-11996  
u.v. absorption, radiation-produced 9-5921  
V<sub>k</sub> centres, optical reorientation temp. dependence 9-16106

**Potassium compounds continued**  
**potassium chloride continued**

- V<sub>k</sub> colour centre lattice effect on optical absorpt. 9-9720  
vacancy breakdown under self diffusion 9-18461  
vacancy conc. in thermal equilibrium 9-3325  
X irradiated, defect production, optical absorpt. meas. 9-18462  
X-ray luminescence stress dependence and effect of Cu impurity 9-3932  
X-ray transmission anomalous, dislocation density effects 9-1746  
<sup>40</sup>Ar diffusion flux, elec. fields effects 9-11897  
Au epitaxial film in u.h. vacuum 9-7310  
Ca doped, thermoluminescence of Z<sub>1</sub>-centres after X-irradiation 9-14088  
ESR of HCN<sup>-</sup> obs. at 4°K 9-13358  
KCl:Ag, forbidden transitions in opt. abs. 9-12381  
KCl:Ba<sup>2+</sup>, yield point and dislocation mobility temp. depend. 9-5363  
KCl:(Ca, Sr or Ba), fluorescence of Z<sub>1</sub> centres 9-5962  
KCl:Cd, coloured, optical, c.s.r. and elec. studies 9-5925  
KCl:Co<sup>2+</sup>, F-centres, growth and bleach at room temp. 9-5386  
KCl:Eu, radical recombination luminescence, atomic H excited 9-3920  
KCl:Eu<sup>2+</sup>, absorption and emission spectra, multiphonon structure, lattice freq. shift effects 9-16410  
KCl:Mn, u.v. band shifts on thermal and optical bleaching rel. to those in highly pure KCl 9-14053  
KCl:Mn<sup>2+</sup>, absorption spectra, optical, in range 0.1 to 15 mol% of dopant range 9-5923  
KCl:Mn<sup>2+</sup>, charge transfer spectra 9-3892  
KCl:NO<sub>2</sub><sup>-</sup>, vibration structure in absorpt. and luminescence spectra at 4.2°K 9-16432  
KCl:OH<sup>-</sup>, dissociation and U<sub>2</sub> decomposition 9-18480  
KCl:Pb, Rayleigh scatt. by single crystal 9-19993  
KCl:Pb, single slip line, nature 9-14948  
KCl:S<sub>2</sub><sup>-</sup>, luminescence at 4.2°K 9-14078  
KCl:Sr, circular dichroism of Z<sub>1</sub>-centres 9-18692  
KCl:SrCl<sub>2</sub>, ionic transport, five-defect model 9-13914  
KCl:Tb<sup>3+</sup>S<sub>2</sub><sup>-</sup>, luminesc. centres, models 9-1846  
KCl:Tb<sup>3+</sup>Se<sub>2</sub><sup>-</sup>, luminesc. centres, models 9-1846  
KCl:Ti<sup>4+</sup>, lattice distortion and binding energy of Ti<sup>4+</sup> with foreign anions 9-3296  
KCl:CaCl<sub>2</sub>-H<sub>2</sub>O soln., isopiestic vapour press. meas., osmotic and activity coeffs. 9-21187  
KCl-Eu and KCl-Sb phosphors with wide forbidden zone, radical recombination luminescence, mech. 9-16428  
KCl-KBr mixed crystal, F centre decay rate and thermal stability obs. 9-9721  
KCl-KBr mixed crystals, Frenkel defect production and volume expansion obs. in coloration process on X-irradiation 9-21331  
KCl-KBr solid soln., removal of divalent cation impurities by introduction of anion-replacing impurities 9-16053  
KCl-KBr system, interdiffusion process, role of anion-cation pair vacancies 9-5411  
KCl-LiCl mixed crystal, ENDOR of A centres 9-12519  
K-(Na-KCl)-NaCl system, light absorpt. by colloidal particles 9-1725  
Kee:NaCl, F centres in additive coloration 9-21344  
Li, doped, paraelec. dipole equilibrium directions and elec. moment by electro-caloric eff. 9-21532  
Mn<sup>2+</sup> at cation vacancies, superhyperfine struct in e.p.r. spectrum 9-5988  
NO<sub>2</sub><sup>-</sup> impurity local vibration quantum, decomposition time into phonons 9-15000

**Potential energy, gaseous molecules** *see Molecules/intermolecular mechanics***Potential energy, single molecules** *see Molecules/internal mechanics; Molecules/vibration***Potentiometers** *see Electrical measurement***Powder diffraction cameras** *see X-ray crystallography/apparatus***Powder metallurgy** *see Metallurgy; Sintering***Powders**

- See also Granular structure; Particle size; Sintering; Surface measurement*  
airborne in duct, mass flowmeters 9-3136  
bed, bottom pressure with applied ext. pressure 9-17322  
brittle inorganic crystalline, shock-wave prep., patent 9-9668  
compacts, ejection pressures and strengths 9-5476  
glass beads, thermal conductivity in vacuum, 100 to 500°K 9-15020  
graphite, compactibility to form reactor fuel rods 9-2797  
graphite, mixtures, particle size distrib. and shape factor, statistics 9-7427  
graphite, surface struct. and adsorpt. of O<sub>2</sub> and H<sub>2</sub> 9-1091  
graphitic carbon, g-factor anisotropy, e.p.r. determ. 9-8014  
hexagonal, temperature diffuse scattering 9-11814  
lamp black, raw mat. for C products, amount of binder needed 9-7590  
mechanical model for fundamental aspects of behaviour 9-21355  
neutron time of flight diffraction, collimator role 9-7397  
neutron time of flight diffractometry, intensity and resolution 9-18437  
packing of solid particles, book 9-11752  
particle formation during atomization by gas stream 9-5221  
perthites, homogenisation during routine thermal treatment of powders 9-18531  
pulverized mats., coatings, determ. of thermal cond. 9-9851  
quartz comminution, net energy input rel. to fineness 9-11953  
quartz comminution, net energy input rel. to fineness 9-7597  
solid particle interacts in sound field, role of microstreaming 9-5192  
steel, pressing and sintering behaviour 9-17339  
X-ray diff., line profile anal., computer program 9-18438  
Al Sn prealloyed, atomizations 9-18536  
Al Sn prealloyed, pressing characteristics 9-18501  
Al<sub>2</sub>O<sub>3</sub>, initial stage sintering kinetics 9-7586  
Al<sub>2</sub>O<sub>3</sub>, sintering kinetics 9-7585  
BaTiO<sub>3</sub>, discoloration, grain size effects 9-21619  
BeO, sintering and inhibition by adsorbed phosphate, crystallite growth obs. 9-17241  
C, actual Hall effect calc. from measured apparent one 9-7737  
C, sintering and graphitization by elec. discharge 9-7610  
Cr, long range magnetic order by n diff. 9-14009  
Cu, particle formation during atomization by gas stream 9-5221  
Fe magnetization reversal, particle agglomeration effect 9-3822  
Fe porous, shock compression in region of incomplete compaction 9-11948  
Fe<sub>3</sub>O<sub>4</sub>, magnetization reversal, particle agglomeration effect 9-3822  
6Fe<sub>2</sub>O<sub>3</sub>.PbO, magnetoplumbite, intrinsic ferromag. resonance 9-1848  
Mg, compacted with 1% O<sub>2</sub>, high temp. creep 9-17311  
MgAl<sub>2</sub>O<sub>4</sub> spinel, active, characterization and sintering 9-3464  
MgAl<sub>2</sub>O<sub>4</sub>, initial sintering kinetics 9-1321



**Powders continued**

- MgAl<sub>2</sub>O<sub>4</sub> spinels, Prep. by decomposition 9-3242  
 MgO, dense, thermal conductivity in N<sub>2</sub> gas 9-15026  
 Mn-Ca alloys, magnetization and coercive force, particle size depend. 9-12239  
 Ni-Al mixtures, exothermic effs. during sintering 9-17324  
 Ni-Al mixtures, sintering, exothermal effs. on Al content and porosity 9-17325  
 Ni-on-Si catalysts, finely divided in direct and alternating fields, superparamagnetism 9-21569  
 Ni, particle size from X-ray powder diffraction line broadening 9-3303  
 Pb, particle formation during atomization by gas stream 9-5221  
 Sb<sub>2</sub>Te<sub>3</sub>-Bi<sub>2</sub>Te<sub>3</sub>, grain size, impurity content and processing effects on thermal conductivity 9-19867  
 SnO<sub>2</sub>, cassiterite, elec. cond., press. depend. to 90 kg/cm<sup>2</sup> 9-13877  
 ThO<sub>2</sub>, thermal conductivity in various gases 9-15031  
 UO<sub>2</sub>, densification, powder morphology and energy effects 9-3465  
 Y Fe garnet, strain induced by various milling treatments 9-5453

**Praseodymium**

- coping of La and Th cpds., effect on supercond. 9-13857  
 crystal, d.h.c.p., Fermi surface, rel. to mag. ordering and structure 9-5615  
 ions, PrIII 4f<sup>3</sup> energy levels, mag. params. 9-4831  
 multiplets of 4f<sup>3</sup>5d config., overlapping phenom. 9-11387  
 Pr<sup>3+</sup> crystal fields shielding 9-7695  
 Pr<sup>3+</sup> in AlLaO<sub>3</sub>, visible and u.v. excitation of fluorescence 9-18724

**Praseodymium compounds**

- thiulphate, thermal resistivity mag. field dependence, 0.4-4°K, anomalies 9-13811  
 PrAl<sub>3</sub>, mag. props. 9-7898  
 Pr-La alloys, mag. susceptibility rel. to temp. and field strength 9-17449  
 Pr-Y alloys, mag. susceptibility rel. to temp. and field strength 9-17449  
 PrBi nuc. mag. cooling, hyperfine enhanced low temp. prod. 9-4185  
 PrCl<sub>3</sub>, active phonon Raman spectra 9-3903  
 PrCl<sub>3</sub>, adjusting poles and zeros of dielec. dispersion to fit reststrahlen 9-5876  
 PrCl<sub>3</sub>, cryst. field, charge penetration and covalency contribs. 9-10159  
 PrF<sub>3</sub>, vapour press., ht. of sublimation 9-9597  
 PrF<sub>3</sub> paramag. single cryst., spin density, anomalous temp. depend. 9-1877  
 PrMnO<sub>3</sub>, crystal and antiferromagnetic structures 9-19717

**Precipitation**

- See also Atmosphere/precipitation*  
 age hardening, book 9-11951  
 coprecipitation for hexagonal ferrite preparation 9-5277  
 graphite in steel, effect of Ca 9-19838  
 hydrides, at grain boundaries in Zircaloy 2 9-19754  
 morphology theory application to massive transformation 9-3485  
 Nimonic alloys,  $\gamma'$ -phase dissolution, recovery after ageing 9-13765  
 particle coarsening theory, further applic. 9-11954  
 particle coarsening theory, further applic., comments 9-11955  
 from polymer solutions, conc. determ. by angular light scatt. 9-14870  
 steel, austenitic,  $\gamma'$  precip., resist changes 9-1319  
 steel, austenitic stainless, ferrite and sigma-phase formation 9-14989  
 steel, austenitic stainless, of  $\gamma'$  9-5517  
 steel, austenitic stainless, Widmannstatten M<sub>23</sub>C<sub>6</sub> precip., nucleation and growth 9-1331  
 steel, H36x12TYu,  $\gamma'$ -phase segregation, form and bonding to matrix particles 9-9789  
 three-dimensional macroperiodic lattices formed by regularly distrib. occurrences in new phase, theory 9-3245  
 Ag-Cu solid solns, supersaturated, substructure changes during decomposition 9-1339  
 Ag-Cu solid solutions, supersaturated, discontinuous, kinetics investig. 9-21399  
 Ag-(10 wt.%) Mn-(1.5 wt.%) Sb alloys, solid soln. decomposition, work hardening effects 9-1326  
 Ag solid, periodic, expt. 9-21405  
 Ag solid, periodic, mathematical modification 9-21406  
 Al-(Ag-Cu) alloys, electron microscopic study, use of different forms of contrast 9-7605  
 Al-Cu alloy,  $\theta'$  structure, lattice parameters determ. 9-11834  
 Al-Cu alloys, deformed, recrystallization 9-21400  
 Al-Cu alloys, inhomogeneities, correl. with lattice strains and lattice const. 9-9783  
 Al-Cu solid solns., of Cu elec. resistivity changes 9-21482  
 Al-Zn alloys precipitation reversion studies, miscibility gap for Guinier-Preston zones obs. 9-21393  
 Al-Zn solid solutions, resistivity 9-21480  
 Al-Zn(Cu)-Mg alloys, electron microscopic study, use of different forms of contrast 9-7605  
 Al-Zr alloys, in age-hardening 9-13762  
 Al, phase formation by ion implantation 9-11956  
 Al-7wt.%Mg alloy, at grain boundaries, electron microscopy 9-19832  
 Al<sub>2</sub>O<sub>3</sub>-Ti<sub>2</sub>O<sub>3</sub> solid solns., and struct., obs. 9-1340  
 Cd separation from Cu, Zn, in pyrophosphate complex 9-18748  
 Co particles in Cu-Co solid solns., distribution function in superparamagnetic range 9-5803  
 Cu-Ag alloys, rel. to stacking faults growth 9-11958  
 Cu-Co mixed crystals, nucleus formation at dissociation 9-14988  
 Cu-Cr alloy, f.c.c., effect on recrystallization texture formation 9-21391  
 Cu-GaAs supersaturated solid solns. 9-5511  
 Cu-In alloys, discontinuous kinetics 9-9797  
 Cu-(2.4 wt.%)Mg alloy, in hardening mechanisms 9-1329  
 Cu-Zn alloy,  $\alpha_1$ -plates, morphology and crystallography correlation 9-11842  
 Fe-(23 at.%)Be, structure changes during ageing, study by transmission e. microscopy 9-17343  
 Fe-C alloys, kinetics, infl. of age-hardening rate 9-9798  
 InAs-Cu(Au, Ag) solid solutions, effect of dislocations 9-11967  
 Mg (3 wt.%)Zn alloy, and clustering kinetics 9-5505  
 MgAl<sub>2</sub>O<sub>4</sub> spinel powders, Prep. by decomposition 9-3242  
 MgO-Al<sub>2</sub>O<sub>3</sub> Cr<sub>2</sub>O<sub>3</sub>, cryst. solns., kinetic, obs. 9-3493  
 MgO single cryst., effect of magnesioferrite precipitates on mech. props. 9-7573  
 Ni base alloys,  $\gamma'$ , -hardened, slip and climb processes 9-7579  
 Ni-(12 at.wt.%)Ti alloy, behaviour study 9-11959  
 Pb Ni alloys, radiation-induced, small angle X-ray and n. scatt. meas. 9-9805  
 Pu(IV)WO<sub>4</sub> from aqueous solns. 9-16474  
 Ra-Ba iodate mixed cry., solid and liq. phase, Ra distrib. determ. 9-18771

**Precipitation continued**

- Ra-Ba oxalate mixed cry., solid and liq. phase, Ra distrib. determ. 9-18771  
 Si-Sb, of Sb solid soln. during annealing 9-1333  
 TiO<sub>2</sub>-SnO<sub>2</sub> crystalline soln., annealed at 850°C and 1000°C, mech. of separation and modulated struct. 9-7602  
 (U, Pu)C fuels, prep. by coprecipitation 9-6939  
 $\alpha$ -U, of UAl<sub>3</sub> from supersaturated soln. of Al 9-11960  
 $\alpha$ -Zr, of hydrides, and H solid solubility, obs. 9-16148

**Pressure**

- See also Atmospheric pressure and density; High pressure phenomena and effects; Radiation pressure; Vapour pressure*  
 axial compression of circular cylindrical shells, creep buckling 9-17761  
 axial compression of circular cylindrical shells, effects of unreinforced circular cutouts on buckling 9-16710  
 cylinders, reln. between ultimate press. and wall thickness 9-5473  
 jet, turbulent shear flow, field characteristics determ. 9-19574  
 losses due to contact resistance in liquid metal flow in circular tubes in trans. mag. field 9-9328  
 sphere, empty, in gas, collapse 9-936  
 on spindle in inviscid liquid flow 9-11664  
 superconducting materials properties, effects 9-9935  
 supercritical, on fluids, their heat transfer coeffs. 9-20998

**Pressure measurement**

- See also Manometers; Vacuum gauges; Vapour pressure measurement*  
 acoustic probe for hypersonic re-entry vehicle 9-4082  
 gas, low, determ. by electron scatt. meas. 9-12849  
 in gaseous diffusion of hydrocarbons 9-964  
 indicator for recording Hg manometer levels at regular intervals 9-6227  
 ionization gauge, i.p. meas. in isothermal and nonisothermal recipients 9-10593  
 low, book 9-6267  
 multiport thermocouple gauge for up to 1 atm. 9-6273  
 Pirani gauge, microminiature, 0.1-10 torr 9-2101  
 thermistor micro-Pirani gauge, circuitry 9-242  
 total, limitations of ionization gauges 9-12810  
 transducer, capacitive diaphragm, for differential vac. gauge 9-6226  
 H plasma, infinite column, press. increase and total thermal cond. calc. 9-11540  
<sup>3</sup>H ionisation gauge, for reactive gases 9-2131  
 Hg manometer, h.p. differential 9-6272

**Prisms, optical**

- Glan-Thompson and Rochon prisms, modified forms, polarizers and polarizing beam splitters 9-10905  
 holographic Foucault knife edge test 9-2417  
 laser beam expansion in one dimens. 9-4485  
 of Ohara glass, dispersion between F and C lines, use of Hg 'e' line as mean reference 9-7935  
 polarising, for i.r. region, 2.6-5  $\mu$  9-17886  
 Rayleighs expression for dispersion between F and C lines 9-6541  
 rectangular prism, total-reflection, for smoothly rotating light source image 9-16793  
 reflecting, ray path rel. to linear glass heterogeneity 9-10889  
 substrate for incidence angle meas. 9-10888

**Probability**

- See also Random processes; Statistical analysis*  
 conditional, analysis of nuclear reactor noise 9-20845  
 gaussians fitting to peaks in nuclear spectrometry, max. probability method 9-13160  
 Markov processes in treatment of colmatage 9-5202  
 model for rad. transfer in spherical shell atmosphere 9-14370  
 Monte Carlo method for generating peripheral events of particle prod. 9-20607  
 population injury model for random re-entry of satellite carrying radioactive mats. 9-20127  
 stochastic theories in quantum mechanics, anal. using Feynman integral 9-16694

**Procopiu effect** *see Films, solid; Magnetolectric effects; Magnetomechanical effects***Programming** *see Calculating apparatus/digital computer programmes***Projectiles** *see Ballistics***Projectors, optical**

No entries

**Promethium**

No entries

**Promethium compounds**

- <sup>147</sup>Pm<sub>2</sub>O<sub>3</sub> microspheres, high density, production by r.f. induction plasma heating 9-2795  
 Pm (III) oxalate, decomposition, and formation of oxide, thermal analysis 9-2790  
 Pm<sub>2</sub>O<sub>3</sub>-Sm<sub>2</sub>O<sub>3</sub>, thermal and elec. prop. meas., rel. to <sup>147</sup>Pm as power source 9-2790

**Prominences, solar** *see Sun/prominences***Propagation** *see Acoustic wave propagation; Electromagnetic wave propagation***Propagators** *see Field theory, quantum; Quantum electrodynamics***Proportional counters** *see Counters/proportional***Prospecting** *see Geophysical prospecting***Protactinium**

- emission spectrum, 3  $\mu$  to 4000 Å, and level system 9-15814  
 spectra, emission, from 3  $\mu$  to 4000 Å 9-19403

**Protactinium compounds**

- Fe-Pd alloys, f.c.c., Curie temp. pressure dependence 9-12289  
 Pa V hydrated oxide u.v. absorption bands obs. 9-21616  
 $\beta$ -PaBr<sub>3</sub>, crystal structure 9-14923

**Proteins**

- albumen, dilute solns., thermal cond. rel. to displacement vel. 9-9506  
 albumin, bovine serum, adsorbed monolayers, water permeability, obs. 9-7262  
 bovine serum albumin film at air-water interface, thickness rel to spreading or adsorption 9-9477  
 carboxypeptidase A, NMR studies 9-17067  
 cytochrome c, Mossbauer spectra 9-831  
 dioxynolionucleic acid, (DNA), X ray diffraction study 9-7093  
 DNA, dilute solns., thermal cond. rel. to displacement vel. 9-9506  
 DNA, double strand scission induced by radiation 9-21991  
 DNA, sodium salt, elec. conductivity 9-1459

**Proteins continued**

- enzymes, noncavitating u.s. effects 9-4140  
 ferrimyoglobin complexes, single-cryst. polarized absorpt. spectra 9-3899  
 fluorescence and phosphorescence under u.v. excitation 9-15905  
 fluorescence spectroscopy 9-18224  
 free radical formation under x-irradiation 9-4013  
 globular, intermol. forces in heat aggregation process, correl. with denaturation 9-18222  
 hen egg-white lysozyme, NMR studies 9-17068  
 histidine residue, struct. and binding sites, n.m.r. obs. 9-7092  
 phase refinement by Karle-Hauptmann tangent formula 9-13667  
 rhodopsin, opsin-chromophore intramol. energy transfer 9-9299  
 serum, electrophoresis medium for improved resolution, patent 9-10566  
 structure analysis by c. diff. 9-14936  
 thymine in alkali soln., fluoresc. excitation spectrum, wavelength depend. of quantum yield 9-11706  
 water permeability of adsorbed monolayers, obs. 9-7262

**Proton magnetic resonance** *see* Nuclear magnetic resonance and relaxation**Proton spectra**

- $^{27}\text{Al}(\text{p},\text{p})^{26}\text{Mg}$ , photoproton, from 26.6 MeV bremsstrahlung 9-15750  
 $^{12}\text{C}$  energy spectra of fast photoprotons for bremsstrahlung 50 to 80 MeV 9-2647  
 $^{63}\text{Cu}(\text{p},\text{p})^{62}\text{Ni}$ , photoproton, from 26.6 MeV bremsstrahlung 9-15752  
 $^{65}\text{Cu}(\text{p},\text{p})^{64}\text{Ni}$ , photoproton, from 26.6 MeV bremsstrahlung 9-15752  
 $^4\text{He}$  states obs. in  $^4\text{He}(\text{p},\text{p})^4\text{H}$  expt. 9-16937

**Protonium** *see* Protons and antiprotons**Protonosphere** *see* Atmosphere/upper**Protons and antiprotons**

- See also* Cosmic rays/protons; Nuclear reactions and scattering due to protons; Nucleons and antinucleons  
 Bragg curve shape, particle interaction eff. 9-15036  
 density in neutron stars from Brueckner-theory calc. 9-18865  
 earth's outer radiation belt, low energy p lifetimes 9-10415  
 energy losses compared with deuterons 9-21452  
 form factor, as three-quark system 9-20610  
 form factors, e.m., fit in terms of reson. 9-6685  
 magnetic monopole moment, upper limit obs. 9-8751  
 n-p mass difference, theory using nucleon form factors 9-13139  
 photoprotons, fast, energy spectra, form  $^{12}\text{C}$  9-2647  
 protons, outward flow from Earth's bow shock 9-8188  
 in solar particle streams, discussion 9-16620  
 structure from elastic scatt. of  $\pi,\text{K},\text{p}$  9-18009  
 transition metals, ( $Z=21-30$ ), stopping power meas. at 5-12 MeV 9-17364  
 p-n mass difference, contribution by A2 Regge pole 9-15640  
 p-n mass difference calc. in reciprocal bootstrap model 9-15639  
 $\text{pp}\rightarrow\pi^+\pi^-\pi^0$  annihilation channel, multi-Regge model description, 5.7 GeV/c 9-14522  
 $\pi\text{-p}\rightarrow\text{pp}'\rho^-$  backward prod. diff. cross section meas.: 8, 16 GeV/c 9-20647  
 $\pi\text{-p}$ , six prong, transverse-momentum distrib., CM ang. distrib., ang. correl., 7.0 GeV/c 9-6669  
 A1, dechannelling at stacking faults, H accumulation 9-16102  
 Ca, stopping power meas. at 5.12 MeV 9-17364  
 $^{52}\text{Cr}(\text{p},\text{p})^{51}\text{Cr}$ , 5.7-6.0 MeV, p polarization 9-4776  
 Ge transmission along  $\{100\}$  and  $\{110\}$  channels in crystal lattice, energy and angular distributions 9-16192  
 Si, energy-loss straggling 9-13816  
 Si transmission along  $\{100\}$  and  $\{110\}$  channels in crystal lattice, energy and angular distributions 9-16192  
 $\text{SiO}_2$ , channel of higher refractive index form., rel. to optical waveguides 9-20556

**absorption**

- bubble chamber range energy relation 9-458  
 $^3\text{H}(^4\text{He},\text{p})^4\text{He}$ , 15.8 MeV proton total react. cross section using associated particle method 9-16957

**angular distribution**

- p<sub>1</sub> group, p<sub>1</sub>-y ang. correlations, Butler theory agreement, ang. distrib. 955 keV  $\gamma$  comparison 9-2755  
 photoprotons, energy and ang. distrib. obs. in giant reson. region from  $\text{C}^{12}(\text{p},\text{p})\text{B}^{11}$  react. 9-11270  
 $^{10}\text{B}(\text{d},\text{p})^{11}\text{B}$ , p<sub>1</sub> ang. distrib. and differential cross sections meas., comparison with theory 9-9060  
 $^{89}\text{Y}(\text{p},\text{p}')^{\text{inelastic}}$  scatt.,  $E_{\text{p}}=24.5$  MeV, obs. 9-19307  
 $^{64}\text{Zn}(\text{n},\text{p})^{64}\text{Cu}$  reaction, and proton energy spectra 9-6887  
 $^{64}\text{Zn}(\text{n},\text{p})^{64}\text{Cu}$  reaction, and proton energy spectra 9-6887

**antiprotons**

- pn scatt., elastic cross-sections, dip-bump structure 9-416  
 pp scatt., charge-exchange, Regge-pole  $\pi$ -conspiracy model 9-11098  
 pp scatt., elastic cross-sections, dip-bump structure 9-416

**detection, measurement**

- discrimination  $\alpha\text{-p}$  9-19226  
 Ilford K-5 emulsion, analysing power for polarized p, 10-50 MeV 9-467  
 organic scintillator response, photomultiplier meas. 9-6722  
 recoil from n-irrad. bone tissue interface 9-15379  
 $^{75}\text{Br}$  compound nuclei from  $^{12}\text{C}+^{63}\text{Cu}$ , p and  $\alpha$  emission energy comparison 9-6828  
 $^{75}\text{Br}$  compound nuclei from  $^{26}\text{O}+^{59}\text{Co}$ , p and  $\alpha$  emission energy comparison 9-6828

**effects**

- crystal, thin, channelling 9-7686  
 in crystals, single 9-1414  
 defects in irradiated material, spatial distribution 9-13668  
 D.N.A., alkali denaturation 9-8300  
 graphite block area density fluctuations meas. using 147 MeV beam 9-19693  
 oxide films on  $\text{Al}_2\text{O}_3$ , charact. X-ray production on 100 keV irrad. rel. to surface density meas. 9-13575  
 spin lattice relax. in  $\text{PH}_4\text{I}$  and  $\text{PdI}$  9-16385  
 transition rad. in opt. region from passing Al and Ag foils, relativistic 9-9860  
 Al, pitting and blistering, orientation dependence 9-9604  
 Au, excitation of 1300 Å continuum 9-9133  
 Au, energy structure in axial channelling at 30 keV 9-7690  
 $\text{CO}_2$  laser power increase 9-15507  
 Cu stress-induced ordering of point defects near  $10^4\text{K}$  9-9755  
 Fe nucleon-meson cascade initiated by 3 GeV p 9-20853  
 Ge, tunnelling of 6.72 MeV protons 9-21448  
 H atom excitation, total cross section 9-9156

**Protons and antiprotons continued****effects continued**

- KBr, tunnelling of 6.72 MeV protons 9-21448  
 KCl, tunnelling of 6.72 MeV protons 9-21448  
 KCl(Br), high-energy protons channelling 9-7680  
 KIO<sub>3</sub>, p irradiated, thermal annealing of radiodine recoils 9-16193  
 NaCl, high-energy protons channelling 9-7680  
 NaCl, tunnelling of 6.72 MeV p 9-21448  
 $\text{Pb-H}_2\text{O}$  system n yield under bombard. by 400, 500 and 660 MeV p 9-19364  
 Si, tunnelling of 6.72 MeV protons 9-21448

**interactions***See also* Nuclear reactions and scattering due to protons

- 13.8 GeV with emulsion nuclei, obs. 9-4808  
 double  $\pi$  photoprod. on p below 1 GeV, isobar excitation investig. 9-2502  
 with hypothetical radiation, range of coupling constants based on energy balance of sun 9-10978  
 with hypothetical zero-mass pseudoscalar meson, range of coupling constants based on energy balance of sun 9-10978  
 K<sup>+</sup>p elastic scatt., backward direction, 2.76 BeV/c 9-4621  
 pN comparison with multiparticle prod. in collisions with light emulsion nuclei 9-6693  
 $\pi^+\text{p}$  elastic scatt. polarisation obs. 5.15 GeV/c 9-8854  
 $\alpha\text{-p}\rightarrow\pi^+\pi^-$ , recoil p polarization 9-415  
 $\text{e}^+\text{-p}\rightarrow\pi^+\pi^-$ , asymmetry calc. by  $\pi$  e.m. form 9-11000  
 $\text{p-p}$ , cross section at high energy, sum rules and vector dominance model 9-6596  
 $\text{p-p}$  interactions in H<sub>2</sub> bubble chamber, 0.3-5.8 GeV, meson and baryon resonance obs. 9-11071  
 $\text{p-p}\rightarrow\Delta^{++}(1236)\pi^-$ , theory discussed, low energies 9-11049  
 $\text{p-p}\rightarrow\Delta^{++}\pi^-$ , expt. comparison with intermediate isobar model  $E_{\text{p}}\leq 1.8$  GeV 9-19207  
 $\text{p-p-K}^+\Lambda$ , forward cross section prediction by  $\text{SU}(6)\text{wE}\gamma=5.16$  GeV 9-8894  
 $\text{p-p-K}^+\Sigma^0$ , forward cross section prediction by  $\text{SU}(6)\text{wE}$ ,  $E_{\text{p}}=5.16$  GeV 9-8894  
 $\text{p-p}\rightarrow\text{p}'\gamma$  by polarised photons, in c.m. system and first reson. region, differential cross sections, comparison with isobaric model 9-16822  
 $\text{p-p}\rightarrow\Delta^{++}\pi^-$ , vector dominance assumption for hadron e.m. current 9-16909  
 $\text{p-p}\rightarrow\pi^0\text{p}$ , test for current algebra 9-2504  
 $\text{p-p}\rightarrow\pi^+\text{n}$  at 300-750 MeV, absence of  $\text{P}_{11}$  resonance at 1466 MeV 9-2503  
 $\text{p-p}$ , validity in Chou-Yang high-energy scatt. model 9-14520  
 $\text{p-p-p}$ ,  $2\pi$  exchange model, cross section and  $\rho^0$  decay ang. distrib. calc.,  $E_{\text{p}}=4.4$  GeV 9-14468  
 $\text{p-p}\rightarrow\Delta^{++}(1236)$  cross section meas.,  $t$  depend. determ., 5-16 GeV 9-20642  
 K  $\text{p}\rightarrow\text{K}^*\Delta$ , quark model expt. test, hi high energies 9-20633  
 K  $\text{p}\rightarrow\Sigma$  decay modes obs. 9-20673  
 K<sup>+</sup>p, multi-body final states studied,  $K_{\text{K}}=5$  GeV/c 9-19200  
 K<sup>+</sup>p $\rightarrow\text{K}^*\text{N}^*$ ,  $\pi$  trajectory quantum numbers determ., 0(3,1) symmetry,  $\text{P}_{\text{lab}}=3.5-5$  GeV/c 9-20635  
 Kp, low energy, coupling constant tested in dispersion relation for K<sup>+</sup> p scatt. 9-6652  
 K p, total and differential cross sections, 10 GeV/c 9-4617  
 K  $\text{p}\rightarrow 2$  charged particles, production, effective mass and decay distrib. at 2.63, 2.70 GeV/c 9-8820  
 K  $\text{p}\rightarrow\text{K}^+\text{p}$ , cross section determ.,  $\text{M}_{\text{K}}=777-1226$  MeV/c 9-15612  
 K  $\text{p}\rightarrow\text{K}^0\text{n}$ , cross section meas.,  $\text{M}_{\text{K}}=7.7$  GeV/c 9-17978  
 K  $\text{p}\rightarrow\text{K}^0\text{n}$  Regge pole analysis 9-6638  
 K  $\text{p}\rightarrow\text{K}^0\text{n}$ , cross section determ.,  $\text{M}_{\text{K}}=777-1226$  MeV/c 9-15612  
 K  $\text{p}\rightarrow\text{K}^*(1420)\text{n}$ , spin density matrix elements, prod. mech.,  $\text{M}_{\text{K}}=4.57$  BeV/c 9-17999  
 K  $\text{p}\rightarrow\text{K}^*(890)\pi\text{N}$ , spin density matrix elements, prod. mech.,  $\text{M}_{\text{K}}=4.57$  BeV/c 9-17999  
 K  $\text{p}\rightarrow\Lambda\pi^0$ ,  $\Sigma^+\pi^-$  cross sections determ.,  $\text{M}_{\text{K}}=777-1226$  MeV/c 9-15611  
 K  $\text{p}\rightarrow\Sigma\pi$ , hyperon resonance interference effects 9-13145  
 K  $\text{p}\rightarrow\Sigma\pi$  partial wave analysis, resonance formation in mass region, 1.6-1.8 GeV 9-8822  
 K $\text{p}\rightarrow\text{Y}_1(1385)\pi\eta$  boson reson. of mass 980 MeV, at 5.5 GeV/c 9-8869  
 K  $\text{p}\rightarrow\eta\Lambda(\Sigma^0)$  cross-section 9-6638  
 K  $\text{p}\rightarrow\text{p}\text{K}^*$ , strange boson prod. cross section obs., 565-670 MeV 9-8821  
 K  $\text{p}\rightarrow\pi^+\Sigma^+$  Regge pole analysis 9-6638  
 K  $\text{p}\rightarrow\pi^0\Lambda$  Regge pole analysis 9-6638  
 K<sup>+</sup>p,  $\text{S}+1$  baryonic resonances search 9-2498  
 K<sup>+</sup>p $\rightarrow\text{K}^0\text{N}^{*++}(1236)$ , density matrix elements,  $t$ -distributions, 12.7 GeV/c 9-15613  
 K<sup>+</sup>p $\rightarrow\text{K}^{*0}(890)\text{N}^{*++}(1236)$ , density matrix elements,  $t$ -distributions, 12.7 GeV/c 9-15613  
 K<sup>+</sup>p $\rightarrow\text{p}\text{K}^*(890)$ , density matrix elements,  $t$ -distributions, 12.7 GeV/c 9-15613  
 $\text{pd}\rightarrow\text{He}\pi^0$  diff. cross section,  $\text{pd}^3\text{He}$  vertex form factor meas.  $E_{\text{p}}=1.515$  BeV 9-8895  
 pN, 24 GeV/c, velocity space transform method of analysis 9-15654  
 pn data compilation 1-27 GeV/c 9-6695  
 $\text{P}\rightarrow\pi^+\pi^-\pi^0$ , helicity density matrix depend. on  $\text{M}_{\pi\pi}$  9-16878  
 $\text{pp}\rightarrow\pi^+\pi^-\pi^+\pi^0$  phase space distrib., spin and parity of resonance 9-2521  
 $\pi\text{ p}$  at 17 GeV,  $\text{o}^-$  and heavy resonance prod. obs. in nuclear emulsion stars 9-20648  
 $\pi\text{ p}\rightarrow\text{A}_2^+\text{p}\eta\pi^0$ , 2.26 GeV/c evidence for intermediate prod. of  $\text{A}_2^+$  and  $\text{p}^-2^+$  for it. 9-14509  
 $\pi\text{ p}\rightarrow\eta\text{n}$ , A<sub>2</sub> exchange domination, Regge theory test 9-14506  
 $\pi\text{ p}\rightarrow\pi^+\pi^-\text{n}$ , 360-780 MeV, amplitudes of N<sup>\*</sup> production 9-20676  
 $\pi\text{ p}\rightarrow\text{p}\pi^0$ , ang. distrib. meas.,  $E_{\text{p}}=2.7$  GeV/c 9-14508  
 $\pi\text{ p}\rightarrow\text{p}\pi^0$ , density matrix elements calc.,  $\text{M}_{\text{K}}=4$  GeV/c 9-20646  
 $\pi$  and N<sup>\*</sup> isobar prod., 6.94 GeV/c 9-8903  
 $\pi$  review of inelastic processes 9-6664  
 $\pi\text{ p}$ , 7.5 GeV with identified proton, use of velocity space images in kinematics study 9-13128  
 $\pi\text{ p}$ , reson prod. at 6 BeV/c 9-8839  
 $\pi\text{ p}\rightarrow\Delta^{++}(1236)\pi^-\pi^-$ ,  $\pi^-\pi^-$  effective mass, scatt. length, 3.25 GeV/c 9-17986  
 $\pi\text{ p}\rightarrow\text{K}^0\Lambda(\Sigma^0)$  Regge pole analysis 9-6638  
 $\pi\text{ p}\rightarrow\Lambda\bar{\Lambda}$  n, 7 and 12 GeV/c peripheral prod. of  $\Lambda\bar{\Lambda}$  and  $\text{n}\bar{\Lambda}$  9-11057  
 $\pi\text{ p}\rightarrow\eta\text{n}$  Regge pole analysis 9-6638  
 $\pi\text{ p}\rightarrow\pi^+\text{p}'$ , cross section, p spectra obs.,  $E_{\text{p}}=340$  MeV 9-11059  
 $\pi\text{ p}\rightarrow\pi^0\text{n}$  Regge pole analysis 9-6638  
 $\pi\text{ p}\rightarrow\text{K}^+\Sigma^+$  Regge pole analysis 9-6638  
 $\pi^+\text{p}\rightarrow\pi^+\text{p}\pi^0$ , 2.34 GeV/c, p<sup>+</sup> and N<sup>+</sup> prod. 9-15624



Protons and antiprotons continued  
interactions continued

$\pi p \rightarrow \Lambda \Lambda n$ , at 7 and 12 GeV/c 9-6667  
 $\pi p \rightarrow pA_2$ , 2.6 GeV/c,  $A_2$  resonance shape, splitting confirmed 9-11058  
 $\pi^+\pi^-d \rightarrow \pi^0 p$ , 2.15 BeV/c for  $|k| < 10 \mu^2$  obs., comparison with  $\pi^+\pi^-$  prod., meas. of  $2\pi^+$  cross section 9-2509  
 $\rho$  from  $\pi^+\Lambda$ , mass spectrum obs. for centre of mass energy 2050-3500 MeV 9-11093  
Li emulsion, hammer track emission, energy spectra obs., 20 GeV/c 9-4636  
 $\pi p \rightarrow \pi^+\pi^0 p$ , low momentum transfers to p obs.,  $M_\pi=2.77$  GeV/c 9-17984  
 $\pi^+\pi^-\pi^0\Delta^{++}$  Regge-pole analysis 9-2512

protons and antiprotons  
interactions, proton-proton  
No entries

Protons and antiprotons  
interactions, proton-proton

12.5 GeV/c, differential cross-section for  $\pi^+$  prod. 9-370  
20 GeV, dynamic characteristics of secondary particles 9 15641  
 $\rightarrow$ YKN, one-boson exchange model parameters applic. 9-8893  
annihilation, quark model for pseudoscalar meson prod., 9-11026  
bremsstrahlung, co- and noncoplanar, pot. model calc., kinematic analysis 9-6692  
Bremsstrahlung at 3.2 and 10 MeV, theory 9-13143  
bremsstrahlung at 47 MeV, cross-section obs. 9-10972  
high-multiplicity at 10 GeV/c, cross-sections, prod. of  $\Delta^{++} \rightarrow p\pi^+$  obs. 9-6694  
Regge fits, partial wave projections and Argand-diagram loops 9-18010  
single-isobar prod. at 28.5 GeV/c, enhancement near 1400 MeV 9-11090  
spectra of secondary particles, analysis in 2-temp. statistical model 9-8896  
 $ss\ p\bar{p} \rightarrow \pi^+\pi^-\pi^+\pi^-\pi^0$  decay of isosinglet resonance to  $4\pi$  9-13131  
strange particle production at 8 BeV/c 9-2532  
pn annihilation in D<sub>2</sub> bubble chamber,  $\pi^+\pi^-\pi^0$  state obs. 9-20671  
 $pp \rightarrow K^-K^-$  cross section meas. near 2 GeV/c 9-11092  
 $pp \rightarrow KK^*(K^*)$ , at rest, upper limit for annihilations 9-402  
 $pp \rightarrow >1$  neutral part., at 10 GeV/c, cross-sections, prod. of  $\Delta^{++} \rightarrow p\pi^+$  obs. 9-6694  
 $pp \rightarrow d\pi^+$ , forward differential cross sections, 3.4 to 12.3 GeV/c 9-407  
 $pp \rightarrow nn$  at 5.6, 7.9, GeV/c 9-8891  
 $pp \rightarrow pN^*$ , 19.2 GeV/c obs. 9-11114  
 $pp \rightarrow pN^*$ , review of data up to 30 GeV/c 9-6696  
 $pp \rightarrow pn \rightarrow p\pi^+$ , cross section;  $\Delta^{++}$  (1236) prod., resonance prod. in  $p\pi^+\pi^+\pi^-$  at 10 GeV/c 9-16901  
 $pp \rightarrow pn\pi^+$ , pion exchange and  $\pi N$  enhancement, double Regge-pole model anal. 9-11091  
 $pp \rightarrow pn\pi^+\pi^+\pi^-$  at 10 GeV/c, cross-sections, prod. of  $\Delta^{++} \rightarrow p\pi^+$  obs. 9-6694  
 $pp \rightarrow pp\omega, pp\eta$  and  $pp\pi^0$ , cross-sections corrected for unobserved decay modes 9-16901  
 $pp \rightarrow pp\pi^+\pi^-\pi^+\pi^-$  at 10 GeV/c, cross-sections, prod. of  $\Delta^{++} \rightarrow p\pi^+$  obs. 9-6694  
 $pp \rightarrow pp\pi^+\pi^-$ , cross section,  $\Delta^{++}$  prod., resonance prod. in  $pp\pi^+\pi^-\pi^0$ , at 10 GeV/c 9-16901  
 $pp \rightarrow pp\pi^+\pi^-$ , distrib. anal. by multi-Regge-pole exchange model,  $E_p=16$  GeV/c 9-16902  
 $pp \rightarrow pp\pi^+\pi^-$ ,  $\pi^+\pi^-$  reson states prod. for  $E_p=24.8$  GeV/c 9-8878  
 $pp \rightarrow pp\pi^+\pi^-\pi^-$  at 10 GeV/c, cross-sections, prod. of  $\Delta^{++} \rightarrow p\pi^+$  obs. 9-6694  
 $pp \rightarrow \pi^+\pi^-d$  and  $\rightarrow \pi^+np$ , relationship, calc. 9 406  
 $pp \rightarrow \pi^+\pi^-$  cross section meas. near 2 GeV/c 9-11092  
 $pp \rightarrow \pi^+\pi^+\pi^-\pi^-$  annihilation channel, multi-Regge model description, 5.7 GeV/c 9-14522  
 $pp \rightarrow \pi^+\pi^+\pi^-\pi^+\pi^-$  decay of isosinglet resonance to  $4\pi$  9-6676  
 $pp \rightarrow \pi^+\pi^+\pi^-\pi^+\pi^-\pi^0$ , obs. of  $\eta\pi^+$  and  $\eta^0\pi^+$  effective mass distrib., peak interpretations 9-14518  
 $pp(n) \rightarrow pp\pi^+\pi^+(n)$ ,  $N^*(1400)$  and  $\bar{N}^*(1400)$  enhancements, evidence of prod.,  $E_p=2.8$  GeV/c 9-11112  
 $\pi$ , single prod. channels, and cross sections, 6.92 BeV/c 9 8892  
H target,  $p\pi\pi$  decay mode of  $N_{1/2}^*(1400)$  reson. obs. 9-6708

magnetic moment

No entries

polarization

20 MeV scatt., correspond. to Y-IV fits 9-411  
in deuteron photodisintegration,  $E_p=282$  to 405 MeV 9-17938  
Pd scatt. at 198 MeV, obs. 9-6698  
in pp elastic scatt. at 5.15 GeV/c for large momentum transfers 9-413  
 $\alpha p \rightarrow p\pi^0$ , recoil p polarization 9-415  
p new source in Univ. Minnesota lin. accel. 9-2619  
in pd elastic scatt. at 22.7 MeV 9-8899  
 $^{208}\text{Pb}(p,p)$ , polarization of elastically and inelastically scatt. protons 9-20780  
 $^{12}\text{C}(p,p)$  polarization meas.,  $E_p=1.3$  MeV 9-11282  
 $^4\text{He}$  scatt. obs. at 540 MeV 9-9022  
 $^6\text{Li}$ , ( $p, ^3\text{He}$ ) $^6\text{He}$  particles ang. distrib. obs., 0.4-3.2 MeV 9-588  
 $^{24}\text{Mg}(p,p)^{24}\text{Mg}$ , 5.7-6.0 MeV, p polarization 9-4776  
 $^{58}\text{Ni}(p,p)^{58}\text{Ni}$  5.7-6.0 MeV, p polarization 9-4776

production

cyclotron, isochronous ring with radial sectors, orbital props. 9-13176  
energy spectrum of photo-p in  $^4\text{He}(p, p)^3\text{H}$  reactions 9-4768  
generator, electrostatic charge-transfer prod. 0.5 keV, 1 mA beam 9-11089  
source, coefficient for utilization of H mol. and atoms studied 9-13142  
 $\pi^+\pi^-$  mass enhancement, 1470 MeV, from 28 GeV/c p on Ne 9-15619  
 $^{40}\text{Ca}$ , photoproton energy and ang. distrib. 9-2716  
 $^{56}\text{Fe}$ , photoproton measurement 9-2716  
 $^{55}\text{Mn}$ , photoproton energy and ang. distrib. 9-2716  
 $^{23}\text{Na}$ , photoproton energy and ang. distrib. 9-2716  
 $^{31}\text{P}$ , photoproton energy and ang. distrib. 9-2716  
 $^{32}\text{S}$ , photoproton energy and ang. distrib. 9-2716

scattering

Compton, sum rules 9-15642  
Compton eff, virtual proton, with 3-3 resonance, contrib. to bremsstrahlung variable rel. to quantum electrodynamics 9-16807  
cubic crystals, rel. to blocking pattern construction 9-19697  
K<sup>+</sup>p, elastic cross section calc.,  $M_\pi=4.6$  GeV/c 9-20640  
large angle cross-section momentum transfer depend 9-2534  
microscope for crystallography 9-3272

Protons and antiprotons continued  
scattering continued

multiple Coulomb scatt. in nuc. emulsions, primary p beam exposure 5-24 GeV/c 9-4637  
in nuclear emulsions, multiple coulomb, scatt. at 19.8 GeV/c 9-14537  
Regge cuts, Wu-Yang hypothesis and amplitude calc. 9-414  
vector meson-proton, momentum transfer dependence, elastic, from photoprod. data 9-11076  
ep, polarization-odd effects,  $E_\gamma \approx 10$  GeV 9-14471  
e<sup>+</sup>p, Tanikawa-Watanabe model checked, new variant introduced 9-335  
 $K^+$ p, hard core and single imag. Yukawa pot. term fit,  $E_\pi=2-20$  GeV/c 9-14503  
 $K^-$ p, polarization meas., fit to 5 Regge-pole model,  $M^*=2-2.4$  GeV/c 9-16867  
 $K^+$ p backward, 1.0 to 2.5 GeV/c 9-2499  
 $K^+$ p low-energy s wave dynamics, singularities contribution calc. 9-8824  
 $K^+$ p resonance in  $p_{1/2}$  state, evidence 9-4030  
 $K^+$ p, cross sections meas.,  $E_\pi=3.55$  GeV/c 9-16883  
 $K^+$ p, partial-wave projections of Regge fits, Argand-diagram loops 9-18010  
 $K^+$ p, real part of amplitude calc. using dispersion relations 9-13124  
 $K^+$ p superconvergent dispersion relation to test self consistency of coupling constant for  $K\rho$  interactions 9-6652  
 $\mu p$ , polarization-odd effects,  $E_\mu=10$  GeV 9-14471  
 $\mu^+p$ , Tanikawa-Watanabe model checked, new variant introduced 9-335  
 $p\alpha$ , quasifree, in  $^7\text{Be}(p,\alpha)^4\text{He}$  react. at 57 MeV 9-14611  
 $p\alpha$  and  $^6\text{Li}(p,\alpha)^3\text{He}$  ang. distrib. comparisons,  $E_p=61.5$  MeV 9-16959  
pn, elastic cross sections, dip- bump struct. compared with pp scatt. 9-416  
pn charge-exchange, Regge-pole  $\pi$  conspiracy model 9-11098  
pn triple scatt., parameters calc., polarization meas. 425 MeV 9-11095  
 $pn \rightarrow np$  cross section  $\ll$  pp scatt. 9-2531  
pp, resonance formation 9-409  
pp charge-exchange, Regge-pole  $\pi$ -conspiracy model 9-11098  
pp energy-depend fluct. in backward hemisphere elastic scatt., interpretation rel. to boson resonances. 9-2537  
 $\pi^+p$ , cross sections meas.,  $E_\pi=2.8-3.6$  GeV/c 9-16883  
 $\pi^+p$ , partial-wave projections of Regge fits, Argand-diagram loops 9-18010  
 $\pi^+p$  two-pole and pole-and-cut fits 9-6633  
W, shadows, asymmetric, prod. in Coulomb scatt, 190, 350 and 500 keV 9-15038

scattering, proton deuteron

polarisation obs. at 22.7 MeV 9-8899  
cross section, amplitude calc., 1-10 GeV 9-2535  
cross section obs., 1-3.5 GeV 9-2536  
D-wave eff., at high energy 9-8901  
small angle, momentum range 1.3 to 1.5 GeV/c 9-4639

scattering, proton-proton

20 Mev, polarization correspond. to Y-IV fits, compared with Suclay and Livermore fits 9-411  
amplitude, real part of forward, in high-energy region dispersion relation calc. 9-8897  
angular distrib. meas., p substructure model anal.,  $M_p=5-21$  GeV/c 9-20669  
angular distrib. structure at high energies 9-8902  
Born term unitarizing correction bounds, generalized dispersion model 0-300 MeV 9-11099  
bremsstrahlung cross-section meas., photon ang. distrib. 9-8900  
bremsstrahlung cross-section obs., 3.2 MeV 9-412  
cross section, amplitude calc., 1-10 GeV 9-2535  
cross section  $\gg$  for  $pn \rightarrow np$ , using Regge pole model 9-2531  
elastic, 3-7 GeV/c, comparison with np scatt 9-420  
elastic,  $\epsilon$  9.92 BeV/c 9-8892  
fifth interaction possibility 9-6619  
high-energy at  $\sim 6(\text{GeV})^2$ , large angle data obs., Pomeranchukon contribution, rel. to  $\pi$  trajectory 9-4638  
hybrid model for elastic scatt., applic. 9-13114  
impact parameter representation study at high-energy large-angle 9-11096  
inelastic, at 12.5 GeV/c 9-408  
at large momentum transfers, Regge and Pomeranchuk trajectories deduced, differential  $\chi$ -sections and consequences for polar 9-16903  
with meson single prod.,  $SU(6) \times O(3)$  quark model 9-8762  
missing mass expts. rel. to shadow effects in p scatt. of nucleus, 5-15 GeV/c 9-9020  
 $O(4)$ , scalar interaction model 9-2533  
oscillations of high energy cross-section as function of momentum transfer 9-20670  
phase shift analysis, ang. distrib. obs., 6-10 MeV 9-6697  
polarisation at low energy 9-11100  
polarization in elastic scatt. at 5.15 GeV/c for large momentum transfers 9-413  
on polarized p target, triple scatt. depolar. transfer parameter meas. 9-14521  
quasiquasical, high energies, S-matrix 9-2466  
quasiquasical, high energies, S-matrix 9-13100  
Regge theory confirmed at large angle and high energy 9-15644  
relativistic off-shell integral eqn. derivation, meson exchange numerical calc. 9-15643  
resonance production, studied, diff. cross section meas.; 12.5, 30 GeV/c 9-11097  
and structure of p 9-18009  
N-N potential, vel. depend. term, phase shift anal. 9-13144  
pp, forward amplitude, real part, in high-energy region dispersion relation calc. 9-8897  
pp differential cross section and polarization distrib., elastic at 1.73, 2.13, 2.37, 2.97 GeV/c 9-11094  
 $pp \rightarrow d\pi^+$ ,  $\pi$  and nucleon exchange models compared, 2.8-3.9 GeV 9-410  
 $pp \rightarrow pN^*$ , selection rules for spin and parity, nucleon pole graphs cancel 9-8898  
 $pp \rightarrow pn^*(1400)$  where  $N^*(1400) \rightarrow n\pi^+$  or  $p\pi^0$ , OPE model 9-11113  
pWp, elastic cross-sections, dip-bump struct. compared with pn scatt. 9-416

scattering proton-deuteron

No entries

Pseudopotential methods see Crystal electron states

Pulsars see Cosmic radiations, radiofrequency

Pulse generators see Circuits

Pulse-height analysers see Counting circuits

**Pumps**

- See also *Vacuum pumps*  
 electrostatic, efficiency 9-9461  
 molecular sieve, pumping speed 9-14298  
 turbomolecular, accommodation process 9-937

**Purkinje effect** see *Vision***Pyroelectricity**

- i.r. receiver, sensitivity 9-19933  
 thermometer for temp. change or rate meas. at low temps. 9-19100  
 tourmaline, in X-ray absorpt. detection 9-18973  
 triglycine selenate, coeff. temp. dependence near Curie temp. 9-13923

**Pyrolysis** see *Chemical reactions***Pyrometers**

- error due to absorbing particles over high-temp. source 9-8535  
 i.r., design and use, book 9-19081  
 line-reversal, self balancing, 1200° 2000°C 9-8536  
 optical, appl. of Si integrating light detector 9-10756  
 optical, for temp. control utilising two thermistors 9-4368  
 optical and thermoelec. thermometry of small spherical metal crystals 9-20462  
 photoelectric, error in temp. of graphite surface due to soot 9-8535  
 thermal imaging detectors 9-2247  
 two-colour, for colour temp. meas. 9-8538

**Quadrupole crystal field interactions** see *Crystals/hyperfine field interactions***Quadrupole moments, molecular** see *Molecules/moments***Quadrupole moments, nuclear** see *Nucleus/electric moment***Quanticule theory (of chemical binding)** see *Bonds***Quantization** see *Field theory, quantum/quantization; Quantum theory/quantization***Quantum chemistry**

- early history 9-10306  
 first order perturbation method, modification for spin-factorable syst. with unknown eigenfunctions 9-16990  
 Hartree-Fock theory, conservation of total momentum, and complex wavefunctions 9-13275  
 isoelectronic systems, scaling of SCF wavefunctions 9-749  
 mathematical and physical aspects, distinction 9-10305  
 nucleic acids, submolecular structure 9-14728  
 proton-transfer reactions in solution, quantum mech. tunnelling through parabolic energy barriers 9-20030  
 variation-perturbation theory of inductive effect in saturated mol. 9-11443  
 H+H<sub>2</sub> reactive scatt., quantum mechanics 9-10317

**Quantum counters** see *Photons; Radiation detectors***Quantum electrodynamics**

- See also *Electrodynamics; Electromagnetism*  
 asymptotic gravitational field of 'electron' 9-4238  
 atoms: neutral hydrogenic, e.m. and electrostatic fields contribution to interaction energy 9-9150  
 Bloch bands at finite and zero fields, adiabatic connection 9-13088  
 catastrophic processes, Lorentz and Coulomb gauge invariance 9-14459  
 causal propagator products, momentum-space representation 9-2440  
 charge quantization and nonintegrable Lie algebras 9-10956  
 charge singularities due to positronium formation 9-336  
 conducting spherical shell e.m. zero pt. energy, invalidation of Casimir model 9-16809  
 Dirac's relation between elec. and mag. charge strengths, generalization 9-8701  
 Dirac eqn. in magnetic field, soln. 9-6573  
 dressed vacuum, Schrodinger stationary-state eqn., soln. 9-13089  
 electric charge motion in mag. monopole field 9-10956  
 electromagnetic zero-pt. energy and retarded dispersion forces, relation to classical e.m. field 9-16808  
 electron in elec. dipole field, ground-state energy eigenvalues and eigenfunctions 9-4554  
 electron interactions in monochromatic e.m. wave background field, quantum intensity-dependent freq. shift 9-296  
 electron motion in special e.m. fields 9-298  
 expansion parameter and muon anomalous magnetic moment 9-8702  
 Feynman integrals, asymptotic approx. rel. to photon and e self-energy graphs 9-14308  
 formulation, finite, for S-operator, applic. 9-13087  
 free field, in presence of randomly fluctuating field, resemblance to classical electrodynamics 9-16808  
 gauge-independent, spinor and e.m. field interaction 9-14458  
 geons, Klein-Gordon: stability and unsymmetrical gravitational collapse 9-10458  
 Green's function mass-shell singularities in soft- and hard-photon momentum space 9-8699  
 gyromagnetic ratio of  $\mu$  and  $e$ , sixth-order contrib., calc. from fourth-order vacuum polar 9-16826  
 infrared divergences, soft-photon asymptotic states, Green's functions, reduction formulae 9-16810  
 infrared divergences, use of asymptotic photon states belonging to non-Fock representations 9-2438  
 interaction with e.m. field, scale transform. and dynamical invariance 9-2448  
 Lagrangian form shows weak nonlinearity of field eqn. 9-297  
 Lagrangian proposed which allows electron and photon to be bound states of electron and positron 9-4555  
 length quantum, free-particle wave eqn: formulation 9-8700  
 Maxwell's equations, structure, invariance 9-20582  
 muonic atoms, vacuum polarisation contribution to nuclear polarisation 9-13320  
 photon-graviton conversion in e.m. field 9-61  
 plasma physics theory 9-18302  
 present status 9-6572  
 radiation from charge moving in mag. and plane wave field 9-17927  
 radiative corrections, review 9-17928  
 relativistic particle in mag. field, dynamical symmetry 9-14460  
 scattering operator matrix elements derivation for coherent soft-photon states, i.r. divergences 9-10962  
 Schrodinger theory, random fluct., connection with classical mechanics 9-16808  
 Schwinger terms and interaction hamiltonian var. 9-10958  
 self-consistent spinor field theory disagreement with Lamb shift meas. 9-10957

**Quantum electrodynamics continued**

- small distances, validity test 9-6575  
 Sturm-Liouville coupled eqns., electron in field of 2 fixed charges 9-19182  
 vacuum magnetic moment of an electron moving in homogeneous mag. field 9-19181  
 vacuum polarization, effs. on D-wave  $\alpha$ - $\alpha$  scatt. 9-11119  
 validity 9-17994  
 validity discussed, book 9-4556  
 validity test, e pair prod. by  $\gamma$  on C 9-8754  
 virtual-proton Compton effect and  $e(\mu)$ -p bremsstrahlung as tests 9-16807  
 e, free relativistic, stationary states, Rayleigh-Ritz procedure for determ. 9-6574  
 $\mu$  pair production from  $\gamma\gamma$  interaction, differential cross section meas., theory test 9-20583

**Quantum electronics** see *Lasers; Masers; Photons; Quantum optics***Quantum field theory** see *Field theory, quantum***Quantum fluids**

- electron gas, ground state energy, parametric approach 9-10675  
 electron liq., degenerate, conductivity tensor calc. using Maxwell's eqns. 9-20367  
 electron liquid, degenerate, dynamic spin susceptibility calc. 9-20368  
 Fermi Bose, phenomenological theory 9-12903  
 fugacity density relation for ideal gas, exact inversion, Hilbert problem 9-10670  
 interacting, strongly, theoretical formalism for calc. of props. 9-10671  
 plasma, low density, free energy interpolation 9-13415  
 plasmas, quantum levels occupancy 9-7136  
 relativistic gas, energy transfer and radiation 9-17742  
 spin systems, thermodynamics 9-16695  
 H<sub>2</sub> crystal, wide range of physical and computational utility 9-15436  
<sup>3</sup>He interacting system of atoms, spin diffusion coeff. 9-6337  
<sup>4</sup>He, phonon dispersion from hydrodynamic Hamiltonian 9-5203

**boson systems**

- atoms, adsorbed monolayers on cryst., thermodyn. props. 9-5255  
 Bose gas, charged at absolute zero 9-12899  
 Bose gas, particle no. fluctuation, at and below condensation temp. 9-14365  
 Bose statistics, derivation from quantum mechanics 9-16698  
 boson expansion of fermion pair operators, degenerate model, interpretation of parameter  $\gamma^0$  and its applic. to quadrupole interac. 9-8448  
 charged boson gas at abs. zero, free energy 9-8428  
 condensed interacting, external perturbation 9-102  
 diagram technique near Curie pt. and phase transition of second kind 9-12900  
 dynamics, quantum and Hartree wave theory 9-19004  
 Fermi-Bose fluid mixtures, phenomenological theory 9-12903  
 gas, 2D, condensation temp. 9-19002  
 gas, nonideal, free energy calc. using effective pot. 9-10668  
 gas, temp. depend. of  $C_p$ ,  $K$ , rel. to off diagonal long-range order 9-16697  
 grand canonical partition function, functional integral representation 9-8447  
 interacting, strongly, theoretical formalisation of strongly interac. mixed and Fermi gases 9-10671  
 lattice struct. arrangement model, analysis 9-4247  
 many boson model, exactly solvable 9-14364  
 mass operator, imaginary part determ. and applic. to phonons in ferromagnet 9-21574  
 mass operator, real part determ. and applic. to ferromagnet 9-20358  
 pair distrib. function using cluster function formula 9-4251  
 perturbation expansion of wave function 9-2174  
 principle of compensation of dangerous diagrams, obtained by maximum overlap 9-14362  
 principle of compensation of dangerous diagrams, obtained from four criteria 9-14363  
 SU(1,1) quasi-spin formalism, in spherical field 9-103  
 thin film, transition from  $\approx$  to 2D behaviour 9-19002  
 two-level system coupled to Bose gas with Einstein spectrum, exact diagonalization of Hamiltonian, simple method 9-20365  
 He, superfluid, hard-sphere Bose gas model 9-3143  
 He II, v.e. ion mobility obs.  $T < 0.5^\circ\text{K}$ , inelastic phonon scatt. contrib. He, liq.  $1/b||c||$  9-1059  
 He liquid films, Bose-Einstein gas model 9-3142

**fermion systems**

- atoms, adsorbed monolayers on cryst., thermodyn. props. 9-5255  
 boson expansion of fermion pair operators, degenerate model, interpretation of parameter  $\gamma^0$  and its applic. to quadrupole interac. 9-8448  
 canonical transformations, unitarity depend. on representation of anticommutation rel. 9-6339  
 charged colliding Fermi particles, Green's functions 9-4252  
 degenerate Boltzmann equation soln. 9-14367  
 density correlation function, diagrammatic expansion 9-15438  
 density matrix structure 9-20366  
 electron liquid degenerated, spin-wave and plasma-wave propag. ang. depend. 9-4254  
 Fermi liquids spin echoes in terms of spin waves 9-12901  
 Fermi statistics, derivation from quantum mechanics 9-16698  
 Fermi-Bose fluid mixtures, phenomenological theory 9-12903  
 fluid, one-dimens., with hard core repulsive long range attractive potential, cell model 9-8446  
 fugacity density relation for ideal gas, exact inversion, Hilbert problem 9-10670  
 gas, magnetized, mag. moment 9-8450  
 gas, magnetized, thermodynamics props. 9-8449  
 Hamiltonian diagonalization, generalized uncertainty relns. determ. 9-16699  
 interacting, strongly, theoretical formulation for calc. of props. 9-10671  
 kinetic energy inhomogeneity correction 9-14368  
 kinetic equations in theory of normal charged fluid 9-8452  
 Landau Fermi-liquid parameters, sum rule 9-3559  
 liquid, effects on plasma propagation in metal 9-7719  
 liquid, surface phenomena at zero temp. 9-104  
 liquid, transport coeffs., exact 9-105  
 liquids, mobility of heavy impurities, temp. depend 9-8451  
 paramagnets, non-reduction of unbonded diagrams in fermion presentation of spin operation 9-16329  
 Pauli transformations, unitarity 9-6339  
 Pomeranchuk stability criterion, deriv. by vertex part. method 9-17744



**Quantum fluids** continued**fermion systems** continued

- projection, antisymmetric, in no spin-orbit coupling approximation 9-10669
- Raman scattering of light on spin wave in Fermi liquid, by spin wave 9-19994
- specific heat, logarithmic terms and corrections, connection with micro-scopic theory 9-10673
- spin function construction by spinor invariants 9-14366
- thermodynamic pot. and temp. Green's functions, mean-occupation-number formalism 9-4253
- time inversion operator generalisation 9-2175
- transport coeff., finite temp. corrections 9-12902
- wave functions of condensed states 9-12904
- zero sound in nuclei, obs. by radiative pion capture, possibility 9-5210
- K. Landau Fermi-liquid parameters 9-9912
- liquid, thermal conductivity and spin-diff. coeff. finite temp. corrections calc. 9-106
- Na, Landau Fermi-liquid parameters, sum rule 9-3559
- Na, Landau Fermi-liquid parameters 9-9912

**Quantum generators** *see Lasers; Masers***Quantum mechanics** *see Quantum theory***Quantum optics**

- double resonance technique for ground-state modulation in trivalent rare-earth-doped single crystals 9-3846
- heterodyned Gaussian cmpt with coherent beam, statistics 9-15504
- i.r. quantum counters, thermal noise 9-6499
- Josephson radiation, freq. pulling effects 9-12120
- laser beam, modulated, photon counting distrib. 9-248
- laser light statistics 9-15534
- laser parameters and meas. techniques, book 9-16788
- oflaser, introductory lecture 9-14425
- luminescence, parametric, noncollinear interaction theory 9-14096
- mode, phys. significance of field comparison of classical and quantum-mechanical descriptions 9-14419
- negative absorption in quasiclassical systems 9-19133
- photon-counting distrib. of optical fields, theory of periodic sampling 9-8444
- rare earth i.r. quantum counter, five-level,  $1-2u$  9-10927
- sodium salicylate, absolute quantum efficiency for extreme ultraviolet 9-21652
- three-wave parametric interactions, symmetrical formulation of quantum theory 9-10837
- ultrashort light pulse generation and meas. by mode-locking of Nd:glass laser with saturable dye 9-14427
- Cs vapour, photon echoes 9-10848

**Quantum statistics** *see Statistical mechanics/quantum***Quantum theory**

- See also Electron theory; Field theory, quantum; Elementary particles*
- 3nj coeffs. of  $R_3$ , closed formula 9-20865
- accidental degeneracy, conditional invariance 9-73
- adiabatic potential calc., use of perturbation theory 9-10637
- algebra of observables, continuous representations of symmetry groups 9-45
- angular momenta, topological characteristics 9-10642
- angular momentum, book 9-2162
- angular momentum operators, construction of orthonormal basis 9-8409
- arbitrary dissipative systems, Fokker-Planck eqn. 9-10666
- atom, effective potential eqns. with oscillatory correction 9-2808
- atomic oscillator strengths, quantum-mech. approach to regularities 9-11377
- atoms field calc. on 3rd row periodic syst., Hartree-Fock pot. comparison 9-4826
- Bethe-Goldstone eqns., atomic, soln. for electronic pair-correlation energies of ground states 9-11383
- Born-Oppenheimer approx. validity test 9-17720
- Clebsch-Gordan coeffs., negative quasibinomial representations 9-6322
- Clebsch-Gordan coeffs., quasibinomial representation by Regge square 9-6321
- coherent state P-distrib., conservation with respect to time 9-10635
- correspondence identities for quantum and classical mech., low quantum no. 9-4866
- for Cotton-Mouton effect of paramag. complexes in solution 9-9183
- Coulomb approx., applic. in molecular transitions calc. 9-13333
- diagram technique in theory of multiple scatt. 9-6699
- diamagnetic molecules, of electric birefringence 9-745
- Dirac approach, university text book 9-10600
- Dirac formalism and extension of Hilbert space 9-17718
- dispersion forces, second- and third-order energies 9-13273
- dissipation, multichannel problems, quasi-classical approx. 9-10636
- dissipation, multichannel problems, quasi classical approx. 9-20321
- dualism of particles and waves, dialogue 9-14350
- dynamical groups, limitable, general theory and spinless model 9-17719
- eigenvalues of self adjoint diff. operators, iterative procedure of calc. 9-4928
- elementary length theory relationship 9-16680
- energy levels, crossing 9-4239
- energy-level density, path representations, Feynman form 9-20322
- evolution of quantum states, free time 9-4234
- fluids, perturbation theory, deviations from classical behaviour 9-10643
- fluorene and derivs., electronic structure calc. rel. to absorpt. spectra 9-3106
- fluorene and derivs., electronic structure calc. rel. to absorpt. spectra 9-3107
- fluorene iodo-derivs., electronic structure calc. rel. to absorpt. spectra 9-3108
- fluorenone and derivs., electronic structure calc. rel. to absorpt. spectra 9-3107
- fluorenone and derivs., electronic structure calc. rel. to absorpt. spectra 9-3106
- fluorenone iodo-derivs., electronic structure calc. rel. to absorpt. spectra 9-3108
- force, exam. of the concept in wave mechanics 9-12827
- four-particle problem, configuration- space approach using Schrodinger eqn. 9-14346
- fundamental principles of quantum mechanics, book 9-12882
- of galvanomagnetic electron-impurity system 9-5601

**Quantum theory** continued

- of galvanomagnetic electron-phonon system 9-7700
- of gravitation, supplementary conditions 9-2139
- gravitational, canonical and covariant 9-18992
- harmonic oscillator, coherent state with time-depend. freq. 9-8416
- harmonic oscillator, relax. to thermodynamic equilb. 9-81
- harmonic oscillator, unity operator expansion in coherent states subset 9-12887
- harmonic oscillators, class of exact invariants 9-14347
- harmonic oscillators, linear system, stochastic types of motion 9-8414
- harmonic oscillators, two coupled, validity of rotating-wave approx. 9-10644
- two harmonic-oscillator wave functions, overlap integral, applic. to mol. spectra 9-15840
- Hartree-Fock approx. in finite nuclei 9-11230
- Heisenberg's uncertainty principles; demonstration 9-20332
- hydrodynamic model of Pauli eqn. 9-71
- information, quantum-mech. axiomatic definition 9-12885
- inverse square law potential, unitary transformations 9-6325
- ion-atom collisions, parametric treatments comparison for low and high impact vel. 9-11407
- Josephson oscillator, including noise 9-12119
- ladder operators, self-adjoint, applic. to angular-momentum 9-14344
- oflaser, introductory lecture 9-14425
- level crossing, application of effective tensor operator 9-6951
- Levinson theorem for charged particles, proof 9-15431
- magnetic charge, photon source model 9-10597
- of magnetoacoustic amplification in semiconds. 9-16171
- matrix mechanics, numerical techniques 9-76
- measurement problem, ergodic theory of macrosystems development 9-18976
- mechanics, axiomatic foundation of orthomodular lattice of linear operators 9-6314
- mechanics, matrix methods appl. 9-2158
- mechanics, orthomodular ortholattices theory, semimodularity and logic 9-6319
- mechanics, stochastic theories, anal. using Feynman integral 9-16694
- mechanics as broken Liouville symmetry and dilatations 9-15416
- model eigenvalues, discrete and continuum orbitals, use in calc. of photoioniz. cross-sections of He to Xe 9-9124
- model of two eqns. coupled by  $\alpha/r^2$  potential, threshold law 9-4237
- molecules, operators representing interact. between different types of internal motion 9-740
- momentum operators 9-14343
- negative metric introduction, S-matrix unitarity, divergence difficulties removal 9-14454
- O(4) representations and Wigner coeff. 9-20305
- operations, pure, and meas. 9-17717
- operator lower bound determ. by method of decomposition, speed of convergence 9-12909
- Pauli eqn. with spin-orbit coupling, hydrodynamic model 9-71
- perturbation theory in nuc. matter, eval. of terms, applic. to Pauli correction 9-11186
- perturbation theory not assuming existence of convergent expansions asymptotic props. 9-16686
- perturbation theory of fluids, deviations from classical behaviour 9-10643
- polaron, runaway mode, renormalization of Hamiltonian 9-17372
- position observables for relativistic systems, differential operators d 9-8400
- propositions as a set of evolving filters on a particle beam 9-18995
- quantum mechanical description using Jaynes' irreversible statistical mech. 9-20323
- Racah coefficients, rel. to crossing matrices 9-341
- relativistic elem. syst., position operator defn. 9-6332
- relativity, special, validity in quantum domain 9-2142
- rigorous lower bounds to expectation value of positive operator, determ. 9-6992
- scattering, generalized superperturbation theory 9-8419
- scattering, operators for delay time and time of motion 9-17724
- self-energy operator in infinite system, model function 9-20333
- semiclassical description, form and condition for equivalence 9-2153
- spin-spin contact Hamiltonian and Coulomb interaction 9-9113
- stationary systems, eigenvalues of observables, lower bounds to second order corrections 9-8401
- statistical two-particle density matrix 9-9112
- stochastic theory and quantum mechanics, general integration of fundamental equation. 9-20329
- sum rules, upper and lower bounds determ. 9-8407
- superfluid nuclei, effective external field acting on quasiparticle, calc. 9-481
- superselection rules, commutativity, and complete set of observables 9-17722
- time-dependent interactions, general perturbation and variational methods 9-6323
- of transport phenomena in strong magnetic fields 9-8461
- two centre problem, commutative operators and numbers 9-15842
- two-particle dynamical nonrel. syst., relativistic corrections 9-17915
- two-particle syst. with spin, relativistic c.m. variables 9-17914
- university level textbook 9-10601
- wave mechanics related to relativistic Planck Laue formula 9-17736
- Wigner transition, existence in impure InSb threshold mag. field 9-15100
- WKB method, generalized, second approx. 9-18998
- H, solid, equation of state 9-19850

**application methods**

- 'fifth interaction' Lagrangian for baryon mass differences 9-18005
- boson expansion methods insoluble two-level shell 9-4723
- complex angular momentum theory, signature in perturbation model 9-79
- contact between theory and experiment, properties 9-77
- correction to fifth virial coeff. 9-13486
- correlation functions of irreducible tensor operators 9-20297
- diagrammatic perturbation theory molec. processes 9-7006
- diamagnetic molecules, quantum theory of electric birefringence 9-746
- double linear harmonic oscillator, elementary treatment 9-17723
- ethane, Kerr constant determ. 9-746
- Fermion superselection rule, proof without T invariance assumption 9-20331
- Feynman-Cameron integrals for generalized Schrodinger eqn. 9-8413
- finite difference solution of Schrodinger difference eqns. 9-15430
- harmonic oscillator, one-dimens., effects of finite boundaries 9-5794

**Quantum theory continued****application methods continued**

- harmonic oscillators, statistics, method of steepest descent 9-12886
- harmonic-oscillator pot. well, different single-part freq. case, transformation and its group-theoretical struct. 9-4236
- Hartree-Fock eqn. for simple open-shell case, soln. and stability conditions 9-20917
- Hartree-Fock exchange potentials for electrons in Cu<sup>+</sup> ion, comparison of methods 9-18138
- Hubbard's theory of Mott transition 9-12056
- Hubbard Hamiltonian, degenerate mass operator perturbation theory 9-14345
- Hubbard Hamiltonian, for correlation and mag arrow energy bands 9-12054
- Hubbard Hamiltonian in Mott-insulator calc. on narrow energy bands 9-15051
- hypervirial theorems, off-diagonal constraints 9-2159
- interchange theorems in degenerate perturbation theory 9-8412
- invariant amp construction for interac. of part. with any spin 9-4568
- Lee model, 2V sector, dispersion methods 9-16844
- many-particle system, interacting, probability of excitation of eigenstates 9-16696
- methane, Kerr constant determ. 9-746
- molecular vibr. rot. Hamiltonian, simplification 9-17014
- N-N realistic potential, self-consistent method for core polar correct 9-6755
- n.m.r. high resolution spectra 9-16756
- nonlocal interactions, analytic props. of Si(K) functions 9-4240
- nuc. two-level shell model, boson expansion methods and time-depend Hartree-Fock theory relationship 9-6780
- one-dimensional problems, matrix elements calc. 9-12883
- perturbation analysis of reactor buckling meas. 9-11351
- perturbation eqns., iterative soln. 9-6324
- perturbation theory, comparison of first-order operators 9-8408
- perturbation theory, operator eqns., applic. to harmonic oscillator 9-72
- perturbation theory, self-consistent, and molec. struct. 9-17016
- perturbation theory, self-consistent, and molec. struct. 9-11446
- perturbation theory for atom or molec. exchange interactions 9-9108
- perturbation theory for celestial dynamical systems 9-6106
- perturbation theory for families of Regge trajectories 9-15598
- perturbation theory Ladder approx. with scalar part., Regge trajectories eval. 9-4603
- perturbation theory upper and lower bounds using linear programming 9-8410
- perturbation treatment in conjunction with localized bond orbitals, for mol. electr. energy calc. 9-13332
- phase space probabilities expansion into classically deterministic parts 9-18997
- phase-space analysis of time-correlation functions 9-12881
- potential  $(x^4 - bx^2)$ , energy corrections 9-6320
- potential well bound states in Schrodinger eqn., numerical results 9-20326
- quantum mechanical systems, applic. of finite group theory, book 9-6292
- Rayleigh Ritz procedure for stationary e states in quantum electrodynamics 9-6574
- Rayleigh-Schrodinger perturbation theory, diagrammatic method 9-16685
- relaxation, quantum theory applied to mag. resonance phenomena 9-15428
- renormalization of N-quantum approx. in field theory 9-2441
- S function selection for vibrational-rotational energy operator, polyatomic mols. 9-2849
- separability and invariance ladder operators, Kepler problem in prolate spherical coords. 9-78
- T-matrix study of many-body scatt. situation, analytic props., geom. of contour distortion, nonperturbative treatment 9-2463
- uncertainty relations interpretation 9-16687
- unimolecular rate const., model studies 9-20324
- variation perturbation methods for highly excited atomic states 9-15833
- variational, upper bounds to excited-state energies 9-2156
- variational form of Van Vleck degenerate perturbation theory 9-8411
- WKB method, second soln. 9-2160
- H<sub>2</sub>, Kerr constant determ. 9-746
- H atom g.s., oscillator strength sum rules upper and lower bounds calc. 9-8407
- H<sub>2</sub>, oscillator strength sum rules upper and lower bounds calc. 9-8407
- perturbation calc. on var. of H-bond energies with intermol. distance 9-11447

**many-particle systems** see *Helium/liquid; Quantum fluids; Statistical mechanics/quantum; Superconductivity; Superfluidity*

**quantization**

See also *Field theory, quantum/quantization*

- exact, conditions 9-12884
- gravitation, locality postulate 9-14334
- Hall effect, transverse in thin layer 9-7732
- hydrodynamics, commutation relation 9-15912
- Kepler problem, in prolate spherical coords. 9-78
- magnetic monopole electric charge from soluble model, interacting particles 9-17913
- Ostrogradsky's mechanics, ambiguity resulting from non-unique Lagrangian 9-8402
- second quantization method applied to investigate matrix elements of Breit eqn. 9-9119
- spin, by path integration 9-17916
- sub-quantum level of matter, hypothesis 9-2161
- wave eqn. for neutral particles with arbitrary spin 9-6579

**wave equations**

- analytic solution, approximate 9-10641
- atom, Hartree-Fock Hamiltonians, perturbation expansions of at. non-relativistic eigenfunctions 9-4827
- atoms, two Coulomb centres problem at large separ., multipole expansion energy, quasi-crossings of curves 9-4829
- book 9-19
- Born approx. cross-sections for He excitation by fast e 9-13317
- boson fields, two coupled massive, bound states 9-2157
- boson system, perturbation expansion 9-2174
- bound-state electron hidden momentum equivalent to mag. charges 9-669
- bremsstrahlung matrix element, in potential model, soft photon theorem 9-16816

**Quantum theory continued****wave equations continued**

- charged part. single channel scatt., Levinson theorem, quantum defect. 9-6316
- correlated wavefunctions, symmetry props. 9-6950
- diatomic two-electron mol., large Z asymptotic wavefunction 9-17015
- Dirac's relativistic eqn., applic. to part. with spin props. 9-15427
- Dirac, single particle interpretation with infinite set of pictures 9-20325
- Dirac-Hestenes, some solutions 9-6311
- eigenvalues of  $1sns$   $^{1,3}S$  states of He sequence, relativistic corrections 9-13316
- electronic wave functions, from modified local-energy method, accuracy of energies 9-2154
- Feynmann-Schrodinger eqn., statistical sampling method, perturbation potentials corrections 9-16684
- first order perturbation method, modification for spin-factorable syst. with unknown eigenfunctions 9-16990
- free particle wave function, asymptotic expression for large values of time 9-2155
- Gaussian wave packet, evolution in time 9-74
- generalized nonlinear eqn. 9-17721
- generator coordinate method rel. to quasi boson approx. 9-6767
- Hamilton operator spectrum function from scattering theory 9-18996
- Hamilton Jacobi and Schrodinger eqns., possibility of coincidence between solutions 9-10640
- harmonic oscillators, two coupled, validity of rotating wave approx. 9-10644
- Hartree-Fock, for He with non-orthogonal orbitals 9-4875
- Hartree-Fock, projected, for  $^{12}C$  and  $^{11}B$  9-6852
- Hartree-Fock, time dependent, new deriv. 9-11379
- Hartree-Fock, unrestricted, for electron and proton excitation of He 9-4878
- Hartree-Fock, unrestricted,  $Z^{-1/2}$  expansion for Li ground state 9-4828
- Hartree Fock and Hartree Hamiltonians, perturbation expansions 9-4827
- Hartree-Fock matrix for MgF first excited electronic state calc. 9-4930
- Hartree Fock numerical results for atoms He to Rn 9-9114
- Hartree-Fock scheme inner-electron rearrangement 9-4826
- Hartree-Fock soln. for Q force in nuc. shells, ang. momentum projection obs. 9-14544
- infinite-component, mag. moments and charge radii for states 9-20609
- integration, perturbation theory of semigroups 9-8406
- isoelectronic systems, scaling of SCF wavefunctions 9-749
- Klein Gordon, perturbed, unitarity of dynamical propagators 9-16683
- Klein-Gordon eqn., calculation of states 9-6313
- Lanczos spin tensor, spinor approach 9-13111
- Majorana eqn., deriv. from irreducible Poincare-representations 9-4235
- mechanical interpretation, Schrodinger eqn. rel. to Markoff process with stochastic force 9-8404
- molecular wave functions, arbitrary, localized orbitals 9-13329
- movement of centre of gravity of wave packet centred on large quantum no., for particle between two planes 9-10639
- neutral particles with arbitrary spin, covariance and quantization 9-6579
- in one-dimens. doubly periodic pot., calc. method and some results 9-12828
- operator, finite rotation, partial wave expansion, Rayleigh waves analogy 9-75
- overlap matrix elements and related integrals for H<sub>2</sub><sup>+</sup> in one-centre approx. 9-11462
- particle number conserving ground state, for nuclear pairing theory 9-6752
- Pauli-principle restriction on Bopp two matrix for atomic ground states 9-15807
- polynomial construct. for wave functions for three-body syst. 9-15429
- quantum wave functionals 9-6318
- relativistic, 5-dimensional approach 9-10955
- for scattering of plane wave by hard sphere, numerical evaluation 9-15407
- Schrodinger's difference eqn. for two relativistic particles 9-20595
- Schrodinger, approximate analytic solution 9-10641
- Schrodinger, emergence from new formulation of stochastic theory 9-2172
- Schrodinger, for metal band struct. and Fermi surface 9-13828
- Schrodinger, generalization, and rel. variable elimination in config. space 9-12893
- Schrodinger, generalized, approximation of Feynman-Cameron integrals 9-8413
- Schrodinger, one dimens., soln. by continued fractions 9-8403
- Schrodinger, potential, establishment from scattering data 9-16682
- Schrodinger, potential well bound states, numerical evaluation 9-20326
- Schrodinger, symmetry operator from group props. investigation 9-8368
- Schrodinger and Hamilton-Jacobi eqns., possibility of coincidence between solutions 9-10640
- Schrodinger difference eqn., finite difference calc., two bodies without interac. 9-15430
- Schrodinger eqn. 2-3-dimens. numerical soln. 9-4911
- Schrodinger eqn., configuration space approach to 4-particle problem 9-14346
- Schrodinger eqn. for diatomic system, separation of rot. coords. 9-14682
- Schrodinger eqn. in Riemannian manifold, kinetic part 9-16681
- Schrodinger Jost function, analytical props. for a more general class of potentials 9-14348
- Schrodinger many-particle operator with combined Zeeman and Stark eff. 9-20330
- Schrodinger separable solns. of Einstein spaces 9-18977
- Schrodinger stationary-state eqn. for dressed vacuum, soln. 9-13089
- Schrodinger type, almost-periodic solns. 9-8405
- second order relativistic generalized eqn. 9-14342
- Slater transform functions, construct. 9-19389
- Slater-type one-electron functions, exchange approx. 9-10638
- spinor field, 8-component, with 4-vector currents and invariants, relationship 9-19184
- spinors, covariant formalism in fermion-fermion scatt. 9-4565
- textbook 9-20
- variational method for scattering phase shifts, analysis w.r.t. other methods 9-11404
- with velocity dependent pots., analytic behaviour of S-matrix 9-6315
- wave function for 2N- electron system, strongly orthogonal geminal product, refinement 9-11444
- wave function of e<sup>-</sup> He<sup>+</sup> syst., expansion and convergence for 1s-2s excitation cross section 9-15834
- $\pi\pi$  partial wave amp. study, potential in Born approx. correct. 9-6675



**Quantum theory continued****wave equations continued**

- Be<sup>+</sup> variational calc., multiplets and config. 9-4884  
 inter- electronic correl. functions, condition removing degeneracy 9-20327  
 Hartree-Fock approx. by perturb. theory, oscillator strengths of dipole transition between  $1s^2 3d^2 L$  state 9-9125  
 He, Hartree-Fock, numerical results 9-9114  
 He multiplets with non-orthogonal orb. Hartree-Fock eqn. and perturbation treatment, Hellmann-Feynman formula anal. 9-4875  
 He variational calc., multiplets and config. 9-4884  
 integral Hellmann Feynman theorem 9-2867  
 Rn, Hartree-Fock, numerical results 9-9114

**Quarks**

- baryon, meson mass model 9-2526  
 baryon model, rel. to energy levels and short-range interaction 9-6680  
 current algebra representation for charge densities in meson models 9-2473  
 and elementary particle theory 9-13109  
 elementary review for teaching 9-15411  
 e.m. quantities, relations using current algebra agreeing with quark model 9-2475  
 form factor of proton as a system of three quarks 9-20610  
 free effective model, meson current algebra 9-20629  
 hadron scatt. cross sections, quark model multiple-scatt. contributions 9-8787  
 hyperon nonleptonic decay model ambiguities 9-2541  
 integrally charged, rel. to  $\pi^0 \rightarrow 2\gamma$  and  $\eta \rightarrow 2\gamma$  9-2500  
 interactions, nucleon form factors calc. from fermi statistics 9-8763  
 leptonic, in cosmic rad., underground search obs. 9-15653  
 meson decay, strong, recoil and rescatt., eff. in strong decays, width meas. 9-16858  
 meson decays, relativistic quark model 9-17969  
 and meson spin-orbit mass splitting 9-4608  
 model, quark diquark with broken SU(6), use in investigation of e.m. props. of baryons 9-16898  
 model, rel. to double charge on hypercharge exchange processes 9-6615  
 model for additivity and algebra of vector charges 9-14478  
 model for mesons and baryons 9-10992  
 model for pseudoscalar meson production in proton-antiproton annihilation 9-11026  
 model of particle interaction 9-11006  
 model prediction for vector meson production 9-20658  
 model predictions about high-energy scatt., simplified derivation 9-4591  
 nonlinear theory, decay constants and magnetic moments of mesons and baryons 9-20611  
 nonlocal particle theory, De Sitter metric appl. 9-8764  
 paraquark harmonic oscillator shell model for baryons 9-19206  
 use in predicting isospin and U spin dependence of hadron-nucleon total cross sections 9-16855  
 QQQ model for meson-baryon interactions 9-2490  
 quark-antiquark meson, Heisenberg-type scalar field theory model 9-8761  
 quasi independent, in baryon model 9-13137  
 Regge quark-model description of  $\pi p$ , Kp charge-exchange react. 9-13127  
 Regge trajectory domination by high-energy scatt. 9-20608  
 Reggeization, invariant of U(6)×U(6) system for reduction of parameter 9-6634  
 reggeization of quark number 9-19194  
 relativistic e/3 and 2e/3, search in cosmic rad. and upper limits of flux 9-2553  
 relativistic model for mesons 9-14495  
 search, elementary review 9-6613  
 spectroscopic search for +2/3 quark and  $\epsilon$  atom formation in plankton, cil drops 9-8765  
 spin, hidden in baryon model 9-2474  
 SU(3) chiral dynamics from generalization of SU(2) 9-344  
 n SU(6) framework, substitution q for q 9-6614

**Quartz**

- $\alpha$ , optical rotary power, variations due to pressure and temperature 9-12341  
 $\alpha$ , Z-cut, vacuum u.v. reflectance temp. eff. 9-3853  
 $\alpha$ -quartz, polariton Raman scattering intensities 9-12436  
 eff. of acoustic waves, finite-amplitude 9-11994  
 birefringence meas., Soleil-Babinet compensator method 9-5880  
 citrine, irradiated, colouring mechanism 9-1237  
 colour centre formation in  $\alpha$ -irrad  $\alpha$  modification, thermoluminescence and dielec. behaviour 9-13701  
 colour centres, nonthermoluminescent smoky, in  $\alpha$ -quartz, nature and formation mechanism 9-5393  
 conductivity, elec., in constant elec. field, of natural and synthetic mat 9-1569  
 crystal, harmonics of 285.7 kHz, detection methods 9-15459  
 crystal, in laser wavelength selection device 9-10857  
 crystal microbalance holder for low-temp. vacuum 9-12814  
 defects revealed by etching and Ag decoration in elec. field 9-13682  
 dielectric consts. 8-140 GHz meas. accuracy of impedance method 9-3696  
 diffusion paths, decorated 9-18488  
 elastic constants, higher-order, in fused fibres, meas. using finite deforms. 9-5419  
 elastic consts., temp. depend., impurity eff. 9-5424  
 elastic surface waves attenuation in cryst. quartz, 316 and 1047MHz, 42-300°K 9-9745  
 elastic wave at surface of  $\alpha$ -crystal, second-harmonic generation 9-11916  
 elastic waves, u.s., attenuation, calc. 9-3405  
 epitaxy of polyamides 9-1158  
 etchants, selective 9-1128  
 faces, first order prism, microtopographical studies 9-9636  
 fused, far i.r. absorpt. 9-10209  
 glass, e.p.r. of  $Ti^{3+}$  9-21664  
 hydrothermal synthesis in Fe-lined vessel 9-13605  
 hypersonic attenuation by thermal Brillouin scattering 9-12000  
 i.r. spectrum of  $\alpha$ -quartz 9-3878  
 light scattering spectrum rel. to hypersonic wave velocity determ. 9-1811  
 magnetic susceptibility obs., and Suprasil 9-19949  
 neutron beam, diffracted, time modulation by crystal vibrated by h.f. pulse 9-21307  
 opalescence, critical obs. and interpretation 9-10181  
 partial polarization of light 9-7938

**Quartz continued**

- phonons, coherent optical, of 100W, generation 9-12320  
 piezoelectric plate, acoustic transmission coeffs. 9-4321  
 piezoquartz, Cherenkov generation of ultra and hypersound 9-10054  
 polarized light Rayleigh scatt. by defects, in optical active cryst., obs. 9-12340  
 $\alpha$ -quartz,  $\gamma$ -irrad., nonthermoluminescent smoky, colour centres, nature and formation mechanism 9-5393  
 $\alpha$ -quartz, elastic const. calc. from force field const. 9-19779  
 quartz, i.r. generation on stimulated Raman scatt. at 10°K 9-7983  
 quartz comminution, net energy input rel. to fineness 9-7597  
 quartz comminution, net energy input rel. to fineness 9-11953  
 Raman, Brillouin and Rayleigh scattering, temp. depend. 9-12445  
 Raman scattering, polariton intensities,  $\alpha$ -quartz 9-12436  
 Raman spectra, one- and two-phonon excitations coupling evidence 9-1361  
 Raman spectrum, u.s. induced enhancements 9-21636  
 reliability under unfavourable weather conditions 9-21825  
 synthetic, growth of first order prism faces, microtopographical studies 9-9636  
 thermal conductivity in pure fused material, precise determ., 0-500°C 9-15028  
 thermodynamics of non-linear electro-elasticity relations 9-17294  
 transducer, coherent phonon fusion 9-3511  
 ultrasonic absorption, temp. depend., optical determ. 9-12001  
 u.s. wave, two pure transverse mode generation at 9.4GHz in x-cut bar 9-5548  
 valence bond approximation; applic. to u.v. spectrum anal. 9-5266  
 vibrating crystal, diffraction of neutrons 9-3516  
 X-cut, ultrasonic harmonics production 9-9824  
 as lowpass n vel. filter, transparency determ.,  $\lambda_0=1.5\text{Å}$  9-11105  
 H-banded OH in synthetic quartz, characts. from i.r. spectra 9-5267

**Quartz resonators see Piezoelectric oscillations; Resonators; Transducers****Quasars****See also Cosmic radiations, radiofrequency; Cosmology; Galaxies; Stars**

- 3C191, absorption spectrum, curve of growth analysis, model 9-12736  
 3c273, opt. variability, random event model applic. 9-6151  
 3C273, proper motion data and minimum distance 9-2029  
 3C273 radioemission of A and B components at 3.9 cms 9-4109  
 3C287, proper motion data and minimum distance 9-2029  
 3C 273: optical variability stat. anal. 9-2027  
 3C 273, opt. polariz., obs. 9-21912  
 3C 273, polarization, 9.55 mm 9-20205  
 3C 286, no opt. polariz., obs. 9-21912  
 3C 454.3 red shift obs. with contact image-converter tube 9-12733  
 3C 48, no opt. polariz., obs. 9-21912  
 0159-11 red shift obs. with contact image-converter tube 9-12733  
 0350-07 red shift obs. with contact image-converter tube 9-12733  
 absorption lines as function of red shift 9-15326  
 from blue object obs. in high galactic latitudes 9-16552  
 characteristics obs. due to optical distortion of light intervening galaxies 9-6152  
 distances, space distrib. and luminosity function 9-15325  
 energy sources from obs. of relativistic effects of non-thermal cosmic sources 9-18885  
 HZ29, radio luminosity obs. 9-21913  
 jets, rel. to line spectrum explanation 9-17629  
 opposite radio sources, cosmological test 9-20211  
 optical positions 9-18887  
 optical variability, systematic survey 9-20206  
 radiation spectra, e and photon synchrotron rad. and inverse Compton scatt. interpretation 9-10505  
 radio spectra, steepness rel. to angular size, brightness rel. to size, polarized ones unresolved 9-12738  
 receding or circulating, comments 9-4110  
 red shift, complex distrib., interpretation 9-18888  
 red shift, cosmological interpretation with  $\Lambda \neq 0$  Cosmology [ $\Lambda \neq 0$  explains quasar red shift] Astronomical spectra [red shift in quasars explained in cosmological model with  $\Lambda \neq 0$  b/c/ 9-14229  
 screening probabilities in universes with positive cosmological const. 9-20134  
 spectra, H $\beta$  emission line width rel. to ionization mech. 9-6111  
 spectra, weak absorpt. line identification 9-2028  
 spectra compared with radio galaxies' 9-20207  
 spectroscopic meas. of emitted light, rel. to verification of equivalence principle 9-1984  
 stage in evolution of galaxies 9-15327  
 structure and positions, 21 sources 9-16592  
 theory for enormous energy 9-17628  
 X-radiation flux calculation 9-4108  
 3C 273, emission-line region, models, H, He, O, Ne, Mg, Fe rel. abund. obs. 9-16594

**Quasi-particles see Excitons; Magnons, Phonons, Polarons, etc.****Quenching, optical see Luminescence****Quenching, thermal see Heat treatment****Racah coefficients see Quantum theory****Radiation**

- See also Acoustic radiations; Bremsstrahlung; Cherenkov radiation; Electromagnetic waves; Electrons/radiation; Emissivity Radiative transfer; Stars/radiation; Sun/radiation; Sunlight*  
 alkali halides ionic crystals, shock compressed, temp. above 1 eV 9-14970  
 atmosphere of Southern Norway, instrument calibration 9-8172  
 $\beta$ , expt. for eval. of phys. props 9-6255  
 blackbody, scalar representation of coherence props. 9-20468  
 boson in plane wave e.m. field, classical and quantum theory analysis 9-6414  
 of charged particle, external field in general relativity 9-17710  
 e.m., in moving medium, Green's functions derived 9-14402  
 e.m. in general relativity first approx. 9-6307  
 emission from charged particles in diffraction grating vicinity, review 9-15486  
 fields, generation from empty gravitational fields 9-60  
 from moving charged particle in ferrite 9-5845  
 gas, non-equilibrium plane-parallel layers, growth curve 9-19586  
 gravitational, from vibrating source, soln. for double series approx., incoming radiation 9-8387  
 gravitational, primordial black-body, present temp. 9-15266

**Radiation** continued

- interaction with matter, kinetic eqn. for quasiparticles to order  $\lambda^4$ , applic. 9-11389
- ionic crystals, shock-compressed, temp. above 1 eV 9-14971
- in ionized gases, spectrum depend on photon momentum distrib. 9-13458
- ionized gases, thermodynamic function calc. 9-13459
- i.r., essentials of modern physics, applic. to lab. problems, book 9-15476
- i.r. basis principles and applic. to technology, book 9-19081
- metals, thermal, rel. to optical and elec. props. 9-21433
- oscillating electric dipole in motion in dispersive medium, complex Doppler effect analysis 9-4400
- particulate, expt. for eval. of phys. props. 9-6255
- plane wave fronts, dynamical props. 9-14403
- plasmons, tangential surface, radiative decay 9-7720
- scalar one-dimensional, directivity theory 9-10623
- Smith-Purcell, from narrow tape helix, self-consistent investig. 9-12961
- $\alpha$ , expt. for eval. of phys. props. 9-6255
- B, expt. for eval. of phys. props. 9-6255

**heat**

- absorption behind main shock front, effect 9-20439
- atmosphere, variations 9-21772
- blackbody, ideal, behavior 9-19082
- ceramic coatings, exposure to Mars dust storm V groove control surface development 9-1386
- composite heat transfer in non-gray medium 9-6394
- from cylindrical cloud of particles, Monte Carlo analysis 9-20371
- disc, with smallest ratio of weight to radiated heat, section profiles and dimensions 9-8520
- disperse layers at high temp., separation of radiant component of thermal cond. 9-9561
- effect on hypervelocity boundary layer flat plate flow 9-19576
- film, 1-dimens, growth from vapour, heat transfer 9-21248
- flames used in MHD conversion, meas. 9-17851
- flux intensity distrib. on contact surfaces of moving bodies, cutting tool appl. 9-19083
- gas, stagnant, eff. on laminar free convection from heated vertical plate 9-7229
- gas, stagnant hot layer surrounded by cold gas capable of abs. and emission, transient energy transfer 9-11659
- gas, temp. distrib. Monte Carlo calc. 9-7226
- grey gas between parallel black walls, radiative layers adjacent to walls in optically thick situation 9-10682
- heat wave distrib. modelling using non-linear electric circuits 9-20444
- interchange between direction depend characts. of arranged surfaces, Monte Carlo study 9-157
- interference film shielding, optical thickness computer calc. 9-4513
- i.r. gaseous rad., large path length limit 9-19585
- i.r. sensitive emulsion, hypersensitization 9-4544
- i.r. source of uniform intensity 9-8521
- from irrus clouds, 8-13 m region, physical model 9-6074
- luminance and colour temperatures, computing formulae 9-8534
- methane gas, i.r. rad., large path length limit 9-19585
- oxide on metal composites, film growth and rad. props. 9-19985
- radiator in heating system with one feed, working characts. 9-2245
- radiometry and photometry units, definitions and conversion factors 9-10749
- reflection, Kramers-Kronig phase angle partitioning, systematic error disclosure 9-10897
- resin, ion-exchange, irrad. effect 9-6021
- Sky, cirrus clouds rel. radiance 9-16530
- in spherically symmetric medium, transfer calc. by planar slab tech. and differential approx. 9-8519
- steel, stainless, exposure to Mars dust storm, V-groove control surface development 9-1386
- Stephan Boltzmann law, expt. verification 9-4207
- from supersonic gas flow round blunt cone 9-13479
- terrestrial, 7-26  $\mu$ , spectral intensity rel. latitude, Cosmos 45 and 65 obs. 9-21787
- terrestrial, 7-27  $\mu$ , angular and spectral distributions, Cosmos obs. 9-21786
- transfer, parallel plates in anisotropically scatt. atm. 9-10752
- transient combined conduction-rad. in optically thick semi-infinite grey medium 9-6393
- wall losses from oil fired MHD generators 9-15496
- Al exposure to Mars dust storm, V-groove control surface development 9-1386
- CO<sub>2</sub> gas, i.r. rad., large path length limit 9-19585
- CO gas, i.r. rad., large path length limit 9-19585
- H<sub>2</sub>O gas, i.r. rad., large path length limit 9-19585
- Ti exposure to Mars dust storm, V-groove control surface development 9-1386

**Radiation belts** *see Atmosphere/radiation belts***Radiation chemistry** *see Chemical effects of radiations/ionizing radiations; Radiochemistry***Radiation damage** *see Physical effects of radiation***Radiation detectors**

- See also Bolometers; Photometry; Radioactivity measurement*
- 100 1000 A with inert gas ionization chamber and thin metal film 9-19227
- actinograph for meas., sensitivity and calibration 9-21773
- calibration for Southern Norway climate obs. 9-8172
- carbon blacks applic., optical props. evaluation, book 9-12324
- fluorescence monitoring by glass dosimeter specimens, patent 9-12461
- gas-flow counter, study of short emissions in extreme ultraviolet 9-5043
- infrared, thin film receiver performance, effect of thermal conduction 9-6395
- i.r., design and use, book 9-19081
- i.r., device characteristics 9-2246
- i.r., response time using InAs laser 9-2383
- i.r., using superconductor junction with 10 A insulating layer 9-7782
- i.r. analyzer using multi-attenuated total reflectance 9-15478
- i.r. camera, hypersonic wind tunnel heat transfer obs. 9-160
- i.r. image converter tube, piezoelec. power supply 9-10751
- i.r. quantum counter, rare-earth, five level, 1-2  $\mu$  9-10927
- i.r. radiometers for airborne surface temp. meas. 9-2249
- i.r. receiver, sensitivity 9-19933
- metal blacks applic., optical props. evaluation, book 9-12324
- optico-acoustic chambers, absorpt. index rel. to length, and conc. of gas 9-6555

**Radiation detectors** continued

- photoelectric, selective, for 15-90 nm. region 9-2410
- pneumatic receiver with strain-gauge sensing element 9-158
- position sensitive detector of ionizing radiation 9-445
- pyroelectric, for thermal imaging 9-2247
- pyroelectric i.r. receiver, sensitivity 9-19933
- pyroelectric i.r. receiver, sensitivity 9-19933
- responsivity, source detector spectral matching factors 9-10909
- sampling radiometer, theory and expt. 9-16739
- scintillation camera, output recording method 9-10948
- thermal imaging with real time picture presentation 9-2248
- up-converter IR detector, noise characteristics and optimization, comparison with photoconductive detector 9-20441
- u.v., as sensitive secondary standard 9-17894
- whole body, stable, low-background counter, uniform detection geom. 9-20260
- Ge:Ga photoconductive, spectral response 9-3745
- Ge, optimal thickness of sensitive layers 9-10073
- Hg, <sup>2</sup>Cd<sub>2</sub>Te alloy, photoconductive i.r. detector 9-8522
- InSb NiSb, anisotropic, as i.r. detector 9-6396
- n-InSb i.r., response to night sky background 9-6086
- Si barrier layer for 10 to 30 kV X-ray meas. characts. 9-13172
- Si light detector, integrating, applied to optical pyrometry 9-10756
- Sr<sub>1-x</sub>Ba<sub>x</sub>Nb<sub>2</sub>O<sub>6</sub> ferroelectric, infrared detector, fast and sensitive 9-3714

**Radiation effects** *see Biological effects of radiations; Chemical effects of radiations; Physical effects of radiations***Radiation monitoring**

- See also Dosimetry*
- activation analysis for competing reactions by using reactor neutron flux 9-6036
- film badges calibration, using low activity <sup>226</sup>Ra or <sup>137</sup>Cs sources in transportable facility 9-20756
- first-flight escape probs. for bodies with central black region 9-19381
- monitor with adjustable alarm, for radiotherapy unit 9-14279
- neutron flux monitoring in TRIGA-II reactor using <sup>238</sup>U(n,p) and <sup>238</sup>U(n,2n) reactions 9-6934
- in reactor vertical channel, use of polyethylene,  $\gamma$  absorption 9-661
- reactor vertical channels, use of cellulose diacetate for  $\gamma$ , n meas., determ. of n volumetric field 9-660
- Rossi- $\alpha$  expt., background counts 9-19382
- waste drums, <sup>239</sup>Pu content scanning 9-2776
- X-ray, with sealed ionization chamber 9-18971
- p synchrocyclotron, 660 MeV, nearby neutron spectra obs. 9-478
- <sup>244</sup>Pu, liq. scintillation technique 9-18082
- <sup>224</sup>Ra determ. of purity of samples used on patients 10 years ago from patent-monitoring 9-12783
- <sup>39</sup>Ko, thermal neutron activation cross section w.r.t. <sup>197</sup>Au 9-9044
- LiOH reactor shield, fast neutron transmission through partially penetrating channel 9-636

**Radiation pressure**

- See also Acoustic streaming*
- acoustic, farfield, from infinite elastic plate excited by transient pt. loading 9-10728
- acoustic, on hemispherical meniscus 9-19856
- critical, in heat, mass, transfer processes, acoustically stimulated 9-5228
- laser beam, effects on laser-produced plasma 9-18299
- noise, above infinite plane baffle, cross spectral density 9-4314
- noise, on recessed plane baffle 9-4315
- solar, effect on two artificial satellite models 9-18825
- solar, on interplanetary matter 9-21953

**Radiation protection**

- See also Radiation monitoring*
- for  $\gamma$ -rays scattered by various shielding barriers 9-574
- concrete shielding, attenuation of scattered neutrons from 660 MeV proton synchrocyclotron 9-479
- flexible alloy-elastomeric matrix, patent 9-9098
- glovebox system for radioactive material spectrophotometry 9-6562
- leakage rad. from annular ducts, distrib. of flux and dose rate around duct 9-13272
- monitor with adjustable alarm, for radiotherapy unit 9-14279
- neutron (14 MeV) attenuation in steel and polyethylene 9-18949
- neutron radiographic scatter factors, determ. for several materials 9-2801
- passive barrier beneath reactor vessel, as safety device against melt-through 9-18124
- phantom, n flux density within and around 9-2092
- polystyrene, thick foamed, for radioactive transport packaging 9-21993
- reactor shielding technique, development 9-6943
- resins to minimize radiation damage on electrical insulation 9-19379
- self shielding factors for arrays of moderator and absorber slabs 9-633
- shield, optimal form and content, calc. by Monte Carlo method 9-11371
- shield, thermal and mechanical, ventilated, for flask containing heat emitting source 9-20258
- shielding a reactor, Monte Carlo integration of adjoint  $\gamma$ -ray transport eqn. 9-19356
- shields, fast neutron obs., co-ordination of ZnS(Ag) plexiglass and Basson detectors 9-659
- spacecraft shielding against nucleon-meson cascade 9-8890
- steel shielding, measurement of dose fields of mixed radiation 9-2091
- transport capsule for irrad. specimens, design and testing 9-21994
- vessel for irradiation of organic mats. 9-6200
- waste drums, <sup>239</sup>Pu content scanning 9-2776
- from X-ray diffraction equipment, hazards and precautions 9-16633
- $\gamma$ -ray leakage through zig-zag slit in Pb shield 9-15381
- $\mu$ , laminated shield, absorption rates in Pb. Fe: thickness depend. 9-2782
- $\gamma$  penetration through heterogeneous barriers, perturbation calc. 9-20842
- $\gamma$  shielding, detector response functions, Monte Carlo calc. with linear energy transform. 9-18028
- $\gamma$  transmission by polyethylene and Fe slabs 9-21447
- $\mu$ , high energy, cylindrically sym. shield no mag. field for p. accelerator 9-4696
- n penetration, calc. and expt. methods and obs. review 9-11104
- n shielding materials, total cross sections minima, 1-11 MeV 9-15760
- <sup>232</sup>Cf n source, design data and shielding requirements 9-14634

**Radioactive recombination** *see Luminescence***Radiative transfer**

- atmosphere, stellar and planetary 9-8654
- atmosphere, temp. profile determ. from outgoing radiance 9-12580



**Radiative transfer** continued

- atmosphere, turbulent, modulation function rel. image averaging time 9-15247  
 atoms, K and L shells, radiative decay rate of vacancies 9-18132  
 Chandrasekhar's X and Y functions integro-differential eqns., derivation 9-6346  
 between concentric spheres, method of regional averaging, exam. 9-10681  
 diffuse reflection from a plane-parallel atmosphere, method of doubling thin layers 9-15338  
 diffusion in medium of large optical thickness with nonisotropic scatt. 9-4261  
 electric arcs, high press., temp. profiles calc. using diff. approx. 9-19566  
 equations, integro-differential, solution 9-16748  
 free-electron atmosphere, solution of equation 9-15305  
 gas between parallel plates, eff. of surface emission by non-black surfaces 9-19080  
 heat, from cylindrical cloud of part., Monte Carlo analysis 9-20371  
 heat, from plane, grey gas, eff. on hypersonic shock layer, soln. 9-21121  
 heat, in layer of absorbing medium 9-2180  
 heat, parallel plates in anisotropically scatt. atm. 9-10752  
 hot radiating gas, transient, to and from surrounding cold gas 9-11659  
 Legendre polynomial representation of transport equation, difference methods 9-113  
 luminescent mixed soln., fluorescence spectra obs. 9-13532  
 in magnetoactive plasma, rad. transfer eqn. 9-15923  
 Milne's problem, soln. by Duhamel's principle giving Hopf-Bronstein reln. 9-10456  
 non-grey, equivalence with Milne problem 9-10679  
 non-grey absorbing gas between parallel plates 9-19006  
 nongray boundary layers, interaction near lower stagnation point 9-19087  
 in optically thick grey gas between parallel black walls 9-10682  
 in planetary atm., solns. to eqns. 9-12746  
 planetary atmosphere, gray optically thick, in radiative convective equil., investg. 9-15337  
 in planetary atmospheres, solution 9-21933  
 in plasma reson. lines and recomb. continuum, stationary and non-stationary problem, diff. and anti-diff. approx. 9-19527  
 radiative opacity calc., using new algorithm for high-speed digital computers 9-14204  
 in Rayleigh scatt. atmosphere, soln. 9-19007  
 residual intensities, calc. for interlocked multiplets using approx. H-function 9-10485  
 semiconductors, laser flash illumination, induced stress effects 9-9776  
 in shock wave, moving in opposite direction 9-20439  
 Sokolov method applic. 9-15440  
 solution of problem using invariant  $S_n$  method 9-15441  
 in spherical shell atmosphere with perfectly absorbing core, probabilistic model 9-14370  
 stellar atmosphere, approximate soln. 9-8241  
 stellar atmosphere, modification due to obs. on fluctuations near solar sunspots and granules 9-15303  
 transport equation, isotropic scatt. 9-20372  
 $N_2$  plasma, thermal rad.  $0.5 \rightarrow 1.1 \mu$ , intensity meas. 9-19524  
 Na atom atmos. rel. to spectral line formation 9-19391  
 O atom atmos. rel. to spectral line formation 9-19391

**Radiators** see *Electromagnetic waves/radiators; Transducers*

**Radicals** see *Free radicals*

**Radioactive dating**

- chondrites,  $^{129}\text{I}$   $^{129}\text{Xe}$  formation intervals and cooling rates 9-6183  
 mica minerals, fission track ages 9-4037  
 mica minerals, fission track ages 9-16523  
 tritium type, synthesis of benzene for sensitivity enhancement 9-11247  
 $^{14}\text{C}$ , benzene synthesis for sensitivity enhancement of scintillation counter 9-11247  
 $^{36}\text{Cl}$ , synthesis of  $\text{SiCl}_4$  solvent for sensitivity enhancement 9-11247  
 K-Ar young, precision rel. Ar air contamination 9-12571

**Radioactive tracers**

- bibliography covering preparation, application and measurements 9-14144  
 biological systems, steady-state, occupancy principle 9-17672  
 blood plasma  $^{59}\text{Fe}$  clearance meas. 9-15382  
 in chemical analysis, review 9-20072  
 cystine,  $^{99m}\text{Tc}$ -labeled, prep., and distrib. in mice 9-21989  
 flow, open channel meas. by continuous sampling method 9-19593  
 labelled, organic compounds, review of stability 9-14145  
 labelled compounds, stability and storage, review 9-14146  
 methionine, prep., and distrib. in mice 9-21989  
 polypeptide, prep., and distrib. in mice 9-21989  
 $^{131}\text{I}$ , ocean surface interact. and mixing obs. 9-18789  
 $^{40}\text{K}$  physics laboratory expt. 9-2108  
 $^{18}\text{O}$ , data handling, isotopic abundance calc. 9-6035  
 $^{31}\text{Si}$  for determ. of etch rate in Si 9-16051  
 $\text{SiO}_2$ , Na ion contamination, expt. results rel. to theory 9-17547

**Radioactivity**

See also *Alpha-particles; Beta-rays, Gamma-rays; Atmosphere/radioactivity; Beta-decay theory; Chemical analysis, radioactive; Chemical effects of radiations/ionizing radiations; Fallout; Geophysical prospecting; Nuclear decay theory; Nuclear bombardment targets; Nuclear excitation; Nuclear reactions and scattering; Radiochemistry*

- $\beta$  sources for electronic meas. systems 9-554  
 glovebox system for radioactive material spectrophotometry 9-6562  
 neutron sources, improvement in absolute calibration 9-11106  
 nuclear stability in 158 neutrons region 9-4805  
 rocks with radioactive impurities, energy distrib. of  $\gamma$  spectra 9-8157  
 rocks with radioactive impurities, Pb-Cu-Cd filter for obs. of  $\gamma$ -spectra 9-6054  
 in satellite, population injury probability for random re-entry 9-20127  
 super heavy nuclei with  $Z > 104$ , prolate spheroid, instability in liquid-drop model 9-551  
 superheavy nuclei,  $A \approx 298$ ,  $\alpha$  and spontaneous fission half-life theoretical estimate 9-14590  
 Vosges rocks, conc. of Ru, Th and K 9-20080  
 $\beta$  source, spherical, shielded, efficiency calc. 9-549  
 $^{210,212}\text{Bi}$ , deduced L-subshell ratios for M1 transitions 9-14570  
 $^{110m}\text{Ag}$ , 530 keV allowed  $\beta$  transition,  $\beta$ - $\gamma$  correl. obs. 9-6841  
 $^{180}\text{Re}$ , 20 hr., nonexistence 9-13196

**Radioactivity** continued

- $^{170}\text{Tm}$ ,  $\beta$  spectra of transitions  $1^- \rightarrow 0^+$ , form 9-16948  
 $^{170}\text{Tm}$ , from  $^{169}\text{Tm}(n, \gamma)$ , relative M line intensities in pure E2 transitions 9-6838  
 $^{170}\text{Tm}$  first forbidden decay,  $\beta$ - $\gamma$  correl. obs. 9-15738  
 $^{141}\text{Ce}$ , 435 keV first forbidden  $\beta$  transition,  $\beta$ - $\gamma$  correl. obs. 9-6841  
 $^{131}\text{I}$ ,  $\beta$ - $\beta'$  decay product annealing in  $\text{H}_2\text{TeO}_6$  9-7584  
 $^{212}\text{Bi}$  decay, high energy  $\gamma$ -radiation 9-11254  
 $^{252}\text{Cf}$  as neutron source 9-2692  
 $^{132}\text{I}$ , new high energy gammas, obs. 9-18081  
 $^{17}\text{Lu} \rightarrow ^{172}\text{Yb}$  decay, sign of  $\delta$  for E2+M1 multipole mixture in  $\gamma$  transition, 1093 KeV 9-561  
 $^{12}\text{Sb}$ , first-forbidden  $\beta$  transitions, nuc. matrix elements parameters, agree with single-part. predictions 9-2705  
 $^{182}\text{Ta}$ , from  $^{181}\text{Ta}(n, \gamma)$ , relative M line intensities in pure E2 transitions 9-6838  
 $^{133}\text{Ba}$  decay,  $\gamma$  energy meas. with Ge(Li) detect. 9-2695  
 $^{133}\text{Ba} \rightarrow ^{133}\text{Cs}$ ,  $\gamma$  energy and intensity meas. 9-8981  
 $^{133}\text{Ba} \rightarrow ^{133}\text{Cs}$ ,  $\gamma$  energy and intensity meas. 9-8981  
 $^{233}\text{Pa}$ , KLL Auger spectra, obs. in  $\beta$ -decay 9-2817  
 $^{113}\text{Sn}$  decay,  $\gamma$  energy meas. with Ge(Li) detect. 9-2695  
 $^{233}\text{U}$  thermal fission products, time var. of mean  $\beta$  activity 9-11338  
 $^{14}\text{Cs}$ , 662 keV allowed  $\beta$  transition,  $\beta$ - $\gamma$  correl. obs. 9-6841  
 $^{154}\text{Eu}$  440 to 1280 keV transitions, e spectroscopy studies, conversion e intensities, and coeffs. 9-2700  
 $^{154}\text{Cd}$  K e intensities, evidence for new  $O^+$  level 9-2668  
 $^{140}\text{Ho}$   $\beta$  decay,  $^{164}\text{Er}$  91.5 keV E2 transition,  $\alpha$  obs. 9-2669  
 $^{14}\text{Pr}$ , deduced L-subshell ratios for M1 transitions 9-14570  
 $^{173}\text{Hf} \rightarrow ^{173}\text{Lu}$  L Auger spectrum, line energy and intensities, fluorescence yields 9-9007  
 $^{233}\text{Pa}$ , decay props. 9-16963  
 $^{235}\text{U}$  thermal fission products, time var. of mean  $\beta$  activity 9-11338  
 $^{166}\text{Ho}$ ,  $\beta$ - $\gamma$  ang. correl.  $\text{Pa}(\cos \theta)$  depend. 9-6844  
 $^{166}\text{Ho}$ , deduced L-subshell ratios for M1 transitions 9-14570  
 $^{166}\text{Ho}$ , from  $^{165}\text{Ho}(n, \gamma)$ , relative M line intensities in pure E2 transitions 9-6838  
 $^{236}\text{Pa}$ , decay props. 9-16963  
 $^{18}\text{Re}$ ,  $\beta$  spectra of transitions  $1^- \rightarrow 0^+$ , form 9-16948  
 $^{137}\text{Cs}$ ,  $\beta$ -branching ratio and internal conversion coeffs. 9-4762  
 $^{237}\text{Pa}$ , decay props. 9-16963  
 $^{17}\text{Re}$ , neutron-deficient, decay charact., positron emitter 9-13196  
 $^{198}\text{Au}$  first-forbidden  $\beta$  transitions, nuc. matrix elements parameters, agree with single-part. predictions 9-2705  
 $^{198}\text{Au}$ ,  $\beta$ -decay, longitudinal depolarization of  $\beta$ -rays in source 9-15740  
 $^{198}\text{Au}$  electron flux spectra in Al 9-18571  
 $^{238}\text{Pa}$ , decay props. 9-16963  
 $^{178}\text{Re}$ , neutron-deficient, decay charact., positron emitter 9-13196  
 $^{228}\text{Th} \rightarrow ^{212}\text{Po}$ , low energy  $\gamma$  radiation rel. to multipolar character of  $^{212}\text{Po}$  9-13212  
 $^{239}\text{Pu}$  thermal fission products, time var. of mean  $\beta$  activity 9-11338  
 $^{179}\text{Re}$ , neutron-deficient, decay  $\beta$  capture, charact. 9-13196  
 $^{129}\text{Te}$  isomeric transition product annealing in  $\text{H}_2\text{TeO}_6$  9-7584  
 $^{26}\text{Al}$  in Greenland ice, obs. 9-10380  
 $^{77}\text{As}$ , new energy  $\gamma$ 's, obs. 9-566  
 $^{13}\text{B}$ , delayed neutrons in  $\beta$ -decay 9-11250  
 $^{10}\text{Be}$  in Greenland ice, obs. 9-10380  
 $^{11}\text{CO}$  preparation for medical use 9-21990  
 $^{58}\text{Co}$ , 485 keV allowed  $\beta$  transition,  $\beta$ - $\gamma$  correl. obs. 9-6841  
 $^{58}\text{Co}$ , (475 keV,  $2^+ \rightarrow 2^+$ ,  $\beta^+$ ) (0.810 MeV,  $\gamma$ ) 9-15743  
 $^{60}\text{Co}$  sources, arrangement geometry for irradiation of conical plastic objects 9-548  
 $^{64}\text{Cu}$  electron flux spectra in Al 9-18571  
 $^{65}\text{Ga}$ , rel. to low energy excited states of  $^{65}\text{Zn}$  9-19291  
 $^{66}\text{Ga}$  gaseous source preparation method 9-18084  
 $^{85}\text{Kr}$  source, thin, preparation 9-2706  
 $^{85}\text{Kr} \rightarrow \text{Rb}^+$  ion, dipole transition from excited states, lifetimes obs 9-9140  
 $^{99}\text{Mo}$ , ang. correl. of forbidden beta transition  $1/2^+ \rightarrow 1/2^-$  9-6843  
 $^{16}\text{N}$ , e pair emission in decay competition from internal formation 9-6833  
 $^{22}\text{Na}$ ,  $\beta^+$  spectrum, and rest mass of  $\nu$  from  $\beta$ -decay 9-9010  
 $^{90}\text{Nb}$  decay to  $^{90}\text{Zr}$ , energies of low-lying excited levels of  $^{90}\text{Zr}$  9-13205  
 $^{91}\text{Nb}$  decay to  $^{91}\text{Zr}$ , energies of low-lying excited levels of  $^{91}\text{Zr}$  9-13205  
 $^{92}\text{Nb}$  decay to  $^{92}\text{Zr}$ , energies of low-lying excited levels of  $^{92}\text{Zr}$  9-13205  
 $\text{O}^{18}$  preparation for medical use 9-21990  
 O isotope behaviour in the sulphate water system 9-8156  
 $\text{O}^{18}$  preparation for medical use 9-21990  
 Os 2.3 min isotope, evidence for 9-13196  
 $^{56}\text{Sc}$ , (357 keV,  $4^+ \rightarrow 4^+ \beta^-$ ) (1.121+0.889 MeV,  $\gamma$ ), B- $\gamma$  circular polarization meas. 9-15743  
 $^{90}\text{Sr}$  on Earth's surface, rel. to fallout rate 9-17555  
 $\text{SrTiO}_3$   $\beta$  source, spherical, shielded, efficiency calc. 9-549  
 $\text{ThO}_2$ , electrodeposition of gaseous decay products 9-21710  
 $^{90}\text{Y}$ , e pair emission in decay competition from internal formation 9-6833  
 $^{89}\text{Zr}$  78.4h, decay props., energies  $\gamma$  transitions meas. 9-2708

**dating** see *Radioactive dating*

**decay periods**

- $^{198}\text{Au}$  half-life obs. 9-18083  
 activity change calcs. using tables of the function  $\exp(-x)$  9-11248  
 lifetimes, moment method corrected for finite range of integration, reduction of centroid shift 9-2693  
 maximum likelihood estimates of half-life 9-16947  
 population of cascading levels, calc. using diagrammatic mnemonic 9-6258  
 $^{170}\text{Ho}$  isomer, 2.9 min., from  $^{170}\text{Er}(n, p)$  obs. 9-14594  
 $^{180}\text{Re}$ , 20 hr., nonexistence 9-13196  
 $^{241}\text{Am}$ ,  $\alpha$  half-life 9-15741  
 $^{241}\text{Pu}$ , lifetime mass-spectrometric obs. 9-4759  
 $^{243}\text{Am}$  lifetime, comparison of coulometric and mass-spectrometric obs. 9-4760  
 $^{253}\text{Cf}$   $\alpha$  decay spectra, energy and intensity meas. 9-11251  
 $^{233}\text{U}$ , half-life by specific activity methods 9-20759  
 $^{244}\text{Cm}$ ,  $\alpha$  half-life 9-15742  
 $^{244}\text{Pu} \rightarrow ^{136}\text{Ce}$  decay intervals of chondrite dark phases 9-2061  
 $^{124m}\text{Sb}$ , from  $^{127}\text{In}$ ,  $\alpha$  at  $E_\alpha = 14.7$  MeV, lifetime and activation cross-section obs. 9-9038  
 $^{125}\text{I}$ , from  $^{127}\text{In}$ , (3n) at  $E_n = 14.7$  MeV lifetime and activation cross-section obs. 9-9038  
 $^{175}\text{Re}$ , first prod. from  $^{165}\text{Ho}(^{16}\text{O}, 6n)$  and  $^{159}\text{Tb}(^{22}\text{Ne}, 6n)$  9-14633  
 $^{155}\text{Sm}$  from  $^{154}\text{Sm}(n, \gamma)$ ,  $\beta$  decay, half-life meas. 9-16949  
 $^{185}\text{W}$ , 1.7 min., identification of isomeric level 9-16941

**Radioactivity continued****decay periods continued**

- <sup>123</sup>Xe, and scheme 9-4755  
<sup>155</sup>Eu from <sup>157</sup>Sm, lifetimes of excited states determ. 9-559  
<sup>136</sup>I  $\beta$  decay,  $\gamma$  spectra obs., energy levels, lifetime determ. 9-20762  
<sup>126</sup>In, from <sup>127</sup> $\Sigma$ (n,2n) at  $E_n=14.7$  MeV, lifetime and activation cross-section obs. 9-9038  
<sup>176</sup>Lu  $\rightarrow$  <sup>178</sup>Hf;  $\beta\gamma$  and  $\gamma\gamma$  coincidence meas., decay scheme determ. 9-9008  
<sup>176</sup>Re, first prod. from <sup>165</sup>Ho(<sup>16</sup>O,n) and <sup>138</sup>Tb(<sup>22</sup>Ne,5n) 9-14633  
<sup>127m,2</sup>Xe and scheme 9-4755  
<sup>197m</sup>Au, lifetime and cross section for reactor n scatt. 9-9009  
<sup>117</sup>Cd  $\rightarrow$  <sup>117</sup>In,  $\beta$  decay characts. 9-20761  
<sup>147</sup>Sm,  $\alpha$  emission, energy determ. 9-2699  
<sup>127</sup>Tc, from <sup>127</sup>In, p) at  $E_n=14.7$  MeV, lifetime and activation cross-section obs. 9-9038  
<sup>128</sup>I, from <sup>127</sup>I(n,  $\gamma$ ) at  $E_n=14.7$  MeV, lifetime and activation cross-section obs. 9-9038  
<sup>148</sup>Sm,  $\alpha$  emission, energy determ. 9-2699  
<sup>218</sup>U spontaneous decay rate from accumulation of Xe in U materials 9-20812  
<sup>129g</sup>Te  $\rightarrow$  <sup>129</sup>I,  $\gamma$  spectra obs. 9-18080  
<sup>129m</sup>Te  $\rightarrow$  <sup>129</sup>I,  $\gamma$  spectra obs. 9-18080  
<sup>129</sup>I  $\rightarrow$  <sup>129</sup>Xe decay intervals of chondrite dark phases 9-2061  
<sup>149</sup>Sm,  $\alpha$  emission, energy determ. 9-2699  
<sup>76</sup>As 46 keV state, obs. 9-4750  
<sup>64</sup>Ca, half life obs. 9-6842  
<sup>20</sup>F, from <sup>23</sup>Na(n, $\alpha$ ) at 14.7 MeV, lifetime obs. 9-6883  
<sup>69</sup>Ge  $\rightarrow$  <sup>69</sup>Ga,  $\beta$ ,  $\gamma$  spectra meas. 9-18085  
<sup>69</sup>Zn  $\rightarrow$  <sup>69</sup>Ga,  $\beta$ ,  $\gamma$  spectra meas. 9-18085  
<sup>56</sup>Mn half life obs. 9-18083  
<sup>89m</sup>Y lifetime and cross-section for reactor n scatt. 9-9009  
<sup>12</sup>N, prod. from Van de Graaff 3 MeV d beam 9-6745  
<sup>15</sup>O  $\rightarrow$  <sup>15</sup>N  $\beta$ -decay calc. 9-6789  
<sup>70</sup>Se, from <sup>59</sup>Co(<sup>4</sup>N,3n) at  $E_{\text{lab}}=140$  MeV, obs. 9-9012  
<sup>84</sup>Se from <sup>235</sup>U fission,  $\beta$ ,  $\gamma$  spectra meas. 9-19300  
 Sn isotopes, separation from other fission products and half-life determ. 9-11335  
<sup>95</sup>Zr  $\rightarrow$  <sup>95</sup>Nb,  $\beta$  and  $\gamma$  spectra meas. 9-15744

**decay schemes**

- $\beta$  decay of heavy nuclei, hindrance factors and influence of giant dipole reson. 9-14591  
<sup>110m</sup>Ag,  $\gamma$  energy obs. 9-6834  
<sup>170</sup>Ho isomer, 2.9 min., from <sup>170</sup>Er(n,p) obs. 9-14594  
<sup>130</sup>I ground state, rel. to  $\gamma$ - $\gamma$  angular correls. in <sup>130</sup>Xe 9-8980  
<sup>140</sup>La,  $\beta$ - $\gamma$  directional correlation from outer group, matrix elements determ. 9-20765  
<sup>140</sup>La  $\rightarrow$  <sup>140</sup>Ce, energy levels, spin and parity assigned from pair-conversion positrons 9-2666  
<sup>160</sup>Tb, decay to levels in <sup>160</sup>Dy 9-2701  
<sup>170</sup>Tm,  $\beta$ -transitions, use of CVC theory, superfluid corrections 9-6839  
<sup>111m</sup>Pd  $\rightarrow$  <sup>111</sup>Ag, G spectra meas., energy levels, spin and parity determ. 9-20760  
<sup>161</sup>Gd  $\rightarrow$  <sup>161</sup>Tb,  $\beta$ , obs. 9-9006  
<sup>161</sup>Gd  $\rightarrow$  <sup>161</sup>Tb,  $\beta$ -decay obs. 9-19297  
<sup>131</sup>La investigation by Ge(Li) and Si(Li) spectrometers and coincidence methods 9-2697  
<sup>231</sup>Pa  $\rightarrow$  <sup>227</sup>Ac,  $\gamma$  spectra obs.; levels, transitions, rotational structure determ. 9-14579  
<sup>111</sup>Pd, using scintillation spectrometer 9-9004  
<sup>111</sup>Pd  $\rightarrow$  <sup>111</sup>Ag,  $\gamma$  spectra meas., energy levels, spin and parity determ. 9-20760  
<sup>111m</sup>Pd, scintillation spectrometer 9-9004  
<sup>241</sup>Pu  $\alpha$ -decay,  $\gamma$  and  $\alpha$ -part. transition energies and intensities, applic. to <sup>237</sup>U energy levels, and half-life meas. 9-6815  
<sup>111</sup>Sn  $\rightarrow$  <sup>111</sup>In,  $\gamma$  de-excitation, new transitions 9-19293  
<sup>161</sup>Tb  $\rightarrow$  <sup>161</sup>Dy, B<sup>-</sup>, 6.9 days obs. 9-9006  
<sup>112</sup>Ag  $\rightarrow$  <sup>112</sup>Cd, energy levels, spin and parity determ. 9-13208  
<sup>127</sup>I, from  $\gamma$ -ray study 9-11222  
<sup>127</sup>Sb, negaton spectrum obs. 9-556  
<sup>187</sup>Ta,  $\gamma$  energy obs. 9-6834  
<sup>162</sup>Tb,  $\beta$  and  $\gamma$  radiations, investigation 9-2702  
<sup>232</sup>Th to <sup>232</sup>U, age of the Galaxy obs. 9-16554  
<sup>192</sup>Tl  $\rightarrow$  <sup>192</sup>Hg,  $\gamma$  and conversion-e spectra obs., energy levels determ. 9-4740  
<sup>103</sup>Ag, half-lives of  $\beta$  and  $\gamma$ , assignment of levels and transitions 9-18078  
<sup>143</sup>Ce decay to <sup>143</sup>Pr, role of weak transitions 9-15720  
<sup>143</sup>Pr energy levels populated in <sup>143</sup>Ce decay, role of weak transitions 9-15720  
<sup>143</sup>Sm  $\rightarrow$  <sup>143</sup>Pm, inv. of low-lying levels of <sup>143</sup>Pm 9-8983  
<sup>214</sup>Bi, h $\gamma$   $\gamma$  radiation 9-11255  
<sup>214</sup>Bi  $\rightarrow$  <sup>214</sup>Po,  $\gamma$  spectra, 1.1 to 3.3 MeV, 4-5 keV resolution 9-13211  
<sup>154</sup>Eu  $\rightarrow$  <sup>154</sup>Gd, E0 transitions, conversion coeff. determ. from  $\gamma$  spectra meas. 9-13210  
<sup>124</sup>Fr  $\rightarrow$  <sup>210</sup>At,  $\alpha$  decay of isomers, energy levels determ. 9-4758  
<sup>124</sup>I 9-13209  
<sup>144</sup>Pm  $\alpha$  capture decay 9-6836  
<sup>144</sup>Pm  $\rightarrow$  <sup>144</sup>Nd,  $\gamma$ 's obs., Nd energy levels determ. 9-517  
<sup>144</sup>Pr, using scintillation spectrometer 9-9005  
<sup>144</sup>Pt, suggestion, from <sup>144</sup>Ir  $\gamma$  decay results 9-15739  
<sup>124</sup>Sb,  $\gamma$  energy obs. 9-6834  
<sup>124</sup>Sb  $\rightarrow$  <sup>124</sup>Te,  $\gamma$  spectra meas., levels determ. 9-18079  
<sup>164</sup>Tm  $\rightarrow$  <sup>164</sup>Er,  $\gamma$  transition,  $I^\pi=0^+$ ,  $K=0$  levels in <sup>164</sup>Er determ. 9-521  
<sup>165</sup>Dy  $\rightarrow$  <sup>165</sup>Ho 9-2703  
<sup>175</sup>Hf  $\rightarrow$  <sup>175</sup>Lu,  $\gamma$ - $\gamma$  angular correlations 9-4738  
<sup>115</sup>Sb  $\rightarrow$  <sup>115</sup>Sn,  $\gamma$  spectra obs., energy levels determ. 9-14592  
<sup>123</sup>Sb,  $\gamma$ -ray study for <sup>123</sup>Te level scheme 9-15736  
<sup>155</sup>Sm from <sup>154</sup>Sm(n, $\gamma$ ),  $\beta$  decay, half-life,  $\gamma$  energies and intensities, deduced levels 9-16949  
<sup>123</sup>Xe, and lifetime 9-4755  
<sup>135</sup>Xe  $\rightarrow$  <sup>135</sup>Cs, levels and spin determ. from  $\gamma$  meas. 9-19296  
<sup>206</sup>Bi,  $\gamma$  energy obs. 9-6834  
<sup>160</sup>Ho,  $\beta$ - $\gamma$  ang. correlation obs., attenuation for solid, liquid HoCl<sub>3</sub> compared 9-560  
<sup>160</sup>Ho,  $\gamma$ - $\gamma$  correlation, temp. effect obs. in crystals of lanthanum ethyl sulfate 9-19298  
<sup>136</sup>I  $\beta$  decay,  $\gamma$  spectra obs., energy levels, lifetime determ. 9-20762  
<sup>176</sup>Lu  $\rightarrow$  <sup>176</sup>Hf;  $\beta\gamma$  and  $\gamma\gamma$  coincidence meas., half-life determ. 9-9008  
<sup>186</sup>Re,  $\beta$ -transitions, use of CVC theory, superfluid corrections 9-6839  
<sup>106</sup>Rh, conversion electrons and  $\gamma$ -spectrum obs. 9-555  
<sup>106</sup>Rh, 30s. level scheme of 19 levels 9-4753  
<sup>116</sup>Sb  $\rightarrow$  <sup>116</sup>Sn,  $\beta$ ,  $\gamma$  spectra obs. 9-11249

**Radioactivity continued****decay schemes continued**

- <sup>156</sup>Sm  $\rightarrow$  <sup>156</sup>Eu, lifetimes of excited states determ. 9-559  
<sup>116</sup>Te  $\rightarrow$  <sup>116</sup>Sb,  $\beta$ ,  $\gamma$  spectra obs. 9-11249  
<sup>196</sup>Tl  $\rightarrow$  <sup>196</sup>Hg,  $\gamma$  and conversion-e spectra obs., energy levels determ. 9-4740  
<sup>166</sup>Tm  $\rightarrow$  <sup>166</sup>Er  $\gamma$  energy obs., spin, parity and energy levels assigned 9-2704  
<sup>127m,2</sup>Xe, and lifetime 9-4755  
<sup>177</sup>Lu,  $\beta$ ,  $\gamma$  transitions obs. 9-15725  
<sup>177</sup>Lu  $\rightarrow$  <sup>177</sup>Hf, internal conversion studies of 113 keV transition 9-524  
<sup>187</sup>Re  $\rightarrow$  <sup>187</sup>W,  $\gamma$  angular correlation meas., spin values determ. 9-20766  
<sup>117</sup>Sb  $\rightarrow$  <sup>117</sup>Sn,  $\gamma$  spectra meas., energy levels, spin and parity determ. 9-13194  
<sup>227</sup>Th  $\rightarrow$  <sup>227</sup>Ra, internal conversion obs. rel. to <sup>223</sup>Ra energy level transitions 9-6812  
<sup>208</sup>At,  $\gamma$  obs. and lifetime meas. 9-531  
<sup>208m</sup>Bi from ( $\gamma$ ,n) reaction, half life and energy meas. 9-11217  
<sup>158</sup>Er  $\rightarrow$  <sup>158</sup>Ho, new levels, mass difference 9-11252  
<sup>128</sup>I 9-19294  
<sup>148</sup>Pm,  $\beta$ - $\gamma$  directional correlation 9-558  
<sup>186</sup>Re,  $\beta$ -transitions, use of CVC theory, superfluid corrections 9-6839  
<sup>186m</sup>Tb from ( $\gamma$ ,n) reaction, half life and energy meas. 9-11217  
<sup>228</sup>Th and <sup>226</sup>Ra,  $\alpha$ - $\alpha$  ang. cor. 9-6840  
<sup>198</sup>Tl  $\rightarrow$  <sup>198</sup>Hg,  $\gamma$  and conversion-e spectra obs., energy levels determ. 9-4740  
<sup>208</sup>Tl, population of levels of <sup>208</sup>Pb 9-13197  
<sup>235</sup>U to <sup>235</sup>U, age of the Galaxy obs. 9-16554  
<sup>129g</sup>Te  $\rightarrow$  <sup>129</sup>I, energy levels, spin and parity determ. from  $\gamma$  spectra 9-18080  
<sup>129m</sup>Te  $\rightarrow$  <sup>129</sup>I, energy levels, spin and parity determ. from  $\gamma$  spectra 9-18080  
<sup>129m</sup>Te  $\rightarrow$  <sup>129</sup>I, rel. to excited states of <sup>129</sup>I 9-15717  
<sup>129m</sup>Xe,  $\gamma$ - $\gamma$  directional correlation 9-19295  
<sup>199</sup>Au obs. with  $4\pi$  spectrometer 9-562  
<sup>13</sup>Ba first-forbidden  $\beta$  decay, spectral shape factor, directional correlation meas. 9-20763  
<sup>139</sup>Ba to levels in <sup>139</sup>La to study struct. of N-82 isotones 9-8982  
<sup>139m</sup>Nd,  $\beta$ -decay, 9-6835  
<sup>11</sup>Te isomers, from  $\gamma$ - $\gamma$  coincidence spectra 9-4754  
<sup>35</sup>Ar  $\rightarrow$   $\text{e}^-$  vector coupling coeff. G obtained 9-564  
<sup>75</sup>Br from <sup>12</sup>C, <sup>63</sup>Ca, <sup>16</sup>O + <sup>59</sup>Co, decay independence mode of formation 9-6828  
<sup>10</sup>C  $\rightarrow$  <sup>10</sup>B,  $\gamma$  spectra meas., branching ratio determ. 9-18086  
<sup>11</sup>C superallowed positron decay, internal bremsstrahlung meas. 9-20733  
<sup>47</sup>Ca, intensities of inner  $\beta$  groups 9-565  
<sup>47</sup>Ca  $\rightarrow$  <sup>47</sup>Sc,  $\gamma$  spectra meas. 9-20767  
<sup>37</sup>Cl gamma transition, following  $\beta$  decay, <sup>37</sup>S meas. into Ge(Li) detector 9-2707  
<sup>57</sup>Co, Moseley's law demonstration apparatus 9-3  
<sup>62</sup>Co isomers,  $\beta$ ,  $\gamma$  spectra obs. 9-14589  
<sup>62</sup>Co  $\rightarrow$  <sup>62</sup>Ni,  $\gamma$  spectra obs. 9-16950  
<sup>51</sup>Cr 9-9011  
<sup>5</sup>Cu,  $\gamma$  spectra obs. 9-20768  
<sup>64</sup>Ga  $\rightarrow$  <sup>64</sup>Zn levels determ., evidence for 0<sup>+</sup> stat  $\rightarrow$   $\gamma$  9-4749  
<sup>69</sup>Ge  $\rightarrow$  <sup>69</sup>Ga,  $\gamma$  spectra,  $\beta$  meas., half life determ. 9-18085  
<sup>76</sup>Ge,  $\gamma$  spectra study, assignment of transitions in level scheme of <sup>76</sup>As 9-11256  
<sup>76</sup>Ge,  $\gamma$  spectra study, assignment of transitions in level scheme of <sup>76</sup>As 9-11256  
<sup>40</sup>K, tracer exp. 9-2108  
<sup>41</sup>K  $\rightarrow$  <sup>41</sup>Ca,  $\gamma$  spectra meas., levels determ. 9-19299  
<sup>87</sup>Kr,  $\beta$  decay, 1.3 h., to <sup>87</sup>Rb, isotope sep., construct. of consistent level schemes 9-13213  
<sup>87</sup>Kr,  $\beta$  decay, 2.8 h., to <sup>87</sup>Rb, isotope sep., construct. of consistent level schemes 9-13213  
<sup>27</sup>Mg  $\rightarrow$  <sup>27</sup>Al,  $\gamma$  spectrum obs. with Ge(Li) spectrometer 9-14595  
<sup>96m</sup>Mo  $\rightarrow$  <sup>96</sup>Tc,  $\gamma$  spectra meas. 9-15731  
<sup>96m</sup>Tc isomeric pair, rel. to levels of <sup>96</sup>Mo 9-6831  
<sup>69m</sup>Zn  $\rightarrow$  <sup>69</sup>Ga,  $\beta$ ,  $\gamma$  spectra meas. 9-18085  
<sup>69m</sup>Zn  $\rightarrow$  <sup>69</sup>Ga,  $\gamma$  spectra,  $\beta$  meas., half life determ. 9-18085  
<sup>96</sup>Nb, rel. to levels of <sup>96</sup>Mo 9-6831  
<sup>87</sup>Rb 3rd forbidden  $\beta$ -decay, shape explanation 9-14597  
<sup>87</sup>Rb,  $\beta$  decay, 15 min., to <sup>87</sup>Sr, isotope sep., construct. of consistent level schemes 9-13213  
<sup>84</sup>Se from <sup>235</sup>U fission,  $\beta$ ,  $\gamma$  spectra meas. 9-19300  
<sup>95</sup>Tc isomers to levels in <sup>95</sup>Mo,  $\gamma$  energies and intensities 9-14599  
<sup>89</sup>Zr isomers,  $\gamma$  energies and intensities,  $\beta$  levels deduced 9-14598  
<sup>95</sup>Zr  $\rightarrow$  <sup>95</sup>Nb,  $\beta$  and  $\gamma$  spectra meas. 9-15744

**electron capture**

- <sup>54</sup>Mn, K electron capture rates and decay, half-lives 9-4761  
<sup>52</sup>K, K-electron capture rates, branching ratio and positron rate 9-4761  
 decay energy meas. from inner bremsstrahlung spectrum, undergraduate laboratory exp. 9-12833  
 e pair formation, competition between decay and K-capture 9-6833  
<sup>210</sup>At pair formation, competition between decay and K-capture 9-6833  
<sup>180</sup>Os, neutron deficient, decay charact. 9-13196  
<sup>181</sup>Os, neutron deficient, decay charact. 9-13196  
<sup>111</sup>Sn  $\rightarrow$  <sup>111</sup>In, of <sup>111</sup>Sn leading to different excited levels of <sup>111</sup>In 9-19293  
<sup>182</sup>Os, neutron deficient, decay charact. 9-13196  
<sup>182</sup>Os, neutron deficient, decay charact. assoc. with positron group 9-13196  
<sup>113</sup>Ba, 222 keV  $\gamma$  transition obs. 9-15737  
<sup>133</sup>Ba  $\rightarrow$  <sup>133</sup>Cs 437 KeV level, (L+M+...)/K capture ratio obs. 9-14593  
<sup>133</sup>Ba  $\rightarrow$  <sup>133</sup>Cs  $\gamma$  spectra obs. 9-557  
<sup>127</sup>Xe, branching at 618 keV, and total transition energy 9-4755  
<sup>139</sup>Ce, K capture probability 9-4756  
<sup>65</sup>Cu 1114 MeV level from <sup>65</sup>Zn decay, L/K e capture ratio determ. 9-6826

**protection see Radiation protection****Radioactivity measurement**

- See also Dosimetry; Radiation monitoring; and the specific radiation, e.g. Gamma rays*  
 $\beta$ - $\gamma$  coincidence method of meas. carrier-containing decay rates 9-20758  
<sup>14</sup>C activity in <sup>14</sup>CO<sub>2</sub>, direct meas. in liq. scintillation counter 9-20764  
 air, fallout concentration from automatic dust monitor 9-8181  
 Al<sub>2</sub>O<sub>3</sub> film as support, patent 9-13163  
 blood plasma <sup>59</sup>Fe clearance meas. 9-15382  
 counting times 9-20755  
 disintegration rate of sources, coincidence resolving time, comparison methods 9-18039



**Radioactivity measurement continued**

- graphite structure resolution 9-3246
- radionuclide mixtures, short-lived, dead-time corrections 9-18076
- scintillography methods 9-15735
- soil, by  $\gamma$ -ray spectrometer calibration 9-18030
- standards of activity and list of isotopes available from Radiochemical Centre 9-18768
- time intervals in large numbers, standard freq. pulse storage method 9-20753
- X-rays from  $\beta$ -emitters, expt. conditions for detec. 9-15734
- $\beta$  sources, energy release evaluation by G-M counter 9-9003
- $^{14}\text{C}$  and  $^3\text{H}$  autoradiography, simultaneous, correlation with gas counting 9-21995
- $^{64}\text{Cu}$  in biological materials by n activation, simul.  $^{56}\text{Mn}$  meas. 9-18783
- $^3\text{H}$  and  $^{14}\text{C}$  autoradiography, simultaneous, correlation with gas counting 9-21995
- $^3\text{H}$  emission from Ti target, for  $^3\text{H}$  estimation of air by liq. scintillators 9-8138
- $^{56}\text{Mn}$  in biological materials by n activation, simul.  $^{64}\text{Cu}$  meas. 9-18783
- Rn/Th ratio in soil gas 9-1935

**apparatus**

- See also Partiele detectors*
- $\text{Al}_2\text{O}_3$  film as support, patent. 9-13163
- coincidence resolving time of disintegration rate of sources comparison method 9-18039
- foil transportation to counters using converted automatic slide projector 9-13206
- liquid scintillators, practical requirement 9-2579
- photographic films 9-2691
- Physics Exhibition, London, 1968, review 9-439
- proportional counter re-entrant well gas flow for solutions with radioactive nuclei 9-15733
- sample changer in radioactive meas., use of slide projector 9-22017
- scintillation counters, adapter for wells, patent 9-15692
- scintillation counting system for  $^{55,59}\text{Fe}$  in blood plasma 9-16634
- scintillation guard detectors, plastic, for low-activity  $\beta$  meas. 9-13168
- semiconductor counters 9-452
- $\text{Ge}(\text{Li})$  drifted diode, fallout meas. 9-550
- $\text{Ge}(\text{Li})$   $\gamma$ -ray detector, directional-correl. attenuation factors 9-16922
- $^{85}\text{Kr}$  and  $\text{Xe}$  charcoal traps, calibration method 9-2711
- Mn, cosmic dust particles, X-rays 9-16919
- Ni, cosmic dust particles, X-rays 9-16919

**Radioastronomy**

- See also Cosmic radiations, radiofrequency; Sun/radiation, radiofrequency*
- aerial for lunar occultation obs. at 81.5 MHz 9-20252
- cosmic microwave background radiation meas. technique 9-8223
- cosmic radiation, linear polarization meas. method, corrections 9-6155
- CP1133, upper limit to continuous emission at various pulse intensities 9-14230
- CP1919 pulsating source, optical search 9-21917
- deep sky survey at 408 MHz, Bologna cross-type radio telescope 9-8267
- extragalactic sources, number count formula derivation and use 9-12741
- fan beam obs. of 7 intense sources 9-14228
- flux density and spectra of 480 discrete sources, 5 GHz (6 cm) obs. 9-10503
- Galactic radio halo, existence 9-16557
- galaxies, three, small dia. radio and optical features, relationship 9-14192
- high freq. sources not listed in 4C catalogue, investigation 9-14231
- HII region, NGC281 and an unnamed nebula, obs. 9-10468
- intercontinental baseline interferometry 9-17627
- interferometers, two-element type, response to partially coherent field 9-14276
- interferometer of  $10^5$  wavelengths baseline, phase stable 9-12774
- interferometric meas. of celestial spectra 9-20251
- interplanetary scintillation investigation of solar wind plasma irregularities 9-20244
- ionosphere E level, sporadic irregularities, producing radio scintillations 9-8205
- Jupiter, radio emission data, artificial periodicities 9-2050
- l.f. Q meter for space vehicle antenna impedance characts. 9-4083
- lunar occultations at 81.5 MHz, aerial and expt. procedure 9-20252
- Mars, rad. obs. at 1.55 and 0.95 cm, rel. to average temp. 9-8278
- moon, r.f. spectra, influence of temp. depend. of mat. props. 9-2042
- NGC 1052, 178MHz flux density meas., 2-component source model suggestion 9-6113
- NGC 4278, 178MHz flux density meas., shape depend. on thermal absorption 9-6113
- NRAO 591/593 radio nebula, struct. and analysis 9-20164
- optical counterparts of 78 identified sources, accurate positions 9-12735
- Parkes obs. corrected by those at Molonglo 9-16598
- planet surface reflectivity to radar, allowance for scatt. 9-2085
- planetary nebulae at 408 MHz, thermal spectra obs. 9-15279
- polarization, high resolution measurements at 408 MHz of region around  $\mu^1=140^\circ$ ,  $\mu^2=+10^\circ$  9-21860
- polarization distrib. in radio sources, interferometric meas. 9-12734
- positions of 78 identified sources 9-12735
- pulsars, plasma parameters affecting radiation 9-6148
- pulsars, pulse structure 9-6147
- pulsating radio star, optical pulse obs. 9-21916
- radar obs. of under dense meteor trails for calc. of mass distrib. of meteoroids 9-15348
- radioheliograph 1 for instant complete one-dimens. pictures at 169 MHz 9-10561
- radiolines of interstellar NO molecules 9-17626
- scintillating sources, optical identification 9-21915
- solar corona radio-wave scatt., statistical ray anal. 9-15369
- solar emission, S-component, spectrum and diameter obs., 3.3 mm-21 cm wavelengths 9-14253
- solar radio emissions, book 9-8289
- space exploration fluxgate magnetometer sensor 9-4125
- spectral line interferometry with independent time standards at stations 845 km apart 9-6145
- telescope, NRAO 300 ft, beam shape and irregularities, influence on 21 cm line obs. 9-6197
- telescope, Onsala, Sweden, maser radiometer system 9-8296
- variation, possible, from NGC 1672 9-21849
- Venus, 8.6 mm brightness temp., phase depend. 9-12752
- v.h.f. fades, high latitude, rel. to auroral disturbance 9-2026
- Vulpecula pulsating source, pulse struct. obs. 9-18891

**Radioastronomy continued**

- H.r.f. recombination lines rest freq. 9-12732
- He r.f. recombination lines rest freq. 9-12732
- OH radio emission from infrared stars, obs. 9-21892

**Radiocarbon dating** *see Radioactive dating***Radiochemistry**

- See also Chemical analysis/radioactive; Chemical effects of radiations/ionizing radiations; Radioactive tracers*
- cytosine-5- $^3\text{H}$ , free radicals formed by decay of constituent T atom 9-1928
- enzyme assay, review 9-14148
- hot-atom reaction yield and energy distrib. 9-1915
- isotope exchange determ. in aqueous solns. 9-8053
- labelled compounds, stability and storage, review 9-14146
- manganese montmorillonite, Szilard-Chalmers reaction 9-10368
- nuclides of high specific alpha activity, cells and equipment for separation 9-14677
- purity of labelled compounds, review 9-14147
- reactions in nuclear reactors 9-21729
- standards of activity review and list of isotopes available from Radiochemical Centre 9-18768
- Szilard-Chalmers reaction in manganese montmorillonite 9-10368
- $^{80}\text{Br}$  nuclear isomers separation at metal surfaces 9-18769
- Cl trace determination in uranyl salts 9-8113
- $^{51}\text{Cr}$  species in n irradi.  $\text{Cr}(\text{III})$  tris-acetylacetonate, thermally annealed, obs. 9-16504
- $\text{H}^{14}\text{CN}$  meas. in HCN from  $\text{N}_2$ -methane fission fragment irradi. 9-18770
- $\text{NpF}_4$  fluorination with  $\text{F}_2$ ,  $\text{BrF}_3$ ,  $\text{BrF}_5$ , at  $250^\circ\text{C}$  400°C obs. 9-6026
- Ra-Ba iodate mixed cry., solid and liq. phase, Ra distrib. determ. by precipitation technique 9-18771
- Ra-Ba oxalate mixed cry., solid and liq. phase Ra distrib. determ. by precipitation technique 9-18771
- ThC reaction with  $\text{HNO}_3$ , obs. 9-6027
- UC reaction with  $\text{HNO}_3$ , obs. 9-6027
- UN reaction with  $\text{HNO}_3$ , obs. 9-6027
- Xe bromides, formation in  $\beta$ -decay of  $^{133}\text{I}$ Br $_2$ , Mossbauer effect 9-4016

**Radiography**

- See also Luminescent devices; X-ray tubes*
- autoradiography, bibliography 9-14144
- film, industrial, detail visibility 9-4546
- graphite structure resolution 9-3246
- of highly active samples using special film 9-2691
- neutron, and appls., review 9-17673
- neutron, display of results by direct viewing of scintillating plate 9-10951
- neutron scatter factors, exptl. results for steel, U and Pb 9-2801
- radioisotope camera, theory of pinhole collimator 9-11428
- stereo-, using holographic techniques 9-14440
- three-dimensional X-ray holography 9-12781
- whole-body, stable, low-background counter, uniform detection geom. 9-20260
- X and electron irradi., 35 MeV linear acceleration 9-2093
- X-ray fluorescent screens, random noise 9-12817
- x-ray generator, diagnostic meas. of peak voltage 9-4143
- $\alpha$  autoradiography, improved resolution for Pu distrib. by use of thin absorber 9-19374
- $\alpha$  track autoradiography of submicron aerosol particles with electron microscope 9-15693
- $^{14}\text{C}$  and  $^3\text{H}$  autoradiography, simultaneous, correlation with gas counting 9-21995
- $^3\text{H}$  and  $^{14}\text{C}$  autoradiography, simultaneous, correlation with gas counting 9-21995

**Radiolysis** *see Chemical effects of radiations/ionizing radiations***Radiometer gauges** *see Vacuum gauges***Radiosondes** *see Meteorological instruments***Radiosources** *see Cosmic radiations, radiofrequency***Radiostars** *see Cosmic radiations, radiofrequency; Stars***Radiotelescopes** *see Radioastronomy***Radiowave propagation** *see Electromagnetic wave propagation***Radiowave spectra** *see Nuclear magnetic resonance and relaxation; Paramagnetic resonance and relaxation; Spectra***Radium**

- concentration in Vosges rocks by gamma spectrometry 9-20080
- $^{224}\text{Ra}$  determ. of purity of samples used on patients 10 years ago from patent monitoring 9-12783

**Radium compounds**

- Ra-Ba iodate mixed cry., solid and liq. phase, Ra distrib. determ. by precipitation technique 9-18771
- Ra-Ba oxalate mixed cry., solid and liq. phase, Ra distrib. determ. by precipitation technique 9-18771
- RaD-Be n source, He diffusion cloud chamber obs. of energy spectrum 9-8907

**Radium emanation** *see Radon***Radon**

- adsorption on polystyrene aerosols prop. to aerosol surface area 9-7287
- daughter products, short lived, conc. in atm.,  $\alpha$ -spectrometry method 9-20092
- $^{222}\text{Rn}$ , atmospheric, effect on personnel dosimeters 9-12782
- Rn/Th ratio in soil gas, meas. 9-1935

**Rain**

- See also Condensation; Snow*
- pluviometry of continuous emission effect of  $\text{AgI}$  nuclei 9-1937
- radiowave dispersion and weakening for rain of various origins 9-6081
- effect on underwater noise level 9-12939

**Raman spectra** *see Scattering/light, Raman spectra***Ramsauer effect** *see Electron beams; Electrons/absorption; Energy of particles***Random functions** *see Random processes***Random processes**

- See also Brownian motion; Fluctuations; Statistical analysis*
- electron motion in an electric field 9-4243
- error, explicit calc. for unfolded spectra obtained by foil activation 9-4241
- Markov random flight soln., e energy distrib. in gas discharge 9-5080
- matrix, random, probability distrib. 9-4242
- off-lattice self-avoiding random walks, geometric props. 9-12891
- optical, in fundamental optical systems, math. description 9-14444
- Poisson compound processes, props. and applic 9-20335

**Random processes continued**

- stochastic aspects of interplanetary mag. lines of force 9-21952  
 stochastic linear, passive transforms 9-6326  
 stochastic model of interstellar mag. field 9-20150  
 vibration, first-passage problem, series soln. 9-17731

**Range of particles** *see Energy loss of particles***Rare earth compounds**

- See also The compounds of the individual metals; Ferrites*  
 chlorides, electronic Raman eff. 9-12356  
 cobalt intermetallic cpds., permanent magnets 9-13963  
 cobalt-rare earth intermetallic cpds., mag. resonance at 9.3 GHz 9-14100  
 concentration and stability const. determ., spectrographic method 9-21738  
 conductivity character 9-16226  
 equiatomic rare-earth-Al cpds., n.m.r. and susceptibility 9-3969  
 ethyl sulphates, zero-field splitting of  $Gd^{3+}$  9-1859  
 gallates, paramagnetic with garnet structure, magnetostriction, 4.2-60°K 9-21571  
 garnets: rare-earth, electronic and vibrational Raman eff. obs. 9-12434  
 germanates, paramagnetic with garnet structure, magnetostriction, 4.2-60°K 9-21571  
 germanides, conductivity, change in character with temp. 9-12091  
 with group V anions, electronic and magnetic props., review 9-18598  
 halides, crystal field stabilization energy rel. to spin-orbital interaction 9-21453  
 halides, e.p.r. of pairs of coupled ions for energy transport mechanisms 9-7697  
 hexaborides, mag. ordering correl. with electron struct. 9-19943  
 interband mixing, exptl. evidence from Knight shift and susceptibilities meas. 9-14116  
 ions, quenching interactions in Na rare-earth tungstates 9-16436  
 ions, trivalent, in Yb<sup>3+</sup> cryst., effect of cubic cryst. field on mag. props. 9-16327  
 i.r. quantum counter/image converter, five-level, 1-2  $\mu$  9-10927  
 lanthanide aluminides,  $Ln_2Ln^{3+}_2Al_3$ , Laves phase cpds., mag. props. 9-12247  
 Lanthanide metals with Ni, 2:17 intermetallic cpds. magnetic props. 9-10091  
 lanthanides, trifluorides, melt growth 9-9648  
 magnesium nitrates, high resolution of crystal field lines in far i.r. 9-5862  
 manganites, perovskite-type, crystal and mag. structures 9-19717  
 orthoferrites, antiferromagnetism vector, reorientation 9-15159  
 orthoferrites, complex polar Kerr effect, u.v. meas. 9-1738  
 orthoferrites, metamagnetic props. 9-16383  
 orthoferrites, weak field magnetization 9-19969  
 oxides:  $Eu^{3+}$ , luminescence and emission spectra, crystal field interpretation 9-10205  
 oxides, colouration of glasses, obs. 9-3856  
 oxides as  $UO_2$  additives rel. to high temp. stability in H atm. 9-3979  
 oxyfl. fluorides, absorpt. spectra rel. to struct., 220-5000  $cm^{-1}$  9-16411  
 oxysulphates,  $Eu^{3+}$ -activated, prep. and luminescence 9-21647  
 sulphates,  $Eu^{3+}$ -activated, prep. and luminescence 9-21647  
 sulphides,  $Eu^{3+}$ -activated, prep. and luminescence 9-21647  
 trichloride crystals, i.r. fluorenc, and exciton migration rates 9-10243  
 vanadates, activated by  $Sm^{3+}$ ,  $Eu^{3+}$  and  $Dy^{3+}$ , luminescence spectra 9-20003  
 Fe-rare earth intermetallics, cubic Laves, Mossbauer study of hyperfine fields 9-7958  
 $Ln_2Me^{4+}Me^{3+}O_8$ , crystal struct., and fluorenc., ( $Ln=La, Gd, Y, Lu, Me^{4+}=Si, Ge, Ti, Me^{3+}=Mo, W$ ) 9-13638  
 $Pd_2O_4$ , ternary oxides, ( $A_2Pd_2O_7$ , A=rare earth), pyrochlore struct., prep. at 3 kbar 9-5274  
 $Pt_2O_4$ , ternary oxides, ( $A_2Pt_2O_7$ , A=rare earth), pyrochlore struct., prep. at 3 kbar 9-5274  
 $R_{1/2}Na_{1/2}MoO_4$ , R=Gd, Tb, Dy, Ho, Er, Tm, and Yb, paramagnetic susceptibility 9-3779  
 $T_2Al_2$  (T=rare earth or metal), mag. props. 9-1646  
 $T_2Ni$  (T=rare earth or Y), mag. props. 9-3775

**Rare earth metals***See also The individual metals*

- electroluminescence of metal mols. in II-VI compounds, by e impact 9-5975  
 galvanomagnetic effects below Neel temp. 9-1709  
 in group II-VI compounds, e.p.r. 9-1854  
 ions, indirect exchange interactions 9-1715  
 ions in aq. soln., nonradiative energy transfer 9-9524  
 ions in crystals,  $4f^n-4f^{n-1}5d$  spectra 9-12371  
 magnetic anisotropy and exchange interactions 9-1645  
 magnetic structure and form factor meas. by n. diff. 9-13971  
 positron-electron ranges 9-12036  
 soda lime glass: rare earths, visible fluorescence 9-3926  
 spectra, extra lines and covalency 9-19982  
 trivalent aquo ions, electronic energy levels 9-16017  
 trivalent ions, i.r. lifetimes in trichloride crystals. 9-10243  
 trivalent ions in single crystals, ground-state modulation using optical double resonance 9-3846  
 u.s. attenuation in helical spin state, inc. below Neel temp. 9-1379  
 X-ray absorpt. coeff. determ. for 4d e, Niv<sub>v</sub> edge studied, 50-500 MeV 9-10228  
 in  $GdCl_3$ , magnetic eff. 9-12270  
 in  $Gd_2O_3$ , by X-ray luminescence analysis 9-16514  
 in  $SrTiO_3$ , dielectric relaxation 9-3699  
 in  $Y_2O_3$ , analysis by X-ray excited fluorosc. spectra 9-16514

**Rare gases** *see Inert gases***Rayleigh scattering** *see Scattering/light***Rayleigh waves** *see Elastic waves; Seismic waves***Re(h)binder effect** *see Mechanical strength; Surface phenomena***Reaction kinetics***See also Catalysis; Chemical reactions; Exchanges, Chemical; Explosions*

- acetonitrile, ion-mol. reactions, ion cyclotron reson. 9-20034  
 alkali atom beams, with polyhalide mols. 9-9307  
 alkali atom beams, with polyhalide mols. 9-7096  
 alkali-halogens, harpooning 9-1888  
 alkyl fluorides, activated, decomposition obs. 9-10331  
 analog simulation, expt. for college students 9-17679  
 aromatic hydrocarbons, cation-anion annihilation react. in electrochemilum. 9-14701  
 Breit-Wigner resonances, effects 9-3985

**Reaction kinetics continued**

- chloroethane- $d_0$  and - $d_4$  chem. activated, isotope effects in unimolec. reactions 9-3990  
 classical mech. of reactions in two dims. 9-8056  
 competitive unimolec. decomp. of chem. activated radicals 9-1890  
 condensation polymerization 9-2923  
 condensed phases 9-21679  
 1,2-dichloroethane- $d_0$  and - $d_4$  chem. activated, isotope effects in unimolec. reactions 9-3990  
 diffusion-controlled reactions, statistical mech. 9-8057  
 diffusion-controlled reactions in porous media 9-1904  
 droplet, liq. fuel, burning in oxidising atm., variable prop. effs. 9-21688  
 droplet in small Peclet number flow, decomposition burning, soln. 9-21687  
 elastic scatt. in reactive systems 9-1894  
 exothermic, 'nearest resonance' tech. for interchange reaction rate calc. 9-6000  
 gas, thermal, monoenergetic atom collisions 9-12524  
 gas reactions in mixtures with inert gases 9-1893  
 graphite, ZTA, reaction rates with gases at 1400° to 3000°K 9-8064  
 graphite pyrolytic B, activation energies and graphitization 9-8059  
 Graphon, activated, chemisorption of  $O_2$  rel. to temp. 9-8079  
 Graphon, cleaned activated surface, chemisorption of  $O_2$  from 25 to 400°C 9-10335  
 heterogeneous catalytic gas reactions, mass transfer factors calc. 9-21690  
 hexafluoroacetone photolysis, rate constants for primary process 9-1923  
 hot atom reaction yield and energy distrib. 9-1915  
 hydration of negative ions in gas phase 9-1896  
 instabilities, time evolution 9-16475  
 ion exchangers, diff. and reaction coupling 9-17510  
 ion-molecule, in flowing afterglow system 9-3983  
 ion-molecule, venetian blind particle multiplier appl. 9-1886  
 ion-molecule reactions, spectator mechanism 9-10314  
 ion-molecule reactions in 50MHz discharge 9-9350  
 ketene with atomic H and O 9-1899  
 light scatt. from reacting mixtures 9-5999  
 low-kinetic energy collision-induced dissociation 9-9406  
 mass spectrometry of v. fast reactions 9-10334  
 metal oxidation, rel. to electronic and ionic diffusion in large surface charge and space-charge fields 9-9620  
 methyl iodide, reaction with electronically excited I atoms 9-1924  
 natural collision coords. 9-5998  
 nonisothermal measurements, calc. methods for reaction order, activation energy and frequency factor determ. 9-21682  
 potassium dipicrylamine, aqueous system, and crystallization in condensed phases 9-21679  
 propyl rupture in chem. activated radicals 9-1890  
 rate const. from transient conc. profile, by mass spectrometry 9-16477  
 reactive collisions, perturbed Morse oscillator calc. 9-16479  
 reactive coperturbed Morse oscillator approx. 9-10313  
 reactive scattering, phenomenological anal. 9-10315  
 recombination-dissoc., nonequilibrium, effects 9-2919  
 resonance tunnelling reactions 9-6001  
 rhodium thiocyanate complexes and exchanges, activation energy determ. 9-8052  
 sea water-LiH react., high-pressure, gas prod., obs. 9-20041  
 solid gas, model compared with diffusional model 9-21680  
 stochastically distrib. second-order reactants decay, third-order closure 9-21683  
 thermomechanical theory of reacting mixtures 9-3984  
 vacancy-interstitial in f.c.c. lattice, diffusion-controlled, unified formalism 9-1201  
 B pyrolytic graphite, activation energies and graphitization 9-8059  
 C<sup>+</sup> with N<sub>2</sub> and O<sub>2</sub> 9-14122  
 C surface, reversible exchange of O between CO<sub>2</sub> and CO 9-8051  
 Ca, oxidation 9-10340  
 Cr<sub>2</sub>O<sub>3</sub> and MgO, effect of processing parameters 9-3986  
 D+O<sub>2</sub>, rate const., activation energies and branching step kinetics 9-14129  
 Fe-Cr alloys, oxidation 9-20044  
 Fe<sub>2</sub>O<sub>3</sub>, interaction with MgO 9-3988  
 H<sub>2</sub>-H<sub>2</sub> bimolec. exchange reaction 9-770  
 H isotope effects, test for transition-state models 9-12525  
 H olefins, Lyman- $\alpha$  re-emission meas., rate const. 9-12527  
<sup>3</sup>H (recoil) with n-butane, n-pentane and neo-pentane, kinetic theory calc., reactivity integral 9-21684  
 H<sub>2</sub>, atom-formation rates behind shock wave, effect of added O<sub>2</sub> 9-1902  
 H<sub>2</sub> + inert gases, photoionization ion-mol. reactions 9-17132  
 H<sub>2</sub> + DI + 2I + HD, energy requirements 9-8068  
 H<sub>2</sub>S, homogeneous reaction with D<sub>2</sub> 9-3981  
 H+Br<sub>2</sub>→HBr+Br, perturbed Morse oscillator calc. 9-16479  
 H+Br<sub>2</sub>→HBr+Br, quantum-mech. calc. 9-10313  
 H+Cl<sub>2</sub> explosion laser 9-2374  
 H+H<sub>2</sub>, rate const., correl. with theoretical H<sub>3</sub> potential surface 9-10311  
 H+H<sub>2</sub>, two-dimensional, rot. energy calc. 9-10318  
 H+H+M→H<sub>2</sub>+M, thermolecular recomb. kinetics, resonance theory 9-17005  
 H<sub>2</sub>+I<sub>2</sub>, low-temp. mechanism 9-10320  
 H<sub>2</sub>+I<sub>2</sub>, mechanism 9-10321  
 H<sub>2</sub>+I<sub>2</sub>, transition state 9-10319  
 H+O<sub>2</sub>, rate const., activation energies and branching step kinetics 9-14129  
 K+Br<sub>2</sub>, molec. beams, quasiclassical trajectory calc. 9-10323  
 Li crossed-beams with Cl<sub>2</sub>, ICl, Br<sub>2</sub>, SnCl<sub>4</sub> and PCl<sub>5</sub>, mass effects 9-17512  
 LiH-sea water react., high-pressure, gas prod., obs. 9-20041  
 MgO, interaction with Fe<sub>2</sub>O<sub>3</sub> 9-3988  
 MgO and Cr<sub>2</sub>O<sub>3</sub>, effect of processing parameters 9-3986  
 N<sub>2</sub>H<sub>4</sub> decomp. in glow discharge 9-14125  
 N<sub>2</sub><sup>+</sup> reaction with H<sub>2</sub>, D<sub>2</sub>, and HD 9-17513  
 NiF<sub>4</sub>, thermal dissociation in shock waves 9-1903  
 NH<sub>4</sub>ClO<sub>4</sub>, thermal decomp., effects of X- and  $\gamma$ -irrad. 9-4011  
 NH<sub>4</sub>ClO<sub>4</sub>, thermal decomp., effects of X- and  $\gamma$ -irrad. 9-4012  
 NO-catalysed recombination of radicals in premixed flames 9-14121  
 NO+O chemiluminesc. in expanding flow, effect of molec. clusters 9-20031  
 N<sub>2</sub><sup>+</sup>+D<sub>2</sub>, product energy and ang. distrib. obs. 2.3 to 11.6 eV 9-10325  
 N<sub>2</sub><sup>+</sup>+H<sub>2</sub>, product energy and ang. distrib. obs. 2.3 to 11.6 eV 9-10325  
 N<sub>2</sub><sup>+</sup>+HD, product energy and ang. distrib. obs. 2.3 to 11.6 eV 9-10325  
 N+NO→N<sub>2</sub>+O fast atom reactions, use of time-of-flight mass spectrometer 9-21681



**Reaction kinetics** continued

- O<sub>2</sub>-low-energy reactions with H<sub>2</sub> and D<sub>2</sub> 9-9401
- O<sub>2</sub> atoms, molecules, ozone, review of kinetics 9-15212
- O<sub>2</sub> atomization on Pt 9-1908
- O(<sup>3</sup>P)+CS<sub>2</sub>→SO+CS<sub>2</sub>, product vibr. energy, expt. and computation 9-10327
- O+NO<sub>2</sub>→NO+O<sub>2</sub> 9-21681
- (Pb, Sr)-(Ti, Zr)O<sub>3</sub>, solid solution formation 9-1892
- PbZrO<sub>3</sub>-PbTiO<sub>3</sub> in PbO-ZrO<sub>2</sub>-TiO<sub>2</sub>-Nb<sub>2</sub>O<sub>5</sub> system 9-8098
- Re, attack by O and O<sub>2</sub> at high temp. 9-17529
- SO<sub>2</sub>, electronically excited, formation on surfaces 9-6009
- SiO<sub>2</sub> colloids, coagulation with hydrolyzed Al(III), rate determining step 9-9570
- UC, thermal dissoc. 9-1897
- U(IV)-U(VI) electron exchange in HCl 9-6007
- Y Fe garnet, Gd<sup>3+</sup>, Al<sup>3+</sup>, and Cr<sup>3+</sup>, pressure sensing 9-1688
- ZrCl<sub>4</sub> with Zr, obs. at various temps. 9-1898

**Reactors** *see Nuclear reactors, fission; Nuclear reactors, fusion***Recombination** *see Ions, recombination; Semiconductors***Recombination radiation** *see Luminescence***Recording**

- 3D, use of photographic emulsion 9-20569
- digital, i.r. gas phase intensities 9-8670
- erasable trace methods reviewed 9-12801
- hydrometeorological events, digital multichannel instrument 9-16527
- indicator for recording Hg manometer levels at regular intervals 9-6227
- intensity-modulated syst., for u.s. diagnosis, eval. and differences of records 9-6205
- magnetic tape, pulse stat. fluct. and stochastic approach information capacity meas. 9-4352
- magnetization vs. temp., continuous, apparatus for hysteresis loop tracer 9-14286
- microwave spectrum, frequency markers 9-2283
- scintillation camera output on analogue mag. tape 9-10948
- small modulated light signals in large uniform background 9-10922
- sound, from flames, photometric 9-16734
- sounds prod. in nest of oriental hornet, origin, phys. parameters and significance 9-8512
- sparks, in Cartesian coordinates, external acoustic pickups 9-462
- underwater sounds of migrating gray whales 9-4350
- CO<sub>2</sub> laser beam profile using foamed polystyrene 9-13010

**Recrystallization (metals)** *see Heat treatment***Rectifiers**

- See also Electron tubes; Semiconducting devices*
- controllable and non-controllable, efficiency of 9-13897
- diodes, nonlinearity and noise, thermodynamic relationship rel. to rectification mechanism 9-12165
- flame on electron flow between electrodes 9-226
- metal-GaAs point contact, rectifying barrier structure 9-12163
- Au-GaAs surface barrier junctions, elec. props. 9-10009
- Hg arc, characts. rel. to 'equiv. press.' use, obs. 9-13473
- ZnS:Cu electroluminescent capacitors, current rectification 9-15195

**Red giants** *see Stars***Red shifts** *see Astronomical spectra; Cosmology; Relativity/general***Reflectance** *see Reflectivity***Reflection**

- See also Neutrons/reflection; X-ray reflection*
- antireflection coatings of small optical elements, cathode sputtering methods 9-13049
- electrons, inelastic, calc. at moderate energies 9-1410
- glare impression, influence of geometry and high luminance light 9-12798
- i.r. reflectography, for examination of paintings 9-2250
- seismic waves in laminated medium with arbitrary depth distrib. 9-20076

**acoustic waves**

- See also Echo; Reverberation*
- anechoic room, averaged press. refl. coeff. meas. 9-2231
- delayed reflections, statistics 9-2216
- immersed spheres and cylinders, hollow, percussion response 9-6385
- multilayered ocean bottom, sediment sound-speed obs. 9-2215
- phase shift at turning point 9-2210
- piezoelectric plate, acoustic transmission coeffs. 9-4321
- piezoelectric semiconductor, from acoustoelec. domains 9-18559
- pipe, open-ended, circular, ray method 9-2213
- pulse response of room, reln. with diffusivity of stationary field 9-4327
- ray transmission in underwater acoustic duct with curved bottom 9-2214
- at rough liquid-solid interface, of plane harmonic wave 9-4328
- on rough surface, generalised boundary condition for multiple scatter 9-10731
- in stratified medium with overlying fluid, phase shifts and pulse deform. 9-2209
- at water-viscoelastic medium boundary, coeff. calc. 9-16731
- CdS, piezoelectric, from acoustoelec. domains 9-18559

**acoustic waves, ultrasonic**

- finite amplitude wave distorted by refl. computer model 9-2212
- by magnetized metals and ferromag. dielectrics, plane of polarization rot. and ellipticity appearance 9-3525
- phase shift, finite amplitude waves, various interfaces 9-2211

**electromagnetic waves**

- diffuse, by random rough surface 9-12957
- diffuse reflection from a plane-parallel atmosphere, method of doubling thin layers 9-15338
- enus, radar obs., variations 9-10529
- from plasma, magnetoactive, inclined incidence 9-879
- Goos-Hanchen shift by Poynting vector calc.: prediction of shift for elliptically polarized incident wave 9-12958
- insulator matt surface radiation scatt. matrix in diffraction approx. 9-8548
- interface, diffused, refl. and transmission coeffs. 9-10771
- by ionosphere F region, oblique 9-21817
- ionospheric, specular component, statistical variations 9-10426
- ionospherically reflected radio waves, horizon focusing effects 9-4392
- lateral shift of circularly polarised incident beam, theor. prediction 9-16751
- materials characts. meas. for varying thickness, e.m. coeffs. 9-12953
- metallic electron plasmas 9-16395
- microwave, e density meas. in shock-wave plasma 9-11585
- multilayer absorbing system, soft X-ray region 9-10772
- plane, from conducting surface with moving uniaxial sheath 9-185

**Reflection continued****electromagnetic waves** continued

- in plasma, coeffs. before and after cut-off, formulae assuming trapezoidal electron density distrib. 9-11560
- by plasma, moving compressible, solns. for E and H waves 9-11559
- at plasma, moving layer 9-21070
- plasma diagnostics, relativistic effects 9-17115
- pulse signal, from plane boundary of absorbing medium 9-4391
- radio waves, from shock waves prod. by explosion region 9-156
- semiconductor with carriers inelastically scattered on optical phonons, h.f. effects 9-13879
- semiconductor with carriers inelastically scattered on optical phonons, h.f. effects 9-1528
- signals oblique reflection from ionosphere, statistical model 9-4390
- surface of uniaxial crystals with electron plasma 9-21602
- synchrotron polarization Stokes params. 9-2276

**light**

- See also Films, solid/optical properties; Mirrors*
- absorbing media, generalized laws 9-20544
- antireflection coatings, broadband, refractive indices 9-14028
- Bragg, of laser light in Q-switching liquid 9-8629
- colour changes with temp., cell for obs. 9-20559
- dielectric film, inhomogeneous, theory 9-15542
- dielectric layers, dispersion of phase shift, use of Kramers-Kronig relns. 9-1734
- dihedral mirror, optical path length rel. to rot. 9-4502
- dihedral mirror, image locations and optical path length rel. to rot. 9-4503
- dispersive semi-infinite medium, of diffuse light, coeffs. 9-17887
- film, thin, and transmission formulae rel. to refractive index 9-12333
- focus of reflected image, reciprocal optical system for meas. 9-10894
- group II-IV cpds., method for crystal orientation 9-18408
- Helmholtz eqn., first two terms in asymptotic series 9-13041
- immersion and echelon grating, analogy 9-13053
- InAs, spectra 9-3877
- incidence angle meas. using prism-substrate 9-10888
- interfacial, diffuse illumination and reflectance 9-19162
- i.r., Kramers-Kronig phase angle partitioning, systematic error disclosure 9-10897
- i.r. materials, bibliography 9-12332
- i.r. materials, spectra, 2-50  $\mu$  9-12366
- laser, coefficient diminution for solids 9-21603
- laser beam, by KDP crystal 9-10854
- multilayer surfaces, minimization of apparent curvature 9-4511
- from natural surfaces (soil, desert sand, white sand and water), polarization features 9-1939
- optical storage effect in mixed liquid crystals, electric-field controlled 9-3099
- oxide films on Cu, ellipsometric meas. 9-16043
- parabolic reflector wavefronts for off-focal source 9-2400
- prisms, effect of linear glass heterogeneity on ray path 9-10889
- sky radiation, by ground, spectral distribution meas. 9-20091
- in Sofica and Brice-Phoenix light scatt. photometers, comparison rel. to errors 9-14832
- solids structure determ. 9-13564
- steel galvanized, reflectances of oxide films of variable roughness and thickness 9-19985
- superconducting films specular and diffuse 9-7767
- total internal, transient filter processes calc. 9-2412
- Venus, albedo, depend. on u.v. wavelength 9-21946
- Ag-Mn(Pd), rel. to resonant states 9-7937
- As<sub>2</sub>(Se)<sub>3</sub>, spectra during transition from crystalline to glassy state 9-10192
- Au-Pd, rel. to resonant states 9-7937
- Au, modulation of attenuated total reflection spectrum 9-5900
- CaBe, meas. rel. to refractive index, extinction coeff. and absorpt. coeff. 9-5866
- Cu-Mn(Pd), rel. to resonant states 9-7937
- CuCl, excitonic spectrum, Zeeman eff., low temp. 9-14044
- CuS layers, i.r., rel. to elec. cond. and stoichiometry 9-1736
- Fe<sub>2</sub>O<sub>4</sub>, coeff. rel. to wavelength and elec. cond. 9-10171
- n-GaAs, impurities effect, 297° to 4°K 9-21621
- GaAs spectra, modulation by surface field obs. 9-10172
- n-GaSb, i.r., rel. to electron masses 9-3852
- (93.5-6.5at%)Ge-(7.6-92.4at%)Si, electroluminescence spectra 9-14045
- Ge, multiple total internal, rel. to surface investig. 9-21622
- Ge, polarized light meas., 310 and 550 Å 9-12334
- Ge, reflectance, e beam modulated for band structure studies 9-9989
- HgCr<sub>2</sub>S<sub>4</sub>, ferromagnetic, diffuse reflection spectrum 9-1781
- InAs, magneto plasma-phonon interaction from Kramers-Kronig analysis of reflection spectra 9-12363
- KMgF<sub>3</sub>-KNiF<sub>3</sub> mixed crystals, i.r. data in lattice vibr. determ. 9-13789
- Mg Mn ferrite, coeff. rel. to wavelength and elec. cond. 9-10171
- Ni Fe ferrite, coeff. rel. to wavelength and elec. cond. 9-10171
- Ni Zn Fe ferrite, coeff. rel. to wavelength and elec. cond. 9-10171
- RbI magneto reflection dichroism, Zeeman effect irregularity 9-7949
- Sb<sub>2</sub>S<sub>3</sub>, spectra rel. to direct and indirect transitions 9-3895
- TiCl<sub>3</sub>, spectra in far i.r. 9-3879
- TiSe, spectra, interpretation using electron energy spectra and chemical binding model 9-5903
- TiTe<sub>2</sub>, semiconducting, meas. rel. to optical energy gap calc. 9-14046
- V<sub>2</sub>Ps, spectra, for band structure determ. 9-19984
- VO<sub>2</sub>, spectra, for band structure determ. 9-19984
- Zn, reflectances of oxide films of variable roughness and thickness 9-19985
- ZnSnP<sub>2</sub>, chalcopyrites and sphalerites, spectra rel. to band structure 9-5931
- ZnSnP<sub>2</sub>, i.r. spectra and optical constants of chalcopyrite and sphalerite structures 9-5904

**reflectivity**

- See also Diffusion/light; Films, solid/optical properties; Optical constants*
- carbon blacks, tabulated values, book 9-12324
- clouds, high altitude, models, 2.5-3.5  $\mu$  9-12582
- diffuse reflectance, simple apparatus for meas. at low temps. 9-4525
- ebonite, diminution for laser radiation 9-21603
- elimination of, solid laser material, use of thin dielectric films 9-10864
- graphite, spectral reflectance, high temp. 9-20560
- Mars, surface particle size effects on albedo 9-18911
- metal blacks, tabulated values, book 9-12324
- metallic electron plasmas 9-16395
- near-infrared, laboratory ice clouds 9-12584

**reflectivity** continued

- planet surface, to radar, allowance for scatt. 9-2085
- quartz, u.v. spectrum, applic. of valence bond approximation to analysis 9-5266
- $\alpha$ -quartz, Z-cut, vacuum u.v. reflectance rel. to temp. 9-3853
- reflectometer, single beam, for spectrographic meas. 9-10942
- semiconductor, plasma edge reflection meas. rel. to carrier conc., effective mass, scattering time and conductivity determ. 9-7792
- semiconductors, enhancement by Q-switched ruby lasers 9-15163
- semiconductors, thermoreflectance 9-14041
- Ag, near plasma edge by derivative optical spectroscopy 9-1758
- Ag<sub>2</sub>SnFeS<sub>4</sub>, hocrartite 9-19705
- Al diminution for laser radiation 9-21603
- As<sub>2</sub>S<sub>3</sub> semiconductor film Ag system, sensitivity depend. on thickness of semicond. layer 9-1735
- Au-Fe dilute alloys, of light, band gap var. 9-21604
- BaSO<sub>4</sub> optical sphere paint 9-5875
- BiTiO<sub>3</sub>, reflectance spectra obs. of grain boundary contribution to dielec. props. 9-3707
- Bi<sub>2</sub>Te<sub>3</sub> molten, photon, energy 0.5-4 eV rel. to electronic struct. 9-16002
- C diminution for laser radiation 9-21603
- CdAs<sub>2</sub>, tetragonal, spectra 9-19983
- CdO, single and polycrystals, up to 13 eV 9-3886
- CdP, tetragonal, spectra 9-19983
- CdSb, optical spectra, 300° and 77°K 9-14042
- CdSb and CdTe molten, photon, energy 0.5-4 eV, rel. to electronic struct. 9-16002
- Cd<sub>1-x</sub>Se<sub>x</sub>, u.v. spectra at 90°K 9-10187
- Cu diminution for laser radiation 9-21603
- GaAs:Te, i.r. spectrum rel. to longitudinal-optical-phonon-plasmon coupling 9-21615
- n-InAs, coupled collective cyclotron excitation-longitudinal optical phonon modes, reflectivity meas. 9-12151
- InSb, spectrum, rel. to exciton effects at hyperbolic crit. pts. 9-5901
- LaCl<sub>3</sub>, restrahlen data rel. to location of poles and zeros of dielec. dispersion 9-5876
- NaNO<sub>3</sub>, i.r., rel. to temp. dependent vibrational modes 9-5902
- PrCl<sub>3</sub>, restrahlen data rel. to location of poles and zeros of dielec. dispersion 9-5876
- Sb<sub>2</sub>S<sub>3</sub>, spectra, polarization eff. 9-18700
- Sb<sub>2</sub>Se<sub>3</sub>, spectra, polarization eff. 9-18700
- Se amorphous, in vacuum ultraviolet 9-12335
- Se<sub>1-x</sub>Te<sub>x</sub>, spectra, i.r. active lattice bands 9-12365
- Si, thermoreflectance spectrum, 3-6 eV region 9-10189
- Sn diminution for laser radiation 9-21603
- SrF<sub>2</sub>, u.v. spectrum, from (111) planes 9-1761
- Te, spectrum in fundamental absorpt. region, 10-300°K 9-21630
- ThO<sub>2</sub> spectral reflectance, high temp. 9-20560
- TiO<sub>2</sub>, role of P<sub>2</sub>O<sub>5</sub> 9-3854
- W spectral reflectance, high temp. 9-20560
- ZnAs<sub>2</sub>, tetragonal, spectra 9-19983
- ZnP<sub>2</sub>, tetragonal and monoclinic, spectra 9-19983
- ZnSb, optical spectra, 300° and 77°K 9-14042
- ZnSe, data rel. to freq., electronic band structure computation 9-18701

**Refraction**

- ocean waves, grid and projection problems in numerical calc. 9-21754
- seismic waves, profile in Coral Sea Basin 9-10375

**acoustic waves**

- See also Dispersion/acoustic*
- lenses, Luneburg, variable density, theory 9-19064
- lenses, perfect focusing spherically symm., characts. 9-19063

**acoustic waves, ultrasonic**

- at interfaces with attenuation, wave models 9-20431

**electromagnetic waves**

- See also Electromagnetic wave propagation*
- atmosphere lowest km., over India, seasonal variations 9-4060
- ionosphere, for various conditions 9-21799

**refraction****light**

- See also Double refraction*
- absorbing media, generalized laws 9-20544
- beams, large-scale self-trapping in paraxial ray approx., variance of self-focusing beam 9-10895
- deflection of ray by plane-parallel glass plate with radially nonuniform steady temperature distribution 9-13042
- general-relativity bending round mass pt., radial 'free-fall' thought expts., validity 9-58
- in Moire interferometry with embedded grids 9-19164
- n dielectric films with different optical properties, polarized light, theory 9-7939
- ray tracing in inhomogeneous media 9-10886

**Refractive index**

- in accelerated systems of reference 9-16764
- atmospheric waves, gradient rel. structure const. for various types of waves 9-1874
- e.m. waves in stationary field 9-184
- gas mixtures, rel. to long range atom-mol. interactions 9-9304
- glasses, K108, LK6 and T411 at liquid hydrogen temperature 9-14026
- optical glass, mean reference index line 9-14447
- particles, subnanogram, determ. 9-12330
- solids, gradual variation using multilayer anti-reflection coatings 9-5874
- X-rays, rel. to anomalous dispersion meas. 9-1729
- GeO<sub>2</sub> glass, spectrum of relaxation times 9-3851
- NaNO<sub>3</sub> and polarizability, anisotropic, of NO<sub>2</sub> 9-3855
- Nb<sub>2</sub>O<sub>7</sub>Cl<sub>3</sub> and dielec. constants for principal crystal axes 9-10030
- SrTiO<sub>3</sub> transition metal, photochromic change 9-10170
- Xc fluid isochores, for temp., density depend. of molar polarization 9-4939

**light**

- See also Dispersions, optical; Double refraction; Optical constants*
- complex, behaviour in isotropic plasma 9-15408
- dispersion, anomalous, meas. method for absorbing body 9-7934
- effective, of interference filter, as performance criterion 9-8664
- film, thin, rel. to reflection and transmission formulae 9-12333
- Ga films, liquid 9-3192
- glass, silicate and borosilicate, rel. to chem. composition over wide temp. and wavelength range 9-14027
- interferometric meas. 9-12181
- i.r. materials, bibliography 9-12332

**Refractive index** continued**light** continued

- isopentane, high-pressure effect 9-5170
- liquids, laser-illuminated, anomalies caused by self-focussing and electrostriction 9-9511
- mesitylene, high-pressure effect 9-5170
- optically pumped medium with near-reson. r.f. irradi. 9-2407
- ruby: Cr<sub>2</sub>O<sub>3</sub>, changes due to population inversion 9-10168
- soda-lime-silica, glasses, rel. to structure and Ca coordination 9-1079
- Ar, solid, 3612 to 6439 Å, rel. to dielec. props. 9-7832
- Ar spectral line displacement, oscillator strength meas., 2300-1100 Å 9-9454
- B<sub>2</sub>O<sub>3</sub> glass, rel. to relax. times spectrum 9-3850
- BeO, molten 9-17210
- BiTiO<sub>3</sub>O<sub>12</sub> crystals, optically induced changes, obs. with internally formed holograms 9-19976
- CCL<sub>4</sub>, He-Ne laser beam induced index change associated with thermal blooming, interferometric observation 9-18361
- CaBa<sub>2</sub> and refractive index, extinction coeff. and absorpt. coeff. from reflection meas. 9-5866
- CaMgCo<sub>4</sub>, pressure dependence 9-16393
- CaWO<sub>4</sub>, pressure dependence 9-16393
- CdS, for spontaneous polarization estimation 9-16393
- CdS:Se<sub>1-x</sub>, and birefringence dispersion 9-18691
- CuCl, from thin film interference spectra, temp. dependence 9-1728
- Eu chalcogenides, temp. and mag. field depend. 9-16391
- Eu chalcogenides, temp. dependence 9-12328
- KH<sub>2</sub>PO<sub>4</sub>, pressure dependence 9-16393
- KNO<sub>3</sub>, orthorhombic, principal, temp. depend. 9-5871
- Kr, solid, 3612 to 6439 Å, rel. to dielec. props. 9-7832
- LiTa(Nb)O<sub>3</sub>, reduction in laser induced inhomogeneity rel. to OH content 9-5870
- MgF<sub>2</sub>, inhomogeneity 9-5872
- NH<sub>4</sub>H<sub>2</sub>PO<sub>4</sub>, pressure dependence 9-16393
- PbSe epitaxial films, calcs. from transmission meas. 9-5863
- sBr, indices 9-10169
- Se amorphous film in vacuum u.v. 9-12335
- SiC films, microwave-discharge prepared 9-21601
- SiO<sub>2</sub>, channel of higher index formed by proton channeling, rel. to optical waveguide prod. 9-20556
- SiO<sub>2</sub> pyrolytic films, ht. treatment dependence 9-3195
- TiO<sub>2</sub> rutile, pressure dependence 9-16393
- Xe, solid, 3612 to 6439 Å, rel. to dielec. props. 9-7832
- ZnS(O), for spontaneous polarization estimation 9-7936

**Refractive index measurement**

- fluids, optical cell for temp. depend. meas. 9-13060
- glass, use of goniometer, differential technique 9-12331
- He gas, method 9-21138

**Refractometers**

- critical angle measurement range, extension using high refractivity glasses 9-13064

**Refractories** *see High-temperature phenomena and effects***Refrigerators** *see Low-temperature production***Regge poles** *see Elementary particles/scattering***Relativity**

- bremsstrahlung of relativistic particles, quasiclassical theory 9-8745
- Dirac eqn., Hamiltonian and use of octonians 9-2141
- disperse materials with heat transfer, dynamics 9-17705
- Einstein algebraically special space with translation group 9-56
- Einstein gravitation, gauge theories of massive and massless tensor fields 9-85
- Einstein universe, supercharge scale model 9-12657
- evaluation of some aspects 9-10628
- faster than light velocities not prohibited, book 9-12877
- flow, relativistic, of viscous fluid 9-18243
- four-vector teaching advantages 9-2
- Galilean-invariant theories construction, infinite momentum 9-17704
- groups in finite geometry approximating the Euclidean 9-8371
- history, influence of Poincaré 9-6248
- irreversible processes theory and superfluidity 9-3144
- Kennedy-Thorndike expt., interpretation 9-12876
- Lorentz transformation simple derivation 9-2113
- M.H.D., shock waves time orientation and compressibility hypothesis 9-21030
- particle orbits, Newtonian-like eqns. 9-2186
- Petrov type space-time evolution 9-17703
- Poincaré's math. contributions to relativity and Poincaré stresses 9-15399
- radio-wave frequency change during propag. on earth's surface, not due to its mass 9-17702
- restricted, particle-scalar field coupling, trajectory of eqn. of motion studied 9-12875
- space-times, asymptotically flat, total invariants 9-8382
- thermodynamical quantities, transformation laws 9-14392
- university-level textbook 9-12843

**general**

- See also Cosmology; Gravitation; Space time configurations*
- annual parallaxes theory 9-62
- asymptotic flat time-space curvature tensor and conformal curvature tensor 9-20315
- axisymmetric electromagnetic radiation in first approx. 9-6307
- Brand-Dicke theory for perfect fluid in radiation field, time-depend. problem 9-8393
- Brans-Dicke theory and post-Newtonian eqn. of hydrodynamics for non-viscous fluid 9-19497
- Cauchy's problem for relativistic eqns. in perfect fluid and pure matter 9-10629
- conformal tensor discontinuities across hypersurface 9-14333
- cosmology model with radiation and dust, relativistic, general theory 9-14187
- cylindrical electrovac fields, stationary props. and extension of Weyl's theorem 9-14332
- cylindrically symmetric distrib. of matter and mag. energy, possible equilibria 9-2148
- double-series approx. method, exact soln., wave tails 9-8387
- dust, charged, spherically symmetric distrib. 9-8386
- Einstein's eqns., Hamiltonian-Jacobi and Schrödinger separable solns. 9-18977
- Einstein's equations, singularity of spherically symmetrical solutions 9-16671



**Relativity continued**  
**general continued**

- Einstein's equations in axi-symmetric case 9-14339  
Einstein's field eqns., Schwarzschild's interior soln., nonstatic analogs 9-16676  
Einstein's field eqns., solns. matched with Schwarzschild's exterior soln. 9-59  
Einstein's field eqns., type-D soln., finite rotating body of perfect fluid 9-6304  
Einstein field eqns. relations between McVittie and other solns. 9-17707  
Einstein tensor and spherical symmetry 9-2150  
Einstein-Maxwell eqns., conformal plane soln. 9-15423  
e.m. fields, stationary, Einstein-Maxwell equations soln. 9-14337  
empty metrics with shearing hypersurface orthogonal eigenvector 9-15422  
field energy +ve definiteness, variational method anal. 9-12879  
field equations 9-14340  
fluid, viscous, relativistic props. 9-18232  
fluid sphere at mech. and thermal equilibrium 9-7104  
fluid spheres, regularity and boundary conditions 9-8384  
Fresnel drag in semiconductors, prod. by e motion, meas. 9-5685  
gravitation eqns. in homogeneous, completely anisotropic model 9-4230  
gravitation theory, proposed verification by means of earth orbiting gyro-scope 9-10634  
gravitational 'bounce' 9-16675  
gravitational field eqns. for general spherically symmetric metric form 9-15426  
gravitational radiation, energy impulse tensor applic. 9 10631  
gravitational waves, reality considerations 9-10632  
Hamiltonian-Jacobi and Schrodinger separable solns. of Einstein's eqn. 9-18977  
hypersurface, conformal tensor discontinuities 9-14333  
inertial-gravitational field, eqns 9-8385  
Kerr metric, interpretation of parameters 9-2144  
Kerr rot. metric, angular momentum of source 9-6301  
layers, surface analysis of motion 9-17708  
light, ball bending round mass pt., radial 'free-fall' thought expts., validity 9-58  
Lorentzian 4D manifolds with local isotropy 9-20317  
Mach's principle and Fermions 9-20592  
Machian effects of rotating bodies 9-66  
matching of two Riemannian metrics 9-59  
Maxwell's equations, structure, invariance 9-20582  
Maxwellian form of field eqns. 9-15444  
momentum and energy conservation laws formulation, Komar generator 9-14338  
multipole, e.m., non-gravitating relativistic behaviour 9-17716  
multipole particles in equilibrium in external field, conditions determ. 9-17712  
Newton's law derived from general relativity 9-8391  
optical scalars, subpace-curvature reinterpretation 9-2151  
oscillating perfect-fluid sphere with uniform density 9-17714  
perihelion shift, isotropic coordinates calc. 9-2143  
Petrov classification related to critical point theory 9-14335  
phase-space formalism, hypergeometrization method 9-14331  
plane fronted waves, embedding in 6D space 9-64  
power counting theorem proof for case of Euclidean metric 9-18993  
pulsar test 9-8268  
quasi-static axisymmetric system, energy transfer via gravitational interactions. 9-16678  
radiating charged particle, external field 9-17710  
radiation fields, generation from empty gravitational fields 9-60  
recurrent conformal spaces, appl. to Maxwell-Einstein eqn. soln. 9-10630  
Riemannian metric which satisfies field eqns. of gravitation 9-8388  
Riemannian manifold, Schrodinger eqn. deriv. 9-16681  
Riemannian space-time, correspondence between field theories and direct interparticle action theories 9-16677  
Riemannian structure of space-time 9-6295  
rotating body of finite fluid, interior soln., type D for Einstein's field eqns. 9-6304  
rotating disc, space-time interior and exterior soln. 9-6306  
rotational motions of planets 9-10518  
Schwarzschild's interior soln. of field eqn., nonstatic analogs 9-16676  
Schwarzschild's problem, interpretation of coordinates 9-2145  
Schwarzschild soln. independence of spatial stresses 9-4228  
Schwarzschild solution, extension 9-17709  
Schwarzschild spheres, stability to radial perturbations 9-6303  
singularities, local description by means of 'g boundary' 9-65  
singularity of, geodesic completeness 9-63  
space-time metric, special type related to plane matter source 9-10633  
spinor structure, definition and implications 9-12880  
star exterior radiation field, energy-momentum tensor 9-20171  
stellar models with non-radial pulsations, emission of gravitational waves 9-18849  
Tangherlini's argument leading to Schwarzschild's metric, inconsistency of postulates 9-12878  
test rel. to shift of pulsar freq. 9-8395  
thin shells, space-time metric rel. to plane source 9-15424  
universe, stationary, energy considerations 9-20319  
vacuum Riemann tensor, algebraic struct. using a (2+1) spinor formalism 9-2149  
vacuum solutions, type-null 9-8392  
variable mass body, equations of motion 9-17715  
variational formulation including full Bianchi identities 9-6298  
white dwarf instability, caused by relativistic effects? 9-14200

**special**

- 4-vectors, by automated tutoring 9-7  
and Abraham Lorenz electron 9-6468  
for cosmic radio sources, determ. of nature of radiation 9-4107  
diffusion eqn. 9-6343  
ehrenfest's paradox erroneous assumptions about Minkowski's space-time 9 10684  
fluid motion, stress forces in fundamental eqn. 9-7099  
in quantum domain, validity 9-2142  
Lorentz group, possibilities of generalization 9-4227  
Lorentz transform., derivation assuming it to be once differentiable 9-15410  
Lorentz transformation, direct derivation 9-10627  
Lorentz-invariance equilibrium distribns. in stat. thermodynamics 9-10653  
Lorentz-invariance of S matrix, consistency with faster-than-light propag. of part. and wave motions 9-16670

**Relativity continued**  
**special continued**

- Maxwell's eqns., relativistic treatment 9-4384  
monads equivalence and reciprocity principles 9-14329  
nonlinear space time, rel. to Lorentz group 9-8383  
rotating disc applic. 9-14330  
scattering of 3 point particles, max. no. of binary collisions 9-17706  
space-like reflections on hyperplanes coupling with Poincare group, translation subgroup construct. 9-16669  
tensor technique, non-component in Minkowski space 9-8365  
thermodynamics, momentum and energy Lorentz transformation by 4-vector 9-10650  
thermodynamics, temp. transforms and moving thermometers 9-57  
thermodynamics in an elastic medium, separation of mechanical and heat transfer tensors 9-10746  
time definition necessary to predict results about rates of clocks 9-10628  
timelike reflection, through spacelike hyperplanes, coupling between time reversal and Poincare group 9-16668  
twin paradox revisited 9-6296

**unified field theories**

- curvature tensor of asymptotically flat space time 9-8397  
Einstein's field equations, factorizability 9-6309  
Einstein-Maxwell eqn, Godel-type soln using equiv. Rainich eqns. 9-6308  
Einstein-Maxwell eqns., generation of new solns. from old 9-14341  
e.m. fields, non-static; Rainich eqns. considered 9-8398  
field theories, equivalence 9-16806  
gravitational, Einstein eqns., axially symmetric soln. 9-16666  
gravitational, Kerr family, global struct. causal behaviour 9-16679  
gravitational, Kerr family, global struct. causal behaviour 9-6310  
gravitational field, first-order equation 9-4233  
gravitational field, when Einstein principle of equivalence obeyed 9-70  
Poisson brackets of constraints 9-2152  
solutions for pressure-free matter with local rot. symm. in presence of e.m. field 9-8399  
Tangherlini argument, counterexample 9-18994

**Relaxation**

- See also Acoustic wave propagation. Dielectric phenomena: Elastic relaxation; Ferroelectric phenomena; Ferromagnetic relaxation; Molecules/relaxation; Nuclear magnetic resonance and relaxation; Paramagnetic resonance and relaxation*  
alkali halides, one phonon, of OH 9-5534  
crystal lattice near vacancy 9-19742  
crystals, max. and min. numbers of jump freq. involved in relax. proc. 9-21328  
dielectric, book 9-2298  
dielectric, of liqs. containing polar mols. with rotating groups 9-11708  
dielectric, of o. m. dihalobenzenes 9-9543  
electrons, high density, freq. depend. of relax. time 9-1437  
hard-sphere gas, discrete spectrum of linearized Boltzmann eqn. 9-4256  
ice, strain relaxation, exptl. investigation 9-16129  
lightning stepped leaders, lab. corroboration with theory 9-4059  
liquid, light scatt. by density fluctuations 9-1010  
liquids under high press., u.s. studies 9-17205  
Mawell-Lorentz gas in elec. field 9-6341  
mechanical, time measuring in thin thermoplastic layers 9-5436  
mirrors, curved, elastic deform. meas. by dynamic relax. 9-10695  
molecular, stochastic model 9-86  
m.o.s. capacitors, inversion layer transient response, types of relaxation mechanisms 9-12172  
plasma, dense, and amplification of radiation 9-14761  
plasma, dense, and amplification of radiation 9-2966  
plasma, low-temp., effect of inelastic collisions 9-5005  
plasma, with dynamic shielding, Balescu Lenard eqn. 9-5002  
plastic stress, time depend. 9-5433  
polycrystals, diffusion relax. theory 9-3403  
polymers, activation energies temp. depend. 9-9753  
polymers, mechanism, e microscopic obs. 9-7535  
polytetrafluoroethylene, and transitions, pressure dependence from u.s. absorpt. and thermal expansion meas. 9-3406  
stellar rotating systems 9-4105  
stress and strain meas., modified Ke torsional pendulum 9-3402  
thermal, in <sup>4</sup>He vapour press. bulb 9-13563  
thermal in N<sub>2</sub> with wet CO<sub>2</sub> as impurity, Kundt's tube obs. 9-13492  
(u.g.) isotope pairs with I=1/2, behaviour and Schmidt correlation 9-17007  
waves, propagating zone between them and compression waves in visco-elasto-plastic half space 9-12932  
Ar, ionized shock front behaviour 9-14798  
Au-Cu alloys, Zener meas. of short-range order 9-19804  
CdSe i.f. oscillations of photocurrent 9-5762  
Cu, surface terrace vacancies 9-21330  
n-InSb surfaces, phen. at high elec. fields 9-19916  
KCl, one-phonon, of OH<sup>-</sup> 9-5534  
KCl effects with Ni<sup>2+</sup> and Cu<sup>2+</sup> 9-1577  
KI, paraelastic, mass depend. 9-9752  
LiF, effects at low freqs., 30°-180°C 9-12185  
Mg-Cd alloys, Zener relax. rel. to internal friction 9-11913  
MnO:Li, dipole relaxation and loss 9-12187  
NaCl effects with Ni<sup>2+</sup> and Cu<sup>2+</sup> 9-1577  
O<sub>2</sub> vibr., from acoustic wave absorpt. in O<sub>2</sub>-CH<sub>4</sub> mixtures 9-21137  
PbZrO<sub>3</sub>, and spontaneous polarization 9-5748  
Se, crystalline and amorphous states 9-19926  
*r*-Ti, spectrum, effect of H content 9-7534  
TiO<sub>2</sub>, dipole process, rel. to variation in dielectric constant in reduced samples 9-1601

**Remanence** *see Magnetization state***Renner effect** *see Molecules***Replica techniques** *see Electron microscopy***Reproduction** *see Sound reproduction***Resistance, electrical** *see Conductivity, electrical***Resistance thermometers** *see Thermometers/resistance***Resistivity** *see Conductivity, electrical***Resolving power, optics***See also Optical instrument testing*

- in Fourier spectroscopy, rel. noise and instrumental factors 9-19171  
image quality in terms of optical transfer functions, significance of phase 9-10892  
imaging systems, resolution measure 9-20541  
i.r., spectrometer, enhancement 9-10940  
microscope, demonstration of role of diff. pattern 9-12839

**Resolving power, optics continued**

- photography, periodic bar pattern reproduction 9-15563
- resolution of incoherent objects by background-limited optical system 9-20542

**Resonance, elementary particles** *see* *Baryons/resonances; Hyperons/resonances; Mesons/resonances***Resonance, magnetic** *see* *Magnetic resonance and relaxation***Resonance spectra** *see* *Spectra***Resonators**

- axial flow compressor stage, acoustic resonance by periodic wake shedding 9-17799
- confocal split, mode formation and selection 9-8596
- dielectric tube, for i.r. and submm. wave lasers 9-2368
- double-cavity device for inversion coeff. meas. on ruby:  $\text{Cr}^{3+}$  9-10853
- earth-ionosphere, natural freq. diurnal var. rel. mag. field 9-21797
- e.m. cavities, effect of rot. movement on field 9-10762
- e.m. coupling between  $\text{Nd}^{3+}$  doped laser resonator and glass-fibre waveguide 9-14434
- external, in semiconductor laser, rel. to power and directivity of coherent radiation 9-14436
- Fabry-Perot with slightly tilted mirrors 9-16795
- focusing elements, effects on dynamics of Nd glass laser 9-6526
- Helmholtz, influence of medium on acoustic props. 9-15467
- for laser, 4 mirror T form, longitudinal vibration selection 9-20518
- laser cavity for increased coherence 9-8595
- with layered dielectric walls, tolerance determ. in construction 9-15485
- microwave, Fabry-Perot, used in anisotropic plasma diagnostics 9-7167
- with multilayer dielectric walls, effects of large power super-high freq. field on characts. 9-8565
- near-hemispherical, stimulated emission at 6401 Å in active He Ne discharge 9-20520
- nonconfocal, with cylindrical mirrors, natural freq. aberration depend. 9-4460
- open, of two plane circular mirrors, calc. of freqs., amps. and energy losses of modes 9-10856
- open, with large Fresnel diffraction number, proper freqs. and diffraction losses 9-12955
- open, with non-spherical mirrors, axial modes selection 9-4386
- open, with plane circular mirrors, freqs., energy losses and e.m. fields of modes 9-6507
- optical, Michelson-type, mixed-polarization modes 9-12844
- optical, spherical: diffraction eff. 9-8598
- optical confocal and semiconfocal, diff. losses 9-4461
- parametrically-coupled oscillations, self-excitation in optical range 9-4457
- perfect conductor in mag. field, parametric magnetoelastic resonance 9-8508
- piezoelectric, perfect, self-excited 9-12201
- plane mirror, inhomogeneous, effect on laser radiation ang. distrib. 9-2367
- quasi-optic imaging, for plasma diagnostics 9-21080
- Raman laser, pulse shapes and spatial modes, theory and experiment 9-19141
- Raman scatt. spectra, effect of resonator on intensity distribution 9-4536
- resonator interferometry of pulsed gaseous submillimeter wave lasers 9-20292
- ruby laser, spherical, generation autostripping 9-15527
- single-mode, open-cavity for high Q 9-4456
- toroidal, voltage meas. in gap in metre range 9-2625
- with nonlinearly absorbing element, shortening of duration of light pulse 9-4499
- He Ne laser, 3 mirror resonator, radiation generation at 0.63 and 3.39  $\mu$  9-6519
- He Ne laser cavity, longitudinal and transverse modes, simultaneous phase-locking 9-6505
- Nd glass laser, circularly polarized modes 9-2380

**acoustic** *see* *Acoustic resonators***electromagnetic** *see* *Electromagnetic oscillations***Reverberation**

*See also Architectural acoustics; Echo*

- correction term in time meas., evaluation by simple analog computing circuit 9-4356
- fluctuations of sound with position in room, stat. at high freq. 9-10741
- integration method of meas. 9-15472
- noise, response of supersonic transport fuselage 9-20435
- regenerative, due to feedback in rooms, obs. 9-2233
- regenerative, due to feedback in rooms, theory 9-2232
- regenerative, sound amplification in closed rooms 9-4355
- sonar in channels and ducts, normal-mode 9-2225
- sonar optimum waveforms for correl. detect., reverberation-limited conditions 9-4349
- sound tube, variation in natural frequency, meas. 9-15465

**Reviews**

- alkaline earth oxides, defects 9-9693
- anthracene, triplet excitons 9-5623
- of architectural acoustics, history 9-4361
- arcs, low-pressure, positive column props. in longit. mag. field 9-3022
- astronomical instrumentation development (1918-68) 9-6195
- atmospheric pollution 9-4050
- atom collision processes 9-6988
- aurora, spectroscopic studies (since 1960) 9-15251
- biomagnetism 9-8299
- biomedical instrums., Physics Exhibition, London 1968 review 9-4136
- bubble chambers, largest in world 9-19248
- carbides, microstructure and mechanical behaviour 9-19704
- carbohydrates, i.r. spectroscopy 9-2897
- Cepheid variables 9-8253
- ceramic sintering, solid-state, research 9-7582
- chemical analysis physical methods, Physics Exhibition, London 1968 review 9-4021
- colorimetry 9-6551
- concrete fatigue and effect upon prestressed beams, review 9-18519
- contact ionization 9-7322
- cosmic ray intensities underground 9-16912
- cosmic ray variations and solar wind dynamical origin 9-17660
- cosmology, evolutionary 9-15272
- cosmology (1917-1967) 9-17604
- coupling of space-line and internal symmetry groups 9-6582
- creep behaviour of crystalline solids at elevated temps. 9-7547

**Reviews continued**

- critical bands in human auditory processing 9-18953
- cryoelectronics 9-8317
- Cryogenics, Physics Exhibition, London (1968) 9-4186
- crystal growth of organic compounds and mechanism for melt grown single crystals 9-13600
- crystal structure, electron diffraction determ. 9-5304
- dielectric, condensed, shock compressed, optical characteristics 9-16285
- dielectric properties of solids 9-13911
- dynamics of plastic deformation 9-10706
- education, objective testing 9-4205
- electrical meas., Physics Exhibition, London (1968) 9-2300
- electroluminescence and photoconductivity 9-10065
- electron diff., low energy 9-15501
- electron diffraction cameras 9-230
- electron emission by solids, due to atom bombard. 9-3760
- electron emission by solids, due to atom bombard. 9-16321
- electron microscopy, scanning 9-10820
- electron spin polarization by low-energy scatt. from unpolarized targets, review 9-18148
- elementary particle progress (1932-67) 9-8704
- elementary particles 9-4560
- elementary particles 9-20588
- Engel-Brewer theories of metals and alloys 9-9667
- enzyme assay, radiochemical 9-14148
- equations of state 9-11740
- experimental design technique 9-8310
- fast breeder reactor technology 9-635
- fatigue, cycle dependent, research progress 9-19783
- ferroelectricity and crystal-lattice dynamics 9-13917
- ferromagnetism, magnetization and band model 9-19950
- fields, centrifugal, creation and use 9-10686
- flame emission and atomic absorption spectrometry 9-18774
- fundamental heavy particles, hadron and lepton triplets 9-15589
- galactic evolution 9-12669
- gases, volumetric props. 9-9439
- heat transfer 9-20446
- holography 9-252
- hydroscience advances 9-15241
- ionosphere studies of the last decade 9-4075
- ionosphere topside sounding 9-18813
- ionospheric components with different temperatures, popular, paper 9-21796
- isotope separation, e.m. and r.f. 9-13161
- isotope separation techniques 9-20904
- Kapitza resistance between liquid  $^4\text{He}$  and metals 9-18379
- labelled compounds, purity 9-14147
- labelled compounds, stability and storage 9-14146
- labelled compounds, stability and storage 9-14146
- laser beam absorption in the lower atmosphere 9-2386
- lasers, solid-state 9-13026
- leptons, polarized, scatt. by hadrons at high energy 9-17944
- light scattering from solid state plasmas, classical theory 9-16425
- liquid scintillation counting 9-13169
- magnetospheric particles and fields 9-8190
- mass spectrometers, limits on measurement 9-728
- measurement standards at NPL 9-8346
- meson-nucleon scatt. up to 30 GeV/c 9-11030
- metals, e.m. wave propag. in mag. field 9-5625
- meteorites, metallurgy 9-6186
- meteorological instrum. (1918-1968) 9-4046
- microstrain, X-ray diffraction meas. 9-3410
- molecular structure determ. from NMR in liq. crystals 9-18171
- muons and muonium 9-6607
- navigational instruments (1918-68) 9-2107
- neutrino physics 9-4584
- neutron penetration, calc. and expt. methods and obs. 9-11104
- neutron radiography and applications 9-17673
- Ni and alloys, prep., properties and uses 9-7581
- noise, under-ice, oceanic 9-6390
- nonlinear mechanics 9-20376
- nuclear fission 9-16968
- nuclear forces, dispersion theory application 9-6759
- nuclear fusion reactor, progress towards 9-11327
- nuclear giant resonant states, shell model 9-6256
- nuclear potential, one and two pion exchange potentials reviewed 9-6757
- nuclear radiation meas., Physics Exhibition, London (1968) 9-439
- nuclear reactions,  $E > 100$  MeV 9-16951
- nuclear SU(3) model 9-19268
- nucleic acids, submolecular structure, quantum chemistry 9-14728
- observational cosmology 9-18832
- one-boson-exchange model for nuclear forces 9-6758
- optical systems, Physics Exhibition, London, (1968) 9-273
- optics in Czechoslovakia 9-10883
- Pb isotope analysis methods 9-8115
- piezoelectric semiconductors, acoustic properties, theory 9-13793
- plasma generation, containment, diagnostics 9-7132
- plasma sources of ions of high-melting elements 9-2981
- plastic strain measurements, special techniques 9-17304
- plasticity of simply supported circular rigid plastic plate dynamically loaded 9-137
- point defects in solids 9-13676
- polymers, structure and physical props. infl. on dielectric props., review 9-19925
- potential model approach to nuclear forces 9-6756
- quantum ergodic theory developments 9-20348
- quarks, search 9-6613
- radiation emission from charged particles in diffraction grating vicinity 9-15486
- radiative corrections 9-17928
- radioactive isotope dilution analysis 9-18784
- radioactive tracers in chemical analysis 9-20072
- rare earth compounds with group V anions, electronic and magnetic props. 9-18598
- rare gas crystals, physical props. 9-13567
- reactor fuel, ceramic, evolution and high burn up behaviour 9-2787
- scattering of elem. parts. at high energy, models 9-6578
- semiconductor detectors 9-16921
- semiconductor devices, modern developments 9-5714
- semiconductor spectrometers 9-13161



**Reviews continued**

semiconductors, charge carrier recombination mechanism 9-3549  
 solar system, origin 9-10507  
 solar system, theories of origin 9-15334  
 solid, resonance lines inhomogeneous broadening 9-18689  
 solid-state and molecular theory (1900-66) 9-9598  
 spark and streamer chambers 9-19250  
 spectra of heavy elements, isotope effect 9-19394  
 spectrophotometers, i.r. 9-280  
 standards of activity and list of isotopes available from Radiochemical Centre 9-18768  
 star cluster proper motion 9-15321  
 star distances meas. by parallax method 9-15262  
 Stark effect in atoms 9-13284  
 steel welds, hot cracks 9-13739  
 stellar energy production, C cycle 9-6126  
 stress-corrosion cracking of high strength steels 9-9757  
 striations 9-15961  
 striations in plasma discharge 9-15945  
 superconducting magnets 9-16250  
 superconductors, hard 9-16238  
 superconductivity, resonating valence-bond theory 9-17381  
 superconductors, type II 9-3590  
 symmetry, Amer. J. Phys. resource letter 9-6584  
 three-particle scatt., recent work on nonrelativistic theory 9-19198  
 unfolding measured distributions 9-20298  
 vacuum deposition of metallic films, techniques 9-7340  
 vacuum gauges and their calibration, review 9-8330  
 vapour pressure measurement methods for water and other liquids 9-14885  
 $\alpha\pi$  interaction 9-15649  
 e probe microanalyser and its applications to medicine 9-4142  
 ep scatt., radiative corrections 9-20603  
 KN inelastic processes above 2.4 GeV/c with more than two particles in final or intermediate state 9-11042  
 $\mu\mu$  scatt., radiative corrections 9-20603  
 NN inelastic processes 9-6690  
 NN scatt. in 50 MeV region, expts. 9-6689  
 $\pi\pi$  inelastic processes 9-6664  
 As<sub>2</sub>S<sub>3</sub> glasses, development since 1950 9-3175  
 CO<sub>2</sub>-N<sub>2</sub> laser, vibrational relax. data, kinetic model 9-15509  
 CO<sub>2</sub>, review 9-15514  
 GaAs semiconducting props. and applics. 9-19910  
 He II fluctuations and correlations, statistical theory 9-21238  
 O, kinetics of various gas reactions involving O, O<sub>2</sub> and O<sub>3</sub> 9-15212  
 SiH<sub>4</sub>, silane, applic. to semicond. mats. fabrication 9-5713  
 Zr alloys oxidation in high temp. H<sub>2</sub>O, irradi effects. 9-10343

**Reynolds number** *see Flow; Hydrodynamics*

**Rhenium**

adsorption and desorption of O from polycryst. filament, thermionic meas. 9-11787  
 diffusion in W surface, effect of elec. field 9-13707  
 magnetic susceptibility, 7-1875°K 9-5801  
 n.q.r. in KReO<sub>4</sub> 9-3974  
 oxidation at high temp. by O and O<sub>2</sub> 9-17529  
 paramagnetic susceptibility, Hall effect, elec. resistance, temp. depend. 9-15072  
 Ptand Re, thermal desorption spectra, high resolution, of He 9-11783

**Rhenium compounds**

[Re(py)<sub>4</sub>O]<sup>+</sup>, spectra, effect of solvent on peak positions, 330-880 mμ 9-5172  
 CeB<sub>6</sub>-Re, elec. props. 9-9919  
 CeB<sub>6</sub>-Re, elec. props. temp. dependence 9-9920  
 Mo-Re alloys, elastic constants, -190 to +100°C 9-11905  
 Re-rare earth metal, ferromag. 9-13949  
 Re-transition metal, paramag. susceptibility, temp. independ. 9-13949  
 ReF<sub>7</sub>, vibr. spectra 9-2871  
 ReO<sub>3</sub>, De Haas-Van Alphen effect, meas. 9-7728  
 ReO<sub>4</sub><sup>-</sup> vacuo u.v. spectra study 9-19483  
 ReO<sub>3</sub>, NMR of <sup>185</sup>Re, Knight shifts and spin relax. rates 9-12512  
 Re<sub>2</sub>[CO]<sub>10</sub>, quadrupole coupling 9-3975  
 W-(26 wt.%) Re alloy, thermal conductivity and elec. resistivity, 300 to 2200°C 9-15035  
 W-Re alloys, prod., patent 9-13772  
 W-Re alloys, superplasticity 9-18507

**Rheology**

*See also Plasticity; Viscoelasticity*  
 clay, rel. to colloidal materials 9-1314  
 colmatage, treatment using Markov processes 9-5202  
 convection in cavity with variable upper wall temp. 9-19514  
 deformable media, thermodynamics, fluidity equations development 9-8478  
 elastic liquids, properties, models, linear and nonlinear behaviour 9-18332  
 fluid behaviour in pipes 9-853  
 liquids, self-aligning platens for Weissenberg Rheogoniometer 9-3064  
 microrheometer for meas. tensile strength of wood fibres 9-5472  
 non-linear behaviour simulation, integration in numerical analysis 9-17757  
 Nujol/water emulsions, stabilized, changes in aging 9-5201  
 paraffins, rheological props. 9-5416  
 plane problems in elastostatics of non-homogeneous solids, anal. 9-4273  
 polymer solids, sinusoidal strain excitation obs. with X-ray diffractometer 9-7536  
 polymeric microcrystal gels, rel. to particle size distrib., high yield values 9-9571  
 polyvinyl alcohol aqueous soln., rheological props. by flow birefringence 9-17172  
 relationships in nonlinear theory of viscoelasticity 9-843  
 solid, incompressible elastic-perfectly plastic, plane radial flow 9-20383  
 surface meas., comp. of linear and annular canal viscometers 9-7257  
 surface movement due to inclined layer excavation 9-19016

**Rhodium**

thermal expansion and lattice parameter determ. by X-ray diffraction, 28-587°C 9-16182

**Rhodium compounds**

Fe-Rh alloy, e.s.r. meas. rel. to antiferromag.ferromag. transition 9-16455

**Rhodium compounds continued**

Ir-Rh alloys, mag. susceptibility comp. and temp. dependence, 6-1850°K 9-13947  
 Mo-Rh alloys, low temp. sp. ht. 9-17354  
 Ni Rh, ferromagnetic behaviour 9-5821  
 Ni-Rh, mag. behaviour 9-16351  
 (63wt.%)Ni-(37wt.%)Rh anomalous low temp. sp. ht. near crit. conc. for ferromag. 9-16176  
 Pd-Rh alloys, dil., mag. susceptibility meas. rel. to impurity scatt. and electron density states 9-13986  
 Pt-Rh alloys, photoelectric  $\gamma$  cross-sect. by dis. and calc. 9-18654  
 Pt/Pt-(13 at:wt.%)Rh thermocouple, stress effect on thermal e.m.f. 9-12208  
 Rh-Pd-Ag, alloy, electron reflection, 200-800eV, energy loss spectra obs. 9-16194  
 Rh-Pd, Fe impurities, magnetic and transport processes 9-3766  
 Rh complex, RhCl(C<sub>6</sub>H<sub>6</sub>), crystal and mol. structure 9-13647

**Riemann-Cristoffel tensors** *see Relativity; Tensors*

**Righi-Leduc effect** *see Magneto-thermal effects*

**Ring currents** *see Atmosphere; Ionosphere*

**Riometers** *see Ionosphere measuring apparatus*

**Rochelle salt**

dielec. conds., temp. var. 9-3700  
 dielectric constant temp. dependence from meas. at 9 GHz 9-10051  
 e.p.r.,  $\gamma$  irradiated single crystal, analysis of centre no.1 9-3953  
 ferroelectricity, Ising model with two phase transitions 9-5754  
 growth, impurity effects, reln. to pH of soln. 9-13601  
 i.r. absorpt. tartrates, i.r. absorpt. spectra in thin crystal textures, temp. dependence, -195 to 51°C 9-1803  
 lattice defects, effect on dielec. props. 9-7486  
 spin-lattice relax. of <sup>23</sup>Na and <sup>2</sup>D 9-10155

**Rock magnetism**

anisotropy by portion pendulum method 9-18818  
 Antarctic reversals rel. to climatic and faunal changes 9-12649  
 earth's mag. field local gradient rel. underground conductivity structure 9-17594  
 earth, Permian, radius calc. by palaeomeridian method 9-17553  
 field reversals attributed to cosmic ray variation 9-10444  
 haematite content, sediments, susceptibility rel. ferrous and ferric content 9-12647  
 lavas of Etna, rel. to orientation from 1300 to 1800 of terrestrial mag. field in Sicily 9-17591  
 lavas of Flores Islands 9-8214  
 lunar, Sinus Medii Surveyor 6 obs. 9-21924  
 maghemite and hematite, intergrown, remanent mag. direction and intensity 9-7886  
 magnetite, stress control of magnetization, implications 9-21586  
 magnetite, volume magnetostriction 9-21836  
 magnetite bearing rocks, remanent magnetization rel. uniaxial compression 9-18822  
 ocean sediment cores, mag. susceptibility stratigraphy 9-12648  
 palaeomagnetic data rel. to rotation of Africa 9-21750  
 palaeomagnetic data rel. to rotation of Africa 9-17557  
 palaeomagnetic directions and pole positions, data table 9-18820  
 palaeomagnetic field, intensity 100-2500 m.y. ago 9-16547  
 polarity reversal rel. oxidation state 9-18819  
 pyrrhotite, Fe<sub>0.85</sub>S and Fe<sub>0.9</sub>S, magnetic phases 9-18821  
 remanance in monodomain grains obs. on Neel thermal activation theory 9-3791  
 stress control of magnetization in magnetite and Ni, implications 9-21586  
 titanomagnetite, natural, susceptibility of fine grain assemblage rel. uniaxial compression 9-21587  
 volcanic, charact. rel. ellipsoidal particle model 9-16544  
 volcanic, unoxidized, ancient field intensities determ. 9-17592  
 volcanic lava of Miocene period, rel. to inversion of Earth's mag. field 9-10442  
 Fe-T: oxides in basalts 9-16545  
 FeOOH, Fe<sub>2</sub>O<sub>3</sub> system, chemical remanent magnetization 9-16546  
 Ni polycrystallites, remanent magnetization rel. uniaxial compression 9-18822

**Rockets**

chambers, v.l.f. pressure oscs., obtained by anal. of acoustic modes 9-6402  
 deep-space probes, optical tracking by specular refl. of sunlight from plane mirror surfaces 9-6100  
 exhaust noise, high alt. wind profile meas. 9-4054  
 ionosphere D-region temperature and electron density meas. 9-12621  
 motors, graphite throat inserts, quality control techs 9-7568  
 motors, solid propellant, non-destructive testing of erosion resistant graphite 9-11936  
 rocket-released probes, instantaneous orientation determ. from signal polarization anal. 9-6099

**Rolling** *see Forming processes*

**Rotating bodies**

*See also Angular velocity measurement; Centrifuges; Earth/rotation; Gyroscopes*  
 axial deviation, meas. for purpose of correction 9-6355  
 disc in non-Newtonian liquid, mass transfer 9-16705  
 electric fields, rotation-induced, near metals 9-198  
 fluid, stratified, spin-down rel. to solar oblateness 9-10539  
 free solid with liquid filling, circular motion stability in force field of two stationary attracting centres 9-12913  
 geodesic motion of rotating source in field 9-14328  
 helical motions in fluid of body bounded by multiply connected surface 9-10689  
 liquid, surface waves 9-21170  
 Machian effects in general relativity 9-66  
 n.m.r. solid specimen, effect on bilinear spin interactions 9-8036  
 nonlinear systems, rotational and oscillatory solutions with several degrees of freedom 9-10722  
 polytropic compressible cylinders, equilibrium 9-18847  
 potential on rotor 9-207  
 satellite, equatorial, in gravitational field, anomalistic and sidereal period in co-ordinate and proper time 9-10446  
 shell, cylindrical, immersed in gas, flutter rel. to centrifugal and Coriolis forces 9-10688  
 solid, with viscous liq. filled cavity, linearized model 9-8471

**Rotation, molecular** *see Molecules/rotation*

**Rotatory power, dispersion** *see Optical rotation***RS coupling** *see Atoms; Spectral atoms***Rubber**

- chloroprene rubbers, crystallization kinetics, obs. 9-11796
- friction on wet surfaces 9-3458
- light scattering, polarized, anal. using annular spherulite model 9-7940
- poly(n alkyl methacrylate), stress-strain-time, relation 9-18396
- polymers, rubber-like, non linear deformation, evaluation of Rivlin's strain energy function 9-19784
- statistical mech. of crosslink orientation 9-16114
- uniaxially stretched, length of statistical segment calc. 9-19781

**Rubidium**

- addition to liquid Na, effect on e.p.r. 9-13541
- atom,  $^{87}\text{Rb}$ , vapour, optically pumped, microwave light emission 9-679
- atom, fine structure transitions in Rb-He collisions 9-11411
- atoms on W and Pt surfaces, meas. of positive surface ionization coeff. 9-5786
- conductivity, electrical, temp. var. calc., comparison with expt. 9-16231
- electron mean free path, resist. obs. 9-18582
- electron-spin susceptibility from Knight shift meas. in liquid binary alkali metal alloys 9-13542
- Electronic structure calcs. using Wigner-Seitz cell method and polymorphic transitions 9-5614
- isotope thermotransport, temp. depend. 9-9491
- Matthiessen rule deviation of thin wires, liq. He temp. 9-16233
- optical pumping and spin exchange signals with Ag, Li, H, N and elec trons 9-14422
- thin films, opt. absorption 9-12384
- vacancy-produced lattice distortion, calc. by method of lattice statics 9-21332
- Rb-Sr cosmochemistry in solar system 9-21919
- Rb magnetometer, self oscillating long term stability, simultaneous mag netic field measurements 9-15498
- $^{85}\text{Rb}$  atom collisions, spin-exchange cross-section obs. 9-9152
- $^{85}\text{Rb}$  atoms nuclear and electronic g factors ratio, obs. 9-6971
- $^{85}\text{Rb}$  maser oscillation of optically pumped vapour, expt. arrangement 9-4449
- $^{85}\text{Rb}$  relative isotope shift by atomic beam technique obs. 9-4852
- $^{87}\text{Rb}$  atom collisions, spin exchange cross-section obs. 9-9152
- $^{87}\text{Rb}$  atoms nuclear and electronic g factors ratio, obs. 9-6971
- $^{87}\text{Rb}$  relative isotope shift by atomic beam technique obs. 9-4852
- $\text{Rb}^+$ , free atomic, nuclear moment obs. 9-11399
- $\text{Rb}^+$  chem. shift in aqueous soln., obs. 9-6971
- $\text{Rb}^+$  excitation from  $^{85}\text{Kr}$   $\beta$  decay, dipole transitions from excited states, lifetimes obs. 9-9140
- $\text{Rb}^+$ -inert gas nearly adiabatic thermal collisions, excitation transfer, Stuckelberg's formula and difficulties 9-18154

**Rubidium compounds**

- silicate glass, viscosity, stress depend.,  $10^{14}$ – $10^{16}$  poise 9-3422
- (Ag+Rb or Cs) $\text{NO}_3$ , molten, thermoelec. power 9-3119
- Rb-Cs liquid binary alloy, electron-spin susceptibility from Knight shift meas. 9-13542
- $\text{Rb}_2\text{MnCl}_4 \cdot 2\text{H}_2\text{O}$ , antiferromag., nuclear spin lattice relax. of  $^{87}\text{Rb}$ ,  $^{85}\text{Rb}$ ,  $^{13}\text{Cl}$  and  $^1\text{H}$  9-21597
- $\text{Rb}_2\text{ZrCl}_6 \cdot \text{Os}^{4+}$ , optical spectra at 4.2°K 9-14055
- $\text{Rb}_2\text{BeF}_6$   $^{19}\text{F}$  NMR rel. to hindered motion in structure 9-16466
- $\text{RbBr} \cdot \text{Mn}^{2+}$ , charge transfer spectra 9-3892
- $\text{RbBr} \cdot \text{Ti}(\text{Pb})$ , absorption spectra, new band 9-10207
- $\text{RbBr}$ , stress-optical dispersion meas. 9-5873
- $\text{RbBr}$  films, emission in far i.r. 9-15175
- $\text{RbCl} \cdot \text{Ag}$ , paraelec. dipole equilibrium directions and elec. moment by elec tro-caloric eff. 9-21532
- $\text{RbCl} \cdot \text{CN}^-$ , tunneling states of  $\text{CN}^-$  ions 9-10040
- $\text{RbCl} \cdot \text{S}^-$ , luminescence at 4.2°K 9-14078
- $\text{RbCl}$ , valence and conduction band, Schrodinger eqn. soln., Brillouin zone symmetry 9-3554
- $\text{RbCl}$  exchange reaction with Cs and K mol. beams 9-10310
- $\text{RbCl}$  films, emission in far i.r. 9-15175
- $\text{RbCl}$  optical absorption of  $\text{V}_A$  center, lattice effect 9-9720
- $\text{RbCl}$  sp. ht., phonon branches calc. from shell model lattice dynamics 9-7633
- $^{85}\text{Rb}^{35}\text{Cl}$ , r.f. Stark spectrum, mol. beam elec. resonance meas. 9-7036
- $\text{RbF}$ , second-order Raman spectra calc. for vibration spectra computation 9-12429
- $^{85}\text{RbF}$ , r.f. Stark spectrum, mol. beam elec. resonance meas. 9-7036
- $^{87}\text{RbF}$ , r.f. Stark spectrum, mol. beam elec. resonance meas. 9-7036
- $\text{RbF}(\text{U})$  luminescence total intensity temp. var.,  $\alpha$ ,  $\Delta E_1$ ,  $\Delta E_2$  calc. 3650 Å 9-10240
- $\text{RbFeF}_3$ , mag. props. in strong pulsed fields, 4.2–106°K 9-16362
- $\text{RbFeF}_3$ , Cotton mott effect and mag. structures at 77 and 200°K 9-3771
- $\text{Rb}_2\text{FeF}_4$ , antiferromagnetic planar susceptibility and long-range order 9-7922
- $\text{RbH}_2\text{PO}_4$ , specific heat, -141 to -120°C 9-9845
- $\text{RbH}_2\text{PO}_4$  paraelectric phase, n.m.r. of  $^{87}\text{Rb}$  9-16469
- $\text{RbI} \cdot \text{Ti}(\text{Pb})$  absorption spectra, new band 9-10207
- $\text{RbI}$ , apparent molal expansibility and volume obs. 9-986
- $\text{RbI}$ , photoemission spectra, L-bands and exciton bands 9-3759
- $\text{RbI}$ , stress-optical dispersion meas. 9-5873
- $\text{RbI}$  magneto-reflection dichroism, Zeeman effect irregularity 9-7949
- $\text{RbI}(\text{Ti}^3+)$  crystals, X-ray treated,  $\text{V}_A$  centre spectra obs., e.p.r. spectra obs. 9-20028
- $\text{RbMg}_{1-x}\text{Co}_x\text{F}_3$ ,  $x=0.35$ – $0.68$ , ferrimagnetism obs. 9-7912
- $\text{RbMnCl}_3$ , antiferromagnetic, from e.s.r. studies of  $\text{MnCl}_2$ -alkali chloride fused mixtures 9-13948
- $\text{RbMnF}_2$ , ENDOR obs. 9-21674
- $\text{RbMnF}_3$ , antiferromagnet, critical fluctuations, e.p.r. studies 9-18735
- $\text{RbMnF}_3$ , elastic constants from u.s. attenuation meas. 9-21431
- $\text{RbMnF}_3$ , antiferromagnet, luminescence enhancement in mag. fields 9-1824
- $\text{RbMnF}_3$ , antiferromag. Zeeman effect anisotropy 9-1795
- $\text{RbMnF}_3$ , antiferromagnetic, magnon sideband shapes, Green function theory 9-12313
- $\text{RbMnF}_3$ , antiferromagnetic domains 9-17465
- $\text{RbMnF}_3$ , Raman scattering spectra and two-magnon absorption, Green's function method 9-12435
- $\text{RbMnF}_3$ , spin wave theory and low temp. magnetization 9-16382
- $\text{RbMnF}_3$ , two-magnon Raman spectra 9-12425
- $\text{Rb}_2\text{MnF}_4$ , optical transitions 9-10208
- $\text{Rb}_2\text{Mn}_2\text{Ti}_2\text{O}_4$ , ( $0.60 < x < 0.80$ ), isomorphs, cry. structure 9-3306

**Rubidium compounds continued**

- $\text{RbNO}_3$ , electrical conductance at phase transformations 9-16254
- $\text{RbNO}_3$ , ionic diffusion by n.m.r. line width rel. to temp. 9-19770
- $\text{RbNO}_3$ , interdiffusion in dilute solns. of  $\text{AgNO}_3$  9-7261
- $\text{RbNO}_3$ , polymorphism 9-5520
- $\text{RbNi}_{1-x}\text{Co}_x\text{F}_3$ , mag. props. in strong pulsed fields, 77 4.2°K 9-16362
- $\text{RbNiF}_3$ , Co substituted, magneto-optical props. 9-5882
- $\text{RbNiF}_3$ , ferrimagnetic resonance, 77-200°K 9-12496
- $\text{RbNiF}_3$  Raman spectrum and exchange interactions 15-300°K using Ar laser 9-10222
- $\text{RbPaF}_6$  crystal structure 9-14925
- $\text{RbPbCl}_3$ , formation in vaporization of  $\text{PbCl}_2$ + $\text{RbCl}$  mixtures, thermodynamic props. from mass spectra 9-19442

**Ruby**

- colour centres, nature 9-5382
- depolarization of light scattered through small angles 9-5877
- electron spin-spin interactions, connection with plarization and nuclear spin relax. 9-15160
- e.p.r., elec. field effect 9-10275
- e.p.r. line broadening, n.m.r. saturation eff. 9-1853
- laser, assembly, two-frequency generation, near and far zones 9-8624
- laser, basic parameters and properties 9-13030
- laser, component generation 9-14433
- laser, Czochralski, energy output degradation 9-15528
- laser, diffraction modulator utilizing standing ultrasonic waves 9-13029
- laser, experimental upper limit to time of nonradiative relaxation between  $^4\text{T}_2$  and  $^4\text{E}$  states 9-12851
- laser, mode-locked, achievement of minimum attainable pulse duration 9-20501
- laser, Q-switched, prod. 300 MW pulse 9-10866
- laser, Q-switched, single mode passive, dynamic behaviour 9-14432
- laser, self Q-switching at 77°K 9-12852
- laser, spherical resonator, generation autostripping 9-15527
- laser, two-rod assembly, reln. between output and design parameters 9-8623
- laser light, Rayleigh scatt. and depolarization by neutral gases 9-14435
- laser losses, passive and active, meas. 9-8625
- laser pulse, spectrum 9-4477
- laser spectrum narrowing, internal freq. modulation 9-4478
- lattice defects, e.p.r. and X-ray investigation 9-9694
- maser, broad band traveling-wave, intrinsic spot noise temp., spectral char. act. 9-6501
- maser, with optical pumping, generated power rel. to pumping intensity 9-4451
- optical homogeneity, surface and volume scattering, surface damage, connection with laser-emission characteristics 9-20522
- optical homogeneity of crystals, rel. to divergence of laser radiation 9-5885
- optical spectra, Cr conc. dependent line shifts 9-1767
- optical-microwave double-resonance studies 9-10163
- refractive index change due to population inversion 9-10168
- relaxation process study, applic. of mag. field prod. as rectangular pulse 9-10807
- self-absorpt. of R lines, 4.2-300°K 9-16435
- spin-lattice calcs. from ground state of ferrous ion 9-12315
- spin-relaxation conc. depend. He temp. 9-18686
- $^{27}\text{Al}$  doped, dynamic nuclear polarization 9-5991
- $^{27}\text{Al}$  NMR at center of  $\text{Cr}^{3+}$  ESR line, nuclear quadrupole coupling constant not obs. 9-10301
- $^{27}\text{Al}$  parametric mag. nuclear spin saturation, obs. 9-10300
- $\text{Al}_2\text{O}_3 \cdot \text{Cr}^{3+}$ , two-photon transitions in e.p.r. spectrum 9-16453
- $\text{Cr}^{3+}$ , e.p.r., optical detection in excited state  $\text{E}(\text{E})$  and ground state  $^4\text{A}_2$  9-20018
- Cr ion pair e.p.r. spectrum 9-18734
- $\text{Cr}_2\text{O}_3$  doped, refractive index change due to population inversion 9-10168
- $\text{MgO}$ , crystal-field parameters, isotope effects 9-12040

**Russell-Saunders coupling** *see Atoms; Spectral atoms***Ruthenium**

- Ru, deformed, domain size distrib. from X-ray line profiles 9-7447

**Ruthenium compounds**

- Mo-Ru alloys, low temp. sp. ht. 9-17354
- Ru complex, nitrogenpentammineruthenium (II) dichloride and related salts, cry. structure 9-7448
- $\text{RuC}$ , gaseous, disoc. energies, mass spec. determination 9-14726
- $\text{RuO}_3$ , magnetoresistance meas. 9-16234
- $\text{RuO}_2$ , Azbel-Kaner cyclotron resonance in  $\{110\}$  plane 9-7725
- $\text{RuO}_2$ , elec. conductivity rel. to phases, comp. and  $\text{O}_2$  partial pressure, -190°C-1000°C 9-1470

**Rutile** *see Titanium compounds***S-matrix theory***See also Dispersion relations*

- analytic, strong interaction dynamics, book 9-11008
- causality, unitarity and analyticity 9-19197
- Coulomb-nuclear, asymptotic behaviour in left-half  $\lambda$ -plane 9-13215
- coupling of space-line and internal symmetry groups 9-6582
- current formalism, Pugh's integral equations, derivation without interacting field 9-4551
- gauge principle rel. to zero mass  $\pi$  9-8844
- internal symmetries scatt. for pseudoscalar mesons scatt. 9-8771
- for Kondo effect, proof of complete equivalence with Green's function approach 9-7701
- in Lee model, second sector connected, diagonalization 9-2446
- Lee model calc. coupled integral eqns. 9-6592
- mass shell, causality conditions and consequences 9-16818
- quasiclassical scattering at high energies 9-13100
- quasiclassical scattering at high energies 9-2466
- S, reconstructed from N/D threshold behaviour and subtracted eqns. 9-4597
- Schrodinger eqn. with velocity-dependent pots., analytic behaviour of S matrix 9-6315
- space-time description of high energy interactions 9-15576
- spin and statistics connection, including crossing, Hermitian analyticity 9-17937
- three-body S-states with Coulomb interactions 9-323
- unitarity, negative metric introduction, divergence difficulties removal 9-14454
- unitarity in field theories with derivatives 9-2437
- $\pi\text{N}$  scatt., appl. of approx. method for evaluating S-matrix 9-8843



**Safety precautions** *see* **Radiation protection**

**Sakata model** *see* **Elementary particles**

## Samarium

- atom incoherent  $\gamma$ -scatt. from K-shell electron obs. 9-712
- conduction e. density at nucleus 9-16211
- $^{147}\text{Sm}$ , hyperfine interact. consts. in J=5 states 9-6973
- $^{149}\text{Sm}$ , hyperfine interact. consts. in J=5 states 9-6973
- $\text{Sm}^{3+}$  activation in rare earth vanadates, luminescence spectra 9-20003
- $\text{Sm}^{2+}$ , spectra in optically pumped  $\text{SrF}_2$  and  $\text{SrCl}_2$  9-10210
- $\text{Sm}^{2+}$  in  $\text{SrF}_2$ , vibronic transitions and Zeeman effect 9-10212
- $\text{Sm}^{3+}$  in  $\text{KTaO}_3$  and  $\text{KTa}_{1-x}\text{Nb}_{1-x}\text{O}_3$ , fluorescence 9-10242
- in  $\text{SrTiO}_3$ , photoluminescence 9-21648

## Samarium compounds

- dibenzoylmetanate, luminescence props. 9-16016
- $\text{Sm}_2\text{Co}_{17}$ ,  $^{153}\text{Eu}$ , hyperfine interactions meas. 9-14040
- $\text{Sm}_2\text{Ni}_{17}$ ,  $^{153}\text{Eu}$ , hyperfine interactions meas. 9-14040
- Sm Fe garnet, sub-lattice magnetization sign reversal 9-1691
- $\text{SmAlO}_3$ , specific heat at low temps rel. to  $\lambda$  transitions in mag. ordering 9-7655
- $\text{SmCrO}_3$ , specific heat at low temps. rel. to Schottky anomaly 9-7655
- $\text{SmFe}_{12}$ ,  $^{153}\text{Eu}$ , hyperfine interactions meas. 9-14040
- $\text{SmFeO}_3$ , spin re-orientation phase transition 9-16372
- $\text{SmNi}$ , paramagnetism indep. of temp. 9-3775
- $\text{Sm}_2\text{O}_3$ , structural stabilization with  $\text{WO}_3$  9-17326
- $\text{SmO}_3$  microspheres, high density, production by r.f. induction plasma heating 9-2795

**Sampling** *see* **Statistical analysis**

## Sand

- sandstones, thermal conductivity calc. for unconsolidated sand, phase distrib. 9-3542
- thermal conductivity, calc. 9-3539
- water-sand suspension, pipeline flow, conc. gradient meas. 9-9563

## Satellites, artificial

- attitude-stabilization system, damping improvement by elastic dumbell 9-14179
- Doppler frequency difference of emitted radio waves, numerical analysis 9-21793
- drag coeffs., separation from atmos. density, expts. 9-10452
- equatorial, in gravitational field, anomalous and sidereal period in co-ordinate and proper time 9-10446
- flight theory, book 9-4081
- four-body problem sun-moon-earth-satellite 9-18834
- gyroscope orbiting earth, proposed verification of Einstein's theory of gravitation 9-10634
- heat balance test vacuum chambers at Noordwijk 9-12651
- inversion radiometric meas., atmosphere 9-4045
- ionospheric trail, kinetic analysis 9-12606
- Luna-11, for 30 KeV electron recording in circumlunar space 9-18899
- lunar, motion rel. to rad. press. of solar, lunar e.m. rad. 9-2040
- lunar orbits classification, long period and secular eff. due to earth 9-2045
- meteorological appls. and requirements 9-21755
- meteorological observations, problems 9-21756
- orbit determ. from three angular meas., two-parameter iteration method 9-8218
- orbit expansion by microthrust, results description 9-17597
- orbit expansion by microthrust, transfer time and fuel mass, Fortran computer programme 9-20130
- orbit with large inclination and eccentricity, elimination of short period terms 9-12652
- orbital transfer, minimum impulse calc. using minimization algorithm 9-10451
- orbits, effect of atm. rot. 9-17596
- orbits, real flight, connection with orbital manoeuvres 9-18827
- orbits, near resonance with tesseral harmonics, long-period behaviour 9-10448
- orbits, two stable and periodic, about Earth-Moon triangular points, sun perturbed 9-10449
- Pioneer 6, solar wind- magnetic fields interaction, obs. compared with theory 9-2063
- planar librational motion stability, accuracy of numerically generated integral manifolds 9-8217
- radio beacon transmissions, electron content measurements in ionosphere 9-20109
- random re entry, population injury probability if carrying radioactive mats. 9-20127
- rotation of orbital plane due to thrust orthogonal to radius and velocity vectors 9-20129
- scintillation at high latitudes, possible relation to precipitation of soft particles 9-10429
- scintillation transmissions in F-region, equatorial irregularity belt 9-12637
- solar radiation press. effect on two models 9-18825
- solution, using methods of Von Zeipel and Brouwer, in book 9-14188
- stability, libration about equilb. position, influence of space environment factors, book 9-20380
- terrestrial light sources intensity comparison 9-21751
- Vinti's spheroidal theory, improvement of mean orbital elements in absence of obs. data 9-10450

**SC (sudden commencement)** *see* **Magnetic storms**

**Scalers** *see* **Counting circuits**

## Scandium

- atoms and ions, bibliography of spectra 9-13287
- electron structure, rel. to diamag. susceptibility 9-1878
- film on (110) face of W, electron and absorpt. props. 9-1115
- films on W(110), structure, LEED obs. 9-1100
- magnetic susceptibility, form with two overlapping bands 9-10098
- n.m.r., relaxation anisotropy in metal 9-12514
- Fermi surface and energy bands using augmented- plane wave method 9-7714

## Scandium compounds

- alloys with mag. impurities, long range antiferromag. spin correl. 9-5856
- Sc-Er alloys, mag. structure comp. dependence 9-5802
- Sc-Gd alloys, n.m.r. and mag. susceptibility, rel. to conduction-electron polarization 9-12513
- Sc-Ho alloys, mag. structure comp. dependence 9-5802
- Sc-Tb alloys, mag. structure comp. dependence 9-5802
- $\text{Sc}_2\text{O}_3$ , crystal structure refinement 9-21321
- ScAl<sub>3</sub> and ScAl<sub>2</sub>, Knight shift mechanism and e structure of Sc 9-1878

## Scandium compounds continued

- $\text{Sc}(\text{NO}_3)_3$  solns., critical coagulation and stabilization concs. for AgBr sols 9-9569
- $\text{Sc}_2\text{O}_3\cdot\text{Bi}^{3+}$ , fluorescence spectra 9-3927
- $\text{ScO}$ , mols. blue-green emission system rot. analysis, obs. 9-4937
- $\text{Sc}_2\text{O}_3$ , elec. conductivity rel. to defects, 700-1600°C 9-1583
- $\text{ScOF}$ , monoclinic, electrostatic energy and anion ordering 9-11790

## Scattering

- aerodynamic, on complex shapes, matrix theory 9-14809
- amplitude, restrictions on high energy behaviour 9-8694
- asymptotic condition based on physically motivated topology 9-6312
- atom collisions, total cross-section calc., stepfunction model 9-20995
- atom-molecule, quenching of glory extrema 9-839
- atoms, repulsive inverse-power potential calcs. 9-705
- Born series for transition amplitudes, convergences 9-8417
- chemically reactive systems, elastic scatt. 9-1894
- elastic, perturbation effects, Stueckelberg formulation for transition probabilities 9-18989
- elastic pulses by rigid obstacles, retarded pot. calc. 9-2199
- Faddeev theory and reln. with projection operator formalism 9-20581
- fluid, multiply relaxing 9-1010
- glory, and diffr. peaks, uniform approx. 9-17699
- integral formulation, extension to Coulomb interac. 9-17725
- interpolation formulas of Lagrange form, construction of integral eqns. 9-8418
- isotropic transport, weak convergence to Brownian motion 9-17748
- Jost function, analytical props. for a more general class of potentials 9-14348
- Jost-soln. phase shift to approach potential 9-10960
- liquid, multiply relaxing 9-1010
- low frequency, hard and soft bodies far field calcs. 9-2138
- Milne problem in infinite slab geometry, depend. of asymptotic characteristics on scatt. operation 9-54
- molecular beams, transformation relationships from c.-of.-m. to lab. obs. 9-2932
- molecular beams by metal surfaces 9-3184
- molecules, inelastic, semiclassical theory 9-2929
- multiple, of waves in irregular media, spatial autocorrel. functions 9-20313
- multiple, variational technique 9-12873
- N-particle scattering amplitudes, nonrelativistic, integral eqns. derivation 9-14361
- N-particle syst., Hilbert space formulation of classical mech. 9-17740
- particle-bound-state scatt., compact operators method, one channel case 9-17726
- particles in infinite medium, multiple many-directional sources 9-12905
- phase shifts, superturbation theory, rapidly convergent 9-8419
- phase shifts in perturbation theory solution of Baker-Cambell-Hausdorff problem 9-18999
- of plane waves by singular potentials without using Lipman-Schwinger integral eqn. 9-53
- plane wave, quantum mechanical, from hard sphere, numerical evaluation 9-15407
- pole configuration in complex momentum plane for spherically symmetric potential 9-6315
- potential, appl. of inverse function of prod. of two Bessel functions 9-14325
- potential, bounds established from variational expression involving S-wave phase shifts 9-16688
- potential, high energy fixed angle, study 9-14326
- potential, local, of finite radius, nonrelativistic sum rules derived from causality condition of Wigner and Van Kampen 9-14349
- potential  $V(r)=g^2/r^4$  analytical props of scatt. amplitude 9-8792
- potentials, static; upper and lower bounds on scatt. lengths 9-17917
- quantum operators for delay time and time of motion 9-17724
- Rayleigh atmosphere, radiative transfer, soln. 9-19007
- reactive, phenomenological anal. 9-10315
- S-wave potential theory applic., pole approx. 9-15565
- of scalar waves by a convex transparent object with surface irregularities 9-52
- Schrodinger time depend. theory, screening 9-82
- small-angle, resolution errors, correction using Hermite function 9-11811
- variational method for phase shifts, analysis w.r.t. other methods 9-11404
- waves, low-freq., thro' aperture in soft screen, expansion and study of formulae 9-20311
- waves by fluctuating potentials system 9-8376
- Weinberg's quasi particle theory applied to standing waves leading to reactance matrix K 9-8375
- H-H<sub>2</sub>, elastic, quantum theory 9-2936
- He, elastic, from He and Ar, differential cross-section 9-727
- K, by Xe, Ar, Ne, He, H<sub>2</sub>, in thermal energy range, total cross section meas. 9-11413
- Li-Hg atomic beams, interatomic potential 9-15827

## acoustic waves

- backscatt. near grazing incidence from shallow water bottom 9-15237
- Brillouin, of temporally absorbed hypersonic waves, vel. dispersion calcs. 9-10732
- by compliant cylinder inhomogeneous, N-layer/gas or liq. 9-4329
- by cylinders, soft, creeping waves scatt., pulse shape changes 9-2218
- ellipsoids and cylinders, pulse form 9-2220
- hypersonic, temporally absorbed, vel. dispersion in Brillouin scatt. 9-10732
- by moving fluid cylinder, characteristics, magnitudes and rad. patterns, eff. of var. in angle of incidence 9-4331
- multiple, in reflection on rough surface, generalized boundary condition 9-10731
- from ocean surface, coherence of reradiated signals, theory 9-15999
- oceanic layer, Slope Water region, due to Myctophid fish schools 9-4040
- plane waves through array of scatterers 9-17800
- sound by sound, superposed parallel beams in liq. 9-4330
- sound pulses, f.m., by spherical elastic shells in water, freq. depend., echo struct., cross-correlations 9-4332
- spindle, nose-on incidence, Dirichlet calc. 9-10733
- in waveguide scattering of sound waves with resulting change of mode and absorption 9-17801

## acoustic waves, ultrasonic

- Mandel'shtam-Brillouin scattering amplification 9-5542
- Raman, in ferromagnet with strong magnetostriiction 9-5543

**electromagnetic waves**

- beam wave, by spherical object 9-6425
- bistatic, matrix analysis 9-19111
- Bragg, microwave analogue model modification 9-6
- conducting cylinder coated with moving uniaxial medium 9-12960
- conductor, cylindrically symmetric, plane waves scatt., exact soln. 9-8553
- from conductors, arbitrary shape, exact soln. 9-17834
- corrugated structures, TM plane wave solution 9-8554
- electric field, total, inside and outside non-mag. scattering bodies 9-19112
- by ferrite cylinder, dipolar resonance effect 9-19110
- in ferromagnets with small mag. anisotropy, anomalous 9-13972
- ferromagnets with weak magnetic anisotropy 9-18677
- finite perfectly conducting wedges, numerical results for radar cross section 9-6426
- groundwave by terrain features, two-dimensional analysis 9-8551
- $\theta$ -pinch in static magnetic field, incoherent microwave scatt., oscillations obs. 9-21087
- ionospheric, coherence ratio meas. 9-10425
- isotropic, from point source in finite spherical atmosphere 9-17835
- meas. at 15.7 GHz for troposphere structure study 9-1942
- metallic filament, thin and short, broadband backscattering 9-6431
- microwave, by turbulent plasma 9-9369
- microwaves in atmosphere, obs. 9-21780
- by neutrons, unpolarized, mathematical exam. 9-2280
- paramagnets in strong mag. field 9-21568
- plane, monochromatic, by uniformly expanding conducting sphere 9-20474
- plane wave by perfectly conducting wire, back-scatt. cross-sections modification by central loading 9-15487
- plane wave scatt. by linearly varying surface impedance 9-8552
- plane waves by moving conducting bodies, Doppler effect 9-188
- plane-polarized, by two equal spherical particles, inc. elec. and mag. dipole effects 9-14404
- planet surface, effect on radar reflectivity 9-2085
- plasma, turbulent; transport eqn. 9-9363
- plasma in strong fields, theory 9-14773
- radio, moon's surface 9-18901
- rough surface slope probability density function 9-266
- scattering by turbulent pulsations in inhomogeneous magnetoactive plasma 9-11562
- semiconductor, mag., by anomalous fluctuations of spin waves in elec. field 9-5814
- sphere, imperfectly conducting with positive and negative  $\epsilon$ , numerical results 9-19113
- spheres, imperfectly conducting, theory 9-19114
- spherical particles, isotropic, calc. by trigonometric expansions of Mie ang. functions 9-20473
- surface with slight roughness tilted away from reference plane, fields and scattered power 9-6427
- transient and impulse response approximations, interpretation 9-6428
- transmission and reflection by absorbing shell of arbitrary shape, boundary conditions 9-6424

**light**

*See also Diffusion, light*

- acrolein and deuterio-derivs., vibratory spectra 9-11491
- aerosol single particle, influence of collecting lens aperture 9-14864
- n-alkanes, depolarized, determ. of molec. optical anisotropy 9-14830
- anisotropic, for turbid medium boundary illuminated by narrow beam 9-5193
- anisotropic discs, polarized components theory 9-15168
- on anisotropic particles 9-12746
- atmosphere, semi infinite, brightness coeff. 9-2046
- atmospheric droplets, physical props. using Mie theory and laser radar return 9-10870
- atoms, interference of excited states considerations 9-683
- bacteria identification by differential scatt. 9-12780
- bacteria suspension in salt soln., osmotic vol. changes study 9-14867
- benzene, liq. and cryst., combination scatt., absolute cross-sections 9-1732
- binary mixtures, long range correlation effects 9-3105
- binary systems with arbitrary mixability of components, activity coeff. determ. 9-18362
- brightness decrease of light emitting objects in scattering media 9-20549
- carbon tetrachloride, relax. determ. 9-3100
- chemically reacting mixtures 9-5999
- cholesteryl myristate liq. cryst., rel. to orientation fluctuations 9-14851
- cholesteryl myristate mesophases, cholesteric, smectic and solid, light scattering props. 9-19633
- clouds, diffuse reflection and transmission 9-21770
- clouds, photographic obs. of the "Glory", Hawaii 9-14162
- coiled molecules, asymptotic behaviour 9-17209
- colloidal suspensions, forward scatt. rel. to particle size for strongly absorbing subst. 9-14865
- colloidal systems, nonlinear due to particle orientation, multiharmonic due to optical deform. 9-14866
- combinational, on Landau levels in semiconductors 9-1744
- corundum, synthetic, Tyndall scatt. rel. to microscopic and colloidal inclusions distrib. 9-1730
- crystals, by light, cross-section rel. to nonlinear polarizability 9-1720
- cyclohexane-aniline binary mixture, long range correlation effects 9-3105
- diacetyl and deuterio-derivs., vibratory spectra 9-11491
- diatomic mols., resonance scatt. in external fields rel. to excited level characts 9-750
- diffuse spectra, double-beam attachment to spectrophotometer for meas. 9-10904
- diffusion theory in scattering media 9-2405
- Einstein's eqns., microscopic extensions 9-13331
- Einstein eqns., microscopic theory 9-13330
- electrons and monatomic gases, using Dirac's noncovariant theory of radiation 9-20550
- from ethanol-water, methanol mixtures, Rayleigh ratios and depolar., anisotropic scatt. contrib. 9-21209
- extrapolation of data to zero scatt. angle, inherent problems 9-14874
- films, by small metallic particles, comparison with absorption 9-15166
- fission track density meas. in dielectric detector 9-6736
- Fraunhofer region, wave eqn. soln. for inhomogeneous media 9-6550
- gas, monochromatic light resonant scatt., freq. distrib. and interference 9-21140
- glass, phase-separated, meas. of diffusion coeffs. 9-14954

**Scandium compounds continued****light continued**

- glyoxal and deuterio-derivs., vibratory spectra 9-11491
- goniophotometer, measurement of scattering characteristics of various objects 9-13054
- hectorite solutions, in elec. field, rel. to particle struct. and elec. anisotropy 9-14861
- heterodisperse systems of isotropic spheres, computer calc. 9-11725
- for holography, three beam 9-20538
- by igneous rocks, spectral obs., Stokes parameters 9-17476
- inert gas, Rayleigh radiation depolarization, cage model 9-21139
- integral for average power from rough surface 9-266
- interaction of light with insulating crystals 9-12351
- inverse, geometric optics limit 9-10893
- ionic crystals, Rayleigh scattering from surface modes, cross sections 9-12393
- ionic crystals, using Divae's noncovariant theory of radiation 9-20550
- Irran I, angular distrib., i.r. obs. 9-12325
- with known coherence function, eqn. for intensity derived 9-8655
- laser beam, optical saturation theory 9-20530
- laser beam, self beating tech. for study of motions in colloids and macromols. in soln. 9-14875
- in laser generation, effect on characts. and oscillation modes 9-8599
- laser measurements in mesosphere and above 9-12587
- leuco-sapphire, Tyndall scatt. rel. to colloidal inclusion distrib. 9-1730
- liquid, orientational relax. determ. by Rayleigh scatt. 9-1009
- liquid, Rayleigh line spectrum rel. to mol. vib. 9-2888
- liquid crystals, nematic, electro-optic dynamic scatt., obs. 9-9510
- liquid studies 9-11676
- liquid surface, stimulated, theory 9-1012
- liquids, activity coeff. determ. 9-9487
- liquids, anti-Stokes generation in trapped filaments of light 9-3102
- liquids, hole theory 9-21206
- liquids, molecular theory 9-18360
- liquids, pure, Rayleigh scatt. and depolarization, temp. depend. 9-14849
- liquids, Rayleigh ratio and depolarization factors rel. to molec. interactions 9-14850
- liquids, thermally excited shear waves producing peaks 9-21211
- macromolecular solutions, critical opalescence 9-16027
- macromolecules, flexible, excluded vol. effects 9-17208
- macromolecules, flexible coil, spectral distrib. 9-3101
- macromolecules, optically anisotropic, spectrum 9-1011
- medium with moving boundary, applic. to Nova phenomena 9-19165
- in a medium with nonlinear polarizability 9-13055
- from methanol-water, ethanol mixtures, Rayleigh ratios and depolar., anisotropic scatt. contrib. 9-21209
- molecular backscatter of laser rad. from turbulent air 9-21141
- molecular theory, liquids 9-18360
- neutral gases, Rayleigh scatt. of ruby laser light and depolarization 9-14435
- non-coherent, Doppler redistribution functions in moving atmosphere 9-16565
- noncoherent, in fundamental absorption region 9-1733
- oil-in-water emulsions, matched with specific turbidity, rel. to globule-size distrib. 9-14869
- one component system near critical point, rel. to density gradient 9-18387
- orientation fluctuation in dipolar media, phenomenological 9-15164
- by particles in fluid 9-16026
- photometer, calibration 9-271
- from plasma in mag. field 9-16397
- by plasma in magnetic field 9-2975
- polydisperse rod solns., distrib. curves from intensity decay in elec. field 9-14860
- polymer films, polarized light, model of annular spherulites 9-7940
- polymer in good solvent, determ. of polydispersity index 9-14862
- polymer latexes, particle size, computer analysis 9-17223
- polymer single crystals grown in soln., rel. to kinetics and optical anisotropy 9-15168
- polymer solutions, dilute, precise data, photometer 9-16003
- polymer solutions in turbidimetric titration, conc. determ. of precipitated particles 9-14870
- poly- $\alpha$ -methylstyrene solns., ang. depend. and radius of gyration determ. 9-14874
- polystyrene in cyclohexane, macromolecular solutions, critical opalescence 9-16027
- quartz, by hypersonic waves, Mandel'shtam-Brillouin component freq. 9-1811
- quartz, critical, opalescence, obs. and interpretation 9-10181
- quartz, optically active, polarized light Rayleigh scatt. by defects, obs. 9-12340
- quartz, Rayleigh scattering, Temp. depend. 9-12445
- Rayleigh, from circularly birefringent media 9-19166
- Rayleigh, in liquids, stimulated thermal 9-9512
- Rayleigh scattering stellar atmosphere, finite plane-parallel, albedo problem 9-18877
- resonance scatt., applic. of quasiparticle kinetic eqn. to order  $\lambda^6$  9-11389
- resonance variation of coherent props., in many level system 9-8638
- rough surface, rotation of polarization plane rel. to radial angle of obs. 9-8656
- ruby, depolarization of light scattered through small angles 9-5877
- ruby laser beam incident on neutral gas, depolarization ratio determ. 9-9453
- S, La Mer sols, analysis of particle size distrib. and number conc., time depend. 9-14871
- salts, polycrystalline, combination scatt. spectra in i.f. region, temp. phase dependence 9-12367
- shock tubes, effect on emission meas. 9-2235
- small angle, phase function 9-17570
- Sofica and Brice-Phoenix photometers, reflection effects, anal. of ang. scatt. data 9-14832
- from solid state plasmas 9-16425
- solids, spectra, conference 9-10190
- by spacecraft (manned) debris atm. 9-20124
- spectrum near critical point by fluctuations 9-11742
- starch granules, rel. to average diameter and fluctuations in anisotropy 9-15167
- statistical copolymers, heterogeneity parameters 9-19487
- stilbene, liq. and cryst., combination scatt., absolute cross-sections 9-1732



**Scandium compounds continued****light continued**

- stimulated, effect of self-focussing of inhomogeneous laser beams 9-14438  
 stimulated, thermal, picosecond regime, in absorbing liqs. and some glasses 9-11697  
 stimulated Rayleigh-wing scattering theory 9-4893  
 stimulated scatt., saturation and depletion 9-14420  
 in system when second medium is optically homogeneous, and surface of divider is smooth 9-265  
 transfer eqn. method and Buger-Lambert-Beer eqn. method, comparison 9-267  
 transient, mean multiplicity rel. to photon diffusion 9-17890  
 transient luminescence of optical layers, kinetics analyzed 9-8648  
 trilinear processes, geometrical model 9-10838  
 troposphere, polarized, comparison with zodiacal polarization 9-1938  
 turbulent medium, time-dependent autocorrelation functions 9-19631  
 twilight, colour rel. stratospheric dust 9-21776  
 two-phonon scattering, electronic terms in spectrum 9-11982  
 from water methanol, ethanol mixtures, Rayleigh ratios and depolar., anisotropic scatt. contrib. 9-21209  
 yeast cells in water, small ang. depend., comparison with Mie theory 9-14868  
 AeSb, from single particle electron and hole excitations 9-12443  
 Ar, gaseous, due polarizability charge prod. in colliding atom pairs 9-959  
 CO<sub>2</sub>, depolarization and Krishnan effect near critical point 9-961  
 CO<sub>2</sub>, depolarized Rayleigh line width meas. for reorientation cross-section calc. 9-13345  
 CdTe, from single particle electron and hole excitations 9-12443  
 Cu thin films, 2200 to 5400 Å 9-17478  
 Eu chalcogenides, magnetic domains effects 9-12328  
 EuS, diffuse, by ferromag. domains 9-10180  
<sup>57</sup>Fe, Rayleigh scatt., spin depend., interference with Mossbauer scatt. 9-7959  
 GaAs, from plasmons and phonons 9-12353  
 GaAs, from single particle electron and hole excitations 9-12443  
 H<sub>2</sub>, depolarized Rayleigh line width meas. for reorientation cross-section calc. 9-13345  
<sup>3</sup>He-<sup>4</sup>He liquid mixtures, by entropy fluctuations and second sound 9-5204  
 InP from single particle electron and hole excitations 9-12443  
 KCl:Pb, Rayleigh scatt. by single crystal 9-19993  
 Kr, gaseous, due to polarizability charge prod. in colliding atom pairs 9-959  
 N<sub>2</sub>, liq., stimulated combinational, energy and time characts. 9-1013  
 N<sub>2</sub> depolarized Rayleigh line width meas. for reorientation cross-section calc. 9-13345  
 NH<sub>4</sub>Cl, critical harmonic scattering 9-12444  
 NaClO<sub>3</sub>, cryst. and powder, combination scatt., absolute cross-sections 9-1732  
 SF<sub>6</sub>, depolarization, including Krishnan effect near critical point 9-961

**light, Brillouin spectra**

- Cummins Gammon formulas based on hole theory 9-21206  
 introductory paper in conference 9-12447  
 paramagnetic crystals 9-12449  
 by phonons in presence of heat flow in insulating cry. Stokes and anti-Stokes Brillouin intensities diff. 9-16162  
 polarization selection rules for crystals 9-12448  
 polymeric solids, relaxational structure transitions 9-12450  
 quartz, hypersonic attenuation, temp. depend. 9-12000  
 quartz, temp. depend. 9-12445  
 silicate glasses, fine structure 9-3908  
 stimulated, rel. to u.s. generation study 9-10836  
 Stokes line, forward first, vanishing 9-1810  
 toluene, line widths using laser and interferometer 9-9521  
 p-(o-) xylene, line widths using laser and interferometer 9-9521  
 CS<sub>2</sub>-CCl<sub>4</sub> mixtures, hypersonic velocity meas. 9-3095  
 CdS, acoustoelec. domain propag. obs. 9-1517  
 CdS, for acoustoelectric interaction analysis 9-12010  
 CdS, photoconducting, acoustic flux distrib., obs. 9-3907  
 CdS acoustoelec. eff. study at microwave freq. 9-12013  
 CdS laser induced scattering 9-3906  
 GaP, digital recording method 9-12446  
 He II, stimulated Mandelstam-Brillouin scatt., rel. to sound propag. 9-14879  
 KBr, component linewidth 9-12451  
 KH<sub>2</sub>PO<sub>4</sub>, study of ferroelectric phase transition 9-12198  
 KH<sub>2</sub>PO<sub>4</sub>, ferroelec. transition at 122°K 9-5750  
 LiNbO<sub>3</sub> 9-12452  
 MgO:Ni microwave, acoustic phonon bottleneck, direct obs. 9-9819  
 NH<sub>4</sub>Cl, Rayleigh-Brillouin spectra 9-16426  
 ZnO acoustoelec. eff. study at microwave freq. 9-12013

**light, Raman spectra**

- antiferromagnets, two magnon pairing effects 9-12435  
 benzene, stimulated by focused low power ruby laser beam 9-5171  
 cross-sections, in crystals and crystalline powders 9-12428  
 crystals, elec. field induced i.r. absorpt. and Raman scatt. 9-16420  
 electronic transition selection rules where appropriate point group is double group 9-3905  
 excitation of induced lines with high generation thresholds 9-4897  
 field induced 9-12400  
 first-order, by polar lattice vibrations 9-12391  
 gases, stimulated combinational, effect of collisions 9-13324  
 generation of freq. differences, conditions 9-4896  
 impurity centre, resonant secondary radiation, infl. of depend. of electronic matrix element on vib. coords. 9-15179  
 impurity-containing crystals, lattice scatt., microscopic theory 9-12402  
 indicatrix asymmetry, intensity depend. on direction 9-4899  
 induced combinational on i.r. active transitions 9-10218  
 intensity, molec. theory 9-733  
 intensity distribution, effect of resonator 9-4536  
 laser, stimulated, high conversion efficiency, quantitative investigation 9-20533  
 laser scattering 9-12390  
 laser excited at 50 cps pulse frequency, signal-noise ratio improvement 9-6560  
 laser-induced instabilities, growth rates 9-11699  
 line width broadening calc. 9-18163  
 liquid, transient stimulated scatt., laser line breadth determ. 9-13527  
 liquids, stimulated by focused low power ruby laser beam 9-5171  
 magnons and their interactions, Raman scatt. obs. 9-12425

**Scandium compounds continued****light, Raman spectra continued**

- nitrobenzene, stimulated by focused low power ruby laser beam 9-5171  
 photon counting system for Raman spectroscopy 9-10818  
 in planetary atmospheres, rotational Raman scatt. 9-15335  
 by polaritons in polyatomic crystals 9-12392  
 polarized, applic. to electr. symmetries calc. 9-17021  
 rapid scanning spectrometry techniques 9-10938  
 receiver choice 9-282  
 review 9-2838  
 scattering tensor for combinations and overtones 9-12394  
 selection rules for Raman effect 9-13323  
 semiconductors, by Landau levels 9-12398  
 semiconductors, by Landau levels 9-12397  
 semiconductors, from magnetoplasma waves 9-12415  
 semiconductors, shallow impurity states, mag. field eff. 9-12396  
 single crystal, chemical implications of laser spectroscopy, with examples 9-21633  
 solids, impurity induced 9-12401  
 spectrometers using laser beams, patent 9-17899  
 stimulated Raman effect, theory 9-9169  
 s-tetrazine-d<sub>8</sub> and d<sub>2</sub>, fundamental vibr. freqs. determ. 9-11500  
 vibrational relaxation of excited luminescence centre 9-12403  
 zinc-blende and wurtzite type crystals, by TO and LO phonons 9-12441  
 Ar laser spectroscopic system 9-15559  
 CS<sub>2</sub>, stimulated by focused low power ruby laser beam 9-5171  
 CdCr<sub>2</sub>Se<sub>4</sub>, ferromagnetic 7°-295°K 9-12409  
 aser, pulse shapes and spatial modes, theory and experiment 9-19141  
 Se-S<sub>8</sub> bond energy diff., force const., fundamental modes assignment 9-20941
- light, Raman spectra, inorganic**
- alkali fluorides, second-order calc. for vibration spectra computation 9-12429  
 alkali halide crystals, of O<sub>2</sub><sup>-</sup> ion 9-10220  
 antiferromagnet, two spin-wave, i.r. absorption 9-12395  
 calcite, stimulated, anti-Stokes components 9-1770  
 cubic single crystals, second order Raman-laser spectrum 9-12421  
 diamond, elec. field eff. 9-12406  
 F-centres in alkali halides, Raman spectra 9-12404  
 ferroelectric crystals, from soft optic mode 9-12405  
 1-fluoro-2-haloethanes, rot. isomers 9-812  
 garnets: rare-earth, electronic and vibrational Raman eff. obs. 9-12434  
 glass, low expansion, CER-VIT, fused silica, ULE and Corning heat absorbing glass 9-12417  
 glycerol, using 4880 Å Ar laser 9-15890  
 halides, by hydroxyl ion 9-12432  
 In chlorides, fused, structure obs. 9-21215  
 ionic crystals, from surface modes, cross sections 9-12393  
 metals, inelastic scatt. theory, opt. phonons 9-1759  
 metals, polyatomic, scatt. by opt. vibration modes, theory 9-12399  
 MnF<sub>2</sub>:Ni<sup>2+</sup> (F<sup>2+</sup>), from magnetic excitations 9-12427  
 Na<sub>2</sub>[Fe(CN)<sub>5</sub>NO].2H<sub>2</sub>O, single crystal 9-19995  
 quartz, one- and two-phonon excitations coupling evidence 9-1361  
 quartz, stimulated, rel. to i.r. generation at 10°K 9-7983  
 quartz, temp. depend. 9-12445  
 quartz, u.s. induced enhancements 9-21636  
 rare-earth chlorides, electronic eff. 9-12356  
 semiconductors, theory rel. to plasmon-phonon interaction 9-3901  
 spin-Raman susceptibility by means of spin-wave instabilities 9-10143  
 sulphates, molten 9-16005  
 Y<sub>3</sub>Al<sub>5</sub> garnet, optical phonon investigation 9-3512  
 zinc-blende, second order Raman-laser spectrum 9-12421  
 AlN, excited by He-Ne laser 9-1805  
 AuAl, frequency of observed line 9-1804  
 BN and BP, excited by He-Ne laser 9-1805  
 BaBrF 9-5934  
 BaClF 9-5934  
 Ba<sub>2</sub>NaNb<sub>3</sub>O<sub>15</sub>, stimulated, gain coeffs. 9-5936  
 Ba, frequency of observed line 9-1804  
 Bi, by optical modes, linewidths, temp. depend. 9-12442  
 Bi chlorides, fused, structure obs. 9-21215  
 C<sub>2</sub>N<sub>2</sub>, solid 9-16164  
 CF<sub>3</sub>OF liquid, freq. assignments, thermodynamic props. calc. 9-19465  
 CM<sub>3</sub>N type mol., intensities rel. to symmetry props. 9-734  
 CN<sup>-</sup> in alkali halides 9-12407  
 CS<sub>2</sub>, stimulated Raman scatt., periodic fine struct. 9-21212  
 CS<sub>2</sub>, polarized band intensities, influence of solvent 9-13528  
 CaF<sub>2</sub>-SrF<sub>2</sub> mixed crystal, from point defects 9-12408  
 Ca(NH<sub>4</sub>SO<sub>3</sub>)<sub>2</sub> 9-12458  
 Ca(NO<sub>3</sub>)<sub>2</sub>-Ba(NO<sub>3</sub>)<sub>2</sub>-Sr(NO<sub>3</sub>)<sub>2</sub> binary fused systems, structure obs. 9-17186  
 CdCr<sub>2</sub>Se<sub>4</sub>, ferromagnetic, Raman scattering 9-12410  
 CdCr<sub>2</sub>Se<sub>4</sub>, Raman scatt. 9-16421  
 CdS, powder, cross section, temp. depend. 9-12428  
 CdS, resonant eff. 9-12411  
 CdS, spin-flop scatt. in mag. field 9-10219  
 CdS, Se<sub>1-x</sub>S<sub>x</sub>, line width, and intensity, temp. depend. 9-12437  
 CeCl<sub>3</sub>, active phonon spectra 9-3903  
 CeCl<sub>3</sub>, electronic eff. 9-12356  
 CoF<sub>2</sub>, two-magnon pairing eff. 9-12435  
 CsBr sp. ht. calc. from freq. spectra 9-7633  
 CsCl sp. ht. calc. from freq. spectra 9-7633  
 CsF, second order calc. for vibration spectra computation 9-12429  
 CsF sp. ht. calc. from freq. spectra 9-7633  
 CsI, second order spectra 9-17481  
 CsI sp. ht. calc. from freq. spectra 9-7633  
 CuCl, second order Raman-laser spectrum 9-12421  
 D<sub>2</sub>P(BH<sub>3</sub>)<sub>2</sub><sup>-</sup>, vibr. modes and P B force const., obs. 9-18183  
 Eu<sup>3+</sup>, scattering tensor of transitions rel. to hosts crystal field symmetry 9-21634  
 FeF<sub>3</sub>, magnon-magnon interactions and excitations 9-12425  
 n-GaAs, e plasma in mag. field 9-14060  
 GaAs, from electron spin-density fluctuations 9-12414  
 GaAs, from magnetoplasma waves 9-12415  
 GaAs, line width, and intensity, temp. depend. 9-12437  
 GaAs optical phonons obs., Ar laser excitation 9-12419  
 GaAs<sub>x</sub>Pi<sub>1-x</sub>, from lattice vibrations 9-12416  
 GaP, digital recording method 9-12446  
 GaP, powder, cross-section, temp. depend. 9-12428  
 H<sub>2</sub>, intensity theory 9-733  
 H<sub>2</sub>P(BD<sub>3</sub>)<sub>2</sub><sup>-</sup>, vibr. modes and P B force const., obs. 9-18183

**Scattering continued****light, Raman spectra, inorganic continued**

- H<sub>2</sub>P(BH<sub>3</sub>)<sub>3</sub>, vibr. modes and P B force const., obs. 9-18183  
 H<sub>2</sub>S and D<sub>2</sub>S, polycryst. phases 9-5935  
 He, liquid, theoretical model 9-11734  
 IF<sub>3</sub> 9-2871  
 InAs, optical phonons obs., Ar laser excitation 9-12419  
 InP optical phonons obs., Ar laser excitation 9-12419  
 InSb, by LO phonons, resonance enhanced, elec. field induced 9-12420  
 InSb, photon energies near the E<sub>g</sub> energy gap 9-1806  
 InSb optical phonons obs., Ar laser excitation 9-12419  
 KAg(CN)<sub>2</sub>, rel. to lattice vibrs. and Ag(CN)<sub>2</sub><sup>+</sup>, obs. 9-16166  
 KBr, second order Raman-laser spectrum 9-12421  
 KF, second-order calc. for vibration spectra computation 9-12429  
 K<sub>2</sub>H<sub>2</sub>PO<sub>4</sub>, H<sub>2</sub>PO<sub>4</sub><sup>-</sup> ion structure obs. in ferroelec. and paraelec. states 9-18652  
 K<sub>2</sub>H<sub>2</sub>PO<sub>4</sub>, by polarization fluctuations 9-12423  
 K<sub>2</sub>H<sub>2</sub>PO<sub>4</sub>, dielectric phase transition data 9-12422  
 K<sub>2</sub>I, second order Raman-laser spectrum 9-12421  
 KNO<sub>3</sub>-Ca(NO<sub>3</sub>)<sub>2</sub> melts, NO<sub>2</sub> Raman frequencies 9-9516  
 KNO<sub>3</sub>, phases I, II and III 9-14061  
 KNO<sub>3</sub>, dielectric phase transition data 9-12422  
 KNO<sub>3</sub>, in phases I, II, and III 9-12424  
 KTaO<sub>3</sub>, elec. field induced first-order scatt. in paraelec. crystals 9-5938  
 KTaO<sub>3</sub>-K<sub>2</sub>NbO<sub>5</sub> solid solutions 9-12433  
 LaBr<sub>3</sub>, compared with LaCl<sub>3</sub> 9-3904  
 LiF, by ultra microscopic centres, multiple-phonon processes 9-5937  
 LiF, ideal lattice spectra generation due to anomalous polarization at surface of ultramicroscopic scatt. centres 9-16422  
 by LiNbO<sub>3</sub> polaritons, stimulated 9-21635  
 Li<sup>+</sup>NbO<sub>3</sub>, stimulated, gain coeffs. 9-5936  
 Mg, by optical modes, line widths, temp. depend. 9-12442  
 MgO, agreement with two phonon density of state curve 9-11988  
 MgO, agreement with two phonon density of state curve 9-9820  
 MnF<sub>2</sub>:Fe<sup>2+</sup> 9-10221  
 MnF<sub>2</sub>:Ni, magnons localized on Ni ions 9-12426  
 MnF<sub>2</sub>:Ni<sup>2+</sup>, low temp obs. 9-10221  
 MnF<sub>2</sub>:Ni, magnons, localised, obs. 9-14062  
 MnF<sub>2</sub>, magnon-magnon interactions and excitations 9-12425  
 Mo(IV) Cl<sub>6</sub> 9-7982  
 MoSe<sub>2</sub>, rel. to vibrs., laser obs. 9-15859  
 N<sub>2</sub> liquid, obs. using laser beam 9-21216  
 NCl<sub>3</sub>, i.r. 9-9222  
 (NH<sub>4</sub>)<sub>2</sub>MoO<sub>4</sub>, rel. to vibrs., laser obs. 9-15859  
 (NH<sub>4</sub>)<sub>2</sub>MoS<sub>4</sub>, rel. to vibrs., laser obs. 9-15859  
 (NH<sub>4</sub>)<sub>2</sub>WO<sub>4</sub>, rel. to vibrs., laser obs. 9-15859  
 NH<sub>4</sub>Br, vibrational, of order-disorder transition 9-11973  
 NH<sub>4</sub>Br, order evolution at  $\lambda$  transition 9-11972  
 NH<sub>4</sub>Cl, vibrational, of order-disorder transition 9-11973  
 NH<sub>4</sub>H<sub>2</sub>PO<sub>4</sub>, dielectric phase transition data 9-12422  
 NO<sub>2</sub> in alkali halides 9-12407  
 Na<sub>2</sub>Al<sub>2</sub> cryolite, liq., complex ion identification 9-1017  
 NaBr, of F centres 9-12431  
 NaBr, of F-centres 9-12404  
 NaCl, second order, 90°K 9-12430  
 NaCl, second order Raman laser spectrum 9-12421  
 NaClO<sub>3</sub>, powder, cross-section, temp. depend. 9-12428  
 NaF, second-order calc. for vibration spectra computation 9-12429  
 NaI, second order spectra 9-17481  
 NaNH<sub>2</sub>SO<sub>3</sub> 9-12458  
 NaNO<sub>3</sub>-Ca(NO<sub>3</sub>)<sub>2</sub> melts, NO<sub>2</sub> Raman frequencies 9-9516  
 NaTaO<sub>3</sub>-KTaO<sub>3</sub> solid solutions 9-12433  
 NSF<sub>3</sub>, rel. to Coriolis const. and thermodynamic functions, i.r. obs. 9-15862  
 O<sub>2</sub>, liquid, obs. using laser beam 9-21216  
 O<sub>2</sub> in alkali halide crystals. 9-1807  
 OH<sup>-</sup> in alkali halides 9-12407  
 PH<sub>3</sub>Br, laser-Raman spectra, barriers to PH<sub>3</sub><sup>+</sup> rot. obs. 9-15865  
 PH<sub>3</sub>Cl, laser-Raman spectra, barriers to PH<sub>3</sub><sup>+</sup> rot. obs. 9-15865  
 PH<sub>3</sub>I, laser-Raman spectra, barriers to PH<sub>3</sub><sup>+</sup> rot. obs. 9-15865  
 PH<sub>3</sub>I and PD<sub>3</sub>I, far i.r., polycryst. 9-1794  
 n PbTe, electron spin flip Raman scatt. 9-18715  
 PbTiO<sub>3</sub> 9-12433  
 Pd(II) selenourea complexes, vibr. modes, obs. 9-15867  
 Pd(II) thiourea complexes, vibr. modes, obs. 9-15867  
 PtCl<sub>3</sub>, active phonon spectra 9-3903  
 Pt(NH<sub>3</sub>)Cl<sub>3</sub>, rel. to metal-ligand vibr. and Pt-Cl bands, obs. 9-15868  
 Pt(CO)Cl<sub>3</sub>, rel. to metal-ligand vibr. and Pt-Cl bands, obs. 9-15868  
 Pt(II) selenourea complexes, vibr. modes, obs. 9-15867  
 Pt(II) thiourea complexes, vibr. modes, obs. 9-15867  
 RbCl sp. ht. calc. from freq. spectra 9-7633  
 RbF, second-order calc. for vibration spectra computation 9-12429  
 RbMnF<sub>3</sub>, magnon-magnon interaction and excitation 9-12425  
 RbMnF<sub>3</sub>, two-magnon pairing eff. 9-12435  
 RbNiF<sub>3</sub> spin excitations, 15-300°K using Ar laser 9-10222  
 ReF<sub>3</sub> 9-2871  
 SO<sub>2</sub>BrF, vibr. assignments from Cs model, obs. 9-15870  
 Si, line width, and intensity, temp. depend. 9-12437  
 SiC, phonon dispersion curves in polytypes 9-3509  
 SiO<sub>2</sub>, fused, rel. to calculated SiO<sub>4</sub> mol. vibrations 9-14694  
 SrClF 9-5934  
 SrTiO<sub>3</sub>, 110°K, phase transition, mechanism evidence 9-11968  
 SrTiO<sub>3</sub>, elec. field-induced first-order scatt. in paraelec. crystals 9-5938  
 SrTiO<sub>3</sub>, spatial variation below 110°K 9-16423  
 SrF<sub>2</sub>-Ca, Raman scattering of green coloured crystals 9-12438  
 TbAl garnet, electronic transitions of Tb<sup>3+</sup> 9-10223  
 TiCl<sub>4</sub>, liq., molec. assoc. and isotope effects 9-1021  
 TiBr, second order spectra 9-17481  
 TlI, pressure depend., induced phase transitions and phonon freq. shifts 9-18716  
 TmGa garnet, oriented crystal, laser induced phonon spectra 9-12439  
 WSe<sub>2</sub>, rel. to vibrs., laser obs. 9-15859  
 XeO<sub>3</sub>F<sub>2</sub> 9-791  
 Y Ga garnet, electronic transitions selection rules rel. to double group, D<sub>2</sub> 9-3905  
 YAl garnet 9-10223  
 YF, garnet, spin Raman susceptibility by means of spin-wave instabilities 9-10143  
 Zn, by optical modes, line widths, temp. depend. 9-12442  
 ZnS, Brillouin zone scattering 9-12440  
 ZnSe, resonant eff. 9-12411

**Scattering continued****light, Raman spectra, organic**

- p-dichlorobenzene, librational amplitudes 9-10224  
 acetaldehyde-2,2,2-d<sub>3</sub> 9-2889  
 acetyl chloride, absolute intensities, obs. and theory 9-2890  
 anthracene, rel. to lattice vibr. intensities, obs. 9-18551  
 anthracene, vibrational study 9-18196  
 anthracene cryst., polarization 9-15180  
 benzene, laser induced instabilities, growth rates 9-11699  
 benzene, powder, cross-section, temp. depend. 9-12428  
 benzene, thermo-spectrum of stimulated 8050 Å line, fine structure period 9-1022  
 benzene substitute, vib. freq. assignment 9-7051  
 benzil crystal 9-5939  
 benzoyl chloride, in liq. solid and gaseous state 9-11481  
 2-bromo propionitrile, vib. freq. assignments, semiquantitative polariz. data obs. 9-20975  
 bromocyclobutane, ring-puckering vib. and potential functions determ. 9-20957  
 bromonitromethane and d<sub>2</sub> analogue, vibr. assignments, obs. 9-15893  
 carbazole 9-9252  
 carbon tetrachloride l.f. motions in liq. 9-9518  
 carbon tetrafluoride, liq. and cryst. 9-1023  
 2-chloro propionitrile, vib. freq. assignments, semiquantitative polariz. data obs. 9-20975  
 chlorocyclobutane, ring-puckering vib. and potential functions determ. 9-20957  
 chloroform, effect of intermolec. interactions on isotope struct. 9-7266  
 chloronitromethane and d<sub>2</sub> analogue, vibr. assignments, obs. 9-15893  
 Chymotrypsin, obs. 9-5940  
 Coumarin, solid and molten, relative intensities 9-11483  
 cyclobutanol, ring pucker vib. and potential functions determ. 9-20957  
 cyclohexane, new spectral components of stimulated scatt. 9-1809  
 cyclohexane, solid phases 9-1801  
 cyclopentadiene: intensity, depolarization, width of line obs. in liquid, 30±5°C 9-4963  
 dibromomethane, d<sub>2</sub>, d<sub>1</sub> and d<sub>3</sub> 9-15886  
 trans-1,4-diodocyclohexane, vibrational spectra and rotational isomerism 9-17482  
 diketene, ring pucker vib. and potential functions determ. 9-20957  
 dimethyl diselenide 9-9264  
 N, N-dimethylacetamide, 3100 250 cm.<sup>-1</sup> obs. 9-4957  
 N, N-dimethylformamide, 3100 250 cm.<sup>-1</sup> obs. 9-4957  
 dimethylsulfoxide, rel. to intermol. interaction in solns., i.r. obs. 9-18365  
 1,3 dioxolane 9-809  
 dye solns., i.r. resonance stimulated, rel. to light generation 9-5169  
 furan: intensity, depolarization, width of line obs. in liquid, 30±5°C 9-4963  
 imidazole cryst., l.f. spectrum 9-16424  
 isobutene, -d<sub>2</sub>: moments of inertia calc., isotopic bands assignment 9-7055  
 lithium acetate dehydrate, meas. in polarized light 9-10225  
 lithium methanesulphonate 9-18218  
 Lysozyme, obs. 9-5940  
 methane, halogen substituted, intensities calc. by bond polarizability theory 9-13387  
 methyl iodide liq. phase, band width C-1 stretching vibrs. 9-4959  
 methylamine, solid and matrix isolated 9-10215  
 naphthalene, rel. to lattice vibr. intensities, obs. 9-18551  
 naphthalene cryst., polarization 9-15180  
 pentafluorotoluene, vib. spectra, assignments 9-11498  
 pepsin, obs. 9-5940  
 perfluorotoluene, analysis and vib. modes assignment 9-20973  
 polarized band intensities, solvent and concentration effects 9-13528  
 polyethylene, crystalline 9-10226  
 polyethylene rel. to B<sub>2</sub>g methylene wagging freq., obs. 9-14063  
 polyoxymethylene, hexagonal, orthorhombic, deutero, and vib. assignments 9-14064  
 $\beta$ -propiolactone, ring-puckering vib. and potential functions determ. 9-20957  
 propionitrile, vib. freq. assignments, semiquantitative polariz. data obs. 9-20975  
 pyridine, induced scatt., effects of dissolved subst. 9-3109  
 pyrrole: intensity, depolarization, width of line obs. in liquid, 30±5°C 9-4963  
 resonance stimulated, in liq. dye solns., rel. to light generation 9-5169  
 sodium methanesulphonate 9-18218  
 stilbene, powder, cross-section, temp. depend. 9-12428  
 thiophene: intensity, depolarization, width of line obs. in liquid, 30±5°C 9-4963  
 thiophene liq. phase, vib. bands 9-3110  
 trichloromethyl cyanide, effect of intermolec. interactions on isotope struct. 9-7266  
 trichloromethyl fluoride, effect of intermolec. interactions on isotope struct. 9-7266  
 triethylphosphine selenide, fundamental vibrations assignment 9-18204  
 triethylphosphine sulfide, fundamental vibrations assignment 9-18204  
 triglycine sulphate, l.f., near Curie point 9-1808  
 trimethylene oxide, vibration mode characterization 9-17483  
 urea, rel. to cryst. lattice vibrations 9-17351  
 BaTiO<sub>3</sub>, single domain, rel. to mode damping 9-3902  
 CCl<sub>4</sub>, mol. symmetry and Jahn Teller eff. obs. 9-4950
- X-rays** see *X-ray scattering*  
**Scattering, elementary particles** see *Elementary particles/scattering*  
**Scattering, nuclear** see *Nuclear reactions and scattering*  
**Scattering, particles**  
 See also *Collision processes; Energy loss of particles; Field theory; quantum interactions; Elementary particles/scattering; Nuclear forces; Nuclear reactions and scattering; Particle tracks; S matrix theory; and under individual particles, e.g. Alpha particles*  
 angular momentum, tensor form, classical mech. and quantum field theory investigation of eff. 9-16803  
 backscattering of electrons in gas discharge tubes 9-19526  
 charged, by random e.m. fields 9-16773  
 charged, elastic scatt. from polar, quadrupole moment, DWBA and WKB techniques 9-2642  
 charged particle emission from crystals, angular distrib. mass dependence, transition to classical limit 9-7863  
 Coulomb nuclear S-matrix study, asymptotic behaviour in scattering plane 9-13215



**Scattering, particles continued**

- elastic, transition matrix, unitarized Born approx. soln. 9-4577
- exclusion principle and equivalent potential, neutral complex particles 9-568
- high energy, quark model predictions, simplified derivation 9-4591
- high energy particles scatt. by plane, distribution 9-16765
- ions, channeled, rel. to stopping powers 9-5586
- ions, heavy, Coulomb back scatt. for foil thickness meas. 9-5234
- Klein-Gordon eqn., nonlinear, time and local energy decay 9-302
- w.r.t. modified Gaussian potential 9-11175
- nuclear emulsions, scatt. factor determ. for different cell lengths 9-20712
- single-channel, Levinson theorem and Coulomb field, quantum defect. 9-6316
- small angle, and peak formation 9-19301
- on surface and detection of surface phonons, for structure determ. 9-21256
- transport eqn. soln. singularities on interfaces 9-8463
- uniform density beam, perpendicular to rectangular edge of slit 9-20493
- Cs<sup>+</sup> slow ions by W surface 9-5231

**Schizons** *see* *Elementary particles; Field theory, quantum/interactions, weak*

**Schlieren systems**

- photographs of pulsed circumferential waves on Al cylinders 9-3521
- SF<sub>6</sub> a.c. are characteristics filmed by laser-Schlieren technique 9-17881

**Schottky defects** *see* *Crystal imperfections/vacancies*

**Schottky effect (noise)** *see* *Electron tubes; Noise/electrical; Semiconducting devices*

**Schrodinger equation** *see* *Quantum theory/wave equations*

**Schwarzschild space** *see* *Cosmology; Gravitation; Relativity/general*

**Scintillation** *see* *Luminescence*

**Scintillation chambers** *see* *Luminescence chambers*

**Scintillation counters** *see* *Counters/scintillation*

**Seals**

- calorimeter gasket, low-mass, for vacuum 0.8°-400°K. 9-2271
- glass-ceramic, for sealing Al tubing or plates to Pt or Mo. 9-18969
- glass-metal, kovar parts holder 9-4199
- glass-metal adhesion theory 9-1335
- glass-metaloxide-metal, wettability, adhesion and atom movements 9-7599
- high press., C-ring plus Al foil rings 9-2100
- metal-to-ceramic, brazing with Cu-Ag alloys 9-13766
- plate, circular, for compressible liquid, stress analysis 9-8476
- ultra-high vacuum polyimide application 9-16651
- vacuum sealing between turned surfaces, analysis 9-6243
- Viton 'A' elastomers for high vacuum 9-16652
- AgCl, to glass, improved technique avoiding metallization 9-2102
- Al tubing or plates to Pt or Mo, glass-ceramic seal 9-18969
- CaF<sub>2</sub> on steel, high pressure and high temp. 9-6233

**Seawater**

- condensation nuclei production, influence of monomolecular surface films 9-6066
- near-surface acoustic waves, surface coupled losses 9-12573
- radiant transfer, meas. and applic., book 9-15240
- surface water, oxygen saturation, NE Pacific 9-6067
- temperature variations resulting from hurricanes 9-6064
- waves, breaker type classification on 3 lab. beaches 9-10382
- wind driven waves, onset 9-6065
- <sup>7</sup>Be tracing of surface interac. and mixing processes 9-18789
- LiH-seawater react. kinetics high press. gas prod., torpedo recovery syst. obs. 9-20041

**Second sound** *see* *Helium/liquid, sound propagation*

**Secondary electron emission** *see* *Electron emission/secondary*

**Sedimentation**

- clay, deflocculation mechanism rel. to colloids 9-3134
- coastal streams sediment content due to erosion 9-21753

**Seebeck effect** *see* *Thermoelectricity*

**Seidel theory** *see* *Aberrations, optical*

**Seignette salt** *see* *Rochelle salt*

**Seignettelectric materials** *see* *Ferroelectric materials*

**Seismic waves**

- See also Seismology*
- amplitude ratio for aerial and underground explosions 9-6042
- compressional, incident on rigid quarter-space, diffraction and reflection theory 9-20424
- compressional, velocity, porous media at permafrost temperatures 9-4035
- Coral Sea Basin refraction profile obs. 9-10375
- core-mantle boundary props., obs. of PcP 9-8143
- decoupling by a shot generated cavity, Sterling expt. 9-8144
- delay time correl. with other geophysical data 9-12563
- in earth core, perturbation by magnetic field 9-14150
- earth interior model, body waves, anelasticity and spectra 9-12567
- electrostatic sources, description and geoaoustic applic. 9-12560
- frequency-wave-number spectra determ. using arrays 9-18786
- gravity waves, long, on rot. earth, e.m. analogies of eqns. 9-17550
- multimode propagation, analysis in presence of noise, digital technique 9-8147
- P, velocity distribution and implications 9-17551
- PcP rel. core-mantle, boundary props., obs. 9-8143
- PKP amplitude/period ratio near caustic 9-16519
- production by non-explosive methods, advantages 9-6048
- Rayleigh, particle motion in solid, Caloi theory extension 9-14151
- reflection and transmission in laminated medium with arbitrary depth distrib. 9-20076
- in rocks and minerals, measurement of velocity at high static pressures 9-12572
- sonic boom coupled, obs. 9-2236
- sonic boom generated, obs. 9-2239
- velocity calc. using Birch's eqn. state 9-16516
- C<sub>1</sub>/Somigliana waves for study of earth's crust 9-12562

**Seismographs** *see* *Seismology*

**Seismology**

- See also Geophysical prospecting; Seismic waves*
- aftershocks, focal depths 9-12561
- Birch's eqn. state, appl. 9-16516
- continental drift controversy 9-10374
- crustal structure, refraction methods, Missouri 9-8149

**Seismology continued**

- crustal structure, refraction methods, Missouri 9-10376
- earth tide obs. with diamag. suspended tiltmeter 9-2140
- earthquake foreshocks, stress and mainshocks, reln. 9-16518
- earthquake phenomena rel. secular mag. field var. 9-17587
- earthquake risk, calc. 9-12559
- earthquakes, deep, rel. sizes of multipolar components 9-8146
- earthquakes, shallow focus, origin time determ., applic. of P<sub>n</sub> and S<sub>n</sub> phases 9-8140
- explosions, above ground, seismic effect 9-8141
- GEDESS, computer program for seismic recordings processing 9-8148
- and global tectonics 9-8142
- laser interferometric earth strain meas. 9-10373
- lunar, rel. meteoritic impacts 9-17638
- major earthquakes, distribution relative to solar and lunar tides and other cosmic forces 9-21747
- models and deterministic operators, marine reverberations 9-6043
- noise, stationarity 9-6044
- ocean bottom microseisms rel. waves and weather 9-10383
- p wave station anomalies and structure of upper mantle 9-16517
- seismic displacement near a fault 9-6045
- seismic observatory, Ellesmere Island, Canada, 1965-6 obs. 9-6047
- seismic waves generated by sonic booms, obs. 9-2236
- seismic waves generated by sonic booms, obs. 9-2239
- spectra of acoustic and seismic signals generated by underwater explosions 9-6046
- underground explosions, mathematical model 9-19079
- upper mantle partial melting, effect on seismic variables 9-8145
- C<sub>1</sub>/Somigliana waves for study of earth's crust 9-12562

**Selenium**

- amorphous, electric conductivity temp. depend rel. to heat treatment and Na atom admixtures 9-3572
- amorphous, optical properties in vacuum ultraviolet 9-12335
- amorphous Faraday effect 9-3861
- in biological mats., instrumental neutron-activation anal. 9-21743
- book 9-11753
- crystallized nonthermally, structure and props. 9-9806
- diffusion in InSb 9-18486
- elastic constants tensor in trigonal selenium 9-17297
- film, amorphous, photogeneration, field controlled and free-carrier transport 9-3729
- film, wavelength depend. of optical transmittance in vacuum u.v. 9-10166
- films, glassy, thermally stimulated conductivity 9-3726
- impurities, metallic, effects on conductivity in phase transition region 9-12103
- liquid, obs. of u.s. vel. 9-1007
- positron annihilation radiation, angular correlation calc. from atomic Hartree-Fock orbitals 9-5638
- relaxation in crystalline and amorphous states 9-19926
- solar u.v. sensor 9-10075
- sols, preparation, particle-size distrib. anal. by absorpt. spectra 9-14872
- space-charge limited currents in single cry. 9-21479
- thermoelectric props. at phase transitions, effect of impurities 9-18368
- thin films, space charge limiting currents, conduction, Fermi level 9-12191
- trigonal, elastic constants tensor 9-17297
- vitreous, thermal expansion, -190° to +30°C 9-19865
- X-ray spectra and electronic structure 9-14067
- Al-Se-Al thin film structure, negative resistance 9-13908
- photogeneration of carriers, vitreous 9-7851
- Se:Br polycrystal photocond. obs. and theory 9-13931
- Se:Ge, amorphous, phonon thermal conductivity 100-300°K 9-1407
- Se:SeO<sub>2</sub>, i.r. spectrophotometric study 9-5898
- Se-CdSe p-n junction, Cl impurity effects on characts. 9-10010
- Se-CdSe p-n junctions, Tl impurity conc. eff. on characts. 9-5721
- Se-Cu-Ag system, thermodynamics 9-18562
- Se<sub>2</sub><sup>-</sup>, luminesc. spectra in KI crystals 9-14082
- Se VIII ion, vacuum u.v. spectrum 9-2813
- SeS<sub>2</sub>, luminesc. spectra in KI crystals 9-14082

**Selenium compounds**

- selenides, book 9-11753
- Zr-Se alloys, hydrided, mech. props. 9-19805
- As<sub>2</sub>Se<sub>3</sub> glass, optical absorption, various initial purities 9-12352
- Au-Se system, phase relationships 9-21411
- Bi-Se alloy, vitreous, thermal props. 9-3153
- OSe halides, mean vibr. amplitude calc. 9-7037
- PbSe thin films, spectral absorption structure and phase composition 9-14021
- <sup>100</sup>Se isomeric ratios for fast neutron radiative capture 9-595
- SeD diffuse spectra, g.s. dissociation determ., 3000-3250 Å 9-18193
- SeF<sub>4</sub> isotopes microwave spectra, isotopes, rotn. const., dipole moment, structure parameter determ. 9-18191
- SeH diffuse spectra, g.s. dissociation determ., 3000-3250 Å 9-18193
- SeO<sub>2</sub>, i.r. spectrum and molecular structure 9-19447
- SeO<sub>2</sub> humidity probe, electrolytic 9-4174
- SeO<sub>3</sub> in Se, i.r. spectrophotometric study 9-5898
- SeOCl<sub>2</sub>, circulating liq. laser system containing Nd 9-13022
- SeOF<sub>2</sub> isotopes, microwave spectra obs., rotn. const. and dipole moment determ. 9-18192
- Se<sub>1-x</sub>Te<sub>x</sub>, i.r. active lattice bands 9-12365
- Te-Se alloy, non-linear optical phenomena 9-10160

**Self-diffusion** *see* *Diffusion in gases, in liquids, in solids*

**Semi-insulating materials (high-resistivity semiconductors)** *see* *Semiconducting materials*

**Semiconducting devices**

- See also Counters/semiconductor; Lasers/semiconductor; Masers*
- bulk negative mobility, operation modes from small signal theory 9-1553
- coolers of liquid flows, optimum construction 9-21544
- cryoelectronic 9-8317
- detector, development and prospects 9-4672
- doped oxides as diffusion sources for fabrication 9-5394
- doping by ion implantation 9-5669
- electronic properties of solids rel. to junction and transistor operation, book 9-18631
- etching of masks, photolithographic process 9-19918
- Gunn, with one part acting as isolator, patent 9-10022
- Gunn effect, bibliography from 1954 9-9970
- Gunn effect oscillators, two domain transit 9-1560
- Gunn generators and appl. 9-5733

**Semiconducting devices continued**

- ion implantation doping photolithographic device for prod. of etched device patterns 9-19918
- microwave oscillators, generalization of theory 9-5715
- modern developments, review 9-5714
- m.o.s. structures, radiation effects in modified oxide insulators 9-17420
- multivibrator for optoelectrical oscillations based on semiconductor laser and photodiode 9-3669
- oscillator, helical instability, effect of small transverse perturbation 9-10005
- oscillator, helical instability mechanism 9-5718
- oscillator-type apparatus, signal transformation 9-12162
- Ovonic threshold switches, radiation hardness 9-17402
- photoelectric, design introduction, book 9-15142
- piezoelectric, acoustic wave amplification and acoustoelect. effects 9-5549
- power transistor structure, thermal instability 9-18640
- production, microscope refinements and applications 9-8661
- radiography as quality control technique 9-5716
- Schottky barriers, normalized thermionic-field emission 9-15144
- Si detectors for 10 to 30 kV X-ray meas., characts. 9-13172
- strain gauge, calibration 9-5441
- switches, amorphous, characts. and fabrication rel. to crystalline semi-conds. 9-1551
- thermistor, new PTC-material 9-1554
- thermistor gauge for meas. of vel. in rarefied gases 9-5105
- thin film application in integrated circuits, technology, book 9-18402
- thyristor for temp. control in furnace 9-174
- two-layer structure, properties control by superhigh freq. 9-14008
- two-layer structures, impedance, theoretical dependences 9-13898
- GaAs, flash X-ray and fast neutron effects 9-17403
- GaAs, review 9-19910
- GaAs bulk and epitaxially grown oversized samples, hybrid Gunn-LSA mode oscillation experiments 9-5736
- GaAs Gunn oscillator, 1 kw from 1 to 10 GHz 9-3685
- n-GaAs Gunn oscillators, sheet-type, reduced domain build-up 9-10023
- GaAs l.f. oscils., appl. 9-5717
- GaAs oscillators, microwave instabilities 9-10006
- Ge, oscillator, frequency of helical instability 9-1561
- n-Ge oscillator, helical instability mechanism 9-5718
- InAs film used in Hall e.m.f. transducers 9-10007
- Mo-Si Schottky diode, from chem. deposition of Mo on Si 9-6010
- Si, films for use as image analyzer tube targets 9-8587
- Si mosaic crystal with low dislocation density, prod., patent 9-13596
- SiC varistors, current dependence of voltage non-linearity 9-7817
- ZnSb-constantan, thermoelements, diffusion phenomena and phase transitions. X-ray microprobe analysis 9-10062

**diodes**

- base impedance due to Dember effect 9-5719
- charge storage discriminator, use in fast coincidence syst. 9-2609
- double injection, conduction mechanism in unstable range 9-5727
- double injection, noise and equivalent circuit 9-15115
- electroluminescent, efficiency and electron-hole recomb. 9-12139
- epitaxial doping density vs. depth meas. 9-18623
- forward characteristics meas. technique 9-7824
- Gunn, direct series operation, above critical  $n\lambda_L$  products, computer simulations 9-5734
- Gunn, with angular geometry, domain propag., theoretical anal. 9-13906
- Gunn effect domain formation controlled by complex load 9-12132
- IMPATT, passivated metal-semiconductor, microwave oscils. 9-15117
- laser, spontaneous emission linewidth rel. to temp. 9-246
- as light sources 9-12166
- mesa, diffusion current, effect of surface recombination and deceleration field in base 9-17405
- negative resistance, V-I characts., theoretical study 9-5724
- nonlinearity and noise, thermodynamic relationship 9-12165
- p-n junction, appl. to high-energy dosimetry 9-14534
- photodiodes, eff. of r.f. bias on microplasma 9-10076
- photovoltaic effects in impurity absorpt. region 9-3740
- point, equivalent circuit with microwave freq. dependent components 9-13903
- point contact, barrier lowering and current change due to mechanical pressure 9-18635
- Read, conduction current, transient behaviour from small signal to large signal oscillations 9-5726
- Read, large signal analysis 9-15116
- reverse-biased, characts. obs. by diffusion current distinguishing method in p-n junctions 9-17404
- Schottky, breakdown microprocesses 9-18634
- Schottky barrier, thermionic and thermionic-field emission, Richardson const. and tunneling eff. mass 9-21524
- Schottky barrier, thermionic emission, Richardson constant 9-15145
- Schottky barriers' differential resistance, effect of ellipsoidal energy surface 9-13904
- Schottky-barrier, effect of surface polishing on stress sensitivity 9-5725
- tunnel, determ. of impurity conc. in alloyed region 9-5731
- Au-n-Si surface barrier, rectification characts. rel. to surface states 9-21525
- CdO-p-Si, photoelec. and rectification characts. and spectral response curve 9-5728
- GaAs-Pd Schottky, electron-phonon coupling in barrier 9-7825
- p-GaAs, electroluminescence, 300°K and 77°K 9-21659
- GaAs, Zn-implanted, formation of deep trapping levels, eff. on elec. characts. 9-19920
- GaAs alloy tunnel, I-V characts. in high crossed elec. and mag. fields 9-10019
- p-GaAs alloyed, electroluminescent props. 9-7996
- GaAs double injection, doping effects on characts. rel. to trapping levels 9-18636
- n-GaAs Gunn, mag. field effect on l.f. oscillations 9-5737
- GaAs Gunn, small transverse dimensions, effect on operation 9-5735
- GaAs Gunn, subcritically doped, stability and reflection gain 9-7829
- p-GaP:O-Zn, electroluminescent, epitaxial growth, patent 9-10257
- GaP, light source 9-12166
- GaP, source of red radiation, prep. and characts. 9-3679
- GaP electroluminescent, minority carrier lifetime 9-12491
- GaSb tunnel, I-V characts. in high crossed elec. and mag. fields 9-10019
- Ge, alloyed, velocity of surface recombination in base, dependence on injection level 9-18637

**Semiconducting devices continued**

- diodes continued
- n-Ge, Schottky barriers' differential resistance, effect of ellipsoidal energy surfaces 9-13904
- Ge, temperature measurement 9-4376
- Ge tunnel, I-V characts. in high crossed elec. and mag. fields 9-10019
- Ge(Li) drifted diode, fallout meas. 9-550
- p-Ge-n-Si heterojunctions, I-V characts. 9-3201
- GaAs: P light source 9-12166
- InSb, carrier generation recombination in space-charge region, applic. of theory 9-3674
- Mo-Si Schottky, from chem. deposition of Mo on Si 9-6010
- Mo-Si Schottky diode, from chem. deposition of Mo on Si 9-6010
- Pb<sub>1-x</sub>Sn<sub>x</sub>Te:Bi diode laser with low threshold currents 9-20529
- Si: Au p<sup>+</sup>-n-n<sup>+</sup>, forward transient characts. 9-16282
- Si: Cd, with negative resistance 9-18633
- Si: P, laser-irrad. production, structural and elec. characts. 9-18638
- Si: Zn, with negative resistance, characts. 9-17406
- p-n Si, Li containing, e-irradiated, room temp. recovery kinetics 9-17407
- Si, n irradiated, majority and minority carrier trapping by capacitance recovery 9-17408
- Si, n, irrad. effects on I-V characts. 9-10018
- Si avalanche, multiplication effects on noise, measurements 9-5730
- Si avalanche, multiresonant oscillator in 1.5 to 11 GHz range 9-5729
- Si avalanche, p<sup>+</sup>n spherical, junction, multiplication props. 9-7820
- Si avalanche diode as  $\nu$  detector 9-13171
- Si IMPATT, X-band, fast n effects on d.c. and microwave characts. 9-17409
- Si p-i-n, avalanche induced relaxation oscillations, computer calcs. 9-16281
- Si p<sup>+</sup>n junction, d.c. characts. pressure and temp. dependence 9-10011
- Si photodiode, p-i-n, u.v. response obs. 9-12217
- Si Read and p-n-n<sup>+</sup> IMPATT, computer simulation under large signal conditions 9-12164
- 9-10017

**junctions**

- alloyed mosaics on Si for use in image analyzer tubes 9-8586
- formation by diffusion of Ni and Cl into p-PbTe at 700°C 9-19767
- Josephson, I-V characteristic meas., current sweep circuit 9-205
- luminescent emission 9-17486
- metal-semiconductor, WKB approx. for tunnelling 9-7821
- metals-semiconductor-metal tunnelling, effect of band structure 9-13901
- n-n heterojunction, differential capacitance 9-15112
- n-type epitaxial films on p<sup>+</sup> substrates, hole diffusion length meas. using laser 9-3616
- np<sup>+</sup>, abrupt, recombination current from transition region, numerical calc. 9-7818
- operation rel. to electronic props. of solids, book 9-18631
- p<sup>+</sup>-n, forward steady state, numerical soln. 9-3676
- p<sup>+</sup>-n, non-uniformly illuminated, linearized time-dependent case 9-3672
- p-n, asymmetrical, carrier generation-recombination in space charge region 9-3674
- p-n, depletion layer and capacitance calc. 9-15113
- p-n, depletion layer width rel. to voltage 9-1555
- p-n, diffusion current distinguishing method, applic. to reverse-biased diode characts. investig. 9-17404
- p-n, doping profile determination from harmonic generation measurements 9-7822
- p-n, epitaxial growth by UHV sublimation 9-13899
- p-n, inhomogeneities, causes and investigation methods 9-13900
- p-n, intrinsic conduction onset temp. determ. from characteristic 9-10008
- p-n, one-dimensional solution, accurate numerical, under arbitrary transient conditions 9-3673
- p-n, photoelectric field, lateral, effect of background illum. 9-16279
- p-n, planar passivated, avalanche drift instability 9-18632
- p-n, Si, light emission characteristics in light pulsing in delayed coincidence syst. 9-2606
- p-n diode, appl. to high-energy dosimetry 9-14534
- p-n-p structure, switching-off by reverse anodic voltage, theory 9-3670
- photoelec. response rel. to narrow light beam displacement 9-7850
- pn<sup>+</sup>, abrupt, recombination current from transition region, numerical calc. 9-7818
- properties rel. crystallographic defects 9-19919
- Al-Al<sub>2</sub>O<sub>3</sub>-Bi: Pb(Te), tunnelling characts. 9-5722
- AlAs-GaAs epitaxial heterojunction structures, coherent radiation 9-10868
- n-AlGa<sub>1-x</sub>As-p-GaAs heterojunction, injection properties 9-3671
- Au-Ag alloy film on n-Si Schottky barrier, characts 9-3675
- Au-GaAs surface barrier, elec. props. 9-10009
- Au-GaAs Schottky barriers, capacitance meas. 9-5720
- CdCr<sub>2</sub>Se<sub>4</sub> ferromagnetic spinel, single crystal, fabrication and characts. 9-10014
- CdO-p-Si, photoelec. and rectification characts. and spectral response curve 9-5728
- CdS-n-Ge, anomalous breakdown, temp. depend. of elec. props. 9-5723
- CdSe-n-Ge, anomalous breakdown, temp. depend. of elec. props. 9-5723
- CdTe, p-n, recombination-generation mechanism 9-21522
- GaAs-Pb, hole-TO-phonon interac. 9-1556
- GaAs-metal point contact, rectifying barrier structure 9-12163
- n-GaAs, Schottky barriers, current mechanisms 9-21519
- GaAs p-n epitaxial, high-efficiency electroluminescence 9-15192
- p-n GaP: N green electroluminescence 9-3938
- GaP p-n structures, radiation spectrum control 9-5952
- Ge, intrinsic layer between p and n regions, one carrier space charge limited currents 9-21523
- Ge, n-p<sup>+</sup> and p-n<sup>+</sup>, avalanche multiplication parameters determ. 9-1559
- Ge, narrow p-n, reactive characts. in breakdown region 9-15110
- p-Ge-n-Si heterojunctions, I-V characts. 9-3201
- GeTe-GaAs tunnel junction, neg. resistance Schottky-type barrier props. 9-15119
- Se-CdSe p-n, Cl impurity effects on characts. 9-10010
- Se-CdSe p-n, Ti impurity conc. eff. on characts. 9-5721
- Si: Au, p-n, impedance and other props rel. to Au conc. 9-21521
- Si: Li p-n electron-irradiated, recombination velocity, Li impurity effects 9-9998
- Si-Si between crystal and amorphous, V-I characteristics and barrier capacity depend. 9-3677
- Si, abrupt p-n, avalanche multiplication, theoretical analysis 9-7819
- Si, p-n,  $\gamma$ -radiation effect on parameters and structure 9-16280
- Si p-n, breakdown and effect on reverse I-V characts. 9-21520
- Si p-n, probe meas. 9-10012



Semiconducting devices continued  
junctions continued

- Si p-n avalanche, temp. and current distrib. 9-3678  
 Si p<sup>+</sup>-n, avalanche photomultiplication, effect of donor density 9-15114  
 Si p<sup>+</sup>-n, d.c. characts. pressure and temp. dependence 9-10011  
 Si p<sup>+</sup>-n spherical, multiplication props. 9-7820  
 Si p-n, abrupt, differential resist. in avalanche mode 9-7823  
 SiC:B, p-n, electroluminescent energy spectrum, 77-300°K 9-18727  
 SiC:CdSe p-n, production technology and props. 9-10013  
 SiC, p-n, prep. by growth from solns. in rare-earth elements 9-16056  
 SiC diffusional p-n, light sum relax. 9-10241  
 SiC p-n, solution grown 9-13902  
 Si(Li), recovery behavior after p-irrad 9-15111  
 Si-SiC p-n heterojunctions, construction and energy band diagram 9-10015  
 ZnSe<sub>x</sub>Te<sub>1-x</sub>, p, n, diffusion barriers for native acceptor defects 9-10016  
 ZnTe, electroluminescence 9-7997  
 ZnTe with photo-n-p junctions, light-emitting mechanism 9-10083

## transistors

- alloy junction, inverse  $\alpha$  characts. and reln. to forward  $\alpha$  at different injection levels 9-21526  
 bipolar, as linear amplifying elements, response time using equivalent circuit 9-15494  
 bipolar, low dose ionization-induced failures 9-17411  
 bipolar, planar, prediction and selection techniques for radiation effects 9-17410  
 bipolar, v.h.f., limitations of power output capability 9-13905  
 converted, control of parameters by varying composition of emitter alloy 9-21527  
 diffusion-action, saturation current characteristics 9-10020  
 use in digital word generator 9-14288  
 epitaxial field effect, pinching phenom. 9-1557  
 excess current generation due to reverse bias p-n junction stress 9-10021  
 f.e.t., as linear amplifying element, response time using equiv. cct. 9-15494  
 f.e.t., conc. dependence of carrier mobility 9-12168  
 f.e.t., pinched-mode operation, development of device-oriented model 9-19923  
 f.e.t., thin film, insulator layer, ionic mobility 9-3681  
 field-effect transistors, analogue calc. of characts. 9-16283  
 j.f.e.t., abnormal current changes 9-7828  
 MOS, 1/f noise 9-7816  
 m.o.s., characts., effects of traps in semiconductor 9-5732  
 m.o.s., drain current temp. dependence 9-7826  
 m.o.s., interface states, eff. on characts. 9-12173  
 m.o.s., process techniques and space radiation effects, interrelation 9-19924  
 m.o.s., saturation drain conductance, correlation of expts. with two-section model theory 9-12175  
 m.o.s.f.e.t.'s, neutron radiation effects, theory and experiment 9-17419  
 m.o.s.f.e.t.'s, radiation damage study using bias-temperature treatments 9-17421  
 MOSFET used to construct He temp. preamplifier 9-6439  
 operation rel. to electronic props. of solids, book 9-18631  
 p-n-p alloy junction, minority carrier lifetime in base 9-1558  
 resonant gate in m.o.s.t., elastic beam analogue analysis 9-19922  
 Al<sub>2</sub>O<sub>3</sub>-Si m.o.s.f.e.t., fabrication and characts. 9-17412  
 Ge, n-p-n- and p-n-p, avalanche multiplication parameter determ. 9-1559  
 Ge alloyed, avalanche multiplication characts., anomalies caused by surface and volumetric effects 9-3682  
 Si, B diffusion in oxygen during fabrication 9-14959  
 Si, n-channel normally-off insulated-gate field-effect, characts. 9-3684  
 Si, n bombarded, radiation and annealing characts. 9-17415  
 Si, n induced base current, recombination statistical model 9-17414  
 Si, n radiation eff. on second breakdown and thermal behaviour 9-17416  
 Si, recovery of gamma dose failures during life testing 9-17418  
 Si m.o.s., interface charges effect on channel conductance 9-12177  
 Si p-n, e irradiated, effect of Si<sub>3</sub>N<sub>4</sub> passivation 9-17417  
 Si p-n planar, n-pulse irradiated, rapid annealing data 9-17413  
 Si p-n planar, double diffused, current amplification factors, structural causes of spread 9-3683

## tunnel and interface devices

- diode, determ. of impurity conc. in alloyed region 9-5731  
 diode, oscillations in switching mode, critical freq. separating switching and oscill. modes 9-18639  
 diode, transistor ring counter 9-2587  
 diode in discriminator for fast scin. counter pulses 9-2580  
 discriminator of amplitude and zero crossing detector, circuit 9-18040  
 Esaki diode pair applic. 9-2602  
 excitation spectrum, collective-modes, theory 9-12169  
 m.i.m. cahtode, effect of dielectric props. on energy distribution of electron emission 9-18661  
 m.i.m. dielectric traps, emission, transfer ratio 9-1419  
 m.i.m. structure, capacitance and I-V characts., oxide thickness depend. 9-18642  
 m.i.m. structures, film thickness fluctuations and elec. field penetration 9-3688  
 m.i.m. structures with SiO<sub>2</sub>/Al<sub>2</sub>O<sub>3</sub> layers, polarisation effects in dielectric 9-3717  
 m.i.m. system, dielectric influence on angular emission of electrons 9-3687  
 m.i.s. capacitance, density of slow states from charge meas. on applying linearly increasing voltage 9-10024  
 m.i.s. structures, e. irrad. eff. on density of surface states 9-12171  
 m.i.s. structures, process techniques and space radiation effects, interrelation 9-19924  
 m.i.s. structures with SiO<sub>2</sub>/Al<sub>2</sub>O<sub>3</sub> layers, polarisation effects in dielectric 9-3717  
 m.o.s. varactor, freeze-out characts. 9-10025  
 M.O.S., injection and migration of charges in oxide 9-5741  
 m.o.s., inversion layer mobility, rel. to misfit dislocation 9-3339  
 m.o.s., ionizing radiation effects 9-18643  
 m.o.s. capacitors, inversion layer transient response, types of relaxation mechanisms 9-12172  
 m.o.s. capacitors, low-temperature hysteresis effect caused by surface-state trapping 9-18644  
 m.o.s. structure, calc. of immobile part of space-charge 9-12174  
 m.o.s. structures, high density of surface states by capacity var. rel. to frequency 9-21528  
 m.o.s. system properties, influenced by SiO<sub>2</sub> structure 9-7830  
 m.o.s. transistors, interface states eff. on characts. 9-12173

## Semiconducting devices continued

## tunnel and interface devices continued

- m.o.s.t. characts., effects of traps in semiconductor 9-5732  
 m.o.s.t. saturation drain conductance, correlation of expts. with two-section model theory 9-12175  
 P.V.K.-metal interface, photoemission of holes into insulators 9-5739  
 surface charge wave propag. in s.i.s. structure 9-15118  
 tunnel-diode sensor for peak current meter 9-16759  
 AL-Al<sub>2</sub>O<sub>3</sub>-Au structures, photovoltaic props., annealing effect 9-7861  
 Al-Al<sub>2</sub>O<sub>3</sub>-Au, capacitance and I-V characts., oxide thickness depend. 9-18642  
 Al-InSb-Al thin film structures, V-I characts. 9-18641  
 Al-Se-Al thin film structure, negative resistance 9-13908  
 Al-SiO-Al system, I-V charact., and temp. dependence 60 to -185°C 9-1562  
 Al-SiO<sub>2</sub>-Si, injection and migration of charges in oxide 9-5741  
 Al-phosphosilicate glass-degenerate Si structure tunnelling conductance peaks 9-16284  
 Al<sub>2</sub>O<sub>3</sub>-Si m.o.s.f.e.t., fabrication and characts. 9-17412  
 Al-Al<sub>2</sub>O<sub>3</sub>-Al junctions, potential barrier shape 9-15120  
 Au-CaF<sub>2</sub>-CdSe m.i.s. capacitors, surface states, obs. 9-5740  
 Au-InSb-Au structures, V-I characts. 9-18641  
 Au-SiO<sub>x</sub>-CaF<sub>2</sub>-CdSe m.i.s. capacitors, surface states, obs. 9-5740  
 Au-SiO<sub>x</sub>-CdSe m.i.s. capacitors, surface states, obs. 9-5740  
 GaAs diodes, high-power epitaxial, prep. and characts. 9-12167  
 GaAs-metal point contact, breakdown 9-3686  
 GaAs, fabrication by micropulse alloying method, recombination rad. detect. 9-7827  
 GaAs alloy diodes, I-V characts. in high crossed elec. and mag. fields 9-10019  
 GaSb diodes, I-V characts. in high crossed elec. and mag. fields 9-10019  
 Ge-metal contacts, e. and phonon tunnelling spectroscopy 9-13909  
 Ge diodes, I-V characts. in high crossed elec. and mag. fields 9-10019  
 GeTe-GaAs tunnel junction, neg. resistance Schottky-type barrier props. 9-15119  
 Al-Al<sub>2</sub>O<sub>3</sub>-Bi-Pb(Te) junctions, tunnelling characts. 9-5722  
 Si-SiO<sub>2</sub> structures, C-V characts. rel. to improved m.o.s. transistors 9-5742  
 Si-SiO<sub>2</sub> interface, recombination carrier velocity, reduction due to heat treatment in H 9-12170  
 Si-SiO<sub>2</sub> interfacial stress, rel. to interface states 9-12176  
 Si m.o.s. transistors, interface charges effect on channel conductance 9-12177  
 Si (degenerate)-phosphosilicate glass-Al structure tunnelling conductance peaks 9-16284  
 SiC backward diode operating from 77° to 1000°K 9-19921  
 SiO<sub>2</sub>, Na ion contamination rel. to m.o.s. dev. stability 9-17547  
 SiO<sub>x</sub> in m.o.s. devices, electrical properties, effect of water 9-7838  
 SiO<sub>2</sub> pyrolytic films, I-V characts. in m.i.s. structure, dependence on ht. treatment 9-3195  
 GaAs:Ge(Zn), degradation during forward operation and in high temp storage 9-3680

## Semiconducting materials

- See also Magnetolectric effects; Photoconductivity; Photovoltaic effects; Semimetals*  
 alcohols, liquid, cond., 20°C 9-13538  
 alloys, lattice thermal conductivity 9-15015  
 alloys with stoichiometric vacancies, thermal conductivity 9-17358  
 aminoacids, single cry. and polycrystalline, protein semicond. study 9-21510  
 amorphous and liq., international colloquium, Bucharest (1967) 9-18614  
 anthracene, dark conductivity electrode dependence 9-15094  
 aromatic subst., electrode injection of charge carriers 9-21509  
 n- Bi<sub>2</sub>Te<sub>3</sub>, Fermi surface shape discrepancy, galvanomagnetic data recal. 9-1427  
 copper phthalocyanine, e. drift mobilities 9-17393  
 copper phthalocyanine, hopping and band conduction mechanisms 9-19915  
 crystal chem. information, tabular reduction 9-16073  
 crystal, wurtzite group; u.s. surface wave amplification coeff. derived 9-12007  
 decay of photoconductivity of II-VI compounds 9-1622  
 detector, boundary var. of drift region, expt. and theory 9-4674  
 diamond, natural, nature of acceptor centre 9-12135  
 dielectric function 9-19909  
 doping by ion implantation 9-5669  
 electric props. of layer, using e.m. field 9-3568  
 fabrication, applic. of SiH<sub>4</sub>, silane, review 9-5713  
 ferroelectric, elec. induction wave theory 9-16257  
 ferroelectric, electric induction waves at temps. above first order transition 9-16258  
 ferroelectric, transverse optical phonon amplification by carrier drift 9-19929  
 ferroelectrics with semicond. props., instability possibility 9-5666  
 films, charact., use of surface elastic vib. meas. method 9-18625  
 galvanomagnetic effects in presence of small number of free carriers 9-13878  
 p-GaP, photoluminescence, voltage pulse modulation 9-5758  
 glass, chalcogenide and transition metal oxide 9-1523  
 glasses, chalcogenide, e props. rel. to energy levels and progressive crystn. model 9-3611  
 group II-VI compounds, band structure calc., Green's function method 9-21467  
 group III-V compounds, magnetophonon effect 9-21513  
 group IV and III V, nonlinear optical coefficients 9-14024  
 Gunn effect domain formation controlled by complex load 9-12132  
 h.f. effects with carriers inelastically scattered on optical phonons 9-1528  
 h.f. effects with carriers inelastically scattered on optical phonons 9-13879  
 III-V-type phosphides, energy struct. from X-ray L<sub>2,3</sub> emission bands 9-5944  
 InAs, X-ray-K-absorption edge shifts 9-21638  
 laser flash illumination, induced stress effects 9-9776  
 layered system, drifting carriers, interaction with surface elastic waves 9-5435  
 lipid films, dry, activation energy and conductivity meas. 9-12138  
 liquid and amorphous, international colloquium, Bucharest (1967) 9-18614  
 magnesium phthalocyanine, hopping and band conduction mechanisms 9-19915  
 magnetoabsorption oscillations associated with interband transitions rel. to exciton states 9-5918

**Semiconducting materials continued**

naphthalene, current flow charact. 9-18621  
 Naphthazarine-Cu-Chelate elec. conductivity 9-3636  
 organic, conductivity mechanism 9-9982  
 organic, hopping and band conduction mechanisms 9-19915  
 organic, long-chain mol.s., Overhauser phase and bond alternation 9-4972  
 oxides, adsorbed Ag photolytic reduction mechanism 9-6017  
 oxides, effect of pressure on conductivity 9-1522  
 photoeffects, in materials and allied devices with quadratic volume recombination 9-1608  
 piezoelectric, acoustic properties, theory, review 9-13793  
 piezoelectric, acoustic props., theory, review 9-13793  
 polymers, organic film-forming, props. description 9-14730  
 resistivity meas. instrument, four-probe 9-12134  
 rhodamine-B films, linear and quadratic recombination of photocarriers 9-12213  
 sintered alloys, thermal conductivity 9-16183  
 surface gas chemisorption, electronic theory 9-16483  
 surface space charge conductivity 9-21459  
 switching, reversible in disordered mats. 9-12140  
 tetra cyanonodimethane derivatives, e.p.r. and thermal conductivity rel. to moving excited states 9-12505  
 titanates, superconductivity 9-3598  
 ultrasound generation in Gunn eff. 9-1524  
 wurtzite type, piezoelectric surface oscils. 9-7646  
 Al and p-, n- semicond., composites, conductivity meas. 9-16260  
 AlSb, light scattering from single particle electron and hole excitations 9-12443  
 As<sub>2</sub>Se<sub>3</sub>, glassy, pulse I-V charact. 9-3617  
 As<sub>2</sub>S<sub>3</sub> film-Ag system, light sensitivity depend. on thickness of semicond. layer 9-1735  
 As<sub>2</sub>S<sub>3</sub>(Se<sub>2</sub>) films, photosensitivity rel. to frequency of incident radiation 9-3731  
 As<sub>2</sub>Se<sub>3</sub>-metal oxide glasses, structure and cond. mechanism 9-1521  
 B, conductivity and charge carrier conc. meas. in breakdown region 9-12143  
 Ba<sub>1-x</sub>La<sub>2x/3</sub>TiO<sub>3</sub>:Fe<sub>2</sub>O<sub>3</sub>, polycrystalline, contrast to barium bismuth titanate 9-3608  
 BaTiO<sub>3</sub>, I-V charact., 200-500°C, 0.01-100 Hz 9-3618  
 BaTiO<sub>3</sub>, elec. cond. rel. to O partial press., 800-1200°C 9-1512  
 BaTiO<sub>3</sub> ceramic for PTC-thermistor 9-1554  
 BaTiO<sub>3</sub> surface, chemisorption of O<sub>2</sub> causing change in electron affinity 9-3648  
 Bi-Sb alloy, transition to metal, mag. field and Sb conc. depend., 4-77°K 9-1513  
 Bi, mag. susceptibility lattice and charge carrier components 9-7876  
 Bi<sub>2-x</sub>Sb<sub>x</sub>Te<sub>3-x</sub>Se<sub>x</sub>, mixed-crystal form. limits 9-14985  
 Bi<sub>2</sub>Te<sub>3</sub>, n and p type, band struct. 9-3637  
 Bi<sub>2</sub>Te<sub>3</sub> molten, optical props. rel. to electronic struct. 9-16002  
 Bi<sub>2</sub>Se<sub>3</sub>, nonohmic conductivity, K 9-3619  
 Bi<sub>2</sub>Te<sub>3</sub>S<sub>2</sub>, semimetal to semiconductor transition, size effect quantization 9-16230  
 Bi<sub>2-x</sub>Sb<sub>x</sub>, mag. susceptibility lattice and charge carrier components 9-7876  
 Bi<sub>2</sub>Sb<sub>3</sub>, (x=97,90; y=3,10), band parameters from galvanomag. meas. 9-1533  
 n-Bi<sub>2</sub>Te<sub>3</sub>, de Haas-van Alphen effect 9-9913  
 BiTeBr, band structure from elec. and optical props. 9-21512  
 Bi-Sb alloy, longit. magnetoresist. anomalies in mag. fields up to 500 kOe at liq. He temp. 9-1514  
 cd,Hg<sub>1-x</sub>Te graded gap structures, photocarrier transport 9-18619  
 CdAs<sub>2</sub>-Zn<sub>2</sub>As<sub>2</sub> system, solid-soln. growth and electronic props. 9-13882  
 CdCr<sub>2</sub>Se<sub>4</sub> ferromagnetic spinel, single crystal p-n junction 9-10014  
 CdF<sub>2</sub>:Eu or In, absorpt. spectra, electrical resistivity and Hall coeff. 9-5672  
 CdGeAs<sub>2</sub>, In, Te, Cu and Ga impurity effect on conductivity 9-18618  
 CdGeAs<sub>2</sub>, radiative recombination 9-5951  
 CdGeAs<sub>2</sub>, radiative recombination 9-5951  
 CdGeP<sub>2</sub>(As), generation of second harmonic 9-9969  
 Cd<sub>1-x</sub>Mn<sub>x</sub>S (x<0.4), e. mobility exam. 9-1516  
 CdO-p-Si, diode, photoelec. and rectification charact. and spectral response curve 9-5728  
 CdO-p-Si junctions, elec. and optical charact. 9-5728  
 CdS-Cl, impurity conduction at low temp. 9-3620  
 CdS:In degenerate, evaporated films, mobility studies 9-12145  
 CdS, acoustoelec. domain formation 9-1515  
 CdS, acoustoelectric domain propag. from Brillouin scatt. obs. 9-1517  
 CdS, acoustoelectric effect, u.s. attenuation and trapping 9-7650  
 CdS, acoustoelectric effect of amplified acoustic oscillations, multitransit noise 9-3530  
 CdS, anisotropic piezoelectric, acoustoelec. effect 9-12009  
 CdS, conductivity storage, model 9-13929  
 CdS, contacts with In and In-Ga resistive props. 9-3613  
 CdS, current noise induced by electron-phonon interaction 9-5686  
 CdS, depolarization field eff. on electron-elastic props. 9-17439  
 CdS, direct e-hole recomb., photoexcitation 9-16261  
 CdS, e-irrad., recombination radiation 9-3915  
 CdS, exciton absorption infl. of strong elec. field 9-19988  
 n-CdS, generation and reception of ultrasound 9-3609  
 CdS, luminescence, green edge, mechanism, and luminescence centre parameters 9-14075  
 CdS, phonon-assisted exciton transitions 9-5966  
 CdS, photosensitive, field-effect 9-10067  
 CdS, piezoelectric, acoustoelectric domains, sound reflections 9-18559  
 CdS, spatial and time variation of elec. fields 9-13874  
 CdS,Se<sub>1-x</sub>, photoconductive, acoustoelec. domain 9-3529  
 CdS crystal, Rayleigh wave, electron interaction 9-5697  
 CdS electronic energy states of dislocations 9-7487  
 CdS laser, electron-beam-pumped, standing waves and single-mode room temp. laser emission 9-19151  
 CdS oriented films, charact., use of surface elastic vib. meas. method 9-18625  
 CdS photoluminescence, orange, red and i.r., mechanism, and centre parameters 9-5976  
 CdS platelets, h.f. acoustoelec. currents and departure from Ohm's Law 9-13798  
 CdS,Se<sub>1-x</sub>, Raman spectra line width, lattice vibrations, temp. depend. 9-12437  
 CdS,Se<sub>1-x</sub> films, structure defects effects on elec. props. 9-9973  
 CdSb, Ag doped, field emission 9-3751

**Semiconducting materials continued**

CdSb, doped, conductivity, Hall effect and magnetoresistance, 2.2-77°K 9-9972  
 CdSb and CdTe molten, optical props. rel. to electronic struct. 9-16002  
 p- CdSb valence band investigation using transverse thermoelec. power meas. 9-16269  
 CdSe, phonon-assisted exciton transitions 9-5966  
 CdSe, photoluminescence, mechanism of  $\lambda_m=0.82 \mu$ , and parameters of luminescent centres 9-10234  
 CdSe film, encapsulated, flat band condition, Hall effect 9-3649  
 CdSiAs<sub>2</sub>, generation of second harmonic 9-9969  
 CdSnP<sub>2</sub>, generation of second harmonic 9-9969  
 CdTe:Li, Hall coeff. and elec. conductivity, temp. depend. meas. rel. to effect of dopant 9-12156  
 p-CdTe:P, film, resistivity meas. 9-15089  
 CdTe, band structure calc., Green's function method 9-21467  
 CdTe, conductance, temp. dependence rel. to ambient partial pressure 9-3644  
 n-CdTe, high-resistivity, conductivity temp. dependence rel. to band structure 9-3621  
 CdTe, light scattering from single particle electron and hole excitations 9-12443  
 n-CdTe, optical absorpt. by free carriers 9-5916  
 CdTe, p-n junctions, recombination-generation mechanism 9-21522  
 CdTe, phonon-assisted exciton transitions 9-5966  
 n-CdTe, photoconductive, oscillatory, from shallow donors 9-5763  
 CdTe elec. and galvanomag. props., theory 9-3622  
 CoO:Li elec. conductivity and thermoelec. power rel. press. and temp. 9-21506  
 CoO, optical absorpt. of small polarons in near and far i.r. 9-5929  
 Cu<sub>2</sub>O single cryst. layer, space-charge-limited current 9-16262  
 CuCl radiative recomb., low temp., laser u.v. excitation 9-16430  
 Cu<sub>2</sub>O, conductivity and thermoelec. power rel. press. and temp. 9-21506  
 Cu<sub>2</sub>S layers, cond. rel. to i.r. reflection and transmission 9-1736  
 Cu<sub>2</sub>Se, electrical conductivity rel. to phase transformation 9-17390  
 EuO<sub>2</sub>, elec. cond. 9-7796  
 EuO, elec. cond., 9-7797  
 FeCr<sub>2</sub>Se<sub>4</sub>, conductivity rel. to effect of interactions between d shells of transition element 9-16253  
 Fe<sub>2</sub>O<sub>3</sub>:Ti, conductivity and thermoelec. power rel. press. and temp. 9-21506  
 n-Ga<sub>1-x</sub>P<sub>x</sub>Te, Se, Hall effect, of two kinds of carriers 9-3623  
 GaAs<sub>1-x</sub>P<sub>x</sub>Se, props. from temp. depend. of Hall effect 9-21500  
 n-GaAs<sub>1-x</sub>P<sub>x</sub>(S)(Te), press. depend. of resistivity at 77° 9-16266  
 GaAs<sub>1-x</sub>P<sub>x</sub>S and Te doped, Hall coeff. and resist. rel. temp., 55 to 400°K 9-12150  
 GaAs<sub>1-x</sub>P<sub>x</sub> electron radiation damage, cathodoluminescence study 9-18570  
 Ga<sub>1-x</sub>In<sub>x</sub>As alloys, E<sub>i</sub> interband transition energies 9-9987  
 GaP:B, Zn, photoluminescence and electroluminescence mechanisms rel. to reactions in doping 9-3940  
 GaP:Cd (Zn), thermal ionization energies of acceptors 9-5696  
 GaP:N, optical absorpt. rel. to theory of isoelectronic impurities 9-7801  
 GaP-O<sup>-</sup>, i.r. radiative capture of electrons at ionized oxygen donors 9-12464  
 n-GaP:S(Te) and undoped, epitaxial, edge luminescence, intrinsic and extrinsic, 80°-300°K 9-12480  
 GaP:Zn, Fermi levels as a function of hole concentration function, 1040°C solid solubility isotherm of Zn 9-7715  
 GaP, bound electron states, symmetry 9-1520  
 GaP, breakdown oscillations, induced impurity, and obs. of traps higher than indirect band edge 9-5695  
 GaP, electron radiation damage, cathodoluminescence study 9-18570  
 GaP, luminescence concentration quenching and the impurity-band Auger model 9-8000  
 GaP, luminescence near indirect transition in multiphoton excitation case, 4.2°K and 77.3°K 9-10236  
 GaP, vapour-grown, elec. props. rel. to substrates 9-12148  
 GaP, X-ray-K-absorption edge shifts 9-21638  
 GaP diode sources of red radiation, prep. and charact. 9-3679  
 GaP donor-acceptor electron recombination luminescence, multipole field effects 9-10266  
 GaP doped epitaxial films, photoluminescence 9-10237  
 GaP-p-n structures, radiation spectrum control 9-5952  
 GaS, indirect energy gap by opt. absorption spectra 9-18622  
 n-GaSb:Te, transport props. from Faraday effect, Hall effect and conductivity meas. 9-10177  
 n-GaSb-InSb mixed crystal, conduction bands, resistivity, Hall effect and piezoresistance investigation 9-5690  
 GaSb, band structure calc. using nonlocal pseudopotential 9-1534  
 GaSb, radiative recombination excited by 20 KeV electron beam 9-21645  
 GaSb, X-ray-K-absorption edge shifts 9-21638  
 GaSb cond. bands from free carrier Faraday rot. obs. 9-13889  
 GaSb tunnel diodes, I-V charact. in high crossed elec. and mag. fields 9-10019  
 GaSe-metal layer, surface barriers 9-5699  
 GaSe, indirect energy gap by opt. absorption spectra 9-18622  
 GaSe<sub>1-x</sub>S<sub>x</sub>, indirect energy gap by opt. absorption spectra 9-18622  
 GaTe film, charge carrier mobility 9-13883  
 GraP, electroluminescent diodes, minority carrier lifetime 9-12491  
 p-Ge:Ga, Li, interimpurity radiation recombination, Li-Ga ion pair effects 9-3919  
 Ge, Hall mobility after deformation, dislocation band model 9-18628  
 Ge surface props. on adsorpt. of Cu from electrolyte 9-5704  
 GeTe-GaAs tunnel junction, neg. resistance Schottky-type barrier props. 9-15119  
 Hg<sub>1-x</sub>Cd<sub>x</sub>Te alloy, photoconductive i.r. detector 9-8522  
 n-Hg<sub>1-x</sub>Cd<sub>x</sub>Te ionized-impurity scattering of conduction electrons at 4.2°K, calcs. 9-13884  
 HgS, e. drift mobility determs. 9-5691  
 n-HgSe, de Haas-Van Alphen and Shubnikov-De Haas eff. in strong mag. fields 9-16218  
 p-HgTe, effective hole mass at 95°K 9-9985  
 n-HgTe, elec. conductivity and Hall effect in strong elec. field 9-3626  
 n-HgTe, magnetoresistance quantum oscils. 9-3625  
 InAs:Cd, Cd ionization energy conc. dependence 9-3646  
 InAs:Cd compensated, intrinsic, e. density lifetime temp. dependence rel. to recombination at Cd levels 9-3630  
 n-InAs:Te, injection laser, self modulation obs. 9-254  
 InAs, 4.2°K, doped, cond. band 9-1535



**Semiconducting materials continued**

n-InAs, coupled collective cyclotron excitation-longitudinal optical phonon modes, reflectivity meas. 9-12151  
 InAs, effective mass carrier density dependence at 78°K 9-3639  
 p-n-InAs, electoreflectance meas., spectra behaviour, p- to n-like changeover 9-9987  
 InAs, energy-momentum reln. in forbidden gap 9-1537  
 InAs, Hall effect, anomalous 9-15091  
 n-InAs, magnetoresistance oscill. maxima fine structure at 1.6°K 9-1530  
 InAs, photomagnetic Gurevich-Firsov oscillations 9-3743  
 n-InAs, quantum thermomag. effects 9-3629  
 InAs, Raman spectra of optical phonons, Ar laser excitation 9-12419  
 InAs diode lasers, generation threshold dependence on resonator length 9-15532  
 InAs epitaxial films, e. mobility and conc., thickness dependence 9-1532  
 InAs film for Hall emf. transducers 9-10007  
 InAs films, magnetoresistance 9-9980  
 InAs laser, used for i.r. detector response time meas. 9-2383  
 n-InAs magnetophonon effect 9-21513  
 In<sub>1-x</sub>Ga<sub>x</sub>As, solid solutions, elec. resistivity and Hall coeff. meas. for energy structure and Debye temp. calc. 9-3640  
 In<sub>1-x</sub>Ga<sub>x</sub>P, photoluminescence, i.r. and visible 9-12488  
 n-In<sub>2</sub>O<sub>3</sub> film, photoconductivity 9-15138  
 n-InP, compensated, magnetoresistance and Hall effect 9-3627  
 InP, electron effective mass depend. on their density 9-9979  
 InP, epitaxial films, stacking disorder 9-9617  
 InP, light scattering from single particle electron and hole excitations 9-12443  
 InP, Raman spectra of optical phonons, Ar laser excitation 9-12419  
 InS<sub>2</sub> field emitter, field distrib. and rate of pot. fall calc., electron multiplication mechanism 9-17447  
 InSb, current flow on optical absorption 9-3843  
 Mg<sub>2</sub>As<sub>2</sub>, props. 9-16267  
 Mg<sub>2</sub>Ge, electoreflectance spectra, 1.5-4.5 eV 9-12364  
 Mg<sub>2</sub>Si, electoreflectance spectra, 1.5-4.5 eV 9-12364  
 Mg<sub>2</sub>Sn, electoreflectance spectra, 1.5-4.5 eV 9-12364  
 p-MnO, Hall mobility of electrons and holes at high temp. 9-12152  
 Ni-Alumina powdered mixture, 20-320°C in atm. of H, He, O, n or p-type depend. on Ni content 9-13887  
 Ni-chromium oxide mixture, semicond. obs. 9-13887  
 Ni-Fe ferrite, conductivity mechanism 9-3632  
 NiCr<sub>2</sub>Se<sub>4</sub>, conductivity rel. to effect of interactions between d shells of transition element 9-16253  
 NiO:Li elec. conductivity and thermoelec. power rel. press. and temp. 9-21506  
 NiO, high-temp. defect struct. and elec. props 9-3571  
 NiO, optical absorpt. of small polarons in near and far i.r. 9-5929  
 Pb<sub>1-x</sub>Sn<sub>x</sub>Te:Bi diode laser with low threshold currents 9-20529  
 Pb<sub>1-x</sub>Sn<sub>x</sub>Te alloys, cation-rich, excess carrier conc., comp. and annealing temp. dependence 9-3634  
 Pb<sub>1-x</sub>Se<sub>x</sub>, generation of coherent laser radiation, 4-6.5 μ range 9-2384  
 p-PbSe, carrier density dependence of thermopower 9-3724  
 p-PbSe, carrier mobilities 9-3633  
 PbSe, conduction band dispersion relation 9-3642  
 p-PbSe, band structure from temp. dependence of elec. props. 9-3643  
 Pb<sub>1-x</sub>Sn<sub>x</sub>Te, resistivity and Hall coeff. temp. dependence, 4-300°K, rel. to band-inversion 9-13890  
 n-PbTe:Gd, Mn, thermoelectric power, thermal and elec. conductivity, temp. depend. 9-13876  
 p-PbTe:Fe:Mn, thermoelec. power, thermal and elec. cond. temp. depend. obs. 9-13876  
 PbTe-PbS solid solutions, valence band structure, from Hall coeff., elec. conductivity and thermoelec. power meas. 9-21514  
 p-PbTe, diffusion of Ni and Cl, 700°C, junction formation 9-19767  
 PbTe, helicon propag., high-field, anisotropy 9-5631  
 PbTe, Nernst-Ettinghausen effect, transverse, in mixed conduction region 9-15132  
 RbNO<sub>3</sub>, conductance at phase transformations 9-16254  
 Sb, electromechanical eff., sign inversion 9-5675  
 Sb<sub>2</sub>Se<sub>3</sub>, needle-like crystals, I-V characts, resistivity, band structure and intrinsic conduction 9-1194  
 SbSi, ferroelec., interphase formation, eff. of nonequilibrium carriers 9-5752  
 SbSi, ferroelec., interphase formation, eff. of nonequilibrium carriers 9-5752  
 Se-CdSe p-n junction, Cl impurity effects on characts. 9-10010  
 Se-CdSe p-n junctions, Tl impurity conc. eff. on characts. 9-5721  
 Si-p, piezoresistance and mag. susceptibility, 1.5 to 500°K 9-10000  
 Si-Ge-B alloy, conductivity and thermoelec. props. 9-15133  
 SiC-B p-n junctions, electroluminescent energy spectrum, 77-300°K 9-18727  
 SiC-CdSe p-n junction, production technology and props. 9-10013  
 n-SiC, photoconduction, 77°K 9-13932  
 n-SiC, sublimation process, effect of time and temp. 9-18416  
 SiC crystal growth and p-n junction prep. from solns. in rare-earth elements 9-16056  
 SiC diffusional p-n junctions, light sum relax. 9-10241  
 SiC p-n junctions, solution grown 9-13902  
 n-SiC semiconductor-to-metal transition 9-15087  
 SiO<sub>2</sub>-Si interface, recombination carrier velocity, reduction due to heat treatment in H 9-12170  
 α-Sn, dielectric singularity in long wave length limit 9-3697  
 SnO<sub>2</sub>, cassiterite powder, elec. cond., press. depend. to 90 kg/cm<sup>2</sup> 9-13877  
 SnSe<sub>2</sub> film, charge carrier mobility 9-13883  
 Sr, metal-semiconductor transition at high pressure 9-18605  
 SrTiO<sub>3</sub>:Nb magnetoresistance rel. to conduction band structure 9-7788  
 SrTiO<sub>3</sub>, ceramics, superconductivity 9-3598  
 Te:Sb, i.r. absorpt. spectrum 9-5930  
 Te, electrical conductivity anisotropy in single crystal 9-19911  
 Te, magnetoresistance, negative, at low temps. 9-3566  
 Te film, activation energy; temp. resistance coeff. thickness depend. 9-7803  
 Ti-Te, liquid, Hall coeff. and mobility, composition and temp-dependence, 340-640°C 9-13537  
 n-TiBiTe<sub>2</sub>, Hall effect and specific conductivity temp. dependence 9-21507  
 TiTe<sub>2</sub>, optical energy gap 9-14046  
 V:O<sub>2</sub>, optical and transport props. 9-18620

**Semiconducting materials continued**

VCr<sub>2</sub>Se<sub>4</sub>, conductivity rel. to effect of interactions between d shells of transition element 9-16253  
 VO<sub>2</sub>, semicond. to metal phase transition, resist. jump 9-16255  
 VO<sub>2</sub>, metal-semiconductor transition 9-1552  
 WSe<sub>2</sub>, n- and p-type, props. 77-295°K 9-5692  
 Y, metal-semiconductor transition at high pressure 9-18605  
 ZnS, band structure calc., Green's function method 9-21467  
 ZnS, I-V characts., built-in field formation rel. to cry. defects 9-15093  
 ZnS, non-equilibrium carrier creation during depolarisation and radiation absorpt. 9-21502  
 ZnSb-constantan, thermoelements, diffusion phenomena and phase transitions, X-ray microprobe analysis 9-10062  
 ZnSe, band structure calc., Green's function method 9-21467  
 n-ZnSe, piezoresistance and piezo-Hall effect 9-5693  
 ZnSe unactivated single crystals, luminescence, λ<sub>m</sub>=0.63 μ band 9-14079  
 ZnSnP<sub>2</sub>, chalcopyrites and sphalerites, band structure from optical spectra 9-5931  
 ZnSnP<sub>2</sub>, mobility of holes rel. to ordering 9-3310  
 ZnTe, band structure calc., Green's function method 9-21467  
 ZnTe, cyclotron resonance from thermally excited holes 9-3635  
 ZnTe, isoelectronic oxygen trap from isotopic substitution and Zeeman expts. 9-18723

**gallium arsenide**  
 Auger recombination 9-15090  
 bulk transferred electron effects 9-3685  
 carrier distrib., equilib., photoluminescent meas. method 9-9974  
 cathodoluminescence in n-type rel. to donor band states 9-12479  
 current oscillations and high-field domain propagation under acoustic amplification 9-19912  
 defects introduced by <sup>60</sup>Co γ irradiation in n-type undoped and Te-doped material 9-13875  
 diffusion improved by exposure to radiation, patent 9-21354  
 diode, alloyed, electroluminescence props. 9-7996  
 diode, Zn-implanted, formation of deep trapping levels, eff. on elec. characts. 9-19920  
 diodes, double injection, doping effects on characts. rel. to trapping levels 9-18636  
 dislocation free, electronic transport props. 9-16099  
 domain, slow, in high resistivity sample 9-7793  
 domains, moving high field, in high resistivity n-type, electro-optic obs. 9-9976  
 elastic constants, temp. depend in heavily doped crystals 9-9742  
 electric-field modulated optical absorpt. in semi-insulating crystals 9-5883  
 electroluminescence, 300°K and 77°K, p-type 9-21659  
 electroluminescence due to acoustoelectric instability of current, n-type 9-7995  
 electron radiation damage, cathodoluminescence study 9-18570  
 epitaxial, far i.r. photocond. 9-7857  
 epitaxial films, photoluminescence of n-type 9-10265  
 epitaxial heavily doped, electron mobility 9-17391  
 film-substrate interface, vapour epitaxial, occurrence of high resistance layer 9-5674  
 films, impurity transfer in vapour growth and carrier-conc. profiles 9-11772  
 free-carrier and exciton radiation recombination 9-10238  
 GaAs:Si epitaxial films, band structure from luminescence spectra 9-5701  
 galvanomagnetic effects of hot electrons, n-type 9-3624  
 Gunn diodes, n-type, mag. field effect of i.f. oscillations 9-5737  
 Gunn diodes, subcritically doped, stability and reflection gain 9-7829  
 Gunn domains, Franz-Keldysh eff. 9-7798  
 Gunn effect charact., influence of nonparabolicity in displaced Maxwellian approx. 9-1519  
 Gunn effect samples non-uniform conductivity effects on behaviour 9-5688  
 Gunn oscillators, sheet-type, reduced domain build-up 9-10023  
 Gunn threshold, calc. 9-1518  
 Hall coeff. and magnetoresistance rel. to 'freezing-out' of electrons, n-type 9-12147  
 Hall eff. and elec. resistivity, temp. and pressure depend., n- and p-type 9-7799  
 Hall effect, 300° to 900°K 9-16264  
 hot electron energy relaxation time 9-9975  
 hot electron magnetophonon effect in n-type epitaxial films 9-16265  
 junction lasers, gain factor and internal loss, annealing and compensation eff. 9-4482  
 laser, bistable operation characts. 9-2382  
 laser, characts. 9-19154  
 laser, e. beam excited, output power and efficiency 9-2381  
 laser, electron-beam pumped, threshold current density and emission spectra, temp. depend. 9-4483  
 laser, injection, threshold current density, effect of external optical coupling 9-4484  
 laser, junction, resonant modes comparison of theoretical and experimental results 9-19152  
 laser, p-n junction injection, characts., obs. 9-15531  
 laser diode c.w., noise 9-247  
 laser radiation absorption 9-3848  
 laser transitions and photon energy 9-3847  
 lasers, injection, construction for cw operation at high temps. 9-8627  
 lifetimes meas. short, of excess carriers, form fluorescence phase shift. 9-1529  
 light scattering from single particle electron and hole excitations 9-12443  
 luminescence, bound- and free-exciton, band- and donor-acceptor, and Auger recombination 9-14077  
 magnetoresistance, undoped, at low temperatures 9-3610  
 metal point contact, breakdown 9-3686  
 metal-GaAs point contact, rectifying barrier structure 9-12163  
 n-type, acoustoelec. domain propag. 9-9835  
 n-type, current instabilities in oriented samples 9-17392  
 n-type, epitaxial films, hot electron magneto phonon effect 9-16265  
 n-type, generation and reception of ultrasound 9-3609  
 n-type, Hall coeff. electron heating dependence 9-12149  
 n-type, Hall effect, 300° to 900°K 9-16264  
 n-type, h.f. photoconductivity phase shift meas. 9-18656  
 n-type, intermediate donor level activation energy by temp. depend of Hall effect 9-3653

### Semiconducting materials continued

#### gallium arsenide continued

- n-type, magnetophonon effect 9-21513
- n-type, space-charge-limited currents and vel.-field characts. 9-5673
- n-type, undoped, magnetoresistance at low temp. 9-3610
- n-type, undoped and Te-doped, defects introduced by  $^{60}\text{Co}$   $\gamma$  irradiation 9-13875
- n-type Faraday effect of free carriers 9-3864
- n-types, luminescence from donor-acceptor pair recombination involving the first excited state of donor 9-12465
- ohmic contacts, vacuum dusting on to hot substrate 9-12161
- optical absorption due to inter-conduction-minimum transitions 9-7932
- optical absorption edge and refl. coeffs., rel. to impurities, 297° to 4°K 9-21621
- oscillations, l.f., appl. 9-5717
- oscillators, microwave instabilities 9-10006
- p-n junction laser with nonlinear passive element in resonator, charact. features of radiation 9-17878
- p-n structures, epitaxial, high-efficiency electroluminescence 9-15192
- p-type, conductivity and capacitance, infl. of constant elec. field 9-3650
- p-type, electroluminescence, 300°K and 77°K 9-21659
- photoconductive lifetime of n-type, diffused with Cu, temp. depend. 9-5765
- photoconductivity, h.f. phase shift meas., n-type 9-18656
- photoconductivity enhancement, elec. and optical, in semi-insulating crystals 9-5766
- photoexcited high-resistivity, current oscillations and high-field domains 9-12210
- Raman scattering, from magnetoplasma waves 9-12415
- Raman spectra line width, and intensity, temp. depend. 9-12437
- Raman spectra of optical phonons, Ar laser excitation 9-12419
- review 9-19910
- Schottky barriers, current mechanisms 9-21519
- Schottky diodes, electron-phonon coupling in barrier 9-7825
- Shubnikov-de Haas oscillations, magnetoresistance, Hall eff., n-type 9-5687
- space-charge-limited currents and vel.-field characts., n-type 9-5673
- substrate, high resistance layer occurrence due to epitaxial film growth on surface 9-11773
- thermal expansion, precision meas. on semi-insulator 25-325°C 9-5570
- transport props., expt. obs. 9-5689
- tunnel diode fabrication by micropulse alloying method, recombination rad. detect. 9-7827
- tunnel diodes, high-power epitaxial, prep. and characts. 9-12167
- tunnel diodes, I-V characts. in high crossed elec. and mag. fields 9-10019
- vapour grown epitaxial layer, light Sn doping 9-15097
- X-ray K-absorption edge shifts 9-21638
- zero field mobility, modified variational calc. 9-9977
- Au-GaAs surface barrier junctions, elec. props. 9-10009
- Au-GaAs Schottky barriers, capacitance meas. 9-5720
- diffusion of Zn, mechanism 9-16111
- n-GaAs:Cr, negative magnetoresistance 9-19913
- GaAs:(Ge,Zn) tunnel diodes, degradation during forward operation and in high temp. storage 9-3680
- GaAs:Ni, p-type, props. 9-15099
- GaAs:Te(Zn diffused) injection laser, threshold current density doping conc. dependence 9-8626
- GaAs-Cs photocathode, photoemission, effect of Sb(Te) on surface 9-12225
- GaAs-InAs laser diodes solid soln. singularities in rad. spectrum 9-8628
- GaAs-Pb, junction, hole TO-phonon interac. 9-1556
- GaAs<sub>0.5</sub>PO<sub>0.5</sub>: Fe trapping phenomena 9-16263
- GaAs diode laser, modulation in an external resonator 9-19153
- Ge-Te-GaAs tunnel junction, neg. resistance Schottky-type barrier props. 9-15119
- Zn diffusion for producing laser diodes p-n junctions 9-17285

### germanium

- acoustic wave generation by elec. field pulses 9-3523
- band structure studies by electron beam modulated reflectance 9-9989
- carrier density gradient, associated instability 9-5707
- carrier distrib. and type, under elec. field, Hall effect study 9-17396
- charge transport in low angle grain boundaries 9-3657
- conductivity, electrical, on ion bombardment 9-7807
- conductivity, electron-beam-induced, terminal voltage change 9-5682
- current carriers, anisotropic scattering, rel. to temp. depend. of mobility tensor, n-type 9-1526
- current instability due to intervalley redistrib. of electrons on heating by elec. field, n-type 9-1545
- current instability in crossed elec. and mag. field 9-7805
- current striction, many valley n-type, theory 9-9995
- depletion effects, non-equib., at electrolyte interface 9-13895
- diffusion improved by exposure to radiation, patent 9-21354
- diode, alloyed, velocity of surface recombination in base, dependence on injection level 9-18637
- dislocations and dislocation diodes, elec. props., bilateral microscopy 9-7806
- electroabsorpt. spectrum rel. to diamag. exciton structure obs. 9-7951
- electromechanical eff., sign inversion 9-5675
- electromechanical effect existence 9-1315
- electron absorpt. coeff. meas. temp. depend. 9-7808
- electron and hole mobility, 300°K 9-17398
- electron heating at surface in strong const. elec. fields, n-type 9-9991
- electron-hole plasma double injection, p-type 9-7804
- etching, surface, effect of impurity and resist. on speed of etching 9-3230
- exciton system, Mott transition from many-electron system to metallic conductivity state 9-3659
- Fermi level, ultimate position rel. to 50 MeV e.-irrad. effects 9-12154
- field effect, role of surface relief 9-1547
- field e.m.f. in n-type material 9-13892
- film, photovoltaic effect, high-voltage, study 9-15141
- film, thermoelectric props., and use as thermoelements 9-16308
- film crystallization by zone melting using SiO<sub>2</sub> and glass coatings 9-3238
- film recrystallized in electron beam, mobility and conc. of current carriers, effect of substrate temp. 9-16271
- films, elec. instabilities at 20.4°K 9-5702
- films, n-type, photoelec. props. 9-3736
- n-Ge:Sb,  $\gamma$ -irrad. induced carrier mobility changes and dopant periodic distrib. effects 9-5705
- n-Ge:Sb(As), electron irradiated, absorpt. edge 9-10200
- Hall effect, longitudinal, p-type 9-15103
- Hall mobility after deformation, dislocation band model 9-18628

### Semiconducting materials continued

#### germanium continued

- high field current fluctuations, n-type 9-16272
- hole low-field mobility and galvanomagnetic props rel. to phonon scatt. 9-5708
- hole mobility in strong elec. fields 9-21515
- hole-phonon coupling const. determ. by cyclotron reson. 9-3551
- impact ionization of impurities 9-15105
- intra-band radiation of hot electrons, n-type b// c// 9-3638
- intrinsic layer between p and n regions, one carrier space charge limited currents 9-21523
- ion implantation, dopant lattice location by C ions backscattering technique 9-18629
- ionization of diamagnetic excitons and quantum eff. in valence band 9-12068
- magnetophonon oscillations of transverse magnetoresist. 9-12158
- magnetophonon oscills. in drag thermoelec. power n-type 9-3722
- metal Ge contacts, e. and phonon tunneling spectroscopy 9-13909
- microwave emission in transverse mag. field 9-15104
- mobility of warm electrons at 78°K, effect of electron-electron collisions, n-type 9-9990
- monocrystals, scanning e beam display of dislocation space charge 9-7390
- n-type, electron damage, orientation and temp. depend. 9-13672
- n-type, field e.m.f. 9-13892
- n-type, high field current fluctuations 9-16272
- n-type, intra-band radiation of hot electrons 9-3638
- n-type, negative differential conductance 9-13891
- n-type, phonon drag effect, influence of electron scattering 9-19917
- n-type, thermo-e.m.f. anisotropy 9-15131
- n-type, thermoelec. power, phonon-drag effect anisotropy parameter 9-12205
- n-type, transient processes after pulsed n. irrad. 9-3654
- n type current instability due to intervalley redistrib. of electrons on heating by elec. field 9-1545
- n-type diodes, surface recombination rates, anisotropic pressure dependence 9-10017
- n-type magnetophonon oscills. in drag thermoelec. power 9-3722
- n-type oscillator, helical instability mechanism 9-5718
- negative differential conductance of n type material 9-13891
- neutron irradiated, impurity photoconductivity kinetics, n-type 9-10072
- oscillator, frequency of helical instability 9-1561
- p-n junctions, reactive characts. in breakdown region 9-15110
- p type, electron-hole plasma double injection 9-7804
- p-type, Hall effect, longit. 9-15103
- p-type, hole mobility in strong elec. fields 9-21515
- p-type, hole recombination at shallow acceptors 9-3655
- p-type, transport props. study using magnetoplasma waves 9-5681
- photosensitivity in thin layers 9-10074
- plastically deformed and irradiated, photoconductivity spectra 9-15137
- radiation detectors, optimal thickness of sensitive layers 9-10073
- radiative recombination at dislocations 9-15183
- resistivity meas. instrument, four-probe 9-12134
- Schottky barriers' differential resistance, effect of ellipsoidal energy surface 9-13904
- slice, carrier injection, transverse mag. field eff. 9-5706
- spin cyclotron reson. free-hole g factor determ. 9-1543
- spin polarized electron scatt. from cyclotron resonance obs. 9-9993
- stopping of Ge\* atoms, band gap effects 9-5589
- surface, non-equilibrium charging 9-21516
- surface elec. props. after exposure to O<sub>2</sub> after heating in vacuo 9-3651
- surface properties on Cu adsorpt. from electrolyte in contact 9-5704
- surface recombination studies using Suhl effect and light injection 9-9988
- surface states, slow relaxation of work function 9-18627
- thermo-e.m.f., n-type 9-15131
- thermoelectric power, phonon drag effect anisotropy parameter 9-12205
- transistors alloyed, avalanche multiplication characts., anomalies caused by surface and volumetric effects 9-3682
- transport props. study using magnetoplasma waves, p-type 9-5681
- tunnel diodes, I-V characts. in high crossed elec. and mag. fields 9-10019
- warm carriers, energy relaxation 9-12159
- X-ray diffraction topography for analyzing crystal faults and stresses in wafer samples 9-9677
- As-doped, u.s. spin reson. of donors 9-5555
- As doped,  $\gamma$ -irradiated, recombination centres 9-17397
- cleaved (111) surface, opt. detection of surface states, 9-1544
- p-Ge:Ga, Li, interimpurity radiative recombination, Li-Ga ion pair effects 9-3919
- Ge:As, complex formation kinetics 9-9992
- Ge:As, e. density modulation by impurity centre field 9-3918
- Ge:A, Ga, nonradiative interimpurity recombination, 4.2°K 9-21646
- Ge:As(Sb), under uniaxial compression, radiative recombination 9-10239
- Ge:As(Sb), under uniaxial compression, effect on long-wavelength intrinsic 'tail' 9-12466
- Ge:Au, electrical noise properties, 80°-300°K, n- and p-type 9-9996
- Ge:Au, n-type, I-V characts., investig., 17° to 35°K 9-18626
- Ge:Cu, n-type, recombination of hot carriers, charact. features 9-21549
- p-Ge:Ga, e. irrad. and annealing effects on conduction mechanism 9-5703
- Ge:Mn, carrier conc. and mobility, variation due to heat treatment 9-3658
- Ge:Sb, resistivity rel. to temp., activation energy rel. to mag. field and deformation 9-3656
- Ge:Zn, e. scatt. by neutralized Zn acceptors, stress effects, 1.5-4.2°K 9-1546
- p-Ge-n-Si heterojunctions, preparation by vacuum evap. and I-V characts. 9-3201
- Ge, chemical polishing apparatus for flat, clean, strain-free surfaces 9-14284
- Ge, magnetoabsorption intensity rel. to exciton absorpt. rise 9-5919
- Ge, photoluminescence in presence of crossed fields, 9-14097
- Ge, quantum effects in cyclotron resonance using c.w. HCN laser 9-14070
- Ge, spin splitting rel. to u.v. absorpt. 9-13893
- n-Ge helicon waves transmission, liq. He temp. 9-16270
- Ge(Li) counter, cylindrical, coaxially-drifted, large sensitive volume, construction 9-6726
- Ge(Li) detector, anomalous effect at 77°K 9-6730
- Ge(Li) detectors characts. and basic expts. with them for undergraduates 9-12824
- Ge(Li) detectors in  $\gamma$  spectrometer system 9-19224



**Semiconducting materials continued****germanium continued**

Ge(Li) diode detector, drift control method 9-4677  
 Si, photoelectron mobility, variation with photon energy 9-13927  
 transistors, n-p-n and p-n-p avalanche multiplication parameter determ. 9-1559

**indium antimonide**

absorption, fundamental, in lightly doped p-type, temp. depend. 9-10202  
 acoustic wave generation by elec. field pulses 9-3523  
 acoustoelectric gain modes origin 9-12011  
 anodic oxide films, resistivity and dielec. const. 9-11770  
 carrier freeze-out effects in strong mag. field 9-1531  
 combined resonance spectra, effects of electron-optical-phonon interact. 9-1742  
 conduction band g-value anisotropy 9-1538  
 current flow effects on optical absorption 9-3843  
 current oscillations, highly sensitive to mag. field, 77°K, n-type 9-15092  
 cyclotron resonance of holes and Landau levels 9-5632  
 diffusion improved by exposure to radiation, patent 9-21354  
 effective electron mass pressure dependence from magneto resistance and thermoelec. power meas. 9-1536  
 epitaxial films, e. mobility and conc., thickness dependence 9-1532  
 film, zone melting by e beam heating 9-14893  
 helicon waves in n-type sample 9-16256  
 hot electron mobility, resonance variation in h.f. magnetic field 9-3550  
 hot electron mobility, resonance variation in h.f. magnetic field 9-13823  
 interaction between drifting carriers and slow e.m. waves 9-9978  
 intrinsic, surface carrier waves 9-15101  
 Landau damping and e scattering by impurities, effect estimated 9-897  
 magnetic freeze-out and evidence for donor impurity band in zero mag. field 9-13885  
 magnetoacoustic amplification, quantum theory 9-16171  
 magnetophonon oscillations of magnetoresistance in strong elec. fields 9-19914  
 n-type, acoustoelectric gain modes origin 9-12011  
 n-type, bounded helicon waves 9-16256  
 n-type, Fermi surface anisotropy, null deflection torque magnetometer obs. 9-3641  
 n-type, galvanomagnetic props. meas., 0.4-4°K 9-12137  
 n-type, localization of electrons by mag. field 9-15100  
 n-type, magnetic freeze-out and evidence for donor impurity band in zero mag. field 9-13885  
 n-type, magnetophonon effect 9-21513  
 n-type, magnetophonon oscillations of magnetoresistance in strong elec. fields 9-19914  
 n-type, microwave emission, anisotropy obs. 9-12136  
 n-type, mm. and sub-mm. radiation absorption, 2.1 and 4.2°K 9-16413  
 n-type, photoconductivity under electron heating conditions 9-10063  
 n-type, photoeffect. in quantizing mag. fields during electron heating by light 9-3744  
 n-type, plasma aftervoltage effects 9-5629  
 n-type, quantum galvanomagnetic phenomena and transport props. 9-13886  
 n-type, quantum thermomag. effects 9-3629  
 n-type, resonant photoconductivity, transport props. 9-17444  
 n-type, temp. dependence of detection props. in microwave region 9-1542  
 n-type, thermoelec. power in transverse quantizing mag. field, phonon drag effects 9-3723  
 n-type conductivity dependence 0.3-20°K 9-3628  
 n-type degenerate crystal, impurity conc. meas. using Burstein eff. 9-3645  
 n-type Faraday effect of free carriers 9-3864  
 noise of hot electrons, 4.K 9-16252  
 p-type, dislocations eff. on elec. props. 9-21505  
 p-type, doped, fundamental absorpt. temp. dependence 9-10202  
 p-type, field-effect at 88°K 9-5700  
 p-type, temp. dependence of Hall coeff., elec. conductivity and carrier mobility 9-3631  
 p-type, thermoelectric power, depend. on carrier density 9-16309  
 photoelectromagnetic effect, short-circuited Demer voltage effects 9-5772  
 pinch, degenerate, stationary state and parameters 9-9983  
 plasma, aftervoltage effects, n-type 9-5629  
 plasma instability, mag. field effect on 70 MHz component, n-type 9-5630  
 radiation absorption, mm. and sub-mm., 2.1 and 4.2°K 9-16413  
 Raman spectra of optical phonons, Ar laser excitation 9-12419  
 resonant photoconductivity, transport props., n-type 9-17444  
 surfaces, relaxation phen. at high elec. fields 9-19916  
 thermoelectric power, depend. on carrier density, p-type material 9-16309  
 thermoelectric power in transverse quantizing mag. field. phonon drag effects, n-type 9-3723  
 thin films, structural, electrical and galvanomagnetic properties 9-3193  
 third harmonic generation enhancement using CO<sub>2</sub> laser, magneto inter-band contrib. 9-257  
 transport parameters temp. depend. interpretation 9-12146  
 De Haas-Van Alphen effect, obs. using pulsed peaks up to 200 kG 9-9914  
 InAs, photomagnetic Gurevich-Firsov oscillations 9-3743  
 n-InSb, photoconductivity due to cyclotron absorpt. 9-5767  
 InSb electron abs. Urbach's law, perturbative and nonperturbative calc. application 9-3603  
 n-InSb i.r. detector, response to night sky background 9-6086

**silicon**

acoustic wave generation by elec. field pulses 9-3523  
 alloyed junction mosaics for use in image analyzer tubes 9-8586  
 annealing of 10 MeV electron damage, carrier conc. and lifetime recovery 9-17399  
 carrier, non-equilibrium, creation during depolarisation and radiation absorpt. 9-21502  
 conductivity depend. on dislocations 9-1548  
 contact resistance of electroless Ni 9-19892  
 current carriers, anisotropic scattering, rel. to temp. depend. of mobility tensor, n-type 9-1526  
 current striction, many valley n-type, theory 9-9995  
 cyclotron resonance between 1.5 and 4.2°K 9-3561  
 deep levels introduced into band structure by 300 KeV electron irradi. 9-7809  
 defect cluster formation electron irradiated, 15 to 45 MeV 9-17400  
 detector, backscatt. and bremsstrahlung, pulse distrib., 300-1200 kev 9-11141  
 detector high voltage operation, improved charge collection 9-4673

**Semiconducting materials continued****silicon continued**

detectors for 10 to 30 kV X-ray meas. characts. 9-13172  
 diffusion improved by exposure to radiation, patent 9-21354  
 diffusion thermal, of Be, resulting elec. and opt. props. 9-10004  
 diodes, n. irradi. effects on I-V characts. 9-10018  
 effective mass approx. for acceptor states 9-18630  
 electrical props. of edge dislocations, effects of contamination 9-5712  
 electron absorption coeff. meas. temp. depend. 9-7808  
 electron drift velocity at high elec. field, temp. depend. 9-10002  
 electron effective mass, field depend. 9-1431  
 electron gas, two-dimensional, effects of tilted mag. field 9-5619  
 electron states at dislocations 9-16274  
 electron transport phenomena, anisotropy at high field 9-10001  
 electron-phonon matrix elements, n-type 9-7814  
 electrons and holes drift velocity at very low temp. 9-10003  
 epitaxial film on spinel, mech. and elec. props. 9-7815  
 epitaxial layers, partial screw dislocations, obs. 9-5369  
 epitaxial technology advances 9-7339  
 etch rate determ. of Si in buffered HF using a <sup>31</sup>Si tracer method 9-16051  
 fabrication, build-in of C 9-3667  
 fast neutron induced resistivity changes at room temp., prediction curves 9-1550  
 Fermi level location, dopant dependency 9-13896  
 Fermi level stabilization and surface states at interface and insulating layers 9-3555  
 field effect, role of surface relief 9-1547  
 films for use as image analyzer tube targets 9-8587  
 gettering of Au and Cu 9-3668  
 ground state energy of P donor, corrected 9-12160  
 Hall mobility and carrier repopulation in n-type at high elec. fields 9-16278  
 heterojunction between crystal and amorphous Si 9-3677  
 high resistivity regions, irradi. with deuterons and  $\alpha$  particles 9-3662  
 impurity atom distributions meas. by differential capacitance technique, mathematical analysis 9-3664  
 irradiated, recombination luminescence 9-7989  
 laser-induced resistivity changes 9-7812  
 magnetoresistance, longitud., in mixed conduction region 9-15106  
 metal-nonmetal transition, resistivity and Hall effect study 9-1472  
 mobility of warm electrons at 78°K, effect of electron-electron collisions, n-type 9-9990  
 monocrystals, scanning e beam display of dislocation space charge 9-7390  
 mosaic crystal, low dislocation density, prod., patent 9-13596  
 n-type, electron-phonon matrix elements 9-7814  
 n-type, heavily P-doped, piezoresistance and mag. susceptibility 9-16276  
 n-type, phonon drag effect, influence of electron scattering 9-19917  
 n-type, phonon drag effect, influence of electron scattering 9-19917  
 n-type, two-dimens. electron gas, effects of tilted mag. field 9-5619  
 n-type dislocation acceptor level energy, from dislocation vel. obs. 9-9713  
 neutron activation analysis, non-destructive 9-20074  
 neutron irradiation defect production, i.r. spectral obs. 9-15177  
 p<sup>+</sup>-n junction, avalanche photomultiplication, effect of donor density 9-15114  
 p<sup>+</sup>n junction diode, d.c. characts. pressure and temp. dependence 9-10011  
 p<sup>+</sup>n spherical junction, multiplication props. 9-7820  
 p-n junction, abrupt, differential resist. in avalanche mode 9-7823  
 p-n junction, avalanching, temp. and current distrib. 9-3678  
 p-n junction,  $\gamma$ -radiation effect on parameters and structure 9-16280  
 p-n junction characts., probe meas. 9-10012  
 p-n junctions, abrupt., avalanche multiplication, theoretical analysis 9-7819  
 p-n junctions, breakdown and effect on reverse I-V characts 9-21520  
 p-type,  $\gamma$ -irradiated, elec. props. changes 9-21518  
 p-type, contact resistance of electroless Ni 9-19892  
 p-type, oscillations induced in photoconductivity and absorpt. spectra and association with A-centres 9-18659  
 p-type, P ion bombard. at 30keV, effects on elec. props. 9-9999  
 p-type contamination in epitaxial layers on corundum substrate 9-3666  
 p-type layers formed by Ga ion-implantation, charge carrier conc. anneal-temp. dependence 9-15108  
 p-type n irradiation-induced defect clusters from Hall effect and conductivity meas. at 76°K 9-17401  
 photoconductivity with In acceptors 9-7859  
 piezoresistance and mag. susceptibility in heavily P-doped material 9-16276  
 radiation conductivity, influence of e bombardment 9-3663  
 radiative spectra from shallow donor- acceptor electron transfer 9-18722  
 Raman spectra line width, and intensity, temp. depend. 9-12437  
 Read and p-n-n<sup>+</sup> IMPATT diodes, computer simulation under large signal conditions 9-12164  
 resistivity meas. instrument, four-probe 9-12134  
 Schottky effect meas. 9-5710  
 Si:Li electron-irradiated, recombination velocity, Li impurity effects 9-9998  
 spin polarized electron scatt. from cyclotron resonance obs. 9-9993  
 surface, atomically clean, nonequilibrium. large-signal field effect, relax. 9-21517  
 surface barrier, high resistivity, holes preferential trapping 9-6725  
 surface elec. props., treated with gaseous HF 9-3661  
 surface inversion layer, Hall mobility of electrons 9-5711  
 surface stabilization using Si<sub>3</sub>N<sub>4</sub> 9-7811  
 transistors, n-p-n planar, double diffused, current amplification factors, structural causes of spread 9-3683  
 vacancies,  $\gamma$ -ray irradiation induced, generation rates 9-5340  
 vapour epitaxy, applic. to device technology 9-13612  
 warm carriers, energy relaxation 9-12159  
 Al-SiO<sub>2</sub>-Si, injection and migration of charges in oxide 9-5741  
 Au-Ag alloy film on n-Si Schottky barrier, characts 9-3675  
 Au doped, conductivity and lifetime of excess carriers anomaly 9-16273  
 Au-n Si surface barrier diodes, rectification characts. rel. to surface states 9-21525  
 B, implantation with improved elec. activity and profiles 9-16277  
 B implantation, range and distribution, capacitance method 9-5709  
 diodes, Zn-compensated, with negative resistance, characts. 9-17406  
 p-Ge-n Si heterojunctions, preparation by vacuum evap. and I-V characts. 9-3201  
 N ion implantation on p-type monocrystal, 20≤E≤215 keV 9-15107  
 n-Si:As, semicond. to-metal transition 9-15087

**Semiconducting materials** continued**silicon** continued

- Si: Au, conductivity recovery after majority carrier sweep-out by trapped space charge 9-18615  
 n-Si: Au, electrical noise properties, -300°K 9-9996  
 Si: Au, p-n junctions, impedance and other props. rel. to Au conc. 9-21521  
 Si: Au, recombination of hot electrons 9-9997  
 p-Si: B, recombination centres from  $\gamma$ -irrad. and annealing 9-3665  
 Si: Cd diodes, with negative resistance 9-18633  
 Si: P, ESR line shift 9-3959  
 n-Si: P, i.r. absorption, dopant eff. on carrier mechanisms 9-18710  
 Si: P, majority-carrier density dependence of neutron dose, infl. of A and E centres 9-1549  
 Si: P, metal-nonmetal transition, eff. on NMR props. 9-15109  
 p-Si: P, radiation damage dependence on n. energy spectrum 9-3660  
 n-Si: P, semicond. to-metal transition 9-15087  
 Si: P diodes, laser-irrad. production, structural and elec. characts. 9-18638  
 Si: SiO<sub>2</sub>, band structure, diagram 9-18587  
 Si: SiO<sub>2</sub>, structures, C-V characts. rel. to improved m.o.s. transistors 9-5742  
 Si-SiC<sub>2</sub> interface, heat-treated, C-V characts., freq. depend. 9-7813  
 Si-SiO<sub>2</sub> interface, recombination carrier velocity, reduction due to heat treatment in H 9-12170  
 Si-SiO<sub>2</sub> interface states 1/f type noise, quantitative theory 9-5738  
 n-Si, deviations from Ohm's law in high electric fields 9-16275  
 Si, photoelectron mobility, variation with photon energy 9-13927  
 n-Si radiation damage studies, preparation of thin specimens 9-13815  
 Si(Li),  $\beta$ -spectrometer, energy resolution, effect of inhomogeneities 9-14530  
 Si(Li) junctions, recovery behaviour after  $\gamma$ -irrad 9-15111

**Semiconductor lasers** *see Lasers/semiconductor***Semiconductors**

*See also Crystal electric states; Magnetolectric effects; Photoconduction; Photovoltaic effects*

- A<sup>II</sup>B<sup>VI</sup>, phonon-assisted exciton transitions 9-5966  
 acoustic amplification, eff. of elec. field redistribution 9-12006  
 acoustic attenuation and amplification in piezoelectric and ferroelectric semiconductors 9-18553  
 acoustic waves, anomalous fluctuations in external electric field 9-5670  
 acoustoelectric effect in magnetic fields, theory 9-1384  
 acoustoelectric effect theory accounting for anisotropic dielec. and piezoelec. props. 9-12009  
 aminoacids, single cry. and polycrystalline, protein semicond. study 9-21510  
 anisotropic, current control 9-3615  
 anisotropic, photosensitivity from I-V characts. 9-15134  
 aromatic, electrode injection of charge carriers 9-21509  
 Auger recombination model modification 9-7800  
 band-tail spreading energy determ. method using lasers 9-1541  
 binary, atomic displacement energies 9-12133  
 capture level determ. by thermally stimulated current method 9-19879  
 carrier, non-equilibrium, creation during depolarisation and radiation absorpt. 9-21502  
 carrier density, equilibrium, in presence of 2 types of local level 9-5678  
 carrier transport in elec. field, flux method applic. 9-5677  
 charge carrier recombination mechanism 9-3549  
 chemisorption, different forms, applic. of Landsberg trapping statistics 9-3992  
 complex dielectric constant calculation 9-5668  
 conductivity, electron-beam-induced, terminal voltage change 9-5682  
 crystals adjacent to piezoelectrics, acoustic surface wave amplification 9-9833  
 current carriers, anisotropic scattering 9-1526  
 current column and S-shaped I-V characts. 9-1527  
 current fluctuations, voltage on sample and p.d. between bands, theory 9-15083  
 defects, radiation induced, factors influencing stability 9-17388  
 degenerate, photoelec. phenom. theory when e. heated by light 9-12209  
 degenerate, plasmon mechanism of superconductivity 9-15077  
 diamagnetic susceptibility, statistical model 9-10096  
 diamagnetic susceptibility rel. to that of semimetal 9-10097  
 dielectric function 9-19909  
 domain motion, steady-state, in systems with drift nonlinearity, stability 9-21498  
 domains, static electrical, in semicond., with hot holes 9-3614  
 domains, stationary and non-stationary high-field, in semi-insulators, int. conditions for transitions 9-12142  
 doped oxides as diffusion sources for fabrication 9-5394  
 doping by ion-plantation, no radiation damage to surface, patent 9-9986  
 in electric and magnetic fields, conductivity 9-15088  
 electron absorption, coeffs. Urbach's law, perturbative and nonperturbative method, weak and strong interactions 9-3603  
 electron energy spectrum, impurity effect 9-15095  
 electron energy spectrum and mobility in a thin film with a nonideal boundary 9-13873  
 electron-hole scattering at high injection levels 9-5676  
 electron-phonon interaction and i.f. oscillations, n-type 9-7790  
 electroreflectance, anomalous Franz-Keldysh eff. 9-1511  
 electrothermal domains, theoretical analysis 9-13871  
 epitaxial doping density vs. depth meas. 9-18623  
 exciton, interaction with charged centre 9-19881  
 exciton line excitation on light absorpt. in mag. field 9-1763  
 excitons, bound, spectra 9-21470  
 ferromagnetic, helicon waves, film thickness effect 9-1539  
 ferromagnetic, magnetoelastic wave amplification 9-5829  
 ferromagnetic, spin wave amplification 9-10110  
 field effect and photoconductivity relax. phenomena 9-10064  
 films, conductivity, quantum oscillations rel. to mag. field 9-5679  
 flexure-drift resonance 9-18617  
 Frenkel' pairs, formation under hard radiation 9-3328  
 Fresnel drag prod. by e motion, meas. 9-5685  
 galvanomagnetic effects in presence of small number of free carriers 9-13878  
 graded mixed, electronic states and transport, theory 9-21511  
 Gunn effect, bibliography from 1954 9-9970  
 Gunn effect, explanatory account 9-5683  
 Gunn effect under s.c.l. conditions 9-1510  
 Hall effect, isothermal in intrinsic semicond. for weak mag. field 9-7787  
 Hall effect and related props., book 9-13880  
 Hall effect calc., if heavily doped and at low temp. 9-12155  
 Hall effect when polarons are charge carriers 9-18616  
 heat transport using polaron model 9-7791  
 h.f. permittivity, spatial dispersion 9-19908  
 high permittivity, phonon drag by electrons, theory 9-17366  
 homopolar, low temp. effects due to local states 9-1425  
 hopping conduction, meas. by a.c. method, model 9-15084  
 impurities, isoelectronic, theory 9-7801  
 impurity band conduction with strong electron correlations 9-7704  
 impurity states, model for metal-nonmetal transition 9-15098  
 inclusions, rel. to supercond. enhancement 9-9940  
 inhomogeneous, electrical conductivity theory 9-21504  
 instability, i.f., rel. negative resistance 9-7793  
 instability of hot electrons in crossed elec. and mag. field 9-21501  
 internal photo-effect, investigation by condenser method 9-13926  
 intrinsic, surface carrier waves 9-15101  
 intrinsic conduction onset temp. determ. from p-n junction charact. 9-10008  
 ion implantation, lattice disorder and electrical effects 9-17395  
 i.r. generation, 75-100 $\mu$ , free-carrier magneto-optical eff. 9-18694  
 Landau level Raman scattering 9-12398  
 Landau level Raman scattering 9-12397  
 Landau levels, combinational scattering of Light 9-1744  
 at Leningrad Physicochemical Institute, historical account of investigations 9-7785  
 LSA mode oscills. 9-5684  
 magnetic, electron effective mass, magnon corrections 9-18584  
 magnetic, e.m. wave and slow neutron scattering by anomalous fluctuations of spin waves in elec. field 9-5814  
 magneto optical phenomena, nonlinear 9-5881  
 magnetoplasma wave propag. in two-carrier system, p-type 9-5681  
 many-valley, absorption and amplification of sound 9-1372  
 many-valley, acoustoelectric effect in quantizing mag. fields 9-1385  
 many-valley, interaction of sound with conduction electrons 9-1371  
 many-valley, two stream instability in hot-electron systems 9-15096  
 many-valley, u.s. absorpt. and amplification oscills. due to inelastic scatt. of electrons 9-7644  
 microwave conductivity, non-ohmic, meas. 9-15102  
 microwave second harmonic generation and sum and difference frequency at low temperatures 9-3604  
 misfit disloc. in inversion layers 9-3339  
 mobility, field-dependent, theory 9-9971  
 n-type epitaxial films on p<sup>+</sup> substrates, hole diffusion length meas. using laser 9-3616  
 n-type group IV, semicond. to-metal transition 9-15087  
 Nernst-Ettinghausen effect, effect of collisions between carriers 9-15129  
 neutron bombarded, carrier scattering from defects 9-17389  
 noise, excess, rel. to anisotropic current instability 9-21497  
 nondegenerate, steady-state diffusion eqns. in space-charge regions with large elec. fields 9-16259  
 nondegenerate, steady-state galvanomagnetic effects, coupled current densities 9-13872  
 nuclear polarization by hot carrier flow in crossed static and mag. fields 9-15042  
 Ohm's law deviations 9-3605  
 Ohm's law violation 9-7786  
 optical absorption, elec.-current-flow induced polarization effect, theory 9-14035  
 organic, kinetic transport coeff. theory, weak-field magnetoresistance approximation 9-21508  
 organic, pre-exponential factor 9-13888  
 p-type, magnetoplasma wave propag. in two-carrier system 9-5681  
 phase meter for subnanosecond electronic processes 9-20483  
 photoconductivity, subject to high illumination intensities 9-1609  
 photomagnetic effect, increase rel. to pair generation rate 9-1621  
 piezo-, sonic waves, theory of fluctuations 9-18552  
 piezoelectric, acoustoelectric domains, sound reflections 9-18559  
 piezoelectric, acoustoelectric gain and current, non-linear theory 9-5558  
 piezoelectric, acoustoelectric gain and current, nonlinear theory 9-16173  
 piezoelectric, coupled acoustic-plasma waves 9-9968  
 piezoelectric, current fluctuations in acoustoelec. steady state 9-5559  
 piezoelectric, depolarization field eff. on electromechanical props. 9-17438  
 piezoelectric, free-carrier Faraday effect at microwave freq. 9-14030  
 piezoelectric, minority carriers in u.s. amplification 9-11999  
 piezoelectric, nonlinear amplification and automodulation of sound 9-12141  
 piezoelectric, ultrasonic surface waves 9-7646  
 piezoelectric, u.s. amplification in a magnetic field 9-3526  
 pinch, degenerate, stationary state and parameters 9-9983  
 pinch-like instabilities and turbulence 9-5694  
 plasma, light scattering in mag. field 9-16397  
 plasma, overheating instability, theory 9-3607  
 plasma, transition to paramag. 9-3606  
 plasma edge reflection meas. rel. to carrier conc., effective mass., scattering time and conductivity determ. 9-7792  
 plate in liquid, piezoelectric, acoustic wave amplification 9-18556  
 polar, acoustoelec. effect 9-5560  
 polar, hot-electron galvanomagnetic coeffs. 9-5680  
 polar, microwave electron mobility, steady field heated, non-parabolic dispersion law 9-1525  
 polar, zero field mobility calc. if no universal relax. time exists 9-9977  
 polarization, establishment times 9-21499  
 positron annihilation 9-17374  
 Raman scatt. theory rel. to plasmon-phonon interaction 9-3901  
 Raman scattering from magnetoplasma waves 9-12415  
 Raman scattering of shallow impurity states, mag. field eff. 9-12396  
 recombination radiation, instrument for spectra study 9-12157  
 recombination through exciton states, kinetics 9-14071  
 reflectivity enhancement by Q-switched ruby lasers 9-15163  
 semi-insulator, domains, stationary and non-stationary, crit. conditions for transitions 9-12142  
 semiconductor, carrier interaction with neutral centre 9-19881  
 semiconductors, exciton absorpt. in crossed elec. and strong mag. fields 9-10174  
 semimetal-semicond. transition, possible anomalies 9-15045  
 shallow surface states, theory 9-16213  
 size effect in sandwich structures 9-5667  
 solid solutions, optical absorption and luminescence edges 9-3880  
 spin polarized e. scatt. from cyclotron resonance obs. 9-9993



**Semiconductors** continued

- superconducting behaviour 9-19894
- surface covered with water, charge relaxations 9-4057
- surface recombinant flying spot method, improved 9-3647
- surface recombination rate, non-equilib. carrier density dependence 9-5698
- surface transport, two- dims. 9-18624
- survey of work by M.Moldovanova 9-16251
- thermoelectric power, longitudinal, in quantizing mag. field 9-16305
- thermorefectance in band structure exam. 9-14041
- thin plates, conductivity, many-valley energy spectrum of carriers 9-9925
- trace metal analysis 9-8114
- transport phenomena research, nuclear- electronic technique 9-15085
- transport properties analysis from combined conductivity and Seebeck-effect plots 9-21503
- two-layer structure, properties control by superhigh freq. 9-14008
- two-layer structures, impedance, theoretical dependences 9-13898
- two-valley, stability of state with negative differential conductivity under small perturbations 9-16268
- ultrasound damping in h.f. elec. field, oscillatory charact. 9-1377
- U.S. propagation in presence of a.f. elec. field 9-11998
- velocity saturated, coupled-mode instabilities 9-13881
- Zone melting process for crystal production, mathematical model 9-9649
- K<sub>2</sub>P<sub>2</sub>O<sub>7</sub>-V<sub>2</sub>O<sub>5</sub> glass, effect of thermal treatment on a.c. props. 9-3612

**Semimetals**

- acoustoelectric effect in magnetic fields, theory 9-1384
- acoustoelectric effect in quantizing mag. fields 9-1385
- acoustomagnetic field instability at low temps. and acoustomagnetic waves 9-15004
- de Haas-van Alphen effect, quasi-local level effects 9-1444
- degenerate, plasmon mechanism of superconductivity 9-15077
- with electron-hole pairing, diamagnetic properties of isotropic model 9-10097
- film with nonideal boundary, electron spectrum and mobility 9-13873
- inclusions, rel. to supercond. enhancement 9-9940
- magnetoresistance 9-15066
- thin plates, conductivity, many-valley energy spectrum of carriers 9-9925
- As, current carrier conc., pressure depend 9-15069
- Bi-Sb alloy, semiconducting to metal transition, rel. to mag. field and Sb conc., 4-77°K 9-1513
- Bi, mag. susceptibility meas. rel. to semimetal-semiconductor transitions 9-7876
- Bi, TeS<sub>2</sub>, semimetal to semiconductor transition, size effect quantization 9-16230
- Bi<sub>1-x</sub>Sb<sub>x</sub>, mag. susceptibility meas. rel. to semimetal-semiconductor transitions 9-7876
- Cr<sub>11</sub>Ge<sub>18</sub>, with hole type conductivity 9-5799
- InSb, negative magnetoresistance and localized spins 9-9932
- P, Hittorf's, atomic crystal structure 9-13646
- Se metallic impurities effects on conductivity in phase transition region 9-12103
- Sr, metal-semiconductor transition at high pressure 9-18605
- Te, Shubnikov-de Haas effect 9-7729
- Y, metal-semiconductor transition high pressure 9-18605

**Series**

- convergence by methods of least squares and Bubnov-Galerkin 9-12908
- Lindstedt's, on computer 9-8357
- literal, applic. to lunar theory 9-10508
- non-orthogonal expansions remedy for difficult calc. of Gramm's determinant 9-12856
- polynomial expansion, optimized for scatt. amplitudes, convergence and mapping 9-16665
- separable expansion for off-shell two-body t matrix with Coulomb pot. 9-13306
- Sudarshan expansion for diagonal coherent-state weight functional, convergence 9-6275
- tabulated, book 9-10683

**Sferics** *see Atmospherics***Shadow universe** *see Cosmology; Elementary particles***Shear strength** *see Mechanical strength/shear***Shell model** *see Nucleus/model***Shielding** *see Radiation protection***Shock tubes**

- electromagnetically driven, shock front form meas. 9-6391
- electrothermal, shock development 9-20437
- e.m., plasma flow obs. 9-14765
- e.m., precursor effects, obs. 9-9360
- gas wake velocity, meas. from induced e.m.f. 9-2238
- for mass spectrometry analysis sampling 9-21110
- MHD power generation obs. elec. field prod. by interacting gas flow and mag. field 9-20488
- MHD-augmented, meas. techniques 9-17813
- rectangular, press. up to 1500 lb in<sup>-2</sup>, vacuum down to 10 $\mu$  torr 9-12942
- scattered radiation, effect on emission meas. 9-2235
- Ar gas wake velocity, meas. from induced e.m.f. 9-2238
- Cr I, II radiation absolute g $\nu$ -values calc. 9-19399
- Xe gas wake velocity, meas. from induced e.m.f. 9-2238

**Shock waves**

- See also Detonation; Explosions; Plasma/shock waves; Supersonic flow*
- aerial, inducing wave in solid, diffraction, polariscopic investigation 9-19077
- in air, interaction with liquid fuel surface, and ignition process 9-14127
- blast waves, variable-energy 9-12941
- collisionless, mag. field capture and plasma containment, expts. 9-15932
- converging, cylindrical ionizing shock in applied axial mag. field, theory 9-18284
- cylindrically and spherically symm., prod. in relaxing gases 9-19568
- detached, axially symmetric, numerical calc. of flow 9-17150
- detached shock calculation by 2-order finite differences 9-946
- detonation, propagation in space with conical cutout 9-13476
- detonation vels. by a multichannel time intervalometer 9-155
- detonation waves, plane and spherical, from solid explosives, finite difference soln. of behaviour 9-20440
- electromagnetically driven, plasma electron density meas. by microwave reflection 9-11585
- envelope, conditions and stability 9-154
- explosion region, rel. to radio reflections 9-156
- flow at distance from object at sonic speed, asymptotic theory 9-8515
- flow behind shock wave, asymptotic expansion 9-21130

**Shock waves** continued

- flow behind wave in gas passing body 9-13477
- formation in radiation-gas-dynamics 9-11651
- front form meas. in e.m. driven shock tube 9-6391
- gas-particle mixture, propag. eff. of finite particle volume 9-9450
- hypersonic flow over wedge, of diatomic gas 9-19572
- hypersonic shock layer, eff. of radiative heat transfer from grey gas, soln. 9-21121
- hypersonic viscous flow past semi-infinite flat plate with sharp leading edge, analysis 9-21004
- interaction problems 9-941
  - interaction with turbulent mixing region 9-19578
- interplanetary, hydromag., math. anal. 9-8286
- in interstellar medium with cosmic rays 9-1988
- ionizing, gas velocity variation 9-18321
- large-amplitude periodic shock-fronted press. waves, generation in resonant tube 9-8517
- lengthening caused by their propag. to high altitudes 9-17815
- liquid-solid impact pressure and wave velocity 9-8516
- longitudinal, in hyperelastic media, thermodynamics 9-8514
- MHD, for non-viscous fluids, structure 9-7127
- in O<sub>2</sub>, interaction with liquid fuel surface, and ignition process 9-14127
- obstacle moving with speed of sound, flow at infinity in front of shock wave 9-19060
- pattern assoc. with turbulent boundary-layer separation ahead of cylinder 9-7214
- phase changes and pulse deformations, comments 9-19078
- physics, and high-temperature hydrodynamic phen., book 9-11645
- in polytrope with poloidal mag. field, propag. 9-10471
- position determ. from pitot tube expts. 9-19076
- production in relaxing gases 9-19568
- propagation, detonation: 3D gas flow by regions of rest 9-21124
- quasi-, in electron beam 9-227
- secondary, production due to radiation absorption behind main front 9-20439
- sharp cone drag coeffs. at supersonic speed, correl. 9-7217
- solar corona, generating radio bursts 9-10555
- solar wind, front due to flare plasma 9-2078
- in solids, vel. of sound, density and press., empirical relnshp 9-4362
- sonic boom, coupled seismic wave obs. 9-2236
- sonic boom, seismic wave generation obs. 9-2239
- sonic boom, strength and propag., effects of winds and inhomogeneous atmos. 9-10397
- sonic flow about axisymm. object at large distance behind shock wave 9-19074
- sonic-boom press. waveforms, spikes 9-4063
- spherical, in visco-elasto-plastic half-space, reflected irrotational wave as plastic stress wave 9-12932
- sun flare generated, energy deposition in solar wind 9-10551
- velocity, position meas., microsec. response system, electrical impedance change of stream 9-2237
- velocity field due to shock waves incident on stationary thin symmetric body 9-5101
- velocity in solids, relation with ht. of sublimation 9-13722
- in water, energy calc. 9-3047
- yield of underground explosions, peak-stress gauge for meas. 9-10744
- H-O, explosive gas, interact. between waves and flame kernels 9-1901
- N<sub>2</sub>-Ne mixture, shock front u.v. radiometry 9-21142

**effects**

- air, ionization, conductivity meas. 9-915
- Alfven, in viscous fluid of finite elec. cond. 9-11532
- alkali halides ionic crystals, compressed, nonequilibrium radiation, temp. above 1 eV 9-14970
- borosilicate glass-metal steel composite, thermal shock resistance 9-1273
- boundary layer obtained at wall, recovery factors from frictional stress and heat transfer 9-21129
- ceramic-metal composite, thermal shock resistance 9-1273
- compression in crystals, microsecond X-ray exposures 9-11815
- condensor circuit under compression, current and elec. relax. calc. 9-200
- dielectric, compressed, optical characteristics, review 9-16285
- dynamic response of cyl. shell: soln. 9-20438
- Galaxy, cluster, degree of gas ionization 9-4088
- gases, diatomic, vibr. dissoc. relax. behind shock wave 9-13483
- gases, ionizing wave fronts, propag. and struct 9-14797
- ionic crystals, compressed, nonequilibrium radiation temp. above 1 eV 9-14971
- magnetic flux compression by explosion, recoil phase 9-12972
- M.H.D., relativistic, compressibility hypothesis and waves time orientation 9-21030
- polyacrylamide, solid, shock wave polymerization obs. 9-15218
- powder, brittle inorganic crystalline, prep., patent 9-9668
- refractory metals, vapour press. meas. 9-9596
- solids, compression Hugoniot's, correlation of two universal expressions 9-5434
- sonic bang intensities in stratified still atmosphere 9-17816
- sonic bangs, eff. on visual task performance 9-15474
- sonic booms, farfield spectrum 9-17814
- two dimensional objects 9-19075
- Al porous, shock response on compaction, computer simulation 9-5437
- Al splash generation by detonation wave impact 9-5438
- Al<sub>2</sub>O<sub>3</sub> alumina ceramics, strength effect in shock compression 9-7563
- Ar, relax. phenomena in ionized shock front 9-14798
- Br<sub>2</sub>, dissoc. rate determ. by two-body emission 9-19480
- br<sub>2</sub>, dissoc. rate determ. by two-body emission 9-13394
- Br<sub>2</sub>, dissociation 9-13395
- CO<sub>2</sub>, vibr. relax. in shock-tube 9-759
- Cl<sub>2</sub>, radiative recomb. 9-9289
- Cu-(30 at.wt.%) Zn alloy, induced deformation faults 9-13681
- Cu, porous, compression 9-11920
- Fe, armco, effect on residual mag. props. 9-13980
- Fe, hardened, twins and complementary twins 9-13695
- Fe porous, shock compression in region of incomplete compaction 9-11948
- H<sub>2</sub>-O<sub>2</sub>-Ar mixture, detonation initiation, reaction mech. 9-14128
- H<sub>2</sub>O, electrical polarization, shock-induced, mechanism 9-1037
- H<sub>2</sub>, dissoc. rates 9-1902
- HCl decomp. 9-8077
- N<sub>2</sub>O, vibr. relax. in shock tube 9-775
- N<sub>2</sub>, vibr. dissoc. relax. behind shock wave 9-13483
- N<sub>2</sub>F<sub>4</sub>, thermal dissoc. 9-1903

**Shock waves continued**  
**effects continued**

- O<sub>2</sub> vibr., dissoc. relax. behind shock wave 9-13483  
Ti-Ar mixtures, ionization of Ti 9-19556

**Shot noise** *see Noise/electrical***Showers** *see Cosmic rays/showers and bursts***Shubnikov-de Haas effect** *see Magnetoresistance***Silicon**

*See also Semiconducting devices; Semiconducting materials/silicon*

- annealing kinetics, activation energy and entropy 9-7505  
atomic energy levels and multiplet data tables 9-9123  
atoms and ions, bibliography of spectra 9-13287  
Bragg condition, depend. of extinction distance on deviation 9-13649  
condensation of Au on (111) surface 9-1094  
contact substrate for Ba and Cs 9-13907  
crystal, filamentary growth from soln. in tin, resistivity 0.01 ohm-cm 9-9644  
crystal growth methods 9-9651  
crystallization front fluctuation during growth by Czochralski technique 9-5280  
defect activation by neutron, energy  $1.2 \pm 0.1$  eV from annealing studies 9-1275  
defect cluster formation electron irradiated, 15 to 45 MeV 9-17400  
defects in e. irradi., n-type mat., photoconductivity meas. after stress-induced dichroism of defects 9-21340  
diffusion improved by exposure to radiation, patent 9-21354  
diffusion in liquid Al, temp. depend. of coeff. 9-9496  
diffusion of B in oxygen ambient rel. to transistor fabrication 9-14959  
diffusion of Ga, retarded 9-5413  
diffusion of Ga, retarded 9-5412  
dislocation generation and concentration during growth 9-1224  
divacancy-associated energy levels: photoconductivity studies of defects 9-3327  
effective mass approx. for acceptor states 9-18630  
electromechanical effect, kinetics 9-1314  
electron irradi., Li defect complex, i.r. spectroscopic study 9-13673  
electron states, applic. of Kohn potential 9-1417  
electron-phonon matrix elements, n-type 9-7814  
epitaxial film growth, equilibria of nuclei formed during H<sub>2</sub> reduction of SiCl<sub>4</sub> 9-11774  
epitaxial growth, continuous method, and thermodynamical anal. 9-14896  
epitaxial growth, light irradiation effects 9-11808  
epitaxial growth in horizontal reactors, theory 9-7378  
epitaxial layers, partial screw dislocations, obs. 9-5369  
evaporation by vacuum-arc discharge evaporation 9-17244  
film epitaxial, chemically grown, nucleation kinetic meas. on (100) surfaces, using molecular beam techniques 9-21298  
films, electron microscope obs., 700-1000°C 9-14899  
ground state energy of P donor, corrected 9-12160  
growth on (111)Si in ultrahigh vacuum, surface processes 9-5276  
heavily doped, lattice periodicity meas., X-ray diffraction exam. 9-5320  
heavy particle range-energy table 9-7693  
ionization energy levels of Zn, existence problem 9-15058  
ionization equilibrium in low-density plasma 9-15820  
i.r. lattice absorption 9-3510  
K<sub>a</sub> X-ray satellites in fluoresc. spectra of Mg in oxides and metals 9-3933  
Kikuchi line anomalies rel. to structural defects 9-18445  
Laue-case profile, variation with thickness from a thin crystal 9-5328  
light detector, integrating, applied to optical pyrometry 9-10756  
mean excitation potentials from stopping power data 9-9135  
neutron irradiation defect production, i.r. spectral obs. 9-15177  
nitridation in preparing Si<sub>3</sub>N<sub>4</sub> films 9-21281  
one-phonon band-mode i.r. absorption by impurity resonances 9-5915  
opacity, eff. on A- and B-star atmospheres 9-18848  
oxidation, thermal, effect of oxidation conditions 9-10341  
Pendellosing interf. fringes in n diff. obs. 9-9663  
phonon-assisted transitions determ. by derivative optical spectroscopy 9-1758  
photoconductivity and absorpt. spectra, oscillations associated with A-centres 9-18659  
photoconductivity studies of defects: divacancy-associated energy bands 9-3327  
photoemission of electrons and holes into Si<sub>3</sub>N<sub>4</sub> thin layers 9-10081  
plastic deformation, single crystals, rel. elec. erosion 9-5350  
positron annihilation radiation, angular correlation calc. from atomic Hartree-Fock orbitals 9-5638  
proton energy-loss straggling 9-13816  
proton irradiated, fringe contrast on X-ray topograph, application of Takagi's dynamic theory 9-3354  
proton transmission along {100} and {110} channels in crystal lattice, energy and angular distributions 9-16192  
proton tunnelling, 6.72 MeV 9-21448  
reference crystals for double-crystal topography 9-7387  
Schottky diode fabrication by chem. deposition of Mo 9-6010  
single crystal solar cell, development survey 9-2320  
solar cell charact. rel. to temp. and solar intensity 9-4423  
solar cells, 1 MeV electron damage 9-4422  
solar cells, fabrication performance and terrestrial applications 9-2318  
spectra, far u.v., band structure effects and many-particle scatt. corrections 9-12378  
spectra, p<sup>2</sup>-p<sup>3</sup> transition line oscillator strength in isoelectronic sequence 9-9122  
sputtering by Ar ions, detection 9-19873  
stopping channelled atomic particles, Z, ocs and size effect 9-5583  
stress patterns on X-ray micrographs, analytical description 9-11873  
substrate for epitaxial Ge layer growth by vacuum evap. 9-3201  
surface evolution by H atoms and their effect on latent image formation in photographic emulsions 9-18045  
surface passivation by SiO<sub>2</sub> film prep. 9-18404  
surface struct., (111) LEED pattern indicating impurity presence 9-5327  
surface structure, (111), Ni induced, LEED study 9-21262  
surface structure, (111), Ni induced, LEED study 9-21261  
thermal oxidation, and interdepend. between thickness of layer and exptl. conditions 9-3993  
thermodesorption, real surface 9-5260  
thermoreflectance spectrum, 3-6 eV region 9-10189  
vacancies, p-ray irradiation induced, generation rates 9-5340  
web growth processes and defects, thermal interaction effects 9-9646

**Silicon continued**

- X-ray interference fringes by an incident plane wave, Si single crystal, wedge-shaped 9-3307  
Zone-melt crystals, liq. zone motion in mutually perpendicular thermal and elec. fields 9-9650  
B diffusion at 1070 to 1190°C 9-13708  
B diffusion using BBr<sub>3</sub> liquid source, 1100-1200°C 9-1254  
B implantation, range and distribution by capac. method 9-5709  
Bi implanted layers, elec. behaviour by sheet Hall effect meas. 9-7810  
in Fe-Cr-Ni alloy, austenitic, in oxidizing acids, effect on corrosion resistance 9-17535  
Ni-on-Si catalysts, finely divided in direct and alternating fields, superparamagnetism 9-21569  
Pion channelling, effect of defects 9-9708  
Si:As(Sb), irradi., impurity-vacancy pairs, e.p.r. and endor exam. 9-5341  
Si:B, P, radiation defects, kinetics of thermal annealing 9-21327  
Si:Cu, n-irrad. induced defects generation rate, effect of impurities and dislocations 9-5335  
n-Si:P, irradiated, thermal donor formation 9-21333  
Si:P, metal-nonmetal transition, eff. on NMR props. 9-15109  
Si:P, point defects and microhardness, reln. 9-5486  
Si:Sb, solid soln, precip. of Sb during annealing 9-1333  
Si, photoelectron mobility, variation with photon energy 9-13927  
Si detector and parallel FET preamp., internal conversion e meas. 9-20703  
Si discs research, using X-ray topography 9-1196  
Si I and II spectral lines, relative oscillator strengths 9-19404  
Si IV, absolute oscillator strengths for important transitions 9-15808  
Si IV, semiempirical atomic core potentials, coeffs. 9-19397  
n-Si phonon drag eff., inf. of e scatt. anisotropy 9-19917  
Si photodiode, p-i-n, u.v. response obs. 9-12217  
SiI radiation, Stark and van der Waals level broadening constants 9-13293  
with SiO<sub>2</sub> surface films, X-ray dynamical diff. effects rel. to induced strain, obs. 9-9612

**Silicon compounds**

*See also Quartz*

- $\beta$ -cristobalite, highly-strained metastability at room temp. 9-1348  
cristobalite, internally nucleated in vitreous silica, crystallization kinetics 9-18426  
cristobalite, surface states, H<sub>2</sub>-D<sub>2</sub> equilibration activity and pH<sub>2</sub> conversion 9-3188  
lithium aluminosilicate, thermal expansion dependence on TiO<sub>2</sub> catalyst content 9-13804  
metal silicides, thermal cond. meas., electric and grid 9-21443  
quartz, surface states, H<sub>2</sub>-D<sub>2</sub> equilibration activity and pH<sub>2</sub> conversion 9-3188  
SiC:Al, luminescence of Al centre, dependence of recombination rates on the intensity of the light excitation 9-5949  
silica, density checking by statistical method 9-13712  
silica, surface states of quartz, cristobalite and silicic acid forms, comparison 9-21260  
silica, vitreous, acoustic props., thermal treatment and impurity-ion conc. effects 9-15001  
silica, vitreous, configurational entropy of random network model 9-14887  
silica, vitreous, critical evaluation of thermal conductivity literature 9-15029  
silica, vitreous, internally nucleated, crystallization kinetics 9-18426  
silica, vitreous, ionizing-radiation-induced dilatation, impurity effect 9-14961  
silica composite, prestressed and reinforced with W wires, props. 9-7569  
silica gel, effect of adsorbed H<sub>2</sub>O on elec. cond. 9-13915  
silica gel, radiolysis of adsorbed hydrocarbons 9-20063  
silicate and borosilicate glasses, thermo-optical properties over wide range of temperature and wavelength 9-14027  
silicate glass: rare earth doped, acoustic paramag. absorpt. 9-5544  
silicate glass, Sn containing, properties 9-13569  
silicates, bonding from X-ray K-emission spectroscopy 9-13589  
silicic acid, surface states, H<sub>2</sub>-D<sub>2</sub> equilibration activity and pH<sub>2</sub> conversion 9-3188  
tetrasilicates, elec. conductivity 9-15062  
trimethylethoxysilane, vibratory spectra from i.r. absorpt. 9-11495  
zeolite fore vacuum pump which also serves as Dewar for cooling agent 9-12808  
zeolites of Faujasite type, chem shift of <sup>13</sup>Cs reson. 9-4924  
Al-Si alloy, eutectic, transverse bands rel. to directional solidification and mag. field 9-5313  
Cr-O systems, phase diagrams, high temp. 9-1351  
Cr-SiC system, composition and phases 9-1328  
Cu-Si alloy, stacking fault energy meas., composition and temp. dependence 9-11887  
Cu-Si solid soln., deformed, elec. resistivity decrease 9-16224  
Fe-Si alloy, eff. of dislocation network on plastic strain 9-16098  
Fe-3 wt.%Si with Goss-texture, irreversible magnetization process and Barkhausen effect 9-13977  
Fe-Si-Zn system, constitution anal. using mag. and X-ray techs. 9-11975  
Fe-Si, coercive forces and mag. susceptibility 9-16360  
Fe-Si, eutectic crystal behaviour below eutectic pts. 9-5213  
Fe-Si, with Goss or cube texture, hysteresis losses rel. to grain size 9-12237  
Fe-Si, grain oriented, basic expts. on nature of anomalous losses 9-12242  
Fe-Si, grain oriented, meas. using ceramic displacement 9-12293  
Fe-Si, phase diagram 900 1200°C for 30 to 40 at.%Si 9-11974  
 $\alpha$ -Fe-Si, superlattice phases, equilibria and transforms. 9-11965  
Fe-Si alloy, crystals, oxidation kinetics, optimal exam. 9-21277  
Fe-Si alloy, embrittlement, effect of cold rolling 9-1311  
Fe-Si alloy, high temp. sp. ht., mag. susceptibility temp. depend., up to 1870°K 9-7601  
Fe-Si alloy, oxide film effect on max. permeability 9-10092  
Fe-Si alloy crystals, oxide film structure 9-21278  
Fe-Si alloys, ferromag. resonance 9-8004  
Fe-Si alloys, Hall effect and resistivity temp. and comp. dependence 9-9921  
Fe-Si alloys, magnetic props., anisotropy, eff. of surface Ni films 9-13990  
Fe-Si alloys, thin foils, antiphase boundaries contrast in superlattice reflections 9-11849  
Fe-Si alloys, X-ray fluorescence 9-14080  
Fe-Si frame m monocrystal, negative Barkhausen jumps, occurrence during magnetization 9-1672



## Silicon compounds continued

- Fe-(3wt. %) Si alloy, magnetoelastic attenuation of vibrations, eff. of temp. 9-11915
- Fe-(3wt. %) Si alloy polycrystals, twinning and effects on brittleness 9-1124
- Fe-6.5% Si, zero magnetostriction,  $n$  induced mag. viscosity, obs. 9-19952
- Fe-(7.5 at%) Si, self-diffusion near Curie temp., activation energy rel. to elastic modulus 9-5402
- Fe-Si ordered ferromag. alloys, spin-wave excitations, dispersion law, Heisenberg model 9-18674
- FeO-SiO<sub>2</sub>, thermoelec. power, 1150-1470°C 9-1606
- Fr-Si alloys, dislocation velocity stress dependence, temp. and comp. effects 9-7488
- (93.5-6.5at%) Ge-(7.6-92.4 at%) Si, electroreflectance spectra 9-14045
- Ge-Si alloys,  $n$ -irrad. effects on thermoelec. props. 9-7849
- Li-Si detector for spark-chamber triggering 9-20701
- Li<sub>2</sub>O-Al<sub>2</sub>O<sub>3</sub>- $n$  SiO<sub>2</sub> ( $4 \leq n \leq 10.0$ ) solid solns., thermal expansion behaviour 9-3537
- Ni-Co-Si alloy, Nicosi, magnetostrictive, anisotropy, static and dynamic props. 9-5830
- NiSi<sub>x</sub>, ( $x=1, 2$ ), X-ray spectral determ. of Ni 3d-band structure 9-3911
- Si-Au alloys, i.r. impurity photocond. of Si surface 9-15140
- Si-Fe sheets, common and grain orientated, remagnetization domain effects 9-15151
- Si-Ge-B alloy, thermoelec. props. and conductivity 9-15133
- Si-O systems, phase diagrams, high temp. 9-1351
- Si-SiO<sub>2</sub>, band structure, diagram 9-18587
- Si-Te vapour system, partial press. and thermodynamic props. 9-7307
- Si<sub>3</sub>N<sub>4</sub> film preparation by direct nitridation of Si substrates 9-12281
- Si<sub>3</sub>N<sub>4</sub> films, d.c. conduction and complex dielec. constant 9-19927
- Si<sub>3</sub>O<sub>8</sub><sup>2-</sup> polymerized, distrib. in binary silicate melts 9-19612
- Si complex, tetrafluorobispyridinesilanes (IV), crystal and mol. structure 9-13648
- SiBi<sub>2</sub>O<sub>20</sub>, synthesis and properties 9-18648
- SiBr<sub>4</sub> molecule, emission spectrum 9-2882
- SiC:B p-n junctions, electroluminescent energy spectrum 9-18727
- SiC-CdSe p-n junction, production technology and props. 9-10013
- SiC-HfB<sub>2</sub>(ZrB<sub>2</sub>) mixtures, bend strength and elastic modulus rel. to grain structure 9-1259
- $\beta$ -SiC, absorption and luminescence spectra rel. to exciton states 9-3900
- $\beta$ -SiC, diffuse X-ray scatt. 9-1195
- SiC, epitaxial films, blue photo- and electroluminescence 9-5972
- SiC, exchange interactions of N donors 9-19972
- $\alpha$ -SiC(6H),  $n$ -type, optical absorption 80°K-1100°K 9-12387
- SiC, phonon dispersion curves by Raman scattering, polytypes 9-3509
- $n$ -SiC, photoconduction, 77°K 9-13932
- $\alpha$  SiC, photoluminescence and phosphorescence quantum yields 9-3929
- SiC, screw dislocations clusters rel. to Frank's growth mechanism 9-18477
- SiC, sublimation process, eff. of time and temp. 9-18416
- SiC, type 120R, direct structure determ. 9-19724
- SiC crystal growth and p-n junction prep. from solns. in rare-earth elements 9-16056
- SiC crystallites on Si(111) surface obs. by electron diffraction 9-5288
- SiC diffusional p-n junctions, light sum relax. 9-10241
- SiC epitaxial layers, X-ray topography 9-3202
- $\beta$ -SiC field ion images, description 9-12988
- SiC filaments, continuous vapour deposited, microstruct. obs. 9-9683
- SiC films, microwave discharge preparation, optical and elec. props. 9-21601
- SiC p-n junctions, solution grown 9-13902
- SiC particle growth in carbon star atms., calc. 9-18852
- $n$ -SiC semicond.-to-metal transition 9-15087
- SiC structure of 6H types 9-16080
- SiC varistors, current dependence of voltage non-linearity 9-7817
- SiC whisker growth 9-3241
- SiCl<sub>4</sub>-NH<sub>3</sub>-H<sub>2</sub> system, thermodynamic study rel. to vapour growth of SiN film 9-5250
- SiCl<sub>4</sub>-H<sub>2</sub> vapour-gas system, conc. ratio in saturator of epitaxial equipment 9-21301
- SiCl<sub>4</sub>, free radical, i.r. spectrum 9-10352
- SiCl<sub>4</sub>, synthesis for <sup>36</sup>Cl dating, sensitivity enhancement for scintillation counter 9-11247
- SiCl<sub>4</sub> molecule, infrared absorption bands obs., bond moments calc. 9-2860
- SiCl<sub>4</sub> neg. ion form. by electron impact 9-3008
- SiD<sub>2</sub>Cl<sub>2</sub> vapour, i.r. absorpt. spectrum and fundamental freqs. 9-13369
- SiD<sub>2</sub>Cl<sub>2</sub> vapour, i.r. absorpt. spectrum and fundamental freqs. 9-13369
- SiF<sub>4</sub>, carbon tetrafluoride, photoelec. spectrum, band assignments from orbital obs. 9-19462
- SiF<sub>4</sub>, force field calc. 9-20942
- SiF<sub>4</sub> molecule, infrared absorption bands obs., bond moments calc. 9-2860
- SiFBr<sub>3</sub> microwave spectra, 30-40 GHz 9-10230
- <sup>28</sup>SiF<sub>2</sub> centrifugal distortion const. calc. 9-17041
- <sup>28</sup>SiF<sub>2</sub>H centrifugal distortion const. calc. 9-17041
- SiH<sub>4</sub>-NH<sub>3</sub>-H<sub>2</sub> system, thermodynamic study rel. to vapour growth of SiN film 9-5250
- SiH<sub>2</sub>F<sub>2</sub> vac. u.v. photolysis, matrix isolation of SiF<sub>2</sub> 9-15903
- SiH<sub>2</sub> free radical, absorpt. spectrum, rotational struct. of three bands 9-7084
- SiH<sub>4</sub>, silane, applic. to semicond. mats. fabrication, review 9-5713
- SiH<sub>5</sub><sup>+</sup> formation in ionized SiH<sub>4</sub>-CH<sub>4</sub> mixtures 9-13452
- SiH<sub>2</sub>Cl<sub>2</sub>, matrix-isolation vac. u.v. photolysis 9-10352
- SiH<sub>2</sub>Cl<sub>2</sub> vapour, i.r. absorpt. spectrum and fundamental freqs. 9-13369
- SiL, u.v. absorption spectra, new band obs. 9-17030
- SiN, elec. cond. processes of Frenkel-Poole emission, field ionization and trap hopping 9-7834
- SiN film, vapour growth from SiH<sub>4</sub>-NH<sub>3</sub>-H<sub>2</sub> and SiCl<sub>4</sub>-NH<sub>3</sub>-H<sub>2</sub> systems 9-5250
- Si<sub>3</sub>N<sub>4</sub>, stabilization of Si surfaces 9-7811
- Si<sub>3</sub>N<sub>4</sub> films, prep. by SiH<sub>4</sub>+NH<sub>3</sub> gas phase reaction, mol. structure and cracks 9-3194
- Si<sub>3</sub>N<sub>4</sub> films, production from stain films on Si and resistivities 9-3205
- Si<sub>3</sub>N<sub>4</sub> thin layers, photoemission of electrons and holes from Si and Al 9-10081
- SiO-Al condensers, breakdown voltage rel. to thickness 9-17430
- SiO<sub>2</sub>-Si system, prep. by thermal oxidation of Si 9-3993
- SiO<sub>2</sub>-ZrO<sub>2</sub>-Al<sub>2</sub>O<sub>3</sub> system, phase diagrams; for Corhart-ZAC type refractories 9-13784

## Silicon compounds continued

- SiO<sub>2</sub>-Al<sub>2</sub>O<sub>3</sub>-Cr<sub>2</sub>O<sub>3</sub> system, phase equilib., data 9-19655
- SiO<sub>2</sub>-Al<sub>2</sub>O<sub>3</sub> binary oxide film deposition on pyrolytic decomposition of trimethylsiloxy-aluminium-isopropoxide 9-21272
- SiO<sub>2</sub>, fused, optical waveguide prod. by proton channeling changing refractive index 9-20556
- SiO<sub>2</sub>, fused, u.s. elastic waves attenuation, calc. 9-3405
- SiO<sub>2</sub>, permeation of H molecules and ions 9-3388
- SiO<sub>2</sub>, photolithographic device for prod. of etched patterns 9-19918
- SiO<sub>2</sub>, vitreous, thermal conductivity, critical evaluation of literature 9-15029
- SiO<sub>2</sub> epitaxial films on Si, elastic anisotropy of edges from contrast fields on X-ray topographs 9-1107
- SiO<sub>2</sub> film deposition at low-temps. by decomposition of organo silicate 9-18405
- SiO<sub>2</sub> film deposition at low temps. by NO<sub>2</sub> process 9-18403
- SiO<sub>2</sub> films, prepared by SiH<sub>4</sub> oxidation, characteristics and applic. to Si surface passivation 9-18404
- SiO<sub>2</sub> glass, thermal cond., 0.5 to 4.2 K 9-19868
- SiO<sub>2</sub> suspension, particle-diameter distrib., for  $d < 1000$  Å, X-ray scatt. determ. 9-14873
- SiO<sub>4</sub> mol. in fused silica, vibration spectra calc. 9-14694
- SiO amorphous film, transparent hole formation mechanism 9-19668
- SiO deposition, magnetic thin element preparation, patent 9-19669
- SiO film in m.i.m. structure, elec. conductivity 9-1562
- SiO films, rel. microscopic surface roughness 9-21531
- SiO films in thin film condensers, elec. strength thickness dependence 9-10043
- SiO<sup>+</sup>, spectral band struct. round 3840 Å, and from 4300-4100 Å 9-4938
- SiO<sub>2</sub>, B diffusion in, 1070 to 1190°C 9-13708
- SiO<sub>2</sub>, contamination of Na ions, radio tracer results rel. to theory 9-17547
- SiO<sub>2</sub>, mean excitation potentials from stopping power data 9-9135
- SiO<sub>2</sub>, r.f. sputtering in Ar with O<sub>2</sub> impurity 9-7332
- SiO<sub>2</sub>, sintered fused silica, fluorination strengthening 9-1304
- SiO<sub>2</sub>, space charge buildup and release with 0 to 30 keV electron irradiation 9-12192
- SiO<sub>2</sub>, vitreous silica, radiation compaction 9-11921
- SiO<sub>2</sub>, X-ray emission by proton bombardment 9-7984
- SiO<sub>2</sub>-Al<sub>2</sub>O<sub>3</sub> catalysts, particle size of deposited Ni 9-1909
- SiO<sub>2</sub> colloids, coagulation with hydrolyzed Al(III), kinetics rel. to destabilization and particle collisions 9-9570
- SiO<sub>2</sub> in crystallization by zone melting of Ge semiconducting thin films 9-3238
- SiO<sub>2</sub> films, i.r. abs. variation, influence of heat treatment 9-12386
- SiO<sub>2</sub> films, thickness meas. over small geometries 9-11767
- SiO<sub>2</sub> gels, diffusion coeffs. rel. to pore size anal. 9-9572
- SiO<sub>2</sub> glass, diffusion of Na, 170-1000°C 9-17291
- SiO<sub>2</sub> layer on Si, electrolysis 9-4008
- SiO<sub>2</sub> particles, dragging by migrating grain boundaries in Cu 9-1233
- SiO<sub>2</sub> pyrolytic films, prop. changes on heat treatment 9-3195
- SiO<sub>2</sub> structure influence on m.o.s. system 9-7830
- SiO<sub>2</sub> thin layers, polarisation effects in m.i.m. and m.i.s. structures 9-3717
- SiO<sub>2</sub> electrical properties, effect of water 9-7838
- SiO<sub>x</sub> films, evaporated, u.v. irrad. effects on optical and dielec. props. 9-5868
- Si-SiC p-n heterojunctions, construction and energy band diagram 9-10015
- Sr-O system, phase diagram 9-18382
- ZnO/Si resin electrophotographic films, characts. 9-15564

## Silver

- additions to Al-Cu-Cd alloy, effect of  $\theta'$  precip. 9-1327
- adsorption of S, surface instability 9-9624
- aerosol, condensation, particle surface area, obs. 9-5197
- in alkali halide crystals, paramag. reson. of stabilized atoms 9-14108
- band structure and electronic props. 9-13830
- catalyst,  $\gamma$ -irrad. effect on work function 9-12219
- colloidal, in KCl, optical extinction coeff. rel. to annealing 9-5924
- compacts, effect of O<sub>2</sub> on sintering rate 9-5498
- de Haas-van Alphen effect, mag. interaction, obs. 9-5635
- Debye temp. by slow c. diffn. on (111) face 9-3532
- deformed at room temp., elec. resistance rel. to temp. 9-19890
- dielectric constants, electroreflectance changes, modulated ellipsometric meas. 9-10035
- diffusion and solubility in InP 9-5409
- diffusion in liquid Ga 9-13516
- diffusion of In, grain-boundary and dislocation, temp-dependence, 180-100°C 9-3375
- elastic constants, higher-order, from finite deform. meas. 9-5419
- electrochemical sulphurization cells 9-17538
- electrode, dipping expts., Biliter pot. 9-15227
- electrodeposition from aqueous solution, nucleating ability of substrate grain boundaries 9-20060
- electron emission, secondary, multiple distrib. 9-5782
- electron scattering, inelastic, in LEED obs. 9-21451
- electronic structure, calc. at two values of lattice const. 9-5611
- electronic structure, calc. at two values of lattice const., model Hamiltonian 9-5612
- epitaxial growth on cleavage face of mica 9-5242
- epitaxial growth on KCl, KBr and KI crystals 9-7377
- f.c.c., rolling texture formation by slip and mechanical twinning 9-19815
- film, attenuation length of hot electrons, meas. 9-12043
- film, Hall coeff., normalized conductivity, thickness depend. from Fuchs-Sondheimer theory 9-7331
- film, photoexcited surface plasmon radiative decay 9-17373
- film, second optical harmonic excitation, eff. of thickness 9-19974
- film, temperature during evaporation 9-17243
- films, single crystal, size effect on elec. resist. 9-5640
- films, vacuum-deposited, electron microscope obs. on sulphuration 9-11765
- granular film, opt. parameters  $v$ ,  $\chi$  and  $d$  9-16398
- halides, dielec. dispersion obs.; lattice structure and forces calc. 9-16074
- Hall coeff. determ. 4.2-300°K 9-5651
- h.f.s. of  $4d^9 5s^2 D_{3/2} \rightarrow 4d^{10} 5p^1 P_{1/2}$  transition at  $X=19372 \text{ Å}$  9-19395
- impurity distribution in ZnS crystals grown from melt 9-18429
- ion diffusion in Pyrex glass and exchange between two-phase structure 9-14958
- ion in molten salt, plane source method for meas. interdiff. coeff. 9-5150
- ion mobility in Ti, 1123-1623°K 9-9733
- ionic core radii calc. and orthogonality corrections 9-19682

**Silver continued**

- ions, adsorption on  $\text{TiO}_2$  in aqueous and methanolic solns. 9-10348  
 ions on anionic sites in alkali halides giving rise to B bands 9-5387  
 irradiated, black-spot damage, nature 9-18459  
 island film, light scatt. and absorpt., comparison with theory 9-15166  
 liquid, diffusion of O, electrochem. meas. 9-11690  
 magnetic domains due to de Haas-van Alphen magnetization, n.m.r. obs. 9-1664  
 magnetoresistances, elec. and thermal, 80-130°K 9-5636  
 membrane, mass spectra comparison of evolved and diffused  $\text{O}_2$  9-11663  
 migration activation energy along natural cleavage surface in mica 9-11892  
 molten, wetting of Fe alloys 9-13508  
 overlayer on Cu(100), struct. 9-1085  
 particles, micron-sized, temp. rise due to e. beam heating in e. microscope 9-11822  
 periodic precipitation, expt. 9-21405  
 periodic precipitation, mathematical modification 9-21406  
 quartz decoration in elec. field post-etching rel. to defect obs. 9-13682  
 reflectivity near plasma edge by derivative optical spectroscopy 9-1758  
 rolling texture formation by slip and twinning 9-3426  
 self-diffusion, effect of electron bombardment 9-5398  
 self-diffusion, infl. of bound divacancies on isotope eff. 9-18487  
 self-diffusion in polycryst. 9-5397  
 and p-, n- semiconductor composites, conductivity meas. 9-16260  
 on semiconductor oxides, adsorbed, photolytic reduction mechanism 9-6017  
 slip, double coplanar, rel. to flow stress theories 9-5471  
 solid soln. with Au, Cd, Zn, In, Ge, Ti and Sb, thermoelectric powers 9-1604  
 specific heat and Gruneison parameter calcs. 9-9842  
 spectrophotometric determ. in aqueous and non-aqueous media 9-6029  
 spin exchange signals with Rb in optical pumping 9-14422  
 stacking fault energy, formation from dislocation loop dissociation during plastic deformation 9-3343  
 stored energy data anal. by Kuhlmann-Wilsdorf theory 9-9780  
 surface plasma waves, nonradiative, excitation by evanescent wave in total reflection in prism 9-5602  
 surface state variation of (111) face 9-7357  
 thermal expansion interferometric meas., Gruneisen parameters calc. 9-19863  
 thermodynamic props. evaluation and literature data analysis, 0°-300°K 9-12015  
 thin films, absorption band shift 9-17479  
 thin metallic layers, abs. spectra, fine struct. 9-19172  
 Ag-Au diffusion couples, Kirkendall effect mechanism 9-19762  
 Ag-Se-Cu system, thermodynamics 9-18562  
 Ag-Cs/Cl,  $\text{NO}_2$  liquid-liquid and solid-liquid equilibria 9-18380  
 Ag, phonon dispersion meas. 9-11983  
 Ag, self-diffusion, influence of traces of  $\text{O}_2$  and S 9-3376  
 Ag, stacking fault energy meas. by different techniques 9-13694  
 Ag(111), scatt. of Ar and Xe atomic beams 9-3187  
 $\text{As}_2\text{S}_3$  semiconductor film-Ag system, light sensitivity depend. on thickness of semicond. layer 9-1735  
 in  $\text{CdCr}_2\text{Se}_4$ , effects on ferromag. resonance 9-16451  
 magnetic surface quantum state transitions 9-7717  
 magnetic surface quantum state transitions 9-7717  
 $^{14}\text{N}$  ions passing thro., range-energy relations 9-9869  
 NaCl:Ag, activator glow output and X-ray lum. spectra temp. dependence, 77-600°K 9-3922  
 in NaCl Ag<sup>+</sup>V<sup>-</sup>e complexes (V=anion vacancy) 9-5928

**Silver compounds**

- alloys, resist.-conc. depend. 9-16223  
 halide, photographic emulsion, open-cell cellular form, 10-95 vol.% void, support method, patent 9-20571  
 halide emulsions for oscillograph recording, preparation, patent 9-21232  
 halide photographic emulsions, dye-sensitized, patent 9-8677  
 halides, abs. spectra, fine struct. 9-19172  
 halides and alkali molybdates, molten, miscibility gaps 9-17192  
 halides in photography, role of holes 9-17901  
 halides photographic processing, limiting factor for Ag, water and colloid binders 9-17902  
 lutidine nitrate complex, space group and unit cell dimens. 9-11832  
 lutidine nitrate complex, unit cell dimens. from powder diff. data 9-13624  
 oxide deposits, anodically formed in KOH soln., texture, growth and orientation 9-17539  
 photodevelopable halide emulsions, optically sensitized method, patent 9-8680  
 thiophene, effect of substituted derivatives on p(CH) deformation vibrations 9-7057  
 Ag/AgCl fuel cell, electrode e.m.f. dependence on Cl pressure 9-6462  
 Ag-Al alloys, transition of Gd 4f electrons from bound to virtual levels 9-1462  
 Ag-Al system, hexagonal  $\zeta$ -phase, stacking-fault energy calc. from thermodynamic data 9-19750  
 Ag-Al system, hexagonal  $\zeta$ -phase, stacking fault energy, exptl. determ. 9-19751  
 Ag-Au:Yb, Kondo effect 9-9929  
 Ag-Au alloys, sp. ht. below 3°K 9-12018  
 Ag-Cu solid solns, supersaturated, substructure changes during decomposition 9-1339  
 Ag-Cu solid solutions, supersaturated, discontinuous precip. kinetics investigation 9-21399  
 Ag-In alloys, dil., band structure 9-15052  
 Ag-Mn alloy film, transmission, reflection and absorpt. coeffs., rel. to resonant states 9-7937  
 Ag-Mn alloys, phonon electron scattering coeff. from electronic thermal conductivity 9-3505  
 Ag-Mn solid solutions, stacking fault energies 9-7492  
 Ag-Pd alloy film, transmission, reflection and absorpt. coeffs., rel. to resonant states 9-7937  
 Ag-Pd alloys, faulting in severely cold-worked filings, X-ray meas. 9-7493  
 Ag-Sb alloys, hexagonal (B-phase), stacking-fault densities 9-1230  
 Ag-Sn solid solns., Mossbauer effect, plastic deform. and annealing effects 9-1750  
 Ag-Zn alloys, stacking fault energy meas. by different techniques 9-13694

**Silver compounds continued**

- Ag-Zn alloys characteristic temp., Gruneisen eqn., Debye function 9-19861  
 Ag-(10 wt.%) Mn-(1.5 wt.%) Sb alloys, solid soln. decomposition, work hardening effects 9-1326  
 $\alpha$ -Ag<sub>2</sub>S crystal structure, analogy with  $\beta$  phase 9-19706  
 $\alpha$ -Ag<sub>2</sub>Se crystal structure, analogy with  $\beta$  phase 9-19706  
 $\alpha$ -Ag<sub>2</sub>Te crystal structure, analogy with  $\beta$  phase 9-19706  
 $\alpha$ -Ag<sub>2</sub>AuS<sub>2</sub> crystal structure, analogy with  $\beta$  phase 9-19706  
 $\alpha$ -Ag<sub>2</sub>AuSe crystal structure, analogy with  $\beta$  phase 9-19706  
 $\alpha$ -Ag<sub>2</sub>AuTe crystal structure, analogy with  $\beta$  phase 9-19706  
 Ag<sub>2</sub>GeS<sub>4</sub> (argyrodite), microhardness and photomechanical eff. 9-14982  
 Ag<sub>2</sub>SnS<sub>4</sub> (canfieldite), microhardness and photomechanical eff. 9-14982  
 Ag halide layer litho development, patent 9-20572  
 Ag-Sb series, X-ray spectra K $\alpha$  line shift 9-14066  
 AgAl gaseous mol., rot. analysis of bands 9-17026  
 Ag<sub>2</sub>AsS<sub>3</sub>, entropy of fusion, thermal expansion and phase transform, 30°K to melting point 9-13782  
 Ag<sub>2</sub>AsS<sub>3</sub>, proustite, optical props in i.r. 9-1727  
 Ag<sub>2</sub>AsS<sub>3</sub> (proustite), second harmonic generation 9-6540  
 AgBF<sub>4</sub>-l-pentene, phase equilibria 9-21242  
 AgBr, adsorption of gelatin 9-7343  
 AgBr, electron mobility determ. 9-15123  
 AgBr electroluminesc. spectrum and mechanism, 80°K 9-12483  
 AgBr film, photocurrent maxima and their origin 9-21545  
 AgBr microcrystals from gelatin adsorption 9-3214  
 AgBr solns, critical coagulation and stabilization concs. for  $\text{Sc}(\text{NO}_3)_3$  solns. 9-9569  
 AgBr suspension, surface area meas. from cyanine dye ads. obs. 9-20566  
 AgCl:Fe<sup>3+</sup>, e.s.r. study 9-5980  
 AgCl:I<sup>-</sup>, excited state structure of I centre 9-12057  
 AgCl:Mn<sup>2+</sup>, luminescence and e.p.r. spectra temp. depend. 9-21642  
 AgCl-glass seal, simplifying improvement 9-2102  
 AgCl, adsorption-sensitive mechanical behaviour 9-13738  
 AgCl, irradiated, 2°-250°K colloid prod., phonon scattering investig. 9-9692  
 AgCl, pressure-induced photoluminescence 9-12462  
 AgCl, transverse slip system at -183 and 22°K 9-1295  
 AgCl electroluminesc. spectrum and mechanism, 80°K 9-12483  
 AgCl excitons, absorpt. spectra anal. 9-9903  
 AgCl film, photocurrent maxima and their origin 9-21545  
 AgCl luminescence centres, temp. and press. dependence 9-3913  
 AgCl single crystals, slightly bent, annealing behaviour, rel. to sub-structure 9-5497  
 AgF<sup>+</sup>, magnetic long-range ordering 9-10117  
 AgGaS<sub>2</sub>, non-enantiomorphous, optical activity obs. 9-12339  
 AgI, hexagonal, linear compressibility for 8 crystal directions 9-7540  
 $\beta$ -AgI, powders and single crystals, n.q.r. coupling constant of  $^{127}\text{I}$  9-18745  
 AgI film, photocurrent maxima and their origin 9-21545  
 $\alpha$ -AgI high-temp. phase, absorpt. meas. 8.6-10.1 GHz, 20-160°K 9-5911  
 AgI nuclei, effects on pluviometry of continuous emission 9-1937  
 AgI suspension, surface area meas. from cyanine dye ads. obs. 9-20566  
 AgN<sub>3</sub>, photo e.m.f. meas. 9-10066  
 AgNO<sub>3</sub>, dilute solns., interdiffusion in alkali nitrates 9-7261  
 AgO shock wave expt. 9-16516  
 Ag<sub>2</sub>O luminescence bands obs. 9-1823  
 AgPd, photoemission, electron energy distribution meas. 9-1628  
 Ag<sub>2</sub>S-As<sub>2</sub>S<sub>3</sub> system, phase diagram for proustite, smithite and pyrrargyrite growth 9-17255  
 Ag<sub>2</sub>S, spec. heat, -70 to 550°K 9-5566  
 Ag<sub>2</sub>SbS<sub>3</sub>, pyrrargyrite, optical props in i.r. 9-1727  
 Ag<sub>2</sub>Se, spec. heat, -70 to 550°K 9-5566  
 (Ag+Rb or Cs)NO<sub>3</sub>, molten, thermoelec. power 9-3119  
 Al-Ag<sub>2</sub>Al eutectic alloys, preferred orientation development during growth 9-1123  
 Al-Ag alloy, liquid quenching, depend. of Ag solid solubility 9-19831  
 Al-Ag alloys, soft X-ray emission spectra, interpretation 9-15181  
 Al-(5 wt.%)Mg-(0.4 wt.%) Ag alloy, precipitate-free zone, light and electron microscopy obs. 9-18537  
 Au-(50 at.%)Ag alloy, short range order, quenched in vacancies 9-3324  
 Au-(54.4at.%)Ag alloy, surface self-diffusion 9-17283  
 Au-Ag alloy film on n-Si Schottky barrier, characts 9-3675  
 Cu-Ag alloy, brazing for metal-to-ceramic seals 9-13766  
 Cu-Ag alloy hollow cathode discharge, spect. study 9-19559  
 Cu-Ag alloys, precipitation assoc. with stacking faults growth 9-11958  
 KNO<sub>3</sub>-AgNO<sub>3</sub>, molten mixtures, vibr. spectra and struct. 9-1019  
 (Li<sub>2</sub>Ag)<sub>2</sub>SO<sub>4</sub>b.c.c., Li<sup>+</sup> and Ag<sup>+</sup> diff. coeffs., 470-550°K 9-17287  
 Pd-Ag alloy tube for ion sources, H<sub>2</sub> permeation rate meas. 9-21353  
 Pd-Ag alloys, dil., mag. susceptibility meas. rel. to impurity scatt. and e density of states 9-13986  
 Pd-Ag alloys, low-temp. Hall effect 9-12102  
 Rh-Pd-Ag alloy, electron reflection, 200-800eV, energy loss spectra obs. 9-16194

**Sinanoglu's theory see Atoms/structure****Sintering**

- ceramics, solid-state, research review 9-7582  
 cordierites, thermal expansion, bending strength 9-21404  
 devitrifiable frit, production of cordierite bodies 9-7315  
 glass, kinetics, effect of particle shape 9-19820  
 glass powder compacts, effect of particle shape 9-7314  
 metal single crystals, bicrystals and tricrystals, special growth technique 9-21300  
 in metallurgy, elementary review 9-3474  
 metals and ceramics, vol., grain boundary and surface diffusion contributions 9-1246  
 nuclear fast oxide fuels, pin design 9-11363  
 shape sensitivity of initial eqns. 9-19816  
 spherical particle rotation rates under grain boundary torque 9-13751  
 steel powders 9-17339  
 undervacuum 9-18530  
 Ag compacts, effect of  $\text{O}_2$  on rate 9-5498  
 Al-CuO, effect on lattice parameter and hardness due to CuO reduction 9-3463  
 Al, in presence of liquid phase, effect of Cu additions 9-16141  
 Al, sintered, grain boundary maximum of internal friction 9-1266  
 Al<sub>2</sub>O<sub>3</sub>, powder initial stage kinetics 9-7586  
 Al<sub>2</sub>O<sub>3</sub>, powder mixtures, kinetics 9-7585  
 Al<sub>2</sub>O<sub>3</sub>-BaO glass ceramics, rel. to glass composition 9-3171



**Sintering continued**

- Al<sub>2</sub>O<sub>3</sub>, mech., thermal, electrical and chemical props., rel. to microstructure 9-1256  
 BaTiO<sub>3</sub>:Ta<sub>2</sub>O<sub>5</sub>, effect of firing atmosphere pressure and temp., on electrical props. 9-1590  
 BaTiO<sub>3</sub>, initial soak effect on elec. props. 9-3708  
 BaTiO<sub>3</sub>, kinetics rel. to resistivity and point defect conc., 600° to 1400°C 9-1589  
 BeO, and inhibition by adsorbed phosphate, crystallite growth obs. 9-17241  
 C powders, by elec. discharge and graphitization 9-7610  
 Cr oxide, and calcination study 9-1320  
 Fe and Fe<sub>2</sub>O<sub>3</sub>, rel. to vol., grain boundary and surface diffusion 9-1246  
 Li ferrites, Ca substituted, temp. reduction 9-1684  
 LiF rel. to vol., grain boundary and surface diffusion 9-1246  
 MgAl<sub>2</sub>O<sub>4</sub> spinel, active, and powder characterization 9-3464  
 MgAl<sub>2</sub>O<sub>4</sub> powders, initial stage kinetics 9-1321  
 MgO-Al<sub>2</sub>O<sub>3</sub>-SiO<sub>2</sub> phase composition and cordierite formation, 800-1400°C 9-21409  
 Mn<sub>2</sub>O-Al<sub>2</sub>O<sub>3</sub>, initial sintering, 1450-1650°C 9-18533  
 Ni-Al powder mixtures, exothermal effs. on Al content and porosity 9-17325  
 Ni-Al powder mixtures, exothermic effs. 9-17324  
 PbO.6Fe<sub>2</sub>O<sub>3</sub>, orientation, preferred, rel. to increase 9-19817  
 ThO<sub>2</sub>-PuO<sub>2</sub> sintering in Ar at 1600°C, in air and in wet and dry H<sub>2</sub> 9-19822  
 UO<sub>2</sub>-Nb ceramets, high-loaded, rel. to fabrication 9-3475  
 UO<sub>2</sub> pellets, sintered, powder morphology and energy effects on densification 9-3465  
 UO<sub>2</sub> sintered pellets, quality control rel. to stoichiometry, density and struct. 9-2796  
 W compacts, grain growth analysis 9-7583  
 Y Fe garnet:Gd<sup>3+</sup>, Al<sup>3+</sup>, and Cr<sup>3+</sup>, pressure, reaction kinetics 9-1688  
 ZnO, densification and grain growth 9-19825  
 ZnO, density decrease and pore growth during final stage of process 9-19826  
 ZnO, under applied pressure, time-temp.-density relations 9-7593

**Skin effect**

- metal films, anomalous, theory 9-1447  
 metals, anomalous, bandstructure effects 9-13840  
 nonlinear, theory 9-18595

**Sky brightness**

- See also Airglow; Twilight*  
 background near satellite, interference with corona and zodiacal obs. 9-10560  
 colour excesses var. in Kapteyn's Selected Area 4, photographic obs. 9-8243  
 Kapteyn's Selected Area 4, colour excesses var. determ. photographically 9-8243  
 morning, irregular pulsations, airborne obs. 9-17567  
 night, polarization, zodiacal cloud model 9-10412  
 H $\alpha$  line in night sky, obs. 9-1952  
 O $\lambda$ ( $\Delta\epsilon$ - $\Sigma\epsilon$ ) 0,1 band obs. in day airglow 9-14167

**Slidrules** *see Calculating apparatus***Slip**

- in one plane system, production by selective hardening 9-1294  
 plastic slipline fields, mass-flux method for dimensions deduction 9-17777  
 secondary, nature and detection by macroscopic meas. 9-14978  
 trace analysis in e microscope and foil thickness determ. without specimen tilt determ. 9-7330  
 turbulent flow, wall effects, anomalous, and associated drag reduction 9-21007  
 Ag, f.c.c., in rolling texture formation 9-19815  
 Ag-rolling texture formation 9-3426  
 Ag double coplanar, rel. to flow stress theories 9-5471  
 AgCl, transverse system at -183 and 22°C 9-1295  
 Al, band continuity across grain boundaries 9-7498  
 Al, quenched-hardened, slip bands behaviour in plastic deformation 9-11924  
 $\beta'$ -AuZn, b.c.c. geometry from optical microscopy studies 9-13692  
 $\alpha$ -U, from dislocation energies and easy glide parameters 9-1226  
 Be, high-purity, along basal plane in plastic deformation, 4.2-300°K 9-1282  
 Cu-Ti-Al alloys, hardening during slip mechanism 9-17319  
 Cu-Ti alloys, hardening during slip mechanism 9-17319  
 Cu, dislocation slip association with magnetomechanical behaviour during fatigue deformation 9-17308  
 Cu, easy glide, rel. to deform. 9-5373  
 Cu, f.c.c., in rolling texture formation 9-19815  
 Cu, formation of rolling texture, orientation changes and deform. bands 9-9777  
 Cu monocrystal, secondary, from compression deformation parameters 9-3427  
 Fe, activation parameters rel. to neutron irradiation 9-1296  
 KCl:Pb, single slip line, nature 9-14948  
 LiF, band dislocation structure during annealing 9-11886  
 LiF slip deformed along on system of crystallographic planes, mech. props. and dislocation struct. 9-5364  
 Lif, line structure determ. using layered polishing and etching and stat. analysis 9-1297  
 Mg:Cd, polycryst., basal 9-5459  
 Mo crystals, surface bands, study by optical microscopy 9-7546  
 Mo foils, geometry study by tensile deform. under electron microscope 9-5460  
 Ni-base alloys,  $\gamma'$ , precipitation-hardened, and climb processes 9-7579  
 Ni, dislocation slip association with magnetomechanical behaviour during fatigue deformation 9-17308  
 Sb<sub>2</sub>Se<sub>3</sub>, needle-like crystals, planes rel. to growth 9-1194  
 Ti during deformation caused by drawing 9-19802  
 $\alpha$ -U, modes rel. to cryst. struct. and elastic const. 9-1228  
 $\alpha$ -U, planes and directions, temp. depend. 9-1298  
 $\alpha$ -U, single crystals, slip planes rel. to orientation, 600-1800°C 9-9762  
 Zn-Al alloy, superplastic, rel. to deformation mech. 9-11858  
 Zn, {1122} <1123> system, dislocation mobility 9-5371  
 Zn, basal dislocations, incorporation in {1012} twins 9-18474  
 Zn, forbidden basal, plastic deform. and rupture 9-11932  
 Zn single crystals, basal deformation 9-18512  
 ZnS, rotational, and twist boundaries 9-5348

**Smectic phase** *see Liquid crystals***Smokes** *see Aerosols***Snoek effect** *see Crystal imperfections/interstitials; Elastic relaxation***Snow**

- electrical meas. in snowstorms, instrumentation 9-16528  
 electrolytic conductivity 9-12570  
 measurements of electrical characteristics of snowstorms 9-12577  
 neutron monitor intensity, effect of snow 9-19211

**Sodium**

- absorption and energy loss in the Hartree approximation 9-3844  
 adsorption on W, work function meas. by field-emission electron projector 9-1112  
 atom, fine structure transitions in Na-He collisions 9-11411  
 atom admixtures in Se, effect on electric conductivity 9-3572  
 atoms adsorbed on W(110), bonding between layers 9-1113  
 atoms and ion, bibliography of spectra 9-13287  
 boiling heat transfer with natural convection, obs. 9-17231  
 conductivity, electrical, temp. var. calc., comparison with expt. 9-16231  
 decarburization and surface graphitization effect on contact with steel at 600°C 9-16150  
 diffusion in SiO<sub>2</sub> glass, 170-1000°C 9-17291  
 donors in carbon black P33, effect on c.s.r. in range 1800°-2400°C 9-8019  
 doping C blacks, effect on Hall coeff. and mag. susceptibility 9-7739  
 e-e scatt. and resistivity low temp. depend. 9-1463  
 e.p.r. of particles, 1.6-200°K 9-20022  
 Fermi surface from helicon Doppler-shifted cyclotron resonance meas. 9-12060  
 film, optical and photoelectric props. rel to electronic structure 9-17472  
 ion beam production by charge exchange with 5-40 KeV p beam 9-233  
 ion diffusion in Pyrex glass and exchange between two-phase structure 9-14958  
 K $\alpha$  X-ray satellites in fluoresc. spectra of Na in NaF 9-3933  
 Landau Fermi-liquid parameters 9-9912  
 Landau Fermi-liquid parameters, sum rule 9-3559  
 lifetime of <sup>32</sup>P resonance state meas. phase shift method 9-6977  
 liquid, Alfvén-wave resonances 9-2955  
 liquid, dilation effect on irrad. graphite rel. to dose and stress 9-6003  
 liquid, dilation effect on neutron irrad. graphite 9-7661  
 liquid, e.p.r., eff. of Rb, Tl and Cs additions 9-13541  
 liquid, isothermal compressibility 9-19596  
 liquid, isothermal compressibility 9-19596  
 liquid, neutron scatt. analysis in terms of atomic displacement 9-21185  
 liquid, self diffusion constant volume and pressure 9-3089  
 liquid, solubility of oxygen 9-19610  
 liquid and solid, electron-electron interaction eff. on optical absorption 9-21628  
 martensitic transform 9-1346  
 melt, corrosion transfer of C from unstabilized to stabilized steel 9-10345  
 melt struct., Mg impurities, nucl. reson. fluoresc. study 9-7278  
 molecules excitation in -N<sub>2</sub>, H<sub>2</sub>, HD, D<sub>2</sub> collisions, <sup>32</sup>P<sub>1/2</sub>=<sup>32</sup>P<sub>3/2</sub> transfer cross section, obs. 9-9309  
 particles, e.p.r., 1.6-300°K 9-20022  
 reactor, fast, Na void reactivity effects calc. 9-15791  
 -seeded plasmas, emission spectra 9-19537  
 spark source mass spectrographic analysis 9-8121  
 thermal expansion coeff. calc. from pseudopotential theory 9-12023  
 thermodynamic props., anharmonic contribs., simplified theory 9-7652  
 thin film, ultraviolet transmittance 9-5867  
 upper atmospheric, twilight obs., seasonal var. of abund. 9-12595  
 vacancy relaxations in b.c.c. crystals 9-9702  
 vacancy-produced lattice distortion calc. by method of lattice statics 9-21332  
 vapour, discharges, low-pressure characts. 9-21113  
 X-ray emission spectra, anomalies in edges of L<sub>23</sub>-spectrum 9-1817  
 X-ray emission spectra, applic. of Green's function method 9-7985  
 X-ray spectra, K $\alpha$ - $\alpha$  satellites, relative intensity 9-18717  
 K-Na-KCl-NaCl system, light absorpt. by colloidal particles 9-1725  
 Na-N<sub>2</sub> beam interaction, excitation energy transfer, obs. 9-9308  
 Na-NH<sub>3</sub> solns., microwave dielec. consts., temp.-variation studies, nonmetal-to-metal transition 9-14854  
 Na-NH<sub>3</sub> conc. solns., <sup>23</sup>Na and <sup>14</sup>N Knight shifts 9-3125  
 Na, interband absorptions, influence of pseudopotential Fourier coeff. V<sub>200</sub> 9-1793  
 Na<sup>+</sup>, <sup>4</sup>S state, electron scatt., nonrelativistic partial wave analysis 9-18147  
 Na<sup>+</sup> emission from Ni and Pt ribbons, thermionic, effect of deformation 9-21554  
<sup>23</sup>Na, h.f.s. of 3 <sup>2</sup>P<sub>3/2</sub> and 4 <sup>2</sup>P<sub>3/2</sub> states, from level crossing expts. 9-6970  
<sup>23</sup>Na atom collisions, spin-exchange cross-section obs. 9-9152  
 positron lifetimes in solid and liquid 9-7731

**Sodium compounds**

- citrates, crystallized from aqueous soln. at 25°C, crystal structure 9-19720  
 halide films, i.r. spectra of adsorbed N<sub>2</sub>O 9-19443  
 halides, lattice dynamics and ionic deformation 9-13791  
 Kurrol salt, type A, (NaPO<sub>3</sub>)<sub>x</sub>, crystal structure refinement 9-11851  
 Na<sub>2</sub>HPO<sub>4</sub>.5H<sub>2</sub>O X-irrad. crystals, e.p.r. of PO<sub>4</sub><sup>3-</sup> 9-14113  
 Na<sub>2</sub>[Fe(CN)<sub>5</sub>NO]2H<sub>2</sub>O, single crystal, Raman spectrum 9-19995  
 periodates, crystallized from aqueous soln. at 25°C, crystal structure 9-19720  
 salt solutions, concentration depend. of <sup>23</sup>Na resonance amplitudes 9-11722  
 selenites, crystallized from aqueous soln. at 25°C, crystal structure 9-19720  
 sodalite, synthetic, interaction with Na vapour, sorption and colour centre formation 9-5262  
 3NaF-Al<sub>2</sub>F<sub>3</sub>-Al<sub>2</sub>O<sub>3</sub>, melt, surface tension, influence of CO<sub>2</sub> in furnace 9-11689  
 6(NaAlSiO<sub>4</sub>)8H<sub>2</sub>O, interaction with Na vapour, sorption and formation of colour centres 9-5262  
 (aPO<sub>3</sub>)<sub>x</sub>, Kurrol salt, type A, crystal structure refinement 9-11851  
 KNO<sub>3</sub>-NaNO<sub>3</sub> liquid, obs. of u.s. vel. 9-1007  
 LiF-NaF, growth by Czochralski technique, preferred <100> texture 9-1123  
 Na-Bi liquid alloy, density meas. 9-5145  
 Na-Cs liquid binary alloy, electron-spin susceptibility from Knight shift meas. 9-13542  
 Na-P zeolite, self-diffusion of water 9-5130  
 Na Pb liquid alloy, density meas. 9-5145  
 Na<sub>2</sub>B<sub>4</sub>O<sub>7</sub>-SiO<sub>2</sub> glasses, phase separation rel. to thermal expansion 9-1083

**Sodium compounds** continued

- Na<sub>2</sub>Cd<sub>3</sub>[Si<sub>3</sub>O<sub>10</sub>], crystal structure 9-21317  
 Na<sub>2</sub>ZrO<sub>3</sub>, crystallographic data, X-ray and optical 9-19721  
 Na<sub>2</sub>Al<sub>6</sub>, cryolite, liq. complex ion identification 9-1017  
 Na<sub>2</sub>Fe(CN)<sub>6</sub>, affect on NaCl crystal growth and characteristics 9-18415  
 Na dodecyl sulphate adsorbed monolayers water/permeability, obs. 9-7262  
 Na polyethylenesulphonate solns., transient elec. birefringence 9-16004  
 Na rare earth tungstates, quenching interactions of rare-earth ions 9-16436  
 Na silicate glasses, photochromic colour centres, kinetics 9-3369  
 Na stearate soap, extruded, struct., e microscope obs. 9-5225  
 Na tallow-coconut soap, extruded, struct., e microscope obs. 9-5225  
 NaAlSi<sub>3</sub>O<sub>8</sub>-KAlSi<sub>3</sub>O<sub>8</sub> system, incipient exsolution and inversion phenomena, electron optical study 9-21318  
 Na<sub>2</sub>As, n.m.r., powder 9-1875  
 NaBF<sub>4</sub>, crystal structure refinement 9-11852  
 Na<sub>2</sub>B<sub>4</sub>O<sub>7</sub>·10H<sub>2</sub>O, borax, effect on growth rate of alum. crystals from soln. 9-13602  
 NaBa<sub>2</sub>Nb<sub>2</sub>O<sub>11</sub>, ferroelec. transition temp. rel. to lattice structure 9-1594  
 Na<sub>2</sub>BeF<sub>6</sub>, <sup>19</sup>F NMR rel. to hindered motion in structure 9-16466  
 NaBr: Ag<sup>+</sup> solns., absorpt., luminesc. and excitation spectra 9-1020  
 NaBr, F-centre absorpt., temp. depend. 9-17280  
 NaBr, F-centre Raman spectra 9-12431  
 NaBr, impurity distrib. coeff. during zone melting 9-3239  
 NaBr, Raman spectra of F centres 9-12404  
 NaBr in NaCl-NaBr mixed crystals, NMR meas. of elec. field gradient at Na<sup>23</sup> nuclei 9-8048  
 NaBrO<sub>3</sub> n.q.r., temp. depend. of <sup>79</sup>Br freq. 9-10304  
 NaBrO<sub>3</sub> single crystal elastic constants, U.S. pulse echo meas. 9-13715  
 Na<sub>2</sub>Cd<sub>3</sub>[Si<sub>3</sub>O<sub>10</sub>], crystal structure rel. to existence of [Si<sub>3</sub>O<sub>10</sub>] group 9-5323  
 NaCl:Ag, Ag<sup>+</sup>V<sup>-</sup>e complexes (V<sup>-</sup>=anion vacancy) 9-5928  
 NaClO<sub>2</sub>, dielectric loss meas. and dipole moment found 9-3698  
 NaCl type alkali halides elastic const. calc. from interatomic parameters 9-7518  
 NaClO<sub>3</sub>, cryst. and powder, combination light scatt., absolute cross-sections 9-1732  
 NaClO<sub>3</sub>, Raman spectra cross sections, temp. depend. 9-12428  
 NaClO<sub>3</sub> elastic const. from u.s. vels. along arbitrary directions 9-7522  
 NaClO<sub>3</sub> mono- and polycrystals, in n.q.r., effect of elastic actions and mag. field 9-15211  
 NaClO<sub>4</sub>, n.m.r. of aq. solns., hydration determ. 9-17220  
 NaClO<sub>4</sub> elec. cond. in dioxane-water mixtures at 25°C ion-solvent interactions 9-11717  
 NaCrS<sub>2</sub>, antiferromagnet below 18°K 9-7921  
 NaCr(SO<sub>4</sub>)<sub>2</sub>·12H<sub>2</sub>O, crystal structure and classification 9-7445  
 Na<sub>2</sub>(SeO<sub>3</sub>)<sub>2</sub>, dielectric and optical props. for low temp. ferroelec. phase transition 9-17434  
 Na<sub>2</sub>(SeO<sub>3</sub>)<sub>2</sub>, ferroelectric transitions from NMR temp. dependence meas. 9-17435  
 NaF:H<sup>+</sup> thin film, frequency shift of localized mode by surface polarization 9-19852  
 NaF:Li, ENDOR spectrum of self-trapped hole associated with Li<sup>+</sup> impurity 9-10286  
 NaF-ZrF<sub>4</sub>-ZrO<sub>2</sub>, melt, surface tension, influence of CO<sub>2</sub> in furnace 9-11689  
 NaF-ZrF<sub>4</sub> mixture, melt, solubility of ZrO<sub>2</sub> rel. to ZrF<sub>4</sub> content 9-17194  
 NaF, dispersion curves determ. by diffuse X-rays scattering 9-1731  
 NaF, ENDOR spectrum of V<sub>k</sub> centre 9-10285  
 NaF, elastic const., meas. by audio freq. reson. method, 20-700°C 9-5423  
 NaF, elastic const., meas. by static, reson. and u.s. techniques 9-5422  
 NaF, electron colour centres, elec. field effects on no-phonon lines and point symmetry 9-18481  
 NaF, F<sub>2</sub><sup>+</sup> colour centres, linear Stark eff. of no-phonon transitions 9-19759  
 NaF, impurity effects on F to M conversion 9-5391  
 NaF, irradi., thermoluminescence rel. to colour centres and d.c. resistivity 9-14092  
 NaF, M<sup>+</sup> centre formation kinetics and optical props. 9-5392  
 NaF, R<sub>2</sub> zero-phonon absorpt. line, effects of uniaxial stress, moment anal. 9-7504  
 NaF, second-order Raman spectra calc. for vibration spectra computation 9-12429  
 NaF, specific heat, meas. and related thermodynamic props., 20°-300°K. 9-5568  
 NaF, X-ray scatt. factors using approx. model for overlap charge density 9-3298  
 NaF films, chemisorption of p-benzoquinone, i.r. spectra 9-8084  
 NaFe<sub>2</sub>(OH)<sub>4</sub>(SO<sub>4</sub>), magnetic properties of Jarosites 9-5800  
 NaH<sub>2</sub>(SeO<sub>3</sub>)<sub>2</sub>, thermal expansion coeff. meas., ferroelec. transition at Curie point 9-9849  
 NaH<sub>2</sub>(SeO<sub>3</sub>)<sub>2</sub>, crystal structure 9-3300  
 NaH<sub>2</sub>(SeO<sub>3</sub>)<sub>2</sub>, ferroelectric transitions from NMR temp. dependence meas. 9-17435  
 NaI-Tl, scintillations, electron-hole and exciton mechanisms, photomodelling 9-20008  
 NaI, excitonic energy transfer to Q and Tl centres during luminescence 9-20000  
 NaI, intrinsic photoluminescence, exciton states 9-3943  
 NaI, photoemission spectra, L-bands and exciton bands 9-3759  
 NaI, r.f. Stark spectrum, mol. beam elec. resonance meas. 9-7036  
 NaI, scintillation response to neutrons determ. 9-20699  
 NaI, second order Raman scattering spectrum 9-17481  
 NaI, unactivated, scintillation counter design and performance 9-19232  
 NaI, X-ray L<sub>III</sub> absorpt. of I, spectrograms 9-12455  
 NaI crystal photomultiplier tube combinations, packaging techniques 9-19129  
 NaI first rotational state h.f.s. level transitions r.f. spectrum obs., mol. const., determ. 9-9226  
 NaI ionic cryst., dielec. saturation 9-1582  
 NaI phonon frequency pres. depend. meas. 9-7713  
 NaI<sub>2</sub>O<sub>4</sub>, X-ray L<sub>III</sub> absorpt. of I, spectrograms 9-12455  
 NaI(Tl) crystal, as fast neutron detector in time-of-flight app. 9-13170  
 NaI(Tl) crystal, scintillation props. rel. to size 9-2577  
 NaI(Tl) internal sources for 1 keV event detection 9-4676  
 NaI(Tl) scintillation Compton spectrometer, electronic cct., response and theor. calc. 9-19239  
 NaI(Tl) scintillation  $\gamma$  background monitor appl. 9-4670

**Sodium compounds** continued

- NaI(Tl) scintillator, optical nonuniformity obs. 9-12482  
 NaI(Tl) stopping power and luminescent-response calcs. 9-12035  
 NaInS<sub>2</sub>:Cr<sup>3+</sup>, e.p.r. rel. to hyperfine structure of Cr<sup>3+</sup> with coplanar In<sup>3+</sup> ions 9-10287  
 NaInS<sub>2</sub>, paramagnetic resonance of Cr<sup>3+</sup> 9-8029  
 NaK seeded Ar, flowing, electrostatic probe meas. of I-V characts. 9-20487  
 NaKNbO<sub>3</sub>, ferroelectric ceramics, polarized optical retardation 9-1743  
 NaMg<sub>2</sub>CrSiO<sub>10</sub>, khrinovite, obs. in meteorites 9-18922  
 Na<sub>2</sub>Mn<sub>2</sub>Si<sub>2</sub>O<sub>7</sub>, synthetic crystal structure determ. by Fourier-transformation of minimum function 9-11831  
 NaNH<sub>2</sub>·SO<sub>3</sub>, Raman and i.r. spectra 9-12458  
 NaNO<sub>2</sub>-alkaline earth nitrate molten mixtures, absorpt. 9-13530  
 NaNO<sub>3</sub>, elastic const. and force fields 9-19780  
 NaNO<sub>3</sub>, i.r. spectrum and lattice vibrations 9-21614  
 NaNO<sub>3</sub>, liquid, oscillatory temp. instabilities 9-14845  
 NaNO<sub>3</sub>, two-phonon absorpt. spectrum 9-16169  
 NaNO<sub>3</sub> molten salt, <sup>22</sup>Na mobility meas. by paper electrophoresis 9-19614  
 NaNO<sub>3</sub>, ferroelec., etching of domains and dislocations rel. to polarization 9-15125  
 NaNO<sub>3</sub>, temp. dependent vibrational modes 9-5902  
 NaNO<sub>3</sub>, refractive index and anisotropic polarizability of NO<sub>2</sub> 9-3855  
 NaNO<sub>3</sub>, interdiffusion in dilute solns. of AgNO<sub>3</sub> 9-7261  
 NaNO<sub>3</sub>,  $\lambda$  transition, u.s. and i.r. meas. 9-1369  
 NaNO<sub>3</sub> fused, elec. conductance meas., by two-probe d.c. method 9-17845  
 NaNbO<sub>3</sub>-KNbO<sub>3</sub> system, thermal phase composition and boundaries, thermal and X-ray diff. meas. 9-7621  
 NaNbO<sub>3</sub>, heat of transition at 372, 527, 576 and 640°C 9-14993  
 NaNiF<sub>3</sub>, lattice const. determ. from single cryst. X-ray photographs 9-5299  
 NaNiF<sub>3</sub>, mag. structure 9-5855  
 Na<sub>2</sub>·NiO<sub>3</sub>, crystal structures 9-13644  
 Na<sub>2</sub>O-SnO<sub>2</sub>-SiO<sub>2</sub> glass, Sn valence states from Mossbauer effect 9-1751  
 Na<sub>2</sub>O-ZnO-SiO<sub>2</sub> glasses, i.r. absorpt. spectra, structural interpret. 9-3894  
 NaO<sup>+</sup>, prod. from Na+O<sub>2</sub> in merged beams 9-909  
 NaOH aqueous soln., hydrolysis effect on UC 9-16482  
 NaPO<sub>3</sub>+KPO<sub>3</sub> and NaPO<sub>3</sub>+Ca(PO<sub>3</sub>)<sub>2</sub> surface tension of molten mixture obs., surface heat of mixing estimation 9-21191  
 Na<sub>2</sub>PO<sub>4</sub>, X-ray L<sub>2,3</sub> emission bands and energy struct. 9-5944  
 Na<sub>2</sub>(PO<sub>3</sub>)<sub>2</sub> soln., aq., u.s. vel. depend. on concn. 1.48-10.37 MHz 9-5162  
 NaPbCl<sub>3</sub>, formation in vaporization of PbCl<sub>2</sub>+NaCl mixtures, thermodynamic props. from mass spectra 9-19442  
 NaSH, elec. dipole-dipole interact. bet. SH<sup>-</sup> ions 9-17038  
 Na<sub>2</sub>Sb, n.m.r., powder 9-1875  
 Na<sub>2</sub>Sb<sub>2</sub>·9H<sub>2</sub>O crystal growth from solution 9-13603  
 NaTaO<sub>3</sub>-KTaO<sub>3</sub> solid solutions, Raman spectra 9-12433  
 Na<sub>2</sub>Ta<sub>2</sub>[Si<sub>2</sub>O<sub>7</sub>]<sub>2</sub>·Si<sub>2</sub>O<sub>7</sub>·nH<sub>2</sub>O, vinogradite, crystal structure determ. by Fourier-transformation of minimum function 9-11831  
 Na<sub>2</sub>WO<sub>4</sub>, crystal structure and isotypism 9-14919  
 Na<sub>2</sub>WO<sub>4</sub>, melts for growing Y Fe garnet crystals 9-1150  
 Na<sub>2</sub>Y(WO<sub>4</sub>)<sub>3</sub> crystal growth and structure 9-1150  
 Na<sub>2</sub>ZnGeO<sub>4</sub>, synthetic D phase, crystal structure 9-13643  
 Na<sub>2</sub>ZrSiO<sub>3</sub>, electroluminescence 9-10258  
 Na<sub>2</sub>[Fe(CN)<sub>5</sub>NO]<sub>2</sub>·H<sub>2</sub>O as standard ref. mat. for chemical shift of Fe cpds. in Mossbauer spectroscopy 9-3872  
 Nd<sub>2</sub>O<sub>3</sub>, structural stabilization with WO<sub>3</sub> 9-17326  
 Ni-Ta(Nb) alloy systems, galvanomagnetic eff. 9-3790

**sodium chloride**

- absorption and reabsorption currents in single crystals 9-10037  
 adsorption of In and In migration path e. microscope determ. 9-1111  
 adsorption of water, effect of prior exposure to HCl, CO<sub>2</sub> and H<sub>2</sub>O vapour 9-19678  
 bicrystals, barrier effect of complex boundaries 9-19755  
 channelling of high-energy protons 9-7680  
 coalescence of Au particles rel. to surface heterodiffusion 9-19765  
 colour centre obs. using chemical method 9-16109  
 colour centres (F- and M-) rational accumulation kinetics in whiskers of different origin 9-13700  
 complex boundaries in bicrystals, barrier effect 9-19755  
 creep at elevated temps. 9-1293  
 crystal, isothermal diffusion of Sr<sup>2+</sup> and Co<sup>2+</sup>, Soret eff. 9-21348  
 crystal, piezoelectric eff. meas., temp. depend. determ. 9-15128  
 crystal, static Greens tensor function calc. 9-7446  
 crystal cleavage apparatus for production of clean film in vacuum 9-1097  
 crystal disloc. interaction, Gyalai-Hartly effect on ionic cond. 9-12194  
 crystal growth, effect of NaFe(CN)<sub>6</sub> 9-18415  
 crystalline, thermodynamic props. from lattice dynamics 9-16174  
 defects determ. from electron centres form. 9-7474  
 diffusion of Cu ions, temp. dependence, 350°C-650°C, rel. to ion size effects 9-1250  
 discharge development in plates with polyethylene barrier 9-1586  
 dislocation etch pits obs. on crystals deformed along cube plane 9-5367  
 dislocation movement in electric fields 9-3350  
 dislocation processes during creep deform. and heating 9-1223  
 dislocation substructure, intergranular, formation during growth from melt 9-21296  
 dispersion curves, on basis of simple shell model 9-11989  
 edge dislocation, atomic calc. of core-structure, core-energy and Peierls stress 9-13690  
 edge dislocation kinks, born model 9-18472  
 elastic const., meas. by audio freq. reson. method, 20-700°C 9-5423  
 elastic const., meas. by static, reson. and u.s. techniques 9-5422  
 electrical microbreakdown on cleaved surfaces, visualization 9-9638  
 electronic band structure investigations using six different potentials 9-15056  
 electronic struct. and molec. props. 9-2872  
 epitaxial growth of CdSe films on (111) surface 9-7338  
 e.p.r. of stabilized Ag atoms 9-14108  
 etch surfaces/Onothermal treatment 9-7366  
 evaporation of single crystals, mechanism 9-11751  
 exciton states, models 9-1432  
 F-centre production by u.v. irradi. 9-1235  
 F-centres,  $\gamma$ -induced, bleaching by laser irradi., 10.6  $\mu$  9-11889  
 F-centres, surface, state of localized electrons 9-16108  
 F-colouring, x- or  $\gamma$ -ray irradi., room temp. 9-3368  
 film, emission in far i.r. 9-15175



**Sodium compounds** continued**sodium chloride** continued

- film, on Al film, electron transport meas. by intensity of photoelectrons emitted by Al 9-19939  
 films, absorption in 25-50 eV region, substrate and exposure to air effects 9-7978  
 films, far i.r. absorpt., spectra, virtual mode analysis 9-1791  
 impurity distrib. coeff. during zone melting 9-3239  
 impurity-induced far-i.r. absorpt., monovalent 9-21627  
 internal friction, time depend. 9-7530  
 internal friction temp. dependence, 150-300°K 9-3399  
 ionic surface states from band-edge method 9-5618  
 luminescence in 800 1000 V fields 9-16433  
 luminescence of thin layers in strong elec. fields 9-3921  
 microcrystal, lattice const. and energies study 9-17270  
 Ni zero-phonon line, strain broadening 9-1792  
 nucleation centres of condensed phase 9-18425  
 orthogonalized-plane-waves calcs. 9-13832  
 proton tunnelling, 6.72 MeV 9-21448  
 Raman spectrum, second order, 90°K 9-12430  
 Raman-laser spectrum, second order 9-12421  
 relaxation effects with  $\text{Ni}^{2+}$  and  $\text{Cu}^{2+}$  9-1577  
 rocksalt substrate for condensation of Au atomic beam 9-14897  
 solutions in glycerol, elec. cond., dielec. relax. and viscosity 9-9548  
 substrate for epitaxial Al films, defect effects on film orientation 9-1105  
 thermal activation and emission mechanism during exoelectron emission 9-1626  
 thermal lattice vibrations 9-21425  
 thermodynamic functions of ionic crystal 9-17253  
 thermoluminescence rel. to colour centres and d.c. resistivity in irradiated crystals 9-14092  
 u.s. velocity and attenuation in crystals containing  $\text{CN}^-$  9-11996  
 vacancy breakdown under self-diffusion 9-18461  
 whiskers, 4-50  $\mu$  thick, ionic cond. 150°-600°C obs. 9-15124  
 X-ray scatt. factors using approx. model for overlap charge density 9-3298  
 n irradiation effect, behaviour of  $^{35}\text{S}$  9-6023  
 luminescence quenching, ionic temp. mechanism and decay law 9-3928  
 NaCl:  $\text{Ag}^+$  solns., absorpt., luminesc. and excitation spectra 9-1020  
 NaCl:  $\text{Sr}^{2+}$ , dislocation velocity 9-1222  
 NaCl:Ag, activator glow output and X-ray lum. spectra temp. dependence, 77-600°K 9-3922  
 NaCl:BaCl<sub>2</sub>, solution hardening 9-3455  
 NaCl:Ca<sup>2+</sup>, vacancy conc. by density change 9-9703  
 NaCl:CaCl<sub>2</sub>, internal friction and Young's modulus rel. to temp., freq., strain amplitude, meas. apparatus 9-5428  
 NaCl:Mn<sup>2+</sup>, X-irrad., e.p.r. spectrum 9-21667  
 NaCl:Mn<sup>2+</sup>, absorption spectra, optical, in range 0.1 to 15 mol% of dopant range 9-5923  
 NaCl:Mn<sup>2+</sup>, impurity-vacancy assoc. from ionic conductance and diffusion meas. 9-1202  
 NaCl:OH<sup>-</sup>, i.r. absorpt., 0.6-4.2°K 9-16415  
 NaCl:Pb, luminous flux scattered at ambient temp. after thermal annealing 9-19979  
 NaCl:NaBr mixed crystals, NMR meas. of elec. field gradient at Na<sup>23</sup> nuclei 9-8048  
 NaCl, edge dislocation, abrupt jog energies 9-18473  
 NaCl-Fe system, complex e.s.r. spectra after X-irrad. 9-20023

**Sofar** see *Sound ranging***Sogicons** see *Semiconducting devices***Soil**

- acid, kaolinitic clay search; Cl, T ions as groundwater tracers 9-18787  
 lunar, density meter-penitrometer of automatic lunar station Luna-13 9-6157  
 lunar, relative cleanliness as meas. of strength 9-16606  
 lunar surface, density 9-6168  
 moisture movement in horizontal column under applied pressure 9-6056  
 moon, struct., surveyor I and III obs. 9-15336  
 organic, removal by oxidation, effect of catalyst bearing porcelain enamels 9-1910  
 radioactivity meas.,  $\gamma$ -ray spectrometer calibration 9-18030  
 surface density gauge, influence of air gap 9-5227  
 unsaturated water movement from cylindrical source, unsteady flow 9-10381  
<sup>10</sup>Be, <sup>7</sup>Be cosmogenic prod. rate determ. by radioactivity meas. in soil. 9-4062  
 Rn/Th ratio in gas, closed-circuit meas. 9-1935

**Solar activity** see *Sun; Sunspots***Solar batteries** see *Electricity, direct conversion***Solar cells** see *Electricity, direct conversion/solar cells***Solar constant** see *Sunlight***Solar corona** see *Sun/corona***Solar corpuscular streams** see *Sun/radiation corpuscular***Solar eclipses** see *Sun/eclipses***Solar flares** see *Sun/flares***Solar furnaces** see *Heating; High-temperature phenomena and effects***Solar noise** see *Sun/radiation, radiofrequency***Solar prominences** see *Sun/prominences***Solar system**

- See also *Planets, etc.*  
 comet belt beyond Neptune, influence on motions of periodic comets 9-15347  
 comets total energy change on passing through 9-10533  
 Copernican theory described 9-15333  
 earth moon and planets, introductory book 9-14234  
 Earth-moon system, particle motion near L4 libration point, nonlinear stability anal. 9-10447  
 elements age and r-process intensity 9-21919  
 environments, planetary and interplanetary 9-4113  
 evolution 9-20214  
 fluid mass calc. of secularly stable equilibria, formation of satellites 9-12749  
 formation, book 9-8220  
 mass distrib. from spinning disc evolution theory 9-2037  
 meteoroid distribution function near ecliptic 9-17648  
 origin, review of theories 9-15334  
 origins, book reviewing various theories 9-14233  
 planetary orbits, Hilda group and Hecuba gap 9-15339  
 planetary rotational motion in general relativity 9-10518

**Solar system** continued

- resonant structure 9-17635  
 satellite motion, canonical eqns. for intermediate orbits 9-17641  
 satellite systems, basic scheme revision for Janus (Saturn satellite X) 9-10523  
 satellite systems, orbital period reln. and commensurability 9-16608  
 Sun-Jupiter system, natural families of periodic orbits 9-6108  
 theories of origin reviewed 9-10507  
 Rb-Sr cosmochronology 9-21919

**Solar wind** see *Sun/radiation, corpuscular***Solid solutions**

- See also *Alloys; and under compounds of the individual elements. Solid solutions such as Au-Cu, Au-Cu-Zn are indexed under compounds of the named elements, i.e. 'Gold compounds', 'Copper alloys', 'Zinc compounds' in these examples*  
 ageing, lattice parameter variation, data analysis 9-11829  
 ageing, variation in lattice constants, theory 9-11828  
 alloys, f.c.c., strengthening rel. to dislocation motion 9-7598  
 anthracene in naphthalene, fluorescence decay pattern 9-12471  
 antiphase domains, equilib. boundaries, theory allowing for short-range -order 9-1163  
 benzophenone-naphthalene, phosphorescence decay at 77°K 9-12476  
 binary metal, interdiffusion coeff., conc. depend. 9-3374  
 $\beta$ -brass type, ordered, adsorpt. in surface layers 9-3211  
 creep behaviour at elevated temps. 9-7547  
 Cu-Sn, structural changes during eutectoid decomposition 9-7613  
 dibenzenechromium cation, ESR spectra meas. 9-19459  
 dilute, Friedel oscillations and short-range order 9-3244  
 dissociative, interface hardening and softening 9-3477  
 electrophotoluminescence of rigid org. solns. 9-16447  
 eutectic crystal behaviour below eutectic pts. 9-5213  
 f.c.c. metal, anomalous after-effect 9-1325  
 $\beta$ -fluoronaphthalene-naphthalene, block structure 9-1334  
 hardening theory, shear modulus parameter 9-3470  
 impurity-drag effect rel. to grain growth kinetics 9-5342  
 InAs-Cu(Ag, Au), precipitation effect of dislocations 9-11967  
 multi-component substitutional, resistance to dislocation motion, effect of short-range order 9-9709  
 naphthalene in anthracene, fluorescence decay pattern 9-12471  
 nickel-cobalt disilicides, lattice parameters, densities, thermal expansion and elec. conductivity 9-3480  
 nucleation of new phase, theory 9-1151  
 oxides, ionic, binary solns., interaction and substitutional disorder 9-17333  
 oxides, ionic, binary solns., pair interactions 9-17334  
 phonons, boundary scatt. 9-1359  
 polyacene, energy transfer, bibliography for 1967 9-7986  
 primary, struct. rel. to Law of Corresponding States 9-5293  
 quartz, growth in MgO-Al<sub>2</sub>O<sub>3</sub>-SiO<sub>2</sub> glass 9-11797  
 semiconductors, optical absorption and luminescence edges 9-3880  
 short range order and size effect, kinematical diffraction theory 9-3251  
 superlattice formation, field ion microscope obs. 9-7402  
 Zircaloy-4, dissolution kinetics of dispersed hydride platelets 9-17336  
 Ag-Au, Cd, Zn, In, Ge, Ti and Sb, thermoelec. powers 9-1604  
 in Ag-(10 wt.%) Mn-(1.5 wt.%) Sb alloy, decomposition, effect of work hardening 9-1326  
 Ag-Cu, supersaturated, discontinuous precip. kinetics investig. 9-21399  
 Ag-Cu, supersaturated, substructure changes during decomposition 9-1339  
 Ag-Mn, stacking fault energies 9-7492  
 Ag-Sn, Mossbauer effect, plastic deform. and annealing effect 9-1750  
 Al-, Ag-, Au-, and Zn-rich, vacancy-impurity binding energies 9-9698  
 Al-Cu solid solns., supersaturated and deformed, elec. resistivity changes after Cu precip. 9-21482  
 Al-Mn alloy, decomposition interaction with alloy recrystallization 9-1153  
 Al-Zn, resistivity during precipitation 9-21480  
 Al in  $\alpha$ -U, supersaturated, precipitation 9-11960  
 Al<sub>2</sub>O<sub>3</sub>:Ti, precip. and struct. obs. 9-1340  
 Bi<sub>2</sub>-Sb<sub>2</sub>Te<sub>3</sub>-Se<sub>2</sub>, mixed-crystal form. limits 9-14985  
 CO-N<sub>2</sub>, equilibrium vapour press. meas. 9-21253  
 CaO-FeO-Al<sub>2</sub>O<sub>3</sub>, X ray and microscopic obs., 1050° and 1200°C. 9-16147  
 Cd-Sb-Zn system, formation, structure and thermo-e.m.f. 9-19835  
 Cd<sub>3</sub>As<sub>2</sub>-Zn<sub>3</sub>As<sub>2</sub> system, growth and semicond. props. 9-13882  
 Cu-Al crystals, hardening 9-13767  
 Cu-(2.5 wt.%)Be, decomposition, effect of electron bombardment 9-5501  
 Cu-Co, distribution function of precip. Co particles in super paramagnetic range 9-5803  
 Cu-GaAs supersaturated, elec. cond., Hall effect and microhardness meas. for precipitation study 9-5511  
 Cu-Ge, mechanical twinning, structure and distribution 9-17254  
 Cu-Mn, stacking fault energies 9-7492  
 Cu-Pd, ordered and disordered, magnetoresistance variation 9-21483  
 Cu-Si, deformed, elec. resistivity decrease 9-16224  
 Cu-Sn, Mossbauer effect, plastic deform. and annealing effect 9-1750  
 Cu<sub>0.75</sub>Ag<sub>0.25</sub>, Mossbauer effect, plastic deform. and annealing effects 9-1750  
 CuBr-CuCl, exciton absorpt. and emission spectra at 8 and 80°K 9-1775  
 CuK<sub>2</sub>(SO<sub>4</sub>)<sub>6</sub>H<sub>2</sub>O, dilution with ZnK<sub>2</sub>(SO<sub>4</sub>)<sub>6</sub>H<sub>2</sub>O effect on spectra 9-10199  
 Dy<sub>2</sub>O<sub>3</sub> in ZrO<sub>2</sub>, UO<sub>2</sub> near their melting points 9-3476  
 Fe-Al, heterogeneous, n-irrad. effects on elec. resistivity rel. to ordering changes 9-1465  
 Fe-Be, Mossbauer eff., elec. field gradient variation 9-17477  
 Fe-C, point defects studied by mag. after effect meas. 9-5333  
 Fe<sub>2</sub>TiO<sub>4</sub>-Fe<sub>3</sub>O<sub>4</sub> initial susceptibility of fine grain assemblage rel. axial stress 9-18680  
 Fe<sub>2</sub>O<sub>3</sub>-Cr<sub>2</sub>O<sub>3</sub>, reduction behaviour at high temp. 9-17332  
 FeO-MgO, magnetic susceptibility 9-5806  
 Fe<sub>2</sub>O<sub>4</sub>-Co<sub>2</sub>O<sub>3</sub> spinel, syst. free energies of formation, oxidation reduction enthalpies for ions 9-13769  
 Fe<sub>2</sub>O<sub>4</sub>-Mn<sub>2</sub>O<sub>4</sub> spinel, syst. free energies of formation, oxidation-reduction enthalpies for ions 9-13769  
 Fe-C, electrical resistivity recovery mechanism after e irrad. 9-19891  
 Ge-As, decay causing defect appearance 9-14937  
 HD-O-H<sub>2</sub>, dilute, spin relax time calc. 9-21596  
<sup>4</sup>He in <sup>3</sup>He, mag. susceptibility at high dilution, obs. 9-1062  
 HgS, Se<sub>1-x</sub> (0≤x≤0.4), kinetic props. investigation 9-1332

**Solid solutions continued**

- $\text{In}_{1-x}\text{Ga}_x\text{As}$ , elec. resistivity and Hall coeff. meas. for energy structure and Debye temp. calc. 9-3640  
 KBr-RbBr(NaBr,KCl) evap. films, intrinsic spectra 9-10204  
 KCl-KBr, removal of divalent cation impurities by introduction of anion-replacing impurities 9-16053  
 $\text{Li}_2\text{O} \cdot \text{Al}_2\text{O}_3 \cdot n\text{SiO}_2$  ( $4 \leq n \leq 10.0$ ), thermal expansion behaviour 9-3537  
 $\text{Li}_x\text{Ni}_{1-x}\text{O}$  system, lattice parameter comp. dependence 9-1191  
 Mg-Cd single crystal, hardening investig. conc. and temp. depend. 9-21378  
 $\text{Mn}_3\text{O}_4 \cdot \text{Co}_3\text{O}_4$  spinel, syst. free energies of formation, oxidation-reduction enthalpies for ions 9-13769  
 $\text{N}_2$ -CO, equilibrium vapour press. meas. 9-21253  
 Ni-W, impurity atom causing distortion of matrix lattice 9-5345  
 $\text{Ni}_3\text{Al}$ , sheet, yield stress, e. irradi. eff. 9-5502  
 (Pb, Sr)-(Ti, Zr) $\text{O}_3$ , formation by solid state reactions 9-1892  
 PbS-PbSe, microindentation hardness rel. to comp., obs. 9-7580  
 PbS-PbTe, microindentation hardness rel. to comp., obs. 9-7580  
 PbTe-PbS, valence band structure, from elec. meas. 9-21514  
 PbTe-PbS effective density-of-states mass rel. to carrier density and temp. 9-9897  
 PtCo alloys, superlattice formation, field-ion microscope obs. 9-7402  
 Si-Sb, precip. of Sb, during annealing 9-1333  
 Si-Ge-B alloy, thermoelec. props. and conductivity 9-15133  
 Ta-W alloy, monotonic strengthening 9-3433  
 ThC-UC, elec. resist., thermoelec. power and Hall coeff. 9-3573  
 $\text{TiO}_2 \cdot \text{SnO}_2$  crystalline soln., annealed at 850°C and 1000°C, mech. of separation and modulated struct. 9-7602  
 $\text{TiO}_2 \cdot \text{SnO}_2$  system, phase separation kinetics, 850-1200°C 9-3494  
 (U,Ce)N, prep. and UN-CeN miscibility, 1800°C 9-9791  
 (U,Nd)n, prep. and UN-NdN miscibility, 1800°C 9-9791  
 UP-US, in paramagnetic state,  $^{31}\text{P}$  Knight shifts 9-10296  
 $\text{Y}_2\text{O}_3 \cdot \text{ThO}_2$  mech. props. 9-3456  
 $\text{YbNbTiO}_4$ , NdNbTiO<sub>4</sub> 9-18538  
 $\text{Zn}_x\text{Hg}_{1-x}\text{Te}$ , energy band structure, from elec. and optical data 9-7716  
 $\alpha$ -Zr-H, hydrides precip. and H solid solubility, obs. 9-16148  
 $\text{ZrO}_2 \cdot \text{Y}_2\text{O}_3$  mixed crystals,  $\text{H}_2\text{O}$  vap. solubility, 900 and 1000°C 9-17335

**Solidification** *see Freezing***Solids**

- See also Crystals; Films, solid; Metals; Plastics; Powders; Semiconductors; Vitreous state*  
 free positron lifetime, effective no. of annihilation electrons per atom 9-5637  
 laser beam thermal self-defocusing and self-focusing in solids 9-17880  
 laser interferometric determination of dynamic response induced by charged particle interaction 9-17348  
 refractory compounds, fundamentals, book 9-5222

**structure**

- See also Crystal structure; Electron diffraction examination of materials; Electron microscope examination of materials; Granular structure; Neutron diffraction examination of materials; X-ray examination of materials*  
 alite composition in Portland cement clinker 9-18393  
 ceramics, interaction of microstruct., features with cracks 9-3445  
 ceramics, rel. to fired properties 9-7312  
 glass, rel. to pair correlation functions 9-1078  
 glass bonded cordierite bodies sintered from devitrifiable frit, and props. 9-7315  
 glass formation, Madelung const. as indicator 9-1082  
 light reflection technique 9-13564  
 magnesia refractory, creep rel. to microstructure, bonding and composition, 1450-1550°C 9-3423  
 ordering forces range in struct. with long range order 9-1162  
 polyethylene, change due to redrawing 9-17238  
 PVC, supermolecular structures, plate-like crystals 9-16088  
 all-trans retinal data, crystallography 9-3218  
 steel, Kh12ND, welds, effect of Cr content 9-14984  
 steels, welded high-strength structural, occurrence of massive ferrite in heat-affected zones which corrode in sea-water 9-21402  
 water in hydrates, i.r. spectra 9-1779  
 $\text{Al}_2\text{O}_3 \cdot \text{Y}_2\text{Al}_2\text{O}_3$ , microstructures formed by controlled solidification from melt 9-3285  
 $\text{Al}_2\text{O}_3$  refractory, rel. to radome fabrication 9-7311  
 Cr-SiC system, composition and phases 9-1328  
 Fe particles, anomalies from X-ray exam. 9-5199  
 $\text{Fe}(\text{OH})_3$  colloid oxidation prods., Cu(II) effects, obs. 9-6014  
 $\text{GeO}_2 \cdot \text{SiO}_2$  glass, binary 9-3172  
 $\text{LiO}_2 \cdot \text{SiO}_2 \cdot \text{Li}_2\text{O} \cdot \text{Al}_2\text{O}_3 \cdot 4\text{SiO}_2$ , glasses, isostructure and correlation 9-21254  
 $\text{LiO}_2 \cdot \text{SiO}_2 \cdot \text{Li}_2\text{O} \cdot \text{Al}_2\text{O}_3 \cdot 4\text{SiO}_2$ , glasses, isostructure and correlation 9-3177  
 MgO brick, microstructure and phases 9-3170

**theory**

- 1900 66, review 9-9598  
 Boskovic, R.J., (1748) 9-16034  
 effective ionic radii, for bond and unit cell calc. 9-7354  
 effective mass concept, matrix singularity 9-1075  
 Einstein, temp. depend. of sp. ht. 9-7367  
 electron-ion system, circular one-dimen. model, random phase approx. 9-10665  
 electron-ion system, circular one-dimen. model, random phase approx. 9-10664  
 electronic and vibrational spectra, unified presentation 9-1757  
 hard spheres, mixture of two sizes excess free energy 9-2178  
 hard sphere and square-well mols., free-path distrib. and collision rates 9-8457  
 light-bound e interactions and quasiparticles kinetic eqn. 9-1416  
 non-crystalline, elementary excitations, dispersion relations 9-9813  
 one electron wave function calc. including many-body aspects 9-5608  
 pair correlation functions, one-dimensional calc. and rel. to glass structure 9-1078  
 phonon gas, heat-pulse propag. theory 9-9852  
 pseudopotential method 9-13817  
 pseudopotential method rel. to effective mass approx. 9-12052  
 scattering, many-channel, by localized potential, total displaced charge 9-5598  
 solid state phenomena, effect on electronics 9-5592  
 spin dynamic polarization, unitary theory 9-17471  
 thermal and elastic waves at hypersonic freqs., unified theory 9-11914

**Solids continued****theory continued**

- trap analysis, extensions to method by thermally stimulated conductivity curves 9-5595  
 volume processes, secondary ion emission exam. 9-16187  
 H-bonded, two-dimens., transfer matrix rel. to anisotropic Heisenberg chain 9-1120  
 $\sigma$ -H<sub>2</sub>, angular momentum RPA 9-20580  
 H<sub>2</sub> quantum crystal, wide range of physical and computational utility 9-15436  
 S, charge carrier transport 9-5603

**Solids** *see Transducers***Sols***See also Colloids; Sedimentation*

- AgBr, coagulation and stabilization in  $\text{Sc}(\text{NO}_3)_3$  soln, critical concs. 9-9569  
 Au, light scatt. and absorption 9-15166  
 Au, particle-diameter distrib. for  $d < 1000$  Å, X-ray scatt. determ. 9-14873  
 S, La Mer type, particle size distrib. and number conc., time dependence 9-14871  
 Se, preparation, particle size distrib. anal. by comparing expt. spectra with theor. curves 9-14872

**Solubility***See also Phase equilibrium*

- Ag halides-alkali molybdates, molten, miscibility gaps 9-17192  
 alcohols, 1- and 2-, films on water, dissolution rate 9-5144  
 alkali halide in organic solvent binary mixture, rel. to dielec. constant of solvent mixture 9-14834  
 dissolution studies, use of phase diagrams 9-17226  
 liquid metals, limited mutual concns. 9-17189  
 metallic salts in organic solvents 9-7253  
 naphthalene in compressed ethane and  $\text{N}_2\text{O}$  9-13485  
 polar org. cpds, in water, calc. from interfacial tension 9-9494  
 polyurethane films, resistance to degradation improved by high cross-link density, chem. content effect 9-14983  
 soda-lime-silica glasses, of  $\text{H}_2\text{O}$  vapour, rel. to structure 9-1079  
 water-ethylene glycol system, of Ar, and thermodynamics 9-19611  
 Zircaloy 4, of H, rel. to dissolution kinetics of hydride platelets 9-17336  
 Al, of Pu 9-11957  
 Al, pure, of H<sub>2</sub> and D<sub>2</sub>, 400°-600°C, validity of square root law 9-9787  
 CdS-Au-S, vapour pressure investigation 9-3380  
 CdSe, of P, and diffusion meas., 900 and 950°C, Cd partial pressure dependence 9-11895  
 CdTe, of Cu, and diffusivity meas., 97-300°C rel. to  $\text{Cu}_2\text{Te}$  film formation 9-11896  
 CdTe, of P, and diffusion meas., 800-1000°C, Cd partial pressure dependence 9-11895  
 $\alpha$ -Fe, of C 9-9788  
 $^3\text{He}$  in  $^4\text{He}$  at 0°K 9-13549  
 InP, of Au, 600° to 850°C, and diffusion 9-14956  
 InP, of Cu, 600° to 900°C 9-5410  
 InP of Ag, depend. of P vapour pressure, 500°-900°C 9-5409  
 N<sub>2</sub>, in alloyed ferrites 9-5395  
 O<sub>2</sub> in liquid sodium 9-19610  
 Pu in Ni 9-19768  
 Pu liquid, of Ti, V, Cr, Mn, Zr, Nb and Mo, 700 to 1000°C 9-11685  
 SrO-ZrO<sub>2</sub> system, solid, phase equilibria 9-1352  
 Ti<sub>2</sub>Al<sub>2</sub>O<sub>7</sub>, structure and precip. obs. 9-1340  
 Zn<sup>2+</sup> doped crystals, rel. to determ. of free energy of association of Zn<sup>2+</sup> vacancy complexes 9-17277  
 $\alpha$ -Zr, H solid solubility, obs. 9-16148  
 ZrO<sub>2</sub>·Y<sub>2</sub>O<sub>3</sub> mixed crystals, of  $\text{H}_2\text{O}$  vap., 900-1000°C 9-17335  
 ZrO<sub>2</sub>, in NaF-ZrF<sub>4</sub> melts, rel. to ZrF<sub>4</sub> content, effect on melting point 9-17194

**Solution energy** *see Heat of solution***Solutions***See also Heat of solution; Liquids; Solid solutions*

- acid-base solvents, molten carbonate electrolytes 9-10347  
 activity coefficient, using light scatt. data 9-9487  
 aqueous, in packed beds, static hold-up, rel. to liq. metals 9-17180  
 azeotropic solvents with low solute conc., luminescence yield and radiative transfer 9-9525  
 benzene, solvent effects on fluoresce. 9-16012  
 benzene-poly(methylmethacrylate) solns., nuclear relax. 9-9558  
 binary, phase separation, microcalorimetry 9-17191  
 birefringence, quantum field theory 9-11696  
 carboxylic acid-water mixture, dielectric const. and loss anomalous var. 9-7271  
 critical model mixture of Gaussian mols. 9-3080  
 cyclohexane, F depend on mol. wt. 9-14838  
 dispersion of solute in m.h.d. laminar flow between parallel plates 9-17094  
 dye mols., solvent depend of position and intensity of absorpt. bands 9-7075  
 electrolyte, Poisson Boltzmann eqn., variational soln. 9-7252  
 electrolytes, equilibrium props., theory 9-8454  
 electrolytes in non-aq. solvents, interionic vibr. spectra 9-9514  
 electrolytic, sound absorpt obs., 0.3 to 2.8 GHz 9-18761  
 energy migration due to electric dipole-dipole interactions, dynamics 9-9486  
 ethane,  $\gamma$ -radiolysis at -78°C, products obs. 9-21726  
 ethylene-d<sub>8</sub>/ethylene-d<sub>4</sub>, partition function 9-17232  
 di-(2-ethylhexyl)Na sulfosuccinate in n-octane, p.m.r. study of phases formed by  $\text{H}_2\text{O}$  addition 9-9559  
 Faraday effects, quantum field theory 9-17206  
 field-flow fractionation, nonequilibrium 9-848  
 fluorescent, for Ross filter balancing in X-ray studies of liqs. 9-15986  
 gas mixing, stopcock 9-22013  
 heated body dissolving in free fluid, thermal cond. and diffusion eqns. 9-1005  
 hydration, negative, nucl. mag. relax. study 9-17190  
 ionic, elec. forces between immersed uncharged plates 9-16484  
 isooctane-nitroethane, conc. fluctuation kinetics, near critical stratification point from acoustic dispersion obs. 9-984  
 liquid mixtures, effect of vol. change on viscosity prediction 9-990  
 liquid-liquid immiscibility in aq. salt solns. at low temp. 9-15988  
 macromolecular, elec. birefringence, orientation factor tables 9-9541  
 of macromolecules, transport props. study via scatt. laser light 9-14875  
 metal deposition, study with rotating disc electrode system 9-2308



**Solutions** continued

- metal-NH<sub>3</sub>, Hall effect 9-1041  
 molar ratio curves, new plotting method 9-17506  
 molten salt mixtures, nonideality and association 9-9484  
 nonionic detergents in water, thermodynamic functions of mixing, and temp-comp. phase diagrams 9-9485  
 nuclear screening, effect of mag. anisotropic solvent mols. 9-9552  
 organic, C-Cl and C-Br stretching vibrs. 9-14697  
 poly(vinyl chloride), mol. wt., macromol. dimens. and segments optical anisotropy determ. 9-14837  
 polyelectrolyte solns., dielectric dispersion props. at 25°C and 40-100 kHz 9-16018  
 polyisobutylene, F depend on mol. wt. 9-14838  
 polymer, damped torsional oscillator model 9-21188  
 polymer, dilute, Huggins const. from relax. spectrum 9-15993  
 polymer, electroconductivity and ion mobility, molecular theory 9-18369  
 polymer, excluded vol. effects on limiting viscosity number 9-9489  
 polymer, Flory-Mandelkern invariant, depend on mol wt. 9-14838  
 polymer, fractionation 9-15991  
 polymer, fractionation, mol. wt. distrib. determ. 9-15992  
 polymer, high, electron microscope study 9-14836  
 polymer, multicomponent, liq.-liq. phase separation 9-11686  
 polymer, multicomponent, liq.-liq. phase separation 9-15990  
 polymer, multicomponent, liq.-liq. phase separation 9-7256  
 polymer, non-athermal, adsorp. at solid surface numerical solns in parallel-layer model 9-18400  
 polymer, viscometer, Zimm-Crothers, modification 9-21190  
 polymer chain, mean-square, displacement function 9-985  
 polymer chains, bead-and-spring model 9-7255  
 polymer dilute, showing drag reduction turbulent heat transfer 9-1006  
 of polymeric dielectrics, electroconductivity 9-21222  
 polymers, in general vel. field, exact soln. 9-14835  
 polymers in good solvent, polydispersity index from light scatt. 9-14862  
 polystyrene in benzene, F depend. on mol. wt. 9-14838  
 proton-transfer reactions, computations on quantum-mech. tunnelling through parabolic energy barriers 9-20030  
 with radioactive nuclei re-entrant well gas flow proportional counter 9-15733  
 Raoult's and Henry's laws, definitions 9-983  
 sodium humate, small-angle X-ray scatt. analysis 9-9480  
 solvated electrons, dielec. model 9-1035  
 solvent effects on intensities of polarised Raman bands 9-13528  
 surfactant, aqueous, surface tension measuring instrument 9-15982  
 water-[25%] carboxymethylcellulose, non-Newtonian film flow on rotating disc surface 9-21181  
 AgNO<sub>3</sub>, dilute, interdiffusion in alkali nitrates 9-7261  
 Al complexes in AlCl<sub>3</sub>-acetonitrile solns., n.m.r. 9-5189  
 CS<sub>2</sub>-CCl<sub>4</sub> mixtures, volume relax. 9-3095  
 Co(II), solvation determ. by <sup>17</sup>O n.m.r. 9-3123  
 H<sub>2</sub>O-KCl-CaCl<sub>2</sub>, activity coeffs. 9-21187  
 H halides in cyclohexane, rotational motion of molecules 9-9488  
 H<sub>2</sub>O-NH<sub>3</sub>, X-ray diffraction and struct. 9-3078  
 H<sub>2</sub>O-D<sub>2</sub>O, disproportionation 9-1891  
 K<sub>2</sub>SiO<sub>3</sub>, cryoscopic determ. 9-982  
 KCNS and alkali halides, molten, eutectic comps. 9-17193  
 Li non-aqueous salts, U.S. vel., molal and adiabatic compressibility determ. 9-7254  
 LiCl-H<sub>2</sub>O system, liq.-liq. immiscibility at low temp. 9-15988  
 LiCl, nuclear spin-lattice relax. 9-1046  
 Na salts, aqueous, concentration depend. of <sup>23</sup>Na resonance amplitudes 9-11722  
 Ni(II) in methanol, p.m.r. and solvation 9-9554  
 Ni(II) ions in dimethyl sulphoxide, proton relax. 9-9555

**Sonar** *see Sound ranging***Sonic boom** *see Aerodynamics; Shock waves/effects***Sonoluminescence** *see Luminescence/liquids and solutions***Soret effect** *see Diffusion in liquids, thermal***Sorption***See also Adsorption*

- area change following adsorption, BET method with Kr, correction 9-21255  
 benzene on silica gel, sorption and dielec. isotherms, analysis 9-21288  
 p-benzoquinone on NaF and BaF<sub>2</sub> films, chemisorption, i.r. spectra 9-8084  
 chemisorption on semiconductors, applic. of Landsberg trapping statistics 9-3992  
 desorption process, exponential tempering function appl. 9-3179  
 diamond, chemisorption of H, F, Cl, Br and O, heats of wetting, e.s.r. and i.r. spectra 9-8083  
 glass, vacuum pump 9-8329  
 graphite, I desorpt. in vacuum and Ar, and adsorp., 27-1100°C 9-9626  
 Graphon, activated, chemisorption of O<sub>2</sub>, rel. to temp. 9-8079  
 Graphon, room-temp. chemisorpt. of O<sub>2</sub>, after degassing 9-8082  
 Graphon chemisorpt. of O<sub>2</sub> from 25 to 400°C on cleaned activated surfaces 9-10335  
 high vacuum system with adsorbing walls 9-7222  
 metal oxide crystals, of orthophosphate 9-21689  
 osmotic reversibility violation, membrane swelling 9-17203  
 oxygen on anthracite, influence on e.p.r. 9-10273  
 polyamides, aromatic, depend. of electrical conductivity 9-7094  
 of radioactive materials by coal humic acid 9-6008  
 semiconductor surface gas chemisorption, electronic theory 9-16483  
 silica, surface sites for o- to p-H<sub>2</sub> conversion and H<sub>2</sub>-D<sub>2</sub> exchange reactions on quartz, cristobalite and silicic acid forms 9-21260  
 thermal desorption spectra, analysis 9-14900  
 vacuum breakdown, description mechanism 9-7203  
 vacuum pumps, Polish developments 9-10589  
 zeolites, Linde-A type, of water, enthalpies and entropies 9-9623  
 C, active, chemisorpt. of SO<sub>2</sub> 9-8081  
 C chemisorption of dry O<sub>2</sub> and in acid, study of basic surface complexes 9-8080  
 CO from He coolant, removal by molecular sieves 9-19373  
 Cu film, H<sub>2</sub>O chemisorption, 77° and 273°K 9-17519  
 Fe, angular distrib. of H<sub>2</sub> mols. desorbed from surface 9-7349  
 Fe<sub>2</sub>O<sub>3</sub>-Al<sub>2</sub>O<sub>3</sub>, chemisorption of hydrogen and water vapour, effect on elec. cond. and thermoelec. power 9-20036  
 Fe<sub>2</sub>O<sub>3</sub>-Cr<sub>2</sub>O<sub>3</sub>, chemisorption of hydrogen and water vapour, effect on elec. cond. and thermoelec. power 9-20036

**Sorption** continued

- Fe<sub>2</sub>O<sub>3</sub>, chemisorption of hydrogen and water vapour, effect on elec. cond. and thermoelec. power 9-20036  
 Fe film, H<sub>2</sub>O chemisorption, 77° and 273°K 9-17519  
 Ge, thermodesorption, real surface 9-5260  
 H, at gas electrode in u.s. field, thermodynamic interpretation 9-5165  
 H<sub>2</sub>O, from He coolant, removal by molecular sieves 9-19373  
 KCl, desorption of neutral species from surface on low energy e. irradi. 9-7327  
 MgO, of water vapour, effects on mech. props. 9-18506  
 Mo, desorption of O from polycryst. filaments, thermionic meas. 9-11787  
 Na on silica gel, isotherm eval. and analysis 9-21288  
 6(NaAlSiO<sub>3</sub>)<sub>8</sub>H<sub>2</sub>O, interaction with Na vapour, colour centres 9-5262  
 Nb (110) surface chemisorption of hydrogen, LEED exam. 9-15215  
 Ni-Cr<sub>2</sub>O<sub>3</sub> catalyst, H desorpt. rel. to H<sub>2</sub>O-H isotopic exchange, obs. 9-16046  
 Ni, angular distrib. of H<sub>2</sub> mols. desorbed from surface 9-7349  
 Ni, surface diffusion of chemisorbed H 9-1086  
 O, by polyolefins, automatic recording apparatus 9-1116  
 O chemisorption, form. of electronically excited SO<sub>2</sub> layer 9-6009  
 O<sub>2</sub> chemisorption on BaTiO<sub>3</sub> surface, variation in electron affinity 9-3648  
 Pd, angular distrib. of H<sub>2</sub> mols. desorbed from surface 9-7349  
 Pt, desorption of O atoms 9-1908  
 Ptand Re, thermal desorption spectra, high resolution, of He 9-11783  
 PuFe, by LiF for recovery and purification 9-5254  
 Re, desorption of O from polycryst. filaments, thermionic meas. 9-11787  
 Si, thermodesorption real surface 9-5260  
 Ti film, of N<sub>2</sub> all-metal meas. apparatus 9-13588  
 UC, of Kr, fission induced, mechanism 9-16047  
 W, desorption of O, thermionic meas. 9-11786  
 W, desorption of O from polycryst. filaments, thermionic meas. 9-11787  
 W (100) surface, desorption of inert gases on heating 9-5263  
 W ribbons, chemisorption of O<sub>2</sub> 9-12539  
 Zn, ht. of chemisorption of O<sub>2</sub> 9-17530

**Sound** *see Acoustics***Sound field** *see Acoustic radiators; Acoustics; Intensity measurement/acoustics***Sound ranging**

- clipped-digital tech., sequential processing of sonar signals 9-4354  
 gray whales, migrating, underwater sounds, detection using hydrophone array 9-4350  
 ocean, channel with parabolic profile, range focusing 9-6061  
 ocean, signals, optimum array detection tech. 9-8161  
 signal detection, clipped-dig. tech. for sequential processing 9-4354  
 sonar normal-mode reverberation in channels and ducts 9-2225  
 sonar optimum waveforms for correl. detect., reverberation limited conditions 9-4349

**Sound recording** *see Recording***Sound reproduction***See also Acoustic radiators; Recording; Transducers*

- feedback in rooms, regenerative reverberation effects, obs. 9-2233  
 feedback in rooms, regenerative reverberation effects, theory 9-2232  
 loudspeaker-microphone reactive coupling, avoidance 9-17804  
 sirens in built-up and rural areas, sound attenuation meas. 9-15460

**Space charge**

- benzene dosimetry, subject to high intensity electron pulses 9-1925  
 clouds, expansion and shrinkage 9-10786  
 current and potential related in cylindrical co-ordinates, Child's eqn. 9-193  
 cyclotron centre, ion vertical motion calc. 9-4699  
 electron beam instabilities due to virtual cathodes 9-2336  
 electrostatic, of interplanetary grains 9-20234  
 Gunn effect, explanatory account 9-5683  
 oscillations, LSA mode 9-5684  
 p-n junction, asymmetrical, carrier generation-recombination 9-3674  
 plasma in nonuniform axial mag. field, acceleration 9-7146  
 positive column theory including space-charge effects 9-5079  
 in semiconductor calculations of complex dielectric constant 9-5668  
 semiconductor surface, conductivity 9-21459  
 in solid, transport noise decomp. 9-4411  
 synchrotron, effects on frequency 9-2624  
 in thermionic conduction stabilization due to effect on cathode temp. change 9-16770  
 waves in partially ionized plasma, dispersion rel. to ionospheric irregularities 9-12616  
 Cu<sub>2</sub>O single cryst. layer, limited current 9-16262  
 Ge monocrystal dislocations, scanning e beam display 9-7390  
 PbO, red, vapour-deposited layers, space-charge- limited photocurrent 9-15139  
 Si monocrystal dislocations, scanning e beam display 9-7390  
 ZnO surface layers, electroreflectance obs. 9-16290

**gas**

No entries

**solid**

- absorption and reabsorption currents in single crystals 9-10037  
 SbSi, SCL currents rel. to trapping centres 9-10038  
 semiconductor-semiconductor structures structure, calc. of immobile part 9-12174  
 surface charge wave propag. in s.i.s. structure 9-15118  
 Ge monocrystal dislocation, display by scanning e beam 9-7390  
 Se single cry., space-charge limited currents, trapping levels and density obs. 9-21479  
 Si monocrystal dislocation, display by scanning e beam 9-7390  
 SiO<sub>2</sub>, buildup and release with 0 to 30 keV electron irradiation 9-12192

**Space groups** *see Crystal structure, atomic***Space research***See also Atmosphere*

- artificial plasma clouds released by rocket 9-6090  
 Surveyor 3, TV observations 9-10513  
 surveyor 3 landing 9-10511  
 ultrahigh vacuum system 9-20285  
 wind spectrometer expt. for Apollo astronauts on lunar surface 9-20236  
 CdS, thin films solar cells 9-2319  
 liquid applics. 9-8318

**Space vehicles***See also Rockets; Satellites, artificial*

- ablation materials, rapidly charred, testing technique 9-11935  
 contamination threat to Mars 9-17643

**Space vehicles continued**

- equation of motion while approaching and meeting on orbits 9-4268  
 flight parameters, autonomous determination 9-18824  
 lifting re-entry, three-dimens. laminary boundary-layer eqns. 9-17595  
 lunar orbiting, meteoroid hazard 9-21950  
 manned, light scatt. by their debris atm. 9-20124  
 Mariner IV, Mars atmosphere analysis by integral inversion of occultation data 9-2053  
 mass-exhaust velocity variations in free space 9-10445  
 motion near L4 libration point of Earth-Moon system nonlinear stability anal. 9-10447  
 motion near L4 point of Earth-Moon system, in VRFB model with inclination, influence of choice of consts. 9-8216  
 multi-impulse flights, optima, close quasi circular noncoplanar orbits 9-18826  
 navigation Earth-Mars, influence of uncertainty in Mars mass 9-20126  
 orbits which return to earth, analysed 9-14178  
 persistent roll resonance on re-entry boundary conds. 9-20128  
 phenolic nylon, ablation study 9-20125  
 Pioneer 6, obs. of steady-state magnetosheath 9-1977  
 power supply, reactor with heat pipes and thermionic diodes 9-11357  
 re-entry mechanics, second-order soln. extension 9-12650  
 shielding against nucleon-meson cascade 9-8890  
 Teflon, ablation study 9-20125  
 trajectories of flight to moon and return to earth 9-18823  
 Venera 4 obs. of Venus atmosphere 9-17644

**Instrumentation**

*See also Rockets; Satellites, artificial*

- acoustic probe for press. fluctuations, hypersonic re-entry vehicle 9-4082  
 camera, ballistic, determ. of geographical coords., method 9-20573  
 i.f. Q meter for antenna impedance characts. 9-4083  
 lunar soil-density meter-penetrrometer of automatic lunar station Luna-13 9-6157  
 lunar surface density meas., of automatic station Luna 13 9-6158  
 OGO-5 spark-chamber telescope, for  $\gamma$  astron. 9-20253  
 orbiting optical telescope, possibility 9-17669  
 radio communication during re-entry 9-21837  
 for re-entry flight in known plasma environment, evaluation in subsonic plasma tunnel 9-21074  
 spectrometer, for auroral electron and proton flux, calibration 9-8219  
 n-InSb i.r. detector, night sky background radiation obs. 9-6086

**Space time configurations**

- asymptotic flat time-space curvature tensor and conformal curvature tensor 9-20315  
 asymptotically flat, asymptotic behaviour of curvature tensor 9-8397  
 asymptotically flat, total invariants 9-8382  
 charged body, isolated, in isotropic co-ords. 9-20316  
 class I, spherically symmetric, Riemann curvature tensor condition and electromagnetism 9-17701  
 conformal plane, rel. to strength of producing e.m. field 9-15423  
 cylindrically symmetric space-time, perfect fluid distribution 9-8465  
 de Sitter space-time, scalar field, quantum theory, quasiclassical motion condition 9-17904  
 dyadic formalism applied to spatially homogeneous world models 9-4231  
 Eddington, symmetry props. and reality conditions 9-12874  
 Einstein's eqns., Hamiltonian-Jacobi and Schrodinger separable solns. 9-18977  
 elementary particle high energy interacs. space-time description 9-15576  
 embedding obtained 9-64  
 empty, and curved, validity of Huygens' principle 9-20312  
 empty, with shearing hypersurface orthogonal eigenvector 9-15422  
 general space of variables, iteration calcs. speeded up 9-12869  
 generalized Einsteinian space-times, condition for unique soln. to Cauchy problem 9-16672  
 hyperplanes, coupling between Poincare group and spacelike reflections, translation subgroup construct. 9-16669  
 hyperplanes, timelike reflection, coupling between time reversal and Poincare group, eqn. of motion and consistency relations derived 9-16668  
 isometries, Killing horizons and orthogonally transitive groups 9-14336  
 Kerr metric, interpretation of parameters 9-2144  
 Killing fields, generalisation to almost symm. spaces 9-17711  
 kinematical groups, classification and physical meaning 9-14327  
 light, fall bending round mass pt., radial 'free-fall' thought expts., validity 9-58  
 Lobachevskii-Einstein velocity space, for analysis of cosmic particle jets 9-18018  
 Markov processes, non-stationary, and space time 9-20339  
 Minkowski's space-time, erroneous assumption rel. to Ehrenfest's paradox 9-10684  
 Minkowski form of e.m. part of energy-momentum tensor supported 9-16764  
 Minkowski space, simplified formalism for tensor analysis 9-8365  
 neutrino, Penney's geometric theory 9-4586  
 odd-dimensional, TCP theorem breakdown 9-17925  
 optical scalars, subspace curvature reinterpretation 9-2151  
 paracompact manifolds modelled on Hilbert space, Green's theorem 9-15417  
 power counting theorem, proof for Minkowski metric 9-16673  
 power counting theorem proof for case of Euclidean metric 9-18993  
 relativistic invariant distributions and space-time props. 9-294  
 Riemannian, motion of free particles in gravit. and e.m. fields 9-6295  
 rotating disc, interior and exterior soln. 9-6306  
 Schwarzschild surface, generalization to arbitrary and static stationary metrics 9-6302  
 space-like reflections on hyperplanes, coupling with Poincare group, translation subgroup construct. 9-16669  
 thin shells, space-time metric rel. to plane source 9-15424  
 timelike reflection, through spacelike hyperplanes, coupling between time reversal and Poincare group 9-16668  
 transformations rel. to Lorentz group 9-8383  
 universe, stationary, general relativity energy considerations 9-20319  
 vacuum Riemann tensor, as series of intersecting manifolds nested in four-dimens. projective space 9-2149

**Spallation** *see Nuclear spallation***Spark chambers**

- acoustic, in telescope for  $\gamma$  astron. 9-20253  
 background particle effects 9-11159  
 digitized, search for Crab nebula  $\gamma$  emission 9-8232  
 electrodes, 'double' wire 9-4693

**Spark chambers continued**

- high pressure, 1/6 atm., characteristics 9-2614  
 improved isotropic behaviour due to perpendicular high voltage electrodes 9-11160  
 momentum anal., large solid angle, apparatus array 9-20711  
 proportional multiwire, readout systems 9-4692  
 review, including streamer chambers 9-19250  
 reviewed in book 9-6739  
 streamer, first uses 9-2615  
 streamer, kinematical resolution, unobs. interaction vertex events 9-18043  
 streamer, operation rel. to delay time between pulse application and cosmic particle passage 9-11158  
 streamer, specific primary ionization, meas. of relativistic increase 9-464  
 streamer chamber with large interelectrode gap, supply generator 9-463  
 with ten cm. gap used to investigate resonance radiation decay 9-11156  
 trigger, Li-Si solid state detector and  $\pi^-$  interaction, 6 GeV/c 9-20701  
 TV method of information extraction 9-8941  
 wire, filmless, external acoustic pickups recording sparks in Cartesian coordinates 9-462  
 wire, magnetostrictive, characteristics 9-13175  
 wire, use of ceramic thyatron pulse generator 9-8943  
 wire digitized with number of wire directly delivered in binary code 9-11157  
 $\gamma$  cosmic rays detection apparatus 9-6715

**Spark counters** *see Counters/spark***Sparks, electric**

*See also Breakdown, electric; Lightning*

- in air, laser prod. in 200 kG mag. field, obs. 9-7205  
 n butane, laser prod. in 200 kG mag. field, obs. 9-7205  
 crystallization nuclei production at surface of aqueous soln. 9-18428  
 development, obs. of new process 9-7207  
 expansion of fast gliding spark 9-7208  
 forming process, cylindrical shell and circular diaphragm deform. 9-19828  
 halides specimen introduction and line intensity reln. with S 9-9126  
 laser induced, holographic investigation 9-5092  
 laser prod., in air, butane, He, in mag. field 9-7205  
 magnetic field effect on formation time 9-18316  
 production by train of mode-locked laser pulses 9-11636  
 sintering and graphitization of C powders 9-7610  
 spark cutter, electronic 9-6230  
 spark timer, synchronous, solid-state 9-6455  
 spark transition in negative ion and free electron gases, asymmetrical fields 9-18317  
 spectral lines distrib. along discharge channel, obs. 9-18318  
 trigatron spark gap discharges with long time lags to breakdown 9-13460  
 triggering of pressurized gap by laser beam 9-13471  
 underwater, laser induced 9-9420  
 ArI, II, atomic and ionic line shifts in discharges 9-5093  
 Cu electrode erosion in spark discharge under Ar atmos. 9-17141  
 He, laser prod. in 200 kG mag. field, obs. 9-7205  
 S specimen introduction and line intensity reln. with halides 9-9126  
 TiO<sub>2</sub> ceramics, influence of voltage polarity 9-10157

**Specific heat**

*See also Thermodynamic properties*

- alkali halide crystals, Debye temp. rel. to lattice props., interac. pot. calc. 9-12019  
 Bose and Fermi atom adsorbed monolayers on cryst., heat capacity 9-5255  
 boson gas divergence with falling temp. rel. to off diagonal long-range order 9-16697  
 calorimetry, steady state, a-c temperature 9-7653  
 Einstein's theory, simplification for teaching purposes 9-6263  
 Einstein solid, temp. depend. 9-7367  
 equations, tabulated 9-3053  
 Fermi liquid, logarithmic terms and corrections, calc. 9-10673  
 fluid near critical pt. 9-1067  
 Ising model, three-dimensional, critical behaviour below T<sub>c</sub> 9-21573  
 Ising model, two-dimens., with random impurities 9-12253  
 liquids calorimeter for meas. 9-13523  
 metals with paramagnetic impurities, electron interactions effects 9-9876  
 rel. to two-point correlation 9-96  
 H<sub>2</sub>O discontinuous changes near 4°C, rel. to phase transform. 9-11681  
<sup>3</sup>He <sup>4</sup>He solns., during HeI-He II transition 9-9576  
 Pd-Ni dilute alloys, nearly magnetic centres 9-1398

**gases**

- molar ht. capacity relationship 9-17159

**liquids**

- Cv. from partition function of cybotactic group 9-7247  
 electrical heating continuous-flow meas. method 9-21196  
 glass, inorganic, heat capacity in supercooled liq. state 9-13801  
 measurement, new method for low temps. 9-5564  
 metals, calorimetric determ. up to 1900°K 9-9838  
 non-associated, temp.-variation at const. vol. comparison with viscosity 9-18357  
 Cu fused, thermal capacity at high temperatures 9-9505  
 Ga, fused, thermal capacity at high temperatures 9-9505  
 He II, superfluid, size effects 9-21236  
<sup>3</sup>He, obs. by differencing method 20-150 m°K 9-13548  
 Li, m.p. to b.p. 9-21197

**solids**

- alloys, dil. non-magnetic, electron-phonon interaction effect 9-1495  
 calorimeter for dynamic meas., 4-150°K 9-19860  
 cerium ethyl sulphate, anomalous phonon effects 9-7658  
 cubic crystals, Debye characteristic temp. at T=0 9-5565  
 CuSO<sub>4</sub>·5H<sub>2</sub>O, ht. capacity in mag. fields, 0.4°-4.2°K 9-9840  
 Debye characteristic temp. at T=0 for cubic crystals 9-5565  
 diamond 9-18443  
 dielectric, infl. of elec. field 9-19858  
 Dy, lattice sp. ht. calc. from phonon freq. distrib. curves 9-16165  
 dysprosium ethyl sulphate, 1°K to 0.13°K temp. range 9-1669  
 electron gas, displacement and collective variables calc. method, low temp. 9-21475  
 electron mass temp. dependence determ. 9-16217  
 ferroelectrics, displacement-type, calcs. from statistical theory 9-21536  
 ferromagnet, spin-phonon interaction influence 9-12017  
 glass, inorganic, heat capacity in glassy and supercooled liq. state 9-13801



Specific heat continued  
solids continued

graphite, 13°-300°K 9-16175  
Gruneisen parameter, quasi-harmonic, relations determining vol. depend 9-9850  
Gruneisen parameters for acoustic waves in uniaxial crystals from third order elastic constns. 9-5572  
Laves phase cpds., Debye temp. and radius ratio of component atoms 9-9836  
magnetic anisotropy infl., Heisenberg model 9-18671  
manganese acetate tetrahydrate, heat capacity, 0.4-20°K 9-12020  
measurement, new method for low temps. 9-5564  
metals, calorimetric determ. about 300°K 9-9838  
Mie-Gruneisen eqn. of state, simple derivation 9-1400  
molybdenum carbides, supercond., heat capacities, 1.5-20°K 9-1396  
polymers in crystalat construction, 1.7-4°K 9-2925  
quinol hydrogen cyanide clathrate, ht. capacity temp. dependences rel. to phase transition 9-1578  
singularity nature near second kind phase transition points, imperfections eff. 9-9837  
transition metals, electron heat rel. to d-electrons per atom 9-3534  
Ag-Au alloys, below 3°K 9-12018  
Ag-Zn alloys, Debye function, Gruneisen eqn., characteristic temp. 9-19861  
Ag, and Gruneisen parameter calcs. 9-9842  
Ag<sub>2</sub>S, -70 to 550°K 9-5566  
Ag<sub>2</sub>Se, -70 to 550°K 9-5566  
Al, Gruneisen parameter volume dependence 9-15010  
Al, heat capacity, const. vol., and Gruneisen parameter, anharmonic effects, data anal. 9-21434  
Al, heat capacity using adiabatic calorimeter in range 25-500°K 9-12014  
Al, vacancy formation contributions, 330°-890°K 9-7654  
Al, X-ray Debye temp. from n. scatt. obs. 9-7639  
Al<sub>2</sub>O<sub>3</sub>, and Gruneisen parameter, pressure variations 9-11919  
Al<sub>2</sub>O<sub>3</sub>, heat capacity using adiabatic calorimeter in range 25-500°K 9-12014  
Au, and Gruneisen parameter calcs. 9-9842  
AuMn, in Neel temp. pressure dependence thermodynamic valuation 9-1699  
CO, 4.2°K-0.8°K, study of results w.r.t. residual entropies of CO and NO 9-15007  
CO, anomaly due to O<sub>2</sub> impurity 9-1392  
CoCl<sub>2</sub>, 1.8-4°K, rel. to mag. props. of lamellar antiferromagnets 9-1393  
CoCl<sub>2</sub>·6H<sub>2</sub>O, finite lattice heat capacity, eff. on antiferromagnetic relaxation 9-8006  
CsBr, meas. and related thermodynamic props., 20°-300°K. 9-5568  
CsBr phonon branches calc. from shell model lattice dynamics 9-7633  
CsBr(l), heat capacity analysis in terms of lattice freq. spectrum 9-9839  
CsCl, and lattice dynamics 9-7634  
CsCl, phonon branches calc. from shell model lattice dynamics 9-7633  
CsF phonon branches calc. from shell model lattice dynamics 9-7633  
CsI phonon branches calc. from shell model lattice dynamics 9-7633  
Cu-Be alloys, temp. depend. during ageing 9-13763  
Cu-Cr, susceptibility, Kondo transition 9-19942  
Cu-Fe alloys, dil., mag. contribution 9-18563  
Cu-Pd alloys, changes in low temp. values from changes in short-range order 9-9844  
Cu-Sb phases, low temp. 9-12122  
Cu-Zn alloys, Debye function, Gruneisen eqn., characteristic temp. 9-19861  
Cu, 1-30°K 9-9843  
Cu, and Gruneisen parameter calc. 9-9842  
Cu excess, temp. dependence, 300-1200°K, analysis 9-1394  
Cu<sub>2</sub>MnAl(Sn), Heusler alloys, low temp. meas. rel. to hyperfine fields 9-9841  
Cu<sub>2</sub>S, -70 to 550°K 9-5566  
Dy, lattice sp. ht. calc. from phonon freq. distrib. curves 9-7635  
Er, lattice sp. ht. calc. from phonon freq. distrib. curves 9-16165  
Er, lattice sp. ht. calc. from phonon freq. distrib. curves 9-7635  
EuS rel. to scaling laws and impurity effects near critical point 9-16345  
Fe-Si alloy, high temp. sp. ht., mag. susceptibility temp. depend., up to 1870°K 9-7601  
Fe-base dilute alloys, electronic component for band struct. rel. to origin of ferromagnetism 9-13800  
Fe, mag. field effect near Curie temp. 9-13802  
Fe<sub>2</sub>Se<sub>8</sub>, electronic component band magnetism interpretation 9-21484  
FeCl<sub>3</sub>, thermal shift, precision Mossbauer meas., 83-350°K 9-16402  
Ga near its melting point 9-21435  
GaAs, 1/30°K 9-9843  
GaSb, 1-30°K 9-9843  
Gd, lattice sp. ht. calc. from phonon freq. distrib. curves 9-7635  
Gd, lattice sp. ht. calc. from phonon freq. distrib. curves 9-16165  
GdCrO<sub>3</sub>, low temp. meas. rel. to  $\lambda$  transitions in mag. ordering 9-7655  
Gg, Gruneisen parameter and anharmonicity 9-14999  
Hg, effective electron mass temp. dependence determ. 9-16217  
Ho, hyperfine interaction from meas., 0.03-0.5°K 9-21600  
HoN 9-5567  
In-Pb superconducting alloys, type II, temp. dependence, 1.5-4.2°K rel. to Maki parameter determ. 9-21493  
InAs, 1-30°K 9-9843  
In<sub>1-x</sub>Ga<sub>x</sub>As, solid solutions Debye temp. calc. from energy structure and Hall coeff. meas. 9-3640  
InSb, 1-30°K 9-9843  
KMnCl<sub>3</sub>·2H<sub>2</sub>O, antiferromagnetic, 1.0°K-6.8°K 9-1395  
LuN 9-5567  
 $\alpha$ -Mn, heat capacity from 0.2 to 0.4°K 9-7657  
MnTiO<sub>3</sub>, ht. capacity, 30° to 300°K 9-3533  
N<sub>2</sub>, 4.2°K-0.8°K, study of results w.r.t. residual entropies of CO and NO 9-15007  
N<sub>2</sub> crystals, and Debye temp. calc. from sound velocity meas. 9-3519  
N<sub>2</sub>, anomaly due to O<sub>2</sub> impurity 9-1392  
NO, 4.2°K-0.8°K, study of results w.r.t. residual entropies of CO and NO 9-15007  
NaF, meas. and related thermodynamic props., 20°-300°K. 9-5568  
Nb-C system, electronic, and Debye temp., effect of C conc. and cryst. struct. 9-1397  
Nb-C system, supercond., heat capacities, 1.5-18°K 9-1397  
Nb-Ta alloys, electronic sp. ht. and superconducting props. 9-13866  
Nb, X-ray Debye temp. determ. from n. scatt. obs. 9-7639  
Ni-Fe alloys, f.c.c., and elastic constns., 4.2°K 9-5421

Specific heat continued  
solids continued

(63wt.%)Ni-(37wt.%)Rh anomalous low temp. sp. ht. near crit. conc. for ferromag. 9-16176  
Ni, and elastic constns., 4.2°K 9-5421  
Ni, electronic sp. ht. calc., 0-300°K 9-16177  
Ni, mag. field effect near Curie temp. 9-13802  
NiF<sub>2</sub>, spin wave contrib., 0.36-50°K 9-15006  
 $\alpha$ -NiSO<sub>4</sub>·6H<sub>2</sub>O, 0.4°-4.2°K, 0-90 kG fields 9-19862  
O<sub>2</sub>, 4.2°K-0.8°K, study of results w.r.t. residual entropies of CO and NO 9-15007  
O<sub>2</sub> crystals, and Debye temp. calc. from sound velocity meas. 9-3519  
Pb, heat capacity, const. vol., and Gruneisen parameter, anharmonic effects, data anal. 9-21434  
Pb, heat capacity using adiabatic calorimeter in range 25-500°K 9-12014  
Pb, X-ray Debye temp. from n. scatt. obs. 9-7639  
Pd-Co alloys, 1.4 to 4.2°K 9-16178  
Pt-Co alloys, 1.4 to 4.2°K 9-16178  
Pt, low temp. ht. capacity 9-17355  
PuO<sub>2</sub>, ht. capacity 192°-1400°K 9-16179  
RbCl, phonon branches calc. from shell model lattice dynamics 9-7633  
RBH<sub>3</sub>PO<sub>4</sub>, -141 to -120°K 9-9845  
Sb, rel. to electron scatt. mechanism 9-9856  
SmAlO<sub>3</sub>, low temp. meas. rel. to  $\lambda$  transition in mag. ordering 9-7655  
SmCrO<sub>3</sub>, low temp. meas. rel. to Schottky anomaly 9-7655  
Ta-C system, electronic and Debye temp., effect of C conc. and cryst. struct. 9-1397  
Ta-C system, supercond., heat capacities, 1.5-18°K 9-1397  
Tb, hyperfine interaction from meas., 0.03-0.5°K 9-21600  
Tb, mag. contrib., temp. depend., and magnetization 9-12292  
TiO<sub>2-x</sub>, reduced rutile, 0.3-20°K, stoichiometry dependence rel. to band structure 9-21436  
U-bearing fuels, and heat contents 9-17356  
U<sub>3</sub>O<sub>8</sub>, rel. to phase transition mechanism obs. 9-3495  
UN, 1.3-4.6°K 9-17357  
U<sub>3</sub>O<sub>8</sub>, ht. capacity 1.6°-24°K 9-9846  
US<sub>2</sub>, heat capacities and thermodynamic props., 5 to 350°K 9-16082  
US<sub>3</sub>, heat capacities and thermodynamic props., 5 to 350°K 9-16082  
V, Debye charact. temp. from Bloch-Gruneisen relation 9-9847  
ZnSnP<sub>2</sub>, Debye temp. rel. to ordering 9-3310

Spectra

See also Absorption/light; Astronomical spectra; Atmospheric spectra; Chemical shift; Colour; Mass spectra; Scattering/light, Raman spectra; Spectrochemical analysis; Spectroscopy; Stark effect; X-ray spectra; Zeeman effect  
absorption, glass tinted with transition metal ions, high temperature changes 9-14052  
anisotropic insulating crystals, band struct. invest. 9-10185  
arcs, line pairs, matrix effect 9-15966  
astronomical radiossources, at wavelengths (5 GHz/6 cm) 9-10503  
auroral studies since 1960, review 9-15251  
benzene, thermo-spectrum of stimulated Raman 8050 Å line, fine structure period 9-1022  
critical point determ. by derivative optical spectroscopy 9-1758  
crystals, impurities, local oscillations and broadening of phonon free lines 9-7961  
crystals, Urbach rule for localized excitations, theory 9-5905  
D-band based on Hubbard's theory and mag. field effect 9-16407  
dielectric, internal photoeffect with atomic centres 9-10231  
electric wire explosion later stages, temp. and e. density distrib. 9-9346  
electronic and vibrational, unified presentation 9-1757  
emission, line form meas. using visibility curves 9-4537  
emission, solid particles in vacuum 9-5908  
e.s.r., line shapes, Gaussian and Lorentzian, comparison 9-4407  
exploding wires, confined, optical and elec. meas. 9-18287  
Fourier transforms data anal. by computer 9-20296  
frustrated total internal reflection, adapter for spectrophotometer 9-13074  
impurity, due to electron-localized vibration interaction, theoretical analysis 9-1762  
impurity absorption band profiles, transitions to degenerate local levels 9-3881  
impurity atom or mol. in solid, antiresonance in absorpt. 9-1765  
impurity crystals, vibrational structure of vibronic spectrum, double adiabatic approximation 9-17349  
insulators, exciton effects in inter-band absorpt. 9-1572  
ions in cubic crystals, Zeeman, intensities for  $\Gamma_6 \rightarrow \Gamma_8$  and  $\Gamma_7 \rightarrow \Gamma_8$  transitions 9-5895  
i.r., multi-attenuated total reflectance analyser 9-15478  
i.r. absorpt., impurity-induced, molecular coupling 9-7966  
Jahn-Teller induced optical transitions 9-7928  
laser beam, electro-optical Doppler-shift-modulated, analysis 9-4497  
level crossing, application of effective tensor operator 9-6951  
light scattering spectra of solids, conference 9-10190  
lightning leader, stepped, slitless spectrograph obs. 9-21777  
line structure determ. using electrostrictively Fabry-Perot interferometer 9-15552  
line-shape for A-doubling transitions 9-9104  
microwave, frequency markers on record chart 9-2283  
molecular cry., electr. abs. spectra, exciton config. construct. 9-21617  
molecular systems, group theory classification of states in calcs. 9-14679  
multiphonon structure in absorpt. and emission, lattice freq. shift effect 9-16410  
optical bands in vibrational systems with degeneracy 9-15172  
organotin cpds., X-ray irradi., e.s.r. investigation of radicals formed 9-7592  
Paschen-Back effect of R lines in TiCr<sub>2</sub> alum. 9-3896  
photons scattered from point source near air-ground interface 9-19189  
plasma, nonuniform, spectral temp., Boltzmann plot investg. 9-17099  
plasma high frequency turbulence and acceleration of sub-cosmic rays 9-14775  
plasma high frequency turbulence and acceleration of sub-cosmic rays 9-2976  
polyatomic many-electron systems, determ. of allowed multiplets 9-13338  
random band models with pure Doppler shaped lines, behaviour for several irradiance distribns. 9-10932  
resonance energy transfer in condensed media from many-particle view-point 9-5621  
ruby laser pulse 9-4477  
seismic, frequency-wave-number, determ. using arrays 9-18786

## Spectra continued

- semiconductors, bound excitons 9-21470  
 solids, optical interactions, theory, book 9-14023  
 solids with deep impurities, decay modes with coherent resonant-energy transfer 9-9889  
 solvent Stark effect temperature dependence 9-21210  
 strong absorpt. band region, dispersion determ. from refl. and transmission data, applicability 9-259  
 thermal desorption, analysis 9-14900  
 turbulence-like in a beam-plasma system 9-3003  
 Urbach's rule, theory rel. to quantum transition from vibr. sub-level to e excitation level 9-1766  
 vibrational, of interacting dislocation segments, in long-wave approximation 9-16095  
 vibrational structure of impurities from radiation spectrum 9-16408  
<sup>208</sup>At decay scheme calc. from  $\gamma$  obs. 9-531  
<sup>208</sup>Po, energy levels determ. from  $\gamma$  obs. 9-531  
 Cd<sup>2+</sup>, complex combinations with the ions SO<sub>4</sub><sup>2-</sup>, Cd<sup>2+</sup> SCN and the amines aniline, benzidine,  $\beta$ -naptyl-amine, o-toluidine and m-toluidine, infrared spectra 9-6969  
 Hg<sup>2+</sup>, complex combinations with the ions SO<sub>4</sub><sup>2-</sup>, Cd<sup>2+</sup> SCN and the amines aniline, benzidine,  $\beta$ -naptyl-amine, o-toluidine and m-toluidine, infrared spectra 9-6969  
 Kf(Cl), photoemission, evidence for L-bands 9-3757  
 Si phonon-assisted transitions determ. by derivative optical spectroscopy 9-1758  
 Zn<sup>2+</sup>, complex combinations with the ions SO<sub>4</sub><sup>2-</sup>, Cd<sup>2+</sup>SCN and the amines aniline, benzidine  $\beta$ -naptyl-amine, o-toluidine and m-toluidine, infrared spectra 9-6969

## atoms

See also Atoms/excitation; Atoms/structure

- <sup>2</sup>P-<sup>2</sup>P transitions in np and np<sup>2</sup> (n=2-6) configurations 9-13286  
 absorption, collision-induced, effect of dispersion on exponential dipole moment model 9-4860  
 absorption, suitable flame sources 9-10944  
 absorption microwave and i.r. analysis of atomic and molecular species in hypervelocity wake 9-19577  
 absorption spectroscopy and flame emission 9-279  
 alkali and noble-gas atoms, bound state, obs. 9-18142  
 all elements from H to V including ions, bibliography 9-13287  
 Ar X-XIII, u.v. lab. and solar coronal obs. 9-6972  
 collective vibrations of atom electrons in dense medium model, interpretation 9-11380  
 electronic partition functions, 1500-7000°K, 73 elements 9-20873  
 excitation of elementary emitters in a nonuniform broadened line 9-13285  
 excitation of elementary emitters in a nonuniform broadened line 9-2812  
 fine structure, matrix elements of Breit eqn. investigated by second quantization method 9-9119  
 flame emission and atomic absorption spectrometry, review 9-18774  
 gas-He mixture vacuum u.v. flow lamps, microwave excited 9-8665  
 halides in spark discharge line intensity reln. with S 9-9126  
 heavy atoms, inclusion of mag. interaction in energy level calc. 9-11382  
 hydrogenic line broadening, rel. to strong collisions 9-15804  
 hyperfine structure and level crossing 9-6957  
 after interaction with e.m. radiation, rel. to plasma spectroscopy, book 9-15936  
 ionized vapours, oven-discharge tube combination 9-19393  
 isotope effect in heavy elements, review 9-19394  
 Lamb shift, failure of self-consistent field theory of quantum electrodynamics 9-10957  
 Lamb shift, use in investigation of O(4) symmetry and Coulomb problems 9-17004  
 level multiplets, overlapping phenom. 9-11387  
 line formation, integral eqns. for source functions 9-19390  
 line pressure shift 9-15803  
 muonic, with odd-mass nuclei, effect of single particle excitation 9-18162  
 noble-gas and alkali atoms, bound states, obs. 9-18142  
 O emission mechanism suggested for tropical night airglow 5577 and 6300 Å 9-8191  
 optical dipole transition between adjacent degenerate states 9-4825  
 oven-discharge tube combination for ionized vapours spectroscopic studies 9-19393  
 p<sub>3/2</sub> levels, splitting by elec. field gradients, photoelectron and internal conversion spectroscopy 9-670  
 partial Corbion diagrams of astrophysical interest 9-13282  
 photon non-coherent scatt. in spectral lines, redistrib. functions 9-19392  
 plasma, atomic line broadening calc., Green's function theory 9-19523  
 in plasma, quantum theory of pressure broadening 9-2965  
 plethysm applied to atomic spectroscopy 9-9118  
 positronium in water, magnetic quenching, hyperfine energy splitting 9-2807  
 red satellite bands, interpretation 9-2811  
 resonance scatt. line splitting under strong monochromatic e.m. irradiation 9-4849  
 resonances, configuration interaction theory, eff. of overlapping 9-11405  
 Stark effect, line broadening, electron contribution 9-667  
 symmetrical self-reversed contour calc. with radial dependence of plasma parameters 9-2809  
 textbook 9-19387  
 two-particle operators, symmetry classification 9-20868  
 two-photon decay rate of singlet and triplet metastable states of He isoelectronic sequence 9-20870  
 X-ray forbidden transitions, classification 9-15805  
 X-ray forbidden transitions, classification 9-15806  
<sup>6</sup>Li Stark effect shifts in plasma rel. to high temp. meas. 9-8539  
<sup>133</sup>Cs, resonance lines in CsI spectrum, isotope shift against <sup>133</sup>Cs 9-6962  
<sup>200</sup>Hg, vapour, effect of detecting light beam on modulated absorption and dispersion signals 9-673  
<sup>201</sup>Hg, Zeeman degeneracy under non resonant light radiation 9-11393  
<sup>213</sup>Pa, KLL Auger spectra, obs. in  $\beta$ -decay 9-2817  
<sup>147</sup>Sm, hyperfine interact. consts. in J=5 states 9-6973  
<sup>149</sup>Sm, hyperfine interact. consts. in J=5 states 9-6973  
 Ag I h.f.s. of 4d<sup>5</sup>5s<sup>2</sup>D<sub>3/2</sub>-4d<sup>4</sup>5p<sup>2</sup>P<sub>1/2</sub> transition at  $\lambda$ =19372 Å 9-19395  
 Al, and Pt excitation inhibition in Pt-Al mixture, discharge obs. 9-18134  
 Al optical resonance transitions, lifetime measurements, phase shift method 9-11392  
 Ar, absorption, near Li, III edge 9-4837  
 Ar, Auger spectra of L<sub>2</sub> and L<sub>3</sub> shells 9-6978  
 Ar, discharge, continuous spectrum in positive column 9-924  
 Ar, excitation by He<sup>+</sup> impact, E<sub>th</sub>=0.3-10-keV 9-20887

## Spectra continued

## atoms continued

- Ar, line intensities in L<sub>2</sub>MM and L<sub>3</sub>MM spectra, calc. using Rubenstein's transition amplitudes 9-4856  
 Ar, proton excitation of 1300-Å continuum 9-9133  
 Ar, radial distrib. of excited species in capillary discharge 9-13461  
 Ar excitation by protons, 4 MeV, continua intensity depend. on press. determ. 9-20883  
 Ar I, 5p levels, electronic excitation, experimental lifetimes 9-15819  
 Ar I, II, broadening of spectral lines in spark plasma 9-5093  
 Ar I, i.r.-transition arrays, transition probabilities and oscillator strengths 9-20880  
 Ar I, radiative lifetimes in resonance series 9-11390  
 Ar I, resonances obs. in photo-ionization continuum 9-13297  
 Ar I, transition probabilities meas. for 26 lines, 3000-6500 Å 9-19396  
 Ar I, i.r. lines in plasma torch sustained at h.f., Stark effect 9-9375  
 Ar II, relative transition probabilities 9-20876  
 Ar II line, in plasma, shift and shift-to-width ratio rel. to electron temp. and density 9-5031  
 Ar refractive index and resonance line oscillator strength obs., 2300-1100 Å 9-9454  
 ArI isoelectronic sequence, Hartree-Fock calcs. of forbidden lines rel. to the spectrum of the corona 9-15368  
 As VII, vacuum u.v. region 9-2813  
 B I level crossing determ. of lifetime of 2S2P <sup>2</sup>D<sub>3/2,5/2</sub> states 9-6964  
 Ba-II, 1400-2000 Å and 4100-4600 Å, abs. oscill. strengths 9-6960  
 Ba I, two-electron spectra, config. mixing and oscillator strengths 9-19398  
 Ba II, resonance lines, 6p <sup>2</sup>P<sub>3/2,1/2</sub>-s<sup>2</sup>S<sub>1/2</sub>, h.f.s. 9-6961  
 Be Stark effect shifts in plasma rel. to high temp. meas. 9-8539  
 Bi, multipole lines, hyperfine structure 9-15810  
 C, p<sup>2</sup>-ps transition line oscillator strength in isoelectronic sequence 9-9122  
 C IV, absolute oscillator strengths 9-15808  
 Ca I, two-electron spectra, config. mixing and oscillator strengths 9-19398  
 Ca III, revised and extended anal. 9-18136  
 Ca XIII-XV, solar coronal u.v. obs. 9-6972  
 Cd, holographic, obtained with Lloyd's mirror 9-4496  
 Cl, neutral, Stark broadening of four multiplets 9-6966  
 Cl affinity continuum, u.v. region 9-9128  
 Cl IX-XIII, u.v. lab. and solar coronal obs. 9-6972  
 Cl in 2,4-dichloroaniline, Zeeman quadrupole spectra obs. 9-20958  
 Cl in CCl<sub>4</sub>, KLL Auger spectrum obs. 9-14668  
 Co, core-electron energy levels and state density, X-ray photoelectron obs. 9-1813  
 Cr I, II absolute g<sub>f</sub>-values, shock tube radiation source 9-19399  
 Cs, doublet suppression in foreign gases 9-13288  
 Cs 8943 Å line, temp. and press. eff. of Ar, Ne; line broadening meas. 9-19400  
 Cs broadening of second doublet by inert gases 9-2814  
 Cs isotopic shift of D<sub>1</sub> line determ. 9-18137  
 Cu, core-electron energy levels and state density, X-ray photoelectron obs. 9-1813  
 Cu I, hyperfine struct. in 4p <sup>2</sup>P<sub>3/2</sub>-state, level-crossing and Stark effect meas. 9-4836  
 Cu VII-XII, Hartree-Fock calcs. rel. to Sun's coronal spectrum 9-15368  
 Cu,II relative transition prob. of resonance lines meas. 9-13289  
 Fe, core-electron energy levels and state density, X-ray photoelectron obs. 9-1813  
 Fe, emission line shift prod. by Ar and He, obs. 9-6963  
 Fe group, doubly ionized atoms, config. 3d<sup>4</sup>4p in 3rd spectra, energy levels, interac. parameters 9-18139  
 Fe I reson. line  $\lambda$ =3720, absolute oscillator strength 9-18140  
 Fe IX-XIV, identification of 3d-4p and 3d-4f transitions in solar spectrum 9-6191  
 Fe XII, transition probabilities for various excited states 9-15809  
 H, <sup>2</sup>P<sub>3/2,1/2</sub>-<sup>2</sup>S<sub>1/2</sub> transition, oscillator strength expt. estimate 9-11416  
 H, Balmer lines H <sub>$\alpha$</sub>  and H <sub>$\beta$</sub> , for conc. in plasma determ. 9-7144  
 H, gaseous, line broadening of intense laser radiation 9-13291  
 H, H<sup>+</sup>, H<sup>-</sup>, absorption coeffs. 9-19410  
 H, hyperfine pressure shifts in Kr and Xe 9-9155  
 H, line widening by plasma electrons 9-2010  
 H, optical polarizability, bounds calc. 9-2825  
 H, recombination lines, partial maser effect in nebular plasma 9-8231  
 H, two-photon bound-bound transitions 9-13310  
 H I, interference between fine structure levels, interpret. 9-20897  
 H quenched from 2S state, polarized radiation fraction calc. 9-20896  
 He-Ar mixtures, collision-induced absorpt. 9-2829  
 He-Ne mixture, 6328 Å Ne line, homogeneous linewidth meas., using non-linear travelling wave interaction technique 9-2824  
 He, differential scatt. cross-section for 25 60-eV e impact 9-9142  
 He, e bombardment, transitions obs. 3230-20582 Å 9-6994  
 He, positive column of discharge emission intensity rel. to validity of theory 9-925  
 He, u.v. reson. lines from sun, intensity calc. 9-12763  
 He, Ar plasma, Doppler broadening of He ion lines 9-2830  
 He I, 2 <sup>2</sup>P-4 <sup>3</sup>P, <sup>3</sup>D, <sup>3</sup>F transitions, electron and ion Stark broadening 9-20899  
 He I line, plasma electronic temp. meas. 9-5042  
 He II, interference between fine structure levels, interpret. 9-20897  
 He low-pressure afterglow, time-depend. behaviour of 10830 Å line 9-18315  
 He metastable (<sup>3</sup>S), decay 9-15832  
 He Stark effect shifts in plasma rel. to high temp. meas. 9-8539  
 He to Xe photo-ionization cross-sections, using model eigenvalues and their discrete and continuum orbitals 9-9124  
<sup>3</sup>He, fine struct. and h.f.s. of 2<sup>3</sup>P states 9-9158  
 in He-Ne laser, emission line intensities modification rel. to population inversion, obs. 9-17873  
 Hg, holographic, obtained with Lloyd's mirror 9-4496  
 Hg, line profile alteration by high power laser pulse 9-11394  
 Hg, magnetic depolarization of resonant light backscattered by 6<sup>3</sup>P<sub>1</sub> state, effect of Hg-Hg collisions 9-674  
 Hg-Xe arcs, far i.r. source 9-19564  
 Ho II nuclear magnetic dipole moment 9-15821  
 K, 4<sup>2</sup> level Stark effect obs. by atomic beam technique 9-13290  
 K, electric octupole 4<sup>2</sup>S-4<sup>2</sup>F transition excited by e impact 9-4839  
 K, enhanced 2-photon emission between 6S and 4S levels 9-20886  
 K XIV, solar coronal u.v. obs. 9-6972



**Spectra continued**  
**atoms continued**

- KII resonance line excitation in slow collisions between  $K^+$  and He 9-14676  
 KII resonance lines excitation in slow collisions between  $K^+$  and He 9-2834  
 K XI-XIII, u.v. lab. and solar coronal obs. 9-6972  
 Kr excitation by  $He^+$  impact  $E_h=0.3-10$  keV 9-20887  
 Kr I, visible 5s-5p array, transition probabilities and oscillator strengths 9-20880  
 Li, doubly excited states 9-13299  
 Li, isoelectronic sequence, dipole transitions between  $1s^2 3^2 L$  states, oscillator strengths by perturbation theory 9-9125  
 Li, self-broadening of 2S-2P reson. line emitted by exploding wire 9-16996  
 Li, Stark effect shifts in plasma rel to high temp. meas. 9-8539  
 Li in noble-gas matrices, 3500-8000 Å, 4.2-40.0°K 9-4840  
 Li isoelectronic sequence continuous absorption 9-19402  
 MgI, radiation, Stark and van der Waals level broadening constants 9-13293  
 Mn I in long period variables 9-21894  
 N, compressed, line broadening of intense laser radiation 9-13291  
 N, Stark effect shifts in plasma rel. to high temp. meas. 9-8539  
 N I multiplex, transition probabilities meas. in far u.v. 9-16995  
 N II, radiative lifetimes, ultraviolet multiplets, phase shift measurement technique 9-11386  
 N second positive bands, excitation by e impact, absolute cross-sections, relative intensities of diff. vibr. bands. 9-13300  
 N V, absolute oscillator strengths 9-15808  
 Na-seeded plasmas, emission spectra, series lines investig. 9-19537  
 Na in solid benzene, for investigation of interstellar absorpt. bands 9-18882  
 $^{23}Na$ , h.f.s. of  $3^2 P_{3/2}$  and  $4^2 P_{3/2}$  states from level-crossing expts. 9-6970  
 Ne, excitation by  $He^+$  impact  $E_h=0.3-10$  keV 9-20887  
 Ne, optical absorption meas. of atom density formed by luminescent discharge 9-6967  
 Ne 6328 Å, homogeneous linewidth meas., using nonlinear travelling wave interaction technique 9-2824  
 Ne I, i.r.-transition arrays, transition probabilities and oscillator strengths 9-20880  
 Ne I, II, III states radiative lifetimes, u.v. obs. 9-4844  
 Ne II, 3p and 3d levels, lifetime determ. 9-20877  
 NeI 3d-4f lines meas.  $2p^2 5f$  config. derived. 9-15813  
 Ni, core-electron energy levels and state density, X-ray photoelectron obs. 9-1813  
 Ni, IV, by vacuum spectrograph 9-4845  
 Ni, IV, sextet and quartet system, intercombination 9-4846  
 O I, Stark effect calc. and displacement and splitting obs. 9-2821  
 O VI, absolute oscillator strengths 9-15808  
 p hyperfine structure, Brueckner-Goldstone many-body theory 9-678  
 Pa, emission, 3  $\mu$  to 4000 Å, and level system 9-15814  
 Pa, emission, from 3  $\mu$  to 4000 Å 9-19403  
 Pb, and reson. interaction with Pt, obs. 9-18134  
 Pb muonic transitions, Eisenberg-Kessler calc. of intensities 9-11430  
 Pr III, multiplets of  $4f^2 5d$  config., overlapping phenom. 9-11387  
 Pt, core-electron energy levels and state density, X-ray photoelectron obs. 9-1813  
 Pt, excitation inhibition by Al and reson. with Pb, obs. 9-18134  
 Pu cpds., core  $p_{3/2}$  levels, splitting, internal elec. field gradients, photoelectron and internal-conversion spectroscopy 9-670  
 $^{85}Rb$  relative isotope shift by atomic beam technique obs. 9-4852  
 $^{87}Rb$  relative isotope shift by atomic beam technique obs. 9-4852  
 $^{87}Rb$  vapour, optically pumped, microwave light modulation 9-679  
 S IX-XII, u.v. lab. and solar coronal obs. 9-6972  
 S in spark discharge line intensity reln. with halides 9-9126  
 ScI radiation, Stark and van der Waals level broadening constants 9-13293  
 Se VIII, vacuum u.v. region 9-2813  
 Si,  $p^2$ - $p^2$  transition line oscillator strength in isoelectronic sequence 9-9122  
 Si I and II lines, relative oscillator strengths 9-19404  
 Si IV absolute oscillator strengths 9-15808  
 SiI, atomic energy levels and multiplet data tables 9-9123  
 Th cpds., core  $p_{3/2}$  levels, splitting, internal elec. field gradients, photoelectron and internal-conversion spectroscopy 9-670  
 Th I, energy levels, odd and even 9-11388  
 Ti II, line strengths for transitions bet.  $(3d^3+3d^2 4s)$  and  $3d^2 4p$  config. 9-14666  
 Tm, i.r. laser emission in vapour 9-2818  
 U, M emission, meas. and comparison 9-6968  
 U cpds., core  $p_{3/2}$  levels, splitting, internal elec. field gradients, photoelectron and internal-conversion spectroscopy 9-670  
 V IV, V levels determ. from condensed spark and hollow cathode discharge 9-2820  
 Xe, isotope shifts of 20 i.r. laser lines 9-15811  
 Xe excitation by  $He^+$  impact  $E_h=0.3-10$  keV 9-20887  
 Xe I, isotope shift in visible lines 9-16997  
 Yb, i.r. laser emission in vapour 9-2818  
 Zn II 4924 LB, de-excitation in pulsed discharges with Zn bimetal electrodes, obs. 9-15963  
 Zn vapour, vacuum u.v., photo- and auto-ioniz. proc., abs. cross-section meas. 9-13453

**inorganic liquids and solutions**

- electrolytes in nonaq. solvents, interionic vibr. spectra 9-9514  
 polymethine dye solns., generation, excited by Nd-glass laser emission ( $\lambda=1.06 \mu$ ) 9-1014  
 rare earths, trivalent aq. ions, electronic energy levels 9-16017  
 spectral broadening of light propag. in self-trapped filaments through liquids with large optical Kerr constants 9-13526  
 spectrophotometer attachment for low temp. to -96°C 9-10943  
 sulphates, molten, i.r. 9-16005  
 water, interpretation of spectra 9-9170  
 $[Fe(py)_4O_2]^{2+}$ , effect of solvent on peak positions, 330-880  $\mu$  9-5172  
 BeO, molten, visible region, absorption index meas. 9-17210  
 $Eu^{3+}$  in aq. soln., electronic energy levels 9-16006  
 H<sub>2</sub> in liq. Ar, collision-induced absorpt., liq. cell model 9-21214  
 H<sub>2</sub> in liq. Ar, collision-induced absorpt., liq. cell model 9-21213  
 H<sub>2</sub>O, i.r. liquid model interpretation 9-13529  
 H<sub>2</sub>O<sub>2</sub> absorpt. spectra and kinetics in HClO<sub>4</sub> soln. 9-9515  
 H<sub>3</sub>O<sup>+</sup> ion in SO<sub>2</sub> soln., vibration 9-2865  
 Hg, absorption, electron-electron interactions eff. 9-21628

**Spectra continued****inorganic liquids and solutions continued**

- $KNO_3$ -M( $NO_3$ )<sub>2</sub>, (M=Ba, Sr, Ca), mixture, absorpt. composition depend. 9-1018  
 $KNO_3$ -AgNO<sub>3</sub> molten mixtures 9-1019  
 LiBr: Ag<sup>+</sup>, and luminesc. and excitation 9-1020  
 LiCl: Ag<sup>+</sup>, and luminesc. and excitation 9-1020  
 Na, absorption, electron-electron interaction eff. 9-21628  
 NaBr: Ag<sup>+</sup> solns., spectra, and luminesc. and excitation spectra 9-1020  
 NaCl: Ag<sup>+</sup> solns., spectra, and luminesc. and excitation spectra 9-1020  
 NaNO<sub>3</sub>-alkaline earth nitrate molten mixtures, absorpt. 9-13530  
 P<sub>4</sub>O<sub>6</sub>,  $^{31}P$  spin-lattice relax 9-9231  
 POCl<sub>3</sub>-SnCl<sub>4</sub> mixture,  $NO_3^+$ ,  $Eu^{3+}$ ,  $Tb^{3+}$  in soln., fluorescence and radiative lifetime of ions 9-21217  
 Pb-BiCl<sub>3</sub> molten mixtures, absorption for reaction study 9-13531  
 Se sols, absorption, expt. compared with theory rel. to particle size distrib. 9-14872  
 SnI<sub>4</sub> in dioxane, visible and u.v. absorpt. 9-18363
- inorganic molecules**  
*See also Molecules*  
 electronic spectra, book 9-11453  
 gas absorption coeff. meas. from CO<sub>2</sub> laser rotational competition and Lamb dip study 9-13009  
 infrared absorption in rare gas mixtures 9-4914  
 rare earth magnesium nitrates, crystal field lines in far i.r. 9-5862  
 rotational line intensities in  $^2\Sigma$ - $^2\Sigma$  electronic transitions 9-2880  
 torsion-vibr.-rot. interaction in rot. spectra 9-7004  
 transition metal pyridine-2-carboxamide chelates, i.r., syntheses of chelates 9-14695  
 Ar pulsed discharge, time-resolved laser spectrum 9-13002  
 B halides, pure and mixed, i.r. obs. and vib. modes assignment 9-7014  
 BF<sub>3</sub> isotopes,  $\nu_3$  bands meas., rotn. fine structure determ. 9-17027  
 BiBr, visible A-X system, rotational anal. 9-18176  
 BiF, rotational analysis of 3050-3250 Å syst. electronic state struct. deduced 9-4919  
 Bi<sub>6</sub>(OH)<sub>12</sub><sup>6+</sup> polynuclear metal complex vib. obs. 9-11455  
 CCl<sub>4</sub>, infrared, absorption bands, integrated intensities obs. 9-2860  
 CF<sub>4</sub>, infrared, absorption bands, integrated intensities obs. 9-2860  
 CO, Frank-Condon factors in ioniz. transitions 9-4934  
 CdF<sub>2</sub>:at1%Er<sup>3+</sup> blue fluorescence, excitation mechanisms, opt. double resonance proc. 9-3925  
 Cu(II) complex of  $\alpha$ -hydroxy-carboxylic acid, i.r. absorption obs. 9-15851  
 GeCl<sub>4</sub>, infrared absorption bands, integrated intensities obs. 9-2860  
 H<sub>2</sub>, transition absorption coeff. calc., dipole moment depend. on rotn. state 9-19431  
 H<sub>2</sub>, Frank-Condon factors in ioniz. transitions 9-4934  
 H<sub>2</sub>, Raman spectra, collisions, line width of S<sub>0</sub>(0) and S<sub>0</sub>(1) 9-2864  
 H<sub>2</sub>O<sup>+</sup> ion in SO<sub>2</sub> solution, vibration 9-2865  
 H<sub>2</sub>S, rotational absorption 10-125 cm<sup>-1</sup> obs., comparison with theory 9-7026  
 LaF<sub>3</sub> vapour discharge, band system obs. 3000-3350 Å 9-9217  
 NH<sub>3</sub>, microwave echoes 9-13362  
 NO, 1-0 vib.-rot. bands: absorption, Zeeman and mag. rot. spectra obs. 9-9225  
 NO, Frank-Condon factors in ioniz. transitions 9-4934  
 NO<sup>+</sup>(A<sup>1</sup> $\Sigma^+$ -X<sup>1</sup> $\Sigma^+$ ) band system, Frank-Condon factors in ioniz. transitions 9-4934  
 O<sub>2</sub>, Franck-Condon factors in ioniz. transitions 9-4934  
 PH, absorption in vacuum u.v., new band systems, rot. analysis 9-9232  
 PO rotational analysis of D and D' states 9-2878  
 P<sup>18</sup>O isotropic bands and shifts 9-2878  
 Pb<sub>6</sub>(OH)<sub>12</sub><sup>4+</sup> polynuclear metal complex vib. obs. 9-11455  
 S-S<sub>8</sub> bond energy diff., force const., fundamental modes assignment, i.r. spectra 9-20941  
 SeD, diffuse, g.s. dissociation energy determ. 3000-3250 Å 9-18193  
 SeF<sub>4</sub> isotopes, rotn. const., dipole moment structure parameter determ., 8000 - 40000 MHz 9-18191  
 SeH, diffuse, g.s. dissociation energy 3000-3250 Å 9-18193  
 SeOF<sub>2</sub> isotopes, microwave obs., rotn. const. and dipole moment determ. 9-18192  
 SiCl<sub>4</sub>, infrared absorption bands, integrated intensities obs. 9-2860  
 SiF<sub>4</sub>, infrared absorption bands, integrated intensities obs. 9-2860
- inorganic molecules, diatomic**  
 emission-absorption intensity ratio temp. meas., thermal non-equl. conditions, theor. investig. 9-20906  
 AgAl gaseous mol., rot. analysis of bands 9-17026  
 AlD absorpt., X $\Sigma^+$ -A<sup>1</sup> $\Pi$  transition intensities 9-18173  
 AlH absorpt., X $\Sigma^+$ -A<sup>1</sup> $\Pi$  transition intensities 9-18173  
 AlO blue-green system, relative band strengths, eff. of self-abs. on emission, comparison with synthetic spectra 9-19426  
 AlO visible and u.v. bands, isotope shift studies 9-13341  
 BF, rotational analysis of 14900 cm<sup>-1</sup> band, assignment as e $\Sigma$ -b $\Sigma$  transition 9-13343  
 BaD, absorption, 4000-3000 Å, extension of F $\Sigma$ -X $\Sigma^+$  system 9-4917  
 BaH, absorption, 4000-3000 Å, extension of F $\Sigma$ -X $\Sigma^+$  system 9-4917  
 BaO, A $\Sigma^+$ -X $\Sigma^+$  band syst., Franck-Condon factors 9-13344  
 BeF, Frank-Condon factors r-centroids for A $\Sigma^+$ -X $\Sigma^+$  system 9-7016  
 BiBr emission bands obs. 9-2858  
 BiI emission, new B-a transition obs. 9-7017  
 C<sub>2</sub>, analysis of Swan bands 9-14686  
 C<sub>2</sub>, new system of simple  $\Sigma$ - $\Sigma$  bands in 4800-6000 Å region 9-4985  
 CN, electron emission spectrum dipole moments of X( $\Sigma^+$ ) and B( $\Sigma^+$ ) states calc. 9-15850  
 CN, in active N flames, absorpt. determ. of ground-state conc. 9-826  
 CO, (A<sup>1</sup> $\Pi$ -X $\Sigma^+$ ) syst. in absorption at high resolution in vacuum u.v. 9-18178  
 CO, branching ratio investigation, 1500 to 2600 Å 9-11460  
 CO, high-resolution widths of self-broadened lines 9-13346  
 CO, u.v. absorpt., study of B-X and C-X transitions 9-11456  
 CO differential scatt. cross-section for 25-60 eV impact 9-9142  
 CO i.r. transmission functions 9-17031  
 $^{12}C^{18}O$ , Angstrom bands in visible region 9-9197  
 CaH, absorpt., A<sup>2</sup> $\Pi$ -X $\Sigma^+$  and B $\Sigma^+$ -X $\Sigma^+$  systems 9-18180  
 Cd band, 4130-4800 Å, electronic transition (B) $\Sigma^+$ -(X) $\Sigma^+$ , spectrographic obs. 9-4920  
 Cl<sub>2</sub>, radiative recombination spectrum studied 9-20891  
 Cs<sub>2</sub>, i.r. absorpt. 9-4923  
 CsBr, dissoci., time-resolved spectra 9-822  
 Cs<sup>35</sup>Cl, r.f. Stark effect, mol. beam elec. resonance meas. 9-7036  
 CsF r.f. Stark effect, mol. beam elec. resonance meas. 9-7036

## Spectra continued

## inorganic molecules, diatomic continued

- CuCl band system, r-centroid, Franck-Condon eff. determ. 9-4925  
 CuO, and orange red region study using  $^{18}\text{O}$  9-20927  
 $\text{D}_2$  in solid Ar, 77°K, fundamental band 9-14687  
 $\text{D}_2$ , electronic field induced, 0-600 psi, fundamental vib.-rot. band lines 9-13354  
 DCL, i.r., higher J rotational struct. 9-13357  
 DH, electric field induced, 0-600 psi, fundamental vib.-rot. band lines 9-13354  
 GeCl, new band system 9-763  
 GeI, u.v. absorption spectra, new band obs. 9-17030  
 $\text{H}_2$ -He mixture, press.-induced i.r. spectrum, vel. and force correlations, deriv. of moment relations 9-9203  
 $\text{H}_2$ , with new photoelectron spectroscopy 9-17898  
 $\text{H}_2$ ,  $\text{H}_2^+$ , absorption coeffs. 9-19410  
 $\text{H}_2$  in solid Ne, 4°K, fundamental band 9-14687  
 $\text{H}^{79}\text{Br}$ , 2-0 vib.-rot. band lines, dipole matrix elements 9-15853  
 $\text{H}$  quasi-mols., continuous absorpt. rel. to stellar spectra 9-6189  
 $\text{H}_2$ , electric field induced, 0-600 psi, fundamental vib.-rot. band lines 9-13354  
 $\text{H}_2$ , differential scatt. cross-section for 25-60 eV e impact 9-9142  
 $\text{H}_2$  gas, press.-induced pure rot. i.r. abs. band analysis, obs. of blue freq. shift 9-11461  
 HBr, gas-phase far-u.v. absorpt. 9-20929  
 HCl, i.r., higher J rotational struct. 9-13357  
 HCl, i.r., press.-induced shifts, j-depend., elastic cross-section expansion 9-17012  
 HCl, vibration rotation spectrum, density and linewidth 9-18182  
 HF, i.r., higher J rotational struct. 9-13357  
 HF<sup>+</sup> photoelectron spectrum, Hartree-Fock calc. 9-19434  
 HGH, analysis of spectrum 9-14689  
 HI, gas-phase far-u.v. absorpt. 9-20929  
 $\text{He}_2$ ,  $\text{D}^2\Sigma^-$ ,  $\text{B}^1\Pi_g$  band system transition prob. Franck-Condon factors calc. 9-9215  
 $\text{He}_2$ , excitation of band spectrum in discharge and recombination 9-5082  
 $\text{I}_2$  in different solvents, absorption maxima of visible band 9-19634  
 $\text{I}_2$  in hydrocarbon solvents, contact charge-transfer spectra 9-19435  
 $\text{K}_2$ , laser-induced fluoresc. 9-15856  
 Li halides, absorpt. below 300 cm<sup>-1</sup> 9-9220  
 $\text{MgCl}_2$ ,  $^2\Pi_{1/2}$  rot. anal. of  $\text{A}^2\Pi_{1/2} \rightarrow \text{X}^2\Sigma^+$  system,  $\lambda\lambda 3950$ -3600 LB 9-11465  
 MgF, Franck-Condon factors for B-X and C-X systems 9-11466  
 $\text{N}_2$ , abnormal rot. energy distrib. in  $\text{C}^3\Pi_u$ - $\text{B}^3\Pi_g$  bands 9-778  
 $\text{N}_2$ , absorption,  $\text{b}^1\Pi_u$ - $\text{X}^2\Sigma^+$  syst. high resolution, 795-1015 LB 9-14690  
 $\text{N}_2$ , band strengths calc. of Halevi's correction 9-19437  
 $\text{N}_2$ ,  $\text{C}^3\Pi_u$ - $\text{B}^3\Pi_g$  transition on pulsed laser action, optical gain meas. 9-781  
 $\text{N}_2$  adsorbed on silica-supported Ir, i.r. spectra 9-20934  
 $^{14}\text{N}_2$ , intensity alternations in second positive bands ( $\text{C}^3\Pi_u$ - $\text{B}^3\Pi_g$ ) 9-18188  
 $^{15}\text{N}_2$ , intensity alternations in second positive bands ( $\text{C}^3\Pi_u$ - $\text{B}^3\Pi_g$ ) 9-18188  
 $\text{N}_2$ ,  $\text{C}^3\Pi_u$ - $\text{B}^3\Pi_g$ (0,0) stimulated transitions, high resolution study 9-2873  
 $\text{N}_2$ , forbidden vibr. transitions in electron-impact spectra 9-9228  
 $\text{N}_2$ , in discharge, intensity of first neg. bands reduced by  $\text{O}_2$  traces 9-5111  
 $\text{N}_2$ , differential scatt. cross-section for 25-60 eV e impact 9-9142  
 ND,  $\text{c}^1\Pi_u$ - $\text{b}^1\Sigma^+$  band system, characts. 9-4931  
 NH,  $\text{c}^1\Pi_u$ - $\text{b}^1\Sigma^+$  band system, characts. 9-4931  
 NO,  $\gamma$  and  $\beta$  band syst., RKR Franck-Condon factors 9-20933  
 NO, mag. rot. spectra of 1-0 vib.-rot. band 9-9221  
 NO, near i.r., transitions betw. Rydberg states, oscillator strengths 9-19439  
 NO, near i.r. mag. rot. calc. 9-2877  
 NaI r.f. Stark effect, mol. beam elec. resonance meas. 9-7036  
 $\text{O}_2$ , with new photoelectron spectroscopy 9-17898  
 $\text{O}_2$ , high resolution electron-energy-loss spectrum 9-784  
 $\text{O}_2$ , oscillator strength of Schumann-Runge band obs. 9-19444  
 $\text{O}_2$ , absorption, 1750 to 2020 Å at 300, 600 and 900°K 9-14692  
 $\text{O}_2$ , forbidden vibr. transitions in electron-impact spectra 9-9228  
 $\text{O}_2$ , microwave, rotational transition obs. 9-9229  
 $\text{O}_2$ , Schumann-Runge system, 3000-18000°K. Stark broadening 9-11471  
 $\text{O}_2$ , photoelectron spectra, high vibrational excitation in ground state 9-17039  
 $\text{O}_2$ ( $\text{A}^2\Sigma_u^+$ - $\text{X}^2\Sigma_g^-$ ) Herzberg I band system, source in Ar-4% $\text{O}_2$  afterglow 9-4933  
 OH, (0,0) (A-X) u.v. transition, collision broadening cross-sections, line-widths, low temp. 9-19484  
 OH<sup>+</sup> fine structure obs. 9-18189  
 OH (4-1) and (5-2) bands in night airglow spectrum 9-20101  
 OH radical, Hanle eff. in  $^2\Sigma^+(\nu=0)$  state obs., g-factor-lifetime product determ. 9-20984  
 $\text{P}^{18}\text{O}$ , isotope shift studies of u.v. and visible bands 9-18190  
 $\text{P}^{18}\text{O}$ , isotope shift studies of u.v. and visible bands 9-18190  
 $\text{P}_2$ ,  $\text{C}^1\Sigma_u^+$ - $\text{X}^1\Sigma_g^-$  system bands, rot. analysis 9-9230  
 PbBr, A-X system rot. analysis, obs. 9-4935  
 PbBr emission spectra up to 6100 Å, dissociation energy calc. 9-4936  
 $^{85}\text{Rb}^{35}\text{Cl}$  r.f. Stark effect, mol. beam elec. resonance meas. 9-7036  
 $^{85}\text{RbF}$ , r.f. Stark effect, mol. beam elec. resonance meas. 9-7036  
 $^{85}\text{RbF}$  r.f. Stark effect, mol. beam elec. resonance meas. 9-7036  
 $\text{ScO}$ , blue-green emission system rot. analysis, obs. 9-4937  
 $\text{SiBr}^+$ , emission 9-2882  
 SiF, rot. analysis of (0,0) band 9-11474  
 SiI, u.v. absorption spectra, new band obs. 9-17030  
 $\text{SiO}^+$ , band struct. in 4300-4100 Å region, and near 3840 Å 9-4938  
 SnCl, visible band system 9-789  
 VO, ground state, perturbation caused by mag. hyperfine interac. 9-19449  
 VO emission, 29 new bands, vib. consts. estimated 9-7039  
 $\text{Xe}_2$ , continuum decay rate 9-926

## inorganic molecules, diatomic, radiofrequency

See also Nuclear magnetic resonance and relaxation; Paramagnetic resonance and relaxation

- $^7\text{LiD}$  rot. line J=0-1 in ground vibr. and first excited states, microwave obs. 9-13361  
 $^7\text{LiD}$  rot. vibr. and pot. constants determ. 9-18184  
 $^6\text{LiD}$  rot. line J=0-1 in ground vibr. and first excited states, microwave obs. 9-13361  
 $\text{LiF}$ , rot. vibr. and pot. constants determ. 9-18184  
 $\text{LiH}$ , calc. of mol. constants from microwave obs. of LiD. 9-13361

## Spectra continued

## inorganic molecules, diatomic, radiofrequency continued

- ND, 0-0 band or  $\text{A}^2\Pi_{1/2}$ - $\text{X}^2\Sigma^+$  system, rot. analysis 9-19440  
 NaI, first rotational state h.f.s. level transitions studied, consts. determ. 9-9226  
 OH, in interstellar space 9-18879  
 $\text{SnTe}$ , microwave rot. spectrum, 27 isotopic mols. 9-2883  
 $\text{SnTe}$ , microwave rot. spectrum, 27 isotopic mols. 9-15873  
 NO, many quanta transitions between A doublet components 9-14691
- inorganic molecules, polyatomic**
- carbon tetrafluoride, photoelectron spectroscopy, ioniz. pot. calc. 9-13457  
 diborene hydrazine, i.r., for struct. 9-11463  
 hydrazine diborene, i.r., for struct. 9-11463  
 isotopic freq. shifts in linear and octahedral mols. 9-15847  
 metalorganic phenyls, O atm. and metal at. wt. effects, 77 and 290°K 9-15848  
 pentafluorodistannates (II),  $\text{Sn}_2\text{F}_7^-$  ion analysis, vib. assignments 9-20985  
 transition metal carbonyls, u.v. absorpt., 77 and 300°K 9-19448  
 transition-metal dichlorides, matrix isolated charge-transfer spectra 9-15858  
 transition-metal dihalides, i.r. absorpt. of monomers and dimers 9-15857  
 water, partially deuterated, i.r., line shape of OD absorpt. 9-14688  
 water, photoelectron, vibrational fine structure, bonding, ionization pot. 9-17895  
 Au complex, dicyanodihaloaurate, charge transfer 9-20921  
 $\text{BO}_2^-$  molecular ion, i.r. absorption in alkali halide crystals 9-14685  
 $\text{CO}_2$ , abs. band at 6970 cm<sup>-1</sup> 9-758  
 $\text{CO}_2$ , self and  $\text{N}_2$  broadenings of rot. lines of 15 and 4.3  $\mu$  bands, width meas. 9-19494  
 $\text{CO}_2$ , 4.3  $\mu$  absorpt. and emission obs. 9-9200  
 $\text{CO}_2$ , i.r. band low resolution emissivity, theory and expt. 9-17028  
 $\text{CO}_2$ , rotational lines, in laser vib. state 9-8610  
 $\text{CO}_2$ , calculation rel. obs. 9-4927  
 $^{12}\text{C}^{18}\text{O}_2$ , i.r., vib.-rot. bands and rot. consts. 9-13348  
 $^{13}\text{C}^{18}\text{O}_2$ , i.r., vib.-rot. bands and rot. consts. 9-13348  
 $\text{Ca}(\text{H}_2\text{PO}_4)_2 \cdot \text{H}_2\text{O}$  and deuterated analogue,  $\text{H}_2\text{PO}_4^-$  and  $\text{H}_2\text{O}$  vibr., 4000-200 cm<sup>-1</sup> 9-15872  
 $\text{Ca}(\text{NH}_4\text{SO}_4)_2$ , Raman and i.r. interpretation 9-12458  
 Cd complexes of triphenylphosphine, i.r. spectra, vib. assignments 9-20944  
 Co complex,  $[\text{CoX}_2\text{L}]$  and  $[\text{CoL}_4]$  ( $\text{ClO}_4$ ), ( $\text{X}=\text{Cl}$ , Br, I and L=2-thiazolidine) i.r. and electronic spectral studies 9-20926  
 CsOH matrix-isolated, i.r. 9-761  
 Cu (II) chelates, mixed, absorpt. spectra study 9-13350  
 Cu acetylacetonate complex, u.v. and visible spectra, Wolfsberg-Helmholtz calc. 9-17029  
 CuH, absorption in far ultraviolet, new band system, rot. analysis 9-9201  
 Cu(II) complexes, bis(thiosemicarbazono) Cu(II) and others 9-2861  
 $\text{D}_2(\text{BH}_3)_2^+$ , vibr. modes and P-B force const., i.r. obs. 9-18183  
 $\text{D}_2\text{S}$ , pure rot. absorpt. spectra, analysis 9-20928  
 $\text{D}_2\text{O}$ , photoelectron vibrational fine structure bonding 9-17895  
 $\text{F}^{19}\text{Cl}/\text{F}^{35}\text{Cl}$ , 5200-4600 Å, investigation of  $\text{O}^+ \cdot \Sigma^+$  system 9-2862  
 GeF<sub>4</sub>, u.v. absorption, rel. to bending freqs. 9-13351  
 $\text{H}_2\text{O}$  vapour, line shape of rot. transition at 22GHz, dispersion studies, Lorentzian behaviour 9-19432  
 $\text{H}_2\text{O}$  vapour, width and intensity of  $\lambda_{\nu}^{-1}=12.67\text{cm}^{-1}$  spectral line 9-771  
 $\text{H}_2(\text{BD}_3)_2^+$ , vibr. modes and P-B force const., i.r. obs. 9-18183  
 $\text{H}_2(\text{BH}_3)_2^+$ , vibr. modes and P-B force const., i.r. obs. 9-18183  
 $\text{H}_2\text{S}$ , far i.r. 9-20928  
 HCN, laser emission line at 12.85  $\mu$  9-2869  
 $\text{H}_2\text{CO}$ , transmission function calc., 1-7  $\mu$  9-2866  
 HN<sub>3</sub>, and D derivs., i.r. study of rotational consts. 9-13355  
 HNCO, and D derivs., i.r. study of rotational consts. 9-13355  
 HNCS, and D derivs., i.r. study of rotational consts. 9-13355  
 HNO<sub>2</sub>, vibration spectra at 77°K 9-7029  
 $\text{H}_2\text{O}$ , laser emission lines at 4.77  $\mu$ , 11.83  $\mu$  and 11.96  $\mu$  9-2869  
 $\text{H}_2\text{O}$  i.r. transmission functions 9-17031  
 $\text{H}_2\text{O}$  vapour, vibrational-rotational fine struct. 9-4926  
 $\text{H}_2\text{O}$  calculation rel. obs. 9-4927  
 Hg complexes of triphenylphosphine, i.r. spectra, vib. assignments 9-20944  
 $\text{H}_2\text{O}_2$ , 1200 2000 Å, abs. coeff. 9-7022  
 $\text{I}_2$  charge-transfer with H<sub>2</sub>S and benzene in solid matrices 9-12380  
 IF<sub>7</sub>, i.r. 9-2871  
 IrF<sub>6</sub>, electronic spectrum, Jahn-Teller progressions 9-772  
 Li halide dimers and trimers, i.r. absorpt. 9-9220  
 Li salicylaldehyde complexes, i.r. spectra 9-7028  
 $\text{MnO}_4^-$ , vacuo u.v. spectra, bands, rel. MO description and behaviour 9-19483  
 $\text{MoSe}_4^{2-}$ , vibrs. and force consts., i.r. obs. 9-15859  
 $\text{N}_2\text{O}$ , u.v. absorption spectrum, interpretation 9-15863  
 NCl<sub>3</sub>, i.r. 9-9222  
 NFCl<sub>2</sub>, i.r. 9-19441  
 NH<sub>3</sub>, rotation-inversion, K splitting 9-13367  
 $\text{N}_2\text{H}_4$ , 1200 2000 Å, abs. coeff. 9-7022  
 $\text{NO}_2$ , electronic, nonempirical SCF calc. 9-776  
 $\text{N}_2\text{O}$ , electronic spectrum, MO calc. 9-7031  
 $\text{N}_2\text{O}$ , rotational line J=5-6, broadening by foreign gases 9-13365  
 NOCl, i.r. absorpt., isotopic species 9-777  
 NSF<sub>3</sub>, e absorpt., rel. to Coriolis consts. and thermodynamic functions, i.r. obs. 9-15862  
 $\text{NaNH}_2\text{SO}_3$ , Raman and i.r. interpretation 9-12458  
 $\text{Nd}^{3+}$  complexes, hypersensitivity, environmental effects on f-f transitions 9-782  
 $\text{Ni}(\text{CH}_3\text{COO})_2 \cdot 2\text{H}_2\text{O}$ , electronic abs. spectrum 9-783  
 OH, stellar, 18 cm radiation, stimulated, elementary model 9-12727  
 $\text{PH}_4\text{Br}$ , laser-Raman spectra, barriers to  $\text{PH}_4^+$  rot. obs. 9-15865  
 $\text{PH}_4\text{Cl}$ , laser-Raman spectra, barriers to  $\text{PH}_4^+$  rot. obs. 9-15865  
 $\text{PH}_4\text{I}$ , laser-Raman spectra, barriers to  $\text{PH}_4^+$  rot. obs. 9-15865  
 (PNCu<sub>2</sub>), vibrational spectrum, assignment of fundamental freq. 9-14693  
 $\text{PbF}_2$ , u.v. absorpt. 9-9236  
 Pd complex, Pd X<sub>2</sub>2RCN (X=Cl or Br and R=Me or Ph), vibrational spectra 9-20937  
 Pd(II) selenourea complexes, vibr. modes, i.r. and laser Raman obs. 9-15867  
 Pd(II) thiourea complexes, vibr. modes, i.r. and laser Raman obs. 9-15867  
 $\text{Pt}_2\text{Cl}_4(\text{PEt}_3)_2$  rel. to Pt-Cl and ligand stretching vibrs., far i.r. 9-15869  
 $\text{Pt}_2\text{Cl}_4(\text{AsEt}_3)_2$  rel. to Pt-Cl and ligand stretching vibrs., far i.r. 9-15869



## Spectra continued

## inorganic solids continued

quartz, extreme i.r., 9-3878  
quartz, H-bonded OH, characts. from i.r. spectra 9-5267  
quartz, u.v., applic. of valence bond approximation to analysis 9-5266  
rare earth crystals, extra lines and covalency 9-19982  
rare earth ions in crystals,  $4f^n \rightarrow 4f^{n-1}5d$  spectra 9-12371  
rare earth oxy. fluorides, absorpt. rel. to struct. 220-5000 cm<sup>-1</sup> 9-16411  
ruby, Cr conc. dependence line shifts 9-1767  
rutile, i.r. study of hydroxyl group 9-7963  
rutile structure crystals, vibrational h spectra, dipole freq. behaviour 9-18549  
rutile structure crystals, vibrational spectra, dipole freq. behaviour 9-7636  
semiconductor oxides rel. to adsorbed Ag photolytic reduction, visible and i.r. 9-6017  
semiconductor solid solutions, absorption edge width 9-3880  
semiconductors, A<sup>I</sup>B<sup>VI</sup> exciton transitions, phonon-assisted 9-5966  
semiconductors, exciton absorpt. in crossed elec. and strong mag. fields 9-10174  
semiconductors, thermorefectance 9-14041  
sericite clay, i.r. absorpt. 3800-700 cm<sup>-1</sup> obs. 9-12372  
silica, fused, Ti-doped, radiation-induced absorpt., rel. to trapping mechanism 9-1777  
silicate glass, absorption, interconversion of Eu<sup>2+</sup>=Eu<sup>3+</sup> 9-14051  
silicate glass, Fe<sup>3+</sup> activated, absorpt. bands 9-10264  
Spectra, inorg. solids [borosilicate glass, Fe<sup>3+</sup> activated, absorpt. bands] Glass [phosphate, Fe-activated, luminesc. spectra and absorpt. bands] [silicate, Fe-activated, luminesc. spectra and absorpt. bands] [borosilicate, Fe-activated, luminesc. spectra and absorpt. bands]  
solids 00000000000000000000000000000000 complexes .rel.to.interplanar.bonding 00000000000000000000 0008021h030000000000001844 9-10264  
tetracyano complexes, rel. to interplanar bonding 9-18441  
tourmaline, absorption for colour origin and change on heating 9-15171  
transition metals, second and third series, electron energy loss spectra 9-15040  
transition-metal octahedral complexes, intensities 9-14056  
transition-metal tetrahedral complexes, charge-transfer spectra 9-1764  
Tutton salt crystals, three, Ni<sup>2+</sup> absorpt. 9-12369  
uranly nitrate, uniaxial and biaxial, polarized i.r. absorpt. 9-16417  
Y<sub>3</sub> Al garnet Raman, optical phonon investigation 9-3512  
2PbO.SiO<sub>2</sub> glass, i.r., rel. to struct. and phase transforms. in 30°C region 9-7321  
Ag granular films, anomalous absorpt., rel. to grain size 9-5912  
Ag halides, far i.r. transmission obs.; lattice structure and forces calc. 9-16074  
Ag thin metallic layers and halides, fine struct. obs. in absorption spectra 9-19172  
AgCl absorption, existence of direct excitons 9-9903  
Al-Y garnet,  $^4A_{1g} \rightarrow ^2E_g$  transition in Nd<sup>3+</sup>, vib. mechanism due to ion-phonon relax. 9-10186  
Al<sub>2</sub>O<sub>3</sub>:Co(Ti), spectra adsorption, rel. to valence state of dopant 9-14908  
Al<sub>2</sub>O<sub>3</sub> anodic film, freshly and evacuation prepared samples comparison 9-18703  
Al<sub>2</sub>O<sub>3</sub>:Cr<sup>3+</sup>, optically pumped, absorption 9-7967  
Al<sub>2</sub>O<sub>3</sub>:V<sup>4+</sup>, far i.r. 9-1768  
AlSiB derivative spectrum of indirect excitons 9-18702  
AlSiOs, kyanite, absorpt. and e microprobe obs. 9-10191  
As<sub>2</sub>S<sub>3</sub>(Se<sub>2</sub>), absorption and reflection during transition from crystalline to glassy state 9-10192  
Au, attenuated total reflection, electromodulation 9-5900  
BaF<sub>2</sub> conc. dependence of Nd<sup>3+</sup> 9-15161  
Ba:MgGe:O:Nd<sup>3+</sup>, and laser action 9-5914  
BaTiO<sub>3</sub>, reflectance, obs. of grain boundary contribution to dielec. props 9-3707  
BaTiO<sub>3</sub>-electrode interfaces, of light generated during polarization reversal 9-12346  
Bi films, transmission, rel. to quantum size effect 9-7969  
BiI<sub>3</sub> crystals, absorption 9-3884  
C, absorpt. coeffs in region 17.6 to 250 Å 9-1769  
CaIn<sub>2</sub>, i.r. lattice vib. 9-16164  
CN<sup>-</sup> in alkali halides, i.r. vibration-libration absorption band, elec. field effects 9-3857  
CO, frosts on Cu and Cat-A-Lac black paint surfaces, reflectance, 0.36 to 1.15 μ 9-10188  
Cs<sub>3</sub>(PO<sub>4</sub>)<sub>2</sub>F:Nd<sup>3+</sup>, absorpt. and luminescence at 300, 77 and 4.2°K 9-18709  
Cs<sub>2</sub>(CrO<sub>4</sub>. PO<sub>4</sub>)Cl, 80°K cryst. spectrum 9-3885  
CeF<sub>3</sub>:Gd<sup>3+</sup>, Zeeman data of Gd<sup>3+</sup> in sites of cubic symmetry 9-10196  
CeF<sub>3</sub>:Ho<sup>3+ (+)</sup>, mag. circular dichroism in absorpt. bands 9-1737  
CeF<sub>3</sub>:Eu<sup>3+</sup>, Zeeman effect and fluorescent lifetime meas.. temp. depend. 9-14050  
CeF<sub>3</sub>:(La,Ce,Gd,Tb) linear dichroism of absorption band 9-14048  
CeF<sub>3</sub>, conc. dependences of Nd<sup>3+</sup> 9-15161  
CeO:Ni<sup>2+</sup>, electronic absorption 9-10195  
CeSn(OH)<sub>6</sub>, crystal structure obs. 9-19709  
CaWO<sub>4</sub>:Th<sup>3+</sup>, ground term energy level analysis 9-12373  
CaWO<sub>4</sub>:Nd<sup>3+</sup>, Landé factor of excited state by Cotton-Mouton eff. 9-18698  
Cd,Hg<sub>1-x</sub>Te graded gap structure, transmission, rel. to photocarrier transport 9-18619  
CdAs<sub>2</sub>, tetragonal, reflectivity 9-19983  
CdF<sub>2</sub>:In or Eu, absorpt. spectra 0.2 to 15 μ 9-5672  
CdF<sub>2</sub>:Yb<sup>3+</sup> 9-1771  
CdInS<sub>2</sub>:Nd<sup>3+</sup> or Er<sup>3+</sup>, narrow line absorption and emission 9-14081  
Cd<sub>1-x</sub>Mn<sub>x</sub>S ( $x \leq 0.4$ ), absorpt. 9-1516  
CdP, tetragonal, reflectivity 9-19983  
CdS:Tm(Cu) phosphors fired in S atmosphere i.r. luminescence 9-5977  
CdS, absorption due to intrinsic defects 9-3887  
CdS, edge emission bands 9-15188  
CdS, exciton absorption, infl. of strong elec. field 9-19988  
CdS, exciton transitions, phonon-assisted 9-5966  
CdS, excitons, correlation between intrinsic absorpt. and emission 9-14049  
CdS edge emission, green and blue, at 4.2°K 9-14074  
CdS, Se<sub>1-x</sub> films, absorpt. structure defects effects 9-9973  
CdSb, optical reflectivity 300° and 77°K 9-14042  
CdSe, exciton transitions, phonon-assisted 9-5966  
CdSe, i.r. absorpt. and refl. rel. to effective mass of cond. electrons

- alkali chlorides,  $\text{Cl}^- \text{L}_{23}$  absorption spectra rel. to x-ray excitation, electronic band structure and two electron excitation 9-1815
- alkali halide crystals, i.r. absorpt. rel. to lattice props. interac. pot. calc. 9-12383
- alkali halide mixed phosphors, absorption spectra of isostructures, interpretation 9-15176
- alkali halides, B. bands due to Ag ions on anionic sites, splitting and characts. 9-5387
- alkali halides, B centres due to reg. charged Ag ions on anion sites, model and props. 9-5387
- alkali halides, far i.r. transmission obs.; lattice structure and forces calc. 9-16074
- alkali halides, two-quantum excitations 9-21618
- alkali halides, u.v. absorpt. coeff. rel. to conc. of  $\text{OH}^-$  ion 9-7374
- alkaline earth oxides, defect studies, review 9-9693
- alkaline earth phosphates, glasses, of iron 9-15173
- alkaline-earth tungsates, u.v.-induced absorpt peak wavelengths, lattice constant dependence 9-5913
- aluminoborate glass: Tl, radiation-induced absorpt., rel. to trapping mechanism 9-1777
- anatase, i.r. study of hydroxyl group 9-7963
- characteristic electron energy loss, of transition metals, second and third series 9-15040
- coal, absorpt. band at  $1600 \text{ cm}^{-1}$ , rel. to aromatic structs. or conjugated chelated carbonyls 9-7964
- corundum:Fe(Ni), absorpt. dependence on oxidation-reduction conditions during growth 9-1132
- diamond, absorpt. of neutral vacancy 9-10194
- diamond, i.r. and u.v. obs., lum., electr., obs. 9-18443
- diamond, one-phonon band- mode i.r. absorption by impurity resonances 9-5915
- diamond with chemisorbed H, F, Cl, Br and O, i.r. obs. 9-8083
- diamonds, absorption in i.r., u.v. and visible region, participation of Al impurities 9-19987
- electronic spectra, book 9-11453
- n-Ge intraband radiation of hot electrons 9-3638
- glass:  $\text{Co}^{2+}$  absorption obs., structural features determ. 9-10193
- glass:  $\text{Na}^{+}$  absorption obs., structural features determ. 9-10193
- graphite, pyrolytic, visible to i.r. range, correl. with struct. anisotropy 9-7970
- graphite, rel. to longit. and transverse dielec. constants 9-7971
- hydrates, i.r. spectra, water struct. 9-1779
- hydrogen-bonded crysts., i.r. spectra, theory 9-15170
- ice, pure, absorpt. props. for  $1\text{s} \rightarrow 2\text{p}$  transition of bound electron 9-5613
- ice II, V and IX, far i.r. 9-1778
- ice VI, i.r. 9-10201
- III-V compounds, reflectance, spin-orbit splittings, 3.5-7.5 eV 9-5899
- illite clay, i.r. absorpt.  $3800\text{-}700 \text{ cm}^{-1}$  obs. 9-12372
- l.r. absorption and temperature dependence by localized vibrational modes 9-7630
- l.r. emission from particulate surfaces of various grain types 9-7965
- l.r. materials, refl. and transmission,  $2\text{-}50 \mu$  9-12366
- l.r. resonant-mode freq. shifts on uniaxial stress 9-5922
- kaolin clay, i.r. absorpt.  $3800\text{-}700 \text{ cm}^{-1}$  obs. 9-12372
- matrix-trapped diatomic mols., effect of localized lattice vibr. 9-3883
- montmorillonite clay, i.r. absorpt.  $3800\text{-}700 \text{ cm}^{-1}$  obs. 9-12372
- phenazine single crystals, absorption rel. to carrier generation 9-7860

## Spectra continued

## inorganic solids continued

- Cd,  $\text{Se}_{\text{Cd}}$ , u.v. reflectivity, at 90°K 9-10187  
 CdTe:  $\text{I}^{2+}$ , abs., and e.s.r. 9-1772  
 CdTe, exciton transitions, phonon-assisted 9-5966  
 $\text{ClO}_4^-$  in alkali halides, i.r. absorpt. temp. dependence, 300-700°C rel. to impurity ion symmetry 9-18704  
 Co, core-electron energy levels and state density, X-ray photoelectron obs. 9-1813  
 CoO, i.r. absorption, nature of nonstoichiometry 9-19989  
 CoO, semiconducting, optical absorpt. of small polarons in near and far i.r. 9-5929  
 $\text{CoO}_{1.85}$ , i.r. absorption 9-19989  
 $\text{CoWO}_4$ , long-wave i.r. absorpt., band identification and spin wave spectrum 9-1773  
 Cr:  $\text{K}\alpha_1$  line, intensity distribution X-ray spect., energy level struct. 9-10227  
 $\text{Cr}_2\text{O}_3$ , i.r. 9-18705  
 $\text{Cs}_2\text{HfCl}_6\cdot\text{Os}^{4+}$ , at 4.2°K 9-14055  
 $\text{Cs}_2\text{ZrCl}_6\cdot\text{Os}^{4+}$ , at 4.2°K 9-14055  
 Cs films, (2300-11000 Å), absorpt. 9-15174  
 $\text{Cs}_2\text{UBr}_6$ , rel. to vibronic and electronic structure 9-7972  
 $\text{Cs}_2\text{UC}_6$ , polarized vibronic spectrum analyzed 9-7972  
 Cu/Mg electric exploded wire, temp. and e. density meas. in later stages 9-9346  
 Cu, core-electron energy levels and state density, X-ray photoelectron obs. 9-1813  
 Cu films, anomalous absorpt. rel. to ambient conditions 9-10198  
 Cu halide complexes with n-heterocyclic ligands, diffuse reflectance and far i.r. rel. to struct. 9-14043  
 CuBr-CuCl solid solns., exciton absorpt. and emission at 8 and 80°K 9-1775  
 CuCl, excitonic refl., Zeeman eff., low temp. 9-14044  
 CuCl, far i.r. 9-1774  
 CuCl, Faraday rotation, sign reversal 9-12374  
 $\text{CuCl}_2\cdot 2\text{H}_2\text{O}$ , i.r. vibrations, study 9-7973  
 $\text{CuK}_2(\text{SO}_4)_6\cdot 6\text{H}_2\text{O}$ , solid dilution effect 9-10199  
 $\text{Cu}_2\text{O}$ , i.r. absorpt. at 110°K rel. to bound states 9-12375  
 $\text{Cu}_2\text{O}$ , transitions to  $n=1$  exciton, elec. fields effects 9-12376  
 $\text{CuSO}_4\cdot 5\text{H}_2\text{O}$ , i.r. vibrations, study 9-7973  
 $\text{DyCl}_3$ , abs. in far i.r. 9-1776  
 $\text{DyCl}_3$ , absorpt. in far i.r. 9-1776  
 $\text{DyFeO}_3$ , absorpt.,  $1.2\leq T\leq 4.2^\circ\text{K}$  and  $T=77^\circ\text{K}$  9-21620  
 ErCl<sub>3</sub>, abs. in far i.r. 9-1776  
 Fe, core-electron energy levels and state density, X-ray photoelectron obs. 9-1813  
 $\text{FeBO}_3$ , calcite struct., i.r., rel. to charact. absorpt. bands of (BO<sub>3</sub>) groups 9-5272  
 $\text{FeF}_2$ , vibrational, critical dipole freq. behaviour 9-18549  
 $\text{FeF}_2$ , vibrational, critical dipole freq. behaviour 9-7636  
 GaAs:Te, i.r. reflectivity rel. to longitudinal-optical-phonon-plasmon coupling 9-21615  
 n-GaAs, absorption and reflection, influence of impurities, 297° to 4°K 9-21621  
 GaAs, edge absorption of mechanically polished surface 9-12379  
 GaAs, far i.r. absorption and photoconductivity of shallow donor 9-12377  
 GaAs, photoemissive yields rel. to energy-band model 9-5917  
 GaAs, uniaxially stressed, inter-valence band transitions 9-18706  
 GaAs laser, electron-beam pumped, emission, and threshold current density, temp. depend. 9-4483  
 Ga<sub>1-x</sub>In<sub>x</sub>As, i.r. reflection, mixed-crystal behaviour 9-1760  
 GaP:N, absorpt. rel. to theory of isoelectronic impurities 9-7801  
 GaP, Brillouin, Raman and i.r. 9-12446  
 GaP, dispersion in the nonlinear susceptibility near the reststrahl band 9-7962  
 GaP, vapour-grown, rel. to substrates 9-12148  
 GaSe absorption fine structure of monocrystals, photoelectric determ. 77°K 9-10203  
 Gd, absorption bands in ferromagnetic and paramagnetic states 9-16412  
 $\text{GdCl}_3\cdot\text{Er}^{3+}$ , Zeeman effect 9-3888  
 $\text{GdCl}_3$  magnon density obs. in optical spectrum 9-7947  
 $\text{Gd}_2\text{O}_3\cdot\text{Eu}^{3+}$ , emission, crystal field interpretation 9-10205  
 n-Ge:Sb (As), electron irradiated, absorption edge 9-10200  
 Ge:Zn<sup>+</sup>, excitation spectrum and stress behaviour 9-7974  
 (93.5-6.5at%)Ge: (7.6-92.4 at%) Si, electroreflectance spectra 9-14045  
 Ge-metal contacts, e. and phonon tunneling spectroscopy 9-13909  
 n-Ge, absorpt. by grain boundaries 9-21623  
 Ge, edge absorption, infl. of temp., 4-400°K 9-3891  
 Ge, edge absorption of mechanically polished surface 9-12379  
 Ge, electroabsorpt. rel. to diagm. exciton structure obs. 9-7951  
 Ge, far u.v., band-structure effects and many-particle scatt. corrections 9-12378  
 Ge, i.r. lattice absorption 9-3510  
 Ge, magnetoabsorpt. oscillations associated with interband transitions, and exciton states 9-5918  
 Ge, magnetoabsorption intensity rel. to exciton absorpt. rise 9-5919  
 Ge, quantum effects in cyclotron resonance using c.w. HCN laser 9-14070  
 Ge, u.v. absorpt., rel. to spin splitting calcs. 9-13893  
 Ge, uniaxially stressed, inter-valence band transitions 9-18706  
 Ge absorption edge shape, electric field eff. 9-3890  
 H<sub>2</sub>, rel. to pair interaction between ortho-molecules 9-17504  
 $\text{HNO}_3$ , vibration spectra at 77°K 9-7029  
 H<sub>2</sub>O frosts on Cu and Cat-A-lac black paint surfaces, reflectance, 0.36 to 1.15μ 9-10188  
 $\text{HANO}_2$ , i.r. reflectivity rel. to temp. dependent vibrational modes 9-5902  
 Hg (CN)<sub>2</sub>, far i.r. 9-1780  
 Hg halides, far i.r. 9-1780  
 $\text{HgCr}_2\text{S}_4$ , ferromagnetic, diffuse reflectance 9-1781  
 Hgl<sub>2</sub>, electroabsorption and electroreflectance near fundamental edge 9-12350  
 HgO, far i.r. 9-1780  
 HgS, far i.r. 9-1780  
 HoFeO<sub>3</sub>, absorpt., near i.r., T=1.2, 4.2, 20 and 77°K 9-21624  
 In<sub>3</sub>S:Nd<sup>3+</sup> or Er<sup>3+</sup>, narrow line absorption and emission 9-14081  
 p-j-InAs, electroreflectance spectra behaviour 9-9987  
 InAs, reflection, Kramers-Kronig analysis of magnetoplasma-phonon interaction 9-12363  
 InAs, reflection spectra 9-3877

## Spectra continued

## inorganic solids continued

- InSb, combined resonance, effects of electron-optical-phonon interact. 9-1742  
 n-InSb, degenerate, Burstein eff. in meas. impurity conc. 9-3645  
 p-InSb, doped, fundamental absorpt. temp. dependence 9-10202  
 InSb, edge absorption of mechanically polished surface 9-12379  
 InSb, Sb, radiation absorption, mm. and sub-mm., 2.1 and 4.2°K 9-16413  
 InSb, reflectivity, rel. to exciton effects at hyperbolic crit. pts. 9-5901  
 $\text{K}_2\text{PtCl}_6\cdot\text{Os}^{4+}$ , at 4.2°K 9-14055  
 K film, plasma resonance transmission obs. 9-12382  
 KAg(CN)<sub>2</sub> rel. to lattice vibrations, and Ag(CN)<sub>2</sub><sup>-</sup>, i.r. obs. 9-16166  
 KBr: impurity defects, far i.r. absorpt., discontinuities obs. 9-19990  
 KBr:Li<sup>+</sup>, far i.r. resonance line shift induced by electric field 9-1784  
 KBr:Li<sup>+</sup>, far i.r. resonant-mode freq. shifts on uniaxial stress 9-5922  
 KBr:NO<sub>2</sub><sup>-</sup>, absorption and luminescence at 4.2°K, vibrational structure 9-16432  
 KBr-K1:Ti type phosphors, absorption spectra of isostructures, interpretation 9-15176  
 KBr-RbBr(NaBr,KCl) solid solutions, evap. films, intrinsic absorption 9-10204  
 KBr, i.r. eigenfrequency pressure dependence, 1-35 kbar 9-5897  
 KBr, with NO<sub>2</sub><sup>-</sup>, NO<sub>3</sub><sup>-</sup> impurities, following exposure to u.v. light 9-5581  
 KBr film, emission in far i.r. 9-15175  
 KBr with H<sup>-</sup> ions, far-infrared abs. 9-10184  
 KCl:Ag, forbidden transitions 9-12381  
 KCl:Eu<sup>2+</sup>, multiphonon structure in absorpt. and emission, lattice freq. shift effects 9-16410  
 KCl:Mn, u.v. band shifts on thermal and optical bleaching rel. to those in highly pure KCl 9-14053  
 KCl:Mn absorption bands, u.v. due to X-irradiation 9-3893  
 KCl:Mn<sup>2+</sup>, absorption, in range 0.1 to 15 mol% of dopant conc. 9-5923  
 KCl:NO<sub>2</sub><sup>-</sup>, absorption and luminescence at 4.2°K, vibrational structure 9-16432  
 KCl, absorption, colour centres representation 9-5920  
 KCl, extinction coeff. of colloidal Ag rel. to annealing 9-5924  
 KCl, i.r. eigenfrequency pressure dependence, 1.35 kbar 9-5897  
 KCl, paraelectric resonance spectroscopy, theory and expt. 9-13916  
 KCl small crystals and films, i.r. absorpt. size- and shape-dependence 9-21626  
 $\text{KClO}_4$ , absorption of Cl<sub>2</sub><sup>-</sup> molecular ion, X-irradiated crystal 9-21625  
 $\text{K}_2\text{CrO}_4$ , abs. eff. of uniaxial compression, 20°K 9-10206  
 $\text{KH}_2\text{PO}_4$ , i.r., meas. 9-5896  
 KI:Ag<sup>+</sup>, far i.r. resonant-mode freq. shifts on uniaxial stress 9-5922  
 KI:NO<sub>2</sub><sup>-</sup>, absorption and luminescence at 4.2°K, vibrational structure 9-16432  
 KI, fundamental absorption band, elec. field effects 9-1783  
 KI, vibrational, of U<sub>1</sub>-centres 9-5388  
 KI with NO<sub>2</sub><sup>-</sup>, NO<sub>3</sub><sup>-</sup> impurities, following exposure to u.v. light 9-5581  
 KI cry. with H<sup>-</sup> ions, far-infrared abs. 9-10184  
 $\text{KMgF}_2$ :K:NiF<sub>3</sub> mixed crystals, i.r. reflection and transmission in lattice vib. determ. 9-13789  
 $\text{KMn}_{1-x}\text{Ni}_x\text{F}_3$  single cryst., electron-magnon transitions in abs. spectra 9-1785  
 $\text{K}_2\text{NiF}_4$ , absorption, comparative study with  $\text{KNiF}_3$  9-7976  
 K<sub>2</sub>Cd, absorption 9-5925  
 KCl:Mn<sup>2+</sup>, charge transfer spectra 9-3892  
 LaF<sub>3</sub>:Nd<sup>3+</sup>, deform. and dipole dipole broadening of Nd<sup>3+</sup> lines 9-1786  
 LaSb films, absorpt. thickness dependence 9-3897  
 LiF:Mg, photoemission 9-3758  
 LiF, absorpt., thermal treatment effects rel. to effects on thermoluminescence 9-5969  
 LiF, emission due to lattice vibrations 9-7977  
 LiF, R<sub>2</sub> zero-phonon line, 4.2°K, moment analysis of Stark effect 9-14054  
 Lu<sub>2</sub>O<sub>3</sub>:Eu<sup>3+</sup>, emission field interpretation 9-10205  
 MgAl<sub>2</sub>O<sub>4</sub>:Cr<sup>3+</sup>, absorption and fluorescence 9-18708  
 MgF<sub>2</sub>:Co<sup>2+</sup>, far i.r. spectrum of Co<sup>2+</sup> ion pairs 9-1788  
 MgF<sub>2</sub>, vibrational, critical dipole freq. behaviour 9-18549  
 MgF<sub>2</sub>, vibrational, critical dipole freq. behaviour 9-7636  
 MgF<sub>2</sub>, n-irradiation-induced vacuum u.v. absorpt. 9-1787  
 Mg:Ge, electroreflectance meas., 1.5-4.5 eV 9-12364  
 MgO:Cr<sup>3+</sup>, line shift temp. dependence interpretation 9-12470  
 MgO:Fe<sup>2+</sup>, absorption bands, pressure shift, and dynamic Jahn-Teller effect 9-5927  
 MgO, polarization, of trigonal colour centres, exam. under uniaxial stresses 9-5389  
 Mg<sub>2</sub>Si, electroreflectance meas., 1.5-4.5 eV 9-12364  
 Mg<sub>2</sub>Sn, electroreflectance meas., 1.5-4.5 eV 9-12364  
 Mn ferrites, i.r. spectra analysis for equilibrium position in cation distribution 9-3876  
 Mn<sub>1-x</sub>Co<sub>x</sub>F<sub>2</sub> mixed crystals, electron-magnon transitions from absorption spectrum 9-15158  
 MnF<sub>2</sub>, vibrational, critical dipole freq. behaviour 9-18549  
 MnF<sub>2</sub>, vibrational, critical dipole freq. behaviour 9-7636  
 MnF<sub>2</sub>, mag. dipole absorpt. 9-1789  
 Mn<sub>1-x</sub>Ni<sub>x</sub>F<sub>2</sub> mixed crystals, electron-magnon transitions from absorption spectrum 9-15158  
 MnO crystal film, absorpt., 280-1000nm at 300 and 77°K 9-1797  
 MoS<sub>3</sub>, hexagonal and rhombohedral crystals, optical absorption props. 9-1798  
 (NH<sub>4</sub>)<sub>2</sub>CrO<sub>4</sub>, abs. eff. of uniaxial compression, 20°K 9-10206  
 $\text{NH}_4\text{H}_2\text{PO}_4$ , i.r., meas. 9-5896  
 NO<sub>2</sub><sup>-</sup> in potassium halides, absorption and luminescence at 4.2°K, vibrational structure 9-16432  
 Na, absorption, electron-electron interactions eff. 9-21628  
 Na, interband absorptions, influence of pseudopotential Fourier coeff. V<sub>300</sub> 9-1793  
 NaCl:Ag, Ag<sup>+</sup>-V<sub>e</sub> complexes (V<sub>e</sub>=anion vacancy) 9-5928  
 NaCl:Mn<sup>2+</sup>, absorption, in range 0.1 to 15 mol% of dopant conc. 9-5923  
 NaCl:OH<sup>-</sup>, i.r. absorpt., 0.6-4.2°K 9-16415  
 NaCl, monovalent-impurity-induced far-i.r. absorpt 9-21627  
 NaCl film, emission in far i.r. 9-15175  
 NaCl films, 25-50 eV region, substrate and exposure to air effects 9-7978  
 NaCl films, far i.r. absorpt., virtual mode analysis 9-1791  
 NaF:H<sup>-</sup> thin film, surface polarization for frequency shift of localized modes 9-19852  
 NaF, R<sub>2</sub> zero-phonon absorpt. line, moment anal. of uniaxial stress effects 9-7504  
 NaI:Cl<sup>-</sup>, Stark-effect, second order, reson. mode freq. shift 9-7637  
 NaNO<sub>3</sub>, i.r., and lattice vibrations 9-21614



**Spectra continued****inorganic solids continued**

NaNO<sub>3</sub>, i.r. absorpt. at  $\lambda$  transition 9-1369  
 Nb V hydrated oxide u.v. absorption bands obs. 9-21616  
 Nd(IV) weak-field fluoride complexes, electronic spectra 9-16416  
 Ni, core-electron energy levels and state density, X-ray photoelectron obs. 9-1813  
 NiO, semiconducting, optical absorpt. of small polars in near and far i.r. 9-5929  
 Os<sup>4+</sup> in single cubic crystals, at 4.2°K 9-14055  
 Pbl and Pdl, far i.r. 9-1794  
 Pa V hydrated oxide u.v. absorption bands obs. 9-21616  
 Pbl<sub>2</sub>, electroabsorption and electroreflectance near fundamental edge 9-12350  
 PbO-SiO<sub>2</sub>-K<sub>2</sub>O glasses, u.v.-induced luminescence at 120°K 9-10267  
 Pb(OH)Cl formation, i.r. absorption spectra and thermogravimetric anal. 9-21632  
 PbTe, magneto reflection spectra of coupled plasmon-phonon modes 9-18699  
 phosphate glass: Fe<sup>3+</sup> activated, absorpt. bands 9-10264  
 Pt, core-electron energy levels and state density, X-ray photoelectron obs. 9-1813  
 Rb:ZrCl<sub>6</sub>:O<sup>4+</sup>, at 4.2°K 9-14055  
 Rb thin films, absorption 9-12384  
 RbBr:Mn<sup>2+</sup>, charge transfer spectra 9-3892  
 RbBr:Ti(Pb), absorption, new band 9-10207  
 RbBr film, emission in far i.r. 9-15175  
 RbCl film, emission in far i.r. 9-15175  
 RbI:Ti(Pb), absorption, new band 9-10207  
 Rb:MnF<sub>4</sub>, transitions rel. to antiferromag. structure 9-10208  
 Sb<sub>2</sub>Se<sub>3</sub>, reflectivity, polarization eff. 9-18700  
 Sb<sub>2</sub>S<sub>3</sub>, reflectivity, polarization eff. 9-18700  
 Sbl<sub>3</sub>, absorpt., 95-293°K and reflection, room temp. rel. to direct and indirect transitions 9-3895  
 Sb<sub>2</sub>Se<sub>3</sub>-I mixed crystals, absorption edge position 9-12385  
 Se:SeO<sub>2</sub>, i.r. spectrophotometric study 9-5898  
 Se<sub>1-x</sub>Te<sub>x</sub>, i.r. active lattice bands 9-12365  
 n-Si:P, i.r. absorption, dopant effect on carrier mechanisms 9-18710  
 p-Si, e. irradi., oscils. in absorpt. spectrum rel. to A-centres 9-18659  
 Si, electron irradiated, i.r. spectral study of Li defect complex 9-13673  
 Si, far u.v., band-structure effects and many-particle scatt. corrections 9-12378  
 Si, i.r. lattice absorption 9-3510  
 Si, n-irrad., i.r. absorpt. rel. to radiation-induced defects 9-15177  
 Si, one-phonon band-mode i.r. absorption by impurity resonances 9-5915  
 Si, thermorefectance, 3-6 eV region 9-10189  
 $\alpha$ -SiC 9-12387  
 $\beta$ -SiC, absorption and luminescence rel. to excitation states 9-3900  
 SiO<sub>2</sub>, fused, i.r. absorpt. rel. to calculated SiO<sub>2</sub> mol. vibrations 9-14694  
 SiO<sub>2</sub>, pyrolytic films, i.r. absorpt., ht. treatment dependence 9-3195  
 SrCl<sub>2</sub>:Sm<sup>2+</sup>, optically pumped 9-10210  
 SrF<sub>2</sub>:Sm<sup>2+</sup>, optically pumped 9-10210  
 SrF<sub>2</sub>:Sm<sup>2+</sup>(Eu<sup>2+</sup>), vibronic transitions and Zeeman effect 9-10212  
 SrF<sub>2</sub>, conc. dependence of Nd<sup>3+</sup> 9-15161  
 SrF<sub>2</sub>, u.v. reflectivity, from (111)-planes 9-1761  
 SrS:Zr phosphors, Zr activated decay and thermoluminescence 9-3936  
 SrTiO<sub>3</sub>:Cr<sup>3+</sup>, Cr R lines spectral shift, 4 kV/cm electric field, 4.2°K 9-3709  
 SrTiO<sub>3</sub>:Mo(Fe or Ni), reversible photochromic changes, model verification 9-19980  
 SrTiO and OD absorpt. bands 9-10211  
 Tb(OH)<sub>3</sub>, Tb<sup>3+</sup> crystal field parameters determ. from absorpt. and fluorescence meas. 9-14019  
 Te:Sb, i.r. absorpt. 9-5930  
 Te, reflectivity, in fundamental absorpt. region, 10-300°K 9-21630  
 Ti complex, hexaaxial Ti(III) iodide, Jahn-Teller effect 9-14057  
 TiO<sub>2</sub>, vibrational, critical dipole freq. behaviour 9-18549  
 TiO<sub>2</sub>, vibrational, critical diode freq. behaviour 9-7636  
 TiO<sub>2</sub>, doped, rel. to electronic props. 9-9706  
 Ti halides, far i.r. transmission obs.; lattice structure and forces calc. 9-16074  
 TiCl<sub>3</sub>, absorption and reflection in far i.r. 9-3879  
 TiCr alum., Paschen-Back effect of R lines 9-3896  
 TlSe, reflection, interpretation using electron energy spectra and chemical binding model 9-5903  
 UO<sub>2</sub> nitrates, i.r., vibrations of UO<sub>2</sub> ions and NO<sub>3</sub> groups 9-7979  
 V<sub>2</sub>O<sub>4</sub>, absorption edge, temp. depend. 9-18620  
 V<sub>2</sub>P<sub>3</sub>, reflection, for band structure determ. 9-19984  
 VO<sub>2</sub>, absorpt. below semiconductor-metal transition point 9-18712  
 VO<sub>2</sub>, reflection, for band structure determ. 9-19984  
 VO<sub>2</sub>, reflectivity and transmission spectra, for both sides of semicond.-metal transition temp. 9-12329  
 WO<sub>3</sub>, vibration 9-18550  
 XeO<sub>2</sub>F<sub>2</sub> 9-791  
 YOH<sub>3</sub>:Tb, Tb<sup>3+</sup> crystal field parameters determ. from fluorescence and absorpt. meas. 9-14019  
 Y<sub>2</sub>O<sub>3</sub>:Eu<sup>3+</sup>, emission, crystal field interpretation 9-10205  
 ZnAl<sub>2</sub>O<sub>4</sub>:Cr<sup>3+</sup>, absorption and fluorescence 9-18708  
 ZnAs<sub>2</sub>, tetragonal, reflectivity 9-19983  
 ZnF<sub>2</sub>, vibrational, critical dipole freq. behaviour 9-18549  
 ZnF<sub>2</sub>, vibrational, critical dipole freq. behaviour<sup>a</sup> 9-7636  
 ZnIn<sub>2</sub>S<sub>4</sub>:Nd<sup>3+</sup> or Er<sup>3+</sup>, narrow line absorption and emission 9-14081  
 ZnP<sub>2</sub>, tetragonal and monoclinic, reflectivity 9-19983  
 ZnS:Co(Ni), bond nature effects in stacking faults 9-1796  
 ZnS:Cu, electroluminesc., freq. depend 9-10259  
 ZnS:Cu single crystal, induced i.r. absorption obs., 1-3  $\mu$  9-10213  
 ZnS, two photon absorption near band gap 9-12388  
 ZnSb, optical reflectivity, 300° and 77°K 9-14042  
 ZnSe, anomalous electro-reflectance signals near fundamental edge 9-16409  
 ZnSe, reflectivity data rel. to freq., electronic band structure computation 9-18701  
 ZnSn(OH)<sub>6</sub>, crystal structure obs. 9-19709  
 ZnSnP<sub>2</sub>, chalcopyrites and sphalerites, absorpt., photoluminescence and reflection, rel. to band structure 9-5931  
 ZnSnP<sub>2</sub>, i.r. reflection and opt. constants of chalcopyrite and sphalerite structures 9-5904  
 ZnWO<sub>4</sub>, absorpt. and i.r. emission, of Cr<sup>3+</sup> ions, theory 9-14058

**inorganic solids, radiofrequency**

See also Nuclear magnetic resonance and relaxation; Paramagnetic resonance and relaxation

fluorotribromosilane, microwave, 30-40 GHz 9-10230  
 Al<sub>2</sub>SiO<sub>5</sub>:Fe<sup>3+</sup> maser props. 9-14069

**molecules**

absorption, rel. to lifetime of excited state 9-2841  
 absorption and emission in i.r. region, simultaneous obs. 9-4898  
 absorption band absolute intensity obs. in gas, condensed phases 9-9172  
 absorption microwave and i.r. analysis of atomic and molecular species in hypervelocity wake 9-19577  
 allowed molecular multiplets set up from prescribed atomic states, general method 9-14679  
 characteristic vibrations, defn. 9-18166  
 collision line broadening, influence of proper vol. 9-2839  
 copper acetate monohydrate, anomalous optical behaviour, symmetry interpretation 9-7043  
 diatomic, matrix trapped, effect of localized lattice vibr. 9-3883  
 9,10-dichloroanthracene dimer, fluorescence, temp. depend. 9-13322  
 dimeric syst., weakly coupled, fluorescence, temp. depend. 9-13322  
 dimers, vibronic energy calc. of absorpt. spectra 9-736  
 dissolved in nematic liq. cryst., n.m.r. obs. 9-19609  
 Doppler spectrum saturation 9-958  
 electric-field-induced, excited-state dipole moment from line shape 9-732  
 emission type anal. rel. to identification of groups in org. cpds 9-9370  
 emission-absorption intensity ratio temp. meas., thermal non-equil. conditions, theor. investig. 9-20906  
 Hont-London factors for  $^3\Phi \rightarrow ^3\Delta$  systems 9-18164  
 after interaction with e.m. radiation, rel. to plasma spectroscopy, book 9-15936  
 intermolecular interactions, effect on spectra 9-2840  
 i.r. absorption in gas mixture, humidity determ. 9-4915  
 i.r. intensity calc., dipole length and dipole velocity 9-4894  
 i.r. lines, press. induced shifts, j-depend., elastic cross-section expansion 9-17012  
 level degeneracy rel. to self-induced transparency effect 9-261  
 liquid, Rayleigh line, rel. to mol. vib. 9-2888  
 Lorentzian bands, convolution and deconvolution, math. theory 9-20907  
 microwave intensity law 9-11433  
 NMR, involving single and double quantum transitions, spin ticking 9-9192  
 overlap integral of two harmonic-oscill. wave functions applic. 9-15840  
 overlapping line broadening 9-17010  
 photoelectron molecular spectroscopy with high resolution 9-17898  
 polarizability of excited mols. from solvent shift 9-14683  
 polyatomic, electron-vibronal, degeneracy eff. on intensity distribution 9-9173  
 polyatomic, i.r., use in structural group and with Boolean algebra and computers 9-6998  
 polyatomic many-electron systems, determ. of allowed multiplets 9-13338  
 Stark modulation absorption system 9-6435  
 stimulated Rayleigh-wing scattering theory 9-4893  
 triplet state of donor and acceptor, demonstration of resonance transfers of type T<sub>g</sub> → T<sub>a</sub>\* 9-17011  
 triplet-triple absorpt. studies, optimization of expt. criteria 9-11434  
 vibration, intermolecular interactions eff., mechanics, electrooptical eff. discussed 9-9177  
 Zeeman eff. in rot. microwave region,  $\lambda=1-10$  cm 9-11435  
 CF<sub>3</sub> containing groups, NMR, spin syst. study, use of composite part. basis functions 9-20908  
 CO<sub>2</sub> laser Lamb dip and rotational computation study, stabilization and gas absorption coeff. meas. appln. 9-13009  
 H-bonded subst., interpretation of spectra 9-9170  
 H<sub>2</sub>O, group theory classification of states 9-14679  
 He metastable ( $^3\Sigma_u^+$ ), decay 9-15832  
 Mg; mols. and quasimols. absorpt., 2852 Å 9-18328

**organic molecules and substances**  
 See also Molecules

4-Fluoro-3-chloro aniline, u.v. absorpt. obs. in solid and gaseous states 9-814  
 4,5-methylenephenanthrene react. with alkali metal, investig. of carbanions MH<sup>-</sup> and H<sub>2</sub>MH 9-19468  
 o-, m- and p-nitroaniline, chelation and complex formation 9-17060  
 o-, m- and p-TERPHENYL, FAR U.V. 9-818  
 3,4,5-trichloro-2,6-difluoropyridine fluorine spectrum, N.M.R. band-shape, coupling const. 9-9239  
 acetylene, differential scatt. cross-section for 25-60 eV impact 9-9142  
 acetylene, emission, two new band systems of CH<sup>+</sup> 9-18208  
 acetylenes, 584 Å photoelectron spectra, obs. 9-4945  
 amino-pyridines, vapour-phase u.v. absorpt. 9-14699  
 amino-pyrimidines, vapour-phase u.v. absorpt. 9-14699  
 anisole and monohalogen deriv., vibrational spectra, torsional barriers calc. 9-14700  
 anthracene, effect on absorption spectra of crystallization and vitrification of solvent 9-2893  
 anthracene, p-irradiated, of paramagnetic centres 9-3963  
 anthracene complexes with tetra halo p-benzoquinone, cryst. 9-1799  
 anthracene in solns. rel. to singlet excited states polarizability, obs. 9-15879  
 anthracene mol. cry., electr. abs. spectra, exciton config. construct. from orbitals 9-21617  
 aromatic, heteroaromatic mols., perturbations between electronic states 9-2894  
 aromatic, polarizability of excited mols. from solvent shift 9-14683  
 aromatic hydrocarbons, extinction coeffs. of triplet-triplet transitions 9-1800  
 aza-acetylenes, 584 Å photoelectron spectra, obs. 9-4945  
 $\beta$  fluoronaphthalene-naphthalene solid soln., rel. to block structure 9-1334  
 $\alpha$ -benzalazo-(anisol- $\alpha'$ -naphthylamine), weak traces rel. to natural or liq. cryst. state 9-7980  
 benzaldehyde, 3715 Å  $\pi \rightarrow \pi^*$ -system, allowed and forbidden 9-9245  
 1,2-benzanthracene, excited singlet absorpt., laser photolysis and spectroscopy 9-20952  
 benzene, doubled thermo-spectrum of 8050 Å stimulated Raman line 9-14703  
 benzene, electronic, SCF MO and CI calc. 9-9246  
 benzene, to test validity of Kramers-Kronig eqns. 9-3104

## Spectra continued

## organic molecules and substances continued

- benzene luminescence in cyclohexane, mol. symmetry determ., 77°K 9-4948
- benzene vapour,  $B_{1u} \leftarrow A_{1g}$  transition, fluorescence obs. 9-19450
- benzenes, monosubstituted, CNDO calc. 9-7052
- benzenes, substituted with electron-donating groups, triplet-triplet absorpt. 9-9248
- benzenes containing OH and NH<sub>2</sub> groups, substituted, singlet-triplet transitions 9-9244
- benzoic acid, absorption, in polarized light 9-10214
- benzophenone, absorpt. spectrum, second triplet state obs. 9-15881
- benzophenone, triplet-singlet absorpt. at 4.2°K 9-10251
- benzophenones, protonated, NMR, isomer obs. and config. 9-20953
- 2,1,3-benzothiadiazole, rot. band contours in 3280 Å electronic system 9-15884
- benzoyl chloride, Raman and i.r. spectra in liq., solid and gaseous states 9-11481
- benzyl acetate, u.v. absorpt. spectra in gaseous liq. and solid states 9-18198
- 4-bromo-testosterone acetate, singlet-triplet states 9-11487
- o-bromoaniline, vapour, absorpt., 3025-2827 Å 9-4946
- m-bromoaniline, vapour, absorpt., 3033-2783 Å 9-4946
- bromostyrene, o-, p-, m-, near u.v. and i.r. 9-819
- butane, electron impact 9-9265
- D-camphor, during phase transition 9-3148
- carbanions MH<sup>-</sup> and H<sub>2</sub>MH<sup>-</sup> of 4,5-methylenephenanthrene, investig. 9-19468
- carbazole, vapour,  $\pi \rightarrow \pi^*$  transition assignments 9-13384
- carbon tetrafluoride photoelec. spectrum, band assignments from orbital obs. 9-19462
- carbonyl cpds., conjugate, E.S.R. calc. of  $\pi$ -e spin densities, Pariser-Parr-Pople methods 9-9255
- carbonyl cpds., conjugated, electr. struct., Pariser-Parr-Pople methods 9-9254
- chloranil radical anion 9-5173
- 1-chloro-9,10-anthraquinone vapour absorption, 90-150°C 9-18202
- p-chlorophenol u.v. emission and absorption obs. 9-2898
- chlorophyll b, two phase system, absorption and fluorescence 9-16418
- 4-chloropyridine vapour, u.v. absorpt. spectra 9-9257
- chromophore identification and conc. determ. by absorption 9-18713
- conjugated systems, molecular orbital theory, book 9-13370
- 2-cyanoethylsilanes, NMR, analyses and parameter predictions 9-20960
- cyclobutane, -d<sub>4</sub>, vibration mean square amplitude, 300°K 9-9259
- cyclohexane, cold-neutron scatt. study of mol. motions in liq. and solid phase 9-14707
- cyclopentadiene and deuterio-derivs., vibration 9-2904
- cyclopentane, cold-neutron scatt. study of mol. motions in liq. and solid phase 9-14707
- cyclopropane-D<sub>6</sub>, i.r. vib.-rotn. bands anal. 9-18217
- di(benzo[a]anthracene) photodimer, electronic spectrum 9-13381
- diaryl carbonium ions, u.v. and PMR 9-14709
- 1,1-diarylprenes, methyl substituted, electr. spectra, config. assignments 9-11486
- diazomethyl, trapped radical, vibrational absorption 9-20970
- dibenzofuran, vapour,  $\pi \rightarrow \pi^*$  transition assignments 9-13384
- 2,4-dichlorotoluene, near u.v. absorption, -10° to 80°C 9-20955
- m-difluorobenzene, u.v. emission obs., 2500-300 Å 9-7066
- 4,4'-diiodobenzophenone, absorpt. spectrum 9-15881
- $\beta$ -diketones, absorpt. under strong optical excitation 9-17051
- 3,4-dimethoxyacetophenone and substituted acetophenones (II; n=1-3), u.v. absorption spectrum 9-14714
- dimethylaniline, u.v., C band assignment 9-15892
- dimethyl ether, valence force field calc. using vib. freq. of (CH<sub>3</sub>)<sub>2</sub>O, (CD<sub>3</sub>)<sub>2</sub>O and CH<sub>3</sub>OC(D<sub>3</sub>) mols. 9-20968
- 2,6-dimethyl naphthalene, temp. effect on first electronic transition 9-15178
- 2,6-dimethyl-1,4-phenylpyridine, absorpt., rel. to bonding and rotation 9-9273
- 4-dimethylamino-4'-nitrodiphenyl + propyl alcohol in frozen decaline soln., fluorescence obs. 9-7071
- 4-dimethylamino-4'-nitrodiphenyl + acetone in frozen decaline soln., fluorescence obs. 9-7071
- m-dinitrobenzene soln. in tetrahydrofuran, e.s.r. photoinduced spectra 9-11497
- o-dinitrobenzene soln. in tetrahydrofuran, e.s.r. photoinduced spectra 9-11497
- p-dinitrobenzene soln. in tetrahydrofuran, e.s.r. photoinduced spectra 9-11497
- o-, m-, p-dinitrobenzene soln. in tetrahydrofuran, e.s.r. photoinduced spectra 9-9276
- dioxycoumarins, (6,7 and 7,8) u.v. in alcohol solns., absorpt. bands 9-7062
- 9,10-diphenylanthracene, singlet-triplet abs. spectra, obs. lowest triplet state 9-11484
- diphenylene oxide, frozen paraffin solns., conc., effect on absorption spectra 9-2913
- diphenylene oxide in paraffins, absorpt. and conds. for Shpolskii effect 9-1802
- diphenylene oxide soln. fluorescence, conc. depend. 9-9279
- divinylbenzene soln. absorpt. bands 9-801
- dye soln. stimulated fluorescence detection method, 720-900 nm 9-9241
- dyes, elec. field effect on optical absorpt. of mols. 9-7041
- dyes, solvent depend. of position and intensity of absorpt. bands 9-7075
- eosin-blue in solvents, fluorescence and absorption, dimer formation, dipole moment determ. 9-13535
- EPR, tetramethyl-2, 2, 6, 6-piperidinol-4-oxyl-1, in polyisoprene and polybutadiene 9-9296
- erbium tricyclopentadiene, absorpt. at liq. He temp. 9-3898
- E.S.R., carbonyl cpds., conjugate calc. of  $\pi$ -e spin densities 9-9255
- ethane, electron impact 9-9265
- ethanes, 1,1-di-substituted, vibratory, calc. and interpret. 9-15889
- ethane and ethene-d<sub>4</sub>, far u.v. 9-813
- ethylene, Rydberg states obs. in Kr matrix 9-14710
- ethylene epifluoride, rotational spectrum, Cs symmetry mol. prediction 9-19464
- ferricytochrome C single cryst. in polarized light, 3700-7500 Å 9-11489
- ferrimyoglobin complexes, single-cryst. polarized absorpt. 9-3899
- ferrimyoglobin complexes, single-cryst. in polarized light, 3700-7500 Å 9-11489

## Spectra continued

## organic molecules and substances continued

- ferrocenes, substituted, electronic absorpt., and photodecomposition 9-20964
- fluorene, vapour,  $\pi \rightarrow \pi^*$  transition assignments 9-13384
- fluorene and derivs., u.v. absorpt. in soln., rel. to electronic structure 9-3106
- fluorene and derivs., u.v. absorpt. in soln., rel. to electronic structure 9-3107
- fluorene iodo-derivs., absorpt. rel. to electronic structure 9-3108
- fluorenone and derivs., u.v. absorpt. in soln., rel. to electronic structure 9-3106
- fluorenone and derivs., u.v. absorpt. in soln. rel. to electronic structure 9-3107
- fluorenone iodo-derivs., absorpt. rel. to electronic structure 9-3108
- fluorescein, emission and absorpt. rel. to species, 80 and 300°K 9-1034
- fluoroacetic acid, microwave, rot. const. and centrifugal distortion parameters 9-13371
- p-fluoroaniline, i.r. absorption and near u.v. emission spectra, correl. and comp. of ground state vib. freq. 9-14711
- $\beta$ -fluoronaphthalene vapour, absorpt. and emission obs. 9-4954
- formic acid, Zeeman effect and Stark Zeeman effect 9-2909
- hexahelicene, low-temp. absorpt. 9-15165
- hydrocarbons, nanosecond absorption spectroscopy using laser beam photolysis 9-19170
- 8-hydroxy-1-(p-nitrobenzyl) pyridinium hydroxide anhydro salt, absorption spectra, intensity and solvent eff. 9-11492
- 8-hydroxy-1-methylquinolinium hydroxide anhydro salt, absorption spectra, intensity and solvent eff. 9-11492
- interaction potential with solvent, polarization change during optical excitation 9-9249
- intersystem crossing rate constant from lowest excited singlet to lowest triplet state, exptl. determ. 9-19452
- mercaptals in n-hexane and propan-2-ol soln., absorptions study 9-14715
- methane, 3.39  $\mu$  line, press. shift and broadening, laser-saturated mol. absorpt. study 9-11496
- Methane, electron impact 9-9265
- methane, emission, two new band systems of CH<sup>+</sup> 9-18208
- 3,4-methoxyacetophenone, u.v. absorption spectrum 9-14714
- methyl chloride, parallel component of 2<sub>u</sub> band near 6015 cm<sup>-1</sup> 9-20971
- methyl fluoride, 2<sub>u</sub> band around 6000 cm<sup>-1</sup> 9-2911
- methyl iodide, rotational Zeeman effect 9-2910
- methyl red dye, electrochromic effect (Stark Effect) 9-16419
- methyl thiocyanate, torsional fine struct. in rot. spectrum 9-4958
- 2-methyl triethylenediamine (II), u.v., vib. struct. of electr. transition 9-11476
- 2-methyl-9,10-anthraquinone 9-19991
- mono-olefins, absorption features explanation by  $\pi \rightarrow \pi^*$  transition 9-9274
- 1-naphthaldehyde, free and -ICI complex, C=O stretching freq. solvent depend. 9-15894
- naphthalene, emission, phonon structure 9-18714
- naphthalene, flash spectroscopy with triggered laser excitation 9-2885
- naphthalene, triplet state, ENDOR meas. 9-7073
- naphthalene in benzophenone crystal, triplet-triplet absorption 9-9275
- naphthalene in solns. rel. to singlet excited states polarizability, obs. 9-15879
- 1-naphthol, excited, H-bonded, absorpt., fluoresc. and phosphoresc. 9-9519
- n-O-nitroaniline in O-xylol, proton-donor effects, obs. 9-11698
- nitrobenzene, soln. in tetrahydrofuran, e.s.r. photoinduced spectra 9-11497
- nitrobenzene soln. in tetrahydrofuran, e.s.r. photoinduced spectra 9-9276
- nitrobenzene-aniline complex, absorption bands and interaction mechanism 9-17061
- nitrobenzene-phenol complex, absorption bands and interaction mechanism 9-17061
- NMR of symmetrical three-spin syst., relaxation eff. 9-9191
- NMR, tetraiodomethane, <sup>13</sup>C chemical shift 9-9282
- NMR, trifluoroacetic acid, chemical shift anisotropic 9-9286
- orbital calc. method MOLKAO, applic. 9-20946
- Osmium complexes with phenyl and pyridine ligands 9-7981
- oxalyl bromide, vapor phase absorption meas., 3200-4400 cm<sup>-1</sup> 9-18212
- para-bromobenzonitrile vapour, u.v. absorption, i.r. obs., fundamentals assigned 9-7054
- para-dichlorobenzene, singlet-triplet transition obs., spin-orbit coupling study 9-19451
- pentaerythritol derivs., vibr. spectra 4000-400 cm<sup>-1</sup> 9-17053
- pentafluorobenzene, microwave region, rot. const. and bond distances obtained 9-2907
- perfluorocyclobutane vibration mean square amplitude, coriolis const., 300°K 9-9259
- perfluorocyclobutane, NMR, spin syst. study, use of composite part. basis functions 9-20908
- pharmaceutical products, absorption spectra 9-5910
- phenanthrene in benzophenone crystal, triplet-triplet absorption 9-9275
- phenol, rotational band contour of O-O band at 2750 Å, computer fit 9-18213
- phenol blue dye, electrochromic effect (Stark effect) 9-16419
- phenoxy-nitroxide biradical, ESR spectrum studies 9-13397
- photoelectron spectra, ionization potential determ. 9-21109
- phthalocyanine, metal-free, polymorph characterization 9-19736
- picolines, combination scattering, freq. shift and line widening 9-18216
- polyacene solid solns., energy transfer, bibliography for 1967 9-7986
- polymer solns., dilute, Huggins const. from relax. spectrum 9-15993
- polymers, vac. -u.v. absorpt., exciton theory 9-10216
- polymethylmethacrylate, absorpt. in excited state 9-10217
- polystyrene in benzene, proton-donor effects obs. 9-11698
- porphyrins, intercombination transitions quantum output meas. using heavy atom effect, obs. 9-15877
- propane, electron impact 9-9265
- purines, 2-, 6- and 8-substituted, electronic struct., SCF MO CI calcs. 9-9280
- pyridine oriented in nematic phase, N.M.R. meas., inter-p distance ratios obs. 9-9277
- pyridines, monosubstituted, CNDO calc. 9-7052
- containing quadrupolar nuclei, N.M.R. band-shape, coupling const. 9-9239
- quinclidine 9-2918
- quinclidine (II), u.v., vib. struct. of electr. transition 9-11476
- salicylic acids, substituted, rel. to intramol. H-bonding in lowest excited singlet states 9-19474



**Spectra continued****organic molecules and substances continued**

- shifts due to solvent solute relax., time-resolved nanosec. emission spectroscopy studies 9-13534  
 solvent shifts of electronic spectra of polar conjugated systems 9-5174  
 stilbene, absorption and fluorescence 9-4961  
 absorption spectra for lowest triplet state 9-19476  
 terephthalic acid, aldehyde and acid chloride, absorpt. bands 9-801  
 tetramethyl-2, 2, 6, 6-piperidinol-4-oxyl-1, in polyisoprene and polybutadiene EPR 9-9296  
 s-tetrazine, 5515 Å band, high resolution study 9-13390  
 thiophene derivatives, vibration deformation frequencies, effect of solvents 9-821  
 thiourea, mol. dynamics by inelastic n scatt. 9-4962  
 o-, m-, p- tolaldehydes in liquid phase, vibrational spectra, assignments of freq. 9-11501  
 torsion-vibr. rot. interaction in rot. spectra 9-7004  
 triacetylbenzene soln., absorpt. bands 9-801  
 3,4,5-trichloro 2,6- difluoropyridine F spectrum, bandshape and coupling const. 9-9239  
 trichloroethylene, u.v. absorption spectrum, nature of transitions 9-20956  
 triethylenediamine 9-2918  
 triethylenediamine (I), u.v., vib. struct. of electr. transition 9-11476  
 trifluoroacetic acid, <sup>19</sup>F NMR, chemical shift-anisotropy 9-9286  
 trimethylamine -H<sub>2</sub>, D<sub>2</sub>, Coriolis coupling coeff. for degenerate vib. assignments and amp., valence force field calc. 9-20980  
 trinitrobenzene soln. in tetrahydrofuran, e.s.r. photoinduced spectra 9-9276  
 trinitrobenzene soln. in tetrahydrofuran, e.s.r. photoinduced spectra 9-11497  
 triphenylene, electronic, 'mol. in mol.' method appl. 9-18214  
 tryptaflavine, radical in soln. absorption band detection, 380 nm 9-9285  
 uranin, emission and absorpt. rel. to species, 80 and 300°K 9-1034  
 uranyl-EDTA complex, emission obs. 9-14723  
 valence freq. var. in vap.-liq. transition of diat. groups 9-7040  
 vinyl esters, vibrational, freq. and intensities determ. 9-9287  
 viscose, and stable derivatives, ultraviolet 9-14852  
 CF<sub>3</sub>OF, i.r. and vib. obs., freq. assignments, thermodynamic props. calc. 9-19465  
 CF<sub>3</sub>COOH HCOOH microwave abs. in the region of rot. transition J=8-7, K struct., dipole moment meas. 9-4941  
 CH<sub>3</sub> scanning microwave echo box spectrometer, 10 cm 9-2284  
<sup>12</sup>CH<sub>4</sub>, Franck-Condon factor and r-centroids for C→X band system 9-7058  
 GeF<sub>4</sub>, carbon tetrafluoride photoelec. spectrum band assignments from orbital obs. 9-19462  
 OH, scanning microwave echo box spectrometer, 4.7, 6.0 GHz 9-2284  
 SiF<sub>4</sub>, carbon tetrafluoride photoelec. spectrum, band assignments from orbital obs. 9-19462  
 Ti<sub>2</sub>(OR)<sub>4</sub>, R-ethyl and normal propyl, polynuclear metal complex vib. obs. 9-11455

**spectra****organic molecules and substances, infrared**

- o-, m-, p- anisaldehyde in liquid state, benzene ring vib. freq. determ. 9-7047  
 3,4-benzopyrene, anthracene vibrs. rel. to mol. struct. obs. 9-15883  
 p- and m- chlorophenols, assoc. effects in soln. 9-1024  
 o- and m- chlorotoluenes absorption, 700-4500 cm<sup>-1</sup> spectrophotometric obs. 9-7059  
 2,4-, 2,5-, 2,6- dichlorotoluenes, absorption spectra, assignments of fundamental vib. 9-11485  
 2,5- dihydrothiophene 9-820  
 1,2- diiodotetrafluoroethane, rel. to rot. isomers, obs. 9-15887  
 o-, m-, p- tolaldehydes in liquid phase, absorption spectra, assignments of vib. freq. 9-11501  
 2,6-dichlorotoluene 9-17049  
 acetaldehyde-2,2,2-d<sub>3</sub> 9-2889  
 acetanilide and deuterio derivatives, absorpt., 50-300 cm<sup>-1</sup> 9-18195  
 acrolein and deuterio-derivs., vibratory spectra 9-11491  
 alcohol, chlorosubstituted; monomeric mols. in CCl<sub>4</sub>, i.r. absorption fine structure obs. 9-9242  
 alkanes, chlorinated, C-H valence freq. 9-7044  
 alkanethiols, torsional band obs. in far i.r. 9-11488  
 alkylamines, torsional band obs. in far i.r. 9-11488  
 amine-halogen charge-transfer complexes 9-2892  
 anilines, substituted, molec. assoc. in soln. 9-934  
 aromatic hydrocarbon bases, H-bonded complexes 9-4942  
 benz-1,2,3- thiadiazoles, monosubstituted, absorpt. 9-18200  
 benzene, cryst., vib. splittings due to intermolec. forces 9-5932  
 benzene, energy transfer in excited electronic states 9-15880  
 benzene, rot. const. from near i.r. vibr. band 9-7050  
 benzene in Ar matrix, multiplet structure analysis 9-18199  
 benzene substitute, vib. freq. assignment 9-7051  
 benzene sulphonylchloride, optical density of absorpt. bands, effect of substitutions 9-7053  
 benzenesulphonamide and benzene-d<sub>3</sub> analogue, 4000-400 cm<sup>-1</sup> 9-14704  
 benzenesulphonamide and benzene-d<sub>3</sub> analogue, 4000-400 cm<sup>-1</sup> 9-14704  
 benzenesulphonyl chloride and benzene-d<sub>3</sub> analogue, 4000-400 cm<sup>-1</sup> 9-14704  
 biphenyl, absorption, temp. depend. 9-18215  
 2-bromo propionitrile, vib. spectra and freq. assignments, semiquantitative polariz. data obs. 9-20975  
 bromocyclobutane, ring-puckering vib. and potential functions determ. 9-20957  
 bromonitromethane and d<sub>2</sub> analogue, vibr. assignments, obs. 9-15893  
 β-bromostyrene 9-18201  
 n-butane, electrooptical parameters for C-H, C-C bonds polar props. calc. 9-4960  
 carbazole 9-9252  
 carbohydrates, review 9-2897  
 carbon tetrafluoride, liq. and cryst. 9-1023  
 cellulose films, regenerated, drying and temp. effects rel. to 25°C phase transition 9-11509  
 chlorinated tetrahedral mols., matrix-isolated 9-2900  
 2-chloro propionitrile, vib. spectra and freq. assignments, semiquantitative polariz. data obs. 9-20975  
 chloroanthraquinone, derivatives in solid phase 650-4000 cm<sup>-1</sup> 9-7060  
 chlorocyclobutane, ring-puckering vib. and potential functions determ. 9-20957  
 chloroform, effect of molec. interactions on vibr. freqs. 9-808

**spectra continued****organic molecules and substances, infrared continued**

- chloronitromethane and d<sub>2</sub> analogue, vibr. assignments, obs. 9-15893  
 cresyl phosphates, P=O band splitting, 20-140°C, 400-3600 cm<sup>-1</sup> 9-18364  
 cupric halide: dialkylamine complexes 9-13379  
 cyclobutanol, ring-puckering vib. and potential functions determ. 9-20957  
 cyclohexane, solid phases 9-1801  
 cyclohexanes, monohalosubstituted, vibratory, interpretation 9-9262  
 cyclopentane, pseudorotation 9-9260  
 cyclopentane in Ar matrix, multiplet structure analysis 9-18199  
 cyclopropylcarbonyl chloride 9-794  
 diacetyl and deuterio-derivs., vibratory spectra 9-11491  
 diaryl glycol acid amides, basic, absorpt., obs. 9-18197  
 dibromocarbene in solid Ar 9-810  
 dibromomethane, d<sub>2</sub>, d<sub>1</sub> and d<sub>2</sub> 9-15886  
 dideuteroacetylene, 4.1 μ bands analysis, obs. 9-13372  
 diethyl ether and deuterated analogues 9-14708  
 trans-1,4-diiodocyclohexane, vibrational spectra and rotational isomerism 9-17482  
 diketene, ring-puckering vib. and potential functions determ. 9-20957  
 N, N- dimethylacetamide, 3100-250 cm<sup>-1</sup> obs. 9-4957  
 N, N- dimethylformamide, 3100-250 cm<sup>-1</sup> obs. 9-4957  
 2,3- dimethylnaphthalene single crystals, absorption 9-5933  
 1,3- dioxolac 9-809  
 diphenyl, single cry., polarized abs. spectra, comparison with soln. spectra 9-19992  
 diphenyl sulphone and benzene-d<sub>3</sub> analogue, 4000-400 cm<sup>-1</sup> 9-14704  
 ethyl isocyanide, vibr. and rot., 4000-200 cm<sup>-1</sup> 9-18205  
 ethyl pyridines, m liquid phase, obs. and explained in terms of ground state vibrations 9-1026  
 ethylene oxide (d<sub>4</sub>), vibratory, interpretation and force constants calc. 9-9268  
 ethylenes interac. with OH-containing cpds., bond obs. 9-18751  
 fluorene, vibr. anal. 9-14712  
 1- fluoro- 2-haloethanes, rot. isomers 9-812  
 p- fluoroaniline, i.r. absorption and near u.v. emission spectra, correl. and comp. of ground state vib. freq. 9-14711  
 p- fluorostyrene, 250-4000 cm<sup>-1</sup>, liq. phase, spectrophotometer obs. 9-4955  
 glyoxal and deuterio-derivs., vibratory spectra 9-11491  
 haloethanes, monosubstituted, vibratory spectra interpretation 9-9269  
 n-hexane, electrooptical parameters for C-H, C-C bonds polar props. calc. 9-4960  
 hydrocarbons, correl. in rocking vib., applic. to macromol. syst. 9-20965  
 hydrogen-bonded crystals, theory 9-15170  
 intensity calc., dipole length and dipole velocity 9-4894  
 isobutene, d<sub>2</sub>s; moments of inertia calc., isotopic bands assignment 9-7055  
 liquids, absorption band width temp. depend. 9-9517  
 lithium methanesulphonate 9-18218  
 methane, 3.39 μ line perturbed by inert gases 9-15891  
 methane, 9050 cm<sup>-1</sup> absorpt. band 9-9271  
 methyl bromide, vibration-rotation spectrum, interpretation near 6000 cm<sup>-1</sup> 9-18211  
 methyl iodide (d<sub>3</sub>), solvent eff. on abs. intensities 9-18209  
 methylamine, solid and matrix isolated 9-10215  
 3- methylcholanthrene, absorpt. rel. to quasi-line luminesc., 77°K 9-16434  
 methylene bromide, polarized cryst. 9-17480  
 methylethoxymethanes, vibratory spectra 9-11495  
 molecules, finite chain, band freqs. rel. to length and end groups 9-15875  
 monochloroacetylene HCC<sup>35</sup>Cl and HCC<sup>37</sup>Cl, ν, band struct. 9-17045  
 N-methylacetamide, absorpt., 50-300 cm<sup>-1</sup> 9-18195  
 naphthalene, cryst., vib. splittings due to intermolec. forces 9-5932  
 naphthalene, energy transfer in excited electronic states 9-15880  
 nonpolar liquids, for i.r. absorpt. 9-7268  
 pentafluorobenzyl and pentafluorobenzylidene halides, vib. modes and freq. 9-20974  
 pentafluorotoluene, vib. spectra, assignments 9-11498  
 n-pentane, electrooptical parameters for C-H, C-C bonds polar props. calc. 9-4960  
 perfluorotoluene, analysis and vib. modes assignment 9-20973  
 phenanthrene, energy transfer in excited electronic states 9-15880  
 phenol-quinone system, intermol. interaction 9-2912  
 polar liqs., far i.r. absorpt. 9-1016  
 poly [3,3-bis (chloromethyl) oxacyclobutane], and structure 9-17071  
 polyets, aliphatic i.r. 9-9301  
 praseodymium ethyl sulphate, crystal field lines in far i.r. 9-5862  
 propane, electrooptical parameters for C-H, C-C bonds polar props. calc. 9-4960  
 β-propiolactone, ring-puckering vib. and potential functions determ. 9-20957  
 propionitrile, vib. spectra and freq. assignments, semiquantitative polariz. data obs. 9-20975  
 pyrazine, cryst., far i.r. 9-1363  
 pyridine and water in CCl<sub>4</sub>, equilib. const. temp. depend. 9-20976  
 p quaterphenyl, single cry., polarized abs., spectra, comparison with soln. spectra 9-19992  
 sodium methanesulphonate 9-18218  
 sulphonyl chlorides, aromatic, substituted, SO<sub>2</sub> antisymmetric stretching vib. band, obs. 9-15876  
 tartrates, temp. dependence in thin crystal textures, -195 to 51°C 9-1803  
 thiophene, effect of substituted derivatives on ν(CH) deformation vibrations 9-7057  
 tolaldehydes, isomeric, liq. phase, 400-4600 cm<sup>-1</sup> 9-9520  
 toluene, energy transfer in excited electronic states 9-15880  
 tribromomethyl radical in solid Ar 9-810  
 tricarboxylatostannates (II), assignment of skeletal vibrations 9-14722  
 triethylphosphine selenide, fundamental vibrations assignment 9-18204  
 triethylphosphine sulfide, fundamental vibrations assignment 9-18204  
 trifluoromethylfluorophosphorane 9-2916  
 trimethylene oxide, abs. and Raman scattering 9-17483  
 trimethylethoxysilane, vibratory spectra 9-11495  
 urea, rel. to cryst. lattice vibrations 9-17351  
 CH<sub>4</sub> transmission functions 9-17031  
 N<sub>2</sub>O, adsorbed on NaCl, NaBr, NaI films 9-19443  
 phenols, two-substituted, NO<sub>2</sub> group vibrs. rel. to H bond form., obs. 9-15896

**Spectra****organic molecules and substances, radiofrequency**

- See also Nuclear magnetic resonance and relaxation; Paramagnetic resonance and relaxation*
- 1-chloro-1,1-difluoroethane 9-13377  
 cyclobutanone 9-805  
 cyclohexene 9-9261  
 cyclopropyl bromide 9-2905  
 1,1-difluoro-2-chloroethylene 9-2906  
 dimethylazirine 9-9263  
 ethyl isocyanide 9-13383  
 ethylene sulphide 9-20961  
 ethylenimine, for  $^{14}\text{N}$  quadrupole coupling constant determ. 9-20962  
 methanesulfonylchloride, microwave, also quadrupole coupling constants, dipole moment 9-11700  
 methylenecyclobutane 9-11493  
 methyltribromosilane, microwave, 30-40 GHz 9-10230  
 nitrosomethane 9-817  
 n.m.r. of four-spin systems, analysis of complex spectra 9-20918  
 polar liqs., u.r.f. absorpt. 9-1016  
 propane, reanal. 9-2915  
 $\text{CF}_3\text{CCl}_2$ , 15-40 GHz 9-15888  
 $\text{CF}_3\text{COOH}$ -HCOOH, K splitting obs. linewidth determ. 9-19463

**Spectral line breadth**

- See also Doppler effect; Stark effect; Zeeman effect*
- atomic, inhomogeneous broadening, upper laser threshold disappearance 9-13295  
 atoms in dense plasma, optical thickness var. with profile 9-9121  
 binary mixtures, long range correlation effects 9-3105  
 broadening calc. of Raman scatt. and quadrupole absorption 9-18163  
 collision broadening, influence of proper mol. vol. 9-2839  
 collision broadening, role of interatomic repulsion 9-13305  
 crystals, impurity spectra, phonon-free lines, and local oscillations 9-7961  
 cyclohexane-aniline binary mixture, long range correlation effects 9-3105  
 $\delta$  Ceti star, H and He equivalent widths and atm. density 9-2009  
 detector response time distortion effects 9-4655  
 2,6-dimethyl naphthalene, temp. effect on first electronic transition 9-15178  
 divergence and distortion, double crystal spectrometer, X-ray spectra 9-1756  
 Doppler broadening integrals and error function relatives, Voigt functions computation 9-15415  
 dynamic distortion of inhomogeneously broadened e.p.r. line 9-1855  
 effective, of spectral photographic line recorded profile 9-16508  
 electric-field-induced spectra, excited-state dipole moment determ. 9-732  
 emission, form meas. using visibility curves 9-4537  
 e.p.r., inhomogeneously broadened, discrete saturation 9-8561  
 e.p.r., inhomogeneously broadened, discrete saturation 9-17839  
 e.p.r. line broadening, n.m.r. saturation eff. 9-1853  
 e.p.r. of radicals in solid-phase, applicability of inhomogeneous line-broadening theory 9-829  
 e.s.r., line shapes, Gaussian and Lorentzian, comparison 9-4407  
 excitation of elementary emitters in a nonuniform line 9-13285  
 excitation of elementary emitters in a nonuniform line 9-17839  
 homogeneous, meas. using nonlinear travelling wave interaction technique 9-2824  
 hydrogenic line broadening, rel. to strong collisions 9-15804  
 Kubo-Anderson model generalization, a stochastic theory 9-7931  
 laser, determ. with pulse duration, from transient Raman scatt. 9-13527  
 laser, gas, natural width, and freq. fluctuations 9-14428  
 laser diode, spontaneous emission, temp. dependence 9-246  
 line formation, integral eqns. for source functions 9-19390  
 line-shape for A-doubling transitions 9-9104  
 Lorentzian mag. resonance transitions, unsaturated, effect of modulation broadening on shape 9-4404  
 methane, laser saturation of absorpt. for 3.39  $\mu$  line press. shift and broadening 9-11496  
 methane, press. broadening and shift of 3.39  $\mu$  line perturbed by inert gases 9-15891  
 methyl fluoride,  $2\nu_4$  band around 6000 $\text{cm}^{-1}$  9-2911  
 microwave quadrupole moments determ. 9-9195  
 molecular line shapes, theory 9-9168  
 natural, determ. by method of total absorpt. 9-2810  
 NMR fine-structure lines, diagonal sum methods used to calculate characteristic features 9-20477  
 organic cpds., C-Cl and C-Br vibr. bands, gas and soln. 9-14697  
 overlapping line broadening 9-17010  
 Permalloy films, ferromag. reson. linewidth thickness depend. 9-8005  
 photoelectron molecular spectroscopy with high resolution 9-17898  
 picolines, combination scattering spectrum, widening and freq. shift 9-18216  
 plasma, and intensities, changes on disturbance of e. energy maxwellian distrib. 9-9368  
 plasma, atomic line broadening calc., Green's function theory 9-19523  
 plasma, electron impact broadening of spectral lines, improvements 9-21055  
 plasma, line broadening theory, ion microfield distrib. 9-18292  
 quadrupole absorption, broadening calc. 9-18163  
 red satellite bands in at. spectra, prediction using quasi-static theory of press. broadening 9-2811  
 reflection echelon, line-shape parameters determ., graphic technique 9-4517  
 solid, resonance lines inhomogeneous broadening, review 9-18689  
 Stark effect due to laser irradiation, doublet shape obs. 9-6955  
 Stark emission line broadening, effect of time fluctuations of microscopic elec. field 9-19383  
 stochastic theory, Kubo-Anderson model generalization 9-7931  
 symmetrical self-reversed contour calc. with radial dependence of plasma parameters 9-2809  
 X-ray emission, meas. three-v.s. two-crystal spectrometer 9-1820  
 Ar I, II, broadening of spectral lines in spark plasma 9-5093  
 $\text{AsO}_4^{3-}$ , 202.5  $\mu\text{m}$  obs., soln. strength depend., u.v. absorption 9-3103  
 $^{10}\text{B}$ ,  $\pi \rightarrow$  mesic atom, 2p-1s transition natural line width meas. 9-9050  
 $^{11}\text{B}$ ,  $\pi \rightarrow$  mesic atom, 2p-1s transition natural line width meas. 9-9050  
 $^{10}\text{Be}$ ,  $\pi \rightarrow$  mesic atom, 2p-1s transition natural line width meas. 9-9050  
 $^{11}\text{C}$ ,  $\pi \rightarrow$  mesic atom, 2p-1s transition natural line width meas. 9-9050  
 CO, high-resolution coeffs. of self-broadened lines 9-13346  
 CO, self-broadening coeffs. using CO<sub>2</sub> laser radiation 9-4921  
 CO<sub>2</sub>, abs. band at 6970  $\text{cm}^{-1}$  9-758

**Spectral line breadth continued**

- CO<sub>2</sub>, self and N<sub>2</sub> broadenings of rot. lines of 15 and 4.3  $\mu$  bands, width meas. 9-19494  
 CO<sub>2</sub>, depolarized Rayleigh line, mol. reorientation cross-section calc. 9-13345  
 CO<sub>2</sub> laser, and small-signal step response 9-13005  
 Cl, neutral atom, Stark broadening 9-6966  
 Cs 8943 Å line, temp. and press. eff. of Ar, Ne; line broadening meas. 9-19400  
 Cs second doublet, broadening by inert gases 9-2814  
 (Cu+Zn)K<sub>2</sub>(SO<sub>4</sub>)<sub>6</sub>H<sub>2</sub>O crystals, magnetically dilute, e.p.r. line width, theory and expt. 9-15201  
 $^{57}\text{Fe}$  Mossbauer narrow-line sources, prep., and investigation of causes of line broadening 9-5891  
 H, widening by plasma electrons 9-2010  
 H<sub>2</sub>O, atmospheric,  $\lambda/\nu = 12.67 \text{ cm}^{-1}$  line obs. 9-771  
 H Balmer lines in strong mag. field in plasma, Stark-broadening obs. 9-17110  
 H<sub>2</sub>, depolarized Rayleigh line, mol. reorientation cross-section calc. 9-13345  
 H<sub>2</sub> Raman collisional narrowing and broadening of Se(0) and Se(1) lines 9-2864  
 He Ne laser, collision broadening, effect on mag. resonance 9-10861  
 He  $2^3\text{P}-4^3\text{D}$  and  $2^3\text{P}-4^3\text{D}$  lines, observations of plasma satellites 9-725  
 He I,  $2^3\text{P}-4^3\text{P}$ ,  $3^3\text{D}$ ,  $3^3\text{F}$  transitions, electron and ion Stark broadening 9-20899  
 He I line broadening in plasma by electron impact, theory 9-21073  
 HeII, Doppler broadening in low pressure arc 9-2830  
 Hg, profile alteration by high power laser pulse 9-11394  
 LaF<sub>3</sub>:Nd<sup>3+</sup>, deform. and dipole dipole broadening of Nd<sup>3+</sup> lines 9-1786  
 Li, self-broadening of 2S-2P reson. line emitted by exploding wire 9-16996  
 $^6\text{Li}$ ,  $\pi \rightarrow$  mesic atom, 2p-1s transition natural line width meas. 9-9050  
 $^7\text{Li}$ ,  $\pi \rightarrow$  mesic atom, 2p-1s transition natural line width meas. 9-9050  
 Mg-Mn polycrystalline ferrite spinel, ferriimag. reson. line broadening mechanism and temp. dependence 9-1852  
 MgI radiation, Stark and van der Waals level broadening constants 9-13293  
 N<sub>2</sub>, depolarized Rayleigh line, mol. reorientation cross-section calc. 9-13345  
 N<sub>2</sub>O, rotational line J=5 $\rightarrow$ 6, broadening by foreign gases 9-13365  
 Na atom atmosphere spectral line formation and radiative transfer 9-19391  
 NaCl, Ni zero-phonon line, strain broadening 9-1792  
 Ni-Zn polycrystalline ferrite spinel, ferriimag. reson. line broadening mechanism and temp. dependence 9-1852  
 O<sub>2</sub> elevated temperature, 1750 to 2020 Å 9-14692  
 O atom atmosphere, spectral line formation and radiative transfer 9-19391  
 O<sub>2</sub>, Stark broadening in Schumann-Runge system, relax treatment 9-11471  
 OH linewidths in (0,0) (A $\rightarrow$ X) u.v. transition, collision broadening obs., low temp. 9-19484  
 Scl radiation, Stark and van der Waals level broadening constants 9-13293

**Spectrochemical analysis**

- See also Chemical analysis/by mass spectrometry; Spectroscopy*
- afatoxins B<sub>1</sub> and G<sub>1</sub>, fluorescence and phosphorescence for presence determ. 9-6201  
 arc source, continuous a.c. 9-18777  
 atomic absorption spectroscopy, spectral line interferences 9-15233  
 atomic absorption system based on high-temp. graphite tube furnace, operating conds. 9-14142  
 atomic partition functions in Boltzmann and Saha eqns., significance 9-17545  
 atomic spectroscopy, internal standardization, theoretical principles 9-16507  
 cements, composition and hydration 9-14123  
 diffuse reflectance spectroscopy, reflectometers, colorimeters and reflectance attachments 9-18773  
 flame emission and atomic absorption spectrometry, review 9-18774  
 flame emission spectroscopy, advances 9-6032  
 flame fluorescence spectrometry, atomic resonance intensity and analytical curves 9-21737  
 fluorescence methods, book 9-6997  
 gas mixtures, i.r. pseudo matrix isolation technique 9-18775  
 geological samples in d.c. arc, borate fusion method 9-21734  
 hollow cathode, evap. and excitation zones separation 9-16509  
 hydrocarbons, polycyclic, by quasi-line fluoresc. obs. 9-18780  
 with interferometer, Fabry-Perot, spectrograph combination 9-18776  
 laser induced Raman spectra of crystalline Lysozyme, pepsin and  $\alpha$ -Chymotrypsin 9-5940  
 laser microprobe 9-21731  
 microwave and i.r. analysis of atomic and molecular species in hypervelocity wake 9-19577  
 neoprene, Si inclusions, laser microprobe obs. 9-12552  
 organic cpd. purity by n.m.r. 9-21733  
 plasma jet method for metal impurities in inorganic liquids 9-6028  
 plasma torch, r.f. induction coupled, atomic spectrometry appls. evaluation 9-21735  
 pyromellite micro additives, obs. 9-18781  
 rare earth complexes, conc. and stability const. determ. method 9-21738  
 solutions, isosbestic points, no. of components determ. 9-20068  
 solutions, pneumatic nebulizer for dry aerosol prod. 9-21736  
 spectral photographic line recorded profile, effective line breadth 9-16508  
 spectrophotometer, automatic scanning, for Na, K, Ca, Mg in clinical samples 9-16512  
 spectrophotometer flow cell holder 9-4024  
 spectrophotometer, difference, for isolated absorpt. band meas. 9-16510  
 steel, mild, by X-ray fluorescence 9-6034  
 steel, of Mo using vacuum spectrometer 9-20069  
 steel, stainless, cleaning in vacuum, emitted gas exam. 9-20070  
 steel foils X25T, H41XT, X25Yu5 and Cr-Ni, N meas., obs. 9-18778  
 X-ray, error minimization in sample prep. theory 9-4025  
 X-ray, inter-element effects, computer prediction 9-4026  
 X-ray fluorescence, sample area effects on intensity meas. 9-8132  
 Ag, trace determ. in aqueous and non-aqueous media 9-6029  
 Au III spectrophotometric determ. with o-phenylenediamine 9-12551  
 BBrs, liquid, using plasma jet 9-6028



**Spectrochemical analysis continued**

- BaF<sub>2</sub>, optical, metal impurities extraction and meas. 9-16513  
 Bi<sup>3+</sup> in HCl, HBr, chem. analysis by luminesc., 77°K 9-16511  
 Bi<sup>3+</sup> in HCl, HBr by luminesc., 77°K 9-16511  
 Br<sub>2</sub>, dissociation rates in shock waves 9-19480  
 Br<sub>2</sub>, dissociation rates in shock waves 9-13394  
 C-C groups in org. cpds. by molec. spectral anal. in plasma discharge 9-9370  
 C surface groups, I.R. spectrometry and pyrolytic volatile anal. 9-7325  
 CO<sub>2</sub>, i.r. gas analyser calibration 9-4027  
 Co in rock, spectrophotometry 9-16525  
 Fe, of Mo using vacuum spectrometer 9-20069  
 Gd<sub>2</sub>O<sub>3</sub> for rare earths by X-ray excited fluoresc. 9-16514  
 NO<sub>2</sub>-Acetylene flame for atomic absorption spectroscopy impurities 9-6030  
 N<sub>2</sub>O-acetylene flame appl. in atomic absorpt. spectrometry 9-10366  
 N<sub>2</sub>O<sub>4</sub>, iron content determ. by atomic absorption spectroscopy 9-4028  
 Ni in rock, spectrophotometry 9-16525  
 Pb, Cu, Bi in boiling mixture separation by chromatography followed by spectrophotometric determ. 9-18779  
 Pb<sup>2+</sup> in HCl, HBr, chem. analysis by luminesc., 77°K 9-16511  
 Pb<sup>2+</sup> in HCl, HBr by luminesc., 77°K 9-16511  
 Sb<sup>3+</sup> in HCl, HBr, chem. analysis by luminesc., 77°K 9-16511  
 Sb<sup>3+</sup> in HCl, HBr by luminesc., 77°K 9-16511  
 Se<sup>4+</sup> in HCl, HBr, chem. analysis by luminesc., 77°K 9-16511  
 Se<sup>4+</sup> in HCl, HBr by luminesc., 77°K 9-16511  
 SrF<sub>2</sub>, optical, metal impurities extraction and meas. 9-16513  
 Te\* in HCl, HBr, chem. analysis luminesc., 77°K 9-16511  
 Ti<sup>4+</sup> in HCl, HBr by luminesc., 77°K 9-16511  
 UO<sub>2</sub> matrix, determ. of impurities by d.c. arc method 9-21085  
 UO<sub>2</sub>, sintered, stainless steel inclusion, laser microprobe obs. 9-12552  
 UO<sub>2</sub>, W microdiffusion, laser microprobe obs. 9-12552  
 Y<sub>2</sub>O<sub>3</sub> for rare earths by X-ray excited fluoresc. 9-16514

**Spectrometers**

- See also Mass spectrometers; Monochromators; Particle spectrometers; Spectrophotometers; X-ray spectrometers*  
 atomic absorption and flame emission methods 9-2424  
 c.w. acoustic mag. reson., freq. locking device 9-19115  
 Czerny-Turner and Ebert grating, multiply dispersed stray light and elimination 9-10933  
 electronic scanning, rapidly changing spectra 9-4538  
 Fabry-Perot, rapid scanning characts. 9-10935  
 Fabry-Perot interferometer, electrostrictively scanning 9-15552  
 Fabry-Perot interferometer, thermal scanning 9-2425  
 Fourier, measurements in 0.4-2.5  $\mu$  region 9-15555  
 grazing-incidence spectrography, absolute intensity calibration, 10-120 Å 9-8668  
 high resolution in i.r., precise calibration 9-17897  
 interference, selective amplitude modulation 9-13070  
 i.r. rapid scan, modifications 9-10934  
 laser homodyne, for particle size meas. 9-17224  
 laser-Raman spectrograph, S<sub>0</sub> fundamental modes determ. 9-20941  
 low-cost construction, instructional applications, optical properties of semiconductor 9-8339  
 Mossbauer, meas. of small isomer shifts 9-19222  
 multislit, sequential encoding 9-10884  
 NMR, high resolution, adaption for heteronuc. double and multiple reson. expts. 9-8669  
 n.m.r., using superconducting magnet, description, performance 9-12962  
 photoelectron molecular spectroscopy with high resolution 9-17898  
 prism, computerized calibration of wavelength drive 9-2428  
 radiant flux analysis, patent 9-13072  
 Raman effect applications, using laser beam, patent 9-17899  
 rapid scan, transient plasma diagnostics 9-11583  
 rapid scanning, for Raman spectra, techniques and advances 9-10938  
 rapid scanning, performance in emission and absorption 9-10936  
 rapid scanning, wide range for emission and absorption meas. 9-10939  
 reflectometer, integrating sphere with laser source, for meas. up to 2500°K 9-20560  
 spectrograph, vacuum grating, 900-2500 Å wavelength region, ultraviolet source, study of plasma jet in rarefied atmosphere 9-5030  
 NaI, scintillation, in Linac thick target bremsstrahlung spectra meas. 9-16926

**accessories**

- comparator, combinational scatt. spectra with standard lines 9-8671  
 digital stabilizer 9-20561  
 fluorimeter, refl. for Techtron AA3 spectrophotometer 9-2429  
 frequency locking device for c.w. acoustic mag. reson. spectrometers 9-19115  
 furnace-cell multipass, high temperature 9-283  
 grating mount for dual axis motion, plane, patent 9-17900  
 for i.r. gas phase intensities, digital data processing system 9-8670  
 low temp. cell, long path 9-6232  
 quadrupole lens syst., opt. diagrams in prism spect. 9-2566  
 receiver for Raman spectroscopy 9-282  
 rectangular prism, total reflection, for smoothly rotating light source image 9-16793  
 reflectance, transmittance, meas., single beam device 9-10942  
 sample exchange device, automatic, for UR10 i.r. spectrophotometer 9-15553  
 spectrochronograph, rotating disc with slits for scanning spectrum 9-13073  
 wavelength drive, computerized calibration 9-2428  
 wavelength modulation device for monochromators 9-15557  
 wavelength modulation device for monochromators 9-6561  
 Be brass photocathode for He lines meas. on HL<sub>A</sub> background 9-15560  
 LiF photocathode for He lines meas. on HL<sub>A</sub> background 9-15560

**Spectrometers, radiofrequency**

- See also Nuclear magnetic resonance and relaxation/measurement; Paramagnetic resonance and relaxation/measurement*  
 for antiferromagnetic resonance in 2 mm range 9-10780  
 cryostat, liquid cell with thermistor amplifier feedback control 9-6438  
 for double resonance phenomena 9-6434  
 echo box, scanning, gaseous chemical 9-2284  
 e.p.r., basic design, freq. control systems and electronic circuitry, book 9-15489  
 e.p.r., modification to tone-burst modulation scheme rel. to precise relax. time meas. 9-14409  
 e.p.r., sensitivity using parametric and maser, preamplifiers 9-10781  
 e.p.v., sensitivity using parametric and maser preamplifiers 9-10782

**Spectrometers, radiofrequency continued**

- ESR pulsed and <sup>3</sup>He cryostat, relax. times 1  $\mu$  sec. meas. 0.24-4.2°K 9-4190  
 field-locked n.m.r., appl. to r.f. mag. field meas. 9-218  
 high pressure spectrometer for meas. to 10<sup>4</sup> kg/cm<sup>2</sup> 9-10783  
 ligand-ENDOR spectrometer 9-2290  
 magnetic double focusing, for ang. correl. meas. 9-6841  
 n.m.d.r., mag. field fluctuations and resonance condition stabilization 9-17842  
 NMR, high resolution 9-16757  
 NMR, twin-T bridge, automatically stabilized 9-15488  
 nuclear acoustic resonance detector, c.w. transmission 9-2288  
 phase-lock klystron stabilization 9-787  
 Q band ESR, versatile instrument with improved sensitivity and resolution 9-6433  
 super-regenerative, for n.q.r. distortion 9-6440  
 ultrasonic vel. change meas., freq. modulation c.w. technique 9-2289

**Spectrophotometers**

- adapter for obtaining frustrated total internal reflection spectra 9-13074  
 astronomical, single-photon counting 9-12775  
 for attenuation coeff. of optical glass meas. 9-2422  
 cell construction with spacing < 10  $\mu$  9-10941  
 for clinical samples Na, K, Mg, Ca meas., automatic scanning spectrophotometer 9-16512  
 double beam attachment to allow meas. of diffuse scatt. spectra 9-10904  
 double-beam absorpt., for far u.v. 9-2426  
 flow cell holder, improved 9-4024  
 glovebox system for radioactive material spectrophotometry 9-6562  
 infrared, UR10, device for automatic exchange of samples 9-15553  
 laser Raman, redesign and construction 9-19168  
 low temp. attachment for liq. spectra meas. down to -96°C 9-10943  
 micro, rapid recording, 2500-8000 Å 9-2427  
 phosphorescope, life time measurements of delayed luminescences of molecular crystals 9-5961  
 rapid scan flash, flying spot light source, mag. storage 9-10937  
 spectrophospho-fluorimeter, sensitive, construction details 9-15554  
 survey of i.r. instruments available in USA 9-280  
 Techtron AA3, fluorimeter attachment 9-2429  
 BaSO<sub>4</sub> coating on integrating spheres, luminous reflectance 9-5875

**Spectrophotometry**

- See also Colorimetry*  
 o, m-, p- anisaldehyde mol. in liquid state, vib. i.r. absorption spectra obs. 9-7047  
 astronomical faint sources by photon counting and d.c. current meas. 9-12772  
 chlorophyll-a and I<sub>2</sub> in methanol soln., reversible photochemical oxidation study 9-18974  
 o- and m- chlorotoluenes i.r. absorption spectra, 700-4500 cm<sup>-1</sup> obs. 9-7059  
 colour changes with temp., cell for obs. 9-20559  
 difference, for quantitative meas. of isolated absorpt. band 9-16510  
 filters, transmittance meas. 9-6556  
 flame, quantitative addition of metals to low pressure flame by exploding wire 9-17896  
 p-fluorostyrene, i.r. spectra, 250-4000 cm<sup>-1</sup>, liq. phase 9-4955  
 gas absorber spectrophotometric cell apparatus 9-281  
 gas cell, long path, for Perkin-Elmer model 225 spectrophotometer 9-4540  
 radioactive material, glovebox system 9-6562  
 serving laboratory equipment 9-2423  
 sun, photosphere, heavier elements with ground state configurations s<sup>2</sup>, s<sup>2</sup>p, s<sup>2</sup>p<sup>2</sup> abundance 9-12768  
 $\sigma$  Boo F-star F-star, atmosphere metal deficiency determ. 9-20176  
 Zodiacal light, theor. Fraunhofer line profile, presence 9-12761  
 Au III spectrochem. determ. with o-phenylenediamine 9-12551  
 Se:SeO<sub>2</sub>, i.r. study 9-5898

**Spectroscopy**

- See also Spectra; Spectrometers; Spectrophotometry*  
 absorption, applic. of Kubelka-Munk theory 9-16797  
 absorption, atomic, and flame emission 9-279  
 absorption for meas O conc. in upper atmosphere 9-4064  
 astronomical, multiplex method 9-4539  
 astronomical, optical methods, resolution and system acceptance 9-15370  
 atomic, h.f.s. and level crossing 9-6957  
 atomic absorption, spectral line interferences 9-15233  
 Auger emission, using The dispenser cathode C evaporation 9-7867  
 beam foil, atomic oscillator strengths, systematic trends in isoelectronic sequences 9-19388  
 beam foil, mean life meas. of electronic levels 9-19405  
 beam foil, review and bibliography 9-19169  
 cell, low temp., for u.v. and visible region absorpt. spectroscopy 9-15558  
 coherent detection, description and astronomical appl. 9-15370  
 difference- $\nu$ -spectrometry, theor. and exptl. investigations 9-13162  
 diffuse scatt. spectra, double-beam attachment to spectrophotometer for meas. 9-10904  
 discharges, pulsed, sampling technique for time-resolved meas. 9-10930  
 emission, review 9-2418  
 error bounds, upper and lower, from equilibrium moments of spectral density 9-8435  
 excited species in a plasma, radial distrib. meas. technique 9-13461  
 far i.r. sub mm and mm techniques, book 9-4405  
 flame emission analysis, advances 9-6032  
 flash, with triggered laser excitation, applic. to study of naphthalene fluorescence, of proteins 9-18224  
 Fourier, noise and resolution 9-19171  
 grating spectra Lyman ghosts, intensity and removal 9-10929  
 grating spectrograph, determ. of instrumental profile using laser 9-13071  
 i.r., response function for resolution enhancement 9-10940  
 i.r., review 9-2419  
 i.r., sample holder for heterogeneous reaction analysis 9-20280  
 i.r., very-far, region, development 9-15551  
 i.r., wavelength standards, book 9-10928  
 i.r. of planets 9-8298  
 laser photolysis, for nanosecond reaction meas. 9-6559  
 light absorption, review 9-2420  
 multi-parameter digital 8-channel analyzer 9-457  
 nanosecond absorption spectroscopy using laser photolysis 9-19170  
 nuclear, fitting of gaussians to peaks by max. probability method 9-13160  
 paraelectric resonance 9-13916

**Spectroscopy** continued

- photographic calibration data, processing method 9-12802  
 photographic plate, double intensification of line blackening 9-8673  
 plasma diagnosis by spectroscopic methods 9-14784  
 plethysm, a method of simplifying the mathematics of complex spectra 9-9118  
 Raman, 50 cps ruby laser excited, signal-noise ratio improvement 9-6560  
 Raman, apparatus with laser excitation 9-16798  
 Raman, choice of receiver 9-282  
 Raman, of single crystals, using laser excitation, chemical implications with examples 9-21633  
 rapid scan, instruments and technological advances 9-10931  
 semiconductor recombination radiation, instrument for study 9-12157  
 techniques, high resolution, appl. laser physics and space research 9-15556  
 time-resolved, equipment and methods 9-6558  
 tunnel junction, collective excitations 9-12169  
 unfolding iterative, of Compton spectra 9-19223  
 u.v. review 9-2421  
 Ar-SF<sub>6</sub> plasma, oscillator strengths of 44SI and 9SII lines, 1100-2000 Å 9-7160  
 CdI band spectra, 4130-4800 Å, electronic transition (B)<sup>2</sup>Σ-(X)<sup>2</sup>Σ<sup>+</sup>, spectrographic obs. 9-4920  
 Hg ion mechanism formation in the column low-press. discharge study 9-5083

**light sources**

- acetylene-N<sub>2</sub>O+air flame for atomic absorpt. meas. 9-10944  
 atomic fluorescence flame spectrometry, electrodeless discharge lamps, preparation and operation improvements 9-16799  
 flame, intermittent nebulization using immersion principle 9-284  
 flying-spot, for Warsaw flash spectrophotometer 9-10937  
 i.r. very-far, laser and conventional sources 9-15551  
 laser spark for highly ionized atoms 9-18145  
 methane-68.7%FI flame, temp., calc. and obs. 9-15561  
 organic dye lasers, tunable, characts. 9-20562  
 plasma jet and arc, interelement effects, obs. 9-20563  
 propane-butane-N<sub>2</sub>O flame for atomic absorpt. meas. 9-10944  
 temperature nonuniformity eff. on atomic spectrum 9-19396  
 vacuum ultraviolet for spectrophotometric and spectrographic measurements 9-4542  
 vacuum u.v. gas mixture flow lamps, microwave excited 9-8665  
 Ar laser system for low intensity sources 9-15559  
 HCN laser in sub. m.m. resonance spectrometer 9-14070  
 N<sub>2</sub>O-acetylene flames, temp. distrib., obs. 9-15562  
 Ta electrodes source, constant intensity line spectrum over 40-600 nm range 9-13075

**Spectroscopy, radiofrequency**

- See also Nuclear magnetic resonance and relaxation; Paramagnetic resonance and relaxation; Spectrometers, radiofrequency*  
 computer calc. of rigid rotor energy levels 9-20911  
 microwave, applic. to physical chemistry 9-17508  
 microwave, Stark modulation absorption system 9-6435  
 microwave intensity law 9-11433  
 microwave modulated, double reson. and Stark spectrometers, line shapes and press broadening 9-12963  
 microwave spectrum, frequency markers on record chart 9-2283  
 mm, sub mm and far i.r. techniques, book 9-4405  
 n.q.r., Zeeman effect thyristor modulator 9-6441  
 optical r.f. double reson. for short-lived molec. states 9-8559  
 spectral analysis, setup for visual recording 9-15490  
 spin echoes in weak fields, method 9-4403

**Speech**

- See also Hearing*  
 acoustic speech signal, effects due to task induced stress 9-4148  
 analysis by loudness analyser 9-19068  
 analysis-synthesis system based on homomorphic filtering 9-20262  
 connected, segmentation procedure 9-6211  
 diphthongs, duration and formant freq. meas., eff. of speaking rate 9-15385  
 fundamental tone, correlation method for investigation 9-18951  
 intelligibility tests, comparison using 3 types of distortion 9-4149  
 level measure, threshold-indep., equiv. peak level 9-4147  
 noise interfering aspects and freq. weighting contours 9-8304  
 pitch synchronous analysis for natural vowels 9-12785  
 primate vocalizations and human linguistic ability 9-15386  
 respiratory vox. in normal speech, influence of consonants type 9-20263  
 speaker's sex, identification from voiceless fricatives 9-8303  
 speaker sex identification, from isolated whispered vowels 9-12786  
 synthesis, by rule, factors affecting prosodic features 9-16636  
 synthesizers, matching range of vowel acoustic parameters 9-6212  
 voice pitch, variation as discriminatory cue for consonants 9-18952

**Spherical aberration** *see Aberrations, optical***Spicules** *see Sun/prominences***Spin** *see Elementary particles; Hyperons/spin and parity;***Mesons/spin and parity; Nucleus/spin and parity; Rotating bodies****Spin echo** *see Nuclear magnetic resonance and relaxation***Spin waves** *see Ferromagnetism/spin-wave theory***Spin-lattice relaxation** *see Crystals/lattice mechanics; Magnetic resonance and relaxation***Spinors** *see Quantum theory, wave equations***Spions (pions with spin)** *see Pions***Spirality** *see Elementary particles; Field theory, quantum***Sporadic-E** *see Ionosphere/E-region***Sprays**

- See also Aerosols; Drops; Jets*  
 dryer with superheated vapour, model 9-3071  
 nuclear reactor containers, spray cooling 9-20849

**Sputtering** *see Elementary particles***Sputtering**

- antireflection coatings on small optical elements 9-13049  
 cathode shielding to minimize sputtering in discharge expts. 9-7197  
 diatomic compounds, by low-energy Li<sup>2+</sup> ions 9-7678  
 dielectric, film, yield and thickness meas. 9-13581  
 films, metallic, formation and physical properties, influence of residual gases 9-3203  
 garnet films, prep. by sputtering 9-5248  
 insulating film deposition in r.f. discharge 9-3204  
 ion formation and emission mechanism 9-18666

**Sputtering** continued

- metal films, at low voltages rel. to elec. props. 9-12097  
 Penning discharge, prod. and analysis of metallic ions 9-3020  
 proton, beam prod. apparatus, 500 eV to 8 keV 9-19252  
 quartz, ratios, and bond enthalpy evaluation of flint glass 9-17361  
 rel. to high energy neutral atoms prod. by scatt. of ions 9-2806  
 sputter-ion pump, effectiveness on He 9-8326  
 of Au single cry., (111) surface, under bombardment by heavy ions, directional eff. 9-13814  
 Cu by 400 and 600 keV Ar ions, mechanism 9-7682  
 GaAs, ejection patterns in low-energy sputtering, 50-525°C, orientation dependence 9-9866  
 GaP, ejection patterns in low-energy sputtering, 50-525°C, orientation dependence 9-9866  
 Gd Fe garnet film, prep. 9-5248  
 Ge, cathode coeffs., meas. for bombarding inert gas ions 9-15037  
 KI, on u.v. irradi. rel. to defect formation mechanism 9-14952  
 Mo, cathodic with 70 keV Ar ions, eff. of target cooling 9-19871  
 Ni-Cr films, bias-sputtered, preferred orientation 9-21265  
 Pb, efficiency for 30-75 keV Pb ions 9-9870  
 PbZrO<sub>3</sub>-PbTiO<sub>3</sub>, ferroelec. films, dielectric loss and strength 9-1596  
 Si single crystals by Ar ions, and detection 9-19873  
 SiO<sub>2</sub>, r.f. in Ar, effect of O<sub>2</sub> impurity in gas 9-7332  
 TaN<sub>x</sub> film prep., rel. to structure and props. of highly nitrated mat. 9-13578  
 W, cathodic with 70 keV Ar ions, eff. of target cooling 9-19871

**Stacking faults** *see Crystal imperfections***Standards**

- See also Constants; Units*  
 acceleration due to gravity, Nat. Bureau Standards, USA 9-26  
 alcohols, thermal conductivity data considerations for standard reference materials 9-14847  
 alloys, radiochem. pure, prod. for neutron activation anal. 9-16645  
 chemical shift in Mossbauer spectroscopy of Fe cpds., standard ref. mat. 9-3872  
 elasticity, moduli meas. by dynamic method 9-1263  
 frequency, atomic hydrogen maser development 9-12991  
 frequency, beam laser, construction possibilities 9-8593  
 glass beads, low thermal conductivity range standard 9-15014  
 hardness, international uniformity of measurement 9-9773  
 hydrophone calibration, international 9-2227  
 irradiance, international comparison of measurements 9-13058  
 length, use of laser interferometry 9-2127  
 length and time, metrology methods comparison 9-10605  
 measurements at NPL, review 9-8346  
 neutron meas., role of N.B.S. 9-9102  
 of radioactivity, review 9-18768  
 radiometric scales, international comparison 9-10911  
 temperature, primary: acetylene-air flame, (2600±3K) 9-10757  
 temperature, secondary: acetylene-air flame line reversal at 2500(±2)K 9-12951  
 thermal conductivity, high temp. development 9-15013  
 wavelength, i.r., book 9-10928  
 X-ray diffraction powder patterns, standard 9-11809  
 CO<sub>2</sub> vapour pressure, 0°C, dynamic meas. method 9-3037  
 He-Ne laser as absolute wavelength standard, problem 9-13014  
 Na<sub>2</sub>[Fe(CH<sub>3</sub>)NO<sub>2</sub>]<sub>2</sub>·H<sub>2</sub>O standard ref. for chemical shift of Fe cpds. 9-3872  
 Pt resistance thermometers, calibration point requirements 9-4378

**Stark effect**

- atoms, review 9-13284  
 broadening of emission lines, effect of time fluctuations of microscopic elec. field 9-19383  
 formic acid, and Stark Zeeman effect on rotational lines 9-2909  
 formic acid, Zeeman effect and Stark Zeeman effect 9-2909  
 H<sub>2</sub> test of broadening at high electron density 9-714  
 hydrogenic line broadening, rel. to strong collisions 9-15804  
 line broadening, electron contribution 9-667  
 methyl red dye interaction with solid polymer 9-16419  
 microwave spectroscopy, high temp., Stark modulation absorption system 9-6435  
 phenol blue dye interaction with solid polymer 9-16419  
 Schrodinger many particle operator with combined Zeeman and Stark eff. 9-20330  
 shifts in atomic plasma spectral lines, rel. to high temp. meas. 9-8539  
 solvent, temperature dependence 9-21210  
 Ar I i.r. lines in plasma torch sustained at h.f. 9-9375  
 Cl, neutral atom, line broadening 9-6966  
 Cs<sup>35</sup>Cl r.f. spectrum mol. beam elec. resonance meas. 9-7036  
 CsF r.f. spectrum, mol. beam elec. resonance meas. 9-7036  
 Cu I, hyperfine struct. in 4p <sup>2</sup>P<sub>3/2</sub> state, of level-crossing signal in meas. 9-4836  
 H, H<sub>2</sub> line broadening for radial temp. distrib. of arc plasma 9-21051  
 H<sub>2</sub> test of broadening at high electron density 9-715  
 H atom energy levels determ. 9-20894  
 H Balmer lines in strong mag. field in plasma, Stark-broadening obs. 9-17110  
 He, singly ionized, Stark-mixing signals in n=4 term 9-20901  
 He I, 2 <sup>3</sup>P-4 <sup>3</sup>P, <sup>3</sup>D, <sup>3</sup>F transitions, electron and ion Stark broadening 9-20899  
 K, 4p<sup>2</sup> level Stark effect obs. by atomic beam technique 9-13290  
 KH<sub>2</sub>AsO<sub>4</sub>, of <sup>75</sup>AsNQR 9-12521  
 LiF, linear eff. of no-phonon transitions of F<sub>2</sub><sup>+</sup> colour centres 9-19759  
 LiF, R<sub>2</sub> zero-phonon line, 4.2°K 9-14054  
 NS radical, gas phase 9-7082  
 NaF, linear eff. of no-phonon transitions of F<sub>2</sub><sup>+</sup> colour centres 9-19759  
 NaI:Cl<sup>-</sup>, lattice resonant mode freq. shifts 9-7637  
 NaI r.f. spectrum, mol. beam elec. resonance meas. 9-7036  
 O I lines, displacement and splitting obs. 9-2821  
 O<sub>2</sub>, broadening in Schumann Runge system, relax. treatment 9-11471  
<sup>85</sup>Rb<sup>35</sup>Cl r.f. spectrum, mol. beam elec. resonance meas. 9-7036  
<sup>85</sup>RbF r.f. spectrum, mol. beam elec. resonance meas. 9-7036  
<sup>87</sup>RbF r.f. spectrum, mol. beam elec. resonance meas. 9-7036

**Stars**

- See also Nebulae; Novae; Sun*  
 14 Aur, photometric and radial velocity meas. results 9-14217  
 A<sub>0</sub>-G<sub>5</sub> type, three-dimensional representation construct. 9-21868  
 Am, applic. of three-dimensional representation 9-21868



## Stars continued

angle of inclination of axis, determ. from spectral absorption width. 9-2012  
 atmosphere, adiabatic temp. gradient, in F-stars 9-15292  
 atmosphere, breakdown of ionization equilibrium calcs. 9-19529  
 atmosphere, monochromatic source function iteration 9-8238  
 atmosphere, non-equilibrium phenomena 9-21865  
 atmosphere, plane-parallel finite Rayleigh-scatt., rad. field construct. and soln. 9-18877  
 atmosphere, radiative transfer 9-8654  
 atmosphere, shock wave structure, press. depend., nomogram calc. 9-19533  
 atmospheres, scaled solar models in contrast to grey-body temp. distrib. models 9-21887  
 atmospheres, spectra, line- blanketing eff. for pure abs. and non-coherent scatt. 9-16587  
 AU Puppi eclipsing binary system, photoelec. study 9-10496  
 B<sub>0</sub>-B<sub>5</sub> stars, parameter of vel. of rot. 9-21866  
 Be, rotational distrib. rel. to abs. absorption widths 9-2011  
 binaries, Cepheids, new radial velocity obs. 9-16586  
 binaries, eclipsing, dimensions of 34, posn. on Hertzsprung-Russell diagram 9-10499  
 binary, angular separation <15", empirical distrib. 9-12722  
 binary, H.D. 208947, orbital elements and dimensions 9-8260  
 binary, origin from statistical and observed distrib. 9-12714  
 binary, spectroscopic, H.R. 8800, apsidal motion, further evidence 9-12721  
 binary and rotating, photometric distinction 9-10473  
 binary spectroscopic systems, catalogue of orbital elements 9-8261  
 binary systems, distrib. of periastron longitudes in the Sixth Catalogue 9-14225  
 blue, faint; lum., colour, motion and distrib. photometric study 9-14202  
 Centaurus, supernova remnant 9-15328  
 Cepheid variables, review of theory 9-8253  
 Cepheids, new radial velocity obs. 9-16586  
 Cepheus IV association, bibliography 9-8259  
 Cepheus region, extinction law 9-10500  
 classical cepheids, nature and causes of pulsation 9-21899  
 Classical Cepheids, space distrib. indicating Galactic structure 9-12664  
 cluster, very young in neighbourhood of Orion Nebula, obs., turnoff point calc. 9-15316  
 cluster NGC 3680, UVB obs. of 79 stars 9-12715  
 cluster proper motion, review 9-15321  
 cluster structure theory 9-10497  
 cluster velocities, generalization to n dimensions of Abazumian's integral eqn. 9-33  
 clusters, ages and chem. composition rel. to late-type stars 9-17613  
 clusters, open: age determ. method, parameter introduced 9-8257  
 clusters, Terzan 3-8, in central region of Milky Way 9-16584  
 clusters and binaries, possible existence of intermediate groupings 9-14226  
 γ-Cygni, radio source obs. at 9.3 and 2.8 cm, correl. with optical phenomena 9-16597  
 δ Ceti, atmos. e density from H and He line widths 9-2009  
 diameter meas. using refraction at Moon's edge 9-2002  
 diametric determ using refraction at the moon's edge 9-2003  
 distance, parallax meas., history 9-15262  
 dwarfs, white, late-type, lum., colour, motion and distrib. photometric study 9-14202  
 dynamical friction in the approx of general relativity 9-12716  
 early-type, atm. He non-local thermodyn. equilib. statistical mechs. 9-6123  
 encounters and escapes 9-20144  
 F-stars, atmospheres, adiabatic temp.-gradient 9-15292  
 flare, UV Ceti, unusual activity obs. 9-18869  
 flare, YZ Canis Minoris, seven flares obs. 9-12675  
 flare stars in Coal Sack 9-16588  
 ζ aurigae, eclipse, 1963 4, photoelectric obs. 9-6140  
 Galactic south pole region, proper-motion stars, blue objects and eclipsing binaries UVB obs. 9-8225  
 gaseous self-gravitating rotating cloud model, adiabatic index=4/3 9-20169  
 general relativity theory, exterior radiation field energy-momentum tensor 9-20171  
 globular cluster M69, colour-magnitude diagram and metal abundance 9-6139  
 globular clusters near M87 9-12720  
 gravitational field generated by gas, Einstein- Liouville eqns. isotropic solns. 9-14358  
 gravitational stability of rotating anisotropic systems 9-2004  
 HD135240, binary, orbit computation 9-20195  
 HD35921, proved to be an eclipsing variable 9-14221  
 HD93403, binary, orbit computation 9-20195  
 H.D. 208947, orbital elements and dimensions 9-8260  
 HII regions exciting stars, Lyman-visual colours, obs. 9-6118  
 horizontal branch, applic. of three-dimensional representation 9-21868  
 H.R. 8800 spectroscopic binary, apsidal motion, further evidence 9-12721  
 HR diagram, stellar rotation depend. 9-21867  
 Hyades, colour, six-colour obs. 9-20178  
 Hyades, distance, and mass-luminosity relation 9-21911  
 Hyades stars, charts 9-15315  
 IC1805, cluster, large W-component, space vel. and absolute proper motion 9-20199  
 image motion mean power spectrum, refraction anomalies 9-12679  
 images, visibility in perfect records and photographs 9-19175  
 i.r., produced by interaction by stars and interstellar clouds 9-6136  
 i.r. survey results, southern sky at 2.2μ 9-6120  
 local group assignment of O to B9 spectral group 9-12674  
 luminosity function and density, near sun 9-6121  
 M39 cluster, struct. determ. from astrophot count 9-2019  
 M 13 globular cluster, UVB data and proper motions 9-2018  
 M giants, space distrib. and densities rel. to Galactic disc distrib. 9-20152  
 magnetic field generation by viscous forces in non-uniformly rotating plasma 9-6114  
 magnetoacoustic waves generation by stellar wind- surrounding gas interaction 9-21861  
 map, from lunar sky, ecliptic coordinate system 9-18846  
 meridian obs., Copenhagen Univ. (1964-7) 9-10470  
 model, vibration and secular stability near dynamic instability 9-12678

## Stars continued

motion and variation obs. 9-6196  
 motion in gravitational field of condensed interstellar gas 9-17625  
 neutron, configurations calc. by Newton gravitational theory 9-20182  
 NGC457, cluster, large W-component, space vel. and absolute proper motion 9-20199  
 NGC581, cluster, large W-component, space vel. and absolute proper motion 9-20199  
 NGC 2533, UVB photographic magnitudes, colour excess, spectral classes obtained 9-6130  
 NGC 2567, UVB photographic magnitudes, colour excess, spectral classes obtained 9-6130  
 NGC 2571, UVB photographic magnitudes, colour excess, spectral classes obtained 9-6130  
 NGC 6334; OH radiolines emission obs. 9-18845  
 NGC 7142, bright stars of main sequence, colour-magnitude diagram 9-2001  
 NGC 7261, galactic cluster, distance, age, physical members, photometry obs. 9-14224  
 non-static fluid spheres without energy flow 9-17713  
 nuclear reactions (triple-alpha), at high temps., reaction rates 9-6125  
 O to B9 spectral type, local group assignment 9-12674  
 OB in northern Milky Way, distribution 9-8234  
 orbit perturbation by gas cloud, motion inclined to galactic plane 9-16555  
 Ori A; OH radiolines emission obs. 9-18845  
 oscillations, eff. of rot., polytropic compressible cylinders 9-18847  
 p Velorum, binary, orbital elements 9-20196  
 parallax and proper motion stars, 4, UVB PHOTOMETRY 9-12700  
 parallax determs., summary of results from past 30 years 9-14196  
 parallaxes and proper motions of nine stars, from plates taken with Van Vleck refractor 9-15281  
 peculiar A stars, origin rel. to mass transfer by type II supernova explosion 9-16572  
 Persei, h and χ double cluster, colour-magnitude diag. struct. 9-2020  
 h and χ Persei Be stars in double cluster, rotation 9-21869  
 Perseus spiral arm in dirc Cassiopeia A mag. fields of order 2×10<sup>-5</sup>G determ. 9-2025  
 Pleiades, optical backscattering functions 9-21882  
 polytrope with poloidal mag. field, shock wave propag. 9-10471  
 polytropic compressible cylinders in rot., equil. and oscillations 9-18847  
 population II, applic. of three-dimensional representation 9-21868  
 Population II models, near main sequence, uncertainties 9-21870  
 proper motion program of Lowell observatory, XI 9-15286  
 pulsars, plasma parameters affecting radiation 9-6148  
 pulsars, pulse structure 9-6147  
 pulsating possible application to spatial navigation 9-12707  
 pulsating stars, nature and causes, review 9-21899  
 pulsation of massive stars 9-2014  
 pulsations, useful boundary condition, for calculations 9-21898  
 R (interstellar absorpt. ratio) found to be valid for distances>1kpc 9-15284  
 radii, photometric computations for 46 stars 9-12673  
 radiosources in clusters of galaxies 9-4104  
 red giant helium core, partially degenerate evolution 9-12684  
 relaxation time of rotating stellar systems 9-4105  
 rotating and binary, photometric distinction 9-10473  
 rotating connective models with rad. press., construct. 9-18850  
 rotating syst., gravitational instability 9-17611  
 rotating systems, relaxation time 9-4105  
 rotation, determ. from line profile 9-2005  
 rotation, eff. on positions in HR diagram 9-21867  
 rotation of configurations, Einstein's theory applic. 9-20170  
 rotation several-colour photometric eff. w.r.t. spectral type 9-21866  
 rotational braking due to stellar wind 9-2006  
 RR Lyrae variables, nature and causes of pulsation 9-21899  
 Ru 58, UVB photographic magnitudes, colour excess, spectral classes obtained 9-6130  
 satellite components of line formation in differential rotation 9-15283  
 self-gravitating stellar systems, extremal props. 9-15290  
 Sixth Catalogue binaries, distrib. of periastron longitudes 9-14225  
 sky survey, twenty year programme for two Schmidt's suggested 9-18946  
 space motions of 430 bright F-type 9-15289  
 stellar system, numerical study 9-20193  
 stellar systems, radial mass flow 9-2021  
 subdwarfs, applic. of three-dimensional representation 9-21868  
 subdwarfs, colour, six-colour obs. 9-20178  
 subdwarfs, obs. in photometric studies of blue objects in high galactic latitudes 9-16552  
 symbiotic, spectra, light curves and nature 9-15282  
 σ Boo atmosphere metal deficiency determ. 9-20176  
 Terzan 3-8, six new clusters, in central region of Milky Way 9-16584  
 thermonuclear react. rates at high densities 9-16570  
 Tr1, cluster, large W-component, space vel. and absolute proper motion 9-20199  
 transit moments, phase photoelectric dev. for registration 9-2000  
 type G5 to K3, Wilson's, relns. between spectral type, effective temp. and colours 9-10480  
 V448 Cygni binary, UVB photoelectric study 9-21908  
 V453 Cygni binary, UVB photoelectric study 9-21908  
 variable, book 9-15313  
 variable, eclipsing systems, absolute dimensions, parameter obs. 9-21893  
 variable, spherical hydrodynamics and radiation diffusion coupled eqns. soln. 9-4103  
 variables, eclipsing, coeff. of darkening to edge and elements of orbits 9-4102  
 variables, of the Orion nebula, comparative study 9-18867  
 variables in YZ Cnc region 9-20189  
 variation in possible optical counterpart of pulsar 9-6149  
 visual binaries, dynamical parallaxes, new elements, orbit computations 9-6144  
 W3, 49, 51, 75; OH radiolines emission obs. 9-18845  
 W Ursae Majoris type, discovery of new star 9-12710  
 W Virginis, nature and causes of pulsation 9-21899  
 white dwarf models, rotating, pulsation periods 9-17618  
 white dwarfs, rapidly rot., models, stable and unstable oscillations 9-16581  
 white dwarfs, supercond. transition 9-15285  
 wind, gas motions and interactions with nebulae 9-4094  
 Wolf-Rayet, distances and distrib. galactic plane 9-16556

## Stars continued

Wolf-Rayet, heavily obscured, search in Cygnus OB2 assoc. 9-20197  
 Wolf-Rayet and OB, comparative distrib. 9-21862  
 YZ Cnc region, obs. of variables 9-20189  
 ZC1137, grazing occultation obs. 17 Sep 1968 9-18851  
 $e^-e^+ \rightarrow \nu\nu$ , energy loss rate and  $\nu$  luminosity 9-10477  
 $\gamma\gamma \rightarrow \nu\nu$ , energy loss rate 9-10477  
 Be, in H and  $\gamma$  Persei, rotation 9-21869  
 C, SiC particle growth in atm., calc. 9-18852

## composition

## See also Elements/origin

3 centauri A, metal abundances 9-14199  
 Am, chemical comp. 9-21874  
 Ap, chemical comp. 9-21874  
 early-type, six, derivation of H/He ratio 9-14206  
 F type, seven, four classified normal showing metallic characts. 9-18860  
 graphite particle formation in C type Mira variables 9-18853  
 horizontal branch stars, primordial He abund. 9-21880  
 hot superdense hydrodynamically stable, limiting mass at equilib. determ. 9-20168  
 Hyades moving group, metal-abund. homogeneity and absolute magnitudes 9-21907  
 K giants, metal abundances determ. from photometric study 9-16567  
 K giants temp. calibration from photometric study 9-16567  
 main sequence massive type, initial chem., influence 9-2007  
 metallicity indicator, Borgman-LPL  $\alpha$  index 9-12696  
 Mira variables, formation of graphite particles in atmosphere 9-2017  
 neutron, configurations calc. by Newton gravitational theory 9-20182  
 neutron matter energy density, relative proton no. 9-18865  
 NGC 6231 open cluster, photometric data for 34 stars 9-18876  
 nucleosynthesis, astronomical evidence 9-21878  
 polytropes, slowly rotating, review of theory 9-15288  
 RR Lyrae, primordial He abund. 9-21880  
 Sirius B, white dwarf, H abund. from obs. of nuc. react. rates at high densities 9-16570  
 C, at south galactic pole cap, obs. 9-21886  
 C type Mira variables, graphite particle formation 9-18853  
 Ca II emission in spectra of  $\gamma$  Virginis 9-21885  
 Mg abundance in B stars, calc. 9-8237  
 Omicron Andromedae, H and He abundances from spectrographic obs. (1961-1966) 9-14218  
 SiC particle growth in carbon star atms., calc. 9-18852

## evolution

a5.6  $M_{\odot}$  in He burning phase, pulsation, radiation eff. 9-16573  
 Am 9-21874  
 Ap 9-21874  
 binaries, early, away from main sequence 9-15320  
 binary,  $1M_{\odot}+2M_{\odot}$  evolution through red giant to white dwarf stage 9-12723  
 binary, in galactic field, statistical test 9-20190  
 binary syst., close, parameter obs. from absolute dimensions of eclipsing syst. 9-21893  
 carbon burning model, heavy neutrino emission due to previous He burning stage 9-12682  
 clusters, open, 25-48 stars, under influence of galactic field 9-20191  
 clusters, spherical, using numerical technique of concentric shells 9-20192  
 collapse due to energy losses by neutrino rad., asymptotic automodel solns. 9-17614  
 colour magnitude distribution of yellow and red giants, age depend. 9-6131  
 early-type, rot. vel. correl. with space vel. 9-14198  
 early-type stars, book 9-12685  
 energy production, C cycle 9-6126  
 formation, collapse of interstellar gas clouds, importance of thermodynamics 9-20175  
 formation near apogalacticon, conformation 9-12683  
 formative processes, book 9-8220  
 gaseous self-gravitating rotating cloud, rarefied ellipsoidal envelope formation 9-20169  
 globular clusters, origin 9-14222  
 Hertzsprung-Russell diagram, calibration, difficulties with stars later than F0. 9-10476  
 Hertzsprung-Russell diagram, calibration, difficulties with stars later than F0 9-21877  
 homogeneous, of mixed stars on left of Hertzsprung-Russell main sequence 9-10474  
 infant stars, popular article 9-16574  
 in interstellar clouds, study using viral theorem 9-20200  
 from interstellar gas, dynamical theory of disruptive forces 9-21909  
 late-type, main sequence position, ages and chem. composition 9-17613  
 main sequence massive type, initial chem. composition influence 9-2007  
 massive blue stars, H-poor, pulsational instabilities 9-18855  
 neutrino emission, energy losses 9-15294  
 neutrino emission ion collapse 9-6124  
 neutron, detect, by Weber's gravitational wave receiver, Brans-Dicke theory prediction 9-20183  
 neutron, thermal and vibr. energy, rel. to age and detection 9-8250  
 planetary nebulae stage between He and burning 9-2008  
 pre-main sequence, of one solar mass, influence of convection inhibition 9-18856  
 protostar of one solar mass, in transparent stage, density-temp-diagram rel. to contraction 9-10478  
 red supergiants, neutrino emission, core contraction and He burning study 9-20174  
 self-gravitating system in extended phase, relaxation eff. 9-16571  
 self-gravitating systems, violent relax. phase, equilibrium considerations 9-21875  
 shell burning, evolution of instabilities 9-4098  
 stability and minimum energy configuration determ. from Vlasov eqn. 9-10479  
 stellar systems, one-dimensional, computer model 9-20194  
 thermonuclear energy production 9-18857  
 three-star system, evolution 9-10495  
 triple-star system, orbits dynamic description 9-21879  
 variable, eclipsing syst., parameter obs. from absolute dimensions data 9-21893  
 rel. to vibration and secular stability near dynamic instability 9-12678  
 W-stars, H-poor, blue colour obs. pulsational instabilities 9-18855  
 white dwarfs, general relativistic instability 9-14200

## Stars continued

## evolution continued

$pe^+p \rightarrow \pi^0\nu$ , detailed rate calc. 9-10475  
 $pp \rightarrow \pi^0\nu$  detailed rate calc. 9-10475  
 ${}^7\text{Be}(e^-)\gamma$ Li, effects of plasma and bound electron screening negligible 9-15293  
 C burning, following He burning, model 9-2008  
 Fe stars, pure, eff. of neutrino loss 9-18854  
 H poor massive blue stars, pulsational instabilities 9-18855  
 He shell burning models with CO core 9-2008  
 ${}^{14}\text{N}(p,p'){}^{14}\text{O}$ , possibility, CN cycle products abundance examined 9-2732  
 ${}^{16}\text{O}$  rapid addition to core, nuc. reaction mechanism 9-6125

## magnetism

## See also Sun/magnetism

early-type, surface fields prod. in convective core 9-8236  
 field which accelerates rot. until onset of instability and then returns star to initial state 9-10472  
 HD 10783, mag. variations 9-14216  
 white dwarfs, rotating, internal field rel. to radius 9-6122

## radiation

## See also Cosmic radiations, radiofrequency; Sun/radiation

4 Canum Venaticorum, photoelec. UVB obs. 9-14220  
 A- and B-type, near North Galactic Pole, photoelec. photometry obs. 9-12688  
 AG stars, photoelectric data 9-10483  
 B327 reddened cluster, obs. 9-20198  
 binaries, eclipsing, light curves, coeffs. of darkening to the edge 9-17623  
 BR Cygni, eclipsing binary, photometry, period, orbital elements 9-10493  
 Brans-Dicke radiation-zone, an observable peculiarity 9-20183  
 BV357, eclipsing binary, photometric study 9-14203  
 BV 332 Cygni, eclipsing binary, orbital elements, ephemerides, ratio of radii 9-10494  
 BV 412 Cygni, eclipsing binary, orbital elements, ephemerides, ratio of radii 9-10494  
 BV photoelec. photometry of 368 northern stars 9-10481  
 Cassiopeia A, emission 9-12689  
 Cepheid variables, pulsations of outer envelopes, comparison with theoretical models 9-8255  
 CH Cygni, rapid variations, photoelec. obs. 9-18871  
 classical cepheids in the Galaxy, fundamental data catalogue 9-6137  
 cluster Pis 20 9-18875  
 CM Lacertae, eclipsing binary, photoelec. UVB obs. 9-21903  
 collisional excitation and ionisation rates for model-atmospheres 9-15302  
 continuous thermal rad., Planck function representation rel. to  $\text{H}^-$  dissociation equilib. 9-17612  
 CY Aqr variable, period study of cycle from epochs of rising branch 9-20185  
 Cygnus X-1, x-ray flux time vars., obs. 9-6127  
 diffusion and spherical hydrodynamics coupled eqns. soln. 9-4103  
 DS Andromedae, photoelec. obs. 9-21904  
 dwarf cepheid HD 199757, amp. of light variation, period decrease 9-6138  
 flare stars in Coma cluster region 9-18870  
 flares, spurious photoelec. obs. 9-14213  
 general-relativistic models with non-radial pulsation, gravitational waves props. 9-18849  
 giant yellow and red, colour-magnitude distribution, age depend. 9-6131  
 gravitational waves from general-relativistic model with non-radial pulsation 9-18849  
 horizontal branch stars, luminosity in He burning-phase 9-21880  
 hyades moving group, absolute magnitudes 9-21907  
 intensity numerical calc. for given source function 9-12701  
 interlocked multiplet lines, calc. in M-E model using approx. H-function 9-10485  
 late-type, polarization changes correl. with brightness 9-15304  
 luminosity indicator,  $H\alpha$  line suggested 9-12690  
 Ly 2 colour excess, photographic magnitude determ. in UVB system 9-6129  
 multiple systems, magnitude obs. 9-8263  
 NGC 457, photographic photometry of 171 stars 9-21906  
 NGC 5617 colour excess, photographic magnitude determ. in UVB system 9-6129  
 NGC 5927 cluster, suspected variable 9-21896  
 NGC 6231 open cluster, photometric data for 34 stars 9-18876  
 non-coherent scatt., Doppler redistribution functions in moving atmosphere 9-16565  
 photometric UVB obs. of stars in two associations in Large Magellanic cloud 9-14223  
 Pis 20 cluster, obs. 9-18875  
 polarization, interstellar, spherical harmonic anal., applic. to Galactic mag. field investigation 9-12665  
 polarization variability, explanation by interstellar dust distrib. 9-15322  
 Puppis-Vela border region, UVB photometry, no colour excess in 1 kpc 9-6119  
 radiative opacity calc., using new algorithm for high-speed digital computers 9-14204  
 radiative transfer eqn. for continuum radiation, modification 9-15303  
 radiative-transfer eqns. for electron scatt. stellar atmosphere, soln. 9-15305  
 red variables, polarization change with wavelength 9-17615  
 RR Lyrae, field, luminosity in He burning-phase 9-21880  
 RT Lacertae, eclipsing binary, study of variable asymmetric light curves 9-15318  
 RZ Pyxidis, photoelec. obs. 9-21904  
 S Velorum, u.v. excess of secondary component, UVB obs. 9-21905  
 Sagittarius A, radio source, lunar occultations obs. 230-2400 MHz, spectral index calc. 9-16595  
 Sco X-1, Apr 1968 obs. 9-10492  
 SCO x-1, x-ray flux time vars., obs. 9-6127  
 synchrotron spectra assoc. with hard electron spectra 9-17616  
 Tr 12 colour excess, photographic magnitude determ. in UVB system 9-6129  
 TT Herculis, eclipsing variable, new times of minima, and photoelec. obs. 9-15317  
 UV Ceti flare star, optical and radio obs., Australasia (Sept.-Oct. 1967) 9-12687  
 V 836 Cygni, eclipsing binary, orbital elements, ephemerides, ratio of radii, variations in light curve 9-10494  
 variables, long-period, UVB obs. 9-21900  
 VZ Cancri variable, period 9-21897  
 Wolf-Rayet, rapid light variations, search 9-21890



## Stars continued

## radiation continued

WUMa, light curves calc. from short model 9-8252

X-ray sources sco X-1 and cyg X-2, r.f. emission obs. 9-8271

YZ Cas light curve for eclipsing system, interpretation and algorithm soln. 9-17622

C stars visual absolute magnitudes 9-18863

OH radio emission from infrared stars, obs. 9-21892

## spectra

3 Centauri A, rel. to microturbulence and metal abundances 9-14199

3C191, absorption spectrum, curve of growth analysis, model 9-12736

9 Chamaeleontis eclipsing binary, radial vel. curve and orbital elements, from spectrograms 9-12718

306 bright southern stars, photoelectric magnitudes and colours 9-12692

 $\chi$  Persei starlight polarization, photographic meas. 9-14205

(B-V) color and radiation temp. empirical relation from obs. of eclipsing variables 9-12676

A0 IV type, search for 'windows' for continuum depth defining 9-18858

A3V, in binary 57 Pegasi, photometric obs., standard absolute visual magnitude rel. to M4IIIa 9-6142

A5V type, search for 'windows' for continuum depth defining 9-18858

 $\alpha$  Del H $\beta$  obs. and compared with theory 9-12697 $\alpha$  Leo, H $\beta$  obs. and compared with theory 9-12697

A stars, peculiar, metallic-line and 10 others 9-21889

A stars with large  $m_i$  indices, classification 9-15300

A-type in north galactic pole region, survey 9-10482

absorption in Kapteyn's Selected Area 19, obs. 9-16589

absorption lines, method of computation of contours 9-4099

Ap. color-index freq. distrib., probably with rot. vel. &lt;90 km/sec. 9-12702

atmosphere, line blanketing eff. for pure abs. and non-coherent scatt. 9-16587

atmosphere emission line profiles calc. by Monte Carlo methods 9-6132

atmospheres of finite opt. thickness, formation of emission lines 9-15296

RT Aurigae, anal. of atm. parameters 9-20186

AX Cir-BV 428, Cepheid variable, 3-colour photometry, dist., dimens. 9-12713

B0.5V type, search for 'windows' for continuum depth defining 9-18858

B1985, emission line in u.v. 9-12686

 $\beta$  Orionis, time variation of H $\alpha$  profile 9-10487

B-type star in M13 globular cluster 9-15314

BaII and N, rel. to temp. sequence 9-6128

Be, absorption width rel. to rotation 9-2011

binaries, eclipsing, light curves, coeffs. of darkening to the edge 9-17623

binary, blending effect in spectroscopic spectra meas. 9-16585

binary, spectroscopic, H.R. 8800, apsidal motion, further evidence 9-12724

binary 57 pegasi, extraction of fainter component photometric obs., standard absolute visual magnitude 9-6142

blue objects, H $\beta$  emission line width rel. to ionization mech. 9-6111Borgmann-LPL $\alpha$  index as metallicity indicator 9-12696

bright southern stars, photoelectric magnitudes and colors 9-12693

broadening used to determ. rotation 9-2005

BV 544 photoelectric study, period calc. 9-8256

 $\gamma$  Peg H $\beta$  obs. and compared with theory 9-12697

C type stars, i.r., qualitative analysis 9-15295

 $\gamma$  Virginis, Ca II emission obs. 9-21885 $\gamma$ -Cassiopeiae, (1911-1966) 9-14211

Ru Camelopardalis UVB photometric study (Feb. 1966-June 1968) 9-21902

vz Cancri, photoelectric spectrometry and spectroscopic obs. 9-8245

carbon-star, study based on C-classification 9-6134

CD-38° 10980, bright, new white dwarf 9-14212

cephid variables V Carinae, U Carinae, IT Carinae and W Sagittarii 9-18868

Cepheus, interstellar reddening, no difference between O and B stars 9-15324

Cepheus OB2 assoc., spectral classification and UVB photometry obs. 9-15297

at classification dispersion, interrelated objective-prism and slit spect. 9-21891

Cr 185 cluster, UVB magnitudes, spectral class of brightest stars 9-16583

CrB(Ap), and element abundance and distrib. 9-20180

CZ Aquarii binary syst., photometric study 9-12724

 $\delta$  Cas H $\beta$  obs. and compared with theory 9-12697 $\delta$  Ceti, H and He lines equiv. widths determ. 9-2009

dwarfs, late type, effective temp. 9-15307

dwarfs, red; photometric study 9-16576

E-region stars, 520, U.B. photometry 9-14207

early-type, line form, with noncoherent scatt., model atm. calc. 9-8242

early-type stars, book 9-12685

eclipsing binary AU Puppis 9-12694

eclipsing binary W Corvi, UVB obs. magnitudes, soln. for light curve 9-12719

eclipsing variable 31 Mensae (HR 2059) 3-colour photometry 9-14208

eight-color system, based on Borgmann, for 985 bright stars 9-15308

Eta  $\eta$  Carinae, 1947-49, anal. 9-18861

EX Hydrae, photometry, orbital observations and minimum changes 9-21881

F2IV type, search for 'windows' for continuum depth defining 9-18858

F and G subdwarfs, Lyman- $\alpha$  wing opacity, eff. on temp. scale and He content 9-18859

F type, seven, four classified normal showing metallic characts. 9-18860

flare star, UV Cet, continual photoelectric monitoring 9-21901

Fraunhofer line saturation, definitions 9-18862

GOV type, search for 'windows' for continuum depth defining 9-18858

 $\zeta$  Geminorum, Cepheid, spectrophotometric anal. 9-20188

h Persei starlight polarization, photographic meas. 9-14205

 $\eta$  UMa H $\beta$  obs. and compared with theory 9-12697

HD87892, central star of planetary nebula NGC 3132, obs. 9-14194

HD 10783, light, mag. and radial vel. var. 9-14216

HD 109995 brighter horizontal branch A star, analysis 9-15301

HD 125248 mag. variable, probably spectroscopic binary 9-20187

HD 125823, spectral changes over 9 days 9-16578

HD 1909 manganese star, material abundance 9-12691

HD 199757 photoelectric study, period calc. 9-8256

HD 202904, half widths of Balmer emission lines 9-10486

HD 221568 A-type, absorpt. line profile, radial vel., composition deduced 9-8244

HD 25329, subdwarf, line profiles obs., H-to-metal ratio 9-15299

HD 4778, light variation with period of 2.<sup>d</sup>156 obs. 9-12712

## Stars continued

## spectra continued

HD 86986 brighter horizontal branch A star, analysis 9-15301

HD 87643, slit-spectroscopic and photoelectric photometry 9-20179

Hont-London factors for  $^3\Phi^3\Delta$  systems 9-18164

H.R. 8800 spectroscopic binary, apsidal motion, further evidence 9-12721

i.r., produced by interaction by stars and interstellar clouds 9-6136

KS Persei, obs. 9-12703

L 1159-16, large proper-motion star, UVB obs. 9-14214

Lacertae OB 1 association, peculiar stars obs. 9-12699

late-type, polarization correl. with brightness 9-15304

LB3209, obs. rel. to radial velocity 9-21884

M13 globular cluster, B-type star obs. 9-15314

M4IIIa giant 57 Pegasi, absolute visual magnitude mass limit, photometric obs. 9-6142

M87, objects nearly obs., probably globular clusters 9-12720

M 13 globular cluster, UVB data and proper motions 9-2018

M type stars, i.r., qualitative analysis 9-15295

M-type, bright, MK spectral types 9-6133

magnetic stars, photometric behaviour 9-15298

MH $\gamma$ , 328-116 (V1016 Cyg), peculiar object 9-20181

model atmospheres, line blanketing 9-21887

multiple systems, magnitude obs. 9-8263

multiplex analysis method 9-4539

NGC2024 number 1, and photometric comparison with  $\theta^2$  Ori B 9-14210

NGC 1068, (Seyfert galaxy nucleus), spectrophotometric study 9-18838

NGC 2483 cluster, distance and age estimated 9-8258

NGC 2489 cluster, distance and age estimated 9-8258

NGC 2546, cluster, UVB magnitudes, spectral class of brightest stars 9-16583

NGC 2579, probably not a real star cluster 9-16583

NGC 3516, (Seyfert galaxy nucleus), spectrophotometric study 9-18838

NGC 4151, (Seyfert galaxy nucleus), spectrophotometric study 9-18838

Nova Vulpeculae 1968, spectrum 9-15310

O, B-type stars, classification of 239 examples 9-12695

OB supergiants, strong line profiles in hot extended atmos. computation 9-16569

Omicron Andromedae, anal. of spectrographic obs. (1961-1966), correl. shell structure 9-14218

opacity, hydrogenic approx. validity 9-16577

parallax and proper motion stars, 4, UVB PHOTOMETRY 9-12700

partition sums, quick method of evaluating 9-21863

Pii cluster, UVB magnitudes, spectral class of brightest stars 9-16583

planetary nebulae, calc. of electron densities from S II line 9-14195

polarimetric stars, obs. on 25 rel. to determ. of instrumental polarization in telescopes 9-12776

polarized starlight, technique for isolating non-interstellar component 9-18942

pulsar corona, oscillations and radiations 9-4095

 $\zeta$  Puppis, far u.v. spectra, abs. and emission lines obs. 9-20177

Puppis UVB photometric study 9-17619

R Coronae Borealis, obs. 9-12703

red variables, polarization change with wavelength 9-17615

RGU system new transformation eqns. to UVB system 9-14197

RR Lyrae, UVB obs. 9-12698

 $\rho$  Cassiopeiae, obs. 9-12703

Sco X-1, synchrotron, assoc. with hard electron spectra 9-17616

SCO x-1 x-ray rel. to struct. obs. 9-8270

Scorpio-Centaurus assoc., photometric study 9-14201

Simeiz 130, spectra of H $\alpha$ -emissive objects 9-1995

southern, slit-spectroscopic and photoelectric photometry 9-20179

SS II, photoelectric obs. of rapid magnitude variations 9-12709

ST Canum Venaticorum 9-12698

standard spectrophotometric, energy distrib. calibration 9-8248

Stebbins and Whitford 6-colour photometry, relation between G-R and R-I 9-15307

synbiotic, and light curves, rel. to nature 9-15282

T Coronae Borealis, equivalent width meas., electron density and atmospheric depth calc. 9-15306

T velorum, visual obs. 9-14209

Tonantzintla list early stars, survey near S. Galactic Pole, spectral classification 9-21888

two colour diagrams, dispersion rel. to absorbing matter in Galactic spiral arm 9-10498

 $\tau$  Cygni, photoelectric investigation 9-21864

UVB, Uc photometry 8000 members of Blanco-Fitzgerald catalog 9-8247

UU Virginis, UVB obs. 9-12698

UV Piscium binary syst., photometric study 9-12724

u.v. radiation from early type, effects on molecular by hydrogen clouds 9-8246

V701 Sco photoelectric study, period calc. 9-8256

V carinae, visual obs. 9-14209

variables long period, obs. on 13 stars 9-12711

 $\nu^2$  Velorum, far u.v. spectra 9-20177

white dwarfs, power-spectrum analysis 9-16575

Wolf-Rayet, interstellar reddening 9-18884

Wolf-Rayet binary HD 186943, revised period, orbital elements 9-12717

Wolf-Rayet binary HD 193928, orbital elements determ. 9-12717

Wolf-Rayet binary HD 211853, orbital elements 9-12717

Wolf-Rayet binary HD 68273, radial vel. of emission and absorption lines 9-15319

Wolf Rayet eclipsing binary HD 193576, orbital elements determ., masses 9-18874

Wolf-Rayet eclipsing binary variable absorpt. line 3872Å obs. 9-15312

Wolf-Rayet in Magellanic Cloud, five-colour narrow band photoelectric obs., absolute magnitude 9-10484

 $\chi$  Cygni, i.r., analysis, CN mol. lines, radial velocity for other lines 9-18864

XX Camelopardalis, obs. 9-12703

YY Eridani, eclipsing binary, B, V light curves, gradual lengthening of period 9-21895

YZ Cas light curve for eclipsing system, interpretation and algorithm soln. 9-17622

 $\omega$  Centauri, brightest variable obs. 9-2016 $\lambda$  Tauri, orbital elements, redetern. 9-6135

Be stars, half-widths of Balmer emission lines, and shell stars 9-10486

C stars, 26 in Auriga, positions colors obs. 9-14215

H, spectral line widening by plasma electrons 9-2010

**Stars continued****spectra continued**

- H quasi-mols. continuous absorpt. effects 9-6189  
 H $\alpha$  line obs. in 951 stars, suggested luminosity indicator 9-12690  
 H $\gamma$  I 4471 absorption width not useful for determ. of angle of inclination 9-2012  
 Mg II 4481 absorption width not useful for determ. of angle of inclination 9-2012  
 Mn I spectrum in long period variables 9-21894

**structure**

- 3 Centauri A, microturbulence deduced from high-resolution spectrogram 9-14199  
 A-star atmospheres, eff. of Si opacity on emergent fluxes and H-line profiles 9-18848  
 Alfvén wave generation, radiation loss effects 9-18279  
 Ap, probably with rot. vel. <90 km/sec. 9-12702  
 $\eta$  Aquilae, cepheid variable, model atmospheres and mass loss processes 9-16582  
 atmosphere, finite extended, radiative transfer eqn. 9-8241  
 atmosphere of F-stars, approx. model 9-4097  
 B-star atmospheres, eff. of Si opacity on emergent fluxes and H-line profiles 9-18848  
 binaries, early, rotational vel. obs., departures from axial orbital synchronism 9-15320  
 binary, H.D. 208947, orbital elements and dimensions 9-8260  
 binary close, with the third component, stability 9-18834  
 clusters, stellar density distrib. 9-17620  
 early-type stars, book 9-12685  
 eclipsing binary WCorvi, revised ephemeris, soln. for primary eclipse 9-12719  
 energy depend. on ang. rel. distrib. 9-10472  
 envelopes of Be stars, model 9-21871  
 F and G subdwarfs, He content, eff. of Lyman- $\alpha$  wing opacity 9-18859  
 F-stars, approx. model atmospheres 9-4097  
 globular clusters, count data, crowding eff. density profile 9-6141  
 H.D. 208947, orbital elements and dimensions 9-8260  
 instabilities, white dwarf to neutron star density range 9-20172  
 M39 cluster, astrophot count 9-2019  
 main sequence, from chemically homogeneous models, procedure 9-20173  
 main-sequence, effect of line absorption 9-21883  
 model with infinite pressure at center, exact soln. 9-4096  
 neutron, supermassive and white dwarf, slowly rot., equilib. config. 9-8249  
 neutron critical radius above which gravitational collapse cannot be stopped 9-2013  
 non-LTE model atmospheres, radiative equilibrium with Lyman-Alpha 9-21872  
 OB supergiants, atmospheric model and computing strong line profiles 9-16569  
 OB supergiants, expanding atmos., temp. and vel. field proposals 9-16568  
 Omicron Andromedae, shell structure core, with spectrographic obs. (1961-1966) 9-14218  
 Pleiades cluster, stellar density distrib. 9-17621  
 polytropes, non radial oscillations, mode obs. 9-15287  
 polytropes, slowly rotating, review of theory 9-15288  
 polytropes radial oscill., central density and mass conc. effects 9-2015  
 Population II, carbon abundance 9-12677  
 population II, main sequence structures from chemically homogeneous models 9-20173  
 Population II models, near main sequence, uncertainties 9-21870  
 red giants; masses in globular clusters 9-17620  
 rotating connective models with rad. press., construct. 9-18850  
 rotating disks, thin, overstabilities 9-16566  
 rotationally distorted stars, perturbation technique applied to structural investigations 9-15291  
 RR Lyrae type, masses 9-17620  
 spherical stationary systems with purely radial velocities 9-12680  
 superdense, equation of state, possible 'third' family 9-8251  
 symbiotic variables both shock and radiative excitation suggested 9-15311  
 T Coronae Borealis atmospheric depth calc. from Fe XIV transitions 9-15306  
 triple system Zeta Aquarii, orbit computation, effects of coupling, stability of configuration 9-6143  
 white dwarfs, rotating, radius rel. to mag. field 9-6122  
 Wolf-Rayet binary HD 68273, orbital eccentricity, large W-component from 127 spectrograms 9-15319  
 Wolf-Rayet eclipsing binary HD 193576, orbital elements determ., masses 9-18874  
 $\gamma$  Cygni, shock wave disturbances suggested by spectra 9-18864  
 YY Eridani, eclipsing binary, gradual lengthening of period 9-21895  
 C burning, models, Henyey method calc. 9-8240  
 He, model atmospheres constructed, 16,000-30,000°K; He, Si spectra computed 9-8239

**Stars (nuclear) see Particle track visualisation****Statistical analysis**

- See also Measurement/errors; Probability; Random processes*  
 analogue counter with up-dated histogram display 9-2182  
 attenuation of correlation, comments on the principle 9-15443  
 Bose and Fermi statistics, derivation from quantum mechanics 9-16698  
 $\gamma$ -ray perturbation by small hollow, Monte-Carlo calc. 9-19190  
 gamma-ray Monte Carlo calcs., linear energy transform. 9-18028  
 geophysics, moving random patterns correl. analysis 9-12555  
 geophysics, moving random patterns dispersion analysis 9-12556  
 Kullback information modification and relation to Gibbs' entropy 9-17727  
 least-squares fitting of straight line when errors in both coords. 9-2181  
 Monte Carlo, analytical method to determ. effect of set of input variables on output variable 9-16689  
 Monte-Carlo method, algorithmic, appl. to light beam propagation theory 9-2398  
 sound fluctuations in reverberant room 9-10741

**applications**

- See also Counters/statistical analysis*  
 atomic very high energy level population thermodynamic equilibrium shifts calc. 9-6956  
 bimolecular exchange reactions 9-10307  
 blackbody radiation, scalar representation of coherence props. 9-20468  
 climatology, Markov chain, order of dependency, test procedure 9-8167

**Statistical analysis continued****applications continued**

- diamagnetic susceptibility, model 9-10096  
 diffusion process in condensed systems, theory 9-13703  
 dislocation velocity, pinning centre conc. and shear stress dependence 9-1209  
 doorway states, density calc. and expl. detection 9-11195  
 ensembles of random matrices, method of predicting nuclear energy levels, calc. of nearest neighbour spacing distrib. 9-8949  
 entropy error parameters 9-8348  
 ergodic Markov chain for atomic-state populations, stat. equil. eqn. soln. 9-14661  
 gaussians fitting to peaks in nuclear spectrometry, max. probability method 9-13160  
 graphite powder mixtures, particle size distrib. and shape factors 9-7427  
 hydrodynamic equations of grad-type, derivation 9-3036  
 ionosphere E $\alpha$ , appl. correl. methods 9-21815  
 laser light, model 9-10847  
 linear correlaon analysis in astronomy 9-18941  
 log-normal distribution for flux fluctuations received after propag. in random media 9-14400  
 Markov chains for estimation of functional from integral eqns. 9-12857  
 maximum likelihood tech. for fitting counting distrib., applic. to sum of two exponentials with const. background 9-13156  
 maximum likelihood tech. for fitting counting distrib., applic. to ang. distrib. 9-8929  
 molecular dissociation energies, Monte-Carlo calcs. 9-7076  
 moment method correction in lifetime analysis and centroid shift reduction 9-2693  
 Monte Carlo analysis of radiative ht. transfer from cyl. cloud of part. 9-20371  
 Monte Carlo computer program for multi-nucleon stimulated decay of heavy hyperfragments 9-18063  
 Monte Carlo method for e scattering in metallic targets 9-7683  
 Monte Carlo method in transport coeff. calc. 9-4258  
 Monte Carlo program for determ. of energy spectrum of photoneutron sources 9-19303  
 Monte-Carlo method in calc. ionization cross-sections for H 9-7186  
 multivariate, to U ore prospecting 9-4036  
 paramagnetic centre distrib. statistics from relax. parameters of inhomogeneously broadened c.p.r. lines 9-1754  
 photographic granularity, stat. model. 9-19173  
 photon-counting distrib. of optical fields, theory of periodic sampling 9-8444  
 polymer chains, Monte Carlo calc. 9-833  
 reactants, stochastically distrib. second-order, decay, third-order closure 9-21683  
 rings on tetrahedral lattice, Monte Carlo calc. 9-8423  
 silica, density checking 9-13712  
 stochastic Born series for sound propag. in random media 9-14384  
 stochastic linear, passive transforms 9-6326  
 transmission lines, e.h.v., noise characts. 9-6446  
 triple coincidence circuit parameters using computer programme 9-20707  
 X-ray emission from e excited targets, computational methods 9-8337  
 X-ray transport codes, Monte-Carlo, effect of e. momenta in calcs. 9-4260  
 $^{125}_{53}\text{I}$ , defect ordering and temp. dependence, statistical model 9-1203  
 $^{125}_{53}\text{I}$ , Monte Carlo calc. and neutron diffusion in cylindrical geometry 9-20822  
 KI(Br $^{-}$ ,Cl $^{-}$ ), randomly doped, calc. of frequency spectrum 9-5312  
 LiF, excess elec. charges 9-1568  
 LiF, slip line structure from layered polishing and etching technique 9-1297  
 LiF thermoluminescent dosimeters, pre-annealing effects 9-14090

**Statistical mechanics**

*See also Lattices, theory and statistics; Quantum fluids*

- Abelian group violation in second-order transitions 9-10657  
 atomic very high energy level population thermodynamic equilibrium shifts calc. 9-6956  
 Bogolyubov distrib., power-density expansion of 2-ptcle. distrib. fn. 9-8445  
 Boltzmann's H function, alternation in sign of time derivatives 9-8422  
 Boltzmann's H theorem based on coarse graining 9-10651  
 Boltzmann eqn., unique soln. to Couette problem 9-20342  
 Boltzmann eqn. approx., monoenergetic, for neutron transport theory 9-18112  
 Boltzmann gas, dil., kinetic eqn. for the self-correlation function  $G_e(r,t)$  9-12889  
 Boltzmann to Gibbs statistic transition, refinement 9-10648  
 Casimir-Onsager reciprocal rels. 9-6335  
 charged-parti, equilibrium props. 9-8454  
 classical, gas, equilibrium approach, transport coeffs. density expansions non-existence 9-20354  
 classical systems, mechanical equilibrium 9-10663  
 compatibility properties of stationary systems 9-8430  
 continuous phase transitions, generalized Landau theory 9-95  
 cosmic ray gas, interplanetary, particle distrib. and motion 9-14245  
 critical phenomena, Ornstein-Zernike eqn. generalization 9-12897  
 diffusion process in condensed systems, theory 9-13703  
 diffusion-controlled chem. reactions 9-8057  
 dumbbells, one-dimens. array, exact occupation kinetics 9-14354  
 Dzialoshinski vector D $^{-}$  for ferromagnet, calc. 9-1656  
 electrolytes, ion distrib. 9-10346  
 electron motion in a random electric field 9-4243  
 ensembles, asymptotic equivalence for real system 9-20349  
 ensembles, relationship to thermodynamic functions 9-12831  
 entropy evolution in spin systems and non Markovian effects 9-20356  
 entropy-production theory, non-isolated system 9-20353  
 ergodic theory, classical 9-20347  
 error bounds, upper and lower, from equilibrium moments of spectral density 9-8435  
 exact master eqn., Markovian 9-94  
 fluctuation-dissipation theorem for nonlinear media 9-14356  
 fluid, cell model with infinite potential 9-14742  
 fluid, classical, one-dimens., Yang-Lee distrib. of zeros 9-8443  
 fluid, relativistic scalar, thermodynamics 9-6330  
 fluids, theory of dynamics for large spatial gradients and long memory 9-9315  
 foundations and application, conference, Copenhagen (1966) 9-20346  
 fugacity expansions convergence for classical systems 9-20351  
 functional formalism, canonical equilibrium statistics 9-10647



**Statistical mechanics continued**

- functional formalism, dynamics of Ursell-Mayer correl. functions 9-10646
- Gibbs classical, relativistic generalization for thermodynamics 9-10650
- Gibbs entropy as measure of uncertainty at microscopic level 9-6328
- Gibbs paradox, general solution and applic. to diffusing ideal gas mixture 9-11657
- Gibbs-Bogoliubov inequality rel. to bounds of configurational free energy 9-2170
- graphs used, including nonadditivity effects 9-92
- Green's functions, thermodynamic, for the Ising chain 9-14352
- Green functions, many-time, calc. using resolvent operator 9-6333
- hard disks and spheres, high density equation of state and entropy 9-8459
- hard spheres, mixture of two sizes excess free energy 9-2178
- hard-core fluid, 1D translational invariance props. 9-17745
- hard-sphere gas continuum eigenfunctions 9-8456
- hard-sphere square-well systems, N depend. in Monte Carlo calc. 9-14369
- Heisenberg antiferromag, resonance phenomena, statistical-mechanical theory 9-5979
- Heisenberg ferromagnet 9-21579
- Heisenberg model, 2D, long range order 9-19002
- Heisenberg model, anisotropic, analyticity props. 9-19000
- interacting particles system, nonanalytic points of Green's function 9-20357
- introduction for undergraduates 9-17680
- inverse problem, picking distrib. function and determ. pot. which could give rise to it 9-12898
- irreversibility 9-15433
- irreversible, perturbative approach 9-20334
- irreversible processes, multiple-time-scale theory 9-2169
- irreversible processes, operator projection method 9-16692
- Ising chain, Green's thermodynamic functions 9-14352
- Ising lattice membranes, steady-state props. 9-88
- Ising model, theory 9-17735
- Ising system approximate method 9-2165
- Langrange multipliers avoidance in introductory courses 9-4250
- lattice models of hard-core molcs, phase diagram 9-8458
- lattice-gas, 1D, equil. state, dynamical syst. 9-14351
- Lennard-Jones type potential systems, analytic props. 9-15435
- linear systems, simplified matrix method 9-8432
- Liouville eqn., soln. for plasma in external inhomogeneous e.m. field 9-10654
- Liouville eqn. for collisionless syst. of gravitationally interact. part., soln. 9-18833
- Liouville equations rel. to one-particle distrib. function 9-14358
- liquid-gas transition, dynamics of associated critical fluctuations 9-21244
- liquids, coherence time, autocorrelation func. and transport coeffs. determ. 9-20364
- long range order in 1D systems, condition 9-19002
- many-body system, classical, direct space-time correl. function 9-10667
- Markov process on compact manifold 9-20340
- Markov processes, non-stationary, and space-time 9-20339
- Markov-Gaussian process, asymptotic methods for investigation of inter-sections 9-84
- Markovian critical oscillator, Kassel theory extension 9-8442
- Maxwell-Lorentz gas in elec. field, relaxation 9-6341
- Mayer's graphical expansions, estimation methods of deg. 0 and 1 9-8437
- Mayer's graphical expansions, estimation methods of deg. 2, results 9-8438
- molecules, nonspherical polar 9-20915
- multipole particle mixed systems, statistical theory, group decomposition 9-20360
- non-equilibrium, and gravitating stellar systems 9-20145
- nonconserved mutual exchange systems, kinetic eqn. 9-2171
- nonequilibrium expansion procedure 9-8433
- nonidentical particles, interference 9-2452
- nonidentical particles, interference 9-13095
- nucleation rates theory, and metastable phase decay rates 9-101
- Onsager's reciprocal relations, with coeffs. depend. on intensive props. 9-16701
- Onsager relations and Pauli eqn. rel. to elec. conductivity 9-8439
- Ornstein-Zernike rel. for disordered fluid 9-14740
- paramagnetic spin system, isolated, nonlinear response 9-93
- particles, suspended in gas stream, phase local pulsating motions 9-89
- Percus-Yevick eqn. for hard spheres with surface adhesion 9-4257
- perturbation theory and local compressibility approx. 9-90
- phase transition, solid-fluid 9-20355
- phase transitions and distrib. of temperature zeros of the partition function examples 9-10660
- phase transitions and the distribution of temperature zeros of the partition function 9-10659
- phase transitions in one-dimensional systems, analysis 9-1065
- phase transitions in triangular lattice gas 9-107
- plasma, turbulent, particle orbits rel. to elec. field fluctuations and diffusion coeff. 9-11548
- plasma bremsstrahlung radiation, correl. function 9-7133
- polymers, cross-linked 9-11755
- quantum spin systems, thermodynamics 9-16695
- quasi-particle description, formal properties 9-16691
- radiating systems, nonequilibrium, time dependent behaviour 9-10652
- relativistic reciprocal relations betw. transport phen. 9-11655
- and religious cosmology 9-15268
- rings on tetrahedral lattice, thermodynamics, Monte Carlo calc. 9-8423
- rubber network, crosslink orientation 9-16114
- scalar hydrodynamics and gravitation 9-21000
- state critical phenomena, theory 9-10655
- stochastic relativistic processes in  $\mu$ -space, covariant treatment without particularized time-variable 9-14355
- temperature, relativistic transformation 9-2173
- thermodynamic pot. and temp. Green's functions, mean-occupation-number formalism 9-4253
- thermodynamics, relativistic, temperature transforms, moving thermometers 9-57
- thermodynamics, relativistic statistical, Lorentz-invariance equilibrium dis-tribs., formalisms 9-10653
- transport coeffs. density expansions, logarithmic terms 9-20370
- two-point correlation and sp. ht. 9-96
- ultradense matter, acoustic waves faster than light 9-6384
- university level textbook 9-10601

**Statistical mechanics continued**

- van der Linden's proof, equilibrium ensembles asymptotic equivalence 9-20344
- Viasov eqn., dispersion rels. 9-8429
- Vlasov eqn. for classical fluids, derivation from Liouville eqn. 9-8440
- zero sound in classical liquids 9-100
- He II, fluctuations and correlations, review 9-21238
- KH<sub>2</sub>PO<sub>4</sub> Slater model, one-dimens. analogue 9-6257
- quantum**
- adsorbed H isotopes, partition function 9-13586
- Birkhoff and von Neumann's interpretation 9-16693
- Boltzmann gas, dense charged, near abs. zero, free energy 9-8428
- bose condensation and shock waves in photon spectra, ionized plasma 9-14766
- Bose fields for integral spin part., fundamental theorem 9-17926
- Brownian motion in phase-space, Schrodinger-type prob. amplitude 9-12893
- correspondence identities for quantum and classical mech., for low quantum no. 9-4866
- Coulomb attraction, two-particle density matrix, path-integral calc. 9-9354
- Coulomb interact. systs., binary Slater sums, distrib. functions 9-11536
- critical phenomena, microscopic analysis 9-12888
- critical phenomena, microscopic analysis 9-83
- density matrices in many-fermion syst. 9-20359
- detection of coherent radiative signal and error probabilities 9-8431
- distribution functions and binary Slater-sums for Coulomb mutual exchange system 9-6329
- dust, spherically symmetric charged distrib., expansion and perturbation eff., gen. relativity 9-8386
- electron gas, quantum mech. distrib. functions 9-4255
- electron gas, relativistic, in intense mag. field 9-8453
- entropy of states, mean 9-8436
- ergodic problem and Gibbs formalism for non-relativistic systems 9-10649
- ergodic theory, development, review 9-20348
- Fermi fields for half-integral spin part., fundamental theorem 9-17926
- Fermi gas, magnetized, thermodynamic props. 9-8449
- fermions interacting in one-dimension, remarks on theory 9-17743
- Feynmann-Schrodinger eqn., statistical sampling method, perturbation potentials corrections 9-16684
- Fokker-Planck exact generalized eqn., arbitrary non- and dissipative quantum system 9-10661
- fugacity expansion convergence 9-20352
- hard-sphere gas, discrete spectrum for linearized Boltzmann eqn., relax. modes 9-4256
- harmonic oscillators, linear system, stochastic types of motion 9-8414
- Heisenberg anisotropic chain rel. to H-bonded cryst. 9-1120
- interacting, probability of excitation of eigenstates 9-16696
- interaction angular momentum, tensor form, classical mech. and quantum field theory investigation of eff. 9-16803
- intermolecular forces, effect of molec. identity 9-2930
- intermolecular two-temp. potentials, effect of molec. identity 9-2931
- introduction for undergraduates 9-17680
- invariant partial states, existence and extension 9-91
- Ising spin model with 5 transition points 9-5795
- Jaynes' irreversible stat. mechanics used in quantum mechanical description of reality 9-20323
- kinetic eqn. for quasiparticles to order  $\lambda^*$  in problem of interac. bet. rad. and matter 9-11389
- kinetic eqn. rel. to Darwin Hamiltonian, electrons with mag. interac. 9-97
- Liouville eqn., applic. of complementary variation principle for  $\Delta\phi=f(\phi)$  9-19001
- locally normal states 9-20341
- many body problem, particle group functions treatment 9-15437
- many-particle system collective motion, generator coordinate theory 9-6766
- Markoff process with stochastic force rel. to Schrodinger eqn. 9-8404
- n-body problem with spin-orbit and Coulomb interac., resolvent study, use of modified Fredholm theory 9-17739
- nonperturbation T-matrix study, analytic props., geom. of contour distortion 9-2463
- nuclear matter, superfluid transition critical temp. 9-488
- of individual systems rel. to infinite systems statistical props. 9-2168
- open systems, nonequil. generalized master eqn. 9-6331
- operator expectation values for transitions within ensembles in pure states, method 9-20343
- oscillators, driven, reservoir coupled 9-10656
- parastatistics applied to quark model of baryon 9-6680
- plasma, fully ionized quantum, eqn. of state 9-860
- plasma, low density, free energy derivation from exact scatt. phase shift 9-7138
- plasma, relativistic phase-space symmetries in Minkowski space 9-859
- quasi-two-body react., parity exchange, splitting of cross-section 9-4569
- radial distribution functions for hydrogenous plasma in equil. 9-18269
- rate eqns., oscillatory solutions 9-6334
- relativistic elem. syst., position operator defin. 9-6332
- resonance energy transfer in condensed media from many-particle view-point 9-5621
- rotational motion of syst. of n mass points 9-6338
- RPA validity in solvable two-mode nuclear model 9-6762
- Schrodinger many-particle operator with combined Zeeman and Stark eff. 9-20330
- specific heat, Einstein's theory, simplification for teaching purposes 9-6263
- spectral density technique 9-98
- stochastic theories in quantum mechanics, anal. using Feynman integral 9-16694
- stochastic theory, new formulation 9-2172
- sums conversion to integrals, validity 9-4249
- susceptibility tensors, isothermal, adiabatic and isolated static, bounds 9-5793
- Thomas-Fermi eqn., applic. of complementary variation principle for  $\Delta\phi=f(\phi)$  9-19001
- transitions, multiple real 9-16696
- vinial coeff., second, quantum corrections at high temps. 9-17746
- and wave mechanics, relationship 9-17736
- H<sub>2</sub> quantum crystal, wide range of physical and computational utility 9-15436

**Statistical mechanics** continued**quantum** continued<sup>3</sup>He liquid, Landau parameter estimated from quasiparticle transport eqn.

T=0 9-106

<sup>3</sup>He surface waves 9-104**Statistical thermodynamics** see *Statistical mechanics***Steady-state theory** see *Cosmology***Steam**

corrosion of graphite, diffusion-convective soln. rel. to reactor appl. 9-9095

corrosion of U fuel element in steam-water system, 285°C 9-11361

oxidation of UO<sub>2</sub> by steam, 885-1835°C 9-3397

thermodynamic properties, tables 9-3053

thermodynamic props. rel. to press., analytical approx. for saturated steam 9-17160

two-phase flow in channel, steam vol. fraction, &lt;2000 psi 9-11646

CO<sub>2</sub> gas, i.r. rad., large path length limit 9-19585D<sub>2</sub>O gas, P<sub>1</sub>-moment of total scattering probability 9-20792D<sub>2</sub>O, virial coeffs., 150°-500°C 9-7224**Steel**

1Kh18N10T, welded joints, corrosion resistance enhancement by quenching 9-16142

60Kh3G8N8V, hot working effects on stress-corrosion cracking susceptibility 9-3449

AISI 4340, environmental cracking 9-19812

alloys, strength without brittleness 9-5491

aluminization by vacuum evaporation 9-13584

analysis by X-ray fluorescence of mild steels 9-6034

annealing of cold-worked Cr-Mn-N steel, structural changes 9-13776

austenite recrystallization in slightly hypoeutectoid carbon steel during hot working 9-16145

austenite to martensite phase transform., dilation coeff. variation 9-5507

austenitic, creep crack nucleation and growth 9-13740

austenitic, exoelectron emission during cyclic loading 9-13937

austenitic, heat treatment to improve corrosion resistance, patent 9-13755

austenitic, oxidation in CO<sub>2</sub>, thermal cycling effects 9-17528austenitic, resist. changes accompanying  $\gamma'$  precipitation 9-1319

austenitic, stainless, ferrite and sigma-phase formation 9-14989

austenitic stainless, precip. of  $\gamma'$  9-5517

austenitic stainless, strengthening by strain hardening due to phase transform. 9-5499

austenitic transformations, C redistrib. law 9-3490

C, slightly hypoeutectoid, austenite recrystallization during hot working 9-16145

C transfer from unstabilized to stabilized steel in Na melt 9-10345

carbon, ductility and strength depend. on hydrostatic press. and temp. 9-5478

cast, repair welded, fatigue props. 9-17316

casting, embrittlement due to welding, effects of conditions and structure 9-17317

cleavage fracture, hydrostatic stress effects in mild and low-C, Mn steels 9-17318

coercive force in transformer steel single crystals, dependence on dislocation structure 9-13988

compression, dynamic, resistance at high strain rates 9-21365

in concrete, restrained expanding, bonding 9-18500

corrosion, outdoor exposure, eff. of orientation of specimens 9-20055

corrosion behaviour of stainless steel, in high temp. water and superheated steam 9-17536

corrosion by CuSO<sub>4</sub> 9-20057

corrosion by organic acids 9-20056

corrosion by S of ferritic Cr steels, 600-1000°C 9-18759

corrosion by sulphate-reducing bacteria 9-17537

corrosion chemistry of austenitic Cr-Ni steel following neutron irradiation 9-21701

corrosion in H<sub>2</sub>SO<sub>4</sub> soln., from polarization data 9-21698

corrosion of pipes under flow conditions, mass transfer correlation with temp. effects 9-21696

corrosion of stainless-steel tube, vented, on exposure to CO<sub>2</sub>-CO mixture in nuclear reactor 9-15221

corrosion pit nucleation in stainless steel, effect of sulphide inclusions 9-21700

corrosion resistance of welded joints, enhancement by quenching 9-16142

crack growth in H and water environments, comments 9-5484

cracking, environmental, in AISI 4340 steel 9-19812

cracking of grain boundary carbide films in 1.4%Mn steel 9-19811

creep crack nucleation and growth in austenitic steel 9-13740

creep tests by deformation with ball 9-5468

cylinder, tensile strain parameters, Bridgman's observational relationship 9-9768

cylindrical shell, thin walled, external press., collapse press. and failure modes determ. 9-18490

decarburization and surface graphitization on contact with Na at 600°C 9-16150

deformation props. under alternate tension and shear above plastic limit 9-11927

deformation resistance in E1702 steel, effect of grain size 9-9760

deformation resistance temp. dependence anomaly in aged N36KH12TYU samples 9-21372

degassing in vacuum 9-13747

dislocation structure on deform. structure in N36KH12TYU 9-3347

ductile fracture criteria, study using AI model 9-18516

E1702, aged and quenched, resistance to deform., effect of grain size 9-9760

electrical sheet, volt-amp. meas. accuracy, air flux correction 9-1466

electrotechnical, hot-rolled, structures of reduced oxide films 9-6012

fatigue fracture, study of surface patterns formed 9-5480

fatigue strength under composite stress including h.f. vibs. 9-5474

ferritic Cr, corrosion by S, 600-1000 °C 9-18759

fracture surfaces with cracks of 'flocule' type, metallographic and X-ray diffraction investigation 9-5483

galvanized, oxide film growth and thermal rad. props. 9-19985

graphite precipitation, effect of Ca 9-19838

H36x12TYu, gamma-phase segregation, form and bonding to matrix particles 9-9789

heat-affected zones in rolled, Nb-treated, low C, Mn steels 9-19819

heat-affected zones of welded high-strength structural steels corroding in sea-water, occurrence of massive ferrite 9-21402

**Steel** continued

hematite, reduction rate of dense sphere by hydrogen, mathematical model 9-20046

hot cracks in welds 9-13739

internally oxidised electrotechnical, mag. props. 9-13989

Kh12ND, welds, structure and properties, effect of Cr content 9-14984

Kh18N10T, creep tests by deformation with ball 9-5468

length meas., zero change at hardening and austempering 9-9778

low C, diffusion of Cr 9-5407

low C, diffusion of Cr 9-5406

magnetic props. of internally oxidised electrotechnical steel 9-13989

martensite, C-bearing, heat evolution during room-temp. ageing 9-1344

martensite, carbon-dislocation interaction 9-1218

martensite, deformed and from cold-worked austenite, thermal effects of ageing 9-7595

martensitic, ferritization by 1% Ti addition 9-16140

martensitic stainless, grindability, effect of C content 9-17323

mild, analysis by X-ray fluorescence 9-6034

mild, corrosion by sulphate-reducing bacteria 9-17537

mild, cylinders, reln. between ultimate press. and wall thickness 9-5473

mild, effect of hydrostatic stress on cleavage fracture 9-17318

mild, elastoplastic stress and deform. on thermal cycling of plates 9-5450

mild, explosively loaded, effect of grain size on dynamic yielding 9-3439

mild, oxidation, effect of air speed 9-21694

molten, decarbonizing and deoxidizing, vacuum techniques 9-18530

Mossbauer effect, influence of plastic deformation 9-19981

N36KH12TYU, aged deformation resistance temp. dependence anomaly 9-21372

N36KH12TYU, disloc. structure on deform. ageing 9-3347

neutron (14 MeV) attenuation, with polyethylene as radiation shield 9-18949

neutron radiographic scatter factors 9-2801

nitride layer formation in Cr-Ni steel in intermediate stages of  $\gamma$ - $\alpha$  transformation 9-13775OKh32N8, quench-hardened,  $\delta$ -ferrite decomp. during tempering 9-1343

oxidation of mild steel, effect of air speed 9-21694

pearlite to austenite, edgewise growth rate 9-11964

phase transitions from Mossbauer obs. 9-16151

pitting corrosion of austenitic Cr-Ni stainless, in H<sub>2</sub>SO<sub>4</sub> containing H<sub>2</sub>S 9-20054

plastic deformation accompanying fracture, localisation and intensity by X-ray diffr. anal. 9-11922

plates, clamped, plastic deform. due to projectile impact 9-1279

Poisson's ratio for plastic deformation 9-21373

powder, pressing and sintering behaviour 9-17339

Poynting-effect problem, numerical soln. 9-5444

for reactor melting pot, corrosion resistance 9-651

Robertson crack arrest test 9-19809

rod in water reflector of reactor, fast reflection 9-18125

rolled, austenite retention determ. from diffracted intensities corrected for texture effects 9-1317

Seal to CaF<sub>2</sub> at high press and temp. 9-6233

sheets, limiting speed of ductile crack propagation 9-18524

solution of atmospheric gases during spontaneous surface cleaning 9-21283

stacking faults in austenitic Cr-Mn-N steel 9-18476

stainless, cleaning in vacuum, emitted gas exam. 9-20070

stainless, corrosion in high temp. water and superheated steam 9-17536

stainless, corrosion pit nucleation, effect of sulphide inclusions 9-21700

stainless, fine structure of spots caused by wedge shaped crystal parts, expl. rel. to theory 9-13620

stainless, foil, for zero point calibration in Fe-Cr alloy Mossbauer spectroscopy 9-19973

stainless, fuel cladding, burst strength rel. to thickness and defects obs. 9-15799

stainless, localized deformations during ductile fracture 9-17315

stainless, Mossbauer eff., infl. of plastic deformation 9-19981

stainless, outgassing at 10<sup>-7</sup> to 10<sup>-10</sup> torr 9-14299

stainless, thermal control surface for Mars Lander, protection from dust storm 9-1386

stainless, thermal radiation props., meas. by cyclic incident radiation 9-5562

stainless, thin films, microtwins prod. by mechanical abrasion 9-3228

stainless 304 film, interfacial free energies, investg. by electron transmission and diffr. microscopy 9-1231

steel, austenitic stainless, Widmannstätten M<sub>23</sub>C<sub>6</sub> precip., nucleation and growth 9-1331

steel, case-hardening, insonation effects 9-19845

steel, var. residual austenite content, residual stress 9-3415

steel-Al interface, directional heat transfer rel. to surface conds. 9-13809

stiff string, normal vibr. modes 9-2198

stress-corrosion cracking of high strength samples 9-9757

stress-corrosion cracking susceptibility, hot-working effects 9-3449

structural changes depend. on temp. after laser irradiation 9-5418

structural recrystallization studies by vacuum metallography 9-1154

tempered, alloyed with W, orientation of carbide phases 9-5504

tensile fracture behaviour as a function of pressure 9-18518

tensile strength, notch effect rel. to inclination angle 9-9769

transformer, cold-rolled, recrystallization 9-1155

transformer, commercial grade, secondary recrystallization, role of surface energy 9-13752

transformer, free energy of grain boundaries, variation rel. to crystal misalignment angle 9-3291

transformer, secondary recrystallization, kinetics, initial grain size 9-9792

transformer, single crystals, coercive force, depend. on dislocation structure 9-13988

transformer, sp. losses mag. induction amplitude dependence, texture effect 9-1676

type 304, thermal expansion obs. using gas-activated acoustic dilatometer 9-15009

vacuum melting and casting 9-5493

welded box columns, ultimate strength 9-14979

welding joints with Cu or Cu alloys, crack formation and melting of base materials 9-21397

welds, structure and properties, effect of Cr content 9-14984

wire, energy dissipated during fatigue cycling, calorimetric study 9-13717

X-ray absorpt., 6MV primary radiation 9-7681

yield and fracture behaviour, Al-killing effect in 0.16-0.2C, 0.65-0.75 Mn steel 9-19795

yield point directionality in strain-aged steels 9-17307



Steel continued

Al coatings, struct., composition and adhesion, effect of condensation temp. 9-21282  
Cr-Mn-N. cold-worked, structural changes during annealing 9-13776  
Cr-Mn-N austenitic, X-ray meas. of stacking faults 9-18476  
Cr-Mo, creep, and creep rupture of pressurized cylinders 9-18509  
Cr-Ni, formation of structure of nitride layers, mechanism 9-13775  
Cr-Ni stainless austenitic, pitting corrosion in H<sub>2</sub>SO<sub>4</sub> containing H<sub>2</sub>S 9-20054  
Cr diffusion layers forming protective coatings, structure and metallography 9-11769  
Fe-Ni-Si-C, fracture of martensite, eff. of plate size, ageing and temp. 9-18517  
Mn, 1.4%, cracking of grain boundary carbide films in 1.4%Mn steel 9-19811  
Mn, low C, Nb-treated, rolled, heat-affected zone props. 9-19819  
12% Mn, martensitic transformation produced by cold working obs. by transmission electron microscopy 9-5516  
Mo content determ. using vacuum spectrometer 9-20069  
N spectrochem. analysis in X25T, H41XT, X25Yu5 and Cr-Ni foils, obs. 9-18778  
Re,  $\gamma$ -martensite formation at -180°C 9-9800  
Si, commercial grade sheets, mag. field annealing eff. 9-13753  
V, secondary hardening on tempering, high dislocation density as preferential nucleation sites 9-17328

**Stellar atmospheres** see *Stars*

**Stellar clusters** see *Stars*

**Stellar composition** see *Stars/composition*

**Stellar evolution** see *Stars/evolution*

**Stellar motion** see *Celestial mechanics; Stars*

**Stellar structure** see *Stars/structure*

**Stellarator** see *Plasma/devices*

**Stereoisomerism** see *Isomerism*

**Stereophonic sound** see *Acoustics*

**Steroscopy** see *Vision*

**Stimulated emission** see *Lasers; Luminescence; Masers*

**Stimulated Raman scattering** see *Lasers; Scattering/light, Raman spectra*

**Stochastic processes** see *Probability; Random processes; Statistical analysis*

**Stokes flow** see *Flow; Hydrodynamics*

**Stokes law, fluids** see *Flow; Viscosity*

**Stokes law, optical** see *Luminescence*

**Stokes lines** see *Luminescence; Scattering/light, Raman spectra; Spectral/molecules*

**Stopping power** see *Energy loss of particles*

**Storage devices**

memory, applic. of coercive force increment in mag. coupled structs. 9-3811  
memory, high density, rel. to specifications and yields of composite mag. films 9-3810  
optical, Lippman emulsion three-dimens. memory 9-10916  
optical random access fixed store 9-2408  
Gd garnet, static and dynamic props. meas. 9-10139  
Ni-Fe films, uniaxial, analog, storage using non-uniform fields 9-5844  
Ni rod, memory, coercive force isothermal remanent magnetization, variation with internal stress 9-5828

**Storage rings** see *Particle accelerators/accessories*

**Storms** see *Atmosphere/movements; Magnetic storms; Thunderstorms*

**Strain effects** see *Deformation; Elastic deformation; Plastic deformation*

**Strain gauges**

balance, method of reducing signal interaction 9-5443  
dosimetry, measurement of thermal expansion of irradiated material 9-16923  
high temp. operation, resistance materials 9-3409  
high-temperature resistance, use of precious metal alloys 9-13723  
measurements, book 9-6267  
peak-stress gauge for determining the yield of underground nuclear explosions 9-10744  
reactor pressure tubes, creep meas. 9-4818  
semiconductor, calibration and characteristics 9-5441  
start-up thermal strains meas. in steam power station plant 9-5442  
X-ray diffraction, tensile loading device 9-11918  
X-ray method for cry. lattice thermal expansion, piezoelectric const. determ. 9-3262  
Cu-Ni resistance alloys for high temp. strain gauges 9-3409

**Strain hardening** see *Work hardening*

**Strange particles**

creation in  $\pi$ N collisions at high energy 9-11053  
final states with two or more, from K-p at 4.25 GeV/c 9-11041  
photoformation on p and n near threshold 9-8908  
pp, 8 BeV/c, production 9-2532  
 $\Xi(1815)$  with strangeness S=-2, evidence for existence 9-11116

**Strangeness** see *Elementary particles; Field theory, quantum*

**Stratosphere** see *Atmosphere*

**Streamers** see *Discharges, electric*

**Strength** see *Electric strength; Mechanical strength*

**Stress analysis**

See also *Bending; Photoelasticity; Strain gauges; Torsion*  
anisotropic media, dislocation fields, analytic solns. 9-7481  
bars, under periodic axial loading, finite element soln. of stability for various end conds. 9-6373  
beam, crack end stress concentration 9-16136  
beam impacted by elastic bar 9-6658  
bending, uniform, of anisotropic plastic plate 9-4279  
bending of plates, Reissnerian algorithms in refined theories 9-14374  
bending of thin layered plates 9-10701  
buckling conditions for columns supported laterally by side-rails 9-20387  
cantilever beams, tapered, with perpendicular load, computer analysis 9-17762  
circular disk with 2 parabolically distrib. loads on its circumference 9-6360  
complex structure, coupling of substructs. and use of basic mass and stiffness matrices in dynamic anal. 9-12925  
cosserat plates, load-induced stress singularities 9-12915  
Coulomb material, short cylinders, analysis 9-20386

**Stress analysis continued**

creep, elastic analogue for all time-independ. boundary conditions 9-21376  
creep buckling of circular cylindrical shells 9-17761  
cylindrical bar under band-press., 3D photoelastic anal. 9-20401  
cylindrical shell, finite curved element, stiffness matrix and load vectors 9-16712  
cylindrical shell, stress distrib. around circular cutout, soln. and boundary condition 9-19018  
cylindrical shell under radial press. difference, elastic-plastic anal of collapse 9-17771  
cylindrical shells, axially compressed, buckling problem, influence of small imperfections 9-19031  
dams, arch, pot. distrib. using matrix displacement method 9-16717  
dielectric spherical shell, compressible, radial deforms. 9-125  
disc, stress function along free edges, boundary conditions 9-12916  
disc in plane stress, discontinuous boundary-value Prandtl eqn. 9-10694  
disc of constant thickness, due to thermal nucleus in sector  $\Delta\alpha$  9-20390  
discontinuity, stress surfaces, relations in 3D rigid-plastic bodies 9-17778  
discrete structural systems, non-linear perturbation analysis 9-17759  
distribution in shallow cone 9-14373  
edge dislocation strain field analysis 9-3341  
edge restraint coupling on ring-supported cylinders, effect on buckling 9-20395  
elastic, homogeneous, isotropic, centro-symmetric body, stress function determ. 9-4275  
elastic body, electrically conductive, in mag. field, asymm. stress possibility 9-21564  
elastic embedded filament under longitudinal force, shear stresses and discontinuities 9-16711  
in elasticity, planar, without intermediate calc. of constraining forces 9-17756  
elasto-plastic matrix, formulation using 'initial stress' finite element approach 9-8484  
elastomer, stress due to sinusoidal oscillations superposed on finite strain 9-19052  
equilibrium cracks under harmonic loading 9-10697  
extension of space containing plane annular slit 9-17768  
finite element methods for solid continua 9-8468  
fluids, forces in relativistic motion 9-7099  
graphite, tensile stress relax., 2000°-2700°C 9-7532  
heterogeneous cone under axial load, equilibrium 9-20402  
h.f. elastic waves in bars under damped sinusoidal loading, photoelastic anal. 9-19058  
holographic interferometer 9-6365  
hyperstatic systems, appl. of photoelasticity 9-20396  
inclusion, eccentric circular, in a circular region 9-2191  
inhomogeneous anisotropic cyl. shells, buckling stress due to bending 9-20384  
instability under applied moment of angle section beam 9-20388  
isotropic materials with memory, use of symmetry in constitutive eqns 9-128  
membrane, anal. by reduction of biharmonic boundary value problem to direct method 9-19015  
membranes, curved 9-6354  
microcracks, dead-end, fields 9-18521  
multilayer sandwich beams, bending inc. rigidity of face layers 9-20393  
Nimonic alloy, critical shear stress changes on structural changes rel. to precip. hardening mechanism 9-3469  
nonlinear stress conc. and crack propagation 9-16709  
orthotropic shells of revolution, prestressed, under axisymmetric loading 9-20394  
panel in supersonic stream, stability boundaries, Liapunov anal. 9-21127  
parallelogram plate element in bending 9-16713  
photoelastic, 'freezing' deformation method 9-14378  
photoelastic, of plate with reinforced circular hole 9-10691  
plane frames, failure loads evaluation using elastic and plastic load-deform. characts. 9-126  
plane strain deformation of elastic mat., class of exact solns. 9-10692  
plastic instability of thick-walled tubes with closed ends 9-20411  
plate, circular, sealing compressible liquid 9-8476  
plate, thick circular, three-dimens. elastic stability 9-8481  
plate bending, conforming quartic triangular element 9-8483  
plate bending, refined triang. finite element 9-15451  
plates, large deflection anal. by finite element method 9-8485  
plates, yield point loads, upper and lower bounds, numerical anal. 9-19032  
plates with notches and holes, rel. to force and dislocation singularities 9-5440  
potential distrib. in structure using matrix displacement method 9-16717  
propagating jumps, infl. of heat conduction 9-16708  
resonators, disc and ring, radial, torsional vibr. modes 9-4271  
ribbon, rigid, excited by plane waves, singular solution 9-143  
shear stress on shear plate calc. 9-6361  
shear stress/shear rate relationship, fluid laminar pipe flow 9-853  
shell, circular cylindrical radial displacement under random press., statistical characts. 9-6371  
shell, cylindrical, axisymmetric creep buckling collapse 9-8473  
shell, helicoidal, stresses, stiffness coeff. calc. 9-19024  
shell, stress function along free edges, boundary conditions 9-12916  
shell, thin, boundary value problem, stress and strain functions determ. 9-17751  
shell, thin cylinder, inconsistencies of Donnell and Morley eqns. 9-8477  
shells, around curvilinear holes 9-4272  
shells, translation, elastic theory 9-20405  
solid, linear viscoelastic, divergent pulses 9-13716  
Statics, collapse analysis of framework systematic selection of redundant force 9-118  
steel, low-carbon, ratio of dynamic yield stress to quasi-static yield stress 9-21365  
strain amplitude, critical, temp. depend 9-3408  
strain distrib. expt. methods, comparison 9-8475  
stress distribution around loaded bolt in axially loaded bar 9-16721  
strip specimen, continuous distrib. rel. to bending 9-19787  
structural analysis, direct stiffness solns., round off errors in computation 9-8474  
surface isotropic with cylindrical hole, stress concentration using dipolar field eqns. 9-19028  
thermal, axisymmetric, in spheroidal shell 9-8497  
thermal, by variational principle, linear viscoelastic body 9-4281

# Stress analysis continued

- thermal end stress in long circular rod 9-19042
- thermal in temp.-dependent viscoelastic body 9-19036
- thermal stresses in solid weakened by external crack 9-17302
- thermoelastic stress wave generation by absorpt. of impulse e.m. rad. 9-16723
- thermoelastic wave propagation in inhomogeneous half-space, discontinuity anal. 9-20423
- thick plates, multi-moment theory of equilibrium 9-10690
- thin elastic isotropic shells, finite-element analysis for static small-deflection behavior 9-20392
- thin elastic shells precrack deformation, correlation theory 9-17767
- three-dimensional photoelastic, design of stress-freezing oven applic. 9-20401
- three-dimensional stress conc. round cyl. hole in semi-infinite elastic body, soln. and boundary values 9-20403
- three-dimensional stress conc. round cyl. hole in semi-infinite elastic body, soln. and boundary values 9-20404
- torus, pressurized, role of initial displacements in analysis by bending theory 9-134
- two dissimilar materials bonded over one face, stress analysis when subject to normal and shear loading 9-20406
- vice for inducing high uniaxial compressive stresses in crystals 9-1165
- waves on spherical shell 9-12931
- Be, high purity, critical shear stress for slip along basal plane in plastic deform., 4.2-300°K 9-1282
- Ni-Al alloys, critical shear stress changes on structural changes rel. to precip. hardening mechanism 9-3469
- Si, patterns on X-ray micrographs, analytical description 9-11873

# Stress effects

- alkali halides: divalent cations, crit. shear stress rel. to impurity-vacancy-dipole agglomerate and precip. 9-5372
- alkaline earth sulphides, thermally induced coloring 9-1745
- alloys, defect structures, shear-induced softening, response to stress 9-21335
- alloys, internal friction at large strain amplitudes 9-16118
- bending of strip specimen by continuous distrib. 9-19787
- crack, Griffith, intensity factors for asymmetrically loaded surfaces 9-18523
- crystals strained by thin films, Lang topographs, contrast asymmetries 9-5292
- cylindrical shell under concentrated loading 9-20385
- disk with circular hole, creep under equal biaxial loading 9-5469
- dislocation groups mobility 9-11876
- graphite, fracture under torsional and biaxial stresses 9-7565
- graphite, highly-oriented, tensile and compressive creep rates 9-7552
- graphite, under compression, acoustic noise emission 9-7641
- lubricant, solid film, pressure effects on friction coeff. 9-16138
- mechanical, rel. to Barkhausen discontinuities 9-5827
- metal beam, dynamic load factor, solid viscosity effect 9-4280
- metals, electrochemical dissolution during yielding 9-1914
- metals, internal friction at large strain amplitudes 9-16118
- Mg disk with circular hole, creep under equal biaxial loading 9-5469
- microstrain, X-ray diffraction obs. 9-3410
- microstrain studies, elastic modulus reduction and reverse strain 9-16122
- paraffin film lubricant on steel, pressure effects on friction coeff. 9-16138
- permalloy, mechanical, rel. to Barkhausen discontinuities 9-5827
- plate with elliptic inclusion, cavitations 9-19029
- polycaprolactam fibres, photomechanical degradation and lifetime 9-11937
- polyethylene terephthalate, deform. bands prod. by tensile and shear tests 9-5463
- polymer, crystallization under shear stress, rel. to unstable flow mechanism 9-17236
- polymer organic solids, shear stress eff. 9-21366
- polymethylmethacrylate, damage under extreme loads during laser-illumination 9-16137
- polystyrene, damage under extreme loads during laser-illumination 9-16137
- semiconductor point contact diode, barrier lowering and current change due to mechanical pressure 9-18635
- shell, cylindrical, dynamic buckling in sustained axial compressive flow 9-138
- shells, cylindrical and spherical, buckling under press., analysis 9-20399
- shells, oval cylindrical; buckling and initial postbuckling under axial compression 9-133
- silk fibres, photomechanical degradation and lifetime 9-11937
- slip, secondary, rel. to detection by macroscopic meas. 9-14978
- solids, shock compressed, empirical reln. between sound vel., density and press. 9-4362
- steel, austenitic stainless, strain hardening due to phase transform, strengthening eff. 9-5499
- steel, high strength, stress-corrosion cracking 9-9757
- steel, loc C, on fatigue strength, eff. of composite stress including h.f. vibs 9-5474
- steel, mild and low-C, Mn, effect of hydrostatic stress on cleavage fracture 9-17318
- steel, surface topography near fatigue fracture 9-5480
- uniaxial, piezoelec. props. meas., high compression vice 9-1165
- viscoplastic ductile creep failure 9-8495
- waves, transverse in an elastic medium due to surface forces, use of Heaviside function 9-8505
- wind stress on water surface, waves obs. 9-21169
- Ag, triangular Frank dislocation loops, induced dislocation, dynamical treatment 9-3343
- Al, dislocation densities and configuration 9-21338
- Al, dislocation viscous drag at high strain rate, 10°K, 77°K, 300°K AND 500°K 9-1214
- Al cylinders, reln. between ultimate press. and wall thickness 9-5473
- Al fatigued, form d. cell structs., and dislocation patches 9-5347
- Au, triangular Frank dislocation loops, induced dislocation, dynamical treatment 9-3343
- Au film lubricant on steel, pressure effects on friction coefficient 9-16138
- BaS, induced coloration obs. 9-1745
- Be, compressive deform. investig. 9-11926
- C, pyrolytic and glassy, stress depend. of tensile creep rate 9-7550
- CaS, induced coloration obs. 9-1745
- Cr, magnetostriction on stress-cooling rel. to ordering obs. 9-1700
- Cr, deformed, dislocation arrangement in stress-applied state, electron microscope obs. 9-14946
- Cu, strain hardening study 9-18499

# Stress effects continued

- Cu, triangular Frank dislocation loops, induced dislocation, dynamical treatment 9-3343
  - Cu stress-induced ordering of point defects near 10°K 9-9755
  - Fe-Si, mechanical, rel. to Barkhausen discontinuities 9-5827
  - Fe in remanent state, elastic tensile stress effects on magnetostrictive props. 9-19956
  - Ge:Zn, on e. scatt. by neutralized Zn acceptors 9-1546
  - Ge:Zn<sup>+</sup> excitation spectrum 9-7974
  - KBr:Li<sup>+</sup>, far i.r. resonant-mode freq. shifts 9-5922
  - KCl:(Cu), X-irrad. luminescence 9-3932
  - KCl dislocation processes during creep deformation 9-1223
  - K<sub>2</sub>CrO<sub>4</sub>, uniaxial compression eff. on abs. spectra, 20°K 9-10206
  - KI:Ag<sup>+</sup>, far i.r. resonant-mode freq. shifts 9-5922
  - LiF, cold-worked, microstrains and crystallite size, evaluation from X-ray diff. line profiles 9-13640
  - LiF, polycrystalline, creep behaviour, 300°-550°C 9-11933
  - LiF slip deformed, dislocation structure, obs. 9-5364
  - Mg alloy disk with circular hole, creep rupture under uniform radial tension 9-7554
  - Mg alloy disk with circular hole, creep rupture under uniform radial tension 9-7554
  - MgO, rel. to creep 9-19799
  - MoS<sub>2</sub> film lubricant on steel, pressure effects on friction coefficient 9-16138
  - (NH<sub>4</sub>)<sub>2</sub>CrO<sub>4</sub>, uniaxial compression eff. on abs. spectra, 20°K 9-10206
  - NaCl, dislocation processes during creep deformation 9-1223
  - NaCl, N<sub>2</sub> zero-phonon line, strain broadening 9-1792
  - NaF, uniaxial, on R<sub>2</sub> zero-phonon absorpt. line 9-7504
  - Ni-base alloy, wrought, cycling effect on creep behaviour, 955°C 9-18511
  - Ni mechanical, rel. to Barkhausen discontinuities 9-5827
  - Pt/Pt-(13 at. wt.%)Rh thermocouple, thermal e.m.f. 9-12208
  - Rb silicate glass, rel. to viscosity, 10<sup>14</sup>-10<sup>16</sup> poise 9-3422
  - Si-SiO<sub>2</sub> interfacial stress, rel. to interface states 9-12176
  - Sn Fermi surface, effects of tension 9-15057
  - SrS, induced coloration obs. 9-1745
  - SrTiO<sub>3</sub>, induced dichroism at absorption edge 9-3858
  - Ti(6 wt.%)Al(4 wt.%) V alloy, fatigue-cracked, load relaxation, effect of methanol 9-19786
  - Ti, polycryst., rel. to microstrain distrib. 9-16125
  - U(10 wt.%)Mo alloy, stress-corrosion cracking, effects of heat treatment and ambient atmospheres 9-21384
  - ZnS, torsional, prod. of low angle twist boundaries 9-5348
- Stress measurement** *see* **Strain gauges**
- Stress-strain relations**  
*See also* **Elastic constants**
- Armco iron, yield and flow stresses, temp. and strain-rate dependence at low temps. 9-1285
  - concrete, curves for short-term loading and deformation 9-16121
  - crystal containing plastic deformation 9-14968
  - curve, rel. to transient work hardening phenomena in crystals with edge dislocation dipole clusters 9-1322
  - cylindrical shell, plane-strain dynamic response 9-19023
  - for deformation studies of real materials, book 9-14973
  - disc of constant thickness, state due to thermal nucleus in sector Δα 9-20390
  - elastic, workhardening solids 9-18497
  - elastoplastic propag. along bar heated at one end 9-19057
  - graphite, RVD, tensile and compressive curves, with and across-grain dirns., to 5500°F 9-7537
  - graphite, torsional and biaxial relations, fracture at room temp. 9-7565
  - graphite, under compression, rel. to noise emission 9-7641
  - graphite relax. of tensile stress in across-grain specimens, 2000-2700°C 9-7533
  - metal welding areas rel. to feasibility of spot cold welding brittle mats. 9-21362
  - microstrain studies, reverse strain and elastic modulus reduction 9-16122
  - nonlinear, generalization of kinematic hardening 9-20408
  - piezoelectric semiconductors, depolarization field eff. 9-17438
  - plastic materials, medium strain rate, compression testing 9-17300
  - in plastics, fibre-reinforced 9-1278
  - polyethylene terephthalate, behaviour 9-1287
  - Poynting-effect problem, numerical soln. 9-5444
  - rubber cylinders, surface strain distrib. under shear 9-7538
  - shear stress on shear plate calc. 9-6361
  - steel, strain rate sensitivity at 1055°C 9-21365
  - tensile device for electron microscopic observation 9-3407
  - thin plate, perforation limits for cylindrical projectiles, simple determ. 9-20381
  - two dissimilar materials bonded over one face, stress analysis when subject to normal and shear loading 9-20406
  - AgCl, in transverse slip system exam. at -183 and 22°C 9-1295
  - Al, strain rate history, dislocation theory of intersections 9-18498
  - Al 1100 at 300°F, time-dependent uniaxial stress, strain depend. on stress history 9-21363
  - CdS, depolarization field eff. on electro-elastic props. 9-17439
  - Cu-Al crystals meas. rel. to solid soln. hardening 9-13767
  - Cu, curves, strain hardening study 9-18499
  - Cu, in fatigue hardening 9-13737
  - Cu polycrystalline, in plastic deformation rel. to mechanism 9-1284
  - Fe, in Luders front propagation accompanying yield-point phenomenon 9-19785
  - Fe, Ferrovac-E, pre-macro yield region, plastic strain rate variation with stress 9-17347
  - Fe, strain rate effect on resistance to plastic defo. 9-9759
  - Fe-30 wt% Cr, parameters 9-1286
  - LiF, u.s. deformed, internal stress distrib. on external stress changes, dislocation mechanism 9-16128
  - Mg-Cd alloy, ordering speed, effect 9-16156
  - MgO, linear rate depend. in creep 9-1292
  - Nb-W alloys, strain rate and temp. depend. of flow stress 9-3411
  - NiAl, diagram for strain hardening stages 9-13761
  - TaC, strain due to comp. gradient, X-ray meas. 9-1271
  - Ti, polycryst., microstrain distrib. under complex stress 9-16125
  - α-Ti hardening, effect of strain rate, temp. and purity 9-5487
- Stresses, internal**  
alkali halides: divalent cation, crit. shear stress, non clustering impurity ion-vacancy pairs 9-3413  
bending of thin layered plates 9-10701



**Stresses, internal continued**

- ceramics, thermal-stress resistance 9-1275  
 ceramics, with compressive surface layers, residual stress meas. 9-3414  
 $\beta$ -cristobalite, metastability at room temp. 9-1348  
 cylindrical bar under band-pressure, 3D photoelastic anal. 9-20401  
 dislocation loops, and line tensions 9-19748  
 displacement fields around dislocation loops 9-14942  
 elastomeric body with predetermined density variation, X-ray apparatus for meas., patent 9-21364  
 ferromagnetic crystal, uniaxial, reversible magnetiz. curve and magnetostriiction 9-13979  
 in films condensed, obs. during condensation and annealing 9-21266  
 fracture markings, transverse, generated by unsteady cleavage velocities 9-1211  
 glide dislocation arrays, coaxial circular associated stress fields 9-5351  
 graphite, creep strain at 2500°C and micro-struct. changes 9-7545  
 inclusion, eccentric circular, in a circular region 9-2191  
 inhomogeneous anisotropic cyl. shells, buckling stress due to bending 9-20384  
 ionic, attractive press. fourth power rel. to interionic distance, derivation 9-21290  
 isotropic elastic semi-infinite disc, stresses and displacements due to heating, eval. 9-19040  
 metals, b.c.c., flow stress, 10-300°K 9-13732  
 metals compressed by liqs., theoretical study 9-5446  
 microcracks, dead-end, fields 9-18521  
 microstrain, X-ray diffraction obs. 9-3410  
 Newtonian fluid, indentation by right circular cyl., solns. 9-19035  
 non-uniform fields and dislocations pile-up, analysis 9-5352  
 orthotropic plate, meas. of two principal residual stresses 9-5445  
 permalloy films, annealing and substrate temp. effects 9-13724  
 plate, series expressions for displacement vector 9-15453  
 poly(vinyl alcohol) networks in swelling equil., energy component 9-21356  
 due to random distribution of dislocations 9-5447  
 relaxation, meas., modified K<sub>e</sub> torsional pendulum 9-3402  
 slip, secondary, rel. to detection by macroscopic meas. 9-14978  
 solid, dislocations mobility 9-7483  
 steel, var. residual austenite content 9-3415  
 steel plates, mild, elastoplastic stress on thermal cycling 9-5450  
 strip, elastic, in contact with two rollers 9-20382  
 thermal, axisymmetric, in spheroidal shell 9-8497  
 thermal stresses in solid weakened by external crack 9-17302  
 thermoelastic, production mechanism in solids on pulsed energy input 9-13725  
 Al<sub>2</sub>O<sub>3</sub>, with compressive surface layers, residual stress meas. 9-3414  
 Bi film, evaporated, during and after deposition 9-5449  
 CaSO<sub>4</sub>·2H<sub>2</sub>O, dispersed porous mat., microstresses on pressing giving plastic deform., X-ray exam. 9-1276  
 $\gamma$ -CuI films rel. to thermal expansion coeff. incompatibility with substrate, obs. 9-16126  
 $\alpha$ -Fe, dipolar strains of C and N 9-9739  
 Fe, flow stress, 10-300°K 9-13732  
 Fe, long range increasing rel. to neutron irradi. 9-1296  
 Ga evap. films, 10-170°K 9-16127  
 Ga film, amorphous and cryst., homogeneous mech. stresses 9-5451  
 Li/F, u.s. deformed. distrib. on external stress changes, dislocation mechanism 9-16128  
 Mg(OH)<sub>2</sub>, dispersed porous mat., microstresses on pressing giving reversible elastic deform., X-ray exam. 9-1276  
 Mo, interstitial impurity content for favorable orientation 9-5452  
 NaCl, rel. to dislocation movement in electric field 9-3350  
 Ni-Al alloy, critical shear stress, conc. depend 9-9756  
 Ni, effect on memory, coercive force, isothermal remanent magnetization 9-5828  
 Sb condensed films, obs. during condensation and annealing 9-21266  
 Si prod. by SiO<sub>2</sub> surface films, rel. to X-ray dynamical diff. effects, obs. 9-9612  
 $\alpha$ -U, and creep rel. to surface oxidation, obs. 9-9765  
 W, compressed lightly, strain inhomogeneities 9-1277  
 Y Fe garnet, powder, strain induced by various milling treatments 9-5453

**Striations** see *Discharges, electric*

**Stripping reactions** see *Nuclear reactions and scattering*

**Stroboscopes**

- viewing system for cine film 9-2431

**Strong interactions** see *Elementary particles/interactions, strong; Field theory, quantum/interactions, strong*

**Strontium**

- electron energy loss meas. in plasmon excitation obs. 9-3547  
 electron prod. in H<sub>2</sub>-N<sub>2</sub>-O<sub>2</sub> flames, meas. by enthalpy changes and equilib. consts. 9-12534  
 energy-band struct. and Fermi surface under press. 9-15054  
 liquid, surface tension and density, temp. dependence obs. 9-5149  
 melt struct., Mg impurities, nucl. reson. fluoresc. study 9-7278  
 metal-semiconductor transition at high pressure 9-18605  
<sup>87</sup>Sr standardization for 1318A ionization chamber calibration 9-20695  
 Rb-Sr cosmochronology in solar system 9-21919  
 Sr<sup>2+</sup> ions, isothermal diff. in pure NaCl crys., Sorot eff. 9-21348  
<sup>86</sup>Sr, diffusion in K<sub>2</sub>O-SrO-SiO<sub>2</sub> glass 9-1249  
<sup>86</sup>Sr diffusion in BaF<sub>2</sub>, CaF<sub>2</sub> and SrF<sub>2</sub> 9-3379  
 Sr<sup>2+</sup> in NaCl, dislocation velocity 9-1222

**Strontium compounds**

- hydroxides, gaseous, dissoc. energies and conc. in fuel-rich H<sub>2</sub>+O<sub>2</sub>+N<sub>2</sub> flames 9-17517  
 CaF<sub>2</sub>-SrF<sub>2</sub> mixed crystal, Raman scattering from point defects 9-12408  
 SôF<sub>2</sub>-Ca, Raman scattering of green coloured crystals 9-12438  
 Sr<sub>2-x</sub>Mg<sub>x</sub>P<sub>2</sub>O<sub>7</sub> system, crystallographic character 9-18453  
 Sr<sub>2</sub>TiSi<sub>2</sub>O<sub>8</sub>, isomorphous with Ba<sub>2</sub>TiSi<sub>2</sub>O<sub>8</sub>, fluoresc. 9-14083  
 Sr<sub>1-x</sub>Ba<sub>x</sub>Nb<sub>2</sub>O<sub>6</sub> ferroelectric, infrared detector, fast and sensitive 9-3714  
 (Sr<sub>0.8</sub>Ba<sub>0.2</sub>)Zn<sub>2</sub>Fe<sub>2</sub>O<sub>4</sub>, angular spin ordering from neutron diffraction meas. 9-10140  
 SrCl<sub>2</sub>:Sm<sup>2+</sup> optically pumped, spectra 9-10210  
 SrCl<sub>2</sub>:Tm<sup>3+</sup>, reduction of Tm<sup>3+</sup> to Tm<sup>2+</sup> on  $\gamma$ - and e-irrad., e.s.r. obs. 9-10277  
 SrCl<sub>2</sub>, e.s.r. of Er<sup>3+</sup> and Yb<sup>3+</sup> 9-1863  
 SrClF, Raman spectra 9-5934  
 SrCo<sub>1-x</sub>Ti<sub>x</sub>FeO<sub>9</sub>, hexagonal ferrite, mag. exchange anisotropy 9-10136  
 Sr<sub>1-x</sub>Eu<sub>x</sub>(PO<sub>4</sub>)<sub>2</sub>SiO<sub>4</sub>, energy transfer between Eu<sup>2+</sup> in non-equivalent sites 9-15189

**Strontium compounds continued**

- SrF<sub>2</sub>:Dy<sup>2+</sup>, luminesc. and lasing props. 9-7990  
 SrF<sub>2</sub>:Er<sup>3+</sup>, luminescence spectra 9-3916  
 SrF<sub>2</sub>:Eu<sup>2+</sup>, e.p.r., hyperfine coupling constant of <sup>151</sup>Eu<sup>2+</sup>, temp. depend. 9-12502  
 SrF<sub>2</sub>:Nd<sup>3+</sup>, interaction mechanism of Nd<sup>3+</sup> ions and nature of conc. quenching 9-15161  
 SrF<sub>2</sub>:Sm<sup>2+</sup>, optically pumped, spectra 9-10210  
 SrF<sub>2</sub>:Sm<sup>2+</sup> (Eu<sup>2+</sup>), vibronic transitions and Zeeman effect 9-10212  
 SrF<sub>2</sub>:Tm<sup>3+</sup>, phonons generated by spin-lattice relaxation obs. 9-1714  
 SrF<sub>2</sub> diffusion of <sup>89</sup>Sr 9-3379  
 SrF<sub>2</sub>, hyperfine consts. of F-centre, endor meas. 9-1234  
 SrF<sub>2</sub>, optical spectrochem. meas. of metal impurities 9-16513  
 SrF<sub>2</sub>, u.v. reflectivity spectrum from (111)-planes 9-1761  
 SrFe<sub>12-x</sub>Ga<sub>x</sub>O<sub>19</sub>, Ga partial substit. of Fe, effect on saturation magnetization 9-16373  
 SrMoO<sub>4</sub>, scheelite-type, two-photon laser excitation of luminescence and damage processes 9-1825  
 Sr(NO<sub>3</sub>)<sub>2</sub>-Ca(NO<sub>3</sub>)<sub>2</sub>-Ba(NO<sub>3</sub>)<sub>2</sub> binary fused systems, Raman spectra obs. of structure 9-17186  
 SrO-ZrO<sub>2</sub> system, phase equilibria, melting points, solid solubility 9-1352  
 SrO, computed ground state props. in molecular orbital approx. 9-7015  
 SrO, F-centres, Faraday rotation studies 9-3362  
 SrO.4Fe<sub>2</sub>O<sub>3</sub>.1.6Cr<sub>2</sub>O<sub>3</sub>, anisotropy of paramagnetic line point 9-12248  
 SrS:Bi electron trap depth determ. from thermoluminescence decay 9-1840  
 SrS:Zr phosphors, Zr activated decay and thermoluminescence spectra 9-3936  
 SrS, shear-induced coloration, obs. 9-1745  
 Sr<sub>2</sub>O<sub>4</sub>.4H<sub>2</sub>O, optical activity in vibration-transition region 9-7941  
 SrTiO<sub>3</sub>:Cr<sup>3+</sup>, Cr R lines spectral shift, 4 kV/cm electric field, 4.2°K 9-3709  
 SrTiO<sub>3</sub>:transition metal, photochromic refractive index change 9-10170  
 SrTiO<sub>3</sub>:Fe<sup>3+</sup>, cubic splitting temp. dependence, 123-773°K 9-18742  
 SrTiO<sub>3</sub>:Mo(Fe or Ni), reversible photochromic changes, observations and model 9-19980  
 SrTiO<sub>3</sub>:Nb magnetoresistance rel. to conduction band structure 9-7788  
 SrTiO<sub>3</sub>, growth from silica flux 9-14907  
 SrTiO<sub>3</sub>, superconductivity 9-3598  
 SrTiO<sub>3</sub>, transition-metal doped, photochromic parameters for electro-optic applications 9-19978  
 SrTiO<sub>3</sub>  $\beta$  radioactive source, efficiency calc. 9-549  
 SrTiO<sub>3</sub>, 110°K phase transition, soft phonon modes and interactions 9-11968  
 SrTiO<sub>3</sub>, anomalous hypersonic attenuation above 100°K 9-12002  
 SrTiO<sub>3</sub>, Raman scatt., elec.-field-induced 9-5938  
 SrTiO<sub>3</sub>, Raman spectrum, spatial variation below 110°K 9-16423  
 SrTiO<sub>3</sub>, rare-earth, dielectric relaxation, activation energy, obs. 9-3699  
 SrTiO<sub>3</sub>, stress induced dichroism at absorption edge 9-3858  
 SrTiO<sub>3</sub>, tetragonal rot. of TiO<sub>6</sub> octahedra as charact. struct. transition 9-1349  
 SrTiO<sub>3</sub>, transition metal doped, photoinduced reversible charge transfer 9-7955  
 SrTiO<sub>3</sub> free carrier absorpt. obs. using two-photon excitation 9-12199  
 SrTiO<sub>3</sub> single cry., linear thermal expansion coeff. 9-12024  
 SrTiO and OD absorpt. bands 9-10211  
 SrTiO<sub>3</sub>, photoluminescence in undoped and Sm- and Cr-doped crystals 9-21648  
 SrWO<sub>4</sub>, phototropy, green after irradi. by u.v. light 9-3866

**Structure factors** see *Crystal structure, atomic; X-ray crystallography*

**Structure of matter** see *Crystal structure; Liquids/structure; Solids/structure*

**SU(3) group theory** see *Elementary particles/symmetry; Field theory, quantum/interactions, strong; Group theory*

**Sublimation**

See also *Heat of sublimation; Vaporization*

- alkali metal sulphates, and thermal decomposition, mass spectrometric studies 9-19663  
 apparatus for large-scale sublimation 9-21251  
 boundary layer flow, convective with surface sublimation 9-17147  
 cathode, meas. by quartz crystal oscillator 9-3755  
 at hypersonic boundary layer, Lewis number=1, determ. of rate 9-7309  
 ice, and crystallization in vacuum 9-19665  
 ice, in vacuum, crystn. on subliming layer surface 9-17234  
 ice, in vacuum, heat and mass transfer mechanisms 9-17233  
 ice, nature in vacuum 9-19664  
 kinetic energy of escaping vapour mols. 9-1074  
 kinetics, principles and exptl. techniques 9-18390  
 naphthalene, mass transfer to air, eff. of transverse vibrations 9-21250  
 phenonol, mass transfer to air, effect of transverse vibrations 9-21250  
 relationship with shock-wave velocity 9-13722  
 UHV for epitaxial growth of p-n junctions 9-13899  
 $\alpha$  emitters in foils, meas. using  $\alpha$  spectrometer 9-8931  
 GaN, kinetic energy of vapour mols. 9-1074  
 PbTe, data for weight-loss at high temps. 9-3159  
 Pu and U, separation by fractional sublimation 9-20857  
 PuO<sub>2</sub>, volatilization behaviour, mass spectrometric study, 1980-2350°K 9-3160  
 SiC, eff. of time and temp. 9-18416  
 SnO<sub>2</sub>, crystal growth process for new electrolum. material 9-15193  
 SnPbTe<sub>2</sub>, vapour equil. obs. from mass spectrometric-Knudsen cell exam. 9-18391  
 ZrO<sub>2</sub>-CaO solid solution, CaO volatilization rel. to stabilization of ZrO<sub>2</sub> ceramics 9-21252  
 ZrO<sub>2</sub>-Y<sub>2</sub>O<sub>3</sub> solid solution, YO volatilization rel. to stabilization of ZrO<sub>2</sub> ceramics 9-21252

**Sudden commencement** see *Magnetic storms*

**Suhl effect** see *Hall effect; Semiconductors*

**Sulphur**

- adsorption by Ag, surface instability 9-9624  
 atoms and ions, bibliography of spectra 9-13287  
 carrier transport and generation 9-7703  
 evaporation rate from molten iron under vacuum 9-19658  
 isotope ratio meas., balance method, problems 9-19417  
 La Mer sols, particle size distrib. and number conc., time dependence 9-14871  
 liquid, density discontinuity near 160°C  $\lambda$ -transition 9-9479  
 liquid and solid, electronic transport 9-5603

**Sulphur** continued

- S<sup>+</sup> trapped impurity in alkali halide crystals, e.s.r. spectra 9-3954  
 spectral lines intensities rel. with halides 9-9126  
 traces in Ag, influence on self-diffusion 9-3376  
 X-ray L<sub>2,3</sub> emission spectrum in sulphates and sulphides, obs. 9-20940  
 S<sub>2</sub><sup>+</sup>, luminesc. spectra in KI crystals 9-14082  
 S<sub>2</sub><sup>+</sup> centre in alkali halides, luminescence at 4.2°K 9-14078  
 S<sub>2</sub>-S<sub>2</sub> bond energy diff. and force consts., 9-parameter potential function 9-20941  
 S IX-XII, u.v. spectrum obs. 9-6972  
<sup>32</sup>S, at. mass using high resolution spectrometer 9-11414  
 SI ground configuration, level values and interaction parameters 9-20885

**Sulphur compounds**

- dithionate crystals, optical activity in vibration-transition region 9-7941  
 fluorine cpds., <sup>19</sup>F n.m.r. 9-762  
 penta-atomic heterocyclic cpds., model for  $\pi$  electron spectra 9-4944  
 SCO<sup>+</sup> X<sup>2</sup>I and X<sup>2</sup>II<sup>+</sup> states, spin-orbit coupling constants calc. 9-15845  
 sulphates, molten, vibr. spectra 9-16005  
 sulphates, S L<sub>2,3</sub> X-ray emission rel. to electron transitions and bonds, obs. 9-20940  
 sulphides, S L<sub>2,3</sub> X-ray emission rel. to electron transitions and bonds, obs. 9-20940  
 thiosulphate, residual, in gelatin, colorimetric analysis 9-6563  
 Ar-SF<sub>6</sub> plasma, oscillator strengths of 44SI and 92II lines, 1100-2000 Å 9-7160  
 HgS optical, non-linear, phenomena 9-10160  
 OS halides, mean vibr. amplitude calc. 9-7037  
 PbS polycrystalline photoresistors, V-I, luminous charact. and absolute spectral sensitivity 9-13935  
 PbS thin films, spectral absorption, structure and phase composition 9-14021  
 S<sub>2</sub>O<sub>3</sub> ion, mean square amplitudes of vibration 9-20943  
 S<sub>2</sub>O<sub>4</sub> ion, mean square amplitudes of vibration 9-20943  
 S<sub>2</sub>O<sub>6</sub> ion, mean square amplitudes of vibration 9-20943  
<sup>31</sup>S<sup>16</sup>O<sub>2</sub>, rotation spectra, Hertzian, second-order 9-20938  
 S<sub>2</sub>Br<sub>2</sub>, Raman and far-i.r. spectra 9-9234  
 S<sub>2</sub>Cl<sub>2</sub>, mean amplitudes of vibr. 9-9235  
 SF<sub>6</sub>, depolarization of scatt. light, with Krishnan effect near critical point 9-961  
 SF<sub>6</sub>, gas, optical nutation effect on rot.-vib. transition 9-788  
 SF<sub>6</sub>, Kerr eff. obs. at various pressures, second Kerr virial coeffs. obtained 9-21144  
 SF<sub>6</sub>, gas, thermal electron attachment rates 9-3007  
 SF<sub>6</sub>, gaseous, heat conductivity, Senftleben-Beenakker effect 9-9446  
 SF<sub>6</sub>, oscillation relax. temp. depend. 10°C to 215°C 9-2879  
 SF<sub>6</sub>, saturable absorption for CO<sub>2</sub> laser line 9-11473  
 SF<sub>6</sub>, vibrational relax. times, temp. depend. 9-4953  
 SF<sub>6</sub> a.c. arc characteristics filmed by laser-Schlieren technique 9-17881  
 SF<sub>6</sub>, dissolved in mineral oil, elec. breakdown effect 9-11711  
 SH<sup>+</sup> singlet-triplet intercombination separation, calc. 9-2874  
 SO, rotational line intensities in <sup>3</sup>Σ<sup>+</sup>Σ<sup>+</sup> electronic transitions 9-2880  
 SO<sub>2</sub>, photoionization 9-905  
 SO<sub>2</sub> isotopic molecules, rotation spectra 9-20939  
 SO<sub>2</sub>BrF, vibr. assignments, Raman and i.r. obs. 9-15870  
 SO<sub>4</sub> ion, mean square amplitudes of vibration 9-20943  
 SO radical, Zeeman effect of J, K=0, 1-1, 0 and 2, 2-2, 3 rot. transitions 9-13399  
 SO<sub>2</sub>, chemisorption on O<sub>2</sub>-free active carbon surface 9-8081  
 SO<sub>2</sub>, luminesc. and radiationless transitions 9-2881  
 SO<sub>2</sub>, submillimeter laser, with He addition, generating at 0.141 and 0.193 mm 9-244  
 SO<sub>2</sub> cryst., spontaneous elec. polarization 9-13842  
 SO<sub>2</sub> fluorescence from lowest excited electronic state, lifetime obs. 9-7038  
 SO<sub>2</sub> phosphorescence intensity depend. on temp., 4-100°K, intersystem crossing 9-15190  
 SO<sub>2</sub> reaction with free radicals in  $\gamma$ -irrad. propionamide, n-butyramide and isobutyramide 9-12538  
 SO<sub>2</sub> vapour, fluoresc. and phosphoresc. 9-9233  
 SO<sub>2</sub> solution containing H<sub>3</sub>O<sup>+</sup> ions, vibration spectra 9-2865  
<sup>31</sup>SO<sub>2</sub> isotopic molecules, rotation spectra 9-19446

**Sum rules** see *Elementary particles/theory*

**Sun**

- See also *Sunspots*  
 active, radio emissions, book 9-8289  
 activity, contrib. to zodiacal light 9-20239  
 activity, optical and radio obs. (1966) 9-18936  
 activity rel. ionosphere parameter vars. during SC mag. storm 9-17580  
 activity rel. to Jupiter's great red spot brightness 9-15343  
 atmosphere, Joule mag.-field dissipation, energy release 9-16629  
 atmospheric dynamics, jet streams, Rossby and Haurwitz waves 9-8294  
 bursts at 7 GHz, flux and polarization distrib. 9-14252  
 chromosphere, dark mottles, size, shape, evolution, high-resolution photo. obs. 9-14272  
 chromosphere, gas viscosity coeff. calc. 9-14270  
 chromosphere, lower, densities in regions of ionized metal radiation 9-4127  
 chromosphere, structure in form of bright streaks 9-17667  
 chromosphere, sunspot, filaments and plagues, VAI rot. maps key 9-15366  
 chromosphere, sunspots, filaments, plagues and prominences, rot. 1525 9-18925  
 chromospheric fine struct., intensity meas. in Lyman- $\alpha$  line 9-16628  
 chromospheric heights, meas. method 9-15365  
 chromospheric heights, meas. method 9-10553  
 chromospheric mag. fields and supergranulation 9-21978  
 continuum intensity at  $\lambda=20.15 \mu$  rel. to absolute meas. of brightness temp. at disc. centre 9-10554  
 Einstein's gravitational field eqns. solved and parameters determ. 9-10538  
 evolution and destruction of elements rel. to abundances of Li, Be and B 9-15353  
 evolutionary model construct. and obs. 9-20237  
 faculae, chromospheric, area and intensity by H and Ca radiation 9-18927  
 flocculi, variation in size from centre to limb of disc 9-14257  
 IQSY and solar-terrestrial research 9-8287  
 local solar motion in studies of distant objects kinematics 9-18839  
 model convection theory rel. to granule generation 9-14261  
 modulation of galactic cosmic rays 9-14185  
 oblateness, rotating core rate and ang. vel. 9-2064

**Sun** continued

- oblateness, stratification and spin-down 9-10539  
 photosphere, CO dissoc. by electr. collision 9-17662  
 photosphere, convective motions 9-21970  
 photosphere, turbulence study 9-15359  
 photospheric brightness differences w.r.t. supergranulation 9-14259  
 photospheric network from Fraunhofer spectra 9-18937  
 photospheric phenomena correl. to radio obs. at 239 MHz, (1966) 9-18936  
 quiet, radio emissions, book 9-8289  
 radio echoes rel. to corona inaccessible layers 9-4128  
 rotation rel. to neutrino flux 9-10546  
 solar activity forecasting, use of determined-probabilistic learning information syst. 9-2087  
 solar constant determ. from many spectrum results 9-10537  
 solar wind, dynamical origin, cosmic ray variation 9-17660  
 spicules, spectral obs. of height differentiation 9-15367  
 supergranules in convection model of atm. 9-14261  
 velocity fields in chromosphere, H $\alpha$  doppler shift investigation 9-18940  
 wind and geomagnetic impulses relation 9-10439  
<sup>B</sup> decay near solar centre, convection in core, e capture 9-21966  
 Ba abundance, hyperfine structure eff. 9-14249  
 CO dissociation by electronic collision in photosphere 9-17662  
 Ca abundance, hyperfine structure eff. 9-14249  
 Ca H, K and subordinate lines formation in chromosphere 9-21979  
 Cl abundance, first obs. 9-15354  
 Cu abundance, hyperfine structure eff. 9-14249  
 Cu abundance determ. 9-13289  
 He, rel. abund., upper rel. to lower limit 9-2075  
 Mn abundance, hyperfine structure eff. 9-14249  
 V, abundance, hyperfine structure eff. 9-14249

**corona**

- 1966, Nov. 12 eclipse, i.r. outer corona obs. 9-21982  
 brightness at 2.13  $\mu$ , study 9-20248  
 concentric ellipse multi-arch syst. 1962, Feb 4 9-2083  
 eclipse obs. lines, Hartree-Fock calc. of possible candidates in ArI isoelectronic sequence 9-15368  
 electron densities 9-14274  
 electron density profile by radiowave scatt., statistical ray anal. 9-15369  
 expanding, ionization processes 9-8290  
 Fraunhofer lines, obliteration by electron scatt. 9-21980  
 gas, viscosity coeff. calc. 9-14270  
 heating by magneto-gravity waves 9-21981  
 heavy ion diffusion, theory 9-10557  
 inaccessible layers rel. to radio echoes 9-4128  
 ionization equilibrium for elements C-Ni 9-20238  
 K-component intensities 9-14274  
 around limb, distribution of the line intensity 5303 Å 9-2080  
 magnetic field, radio emitting electron energy from Type 4 solar radio burst determ. 9-17668  
 North-South asymmetry 9-14274  
 observational difficulties due to background brightness near satellite 9-10560  
 polarization-interference filters with thermoptically compensated steps for the observation of corona 9-4130  
 pulsar study proposed 9-8268  
 radar studies and a mechanism of formation of a reflection signal 9-4129  
 radiowave scatt., statistical ray anal. 9-15369  
 shape in eclipse, and luminosity of moon 9-15352  
 shock waves and mag. field for type II radio bursts 9-10555  
 structure interpretation, streamers rel. to mag. field struct. 9-2084  
 temperature,  $1.92 \times 10^6$  overall meas. 9-14274  
 temperature calc. using collisional ionization cross-sections for Fe ions 9-10556  
 type IV bursts, calc. of gyro-synchrotron emission from electrons in coronal mag. field 9-17658  
 visible line identifications, survey 9-2082  
 X-ray emission 16-40 Å obs. during 12 Nov 1966 eclipse 9-17654  
 O VI emission, presence in corona 9-2081  
 O VIII Ly- $\alpha$  and Ly- $\beta$  rad. ratio, temp. depend. 9-16630

**eclipses**

- 1962 Feb 4, concentric ellipse multi-arch system in corona 9-2083  
 1965 May 30, rel. to corona structure 9-2084  
 1966, Nov. 12, total eclipse 9-12760  
 1966, Nov. 12, Brazil, preliminary results 9-14247  
 1966, Nov. 12, ephemeris time determ. and radius of lunar umbra 9-17636  
 1966, Nov. 12, partial obs. in Brazil at  $\lambda=100$  cm 9-2065  
 1966, record of obs. at Mendon 9-14248  
 1966, May 20, radioastronomical obs. 9-15360  
 corona shape, and luminosity of moon 9-15352  
 Fraunhofer lines in inner corona obs., obliteration by electron scatt. 9-21980  
 partial, response of ionospheric and exospheric e contents 9-10427

**flares**

- 3.3 mm bursts associated with flares 9-17657  
 1958-65, 2907 flares obs., statistical analysis 9-15363  
 1966, 28 Aug. 1522 UT, decametric r.f. spectra 9-21965  
 1966, Aug. 28, positron, X-ray and u.v. rad. from ionos. disturbance data, time depend. burst 9-2079  
 1966, Aug. 28 and 30, Mount Wilson Observatory 9-14268  
 in 23 and 28 May 1967 solar particle events 9-18939  
 Bartels' active longitudes, sector boundaries and flare activity 9-14269  
 $\gamma$ -spectra as a possible indicator of chemical composition of solar atm. 9-10550  
 chromospheric, correl. to radio bursts at 239 MHz, 1966 obs. 9-18936  
 cosmic rays, associated ionospheric disturbances 9-16539  
 development, early phase, chromospheric explosion model investigation 9-16627  
 earth's ozonosphere, effects on 9-21757  
 electron, radio and X-ray emission obs. in interplanetary space 9-10552  
 electron events obs. on earth 9-17661  
 electron inner radiation belt addition after solar flare event 9-8195  
 evolution from filaments 9-10549  
 H $\alpha$  obs. and flare distrib. asymmetry 9-21958  
 in magnetic features of active regions, evolution 9-15362  
 Oct-Dec 1967 obs. 9-10540  
 photography, fine struct. 9-21976  
 plasma transport to earth, solar wind shock front prod. 9-2078  
 polarization and e density in spray, 11 Jul 1966 9-8292



**Sun continued****flares continued**

- processes and description, book 9—8220
- radio bursts at 3 mm and H $\alpha$  emission 9—17665
- shock wave generation, energy deposition in solar wind 9—10551
- sunspot area relationship 9—14265
- sunspot area relationship, amendment 9—14266
- synchrotron and X-ray emission 9—21975
- theory, and related phenomena 9—17664
- transient associated solar atm. phenomena 9—8293
- X-ray flux calc. for temp.,  $7 \times 10^7$ – $10^{10}$  K, comparison with expt. 9—17655
- X-ray obs., 1964-7, atlas 9—16619
- X-ray obs. (8 June 1968) 9—18928

**magnetism**

- axisymmetric mag. field of differentially rotating sun, topology obs. 9—18935
- Bartels' active longitudes, sector boundaries and flare activity 9—14269
- chromospheric field struct. and supergranulation 9—21978
- coronal field determ. from type IV burst 9—17658
- field, stochastic aspects of lines of force, applic. to cosmic ray propag. 9—21952
- field development in active sunspot regions 9—21973
- field meas. by photoelectric magnetographs, photographic methods comparison 9—2066
- field of two active prominences, obs. 9—15364
- field over sun, pattern obs. 9—18926
- field which accelerates rot. until onset of instability and then returns sun to initial state 9—10472
- hydromagnetic eqns. for axisymmetric field of differentially rot. sun 9—18935
- local field correlation with central intensity of Fraunhofer lines, obs. 9—16616
- local fields correl. with H $\alpha$ , K $\beta$  line intensities 9—21957
- quiet sun, background and Ca K-emission fields distrib. and struct., obs. 9—6193
- Rossby waves, as hydromag. dynamos 9—6194
- sunspot fields, formation mechanism 9—2076
- sunspot vicinity, mag. 'knot' obs. 9—14264
- supergranulation zone, mag. fields in convective cells 9—21969

**prominences**

- 1967, Sept.-Oct. obs. at Mendon 9—14263
- eruptive prominence on solar disk, (29 Jan. 1968) 9—16625
- magnetic field of two active prominences 9—15364
- oscillatory phenomena, model explaining periods, damping time and shape 9—14267
- spicules, obs. techniques and m.h.d. models 9—12770
- spicules, three dimen. H $\alpha$  pictures 9—16626
- surge, acceleration mechanism 9—21977
- variation with latitude and solar activity cycle (1933-1960) 9—20247

**radiation***See also Sunlight*

- 44-60 Å flux, obs. by Solrad 6, 7 and 8 satellites 9—17653
- absorption by earth's atmosphere 9—12585
- in atmosphere, airborne polarimeter 9—13056
- atmosphere density changes, delay following solar activity 9—8184
- coronal X-ray emission 16-40 Å obs. during 12 Nov 1966 eclipse 9—17654
- cosmic ray, intensity increase, 28 Jan., 1967 9—12646
- e.m., press. eff. on lunar satellites motion 9—2040
- facular plages, Aug-Sept. 1967 obs. 9—20245
- flare of 8 June 1968, X-ray obs. 9—18928
- heliograph records, Uccle (1967) 9—10541
- intensity emitted, computer soln. of integral eqns. 9—20243
- limb brightening obs. at 1.2 mm 9—14273
- localized enhancement at 1.2 mm 9—15361
- and modulation of ionospheric riometer absorption 9—20111
- photosphere model with two stream granulation representation 9—14260
- pressure, effect on interplanetary matter 9—21953
- radio bursts, rel. to sunspot type during sunspot min. 9—21972
- solar atmosphere, structure and emissions, IQSY obs. 9—8295
- solar constant, direct determination 9—21959
- spectral line profile, progressive Alfvén waves effects 9—2069
- synchrotron and X-ray emission from electrons in flares 9—21975
- thermospheres, planetary, response to heating 9—8185
- u.v., effect on nightglow brightness (1957-63) 9—20100
- u.v. images from orbiting observatory 9—17651
- wind, during geomagnetic storm, Vela satellite obs. 9—10408
- wind, ionic components 9—8290
- X-ray, 'Cosmos-166' investigation 9—21960
- X-ray and synchrotron emission from electrons in flares 9—21975
- X-ray bursts, time characts. and associated microwave bursts 9—14251
- X-ray flares, 1964-7, atlas 9—16619
- X-ray flux, upper limits from 50-290 keV cosmic rays obs. 9—6717
- X-ray flux calc. for temp.,  $7 \times 10^7$ – $10^{10}$  K, comparison with expt. 9—17655
- X-ray source on Sun identified during 12 Nov. 1966 eclipse, using D layer ionization 9—18929
- X-rays, 77-210 keV, OSO-III satellite (1967) obs. 9—18930
- CVI ion X-ray emission, rocket-borne cry. spectrometer meas. [cc N VII ion X-ray emission, rocket-borne cry. spectrometer meas.] C [cc C VI ion solar X-ray emission, rocket-borne cry. spectrometer meas.] N [cc N VII ion solar X-ray emission, rocket-borne cry. spectrometer meas.] 9—12676
- 032905243(2 05344—032(053m242 230 0008022
- 0300000(08000016630 9—12676
- O VIII Ly- $\alpha$  and Ly- $\beta$  rad. ratio, from corona, temp. depend. 9—16630

**radiation, corpuscular**

- central convection and solar neutrinos 9—21966
- cooling, inertial and temp. anisotropy 9—17659
- cosmic ray modulation spectrum in interplanetary space 9—17606
- cosmic-rays, low-energy latitude-intensity structure and pitch-angle distrib. 9—10441
- cycle variations, polar cap absorption indices, solar protons daily meas. 9—21967
- diamagnetic cavity behind Moon, Explorer obs. 9—10547
- electrons, relativistic, obs. from solar flares 9—17661
- energy dissipation, earth's atmosphere, PCA 3914 and 5577 Å light emission calc. 9—20102
- flow, mag. fields interaction, Pioneer 6 obs. compared with theory 9—2063
- geomagnetic field, interaction, pioneer 6 obs. 9—1977
- ionosphere F region effects, day and night (Mar 21-5, 1966) 9—21821
- modulating cloud causing Forbush-decrease, transit time 9—1980

**Sun continued****radiation, corpuscular continued**

- modulation of cosmic rays, possible anisotropy of w.r.t. helio-latitude 9—21832
  - neutrino flux rel. to rotation of core 9—10546
  - neutrino fluxes mixing effect 9—4126
  - neutrinos, detect. 9—18934
  - neutrinos, identification and flux-cross section prod. 9—10544
  - neutron transport on Earth's atmosphere 9—10396
  - rel. to nightglow brightness maxima (1957-63) 9—20100
  - penetration to geomagnetic equator, p,  $\alpha$  obs. 9—1978
  - plasma irregularities from interplanetary scintillation investigation 9—20244
  - pressure, effect on artificial satellite models 9—18825
  - proton and electron flux, ATS-1 omnidirectional spectrometer obs. 9—21968
  - proton events, small, effect on D region ionization, partial refl. obs., (Feb. 1965) 9—14175
  - solar wind, angular momentum rel. to l.f. plasma fluctuations 9—6192
  - solar wind electrons, Vela 4 meas. 9—10545
  - streams, long lived, of electrons and protons, discussion 9—16620
  - v.l.f. emission during the great disturbance of 25-26 May 1967 9—1979
  - wind, ioniz. stages of He and O 9—14255
  - wind, speed and directional fluctuation determ. from waviness in tail of comet Morehouse 1908 III 9—14256
  - wind interaction with magnetosphere rel. micropulsations 9—20118
  - wind particles, direct obs. (1962-67) 9—15358
  - wind spectrometer expt. for Apollo astronauts on lunar surface 9—20236
  - $\nu$  flux, upper limit, rel. to initial He abund. 9—2075
- radiation, radiofrequency**
- 3.3 mm bursts associated with flares 9—17657
  - burst, 1959, June 9, radio at decametric f, Type IV continuum, obs. 9—2074
  - burst, decimeter peaking near 1000 MHz, 6 March 1968 9—10542
  - burst activity index at 10-7 cm. 9—21964
  - bursts, 6-11 Jul 1968, metre and decametre obs. 9—21962
  - bursts, impulsive at 2800 MHz, index of impulsiveness, mag. field relation 9—2073
  - bursts, microwave type IV, flux density and decay times, time variations 9—10543
  - bursts, microwave up to 35 GHz, spectra 9—18933
  - bursts, monochromatic-to-spectral conversion classification 9—21963
  - bursts, moving type IV, spectral study and eff. of plasma on synchrotron emission 9—18932
  - bursts, stationary type IV, structure of sources 9—18931
  - bursts, type III, noise, at hectometer wavelengths 9—20242
  - bursts, type III, polarization degree depend. on heliographic longitude 9—2072
  - bursts, type IV, characts. rel. to electron accel. and synchrotron emission 9—12765
  - bursts, type IV, time depend. of Razin spectra 9—20241
  - bursts at 3 mm from flares and H $\alpha$  emission 9—17665
  - cosmic rays, radio emissions, eff. book 9—8220
  - eclipse (20 May 1966) observations 9—15360
  - flare, 28 Aug, 1966: 1522 UT, decametric r.f. spectra 9—21965
  - flares, chromospheric, correl. to radio bursts at 239 MHz, 1966 obs. 9—18936
  - floculi and spots at  $\lambda=16$  cm 9—2071
  - flux, daily relative to sunspot number, spectral analysis 9—18938
  - intensities in 3.6-4 mm., comparison with moon's radiations 9—8288
  - microwave bright regions, directivity 9—15357
  - noise-storm enhancements, structure of sources 9—18931
  - Oct-Dec 1967 obs. 9—10540
  - one-dimensional pictures at 169 MHz with new radioheliograph 9—10561
  - photospheric phenomena correl. to radio obs. at 239 MHz, (1966) 9—18936
  - radio emissions, book 9—8289
  - radioheliograph, 80 MHz, second-by-second picture production of sun, Australian project 9—4125
  - S-component emission, spectrum and diameter of source, 3.3 mm→21 cm wavelengths 9—14253
  - storms, meter-wave, cyclotron mechanism 9—17656
  - Type 4 burst electron energy in coronal magnetic field determ. 9—17668
  - type II bursts rel. to shock waves and mag. field above corona 9—10555
  - type III, interplanetary accompaniment to solar flare electrons 9—10552
  - type III bursts, solar longitude and distance from sun 9—12766
  - type IV bursts, calc. of gyro-synchrotron emission from electrons in coronal mag. field 9—17658
  - variation due to bremsstrahlung and cyclotron mechanism 9—2070

**spectra***See also Sun/corona; Sun/flares; Sun/prominences*

- 5303 Å line, emission calc. 9—14274
- absorption-line red-shifts, interpretation 9—15356
- acoustic waves, short period, propag. in photosphere, effect on line profiles 9—16617
- $\gamma$ -spectra as a possible indicator of chemical composition of solar atm. 9—10550
- chromosphere, H lines, decrease in intensity 9—17666
- chromosphere vel. field, temporal characts. by H $\alpha$  doppler shifts 9—18940
- chromospheric fine struct., intensity meas. in Lyman- $\alpha$  line 9—16628
- continuum emission study, 1950→3000 Å 9—17650
- corona eclipse obs. lines, Hartree-Fock calc. of possible candidates in Ar I isoelectronic sequence 9—15368
- energy distribution, 1800Å-4 mm, mean of many results 9—10537
- equivalent widths analysis, new method 9—16621
- flare, 28 Aug, 1966: 1522 UT, decametric r.f. spectra 9—21965
- Fraunhofer lines, correlation between central intensity and local magnetic field 9—16616
- Fraunhofer lines, variation with sunspot number 9—12762
- Fraunhofer lines in inner corona, obliteration by electron scatt. 9—21980
- hyperfine rel. to determ. of solar abundances 9—14249
- i.r. and brightness temp., balloon obs. 9—20240
- line profile, progressive Alfvén waves effects 9—2069
- local mag. fields correl. with H $\alpha$ , K $\beta$  line intensities 9—21957
- Lyman- $\alpha$  variations, March and May 1966, correl. to solar activity 9—14250
- microwave bright regions, directivity 9—15357
- photosphere, heavier elements with ground state configurations  $s^2$ ,  $s^2p$ ,  $s^2p^2$  abundance 9—12768
- photospheric, forbidden Fe II lines 9—14258
- photospheric, weak mol. and atomic lines detect. 9—16622

**Sun continued****spectra continued**

- photospheric brightness differences w.r.t. supergranulation 9-14259  
 spicules, spectral uniqueness of each spicule, velocities, anomalously broad H, K lines 9-15367  
 u.v. appl. high resolution spectroscopy to meas. 9-15556  
 X ray deka-keV burst, theory 9-21961  
 X-ray emission distribution from ionospheric absorption meas. 9-16618  
 Zeeman determ. of radial velocities in sunspot penumbrae, slight flaring 9-16623  
 Ar, coronal 4412 Å emission line obs. in  $\theta$ -pinch 9-7162  
 B abundance lower than previously admitted 9-15353  
 Ba abundance calc. 9-2068  
 Be abundance in atm. 9-14271  
 Be abundance lower than previously admitted 9-15353  
 Ca abundance calc. 9-2068  
 Ca II K-line and H $\alpha$  simultaneous obs. method 9-17652  
 Ca red auto ionizing lines, oscillator strengths 9-15355  
 CII line identified 9-15354  
 Fe I 5250 Å line, effect of short period acoustic waves in photosphere 9-16617  
 Fe IX-XIV, identification of 3d-4p and 3d-4f transitions in lines between 170 and 70 Å 9-6191  
 H quasi-mols. continuous absorpt. effects 9-6189  
 H $\alpha$  and Ca II K-line, simultaneous obs. method 9-17652  
 H $\alpha$  doppler shift investigation of chromosphere vel. field 9-18940  
 H $\alpha$  line, wing obs. for population of  $n=2$  and  $n=3$  levels 9-12764  
 H $\alpha$  obs. and flare distrib. asymmetry 9-21958  
 H $\alpha$  three dimen. pictures of spicules 9-16626  
 He. 584 and 537 Å reson. line intensities from model atom calcs. 9-12763  
 Li abundance lower than previously admitted 9-15353  
 Mg abundance calc. 9-2068  
 Mg I multiplets, 1-2  $\mu$ , 30 km balloon obs. 9-6190  
 O $_2$  photospheric, applic. of new method for equivalent widths analysis 9-16621  
 S forbidden lines in Fraunhofer spectrum 9-18924  
 Sr abundance calc. 9-2068

**Sunlight**

- See also Sky brightness  
 absorption by earth's atmosphere 9-12585  
 actinograph for meas., sensitivity and calibration 9-21773  
 radiation in N.Norway & Spitzbergen 9-21773

**Sunspots**

- 16 month periodicity and in earth mag. field, obs. 9-1976  
 26 month periodicity and in earth mag. field, obs. 9-1976  
 1967, Sept.-Oct. obs. at Mendon 9-14263  
 Alfven waves effect on solar spectral line profile, application area changes rel. to flare occurrence, amendment 9-2069  
 area changes rel. to flare occurrence 9-14266  
 area changes rel. to flare occurrences 9-14265  
 centre-limb intensity profiles, 2D radiative transfer analysis, struct. deductions 9-16624  
 chromosphere, rot. 1525, map 9-18925  
 chromosphere, VAI rot. maps, key 9-15366  
 classifications, Catania and Zurich, comparison 9-20246  
 fibrils, behaviour obs. 9-17663  
 force-free magnetic fields, behaviour 9-10548  
 Fraunhofer lines, variation with sunspot number 9-12762  
 intensities, monochromatic, photoelec. meas. with Coude refractor, scatt. light correction 9-2077  
 latitude distribution, slow increase in last 5 sunspot cycles. 9-14262  
 magnetic 'knots' near sunspots, obs. 9-14264  
 magnetic field development in active regions 9-21973  
 magnetic field formation mechanism 9-2076  
 model computation, mag. field, gas press. and temp. determ. 9-21974  
 with normal Zeeman triplet, polarization rel. to Faraday rotation 9-12769  
 number, daily relative to solar flux, spectral analysis 9-18938  
 Oct-Dec 1967 obs. 9-10540  
 photometric obs. with pinhole device to reduce diffracted light 9-8291  
 radial vel. (Evershed effect) determ. 9-16623  
 radio bursts, rel. to sunspot type during sunspot min. 9-21972  
 relationship with ionospheric index IF2 9-6094  
 Fe I and Fe II, curve of growth calcs., equivalent widths interpretation 9-21971  
 Ti I and Ti II, curve of growth calcs., equivalent widths interpretation 9-21971

**Superconducting devices**

- bolometer, temp. stabilization by electronic means 9-12952  
 coils, multilayer, flux jumps and internal phenomena 9-9964  
 coils, stabilization studies 9-18613  
 cryoelectronic 9-8317  
 d.c. transformer, eff. of current distrib. in type II supercond. thin film 9-13858  
 d.c. transformer, phase incoherence 9-5660  
 high mag. field production, book 9-2325  
 interfaces, superconductor-normal-metal, theory 9-9965  
 interference grating 9-19900  
 i.r. detection using 10 Å insulating layer between superconductors 9-7782  
 Josephson current, destruction by fluctuations 9-13870  
 Josephson current, self-field modified, mag. field dependence 9-9963  
 Josephson junction, cylindrical, theory 9-19906  
 Josephson junctions, coupled, as far i.r. coherent source 9-3601  
 Josephson junctions, relax. oscils. 9-19907  
 Josephson junctions array, resistive transition tailing 9-7784  
 Josephson oscillator, quantum mechanical theory including noise 9-12119  
 Josephson tunnel junction, I-V characteristic meas., current sweep circuit 9-205  
 Josephson tunnel junctions, dV/dI characts. 9-15081  
 lens with Ho poles, cardinal elements and aberration coeffs. 9-14417  
 magnet, in n.m.r. spectrometer, description, performance 9-12962  
 magnets for high-energy physics 9-12121  
 quantum interference magnetometer response to magnetic Johnson (thermal) noise from conducting environment 9-7783  
 resonator-solenoid, design 9-19905  
 solenoids 9-18610  
 transformer, thin film d.c., mag. field and temp. depend. 9-3602  
 tunnel contacts, small cross-section, Josephson eff. 9-15082  
 tunnel junctions, d.c. Josephson effect rel. to strong-coupling 9-12131  
 Al-Al $_2$ O $_3$ -In tunnel junction, rel. to energy gap anisotropy obs. in In 9-3596

**Superconducting devices continued**

- Al-Al $_2$ O $_3$ -Bi tunnel junctions with ultrathin Bi films, I-V characts. 9-9966  
 Al tunnel junctions in meas. of phonon spectrum of granular mat. 9-9817  
 Pb-Cu-Pb sandwiches, resist. studies with Pb in supercond. state 9-13862  
 Pb tunnel junctions, d.c. Josephson effect, strong-coupling effects 9-12131  
 Sn-SnO-Sn Josephson junctions, relax. oscils. 9-19907  
 Sn tunnel junctions, d.c. Josephson effect, strong-coupling effects 9-12131

**Superconducting magnets**

- composite conductors strengthening for construction 9-19904  
 elementary review 9-1509  
 enthalpy stabilization of flux motion 9-3600  
 for MHD generators, model 9-15497  
 review of materials, elec. and mag. characts. and stability 9-16250  
 saddle-shaped, construction and test for MHD generator 9-19903  
 supply, with supercond. rectifier 9-7781  
 He liquid applic. 9-8318  
 Nb $_3$ Sn, permanent, possibilities, advantages and disadvantages 9-7771

**Superconducting materials**

- alkali metals 9-5661  
 alloys, dil. mag., ultra-high critical field 9-21488  
 alloys, non-transition metal Cu $_3$ Au-type, T $_c$  W-like depend. on number of valence electrons 9-12123  
 alloys, properties review with theory 9-9946  
 with anisotropic conduct. and mag. props., patents 9-9967  
 anomalous, theoretical considerations 9-21487  
 behaviour in varying field 9-15078  
 composite, maximum completely stabilized current density 9-3584  
 crystallites, small coated with polarizable material 9-5654  
 d.c. Josephson effect rel. to strong-coupling 9-12131  
 ferromagnetic, effect of impurities on existence of inhomogeneous state 9-9943  
 film magnetization phase transitions described 9-12231  
 films, superposed, coupled motion of vortices 9-7777  
 hard, review 9-16238  
 impure, Josephson effect 9-9949  
 impurity band growth in energy gap, classical spin supercond. 9-5606  
 magnetic behaviour and effect of temperature and substitutional Mo 9-1474  
 with magnetic impurities, ultrahigh critical fields 9-21488  
 metal, alkali; electron-phonon interaction contrib. to density of states 9-19901  
 metals, properties review with theory 9-9946  
 mixed state, reactor irradiated, dissipative processes 9-3587  
 mixed state, reactor irradiated, dissipative processes 9-13850  
 molybdenum carbides, heat capacities, 1.5-20%K 9-1396  
 with paramagnetic impurities, dynamic props., model 9-13856  
 properties, effect of pressure and comparison with theory 9-9935  
 quantum electronics props. demonstrated 9-13849  
 T $_c$  depression meas., 3d-transition element impurities 9-21486  
 thin films, critical fields 9-1485  
 thin films, critical fields 9-13854  
 titanates, semicond. 9-3598  
 tubes, mag. field enhancement 9-15075  
 (86 at %)(n(14 at %)) TL mech. effects, type II superconds. 9-16245  
 Al-Al $_2$ O $_3$ -Bi tunnel junctions with ultrathin Bi films, I-V characts. 9-9966  
 Al films, dependence of critical temperature and energy gap on thickness 9-1497  
 Al films, dependence of critical temperature and energy gap on thickness 9-15080  
 Al granular, tunneling meas. of phonon spectrum 9-9817  
 Al $_2$ (Os $_{1-x}$ Ru $_x$ ) monoclinic phase, transition temps. 9-13852  
 Be thin films, below 7°K, e. diff. study 9-13863  
 Bi, films, resistive transition thickness dependence 9-9955  
 Cd, and band structure from single pseudopotential 9-13827  
 Ce high-pressure phase > 50kbar, mag. ordering and supercond. props 9-3595  
 CeCo $_5$  phase, T $_c$ , press. depend. 9-3594  
 Cu-Sb phases and absence of antiferromagnetism in Cu $_3$ Sb 9-12122  
 Cu $_3$ Au-type alloys of non-transition metals, T $_c$  W-like depend. on number of valence electrons 9-12123  
 GeTe, transition temp. carrier-conc. dependence rel. to intervalley transitions 9-21494  
 H in metallic phase, possible high temp. superconductor 9-9956  
 Hf, absence of superconductivity in bulk material 9-12124  
 Hg: Cd crystals, attenuation, ultrasonic 9-7772  
 Hg crystals, attenuation, ultrasonic 9-7772  
 In/Th superimposed films, proximity effect 9-17384  
 In-Hg(Cd) dilute alloys, transition temp. impurity conc. dependence rel. to phonon spectra changes 9-5533  
 In-Pb alloy, thermal conductivity meas. down to 0.4°K rel. to phonon scatt. mechanism 9-21444  
 In-Pb alloy, upper critical field, anomalous values 9-1498  
 In-Pb alloys, transition temp. depend. rel. to Fermi surface interactions 9-21491  
 In-Pb alloys, type II, specific heat temp. dependence, 1.5-4.2°K rel. to Maki parameter determ. 9-21493  
 In-Pb system, pressure depend. of superconducting critical temp. 9-16246  
 In-Tl alloy, upper critical field, anomalous values 9-1498  
 In, conductivity in normal state from meas. on superconductor 9-9933  
 In, energy gap anisotropy 9-3596  
 In, type-I, Grueneisen functions determ. 9-21440  
 In, very-high-impurity, thermal-resistivity ratio, 1.5-4.2°K 9-12101  
 In single spheres, superheating and supercooling props. 9-21495  
 InSb, metallic, with anisotropic upper critical field, props. 9-21492  
 Ir-based dilute alloys, localized spin fluctuations 9-1499  
 La:Ce(Gd) transition temperature, pressure dependence 9-1486  
 La $_2$ -xGd $_x$ Al, transition temp., anomalous behaviour 9-7773  
 La cpds.: Pr and Tm mag. impurities effect 9-13857  
 LaSn $_2$ : Gd, critical temp. reln with normal-state mag. props. 9-1478  
 Mo-Fe alloys, dil. rel. to Kondo effect 9-1500  
 Mo-34 at.%W: Re, lower critical field depend. on normal state resistivity 9-7770  
 Nb $_6$ Ti wires, preparation of foil samples for electron microscope exam. 9-16071  
 Nb-C system, heat capacities, 1.5-18°K, rel. to effect of C conc. and cryst. struct. on T $_c$  9-1397  
 Nb-Ta alloys, transition temp. and electronic spec. heat 9-13866  
 Nb-Ti alloys, influence of structure 9-12125



**Superconducting materials continued**

- Nb-Ti alloys,  $T_c$  and  $H_c$  meas. 9-1504  
 Nb (44wt.%)Ti wire, microstructure obs. 9-18450  
 Nb-Zr-Ti alloys,  $T_c$  and  $H_c$  meas. 9-1504  
 Nb-Zr alloys, eff. of hydrostatic pressure on critical current 9-15074  
 Nb-Zr tube, flux penetration 9-7774  
 Nb (25 at. %) Zr wire, critical surface defn. between normal and supercond. state 9-13867  
 Nb<sub>3</sub>Al, sintered, Ginzburg-Landau parameter and mag. field penetration depth calc. 9-18611  
 Nb<sub>3</sub>Al, with V partial substitution, transition temp. 9-7778  
 Nb<sub>3</sub>Ga, with V partial substitution, transition temp. 9-7778  
 Nb<sub>3</sub>Sn, sintered, Ginzburg-Landau parameter and mag. field penetration depth calc. 9-18611  
 Nb<sub>3</sub>(Al,Ge) system above 20.5°K, obs. 9-12128  
 Nb<sub>3</sub>(M<sub>1-x</sub>N<sub>2</sub>)<sub>2</sub>, solid solns. (M,N=Al, Ga, Ge, In and Sn) transition temp. reln with microhardness 9-5664  
 NbN, energy gap meas. 9-12127  
 Nb<sub>3</sub>Sn composite tapes and appl. mag. field production 9-5663  
 Nb<sub>3</sub>Sn ribbon, critical surface definition between normal and superconducting state 9-13867  
 NbTi, effective resistivity during mag. field step transmission 9-9957  
 NbTi wire, pinning force, depend. on mag. fields 9-12118  
 Nb<sub>3</sub>Zr wire, pinning force, depend. on mag. fields 9-12118  
 Nb-Ti alloy props. and appl. mag. field production 9-5663  
 P, at 170-260 kbar 9-1505  
 Pb-Cu-Pb sandwiches, resist. studies with Pb in supercond. state 9-13862  
 Pb-In(Bi) alloys, dirty type-II, h.f. surface impedance in surface-sheath regime 9-12113  
 Pb-(1.89wt.%) Ti alloy with Ginzburg Landau parameter near  $1/\sqrt{2}$ , flux line lattices in intermediate state 9-16248  
 Pb-Ti alloys, type II, flux pinning by grain boundaries 9-3597  
 Pb thin films, critical temp. gradient and critical current density 9-18609  
 PbHg, type II, interaction between vortex lines and ferromag. inclusions 9-9958  
 Sn-Sb(In)(Zn), impurity effects on critical-field curve 9-9961  
 Sn-Sb(In)(Zn)(Cd), impurity effects on residual resistivity anisotropy, ideal resistivities and derivations from Matthiessen's Rule at 77 and 273°K 9-9962  
 Sn, conductivity in normal state from meas. on superconductor 9-9933  
 Sn, d.c. Josephson effect rel. to strong coupling 9-12131  
 Sn, energy-gap effects on thermal conductivity, calc. 9-9857  
 Sn, energy gap, effect of high pressure 9-12129  
 Sn, energy gap pressure dependence, u.s. attenuation meas. 9-17385  
 Sn, magnetic transitions of thin films and foils 9-7775  
 Sn, single crystals, u.s. absorpt. at 500 kHz, temp. depend. 9-21496  
 Sn, type-I, Gruneisen functions determ. 9-21440  
 Sn depairing of thin films 9-1506  
 Sn films, quantum size effects 9-5832  
 Sn films, superposed, coupled motion of vortices 9-7777  
 Sn films, type II, switch from thin to bulk behaviour 9-16249  
 Sn single spheres, superheating and supercooling props. 9-21495  
 SnTe, transition temp. carrier-conc.-dependence rel. to intervalley transitions 9-21494  
 SrTiO<sub>3</sub>, semicond. ceramics 9-3598  
 Ta-C system, heat capacities, 1.5-18°K, rel. to effect of C conc. and cryst. struct. on  $T_c$  9-1397  
 Ta, surface nucleation and bulk supercooling fields meas. 9-17386  
 Ta, type-I, Gruneisen functions determ. 9-21440  
 Th cpds., Pr and Tm mag. impurities effect 9-13857  
 Ti-(47 wt.%)Nb alloy, props., dependence on structure 9-13865  
 Ti-Nb alloys, phase transformations 9-1507  
 TiO<sub>x</sub>, transition temp. increase due to quenching 9-21392  
 Ti, U.S. attenuation in high-purity material 9-12003  
 $\alpha$ -U-Mo alloys, pressure dependence, 0-10 kbar 9-12130  
 $\alpha$ -U isotope effect 9-1487  
 V-(Sat.wt.%)Ta, type II, u.s. absorpt. in intermediate purity state 9-18612  
 V, isolated-vortex state near  $H_{c1}$  from u.s. attenuation obs. 9-17387  
 V, mixed state, u.s. attenuation 9-12005  
 V, type II, flux flow resistance and  $\kappa_2(T)$  parameter 9-1508  
 V<sub>3</sub>Ga, (Al, In, Si or Ge partial substitution), transition temp. 9-7778  
 V<sub>3</sub>Ga, sintered, Ginzburg-Landau parameter and mag. field penetration depth calc. 9-18611  
 V<sub>3</sub>Si, sintered, Ginzburg-Landau parameter and mag. field penetration depth calc. 9-18611  
 V<sub>3</sub>Si, with (Al, Ga, In or Ge partial substitution), transition temp. 9-7778  
 (V,Mn)<sub>3</sub>Si ternary cpds., with high transition temp. 9-3599  
 $\beta$ -W, films, characts. 9-13869  
 Zn, and band structure for single pseudopotential 9-13827  
 Zn, u.s. attenuation 9-1381  
 Zr-Nb alloys, transition temp. and upper critical field 9-18606  
 Zr-V alloy, upper critical field and transition temp. 9-5665

**lead**

- conductivity in normal state from meas. on superconductor 9-9933  
 d.c. Josephson effect rel. to strong-coupling 9-12131  
 electron drag, and flow stress, in transition, 4.2°K 9-1502  
 energy gap variations with temp., tunneling meas., advanced laboratory expt. 9-12830  
 films and foils, superconducting, magnetic transitions 9-7780  
 Josephson voltage freq. relations comparison with Sn and In 9-9960  
 magnetic props. study, flux penetration depend. on surface condition 9-13861  
 magnetic transitions of thin films and foils 9-7780  
 transition temp. meas. by C resistance thermometer 9-19101  
 transition temp. pressure dependence 9-9959  
 type-I, Gruneisen functions determ. 9-21440  
 Pb/Th superimposed films, proximity effect 9-17384  
 Pb-Cu-Pb sandwiches, resist. studies with Pb in supercond. state (98 at. %) Pb (2 at. %) In, type II, flux jump size distrib. 9-1480

**niobium**

- anisotropy in upper critical field, precision meas. 9-12126  
 de Haas-van Alphen oscills., Fermi surface model 9-7727  
 electron drag, and flow stress, in transition, 4.2°K 9-1502  
 films, reactively sputtered, transition temps. process parameter dependence 9-5662  
 hysteresis in u.s. attenuation near  $H_{c1}$  9-9831  
 intrinsic type-II superconductivity 9-19899  
 magnetic props. study, flux penetration depend. on surface condition 9-13861  
 sheath supercond., critical phenomena 9-19902

**Superconducting materials continued****niobium continued**

- surface critical current, temp. and orientation dependence 9-16247  
 surface impedance near  $H_{c2}$  map-field and depend. ang. 9-1479  
 surface structure and a.c. losses 9-13864  
 type II, a.c. losses, effect of static mag. field 9-1501  
 wires, critical state equation 9-1503  
 films, reactively sputtered in presence of N<sub>2</sub>, critical current densities 9-7742  
 Nb-Zr and Lipowitz alloy plates, mag. flux penetration 9-9952  
 Nb<sub>3</sub>Sn and Nb-Ti plates, mag. flux penetration 9-9952

**Superconductivity**

- abs. of transverse U.S. phonons near  $T_c$ , relaxation of Ginzburg-Landau parameter 9-3586  
 alloys, dil. non-magnetic, electron-phonon interaction effect on  $T_c$  9-1495  
 anomalous, theoretical considerations 9-21487  
 anomalous electrical conductivity above  $T_c$  9-17380  
 BCS model, soln by quantum statistical spectral density technique 9-98  
 BCS-spin model, thermodynamic representations, time evolution and vacuum props. 9-7762  
 behaviour in varying field 9-15078  
 critical behaviour of singular quantities near second-order transition line 9-16195  
 critical field of surface 9-15073  
 critical field of surface 9-3588  
 critical fluctuation, dynamic, above transition point 9-9941  
 critical phenomena, dynamic 9-9939  
 critical supercooling field, increase by paramag. impurities 9-9937  
 current distrib. in thin strip, analytical soln. 9-9938  
 current ring supported in mag. field, stability 9-19896  
 electron gas in spin density wave state as carrier 9-7763  
 electron mechanism, theory 9-9947  
 electron-phonon interaction h.f. effect 9-3589  
 electron-phonon interaction h.f. effect 9-13853  
 enhancement by semi-metallic or semicond. inclusions 9-9940  
 enhancement by phonon spectrum changes in small particles layers 9-5529  
 equilibrium approach rel. to Cooper pair density relax. 9-7789  
 film, thin in surface parallel mag. fields, eqn. for critical field 9-7767  
 film, transport current distrib. inhomogeneity 9-7758  
 film carrying current 9-16239  
 films, layered metallic, enhancement 9-7765  
 fluctuation of current density at threshold using Ginzburg-Landau theory 9-9951  
 fluctuations due to paramag. impurities 9-7764  
 flux line lattices in intermediate state of superconductors with Ginzburg Landau parameters near  $1/\sqrt{2}$  9-16248  
 gap equation, existence proof 9-19895  
 granular superconductors, microwave props. 9-12107  
 high temperature, possible means of production, exciton mechanism 9-7757  
 high-temp., thermal phonon, effect on transition temp., 9-1484  
 hollow microcylinder, fluxoid quantization and field-induced depairing 9-12273  
 Intermag. conference, Washington, D.C., April 1968 9-3774  
 Intermag. conference, Washington, D.C., April 1968 9-7883  
 Intermag. conference, Washington, D.C., April 1968 9-3773  
 intermediate state, dynamic thermal effects 9-1475  
 i.r., very-far, new techniques 9-15551  
 Josephson effect, 10 Å insulating layer between superconductors 9-7782  
 Josephson effect, thinning interpretation 9-3585  
 Josephson effect in very impure superconductors 9-9949  
 Josephson junction, radiation, freq. pulling effects 9-12120  
 Josephson tunnelling effect, theory 9-9944  
 jump temperature obs. under pressure at 0.1°K 9-5653  
 Kim-Anderson flux flow where  $K \sim 1$  9-18608  
 low-pass filter for mag. field meas. 9-10811  
 magnetization of hollow tube in sheath state 9-1483  
 metallic alloys, dil. with magnetic impurities, below Kondo temp., critical temp. and energy gap meas. 9-7779  
 metals and alloys, rel. to positron annihilation 9-12078  
 microscopic theory rel. to basic physical ideas involved 9-18607  
 nonlocal superconductors in mag. field, theory 9-7766  
 normal region motion along superconducting strip 9-16242  
 nucleation above  $H_{c2}$  9-21489  
 one-dimensional system, theory 9-9948  
 order parameter in transition region 9-16243  
 with paramagnetic impurities, dynamic props., model 9-13856  
 with paramagnetic impurities, electron interaction effect on transition temp. and gap 9-1476  
 phase boundary between normal and supercond. regions, dynamics of current flow 9-12110  
 photoinduced, theoretical exam. 9-5656  
 proximity effect, tunneling model 9-17379  
 proximity effect theory, expt. tests 9-17384  
 quantum electronics props. demonstrated 9-13849  
 quasi one-dimensional structures, theory 9-15076  
 quasiclassical theory, penetration depth rel. to field strength 9-13855  
 resistance jump in cylinder with current and phenomenological interpretation of Meissner effect 9-1481  
 resistivity in normal state near transition temp., Ginzburg-Landau theory 9-5657  
 resistivity meas. device, 5-100°K 9-2301  
 resonating-valence-bond theory reviewed 9-17381  
 second-order transition line, critical behaviour of singular quantities in its neighbourhood 9-16195  
 semiconductors 9-19894  
 semiconductors and semimetals, plasmon mechanism 9-15077  
 shear-wave attenuation near  $T_c$ , nonlinear effect 9-7760  
 shielding and field-retaining properties of hollow cylinders 9-7768  
 small size, nuclear spin relax 9-1712  
 soft surfaces and size effect 9-7761  
 solders, obs. 9-12805  
 stars, white dwarfs, transition props. and temp. 9-15285  
 superconducting and normal metals in adjacent layer systems, proximity effect 9-9945  
 superconductor, 2-dimens., electrical conductivity temp. depend. near  $T_c$  9-21490  
 superfluid exponent  $\zeta$  from self-consistent Landau-Ginzburg theory 9-10658  
 surface, critical field and surface layer structure 9-3588

# Superconductivity continued

- surface, critical field and surface layer structure 9-15073
- surface, theoretical and experimental review 9-9936
- surface current equilibria in applied fields 9-9942
- surface impedance and the effect of a static magnetic field 9-12111
- teaching expts., flux quantization and Josephson effect 9-2123
- temperature-dependent interaction and thermodynamic props. 9-12109
- thermal conductivity, anomalies due to impurity spin ordering 9-12108
- transformation point rel. to m.p. 9-16236
- transition temp., effect of lattice disorders 9-5655
- transition temp., one-body interaction eff. 9-9950
- tube, hard, flux penetration 9-7774
- tunneling density of states, current effect including mean free path 9-7759
- tunneling in anisotropic supercond. 9-1477
- tunneling in anisotropic supercond. 9-13851
- two-band, infl. of normal d band on s band 9-16240
- two-band superconductors with nonmagnetic impurities, upper critical field 9-16241
- type I, hollow cylinder, shielding and field retaining properties 9-7768
- type I, propag. of transverse sound, theory 9-1376
- type I, thin films, critical temp. gradient and critical current density 9-18609
- type-I, Gruneisen functions determ. 9-21440
- u.s. absorption, rel. to strong  $\epsilon$ -phonon interaction, theory 9-1373
- u.s. attenuation anomaly in strong coupling and impure superconductors 9-13796
- vortex line obs. using transmission e. microscopy 9-7393
- zero-freq. currents, stability, in simply connected superconductors 9-1482
- In Josephson voltage-freq. relations, comparison with Sn and Pb 9-9960
- Pb-Cu-Pb sandwiches, resist. studies with Pb in supercond. state 9-13862
- Pb Josephson voltage-freq. relations comparison with Sn and In 9-9960
- Sn-In alloy, resonant freq. of tank cct. with specimen as core and a.c. mag. susceptibility 9-16237
- Sn, Josephson voltage freq. relations, comparison with Pb and In 9-9960
- Sn film, Cu added, tunnel junction meas. for critical temp. determ. 3.5-7°K 9-7776
- Sn film, disordered, invest. by superconducting tunnelling 9-13868
- $\alpha$ -U isotope effect 9-1487
- V<sub>1</sub>Si type cpds, anomalous props based on energy band model 9-1496
- type II**
  - Abrikosov's vortex structure, stability 9-3591
  - alloys, lower int. field depend. on normal state resistivity 9-7770
  - bound excitations of single vortex 9-1488
  - core model, explanation of Hall effect and resistivity in mixed state 9-12117
  - critical parameters of thin cylinder coated with normal metal 9-12116
  - critical-state model, generalized 9-7769
  - current-carrying capacity, surface temp. gradient eff. 9-13859
  - density of states, theory 9-12115
  - destruction by current, intermediate state resistance transition 9-1489
  - electrodynamics, London eqn. in Schubnikov state 9-9954
  - excitation spectrum of fluctuation in order parameter, study using time-depend. Ginzburg-Landau eq. 9-3591
  - ferromagnetic inclusions interaction with vortex lines 9-9958
  - films, switch from thin to bulk behaviour 9-16249
  - flux motion, review 9-3590
  - flux-trapping model showing magnetization behaviour 9-3593
  - fluxoids, formation of super-radiative induction and echo signals 9-19897
  - hard superconductors, review 9-16238
  - magnetic flux penetration 9-9952
  - magnetic props., resonance scatt. effect 9-15086
  - magnetization meas., vibrating coil magnetometer 9-1491
  - magnetostriction 9-5658
  - mixed state, core model explaining Hall effect and resistivity 9-12117
  - nuclear spin relax. rate near upper critical field, theory 9-7923
  - orbital quantization effects on critical fields 9-12114
  - order parameter, thermal critical fluctuation observable in very dirty superconductors 9-3592
  - peak effect, infl. of small oscillating magnetic fields 9-1492
  - peak effect, possible mechanism 9-16244
  - periodic structures, exptl. investigation by  $\mu$ -mesons 9-1493
  - phase transition, anomalous 9-19898
  - pinning force, depend. on mag. fields 9-12118
  - r.f. flux penetration, mag. field dependence 9-12112
  - surface resistance 9-5659
  - surface supercond. destruction by h.f. field 9-15078
  - surface-impedance, h.f., in dirty superconductors in surface-sheath regime 9-12113
  - thermal conductivity, in mixed state 9-21442
  - thermodynamic effects, heat current 9-9953
  - thin film, current distrib., eff. in d.c. superconducting transformer 9-13858
  - transition of homogeneous cylinder under infl. of axial current, mag. field distribution 9-17382
  - type II, surface current effect 9-19893
  - u.s. absorption in intermediate purity state 9-18612
  - voltage generation by vortex motion 9-15079
  - vortex scattering of BCS single-particle excitations in clean superconductor 9-17383
  - vortices, theory 9-13860
  - In-Pb alloys, specific heat temp. dependence, 1.5-4.2°K rel. to Maki parameter determ. 9-21493
  - InSb, metallic, with anisotropic upper critical field, props. 9-21492
  - Nb, intrinsic 9-19899
  - Nb magnetic flux penetration depend. on surface condition, intermediate state formation 9-13861
  - NbTi, effective resistivity during mag. field step transmission 9-9957
  - NbTi wire, pinning force, depend. on mag. fields 9-12118
  - Nb<sub>2</sub>Zr wire, pinning force, depend. on mag. fields 9-12118
  - Pb-Tl alloys, flux pinning by grain boundaries 9-3597
  - Pb magnetic flux penetration depend. on surface condition, intermediate state formation 9-13861
  - PbHg, ferromagnetic inclusions interaction with vortex lines 9-9958
  - Pb<sub>1-x</sub>Bi<sub>x</sub> resistivity minimum, 9-1490
  - Pb<sub>1-x</sub>Tl<sub>x</sub> thermal dissipation 9-1490
  - V, flux flow resistance and  $\kappa_2(T)$  parameter 9-1508
  - V, mixed state, u.s. attenuation 9-12005

# Supercooling

- aerosols, probability of crystallization 9-11727

# Supercooling continued

- D-camphor in liquid-solid phase transition studies 9-3148
- cholesteryl ester crystal static dielectric const. temp. var. 9-9539
- cloud, ice crystal dielec. polarity rel. to temp. 9-12183
- interface melted subst. and crystal, rel. to surface energy changes 9-7323
- metal melt, stable solid nucleus growth 9-13559
- superconductor, critical field, increase by paramagnetic impurities 9-9937
- temperature difference curves 9-1068
- Ge epitaxial film, droplets rel. to growth 9-13580
- H<sub>2</sub>O, homogeneous nucleation temp. 9-7301
- Ta, surface nucleation and bulk supercooling fields meas. superconductivity 9-17386
- Superexchange** *see Antiferromagnetism; Exchange interactions*
- Superfluidity**
  - See also Helium/liquid; Quantum fluids*
  - boson system, grand canonical partition function, functional-integral representation 9-8447
  - flow through channels, thermodynamic stability 9-18377
  - Helmholtz resonator, master eqn. 9-4337
  - ion trapping in rotating liq. He 9-9582
  - long range order in 2D 9-19002
  - nuclear matter, critical transition temp. 9-488
  - phenomenological theory, validity 9-18670
  - relativistic theory of irreversible processes 9-3144
  - He, density, temp. depend. eqn. for 1.2°K ≤ T ≤ T<sub>λ</sub> 9-7297
  - He, hard-sphere Bose gas model 9-3143
  - He, liquid, dynamical critical phenomena at  $\lambda$  transition 9-9575
  - He, possibility of two critical velocities 9-2959
  - He, rot., trapped negative ions mobility on vortices, 0.8-1.6°K 9-5207
  - He energetic neutral excitation, prod. of charged part. at surface 9-11735
  - He films, unsaturated, superfluidity without superflow 9-19653
  - He II, applic. of thermodynamic stability criterion 9-18377
  - He II, critical heat flux close  $\lambda$  transition 9-18378
  - He II, density increase due to turbulent flow 9-5208
  - He II second-sound damping in T<sub>λ</sub> region 9-3146
  - He liq., critical flow rate through narrow pores 9-11737
  - He liq., energy dissipation in flow, critical vel. obs. 9-11736
  - He liq., thermal conductivity near transition 9-1054
  - He second critical velocity in narrow annulus 9-1057
  - He under press., trapping lifetime of negative ions 9-13551
  - <sup>4</sup>He, logarithmic corrections to theory of  $\lambda$ -transition 9-16029
  - He<sup>+</sup> thermal conductivity meas. of pure and in sol. of He<sup>3</sup>, 0.035-0.5°K b/l c// 9-3145
  - <sup>3</sup>He-<sup>4</sup>He solution, sound propag. in narrow channels 9-13553
  - HeII, mutual friction near superfluid transition, evidence from heat flow obs. 9-11738
  - II, atomic admixtures, adsorpt. on quantized vortices 9-1060
- Superlattice structure** *see Alloys; Crystal structure, atomic; Solid solutions*
- Supernovae** *see Novae*
- Superparamagnetism** *see Ferromagnetism*
- Supersonic flow**
  - See also Shock waves*
  - air jets, eff. of acoustic feedback on spread and decay 9-21126
  - air-H<sub>2</sub> mixture, flame propag. 9-16747
  - axisymmetric near wake, approx. pressure-angle calc. procedure 9-7215
  - base pressure for 9° cones, local flow effects 9-17151
  - past blunt bodies, numerical calc. of detached shock problem 9-17150
  - round blunt cone, producing radiation 9-13479
  - blunted cones and wedges, asymptotic theory 9-9437
  - boundary layer plate flow, effects of thermal rad. 9-19576
  - cone, near-wake flowfield with injection, effect of species and nozzle locations 9-21128
  - delta wing, minimum drag with finite leading-edge velocity 9-11653
  - detached shock calculation by 2-order finite differences 9-946
  - gases in hypervelocity nozzles, meas. of viscosity, Reynolds number and atom conc. 9-9434
  - heat transfer to cavity, mass addition eff. 9-159
  - heat transfer to wavy wall 9-11642
  - hypersonic flow over wedge, of diatomic gas 9-19572
  - integral correlation method calc. 9-9428
  - jet, separation of gas mixture 9-21145
  - luminous flow around bodies, exptl. data 9-5107
  - Mach number infinite, one dimens. unsteady flow past bodies, downstream soln. 9-849
  - method of characteristics for 3D flow 9-13475
  - nonstationary pressure vibr. of rectangular plate 9-4298
  - panel, two-dimensional, stability boundaries, Liapunov anal. 9-21127
  - perturbation of rotating body in air 9-949
  - plasma, magnetic Laval nozzle, modification of B field config. of Q device 9-2980
  - reduction of 3-D to 2D hyperbolic differential eqn. 9-13480
  - sharp cone drag coeffs., correlation 9-7217
  - shell, cylindrical, unsteady oscils. 9-7220
  - three-dimensional, of nonviscous gas 9-14807
  - three-dimensional, past segment-shaped body, pattern 9-5100
  - transpiration cooling of porous wall, Mach number effect on temp. distrib. 9-20457
  - turbulence characts. of Mach 3 body wake 9-11652
  - turbulent base flows behind rearward facing step, integral near-wake anal. 9-9431
  - turbulent boundary layer, effect of streamwise wall curvature on heat transfer 9-14811
  - turbulent boundary-layer separation ahead of cylinder, associated shock pattern 9-7214
  - turbulent wake behind sharp slender cone 9-17152
  - vibration, forced, of finite plate 9-8504
  - CO<sub>2</sub> jet, e diff. for existence of crystals and free molecules 9-11459
  - H<sub>2</sub>-O mixture, detonations propagation 9-19582
  - H<sub>2</sub>-N<sub>2</sub> jet, separation of gases 9-21145
  - He, low-density, visualization with fluoresc. and afterglow methods, elec. ion beam excited 9-21131
- Supersonics** *see Ultrasonics*
- Surface diffusion** *see Diffusion in liquids; Diffusion in solids; Surface phenomena*
- Surface energy**
  - See also Crystal electron states/surface*
  - alloys, embrittled by enrichment of boundaries with impurities, grain boundary 9-11922



**Surface energy continued**

- bubble contact angle with liquid, investigation using deflection of light beam 9-21178
- crystal, bulk free energy rel. to equilib. shape 9-13595
- glass, fracture surface energy 9-1306
- interface melted subst. and crystal rel. to supercooling 9-7323
- metals, h.c.p., interface, anisotropy 9-21257
- metals, solid liquid interfacial free energies, absolute determ. 9-11759
- phenol formaldehyde resin carbons, contact pot. difference rel. to heat treat ment temp. 9-7324
- silica, comparison of quartz, cristobalite and silicic acid forms 9-21260
- steel, commercial grade transformer, role in secondary recrystallization 9-13752
- steel, stainless 304 film, interfacial free energies, investig. by electron trans mission and diff. microscopy 9-1231
- Ag S system, variation with crystallographic orientation 9-9624
- Bi, absolute solid liquid interfacial free energies 9-11759
- Cd, interfacial energy during growth from melt 9-18401
- Fe, effect of O<sub>2</sub> adsorption 9-9603
- LiF fracture, rel. to dynamical cleavage processes 9-13741
- Zn, solid vapour interface, anisotropy from inert gas bubble shapes, 130-300°C 9-21257

**Surface ionization** *see Ionization, surface***Surface measurement**

- See also Area measurement*
- density gauge, influence of air-gap 9-5227
- surface area and porosity calc. from gas adsorpt. isotherms for C black 9-7348
- temperature of substrates on hotplate used for epitaxial growth 9-11807
- AgBr suspension, surface area meas. from cyanine dye ads. obs. 9-20566
- AgI suspension, surface area meas. from cyanine dye ads. obs. 9-20566
- C blacks, cumulative area calc. from gas adsorpt. isotherms 9-7348

**Surface phenomena**

*See also Adsorption; Capillarity; Catalysis; Electron emission; Films; Ionization, surface; Liquid waves/surface; Sorption*

- 'optical' discharges produced by single laser pulses on non absorbing surfaces 9-5785
- adhesion of solid surfaces formed by cleavage in ultrahigh vacuum 9-3186
- area change following adsorption, BET method with Kr, correction 9-21255
- axisymmetric stress wave propag. across cylindrical solid fluid, interface 9-3182
- bending, stretching and shearing of an orthotropic simple solid, supported by surface traction 9-19027
- contact ionization, review 9-7322
- contact region of hard ball rolling on viscoelastic plate 9-12924
- crack, Griffith, asymmetrically loaded, stress intensity factors 9-18523
- creepage flashover discharge, effects of conducting metallic barrier 9-10041
- cristobalite, surface states, H<sub>2</sub>-D<sub>2</sub> equilibration activity and pH<sub>2</sub> conver sion 9-3188
- crystal states, role in unified model of oxide cathode 9-5776
- defects in aerospace structures, i.r. detection 9-3444
- desorption, diffusion processes, appl. of exponential tempering function 9-3179
- diffusion, effect on gaseous isotope separation efficiency 9-7236
- diffusion, importance in crystal growth from solution 9-18418
- diffusion laws, theoretical study 9-9725
- elastic, stability of liquid laminar boundary layer 9-14822
- elastic infinite surface with cylindrical hole, stress analysis 9-19028
- electrical double layers in fused alkali metal nitrates 9-21707
- electrolyte conductor interface, eff. of elec. double layer on reflectance and ellipsometry 9-14136
- Fermi liquid at zero temp. 9-104
- ferromagnetic thin films, resonance peak 9-5834
- fluid solid, momentum and heat transfer in regular packings 9-5229
- fluid/solid, isotopic method for movement investigation 9-3185
- gas-filled interactions, three- dims. model 9-3183
- gas-surface reactions, book 9-5230
- gas-surface second virial coeff., quantum corrections 9-9601
- glass, adhesion of colloidal hydrous Fe<sub>2</sub>O<sub>3</sub>, effect of stirring 9-9567
- graphite, complexes formed during irradi. in CO<sub>2</sub>/CH<sub>4</sub> mixtures 9-8065
- graphite, interaction potentials for polar mols. 9-1090
- graphite, triple point press. and temp., solidus-liquidus interface 9-1092
- graphite, wettability by BaF<sub>2</sub>-CaF<sub>2</sub> eutectic 9-7326
- heat, mass, transfer processes, critical sound press. in acoustic stimulation 9-5228
- heat transfer, synthesis techniques 9-20451
- heat transfer obs. from rough and smooth tubes 9-19102
- interaction with gas atoms, theory 9-1088
- interface growth, solution where diffusion coeff. is conc. dependent 9-1087
- Johnsen-Rahbek effect, simple theory 9-16040
- liquid, flame propag., induction period 9-4372
- liquid, flame propag., steady-state conditions 9-6404
- liquid, flame propag., theoretical model 9-4373
- liquid, shallow, drop splashing 9-11675
- liquid, stimulated light scatt. 9-1012
- liquid-solid impact pressure and shock wave vel. 9-8516
- liquid-vapour interface, transient movement, u.s. meas. technique 9-11746
- metal, adhesion time and surface diffusion of inert gases 9-21347
- metal, sound excitation by e.m. waves 9-1367
- metal microcontacts, real area and number of contact points 9-17303
- metal oxidation, controlled by surface reaction, logarithmic law 9-14131
- mica, van der Waals forces, normal and retarded, direct meas. 9-18398
- molecular beam scatt. by metals 9-3184
- natural surfaces (soil, desert sand, white sand and water), polarization features of reflected light 9-1939
- phonon vibrations, phase shift solution 9-21418
- photoelectric properties change in the oxidation process 9-5760
- plasmon reson. effects in grating diff. light 9-4520
- polar molecules, surface force action and i.r. determ. of interfacial region thickness 9-13515
- potential on conducting or semiconducting surface, probe for meas. 9-4413
- pyrrole between polyethylene supports, surface forces and i.r. determ. of

**Surface phenomena continued**

- quartz, surface states, H<sub>2</sub>-D<sub>2</sub> equilibration activity and pH<sub>2</sub> conversion 9-3188
- repulsive forces by charged double layers on solid surfaces 9-18399
- rough liquid solid interface, reflection of plane harmonic sound wave 9-4328
- sapphire, wetting by liq. Al, effect of nature of surfaces 9-19622
- scalar wave scatt. by a convex transparent object with surface irregulari ties 9-52
- semiconductor covered with water charge relaxations 9-4057
- semiconductors, recombination velocity, flying spot method, improved 9-3647
- silicic acid, surface states, H<sub>2</sub>-D<sub>2</sub> equilibration activity and pH<sub>2</sub> conversion 9-3188
- solid adsorption from non- athermal polymer solns, numerical solns in parallel-layer model 9-18400
- solid liquid interfacial reaction between 18-8 stainless steel and aluminium 9-1089
- steel, topography in fatigue fracture 9-5480
- stress and tension, difference, physical significance 9-21258
- structure of condensing vapours at solid surfaces 9-18351
- superconductors, type II, surface resistance 9-5659
- temperature distrib. in solid and liquid phases and position of interface as function of time 9-9588
- thermal accommodation coeff. and lattice anharmonicity 9-9602
- thermodynamics of charged and polarized layers, book 9-10662
- triglycine sulphate cryst., layers rel. to dielec. const. 9-5753
- vacuum metallurgy 9-8324
- Ag(111), scatt. of Ar and Xe atomic beams 9-3187
- Al<sub>2</sub>O<sub>3</sub>, sapphire, wetting by liq. Al, effect of nature of surfaces 9-19622
- Al films, effect on energy losses of electrons 9-5588
- Au, self diffusion 9-21349
- Au, surface stress determ. 9-21259
- C, reactivity with radicals, and surface groups obs. 9-8058
- CdS crystal, Rayleigh wave, electron interaction 9-5697
- CdSe, u.s. surface wave amplification, expt. method 9-7648
- Cu, self diffusion, infl. of Pb vapour 9-17284
- Cu adhesion time of inert gases 9-21347
- Fe, corrosion inhibition, transition state in inhibitor ionc. versus surface coverage 9-15223
- GaAs film substrate interface, vapour epitaxial, occurrence of high resis tance layer 9-5674
- Ge-Al system, 'unipolar' diffusion 9-5408
- n- Ge, depletion effects, non-equilib., at electrolyte interface 9-13895
- Ge, field effect, role of surface relief 9-1547
- Ge, on Cu adsorpt. from electrolyte 9-5704
- Ge, recombination studies using Suhl effect and light injection 9-9988
- <sup>3</sup>He-<sup>4</sup>He interfacial surface tension 9-18376
- Hg/aqueous soln. interface, specific adsorption of Cl<sup>-</sup> ions 9-17246
- InP clean surface, photoclec. field near threshold 9-16319
- n-InSb, relaxation at high elec. fields 9-19916
- NaCl cleaved surface, electrical microbreakdown visualisation 9-9638
- NaF:H, thin film, polarization for frequency shift of localized mode 9-19852
- Nb (25 at.%) Zr wire between normal and supercond. state, critical defn. 9-13867
- Nb<sub>3</sub>Sn ribbon, between normal and superconducting state, critical definition 9-13867
- Ni, surface diffusion of chemisorbed H 9-1086
- Pt, accommodation coeffs. of air, N<sub>2</sub>, O<sub>2</sub>, press. depend. 9-16039
- Pt, atomization of O<sub>2</sub> 9-1908
- SO<sub>2</sub>, electronically excited, formation on surfaces 9-6009
- Si-SiO<sub>2</sub> interfacial stress, rel. to interface states 9-12176
- Si, atomically clean, nonequilib. large-signal field effect, relax. 9-21517
- Si, field effect, role of surface relief 9-1547
- Si, passivation by SiO<sub>2</sub> film prep. 9-18404
- Si, stabilization using Si<sub>3</sub>N<sub>4</sub> 9-7811
- Si, treated with gaseous HF, elec. props. 9-3661
- Si m.o.s. transistors, interface charges effect on channel conductance 9-12177
- inSi growth on (111)Si in ultrahigh vacuum 9-5276
- Ti on W, anomalous migration 9-5264
- TiO<sub>2</sub>, electrochem. double layer model study from differential capacity curves 9-9606
- W, O<sub>2</sub> interaction 9-9600
- W single crystal, scatt. of slow Cs<sup>+</sup> ions 9-5231

**Surface structure**

- alloys, composition due to chem. modification, relevance to corrosion 9-16037
- analysis by optical simulation of LEED patterns 9-13570
- asperities for field emission, density mapping technique 9-3750
- aspherical, quality control using interferometers 9-4512
- corundum ceramics, damage on cutting and grinding from X-ray analysis 9-13574
- crystals, electron diffraction, low energy, matrix formulation 9-5302
- defect distribution in ion crystal near interface 9-17274
- electron diff. study, low energy 9-15501
- electropolishing, jet, of e microscope specimens, modification 9-16069
- etch pits, slope 9-21341
- film, evaporated, roughness effect on thickness meas. by Tolansky method 9-5235
- of films deposited on glass, mass spectrographic studies 9-7333
- glass, laser radiation damage 9-3176
- glass, leached layer formation kinetics 9-13573
- glasses, laser induced damage, mechanism 9-14891
- graphite, freshly powdered 9-1091
- graphite, surface complexes after radiolytic oxidation, stability 9-8087
- graphite spheron 6, surface complexes formed by contact with air at high temp. 9-8088
- ice, revised model 9-9478
- ionic crystals in contact with aq. soln., intrinsic defect depletion and accu mulation 9-14890
- juvenile, rel. to controlled internal fracture production by plastic extrusion method 9-13572
- juvenile, rel. to controlled internal fracture production by plastic casing method 9-13571
- macroreticular ion exchange resins, pore structure determ. 9-14892
- metal, faceted, LEED patterns 9-11794
- metal films, roughness effect on resistivity thickness dependence 9-9928
- metal overlayers 9-1084

**Surface structure continued**

- metal overlayers, LEED 9-1085  
 metals, effect on emissivity and optical const. 9-21433  
 p-n junctions, imperfections 9-13900  
 particle beam collimation from accelerator, scanning, anal. 9-18435  
 particle scattering, and surface phonons detection methods 9-21256  
 polypeptides, synthetic, monolayers, air/water interface 9-834  
 quartz, topography of crystals grown hydrothermally in Fe-lined vessel 9-13605  
 scanning system for use with e microprobe X-ray analyzer 9-11821  
 silica, comparison of quartz, cristobalite and silicic acid forms 9-21260  
 silica gel 9-19667  
 steel, electrotechnical hot-rolled, reduced oxide films 9-6012  
 steel-Al interface, surface props. effect on directional heat transfer 9-13809  
 water, revised model 9-9478  
 X-ray goniometer, double crystal 9-1170  
 Ag overlayer on Cu(100) 9-1085  
 Al, pitting and blistering on p-irrad., orientation dependence 9-9604  
 Al electrode, erosion by impulse accelerator plasmas 9-9412  
 Al electrode erosion by impulse accelerator plasmas 9-9411  
 Au(100), atomic arrangement 9-1084  
 C, pyrolytic, rubbed, orientations development and reln. to friction and wear 9-11758  
 C, superficial pore sizes rel. to He adsorption 9-7347  
 C surface groups, anal. by i.r. spectrometry and pyrolytic volatile anal. 9-7325  
 CdS thin film, u.h. vacuum system for preparation and expt. 9-16038  
 Cu, defects, relaxation, migration and formation energies 9-21330  
 Cu, influence on fatigue at low amplitudes 9-16135  
 Cu electrode, erosion by impulse accelerator plasmas 9-9412  
 Cu electrode erosion by impulse accelerator plasmas 9-9411  
 Cu spherical single crystals, O<sub>2</sub> ads. 9-5259  
 Fe-Cr-Mn alloy, effect on oxidation resistance 9-5503  
 Fe-Cr alloys, oxide growth micro-roughness 9-18755  
 Fe(CO)<sub>5</sub> powder, roughness effects on X-ray integrated intensities 9-11845  
 GaAs, mechanically polished, edge absorption correl. with thickness 9-12379  
 Ge, chemical polishing apparatus for flat, clean, strain-free surfaces 9-14284  
 Ge, internal reflection, multiple total, and field-effect technique investig. 9-21622  
 Ge, mechanically polished, edge absorption correl. with thickness 9-12379  
 Ge monocrystal, dislocation space charge display by scanning e beam 9-7390  
 InSb, mechanically polished, edge absorption correl. with thickness 9-12379  
 KCl, dissociation on e. irrad. at low temps. 9-7327  
 LiF, dislocation formation during annealing 9-11884  
 Mo electrode erosion by impulse accelerator plasmas 9-9411  
 Nb, superconducting, and a.c. losses 9-13864  
 Ni evap. films on glass, X-ray texture investigation 9-7336  
 Pb cryst., specular LEED 9-11760  
 Pd cryst., specular LEED 9-11760  
 Pt cryst. specular LEED 9-11760  
 Si (111), Ni induced, LEED study 9-21261  
 Si (111), Ni induced, LEED study 9-21262  
 Si (111) LEED pattern indicating impurity presence 9-5327  
 Si (111) surface, Au decoration 9-1094  
 Si monocrystal, dislocation space charge display by scanning e beam 9-7390  
 Sn single crystals growing from liquid, cellular 9-1126  
 Te clean surfaces, LEED study. 9-21263  
 Ti, impurity effects in pore formation in welds 9-16146  
 W, roughness effects on thermal radiation in normal and off-normal directions 9-5577  
 W cathode, hair-pin, during pre-breakdown conditioning, electron optical obs. 9-11633  
 Zn, slope of etch pits 9-21341  
 ZnS, diffus patterns in slow e diffr. from cleaved faces 9-9607

**Surface tension**

- See also Capillarity*  
 alcohols on water, interfacial tension calc. from spreading press. 9-9494  
 aqueous solutions and liquid metals in packed beds, static hold-up, obs. 9-17180  
 binary liquid mixtures, theory 9-7245  
 of binary low density of liquid mixtures 9-7238  
 binary organic liquid mixtures 9-19623  
 cavitation bubbles, influence on collapse velocity 9-9467  
 contact angle and spreading on solids and liquids, adsorpt. model 9-7259  
 decrease at interfacial film 9-18348  
 drop, incompressible fluid, revolving, shape and energy 9-14825  
 drop, incompressible fluid, revolving, stability 9-14826  
 fluxes, and interface tension between them and armco iron 9-14889  
 liquid, layer thickness and temp. depend. 9-7258  
 liquid bridges between sphere and plane and two spheres 9-21174  
 liquid metals, temp. depend. 9-17199  
 polymers, critical values derived from molecular constitution by modified Hildebrand-Scott eqn. 9-16041  
 sessile drop, contact angle calc. from max. radius and radius at plane of contact 9-9475  
 shadow-sausage eff., meniscus shape derivation 9-3086  
 sieve-plate distillation, effects 9-17179  
 sodium lauryl sulphate, black film, contact angles with bulk liq., and expansion kinetics 9-19602  
 solids, stress and tension, difference, physical significance 9-21258  
 surface-active agents in hydroerosion of metals 9-9775  
 variation effects on two-phase flow 9-21151  
 water-hydrocarbon liquid interfacial interaction energy rel. to hydrocarbon orientation 9-7260  
 wave patterns on surface of shallow depth 9-18340  
 waves, water, due to heaving circular cylinder, depend. 9-21171  
 at He-<sup>4</sup>He interface 9-18376  
 3NaF-Al<sub>2</sub>F<sub>3</sub>-Al<sub>2</sub>O<sub>3</sub>, melt, rel. to Al<sub>2</sub>O<sub>3</sub> content and CO<sub>2</sub> in furnace 9-11689  
 Ag compacts, effect of O<sub>2</sub> 9-5498  
 Au, rel. to stress determ. 9-21259  
 Ba, temp. dependence obs. 9-5149

**Surface tension continued**

- Ca, temp. dependence obs. 9-5149  
 H<sub>2</sub>O condensed droplet, in nucleation theory 9-7304  
 KPO<sub>3</sub>, molten, obs. 9-21191  
 Li, m.p. to b.p. 9-21197  
 LiPO<sub>3</sub> and LiPO<sub>3</sub>+NaPO<sub>3</sub>, molten mixtures obs. 9-21191  
 Mg, temp. dependence obs. 9-5149  
 NaF-ZrF<sub>4</sub>-ZrO<sub>2</sub> melts, rel. to ZrO<sub>2</sub> content, and CO<sub>2</sub> in furnace 9-11689  
 NaPO<sub>3</sub>+KPO<sub>3</sub> and NaPO<sub>3</sub>+Ca(PO<sub>3</sub>)<sub>2</sub>, molten mixture, obs. 9-21191  
 Sr, temp. dependence obs. 9-5149

**Surface tension measurement**

- apparatus for exact determ 9-5148  
 surfactant, aqueous, solns., instrument 9-15982

**Surface texture** *see Surface structure***Surveys** *see Reviews***Suspensions**

- See also Aerosols; Sedimentation; Sols*  
 acoustic attenuation rel. to freq. and conc. 9-3141  
 bacteria in salt soln., osmotic vol. changes study by light scatt. 9-14867  
 colloidal, light absorption, extinction coeff. and forward scatt. rel. to particle size, for strongly absorbing subst. 9-14865  
 colmatage, treatment using Markov processes 9-5202  
 of dumb-bell shaped particles, dissipation and intrinsic viscosity 9-17084  
 dust in gas, conducting, plane parallel flow 9-13410  
 electrophoresis in liq. of low permittivity 9-16025  
 flow, eff. of particles on solid boundaries 9-18508  
 flow, pulsatile and oscill., through tubes, particle interactions 9-5195  
 flow, pulsatile and oscill., through tubes, particles radial migration 9-5194  
 gas-solids, turbulent flow study at high Reynolds number 9-3131  
 impulse breakdown mechanism 9-11724  
 ionized, recombination coeffs. and transport props. 9-3132  
 laser beam absorpt. anomalies in scatt. medium 9-3128  
 macromolecular mixture, mass separation method, centrifugal field tests 9-7285  
 macromolecular mixture, mass separation method, gravitational tests 9-9564  
 macromolecular mixture, mass separation method, theory 9-7284  
 non-Newtonian flow computer simulation 9-3129  
 particle distrib. rel. to flow rate 9-3039  
 particle separation by electronically sensed vol. 9-11728  
 particles precipitated from polymer soln., light scatt. rel. to conc. 9-14870  
 pipeline flow, conc. gradient meas. by  $\gamma$ -radiation technique 9-9563  
 polymers in non-polar solvents, spherical suspension model 9-14855  
 PVC grains, in suspension, effect of porosity on interaction with plasticizer 9-21231  
 spheres in vertical tube at high Reynolds number 9-21229  
 stratospheric dust, near twilight 9-21776  
 tobacco mosaic virus-III soln., distrib. curve from light scatt. in elec. field 9-14860  
 turbulence, decaying isotropic, distortion of energy spectrum due to suspended particles 9-2948  
 viscosity, refinement of theoretical calcs. 9-1049  
 yeast cells in water, small ang. depend. of light scatt., comparison with Mie theory 9-14868  
 SiO<sub>2</sub>, particle diameter distrib., for d<1000 Å, X-ray scatt. determ. 9-14873

**Suzuki atmospheres** *see Crystal imperfections/dislocations***Switching time, ferroelectric** *see Ferroelectric materials; Ferroelectric phenomena***Switching time, ferromagnetic** *see Ferromagnetism; Magnetic properties of substances/ferromagnetic***Symbols** *see Nomenclature and symbols***Synchrocyclotrons** *see Particle accelerators/cyclotrons***Synchrotron radiation**

- electron in hollow cylindrical resonator, forced radiation 9-2469  
 gyrosynchrotron rad. of electrons in Sun's corona 9-17658  
 from plasma hot e, spectrum, 0.2-4 mm 9-11566  
 reabsorption 9-10502  
 Sco X-1, spectra assoc. with hard electron spectra 9-17616  
 in solar bursts, moving type IV, spectra and eff. of plasma on emission 9-18932  
 in solar flares, generation from electrons 9-21975  
 e polarization, elliptical, in magnetic field, high-speed photography obs. 9-4587  
 e., polarization, 500-1000 Å, 6 GeV 9-10979

**Synchrotrons** *see Particle accelerators/synchrotrons***Szilard-Chalmers reactions** *see Radiochemistry***Tables, mathematical**

- angular correl. coeffs. for radiative transitions from aligned nuclei 9-6782  
 integrals, series and products, book 9-10683  
 Kepler's eqn., table of E-M 9-19008  
 orientation factor for elec. birefringence in macromol. soln. 9-9541  
 specific heat equations 9-3053  
 structural problem, Shingo modified functions table 9-4264  
 $\gamma$  ang. distrib. coeffs. from aligned nuclei 9-6781

**Tables, physical** *see Collections of physical data***Tachometers** *see Angular velocity measurement***Tandel** *see Dielectric devices***Tantalum**

- atom, incoherent  $\gamma$ -scatt. on K shell electron obs. 9-712  
 cavity, Cs plasma production, 1400°K 9-11591  
 electrodes for high source, constant intensity line spectrum over 40-600 nm range 9-13075  
 fibre bundles, tensile props. at 1000°F 9-18515  
 films, cathode sputtered, structure and elec. resistance 9-3196  
 films, deposition in reactive cathodic pulverisation and three-dimens. equilib. diag. 9-3197  
 films, thin and very thin structure 9-1101  
 internal friction, dynamic modulus and creep up to 2000°C at low freq. 9-14965  
 ions produced by hypervelocity impact, mass analysis 9-10084  
 superconducting, type-I, Gruneisen functions 9-21440  
 superconductivity, surface nucleation and bulk supercooling fields meas. 9-17386  
 surface self-diffusion, field e microscope obs., 1200°K-1400°K 9-1255  
 u.s. damping, relax. peaks activation energy rel. to prestraining 9-5546  
 H interstitial impurity precipitation rel. to nuclear-acoustic-reson. linewidth temp. depend. anomalies 9-21334



**Tantalum compounds**

- alloys, chem. vapour deposition of  $\alpha$ -Al<sub>2</sub>O<sub>3</sub> 9-1108  
 Ta-C hypereutectic, thermal shock resist., fabrication and mech. and thermal props. 9-3168  
 in BaTiO<sub>3</sub>, sintering, effect of firing atmosphere pressure and temp., on electrical props. 9-1590  
 C-Ta alloy, reinforced, commercial development 9-3467  
 CeB<sub>6</sub>-Ta, elec. props. 9-9919  
 CeB<sub>6</sub>-Ta, elec. props. temp. dependence 9-9920  
 Fe-Ta alloys, ferromagnetic magnetization 9-18679  
 Nb-Ta alloys, superconducting props. and electronic spec. heat 9-13866  
 Ni-Ta alloy system, galvanomagnetic eff. 9-3790  
 Ta-C system, supercond., heat capacities, 1.5-18°K 9-1397  
 Ta-H(D) solid solns., n scatt. study of structure and phase transitions 9-7449  
 Ta-Hf-C microcomposite, thermal shock resist., fabrication and mech. and thermal props. 9-3168  
 Ta-W solid solution alloy system, monotonic strengthening 9-3433  
 Ta-X-Al alloys, (X=Fe, Co, Ni, Cu, Cr, Mo),  $\mu$ -phase extension and  $\mu'$ -phase occurrence 9-19844  
 Ta-base alloys, creep-rupture props., comparative mech. behaviour 9-14977  
 Ta<sub>2</sub>O<sub>3</sub>, thin films, interference peaks, elec. field induced shift 9-19975  
 Ta<sub>2</sub>O<sub>3</sub> films, ionic conduction mechanism for high field 9-16291  
 TaB<sub>2</sub> cathode, thermionic properties 9-5778  
 TaC, fast n irradi., fracture and vol. changes, 10<sup>21</sup> n/cm<sup>2</sup> 9-9862  
 TaC, strain due to comp. gradient, X-ray meas. 9-1271  
 TaC, thermal conductivity, electron beam meas.,  $\leq 2250^\circ\text{C}$  9-7665  
 TaC<sub>0.75</sub>, partial dislocations bounding stacking faults 9-9714  
 TaN<sub>x</sub>, sputtered, highly nitrified films, prep., props. and structure 9-13578  
 TaNiB, crystal structure 9-1193  
 TaO<sub>2</sub> protective film on Ta in high temp. HNO<sub>3</sub> acid and ag. CuCl<sub>2</sub> soln. 9-21267  
 Ta<sub>2</sub>O<sub>3</sub>, deposition in reactive cathodic pulverisation and three-dimens. equilib. diag. 9-3197  
 V-(5at.wt.%)Ta, intermediate purity type II superconductor, u.s. absorpt. 9-18612

**Targets** *see Nuclear bombardment targets***Teaching**

- A-level physics textbook with modern approach 9-20289  
 angular velocity of orthogonal curvilinear frame, mnemonic 9-6350  
 atomic spectra textbook 9-19387  
 batteries connected in parallel 9-6444  
 chemical kinetics expt. analog simulation for college students 9-17679  
 crystallography, close packing in b.c.c. and simple cubic systems 9-21302  
 dynamics textbook for upper forms at school 9-10604  
 earth's crust, present day experimentation lecture 9-20288  
 electrostatics, dielec. sphere near conducting plane 9-12826  
 experiments for students of astrophysics, book 9-18975  
 Fermi's (1934) paper on  $\beta$ -decay, complete translation 9-15409  
 Feynman diagrams, instructive simple example 9-4557  
 force, momentum change and motion, discussion 9-12835  
 formulae and data of use to first year engineering students 9-14303  
 gravitation, nonlinear, example 9-6297  
 inductance,  $L_1L_2 \geq M^2$ , derivation and physical significance 9-12825  
 Klein-Gordon equation, nonlinear, discussion, for undergraduates 9-12829  
 Mercury orbit calc., geometric expt. for students 9-12834  
 metals electronic props., teaching aids and literature review 9-8343  
 MHD, interaction between flow and field 9-15412  
 molecular bonding, symmetry effects 9-14302  
 molecular orbital models for structure and props of matter 9-14300  
 nuclear engineering courses, Univ. Rio de Janeiro (196) 9-10599  
 nuclear reactors, literature and teaching aids review, college 9-2272  
 oceanography for nongenie major 9-8158  
 organic cpds. with metallic conduction props., Liversidge Lecture, Sydney 1966 9-7756  
 physics, elementary, individual work approach 9-6250  
 physics, suggested course improvements 9-6251  
 quantum theory of double linear harmonic oscillator 9-17723  
 quarks 9-15411  
 rational mechanics, university level textbook 9-10603  
 simple harmonic motion, oscillators forced and coupled, book 9-10716  
 specific heat, Einstein's theory, simplification 9-6263  
 statistical mechanics, introduction for undergraduates 9-17680  
 Stokes' law, lab. work 9-19616  
 thermodynamics, connection with statistical mechanics 9-12831  
 thermodynamics, Emden's theorem, simple proof 9-12838  
 transport phenomena in general physics course, method for analysing and illustrating phenomena 9-17747  
 wave functions in one-dimens. doubly periodic pot. 9-12828  
 wave mechanics, the concept of force 9-12827  
 waves, longitudinal, transverse, e.m., Fourier methods and diffraction, book 9-10716  
 X-ray crystallography, scientific American article 9-16653  
 CO<sub>2</sub> bonds, model from orbital theory 9-14301  
 O<sub>2</sub> bonds, model from orbital theory 9-14301

**demonstrations**

- atomic physics, experiments and projects, book 9-2120  
 automated tutoring, discontents, special relativity applic. 9-7  
 ball pendulum 9-4210  
 ballistic pendulum expt. using blowgun 9-14  
 Bragg scatt., microwave analog models modification 9-6  
 centripetal force pendulum 9-6351  
 chemical exchange kinetics, n.m.r. application 9-8344  
 classical system, dissipative, time-translational invar. equation of motion 9-2187  
 counters, proportional, position sensitive, for undergraduate laboratory 9-12841  
 crustal structure model 9-14902  
 crystal symmetry operations 9-18431  
 elastic band and toothpick model for wave propag. 9-12837  
 elastic collisions using superballs 9-4206  
 electric field mapping, computer program and expts. 9-2124  
 electrical experiments and projects, book 9-2119  
 electron capture, decay energy from inner bremsstrahlung spectrum under-graduate laboratory expt. 9-12833  
 electronics lab. course 9-10  
 electrostatic voltmeter, cylindrical, built around air track 9-4202

**Teaching continued****demonstrations continued**

- electrostatics, with vibrating reed electrometer 9-2117  
 e.m. field theory, classical, undergraduate expts. 9-2121  
 fluid dynamics; extent of concepts, teaching 9-2109  
 Fresnel convection coeff. in dispersive medium 9-17  
 Gaussian wavepacket, evolution in time, alternative derivation 9-74  
 gravitational lens simulator 9-12836  
 Heisenberg's uncertainty principle 9-20332  
 impedance, complex, vector meter for undergraduate laboratory 9-12832  
 impulse experiment with linear air track 9-4265  
 inelastic collisions, locking air track glider bumpers 9-4209  
 interferometric expts. in acoustics, optics and at super-high frequencies 9-8338  
 kaleidoscope for point group symmetry demonstration 9-13048  
 laser source, optical and X-ray diffraction effects 9-15405  
 Lenz-Schiff argument, counter example on light-bending round mass point 9-58  
 liquid simulator, oil-covered ball bearings on vibrating rough-molded glass 9-11677  
 Lorentz transformation simple derivation 9-2113  
 Malus law of light polarization 9-15406  
 mechanics, generalised 9-2115  
 mechanics computer programmes, 1130 FORTRAN 9-2110  
 microscope resolving power, role of diff. pattern 9-12839  
 microwave diff. expts., atomic stacking models 9-16  
 molecular vel. determ by gas effusion intermediate laboratory expt. 9-12823  
 normal modes of symmetrical vib. syst. rel. to group theory 9-9  
 optical rotatory dispersion in transparent media 9-20287  
 organic vapour diffusion in air 9-8340  
 parametric resonanc apparatus 9-10715  
 particulate rad., expt. for eval. of phys. props. 9-6255  
 physical optics of slits 9-15404  
 physics, as a career, declining interest, stat. 9-2111  
 Ramsaver-Townsend effect using Xe thyratron 9-2125  
 relativity, four-vector formulation 9-2  
 resistance variation at low temps., elementary expt. 9-12842  
 resonance phenomena, apparatus for freq. response curves demonstration 9-4  
 Stephan-Boltzmann law, expt. verification 9-4207  
 superconductive tunneling, advanced laboratory expt. 9-12830  
 superconductivity, flux quantization and Josephson effect 9-2123  
 surface charges on conductors carrying steady currents 9-8  
 thermogalvanic energy conversion, thermocell configs. 9-2557  
 vacuum apparatus 9-17678  
 vapour density meas. apparatus for student use 9-20286  
 vector potential expansion, elim. of monopole term. 9-11  
 velocity of light meas. undergraduate expt. 9-4208  
 vertical force table 9-15  
 vibrating wire, Eigenvalue problem introduction 9-2112  
 vibrations of circular membrane using mag. driven mesh 9-2116  
 wave and particle experiments for students 9-4211  
 weightlessness 9-8379  
 X-rays, using radioisotope source, undergraduate expts. 9-2122  
<sup>57</sup>Co, Moseley's law demonstration apparatus 9-3  
 Ge(Li) detectors characts. and basic expts. with them for undergraduates 9-12824  
<sup>40</sup>K radioactivity, tracer expt. 9-2108  
<sup>7</sup>Li (p,d)<sup>6</sup>He, student exercise 9-9030

**Technetium**

No entries

**Technetium compounds**

- TcO<sub>4</sub><sup>-</sup> vacuo u.v. spectra study 9-19483

**Tektites** *see Meteorites***Telescopes**

- cosmic ray, mobile, for vertical flux intensity 9-19212  
 periscopic, dual power and light level 9-4522  
 range, used in acceleration neighbourhood, remote controlled absorber-system 9-4669  
 spark-chamber telescope for  $\gamma$  astronomy 9-20253

**astronomical***See also Radioastronomy*

- 84in reflecting, interferometric tests, opt. path difference, primary astigmatism and deviation of wavefront meas. 9-6198  
 150-inch, Kitt Peak and Cerro Tololo, construction 9-18944  
 automation appl. 9-12777  
 Bologna cross-type radio telescope, deep sky survey at 408 MHz 9-8267  
 Cassegrain, corrector systems 9-6199  
 Cassegrain d-camera, systematic errors 9-14278  
 Cassegrain d-camera, systematic errors 9-15375  
 i.r., 62 inch 9-10563  
 maser radiometer system for 84 ft radio telescope, Onsala, Sweden 9-8296  
 Metcalf refractor at Boyden observatory, photometric centre correction 9-10562  
 NRAO 300-ft, beam shape and irregularities, influence on 21 cm line obs. 9-6197  
 orbiting, high-resolution, possibility 9-17669  
 photometric, computer controlled 9-14277  
 photometric telescopes, design 9-15374  
 polarization, determ. list of 25 polarimetric stars within 20 pc of sun 9-12776  
 transit, errors inherent in micrometer screw asymmetry 9-18943  
 Vienna Univ. refractor, accessories for astrophotometry 9-8297  
 X-ray, grazing incidence, progress review 9-21986

**Tellurium**

- absorption edge, i.r., effect of Sb impurities 9-18711  
 alloying addition to Pb, effect on strength 9-1303  
 diffusion in CdTe, self-diffusion mechanism 9-1244  
 diffusion in ZnTe 9-14960  
 electrical conductivity anisotropy in single crystal 9-19911  
 electromechanical effect 9-18525  
 epitaxial growth on Cu(111) surface, LEED study 9-21270  
 film, wavelength depend. of optical transmittance in vacuum u.v. 9-10166  
 films, orientation from X-ray analysis rel. to piezoelec. coeff. 9-14894  
 films on insulating substrates (mica, glass, teflon), field effect relax. obs. 9-7840  
 magnetoresistance, negative, at low temps. 9-3566  
 optical properties in fundamental absorption region 9-21630

**Tellurium continued**

- phonons, optical and dynamic charge in trigonal systems 9-3508
- piezoelectric coeff.  $D_{14}$  determ. 9-16303
- piezoresistance coeff., pressures lowering symmetry 9-3716
- quantum oscillations of photomagnetic effect 9-1624
- semicond. props. film, activation energy temp. resistance coeff. thickness depend. 9-7803
- Shubnikov-De Haas eff. obs. 9-9915
- shubnikov-de Haas effect 9-7729
- surfaces, clean. LEED study 9-21263
- thermoelectric props. at phase transitions, effect of impurities 9-18368
- u.s. absorption, freq. and temp. depend. 9-9832
- U.S. attenuation in superconducting high-purity material 9-12003
- Young's modulus of square rods, torsional modulus of circular rods 9-19776
- <sup>125</sup>Te, nuclear mag. relax. obs. and mechanism 9-10299
- <sup>125</sup>Te Mossbauer effect in Te cpds. 9-16405
- in CdGeAs<sub>2</sub>, effect on conductivity 9-18618
- GaAs-Cs photocathode, effect of Te on photoemission 9-12225
- in GaAs(Zn-diffused) injection laser, doping effects on threshold current density 9-8626
- Te:Sb, i.r. absorpt. spectrum 9-5930
- Te:Sb, thermal conductivity of Sb-doped material, 100-600°K, mechanism 9-13810

**Tellurium compounds**

- aqueous solns.,  $\gamma$  radiolysis 9-15230
- PbAsTlOs, supercond. thermal dissipation 9-1490
- Bi:Sb-Te system, intermetallic cpds., mag. anisotropies and susceptibilities temp. dependence 9-13945
- Mg-Te system, MgTe phase formation 9-17341
- Pb<sub>2</sub>Sn<sub>1-x</sub>Te alloys, cation-rich, excess carrier conc., comp. and annealing temp. dependence 9-3634
- Pb<sub>100</sub>TlO resistance minimum in supercond., thermal dissipation 9-1490
- Se-Te alloy, non-linear optical phenomena 9-10160
- Te-Tl alloys, enthalpies of formation 9-17514
- p-TeO<sub>2</sub>, a new piezoelectric material 9-7846
- Te-Tl, liquid, Hall coeff. and mobility, composition and temp-dependence, 340-640°C 9-13537

**Temperature**

- See also High-temperature phenomena and effects; Low-temperature production*
- cylindrical wall, heat-insulated, approx. calc. using Grover nomogram 9-14396
- ion, ionosphere, diurnal variation, results from Thomson scatter spectra, Arecibo 9-10417
- optical pumping to define equilibria at arbitrary distances from Boltzmann equilibrium 9-168
- relativistic transform, from statistical mech. of ideal relativistic gas 9-2173
- stability control  $\pm 0.003^\circ\text{C}$  from 75-200°C in X-ray scatt. expt. 9-2263
- He liq. controller, integrated semicond. circuits 9-11733

**Temperature control** *see Cryostats; Thermostats***Temperature distribution**

- body under non-linear thermal conductivity conditions 9-14397
- on contact surfaces of moving bodies, cutting tool appl. 9-19083
- crystal-melt system surface, meas. device 9-3237
- cylinder, infinite with moving heat boundary, nonaxi-symm. field 9-19099
- cylinder, lateral wall with mixed Dirichlet and radiation conds. 9-8537
- cylinder, solid, solar radiation heating 9-10758
- cylindrical shell with heat transfer to inner surface and insulated on outer surface 9-20458
- field, air, adaptation to case of sea 9-6060
- field in rotating radial circular pipes, with laminar fluid flow 9-13518
- flame in condensed phase, temp. and conc. fields, rate of burning 9-8530
- fluid laminar flow between parallel walls, circular pipe, suction eff. 9-4990
- gas, radiant, Monte Carlo calc. 9-7226
- gases, behind detonation fronts, meas. 9-2240
- heat-generating polygonal cylinder with central circular hole 9-20450
- hollow cylinder with boundary conds. of fourth kind on external surface 9-8529
- in conducting plane layer, and e.m. oscillations 9-182
- of light source, computer calculations 9-10913
- liquid, hydrodynamic flow patterns in horizontal layers at natural convection 9-21195
- liquid, viscous, exponential heating superposed on steady temp. between confocal cycls. 9-11691
- liquids, boiling, local temp. fluctuations 9-19661
- lunar surface, Surveyor 5 obs. 9-21926
- plasma column, and density meas. 9-13436
- plasma-jet, inductive, radial distribution, analogic analysis 9-21079
- porous wall in transpiration cooling, effect of Mach number and blowing parameter 9-20457
- in pulled crystals, analysis 9-11802
- radial, in a.c. arcs, meas. 9-11637
- reactor coolant channel axial temp. distrib. 9-19344
- rotating annulus of heated fluid, rel. heat transfer 9-21013
- in rotating cylinder with steady pt. heat source at surface, soln. 9-20459
- rough and smooth tubes, obs. 9-19102
- at solid liquid interface with phase transforms, as function of time 9-9588
- Spalding function for continuous and source heat flux, recalc. 9-169
- steel, in area of laser-radiation action, exptl. verification 9-5418
- in thermocouple sample in isotropic medium, effect of thermocouple on sample temp. 9-15011
- transient fields in channel considering heat transfer fluid and wall metal 9-14841
- Ar plasma jet, spectroscopy 9-11582
- H<sub>2</sub>-N<sub>2</sub>-O<sub>2</sub> flame, atm. press., using thermocouple probe and optical method 9-15480
- in NaNO<sub>2</sub>, liquid, oscillatory instabilities 9-14845
- in Si avalanching p-n junction 9-3678

**Temperature measurement**

- See also Pyrometers; Thermocouples; Thermometers*
- atmospheric surfaces, using i.r. radiometers 9-2249
- book 9-6267
- eddy current method 9-20460
- flame as primary standard, acetylene-air, (2600 $\pm$ 3K) 9-10757
- in hollow cathode discharge lamp, difference from atomic and ionic spectral lines 9-9413
- inductive thermometry 9-20460

**Temperature measurement continued**

- i.r. radiometric microscope 9-2262
  - kelvin, (K), definition 9-10606
  - metal crystals, small spherical, optical and thermoelectric thermometry 9-20462
  - metals, non-destructive methods: inductive and eddy current 9-20460
  - microcircuits, i.r. techniques 9-4375
  - microwave meas. of plasma temp. 9-11587
  - moths, night flying 9-4132
  - in n.m.r., with spinning thermistor 9-17841
  - ocean, dragged thin film resistance thermometer behaviour 9-6062
  - plasma, photoelectronic spectral intensity technique 9-9377
  - plasmas, non-thermal equilibrium 9-2962
  - from polarized radiation components intensities 9-17830
  - practical scales from 11° to 273°K 9-15482
  - solid surfaces, increasing the accuracy of limited meas. by 'regularisation' method 9-10759
  - steady-state method using calibrated thermopile for oxide surface temp. determ. 9-1404
  - substrate surface temp. on hotplate used for epitaxial growth, thermocouple meas. 9-11807
  - surface thermal detector design, electrothermal analogy method 9-8533
  - thermodynamic scale, He gas thermometer determ. -183° to +100°C 9-17829
  - thermometer probe, using dual transistor 9-10797
  - Venus, 8.6 mm brightness temp., phase depend. 9-12752
  - using Ge diode 9-4376
  - He liquid, appl. of Ce-Mg nitrate powder thermometer 9-172
  - MgO flame radiative meas. 9-6405
  - NH<sub>4</sub>ClO<sub>4</sub>, deflagration, surface temp. meas. from orthorhombic-cubic transition thickness 9-10755
  - Pd-Fe alloys, ferromag. ordering temp. by resist. obs. 9-5818
  - Pt resist. thermometer, bridge circuit for direct reading 9-15481
- spectral methods**
- acetylene-air flame, line reversal at 2500( $\pm$ 2°)K as secondary temp. standard 9-12951
  - colour, rel. to luminance and true temps., two-colour pyrometer obs. 9-8538
  - diagrams from stark effect shifts in plasma spectral lines 9-8539
  - electric wire explosion later stages, and e. density distrib. 9-9346
  - flame, line reversal appl. problems 9-16744
  - gases, line reversal and excitation temp. in low pressure flames 9-9449
  - hot gases 9-7230
  - luminance and colour temperatures, computing formulae 9-8534
  - nonresolved spectra densitometry 9-8531
  - optical pyrometry, appl. of Si integrating light detector 9-10756
  - Ar low pressure hot cathode discharge 9-9419
  - CN, nonresolved spectra densitometry, obs. 9-8531
  - Cu/Mg electric exploded wire, and e. density distrib. 9-9346
  - H<sub>2</sub>, low pressure flames, line reversal and excitation temp. 9-9449

**Tensile strength** *see Mechanical strength/tensile***Tensors**

- curvature, of asymptotically flat space time 9-8397
- Einstein tensor and spherical symmetry 9-2150
- energy, in thermodynamics of non-relativistic fluids 9-17738
- formalism simplified, elimination of component form. 9-8365
- a Galilean tensor calculus 9-14307
- Gell Mann d- and f-tensors of SU(3), algebraic props. 9-17691
- Hilbert spaces, continuous products and generalized random fields 9-14317
- Lanczos spin tensor, spinor approach 9-13111
- Lorentz covariant distrib. of four vector variables 9-14314
- membranes, curved, stress anal. 9-6354
- operators, irreducible, props. of correlation functions 9-20297
- operators grad and grad\*, applic. in general system of coordinates 9-10613
- Riemann, discontinuities across hypersurface 9-14333
- separation of heat transfer and mechanical tensors in relativistic thermodynamics 9-10746

**Terbium**

- band structure rel. to mag. ordering 9-16212
- doping of YFe garnet, effect on Bloch wall mobility 9-13975
- elastic moduli and u.s. attenuation rel. to mag. transitions 9-7517
- ferromagnetic spin fluctuations decay rates rel. to anisotropy 9-16347
- hyperfine interactions from specific heat meas., 0.03-0.5°K 9-21600
- internal conversion coeff. in M-shell allowing for screening, semiempirical method 9-9127
- L-spectrum, new lines 9-1822
- magnetic structure and form factor meas. by n. diff. 9-13971
- magnetization and mag. specific heat 9-12292
- thermal conductivity study of polycryst. and single cryst., 1°-4°K 9-9858
- X-ray diagram lines, new, in L emission spectrum 9-13294
- Tb<sup>3+</sup>, e.p.r. in BaF<sub>2</sub> 9-20014
- Tb<sup>3+</sup> in POCl<sub>3</sub>-SnCl<sub>4</sub> soln., fluorescence spectra and radiative lifetimes 9-21217
- Tb<sup>3+</sup>, electronic Raman transitions 9-10223
- Tb<sup>3+</sup> in CaWO<sub>4</sub>, ground term energy level analysis 9-12373
- Tb<sup>3+</sup> in hydroxides, crystal field parameters from absorpt. and fluorescence meas. 9-14019

**Terbium compounds**

- Ho (80 wt.%)Tb, alloy single crystal, antiferromagnetism 9-16377
- La-Tb, dil. alloys, n. diff. and susceptibility meas. 9-17454
- Sc Tb, mag. structure comp. dependence 9-5802
- Tb<sup>3+</sup> chelates, <sup>241</sup>Am-doped,  $\alpha$ -particle fluoresc. 9-1829
- TbAl, n.m.r. of <sup>27</sup>Al, Knight shift and susceptibilities, temp. depend. 9-3969
- TbAl garnet, electronic Raman transitions 9-10223
- TbFeO<sub>3</sub>, metamagnetic props. 9-16383
- Tb(OH)<sub>3</sub>, Tb<sup>3+</sup> crystal field parameters determ. from fluorescence and absorpt. meas. 9-14019
- TbP, lattice deformation at Neel pt. 9-12309

**Terrestrial electricity** *see Earth/electricity***Terrestrial heat** *see Earth/heat***Terrestrial magnetism** *see Earth/magnetic field; Magnetic storms***Tetraneutrons** *see Neutrons***Thallium**

- addition to liquid Na, effect on e.p.r. 9-13541
- in alkali halides, activated, quantum efficiency of F- and Tl<sup>0</sup>-scintillations 9-16445



### Thermal expansion continued

**thermal expansion** continued

Mie-Grüneisen eqn. of state, simple derivation 9-1400  
nickel-cobalt disilicide solid soln. 9-3480  
niobates, rel. to interatomic bonds 9-7659  
organic glass, 10-300°K 9-21437  
petroleum cokes, X-ray diffr. peaks rel. to vol-expansion and closed pore vol. 9-7457  
polytetrafluoroethylene, transitions and relax. pressure dependence determ. 9-3406  
PVC, stretched uniaxially, thermal and mechanical props. anisotropy 9-19781  
pyrocarbons, reproducible compressed samples, coeffs. in a and c crystallographic directions 9-7596  
soda-lime-silica, glasses, rel. to structure and Ca coordination 9-1079  
 $\beta$ -spodumene-SiO<sub>2</sub> solid solns., behaviour 9-3537  
steel, type 304, gas-actuated acoustic dilatometer meas. and obs. 9-15009  
superconductors, type-I, Grüneisen functions 9-21440  
temperature and volume dependence of coefficient 9-12021  
transition metal carbides, stoichiometry dependence 9-21374  
vitrocarbon, rel. to heat treatment temp. 9-7318  
Ag-Zn, alloys, Debye function, Grüneisen eqn., characteristic temp. 9-19861  
Ag, interferometric meas., Grüneisen parameters calc. 9-19863  
Ag, meas. by convection heated furnace with X-ray diffractometer 9-13803  
Ag<sub>3</sub>AsS<sub>3</sub>, anisotropic around 150°C 9-13782  
Al, Grüneisen parameter, anharmonic effects, data anal. 9-21434  
Al, Grüneisen parameter volume dependence 9-15010  
Al base alloys, low temp. 9-19864  
Al<sub>2</sub>O<sub>3</sub>, Grüneisen parameter and vol. coeff., pressure variations 9-11919  
Au, anomalous, below 8°K and lattice Grüneisen gamma 9-16180  
Au, Grüneisen parameter and spec. ht. calcs. 9-9842  
AuMn, in Neel temp. pressure dependence thermodynamic valuation 9-1699  
B, pyrolytic graphite, rel. to B content 9-7515  
Ce, anomalous, rel. to isomorphism theory 9-3225  
Cr lattice relaxation due to rapid heating through Neel temp. 9-21417  
CsBr, temp. dependence 9-12022  
Cu-Ni alloys, lattice constant temp. dependence from X-ray meas. over conc. range 9-19955  
Cu-Zn alloys, Debye function, Grüneisen eqn., characteristic temp. 9-19861  
Cu, Grüneisen parameter and spec. ht. calcs. 9-9842  
Cu, meas. by convection heated furnace with X-ray diffractometer 9-13803  
Cu base alloys, low temp. 9-19864  
 $\gamma$ -CuI films and substrates, incompatibility rel. to internal stresses, obs. 9-16126  
Fe, lattice parameter anomalies at Curie point 9-5569  
Fe base alloys, low temp. 9-19864  
Fe particles, from X-ray exam. 9-5199  
Ga<sub>2</sub>Se<sub>3</sub>, temp. depend. 9-18564  
GaAs, semi-insulating, precision meas, 25-325°C 9-5570  
Gd, near T<sub>c</sub>, study of impurity effects on high order phase transitions 9-1399  
Ge, dilatometric study of point defects at thermodynamic equilibrium 9-3331  
Ge, Grüneisen parameter and anharmonicity 9-14999  
H<sub>2</sub>O, coeff. rel. to phase transform. 9-11681  
He II, liquid, 0.85-2.0°K, from capacitance meas 9-16028  
In, superconducting, type-I, Grüneisen functions 9-21440  
In<sub>2</sub>Te<sub>3</sub>, temp. depend. 9-18564  
K, coeff. calc. from pseudopotential theory 9-12023  
Kr, crystalline, near triple point 9-9848  
Li<sub>2</sub>O-Al<sub>2</sub>O<sub>3</sub>-n SiO<sub>2</sub> (4 < n < 10.0) solid solutions, behaviour 9-3537  
Li<sub>2</sub>SO<sub>4</sub> polycryst., 200-550°C and 600-750°C 9-7664  
Mg<sub>2</sub>Si, linear, coeffs., 25-300°K 9-18564  
MnP, compressibility and temp. depend. 9-15149  
MnP single cryst., anisotropic linear, rel. to change in atomic dist. and mag. ordering 9-16181  
Na, coeff. calc. from pseudopotential theory 9-12023  
Na<sub>2</sub>B<sub>6</sub>O<sub>13</sub>-SiO<sub>2</sub> glasses, rel. to phase separation 9-1083  
NaH<sub>3</sub>(SeO<sub>3</sub>)<sub>2</sub> Fizeau interferometric technique, 4 directions -30-140°C 9-9849  
Nb-Zr-Ti alloy, 10-200°K 9-21437  
NbC-C composite, effect of particle size and C source powders 9-3391  
NbC-graphite composite system, rel. to effect of processing parameters 9-3161  
Ne, single crystals, isotope effects in lattice constant 9-7624  
Ni-Cr alloys, X-ray study up to 900°C 9-21438  
Ni base alloys, low temp. 9-19864  
Pb, Grüneisen parameter, anharmonic effects, data anal. 9-21434  
Pb, superconducting, type-I, Grüneisen functions 9-21440  
Pd:Ni alloy, paramagnetic, low-temp., crit. conc., log. singularity, temp. depend anomaly 9-1642  
Pd, interferometric meas., Grüneisen parameters calc. 9-19863  
Pd-low temp., crit. conc., log. singularity, temp. depend anomaly 9-1642  
Pm<sub>2</sub>O<sub>3</sub>-Sm<sub>2</sub>O<sub>3</sub>, rel. to <sup>147</sup>Pm as power source, 70-1030°C 9-2790  
Rh, dterm. by X-ray diffraction, 28-587°C 9-16182  
Sb, and lattice parameters 28-220°C obs. 9-21439  
Se, vitreous, -190° to +30°C 9-19865  
Sn, superconducting, type-I, Grüneisen functions 9-21440  
SrTiO<sub>3</sub> single cryst., linear expansion coeff. 9-12024  
Ta, anomalies due to interstitial hydrogen impurities precipitation 9-21334  
Ta, superconducting, type-I, Grüneisen functions 9-21440  
V, anomalies due to interstitial hydrogen impurities precipitation 9-21334  
Zn, meas. by convection heated furnace with X-ray diffractometer 9-13803  
Zr-U-H system, meas. for phase boundaries investigation 9-14995  
ZrSiO<sub>4</sub>, X-ray diffraction and dilatometric methods 9-5571  
ZrZn<sub>2</sub>, Invar-type ferromagnet, mag. contrib. to low temp. thermal expansion. 9-21580





**Thermodynamic properties continued**

- NSF<sub>3</sub>, from i.r. absorpt. and Raman obs. 9-15862  
 Na, anharmonic contribs., simplified theory 9-7652  
 NaCl crystalline, from lattice dynamics 9-16174  
 NaCl crystals, thermodyn. functions 9-17253  
 NaF, from low temp. sp. Ht. meas. 9-5568  
 NaNbO<sub>3</sub>-K<sub>2</sub>NbO<sub>3</sub> system, phase composition and boundaries from calorimetric determ. 9-7621  
 NaPbCl<sub>3</sub>, enthalpy and free energy of formation in vaporization of PbCl<sub>2</sub>+NaCl mixtures 9-19442  
 Ne, solid, improved self-consistent phonon theory 9-12016  
 Pb, anharmonic effects, data analysis 9-21434  
 PuO<sub>2</sub>, 192°-1400°K 9-16179  
 RbPbCl<sub>3</sub>, enthalpy and free energy of formation in vaporization of PbCl<sub>2</sub>+RbCl mixtures 9-19442  
 Si-Te vapour system 9-7307  
 Si, E-centre annealing kinetics, activation energy and entropy 9-7505  
 SiN film, vapour growth study for SiH<sub>4</sub>-NH<sub>3</sub>-H<sub>2</sub> and SiCl<sub>4</sub>-NH<sub>3</sub>-H<sub>2</sub> systems 9-5250  
 Ta-Hf-C microcomposite, thermal shock resist., and development 9-3168  
 UF<sub>6</sub>, evaluated from exptl. data analysis. 9-2786  
 UO<sub>2</sub>, enthalpy, 1200-3260°K 9-3151  
 UO<sub>2</sub>, Gibbs energy function and entropy, 5 to 350°K 9-16082  
 UO<sub>2</sub>, Gibbs energy function and entropy, 5 to 350°K 9-16082  
 Zn<sup>2+</sup>-vacancy complex formation, free energy of association determ. from solubility data 9-17277  
 Zn halides, mols. 9-792

**Thermodynamics**

- See also Atmosphere/thermodynamics; Entropy; Equations of state; Statistical mechanics*  
 'exergy' and 'entropy', confusion of terms 9-2244  
 biopolymers, statistical-thermodynamic theory 9-14732  
 Boltzmann equilibrium, use of optical pumping to define other equilibria 9-168  
 canonical relationship to statistical mechanics 9-12831  
 Casimir-Onsager reciprocal rels. 9-6335  
 charged and polarized layers, book 9-10662  
 of chemical reactions, data evaluation computer program, CHAFFER 9-20279  
 classical, of irreversible processes as a special case of entropy free thermodynamics 9-8518  
 convexity of thermodynamic functions 9-4364  
 corresponding states theorem, extensions 9-16738  
 deformable media, fluidity equations development 9-8478  
 Ehrenfest relation and second-order phase transitions 9-8441  
 Emden's theorem, simple proof for log P-log V plot 9-12838  
 flow, responses to forces, press. tensor and heat-current vector 9-9315  
 fluid, relativistic scalar, thermodynamics 9-6330  
 fluids, non-relativistic, energy tensors 9-17738  
 gases, volumetric props. 9-9439  
 generalization of square 9-13  
 Gibbs entropy as measure of uncertainty at microscopic level 9-6328  
 Green's functions for Ising chain 9-14352  
 hadron coll. at high-energy, global and boiling pt. aspects 9-4596  
 Heisenberg antiferromagnet, fluctuations decay 9-12305  
 Heisenberg linear chain, anisotropic, free energy lower bound 9-12263  
 homotopy and energy balance 9-6392  
 inherently macroscopic processes, theory applic. to heat and active transport 9-17737  
 Klein's theorem for thermodynamic functions, correction 9-21049  
 Maxwell's relations, derivation 9-2242  
 melting, Lindemann hypothesis, thermodynamic consequences 9-19657  
 molecules of different sizes, mixtures, free energy, stat. calc. 9-20993  
 nonlinear theory of viscoelasticity 9-843  
 phase transitions and distrib. of temperature zeros of the partition function examples 9-10660  
 phase transitions and the distribution of temperature zeros of the partition function 9-10659  
 phase transitions and zeros in complex temperature plane 9-9585  
 phase transitions and zeros in several physical variables 9-9584  
 phase transitions of second kind, eff. of sample nonuniformity 9-15005  
 Planck-Laue formula confirmed 9-17736  
 power cycle, super-critical 9-17819  
 quantum spin systems 9-16695  
 quasi-equilibrium thermal cond., struct. of compatibility parameter 9-8430  
 radiating systems, nonequilibrium, time-dependent behaviour 9-10652  
 relativistic, momentum and energy transfer transform under Lorentz transformation as components of 4-vector 9-10650  
 relativistic, temperature transform laws and moving thermometers 9-57  
 relativistic in an elastic medium, separation of mechanical and heat transfer tensors 9-10746  
 relativistic statistical, Lorentz-invariance equilibrium distribs., formalisms 9-10653  
 relativistic transformation laws of quantities 9-14392  
 and religious cosmology 9-15268  
 rods, plates, shells, non-linear theory, approximation methods 9-15432  
 second law, and adiabatic surfaces intersection 9-2243  
 spin systems, negative heat conduction 9-12896  
 state critical phenomena, theory 9-10655  
 statistical function limit, rigorous result 9-20350  
 structure transforms. 9-5508  
 superfluid exponent  $\zeta$  from self-consistent Landau-Ginzburg theory 9-10658  
 systems with coupled Pfaffians, existence of absolute temp. 9-10748  
 university level textbook 9-10602  
 zeolites, sorption of water, enthalpies and entropies 9-9623

**applications**

- adsorption of pure and mixed hydrocarbons, 2-D equation of state 9-9629  
 critical points in phase transform., unified theory 9-11741  
 crystallization, nonequilib. distrib. coeffs. 9-16054  
 electric power generation, engine based on super-critical power cycle 9-17819  
 flow of binary soln. through membrane 9-9499  
 nuclear spin systems at negative absolute temp. 9-11201  
 paramagnetic system in mag. fields, steady state 9-14353

**Thermoelasticity**

- acousto-thermal eff., phenomenological theory 9-13794  
 coupled thermoviscoelasticity, theory 9-6367

**Thermoelasticity continued**

- cylinder, aeolotropic with rigid insulation, thermal stress calc. 9-10714  
 cylinder, hollow, transversely anisotropic, transient problem, temperature-dependent properties 9-20414  
 discontinuity propag., 16 different problems 9-19043  
 dynamic, Lagrangian formulation for mixed boundary conditions 9-10713  
 intercrystalline internal friction, Karman correlation function 9-3396  
 isotropic elastic semi-infinite disc, stresses and displacements due to heating, eval. 9-19040  
 Lagrangian formulation, Biot method generalized 9-10712  
 laser beam destruction of brittle homogeneous transparent medium 9-19869  
 linear coupled, approx. solns. 9-19041  
 membrane, temp. field determination 9-14380  
 plate, solid circular, quasi-static thermal deflection in axisymmetric case 9-141  
 poly(vinyl alcohol) networks in swelling eqn., props. 9-21356  
 self-gravitating globes, thermoelastic deforms., explicit form of governing eqns. 9-6170  
 semi-space, bounded by rough surface, thermoelastic field calc. 9-4282  
 shell, spheroidal, axisymmetric thermal stresses 9-8497  
 skew plates deformation, equations 9-142  
 stress and displacement fields in elastic solid weakened by external circular crack 9-17302  
 stress distrib. in inhomogeneous elastic rods 9-10710  
 stress distrib. in transversely isotropic body 9-10709  
 in stress production mechanism in solid on pulsed energy input 9-13725  
 stress waves, generation by penetration and absorpt. of impulsive e.m. rad. 9-16723  
 thermo-magneto-microelasticity 9-10711  
 wave propagation in inhomogeneous half space, anal. of discontinuities 9-20423  
 wave-motion in infinite body, generalized Kirchhoff eqn. 9-4283  
 Cd hexagonal crystal, thermal and electronic attenuations and dislocation drag 9-19853  
 DIO<sub>3</sub>, and piezoelectric and elastic props. rel. to bonding 9-12202  
 HIO<sub>3</sub>, and piezoelectric and elastic props. rel. to bonding 9-12202

**Thermoelectric conversion** *see Electricity/direct conversion***Thermoelectricity***See also Thermocouples*

- alkali metals, used to investigate Heine-Abarenkov pseudopotential 9-10061  
 alloy, dilute, low temp. thermopower depend. on solute ion virtual recoil 9-1603  
 alloys, binary and ternary, study rel. to spin subband thermoelec. power determ. 9-3718  
 alloys, liquid, thermoelec. power 9-9546  
 alloys, non-transition metal Cu<sub>3</sub>Au-type, T<sub>e</sub>, thermoelec. power, W-like depend. on number of valence electrons 9-12123  
 cooling of baffles for rotary pump backstreaming reduction 9-4196  
 current curves, stimulated, rel. to thermoluminescence 9-13924  
 ferromagnetic alloys, e.m.f., magnon drag eff., low temp. 9-13951  
 ferromagnetic metals, thermo-e.m.f. due to e. scatt. on spin-waves allowing for interzone transitions 9-3719  
 film, epitaxial, power, theory 9-15130  
 graphite, pyrolytic, Seebeck coeff. above room temp., temp depend. 9-10060  
 graphite, SP-1, effect of B(to 1%ppm) on power, temp. depend. 9-7848  
 graphite flakes, absolute power in range 77 to 300°K 9-7847  
 graphite nitrates, power peak in  $\lambda$  transform. region, rel. to cryst. struct. 9-7607  
 metal films, power, and mean free path effects 9-13925  
 metals, liquid, thermo-e.m.f. and electroconductance, correlation in approximation of weakly bound electrons theory 9-3117  
 metals with paramagnetic impurities, electron interactions effects 9-9876  
 Peltier effect cooling device for photocathodes 9-4444  
 Peltier heating and cooling for atomic kinetics of solidification 9-3152  
 resolving capacity of thermally stimulated current method 9-19879  
 Seebeck effect curves and combined conductivity, applic. to analysis of semiconductor props 9-21503  
 semiconductor, longitudinal power, in quantizing mag. field 9-16305  
 semiconductors, rel. to Hall effect, book 9-13880  
 thermal battery for cooling liq. flows, optimum efficiency rel. to geometry of elements 9-21544  
 thermionic diodes outside reactor, with heat pipes, as space power supply 9-11357  
 thermocouple, n-irrad., influence on calibration 9-4377  
 thermogalvanic energy conversion demonstration, thermocell configs. 9-2557  
 3d transition metals in liq. Sn, powers and elec. resistivity 9-16021  
 two band model, analysis of power 9-3718  
 Ag solid soln. with Au, Cd, Zn, In, Ge, Tl and Sb, thermoelec. powers 9-1604  
 (Ag+Rb or Cs)NO<sub>3</sub>, molten, thermoelec. power 9-3119  
 Al, power and resistance, effect of high pressure 9-16306  
 AlSb, power, 2°-500°K 9-7794  
 As<sub>2</sub>Se<sub>3</sub>-metal oxide, semiconductor, glasses, Seebeck coeff., obs. 9-1521  
 Au-Cr, dilute, positive hump of power 9-3720  
 Au-(0.03 at.%)Fe alloy, thermoelec. power, 0.35°K-10°K, mag. field (0-77 kOe) dependence 9-1605  
 Au, power and resistance, effect of high pressure 9-16306  
 Ba ferrite polycrystals, Seebeck coeff. Fe<sup>2+</sup> content dependence 9-12086  
 BaTiO<sub>3</sub>, paraelectric, thermocurrents rel. to point defects 9-5756  
 Be, eff. of metallic impurities at phase transitions 9-18368  
 Bi-Sb alloy, figure of merit and Seebeck coeff. 9-12026  
 Bi, props. at low temp. 9-10059  
 Ca V Bi Fe garnet, conduction mechanism by conductivity and thermoelec. power meas. 9-1458  
 Cd-Sb-Zn system solid soln. 9-19835  
 CdAs<sub>2</sub>-Zn<sub>3</sub>As<sub>2</sub> system, of solid solns. grown 9-13882  
 CdSb, transverse power meas. for valence band investigation 9-16269  
 n-CdTe, high-resistivity, thermally stimulated currents 9-3621  
 CeB<sub>6</sub>-M, (M=Hf, Ta, W and Re), temp. dependence 9-9920  
 CeB<sub>6</sub>-M, (M=Hf, Ta, W and Re), thermo-emf comp. dependence 9-9919  
 CoO:Li power rel. press. and temp. 9-21506  
 Cr Ni alloys, power, max. due to antiferromagnetic ordering for low Ni content 9-3721  
 Cr, Seebeck coeff., 77 to 400°K 9-15024

**Thermoelectricity** continued

- Cu-Sn, liquid, absolute power, as function of temp. and composition 9-7274  
 Cu, thermopower calcs. 9-12204  
 Cu<sub>2</sub>Au-type alloys of non-transition metals, thermoelec. power, W-like depend. on number of valence electrons 9-12123  
 Cu<sub>2</sub>O, power rel. press. and temp. 9-21506  
 Fe<sub>2</sub>O<sub>3</sub>-Al<sub>2</sub>O<sub>3</sub>, thermoelec. power, effect of chemisorbed water vapour and hydrogen 9-20036  
 Fe<sub>2</sub>O<sub>3</sub>-Cr<sub>2</sub>O<sub>3</sub>, thermoelec. power, effect of chemisorbed hydrogen and water vapour 9-20036  
 Fe<sub>2</sub>O<sub>3</sub>, thermoelec. power, effect of chemisorbed water vapour and hydrogen 9-20036  
 Fe hysteresis in thermoelec. e.m.f. rel. to  $\alpha$ - $\gamma$  phase transition 9-17340  
 FeCr<sub>2</sub>Se<sub>4</sub>, thermoelec. power rel. to effect of interactions between d shells of transition element 9-16253  
 Fe<sub>2</sub>O<sub>3</sub>:Ti, power rel. press. and temp. 9-21506  
 FeO, FeO SiO<sub>2</sub>, FeO-CaO, thermoelec. power, 1150-1470°C 9-1606  
 GaP, power, 2°-500°K 9-7794  
 GdAl<sub>3</sub>, thermoelec. power temp. dependence, ferromag. ordering effects 9-16307  
 Ge-Si alloys, n-irrad. effects on props. 9-7849  
 n-Ge, drag thermoelec. power, magnetophonon oscils. 9-3722  
 n-Ge, force tensors from infl. of e scatt. anisotropy on phonon drag eff. 9-19917  
 n-Ge, thermo-e.m.f. anisotropy 9-15131  
 n-Ge, thermoelec. power, phonon-drag effect anisotropy parameter 9-12205  
 Ge film, props. and use as thermoelements 9-16308  
 GeTe-MnTe alloys, power, 2.5 to 110°K, extended to 350°K 9-5757  
 GeTe alloys, power, 2.5 to 110°K, extended to 350°K 9-5757  
 Hg, liquid, thermoelec. power, vol. depend. meas., pressure up to 1000 bars, 20-120°C 9-1040  
 HgSe, power, Lorenz number, 80°-400°K 9-5642  
 InP, power, rel. to effective mass of electron 9-9979  
 n-InSb, thermoelec. power in transverse quantizing mag. field, phonon drag effects 9-3723  
 InSb, thermoelec. power meas. in effective electron mass pressure dependence determ. 9-1536  
 p-InSb, thermoelectric power depend. on carrier density 9-16309  
 KBr:Ba<sup>2+</sup>, thermoelec. power and ionic conductivity 9-1607  
 KBr:OH, dipole equilibrium directions and elec. moment 9-21532  
 KCl:Li dipole equilibrium directions and elec. moment 9-21532  
 Mg and alloys, 5 300°K 9-12206  
 Mn-Fe spinel effect of Mn<sup>2+</sup> clusters on Seebeck coeff. 9-1206  
 MnP, power temp. dependence, 4.2-500°K rel. to s-d exchange interaction 9-1456  
 Ni-Co alloys, absolute thermo e.m.f., eff. of plastic deformation 9-21543  
 Ni-Fe alloys, absolute thermo e.m.f., eff. of plastic deformation 9-21543  
 Ni, power and resistance, effect of high pressure 9-16306  
 Ni and alloys, power, and struct. of 3d zone 9-12207  
 Ni and Ni alloys, thermo-e.m.f. and structure of 3d-zone 9-16310  
 Ni-Fe ferrite, thermal e.m.f., rel. to conduction mechanism 9-3632  
 NiCr<sub>2</sub>Se<sub>4</sub>, thermoelec. power rel. to effect of interactions between d shells of transition element 9-16253  
 NiO:Li, power rel. press. and temp. 9-21506  
 NiO, seebeck coeff. 1000°-1600°C obs. 9-3571  
 p-PbSe, power, temp. dependence for band structure determ. 9-3643  
 p-PbSe, thermopower power dependence on carrier density 9-3724  
 p-PbTe:Fe,Mn, temp. depend. obs. 9-13876  
 n-PbTe:Gd,Mn, temp. depend. obs. 9-13876  
 PbTe-PbS, solid solutions, power, rel. to valence band structure 9-21514  
 PbTe-PbS solid solns., power 9-9897  
 PbTe, design parameters 9-3725  
 Pd-Au alloys, thermoelec. power, high temp. 9-15027  
 Pt-Pd-Au alloys, thermoelec. power, high temp. 9-15027  
 Pt, power and resistance, effect of high pressure 9-16306  
 Pt/Pt-(13 at.wt%)Rh thermocouple, stress effect on e.m.f. 9-12208  
 RbCl:Ag, dipole equilibrium directions and elec. moment 9-21532  
 Se, eff. of metallic impurities at phase transitions 9-18368  
 Se films, glassy, thermally stimulated conductivity 9-3726  
 Si-Ge-B alloy, power, figure of merit, and conductivity 9-15133  
 n-Si force tensors from infl., of e scatt. anisotropy on phonon drag eff. 9-19917  
 SnTe-Sb<sub>2</sub>Te<sub>3</sub> system, composition and temp. dependence 9-12153  
 Te, eff. of metallic impurities at phase transitions 9-18368  
 Te film, power thickness depend. 9-7803  
 Th, Seebeck coeff. anisotropy and temp. dependence rel. to mag. props. 9-13843  
 ThB<sub>4</sub> polycrystals, obs. 9-1471  
 ThB<sub>4</sub> polycrystals, obs. 9-1471  
 ThC-UC solid solns., power, and elec. resist. and Hall coeff. 9-3573  
 Ti<sub>2</sub>S<sub>3</sub>(Se<sub>2</sub>)<sup>2-</sup> cpds, MTi<sub>2</sub>X<sub>4</sub> (M=Fe, Co, Ni), Seebeck coeff. 9-9934  
 TiTe<sub>2</sub>, semiconducting, power meas. rel. to optical energy gap determ. 9-14046  
 Tm, Seebeck coeffs. 5 300°K rel. to Neel temp. and mag. superzones 9-14014  
 UN, Seebeck coeff., rel. to electronic and lattice contrib. to thermal conductivity, 77-400°K 9-7675  
 UO<sub>2</sub>:SiO<sub>2</sub> system, thermo-e.m.f., effect of fission fragments 9-7743  
 VCr<sub>2</sub>Se<sub>4</sub>, thermoelec. power rel. to effect of interactions between d shells of transition element 9-16253  
 WS<sub>2</sub> single crystal, thermoelec. power obs. 300°-820°K 9-16311  
 Y, anisotropy of e.m.f., 300-3°K 9-15064  
 Y-Fe garnet, conduction mechanism by conductivity and thermoelec. power meas. 9-1458  
 ZnSb, e.m.f. anisotropy 9-9923  
 ZrO<sub>2</sub>, power, rel. to defects, 800-1600°C 9-3703

**Thermoluminescence**

- aromatic hydrocarbons in boric acid glass 9-17493  
 diamond, synthetic, disperse nitrogen impurity effects 9-3935  
 diamonds, artificial, with B impurity, and phosphorescence 9-21651  
 dosimeter, dose and dose rate dependences, theoretical interpret. 9-5978  
 dosimetry, book 9-11144  
 dosimetry, noise limitations for low radiation dosage 9-14533  
 dosimetry, solid state Bragg-Gray cavity chamber appl. 9-20704  
 duren, after photoionization in methylcyclohexane glass 9-17494  
 duren in rigid glass, following photoionization 9-21655  
 fluorescein in boric acid glass, and photoconductivity 9-16314  
 glow curves, intensity var., tabulation of expected characs. 9-3934

**Thermoluminescence** continued

- heat rate controller 9-2267  
 moon 9-6165  
 non-constant recombination lifetime, rel. to thermally stimulated current curves 9-13924  
 $\alpha$ -quartz,  $\gamma$ -irrad., rel. to smoky centre formation 9-13701  
 spectra, emission, new method of meas. 9-16444  
 starting temp. variation, importance on expts. 9-21656  
 Al<sub>2</sub>O<sub>3</sub> films, 500 to 6000Å,  $\gamma$  irradiated, traps study 9-17429  
 BaF<sub>2</sub>:rare earth, paramag. hole centres interpretation 9-10252  
 BaS:Cu phosphor, decay rel. to calc. of electron trap depths 9-1840  
 CaF<sub>2</sub>:Ho<sup>3+</sup>, X-irrad., glow peak spectral distrib. 9-21657  
 CaF<sub>2</sub>, irradi., rel. to colour centres and d.c. resistivity 9-14092  
 CaF<sub>2</sub> thermoluminescent dosimeter 9-2599  
 CaS:Ce phosphor, rel. to trap depths. 9-21546  
 CaWO<sub>4</sub> single cry., comp. with thermally stimulated current, origin of defect states investig. 9-12042  
 CaWO<sub>4</sub>, paramagnetic colour centres 9-19757  
 CdSe, radiation emission after applic. of a.c. elec. field 9-3939  
 KCl:Ca, Z<sub>1</sub>-centres after X-irradiation 9-14088  
 KCl:Mn F<sub>1</sub>-centres suppressed by Mn presence 9-3893  
 KCl, irradi., rel. to colour centres and d.c. resistivity 9-14092  
 LaF<sub>3</sub>:Mg:Ca, rel. to colour centres 9-21658  
 Li<sub>2</sub>B<sub>4</sub>O<sub>7</sub>:Mn as material for thermoluminescent dosimetry 9-20006  
 Li<sub>2</sub>B<sub>4</sub>O<sub>7</sub>:Mn, emission spectra, apparatus and results 9-18726  
 LiF, characts. after reactor irradiation, rel. to dose 9-17492  
 LiF, irradi., rel. to colour centres and d.c. resistivity 9-14092  
 LiF, thermal treatment effects rel. to effects on optical absorpt. 9-5969  
 LiF (TLD-100), emission spectra, apparatus and results 9-18726  
 LiF dosimeters, influence of pre-annealing on precision meas., statistical anal. 9-14090  
 LiF dosimeters, isotopic effect. 9-14091  
 LiF dosimeters, thermal history influence, pre-annealing technique for precision meas. 9-14089  
 LiF dosimetry, design of reader 9-2090  
 LiF dosimetry application, toxicity 9-15384  
 LiF spectra, new method of meas. 9-16444  
 MgO, plastic deformation eff. 9-18740  
 Na<sub>2</sub>O-Al<sub>2</sub>O<sub>3</sub>-GeO<sub>2</sub> glass, study of  $\gamma$ -induced colour centres 9-18482  
 NaCl, irradi., rel. to colour centres and d.c. resistivity 9-14092  
 NaF, irradi., rel. to colour centres and d.c. resistivity 9-14092  
 PbCl<sub>2</sub> 9-10253  
 SiO<sub>2</sub> films, 500 to 6000Å,  $\gamma$  irradiated, traps study 9-17429  
 SrS:Bi phosphor, decay rel. to calc. of electron trap depths 9-1840  
 Sr:Zr phosphors, excited by W filament lamp, trap depth calc. 9-3936  
 Y<sub>2</sub>O<sub>3</sub>:Eu(Dy),  $\gamma$ -ray thermoluminescence,  $\gamma$ -ray induced 9-12478

**Thermomagnetic effects** see *Magnetothermal effects***Thermometers**

- See also *Pyrometers; Thermocouples*  
 halite, x-ray crystallography 9-1169  
 i.r. radiation, portable, for sensing biological environment 9-4131  
 moving, temp. transforms in relativistic thermodynamics 9-57  
 probe, using dual transistor 9-10797  
 pyroelec., for low temp. 9-19100  
 Ce Mg nitrate, powder and cryst. sphere, temp. comparison 9-172  
 Ce<sub>2</sub>Mg<sub>3</sub>(NO<sub>3</sub>)<sub>12</sub>, shape factors from demagnetizing factors meas. 9-15395  
 Pt resist. thermometer, bridge circuit for direct reading 9-15481

**resistance**

- carbon type, sensitivity variation, calibration 9-19101  
 potentiometers, advantage over resistance bridge, method of application 9-173  
 Pt, calibration tables, 2-273.15°K 9-2264  
 thermistor, circuitry for micro-Pirani pressure gauge 9-242  
 thin film at stagnation point in liquid flow, frequency response 9-6062  
 C, new interpolation formula 9-2261  
 Pt, calibration, liq. He cryostat 9-2265  
 Pt, comparison with standard, 63°K to 373.15°K 9-4378  
 Pt, comparison with standard, 63°K to 373.15°K 9-4379  
 Pt, miniature, stability and calibration 9-6407

**Thermonuclear devices** see *Plasma/devices***Thermonuclear reactions**See also *Elements/origin; Nuclear fusion*

- Thermonuclear reactions** see *Elements/origin; Nuclear fusion*  
 pulsational instability, nuclear-energized, criterion 9-21876  
 in stars, react. rates at high densities 9-16570  
 stellar energy prod. and evolution 9-18857  
 triple-alpha, in stellar atmospheres, reaction rates at high temps. 9-6125  
 C burning in stars, heavy neutrino emission due to previous He burning stage 9-12682  
 LiD surface, thermonuclear neutron emission at Nd-glass laser beam focus 9-13245

**Thermopiles** see *Thermocouples***Thermosphere** see *Atmosphere/upper; Ionosphere***Thermostats**See also *Cryostats*

- closed loop, stable to 0.001°C 9-17831  
 control with optical pyrometer using two thermistors 9-4368  
 controller incorporating variable sensitivity and proportional control 9-6408  
 furnace temp. controller using thyristors 9-174  
 gas flow temp. control, motor driven metering valves 9-20463  
 heat rate controller for thermoluminescent studies 9-2267  
 wires, small dia., programmable temp. control 9-10760  
 Cd thermal switch for mag. refrigerator 9-175

**Theta pinch** see *Plasma/confinement***Thickness measurement**See also *Particle size*

- adsorption layers on single crystal faces, by ellipsometry 9-9609  
 bovine serum albumin film at air-water interface, rel. to spreading or adsorp. 9-9477  
 ceramic deposition, electrophoretic, probe electrode technique 9-12966  
 dielectric, spattering yield 9-13581  
 dielectric film, spattering yield 9-13581  
 electrolytically sectioned metal film 9-11763  
 fibre diameters using cell interferometer, and Edser-Butler fringes 9-4213  
 film, liquid, adhering to cylinder withdrawing from Newtonian liquid baths 9-18347  
 film, thin, appl. of small freq. change detector cct. 9-12968



**Thickness measurement continued**

- film by electron microprobe analyzer 9-3190
- film coating on rough surface, luminescent method 9-10609
- films, evaporated, by Tolansky method, influence of surface roughness 9-5235
- films, solid, x-ray direct counting precision method 9-1098
- films, solid using quartz oscillator 9-11764
- films, transparent, on reflective substrates, phase-shift corrections 9-7329
- films, using quartz-crystal monitors, acoustic wave analysis of operation 9-11761
- films, vacuum-deposited apparatus 9-5232
- films grown on rough surfaces, technique 9-5236
- films on microstructures, nondestructive meas. (10 nm-10  $\mu$ m) 9-3191
- foil, by Coulomb back scatt. of heavy ions 9-5234
- foils in e. microscope from slip trace analysis without specimen tilt determ. 9-7330
- glaciers, using radar method 9-6055
- metal films, rel. to mean free path of conduction electrons 9-13925
- metal films, self-supporting by e transmission 9-9608
- microscopic height differences by reflection electron microscopy 9-4217
- oxide films, by triton irradi. 9-2758
- oxide films on Cu, ellipsometric meas., and reflection eqns. 9-16043
- target, by energy loss of transmitted  $\alpha$  particles 9-2560
- target monitor 9-19218
- Au films grown on rough surfaces, technique 9-5236
- C films, by e. microscopy of transverse sections and optical density meas. 9-11766
- Cr coating on brass, from flash spectra produced by laser interaction 9-11762
- In condensed films of subcritical thickness, e microscope determ. 9-18383
- MgF<sub>2</sub>, evaporated film, use of zero-order reflectance formula 9-5872
- Pb film, by ionization gauges 9-21264
- SiO<sub>2</sub> films, over small geometries 9-11767
- Sn film, by ionization gauges 9-21264

**Thin films** *see* **Films; Films, solid****Thirring model** *see* **Elementary particles; Field theory, quantum****Thixotropy**

No entries

**Thomas-Fermi method** *see* **Atoms/structure****Thomson effect** *see* **Thermoelectricity****Thorium**

- concentration in Vosges rocks by gamma spectrometry 9-20080
- de Haas-van Alphen eff. obs., electronic and Fermi surface structure determ. 9-21466
- electromigration of adsorbed atoms on W(113) face 9-17250
- hydrolysis in NaNO<sub>3</sub> and NaClO<sub>4</sub> solns., obs. 9-12529
- $p_{1/2}$  level splitting by internal elec. field 9-670
- Th/In(Pb) superimposed films, superconducting proximity effect 9-17384
- Th-U-N system phases  $\geq 50$  at.% N, 1000°C 9-16157
- Th I, atomic energy levels, present state of anal. 9-11388

**Thorium compounds**

- alkali metal vanadates, Eu<sup>3+</sup> activated, luminescence 9-20002
- complex of thiocyanate, paper chromatographic method for separation and identification 9-18772
- thallous halides, pressure effect on the polymorphism and melting point 9-7622
- Pr and Tm doping effect on supercond. 9-13857
- Th<sub>2</sub>(N<sub>2</sub>O)<sub>x</sub>, (X=P, As, Se and S), crystal structure 9-14928
- ThC UC solid solns., elec. resist., thermoelec. power and Hall coeff. 9-3573
- ThC, chem. reaction with HNO<sub>3</sub>, obs. 9-6027
- ThC cathode thermionic emission and evaporation props. 9-3754
- Th(ClO<sub>4</sub>)<sub>4</sub>, aq. soln., X-ray diffraction study, Th co-ord. no.determ. 9-11683
- Th(HClO<sub>4</sub>)<sub>2</sub>, aqueous soln., X-ray diff. study, Th co-ord., no. determ. 9-11683
- ThN, <sup>14</sup>N n.m.r. 9-10295
- ThN, dissoci. energy 9-824
- ThO<sub>2</sub>:<sup>155</sup>Gd<sup>3+</sup>, hyperfine coupling temp. dependence 9-8031
- ThO<sub>2</sub>:PuO<sub>2</sub> sintering in Ar at 1600°C, in air and in wet and dry H<sub>2</sub> 9-19822
- ThO<sub>2</sub> (1.3 wt.%)UO<sub>2</sub>, thermal cond. changes, irradi. induced, annealing 9-7676
- ThO<sub>2</sub>, electrodeposition of gaseous decay products 9-21710
- ThO<sub>2</sub> powder, thermal conductivity in various gases 9-15031
- ThO<sub>2</sub> spectral reflectance, high temp. 9-20560
- ThO<sub>2</sub>, e.p.r. of Gd<sup>3+</sup>, low field spectrum 9-12503
- ThO<sub>2</sub> film, grain growth and crystallization 9-5251
- ThP, <sup>31</sup>P n.m.r. 9-10295

**Thulium**

- doping of La and Th cpds., effect on supercond. 9-13857
- L emission spectrum, five new lines 9-4847
- transport properties 9-14014
- <sup>169</sup>Tm in Tm Ga garnet, NMR at 4°K 9-1880
- <sup>169</sup>Tm NMR in thulium ethyl sulphate 9-1879
- Tm<sup>3+</sup> crystal fields shielding 9-7695
- Tm<sup>3+</sup> in CaF<sub>2</sub>, covalency evidence 9-11791
- Tm<sup>3+</sup> in Sr F<sub>2</sub> phonons generated by spin-lattice relaxation obs. 9-1714
- Tm<sup>3+</sup> production in SrCl<sub>2</sub>:Tm<sup>3+</sup> and CaO:Tm<sup>3+</sup> on  $\gamma$ - and e-irrad., e.s.r. obs. 9-10277
- Yb, i.r. laser emission in vapour 9-2818

**Thulium compounds**

- thulium ethyl sulphate, p.n.r. spectra 9-15206
- Tm Ga garnet, <sup>149</sup>Tm NMR at 4°K 9-1880
- TmAl<sub>3</sub>, mag. props. and cryst. elec. field 9-16334
- TmFe garnet, sublattice magnetization by <sup>57</sup>Fe n.m.r. 9-21671
- TmFeO<sub>3</sub>, microwave absorpt meas., interpretation in two-sub-lattice model 9-7914
- TmGa garnet, oriented crystal, phonon spectra, laser induced 9-12439
- Tm<sub>2</sub>Ni, ferromagnetic props. 9-3775

**Thunderstorms**

- See also Lightning*
- discharges, theory based on turbulent generation of electric fields 9-6469
- isolated, potential gradient and radar echoes 9-15245

**Thyratrons** *see* **Gas discharge tubes****Tides** *see* **Atmosphere/movements; Ionosphere; Oceanography****Time interval measurement**

- circuit for fast meas. of short time intervals 9-4218

**Time interval measurement continued**

- in large numbers, radioactive decay, standard freq. pulse storage method 9-20753
- multichannel time intervalometer for detonation vels. in explosives 9-155
- time-amplitude converter errors, compensation 9-11447
- time-lag, nanosecond, random, automatic meas. 9-6719
- timing circuit for rotating-prism Q-switched laser 9-2364

**Time measurement**

- atomic hydrogen maser, standards 9-12991
- and frequency, book 9-6267
- frequency, by quadrant electrometer 9-6270
- metrology methods comparison 9-10605
- second, (S), definition 9-10606
- variant and invariant filters, application to time analysis on  $\gamma$  rays 9-19236

**Tin**

- addition to Al-10wt.%Zn, infl. on ageing characts. 9-17329
- atom,  $\gamma$ -ray total cross sections, 280 keV 9-16999
- atom incoherent  $\gamma$ -scatt. from K-shell electron obs. 9-712
- band struct. of grey Sn 9-13833
- bond to transition metal nature 9-16048
- cellular structure on face of single crystals growing from liquid 9-1126
- conductivity in normal state from meas. on superconductor 9-9933
- containing silicate glasses, properties 9-13569
- crystal-melt system surface temp. distrib. meas. apparatus rel. to solidification obs. 9-2327
- dopant diffusion in ZnSb-constant semiconductor thermoelements, X-ray microprobe analysis 9-10062
- doping in vapour grown GaAs epitaxial layer 9-15097
- evaporation rate and film thickness meas. by ionization gauges 9-21264
- evaporation rate from molten iron under vacuum 9-19658
- Fermi surface, effects of tension 9-15057
- film, critical conducting thickness, 100-400°K 9-3577
- film, Cu added, tunnel junction meas. for critical temp. determ. 3.5-7°K 9-7776
- film, disordered, invest. by superconducting tunnelling 9-13868
- grey, conduction and valence bands at k=0, excitonic transition, critical temp. 9-15047
- Josephson voltage-freq., relations with comparison Pb and In 9-9960
- liquid, impurity states, localized, elec. resistivities and thermopowers of 3d-transition metals 9-16021
- liquid, ordered structural region size estimation by X-ray scatt. 9-17187
- liquid, self-diffusion, applic. of 'fluctuation' theory 9-5151
- melt struct., Mg impurities, nucl. reson. fluoresc. study 9-7278
- plasticity in contact with binary alloy, alloy comp. dependence 9-9761
- reflection coeff. diminution for laser light 9-21603
- resonant  $\gamma$  radiation, diffraction in Bragg scattering by nuclei and electrons 9-21612
- solid and liq., mag. susceptibility 9-21563
- solidification, thermal wave technique 9-5217
- superconducting, energy gap, effect of high pressure 9-12129
- superconducting, type-I, Gruneisen functions 9-21440
- superconducting energy gap pressure dependence, u.s. attenuation meas. 9-17385
- superconducting energy-gap effect on thermal conductivity, calc. 9-9857
- superconducting films, depairing 9-1506
- superconducting films, quantum size effects 9-5832
- superconducting films, superposed, coupled motion of vortices 9-7777
- superconducting films, type II, switch from thin to bulk behaviour 9-16249
- superconducting films and foils, magnetic transitions 9-7775
- superconducting single spheres, superheating and supercooling props. 9-21495
- superconducting single crystals, u.s. absorpt. at 500 kHz, temp. depend. 9-21496
- superconductor, d.c. Josephson effect rel. to strong-coupling 9-12131
- thermal conductivity, normal and supercond. state 9-15030
- white, preferred orientation investigation by galvanomagnetic effects 9-16050
- white, tetragonal, freq. distrib. function calcs. 9-7631
- in GaAs, luminescence rel. to impurity band structure and effects 9-12463
- Na<sub>2</sub>O-SnO<sub>2</sub>-SiO<sub>2</sub> glass, valence states from Mossbauer effect 9-1751
- Sn:Sb(In/Zn), impurity effects on critical-field curve 9-9961
- Sn:Sb(In/Zn/Cd), impurity effects on residual resistivity anisotropy, ideal resistivities and derivations from Matthiessen's Rule at 77 and 273°K 9-9962
- Sn-SnO-Sn Josephson junctions, relax. oscills. 9-19907
- $\alpha$ -Sn, dielectric singularity in long wave-length limit 9-3697
- Sn, white, 'Shubnikov-de Haas' oscillations, explanation in terms of mag. breakdown 9-3564
- Sn<sup>4+</sup> in V<sub>2</sub>O<sub>5</sub>, Mossbauer exam. using <sup>57</sup>Fe 9-21613

**Tin compounds**

- Al-Sn prealloyed powders, pressing characteristics 9-18501
- $\beta$ -Cu-Sn martensitic transformation 9-1338
- organic, X-ray irradi., e.s.r. investigation of radicals formed 9-7592
- pentafluorodistannates (II), vib. spectrum, Sn<sub>2</sub>F<sub>7</sub><sup>-</sup> ion analysis 9-20985
- SnSe, film, charge carrier mobility 9-13883
- $\beta$ -stannic acid, colloid solns., effect of viscosity on reson. absorpt. of  $\gamma$ -quanta 9-3138
- <sup>119</sup>Sn Mossbauer isomer shifts, correl. with electronic props. 9-11475
- Al-Sn prealloyed powders, atomizations 9-18536
- Bi-Sn alloys, electron transitions, pressure-induced, 4.2-295°K 9-9892
- Cu-Sn, liquid, electron transport, Ziman theory and exptl. data. comparison 9-7274
- Cu-Sn alloys, equilibrated, grain boundary segregation, electron microprobe obs. 9-11843
- Cu-Sn alloys, isomeric shift of <sup>119</sup>Sn in Mossbauer spectrum 9-5888
- Cu-Sn bronzes, electrodeposition from Cyanide stannate bath 9-4006
- Cu-Su alloy, grain boundary segregation, electron microprobe obs. 9-5378
- Cu<sub>2</sub>MnSn, Heusler alloys, low temp. sp. ht. meas. rel. to hyperfine fields 9-9841
- Pb-Sn alloy, liquid, ordered structural region size estimation by X-ray scatt. 9-17187
- Pb-7 at.% Sn cellular reaction kinetics 9-14906
- Pb-Sn- $\gamma$ -Te alloys, cation-rich, excess carrier conc., comp. and annealing temp. dependence 9-3634
- Pd/MnSn Heusler alloy, internal field at <sup>119</sup>Sn site 9-16404
- Sb-Sn alloys, galvanomagnetic eff. and band structure 9-3841

**Tin compounds continued**

- Sn-In alloys, superconductivity; resonant freq. of tank cct. with specimen as core and a.c. mag. susceptibility 9-16237  
 Sn-Ni alloys, electrodeposited, structure, composition and thermal stability rel. to acid bath conditions 9-14926  
 Sn Zn molten, foreign diff. coeffs. 9-17201  
 Sn Zn strations, lineage structures, melt-grown crystals 9-1225  
 Sn-F<sub>3</sub><sup>-</sup> ion in pentafluorodistannates (II), vibrational spectrum 9-20985  
 SnCl<sub>2</sub>, visible band system 9-789  
 SnCl<sub>4</sub>, Mossbauer study of reactor radiation eff. 9-5582  
 SnF<sub>2</sub>, u.v. absorpt. spectra 9-9236  
 SnI<sub>4</sub>, absorpt. spectrum in dioxane, visible and u.v. 9-18363  
 SnI<sub>4</sub>, Mossbauer effect and lattice dynamics 9-1365  
 SnI<sub>4</sub> structure type, morphology theoretical 9-9637  
 SnM<sub>2</sub>O<sub>4</sub>, (M=Co, Mg, Zn, Mn), oxides, spinels, Mossbauer spectra 9-1752  
 SnO<sub>2</sub>:Fe<sup>3+</sup>, e.s.r. spectrum 9-17497  
 SnO<sub>2</sub>, Mossbauer resonance line form 9-1753  
 SnO<sub>2</sub>, Mossbauer study of reactor radiation eff. 9-5582  
 SnO<sub>2</sub>, cassiterite powder, elec. cond., press. depend. to 90 kg/cm<sup>2</sup> 9-13877  
 SnO<sub>2</sub>, crystal growth process for new electrolum. material 9-15193  
 SnO<sub>2</sub>, weak-field magnetoresistance rel. to electronic props. 9-9981  
 SnO<sub>2</sub>, Zeeman effect and symmetry of exciton 9-1433  
 SnO<sub>2</sub> transparent electrode, electron transfer with optically excited mol. in soln., photocurrent obs. 9-16486  
 SnPbTe<sub>2</sub>, sublimation, vapour equilib. obs. from mass spectrometric-Knudsen cell exam. 9-18391  
 SnS<sub>x</sub>, pellets obtained by compression, electronic props. 9-19887  
 SnTe-Sb<sub>2</sub>Te<sub>3</sub> system, Hall effect, cond. and thermoelec. props., temp. dependence 9-12153  
 SnTe, elastic constants 9-11907  
 SnTe, microwave rot. spectrum, 27 isotopic mols. 9-2883  
 SnTe, microwave rot. spectrum, 27 isotopic mols. 9-15873  
 SnTe, superconductivity carrier-conc. dependence 9-21494  
 Ti-(5wt.%) Al-(2.5wt.%) Sn alloys, hot salt cracking 9-21383  
 Ti-Sn alloys, binary, hot salt cracking 9-21383  
 Zn(ClO<sub>4</sub>)<sub>2</sub>·6H<sub>2</sub>O·Mn<sup>2+</sup>, ESR in a parallel and perpendicular configuration 9-8032

**Titanium**

- adsorbed layer on W, anomalous migration 9-5264  
 adsorption of bromide, <sup>80</sup>Br nucl. isomers separation 9-18769  
 antichathode, primary X-ray emission, distrib. in depth 9-5946  
 atoms and ions, bibliography of spectra 9-13287  
 cold-rolled, anisotropy of Young's modulus 9-11908  
 ductility and strength depend. on hydrostatic press. and temp. 9-5478  
 elasticity modulus, eff. of hydrogen 9-11910  
 evaporation controlled from thermoelectronic emission 9-12811  
 ferritization of martensitic steel 9-16140  
 film, N<sub>2</sub> sorption, all-metal meas. apparatus 9-13588  
 film for getting H impurities in He discharge tube 9-3021  
 growth, hexagonal single crystals, e beam zone melting 9-11804  
 ionization by shock waves in Ti-Ar mixtures 9-19556  
 microstrain distrib. in polycryst. under complex stress 9-16125  
 mobility of Ag ions, 1123-1K 9-9733  
 morphology of vapour-deposited foils, eff. of deposition rate and temp. 9-14927  
 Mossbauer eff. of <sup>57</sup>Fe, high pressure eff. at room temp. 9-21610  
 oxidation, early stage mechanism 9-14133  
 slip and twinning during deformation caused by drawing 9-19802  
 thermal control surface for Mars Lander, protection from dust storm 9-1386  
 thin film, infl. of thickness and substrate temp. on elec. conductivity and structure 9-5238  
 welds, pore formation, surface impurity effects 9-16146  
 X-ray emission spectra, K and L<sub>III</sub> bands rel. to band structure 9-1821  
 X-ray L<sub>II</sub>, III spectra pure metal, oxides, nitride carbide and boride 9-19999  
 X-ray spectra, K- and L- emission bands, rel. to electron struct. 9-10229  
 addition to brazes for promotion of wetting of oxides 9-3180  
 In Al<sub>2</sub>O<sub>3</sub>, effect of valence state on growth and colour 9-14908  
 In Al<sub>2</sub>O<sub>3</sub>, solubility, precip. and struct. obs. 9-1340  
 D<sup>+</sup> backscattering energy distrib. 9-12037  
 H diffusion at 78°K following 35 KeV implantation 9-21352  
 α-Ti, deformation dynamics, effect of grain size 9-3420  
 α-Ti, relaxation spectrum, effect of H content 9-7534  
 β-Ti, self-diffusion, 900-1C 9-9732  
 α-Ti, strain hardening, effect of strain rate, temp. and purity 9-5487  
 Ti<sup>3+</sup>, e.p.r. in quartz glass 9-21664  
 Ti I and Ti II sunspot lines curve of growth calcs., equivalent widths interpretation 9-21971  
 Ti II, line strengths for transitions bet. (3d<sup>3</sup>+3d<sup>2</sup>4s) and 3d<sup>2</sup>4p config. 9-14666  
<sup>46</sup>Ti in CaF<sub>2</sub>, valency determ. using e.p.r. 9-10276  
 Ti<sup>2+</sup> in CdTe, optical absorption and e.s.r. 9-1772  
 Ti<sup>3+</sup>, doped corundum, catalytic activation of H<sub>2</sub>-D<sub>2</sub> exchange 9-8085  
 Ti<sup>3+</sup> in AlCl<sub>3</sub>, e.s.r. 9-12499  
 V-Ti alloys, creep and stress-rupture behaviour 9-19801

**Titanium compounds**

- alloy, age-hardenable, composition and props. patent 9-13771  
 alloy, stress-corrosion cracking, electrochemical mechanism 9-19813  
 alloy welds, pore formation, surface impurity effects 9-16146  
 alloys, high-strength, fatigue strength loss on Ni and Cr plating 9-3442  
 anatase, activity coeffs. of adsorbed N<sub>2</sub>-O<sub>2</sub> mixtures 9-7350  
 anatase, i.r. spectrometric study of hydroxyl group 9-7963  
 complex of thiocyanate, paper chromatographic method for separation and identification 9-18772  
 metal-like, X-ray spectra obs. rel. to band structure calcs. 9-3912  
 rutile, e.p.r. of ions with d<sup>1</sup> shells rel. to internal crystal field 9-16460  
 rutile, hypersonic attenuation 9-13797  
 rutile, i.r. spectrometric study of hydroxyl group 9-7963  
 rutile, lattice energy, anion dipole contrib. 9-9630  
 rutile, reduced, paramag. centre-charge carrier interaction 9-1864  
 Ticonal 2000, sintered alloy in high coercivity state, structure 9-3302  
 titanium-aluminium acetylacetonate, mixed cryst., spin-lattice relax. 9-16386  
 X-ray L<sub>II</sub>, III spectra pure metal, oxides, nitride carbide and boride 9-19999  
 9-1584  
 Cu-Ti-Al alloys, hardening during slip mechanism 9-17319

**Titanium compounds continued**

- Cu-Ti alloys, hardening during slip mechanism 9-17319  
 Fe-Ni-Ti, mechanical props. improvement by ageing 9-11928  
 Fe-Ti: oxides in basalts, composition 9-16545  
 Fe-Ti alloy system, Laves phase magnetism, conc. depend. 9-7897  
 Nb-Ti alloy, deform. effects, X-ray powder diffraction studies 9-11930  
 Nb-Ti alloy, dislocation structure after annealing at 1250-1500°C 9-5368  
 Nb-Ti alloys, superconductivity, influence of structure 9-12125  
 Nb (44wt.%)Ti superconducting wire, microstructure obs. 9-18450  
 Nb-Zr-Ti alloy, thermal expansion, 10-300°K 9-21437  
 Ni-Al-Ti, coherency hardening, comments 9-11946  
 Ni-Al-Ti alloy, coherency hardening 9-11945  
 Ni-Cr-Ti alloys, internal friction temp. dependence 9-14966  
 Ni-Cr-W-Co-Al-Ti, with borophoric addition, mech. props., effect of grain boundary composition 9-5475  
 Ni-Ti, equi-atomic, martensite transform. 9-7615  
 Ni-Ti alloy, X-ray emission L<sub>III</sub> bands of Ni, structure 9-12456  
 Ni-(12 at.wt.%)Ti alloy, precipitation behaviour 9-11959  
 Ti (5wt.%) Al-(2.5wt.%) Sn hot salt cracking 9-21383  
 Ti (6 wt.%)Al-(4 wt.%) V alloys, fatigue-cracked, load relaxation, effect of methanol 9-19786  
 Ti-Al, α-phase, single crystals, e beam zone melting 9-11804  
 Ti-Al alloys, binary, hot salt cracking 9-21383  
 Ti-Cr alloys, β-stabilized, resistance anomaly, 4.2°-473°K 9-12104  
 Ti-Cu alloys, spot-cooled, new non-crystalline phases 9-5523  
 Ti-Mo alloys, U diffusion 9-19769  
 Ti (47 wt.%)Nb alloy, superconducting props., dependence on structure 9-13865  
 Ti-Nb alloys, superconducting, phase transformations 9-1507  
 Ti-Pd system, crystal structures of Ti<sub>2</sub>Pd<sub>3</sub>, Ti<sub>3</sub>Pd<sub>2</sub>, TiPd<sub>2</sub>, TiPd<sub>3</sub> 9-19725  
 Ti-Pt system, crystal structure of Ti<sub>3</sub>Pt<sub>5</sub> 9-19725  
 Ti-Sn alloys, binary, hot salt cracking 9-21383  
 Ti<sub>2</sub>O<sub>3</sub> electrical transition, semiconductor-semimetal model 9-15060  
 β-Ti alloy, VT15, elasticity modulus, eff. of hydrogen 9-11910  
 Ti complex, hexaurea Ti(III) trioxide, crystal spectra, Jahn-Teller effect 9-14057  
 Ti V alloy, decomposition of martensite during continuous heating 9-5494  
 Ti<sub>3</sub>Au-Ti<sub>3</sub>Pt system, phase relationships, transformations and ordering 9-5521  
 TiB<sub>2</sub> irradiated by thermal neutrons, investigation of stability 9-1409  
 TiC, fast n irradi., fracture and vol. changes, 10<sup>21</sup> n/cm<sup>2</sup> 9-9862  
 TiC, X-ray K-bands of C, rel. to electron struct. 9-10229  
 TiC ceramic crystals, recryst. forging and annealing 9-3482  
 TiCl<sub>4</sub>, molec. assoc. and Raman spectra 9-1021  
 TiFe<sub>2</sub>, magnetic props. in homogeneity range temp. depend. of Curie temp. and saturation magnetization 9-3799  
 TiO<sub>2</sub> aqueous soln., interface, double layer thermodyn. and H<sup>+</sup>, OH<sup>-</sup> adsorpt., obs. 9-7351  
 TiO<sub>2</sub>, heats of formation of point defects 9-12726  
 TiO<sub>2</sub>:SnO<sub>2</sub> crystalline soln., annealed at 850°C and 1000°C, mech. of separation and modulated struct. 9-7602  
 TiO<sub>2</sub>:SnO<sub>2</sub> system, phase separation kinetics, 850-1200°C 9-3494  
 TiO<sub>2</sub>:x, reduced rutile, specific heat and paramagnetic susceptibility 9-21436  
 TiO<sub>2</sub>, rutile structure, vibrational spectra, critical dipole frequency behavior 9-18549  
 TiO<sub>2</sub>, rutile structure, vibrational spectra, critical dipole frequency behavior 9-7636  
 TiO<sub>2</sub>, changes in lattice parameters, density, vacancies due to quenching 9-21392  
 TiO<sub>2</sub>, adsorpt. isotherms, diff. capacity curves and electrochem. double layer model 9-9606  
 TiO<sub>2</sub>, domain boundaries and stacking faults 9-5376  
 TiO<sub>2</sub>, doped, electronic defect structure rel. to optical and elec. props. 9-9706  
 TiO<sub>2</sub>, in aqueous and methanolic solns, adsorpt. of Ag ions 9-10348  
 TiO<sub>2</sub>, interstitial L<sub>1</sub> diffusion 9-9705  
 n-TiO<sub>2</sub>, interstitially doped, e.p.r. 9-9704  
 TiO<sub>2</sub>, opacified porcelain enamels, role of P<sub>2</sub>O<sub>5</sub> on colour and reflectance 9-3854  
 TiO<sub>2</sub>, orthorhombic (Brookite), Van Vleck paramagnetism 9-10099  
 TiO<sub>2</sub>, partially reduced, e.s.r. of adsorbed O<sub>2</sub> 9-17249  
 TiO<sub>2</sub>, reduced, variations of dielectric constant and loss 9-1601  
 TiO<sub>2</sub>, rutile, refractive index, pressure dependence 9-16393  
 TiO<sub>2</sub>, transition metal doped, photoinduced reversible charge transfer 9-7955  
 TiO<sub>2</sub> catalyst, effect on thermal expansion of lithium aluminosilicate 9-13804  
 TiO<sub>2</sub> ceramics, surface spark discharge, influence of voltage polarity 9-10157  
 TiO<sub>2</sub> rutile and anatase forms, colorimetric obs. 9-15169  
 TiO<sub>2</sub> single cry., normal, reduced and specially reduced, dielec. props. at room temp. 9-12188  
 Ti<sub>2</sub>O<sub>3</sub>, elec. props. 9-5646  
 Ti<sub>2</sub>S<sub>2</sub>(Se<sub>2</sub>)<sub>2</sub><sup>-</sup> cpds, MTi<sub>2</sub>X<sub>4</sub>, (M=Fe, Co, Ni), elec. and structural props. 9-9934  
 U-Ti alloys orthorhombic, metastable phases 9-19823  
 V-Ti-Nb alloys, creep and stress-rupture behaviour 9-19801

**Torquemeters** *see Mechanical measurement***Torsion**

- See also Elastic constants; Stress analysis*  
 adhesive bonded joints, shear props., napkin-ring apparatus 9-3395  
 bar, prismatic, formal soln. from mapping function in power series 9-8469  
 curvilinearly aeolotropic cylinder, with elastic symmetry, Saint-Venant problem 9-19019  
 cylinder, circular isotropic viscoelastic, quasi-static soln. 9-140  
 cylinder, orthotropic, torsional rigidity bounds 9-8490  
 elastic cylindrical Cosserat surface 9-17752  
 elastic-plastic, numerical methods, 9-19033  
 flexure of aerofoils in cascade, flutter theory and expt. 9-7219  
 plastic bar with jump in homogeneity, sand hill analogue 9-14372  
 plastic waves in metals, vel. meas. 9-16724  
 vibration in inhomogeneous linear elastic continuum 9-20418  
 9-147

**Total cross-sections** *see under individual particles, no subheading***Townsend coefficient** *see Ionization/gases*



**Tracers**

- See also *Radioactive tracers; Radiochemistry*  
diffusion in solid Kr, obs. by isotope exchange techniques,  $90^\circ < T < 115^\circ \text{K}$  9-9731  
fluorescence detector for on line water contamination monitoring 9-4022

**Transducers**

- See also *Acoustic generators; Acoustic receivers; Microphones; Sound reproduction*  
alignment device for A scan echoencephalography 9-6208  
antiferroelec., ferroelec., generation of acoustic transients in  $\text{H}_2\text{O}$ , press. pulses obs. 9-4341  
electroacoustic, four-terminal network closed on reactive load 9-15468  
electrodynamic for intensity meas. of u.s. pulses in liquids 9-9507  
for hydrometeorological multichannel digital recorder 9-16527  
hydrophone, small low freq. omnidirectional broad-band, design 9-14390  
for laser resonator i.r. field distrib. meas., thermotransducer 9-15506  
liquid two phase pipe flow, presence, movement detection 9-5129  
magnetoelastic, transformer type, error reduction 9-8353  
 $\text{PbZrO}_3$ - $\text{PbTiO}_3$  piezoelec., for broad-band acoustic noise meas. 10-100 kHz 9-2228  
piezoelectric polymer due to uniaxial orientation of crystallites 9-2926  
planar array, acoustic field study, vib. and synthesis 9-4296  
pressure, in random sound field of infinite plate 9-4338  
Sell type, for temp. depend. of oscill. relax. in acoustic absorpt. 9-2879  
signal interaction reduction 9-5443  
sonar, vib. analysis by holographic interferometry 9-4353  
u.s. immersion scanner, use in symmetrical scanning of head 9-6207  
u.s. two dimensional visual., design and tech., use in medical diagnosis 9-6204  
u.s. visual, of images, eff. of skull on echoencephalographic B and C scans, mislocalization in range of images and azimuth 9-6206  
CdS evaporated film n. irr. effects on acoustic performance 9-15002  
CdS multilayer piezoelec. type, method of c axes flipping 9-10055  
GaAs ultrasonic 9-17795  
InAs film, Hall e.m.f. application 9-10007  
 $\text{YFeF}_3$ , e.m. sound conversion by linear magnetostriction 9-16170  
TiFe garnet, epitaxial film on YAl garnet, shear wave generation at micro wave freqs. 9-10141  
ZnS multilayer piezoelec. type, method of c axes flipping 9-10055

**Transformations** see *Phase transformations***Transformations, mathematical**

- Bogoliubov transf. in quasi free states of C.C.R. algebras 9-16811  
CHF primaries, colorimetric relationships 9-20555  
for convergence of optimized polynomial expansion 9-16665  
deconvolution, error due to finite limits 9-4221  
Fhrenfest relations, for second order phase, new deriv. 9-8441  
films, magnetic thin, Tyablikov-Bogoliubov diagonalization method, applic. 9-5835  
finite integral transforms, for soln. of eqns. with general boundary conds. 9-8528  
Fourier, d dimensional, asymptotic behaviour 9-10619  
Fourier, spectral data anal. by computer 9-20296  
Korteweg de Vries eqn. related to similar non linear eqn. 9-6278  
Laplace, inversion in terms of Jacobi polynomials, applic. to vibs. of elastic bodies 9-17787  
Laplace method in high temp. asymptotic expansions for second virial coeff. 9-17746  
Lorentz, derivation assuming it to be once differentiable 9-15410  
Lorentz for momentum and energy in relativistic thermodynamics 9-10650  
Mangler's transformation in magnetogasdynamics 9-17093  
nonlinear space time, rel. to Lorentz group 9-8383  
phase, second order, Ehrenfest relations, new deriv. 9-8441  
plane steady motion of perfect gas, invariant transformation of equations 9-18323  
in quantum field theory, relativistic, symmetry operations rel. to spontaneously broken symmetries 9-16805  
relativistic, for temp., from statistical mech. of ideal relativistic gas 9-2173  
Stieltjes, asymptotic behaviour 9-14313  
Stieltjes transforms, asymptotic behaviour similar to that of corresponding function 9-17683  
unitary, appl. to nuclear matter 9-4718  
Young and Mills field rel. to conformal group 9-16657

**Transistors** see *Semiconducting devices/transistors***Transition metal compounds**

- alloys, thermodynamic props. 9-17353  
alloys, variation in no. of 3p, 3d electrons meas. by X-ray spectroscopy 9-19877  
borides, physical and mechanical props. 9-7510  
carbides, ordering structures 9-17272  
carbides, physical and mechanical props. 9-7510  
carbides of group IVB and VB metals, mech. props. 9-21374  
carbonyls, electronic structure, SCCO Mo calc. method 9-19448  
chelates, phosphoresc. 9-1837  
complexes, molecular orbital interpretation of X ray K-absorpt. spectral data 9-14065  
complexes, trinuclear, containing Cu, antiferromag. 9-10148  
complexes, unrestricted Hartree-Fock molecular orbital treatment 9-12232  
dichlorides, matrix isolated charge-transfer spectra 9-15858  
dihalides, bending freqs. and dimer modes in i.r. spectra 9-15857  
electrode, made by pressing in powdered form transition metal with transition metal comp., patent 9-12970  
liquid alloys, elec. and mag. props. 9-5186  
metal atom clusters, electron in box theory 9-748  
metal-like, X-ray spectra obs. rel. to band structure calcs. 9-3912  
moderator material for reactors 9-14655  
nitrides, group III-VI, diatomic, disoc. energies 9-824  
nitrides, ordering structures 9-17272  
nitrides, physical and mechanical props. 9-7510  
octahedral complexes, absorpt. spectra intensities 9-14056  
oxide halides of heavy metals, metal-oxygen stretching frequencies 9-19475  
oxides, mechanisms for metal-nonmetal transitions 9-15122  
oxides, semiconductors, effect of pressure on conductivity 9-1522  
point defects and phase stability 9-5332  
pyridine 2-carboxamide chelates, i.r. spectra and syntheses of chelates 9-14695

**Transition metal compounds continued**

- sulfides, mechanisms for metal-nonmetal transitions 9-15122  
tetrahedral complexes, charge-transfer spectra 9-1764  
 $\text{NiFe(Mn)}$ -based ternary alloys with transition metal, electronic structure and ordering processes 9-19834

**Transition metals**

- 3d, in liquid Sn, elec. resistivity and thermopowers 9-16021  
3d-, in liq. Sb, mag. susceptibilities and localized impurity states 9-1043  
atomic binding on W surface 9-9628  
atoms, ground states, configs. and truncated orbital bases. 9-2815  
atoms and ions, Slater-Condon integrals, calc. 9-4823  
bond to tin, nature 9-16048  
bonding and structures 9-18577  
elastic moduli and band structure correlations 9-19773  
electroluminescence of metal mols. in II-VI compounds, by e impact 9-5975  
e.p.r. of ions in crystals, book 9-14107  
Hall effect, anomalous, rel. to Fermi surface structure 9-1461  
impurities in other metals, localised mag. mom. 9-7874  
Mossbauer effect, of  $^{57}\text{Fe}$ , isomer shift 9-12357  
resistivity anomaly of dil. metallic solns. 9-16229  
solubility of seven elements in liquid Pb, 700 to 1000°C 9-11685  
spectra, charact. electron energy loss, of second and third series 9-15040  
spin-orbit coupling effect on electronic structure and mag. props. 9-16201  
stopping power of elements  $Z=21-30$  for 5-12 MeV protons and deuterons 9-17364  
transition metals, electron heat rel. to d-electrons per atom 9-3534  
work function, resistivity and Hall constant rel. to electronic structure 9-10078  
in CsI, impurity effect on strength 9-18514  
in Fe-base alloys, electronic sp. ht. for band struct. rel. to origin of ferromagnetism 9-13800

**Transition**

- 100-1000 Å radiation by thin films of Bi, In, Ti, rel. to detection 9-19227  
electrons, coeff. calc. at moderate energies 9-1410  
e.m. waves, plane, by moving compressible plasma fluid, solns. for E and H waves 9-11559  
e.m. waves by diffused interface, refl. and transmission coeffs. 9-10771  
seismic waves in laminated medium with arbitrary depth distrib. 9-20076  
Ge, X-ray anomalous, integrated characts. 9-3889  
KCl, X-ray, anomalous, dislocation density effects 9-1746

**acoustic waves**

- See also *Acoustic wave propagation*  
double walls with air separation and no edge coupling 9-17811  
ducts, due to reflection, meas. rooms 9-15464  
flexural wave propag. in plate submerged in liquid with obstruction 9-17794  
by floors, single-layer, of impact noise 9-4357  
ice, attenuation of multiply reflected pulses for longit. and transverse waves 9-5545  
inhomogeneous gas medium, amplification by transition radiation effect 9-4333  
intensity expression in ray acoustics 9-17796  
intensity loss due to ray spreading in inhomogeneous media, differential eqns. 9-15462  
through laminated plate reinforced by elastic stiffness members in one direction 9-4318  
plane waves through array of scatterers 9-17800  
pulsed circumferential waves on Al cylinders, obs. 9-3521  
quartz piezoelec. plate, transmission, refl. coeffs. 9-4321  
rods to infinite plates, meas. 9-6382  
slots, narrow, for diffused sound 9-19065  
slots, narrow, in corners 9-19066  
viscous media, lumped-element transmission line analogue 9-18359  
CdS evaporated film transducer, n. irr. effects on acoustic performance 9-15002

**acoustic waves, ultrasonic**

- through optical-contact bonds at room temp. at GHz freq. 9-10730  
quartz bar x-cut, two pure transverse modes generation at 9.4 GHz 9-5548  
quartz transducer, coherent phonon fusion 9-3511  
semiconductor, damping in h.f. elec. field, oscillatory character 9-1377  
Mo prestrained, damping, activation energy of relax. peaks 9-5546  
Ta prestrained, damping, activation energy of relax. peaks 9-5546

**electromagnetic waves** see *Electromagnetic wave propagation***light**

- See also *Absorption/light; Filters, optical*  
absorbing medium, self-induced transparency reflects, level degeneracy 9-261  
atmosphere, anisotropic scatt. cloud 9-6076  
carbon blacks, transmittance meas., tables, book 9-12324  
dielectric film, inhomogeneous, theory 9-15542  
diffuse, through spherical, inhomogeneous, scatt. shell 9-8654  
fiber elements, effect of interdiffusion of glass 9-13065  
in filaments, trapped, self-modulation, self-steepening and spectral development 9-13526  
film, 90 nm thick, meas. luminescent substrate appl. 9-10166  
film, thin, and reflection formulae rel. to refractive index 9-12333  
free-electron-like foils, dielec. response 9-14022  
Fresnel convection coeff. in dispersive medium 9-17  
through gas lenses, distortion of shuttled gaussian pulse obs. 9-5118  
glasses, rare earth oxide coloured 9-3856  
graphite, colloidal 9-1050  
i.r., image-spoiling props. of materials 9-4510  
i.r. materials, bibliography 9-12332  
i.r. materials, spectra, 2-50  $\mu$  9-12366  
laser mirror, optimization 9-4455  
metal blacks, transmittance meas., tables, book 9-12324  
metal films, thin, determ. of optical constants 9-3849  
in nonlinear medium, of intense beam 9-2399  
phthalocyanine aluminum chloride solns., dimeric, decrease of transmittance in intense light flux 9-1025  
polyethylene terephthalate, change in extinction direction in deform. bands 9-5463  
spectroscopic single beam device for transmittance meas. 9-10942  
Ag Mn(Pd), rel. to resonant states 9-7937  
Au Pd, rel. to resonant states 9-7937  
Bi films, rel. to quantum size effect 9-7969

**Transmission continued**  
**light continued**

- C films, optical density meas. in thickness meas. 9-11766  
 C particles in N<sub>2</sub> stream, cross section 9-11726  
 CH<sub>4</sub> vapour, i.r. spectral transmission functions 9-17031  
 CO vapour, i.r. spectral transmission functions 9-17031  
 CaB<sub>6</sub>, extinction coeff., refractive index and absorpt. coeff. from reflection meas. 9-5866  
 Cd<sub>0.81</sub>Te graded gap structure, spectra rel. to photocarrier transport 9-18619  
 Cu-Mn(Pd), rel. to resonant states 9-7937  
 Cu<sub>2</sub>S layers, i.r., rel. to elec. cond. and stoichiometry 9-1736  
 Fe<sub>3</sub>O<sub>4</sub> new colloidal soln. in mag. field, time depend. 9-5200  
 Ga films, liquid, extinction coeff. 9-3192  
 H<sub>2</sub>CO<sub>3</sub>, gas, transmission function calc., 1-7  $\mu$  9-2866  
 H<sub>2</sub>O vapour, i.r. spectral transmission functions 9-17031  
 n-InSb, degenerate, Burstein eff. in meas. impurity conc. 9-3645  
 K film, plasma resonance transmission obs. 9-12382  
 K thin film, ultraviolet transmittance 9-5867  
 KMgF<sub>3</sub>-KNiF<sub>3</sub> mixed crystals, i.r. data in lattice vibr. determ. 9-13789  
 Li thin film, ultraviolet transmittance 9-5867  
 LiTaO<sub>3</sub>, extinction ratios rel. to birefringence and light modulation 9-10178  
 Na thin film, ultraviolet transmittance 9-5867  
 PbSe epitaxial films, 0.5-6 eV, thickness dependence, 180-550 Å 9-5863  
 SiC films, microwave-discharge prepared 9-21601  
 TiTe<sub>2</sub>, semiconducting, meas. rel. to optical energy gap calc. 9-14046

**Transmission lines, r.f.** *see* **Electromagnetic wave propagation/guided waves****Transparency**

- See also* **Optical constants; Transmission/light**  
 atmosphere, spectra, 0.59 to 15  $\mu$  for paths up to 2.6 km 9-6077  
 bromophthalocyanine solns., clearing effect of Nd laser beam 9-1015  
 colloidal suspensions for magnetic fields examination, extinction index 9-1051  
 phthalocyanine aluminium chloride, decrease in intense light flux 9-1025  
 plexiglass, reduction on contact with dense plasma 9-10179  
 self-induced, consequences of different phase and signal velocities 9-15541

**Transport processes**

- See also* **Diffusion; Kinetic theory; Liquids/theory; Radiative transfer; Solids/theory; Statistical mechanics**  
 active, applic. of theory of inherently macroscopic processes 9-17737  
 air-water system, degassing in sound field, influence of static press. and temp. 9-5161  
 atmosphere, elec. conductive, weak discontinuity propag. 9-21761  
 atmosphere, upper, matter fluxes and diurnal temp. vars. 9-17575  
 Boltzman's eqn. for e. component, transformation, applic. to hard inactive sphere model of weakly ionized gas in a.c. field 9-15921  
 Boltzmann's eqn., generalizations 9-4986  
 Boltzmann's eqn. for e component, transformation, applic. to Lorentz gas 9-13412  
 Boltzmann and other eqns., solns. 9-8421  
 Boltzmann eqn., quantum-mechanical description, avoidance of singular and non-physical terms 9-19336  
 Boltzmann eqn. soln. for gas flow along pipe with mol. mean free path rel. to tube diameter 9-943  
 Boltzmann gas, dil., kinetic eqn. for the self-correlation function  $G_R(r,t)$  9-12889  
 Boltzmann linearized eqn., initial and boundary conditions, normal solns. 9-19498  
 Boltzmann-Landau equation, Chapman-Enskog first order approx. 9-17729  
 Boltzmann-Landau equations, transport coeffs. 9-17730  
 boundary layers with mass transfer, exptl. studies 9-19496  
 Brownian motion and diffusion of spins 9-12895  
 coefficient calculation from mathematical experiment 9-4258  
 colloidal solutions, dynamics study by spectral distrib. of scatt. laser light 9-14875  
 conductivity electrical or thermal stream variant of finite difference approach 9-110  
 degenerate Fermi syst. Boltzmann eqn., soln. 9-14367  
 dense-gas theory, power-density expansion of 2-ptcle distrib. fn. 9-8445  
 density expansions of coefficients, logarithmic terms 9-20370  
 dipolar gases, and equilb. props. 9-5110  
 effusion from effusion oven, vapour-solid interactions 9-940  
 electrical and magnetic fields, crossed, semiclassical and quantum theories 9-8461  
 electrolytic solutions, concentrated 9-21705  
 electron gas, weakly ionized, in d.c. mag. field 9-10676  
 electrons, localization in ordered and disordered systems, percolation of classical particles 9-10678  
 elementary theory appl. to gas between moving strip and fixed place 9-8460  
 energy transfer of thermal radiation btw. two dielectrics 9-7677  
 equation, generating functions for exact soln. 9-17728  
 equation, soln. singularities on interfaces 9-8463  
 Fermi liq., exact coeffs. 9-105  
 flux stability in slab reactors, applications of differential equations theory 9-9090  
 free convection mass transfer at vertical mesh electrodes 9-14137  
 gas, hard-sphere, continuum eigenfunctions 9-8456  
 gas, rigid sphere, Boltzmann, Eqn. soln. 9-8455  
 gaseous mixtures, combination rules 9-9458  
 gases, charged particles 9-19588  
 gases, dense 9-21132  
 hard-sphere and square-well mols., free-path distrib. and collision rates 9-8457  
 heat transfer bibliography 9-19085  
 hot gases, contrib. of non-resonance non-elastic collisions of atoms and mols. 9-14819  
 inert gases, transport coeff. calc. from Boltzmann eqn. 9-13496  
 inert gas liquids, theory 9-9490  
 Ising lattice membranes, steady-state props. 9-88  
 isotropic scatt., weak convergence to Brownian motion 9-17748  
 liquids, applic. of Prigogine-Nicolis-Misguich theory 9-9490  
 magnetic field, strong, semiclassical and quantum theories 9-8461  
 magnetopause boundary layer 9-10402  
 as Markov chain, nonlinear functionals and ensemble nonstants 9-109  
 mass, in cnoidal waves 9-8163  
 mass, interfacial turbulence induced by Maragoni effect. 9-17177  
 mass and heat, from suspended bodies in shear flow 9-20452

**Transport processes continued**

- mass and momentum, bounds, turbulent flow between parallel plates 9-17749  
 mass injection effects on near-wake flowfield of cone 9-21128  
 mass transfer, elec. analogue circuit, also heat transfer 9-17822  
 mass transfer, free-convection, and heat transfer, limiting cases 9-16740  
 mass transfer, non-stationary, appl. 9-2259  
 mass transfer, non-stationary, elec. simulation of boundary conditions 9-20443  
 mass transfer, nonlinear unsteady-state eqns, reduction to equivalent linear eqns. 9-20444  
 mass transfer and wake phenomena 9-15983  
 mass transfer by gases, using porous spheres 9-939  
 mass transfer coefficients for simultaneously rotating and translating sphere 9-21228  
 mass transfer coeffs. for reverse osmosis process design 9-18356  
 mass transfer factors for heterogeneous catalytic gas reactions 9-21690  
 mass transfer from rotating disc to non-Newtonian liquid 9-16705  
 mass transfer in drying in liq. media 9-3154  
 mass transfer in drying of ground paste like materials 9-17823  
 mass transfer in laminar co-current flow of two liqs., across moving inter. face 9-13501  
 mass transfer mechanism in ice sublimation in vacuum 9-17233  
 mass transfer round sphere, diffusion boundary layer from forward stagnation point to point for separation 9-13495  
 mass transport from rotating disc into power-law liquids 9-19624  
 material in soln, during electrolytic reaction with rotating electrodes 9-20058  
 membranes, characts. of ultrafine capillaries 9-997  
 Milne's problem, soln. by Duhamel's principle giving Hopf-Bronstein reln. 9-10456  
 Milne problem in non grey radiative transfer 9-10679  
 moisture transfer in capillary-porous substances 9-18336  
 momentum transfer in regular fluid-solid packings 9-5229  
 momentum transfer in turbulent conical confined jet 9-18342  
 momentum transfer near wall, effect of transpiration 9-13519  
 Monte-Carlo X-ray transport codes effect of e. momenta in calcs. 9-4260  
 multicomponent Margules eqns. 9-108  
 neutron, coherence function for two-node reactor models 9-18111  
 neutron, cylindrical geometry, method for soln. of multigroup P<sub>3</sub> eqns. 9-20836  
 neutron, equations, numerical methods of solution using P<sub>n</sub> approximation 9-11344  
 neutron, low energy, book 9-13258  
 neutron, monoenergetic half-space and slab problems, Case's method 9-20830  
 neutron, multigroup diff. theory, reality of eigenvalues for bare reactors 9-20834  
 neutron, static eigenvalue problem in Boltzmann eqn., Monte Carlo technique for soln. 9-20832  
 neutron, theory in USA, 1967 status 9-6928  
 neutron behaviour in transport and diff. regions of D-lattice, cruciform control rod worth calc. 9-19354  
 neutron coupled cone coherence function in Argonaut reactor 9-19351  
 neutron diffusion length problem in finite slab 9-20833  
 neutron in slab geometry, discrete ordinates numerical integration method 9-15788  
 neutron Milne problem, solution by Kofink's method 9-20830  
 neutron reactor kinetics, modification of Liapunov's direct method due to Lasalle 9-20839  
 neutron soln. for multiplying slab by Laplace transformation 9-20831  
 neutron transport eqn., 2-group numerical solns. to Milne and constant source problems 9-20827  
 neutron transport eqn., explicit behaviour of quantum correction terms at very low energy 9-13264  
 neutron transport eqn., two-group, with isotropic scatt. 9-19337  
 neutron transport eqn. one-velocity in one dimension, stabilized march technique of soln. 9-20828  
 neutron wave propag. in heterogeneous multiplying medium, solns., behaviour 9-19332  
 neutrons, slabs and cylinders, time of flight meas. of thermal neutron spectra 9-20835  
 neutrons in non-uniform media, operator spectrum 9-11343  
 noise, decomp. under space charge conditions 9-4411  
 particles in infinite medium, multiple many-directional sources 9-12905  
 phonon, in dielectric anharmonic crystals, by Green's function methods 9-21421  
 phonon system, interacting 9-7632  
 plane, unlimited region, integro-differential eqn. soln., straight line convergence method 9-16654  
 plasma, partially degenerate, coeff. calc. 9-5004  
 plasma, study using semi-classical quantum potential 9-19525  
 plasma in external inhomogeneous e.m. field, master eqn. 9-10654  
 plasmas, charged particles 9-19588  
 quantum theory of transport coeffs. 9-13819  
 radiative transfer with isotropic scatt., transport equation 9-20372  
 reactor kinetics, two-time doublet Boltzmann eqn. 9-6931  
 relativistic gas, energy transfer by material particles 9-17742  
 relativistic reciprocal relations 9-11655  
 Rossi- $\alpha$  expts., space depend. eff. 9-19338  
 semiconductor mobility, field-dependent, theory 9-9971  
 stationary systems, compatibility concept. rel. to generalized intensive parameters 9-8430  
 steel pipe corrosion under flow conditions, mass transfer correlation with temp. effects 9-21696  
 teaching in general physics course, method for analysing and illustrating phenomena 9-17747  
 transpiration cooled porous flat plate in stream of air or CO<sub>2</sub> 9-20453  
 tropopause, laminar transfer of material across 9-6070  
 turbulent fluid, prediction with simple model, appl. to bulk behaviour 9-11661  
 two-phase materials, bounds on coeffs. 9-4259  
 unsteady equation, fundamental soln. in solid geometry 9-17750  
 vapour migration in capillary-porous bodies 9-962  
 variational principle, first and second kind of boundary value problems in momentum transport, heat and mass transfer processes 9-6342  
 Vladimirov functional, tensor form of spherical harmonics 9-8462  
 $\gamma$  transport eqn. Monte Carlo integration 9-19356  
 n transport eqn. in plane geometry multigroups, eigensolutions by Case's method 9-20826



**Transport processes continued**

- n wave propag., convergence of eigenfunction analysis 9 20854
- Ar, Rinsmaier gas kinetic electron collision integrals 9 17000
- Cu Sn, liquid, electron transport, Ziman theory and expl. data comparison 9 7274
- H<sub>2</sub>, ionized, transport coefficients at 0.01, 0.1, 1 and 10 atm. pressures and up to 5000°K 9 18309
- K, liq., isotope thermotransport, temp. depend. 9 9491
- K<sub>2</sub>SO<sub>4</sub>-Li<sub>2</sub>SO<sub>4</sub> (41.90 equiv.%), molten isotope effects of electro migration 9 7612
- (Pt-H) electrodes oxidation in H<sub>2</sub>SO<sub>4</sub>, mass transport obs. 9 16485
- Rb, liq., isotope thermotransport, temp. depend. 9 9491
- Rh-Pd alloys, Fe impurities, magnetic props. 9 3766
- Tl, rel. to mag. props. 9 13843
- Tl bearing liquid metal immiscible solvent metal system, mass transfer meas., rel. to extraction processes 9 16473

**Trapped free radicals** *see Free radicals*

**Traps** *see Crystal electron states/impurity states and effects; Crystal imperfections; Semiconductors*

**Travelling wave tubes** *see Electron tubes*

**Trielectronic emission** *see Electron emission*

**Trielectroactivity**

Hg insulating material, effect of applied electric field 9 5755

**Triboluminescence** *see Luminescence*

**Trions (<sup>3</sup>He, <sup>3</sup>Li)** *see Helium 3; Tritons*

**Tripole point** *see Critical constants, thermal*

**Tritium**

- in air, estimation by liq. scintillators, Ti target emission meas. 9 8138
- ions as groundwater tracers for kaolinitic clay in acid soil detection 9 18787
- radioactive source, thin, preparation 9 2706
- recoil atoms, react., with n butane, n pentane and neo pentane 9 21684
- scintillation (liq.) counting, low level, apparatus 9 20696
- in Ar, hyperline splitting press. shift, obs. 9 4870

**Tritium compounds** *see Hydrogen compounds***Tritons**

*See also Nuclear reactions and scattering due to/tritons*

- binding energy calc., realistic local potentials 9 13150
- binding energy calc., from N-N interaction potential 9 13140
- binding energy calc., using separable representation of two nucleon interactions 9 13141
- properties calc., from matrix elements from N-N phase shifts 9 16911
- <sup>3</sup>He binding energy, with tensor forces and hard shell repulsion 9 8979
- <sup>3</sup>He(p,n)<sup>3</sup>He, 2.5-3.0 MeV, ang. distrib. obs. 9 20783

**Interactions**

oxide films, rel. to thickness determ. 9 2758

**Scattering**

No entries.

**Troposphere** *see Atmosphere***Tungsten**

- (100) surface, adsorp. and decomp. of NH<sub>3</sub> 9 1114
- with adsorbed Y atoms in equilib. conc., elec. field effects 9 21287
- adsorption and desorption of O from polycryst. filament, thermionic meas. 9 11787
- adsorption and nucleation of H<sub>2</sub> 9 21284
- adsorption and desorption of O, meas. via work function and thermionic emission changes 9 11786
- adsorption of Ba on (100) face, effect on work function 9 19680
- adsorption of Ba on oriented surfaces 9 9627
- adsorption of CO<sub>2</sub> on (110) and (111) faces, effect of partial coverage with O 9 3217
- adsorption of C atoms, meas. via thermionic emission props. 9 11785
- adsorption of H, field emission patterns of phases 9 19677
- adsorption of Na, work function meas. by field emission electron projector 9 1112
- adsorption of Na atoms on (110) face, bonding between layers 9 1113
- adsorption of O<sub>2</sub> on (100) face, two layer process at room temp. 9 21286
- adsorption of U monolayer films on (100), (110) and (111) oriented faces, work function meas. by photoelec. and contact potential diff. methods 9 14901
- adsorption of Y, migration and evaporation 9 3216
- binding of transition metal atoms on cryst. surface 9 9628
- brittleness temp. threshold, gaseous impurity effect 9 1309
- enthotic sputtering with 70 keV Ar ions, eff. of target cooling 9 19871
- chemisorption of P<sub>2</sub> 9 12539
- colour, lumiance and true temps. conversion tables 9 8538
- creep of polycrystalline material at high temps. 9 13733
- de Haas Van Alphen eff. and Fermi surface 9 3565
- desorption of inert gases from (100) surface on heating 9 5263
- diffusion of adsorbed Re on surface, effect of elec. field 9 13707
- dislocation redistribution during annealing and deformation 9 13688
- dislocations from field ion micrographs 9 9715
- electron irradi. at 240 MeV, cavity and interstitial prod. 9 1204
- emission, auto., stabilization by Ge coating 9 21551
- Fermi surface area, expl. estimation from size effect meas. 9 12062
- fibre bundles, tensile props. at 1000°F 9 18515
- field e microscope, emission, effect of adsorbed Al 9 11784
- field emission tip, heated, effect of O<sub>2</sub> on electron current 9 12220
- field emission patterns for H<sub>2</sub> adsorption 9 5775
- field evaporation in ion microscope, surface atoms cohesion 9 5784
- films, vacuum deposited, on glass and polycryst. foil, structure and contact p.d. between 9 5239
- foil preparation for electron microscope exam. 9 16071
- fracture, intergranular, influence of oxygen 9 16134
- fusion curves up to 50 kbars, meas. by optical techniques 9 7299
- internal friction freq. dependence at 1400-2500°K 9 3401
- ion emission, positive, further obs. 9 19940
- ion source in arc discharge 9 232
- ions, field evaporated, charge state, obs. 9 10085
- ions, field evaporated, charge state, obs. 9 5783
- irradiated and annealed, vacancy dislocation loops 9 7491
- magnetoresistances, elec. and thermal, and phonon cond., 80-130°K 9 5636
- migration of H<sub>2</sub>, N<sub>2</sub> and CO<sub>2</sub> in second layer, with trapping on first layer sites 9 11900
- neutron irradiated, high temp. recovery 9 13812
- neutrons, fast, space, energy and angular distrib. 9 19329
- oxidation at room temp. 9 10342

**Tungsten continued**

- photocathode u.v. quantum efficiency, e irradi. effects, 1-2 MeV 9-12224
- polycrystalline, penetration and capture of low-energy inert gas ions 9 5590
- scattering of Cs<sup>+</sup> by surface 9-5231
- shadows produced in Coulomb scatt. of protons, asymmetry, 190, 350 and 500 keV 9-15038
- sintering, grain growth analysis 9-7583
- spectral reflectance, high temp. 9-20560
- stacking faults, from field ion micrograph analysis 9-9717
- stopping channelled atomic particles, Z<sub>1</sub> oscs and size effect 9-5583
- strain inhomogeneities in lightly compressed crystals 9-1277
- substrate for Pd films on (110) face, film structure from LEED 9-1135
- superconductivity in films of β-W 9-13869
- surface ionization coeff. for K atoms 9-5786
- target in X ray tube, ratio of K charact. to total radiation 9-2103
- thermal conductivity, new meas. rel. to reference standard, comment 9 162
- thermal radiation in normal and off-normal directions, surface roughness effects 9 5577
- thermionic e emission CO<sub>2</sub> laser, induced 9-10079
- thermionic emission of pyroelectric coatings 9-5779
- wires, recrystallization phenomena, investigation using simple electron optics apparatus 9-3247
- wire, high temp. vacuum tensile fatigue, temp. depend. 9-7570
- wires for prestressing and reinforcement of silica composites 9-7569
- γ heating, thin detector in reactor water shield 9-12038
- C diffusion from UC, 1000-1800°K, layer thickness calc. 9-19764
- NH<sub>3</sub> adsorption and decomposition on (211) surface 9-19679
- O interface, acousto-optical effect under thermal irradi., mechanism 9 3181
- O<sub>2</sub> interaction with W ribbon, obs. by flash method 9-9600
- Sc film absorbed on (110) face, electron and absorption props. 9-1115
- TiO<sub>2</sub> adsorbate, anomalous migration 9-5264
- W carrier, evaporation of larger amount of metal 9-11749
- W filaments, electrotransport and life 9-15071

**Tungsten compounds**

- alloys, replacement of W by Cr and Mo 9-19842
- tungstates, dipole dipole interactions 9-1362
- CaWO<sub>4</sub>:Nd<sup>3+</sup> solid laser, sun-pumped, 130 mW power output 9-13031
- CaWO<sub>4</sub>, refractive index, pressure dependence 9-16393
- CeB<sub>6</sub>, W, elec. props. 9-9919
- CeB<sub>6</sub>, W, elec. props. temp. dependence 9-9920
- Fe-W alloys, wetting with molten Ag 9-13508
- Nb-W alloys, solution hardening and deformation 9-3411
- Ni Cr-W-Co-Al Ti alloy, with horophilic addition, mech. props. effect of grain boundary composition 9-5475
- Ni-W solid solutions, impurity atom causing distortion of matrix lattice 9 5345
- Ta-W solid solution alloy system, monotonic strengthening 9-3433
- W (26 wt.%) Re alloy, thermal conductivity and elec. resistivity, 300 to 2200°C 9-15035
- W-Re alloys, prod., patent 9-13772
- W-Re alloys, superplasticity 9-18507
- W-Sm oxide cermet, thermal conductivity, electron beam meas., ≤2000°C 9 7665
- β-W compounds, electrical resistivity 9-18604
- WC-Co alloys, compressive creep deformation at elevated temps. 9-7555
- WC, fast n irradi., fracture and vol. changes, 10<sup>21</sup> n/cm<sup>2</sup> 9-9862
- WC monocrystal growth from Co flux by Czochralski technique 9-5281
- W-C-WC structure when carburizing in field ion microscope 9-1175
- W(CO)<sub>6</sub>, negative ion metastable transitions 9-3015
- WC-NbC (10 wt. %)Co sintered alloy, eff. of C content on phase props. 9 13779
- WC<sub>16</sub>, crystal structure 9-19726
- W<sub>18</sub>U<sub>2</sub> mixture, liquid vapour phase equilib. determ., 1520-2660 mm Hg 9-21246
- WO<sub>3</sub>, growth of plates from vapour 9-1137
- WO<sub>3</sub>, vibration spectrum 9-18550
- WO<sub>3</sub>, structural stabilization of Sm<sub>2</sub>O<sub>3</sub>, Gd<sub>2</sub>O<sub>3</sub> and Nd<sub>2</sub>O<sub>3</sub> 9-17326
- WS<sub>2</sub>, single crystal, thermoelec. power obs. 300°-820°K 9-16311
- WSe<sub>2</sub>, v. vibrs. and force const., Raman and i.r. obs. 9-15859
- WSe<sub>2</sub>, n and p type semiconducting props., 77-295°K 9-5692

**Tuning forks** *see Vibrating bodies***Tunnel diodes** *see Semiconducting devices/tunnel and interface devices***Turbidimetry** *see Chemical analysis***Turbidity** *see Scattering/light; Suspensions***Turbulence**

*See also Cavitation; Flow; Vortices*

- aerodynamic boundary layer separation in front of step 9-11648
- air, flow in rounded corner triangular duct, local friction and heat transfer coeffs. 9 13491
- air, heat transfer from solid spheres, importance of turbulence parameters 9 17162
- air, molecular backscatter of laser rad., density and vel. fluct. obs. 9 1144
- air flow across vertical cylinders with condensation of water and methanol 9 1070
- annulus, concentric, analysis of fully developed turbulent flow 9-18337
- atmosphere, laser beam phase fluctuations, interferometry 9-10869
- atmospheric, weak optical strength, observation 9-16531
- atmospherics, effects on phase and frequency of optical waves 9-14161
- base pressure data for 9° cones, local flow effects 9-17151
- boundary layer, drag coeffs. on plate, evaluation of Coles' theory 9 17145
- boundary layer, viscous region 9-18246
- boundary layer flow with press. grad., heat transfer and possibly mass transfer 9-17144
- boundary layer on rough plate, skin friction coeff. 9-18338
- boundary layers, intensities 9-9319
- bounded jet, mixing characts. 9-21173
- Burger's model correl. function, functional integral numerical calc. 9 11526
- Burgers model fluid, a successive approximation 9-2946
- in channel flow, from kinetic damping force due to dynamical vibs interact. with proper turbulence 9-9427
- in confined equilb. flows, shear stress distrib. 9-19594
- conical confined water jet, momentum transfer 9-18342

**Turbulence** continued

- cored channel, non-Newtonian eff. in flows of visco elastic liquids 9-21023
- decaying isotropic, distortion of energy spectrum due to suspended particles 9-2948
- differential equation, second order approx., for fluid motion 9-11669
- diffusion effects in inhomogeneous plasma flow 9-18265
- electrodynamic, in conducting media, e.m. field behaviour 9-7130
- electrodynamics, in conducting media, e.m. field behaviour 9-7131
- flow, swirling inlet in circular pipe, theoretical conditions 9-17176
- flow between parallel plates, bounds on transport of mass and momentum 9-17749
- flow around cylinder, electrochem. meas. of velocity grads. at wall 9-17086
- flow in concentric annuli, velocity profile and reln. between friction factor and Reynolds number 9-11522
- fluid, electronic, for instantaneous meas. of time mean products and squares 9-4987
- fluid, transport props. prediction with simple model 9-11661
- fluid in channel, turbulent heat transfer coeff. calc. 9-17081
- four-wave processes, general weak turbulence theory 9-16664
- friction coeff. for turbulent flow through smooth pipes 9-14746
- gas, heat transfer rel. to variability of physical props. 9-9443
- gas flow frequency spectrum by laser beam 9-19062
- gas in circular adiabatic pipe efficiency of gas screen 9-938
- half-jet, mixing along curved streamline, rel. and press. distrib. 9-14749
- heated air flow in diffusers, friction in pre separation and heat transfer in separation regions 9-9425
- Heisenberg's statistical theory and eqns. of motion of flow 9-7112
- homogeneous, vibration of beam in air flow 9-119
- hot wire meas. of small-scale structure 9-947
- interfacial, mass transfer, induced by Marangoni effect. 9-17177
- interference fringe photometric obs. 9-10908
- jet, plane wall type in moving stream, meas. of mean and fluctuating props. 9-15573
- jet mixing in coflowing stream 9-21001
- jet of conducting liquid, axial symmetry in a longitudinal magnetic field 9-21045
- kinetic energy vertical transport measurement in air layer near ground with sonic anemometer 9-15242
- laminar-turbulent transition in two-dimens. channel 9-13505
- laser radiation space coherence atmos. turbulence dependence 9-2385
- liquid flow in tube, onset of fluidization with heat transfer 9-9466
- liquid metal flow, mag. field eff. on velocity pulsations 9-7125
- lubrication, possibilities of universal velocity laws 9-11668
- magnetic field of bounded medium, dynamics 9-8541
- MHD, effect on Lorentz field strength and Hall coeff. 9-9335
- MHD, two-dimens., in Ohm's law governed system 9-11533
- MHD channel with non-conducting wall, turbulent boundary layer calc. 9-7128
- MHD flow, axially-symmetric, in vortex chamber for large Hartmann numbers 9-7126
- MHD flow in pipes, unified semiempirical theory 9-7122
- mixing of two-coaxial gas streams, mass diffusion processes 9-7234
- plasma, collisionless, diagrammatic theory 9-5009
- plasma, fluctuations spectrum, calc. 9-5001
- plasma, many-particle quasilinear distrib. functions 9-5000
- plasma in mag. field, diffusion coeffs. rel. elec. field vars. and particle orbits 9-11548
- pressure pulsations on plate surface below a turbulent boundary layer, characteristics computation 9-971
- ray displacement in turbulent medium 9-6417
- reactor coolant, heat transfer from fuel rod array 9-639
- shock wave interaction with turbulent mixing region 9-19578
- in solar photosphere 9-15359
- spectral data in 2 dimens. boundary layer developed on wind tunnel floor 9-19508
- statistical theory of an incompressible fluid with a large Reynold's number 9-13503
- statistical theory of an incompressible fluid with a large Reynolds number 9-3068
- sublayer temperature distrib. including wall injection and dissipation 9-13519
- n supersonic base flows behind rearward-facing step, integral near-wake anal. 9-9431
- supersonic boundary layer, effect of wall curvature on heat transfer 9-14811
- suppression by transverse magnetic fields in tubes of special shape 9-21044
- theory, convergent approximants to infinite series 9-4992
- tube flow with axially varying heat flux, Nusselt number prediction 9-13487
- turbulent boundary-layer ht. transfer in supersonic dissociated air, exptl. investig. 9-21120
- two-stream jet-mixing region, similarity parameter 9-7216
- unstrained free flow, spreading and contraction at transition boundaries 9-21016
- velocity meter, cold tip, for vel. fluctuations 9-13502
- viscous sublayer, longit. intensity eqn. 9-21166
- vortex flow in slots with laminar flow above, control expt. rel. to disturbances 9-13499
- wake, axisymmetric, of Mach 3 body 9-11652
- wakes, determ. of molecular mixing lengths 9-7211
- wall effects, anomalous, and associated drag reduction 9-21007
- water free convection boundary layer formed near hot plate, structure 9-21167
- water with added soluble polymers, mechanism to account for damping effect 9-7242
- wave behind hypervel. sharp slender cone 9-17152
- wind wave interac., wind profile surveys, drift current and water surface obs. 9-21169
- zeta plasma, density fluctuations, theory and experimental observations 9-21081
- Ga liquid in channels with conducting walls, resistance during transition from laminar to turbulent flow 9-9336
- He II in flow, leading to density increase 9-5208
- Hg pipe flow in strong longit. mag. field, struct. and transition region effects 9-14753
- N<sub>2</sub>+ air jet at 4000-6000°K, total press. profiles for round and rectangular nozzles 9-9433

**Turbulent flow** *see* **Flow****Twilight**

- See also Atmospheric spectra; Zodiacal light*
- colour rel. stratospheric dust, models 9-21776
- resonance emissions due to upper atm. Na, Li and K. seasonal var. of abundances 9-12595
- temp. distrib. in upper atmosphere from zenith sky intensity meas. 9-8183
- He emission rel. to geomagnetic activity 9-1951
- OI green emission spectra at mid latitude 9-12600

**Twinning** *see* **Crystals, twinning****Twistors** *see* **Calculating apparatus; Magnetic devices****Two-phase flow** *see* **Flow/two phase****Type II superconductors** *see* **Superconductivity/type II****Ultracentrifuges** *see* **Centrifuges****Ultrasonics**

- See also separate headings, e.g. Absorption*
- aerosol crystallization in ultrasonic fields 9-18374
- attenuation meas., buffer-rod syst. 9-8513
- attenuation meas. by pulse method 9-10740
- of crystals, preparatory orientation and polishing 9-3515
- diagnosis, intensity modulated recording syst., eval. and differences of records 9-6205
- diagnostic applic. to eye, intraocular distances, improvement in meas. 9-10577
- diagnostic in obstetrics and gynecology 9-6209
- diff. of light by u.s. waves, holographic investigation 9-2406
- echo impulse method for meas. absorption in liquids 9-153
- echoencephalography, A-scan, transducer alignment device 9-6208
- flow det. using transducerless generation in mag. field 9-7469
- generation by stimulated Brillouin effect 9-10836
- harmonics production in quartz bar 9-9824
- health aspects of cleaning and cutting 9-18947
- heating effect on u.s. treatment of metal surfaces 9-10739
- image reception, use of electrokinetic target 9-4346
- immersion scanner, use in symmetrical scanning of head 9-6207
- industrial and medical application hazards 9-4348
- intensity in liquids, electrodynamic transducer for meas. 9-9507
- interaction with light rel. to use as optical signal processor 9-6389
- liquid diffusion systems, u.s. standing wave freezing-in by conc. zone effect 9-18358
- liquid studies 9-11676
- liquid-vapour interface, transcendent movement meas. using pulse technique 9-11746
- medical and industrial application hazards 9-4348
- photosensitive layer, representation of 18-70 KHz range 9-17807
- plastic waves, in metals, probe 9-11923
- probe calibration method 9-9507
- pulse echo attenuation comparator 9-10734
- sorption at gas electrode in u.s. field, thermodynamic interpretation 9-5165
- standing ultrasonic wave diffraction modulator for ruby laser 9-13029
- superposed-wave diffraction of light, calc. 9-17889
- temperature switch 9-10739
- theory and application, book 9-6381
- u.s. displacement amplitude, variable gap capacitive detector 9-1368
- velocity change meas., freq. modulation c.w. technique 9-2289
- visualization of images, eff. of skull on echoencephalographic B and C scans, mislocalization in range of images and azimuth 9-6206
- visualization of tissue, new scanning and presentation methods, applic. to brain exam. 9-6220
- visualization syst., two-dimensional, design and tech., use in medical diagnosis 9-6204
- GaAs transducers 9-17795
- GeAs, spin reson. of As donors 9-5555
- Gc, irradiation acceleration of Sb diffusion 9-1247
- KCl oscillations, transformation to electrical oscillations 9-12012
- Li salts, non-aqueous soln., U.S. vel., molal and adiabatic compressibility determ. 9-7254

**Ultraviolet detectors** *see* **Radiation detectors****Ultraviolet sources** *see* **Light sources****Umklapp process** *see* **Crystals/lattice mechanics****Uncertainty** *see* **Indeterminacy; Probability****Undor** *see* **Electron theory; Field theory, quantum****Unified field theory** *see* **Relativity/unified field theories****Unimolecular layers** *see* **Adsorbed layers****Units**

- See also Constants; Dimensions. Nomenclature and symbols*
- astronomical, Doppler shift of galactic spectral features of neutral hydrogen at 21 cm 9-10559
- definitions, SI basic units 9-10606
- electric and mag. quantities, relations in Gauss and SI system 9-20290
- e.m., humorous note 9-15413
- magnetic and elec. quantities, relations in Gauss and SI system 9-20290
- radiometric scales, international comparison 9-10911
- transformation between different systems, dimensionally correct method 9-6266
- X-ray wavelength, x unit, history 9-4214

**Upper atmosphere** *see* **Atmosphere/upper; Ionosphere****Uranium**

- See also Nuclear fission/uranium*
- adsorption on W (100), (110) and (111) oriented faces, work function meas. by photoelec. and contact potential diff. methods 9-14901
- atomic lines, M series, meas. and comparison 9-6968
- Auger spectra obs. 9-9141
- corrosion of fuel element with defective Zircalloy-2 cladding in steam water system, 285°C 9-11361
- critical assembly, water-graphite moderated with enriched U, buckling, obs. 9-19348
- cylinders, with minimum <sup>235</sup>U enrichment, criticality anal. 9-9096
- density changes on thermal cycling between 400 and 600°C 9-19771
- depleted silt between borated polyethylene, spatially depend. resonance neutron spectra 9-16987
- diffusion in Al at infinite dilution 9-17282
- diffusion in UC and mechanism, 1505.1863°C 9-11899
- fission gas bubble behaviour rel. to post-irrad. annealing and stress 9-11336
- ignition in O<sub>2</sub> and air, irradi. effects, 20% enriched U, obs. 9-10332
- inclusions in grain boundaries of UC, dihedral angles 9-11855



**Uranium continued**

- irradiated, annealing in NaK under high hydrostatic press. and temps., technique 9-19824  
 irradiated, n, length and electrical resistivity changes 9-3574  
 isotope abundance ratio meas., surface ionization method 9-19416  
 metal production by C reduction of  $\text{UO}_2$  in vacuum 9-14134  
 natural U graphite lattice, infinite multiplication factor meas. by null reactivity method 9-13266  
 neutron radiographic scatter factors 9-2801  
 ore prospecting, mathematical methods appl. 9-4036  
 in organic solns., chemical analysis 9-1929  
 $p_{1/2}$  level splitting by internal elec. field 9-670  
 polycrystals, elastic constants and u.s. attenuation meas., 4.2 300°K 9-11909  
 prospecting, use of isotopic composition of Pb 9-20079  
 reactor fuel element in contact with can, thermal resistance 9-1408  
 reactor fuel elements state comparison by U equiv. contents calc. 9-16983  
 separation from fission products by eutectic freezing of uranyl nitrate-hexahydrate 9-18749  
 separation from Pt by fractional sublimation in reactor fuel 9-20857  
 vapour press. obs., heat of sublimation calc. 9-16033  
 viscous displacement at grain boundaries during creep 9-19800  
 $^{235}\text{U}$  isotope contents,  $\alpha$  spectra, semicond. detector meas. 9-2835  
 $^{235}\text{U}$  graphite critical assemblies, leakage anal. and cross-sections 9-18122  
 $^{235}\text{U}$  ternary fission following n bombardment 9-20815  
 $^{235}\text{U}$  fission resonance in homogeneous system, temp. depend. 9-19324  
 $^{235}\text{U}$  isotope contents,  $\alpha$  spectra, semicond. detector meas. 9-2835  
 $^{235}\text{U}$  reactor cores, moderated or unmoderated, criticality data 9-14650  
 $^{238}\text{U}$  absorption near Na resonance, self-shielding factor 9-2798  
 $^{238}\text{U}$  fission fragments causing microbubbles in water, acoustic detect. method 9-21204  
 $^{238}\text{U}$  isotope contents,  $\alpha$  spectra, semicond. detector meas. 9-2835  
 $^{238}\text{U}$  ternary fission following n bombardment 9-20815  
 $\alpha$ -U, dislocation energies and easy glide parameters rel. to slip systems 9-1226  
 Th-U-N system phases,  $\geq 50$  at.% N, 1000°C 9-16157  
 Ti-Mo alloys, U diffusion 9-19769  
 U-graphite assemblies, enriched, accurate criticality meas. 9-18121  
 U-D $_2$ O lattice with Pu in fuel, n thermalization, model 9-16974  
 U-H $_2$ O reactor assembly, fuel loading and critical mass expt. 9-18120  
 U-H $_2$ O subcritical assembly with n source, params., obs. 9-11347  
 U-Zr-C phase diagram, 1700-2000°C 9-11976  
 $\alpha$ -U, growth under irradi. at 25°C 9-7371  
 $\alpha$ -U, neutron irradi. defects and Matthiessen's rule 9-16089  
 $\alpha$ -U, precipitation of  $\text{UAl}_3$  on heating, kinetics 9-11960  
 $\alpha$ -U, slip modes rel. to dislocation parameters and elastic const. 9-1228  
 $\alpha$ -U, slip planes and directions, temp. depend. 9-1298  
 $\alpha$ -U, superconducting, isotope effect 9-1487  
 $\alpha$ -U creep and internal stresses rel. to surface oxidation, obs. 9-9765  
 $\alpha$ -U neutron-induced growth at low doses, mechanism 9-19870  
 U underground leaching from water-bearing deposits 9-20081

**Uranium compounds**

- ammonium uranyl sulphate, electronic and infrared absorp. spectra 9-1790  
 complex of thiocyanate, paper chromatographic method for separation and identification 9-18772  
 fission gas increase with thermal n flux, and decrease of solid fission products 9-11337  
 in reactor fuels, heat contents and specific heats 9-17356  
 Sical F1, n induced swelling, 500 MWd/t 9-16188  
 Sical F2, n induced swelling, 500 MWd/t 9-16188  
 $\text{UO}_2$ -rare earth oxides, high temp. stability in H atm. 9-3979  
 uranyl nitrate, polarized i.r. absorpt. spectra, uniaxial and biaxial crystals. 9-16417  
 uranyl salts, Cl trace determ. 9-8113  
 $^{235}\text{U}$  fast n fission cross-section ratio n energy range 0.3-2.5 MeV 9-623  
 $^{235}\text{UO}_2$ -97 wt.%ThO $_2$  fuel, thermal flux shape and reflector savings 9-19371  
 $^{235}\text{U}$  enriched assemblies, statistical wt determ. 9-642  
 $^{235}\text{U}$  fast n fission cross-section ratio n energy range 0.3-2.5 MeV 9-623  
 ThC-UC solid solns., elec. resist., thermoelec. power and Hall coeff. 9-3573  
 ThO $_2$  (1.3 wt.%UO $_2$ ), thermal cond. changes, irradi. induced, annealing 9-7676  
 U-(Fe,Al),  $\beta$ -quenched, recrystallization after annealing 9-3466  
 U-H $_2$ O subcritical syst., pulsed neutron determ. of 2 group reactor-physical parameters 9-16984  
 U-Mo-Al-Sn, n induced swelling, 500 MWd/t 9-16188  
 U-Mo 1,1, n induced swelling, 500 MWd/t 9-16188  
 $\alpha$ -U-Mo alloys, supercond. props. pressure dependence, 0-10 kbar 9-12130  
 U-(10 wt.%Mo) alloy, stress-corrosion cracking, effects of heat treatment and ambient atmospheres 9-21384  
 U-Nb alloys, electrolytic etching in conc. aqueous citric acid, potentiostatic method 9-1129  
 U-Ti alloys orthorhombic, metastable phases 9-19823  
 U-UMn $_2$ -UF $_6$  system phase equilibrium 9-1353  
 (U, Pu)C, synthesis from U-Pu alloy and fabrication of pellets 9-2791  
 (U, Pu)C fuels, prep. by coprecipitation 9-6939  
 (U, Zr)C solid solns., lattice params. rel. to comp., obs. 9-11976  
 (U,Ce)n solid solns. prep. and UN-CeN miscibility, 1800°C 9-9791  
 (U,Nd)N solid solns. prep. and UN NdN miscibility, 1800°C 9-9791  
 (U,Pu)O $_2$  microphases, techniques for ceramography and alpha autoradiography 9-3309  
 U $_2$ N $_2$ X, (X=P, As, Se and S), crystal structure 9-14928  
 U $_3$ N $_3$ ,  $\alpha$  and  $\beta$  phase relations 9-16159  
 U $_3$ O $_8$  matrix, spectrochem. determ. of impurities by d.c. arc method 9-21085  
 UP $_4$ , enthalpies of formation, qualitative method of differential thermal analysis 9-19368  
 U $_3$ Si alloys, approx., effect of C on  $\delta$ -peritectoid reaction 9-16158  
 U $_4$ O $_9$ , phase transition mechanism obs. in sp. ht. meas. 9-3495  
 UAl $_3$  UMn $_2$ -UF $_6$  system, phase equilibrium 9-1353  
 UAs, antiferromagnetism, neutron diffraction study 9-3837  
 UC-D $_2$ O lattice fast fission ratio, ECO reactor obs. 9-11355  
 UC, arc cast and sintered, thermal conductivity, radiation eff. 9-15034  
 UC, chem. reaction with HNO $_3$ , obs. 9-6027  
 UC, diffusion of U and C, and mechanisms, 1266-1863°C 9-11899

**Uranium compounds continued**

- UC, dihedral angles of U inclusions in grain boundaries 9-11855  
 UC, fabrication of stabilized compacts 9-20847  
 UC, Kr sorption, fission induced, mechanism 9-16047  
 UC, reactions with NaOH aqueous soln. 9-16482  
 UC, thermal diffusivity, USNRDL flash technique 9-15032  
 UC, thermal dissociation. 9-1897  
 UC diffusion of C into Mb and W, 1000-1800°C 9-19764  
 U $_2$ C $_3$  form. in UC-UC $_2$  melt, reactions rel. to grain orientation, 1350°C 9-12530  
 UCl $_4$ -KCl-NaCl eutectic diagram predicted and confirmed by X-ray diffraction 9-11969  
 UCl $_4$ -NaCl eutectic diagram predicted, confirmed by X-ray diffraction 9-11969  
 UCo $_3$  and other PuNi $_3$ -type cpds, unit-cell constants 9-7451  
 UF $_6$ -WF $_6$  mixture, liquid-vapour phase equilib. determ., 1520-2660 mm Hg 9-21246  
 UF $_6$ , gaseous, heat conductivity, Senftleben-Beenakker effect 9-9446  
 UF $_6$  thermodynamic properties evaluated from analysis of available experimental data. 9-2786  
 UF $_6$ X (X=Li, Na or Cs), paramag. reson. study 9-3960  
 UFeO $_4$ , Mossbauer effect and neutron diff. study of magnetic ordering 9-3873  
 U $_3$  antiferromagnetic, I $^{127}$  nuclear quadrupole resonance 9-1885  
 U(IV)-U(VI) electron exchange in HCl 9-6007  
 UN, chem. reaction with HNO $_3$ , obs. 9-6027  
 UN, sp. ht., 1.3-4.6°K 9-17357  
 UN, thermal conductivity, elec. resist. and Seebeck coeff., 77-400°K 9-7675  
 UN, thermal diffusivity from 20 to 1000°C by laser pulse method 9-13269  
 UN, vaporization reactions and U, N $_2$  vapour partial pressures 9-7308  
 UN microspheres, prep. by carbothermic reduction of UO $_2$  in N atm. 9-2794  
 UNO, gaseous mol., mass spectrometric obs. 9-790  
 UO $_2$ -GdO $_2$ , phase diagram 9-3979  
 UO $_2$ -Nb-H system compatibility 9-6941  
 UO $_2$ -(20 wt.%)PuO $_2$  fuel, stoichiometry rel. to temp. gradient 9-2788  
 UO $_2$ -Ta-H system compatibility 9-6941  
 UO $_2$ -UCl $_4$ -KCl, X-ray examination 9-16986  
 UO $_2$ -puO $_2$  reactor fuel, stoichiometry, effect of external O sink 9-2789  
 UO $_2$ -H $_2$ O lattice, subcritical multiplying medium, diffusion constants determ. 9-18127  
 UO $_2$ -Nb cermet, high loaded fabrication by sintering 9-3475  
 UO $_2$ -SiO $_2$  system, elec. props., effect of fission fragments 9-7743  
 UO $_2$ -SiO $_2$  system, thermal cond. and resist., 100-800°C 9-16186  
 UO $_2$ , 90% enriched, -Ni fuel element plates, irradi. stability, 1.9-30% burn-up 9-19362  
 UO $_2$ , cation self-diffusion 9-16113  
 UO $_2$ , densification, powder morphology and energy effects 9-3465  
 UO $_2$ , effective reson. integral of rad. and cluster. obs. 9-19366  
 UO $_2$ , grown by solar furnace 9-16057  
 UO $_2$ , n space energetic distrib. 9-653  
 UO $_2$ , reduction by C in vacuum to produce metal U 9-14134  
 UO $_2$ , sintered, thermal conductivity, radiation eff. 9-15034  
 UO $_2$ , with cracks, thermal diffusivity, flash method suitability 9-15033  
 UO $_2$  base elements, influence of filling gas and radial distance between fuel and can 9-656  
 UO $_2$  cermet, isothermal Young's modulus 9-19777  
 UO $_2$  cry. prep. by thermal decomposition of UOCl $_2$  dissolved in molten UCl $_4$  9-19686  
 UO $_2$  crystallization from melt by electrolysis 9-19690  
 UO $_2$  single crystal prepared by induction heating of rod, with rotation and elevation 9-21297  
 UO $_2$  unenriched barrier beneath reactor core, as safety device against melt-through 9-18124  
 UO $_2$ -D $_2$ O lattices, fast fission ratio, obs. 9-19349  
 UO $_2$ , crystallographic changes at para-antiferromag. transition, X-ray diff. obs. 9-7890  
 UO $_2$ , enthalpy and heat of fusion, 1200-3260°K 9-3151  
 UO $_2$ , fission gas release around 2000°C and grain growth 9-13250  
 UO $_2$ , flow of single crystals, slip planes rel. to orientation, 600-1800°C 9-9762  
 UO $_2$ , n-irradi., elec. conductivity n flux dependence 9-1457  
 UO $_2$ , oxidation by steam, 885-1835°C 9-3997  
 UO $_2$ , reprocessing of irradiated fuels, by fluorinating with BrF $_3$  and F $_2$  9-6944  
 UO $_2$ , sintered, exaggerated grains and growth mechanism, obs. 9-11798  
 UO $_2$ , sintered, stainless steel inclusion, laser microprobe analysis obs. 9-12552  
 UO $_2$ , W microdiffusion, laser microprobe analysis obs. 9-12552  
 UO $_2$ , yield and flow in compression, rel. to temp. 600°-2000°C 9-11931  
 UO $_2$ , Young's modulus, cylindrical samples, Forster technique 9-1264  
 UO $_2$  containing Dy $_2$ O $_3$  dispersion, behaviour at high temps. 9-3476  
 UO $_2$  fuel pellets, microstruct. after irradi., defects, gas bubbles and grain growth 9-11856  
 UO $_2$  fuel rod fabrication by vibratory compaction 9-6942  
 UO $_2$  fuels, O redistrib. 9-11360  
 UO $_2$  heated, electrical resistivity, local meas. for fission prod. diffusion profile determ. 9-5647  
 UO $_2$  n irradi. behaviour rel. to initial structure and props. 9-2787  
 UO $_2$  nitrates, i.r. spectra and vibrations of UO $_2$  ion 9-7979  
 UO $_2$  oxidation and reduction in CO $_2$ -CO mixtures, surface controlled, 977-1400°C 9-3998  
 UO $_2$  sintered pellets, quality control rel. to stoichiometry, density and struct. 9-2796  
 UO $_2$  targets, large surface, prep. technique 9-13157  
 UO $_2$  targets, defect ordering and temp. dependence, statistical model 9-1203  
 U $_4$ O $_9$ , ht. capacity 1.6°-24°K, mag. entropy 9-9846  
 U $_4$ O $_9$ , superlattice reflections 9-7450  
 UO $_2$ (NO $_3$ ) $_2$ ·6H $_2$ O, excimer migration and quenching during cooling 9-5620  
 UO $_2$ ·SO $_3$ ·H $_2$ O effect of D $_2$ O substitution on fluorescence lifetime 9-1830  
 UO $_2$ -Mo cermet, isothermal Young's modulus 9-19777  
 UO $_2$ ·2H $_2$ O·ThO $_2$ , magnetic susceptibilities of nonstoichiometric samples 9-13950  
 UP-US solid solns. in paramagnetic state,  $^{31}\text{P}$  Knight shifts 9-10296  
 UP $_2$ , enthalpies of formation, qualitative method of differential thermal analysis 9-19368  
 (U $_0.85$ Pu $_0.15$ )C pellets, low density, prep. by reproducible process 9-6938

**Uranium compounds** (continued)

- US<sub>2</sub>, sto US<sub>2</sub>, cryst. struct., phases and mag. props. 9-16081  
 US<sub>2</sub>, heat capacity and thermodynamic props., 5 to 350°K 9-16082  
 US<sub>2</sub>, heat capacity and thermodynamic props., 5 to 350°K 9-16082  
 USe<sub>2</sub>, to USe<sub>2</sub>, cryst. struct., phases and mag. props. 9-16081  
 UX, magnetic properties with elements of the V B and VI B groups 9-7882  
 Ual, precipitation from  $\alpha$ -U on heating, kinetics 9-11960  
 UO<sub>2</sub>-ZrO<sub>2</sub>, Young's modulus, cylindrical samples Forster technique 9-1264  
 uo<sub>2</sub>, swaged, microstruct. changes on irradiation to burnup of 3,000 MWD/J-U 9-11358

**Urey-Bradley forces** *see* *Molecules/internal mechanics***V-centres** *see* *Colour centres***V particles** *see* *Hyperons; Mesons***Vacancies** *see* *Crystal imperfections/vacancies***Vacancy breakdown** *see* *Diffusion in solids***Vacuum apparatus***See also* *Seals*

- calibration chamber, servocontrolled gas inleak syst., design and development 9-19575  
 chamber for space plasma simulation 9-14296  
 chambers for satellite heat balance tests at Noordwijk 9-12651  
 electric quadrupole mass filter for high vacuum meas. 9-8334  
 glass, use of heat shrinkable sleeve in lubricant free connector 9-16649  
 all glass system 10<sup>-10</sup> torr 9-14295  
 mass spectrometer for residual atmos. analysis in vacuum systems 9-8119  
 measuring systems 9-4193  
 microbalance of pivot type 9-10612  
 for plasma machine, toroidal 9-8328  
 quartz crystal low-temp. microbalance holder 9-12814  
 rotatable multiple sample mount for bakeable syst. 9-12813  
 rotator, multiple for ultra high vac., manual or automatic op. 9-4200  
 simple, for lecture expt. 9-17678  
 target chamber for light ion beam accelerator 9-11165  
 vacuum line, articulated 9-16650  
 valve, bellows-sealed, for reactive gases at moderately high press. 9-18964  
 valve, self-centering, metallic with elastic filler 9-12812  
 valve, variable leak, modification to permit continuous high temp. operation in mass spectrometer 9-19385  
 for Van de Graaff accelerator 9-6749

**Vacuum gauges**

- Bayard-Alpert, controller 9-18968  
 Bayard-Alpert, ionization, sensitivity meas. with mol. beam probe 9-4198  
 Bayard-Alpert, with ion-electron converter and counter 9-8331  
 Bayard-Alpert ionization, sensitivity, variations, end-cap effect 9-6242  
 and calibration of high vacuum gauges, review 9-8330  
 differential, capacitive diaphragm press. transducer appl. 9-6226  
 hidden collector, sensibility 9-6241  
 ionization, high pressure, calibration 9-4197  
 ionization, hot filament, behaviour of H<sub>2</sub> at press. near 10<sup>-11</sup> Torr 9-10591  
 ionization, low press. meas. in isothermal and nonisothermal recipients 9-10593  
 ionization, of JG type, energy supply conditions and electric props. 9-6239  
 ionization, total press. meas., limitations 9-12810  
 ionization meas. of Pb and Sn evaporation rate and film thickness 9-21264  
 magnetron ionization, striking characteristics in He, 1.9x10<sup>-7</sup> torr-7x10<sup>-10</sup> 9-6240  
 test equipment and procedures 9-10592  
<sup>3</sup>H, ionisation, for press. of reactive gases 9-2131

**Vacuum polarization** *see* *Quantum electrodynamics***Vacuum pumps**

- in accelerators, linear, effect on conductance and pressure 9-6743  
 axial flow molecular pump with rotor with single blade row, performance 9-17676  
 cold diffusion, CO<sub>2</sub> as working medium 9-4168  
 cryogenic pumping of H<sub>2</sub> in ultrahigh vacuum systems 9-6238  
 cryopumping, utilizing He-cooled surfaces 9-8318  
 diffusion pump equation, numerical soln. 9-22021  
 equipment evolution and performance 9-18967  
 ionic, residual atmosphere after pumping 9-10588  
 oil in diffusion pump vapour jet, mol. velocity distrib. after impact 9-20994  
 properties and design calculations 9-15396  
 pumpdown time determ. using model, scaling laws 9-8322  
 rotary, thermoelectrically cooled baffles 9-4196  
 rotary, types and characteristics 9-22020  
 sorption, glass low pressure prod. 9-8329  
 sorption, Polish developments 9-10589  
 speed and current evacuation, magnetic-discharge pumps 9-4194  
 sputter-ion and Redhead gauge, appendage pumps comparison 9-12809  
 sputter-ion pump, effectiveness on He 9-8326  
 turbo-molecular, applic. to He leak detector sensitivity improvement 9-22022  
 ultrahigh, cooled T, sorption 9-4195  
 vapour, back-diffusion of oil 9-8327  
 zeolite fore vacuum pump which also serves as Dewar for cooling agent 9-12808  
 H<sub>2</sub> residual atm. in sputter-ion and non-evaporable getter pumped systems 9-14297

**Vacuum technique**

- continuously pumped systems 9-10590  
 crystal cleavage repetition apparatus 9-1097  
 deposition of thin films, differential ion pumping 9-12816  
 design and technology, book 9-16648  
 dictionary with definitions in six languages 9-10587  
 electrical discharges, apparatus for investigation from 10<sup>-8</sup> torr to 4 atmos. 9-3019  
 electron microscope, modifications for ultrahigh vacuum work 9-6485  
 film deposition, metallic, review 9-7340  
 films, metallic, formation and physical properties, influence of residual gases 9-3203  
 Geiger-Müller counter for u.h. vacuum systems 9-18033

**Vacuum technique** (continued)

- gettering on Ti film, removal of H impurities from He discharge tube 9-3021  
 glass systems assembling without vacuum grease 9-16649  
 high vacuum system with adsorbing walls, gas kinetics 9-7222  
 mass spectrometer, miniature for identification of all vapours 9-8333  
 measuring systems 9-4193  
 metal outgassing at 10<sup>-7</sup> to 10<sup>-10</sup> torr 9-14299  
 metallurgical melting and casting 9-5493  
 metallurgy, thermodynamic aspects 9-8325  
 metallurgy, physico-chemical aspects 9-18530  
 microfurnace for e microscope specimens 9-14292  
 model for determ. of pumpdown time, scaling laws 9-8322  
 molecular conductance and flow as temp. indep. substitutes for gaseous conductance and flow 9-8323  
 polyimide seals for u.h. vacuum 9-16651  
 problems at Industrial Institute of Electronics 9-10584  
 pumped systems and leak detection, book 9-10586  
 reactive metal vacuum-induction melting in water-cooled crucibles 9-13746  
 seals, glass-ceramic, for Al to Pt or Mo. 9-18969  
 shock tubes, rectang., down to 10<sup>0</sup> torr 9-12942  
 sputtering of insulator films in r.f. discharge 9-3204  
 surface phenomena in metals 9-8324  
 ultra-high systems, design and technology, book 9-16648  
 ultrahigh vacuum system, space physics research laboratory 9-20285  
 universal motion device for use in ultrahigh vacuum 9-8332  
 vacuum degassing of alloys and steels 9-13747  
 Viton 'A' elastomer seals 9-16652  
 water vapour and O<sub>2</sub> trapping by Cs vapour injection 9-10585  
 Be purification by vacuum melting followed by distillation and simultaneous deposition to sheet in e beam furnace 9-13748  
 Cu-Al alloy, brazing for metal-to-ceramic seals 9-13766  
 Fe, carburization under vacuum 9-14124  
 H impurity removal from He discharge tube, gettering and pumping through Pd membrane 9-3021  
 He leakproofing control and leak detection 9-18970  
 Hg vapour drag effect in pressure region of transition flow, accurate meas. 9-6237  
 Ni-Cr-Cu-Al alloy, vacuum fractionation model. 9-7342  
 SiO films, resistance-heat and e-gun evaporated comparison of props. 9-3206  
 Ti film evaporation for getter ion pump, control through thermoelectron emission 9-12811  
 U metal production by C reduction of UO<sub>3</sub> in vacuum 9-14134

**Vacuum tubes** *see* *Electron tubes***Valence bands** *see* *Crystal electron states/band structure***Valency**

- benzene-d<sub>6</sub> in active solvent, C-D valence vib. integrated intensities 9-4949  
 cyclohexane-d<sub>12</sub> in active solvent, C-D valence vib. integrated intensities 9-4949  
 CaF<sub>2</sub>, <sup>48</sup>Ti, e.p.r. determ. 9-10276  
 MnCO<sub>3</sub>, covalency and exchange polarization 9-15156  
 UO<sub>2.17</sub>-Y<sub>2</sub>O<sub>3</sub>, mean U valency, rel. to mag. susceptibility data 9-13950

**Valves, thermionic** *see* *Electron tubes***Van Allen radiation** *see* *Atmosphere/radiation belts***Van de Graaff generators** *see* *High voltage techniques; Particle accelerators/linear***van der Waals forces** *see* *Atoms; Kinetic theory; Molecules/intermolecular mechanics; Solids***Vanadium**

- atoms and ions, bibliography of spectra 9-13287  
 Debye charact. temp. from Bloch-Grüneisen relation 9-9847  
 diffusion of Fe and isotope-effect parameter of <sup>55</sup>Fe and <sup>59</sup>Fe 9-9734  
 Fermi surface anisotropy from magnetoresistance 9-12105  
 films, nucleation, growth and structure obs. in e. microscope 9-19672  
 Mossbauer eff. of <sup>51</sup>Fe, high pressure eff. at room temp. 9-21610  
 point defects, rel. to elec. resistivity recovery peak 9-11871  
 solar abundance determ., including hyperfine structure 9-14249  
 spectra, IV and V, levels determ. from hollow cathode discharge 9-2820  
 stopping of slow recoil Cr atoms 9-19875  
 superconducting, type II, flux flow resistance and  $\kappa_2(T)$  parameter 9-1508  
 superconducting, type II, nuclear spin relax. rate near upper critical field 9-7923  
 superconductor, isolated-vortex state near H<sub>c1</sub> from u.s. attenuation obs. 9-17387  
 u.s. attenuation in mixed superconducting state 9-12005  
 X-ray emission spectra, K and L<sub>23</sub> bands rel. to band structure 9-1821  
 X-ray spectra, K- and L- emission bands, rel. to electron struct. 9-10229  
 H interstitial impurity precipitation, effect on elastic props. and thermal expansion 9-21334  
<sup>51</sup>V in VH<sub>2</sub>(x<2), n.m.r. 9-3970  
<sup>51</sup>V<sup>2+</sup>, spin Hamiltonian from ENDOR in MgO 9-12520  
 V<sup>2+</sup> in cubic fields, effect of dynamic phonon interaction on hyperfine fields 9-5531  
 V<sup>3+</sup> doped corundum, catalytic activation of H<sub>2</sub>-D<sub>2</sub> exchange 9-8085  
 V<sup>3+</sup> in CaF<sub>2</sub>, electron-nuclear double resonance 9-16472

**Vanadium compounds**

- metal-like, X-ray spectra obs. rel. to band structure calcs. 9-3912  
 oxides crystallization, from oxychloride hydrolysis 9-3234  
 steel, secondary hardening on tempering, high dislocation density as preferential nucleation sites 9-17328  
 Au-V dil. alloys, mag. props. temp. dependence 9-12267  
 Co-V alloys, n.m.r. of <sup>59</sup>Co 9-15204  
 Fe V alloy, diffusion of Cr 9-5404  
 Fe-V alloys, Hall effect and resistivity temp. and comp. dependence 9-9921  
 Fe-V alloys, itinerant electron ferromagnetism evidence 9-3797  
 Nb-V alloy, deform. effects, X-ray powder diffraction studies 9-11930  
 Ni-V alloy, X-ray emission L<sub>23</sub>-bands of Ni, struct. 9-12456  
 Ni<sub>3</sub>V alloy, ordering transition 9-13781  
 oxides, crystalline and glassy, electronic conductivity rel. to structure 9-3702  
 Ti-6 wt.%Al-4 wt.% V alloy, fatigue cracked, load relaxation, effect of methanol 9-19786  
 Ti V alloy, decomposition of martensite during continuous heating 9-5494  
 V-Mn alloys, <sup>51</sup>V and <sup>55</sup>Mn Knight shift 9-21672



**Vanadium compounds continued**

V-N solid solns., internal friction 9-19788  
V-O solid solns., internal friction 9-19788  
V-(Sat.wt.%)Ta, intermediate purity type II superconductor, u.s. absorpt. 9-18612  
V-Ti alloys, creep and stress-rupture behaviour 9-19801  
V-ti-Nb alloys, creep and stress-rupture behaviour 9-19801  
V<sub>2</sub>O<sub>3</sub>, Hall effect in metallic conduction region, at 200-320°K 9-18603  
V<sub>2</sub>O<sub>4</sub>, optical and transport props. 9-18620  
V<sub>2</sub>O<sub>5</sub>:Fe<sup>3+</sup>, Sn<sup>4+</sup>, Mossbauer effect of <sup>57</sup>Fe and <sup>119</sup>Sn 9-21613  
V<sub>2</sub>O<sub>5</sub>, band structure from reflection spectra 9-19984  
V<sub>3</sub>Ga sintered, Ginzburg-Landau parameter and mag. field penetration depth calc. 9-18611  
V<sub>3</sub>Ga with Al, In, Si or Ge partial substitution, supercond. props. 9-7778  
V<sub>3</sub>Si sintered, Ginzburg-Landau parameter and mag. field penetration depth calc. 9-18611  
V<sub>3</sub>Si with Al, Ga, In or Ge partial substitution supercond. props. 9-7778  
V carbide melt, C saturated, reaction with disordered carbons rel. to catalytic graphitization 9-12531  
VC melt, reaction with disordered C to form graphite 9-7617  
VC<sub>0.88</sub>, X-ray K-bands of C, rel. to electron struct. 9-10229  
VCr<sub>2</sub>Se<sub>4</sub>, physical props., effect of interactions between d shells of transition element 9-16253  
VH<sub>2</sub>(x<2), n.m.r. of <sup>51</sup>V and proton 9-3970  
(V,Mn)<sub>2</sub>Si ternary cpd. with high superconducting transition temp. 9-3599  
VO, ground state, perturbation caused by mag. hyperfine interac. 9-19449  
VO, heats of formation of point defects 9-17276  
VO, X-ray K bands of O, rel. to electron struct. 9-10229  
VO<sub>2</sub>, absorpt. spectrum below semiconductor-metal transition point 9-18712  
VO<sub>2</sub>, band structure from reflection spectra 9-19984  
VO<sub>2</sub>, electronic phase transitions and nature of 'metallic' state 9-15048  
VO<sub>2</sub>, semicond. to metal phase transition, resist. jump 9-16255  
VO mol., emission spectra, 29 new bands, vib. consts. estimated 9-7039  
VO potential energy curves and dissociation energies, transitions predicted 9-7079  
VO<sub>2</sub>, metal-semiconductor transition 9-1552  
VO<sub>2</sub>, photoemission quantum yield and energy distrib. curves 9-12227  
VO<sub>2</sub>, reflectivity and transmission spectra, for both sides of semicond.-metal transition temp. 9-12329  
VO<sup>2+</sup>, e.p.r. in KNO<sub>3</sub> and CsNO<sub>3</sub> crystals. 9-3961  
VO<sup>2+</sup> complexes,  $\pi$ -bonding by equatorial O, study by proton n.m.r. 9-13590  
V<sub>2</sub>O<sub>3</sub>, phase transition for strong electron phonon interaction, applic. of theory 9-9884  
VOF<sub>3</sub><sup>2-</sup>, e.s.r. and electronic struct. 9-14114  
VS, 2nd-order phase transition in one-phase region 9-9807  
V<sub>6</sub>Si<sub>6</sub> on Si, transmission e. microscope exam. 9-9613  
Vn, X-ray K-bands of N, rel. to electron struct. 9-10229  
Zr-V alloy, upper critical field and transition temp. 9-5665

**Vaporization**

*See also Boiling; Condensation; Distillation; Evaporation; Heat of vaporization; Vapour pressure*  
droplet in small Peclet number flow, adiabatic vaporiz. and decomposition burning, soln. 9-21687  
dryer with superheated vapour, model 9-3071  
powder particle formation during atomization by gas stream 9-5221  
vapour density meas. apparatus for student use 9-20286  
vapour film of uniform thickness, 1-dimens. growth 9-21248  
As single crystals., rates and coeff. 9-11750  
Ca, mass spectrometric study 9-19386  
CaH<sub>2</sub>, mass spectrometric study 9-19386  
CdO, kinetics, knudsen effusion study 9-3158  
Cu, powder particle formation during atomization by gas stream 9-5221  
<sup>3</sup>He-<sup>4</sup>He solns., during HeI-He II transition 9-9576  
Mg, mass spectrometric study 9-19386  
MnH<sub>2</sub>, mass spectrometric study 9-19386  
Pb, powder particle formation during atomization by gas stream 9-5221  
PbCl<sub>2</sub>+ACl (A=Na, K, Rb, Cs.), mixtures, mass spectra rel. to thermodynamic props. 9-19422  
PbZrO<sub>3</sub>, PbTiO<sub>3</sub>, vaporization of hot-pressed pellets, 780-1250°C 9-3156  
PuO<sub>2</sub>, volatilization behaviour, mass spectrometric study, 1980-2350°K 9-3160  
UC, thermal dissoc. 9-1897  
UN, decomp. reactions and U, N<sub>2</sub> vapour partial pressures 9-7308  
ZnCl<sub>2</sub>, ZnBr<sub>2</sub> and ZnI<sub>2</sub> 9-7306

**Vapour density** *see Density/gases*

**Vapour pressure**

*See also Humidity; Vaporization*  
alkanes, and critical press. and temp. correl. with acentric factor and molec. struct. 9-18381  
ethylene-d<sub>2</sub> and -d<sub>4</sub> 9-17232  
gas counterflow phenomenon used for quantitative analysis of volatile liquid 9-12550  
radioactive elements in cyclotron target, optimum evaporative separation conditions 9-18392  
Ar, liq., and comparison with liq. Kr, Xe 9-11748  
H<sub>2</sub>O-KCl-CaCl<sub>2</sub> soln., isopiestic meas. 9-21187  
<sup>4</sup>He, bulb. thermal relax. obs. 9-13563  
Kr liq., and comparison with liq. Ar, Xe 9-11748  
PrF<sub>3</sub> 9-9597  
Si-Te system, partial press. of Te<sub>2</sub> and SiTe 9-7307  
SnPbTe<sub>2</sub>, Knudsen cell exam. of equilb. sublimation 9-18391  
U obs., heat of sublimation calc. 9-16033  
Xe liq., and comparison with liq. Kr, Ar 9-11748

**Vapour pressure measurement**

boiling point method, modification of that of Ramsay and Young 9-3157  
bromobenzene, 16 torr-atmospheric pressure, by new method 9-3157  
chlorobenzene, 16 torr-atmospheric pressure, by new method 9-3157  
cut-off valve control to prevent contamination 9-1073  
and diffusion coeff., simultaneous absorpt. method 9-13562  
n-hexadecane, 0.02-200 torr., by new method 9-3157  
liquids, meas. methods review 9-14885  
refractory metals, high temp., shock-tube method 9-9596  
water, and other liqs., meas. methods review 9-14885  
water, dielectrically heated psychrometer 9-18389

**Vapour pressure measurement continued**

Ar+N<sub>2</sub> liquid-vapour equil. syst., 10atm. 9-17228  
CO-N<sub>2</sub> solid solns., equilibrium press. 9-21253  
CO<sub>2</sub>, 0°C, dynamic method 9-3037  
N<sub>2</sub>-CO solid solns., equilibrium press. 9-21253  
N<sub>2</sub>+Ar liquid-vapour equil. syst., 10 atm. 9-17228

**Variable stars** *see Stars*

**Variational calculus** *see Mathematics*

**Variational method** *see Quantum theory/application methods*

**Vavilov-Cherenkov radiation** *see Cherenkov radiation*

**Vectons (vector mesons)** *see Mesons*

**Vectors**

generalized derivatives for systems with multiple relative motion 9-124  
octets of SU(3), algebraic props. 9-17691  
operators grad and grad\*, applic. in general system of coordinates 9-10613  
space, complex related simple geometric structure 9-38  
and statics, book for students 9-4821  
textbook 9-20

**Velocity**

air, effect on oxidation of mild steel 9-21694  
shock-wave and particles, in solids, relation with ht. of sublimation 9-13722  
sonic, compact equation for nonideal gases, applicable for z values down to 0.80 9-13482

**acoustic waves**

*See also Dispersion, acoustic; Helium/liquid, sound propagation; Shock waves*  
air, approximation for, in terms f press. and enthalpy 9-10386  
alcohols, primary aliphatic, along saturation line 9-16001  
cyclopropane and ethylene, rel. to vibrational relax. times, -70-150°C 9-4953  
dielectric, ingl. of elec. field on velocity, attenuation and second harmonic generation 9-19858  
duralumin-water laminate, velocity of sound variation 9-3518  
Epstein profile, general, ray theory 9-2207  
in gas, second virial coeff. determ. 9-21235  
n-heptane, for thermodynamic props. determ. 9-17204  
l.f., in wet porous medium 9-5541  
liquified gas solutions by interferometric methods 9-5159  
metals, contributing factors rel. to realistic model 9-21428  
natural sea floor sediments, 15-1500 kHz 9-4031  
natural sea floor sediments, 15-1500 kHz 9-8160  
polycapraamide oriented fibres, coefficient of absorption by travelling wave method in a wide range of temps. 9-5540  
quartz, hypersonic, from light scatt. spectral analysis 9-1811  
semiconductors, many-valley, correction by interaction of sound with conduction electrons 9-1371  
silicon, vitreous, thermal treatment and impurity-ion conc. effects 9-15001  
in solids, shock-compressed, empirical reln. with density and press. 9-4362  
in ultradense matter, above the speed of light 9-6384  
Ar-O system, liquefied, interferometric meas. 9-9508  
Ar-methane, liquid solution, by interferometric method 9-5159  
Ar range dependence at very low press. 9-15973  
CdS, photoconductive, meas. by composite-bar method 9-17439  
H<sub>2</sub>SO<sub>4</sub>, aqueous mixture, molecular, and compressibility 9-16000  
He II, critical region 9-5209  
<sup>4</sup>He, liquid, and struct. factor, calc. 9-5205  
LaF<sub>3</sub>, meas. using Bragg diff. of light 9-9826  
MgO, polycrystalline, porosity dependence by resonant sphere method 9-18494  
in N<sub>2</sub>-wet CO<sub>2</sub> mixture, for thermal relax. freq. of N<sub>2</sub> 9-13492  
N<sub>2</sub> crystals, rel. to thermal and elastic props. 9-3519  
O<sub>2</sub> crystals, rel. to thermal and elastic props. 9-3519  
Pd alloys doped with transition elements 9-7642  
SF<sub>6</sub>, rel. to vibrational relax. times, -70-150°C 9-4953

**acoustic waves, ultrasonic**

*See also Dispersion, acoustic/ultrasonic*  
alkali halides containing CN<sup>-</sup>, and attenuation 9-11996  
benzene, along saturation line 9-9509  
benzene-O<sub>2</sub> mixture, molecular relaxation meas. 9-2901  
carbon tetrachloride, relax. determ. 9-3100  
m-cresol, variation along state isotherms, isobars and isochors 9-5164  
electrolytes, simple and complex ternary systems, rel. to molar conc. 9-15998  
ethylene glycol, variation along state isotherms, isobars and isochors 9-5164  
freshwater fish tissue, by pulse-echo tech., eff. of freezing 9-4323  
glycerol mixtures, temp. and freq. depend. 9-11693  
hydrocarbon gases, effect of temp. on rot. and vibr. relax. 9-957  
in eutectic liquid mixtures 9-986  
liquid, multiple relax. and light scatt. 9-1010  
measurement of very small change, f.m. c.w. technique 9-2289  
methane, solid, temp. depend., rel. to disorder 9-1370  
in polycrystalline metallic probe, effect of mag. field parallel to propag. direction 9-21429  
quartz bar, x-cut, generated at 9.46 Hz 9-5548  
CO<sub>2</sub>-O<sub>2</sub> mixture, molecular relaxation meas. 9-2901  
CS<sub>2</sub>-CCl<sub>4</sub> mixtures, volume relax. 9-3095  
Co, anomalies at high temp. 9-5547  
KCl, KBr and KI containing CN<sup>-</sup>, and attenuation 9-11996  
KH<sub>2</sub>PO<sub>4</sub>, in paraelec. region 9-21430  
N<sub>2</sub>-CO<sub>2</sub> gaseous mixtures at 95 atm., 31-100°C 9-9451  
NaCl containing CN<sup>-</sup>, and attenuation 9-11996  
NaNO<sub>3</sub>, at  $\lambda$  transition 9-1369  
Ni, anomalies at high temp. 9-5547  
Ni ferrites, hysteresis of u.s. vel. 9-9828  
Ni ferrites, temp. depend. minimum obs., mag. polarization eff. 9-9827  
Se liquid, obs. 9-986

**light**

acoustic waves faster than light in ultradense matter 9-6384

**Velocity analysis, particles** *see Particle velocity analysis*

**Velocity measurement**

*See also Angular velocity measurement; Stroboscopes*  
Alfven waves, compressional and torsional, under identical plasma conditions 9-21098

# Velocity measurement continued

cold tip meter, for turbulent vel. fluctuations 9-13502  
Dopplermeter, laser, new theoretical model 9-12848  
droplets in air stream, photographic technique 9-18346  
explosive, detonation, multichannel e counter chronograph 9-155  
gas flow profiles, optical tech. using ring laser 9-19569  
gas wave in shock tube, from induced e.m.f. 9-2238  
gases, rarefied, with thermistor gauge 9-5105  
heated element or skin friction gauges 9-5106  
projectile, metallic, gauge 9-2130  
velocity meas. of gases with variable fluid props. 9-15967  
waves, plastic, torsional, through stressed metal, velocity expt. determ. 9-16724  
wind, hot-wire anemometer 9-18791

# acoustic waves

in highly absorbent mats., compound piezoelec. vibrator 9-7523  
in liquids, by sing- around velocimeter, errors due to circuit reversal time 9-5153  
liquids, small quantities, a resonator method 9-5155  
H<sub>2</sub>O at 34°C, theoretical correction of errors 9-8511

# acoustic waves, ultrasonic

diffraction effects in u.s. devices with plane radiators 9-14385  
liquids, phase comparison method for small vel. differences 9-6383  
for NaClO<sub>3</sub> elastic consts. determ. 9-7522

# light

radio interferometric method 9-8642  
undergraduate expt., direct meas 9-4208

# Venus see Planets

# Verdet constant see Magneto-optical effects

# Verneuil process see Crystals/growth

# Vertex functions see Elementary particles; Field theory, quantum; Functions

# Vibrating bodies

See also *Crystals/lattice mechanics; Elastic waves; Pendulums; Piezoelectric oscillations*  
bar, axial vibs., optimal design for specified minimum cross-section 9-8499  
bars, under periodic axial loading, finite element soln. of stability for various end conds. 9-6373  
beam, Bernoulli-Euler, nonhomogeneous, parametric excitation 9-19046  
beam, clamped or free, semi-infinite, transverse motion 9-19047  
beam, wedge-shaped, transverse vibr., eigenvalue bounds 9-12929  
beam in turbulent air flow, effect of normal loading in time and space 9-119  
boundary, acoustic-field study of planar transducer and hydrophone arrays, synthesis problem 9-4296  
box structures, sine series theoretical soln. 9-8502  
cantilever beams with end support, transverse vibr. analysis using Bernoulli Euler eqns. 9-10721  
cantilever elastic, torsional stability under dynamic axial loading 9-147  
circular plate clamped at edge, eigenvalue estimation 9-14381  
circular plates, forced vib., finite integral transform determination 9-19051  
circular ring, dynamic response, applic. of series expansion of ultraspherical polynomials in anal. 9-17787  
combined struct., lin. elastic, normal modes and natural freq., scaling factors 9-4294  
complex structure, free vib. anal. using coupling of substructs. and mass and stiffness matrices 9-12925  
conical and cylindrical shells, laterally excited, transmission charact. 9-10719  
cylindrical shell, infinitely long, nonlinear vibs., asymptotic behaviour of finite shells 9-6372  
damping capacity meas. circuit 9-4297  
disc, finite, isotropic, axially symmetric vibs. 9-4290  
dynamic response of structural members, normal-mode solns. with time-depend. in-span conditions 9-10720  
elastic beam analogue analysis of resonant gate in m.o.s.t. 9-19922  
elastic free-free, natural freq. and modes determ. from integral eqn. 9-4292  
elastic plate, sound field near plate, spatial correl. characts. 9-4309  
elastic plates, formed motion, soln. method 9-19053  
elastic shell filled with non-viscous compressible fluid 9-15457  
elastic solid containing penny-shaped crack, torsional vib., soln. of axisymmetric eqn. 9-4304  
flow over flexible plate, nonlinear flutter theory 9-11650  
in fluid, elastico-viscous, damping force calc. 9-14745  
free free bar with arbitrary press. pulse at one end, propag. of stress wave 9-17791  
frictional force meas. during vibration 9-6349  
mechanical oscillator, third order, motion and solns. 9-19048  
membrane, non linear wave equat. anal. 9-6375  
membranes loaded by air layer, config. soln. 9-4286  
multistorey structures, digital computation 9-10724  
non-uniform rods, reson. freqs. calc. by flexural impedance method 9-4289  
nonlinear systems, rotational and oscillatory solutions with several degrees of freedom 9-10722  
normal modes and natural frequencies, systematic relax. method for determ. 9-4293  
orthotropic circular plates of variable thickness, natural freqs. 9-20416  
with oscillators, nonlinear, moving a surface, vibs. stability and damping 9-10723  
particle in plane restrained by two springs 9-4267  
pendulum, elastic, asymptotic and analog computer solns. 9-16727  
plate, circular, inhomog. with central hole, forced vibr. 9-8500  
plate, circular, inhomog. with central hole, forced vibr. 9-10725  
plate, clamped, bounding eigenvalues determ. 9-17788  
plate, finite, in supersonic plane flow 9-8504  
plate, flat, rectang., excited by turbulent flow, anal. 9-12928  
plate resonance response to multi-mass moving system 9-20415  
plate systems, natural freq. calc., Bolotin edge effect method 9-8501  
plate tensioned with fatigue crack rel. to aeroplane fuselage 9-15458  
plates, elastic, nonlinear response to pulse excitations 9-148  
plates, hologram reconstruction, record, high index fringes. 9-4291  
plates, rhombic, fundamental freq., obs. 9-2197  
quartz crystal, harmonics of 285.7 kHz, detection methods 9-15459  
rectangular plate, nonstationary press. in 3-dimens. supersonic flow 9-4298

# Vibrating bodies continued

resonators, disc and ring, radial, torsional modes 9-4271  
ribbon, rigid, excited by plane waves, singular solution 9-143  
rigid circular die, on an elastic half space, eff. of rotatory vib. 9-4295  
shake tables, noise, generation and radiation characts. 9-4358  
sheets, thin, decay time constants 9-19044  
shell, cylindrical in external or internal supersonic flows 9-7220  
shell, cylindrical ring-reinforced; dynamic response to press-change in surrounding medium 9-149  
shell, infinite, dynamic response, applic. of series expansion of ultraspherical polynomials in anal. 9-17787  
shell (thin dome of revolution) nonsymmetric elastic vibrations 9-19054  
shells, circular cylindrical, due to gyroscopically induced inertia loads 9-12927  
shells, cylindrical semi-infinite; soln. with space and time var. 9-150  
shells, orthotropic, laminated cylindrical, free vibr. 9-10717  
shells, small perturbations, buckling and vibration 9-19025  
shells, thin, elastic, spherical, surrounding fluid effect on free axisymm. vibs. 9-16725  
shells, thin, orthotropic, oblate, spheroidal, free vibs., soln. 9-20420  
skew membranes, natural frequencies and mode shapes 9-10718  
solid in fluid stream, energy transfer meas. 9-144  
sound radiation at surface, integral eqns. and iterative solns. 9-16730  
sound radiation generation mechanism, theoretical and experimental investigation 9-4335  
spheroids, prolate elastic, and shells, torsional vibs. 9-2196  
spinning membrane disks, large amp. axisymmetric transverse vib. 9-19050  
stiff steel strings, normal vibr. modes 9-2198  
strings, equation assuming monotonically increasing boundary conditions 9-20421  
strip, flexurally vibr. in infinite baffle, radiation impedance 9-4287  
undamped non-linear spring mass syst. subjected to const. force excitation, transient response 9-19049  
uniform rectangular curved panels, free vibrations, soln. 9-20417  
wedge, cone, free and forced transverse vib., freq. eqn., mode shapes determ. 9-19045

# Vibration, molecular see Molecules/vibration

# Vibrations

See also *Acoustics; Damping; Oscillations; Vibrating bodies; Waves*  
anti-vibration instrument mounting 9-20281  
bar, optimal design for specified minimum cross-section, for axial vibs. 9-8499  
bars, under periodic axial loading, finite element soln. of stability for various end conds. 9-6373  
circular plates, forced vib., finite integral transform determination 9-19051  
circular plates, orthotropic of variable thickness, natural freqs. 9-20416  
cylindrical shell, infinitely long, nonlinear vibs., asymptotic behaviour 9-6372  
dislocations, parallel edge, self-vibrations 9-5355  
flexural, of symmetrical multi-layer beams, viscoelastic damping 9-16726  
flexural, rel. to Young's modulus determ., errors due to shear and rotatory inertia 9-13713  
free, of laminated orthotropic cylindrical shells 9-10717  
matrix anal. using the A-P algorithm 9-20373  
non-linear, travelling threadline 9-6374  
non-linear problems, equivalent linearisation for soln. by differential eqns. 9-17784  
normal mode, existence in nonlinear system 9-17783  
normal modes of symmetrical vib. syst. rel. to group theory 9-9  
parametric resonance apparatus for teaching demonstrations 9-10715  
planar array and synthesis, acoustic field study 9-4296  
plate, infinite, impedance to longit. force 9-4288  
quartz crystal, diffraction of neutrons 9-3516  
random, first-passage problem, series soln. 9-17731  
reducing materials in construct. industry, performance and economics 9-17782  
rotational-oscillatory systems excited by high frequency drives 9-12930  
rotatory, rigid circular die on elastic half space, eff. 9-4295  
of skew membranes, natural frequencies and mode shapes 9-10718  
spinning membrane disks, large amp. axisymmetric transverse vib. 9-19050  
teaching demonstration, mag. driven circular mesh 9-2116  
torsional, in inhomogeneous, linear, elastic continuum 9-20418  
vertical and torsional, in stratified inhomogeneous, non-linear, nonelastic medium 9-20419  
vibrosopes, fixed frequency, evaluation tests 9-6370  
wire, Eigenvalue problem introduction 9-2112

# excitation

linear structure, point trajectory calc. 9-8503  
linear systems, resonant and non-resonant case 9-146  
mechanical systems random excitation, creep depend. 9-21377

# measurement

See also *Seismology*  
beam systems, vibr. transmission 9-8498  
by holographic interferometry, stroboscopic 9-8634  
holographic method, verification 9-4285  
interferometric analysis by projected fringes 9-6369  
by interferometry, opt. holographic, applic. to sonar transducer 9-4353  
normal modes and natural freq. of combined struct. 9-4294  
normal modes and natural frequencies, systematic relax. method for determ. 9-4293  
plate, by interferometric method 9-15456  
solid in fluid stream, energy transfer meas. 9-144  
transverse, of cantilever beams with end support, analysis using Bernoulli-Euler eqns. 9-10721

# Vibronic states see Molecules/electronic structure; Molecules/vibration

# Vidicons see Electron tubes

# Viral coefficients see Equations of state

# Virtuons (virtual phonons) see Crystals/lattice mechanics

# Viscoelasticity

See also *Plasticity*  
constitutive eqn. based on Cauchy-Green strain tensor for second order fluid 9-6366  
contact problems, solution of integral eqn. for certain problems 9-19038  
contact region of hard ball rolling on viscoelastic plate 9-12924  
coupled thermoviscoelasticity, theory 9-6367



**Viscoelasticity** continued

- cylinder, circular, isotropic; quasistatic soln. for torsion. non-linearity effects 9-140  
 cylinders, dissimilar, rolling contact 9-10708  
 elastic-visco-plastic medium, propag. of loading and unloading waves 9-6379  
 elastomer, stress due to sinusoidal oscillations superposed on finite strain 9-19052  
 eye lens, dynamic props. 9-18958  
 flow through tubes, efflux perturbation 9-15913  
 fluid, steady laminar flow through porous walls 9-5128  
 fluid flow down inclined plane, stability 9-2944  
 fluids, with finite deformations, kinematics 9-12923  
 half-plane boundary, motion of rigid stamp 9-17781  
 hexachlorobiphenyl liq. with inert-gas infusion 9-15996  
 linear thermo-viscoelasticity theory, correspondence principle, mixed boundary value problems 9-16662  
 liquid with inert-gas infusion 9-15996  
 metal cantilever beam, transverse oscs. rel. to solid viscosity effect on dynamic load factors 9-4280  
 Newtonian fluid, indentation by right circular cyl., solns. 9-19035  
 nonlinear theory, kinematics, thermodynamics and rheological relationships 9-843  
 plastics, glass reinforced, behaviour with reference to adhesion 9-17237  
 polyethylene terephthalate monofibres, effect of orientation 9-9750  
 polymer melts, apparatus for meas. 9-3069  
 polymer solutions and melts, nonlinear model 9-21168  
 polymers, relax., thermodynamic description 9-9754  
 quadratic yield condition in elastoviscoplastic materials 9-8496  
 rod under body force and deforming mag. field, disturbance propagation 9-21360  
 shock waves, spherical, in visco-elasto-plastic half-space 9-12932  
 solid, linear, divergent stress pulse analysis 9-13716  
 sphere, gravitating, oscs. and vel. field, soln. 9-18235  
 string, 3-element, subject to transverse impact, transverse and longitudinal wave coupling 9-20427  
 temperature depend body thermal stresses 9-19036  
 thermodynamic restrictions in continuous media 9-19037  
 variational principle for thermal stresses in linear viscoelastic body 9-4281  
 viscous drag and secondary flow in granular beds 9-13406  
 wave, elastic, propag., equation 9-17790  
 wave, propag. along bar, with realistic props. 9-19039  
 Na stearate -19.7 to 35.7% H<sub>2</sub>O, rel. to struct., shear creep obs., 5-60°C 9-5470

**Viscometers**

- air turbine, variable shear stress, modification 9-11688  
 capillary for vapours 9-19589  
 cone and plate, flow curve determ. 9-4991  
 cone and plate, geometry of cones 9-17082  
 cone-and-plate, secondary flow effect on meas. 9-19615  
 linear and annular canal, comparison for surface rheological meas. 9-7257  
 linear oscill., design and performance 9-19617  
 portable, measuring power needed to maintain const. torsional vib. amplitude 9-988  
 probe capillary, for samples < 1ml 9-3082  
 Zimm-Crothers, modification 9-21190

**Viscoplasticity** see *Plasticity***Viscosity**

- chain polymers, intrinsic 9-4975  
 colloid solns., effect on resonance absorpt. of  $\gamma$ -quanta 9-3138  
 couette fluid flow var. with mag. field, press. gradient 9-2958  
 detonation, influence of viscosity on LVD 9-16737  
 Fermi liq., transport coeffs. expressed as rapidly converging series 9-105  
 fluid, decay of discontinuity line, secondary vortex occurrence 9-13405  
 fluid, non-Newtonian, viscometric flow, book 9-11529  
 friction in pre-separation region of turbulent boundary layer in diffuser with hot air flow 9-9425  
 glass, rel. to microhardness, indentation tests 9-18527  
 glycerine, acoustic wave damping, dispersion calc. 9-19513  
 high polymer molecules, mechanical entanglements 9-19488  
 hypersonic viscous flow over slender bodies with sharp leading edges, solns. 9-18236  
 hypersonic viscous flow past semi-infinite flat plate with sharp leading edge, analysis 9-21004  
 linear shear flow, lift tensor for three-dimens. body and maximum dissipation 9-17084  
 measurements, book 9-6267  
 metal beam, dynamic load factor, solid viscosity effect 9-4280  
 N-methylpropionamide solutions, relative viscosity and apparent molal volume 9-19620  
 Navier-Stokes eqns., canonical form derived using Clebsch transformation 9-21002  
 optical glass in the softening and annealing range 9-5147  
 organic materials, temp. depend. at const. pressure 9-14839  
 plasma, collisionless, in mag. field, stress tensor expression 9-21061  
 polystyrene, melt viscosity, eff. of press., analysis 9-18385  
 porcelain enamel frits 9-17196  
 region of turbulent boundary layer 9-18246  
 shear stress distrib. in confined equilib. turbulent flows 9-19594  
 soda-lime-silica, glasses, rel. to structure and Ca coordination 9-1079  
 Stokes' law, expt. investigations 9-19616  
 suspension, refinement of theoretical calcs. 9-1049  
 turbulent boundary layer, drag coeffs. on plate evaluation of Coles' theory 9-17145  
 variable, in fluid layer, anal. of slow thermal convection 9-6039  
 B<sub>2</sub>O<sub>3</sub> glass, rel. to relax times spectrum, 10<sup>10</sup>-10<sup>14</sup> poise 9-3850  
 Rb silicate glass, stress depend., 10<sup>14</sup>-10<sup>16</sup> poise 9-3422

**gases**

- binary mixtures, combination rules test 9-9458  
 ter-butyl alcohol, 30°-200°C obs. for intermol. force determ. 9-13497  
 capillary viscometer 9-19589  
 dense, quadrupole-quadrupole interact. eff. on initial press. depend. 9-5112  
 diethyl ether, 30°-200°C obs. for intermol. force determ. 9-13497  
 ethyl acetate, 30°-200°C obs. for intermol. force determ. 9-13497  
 hard sphere, correction for suspended large heavy Brownian particles 9-14820

**Viscosity** continued**gases** continued

- in hypervelocity nozzles, from meas. of heat-transfer rates at stagnation points 9-9434  
 mixture, modification of Brokaw's calc. method 9-963  
 polar and nonpolar mixture, calc. method 9-5122  
 sharp cone drag coeffs. at hyper- and super-sonic speeds, correl. 9-7217  
 sphere moving in circular path, obs. on forces 9-17197  
 temp depend. investigation by law of corresponding states 9-9456  
 temperature dependent, influence on laminar boundary-layer stability 9-11687  
 viscometric flow with heat generation, temp. depend. 9-9457  
 wall shear stress for laminar boundary layer, shock induced, rel. to recovery factors 9-21129  
 BF<sub>3</sub>, coeff. depend. on B isotopic composition and temp. 9-21146  
 NH<sub>3</sub>, coeff. depend. on N isotopic composition and temp. 9-21146  
 NO, coeff. depend. on N isotopic composition and temp. 9-21146

**liquids***See also Lubrication; Superfluidity*

- alloys, rel. to concentration, near eutectic temp. 9-15995  
 binary soln., calc. from Eyring's reaction rate theory 9-993  
 borates, binary, 10<sup>4</sup>-10<sup>8</sup> poise, rel. to struct. 9-3083  
 round cavitation bubbles, influence on collapse velocity 9-9467  
 chlorobiphenyls, thermal variation 9-13514  
 cone-and-plate viscometer meas., effect of secondary flow 9-19615  
 o-cresol, rel. to glass transition, 10<sup>3</sup>-10<sup>14</sup> poise 9-3084  
 m-cresol, shear coeff. rel. to pVT state 9-5164  
 near critical point bulk and shear viscosities 9-991  
 1,4-dibromobutane in benzene-paraffin mixtures, viscosity depend. of dielec. relax. times 9-1712  
 1,3-dibromopropane in benzene-paraffin mixtures, viscosity depend. of dielec. relax. times 9-1712  
 elastico-viscous, flow between rotating spheres, asymptotic soln. 9-9469  
 electrolytes, theory of B-coeffs. 9-19619  
 ethylene glycol, shear coeff. rel. to pVT state 9-5164  
 flow, incompressible plane, around an object, solns. to Navier-Stokes eqn. 9-21154  
 flow about parabolic object 9-21161  
 flow through particle assemblages at intermediate Reynolds nos. 9-9492  
 force on sphere moving unsteadily along circular path 9-19618  
 glass-forming liquids, 10<sup>3</sup> to 10<sup>14</sup> poise 9-3084  
 glycerine, rel. to glass transition, 10<sup>3</sup>-10<sup>14</sup> poise 9-3084  
 heating in plane and circular flow between moving surfaces 9-987  
 hexachlorobiphenyl with inert-gas infusion 9-15996  
 inert gases, shear viscosity theory 9-9490  
 inviscid fluid in tank, effect on free surface oscs. 9-11671  
 mixture, effect of vol. change on prediction 9-990  
 molten salts, data collection 9-11714  
 molten salts, significant-struct. theory 9-978  
 non-associated, temp. depend. comparison with temp. variation of heat capacity at const. vol. 9-18357  
 nucleate bulk boiling, effect on loss of hydrodynamic stability 9-7305  
 Nujol/water emulsions, stabilized, rel. to aging 9-5201  
 phenol-benzene, calc. from Eyring's theory model 9-993  
 $\alpha$ -phenyl, rel. to glass transition, 10<sup>3</sup>-10<sup>14</sup> poise 9-3084  
 phenyl salicylate, rel. to glass transition, 10<sup>3</sup>-10<sup>14</sup> poise 9-3084  
 polydiphenylpropene-polystyrene graft copolymers 9-994  
 polymer melts, and glass transition, theories 9-3085  
 polymer melts, viscoelasticity 9-3069  
 polymer monodisperse system, intrinsic viscosity shear rate dependence 9-19621  
 polymer solns., excluded-vol. effects on limiting viscosity number 9-9489  
 polymethylmethacrylate, dilute solns., non-Newtonian variations 9-17198  
 polymethylmethacrylate-polystyrene graft copolymers 9-994  
 polystyrene, dilute solns., non-Newtonian variations 9-17198  
 porcelain enamel frits 9-17196  
 Prandtl equation for flow round a smooth body, critical point investigation 9-13513  
 rodlike mols. in soln., theory 9-989  
 sphere moving in circular path, obs. on forces 9-17197  
 stability characteristics, long-wave disturbances 9-3072  
 surface, meas., linear and annular canal viscometers comparison 9-7257  
 temperature dependent, influence on laminar boundary-layer stability 9-11687  
 two-component systems 9-21189  
 viscoelastic liq. with inert-gas infusion 9-15996  
 viscometer, linear oscill., design and performance 9-19617  
 viscometer, probe capillary, for samples < 1ml 9-3082  
 viscometer, rotational for non-Newtonian liquids 9-5146  
 viscometer, Zimm-Crothers, modification 9-21190  
 viscometric flow with heat generation, temp. depend. 9-9457  
 viscous heating of power-law liquid in plane flow 9-3081  
 water, anomaly below 30°C explained 9-992  
 B<sub>2</sub>O<sub>3</sub>, 10<sup>4</sup>-10<sup>8</sup> poise, rel. to struct. 9-3083  
 B<sub>2</sub>O<sub>3</sub> molten glass, inadequacies of theories 9-9493  
 CCL<sub>4</sub>-cyclohexane, calc. from Eyring's theory model 9-993  
 Cd, dilatational, existence from temp. depend. of sound absorpt. 9-5163  
<sup>4</sup>He, 14-31°K and pressures up to 100 atm. 9-1056  
 In, dilatational, existence from temp. depend. of sound absorpt. 9-5163  
 Li, m.p. to b.p., and Prandtl number 9-21197  
 NaCl-glycerol solns. 9-9548  
 Pb, dilatational, existence from temp. depend. of sound absorpt. 9-5163  
 Zn, dilatational, existence from temp. depend. of sound absorpt. 9-5163

**Visibility** see *Atmospheric optics***Vision***See also Colour vision; Eye*

- acuity, effect of grating size on threshold contrast 9-12793  
 acuity, vernier, apparatus for meas. in white and coloured light 9-20273  
 acuity, when tracking target, speed depend. 9-20271  
 acuity and critical flicker frequency in 6 animals 9-22011  
 acuity thresholds in narrow band chromatic illumination of gratings 9-20270  
 autokinesis, physiology of eccentric fixation 9-14282  
 backward masking, temporal summation 9-21998  
 binocular fixation, interplay of drifts and flicks. 9-18960  
 brightness, apparent, as function of retinal locus 9-20274  
 brightness contrast perception, xerographic model 9-22004  
 brightness discrimination with stabilized retinal image 9-12794  
 brightness of ramp stimuli as functional plateau and grad. widths 9-12791

**Vision continued**

- cat's controlled by central mechanisms 9-22008
- cat's evidence for central inhibition of retinal function 9-22009
- cortical response at different locations, binocular addition 9-20272
- cortical response to flicker in rabbits 9-22002
- critical flicker frequency, underlying mechanism 9-22002
- critical flicker frequency meas. in 5 rabbits 9-22012
- distance, direction estimates by extra-foveal retinal areas, eye movements improving accuracy 9-14283
- distance perception and retinal disparity 9-22001
- electroretinogram, signals 9-18957
- equivalent luminance of any light, as function of scotopic and photopic luminances 9-14446
- excitability rel. spatial and luminance factors 9-12790
- extra-foveal spectral sensitivity, depend. on retinal illumination 9-22005
- frog, dark adaptation of single units of retina following bleaching 9-22010
- glare impression, influence of geometry and high luminance light 9-12798
- Hermann-grid effect, border-visibility study 9-22000
- human, spatial brightness interact., perturbation approach and transfer function 9-15390
- human foveal vision, origin of dark noise 9-15391
- interaction between scotopic light stimuli in peripheral retina 9-18959
- laser illumination under low atmospheric transparency 9-4548
- lateral masking, interference 9-20268
- molecular basis 9-4167
- optimum signal luminance for normal and proton observers 9-4169
- quality effect on sunspot group classifications 9-20246
- retinal image, role of various eye elements 9-10578
- rod-cone interrelation, summation-index technique 9-21999
- shadow-caster for binocular stereopsis testing 9-12792
- single cone response recording site, electrode marking technique 9-12797
- snail, selection of darker area 9-20277
- spatial sine-wave responses of visual system 9-22003
- stereoscopic shadow-caster, theory and applics. 9-12792
- target visibility rel. to  $\alpha$ -occurrence in encephalogram 9-15392
- threshold for test line perception increased by presence of adjacent inducing fields 9-20269

**Vitreous state**

- See also Glass*
- polymers, glass transition 9-3085
- silica, acoustic props., thermal treatment and impurity-ion conc. effects 9-15001
- silica, configurational entropy of random network model 9-14887
- silica, impurity effect on ionizing radiation induced dilatation 9-14961
- silica, internally nucleated, crystallization kinetics 9-18426
- silica, thermal conductivity, critical evaluation of literature 9-15029
- systems and related crystalline compounds, new nomenclature for structure description 9-16035
- vitrocarbon, elec. resistivity, crystallite spacing, elastic constns. rel. to heat treatment temp. 9-7318
- As<sub>2</sub>Se<sub>3</sub>, glassy, pulse I-V characs. 9-3617
- C, glass-like, from pyrolysis of non-melting resins, study rel. to heat treatment state 9-7319
- C, glassy, characs. rel. to fabrication factors 9-7317
- C, glassy, industrial applic. in Japan 9-7316
- C, oxidation in CO<sub>2</sub> and O<sub>2</sub>/Ar mixtures, at 1500-3000°K, rate compared with graphite 9-8091
- C glass monofilament, prep. from thermo-setting resins 9-7320
- Se:SeO<sub>2</sub>, i.r. spectrophotometric study 9-5898
- Se, thermal expansion, -190° to +30°C 9-19865
- Se films, glassy, thermally stimulated conductivity 9-3726
- Se photogeneration of carriers 9-7851
- SiO<sub>2</sub>, thermal conductivity, critical evaluation of literature 9-15029
- SiO<sub>2</sub>, radiation compaction 9-11921

**Vlasov equation** *see Plasma***Vocoders** *see Speech***Voigt effect** *see Magneto-optical effects***Volta effect** *see Contacts, electrical***Volume measurement**

- dilatometer, autographic attachment 9-22015

**Vortices**

- See also Cavitation; Turbulence*
- conjugate solutions for flow 9-19503
- external vorticity, effect on stagnation-point heat transfer at high Prandtl number 9-20448
- gas flow, vorticity rel. to dissipative boundary layer 9-14808
- jet-driven flow, hydromagnetic stabilization 9-21043
- plane vortex sheet, stability rel. to compressibility and mag. field applic. 9-21101
- quantized lines and rings, model many-body wave functions, energy and velocity calc. 9-11732
- secondary, from discontinuity line decay in viscous fluid 9-13405
- stagnation criterion, importance of maximum swirl angle 9-17146
- Taylor's, in wide gap, heat exchange, analytical investigations 9-15479
- two-phase, gas-jet driven, flow velocity distrib. model 9-4993
- vortex ring creation in liq. He by positive ions, critical vel. 9-9579
- in He superfluid, trapped negative ion mobility, 0.8-1.6°K 9-5207
- II, liq., quantized, absorpt. of atomic admixtures 9-1060

**Water**

- See also Ice; Seawater; Steam*
- absorption, 100 to 1000 GHz 9-17164
- addition to Aerosol OT in n-octane solns, p.m.r. study of clear and turbid phases formed 9-9559
- adsorbed on silica gel, elec. cond. 9-13915
- adsorbed on sugar carbon, p.m.r. relaxation times 9-5257
- adsorbed onto synthetic Linde type-A zeolite, permittivity and loss factor 9-17427
- adsorbed onto synthetic zeolite, permittivity and loss factor 9-17426
- adsorption on NaCl, effect of prior exposure to HCl, CO<sub>2</sub> and H<sub>2</sub>O vapour 9-19678
- air-water interface, thickness of bovine serum albumin film 9-9477
- air-water system, degassing in sound field, influence of static press. and temp. 9-5161
- air/water interface, equation of state of ionized monolayers, for low surface press. 9-9500
- albumin, bovine serum, adsorbed monolayers permeability, obs. 9-7262
- alcohols, 1- and 2-, films dissolution rate on surface 9-5144
- bubble columns, gas hold-up and water axial dispersion coeff. 9-21175

**Water continued**

- t-butyl alcohol-water mixtures, u.s. absorpt. and relax. curves anal. 9-19630
- chemisorption on Fe and Cu films, 77° and 273°K 9-17519
- cometary atmospheres 9-4123
- contaminant in the coolant, removal by molecular sieves 9-19373
- content determination, interference filter analyzer, near infrared absorption 9-14140
- in continental crust, lower, saturation rel. elec. conductivity 9-12569
- convection from vertical circular heated cylinder 9-19093
- corrosion of U fuel element in steam-water system, 285°C 9-11361
- of crystallization, optical activity in vibration-transition region 9-7941
- deuterium solvent isotope effs. 9-21678
- diffusion of H<sub>2</sub>O in D<sub>2</sub>O examined by means of n radiography 9-11367
- dipole moment of mol. in first hydration shell of monovalent ion 9-5077
- drops, applic. of electrostatic theory of dielec. sphere 9-12826
- drops, uncharged, free fall in electric field, charge transfer between drops 9-14160
- duralumin-water laminate, velocity of sound variation 9-3518
- electrical polarization, shock-induced, mechanism 9-1037
- environment for slow crack growth in steels 9-5484
- equation of state, limitations and extensions of Rice and Walsh results 9-11680
- flow, unsteady, in open channels 9-7241
- flow of air-water mixture in tube, characteristics of disturbed region 9-18331
- freezing, step growth 9-5216
- heavy, diffusion of H<sub>2</sub>O in, examined by means of n radiography 9-11367
- heavy oxidation by peroxodisulphate 9-18756
- hydrated electrons, e.s.r. detect 9-1044
- hydration of ions, enthalpies 9-14904
- hydrosolence advances, review 9-15241
- ice water system, <sup>35</sup>S-<sup>35</sup>S conversion of positronium in positron annihilation mechanism 9-12079
- immersion effects on adhesion of Au particles to cellulose or polyester 9-9605
- ion product const. determ., thermodynamics considered 9-16487
- Kerr constants temp. dependence, 5-55°C at 365 mμ 9-19632
- laminar boundary layers with adverse press. grad., heat flow 9-21163
- aser, meas. of far i.r. power using liq. load calorimeter 9-17875
- light, oxidation by peroxodisulphate 9-18756
- liquid, cell theory applic. assuming electrostatic intermolec. potential 9-19606
- magnetic susceptibility, temp. depend. 9-5188
- and methanol, simultaneous condensation from turbulent air flow 9-1070
- microbubbles created by <sup>238</sup>U fission fragments, detect. by acoustic wave absorpt. 9-21204
- mixtures, methanol and ethanol, light scatt. 9-21209
- molecular diffusion in hydrated crystals, effect on NMR spectrum 9-1241
- molecule, centrifugal distortion effects 9-15855
- molecule, group theory classification of states 9-14679
- molecule, Hamiltonian constns. for vib. states 9-7024
- molecule, one electron props. and electronic struct. 9-9208
- molecule, one-electron props. of near Hartree-Fock wavefunctions 9-9207
- molecule, vib. force constants determ. 9-13326
- molecule, wave functions of vibrating state 9-9205
- molecule nuclear corrections to expectation values, zero-point vibr. effects 9-9209
- molecules, spectra calc. rel. obs. 9-4927
- molecules diffusion in hydrates and NMR spectra 9-1242
- molecules diffusion in hydrates and NMR spectra 9-13704
- neutron diffusion and extrapolation lengths, stationary meas. 9-9079
- neutron moderation, spectra obs. 9-18574
- neutron reflector, effect of steel rods 9-18125
- neutron scatt. in mixture of light and heavy water 9-19377
- neutron thermal diffusion parameters using pulsed method 9-19341
- neutron thermalization in light water, Nelkin model modification 9-20856
- neutron thermalization params., obs. 9-6701
- neutrons, fast, space, energy and angular distribs. 9-19329
- n.m.r. relaxation times of protons adsorbed on sugar carbon 9-5257
- nonionic detergent solns, thermodynamic mixing junctions and temp.-comp. phase diagrams 9-9485
- nucleation theory, embryonic droplet surface free energy 9-7304
- oil/water interface, equation of state of ionized monolayers, for low surface press. 9-9500
- partially deuterated, i.r. spectrum, line shape of OD absorpt. 9-14688
- permittivity and conductivity meas., freq. limit by "electrodeless" method 9-14853
- phase transform, at critical temp. 9-11681
- phase transitions in atmos., kinetics rel. to droplets and ice behaviour in clouds, book 9-20088
- phenol-water system, diff. const. temp. depend., photon correlation method 9-9497
- photoelectron spectroscopy, vibrational fine structure 9-17895
- polymer addition, soluble, mechanism to account for turbulence damping effect 9-7242
- pool boiling, effects of high press. and accel. 9-13560
- pool boiling, saturated, crisis mechanism at high heat fluxes 9-13561
- protein adsorbed monolayers permeability, obs. 9-7262
- reactor, high flux, effect of water density on reactivity 9-646
- role in earth's thermal history 9-6041
- sand water suspension, pipeline flow, conc. gradient meas. 9-9563
- shallow channel, motion 9-972
- shock waves, energy calc. 9-3047
- in soil, unsaturated, movement from cylindrical source unsteady flow 9-10381
- sorption on zeolites, Linde-A, enthalpies and entropies 9-9623
- sound field, asymptotic soln. for shallow water 9-19061
- sound velocity meas. at 34°C, theoretical correction of errors 9-8511
- spectra, interpretation 9-9170
- spreading press. of alcohols, rel. to interfacial tension, work of adhesion and solubility 9-9494
- structure in solid hydrates, i.r. spectra 9-1779
- super, structure and props., theory 9-14828
- surface structure, revised model 9-9478
- surface wave instability on air flow over surface 9-17154
- swirling flow through conical pressure nozzles, measurement of rotational velocity 9-18343
- thermodynamic properties, tables 9-3053



**Water** continued

- thermodynamic props. rel. to press., analytical approx. 9-17160  
 total neutron cross section, precision meas. 9-16988  
 turbulent free convection boundary layer formed near hot plate, structure 9-21167  
 ultrasonic absorption 9-153  
 u.s. light diff. spectra, interferometric meas. method 9-10903  
 vapour, atm., width and intensity of the  $A_{H_2O}$   $^{12.67\text{cm}^{-1}}$  line 9-771  
 vapour, electron collision freq. calc. 9-13352  
 vapour, i.r. spectral transmission function 9-17031  
 vapour, laser, monochromatic rad., strongly linearly polarized, 118.6  $\mu$  9-19111  
 vapour, laser relaxation phenom. 9-8612  
 vapour, oxidizing effect on graphite, at high temp. 9-8095  
 vapour, spectr., vibrational rotational line struct. 9-49226  
 vapour, sub mm. laser, with H as buffer 9-20512  
 vapour effect on mech. props. of MgO 9-18506  
 vapour laser, emission lines at 4.77  $\mu$ m, 11.83  $\mu$ m and 11.96  $\mu$ m 9-2869  
 vapour laser, proposed transmission assignments, expt. test 9-8611  
 vapour pressure meas., dielectrically heated psychrometer 9-18389  
 vapour solubility in ZrO<sub>2</sub>, Y<sub>2</sub>O<sub>3</sub> solid soln., 900 and 1000°C 9-17335  
 vapour trapping in vacuum device by Cs injection 9-10585  
 vapour air mixtures, condensation on cool surfaces, conds. for fog formation 9-9591  
 velocity meas. with heated element or skin friction gauges 9-5106  
 vibrational dynamics, and i.r. spectrum of liquid 9-13529  
 viscosity anomaly below 30°C explained 9-992  
 water hydrocarbon liquid interfacial interaction energy rel. to hydrocarbon orientation 9-7260  
 water-methanol system, mass transfer from single bubbles under distillation conditions 9-18329  
 wave patterns on surface of shallow depth 9-18340  
 wave potentials expansion at great distances 9-18341  
 waves due to heaving circular cylinder, surface tension effect 9-21171  
 $\pi$  interac., effective atomic number determ., 30 1332 keV 9-9865  
 $\pi$  beam energy loss spectrum and Bragg curve calc. 9-21223  
 B poisoned, decay of thermal neutrons 9-14644  
 Cd poisoned, decay of thermal neutrons rel. to non 1/v absorber 9-14644  
 D<sub>2</sub>O, Kerr constants temp. dependence, 5-55°C at 365  $\mu$ m and 436  $\mu$ m 9-19632  
 D<sub>2</sub>O circulation loop at MZFR Karlsruhe reactor, fuel pin irradiation facility 9-14656  
 D<sub>2</sub>O, modes of motion from slow neutron inelastic scatt. obs. 9-13500  
 D<sub>2</sub>O, photoelectron spectroscopy, vibrational line 9-17895  
 D<sub>2</sub>O diffusion of H<sub>2</sub>O in, examined by means of x-radiography 9-11367  
 H<sub>2</sub>O KCl-CaCl<sub>2</sub> soln., isopiestic vapour press. meas., osmotic and activity coeffs. 9-21187  
 H<sub>2</sub>O vapour, line shape of rot. transition at 22GHz, dispersion studies, Lorentzian behaviour 9-19432  
 in HF, pulsed electrolysis 9-21715  
 H<sub>2</sub>O, supercooled, homogeneous nucleation temp. 9-7301  
 H<sub>3</sub>O<sup>+</sup> ion in SO<sub>4</sub> solution, vibration spectra 9-2865  
 H<sub>2</sub>O (D<sub>2</sub>O), disproportionation 9-1891  
 mol., mag. susceptibility calc. 9-744  
 Na P zeolite, self diffusion of water 9-5130  
 on Na bentonite amine complexes, vapour adsorpt., rel. to hydrophilic hydrophobic props., obs. 9-5261  
 Na dodecyl sulphate adsorbed monolayers permeability, obs. 9-7262  
 structure of NH<sub>3</sub> solns., X-ray diffraction 9-3078  
 U H<sub>2</sub>O nuclear reactor assembly, fuel loading and critical mass expt. 9-18120  
 vapour laser, pulsed Brewster window, operating between 20 and 120  $\mu$  9-13013  
 with D<sub>2</sub>O, and soln. of paramagnetic ions, proton relaxation time 9-1045

**Wave equations, quantum theory** *see* *Quantum theory/wave equations*

**Wave functions** *see* *Quantum theory/wave equations*

**Wave mechanics** *see* *Quantum theory*

**Wavefront reconstruction imaging** *see* *Diffraction/light; Holography; Optical images*

**Waveguides** *see* *Electromagnetic wave propagation/guided waves*

**Waves**

- See also* *Acoustic waves; Elastic waves; Electromagnetic waves; Liquid waves; Magnetohydrodynamics; Seismic waves; Shock waves*  
 acoustic internal gravity waves 9-7115  
 atmospheric, structure const. rel. refractive index and gradient of refractive index in surface layer 9-8174  
 axisymmetric, in cylindrical shells in sustained axial compressive flow 9-138  
 breaker type classification on 3 lnb. beaches 9-10382  
 capillary gravity waves, weak reson. interaction, variational method 9-21024  
 e. plasma, dispersion and damping 9-17104  
 elastic/visco plastic medium reflection from non deformable plane soln. 9-10622  
 in elastic plastic medium during fatigue 9-136  
 electrodynamics 9-9311  
 electron plasma, dispersion 9-18304  
 fluid, compress. stratified, over channel, long waves 9-21025  
 fluid, two dimensional internal waves in stratified fluid 9-19512  
 fluid layer heated from above, stability 9-11530  
 four wave processes, general weak turbulence theory 9-16664  
 generation, transverse plasma modes, non linear wave wave interaction 9-18306  
 Gerstner, Fourier decomposition and related identities 9-7243  
 harmonic in laminates, continuum theory 9-20428  
 Huygens' principle, validity in curved and empty space times 9-20312  
 induced, in solid by aerial shock wave, diffraction, polariscopic investigation 9-19077  
 inelastic medium, three methods of soln. 9-4284  
 in inhomogeneous, anisotropic media, dispersion relation and energy transfer 9-18305  
 ion acoustic, excitation in non isothermal plasma under skin effect conditions 9-5033  
 Lee, in stratified flow with semicircular obstacle 9-17080  
 longitudinal transverse radial cylindrical, propagation in nonhomogeneous elastic/visco plastic medium 9-4225  
 MHD, shallow liquid, propagation of surfaces 9-14751  
 model, using elastic bands, for demonstrating propag. effects 9-12837  
 modulated, in nonlinear dispersive media 9-49

**Waves** continued

- negative energy, associated with a loss-cone velocity distribution 9-2938  
 non linear equat., vibr. membrane anal. 9-6375  
 nonuniform medium, short-wave asymptotics of Green's function 9-8378  
 plastic, combined longit. and torsional, speeds of elastic-plastic boundaries 9-19059  
 plastic, in metals, u.s. probing 9-11923  
 plastic, torsional, through stressed anal. velocity expt. determ. 9-16724  
 proper, damping in plate with rough walls 9-50  
 Rossby, weak westerly wind waveguides, vertical propagations 9-18798  
 scalar, diffraction by circular diaphragm 9-51  
 scalar, scatt. by a convex transparent object with surface irregularities 9-52  
 scattering, low-freq., thro' aperture in soft screen, expansion, study of formulae 9-20311  
 scattering., multiple, in irregular media, spatial autocorrel. functions 9-20313  
 scattering by system of fluctuating potentials 9-8376  
 short, refl. coeff. calc. for variable medium 9-8377  
 surface, conducting fluids, microwave resonator theory 9-2941  
 surface wave propag., high freq., theory and eqns. 9-18988  
 systems with travelling waves, amplification of non-stationary discontinuity waves 9-6368  
 transverse, in an elastic medium due to surface forces, use of Heaviside function 9-8505  
 transverse, longitudinal, on transmission lines, more than one dimension, text book 9-10716  
 viscoelastic bar with realistic props. 9-19039  
 wave and particle experiments for students 9-4211  
 surface, on Hg liquid microwave resonator, obs. Navier Stokes eqn. 9-2942

**Waxes**

- cratering, high-speed in wax and plasticine 9-20410  
 paraffin, moderation of neutrons, spectra obs. 9-18574

**Weak interactions** *see* *Elementary particles/interactions, weak; Field theory, quantum/interactions, weak*

**Wear**

- abrasive, mechanism 9-18528  
 cylinder, viscoelastic hollow in elastic casing, inner surface ablation, axial plane strain 9-17320  
 metal hydroerosion, effect of surface-active agents 9-9775  
 metals, role of oxygen in eff. of additive surface-active substances 9-18529  
 plastic, crystalline, resistance tests 9-11947  
 polytetrafluorethylene, and friction 9-5488  
 surface, flow, eff. of particles on solid boundaries 9-18508  
 $\alpha$  Al<sub>2</sub>O<sub>3</sub>, abrasion resistance rel. to ZrO 9-3457  
 Be-Co alloy, rel. crystal structure and atomic ordering 9-19814  
 C, pyrolytic, rubbed, rel. to surface orientations 9-11758  
 Fe-Co alloy, rel. crystal structure and atomic ordering 9-19814  
 ZrO abrasion resistance rel. to  $\alpha$  Al<sub>2</sub>O<sub>3</sub> 9-3457

**Weather** *see* *Meteorology*

**Weighing** *see* *Balances; Mechanical measurement*

**Weissenberg cameras** *see* *Cameras; X-ray crystallography/apparatus*

**Welding** *see* *Forming processes*

**Wentzel-Kramers-Brillouin method** *see* *Quantum theory*

**Wertheim effect** *see* *Magnetomechanical effects*

**Wetting**

*See also* *Capillarity*

- cermets, high temp., of ceramic by refractory metal 9-18535  
 contact angle and spreading on solids and liquids, adsorpt. model 9-7259  
 diamond with chemisorbed H, F, Cl, Br and O, heat of wetting obs. 9-8083  
 glass metal oxide-metal system, rel. to atom movements and adhesion 9-7599  
 graphite, by BaF<sub>2</sub>-CaF<sub>2</sub> eutectic 9-7326  
 of plate of circular orifice through which droplets are formed, effect on system parameters 9-18344  
 sapphire, by liq. Al, effect of nature of surfaces 9-19622  
 Al<sub>2</sub>O<sub>3</sub>, adhesion to metals and alloys, rel. to wettability 9-1336  
 Fe-Mo alloys, with molten Ag 9-13508  
 Fe-W alloys, with molten Ag 9-13508  
 oxides, promotion by addition of Ti to brazes 9-3180

**Whiskers** *see* *Crystals/whiskers*

**Whistlers** *see* *Atmospheres; Ionosphere*

**White dwarfs** *see* *Stars*

**Wiedemann effect** *see* *Magnetomechanical effects; Magnetostriction*

**Wiedemann-Franz law** *see* *Conductivity, electrical/solids; Conductivity, thermal/solids*

**Wien effect** *see* *Conductivity, electrical/liquids, electrolytic*

**Wigner coefficients** *see* *Quantum theory*

**Wigner effect** *see* *Physical effects of radiations*

**Wilson cloud chambers** *see* *Cloud chambers*

**Wind**

- air earth current measurements 9-10387  
 anemometer, sonic, vertical component sensor 9-15246  
 in atmosphere below macroscale, power spectrum 9-18799  
 atmospheric circulation in meteor zone 9-12599  
 atmospheric motion, 70 to 100 km, in S. hemisphere, drift meas. of seasonal variations 9-12613  
 easterly surface winds, eff. of earth's rot. and surface movements 9-21768  
 effect on sonic boom strength and propag. 9-10397  
 fall reversal, power and middle stratosphere, northern hemisphere 9-15244  
 high alt. meas. from rocket exhaust noise 9-4054  
 hurricanes, effect on sea surface temp. 9-6064  
 interlevel, velocity prediction by linear regression of statistical data 9-17565  
 ionospheric, r.m.s. velocity and shear, 90 to 150 km, stat. anal. procedure 9-12617  
 ionospheric, statistics of time shifts in meas. 9-1966  
 ionospheric north-south neutral wind causing ionization day and night reversal 9-18815  
 ionospheric profiles, dynamic model 9-4078  
 in lower ionosphere, solar cycle dependence 9-10430

**Wind continued**

- neutral, profiles in E-region, expt. comparison with radio drift meas. 9-15255
- neutral atmosphere and plasma movement in ionosphere 9-12611
- in polar belt, eff. of earth's rot. and surface movements 9-21768
- profiles above Sardinia, results from ESRO skylark launches (Sep. and Oct. 1965) 9-12576
- siren signals in town and country obs. wind effects 9-15460
- speed fluctuations, macroscale, power spectra, mean turbulent kinetic energy 9-21762
- tangential stress on sea surface 9-12578
- thermospheric, obs. during geomagnetic storm 9-4053
- velocity meas. hot-wire anemometer 9-18791
- velocity var. with height in turbulent elec. conducting atmosphere 9-21766
- weak westerly waveguides, Rossby waves, vertical propagation 9-18798
- westerly zonal, eff. of earth's rot. and surface movement 9-21768
- wind-wave interact., wind profile surveys, drift current and water surface obs. 9-21169
- zonal, quasi-biennial oscillation theory 9-21767

**WKB method** *see* Quantum theory**Wolfram** *see* Tungsten**Wood**

- fibres, microrheometer for meas. tensile stress 9-5472
- orthotropic plate, meas. of two principal residual stresses 9-5445
- piezoelectric modulus, temp. dispersion 9-15127

**Work function**

- See also Electron emission*
- cathode, effect of Ba adsorpt. 9-3752
- metallic surface, polycrystalline, distribution function 9-19937
- transition metals, rel. to electronic structure 9-10078
- Ag catalyst,  $\gamma$ -irrad. effect, oxygen or ethylene atm., 20 and 120°C 9-12219
- Au on Ba, double film on Nb, contact potential difference 9-1093
- EuSe, and cathodoluminescence 9-5970
- Ge surface states, slow relaxation phenomena 9-18627
- NH<sub>3</sub> adsorption and decomposition on W(211) surface, work function change 9-19679
- Na atoms adsorbed on W crystal, meas. by field-emission electron projector 9-1112
- Ni faces, (111), (100) and (110) faces 9-1625
- Sc film on (110) face of W, rel. to absorption props. 9-1115
- TaB<sub>3</sub> cathodes 9-5778
- ThC cathode, calc. 9-3754
- ThC thermionic cathode, calc. 9-3754
- U monolayer films on (100), (110) and (113) oriented faces of W, meas. by photoelec. and contact potential diff. meas. 9-14901
- W-O surface, metastable Ar, Xe, N<sub>2</sub>, H<sub>2</sub> impact, effect on secondary e emission and ionization 9-11409
- W, (100) face, eff. of adsorbed Ba 9-19680
- W, rel. to O adsorption and desorption 9-11786
- W, with Ba adsorbed on oriented surfaces 9-9627
- W surface, metastable Ar, Xe, N<sub>2</sub>, H<sub>2</sub> impact, effect on secondary e emission and ionization 9-11409

**Work hardening**

- See also Cold working; Surface structure*
- b.c.c. metals, flow stress, inherent lattice or solution hardening 9-3429
- b.c.c. metals, flow stress, inherent lattice or solution hardening 9-3430
- dislocation groups mobility, effect on theory 9-11876
- dissociative solid solns., interface hardening and softening 9-3477
- elastic solid, stress-strain relations 9-18497
- generalization for nonlinear stress/strain law 9-20408
- intersection jogs role, in L1<sub>2</sub> structure 9-16094
- Kuhlmann-Wilsdorf theory of analysis from stored energy data, comments on new formulation 9-9781
- metal, f.c.c., crystals, Kuhlmann-Wilsdorf theory of analysis, new formulation 9-9780
- metal, f.c.c. crystals, Kuhlmann-Wilsdorf theory of analysis, comments on new formulation 9-9781
- solid solution hardening theory, shear modulus parameter 9-3470
- steel, 60Kh3G8N8V, hot working effects on stress-corrosion cracking susceptibility 9-3449
- steel, V, on tempering, high dislocation density as preferential nucleation sites 9-17328
- steel, zero change in length 9-9778
- superconductivity composite conductors strengthening for large magnet construction 9-19904
- superlattices, mechanism 9-13758
- transient phenom. in crystals with edge dislocation diode clusters 9-1322
- Ag-(10 wt.%) Mn-(1.5 wt.%) Sb alloy, effect on decomposition of solid solution 9-1326
- Al-Zn alloys Guinier-Preston zone miscibility gap obs. in precipitation reversion studies 9-21393
- Cu-Ga single crystal, curve, transition from stage I to stage II, X-ray investig. 9-13760
- Cu<sub>3</sub>Au, mechanism rel. to superlattice structures 9-13758
- Fe, n-irrad. and plastic prestraining characts. 9-3468
- Ni-Fe-based alloys, deformational hardening coeff. change on isothermal ordering 9-9741
- Ni<sub>3</sub>Fe mechanism rel. to superlattice structures 9-13758
- V steel, secondary hardening on tempering, high dislocation density as preferential nucleation sites 9-17328

**X and gamma-ray astronomy**

- 3c273 X-ray luminosity obs. 9-12744
- $\gamma$  lines from young supernova remnants due to radioactive decay of Ni<sup>64</sup> 9-16579
- CEN X-R-2, Apr. 1967 obs. 9-12743
- Cen XR-2, high energy X-rays, spectrum and intensity 9-18895
- Cen XR-2, high temp. component, rel. to nova-like model 9-20212
- cosmic X-ray flux, 50-290 keV, upper atm. obs. 9-6717
- Crab nebula,  $\gamma$  search by digitized spark chamber 9-8232
- crab nebula  $\gamma$  detection by digitized spark chamber 9-8232
- Crab nebular and SCO X-1 soft X-ray spectra 9-21918
- Cygnus  $\gamma$  source, evidence 9-8272
- Cygnus X-2, origin of broad, wingless H $\gamma$  absorption line profile 9-14232
- galactic X-ray sources in hydromag. waves 9-20213
- Lupus XR-1 spectral power law, invariance with time 9-18930
- M87 X-ray luminosity obs. 9-12744
- quasars, flux calculation 9-4108

**X and gamma-ray astronomy continued**

- radiogalaxies, flux calculation 9-4108
- SCO XR 1, Apr. 1967 obs. 9-12743
- SCO XR 1, photoelec. spectrum scans and i.r. photometric obs. 9-18893
- solar deka keV X-ray burst, theory 9-21961
- in solar flares, generation of X-ray and synchrotron emission from electrons 9-21975
- solar X-rays refl. in atm., Apr. 1967 obs. 9-12743
- spark-chamber  $\gamma$  telescope 9-20253
- spectra of GX3+1, GX354-5 and Sco XR-1 X-ray sources 9-18894
- X-ray sources sco X-1 and cyg X-2 9-8271
- x-ray spectra analysis, programme 9-8270

**X-ray absorption**

- See also X-ray spectra/absorption*
- coherence in the diffraction of a three-dimensional lattice 9-3254
- concrete, 6MV primary radiation 9-7681
- K-shell by various metals, meas. method 9-18172
- steel, 6MV primary radiation 9-7681
- tourmaline, pyroelectric detection 9-18973
- Pb, 6MV primary radiation 9-7681

**X-ray analysis** *see* Chemical analysis/X-ray; Crystal structure, atomic; X-ray crystallography**X-ray astronomy** *see* X and gamma-ray astronomy**X-ray characteristic temperature** *see* Specific heat**X-ray crystallography**

- For results of structure analysis see Crystal structure, atomic*
- b.c.c. metals, coherent scatt. regions in presence of packing defects on {110} plane 9-13677
- Bragg angle H $^{\circ}$ (460) of NaCl crystal dependence on temp. for Cu K $\alpha$ 1, radiation thermometer 9-1169
- Bragg intensity correction for thermal diffuse scatt. 9-19702
- coherence in the diffraction of a three-dimensional lattice 9-3254
- diffraction powder patterns, standard 9-11809
- diffraction topography, method using monochromatic divergent beams made by curved crystal. 9-5300
- dislocation-containing crystals, diffraction, method of moments, applic. to theory 9-13618
- dispersion curves of NaF crystal by diffuse X-rays scatt. 9-1731
- goniometer, single-crystal, high-temp. furnace attachment 9-5298
- introductory article for students from scientific American 9-16653
- lattice consts. determ. from single cryst. X-ray photographs 9-5299
- microsecond exposures suitable for study of shock wave compression 9-11815
- powder patterns from hexagonal crystals, temp. diffuse scatt. 9-11814
- powder specimens, flat absorpt. factor error due to incident beam divergence 9-3258
- solid solutions with short range order and size effect, kinematical diffraction theory 9-3251
- wave fields diffracted by slit inside perfect crystal 9-7379
- Al, Debye temp. from n. scatt. obs. 9-7639
- Ge, X-ray anomalous transmission, integrated characts. 9-3889
- He, b.c.c. and h.c.p., Debye-Waller factor with short range correlations 9-5212
- KCl, anomalous transmission, dislocation density effects 9-1746
- Nb, Debye temp. from n. scatt. obs. 9-7639
- Pb, Debye temp. from n. scatt. obs. 9-7639
- Si Bragg condition, depend. of extinction distance on deviation 9-13649
- Si discs research, using X-ray topography 9-1196

**apparatus**

- See also X-ray monochromators; X-ray spectrometers*
- camera, back-refl. focusing, diff. line width geometry 9-1167
- camera, back-refl. focusing for polycryst. meas. 9-3257
- camera, low temp. 9-7388
- camera, powder diffraction, modified allowing short exposure time 9-16067
- camera for liquid crystal investigations 9-13512
- Debye-Scherrer high temp. camera 9-3260
- diffraction camera for three-dimens. data fast recording 9-1166
- goniometer, double crystal 9-1170
- goniometer, optical, for Lane orientation 9-3261
- goniometer for cylindrical specimens partial pole figure determ. 9-11816
- goniometer sample mount, orientation and machining 9-11817
- lattice strains, thermal expansion, piezoelectric const. determ. by strain-meter 9-3262
- small-angle scatt. meas. at low temp. 9-3259
- spectrometer, spectral 'window', effective size determ. 9-5297
- Weissenberg goniometer modification for comparison of lattice consts. 9-13619

**calculation apparatus**

- computer program for correction to Bragg intensity due to thermal diffuse scatt. 9-19702

**calculation methods**

- atom form factor determ. from vanishing second order reflection in high voltage electron diff. 9-9676
- Debye-Scherrer rings, radial freq. distrib. of interference spots 9-3252
- diffraction, spatially-inhomogeneous dynamic problem, generalized two-wave approx. 9-7389
- diffraction line profile anal., deformed polycrystalline material, computer program 9-18438
- diffraction profile centroid computation, simplified method 9-7399
- diffractionometer - collected data, least squares weighting schemes, effect of random setting errors 9-13621
- distorted crystals, Pendellosung fringes, computer calc. 9-9664
- electron density maps, thermal parameters effects 9-3249
- electron density maps from line profile analysis 9-3253
- Fourier transform, of time-independent Patterson function in reln. between X-ray scatt. and Mossbauer effect 9-7385
- Fourier-transformation of minimum function in determ. crystal structures 9-11831
- interference linewidth, approximation with standard sample 9-9656
- Karle-Hauptmann tangent formula for phase refinement, protein-model test 9-13667
- molecule, planar or partly planar, orientation in crystal plane, determ. 9-9654
- moments of lines, applied to fine structure determ. 9-18439
- Patterson function, 3-dimens., integral charact., analyt. representation 9-1177
- planar molecules in cry. structure, modified 2-dimens. data construction 9-18440



**X-ray crystallography continued****calculation methods continued**

- powder diagram indexing, computer-based 9-1176  
 powder pattern indexing for orthorhombic polycrystalline mats. 9-11813  
 powder photograph indexing and cell dimens. refinement computer programme 9-5311  
 power pattern indexing, triclinic case, theory 9-3250  
 stereo plotting of 3 dimens. c. density 9-13622  
 Takagi's dynamical theory, appl. to moiré fringe contrast on topographs of Si 9-3354  
 Takagi's dynamical theory appl. to stacking-fault topography fringe contrast 9-3353  
 temperature parameters, systematic errors from bonding effects 9-3274  
 thermal diffuse scatt. corrections in measured integrated intensities from cubic single crystals 9-18543  
 Zachariasen's extinction correction appl. to visually estimated intensity data 9-7398

**structures** *see Crystal structure, atomic***technique**

- anomalous scatt. by centrosymmetric structures 9-11825  
 Bond, for lattice parameter determ., specimen and beam tilt errors 9-7384  
 centrosymmetric structure analysis using anomalous scatt. 9-11825  
 diffracting plane shapes from Laue technique 9-9659  
 diffraction, photographic, meas. accuracy 9-19694  
 diffractometric powder analysis of plate-like particles, correction for preferred orientation 9-11812  
 diffractometry, intensity meas. reproducibility 9-7383  
 dislocations, axial screw, detection in whiskers using  $K_{\alpha}$  X-radiation 9-14944  
 double-crystal topography, Si reference crystals 9-7387  
 lattice parameter relative meas., new double crystal arrangement technique 9-21305  
 powder diffractometry, line broadening in particle size determ. 9-3303  
 structure factor meas., optimum strategy 9-7386

**X-ray diffraction**

- See also X-ray crystallography; X-ray scattering*  
 apparatus, patent 9-10581  
 Borrmann effect, ordering effects 9-3255  
 camera for three-dimens. crystallographic recording 9-1166  
 counter meas., review 9-2593  
 by crystal, distorted, scattering amplitude for a wave packet of finite size 9-3256  
 Debye-Scherrer rings, radial freq. distrib. of interference spots 9-3252  
 diffractometer, monochromator for use with 9-8335  
 diffractometer for studying rheo-optical behaviour of polymeric crystals 9-7536  
 dioxynolionucleic acid, (DNA), X-ray diffraction study 9-7093  
 dislocation-containing crystals, method of moments, applic. to theory 9-13618  
 elastic strain, tensile loading device 9-11918  
 epitaxial layer structure determ. 9-3198  
 glass grating, reflection efficiencies in soft region, Rayleigh Fano theory 9-10901  
 grating for electron probe microanalysis 9-9661  
 grating reflectivity in ultrasound region 9-6549  
 gratings, ruling methods, props. and appls. 9-6548  
 image intensifier system 9-3263  
 impurities, trace, effect of 9-7475  
 intensity meas. reproducibility 9-7383  
 by lattice, three-dimensional, account taken of the coherence of X-rays 9-3254  
 Laue camera, for vacuum at high temp. 9-8336  
 Laue-case profile, variation with thickness from a thin Si crystal 9-5328  
 line profile anal., deformed polycrystalline material computer program 9-18438  
 microsecond exposures suitable for study of shock wave compression 9-11815  
 for microstrain obs. 9-3410  
 monochromatic patterns on polaroid film, fluorescent screens 9-3264  
 optical and X-ray effects demonstration by laser source 9-15405  
 petroleum cokes, 'doublet' (00l) peaks, rel. to vol. expansion and closed pore vol. 9-7457  
 photographic, meas. accuracy 9-19694  
 polycrystal, lattice parameter determ. over unsolved double lines 9-9655  
 polycrystal, linewidth formation geometry 9-9657  
 powder analysis of platelike particles, correction for preferred orientation 9-11812  
 powder patterns, standard 9-11809  
 profile centroid computation, simplified method 9-7399  
 radiation hazards from equipment, dose rates, precautions 9-16633  
 refractive index meas. rel. to anomalous dispersion meas. 9-1729  
 review 9-3248  
 shapes of diffracting planes by Laue technique 9-9659  
 solid solutions with short range order and size effect, kinematical theory 9-3251  
 spatially-inhomogeneous dynamic problem, generalized two-wave approx. 9-7389  
 topography, method using monochromatic divergent beams made by curved cryst. 9-5300  
 wave fields diffracted by slit inside perfect crystal 9-7379  
 $\text{Fe}_3(\text{CO})_{11}\text{P}(\text{C}_6\text{H}_5)_3$  crystal structure determ. 9-21314  
 Ge wafers, topography for analysis of crystal faults and stresses 9-9677  
 Mn  $K_{\alpha}$  from  $^{57}\text{Fe}$  source, lab. Debye-Scherrer camera 9-3265  
 Si, thin crystal, Laue-case profile, variation with thickness 9-5328  
 Si with  $\text{SiO}_2$  surface dynamical diff. effects rel. to induced strain, obs. 9-9612

**X-ray diffractometers** *see X-ray crystallography/apparatus***X-ray examination of materials**

- See also Chemical analysis/X-ray; Radiography*  
 b.c.c. metals, coherent scatt. regions in presence of packing defects on {110} plane 9-13677  
 binary  $\sigma$  phases, n. radiation damage 9-11868  
 carbon black, electron momentum density determ. 9-18581  
 carbons, non-graphitizing, composite profiles rel. to characts. 9-9672  
 cementite particles from growth in tempered iron martensite 9-19714  
 cements, composition and hydration 9-14123  
 concrete, 6MV primary radiation absorpt. 9-7681  
 corundum ceramics, surface damage on cutting and grinding 9-13574  
 diamond, electron momentum density determ. 9-18581

**X-ray examination of materials continued**

- diffraction topography, method using monochromatic divergent beams made by curved cryst. 9-5300  
 diffusion in solids, radiographic surface analysis 9-14953  
 N, N-diphenylacetamide, crystal structure 9-7461  
 dislocations, partial twinning, on topographs, obs. of sources and reactions 9-7484  
 elastomeric body, X-ray apparatus for internal stresses meas., patent 9-21364  
 film used in radiographic camera (industrial), detail visibility 9-4546  
 graphite, electron momentum density determ. 9-18581  
 graphite, n-irrad., diffuse diffracted intensity obs. 9-7404  
 hexaphenylbenzene modification, crystal structure 9-7462  
 ice III, structure 9-7441  
 impurities, trace, rel. diffraction 9-7475  
 Lang topographs of crystals, strained by thin films, contrast asymmetries 9-5292  
 metals, structural defects and diffusion, autoradiographic obs. 9-9707  
 DL-2-methyl-7-oxododecanoic acid, crystal structure 9-19735  
 modulated structures, obs. of satellites 9-5301  
 Monazite, following heat-treatment 9-3280  
 ophiobolin methoxybromide, crystal structure 9-7466  
 perovskites, high-pressure synthesized, structure 9-18452  
 porous, from scatt. curves 9-1168  
 ruby, investigation of lattice defects 9-9694  
 semiconductor radiography as quality control technique 9-5716  
 semiconductors, Kikuchi line anomalies rel. to structural defects 9-18445  
 shadow microscope, visual image 9-6244  
 stacking fault probability meas. in determining energies 9-13694  
 steel, 6MV primary radiation absorpt. 9-7681  
 steel, Cr-Mn-N, austenitic, X-ray meas. of stacking faults 9-18476  
 steel, rolled, austenite retention determ. from diffracted intensities corrected for texture effects 9-1317  
 steel, stainless, corrosion pit nucleation, effect of sulphide inclusion 9-21700  
 steel with cracks of 'flocule' type, fracture surfaces 9-5483  
 terpenoid,  $\text{C}_{25}$ , ophiobolin methoxybromide, crystal structure 9-7466  
 thiourea nitrate, crystal structure 9-7454  
 triglycine sulphate, topography of 180° domains 9-16301  
 twinned stacking faults, deformational 9-1229  
 ZnO, zincite, Fe entry during hydrothermal growth, distrib. and effect on morphology 9-18419  
 Ag-Pd alloys, faulting in severely cold-worked filings 9-7493  
 Ag-Sb alloys, hexagonal ( $\beta$ -phase), stacking-fault densities, diffraction exam. 9-1230  
 Ag thermal expansion meas. with a convection heated furnace 9-13803  
 Al-Fe binary system, electronic structure 9-3553  
 Al, Lang topography of dislocation densities and configurat. rel. to stress 9-21338  
 Al, liquid, ordered structural region size 9-17187  
 Aln, mean square vibration displacements and at. scatt. factors, 85-670°K 9-11993  
 Au sol., particle-diameter distrib. determ. 9-14873  
 AuMn, phase transform.,  $\beta$ -martensitic f.c.c., caused by cold work and subsequent heating 9-3486  
 BaTiO<sub>3</sub> whiskers, axial screw dislocation detection using  $K_{\alpha}$  X-radiation 9-14944  
 Be, Lane patterns, rel. to compressive deform. investig. 9-11926  
 BeO crystal, inversion twin boundaries from diff. contrast 9-3356  
 Bi perovskites, high-pressure synthesized, structure 9-18452  
 C, heat treated under press. with Cu cpds, composite (002) profiles 9-10595  
 C fibres of carbonized cellulose, preferred orientation 9-7359  
 $\text{CaSO}_4 \cdot 2\text{H}_2\text{O}$ , dispersed porous mat., microstresses on pressing giving plastic deform. 9-1276  
 CdTe, mean square displacements for sub-lattices 9-19711  
 Cr, interference, 293-1100°K 9-21312  
 Cu-Al alloys, annealed, near-order parameters, conc. dependence 9-3479  
 Cu-Ga single crystal, work hardening curve, transition from stage I to stage II 9-13760  
 Cu-Ni alloys, lattice constant temp. dependence over conc. range 9-19955  
 Cu-Si alloy, stacking fault probability meas. in energy determ. 9-11887  
 Cu thermal expansion meas. with a convection heated furnace 9-13803  
 Fe (16wt.%Cr) crystal, corrosion pit nucleation, e. microprobe exam. 9-21697  
 Fe-Ni, hysteresis loops, constant-field, texture effects 9-5825  
 Fe-Ni alloys, diff. study of grain size variation 9-13577  
 Fe particles, thermal expansion and structure anomalies 9-5199  
 Fe(CO)<sub>5</sub> powder, surface roughness and porosity effects on integrated intensities 9-11845  
 GaAs, Kikuchi line anomalies rel. to structural defects 9-18445  
 GaAs<sub>1-x</sub>P<sub>x</sub> epitaxial layers on GaAs, compositional inhomogeneities 9-14895  
 GaAs substrate crystals for epitaxial growth expts., annealing effects, 800°-1200°C 9-11950  
 Gd<sub>2</sub>(MoO<sub>4</sub>)<sub>3</sub> ceramic and single-crystal, structural analyses 9-18446  
 Ge, anomalous transmission, integrated characts. 9-3889  
 Ge, heavily doped, lattice periodicity meas. 9-5320  
 Ge, n-irrad., induced defects, by small-angle scatt. 9-5331  
 H<sub>2</sub>O<sub>2</sub>, space group determ. rel. to double reflexion effect errors 9-11846  
 (HgCd)Te solid solns., mean square displacements for sub-lattices 9-19711  
 $\gamma$ -Hg<sub>2</sub>Se<sub>2</sub>Cl<sub>2</sub>, crystal structure 9-11847  
 HgTe, lattice parameter, bond weakening and lattice vibrations 9-9678  
 HgTe, mean square displacements for sub-lattices 9-19711  
 In, liquid, ordered structural region size 9-17187  
 InSb, defect structure from topography 9-1208  
 KBr-TlBr solid solutions, lattice parameter composition dependence 9-13637  
 KCl, anomalous transmission, dislocation density effects 9-1746  
 KCl, thermal lattice vibrations 9-21425  
 LaAlO<sub>3</sub>, phase transitions and lattice vibrations 9-3504  
 Li<sub>2</sub>O-SiO<sub>2</sub> glasses, rel. to crystallization phases 9-1080  
 LiF, cold-worked, crystallite size and microstrains, evaluation from diff. line profiles 9-13640  
 Mg<sub>2</sub>Cd type alloys, ordering rel. to anomalous change in resistance 9-3570  
 Mg(OH)<sub>2</sub>, dispersed porous mat., microstresses on pressing giving reversible elastic deform. 9-1276

**X-ray examination of materials continued**

- MoZn<sub>22</sub>, crystal structure 9-19719  
 NH<sub>4</sub>Br and ND<sub>4</sub>Br, modifications III and IV, -56° to -192°C 9-16153  
 Na<sub>2</sub>ZrO<sub>3</sub>, crystallographic data 9-19721  
 NaCl, thermal lattice vibrations 9-21425  
 NaNbO<sub>3</sub>/KNbO<sub>3</sub> system, phase compositions and boundaries 9-7621  
 Nb-Ti(V/Zr) alloys, deform. effects, studies 9-11930  
 Ni-Cr alloys, thermal expansion up to 900°C 9-21438  
 Ni-(14.9wt.%)P alloy, electrodeposited, amorphous structure 9-19839  
 Ni alloys, structural defects and Ni self-diffusion, autoradiographic obs. 9-9707  
 Ni powder, particle size from powder diff. line broadening 9-3303  
 Pb-Ni alloys, radiation-induced precipitation, small-angle scatt. meas. 9-9805  
 Pb-Sn alloys, liquid, ordered structural region size 9-17187  
 Pb, 6MV primary radiation absorpt. 9-7681  
 Pb, liquid, ordered structural region size 9-17187  
 Pb perovskites, high-pressure synthesized, structure 9-18452  
 Pt catalyst, alumina-supported, ave. crystallite size and crystalline content 9-17271  
 Pt catalyst, Warren-Averbach tech. for characterization 9-5326  
 PuNi<sub>2</sub>-type cpds, unit cell constants 9-7451  
 Rh complex, RhCl(C<sub>2</sub>H<sub>4</sub>)<sub>2</sub> crystal and mol. structure 9-13647  
 Rh thermal expansion and lattice parameter determ., 28-587°C 9-16182  
 Ru, deformed, domain size distrib. from line profiles 9-7447  
 Ru complex, nongeminalaminoruthenium (II) dichloride and related salts, crystal structure 9-7448  
 Si:P diodes, laser-irrad.-produced, structural characts. 9-18638  
 Si, heavily doped, lattice periodicity meas. 9-5320  
 Si, Kikuchi line anomalies rel. to structural defects 9-18445  
 Si, stress patterns on micrographs, analytical description 9-11873  
 SiO<sub>2</sub>, epitaxial films on Si, elastic anisotropy of edges from contrast fields on topographs 9-1107  
 SiO<sub>2</sub> suspensions, particle-diameter distrib. determ. 9-14873  
 Sn-Ni alloys, electrodeposited, structure, composition and thermal stability rel. to acid bath conditions 9-14926  
 Sn, liquid, ordered structural region size 9-17187  
 Te films, orientation 9-14894  
 Ti alloys, structural defects and Ni self-diffusion, autoradiographic obs. 9-9707  
 UCo<sub>2</sub> and other PuNi<sub>2</sub>-type cpds, unit-cell constants 9-7451  
 UO<sub>2</sub>-UCl<sub>4</sub>-KCl, X-ray examination 9-16986  
 UO<sub>2</sub>, crystallographic changes at para-antiferromag. transition 9-7890  
 W, compressed lightly, strain inhomogeneities using back-reflection divergent beam method 9-1277  
 Zn, chemically attacked, Berg-Barrett obs. of dislocations 9-19749  
 Zn thermal expansion meas. with a convection heated furnace 9-13803  
 ZnS crystals from melt under 50 atm. pressure, structure 9-5329  
 ZnSb-constantan semiconductor thermoelements, diffusion phenomena and phase transitions, microprobe analysis 9-10062

**liquids**

- benzene, X-ray structural anal. 9-5142  
 diffraction studies of simple liquids 9-11676  
 Ross filter balancing, expl. testing method 9-15986  
 sodium humate solns., small-angle scatt. analysis 9-9480  
 H<sub>2</sub>O-NH<sub>3</sub> solns. 9-3078  
 Hg, Hg-Cd, Hg-Pb dil. alloys, X-ray diff. 9-7251  
 Th(ClO<sub>4</sub>)<sub>3</sub>, diffraction study Th co-ord. no. determ. 9-11683  
 Th(HClO<sub>4</sub>)<sub>3</sub>, diffraction study, Th co-ord. no. determ. 9-11683

**microstructures**

- See also Crystal structure/microstructure*  
 $\alpha$ -brass, fibre texture, comparison with n diff. method 9-5490  
 carbons, influence of prep. and standards on results of Warren-Averbach anal. 9-7426  
 graphites, influence of prep. and standards on results of Warren-Averbach anal. 9-7426  
 metals, axial textures, diff. method 9-3289  
 microcamera for phase anal. of microsegregations 9-22025  
 Al-Cu solid solns., supersaturated, substructure changes during decomposition 9-1339  
 Al wire, axial textures, diff. method 9-3289  
 Au-Cu alloy on Au, two-layer films, polycrystalline substructure from Moiré patterns 9-3200  
 C, non-graphitizing, (002) refl. peaks rel. to interlayer spacing and crystallite size 9-5315  
 Cu, cold-rolled, three-dimens. orientation distrib. function of crystallites 9-11841  
 Cu, fibre texture, comparison with n diff. method 9-5490  
 Cu wire, axial textures, diff. method 9-3289  
 Fe 28 wt.% Ni-0.04 wt.% C alloy, martensite grain substructure (fragmented structure) 9-1187  
 K<sub>2</sub>UCl<sub>6</sub>-NaCl eutectic diagram confirmed 9-11969  
 K[Al(Cu)<sub>2</sub>]<sub>2</sub>H<sub>2</sub>O, solid soln., crystal structure by X-ray diff. 9-13636  
 Ni-Cu alloys, interstitial H occlusion 9-12728  
 Ni evap. films on glass, texture investigation 9-7336  
 Ni wire, axial textures, diff. method 9-3289  
 SiC epitaxial layers, topography 9-3202  
 UCl<sub>4</sub>-KCl NaCl eutectic diagram predicted on confirmed by diffraction 9-11969  
 UCl<sub>4</sub>-NaCl eutectic diagram confirmed 9-11969

**molecular structure**

- chain segment shape investigations 9-17064

**X-ray fluorescence** *see Luminescence; X-ray spectra/emission***X-ray measurement**

- See also Dosimetry*  
 6 MV primary radiation, abs. in Pb, steel and concrete 9-7681  
 'Angstrom ruler', use of interferometer 9-10608  
 cavity ionization chamber, beam energy obs. 9-7691  
 correlation factor, accuracy improvement 9-22024  
 counter, proportional, background reduction by pulse shape discrimination 9-19229  
 dosimeter, FD-P8-3 glass, response, 23-40 keV 9-8939  
 ionization chamber meas. for 10-30 kV 9-2105  
 ionization chamber monitor 9-18971  
 tourmaline absorpt., from pyroelectric props. 9-18973  
 x-ray generator, diagnostic meas. of peak voltage 9-4143  
 Si barrier layer detectors for 10 to 30 kV meas., characts. 9-13172

**X-ray microscopes** *see Microscopes***X-ray monochromators**

- crystal for use with X-ray diffractometers 9-8335

**X-ray photoeffect** *see Electron emission/photoelectric***X-ray reflection**

- atmosphere, of solar X-rays, Apr. 1967 obs. 9-12743  
 camera, back-refl. focusing for polycrystals meas. 9-3257  
 by diamonds, intensity differences 9-18443  
 glass mirrors, spectra distribution in proper absorption region 9-21637  
 by multilayer absorbing system 9-10772  
 scatter from refl. surfaces, obs. 9-16394  
 C, non-graphitizing, (002) characts. 2400 3000°C 9-5315

**X-ray scattering**

- See also Compton effect; X-ray diffraction*  
 benzene, liq., scatt. anal. 9-5142  
 carbon black, Compton profile in e. momentum density meas. 9-18581  
 by crystal, distorted, scattering amplitude for a wave packet of finite size 9-3256  
 crystal structural analysis, anomalous scatt. by centrosymmetric structures 9-11825  
 cylindrical symmetry samples, determ. of Porod's invariant using a diaphragm 9-14912  
 diamond, Compton profile in e. momentum density meas. 9-18581  
 graphite, Compton profile in e. momentum density meas. 9-18581  
 graphite, plasmon obs. 9-1818  
 heterogeneity size distribution in solids 9-18432  
 interference fringes by an incident plane wave, Si single crystal, wedge-shaped 9-3307  
 interference intensities, effect of pressure 9-5294  
 lattices, two-dimens., effect of preferred orientation on intensity distrib. of (hk) interferences 9-7360  
 modulated structures, obs. of satellites 9-5301  
 mosaic blocks inferior, low angle, dynamic theory 9-9658  
 Mossbauer effect relationships, from Fourier transform. of time-independent Patterson function 9-7385  
 porous materials, interpretation 9-1168  
 from reflecting surfaces, obs. 9-16394  
 small angle parameters, evaluation by transmission electron microscopy: GP zones 9-13627  
 small-angle, from chain mol., segment shape 9-17064  
 small-angle meas. at low temp. 9-3259  
 temp. stability control  $\pm 0.003^\circ\text{C}$  from 75-200°C 9-2263  
 temperature diffuse, for powder patterns from hexagonal crystals 9-11814  
 Thomson, synchrotron, polarization Stokes params. 9-2276  
 Be, plasmon obs. 9-1818  
 Ge, n-irrad., small-angle scatt. rel. to radiation-induced defects 9-5331  
 Kr, photo-ionization by polarized and unpolarized photons, sub-shell contrib. calc. 9-13455  
 Kr, photoionization, 300-1500 eV subshell cross-sections obs. 9-13454  
 Li, plasmon obs. 9-1818  
 LiF, scatt. factors using approx. model for overlap charge density 9-3298  
 NaCl, scatt. factors using approx. model for overlap charge density 9-3298  
 NaF, rel. to dispersion curves determ. 9-1731  
 NaF, scatt. factors using approx. model for overlap charge density 9-3298  
 Ni, by n-irrad. induced voids, small-angle scatt., obs. 9-9718  
 Si, single crystal, interference fringes by an incident plane wave 9-3307  
 $\beta$ -SiC, diffuse 9-1195

**X-ray spectra**

- See also Atmospheric spectra; Chemical analysis/X-ray*  
 chromium halides, continuous spectrum at high freq. limit in band structure and charact. energy loss meas. 9-16210  
 dispersionless anal. of soft rays using differential refl. filters 9-2104  
 divergence and distortion, double crystal spectrometer 9-1756  
 energy spectra for accuracy improvement of correlation factor 9-22024  
 excitation states, Parratt theory, evidence 9-10227  
 forbidden transitions, classification 9-15806  
 forbidden transitions, classification 9-15805  
 glass mirrors, spectra distribution of X-rays reflected in proper absorption region 9-21637  
 inner bremsstrahlung obs. for electron capture decay energy meas., under graduate laboratory expt. 9-12833  
 KX-radiation from atoms, excited by  $\alpha$ -bombard. 9-677  
 muons in nucleus field, energy levels perturbation calc. 9-731  
 Parratt excitation theory, evidence 9-10227  
 pionic and muonic, condensed state effects 9-3909  
 sun, 'Cosmos-166' investigation 9-21960  
 transition metal alloys, variation in number of 3p 3d electrons meas. 9-19877  
 transition metal cpds., metal-like, rel. to electron structure calcs. 9-3912  
<sup>104</sup>Ag, muonic, isotope shift K lines and RMS radius, comparison with opt. spect. 9-6794  
<sup>106</sup>Ag, muonic isotopes shift of K lines and RMS radius, comparison with opt. spect. 9-6794  
 Ag-Sb series, shift of K $\alpha$  lines 9-14066  
 Al, K $\alpha_{1,2}$  satellites, relative intensity 9-18717  
 Cr cpds., metal-like, rel. to electron structure calcs. 9-3912  
 Cu to Se elements, at end of first long period, and electronic struct. of elements 9-14067  
 Ge, primary and fluorescent L $\alpha_1$ , 2 and L $\beta_1$  lines 9-19997  
 Mg, K $\alpha_{1,2}$  satellites, relative intensity 9-18717  
 Na, K $\alpha_{1,2}$  satellites, relative intensity 9-18717  
<sup>23</sup>Na, pionic and muonic 2p-1s transition energy and natural linewidth 9-6813  
 Ni, interferences in the Curie point neighbourhood, temperature dependence 9-5816  
 NiSi<sub>2</sub>, (x=1, 2), alloys, Ni 3d-band structure 9-3911  
 PbO<sub>2</sub>-based polymorphic systems, spectral sensitivity 9-12457  
 Tb, L-spectrum, new lines 9-1822  
 Tb, L emission spectrum, new diagram lines 9-13294  
 Ti cpds., metal-like, rel. to electron structure calcs. 9-3912  
 V cpds., metal-like, rel. to electron structure calcs. 9-3912

**absorption**

- alkali chlorides, Cl<sup>-</sup> L $\alpha_2$  spectra rel. to x-ray exciton, electronic band structure and two electron excitation 9-1815  
 fine structure, extended, model 9-5942  
 lattice sites of atoms of nearly equal X-ray scatt. power, molecular orbital



**X-ray spectra continued**  
**absorption continued**

- methane in 10.50 Å range 9-15955  
molecular orbital theory in interpreting K-absorpt. data 9-14065  
rare earth metals, X-ray absorpt. coeff. determ. for 4d c, N<sub>iv</sub>, v edge studied, 50 500 MeV 9-10228  
review 9-5941  
transition metal complexes, molecular orbital theory interpretation 9-14065  
Be, K-shell, and electron energy loss spectrum for 20 keV e 9-15182  
BeO, K-shell, and electron energy loss spectrum for 20 keV e 9-15182  
Ca metal, K absorpt. fine structure obs. 9-21639  
CaCO<sub>3</sub>, Ca<sup>+</sup> K-absorpt. fine structure obs. 9-21639  
CaO, Ca<sup>2+</sup> K-absorpt. fine structure obs. 9-21639  
CoSe<sub>2</sub>, chemical bonding study 9-20931  
Cu, K absorpt. edge, shift due to chemical combination 9-12454  
Cu fine structure obs. by bent crystal X-ray spectrograph 9-3910  
GaAs, K edge shifts 9-21638  
GaP, K edge shifts 9-21638  
GaSb, K edge shifts 9-21638  
Ge, L<sub>III</sub> lines 9-19997  
Hg L<sub>III</sub> edge of <sup>200</sup>Hg, chemical shift 9-14068  
HgO, L<sub>III</sub> absorption edge of <sup>200</sup>Hg, chemical shift 9-14068  
I, solid L<sub>III</sub> absorpt. spectrograms 9-12455  
InAs, K edge shifts 9-21638  
K<sub>1</sub>, L<sub>III</sub> absorpt. of I, spectrograms 9-12455  
KIO<sub>3</sub>, L<sub>III</sub> absorpt. of I, spectrograms 9-12455  
KIO<sub>4</sub>, L<sub>III</sub> absorpt. of I, spectrograms 9-12455  
K<sub>2</sub>[Ni(CN)<sub>4</sub>].H<sub>2</sub>O, fine structure of Ni K X-ray absorption observed 9-17484  
Mg, ultrasoft X-ray spectra 9-18718  
MgO, L<sub>II,III</sub> band of Mg and K band of O, rel. to energy struct. 9-18586  
MgO, ultrasoft X-ray spectra 9-18718  
MnFe<sub>2</sub>, (Sc<sub>2</sub>O<sub>4</sub>) ferrites, K absorption edge 9-5945  
MnSe<sub>2</sub>, chemical bonding study 9-20931  
MnZn ferrites of stoichiometric compositions, K- boundary, rel. to comp position 9-16079  
N<sub>2</sub>, absorption structure near K edge 9-20932  
NaI, L<sub>III</sub> absorpt. of I, spectrograms 9-12455  
NaIO<sub>4</sub>, L<sub>III</sub> absorpt. of I, spectrograms 9-12455  
Ni<sub>3</sub>Fe<sub>1-x</sub>, <sup>57</sup>Fe<sup>2+</sup> O<sub>K</sub>, K-absorpt. edge obs., comp. dependence 9-21640  
Ni<sub>3</sub>Zn<sub>1-x</sub>Fe<sub>2</sub>O<sub>4</sub> 9-21640  
Ni(CN)<sub>2</sub>.4H<sub>2</sub>O, fine structure of Ni K abs. obs. 9-17484  
NiCl<sub>2</sub>.6H<sub>2</sub>O, fine structure of Ni K X-ray absorpt. obs. 9-17484  
[Ni(NH<sub>3</sub>)<sub>6</sub>].Cl<sub>2</sub>, fine structure of Ni K X-ray absorption observed 9-17484  
NiO, fine structure of Ni K X-ray absorpt. obs. 9-17484  
NiSO<sub>4</sub>.6H<sub>2</sub>O, Ni K X-ray absorption fine structure obs. 9-17484  
Ti L<sub>II, III</sub> lines from pure metal, oxides, nitride, carbide and boride rel. to band structure 9-19999  
Ti L<sub>III</sub> edge of <sup>48</sup>Ti, chemical shift 9-14068  
TiBr<sub>3</sub>, L<sub>III</sub> absorption edge of <sup>48</sup>Ti, chemical shift 9-14068  
Ti(NO<sub>3</sub>)<sub>3</sub>, L<sub>III</sub> absorption edge of <sup>48</sup>Ti, chemical shift 9-14068  
ZnSe, K absorpt. edge shifts rel. to absorpt. in pure metals 9-5947

**emission**

- alkali aluminosilicate, glasses, rel. to chem. bonding 9-1117  
alloys, monovalent, interpret. rel. to electron states distrib. 9-7705  
Fe-Al alloys, parameters, isomeric shift, electron transitions 9-3871  
insulates, excitation by proton bombardment 9-7984  
ionsphere, correlation with auroral light bursts, v.l.f. hiss, obs. (March 1966) 9-14170  
light metals, theory, Green's function method 9-7985  
linewidth meas., three versus two crystal spectrometer 9-1820  
metals, monovalent, interpret. rel. to electron states distrib. 9-7705  
metals, soft X-ray, anomalies in edges 9-1817  
oxide films on Al<sub>2</sub>O<sub>3</sub>, p-irrad. at 100-keV, rel. to surface density effects 9-13575  
oxides, bonding from K-emission spectroscopy 9-13589  
review 9-5941  
silicates, bonding from K-emission spectroscopy 9-13589  
sphalerite, and diamond: type crystals, rel. to complex structure of hole bands 9-1812  
Z=114, 126 and 140, K, L X-ray energies, relativistic calc. 9-4833  
β-excited characteristic X rays intensity, calc. and obs. 9-19996  
Al-Ag alloys, interpretation of soft X-ray spectra 9-15181  
Al, and oxide, K/β satellite lines, theory 9-1819  
Al, K<sub>α</sub> band shape anode potential dependence, 4.5-20 keV 9-1814  
Al, L<sub>2,3</sub> lines, rel. to plasmaron structure 9-5943  
Al in metals and oxides, K<sub>α</sub> X-ray satellites in fluoresc. spectra 9-3933  
Al<sub>2</sub>O<sub>3</sub>, by proton bombardment 9-7984  
Al<sub>2</sub>O<sub>3</sub> (γ- and γ-), OK bands, fine struct. obs. 9-12453  
AlPO<sub>4</sub>, L<sub>2,3</sub> bands rel. to energy struct. 9-5944  
ClO<sub>2</sub> and ClO<sub>4</sub>, electronic struct. determ. 9-7019  
Cr, K and L<sub>III</sub> bands rel. to band structure 9-1821  
CsI:Ti, excitation intensity effect on luminescence 9-16442  
Fe-Si alloys, fluorescence spectra 9-14080  
Ge and Ge:Ga,Sb, comparison 9-1816  
Li, K-spectrum anomalies due to localized holes 9-1817  
Mg, and oxide, K/β satellite lines, theory 9-1819  
Mg, ultrasoft X-ray spectra 9-18718  
Mg in metals and oxides, K<sub>α</sub> X-ray satellites in fluoresc. spectra. 9-3933  
MgO, L<sub>II,III</sub> band of Mg rel. to energy struct. 9-18586  
Mo K<sub>α</sub>, line width meas. with three cryst. spectrometer 9-1820  
Na, applic. of Green's function method 9-7985  
Na, L<sub>2,3</sub> spectrum anomalies due to localized holes 9-1817  
Na in NaF, K<sub>α</sub> X-ray satellites in fluoresc. spectra 9-3933  
Na<sub>3</sub>PO<sub>4</sub>, L<sub>2,3</sub> bands rel. to energy struct. 9-5944  
Ni K<sub>β</sub>/γ lines, effect of chem. bonding 9-19998  
Ni L<sub>III</sub> bands in Ni, Ni-V, Ni<sub>3</sub>Ti and Ni-Ti alloys, structure 9-12456  
P, and oxide, K/β satellite lines, theory 9-1819  
P, red and black, L<sub>2,3</sub> bands rel. to energy struct. 9-5944  
Pb antihode, distrib. in depth 9-5946  
S, and oxide, K/β satellite lines, theory 9-1819  
S L<sub>2,3</sub> bands in sulphates and sulphides rel. to electron transitions and bonds, obs. 9-20940  
S L<sub>2,3</sub> bands rel. to electron transitions and bonds, obs. 9-20940  
Si, and oxide, K/β satellite lines, theory 9-1819  
Si in metals and oxides, K<sub>α</sub> X-ray satellites in fluoresc. spectra 9-3933  
SiO<sub>2</sub>, by proton bombardment 9-7984  
Ti, K and L<sub>III</sub> bands rel. to band structure 9-1821  
Ti and TiC, K- and L- bands rel. to electron struct. 9-10229

**X-ray spectra continued****emission continued**

- Ti antihode, distrib. in depth 9-5946  
Ti L<sub>II, III</sub> lines from pure metal, oxides, nitride, carbide and boride rel. to band structure 9-19999  
Tm, L emission spectrum, five new lines 9-4847  
U, M emission, meas. and comparison 9-6968  
V, K and L<sub>III</sub> bands rel. to band structure 9-1821  
V, VC<sub>0.88</sub>, VN and VO, rel. to electron struct. 9-10229

**X-ray spectrometers**

- See also Gamma ray spectrometers; X-ray crystallography/apparatus  
divergence and distortion, double crystal spectrometer 9-1756  
ESCA, sensitivity enhancement 9-10594  
for microanalysers, design considerations 9-8133  
resolution improved by crystal curvature 9-17677  
spectral 'window', effective size determ. 9-5297  
spectrographic camera, non destructive sample analysis, 0.5-7 Å 9-2432  
three crystal versus two cryst. for linewidth meas. 9-1820  
vacuum, for 1.5-45 nm spectral region 9-18972  
Ge(Li) ultra high resolution spectrometer, 6 keV-2 MeV 9-4679

**X-ray spectroscopy**

- See also X-ray crystallography; X-ray diffraction  
Crab nebula γ emission scan by telescope 9-21858  
dispersionless spectral anal. of soft X-rays, using differential refl. filters 9-2104  
radioactive β emitters 9-15734  
resonance study, high press. low temp., clamp cell meas. 9-12355  
source-target assembly for X-ray spectrophotometry 9-6033  
<sup>125m</sup>Te as X-ray source 9-22023  
KCl:Mn irradiated, u.v. band obs. 9-3893

**X-ray tubes**

- power supply with technique for energizing tubes for single or double operation, patent 9-15397  
rotary target of 0.05-2% Ti/Zr and 98% Mo alloy with W overlayer, patent 9-12818  
W target, ratio of K charact. to total radiation 9-2103

**X-rays**

- See also Cosmic rays/X-rays; Gamma rays  
from air discharges at atmos. pressure 9-5094  
calibration of Ge(Li) detector by muons 9-19234  
from deuterium plasma, laser produced 9-18293  
emission from e excited targets, computational methods 9-8337  
emission in vacancies in K and L shells of atoms, radiative decay rates 9-18132  
Monte Carlo transport codes, effect of e. momenta in calcs. 9-4260  
muonic from <sup>208</sup>Pb, weak transitions meas., nuc. polarization by μ 9-17009  
from plasma in a mirror field heated by linear turbulent heating 9-2978  
polarization analysis using X-ray monochromator 9-8335  
teaching expts. using radioisotope X-ray source, undergraduate 9-2122  
telescope, grazing incidence, astronomy 9-21986  
x unit of wavelength, history 9-4214  
γ-mesic, 4f-3d and 5g-4f, for nucleus energy, width determ. 9-373  
from He discharges at atmos. pressure 9-5094  
W target tube, ratio of K charact. to total radiation 9-2103

**effects**

- See also Nuclear reactions and scattering due to photons  
anthracene, low energy rays, compared with γ rays 9-6020  
anthracene, photoconductivity 9-3739  
fluorescent screens, random noise 9-12817  
KClO<sub>4</sub>, ClO<sub>2</sub> radical creation, e.p.r. and optical absorption 9-18737  
mammalian cells, survival after exposure to ultra high X-ray dose rates 9-15380  
polymers, carbazole-ring based, e.p.r., rel. to cross linking 9-3965  
proteins, formation of free radicals 9-4013  
radiation hazards from diff. equipment 9-16633  
rat embryo, obs. 9-21992  
sapphire, luminescence under X irrad. 9-1839  
silica, vitreous, ionizing radiation-induced dilatation, impurity effect 9-14961  
teaching expts. using radioisotope source, undergraduate 9-2122  
thiodiglycolic acid, ion formation 9-15202  
Al surface oxide film irrad. causing Al K<sub>β</sub> band shape distortion at anode potential <10 keV 9-1814  
GaAs devices 9-17403  
KBr, coloration process, Frenkel defect production and volume expansion obs. 9-21331  
KBr, volume change due to point defects 9-18460  
KBr-KCl mixed crystals, coloration process, Frenkel defect production and volume expansion obs. 9-21331  
KCl:Ca, thermoluminescence of Z<sub>1</sub> centres after irradiation 9-14088  
KCl, defect production, optical absorpt. meas. 9-18462  
KCl(Ca) crystal coloration mechanism, model 9-14951  
KClO<sub>4</sub>, ClO<sub>2</sub> radical creation, e.p.r. and optical absorption 9-18737  
K<sub>2</sub>Co(CN)<sub>6</sub>, e.p.r. of X-irrad. crystals 9-10278  
LiF, absorption coeff. increase, density decrease 9-5926  
Na<sub>2</sub>HPO<sub>4</sub>.5H<sub>2</sub>O, radicals prod. in irrad. crystals 9-14113  
NaCl, F-colouring 9-3368  
NaCl-Fe system, paramagnetic centres causing complex e.s.r. spectra 9-20023  
PbCl<sub>2</sub>, thermoluminesc. 9-10253  
Xe ionization, ion average charge and abundance determ. 9-11618  
ZnS:Cu, Mn, Cl electroluminescence enhanced 9-10262

**protection see Radiation protection****Xenon**

- accumulation in U, meas. of spontaneous fission decay rate 9-20812  
adsorption and interac. on Cu, 77°K 9-21285  
adsorption of Ne 9-9622  
adsorption on Ni films etched on NaCl 9-17248  
atom, electron scatt. compared with Hg and Ar, rel. to Mott theory and non relativistic approx. 9-19408  
atom, energy loss spectra for keV electrons interaction with electron shell 9-18150  
atom, energy loss spectra for keV electrons interaction with electron shell 9-11398  
atom, excited, time correlation of emitted photons 9-13301  
atomic beam scatt. from Ag(111) 9-3187  
bubbles in Al, distrib. rel. to grain boundary migration 9-657  
chondrite, light dark structure chronology 9-2061

**Xenon continued**

- continuum radiation decay rate 9-926  
 crystal, Debye Waller factors 9-5536  
 crystals, review 9-13567  
 discharge tubes, pulsed, series and parallel connection, obs. 9-11629  
 double current pulse lamp, emission 9-2415  
 elastic constants, at absolute zero, effect of long-range three-body forces 9-11906  
 excitation by e impact, 1470 Å resonance line obs. 9-4853  
 fissionogenic, in chondrites 9-16615  
 gas wake in shock tube, velocity meas. from induced e.m.f. 9-2238  
 ion bombardment of Ge, e. emission and defect formation and annealing 9-18662  
 ion bombardment temp. effect on trapping in oxides and halides 9-19746  
 ion source in arc discharge 9-232  
 ionisation by X-rays, ion average charge and abund. determ. 9-11618  
 ionization, multiphonon, by Nd laser, role of bound states 9-910  
 ionization processes on electron impact 9-14800  
 i.r. laser lines, isotope shift 9-15811  
 liquid, electron pair shower prod. by  $\gamma$  bombard. 9-15584  
 liquid, vapour press. and comparison with that of liq. Ar, Kr 9-11748  
 molar polarizability, temp., density depend. 9-4939  
 optical emission continuum induced by 1470 Å radiation 9-19401  
 photosensitization of HD exchange reaction, mechanism 9-16476  
 plasma, turbulent, elec. conductivity 9-875  
 power spatial transients in thermal reactor, computing algorithm for optical control 9-16982  
 scintillation, light gain in elec. field, geometrical props. 9-689  
 solid, cathodoluminescence in u.v. region 9-1841  
 solid, infl. of lattice anharmonicity on exponential potential parameters 9-16161  
 solid, optical consts. and excitonic struct. from energy loss meas. on electrons 9-7694  
 solid, refractive index rel. to dielec. props., 3612 to 6439 Å 9-7832  
 solid, thermal conductivity temp. depend. for multiphonon interaction 9-15021  
 supersonic jets, intermolecular binding 9-18179  
 Hg-Xe arcs, far i.r. source 9-19564  
 K scatt. in thermal energy range, total cross section meas. 9-11413  
 Xe and Ar mixture, ion pumping effect in ionization tube 9-2354  
 Xe I,  $5p^2(6s+5d)$  and  $5p^2(6p+7p)$  configurations and hyperfine structure 9-20878  
 Xe I, spectrum, isotope shift in visible lines 9-16997  
 Xe III, Hartree-Fock parameters for the  $^1D$  and  $^1S$  terms of configuration  $5s^2 5p^4$  9-9129  
 Xe $^+$ , fine struct. in ioniz. efficiency curves 9-9395

**Xenon compounds**

- bromides, formation in  $\beta$ -decay of  $^{129}\text{IBr}_2$ , Mossbauer effect 9-4016  
 XeO $_2$ F $_2$ , vibr. spectra and structure 9-791  
 (90wt.%)Xe-(10wt.%)CO $_2$  proportional counter gas, pulse shape calcs. 9-19228  
 XeF $_4$  force field, Coriolis coupling, vibration and shrinkage props. 9-14696  
 XeF $_2$ , photoionization and dissociation 9-11617  
 XeOF $_4$  force field, Coriolis coupling, vibration and shrinkage props. 9-14696

**Xerography see Photography****Y-particles see Hyperons/resonances****Yield see Elastic limit; Plastic deformation; Plastic flow****Young's modulus see Elastic constants****Ytterbium**

- atom,  $g$  factors of  $6s6p^3P_1$  and  $6s6p^3P_1$  states 9-15812  
 c.p.r. of dissolved Eu $^{2+}$ ,  $g$ -shift and exchange integral calc. 9-12504  
 photoionization, 1350-2000 Å 9-5065  
 silicate glass coactivation with Ho and Er 9-4476  
 in Ag-Au alloys, Kondo effect 9-9929  
 Yb, i.r. laser emission in vapour 9-2818  
 Yb $^{3+}$ , optical and e.s.r. spectra in CdF $_2$  9-1771  
 Yb $^{3+}$  in CaF $_2$ , covalency evidence 9-11791  
 Yb $^{3+}$  in SrCl $_2$ , e.s.r. 9-1863  
 Yb $^{3+}$  in YVO $_4$ , e.p.r. 9-16461  
 Yb $^{3+}$  paramagnetic scatt. cross section obs. 0.0253 eV 9-4736

**Ytterbium compounds**

- Er $_2$ O $_3$ , magnetic structures 9-17463  
 Eu-Yb, Mossbauer effect 9-7957  
 YbFe garnets, high-field magnetization 9-15154  
 YbH $_2$ , orthorhombic to cubic phase transition, crystallographic study 9-18542

**Yttrium**

- adsorbed atoms in equilib. conc. on W point, elec. field effects 9-21287  
 adsorption on W, and migration and evaporation 9-3216  
 conductivities, elec. and thermal, and thermo-e.m.f., anisotropy, 300-3°K 9-15064  
 metal-semiconductor transition at high pressure 9-18605  
 n.m.r. in metal, 2.2° 300°K 9-12516  
 Zr, positron annihilation rel. to electronic structure 9-18597

**Yttrium compounds**

- YAl-Nd, optical refrigeration 9-1831  
 YVO $_4$ :Nd $^{3+}$ (Dy $^{3+}$ )(Er $^{3+}$ Yb $^{3+}$ ), c.p.r. 9-16461  
 GdVO $_4$ , activated by Sm $^{3+}$ , Eu $^{3+}$  and Dy $^{3+}$ , luminescence spectra 9-20003  
 LaVO $_4$ , activated by Sm $^{3+}$ , Eu $^{3+}$  and Dy $^{3+}$ , luminescence spectra 9-20003  
 Pr-Y alloys, mag. susceptibility rel. to temp. and field strength 9-17449  
 YOH $_3$ :Tb, Tb $^{3+}$  crystal field parameters determ. from fluorescence and absorpt. meas. 9-14019  
 Y-Ce alloys, non dilute, h.c.p., resistance minima rel. to spin-compensated state 9-15063  
 Y $_2$ O $_3$  solid solutions, mech. props. 9-3456  
 Y $_2$ O $_3$  stabilizing additive to ZrO $_2$  ceramics, YO volatilization 9-21252  
 YAl $_3$  garnet, optical phonons by infrared reflection spectra 9-3512  
 Y $_2$ Ln $_2$ Ga $_2$ Fe $_2$ O $_8$ , four magnetic Fe sublattices 9-21591  
 Y Al garnet: Nd $^{3+}$ , luminescence and laser emission, temp. depend. 9-5955  
 Y Fe, magnetoacoustic resonance at 3 and 10-cm bands 9-5557  
 Y Fe garnet:Gd $^{3+}$ , Al $^{3+}$ , and Cr $^{3+}$ , reaction kinetics and mag. props. 9-1688  
 Y Fe garnet:Hf, conduction mechanism by conductivity and thermoelec. power meas. 9-1458

**Yttrium compounds continued**

- Y Fe garnet-type cpds., spin wave theory 9-1690  
 Y Fe garnet, Al-Gd substituted, alignment and microwave props. 9-1685  
 Y Fe garnet, crystal growth from Na $_2$ WO $_4$  melts 9-1150  
 Y Fe garnet, Faraday eff. rotation rel. to mag. field intensity 9-7950  
 Y Fe garnet, Faraday effect, effect of mag. field 9-1740  
 Y Fe garnet, Fe $^{2+}$ -Fe $^{3+}$  equilibrium in flux growth, model 9-1149  
 Y Fe garnet, magnetoelastic waves, excitation and amplification 9-1689  
 Y Fe garnet powder, strain induced by various milling treatments 9-5453  
 Y Ga Fe, magnetoacoustic resonance at 3 and 10-cm bands 9-5557  
 Y Ga garnet, electronic Raman transition selection rules rel. to double group, D $_2$  9-3905  
 YAl garnet:Nd $^{3+}$ , laser efficiency, influence of pump-power level and pump light spectral filtering 9-20526  
 YAl garnet:Nd laser, non-mode-locked, two photon fluorescence displays 9-6527  
 YAl garnet, laser Raman spectra 9-10223  
 Y $_2$ Al $_2$ -Ga $_2$ O $_7$  garnet, cation distrib. 9-11857  
 Y $_2$ Al $_2$ O $_7$ :Nd $^{3+}$ , luminescence and laser emission, temp. depend. 9-5955  
 YAsO $_4$ :Gd $^{3+}$ , e.p.r. 9-21668  
 Y $_2$ ss(Eu, Yb) $_2$ ssAl $_2$ O $_7$ , colour centre formation in optical zone melting 9-1238  
 YF $_3$  garnet, spin Raman susceptibility by means of spin-wave instabilities 9-10143  
 YFe garnet:Hf, characterization of Fe $^{2+}$  9-16388  
 YFe:Tb garnet, Bloch wall ability 9-13975  
 YFe, garnets, nonlinear phenom. during excitation of magnetoelastic waves 9-19970  
 YFe garnet, domain structure and growth defects effects 9-12302  
 YFe garnet, epitaxial, film on YAl garnet, shear wave generation at micro wave freqs. 9-10141  
 YFe garnet, interaction of longitudinal phonons, with spin waves 9-12304  
 YFe garnet, magnetic eqn. of state near Curie point 9-7913  
 YFe garnet, magnetoacoustic resonance 9-16172  
 YFe garnet, magnetoelastic effect 9-12303  
 YFe garnet, nonlinear ferromagnetic resonance instability 9-12495  
 YFe garnet, polycrystalline, magnetostriction effects, control 9-3833  
 YFe garnet, rods, polycrystalline, axially magnetized, magneto-static modes at 9.96 GHz 9-5851  
 YFe garnet, sublattice magnetization by  $^{57}\text{Fe}$  n.m.r. 9-21671  
 YFe garnet, sublattice magnetization calc. by Oguchi method 9-10144  
 YFe garnet diffraction probing of magnetoelastic waves 9-12342  
 YFe garnet rods, magnetoelastic largit. waves, obs. 9-9746  
 YFe garnet rods, parametric amplification of magnetoelastic waves at room temp. 9-14967  
 Y $_2$ Fe $_2$ O $_7$ , Faraday eff. rotation rel. to mag. field intensity 9-7950  
 Y $_2$ Fe $_2$ O $_7$  crystals, elastic wave damping freq. dependence 9-1274  
 YGa garnet:Cr $^{3+}$ , e.p.r. 9-1865  
 YGd garnet, magnetoacoustic resonance 9-16172  
 YMnO $_3$ , dynamic fatigue, rel. to free loads 9-10045  
 Y $_2$ Ni, paramagnetism independ. of temp. 9-3775  
 Y $_2$ O $_3$ :Bi $^{3+}$ , fluorescence spectra 9-3927  
 Y $_2$ O $_3$ :Eu $^{3+}$ , luminescence and emission spectra, crystal field interpretation 9-10205  
 Y $_2$ O $_3$ :Eu(Dy),  $\gamma$ -ray thermoluminescence 9-12478  
 Y $_2$ O $_3$ :Zr dispersions, struct., stability and props. 9-1318  
 Y $_2$ O $_3$ , polycrystalline, Young's and shear moduli, porosity dependence 9-12798  
 Y $_2$ O $_3$ , rare earth traces meas. by X-ray excited fluoresc. spectra 9-16514  
 Y $_2$ O $_3$ , rare earth traces X-ray excited fluoresc., interelement effects, obs. 9-16443  
 YPO $_4$ :Gd $^{3+}$ , cryst.-field determ. by variable-freq. e.p.r. 9-5985  
 YPO $_4$ :Gd $^{3+}$ , zero-field reson. of Gd $^{3+}$  9-8026  
 Y $_2$ TiO $_5$ , orthorhombic, crystal structure rel. to seven- and five-fold coordination 9-7452  
 YVO $_4$ :Gd $^{3+}$ , cryst.-field determ. by variable-freq. e.p.r. 9-5985  
 YVO $_4$ :Gd $^{3+}$ , zero-field reson. of Gd $^{3+}$  9-8026  
 YVO $_4$ :Gd $^{3+}$ , e.p.r. 9-21668  
 YVO $_4$ :Gd $^{3+}$ , e.p.r. 9-21668  
 YVO $_4$ , activated by Sm $^{3+}$ , Eu $^{3+}$  and Dy $^{3+}$ , luminescence spectra 9-20003  
 YVO $_4$ , Verneuil growth 9-18417  
 YnBTiO $_6$ :Nd/NbTiO $_6$  photo studies of system 9-18538  
 ZrO $_2$ :Y $_2$ O $_3$  mixed crystals, H $_2$ O vap. solubility, 900 and 1000°C 9-17335  
 ZrO $_2$ , melting point meas. using solar furnace 9-13557

**Yukawa potential see Field theory, quantum/meson field; Nuclear forces; Scattering****Zeeman effect**

- chalcopyrite, splitting in Mossbauer spectra, 80 700°K 9-5889  
 chlorobenzene,  $^{35}\text{Cl}$  n.q.r. 9-8049  
 formic acid, and Stark Zeeman effect on rotational lines 9-2909  
 ions in cubic crystals, intensities for  $\Gamma_6 \rightarrow \Gamma_4$  and  $\Gamma_7 \rightarrow \Gamma_8$  transitions 9-5895  
 methyl iodide, rotational 9-2910  
 molecules, linear and asymmetric-top, microwave rot. spectra,  $\lambda=1-10\text{cm}$  9-11435  
 normal triplet, polarization rel. to Faraday rotation, appl. to sunspot study 9-12769  
 polarization Stokes params. 9-2276  
 Schrodinger many-particle operator with combined Zeeman and Stark eff. 9-20330  
 spinless two-body system, exact theory 9-14664  
 thyristor modulator for n.q.r. spectroscopy 9-6441  
 Zeeman quadrupole spectra obs. in 2,4-dichloroaniline 9-20958  
 $^{201}\text{Hg}$  atoms, degeneracy under non resonant light radiation 9-11393  
 CaF $_2$ :Gd $^{3+}$ , of Gd $^{3+}$  in sites of cubic symmetry 9-10196  
 CaF $_2$ :Eu $^{2+}$  and fluorescent lifetime meas., temp. depend. 9-14050  
 p-Cl $_2$ - $\phi$ , intensity rel. to static mag. field 9-15211  
 Cs $_2$ UBr $_3$ , rel. to vibronic and electronic structure 9-7972  
 Cs $_2$ UCl $_3$ , rel. to vibronic and electronic structure 9-7972  
 CuCl, on excitonic refl. spectrum, low temp. 9-14044  
 CuFeS $_2$  (chalcopyrite), splitting in Mossbauer spectrum, 80-700°K 9-5889  
 GdCl $_3$ :Er $^{3+}$  9-3888  
 IQ switched laser, energy increase by Zeeman splitting 9-19147  
 RbI magnetoreflection dichroism, Zeeman effect irregularity 9-7949  
 RbMnF $_3$ , antiferromag., doublet splitting, low temp 9-1795  
 SO radical, in microwave spectrum of J, K=0, 1-1, 0 and 2, 2-2, 3 rot. transitions 9-13399  
 SnO $_2$ , exciton, intrinsic, symmetry 9-1433  
 SrF $_2$ :Sm $^{2+}$ (Eu $^{2+}$ ), of vibronic transitions 9-10212

**Zener diodes see Semiconducting devices/diodes**



**Zener effect** *see* **Metals; Semiconducting materials; Semiconductors****Zeta-potential** *see* **Electrokinetic effects****Zinc**

- alloying of Cu effects on brittle fracture 9-9772  
corrosion by  $\text{CuSO}_4$  9-20057  
de Haas-van Alphen effect in pulsed mag. field, oscillation amplitudes meas. 9-10094  
deformation at high strain rates 9-18512  
diffusion in Cu and resulting dislocation arrangements from etch-pit exam. 9-5359  
diffusion in GaAs, mechanism 9-16111  
diffusion in liquid Ga 9-13516  
diffusion in ZnTe 9-14960  
dislocation, mobility in  $\{112\} \langle 11\bar{2}3 \rangle$  slip system 9-5371  
dislocations, in basal slip,  $\{10\bar{1}2\}$  twins, incorporation 9-18474  
dislocations in chemically attacked crystals, Berg-Barrett X-ray obs. 9-19749  
ductility and strength depend. on hydrostatic press. and temp. 9-5478  
electron-phonon mass enhancement, determ. pseudopot. approaches 9-13827  
etch pits slope 9-21341  
excitation of  $4s5s^2S_1$  level, cascade transition line intensities obs. 9-9134  
fracture, brittle, effects of alloying 9-9772  
galvanomagnetic props., anomalous size effects caused by compensation 9-13848  
in GaP, thermal ionization energy 9-5696  
heat of chemisorption of O<sub>2</sub> 9-17530  
ion beam production by charge exchange with 5-40 KeV p beam 9-233  
lattice dynamics, h.c.p. structure 9-3506  
liquid, effective ion ion interaction and dielectric screening 9-18350  
magneto-oscillatory effect analysis by Fourier method 9-16219  
molten, sound absorpt. temp. depend. showing existence of dilational viscosity 9-5163  
oxide film growth and thermal rad. props. 9-19985  
plastic deform. and rupture for forbidden basal slip 9-11932  
positron annihilation radiation from single crystals, 250°C, angular correlation 9-1449  
Raman scattering by optical modes, linewidths temp. depend. 9-12442  
slip relation for basal glide, primary and secondary, in single crystals 9-3345  
solid-vapour surface free energy, anisotropy from inert gas bubble shapes 9-21257  
solid soln. in Ag, thermoelec. power 9-1604  
stopping of slow recoil Cu atoms 9-19875  
structure of liq. from n diff. expts. 9-14011  
u.s. attenuation in normal and superconducting material 9-1381  
vapour, vacuum u.v. spectrum, photo- and auto-ioniz. proc., abs. cross-section meas. 9-13453  
X-ray spectra and electronic structure 9-14067  
Bi-Zn binary liquid metal mixture, critical inelastic slow neutron scatt. 9-19607  
Cu-Zn alloy, elastic moduli var. with annealing time 9-9738  
GaP-Zn, Fermi levels as a function of hole concentration function, 1040°C solid solubility isotherm of Zn 9-7715  
liquid, structure and elec. props. 9-7248  
in Si, low ionization energy levels, existence problem 9-15058  
in Sn, impurity effect on critical-field curve 9-9961  
in Sn, impurity effect on residual resistivity anisotropy, ideal resistivities and deviations from Matthiessen's Rule at 77° and 273°K 9-9962  
 $\text{Zn}^{2+}$ -vacancy complex formation, free energy of association from solubility data 9-17277  
Zn II lines de-excitation in pulsed discharges with Zn bimetal electrodes, obs. 9-15963  
 $\text{Zn}^-$  in Ge, excitation spectrum and stress behaviour 9-7974  
 $\text{Zn}^+$  mobility calc. in parent vapour 9-5067  
 $\text{Zn}^{2+}$ , complex combinations with the ions  $\text{SO}_4^{2-}$ ,  $\text{Cd}^{2+}$  SCN and the amines aniline, benzidine,  $\beta$ -naptyl-amine, o-toluidine and m-toluidine, infrared spectra 9-6969  
 $\text{Zn}^{2+}$  diff. in cubic  $\text{Li}_2\text{SO}_4$ , 600-800°C 9-17288

**Zinc compounds**

- brass, (70/30), fracture behaviour rel. to grain size, pre-strain and strain rate 9-19806  
 $\alpha$ -brass, f.c.c., fatigue mechanism at u.s. freqs. 9-13735  
 $\alpha$  brass, stress dependence of dislocation velocity 9-5358  
complexes of triphenylphosphine, i.r. spectra 9-20944  
halides, vibration spectra and thermodynamics 9-792  
methacrylate, postirradiation polymerization 9-21691  
Sn-Zn, striations, lineage structures, melt-grown crystals 9-1225  
zinc-blende, second order Raman-laser spectrum 9-12421  
Zn complex, tris (2-dimethylaminoethyl) aminezinc (II) bromide, crystal structure 9-3299  
ZnS, hexagonal-cubic phase transform. kinetics 9-14994  
.ZnTe, cyclotron resonance from thermally excited holes 9-3635  
Ag-Zn alloys, stacking fault energy meas. by different techniques 9-13694  
Ag-Zn alloys characteristic temp., Gruneisen eqn., Debye function 9-19861  
Al-Zn-Mg alloy, kinetics of clustering 9-7600  
Al-(10wt.%)Zn, infl. of Su addition on ageing characts. 9-17329  
Al-(78 wt.%)Zn, alloy, superplasticity, mechanism 9-21370  
Al-(20 wt.%)Zn, alloy triple point cracks, nucleation and growth 9-3448  
Al-(0.3at.%)Zn alloys, recovery of resistivity in stages II and III after 2-MeV e. irradi. 9-9696  
Al-Zn alloy, dilute, n.m.r. of  $^{27}\text{Al}$ , quadrupole structure 9-12508  
Al-Zn alloy, superplastic state 9-21369  
Al-Zn alloys, rhombohedral distortion of transition phase, Zn content effect 9-7604  
Al-Zn eutectic alloys, preferred orientation development during growth 9-1123  
Al-Zn precipitation reversion studies, miscibility gap for Guinier-Preston zones obs. 9-21393  
Al-(4.4 at.%)Zn-(0.3 at.wt.%)Be, alloy, Be-vacancy interaction 9-9701  
Al-6.7 at.% Zn alloys, Guinier-Preston zones, formation and reversion 9-13626  
Cd-Sb-Zn system solid solution formation, structure and thermo-e.m.f. 9-19835  
Cd-Zn alloy, carrier scatt. between adjacent branches of hole surface 9-12106  
Cu-Ni-Zn alloys, yield point and plastic deformation rel. to degree of ordering 9-19794

**Zinc compounds continued**

- Cu-Zn, alloy,  $\alpha_1$ -plates, morphology and crystallography correlation 9-11842  
 $\beta_1$ -Cu-Zn alloy, martensitic transformations, effect of n irradiation, heat treatment and deform. 9-5512  
Cu-Zn alloys, characteristic temp., Gruneisen eqn., Debye function 9-19861  
Cu-Zn specific resistance for different compositions 9-1464  
Cu-(30 at.wt%)Zn alloy, shock-induced deform. faults 9-13681  
Fe-Si-Zn system, constitution anal. using mag. and X-ray techs. 9-11975  
film, electroluminescence, excitation mechanism 9-5974  
Mg-(3 wt.%)Zn, clustering kinetics and precip. 9-5505  
Ni-Zn-Co alloy Procopiu effect in bar sample 9-3832  
Sn-Zn molten, foreign diff. coeffs. 9-17201  
Zn-Al alloy, superplastic, microstructure and mech. behaviour 9-11858  
Zn-Al solid solutions, resistivity during precipitation 9-21480  
 $\text{Zn}_2\text{TiO}_4$ :Mn phosphor, spinel struct., co-ord. of  $\text{Mn}^{2+}$  luminesc. centres 9-20005  
 $\text{Zn}_x\text{Hg}_{1-x}\text{Te}$  solid solutions, energy band structure 9-7716  
 $\text{ZnAl}_2\text{O}_4$ : $\text{Cr}^{3+}$ , optical absorption and fluorescence spectrum 9-18708  
 $\text{ZnAs}_2$ - $\text{Cd}_3\text{As}_2$  system, solid-soln. growth and semicond. props. 9-13882  
 $\text{ZnAs}_2$ , tetragonal, reflectivity spectra 9-19983  
 $\text{ZnBr}_2$ , vaporization 9-7306  
 $\text{ZnCl}_2$ -KCl liquid, u.s. vel. obs. 9-986  
 $\text{ZnCl}_2$ , vaporization 9-7306  
 $\text{ZnF}_2$ , rutile structure, vibrational spectra, critical dipole frequency behaviour 9-18549  
 $\text{ZnF}_2$ :rutile structure, vibrational spectra, critical dipole frequency behaviour 9-7636  
 $\text{Zn}_x\text{Fe}_{1-x}\text{Te}$ , elec. conductivity in strong microwave fields 9-12092  
ZnI<sub>2</sub> apparent molar expansibility and volume obs. 9-986  
ZnI<sub>2</sub>, vaporization 9-7306  
 $\text{ZnIn}_2\text{S}_4$ :Nd<sup>3+</sup> or Er<sup>3+</sup> fluorescence 9-14081  
 $\text{ZnIn}_2\text{Te}_4$ , photoconductivity 9-3732  
 $\text{ZnMn}_2\text{Fe}_{2-x}\text{O}_4$  charge distrib. from Mossbauer spectra 9-1119  
 $\text{ZnNH}_4\text{PO}_4$ , crystal lattice structure of two forms 9-21322  
 $\text{ZnO}:\text{Mn}^{2+}$ , e.s.r. spectra at 9.5 and 36 kMc/s 9-1867  
 $\text{ZnO}:\text{Li}$ , radiation-induced paramagnetic centre structure 9-1868  
ZnO, crystal, electroreflectance study of space charge layers, conductivity depend. 9-16290  
ZnO, decay times of u.v. and green emission lines 9-1826  
ZnO, diffusion improved by exposure to radiation, patent 9-21354  
ZnO, red, e.p.r. characterization 9-3962  
ZnO, sintering, densification and grain growth 9-19825  
ZnO, sintering, density decrease and pore growth during final stage of process 9-19826  
ZnO, sintering under applied pressure, time-temp.-density relations 9-7593  
ZnO, zincite, Fe entry during hydrothermal growth 9-18419  
ZnO, Zn excess, optical and elec. props. 9-14059  
ZnO:Si resin electrophotographic films, characts. 9-15564  
ZnO films, structure and props. control during growth process from super-saturated condensate current 9-1103  
ZnO isotopically enriched, for  $^{69}\text{m}\text{Zn}$  prod. 9-18075  
ZnO layers, cathode-deposited, crystal structure rel. to prep. conditions 9-1102  
ZnO polarization, spontaneous estimation from refractive indices and Pockels coeff. 9-7936  
ZnO single crystal, differential capacitance between nonsymmetric contacts 9-17428  
ZnO thin films, growth and electrical resistivity 9-5252  
3 ZnO.P<sub>2</sub>O<sub>5</sub>.4H<sub>2</sub>O (opetie) cryst. grown from ZnPO<sub>4</sub> cements in humid atm. 9-3233  
ZnP<sub>2</sub>, tetragonal and monoclinic, reflectivity spectra 9-19983  
ZnP<sub>2</sub>O<sub>4</sub>, monoclinic, crystallographic data and polymorphism 9-5324  
ZnS:Pt:Cs forward biased Schottky barrier, electron emission 9-16317  
(ZnS-CdS):Cu, recombination luminescence, temp.-time depend. 9-15185  
ZnS Cu, luminophors, temperature dependence of three kinds of the Gudden-Pole effect 9-5959  
ZnS-Cu, luminophors, dependence of three kinds of the Gudden-Pole effect on the light sum 9-5960  
ZnS-Cu phosphors, effect of coactivators 9-3930  
ZnS, birefringent striation in a faulted crystal, phenomenological explanation 9-3859  
ZnS, internal friction, amplitude depend. 9-5429  
ZnSag, scintillation due to  $\alpha$ -particles, amplitude elec. field dependence 9-3937  
ZnS(Ag) single crystals photo luminescence obs. 9-12468  
ZnSb-constantan semi-conductor thermoelements; diffusion phenomena and phase transitions, X-ray microprobe analysis 9-10062  
ZnSb, elec. and thermoelec. props., anisotropy 9-9923  
ZnSb, optical reflectivity spectra, 300° and 77°K 9-14042  
ZnSe-Mn thin films, electroluminescence 9-20009  
ZnSe, anomalous electro-reflectance signals near fundamental edge 9-16409  
ZnSe, band structure, Green's function method calc. 9-21467  
ZnSe, electroluminescence in low-resistivity crystals 9-5973  
ZnSe, exciton emission oscs in excitation spectra 9-12489  
ZnSe, excitons interactions with opt. phonons in photoconductivity 9-10069  
n-ZnSe, piezoresistance and piezo- Hall effect 9-5693  
ZnSe, reflectivity, electronic band structure computation rel. to freq. 9-18701  
ZnSe, X-ray K absorpt. edge shifts rel. to absorpt. in pure metals 9-5947  
ZnSe cathodoluminescence by scanning electron microscope in single crystals 9-3944  
ZnSe epitaxial films, photoluminescence 9-5956  
ZnSe resonant Raman eff. 9-12411  
ZnSe unactivated single crystals, luminescence,  $\lambda_m=0.63 \mu$  band 9-14079  
ZnSe:Te<sub>1-x</sub> p-n junctions, diffusion barriers for native acceptor defects 9-10016  
 $\text{ZnSn}(\text{OH})_6$ , crystal structure from n. diff., i.r. absorpt. and n.m.r. 9-19709  
 $\text{ZnSnP}_2$ , chalcopyrites and sphalerites, band structure from optical spectra 9-5931  
 $\text{ZnSnP}_2$ , i.r. reflection spectra and optical constants of chalcopyrite and sphalerite structures 9-5904  
 $\text{ZnSnP}_2$ , position of P-atom in ordered struct., Debye temp., Hall mobility 9-3310



**Zinc compounds continued**

- ZnTe:Al alloyed junctions, injection electroluminescence 9-15194  
 ZnTe, electronic structure from photoemission obs. 9-7866  
 ZnTe, isoelectronic oxygen trap from isotopic substitution and Zeeman expts. 9-18723  
 ZnTe, self-diffusion of Zn and Te 9-14960  
 ZnTe band structure, Green's function method calc. 9-21467  
 ZnTe epitaxial films on CdS, prep. by vapour transport method 9-5245  
 ZnTe junctions, electroluminescence 9-7997  
 ZnTe with photo-n-p junctions, light-emitting mechanism 9-10083  
 ZnWO<sub>3</sub>:Cu<sup>2+</sup>, e.p.r. line half-width, angular dependence 9-1866  
 ZnWO<sub>3</sub>:MnWO<sub>3</sub> system, e.p.r. spectrum of Mn<sup>2+</sup>, 1.5° to 300°K 9-5989  
 ZnWO<sub>3</sub> absorpt. and i.r. emission of Cr<sup>3+</sup> ions, theory 9-14058  
 ZnWO<sub>3</sub>:Co<sup>2+</sup>, mag. props. anisotropy, 4.2-100°K 9-16326  
 Zn<sub>2</sub>Y, anisotropy of paramagnetic line point 9-12248  
 Zn-Al alloy, superplasticity 9-3428  
 ZnO, acoustoelec. eff., Brillouin scattering study at microwave freq. 9-12013

**zinc sulphide**

- absorption, two-photon, depend. on orientation of polarized light and crystallographic axes 9-21631  
 activatorless luminsors, band edge emission, electro- and photoexcitation 9-10233  
 band structure, Green's function method calc. 9-21467  
 built-in field formation in I-V charact., rel. to cry. defects 9-15093  
 crystal structure, obtained from melt under 50 atm. pressure, X-ray investigation 9-5329  
 diffuse patterns in slow e diff. from cleaved faces 9-9607  
 electroluminescence, i.r. enhanced, temp. depend. 9-14095  
 electroluminescence, polarization, field depend. of radiation energy 9-15191  
 electroluminescence, positive-hole lifetimes and i.r. enhancement 9-14094  
 electroluminescence frequency charact. rel. to CuCl and Mn doping 9-3941  
 electroluminescence of Cu, polarization effect 9-21499  
 electroluminescent, electron emission meas. 9-16446  
 electron microscope obs. 9-7453  
 luminsors, electroluminescence enhanced by X-irradiation 9-10262  
 phosphor, electroluminescence brightness wave-current relations 9-12487  
 phosphors, broad-band luminescences 9-5957  
 phosphors, broad-band luminescences characteristics of pair emission types 9-5958  
 phosphors, electroluminescence on short-pulse excitation 9-12486  
 phosphors, i.r. luminescence and role of cation vacancies 9-12467  
 plexiglass n detector, coord. with Basson type 9-659  
 polarization, spontaneous estimation from refractive indices and Pockels coeff. 9-7936  
 Raman spectra, Brillouin zone scattering 9-12440  
 recombination luminescence, temp.-time depend. 9-15185  
 thin films, optical phonons by e tunneling obs. 9-9814  
 twist boundaries and rotational slip 9-3348  
 two-photon absorption spectrum 9-12388  
 ZnS:Cu, electroluminescence ageing mechanism 9-1844  
 ZnS, hexagonal-cubic phase transform. kinetics 9-7616  
 crystals grown, Zn or S vapour excess, I carrier, luminescence meas. 9-21345  
 doped single crystal, induced i.r. absorption spectra obs., 1-3μ 9-10213  
<sup>64</sup>LiF:ZnS(Ag) polyethylene scintillation detector for subcritical thermal n flux 9-6723  
 transducer, multilayer piezoelec., method of c axes flipping 9-10055  
 ZnO thin films, optical phonons by e tunneling obs. 9-9814  
 ZnS: Cu, electroluminesc., and photoluminesc. of u.v. rad. 9-7998  
 ZnS:Co(Ni), bond nature effects in stacking faults 9-1796  
 ZnS:Cr<sup>3+</sup>, decay behaviour of photo-induced c.s.r. 9-10290  
 ZnS:Cu, Al, electroluminescent regions, radiation charact. 9-3942  
 ZnS:Cu, Cl thin phosphor film, photodiode effect 9-1570  
 ZnS:Cu, I(Cl, Al or Ga) luminescence, blue-Cu, polarization 9-16449  
 ZnS:Cu, trap levels with electrons excited by modulated light, dynamic study of behaviour 9-17487  
 ZnS:Cu,Al, electroluminescence brightness wave temp. and freq. dependence 9-10260  
 ZnS:Cu electroluminesc. spectra, freq. depend. 9-10259  
 ZnS:Cu electroluminescent capacitors, charact. and current rectification applic. 9-15195  
 ZnS:Cu phosphor prep. 9-7991  
 ZnS:Er<sup>3+</sup>, fluorescence 9-10244  
 ZnS:Mn<sup>2+</sup>, e.s.r., effect of elec. field 9-17499  
 ZnS:Cu,Mn basis of film electrolum. capacitors 9-18653  
 ZnS:Mn(Cu, Cl) films, electroluminescence brightness waves, effect of elec. polarization 9-10261  
 ZnS, wurtzite, effective ionic charge magnitude estimation 9-9631  
 ZnS(Ag) crystals, stability of radiation under bombard of α, e. 9-11139  
 Zn(S<sub>100-x</sub>Se<sub>x</sub>):Cu(I), electro and photoluminesc., comparison of spectra 9-10263

**Zirconium**

- adsorption of bromide, <sup>80</sup>Br nucl. isomers separation 9-18769  
 concentration in Be, Mg, Al, Nb alloys by photoactivation 9-1933  
 crack nucleation and propag. rel. to hydride precipitates and deform. 9-3452  
 diffusion of H examined by means of n radiography 9-11367  
 films on graphite, metallographic exam. 9-13579  
 mass transport, thermal, and electromigration, in β-modification 9-13709  
 paramagnetic susceptibility, Hall effect, elec. resistance, temp. depend. 9-15072  
 reaction kinetics obs. with ZrCl<sub>4</sub> 9-1898  
 single crystals, e beam zone melting 9-11804  
 γ scatt., Thomas-Fermi model for electron binding eff. 9-18146  
 U-Zr-C phase diagram, 1700-2000°C 9-11976  
 with Y<sub>2</sub>O<sub>3</sub> dispersed particles, microstruct., stability and props. 9-1318  
 α-Zr, hydrides precip., and H solid solubility obs. 9-16148  
 Zr, positron annihilation rel. to electronic structure 9-18597  
 α-Zr, self-diffusion 9-5414  
 α-Zr, self and impurity diffusion 9-3389  
<sup>90</sup>Zr irradiated, damage rate and distrib. determ., depend on lattice energy 9-17365  
 Zr-H phase boundaries and lattice params. 0.61-0.66 wt.% H 9-16160

**Zirconium compounds**

- alloys, eff. of alloying mat. on struct. and morphology of thin oxide films forms 9-20051

**Zirconium compounds continued**

- alloys, hydride precipitates, orientation 9-19683  
 alloys oxidation in high temp. H<sub>2</sub>O, irradi. effects, review 9-10343  
 alloys with improved corrosion resistance, composition, patent 9-13745  
 complex of thiocyanate, paper chromatographic method for separation and identification 9-18772  
 Zircaloy-2, annealed, effect of irradi. on strain ageing 9-17330  
 Zircaloy-2, diffusion of Cr and Fe 9-19761  
 Zircaloy-2, hydride precipitation at grain boundaries 9-19754  
 Zircaloy-2 fuel cladding, burst strength rel. to thickness and defects obs. 9-15799  
 Zircaloy-4, dissolution kinetics of dispersed hydride platelets 9-17336  
 zirconia, thermal shock resistance, phase comp. effect 9-13742  
 Zr-Se alloys, hydrided, mech. props. 9-19805  
 neutron diff., temp. depend. 9-19326  
 Al-Zr alloys, age-hardening 9-13762  
 C-Zr alloy, reinforced, commercial development 9-3467  
 Cu-Zr alloys, oxidation by CO<sub>2</sub>, resistance behaviour 9-20049  
 Fe (0.2 wt.%) Zr alloy, deformation mechanisms, 77° to 300°K 9-5458  
 LiF-BF<sub>3</sub>:ZrF<sub>4</sub> system, equilib. phase diagram, 350-1000°C 9-16031  
 Nb-Zr-Ti alloy, thermal expansion, 10-300°K 9-21437  
 Nb (25 at.%) Zr wire, critical surface definition between normal and superconducting state 9-13867  
 Nb Zr alloy deform. effects, X-ray powder diffraction studies 9-11930  
 Nb Zr alloys, oxidation by CO<sub>2</sub>, resistance behaviour 9-20050  
 Nb Zr alloys, superconducting, eff. of hydrostatic pressure on critical current 9-15074  
 Zr (2.5 wt.%) Nb corrosion resistance, cold deformation effect 9-647  
 Zr-Cu, alloy, oxidation resistant for use as a coolant 9-20852  
 Zr-Cu alloys, effect of O<sub>2</sub> on ductile-brittle transition 9-11940  
 Zr-Cu alloys (<5 wt.% Cu), phase transforms after quenching and tempering from β phase 9-11970  
 Zr-Nb alloys, superconducting transition temp., critical field and resistivity 9-18606  
 Zr (2.7 wt.%) Nb, irradiation strengthening, effect of Nb 9-5479  
 Zr-1% Nb alloy, radiation resistance, suitability for high flux reactors 9-6937  
 Zr-Ni(Pd, Cu, Co) alloys, spot-cooled, new non-crystalline phases 9-5523  
 Zr-Pt system, crystal structure of Ti<sub>3</sub>Pt<sub>2</sub> 9-19725  
 Zr-U-H system, phase boundaries by elec. resistivity and thermal expansion meas. 9-14995  
 Zr-V alloy, upper critical field and transition temp. 9-5665  
 ZrB<sub>2</sub>, bend strength and elastic modulus rel. to grain structure 9-1259  
 ZrB<sub>2</sub> irradiated by thermal neutrons investigation of stability 9-1409  
 ZrB<sub>2</sub> protective sheath for thermocouples, production 9-15483  
 ZrC, fast n irradi., fracture and vol. changes, 10<sup>21</sup> n/cm<sup>2</sup> 9-9862  
 ZrC, thermionic emission of pyroelectric coatings 9-5779  
 ZrCl<sub>4</sub> reaction kinetics with Zr obs. 9-1898  
 ZrFe<sub>2</sub>-NaF mixture, melt, solubility of ZrO<sub>2</sub> rel. to ZrF<sub>4</sub> content 9-17194  
 ZrFe<sub>2</sub>, ferromagnetic props. in homogeneity range temp. depend. of Curie temp. and saturation magnetization 9-3799  
 ZrN, dissociation energy, ht. sublimation and formation 9-823  
 Zr1wt.%(Nb, tensile strength and ductility, effect of H<sub>2</sub> and extension rates 9-17313  
 (Zr<sub>0.9</sub>Nb<sub>0.1</sub>)<sub>2</sub>Fe<sub>2</sub>, magnetism study using Mossbauer technique 9-16406  
 ZrO<sub>2</sub>:Al<sub>2</sub>O<sub>3</sub>:SiO<sub>2</sub> system, phase diagrams; for Corhart-ZAC type refractories 9-13784  
 ZrO<sub>2</sub>:Sc<sub>2</sub>O<sub>3</sub>, crystal structures of intermediate phases Zr<sub>2</sub>Sc<sub>2</sub>O<sub>11</sub> and Zr<sub>2</sub>Sc<sub>2</sub>O<sub>12</sub> 9-3311  
 ZrO<sub>2</sub>:Y<sub>2</sub>O<sub>3</sub> mixed crystals, H<sub>2</sub>O vap. solubility, 900 and 1000°C 9-17335  
 ZrO<sub>2</sub>:Y<sub>2</sub>O<sub>3</sub> system, phase diagram 9-1354  
 ZrO<sub>2</sub>, abrasion resistance, rel. to α-Al<sub>2</sub>O<sub>3</sub> 9-3457  
 ZrO<sub>2</sub>:CaO solid solution, CaO volatilization rel. to stabilization of ZrO<sub>2</sub> ceramics 9-21252  
 ZrO<sub>2</sub>:Y<sub>2</sub>O<sub>3</sub> solid solution, YO volatilization rel. to stabilization of ZrO<sub>2</sub> ceramics 9-21252  
 ZrO<sub>2</sub>, low density, monolithic structure for thermal insulation systems 9-3543  
 ZrO<sub>2</sub>, phase transition, high-pressure induced 9-19840  
 ZrO<sub>2</sub> crystal, hydrothermal growth, temp. and solvents effects 9-1139  
 ZrO<sub>2</sub> paper-Mo foil, multi thermal insulation systems 9-3543  
 ZrO<sub>2</sub>, elec. conductivity and thermoelec. power rel. to defects, 800-1600°C 9-3703  
 ZrO<sub>2</sub>, hypostoichiometric, O ion diffusivity, 600-850°C 9-17292  
 ZrO<sub>2</sub>, melting point meas. using solar furnace 9-13557  
 ZrO<sub>2</sub>, O<sub>2</sub> diffusion in growing films, 400-500°C 9-9735  
 ZrO<sub>2</sub>, solubility in NaF/ZrF<sub>4</sub> melts, rel. to ZrF<sub>4</sub> content 9-17194  
 ZrO<sub>2</sub> containing Dy<sub>2</sub>O<sub>3</sub> dispersion, behaviour at high temps. 9-3476  
 ZrO<sub>2</sub> films on Zr in O<sub>2</sub> atm., struct. and epitaxy, 300°C 9-9619  
 (ZrO<sub>2</sub>)<sub>2</sub>P<sub>2</sub>O<sub>7</sub>, thermal decomposition, 1450-1700°C 9-3989  
 ZrSiO<sub>4</sub>, thermal expansion by X-ray diffraction and dilatometric methods 9-5571  
 ZrZn<sub>2</sub>, Invar-type ferromagnet. mag. contrib. to low temp. thermal expansion and Curie temp. pressure dependence 9-21580  
 ZrZn<sub>2</sub>, high purity, ferromagnetism 9-12272

**Zodiacal light**

- cometary contrib. and solar activity effects 9-20239  
 Fraunhofer line profiles, theor., in spectrum 9-12761  
 gegenschein and Earth-Moon libration point L<sub>3</sub> 9-21956  
 night sky polarization, zodiacal cloud model 9-10412  
 observational difficulties due to background brightness near satellite 9-10560  
 polarization meas. and comparison with troposphere scatt. polarized light 9-1938  
 radial velocity meas. 9-17649  
 spectrum, theor. Fraunhofer lines 9-12761

**Zonal heating see Atmosphere/thermodynamics****Zone melting and refining**

- anthracene, using triplet lifetime as monitor 9-5282  
 apparatus, patent 9-14285  
 crystal growth by pulling, diffusion effects 9-19687  
 diffusion into crystal from melt moving in solid phase 9-9649  
 distribution coeff. determ. 9-1140  
 metal, refractory, point-focused e beam appl. 9-9647  
 organic liquid technique 9-7373  
 purification possibility in solid state 9-5278  
 Ge semiconductor thin films, crystallization using SiO<sub>2</sub> and glass coatings 9-3238  
 InSb single crystal 9-1147  
 InSb thin films, e beam heating 9-14893



**Zone melting and refining** continued

- KBr, impurity distrib. coeff. 9-3239
- KCl, after heat treatment, for high purity crystals 9-18423
- KCl, impurity distrib. coeff. 9-3239
- KI monocrystal, removal of  $\text{NO}_3^-$ ,  $\text{NO}_2^-$ ,  $\text{SO}_4^{2-}$  impurities 9-3240
- Mo single cryst., rel. to impurity distrib. 9-5344
- NaBr, impurity distrib. coeff. 9-3239
- NaCl, impurity distrib. coeff. 9-3239
- Si crystals, liq. zone motion in mutually perpendicular thermal and elec. fields 9-9650

Si float zone and pulling 9-9651

Ti-Al,  $\alpha$ -phase, single crystals growth, using electron beam technique 9-11804

Ti, single crystals, growth using electron beam technique 9-11804

$\text{Y}_{2.95}(\text{Eu}, \text{Yb})_{0.05}\text{Al}_5\text{O}_{12}$ , optical method, rel. to colour centre formation 9-1238

Zr, single crystals, growth using electron beam technique 9-11804

**Zone plates** see *Diffraction/light*

**Zoology**

No entries

## Information retrieval

Produced by computer-controlled phototypesetting, these abstracts journals cover the world's periodical, conference and book literature and are extending into the fields of

reports and patents. Alphabetical author and subject indexes are given twice yearly.

**Physics Abstracts (PA)**, fortnightly. Individual members of the American Institute of Physics and the Institute of Physics & the Physical Society receive a privilege price if they order through their society.

**\*Electrical & Electronics Abstracts (EEA)** specialises in electrical and electronics engineering. Published monthly.

**\*Computer & Control Abstracts (CCA)**, monthly, covers computer science and technology, control and automation.

£80 (\$US 192) p.a.

£65 (\$US 156) p.a.

£35 (\$US 84) p.a.

\* Combined subscription to EEA/CCA: £80 (\$US 192) p.a.

## Current awareness

Each 'Current Papers' publishes the full bibliographic reference of every abstract in the corresponding abstract journal and is produced by computer-controlled phototypesetting. Individual members of the IEE, AIP, IEEE,

IPPS and IERE, wherever they reside, can obtain Current Papers at special privilege prices if they order through their own society.

**Current Papers in Physics (CPP)**.  
Fortnightly

**Current Papers in Electrical & Electronics Engineering (CPE)**. Monthly

**Current Papers on Computers & Control (CPC)**. Monthly

£4 (\$US 10) p.a.

£7 10s. (\$US 18) p.a.

£5 (\$US 12) p.a.

## CUMULATIVE INDEXES

*Physics Abstracts*—author index for the five years 1955–59 inclusive, bound in one volume, stiff covers and buckram cloth, 750 pp.

£20

*in preparation*

*Physics Abstracts*—subject index for the five years 1955–59 inclusive, bound in one volume, stiff covers and buckram cloth 800 pp.

£20

*Physics Abstracts*—author index for the five years 1960–64 inclusive, bound in four parts, stiff covers and buckram cloth, 2300 pp.

£17 set

*Members: £10 set*

*Physics Abstracts*—subject index for the five years 1960–64 inclusive, bound in two parts, stiff covers and buckram cloth, 2550 pp.

£40 set

*Physics Abstracts*—author index for the four years 1965–68 inclusive, bound in two parts, stiff covers and buckram cloth, 2000 pp.

£25 set

*Physics Abstracts*—subject index for the four years 1965–68 inclusive, bound in three parts, stiff covers and buckram cloth, 3300 pp.

£60 set

*in preparation*

*Electrical Engineering Abstracts*—author index for the five years 1955–59 inclusive, bound in one volume, stiff covers and buckram cloth, 389 pp.

£20

*Electrical Engineering Abstracts*—subject index for the five years 1955–59 inclusive, bound in one volume, stiff covers and buckram cloth, 320 pp.

£15

*Members: £9*

*Electrical Engineering Abstracts*—author index for the five years 1960–64 inclusive, bound in two volumes, stiff covers and buckram cloth, 970 pp.

£12 10s. set

*Members: £7 10s. set*

*Electrical Engineering Abstracts*—subject index for the five years 1960–64 inclusive, bound in one volume, stiff covers and buckram cloth, 950 pp.

£20

*Members: £12*

*Electrical Engineering Abstracts*—author index for the four years 1965–68 inclusive, bound in one volume, stiff covers and buckram cloth, 1000 pp.

£20

*Electrical Engineering Abstracts*—subject index for the four years 1965–68 inclusive, bound in two parts, stiff covers and buckram cloth, 1800 pp.

£35

*in preparation*

*Control Abstracts*—author and subject index combined for the three years 1966–68 inclusive, bound in one volume, stiff covers and buckram cloth, 380 pp.

£15

Subscription renewals, orders, inquiries and changes of address should be sent as follows:

(1) For **Physics Abstracts** and **CPP** from AIP members, wherever they reside, and from the public in the Americas, to the Subscription Department, American Institute of Physics, 335 East 45th Street, New York, NY 10017, USA. Please allow six weeks' notice for changes of address. Send both old and new addresses and include an address label from a recent issue.

(2) For **Electrical & Electronics Abstracts**, **Computer & Control Abstracts**, **CPE** and **CPC** from IEEE members, wherever they reside and from the public in the Americas, to the Fulfillment Manager, Institute of Electrical & Electronics Engineers Inc., 345 East 47th Street, New York, NY 10017, USA.

(3) For all subscriptions not covered by (1) and (2) above, and for all **Cumulative indexes**, to IEE, Savoy Place, London WC2, England. Telephone 01-240 1871, Telex 261176, Telegrams Voltampere London WC2.

All other correspondence should be sent to: IEE Publishing Department, PO Box 8, Southgate House, Stevenage, Herts., England. Telephone Stevenage 3311 (s.t.d. 0438 3311), Telex 261176, Telegrams Voltampere Stevenage.



## Periodicals

**Proceedings IEE**, published monthly, contains papers of industrial and technological interest from engineers and scientists the world over. Each issue comprises three self-contained groups of papers on Electronics; Power; and Control and Electrical Science, and these can be ordered as separate publications—*Electronics Record*, *Power Record*, and *Control & Science Record*.

Subscriptions to *Proceedings IEE*:

£21 p.a. IEE Associates and Associate Members under 28 and  
IEE Students: £2 10s. Other IEE members: £5

Separate copies of individual papers are available when they have been published in the *Proceedings*. Price 2s. each

**Electronics Record** is published every two months, the papers being taken from the two previous issues of *Proceedings IEE*.

£10 p.a. IEE Associates and Associate Members under 28 and  
IEE Students: 25s. Other IEE members: £2 10s.

**Power Record**, quarterly, takes its material from the three preceding issues of *Proceedings IEE*.

£6 p.a. IEE Associates and Associate Members under 28 and  
IEE Students: 15s. Other IEE members: 30s.

**Control & Science Record**, quarterly, includes papers on control and automation and electrical science taken from the three previous issues of *Proceedings IEE*.

£6 p.a. IEE Associates and Associate Members under 28 and  
IEE Students: 15s. Other IEE members: 30s.

**Electronics Letters**, published fortnightly, is an international journal offering speedy dissemination of research and development results in electronics, control and allied subjects, in the form of communications up to about 1200 words in length. Publication is within two to six weeks of receipt, giving the engineer an immediate picture of the latest developments in the field.

£10 p.a. IEE members: £3

**Electronics & Power**, published monthly, is a wide-ranging magazine covering the complete field of interest of electrical, electronics, and control technology by means of articles, product reviews, correspondence, editorial comment and book reviews.

*Electronics & Power*: £8 p.a.  
IEE members: free

**IEE News** is a twice-monthly tabloid newspaper for the professional electrical, electronics and control-systems engineer.

IEE News: £2  
IEE members: free

**Students' Quarterly Journal** is received free of further subscription by all IEE Students, Associates and Associate Members under the age of 30. It caters particularly for the younger member, and specialises in concise, topical articles on the latest advances in electrical, electronics and control engineering.

20s. p.a. Senior members: 10s. p.a.

## IEE Conference Publications

Each conference is organised by one or more of the IEE Divisions, **Power, Electronics or Control & Automation**, or by the **Science & Education Joint Board**. The conferences thus survey the whole ambit of electrotechnology and control.

IEE Conference Publications are internationally recognised as up-to-date, authoritative reviews of development and progress in the various branches of electrotechnology and control with which they deal.

Conference  
Publication  
No.

### 46 International Broadcasting Convention

Part 1, the papers presented: 406 pp. 87 papers. 1968.  
Part 2, the discussion: 108 pp. 8 contributions. 1968.  
Inclusive price £6. members £4

### 47 Nucleonic instrumentation

228 pp. 31 papers. 1968. price £3 10s. members £2 5s.

### 48 Tropospheric wave propagation

251 pp. 31 papers. 1968. price £4 5s. members £2 16s.

### 49 Applications of microelectronics

80 pp. 7 papers. 1968. price £2 10s. members 25s.

### 50 Performance of electrified railways

571 pp. 21 papers. 1968. price £6 10s. members £4 5s.

### 51 Computer-aided design

683 pp. 69 papers. 1969. price £11. members £7 10s.

### 52 Switching techniques for telecommunication networks

482 pp. 103 papers. 1969. price £11 10s. members £7 10s.

### 53 Power thyristors & their application

543 pp. 68 papers. 1969. price £11 10s. members £7 10s.

### 54 Microelectronics

69 pp. 33 papers. 1969. price £5 10s. members £3 12s.

### 55 Computer Science & technology

324 pp. 39 papers. 1969. price £8 10s. members £5 13s.

### 56 Measurement education

167 pp. 32 papers. 1969. price £7. members £4 15s.

Copies and information may be obtained from the  
**Publications Department**  
**IEE, Savoy Place, London WC2**

